Can. J. Chem. Downloaded from www.nrcresearchpress.com by 61.7.252.67 on 09/04/12
For personal use only.

Canadian Journal of Chemistry

Issued by THE NATIONAL RESEARCH COUNCIL OF CANADA

VOLUME 36 JANUARY 1958 NUMBER 1

Symposium on The Structure and Reactivity of Electronically-Excited Species

A REPORT ON A SYMPOSIUM HELD BY THE PHYSICAL CHEMISTRY DIVISION OF THE CHEMICAL INSTITUTE OF CANADA[1]

K. J. LAIDLER AND D. A. RAMSAY

A symposium on the structure and reactivity of electronically-excited species was held at the University of Ottawa under the auspices of the Physical Chemistry Division of the Chemical Institute of Canada on September 5th and 6th, 1957. A number of invited papers were presented, most of these having previously been printed in full and distributed to the participants in advance of the meeting. The sessions were devoted to brief presentations of these invited papers, to presentations of additional work, and to general discussions. A number of the invited papers are being published in the present issue of the Canadian Journal of Chemistry; in this paper we give a general account of the meeting, emphasizing the main matters that were discussed and the main conclusions that were drawn. The papers will be discussed under two main headings, the first dealing with the structures of electronically-excited species and the second with their reactivities.

THE STRUCTURES OF ELECTRONICALLY-EXCITED SPECIES

During recent years considerable efforts have been devoted to the detailed study of the electronic spectra of simple polyatomic molecules. The rapid development of the subject may be seen from the following chronological list of molecules, ions, and free radicals for which rotational and vibrational analyses have been carried out:

Prior to 1940	H_2CO, CO_2^+
1940 to 1950	CS_2, CO_2^+, SO_2, NO_2, ClO_2
1950 to 1957	C_2H_2, HCN, CS_2, H_2CO, CS_2^+, $C_4H_2^+$ 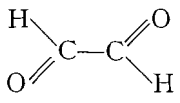 NH_2, HCO, CH_3, HNO

[1]*Manuscript received October 3, 1957.*
Contribution from the Department of Chemistry, University of Ottawa, and the Division of Pure Physics, National Research Council, Ottawa, Canada.
Issued as N.R.C. No. 4538.

There is therefore available at the present time fairly detailed knowledge of the structures of these species in their ground and excited states, and a number of them were discussed at the symposium.

Shapes of Excited Species

An introductory paper dealing with the structures of electronically-excited species was presented by G. Herzberg (National Research Council, Ottawa), who pointed out that the symmetry species and shapes of molecules in electronically-excited states are often considerably different from the corresponding properties in the ground states. For example, C_2H_2, HCN, and CS_2 are linear in their ground states but non-linear in their first electronically-excited states. The free radicals NH_2 and HCO are non-linear in their ground states and linear in their low-lying excited states.

Additional examples of changes of molecular shape or molecular symmetry accompanying an electronic transition were afforded by subsequent papers presented at the meeting. G. W. Robinson and V. E. DiGiorgio (Johns Hopkins University, Baltimore, Md.) presented conclusive evidence that formaldehyde is non-planar in its low-lying excited state, and K. Allison and A. D. Walsh (Queen's College, Dundee) showed that a similar deviation from planar symmetry may occur in one or two of the electronic states involved in Rydberg transitions of formaldehyde. G. W. King (McMaster University, Hamilton, Ont.) discussed the absorption spectrum of glyoxal, and showed that while there is probably very little change in molecular geometry during the transition there is a change of molecular symmetry. In the general discussion period Walsh advanced the idea that NH_2 may not be quite linear in its low-lying excited state. The potential-energy curve may have a small potential maximum in the 180° configuration, and this may account for the negative anharmonicity in the bending vibrations.

The experimental data which have accumulated on the shapes of molecules in electronically-excited states have provided striking support for the general accuracy of the extensive predictions made by Walsh in 1953. The general usefulness of these predictions was underlined by the discussions at the meeting.

Theoretical Treatments of Excited States

R. S. Mulliken (University of Chicago) dealt with the molecular orbital method for computing the energies of electronically-excited states. He suggested that we may be at the dawn of a new era of structural chemistry in which it will be possible to make detailed and reliable calculations of energies and other properties. He presented the results of some recent calculations on CO, N_2, C_2H_2, and several molecules of the AB_2 type, and compared the results with experimental data wherever available. The possibility that certain excited states of AB_2 molecules may have unsymmetrical configurations was discussed, and supporting evidence was cited in the case of the ClO_2 molecule, in which the antisymmetric stretching vibration appears to be excited with considerable intensity in the absorption spectrum.

J. W. Linnett (Oxford University) discussed an apparent discrepancy in viewpoint between simple molecular orbital theories as developed by Walsh and hybridized orbital theories as developed by Pauling. According to the former viewpoint the simplest electronic transition may be regarded as due to the transfer of an electron from one orbital to another, and may be accompanied by a considerable change in molecular geometry. According to the latter viewpoint the shapes of molecules are determined by hybridized groups of electrons, e.g. sp^2, sp^3, rather than by individual electrons. The change of

Can. J. Chem. Downloaded from www.nrcresearchpress.com by 61.7.252.67 on 09/04/12
For personal use only.

shape that may accompany an electronic transition should therefore be regarded as indicating a change of hybridization. By considering possible electron distributions in simple molecules such as N_2, CO, and C_2H_2, Linnett showed that the two methods of approach may differ merely in viewpoint rather than in fundamental concepts.

Multiplicities of Excited States

Considerable discussion centered on the question of the multiplicities of the excited states of various molecules. A. E. Douglas (National Research Council, Ottawa) presented some preliminary results on Zeeman effects which strongly suggested that the excited state of the near ultraviolet bands of CS_2 is a triplet and not a singlet as had previously been assumed. G. W. Robinson and V. E. DiGiorgio discussed some very weak bands of formaldehyde which showed a doublet spacing that does not change appreciably with either vibrational excitation or isotopic substitution. They assigned these bands to a singlet–triplet system and suggested that the rather large doublet spacing may be due to a coupling between the electron spin and residual unquenched orbital angular momentum in the molecule. Further work is clearly required, both theoretically and experimentally, on (1) the Zeeman effect in polyatomic molecules, and (2) spin–orbit coupling in polyatomic molecules.

In connection with the multiplicity problem mentioned above some headway might be made if the theoreticians were to form a more definite view about the f values to be expected for "allowed" and "forbidden" transitions, and if the experimentalists were to begin to measure the integrated intensities of various band systems. It would be valuable to have order of magnitude f values from both points of view.

Theoretical work on the intensity of the $^1A_2 \leftarrow {}^1A_1$ bands of formaldehyde was presented by J. A. Pople and J. W. Sidman* (Cambridge University). The bands are forbidden by the electronic selection rules, and electronic–vibration interaction is usually invoked to explain the existence of the perpendicular bands. This explanation, however, cannot account for the appearance of parallel bands, and Pople and Sidman suggested that the intensity of these bands may be due to an electronic–rotational interaction. They calculated an approximate f value, and thus provided a challenge to the experimentalists to obtain the measured value.

Excited States of Ions

An interesting method for obtaining information regarding the excited states of molecular ions was described in a paper by D. C. Frost and C. A. McDowell (University of British Columbia, Vancouver, B.C.). An essentially monoenergetic source was used in a mass spectrometer, and discontinuities in the curves of ion current *versus* electron energy were observed; these discontinuities yielded information concerning the energies of the excited states of the ions. This approach provides a valuable complement to the usual spectroscopic methods, there being very little spectroscopic information available on the electronic spectra of polyatomic ions. The only spectra obtained so far have been in emission, and the only ions for which detailed analyses have been carried out are CO_2^+, CS_2^+, and $C_4H_2^+$. No absorption spectrum of a molecular ion, whether diatomic or polyatomic, has yet been observed in the gas phase.

The spectra of molecular ions have frequently been investigated in the solid phase, and a paper was presented by J. W. Sidman on the emission and absorption spectra of the nitrite ion in the crystalline state at low temperatures. Information was derived

Now at Department of Chemistry, Cornell University, Ithaca, N.Y.

Can. J. Chem. Downloaded from www.nrcresearchpress.com by 61.7.252.67 on 09/04/12
For personal use only.

concerning the vibrational and lattice frequencies for both the ground and excited states, and the results were compared with the predictions made by Walsh for 18-electron AB_2 systems.

Interaction between Electronic and Vibrational Motions

Two of the papers at the symposium described the rather complex interaction between electronic and vibrational motions in polyatomic molecules. M. H. L. Pryce and U. Öpik (Bristol University) and H. C. Longuet-Higgins and R. A. Sack (Cambridge University) dealt with the dynamical Jahn–Teller effect; this paper was concerned with the vibronic energy levels of a non-linear molecule in a doubly-degenerate electronic state which is split in first order by a doubly-degenerate vibrational mode. Theoretical patterns were presented showing the vibrational structures and intensity distributions expected for bands involved in transitions between a Jahn–Teller distorted state and a non-degenerate electronic state. These predictions should prompt experimentalists to obtain data on transitions of this type.

The second paper along these lines was presented by K. Dressler and D. A. Ramsay (National Research Council, Ottawa) and dealt with the Renner effect in linear polyatomic molecules. This work was concerned with the complex vibronic patterns that may arise as the result of the interaction between electronic orbital angular momentum in a linear polyatomic molecule and the angular momentum associated with the bending vibrations. The analysis of the spectrum of NH_2 suggests that the vibronic levels of a hypothetical Π state split into two groups, half of the levels correlating with the vibronic levels observed in the excited state and the other half with vibrational and rotational levels of the ground state. The interpretation of the experimental results involves a considerable extrapolation of the theory originally developed by Renner, and necessitates further theoretical investigations.

The problem of the transfer of electronic and vibrational energies in weakly coupled systems was discussed both theoretically and experimentally in papers by J. N. Murrell (Cambridge University and University of Chicago) and by D. S. McClure (R.C.A. Laboratories, Princeton, N.J.). The general problem of energy transfer is now being attacked using a variety of experimental techniques, such as ultrasonics, flash photolysis, shock waves, and fluorescence quenching, and information is being obtained concerning the probabilities for the conversion of energy from one form to another.

An important problem of interest to spectroscopists, photochemists, and theoreticians concerns the probability of predissociation in polyatomic molecules. Recent spectroscopic work has shown that the probability of predissociation in a polyatomic molecule depends not only on energy and symmetry considerations, as in a diatomic molecule, but on additional quantum numbers that have no counterpart in a diatomic molecule. Recent work on the ultraviolet spectrum of HCN has shown that the probability of predissociation in the non-linear excited state increases with the quantum number for rotation about the axis of least inertia of the molecule. In the linear excited state of HCO the Σ vibronic levels associated with the various vibrational modes have been found to be stable; the Π, Δ, . . . vibronic levels, on the other hand, are predissociated. Theoretical investigation of these new empirical rules is needed.

THE REACTIVITY OF ELECTRONICALLY-EXCITED SPECIES

The section of the symposium devoted to reactivity was introduced by E. W. R. Steacie (National Research Council, Ottawa), who outlined the role played by electronically-excited species in reaction mechanisms, and gave a brief history of the subject

Can. J. Chem. Downloaded from www.nrcresearchpress.com by 61.7.252.67 on 09/04/12
For personal use only.

of reaction mechanisms with special reference to excited states. He pointed out that in the early days of chain reactions excited species, or 'hot' molecules, were introduced in order to explain certain features of the mechanisms, and that in some cases their introduction was without basis. As time goes on, however, we are learning more and more about the detailed nature of the reactions involving these excited species, and in some cases can make reliable identifications of the species. On the whole rather more is known about the part played by electronically-excited species in flames, but knowledge of their role in thermal, photochemical, and photosensitized reactions is rapidly being gained.

H. Eyring (University of Utah, Salt Lake City) gave a broad review of the subject of reactions of electronically-excited species, and emphasized the importance of treating the reactions theoretically in terms of potential-energy surfaces. He discussed from a theoretical standpoint certain processes involving argon ions, and also the interpretation of the mass spectrum of propane.

Theoretical Treatments

Several papers in the symposium were devoted to the theoretical treatment of reactions involving electronically-excited species. R. A. Marcus (Polytechnic Institute of Brooklyn) presented a theory of unimolecular reactions of electronically-excited molecules. He dealt with the process of excitation of a molecule in its ground state to vibrationally-excited states of the electronically-excited molecule, and also the unimolecular breakdown of the molecule formed. The course of this reaction is represented by a motion on a potential-energy surface, the reaction being the passage over a saddle point. Marcus's final expression for the rate of the reaction involves an activation energy that is independent of the frequency of the absorbing light, and a frequency factor that depends on the frequency of the light. The frequency factor for the unimolecular decomposition of an electronically-excited species will in general be smaller than 10^{13} sec.$^{-1}$, the value typical for molecules in their ground states. A second paper by Marcus dealt with the potentialities and limitations of the flash photolysis method for studying the chemical reactions of excited states.

The decomposition of an electronically-excited molecule was also treated by B. Stevens* (Princeton University). It has been concluded by Sponer and Teller that whereas an optical transition in a symmetrical molecule excites the totally symmetric vibrations, it is the non-totally symmetric vibrations that are usually responsible for the dissociation processes. The unimolecular breakdown of an electronically-excited molecule therefore involves an internal redistribution of vibrational energy, and the rate depends on the magnitude of coupling of the optically active (symmetrical) and dissociative (non-symmetrical) vibrations; this coupling will be a function of the anharmonicity and hence of the energy. The implications of this were worked out in some detail by Stevens, who pointed out that the rate of the dissociation process will vary very considerably with the amount of optical energy given to the molecule. If the amount of energy is small there will be little coupling between the two types of vibration, and therefore a low probability of unimolecular dissociation; as the energy is increased the probability of transfer from the optically active to the dissociative vibrations becomes greater, and the rate of reaction is therefore greater.

A paper by E. K. Gill and K. J. Laidler (University of Ottawa) dealt for the most part with the nature of the reaction

$$Hg^*(^3P_1) + O_2(^3\Sigma_g^-) \rightarrow Hg(^1S_0) + O_2^*.$$

In the past there has been some discussion as to the electronic nature of the oxygen

Now at Esso Research and Engineering Co., Linden, N.J.

Can. J. Chem. Downloaded from www.nrcresearchpress.com by 61.7.252.67 on 09/04/12
For personal use only.

formed in this reaction. Gill and Laidler considered both the experimental evidence and the potential-energy surfaces, and showed that both lead to the conclusion that the oxygen formed is in the $^3\Sigma_u^+$ state. This is the highest electronically-excited state of oxygen for which there is enough energy available in the excited mercury, so that in the reaction there has been a minimal transfer of electronic to vibrational energy. The experimental evidence for this conclusion is that inert gases increase the rate of ozone production in this reaction, which they could hardly do if the excitational energy of the oxygen were to a considerable extent vibrational energy; the inert gases would then readily bring about deactivation. The theoretical treatment of the reaction involves the use of the potential-energy surfaces, and when these are constructed it is seen that there is an easy path for the formation of the $^3\Sigma_u^+$ oxygen.

Experimental Studies of Simple Systems

A number of the papers presented at the symposium dealt with experimental studies of reactions of a very simple type; many of them dealt with reactions involving three atoms, reactions that are very simple to treat theoretically. H. E. Gunning* (Illinois Institute of Technology, Chicago) presented the results of a number of experiments on photosensitization by isotopic mercury atoms. The procedure was to excite Hg^{202} ($^3P_1$) atoms in natural mercury vapor, and to cause them to react with substrates that form solid mercury compounds when the photosensitization process occurs. The solid mercury compounds formed were examined to see whether they were enriched in the Hg^{202} isotope. Such enrichment is evidence for the primary formation of the mercury compound. One group of substances used consisted of halides such as hydrogen chloride, methyl chloride, and carbon tetrachloride; these formed Hg_2Cl_2 on photoexcitation, and there was enrichment of the isotope in every case. It therefore follows that the excited mercury reacts directly with the abstraction of a halogen atom. Three substances which form HgO were studied: water vapor, nitrous oxide, and oxygen. There was very slight isotope enrichment in the case of H_2O, but no enrichment at all with nitrous oxide and oxygen.

During the presentation of his paper Gunning referred to the fact that his more recent results had indicated quite different quenching cross-sections for Hg^{198} and Hg^{202} in their $^3P_1$ states. In the discussion period Shuler pointed out that this was a very surprising result since isotopes would be expected to react at approximately the same rate. There was considerable discussion on this point, but no definite conclusions were drawn.

The chemiluminescence in the system atomic sodium plus atomic hydrogen was discussed in a paper by J. D. McKinley, Jr.,† and J. C. Polanyi‡ (Princeton University), the procedure being to allow atomic sodium to diffuse into a mixture of atomic and molecular hydrogen. The results indicated that the reaction giving rise to luminescence is either $Na+Na+H \rightarrow NaH+Na^*$ or $Na+H+H \rightarrow H_2+Na^*$. In the former case the collision yield is 4×10^{-3}, in the latter case 1×10^{-5}; these figures are based on Bodenstein's method of calculating rates of termolecular collisions.

Two papers dealt with the quenching of the iodine fluorescence spectrum, one by C. L. Arnot and C. A. McDowell (University of British Columbia) and the other by J. C. Polanyi (University of Toronto). When iodine vapor is excited by the green mercury line at 5461 Å there is produced a $^3\Pi$ electronically-excited state of iodine in the 26th vibrational level. On collision with foreign molecules these excited iodine molecules may undergo a transition to the 25th and the 27th vibrational levels, and new fluorescence

Now at Department of Chemistry, University of Alberta, Edmonton, Alta.
†*Now at the National Bureau of Standards, Washington, D.C.*
‡*Now at the Department of Chemistry, University of Toronto.*

Can. J. Chem. Downloaded from www.nrcresearchpress.com by 61.7.252.67 on 09/04/12
For personal use only.

bands appear corresponding to transitions from these levels to ground electronic states. In addition there is the possibility of a direct fluorescence of the electronically-excited molecule in the 26th vibrational state, and it is possible to compare the rate constants for vibrational energy transfer (k_t) with those for fluorescence (k_f), for various added gases. Some ratios of rate constants obtained by Arnot and McDowell are as follows:

Added gas	He	Ne	A	O_2
k_t/k_f (liter mole^{-1})	5.31×10^4	2.69×10^4	1.64×10^4	1.5×10^4

On the assumption that the fluorescence lifetime for the excited iodine is 10^{-8} second, these ratios are approximately ten times as great as would be calculated using the collision theory. There are two possible reasons for this discrepancy: the lifetime of the excited iodine may be less by a factor of ten or so, or the rate constants for the transfer processes may indeed be ten times greater than the collision frequencies. In the discussion of this paper Mulliken pointed out that data are probably available for making a calculation of the lifetime of the excited iodine molecule, so that it should be possible to resolve this problem. In Polanyi's investigation of the system the results were somewhat different; transfer in the case of hydrogen molecules, for example, occurred in one out of every four collisions.

Work on the reaction between nitric oxide and oxygen atoms was described by T. M. Sugden and E. M. Bulewicz (Cambridge University) and by F. Kaufman (Aberdeen Proving Ground, Maryland). When small amounts of nitric oxide are added to a system containing oxygen atoms, such as a flame, a greenish continuum is emitted, and this was studied by Sugden and Bulewicz over a range of temperatures and compositions. It has for some time been believed that the continuum is due solely to the process $NO+O \rightarrow NO_2+h\nu$, and that the intensity of the continuum may be used as a measure of the oxygen-atom concentration in a flame. However, the results of Sugden and Bulewicz showed that nitric oxide catalyzed the combinations of free radicals in flames, and that the intensity of the continuum is determined by more complicated processes than a simple combination of NO and O. The intensity may therefore not be used as a measure of oxygen atom concentrations. Various other reactions giving rise to the formation of NO_2* were considered. Kaufman's work provided rate constants for the reaction $O+NO+M \rightarrow NO_2+M$.

G. J. Minkoff (Imperial College, London) dealt with the mechanism of the thermal decomposition of acetylene, with special references to the role played by electronically-excited states of acetylene. It was pointed out that the relatively large reaction rates observed at the beginning of the induction period are not consistent with previous mechanisms involving the intervention of stable dimers, and that in order to explain the kinetics it is necessary to postulate that a diradical is produced on the surface; this diradical then undergoes a polymerization in the gas phase, with some chain ending occurring on the surface. Minkoff postulated that at lower temperatures the triplet diradical formed is in the *trans* configuration

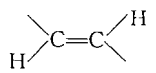

and that this readily undergoes polymerization. At higher temperatures the *cis* form is produced to a greater extent and, owing to the proximity of the hydrogen atoms, readily undergoes dehydrogenation. There was considerable discussion about the nature of the excited states of acetylene, and G. W. King indicated that his work with Ingold showed

Can. J. Chem. Downloaded from www.nrcresearchpress.com by 61.7.252.67 on 09/04/12
For personal use only.

the triplet state of acetylene to be normally in the *trans* form. Mulliken pointed out that the *cis* and *trans* forms should not differ very much in energy.

Elementary Processes in Flames

In addition to that of Sugden and Bulewicz, referred to above, there were two papers dealing with reactions in flames. A paper by H. P. Broida and K. E. Shuler (National Bureau of Standards, Washington) described additional work by these authors on the study of flame temperatures and energy distributions. Their work involved the addition of iron to various flames and a study of the electronic states of the iron, a number of iron lines being examined. The general conclusion was that iron is a good thermometer in that if there is equilibrium in the flame the iron lines provide a reliable temperature for the flame; if on the other hand there is not equilibrium this fact is readily revealed.

T. Carrington (National Bureau of Standards, Washington) described investigations on the electronically-excited ($^2\Sigma^+$) OH radicals in oxyacetylene flames burning at atmospheric and reduced pressures. The results indicate that these electronically-excited radicals are quenched at practically every collision. This is of some interest since non-equilibrium populations of rotational levels of the excited radicals had been observed spectroscopically in certain flames and discharges, and the results have often been assumed to indicate a persistence of the initial rotational distribution. It has been assumed that the OH radicals remain in the excited state for the normal radiative lifetime of the electronic transitions (6×10^{-6} second), and therefore undergo at atmospheric pressure about a thousand collisions before radiating. Carrington's discovery that the quenching efficiency is very high indicates, however, that this cannot be so: the electronically-excited radicals have no chance to undergo a series of collisions. The non-equilibrium distribution cannot therefore be due to the persistence of the rotational levels, and must correspond to the distribution existing when the OH radicals are initially formed. A possible mechanism for the production of abnormal populations of OH* in flames and in discharges through water vapor was suggested by Broida; his explanation is based on the idea, due originally to Niira, that electronically-excited H_2O^* dissociates into OH* ($^2\Sigma^+$) with excess rotational energy. In flames, according to Broida, the excited H_2O is produced in the reaction

$$C + O + H_2O \rightarrow CO + H_2O^*.$$

Reactions of More Complex Molecules

Several papers dealt with reactions involving polyatomic molecules, including the one by Stevens discussed above. J. Heicklen and W. A. Noyes, Jr., (University of Rochester) and H. Okabe (National Research Council, Ottawa) dealt with reactions involving electronically-excited ketone molecules. Heicklen and Noyes showed that the primary processes for simple ketones, such as acetone, are essentially as follows:

(1) The initial absorption of radiation gives rise to a singlet-excited ketone, the vibrational energy of which depends upon the wave length.

(2) Some of the initially excited molecules dissociate, the number depending upon the wave length and the pressure. Others lose vibrational energy by collision to reach the lowest vibrational level of the upper singlet state.

(3) Molecules in the lowest vibrational level in the singlet state may either fluoresce or be converted into a triplet state which rapidly passes into its lowest vibrational level.

(4) Phosphorescence may occur from the lowest vibrational level of the triplet state, but dissociation may occur if molecules are raised to higher vibrational levels of this state.

Can. J. Chem. Downloaded from www.nrcresearchpress.com by 61.7.252.67 on 09/04/12
For personal use only.

There are therefore two methods of dissociation, one of which depends on wave length but only slightly on temperature, the other only slightly on wave length but greatly on temperature. Some work with biacetyl, $CH_3COCOCH_3$, was described, and it was shown that at 4358 Å the decomposition is due to collision between two triplet-excited biacetyl molecules:

$$2CH_3COCOCH_3^* \rightarrow CH_3COCOCH_3 + CH_3CO + CO + CH_3.$$

When a mixture of acetone and biacetyl is irradiated at 3130 Å the light is absorbed solely by the acetone, but fluorescence of biacetyl has been observed. This is attributed to reactions involving transfer of electronic energy on collision, as follows:

$$CH_3COCH_3^* + B \rightarrow CH_3COCH_3 + B^*.$$

A paper on the fluorescence and photolysis of hexafluoroacetone, CF_3COCF_3, was presented by H. Okabe (National Research Council). The excitation of hexafluoroacetone vapor by light of wave length 3130 Å gives rise to strong fluorescence. The variation of the fluorescence efficiency with pressure and the addition of foreign gases suggest that the fluorescence may be principally from the lowest vibrational level of the short-lived singlet-excited state. It is proposed that the molecule is raised to the upper vibrational levels of a singlet-excited state, and subsequently deactivated to the lowest vibrational level of that state, from which it fluoresces. The molecule in the higher vibrational level can dissociate into C_2F_6 and CO. The over-all reaction scheme proposed to explain the results is as follows:

$$\begin{aligned}
CF_3COCF_3 &\xrightarrow{h\nu} CF_3COCF_3^{*n} \\
CF_3COCF_3^{*n} &\rightarrow C_2F_6 + CO \\
CF_3COCF_3^{*n} &\rightarrow CF_3COCF_3 \text{ (internal conversion)} \\
M + CF_3COCF_3^{*n} &\rightarrow CF_3COCF_3^{*0} + M \\
CF_3COCF_3^{*0} &\rightarrow CF_3COCF_3 + h\nu \\
CF_3COCF_3^{*0} &\rightarrow CF_3COCF_3 \text{ (internal conversion)}
\end{aligned}$$

Here $*n$ denotes the nth vibrational level of the singlet excited state, *0 the lowest vibrational level.

In the discussion period the possibility that the singlet-excited state may pass into a triplet-excited state by internal conversion was discussed in some detail.

Can. J. Chem. Downloaded from www.nrcresearchpress.com by 61.7.252.67 on 09/04/12
For personal use only.

Can. J. Chem. Downloaded from www.nrcresearchpress.com by 61.7.252.67 on 09/04/12
For personal use only.

THE LOWER EXCITED STATES OF SOME SIMPLE MOLECULES[1]

R. S. MULLIKEN

ABSTRACT

The present and prospective rapidly increasing usefulness of good LCAO-MO calculations on the electronic states of simple molecules in the interpretation of observed excited states is pointed out. As examples, the observed and predicted states of, in particular, the $\pi^3\pi$ configurations of N_2 and CO are compared with those of C_2H_2 and HCN and with those of CO_2 and CS_2. Further, the results of LCAO-SCF calculations on CO_2 and on O_3 are surveyed, and it is shown how these can be helpful in interpreting and understanding the ground and excited states of AB_2 (expecially AO_2) molecules in general. A new interpretation of the so-called $d\ ^3\Pi$ state of CO as a case $b\ \pi_u^3\pi_g$, $^3\Delta_u$ state is proposed. Tentative interpretations of some of the ultraviolet absorption spectra of C_2H_2, HCN, and of a number of AB_2 molecules are reviewed or suggested, including some discussion of the shapes of excited states. The AB_2 discussion is a revision of one given earlier. Finally, following up a suggestion of Coon, it is pointed out that there exists strong evidence for slightly unequal A—O distances in certain excited states of ClO_2 and SO_2.

INTRODUCTION

Experience shows that any antibonding MO is much stronger in its effects than its corresponding bonding MO. For example, two H atoms in the $\sigma_g1s\ \sigma_u1s$ state repel, two He atoms ($\sigma_g1s^2\ \sigma_u1s^2$) repel, and two coplanar CH_2 groups in C_2H_4 in its first excited states (configuration . . . $(x+x)(x-x)$ in LCAO symbolism) twist to become perpendicular.[2] Further examples are found in molecules AB_2, where as soon as all bonding (and non-bonding) MOs are filled (as in CO_2, NO_2^+, N_3^-, etc.), addition of further electrons causes bending (as in NO_2, O_3, SO_2, ClO_2, excited CS_2, etc.); this gives relief (with energy-lowering) from otherwise strong antibonding. The writer has discussed the double-bond case (8) and the AB_2 cases (9),[3] and A. D. Walsh (16) has treated the AB_2 and a variety of other cases in a comprehensive series of papers which have given marked impetus to the study of the shapes of excited molecules.

Meanwhile new spectroscopic and other data and theoretical LCAO-MO electronic structure computations provide a basis for increased (though not yet thorough) insight into this field. Some of the new evidence and conclusions are reviewed below, in a discussion of some simple linear molecules, and of AB_2 molecules in general. Emphasis is placed first on observed and computed excited electronic states of the prototype molecules CO, N_2, C_2H_2, and CO_2 all of which if or when linear have a lowest or second-lowest excited configuration of the type . . . $\pi^3\pi$. Attention is then given to the low excited states and non-Rydberg spectra of CO_2 and C_2H_2. Finally, a comparison between theoretical computations on the forms and energies of the LCAO-MOs of CO_2 (180°) and O_3 (120°) throws light on the energies and shapes of the spectroscopically known excited states of CO_2, NO_2, and so on. In some excited states of AB_2 molecules, there is evidence of further loss of symmetry ($C_{2v} \rightarrow C_s$) in addition to bending; this can be understood as giving additional relief from antibonding.

[1]*Manuscript received August 16, 1957.*

Contribution from the Laboratory of Molecular Structure and Spectra, Department of Physics, The University of Chicago, Chicago 37, Illinois. This paper was presented at the Symposium on the Structure and Reactivity of Electronically-Excited Species held at the University of Ottawa, Ottawa, Canada, September 5 and 6, 1957.

This work was assisted by the office of Ordnance Research under Project TB2—0001(505) of Contract DA-11-022-ORD-1002 with the University of Chicago.

[2]*See Mulliken (8). In C_2H_4, the twisting is distinctly assisted by hyperconjugation in the twisted form. This is strong enough so that $C_2H_4^+$, even though no antibonding electron is present, probably is only barely or not quite stable toward twisting (10, 17).*

[3]*The acute-angled O_3 model reluctantly adopted there was forced by the then available knowledge of the infrared spectrum. It does not affect the essential features of the paper.*

Can. J. Chem. Downloaded from www.nrcresearchpress.com by 61.7.252.67 on 09/04/12
For personal use only.

THE LOW EXCITED ELECTRONIC LEVELS OF CO, N_2, AND CO_2

To begin, let us consider theory and experiment for the lowest excited configurations of CO and N_2, then of CO_2. The ground states of N_2 and CO may be described as:

[1] N_2: $(\sigma_g 1s)^2\,(\sigma_u 1s)^2\,(3\sigma_g)^2\,(2\sigma_u)^2\,(1\pi_u)^4\,(3\sigma_g)^2$, $^1\Sigma_g^+$;
CO: $(1\sigma)^2\,(2\sigma)^2\,(3\sigma)^2\,(4\sigma)^2\,(1\pi)^4\,(5\sigma)^2$, $^1\Sigma^+$.

Leaving aside the four inner electrons, the theoretically computed forms and energies (i.e. ionization energies or term values) of the ground-state MOs and of the two atomic-valence-shell excited MOs are described in LCAO approximation in Table I. Especially notable are the considerable hybridization in the σ MOs and the resulting strength of bonding in the lowest energy of these, with corresponding weakness of bonding in the last occupied MO, and great strength of antibonding in the excited σ MO. Similar characteristics are found for all other molecules on which theoretical LCAO-MO SCF computations have been made (e.g. CO_2 and O_3, Table V).

TABLE I

FORMS OF N_2 AND CO MOLECULAR ORBITALS*

Nitrogen			ϵ (ev.)		Carbon monoxide			ϵ (ev.)	
MO	Form†		Obs.	Calc.	MO	Form†		Obs.	Calc.
$3\sigma_u$	$h,\ -h$	(A)			6σ	$h,\ -h$	(A)		
$1\pi_g$	$\left\{\begin{matrix} x, & -x \\ z, & -z \end{matrix}\right\}$	(A)	7‡	6‡	2π	$\left\{\begin{matrix} X, & -x \\ Z, & -z \end{matrix}\right\}$	(A)	6‡	
$3\sigma_g$	$h',\ h'$	(b)	15.6	14.8	5σ	$H',\ h'$	(a)	14.0	13.4
$1\pi_u$	$\left\{\begin{matrix} x, & x \\ z, & z \end{matrix}\right\}$	(B)	17.1	15.8	1π	$\left\{\begin{matrix} x, & X \\ z, & Z \end{matrix}\right\}$	(B)	16.6	16.0
$2\sigma_u$	$sh',\ -s-h'$	(a)	18.7	19.9	4σ	$sh,\ H'$	(b)§	19.7	20.0
$2\sigma_g$	$sh,\ sh$	(B)	—	39.5	3σ	$h,\ sh$	(B)	—	43.4

*Based on: C. W. Scherr (J. Chem. Phys. **23**, 569 (1955)) for N_2, R. C. Sahni (Trans. Faraday Soc. **49**, 1 (1953)) for CO.

†The symbols s; h; h' mean 2s; a 2s, 2pσ hybrid with strong end toward the other atom and positive; and a 2s, 2pσ hybrid with weak end toward the other atom and positive (cf. Fig. 1); x and z refer to 2px and 2pz, together comprising 2pπ. The symbols B and b mean strongly or weakly bonding, A and a mean strongly or weakly antibonding.

‡Rough weighted average term values based on excitation energies to various states.

§Observed; calc. is (a).

Theoretically computed energies (N_2), and observed energies and other data (CO, N_2), are given in Table II for the various *states* of the two lowest excited *configurations*. It should be noted that this table incorporates the most recent spectroscopic results and their interpretation, and includes a new identification of the d state of CO as a $^3\Delta_u$ state (cf. Table II footnote). A study of Table II gives confidence that LCAO-MO computations on simple molecules can predict correctly the energy order of the various states of a $\pi^3\pi$ configuration, and even roughly quantitatively the positions of the lower-energy excited states. However, the predicted energy of the $\pi_u^3\,\pi_g$, $^1\Sigma_u^+$ state of N_2 is certainly too high, since the actual energy can surely not exceed the (vertical) 17.5 ev. required to remove a $1\pi_u$ electron entirely. We may nevertheless reasonably conclude from the very high computed value that the vertical energy of the actual state must be rather close to the π_u ionization limit. This is true for the observed state b' identified in Table II as $\pi_u^3\,\pi_g$, $^1\Sigma_u^+$; its vertical energy is roughly 14 or 15 ev. The theory also shows that this one

TABLE II

COMPARISON OF SOME CARBON MONOXIDE AND NITROGEN MOLECULE STATES

	Carbon monoxide*				Nitrogen†				
Confign.	State	Energy (ev.)	ω_e (cm.$^{-1}$)	r_e (Å)	State	Energy (ev.)		ω_e (cm.$^{-1}$)	r_e (Å)
$\pi^{-1}\pi^*$					$b'\ ^1\Sigma_u^+$	12.85	(24.9)	752	1.44
					$w\ ^1\Delta_u$	9.26 (+?)	(9.8)	1548	1.26
	$I\ ^1\Sigma^-$	Near $e\ ^3\Sigma^-$			$a'\ ^1\Sigma_u^-$	8.76 (+?)	(9.0)	1530	1.27
	$e\ ^3\Sigma^-$	8.11	1094	1.39	$^3\Sigma_u^-$	[8.76]	(9.0)		
	$d\ ^3\Delta^*$	7.72*	1138*	1.39*	$^3\Delta_u$	[7.47]	(7.7)		
	$a'\ ^3\Sigma^+$	6.92	1231	1.35	$A\ ^3\Sigma_u^+$	6.17	(6.5)	1460	1.29
$\sigma^{-1}\pi^*$	$A\ ^1\Pi$	8.07	1516	1.24	$a\ ^1\Pi_g$	8.55	(9.1)	1694	1.22
	$a\ ^3\Pi$	6.04	1739	1.21	$B\ ^3\Pi_g$	7.35	(8.1)	1734	1.21
Ground	$X\ ^1\Sigma^+$	0.00	2170	1.128	$X\ ^1\Sigma_g^+$	0.00		2358	1.094

*The CO state d here identified as $^3\Delta$ (Hund's case b) has hitherto been called d $^3\Pi_i$ (Hund's case a), following an analysis by Gerö and Szabo (Ann. Physik, **35**, 597 (1939)) of the d → a emission bands. Although their data are not adequate for a conclusive judgment, the reported structure seems to be entirely compatible with $^3\Delta(b) \rightarrow {}^3\Pi(a)$, and not with $^3\Pi(a) \rightarrow {}^3\Pi(a)$. See G. Herzberg and T. J. Hugo (Can. J. Phys. **33**, 757 (1955)) and Tanaka, Jursa, and Leblanc (J. Chem. Phys. **26**, 862 (1957)), and references there given, for sources of the above data on CO. Because of some uncertainty in the vibrational numbering, ω_e may be somewhat larger, and r_e and the energy somewhat smaller, for d $^3\Delta$.*

†*For sources of the data on N_2, see R. S. Mulliken, in Proceedings of the Conference on Aeronomy (held at Cambridge, Mass., in June, 1956), (Pergamon Press, Ltd., London, 1957), and references there given. Values in brackets are estimated (not observed). Energy values in parentheses are vertical values from LCAO-MO theoretical computations by C. W. Scherr (J. Chem. Phys. **23**, 569 (1955)). Observed energy values are non-vertical; the vertical values would be about 0.5 ev. higher for the $\sigma^{-1}\pi^*$ states, about 1.5 ev. higher for the $\pi^{-1}\pi^*$ states.*

state must be much more ionic in character than all the other $\pi_u^3\,\pi_g$ states, justifying the identification in Table II with an observed state of much larger r_e and smaller ω_e than the others. Further, the theory shows that this $^1\Sigma_u^+$ state is the *only* one of the $\pi_u^3\,\pi_g$ states to which spectroscopic transition from the ground state is allowed by the selection rules (analogously for $\pi^3\,\pi^*$, $^1\Sigma^+$ of CO), but that this one transition should be intense (V, N type). The state identified in Table II with $^1\Sigma_u^+$ is the lowest-energy $^1\Sigma_u^+$ state of N_2 to which an intense transition occurs.[4]

The good agreement of theory and experiment for CO and N_2 lends strong credence to the LCAO-MO theoretically predicted energy order and rough quantitative locations of the states of the excited configurations . . . $1\pi_g^3\,2\pi_u$, . . . $1\pi_g^3\,3\sigma_g$, and . . . $1\pi_g^3\,3\sigma_u$ for linear CO_2 (cf. Table III). The negative computed ϵ values (term values) for $3\sigma_g$ and $3\sigma_u$ (see Table V) of course cannot be taken literally. They may, however, reasonably be interpreted to mean that the actual (necessarily positive) ϵ values for these MOs are small. The computed negative values probably signal a characteristic breakdown of the usual LCAO-MO approximation, based on free-atom Slater AOs, for high-energy LCAO-MOs. Further, such small-ϵ LCAO-MOs should probably be, as it were, dissolved and replaced by Rydberg MOs. Borderline cases between LCAO and Rydberg MOs are known. For example, the LCAO-MO $\sigma_u 1s$ (i.e., $1s_a - 1s_b$) of H_2 is nearly identical in form and

[4]*There should also be another high-energy $^1\Sigma_u^+$ state of (approximately) V type, corresponding to the configuration $\sigma_g^{-1}\sigma_u^*$. Presumably this is present at somewhat higher energies, but possibly the b′ state is $\sigma_g^{-1}\sigma_u^*$ and the $\pi_u^{-1}\pi_g$ V state is at higher energies, or possibly the situation is more complicated and involves mixing of two or more $^1\Sigma_u^+$ states.*

Can. J. Chem. Downloaded from www.nrcresearchpress.com by 61.7.252.67 on 09/04/12
For personal use only.

TABLE III

CARBON DIOXIDE STATES

Linear CO_2 ($D_{\infty h}$)			Bent CO_2 (C_{2v})		
Config. and state		Energy (ev.)*	Config., state, polzn.**	Probable form	Observed†
$\pi_g^3\,\sigma_g$	$^1\Pi_g$	(14.6)	$a_2\,b_2^2\,a_1,\ ^3A_2,\ ^1A_2(f)$	Linear‡	
	$^3\Pi_g$	(14.6)	$a_2^2\,b_2\,a_1,\ ^3B_2,\ ^1B_2(y)$	Linear‡	
$\pi_g^3\,\pi_u$	$^1\Sigma_u^+$	(22.1)	$a_2\,b_2^2\,b_1,\ ^1B_2(y)$	Linear‡	Band systems with maxima at λ1475 (8.2 ev.), $f = 0.004$, bands to at least λ1810; λ1330(9.4 ev.), $f = 0.005$; λ1100, $f = 0.12$. *Identify* λ1475 upper state with $^1\Delta_u$ $^1B_2$, λ1100 level with a Rydberg state or states.
	$^1\Delta_u$	(9.5)	$a_2^2\,b_2\,b_1,\ ^1A_2(f)$	Linear‡	
			$a_2^2\,b_2\,a_1,\ ^1B_2(y)$	Bent	
	$^3\Sigma_u^-$	(9.2)	$a_2^2\,b_2\,b_1,\ ^3A_2$	Linear‡	
	$^1\Sigma_u^-$	(9.2)	$a_2\,b_2^2\,a_1,\ ^1A_2(f)$	Bent	
	$^3\Delta_u$ (case b)	(8.4)	$a_2\,b_2^2\,b_1,\ ^3B_2$	Linear‡	
			$a_2\,b_2^2\,a_1,\ ^3A_2$	Bent	
	$^3\Sigma_u^+$	(7.6)	$a_2^2\,b_2\,a_1,\ ^3B_2$	Bent	
π_g^4	$^1\Sigma_g^+$	0.00	$a_2^2\,b_2^2,\ ^1A_1$	Linear	

*Calculated vertical energies (in parentheses): J. F. Mulligan (J. Chem. Phys. **19**, 1428 (1951)).

†P. G. Wilkinson and H. L. Johnston (J. Chem. Phys. **18**, 190 (1950)), E. C. Y. Inn, K. Watanabe, and M. Zelikoff (J. Chem. Phys. **21**, 1648 (1953)). Unpublished photographs by Dr. P. G. Wilkinson of this laboratory show definite band structure in the λ1475 system.

‡But perhaps slightly unsymmetrical.

**Polarization expected for absorption transition from ground state (*f* means forbidden).

must be identified with the Rydberg (or united-atom) MO $2p\sigma_u$. Again, the C—H antibonding a_1 excited LCAO-MO for CH_4 (or NH_3, or H_2O) strongly resembles and must be identified with the Rydberg MO 3*s*.

We may now conclude that: (1) the $^1\Sigma_u^+$ state of $\pi_g^3\,\pi_u$ for linear excited CO_2 is to be expected only at much higher energies than the others of this configuration, and (2) the $^3\Pi_g$ and $^1\Pi_g$ states of $\pi_g^3\,\sigma_g$ and the $^3\Pi_u$ and $^1\Pi_u$ states of $\pi_g^3\,\sigma_u$ are to be expected only at high energies close to the π_g ionization limit (13.8 ev.), and well above all the $\pi_g^3\,\pi_u$ states except the $^1\Sigma_u^+$. Point (2) makes it fairly certain that Walsh (16) was right in assuming the $3\sigma_g$ MO of CO_2 to be less firmly bound than the $2\pi_u$, reversing the order assumed by the present writer (9) in his 1942 diagram of the orbital energies of AB_2 molecules for apex angle 180°.[5]

Let us next consider the predicted levels of linear and bent CO_2 (Table III) in relation to the observed absorption spectra above 1600 Å. For bent CO_2 (C_{2v} symmetry), the π_g MO of $\pi_g^3\,\pi_u$ must split into an a_2 and a b_2 MO, and the π_u into an a_1 and a b_1.[6] The partial configuration $\pi_g^3\,\pi_u$ thus gives rise to *four* partial configurations yielding four singlet and four triplet states. The latter must be correlated with the several linear-molecule $\pi_g^3\,\pi_u$ states in the manner shown in Table III if we assume that the a_1 excited MO becomes rapidly lower than b_1 on bending, as is indicated by both empirical (9, 16) and now also theoretical (cf. Table V) evidence. It can then be predicted that some of

[5]*The writer in 1942 thought $3\sigma_g$ might be lower because of the large amount of $2s_C$ in it, if strongly antibonding; but Mulligan's LCAO-MO computations show it to be nevertheless of high energy.*

[6]*The orbital notation follows the internationally approved recommendations (J. Chem. Phys.* **23**, *1997 (1955)).*

Can. J. Chem. Downloaded from www.nrcresearchpress.com by 61.7.252.67 on 09/04/12
For personal use only.

these states should be bent, others linear (Table III). There seems to be little doubt that the observed rather weak absorption system with maximum near λ1475 (cf. Table III) represents a transition to a bent $^1\Delta_u B_2$ state, as proposed by Walsh.

The interpretation of the observed second rather weak CO_2 system with maximum near λ1330 then presents a puzzle; Walsh has identified it as the transition to the $^1\Sigma_u^+$ of $\pi_g^3\,\pi_u$ or to the corresponding $^1B_2$ state, but this identification must apparently be rejected because (*a*) the transition is too weak, and (*b*) its upper state should surely be considerably higher in energy in view of Point (1) in the second preceding paragraph. The state in question might conceivably be identified with $^1\Pi_g$ of $\pi_g^3\,\sigma_g$, but this seems to be excluded by (*a*) Point 2 of the second preceding paragraph, and (*b*) the fact that the molecule in this state is expected to be linear, in which case there should be only one relatively strong band in the system, instead of the large number actually observed. A rather plausible identification would be with a transition to a strongly bent $b_1\,a_1^2\,a_1$, $^1B_1$ or $b_1^2\,a_1\,a_1$,$^1A_1$ upper state corresponding to a $^1\Sigma_g^-$ or $^1\Delta_g$ state of the linear-molecule configuration $1\pi_u^3\,2\pi_u$, although one would have expected such a state to be distinctly higher in energy, since the ionization potential of $1\pi_u$ is 3.6 volts higher than that of $1\pi_g$ (cf. Table V).

In the doubtless analogous case of the weak near-ultraviolet CS_2 absorption spectrum, rotational and vibrational analysis seems to show conclusively that the lowest excited singlet level is a bent $^1B_2$ (equilibrium angle about 140° according to Dr. B. Kleman), with rotational perturbations attributable to the predicted (cf. Table III) nearby $^1A_2$ state. Direct transitions to the latter state, being electronically forbidden, should be weaker than to the $^1B_2$. According to a private communication from Dr. Kleman, the bands at the high-frequency end of the near-ultraviolet CS_2 absorption look like a separate system; if so, this might be analogous to the λ1330 CO_2 system.

[*Added after the conference.*—Dr. A. E. Douglas reported at the conference that the low-frequency end of the near-ultraviolet CS_2 spectrum shows a pronounced Zeeman effect, indicating that the excited state is a triplet state. The high-frequency end, which shows no definite evidence of a Zeeman effect, might then have a singlet upper state. These results can be understood without radical revision of the preceding discussion if the upper state of the weak low-frequency bands is the lowest $^3A_2$ of Table III, related to $^3\Delta_u$ of the linear case; its rotational perturbations would be attributed to the second (or possibly both) of the low $^3B_2$ states of Table III. The stronger high-frequency region could then be explained by transitions to the bent $^1B_2$ state related to $^1\Delta_u$ of the linear case. Additional weak transitions to other states listed in Table III might possibly also be present in the observed structure. This revision of the earlier interpretation of the near-ultraviolet CS_2 absorption spectrum is not unreasonable in view of the relatively strong spin–orbit coupling in the sulphur atom (analogous singlet–triplet transitions should be very much weaker and very difficult to observe in CO_2). However, the fact that no indication whatever of the presence of triplet fine structure has been noted in any of the band lines by Liebermann or by Kleman, in spite of the use of high resolution, seems difficult to reconcile with a triplet state for the upper state of the low-frequency near-ultraviolet bands.]

On the basis of the preceding discussion and Table III, it seems fairly safe to conclude (*a*) that the lowest singlet excited states of CO_2 are a bent $^1B_2$ and $^1A_2$ with vibrational zero levels near 7 ev., and (*b*) that the lowest triplet states are corresponding bent $^3B_2$ and $^3A_2$ states near 5–5.5. ev. (Walsh (16) attributes a well-known emission system observed in carbon monoxide flames to a transition from a higher triplet level to one of

Can. J. Chem. Downloaded from www.nrcresearchpress.com by 61.7.252.67 on 09/04/12
For personal use only.

Can. J. Chem. Downloaded from www.nrcresearchpress.com by 61.7.252.67 on 09/04/12
For personal use only.

TABLE IV

COMPARISON OF SOME NITROGEN AND ACETYLENE STATES

Confign. and state		N_2 energy (ev.)*		Linear C_2H_2 energy (ev.)*	Non-linear C_2H_2			
					Confign., state, polzn.†			
					If *trans* (C_{2h})	If *cis* (C_{2v})	Probable form	Observed§
$\sigma_g\pi_g$	$^1\Pi_g$	8.35	(9.1)	(High?)				
	$^3\Pi_g$	7.35	(8.1)	(High?)				
$\pi_u{}^3\pi_g$	$^1\Sigma_u^+$	12.85(?)	(24.9)	(19.98)	$a_u b_u{}^2 b_g, {}^1B_u$ (y, z)	$b_1 a_1{}^2 a_2, {}^1B_2$ (y)	Linear,‡ high energy	
	$^1\Delta_u$	9.26	(9.8)	(8.63)	$a_u{}^2 b_u b_g, {}^1A_u$ (x)	$b_1{}^2 a_1 a_2, {}^1A_2$ (f)	Linear‡	
					$a_u{}^2 b_u a_g, {}^1B_u$ (y, z)	$b_1{}^2 a_1 b_2, {}^1B_2$ (y)	Bent, stably planar	Bands below λ2000; expect *cis* (y) *and trans* (y, z)
	$^3\Sigma_u^-$	[8.76]	(9.0)	(8.02)	$a_u{}^2 b_u b_g, {}^3A_u$	$b_1{}^2 a_1 a_2, {}^3A_2$	Linear‡	
	$^1\Sigma_u^-$	8.76	(9.0)	(8.02)	$a_u b_u{}^2 a_g, {}^1A_u$ (x)	$b_1 a_1{}^2 b_2, {}^1A_2$ (f)	Bent, easy to twist	*Trans*: $\nu_{00} = 5.23$ ev.; $\nu_{max} \simeq 5.7$ ev.
	$^3\Delta_u$	[7.47]	(7.7)	(6.98)	$a_u b_u{}^2 b_g, {}^3B_u$	$b_1 a_1{}^2 a_2, {}^3B_2$	Linear‡	$\nu_{CC} = 1389$; $\nu_{CCH} = 1048$; $r_{CC} = 1.39$ Å; $\theta = 120°$
					$a_u b_u{}^2 a_g, {}^3A_u$	$b_1 a_1{}^2 b_2, {}^3A_2$	Bent, easy to twist	
	$^3\Sigma_u^+$	6.17	(6.5)	(5.94)	$a_u{}^2 b_u a_g, {}^3B_u$	$b_1{}^2 a_1 b_2, {}^3B_2$	Bent, stably planar	
$\pi_u{}^4\sigma_g{}^2$	$^1\Sigma_g^+$	$\nu = 2330$; $r = 1.09$ Å		$\nu_{CC} = 1974$; $\nu_{CCH} = 612$; $r_{CC} = 1.20$				

*Calculated (vertical) values in parentheses. For N_2, C. W. Scherr (*J. Chem. Phys.* **23**, 569 (1955)). For linear C_2H_2, I. G. Ross (*Trans. Faraday Soc.* **48**, 973 (1952)). In both cases, without allowance for configuration interaction. For some additional possibilities in the case of C_2H_2, see text "Added after the meeting".*

†*The MO configurations given of course neglect configuration interaction. Polarization of absorbed light for transition to state is indicated in parentheses (f, forbidden; x, perpendicular to plane; y, parallel to* CC *line for cis, along least axis of inertia for trans).*

‡*Or possibly bent and twisted.*

§*C. K. Ingold and G. W. King (J. Chem. Soc. 2708 (1953)), K. K. Innes (J. Chem. Phys.* **22**, *863 (1954)), and references given there. The transition to the 5.23 ev. state is x-polarized, with an oscillator strength f of about 10^{-4}. See also Ref. 10, and text "Added after the meeting".*

these.) With respect to the higher excited levels, the present survey suggests that considerably more study, both experimental and theoretical, is needed. Similar remarks apply to CS_2.

THE LOW EXCITED LEVELS OF ACETYLENE

The ground-state electron configuration of C_2H_2 should be closely analogous to that of N_2 (cf. [1]) except for the C—H bonding properties of the σ MOs:

$$[2] \qquad C_2H_2\colon\ (\sigma_g 1s_C)^2\,(\sigma_u 1s_C)^2\,(2\sigma_g)^2\,(2\sigma_u)^2\,(3\sigma_g)^2\,(1\pi_u)^4,\ {}^1\Sigma_g^+.$$
$$\qquad\qquad\qquad\qquad\qquad\qquad\qquad\qquad\qquad\qquad \text{HC, CH}\ \ \text{HC, CH}\ \ \text{CC}\ \ \ \text{CC}$$

The capital letters under the last four MOs indicate their probable major bonding characteristics. For spectroscopic purposes, the major difference from N_2 is that $3\sigma_g$, because of its strong C—C bonding function, must be less easily excited than $1\pi_u$, the reverse of what is true for N_2.[7] Hence for linear excited C_2H_2, the $(3\sigma_g)\,(1\pi_u)^4\,1\pi_g$ states, unlike N_2 (Table II), are doubtless definitely above all except perhaps the highest $({}^1\Sigma_u^+)$ of the $(3\sigma_g)^2\,(1\pi_u)^3\,1\pi_g$ states, so that we need consider only the latter. In Table IV, the observed and computed $\pi_u^3\,\pi_g$ states of N_2, and the corresponding computed states for *linear* C_2H_2 (14),[8] are compared. From our experience on CO and N_2 as discussed above, we may place confidence in these computed values for linear C_2H_2 so far as the energy order of the states is concerned, and also very roughly quantitatively. The foregoing considerations furnish a basis for the correlations given in Table IV of these linear-molecule with bent-molecule states of excited C_2H_2, and give some guidance as to the energy order for the bent-molecule states.

Now let us assume, with Walsh (16), that $1\pi_u$ splits into two MOs differing little in energy, namely a_1 and b_1 for C_{2v} (*cis*) symmetry, or b_u and a_u for C_{2h} (*trans*) symmetry, and that $1\pi_g$ splits into one MO whose energy does not change with bending (a_2 for *cis*, b_g for *trans*) and another whose energy decreases strongly with bending (b_2 for *cis*, a_g for *trans*).[9] This assumed behavior on bending is analogous to what happens in AB_2 molecules, where it is definitely known that the low-energy π MOs $1\pi_u$ (bonding) and $1\pi_g$ (non-bonding) split only slightly with bending, while the high-energy antibonding $2\pi_u$ splits very strongly (cf. Table V). The MOs a_2 or b_g from π_g and b_1 or a_u from π_u are antisymmetric to the plane of bent C_2H_2 and necessarily remain strongly bonding and antibonding, respectively, during bending. For C_{2v} (*cis*-bent) C_2H_2, the correlations in Table IV are formally identical with those for CO_2 (Table III) except for the MO labels (a_2 replaces b_2, a_1 replaces b_1, and vice versa, because the configuration here is $\pi_u^3\,\pi_g$ instead of $\pi_g^3\,\pi_u$). For C_{2h} (*trans*-bent) C_2H_2, which has no analogue for CO_2, the correlations are similar, but the selection-polarization rules for allowed spectroscopic transitions from the ground state are distinctly altered. Ingold and King, and Innes, in their thorough analyses of the observed weak absorption band system near λ2200, find transitions only to *trans*-bent ${}^1A_u$ excited molecules (see Table IV) (4, 5). The absence of transitions to *cis*-bent molecules can be explained by the spectroscopic forbiddenness of ${}^1A_2 \leftarrow {}^1\Sigma_g^+$, but there is

[7] *The writer estimates that the ionization potential of $3\sigma_g$ is 20–21 volts, whereas the observed minimum ionization potential of C_2H_2, which must belong to $1\pi_u$, is only 11.3 volts.*

[8] *For further calculations, see Serre (15) and references given there.*

[9] *Ingold and King, on the other hand, assume that $\pi_u b_u$ and $\pi_g a_g$ (or $\pi_u b_1$ and $\pi_g a_2$) both become nearly nonbonding and nearly equal in energy in bent C_2H_4. This results in a very different pattern of predicted excited levels. A consequence is that the lowest ${}^1B_u$ of bent C_2H_2 should be rather far (perhaps 3 ev.) below the lowest ${}^1A_u$ (cf. Fig. 3 on p. 2715 of their papers (4)). Since the transition to this state should then lie in the visible, and be relatively strong, their assumption about the nature of these MOs seems improbable (but see below). However, they are in agreement with Table IV and with Walsh that the configuration of the ${}^1A_u$ upper level of the λ2200 system is $a_u b_u^2 a_g$.*

Can. J. Chem. Downloaded from www.nrcresearchpress.com by 61.7.252.67 on 09/04/12
For personal use only.

TABLE V

MOLECULAR ORBITALS OF OZONE AND CARBON DIOXIDE*

MO	Form		ϵ (ev.)	ϵ (ev.) Compd.	ϵ (ev.) Obs.	Form		MO
$4b_2$	$-h,\ y,\ h$	(A)		(-4.8)	[2est]	$-h,\ Y,\ h$	(A)	$3\sigma_u$
$5a_1$	$-h,\ h,\ -h$	(A)		(-3.1)	[2est]	$-h,\ S,\ -h$	(A)	$3\sigma_g$
$2b_1$	$-x,\ x,\ -x$	(A)		(2.5)	(5appr)	$\begin{Bmatrix}-x,\ X,\ -x\\ -p,\ Z,\ -p\end{Bmatrix}$	(A)	$2\pi_u$
$1a_2$	$x,\ 0,\ -x$	(N)	13.7	11.5	13.73	$\begin{Bmatrix}x,\ 0,\ -x\\ p,\ 0,\ -p\end{Bmatrix}$	(N)	$1\pi_g$
$4a_1$	$-p,\ zh',\ -p$	(a)	14.8					
$3b_2$	$p,\ v,\ -p$	(a)	15.6					
$1b_1$	$x,\ X,\ x$	(B)	21.3	18.8	17.30	$\begin{Bmatrix}x,\ x,\ x\\ p,\ Z,\ p\end{Bmatrix}$	(B)	$1\pi_u$
$3a_1$	$p-s,\ Zh',\ p-s$	(b)	22.8					
$2b_2$	$h',\ y,\ -h'$	(a)	25.2	17.9	18.07	$-s+h',\ y,\ s-h'$	(a)	$2\sigma_u$
$2a_1$	$-s,\ s-h',\ -s$	(A)	32.6	19.4	19.38	$H',\ s,\ H'$	(a)	$2\sigma_g$
$1b_2$	$Sh,\ y,\ -S-h$	(B)	41.0	42.4		$sh,\ y,\ -s-h$	(B)	$1\sigma_u$
$1a_1$	$sh,\ Sh,\ sh$	(B)	47.3	44.9		$hs,\ s,\ hs$	(B)	$1\sigma_g$

*See Fig. 1 for explanation of atomic orbital symbols describing the form of each MO. The symbols B, b, N, a, A respectively mean strongly bonding, weakly bonding, essentially non-bonding, weakly antibonding, and strongly antibonding. Computed quantities based on I. Fischer-Hjalmars (Arkiv. för Fysik, **11**, 529 (1957)) for O_3, and J. F. Mulligan (J. Chem. Phys. **19**, 347, 1428 (1951)) for CO_2. The "observed" ϵ values for the occupied MOs of CO_2 are ionization potentials based on Rydberg series (including the latest unpublished results of Y. Tanaka on $2\sigma_g$) and the CO_2^+ spectrum (for $1\pi_u$). For the unoccupied MOs of CO_2, the ϵ values are approximate average term values appropriate to excited states. Ozone is at the left, carbon dioxide at the right.*

no reason to suppose that *cis*-bent $^1A_2$ molecules cannot exist, although perhaps (4) they may have somewhat higher energy.

Comparing with CO_2, it seems relevant that the intensity of ^1A_u (*trans*) $\leftarrow {}^1\Sigma_g^+$ in acetylene ($f = 10^{-4}$, cf. Table IV footnote), whose analogue $^1A_2 \leftarrow {}^1\Sigma_g^+$ in CO_2 is forbidden, is much less than that of the observed $^1B_2 \leftarrow {}^1\Sigma_g^+$ λ1475 system of CO_2 ($f = 0.004$). This seems reasonable, since $^1A_u \leftarrow {}^1\Sigma_g^+$ of C_2H_2 must acquire its intensity from $^1\Pi_u A_u \leftarrow {}^1\Sigma_g^+$ transitions (through some weak mixing of higher-configuration $^1\Pi_u A_u$ states with our $^1\Sigma_u^- A_u$), while $^1B_2 \leftarrow {}^1\Sigma_g^+$ of CO_2 can acquire its intensity mainly from the predictedly very intense $(\pi^3\pi,\ {}^1\Sigma_u^+)^1B_2 \leftarrow {}^1\Sigma_g^+$ transition (by admixture of $(\pi^3\pi,\ {}^1\Sigma_u^+)^1B_2$ into $(\pi^3\pi,\ {}^1\Delta_u)^1B_2$ on bending).

It can now be predicted that there should be absorption transitions $^1B_2$(*cis*) $\leftarrow {}^1\Sigma_g^+$ and ^1B_u (*trans*) $\leftarrow {}^1\Sigma_g^+$ for C_2H_2, and that these should be much stronger than the ^1A_u (*trans*) $\leftarrow {}^1\Sigma_g^+$ λ2200 system. It seems likely that these predicted transitions can be identified with the rather plentiful confusion of bands, which are relatively weak but stronger than the λ2200 system, extending from near λ2000 for a few hundred angstroms toward shorter wavelengths.[10] A detailed study of these bands, if feasible, would be of great interest. Comparisons with recent work of Herzberg and Innes (3) on HCN will also be valuable; here again, the linear-molecule predicted states of $\pi^3\pi$ configuration should be similar to those of N_2 or CO.

[*Added after the meeting.*—At λ1520 occurs the origin of the first Rydberg transition

[10]*See the extensive discussion in Walsh's paper (16). Further, on the basis of unpublished results, Dr. P. G. Wilkinson estimates a total f value of very roughly 10^{-3} for the bands between λ1900 and λ1550. But Dr. T. M. Dunn of University College, London (private communication), estimates an f value five or ten times larger for these bands. He also estimates a larger f value for the "λ2200" system, and furthermore estimates that the intensity maximum of this system is near λ1900 rather than λ2200.*

Can. J. Chem. Downloaded from www.nrcresearchpress.com by 61.7.252.67 on 09/04/12
For personal use only.

of C_2H_2. This is an intense transition (f = 0.13 according to Moe and Duncan (7)). On the basis of the vibrational structure (essentially only two or three quanta of the C—C stretching vibration) and the appearance of the bands, the excited state here, hence presumably the $^2\Pi_u$ ground state of $C_2H_2^+$, is definitely linear. A report on this transition and on the next group of strong bands near λ1340, going beyond previous work of W. C. Price (12), is in course of preparation by Dr. P. G. Wilkinson. Wilkinson's analysis indicates the presence of a very close group of three upper electronic states for the λ1340 group, of which two seem to be Rydberg states with a nearly but not quite linear configuration, while the third appears to be a non-Rydberg state in which the molecule is *trans*-bent, perhaps to 120°, *and twisted.* (Price assigned this whole group of bands to a single Rydberg transition.) The most likely identification of this bent and twisted state is with the transition to the high-energy ^1B_u state of Table IV which corresponds to the linear-molecule $\pi_u^3\,\pi_g$, $^1\Sigma_u^+$ state. The high intensity (f about 0.17 according to Moe and Duncan for the group of three electronic transitions near λ1340; more or less equally shared by all three) and the energy (9.25 ev., as compared with 12.85 ev. for the supposedly analogous $^1\Sigma_u^+$ of N_2—cf. Table IV) tend to support this identification. However, it is evident that our theoretical understanding is still incomplete. A possibility not considered in Table IV, which perhaps may be important, is that for linear acetylene there exist low excited $^3\Pi_u$ and $^1\Pi_u$ states of configuration $\pi_u^3\,\sigma_u$ involving a strongly antibonding σ_u MO analogous to $3\sigma_u$ of N_2 (cf. Table I) but lower in energy, to which might correspond bent states one of which could be (or could be mixed into) the λ1340 bent upper state. Final conclusions must await further experimental and theoretical study.

In seeking to interpret the four electronic absorption systems of HCN and DCN which Herzberg and Innes (3) observe below λ2000, a qualitative theoretical consideration indicates an electron configuration

[3] $$\underset{\text{CN}}{(1s_N)^2}\,\underset{\text{CH}}{(1s_C)^2}\,\underset{\text{C=N}}{(3\sigma)^2\,(4\sigma)^2\,(1\pi)^4\,(5\sigma)^2}$$

in which the last σ MO (5σ) and the π MO may have about equal ionization potentials, or the 5σ even somewhat less than the 1π. This is in marked contrast to acetylene (cf. [2] and text above) where there seems to be no doubt that the last σ MO ($3\sigma_g$) is very much more tightly bound than the $1\pi_u$ MO. The excited states of HCN for the molecule if it were linear should then resemble closely those of N_2 and CO (cf. Table II) in that the configuration $\sigma^{-1}\pi^*$ would be involved in giving rise to the lowest excited states. On this basis, the bent upper state of Herzberg and Innes' α system might be identified with the $^1A''$ state corresponding to the linear-molecule $\sigma^{-1}\pi^*$, $^1\Pi$ state, while the β, γ, and δ system upper states could be correlated with some of the other states corresponding to $\sigma^{-1}\pi^*$ and $\pi^{-1}\pi^*$. In favor of this identification is the fact that Herzberg and Innes find a considerable increase in the C—H distance in the α upper level, which does not seem to be understandable (and is not found in the λ2200 system of C_2H_2) in terms of any state correlated with a pure $\pi^{-1}\pi^*$ linear-molecule configuration. In $\sigma^{-1}\pi^*$, the C—H distance could be increased if the 5σ MO is somewhat C—H bonding. The interpretation suggested here is open to objections, but may at least point toward some possibilities which should be explored.]

Because of the definite conclusions as to the energy order and other characteristics of the $\pi_u^3\,\pi_g$ states of linear C_2H_2, the correlations and interpretations proposed here are somewhat different from those of Walsh. They also differ considerably from those of

Can. J. Chem. Downloaded from www.nrcresearchpress.com by 61.7.252.67 on 09/04/12
For personal use only.

Ingold and King (4). The present interpretation is in harmony with the observation of a ^1A_u lowest excited state of moderately high energy. It does not, however, offer any explanation as to why the molecule is bent to just 120° in this state. Complete LCAO-MO theoretical calculations on C_2H_2 and HCN, for various geometrical forms and electronic states, should be exceedingly helpful in giving better answers and increased understanding.

THE LOWER-ENERGY EXCITED LEVELS AND SPECTRA OF BENT AB_2 MOLECULES

As is well known, AB_2 molecules with up to 16 valence-shell electrons (CO_2, etc.) are linear in their ground states, but those with more are bent. Recent microwave and other spectroscopic work now affords reliable information on angles and internuclear distances for many of these (cf. Table VI). The bent form of the 17–19 electron molecules can be explained if (*a*) the linear form is stabilized by the net effect of the predominantly bonding and non-bonding MOs occupied by the first 16 electrons, (*b*) the next two electrons go into an MO ($4a_1$) whose energy decreases rapidly with bending, (*c*) the next electron goes into an MO which is little affected by bending (cf. ClO_2). The increased bending in 20-electron molecules like F_2O and Cl_2O may presumably be attributed to decreased s–p hybridization in the halogen outer atoms and other quantitative changes. Recent LCAO-MO theoretical calculations on the electronic structures of CO_2 and O_3, for the experimentally known internuclear distances in each case, throw a great deal of light on the forms of all the MOs involved. A survey of the results, including a simplified rough description of the computed form and energy of each MO occupied in the ground state, as well as of the forms of all valence-shell-AO excited MOs, is presented in Table V (see also Fig. 1). The table has a number of points of interest. In studying it, however, one should keep in mind that the computed results, while good, are only approximate.[11] The reliability of the computed ϵ values can be judged by a comparison of observed and computed values for CO_2—see also Tables II and III. The approximate forms of the MOs are probably fairly reliable in most cases.

The following points are especially relevant here. (1) The linear-molecule $1\pi_u$ and $1\pi_g$ MOs split and change in energy relatively little as a result of bending. (In comparing ϵ values of bent O_3 and linear CO_2 in Table V, it should be kept in mind that the larger nuclear charge on the central atom in O_3 causes a general increase in ϵ values.) (2) The first excited MO $2\pi_u$ of CO_2 splits very strongly to give a $4a_1$ MO whose ϵ in O_3 is as large as the MOs corresponding to $1\pi_g$, and a $2b_1$ MO whose ϵ should not change on bending. We have thus a theoretical explanation of the highly angle-sensitive $4a_1$ MO which is known empirically. One notes that, although the $2\pi_u$ MO is strongly antibonding, and the $2b_1$ remains so, the $4a_1$ for a 120° angle is only weakly antibonding. The very large ϵ of $4a_1$ at 120° is a result which comes out of the theoretical calculation and which perhaps cannot be fully explained in qualitative terms, although it can be partially attributed to the decreased antibonding. (3) The linear-molecule MOs $3\sigma_g$ and $3\sigma_u$ are very high in energy, and go over into even higher energy (at least for the $3\sigma_g$) bent-molecule MOs $5a_1$ and $4b_2$. The thus-indicated ϵ values are so small that, contrary to earlier assumptions (9), these MOs probably may be left out of consideration in the explanation of observed absorption spectra except perhaps at short wavelengths in the vacuum ultraviolet.

The theoretical computations permit considerable improvements in both the writer's and Walsh's AB_2 diagrams with respect to the energies of the various MOs, and give new

[11] *Besides the approximations inherent in the LCAO–MO SCF method, the computations on* O_3 *and* CO_2 *did not specifically take into account the 1s electrons. Further, many of the integrals involved were approximated. On the other hand, the results for* N_2 *in Table I are based on a complete exact LCAO–MO SCF computation.*

Can. J. Chem. Downloaded from www.nrcresearchpress.com by 61.7.252.67 on 09/04/12
For personal use only.

Can. J. Chem. Downloaded from www.nrcresearchpress.com by 61.7.252.67 on 09/04/12
For personal use only.

TABLE VI. SOME IDENTIFICATIONS OF OBSERVED WITH PREDICTED NON-INTERSYSTEM SPECTRA OF NON-LINEAR AB_2 MOLECULES

Predictions*				Observed data,† in the following order for each molecule: with the column heading, α and r (Å) for ground state; below, ΔE_{vert} in ev. (and λ_{max} in Å); polarization; f value (or strength); $\alpha'-\alpha''$; $r'-r''$; $\Delta v_3 > 0$; x_{33} (cm^{-1})					
Transition	Polzn. and strength	$\alpha'-\alpha''$;	$r'-r''$	NO_2 (134°, 1.19)	NO_2^- (116°, 1.23)	O_3 (117°, 1.28)	CF_2	SO_2 (120°, 1.43)	ClO_2 (117°, 1.49)
$2b_1 \leftarrow 4a_1$	x, w	+	+	3 (λ4000); ?; 0.003; to 180° (?); ?; ?	3.54 (λ3500); x; 0.0005; long ν_2' series	(calc. $f = 10^{-4}$) 2.1 (λ6000); ?; 0.6×10^{-4}	Possibly λ3500	3.3 (λ3800); x?; 10^{-6}; +5°; +0.06Å; 2,4 (or 1,2); +9	
$4a_1 \leftarrow 3b_2$	y, s?	−	~0	5.3 (λ2350); y; 0.0007; to 116°; +	($4a_1$ full)	($4a_1$ full)	($4a_1$ full)	($4a_1$ full)	($4a_1$ full)
$2b_1 \leftarrow 3b_2$	f	~0	+		4.27 (λ2900); ?; 0.0004				
$2b_1 \leftarrow 1a_2$	y, s	~0	+	8.7 (λ1450); y?; s	6.05 (λ2050); y; 0.20	(calc. $f = 0.6$) 4.86 (λ2550); y?; 0.086	5 (λ2450); y; s?; +; small; none	4.2 (λ2900); y?; 0.006; −?; large?; 1?, 2,4	3.6 (λ3500); y; s?; −10°(?); +0.22 Å(?); 2,4; +10

*See Table V (ozone) for approximate forms of MOs. The symbols x, y, f respectively refer to transitions polarized perpendicular to the molecule plane, parallel to the B–B axis, or forbidden; w means weak, s, strong. The predicted changes in apex angle α and A—B distance r are based on the bending and bonding properties of the MOs involved.

†*Ground-state data: for* NO_2, *cf. G. E. Moore (J. Opt. Soc. Am.* **43**, *1045 (1953)) and G. R. Bird (J. Chem. Phys.* **25**, *1040 (1956)); for* NO_2^- *(in crystal), M. R. Truter (Acta Cryst.* **5**, *132 (1952)); for* O_3, *cf. R. H. Hughes (J. Chem. Phys.* **24**, *1313 (1956)); for* SO_2, *S. R. Polo and M. K. Wilson (J. Chem. Phys.* **22**, *900 (1954)); for* ClO_2, *J. D. Dunitz and K. Hedberg (J. Am. Chem. Soc.* **72**, *3108 (1950). Spectroscopic data*: NO_2 *absorption, L. Harris and G. W. King (J. Chem. Phys.* **2**, *51, (1934)) and G. Wilse Robinson (report at Ohio State University Spectroscopic Conference (1957)); for* NO_2 *absorption intensities, T. C. Hall and F. E. Blacet (J. Chem. Phys.* **20**, *1745 (1952)) and Harris and King (loc. cit.); for* NO_2 *fluorescence spectrum (probably* $2b_1 \rightarrow 4a_1$*; smaller f (longer lifetime) in emission may be explained by lower transition probability at larger angle), D. Neuberger and A. B. F. Duncan (J. Chem. Phys.* **22**, *1693 (1954)). Note that* $2b_1 \leftarrow 1a_2$ *in* NO_2 *should give rise to two non-intersystem transitions of which an identification is given here for one. For* NO_2^- *in* $Na^+NO_2^-$ *crystal: see W. G. Trawick and W. H. Eberhardt (J. Chem. Phys.* **22**, *462 (1954)), J. W. Sidman (J. Am. Chem. Soc.* **79**, *2669, 2675 (1957)); Sidman's work shows that the λ3500 system is an allowed one in spite of its weakness and confirms the x polarization found by Trawick and Eberhardt. The f values for* NO_2^- *are based on aqueous solution data of H. L. Friedman (J. Chem. Phys.* **21**, *319 (1953)); the λ2900 solution band is apparently much weaker or possibly absent in the crystal, while the λ2100 solution band shows a double peak, and possibly part or most of the f value may belong to a different (charge-transfer) transition.* O_3*: calculated frequencies (not given above) and f values, I. Fischer-Hjalmars (loc. cit. Table V); absorption bands, cf. survey by H. Sponer and E. Teller (Revs. Modern Phys.* **13**, *75 (1941)) and more recent literature. It is here assumed that the very weak reported infrared system is due to impurities (perhaps* O_4*) or is an intersystem transition. Evidence that the bands near λ3500 form a system distinct from the stronger region near λ2550 has also been disregarded.* CF_2 *emission, P. Venkateswarlu (Phys. Rev.* **77**, *676 (1950)), absorption, R. K. Laird, E. B. Andrews, and R. F. Barrow (Trans. Faraday Soc.* **46**, *803 (1950)).* SO_2*: λ3800 system, Russell et al. (ASTIA AD81060), Coffmann et al. (ASTIA AD95806), with J. B. Coon; λ2900 system, N. C. Metropolis (Phys. Rev.* **60**, *295 (1941)) and see P. A. deMaine (J. Chem. Phys.* **26**, *1036 (1957)) for* CCl_4 *solution data from which f value has been computed. The λ2900 system and a stronger absorption region near λ2000 also appear in fluorescence.* ClO_2*: J. B. Coon and E. Ortiz (J. Molecular Spectroscopy (In press, 1957) and Phys. Rev.* **96**, *845A (1954)). In a private communication, J. B. Coon gives* $f = 1.7\times10^{-7}$ *and* 4.3×10^{-3} *respectively for the* SO_2 *λ3800 and λ2900 systems. See also text "added after the meeting".*

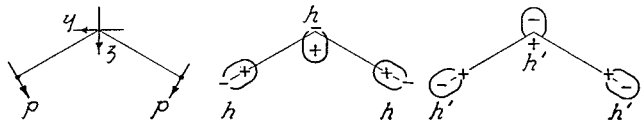

FIG. 1. Schematic diagram to indicate forms of atomic orbitals used in describing O_3 molecular orbitals in LCAO approximation. For any atom, s means $2s$ and x means $2px$, while h and h' respectively refer to various in-plane sp hybrids directed *more or less* toward or away from the center but whose exact forms and orientations vary from case to case. For the middle atom, y and z mean $2py$ and $2pz$ with positive end in the direction shown. For the outer atoms, p means an in-plane $2p$ AO directed *approximately* perpendicular to an O—O bond. The x AO's are antisymmetric to the molecular plane, while all others are symmetric. Double symbols in the descriptions (e.g. sh or $p-s$) are used where hybridization is somewhat minor in importance (e.g. sh means a mixture of s and h, $p-s$ a mixture of p and $-s$). *Capital letters* are used in a few cases to indicate rather strong predominance in the total LCAO-MO.

Fig. 1 applies also to CO_2 if the apex angle is increased from 120° to 180° with the O atom orbitals retaining their orientations to the CO axes; the x and the p_O and z_C AOs now become π AOs.

insight into the forms of the MOs. In combination with new experimental data of the last few years, they have led the writer to review earlier attempts to interpret the electronic absorption spectra of triatomic oxides, and to propose, in Table VI, identifications of known spectra above about λ2000. In this effort, he is indebted to Professors G. W. Robinson, J. B. Coon, and W. H. Eberhardt for suggestions and for information on their current work.

The assignments of observed band systems to MO transitions for the several molecules are to a large extent mutually consistent and consistent with theoretical requirements and expectations (listed under "Predictions"). However, there seem to be some discrepancies which are difficult to explain, and the identifications must therefore still be considered provisional. These difficulties will now be mentioned and commented on briefly.

(1) The SO_2 λ3800 system is so weak that one is tempted to attribute it to a singlet–triplet transition, but if this is correct, the corresponding singlet–singlet transition should be nearby at somewhat shorter wavelengths. Although the λ2900 system fulfills this specification, its $\Delta\alpha$, Δr characteristics are so different as to rule out such a relation. The much stronger bands near λ2000 are too far away. Thus one is left with the assignments in the table. The low intensities of the assigned SO_2 bands, and the fact that we have ignored the strong bands near λ2000 whereas for NO_2 and NO_2^- we have included strong bands at short wavelengths in the assignments, are not entirely satisfactory.

[*Added after the meeting.*—Dr. A. E. Douglas reported at the meeting that the SO_2 λ3800 system shows a pronounced Zeeman effect. This supports its interpretation as a singlet–triplet transition rejected above, but does not answer the contrary argument given above. Douglas finds no Zeeman effect in the λ2900 system; if λ3800 is actually a singlet–triplet transition, λ2900 is probably $2b_1 \leftarrow 4a_1$ (it will be noted that the experimental data in Table VI which would contradict this appear with a ?) and $2b_1 \leftarrow 1a_2$ is probably represented by strong bands near λ2000.]

In the case of *ozone*, the assignments are definitely tentative and need further study (see footnote on O_3 in Table VI). For *all* the molecules, additional non-Rydberg transitions besides those considered in Table VI, involving excitation from the deeper occupied MOs (and possibly also to higher excited MOs), are of course to be expected at shorter wavelengths, and a number of such transitions have certainly been observed. There seems, however, to be no reason why d hybridization for S and Cl in SO_2 and ClO_2 should markedly affect the long wavelength spectra. It should make the MOs $1a_2$ and $3b_2$ somewhat bonding, and strengthen the bonding MOs on the whole.

Can. J. Chem. Downloaded from www.nrcresearchpress.com by 61.7.252.67 on 09/04/12
For personal use only.

(2) The identification of the visible NO_2 bands as $2b_1 \leftarrow 4a_1$ seems to be supported by the work of Robinson (13) and of Eberhardt, but the observed intensity ($f = 0.003$) is higher than expected, and also higher than for the transition identified as $4a_1 \leftarrow 3b_2$ which one might expect to be rather strong. An *alternative identification* would be to attribute the visible bands to $4a_1 \leftarrow 3b_2$, the bands with λ_{max} at about 2350 to $2b_1 \leftarrow 1a_2$, and to suppose that the $2b_1 \leftarrow 4a_1$ bands are present among the visible bands but too weak to be noticed. It should be noted that $4a_1 \leftarrow 3b_2$ is possible only for NO_2 among the molecules in Table VI, since in the others the $4a_1$ shell is filled in the ground state.

(3) While $4a_1$ in NO_2 should be more or less halfway down from $2b_1$ toward $3b_2$ and $1a_2$, as one sees by interpolation between CO_2 and O_3 in Table V, it should in the other molecules (judging from the O_3 calculated results in Table V) be close to $1a_2$ and $3b_2$, and the latter should have ϵ values near 15 ev., while $2b_1$ is expected to have ϵ near 5 ev. Hence the $2b_1 \leftarrow 4a_1$ and $2b_1 \leftarrow 1a_2$ spectra of NO_2^-, O_3, SO_2, and ClO_2 might be expected to have frequencies corresponding to about 10 ev., instead of being in the range 3–6 ev. as observed according to Table VI. However, since an examination of Table V excludes any possibility of alternative MOs which could give smaller predicted excitation energies, we must apparently conclude that the MO identifications are not essentially at fault.

Granting this, it would seem that theoretical calculations based more directly on *electronic states* may be needed to account for the observed spectra. In general, the energies of electronic states can be estimated only roughly by the assumption of a definite fixed orbital energy ϵ for each excited MO. "Configuration interaction" often strongly affects excitation energies. Reorganization when excitation from one to another particular MO involves a large change in charge distribution can also cause energy lowering. When *degenerate* MOs are involved, there are often a number of states covering a wide energy spread, as for example in the $\pi^3\pi$ states of Tables II–IV. While it is true that in bent AB_2 molecules there are no degenerate MOs, one may expect a partial persistence of the widely spread groupings of states that would exist for the degenerate-MO configurations of these molecules if linear. In fact the discussion given above of the excited states as a point of departure was based on this premise. In applying the same approach to the excited states of, say, NO_2 and O_3, one would first compute the energies of the linear-molecule states, then consider what happens on bending. For NO_2, $\pi_g^4\,\pi_u$, $^2\Pi$ would yield the ground state . . . $1a_2^2\,3b_2^2\,4a_1$, $^2A_1$ and the low excited state . . . $1a_2^2\,3b_2^2\,2b_1$, $^2B_1$, while the several states $^4\Pi_g$, $^2\Pi_g$, $^2\Pi_g$, $^2\Phi_g$, and $^2\Pi_g$ of $\pi_g^3\,\pi_u^2$ would give a number of other excited states. For O_3, one would start with the states of $\pi_g^4\,\pi_u^2$ and $\pi_g^3\,\pi_u^3$. In general, *it is important to consider states as well as orbitals.*

A final point of considerable interest which emerges from some of the data on SO_2 and ClO_2 is the probability that these molecules become slightly unsymmetrical (C_s instead of C_{2v} symmetry) when excitation to a $2b_1$ MO occurs. This MO (cf. Table VI) is inescapably antibonding, but its antibonding effect would be expected to be smaller for an unsymmetrical structure—just as, conversely, a bonding electron in a delocalized MO can give stronger total bonding than one localized between two nuclei. The evidence for an unsymmetrical upper state for the ClO_2 band system, first brought to the writer's attention by J. B. Coon (2),[12] and for the λ3800 and λ2900 SO_2 systems, consists in the fact that the (for C_{2v} antisymmetric) frequency ν_3 is more strongly excited in the upper state than could otherwise reasonably be understood; further, that this frequency shows an

[12]*Earlier, Lotmar (6) gave evidence for an unsymmetrical upper state (cf. p. 780) for the* SO_2 *bands near λ2000, in the fact that* $\Delta v_3 > 0$ *seems to occur in fluorescence. However, later work raises some questions as to this evidence (1).*

Can. J. Chem. Downloaded from www.nrcresearchpress.com by 61.7.252.67 on 09/04/12
For personal use only.

exceptionally large positive anharmonicity (cf. x_{33} values in Table VI). If we assume that these upper states *are* unsymmetrical, then in terms of the coordinate Q_3 associated with ν_3 under C_{2v} symmetry, one has a double minimum problem.[13] If the asymmetry is *only slight*, so that the hump between the two minima is very low, the ν_3 vibration levels should still be fairly evenly spaced, as for C_{2v} symmetry. However, the resulting broadened potential curve should result in (*a*) diminishing the effective force constant for small ν_3 vibrations but introducing strong positive anharmonicity, (*b*) permitting transitions $\Delta v_3 = 2, 4 \ldots$ to occur much more strongly than would be possible by Franck–Condon considerations if there were a single minimum. (Also, $\Delta v_3 = 1, \ldots$ can now occur if the transition is *y* or *z* polarized, but probably only very weakly.) The expected results agree with what is observed. For *larger* asymmetry, the situation would change to resemble ordinary inversion doubling as in NH_3; one should then observe strong *negative* anharmonicity, but $\Delta v_3 > 0$ should still occur readily.

One is tempted to connect unsymmetry of an AB_2 excited state with photodissociation into AB + B. Minimum-energy dissociation of AB_2 into AB + B may be effected, with or without initial asymmetry, by suitable simultaneous excitation of the vibrational coordinates Q_1 and Q_3 (and in general also Q_2). The main importance of initial asymmetry for direct photodissociation would be in softening the usual Franck–Condon inhibitions against $\Delta v_3 > 0$. The diffuseness of the high-frequency regions of some AB_2 absorption systems (e.g. the ClO_2 system) may well be due to direct dissociation of this sort at a saddle-point or a saddle-asymptote of the vibrational energy and/or to vibrational predissociation of vibrational levels near and above such a saddle-point, or above such a saddle-asymptote. In other cases, predissociation into a different electronic state having a lower vibrational saddle-point or saddle-asymptote may occur.

REFERENCES

1. CHOW, T. C. Phys. Rev. **44**, 638 (1938).
2. COON, J. B. Bull. Am. Phys. Soc. **2**, 100 (1957).
3. HERZBERG, G. and INNES, K. K. Can. J. Phys. **35**, 842 (1957).
4. INGOLD, C. K. and KING, G. W. J. Chem. Soc. 2708 (1953).
5. INNES, K. K. J. Chem. Phys. **22**, 863 (1954).
6. LOTMAR, W. Z. Physik, **83**, 765 (1933).
7. MOE, G. and DUNCAN, A. B. F. J. Am. Chem. Soc. **74**, 3136 (1952).
8. MULLIKEN, R. S. Phys. Rev. **41**, 751 (1932); **43**, 279 (1933).
9. MULLIKEN, R. S. Phys. Rev. **60**, 512 (1941); Revs. Modern Phys. **14**, 204 (1942).
10. MULLIKEN, R. S. and ROOTHAAN, C. C. J. Chem. Revs. **41**, 219 (1947).
11. ÖPIK, U. and PRYCE, M. H. L. Proc. Roy. Soc. A, **238**, 427 (1957).
12. PRICE, W. C. Phys. Rev. **47**, 444 (1935).
13. ROBINSON, G. W., MCCARTY, M., and KEELTY, M. C. J. Chem. Phys. **27**, 972 (1957), and unpublished work.
14. ROSS, I. G. Trans. Faraday Soc. **48**, 973 (1952).
15. SERRE, J. Compt. rend. **242**, 1469 (1956).
16. WALSH, A. D. J. Chem. Soc. 2260 (1953).
17. WILKINSON, P. G. Can. J. Phys. **34**, 651 (1956).

[13]*Öpik and Pryce (11) have discussed a related situation for a linear* AB_2 *molecule.*

Can. J. Chem. Downloaded from www.nrcresearchpress.com by 61.7.252.67 on 09/04/12
For personal use only.

Can. J. Chem. Downloaded from www.nrcresearchpress.com by 61.7.252.67 on 09/04/12
For personal use only.

EQUIVALENT ORBITALS AND THE SHAPES OF EXCITED SPECIES[1]

J. W. LINNETT

ABSTRACT

The electron distributions in the ground states of C_2H_2, HCO, and NH_2, and in one excited state of each species, have been considered by transforming the simple molecular orbitals into equivalent ones. In the light of these considerations, the shapes and dimensions of the above species in these states have been discussed. It is found that a considerable degree of understanding can be achieved though there is uncertainty in the interpretation in some cases.

INTRODUCTION

The object of this paper is to discuss some ways in which the shapes of molecules and radicals in their ground and excited states are decided by their electronic structures. The molecule C_2H_2 and the radicals HCO and NH_2 will be considered as examples. An extensive treatment of this type of problem has been given by Walsh (10), his approach being that of *simple* molecular orbital (M.O.) theory. This method, in its simple form, implies that the total energy can be represented to a satisfactory approximation by the sum of a number of one-electron energies of values corresponding to the orbitals that are occupied. Clearly this is an overapproximation, for interelectronic effects arising both from their charge and from the consequences of the Pauli principle (i.e. effects of multiplicity) are ignored. To some extent, of course, in drawing diagrams in his papers, Walsh has taken account of these effects, for the graphs of energy against angle are not computed from a number of one-electron calculations but are derived on a more empirical basis.

Simple M.O. theory, because interelectronic effects are ignored, is clearly an oversimplification. This may be particularly serious in the discussion of shapes, for these are, to a large extent, decided by the mutual effects of electrons on one another. For example, methane is tetrahedral because the Pauli principle requires that four electrons with parallel spins in the $2s$ and three $2p$ orbitals of carbon will be, with greatest probability, at the corners of a regular tetrahedron (11). Moreover charge effects favor this shape also. Also NH_3 is pyramidal because of the presence of the lone pair and of the interaction of this with the bonding pairs (7). Consideration of shapes should therefore include interelectron effects as well as one-electron effects, and consequently the simple M.O. procedure is not wholly satisfactory.

The approach used in this paper will be that based on the representation of the molecular wave function in terms of equivalent orbitals which are linear combinations of the basic one-electron molecular orbitals, for these allow an easier appreciation of the electron distribution, and a more reasonable assessment of the effects of electron interactions. This procedure has been used previously by the author to discuss the bonding in the ground and some excited states of the diatomic molecules and ions formed by carbon, nitrogen, and oxygen (5). Equivalent orbitals of this type are to be preferred when electron distributions are being considered (4). It was found that the force constants and bond lengths correlated well with the number of electrons concentrated in the internuclear region, providing the types of orbitals that were occupied were taken into account.

For the diatomic molecules it was shown (5) that the wave function could be transformed in part from an M.O. description to an equal equivalent orbital description, the

[1]*Manuscript received August 16, 1957.*
Contribution from Inorganic Chemistry Laboratory and Queen's College, Oxford University, Oxford, England. This paper was presented at the Symposium on the Structure and Reactivity of Electronically-Excited Species held at the University of Ottawa, Ottawa, Canada, September 5 and 6, 1957.

equivalent orbitals being atomic orbitals if the L.C.A.O. (linear combination of atomic orbitals) approximation was being used for the molecular orbitals. Let us consider a diatomic molecule AB and the orbitals π_1 (bonding) and π_2 (antibonding). There are two degenerate π_1 orbitals, which may be designated π_1^+ and π_1^-, involving $e^{+i\phi}$ and $e^{-i\phi}$ respectively where ϕ is the azimuthal angle. To a first approximation one may write for the molecular orbitals expressions of the type

$$[1] \qquad \begin{aligned} \pi_1^+ &= a.2p\pi_A^+ + b.2p\pi_B^+, \\ \pi_2^+ &= a'.2p\pi_A^+ - b'.2p\pi_B^+, \end{aligned}$$

where a, b, a', and b' are all positive. Suppose that two electrons having parallel spins occupy π_1^+ and π_2^+, and, for the moment, that these are the only two electrons in the molecule. To satisfy the Pauli principle the wave function must be

$$[2] \qquad \begin{vmatrix} \pi_1^+(1).\alpha(1) & \pi_2^+(1).\alpha(1) \\ \pi_1^+(2).\alpha(2) & \pi_2^+(2).\alpha(2) \end{vmatrix},$$

where α is the spin function. The above function can easily be shown to be identical with

$$[3] \qquad \begin{vmatrix} 2p\pi_A^+(1).\alpha(1) & 2p\pi_B^+(1).\alpha(1) \\ 2p\pi_A^+(2).\alpha(2) & 2p\pi_B^+(2).\alpha(2) \end{vmatrix}.$$

So one may equally describe the electrons as being in the atomic orbitals $2p\pi_A^+$ and $2p\pi_B^+$ or as being in π_1^+ and π_2^+. On this basis one may describe the ground state (G.S.) of O_2 either as $\sigma_g^2.\sigma_u^2.\pi_u^4.\sigma_g^2.\pi_g^2$ or as $2s_A.\overline{2s_A}.2s_B.\overline{2s_B}.2p\pi_A^+.2p\pi_B^+.2p\pi_A^-.2p\pi_B^-.(\overline{\pi_u^+}.\overline{\pi_u^-}.\sigma_g.\overline{\sigma_g})$. In the second of these the presence of an electron with a β spin function in the orbital $2s_A$ is represented by $\overline{2s_A}$, while, if the spin wave function is α, the bar sign is omitted (5). This type of procedure will now be used to consider the shape and binding in some polyatomic molecules and radicals in both ground and excited states.

THE GROUND AND EXCITED STATES OF ACETYLENE

Ingold and King (3) have shown that the absorption band system of acetylene in the neighborhood of 2200 Å is due to a transition to an excited state in which the acetylene molecule is bent, having a *trans* configuration and a center of symmetry. They also bring forward good evidence for believing that the bond between the two carbon atoms is probably a three-electron bond and that the symmetry of the state is ^1A_u.

The electronic structure of the ground state of acetylene is analogous to that of nitrogen, which may be represented by $\sigma_g^2.\sigma_u^2.\pi_u^4.\sigma_g^2$. This is equivalent to $2s_A.\overline{2s_A}.2s_B.\overline{2s_B}.(\pi_u^+.\overline{\pi_u^+}.\pi_u^-.\overline{\pi_u^-}.\sigma_g.\overline{\sigma_g})$ and corresponds to a configuration of maximum probability in which each nitrogen nucleus and K-electron core is surrounded by two approximately tetrahedral sets of electrons, there being five in each set, three in the bond region and two on the internuclear axis, both these being outside the bond region and at opposite ends of the molecule (5). The configuration of maximum probability is therefore reminiscent of Baeyer's interpretation of the triple bond. In acetylene the first four electrons of the set $\sigma_g^2.\sigma_u^2.\pi_u^4.\sigma_g^2$ serve to bond the hydrogen atoms to the carbon, and the remaining six the two carbon atoms to one another, the spatial configuration of the electrons being satisfactory for doing this with a linear arrangement of the four nuclei. For N_2, a relatively small excitation of this system can be achieved by transferring one electron from the π_u to a π_g molecular orbital. Only singlet states will be considered here since it is certain that the excited state observed by Ingold and King is a singlet. There are several singlet states described by $\sigma_g^2.\sigma_u^2.\pi_u^3.\sigma_g^2.\pi_g$. They are:

Can. J. Chem. Downloaded from www.nrcresearchpress.com by 61.7.252.67 on 09/04/12
For personal use only.

$$\left.\begin{array}{l}\sigma_g\cdot\overline{\sigma_g}\cdot\sigma_u\cdot\overline{\sigma_u}\cdot\pi_u^{+}\cdot\overline{\pi_u^{+}}\cdot\pi_u^{-}\cdot\sigma_g\cdot\overline{\sigma_g}\cdot\overline{\pi_g^{+}} \\ \text{or}\quad 2s_A\cdot\overline{2s_A}\cdot 2s_B\cdot\overline{2s_B}\cdot\overline{2p\pi_A^{+}}\cdot\overline{2p\pi_B^{+}}\cdot(\pi_u^{+}\cdot\pi_u^{-}\cdot\sigma_g\cdot\overline{\sigma_g})\end{array}\right\}\ {}^1\Delta_u$$

$$\left.\begin{array}{l}\sigma_g\cdot\overline{\sigma_g}\cdot\sigma_u\cdot\overline{\sigma_u}\cdot\pi_u^{+}\cdot\pi_u^{-}\cdot(\overline{\pi_u^{+}}\cdot\overline{\pi_g^{-}}+\overline{\pi_u^{-}}\cdot\overline{\pi_g^{+}})\cdot\sigma_g\cdot\overline{\sigma_g} \\ \text{or}\quad 2s_A\cdot\overline{2s_A}\cdot 2s_B\cdot\overline{2s_B}\cdot(\overline{\pi_u^{+}}\cdot\overline{\pi_g^{-}}+\overline{\pi_u^{-}}\cdot\overline{\pi_g^{+}})\cdot(\pi_u^{+}\cdot\pi_u^{-}\cdot\sigma_g\cdot\overline{\sigma_g})\end{array}\right\}\ {}^1\Sigma_u^{-}$$

[4]

$$\left.\begin{array}{l}\sigma_g\cdot\overline{\sigma_g}\cdot\sigma_u\cdot\overline{\sigma_u}\cdot\pi_u^{+}\cdot\pi_u^{-}\cdot(\overline{\pi_u^{+}}\cdot\overline{\pi_g^{-}}-\overline{\pi_u^{-}}\cdot\overline{\pi_g^{+}})\cdot\sigma_g\cdot\overline{\sigma_g} \\ \text{or}\quad 2s_A\cdot\overline{2s_A}\cdot 2s_B\cdot\overline{2s_B}\cdot(\overline{\pi_u^{+}}\cdot\overline{\pi_g^{-}}-\overline{\pi_u^{-}}\cdot\overline{\pi_g^{+}})\cdot(\pi_u^{+}\cdot\pi_u^{-}\cdot\sigma_g\cdot\overline{\sigma_g})\end{array}\right\}\ {}^1\Sigma_u^{+}$$

For all these the bonding group is $(\pi_u^{+}\cdot\pi_u^{-}\cdot\sigma_g\cdot\overline{\sigma_g})$ so that the bond length would be expected to be about $0.92\times1.40 = 1.29$ Å (cf. Linnett (5), Table 3 (1.40) and Figure 1 (0.92)). No ${}^1\Delta_u$ state has been identified for N_2 but the state designated j (Herzberg (1)) is described as ${}^1\Sigma_u^{+}$ (about 100,000 cm.$^{-1}$ above the G.S.) and the state a' (probably 60,000 cm.$^{-1}$ above the G.S.) is probably ${}^1\Sigma_u^{-}$. The first of these (j) has $r_0 = 1.28$ Å while the second (a') has $r_e = 1.28$ Å. It seems possible therefore that j and a' are to be identified with the corresponding two states described just above.

The three states just described differ in the non-bonding group of two electrons with parallel spins, one in a π_u (bonding) and one in a π_g (antibonding) orbital. The differing groups are:

[5]

$${}^1\Delta_u:\quad \pi_u^{+}\cdot\pi_g^{+}\qquad\qquad (\text{and } \pi_u^{-}\cdot\pi_g^{-})$$

$${}^1\Sigma_u^{-}:\ (\pi_u^{+}\cdot\pi_g^{-}+\pi_u^{-}\cdot\pi_g^{+})$$

$${}^1\Sigma_u^{+}:\ (\pi_u^{+}\cdot\pi_g^{-}-\pi_u^{-}\cdot\pi_g^{+})$$

For the situation in which electrons 1 and 2 occupy the above orbitals the above become, using $\pi_u^{+} = \pi_u\cdot e^{+i\phi}$ and $\pi_g^{-} = \pi_g\cdot e^{-i\phi}$, etc.:

[6]

$${}^1\Delta_u:\ \{\pi_u(1)\cdot\pi_g(2)-\pi_u(2)\cdot\pi_g(1)\}\{\cos(\phi_1+\phi_2)\pm i\sin(\phi_1+\phi_2)\}$$
$$\text{or}\ \{2p\pi_A(1)\cdot2p\pi_B(2)-2p\pi_A(2)\cdot2p\pi_B(1)\}\{\cos(\phi_1+\phi_2)\pm i\sin(\phi_1+\phi_2)\}$$

$${}^1\Sigma_u^{-}:\ \{\pi_u(1)\cdot\pi_g(2)-\pi_u(2)\cdot\pi_g(1)\}\{\cos(\phi_1-\phi_2)\}$$
$$\text{or}\ \{2p\pi_A(1)\cdot2p\pi_B(2)-2p\pi_A(2)\cdot2p\pi_B(1)\}\{\cos(\phi_1-\phi_2)\}$$

$${}^1\Sigma_u^{+}:\ \{\pi_u(1)\cdot\pi_g(2)+\pi_u(2)\cdot\pi_g(1)\}\{\sin(\phi_1-\phi_2)\}$$
$$\text{or}\ \{2p\pi_A(1)\cdot2p\pi_A(2)-2p\pi_B(1)\cdot2p\pi_B(2)\}\{\sin(\phi_1-\phi_2)\}$$

(When considering the symmetry of these last expressions it must be remembered that the bonding group $\pi_u^{+}\cdot\pi_u^{-}$ has the symmetry represented by a negative sign so that the symmetry of the whole group of electrons is the reverse of the symmetry of the pair considered in the expressions [6].) The probability distribution for this non-bonding group in the ${}^1\Delta_u$ state is independent of ϕ_1 and ϕ_2, one electron being on each nitrogen atom. For the ${}^1\Sigma_u^{-}$ state there is one electron on each atom so placed that the highest probability is when the two are in the same plane (i.e. $(\phi_1-\phi_2) = 0$ or π). The ${}^1\Sigma_u^{+}$ state is an ionic state, there being a high probability of both electrons being simultaneously on A or on B. This means that the electron pattern of the ${}^1\Delta_u$ state may be summarized as $sp^3(\sigma\pi^2)$; $sp^2(\sigma)$.* The first group, $sp^3(\sigma\pi^2)$, forms a set like that for a conventional

*The symbolism used here has been described by the author elsewhere (5) and signifies a set of one spin which employs an sp^3 group of orbitals from each atom, the bonding group consisting of three electrons in a σ and two π orbitals, and a second set of the other spin which employs an sp^2 group of orbitals from each atom, the bonding group consisting of one electron in a σ orbital. The atomic orbitals used are given outside the brackets and the bonding orbitals inside the brackets. In addition the orbitals occupied by electrons of one spin are given before the semicolon and those occupied by electrons of the other spin are given after the semicolon.

Can. J. Chem. Downloaded from www.nrcresearchpress.com by 61.7.252.67 on 09/04/12
For personal use only.

triple bond, which has been described above. The second group, $sp^2(\sigma)$, of five electrons involves in the configuration of maximum probability a triangular arrangement round each atom, one electron being between the nuclei (5). In the $^1\Delta_u$ state the plane of the triangular group round one atom is independent of the plane of the group round the other atom (probability independent of ϕ_1 and ϕ_2). For the $^1\Sigma_u^-$ state the electron pattern is also $sp^3(\sigma\pi^2)$; $sp^2(\sigma)$, but the triangular planes of the electrons of the $sp^2(\sigma)$ set tend to lie in the same plane (maximum when $(\phi_1-\phi_2) = 0$ or π). For the $^1\Sigma_u^+$ state the electron pattern is $sp^3(\sigma\pi^2)$; $sp(p^2)^{\frac{1}{2}}(\sigma)$, this being an ionic state.

Consideration of acetylene differs from that of nitrogen in that the location of the protons must also be examined. These protons will be in a particular spatial relation to one another and to the rest of the molecule. For this reason the electronic pattern of the $^1\Delta_u$ states will not be well suited to holding the protons since the electrons of the $sp^2(\sigma)$ set on the two atoms do not tend to have any particular spatial relation with respect to one another with the result that the electron cloud will tend to be too diffuse for binding. In the $^1\Sigma_u^-$ state the two sets are separately well suited to bonding the protons but in different places. The $sp^3(\sigma\pi^2)$ set would tend to bind them in a linear form on the CC axis, but the $sp^2(\sigma)$ set will tend to bind them in a non-linear planar form, either *cis* or *trans*. So this state unmodified is not suited to binding the two protons. However if the electrons of the $sp^3(\sigma\pi^2)$ set, which are outside the central bond region, are displaced towards the directions of the electrons of the $sp^2(\sigma)$ set, two electron pair CH bonds could be formed. But, if this happened without any modification of the $\sigma\pi^2$ group in the central bond region, the electron configuration round each carbon atom would become very unbalanced and this is improbable on the grounds of both charge and spin correlation. The unevenness of the distribution can be remedied to some extent by moving an electron out of the bond region so that the $sp^3(\sigma\pi^2)$ set becomes $sp^2p^{\frac{1}{2}}(\sigma\pi)$, one tetrahedral position on each carbon atom being occupied by only one electron. On this basis, this excited state of acetylene would be expected to be planar and non-linear (probably *trans* because of charge repulsion effects), involving an ordinary electron pair CH bond and a CC bond having three electrons in the bond region (even though it is derived from a state of N_2 having four electrons in the bond region). All these features are observed by Ingold and King, the CC and CH bond lengths being 1.383 and 1.09 Å respectively, the corresponding vibration frequencies being consistent with these values. Moreover, the bending frequency for the excited state is higher than that in the ground state, which would be anticipated for this structure (cf. Walsh (10)). This is the electronic structure suggested by Ingold and King for the excited state, for the $^1\Sigma_u^-$ state of the linear molecule correlates with the ^1A_u state of the bent one and the orbital occupation would also be that expected. The orbitals of *trans* HCCH will now be considered briefly.

The possible molecular orbitals of *trans* HCCH are of the symmetries represented by a_g, a_u, b_g, and b_u; a and b represent orbitals symmetric and antisymmetric to the twofold symmetry axis, and g and u those that are symmetric and antisymmetric to the center respectively. The four singlet excited states which correlate with the $^1\Delta_u$ (^1A_u and ^1B_u), $^1\Sigma_u^-$ (^1A_u), and $^1\Sigma_u^+$ (^1B_u) states are:

$$
\begin{aligned}
&^1A_u\colon a_g\cdot\overline{a_g}\cdot b_u\cdot\overline{b_u}\cdot a_g\cdot\overline{a_g}\cdot \;\vdots\; a_u\cdot b_u\cdot\overline{b_u}\cdot\overline{a_g}\\
&^1A_u\colon a_g\cdot\overline{a_g}\cdot b_u\cdot\overline{b_u}\cdot a_g\cdot\overline{a_g}\cdot \;\vdots\; a_u\cdot\overline{a_u}\cdot b_u\cdot\overline{b_g}\\
&^1B_u\colon a_g\cdot\overline{a_g}\cdot b_u\cdot\overline{b_u}\cdot a_g\cdot\overline{a_g}\cdot \;\vdots\; a_u\cdot\overline{a_u}\cdot b_u\cdot\overline{a_g}\\
&^1B_u\colon a_g\cdot\overline{a_g}\cdot b_u\cdot\overline{b_u}\cdot a_g\cdot\overline{a_g}\cdot \;\vdots\; a_u\cdot b_u\cdot\overline{b_u}\cdot\overline{b_g}
\end{aligned}
\qquad [7]
$$

The orbitals to the right of the dotted line correlate with the $\pi_u^3\cdot\pi_g$ group of the linear

Can. J. Chem. Downloaded from www.nrcresearchpress.com by 61.7.252.67 on 09/04/12
For personal use only.

molecule. The two derived from the $\pi_u^+.\pi_u^-$ group of two electrons with the same spin are in all cases the $a_u.b_u$ pair. The pair derived from the $\pi_u.\pi_g$ set with the other spin differs in the four cases. In the first ^1A_u state it is a $b_u.a_g$ and both these orbitals are concentrated in the plane of the molecule. For the second ^1A_u state both the orbitals ($a_u.b_g$) are concentrated out of the plane of the molecule, the molecular plane being a node. Electrons in these two orbitals are clearly not suited to binding the protons in the molecular plane. With the two ^1B_u states the orbital pairs are $a_u.a_g$ and $b_u.b_g$. In both cases one orbital is concentrated in the molecular plane and the other has that plane as a node. This group will not be suited for binding the atoms in a planar arrangement. So the only state of this set of four which would be expected to provide strong binding for the atoms in a planar arrangement is the first ^1A_u state. This correlates with the $^1\Sigma_u^-$ state, which has just been discussed as providing a suitable basis for the binding, if a modification occurs which leads to the molecule becoming non-linear. The whole interpretation is therefore entirely self-consistent as between the electronic structures of the linear and bent forms (9), and also as between the electronic structure and the observed shape and dimensions.

THE NH_2 RADICAL

The lowest state of a linear NH_2 radical would be expected to be a $^2\Pi$ state having the orbital occupation $\sigma_g.\overline{\sigma_g}.\sigma_u.\overline{\sigma_u}.\pi_u^+.\overline{\pi_u^+}.\pi_u^-$. The orbitals occupied by the electrons of one spin form the set $\sigma_g.\sigma_u.\pi_u^+.\pi_u^-$, which will involve contributions from the $2s$ and three $2p$ orbitals of the nitrogen atom. Therefore it will be expected that there will be a tetrahedral group of four electrons round the nitrogen atom. The orbitals occupied by electrons of the other spin form the set $\overline{\sigma_g}.\overline{\sigma_u}.\overline{\pi_u^+}$, which will involve contributions from the $2s$ and two $2p$ orbitals of the nitrogen atom. Therefore it will be expected that there will tend to be a triangular group of three electrons round the nitrogen atom. Neither of these sets is in fact suitable for binding the atoms in a straight line. However they are both well suited to binding the two protons in directions which are at about 110° with respect to one another. A suitable mutual orientation of the triangle and the tetrahedron can achieve this simultaneously. In fact, NH_2, in the ground state, is found to be non-linear (8), though the angle ($103\frac{1}{3}°$) is smaller than would be expected from the above arguments. Presumably the explanation for this lies in the polarization of the electron cloud round the nitrogen atom as a result of the presence of the protons. Such polarization always tends to cause a reduction in interbond angles (6). The electronic structure then becomes $a_1.\overline{a_1}.b_2.\overline{b_2}.a_1.\overline{a_1}.b_1$ (cf. Walsh (10)).

The two members of the degenerate pair of the $^2\Pi$ ground state of linear NH_2 pass, on bending the molecule in a particular plane, into the configurations $a_1.\overline{a_1}.b_2.\overline{b_2}.a_1.\overline{a_1}.b_1$ and $a_1.\overline{a_1}.b_2.\overline{b_2}.a_1.b_1.\overline{b_1}$. As has been said, the consequence of this, for the ground state, is that the set of four of one spin and the set of three of the other both tend to cause the HNH angle to be about 110°. Moreover, in the ground state, these effects operate in the same plane for both spin sets. In the excited state, the set of four electrons is similar, but the set of three would here tend to bend the molecule in a plane at right angles to that in which the set of four would tend to bend it. The experimental data indicate that the best compromise between these two effects results in the molecule having the lowest energy when it is linear.

THE HCO RADICAL

This is isoelectronic with the NO molecule, which, in the ground state, has the structure $\sigma_1.\overline{\sigma_1}.\sigma_2.\overline{\sigma_2}.\pi_1^+.\overline{\pi_1^+}.\pi_1^-.\overline{\pi_1^-}.\sigma_3.\overline{\sigma_3}.\pi_2^+$. One group of orbitals ($\sigma_1.\sigma_2.\pi_1^+.\pi_1^-.\sigma_3.\pi_2^+$) is

Can. J. Chem. Downloaded from www.nrcresearchpress.com by 61.7.252.67 on 09/04/12
For personal use only.

that characteristic of an ordinary double bond, $sp^3(\sigma\pi)$, and the other group $(\overline{\sigma_1}.\overline{\sigma_2}.\overline{\pi_1^+}.\overline{\pi_1^-}.\overline{\sigma_3})$ is that characteristic of an ordinary triple bond, $sp^3(\sigma\pi^2)$. On passing to a consideration of HCO it is clear that there is no direction from the carbon atom in which two electrons, one from each set, tend to be concentrated. An electron pair CH bond can however be achieved in the same manner as that discussed for the excited state of HCCH, namely by modifying the $sp^3(\sigma\pi^2)$ group to one of $sp^2p^{\frac{1}{2}}(\sigma\pi)$ so that the electrons not in the CO bond region are concentrated off the CO axis. However it would seem that, as with acetylene, this can only be done at the expense of weakening the CO bond; in this case, from a five-electron to a four-electron one. The observed length is 1.20 Å(2), which may be compared with 1.23 for H_2CO, 1.16 for CO_2 and COS, and 1.13 for CO. It is not clear just how the observed lengths should be interpreted. The length is nearer to that in H_2CO than that in CO but it is not certain what allowance should be made for the absence of one proton and one electron compared with H_2CO. A possibility is that the electronic structure is intermediate between that in which the CH bond is an electron pair bond and the CO a four-electron one, and that in which the CH is essentially a one-electron bond and the CO a five-electron bond. This would explain why the CO bond is somewhat shorter than that in H_2CO, why the molecule is bent, but it would suggest that the CH might be somewhat weak. Information on this is not available.

Of the excited state observed by Herzberg and Ramsay (2) three structural features are known: (*a*) the molecule appears to be linear; (*b*) the CO bond length (1.18) is a little smaller than that in the ground state, though still considerably longer than that in CO; (*c*) the CH valence vibration suggests a strong CH bond analogous to those in the ground states of HCN and HCCH.

The lowest state of linear HCO is a Π state and therefore doubly degenerate. If the molecule is bent in a particular plane, these members of the doubly degenerate pair pass into the states $a_1'^2.a_2'^2.a_3'^2.a_1''^2.a_4'^2.a_5'$ and $a_1'^2.a_2'^2.a_3'^2.a_1''^2.a_4'^2.a_2''$ since the degenerate members of the Π pair of orbitals pass into an a' and an a'' orbital (cf. Walsh (10)). The situation appears to be somewhat similar to that in NH_2. That is, for the ground state, both sets of electrons have configurations tending to cause the molecule to bend in the same plane, while, for the excited state, the two sets have configurations tending to cause the molecule to bend in different planes, with the result that the best compromise (i.e. lowest energy) is achieved when the molecule is linear. In this linear configuration the structure of the set of five electrons having the same spin will probably be $sp^3(\sigma\pi^2)$, since this tends to concentrate an electron on the OC axis for binding the hydrogen atom. The other set must remain $sp^3(\sigma\pi)$. However, this will mean that, in the linear excited state, there will be a greater concentration of electrons in the CO bond region than in the bent ground state. This accounts for the CO bond being shorter in the excited than in the ground state, as is observed. However, the strength of the CH bond is surprising.

SUMMARY

From the above discussion it can be seen that considerations of the above kind, which involve transforming the molecular orbitals into orbitals more localized in particular, and if possible separate, regions of space, enable one to draw conclusions about the electron distribution in different states. As a consequence, certain properties of the ground and excited states can be understood. The application of these ideas has been most successful for the states of acetylene involved in the transition observed by Ingold and King. The interpretation of the states of NH_2 and HCO is however less certain in the present state of our understanding of electron configurations.

Can. J. Chem. Downloaded from www.nrcresearchpress.com by 61.7.252.67 on 09/04/12
For personal use only.

ACKNOWLEDGMENT

I wish to thank Dr. D. A. Ramsay for the conversation we had recently in Oxford about his work on HCO and NH_2.

REFERENCES

1. HERZBERG, G. Molecular spectra and molecular structure of diatomic molecules. D. Van Nostrand Co. Inc., New York. 1950. p. 553.
2. HERZBERG, G. and RAMSAY, D. A. Proc. Roy. Soc. (London), A, **233,** 34 (1956).
3. INGOLD, C. K. and KING, G. W. J. Chem. Soc. 2702, 2704, 2708, 2725, 2745 (1953).
4. LENNARD-JONES, J. E. J. Chem. Phys. **20**, 1024 (1952).
5. LINNETT, J. W. J. Chem. Soc. 275 (1956).
6. LINNETT, J. W. and MELLISH, C. E. Trans. Faraday Soc. **50,** 657 (1954).
7. LINNETT, J. W. and POE, A. J. Trans. Faraday Soc. **47,** 1033 (1951).
8. RAMSAY, D. A. J. Chem. Phys. **25,** 188 (1956).
9. ROSS, I. G. Trans. Faraday Soc. **48,** 973 (1952).
10. WALSH, A. D. J. Chem. Soc. 2260, 2266, 2288, 2296, 2301, 2306, 2318, 2321, 2325, 2330 (1953).
11. ZIMMERMANN, H. K. and VAN RYSSELBERGHE, P. J. Chem. Phys. **17,** 598 (1949).

Can. J. Chem. Downloaded from www.nrcresearchpress.com by 61.7.252.67 on 09/04/12
For personal use only.

Can. J. Chem. Downloaded from www.nrcresearchpress.com by 61.7.252.67 on 09/04/12
For personal use only.

THE NATURE OF FORMALDEHYDE IN ITS LOW-LYING EXCITED STATES[1]

G. W. Robinson and V. Erdmanis DiGiorgio

ABSTRACT

Long path length, high resolution spectra in the near ultraviolet of H_2CO and D_2CO at −78° C. have been obtained, and further strong evidence in support of a non-planar excited state is presented. The double-headed bands to the long wavelength side of the singlet–singlet system are shown to belong to the singlet–triplet transition. A vibrational analysis and partial rotational analysis shows the excited triplet state to be very similar to the excited singlet state. The larger C—O stretching frequency in the triplet state may characterize the multiplicity of these states in the simple aliphatic aldehydes and ketones. It is found that the C—O bond order in both states is very nearly 1.5, and striking similarities between the bonding in these states and the C—O bonding in formic acid are pointed out. The similarity between the singlet and triplet excited states may not extend to chemical behavior because of spin correlation rules, but there are no general reasons why the triplet state should be more reactive than the singlet.

INTRODUCTION

Recently an extensive body of experimental evidence has indicated that a rather large difference in geometry exists between the ground and excited state structures of most simple polyatomic molecules. In many instances, even the symmetry properties of the equilibrium configurations are different. For example, acetylene, while linear in its ground state, has a non-linear *trans* configuration in its low-lying excited state (15). Ethylene has a planar structure in the ground state with a very high barrier for internal rotation, but in its low-lying $^1B_{1u}$ state, as well as in its Rydberg states, the molecule exhibits an equilibrium configuration in which the CH_2 groups are no longer coplanar, and the barrier for internal rotation is more nearly that expected for a carbon–carbon single bond (37, 38). The molecules NH_2 (9, 29), HCO (14), and probably NO_2 (31) are bent in the ground state but linear in their low-lying excited states, while for CS_2 (16) and quite likely HCN and CO_2 (34, 35), the opposite holds true. The ammonia molecule has a low-lying electronic state which has a planar configuration (1), and formaldehyde, the topic of this paper, is non-planar in its low-lying excited states (3, 30).

Such changes in geometry are to be expected if the *bonding* electron configuration is changed by the electronic transition. For similar reasons, chemical properties are expected to be quite different in the ground as compared with the excited states of such molecules.

The formaldehyde molecule is an excellent testing ground for the study of these effects. An intimate knowledge concerning the low-lying excited states has intrinsic interest since the molecule is a simple example of a group of molecules on which a considerable number of photochemical investigations have been made (27). Furthermore, the long wavelength system is a prototype of n–π^* transitions which have attracted a great deal of theoretical and experimental interest. Finally, evidence presented here indicates that certain of the long wavelength absorption bands are associated with a singlet–triplet transition in the molecule, so that now the possibility exists of studying in detail the rotational–vibrational structure of a triplet state in a polyatomic molecule.

The first part of the paper discusses in a qualitative way the electronic, structural, and chemical properties of the low-lying excited states of formaldehyde based on the

[1]*Manuscript received August 16, 1957.*

Contribution from Department of Chemistry, The Johns Hopkins University, Baltimore, Maryland. This paper was presented at the Symposium on the Structure and Reactivity of Electronically-Excited Species held at the University of Ottawa, Ottawa, Canada, September 5 and 6, 1957.

Work supported in part by the Office of Ordinance Research, U.S. Army, under Project No. TB2-0001 of Contract No. DA-36-034-ORD-2169.

results of recent spectroscopic investigations. The second part treats briefly the experimental techniques and gives some details concerning the more recent investigations of the singlet–singlet as well as the singlet–triplet systems.

THE GROUND STATE

The absence of inversion doubling in addition to the observed statistical weights of the rotational sublevels definitely shows that the ground state has the well-known planar Y-shaped structure of point group C_{2v} (12). In spite of the large amount of work on formaldehyde and its isotopically substituted species, zero-point vibrations cause some uncertainty to exist in the structural determination (7).

The electronic structure of the ground state has been discussed by Mulliken (23), McMurry and Mulliken (22), and more recently by Walsh (36). The 12 valence electrons are situated in the six lowest-lying molecular orbitals which in approximate order of energy are*

$$(1a_1)^2(2a_1)^2(1b_2)^2(3a_1)^2(1b_1)^2(2b_2)^2(2b_1)^0(4a_1)^0 \ {}^1A_1.$$

Roughly, the nature of these orbitals with respect to molecular bonding is

$1a_1$	$2s$ oxygen, non-bonding
$2a_1$	CH_2, bonding
$1b_2$	CH_2, bonding
$3a_1$	CO, σ bonding
$1b_1$	CO, π bonding
$2b_2$	$2p_y$ oxygen, lone pair non-bonding
$2b_1$	CO, π antibonding
$4a_1$	CO, σ antibonding.

The orbitals $2b_1$ and $4a_1$ are the first two excited orbitals.

Since the low-lying transitions in the molecule are localized in the CO bond, an alternative and fairly useful description regards formaldehyde as a perturbed linear molecule with symmetry axis along the CO direction. In the linear limit the a_1 orbitals correlate with σ-orbitals as does $1b_2$. The pairs $1b_1$ and $2b_2$ as well as $2b_1$ and $3b_2$ (not listed) become degenerate in this limit to form π-orbitals. The correlation diagram will resemble very closely that given by Walsh (35) for HAB molecules except an additional low-lying σ-orbital must be added. The available electrons fill all orbitals up to and including the first π-orbital, which holds four electrons, and the electronic symmetry is thus $^1\Sigma^+$ (perturbed).

THE NEAR ULTRAVIOLET TRANSITIONS

The lowest-lying electronic states in formaldehyde result from excitation of an electron from the non-bonding $2b_2$ orbital into the $2b_1$ excited orbital which is CO antibonding. A triplet state $^3A_2$ and a singlet state $^1A_2$ result. The presence of the antibonding π-electron in both states is expected to cancel approximately the bonding power of a bonding π-electron so that essentially *a three-electron bond results*. The CO linkage is expected to be about intermediate in length between a single and double bond. The HCH angle should be smaller† while the C—H distance should be larger than these same parameters in the ground state. The force constants and vibrational frequencies are well known to change in a similar way (3).

*The notation throughout is that suggested by Mulliken (25).
†The opposite is actually observed.

Can. J. Chem. Downloaded from www.nrcresearchpress.com by 61.7.252.67 on 09/04/12
For personal use only.

Can. J. Chem. Downloaded from www.nrcresearchpress.com by 61.7.252.67 on 09/04/12
For personal use only.

The most interesting effect of the decreased bond order is the lack of stability of the planar equilibrium configuration in these excited states (3, 30), the out-of-plane angle lying about midway between zero degrees and the out-of-plane angle for a tetrahedral structure (55°). Thus, strictly speaking, the electronic wave functions do not transform as representations of C_{2v}, but this is still a good approximation since the molecular orbitals do not feel very strong perturbative effects of the hydrogens. For this reason and for simplicity of discussion we prefer to retain the C_{2v} nomenclature throughout. In those instances where effects arise owing to the slight deviation from C_{2v} symmetry, the appropriate C_s description will be given in parentheses.

Because of the non-planar equilibrium configuration of the excited states, inversion doubling occurs (3, 30). The extremely low observed barriers for inversion indicate that a very small amount of energy stabilization is gained through mixing of carbon $2s$ and $2p_x$ orbitals in the non-planar molecule. The doubling of vibrational levels, many of which are not observed, introduces some uncertainty into the determination of excited state fundamentals.

The chemical properties of these states are quite different from those of the ground state, but *there are no general reasons why the triplet state should be more reactive than the singlet* since both exhibit nearly identical electronic structures. Both have two free valences and may be appropriately described as diradicals. The conservation of electron spin angular momentum (13) may under certain conditions allow one species to be more reactive than the other. For example, it would be predicted that the triplet states, but not the excited singlet states, of aldehydes and ketones would react very rapidly with O_2 ($^3\Sigma_g^-$ ground state), since in the latter case the reaction intermediate can not be produced in its singlet ground state. Such reactions of excited polyatomic molecules have not been discussed to a great extent in the past, but may in certain cases be important as evidenced from recent work (28).

Transitions to the $^{1,3}A_2$ excited states can be observed in absorption, while emission has been observed only for the singlet–singlet transition. These transitions are formally forbidden under the strict C_{2v} selection rules but occur through mixing with nearby electronic states. The strong type-B ($\perp$) bands are actually allowed by the non-planar selection rules (3) but could gain intensity through mixing with the $^1B_2$ state at $\sim$7 ev.

The weaker type-A ($\parallel$) bands are of a kind $^1A_1(^1A') \rightarrow {}^1A_2(^1A'')$ in the total vibronic sense and are strictly forbidden under the C_{2v} as well as the C_s selection rules. These transitions may gain intensity through mixing with a neighboring A_1 state (3), but there is an alternative way of understanding this apparent anomaly.* In the perturbed linear description of formaldehyde, three excited states would result from excitation of an electron to the first excited π-orbital, Σ^+, Σ^-, and Δ, the last probably lying lowest.

*NOTE ADDED IN PROOF.—*According to a paper soon to be published by J. A. Pople and J. W. Sidman, the mixing of A_1 and A_2 electronic states arises through a rotational-electronic interaction. That vibrationally-induced mixing does not occur to give a $\parallel$-type zero–zero band is clear, since there is no fundamental with a_2 symmetry. The viewpoint taken by us that formaldehyde can be considered a perturbed linear molecule with inherent mixing of the originally degenerate electronic states is exactly equivalent to the theory of Pople and Sidman. This was pointed out to us by Professor H. C. Longuet-Higgins in a private discussion. The interaction is the electronic analogue of the coriolis type rotational-vibrational interactions which cause mixing of approximately degenerate vibrational states of different symmetries in polyatomic molecules. The mixing gives rise to vibrational angular momentum which can interact with the rotational angular momentum to produce anomalies in the subband positions and intensities. In the present problem, electronic orbital angular momentum about the C—O axis arises from the interaction. In the absence of spin the perturbation can be detected through intensity anomalies, but in the triplet state, Hund's case-a coupling can occur, and subband positions as well as intensities are affected. The as yet incomplete experimental observations seem to bear out these concepts quite well, but it should be remembered that the observed $\parallel$-type bands could occur in an electric quadrupole transition.

The $^1\Delta$ state correlates with the $^1A_2$ state in the non-linear molecule, and the long wavelength spectrum could be described as a highly perturbed $^1\Sigma^+ \leftrightarrow {}^1\Delta$ transition for which $\Delta K = 0, \pm 1$. Type-C ($\perp$) bands were not observed even though some effort was made to find them. These would be Franck–Condon forbidden since they require excitation of b_2 vibrations in the excited state.

The singlet–triplet transition becomes allowed probably through a spin–orbit perturbation. The orbital part of the perturbation operator transforms as representations of the rotational subgroup $\mathbf{C}_2$, and because of symmetry, matrix elements are non-zero only for certain pairs of interacting electronic states (20). According to these selection rules, the $^3A_2$ state can mix with $^1B_1$, $^1B_2$, and $^1A_1$ states through perturbations by the x, y, and z components, respectively, of the spin–orbit operator. The observed bands resemble double-headed parallel bands having an irregular subband structure (see Fig. 3). Until a complete rotational analysis of these bands is obtained, however, the exact nature of the perturbing state will not be known. At present, it would appear that the z component of the perturbation operator is the one responsible for the mixing. This result is in disagreement with previous theoretical and experimental investigations (21).

EMISSION SPECTRUM

In formaldehyde, as in the higher aldehydes and ketones, the fluorescence and discharge emission spectra are identical (32), and their existence indicates the presence of relatively stable excited states in these molecules. It is well established (3, 30) that *the triplet state is not involved to an observable extent in emission*, and all observed bands have now been explained solely on the basis of the $^1A_2 \rightarrow {}^1A_1$ transition. A good reproduction of the very sharp electrodeless discharge spectrum can be found in the literature (30). As in most polyatomic systems, transitions occur from only a few of the lowest-lying vibrational levels in the excited electronic state. In H_2CO, under the conditions of discharge tube excitation, emission occurs strongly from the vibronic ground level and also from the level in which one quantum of ν_2' has been excited. Much weaker transitions occur from $2\nu_2'$ and also from the 0^- member of the first inversion doublet. The only ground state fundamentals which are involved are ν_4'' and ν_2'', this being in qualitative agreement with the predictions of the Franck–Condon principle.

The vanishingly small emission intensity from the $1^\pm$ inversion doublet in H_2CO is strong evidence in favor of predissociation in this region of the potential energy surface (4). This would set an upper limit to the dissociation energy,

$$H_2CO(^1A_1) \rightarrow H(^2S) + CHO(^2A'),^* \qquad E_{diss} \leqslant 28728 \text{ cm.}^{-1} \text{ (82.1 kcal./mole).}$$

A few remarks about the photolysis of H_2CO at 3650 Å (10) should be made. At dry ice temperature the absorption coefficient is negligible, the 3650 Å Hg line falling between two singlet–triplet bands. However, at temperatures where photochemical experiments must be performed to avoid polymerization, i.e. $T > 100°$ C., there is considerable hot band structure from the $^1A_1 \rightarrow {}^1A_2$ transition in this region. The analysis of the spectrum shows that the primary photochemical process would populate high rotational sublevels of 0^+ or $0^+ + \nu_2'$, these final states lying somewhat higher than 82 kcal./mole. It is therefore probable that the previously reported upper limit of 78 kcal./mole is slightly low. It should be mentioned that in these low-lying regions of the excited state

**The $^2A'$ state is probably the electronic ground state of* CHO *(35). The minimum additional energy needed to produce electronically excited* CHO *is about 10,000 cm.$^{-1}$ (14). See, however, Refs. (4) and (14).*

Can. J. Chem. Downloaded from www.nrcresearchpress.com by 61.7.252.67 on 09/04/12
For personal use only.

potential energy surface, the predissociation is so relatively weak that the rotational fine structure in absorption can be resolved to at least 0.1 cm.$^{-1}$. Even so, the transition probability for predissociation may still be a factor of 10^4 greater than that for the radiative transition. The intermediate dissociative state through which these predissociation processes occur is no doubt the first excited C—H antibonding triplet state since this state would correlate with the correct dissociation products.

The report (11) of two emitting levels, presumably $^1A_2$ as well as $^3A_2$, in acetone is puzzling and may indicate that the complex nature of the potential surfaces in the larger molecules is more advantageous to triplet state population prior to emission.

THE ABSORPTION SPECTRUM

In order to resolve the rotational structure in the weak singlet–triplet transition, collision broadening and hot band overlapping must be reduced to a minimum. To accomplish this, multiple pass techniques at −78° C. were employed both for H_2CO and for D_2CO. The gain in resolution above that obtained under ordinary conditions is striking, the limitation apparently being instrumental resolving power, in this case 250,000.

A multiple pass cell similar to the one described by Bernstein and Herzberg (2) was capable of giving path lengths of up to about 50 meters. The cell was cooled with dry ice, and at this temperature, formaldehyde pressures of 30 mm. Hg could be used. This pressure furnishes more than the necessary meter-atmosphere absorbing path for observation of the singlet–triplet bands. The procedure is also the most convenient for observation of the singlet–singlet system, since it was found that the vapor pressure of the gas over the polymer kept at room temperature is adequate. The rate of polymerization on the mirror surfaces was finite yet sufficiently slow so as not to cause difficulties.

The lack of hot band structure not only aids in the rotational analysis but also permits an unambiguous vibrational analysis to be made. For example, the photographs shown in Fig. 1 leave no doubt as to the hot band nature of the α-band at 27021 cm.$^{-1}$, and also they conclusively show the singlet–triplet bands to be temperature insensitive.

The Singlet–Singlet System

The very nice work of Brand (3) on the vibrational analysis of the emission and absorption systems quite strongly indicates a non-planar excited state. At about the same time, the rotational analysis of the α-band in emission was completed (30, 33) and showed a negative inertial defect, $\Delta = I_C - I_A - I_B$, in the excited state, proving beyond doubt the non-planar structure. The analysis will be published elsewhere (33), but the results are listed in Table I. The structural parameters, except for the HCH

TABLE I

H_2CO PARAMETERS, GROUND AND $^1A_2$ ELECTRONIC STATES

	Ground state (7, 17)		$^1A_2$ state	
I_A	1.792	a.m.u.-Å^2	1.881	a.m.u.-Å^2
I_B	13.015		14.985	
I_C	14.864		16.767	
Δ	+0.057		−0.099	
∠HCH	120°		122°	
C=O	1.22 Å		1.32 Å	
C—H	1.08 Å		1.09 Å (assumed)	
Out-of-plane angle	0°		20°	

Can. J. Chem. Downloaded from www.nrcresearchpress.com by 61.7.252.67 on 09/04/12
For personal use only.

angle and possibly the C—H distance, do lie about midway between Sp^2 and Sp^3 structures, but these must be considered tentative because of the lack of CD_2O data as well as the effect of zero-point vibrations.

The once puzzling 127 cm.$^{-1}$ spacing in the excited state is simply a result of inversion through a very low potential barrier. The first two intense $\perp$-bands of the absorption system are transitions from the ground vibronic state to the 0^- and 1^- members of the inversion doublets, and Brand assigned the weak $\parallel$-bands in this region to similar transitions involving 0^+ and 1^+. Since high dispersion plates taken of the gas at $T >$ 100° C. did not show clearly the presence of 0^+, there was some doubt about this interpretation (30), but the validity of Brand's assignment is completely borne out by a study of the spectrum at $T = -78°$ C. (see Fig. 2). The band marked 0^+, highly overlapped by the ^pP-branches of the A-band (0^-), should have the same lower state as the A-band and the same excited state as the α-band. A partial rotational analysis (19) shows that this is indeed the case. Incidentally, from these analyses an improved value of the out-of-plane bending fundamental in the ground state can be obtained (Table II). The barrier for inversion can be calculated to be ~650 cm.$^{-1}$ (3) from the positions

TABLE II

FUNDAMENTAL FREQUENCIES (cm.$^{-1}$) IN THE GROUND AND EXCITED STATES OF H_2CO AND D_2CO

	H_2CO			D_2CO		
	$^1A_1$	$^1A_2$	$^3A_2$	$^1A_1$	$^1A_2$	$^3A_2$
0^-	—	127	30	—	69	
1^+	—	530	537	—	387	448
1^-	—	951	779	—	669	
2^+	—		1171	—		889
2^-	—			—		
ν_1	2780	2851		2056	2077	
ν_2	1738	1177	1251	1700	1174	1249
ν_3	1503	1321		1106		1086
ν_4	1164.7	683	643	938		
ν_5	2874			2160		
ν_6	1280	899		990	735	

of the doublets, but the value is expected to be very approximate because of the inadequacies of the simple theories for low barriers. This is evidenced by the lack of agreement between barriers computed from CH_2O and CD_2O data. The absence of higher inversion doublets than $1^\pm$ in both H_2CO and D_2CO is caused by the fact that above the barrier the vibrational wave functions are approximately orthogonal with those in the ground electronic state.

In addition to ν_2' and the inversion doublets, the frequencies ν_1', ν_3', and ν_6' also occur weakly in combinations with these. Therefore all fundamentals except ν_5' may be approximately obtained and these are given in Table II along with the ground state values. The C—O stretching frequency 1177 cm.$^{-1}$ is very nearly the same as that observed for C—O in carboxylic acids, and may indicate similar three-electron bonding configurations in the two cases. The otherwise unexplained large value of ν_1' gives further evidence of this.*

**The similarity between the properties of the* CHO *bonding in the* $^1A_2$ *state of formaldehyde and the ground state of formic acid is quite striking:*

	H_2CO ($^1A_2$)	HCOOH
C—H stretch	2855 cm.$^{-1}$	2943 cm.$^{-1}$
C—O stretch	1177 cm.$^{-1}$	1180 cm.$^{-1}$
C—O bond length	1.32 Å	1.312 Å

The "three-electron" nature of the C—O *bond in* HCOOH *is further evidenced by recent microwave work (18).*

Can. J. Chem. Downloaded from www.nrcresearchpress.com by 61.7.252.67 on 09/04/12
For personal use only.

Can. J. Chem. Downloaded from www.nrcresearchpress.com by 61.7.252.67 on 09/04/12
For personal use only.

PLATE I

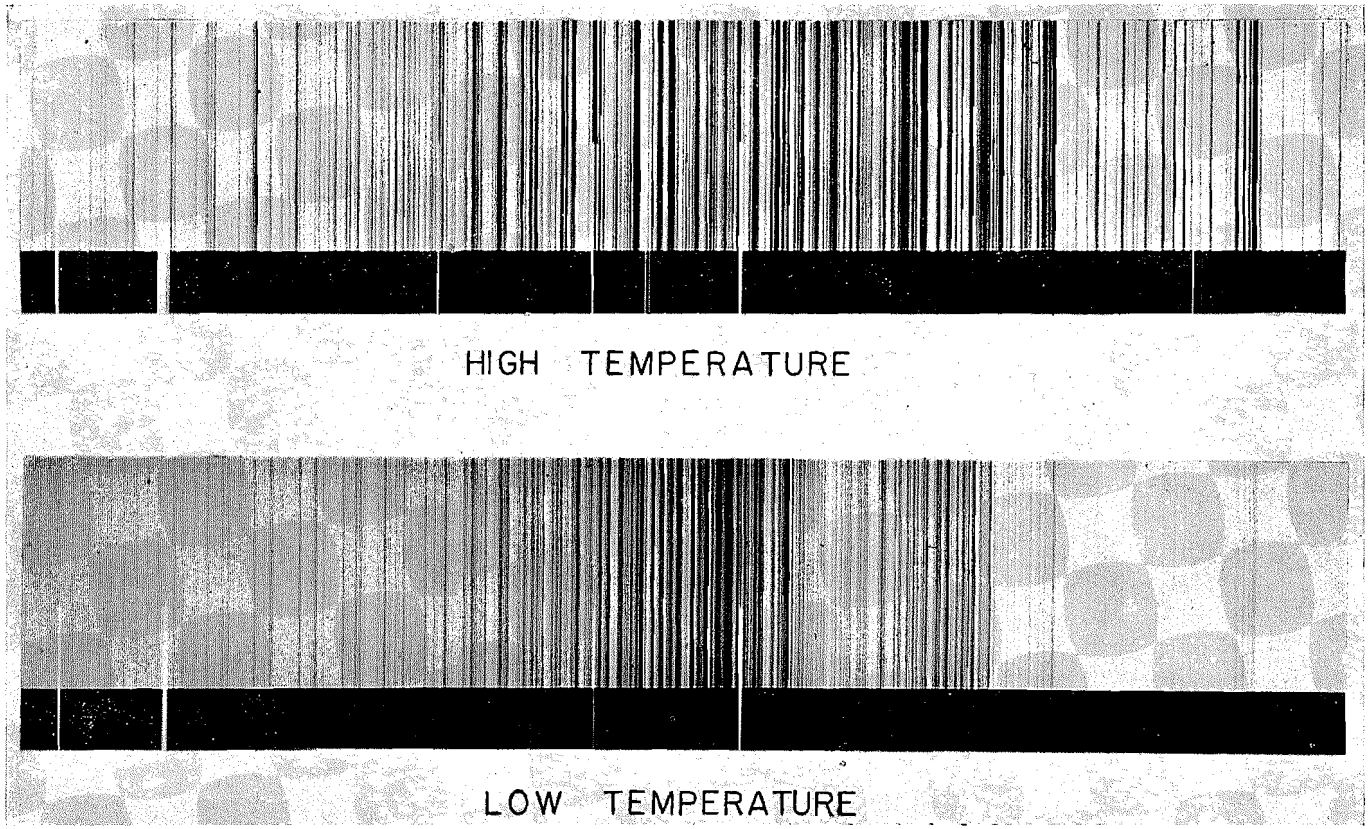

FIG. 1. H_2CO bands at λ3700. (*a*) Spectrum taken at 120° C., 0.1 meter-atm. path. (*b*) Spectrum taken at −78° C., 0.8 meter-atm. path. Notice that the fairly strong ⊥-band (α-band) has lost much of its intensity at −78° C. Directly beneath it is found a weak, temperature insensitive singlet–triplet band.

Can. J. Chem. Downloaded from www.nrcresearchpress.com by 61.7.252.67 on 09/04/12
For personal use only.

PLATE II

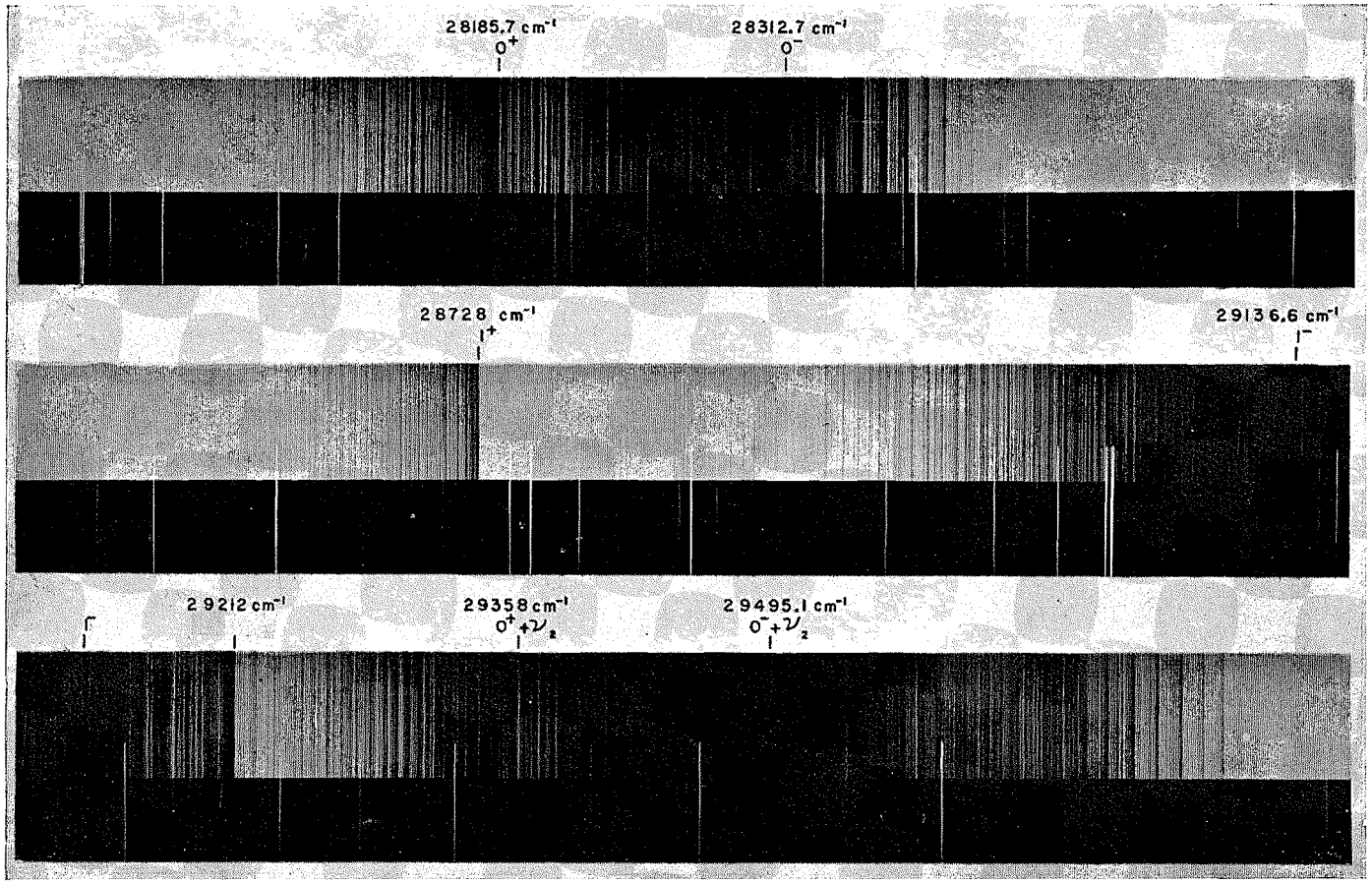

FIG. 2. Inversion doubling in the $^1A_2$ state of H_2CO. The spectrum was obtained at −78° C., 0.2 meter-atm. path. The unmarked parallel band at 29212 cm.$^{-1}$ probably involves excitation of the ν_6 fundamental in the excited state.

Can. J. Chem. Downloaded from www.nrcresearchpress.com by 61.7.252.67 on 09/04/12
For personal use only.

PLATE III

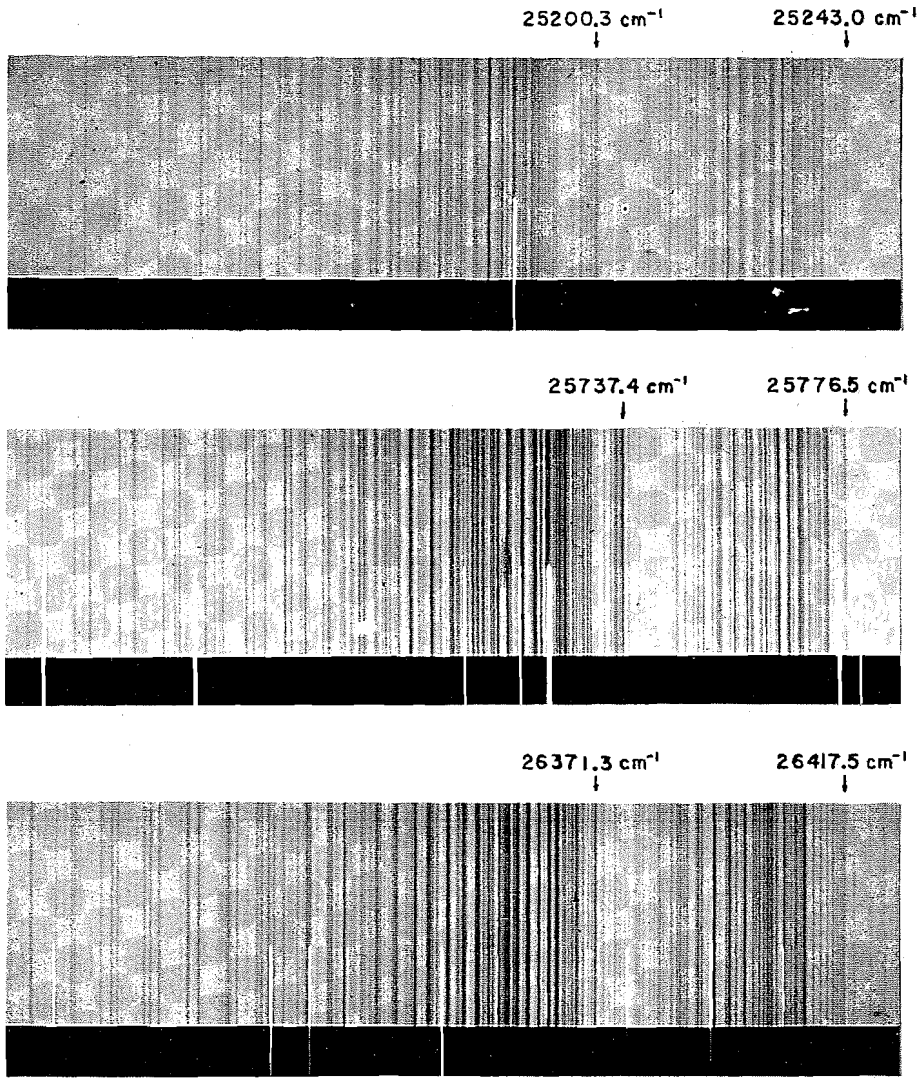

FIG. 3. Some singlet–triplet bands of H_2CO. Spectra taken at −78° C., 0.8 meter-atm. path. The doublet spacing does not change with vibrational excitation nor with isotopic substitution.

Table III lists all bands and their assignments. Since the vibrational pattern can be easily followed down to $\lambda \approx 2500$ Å it is safe to say that *the spectrum in the region 2500 Å $\leqslant \lambda \leqslant$ 3700 Å is caused by a single electronic transition.*

TABLE III

VIBRONIC BANDS OF SINGLET–TRIPLET TRANSITIONS OF H_2CO AND D_2CO

Assignment	H_2CO			D_2CO		
	λ_{air}	ν_{vac}	Int.	λ_{air}	ν_{vac}	Int.
0^+	3967.10	25200.2	m	3948.11	25321.4	w
1^+	3884.32	25737.3	s	3879.53	25769.0	s
2^+	3790.94	26371.2	m	3814.14	26210.8	m
$0^+ + \nu_2$	3775.15	26481.5	w	3762.47	26570.7	w
$1^+ + \nu_3$				3722.60	26855.3	w
$1^+ + \nu_2$	3704.56	26986.1	m	3700.43	27016.2	s
4^+				3689.06	27099.5	ww
$2^+ + \nu_2$	3618.98	27624.2	w	3641.32	27454.7	s
$0^+ + 2\nu_2$	3604.52	27735	w	3597.52	27789.0	w
$1^+ + \nu_2 + \nu_3$				3558.22	28095.9	w

The Singlet–Triplet Transition

The singlet–triplet bands with origins at approximately 3950 Å in H_2CO and D_2CO have been known for some time, being observed independently by Brand (3), Cohen and Reid (5), Coon (6), and Robinson (30). A reproduction of three of these bands in the H_2CO spectrum is given in Fig. 3. The bands are temperature insensitive (Fig. 1), are different in appearance from the usual parallel or perpendicular bands (compare Fig. 2), and do not fit into the established vibronic pattern of the 3650 Å system. These facts indicate that the bands belong to another electronic system, almost certainly to $^1A_1 \rightarrow {}^3A_2$ since they are weak and lie to the long wave-length side of the *lowest predicted* singlet–singlet transition.

High resolution (resolving power $\approx$250,000) photographs were obtained of the H_2CO and D_2CO systems at high and low temperatures. In all, nine D_2CO and eight H_2CO bands were found, many of which lay under hot band structure on the high temperature plates. The bands are "double-headed", *the doublet spacing being about 40±3 cm.$^{-1}$ in all bands of both isotopic species.* Since the magnitude of the spacing does not change on isotopic substitution, and is not highly dependent on vibrational excitation, this is strong evidence that it arises from an electronic, and not a rotational or vibrational origin. The doubling probably is caused by "case-*a*" coupling (13) of electron spin and partially quenched electron orbital angular momentum along the "symmetric top" axis. The electronic angular momentum then couples with the component of rotational angular momentum in this direction to give the observed irregular subband structure. The rotational analysis of the bands is in progress and thus far it has been possible to establish that the constant $\frac{1}{2}(B+C)$ for the $^3A_2$ state is very nearly identical but slightly larger than that of the $^1A_2$ state. This shows, as expected, that the C—O bond distance is quite similar in the two states.

The observed bands measured from the low frequency member of the doublet are listed, together with their vibrational assignments, in Table III. Some temperature sensitive bands of H_2CO, have been observed by Coon (6) at very long path-lengths and moderate dispersion. The observed effects of inversion doubling show that the excited state is non-planar, and from Coon's bands, some of which are analogous to the α-band in the singlet–singlet system, one can calculate the inversion splitting to be

Can. J. Chem. Downloaded from www.nrcresearchpress.com by 61.7.252.67 on 09/04/12
For personal use only.

$0^+ - 0^-$ 30 cm.$^{-1}$
$1^+ - 1^-$ 242 cm.$^{-1}$

which means that the barrier for inversion is somewhat higher in the triplet state than in the singlet state.

The triplet state fundamentals which have been observed are tabulated in Table II along with the singlet state values. The C—O stretching fundamental ν_2' is about 75 cm.$^{-1}$ larger than ν_2' in the excited singlet state. Since this difference is expected to remain fairly constant among the aliphatic aldehydes and ketones, it may provide a good check as to the multiplicity of the excited state in the many instances where only the coarse structure of the spectrum can be resolved.

In conclusion we would like to thank Professor G. H. Dieke for the use of the 21-ft. grating spectrograph on which much of this work was done. We also wish to extend our appreciation to Mr. Maclyn McCarty for helping with the calculations.

REFERENCES

1. BENEDICT, W. S. Phys. Rev. **47**, 641 (1935).
2. BERNSTEIN, H. J. and HERZBERG, G. J. Chem. Phys. **16**, 30 (1948).
3. BRAND, J. C. D. J. Chem. Soc. 858 (1956).
4. BRAND, J. C. D. and REED, R. I. J. Chem. Soc. 2386 (1957).
5. COHEN, A. D. and REID, C. J. Chem. Phys. **24**, 85 (1956).
6. COON, J. B. Symposium on Molecular Structure and Spectroscopy, Columbus, Ohio. 1957.
7. DAVIDSON, D. W., STOICHEFF, B. P., and BERNSTEIN, H. J. J. Chem. Phys. **22**, 289 (1954).
8. DIEKE, G. H. and KISTIAKOWSKY, G. B. Phys. Rev. **45**, 4 (1934).
9. DRESSLER, K. and RAMSAY, D. A. Symposium on Molecular Structure and Spectroscopy, Columbus, Ohio. 1957.
10. GORIN, E. J. J. Chem. Phys. **7**, 256 (1939).
11. GROH, H. J., JR., LUCKEY, G. W., and NOYES, W. A., JR. J. Chem. Phys. **21**, 115 (1953).
12. HERZBERG, G. Infrared and Raman spectra of polyatomic molecules. D. Van Nostrand Co., Inc., New York. 1945.
13. HERZBERG, G. Spectra of diatomic molecules. D. Van Nostrand Co., Inc., New York. 1950.
14. HERZBERG, G. and RAMSAY, D. A. Proc. Roy. Soc. (London), A, **233**, 34 (1955).
15. INGOLD, C. K. and KING, G. W. J. Chem. Soc. (London), 2702 (1953).
16. KLEMAN, B. Symposium on Molecular Structure and Spectroscopy, Columbus, Ohio. 1956.
17. LAWRANCE, R. B. and STRANDBERG, M. W. P. Phys. Rev. **83**, 363 (1951).
18. LERNER, R. G., DAILEY, B. P., and FRIEND, J. P. J. Chem. Phys. **26**, 680 (1957).
19. MCCARTY, M., JR. Unpublished work.
20. MCCLURE, D. S. J. Chem. Phys. **17**, 665 (1949).
21. MCCLURE, D. S. J. Chem. Phys. **17**, 905 (1949).
22. MCMURRY, H. L. and MULLIKEN, R. S. Proc. Natl. Acad. Sci. **26**, 312 (1940).
23. MULLIKEN, R. S. J. Chem. Phys. **3**, 564 (1935).
24. MULLIKEN, R. S. Revs. Modern Phys. **14**, 204 (1942).
25. MULLIKEN, R. S. J. Chem. Phys. **23**, 1997 (1955).
26. NOYES, W. A., JR. Unpublished work.
27. NOYES, W. A., JR., PORTER, G. B., and JOLLEY, J. E. Chem. Revs. **56**, 49 (1956).
28. PORTER, G. B. J. Am. Chem. Soc. **79**, 1878 (1957).
29. RAMSAY, D. A. J. Chem. Phys. **25**, 188 (1956).
30. ROBINSON, G. W. Can. J. Phys. **34**, 699 (1956).
31. ROBINSON, G. W. Symposium on Molecular Structure and Spectroscopy, Columbus, Ohio. 1957.
32. ROBINSON, G. W. Unpublished work.
33. ROBINSON, G. W. and BENEDICT, W. S. Manuscript in preparation.
34. WALSH, A. D. J. Chem. Soc. 2266 (1953).
35. WALSH, A. D. J. Chem. Soc. 2288 (1953).
36. WALSH, A. D. J. Chem. Soc. 2306 (1953).
37. WILKINSON, P. G. Can. J. Phys. **34**, 643 (1956).
38. WILKINSON, P. G. and MULLIKEN, R. S. J. Chem. Phys. **23**, 1895 (1955).

Can. J. Chem. Downloaded from www.nrcresearchpress.com by 61.7.252.67 on 09/04/12
For personal use only.

Can. J. Chem. Downloaded from www.nrcresearchpress.com by 61.7.252.67 on 09/04/12
For personal use only.

EXCITED STATES OF THE MOLECULAR IONS OF HYDROGEN FLUORIDE, HYDROGEN IODIDE, WATER, HYDROGEN SULPHIDE, AND AMMONIA[1]

D. C. Frost and C. A. McDowell

ABSTRACT

The ionization of the molecules of hydrogen fluoride, hydrogen iodide, water, hydrogen sulphide, and ammonia, by essentially monoenergetic electrons, has been studied in a mass spectrometer. The various excited states of the molecular ions of these compounds have been observed and the corresponding energy levels of the ions have been measured. The results are interpreted in terms of the electronic structures of these molecules as given by molecular orbital theory.

INTRODUCTION

The analysis of visible or ultraviolet spectra yields information about the excited states of molecules and free radicals. Almost all of our present data have been obtained in this way. And though a vast amount of such information is available, little of this refers to saturated molecules. There are obvious reasons why this is so, and it will undoubtedly be some time before sufficient spectroscopic data are available to permit the excited states of many saturated molecules to be evaluated. It is now possible, however, to use electron impact methods to obtain some of this much desired information. Recently a new electron impact technique (5, 6) has been used to study the ionization of molecules. This method utilizes essentially monoenergetic electrons with an energy spread of $\sim$0.1 ev., and so it is now possible to determine accurately the energies of the excited states of many molecular ions. These data are now available for molecular ions of nitrogen (6), methane (7), the alkyl halides (7), and several other molecules. In this paper we shall describe some new results for the molecular ions of hydrogen fluoride, hydrogen iodide, water, hydrogen sulphide, and ammonia.

Besides yielding values for the energy levels of the excited states of the various molecular ions, the present studies are of interest for other reasons. They enable the molecular orbital theories of the electronic structures of these molecules to be assessed. Furthermore, it is known from self-consistent field molecular orbital theories (8, 13, 14, 17, 21), that Koopmans' theorem indicates to a good approximation that the energy of an electron in a given molecular orbital is equal to minus the ionization potential referring to the removal of an electron from that orbital; and it follows that once the several ionization potentials of a molecule are known, the energies of the various molecular orbitals are likewise known. The determination of the energies of the molecular orbitals of molecules is important, for by this means there are available further data for the more detailed assessment of the reliability of self-consistent field molecular orbital calculations. As was mentioned earlier, optical spectroscopic studies have not so far yielded much of the desirable information for saturated compounds, and it is perhaps for such molecules that the present studies are particularly important in that now there have become available data which cannot as yet be provided by any other experimental method.

EXPERIMENTAL

The Metropolitan-Vickers M.S.I. mass spectrometer, modified as previously described (6, 7), was used to determine the ionization potentials. As the tube of this instru-

[1]*Manuscript received October 3, 1957.*
Contribution from the Department of Chemistry, University of British Columbia, Vancouver 8, B.C., Canada.
This paper was presented at the Symposium on the Structure and Reactivity of Electronically-Excited Species held at the University of Ottawa, Ottawa, Canada, September 5 and 6, 1957.

ment and the inlet system are largely made of glass, a new gas introduction system had to be provided so that we could study hydrogen fluoride. The new inlet system was made from copper and it extended through a metal–glass seal down into the ionization chamber. At the extremity of the copper inlet tube a small teflon tube was added to provide insulation between the inlet tube and the ion source. A diagram of the inlet system is shown in Fig. 1. It will be noted that only metal gas valves with teflon diaphragms were used.

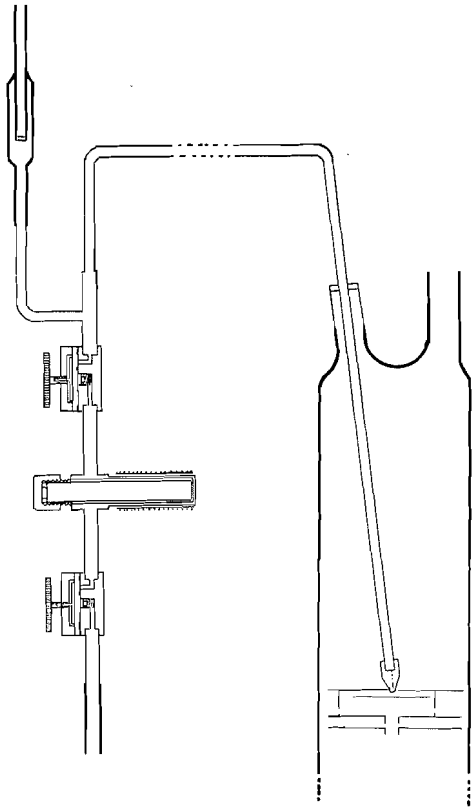

FIG. 1. All-metal inlet system for introducing hydrogen fluoride into mass spectrometer.

The hydrogen fluoride was prepared by heating a dry sample of potassium hydrogen fluoride. The reaction vessel was a copper-lined brass cylinder which could be heated electrically (see Fig. 1).

The hydrogen iodide was prepared by the combination of hydrogen and iodine vapor over a platinized asbestos catalyst in a high vacuum system, the gas being purified by repeated fractionation.

The other compounds used were prepared by normal chemical methods and highly purified before use.

Krypton was used as a calibration gas for all the studies. The ionization potential of krypton was taken as 112914.5 $cm.^{-1}$ (1) or 13.997 v., taking 8066.83 $cm.^{-1}$ equal to 1 v. (2).

EXPERIMENTAL RESULTS

The ionization efficiency curve for hydrogen fluoride is shown in Fig. 2. This shows clearly that there are two ionization processes, one producing the HF^+ ion in its ground

Can. J. Chem. Downloaded from www.nrcresearchpress.com by 61.7.252.67 on 09/04/12
For personal use only.

state, and the other the ion in its first excited state. The averages of many determinations of the two ionization potentials with their standard deviations are given in Table I. Fig. 3 shows the ionization efficiency curve for the formations of the HI^+ ion from hydro-

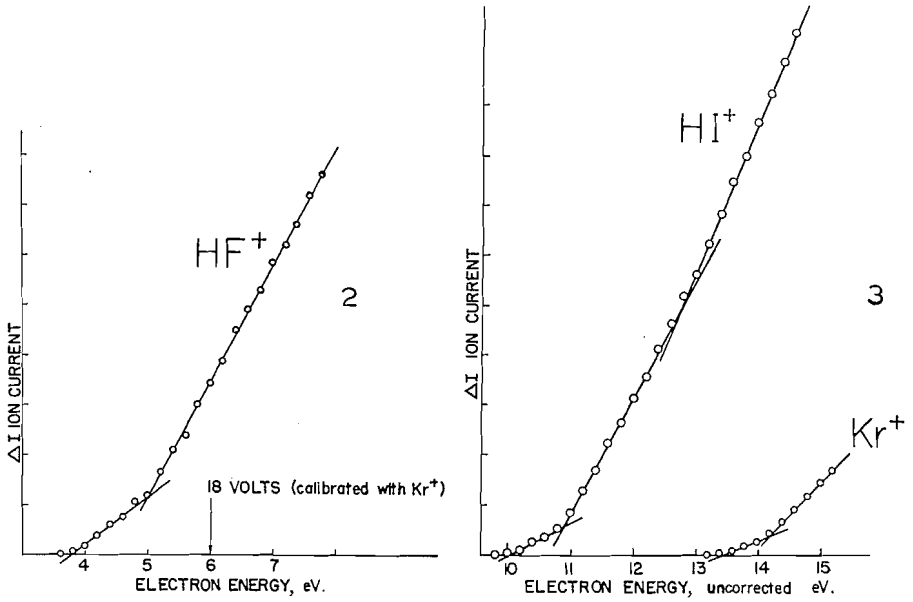

FIG. 2. The ionization efficiency curve for the formation of the HF^+ ion.
FIG. 3. The ionization efficiency curve for the formation of the HI^+ ion.

TABLE I

VERTICAL IONIZATION POTENTIALS OF HYDRIDES

Compound	Ionization potential (v.)	Electronic state of ion
Hydrogen fluoride	15.77±0.02	$^2\Pi_{3/2,1/2}$
	16.91±0.10	$^2\Sigma$
Hydrogen iodide	10.44±0.04	$^2\Pi_{3/2}$
	11.14±0.04	$^2\Pi_{1/2}$
	13.27±0.10	$^2\Sigma$
Water	12.60±0.01	$^2B_1$
	14.35±0.03	$^2A_1$
	16.34±0.06	$^2B_2$
Hydrogen sulphide	10.45±0.03	$^2B_1$
	12.46±0.03	$^2A_1$
	14.18±0.04	$^2B_2$
	16.07±0.05	?
Ammonia	10.40±0.02	$^2A_1$
	15.31±0.04	$^2E_{3/2,1/2}$

gen iodide. Here it is evident that there are three ionization processes. We shall show later that the first two are observed because the spin-orbital components of the $^2\Pi$ ground state of the HI^+ ion have been resolved. The other process refers to the formation of the $^2\Sigma$ first excited state of the HI^+ ion. The values of the ionization potentials for hydrogen iodide are given in Table I. Fig. 4 shows the ionization efficiency curve for the water molecule. The three ionization processes result from the formation of the H_2O^+ ion in its ground $^2B_1$ state, and its two excited states, the $^2A_1$ and $^2B_2$ states. The corresponding ionization potentials are given in Table I. In the case of hydrogen sulphide,

Can. J. Chem. Downloaded from www.nrcresearchpress.com by 61.7.252.67 on 09/04/12
For personal use only.

Can. J. Chem. Downloaded from www.nrcresearchpress.com by 61.7.252.67 on 09/04/12
For personal use only.

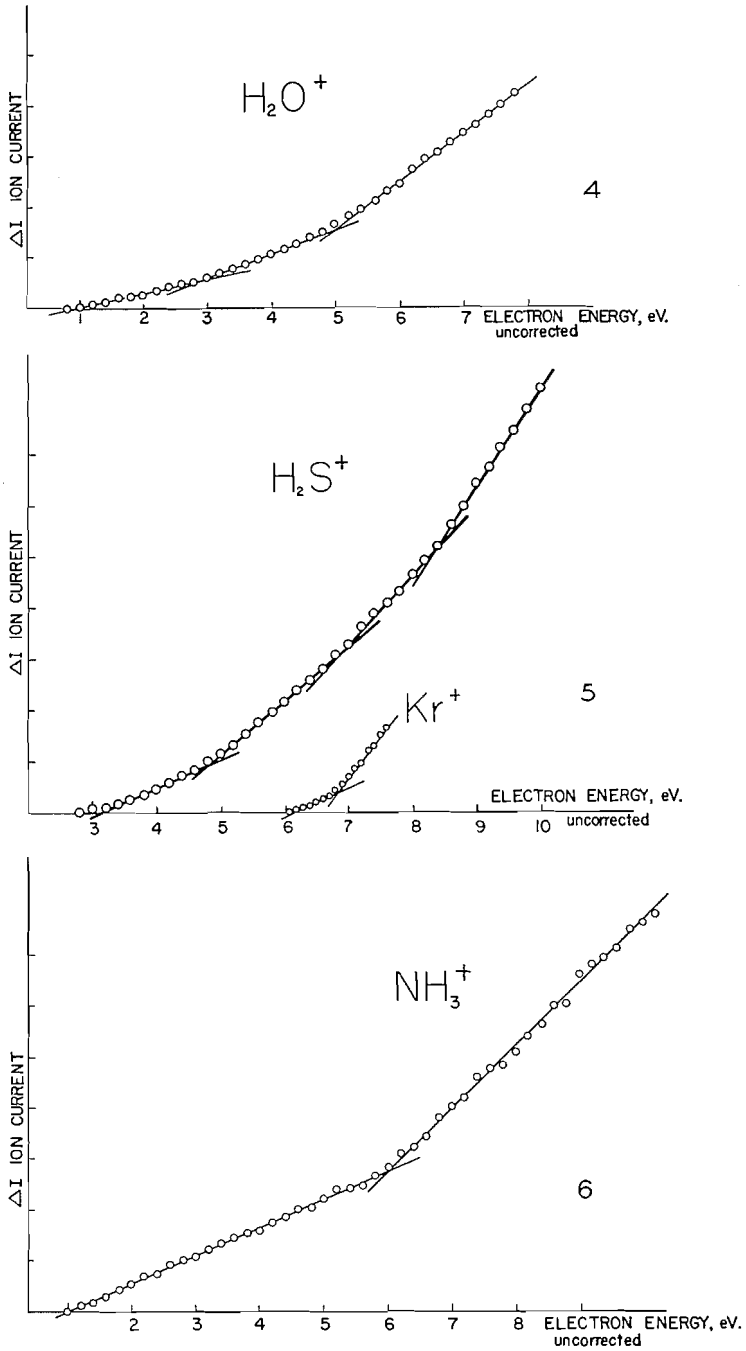

FIG. 4. The ionization efficiency curve for the formation of the H_2O^+ ion.
FIG. 5. The ionization efficiency curve for the formation of the H_2S^+ ion.
FIG. 6. The ionization efficiency curve for the formation of the NH_3^+ ion.

for which the ionization efficiency curve is shown in Fig. 5, besides the processes due to the formation of the H_2S^+ ion in its $^2B_1$ ground state and its $^2A_1$ and $^2B_2$ excited states, an extra ionization process is observed. The origin of this is not clear. The four observed

ionization potentials are listed in Table I. Fig. 6 shows the ionization efficiency curve for ammonia. Here there are clearly two ionization processes. The first refers to the formation of the NH_3^+ ion in its $^2A_1$ ground state, and the second to the formation of the NH_3^+ ion in its first excited ^2E state. The corresponding ionization potentials are listed in Table I.

DISCUSSION

Hydrogen Fluoride

The electronic structure of hydrogen fluoride can be represented by the molecular orbital formula

$$K\ (2s\sigma)^2\ (2p\sigma)^2\ (2p\pi)^4,\ ^1\Sigma^+ \qquad [1]$$

in which the orbitals are written in order of decreasing ionization energy from left to right. The first ionization potential which we have observed to occur at 15.77 ev. will refer to the removal of an electron from the $(2p\pi)$ orbital to form an HF^+ ion in its $^2\Pi_i$ state. This state has two components, $^2\Pi_{3/2}$ and $^2\Pi_{1/2}$, but for fluorine compounds our apparatus cannot resolve these (3). The first excited state of the HF^+ ion will be formed by the removal of an electron from the $(2p\sigma)$ orbital of equation (1) to yield the $^2\Sigma$ state of the ion. The process which we have observed to occur at 16.91 ev. obviously is due to the formation of the HF^+ ion in its first $^2\Sigma$ excited state.

Recently Johns and Barrow (12) reported the observation of the ultraviolet spectra of the DF^+ and HF^+ ions. They concluded that the observed bands were due to transitions between a lower A-state and an upper B-state. The A-state was assumed to arise from the combination H^+ (or D^+) $+F(^2P)$ and was assumed to be the $A\ ^2\Sigma^+$-state. These spectroscopic studies indicate that the $A\ ^2\Sigma^+$-state of the HF^+ ion is 16.88 ev. above the ground $^1\Sigma_g^+$ state of hydrogen fluoride. Our results indicate clearly that the ionization potential which we observe at 16.91 v. is due to the formation of the HF^+ ion in its first excited state, i.e. the $A\ ^2\Sigma^+$ state, and the ionization potential due to the formation of the HF^+ ion in its ground state is 15.77 v. The ground state we take to be the $^2\Pi_i$ state in agreement with the molecular orbital formula [1] and with the spectroscopic data for the molecular ions HCl^+, HI^+, and HBr^+, all of which are known (10) to have $^2\Pi_i$ ground states. It follows, therefore, that bands due to the transitions $A\ ^2\Sigma^+$—$X\ ^2\Pi_i$ and $B\ ^2\Sigma^+$—$X\ ^2\Pi_i$ are still to be found for the DF^+ and HF^+ ions. Our results indicate that the former bands should be found in the near infrared.

Hydrogen fluoride, being a simple molecule with only 10 electrons, has recently been the subject of several extensive theoretical studies. Mueller (16) has reported the results of both a molecular and an atomic orbital treatment, while Kastler (13) has made a very detailed study of this compound from the valence bond standpoint. A self-consistent field molecular orbital treatment using Roothaan's (21) method has been carried out by Duncan (3), and more recently by Hamano (9). Hurley (11) has recently given a detailed discussion of the ground state of this molecule using the method of "atoms in molecules".

With the exception of Duncan's work, nearly all the other authors have chosen either the dissociation energy of the hydrogen fluoride molecule or its dipole moment as data for assessing the accuracy of their calculations. Above, we have mentioned that ionization potentials may be more useful data for comparing the validity of theoretical calculations. Duncan calculated that the first ionization potential of hydrogen fluoride should be 11.3 v. This is very much less than our experimentally determined value of 15.77 v. An examination of Duncan's calculation shows that the method used is probably

Can. J. Chem. Downloaded from www.nrcresearchpress.com by 61.7.252.67 on 09/04/12
For personal use only.

not the best one, and a detailed treatment of the hydrogen fluoride molecule recently carried out by Dr. J. A. R. Coope of this laboratory, using a method analogous to Hurley's "atoms in molecules" treatment, leads to a theoretical value for the first ionization potential which is in very good agreement with the experimental one.

Hydrogen Iodide

The hydrogen iodide molecule may be represented by the molecular orbital equation

$$KLMN\ (5s\sigma)^2\ (5p\sigma)^2\ (5p\pi)^4,\ {}^1\Sigma_g^+. \qquad [2]$$

From this equation it follows that it would require least energy to remove an electron from the non-bonding $(5p\pi)$ orbital, thus forming an ion with the structure . . . $(5p\sigma)$ $(5p\pi)^3$ and so presumably in a ${}^2\Pi_i$ state with spin-orbital components ${}^2\Pi_{3/2}$ and ${}^2\Pi_{1/2}$. Some years ago Price (19) obtained spectroscopic evidence to substantiate this, and also the fact that of the two spin-orbital components, the ${}^2\Pi_{1/2}$ was the upper one. Price observed a Rydberg series for hydrogen iodide with a limit at 89,130 cm.$^{-1}$, i.e. there is an ionization potential at 11.049 v. This limit Price assigned to the ${}^2\Pi_{1/2}$ level of the HI^+ ion. From considerations of the magnitude of the spin-orbital coupling separations of halogen atoms, Price concluded that the ${}^2\Pi_{3/2}$ level of the HI^+ ion should lie about 0.66 ev. below the ${}^2\Pi_{1/2}$ level, i.e. the ionization potential referred to this level should be $11.049-0.66 \approx 10.39$ v. Price was unable to find any Rydberg series which could be satisfactorily established as going to this limit. Our experimental results, shown as the ionization efficiency curve for the HI^+ ion in Fig. 3, do, however, clearly indicate the formation of the HI^+ ion in both the ${}^2\Pi_{3/2}$ and the ${}^2\Pi_{1/2}$ states, as well as an excited state above these. The separation of the spin-orbital components, ${}^2\Pi_{3/2}$ and ${}^2\Pi_{1/2}$, of the ground state of the HI^+ ion we find to be 0.70 ev., a value which is in excellent agreement with that estimated by Price (19), and also with the value we observed earlier for the separation of the spin-orbital components ${}^2E_{3/2}$ and ${}^2E_{1/2}$ of the ground state of the CH_3I^+ ion (3). That this interpretation of the first two processes in the ionization efficiency curve of the HI^+ ion is correct is supported by the photoionization studies of Watanabe (24), who found the first ionization potential of HI to be 10.38 ± 0.02 v. The value which we observed in our experiments is 10.44 ± 0.04 v.

The third ionization process observed at 13.27 v. for the HI^+ ion is obviously to be ascribed to the formation of this ion in its ${}^2\Sigma$ excited state. This state would arise by the removal of an electron from the $(5p\sigma)$ orbital of HI to form the HI^+ ion with the electronic structure . . . $(5p\sigma)^1\ (5p\pi)^4$. It will be recalled that we observed the formation of the HF^+ ion in the corresponding state. It is of interest to compare the value of 13.27 v. for the ionization potential of HI, referring to the production of the HI^+ ion in its ${}^2\Sigma$ excited state, with that of 11.22 v. observed for the formation of the CH_3I^+ ion in its ${}^2A_1$ excited state. Both these states arise by the removal of an electron from the σ-orbitals concentrated mainly along the X—I bond. It is, therefore, to be expected that the corresponding ionization potentials will vary as binding energies of the electrons in these X—I σ-orbitals. The dissociation energies of the X—I bonds can be taken as a rough measure of the binding energies of the electrons in the σ-type orbitals under discussion. The dissociation energy of the hydrogen iodide molecule is 70.44 kcal. mole^{-1} (9), whereas the dissociation energy of the C—I bond in methyl iodide is 52.6 kcal. mole^{-1} (15). This difference reflects that found for the ionization potentials referring to the removal of an electron from the σ-type orbitals along the X—I bonds in these two compounds.

Can. J. Chem. Downloaded from www.nrcresearchpress.com by 61.7.252.67 on 09/04/12
For personal use only.

Can. J. Chem. Downloaded from www.nrcresearchpress.com by 61.7.252.67 on 09/04/12
For personal use only.

Water

The ionization efficiency curve for the water molecule is shown in Fig. 4. Here there are obviously three different ionization processes occurring at 12.60±0.01, 14.35±0.03, and 16.34±0.06 v. It is interesting to note that in early experiments Sugden and Price (22), using a simple ionization tube, found evidence for ionization processes in water at similar voltages. These they attributed to the formation of the water molecule in various excited states. Their technique was, however, rather simple, and as they did not have any means of making mass analysis, they could not be certain that the different ionization processes observed did, in fact, refer wholly to the formation of excited states of the molecular ion species.

The electronic structure of the water molecule in terms of molecular orbital theory can be written as (18, 4):

$$(1a_1)^2\ (2a_1)^2\ (1b_2)^2\ (3a_1)^2\ (1b_1)^2,\ ^1A_1 \qquad [3]$$

Recent self-consistent field molecular orbital calculations by Ellison and Shull (4) have shown that this is the correct order of the orbitals and that the $(1b_1)$ is a pure $2p_x$ orbital of oxygen, the main bonding orbitals being the $(1b_2)$ and $(3a_1)$ orbitals, though $(2a_1)$ has some bonding character also.

This molecular orbital formula for water indicates that the first three states of the H_2O^+ ion should be the $^2B_1$, $^2A_1$, and $^2B_2$ states. These we assume to be those associated with the ionization processes observed at 12.6, 14.35, and 16.34 v. This identification is supported by Ellison and Shull's calculations, which give the energies of the $(1b_1)$, $(3a_1)$, and $(1b_2)$ orbitals for a H—O—H valence angle of 105° as −11.79, −13.20, and −18.35 ev., values which are in reasonable agreement with those which we have determined experimentally. The present assignment agrees with that suggested earlier by Sugden and Price (22). It should perhaps be pointed out that there is no doubt about the accuracy of the identification of the ground state of the H_2O^+ ion as a $^2B_1$ state. It may also be noted that the presently reported value for the first ionization potential of the water molecule is in excellent agreement with the spectroscopic value of 12.56± 0.01 v. obtained by Price (20) from a Rydberg series in the far ultraviolet spectrum of water.

Hydrogen Sulphide

Hydrogen sulphide has the same symmetry, i.e. C_{2v}, as the water molecule and it was of interest to see if the excited states of the molecular ion bore any relation to those observed for the water molecule. The ionization efficiency curve for the formation of the H_2S^+ ion is shown in Fig. 5. This curve is reminiscent of that for the water molecule, though the uppermost ionization process was not observed in that case.

The electronic structure of hydrogen sulphide can be represented by the following molecular orbital formula:

$$(1a_1)^2\ (2a_1)^2\ (1b_2)^2\ (3a_1)^2\ (1b_1)^2\ (4a_1)^2\ (2b_2)^2\ (5a_1)^2\ (2b_1)^2,\ ^1A_1 \qquad [4]$$

The first 10 electrons are in orbitals which approximate to the minor shell $1s^2\ 2s^2\ 2p_x^2\ 2p_y^2\ 2p_z^2$ structure of the sulphur atom. The last eight, in valence shell molecular orbitals, correspond to the last eight electrons in the molecular orbital formula for the water molecule.

From this equation it follows that the first three ionization processes observed for the H_2S^+ ion are due to the formations of the $^2B_1$, $^2A_1$, and $^2B_2$ states of the ion. These we

identify with the ionization potentials observed at 10.45±0.03, 12.46±0.03, and 14.18±0.04 v. It is of interest to note that Sugden and Price (22) observed ionization processes in hydrogen sulphide at 10.5, 12.2, and 14.0 v. and gave a similar interpretation. Again there is no doubt about the accuracy of our identification of the first ionization potential. This refers to the removal of an electron from the $2p_y$ orbital of the sulphur atom. Our value of 10.45 v. is to be compared with the spectroscopic value of 10.47 v. obtained by Price (20) and the result of 10.46 v. obtained by Watanabe (24) from photoionization experiments.

Ammonia

The ionization efficiency for ammonia (Fig. 6) shows the presence of an excited state of the NH_3^+ ion at 4.91 ev. above the first ionization potential. The identification of the two states of the NH_3^+ ion is apparent from the molecular orbital formula for ammonia. Ammonia belongs to the symmetry group C_{3v} and so its molecular orbital formula is:

$$(1a_1)^2\ (2a_1)^2\ (1e)^4\ (3a_1)^2,\ ^1A_1. \qquad [5]$$

The first ionization potential observed at 10.40±0.02 v. obviously refers to the energy required to remove an electron from the non-bonding ($3a_1$) orbital to form a NH_3^+ ion in its $^2A_1$ ground state, assuming that the C_{3v} symmetry is retained in the ion. This value of 10.4 v. for the first ionization potential of ammonia is confirmed by the photoionization work of Watanabe (24), though Walker and Weissler (23) report that their photoionization studies showed that ionization set in at 10.07 v.

The second ionization process which we observed to occur at 15.31±0.02 v. is identified as being due to the formation of the first excited state of the NH_3^+ ion, i.e. the ^2E state, by the removal of an electron from the ($1e$) degenerate orbital of the ammonia molecule. This ($1e$) orbital of ammonia is the main bonding orbital and it spans the three N—H bonds. It is interesting to note that Walker and Weissler (23) found evidence for a second ionization process setting in a little above 15 ev. They were, of course, not able to identify the cause of this, but our results at least show that at this energy there lies the first excited state of the NH_3^+ ion and so Walker and Weissler's observation is at least partly due to the formation of this excited state of the NH_3^+ ion.

ACKNOWLEDGMENT

We wish to thank the National Research Council of Canada for grants in support of this work.

REFERENCES

1. Becker, R. F. and Goudsmit, S. Atomic energy states. McGraw-Hill Book Co., Inc., New York. 1932.
2. Dumond, J. W. M. and Cohen, E. R. Phys. Rev. **82**, 555 (1951).
3. Duncan, A. B. F. J. Am. Chem. Soc. **77**, 2107 (1955).
4. Ellison, F. O. and Shull, H. J. Chem. Phys. **23**, 2348 (1955).
5. Fox, R. E., Hickam, W. M., Kjeldaas, T., Jr., and Grove, D. J. Phys. Rev. **84**, 859 (1951).
6. Frost, D. C. and McDowell, C. A. Proc. Roy. Soc. A, **232**, 227 (1955).
7. Frost, D. C. and McDowell, C. A. Proc. Roy. Soc. A, **241**, 194 (1957).
8. Hall, G. G. and Lennard-Jones, Sir J. Proc. Roy. Soc. A, **202**, 155 (1950).
9. Hamano, H. J. Chem. Soc. Japan, **77**, 985 (1956).
10. Herzberg, G. Spectra of diatomic molecules. D. Van Nostrand Co. Inc., New York. 1950.
11. Hurley, A. Proc. Phys. Soc. A, **69**, 301 (1956).
12. Johns, J. W. C. and Barrow, R. F. Nature, **179**, 374 (1957).
13. Kastler, D. J. chim. phys. **50**, 556 (1953).
14. Koopmans, T. Physica, **1**, 104 (1933).
15. McDowell, C. A. and Cox, B. C. J. Chem. Phys. **20**, 1496 (1952).
16. Mueller, C. R. J. Chem. Phys. **19**, 1498 (1951).

Can. J. Chem. Downloaded from www.nrcresearchpress.com by 61.7.252.67 on 09/04/12
For personal use only.

17. MULLIKEN, R. A. J. Am. Chem. Soc. **77**, 887 (1955).
18. MULLIKEN, R. A. J. chim. phys. **46**, 497, 675 (1949).
19. PRICE, W. C. Proc. Roy. Soc. A, **167**, 216 (1938).
20. PRICE, W. C. J. Chem. Phys. **4**, 147 (1936).
21. ROOTHAAN, C. C. J. Revs. Modern Phys. **23**, 69 (1951).
22. SUGDEN, T. M. and PRICE, W. C. Trans. Faraday Soc. **44**, 108 (1948).
23. WALKER, W. C. and WEISSLER, G. L. J. Chem. Phys. **23**, 1540 (1955).
24. WATANABE, K. J. Chem. Phys. **26**, 542 (1957).

Can. J. Chem. Downloaded from www.nrcresearchpress.com by 61.7.252.67 on 09/04/12
For personal use only.

Can. J. Chem. Downloaded from www.nrcresearchpress.com by 61.7.252.67 on 09/04/12
For personal use only.

THE ELECTRONIC SPECTRA OF CRYSTALLINE TOLUENE, DIBENZYL, DIPHENYLMETHANE, AND BIPHENYL IN THE NEAR ULTRAVIOLET[1]

ROBERT COFFMAN[2] AND DONALD S. MCCLURE[3]

ABSTRACT

The electronic absorption spectra of single crystals of toluene, dibenzyl, diphenylmethane, and biphenyl have been photographed at 20° K. using polarized light in the range 3000 to 2500 Å. The fluorescence spectrum of biphenyl has also been examined. This is the first time that the excited states of biphenyl analogous to the B_{2u} state of benzene have been observed. The main features of the spectra are similar for all four compounds, and the differences may be understood in terms of the weak coupling between the benzene rings of the "double molecules".

I. INTRODUCTION

According to current theory the π-electronic states of the dibenzyl molecule should closely resemble those of the toluene molecule. Any slight differences would have to be ascribed to a mechanical or electronic coupling between the rings in dibenzyl. The electronic component of this coupling should be small because the $-CH_2-CH_2-$ link between the benzene rings is not a conjugative link. Greater differences are expected between toluene and diphenylmethane since only one $-CH_2-$ group separates the rings in the latter. Finally with no intervening "insulating group", as in biphenyl, the spectra may differ greatly.

This series of molecules has been investigated before (2), but only with the aid of solution spectra, and no clear results have been obtained. We have obtained the spectra of single crystals at 20° K. with polarized light. Under these conditions a wealth of detail is observed. In the present article, the experimental results are described, and partial vibrational analyses of the spectra are given. One of us has interpreted further details of the spectra in terms of the electronic and vibrational coupling energies between the benzene rings. This work is reported in the article following this one (12).

An especially interesting discovery made during the course of this work is the existence of a weak, sharp transition in biphenyl. In previous studies of this molecule, only strong continuous absorption regions have been found.

II. EXPERIMENTAL

The polarized spectra of single crystals were obtained using a large Hilger quartz prism instrument. The details have been described previously (10). The spectra were observed at 20° K. At 77° K. they are quite broad and very few details may be resolved. Helium temperatures would probably have given sharper lines than 20° K., and would permit a more precise analysis, which would have been advantageous in several cases.

The biphenyl crystals were flakes grown from the vapor. They had the cleavage plane, the *ab* plane, most fully developed. From the order of interference determined with a quartz wedge in the polarizing microscope, and the value $\Delta n = 0.097$ for the birefringence on the *ab* plane (18), the thickness of the crystals was found. They were usually between

[1]*Manuscript received August 16, 1957.*
Contribution from the Department of Chemistry and Chemical Engineering, University of California, Berkeley, California. This paper was presented at the Symposium on the Structure and Reactivity of Electronically-Excited Species held at the University of Ottawa, Ottawa, Canada, September 5 and 6, 1957.
Work supported in part by the Office of Naval Research under contract N6-ori-211-III.
[2]*Present address: General Electric Co., Electronic Park, Syracuse, New York.*
[3]*Present address: RCA Laboratories, Princeton, New Jersey.*

2 and 5 μ thick, and several millimeters across. A complete structure analysis of the biphenyl crystal does not exist. It is known to have the space group C_{2h}^5 with two molecules per unit cell, and to have the long molecular axis nearly coinciding with the c axis (3, 15). Since $\beta = 94.5°$, the long axis is nearly perpendicular to the ab plane. We therefore expected to be able to observe only the short-axis polarized transitions. We found a polarization ratio of $I_a/I_b = 1.0$ for short-axis transitions. The two molecules per unit cell must be nearly at right angles to each other if we are correct. Krishnan (9) and Dhar (4), using diamagnetic anisotropy and X-ray analysis respectively, obtained values for the molecular orientation parameters which would result in a polarization ratio $I_a/I_b = 1/3.89$ for short-axis transitions and would give appreciable intensity along the a axis for long-axis transitions. Our results are in disagreement with theirs in both respects.

Dibenzyl crystals were grown by cooling a melt held between quartz plates pressed together. Large areas having many crystals all aligned in the same way could be made by remelting most of the crystal and letting it grow again from a small unmelted bit. The value of the birefringence was obtained as approximately 0.13 by measuring the retardation and thickness on some moderately thick crystals grown in the above manner. This number could then be used for the thinner crystals, whose thickness could not be measured directly. The crystal plane developed in these crystals is the ab plane. A very precise X-ray structural study has been made by Jeffrey (8). The theoretical polarization ratio for a short-axis transition in the molecule is $I_a/I_b = 0.65$. No large polarization effects were therefore expected, or found.

Crystals of toluene were grown by allowing the liquid to solidify between quartz plates in a temperature gradient established over a liquid nitrogen bath. Diphenylmethane crystals were grown by allowing the melt to solidify between quartz plates. Its melting point is 26° C., but crystals grew well at 20° C. The diphenylmethane crystals were examined in the polarizing microscope and an area showing uniform orientation of the dielectric axes and low retardation was masked off and used for the experiments. The toluene crystals were examined in the dewar at 77° K. between crossed polaroids. A magnified image of the crystal mass was projected onto a white card, and a large uniformly oriented area was selected. The dielectric axes of this area were oriented vertically and horizontally and the image of the crystal was projected onto the slit of the spectrograph. The areas used were about one millimeter across.

The vapor spectra of these molecules are very complex. That of biphenyl is continuous (1). We examined the vapor spectrum in a 3 meter path after finding the sharp crystal spectrum, but could detect no sharp absorption bands. The spectrum of toluene vapor reported by Ginsburg and Robertson (7) was helpful in the analysis of the crystal spectrum. Robertson and Matsen (17) have reported the spectrum of diphenylmethane, but few details were given. No reports of the spectrum of dibenzyl vapor have been published to our knowledge.

III. RESULTS AND INTERPRETATION

Microphotometer tracings of the absorption spectra obtained are shown in Figs. 1–4. There is no marked dichroism arising from intermolecular interactions, but in the cases of toluene and diphenylmethane there are strong differences between the oppositely polarized spectra arising from molecular orientation. Several plates of the biphenyl spectrum appeared to show a crystal dichroism in the first strong band amounting to 4 cm.$^{-1}$. This is probably real, but since the bands are about 10 cm.$^{-1}$ wide it is hard to be certain of it.

Can. J. Chem. Downloaded from www.nrcresearchpress.com by 61.7.252.67 on 09/04/12
For personal use only.

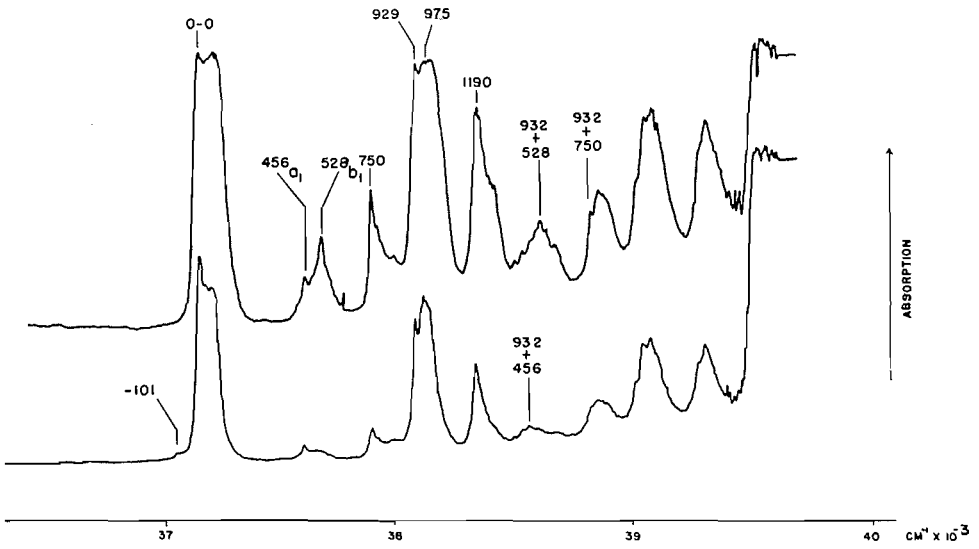

TOLUENE MONO-ORIENTED CRYSTAL ABSORPTION (POLARIZED), 20° K.

FIG. 1. Polarized absorption of oriented toluene crystals at 20° K. Some of the more important features are noted on the microphotometer tracing and others may be identified by reference to Table I.

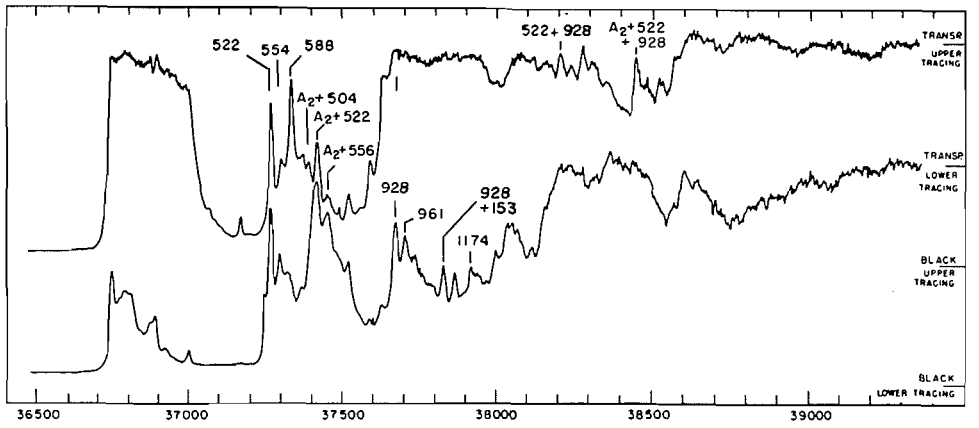

POLARIZED ABSORPTION OF MONO-ORIENTED CRYSTALS OF DIPHENYLMETHANE AT 20 °K.

FIG. 2. Polarized absorption spectrum of diphenylmethane crystal at 20° K. The designation A_2 in the figure is to be interpreted as 2Δ, and equals approximately 150 cm.$^{-1}$.

A. Toluene

The observed lines and their interpretation are given in Table I and the spectrum is illustrated in Fig. 1. The agreement with Ginsburg's analysis of the vapor (7) is excellent if one takes the first strong band of the crystal spectrum, 37155 cm.$^{-1}$, as the 0–0 band. This is 322 cm.$^{-1}$ to the red of the 0–0 band of the vapor. There is a weak band at 37054, 101 cm.$^{-1}$ to the red of the 0–0 band. This is undoubtedly the same sort of band as is found in crystalline benzene, naphthalene, phenanthrene, etc., and probably serves as the origin of fluorescence, although the fluorescence spectrum was not studied. Other than this, there

Can. J. Chem. Downloaded from www.nrcresearchpress.com by 61.7.252.67 on 09/04/12
For personal use only.

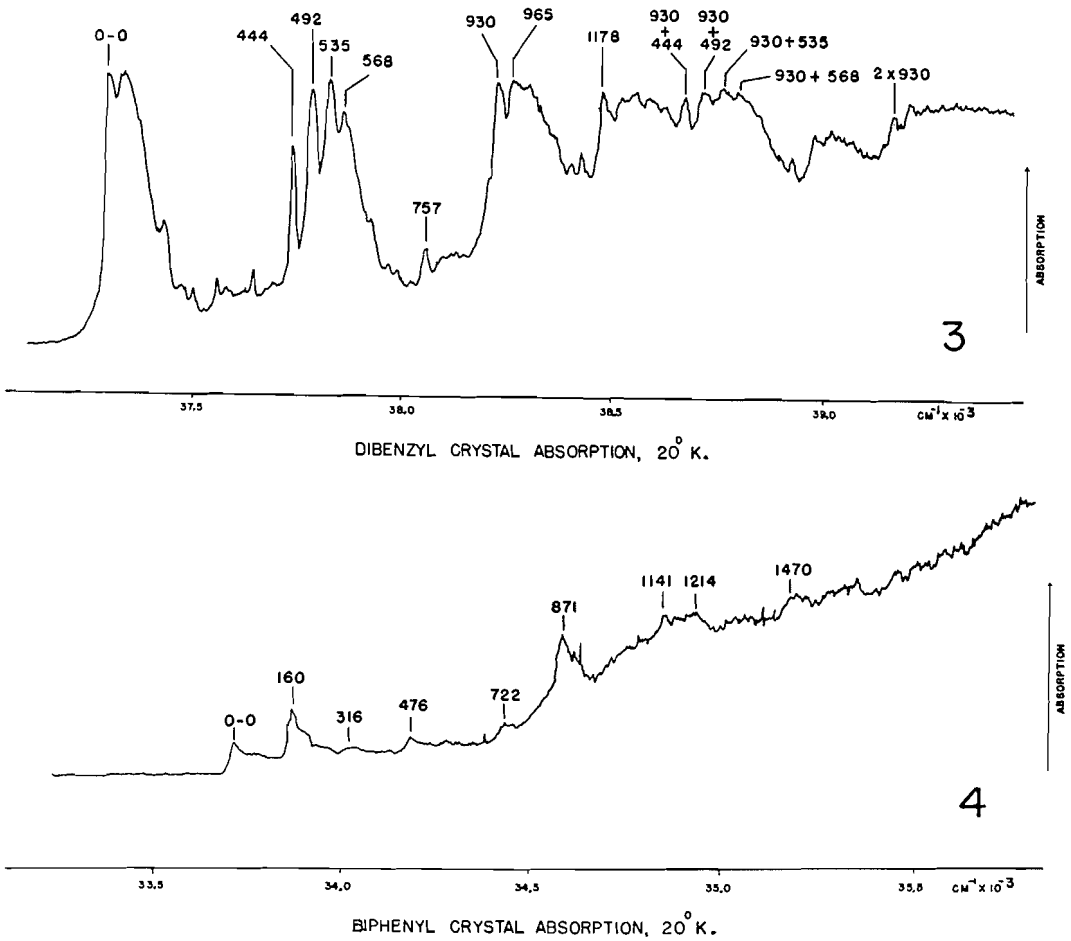

FIG. 3. Absorption spectrum of dibenzyl crystal at 20° K., *ab* plane. The polarized spectrum is the same along the *a* and *b* axes.

FIG. 4. Absorption spectrum of single biphenyl crystal, *ab* plane, at 20° K. The spectra are identical along the two axes except as noted in the text. The background appearing at higher frequencies is probably the long-axis transition giving rise to the well-known continuous absorption of this molecule.

are no distinct crystal effects. The 0–0 band components are at the same energy, so the intermolecular resonance energy is very small.

The most interesting feature of the spectrum is the region where the vibrations analogous to e_{2g} of benzene appear. The 456 and 528 cm.$^{-1}$ peaks respectively represent the a_1 and b_1 components of this motion in point group C_{2v}. The a_1 vibrational addition should be polarized in the same way as the 0–0 band, along the short axis in the molecular plane, while the b_1 band should be polarized along the ring-methyl direction, or long axis. These facts enable one to determine approximately how the toluene molecules are oriented in the crystal. The oriented gas model (fixed, but non-interacting molecules) can be used with confidence here because of the demonstrated absence of strong intermolecular resonance. The polarization of the 528 cm.$^{-1}$ band shows that the long axis is confined to one direction in the projection of the crystal plane we have studied. The polarization of the 456 cm.$^{-1}$ band shows that the short axis prefers the same direction by a factor of about 2. At least two molecules and probably four are needed per unit cell.

Can. J. Chem. Downloaded from www.nrcresearchpress.com by 61.7.252.67 on 09/04/12
For personal use only.

TABLE I

POLARIZED ABSORPTION SPECTRUM OF A TOLUENE CRYSTAL AT 20° K.

The frequency of each band is given, with a probable error of 3 cm.$^{-1}$, in column 1. The intensity in column 2 is indicated by vs = very strong, s = strong, m = medium, w = weak, vw = very weak, sh = shoulder on a stronger band. Most bands are polarized about twice as strongly in one of the crystal directions as in the other. This is indicated by 0 in column 3. The departures from the 2:1 ratio are indicated by + and −. Frequency differences from the 37155 cm.$^{-1}$ band are given in column 4, and the analysis of these differences in column 5. The vibration frequencies used in column 5 are from Ginsburg's work (see Ref. 7). The error given in column 6 is positive if the assigned combination is greater than the observed frequency. Positive deviations could be caused by anharmonicity.

ν (cm.$^{-1}$)	Int.	Pol.	$\Delta\nu$ (cm.$^{-1}$)	Interpretation	Error
37054	vvw	−	−101	Crystal effect	
37155	vs	0	0	0–0, $^1A_1 \rightarrow {}^1B_1$	
37209	vs	0	46	Lattice vib.	
37612	w	0	457	456 a_1 (e_{2g})	−1
37682	m	+	527	528 b_1 (e_{2g})	1
37907	m	0	750	751 a_1	1
37920	w(sh)	0	765		
37988	w(sh)	0	833		
38083	s	0	929	932 a_1	3
38130	s	0	975	965 a_1	−10
38345	ms	0	1190	1189 a_1	−1
38418	w(sh)	+	1263	528+751	16
38506	w(sh)	0	1350		
38540	w(sh)	0	1385	932+456	3
38575	w(sh)	0	1420	965+456	1
38622	m	+	1467	932+528	−7
38680	w	0	1525		
38835	w(sh)	0	1680	932+751	3
38870	m	0	1715	965+751, 1189+528	1, 2
38890	w(sh)	0	1735	751+528+456	0
39025	w(sh)	0	1870	2×932	−6
39060	w(sh)	0	1905	932+456+528	11
39090	m	0	1935	1189+751	5
39280	w(sh)	0	2125	1189+932	−4
39310	m	0	2155	1189+965	−1

Much fine structure appears on the plates, and also in the tracings. This may be evidence for excitation of the methyl group motions.

B. Dibenzyl

Of the three double molecules the spectrum of this one, illustrated in Fig. 3, should bear the most similarity to that of toluene, and should therefore be the easiest to understand. Table II shows the positions of the bands observed and the remarkable similarity of the prominent vibrational intervals to those of toluene. Since no dichroism was observed at the 0–0 band, 37296 cm.$^{-1}$, there must be very little intermolecular resonance. The fluorescence of this crystal could not be observed, possibly because traces of stilbene could not be entirely removed. The stilbene absorption, however, is too weak to interfere with the dibenzyl absorption. A few very weak bands to the red of the 0–0 band remain uninterpreted. Again, of chief interest is the region from 450 to 600 cm.$^{-1}$ from the origin.

The appearance of four bands instead of two in this region is direct evidence for either vibrational or electronic coupling between the rings. The analysis of these bands appears in the following paper.

The totally symmetric frequencies in the rest of the spectrum are very close to those of toluene, as expected. There is evidence that some of these bands are doubled, an indication of vibrational coupling between rings. The 930 cm.$^{-1}$ peak is as sharp as the 929 peak in toluene, so there is probably very little interaction here. But the analogue of the toluene

Can. J. Chem. Downloaded from www.nrcresearchpress.com by 61.7.252.67 on 09/04/12
For personal use only.

TABLE II

ABSORPTION SPECTRUM OF A DIBENZYL CRYSTAL AT 20° K.

The intensities are designated as in Table I. The frequency differences of column 3 are measured from 37296 cm.$^{-1}$, and are analyzed in column 4. Frequencies in parentheses followed by t are toluene frequencies.

ν (cm.$^{-1}$)	Int.	$\Delta\nu$ (cm.$^{-1}$)	Interpretation	ν (cm.$^{-1}$)	Int.	$\Delta\nu$ (cm.$^{-1}$)	Interpretation
36870	vvw			38300	s	1004	
36895	vvw			38322	vw	1026	
37184	vvvw			38338	vw	1042	
37296	vs	0	0–0	38363	vw	1067	
37334	vs	38	0+38	38382	vw	1086	
37365	m	69		38398	vw	1102	
37426	m	130	0+130	38425	vw	1129	
37462	m	166	0+130+38	38435	vw	1139	
37500	m	204		38455	vw	1159	
37530	vw	234		38474	s	1178	a_g (1189t)
37554	w	258		38492	w(sh)	1196	
37565	vw	269		38522	s	1226	
37598	vw	302		38556	s	1260	
37642	w	346		38590	s	1294	
37673	vw	377		38625	s	1329	
37684	vw	388		38675	s	1379	930+444
37698	vw	402		38720	s	1424	930+492
37740	s	444	(456t)	38765	s	1469	930+535
37788	s	492		38795	s	1499	930+568
37831	s	535	(528t)	38872	m (sh)	1576	
37884	s	568		38894	m	1598	
37926	m	630		38925	m	1629	
37970	vw	674		38970	m	1674	
37985	vw	689		39015	m	1719	
38020	vw	724		39032	m	1736	
38053	w	757	a_g (751t)	39046	m	1750	
38087	vw	791		39062	m	1766	
38115	w	819		39082	m	1786	
38140	vw	844		39134	m	1838	
38200	m	904		39160	s	1864	2×930
38226	s	930	a_g (932t)	39200	s	1904	930+959
38265	s	959	a_g (965t)				

975 cm.$^{-1}$ peak appears to be split into 959 and 1004 cm.$^{-1}$. The analogue of 1190 cm.$^{-1}$ in toluene appears to be 1178+1196 cm.$^{-1}$ in dibenzyl. The 750 cm.$^{-1}$ peak is sharp and not split in dibenzyl.

C. Diphenylmethane

The spectrum of a diphenylmethane crystal is considerably more complex than those of toluene and dibenzyl (see Fig. 2). Table III gives the observed bands for two directions of polarization labelled *w* (weakly absorbing) and *s* (strongly absorbing). The crystals studied were in every case too thick to resolve the structure near the origin in the *s* polarization. In the *w* direction, structure could be resolved throughout the entire spectrum. The fact that great differences are observed in the spectra of the two polarizations is very fortunate, since it makes a detailed interpretation possible. We have not obtained accurate intensity measurements, however, and cannot take full advantage of this fact. In the following paper, it will be shown that both the molecular shape and an approximate crystal structure could be obtained from accurate spectral intensity data.

The spectrum may be analyzed, as shown in Table III, if one assumes that there are two origins separated by 150 cm.$^{-1}$, and two superposed spectra nearly identical to dibenzyl spectra. The occurrence of two spectra is interpreted as a result of electronic resonance between the two rings. The details of this interpretation are given in the following paper.

Can. J. Chem. Downloaded from www.nrcresearchpress.com by 61.7.252.67 on 09/04/12
For personal use only.

TABLE III

POLARIZED ABSORPTION SPECTRUM OF A DIPHENYLMETHANE CRYSTAL AT 20° K.

The intensity of each band is given for the weakly absorbing (*w*) component, and the strongly absorbing (*s*) component. Frequency differences are given in column 4, measured from 36742 cm.$^{-1}$. Column 5 gives the interpretation of lines considered as combinations. See Table II of following paper for further details. Frequencies in parentheses designated by t are toluene frequencies.

	Int.				
ν (cm.$^{-1}$)	*w*	*s*	$\Delta\nu$ (cm.$^{-1}$)	Interpretation	Error
36742	m	vs—edge of	0	0–0 $A \rightarrow A$	
36770	m (br)	broad band			
36788	m				
36800	m				
36840	vw				
36867	w				
36887	w		145	0–0 $A \rightarrow B\,(2\Delta)$	
36921	vw				
36996	vw				
37167	vvw	vw			
37246	m	0	504		
37264	s	s	522		
37296	m	m	554	e_{2g} region	
37320	m	0?	578?		
37330	0?	s	588		
37365	w	w	623	?	
37386	0?	w	644	$2\Delta+504$	
37415	s	m	673	$2\Delta+522$	
37449	m	w	707	$2\Delta+556$	
37480	w (sh)	0?	738	$2\Delta+588$	
37516	w	w	774	a_1 (751t)	
37583	vvw	w	841		
37623	vw	s	881		
37670	m	vs—edge of	928	a_1 (932t)	
37703	m	broad band	961	a_1 (965t)	
37728	m		986		
37823	w		1081	928+153	
37862	w		1120	961+159	
37916	w		1174	a_1 (1189t)	
37993	m		1251		
38035	m		1293		
38049	m		1307		
38065	m		1323	1174+149	
38113	m		1371		
38155	s (sh)		1413		
38200	vs	vs	1458	522+928	−8
38230	vs	vs	1488	554+928	−6
38260	vs	vs	1518	588+928	−2
38310	vs	vs	1568	$2\Delta+504+928$	15
38350	vs	s	1608	$2\Delta+522+928$	−7
38385	s	s	1643	$2\Delta+556+928$	−10
38440	s	vs	1698		
38480	s	s	1738		
38520	w	s	1778		
38560	m	s	1818		
38600	s	vs	1858	2×928	−2
38635	s	vs	1893	928+961	−4

D. Biphenyl

The biphenyl absorption spectrum observed on the *ab* plane of a crystal 5.0 μ thick at 20° K. is shown as a tracing in Fig. 4, and the observed features are listed in Table IV. As is well known, the solution and vapor spectra of biphenyl are entirely diffuse, but sharp bands appear in the crystal spectrum. They have the same strength in both the *a* and the *b* directions. These bands are very weak compared to the continuous absorption.

Can. J. Chem. Downloaded from www.nrcresearchpress.com by 61.7.252.67 on 09/04/12
For personal use only.

The order of magnitude of the f-number associated with the weak transition is about 0.001, whereas the solution spectrum of the strong absorption band yields an f-number of 0.44.

TABLE IV

ABSORPTION SPECTRUM OF A SINGLE CRYSTAL OF BIPHENYL AT 20° K.

The interpretation of the frequency differences, measured from 33714 cm.$^{-1}$, may have to be modified as mentioned in the text. Frequencies of polarized Raman lines are given when they are close to an excited state interval (Fruhling, Ref. 6). p = polarized.

ν (cm.$^{-1}$)	Int.	$\Delta\nu$ (cm.$^{-1}$)	Interpretation	Raman
33714	m	0	$^1A_g \rightarrow {}^1B_{2u}$	
33874	s	160		161
33915	sh	201		
34030	w	316		324 p
34190	m	476	316+160	
34280	w	566		
34436	m	722		
34585	vs	871	722+160	731 p
34622	sh	918		
34855	m	1141		1157 p
34882	m	1168		
34928	m	1214		
35184	m	1470		1503 p?
35290	m	1576		1600 p?
35340	m	1726	1576+160	
35455	w	1741		

The first band which can be seen in the spectrum of the 5 μ crystal is as strong as the other bands of the spectrum; yet because of the high symmetry of the molecule, it is not necessarily the true electronic origin of the weak transition. Therefore we studied the absorption of thicker crystals and the fluorescence. In a 50 μ crystal at 77° K., broad absorption appears beginning at about 33200 cm.$^{-1}$, 510 cm.$^{-1}$ to the red of the first sharp band. There is a diffuse maximum at 33310 cm.$^{-1}$.

Pesteil (14) has reported the fluorescence spectrum of biphenyl crystal at 2° K. We studied the spectrum at 77° K. merely to be sure that impurities were not present in our samples and to verify the main features of Pesteil's data. He reports the first fluorescence band to lie at 33340 cm.$^{-1}$. This coincides within the rather large limit of error with our 33310 cm.$^{-1}$ absorption maximum. The band which Pesteil calls the origin of the electronic system is at 32480 cm.$^{-1}$ and is a weak band. We found this to be the first strong band of the spectrum; this is our main disagreement with Pesteil, but the different crystallographic plane used by Pesteil (*ac* plane) and the difference in temperature may explain it. The intervals measured from the 32480 cm.$^{-1}$ band to the other fluorescence bands agree very well with the Raman bands (6), as Pesteil shows.

The origins of progressions in symmetric vibrations in absorption and fluorescence are 1232 cm.$^{-1}$ apart, and the band where weak absorption and weak fluorescence coincide lies 860 cm.$^{-1}$ above the fluorescence origin and 374 cm.$^{-1}$ below the absorption origin. The 860 cm.$^{-1}$ interval is very nearly equal to an infrared frequency (16). Furthermore, a weaker band reported by Pesteil at 32610 cm.$^{-1}$ in fluorescence is 730 cm.$^{-1}$ from the 33340 cm.$^{-1}$ band. The 730 cm.$^{-1}$ interval also appears in the infrared. It seems quite likely therefore that the fluorescence spectrum is a forbidden transition which appears principally through the action of the 860 cm.$^{-1}$ vibration. The forbidden 0–0 band at 33340 cm.$^{-1}$ appears weakly because of the perturbations from the crystal field. The

Can. J. Chem. Downloaded from www.nrcresearchpress.com by 61.7.252.67 on 09/04/12
For personal use only.

33714 cm.$^{-1}$ band is interpreted as the origin of an allowed transition. The 374 cm.$^{-1}$ difference between these two origins may be interpreted in terms of the interaction between the two benzene rings, as is done in the following paper. It would be difficult to call the 1232 cm.$^{-1}$ interval a 1–0+0–1 interval with 860 cm.$^{-1}$ the 1–0 band and 374 cm.$^{-1}$ the 0-1 band because these two frequencies are not comparable in magnitude. A difference of only 10-20% would be expected if this were to be the interpretation.

There is an alternative interpretation of the weak 33340 cm.$^{-1}$ band which must be considered. Similar weak absorption bands have been observed before in molecular crystals such as phenanthrene (11) and naphthalene (13). There is no possibility of interpreting these in terms of an intramolecular resonance. They must be interpreted as fluorescence from the same electronic state as the absorption. The energy separation has not been fully interpreted, but is only present in pure molecular crystals, not in diluted crystals or in other types of solution.

A rigorous experiment to decide between these alternatives would be to use a crystal which is transparent in the region where biphenyl absorbs, and to examine the polarized solid solution spectra of biphenyl in this solvent. We have not done this experiment but instead used a 3-methylpentane glass as the solvent for absorption and emission. The absorption at 77° K. in this glass is continuous, and the point where $\epsilon = 100$ is at approximately 35600 cm.$^{-1}$. The fluorescence bands are quite broad, and the onset of the first one was estimated to be at 34000 cm.$^{-1}$. There is thus a difference of 1600 cm.$^{-1}$ between the onset of absorption and emission. It appears therefore that the gap is not less than in the crystal.

Another difference between biphenyl and the other crystals mentioned is that there is no strong emission beginning from the weak absorption band. As we have pointed out, only very faint emission occurs here, whereas in naphthalene and phenanthrene, the strong allowed band begins here. Therefore the emission observed from biphenyl must be coming from a state different from the state absorbing at 33714 cm.$^{-1}$. We conclude that there is good evidence for the existence of two excited electronic levels, 33340 and 33714 cm.$^{-1}$.

The analysis of the vibrational intervals in the absorption spectrum of biphenyl is given in Table IV. The interpretation of this analysis is not so obvious as in the case of the other molecules we have discussed. In the other cases, the vibrations which were excited in the transition were all analogous to the ones in the toluene spectrum. Even though the excited state of biphenyl can be considered to be derived from the B_{2u} state of benzene and is closely related to it, there must be enough differences to change the vibrational overlap integrals so as to favor other vibrations.

The spectrum may be understood if it is compared to the Raman spectrum (6). There is a line at 161 cm.$^{-1}$ which appears only in the solid and whose nature is not known. It is quite possible that the prominent 160 cm.$^{-1}$ band in the absorption spectrum corresponds to a vibration mode similar to the 161 cm.$^{-1}$ Raman line.

A polarized Raman line at 324 cm.$^{-1}$ corresponding to a totally symmetric vibration could well be the ground state counterpart of the 316 cm.$^{-1}$ interval seen in absorption. Another polarized line of 731 cm.$^{-1}$ could be the analogue of the 722 cm.$^{-1}$ absorption band. The strong 871 cm.$^{-1}$ absorption band has no analogue in the Raman spectrum, however. It is therefore interpreted as the combination 160+722. Other probable associations of Raman and absorption bands are noted in Table IV.

There is an interesting similarity between the types of vibrations excited in the biphenyl spectrum and those excited in the stilbene spectrum (5). These two molecules are similar in that their benzene rings are conjugated, while in dibenzyl and diphenylmethane they

Can. J. Chem. Downloaded from www.nrcresearchpress.com by 61.7.252.67 on 09/04/12
For personal use only.

are not. In both stilbene and dibenzyl the symmetric C—C stretching modes derived from ν_{16}, e_{2g}, 1584 cm.$^{-1}$, and ν_{13}, e_{1u}, 1485 cm.$^{-1}$, of benzene are excited while the frequencies in the neighborhood of 1000 cm.$^{-1}$ analogous to the ν_2, a_{1g}, 992 cm.$^{-1}$, breathing mode of benzene are much less strongly excited. With the unconjugated molecules, exactly the opposite occurs. A simple explanation of this is that polar structures contribute more to the excited states of the conjugated molecules, and these structures, in order to exist, must shrink some bonds and expand others in just the way required to excite the symmetric partners of the degenerate vibrations.

Both stilbene and biphenyl have strongly excited low frequency vibrations. In stilbene these may be explained in terms of totally symmetric bending modes, but there are no such modes in biphenyl, and it does not seem possible to explain the 160 cm.$^{-1}$ interval as a totally symmetric molecular vibration. The lowest such mode should be the vibration of one ring against the other, and this could hardly be below 300 cm.$^{-1}$. (Perhaps the polarized 324 cm.$^{-1}$ line is this mode.) Because the absorption intensity in this transition is very low, it may be that the 160 cm.$^{-1}$ interval represents a non-totally-symmetric vibration which mixes in some other electronic state. But, if our B_{1u} assignment of the 33714 cm.$^{-1}$ state is correct, the 160 cm.$^{-1}$ vibration must be g in order to induce such mixing, and no g vibration of biphenyl could be this low. A possibility is that it represents the addition of a 374+160 = 534 cm.$^{-1}$ frequency to the forbidden electronic origin at 33340 cm.$^{-1}$. The value 534 cm.$^{-1}$ is in the range of the benzene-like e_{2g} vibration. It would have to be the antisymmetric a_1 component since a short-axis transition must be produced (see following paper).

IV. CONCLUSIONS

In all four molecules studied the spectra are produced by transitions closely related to the $^1A_{1g} \rightarrow {}^1B_{2u}$ transition of benzene appearing at 2600 Å. In the spectra of toluene, dibenzyl, and diphenylmethane, the same types of ring vibrations are excited during the transitions. This fact is of importance in analyzing the spectra of the latter two molecules. Quite different types of vibrations are excited in the biphenyl transition. Some of these vibrations are the highest frequency C—C stretching vibrations of the rings, similar to those excited by electronic transitions in stilbene, anthracene, and other conjugated aromatic molecules.

The low temperature spectra under our conditions of high resolution have revealed several important details about the excited electronic states of four related molecules. In each case the magnitude of the electronic and vibrational interactions between the benzene rings of the double molecules may be deduced from the spectra. Details of these interactions are discussed in the following paper.

REFERENCES

1. ALMASY, F. and LAEMMEL, H. Helv. Chim. Acta, **33**, 2092 (1950).
2. BRAUDE, E. A. J. Chem. Soc. 1890, 1898, 1902 (1949).
3. CLARK, G. L. and PICKETT, L. J. Am. Chem. Soc. **53**, 167 (1931).
4. DHAR, J. Indian J. Phys. **7**, 43 (1932).
5. DYCK, R. and McCLURE, D. S. To be published.
6. FRUHLING, A. Ann. Physik, **6**, 401 (1951).
7. GINSBURG, N. and ROBERTSON, W. J. Chem. Phys. **14**, 511 (1946).
8. JEFFREY, G. A. Proc. Roy. Soc. (London), A, **288** (1947).
9. KRISHNAN, K. S., GUHA, B. C., and BANERJEE, S. Phil. Trans. Roy. Soc. London, A, **231**, 235 (1933).
10. McCLURE, D. S. J. Chem. Phys. **22**, 1668 (1954).
11. McCLURE, D. S. J. Chem. Phys. **25**, 481 (1956).
12. McCLURE, D. S. Can. J. Chem. **36**, 59 (1958).
13. McCLURE, D. S. and SCHNEPP, O. J. Chem. Phys. **23**, 1575 (1955).
14. PESTEIL, P. and BARBARON, M. J. phys. radium, **15**, 92 (1954).

Can. J. Chem. Downloaded from www.nrcresearchpress.com by 61.7.252.67 on 09/04/12
For personal use only.

15. PICKETT, L. W. Nature, **131**, 513 (1933).
16. RICHARDS, R. E. and THOMPSON, H. W. Proc. Roy. Soc. (London), A, **195**, 1 (1948).
17. ROBERTSON, W. W. and MATSEN, F. A. J. Am. Chem. Soc. **72**, 5250 (1950).
18. WINCHELL, A. N. The optical properties of organic compounds. 2nd ed. The University of Wisconsin Press, Madison, Wis. 1954.

Can. J. Chem. Downloaded from www.nrcresearchpress.com by 61.7.252.67 on 09/04/12
For personal use only.

Can. J. Chem. Downloaded from www.nrcresearchpress.com by 61.7.252.67 on 09/04/12
For personal use only.

ENERGY TRANSFER IN MOLECULAR CRYSTALS AND IN DOUBLE MOLECULES[1]

DONALD S. MCCLURE[2]

ABSTRACT

The theory of the transfer of electronic energy between two molecules, or between two parts of a "double molecule", is discussed for the case in which vibrational quanta are present. The results are obtained for two limiting cases of weak and strong electronic interaction. Some of the phenomena occurring in the intermediate region are discussed qualitatively. With the aid of these results the spectra of biphenyl, diphenylmethane, and dibenzyl have been analyzed, and the electronic energy exchange parameter has been determined for each. These data are compared with similar data on durene crystal and the paracyclophanes. The electronic energy exchange parameter is given approximately correctly by considering the interaction of electronic transition dipoles except for very close and for very distant molecules.

I. INTRODUCTION

Two kinds of weakly coupled systems in which energy transfer processes have been observed are molecular crystals and "double molecules", i.e. molecules consisting of two identical parts coupled through a weakly conjugating linkage. Recently, high resolution single crystal spectra of several double molecules have been obtained (2). The spectral data are analyzed in this paper and compared with existing information on molecular crystals and other double molecules. Our main purpose is to show what the actual values of these energy transfer parameters are and to make them available for theoretical work.

Vibrational as well as electronic energy transfer has been observed. Effects of intermolecular coupling on vibrations have been observed in infrared spectra of single crystals as well as in electronic spectra. Our main interest in vibrational coupling in this paper will be in the way it interacts with the electronic coupling. This interaction may take any form from a minor splitting of vibrational levels to a major change in the geometry of the system.

Some of the theory of electronic states of weakly coupled systems has been reviewed by Craig (3), who applies it to molecular crystals. In this theory the interaction between the units of the molecular crystal occurs by way of an excitation transfer without necessarily any electron transfer. The intermolecular potential is usually expanded in a multipole series and the leading term is evaluated to determine the interaction energy. In this way Craig (3) calculated the spectrum of the anthracene crystal using the dipole–dipole term and Fox and Schnepp (5) calculated the spectrum of the benzene crystal using the octupole–octupole term. Longuet-Higgins and Murrell (6) have developed a theory which is applicable to "double molecules", since the potential for interaction between the parts is not expanded in a multipole series and allowance is made for electron transfer processes. The energy states of biphenyl, for example, were calculated.

II. ELECTRONIC SPLITTING IN BIPHENYL, DIPHENYLMETHANE, AND DIBENZYL

Schematic representations of the spectra of toluene and the related double molecules are shown in Fig. 1, after the work of Coffman and McClure (2). The original spectra were taken at 20° K. with polarized light and single crystals. Only in the case of biphenyl

[1]*Manuscript received August 16, 1957.*
Contribution from the Department of Chemistry and Electrical Engineering, University of California, Berkeley, California. This paper was presented at the Symposium on the Structure and Reactivity of Electronically-Excited Species held at the University of Ottawa, Ottawa, Canada, September 5 and 6, 1957.
[2]*Now at Radio Corporation of America Laboratories, Princeton, New Jersey.*

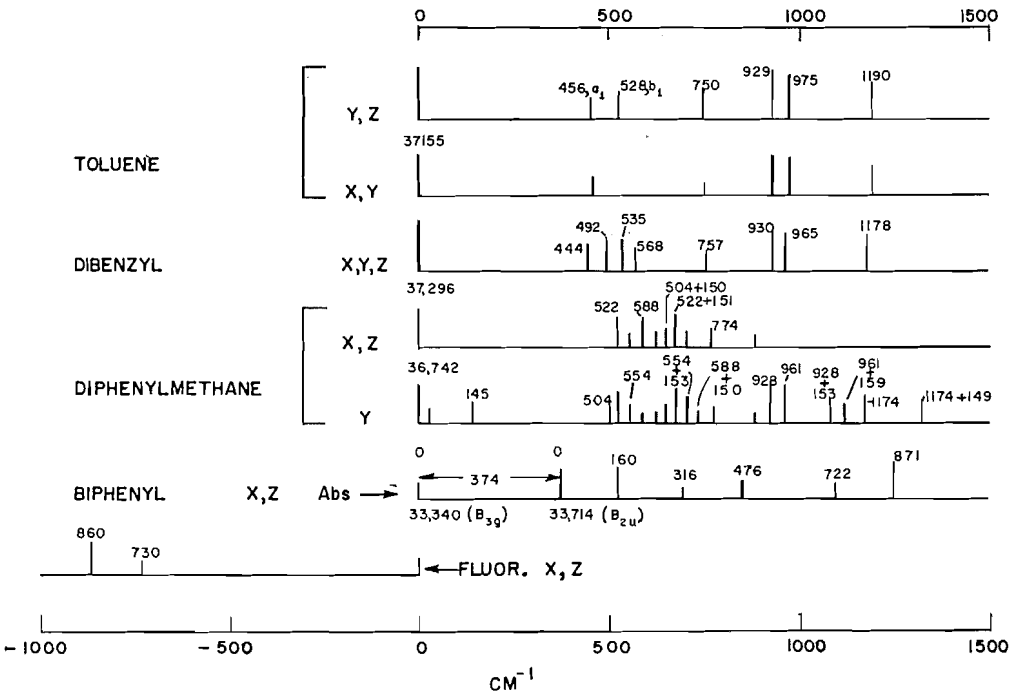

FIG. 1. Schematic drawings of the spectra of toluene and some related double molecules. Vibration frequencies measured from the electronic origins are given.

is it possible to observe the electronic splitting directly, as indicated in the analysis on Fig. 1. In the other two cases, it is possible with the aid of the toluene spectrum for comparison to find the approximate value of the electronic splitting. The molecular shapes and the coordinate systems to be used in the following discussion are shown in Fig. 2.

A. Analysis of the Spectra of Double Molecules

Some simple quantum mechanical problems must be considered first before proceeding to the spectroscopic data. The electronic and vibrational states of double molecules may be written to a first approximation as products of the wave functions of the separate parts. For the ground state $\psi^n = \psi_1^0\psi_2^0$, and for the excited states, corresponding to the mth excited state of the parts,

$$\left.\begin{matrix}\psi_S^m \\ \psi_A^m\end{matrix}\right\} = \frac{1}{\sqrt{2}}(\psi_1^0\psi_2^m \pm \psi_1^m\psi_2^0). \qquad [1]$$

The subscript S goes with the + sign and A with the − sign. The double molecules we are considering have symmetry elements, some of which interchange rings. ψ_S and ψ_A will behave oppositely under such symmetry operations, i.e. one will change sign and the other not. The ± property itself may be considered as a symmetry element in the following general discussion.

In each case the excited state is like the B_{2u} state of benzene and therefore in the individual rings there is a node across the ring passing through the point of substitution. This transition is forbidden in benzene, but allowed in toluene. However the vibrational electronic interaction mechanism active in benzene still induces an appreciable transition moment in toluene as well as in the double molecules under consideration. Our most

Can. J. Chem. Downloaded from www.nrcresearchpress.com by 61.7.252.67 on 09/04/12
For personal use only.

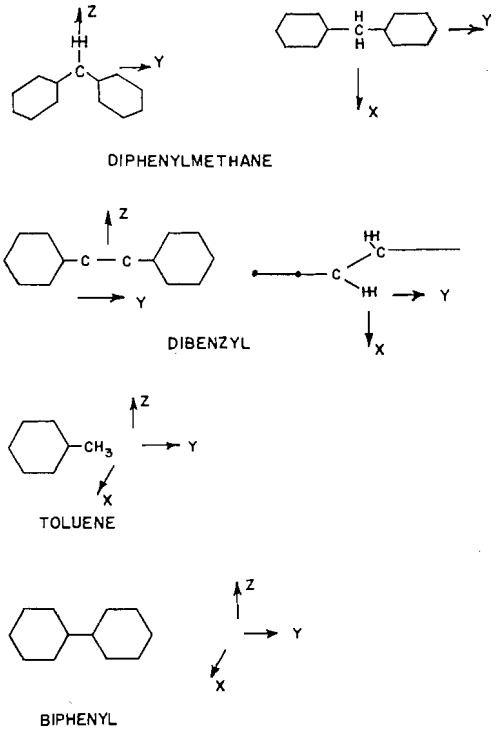

FIG. 2. Coordinate systems and symmetry properties of toluene, dibenzyl, diphenylmethane, and biphenyl. The rings of diphenylmethane are drawn to indicate the foreshortening due to rotation about the C—CH_2 bond.

interesting results will be obtained by analyzing the spectrum in the region where the perturbing vibration appears. In benzene this is an e_{2g} mode of 521 cm.$^{-1}$ which splits in toluene into an a_1 at 456 cm.$^{-1}$ and a b_1 at 528 cm.$^{-1}$ in the excited state. Note that the a_1 mode is lower, since it involves motion of the attached methyl group, while in the b_1 vibration there is a node at the methyl group.

The following problems must now be solved in order to interpret the spectra.

1. Splitting of the Vibrationless Transition in Double Molecules

The hamiltonian for the double molecule may be written as $H_1+H_2+H_{12}$, where H_1, H_2 are the hamiltonian functions for toluene and H_{12} is an interaction potential. Using the wave functions given earlier, the energy of the S state is $D+\Delta$, and of the A state $D-\Delta$, relative to the unperturbed energy as zero. Here D is the displacement of the center of gravity due to the interaction potential, i.e.,

$$D = \int (\psi_1^0 \psi_2^m)^2 H_{12}\, d\tau \qquad [2]$$

and Δ is half the splitting, i.e.

$$\Delta = \int \psi_1^0 \psi_2^m H_{12} \psi_1^m \psi_2^0\, d\tau. \qquad [3]$$

The transition moment is

$$\left.\begin{matrix}\mathbf{M}_S \\ \mathbf{M}_A\end{matrix}\right\} = \frac{\mathbf{M}_1 \pm \mathbf{M}_2}{\sqrt{2}} \qquad [4]$$

Can. J. Chem. Downloaded from www.nrcresearchpress.com by 61.7.252.67 on 09/04/12
For personal use only.

for the S and A states. The vector sum is zero for one of the states in the case of dibenzyl, since it corresponds to a g-state. In diphenylmethane both states may have non-zero components for certain geometries. The displacement, D, will be neglected in later calculations since it does not affect the spectrum.

2. Splitting of Symmetric Vibronic States

Vibrations which are totally symmetric in toluene form two vibrations in the double molecule. They will have different energies because of the mechanical and electronic coupling between the two rings. One can write four product-type vibronic wave functions corresponding to the presence of one vibrating ring and one electronically excited ring in the double molecule. It is important to realize that the ring containing the electronic excitation may or may not contain the vibrational excitation. Another important distinction, discussed in detail by Simpson and Peterson (9), is related to the first. One must distinguish two limiting cases: (1) the electronic interaction between the parts of the molecule results in a splitting which is small compared to the vibrational intervals, (2) the electronic interaction produces a splitting much larger than the vibrational intervals. These are called the weak and the strong coupling cases, respectively. We may now list the wave functions, the first order energies, and the transition probabilities from the ground state for these two limiting cases. This information is given in Table I. It has been assumed throughout that the electronic and vibrational wave functions of each part of the double molecule are exactly the same as those of the related single molecules.

TABLE I

WAVE FUNCTIONS, ENERGIES, AND TRANSITION PROBABILITIES FOR WEAK AND STRONG COUPLING

State	Symm.	Wave function	First order energy	Transition probability
Ground	S	$\psi_1^0\psi_2^0X_1^{00}X_2^{00}$	0	—
m-Electronic	S A	$1/\sqrt{2}.[\psi_1^m\psi_2^0X_1^{m0}X_2^{00} \pm \psi_1^0\psi_2^mX_1^{00}X_2^{m0}]$	$E_m \pm \Delta$	$(\mathbf{M}_1 \pm \mathbf{M}_2)/\sqrt{2}$
Weak coupling:				
m-elect.	S A	$1/\sqrt{2}.[\psi_1^m\psi_2^0X_1^{m0}X_2^{0a} \pm \psi_1^0\psi_2^mX_1^{0a}X_2^{m0}]$	$E_m + V_a^0 \pm \Delta$	$\begin{cases} 0 \\ 0 \end{cases}$
+ a-vibr.	S A	$1/\sqrt{2}.[\psi_1^m\psi_2^0X_1^{ma}X_2^{00} \pm \psi_1^0\psi_2^mX_1^{00}X_2^{ma}]$	$E_m + V_a^m \pm \Delta$	$\begin{cases} (\mathbf{M}_1 \pm \mathbf{M}_2)S_{1a}/\sqrt{2} \\ \end{cases}$
Strong coupling:				
m-elect.	S A	$1/2.[\psi_1^m\psi_2^0 + \psi_1^0\psi_2^m][X_1^{S0}X_2^{Sa} \pm X_1^{Sa}X_2^{S0}]$	$E_S + V_a^S \pm v$	$\begin{cases} (\mathbf{M}_1+\mathbf{M}_2)S_{1a} \\ 0 \end{cases}$
+ a-vibr.	A S	$1/2.[\psi_1^m\psi_2^0 - \psi_1^0\psi_2^m][X_1^{A0}X_2^{Aa} \pm X_1^{Aa}X_2^{A0}]$	$E_A + V_a^A \pm v$	$\begin{cases} (\mathbf{M}_1-\mathbf{M}_2)S_{1a} \\ 0 \end{cases}$

Notes to table:
m = mth excited electronic state of one ring.
a = ath vibrational mode.
ψ_1^m = electronic wave function of ring 1 in state m.
X_1^{ma} = vibrational wave function of ring 1 in electronic state m and vibrational state a.
Δ = electronic coupling energy.
v = vibrational coupling energy.
V_a^m = vibrational energy of ath mode in mth electronic state.
S = Symmetric under ring interchange.
A = Antisymmetric under ring interchange.
E_m = energy of mth electronic state.
$\mathbf{M}_1$ = transition moment of one ring from 0 to m.
$E_S = E_m + \Delta$, $E_A = E_m - \Delta$.
S_{1a} = Franck–Condon overlap integral; a-vibr., ring 1.

Can. J. Chem. Downloaded from www.nrcresearchpress.com by 61.7.252.67 on 09/04/12
For personal use only.

Can. J. Chem. Downloaded from www.nrcresearchpress.com by 61.7.252.67 on 09/04/12
For personal use only.

The qualitative results are these. In the weak coupling limit, the electronic splitting Δ is very small. If it is considered to be zero there are two vibronic states: one having a vibrational quantum in the unexcited ring with its ground state frequency, V_a^0; and the other having a vibrational quantum in the excited ring, with the frequency V_a^m, determined by the force constants of the excited state. Only the second of these states has a non-vanishing transition probability from the ground state. This is a result of vibrational overlap. Two vibronic states separated by 2Δ arise from each one when the first order electronic energy coupling is added.

In the strong coupling limit, there are two widely separated electronic states of the double molecule. In this limit 2Δ is much larger than the vibrational energies. The vibration frequencies V_a^S and V_a^A are characteristic of the force constants of the excited states S and A. The mechanical coupling v between the rings is considered to be small and splits each vibration into a symmetric and an antisymmetric mode. The symmetry of each state is determined by the product of the vibrational and the electronic symmetry, since it is possible to separate the electronic and vibrational wave functions in the strong coupling limit. One of the A states, $S \cdot A$, and one of the S states, $A \cdot A$, have zero transition probability from the ground state because the vibrational overlap factor, $S_{1a} - S_{2a}$, is zero.

Real cases of course fall into the intermediate region. We will not attempt to solve the intermediate coupling problem here, but will only point out those features of it which are important for analyzing the spectra at hand. Intermediate coupling must begin to be considered when the two classes of weak coupling states interact appreciably. This occurs when the value of Δ approaches $V_a^0 - V_a^m$, the difference in energy of a vibration in the ground state and in the mth excited state. These energy differences are of the order of 100 cm.$^{-1}$. In the examples to be discussed later, values of Δ less than and greater than this figure are found. We expect the vibrational intervals to become altered when Δ is in the region of $V_a^0 - V_a^m$.

Simpson and Peterson pointed out that the splitting energy, Δ, in the weak coupling region is proportional to the band intensity of the individual vibronic bands undergoing the interaction, while in the strong coupling limit Δ is proportional to the full electronic band intensity. In the intermediate region the Δ value depends upon matrix elements of electronic interaction between different vibronic states, and so will have a value larger than in the weak coupling limit. The Δ value will begin to increase rapidly when the interacting systems are close enough so that these second order matrix elements become large, that is when Δ is of the order of V_a^m.

Thus we may distinguish two important cases of the intermediate coupling region: (1) $\Delta \approx V_a^0 - V_a^m$ and (2) $\Delta \approx V_a^m$.

In the first region in which $\Delta \approx V_a^0 - V_a^m$, mixing must occur between the two S states, and between the two A states. The transition probabilities are therefore no longer zero and finite respectively, but all four states must have a finite transition probability. The spectrum for small Δ should appear as a lower doublet at $E_m + V_a^m \pm \Delta$ and a weak doublet at higher energies $E_m + V_a^0 \pm \Delta$, since V_a^0 is usually greater than V_a^m. By the time Δ has reached $V_a^0 - V_a^m$, there should be four lines of roughly equal spacing, and having intensities determined only by the orientation of the vectors $\mathbf{M}_1$ and $\mathbf{M}_2$. Thus if the molecular geometry permitted $\mathbf{M}_1 + \mathbf{M}_2$ to equal $\mathbf{M}_1 - \mathbf{M}_2$ all four lines would be of equal intensity.

As the second region is approached there should be no large changes in relative in-

tensity of the four vibronic lines. Somewhere between the second region and the strong field limit, the intensity of two of the lines must decrease. The spectrum now consists of a pair of widely spaced doublets, and one component of each must lose its intensity.

3. Degenerate Vibration in the Excited State

The degenerate vibration is split in the molecule even without energy exchange. One of its components acts like an ordinary totally symmetric vibration while the other induces a forbidden transition by vibrational–electronic interaction. The problem thus reduces to a treatment of the non-totally-symmetric vibration. This vibration induces a transition in the half-molecule, independent of energy transfer. The degenerate vibrations of most interest are derived from the benzene e_{2g} mode. In toluene this becomes a_1 and b_1 (C_{2v}). We will continue to use a and b to designate the totally symmetric and non-symmetric components, respectively.

The energy levels are not appreciably affected by the vibrational mixing of excited states, and the transition probabilities are enhanced in the double molecule to the same extent as in the single molecule.

A possible effect could arise from the fact that vibrational mixing, if it is to produce any enhancement of intensity, must occur between states in weak coupling and states in strong coupling. The result is that the overlap factor, which causes two of the weak coupling states to have zero transition probability, is no longer as effective, and these two states could have a finite transition moment. The induced moment for this case is the moment induced in the single molecule times a vibrational overlap integral, $(X_1^{0a} \cdot X_1^{s0})$. This is similar to the Franck–Condon overlap integral, and may sometimes have an appreciable value. It is probably not an important source of intensity, however, compared to the intermediate coupling effects discussed in Section *2*. The conclusion is therefore that vibrationally induced transitions will act no differently from the direct transitions in the double molecules, and all the considerations of Section *2* apply equally to both.

We may now proceed to the analysis of the spectra.

B. Dibenzyl

The important features of the spectrum of dibenzyl are shown in the diagram of Fig. 1. No splitting of the 0–0 band could be observed, and a direct measure of the coupling between the benzene rings cannot be made. The appearance of four bands related to the e_{2g} vibration of benzene is of considerable interest, however, and permits some estimate to be made of the ring–ring interaction. The interpretation of these bands as arising from the mode related to e_{2g} of benzene seems well justified if one compares the spectrum with that of toluene, diagrammed in Fig. 1 and shown in detail in the preceding paper (2).

The dibenzyl molecule in the crystal has the symmetry C_i, but it is very close to C_{2h}, and selection rules based on C_{2h} are found to be closely obeyed. If we let the ring-interchanging operation defining S and A be the C_2 axis, then the pure electronic state related to B_{2u} of benzene, or A_1 of toluene, will become $A_u(S)$ and $B_g(A)$. Transitions to the A_u state are expected to be as strong as in toluene, and those to the B_g state are forbidden. If a dipole–dipole interaction potential is assumed (Sec. III), one predicts that the B_g state lies below the A_u state.

In the weak coupling limit we would expect to have a spectrum similar to that of toluene. Only two bands would appear in the e_{2g} region. These would correspond to the

Can. J. Chem. Downloaded from www.nrcresearchpress.com by 61.7.252.67 on 09/04/12
For personal use only.

a_1 and b_1 vibrations observed in toluene. The vibronic state containing the a_1 vibration would be $S(A_u)$, the same as the pure electronic transition, while the vibronic state containing the b_1 vibration would be $A(B_u)$. The polarizations would be z and y respectively, in analogy with toluene.

The presence of four bands of comparable intensity can be interpreted by assuming an appreciable excursion into the intermediate coupling region where the vibronic states containing ground state vibrational quanta may gain intensity. If we refer to Table I, and let a and b represent the a_1 and b_1 toluene-type vibrations we would expect the following levels, whose total energies are given to the right, to appear with appreciable intensity:

$$S(A_u) \quad E_m+V_a{}^0+\Delta, \qquad S(A_u) \quad E_m+V_a{}^m+\Delta,$$
$$A(B_u) \quad E_m+V_b{}^0-\Delta, \qquad A(B_u) \quad E_m+V_b{}^m-\Delta,$$

where m represents the B_{2u} type excited state. We know the approximate values of the vibrational quanta to be close to the following values for toluene:

$$V_a{}^0 = 521 \text{ cm.}^{-1}, \qquad V_a{}^m = 456 \text{ cm.}^{-1},$$
$$V_b{}^0 = 622 \text{ cm.}^{-1}, \qquad V_b{}^m = 528 \text{ cm.}^{-1}.$$

The intervals are measured in the spectrum from the electronic S level at $E_m+\Delta$. If we subtract this from the energy formulas for the vibronic levels and substitute the vibrational quanta we obtain a set of theoretical intervals which must be compared to the measured ones. By making the band assignments which appear to be the most consistent we obtain the list of comparisons:

Theor.		Exptl.
521	→	535
$622-2\Delta$	→	568
456	→	444
$528-2\Delta$	→	492

The values for 2Δ are 54 and 36, with an uncertainty of about 14, considering the mismatch of the two intervals which do not involve Δ. We will use $2\Delta = 45\pm14$ cm.$^{-1}$.

C. Diphenylmethane

Neither the true molecular shape nor the crystal structure of this compound is known. The single crystal spectra are strongly polarized, however, and some information about energy transfer within the molecule may therefore be obtained. The spectrum is diagrammed in Fig. 1.

One assumption which seems unlikely to be wrong is that diphenylmethane has a twofold symmetry axis bisecting the C—CH_2—C angle. The angle of rotation ϕ of the phenyl groups about the C(ar)—CH_2 axis is unknown. The C—CH_2—C angle may be assumed to be close to 112°. The molecular geometry and the coordinate system to be used are shown in Fig. 2.

The spectrum in the e_{2g} region has the eight bands which would be predicted for a molecule having no more than C_2 symmetry. Only four would be permitted for C_{2v} symmetry. In the two configurations corresponding to C_{2v}, the phenyl planes are perpendicular or parallel to the C—CH_2—C plane. It is clear then that the angle of rota-

Can. J. Chem. Downloaded from www.nrcresearchpress.com by 61.7.252.67 on 09/04/12
For personal use only.

tion, ϕ, of the phenyl groups around the C—C bond is between 0° and 90° (ϕ will be measured from the perpendicular position).

As in the case of dibenzyl there is no clear evidence for a forbidden electronic origin. In case $\phi = 0$ (C_{2v} geometry) the forbidden transition would be $A_1 \rightarrow A_2$ and the allowed one $A_1 \rightarrow B_2$ (x-polarized). In C_2 geometry with $0° < \phi < 90°$, the A_2 excited state becomes an A state having a transition moment along the z-axis. The B_2 state becomes a B state and gradually loses its x-moment and gains a y-moment as ϕ increases. If a dipole–dipole interaction between the two rings is assumed, the energy of the A and B states as a function of the angle ϕ may be found. The energies are

$$[5] \qquad E\begin{pmatrix} A \\ B \end{pmatrix} = \pm \frac{2M^2}{R^3} (2.308\sin^2\phi - 1),$$

where M is the transition moment in one ring. Both the energies and the transition moments of states A and B are plotted in Fig. 3 as a function of angle. It can be seen

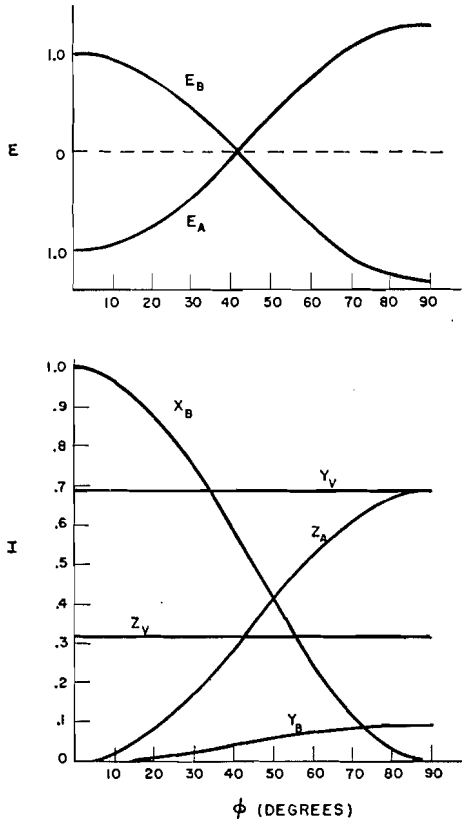

FIG. 3. Upper part: Energies of the A and B electronic states of diphenylmethane as a function of the angle of rotation ϕ.
Lower part: X_B, Y_B, Z_A—probabilities of short-axis transitions in the rings of diphenylmethane along molecular axes (see Fig. 2). Y_V, Z_V—probabilities of long-axis transitions (vibration-induced) along molecular axes.

that the higher state always has the higher transition moment, and that the two states coincide at $\phi = 41°$. The transition moments for vibronic transitions of the a_1-type toluene vibrations have the same polarization properties as the electronic origins, and

Can. J. Chem. Downloaded from www.nrcresearchpress.com by 61.7.252.67 on 09/04/12
For personal use only.

Can. J. Chem. Downloaded from www.nrcresearchpress.com by 61.7.252.67 on 09/04/12
For personal use only.

may therefore be read from Fig. 3. The induced transition moments due to the b_1-type toluene vibrations have polarizations independent of the angle ϕ. These are also plotted in Fig. 3. The intensity of the y-component of the vibrationally induced transition is the same as the vibration-induced intensity in toluene times $\sin^2 56°$. That of the z-component is proportional to $\cos^2 56°$. Further deductions from Fig. 3 may be made after examining the spectrum again.

The region of the spectrum corresponding to the e_{2g} vibration of benzene has its first band at 504 cm.$^{-1}$ from the allowed origin. This is somewhat higher than in toluene, where the first such band is at 456 cm.$^{-1}$. This suggests that the vibration modes of diphenylmethane are not as strictly comparable to those of toluene and benzene as in the case of dibenzyl. Nevertheless we will proceed with a similar analysis since the other prominent vibration frequencies, 928, 961, and 1174 cm.$^{-1}$, are very close to the dibenzyl frequencies 930, 965, and 1178 cm.$^{-1}$.

The bands of the e_{2g} region fall into two groups: 504 to about 580, and 649 to about 700 cm.$^{-1}$. If the second group are to be interpreted as vibrations of a character similar to the first, they must contain an electronic component which results in an energy about 150 cm.$^{-1}$ higher than that of the first group.

This is true not only for the e_{2g} region, but the entire spectrum may be analyzed as a superposition of two nearly identical spectra displaced from each other by 150 cm.$^{-1}$. The three totally symmetric frequencies, 928, 961, and 1174 cm.$^{-1}$, are found repeated at 153, 159, and 149 cm.$^{-1}$ respectively. This is within experimental error of 150 cm.$^{-1}$ because the bands here are somewhat broad. The band analogous to the 750 cm.$^{-1}$ band of toluene seems to be present at 774 cm.$^{-1}$ in diphenylmethane but its high frequency counterpart would fall too close to 928 cm.$^{-1}$ to be distinguishable from it.

A detailed analysis of the vibrational structure in the e_{2g} region may be made. It appears necessary to assume $\phi = 30°$ (approximately) and that the energy of the A state lies below that of the B state. It is also reasonable to identify each vibronic state by means of its strong coupling symbol, because the electronic splitting is large enough to separate two groups of vibronic levels into the states which ultimately go over into strong coupling states. Thus the symmetric and antisymmetric electronic and vibrational wave functions are represented by ψ_S, ψ_A, X_S, X_A respectively. The superscript a or b is added to X in order to indicate the type of vibrational mode. The analysis is shown in Table II.

The analysis is not entirely satisfactory because $X_A{}^a$ must be assumed to lie above

TABLE II

ANALYSIS OF DIPHENYLMETHANE SPECTRUM IN 400–700 cm.$^{-1}$ REGION

State	Symmetry	Intensity and polarization, calc.	Assignment	Polarization observed
$\psi_S X_S{}^a$	B	x, $\cos^2\phi$; y, 0.096 $\sin^2\phi$ M^2	556 + 2Δ	x, y
$\psi_S X_S{}^b$	B	y, $\sin^2 56$ $M_i{}^2$	588 + 2Δ	y
$\psi_S X_A{}^a$	A	z, 0.69 $\sin^2\phi$ M^2	522 + 2Δ	x, y
$\psi_S X_A{}^a$	A	z, $\cos^2 56$ $M_i{}^2$	504 + 2Δ	z
$\psi_A X_S{}^a$	A	z, 0.69 $\sin^2\phi$ M^2	554	x, y
$\psi_A X_S{}^b$	A	z, $\cos^2 56$ $M_i{}^2$	588	z
$\psi_A X_A{}^a$	B	x, $\cos^2\phi$; y, 0.096 $\sin^2\phi$ M^2	522	x, y
$\psi_A X_A{}^b$	B	y, $\sin^2 56$ $M_i{}^2$	504	y

Notes to table: M = direct vibronic transition moment,
M_i = vibrationally induced moment.

It is assumed that intermediate coupling causes enough mixing of states that transitions forbidden in the limiting cases are as strong as the allowed transitions.

$X_A{}^b$. Also the states $\psi_S X_A{}^a$ and $\psi_A X_S{}^a$, which are mixed in the intermediate region, do not have the correct polarization. The relationship between the polarization of a vibration in the first group of bands (superposed on the A origin) and the same frequency in the second group (superposed on the B origin) is correct in all cases, and the absolute polarizations, arising from the assumption that the A state is the lower one, are correct in three cases. Even though certain details do not seem entirely correct, it appears that the splitting between the A and B states, 2Δ, is almost certainly 150 cm.$^{-1}$.

The higher frequency electronic origin could be the band at 145 cm.$^{-1}$ from the first origin. Both origins are much stronger in one component than the other, and in fact the spectrum in one polarization has not been resolved because the crystals used have been too thick.

The diagram of Fig. 3 shows that in order to obtain strong absorption to both the A and B electronic origins in one polarization for ϕ between 20° and 60°, the molecular y-axis must be in the weakly absorbing direction of the crystal, and the x and z axes must both lie in the strongly absorbing direction. For values of ϕ near 80–90°, the x direction could be the weakly absorbing direction with y and z in the strong direction. We do not have good intensity measurements, so cannot say definitely what the molecular configuration is. It should be possible, however, to determine a molecular and a crystal structure from such measurements.

D. Biphenyl

In the experimental observations on the biphenyl crystal, the light was propagated parallel to the long molecular axis. Thus the only π–π transitions which could be observed are along the short axis. This was advantageous in that interference from the very strong long-axis polarized transition $^1A_{1g} \rightarrow {}^1B_{2u}$ was eliminated, and only the weak short-axis transitions could be seen. Using the diagram of Fig. 2 and Herzberg's notation for the group D_{2h}, the states of biphenyl derived from the B_{2u} state of benzene are B_{1u} and B_{3g}. Transitions are permitted from the ground state to the B_{1u} state, but not to the B_{3g} state. The allowed transition should have about the same intensity as the corresponding toluene transition. According to the intensity estimates made from the photographic plates they are approximately the same.

Both fluorescence and absorption have been observed, and direct observation of the two electronic states was therefore possible. The absorption beginning at 33714 cm.$^{-1}$ is interpreted as the $A_g \rightarrow B_{1u}$ transition. According to Pesteil (7), the fluorescence begins at 33340 cm.$^{-1}$ with a series of weak bands, and a series of strong bands begins at 32480 cm.$^{-1}$. The transition moment of the strong bands is along the long axis of the molecule. Our fluorescence experiments (2) essentially confirmed Pesteil's results but did not go as far as his. A broad band having its maximum at about 33310 cm.$^{-1}$ appeared in the absorption spectrum of a crystal 50 μ thick. We think that this is the absorption corresponding to the 33340 cm.$^{-1}$ fluorescence.

The interval between 33340 cm.$^{-1}$ and the strong fluorescence band 32480 cm.$^{-1}$ is 860 cm.$^{-1}$. This is equal to a known infrared absorption band. Its symmetry properties are not known, however. The interpretation is that a 860 cm.$^{-1}$ vibration makes a forbidden transition, whose origin is 33340 cm.$^{-1}$, allowed through vibrational–electronic interaction. The long-axis polarization of the fluorescence is reasonable, since the strongest nearby transitions which may be mixed in by vibration are long-axis polarized. The origin at 33340 cm.$^{-1}$ is interpreted as the $A_g \rightarrow B_{3g}$ transition made allowed by the unsymmetrical crystal field. Since the corresponding allowed $A_g \rightarrow B_{1u}$ transition is the 33714 cm.$^{-1}$ absorption, the B_{1u}–B_{3g} separation is 374 cm.$^{-1}$.

Can. J. Chem. Downloaded from www.nrcresearchpress.com by 61.7.252.67 on 09/04/12
For personal use only.

E. Paracyclophanes

Cram, Allinger, and Steinberg (4) have published the solution spectra of the paracyclophanes, a series of molecules in which two benzene rings are linked together in both para positions by $(CH_2)_n$ groups. The spectra look very similar to a *p*-xylene spectrum when the benzene rings are separated by at least $(—CH_2—)_4$ at both positions. If the rings are any closer a new and weaker band appears to the red. Table III gives the energy difference between the two bands for the compounds studied. These values of ΔE are only approximate because of the breadth of the bands.

TABLE III

INTERACTION ENERGIES BETWEEN BENZENE RINGS

Paracyclophanes						
m	*n*	C_1–C_1'	C_4–C_4'	*R* (separation of ring centers)	ΔE (calc.)	ΔE (obs.)
2	2	1.54	1.54	1.54	632	2400
2	3	1.80	2.26	2.03	278	2700
2	4	2.12	3.16	2.64	126	1600
3	3	2.52	2.52	2.52	142	2800
3	4	2.84	3.41	3.12	78	1950
3	6	3.50	5.27	4.39	28	~0
4	4	3.73	3.73	3.73	44	~0

Other molecules	R_1 (ring center)	R_2 (nearest points)	ΔE_1	ΔE_2	ΔE (obs.)
Biphenyl	4.25	1.45	30	760	374
Diphenylmethane (ϕ = 30°)	4.88	2.56	18	120	150
Dibenzyl	6.66	3.94	8	37	45±14
Durene crystal	6.45		29.6		<5

The weaker absorption band to the red is most probably the forbidden transition of the two which would be expected in the 2600 Å region of the double molecules. If the benzene rings are exactly parallel, this transition is rigorously forbidden in the pure electronic spectrum. Since it is always quite broad, it is probable that it only appears through vibrational–electronic interaction.

Some of the energy differences given in Table III are very large compared to those found for the singly linked double molecules of the previous section. The total intensity of the absorption per ring to both upper states is about right for the $A_g \rightarrow B_{2u}$ transition in *p*-xylene, so that the large splitting is not caused by admixtures of higher excited benzene-like π states. Cram, Allinger, and Steinberg have also calculated the ring–ring distances in these compounds assuming that the bond angles and distances are as nearly "normal" as possible. They point out that the large spectral changes only occur when the rings are closer than the Van der Waals packing distance of 3.40 Å. The distances between corresponding para and para-prime positions in some of these molecules are given in Table III.

F. Molecular Crystals

Crystal structure data are available for benzene and durene, but for very few other crystals containing principally benzene rings. Fox and Schnepp (5) have published an interpretation of the benzene spectrum as observed by Broude, Medvedew, and Prikhotjko (1). The spectrum of the durene crystal in absorption and fluorescence has been studied by Schnepp and McClure (8). There are two molecules per unit cell in

Can. J. Chem. Downloaded from www.nrcresearchpress.com by 61.7.252.67 on 09/04/12
For personal use only.

this crystal and from its geometry some splitting is expected. No dichroism could be found, however, and the splitting must be under 5 cm.$^{-1}$.

III. INTERPRETATION OF THE DATA

A detailed interpretation of the data derived in this article would be of considerable value in learning about the outer parts of the wave functions of the systems considered. The energy transfer phenomena depend predominantly upon the shape of the wave functions in their outer regions. As our main purpose was to establish some valid numbers, only a rudimentary treatment based on the dipole–dipole interaction will be attempted here. An equation similar to eq. [5] is used.

All that is needed to carry out this treatment is a knowledge of the geometry, and the strength of the transition in the individual molecules, or parts of molecules. From the integrated absorption band one may obtain the magnitude of the transition moment (in cm.) through the equation

$$M^2 = 3.97\times10^{-20}\int\epsilon d\nu/\nu,$$

where ϵ is the molar extinction coefficient to base 10. The value of M for toluene is found to be 0.10 Å, and this number may be used in calculations on other compounds containing benzene rings. The full electronic transition moment has been used. The results of the calculations are shown in Table III.

Some of the paracyclophane splitting energies are greater by an order of magnitude than that predicted from the excitation exchange energy. In the two cases, the 3,6 and 4,4 compounds, where no splitting could be observed in the solution spectra, small splittings were calculated. The smallest splitting distinguishable in the solution spectra is roughly 500 cm.$^{-1}$. In the spectrum of the 4,4 compound, some spreading out of the vibrational structure is observable in the solution spectra, and in the low-temperature polarized crystal spectra one expects to see clear evidence for the ring–ring interaction.

The paracyclophanes, which have the very large splittings, all have their benzene rings separated by less then the "packing thickness" of 3.40 Å. Since below this distance there must be considerable π–π overlapping, it is reasonable to find that the dipole–dipole energy does not account for all of the splitting.

For the other double molecules, the dipole–dipole energy gives somewhat better values for the splitting. Taking the distance of separation from the nearest points of the benzene rings gives better values than using the separation of the ring centers. As pointed out by Schnepp and McClure (8), the durene crystal should have an observable dichroic splitting according to the dipole–dipole model. This is the one case in Table III where an overestimate of the interaction energy certainly occurs.

In the calculations for Table III the full electronic moment has been used. Simpson and Peterson (9) have recently shown that one must use only the individual vibronic band moments in the limit of very weak coupling, and the full electronic moment only in strong coupling. The overestimate of the durene energy is probably explainable in this way, as it is a very weakly coupled system.

In diphenylmethane the coupling seems to require use of the full electronic moment. The use of point dipoles is obviously a poor approximation for such closely coupled rings, and the full geometry of the system should be used. This statement also applies to the other molecules where large coupling energies are involved.

The numbers in Table III are believed to be well deserving of further theoretical study.

Can. J. Chem. Downloaded from www.nrcresearchpress.com by 61.7.252.67 on 09/04/12
For personal use only.

REFERENCES

1. BROUDE, V. L., MEDVEDEW, V. C., and PRIKHOTJKO, A. F. Zhur. Eksptl. i Teoret. Fiz. **21**, 665 (1951).
2. COFFMAN, R. E. and McCLURE, D. S. Can. J. Chem. **36**, 48 (1958). (Preceding paper).
3. CRAIG, D. P. J. Chem. Soc. 539 (1955).
4. CRAM, D. J., ALLINGER, N. L., and STEINBERG, H. J. Am. Chem. Soc. **76**, 6132 (1954).
5. FOX, D. and SCHNEPP, O. J. Chem. Phys. **23**, 767 (1955).
6. LONGUET-HIGGINS, H. C. and MURRELL, J. N. Proc. Phys. Soc. (London), A, **58**, 601 (1955).
7. PESTEIL, P. and CABANNES, J. Compt. rend. **235**, 1384 (1952). PESTEIL, P. and BARBARON, M. J. phys. radium, **15**, 92 (1954).
8. SCHNEPP, O. and McCLURE, D. S. To be published.
9. SIMPSON, W. T. and PETERSON, D. L. J. Chem. Phys. **26**, 588 (1957).

Can. J. Chem. Downloaded from www.nrcresearchpress.com by 61.7.252.67 on 09/04/12
For personal use only.

Can. J. Chem. Downloaded from www.nrcresearchpress.com by 61.7.252.67 on 09/04/12
For personal use only.

DIABATIC REACTIONS[1]

HENRY EYRING, GEORGE STEWART, AND RANSOM B. PARLIN

ABSTRACT

The fundamentals of diabatic reactions are briefly reviewed. The two important types of radiationless transitions at the crossover region of two potential surfaces are considered kinetically and rate formulations are given. The first type involves an appreciable activation energy in excess of the heat of reaction. The second does not. The reaction velocity is formulated using the absolute rate theory where the transmission coefficient is interpreted in terms of the Landau–Zener probability approximation. The over-all rate of a sequence of reactions is treated in accordance with the principle that resistances in series are additive. If the second in a sequence of two reaction steps involves a negative activation energy and is slow because of failure to cross to the new surface the resultant repeated passage through the crossover region requires a special formulation of the transmission coefficient, which is given. Whether this transmission coefficient influences the over-all rate or not depends on whether or not it belongs to the rate-determining step.

Quenching reactions are classified in terms of the number of free valences involved, an electron being excited from a saturated molecule conferring radical-like properties on the excited molecule. Excited odd-electron molecules will attract at considerable distances without appreciable activation energy.

The transmission coefficient is discussed in terms of recruitment factors for cases in which the products of a reaction are out of equilibrium.

Hot positive ions resulting from mass spectrographic reactions are indicated as another example of diabatic reactions, and a procedure for treating these by the activated complex theory is briefly mentioned.

Most chemical reactions at low temperatures proceed adiabatically, in the Ehrenfest sense, and so involve no crossing over from one potential energy surface to another (2). Diabatic reactions induced by radiation or by fast particles (2, 3) pass from one surface to another either by absorbing radiation or by a radiationless transition at the crossover region of two potential energy surfaces, or else by spontaneous emission of radiation (5). The Einstein transition probabilities are given by the well-known relations (1, 7)

$$[1] \qquad A_{m\to n} = \frac{8\pi h\nu_{mn}^2}{C^3} B_{m\to n} = \frac{32\pi^3\nu_{mn}^2}{3C^3\hbar} \int \psi_m^* \sum_i e_i \mathbf{r}_i \psi_n d\tau,$$

where the symbols have their usual meaning. A most useful relation for the probability

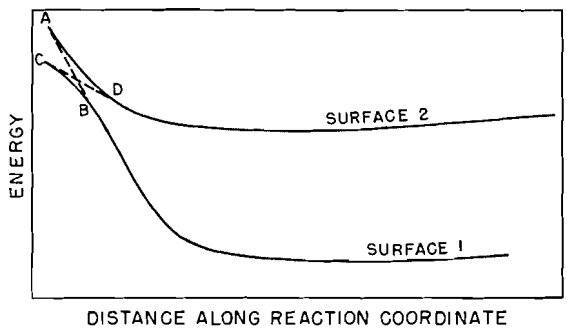

FIG. 1.

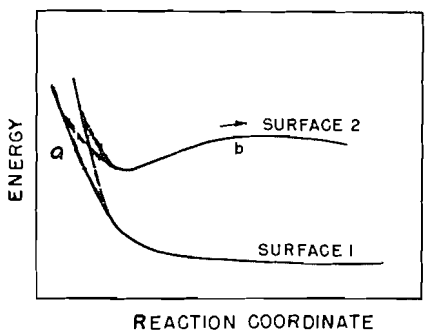

FIG. 2.

[1]*Manuscript received October 3, 1957.*
Contribution from the Department of Chemistry, University of Utah, Salt Lake City, Utah. This paper was presented at the Symposium on the Structure and Reactivity of Electronically-Excited Species held at the University of Ottawa, Ottawa, Canada, September 5 and 6, 1957.

of continuing along one of the dotted curves in Fig. 1 instead of following along a full curve is given by the approximate relationship

$$P = \exp(-4\pi^2\epsilon_{12}^2/hv|S_1-S_2|) \quad [2]$$

due to Landau (4) and Zener (11).

In equation [2], $2\epsilon_{12}$ is the distance between the upper and lower full curves along a vertical line passing through the intersection of the dotted lines. The value of ϵ_{12} is $\int\psi_m^* H^{(1)}\psi_n d\tau$, where ψ_m and ψ_n are the eigenfunctions of H_0 corresponding to the crossing lines and $H^{(1)}$ is the perturbation which shifts the system to the full-lined non-crossing energy surfaces; v is the velocity of approach along the reaction coordinate and S_1 and S_2 are the respective slopes of the two dotted lines. For complicated intersecting surfaces a more exact solution than [2] should be found, but in any case appropriate averages of the parameters in [2] are required to give a mean value for the probability $\bar{P}$. The reaction velocity for passing from surface 2 to surface 1 is

$$v = \prod_i C_i(\mathfrak{H}kT/h)\exp(-\Delta F^{\ddagger}/RT). \quad [3]$$

We will write $\mathfrak{H} = \mathfrak{H}_1\mathfrak{H}_2$, where

$$\mathfrak{H}_2 = 2\bar{P}(1-\bar{P}) \quad [4]$$

and $\mathfrak{H}_1$ will be discussed subsequently. The velocity of the back reaction is

$$v_b = \prod_b C_b(\mathfrak{H}kT/Kh)\exp(-\Delta F^{\ddagger}/RT), \quad [5]$$

where C_b is the concentration of the bth product molecule and K is the equilibrium constant. The other symbols have the same values as in [3].

In Fig. 2 we have a second common type of surface crossing. Here the crossover point is at a lower value of the energy than the final state on surface 2 (to the right of b). In this case we have a specific rate constant at a which we call k_a and at b there is a specific rate constant k_b. The over-all rate is then

$$v = \prod C_i/(k_a^{-1}+k_b^{-1}) = \prod C_i k_a k_b/(k_a+k_b). \quad [6]$$

Again the velocity of the back reaction is

$$v_b = \prod_b (C_b/K)[k_a k_b/(k_a+k_b)]. \quad [7]$$

The rate constants k_a and k_b are each to be calculated as if the other rate-limiting process were absent. More generally, a sequence of any number of reactions has an over-all rate constant equal to the reciprocal of the sum of the reciprocals of the individual rates each calculated as though it were the only rate-determining step. This result is in accordance with the principle that resistances in series are additive (6). In [7] we have $k_b = \mathfrak{H}_b(kT/h)\exp(-\Delta F_b^{\ddagger}/RT)$, where $\mathfrak{H}_b \approx 1$ and $k_a = \mathfrak{H}_a(kT/h)\exp(-\Delta F_a^{\ddagger}/RT)$. We now take $\mathfrak{H}_a = \mathfrak{H}_1\mathfrak{H}_2$, where

$$\mathfrak{H}_2 = \{1-[1-2\bar{P}(1-\bar{P})]^{\nu\tau}\}(\tau\nu)^{-1}. \quad [8]$$

Here τ is the lifetime of the complex which vibrates ν times per second along the reaction coordinate if the only escape of the complex is back to surface 2, that is,

$$1/\tau = (kT/h)\exp[-(\Delta F_b^{\ddagger}-\Delta F_a^{\ddagger})/RT]. \quad [9]$$

The term in [8] which is raised to the power $\nu\tau$ expresses the probability of not transi-

Can. J. Chem. Downloaded from www.nrcresearchpress.com by 61.7.252.67 on 09/04/12
For personal use only.

tioning in $\nu\tau$ tries so that the quantity in brackets expresses the chance of transitioning in $\nu\tau$ vibrations. Consequently $\mathfrak{H}_2$ is the average chance of transitioning per vibration. $\Delta F_a^{\ddagger}$ and $\Delta F_b^{\ddagger}$ are the standard free energies in going from the initial state to the activated states a and b, respectively. $\mathfrak{H}_1$ is the fraction of activated complexes moving from right to left, at equilibrium, which were formed from reactants. $\mathfrak{H}_1$ is discussed subsequently.

TYPE REACTIONS

The reverse of each quenching process is an excitation so that by the principle of microscopic reversibility discussing one is equivalent to discussing the other. When molecules collide there is a tendency for the compressed electron orbits to be promoted as they are promoted in the united atom. Thus, at some interatomic distance one expects a crossing of the non-excited state with the corresponding excited state, as seen in Figs. 1 and 2. Our figures and discussion apply as well to quenching within a molecule as to quenching by collision. In internal quenching the lower surfaces, instead of being flat, turn up like a parabola. This only changes the detailed partition functions to be used but does not modify the above formal considerations.

It is convenient to classify the types of quenching reaction in terms of the number of free valences involved. When an excited saturated molecule is quenched by a second saturated molecule, we have the hole from which the electron was ejected conferring radical-like properties on the excited molecule. Thus the activation energy for collision of such a pair should not exceed a few calories in analogy to the radical reactions $H+H_2 \rightarrow H_2+H$ with 8 calories activation energy, or the reaction $H+Cl_2$ with about 2 calories. The lowering of the activation energy due to the polar nature of the excited molecule leads us to expect low values approaching zero for the activation energy of barrier crossing leading to quenching. At room temperature each 1.3 calories activation energy yields a decrease in the apparent collision cross section by a factor of 10. Such a process is represented in Fig. 1. If the quencher or the excited molecule possesses an odd number of electrons in addition to being excited, two molecules will attract at considerable distance without appreciable activation energy, thus leading to large apparent cross sections. Fig. 2 exemplifies this situation.

THE CHEMICAL BOND AND ACTIVATION ENERGY

An electronic orbital behaves like a fluid sphere or rod of high surface tension which, like any fluid, seeks the lowest possible level of potential energy consistent with minimum surface area. Thus, if there are holes of low potential energy lying in two adjacent atoms and if in addition there is an available electron which by occupying the holes jointly can lower its energy, then the atoms will be drawn together by the electronic orbital, thus forming a chemical bond. Minimum curvature for the orbital means minimizing the kinetic energy, much as minimizing surface area lowers total surface energy for a fluid. Laidler (3) has compiled tables listing a variety of quenching cross sections and explained many of them in terms of the types of potential surfaces which cross. A crossing of surfaces with different multiplicities leads to slow reaction rates because of a small k_a. It is interesting that the observed cross sections are all near enough to ordinary kinetic theory values to preclude activation energies larger than a few calories. Since, however, with competing reactions only the fast reactions are exhibited, we naturally miss such quenching reactions as are relatively slow.

It is natural to expect that the rare gases would be poor quenchers of excited saturated

Can. J. Chem. Downloaded from www.nrcresearchpress.com by 61.7.252.67 on 09/04/12
For personal use only.

molecules or even of excited mercury, not being able to complex with them, whereas excited radicals such as O*H, which can form coordination complexes even with saturated structures, should be quenched by most molecules including the rare gases. The efficiency of the rare earths and transition elements in picking up excitation in the carbon arc is understandable in terms of their unfilled shells, which when excited complex with even saturated molecules making k_a large. Even what Laidler (3) classifies as physical quenching where no new chemical species emerges might well be described as a chemical isomerization in which an excited isomer with its unsaturated valences by being quenched (or by emitting light) changes over into the completely or at least more completely saturated isomer. In this important sense all quenching processes are chemical reactions, each passing through its peculiar activated complex. The quenching molecule, when it emerges unchanged, has served like any other catalyst in providing a changed reaction path, in this case by yielding a crossing of potential surfaces.

Table I lists some of the quenching cross sections found in compilations such as those of Laidler (3). Gases like H_2 and D_2 have quenching cross sections larger than kinetic theory values if they react readily with $Hg(^3P_1)$, thus avoiding a multiplicity change, or if they overcome the multiplicity restriction, by having a long lifetime, τ, for the complex, as is probably true for $Na(^2P)$. $Cd(^3P_1)$, in spite of reacting with the hydrogens, is probably slowed down by a slow multiplicity change.

TABLE I

CROSS SECTIONS, Å²

	$Hg(^3P_1)$	$Cd(^3P_1)$	$Na(^2P)$
H_2	8.6, 6.0	0.67, 3.54	7.4
D_2	8.4, 11.9	0.19, 1.80	
	Unsaturated hydrocarbons		
C_2H_2	23	22	
C_2H_4	48, 26	24.9	44
C_3H_6	31	29	52
C_4H_8-1	33.5	35.2	58
C_4H_8-2	29	30.6	58
C_6H_6	41.9, 59.9	28.4	75
	Saturated hydrocarbons		
CH_4	0.059	0.012	0.11
C_2H_6	0.42	0.024	0.17
C_3H_8	1.6	0.012	0.2
n-C_4H_{10}	4.1	0.064	0.3
n-C_5H_{12}	8.6	—	—
n-C_6H_{14}	16	—	—
n-C_7H_{16}	24	—	—
	Odd electron		
NO	24.7	—	—
	Halogens		
I_2	—	—	40
Br_2	—	—	100

The unsaturated hydrocarbons with their π electrons attract at large distances and then complex strongly enough that $k_a \gg k_b$ because of a long lifetime, τ_1, of the complex or else by an increase in the transition per vibration, $2\bar{P}(1-\bar{P})$. It is interesting that for the quenching of $Na(^2P)$, where chemical changes in the unsaturated hydrocarbons

Can. J. Chem. Downloaded from www.nrcresearchpress.com by 61.7.252.67 on 09/04/12
For personal use only.

do not occur, the quenching cross sections are nevertheless greater than for $Hg(^3P_1)$ and $Cd(^3P_1)$, where H_2 is liberated. One must conclude that long lifetimes, τ, contrive to make $k_a \gg k_b$ and that this is independent of whether there are subsequent chemical changes or not. This indication that the rate-determining step is the "physical quenching" whether or not this is followed by a chemical reaction is interesting in connection with Zemansky's (10) evidence that oscillators which most nearly matched their quantum to the 5.03 kcal. for the change $Hg(^3P_1) \rightarrow Hg(^3P_0)$ were most efficient in the quenching process.

Table I indicates also that for saturated hydrocarbons the rate-determining step for quenching seems to yield roughly similar cross sections whether chemical reactions follow as for $Hg(^3P_1)$ or $Cd(^3P_1)$ or whether they do not as for $Na(^2P)$. This suggests again that the rate-determining step is low for methane because $2\bar{P}(1-\bar{P})$ and/or τ are low. Larger molecules would be expected to complex more readily with the excited atoms and so increase τ and, therefore, the quenching cross section, as is observed. The remaining cases are also in accord with the view that in quenching the rate-determining step is usually without an activation energy and is governed by τ and $2\bar{P}(1-P)$ whether or not it is followed by a subsequent chemical reaction.

THE TRANSMISSION COEFFICIENT, THE CONNECTIVITY OF STATES, AND THE RECRUITMENT FACTORS

We have discussed at some length $\mathfrak{H}_2$, which we will call the diabatic factor in the transmission coefficient $\mathfrak{H}_a = \mathfrak{H}_1\mathfrak{H}_2$. The factor $\mathfrak{H}_1$ is the additional factor required to correct an equilibrium reaction rate expression for non-equilibrium conditions. Ideally we should consider every possible quantum state of a reacting system as a separate species and proceed by the methods made familiar in dealing with chain reactions. Such a procedure yields the set of equations

$$[10] \qquad dc_i/dt = \sum_j (k_{j\rightarrow i}\, c_j - k_{i\rightarrow j}\, c_i),$$

where there are as many equations as there are quantum states. In the general case the k's are functions of the concentrations of various species, the temperature, which isotope is involved, and the radiation density. At equilibrium we have $dc_i/dt = 0$ for all species. In a steady state, dc_i/dt can be taken as zero to a good approximation only for certain intermediates which exist at very low concentrations in the reaction sequence. For those states considered to maintain an equilibrium distribution in spite of the reaction we assume

$$[11] \qquad d\ln c_i/dt = d\ln \textstyle\sum_k c_k/dt = -d\ln \sum_l c_l/dt.$$

This is, of course, a great simplification and never quite true. In [11] $\sum_k c_k$ gives the total concentration of a particular reactant while $\sum_l c_l$ is the concentration of a product; c_i is the concentration of the particular species in the ith quantum state. When one observes that the products of a reaction are out of equilibrium as chemiluminescent spectra often show, it follows by the principle of detailed balance that for the reverse reaction the reacting species would not be withdrawn from the reservoir of states in such a way as to maintain equilibrium exactly. To this extent a mean $\mathfrak{H}_1$ is not exactly true but is still a useful approximation. However, molecular beam experiments such as those of Taylor and Datz (9) will require something better than a mean $\mathfrak{H}_1$ and will be revealing the detailed structure of potential energy surfaces. The various isotopic reactions may have nearly equal mean values of $\mathfrak{H}_1$, in spite of markedly fluctuating transmission coefficients for various states of the activated complex.

Can. J. Chem. Downloaded from www.nrcresearchpress.com by 61.7.252.67 on 09/04/12
For personal use only.

As indicated in equation [10], a particular state recruits its occupants from all other states. We define the recruitment factor for the j to i state with reference to equation [10] as

$$f_{j\to c} = k_{j\to c} c_j^0 / \sum_j k_{j\to i} c_j^0, \qquad [12]$$

where the zero subscript refers to the equilibrium concentration and $\sum_j f_{j\to i} = 1$. Clearly the f's are expressible in terms of partition functions alone. In order that $\mathfrak{H}_1$ should be unity, it is clear that every activated complex corresponding to crossing from reactant to product should recruit only from reactants, since $\mathfrak{H}_1$ is the total recruitment from reactant over recruitments from both reactants and from products. However, if it recruits equally from reactants and products, $\mathfrak{H}_1$ is still one-half. In pathological cases such as in the reaction $H_2 \rightarrow 2H$, the activated complex states moving in the direction reactants to products recruit largely from products. This yields a correspondingly low value for $\mathfrak{H}_1$.

MASS SPECTROGRAPHIC REACTIONS

The activated complex theory has been applied to reactions in the mass spectrograph (8). When an electron knocks another electron out of a molecule and makes a positive ion, this constitutes a Franck–Condon transition from the low potential surface for the molecule up to the surface corresponding to the ion. If the electron removed were completely localized in one bond in the ground state, and if there were no electronic reorganization in the positive ion, then only one bond length would be too short after the transition and the stored up energy would either break the weakened bond or would be insufficient to do so. Instead, the bonds finally broken bear little relation to the bond which must have been the source of the displaced electron. Another way of looking at the situation is that the equilibrium structure of the positive ion usually differs greatly from that of the neutral molecule in many bonds. The result is that, typically, ionization creates a positive ion with several electron volts of energy scattered over many degrees of freedom and only as the Lissajous motion of the mass point concentrates the dissociation energy in a bond does one get dissociation.

Thus, ionization creates a hot positive ion which usually has sufficient energy to break a variety of bonds each with a specific rate constant. The appearance potentials fix the activation energy for the corresponding reactions and the vibration frequencies can be estimated so that one can calculate a corresponding set of rate constants. Thus, for an assumed energy in the molecule, one can calculate the percentage of each of the possible products formed during the time the positive ion stays in the mass spectrograph. If the distribution function of number of ions against energy stored in the ion can be measured, or assumed, or calculated one can predict the mass spectra for a molecule. Much remains to be learned about such measurements and calculations, but enough success has been achieved to indicate that the outlined procedure is on the right track. Hot positive ions with their mobile structure and enormous reactivity seem to constitute one more diabatic province at least partly understood. Characteristically the energy left in electronically excited states crosses over and becomes available as vibrational energy promoting reaction on the lowest state of the positive ion. Molecules like the aromatic hydrocarbons which tend to fluoresce in solution possess groups of states which do not cross effectively with other states and, as would be expected, yield larger percentages of parent ions.

We wish to express our appreciation to the National Science Foundation for their support of this research.

Can. J. Chem. Downloaded from www.nrcresearchpress.com by 61.7.252.67 on 09/04/12
For personal use only.

REFERENCES

1. EYRING, H., WALTER, J., and KIMBALL, G. E. Quantum chemistry. John Wiley and Sons, Inc., New York. 1944. p.115.
2. GLASSTONE, S., LAIDLER, K. J., and EYRING, H. The theory of rate processes. McGraw-Hill Book Company, Inc., New York. 1941.
3. LAIDLER, K. J. The chemical kinetics of excited states. Oxford Univ. Press, London. 1955.
4. LANDAU, L. Physik. Z. Sowjetunion, **46**, No. 2 (1932).
5. LUMRY, R. and EYRING, H. Radiation biology. Vol. 3. *Edited by* A. Hollaender. McGraw-Hill Book Company, Inc., New York. 1956. Chap. I.
6. PARLIN, R. B. and EYRING, H. Ion transport across membranes. *Edited by* H. T. Clarke. Academic Press Inc., New York. 1954. p. 103.
7. PAULING, L. and WILSON, E. B. Introduction to quantum mechanics. McGraw-Hill Book Company, Inc., New York. 1935.
8. ROSENSTOCK, H. M., WALLENSTEIN, M. B., WAHRHAFTIG, A. L., and EYRING, H. Proc. Natl. Acad. Sci. U.S. **38**, 667 (1952).
9. TAYLOR, E. H. and DATZ, S., JR. J. Chem. Phys. **23**, 1711 (1955).
10. ZEMANSKY, M. W. Phys. Rev. **36**, 1919 (1930).
11. ZENER, C. Proc. Roy. Soc. (London), A, **137**, 696; A, **140**, 660 (1933). See also Ref. 1, Chap. 16.

Can. J. Chem. Downloaded from www.nrcresearchpress.com by 61.7.252.67 on 09/04/12
For personal use only.

Can. J. Chem. Downloaded from www.nrcresearchpress.com by 61.7.252.67 on 09/04/12
For personal use only.

REACTIONS INVOLVING ELECTRONICALLY-EXCITED OXYGEN[1]

E. KERRY GILL AND K. J. LAIDLER

ABSTRACT

The various electronically-excited states of oxygen atoms and molecules are briefly considered. Certain reactions involving some of these electronically-excited species are then discussed with reference to the experimental evidence and to the potential-energy surfaces on which they occur. In the case of the mercury-photosensitized formation of ozone from oxygen it is concluded that both experimental evidence and theoretical arguments point to the fact that the oxygen molecule initially formed is in an excited $^3\Sigma_u^+$ state. Consideration is also given to the mechanism of formation of O_2^* in the carbon monoxide flame and in other flames. The reactions

$$O+O_3 \rightarrow 2O_2^*$$

and

$$O_2^*+O_3 \rightarrow 2O_2+O$$

are also discussed briefly.

INTRODUCTION

A considerable number of electronically-excited states of oxygen molecules and atoms are known to exist, and spectroscopic data have provided detailed information about many of them. Several of these excited species are known to be involved in chemical reactions, either as reactants or as products. The purpose of this paper is to refer to a few of the more common reactions of this type, to discuss the evidence for the nature of the species involved, and to consider detailed reaction mechanisms from the standpoint of the method of potential-energy surfaces.

ELECTRONIC STATES

The electronic states of O and O_2 will be mentioned only very briefly, since this matter has been fully discussed elsewhere (14, 15). According to the Wigner–Witmer correlation rules two atoms of oxygen in their ground states (^3P_g) can produce, on combination, 18 different electronic species of the molecule, while one ground state atom plus one in the first excited level (^1D_g) can give an additional 18 species. Only a few of these are stable or relatively abundant, and Fig. 1 shows the potential-energy curves for those states of the molecule that have been observed spectroscopically. The $^1\Sigma_u^-$ and $^3\Delta_u$ states ($^3\Delta_u$ not drawn) have been detected by Herzberg (16).

The ground state of O_2 ($^3\Sigma_g^-$) and the first two excited states ($^1\Delta_g$ and $^1\Sigma_g^+$) have the electronic configuration

$$KK(\sigma_g 2s)^2(\sigma_u 2s)^2(\sigma_g 2p)^2(\pi_u 2p)^4(\pi_g 2p)^2$$

and dissociate to normal ^3P_g atoms as shown in the figure. Additional excited states are formed by the transfer of an electron from the bonding ($\pi_u 2p$) orbital to the antibonding ($\pi_g 2p$) orbital to give

$$KK(\sigma_g 2s)^2(\sigma_u 2p)^2(\sigma_g 2p)^2(\pi_u 2p)^3(\pi_g 2p)^3.$$

This configuration could produce the states $^1\Sigma_u^+$, $^1\Sigma_u^-$, $^1\Delta_u$, $^3\Sigma_u^+$, $^3\Sigma_u^-$, and $^3\Delta_u$, of which $^1\Sigma_u^-$, $^3\Sigma_u^+$, $^3\Sigma_u^-$, and $^3\Delta_u$ have been observed. $^3\Sigma_u^-$ dissociates into $O(^3P_g)+O(^1D_g)$, the rest into ground-state $O(^3P_g)$ atoms.

[1]*Manuscript received August 16, 1957.*
Contribution from the Department of Chemistry, University of Ottawa, Ottawa, Canada. This paper was presented at the Symposium on the Structure and Reactivity of Electronically-Excited Species held at the University of Ottawa, Ottawa, Canada, September 5 and 6, 1957.

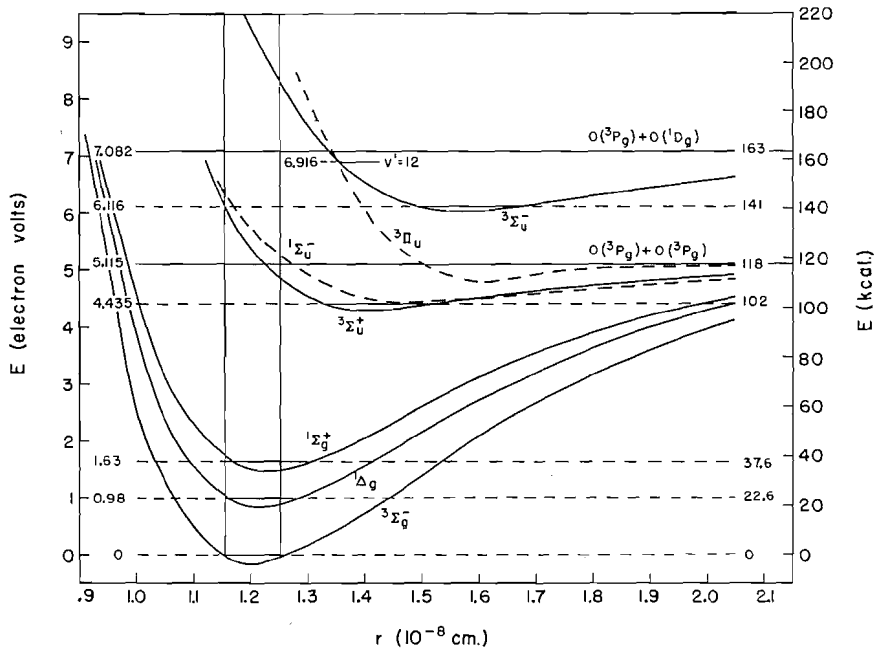

FIG. 1. Potential-energy curves for the ground and excited states of the oxygen molecule.

Fig. 1 also includes a $^3\Pi_u$ curve recently proposed by Wilkinson and Mulliken (34) to account for the predissociation of $O_2(^3\Sigma_u^-)$ into ^3P_g atoms.

THE REACTION $Hg^*(^3P_1) + O_2(^3\Sigma_g^-) \rightarrow Hg(^1S_0) + O_2^*$

Molecular oxygen is an effective quencher for the 2537 Å mercury line, the quenching cross-section being very large (29, 35). This quenching process involves the transition from the $^3P_1$ state of Hg to the $^1S_0$ state, a transition that occurs with an energy liberation of 4.88 ev. or 112.5 kcal. Ozone is produced during the quenching, and it is of interest to consider the state of the oxygen after it has reacted with the excited mercury atom.

In the first place, there is abundant evidence that the reaction is

[1] $$Hg^*(^3P_1) + O_2(^3\Sigma_g^-) \rightarrow Hg(^1S_0) + O_2^*,$$

where O_2^* is an excited state of oxygen, the nature of which is discussed below. The reasons for preferring this reaction to

[2] $$Hg^*(^3P_1) + O_2 \rightarrow HgO + O$$

and

[3] $$Hg^*(^3P_1) + O_2 \rightarrow Hg(^1S_0) + 2O(^3P_g)$$

are briefly as follows. Reaction [2] is exothermic by at least 64 kcal. (32) and is therefore energetically possible; however if it were followed by $O+O_2 \rightarrow O_3$ there would be one molecule of ozone formed from each Hg* atom.† Experimentally at least seven molecules are formed (3, 32), and the reaction $HgO+O_2 \rightarrow Hg+O_3$ is too endothermic to be useful. Reaction [3] can be excluded as being slightly endothermic.

†*Since the* Hg *is converted into* HgO *there can be no re-excitation to* Hg*. *If reaction* [1] *occurs re-excitation is possible and large yields can result.*

Can. J. Chem. Downloaded from www.nrcresearchpress.com by 61.7.252.67 on 09/04/12
For personal use only.

According to the correlation rules $Hg^*(^3P_1)$ and $O_2(^3\Sigma_g^-)$ can combine to give the linear complex HgO_2 in Σ and Π states with singlet, triplet, and quintet multiplicities. Energetically, since 4.88 ev. is available, the O_2^* could be in any one of the four lowest electronic states, namely $^3\Sigma_g^-$ (ground), $^1\Delta_g$, $^1\Sigma_g^+$, and $^3\Sigma_u^+$. All of these states are permitted by the correlation rules, as may be seen as follows:

$$Hg(^1S_0) + O_2^*(^3\Sigma_g^- \text{ or } ^3\Sigma_u^+) \rightarrow HgO_2(^3\Sigma),$$
$$Hg(^1S_0) + O_2^*(^1\Delta_g) \rightarrow HgO_2(^1\Sigma, {}^1\Pi, {}^1\Delta),$$
$$Hg(^1S_0) + O_2^*(^1\Sigma_g^+) \rightarrow HgO_2(^1\Sigma).$$

The question now to be decided is which of these four electronic states of O_2 is actually formed. Various suggestions have previously been made. Mitchell (25) suggested that, since the ground state of oxygen has a vibrational level at 4.86 ev., which corresponds closely to the energy released, this state will actually be formed; in other words, the electronic energy of the mercury will pass almost entirely into vibrational energy of the oxygen. However, recent work has indicated (23, p. 105) that this resonance factor, arising from the matching of energy levels, is not an important one. Volman (33), on the basis of his results (32) on the effect of foreign gases on ozone production, suggested that the oxygen produced was either vibrationally excited $^3\Sigma_g^-$ or a singlet state, and argued against its being the $^3\Sigma_u^+$ state. Finally one of us (see p. 101 of Ref. 23) has tentatively suggested that the most probable process is the one involving the least loss of electronic energy, and from this it follows that the $^3\Sigma_u^+$ state is the one that should be produced.

In the following two subsections we re-examine this problem from both the experimental and theoretical points of view, and conclude that the $^3\Sigma_u^+$ state is probably produced.

Influence of Foreign Gases

The reactions subsequent to reaction [1] and leading to ozone production are

[4] $$O_2^* + O_2 \rightarrow O_3 + O$$

and

[5] $$O + O_2 + M \rightarrow O_3 + M + \text{k.e.}$$

where M is a third body required to carry off the excess energy. Volman's discussion (33) of the probable state of the O_2^* produced in reaction [1] is based on the effects of foreign gases added to the system. A number of such gases were found to increase the rate of ozone production in the mercury-photosensitized reaction, the order of effectiveness being

$$He > A > N_2 > CO_2.$$

These gases play a role in reaction [5] as well as in the reactions

[6] $$Hg^*(^3P_1) + M \rightarrow Hg(^1S_0) + M^*$$

and

[7] $$O_2^* + M \rightarrow O_2 + M^*.$$

This behavior of foreign gases is to be contrasted with their effects on the unsensitized photochemical formation of ozone from oxygen at 1849 Å (32). The foreign gases were in this case found to reduce the role of ozone formation, their order of effectiveness as retarders being the same as above. At this wavelength oxygen dissociates into two normal

Can. J. Chem. Downloaded from www.nrcresearchpress.com by 61.7.252.67 on 09/04/12
For personal use only.

^3P atoms (27, p. 246), either by a direct transition to a repulsive state of O_2 or by a predissociation from the $^3\Sigma_u^-$ state:

[8] $$O_2 + h\nu \xrightarrow{1849\ \text{Å}} O(^3P) + O(^3P)$$

Subsequent processes are

[9] $$O + O_2 + M \rightarrow O_3 + M$$

and

[10] $$O + O + M \rightarrow O_2 + M.$$

The reactions occurring in the sensitized and unsensitized reactions may thus be compared as follows:

Sensitized reaction (accelerated by foreign gases)		Unsensitized reaction (retarded by foreign gases)	
I	$Hg^*(^3P_1) + O_2(^3\Sigma_g^-) \rightarrow Hg(^1S_0) + O_2^*$	VI	$O_2 + h\nu \xrightarrow{1849\ \text{Å}} O(^3P) + O(^3P)$
II	$O_2^* + O_2 \rightarrow O_3 + O$	VII	$O + O_2 + M \rightarrow O_3 + M$
III	$O + O_2 + M \rightarrow O_3 + M$	VIII	$O + O + M \rightarrow O_2 + M$
IV	$Hg^* + M \rightarrow Hg + M^*$		
V	$O_2^* + M \rightarrow O_2 + M^*$		

It is to be noted that in the sensitized reaction M catalyzes the production of ozone as far as III is concerned and inhibits it in IV and V. In the unsensitized reaction M is a catalyst in VII and an inhibitor in VIII.

In the sensitized reaction the foreign gases catalyze the formation of ozone, the inert gases being the most effective. Evidently their effect on III overrides that on IV and V. But if, as Volman asserts, the energy of O_2^* is largely vibrational, these gases would readily bring about deactivation, and no over-all accelerating effect would result. In our view the simplest explanation of the facts is that the excitation energy of O_2^* is largely electronic in nature. If this is the case the quenching to lower electronic states will occur only with difficulty, and hardly at all with the inert gases (20). In order for the ozone-producing reaction II to occur readily the O_2^* must have at least 94 kcal. of energy. If this O_2^* is in the $^3\Sigma_u^+$ state, even if it is in its ground vibrational level it still has more than this amount of energy. In the case of the three lower known electronic states, however, quenching by the foreign gases to the ground vibrational state would produce a molecule having insufficient energy to produce ozone. The facts are therefore completely explained if the $^3\Sigma_u^+$ state is formed, but not if any of the lower states are formed.

We may now consider whether these ideas are also consistent with the facts regarding the unsensitized formation of ozone by 1849 Å radiation, the mechanism for which is given above. To explain the retardation by foreign gases it must be supposed that their effect on reaction VIII is more important than on VII. This is probably due to the relative rates of the reactions; reaction VIII presumably has no activation energy, while Dainton and Kimberley (2) by an indirect method have concluded that VII has an activation energy of 4.3 kcal. Furthermore, in the thermal decomposition of ozone, which probably occurs by the mechanism

[11] $$O_3 + M \rightleftarrows O_2 + O + M,$$

[12] $$O + O_3 \rightarrow 2O_2,$$

[13] $$2O + M \rightarrow O_2 + M,$$

Griffith and McKeown (10) found that He, A, N_2, and CO_2 catalyzed the decomposition;

Can. J. Chem. Downloaded from www.nrcresearchpress.com by 61.7.252.67 on 09/04/12
For personal use only.

this indicates that the last reaction is influenced by M more than is VII. Reaction VIII has not been included in the scheme for the sensitized reaction since there will be a much smaller concentration of oxygen atoms than in the unsensitized process; the over-all rate is very much less.

Volman (33) based his conclusion that O_2^* is *not* in the $^3\Sigma_u^+$ state upon the *relative* effects of the foreign gases, and made no mention of the important fact that increasing their concentration increases the rate. It is of interest that the results indicate the order of the effects of the gases to be the same on III as on VIII.

The conclusion of the present subsection is that the O_2^* produced in reaction [1] is in the $^3\Sigma_u^+$ state, and it would be of interest to have direct spectroscopic evidence of this. In the meantime we will now show that the same conclusion is suggested by the theoretical considerations.

Potential-Energy Surfaces

It is instructive to discuss the mechanism of reaction [1] using the method of potential-energy surfaces. Fig. 2 shows a schematic representation of the surfaces, the method

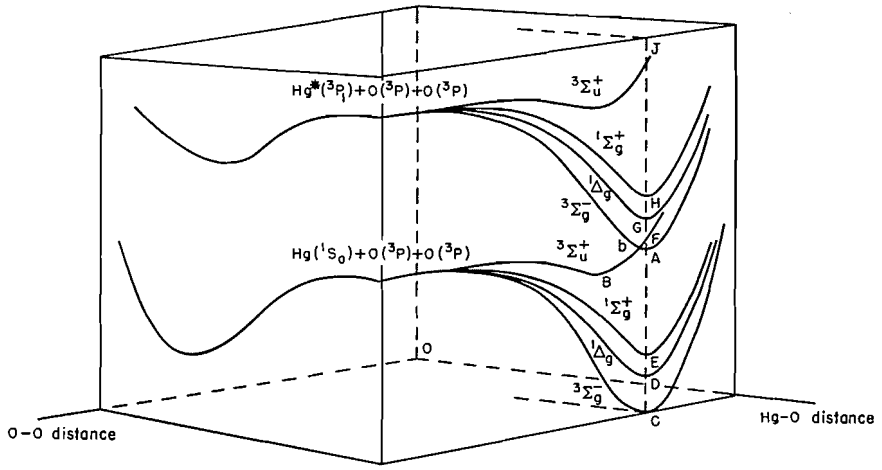

FIG. 2. Potential-energy surfaces for the Hg—O—O system.

employed being that previously used by one of us (20, 21, 22, 23, 24). Point A represents the initial state of the reaction, with $Hg^*(^3P_1)$ and $O_2(^3\Sigma_g^-)$ separated from one another. Points B, C, D, and E represent possible final states, corresponding to Hg ($^1S_0$) together with O_2 in its ground state (point C) or some excited state. Points A, B, C, D, and E are the entrances to valleys that proceed into the cube from the right-hand face.

Consider first the possibility of a transition from A to B, corresponding to the process

$$[14] \qquad Hg^*(^3P_1) + O_2(^3\Sigma_g^-) \rightarrow Hg(^1S_0) + O_2^*(^3\Sigma_u^+).$$

When the potential-energy curves are constructed accurately, using the spectroscopic data, the form of the curves in the region of the points A and B is as shown in Fig. 3. It is to be seen that the crossing point b lies at about the ground vibrational level of the $O_2(^3\Sigma_g^-)$ curve, so that the transition can easily occur even at considerable separations between Hg* and O_2. The potential-energy surfaces therefore confirm our deductions from the experimental results that the O_2 formed will be in the $^3\Sigma_u^+$ state, corresponding to the least transfer of electronic energy into other forms. The fact that the transition

Can. J. Chem. Downloaded from www.nrcresearchpress.com by 61.7.252.67 on 09/04/12
For personal use only.

can occur at large separation is consistent with the very large quenching cross-section observed for the reaction (29, 35).

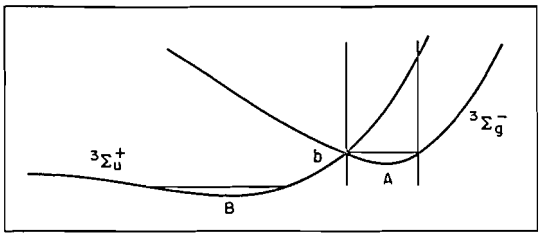

FIG. 3. Enlarged version of a portion of Fig. 2.

If for any reasons the transition to *B* did not occur, the conclusion from the surfaces is that the next most likely possibility is a transition to *E*; failing that, transitions to *D* and *C* could occur. In other words, the system "cascades" through the various electronic states. The evidence for this is as follows. Fig. 4 shows a schematic potential-energy profile through the line *CAJ* in Fig. 2. In this diagram the valley starting at *A*

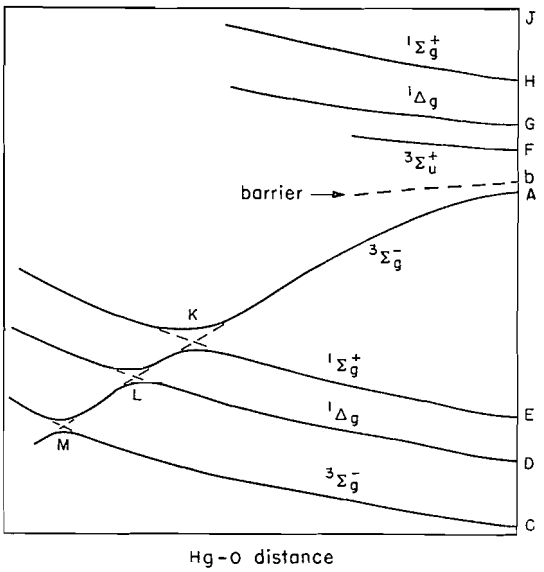

FIG. 4. Potential-energy profile through *CAJ* in Fig. 2. The designations refer to the state of the oxygen molecule.

is represented as going down as the Hg—O distance is decreased; this corresponds to attraction between Hg* and O_2. A number of valleys will start from the points *C*, *D*, *E*, *F*, *G*, and *H*; some of these will correspond to repulsive states and will therefore slope upwards. The dotted line starting at *b* represents the top of the barrier separating the valleys *A* and *B*; this line should not be in the plane of this profile but slightly above it (i.e. corresponding to larger O—O separations).

With regard to the valleys starting at *A*, *C*, *D*, and *E* there is some choice of multiplicities, and it will be assumed that those curves represented in Fig. 4 all correspond to the same multiplicity. The non-crossing rule then provides for resonance splittings, as

Can. J. Chem. Downloaded from www.nrcresearchpress.com by 61.7.252.67 on 09/04/12
For personal use only.

shown at K, L, and M. At the point K a system proceeding in the direction AK may undergo a transition and end up at E. Failing such a transition the next possibility is a transition at L, the system ending up at D. Failing that the oxygen will be in the ground state, at C. These latter possibilities, however, are very unlikely. Although the curves shown in Fig. 4 are only schematic it does not seem to be possible, by modifying the form of the curves, to arrive at conclusions other than those reached above.

To summarize, our conclusion from the potential-energy surfaces is that the order of probabilities for the formation of oxygen in reaction [1] is

$$^3\Sigma_u^+ > {}^1\Sigma_g^+ > {}^1\Delta_g > {}^3\Sigma_g^-.$$

The conclusion that the $^3\Sigma_u^+$ state is the most likely confirms our deduction from the experimental evidence based on the effects of foreign gases on ozone production.

THE REACTIONS $O(^3P) + CO(^1\Sigma_u^+) \rightarrow CO_2^*(^3\Pi)$ AND $CO_2^*(^3\Pi) + O_2 \rightarrow CO_2 + O_2^*$

The reactions

[15] $$O(^3P) + CO(^1\Sigma_u^+) \rightarrow CO_2^*(^3\Pi)$$

and

[16] $$CO_2^*(^3\Pi) + O_2 \rightarrow CO_2 + O_2^*$$

are believed to take place in the carbon monoxide flame. Since the mechanisms and other features of the reactions have recently been discussed (9, 23) only a brief discussion will be given here.

The luminosity of the carbon monoxide flame is too great to be attributed to thermal radiation alone, so that the presence of electronically excited species is to be expected. The ground state of CO_2 is $^1\Sigma_g^+$ (26) and the first excited states probably $^3\Pi$ and $^1\Pi$ in that order. Spectroscopic observation of the flame shows no evidence of any excited CO, and it is therefore believed that CO_2 is formed as above. Since CO is a singlet in its ground state, reaction with a normal (triplet) oxygen atom will necessarily produce excited $CO_2^*(^3\Pi)$, whereas CO_2 ($X\ ^1\Sigma_g^+$) can be formed directly only from an atom in a singlet state:

[17] $$O^*(^1D) + CO(^1\Sigma_u^+) \rightarrow CO_2(X\ ^1\Sigma_g^+).$$

The presence of O atoms in the reaction has been confirmed by Gaydon (6, 7). It is found (8, 11) that $O(^3P)$ atoms do not react with CO on every collision, but the reaction between $O(^1D)$ and CO is much more rapid (28).

If the CO_2 formed in [15] were in the ground state, the process would be exothermic by 126.7 kcal., whereas the actual heat liberated is lower than this by the energy of excitation and is probably about zero (7). The spectral continuum of the flame has been attributed (7) to the association reaction

[18] $$CO + O \rightarrow CO_2^* \rightarrow CO_2 + h\nu.$$

At the same time, the banded structure of the spectrum is due to the Schumann–Runge system

[19] $$O_2^*(^3\Sigma_u^-) \rightarrow O_2(^3\Sigma_g^-).$$

Hornbeck (17) observed that with increasing O_2/CO ratio, the intensity of the continuum decreased while that of the banded structure increased. This would be explained

Can. J. Chem. Downloaded from www.nrcresearchpress.com by 61.7.252.67 on 09/04/12
For personal use only.

by the fact that an increase in O_2 pressure will increase the amount of O_2^* formed in [16] and consequently the intensity of the Schumann–Runge bands. But also the CO_2^* ($^3\Pi$) is brought to the ground state by this radiationless transition and less will be at hand to give the continuum reaction [18] (23, p. 72).

The possibility of physical quenching in [16], with the oxygen remaining in its ground state, is not forbidden by the correlation rules, but consideration of the disposition of the potential-energy surfaces involved (9) shows that it is very unlikely since the $^3\Sigma$ surface lies much below the others with no apparent connection between them.

Two excited electronic states of oxygen have been detected in the flame; one is the $^3\Sigma_u^-$ state which, by passing to the lowest state, gives the Schumann–Runge bands. This state can be formed via triplet complexes, and if ionic surfaces are involved, the process would be (Ref. 23, p. 101):

[20] $$CO_2^*(^3\Pi) + O_2(^3\Sigma_g^-) \rightarrow CO_2O_2(^3\Sigma, {}^3\Pi) \rightarrow CO_2^+O^-O(^3\Sigma, {}^3\Pi) \rightarrow CO_2(^1\Sigma_g^+) + O_2^*(^3\Sigma_u^-).$$

The other state is the $^1\Sigma_g^+$, which can be produced via singlet complexes:

[21] $$CO_2^*(^3\Pi) + O_2(^3\Sigma_g^-) \rightarrow CO_2O_2(^1\Sigma, {}^1\Pi) \rightarrow CO_2^+O^-O(^1\Sigma, {}^1\Pi) \rightarrow CO_2(^1\Sigma_g^+) + O_2^*(^1\Sigma_g^+).$$

THE REACTION $O(^3P) + O^*(^1D) + M \rightarrow O_2^*(^3\Sigma_u^-) + M$

The fact that the Schumann–Runge bands have been observed in the hydrogen (1, 5, 31), carbon monoxide (18), and ammonia (19) flames suggests that there may be a reaction such as

[22] $$O(^3P) + O^*(^1D) + M \rightarrow O_2^*(^3\Sigma_u^-) + M$$

common to all of these flames, by which the $O_2^*(^3\Sigma_u^-)$ is produced (Ref. 23, p. 75). The metastable O^* (^1D) may be produced thermally, from the dissociation of one of the reaction intermediates such as $OH^*(^2\Sigma^+)$, or perhaps, in the case of the CO flame, from

[23] $$CO_2(^1\Sigma^+) \rightarrow CO(^1\Sigma^+) + O^*(^1D).$$

THE REACTIONS $O + O_3 \rightarrow 2O_2^*$ AND $O_2^* + O_3 \rightarrow 2O_2 + O$

The reactions

[24] $$O + O_3 \rightarrow 2O_2^*$$

and

[25] $$O_2^* + O_3 \rightarrow 2O_2 + O$$

are believed to occur in the photochemical decomposition of ozone. The primary process of the scheme must be

[26] $$O_3 + h\nu \rightarrow O_2 + O.$$

From thermal data, ΔH for [26] is 24.1 kcal. corresponding to a wavelength of about 11,800 Å, which would be the infrared limit for a possible dissociation (Ref. 29, p. 144). Shorter wavelengths supply energy for the following reactions:

		ΔH (kcal.)	λ (Å)	
[27]	$O_3 + h\nu \rightarrow O_2(^3\Sigma_g^-) + O(^3P)$	24.1	11,800	I.R.
[28]	$O_3 + h\nu \rightarrow O_2^*(^1\Delta_g) + O(^3P)$	47.1	6,200	
[29]	$O_3 + h\nu \rightarrow O_2^*(^1\Sigma_g^+) + O(^3P)$	62	4,600	Visible
[30]	$O_3 + h\nu \rightarrow O_2(^3\Sigma_g^-) + O^*(^1D)$	70	4,000	
[31]	$O_3 + h\nu \rightarrow O_2^*(^1\Sigma_g^+) + O^*(^1D)$	108	2,600	U.V.

Can. J. Chem. Downloaded from www.nrcresearchpress.com by 61.7.252.67 on 09/04/12
For personal use only.

Consequently, it has been suggested (30) that the O atom of [26] is ^3P when absorption takes place in the visible region, and ^1D when in the ultraviolet.

The experimental work of Forbes and Heidt (4, 12) showed a range of values for the quantum yield ϕ and a complex dependence of ϕ on ozone concentration, total pressure, light intensity, etc. Heidt (13) concluded that activated molecules must play a part in the reaction and found it necessary to postulate an energy chain:

[32] $$O_3 + h\nu \longrightarrow O_2^* + O,$$

[33] $$O + O_3 \longrightarrow 2O_2^*,$$

[34] $$O + O_2 + M \longrightarrow O_3 + M,$$

[35] $$O \xrightarrow{\text{walls}} \tfrac{1}{2}O_2,$$

[36] $$O_2^* + O_3 \longrightarrow 2O_2 + O,$$

[37] $$O_2^* + M \longrightarrow O_2 + M.$$

The rather complicated expression for ϕ that results gives the correct dependence of ϕ on light intensity, pressure, and so forth.

Whether or not the O_2 of [32] is electronically excited depends upon the wavelength used, as seen above. ΔH for reaction [33] is $(-92.3+2E_e)$ kcal. where E_e is the excitation energy of each O_2^* in [33]. Consequently, each oxygen molecule could be in the $^1\Sigma_g^+$ state and the reaction still be exothermic. Now ΔH for reaction [36] is $(25.7-E_e)$ kcal. so that in order for it to be exothermic, $E_e \geqslant 25.7$ kcal. or 1.12 ev.; i.e. O_2^* is $^1\Sigma_g^+$ or a vibrationally excited form of a lower state.

Ozone absorbs weakly in the visible and strongly in the ultraviolet region. The electronic term level of the $^1\Sigma_g^+$ state of O_2 is 38 kcal., which, according to Heidt, corresponds roughly to the difference in energy between the long wave limits of the ultraviolet and visible absorption spectra of O_3, 3500 and 6500 Å (Ref. 27, p. 396). If this also corresponds to the energy difference between two electronic levels of O_3, the upper one of which dissociates spontaneously to O_2+O, then reaction [36] may be expected to be very efficient if the O_2^* is $^1\Sigma_g^+$. It is therefore assumed that this is the electronic state involved.

REFERENCES

1. Broida, H. P. and Shuler, K. E. J. Chem. Phys. **20**, 168 (1952).
2. Dainton, F. S. and Kimberley, H. M. Trans. Faraday Soc. **46**, 629 (1950).
3. Dickinson, R. G. and Sherrill, M. S. Proc. Natl. Acad. Sci. U.S. **12**, 175 (1926).
4. Forbes, G. S. and Heidt, L. J. J. Am. Chem. Soc. **56**, 1671 (1934).
5. Gaydon, A. G. Nature, **164**, 22 (1949).
6. Gaydon, A. G. Proc. Roy. Soc. A, **183**, 111 (1944).
7. Gaydon, A. G. Trans. Faraday Soc. **42**, 292 (1946).
8. Geib, K. H. and Harteck, P. Ber. **66**, 1815 (1932).
9. Griffing, V. and Laidler, K. J. Third symposium on combustion, flame and explosion phenomena. Williams and Wilkins Co., Baltimore, Md. 1949, p. 432.
10. Griffith, R. O. and McKeown, A. J. Chem. Soc. **127**, 2087 (1925).
11. Harteck, P. and Kopsch, V. Z. physik. Chem. (Leipzig), B, **12**, 327 (1931).
12. Heidt, L. J. and Forbes, G. S. J. Am. Chem. Soc. **56**, 2365 (1934).
13. Heidt, L. J. J. Am. Chem. Soc. **57**, 1710 (1935).
14. Herzberg, G. Atomic spectra and atomic structure. Prentice-Hall, Inc., New York. 1937.
15. Herzberg, G. Molecular spectra and molecular structure. Vol. I. Spectra of diatomic molecules. D. Van Nostrand Co. Inc., New York. 1950.
16. Herzberg, G. Can. J. Phys. **31**, 657 (1953).
17. Hornbeck, G. A. J. Chem. Phys. **16**, 845 (1948).
18. Hornbeck, G. A. and Hopfield, H. S. J. Chem. Phys. **17**, 982 (1949).
19. Hornbeck, G. A. See Ref. 23, p. 75.
20. Laidler, K. J. J. Chem. Phys. **10**, 34, 43 (1942).
21. Laidler, K. J. J. Chem. Phys. **15**, 712 (1947).
22. Laidler, K. J. J. Chem. Phys. **22**, 1740 (1954).
23. Laidler, K. J. The chemical kinetics of excited states. Clarendon Press, Oxford. 1955.
24. Laidler, K. J. and Shuler, K. E. Chem. Revs. **48**, 153 (1951).

Can. J. Chem. Downloaded from www.nrcresearchpress.com by 61.7.252.67 on 09/04/12
For personal use only.

25. MITCHELL, A. C. G. J. Franklin Inst. **206**, 817 (1928).
26. MULLIKEN, R. S. J. Chem. Phys. **7**, 14 (1939).
27. NOYES, W. A. and LEIGHTON, P. A. The photochemistry of gases. Reinhold Publishing Corporation, New York. 1941.
28. POPOV, B. Acta Physicochim. U.R.S.S. **3**, 223 (1935).
29. ROLLEFSON, G. K. and BURTON, M. Photochemistry and the mechanism of chemical reactions. Prentice-Hall, Inc., New York. 1939.
30. SCHUMACHER, H. J. J. Am. Chem. Soc. **52**, 2377 (1930).
31. SHULER, K. E. J. Chem. Phys. **19**, 888 (1951).
32. VOLMAN, D. H. J. Am. Chem. Soc. **76**, 6034 (1954).
33. VOLMAN, D. H. J. Chem. Phys. **24**, 122 (1956).
34. WILKINSON, P. G. and MULLIKEN, R. S. Astrophys. J. **125**, 594 (1957).
35. ZEMANSKY, M. W. Phys. Rev. **36**, 919 (1930).

Can. J. Chem. Downloaded from www.nrcresearchpress.com by 61.7.252.67 on 09/04/12
For personal use only.

Can. J. Chem. Downloaded from www.nrcresearchpress.com by 61.7.252.67 on 09/04/12
For personal use only.

PRIMARY PROCESSES IN REACTIONS INITIATED BY PHOTOEXCITED MERCURY ISOTOPES[1]

HARRY E. GUNNING[2]

ABSTRACT

A study has been made of the reaction of $Hg^{202}6(^3P_1)$ atoms, photoexcited in natural mercury vapor, with a number of substrates which form solid mercury compounds in mercury photosensitization. Some data are also given for reactions initiated by $Hg^{198}6(^3P_1)$ atoms. The solid mercury compounds formed were examined for enrichment in the isotope initiating the reaction. Such enrichment would be evidence for the primary formation of the mercury compound.

Three HgO-forming substrates were studied: water vapor, nitrous oxide, and oxygen. The Hg_2Cl_2-forming substrates studied included hydrogen chloride, methyl chloride, methylene chloride, chloroform, carbon tetrachloride, isopropyl chloride, and boron trichloride. One Hg_2Br_2-forming substrate was examined—isopropyl bromide.

Among the HgO-forming substrates only water vapor gave enrichment in Hg^{202} in the HgO product. The Hg^{202} content of the oxide was found to vary from 32 to 35%, depending on reaction conditions, compared to a natural abundance of 29.6%. With water vapor – butadiene mixtures, oxides containing as high as 90% Hg^{202} were obtained. Similar enrichment factors were obtained for $Hg^{198}6(^3P_1)$ reactions.

Hydrogen chloride and the alkyl chlorides yielded calomels containing a maximum of 45% Hg^{202}. Methyl chloride gave similar enrichment factors in Hg^{198} for the $Hg^{198}6(^3P_1)$ reaction. The calomel formed in the boron trichloride reaction showed no enrichment.

Addends such as butadiene and benzene, when added to hydrogen chloride, increased the Hg^{202} enrichment from 45% to 60%.

For those reactions which yield mercury compounds enriched in the initiating mercury isotope, evidence is presented for a single primary process. Failure to obtain pure isotopes is attributed to exchange reactions with adsorbed natural mercury during recovery of the enriched mercury from the product. It is postulated that the addends react with the mercury product and reduce chemisorption of natural mercury on the product.

The significance of these findings in the mechanisms of the reactions studied is discussed.

INTRODUCTION

Mercury-$6(^3P_1)$ photosensitization has been extensively employed as a photochemical technique for the study of free radical reactions in the gas phase. Little, however, is known about the nature of the primary process in such reactions. The situation is complicated by the fact that mercury is polyisotopic, consisting of an even-mass group of isotopes of zero nuclear spin, Hg^{196}, Hg^{198}, Hg^{200}, Hg^{202}, Hg^{204}, together with two odd-mass isotopes, Hg^{199} and Hg^{201}, of nuclear spin 1/2 and 3/2 respectively. These isotopes may differ markedly, one from another, in the efficiency of energy transfer in the collision of the photoexcited isotope with the substrate, and also in the nature of the primary reaction. The problem would clearly be simplified by studying the mechanism of reactions initiated by the $6(^3P_1)$ state of a single mercury isotope. Through a systematic investigation of monoisotopic mercury-photosensitization the importance of nuclear spin and related factors could be assessed.

In many mercury-photosensitized reactions solid compounds of mercury are formed. Thus HgO is a product in the reaction of Hg $6(^3P_1)$ atoms with H_2O, O_2, and N_2O, while Hg_2Cl_2 is formed with alkyl chlorides as substrates, and Hg_2Br_2 with the alkyl bromides. If the solid mercury compound is formed exclusively in the primary process, the product

[1]*Manuscript received August 16, 1957.*
Contribution from the Department of Chemistry, Illinois Institute of Technology, Chicago 16, Illinois
This paper was presented at the Symposium on the Structure and Reactivity of Electronically-Excited Species held at the University of Ottawa, Ottawa, Canada, September 5 and 6, 1957.
This work was supported by the U.S. Atomic Energy Commission under Contract AT(11-1)-43.
[2]*Present address: Department of Chemistry, University of Alberta, Edmonton, Alberta.*

should contain only that mercury isotope which has been excited. If the isotope is photo-excited in natural mercury vapor (Hg^N), any enrichment in that isotope in the solid mercury product will be evidence for primary formation of the product.

Experiments in monoisotopic mercury-photosensitization are performed in general by exposing the substrate gas, presaturated with Hg^N, to the resonance radiation from a quartz electrodeless discharge containing a trace of the mercury isotope to be studied. The even-mass isotopes will emit a single hyperfine component at 2537 Å, and this component will be absorbed by the same isotope in the Hg^N vapor in the reaction cell.

Owing to the small separation in the hyperfine components of the 2537 Å line, *ca.* 0.01 Å, the optical conditions for the unique excitation of a single mercury isotope in Hg^N vapor are very critical. Broadening effects in both emission and absorption must be minimized. An experimental and theoretical study of this problem has recently been made by Osborn, McDonald, and Gunning (3). These authors showed that the lamp must be operated at constant temperatures below 30° C., and that the substrate gas pressure in the reaction system must be kept low to reduce pressure-broadening effects in absorption. Under these conditions it was shown that the observed absorption could be calculated on the assumption that the emission line was a Doppler type, of width determined by the lamp wall temperature, modified by self-absorption, and that the absorption line was a pure Doppler line.

In this paper the results of a number of exploratory studies on various substrates will be presented. The majority of the photosensitizations have been carried out with $Hg^{202}6(^3P_1)$ atoms. However, some data are reported for $Hg^{198}6(^3P_1)$ atoms. Among the HgO-forming substrates, H_2O, N_2O, and O_2 have been studied. The results on a number of calomel-forming substrates will be reported. These include HCl, CH_3Cl, CH_2Cl_2, $CHCl_3$, CCl_4, i-C_3H_7Cl, and BCl_3. Data on one Hg_2Br_2-forming substrate, i-C_3H_7Br, will also be given.

EXPERIMENTAL

The details of the lamp assembly have already been described (2). The quartz electrodeless discharge tubes were 6 mm. I.D. and 25 cm. in length. The excitation was maintained by a 2450 Mc. oscillator. In all runs the lamps were maintained at constant temperature, ±0.1° C., by a sheath of thermostated cooling water. The lamp temperatures used varied slightly with various substrates, within the 25–30° C. range. A number of shapes and sizes of quartz cells were employed in the studies. It was shown that cell dimensions did not influence the enrichments obtained. Most of the data on HCl and the alkyl halides were obtained using ribbon-type quartz cells, with windows 0.1 cm. apart. The data on HgO-forming substrates were obtained with quartz spiral reaction cells with the lamp placed concentric with the coils of the cell. The cells were attached to the reaction system with spherical joints.

A conventional flow system was employed with manometers placed at exit and entrance points to measure the pressure drop across the cell. Flow rates were measured with calibrated capillary flow meters. The stream of substrate gas was presaturated with Hg^N by allowing it to pass through an operating, umbrella-type, mercury diffusion pump.

During the irradiation the solid mercury product deposited in and downstream from the radiation zone. At the end of the run, the product was removed by solution in hydrochloric acid. The acid solution was partially neutralized with sodium hydroxide, and the mercury recovered by deposition on gold wire. The isotopic composition of the mercury was determined *in vacuo* by resonance radiation absorbiometry. This method has already been described (2).

Can. J. Chem. Downloaded from www.nrcresearchpress.com by 61.7.252.67 on 09/04/12
For personal use only.

The particular experimental procedures employed with each substrate will be described in forthcoming publications.

RESULTS

The Reaction of Water Vapor with $Hg^{202}6(^3P_1)$ *Atoms*

Separate studies on the Lorentz-broadening effect of added substrate gas on the contour of the absorption line indicated that total foreign gas pressures should not exceed 50 mm. (3). All runs were therefore performed below 50 mm. pressure.

A large number of runs was carried out with water vapor alone, and in the presence of nitrogen and helium as carrier gases. The percentage of Hg^{202} found in the oxide product varied from 32 to 35%, compared to the natural abundance of 29.6%.

The addition of butadiene to the water vapor stream was found to have a remarkable effect on the enrichments obtained. Some of the preliminary data have already been published (6). Only the basic findings will be noted here. Thus with the progressive addition of higher mole percentages of butadiene to the water vapor, it was found that the enrichment increased markedly, reaching a maximum value of 90% Hg^{202} with a 4:1 mole ratio of water vapor to butadiene.

The Reaction of Water Vapor with $Hg^{198}6(^3P_1)$ *Atoms*

Several experiments have been done on the irradiation of flowing butadiene – water vapor mixtures, presaturated with Hg^N, with a Hg^{198}-electrodeless discharge. Here the photoexcitation process is complicated (3) by the fact that the 201*b* component in absorption is separated from the 198 component by only 0.0011 Å. The Doppler half-width of the emission line is calculated to be 0.0024 Å. Hence the emission line from the Hg^{198} source should simultaneously excite both Hg^{198} and Hg^{201} atoms. In the absorbiometric method of analysis (2), the Hg^{198} source was operated under the same conditions as in the reaction. Hence the analytical data will yield the total enrichment in $Hg^{198}+Hg^{201}$.

For butadiene – water vapor mixtures over the range of 35–45 mole per cent butadiene, the fractional enrichment in $Hg^{198}+Hg^{201}$ was found to vary from 3.21 to 3.13. If the emission line did not appreciably overlap the 201*b* component, these data would correspond to a change in Hg^{198} concentration from the natural abundance of 10.0% to 31.3–32.1%. By analogy with the Hg^{202} reaction, it is expected that high purity Hg^{198} should be obtainable with lower concentrations of butadiene in the stream, using an Hg^{198} source, operated at 0° C.

The Reaction of $Hg^{202}6(^3P_1)$ *Atoms with Nitrous Oxide and Oxygen*

Both nitrous oxide and oxygen form HgO in mercury photosensitization. Enrichment in Hg^{202} in the oxide product would of course be evidence for formation of HgO in the primary process. A large number of runs have been made with these substrates over the pressure range from 0 to 100 mm. In all cases the HgO formed had the normal abundance of Hg^{202}.

The Reaction of $Hg^{202}6(^3P_1)$ *Atoms with Hydrogen Chloride and the Alkyl Halides*

Hydrogen chloride and the alkyl chlorides were found to form deposits of calomel in mercury photosensitization. X-Ray examination of these deposits showed them to consist of Hg_2Cl_2, together with traces of $HgCl_2$.

The calomel was removed from the reaction vessel by solution in concentrated hydrochloric acid. Repeated tests showed that mercury did not detectably dissolve under these conditions. The acid solution was neutralized with sodium hydroxide, and the mercury

Can. J. Chem. Downloaded from www.nrcresearchpress.com by 61.7.252.67 on 09/04/12
For personal use only.

Can. J. Chem. Downloaded from www.nrcresearchpress.com by 61.7.252.67 on 09/04/12
For personal use only.

was recovered by plating on gold. The isotope analysis was done as with the HgO-forming substrates.

Hydrogen chloride was found to form an enriched calomel, containing a maximum of 45% Hg^{202}. The highest yields were obtained at substrate pressures less than 50 mm., and at high flow rates. The low pressures were necessary to eliminate Lorentz broadening effects. The effects of flow rate will be discussed in a later paper.

Free radical acceptor addends such as butadiene, propylene, and benzene were found to increase markedly the enrichment in Hg^{202}. Benzene and butadiene were found to increase the enrichment to 60% Hg^{202}. Propylene was somewhat less effective, yielding calomels containing a maximum of 52% Hg^{202}.

Of the alkyl chlorides, methyl and isopropyl chlorides were the most thoroughly studied. These compounds behaved similarly to hydrogen chloride in that maximum enrichments of 45% were obtained for the pure substrates. The addition of butadiene was found to be almost ineffective in increasing the enrichment in contrast to the hydrogen chloride reaction.

Among the simple alkyl chlorides, it was found that increasing the length of the alkyl chain did not markedly change the enrichment.

The series CH_3Cl, CH_2Cl_2, $CHCl_3$ and CCl_4 was studied in order to determine the effect of increasing chlorine substitution on the Hg^{202} enrichment. The first three members of the series all gave maximum enrichments in the 43–45% range. In proceeding from CH_3Cl to $CHCl_3$ progressively lower pressures had to be used since the Lorentz broadening cross section of the substrate molecule increased with increasing chlorine substitution. Carbon tetrachloride did not form measurable yields of calomel.

One Hg_2Br_2-forming substrate, isopropyl bromide, was studied in order to determine the influence of the type of halogen on the enrichment. The Hg_2Br_2 was found to be enriched to a maximum of 35% Hg^{202}—a markedly lower value than obtained with the chlorides.

Several experiments were done with boron trichloride as the calomel-forming substrate. While good yields of calomel were obtained, no enrichment was detected.

The Reaction of Methyl Chloride with $Hg^{198}6(^3P_1)$ *Atoms*

In this reaction a maximum enrichment factor of 1.5 was obtained, corresponding to an increase in Hg^{198} concentration from 10.0 to 15.0%. As in the case of the reaction of water vapor with $Hg^{198}6(^3P_1)$ atoms, part of this enrichment could be attributed to Hg^{201}.

The Effect of Product Recovery Techniques on Enrichment

It is well known that mercury vapor tends to adsorb readily on its own solid compounds. In the formation of HgO and Hg_2Cl_2 during monoisotopic photosensitization, it was found that appreciable adsorption of Hg^N occurred on the surface of the solid mercury product. It was therefore possible that exchange reactions could occur during the recovery of the product by solution in hydrochloric acid. The importance of exchange reactions was clearly demonstrated by the following experiment: An HgO, 88% enriched in Hg^{202}, was prepared from the reaction of $Hg^{202}6(^3P_1)$ atoms with a water–butadiene mixture. The HgO was recovered by solution in 1:5 acid by volume. After analysis the mercury was dissolved in dilute nitric acid, the oxide was precipitated with base, and the oxide was then redissolved in 1:5 acid. A tiny globule of natural mercury was added to the solution in hydrochloric acid and let stand for an hour. The mercury metal was removed by filtration, and the mercury in the solution was recovered by plating on gold. Analysis showed that the mercury contained only 42% Hg^{202}. Several similar experi-

ments were performed with enriched mercury samples, and it was concluded that exchange was occurring between dissolved Hg^N and the Hg^{202++} ions present in the acid solution.

The exchange reaction between Hg^N (dissolved) and Hg^{202++} was found to increase in rate at higher acid concentrations. These exchange reactions are now being systematically studied.

DISCUSSION

From the data presented here on the reactions of single isotopes, photoexcited in natural mercury vapor, with hydrogen chloride and some simple alkyl halides, it would appear likely that the primary reaction:

$$Hg^i6(^3P_1) + RX \rightarrow Hg^iX + R \quad [1]$$

occurs to an appreciable extent. The fact that the mercury recovered in the Hg^iX product is not a pure isotope might be attributed to one or more of the following factors:

(*a*) The emission line is sufficiently broad to cause photoexcitation of more than one isotopic species.

(*b*) Two primary processes are operative: the isotopically-specific process [1] above, together with

$$Hg^i6(^3P_1) + RX \rightarrow Hg^i + R + X. \quad [2]$$

The X atoms formed in [2] could form Hg^NX by reaction with the Hg^N always present in the reaction cell.

(*c*) Many secondary exchange reactions could occur which would reduce enrichment in the final product. Thus secondary gas-phase reactions of the type

$$Hg^iX + Hg^N \rightarrow Hg^NX + Hg^i \quad [3]$$

could account for the observed enrichments.

(*d*) Exchange reactions could occur in the recovery of the mercury from the product, owing to the presence of adsorbed Hg^N in the product.

The fact that essentially pure Hg^{202} can be obtained from the water–butadiene reaction would indicate that only Hg^{202} isotopes are being photoexcited. This conclusion is further substantiated by the work of Osborn, McDonald, and Gunning (3), on the shapes of the emission and absorption lines.

Sufficient evidence is not yet available to determine the importance of factors (*b*) and (*c*). However, from the data now known, the fact that pure isotopes are not recovered in the mercury product can be reasonably explained by factor (*d*). Thus in the recovery of mercury from the HgX product, it is necessary to dissolve the product in concentrated hydrochloric acid. It has already been shown that Hg^{i++} ions exchange with dissolved Hg^N in acid solution. The rate of the exchange increased markedly with increased acid concentration. The high enrichments obtained in the water reaction were possible only because of the fact that the HgO can be dissolved in dilute acid. The extent to which the exchange reaction would be important would also depend upon the amount of adsorbed Hg^N on the mercury product. Semiquantitative data have now been obtained in this laboratory which indicate that Hg^N adsorbs much more strongly on Hg_2Cl_2 than it does on HgO.

From the foregoing it can be seen that our findings can be explained on the assumption that (1) there is a single primary process and (2) exchange reactions in product recovery cause reduction in enrichment.

The lower maximum enrichment found for isopropyl bromide, compared to the alkyl

Can. J. Chem. Downloaded from www.nrcresearchpress.com by 61.7.252.67 on 09/04/12
For personal use only.

chlorides, may be due to differences in Hg^N adsorption in the product. A more reasonable explanation, however, would be that direct photolysis of the bromide is occurring, with the formation of Hg^NBr from the reaction of Br atoms with the Hg^N present.

The role of butadiene in increasing the enrichment in the hydrogen chloride reaction with photoexcited Hg^{202} and Hg^{198} atoms, an effect much more evident in the water reaction, was at first thought to arise from the suppression of secondary calomel formation. Thus if Cl atoms are formed in the primary process, they would be expected to add rapidly to butadiene, thereby reducing the formation of Hg^NCl. While this possibility has not been eliminated, an alternative explanation is that the butadiene polymer, formed by the interaction of butadiene with R radicals from the primary process, deposits on the calomel product, and protects it from Hg^N adsorption. It has been noted that a thin film of butadiene polymer does indeed form over the calomel (4).

For hydrogen chloride and the alkyl halides studied, our data are consistent with the assumption that reaction [1] is the only primary process operative. The normal mercury-$6(^3P_1)$-photosensitized decomposition of methyl chloride has been studied by Masson and Steacie (1). These authors conclude that reaction [2] is the primary process. It should be emphasized that their conclusions are not in disagreement with ours, since they investigated the reaction at 72–328° C., whereas our work was done at 25–30° C. It would be expected that higher temperatures would favor reaction [2] over reaction [1]. In the reaction of methyl chloride with $Hg^{202}6(^3P_1)$ atoms (5), at 30° C., no hydrogen chloride was detected among the products. This is important evidence that reaction [2] does not occur to an appreciable extent under these conditions.

In the chlorinated methane series, no change of maximum enrichment was observed in methyl chloride through chloroform. In the carbon tetrachloride reaction the quantum yield of calomel formation is apparently very small, since the quantities of calomel obtained were insufficient for analysis, in the same exposure period used for the other chlorinated methanes.

The absence of enrichment in the boron trichloride reaction would indicate that the primary process involves scission into BCl_2+Cl. This reaction is currently under study in this laboratory as a method for synthesizing B_2Cl_4.

Among the three HgO-forming substrates studied—water vapor, nitrous oxide, and oxygen—only water vapor was found to give enrichment. The absence of enrichment in the nitrous oxide reaction would be evidence in favor of the primary cleavage into N_2+O. In the oxygen reaction HgO can be eliminated as a primary product.

A detailed study of the reaction of $Hg^{202}6(^3P_1)$ atoms with water vapor and water vapor–butadiene mixtures will be published shortly (7). The data obtained would favor the primary process:

$$HOH + Hg^{202}6(^3P_1) \rightarrow Hg^{202}OH + H. \qquad [4]$$

The marked effect of added butadiene on the enrichment may be due in part to a suppression of the reaction:

$$Hg^{202}OH + H \rightarrow Hg^{202} + HOH \qquad [5]$$

by virtue of the rapid reaction of H atoms with butadiene. It appears more likely, however, that the butadiene prevents the reduction of HgO by H atoms at the wall. The removal of H atoms should increase the over-all quantum yield of HgO formation, without changing the isotopic composition of the mercury. The butadiene must also serve to eliminate exchange reactions. In this connection it should be noted that HgOH has free radical character. Hence there may be a direct addition reaction between HgOH

Can. J. Chem. Downloaded from www.nrcresearchpress.com by 61.7.252.67 on 09/04/12
For personal use only.

and butadiene. The resulting compound may protect the mercury compound from exchange reactions in product recovery.

CONCLUSIONS

In this paper it has been shown how the technique of monoisotopic photosensitization may be employed to give important information on the primary process in mercury-photosensitized reactions wherein solid mercury compounds are formed as products. Quantum yields are currently being measured for a number of the reactions discussed in this paper. From these data, taken in conjunction with the enrichment values, it should be possible to determine the absolute rate of the primary, isotopically-specific process.

Photosensitization with natural mercury is a complex process owing to the polyisotopic character of natural mercury. The odd-mass isotopes of finite nuclear spin probably differ markedly from the even-mass isotopes in their quenching reactions. Through detailed studies on monoisotopic photosensitization considerable information should be obtained on the factors which determine the nature and rate of primary processes in collisions of the second kind.

ACKNOWLEDGMENTS

The author is deeply indebted to a number of his present and former graduate students whose work is discussed here. He would especially like to thank Dr. C. Cameron McDonald, Dr. Kenton R. Osborn, Mr. Richard Pertel, Mr. John A. Poole, and Mr. John McDowell.

REFERENCES

1. MASSON, C. R. and STEACIE, E. W. R. J. Chem. Phys. **19**, 183 (1951).
2. OSBORN, K. R. and GUNNING, H. E. J. Opt. Soc. Am. **45**, 552 (1955).
3. OSBORN, K. R., MCDONALD, C. C., and GUNNING, H. E. J. Chem. Phys. **26**, 124 (1957).
4. OSBORN, K. R., MCDONALD, C. C., and GUNNING, H. E. To be published.
5. OSBORN, K. R., MCDONALD, C. C., and GUNNING, H. E. To be published.
6. PERTEL, R. and GUNNING, H. E. J. Chem. Phys. **26**, 219 (1957).
7. PERTEL, R. and GUNNING, H. E. To be published.

Can. J. Chem. Downloaded from www.nrcresearchpress.com by 61.7.252.67 on 09/04/12
For personal use only.

Can. J. Chem. Downloaded from www.nrcresearchpress.com by 61.7.252.67 on 09/04/12
For personal use only.

SOME EFFECTS OF INTRAMOLECULAR VIBRATIONAL ENERGY TRANSFER IN COMPLEX FLUORESCENT MOLECULES[1]

B. STEVENS[2]

ABSTRACT

The effects of intramolecular redistribution of vibrational energy on both the fate of an excited complex molecule and the appearance of its electronic spectra are discussed in terms of a three-dimensional energy surface. It is suggested that continuous absorption be used as a criterion for the application of classical methods to intra- and inter-molecular vibrational energy transfer in those cases where fluorescence emission is observed.

INTRODUCTION

The selection rules require that comparatively few vibrations of a polyatomic molecule are excited during an electronic transition (13) and that if the transition is allowed these are totally symmetric (8). Since totally symmetric vibrations lead to the simultaneous rupture of more than one bond if excited sufficiently, it is concluded that normal dissociation into two fragments is brought about by non-totally symmetric vibrations, the ground state energy of which is preserved during the electronic transition (25). If a forbidden transition to the fluorescent state is observed owing to the excitation of a non-totally symmetric vibration as in benzene (26) and naphthalene (24), this vibration is rarely excited sufficiently to cause direct dissociation. Thus the normal photodissociation of polyatomic molecules involves an internal transfer of energy from totally symmetric to non-totally symmetric vibrations.

THE THREE-DIMENSIONAL ENERGY SURFACE

Let us make the generalization that the majority of vibrations of a complex molecule will not be excited during an electronic transition but will be associated with dissociation along one coordinate, whilst the few optically excited vibrations require a much higher energy for a dissociation which produces more than two fragments; these will be referred to as optically inert or dissociative vibrations and optically active vibrations respectively. The energy of the former will be related to the vapor temperature T, whilst that of the latter will be determined by the energy $hc\bar{\nu}$ of the absorbed quantum.

If the vibrations of the excited n-atomic molecule are assumed to be harmonic, its total vibrational energy V is given by

$$\begin{aligned} V &= hc[\bar{\nu}_1(v_1+\tfrac{1}{2})+\bar{\nu}_2(v_2+\tfrac{1}{2})+ \ldots +\bar{\nu}_{3n-6}(v_{3n-6}+\tfrac{1}{2})] \\ &= V_A+V_D, \end{aligned}$$

where v_i and $\bar{\nu}_i$ are the level and frequency of the ith vibration and V_A and V_D are the energy sums of optically active and optically inert vibrations respectively. If we now consider the molecule as a single harmonic oscillator we may write

$$V = k\alpha^2/2 = k(\alpha_A{}^2+\alpha_D{}^2)/2,$$

[1]*Manuscript received September 24, 1957.*
Contribution from The James Forrestal Research Centre, Princeton University, Princeton, New Jersey, U.S.A. This paper was presented at the Symposium on the Structure and Reactivity of Electronically-Excited Species held at the University of Ottawa, Ottawa, Canada, September 5 and 6, 1957.
This research was supported by the United States Air Force under Contract No. AF 33(038)-23976 monitored by the Office of Scientific Research.
[2]*Present address: Products Research Division, Esso Research and Engineering Co., Linden, New Jersey, U.S.A.*

where k has the dimensions of a force constant and α is a vibrational amplitude with optically active and dissociative components α_A and α_D related to V_A and V_D respectively; these components have the properties

$$V_A, \alpha_A = f(\bar{\nu}); \qquad V_D, \alpha_D = f(T).$$

The energy surface of the excited n-atomic molecule may now be represented as a circular paraboloid of radius α at height V above its minimum, with mutually perpendicular horizontal coordinates α_A and α_D. This is shown in Fig. 1 as a series of isoenergetic con-

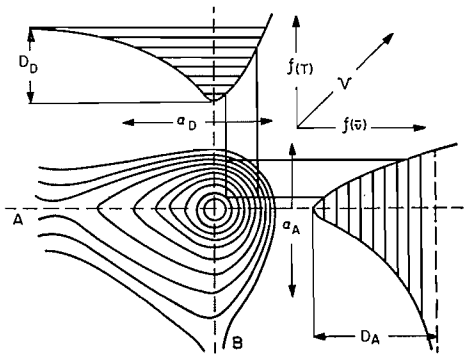

FIG. 1. Three-dimensional energy surface for a complex fluorescent molecule.

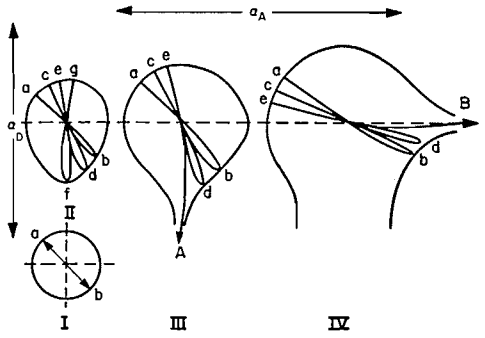

FIG. 2. Isoenergetic contours for four types of vibrational levels recognized in Fig. 1.

tours in which the effects of anharmonic forces are taken into consideration; cross sections showing the variation of surface energy along each coordinate are drawn at the top and to the right of the figure. The effects of anharmonic forces along the α_D coordinate leading to normal dissociation at A when $V \geqslant D_D$ may be expected to be more pronounced than those along the α_A coordinate which requires that $V \geqslant D_A \gg D_D$ for dissociation into several fragments to take place at B.

THE EFFECT OF INTRAMOLECULAR VIBRATIONAL ENERGY TRANSFER ON EMISSION AND PHOTODISSOCIATION

Four types of energy contour recognized in Fig. 1 are shown in Fig. 2. The behavior of the potentially fluorescent molecule in each of the corresponding vibrational levels at pressures so low that collisional perturbation is negligible is discussed below.

(*a*) The lowest vibrational levels produced by the absorption of a frequency $\bar{\nu}$ close to the frequency $\bar{\nu}_0$ of the 0,0 band at the lowest possible vapor temperatures (see Fig. 1) are comparatively free from anharmonic effects and may be represented by contour I of Fig. 2. If we may assume that both vibrational components are in phase at the instant of transition, the vibrational excursion is represented by the line *ababa* . . . and little or no redistribution of energy between the vibrational components takes place during the lifetime τ of the excited molecule. Since $V_A = hc(\bar{\nu}-\bar{\nu}_0) \sim 0$, the characteristic fluorescence spectrum will be emitted.

In benzene the 0,0 band is not observed and higher vibrational levels are produced by the absorption of a frequency greater than $\bar{\nu}_0$. Owing to the high symmetry of this molecule these levels will also have the properties of contour I and the absence of vibrational energy redistribution results in the appearance of the well-known resonance emission (14, 16) originating from the level $V_A = hc(\bar{\nu}-\bar{\nu}_0)$. At higher pressures V_A is collisionally

Can. J. Chem. Downloaded from www.nrcresearchpress.com by 61.7.252.67 on 09/04/12
For personal use only.

reduced to a minimum and the simpler fluorescence spectrum is observed (7); in view of the discussion of contour II below, an increase in either T or $\bar{\nu}$ should produce the same effect. Similar remarks apply to the naphthalene emission spectrum in which progressions from the vibrationally excited upper state are observed at low pressures (24).

(*b*) An increase in either $\bar{\nu}$ or T produces intermediate vibrational levels (Fig. 1) with $V < D_D$ which are represented by contour II of Fig. 2. These are characterized by an increased anharmonicity along the dissociative coordinate α_D, and the initial vibrational excursion may be imagined to precess along *abcde* until it is stabilized along *efgfe* . . . with $V_A \sim 0$ and $V_D = CT + hc(\bar{\nu} - \bar{\nu}_0)$, where C is the molecular heat capacity.[3] If this precession is stabilized within the time interval τ, the virtual independence of the fluorescence spectrum of T and $\bar{\nu}$ at low pressures where $\tau < 1/Z$ is understood (21).

(*c*) Higher vibrational levels with $D_D < V < D_A$ produced by a further increase in T or $\bar{\nu}$ or both have the hypothetical contour III (Fig. 2). Here the precession *abcde* representing the transfer of optically excited vibrational energy allows dissociation at A to compete with fluorescence emission. The probability d of dissociation will depend on the speed of the precession and on the barrier width at A, both of which increase with the over-all energy V. Since $V = f(\alpha_A, \alpha_D)$, the equivalence of thermal and optical contributions to d is evident (19, 20).

(*d*) Contour IV of Fig. 2 corresponds to the highest vibrational levels of the excited molecule with $V > D_A$. Two dissociative possibilities exist and the path followed may be expected to depend on the relative magnitudes of the optically and thermally excited vibrational components. The production of more than two fragments at B requires that $hc(\bar{\nu} - \bar{\nu}_0)$ be greater than CT for the precession to follow the direction *abcde* as shown, and in this respect it is interesting to note the production of C_2H_2 when benzene vapor is photolyzed by the Al spark (1855–2000 Å) (32), whereas at longer wavelengths the principal non-condensible product is H_2 (17, 23). A thermally induced dissociation into three or more fragments would not be expected owing to the much larger probability of normal dissociation at A as the molecule is collisionally activated in its ground state; the absorption of a sufficiently energetic quantum produces this type of level directly and allows both modes of disruption to compete. The variation of the primary photodissociation process with the frequency of absorbed radiation has been previously recognized (18); it appears from this discussion that the controlling factor is the relative magnitude of $V_A(\bar{\nu})$ and $V_D(T)$ rather than $\bar{\nu}$ alone.

THE EFFECT OF INTRAMOLECULAR VIBRATIONAL ENERGY TRANSFER ON THE APPEARANCE OF ELECTRONIC SPECTRA

Beyond a certain frequency limit the discrete absorption spectrum of a diatomic molecule becomes diffuse owing to the onset of predissociation. The lifetime of the excited molecule is reduced by a transition to a dissociated state with the result that the corresponding line width b given by

$$b = h/2\pi\tau$$

is increased. b approaches the separation of vibrational levels as τ is reduced to the order of a vibrational period and the spectrum becomes continuous at shorter wavelengths.

The absorption spectra of polyatomic gases exhibit similar characteristics ranging from sharp bands at long wavelengths, through a diffuse region, to a continuum in the

[3]*It is not suggested that the energy is transferred to the inactive vibrations because these are anharmonic; the anharmonicity allows the internal redistribution of the energy* $hc(\bar{\nu} - \bar{\nu}_0)$ *amongst all vibrations, of which those referred to as inactive are by far the more numerous.*

Can. J. Chem. Downloaded from www.nrcresearchpress.com by 61.7.252.67 on 09/04/12
For personal use only.

direction of higher frequencies (12, 29, 30); the structure at longer wavelengths fades into a continuous background as the temperature is increased (2, 10, 11) and shows a tendency to disappear completely as the molecule becomes more complex. It has been suggested that continuous absorption is due to predissociation in this case also (1, 27), but whilst this is probably true for simpler molecules which cannot be excited to fluorescence in this region, the following arguments suggest that this is not a unique interpretation in the case of more complex systems.

(*a*) As the complexity of a conjugated molecule increases, its absorption spectrum shifts towards the red (5). Since an energy corresponding to approximately 4000 Å is required to break the weaker bonds, absorption in the visible region should be discrete if dissociation alone is responsible for continuous absorption. The structureless bands of organic dyes do not support this criterion.

(*b*) To produce the necessary line broadening τ must be reduced to the order of a few vibrational periods in which case fluorescence emission would no longer be observed. A number of organic vapors can be excited to fluorescence by absorption in the continuous region (19, 29), which in several cases extends over the whole range; it is found moreover that the rate of dissociation is sufficiently slow to compete with emission when the wavelength of absorbed radiation varies by several hundred Å (18, 19).

(*c*) Fluorescence spectra in general exhibit less structure than the corresponding absorption spectra. Since the energy range of the observed emission rarely exceeds 20 kcal., dissociation of the ground state following emission is extremely unlikely (16).

It has been pointed out that the spacing of vibrational levels in polyatomic molecules decreases very rapidly with increasing vibrational energy (15); furthermore, as an increase in molecular complexity usually lowers molecular symmetry, a larger number of vibrations are electronically excited, which, together with a closer spacing of rotational levels due to larger moments of inertia, may well account for the appearance of continuous spectra in these cases (16). The remainder of this discussion will be concerned with the additional hypothesis that the diffuse and continuous spectra of complex molecules are due in part to line broadening.

To produce an appreciable effect, the broadening of vibration–rotational lines must be due to a process taking place within a few vibrational periods following the absorption act, yet allowing fluorescence emission to take place after an interval of approximately 10^{-8} second. This process must be intramolecular since continuous spectra are observed at low pressures (7, 30), and to account for continuous emission it must also take place in the ground state. If we consider that the line width b is determined by the lifetime θ of the individual vibronic states rather than by the lifetime τ of the electronically excited molecule, then such a process could be the internal redistribution of vibrational energy (22). If θ is of the order of 10 vibrational periods, b is approximately 5 cm.$^{-1}$, which, in view of the already close spacing of the numerous vibration–rotational lines, is sufficient to produce a continuous aspect.

A complex molecule has been defined as one in which the probability W of internal energy transfer exceeds $1/\tau$ (22). Since $\theta = 1/W$ and W increases both with molecular complexity and total vibrational energy V, θ has the range of values

$$\tau \geqslant \theta(T, \bar{v}) \geqslant 10^{-13} \text{ second.}$$

Thus we may expect discrete absorption only if this produces vibrational levels with the properties of contour I (Fig. 2), i.e. for simpler molecules at low vapor temperatures in the long-wave region. At shorter wavelengths, higher temperatures, or for more complex

Can. J. Chem. Downloaded from www.nrcresearchpress.com by 61.7.252.67 on 09/04/12
For personal use only.

molecules with larger heat capacities, absorption produces vibrational levels with the contour II, the lifetime θ of the initially formed vibronic state is reduced by internal energy redistribution, and the structure fades into a continuous background. This is the behavior observed.

The continuous nature of emission spectra is similarly explained if the surface in Fig. 1 is used to represent the molecular ground state. The energies of the vibrational components following emission are given by

$$V_A = hc(\bar{\nu}_0 - \bar{\nu}^*),$$

$$V_D = hc(\bar{\nu} - \bar{\nu}_0) + CT,$$

where $\bar{\nu}^*$ is the frequency of emitted radiation. The dependence of V_D on the frequency $\bar{\nu}$ of absorbed radiation arises from the transfer of the optically excited vibrational energy to this component prior to emission. Discrete fluorescence spectra will be observed only if the lowest vibrational levels of the ground state represented by contour I are produced. This requires that both V_A and V_D be small, as is the case at low temperatures for simple molecules with lower heat capacities when both the absorbed and emitted radiations have frequencies close to $\bar{\nu}_0$. These are the conditions under which the discrete emission spectra of benzene (14, 16), toluene (3), benzonitrile (3), fluorobenzene (4), aniline (30), naphthalene (24, 31), and anthracene (28) are observed. Since $\bar{\nu}$ is usually greater than $\bar{\nu}_0$, V_D is larger in the ground state following emission than in the upper state following absorption, with the result that fluorescence spectra are often less discrete than the corresponding absorption.

Thus diffuseness in the electronic spectra of polyatomic fluorescent molecules and of diatomic molecules may be considered as having a common origin if it is accepted that the lifetime of the vibronic states determines the width of vibration–rotational lines. In the former case intramolecular vibrational energy transfer reduces the lifetime of the initially formed vibronic state by changing the energies of the optically active and inactive components, but need not necessarily lead to dissociation. The internal energy transfer requires that a number of isoenergetic vibrational combinations be available for each vibrational level, in which case the levels themselves will be sufficiently closely spaced to account for the observed continuum. The criterion of continuity is largely one of resolution and its appearance may be due to both factors discussed, in which case there is some justification for the following conclusions:

(*a*) Where absorption in the continuous region excites fluorescence, the internal redistribution of vibrational energy is sufficiently rapid for thermal equilibrium to be established between the numerous oscillators within the interval τ (9), and the concept of vibrational temperature (6) is valid.

(*b*) The spacing of vibrational levels in a molecule excited by absorption in its continuous region is sufficiently close for the collisional removal of vibrational energy to be treated as a process of accommodation (6, 20).

(*c*) This classical treatment of vibrational energies cannot be applied to polyatomic molecules excited by absorption in the discrete region.

REFERENCES

1. ALMASY, F. Naturwiss. **20**, 296 (1932).
2. ASUNDI, R. K. and PADHYE, M. R. Indian J. Phys. **23**, 237 (1949).
3. BASS, A. M. J. Chem. Phys. **18**, 1403 (1950).
4. BASS, A. M. and SPONER, H. J. Opt. Soc. Am. **40**, 380 (1950).
5. BAYLISS, N. S. Quart. Revs. **6**, 319 (1952).

Can. J. Chem. Downloaded from www.nrcresearchpress.com by 61.7.252.67 on 09/04/12
For personal use only.

6. BOUDART, M. and DUBOIS, J. T. J. Chem. Phys. **23**, 223 (1955).
7. CUTHBERTSON, G. R. and KISTIAKOWSKY, G. B. J. Chem. Phys. **4**, 9 (1936).
8. DUNCAN, A. B. F. J. Chem. Phys. **3**, 384 (1935).
9. DUSCHINSKY, F. Compt. rend. acad. sci. U.R.S.S. **17**, 179 (1937).
10. HENRI, V. Trans. Faraday Soc. **25**, 765 (1929).
11. HENRI, V. and CARTWRIGHT, C. H. Compt. rend. **200**, 1532 (1935).
12. HENRI, V. and WURMSER, R. J. phys. radium, **8**, 289 (1927).
13. HERZBERG, G. and TELLER, E. Z. physik. Chem. (Leipzig), B, **21**, 410 (1933).
14. INGOLD, C. K. and WILSON, C. L. J. Chem. Soc. 941, 955 (1936).
15. KASSEL, L. S. J. Am. Chem. Soc. **53**, 2143 (1931).
16. KISTIAKOWSKY, G. B. and NELLES, M. Phys. Rev. **41**, 595 (1932).
17. KRASSINA, G. I. Acta Physicochim. U.R.S.S. **10**, 189 (1939).
18. NEPORENT, B. S. Zhur. Fiz. Khim. **13**, 965 (1939).
19. NEPORENT, B. S. Zhur. Fiz. Khim. **21**, 1111 (1947).
20. NEPORENT, B. S. Zhur. Fiz. Khim. **24**, 1219 (1950).
21. NEPORENT, B. S. Zhur. Eksptl. i Teoret. Fiz. **21**, 172 (1951).
22. NEPORENT, B. S. Izvest. Akad. Nauk S.S.S.R. Ser. Fiz. **15**, 533 (1951).
23. PRILESHAJEWA, N. A. Acta Physicochim. U.R.S.S. **10**, 193 (1939).
24. SCHNEPP, O. and MCCLURE, D. S. J. Chem. Phys. **20**, 1375 (1952).
25. SPONER, H. and TELLER, E. Revs. Modern Phys. **13**, 75 (1941).
26. SPONER, H., NORDHEIM, G., SKLAR, A. L., and TELLER, E. J. Chem. Phys. **7**, 207 (1939).
27. TERENIN, A. Acta Phys. Polon. **5**, 229 (1936).
28. TERENIN, A. Acta Physicochim. U.R.S.S. **18**, 210 (1943).
29. TERENIN, A., VARTANYAN, A., and NEPORENT, B. S. Trans. Faraday Soc. **35**, 39 (1939).
30. VARTANYAN, A. Izvest. Akad. Nauk S.S.S.R. Ser. Fiz. **3**, 341 (1938).
31. WEST, W. Ann. N.Y. Acad. Sci. **41**, 203 (1941).
32. WILSON, J. E. and NOYES, W. A., Jr. J. Am. Chem. Soc. **63**, 3025 (1941).

Can. J. Chem. Downloaded from www.nrcresearchpress.com by 61.7.252.67 on 09/04/12
For personal use only.

Can. J. Chem. Downloaded from www.nrcresearchpress.com by 61.7.252.67 on 09/04/12
For personal use only.

STUDIES OF CHEMICAL REACTIONS OF EXCITED SPECIES USING INTENSE LIGHT SOURCES[1]

R. A. MARCUS

ABSTRACT

The use of measurements of the products of flash photolysis as a means for studying the reactions of electronically-excited molecules is discussed. With intense light sources the problem of isolating these reactions from others involving free radicals is simplified. The flash sources also have their limitations, and misleading information which can result from the presence of inert gases is noted. A diagnostic test is proposed for detecting the effects (if any) of a possible adiabatic temperature rise of the flash.

Some recent studies in the author's laboratory are summarized. Evidence is presented that in the flash photolysis of acetone acetyl radicals arise from an excited molecule. Several deactivation processes are described and compared with results from fluorescence studies.

INTRODUCTION

The study of the chemical products of photochemical systems using low light intensities has yielded a considerable body of knowledge about the reactions of free radicals and some information about the behavior of electronically-excited molecules (13, 18). The short-lived species are produced in these systems in a well-defined way at a definite temperature. At the usual wavelengths employed there is no formation of ions which result from many other sources of radiation, nor are there the high temperatures which accompany the use of shock waves for producing these intermediates. Various methods of production and observation of unstable chemical species have been the subject of a recent symposium (19) and survey (10).

A number of detailed investigations have served to point up some of the information which can be derived about the electronically-excited molecules by these low light intensity techniques and at the same time have revealed their limitations. The experimental results show that the problem of distinguishing between the reactions of excited states and reactions involving free radicals is frequently a matter of some difficulty. Several such examples will be discussed.

In the method of flash photolysis, an intense light source is used, such as a flash lamp (11, 12), a spark (7), or an exploding wire (14). In these systems the concentration of the free radicals is so high that radical–radical reactions are usually favored over all others unless the radical is "hot". The reaction products thus become a more direct measure of the primary photochemical steps and of the reactions of the resulting electronically-excited molecules. However, since low intensity light sources have certain compensating features, the two techniques provide complementary rather than alternative approaches for the investigation of the reactions of excited states.

The study of unstable species and their reactions, by spectroscopic observations of the flashed system, has been reviewed recently (12). We shall be principally concerned here, instead, with flash studies based on a determination of reaction products.

[1]*Manuscript received August 16, 1957.*

Contribution from the Department of Chemistry, Polytechnic Institute of Brooklyn, Brooklyn, New York. This paper was presented at the Symposium on the Structure and Reactivity of Electronically-Excited Species held at the University of Ottawa, Ottawa, Canada, September 5 and 6, 1957. A second paper presented at the Symposium, on the theory of internal conversion or dissociation of excited molecules, will be published elsewhere.

This research was supported by the United States Air Force under Contract No. AF 33 (616) 3887, monitored by WCRRC, Aeronautical Research Laboratory, Wright Air Development Center.

Can. J. Chem. Downloaded from www.nrcresearchpress.com by 61.7.252.67 on 09/04/12
For personal use only.

EXAMPLES OF LOW LIGHT INTENSITY STUDIES—THEIR FINDINGS AND LIMITATIONS

In the photolysis of acetone, Noyes and his collaborators have shown that traces of oxygen (*ca.* 0.02 mm.) can quench the fluorescence of a long-lived electronically-excited acetone molecule (3) and can inhibit ethane formation at low light intensities (8, 9). A considerable amount of information was obtained about the latter process, but it is difficult to separate the reactions of oxygen with the excited molecules from those with the methyl radicals. However, from the rate constant estimated in the above study it can be computed that 10 mm. of oxygen will not react with methyl radicals under the usual flash photolysis conditions, thereby permitting the reaction with excited molecules to be studied in the absence of competing free radical processes.

Another important reaction of excited states is unimolecular dissociation. Some evidence described later suggests that acetyl radicals, but not carbon monoxide, may arise from the unimolecular dissociation of an excited acetone molecule which can be quenched by acetone at moderate pressures. This unimolecular reaction undoubtedly has some temperature coefficient, but its amount has not been definitely established. Complicating features occur, such as an increasing dissociation of acetyl radicals themselves with increasing temperature. The study of this system with intense light sources will serve to eliminate the latter reaction and permit an assessment of the temperature dependence of the former. Recently, flash experiments have provided some information on this process (17).

The photolysis of perfluoroacetone has been recently shown to result in the formation of carbon monoxide from an excited perfluoroacetone molecule (2). The unimolecular reaction rate constant was studied as a function of temperature. Since no perfluoroacetyl compound could be detected, it was not certain whether the dissociation first resulted in a short-lived perfluoroacetyl radical or whether there was a direct split into carbon monoxide. Supplementing this study by one employing flash photolysis could serve either to detect the radical or to place a lower limit on the latter's unimolecular rate constant, of the order of 10^6 sec.$^{-1}$ or so (depending on the light intensity).

SOME LIMITATIONS OF FLASH PHOTOLYSIS

While flash photolysis experiments have much to offer, they also have their limitations, whose importance depends upon the purpose for which they are being used. One problem is that of obtaining sufficiently monochromatic light by filters without reducing the intensity unduly and without having to use an inordinate number of flashes. Again, depending upon the flash time, there may be a more or less appreciable departure from steady-state conditions for the transient species. This situation will complicate the mathematical treatment of certain reaction schemes but not that of others. This problem will be analyzed in detail elsewhere.

Computation of variations in the light absorbed accompanying changes in the experimental conditions can be a difficult problem. It was not one in the present study, however, (except at wavelengths below 2000 Å where the absorption of acetone was not proportional to pressure at the pressures employed). The type of light source used in this study serves to alleviate the difficulty. Calculation of absolute quantum yields is a more formidable problem, partly because of the polychromatic nature of the light.

The reaction temperature may be uncertain because of some increase caused by the flash. Its amount can be reduced by increasing the heat capacity of the gaseous system, i.e. by adding large amounts of inert gas. This procedure, we shall see, has resulted in

misleading information when excited states are present. An alternative way is simply to investigate the effects of reducing the intensity and, thereby the temperature rise, of the flash. At these high light intensities, the quantum yields of products would probably not vary with light intensity if no temperature change occurs. Thus, when no intensity effect is found, this is evidence that either temperature changes do not occur or that if they do, their effect on the reaction products is negligible.

STUDIES IN THE FLASH PHOTOLYSIS OF ACETONE

The flash apparatus used in the present experiments (14) was of a standard type, but the customary flash lamp was replaced by an exploding wire. It proved to be convenient, cheap, and reproducible within several per cent. It was found that the light intensity could be easily varied in a known way merely by changing the distance from this line source, a long thin wire, to the axis of a parallel, cylindrical quartz reaction vessel (14). On the other hand, in any experimentation where an extremely large number of flashes is required, a flash lamp is preferable since it can be automatically flashed many times. In most of the experiments reported below the number of flashes varied between one and three, and the total per cent decomposition was about 0.1%. The flash period was fairly long, about 300 μsec.

Preliminary Studies with Unfiltered Light

In some preliminary experiments (15) using light containing radiation of wavelengths near 1900 Å, ethane, carbon monoxide, and methane were measured. No hydrogen was formed. The ratio of ethane to carbon monoxide was greater than one, averaging about 1.25 and indicating the presence of biacetyl.

Using 400 mm. carbon dioxide, the ethane to carbon monoxide ratio fell to about 0.95. Traces of biacetyl (0.1 to 0.7 mm.) also reduced the ratio to slightly below unity, even though they were present in too small an amount to absorb the radiation. When the 1900 Å light was removed by interposing a cellophane filter, these amounts of biacetyl had no effect at all on the products, showing that the electronically-excited molecule which it quenched arises from light in the 1900 Å region.

In the experiments in this and in the following sections the ratio of methane to carbon monoxide was about 0.1. There is evidence from these studies that this methane is not formed from a disproportionation between methyl and acetyl radicals. For example, the acetyl radicals could be reduced to zero concentration by addition of carbon dioxide, without appreciably affecting the methane to carbon monoxide ratio. Instead, the methane appears to arise either from a primary photochemical act or from the collision of a hot methyl radical with acetone. If the primary photochemical step is indeed the origin of the methane at high light intensities, the photolysis of mixtures of acetone and acetone-d_6 should result in the formation of methane and methane-d_4, but not any other deuterated methanes. Such experiments are in progress.

A methane to carbon monoxide ratio of 0.1 has also been obtained in experiments made with a fairly intense light source (1). These authors detected ketene.

In an earlier flash photolysis study using unfiltered radiation (5), Khan, Norrish, and Porter photolyzed acetone to high conversions and in the presence of 480 mm. carbon dioxide. This gas was added to reduce the temperature rise. Their ratio of methane to carbon monoxide was the same as ours but their ethane to carbon monoxide ratio was about 0.9. This is quite consistent with our subsequent results on the deactivating effects of carbon dioxide and of traces of biacetyl. It also serves to indicate the limitations of using inert gases to reduce the temperature rise when excited states are present.

Can. J. Chem. Downloaded from www.nrcresearchpress.com by 61.7.252.67 on 09/04/12
For personal use only.

Studies with Filtered Light

In these experiments (16), a cylindrical cellophane filter was employed. It surrounded the reaction vessel and was protected from the exploding wire by a concentric close-fitting quartz tube. The quantum yields of carbon monoxide and ethane, or more precisely the ratios of each of these products to the acetone pressure, were independent of light intensity when it was varied by a factor of five. The quantum yield of carbon monoxide was constant over a range of acetone pressures varying from 7 to 160 mm. (though there may be a 15% drop at high pressures, ~220 mm.). The yield of ethane decreased markedly with increasing acetone pressure, as in Fig. 1. This curve lies approximately between the curve found by Herr and Noyes at 3130 Å and their curve at 2537 Å

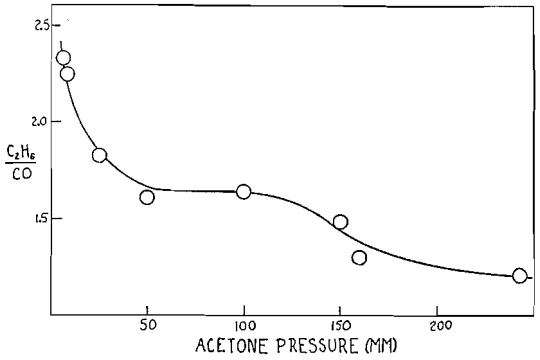

FIG. 1. Plot of ethane to carbon monoxide ratio vs. acetone pressure at room temperature. The point at 100 mm. is the mean of 1.62, 1.65, 1.66.

(4). These authors used low light intensities and worked at constant absorbed intensity to reduce the effects of changing the relative amounts of the secondary free radical reactions as the radical concentration varies. The shape of our curve suggests the presence of two excited acetone states.

Since our yields were independent of the light intensity, either the temperature of the system in these experiments is that of the room or temperature effects can be neglected. We can compare these results, then, with some obtained in fluorescence studies made at a definite temperature.

Acetone has been shown to fluoresce from two excited states, both of which can be quenched by acetone molecules (3). No fluorescence enhancement was reported at any pressure. At 50° C. the quenching occurs appreciably at acetone pressures of about 150 mm. for both states. Studies as detailed as this do not appear to have been reported for 25° C., but the behavior of total fluorescence with pressure is about the same at 25° C. and 50° C. (6). Purely for the present purposes of discussion, it will be assumed that this behavior is also the same for each state at the two temperatures.

From the photolysis studies, in conjunction with those of Herr and Noyes and the foregoing results, it is inferred that the excited state which yields acetyl radicals and is deactivated in the low pressure region of Fig. 1 is probably not responsible for the fluorescence, although the one deactivated in the higher pressure range may be. Carbon monoxide also does not appear to be a product of either fluorescing excited state, unless the fluorescence behavior at 25° C. and 50° C. is rather different.

Studies in Progress

Studies in progress in this laboratory include the effects of added hydrocarbons, of oxygen, and of increased temperature on the lifetime of the excited acetone molecules.

Can. J. Chem. Downloaded from www.nrcresearchpress.com by 61.7.252.67 on 09/04/12
For personal use only.

CONCLUSIONS

The determination of the chemical reaction products of flash photolysis is particularly suited for studying the reactions of electronically-excited molecules. It is shown that the addition of inert gases, for purposes of reducing the possible temperature rise of the flash, has led to misleading information. These gases can deactivate excited molecules and so change the reaction scheme. A preferable procedure, it is suggested, is to test for the effects of any temperature rise, and a diagnostic test is proposed.

Results obtained on the flash photolysis of acetone in several studies in this laboratory are described.

REFERENCES

1. AUSLOOS, P. and STEACIE, E. W. R. Can. J. Chem. **33**, 47 (1955).
2. AYSCOUGH, P. B. and STEACIE, E. W. R. Proc. Roy. Soc. (London), A, **234**, 476 (1956).
3. GROH, H. J., JR., LUCKEY, G. W., and NOYES, W. A., JR. J. Chem. Phys. **21**, 115 (1953).
4. HERR, D. S. and NOYES, W. A., JR. J. Am. Chem. Soc. **62**, 2052 (1940).
5. KHAN, M. A., NORRISH, R. G. W., and PORTER, G. Proc. Roy. Soc. (London), A, **219**, 312 (1953).
6. LUCKEY, G. W. and NOYES, W. A., JR. J. Chem. Phys. **21**, 227 (1953).
7. MAINS, G. J., ROEBBER, J. L., and ROLLEFSON, G. K. J. Am. Chem. Soc. **59**, 733 (1955).
8. MARCOTTE, F. B. and NOYES, W. A., JR. Discussions Faraday Soc. **10**, 236 (1951).
9. MARCOTTE, F. B. and NOYES, W. A., JR. J. Am. Chem. Soc. **74**, 783 (1952).
10. MARCUS, R. A. Ann. N.Y. Acad. Sci. **67**, 661 (1957).
11. NORRISH, R. G. W. and PORTER, G. Nature, **164**, 658 (1949).
12. NORRISH, R. G. W. and THRUSH, B. A. Quart. Revs. (London), **10**, 149 (1956).
13. NOYES, W. A., JR., PORTER, G. B., and JOLLEY, J. E. Chem. Revs. **56**, 49 (1956).
14. OSTER, G. K. and MARCUS, R. A. J. Chem. Phys. **27**, 189 (1957).
15. OSTER, G. K. and MARCUS, R. A. J. Chem. Phys. **27**, 472 (1957).
16. SLAGOWITZ, N. and MARCUS, R. A. Paper presented at Am. Chem. Soc. meeting, New York City, September, 1957.
17. SLAGOWITZ, N. and MARCUS, R. A. Unpublished.
18. STEACIE, E. W. R. Atomic and free radical reactions. 2nd ed. Reinhold Publishing Corporation, New York. 1954.
19. THACHER, H. C., JR. (Consulting Editor). Ann. N.Y. Acad. Sci. **67**, 449–669 (1957).

Can. J. Chem. Downloaded from www.nrcresearchpress.com by 61.7.252.67 on 09/04/12
For personal use only.

CHEMILUMINESCENCE IN THE SYSTEM ATOMIC SODIUM PLUS ATOMIC HYDROGEN[1]

J. D. McKinley, Jr.[2] and J. C. Polanyi[3]

ABSTRACT

When atomic sodium is diffused into a mixture of atomic and molecular hydrogen, a weak chemiluminescence is observed in the gas phase. Visible emission consists of the sodium D lines. The total intensity of the emission, $\sim 5 \times 10^{11}$ photons/second, indicates that only one in 5×10^4 of the sodium atoms entering the reaction vessel is involved in luminescent reaction. In order to account for the rapid fall-off in intensity of the flame away from the nozzle it is necessary to suppose that some non-luminescent reaction is removing sodium atoms in the gas phase. Preliminary experiments suggest that the non-luminescent reaction is $Na + H + H_2 \rightarrow NaH + H_2$, and the luminescent reaction either $Na + Na + H \rightarrow NaH + Na^*$ with collision yield 4×10^{-3} or $Na + H + H \rightarrow H_2 + Na^*$ with collision yield 1×10^{-5}.

This study of chemiluminescence in the gas phase was undertaken to obtain quantitative information concerning the efficiency of energy transfer into an electronic degree of freedom. It is frequently supposed that "energy matching" is important in processes of this type, although there is little direct experimental evidence for this supposition.

The luminescence of sodium vapor in the presence of atomic hydrogen was observed by Bonhoeffer (4), by Mohler (12), and recently by Aynard (1). The technique in every case was to pass dissociated hydrogen from a Wood's tube over hot sodium. Both Bonhoeffer and Mohler found that the luminescence consisted exclusively of the sodium D lines. Aynard, however, found the 3302–3303 Å sodium lines as well and attributed this discrepancy to the fact that earlier workers used wet hydrogen.

In the above investigations it was not possible to distinguish between surface reactions and gas phase reactions. In the present work we have avoided this ambiguity by operating under diffusion flame (13) conditions. The reaction can be confined in this way to the gas phase, and rates can be calculated from the observed diameter of the luminescent flame. This information was supplemented by measurements of emission intensity.

EXPERIMENTAL

The apparatus (Fig. 1) consisted of two separately controlled hydrogen flow systems, one carrying sodium vapor from a saturator, S, into the reaction vessel through a nozzle (0.05 mm. radius), and the other bringing atomic hydrogen from the discharge tube, W, into the reaction vessel.

In each system, cylinder hydrogen flowed through a "Deoxo" catalytic purifier and then through towers of magnesium perchlorate, ascarite, and again magnesium perchlorate. Hydrogen flows were regulated by needle valves and measured with calibrated capillary flow meters.

Prior to an experiment cubes of A.R. sodium, from which the outer layer of oxide had been cut away under benzene, were introduced into the saturator. By moving the sliding furnace, F_1, it was possible to distill the sodium in three stages along the length of the

[1]*Manuscript received August 16, 1957.*
Contribution from the James Forrestal Research Center, Princeton University, Princeton, New Jersey, U.S.A. This paper was presented at the Symposium on the Structure and Reactivity of Electronically-Excited Species held at the University of Ottawa, Ottawa, Canada, September 5 and 6, 1957.
This research was supported by the United States Air Force under Contract No. AF 33(038)-23976 monitored by the Air Research and Development Command.
[2]*Present address: National Bureau of Standards, Washington, D.C.*
[3]*Present address: Department of Chemistry, University of Toronto, Toronto, Canada.*

Can. J. Chem. Downloaded from www.nrcresearchpress.com by 61.7.252.67 on 09/04/12
For personal use only.

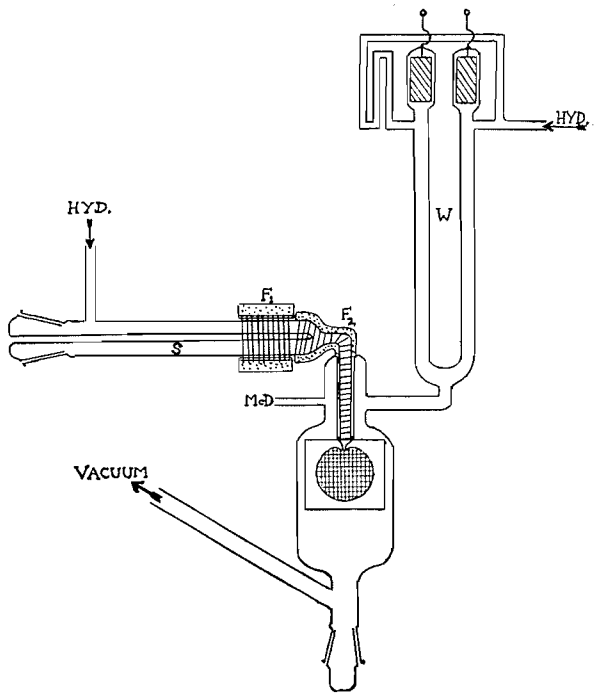

FIG. 1.

saturator. The last distillation resulted in a clean sodium mirror on the walls of the saturator just short of the heating coil F_2. F_2 was continued between the double walls of the central tube of the reaction vessel as far as the internal seal directly above the nozzle. By means of F_2 the central tube and the nozzle were kept at about 350° C. to prevent condensation of sodium.

The pressure of sodium at the nozzle was determined by the temperature of F_1. Since the total pressure in the saturator could be measured on a McLeod gauge (not shown in Fig. 1) the molar flow of sodium into the reaction vessel was calculable using the relationship

$$\text{molar flow of Na} = (\text{vapor pressure of Na in the saturator/total pressure in saturator}) \times \text{molar flow of } H_2 \text{ in saturator.}$$

In order to show that the vapor pressure of sodium in the saturator was the equilibrium pressure corresponding to the temperature of F_1, separate experiments were performed in which a copper gauze cylinder was suspended inside the reaction vessel to catch the sodium issuing from the nozzle in given time at known hydrogen flow rate and known F_1 temperature. The sodium thus collected was washed off the gauze with alcohol, and titrated against standard HCl. The results showed that the hydrogen stream was within 5% of being saturated with sodium. (The copper gauze was found to be necessary since deposition of the sodium on the pyrex vessel resulted in a substantial loss through combination with the glass.)

The hydrogen stream leading to the Wood's tube could be diverted through a water bubbler prior to the flow meter in order to observe the effect of using wet hydrogen.

The current passing through the discharge tube was in the region of 50 ma. at 15,000 volts (0.75 kw.). The percentage decomposition of the hydrogen in the region of the nozzle

Can. J. Chem. Downloaded from www.nrcresearchpress.com by 61.7.252.67 on 09/04/12
For personal use only.

was *ca.* 30%; this was determined in separate experiments by a calorimetric method (9, 14). Typical rates of flow through the saturator and Wood's tube were 3×10^{-5} and 5×10^{-6} moles/second respectively; total pressure in the saturator was *ca.* 6 mm. and total pressure in the Wood's tube and reaction vessel 0.4–0.5 mm.

The region of luminescence could be observed through a plane pyrex window in the reaction vessel.

RESULTS AND DISCUSSION

With pressures of sodium at the nozzle tip from 2.5×10^{-3} to 1.5×10^{-2} mm. (F_1 *ca.* 260°–300° C.), and a rate of inflow of sodium of *ca.* 5×10^{-8} moles/second, an orange-colored luminescent flame was observed centering on the nozzle. The intensity of the emission was such as to be weakly visible in a partially darkened room. The luminescence was weaker at points further from the nozzle, fading into darkness well short of the walls.

After 10 minutes of operation under flame conditions a white deposit began to obscure the window. The deposit was formed in a ring around the reaction vessel along a length corresponding to the flame region. The deposit, a fine powder, could easily be distinguished from the metallic sodium-mirror obtained when the Wood's discharge tube was switched off. This white salt-like deposit is almost certainly sodium hydride.

Concurrently with the appearance of the white deposit a diffuse orange glow was observed at the walls of the reaction vessel. The glow was most intense in its upper region, i.e. at the level of the nozzle, where the deposit of sodium hydride was thickest. This secondary glow obscured the emission from the flame and made photography of the flame impossible. A photograph (*f* 2.5 camera, Eastman Kodak 103aF plates, 25-minute exposure) taken through an interference filter transmitting the sodium D line showed only the secondary luminescence. The flame emission could, however, be weakly detected on the same plate by microdensitometry.

A spectroscopic examination of the luminescence showed only the D line radiation 5890–5896 Å ($3^2P \rightarrow 3^2S$) and the H_α line at 6560 Å (the latter probably originating in scattered light from the Wood's tube). A glass lens focused the luminescence on the slit of a small Hilger constant deviation glass prism wavelength spectrometer, similar to the D-186 (focal length 286 mm., *f* 11) with camera attachment. The dispersion was *ca.* 70 Å/mm. at 5900 Å. Spectrograms were taken on Eastman Kodak I-F plates with 2 hours' exposure. It now seems unlikely that any light entered the spectrometer after the first 30–40 minutes, owing to the formation of the sodium hydride film on the window. The greater part of the light after the first 10 minutes must have come from the secondary emission. With the spectrometer we used we would have been unable to observe the sodium $4^2P \rightarrow 3^2S$ emission at 3302–3303 Å had it been present.

In view of the rapid deposition of NaH and consequent secondary luminescence, observations had to be of a kind that could be completed in the first 5 to 10 minutes after the flame had been started in a clean reaction vessel: namely visual observation and photometric observation.

By visual observation it was found that the size of the flame could be increased either by increasing the pressure of sodium at the nozzle or by decreasing the pressure of atomic hydrogen, which suggests that the luminescent reaction, or its rate-determining reaction, involves these two species.

The fact that the flame falls short of the vessel walls is proof that one of the reagents involved in the luminescence, or its rate-determining reaction, is more plentiful at the nozzle than away from it. This reagent is in all probability sodium.

We have therefore to account for an observed chemiluminescence in the gas phase,

Can. J. Chem. Downloaded from www.nrcresearchpress.com by 61.7.252.67 on 09/04/12
For personal use only.

and consumption of some (or all) of the atomic sodium in the gas phase. Our further observations lead us to believe that these two effects arise from different reactions.

Experiments made with an R.C.A. 5819 photomultiplier tube calibrated against a 200 watt bulb of known color temperature showed that the total hemispherical emission from the flame was *ca.* 5×10^{11} photons/second when the inflow of sodium was 2.4×10^{16} molecules/second. Thus approximately one sodium atom in 5×10^{4} is involved in chemiluminescent reaction.

If the luminescent reaction were to account for the total consumption of sodium, then the ratio of the sodium pressure at the nozzle to that at the edge of the flame (ignoring the gradient due to flow) would be $1/[1-(5\times10^{4})^{-1}] = 1/[1-(2\times10^{-5})]$. In fact (see below) this ratio is *ca.* 1/0.3, from which we conclude that a non-luminescent gas-phase reaction is responsible for the bulk of the sodium consumption.

The true pressure of sodium at the limit of the visible flame can be estimated, since it must be approximately the same as the pressure at the nozzle *when the limit of the flame is at the nozzle*, i.e. when the first trace of flame, right at the nozzle tip, is observed. As already noted, the first luminescence was observed with $F_1 \simeq 260°$ C., i.e. *ca.* 2.5×10^{-3} mm. pressure of sodium at the nozzle. We therefore take this to be the pressure, p_R, of sodium at the edge of the flame.

The flame diameter was found to be 3.8 cm. ($\pm10\%$) in an experiment carried out under the following conditions: H_2 flow through the saturator 3×10^{-5} moles/second, H_2 flow through the Wood's tube 5×10^{-6} moles/second, H flow from Wood's tube 4×10^{-6} moles/second, pressure of H_2 in the saturator 6.5 mm., pressure of sodium in the saturator and at the nozzle 0.0074 mm. (F_1 at 284° C.), pressure of H_2 in Wood's tube and reaction vessel 0.4 mm., pressure of H in reaction vessel 0.04 mm.

No change in flame diameter was observed when the water saturator was switched into the hydrogen stream supplying the Wood's tube. This indicates that the gas-phase chemiluminescence proceeds at the same rate, and presumably by the same mechanism, whether or not water vapor is present. A faster chemiluminescent reaction, for example, would be expected to give a larger flame since it would have an appreciable rate at lower pressures of sodium. (It is not likely that the switch to wet hydrogen would have any instantaneous effect on the H atom concentration in the reaction vessel—time would be needed for water to be adsorbed on the wall.) Some other explanation must therefore be found for the discrepancy between Aynard's results and those of Bonhoeffer and Mohler.

We propose the following reaction scheme:

$$Na + H + H_2 \rightarrow NaH + H_2, \qquad [1]$$

$$Na + Na + H \rightarrow NaH + Na^*, \qquad [2]$$

$$Na + H + H \rightarrow H_2 + Na^*, \qquad [3]$$

in which [1] is the non-luminescent reaction consuming sodium, and either [2] or [3] or both are responsible for the observed luminescence. At a distance r from the nozzle the stationary state requirement is then

$$\delta\, d^2p_{Na}(r)/dr^2 - k_1\, p_{Na}p_H p_{H_2} = 0 \qquad (i)$$

if we ignore the very small amount of sodium that may be consumed by reaction [2]. $p_{Na}(r)$ is the sodium pressure within the interval dr; δ is the diffusion constant of atomic sodium in hydrogen (3.14 cm.^{2}/second (8)). This is a termolecular analogue to the well-known diffusion flame equation (Reference 4). Integration gives

$$k_1 = \delta(\ln p_R/p_0)^2/[p_H\, p_{H_2}(R-r_0)^2], \qquad (ii)$$

Can. J. Chem. Downloaded from www.nrcresearchpress.com by 61.7.252.67 on 09/04/12
For personal use only.

where p_R is the pressure of sodium at the edge of the flame, p_0 is the pressure of sodium at the nozzle, R is the radius of the flame, and r_0 is the radius of the nozzle. Inserting the values listed above gives $k_1 = 1.5\times10^{16}$ cc.^{2} moles^{-2} seconds^{-1}.

This rate constant is only significant as an order of magnitude for k_1, in view of the approximate manner in which p_R was estimated. However, $k_1 \backsim 1\times10^{16}$ cc.^{2} moles^{-2} seconds^{-1} is in good agreement with rate constants obtained for other atomic combination reactions. Farkas and Sachsse (7) obtained $k = 3.4\times10^{16}$ cc.^{2} moles^{-2} seconds^{-1} for H + H + H_2, in quite good agreement with an earlier value of $k = 9\pm2\times10^{15}$ cc.^{2} moles^{-2} seconds^{-1} for the same reaction, due to Steiner and Wicke (17). In addition various workers (5, 6, 15, 16) have obtained (with accuracies to $\pm5\%$) $k \simeq 1\times10^{16}$ cc.^{2} moles^{-2} seconds^{-1} for I + I + M, depending on the nature of M, which is some inert gas; and for Br + Br + A, $k = 2.5\times10^{15}$ cc.^{2} moles^{-2} seconds^{-1} (18).

As an alternative to reaction [1] we have considered the bimolecular reaction

$$Na_2 + H \rightarrow NaH + Na, \qquad [4]$$

$\Delta H = -31$ kcal./mole so that the reaction would be non-luminescent ($3^2P \rightarrow 3^2S$ for sodium requires 48 kcal./mole). However, in order for this reaction to affect the concentration of *atomic* sodium appreciably, it would be necessary for molecular sodium to be replenished by a termolecular reaction, most probably (since H_2 is the most abundant "third body")

$$Na + Na + H_2 \rightarrow Na_2 + H_2. \qquad [5]$$

The minimum rate constant for [5] can be obtained by setting up a stationary state equation in which [5] determines the rate of consumption of sodium. Integration gives $k_5 \geqslant 3\times10^{17}$ cc.^{2} moles^{-2} seconds^{-1}, which is improbably high and would seem to rule out this possibility.

Another possible reaction involving sodium consumption,

$$Na + H_2 \rightarrow NaH + H, \qquad [6]$$

is endothermic and must be very slow since hydrogen is used as an "inert" carrier gas in sodium flame experiments (2, 13, 19).

We therefore consider that on the present evidence reaction [1] is the most likely non-luminescent reaction responsible for the consumption of sodium.

The luminescent reaction

$$NaH + H \rightarrow H_2 + Na^* \qquad [7]$$

is energetically possible ($\Delta H \simeq -56$ kcal./mole) and may be the explanation of the secondary luminescence at the wall. However, there are two reasons for supposing that it is not of major importance in the gas phase (possibly owing to appreciable activation energy). In cases where luminescence arises from reaction among the products formed in a diffusion flame one would not expect to observe, as we did under all flow conditions, the maximum emission at the tip of, or in, the nozzle. Observations on other low-pressure diffusion flames indicate that it is the initial reaction that occurs in this region. If reaction [7] nonetheless accounts for the luminescence, it must be extremely fast, in which case [1] will be the rate-determining reaction for luminescence. Evidence against this comes from our experiments with a photomultiplier tube. We attempted to vary separately the pressure of atomic sodium, atomic hydrogen, and molecular hydrogen. The luminescent intensity was found to be strongly dependent on the first two variables and only weakly on the third. This would not be the case if reaction [1] was determining the rate of luminescent reaction. We conclude that reaction [7] is not the principal luminescent reaction.

Can. J. Chem. Downloaded from www.nrcresearchpress.com by 61.7.252.67 on 09/04/12
For personal use only.

Calculation of the total number of collisions Na + Na + H in the flame and Na + H + H in the flame leads to values of the collision yields for the two luminescent reactions, [2] and [3], in the case that either [2] or [3] predominates. Recent experimental evidence (5) indicates that Bodenstein's method (3) of calculating rates of termolecular collision is as good as any at present available. Accordingly we write

$$\frac{\text{rate of bimolecular collision}}{\text{rate of termolecular collision}} = \frac{\text{mean free path}}{\text{mean molecular diameter}}. \qquad \text{(iii)}$$

The total number of bimolecular collisions Na + H in the flame per second is

$$Z^{\text{Tot.}}_{\text{Na,H}} = Z_{\text{Na,H}}\, p_{\text{H}}\, 4\pi\, N_0 \int_{r_0}^{R} p_{\text{Na}}(r).r^2.dr, \qquad \text{(iv)}$$

where $Z_{\text{Na,H}}$ is the rate of collision at a concentration of 1 mole/cc. So that the total numbers of termolecular collisions are

$$Z^{\text{Tot.}}_{\text{Na,Na,H}} = \frac{Z_{\text{Na,H}}\, Z_{\text{Na,NaH}}\, p_{\text{H}}\, 4\pi\, \sigma_{\text{Na,NaH}}\, N_0}{\bar{c}_{\text{Na}}} \int_{r_0}^{R} (p_{\text{Na}}(r))^2.r^2.dr \qquad \text{(v)}$$

$$= 1.3\times10^{14}\ \text{seconds}^{-1},$$

$$Z^{\text{Tot.}}_{\text{Na,H,H.}} = \frac{Z_{\text{Na,H}}\, Z_{\text{H,NaH}}\, p_{\text{H}}{}^2\, 4\pi\, \sigma_{\text{H,NaH}}\, N_0}{\bar{c}_{\text{H}}} \int_{r_0}^{R} p_{\text{Na}}(r).r^2.dr \qquad \text{(vi)}$$

$$= 4.5\times10^{16}\ \text{seconds}^{-1}.$$

Since the total luminescence is $\backsim 5\times10^{11}$ photons/second, the luminescent collision yield in the case that reaction [2] predominates is $5\times10^{11}/1.3\times10^{14} \simeq 4\times10^{-3}$, and in the case that reaction [3] predominates $5\times10^{11}/4.5\times10^{16} \simeq 1\times10^{-5}$. If both reactions [2] and [3] contribute appreciably to the luminescence these figures are still substantially correct, and in *any* case they represent upper limits for the luminescent collision yields of these reactions.

Table I shows the extent of "energy matching" for the two luminescent reactions under discussion (cf. Kaplan (10) and Aynard (1)).

TABLE I

No.	Reaction	$-\Delta H$, kcal./mole
[2]	$Na + Na + H \rightarrow NaH(v = 0, J = 0) + Na^* 3^2P$	0±1.5*
[3] *a.*	$Na + H + H \rightarrow H_2(v = 0, J = 0) + Na^* 3^2P$	54.5
b.	$Na + H + H \rightarrow H_2(v = 1, J = 0) + Na^{**} 4^2P$	5.2
c.	$Na + H + H \rightarrow H_2(v = 1, J = 5) + Na^{**} 4^2P$	0.2
d.	$Na + H + H \rightarrow H_2(v = 5, J = 0) + Na^* 3^2P$	1.9
e.	$Na + H + H \rightarrow H_2(v = 5, J = 3) + Na^* 3^2P$	0.2

**A. G. Gaydon (Dissociation energies, Dover Publications, 1950) gives D(Na—H) ≈ 47 kcal. G. Herzberg (Spectra of diatomic molecules, D. Van Nostrand, 1950) gives D(Na—H) ≈ 50.5 kcal.; spectroscopic constants for H_2 were taken from Herzberg.*

If one considers all the quantized degrees of freedom of the products to be simultaneously equally available, then a case can always be made for perfect energy matching —certainly to the accuracy to which the energy terms are known. Some additional criterion is therefore required, the simplest being to suppose that the greater the number of degrees of freedom among which the energy must be distributed the less likely is the process. On this basis reaction [2] is favored as against reaction [3].

Can. J. Chem. Downloaded from www.nrcresearchpress.com by 61.7.252.67 on 09/04/12
For personal use only.

Magee and Ri (11), in a theoretical study of reaction [3] according to the semiempirical method, calculate a potential energy surface across which [3] proceeds adiabatically (activation energy $E = 6.5$ kcal./mole) in competition with the non-luminescent reaction [8] on a lower surface ($E = 0$ kcal.),

$$Na + H + H \rightarrow H_2 + Na^*, \quad E = 6.5 \text{ kcal./mole}; \qquad [3]$$

$$Na + H + H \rightarrow H_2 + Na, \quad E = 0 \text{ kcal./mole}. \qquad [8]$$

Making reasonable assumptions about the magnitudes of the transmission coefficients ($\kappa_3/\kappa_8 = 1/0.1$) they calculate that at 200° C. 15 sodium atoms are excited electronically for 1000 which gain only thermal energy. Since $\kappa_8 = 0.1$, this leads to a collision yield of 1.5×10^{-3} at 200° C., or 3×10^{-5} at room temperature, for luminescence due to reaction [3], in good agreement with our figure of *ca.* 1×10^{-5}. It is not possible to say how far this agreement is real until the kinetics of the luminescence have been properly elucidated, preferably over a range of temperatures.

ACKNOWLEDGMENTS

We are indebted to Mr. C. Sadowski of the University of Toronto for assistance with the calculations. We should also like to thank Professor A. G. Shenstone of the Physics Department, Princeton University, for the loan of a spectrograph.

REFERENCES

1. AYNARD, R. Ph.D. Thesis, Sorbonne, Paris (1956).
2. BAWN, C. E. H. Am. Chem. Soc. Repts. **39,** 36 (1943).
3. BODENSTEIN, M. Z. physik. Chem. **100,** 118 (1922).
4. BONHOEFFER, K. F. Z. physik. Chem. **113,** 199 (1924); **116,** 391 (1925).
5. CHRISTIE, M. I., NORRISH, R. G. W., and PORTER, G. Proc. Roy. Soc. A, **216,** 152 (1953).
6. DAVIDSON, N., MARSHALL, R., LARSH, A. E., and CARRINGTON, T. J. Chem. Phys. **19,** 1311 (1951); **21,** 659 (1953).
7. FARKAS, L., and SACHSSE, H. Z. physik. Chem. B, **27,** 111 (1934).
8. HARTEL, V., MEER, N., and POLANYI, M. Z. physik. Chem. B, **19,** 139 (1932).
9. HENKIN, H. and TAYLOR, H. A. J. Chem. Phys. **8,** 1 (1940).
10. KAPLAN, J. Phys. Rev. **31,** 997 (1928).
11. MAGEE, J. L. and RI, T. J. Chem. Phys. **9,** 638 (1941).
12. MOHLER, F. I. Phys. Rev. **29,** 419 (1927).
13. POLANYI, M. Atomic reactions. Williams & Norgate Ltd., London. 1932.
14. POOLE, H. G. Proc. Roy. Soc. (London), A, **163,** 404 (1937).
15. RABINOWITCH, E. and WOOD, W. C. Trans. Faraday Soc. **32,** 907 (1936); J. Chem Phys. **4,** 497 (1936).
16. RUSSELL, K. E. and SIMONS, J. Proc. Roy. Soc. (London), A, **217,** 271 (1953).
17. STEINER, W. and WICKE, F. W. Z. physik. Chem. Bodenstein-Festband, 817 (1931).
18. STRONG, R. L. and WILLARD, J. E. Abstracts, Am. Chem. Soc. Meeting, New York (Sept. 1954), p. 26R.
19. WARHURST, E. Quart. Revs. (London), **5,** 44 (1951).

Can. J. Chem. Downloaded from www.nrcresearchpress.com by 61.7.252.67 on 09/04/12
For personal use only.

Can. J. Chem. Downloaded from www.nrcresearchpress.com by 61.7.252.67 on 09/04/12
For personal use only.

THE QUENCHING OF THE IODINE FLUORESCENCE SPECTRUM[1]

C. ARNOT AND C. A. MCDOWELL

ABSTRACT

The quenching of the iodine fluorescence spectrum by various inert gases and oxygen has been studied with a view to obtaining information on the efficiencies of vibration energy transfer processes in this system. Preliminary results here presented are in agreement with earlier work of Rössler and Eliaschevich and indicate that the transfer processes are very efficient. A kinetic scheme is proposed to account for the various possible quenching and transfer processes and it is shown that this is in agreement with experimental results.

INTRODUCTION

The fluorescence spectrum of iodine vapor excited by the green mercury line 5461 Å was first investigated by Wood (6) (see Fig. 1). It consists of a series of bands stretching from 5461 towards the red. The excited state was shown by Mulliken (2) to be a $^3\Pi_{0_u}$ state which is split into levels by Λ doubling; these two levels behave almost like two independent $^1\Sigma$ states and only one of them (designated by Mulliken as $^3 0_u^+$) combines with the ground state.

On excitation with the narrow green line (Hg 5461) the iodine molecules are raised to the 26th vibrational level (6) of this $^3 0_u^+$ state and the fluorescence bands are produced by the transitions back to the ground state $26' \rightarrow 0''$, $26' \rightarrow 1''$, $26' \rightarrow 2''$, $26' \rightarrow 3''$, etc. The resonance spectrum has been extended as far as the 39th member at 9097 Å (6). The bands under these conditions have only a doublet structure (6).

It has been established that the quenching mechanism by foreign gases is by induced predissociation (3); the iodine molecule is induced by the foreign gas to pass into a repulsion potential energy state.

Transfer of the excited iodine molecule from the 26th vibrational level to other vibrational levels occurs with certain foreign gases, and new fluorescence bands originating from these levels are then observed (see Fig. 2). Rössler (4) showed that the vibrational quantum number only changes by 1 or 2 on these transfer collisions and so molecules are only transferred to the 24th, 25th, 27th, and 28th vibrational levels of the excited state. Change of rotational state also occurs in these transfer collisions and the bands lose their doublet structure and are broadened.

Transfer bands have, in general, only been observed with the rare gases, as the quenching action is much stronger with other gases, and the fluorescence intensity is weakened to a much larger extent.

EXPERIMENTAL

Materials

The rare gases were spectroscopically pure samples provided by the British Oxygen Company. The iodine was purified by sublimation.

Apparatus

The light source was a high intensity low pressure mercury arc with water-cooled electrodes, operated at 25 amp., 180 volts, which was made to a design by Stoicheff (5).

[1]*Manuscript received October 7, 1957.*
Contribution from the Department of Chemistry, University of British Columbia, Vancouver 8, B.C., Canada, and the Department of Inorganic and Physical Chemistry, University of Liverpool, Liverpool, England. This paper was presented at the Symposium on the Structure and Reactivity of Electronically-Excited Species held at the University of Ottawa, Ottawa, Canada, September 5 and 6, 1957.

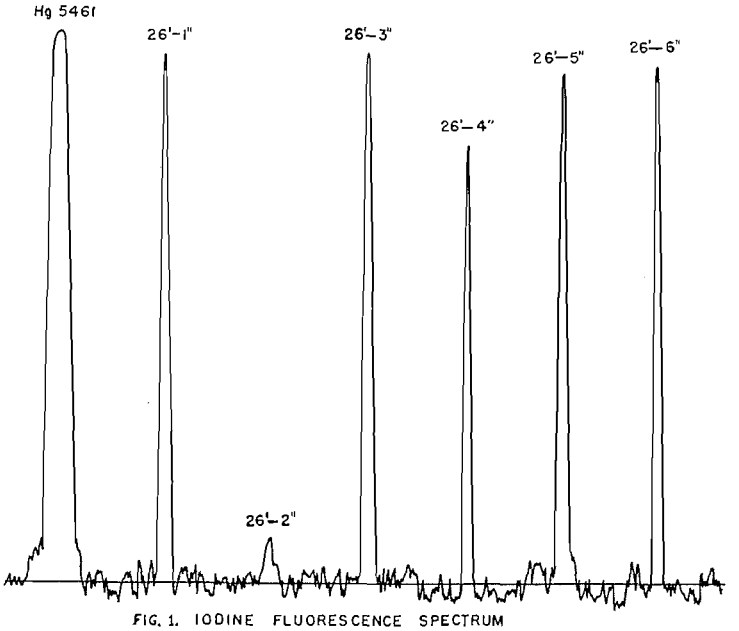

FIG. 1. IODINE FLUORESCENCE SPECTRUM

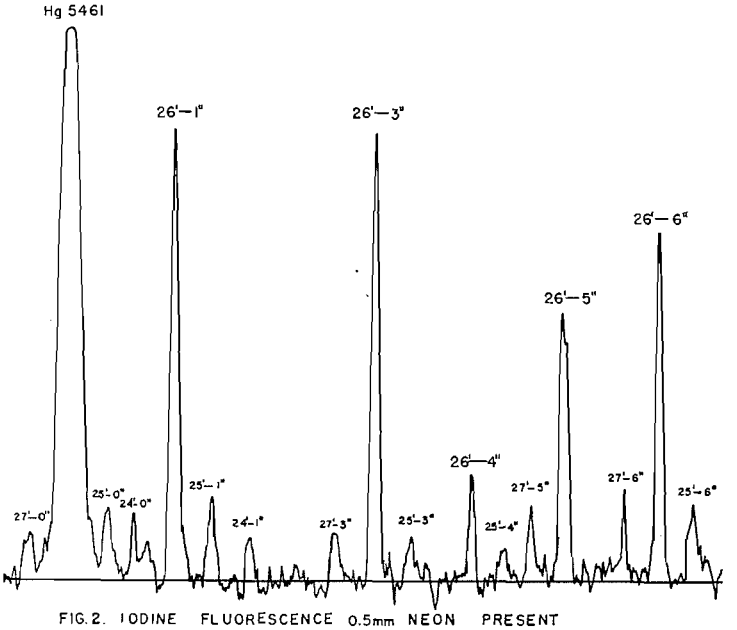

FIG. 2. IODINE FLUORESCENCE 0.5mm NEON PRESENT

FIG. 1. A portion of the fluorescence spectrum of the iodine molecule.
FIG. 2. A portion of the fluorescence spectrum of iodine showing transfer bonds caused by adding 0.5 mm. of neon.

The fluorescence vessel was a glass tube 70 cm. long and 2.5 cm. in diameter with an outer jacket 4.0 cm. in diameter to contain the filter solution. An optical flat at one end of the tube served as a viewing window and the other end of the tube led to a dibutyl phthalate manometer for measuring foreign gas pressure, a gas-introduction apparatus, and vacuum pumps.

Can. J. Chem. Downloaded from www.nrcresearchpress.com by 61.7.252.67 on 09/04/12
For personal use only.

The fluorescence was photographed using a prism spectrograph having a dispersion of 33 Å per mm. The photographic plates were Kodak Scientific Plates type IIaF, which are sensitive to 7000 Å, thus allowing the first 19 bands of the resonance series to be studied. The plates were analyzed using a Hilger microphotometer, the blackening of the plates being recorded on a Leeds and Northrup recorder. The filter solution was a 0.5 *M* $NdCl_3$ solution, which eliminated the yellow mercury lines 5770 and 5790 Å.

The fluorescence tube and arc were mounted side by side and surrounded by a magnesium oxide reflector to cut down exposure times. A set of calibration marks was put on each plate by means of a Hilger calibrated step filter. Under these conditions an exposure time of 2 minutes was satisfactory.

Iodine crystals were contained in a small glass bulb. The system was evacuated with the iodine bulb maintained at a temperature of −80° C. The iodine was then kept at 0° C. while the pumping was continued, and then the system was isolated and the iodine allowed to come to equilibrium with its vapor at 0° C.

Exposures were made of the fluorescence in the absence of foreign gas and at various pressures of foreign gas, the gas being admitted by expansion from a small volume.

For self-quenching data the iodine was allowed to warm up and exposures were made at various iodine pressures, the pressure being measured on a Pirani gauge.

RESULTS AND DISCUSSION

Transfer bands were observed only on the plates with helium, neon, argon, hydrogen, and in some cases oxygen as foreign gas. Of these the intensities of the argon ones were very small and difficult to measure accurately. Even with He or Ne as foreign gas the intensities of the transfer bands were small and could not be accurately measured, as their density of blackening fell in the toe of the calibration curve for the photographic emulsion. With the other foreign gases added (O_2, N_2, Kr, and Xe) the quenching action was stronger.

The data obtained were interpreted in the light of the following kinetic scheme:

M = iodine molecule in ground state
M* = iodine molecule in 26th vibrational level of excited state
M_n^* = iodine molecules in any other level of excited state
X = foreign gas molecules

activation: $$M + h\nu \overset{k_a}{\rightleftharpoons} M^* \quad [1]$$

fluorescence: $$M^* \overset{k_{f_1}}{\rightleftharpoons} M + h\nu \quad [2]$$

$$\overset{k_{f_2}}{\rightleftharpoons} M + h\nu$$

$$\overset{k_{f_3}}{\rightleftharpoons} M + h\nu$$

we shall write $$\sum_n k_{f_n} = k_F$$

self-quenching: $$M^* + M \overset{k_s}{\rightleftharpoons} M + M \quad [3]$$

quenching: $$M^* + X \overset{k_q}{\rightleftharpoons} M + X \quad [4]$$

collisional transfer to some other vibrational level: $$M^* + X \overset{k_{t_1}}{\rightleftharpoons} M_1^* + X \quad [5]$$

$$\overset{k_{t_2}}{\rightleftharpoons} M_2^* + X$$

$$\sum_n k_{t_n} = k_T$$

Can. J. Chem. Downloaded from www.nrcresearchpress.com by 61.7.252.67 on 09/04/12
For personal use only.

back-transfer to 26th level:
$$M^*+X \overset{k_t}{\rightleftharpoons} M^*+X \quad [6]$$
$$M^*+X \overset{k_t}{\rightleftharpoons} M^*+X$$

fluorescence from collisionally excited levels:
$$M^* \overset{k_f}{\rightleftharpoons} M+h\nu \quad [7]$$
$$M_2^* \overset{k_f}{\rightleftharpoons} M+h\nu$$

self-quenching:
$$M_n^*+M \overset{k_s}{\rightleftharpoons} M+M \quad [8]$$

quenching:
$$M_n^*+X \overset{k_q}{\rightleftharpoons} M+X \quad [9]$$

Without foreign gas this scheme leads to the following expression for the intensity of the band of the fluorescence spectrum:

$$F_{0_n} = k_{f_n}[M^*].$$

Since $F_0 = \sum_n F_{0_n}$,

we get
$$F_0 = k_F k_a[M]/(k_F+k_s[M]) \quad [10]$$

and
$$F_{0_n} = k_{f_n} k_a[M]/(k_{f_n}+k_s[M]); \quad [11]$$

hence
$$1/F_{0_n} = k_F/k_a k_{f_n}[M]+k_s/k_{f_n}k_a. \quad [12]$$

A plot of $1/F_{0_n}$ against $1/[M]$ yields an intercept/slope ratio equal to k_s/k_F, and so the self-quenching efficiency of iodine can be determined.

With foreign gas present and where no transfer bands are observed, the above kinetic scheme leads to the following expression for the intensity of the nth band of the spectrum:

$$F_n = k_{f_n}[M^*]$$
$$= k_{f_n}k_a[M]/(k_F+k_s[M]+k_q[X]) \quad [13]$$

and
$$F_{0_n}/F_n = k_F+k_s[M]+k_q[X]/(k_F+k_s[M]) \quad [14]$$
$$= 1+(k_q/k_F)[X]/\{1+(k_s/k_F)[M]\}. \quad [15]$$

From a plot of F_{0_n}/F_n against $[X]$, k_q/k_F can be calculated for each of the foreign gases studied.

Where transfer bands are observed, all the processes 1–9 have to be considered and we can deduce an expression for the over-all kinetic scheme in the following way:

Let R_1 be the ratio of the total fluorescence intensities before and after the addition of foreign gas at a concentration X.

Let R_2 be the ratio of intensities of fluorescence originating from the 26th vibrational level before and after the addition of foreign gas at a concentration X.

Let R_3 be the ratio of intensity of fluorescence from levels other than the 26th level when foreign gas at a concentration X is present.

At equilibrium, $d[M^*]/dt = 0$ and $d[M_n^*]/dt = 0$.

Hence
$$k_a[M] = k_F[M^*]+k_s[M^*][M]+k_q[M^*][X]+k_T[M^*][X]-[X]\sum_n k_{t_n'}[M_n^*], \quad [16]$$

also
$$k_T[M^*][X] = [X]\sum_n k_{t_n'}[M_n^*]+k_F\sum_n[M_n^*]+k_s[M]\sum_n[M_n^*], \quad [17]$$

assuming
$$\sum k_{f_m} = \sum k_{f_l} = \sum k_{f_n} = k_F.$$

Processes involving collisional transfer of energy between the 24th, 25th, 27th, and

Can. J. Chem. Downloaded from www.nrcresearchpress.com by 61.7.252.67 on 09/04/12
For personal use only.

28th vibrational levels have been disregarded since these only lead to the iodine molecule being in a state in which processes identical to those in its previous state can occur and here we are considering the *summation* of intensities originating from these collisionally excited states.

Assuming that $$k_{t_1'} = k_{t_2'} = k_{t_3'},$$

i.e. assuming $$\sum_n k_{t_n'} = Zk_{t_n'} = k_{T'},$$

it follows, therefore, that $k_{t_n'} = k_{T'}/Z$, where Z is the number of occupied levels, i.e. $k_{t'}$ is independent of the vibrational level for back transfer to the original state;

then $$\sum_n k_{t_n'}[M_n^*] = k_{t_n'}\sum_n[M_n^*] = (k_{T'}/Z)\sum_n[M_n^*],$$

then, from [2], $$R_3 = k_F[M_n^*]/k_F[M^*] = k_T[X]/([X]k_{t_n'}+k_F+k_s[M]+k_q[X]) \quad [18]$$

and also, from [2],

$$\sum_n[M_n^*] = k_T[M^*][X]/([X]k_{t_n'}+k_F+k_s[M]+k_q[X]) = [M^*]R_3. \quad [19]$$

Hence $$[X]k_{t_n'}\sum_n[M_n^*] = k_{t_n'}[X][M^*]R_3 = (k_{T'}/Z)[X][M^*]R_3$$

and, substituting in [1], we get

$$k_a[M] = k_F[M^*]+k_s[M^*][M]+k_q[M^*][X]+k_T[M^*][X]-(k_{T'}/Z)[X][M^*]R_3, \quad [20]$$

and the intensity of fluorescence from the 26th level at the concentration of foreign gas

$$[X] = k_F[M^*] = k_Fk_a[M]/(k_F+k_s[M]+k_q[X]+k_T[X]-(k_{T'}/Z)[X]R_3). \quad [21]$$

Since $$F_0 = k_Fk_a[M]/(k_F+k_s[M]),$$

therefore $$R_2 = \{k_F+k_s[M]+k_q[X]+k_T[X]-(k_{T'}/Z)[X]R_3\}/(k_F+k_s[M]). \quad [22]$$

Assuming the probability of back transfer equals the probability of transfer, i.e. $k_T = k_{T'}$, then the following expression is obtained for R_2:

$$R_2 = \frac{1+(k_s/k_F)[M]+(k_q/k_F)[X]+(k_T/k_F)[X](1-R_3/Z)}{1+(k_s/k_F)[M]}. \quad [23]$$

k_T/k_F can be determined from R_1 in the following manner. If we consider that M* is an iodine molecule in any vibrational level of the excited state, then transfer processes may be neglected as they only lead to an excited molecule which undergoes exactly the same processes as in its previous state, i.e. fluorescence, self-quenching, and quenching. We thus obtain the same equation as previously for quenching processes, i.e.

$$R_1 = F_0/F = 1+(k_q/k_F)[X]/\{1+(k_s/k_F)[M]\}. \quad [24]$$

It follows from equation [24] that a plot of F_0/F against the concentration of quenching gas X should be linear with an intercept of unity on the F_0/F axis. In Figs. 3 and 4

Can. J. Chem. Downloaded from www.nrcresearchpress.com by 61.7.252.67 on 09/04/12
For personal use only.

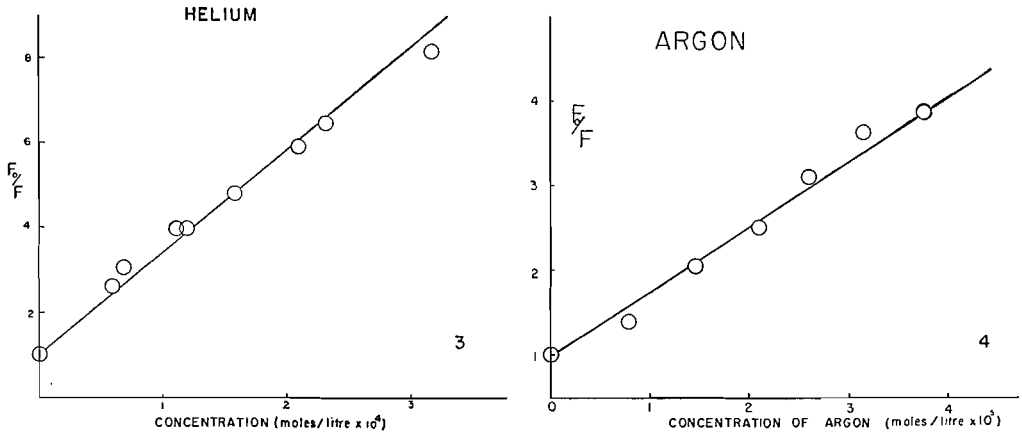

FIG. 3. Plot of F_0/F for the quenching of the fluorescence spectrum of iodine by helium.
FIG. 4. Plot of F_0/F for the quenching of the fluorescence spectrum of iodine by argon.

we show graphs of F_0/F against the concentration of the quenching gas for helium and argon; it will be seen that these are linear and that both intercept the F_0/F axis at unity in agreement with the requirements of equation [24]. It has been found that equation [24] is also obeyed by the gases listed in Table I.

From the slope of the straight line resulting from plotting equation [24] one can calculate the ratio $(k_q/k_F)/\{1+(k_s/k_F)[\mathrm{M}]\}$. Knowing the concentration of the iodine in the experiments and having previously determined k_s/k_F from self-quenching experiments with iodine using self-quenching bands where self-absorption is negligible, one can calculate values for k_q/k_F for each quenching gas studied.

Similarly, by plotting R_2 against the concentration of quenching gas X, one can determine (see equation [23]) the ratio

$$(1-R_3/Z)(k_q/k_F+k_T/k_F)/\{1+(k_s/k_F)[\mathrm{M}]\},$$

and knowing the concentration of iodine in the experiments and having determined R_3 (see definition above), k_q/k_F, and k_s/k_F, one can calculate k_T/k_F, the transfer coefficients, since Z is known, being the number of occupied levels of the excited iodine molecule. The values obtained for the coefficients k_T/k_F for the different gases studied are given in Table I.

TABLE I

COEFFICIENTS FOR THE TRANSFER OF VIBRATIONAL ENERGY IN EXCITED IODINE MOLECULES (T = 20° C.)

Gas	k_T/k_F, liters mole^{-1} experimental	k_T/k_F, liters mole^{-1} theoretical
Helium	5.31×10^4	3.23×10^3
Neon	2.69×10^4	1.66×10^3
Argon	1.64×10^4	1.39×10^3
Oxygen	1.5×10^4	1.37×10^3

The theoretical values quoted for the quenching coefficients in Table I were calculated from the equation

$$k_T/k_F = \frac{p_T N(r_1+r_2)^2}{1000} 8\pi RT\left(\frac{1}{M_1}+\frac{1}{M_2}\right)^{\frac{1}{2}} \qquad [25]$$

Can. J. Chem. Downloaded from www.nrcresearchpress.com by 61.7.252.67 on 09/04/12
For personal use only.

using the following values for the parameters:

$N = 6.023 \times 10^{23}$ molecules liter^{-1}, $r_{He} = 0.98$ Å,
$r_{I_2} = 2.72$ Å, $r_{Ne} = 1.18$ Å,
$r_A = 1.46$ Å, $r_{O_2} = 0.47$ Å;
M_1 = mass of the iodine molecule;
M_2 = mass of the quenching molecule.

The value taken for the lifetime of the excited $^3\Pi_{0_u}$ state of the iodine molecule was $\tau = 10^{-3}$ second and the theoretical values were computed for a pressure of 1 cm.

The experimental data in Table I, which must only be regarded as preliminary, indicate that the transfer of energy in the system studied must be very efficient. Though our data are in agreement with the results of Rössler (4) and Eliaschevich (1), there is, of course, still to be explained the discrepancy between the experimental and theoretical values. It could be that the value of 10^{-8} second assumed for the lifetime of the excited iodine molecule is too short and it should be of the order of 10^{-7} second. Were this so, then the experimental values would be more nearly in agreement with the theoretical ones, which would now be 10 times larger.

ACKNOWLEDGMENTS

The earlier part of this work was carried out in the Department of Inorganic and Physical Chemistry, University of Liverpool, Liverpool 7, England, and we are grateful to Professor C. E. H. Bawn, C.B.E., F.R.S., for providing laboratory facilities. The remainder of the work and the analysis of the photographic plates was carried out in the Department of Chemistry, University of British Columbia, Vancouver 8, B.C. This latter portion was supported by grants from the National Research Council of Canada whom we should like to thank.

REFERENCES

1. Eliaschevich, M. Phys. Rev. **39**, 532 (1932); Physik. Z. Sowjetunion, **1**, 510 (1932).
2. Mulliken, R. A. Revs. Modern Phys. **4**, 1 (1932).
3. Rabinovitch, E. and Wood, W. C. Trans. Faraday Soc. **31**, 689 (1935).
4. Rössler, F. Z. Physik, **96**, 251 (1935).
5. Stoicheff, B. P. Can. J. Phys. **32**, 330 (1954).
6. Wood, R. W. Phil. Mag. **12**, 499 (1906).

Can. J. Chem. Downloaded from www.nrcresearchpress.com by 61.7.252.67 on 09/04/12
For personal use only.

Can. J. Chem. Downloaded from www.nrcresearchpress.com by 61.7.252.67 on 09/04/12
For personal use only.

QUENCHING AND VIBRATIONAL-ENERGY TRANSFER OF EXCITED IODINE MOLECULES[1]

J. C. POLANYI[2]

ABSTRACT

Quenching of I_2^* ($^3\Pi_{0u}^+$) ($v' = 26$) is shown to take place to the exclusion of vibrational-energy transfer in iodine at pressures up to 19 mm. A possible quenching mechanism involving sensitized predissociation of the collision partner is described. Vibrational transfer in collisions with H_2 and D_2 is found to occur at less than every gas kinetic collision. Arguments on general grounds are put forward to support this result, which conflicts with that of earlier workers. Increase in the mass of the isotope is found to bring about increased efficiency of vibrational transfer.

INTRODUCTION

Franck and Wood (1) were the first to observe that the resonance spectrum of iodine vapor excited by the mercury green line is transformed into the complete band spectrum when foreign gases are added. Absorption of the narrow green line obtained from a water-cooled mercury discharge gives rise to the electronic transition $^3\Pi_{0u}^+ \leftarrow {}^1\Sigma_g^+$ resulting for the most part in I_2^* ($v' = 26$; $J' = 35$, 34, 29, and 28) (2, 3). Collisions between I_2^* and added gas may result either in quenching or in transfer to new vibrational and rotational levels of the excited $^3\Pi$ state.

The latter phenomenon is the origin of the effect observed by Franck and Wood. They were able to show that the changes in vibrational quantum number (v') were restricted to ± 1 or ± 2, with roughly equal probability, the changes in rotational quantum number to ± 2. It was clear that if the "transferred spectra" could be compared for a series of foreign gases, relative efficiencies in taking up single vibrational quanta of a known size would be calculable. Eliaschevich (4) made use of this method with H_2 and N_2 as the foreign gases. Rössler (5) performed similar experiments using the inert gases. Both workers calculated the probability of vibrational transfer on the assumption that the lifetime of I_2^* ($^3\Pi$) is 1×10^{-8} second. The calculated number of successful collisions was in every case greater (up to $100\times$) than the number of collisions obtained when the collision cross-section from kinetic theory was used. Rössler found that the transfer probability increased with the atomic weight of the inert gas.

It is generally supposed (see for example Pringsheim (6)) that the effect of increasing iodine pressure is the same as that of adding foreign gas, but there is to the writer's knowledge no experimental evidence for this. Wood and Speas (7) and also Pringsheim (8) investigated the self-quenching of iodine fluorescence at elevated pressures, but did not examine the fluorescent spectrum.

The present work was undertaken in the first place to ascertain the probability of vibrational-energy transfer in collisions I_2^* ($^3\Pi$) ($v' = 26$) $+ I_2$. Secondly it was hoped to obtain an independent check on the large transfer probabilities reported by Eliaschevich and Rössler. At the same time information was sought concerning the effect on transfer probability of a change in mass of the colliding partner in a case where other factors (such as polarizability) remained constant. Hydrogen and deuterium were therefore chosen as foreign gases.

[1]*Manuscript received October 10, 1957.*
Contribution from the James Forrestal Research Center, Princeton University, Princeton, New Jersey, U.S.A. This paper was presented at the Symposium on the Structure and Reactivity of Electronically-Excited Species held at the University of Ottawa, Ottawa, Canada, September 5 and 6, 1957.
This research was supported by the United States Air Force under Contract No. AF 33(038)-23976 monitored by the Air Research and Development Command.
[2]*Present address: Department of Chemistry, University of Toronto, Toronto, Canada.*

EXPERIMENTAL

In the early part of this work an attempt was made to observe the fluorescence using a Raman-type apparatus (see for example Stoicheff (9)). A greatly increased fluorescence intensity was obtained in this way but the method was abandoned because of the considerable self-absorption in the important region of the spectrum up to $v'' = 3$.

The apparatus used is shown in Fig. 1. At first the source was a water-cooled mercury-discharge lamp but it was found that a sufficiently narrow green line could be obtained

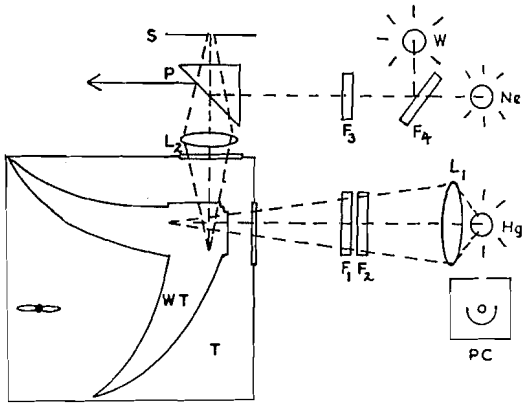

FIG. 1.

using a Mazda medium pressure 250 watt concentrated mercury arc. This lamp was started in a closed container and then operated in the open under an air blower. In this way the discharge was operated at the lowest practicable mercury pressure. The photocell (PC) was a WL930 used to keep a check on the constancy of the mercury lamp intensity.

Condenser lens L focused the light beam on a point about 1.55 cm. inside the double-horned Wood's fluorescence tube (WT), as close as possible to the exit window so as to minimize self-absorption. The Wood's tube shown in the figure was a sealed tube containing only crystals of iodine purified by resublimation. In the experiments where foreign gases were added a Wood's tube was used with a tap which was connected through a fine capillary to minimize absorption of iodine in the tap grease. This tube also differed from the sealed tube in that the ends of the conical limbs were connected to one another by an S shaped length of 6 mm. glass tubing. After the foreign gas had been introduced one limb of the S would be cooled while the other was heated so that the convecting gas would mix with the iodine vapor (for 10–15 minutes). The Wood's tube was immersed in a thermostated water-bath (T). The temperature was controllable to $\pm 0.1°$ C.

The filters F_1 and F_2 consisted of a Baird Multilayer filter with peak transmission at the mercury green line, and a Kodak Wratten No. 77 filter (2% transmission at the yellow line). The fluorescent light was focused by L_2 onto the slit S of a Steinheil spectroscope with three large glass prisms (*ca.* $f/10$), dispersion approximately 40 Å/mm. in the yellow. When the fluorescent spectrum was being observed, prism P was removed in the direction of the arrow (Fig. 1). With P in front of the slit the neon lamp (Ne) or the standard tungsten-filament lamp (W) could be photographed for calibration purposes. (F_3 was a sheet of frosted glass, F_4 a half-silvered mirror.) The neon spectrum was used both for wavelength calibration and for density vs. log exposure calibration. In the latter case a rotating sector not shown in Fig. 1 (Jarrel Ash, J.A. 1660; $I_0/I = 2$) was placed in front of the spectrograph slit. The tungsten lamp was a standard lamp of known color

Can. J. Chem. Downloaded from www.nrcresearchpress.com by 61.7.252.67 on 09/04/12
For personal use only.

temperature; it was used for calibrating the plates for variation in sensitivity with wavelength.

Hydrogen and deuterium were kindly supplied by Dr. P. M. Gundry, Princeton University. The gases had been purified by passage through a palladium thimble.

RESULTS

Fig. 2*a* is the fluorescent spectrum of iodine at 0.43 mm. pressure, photographed on a Kodak 103 aF plate (used for all spectra of Fig. 2) at a 6.5 minute exposure. Fig. 3*a* is the microdensitometer trace of this plate. The spectrum corresponds to that reported by Rank (3) for the iodine emission $^3\Pi_{0u}^+ \rightarrow {}^1\Sigma_g^+$; $v' = 26 \rightarrow v'' = 0, 1, (2), 3 \ldots$. Using a sensitized lN plate and 8.75-hour exposure we were able to photograph this spectrum as far as $v' = 26 \rightarrow v'' = 37$ (8830 Å). The rotational structure of the bands could not be resolved. The possibility that some of the fluorescence originated in $v' = 27$ and $v' = 25$ owing to absorption from wings of the mercury green line cannot be ruled out since the positions of the bands and their relative intensities would not be appreciably different if this were the case. However, the mercury green line did not appear significantly broadened in photographs of the source; promotion to 27′ and 25′ would consequently be expected to be slight.

Fig. 2*b* is the fluorescent spectrum of iodine at 19.2 mm. pressure (84° C.), with 4 hours'

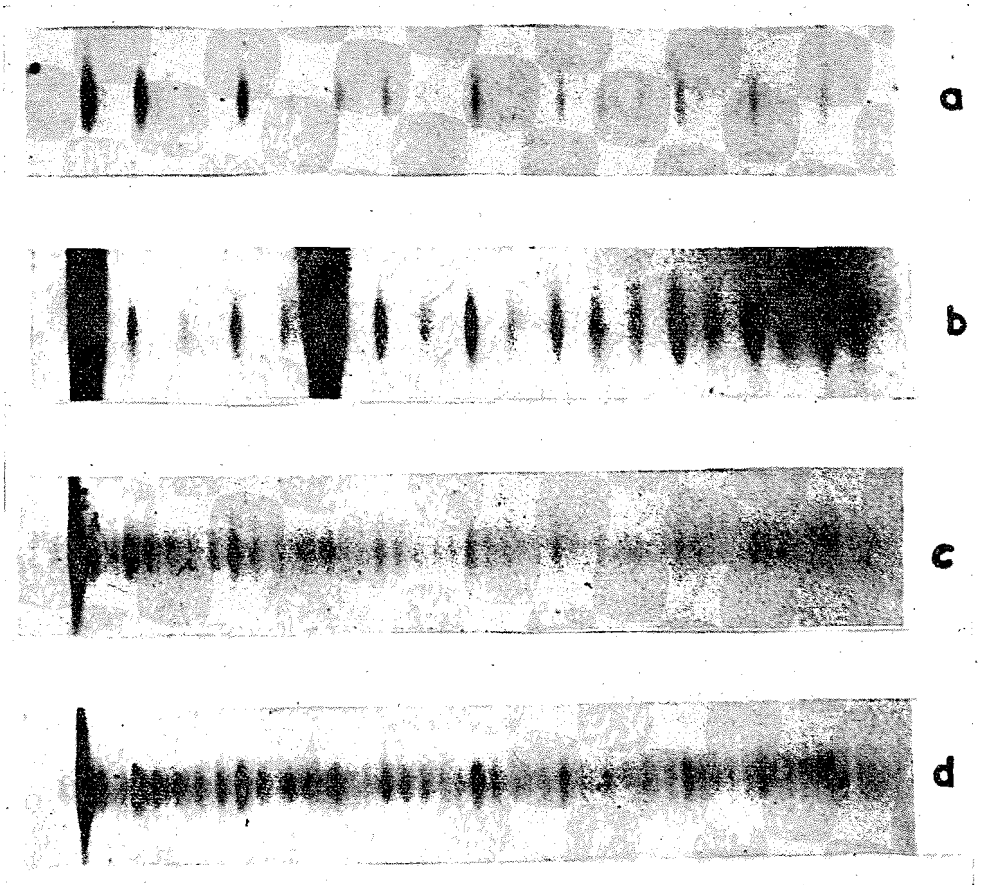

FIG. 2.

Can. J. Chem. Downloaded from www.nrcresearchpress.com by 61.7.252.67 on 09/04/12
For personal use only.

Can. J. Chem. Downloaded from www.nrcresearchpress.com by 61.7.252.67 on 09/04/12
For personal use only.

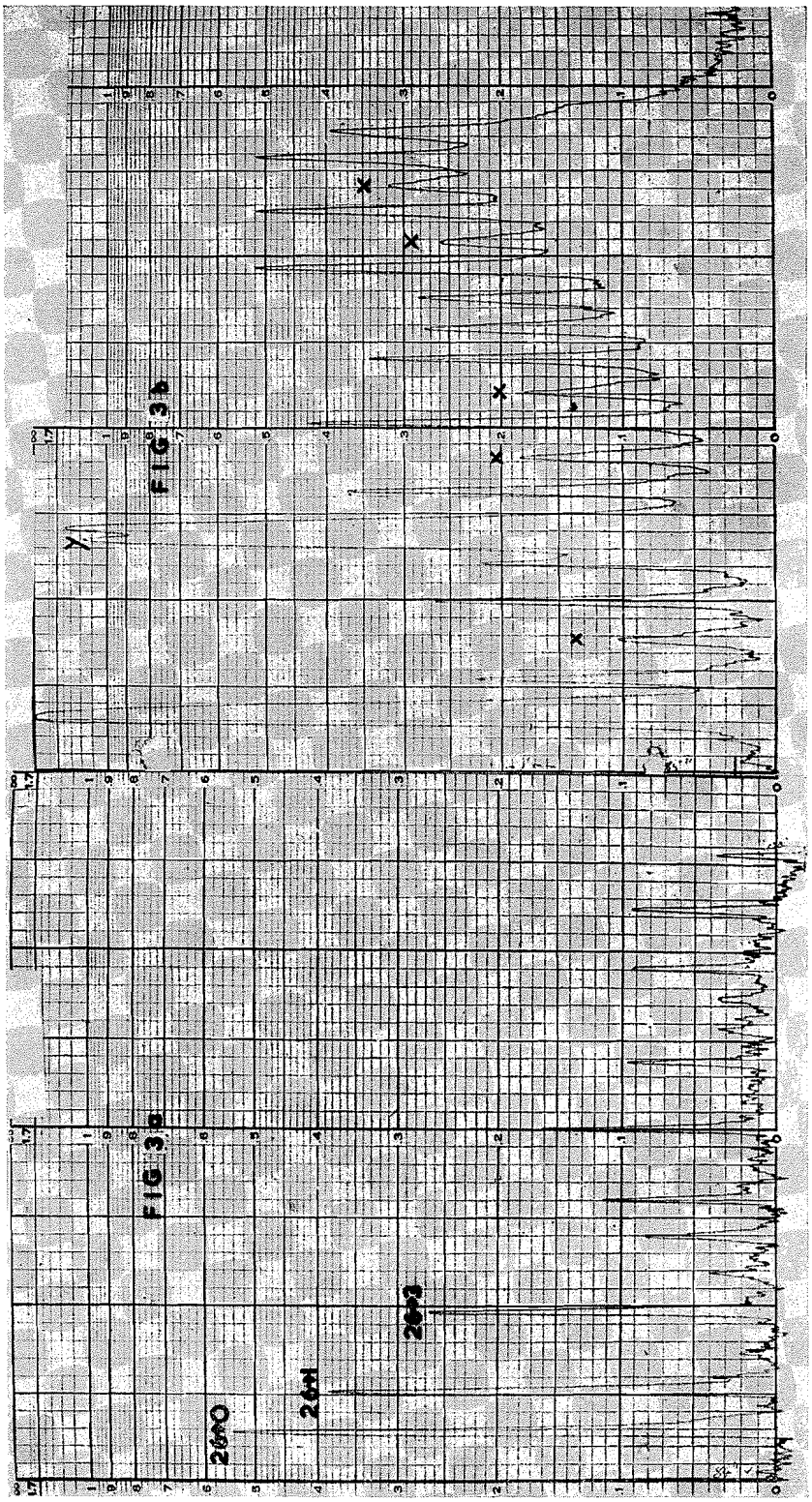

FIG. 3 *a* and *b*.

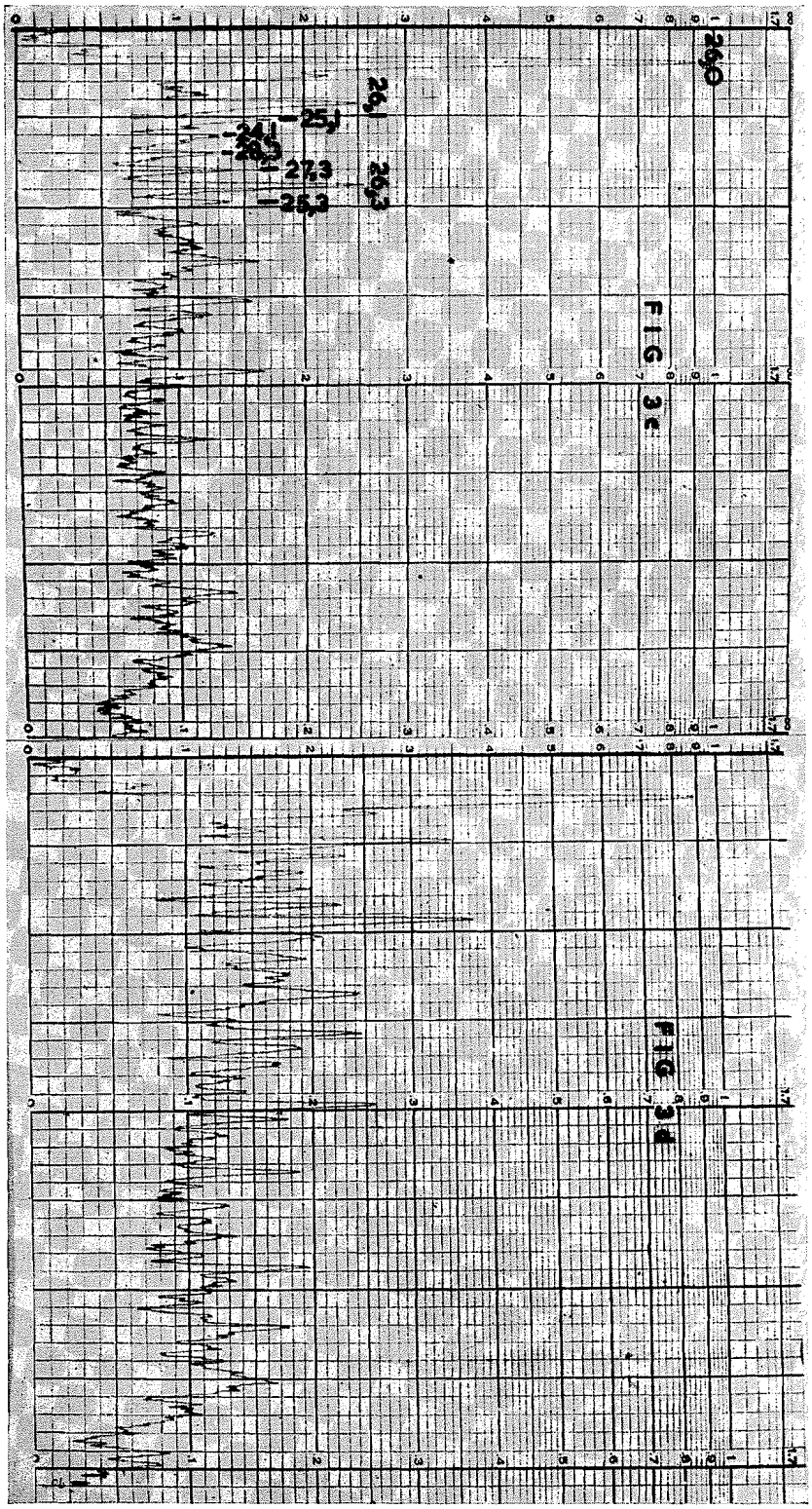

FIG. 3 *c* and *d*.

Can. J. Chem. Downloaded from www.nrcresearchpress.com by 61.7.252.67 on 09/04/12
For personal use only.

exposure. The first band, at 5460 Å, as in all these plates, also contains reflected green light from the mercury discharge lamp. In plate 2*b* the amount of scattered light appears greater relative to the fluorescence since the latter has been much reduced by quenching. Some scattered yellow light (5770 and 5780 Å) from the mercury lamp appears at *Y* on trace 3*b* of plate 2*b*, obscuring the $v' = 26 \rightarrow v'' = 5$ transition.

Three significant changes have occurred in the fluorescent spectrum. The bands are now broader relative to their height. Five new bands have appeared (marked *X* in Fig. 3*b*) at the positions of the missing bands in the low pressure spectrum. Two anti-Stokes bands have appeared, separated from the resonance band by a space approximately equal to the separation between the normal bands, $26' \rightarrow 0''$, $26' \rightarrow 1''$, etc. (these anti-Stokes lines are not shown in 2*b* or 3*b*).

All three changes can be accounted for by supposing (cf. Loomis' (10) detailed analysis of Wood's low pressure spectrum) that the fundamental series of doublets originates in $v'' = 0$ and has no anti-Stokes members. At an elevated temperature the series of doublets originating in $v'' = 1$ and $v'' = 2$ will become important. With the dispersion used in the present work the various orders of the new series of doublets will almost coincide with the orders of the fundamental series. The slight difference in wavelength between the doublets of the new series and those of the fundamental series will result in the observed broadening of the spectral bands. Thus the origin of the first new series $29' \rightarrow 1''$ at 18,341 cm.$^{-1}$ overlaps heavily with the origin of the fundamental series $26' \rightarrow 0''$ at 18,311 cm.$^{-1}$. The anti-Stokes doublets of -1 and -2 order are a part of the series originating in $v'' = 1$ and $v'' = 2$ respectively.

The appearance of the new bands *X* can be explained as follows. It is known that the fundamental series $26' \rightarrow 0''$, $1''$, $2''$ . . . has practically identical doublet intensities to the series $27' \rightarrow 0''$, $1''$, $2''$ . . . and $28' \rightarrow 0''$, $1''$, $2''$ . . . . This is probably due (cf. Pringsheim (6), p. 156) to the relatively high values, v', of the eigenfunctions for all the upper levels (26, 27, 28) resulting in a great number of maxima near the turning points, which are all at nearly the same internuclear separation. It follows from the Franck–Condon principle that the transition probabilities depend largely on the eigenfunctions of the lower states determined by v''. This being the case the transitions $29' \rightarrow 0''$, $1''$, $3''$, $4''$ . . . (but not $2''$, $7''$, $9''$, $14''$, and $16''$) should be observed. Of these, $29' \rightarrow 3''$ will fall very close to the position of the missing line $26' \rightarrow 2''$. The other four new doublets are similarly accounted for by transitions $29' \rightarrow 8''$, $10''$, $15''$, and $17''$.

This leaves no lines unaccounted for and leads us to conclude that vibrational-energy transfer (the Wood effect) does not take place as a result of $I_2^* + I_2$ collisions to any extent even at this high pressure of iodine. The same was found to be true at intermediate pressures of iodine.

Figs. 2*c* and 2*d* are the fluorescent spectra of iodine at 0.43 mm. pressure in the presence of 9.6 mm. of hydrogen and 8.3 mm. of deuterium respectively. The exposure time was 35 minutes in each case. Four new bands are visible between the $v'' = 1$ and $v'' = 3$ bands of the original series. The positions and relative intensities of these bands identify them as arising from transitions $25' \rightarrow 1''$, $24' \rightarrow 1''$, $28' \rightarrow 3''$, $27' \rightarrow 3''$ (in order of increasing wavelength). Immediately to the long wavelength side of $v'' = 3$ of the original series is $25' \rightarrow 3''$. It is evident that the addition of hydrogen or deuterium has the effect of bringing about "transferring" collisions in which $I_2^*(v' = 26) \rightarrow I_2^*(v' = 28, 27, 25, 24)$, i.e. the iodine molecule may lose or gain either one or two quanta.

To interpret the densitometer traces (Figs. 3*c* and 3*d*) it is necessary to assume (see above) that the probability of a transition $v' \rightarrow v''$ is determined, in this region of high v', by v'' alone. The density plot is first converted to an intensity plot making use of the

Can. J. Chem. Downloaded from www.nrcresearchpress.com by 61.7.252.67 on 09/04/12
For personal use only.

calibration marks on the plate, and the area under each band is integrated graphically. The areas obtained for bands having the same v'', but different v', should then be in the ratio of the populations of the v' levels from which they originate. The areas obtained for the bands $28' \rightarrow 3''$, $27' \rightarrow 3''$, $25' \rightarrow 3''$ were the same to within $\pm 10\%$, indicating that a collision results in a change of vibrational quantum number of ± 1 or ± 2 with equal probability. This was the case for both H_2 and D_2.

A closer analysis of the data requires that one take into account that a new vibrational level may be partially converted by further collisions back to the original level. This may be significant for H_2 and D_2 since the quenching probability (which must be distinguished from the vibrational-transfer probability) is low. Rössler (5) (following Eliaschevich's (4) extension of the Stern–Volmer (11) treatment of quenching curves) took this "compound transfer" into account and derived the relationship

$$[1] \qquad I_0/I_p - 1 - \delta\tau p = \epsilon\tau p(1 - B.I_p'/I_p),$$

where I_p and I_0 are the fluorescent intensities of a particular band ($v' \rightarrow v''$) with and without the addition of a pressure p mm. of gas, I_p' is the intensity of some new band arising from vibrational transfer when gas is added: $(v'+1) \rightarrow v''$, $(v'-1) \rightarrow v''$, etc., δ and ϵ are quenching and vibrational-transfer constants such that the probabilities of quenching and transfer are given by δp and ϵp, τ is the mean life of I_2^* ($^3\Pi_{0u}^+$) ($v' = 26$) which we take to be 1×10^{-8} second in conformity with earlier workers, and B is an empirical constant which allows for the fact that the probability of a change in the vibrational quantum number by ± 1 may not be exactly the same as that by ± 2. Rössler found B to be ~ 0.85, only weakly dependent on the ratio of double to single jumps. We have adopted the same value.

The quenching constant δ comes from the expression

$$[2] \qquad Q = 1/(1+\delta p\tau),$$

where Q is the over-all quenching, i.e. the total intensity of the fluorescence in the presence of p mm. of added gas divided by the intensity in the absence of added gas. We have taken Q from the quenching curve for hydrogen obtained by Wood (12).

Q for deuterium is not known. However, we have provisionally calculated ϵ for deuterium on the basis that Q is the same as for hydrogen. This amounts to the assumption that the factor governing the relative quenching efficiencies of hydrogen and deuterium will be the collision duration. If this is the case, then Q at any pressure p must be the same for the two gases since the increased collision duration for D_2 will be exactly offset by the decreased number of collisions. Rössler found that the relative quenching efficiences of the inert gas series could be accounted for in terms of three variables: collision duration, polarizability, and effective cross section. Polarizability will not vary between H_2 and D_2. The effective cross section varies by only 10% from one member to the next of the inert gas series, making a negligible contribution to the variation in Q.

Table I lists the values used for the various quantities in equation [1] (I_0/I_p and I_p'/I_p are mean values) and the values obtained for the vibrational-transfer probability per

TABLE I

For $\tau = 1 \times 10^{-8}$ second

	p, mm.	I_0/I_p	I_p'/I_p	$Z_p \times 10^{-8}$	$\delta \times 10^{-8}$	$\delta p/Z_p$	$\epsilon \times 10^{-8}$	$\epsilon p/Z_p$
H_2	9.6	3.15	0.78	2.78	0.17	0.59	0.16	0.55
D_2	8.3	3.88	0.80	1.69	(0.17)	(0.83)	(0.55)	(2.7)

Can. J. Chem. Downloaded from www.nrcresearchpress.com by 61.7.252.67 on 09/04/12
For personal use only.

collision, $\epsilon p/Z_p$. Z_p is the number of collisions per second suffered by I_2^* at a pressure p of added gas, calculated using $r_{I_2} = 2.7$ Å and $r_{H_2} = r_{D_2} = 1.1$ Å.

DISCUSSION

In the previous section it was observed that quenching collisions $I_2^* + I_2$ take place to the exclusion of vibrational-transfer collisions even up to a pressure of 19.2 mm. of iodine. The question arises as to whether this is a specific effect due to the fact that the colliding partners are both iodine molecules.

It has been established (13) that the quenching of iodine resonance radiation excited by the mercury green line is due almost entirely to predissociation. According to the potential-energy diagram for iodine given by Mathieson and Rees (2) predissociation in normal quenching involves a transition from $^3\Pi_{0u}^+$ ($v' > 24$) to $^3\Sigma_u^+$ (0_u^-) $\rightarrow {}^2P_{3/2} + {}^2P_{3/2}$, normal atoms. Mulliken (14) has suggested that the transition may also be to $^1\Sigma_u^-$ (0_u^-).

In the present case, which involves self-quenching of iodine vapor, it is possible that the process is one in which the $^3\Pi_{0u}^+$ excited iodine molecule transfers its electronic energy to the ground-state I_2 collision partner, which is consequently excited to the lower repulsive state $^3\Pi_{1u}$ and dissociates into normal atoms. This could be characterized as *sensitized predissociation* by analogy with sensitized fluorescence. The transition $^3\Pi_{1u} \leftarrow {}^1\Sigma_g^+$ has actually been observed as a weak absorption in the red. The energy required is about 13 kcal./mole less than that liberated by the Hg-green-line fluorescence of I_2 in falling to the zero vibrational level of the ground state. The 13 kcal. would most probably remain in the quenched iodine molecule as vibrational energy ($v'' \simeq 23$):

$$I_2^* (^3\Pi_{0u}^+)(v' = 26) + I_2 (^1\Sigma_g^+)(v'' = 0) \rightarrow I_2 (^1\Sigma_g^+)(v'' \simeq 23) + I_2\dagger (^3\Pi_{1u}) \rightarrow I_2 + 2I.$$

On the evidence at present available the self-quenching of iodine fluorescence could equally well be due to a collisional transfer of I_2^* ($^3\Pi_{0u}^+$) into the $^3\Sigma_u^+$ (0_u^-) repulsive state, in precisely the same way that the inert gases quench the fluorescence. However, in view of the high efficiency observed for self-quenching it is of interest to note that this quenching is unique in having two reaction paths open to it:

$$I_2^* + I_2 \rightarrow I_2 + I + I \quad \text{(sensitized predissociation)},$$

$$I_2^* + I_2 \rightarrow I + I + I_2 \quad \text{(collisional predissociation)}.$$

In view of uncertainty in the value of δ, and probable error in obtaining I_0/I_p and I_p'/I_p, the value obtained for $\epsilon p/Z_p$ for hydrogen (vibrational-transfer probability per collision) could be in error by a factor of $\times 2$. With these limits of error our conclusion, taking $\tau = 1 \times 10^{-8}$ for I_2^*, is that on the average one to four collisions are needed between I_2^* ($v' = 26$) and hydrogen molecules to bring about a transfer of one or two quanta of vibrational energy into rotational or kinetic energy of H_2.

Eliaschevich (4) obtained a transfer efficiency $25\times$ our highest figure. Though significant differences in experimental technique exist between the two pieces of work they do not seem to account for the large discrepancy between our results and his. Eliaschevich appears to have used the peak height on an intensity vs. λ plot as a measure of band intensity, whereas we have used the integrated area under the band. Self-absorption would be somewhat greater in his experiments, though he used a lower pressure of I_2 (0.17 mm. compared with 0.43 mm.), owing to a 15 cm. long emission path compared with 1–1.5 cm. in our experiments. Our vibrational-transfer probabilities were measured at almost $10\times$ the pressure of H_2 that he used (1.1 mm. compared with 9.6 mm.). It is not expected that

Can. J. Chem. Downloaded from www.nrcresearchpress.com by 61.7.252.67 on 09/04/12
For personal use only.

appreciable Lorentz pressure-broadening would occur even at the higher pressure of hydrogen.

As regards the correct lifetime (τ) to be used for I_2^* $^3\Pi$, Rabinowitch and Wood (13) point out that there is an analogy between $^3\Pi \rightarrow {}^1\Sigma$ for I_2^* emission, and $^3P \rightarrow {}^1S$ for Hg* emission. The Hg* $^3P_1$ lifetime is known to be $\sim 1 \times 10^{-7}$ second (Cd* $^3P_1$ and Zn* $^3P_1$ are respectively $\sim 2 \times 10^{-6}$ and 1×10^{-5} second). The assumption of 10^{-8} for the lifetime of I_2^* seems therefore to be a poor one. If a value of 3×10^{-7} were taken for the lifetime of I_2^*, then even for the case of Xe, for which Rössler obtained the highly improbable effective-collision-radius $r_{I_2} = 20$ Å, vibrational transfer would not occur at more than every gas kinetic collision. According to our results and using $\tau = 3 \times 10^{-7}$ seconds H_2 would have a collision efficiency for vibrational transfer of 1 collision in 55, and D_2 of 1 collision in 11. This seems more plausible than Eliaschevich and Rössler's collision efficiencies, which are $\gg 1$. As is well known, sound-dispersion data, which relate to changes in vibrational quantum number in the region $v \simeq 0$, give collision efficiencies $\ll 1$. "Third-body" data (see for example I + I + argon (15)), which refer to the removal of vibrational quanta in the region $v \sim \infty$, i.e. at the point of dissociation, can best be interpreted on the basis that the collision efficiency is 1. It would be remarkable if the intermediate case for which $v \simeq 26$ (approximately halfway to dissociation) were to have a collision efficiency $\gg 1$.

The value of $\epsilon p/Z_p$ for deuterium has been included in order to show that if, as seems likely, the ratio of quenching probabilities per collision for D_2 and H_2 is the same as the ratio of the collision durations, $\sqrt{(m_{D_2}/m_{H_2})} = 1.4$, then the ratio of the vibrational-transfer probabilities per collision will be approximately 5:1 (deuterium : hydrogen). Increasing vibrational-transfer efficiency with increasing mass of the colliding partner is in agreement with Rössler's work on I_2^* + inert gases. However, in the present case the difference is unambiguously associated with a change in mass.

The accuracy of these results could be greatly improved if heterochromatic microdensitometry were replaced by direct photometry. An attempt by the author to do this failed as a result of inadequate technique: the individual lines could be detected using a 10-stage photomultiplier tube, but the signal to noise ratio was too poor for accurate measurement. With a chopped light-beam and 14-stage photomultiplier these difficulties could probably be overcome.

ACKNOWLEDGMENTS

The author wishes to thank Dr. G. Herzberg of the Division of Pure Physics, National Research Council, Ottawa, and Prof. A. G. Shenstone of the Department of Physics, Princeton University, for their kindness in providing him with spectrographs and with all possible assistance. He is indebted to the David Sarnoff Research Laboratories, Radio Corporation of America, for the use of their recording microdensitometer.

REFERENCES

1. Franck, J. and Wood, R. W. Verhandl. deut. physik. Ges. **13**, 78 (1911); Phil. Mag. **21**, 314 (1911).
2. Mathieson, L. and Rees, A. L. G. J. Chem. Phys. **25**, 753 (1956).
3. Rank, D. H. J. Opt. Soc. Am. **36**, 239 (1946).
4. Eliaschevich, M. Phys. Rev. **39**, 532 (1932); Physik. Z. Sowjetunion, **1**, 510 (1932).
5. Rössler, F. Z. Physik, **96**, 251 (1935).
6. Pringsheim, P. Fluorescence and phosphorescence. Interscience Publishers, Inc., New York. 1949. p. 193.
7. Wood, R. W. and Speas, P. A. Phil. Mag. **27**, 531 (1914); Physik. Z. **15**, 317 (1925).
8. Pringsheim, P. Z. Physik, **4**, 52 (1921).

Can. J. Chem. Downloaded from www.nrcresearchpress.com by 61.7.252.67 on 09/04/12
For personal use only.

9. STOICHEFF, B. P. Can. J. Phys. **32**, 330 (1954).
10. LOOMIS, F. W. Phys. Rev. **27**, 802 (1926); **29**, 112 (1927).
11. STERN, O. and VOLMER, M. Physik. Z. **20**, 184 (1919).
12. WOOD, R. W. Verhandl. deut. physik. Ges. **13**, 72 (1911).
13. RABINOWITCH, E. and WOOD, W. C. J. Chem. Phys. **4**, 358 (1936).
14. MULLIKEN, R. S. Phys. Rev. **46**, 549 (1934); **57**, 500 (1940).
15. (*a*) DAVIDSON, N., MARSHALL, R., LARSH, A. E., and CARRINGTON, T. J. Chem. Phys. **19**, 1311 (1951); **21**, 659 (1953).
(*b*) CHRISTIE, M. I., NORRISH, R. G. W., and PORTER, G. Proc. Roy. Soc. A, **216**, 152 (1953).
(*c*) RUSSELL, K. E. and SIMONS, J. Proc. Roy. Soc. A, **217**, 271 (1953).

Can. J. Chem. Downloaded from www.nrcresearchpress.com by 61.7.252.67 on 09/04/12
For personal use only.

Can. J. Chem. Downloaded from www.nrcresearchpress.com by 61.7.252.67 on 09/04/12
For personal use only.

EXCITED STATES OF ACETYLENE AND THEIR ROLE IN PYROLYSIS[1]

G. J. MINKOFF

ABSTRACT

Previous theories of acetylene pyrolysis are reviewed in the light of recent work by Minkoff, Newitt, and Rutledge. It is shown that the relatively large rates observed at the beginning of the induction period do not agree with mechanisms involving the intervention of comparatively stable dimers. The required kinetic form is obtained, however, if a triplet diradical is produced on the surface in a bimolecular process, followed by gas phase polymerization, with some chain ending on the surface. The detailed mechanism closely resembles Flory's scheme for liquid phase vinyl polymerization. The shape of the radical is discussed, and it is suggested that the *trans*-configuration leads to polymerization, while the *cis* facilitates dehydrogenation.

There has recently been some interest in the reactions of atoms or molecules in excited states (12, 14), and particularly of unsaturated molecules in triplet states. The purpose of this communication is to examine the role played by acetylene, and its polymers, in triplet states, during the pyrolysis of acetylene at temperatures below 500° C., particularly in view of the failure of mechanisms based on ground state molecules and radicals (21). In fact, there has been considerable controversy not only over the proposed mechanisms, but also over the experimental results. As a consequence of some recent work at temperatures below 525° C. (15), it has been possible to select those results which are most likely to be free of unexpected complications, and to propose a simple mechanism to account for most of the observations.

1. REVIEW OF PREVIOUS WORK

The main difficulties indicated in the literature are threefold; the first are concerned with the nature of the products, the second with the effect of surfaces, and the third is related to the effect of nitric oxide and the role of radicals. These will be considered in turn.

Confusion has often arisen regarding the products, since it is frequently stated, for example, that benzene is the main product of pyrolyzing acetylene. The latter result is only obtained under special conditions; the main reaction at low temperatures (i.e. below 500° C.) is polymerization to polycyclic and substituted aromatic compounds (see Ref. 15 for detailed references). Above 7–800° C., this is almost entirely superseded by decomposition to carbon and hydrogen (2). Products in the intervening region vary continuously from hydrogen and methane down to lower aromatics, including benzene, depending mainly on the temperature, but also on other factors. In particular Minkoff, Newitt, and Rutledge have shown that even at low temperatures, polymerization can be replaced by decomposition to carbon and hydrogen when halogen compounds or some metals are added to acetylene.

The elucidation of the mechanism has also been hindered by the differing reports of the effect of packing the reaction vessel with glass or other supposedly inert materials. Schlapfer and Brunner (19), and Frank-Kamenetsky (7), found the rate to be unaffected by increasing the surface-to-volume ratio. Pease (17), however, found the rate to be reduced by *ca.* 30%; Minkoff, Newitt, and Rutledge reported a weaker, but still inhibitory, influence of surface, while Silcocks (20) (who observed reaction to occur at unusually

[1]*Manuscript received August 16, 1957.*
Contribution from the Chemical Engineering Department, Imperial College, University of London, London, England. This paper was presented at the Symposium on the Structure and Reactivity of Electronically-Excited Species held at the University of Ottawa, Ottawa, Canada, September 5 and 6, 1957.

low temperatures) stated that the rate of reaction was considerably increased by packing the vessel. The treatment of the surface can also influence the rate in some circumstances (15, 24) but not in others (7). The different influences could be explained to some extent if both the chain initiation and chain termination were surface dependent, though to different extents. Any modifications of the surface would then have an over-all effect on the rate, which would depend on the relative activity of the surface to each of the two steps.

Random effects cannot be excluded, but the reported surface effects show some correlation with the amount of permanent gases (mostly hydrogen) detected, this being a possible measure of the decomposition reaction. Thus, in the absence of hydrogen, Pease found packing to inhibit the rate; Minkoff, Newitt, and Rutledge, who found only small inhibition, detected approximately 2–3% hydrogen, while the acceleration observed by Silcocks was associated with the isolation of considerable amounts of hydrogen.

Contradictions also exist regarding the presence of radicals. For example, Paneth and Hofeditz (16) found no positive evidence, so that if any radicals participate in the reaction, they may have unusual properties. On the other hand, Minkoff, Newitt, and Rutledge have confirmed the findings of Burnham and Pease (4) and of Frank-Kamenetzky (7), who observed that nitric oxide can almost completely inhibit the polymerization, and that after the nitric oxide has been used up, the reaction proceeds at the normal rate. While this indicates the presence of radicals, there is a sharp contrast with the normal effect of nitric oxide on hydrocarbon pyrolysis (see Ref. 21), since in the latter case, the rate gradually diminishes as more nitric oxide is added; however, some residual reaction is always observed, which the nitric oxide does not inhibit. A further complication is that exactly this behavior was reported for acetylene pyrolysis by Robertson, Magee, Fain, and Matsen (18); however, their measure of the rate was based on the instantaneous concentration of benzene, which occurred as an intermediate. This clearly was not indicative of the required rate, since the results obtained by this method are the only ones which do not give linear plots of log rate against $1/T$ (15). In view of the recent work of Jach and Hinshelwood (11), it is not impossible that the uninhibited reaction was induced by the Freon which was present in the system as an internal standard for the infrared absorption. Presumably, these observations will be of value when a deeper understanding of the reaction has been obtained.

2. KINETIC FEATURES

Most workers agree that the polymerization is, essentially, kinetically of the second order, although an induction period is usually observed (7, 15, 20). It has usually been assumed that the induction period represents the formation of a comparatively stable dimeric intermediate, and its accumulation to a steady state concentration when the rate of formation equals the rate of decomposition. The radicals formed by the decomposition are then supposed to catalyze the polymerization. Various suggestions have been made regarding the nature of the dimer, which has been said to be vinyl acetylene, cyclobutadiene, etc. Clearly, this scheme is formally of the Semenoff degenerate branching chain type, and the rate should therefore increase considerably from an initially very small value. This does not agree with the recent observation (15) that the initial rate, instead of being extremely low relative to the maximum value, is usually 30–50% of the latter. Another difficulty is that, while the initial rate and the maximum rate are both proportional to the square of the initial pressure (15), the length of the induction period is independent of the initial pressure (7, 15) below 500° C.

Can. J. Chem. Downloaded from www.nrcresearchpress.com by 61.7.252.67 on 09/04/12
For personal use only.

A more satisfactory explanation is provided by a slow, bimolecular initiation, followed by a series of comparatively rapid bimolecular addition steps. The molecularity of the initiation step is indicated not only by the dependence of the initial rate on the square of the initial pressure, but also by the similarity of the initial and maximum rates. The relatively small difference between the latter implies that both sets of reactions contribute to the total rate of disappearance of acetylene, throughout the time during which second order kinetics are observed, and both must therefore be second order reactions. It is in fact shown later that the observed kinetic form closely resembles that of liquid phase polymerizations, which have similar mechanisms.

3. IDENTIFICATION OF CHAIN CARRIERS

Only two types of chain carriers can readily be formed from acetylene. One involves the fission of a C—H bond (I), while the other is formed by the "opening" of one of the triple bonds (II):

$$\underset{\text{(I)}}{CH{\equiv}C-} \qquad\qquad \underset{\text{(II)}}{-CH{=}CH-}$$

(No distinction is made at this stage between monomeric and polymeric radicals of each category.) Bimolecular collisions of two acetylene molecules seem at first sight to lead to —CH=CH—CH=CH— (II) rather than to CH≡C—CH=CH— (I), but, once formed, either radical would be able to propagate the polymerization chain. Considerations of the heats of formation (in the absence of activation energies) favor the formation of radical II. Thus, for radical I, the bond energy of the acetylenic C—H has been estimated as being 121 kcal. (25). With regard to II, the energy required to 'open one of the triple bonds' has been variously estimated as being in the region of 30 to 60 kcal. (cf. (5, 26)). A value of 50 kcal. will thus be assumed as being reasonably high. The conversion of the triple C—C bond into a double C—C bond probably implies (see below) a change of bonding orbitals in the C—H bonds from sp to sp^2. According to Walsh, the consequent total weakening requires 20–30 kcal. If this value is added to the 50 kcal. deduced previously, the heat of formation of II from acetylene has an upper limit of *ca.* 80 kcal. and a lower limit of 50 kcal. This is at least 40 kcal. less than is required to form I. The conclusion that C_2H— is more difficult to form than —C_2H_2—, in the absence of an excess of energy, is supported by a number of observations. The lack of effect of ethyl radicals when lead tetraethyl is added suggests that the energy of hydrogen abstraction is high, and this agrees with the lack of effect of oxygen, and with the shortness of extra chains produced by acetyl (or methyl) radicals from the pyrolysis of diacetyl, and of methyl radicals from the photolysis of acetone (23). Furthermore, the negative results of Paneth and Hofeditz suggest II rather than I. The results of photochemical experiments are not directly applicable. Nevertheless, it is clear that when sufficient energy is available to form C_2H—, polymerization proceeds readily; this can occur, for example, in the presence of $Cd(^1P_1)$ (2288 Å, 124 kcal.) or of $Hg(^3P_1)$ (2537 Å, 112 kcal.) (22). However, polymerization is also observed when triplet cadmium atoms (3261 Å, 87 kcal.) are used; Steacie and Le Roy attempted to overcome the difficulty by suggesting that since the heat of formation of cadmium hydride is 15.5 kcal., the reaction

$$Cd(^3P_1) + C_2H_2 \rightarrow CdH + C_2H-$$

can proceed if $D_{C-H(C_2H_2)}$ is not greater than 103 kcal. Since this estimate is much lower than that of other workers, a preferable explanation is that a triplet acetylene diradical is formed, which is responsible for the polymerization.

Can. J. Chem. Downloaded from www.nrcresearchpress.com by 61.7.252.67 on 09/04/12
For personal use only.

Can. J. Chem. Downloaded from www.nrcresearchpress.com by 61.7.252.67 on 09/04/12
For personal use only.

4. THE MULTIPLICITY AND NATURE OF THE RADICAL

The end of the previous paragraph introduced the possibility that the diradical is in the triplet state; this was necessary in the photochemical system because the multiplicity of the triplet cadmium atoms cannot be lost, but must be passed to another atom or molecule (cf. 14).

Since the triplet state, for any configuration, lies energetically lower than the corresponding singlet, the former would be more readily formed at a given temperature, were it not for the Wigner–Witmer spin conservation rules. These prohibit, in simple systems at least, the direct conversion of a singlet into a triplet. However, this restriction can be overcome by perturbing the fields of the system undergoing transition; this could be effected particularly well by a surface. If the suggestion is correct, then the bimolecular initiation reaction will become a surface process. If the polymerization is now visualized as a successive lengthening of the carbon skeleton of the diradical (II), by incorporation of acetylene molecules, then the formation of stable compounds can occur in two ways (other than by mutual destruction of carriers). One of these consists of passing the triplet multiplicity to an acetylene molecule

$$M_m^* + A \rightarrow Prod_m + A^*;$$

this is exactly parallel to the concept of chain transfer in liquid phase polymerization (3, 6); the regeneration of the chain carriers is thus ensured. The other process represents the spontaneous, unimolecular, conversion of a triplet chain carrier into a stable molecule. Again, this would be very slow in the gas phase, because of spin conservation restrictions, but it will readily occur on the surface.

The mechanism thus introduces a partial dependence on the surface of both chain initiation and termination, as was required by the consideration of the effect of surfaces. The apparent irregularities in the latter may further be explained by the difference in kinetic order of the two processes, in view of the fact that the comparisons are usually carried out under only one set of conditions by each worker.

5. MECHANISM

Formally, the mechanism can be represented as follows:

$$\textit{Initiation} \quad A + A \xrightarrow{\text{surface}} \begin{cases} A^x + A^x \\ A^x + A \\ A_2^x \end{cases} \quad \begin{cases} A = C_2H_2 \\ A^x = -C_2H_2- \\ A_2^x = -C_4H_4- \end{cases} \tag{1}$$

$$\textit{Polymerization} \quad A^x + A \longrightarrow A_2^x \tag{2}$$

$$A_n^x + A \longrightarrow A_{n+1}^x \tag{$n+1$}$$

$$\textit{Chain Transfer} \quad A_n^x + A \longrightarrow A^x + M_n \qquad (M_n = \text{stable product}) \tag{3}$$

$$\textit{Termination} \quad A_m^x + A_n^x \longrightarrow \text{Products} \tag{4}$$

$$A_n^x \xrightarrow{\text{surface}} M_n \tag{5}$$

Regarding the initiation reaction, it is not at present possible to decide whether this results in one or more entities, but this does not affect the remainder of the discussion.

Apart from the inherent simplicity, the mechanism is supported by a number of considerations. Thus, it is very similar to the simplified scheme which Flory (6) proposed in 1937 to account for "vinyl" type polymerization in the liquid phase (see Ref. 1, 3 for later refinements). The main steps were: (*a*) formation of a dimeric divalent radical, (*b*) comparatively long polymerization chains, (*c*) chain transfer, similar to reaction (3), and (*d*) chain termination, involving interaction of two chain carriers. (The order of the

last reaction had little effect on the kinetic form deduced.) With some simplifications, graphs of concentration (C) against time have been deduced by the author for various possible ratios of chain termination to chain propagation. In every case, the initial rate is of the same order of magnitude as the maximum rate. From the diagram in Flory's paper, values of $1/C$ have been deduced, and plotted against time; the resulting graphs are identical in form with those reported for acetylene polymerization by Minkoff, Newitt, and Rutledge.

In the liquid phase system, direct evidence has been obtained of the formation of the dimeric radical, by the isolation of an addition compound with a molecule of benzoquinone inhibitor (13):

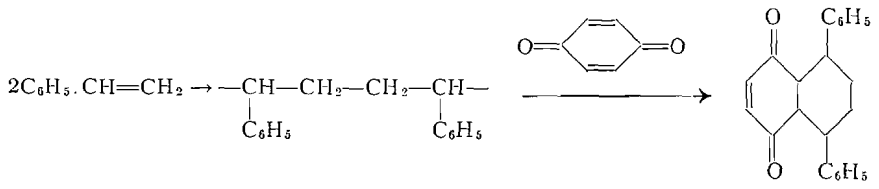

Under these conditions, Bamford and Dewar suggested that there was no need to invoke a triplet state. However, this point of view does not necessarily apply to the gas phase, particularly in view of the need for making the reaction mechanism sensitive to surface.

6. THE SHAPE OF THE TRIPLET STATE

The use of —CH=CH—CH=CH— as a chain carrier is not new (20), but it is only when this radical is considered as a triplet that the effect of surfaces, and of tests for radicals, can be reasonably explained. A further refinement is to predict the conditions leading to polymerization, and to decomposition. This is made possible by Ingold and King's analysis of the U.V. absorption spectrum of acetylene (10), which indicates that the triplet diradical is likely to have the *trans* configuration in the lower state, and the *cis* in a higher one:

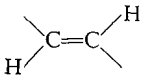

trans

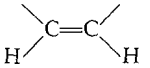

cis

It seems probable that during polymerization the carbon skeleton retains the *trans* shape. To some extent, this is supported by the "staggered" configuration of diacetylene in its upper, singlet, state (Dr. Callomon, private communication). Comparatively long carbon skeletons would then be formed in preference to small cyclic ones. At higher temperatures, however, sufficient energy becomes available for the *cis* configuration to be of importance, thus facilitating both the elimination of molecular hydrogen, and the formation of benzene in considerable amounts (cf. the textbook methods of making benzene by passing acetylene through a red-hot tube).

It is also possible that the effect of halogenated compounds and of metals can be explained in a similar way, by postulating that the change from *trans* to *cis* is facilitated by the free electrons in the metal surfaces, or by the strong electronegativity of the

Can. J. Chem. Downloaded from www.nrcresearchpress.com by 61.7.252.67 on 09/04/12
For personal use only.

halogen atoms. Once the C_2 molecules (or radicals) have been formed in the gas phase, they readily react with acetylene and form carbonaceous deposits (9).

This explanation of the role of halogens seems to be at least as probable as mechanisms based on the so-called affinity of halogen atoms for hydrogen. The latter are difficult to reconcile with the relative bond dissociation energies of 121 kcal. for C—H in acetylene and of 102 kcal. for HCl and even lower for HBr (8).

CONCLUSION

The mechanism presented in this communication explains the greater part of the effects reported below 500° C., and particularly that of surfaces. It has the advantage of treating the polymerization of acetylene in a manner analogous to that generally accepted for vinyl polymerization reactions, and it provides a simple explanation of the change from polymerization to decomposition at low temperatures. More experimental work on the latter aspect would be desirable.

The author acknowledges valuable discussions with Dr. V. Griffing, Dr. G. W. King, Prof. D. M. Newitt, and Dr. P. V. Rutledge.

REFERENCES

1. Bamford, C. H. and Dewar, M. J. S. Proc. Roy. Soc. A, **192**, 309 (1948).
2. Bone, W. A. and Coward, H. F. J. Chem. Soc. **93**, 1197 (1908).
3. Burnett, G. M. Quart. Revs. (London), **4**, 292 (1950).
4. Burnham, H. D. and Pease, R. N. J. Am. Chem. Soc. **64**, 1404 (1942).
5. Cottrell, T. L. The strengths of chemical bonds. Butterworth Scientific Publications, London. 1954.
6. Flory, P. J. J. Am. Chem. Soc. **59**, 241 (1937).
7. Frank-Kamenetzky, D. A. Acta Physicochim. U.R.S.S. **18**, 148 (1943).
8. Gaydon, A. G. Dissociation energies. 2nd. ed. Chapman & Hall, Ltd., London. 1953.
9. Gaydon, A. G. and Fairbairn, A. R. 5th Symposium on Combustion. Reinhold Publishing Corporation, New York. 1955. p. 324.
10. Ingold, C. K. and King, G. W. J. Chem. Soc. 2713 (1953).
11. Jach, J. and Hinshelwood, C. Proc. Roy. Soc. A, **229**, 143 (1955).
12. Kasha, M. and McGlynn, S. P. Ann. Rev. Phys. Chem. **7**, 403 (1956).
13. Kern, W. and Feuerstein, K. J. prakt. Chem. **158**, 186 (1941).
14. Laidler, K. J. Chemical kinetics of excited states. Oxford University Press, Oxford. 1955. p. 93.
15. Minkoff, G. J., Newitt, D. M., and Rutledge, P. V. J. Appl. Chem. (London), **7**, 412 (1957).
16. Paneth, F. and Hofeditz, W. Ber. B, **62**, 1335 (1929).
17. Pease, R. N. J. Am. Chem. Soc. **51**, 3470 (1929).
18. Robertson, W. W., Magee, E. M., Fain, J., and Matsen, F. A. 5th Symposium on Flame and Combustion. Reinhold Publishing Corporation, New York. 1955. p. 628.
19. Schläpfer, P. and Brunner, M. Helv. Chim. Acta, **13**, 1125 (1930).
20. Silcocks, C. G. Ministry of Supply Report 39/R/49 (open).
21. Steacie, E. W. R. Atomic and free radical reactions. Vol. I. 2nd ed. Reinhold Publishing Corporation, New York. 1954. p. 172.
22. Steacie, E. W. R. Ref. 21, p. 423.
23. Taylor, H. S. and Jungers, J. C. Trans. Faraday Soc. **33**, 1353 (1937).
24. Taylor, H. A. and van Hook, A. J. Phys. Chem. **39**, 811 (1935).
25. Walsh, A. D. Discussions Faraday Soc. No. **2**, 18 (1947).
26. Westbrook, E. A., Hellwig, K., and Anderson, R. C. 5th Symposium on Combustion. Reinhold Publishing Corporation, New York. 1955. p. 631.

Can. J. Chem. Downloaded from www.nrcresearchpress.com by 61.7.252.67 on 09/04/12
For personal use only.

THE FLUORESCENCE AND ITS RELATIONSHIP TO PHOTOLYSIS IN HEXAFLUOROACETONE VAPOR[1]

HIDEO OKABE[2] AND E. W. R. STEACIE

ABSTRACT

Hexafluoroacetone vapor, when excited at 25° C. by light of wavelength 3130 Å, gives rise to fluorescence. The fluorescence spectrum starts at about 3470 Å and extends to almost 6000 Å with a maximum at about 4200 Å, independent of pressure over the range 3 mm. to 170 mm. No fine structure is observed. Oxygen has almost no effect on the spectrum, contrary to the cases of acetone and biacetyl vapor, where oxygen causes a marked change. The absorption follows Beer's law between 5 mm. and 50 mm. of hexafluoroacetone pressure and the absorption coefficient has been measured.

The fluorescence efficiency decreases slightly with the addition of less than 1 mm. of oxygen and there stays constant up to an oxygen pressure of 30 mm., indicating that the fluorescence may be principally from the short-lived singlet excited state. The fluorescence efficiency increases with pressure of hexafluoroacetone or with the addition of inert gases such as perfluorobutane, perfluoropropane, hexafluoroethane, or carbon dioxide. The present results may be compared with those of the photolysis, where it was found that the quantum yield of the decomposition decreases with increasing pressure and with added inert gases. A close relationship between the fluorescence and the photolysis suggests itself. A mechanism is proposed to explain the results, which assumes that the molecule is raised to the upper vibrational levels of a singlet excited state, and subsequently deactivated to the lowest vibrational levels of the same state, from which it fluoresces. On the basis of this mechanism it seems possible to correlate the photolysis with the fluorescence.

INTRODUCTION

The photolysis and fluorescence of ketones have been studied extensively for many years (1).

While most photochemical reactions seem to involve principally the dissociation of molecules, in some cases both the dissociation and the fluorescence take place concurrently, when excited species are formed by the absorption of the radiation. In a few cases it seems possible to explain the results in terms of a mechanism which correlates both phenomena (2, 3).

The photolysis of hexafluoroacetone has been studied mainly by Ayscough and Steacie (4). They found that the mechanism of the photolysis by light of wavelength 3130 Å seems to be unusually simple over a wide range of temperatures. By investigating the effect of pressure and of various inert gases on the primary photochemical yields they concluded that the photolysis proceeds by way of an electronically excited species with a considerable lifetime. They found that the photochemical yields decreased with increase of pressure and with the addition of inert gases, which indicates that the excited molecules are deactivated effectively by collision. Since the photochemical yields were always considerably less than unity over the range of pressures studied, the possibility of fluorescence may be suggested as another way of energy dissipation. The study of fluorescence, if it is found, is of interest in order to arrive at a further understanding of the primary process. The present work was undertaken to investigate the hitherto unknown fluorescence of hexafluoroacetone and to correlate it with the photolysis data.

[1]*Manuscript received October 7, 1957.*
Contribution from the Division of Pure Chemistry, National Research Laboratories, Ottawa, Canada. This paper was presented at the Symposium on the Structure and Reactivity of Electronically-Excited Species held at the University of Ottawa, Ottawa, Canada, September 5 and 6, 1957.
Issued as N.R.C. No. 4548.
[2]*National Research Council of Canada Postdoctorate Fellow 1956–58.*

Can. J. Chem. Downloaded from www.nrcresearchpress.com by 61.7.252.67 on 09/04/12
For personal use only.

Can. J. Chem. Downloaded from www.nrcresearchpress.com by 61.7.252.67 on 09/04/12
For personal use only.

EXPERIMENTAL

Hexafluoroacetone hydrate was supplied by Dr. Leitch of this laboratory, to whom we are greatly indebted. It was dehydrated by phosphorus pentoxide, degassed and stored in a blackened bulb behind a mercury cutoff. The fluorocarbons were supplied by E. I. duPont de Nemours and Company. They were purified by trap to trap distillation in the vacuum line, a middle portion being retained, dried by phosphorus pentoxide, and stored behind a mercury cutoff. Oxygen was prepared by heating potassium permanganate and by passing it through liquid nitrogen traps.

The light source was a Hanovia S-500 lamp operated with a Sorensen regulator. The radiation passing through a 10 mm. hole was collimated by a quartz lens of 100 mm. focal length, and passed through the color filter combination of 3 mm. Corning No. 9863, 50 mm. path length of 0.178 M nickel chloride solution, and 30 mm. path length of 0.0025 M potassium chromate solution. The wavelength of the radiation was mainly 3130 Å. That light transmitted by the cell was focused by another quartz lens of 150 mm. focal length on a G.E. 935 photocell and the light intensity measured by galvanometer deflection. The fluorescent radiation was measured at right angles to the incident radiation. After removal of scattered ultraviolet radiation by a Corning No. 738 filter, the fluorescent radiation was focused by a quartz lens on the 1P21 photomultiplier tube of a Farrand photometer. The photocurrent was measured on a galvanometer. A correction for the background radiation, amounting to less than 3%, was applied. It was found that both the fluorescence and the transmission amplifier circuits were stable and reproducible during the run. The intensity of the light source sometimes fluctuated over a long period of time and it was necessary to correct this occasionally during a run by changing the secondary voltage.

The cell employed was similar to that of Hunt and Noyes (5) except that it was made of Pyrex with quartz windows in order to facilitate the replacement of the windows, which were attached to the cell by Apiezon W cement. The cell was T shaped with an internal diameter of 40 mm. and length of 150 mm. The stem of the T was 40 mm. in diameter and tapered down to 10 mm.

A Toepler-type expansion bulb was used for mixing the reactants. Oxygen was stored in a 5 liter bulb and was dosed into the cell by means of a 20 cc. mercury Toepler pump.

Most spectrograms were taken with a Hilger $f/4$ quartz spectrograph. Eastman Kodak 103a-B plates were employed with Kodak D-19 developer. The vacuum line, free of stopcocks, followed the customary design used in this laboratory.

The following measurements were carried out for hexafluoroacetone: (1) I_t^0, the light transmitted by the empty cell; (2) I_t, the transmitted light with the gas in the cell; (3) I_f, the intensity of the fluorescence emerging from the center of the cell; and (4) I_f^0, the intensity of scattered radiation, which was very small and virtually constant so that it was not measured each time.

The fluorescence efficiency, Q, proportional to the absolute quantum yield of fluorescence, was calculated from the following equation:

$$Q = (I_f - I_f^0)/(I_t^0 - I_t).$$

RESULTS

It was found that hexafluoroacetone gives strong fluorescence when excited by light of wavelength 3130 Å. The spectrum starts at about 3470 Å and extends to 6000 Å with a maximum at about 4200 Å (Fig. 1). The main features follow:

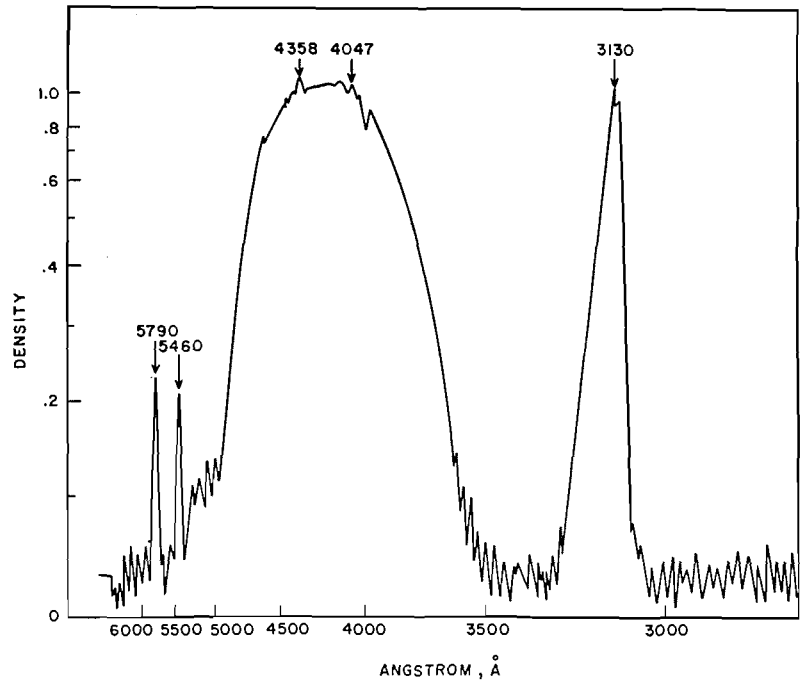

FIG. 1. Microdensitometer tracing of the fluorescence spectrum of hexafluoroacetone vapor excited by light of 3130 Å, using a Kodak 103a-B plate.

(1) The spectrum was independent of pressure of hexafluoroacetone from 3 mm. to 170 mm. at room temperature.

(2) No fine structure was observed with a Hilger high aperture glass spectrograph with a reciprocal linear dispersion of 80 Å/mm.

(3) The same spectrum was also obtained by exciting with light of wavelength 2800 Å or shorter.

(4) Oxygen had almost no effect on the spectrum.

The absorption followed Beer's law well between 5 mm. and 50 mm. and the calculated absorption coefficient k from the equation $I_t = I_t^0\ 10^{-kcd}$, where I_t^0 is the incident intensity, I_t the radiation transmitted, c the concentration in moles per liter, and d the distance in centimeters, was 6.80. The absorption coefficient is about 2.4 times greater than that of acetone at 3130 Å (6). The fluorescence efficiency Q was measured at 25° C. with various pressures of hexafluoroacetone and is given in Table I. It may be seen from

TABLE I

THE VARIATION OF THE FLUORESCENCE EFFICIENCY WITH HEXAFLUOROACETONE PRESSURE AT 3130 Å

P (mm.)	Q	P (mm.)	Q
1.75	6.9	17.0	7.81
4.7	7.7	21.5	8.19
7.3	6.51	25.5	8.31
11.9	7.21	30.5	8.91
15.4	7.40	37.5	8.36

Can. J. Chem. Downloaded from www.nrcresearchpress.com by 61.7.252.67 on 09/04/12
For personal use only.

the table that Q increases with pressure and reaches almost a maximum at about 20 mm. of pressure. This is quite contrary to the case of acetone, where Q decreases with pressure (6, 7), but is similar to biacetyl phosphorescence excited by light of wavelength 3650 Å (8). Fig. 2 shows the effect of oxygen pressure on the fluorescence efficiency Q of

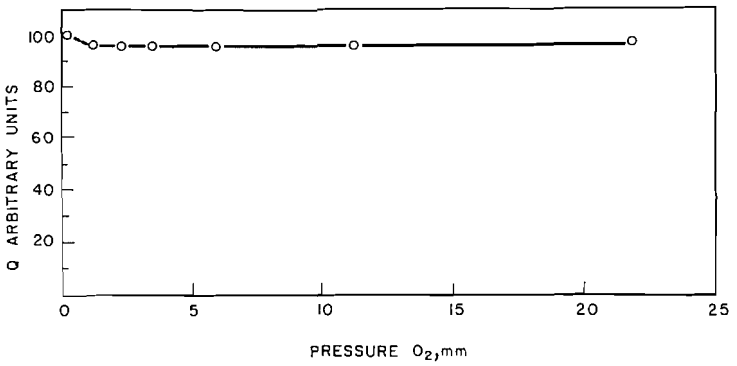

FIG. 2. Variation of fluorescence efficiency of 20 mm. hexafluoroacetone with oxygen pressure at 3130 Å.

20 mm. hexafluoroacetone at 25° C. As is seen from the curve, Q decreases slightly but definitely somewhere in the region below 1 mm. of oxygen pressure and there stays almost constant with further addition of oxygen. This is in marked contrast to acetone (6, 7) or biacetyl (9, 10, 11), where the emission decreased sharply to an almost negligible value with increasing oxygen pressure. The absorption of hexafluoroacetone was also measured and no change was observed with added oxygen.

In order to correlate the photolysis results with the fluorescence, the same inert gases used in the photolysis experiments were added to hexafluoroacetone and the fluorescence efficiency measured. Fig. 3 illustrates the effects of perfluorobutane, perfluoropropane, hexafluoroethane, and carbon dioxide on the fluorescence efficiency Q with 10 mm. of

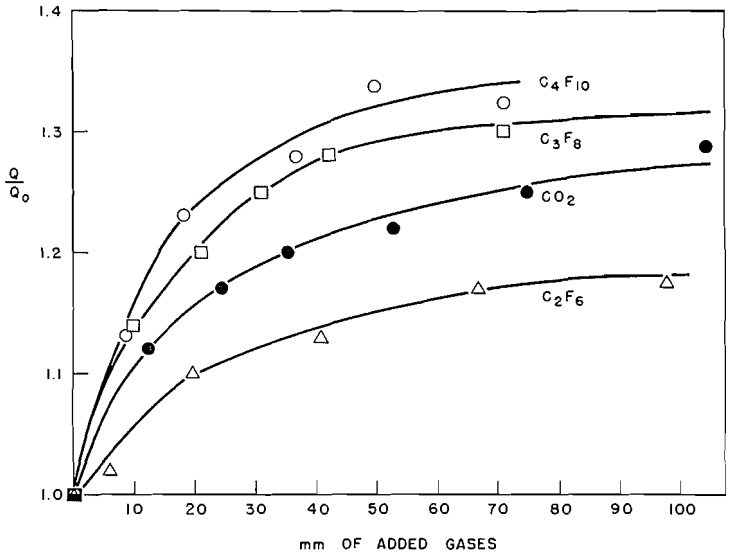

FIG. 3. Variation of fluorescence efficiency of 10 mm. hexafluoroacetone with pressure of added inert gases at 3130 Å.

Can. J. Chem. Downloaded from www.nrcresearchpress.com by 61.7.252.67 on 09/04/12
For personal use only.

hexafluoroacetone at 25° C. It can be seen from the curves that in every case there is an increase of Q with added gases. The order in which the gases increase Q is as follows: perfluorobutane > perfluoropropane > carbon dioxide > hexafluoroethane. Perfluorobutane increases the fluorescence efficiency by almost 30%, and hexafluoroethane by 17% over the range covered. If smaller pressures of hexafluoroacetone were used, a more pronounced effect of added gas would be expected. Apparently neither of the added gases is as effective as hexafluoroacetone itself in increasing the fluorescence efficiency. The intensity transmitted by the empty cell I_t^0 was frequently checked by freezing down the mixtures with liquid nitrogen. No change of absorption occurred in the presence of the added gases. The photolysis data (4) show that the decomposition is reduced by the addition of inert gases and that the efficiency of reduction follows the same order as the efficiency of fluorescence increase, except that the order of carbon dioxide and hexafluoroethane is reversed. This suggests related mechanisms for the fluorescence and the photochemical decomposition.

DISCUSSION

The striking simplicity of the over-all photochemical process at 3130 Å in hexafluoroacetone was reported by Ayscough and Steacie (4). They found that hexafluoroethane and carbon monoxide are the only products and that the quantum yield of decomposition is always less than unity and strongly dependent on pressure and the addition of inert gases. These facts led them to postulate the formation of a long-lived electronically excited molecule as an intermediate, which decomposes by a first order process unless deactivated by collision. Since the quantum yield of dissociation is always less than unity, the energy must be dissipated by some process other than dissociation. These steps may be the internal conversion or the fluorescence or both. No details of this process are known.

The present work revealed the existence of strong fluorescence extending from 3470 Å to 6000 Å with a maximum at about 4200 Å, independent of pressure studied, with incident radiation of 3130 Å. The fluorescence does not seem to originate from perfluorobiacetyl as acetone fluorescence does from biacetyl, because (1) the CO to C_2F_6 ratio is always unity indicating that no CF_3CO radical is formed, (2) no perfluorobiacetyl was found mass-spectrometrically after the sample was photolyzed, (3) the fluorescence spectrum starts almost from the end of the absorption band, and has no resemblance to that of biacetyl fluorescence, and (4) the fluorescence intensity does not change with time, whereas the acetone fluorescence does, owing to the accumulation of reaction product (biacetyl) (5).

The absorption band of the vapor lies between 2450 and 3550 Å (4). Since fluorescence and absorption overlap, the 0–0 band would lie in the region of overlap. This band may tentatively be assigned to 28570 cm.$^{-1}$ (3500 Å). This would be the 0–0 band for the transition in absorption and presumably for the transition in fluorescence from a singlet excited state. By excitation at 3130 Å the molecule will be raised to high vibrational levels, Y_n, of a singlet excited state (see Fig. 4). Since no resonance fluorescence was observed, the molecule must be deactivated rapidly to the lowest vibrational levels, Y_0, of the singlet excited state before it fluoresces. Oxygen has almost no effect on the fluorescence efficiency as well as on the spectrum. By analogy with the cases of acetone and biacetyl, in which the fluorescence from a singlet excited state is not quenched by added oxygen, whereas the phosphorescence from a triplet state is strongly quenched by oxygen (6, 7, 10, 11), it may be assumed that the fluorescence is mainly from the singlet excited state of hexafluoroacetone although no direct evidence has been found.

Can. J. Chem. Downloaded from www.nrcresearchpress.com by 61.7.252.67 on 09/04/12
For personal use only.

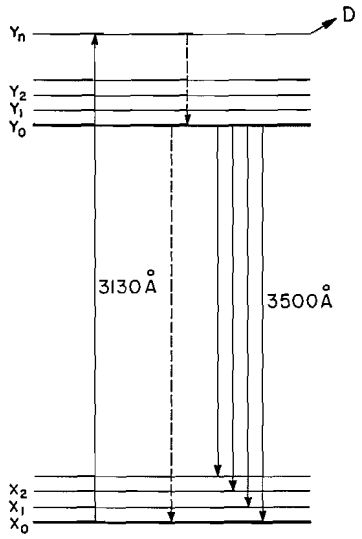

FIG. 4. Energy level diagram of hexafluoroacetone, where X_i is the ith vibrational level of the ground state, Y_i is the ith vibrational level of the singlet excited state, and D is the decomposition process. The full line represents the absorption or fluorescence process and the broken line represents the internal conversion or deactivation process.

The measurement of lifetime of hexafluoroacetone fluorescence is highly desirable in this respect.

It may be of interest to compare acetone and hexafluoroacetone with benzene and fluorobenzene. It was found that benzene shows both fluorescence and phosphorescence, whereas fluorobenzene shows only fluorescence at 77° K. (12). This was attributed to the more rapid transition from the singlet excited to the ground state compared to the radiationless transition to the triplet state in fluorobenzene, relative to that in benzene. This may be the case with acetone and hexafluoroacetone, although integrated extinction coefficients have not been compared in both cases.

From the foregoing discussion, the following process may be written:

[1] $$X+h\nu = Y_n,$$

[2] $$Y_n = C_2F_6+CO,$$

[3] $$Y_n = X,$$

[4] $$Y_n+X = Y_0+X,$$

[5] $$Y_0 = X+h\nu^*,$$

[6] $$Y_0 = X,$$

where X designates the ground state and Y_0 and Y_n, 0th and nth vibrational levels of the singlet excited state of hexafluoroacetone. Either or both steps [3] and [6] may be included. The following equation may be obtained from the above steps:

[7] $$\frac{1}{\phi} = 1+\frac{k_3}{k_2}+\frac{k_4}{k_2}(X),$$

where ϕ is the quantum yield of decomposition and (X) is hexafluoroacetone concentration. The validity of equation [7] may be tested by plotting $1/\phi$ against (X) from the

Can. J. Chem. Downloaded from www.nrcresearchpress.com by 61.7.252.67 on 09/04/12
For personal use only.

photolysis data (4). The plot corresponding to various temperatures gives a series of straight lines with an intercept of unity. This indicates that $k_3 = 0$, that is, there is no first order step other than the decomposition. Therefore the following equations will be obtained:

[8] $$\frac{1}{\phi} = 1+\frac{k_4}{k_2}(\mathrm{X})$$

and

[9] $$\frac{1}{aQ} = \frac{k_5+k_6}{k_5}+\frac{k_2(k_5+k_6)}{k_4k_5}\frac{1}{(\mathrm{X})},$$

where Q is the fluorescence efficiency and a is the ratio of quantum yield of fluorescence to the fluorescence efficiency. Since a is not known, each individual constant can not be obtained. The process may be compared to that for biacetyl when excited by 3650 Å radiation where step [3] should be included since the intercept is always greater than unity (2).

Fig. 5 illustrates the relation between $1/Q$ and $1/(\mathrm{X})$. It may be seen that equation [9] is approximately obeyed. At pressures lower than 5 mm., the plot deviates considerably from linearity, indicating that some other process must be considered. However, the data are not extensive and accurate enough to warrant further discussion of this process.

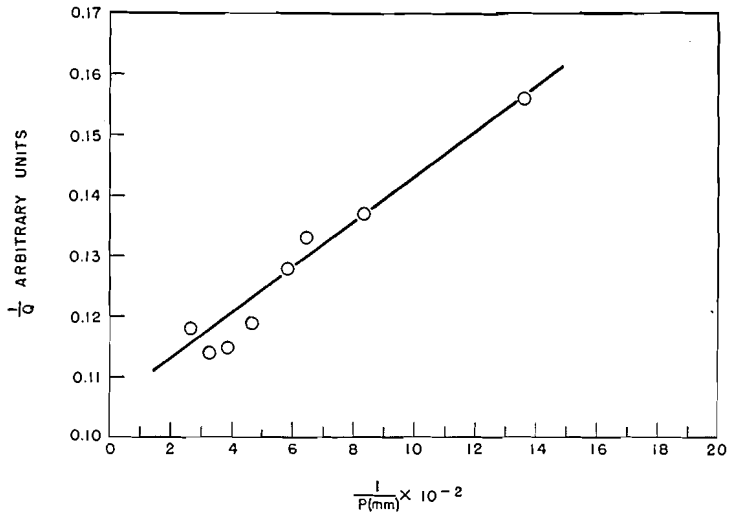

FIG. 5. The dependence of the reciprocal of the fluorescence efficiency on the reciprocal of the hexafluoroacetone pressure at 3130 Å.

The mechanism for hexafluoroacetone fluorescence seems to follow that for biacetyl green phosphorescence excited by light of 3650 Å, but not that for acetone fluorescence excited by light of 3130 Å. It indicates that the self-quenching process $\mathrm{Y}_0 + \mathrm{X} = 2\mathrm{X}$ is small and relatively unimportant compared to the deactivation process [4]. It also follows from the mechanism that

[10] $$\frac{aQ}{\phi} = \frac{k_4k_5}{k_2(k_5+k_6)}(\mathrm{X}).$$

Can. J. Chem. Downloaded from www.nrcresearchpress.com by 61.7.252.67 on 09/04/12
For personal use only.

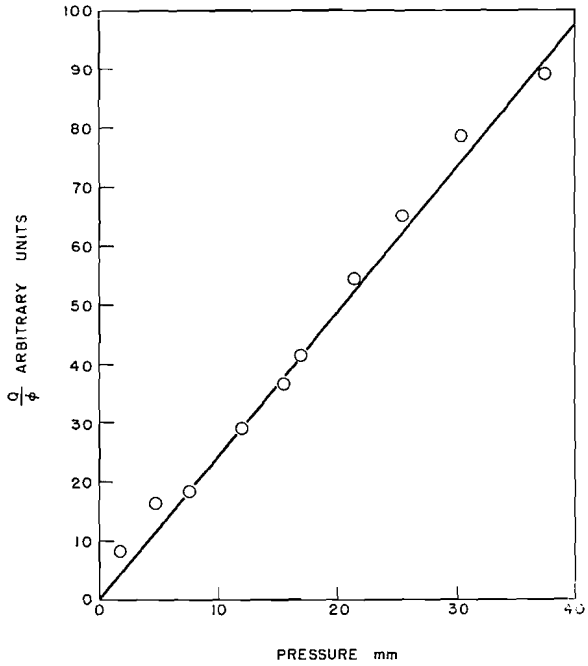

FIG. 6. The dependence of the ratio of the fluorescence efficiency, Q, and the photochemical yield, ϕ, on the pressure of hexafluoroacetone at 3130 Å.

Fig 6 shows the relation between Q/ϕ and (X), the pressure of hexafluoroacetone. The values for photochemical decomposition are taken from Ayscough and Steacie's data (4). As can be seen, a plot of Q/ϕ vs. pressure gives a straight line which passes through the origin. This indicates that the decomposition results almost exclusively from a first order step, and the fluorescence, from a second order step. The positive intercept on the Q/ϕ axis observed with biacetyl (2), indicating that dissociation results from the collision of two excited molecules, does not appear with hexafluoroacetone.

The close relationship between the photolysis and the fluorescence may be seen further from the effect of inert gases.

The hexafluoroacetone has the great advantage that it is possible to compare the effect of inert gas on the photolysis and the fluorescence simultaneously; since firstly it is possible to measure the primary photochemical yields even in the presence of added gas, and secondly the fluorescence yields are large enough to measure, thus making it possible to compare both directly.

In the presence of inert gas, the following step must be added:

[11] $$Y_n + M = Y_0 + M,$$

where M designates inert gases. The following equations may be derived:

[12] $$\frac{1}{\phi} = 1+\frac{k_4}{k_2}(X)+\frac{k_{11}}{k_2}(M),$$

[13] $$\frac{\phi_0}{\phi} = 1+\frac{k_{11}}{k_2+k_4(X)}(M),$$

Can. J. Chem. Downloaded from www.nrcresearchpress.com by 61.7.252.67 on 09/04/12
For personal use only.

[14] $$\frac{aQ}{\phi} = \frac{k_4k_5}{k_2(k_5+k_6)}(\mathrm{X})+\frac{k_5k_{11}}{k_2(k_5+k_6)}(\mathrm{M}),$$

and

[15] $$\frac{Q}{Q_0}\frac{\phi_0}{\phi} = 1+\frac{k_{11}}{k_4(\mathrm{X})}(\mathrm{M}),$$

where (M) represents added inert gas concentration, and ϕ_0 and Q_0, the quantum yield of decomposition and the fluorescence efficiency, respectively, with 10 mm. hexafluoroacetone without added inert gas in the cell. It was shown (4) that ϕ_0/ϕ plotted against (M) gives a series of straight lines. Fig. 7 shows the relation between $(Q/Q_0)(\phi_0/\phi)$ and

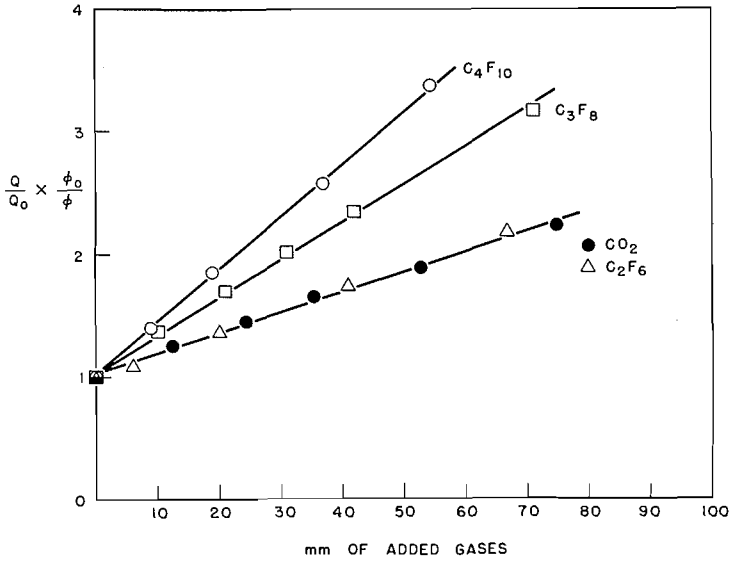

FIG. 7. The dependence of the ratio of the fluorescence efficiency and the primary photochemical yield on the pressure of added inert gases at 3130 Å.

(M). In this figure ϕ_0/ϕ values were taken from the points on the straight line corresponding to each pressure of added inert gas at 78° C., the only temperature for which data are available. It may be seen that a series of straight lines is obtained for each added gas. The slopes of the lines give the rates of deactivation by inert gases relative to that by hexafluoroacetone. The relative rates are 1, 0.42, 0.31, 0.17, and 0.17 for CF_3COCF_3, C_4F_{10}, C_3F_8, C_2F_6, and CO_2 respectively. These values are lower than those obtained from the photolysis data, although their relative orders are the same with the exception of that for CO_2. This is probably due to the fact that ϕ_0/ϕ values are obtained at 78° C. whereas Q/Q_0 values are at 25° C.

The authors wish to thank Mr. G. Ensell for the construction of the cell.

REFERENCES

1. NOYES, W. A., JR., PORTER, G. B., and JOLLEY, J. E. Chem. Revs. **56**, 49 (1956).
2. SHEATS, G. F. and NOYES, W. A., JR. J. Am. Chem. Soc. **77**, 1421 (1955).
3. OKABE, H. and NOYES, W. A., JR. J. Am. Chem. Soc. **79**, 801 (1957).
4. AYSCOUGH, P. B. and STEACIE, E. W. R. Proc. Roy. Soc. A, **234**, 476 (1956).

Can. J. Chem. Downloaded from www.nrcresearchpress.com by 61.7.252.67 on 09/04/12
For personal use only.

5. HUNT, R. E. and NOYES, W. A., JR. J. Am. Chem. Soc. **70**, 467 (1948).
6. LUCKEY, G. W. and NOYES, W. A., JR. J. Chem. Phys. **19**, 227 (1951).
7. GROH, H. J., JR., LUCKEY, G. W., and NOYES, W. A., JR. J. Chem. Phys. **21**, 115 (1953).
8. ALMY, G. M. and GILLETTE, P. R. J. Chem. Phys. **11**, 188 (1943).
9. COWARD, N. A. and NOYES, W. A., JR. J. Chem. Phys. **22**, 1207 (1954).
10. ALMY, G. M., FULLER, H. Q., and KINZER, G. D. J. Chem. Phys. **8**, 37 (1940).
11. GROH, H. J., JR. J. Chem. Phys. **21**, 674 (1953).
12. GILMORE, E. H., GIBSON, G. E., and MCCLURE, D. S. J. Chem. Phys. **20**, 829 (1952).

Can. J. Chem. Downloaded from www.nrcresearchpress.com by 61.7.252.67 on 09/04/12
For personal use only.

Can. J. Chem. Downloaded from www.nrcresearchpress.com by 61.7.252.67 on 09/04/12
For personal use only.

REACTION OF AMINO ALCOHOLS WITH CARBON DISULPHIDE[1]

A. F. McKay, M. Skulski, and D. L. Garmaise

ABSTRACT

ω-Amino alcohols possessing five or more methylene units between the amino and hydroxyl groups on condensation with carbon disulphide gave good yields of 1,3-di-(ω-hydroxyalkyl) thioureas. These symmetrically disubstituted thioureas on oxidation gave the corresponding 1,3-di-(ω-hydroxyalkyl) ureas.

The investigation of the reaction of carbon disulphide with amino alcohols (1) has been extended to the longer chain ω-amino alcohols. The ω-amino alcohols having five or more methylene units between the amino and hydroxy groups combine with carbon disulphide to give 1,3-di-(ω-hydroxyalkyl) thioureas (II). A series of these symmetrical thiourea derivatives II have been prepared and their properties are listed in Table I. 1,3-Di-(5-hydroxypentyl)-thiourea (II, $n = 5$) was isolated as an oil and it was converted directly into the corresponding urea without further purification. The 1,3-di-(5-hydroxy-

$$2HO(CH_2)_nNH_2 + CS_2 \rightarrow HO(CH_2)_nNHC(=S)NH(CH_2)_nOH + H_2S\uparrow$$

I II

$\downarrow H_2O_2$

$$HO(CH_2)_nNHC(=O)NH(CH_2)_nOH$$

$n = 5$–11 III

pentyl)-, 1,3-di-(6-hydroxyhexyl)-, and 1,3-di-(7-hydroxyheptyl)-thioureas were oxidized in alkaline solution with hydrogen peroxide into the corresponding symmetrical urea derivatives III. 1,3-Di-(11-hydroxyundecyl)-thiourea was not oxidized under the same conditions but it was converted into 1,3-di-(11-hydroxyundecyl)-urea by refluxing with ethanolic silver nitrate solution (2).

TABLE I

$HO(CH_2)_nNHC(=X)NH(CH_2)_nOH$

X	n	Yield, %	M.p., °C.	Formula	C Calc.	C Found	H Calc.	H Found	N Calc.	N Found	S Calc.	S Found
O	5	73.2	106.5–108.5	$C_{11}H_{24}N_2O_3$	56.87	57.06	10.41	10.14	12.06	11.96		
S	6	81.5	79.5–80.5	$C_{13}H_{28}N_2O_2S$	56.48	56.49	10.21	10.23	10.14	10.21	11.60	11.42
O	6	68.9	117–118	$C_{13}H_{28}N_2O_3$	59.95	59.75	10.84	10.83	10.76	10.96		
S	7	69.0	82.5–83	$C_{15}H_{32}N_2O_2S$	59.18	59.55	10.59	10.35	9.20	8.96	10.53	9.98
O	7	60.9	122.5	$C_{15}H_{32}N_2O_3$	62.48	62.58	11.19	11.00	9.72	9.71		
S	11	69.3	97–98.5	$C_{23}H_{48}N_2O_2S$	66.28	66.45	11.61	11.81	6.72	6.74	7.69	7.81
O	11	88.3	134.5–136	$C_{23}H_{48}N_2O_3$	68.95	68.80	12.08	12.11	6.99	6.78		

[1]*Manuscript received September 19, 1957.*
Contribution from the L. G. Ryan Research Laboratories of Monsanto Canada Limited, Ville LaSalle, Quebec.

Other urea derivatives prepared for characterizing the amino alcohols were 1-(α-naphthyl)-3-(6-hydroxyhexyl)-urea, 1-phenyl-3-(7-hydroxyheptyl)-urea, and 1-(α-naphthyl)-3-(11-hydroxyundecyl)-urea.

EXPERIMENTAL[2]

5-Aminopentanol-1

5-Aminopentanol-1 (b.p. 119–120° C. at 17 mm.; m.p. 26–28° C.; n_D^{16} 1.4608) was prepared in 45.5% yield by the method of Putokhin (3). The previously reported (3) physical constants are m.p. 26° C., d_4^{17} 0.9488, and n_D^{17} 1.4618.

6-Aminohexanol-1

6-Aminohexanol-1 was prepared by a modification of Wallach's method (4). Metallic sodium (150 g., 6.52 moles) was added to a refluxing solution of caprolactam (30 g., 0.26 mole) in freshly distilled absolute ethanol (1500 cc.) at a sufficient rate to maintain vigorous reflux. The reaction was complete in 1½ hours. The reaction mixture was steam distilled and the distillates were collected in 1 liter fractions. These fractions were acidified with hydrochloric acid and then evaporated to dryness. The first two fractions gave an impure hydrochloride melting at 215–235° C., yield 5.85 g. (16.25%). These crystals were considered to be impure hexamethylenimine hydrochloride, which Wallach reported (4) to melt at 236–237° C. The remaining distillate fractions gave a yellowish colored hydrochloride melting at 63–64° C., yield 28.91 g. (70.9%). This crude material (23.63 g., 0.15 mole) in absolute methanol (500 cc.) was passed through IRA-400 resin (1000 cc. of resin in the hydroxyl form previously washed with methanol) at a rate of 5 cc. per minute. The column of resin was washed with methanol (2500 cc.) and the eluate and washings were taken to dryness *in vacuo* under nitrogen. The product was distilled *in vacuo* under nitrogen. A crystalline product (b.p. 137–139° C. at 20 mm.) was obtained, yield 13.10 g. (42.1%). This crystalline product appeared to be dimorphous with one form melting at 57–58° C. and the other at 75–78° C. Wallach (4) reported a melting point of 55–56° C. Both forms gave one spot with a R_f value of 0.54 when chromatographed on Whatman No. 1 paper with butanol: acetic acid: water (4: 1: 5) solvent.

A sample (0.15 g., 0.001 mole) of 6-aminohexanol-1 was treated with α-naphthylisocyanate (0.218 g., 0.001 mole) in dry benzene (10 cc.). This suspension was refluxed for 1 hour. The gummy precipitate of 1-α-naphthyl-3-(6-hydroxyhexyl)-urea was removed by filtration and then crystallized from boiling acetone (5 cc.). A crop of colorless needles (m.p. 140–141° C.) was obtained, yield 0.265 g. (71.8%). The melting point was not changed by further crystallization. Anal. Calc. for $C_{17}H_{22}N_2O_2$: C, 71.30; H, 7.69; N, 9.78%. Found: C, 71.39; H, 7.83; N, 9.97%.

7-Aminoheptanol-1

Cycloheptanone oxime (b.p. 129–130° C. at 23 mm.) was prepared in 94.4% yield by the method of Pearson and Bruton (5). It was then converted into enantholactam (b.p. 148–150° C. at 10 mm.) in 82% yield by the method of Eck and Marvel (6).

Enantholactam (75.95 g., 0.6 mole) was converted into 7-aminoheptanol-1 hydrochloride by the method described above for the preparation of 6-aminohexanol-1. The first two distillates yielded a brownish oil (20 g.), which is probably impure heptamethylenimine hydrochloride. The residue from distillate fractions 3–7 was obtained as

[2]*All melting points are uncorrected. Microanalyses were performed by Micro Tech Laboratories, Skokie, Illinois.*

Can. J. Chem. Downloaded from www.nrcresearchpress.com by 61.7.252.67 on 09/04/12
For personal use only.

brownish needles melting at 67–75° C., yield 25.06 g. This crude 7-aminoheptanol-1 hydrochloride was dissolved in water (500 cc.) and the solution passed through a column of IRA-400 resin (600 cc. of resin in the hydroxyl form) at a rate of 5 cc. per minute. The column was washed with water (3500 cc.) and the eluate and washings were evaporated to dryness *in vacuo* under nitrogen. A crystalline distillate (b.p. 123° C. at 5 mm.; m.p. 48–53° C.) was obtained from the residue, yield 23.5 g. (29.9%). Wallach (4) reported a melting point of 48–50° C. for 7-aminoheptanol-1. A sample of the 7-aminoheptanol-1 (0.67 g., 0.0051 mole) in dry benzene (10 cc.) was treated with phenylisocyanate (0.61 g., 0.0051 mole). The product (m.p. 79.5–83° C.) was recovered by filtration, yield 1.25 g. (97%). One crystallization from acetone raised the melting point to 87–88° C. Anal. Calc. for $C_{14}H_{22}N_2O_2$: C, 67.16; H, 8.86; N, 11.20%. Found: C, 67.03; H, 8.71; N, 11.22%.

11-Bromoundecanoic Acid

11-Bromoundecanoic acid (m.p. 48° C.) was prepared in 69.9% yield from 11-undecanoic acid by the method of Ashton and Smith (7). The reported (7) melting point is 49.25° C.

11-Aminoundecanoic Acid

The patent procedure (8) for the preparation of 11-aminoundecanoic acid from 11-bromoundecanoic acid gave a 78.4% yield of product melting at 182–185° C. The reported (9) melting point of 11-aminoundecanoic acid is 186–187° C.

11-Aminoundecanoic acid (47 g., 0.23 mole) in 3.5 *N* methanolic hydrogen chloride solution was allowed to stand at room temperature for 16 hours. After most of the methanol was removed *in vacuo*, the crude methyl ester hydrochloride (m.p. 158–161° C.) was recovered by filtration, yield 51.1 g. (86.8%). One crystallization from methanol raised the melting point to 159.5–160.5° C. Anal. Calc. for $C_{12}H_{26}ClNO_2$: C, 57.24; H, 10.14; Cl, 14.09; N, 5.56%. Found: C, 57.33; H, 10.25; Cl, 14.35; N, 5.50%.

11-Aminoundecanol-1

Methyl 11-aminoundecanoate hydrochloride (m.p. 158–161° C.) (22.2 g., 0.088 mole) in methanol (400 cc.) was passed through a column of IRA-400 (OH) resin (400 cc. of resin previously washed with methanol) at a rate of 5–7 cc. per minute. The eluates and washings were evaporated to dryness *in vacuo* under nitrogen. The residue of crude methyl 11-aminoundecanoate melted at 70–85° C., yield 16.2 g. (85.3%). Pellets of metallic sodium (28 g., 1.2 moles) were added to the crude methyl ester (16.2 g., 0.075 mole) in absolute ethanol (500 cc.) at a rate to maintain the alcoholic solution at gentle reflux. After the solution cooled it was diluted with water (250 cc.) to decompose the excess sodium ethoxide. The methanol was removed *in vacuo* under nitrogen and the residual aqueous solution was extracted with chloroform. The chloroform extract was dried over anhydrous sodium sulphate and evaporated to dryness. A residue (m.p. 74–78° C.) of yellowish crystals was obtained, yield 4.0 g. (28.3%). This crude 11-aminodecanol-1 was purified by solution in warm methanol (13.5 cc./g.), and filtration and dilution of the filtrate with water (10 cc.). The final product melted at 71–73° C.

A sample (0.187 g., 0.001 mole) of 11-aminoundecanol-1 in dry benzene on treatment with α-naphthylisocyanate (0.169 g., 0.001 mole) gave 0.286 g. (80.2%) of crude 1-α-naphthyl-3-(11-hydroxyundecyl)-urea (m.p. 126–130° C.). Crystallization from acetone–benzene solution raised the melting point to 131° C. Anal. Calc. for $C_{22}H_{32}N_2O_2$: C, 74.11; H, 9.05; N, 7.86%. Found: C, 73.73; H, 9.05; N, 7.84%.

Can. J. Chem. Downloaded from www.nrcresearchpress.com by 61.7.252.67 on 09/04/12
For personal use only.

The aqueous filtrate from the chloroform extraction gave 16.5 g. of material melting at 197–205° C. This is considered to be the crude sodium salt of 11-aminoundecanoic acid. On treatment with concentrated hydrochloric acid solution it gave 11-aminoundecanoic acid hydrochloride (m.p. 148–149° C.). The latter material did not depress the melting point of a known sample of 11-aminoundecanoic acid hydrochloride (m.p. 148–149° C.).

Reaction of Amino Alcohols with Carbon Disulphide

The amino alcohol (0.05 mole) in absolute alcohol (25 cc). was added dropwise over a period of 20 minutes to a stirred solution of carbon disulphide (0.025 mole) at 5° C.

After the reaction mixture had remained at room temperature for several hours, it was refluxed for 9 to 15 hours. The colored alcoholic solution was treated with Norite A and filtered. The product was recovered by evaporating the filtrate to dryness *in vacuo* under nitrogen. The crystals were purified by crystallizing from a suitable solvent such as ethyl acetate. The properties of the symmetrical 1,3-di-(ω-hydroxyalkyl) thioureas prepared in this manner are given in Table I.

1,3-Di-(ω-hydroxyalkyl) Ureas

Method A

The 1,3-di-(ω-hydroxyalkyl) ureas with the exception of 1,3-di-(11-hydroxyundecyl)-urea were prepared in the manner described below for 1,3-di-(7-hydroxyheptyl)-urea.

To 1,3-di-(7-hydroxyheptyl)-thiourea (3.04 g., 0.01 mole) in alcoholic sodium hydroxide solution (34 cc. containing 0.8 g. of sodium hydroxide) hydrogen peroxide (5.08 cc. of 7.6 molar solution; 0.03 mole) was added dropwise at a temperature of 25–28° C. After the solution had been left at room temperature for 4 hours, it was diluted with water (250 cc.). The crystals (m.p. 121–122° C.) were recovered by filtration and dried, yield 2.77 g. (86.3%). One crystallization from absolute ethanol raised the melting point to 122–122.5° C.

Method B

1,3-Di-(11-hydroxyundecyl)-thiourea was converted in 88.3% yield into 1,3-di-(11-hydroxyundecyl)-urea (m.p. 128–129° C.) by the method of Kjaer *et al.* (2). Two crystallizations from ethyl acetate – ethanol (1:1) solution along with one treatment with Norite A raised the melting point to 134.5–136° C.

REFERENCES

1. Skulski, M., Garmaise, D. L., and McKay, A. F. Can. J. Chem. **34**, 815 (1956).
2. Kjaer, A., Rubenstein, K., and Jensen, K. A. Acta Chem. Scand. **7**, 5181 (1953).
3. Putokhin, N. Trans. Inst. Pure Chem. Reagents (Moscow), No. **6**, 10 (1927).
4. Wallach, O. Ann. **324**, 292 (1902).
5. Pearson, D. E. and Bruton, J. D. J. Org. Chem. **19**, 957 (1954).
6. Eck, J. C. and Marvel, C. S. Org. Syntheses, Coll. Vol. II, p. 76 (1944).
7. Ashton, R. and Smith, J. C. J. Chem. Soc. 435 (1934).
8. Brit. Patent No. 591,027 (August 5, 1947); Chem. Abstr. **42**, 592 (1948).
9. Coffman, D. D., Cox, N. L., Martin, E. L., Mochel, W. E., and Van Natta, F. J. J. Polymer Sci. **3**, 85 (1948).

Can. J. Chem. Downloaded from www.nrcresearchpress.com by 61.7.252.67 on 09/04/12
For personal use only.

THE INFRARED SPECTRA OF MALONATE ESTERS[1]

R. A. ABRAMOVITCH[2]

ABSTRACT

The infrared spectra of a number of malonate esters have been examined. Most of them exhibit two ester carbonyl stretching bands which have been shown not to be due to enolization and conjugate chelation or to association. The influence of α-substituents is discussed, as well as the reason for the splitting of the band.

Can. J. Chem. Downloaded from www.nrcresearchpress.com by 61.7.252.67 on 09/04/12
For personal use only.

During the course of another investigation diethyl 1-methyl-2-cyanoethylmalonate was prepared and its infrared spectrum examined. Two bands were observed at 1742 and 1730 cm.$^{-1}$ respectively which could only be attributed to the carbonyl groups of the ester functions. This was surprising, since Bellamy (5) states that diethyl malonate is essentially normal in its carbonyl frequency. The original authors (24), however, had only measured the spectrum up to 1750 cm.$^{-1}$. Bender and Figueras (7) remarked that diethyl malonate had an unusually broad (25 cm.$^{-1}$) band at 1740 cm.$^{-1}$, and indeed Felton and Orr (10) have recently shown that diethyl malonate exhibits two C=O stretching peaks at 1757 and 1740 cm.$^{-1}$ (in carbon tetrachloride solution). These authors ascribe the splitting either to symmetric and antisymmetric coupling of the two C=O stretching vibrations or to their resonance coupling with an overtone. In view of current interest in the splitting of carbonyl stretching frequencies the spectra of the malonate esters were examined in greater detail.

Vibrational coupling between carbonyl groups (16*a*) has been observed in a number of cases: diacyl and diaroyl peroxides (9), carboxylic acid anhydrides (23), and N,N-diacylamines (1). Recently, it has been suggested that glycidic esters dimerize in non-hydrogen-bonding solvents and that vibrational coupling then occurs between the carbonyl stretching motions of the two ester groups in the dimer (19). It should be pointed out, however, that whereas anhydrides exhibit two Raman bands corresponding to those found in the infrared (16*a*), the malonates, with one exception, show only one Raman shift in this region (18).

Preliminary examinations of some available malonates seemed to indicate that an α-hydrogen was necessary for two bands to appear, which would have pointed towards enolization with subsequent hydrogen bonding as the reason for the second peak. Thus, diethyl diethylmalonate and diethyl 2,2-*trans*-hydrind-5-enylmalonate only showed one band, though the former compound also had a very poorly-defined shoulder on the higher frequency side. Again, Felton and Orr (10) report only one band for diethyl *iso*propylidenemalonate though tetraethyl ethylenetetracarboxylate shows two. There is a large body of chemical evidence indicating that malonate esters have no appreciable enol content (3). In any case, had the second peak been due to a chelated carbonyl group its frequency should have been lower, and not higher, than the normal ester carbonyl stretching frequency. To examine the possibility of enolization and hydrogen bonding, diethyl ethyldeuteromalonate was prepared and compared with diethyl ethylmalonate; if enolization was taking place the position of the hydrogen-bonded carbonyl band would be altered on deuteration. Another possibility considered was that, when

[1]*Manuscript received September 9, 1957.*
Contribution from King's College, University of London, Strand, London, W.C.2, England.
[2]*I.C.I. Research Fellow at King's College. Present address: Chemistry Department, University of Saskatchewan, Saskatoon, Sask., Canada.*

the α-carbon atoms carried two substituents other than hydrogen, steric inhibition of vibrational coupling might occur and this could account for the single band observed in some cases. To investigate this, the spectra of diethyl *tert*-butylmalonate and di-*tert*-butylmalonate were recorded. Finally, a number of α-mono- and di-substituted malonates were examined in which the substituents varied in size and in electron attracting or repelling character.

EXPERIMENTAL

Most of the diethyl malonates used in this study were commercial samples purified by repeated fractional distillation when required. The author wishes to acknowledge gratefully the following gifts of specimens: diethyl 2,2-*trans*-hydrind-5-enylmalonate from Dr. H. B. Henbest; a sample of diethyl 1-acenaphthylmalonate from Dr. R. A. Heacock; and a sample of diethyl 1,1-dimethylprop-2-ynylmalonate from Dr. K. Mackenzie.

Di-*tert*-butylmalonate was prepared according to Backer and Homan (4). Diethyl bis-(2-cyanoethyl)-malonate was prepared according to Bruson and Riener (8) and had m.p. 62°. Diethyl *p*-nitrobenzylidenemalonate, m.p. 94°, was obtained from *p*-nitrobenzaldehyde and diethyl malonate in the presence of piperidine (17). Diethyl *tert*-butylmalonate was prepared in low yield by the action of *tert*-butylbromide on diethyl sodiomalonate (13). Diethyl 1-methyl-2-cyanoethylmalonate was prepared by the action of diethyl malonate on allyl cyanide in ethanolic sodium ethoxide (2).

Diethyl Ethyldeuteromalonate

Diethyl ethylmalonate (5 g., n_D^{23} 1.4150, redistilled, b.p. 212–214°) in absolute ethanol (20 ml.) containing sodium ethoxide (prepared from 0.615 g. sodium) was kept at room temperature overnight and then taken to dryness under vacuum to remove all traces of

TABLE I

ESTER CARBONYL FREQUENCIES (CM.$^{-1}$) OF MALONATE ESTERS AS LIQUID FILMS OR NUJOL MULLS

Diethyl malonate derivative	ν (cm.$^{-1}$)	Mean ν (cm.$^{-1}$)	$\Delta\nu_{C=O}$ (cm.$^{-1}$)
Dihydrogen	1760 (vs), 1742 (vs)	1751	18
Ethyl	1759 (m), 1742 (s)	1750	17
n-Propyl	1754 (s), 1737 (vs)	1745	17
n-Butyl	1757 (s), 1737 (vs)	1747	17
Ethyldeutero	1758 (sh) (m), 1742 (s)	1750	16
Diethyl	1751†(indistinct sh) (m), 1737 (s)	1744	(14†)
1-Acenaphthyl	1757 (sh) (s), 1745 (vs)	1751	12
Phenyl	1762 (s), 1741 (vs)	1752	21
Ethylphenyl	1754†(indistinct sh) (m), 1736 (s)	1745	(18†)
Chloro	1767 (s), 1754 (vs)	1760	13
Bromo	1771 (sh) (m), 1751 (s)	1761	20
Dibromo	1763 (s), 1752 (sh) (m)	1758	11
1,1-Dimethylprop-2-ynyl	1751 (s), 1730 (vs)	1740	21
2,2-*trans*-Hydrind-5-enyl	1730 (br) (vs)	—	—
1-Methyl-2-cyanoethyl	1742 (sh) (s), 1730 (vs)	1736	12
Bis-(2-cyanoethyl)*	1754 (s), 1733 (vs), 1705 (sh) (m)	1743	21
tert-Butyl	1767 (s), 1742 (vs)	1754	25
Acetamido*	1761 (vs), 1745 (sh) (s)	1753	16
p-Nitrobenzylidene*	1739 (vs), 1724 (vs)	1731	15
Thiophenacetamido* (21)	1745	—	—
Di-*tert*-butyl malonate	1751 (sh) (s,) 1739 (vs)	1745	12
Ethyl cyanoacetate	1754 (vs)	—	—
Ethyl acetate	1748 (vs)	—	—

**Nujol mulls.*

†Only approximate position can be obtained, though the presence of a shoulder can be readily seen.

Can. J. Chem. Downloaded from www.nrcresearchpress.com by 61.7.252.67 on 09/04/12
For personal use only.

TABLE II

EFFECT OF DILUTION ON ESTER CARBONYL FREQUENCIES (CM.$^{-1}$) OF DIETHYL ETHYLMALONATE IN CHLOROFORM

Concn. (mg./cc.)	Cell thickness (in.)	ν (cm.$^{-1}$)	% Absorption
50	0.00194	1742 (sh)	81
		1730	90.5
10	0.00970	1742 (sh)	81
		1730	90.5

TABLE III

ESTER CARBONYL FREQUENCIES OF DIETHYL MALONATE DERIVATIVES IN SOLUTION

Compound	$\nu_{C=O}$ (cm.$^{-1}$)	
	Carbon tetrachloride solution	Chloroform solution
Diethyl malonate[a]		1761 (vs), 1742 (vs), 1706 (sh) (vw)
Diethyl malonate[b]	1757, 1740	1747, 1731
Diethyl ethylmalonate[a]	1760 (vs), 1742 (vs), 1709 (sh) (w)	
Diethyl ethyldeuteromalonate[a]	1760 (vs), 1742 (vs), 1709 (sh) (w)	
Diethyl diethylmalonate[a]	1757 (indistinct sh) (s)†, 1742 (vs) $\Delta\nu_{\frac{1}{2}}$ 50 cm.$^{-1}$	
Diethyl bromomalonate[a]	1776 (s), 1754 (vs), 1712 (sh) (w)	
Diethyl dibromomalonate[a]	1767 (vs), 1751 (s), 1712 (sh) (w)	
Diethyl phenylmalonate[a]	1764 (vs), 1743 (vs), 1727 (sh) (s)	
Diethyl ethylphenylmalonate[a]	1739 (vs), 1730 (sh) (s) $\Delta\nu_{\frac{1}{2}}$ 58 cm.$^{-1}$	
Diethyl *tert*-butylmalonate[a]		1761 (s), 1736 (vs), 1701 (sh) (w)
Tetraethyl ethylenetetracarboxylate[b]	1750, 1739	1750, 1737
Tetraethyl ethanetetracarboxylate[b]	1751, 1742	1746, 1737
Diethyl *iso*propylidenemalonate[b]	1726	1719
Ethyl acetate[b]	1744	1733
Ethyl propionate[b]	1740	1728
Ethyl succinate[b]	1740	1732
Ethyl cyanoacetate[b]	1754	1751

[a]*Solutions containing ca. 25 mg./cc. Cell thickness 0.01 in. Average of three determinations.*

[b]*Values taken from the paper by Felton and Orr (10).*

†*Only approximate position could be obtained, though the presence of a shoulder could be readily seen.*

ethanol. The residual solid was treated with redistilled 99.9% deuterium oxide (5 ml.), the product quickly extracted with AnalaR carbon tetrachloride (previously dried over Na_2SO_4), the extract dried (Na_2SO_4), evaporated to dryness, and distilled in the absence of moisture, giving diethyl ethyldeuteromalonate, b.p. 211–212°, n_D^{23} 1.4167.

Diethyl ethyldeuteromalonate (0.5 g., twice redistilled, b.p. 211–212°) in absolute ethanol containing an excess of sodium ethoxide (solution got warm on mixing) was kept at room temperature overnight, evaporated to dryness, and treated with water

Can. J. Chem. Downloaded from www.nrcresearchpress.com by 61.7.252.67 on 09/04/12
For personal use only.

(5 cc.). Extraction with carbon tetrachloride and working up as above gave only a trace of a high boiling product, which proved to be diethyl diethylmalonate, b.p. 222° (I.R. spectrum identical with that of an authentic specimen but different from that of either diethyl ethylmalonate or diethyl ethyldeuteromalonate).

Infrared Spectra

A Grubb-Parsons double-beam spectrometer, type S4, with a sodium chloride prism, was used. The measurements were carried out at slow chart speeds over the 6 μ range (at faster chart speeds the second band may be difficult to detect or appears only as a poorly defined shoulder) though they were carried out from 2 to 15 μ for some individual compounds. Points of interest other than in the 6 μ region are mentioned in the discussion. The frequency scale was calibrated by ammonia vapor bands (accuracy ± 3 cm.$^{-1}$ in the 6 μ region). Carbon tetrachloride and chloroform were analytical reagent grade, thoroughly dried before use. The measurements were carried out at a slit schedule of 1.5 mm. A variable-path cell was used to study the effect of dilution so that when the concentration of the solution was halved, for example, the cell thickness was doubled. The results are summarized in Tables I, II, and III. The relative intensities of the spectral bands are shown in parentheses, *i.e.* (vs) very strong, (m) medium, (w) weak, (sh) shoulder, (br) broad.

DISCUSSION

Most of the compounds examined exhibit two bands in the 5.6–5.9 μ region, with the notable exception of three of these: diethyl diethylmalonate ($\Delta\nu_{\frac{1}{2}}$ 46 cm.$^{-1}$, liquid film), diethyl ethylphenylmalonate, and diethyl 2,2-*trans*-hydrind-5-enylmalonate. The first two of these do have an indistinct shoulder, the first on the high and the second on the low frequency side of the peak respectively, whereas the third gives a broad band ($\Delta\nu_{\frac{1}{2}}$ 45 cm.$^{-1}$). In agreement with the chemical evidence (3), the presence of double peaks in compounds such as diethyl bis-(2-cyanoethyl)-malonate, diethyl *p*-nitrobenzylidene-malonate, and tetraethyl ethylenetetracarboxylate (10), in which no hydrogen atom is present *alpha* to the carbonyl groups, makes the hypothesis that the double peaks are due to enolization and conjugate chelation untenable. In support of this conclusion is the fact that the replacement of an α-hydrogen by a deuterium atom makes no apparent difference to the positions of the two bands in this region. This is seen particularly well when the spectra of diethyl ethylmalonate (I) and diethyl ethyldeuteromalonate (II) in carbon tetrachloride solutions are compared:

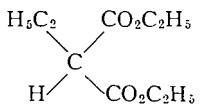

I

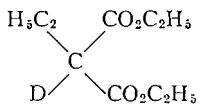

II

If enolization with consequent conjugate chelation had occurred, it would be expected that the positions of these carbonyl peaks would be shifted somewhat, which is not the case:

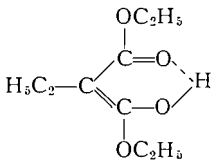

Ia

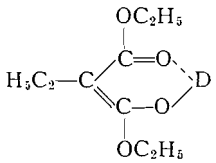

IIa

Can. J. Chem. Downloaded from www.nrcresearchpress.com by 61.7.252.67 on 09/04/12
For personal use only.

Finally, the positions of the two peaks are not in agreement with those expected for chelated and unchelated carbonyl groups (22). On the other hand, some of the malonates which have an α-hydrogen atom do show a weak shoulder at 1700–1712 cm.$^{-1}$ when in solution, whereas those that do not have an α-hydrogen atom (with the exception of diethyl dibromomalonate, which is also abnormal in other respects) do not have this shoulder. This may be evidence of a very small extent of enolization, though other explanations are possible. Gordy (12) attributes a very weak band at 6.12 μ in the spectrum of ethyl malonate to the presence of a very small quantity of enol.

Dilution has no effect on either the position or the intensity of the double peaks (Table II), which means that end-to-end association of molecules, should it exist in the condensed state, is not the cause of the splitting of the C=O band (20). Also, Morris and Young (19) showed that, in a solvent such as chloroform (which was the solvent used in our dilution experiments), their suggested glycidic ester anti-parallel dimers dissociated into single molecules, so that our results indicate the absence also of such an association in the case of malonate esters as the cause of the two carbonyl peaks. It would be interesting to see if the positions and relative intensities of the peaks showed any temperature dependence. There is practically no shift in the positions of the bands on passing from the pure liquid to the solution spectra.

The absence of a second clear-cut peak in the cases of diethyl diethylmalonate and diethyl ethylphenylmalonate does not seem attributable to steric inhibition of vibrational coupling or dipole–dipole interaction between the two carbonyl groups, since when a single large group is present, as in the cases of diethyl *tert*-butylmalonate and diethyl 1-acenaphthylmalonate, as well as in di-*tert*-butylmalonate, the two bands still appear. The positions and the frequency differences between the two bands ($\Delta\nu$ = 11–25 cm.$^{-1}$) do, however, vary with the nature of the α-substituents (the influence of α-substituents is discussed in greater detail below), and a possible explanation is that, in the cases where only a single band or a band and an indistinct shoulder (only approximate position can be obtained) are observed, the two peaks are insufficiently resolved because $\Delta\nu$ is too small. The unusually large band widths at half maximal intensity ($\Delta\nu_{\frac{1}{2}}$) observed support this view.

The variation to a greater or lesser extent of the position of the peaks with the nature of the α-substituent makes it unlikely that resonance coupling of a C=O stretching vibration with an overtone should be the cause of the splitting, though it does not eliminate it as a possibility. Also, the absence of a clear-cut steric effect seems to rule out dipole–dipole interaction as the cause, since this would probably necessitate having the dipoles parallel to each other. A likely explanation for the double peaks seems, on the present evidence, to be symmetric and anti-symmetric coupling of the two C=O stretching vibrations, which would not, presumably, require such restricted steric conditions as would dipole–dipole interaction. Another possible answer, which would also fit in with some of the effects observed with α-halogeno substituents, would be some form of rotational isomerism, e.g. III $\rightleftharpoons$ IV:

III IV

Confirmation (or otherwise) of this possibility might be obtained from an examination

Can. J. Chem. Downloaded from www.nrcresearchpress.com by 61.7.252.67 on 09/04/12
For personal use only.

of the temperature dependence, if any, of the spectra (14). It is hoped to investigate this soon. The vibrational coupling hypothesis would fit in with the positions of the double peaks rather well. Thus, ethyl acetate absorbs at 1748 cm.$^{-1}$, and the introduction of an electron-withdrawing substitutent *alpha* to the carbonyl group raises the C=O stretching frequency by increasing the double-bond character of the carbonyl group. The ester band in ethyl cyanoacetate is at 1754 cm.$^{-1}$ and a similar (though somewhat lesser) effect to that of the cyano group is to be expected by the introduction of an α-ethoxycarbonyl group, as in diethyl malonate, in which the common ester stretching frequency should be *ca.* 1750–1752 cm.$^{-1}$. Splitting of the C=O band precludes the observation of this effect, though two things can be noted: (i) the mean position of the two components (1751 cm.$^{-1}$) is higher than that of the band for ethyl acetate, and (ii) the C=O band is split into two components, one at a frequency higher, and the other at a frequency lower, than the common value expected had no splitting occurred. Such behavior is typical of groups undergoing vibrational coupling (16*a*).

In view of the splitting of the C=O band it is rather difficult to correlate the nature of the α-substituent with its effect on the stretching frequency. It is clearly not justifiable to consider the influence of the substituent on the position of either one of the bands, and the only way is to consider the mean of the two peaks. The use of this frequency in any correlation is of a rather doubtful nature, however, since $\Delta\nu_{C=O}$ varies from one substituent to another and, though vibrational coupling is the most likely explanation of the splitting, other possibilities have not been completely ruled out, as mentioned above. In the case of the monocarboxylic acids and esters, lengthening of the alkyl chain causes a slight fall in the C=O frequency, as in ethyl propionate (1740 cm.$^{-1}$) compared with ethyl acetate (1744 cm.$^{-1}$) (see Table III). This is in line with the electron-repelling character of the methyl group. A similar, though weaker, effect takes place when one of the α-hydrogen atoms in diethyl malonate (1751 cm.$^{-1}$) is replaced by an ethyl group (1750 cm.$^{-1}$), and a still larger fall (in the mean position) occurs when it is replaced by an *n*-propyl group (1745 cm.$^{-1}$). When both α-hydrogen atoms are replaced by ethyl groups the mean frequency falls still further to 1744 cm.$^{-1}$. With a single *n*-butyl substituent the frequency rises slightly to 1747 cm.$^{-1}$ and with a single α-*tert*-butyl substituent it *rises above* the mean value for diethyl malonate, to 1754 cm.$^{-1}$. It appears, therefore, that a steric effect *is* in operation with α-alkyl substituents, and that it acts in opposition to the inductive and hyperconjugative effect of these groups. The nature of this steric effect is not clear (rotational isomerism?), and though it does not inhibit the splitting of the band it seems to raise the mean C=O stretching frequency. (*This, of course, obtains only if the use of the mean of the two frequencies is valid.*) The very slight increase caused by an α-phenyl group (1752 cm.$^{-1}$) could be due either to its –I effect or to its steric effect, and in the ethylphenyl derivative the frequency falls to 1745 cm.$^{-1}$. The –I effect of the α-acetamido group is seen in the increase to 1753 cm.$^{-1}$, whereas the effect of $\alpha\beta$-unsaturation in diethyl *p*-nitrobenzylidenemalonate (1731 cm.$^{-1}$) and in diethyl *iso*-propylidenemalonate (1726 cm.$^{-1}$) is clear. The influence of α-halogens is not straightforward. As is well established, in general, halogenation of the alkyl group *alpha* to a carbonyl raises the C=O frequency, the magnitude of the shift increasing with the increasing dipole moment of the C—X bond (viz. F > Cl > Br > I) (16*b*) (Table IV).

Further, Jones *et al.* (15) showed that while an equatorial bromine atom *alpha* to a keto group in steroidal *cyclo*hexanones causes an increase in the C=O frequency of 13–19 cm.$^{-1}$ by virtue of a Coulombic field effect which outweighs its inductive effect, introduction of a second bromine atom at the same α-carbon atom to form a *gem*-dibromide produces no, or only a slight, further increase, which can be associated with residual

Can. J. Chem. Downloaded from www.nrcresearchpress.com by 61.7.252.67 on 09/04/12
For personal use only.

TABLE IV

Compound	$\nu_{C=O}$ (cm.$^{-1}$)
Acetic acid	1721
Monoiodoacetic acid	1721
Monobromoacetic acid	1730
Monochloroacetic acid	1736

inductive effects (6). Diethyl chloromalonate shows the expected strong increase in frequency (1760 cm.$^{-1}$); in diethyl bromomalonate the increase is still larger (1761 cm.$^{-1}$), which is the reverse of the order expected on the basis of electronegativity (Table IV) (see also Ref. 16*c*). Furthermore, the introduction of a second bromine atom to give diethyl dibromomalonate *lowers* the frequency to 1758 cm.$^{-1}$. It seems likely that the governing factor which produces the first increase is connected with the size of the halogen atom (Br > Cl) and that the second bromine introduced interferes sterically or otherwise with the first bromine–carbonyl interaction. It may be worth noting in this connection that the ratio of the intensities of the two carbonyl peaks is reversed on passing from the monochloro- and monobromo-malonates, to the dibromo-malonate.

The spectrum of diethyl ethyldeuteromalonate was interesting in that no C—D stretching band could be detected. This is not altogether surprising, for two reasons: (i) in most aliphatic hydrocarbons no peak attributable to the stretching vibration of a tertiary C—H bond can be discerned (16*d*), especially in this case, where only one such group exists in the molecule so that its contribution to the integrated absorption intensity on the basis of Francis' equation (11) would be very small; (ii) the force constant of the α-tertiary C—H bond in malonates would be expected to be rather weak and the band would, therefore, be shifted towards the long wave-length region. It may be possible that the additional shift in the same direction caused by substituting deuterium for hydrogen would move the band close to the carbonyl region, where it could not be detected. The presence of the C—D linkage in this compound is readily detected in the 'bending' region of the spectrum, and by a comparison of the spectrum with those of diethyl ethylmalonate and diethyl diethylmalonate over this range. In Table V the abbreviations h = high, l = low, and e = approx. equal intensities have been used to compare very roughly the relative intensities of corresponding peaks in the three compounds.

Some of the peaks present in diethyl ethylmalonate are shifted to lower frequencies

TABLE V

SPECTRA OF LIQUID FILMS OF DIETHYL MALONATE DERIVATIVES

Ethyl (cm.$^{-1}$)	Ethyldeutero (cm.$^{-1}$)	Diethyl (cm.$^{-1}$)
1339 (h)	1339 (l)	1339 (l)
1259 (l)	1259 (h)	—
1235 (l)	1238 (h)	1239 (h)
1209 (e)	1209 (sh)(e)	1209 (e)
1181 (h)	1174 (l)	1174 (sh)(l)
1156 (e)	1142 (e)	1151 (e)
1117 (l)	1125 (h)	1125 (h)
1098 (l)	—	1098 (l)
1093 (sh)	—	—
—	1075	—
1049	—	—
—	1036	—
1026 (e)	1032 (sh)(e)	1024 (e)

Can. J. Chem. Downloaded from www.nrcresearchpress.com by 61.7.252.67 on 09/04/12
For personal use only.

in the deutero compound and the ratio of intensities of some peaks is altered considerably. The spectrum of the deutero compound falls in very nicely as a mixture of parts of the ethyl and parts of the diethyl spectra, as expected.

An interesting reaction was observed when diethyl ethyldeuteromalonate was treated with sodium ethoxide in absolute ethanol (slight heat evolved), kept overnight, and the mixture taken to dryness and treated with water. Instead of the expected diethyl ethylmalonate there was obtained a very small amount of diethyl diethylmalonate, identical in boiling point and infrared spectrum with an authentic specimen. In view of the repeated purifications to which the diethyl ethyldeuteromalonate was subjected, it is unlikely that any diethyl compound was present in it before the sodium ethoxide treatment. The reaction probably involves a disproportionation, as *no* diethyl ethylmalonate was isolated from the product. That the ethyl group should have come from the sodium ethoxide or the alcohol used seems unlikely.

ACKNOWLEDGMENTS

The author wishes to thank Dr. R. N. Jones for a valuable discussion. This work was carried out during the tenure of an I.C.I. Research Fellowship in the University of London.

REFERENCES

1. ABRAMOVITCH, R. A. J. Chem. Soc. 1413 (1957).
2. ABRAMOVITCH, R. A. Forthcoming publication.
3. (*a*) ARNDT, F., LOEWE, L., and GINKÖK, R. Rev. fac. sci. univ. Istanbul, A, **11**, 147 (1946); Chem. Abstr. **41**, 3761 (1947).
   (*b*) EISTERT, B. and REISS, W. Chem. Ber. **87**, 92 (1954).
   (*c*) MEYER, K. H. Ber. **45**, 2864 (1912).
4. BACKER, H. J. and HOMAN, J. D. H. Rec. trav. chim. Belg. **58**, 1054 (1939).
5. BELLAMY, L. J. The infrared spectra of complex molecules. Methuen & Co., Ltd., London. 1954. p. 157.
6. BELLAMY, L. J., THOMAS, L. C., and WILLIAMS, R. L. J. Chem. Soc. 3704 (1956).
7. BENDER, M. L. and FIGUERAS, J. J. Am. Chem. Soc. **75**, 6304 (1953).
8. BRUSON, H. A. and RIENER, T. W. J. Am. Chem. Soc. **65**, 23 (1943).
9. DAVISON, W. H. T. J. Chem. Soc. 2456 (1951).
10. FELTON, D. G. I. and ORR, S. F. D. J. Chem. Soc. 2170 (1955).
11. FRANCIS, S. A. J. Chem. Phys. **18**, 861 (1951).
12. GORDY, W. J. Chem. Phys. **8**, 516 (1940).
13. GRYSZKIEWICZ-TROCHIMOWSKI, E. and GRYSZKIEWICZ-TROCHIMOWSKI, O. Bull. soc. chim. France, **18**, 269 (1951).
14. JONES, R. N., FORBES, W. F., and MUELLER, W. A. Can. J. Chem. **35**, 504 (1957).
15. JONES, R. N., RAMSAY, D. W., HERLING, F., and DOBRINER, K. J. Am. Chem. Soc. **74**, 2828 (1952).
16. JONES, R. N. and SANDORFY, C. Technique of organic chemistry. Vol. IX. Chemical applications of spectroscopy. Interscience Publishers, Inc., London. 1956. (*a*) p. 495, (*b*) p. 474, (*c*) p. 478, (*d*) p. 340.
17. KNOEVENAGEL, E. Ber. **31**, 2593 (1898).
18. KOHLRAUSCH, K. W. F. and SABATHY, R. Monatsh. **72**, 303 (1939).
19. MORRIS, H. H. and YOUNG, R. H. J. Am. Chem. Soc. **79**, 3408 (1957).
20. PARTINGTON, J. R. An advanced treatise on physical chemistry. Vol. V. Longmans, Green and Co., Ltd., London. 1954. p. 384.
21. RANDALL, H. M., FOWLER, R. G., FUSON, N., and DANGL, J. R. Infrared determination of organic structures. D. Van Nostrand Company, Inc., New York. 1949. p. 111.
22. RASMUSSEN, R. S., TUNNICLIFF, D. D., and BRATTAIN, R. R. J. Am. Chem. Soc. **71**, 1068 (1949).
23. THOMPSON, H. W. J. Chem. Soc. 328 (1948).
24. THOMPSON, H. W. and TORKINGTON, P. J. Chem. Soc. 640 (1945).

Can. J. Chem. Downloaded from www.nrcresearchpress.com by 61.7.252.67 on 09/04/12
For personal use only.

Can. J. Chem. Downloaded from www.nrcresearchpress.com by 61.7.252.67 on 09/04/12
For personal use only.

HYDROGEN ABSTRACTION REACTIONS OF DIPHENYLPICRYLHYDRAZYL[1]

A. G. Brook, R. J. Anderson, and J. Tissot Van Patot

ABSTRACT

The stable free radical diphenylpicrylhydrazyl (DPP·) has been found to react quantitatively with ammonia and hydrazine forming nitrogen and diphenylpicrylhydrazine, and less cleanly with hydroxylamine forming diphenylpicrylhydrazine and nitrous oxide. The reactions of DPP· with a variety of amines are not clean, in part owing to the formation of complexes of the amines with the reaction product diphenylpicrylhydrazine. Preliminary investigations of the reactions of DPP· with mercaptans have shown that these otherwise clean reactions have a variable stoichiometry, dependent on the concentration and other reaction conditions.

The stable free radical diphenylpicrylhydrazyl (DPP·), while not in general a powerful dehydrogenating agent, nevertheless shows considerable facility in removing hydrogen atoms attached to a nitrogen atom in a variety of compounds (3). In order to study this behavior further we have investigated the reactions of DPP· with a number of simple compounds having N—H bonds, and also with some mercaptans.

The ability of the radical to abstract hydrogen atoms from nitrogen is evidently a general reaction but a marked variation in the "cleanliness" of the reactions was noted. It was found that DPP· quantitatively converted both ammonia and hydrazine to nitrogen, being itself reduced to diphenylpicrylhydrazine (DPPH), according to the following equations:

$$3\text{DPP}\cdot + \text{NH}_3 \rightarrow 3\text{DPPH} + \tfrac{1}{2}\text{N}_2$$

$$4\text{DPP}\cdot + \text{N}_2\text{H}_4 \rightarrow 4\text{DPPH} + \text{N}_2$$

These reactions occurred relatively rapidly at room temperature and could be followed by collection of the gas evolved, and also by observing the disappearance of the characteristic intense purple color of the radical. The DPPH formed could be isolated practically quantitatively. Typical results are summarized in Table I. Attempts to partially dehydrogenate ammonia to give hydrazine failed, and the volume of gas collected indicated that complete oxidation of one-third of the ammonia occurred.

TABLE I

Reaction of diphenylpicrylhydrazyl with hydrazine and ammonia

Run	DPP·, mM.	H donor, mM.	Solvent	N_2, mM.	% N_2	% DPPH[a]
1	0.80	N_2H_4, 0.20	$CHCl_3$	0.199	99[b]	99.5
2	0.40	N_2H_4, 0.40	$CHCl_3$	0.098	98[c]	99
3	1.20	N_2H_4, 0.20	$CHCl_3$	0.197	98.5[b]	[d]
4	2.74	NH_3, 0.913	GMME[e]	0.453	99.2[c]	98
5	1.81	NH_3, 0.457	GMME[e]	0.448	98[b]	[d]
6	1.37	NH_3, 0.457	GMME[e]	0.448	98[b]	99

[a] *Yield of* DPPH *is the % of* DPP· *recovered as* DPPH *in all cases.*
[b] *Yield based on hydrogen donor.*
[c] *Yield based on diphenylpicrylhydrazyl.*
[d] *Product was a mixture of* DPP· *and* DPPH.
[e] GMME = *ethylene glycol monomethyl ether.*

[1] *Manuscript received July 2, 1957.*
Contribution from the Department of Chemistry, University of Toronto, Toronto, Ontario.

DPP· also reacts rapidly with hydroxylamine but the reaction is not as clean as those above, nor is the stoichiometry as clearly defined. Dilute solutions of the reagents can be "titrated" against one another to a clear orange-brown end point formed as the purple color of the radical disappears. From such experiments the molar ratio of DPP· to hydroxylamine was found to lie between 2.88 and 2.98. From larger runs in more concentrated solutions, carried out to afford reasonable quantities of reduction products and gas for examination, the molar ratio varied from 2.5 to 3.1. The major reduction product again was DPPH, isolated in 89% yield, and the gas was shown by its infrared absorption spectrum to be nitrous oxide. The most reasonable equation representing these data is as follows:

$$6\text{DPP}\cdot + 2\text{NH}_2\text{OH} \rightarrow 5\text{DPPH} + \text{N}_2\text{O} + \text{DPPOH?}$$

However, no product corresponding to 1-hydroxy-1-picryl-2,2-diphenylhydrazine (DPPOH), a known compound (6), was detected although small amounts of other products were isolated by chromatography of the reaction mixture. Since the ratio of DPP· to hydroxylamine and the amount of gas evolved in most cases corresponded fairly well to that predicted by the above equation it seems probable either that any DPPOH formed decomposed during the working up of the reaction or that other reactions are also occurring to a small extent. In support of this reasoning is the fact that more DPP· was converted to DPPH (89%) than is predicted by the equation (83%). These results are listed in Table II.

TABLE II

REACTION OF DIPHENYLPICRYLHYDRAZYL WITH HYDROXYLAMINE AND METHYLAMINE

Run	DPP·, mM.	H donor, mM.	Gas, mM.	Molar ratios DPP/donor	Molar ratios DPP/gas	Products
7	6.34[a]	NH_2OH,[b] 2.31	1.09	2.75	5.8	DPPH, N_2O
8	6.34[a]	NH_2OH,[b] 2.58	1.16	2.46	5.47	DPPH (89%), N_2O
9	6.34[a]	NH_2OH,[b] 2.26	0.65	2.81	9.7	DPPH, N_2O
10	6.34[a]	$MeNH_2$,[a] 3.40	0.607	1.86	10.4	DPPH, N_2?
11	12.7[a]	$MeNH_2$,[a] 6.24	1.02	2.04	12.4	DPPH (50%), N_2?
12	6.34[c]	$MeNH_2$,[c] 3.19	0.36	1.99	17.6	DPPH (46%), N_2?
13	6.34[c]	$MeNH_2$,[c] 3.28	0.30	1.93	20.8	DPPH, N_2?

[a]*Solvent was chloroform.*
[b]*Solvent was methanol.*
[c]*Solvent was benzene.*

DPP· also reacts with a variety of amines but the nature of the reaction is not clear. Titration of very dilute (0.0005 *M*) solutions of the radical and methylamine to an orange end point indicates a molar ratio of radical to amine of 2.0, and the same ratio seems to hold for isopropylamine and *n*-butylamine also. Of the amines investigated only methylamine evolves significant quantities of gas, which by the absence of any characteristic infrared spectrum appears to be nitrogen. However the volume of gas evolved varied markedly with the solvent (see Table II).

From relatively large scale runs in concentrated chloroform solution the main reduction product isolated from all the amines investigated was DPPH, in amounts corresponding to 50–75% of the DPP· originally present. The remaining products were either intractable tars or amorphous solids which had variable and wide melting point ranges which recrystallization failed to improve. All that can be definitely stated about the

Can. J. Chem. Downloaded from www.nrcresearchpress.com by 61.7.252.67 on 09/04/12
For personal use only.

reactions of the radical with these primary amines is that one of the amino hydrogens is readily abstracted by DPP· and that the resulting radical then apparently reacts in a variety of ways, in part with a second equivalent of DPP· and perhaps also with the solvent.

We also investigated to some extent the reaction between DPP· and diethylamine but the stoichiometry of the reaction could not be definitely extablished. In non-polar solvents the reactions were extremely slow while in polar solvents the reaction mixture became a muddy brown-black color as the reaction proceeded instead of the typical clear orange-brown color. Work-up of these reaction mixtures yielded as major products DPPH and a black solid which at about 115°–120° turned red and then melted at 172° as if it were pure diphenylpicrylhydrazine. It was shown that this latter material was a 1:1 complex of diphenylpicrylhydrazine and diethylamine.

The reactions of the radical with amines were much slower than those with the other reagents previously described. This led to the interesting observation that the rates of reduction of DPP· were much more rapid in polar solvents such as methanol or ethanol than in non-polar solvents such as benzene or chloroform, and furthermore, that in the polar solvents the final reaction mixtures were usually an opaque muddy brown color while in the non-polar solvents the reaction mixtures were a clear orange or orange-brown color. It was found that the intensity of this muddy brown color could be markedly changed by dilution, especially with a non-polar solvent, so that the system became clear orange-brown, or that this color could be turned to muddy brown by the addition of more amine solution. These observations are explained if a complex is formed between diphenylpicrylhydrazine and the amine which can dissociate into its components depending on the polarity of the medium and the concentration of the solution.

$$\mathrm{DPPH} + \mathrm{R_2NH} \rightleftarrows \mathrm{DPPH.R_2NH}$$

Such a complex was actually isolated in the case of diethylamine. It is obvious that such complex formation will completely confuse any stoichiometric determinations which may depend on the color of end points.

That the rate of a homopolar reaction should be dependent on the polarity of the medium is not unreasonable, since in these reactions the most probable means for transfer of a hydrogen atom from donor to acceptor is through formation of a complex between the amine and stable free radical (3). Such complexes involving the picryl group of DPP· would be expected to be more readily formed and to be more stable in polar solvents, as are the well-known complexes of amines with polynitroaromatic compounds (8). If hydrogen transfer depends on the formation of such complexes, it is not surprising that dehydrogenation occurs more rapidly in a medium favorable to their formation. Nor is it surprising that DPPH forms similar complexes in polar solvents.

We have also investigated briefly the reactions of DPP· with thiophenol and butyl mercaptan. These reagents react rapidly with the radical but, unlike in the other reactions studied, the molar ratio of DPP· to mercaptan varied markedly, being dependent on the concentration of the solutions and their order of addition. This was particularly noticeable with thiophenol, for in very dilute solution, when the radical was added to the thiophenol, the mole ratio was approximately 1.0 but in concentrated solution with the reverse order of addition the mole ratio was between 1.9 and 2.0. With butyl mercaptan there appeared to be less dependence on the order of addition and the mole ratio varied from 1.0 to 1.15 over a range of concentrations. These results can be explained by assuming the following reactions to be occurring:

Can. J. Chem. Downloaded from www.nrcresearchpress.com by 61.7.252.67 on 09/04/12
For personal use only.

(*a*) DPP· + RSH → DPPH + RS·

(*b*) 2RS· → RSSR

(*c*) DPP· + RS· → DPPSR

The over-all stoichiometric ratio of the reaction depends on the relative importance of reactions (*b*) and (*c*), which depend strongly on concentration and on the various species present in the reaction mixture. In dilute solution, where DPP· is added to thiophenol, reaction (*b*) evidently occurs almost to the exclusion of (*c*), but in concentrated solution, where RS· radicals are being formed in the presence of DPP·, coupling of the unlike radicals occurs (reaction *c*) almost exclusively. When the reactions were worked up it was found that a mixture of compounds was obtained from which DPPH could be separated by chromatography and recrystallization. No success was achieved in isolating the thio derivative DPPSR.

With butyl mercaptan reaction (*c*) was evidently slower than (*b*), since the molar ratio varied over a much smaller range and appeared to be less dependent on the concentration of the reagents or the order of addition. In accord with this, relatively high yields (75%) of DPPH were isolated from the reactions. The kinetics of this reaction, in excess butyl mercaptan, have been reported (7).

It is obviously impossible to speculate at this stage as to the nature of the intermediate radicals produced during the dehydrogenation of hydrazine, ammonia, or hydroxylamine, but it is apparent from the last two cases that dimerization occurs at some stage. It is hoped that further insight into these reactions may be gained by kinetic studies on some of the simpler systems. It is obviously desirable to work with these relatively clean systems, since much of the work reported here is disappointing because of the difficulties found in isolating crystalline products in good yield, thus leaving the conclusions as to the processes occurring in many of the reactions rather speculative.

EXPERIMENTAL

All yields of diphenylpicrylhydrazine (DPPH) are based on the moles of diphenylpicrylhydrazyl (DPP·) reduced.

Materials

DPP· was prepared according to the method of Goldschmidt and Renn (4) as modified by Poirier *et al.* (6). The purple solid was dried *in vacuo* for several hours at 80° to remove the complexed chloroform (5). Anhydrous hydrazine (1) and anhydrous hydroxylamine (2) were prepared by published procedures. All solvents were purified and the liquid amines were distilled. Methylamine solutions were usually prepared by treating a mixture of the appropriate organic solvent and 30% aqueous methylamine solution with sodium hydroxide pellets to remove the bulk of the water. The supernatant liquid was decanted and dried over anhydrous sodium sulphate and then standardized against standard acid using methyl orange indicator. In some cases methylamine was prepared by liberating the amine from methylamine hydrochloride with alkali. Tank ammonia was used. All solutions were freshly prepared and frequently standardized.

Bulk Reactions of DPP·

A. Hydrazine

To 25 ml. of methanol containing 0.00125 mole of hydrazine was added 1.97 g. (0.0050 mole) of DPP· in 25 ml. of chloroform. The violet color of the radical disappeared as the solution successively became violet-red, amber, and finally orange-brown over a

Can. J. Chem. Downloaded from www.nrcresearchpress.com by 61.7.252.67 on 09/04/12
For personal use only.

period of about 1 hour. Evaporation of the solution to dryness gave 1.97 g. (100%) of DPPH, m.p. 171°–172° (dec.), identified by mixed melting point with an authentic specimen. Recrystallization from 1:2 chloroform–ethanol failed to raise the melting point. If more than 4 equivalents of DPP· were added the solution remained purple and unchanged free radical could be recovered.

B. Ammonia

To 25 ml. of methanol containing 0.0013 mole of ammonia was added 1.54 g. (0.0039 mole) of DPP· in 25 ml. of chloroform. After 1 hour the solution was orange-brown and 1.54 g. (100%) of red DPPH, m.p. 171°–172° (dec.), was isolated.

C. Hydroxylamine

To 5.0 g. (0.00634 mole) of DPP· in 35 ml. of chloroform was added in 0.2 ml. aliquots a total of 5.7 ml. (0.00412 mole) of a 0.723 *M* solution of hydroxylamine in methanol. The reaction mixture was stirred magnetically and the reaction vessel was connected to a mercury-filled gas burette so that any gas evolved could be collected and measured. Gas was steadily evolved and the color changed from purple to orange-brown regularly until about 5.5 or 5.7 ml. of hydroxylamine solution had been added. No significant changes on further additions of hydroxylamine occurred. Toward the end of the addition a red solid precipitated from the reaction mixture. About 20 ml. of gas was evolved, which was shown by its infrared absorption spectrum to be nitrous oxide. This spectrum also contained absorption bands due to chloroform vapor so that a comparison was made with a gas sample made up of chloroform vapor and authentic nitrous oxide, which proved to be identical in every respect. The precipitate was filtered off and shown to be 2.52 g. (50.5%) of DPPH, m.p. 171°–172° (dec.). The filtrate was placed on a 3×25 cm. chromatography column of activated alumina and was eluted with several hundred milliliters of chloroform. Evaporation of this eluate to dryness followed by recrystallization from chloroform–ethanol gave an additional 1.96 g. (39.2%, total 89.7%) of DPPH, m.p. 171°–172° (dec.). A black band remained on the column which was eluted with ethanol to give an intense red colored solution. On evaporation to dryness this yielded 0.24 g. of a green-black solid which appeared to decompose at about 88° and which frothed at 120°. It was insoluble in dry benzene or chloroform but was soluble to give an intensely red solution in ethanol or ethyl acetate. It could not be recrystallized from these solvents or solvent pairs, since only gums were formed.

D. Methylamine

To 3.5 g. (0.0089 mole) of DPP· in 25 ml. of chloroform was added an excess (0.0087 mole) of methylamine in 5 ml. of chloroform. The color of the solution changed very slowly over 1–1.5 hours until it became orange-brown. About 25 ml. of gas was evolved. The infrared spectra showed absorption characteristic only of chloroform and methylamine vapors, as shown by comparison of a spectrum made up of these two substances; hence it seems likely that the major part of the evolved gas was nitrogen. To guard against the possibility that the excess of methylamine was responsible for the gas evolved, other runs with a deficiency of methylamine were made. Spectra of the gas evolved in these runs showed only the presence of chloroform and a trace of methylamine, neither of which would account for the volume of gas evolved.

The filtrate from this run was chromatographed on alumina and eluted with chloroform. A total of 2.24 g. (64%) of DPPH, m.p. 171°–172° (dec.), was isolated together with small traces of intractable gums and amorphous solids which could not be purified by crystallization.

Can. J. Chem. Downloaded from www.nrcresearchpress.com by 61.7.252.67 on 09/04/12
For personal use only.

Can. J. Chem. Downloaded from www.nrcresearchpress.com by 61.7.252.67 on 09/04/12
For personal use only.

E. n-Butylamine and Isopropylamine

When 14.2 g. (0.036 mole) of DPP· in 100 ml. of ethanol was treated with 1.85 g. (0.025 mole) of *n*-butylamine the color changed from purple to a muddy brown-black color over a period of 1 hour. Only a trace (1–2 ml.) of gas was evolved. A black precipitate weighing 7.75 g. (55%) of crude DPPH, m.p. 164°–172° (dec.), was filtered off and recrystallized from ethanol–chloroform to yield 6.5 g. (46%) of pure DPPH, m.p. 170°–172° (dec.). The filtrate from the original precipitate was evaporated to dryness, dissolved in chloroform, and chromatographed on alumina to yield an additional 0.9 g. (6%) of DPPH, m.p. 170°–172° (dec.), 0.42 g. of a dark solid, m.p. 205°–207° (dec.), which decomposed on attempted recrystallization from chloroform, and some tars which could not be induced to crystallize.

To 39.4 g. (0.1 mole) of DPP· in 300 ml. of diethyl ether was added 2.95 g. (0.05 mole) of isopropylamine. Over a period of several days the reaction mixture became brown. The suspension was filtered and 31.1 g. of solid was collected. Concentration of the filtrate yielded an additional 2.65 g. of solid. Aliquots of this 33.75 g. of solid were chromatographed on alumina. Elution with benzene of a 5-g. sample led to the isolation of 4.15 g. (83% of sample, 71% yield) of DPPH, m.p. 171°–172° (dec.), whose color was red-brown rather than the characteristic red. Elution with ethanol yielded a second fraction, 0.25 g. of brown-black amorphous material which melted at 184°–200° (dec.). Recrystallization from ethanol–petroleum (b.p. 90°–100°) failed to improve the melting range.

F. Diethylamine

To 0.5 g. (0.00126 mole) of DPP· in 25 ml. of 95% ethanol was added 0.00069 mole of diethylamine in 5 ml. of ethanol. The solution turned brown over 24 hours and a reddish brown after 48 hours. Red crystals were slowly deposited over 4 weeks and were filtered to yield 0.27 g. (54%) of DPPH, m.p. 171°–172° (dec.), identified by mixed melting point. The filtrate was evaporated to dryness and the resulting red-brown gum was redissolved in benzene and chromatographed on alumina. Two fractions were obtained, one of which was 0.04 g. (8%) of crude DPPH, m.p. 154°–170° (dec.), and the second, 0.02 g., melted at 77°–115° (dec.).

Alternatively, 5.00 g. (0.0127 mole) of solid DPP· was treated with about 10 ml. of diethylamine, the excess amine acting as solvent. There was immediate effervescence, the mixture became warm, and the suspension turned brown. After 1 hour 50 ml. of chloroform was added to dissolve the solid which was present. The solution was concentrated and cooled and a total of 0.58 g. (11%) of black crystalline solid was filtered off. This material started to change color at 90° and by 115° was bright red. It finally melted at 171°–172° (dec.), and a mixed melting point with DPPH was not depressed. This material was identical in behavior to the 1:1 complex of DPPH and diethylamine described below.

The remainder of the filtrate was evaporated to dryness under reduced pressure to yield a red gum. Chromatography on alumina yielded 2.0 g. (40%) of DPPH, m.p. 170°–172° (dec.).

Preparation and Identification of DPPH–Diethylamine Complex

To a red solution of 1.00 g. (0.00252 mole) of DPPH in 70 ml. of acetone was added 10 ml. (0.10 mole) of diethylamine. To this dark opaque solution was added 800–900 ml. of water and after it was cooled to 4° for 16 hours, 0.71 g. (61%) of black crystals was filtered off. This material began to change to red at 100° and by 120° was completely bright red. It then melted at 170°–172° (dec.). This material was similar in all respects

Can. J. Chem. Downloaded from www.nrcresearchpress.com by 61.7.252.67 on 09/04/12
For personal use only.

to that described above and a mixed melting point was not depressed. This material is the 1:1 complex of DPPH and diethylamine as shown below.

A 0.40-g. (0.00085 mole) sample of the black complex was heated at 120°–140° for 20 minutes while air was passed over the solid and then bubbled into a known amount of standard acid. The acid was then back-titrated with base, which showed that 0.00084 mole of diethylamine had been collected. The residue, which was a light red solid, weighed 0.33 g. (0.00084 mole) and was shown to be DPPH, m.p. 170°–172° (dec.), by its melting point which was not depressed when admixed with authentic DPPH. Thus the black solid is a 1:1 complex of DPPH and diethylamine, and the diethylamine was recovered in 99% yield. A second experiment gave identical results.

When a small sample of the black complex was dissolved in a few milliliters of chloroform an opaque brown solution was obtained. On dilution, the solution gradually became a clear orange-brown color characteristic of solutions of DPPH. Addition of more diethylamine converted the color back to the opaque brown color. Similarly if the opaque brown solution was shaken with concentrated hydrochloric acid, the solution became a clear orange-brown or red color, depending on the concentration.

When solutions of the complex of approximately the same concentration were made up in ethanol, acetone, and chloroform, the more polar solvents produced darker, browner solutions. Addition of a polar solvent, e.g. ethanol, to the chloroform solution produced an even darker solution, indicating that the opaque brown color was intimately associated with the polar medium.

Titration Experiments with DPP·

A. With Hydroxylamine

Dilute standard solutions of DPP· and hydroxylamine (0.002–0.005 *M*) in benzene or in ethylene glycol monomethyl ether were prepared. Known volumes of the hydroxylamine solution were titrated with the DPP· solution to an end point where a permanent pale purple color persisted. Several runs gave the following values for the molar ratio of DPP· to hydroxylamine: 2.97, 2.88, 2.98, 2.96. Evaporation of these solutions to dryness gave impure material melting at 145–170° (dec.).

B. Methylamine

Similar experiments to those described above carried out in ethanol solution gave the following values for the molar ratio of DPP· to methylamine: 1.91, 2.05, 2.07, 1.97.

C. Thiophenol

To 0.75 g. (0.0019 mole) of DPP· in 10 ml. of chloroform was added slowly a 0.374 *M* solution of thiophenol in ethanol. The color changed rapidly from purple to opaque brown to clear red-brown during the addition of 2.6 ml. (0.00097 mole) (mole ratio 2:1) of the thiophenol solution. Evaporation to dryness and recrystallization from 1:3 chloroform–ethanol yielded 0.30 g. of orange-red solid which appeared to be identical in all respects to DPPH except that the material melted at 132–134° with decomposition. A similar behavior has been previously described (7). Recrystallization failed to improve the melting point markedly. The material was chromatographed on alumina, and elution with benzene and then 1:1 benzene–chloroform yielded the following fractions, with their respective melting points: (1) 0.09 g. (12%), 172–173° (dec.), identified as DPPH by mixed melting point; (2) 0.05 g., 160–164° (dec.); (3) 0.03 g., 150–153° (dec.); (4) 0.05 g., 131–139° (dec.). Recrystallization failed to improve the melting points of the impure fractions.

When an identical run to that above was carried out except that the DPP· was dis-

solved in 100 ml. of chloroform and 50 ml. of ethanol, and the thiophenol solution was diluted 20-fold, 72 ml. (0.00133 mole) of thiophenol (mole ratio 1.43:1) was required to produce a clear orange-brown end point. The products isolated were similar to those described above, and DPPH was obtained in 14% yield.

When approximately 0.01 *M* solutions of the reagents were titrated against one another the mole ratios of radical to mercaptan were 1.09–1.16 when thiophenol was added to DPP·, and 1.00 when the DPP· was added to the thiophenol solution.

D. Butyl Mercaptan

To 0.20 g. (0.0005 mole) of DPP· in 25 ml. of chloroform was added 0.00061 mole of butyl mercaptan in 25 ml. of ethanol. The color changed from purple through opaque red-brown to clear orange-red over a few seconds. The solution was concentrated to yield, after recrystallization, 0.15 g. (75%) of DPPH, m.p. 169–172° (dec.), identified by mixed melting point.

When dilute (0.02 *M*) solutions of DPP· and butyl mercaptan were titrated against one another as described above the moles of radical per mole of mercaptan varied between 1.0 and 1.15, depending on the concentration, but the ratio did not seem to depend on the order of addition of the reagents.

Gas Evolution Experiments

In experiments in which gas evolution was quantitatively determined, the 50 ml. reaction vessel, equipped with magnetic stirrer and maintained at constant temperature by a water bath, was connected by capillary tubing to a 50-ml. burette filled with mercury which was attached to a mercury levelling bulb. The general procedure was as follows. In experiments in which it was established that nitrogen was evolved, all solutions were presaturated with nitrogen. The DPP· dissolved in the major portion of the solvent (concentration approximately 10 ml. per g.) was placed in the reaction flask, the system was closed off, and the solution was stirred and allowed to reach equilibrium. Then the hydrogen donor solution (sufficiently concentrated that the volume added was not more than 20% of the total volume of the system) was admitted from a 5-cc. burette which was attached to the reaction vessel through a ground-glass joint. The mercury levelling bulb was continually adjusted to maintain atmospheric pressure in the reaction flask.

The hydrogen donor solutions were added in arbitrary amounts in the cases of hydrazine and ammonia, after which the volume of gas evolved was measured, or else the hydrogen donor solution was added dropwise until a clear orange-brown end point was obtained, and significant changes in the volume of gas evolved ceased.

Tables I and II summarize the results obtained from a variety of hydrogen donors.

REFERENCES

1. Audrieth, L. F. and Ogg, B. A. The chemistry of hydrazine. John Wiley & Sons, Inc., New York, N.Y. 1951. p. 48.
2. Booth, H. S. Inorganic syntheses. Vol. I. McGraw-Hill Book Company Inc., New York, N.Y. 1939. p. 87.
3. Braude, E. A., Brook, A. G., and Linstead, R. P. J. Chem. Soc. 3574 (1954).
4. Goldschmidt, S. and Renn, K. Ber. **55**, 628 (1922).
5. Lyons, J. A. and Watson, W. F. J. Polymer. Sci. **18**, 141 (1955).
6. Poirier, R. H., Kahler, E. J., and Bennington, F. J. Org. Chem. **17**, 1437 (1952).
7. Russell, K. E. J. Phys. Chem. **58**, 437 (1954).
8. Weiss, J. J. Chem. Soc. 245 (1942).

Can. J. Chem. Downloaded from www.nrcresearchpress.com by 61.7.252.67 on 09/04/12
For personal use only.

Can. J. Chem. Downloaded from www.nrcresearchpress.com by 61.7.252.67 on 09/04/12
For personal use only.

EXCHANGE BETWEEN THALLOUS AND THALLIC IONS IN THE PRESENCE OF SULPHATE ION[1]

D. R. WILES

ABSTRACT

The rates of the exchange reaction between thallous and thallic ions have been measured as a function of sulphate ion concentration, at constant acidity. At high sulphate concentrations, the results agree with those of Brubaker and Mickel, indicating second- and higher-order dependence of the rate on sulphate ion concentration. At low sulphate concentrations, pure first-order dependence on sulphate is found. The inhibitive effect found in some systems is absent. A bridge-transfer mechanism is suggested.

INTRODUCTION

The exchange between thallous and thallic ions in aqueous solution has been studied during the past several years by a number of workers, under a variety of conditions (1, 2, 3, 4, 5). It has generally been found that any change in the nature or number of ligands attached to one or other of the exchanging ions has a distinct effect on the rate of the exchange reaction. This effect amounts, in the case of most of the anionic ligands studied (e.g. hydroxyl, nitrate), to a positive catalysis of the reaction. In other cases (e.g. chloride and cyanide) the exchange rate is markedly decreased at low concentrations of the anion and very greatly increased at higher concentrations.

The present work is an investigation of the nature of the kinetics of the thallous–thallic exchange in perchloric acid solutions containing varying small concentrations of sulphate ion. This work is complementary to that of Brubaker and Mickel (1), who have reported recently on this exchange in somewhat stronger sulphate solutions.

EXPERIMENTAL

Thallous perchlorate was crystallized from a solution of reagent grade thallous nitrate to which had been added a considerable excess of perchloric acid. Crystallization was repeated once from strong perchloric acid, and once from water. Ferric ion was added to the solution of these crystals, and precipitated as hydroxide with ammonia. The thallous perchlorate was twice more crystallized from water, dried for 1 hour at 105°, and dissolved in water to make a stock solution 0.100 molar in thallous ion. This solution showed no darkening on neutralization, which indicated negligible contamination by thallic ion.

The thallic perchlorate solution was prepared from reagent grade thallic oxide which had, in turn, been purified of thallous ion by repeated precipitation with ammonia and redissolution in excess perchloric acid. The purified thallic oxide was dissolved in an excess of perchloric acid, to make a stock solution 0.100 molar in thallic ion, and 4.7 molar in excess acid. Radioactive Tl^{204} in the form of a solution of thallic nitrate was added at an early stage in the purification. Failure to show turbidity on addition of iodide to an aliquot of this stock solution set the limiting concentration of thallous ion at $\ll$0.004 molar, i.e. $\ll$4%. In both these preparations, heating of solutions was kept to a low minimum because of the danger that some chloride ion might be formed as a decomposition product of perchloric acid. Analysis of the solutions was done by precipitation of thallous chromate, which was dried and weighed as such. All other reagents were reagent grade, and were used with no further purification.

[1]*Manuscript received September 23, 1957.*
Contribution from the Department of Mining and Metallurgy, University of British Columbia, Vancouver, B.C. Paper presented at the Annual Conference of the Chemical Institute of Canada, June, 1957.

Can. J. Chem. Downloaded from www.nrcresearchpress.com by 61.7.252.67 on 09/04/12
For personal use only.

Exchange measurements were done by using the radioactive tracer as thallium(III) and observing its appearance in the thallous state. Separation of the thallous ion from the reaction mixture was done by the method of Prestwood and Wahl (5) using sodium chromate as precipitating agent, in an alkaline cyanide medium to prevent precipitation of thallic species. The thallous chromate precipitate was filtered onto tared filter disks, dried, weighed, and mounted on cards with cellulose tape. Counting of these radioactive samples was done with an end-window proportional counter, using a flowing methane–argon gas mixture.

Solutions for exchange measurements were made up to 0.010 M in each of thallic and thallous species, and 3.12 M in total acid (i.e. $[H_2SO_4]+[HClO_4] = 3.12$).* Solutions were made complete but for the thallous ion, and allowed to come to equilibrium with the constant temperature bath before addition of the thallous solution.

The errors involved in this type of work are very difficult to assess. Constancy in the weights of the samples counted made correction for back-scattering and self-absorption unnecessary. Observed activities in these samples are estimated to be in error by no more than 5%. The standard deviation of the measured specific activities of the "infinite time" samples was ±2%. It is thus likely that individual rate measurements are, in general, accurate to about ±10%, and internally consistent to ±5%.

RESULTS AND DISCUSSION

The results of the kinetic studies of the exchange are given in Table I.

Data plotted for the complete range of sulphate concentrations studied are shown in Fig. 1. These data show that the over-all dependence on sulphate concentration is

TABLE I

THALLOUS–THALLIC EXCHANGE RATES
$[Tl(I)] = [Tl(III)] = 0.010\ M$

			Rate×10⁷ (moles l.⁻¹ sec.⁻¹)[b]		
$[SO_4^{=}]$[a]	$[H^+]$[a]	μ[a]	24.2° C.	37.2° C.	50.0° C.
0.0000	3.12	3.12	0.064	0.18	0.50
0.0060	3.13	3.13	0.10		0.70
0.0067	3.13	3.13		0.28	
0.015	3.14	3.14	0.16	0.44	
0.021	3.14	3.15			1.46
0.030	3.15	3.17	0.26	0.70	
0.047	3.17	3.19	0.35	0.97	2.7
0.093	3.21	3.26	0.74	1.7	4.8
0.158	3.28	3.36	1.1	2.9	5.3
0.276	3.40	3.56		5.2	12.4
0.39	3.50	3.72		6.2	19.6
0.49	3.61	3.86		10.5	

[a]*The values of* $[SO_4^{=}]$, $[H^+]$, *and* μ *were computed using the data of Smith (6) for the dissociation of* H_2SO_4. *For values of* $[SO_4^{=}] < 0.05$ *the variations in* $[H^+]$ *and* μ *are* $\leqslant 2\%$, *and are likely insignificant.*

[b]*Rate* $(R) = [Tl(III)][Tl(I)]/([Tl(III)] + [Tl(I)])$. $0.693/t_{\frac{1}{2}}$. *For the concentrations used in the present work,* $R = 5\times10^{-3}$. $0.693/t_{\frac{1}{2}}$.

Consideration of H_2SO_4 as effectively monobasic, for purposes of determining ionic strength, was based upon widely used but evidently inapplicable dissociation data. The author is very grateful to Dr. C. H. Brubaker for drawing attention to work by Smith (6), who has measured the concentration of the various species in sulphuric acid solutions over a wide range of ionic strength. At the ionic strengths used in the present work, Smith indicates a value of 1.3 for the dissociation constant of the bisulphate ion. The present work was, unfortunately, completed without reference to the more recent values. Values of the sulphate concentration reported in this paper were recalculated in accordance with Smith's data. Only at sulphate concentrations of greater than 0.1 M will the ionic strength and acidity vary significantly from the intended 3.12 M.

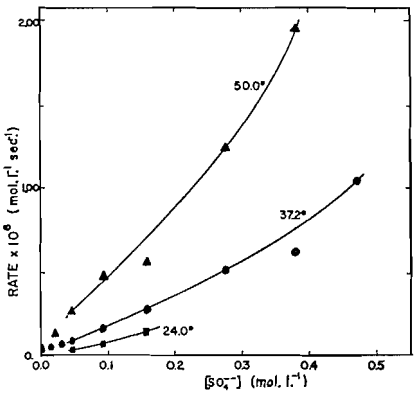

FIG. 1. Thallous–thallic exchange rates.

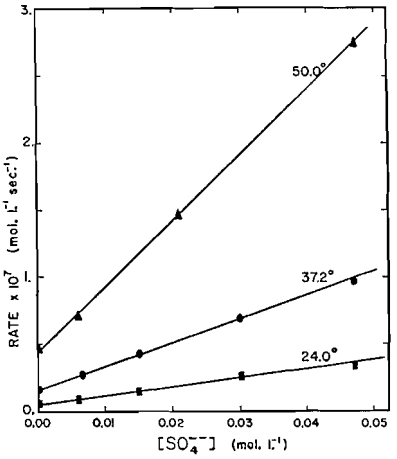

FIG. 2. Thallous–thallic exchange rates at low sulphate concentration.

greater than the first order. This is in agreement with the results of Brubaker and Mickel (1) and indicates that more than one ligand takes part in the rate-determining step.

In Fig. 2 are plotted the exchange data for low values of the sulphate concentration. In this range, the dependence is linear, and the participation of only one sulphate group is indicated at these low sulphate concentrations.

Perhaps the most significant characteristic of the present rate curves is that they do not show the strong negative effect (inhibition) on the exchange found in the chloride (3) and cyanide (4) systems. The sulphate system seems in this respect more to resemble the nitrate (5) system.

From the above results and from the known (1) first-order dependence on each of Tl(III) and Tl(I), it can be inferred that the activated complex contains one ion of each of thallous, thallic, and sulphate. Following the suggestions of Taube (7) and others, in other cases, it seems reasonable that the actual activated complex might well be a bridge type of structure:

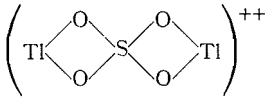

in which case the transfer of two electrons arises from the transfer of a sulphate radical from one thallium atom to the other. This same bridge-transfer mechanism would very likely also be applicable in the case of the more highly complexed species at higher sulphate concentrations.

It is important to point out that the above mechanism is not the only one consistent with the kinetics. Others might be: rapid dissociation of the thallic sulphate complex into a thallous ion and a neutral sulphate radical, dissociation of the bridge structure without transfer of sulphate, direct transfer of electrons by barrier penetration, and still others. The bridge-transfer mechanism seems to be the most attractive of these.

ACKNOWLEDGMENTS

The author is grateful to Drs. R. W. Dodson and J. Halpern for helpful comments, and to the National Research Council for financial support.

Can. J. Chem. Downloaded from www.nrcresearchpress.com by 61.7.252.67 on 09/04/12
For personal use only.

REFERENCES

1. BRUBAKER, C. H. and MICKEL, J. P. J. Inorg. & Nuclear Chem. **4**, 55 (1957).
2. DODSON, R. W. J. Am. Chem. Soc. **75**, 1795 (1953).
3. HARBOTTLE, G. and DODSON, R. W. J. Am. Chem. Soc. **73**, 2442 (1951).
4. PENNA-FRANCA, E. and DODSON, R. W. J. Am. Chem. Soc. **77**, 2651 (1955).
5. PRESTWOOD, R. J. and WAHL, A. C. J. Am. Chem. Soc. **71**, 3137 (1949).
6. SMITH, H. M. Raman spectral study of the dissociation of sulfuric acid in aqueous solution at 25° C. Ph.D. Thesis, University of Chicago. 1950.
7. TAUBE, H., MYERS, H., and RICH, R. L. J. Am. Chem. Soc. **75**, 4118 (1953).

Can. J. Chem. Downloaded from www.nrcresearchpress.com by 61.7.252.67 on 09/04/12
For personal use only.

THE SYSTEMS Li_2SO_4–K_2SO_4–H_2O AND Li_2SO_4–Na_2SO_4–H_2O AT 25° C.[1]

A. N. CAMPBELL AND E. M. KARTZMARK

ABSTRACT

The 25° isotherm of the system Li_2SO_4–K_2SO_4–H_2O shows the existence of the double salt, $Li_2SO_4.K_2SO_4$, whereas that of the system Li_2SO_4–Na_2SO_4–H_2O yields no double salt but extensive solid solution of lithium sulphate in sodium sulphate. On the other hand, a study at 39.5° C. of the latter system shows that the double salt, $Li_2SO_4.Na_2SO_4$, does form at this temperature, accompanied as before by solid solution of lithium sulphate in sodium sulphate. The transition temperature for the reaction

$$Li_2SO_4.H_2O + Na_2SO_4 = Li_2SO_4.Na_2SO_4 + H_2O$$

is 29.3° C. A further transition, of unknown nature, occurs between 49° and 57°.

This paper is the second stage in our study of the system containing the radicals Li_2, Na_2, K_2, Cl_2, SO_4, and water. Our first paper (1) dealt with the system LiCl–NaCl–KCl–H_2O at 25° C. The corresponding system involving the sulphates is Li_2SO_4–Na_2SO_4–K_2SO_4–H_2O. The component ternary systems are Li_2SO_4–Na_2SO_4–H_2O, Li_2SO_4–K_2SO_4–H_2O, and Na_2SO_4–K_2SO_4–H_2O. The system Na_2SO_4–K_2SO_4–H_2O has been investigated by various workers. A complete bibliography is given by Hamid (2). A double salt, glaserite or Penny's salt, is formed, having the composition $3K_2SO_4.Na_2SO_4$. This double salt, however, while it is incapable of forming solid solutions with potassium sulphate, does so, at 25°, to some extent with sodium sulphate. Thus, according to Hamid, the two isothermally invariant ternary solutions, at 25°, are in equilibrium respectively with pure double salt and potassium sulphate and with Glauber's salt and the solid solution of sodium sulphate in double salt.

The systems Li_2SO_4–K_2SO_4–H_2O and Li_2SO_4–Na_2SO_4–H_2O have not previously been investigated, although Nacken (3) has investigated the equilibrium diagram of the anhydrous systems Li_2SO_4–K_2SO_4 and Li_2SO_4–Na_2SO_4. He finds that the former system gives rise to the congruently melting compound $Li_2SO_4.K_2SO_4$ and the latter to the compound $Li_2SO_4.Na_2SO_4$, which cannot exist in equilibrium with the melt. Scacchi (4) and Traube (5) have also obtained $Li_2SO_4.Na_2SO_4$ by crystallization of hot solutions of lithium and sodium sulphates.*

EXPERIMENTAL TECHNIQUE

The technique of solubility determinations is too well known to merit description here but something must be said about the methods of analysis. The only really practical method of determining sulphate radical, viz. barium sulphate precipitation, is notoriously unreliable, particularly in solutions containing alkali ions. Although we used this method we thought it necessary to support it by the use of a purely physical method and for this purpose we chose viscosity. All density and viscosity determinations were made on solutions containing 10 or 20 g. total anhydrous salt in 100 ml. of solution.

[1]*Manuscript received September 13, 1957.*
Contribution from the Chemistry Department, University of Manitoba, Winnipeg, Manitoba.

*NOTE ADDED IN PROOF.—*A paper by L. Cavalca and M. Nardelli (Gazz. chim. ital. **82**, 394–405 (1952)) has just come to hand, in which they have studied the system Li_2SO_4–Na_2SO_4–H_2O at 27° and 45.6° C. They agree with us in finding that the double salt $Na_2SO_4.Li_2SO_4$ does not exist at 27° though it does at 45.6° C. In addition, however, they claim the existence of a double salt $Na_3Li(SO_4)_2.6H_2O$. The existence of such a salt would require that the tie-lines intersect in the body of the diagram and this we feel to be impossible. We point out, in this connection, that prolonged and vigorous stirring is necessary to ensure the attainment of equilibrium.*

Can. J. Chem. Downloaded from www.nrcresearchpress.com by 61.7.252.67 on 09/04/12
For personal use only.

Can. J. Chem. Downloaded from www.nrcresearchpress.com by 61.7.252.67 on 09/04/12
For personal use only.

EXPERIMENTAL RESULTS

The results for the system Li_2SO_4–K_2SO_4–H_2O are shown in Tables I and II. Those for the system Li_2SO_4–Na_2SO_4–H_2O at 25° C. are shown in Tables III, IV, and V.

TABLE I

DENSITIES AND VISCOSITIES OF SOLUTIONS OF LITHIUM SULPHATE AND POTASSIUM SULPHATE, CONTAINING 10 G. ANHYDROUS SALT IN 100 ML. SOLUTION, AT 25° C.

Composition	Density, g./ml.	Relative viscosity (H_2O = 1)
10 g. Li_2SO_4	1.0780	1.6141
10 g. K_2SO_4	1.0736	1.1316
5 g. Li_2SO_4, 5 g. K_2SO_4	1.0757	1.3460
7 g. Li_2SO_4, 3 g. K_2SO_4	1.0766	1.4347
3 g. Li_2SO_4, 7 g. K_2SO_4	1.0749	1.2602

TABLE II

COMPOSITIONS OF SOLUTIONS AND "WET" SOLID PHASES AT 25° C.

Liquid phase		Solid phase		
Wt. % Li_2SO_4	Wt. % K_2SO_4	Wt. % Li_2SO_4	Wt. % K_2SO_4	Nature of solid phase
25.5	—	—	—	$Li_2SO_4.H_2O$
25.8	0.2	—	—	$Li_2SO_4.H_2O$
26.0	0.4	71.2	0.1	$Li_2SO_4.H_2O$
26.7	2.3	61.3	16.8	$Li_2SO_4.H_2O$ + double salt
26.5	2.2	51.7	21.9	$Li_2SO_4.H_2O$ + double salt
26.5	2.4	37.0	45.0	Double salt
24.6	2.8	35.8	46.0	"
18.1	4.1	34.0	42.8	"
12.1	9.2	35.1	55.5	"
12.0	9.2	32.0	49.0	"
11.9	9.0	31.6	48.1	"
11.0	10.3	25.4	61.2	Double salt + K_2SO_4
10.6	10.7	8.8	65.0	K_2SO_4
8.5	10.1	7.4	63.6	K_2SO_4
5.1	10.2	4.1	76.2	K_2SO_4
4.4	9.9	3.7	72.7	K_2SO_4
—	10.7	—	—	K_2SO_4

TABLE III

DENSITIES AND VISCOSITIES OF SOLUTIONS OF LITHIUM SULPHATE AND SODIUM SULPHATE, CONTAINING 20 G. ANHYDROUS SALT IN 100 ML. OF SOLUTION, AT 25° C.

Compositions			
Li_2SO_4	Na_2SO_4	Density, g./ml.	Relative viscosity (H_2O = 1)
0.0	20	1.1608	1.9057
2	18	1.1600	1.9699
4	16	1.1591	2.0369
8	12	1.1575	2.1817
10	10	1.1567	2.2552
14	6	1.1551	2.4231
16	4	1.1542	2.5163
18	2	1.1534	2.6125
20	0	1.1526	2.7016

DISCUSSION

The results of Table II are plotted in Fig. 1. It is obvious that the expected double salt, $Li_2SO_4.K_2SO_4$, is stable at 25° C., although the solution is not congruently saturating; the pure anhydrous double salt decomposes when treated with water to give a mixture of double salt and potassium sulphate. The figure also shows some solid solubility of lithium sulphate in potassium sulphate and of lithium sulphate in double salt.

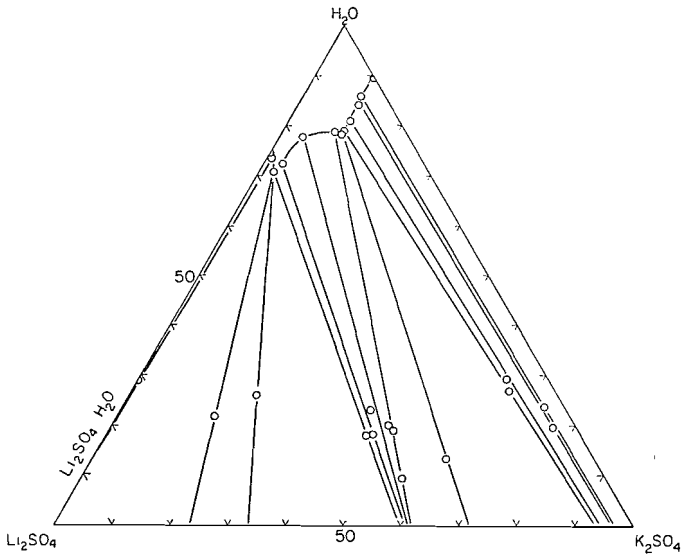

FIG. 1. The system Li_2SO_4–K_2SO_4–H_2O at 25° C.

The figures of Table IV are plotted in Fig. 2. Rather surprisingly, no double salt forms at 25° C. but there is extensive solid solubility of lithium sulphate in sodium sulphate,

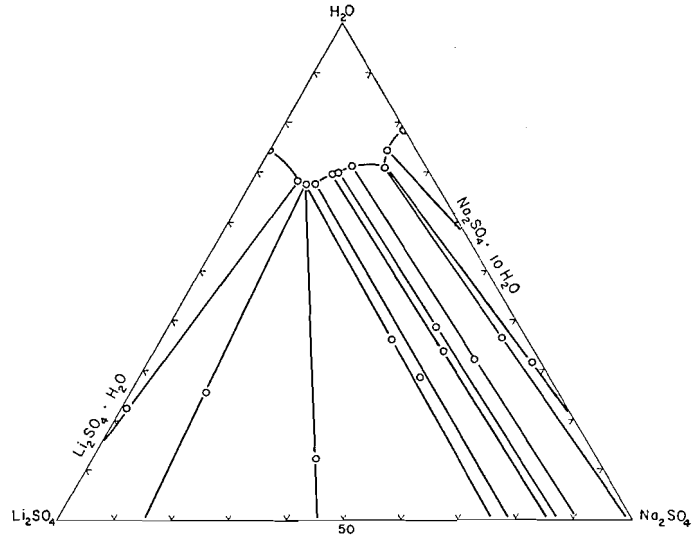

FIG. 2. The system Li_2SO_4–Na_2SO_4–H_2O at 25° C.

Can. J. Chem. Downloaded from www.nrcresearchpress.com by 61.7.252.67 on 09/04/12
For personal use only.

TABLE IV

COMPOSITIONS OF SOLUTIONS AND "WET" SOLID PHASES IN WT. % AT 25.0° C.

Liquid		"Wet" solid		
Na_2SO_4	Li_2SO_4	Na_2SO_4	Li_2SO_4	Nature of solid phase
—	25.5	—	—	$Li_2SO_4.H_2O$
8.0	23.8	0.9	76.7	"
9.9	22.4	13.2	60.8	$Li_2SO_4.H_2O$ + solid solution
9.7	22.8	39.7	48.7	"
9.2	22.9	40.2	23.7	Homogeneous solid solution
11.3	20.8	49.0	22.5	"
14.2	15.7	47.0	14.5	"
15.9	12.9	56.8	11.0	"
21.9	7.8	59.4	4.0	"
22.0	7.0	67.0	1.3	$Na_2SO_4 + Na_2SO_4.10H_2O$
20.4	5.1	41.7	Trace	$Na_2SO_4.10H_2O$
21.7	—	—	—	"

to the extent of, say, 25% lithium sulphate by weight. Because of the difference in crystal structure of lithium sulphate and β-Na_2SO_4, and of the difference in ionic radii of the lithium and sodium ions (6), this result surprised us and we verified it with some care. In one case, a very small solid phase was vigorously stirred with solution for 3 weeks, to ensure true equilibrium, before analysis. We have therefore no doubt of the fact, however surprising it may be. According to Nacken (3), solid α-Na_2SO_4 dissolves extensively in solid α-Li_2SO_4 at temperatures between 600° C. and 850° C., while α-Li_2SO_4 does not dissolve at all (in the solid state) in α-Na_2SO_4. We now find that, in the neighborhood of room temperature, Li_2SO_4 dissolves extensively in β-Na_2SO_4. The question of whether β-Na_2SO_4 dissolves in (anhydrous) β-Li_2SO_4 cannot be answered by this study, because the equilibrium lithium sulphate solid phase is always the monohydrate.

Since the literature indicated, beyond all reasonable doubt, that the double salt, $Li_2SO_4.Na_2SO_4$, does form from hot solution, there must be a transition temperature for the reaction:

$$Li_2SO_4.H_2O + Na_2SO_4 = Li_2SO_4.Na_2SO_4 + H_2O.$$

Accordingly, a dilatometric experiment was carried out, using a bulb charged with a moist equimolar mixture of lithium and sodium sulphates and *m*-xylene as indicator fluid. A marked expansion was observed at 30.0° C. and a less distinct expansion between 49.6° C. and 56.6° C. This was checked by determination of total solubility of an equimolar mixture of lithium and sodium sulphates. The results were:

Temperature, ° C.	Total solubility in wt. %
25	29.0
28.5	32.1
31.4	32.8
39.8	33.3
50.1	34.0
60.3	34.0
67.7	32.3

When the above figures are plotted as total solubility versus temperature, sharp breaks are observed at 29.3° C. and 57.5° C. We did not pursue further the question of the nature of the higher temperature transition.

Can. J. Chem. Downloaded from www.nrcresearchpress.com by 61.7.252.67 on 09/04/12
For personal use only.

After determining the transition temperature to be 29.3° C., we undertook the study of the 39.5° C. isotherm. When the data of Table V are plotted (Fig. 3) in the usual

TABLE V

COMPOSITIONS OF SOLUTIONS AND "WET" SOLID PHASES IN WT. % at 39.5° C.

Liquid		"Wet" solid		
Na_2SO_4	Li_2SO_4	Na_2SO_4	Li_2SO_4	Nature of solid phase
—	25.0	—	—	$Li_2SO_4.H_2O$
5.8	22.6	1.8	70.0	"
9.0	23.4	27.5	43.0	$Li_2SO_4.H_2O$ + double salt
9.3	22.7	22.3	50.6	"
12.2	20.1	41.5	38.5	Double salt
14.7	18.3	38.6	35.0	"
17.0	15.7	43.0	34.5	"
17.0	15.5	51.8	28.2	Double salt + solid solution
17.2	15.4	48.5	19.1	Solid solution
20.2	12.3	52.5	14.5	"
27.4	6.7	68.0	9.1	"
32.5	—	—	—	Na_2SO_4, anhydrous

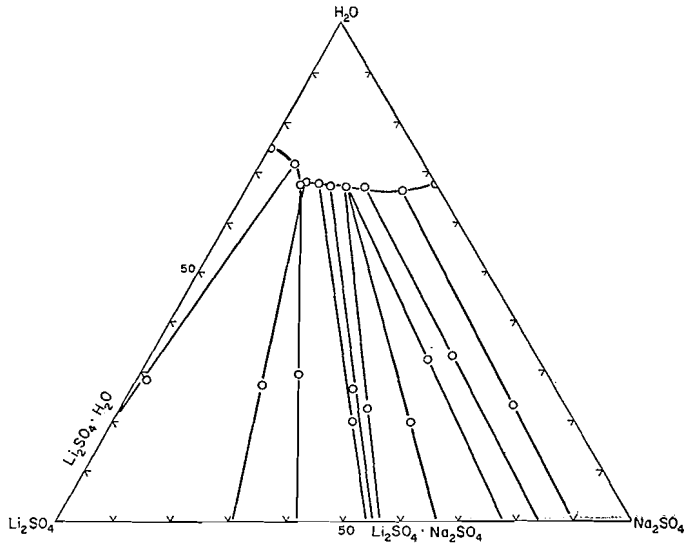

FIG. 3. The system Li_2SO_4–Na_2SO_4–H_2O at 39.5° C.

way, it is apparent that the double salt, $Li_2SO_4.Na_2SO_4$, does indeed form although the region of its existence in contact with solution is small. Like the corresponding lithium–potassium double salt, it is incongruently saturating. The fact that the double salt of lithium–sodium is not stable at room temperature may account for some of the crystallographic difficulties encountered by Traube (5).

REFERENCES

1. CAMPBELL, A. N. and KARTZMARK, E. M. Can. J. Chem. **34**, 672 (1956).
2. HAMID, M. A. J. Chem. Soc. 201 (1926).
3. NACKEN, R. Neues Jahrb. Mineral. Paläontol., Beilage Bd. **24**, 32 (1907).
4. SCACCHI, A. Atti Accad. sci. fis. mat. Napoli, **3** (No. 27), 31 (1868).
5. TRAUBE, H. Neues Jahrb. Mineral., Geol. u. Paläontol. **II**, 62 (1892).
6. WELLS, A. F. Structural inorganic chemistry. 2nd ed. Oxford University Press, London. 1950. pp. 170 and 386.

Can. J. Chem. Downloaded from www.nrcresearchpress.com by 61.7.252.67 on 09/04/12
For personal use only.

PHOTOLYSIS OF ACETONE IN THE PRESENCE OF METHYL-d_3 ACETATE[1]

M. H. J. WIJNEN

ABSTRACT

The photolysis of acetone in the presence of CH_3COOCD_3 has been carried out over the temperature range 151° to 274° C., at different ratios of acetone to methyl acetate and at different light intensities. As activation energies for the abstraction reactions

$$CH_3 + CH_3COOCD_3 \rightarrow CH_4 + CH_2COOCD_3 \quad [2]$$

and

$$CH_3 + CH_3COOCD_3 \rightarrow CH_3D + CH_3COOCD_2 \quad [3]$$

were obtained $E_2 = 10 \pm 0.5$ kcal. and $E_3 = 14 \pm 1$ kcal.

INTRODUCTION

Direct photolysis of CH_3COOCH_3 (5) and CH_3COOCD_3 (6), recently undertaken at this laboratory, indicated a considerable difference in activation energy between the abstraction of a hydrogen atom from the acetyl group and the abstraction of a hydrogen or deuterium atom from the methoxy group in methyl acetate by methyl radicals. In order to study these abstraction reactions in a relatively simple system, acetone was photolyzed in the presence of CH_3COOCD_3.

EXPERIMENTAL

The apparatus and technique were mainly the same as described elsewhere (7). The storage vessels containing acetone and methyl acetate were separated from the reaction vessel by mercury cutoffs. In order to prevent absorption by methyl acetate, the light of the S-500 medium pressure arc was filtered through Corning filter 9700, transparent above 2600 Å. The trideuteromethyl acetate was obtained from New England Nuclear Corporation. Mass spectrometric analysis showed it to contain at least 98% of CH_3COOCD_3. The acetone was obtained from Celanese Chemcel plant and was distilled once *in vacuo* before use.

RESULTS AND DISCUSSION

The results of the experiments carried out at various temperatures for various mixtures of acetone and methyl acetate are given in Table I.

The use of acetone as a source of methyl radicals to study hydrogen abstraction reactions is well established. The following reactions are, therefore, proposed to explain the methane and ethane formation when acetone is photolyzed in the presence of CH_3COOCD_3 at temperatures above 140° C.:

$$CH_3 + CH_3COCH_3 \rightarrow CH_4 + CH_2COCH_3 \quad [1]$$

$$CH_3 + CH_3COOCD_3 \rightarrow CH_4 + CH_2COOCD_3 \quad [2]$$

$$CH_3 + CH_3COOCD_3 \rightarrow CH_3D + CH_3COOCD_2 \quad [3]$$

$$2CH_3 \rightarrow C_2H_6 \quad [4]$$

The following equations may be derived from this reaction mechanism:

$$R_{CH_4}/(R^{\frac{1}{2}}_{C_2H_6}[Ac]) = k_1/k_4^{\frac{1}{2}} + k_2/k_4^{\frac{1}{2}}[MeAc]/[Ac] \quad [I]$$

$$R_{CH_3D}/(R^{\frac{1}{2}}_{C_2H_6}[MeAc]) = k_3/k_4^{\frac{1}{2}} \quad [II]$$

$$R_{CH_4}/R_{CH_3D} = k_2/k_3 + k_1/k_3[Ac]/[MeAc] \quad [III]$$

[1]*Manuscript received August 15, 1957.*
Contribution from the Chemical Division, Research and Development Laboratories, Celanese Corporation of America, Clarkwood, Texas.

Can. J. Chem. Downloaded from www.nrcresearchpress.com by 61.7.252.67 on 09/04/12
For personal use only.

TABLE I

PHOTOLYSIS OF CH_3COCH_3 IN THE PRESENCE OF CH_3COOCD_3

Expt. No.	Temp., ° C.	$[Ac]_i$, molecules/cc. $\times 10^{-17}$	$[MeAc]_i$, molecules/cc. $\times 10^{-17}$	In molecules/(sec. cc.) $\times 10^{-12}$				
				R_{CH_4}	R_{CH_3D}	$R_{C_2H_6}$	R_{CO}	$10^{14}k_3/k_4^{1/2}$
1	151	13.60	—	5.42	—	13.45	17.93	—
2	"	11.90	9.90	5.02	—	11.69	16.30	—
3	"	13.02	14.58	5.63	—	12.00	17.25	—
4	"	10.20	19.50	4.73	—	10.07	14.12	—
5	"	10.43	23.22	5.10	0.07	10.36	14.32	0.94
14	"	7.98	24.12	0.73	0.01	0.22	0.76	0.98
15	"	10.10	32.10	5.00	0.10	7.77	11.50	1.11
16	"	10.08	31.67	2.08	0.03	1.41	2.88	0.81
19	176	15.70	13.80	1.90	0.01	0.25	1.48	1.63
20	"	10.38	17.37	10.53	0.11	9.85	18.10	2.09
21	"	8.15	28.25	7.08	0.15	5.30	10.90	2.28
22	"	9.20	20.30	7.18	0.11	6.22	11.85	2.23
6	208	7.57	4.72	11.80	0.11	6.40	15.50	9.36
7	"	8.90	10.21	16.60	0.23	6.47	18.40	8.84
8	"	8.23	—	11.32	—	6.95	15.50	—
9	"	5.68	10.98	9.58	0.20	4.10	11.70	9.00
17	"	7.62	19.76	13.80	0.31	4.25	13.82	7.55
18	"	5.35	20.83	3.75	0.10	0.50	2.96	9.06
10	274	9.52	6.78	26.20	0.44	2.16	19.20	44.2
11	"	8.12	16.08	24.65	0.84	1.83	18.35	39.0
12	"	9.40	—	21.20	—	2.05	16.35	—
13	"	8.50	20.00	26.68	1.32	2.41	21.95	42.6
23	"	8.09	23.59	20.22	0.92	1.20	15.15	35.8
24	"	16.38	7.25	36.20	0.42	1.70	23.45	44.4
25	"	6.67	20.58	17.90	0.93	1.14	12.60	42.5

The results obtained for $k_3/k_4^{\frac{1}{2}}$ via equation [II] are given in Table I. Within experimental error constant values were obtained for $k_3/k_4^{\frac{1}{2}}$ at constant temperatures. A plot of log $k_3/k_4^{\frac{1}{2}}$ against $1/T$ in Fig. 2 gives an activation energy difference of $E_3-\frac{1}{2}E_4 = 14\pm1$ kcal.

Equation [I] is plotted in Fig. 1. The data show good agreement with the proposed reaction mechanism. The intercepts of the lines in Fig. 1 give values of $k_1/k_4^{\frac{1}{2}}$. These values may also be obtained by photolysis of acetone alone. At three temperatures, runs were carried out photolyzing acetone alone. Values thus obtained are indicated on the ordinate of Fig. 1 and coincide within experimental error with the intercepts obtained by plotting equation [I].

From the slopes of the lines in Fig. 1 we obtain the values of $k_2/k_4^{\frac{1}{2}}$ reported in Table II. A plot of log $k_2/k_4^{\frac{1}{2}}$ against $1/T$ is shown in Fig. 2, together with data obtained for $k_2/k_4^{\frac{1}{2}}$ by direct photolysis of CH_3COOCD_3 (6). From the slope of this plot an activation energy of $E_2 = 10\pm0.5$ kcal. is obtained, assuming $E_4 = 0$ kcal. Plots of equation [III] at 208° and 274° C. give the following values for k_2/k_3 and k_1/k_3: $k_2/k_3 = 23$ and $k_1/k_3 = 54$ at 208° C., $k_2/k_3 = 8$ and $k_1/k_3 = 37$ at 274° C. Small errors in the determination of R_{CH_3D} at low temperatures have a large effect on the ratio R_{CH_4}/R_{CH_3D} and prevent plotting equation [III] at temperatures below 208° C.

Values obtained for the different ratios of rate constants are summarized in Table II.

As activation energy for reaction [2] is obtained $E_2 = 10\pm0.5$ kcal. An activation energy of 10.2 kcal. has been reported by Ausloos and Steacie (1) for the following reaction:

$$CH_3 + CH_3COOH \rightarrow CH_4 + CH_2COOH. \qquad [5]$$

Can. J. Chem. Downloaded from www.nrcresearchpress.com by 61.7.252.67 on 09/04/12
For personal use only.

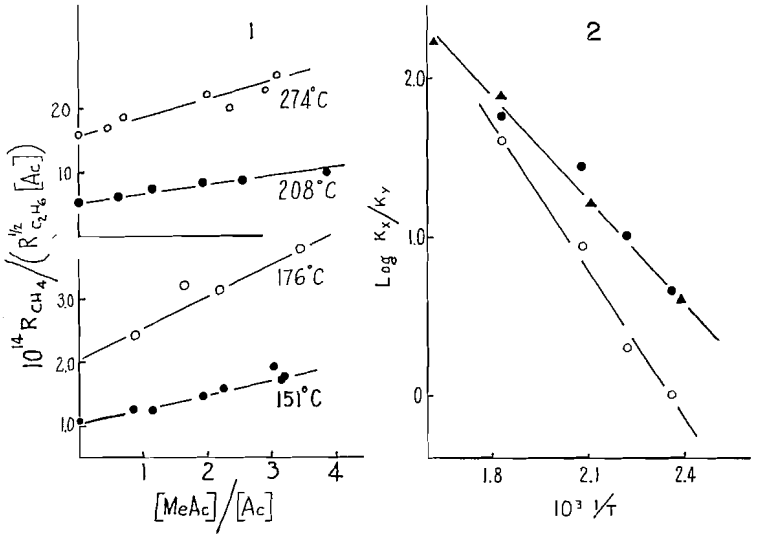

FIG. 1. Plot of $10^{14} R_{CH_4}/(R^{1/2}_{C_2H_6}[Ac])$ versus [MeAc]/[Ac] at various temperatures.
FIG. 2. Plot of $14 + \log k_3/k_4^{1/2}$ (○) and of $12.7 + \log k_2/k_4^{1/2}$ (●, ▲) against $10^3\,1/T$. Data marked by ● are reported in this work, those marked by ▲ were obtained by direct photolysis of CH_3COOCD_3.

TABLE II

RATIOS OF RATE CONSTANTS

Temp., ° C.	$10^{13}\,k_2/k_4^{1/2}$ in molecules$^{1/2}$/sec.$^{1/2}$ cc.$^{1/2}$	$10^{14}\,k_3/k_4^{1/2}$ in molecules$^{1/2}$/sec.$^{1/2}$ cc.$^{1/2}$	k_1/k_3	k_2/k_3
151	2.3	1.0	—	—
176	5.0	2.0	—	—
208	14.0	8.8	54	23
274	30	41.3	37	8

Since in both reactions, [2] and [5], the hydrogen is abstracted from the acetyl group, these values may be considered to be in good agreement.

The experimentally determined activation energy of 14±1 kcal. for the abstraction of a D-atom from the methoxy group in methyl acetate seems high. A direct comparison of the difference in activation energies between the abstraction of a hydrogen from the acetyl and from the methoxy group in methyl acetate is not possible owing to the different hydrogen isotopes in these groups.

Differences in activation energies between the abstraction reactions of H- and D-atoms by methyl radicals have been observed in the case of acetone, where values of 9.7 kcal. (3) were reported for E_6 and 11.3 kcal. (2) for E_7.

$$CH_3 + CH_3COCH_3 \rightarrow CH_4 + CH_2COCH_3 \quad [6]$$

$$CD_3 + CD_3COCD_3 \rightarrow CD_4 + CD_2COCD_3 \quad [7]$$

This difference in activation energies seems mainly caused by the difference in zero point energies between the C—H and C—D bonds, since CH_3 and CD_3 radicals have been suggested (4) to abstract hydrogen atoms with, within experimental error, similar activation energies.

Accepting therefore for the reaction

$$CH_3 + CH_3COOCH_3 \rightarrow CH_4 + CH_3COOCH_2, \quad [8]$$

Can. J. Chem. Downloaded from www.nrcresearchpress.com by 61.7.252.67 on 09/04/12
For personal use only.

an activation energy of 12.5±1 kcal., our results indicate that the abstraction of a hydrogen atom from the acetyl group requires less energy than the abstraction of a hydrogen atom from the methoxy group in methyl acetate.

It is interesting to compare these results with results obtained in the direct photolysis of CH_3COOCH_3 (5). As activation energy for the hydrogen abstraction by methyl radicals was obtained a value of 10 kcal., in agreement with the value of E_2 obtained in the present work. Among the reaction products were found large amounts of methyl propionate, probably formed by the reaction

$$CH_3 + CH_2COOCH_3 \rightarrow C_2H_5COOCH_3. \qquad [9]$$

No evidence could be obtained for the formation of ethyl acetate, indicating that most hydrogen was abstracted from the acetyl group, rather than from the methoxy group in methyl acetate.

These results confirm the conclusion drawn in this work that less energy is required for the abstraction of a hydrogen atom from the acetyl group than from the methoxy group in methyl acetate by methyl radicals.

In addition to the reaction products given in Table I, trace amounts of CD_3H, CO_2, and occasionally CD_4 were observed at 273° C. These products may originate from the thermal decomposition of the CH_2COOCD_3 radical.

Accepting as collision diameters of CH_3 and CH_3COOCD_3 3.5 and 6×10^{-8} cm., respectively, we calculated the steric factor ratios and obtained:

$$P_2/P_4^{\frac{1}{2}} = 1.5\times10^{-3} \text{ and } P_3/P_4^{\frac{1}{2}} = 5\times10^{-3}.$$

These values are of the order of magnitude generally observed in hydrogen abstraction reactions by methyl radicals.

ACKNOWLEDGMENTS

The author acknowledges many helpful discussions with Dr. H. D. Medley during the progress of this work. Special thanks are due to Messrs. R. W. Jarrett and R. H. Guedin for calculation and interpretation of the mass spectrometer data.

REFERENCES

1. Ausloos, P. and Steacie, E. W. R. Can. J. Chem. **33**, 1530 (1955).
2. McNesbey, J. R., Davis, T. W., and Gordon, A. S. J. Am. Chem. Soc. **76**, 823 (1954).
3. Trotman-Dickenson, A. F. and Steacie, E. W. R. J. Chem. Phys. **18**, 1097 (1950).
4. Whittle, E. and Steacie, E. W. R. J. Chem. Phys. **21**, 993 (1953).
5. Wijnen, M. H. J. 131st National Meeting, Am. Chem. Soc., Miami, Florida (April, 1957).
6. Wijnen, M. H. J. To be published.
7. Wijnen, M. H. J. and Steacie, E. W. R. J. Chem. Phys. **20**, 205 (1952).

Can. J. Chem. Downloaded from www.nrcresearchpress.com by 61.7.252.67 on 09/04/12
For personal use only.

Can. J. Chem. Downloaded from www.nrcresearchpress.com by 61.7.252.67 on 09/04/12
For personal use only.

THE STUDY OF HYDROGEN BONDING AND RELATED PHENOMENA BY ULTRAVIOLET LIGHT ABSORPTION

PART I. INTRODUCTION[1,2]

W. F. Forbes and J. F. Templeton

ABSTRACT

Hydrogen bonding, which is known to give rise to dimer formation in benzoic acids and similar compounds, may affect solution spectra by intermolecular and by intramolecular bond formation. Generally environmental factors affecting absorption spectra can be conveniently divided into three types: intermolecular hydrogen bonding between solute molecules only; intermolecular hydrogen bonding between solute and solvent molecules; and environmental effects not involving the formation of hydrogen bonds.

Distinct evidence for these types of interaction is deduced from ultraviolet spectra, and various implications of the spectral analyses are discussed.

INTRODUCTION

Hydrogen bonding has been previously mentioned in this series as a possible cause of certain anomalous spectra (13, 14, 15, 17). Intramolecular hydrogen bonding has previously been used to explain certain features of the ultraviolet spectra of *o*-hydroxyacetophenone and salicylic acid (9, 10). Intermolecular hydrogen bonding would be expected to occur in organic compounds like benzoic acid, firstly because dimer formation in benzoic acids is a well-known phenomenon in infrared spectroscopy (2, 11, 22, 26) and secondly because certain changes in ultraviolet absorption spectra on alteration of the solvent have been ascribed to intermolecular hydrogen bonding (5, 6, 7, 30, 31, 33). Further, the dependence of a number of ultraviolet spectra on solution concentration has been noted by several workers (1, 19, 25, 28, 29, 34).

Intermolecular hydrogen bonding, for which there is therefore some evidence, may be conveniently divided into two types. Intermolecular hydrogen bonding may occur between solute molecules only or may occur between solvent and solute molecules. The former, intermolecular hydrogen bonding between solute molecules only, may be a function of the concentration. Consequently, it may be susceptible to independent investigation, particularly since examples can be selected which largely eliminate intramolecular hydrogen bonding and steric effects. Monosubstituted benzenes and especially benzoic acids provide a satisfactory starting point. The latter have also previously been discussed in this series (18) and it was found that although dimer formation was anticipated, the *B*-bands could as a first approximation be satisfactorily related without considering the effect of hydrogen bonding. The present communication may thus be considered as an extension of this previous study.

The effect of intermolecular hydrogen bonding between solvent and solute molecules and other environmental effects may be investigated by choosing examples in which again steric and intramolecular hydrogen bonding effects are small, and which further do not show the concentration changes ascribed to solute–solute hydrogen bonding. Such examples are available and these will be examined separately.

EXPERIMENTAL

The ultraviolet absorption spectra were determined by standard methods using a Unicam SP 500 spectrophotometer. Intensity readings at different concentrations were

[1]*Manuscript received June 24, 1957.*
Contribution from the Memorial University of Newfoundland, St John's, Newfoundland.
[2]*This paper may also be considered as Part IX of a series of studies on light absorption, Part VIII of which appeared in Can. J. Chem.* **35**, *1049 (1957).*

obtained by using quartz cells of various path length, so that for different concentrations the optical density readings remained similar. For most of the compounds the concentration dependence was determined at least in duplicate over similar concentration ranges and was found to be qualitatively similar.

Compounds were purified by standard methods as described in the literature. Dioxane was purified by the method of Hess and Frahm (24), that is, by refluxing the dioxane with hydrochloric acid in a stream of nitrogen for 12 hours, removing the hydrochloric acid by treatment with potassium hydroxide, and then refluxing the dioxane with sodium for 10 hours. The distilled material, obtained in about 50% yield, was stored under nitrogen. Generally, purification was deemed adequate when additional processing resulted in no further measurable changes in the absorption intensity. Aqueous dioxane solvent mixtures were made up by mixing together the corresponding volume percentages. For example, 75% aqueous dioxane was obtained by mixing 75 volumes of purified dioxane with 25 volumes of distilled water.

The maximal wavelengths and absorption intensities are recorded in Tables I, II, and III. The concentration range was chosen to keep optical density readings between 0.3 and 0.7. Also, since no direct comparison of concentration dependences is intended at present, the reported values are mostly uncorrected. However, care was taken to use well-matched, carefully cleaned, cells, since some pairs of cells gave rise to differences in ϵ of up to 6% on interchanging the cells. For each concentration the observed extinction coefficients were within 2%. Band shapes for the benzoic acid spectra were found to be similar and consequently ϵ_{max} values may be used as measures of the actual absorption intensities.

Errors in a number of earlier determinations (cf. 19) were caused by the following:

(i) Solvents, if kept in some polyethylene bottles, frequently deteriorate on standing. Consequently all-glass bottles were used in preparing and storing solutions. The transmission density was checked for each solvent immediately before use. Further, the cells in each calibrated set were checked against each other before use.

(ii) Difficulties in solvent purification did not permit the determination of density readings in the longer cells without altering the sensitivity. This was particularly pronounced for dioxane. To obtain values for the 4 cm. cells at 230 mμ without altering the sensitivity, about five redistillations were required. As a general rule, the optical density reading in a 1 cm. cell at 250 mμ was 0.5 or less against air; if not, the dioxane was redistilled.

THE DEPENDENCE OF ELECTRONIC ABSORPTION SPECTRA ON CONCENTRATION (INTERMOLECULAR HYDROGEN BONDING BETWEEN SOLUTE MOLECULES ONLY)

For investigating hydrogen bonding and related effects *between solute molecules only*, hexane is a suitable solvent, because of its inactive nature and low dielectric constant. Consequently the main factor influencing the spectra may be the hydrogen bonding between solute molecules, and the intensity change with concentration in hexane as shown in the last examples of Table I may be provisionally assumed to represent a measure of this intermolecular hydrogen bonding.

Using this hypothesis, the data summarized in Table I are in agreement with results deduced by other methods. Thus, diphenyl, aniline, phenol, acetophenone, *p*-methylacetophenone, and methyl benzoate in cyclohexane solution do not show an appreciable intensity increase on increasing the concentration. For diphenyl, acetophenones, and methyl benzoate, this may be related to the inability of these compounds to form a hydrogen bond; and the reported absence of association for acetophenones (27), as

Can. J. Chem. Downloaded from www.nrcresearchpress.com by 61.7.252.67 on 09/04/12
For personal use only.

TABLE I

MAIN ABSORPTION MAXIMA OF COMPOUNDS IN CYCLOHEXANE SOLUTIONS OF VARYING CONCENTRATION*
(Concentration, $c = 6.5\times10^{-6}$–10^{-4} moles/l.; cell lengths in brackets)

Compound	40c (1 mm.)		4c (10 mm.)		c (40 mm.)	
	λ_{max}, mμ	ϵ_{max}	λ_{max}, mμ	ϵ_{max}	λ_{max}, mμ	ϵ_{max}
Diphenyl	246–247	17,400	246	17,200	246–247	17,200
Acetophenone	237–238	12,500	238	12,500	238	12,000
Aniline	233–234	9300	233–234	9200	234	8900
p-Methylacetophenone	246–247	15,000	247	15,200	246–247	14,800
Methyl benzoate	227	12,400	227	12,200	226–227	12,100
Aniline (*C*-band)	286	1920	286	1890	286	1870
Phenol (*C*-band)	264	1420	263	1400	263	1400
	269.5	2200	269.5	2200	269.5	2200
	276	2120	276	2050	276	2040
Benzoic acid	231–232	13,700	230	12,900	228	11,900
p-Toluic acid	241	15,500	239	15,000	236–237	13,400
m-Toluic acid	235	12,500	232–233	10,700	232	9700
o-Toluic acid	234–235	10,900	231–232	10,500	230	10,000
Salicylic acid	241	9500	239	8000	238	7200

**Three concentrations only are reported in this and subsequent tables; intermediate values were obtained at intermediate concentrations.*

judged from infrared and Raman spectral studies, may also be noted in this connection. Aniline also does not exhibit any appreciable concentration dependence, which is perhaps surprising, since the presence of association is suggested from infrared data (21). At least two explanations, however, may be proposed for the discrepancy. In the first place, the change in the amount of intermolecular hydrogen bonding may be small or negligible within the concentration range under investigation, but may be more pronounced in a different concentration range. This suggestion receives strong support since pyrrole and related compounds do not show any appreciable stretching vibration changes, which may be ascribed to hydrogen bonding (21), below a concentration of 10^{-2} moles per liter. By contrast, the present concentration range lies between 10^{-6} and 10^{-2} moles per liter. Secondly, the sensitivity of the method may generally not be sufficient to discern a change, which nevertheless actually occurs.

At this stage the significance of the data may be discussed. For all the early examples listed in Table I an intensity change of between 1 and 5% does in fact occur on increasing the concentration by a factor of 40, whereas a similar intensity change does not occur for some of the compounds listed in Table II. Since this change occurs for all the examples in Table I and also frequently occurs independently of the solvent (see, for example, the spectrum of methyl benzoate in ethanol and in cyclohexane as listed in Table II), it is unlikely to be associated with weak intermolecular hydrogen bonding. Moreover, if we take the accuracy of each ϵ value to be $\pm2\%$ (cf. Experimental), practically all these values are within experimental error. However, the fairly general occurrence of the trend (see Table I) suggests that the slight intensity increase is real. The most probable explanations are therefore that the intensity increase is caused by van der Waal's forces of molecular interaction or merely by errors inherent in the experiments (cf. 3, 4, 12).

Table I also shows that for benzoic acids the situation is different. Apart from the small increase discussed in the previous paragraph, many benzoic acids in cyclohexane solution when the concentration is increased give rise to a more pronounced increase in the observed absorption intensity. Since the changes occur at different wavelengths, they cannot be ascribed to any phenomenon associated with a particular wavelength. Simi-

Can. J. Chem. Downloaded from www.nrcresearchpress.com by 61.7.252.67 on 09/04/12
For personal use only.

larly, the previously discussed small intensity increase is not confined to a limited wavelength range; compare the early examples in Table I, which occur between 227 and 286 mμ. Further, Ungnade and Lamb (34) have noted that similar changes to those described for the *B*-band of benzoic acid occur in the *C*-band of benzoic acid in cyclohexane solution. For example, they report a maximal absorption at 274 mμ, $\epsilon = 1050$ at a concentration of 0.0805×10^{-3} moles per liter, whereas at a concentration of 10.27×10^{-3} moles per liter this absorption occurs at 276 mμ, $\epsilon = 1120$ (34). Lastly, it will be shown in a later section that this intensity decrease is less pronounced for more polar solvents, and this observation again is consistent with the initial assumption which relates these intensity changes to intermolecular hydrogen bonding.

Another example of appreciable intensity change is provided by the concentration dependence of the *C*-band in phenols (28). This dependence has been ascribed to intermolecular hydrogen bonding (28), but possibly for similar reasons as have been mentioned for aniline, no appreciable spectral changes under the conditions of the present experiment are observed.

CONCERNING THE INTERPRETATION OF THE INTENSITY DECREASE

The observed intensity changes in Table I are apparently not accompanied by any large wavelength change. With this in mind, the possible factors causing the observed changes may now be briefly discussed at a more fundamental level. One possible explanation is that intermolecular hydrogen bonding (or generally association), by withdrawing part of the electronic cloud from the carboxyl group, increases the planarity of the molecule (cf. 18). The resulting decreased steric hindrance could account for the increased absorption intensity, and would be expected to give rise to a bathochromic shift (cf. 13, 18).

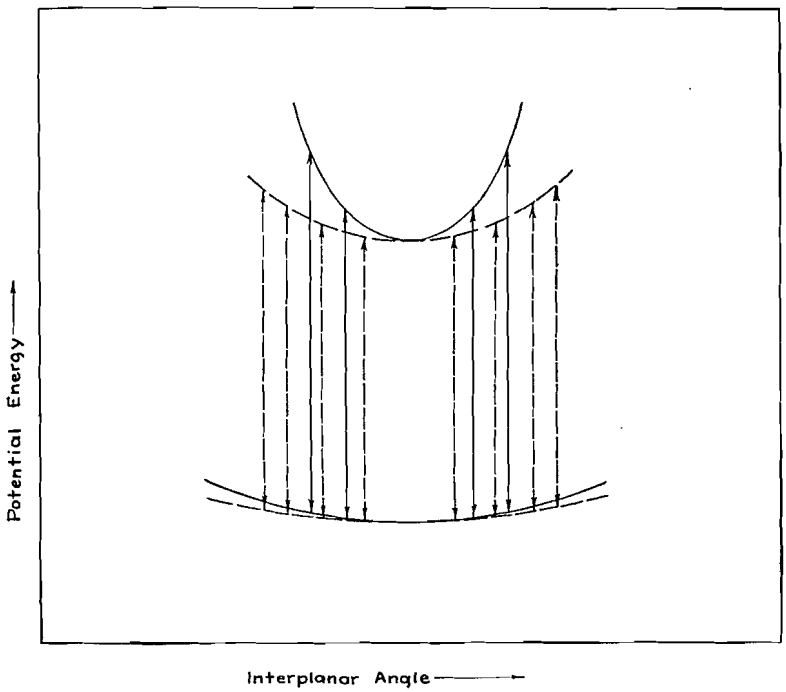

FIG. 1. Schematic representation of potential energy curves and electronic transitions for benzoic acid in the monomeric form (full lines) compared to benzoic acid in the dimeric form (dashed lines).

Can. J. Chem. Downloaded from www.nrcresearchpress.com by 61.7.252.67 on 09/04/12
For personal use only.

Another, not necessarily alternative, interpretation is to assume that association decreases the force constant of twist about the bond linking the carboxyl group to the benzene ring. This might be expected to cause an effect as illustrated in Fig. 1. (Fig. 1 is, of course, an idealization since, for example, it is not certain that the energy level minima of ground and excited states occur at similar interplanar angles.) As shown in the diagram, the decreased force constant is assumed to flatten the energy level curves of the ground and excited states and thereby increases the absorption intensity. This follows, because the proportion of molecules in positions favorable for electronic excitation will be increased. At the same time, the wavelength of maximal absorption normally undergoes a bathochromic shift.

A third explanation is that increased association (involving non-bonded electrons of the carbonyl group) increases the energy of excitation, because of the greater amount of energy required to excite partially bound electrons. Since this greater energy would cause a hypsochromic shift, this is probably not the predominant factor for the compounds studied (see Table I).

The hypothesis that association causes the observed changes, chiefly by varying the force constant, receives support from a number of other independent observations. Thus, in the first place, a smaller force constant—assuming the explanation proposed for the *C*-band (17)—would frequently produce similar changes in both *B*- and *C*-bands. This is in fact observed for benzoic acid.

Next, a similarly altered force constant would be anticipated on introduction of an electron-withdrawing substituent in a molecule in a position such that the main mesomeric interaction remains approximately constant. This is found to be correct. For example, *m*-terphenyl (λ_{max} 252 mμ, ϵ = 44,000) absorbs at the same maximal wavelength as diphenyl (λ_{max} 252 mμ, ϵ = 18,000), but rather surprisingly with more than twice the absorption intensity of diphenyl (23). This suggests that an effect analogous to the above-mentioned association occurs; more precisely, the third phenyl ring may be supposed to weaken the force constant for the central bonds and in this way cause the intensity increase.

Another example may be provided by the previously noted, but unexplained, similarity between the spectra of nitrobenzoic acids and nitrobenzene (18). There, the electron-withdrawing effect of both substituents in nitrobenzoic acids can be supposed to deactivate the benzene nucleus sufficiently to prevent any primary mesomeric interaction. This explains the absence of any appreciable mesomeric interaction between the two substituents in *p*-nitrobenzoic acid as indicated by the lack of any significant wavelength shift. Further, according to the present hypothesis, a secondary effect may now operate which will tend to reduce the force constant of the N-nuclear bond, and thus be responsible for the increased absorption intensity (λ_{max} 258 mμ, ϵ = 11,000) in *p*-nitrobenzoic acid. The meta-isomer absorbs with approximately the same intensity (λ_{max} 255 mμ, ϵ = 7500) as nitrobenzene (λ_{max} 258 mμ, ϵ = 8500), but in this compound a buttressing effect may account for a reduced absorption intensity (16). In the ortho-isomer, steric interactions certainly inhibit the conjugation between the nitro-group and the benzene ring and only an inflection appears at approximately 255 mμ, ϵ = 3500.

A similar explanation may also be used to explain more fundamentally the increased absorption intensity of phenyl benzoate (λ_{max} 230 mμ, ϵ = 15,000) compared with benzoic acid (λ_{max} 227 mμ, ϵ = 11,000; cf. (18)), and other "anomalous" spectral changes. These will be discussed in more detail in a separate communication.

Can. J. Chem. Downloaded from www.nrcresearchpress.com by 61.7.252.67 on 09/04/12
For personal use only.

Can. J. Chem. Downloaded from www.nrcresearchpress.com by 61.7.252.67 on 09/04/12
For personal use only.

THE EFFECT OF INTERMOLECULAR HYDROGEN BONDING BETWEEN SOLUTE AND SOLVENT MOLECULES ON ELECTRONIC ABSORPTION SPECTRA

It has been shown that definite spectral changes, which may be ascribed to association, are observed for benzoic acids in cyclohexane solution. If hydrogen bonding does occur and is responsible for these changes, one would expect that the concentration dependence would normally be greatest in hexane solution. This follows because, in solvents which are able to form a hydrogen bond with the solute molecules, a competitive hydrogen bonding may occur. This in turn presumably reduces the association occurring between solute molecules only, since generally the same substituent of the solute molecule would be involved in both solute–solute and solute–solvent hydrogen bonding. In the limit, as the solute–solvent interaction becomes increasingly more important, no concentration dependence would be observed. Therefore, it might be anticipated that, in the absence of special considerations, concentration dependence varies with the solvent. If concentration dependence occurs in an inert solvent, it may be expected to decrease in the solvent order hexane > ethanol > water.

This hypothesis has been investigated and some of the results are listed in Table II. The data can again be divided into two groups. There are the earlier values in Table II,

TABLE II

CONCENTRATION DEPENDENCE OF ABSORPTION MAXIMA IN DIFFERENT SOLUTIONS
(Concentration, $c = 6.5\times10^{-6}$–10^{-5} moles/l.; cell lengths in brackets)

		$40c$ (1 mm.)		$4c$ (10 mm.)		c (40 mm.)	
Compound	Solvent	λ_{max}, mμ	ϵ_{max}	λ_{max}, mμ	ϵ_{max}	λ_{max}, mμ	ϵ_{max}
Diphenyl	Cyclohexane	246–247	17,400	246	17,200	246–247	17,200
Diphenyl	Ethanol	247	17,300	247	17,200	246	17,300
Aniline	Cyclohexane	233–234	9300	233–234	9200	234	8900
Aniline	Ethanol	234	8200	234	8000	235	7700
Methyl benzoate	Cyclohexane	227	12,400	227	12,200	226–227	12,100
Methyl benzoate	Ethanol	227–228	12,300	227–228	12,100	227	11,700
Benzoic acid	Cyclohexane	231–232	13,700	230	12,900	228	11,900
Benzoic acid	Approx. 0.01 *N* acidic ethanol	226–227	11,400	227–228	11,400	227	11,700
Benzoic acid	0.01 *N* aqueous* HCl	229	10,800	229	11,000	229	11,100
Benzoic acid	Ethanol	227	11,600	227	11,500	227	10,800
Benzoic acid	Water	227	9400	224	8700	223	9300

**Hydrochloric acid has been added to the aqueous solution to avoid ionization, which evidently occurs in the pure aqueous medium as shown by the wavelength displacement to 223 mμ (cf. 34).*

where concentration dependence for both cyclohexane and ethanolic solution is small or absent. As mentioned before, the smallness of these intensity changes renders any conclusions based on them extremely doubtful. However, the indication is, as noted previously, that for some of these compounds changing the solvent does not materially affect the concentration dependence. This in turn indicates that this concentration dependence is not caused by hydrogen bonding. It may also be noted that Raman spectral studies (32) for methyl benzoate in ethanol afford no evidence for hydrogen bonding between methyl benzoate molecules.

For benzoic acid in ethanolic solution the expected decreased concentration dependence is observed. This concentration dependence unfortunately is so small that no decision

can be made concerning its reality. For aqueous solutions of benzoic acid ionization of the acid alters the spectrum (34) and consequently no decision can be made about dimerization. Addition of acid to both aqueous and ethanolic solution apparently inhibits concentration dependence, but the acid—apart from preventing ionization—may clearly also affect the hydrogen bonding. Similar changes are also observed for a number of substituted benzoic acids (20).

These observations are of interest for at least two reasons. First, they support the previous hypothesis, ascribing the spectral changes for benzoic acid in hexane solution to intermolecular hydrogen bonding. If this is so, the smaller concentration dependence or complete absence thereof provides at the same time evidence that hydrogen bonding occurs between solute and solvent molecules. This latter phenomenon is also well established from other physical data. Secondly, the smaller concentration dependence may throw light on the relative strengths of the hydrogen bonding involved. Thus, if *no* concentration dependence is observed in ethanolic solution, it may be supposed that the monomeric acids are under these conditions preferentially stabilized by hydrogen bonds, which are probably more important than the hydrogen bonds making up the benzoic acid dimer (cf. 34). Unfortunately, on the basis of the present data, remembering their qualitative nature (cf. Experimental), no definite decision can be made. There is, however, some indication that in *both* ethanolic *and* aqueous solution intermolecular hydrogen bonding between benzoic acid molecules is entirely inhibited (see Table II for the spectra of benzoic acid in ethanol and water when HCl has been added; cf. also (34)); that is, that any observed concentration dependence in aqueous or ethanolic solution should be ascribed to a changed degree of dissociation for the benzoic acid molecules rather than to dimerization.

THE EFFECT OF OTHER ENVIRONMENTAL FACTORS ON ELECTRONIC ABSORPTION SPECTRA

Under this heading we may group together a variety of other environmental factors which by means of a mechanism other than hydrogen bonding affect the absorption spectra. Their existence is almost self-evident from theoretical considerations, but clear-cut examples of their spectral effects are not always available. At present, we shall confine ourselves to discussing only one example, linking this with other spectral phenomena which also point to these environmental factors as a means of affecting spectra. Additional examples will be discussed in other parts of this series as they arise in the course of discussion.

The example chosen is the spectrum of acetophenone in dioxane–water mixtures and the relevant data are recorded in Table III. Dioxane–water mixtures were chosen partly because the dielectric constant of such solutions is known, and it was in this way hoped to find a relation between the dielectric constant of a solution and one of its characteristic spectral properties. The results show that for acetophenone in various solvent mixtures no concentration dependence is observed. This confirms the expectation that acetophenone under these conditions does not associate with itself (cf. 27). On changing the dielectric constant of the solvent, however another type of change is observed, namely a distinct wavelength shift in the *B*-band of acetophenone. This wavelength shift may either be caused by intermolecular hydrogen bonding of the type discussed in the previous section, or it may be caused by other forces acting on the molecule.

The following suggest that "other" factors also contribute to the observed spectral changes:

Can. J. Chem. Downloaded from www.nrcresearchpress.com by 61.7.252.67 on 09/04/12
For personal use only.

TABLE III

ABSORPTION MAXIMA OF COMPOUNDS IN SOLUTIONS OF VARYING DIELECTRIC CONSTANT

Compound	Solvent	Concentration range	λ_{max}, mμ	ϵ_{max} and percentage deviation
Acetophenone	Dioxane	4×10^{-4} to 1×10^{-5}	239	*12,700±3%
	75% aqueous dioxane	4×10^{-4} to 1×10^{-5}	241	12,300±2%
	50% aqueous dioxane	4×10^{-4} to 1×10^{-5}	243	12,200±2%
	25% aqueous dioxane	4×10^{-4} to 1×10^{-5}	244	12,300±2%
	Water	4×10^{-4} to 1×10^{-5}	244.5	12,100±2%
Acetophenone (*C*-band)	Dioxane	4×10^{-3} to 1×10^{-4}	277	*1010±3%
	75% aqueous dioxane	4×10^{-3} to 1×10^{-4}	277	1060±2%
	50% aqueous dioxane	4×10^{-3} to 1×10^{-4}	278	1120±2%
	25% aqueous dioxane	4×10^{-3} to 1×10^{-4}	278	1200±2%
	Water	4×10^{-3} to 1×10^{-4}	277	1240±2%
Nitrobenzene	Dioxane	8×10^{-4} to 2×10^{-5}	258	8200±2%
	50% aqueous dioxane	6×10^{-4} to 1.5×10^{-5}	264	7800±2%
	Water	8×10^{-4} to 2×10^{-5}	266	7850±2%

*ϵ *values within any particular concentration range are* ±2%.

(i) The location of maximal wavelength changes for the *B*-bands of both acetophenone and nitrobenzene with increase of dielectric constant (see Table III). Wavelength displacements of similar magnitude were observed on altering the solvent from ethanol to water by Ungnade (33), who tentatively ascribes these wavelength displacements to hydrogen bonding. However, if hydrogen bonding were exclusively responsible for the spectral change, one would expect almost every dioxane–water solvent mixture to have sufficient water molecules to ensure suitably solvated structures for all the acetophenone molecules present. It would follow that maximal wavelengths would be expected to alter appreciably on addition of a small amount of water to pure dioxane as solvent; after which addition of water to the solvent mixture should not cause any further spectral change. In fact, the addition of water progressively alters the wavelength of maximal absorption, and there is no indication of any break in the curve relating maximal wavelengths and dielectric constant of the solvent mixtures.

(ii) Infrared data (27) for acetophenone in various solutions failed to show any band doubling, such as would be expected if more than one molecular species were present in solution. Such band doubling *is* observed for various substituted amines and has been ascribed to hydrogen bonding (21).

(iii) It is well known that changing the solvent affects the general shape of an absorption curve in many cases. In one instance at least, an investigation has been carried out to determine whether these changes are due to intermolecular hydrogen bonding. Coggeshall and Lang (8), using the temperature effects in isooctane and ethanolic solutions, conclusively showed that the spectral differences between the two solutions for aniline and phenol do not depend on stable hydrogen bonded complexes.

In concluding this section it should be noted that apart from the existence of other environmental factors, little else can as yet be ascertained about these forces, from electronic absorption spectra. Consequently, no attempt has been made to explain their effects on the *C*-band, which apparently are different from the effect of these forces on the *B*-band (see Table III). For similar reasons steric effects have not been investigated, although steric effects will almost certainly affect such molecular interaction. Finally, the nature of the molecular interaction itself, which probably includes a polar solvent

Can. J. Chem. Downloaded from www.nrcresearchpress.com by 61.7.252.67 on 09/04/12
For personal use only.

effect and the possibility of a change in the molecular entity concerned (for example, benzoic acids in different solvent media), has not been fully elucidated, and the problem evidently requires further consideration.

ACKNOWLEDGMENTS

The authors gratefully acknowledge the receipt of research grants from the National Research Council of Canada and the Research Corporation of New York.

REFERENCES

1. BEINERT, H. J. Am. Chem. Soc. **78**, 5323 (1956).
2. BELLAMY, L. J. The infra-red spectra of complex molecules. Methuen and Co., Ltd., London. 1954. p. 139.
3. BLADON, P., HENBEST, H. B., and WOOD, G. W. J. Chem. Soc. 2737 (1952).
4. BRAUDE, E. A. and TIMMONS, C. J. Photoelec. Spectrometry Group Bull. No. **6**, 139 (1953).
5. BREALEY, G. J. and KASHA, M. J. Am. Chem. Soc. **77**, 4462 (1955).
6. BURAWOY, A., CAIS, M., CHAMBERLAIN, J. T., LIVERSEDGE, F., and THOMPSON, A. R. J. Chem. Soc. 3721 (1955).
7. BURAWOY, A. and THOMPSON, A. R. J. Chem. Soc. 1443 (1953).
8. COGGESHALL, N. D. and LANG, E. M. J. Am. Chem. Soc. **70**, 3283 (1948).
9. CRAM, D. J. and CRANZ, F. W. J. Am. Chem. Soc. **72**, 595 (1950).
10. DANNENBERG, H. Z. Naturforsch. **4b**, 327 (1949).
11. DAVIES, M. and GRIFFITHS, D. M. L. J. Chem. Soc. 132 (1955).
12. EGLINTON, G., JONES, E. R. H., and WHITING, M. C. J. Chem. Soc. 2873 (1952).
13. FORBES, W. F. and MUELLER, W. A. Can. J. Chem. **34**, 1340 (1956).
14. FORBES, W. F. and MUELLER, W. A. Can. J. Chem. **34**, 1542 (1956).
15. FORBES, W. F. and MUELLER, W. A. Can. J. Chem. **35**, 488 (1957).
16. FORBES, W. F. and MUELLER, W. A. J. Am. Chem. Soc. **79** (In press, 1957).
17. FORBES, W. F., MUELLER, W. A., RALPH, A. S., and TEMPLETON, J. F. Can. J. Chem. **35**, 1049 (1957).
18. FORBES, W. F. and SHERATTE, M. B. Can. J. Chem. **33**, 1829 (1955).
19. FORBES, W. F. and TEMPLETON, J. F. Chem. and Ind. 77, 600 (1957).
20. FORBES, W. F. *et al.* Unpublished information.
21. FUSON, N., JOSIEN, M. L., POWELL, R. L., and UTTERBACK, E. J. Chem. Phys. **20**, 145 (1952).
22. FUSON, N., JOSIEN, M. L., and SHELTON, E. M. J. Am. Chem. Soc. **76**, 2526 (1954).
23. GILLAM, A. E. and HEY, D. H. J. Chem. Soc. 1170 (1939).
24. HESS, K. and FRAHM, H. Ber. **71**, 2627 (1938).
25. HIRSHBERG, Y., KNOTT, E. B., and FISHER, E. J. Chem. Soc. 3313 (1955).
26. JONES, R. N. and SANDORFY, C. *In* West, W. Chemical applications of spectroscopy. Interscience Publishers, Inc., New York. 1956. pp. 424–427.
27. JOSIEN, M. L. and LASCOMBE, J. Compt. rend. **239**, 51 (1954).
28. KEUSSLER, V. v. Z. Elektrochem. **58**, 136 (1954).
29. KOIZUMI, M. and MATAGA, N. Bull. Chem. Soc. Japan, **27**, 194 (1954); cf. Chem. Abstr. **49**, 7382 (1955).
30. KUMLER, W. D. J. Am. Chem. Soc. **68**, 1184 (1946).
31. NAGAKURA, S. and BABA, H. J. Am. Chem. Soc. **74**, 5693 (1952).
32. PURANIK, P. G. J. Chem. Phys. **26**, 601 (1957).
33. UNGNADE, H. E. J. Am. Chem. Soc. **75**, 432 (1953).
34. UNGNADE, H. E. and LAMB, R. W. J. Am. Chem. Soc. **74**, 3789 (1952).

Can. J. Chem. Downloaded from www.nrcresearchpress.com by 61.7.252.67 on 09/04/12
For personal use only.

Can. J. Chem. Downloaded from www.nrcresearchpress.com by 61.7.252.67 on 09/04/12
For personal use only.

THE ELECTRIC MOMENTS OF SOME N,N′-DISUBSTITUTED PIPERAZINES[1]

M. V. George and George F Wright

ABSTRACT

The establishment of significant orientation polarizations for a series of symmetrically N-substituted piperazines including N,N′-dichloro-2,5-↑↓-dimethylpiperazine, which was prepared anew, confirms the report of Partington and contradicts that of Hassel. The existence of these moments is not compatible with the postulation of a favored chair conformation especially in consideration of the proton magnetic resonances of N,N′-dimethylpiperazine and N,N′-diformylpiperazine. On the other hand the experiments favor the postulation of flexible conformation for these piperazines.

According to several reviews (8, 2) the "chair" form of six-membered alicyclic compounds is the expected conformation. The reported zero dipole of N,N′-dichloropiperazine (1) is cited in support of this opinion. This evidence seems to be at variance with the report (14) that piperazine and diphenylpiperazine in benzene have moments of 1.47 D. and 0.85 D. respectively. The experimental data kindly furnished to us by Professor Partington seem to be unequivocal. In order to resolve the apparent contradiction we have examined the polarization of a series of piperazines by methods which have been described previously (15, 16). The results are included in Table I.

The values for solutions in benzene are derived by determination of $d\epsilon/d\omega$ (lines marked with unprimed letters, Fig. 1) and $d\bar{V}/d\omega$ (lines marked with primed letters in Fig. 1). Specifically, the dielectric constants (ϵ) and specific volumes ($\bar{V}$) of N,N′-dichloro-2,5-↑↓-dimethylpiperazine are recorded with respect to weight fractions ω for a series of solutions along lines A and A′, Fig. 1. Extrapolation to zero weight fraction gives values conforming closely with $\epsilon = 2.2840$ and $\bar{V} = 1.13795$ for pure benzene at 20°. Therefore calculation for total solute molecular polarization by the method of Halverstadt and Kumler (8) is justified.

In order to calculate the moment of this substance the distortion polarization must be evaluated. Since the additive group refraction (8.6 cc.) derived from the N–Cl linkage in a few liquid chloramines (17) is probably unreliable we have chosen to determine P_{E+A} from the dielectric constant of solid dichlorodimethylpiperazine obtained by extrapolation of apparent ϵ versus pellet thickness (line M, Fig. 2) to zero thickness where "edge effect" is minimal. The distortion polarization by this method (15, 16) is 40.4 cc. in contrast to 44.9 cc. calculated from group refractions. The electric moment calculated from $P_T - (P_{E+A})$ is 0.66 D. while that from $P_T - R_D$ (calc.) is 0.47 D. While the higher value should be considered the more reliable, neither moment conforms with the zero value stipulated for N,N′-dichloropiperazine by Andersen and Hassel (1).

Since these authors did not report experimental details we have redetermined the dielectric constants and specific volumes of benzene solutions containing dichloropiperazine. These values (lines B and B′, Fig. 1) justify the calculation of total molecular solute polarization as 46.3 cc. Unfortunately the distortion polarization (P_{E+A}) cannot be determined directly because the substance explodes in the pellet press. The damage attests to the energy of the N–Cl linkage.

In the absence of the experimental value we have calculated the moment of dichloropiperazine by use of the additive group refraction, and also by correcting the latter R_D by a factor derived from the additive versus the experimental distortion polarization of the dimethyl homologue. The moment (Table I) may be 0.85 D. or 0.71 D.,

[1]*Manuscript received July 23, 1957.*
Contribution from the Department of Chemistry, University of Toronto, Toronto, Ontario.

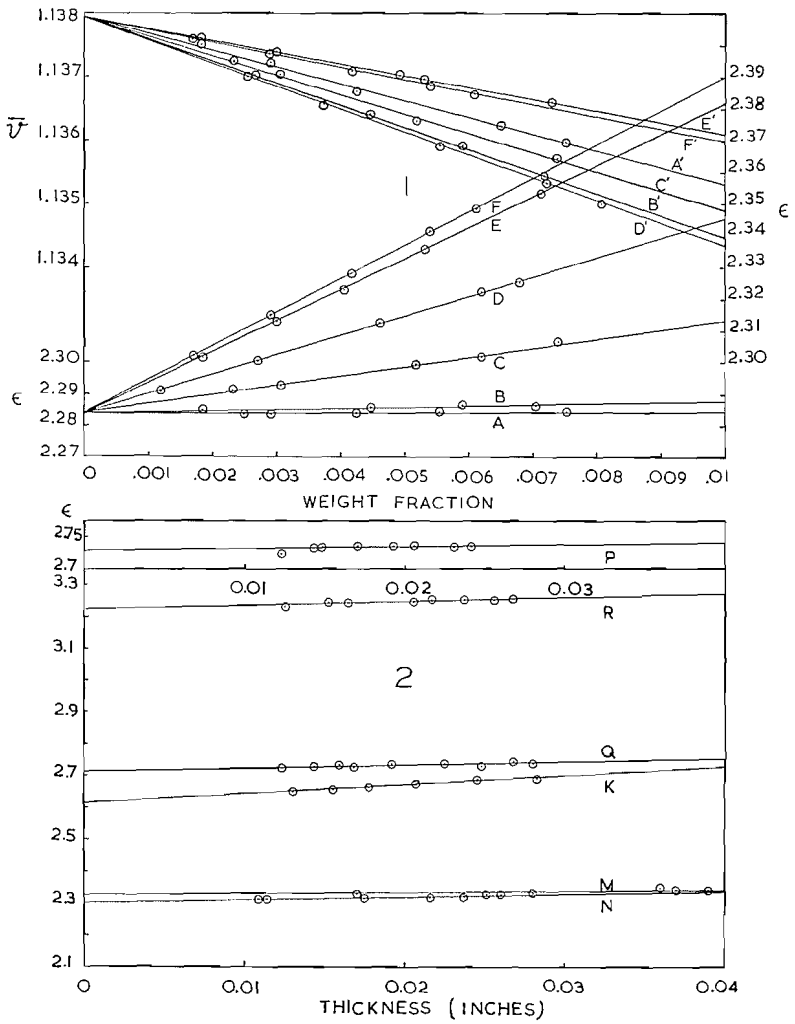

FIGS. 1 and 2.

depending on whether the corrected or the uncorrected additive refraction is applied. Despite the uncertainty one may affirm that the moment of N,N′-dichloropiperazine is not zero, as was reported previously (1). Moreover in view of the low group moment (*ca.* 0.3 D.) which has been assigned to the N–Cl linkage (23, 11) the conformation of atoms in this substance must exist largely in the flexible (so-called boat) form rather than the chair form.

In order to exclude the possibility that the presence of substituent methyl groups might vitiate the comparison between the two dichloropiperazines described above we have determined P_T and P_{E+A} for 2,5-↑↓-dimethylpiperazine from $d\epsilon/d\omega$ (line S, Fig. 3), $d\bar{V}/d\omega$ (line T, Fig. 3), and $d\epsilon/d$(thickness) (line N, Fig. 2). Although we used dioxane solutions the calculated moment (1.55 D.) compares favorably with the 1.47 D. reported by Martin (14) for piperazine in benzene. Furthermore the experimental P_{E+A} (Table I) is reasonably close to the calculated R_D for 2,5-↑↓-dimethylpiperazine. A similar comparison (from line P, Fig. 2) justifies Martin's calculated R_D for diphenylpiperazine. Thus correlations among the distortion polarization of piperazines seem to be reliable.

Can. J. Chem. Downloaded from www.nrcresearchpress.com by 61.7.252.67 on 09/04/12
For personal use only.

In view of Martin's small moment (0.85 D.) for N,N′-diphenylpiperazine it seemed worth while to examine an N-alkyl-disubstituted piperazine. Examination of N,N′-dimethylpiperazine in benzene ($d\epsilon/d\omega$, line V and $d\bar{V}/d\omega$, line U, Fig. 3) shows that its

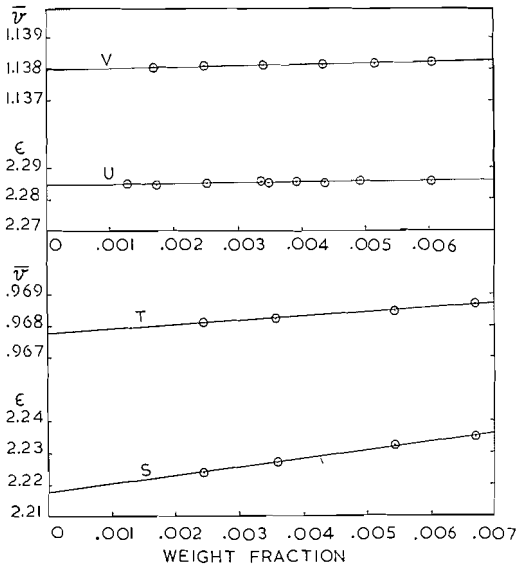

FIG. 3.

moment is low (0.59 D.). The difference between the diphenyl and dimethyl analogues is not unexpected (μ for aniline, 1.58 D., versus μ for trimethylamine, 0.86 D. in benzene), but closer correlation to define constellar differences is not justified without an elaborate study in which temperature and solvent are varied (15).

However it may be noted that a zero moment would be expected for a symmetrical

TABLE I

POLARIZATIONS AND MOMENTS OF PIPERAZINES AND RELATED COMPOUNDS AT 20°±0.05° C.

Compound	Solvent	P_T, cc.	R_D, cc. calc.	Pellet P_{E+A}, cc.	μ, D.
N,N′-Dichloro-2,5-↑↓-dimethylpiperazine	Benzene	49.6	44.9	40.4	0.47 0.66
N,N′-Dichloropiperazine	Benzene	46.3	35.6		0.71 0.85
Piperazine	Benzene				1.47 (14)
N,N′-Diphenylpiperazine	Benzene		74.3	75.2	0.85 (14)
2,5-↑↓-Dimethylpiperazine	Dioxane	85.7	34.9	33.1	1.55
N,N′-Diformylpiperazine	Benzene	195	35.6	43.3	2.72± .03
N,N′-*Bis*-cyanoethylpiperazine	Benzene	433	52.7	60.8	4.23± .02
N,N′-*Bis*-cyanoethyl-2,5-↑↓-dimethylpiperazine	Benzene	470.6	61.5	68.8	4.32± .01
Methyldiformamide	Benzene	68.27	20.3[b]		1.51[d]
N,N′-Dimethylpiperazine	Benzene	41.8	35.5[b]		0.59
Dimethylformamide	Benzene	327	19.9[b] 20.0[a]		3.82[c]

[a] *R_D by additive refraction values.*
[b] *R_D from density and refractive index.*
[c] *Confirms S. Suzuki, Kagaku,* **23**, *535 (1953); Chem. Abstr.* **47**, *11892 (1953).*
[d] *Kindly furnished by Dr. Rae of Stanford University. The proton magnetic resonance spectrum of this liquid at 25° consists of two simple peaks with areas corresponding to an intensity ratio of 2:3. The lesser peak at −140 c.p.s. (relative to water) should be due to the formyl protons while the larger peak at +88 c.p.s. may be attributed to the methyl protons.*

Can. J. Chem. Downloaded from www.nrcresearchpress.com by 61.7.252.67 on 09/04/12
For personal use only.

conformation since the methyl groups would be opposed either in axial or equatorial positions. Since their algebraic sum ought then to be zero, the existence of a real moment belies the postulation of a crown conformation.

Inherent in arguments of this sort is the assumption that a chair conformation, because of its essential stability, contributes so largely to the state of atomic arrangement in a six-membered cyclic molecule that the latter may be described as a static chair form. Such a form, if it is centrosymmetrical, will not be oriented in the electrical field. However, any activated deviation from this centrosymmetry will be observable by fields of frequency higher than those of atomic motion within the molecule. Undoubtedly for this reason Partington has suggested (14) that the observed moments of piperazines are due to axial–equatorial disposition of N,N′-substituents of chair conformations. The *e–a* constellation in IV (Fig. 4) would contribute to orientation polarization while the symmetrical *e–e* conformation, V, or the alternative *a–a* form would not make a contribution.

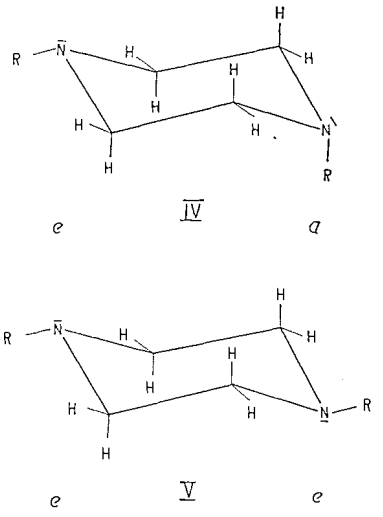

FIG. 4.

The transition from V *e–e* to V *a–a* may be expected to involve an activation energy which is not much less than the 3.6 kcal. specified (3) for the free energy difference between the *a–a* and *e–e* forms of 1,4-dimethylcyclohexane, and this activation energy should not be very different from the free energy difference between Partington's unsymmetrical form, IV, and his symmetrical V *e–e*. In these circumstances the amount of IV should not be great enough to account for the moments observed by Partington and ourselves. Moreover the transition rate from V to IV ought to be of the order of 0.0005 c.p.s. at ordinary temperatures, according to the energies that are involved. For our evaluation of transition rates we are greatly indebted to Dr. H. W. Patton and Mr. J. H. Chaudet of the Tennessee Eastman Company (Division of Eastman Kodak Co.), who determined proton magnetic resonances at 40 Mc. for several of these piperazines.

These workers have reported to us the information that N,N′-dimethylpiperazine shows two simple peaks about 6 cycles apart in the vicinity of 98 c.p.s. relative to water,

Can. J. Chem. Downloaded from www.nrcresearchpress.com by 61.7.252.67 on 09/04/12
For personal use only.

at 25°. They attribute the peak at the higher field position to the protons of the two N-methyl groups, which therefore are equivalent. The peak at the lower field position must be due to the methylene protons. Since these methylene protons in a static six-membered ring ought to be non-equivalent, Patton and Chaudet have cooled the sample to −5° C. in an attempt to separate the peak at lower field position, but without success. Therefore the transition rate must be faster by several orders of magnitude than the modulatory frequency at which resonance is measured. It follows that a chair conformation does not describe N,N′-dimethylpiperazine adequately.

For further variation in the piperazine substituents we have included N,N′-diformylpiperazine as a typical amide. The dielectric constants and specific volumes of its benzene solution are shown as D and D′, Fig. 1. The distortion polarization has been evaluated by the pellet technique (R, Fig. 2). Calculation of P_{E+A} discloses the presence of a high (7.7 cc.) atom polarization if the bond additivity calculation of P_E is reliable. The reliability of the calculated electronic polarization is attested in this instance by the close agreement (Table I) between calculated and observed molecular refractions of the analogous dimethylformamide.

Therefore the atom polarization of diformylpiperazine, specified by pellet measurement, probably is genuine, but one may doubt that it is related to the piperazine ring. More likely this distortion by the external electric field involves the formyl groups. It may be seen in Table I that substances like 2,5-dimethylpiperazine and N,N′-diphenylpiperazine do not display appreciable atom polarization. On the other hand *bis*-N,N′-β-cyanoethylpiperazine (moment calculations from F, F′, Fig. 1, and K, Fig. 2) and *bis*-N,N′-cyanoethyl-2,5-↑↓-dimethylpiperazine (calculations from E, E′, Fig. 1, and Q, Fig. 2) both seem to have atom polarizations comparable in magnitude with that of diformylpiperazine. Presumably the cyano groups, like the formyl group, can be distorted appreciably by a weak electric field at 500 kc. The phenomenon should and will be investigated more thoroughly. At present it is relatively unimportant because it does not affect appreciably the moment (2.72 D.) of diformylpiperazine.

The moment angle of the formylamino group is not known, but it is probably low. Indeed a low formylamino moment angle is exemplified by the value of 1.51 D. found (Table I) for methyldiformamide. Now if N,N′-diformylpiperazine is considered in the sense of two opposed units of dimethylformamide (Table I, 3.82 D.) in which the formyl moment angles are low, then the observed moment (2.72 D.) seems to be high if a symmetrical chair conformation is assumed. In such a structure the formyl groups would be opposed either in axial or equatorial positions. Thus they would largely cancel each other unless random rotation of the formyl group were restricted. Evidence that this restriction does not exist is presented below in order to confirm that the chair conformation for diformylpiperazine is improbable.

The proton magnetic resonance spectrum of N,N′-diformylpiperazine in water at 25° shows the same simplicity as that of N,N′-dimethylpiperazine. The weaker (−115 c.p.s. with respect to water) of two simple peaks has been attributed to the formyl protons, so the stronger peak, at +1.5 c.p.s., must be due to the methylene protons. There is no tendency toward splitting of the peak when the solution of diformylpiperazine is chilled almost to its freezing point. This behavior is different from that of dimethylformamide (19, 24). If the spectrum reported for this latter substance is revised to compare with a 40 Mc. field, a formyl-proton peak exists at −120 c.p.s. and two methyl-proton peaks occur at +80 and +88 c.p.s. relative to water, the respective areas being

Can. J. Chem. Downloaded from www.nrcresearchpress.com by 61.7.252.67 on 09/04/12
For personal use only.

1:3:3. However the rigidity is lost when the sample in the field is heated to 117°, at which temperature only a single peak at about 84 c.p.s. is observed.

It is apparent that the spectrum of diformylpiperazine at 25° resembles that of dimethylformamide at 117°, where the latter is presumed to have free, rapidly rotating methyl groups. Of course diformylpiperazine cannot have this generalized positioning of protons because of its cyclic structure. However an oscillatory motion of the six-membered ring would account for the single methylene peak that Patton and Chaudet observed if this oscillation were more rapid than that of the proton resonance frequency.

But in this circumstance the ring oscillation frequency ought to exceed 100 c.p.s. by at least an order of magnitude. Clearly this rate is incompatible with the oscillation of a "chair" ring for which the transition rate should not exceed 0.01 c.p.s., assuming a rather low transition energy of 2 kcal. The transition rate from "chair" to rigid "boat" is even more unfavorable according to the calculated energies (3). Consideration of Patton and Chaudet's results suggests that the transition energy must not exceed 300 cal. in order to attain a rate of about 1000 c.p.s., at which the substituent proton positions would not be discernible by the N.M.R. modulatory frequency.

It is widely accepted that the crown form of cyclohexane is more stable than is the flexible form (13), although some refinement of calculation suggests that the higher free energy attributed to the flexible form may be exaggerated (9). In fact the electron diffraction patterns of 1,2-dichlorocyclohexane and 1,1,2-trichlorocyclohexane have been interpreted in favor of the flexible form at not-too-elevated temperatures (5). Actually it might be expected that substituent groups would affect profoundly the shape of the ring to which they are attached, and Oosterhof (18, 9) has shown that the dipole moment of 1,4-cyclohexanedione is best explained in terms of a flexible form. This opinion is supported by solid dielectric studies to be reported from the Toronto laboratory, which show that this substance does not have an abnormal atom polarization.

Recently Kumler and Huitric have classified those cyclic types which may be expected to be flexible (12). The inclusion of piperazines among these classes is reasonable. A flattened tetrahedral aspect for the nitrogen atoms should permit the flexibility that is indicated for 1,4-cyclohexanedione. The potential energy barrier due to methylene hydrogen interaction should be significantly less than that postulated for cyclohexane. In this circumstance a transition energy of 300 cal., largely involving compensated bond rotations, may indeed account satisfactorily for the absence of axial and equatorial proton positions in the N.M.R. spectrum. Therefore piperazines are thought to be in flexible conformation.

Within this definition we question whether the term "conformation" is an appropriate description of the saturated six-membered ring of atoms when it is considered in its flexible aspect. These terms imply the existence, during time intervals greater than those of molecular collision rate, of definite static structures. But the flexible ring will assume an infinity of forms and certainly cannot be defined in less than six static structures. None of these six will be equivalent when substituents of different complexity are present. In such circumstances the difficulties of "conformational analysis" are apparent. Perhaps they are not unsurmountable if the use of a static model is abandoned in favor of a dynamic one.

The authors wish to thank the National Research Council and the Defence Research Board of Canada for funds in support of this research and Mrs. Westland, Mr. Podleschka,

Can. J. Chem. Downloaded from www.nrcresearchpress.com by 61.7.252.67 on 09/04/12
For personal use only.

and the Tennessee Eastman Company, Division of Eastman Kodak Company, for extensive experimental aid.

EXPERIMENTAL*

Purification of Solvents

Benzene was washed with concentrated sulphuric acid until the acid layer was colorless and then was dried and distilled by the sodium benzophenone technique (15). The specific volume and dielectric constant were 1.13795 and 2.284 at 20° C. respectively. Dioxane was refluxed with concentrated hydrochloric acid (5 ml./l.) for 6 hours, then neutralized, dried with sodium hydroxide, then refluxed, and finally distilled by the sodium benzophenone technique. The specific volume and dielectric constant at 20° C. were 0.96770 and 2.2175 respectively.

N,N'-Dichloro-2,5-↑↓-dimethylpiperazine

Repeated vacuum sublimation of commercial 2,5-↑↓-dimethylpiperazine gave flakes, m.p. 117–117.5° C. A solution of 5 g. (0.044 mole) in 20 ml. of water was added slowly with stirring to an excess of fresh sodium hypochlorite solution at 0° C. The white precipitate was filtered off, washed with cold water, and dried, 5.8 g. (72%), m.p. 81.5–82° C. Vacuum sublimation raised the melting point to 83.8° C. with 64% recovery. The density at 20° C. was found by flotation to be 1.394. Calc. for $C_6H_{12}Cl_2$: C, 39.4; H, 6.61; N, 15.3. Found: C, 39.7; H, 6.61; N, 15.8.

N,N'-Dichloropiperazine

This compound, prepared in 68% yield, m.p. 71–71.5° C. (21), was crystallized from ether–ethanol (2: 1, 15 ml./g.) and this was vacuum sublimed, m.p. 72° C.

N,N'-Diformylpiperazine

The reported procedure (20) gave a 91.5% yield, m.p. 125–126° C. Repeated crystallization from absolute ethanol (10 ml./g.) raised the melting point to 127.5° C. The density was determined by air displacement to be 1.391.

N,N'-Bis-[2-cyanoethyl]-2,5-↑↓-dimethylpiperazine (25)

To a suspension of 5.71 g. (0.05 mole) of 2,5-↑↓-dimethylpiperazine in 10 ml. of dioxane was added 0.25 cc. of benzyltrimethylammonium hydroxide (40% aq., Triton B) and then 7.18 g. (0.135 mole) of pure acrylonitrile with stirring during 1 hour. The temperature was maintained below 30° C. After subsequent stirring for 8 hours the system was diluted with 20 ml. of water and was extracted with methylene chloride. The methylene chloride extract was dried by magnesium sulphate and then evaporated, leaving 4.1 g. (38%), m.p. 140° C. Crystallization from absolute ethanol (50 ml./g.) using decolorizing charcoal raised the melting point to 147° C. The density (air displacement) was 1.163. Calc. for $C_{12}H_{20}N_4$: C, 65.4; H, 9.16; N, 25.4. Found: C, 65.5; H, 9.05; N, 25.7.

N,N'-Bis-[2-cyanoethyl]piperazine

The detail for preparation of the substance was not reported (6) so it was synthesized essentially as described above, yielding a brown mass which was distilled under reduced pressure. The fraction boiling at 174–176° C. at 6–7 mm. pressure solidified on cooling, and was purified by crystallization from ether (25 ml./g.), m.p. 62–63° C., 59.9% yield. Density determined by air displacement was 1.119.

Melting points have been corrected against reliable standards (see Wright, G. F. Can. J. Technol. **34, 89 (1956)).*

Can. J. Chem. Downloaded from www.nrcresearchpress.com by 61.7.252.67 on 09/04/12
For personal use only.

N,N'-Dimethylpiperazine

The substance was prepared (22) in 40% yield, b.p. 131–132° C. (758 mm.), D_4^{20} 0.861, n_D^{20} 1.4477.

Polarizations of Solutions

Dielectric constants and specific volumes were determined as described previously (16) except that a matching signal of 60 c.p.s. or 120 c.p.s. was read from an oscilloscope instead of a zero beat between V.F.O. and F.F.O. The polarization was calculated by the method of Halverstadt and Kumler (8).

Polarization of the Solids

The method outlined previously (15) was used, the only alteration being the use of a gold amalgam (4.0 g. Hg + 1.5 g. Au). The densities have been determined either by the flotation method (4) or by an air-displacement method. The density of N,N'-diphenylpiperazine by the latter method was 1.158 at 20° C.

Density of Solids by Air Displacement

In order to avoid the errors due to solubility and chemical reactions which are likely to occur when density is determined by flotation an apparatus has been redesigned (shown cross-sectionally in front and top elevations in Fig. 5) for greater precision than

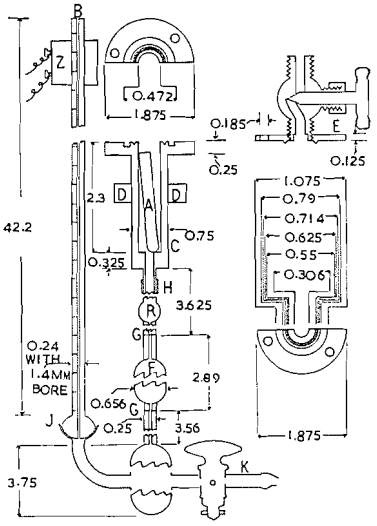

FIG. 5.

was required in the original one (7). The displacement of air by a finely-ground 0.3–1.0 g. sample in weighing tube A is measured by the change in pressure measured in manometer B after a 6-volt buzzer has reduced the column of mercury to a constant height. The brass chamber C, held by clamping block D, is equipped with a flange in which a seating V groove and a sealing square groove (containing a Parker O ring, 0.125 in. width, 0.8125 in. I.D., and 1.0625 in. O.D.) are cut. The V groove matches a V tongue in the flange E which is mated to C by three 10–32 machine screws. This flange, which is equipped for closure by a $\frac{1}{4}$ inch I PS Hoke valve, must be seated carefully with repeated symmetry tests by insertion of feeler stock between the flanges. When properly seated the volume of C, containing the empty sample tube, can be measured to a precision of

Can. J. Chem. Downloaded from www.nrcresearchpress.com by 61.7.252.67 on 09/04/12
For personal use only.

0.04% by compressing air (by means of a levelling bulb, not shown) in front of mercury which fills the bulb F, the volume of which between two fiduciary marks G, G is previously known. A glass–metal seal H connects C and F, via a 2 cc. bulb R above the fiduciary mark. This bulb may be reduced in size to obtain proper volume relationship in the system. With attention to barometric pressure the change in manometric height is determined upon compression when the sample is included inside of C.

Thereupon the density is determined according to the relationship $d = W/L$, where L is the volume occupied by weight W of the sample. Then $L = M - PN/dp_2$, where P is the barometric pressure, dp_2 is the pressure difference (cm. Hg) observed when volume N of bulb F is filled with mercury, after brass chamber C containing the sample is rendered airtight. M is the volume of C containing the empty sample tube and is defined as $M = PN/dp_1$, where dp_1 is the observed pressure difference when mercury fills F without a sample in airtight chamber C.

Both the 12/2 ball joint J attaching the manometer and the stopcock K leading to the levelling bulb must be clamped tightly during the determination. The O ring but not the tongue and groove should be lightly greased in order to ensure airtightness when the flanges are connected. In order to avoid strain on the glass–metal seal during the closure operation the massive brass clamp D must secure C rigidly to the retort stand. Ordinary burette clamps suffice for the remainder of the apparatus.

The method is more arduous than a determination of density by flotation, but it is less subject to error than is the flotation method. For example the flotation of ferric acetylacetonate in aqueous calcium chloride has led to an erroneous value of 1.41 (15). The density by air displacement is 1.382 ± 0.002. A revised flotation in which the medium was hexane plus 1,2-dibromoethane saturated with the ferric compound gave a value of 1.381 ± 0.008. The value is decreased by either method when a crystal contains impenetrable faults, so the sample should be ground finely before analysis.

Polarization Values

Experimentally determined values for $d\epsilon/d\omega$ (α) and $d\bar{V}/d\omega$ (β) for the various piperazine derivatives are recorded as follows: N,N′-dichloro-2,5-↑↓-dimethylpiperazine, $\alpha = 0.05$, $\beta = 0.265$; N,N′-dichloropiperazine, $\alpha = 0.35$, $\beta = 0.355$; methyldiformamide, $\alpha = 2.88$, $\beta = 0.307$; N,N′-diformylpiperazine, $\alpha = 6.14$, $\beta = 0.368$; N,N′-*bis*-cyanoethyl-2,5-↑↓-dimethylpiperazine, $\alpha = 9.62$, $\beta = 0.180$; N,N′-*bis*-cyanoethylpiperazine, $\alpha = 10.61$, $\beta = 0.205$; 2,5-↑↓-dimethylpiperazine, $\alpha = 2.65$, $\beta = 0.140$; N,N′-dimethylpiperazine, $\alpha = 0.11$, $\beta = 0.034$.

The extrapolated values for ϵ from pellet measurements are listed as follows: N,N′-dichloro-2,5-↑↓-dimethylpiperazine, 2.325; N,N′-diformylpiperazine, 3.22; N,N′-*bis*-cyanoethyl-2,5-↑↓-dimethylpiperazine, 2.714; N,N′-*bis*-cyanoethylpiperazine, 2.615; 2,5-↑↓-dimethylpiperazine, 2.306; and N,N′-diphenylpiperazine, 2.730.

REFERENCES

1. ANDERSEN, P. and HASSEL, O. Acta Chem. Scand. **3**, 1180 (1949).
2. BARTON, D. H. R. and COOKSON, R. C. Quart. Revs. **10**, 44 (1956).
3. BECKETT, C. W., PITZER, K. S., and SPITZER, R. J. Am. Chem. Soc. **69**, 2488 (1947).
4. BERNAL, J. D. and CROWFOOT, D. Nature, **134**, 809 (1934).
5. DALLINGA, G. Thesis, Leyden. 1951.
6. FARBENIND., I.G., A.-G. German patent 641,597 (1937); Chem. Abstr. **31**, 5813 (1937).
7. GALLAY, W. and TAPP, J. S. J. Am. Leather Chemists Assoc. **37**, 140 (1942); Chem. Abstr. **36**, 3387 (1942).
8. HALVERSTADT, I. F. and KUMLER, W. D. J. Am. Chem. Soc. **64**, 2988 (1942).
9. HASELBROCK, P. and OOSTERHOF, L. J. Trans. Faraday Soc. **10**, 87 (1951).
10. HASSEL, O. Quart. Revs. (London), **7**, 221 (1953).

Can. J. Chem. Downloaded from www.nrcresearchpress.com by 61.7.252.67 on 09/04/12
For personal use only.

11. KETELAAR, J. A. A. Rec. trav. chim. **62**, 289 (1943).
12. KUMLER, W. D. and HUITRIC, A. C. J. Am. Chem. Soc. **78**, 3369 (1956).
13. KWESTROO, W., MEIJER, F. A., and HARINGA, E. Rec. trav. chim. **73**, 717 (1954).
14. MARTIN, G. T. O. Thesis, London. 1936. pp. 134, 180. PARTINGTON, J. R. An advanced treatise on physical chemistry. Vol. 5. Longmans, Green and Co., London. 1954. p. 538.
15. MEREDITH, C. C., WESTLAND, L. and WRIGHT, G. F. J. Am. Chem. Soc. **79**, 2385 (1957).
16. MEREDITH, C. C. and WRIGHT, G. F. Can. J. Technol. **33**, 182 (1955).
17. MYERS, G. S. and WRIGHT, G. F. Can. J. Research, B, **26**, 257 (1948).
18. OOSTERHOF, L. J. Thesis, Leyden. 1949.
19. PHILIPS, W. D. J. Chem. Phys. **23**, 1363 (1955).
20. ROBSON, J. H. and REINHART, J. J. Am. Chem. Soc. **77**, 2453 (1955).
21. SCHMIDT, A. and WICHMAN, G. Ber. **24**, 3237 (1891).
22. STEWART, H. W. *et al.* J. Org. Chem. **13**, 134 (1948).
23. THEILACKER, W. and FAUSER, K. Ann. **539**, 103 (1939).
24. VARIAN ASSOCIATES. Anal. Chem. **28**, 25A (Aug., 1956).
25. WAGNER, W. F. and KAUFFMAN, W. B. Anal. Chem. **25**, 538 (1953).

Can. J. Chem. Downloaded from www.nrcresearchpress.com by 61.7.252.67 on 09/04/12
For personal use only.

Can. J. Chem. Downloaded from www.nrcresearchpress.com by 61.7.252.67 on 09/04/12
For personal use only.

CRITICAL CONCENTRATION EFFECTS IN POLYMER–POLYMER–SOLVENT SYSTEMS[1]

C. C. Bigelow and L. H. Cragg

ABSTRACT

In various ternary systems of the type polymer A – polymer B – solvent S, a dip or peak has been observed in the $[\eta]$–c_B curve at the critical concentration of polymer B. ($[\eta]$ is the intrinsic viscosity of A in mixed solvent consisting of B and S, and c_B is the concentration of B in this mixed solvent.) It is shown that such a critical concentration effect is most likely to occur when the solvent is poor for polymer B, and will be the larger the poorer the solvent.

Evidence is also presented in support of the hypothesis that if, as is usual, the two polymers repel each other, the effect is a dip if the solvent is good for polymer A and is a peak if the solvent is sufficiently poor for polymer A.

Critical concentrations of polystyrene, polyvinyl acetate, and polymethyl methacrylate (five different samples) have been measured in this way in 12 different ternary systems. These observed critical concentrations are in good agreement with values calculated using the equation previously described, according to which the critical concentration of a polymer is inversely proportional to its intrinsic viscosity in the solution.

INTRODUCTION

In a recent paper (1) we presented evidence to show that a critical concentration can be determined in suitable viscometric experiments with ternary systems of the type polymer A – polymer B – solvent S. ("Critical concentration" here means the concentration of polymer at which the equivalent sphere of a given polymer molecule just touches the equivalent spheres of all of its nearest neighbor molecules of like kind.) If the intrinsic viscosity $[\eta]$ of Polymer A is measured first in pure S and then in a series of mixed solvents (solutions of polymer B in S) successively richer in polymer B, and if these intrinsic viscosities are plotted against c_B, the concentration of polymer B in the mixed solvent, then the resulting curve may exhibit a discontinuity at or very near the concentration calculated to be the critical concentration (c_{crit}) of polymer B in the solution. In four of the five experiments of this type that were reported, the discontinuity took the form of a dip, the curve having the general shape indicated in Fig. 1.

A qualitative explanation of this behavior was proposed, and an equation for calculating critical concentrations was developed with the aid of the Flory-Fox treatment of intrinsic viscosity. According to this equation, the critical concentration of polymer B should be inversely proportional to its intrinsic viscosity in pure solvent S (more strictly, to its reduced viscosity at $c_B = c_{crit}$, but since c_{crit} is very small, this reduced viscosity will differ little from the intrinsic viscosity). This conclusion was tested in experiments with the ternary system polystyrene – polymethyl methacrylate – solvent in which the intrinsic viscosity of polymer B (polymethyl methacrylate in this system) was varied, first by using samples of different molecular weight with the same solvent (*m*-xylene), and then by using two different solvents with the same sample of polymer. The observed critical concentration varied as predicted, and the values agreed remarkably well with the calculated values. (The observed critical concentration is taken to be the concentration c_B at which the discontinuity occurs or, more precisely, the concentration corresponding to the bottom of the dip or the top of the peak.)

In this paper we report and discuss the results of further study of this critical concentration phenomenon.

[1]*Manuscript received September 16, 1957.*
Contribution from the Department of Chemistry, McMaster University, Hamilton, Ontario. This work was done as part of the requirements for the Ph.D. degree, and was financially supported by the National Research Council of Canada.

Can. J. Chem. Downloaded from www.nrcresearchpress.com by 61.7.252.67 on 09/04/12
For personal use only.

PROCEDURE

In the experiments to be reported here, we have (with a few exceptions noted in Table III) used the first of the two methods for determining critical concentrations that were described in the earlier paper (1). This was partly because this "intrinsic viscosity method" is more trustworthy (though much more time-consuming) than the other, but mainly because we were interested in the nature, as well as in the location, of the discontinuity in the $[\eta]$ vs. c_B curve.

Special care was taken in determining intrinsic viscosities. Both η_{sp}/c and $(\ln \eta_r)/c$ were plotted against c_A on a common plot and the curves were extrapolated to a common point at $c_A = 0$ to obtain $[\eta]$. When, as in almost all cases, these curves were straight lines, $[\eta]$ was evaluated by the method of least squares.

RESULTS AND DISCUSSION

I. The Nature of the Discontinuity

(*a*) In all of the experiments reported in the earlier paper, the solvent S was a poor one for polymer B. (By a "poor" solvent we mean here one in which the polymer has a relatively low intrinsic viscosity.) If the explanation of the critical concentration "dip" proposed in the previous paper is correct, a system in which the solvent S is poor for polymer B (and good for polymer A) should give a greater effect than one in which the solvent is good for polymer B (and good for polymer A). In a solvent that is good for it, the molecules of polymer A will be loosely coiled and the effective volume of an isolated molecule will be relatively large. As the critical concentration of polymer A is approached, molecules of polymer B will begin to crowd in on the molecule on all sides; and further increase in concentration will cause contraction of the polymer A molecule or of the polymer B molecules or both (assuming that the two polymers repel each other, as is true of most polymer pairs). If the solvent is poor for polymer B, its molecules will be more tightly coiled, and the density of segments of B in the immediate neighborhood of the A molecule will be higher than if the solvent is good for polymer B. The repulsive forces causing the molecule of A to shrink (and hence its intrinsic viscosity to decrease) will therefore be greater. Conversely, if the solvent is good for polymer B the contraction in volume of the molecule of polymer A (and therefore the decrease in $[\eta]$) might well be so slight as to be undetectable, partly because of the much lower density of B segments at the critical concentration, and partly because such contracting as would occur would be shared by the B molecules.

The validity of these speculations was tested in experiments with the systems listed in Table I. The results are shown graphically in Fig. 3. Toluene and benzene are both *poor* solvents for polyvinyl acetate; experiments 6 and 8 should therefore give measurable effects. Toluene and *m*-xylene are both *good* solvents for polystyrene; in experiments 7 and 9, therefore, the discontinuity should be very small or undetectable. As

TABLE I

TERNARY SYSTEMS IN EXPERIMENTS 6 TO 9
(For identification of polymer samples see Table V)

Experiment	Polymer A	Polymer B	Solvent S
6	PS-3	PV-1	Toluene
7	PV-1	PS-3	Toluene
8	PS-3	PV-1	Benzene
9	PM-4	PS-3	*m*-Xylene

can be seen, unmistakable "dips" do occur in the $[\eta]$–c_B curves for experiments 6 and 8 (and they occur at the calculated critical concentrations, indicated by the arrow) but there is no sign of a "dip" in the curves for experiments 7 and 9.

(*b*) In experiment 5 of the earlier paper (1) the discontinuity in the $[\eta]$–c_B curve was a peak rather than a dip (see Fig. 2 of this paper). In this experiment polymer A was

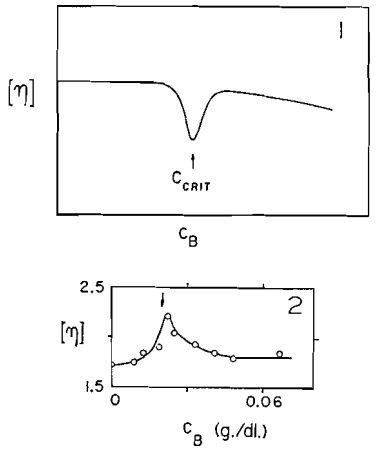

FIG. 1. Viscometric critical concentration effect: idealized curve.
FIG. 2. A critical concentration peak. (System: polystyrene – polymethyl methacrylate – butanone.)

polystyrene, polymer B was polymethyl methacrylate, and the solvent was butanone. This solvent is a poor one for *both* polymers. The shape of the discontinuity was a surprise, but it can be plausibly accounted for in terms of our molecular explanation. If the solvent is a very poor one for the A polymer (as butanone is for polystyrene in experiment 5) the segments of a polymer A molecule will much prefer one another's company to that of solvent molecules, and the polymer molecule will coil up tightly. If the dislike of polymer A for polymer B is less than its dislike of the solvent S, then the fairly uniform environment, consisting of solvent molecules and polymer B segments, that is attained near the critical concentration will be a more favorable environment for the polymer A molecule than pure solvent S. The molecule will therefore expand and $[\eta]$ will increase. Further, as c_B is increased, $[\eta]$ will continue to increase until the critical concentration is reached, after which interpenetration of the two kinds of polymer molecules begins to make the environment within and without the polymer A molecule more nearly the same. Then the molecule of polymer A will begin to contract again, for the mixed solvent is still a poor solvent for the polymer.

One might therefore expect to find a peak with systems in which the solvent S is poor for both polymers and is so poor for polymer A that the mutual repulsion of polymer A segments and solvent S molecules would exceed that of polymer A segments and polymer B segments.

We therefore investigated three additional systems, in which the solvent was at the same time poor for both polymers. These systems are described in Table II and the results obtained with them are shown graphically in Fig. 4. In two of the three experiments (10 and 11) a peak was indeed obtained— and at or very near the concentration calculated to be the critical concentration. In the third (experiment 12) no discontinuity of any kind was observed. This may be because the polymer A – solvent repulsion was not appreciably greater than the polymer A – polymer B repulsion.

Can. J. Chem. Downloaded from www.nrcresearchpress.com by 61.7.252.67 on 09/04/12
For personal use only.

TABLE II

SYSTEMS IN WHICH THE SOLVENT IS POOR FOR BOTH POLYMERS

Experiment	Polymer A	Polymer B	Solvents
10	PS-3	PV-1	Butanone
11	PS-3	PM-5	Ethyl acetate
12	PM-5	PS-3	Ethyl acetate

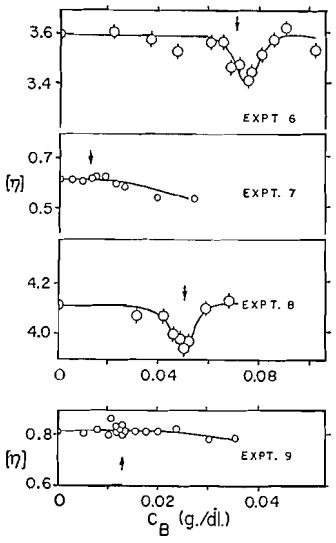

FIG. 3. Effect of goodness of solvent for polymer B. The solvent is poor for B in experiments 6 and 8 and good for B in experiments 7 and 9. (The arrows point to the calculated critical concentrations.)

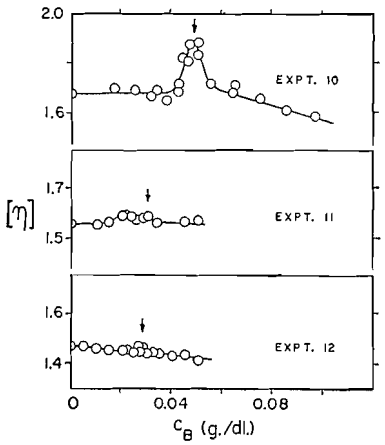

FIG. 4. Critical concentration effects with systems in which the solvent is poor for both polymers. (Arrows indicate calculated critical concentrations.)

(*c*) The success that our hypothesis has had in explaining and predicting experimental findings makes it seem highly probable that the critical concentration effects we have been studying are due to polymer–polymer and polymer–solvent interactions and to their relative magnitudes. So far we have dealt with systems in which the two polymers would be expected to repel each other (see for example the polymer incompatibility studies of Dobry and Boyer-Kawenoki (2) and of Kern and Slocombe (3)). The magnitude of the dip should be greatest when the solvent is good for polymer A and poor for polymer B and when the two polymers repel each other strongly. The magnitude of the effect should be less when the two polymers are more alike than are polystyrene and polyvinyl acetate, or polystyrene and polymethyl methacrylate. A number of experiments have been done which seem to support this idea. The systems investigated are listed in Table III. In all of them the solvent is a poor one for the solvent polymer (polymer B).

In five of the eight experiments (13, 14, 15, 21, and 22) the critical concentration effect, if any, was too small to manifest itself by an unmistakable discontinuity. In each of the other three experiments (16, 19, and 20) a dip was indicated, each time at or near the concentration calculated to be the critical concentration (see Fig. 5). These dips were, however, very small ones, definitely smaller than those observed in systems in which the two polymers were more different chemically. (It is interesting to note

Can. J. Chem. Downloaded from www.nrcresearchpress.com by 61.7.252.67 on 09/04/12
For personal use only.

TABLE III

SYSTEMS IN WHICH THE POLYMERS ARE SIMILAR

Experiment*	Polymer A	Polymer B	Solvent S	Relationship of polymers
13	PM-5	PV-1	Toluene	Both esters
14*f*	PV-1	PM-5	Toluene	Both esters
15	PM-5	PV-1	Butanone	Both esters
16	PV-1	PM-5	Butanone	Both esters
19	PS-4	PS-5	Butanone	Homologues
20	PM-6	PM-7	Ethyl acetate	Homologues
21*f*	PpMeS	PmMeS	Butanone	Isomers
22*f*	PmMeS	PpMeS	Butanone	Isomers

**f indicates that the experiment was done using the flow time method only.*

that with two quite different systems—see experiments 19 and 20—critical concentration effects were observed when the two polymers were two different samples of the same polymer. These experiments provide direct evidence that molecules of the same polymer repel each other and, when crowded close together, cause each other to shrink. Such behavior was postulated on theoretical grounds and some of its consequences discussed by Weissberg, Simha, and Rothman (4). Indeed, they derived an expression for the concentration at which this shrinkage should occur (in a binary system)—though they did not call it a critical concentration—and their expression has the same form as ours.)

II. The Location of the Discontinuity: The Critical Concentration

Although these experiments have been concerned primarily with the nature (shape and magnitude) of the discontinuity, they contribute further evidence that the discontinuity does indeed occur at a critical concentration. In the first paper, proof that a critical concentration effect was being observed was provided by the excellent agreement between observed and calculated values of the critical concentration. The equation for calculating the critical concentration (c_{crit}) was shown to be

$$c_{crit} = 0.0436k^3/[\eta]_B,$$

where k is a (dimensionless) proportionality constant whose value is apparently very close to unity. The constant should have substantially the same value for all the polymers used as polymer A in the systems we have studied, for all of them are flexible linear vinyl polymers. The same equation, viz. $c_{crit} = 0.0436k^3/[\eta]_B$, should therefore apply to all the systems.

The value of c_{crit}, the critical concentration, obtained from the equation is marked on each of the plots by means of an arrow; any dip or peak in the $[\eta]$–c_B curve invariably occurs at or near this point. In Table IV are listed values of the product of the observed critical concentration and the intrinsic viscosity of polymer B. The essential constancy of this product is strong evidence for the validity of our assumptions. Visual evidence of

TABLE IV

OBSERVED VALUES OF THE PRODUCT $[\eta]_B c_{crit}$

Experiment	$[\eta]_B c_{crit}$	Experiment	$[\eta]_B c_{crit}$
1	0.046	8	0.044
2	0.047	10	0.046
3	0.042	11	0.034
4	0.046	16	0.040
5	0.048	19	0.034
6	0.047	20	0.044

Can. J. Chem. Downloaded from www.nrcresearchpress.com by 61.7.252.67 on 09/04/12
For personal use only.

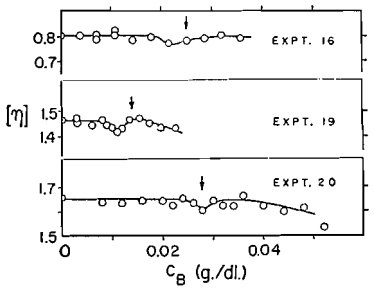

FIG. 5. Critical concentration effects. (Experiment 16, polyvinyl acetate – polymethyl methacrylate – butanone; Experiment 19, polystyrene–polystyrene–butanone; Experiment 20, polymethyl methacrylate – polymethyl methacrylate – ethyl acetate.)

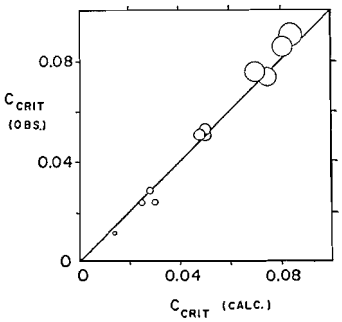

FIG. 6. Plot of observed vs. calculated critical concentrations.

the good agreement between calculated and observed values is afforded in Fig. 6, in which c_{crit}(observed) is plotted against c_{crit}(calculated) for all systems in which a discontinuity has been observed. The agreement would be perfect if the points fell on the 45° line; it is not perfect, but it is surprisingly good.

EXPERIMENTAL

The apparatus and experimental methods were those used previously (1). The intrinsic viscosities of the various polymers used are given in Table V.

TABLE V

INTRINSIC VISCOSITIES OF POLYMER SAMPLES USED

Polymer	Solvent	[η] (dl./g.)
Polystyrene		
PS-3	Benzene	4.13
	Butanone	1.67
	Ethyl acetate	1.55
	Toluene	3.60
	m-Xylene	3.44
PS-4	Butanone	1.67
PS-5	Butanone	3.07
Polymethyl methacrylate		
PM-4	*m*-Xylene	0.81
PM-5	Butanone	1.74
	Ethyl acetate	1.47
	Toluene	1.75
PM-6	Ethyl acetate	1.65
PM-7	Ethyl acetate	1.57
Polyvinyl acetate*		
PV-1	Benzene	0.88
	Butanone	0.80
	Toluene	0.62
Poly(*m*-methylstyrene) and poly(*p*-methylstyrene)*		
PmMeS	Butanone	1.55
PpMeS	Butanone	1.28

We are grateful to Shawinigan Chemicals Ltd., Shawinigan Falls, Que., for providing us with the sample of polyvinyl acetate (Gelva. V-27) and to Dr. R. J. Kern (3), Monsanto Chemical Co., Dayton, Ohio, for the samples of poly(m-methylstyrene) and poly(p-methylstyrene).

Can. J. Chem. Downloaded from www.nrcresearchpress.com by 61.7.252.67 on 09/04/12
For personal use only.

REFERENCES

1. CRAGG, L. H. and BIGELOW, C. C. J. Polymer Sci. **24**, 429 (1957).
2. DOBRY, A. and BOYER-KAWENOKI, F. J. Polymer Sci. **2**, 90 (1947).
3. KERN, R. J. and SLOCOMBE, R. J. J. Polymer Sci. **15**, 183 (1955).
4. WEISSBERG, S. G., SIMHA, R., and ROTHMAN, S. J. Research Natl. Bur. Standards, **47**, 298 (1951).

Can. J. Chem. Downloaded from www.nrcresearchpress.com by 61.7.252.67 on 09/04/12
For personal use only.

Can. J. Chem. Downloaded from www.nrcresearchpress.com by 61.7.252.67 on 09/04/12
For personal use only.

THE SYNTHESIS OF ω-DEOXY-ω-*S*-ETHYL-POLYOLS[1]

J. K. N. JONES AND D. L. MITCHELL[2]

ABSTRACT

Treatment of an aldose diethyl thioacetal with a limited amount of aged Raney nickel catalyst resulted in the reductive cleavage of one thioethyl group. 1-Deoxy-1-*S*-ethyl derivatives of D-galactitol, L-arabitol, L-rhamnitol, and D-glucitol have thus been synthesized and their structures proved. 1-Deoxy-1-*S*-ethyl-L-galactitol has been prepared by the borohydride reduction of 6-deoxy-6-*S*-ethyl-D-galactose.

INTRODUCTION

Reductive desulphurization of aldose thioacetals (1, 2, 3, 4, 5, 6) and aldose thioacetal acetates (1, 7) using an excess of Raney nickel catalyst provides a simple method of preparing 1-deoxy sugar alcohols. In a review, Fletcher and Richtmyer (8) questioned the value of using as high catalyst ratios as have been reported in the literature. They tabulate examples of ratios from 9:1 to 15:1 (grams of Raney nickel catalyst to grams of thioacetal derivative). Generally, the yield of 1-deoxy-polyol or 1-deoxy-polyol acetate varied inversely with the catalyst ratio. The decrease in yield was probably due to adsorption of product on the catalyst. We found that when a catalyst with a low hydrogen content (e.g. W-2 catalyst) was used, and a low catalyst ratio was chosen (*ca.* 5 : 1), a mixture of three compounds resulted. When D-galactose diethyl thioacetal was thus treated, paper chromatographic examination of the product indicated the presence of a fast-moving compound, D-galactose diethyl thioacetal; a slow-moving compound, 1-deoxy-D-galactitol (L-fucitol); and a second sulphur-containing compound (II) which was between these two compounds on the chromatogram. A catalyst ratio was determined, by means of trial experiments in which compound II was the main product of the reaction. In this reaction one thioethyl group of the aldose diethyl thioacetal (I) was replaced by a hydrogen atom to give the monothioethyl derivative (II). Compound II on reductive desulphurization gave 1-deoxy-D-galactitol (L-fucitol) (III).

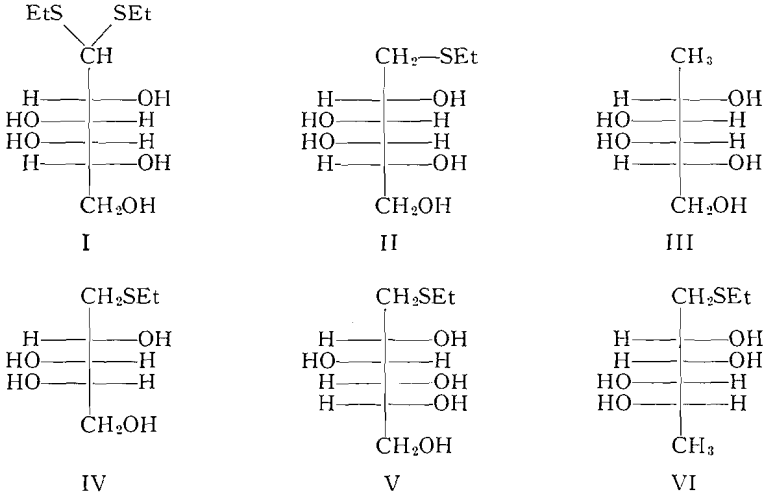

[1]*Manuscript received September 9, 1957.*
Contribution from the Department of Chemistry, Queen's University, Kingston, Ontario.
[2]*Present address: Department of Organic Chemistry, University of Bristol, Bristol 8, England.*

The diethyl thioacetals of D-galactose, L-arabinose, D-glucose, and L-rhamnose were also partially desulphurized, and respectively yielded 1-deoxy-1-*S*-ethyl-(D-galactitol) (II), -(L-arabitol) (IV), -(D-glucitol) (V), and -(L-rhamnitol) (VI). Crystalline acetates of compounds II, IV, and V were also prepared. The yields were not appreciably reduced when large scale experiments were carried out. This result corresponded with the observations of Richtmyer and co-workers (2, 3, 4, 5, 6). Complete reductive desulphurization of compounds II, IV, V, and VI yielded the known ω-deoxy sugar alcohols, which are 1-deoxy-D-galactitol (L-fucitol), 1-deoxy-L-arabitol (L-lyxomethylitol), 1-deoxy-D-glucitol (L-gulomethylitol), and 1,6-dideoxy-L-mannitol respectively.

ω-Deoxy-ω-*S*-alkyl polyols can also be synthesized by the reduction of the corresponding aldose (9). In this manner 6-deoxy-6-*S*-ethyl-D-galactose (6-deoxy-6-thioethyl-D-galactose) (10) was reduced with potassium borohydride to 1-deoxy-1-*S*-ethyl-L-galactitol (6-deoxy-6-*S*-ethyl-D-galactitol). This compound had about the same melting point and magnitude of optical rotation (but in the opposite direction) as the D-isomer. The D- and L-isomers had identical rates of movement on paper chromatograms. The racemate melted at about 10° C. lower than the isomers.

EXPERIMENTAL

Solutions were concentrated under reduced pressure (*ca.* 15 mm.) at a bath temperature of 50° C. or less. Melting points were uncorrected and optical rotations were determined in water unless otherwise stated. Paper chromatography was carried out by the descending method (11) on Whatman No. 1 filter paper using the following solvent systems (v: v): (*a*) ethyl acetate – acetic acid – water (9: 2: 2), (*b*) ethyl acetate – acetic acid – formic acid – water (18: 3: 1: 4), (*c*) *n*-butanol–ethanol–water (3: 1: 1), (*d*) *n*-butanol–pyridine–water (10 : 3 : 3). Non-reducing compounds were detected on paper chromatograms with a silver nitrate spray reagent (12). The rate of movement of the compound on paper chromatograms is quoted relative to that of the solvent front (R_f value) or relative to that of rhamnose (R_{Rh} value).

A standard method of preparing Raney nickel catalyst W-2 (13) was followed exactly. It was stored in ethanol at 0–5° C. This catalyst will be referred to as catalyst (*a*) in these experiments. A catalyst of slightly lower hydrogen content was obtained from the Aldrich Chemical Company.* It was washed free from traces of alkali and was stored in ethanol at 0–5° C. This catalyst will be referred to as catalyst (*b*). The activity of catalysts (*a*) and (*b*) did not change appreciably over a storage period of 4 months.

Preliminary Experiments

Weighed samples (*ca.* 0.5 g.) of D-galactose diethyl thioacetal (14) were dissolved in 75% *iso*propanol (50 ml.). A range of catalyst ratios was chosen (*ca.* 3 : 1 to 8 : 1) and the appropriate volume of Raney nickel catalyst (*a*) was added to the flasks. The mixture was boiled under reflux for 2 hours and cooled. The solutions were filtered from the catalyst and examined by paper chromatography. The catalyst ratio that produced the maximum amount of component with a rate of movement between galactose diethyl thioacetal and fucitol was used in subsequent experiments. Catalyst ratios are expressed in liters of settled volume of nickel per mole of aldose thioacetal.

Preparation of 1-Deoxy-1-S-ethyl-D-galactitol

(i) D-Galactose diethyl thioacetal (3.73 g., 0.013 mole) and Raney nickel catalyst (*a*)

**Aldrich Chemical Co., Inc., Milwaukee 12, Wisconsin.*

Can. J. Chem. Downloaded from www.nrcresearchpress.com by 61.7.252.67 on 09/04/12
For personal use only.

(settled volume 30 ml. equivalent to 2.3 liters/mole) in 75% *iso*propanol (200 ml.) were shaken in a hydrogen atmosphere (pressure *ca.* 800 mm.) for 2 hours at 60° C. and then boiled under reflux on the water bath (100° C.) for an additional 3 hours. The filtered solution was concentrated to a crystalline mass, which was recrystallized from methanol and acetone (5 : 1) to give 1.24 g. (57.5%) of product melting at 151–153° C. (The catalyst was lost accidentally before it could be washed.) The rate of movement on a paper chromatogram ((*a*) R_f 0.47, R_{Rh} 1.70; (*b*) R_f 0.52, R_{Rh} 1.29) was intermediate between galactose diethyl thioacetal and fucitol, and the compound on treatment with silver nitrate spray reagent gave an intense spot which appeared immediately, whereas the spot due to fucitol appeared slowly. The product on recrystallization from methanol gave a chromatographically pure product that had m.p. 149–151° C. and $[\alpha]_D^{25°}$ −9°±2° (*c*, 0.95). Anal. Calc. for $C_8H_{18}O_5S$: C, 42.6; H, 8.1; S, 14.2. Found: C, 42.5; H, 8.1; S, 14.0.

(ii) *Large scale experiment.*—D-Galactose diethyl thioacetal (11.0 g., 0.038 mole) and Raney nickel catalyst (*a*) (83.5 ml. settled volume equivalent to 2.2. liters/mole) in 75% *iso*propanol (1 liter) were boiled under reflux on the water bath (100° C.) for 3 hours. The solution was decanted from the catalyst, which was washed twice with ethanol and separated by centrifugation. The catalyst was digested with ethanol (3 times with 300 ml.) and then with water (2 times with 200 ml.), and the combined washings and decanted solution were filtered through a pad of Celite and evaporated to dryness. Recrystallization from methanol and acetone (5 : 1) gave 5.80 g. (67%) of product in three crops of crystals, m.p. 148–149° C. Duplicate readings gave $[\alpha]_D^{21°}$ −8.2° (*c*, 2.24); $[\alpha]_D^{24°}$ −8.9° (*c*, 2.33).

*1-Deoxy-1-S-ethyl-*D*-galactitol Pentaacetate*

1-Deoxy-1-*S*-ethyl-D-galactitol (88 mg.) in pyridine (1 ml.) was acetylated for 24 hours with acetic anhydride (1 ml.). The product crystallized when it was poured into a slurry of chipped ice and water, and it was collected by filtration. It was dissolved in hot methanol, and the solution was purified with a little charcoal and filtered through a pad of Celite. The filtrate was warmed and an equal volume of hot water was added. After cooling, the crystals in the form of flakes were collected by filtration and washed with cold water. Yield: 117 mg. (60%), m.p. 150.5–151.0° C. $[\alpha]_D^{22°}$ 8°±1° (*c*, 1.1, chloroform). Anal. Calc. for $C_{18}H_{24}O_{10}S$: C, 49.5; H, 6.5; S, 7.3. Found: C, 49.8; H, 6.7; S, 7.1.

*Conversion of 1-Deoxy-1-S-ethyl-*D*-galactitol to* L*-Fucitol*

1-Deoxy-1-*S*-ethyl-D-galactitol (120 mg.) was dissolved in 70% ethanol (10 ml.) containing Raney nickel W-2 catalyst (3 ml. settled volume) and the suspension was boiled under reflux on the water bath (100° C.) for 3 hours. The catalyst was removed by filtration through a pad of Celite, and the filtrate was concentrated to a crystalline mass. The product moved as a single spot on paper chromatograms developed in solvents (*a*), (*b*), (*c*), and (*d*) and had a rate of movement identical with that of L-fucitol prepared by the borohydride reduction of L-fucose. The following R_f and R_{Rh} values were obtained: R_f 0.37, R_{Rh} 1.12 (*a*); R_f 0.39, R_{Rh} 1.07 (*b*); R_f 0.31, R_{Rh} 1.00 (*c*); R_f 0.30, R_{Rh} 0.93 (*d*). Recrystallization from ethanol (3 ml.) gave 33.4 mg. (38%) of fine needles melting at 156.0–156.5° C. The mixed melting point with an authentic specimen was 156.0–156.5° C.

*1-Deoxy-1-S-ethyl-*L*-arabitol*

(i) L-Arabinose diethyl thioacetal (1.50 g., 0.008 mole) (15, 16) and freshly prepared Raney nickel catalyst (*a*) (settled volume 12 ml., 1.5 liters/mole) in 75% *iso*propanol (80 ml.) were boiled under reflux on the water bath (100° C.) for 3 hours. The cooled solution was decanted and the catalyst was washed with ethanol and separated by centrifugation. The catalyst was then digested with ethanol (2×100 ml.) and the combined

Can. J. Chem. Downloaded from www.nrcresearchpress.com by 61.7.252.67 on 09/04/12
For personal use only.

Can. J. Chem. Downloaded from www.nrcresearchpress.com by 61.7.252.67 on 09/04/12
For personal use only.

washings and decanted solution were filtered through a pad of Celite and evaporated to dryness. The crystalline mass was examined by paper chromatography, which indicated the presence of two compounds. The main constituent had a rate of movement of R_f 0.61, R_{Rh} 1.79 (*a*) and the second component had a rate of movement of R_f 0.43, R_{Rh} 1.27 (*a*). The ratio of the two components was visually estimated to be 20 : 1. The crude product was dissolved in hot acetone (40 ml.), filtered, and chilled in the refrigerator. The crystals were collected by filtration and the mother liquors were concentrated to yield a second crop. Yield: 0.71 g. (68%), m.p. 118.5–119.5° C., $[\alpha]_D^{22°}$ −12°±1° (*c*, 2.59). Anal. Calc. for $C_7H_{16}O_4S$: C, 42.8; H, 8.2; S, 16.3. Found: C, 43.1; H, 8.5; S, 16.1.

(ii) L-Arabinose diethyl thioacetal (19.0 g., 0.074 mole) and 75% *iso*propanol (3 liters) were stirred mechanically with aged Raney nickel catalyst of a low hydrogen content (settled volume 250 ml., 3.3 liters/mole) and boiled under reflux on the water bath (100° C.) for 3.5–4 hours. The cooled solution was decanted and the catalyst was treated in the manner described above. Examination of the product by paper chromatography revealed only a single spot (R_f 0.69, R_{Rh} 1.83 (*a*)). The product was recrystallized from acetone–ethanol (3 : 1) to give a total yield of 8.43 g. (58%) in four crops, m.p. 119–120° C., $[\alpha]_D^{26°}$ −12°±1° (*c*, 1.75). Recrystallization from *iso*propanol gave fine needles, m.p. 118.5–119.5° C. When tested in high concentration, a trace of L-lyxomethylitol was revealed on the chromatogram and this impurity was removed by repeated recrystallizations from *iso*propanol, but the melting point remained unchanged (118.5–119.5° C.).

*1-Deoxy-1-S-ethyl-*L*-arabitol Tetraacetate*

The tetraacetate was prepared in the manner previously described for the acetylation of 1-deoxy-1-*S*-ethyl-D-galactitol. Recrystallization from ethanol and water (3 : 1) gave white plates (40%) melting at 58.0–58.5° C., $[\alpha]_D^{26°}$ −35°±1° (*c*, 1.64, chloroform). Anal. Calc. for $C_{15}H_{24}O_8S$: C, 49.4; H, 6.6; S, 8.8. Found: C, 49.5; H, 6.5; S, 8.9.

*1-Deoxy-*L*-arabitol* (L-*Lyxomethylitol*)

1-Deoxy-L-arabitol (7) was prepared in 70% yield by the desulphurization of 1-deoxy-1-*S*-ethyl-L-arabitol in the same fashion as is described for the desulphurization of L-fucitol. The product (0.19 g.) was recrystallized from ethyl acetate (40 ml.), m.p. 128–129° C., $[\alpha]_D^{27°}$ −1.8° (*c*. 1.70), (lit. m.p. 129–131° C., $[\alpha]_D^{30°}$ −1.46° (water) (9)). 1-Deoxy-D-arabitol has a reported m.p. 129–131° C. and a $[\alpha]_D^{20°}$ +0.7° (6).

*1-Deoxy-1-S-ethyl-*D*-glucitol*

D-Glucose diethyl thioacetal (15) (5.0 g., 0.017 mole) in 75% *iso*propanol (600 ml.) was boiled under reflux with aged Raney nickel catalyst (*b*) (50 ml. settled volume, 2.9 liters/mole) in exactly the same manner as is described for the preparation of 1-deoxy-1-*S*-ethyl-D-galactitol in experiment (ii). The crude product, 1.94 g. (51%), contained a trace of 1-deoxy-D-glucitol (paper chromatography), and was recrystallized four times from *iso*propanol. The pure compound had a rate of movement on a paper chromatogram of R_f 0.59, R_{Rh} 1.70 (*a*); R_f 0.61, R_{Rh} 1.53 (*b*); R_f 0.52, R_{Rh} 1.61 (*c*); R_f 0.53, R_{Rh} 1.48 (*d*); a m.p. 107.5–108° C.; and $[\alpha]_D^{26°}$ −29°±1° (*c*, 1.85). Anal. Calc. for $C_8H_{18}O_5S$: C, 42.7; H, 8.1; S, 14.2. Found: C, 42.9; H, 8.2; S, 14.0.

When the experiment was repeated on a larger scale (D-glucose diethyl thioacetal, 23.6 g., Raney nickel catalyst (*b*), 215 ml. settled volume, and *iso*propanol, 3 liters) in the manner previously described for the preparation of 1-deoxy-1-*S*-ethyl-L-arabitol, part (ii), a yield of 9.87 g. (49%) of crude product was obtained. Repeated recrystallizations from *iso*propanol gave 6.9. g. (34%) of pure compound, m.p. 107.5–108° C., $[\alpha]_D^{24°}$ −30° (*c*, 1.89).

*1-Deoxy-1-S-ethyl-*D*-glucitol Pentaacetate*

The pentaacetate was prepared in the manner previously described and was crystallized from methanol and water (1:1) in a 59% yield, m.p. 82° C., $[\alpha]_D^{26°}$ 5°±1° (*c*, 1.1, chloroform). Anal. Calc. for $C_{18}H_{28}O_{10}S$: C, 49.5; H, 6.5; S, 7.4. Found: C, 49.7; H, 6.5; S, 7.4.

*1-Deoxy-*D*-glucitol Pentaacetate*

Reductive desulphurization of 1-deoxy-1-*S*-ethyl-D-glucitol in ethanol with an excess of Raney nickel catalyst (*a*) in the usual manner gave a non-crystalline product which appeared to be chromatographically pure (R_f 0.60, R_{Rh} 1.52 (*a*); R_f 0.28, R_{Rh} 0.95 (*c*); R_f 0.29, R_{Rh} 0.88 (*d*)). It was therefore acetylated and the pentaacetate was recrystallized from ethanol, m.p. 105.5–107° C., $[\alpha]_D^{26°}$ 21°±1° (*c*, 1.26, methanol) (lit. m.p. 105–106° C., $[\alpha]_D^{21°}$ 21° (methanol) (7, 17)).

*1-Deoxy-1-S-ethyl-*L*-rhamnitol*

L-Rhamnose diethyl thioacetal (15) (4.0 g., 0.015 mole) was dissolved in 75% *iso*propanol (600 ml.) and was boiled under reflux with Raney nickel catalyst (*a*) (33 ml. settled volume equivalent to 2.2 liters/mole) for 4 hours. The crude product (1.0 g. (32%)), m.p. 118–119.5° C., was isolated in the usual way. This compound was readily soluble in water, ethanol, and *iso*propanol but it could be recrystallized from a small volume of ethyl acetate. Repeated recrystallizations from ethyl acetate gave flat plates melting at 120.5–121° C. and with $[\alpha]_D^{26°}$ −21.2° (*c*, 1.36). The rates of movement on paper chromatograms were R_f 0.76 (*a*) and R_f 0.73 (*b*). Anal. Calc. for $C_8H_{18}O_4S$: C, 45.7; H, 8.6; S, 15.2. Found: C, 46.1; H, 8.9; S, 15.1.

Reductive desulphurization of this compound in the usual way gave 1,6-dideoxy-L-mannitol. Recrystallization from a small volume of ethyl acetate gave clusters of crystals melting at 146–147° C. and with $[\alpha]_D^{24°}$ 23° (*c*, 1.02) (lit. m.p. 145–146° C., $[\alpha]_D^{20°}$ 22.8° (3)).

*1-Deoxy-1-S-ethyl-*L*-galactitol*

The preparation of 6-deoxy-6-*S*-ethyl-D-galactose described by Baker (10) was followed except that 1,2;3,4-di*iso*propylidene-6-*O*-methanesulphonyl-D-galactose (18) was used as the starting compound. 1,2;3,4-Di*iso*propylidene-6-deoxy-6-*S*-ethyl-D-galactose, $[\alpha]_D^{29°}$ 1.4765, $[\alpha]_D^{26°}$ −85.8° (*c*. 5.90, chloroform), was obtained in 92% yield after purification by high vacuum distillation. The reported constants are: $[\alpha]_D^{24°}$ 1.4795, $[\alpha]_D^{22°}$ −85.7° (chloroform) (10). Mild acid hydrolysis gave a reducing sirup that moved as a single spot on a paper chromatogram (R_f 0.53, R_{Rh} 1.35 (*b*)) (*p*-anisidine spray reagent).

A solution of this sirup (2.6 g. in 25 ml. of water) was added dropwise to a stirred solution of potassium borohydride (0.85 g. in 20 ml. of water). After 2 hours a test portion was neutralized with acetic acid and it gave a negative test with Fehling's solution. The solution was acidified with acetic acid, then percolated through a column of IR-120 (H form) ion exchange resin. The solution and washings were filtered and concentrated to dryness. After six codistillations with methanol, the residue was dissolved in a solution of methanol–acetone (5:1)(15 ml.). Crystals (1.0 g. (39%)) were deposited when the solution was chilled to −20° C. A second recrystallization from methanol–acetone gave a chromatographically pure compound which had a rate of movement on a paper chromatogram identical with that of 1-deoxy-1-*S*-ethyl-D-galactitol in solvents (*a*), (*b*), and (*c*), m.p. 151–153° C., $[\alpha]_D^{24°}$ 8.6 (*c*, 4.18). The racemate melted at 141.5–142.0° C. Anal. Calc. for $C_8H_{18}O_5S$: C, 42.6; H, 8.1; S, 14.2. Found: C, 42.8; H, 8.1; S, 13.9.

The pentaacetate was prepared in 57% yield in the usual way. Recrystallization from methanol–water (5:1) gave flakes melting at 151.0–151.5° C., $[\alpha]_D^{24°}$ −9°±1° (*c*, 1.31

Can. J. Chem. Downloaded from www.nrcresearchpress.com by 61.7.252.67 on 09/04/12
For personal use only.

chloroform). Anal. Calc. for $C_{18}H_{24}O_{10}S$: C, 49.5; H, 6.5; S, 7.3. Found: C, 49.7, H, 6.7; S, 7.2.

ACKNOWLEDGMENTS

The authors thank Dr. W. B. Reid of the Upjohn Company, Kalamazoo, Michigan, for a gift of nickel–aluminum alloy. One of us (D. L. M.) thanks the Ontario Research Foundation for grants which made this investigation possible.

REFERENCES

1. KARABINOS, J. V. and WOLFROM, M. L. J. Am. Chem. Soc. **66**, 909 (1944).
2. HUDSON, C. S. and RICHTMYER, N. K. J. Am. Chem. Soc. **72**, 3880 (1950).
3. RICHTMYER, N. K. and ZISSIS, E. J. Am. Chem. Soc. **74**, 4373 (1952).
4. HUDSON, C. S., RICHTMYER, N. K., and ZISSIS, E. J. Am. Chem. Soc. **73**, 4714 (1951).
5. RICHTMYER, N. K. and ZISSIS, E. J. Am. Chem. Soc. **72**, 129 (1953).
6. RICHTMYER, N. K. and ZISSIS, E. J. Am. Chem. Soc. **76**, 5515 (1954).
7. BOLLENBACK, G. N. and UNDERKOFLER, L. A. J. Am. Chem. Soc. **72**, 741 (1950).
8. FLETCHER, H. G., JR. and RICHTMYER, N. K. Advances in carbohydrate chemistry. Vol. 5. Academic Press, Inc., New York. 1950. p. 1.
9. OVEREND, W. G. and PARKER, L. F. J. Nature, **167**, 527 (1951).
10. BAKER, S. B. Can. J. Chem. **33**, 1102 (1955).
11. PARTRIDGE, S. M. Biochem. J. **51**, 238 (1948).
12. TREVELYAN, W. E., PROCTOR, D. P., and HARRISON, J. S. Nature, **166**, 444 (1950).
13. ORGANIC SYNTHESES. Vol. 21. John Wiley & Sons, Inc., New York. 1941. p. 15.
14. WOLFROM, M. L. J. Am. Chem. Soc. **52**, 2464 (1930).
15. FISCHER, E. Ber. **27**, 673 (1894).
16. WOLFROM, M. L. J. Am. Chem. Soc. **52**, 2464 (1930).
17. GATZI, K. and REICHSTEIN, T. Helv. Chim. Acta, **21**, 914 (1938).
18. HELFERICH, B. and DRESSLER, R. J. prakt. Chem. **153**, 285 (1939).

Can. J. Chem. Downloaded from www.nrcresearchpress.com by 61.7.252.67 on 09/04/12
For personal use only.

Can. J. Chem. Downloaded from www.nrcresearchpress.com by 61.7.252.67 on 09/04/12
For personal use only.

THE RELATION BETWEEN THE SULPHATE AND NITROGEN CONTENT OF UNSTABILIZED CELLULOSE NITRATE[1]

PAUL E. GAGNON, KARL F. KEIRSTEAD,[2] AND BRIAN T. NEWBOLD[3]

ABSTRACT

The sulphate and nitrogen contents of cellulose nitrates prepared from mixed acids containing different amounts of sulphuric acid were compared. The sulphate content showed a tendency to decrease with increasing nitrogen, for instance it was 1.96% for 10.54% and 0.44% for 13.31%. Similar results were obtained with a series of wood cellulose nitrates, for instance 2.40% for 11.01% and 0.91% for 12.47%. With practically the same amount of sulphuric acid in the mixed acid, cellulose nitrates were prepared and the sulphate and nitrogen contents were compared. For unstabilized cotton cellulose nitrates, the sulphate content decreased steadily with increasing nitrogen content. Similar results were obtained with wood cellulose nitrates.

INTRODUCTION

In a recent publication (1) the degree of nitration of cotton linters and wood cellulose was determined when the same mixed acid was used. The sulphate content of the unstabilized cellulose nitrates obtained was shown to be dependent upon the sulphuric acid content of the mixed acid.

Miles (4) has stated that the total sulphate content of cellulose nitrate tends to increase with decreasing nitrogen content. The object of the present work was to determine the relation between the total sulphate and nitrogen contents of both cotton and wood unstabilized cellulose nitrates.

EXPERIMENTAL

Cellulose Nitrate

The procedure for the nitration of cotton linters and wood cellulose was given in a recent publication (2). The methods used to analyze the mixed acids and to determine the sulphate and nitrogen contents of the unstabilized cellulose nitrates were also described in previous papers (1, 3).

RESULTS AND DISCUSSION

In general the total sulphate content of unstabilized cellulose nitrate depends upon several factors, namely, the composition of the mixed acid used to nitrate the cellulose, the nitration conditions, the degree of washing, and the nitrogen content of the cellulose nitrate. The sulphate content has been shown to increase when the proportion of sulphuric acid in the mixed acid increased (1).

In the present work, the sulphate and nitrogen contents of unstabilized cotton and wood cellulose nitrates were determined by good precision methods (1) and compared. The nitrogen contents of the cellulose nitrates varied from 13.3 to 7.7% for cotton, and 13.0 to 7.3% for wood cellulose nitrate.

The sulphate and nitrogen contents of cotton cellulose nitrates prepared from mixed acids containing different amounts of sulphuric acid are compared in Table I. The sulphate content showed a tendency to decrease with increasing nitrogen, for instance

[1]*Manuscript received September 27, 1957.*
Contribution from the Department of Chemistry, Laval University, Quebec, Que., with financial assistance from the Defence Research Board of Canada.
[2]*Present address: Lignosol Chemicals Limited, Quebec, Que.*
[3]*Research assistant, Department of Chemistry, Laval University.*

TABLE I

COMPARISON OF SULPHATE AND NITROGEN CONTENTS OF COTTON AND OF WOOD CELLULOSE NITRATES PREPARED FROM A VARIETY OF MIXED ACIDS

Cotton cellulose nitrates				Wood cellulose nitrates			
Expt. No.	Sulphuric acid in mixed acid, %	Total sulphate, $\%H_2SO_4$	Nitrogen, %	Expt. No.	Sulphuric acid in mixed acid, %	Total sulphate, $\%H_2SO_4$	Nitrogen, %
1	68.25	1.96	10.54	1	73.31	2.40	11.01
2	70.67	1.55	11.66	2	72.50	2.32	11.43
3	"	1.53	11.66	3	"	2.17	11.36
4	71.20	1.17	11.71	4	71.20	2.13	11.44
5	65.40	1.00	11.40	5	72.83	2.12	11.74
6	72.50	0.95	11.60	6	70.67	2.02	10.86
7	"	0.95	11.73	7	71.30	2.01	12.01
8	65.40	0.89	11.35	8	65.40	1.71	10.80
9	65.99	0.85	11.28	9	"	1.62	10.75
10	65.71	0.85	11.52	10	"	1.33	11.67
11	65.40	0.69	11.91	11	70.35	1.30	12.75
12	65.00	0.63	12.14	12	65.40	1.23	11.80
13	65.40	0.58	12.07	13	71.23	1.04	13.00
14	70.35	0.47	13.21	14	65.00	0.93	11.91
15	65.66	0.44	13.31	15	65.66	0.91	12.47

it was 1.96% for 10.54% and 0.44% for 13.31%, but no definite curve can be drawn. Similar results were obtained with a series of wood cellulose nitrates, as shown also in Table I, for instance 2.40% for 11.01% and 0.91% for 12.47%.

The nitrogen contents of the cellulose nitrates given in Table I varied from 13.3% to 10.5%, which is the range for cellulose nitrates used in industry. In the present work, cellulose nitrates containing less than 10.0% nitrogen did not give satisfactory results because they were either swollen or gelatinized to such an extent that it was not possible to attain a reproducible degree of washing.

The nitration conditions and the degree of washing with water for the preparation of the two types of cellulose nitrates mentioned in Table I were very similar; therefore any effects on sulphate content due to the latter can be discounted. The fact that no precise curve could be drawn to show the relation between the sulphate and nitrogen contents of the cellulose nitrates prepared from various mixed acids was thought to be due to the effects of the proportion of sulphuric acid in the mixed acid and that of the nitrogen in the cellulose nitrate. Since it has been shown that the sulphuric acid content of the mixed acid has a profound effect upon the sulphate content (1), it was essential

TABLE II

COMPARISON OF SULPHATE AND NITROGEN CONTENTS OF CELLULOSE NITRATES PREPARED FROM MIXED ACIDS CONTAINING SIMILAR AMOUNTS OF SULPHURIC ACID

		Cotton cellulose nitrate		Wood cellulose nitrate	
Expt. No.	Sulphuric acid in mixed acid, %	Sulphate, $\%H_2SO_4$	Nitrogen, %	Sulphate, $\%H_2SO_4$	Nitrogen, %
1	65.40	1.00	11.40	1.62	10.75
2	"	0.89	11.35	1.71	10.80
3	"	0.69	11.91	1.33	11.67
4	"	0.58	12.07	1.23	11.80
5	65.66	0.44	13.31	0.93	12.47

Can. J. Chem. Downloaded from www.nrcresearchpress.com by 61.7.252.67 on 09/04/12
For personal use only.

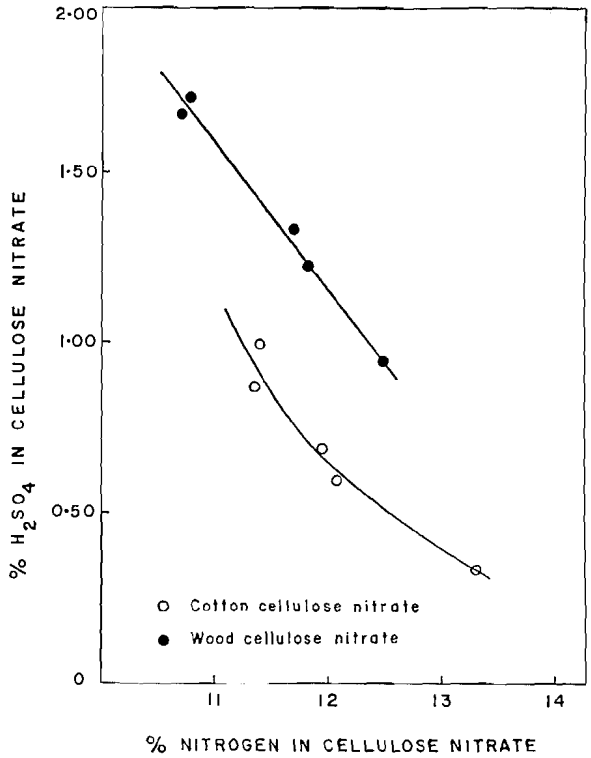

FIG. 1. Relation between sulphate and nitrogen contents of cellulose nitrates prepared from mixed acids containing similar amounts of sulphuric acid.

to remove this factor before determining the sulphate–nitrogen relation. Accordingly, cellulose nitrates were prepared using mixed acids containing an almost constant amount of sulphuric acid, and their sulphate and nitrogen contents were compared. The results for cotton and wood cellulose nitrates are given in Table II and Fig. 1.

For unstabilized cotton cellulose nitrates, the sulphate content decreased steadily with increasing nitrogen content. Furthermore, similar results were obtained for wood cellulose nitrates.

REFERENCES

1. GAGNON, P. E., KEIRSTEAD, K. F., and NEWBOLD, B. T. Can. J. Chem. **36**, 215 (1958).
2. GAGNON, P. E., KEIRSTEAD, K. F., and YAMASAKI, D. Can. J. Technol. **34**, 477 (1957).
3. KEIRSTEAD, K. F. and MYERS, J. Can. J. Chem. **32**, 566 (1954).
4. MILES, F. D. Cellulose nitrate. Clarke, Irwin & Co. Ltd., Toronto. 1955.

Can. J. Chem. Downloaded from www.nrcresearchpress.com by 61.7.252.67 on 09/04/12
For personal use only.

Can. J. Chem. Downloaded from www.nrcresearchpress.com by 61.7.252.67 on 09/04/12
For personal use only.

A CONTRIBUTION TO THE CHEMISTRY OF UNSTABILIZED CELLULOSE NITRATE[1]

PAUL E. GAGNON, KARL F. KEIRSTEAD,[2] AND BRIAN T. NEWBOLD[3]

ABSTRACT

Cotton linters and wood cellulose were nitrated in parallel experiments with a series of mixed acids and the products examined for nitrogen and sulphate content. A higher degree of nitration was obtained with the cotton cellulose, and the sulphate content of the nitrated cotton increased steadily with increasing concentration of sulphuric acid in the nitration medium while the sulphate content of the wood cellulose passed through a maximum value which depended on the degree of nitration. The sulphate content of the cotton cellulose nitrates was higher than that of the wood cellulose nitrates when the nitrations were performed under similar conditions.

INTRODUCTION

The sulphate content of crude, but well washed, cellulose nitrate prepared from mixed acid varies from about 0.2 to 3.0%, expressed as sulphuric acid, according to the composition of the nitric–sulphuric acid mixture. The total sulphate and the proportion of sulphate ester tend to increase with decreasing nitrogen content (2, 4).

The object of the present work was to compare the degree of nitration of cotton linters and wood cellulose obtained when the composition of the mixed acid used was the same, and to establish the relation between the sulphate content of unstabilized cellulose nitrate and the sulphuric acid content of the mixed acid.

EXPERIMENTAL

Cellulose Nitrate

Cotton linters and wood cellulose were nitrated with mixed acids, using the method given in a previous publication (2). The mixed acids were analyzed by standard methods. The total sulphate content in the cellulose nitrates was determined as barium sulphate (3). The nitrogen content was obtained by the Devarda method.

RESULTS AND DISCUSSION

Degree of Nitration

Many nitrations of cotton linters and wood cellulose were carried out using a variety of mixed acids, in order to determine the relation between mixed acid constitution and nitrogen content. Miles (4) states that "the degree of nitration possible in any mixed acid is chiefly a function of acid composition". In the present work, the results obtained were in accord with this statement. The range of mixed acids varied from 65.0 to 73.6% for the sulphuric acid, from 9.0 to 25.5% for the nitric acid, and from 8.4 to 20.4% for the water. The composition of the mixed acids and the corresponding nitrogen contents for the cotton cellulose nitrates together with a few results reported by Miles and Milbourn for ramie fiber cellulose nitrates are given in Table I.

Miles and Milbourn (5) nitrated ramie fiber with a wide range of mixed acids, and expressed their results for the relation between "composition and degree of nitration" in the form of a triangular chart. The results obtained for the nitration of cotton linters

[1]*Manuscript received August 29, 1957.*
Contribution from the Department of Chemistry, Laval University, Quebec, Que., with financial assistance from the Defence Research Board of Canada.
[2]*Present address: Lignosol Chemicals Limited, Quebec, Que.*
[3]*Research Assistant, Department of Chemistry, Laval University.*

TABLE I

MIXED ACID COMPOSITIONS AND NITROGEN CONTENTS OF COTTON CELLULOSE NITRATES

Expt. No.	% H_2SO_4	% HNO_3	% H_2O	% N
1	71.2	20.4	8.4	—*
2	65.7	22.1	12.2	13.3
3	70.4	19.0	10.6	13.2
4	71.3	13.3	15.4	12.8
5	72.8	12.6	14.6	12.2
6	65.0	18.7	16.3	12.1
7	70.7	13.4	15.9	11.7
8	65.7	16.8	17.5	11.5
9	73.3	10.8	15.9	11.4
10†	67.9	13.6	18.5	10.9
11	68.3	12.3	19.4	10.5
12	62.0	25.5	12.5	—*
13	65.0	14.6	20.4	9.7
14†	73.6	9.0	17.4	10.5
15	73.1	9.0	17.9	9.7
16†	70.1	10.0	19.9	9.4
17	70.1	10.0	19.9	9.0

**Product dissolved.*
†*Results of Miles and Milbourn (5).*

in the present work are given in Fig. 1, which is a portion of the triangular chart used by Miles (4), but drawn on a larger scale. Miles's constant nitrogen lines are shown by broken lines and the results of the present work are plotted as individual points over the nitrogen range 9.0 to 13.3%.

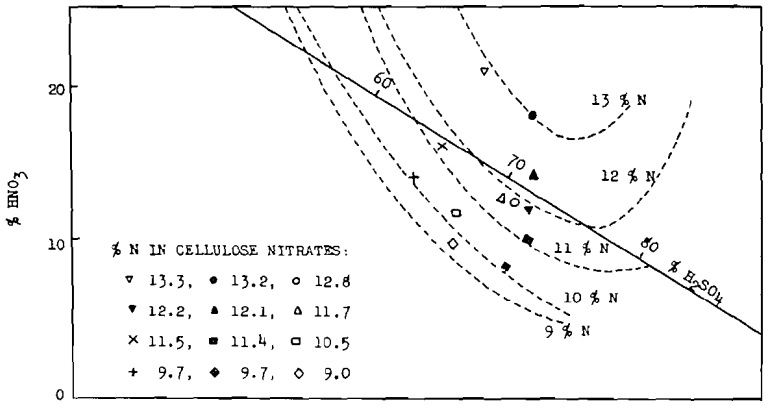

FIG. 1. Mixed acid chart.

Part of the difference in the nitrogen content of cellulose nitrate prepared from ramie fiber and from cotton linters with the same nitric–sulphuric acid, as shown in Table I, experiments 16 and 17, can be attributed to structural differences in the fibers employed. In two experiments, the cellulose nitrate dissolved, a phenomenon encountered by Miles and Milbourn (5).

In order to assess the experimental error involved in attempts to prepare identical cellulose nitrates from the same nitric–sulphuric acid, several duplicate experiments were carried out and the nitrogen determined on each sample. The results are shown in Table II. The mean difference in the nitrogen content of the duplicates was 0.08%

Can. J. Chem. Downloaded from www.nrcresearchpress.com by 61.7.252.67 on 09/04/12
For personal use only.

TABLE II

NITROGEN CONTENTS IN CELLULOSE NITRATES PREPARED BY DUPLICATE NITRATIONS

Expt. No.	Cotton cellulose nitrate, %N		Wood cellulose nitrate, %N	
	Original	Duplicate	Original	Duplicate
1	12.1	11.9	11.7	11.8
2	11.7	11.6	11.4	11.4
3	11.4	11.4	10.8	10.8
4	8.9	9.0	8.5	8.4

and the standard deviation was 0.07. The confidence limits for the difference calculated by the method of Dean and Dixon (1) were 0.08%±0.08, 95% confidence. This difference for duplicates is significantly less than the difference in nitrogen content, 0.4%, found between ramie and cotton cellulose nitrate prepared from the same mixed acid (Table I, expts. 16 and 17).

Further evidence for varying degrees of nitration of different fibers nitrated with the same mixed acid is shown in Table III. A series of mixed acids were used to nitrate

TABLE III

NITROGEN CONTENTS OF CELLULOSE NITRATES

Expt. No.	Cotton cellulose nitrate, %N	Wood cellulose nitrate, %N
1	13.3	12.8
2	13.2	12.8
3	12.8	12.0
4	12.2	11.7
5	12.1	11.9
6	11.7	10.9
7	11.5	10.8
8	11.4	11.0
9	10.5	9.9
10	10.2	10.0
11	9.7	9.7
12	9.4	9.3
13	9.0	8.4
14	8.9	8.5

cotton linters and wood cellulose. The cotton cellulose nitrate almost invariably had a greater nitrogen content than the corresponding wood cellulose. The average difference was 0.4% and the standard deviation was 0.29. The confidence limits for the difference were 0.46%±0.17, 95% confidence.

Assuming the same conditions for nitration, it appears that the percentage of nitrogen obtained from the same mixed acid varies with the nature of the fibers as follows:

ramie, 9.4; cotton linters, 9.0; wood cellulose, 8.4.

Cotton cellulose was nitrated to a higher degree than wood cellulose when the same conditions were employed. The sulphate content of both was dependent upon the composition of the mixed acid. The sulphate content of wood cellulose nitrate was almost always

Can. J. Chem. Downloaded from www.nrcresearchpress.com by 61.7.252.67 on 09/04/12
For personal use only.

higher than that of cotton cellulose nitrate. The different behavior exhibited by cotton and wood cellulose during nitration could be attributed to the different structures. These results agree with the experience of Schur and McMurtrie (6), who found that cotton linters, when nitrated with mixed acid containing 26.0% nitric acid, yielded cellulose nitrate of higher nitrogen content, under the conditions of nitration employed, than did most of the wood pulp samples used. These authors concluded that the behavior of the wood pulps during nitration depended partly on the gross physical form and partly on differences in the physical characteristics of the fibers undergoing nitration.

Sulphate Content

In order to establish the relation between the sulphuric acid content of the mixed acid and the total sulphate content of the cellulose nitrates, many experiments were carried out with cotton linters and wood cellulose, using mixed acids containing amounts of sulphuric acid varying from 65.0 to 73.3%. The sulphate contents of the cellulose nitrates are given in Table IV.

TABLE IV

SULPHURIC ACID IN MIXED ACID AND TOTAL SULPHATE IN CELLULOSE NITRATES

Expt. No.	%H_2SO_4 in mixed acid	Cotton cellulose nitrate		Wood cellulose nitrate	
		%H_2SO_4	%N	%H_2SO_4	%N
1	65.0	1.54	9.7	2.17	9.7
2	68.3	1.86	10.5	2.36	9.9
3	73.3	2.30	11.0	2.40	11.0
4	65.7	0.79	11.5	1.13	10.8
5	70.7	1.53	11.7	1.46	10.9
6	65.0	0.63	12.1	0.93	11.9
7	72.8	2.26	12.2	2.12	12.0
8	71.3	1.13	12.8	2.09	12.0
9	70.4	0.47	13.2	1.30	12.8
10	65.7	0.44	13.3	0.91	12.5

It was found that the sulphate content of wood cellulose nitrate was almost always higher than that of cotton cellulose nitrate, when products prepared from the same mixed acid and containing about the same amount of nitrogen were compared. The mean difference was 0.38% and the standard deviation was 0.29. The confidence limits for the difference were 0.38%±0.21, 95% confidence.

To test the reproducibility of the sulphate determinations, several duplicate experiments were performed and typical results are given in Table V. The mean difference

TABLE V

SULPHATE DETERMINATIONS ON COTTON CELLULOSE NITRATES PREPARED BY DUPLICATE NITRATIONS

Expt. No.	%H_2SO_4 in mixed acid	Total sulphate, %H_2SO_4		Nitrogen, %	
		Original	Duplicate	Original	Duplicate
1	68.3	1.91	1.86	10.8	10.5
2	70.1	1.76	1.62	8.9	8.9
3	70.7	1.53	1.55	11.7	11.6
4	71.3	1.13	1.17	12.0	11.8
5	65.4	1.00	0.89	11.4	11.4
6	65.3	0.69	0.58	11.9	12.1

Can. J. Chem. Downloaded from www.nrcresearchpress.com by 61.7.252.67 on 09/04/12
For personal use only.

in the duplicate sulphate contents was 0.09% and the standard deviation was 0.05. The confidence limits for the difference were 0.09%±0.05, 95% confidence. Similar results were obtained from sulphate analyses of wood cellulose nitrates.

The relation between the sulphuric acid content of the mixed acid and the sulphate content of the cellulose nitrates is shown in Figs. 2 and 3. In Fig. 2, three curves are given for cotton cellulose nitrates of average nitrogen content of 9.4, 11.5, and 12.4%. The sulphate content increases with increasing concentration of sulphuric acid.

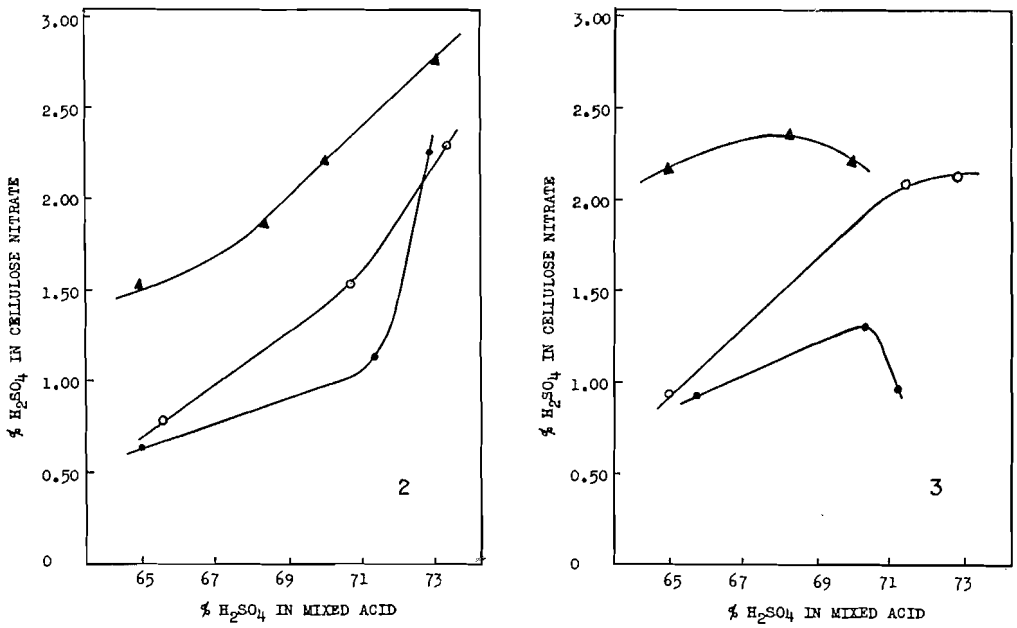

FIG. 2. Relation between $\%H_2SO_4$ in mixed acid and the sulphate content of cotton cellulose nitrates. Av. %N in cellulose nitrate: ● 12.4%, ○ 11.5%, ▲ 9.4%.

FIG. 3. Relation between $\%H_2SO_4$ in mixed acid and the sulphate content of wood cellulose nitrates. Av. %N in cellulose nitrate: ● 12.8%, ○ 11.9%, ▲ 9.4%.

The curves for wood cellulose nitrates (Fig. 3) possess a maximum indicating the optimum concentration of sulphuric acid for the highest sulphate content. For instance, 70.3% sulphuric acid was the optimum concentration for 1.30% sulphate in a wood cellulose nitrate containing 12.8% nitrogen.

Conclusion

The nitrogen and sulphate contents of both cotton and wood cellulose nitrates are shown to be intimately related. The sulphate content of the cellulose nitrates depends upon the formation of sulphate ester, which will be discussed in a forthcoming publication.

REFERENCES

1. DEAN, R. B. and DIXON, W. J. Anal. Chem. **23**, 636 (1951).
2. GAGNON, P. E., KEIRSTEAD, K. F., and YAMASAKI, D. Can. J. Technol. **34**, 477 (1957).
3. KEIRSTEAD, K. F. and MYERS, J. Can. J. Chem. **32**, 566 (1954).
4. MILES, F. D. Cellulose nitrate. Clarke, Irwin & Co. Ltd., Toronto. 1955.
5. MILES, F. D. and MILBOURN, M. J. Phys. Chem. **34**, 2598 (1930).
6. SCHUR, M. O. and MCMURTRIE, J. Paper Trade. J. **16**, 2 (Sept. 23, 1948).

Can. J. Chem. Downloaded from www.nrcresearchpress.com by 61.7.252.67 on 09/04/12
For personal use only.

Can. J. Chem. Downloaded from www.nrcresearchpress.com by 61.7.252.67 on 09/04/12
For personal use only.

AMMONOLYSIS OF 1,2-EPOXYCYCLOHEXANE AND *TRANS*-2-BROMOCYCLOHEXANOL[1]

L. R. HAWKINS AND R. A. B. BANNARD

ABSTRACT

Optimum conditions for the preparation of *trans*-2-aminocyclohexanol by ammonolysis of 1,2-epoxycyclohexane or *trans*-2-bromocyclohexanol are realized by use of a 20-fold excess of aqueous alcoholic ammonia at 100°. Under these conditions formation of secondary amines is minimized. Lower ammonia–reactant ratios, or the use of absolute methanolic ammonia or aqueous ammonia, lead to lower yields of primary amine and higher yields of secondary amines. 1,2-Epoxycyclohexane has been isolated from the interaction of *trans*-2-bromocyclohexanol with aqueous ammonia. The oxide reacts more rapidly with aqueous alcoholic ammonia than the bromohydrin and the rate of conversion of the latter to amine is thus controlled by the rate of conversion of bromohydrin to oxide.

INTRODUCTION

Winstein and Henderson (31) have emphasized that reactions involving *trans*-1,2-halohydrins under basic conditions can proceed via the corresponding oxide as intermediate. If such is the case, approximately equal yields of primary amine should be obtainable from either reactant, and the preferred starting material for preparation of 1,2-aminocyclanols would be the halohydrin rather than the oxide, a synthetic step thereby being eliminated. For the synthesis of a 1,2-aminocyclanol, practical considerations demand that attention be given to the possible intervention of side reactions. Mousseron and Granger (16), for example, found in a number of instances that ammonolysis of alicyclic epoxides or 1,2-chlorohydrins led to formation of considerable quantities of secondary amines together with the desired primary amine. Brunel (4) prepared *trans*-2-aminocyclohexanol by heating 1,2-epoxycyclohexane with a sixfold excess of aqueous ethanolic ammonia at 110–115°. When a twofold excess of ammonia was used, however, the main products were two diastereoisomeric bis-2-hydroxycyclohexylamines (I) of m.p. 114° and 153°, subsequently shown by Mousseron and Granger (16) to be *dl* and *meso* forms respectively.

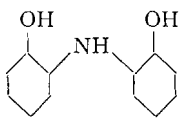

I

Godchot and Mousseron (9), however, studying the same reaction, obtained cyclohexadiene as by-product. Osterberg and Kendall (17) obtained a 61% yield of *trans*-2-aminocyclohexanol by heating *trans*-2-chlorocyclohexanol at 100° with an unspecified excess of aqueous alcoholic ammonia, and reported that omission of the alcohol resulted in formation of secondary and tertiary amines as the main products. They failed, however, to characterize these substances. Wilson and Read (32) studied the same reaction at room temperature, and did not note formation of by-products. Our purpose was to determine whether the halohydrin is the preferred starting material and to establish experimental conditions leading to maximum yield of primary amine, since we required

[1]*Manuscript received July 15, 1957.*
Contribution from Defence Research Chemical Laboratories, Ottawa, Canada. Issued as D.R.C.L. Report No. 220.

certain more complex aminocyclanols in connection with other studies to be described later.

The ammonolysis of 1,2-epoxycyclohexane and *trans*-2-bromocyclohexanol with aqueous alcoholic, aqueous, and absolute methanolic ammonia has been studied at 100° and at room temperature. The influence of these and other variables, such as molar ratio of ammonia to reactant and time of contact, on the yield of primary and secondary amines has been determined.

RESULTS AND DISCUSSION

From Table I it is clear that, within the limits of the variables examined, optimum conditions for conversion of 1,2-epoxycyclohexane and *trans*-2-bromocyclohexanol to

TABLE I

AMMONOLYSIS OF 1,2-EPOXYCYCLOHEXANE AND *trans*-2-BROMOCYCLOHEXANOL

Run number	Reactant*	Medium†	Molar ratio NH_3:reactant	% Yield primary amine	% Yield secondary amine			Experimental conditions
					m.p. 154°	m.p. 126°	Total	
1	Oxide	1	20	86.5	2.0	1.5	3.5	1 hr. 100°
2	Oxide	1	20	85.5	1.9	1.3	3.2	4 hr. 100°
3	Bromohydrin	1	20	76.4			1.7	1 hr. 100°
4	Bromohydrin	1	20	75.6			1.9	4 hr. 100°
5	Oxide	1	5	71.7	10.1	5.3	15.4	1 hr. 100°
6	Oxide	1	5	68.2	11.4	6.1	17.5	2 hr. 100°
7	Bromohydrin	1	5	65.2	7.2	3.1	10.3	1 hr. 100°
8	Bromohydrin	1	5	62.2	8.0	3.3	11.3	2 hr. 100°
9	Oxide	1	20	68.3			Trace	16 hr. R.T.‡
10	Bromohydrin	1	20	56.7			Trace	16 hr. R.T.
11	Oxide	1	20	26.6			Nil	4 hr. R.T.
12	Bromohydrin	1	20	4.4			Nil	4 hr. R.T.
13	Oxide	1	5	64.0	7.0	6.6	13.6	48 hr. R.T.
14	Bromohydrin	1	5	63.9	7.7	6.5	14.2	72 hr. R.T.
15	Oxide	2	20	75.3	2.9	2.4	5.3	1 hr. 100°
16	Oxide	2	20	72.3	2.9	4.6	7.5	24 hr. 100°
17	Oxide	2	2	31.7	25.4	11.7	50.7§	2 hr. 100°
18	Bromohydrin	2	20	47.8	2.8	3.3	6.1	1 hr. 100°

**0.200 mole per run.*
†1, aqueous ethanolic ammonia; 2, aqueous ammonia.
‡Room temperature.
§13.6% of mixed secondary amines was not further purified.

trans-2-aminocyclohexanol are realized by ammonolysis for 1 hour at 100° with aqueous ethanolic ammonia in which the ammonia–reactant ratio is 20:1. Under these conditions the oxide and bromohydrin furnish the primary amine in 85% and 75% yield respectively and formation of secondary amines is limited to 3.5% (runs 1 and 3). In spite of the slightly higher yield of *trans*-2-aminocyclohexanol obtained by the one-step ammonolysis of the bromohydrin (75% vs. 68%), the two-step method, involving prior preparation of the oxide, is preferred because of greater ease of isolation of the product. Prolonging the time of heating has no significant effect on the yield of amines (runs 2 and 4). Use of only a fivefold excess of ammonia, however, causes a marked drop in the yield of primary amine and a corresponding increase in yield of secondary amines (runs 5–8). This result follows from the Law of Mass Action.

The effect of temperature on yield and rate of reaction is illustrated by comparing

Can. J. Chem. Downloaded from www.nrcresearchpress.com by 61.7.252.67 on 09/04/12
For personal use only.

the results of runs 9 to 14 at room temperature with runs 1 to 8 at 100°. It is evident that ammonolysis is much slower at room temperature, as would be expected. However, the results described here for the oxide contrast with Brunel's observation (4) that 1,2-epoxycyclohexane requires several weeks to react with aqueous alcoholic ammonia at room temperature. At room temperature the bromohydrin reacts more slowly than the oxide at both high and low ammonia–reactant ratios. It is thus clear that in the case of bromohydrin, the rate of formation of the intermediate oxide (see below) at room temperature becomes the governing factor.

Aqueous ammonia is a less satisfactory medium for ammonolysis of 1,2-epoxycyclohexane or *trans*-2-bromocyclohexanol than aqueous alcoholic ammonia (runs 15, 16, and 18), presumably because two-phase systems are formed and there is an increased tendency toward formation of 1,2-cyclohexanediol as by-product (4, 20). The especially poor yield from the bromohydrin is to be expected because the intermediate oxide is readily soluble in the bromohydrin. The result reported in run 18 contrasts with Osterberg and Kendall's claim (17) that ammonolysis of *trans*-2-chlorocyclohexanol with aqueous ammonia produces secondary and tertiary amines as the main products. We did not obtain tertiary amines under any of the conditions studied, in agreement with Brunel's (4) results on ammonolysis of 1,2-epoxycyclohexane. Normally, ammonolysis of a 1,2-epoxide or halohydrin in aqueous solution leads to formation of primary, secondary, and tertiary amine together with quarternary ammonium salt (19), but in the present case formation of the last two may be prevented by steric factors. Brunel's (4) observation that treatment of the oxide with a twofold excess of ammonia produces the diastereoisomeric secondary amines as major product has been verified (run 17). Ammonolysis with anhydrous methanolic ammonia causes the yield of primary amine to fall approximately 30% from maximum. This result was not unexpected since water exerts a catalytic effect on the ammonolysis reaction (6, 3, 22) and, moreover, reaction of 1,2-epoxides or 1,2-halohydrins with alcohols under basic conditions leads to formation of glycol monoethers (4, 13, 14). We did not attempt to isolate glycol or glycol monoethers from the ammonolyses but these compounds would undoubtedly be present in small amounts in the distillate collected prior to sublimation of the primary amine.

The reaction of ammonia or amines with 1,2-epoxides in aqueous solution is considered to proceed by an S_N2 mechanism (31, p. 27; 12; 23; 7). The stereochemical course of the reaction of 1,2-epoxycyclohexane with ammonia (15) and the fact that the reaction rate increases (runs 9 and 13) when the concentration of nucleophile is increased (12, p. 321) are in agreement with such a mechanism.

Ammonolysis of *trans*-2-bromocyclohexanol proceeds with over-all retention of stereochemical configuration, and this suggests that 1,2-epoxycyclohexane is an intermediate (27; 30; 31, pp. 11 and 27). The conversion of 1,2-halohydrin to oxide in the presence of a strong base is rapid and almost quantitative (31, p. 8) but there does not appear to be any definite evidence for formation of oxide in the presence of a weak base such as ammonia, other than the kinetic data of Smith and Nilsson (23). On the other hand Elderfield *et al.* (8) and Petrov and Lagucheva (18) have published data which indicate that amination of 1-chloropentanol-2 with diethylamine or ethylene chlorohydrin with 2,5-dichloroaniline does not proceed via an intermediate oxide stage. Therefore, although oxide can intervene (31), this is not always the case and proof must be sought in each instance. In the present study, we treated *trans*-2-bromocyclohexanol with 28% aqueous ammonia at room temperature, obtained 1,2-epoxycyclohexane and ammonium bromide in 38.8% and 41.8% yield respectively, and recovered 43.3% of the bromohydrin. This is the first time to our knowledge than an oxide has actually been isolated from inter-

Can. J. Chem. Downloaded from www.nrcresearchpress.com by 61.7.252.67 on 09/04/12
For personal use only.

Can. J. Chem. Downloaded from www.nrcresearchpress.com by 61.7.252.67 on 09/04/12
For personal use only.

action of a halohydrin and ammonia. This observation, together with the fact that the rate of formation of amine from oxide is greater than from bromohydrin at both high and low ammonia–reactant ratios (runs 9 to 14), leads to the conclusion that the oxide is an intermediate in ammonolysis of *trans*-2-bromocyclohexanol.

The bis-2-hydroxycyclohexylamine of m.p. 126° was reported by Brunel (4) to have m.p. 114°, and it presumably contained a trace of the higher melting diastereoisomer. *meso*-Bis-2-hydroxycyclohexylamine hydrochloride was reported (4) to have m.p. 264°, whereas the *dl*-isomer exhibited a double melting point, the first at 192° and the second at 264°. Brunel (4) suggested that the *dl*-isomer was converted to the *meso*-isomer above its first melting point, melting again at 264°. We have found *dl*-bis-2-hydroxycyclohexylamine to possess a single melting point, 194–195°, and conclude that Brunel's suggestion regarding interconversion of the isomers is incorrect. The hydrobromides of *meso*- and *dl*-bis-2-hydroxycyclohexylamine were prepared and have m.p. 257–258° and 180–182° respectively.

Recently, Guss and Rosenthal (10) reported the preparation of *trans*-2-bromocyclohexanol by bromination of cyclohexene with *N*-bromosuccinimide. We used their method and found that the liquid product frequently darkens rapidly either during distillation or on storage. Similar observations regarding the rapid discoloration of *trans*-2-bromocyclohexanol have been made independently by Schmidt, Schumacher, and Asmus (21), Bedos (1), and Hunter and Marriott (11), all of whom used different methods of preparation. Swarts' observation (25) that *trans*-2-bromocyclohexanol is a solid of m.p. 27° seems to have been overlooked by subsequent workers (10, 26, 28, 29). Guss and Rosenthal's (10) procedure was modified by using a 5 mole % excess of olefin over bromoimide, and *trans*-2-bromocyclohexanol was obtained in 89% yield as a colorless solid of m.p. 27°, after purification by recrystallization from heptane rather than distillation. This product does not discolor on standing in contact with light and air. The colorless solid, if distilled *in vacuo*, discolors much more slowly than preparations made by Guss and Rosenthal's method. This observation suggests that *trans*-2-bromocyclohexanol decomposes slightly on distillation (cf. Swarts (25)) and that the excess of olefin used in our method of preparation is beneficial, possibly in preventing the presence of excess hypobromous acid, which could either cause slight oxidation of the product or lead to formation of *trans*-1,2-dibromocyclohexane as observed by Coffey (5). The latter substance is difficult to obtain in a colorless condition because it undergoes oxidation readily in the presence of air (24). During several ammonolysis experiments in which discolored *trans*-2-bromocyclohexanol was used, explosions occurred. Explosions were not experienced when colorless bromohydrin was used. Boon (2) found the reaction of alkylene dibromides with certain amines to be very exothermic during the initial stage, and it is possible that a trace of *trans*-1,2-dibromocyclohexane present in the bromohydrin is responsible for the observed explosions.

EXPERIMENTAL

All melting points are uncorrected. Microanalyses are by Micro-Tech Labs., Skokie, Ill., and C. E. Reynolds of these Laboratories.

trans-2-Bromocyclohexanol

Guss and Rosenthal's (10) procedure was modified as follows. Cyclohexene (86.2 g., 1.05 moles), water (400 ml.), and N-bromosuccinimide (178 g., 1.00 mole) were placed in a 1-liter three-necked flask equipped with a "trubore" stirrer and thermometer. The mixture was stirred mechanically until the N-bromosuccinimide dissolved and a colorless heavy layer of bromohydrin separated (15 minutes), during which time the

temperature rose to 75°. The two-phase system was allowed to cool to room temperature, the bromohydrin layer was separated, and the aqueous phase extracted with ether (2×100 ml.). The extracts and bromohydrin were combined and the ether removed *in vacuo*. The residue was diluted with heptane (1 liter) and kept at 4° overnight. The precipitated succinimide was removed and the filtrate was allowed to stand overnight at −20°. The colorless crystals of *trans*-2-bromocyclohexanol which separated were collected by suction filtration and washed with ice-cold heptane. Concentration of the mother liquor gave further crops. Yield, 160 g. (89.0%), m.p. 27°. Swarts (25) reports m.p. 27.5°. Calc. for $C_6H_{11}OBr$: C, 40.24; H, 6.19; Br, 44.63%. Found: C, 40.20; H, 6.10; Br, 44.58%. *trans*-2-Bromocyclohexanol prepared as described above has remained colorless for more than 4 months on storage in clear bottles not protected from daylight.

Ammonolysis of trans-2-Bromocyclohexanol

The bromohydrin was treated with aqueous, aqueous ethanolic, or absolute methanolic ammonia in glass or stainless steel pressure vessels at room temperature or 100° for varying lengths of time. Experimental conditions required for maximum yield of *trans*-2-aminocyclohexanol are as follows. *trans*-2-Bromocyclohexanol (35.8 g., 0.200 mole) was heated for 1 hour at 100° with an aqueous ethanolic ammonia solution prepared from 28% aqueous ammonia (270 ml., 4.00 moles) and absolute ethanol (120 ml.). The pale yellow solution was evaporated to dryness *in vacuo* at room temperature. The residual solid was treated with a boiling solution of sodium hydroxide (8.0 g.) in absolute ethanol (100 ml.) for 20 minutes with stirring. The insoluble salt was collected and washed with anhydrous ether (50 ml.). The combined filtrate and washings were evaporated to dryness *in vacuo* at room temperature, and the primary amine (17.6 g., 76.4%) was obtained as a colorless sublimate, m.p. 67–68°, by heating the residue at 80–100° at 1 mm. (McCasland *et al.* (15) report m.p. 68°). *trans*-2-Aminocyclohexanol is hygroscopic and carbonates rapidly. Complete separation of primary amine from the mixture of secondary amines and inorganic salt is not effected and the residue still possesses the characteristic piperidine-like odor of the primary amine. The water-insoluble *meso*-bis-2-hydroxycyclohexylamine (m.p. 154°) was isolated by filtration after the residue from the sublimation was treated with boiling water (100 ml.) and allowed to cool. The *dl*-secondary amine (m.p. 126°) was isolated by evaporation of the filtrate to dryness. The experiment under consideration yielded only 0.36 g. (1.7%) of a mixture of the two secondary amines, m.p. 114–116°. Calc. for $C_{12}H_{23}NO_2$: C, 67.56; H, 10.86%. Found: C, 68.00; H, 11.10%.

1,2-Epoxycyclohexane from Ammonolysis of trans-2-Bromocyclohexanol

trans-2-Bromocyclohexanol (35.8 g., 0.200 mole) was stirred at room temperature for 6 hours in a stoppered flask with 28% aqueous ammonia (20 ml., 0.297 mole). The lower layer was decanted and the aqueous layer extracted with ether (3×10 ml.) and combined with the non-aqueous layer. The ether solution was dried and distilled, yielding 7.6 g. (38.8%) of cyclohexene oxide, b.p. 130°, n_D^{25} 1.4497, and 15.5 g. (43.3%) of *trans*-2-bromocyclohexanol, b.p. 50–52° at 1.5 mm., n_D^{25} 1.5185. Evaporation of the aqueous solution to dryness yielded 8.2 g. (41.8%) of ammonium bromide which contained only a trace of *trans*-2-aminocyclohexanol as revealed by paper chromatography using *n*-butanol – acetic acid – water (25:6:25) as developer and bromcresol green as detector.

1,2-Epoxycyclohexane

1,2-Epoxycyclohexane was prepared in 80% yield from *trans*-2-bromocyclohexanol by the method of Guss and Rosenthal (10), b.p. 130°, n_D^{25} 1.4498.

Can. J. Chem. Downloaded from www.nrcresearchpress.com by 61.7.252.67 on 09/04/12
For personal use only.

Ammonolysis of 1,2-Epoxycyclohexane

1,2-Epoxycyclohexane was ammonolyzed with aqueous, aqueous alcoholic, or absolute methanolic ammonia in glass or stainless steel pressure vessels at room temperature or 100° for varying lengths of time. Experimental conditions which produce maximum yield of *trans*-2-aminocyclohexanol are as follows. 1,2-Epoxycyclohexane (19.6 g., 0.200 mole) was heated for 1 hour at 100° with aqueous ethanolic ammonia solution as described for *trans*-2-bromocyclohexanol. The pale yellow solution was evaporated to dryness *in vacuo* at room temperature. The residue was heated at 80–100° at 1 mm. and *trans*-2-aminocyclohexanol (19.9 g., 86.5%) was obtained as a colorless sublimate, m.p. 67–68°. The two secondary amines were recovered by the method described under ammonolysis of *trans*-2-bromocyclohexanol. More complete recovery and separation of the amines was effected because the process is uncomplicated by the presence of inorganic salt. The *meso*-secondary amine (m.p. 154°) was obtained in 2.0% yield and the *dl*-isomer (m.p. 126°) in 1.5% yield.

trans-2-Aminocyclohexanol Hydrochloride

trans-2-Aminocyclohexanol (23.0 g., 0.200 mole) was dissolved in hot anhydrous benzene (250 ml.) and hydrogen chloride gas was passed into the solution until precipitation was complete. The colorless hydrochloride was collected, washed with anhydrous ether (2×100 ml.), and recrystallized from absolute ethanol (180 ml.), yielding 26.5 g. (87.2%) of colorless *trans*-2-aminocyclohexanol hydrochloride as clusters of fine prisms, m.p. 180–181°. McCasland *et al.* (15) report m.p. 176–177°.

trans-2-Aminocyclohexanol Hydrobromide

trans-2-Aminocyclohexanol (2.88 g., 0.025 mole) was dissolved in anhydrous ether and treated with hydrogen bromide gas as described above. The salt was collected, washed with anhydrous ether, and recrystallized from absolute ethanol (20 ml.), yielding 4.28 g. (92.2%) of fine colorless clusters of needles, m.p. 191–192°. Osterberg and Kendall (17) report m.p. 191°.

trans-2-Acetamidocyclohexanol

trans-2-Aminocyclohexanol (1.00 g., 0.0878 mole) was dissolved in acetic anhydride (5.0 ml.) and a very exothermic reaction occurred. Water (3.0 ml.) was added and the mixture was evaporated to dryness *in vacuo*. The amide was collected and washed with cold anhydrous ether. Yield 1.14 g. (82.4%), m.p. 126–127°. McCasland *et al.* (15) report m.p. 126–127°. Calc. for $C_8H_{15}O_2N$: C, 61.12; H, 9.62; N, 8.91%. Found: C, 61.22, 61.36; H, 9.55, 9.55; N, 8.98, 8.82%.

meso-Bis-2-hydroxycyclohexylamine

This substance had m.p. 145–150° when first obtained from the ammonolysis reactions. Recrystallization from benzene (17 ml./g.) gave colorless platelets, m.p. 154°. Brunel (4) reports m.p. 153°.

meso-Bis-2-hydroxycyclohexylamine Hydrochloride

meso-Bis-2-hydroxycyclohexylamine (1.07 g., 0.005 mole) was dissolved in anhydrous ether (250 ml.) and treated with hydrogen chloride gas as described above. The precipitate was collected, washed with anhydrous ether (3×25 ml.), and recrystallized from absolute ethanol (100 ml.), yielding 1.14 g. (91.2%) of *meso*-bis-2-hydroxycyclohexylamine hydrochloride, m.p. 270–271°, as colorless clusters of prisms. Calc. for $C_{12}H_{24}NO_2Cl$: N, 5.61; Cl, 14.19%. Found: N, 5.68, 5.79; Cl, 14.50, 14.56%. Brunel (4) reports m.p. 264°. This substance sublimes below its melting point.

Can. J. Chem. Downloaded from www.nrcresearchpress.com by 61.7.252.67 on 09/04/12
For personal use only.

meso-Bis-2-hydroxycyclohexylamine Hydrobromide

The hydrobromide was prepared in the same manner as the hydrochloride and recrystallized from absolute ethanol (70 ml.), yielding 1.89 g. (95.5%) of fine colorless needles, m.p. 257–258°. Calc. for $C_{12}H_{24}NO_2Br$: N, 4.76; Br, 27.16%. Found: N, 4.85, 4.91; Br, 27.05, 26.75%.

dl-Bis-2-hydroxycyclohexylamine

This substance usually had m.p. 114–116° when obtained from the ammonolysis reactions. Recrystallization from ethanol–ether or benzene gave colorless needles, m.p. 126°. Brunel (4) previously reported m.p. 114° for this substance. Calc. for $C_{12}H_{23}NO_2$: C, 67.56; H, 10.87; N, 6.57%. Found: C, 67.76; H, 11.20; N, 6.39%. Recrystallization did not effect recovery of all the lower melting isomer in a pure condition. A small portion always remained contaminated with the higher-melting isomer. Such residues usually melted over a 1° range within the region 110–118° and analyzed satisfactorily for secondary amine.

dl-Bis-2-hydroxycyclohexylamine Hydrochloride

dl-Bis-2-hydroxycyclohexylamine (200 mg., 0.000935 mole) was dissolved in anhydrous ether (40 ml.) and the solution treated with hydrogen chloride gas. The precipitate was collected and washed with anhydrous ether (2×10 ml.) yielding 213 mg. (91.0%) of colorless substance, m.p. 193–194°. Calc. for $C_{12}H_{24}NO_2Cl$: N, 5.61; Cl, 14.19%. Found: N, 5.45, 5.59; Cl, 14.34, 14.46%. The double melting point phenomenon previously reported by Brunel (4) for this substance was not observed.

dl-Bis-2-hydroxycyclohexylamine Hydrobromide

dl-Bis-2-hydroxycyclohexylamine (2.00 g., 0.00935 mole) was dissolved in ethanol–ether and treated with hydrogen bromide gas as above. The salt was collected and recrystallized from ethanol–ether yielding 2.1 g. (76.1%) of colorless needles, m.p. 180–182°. Calc. for $C_{12}H_{24}O_2NBr$: C, 48.98; H, 8.22; N, 4.76; Br, 27.16%. Found: C, 48.93, 48.99; H, 8.07, 8.37; N, 5.04, 5.00; Br, 27.10, 27.00%.

REFERENCES

1. Bedos, P. Bull. soc. chim. France, **39**, 292 (1926).
2. Boon, W. R. J. Chem. Soc. 307 (1947).
3. Bortnick, N., Luskin, L. S., Hurwitz, M. D., Craig, W. E., Exner, L. J., and Mirza, J. J. Am. Chem. Soc. **78**, 4039 (1956).
4. Brunel, L. Ann. chim. (Paris) [8], **6**, 200 (1905).
5. Coffey, S. Rec. trav. chim. **42**, 387 (1923).
6. Eastham, A. M. J. Chem. Soc. 1936 (1952).
7. Eastham, A. M., Darwent, B. de B., and Beaubien, P. E. Can. J. Chem. **29**, 575 (1951).
8. Elderfield, R. C., Craig, L. C., Lauer, W. M., Arnold, R. T., Gensler, W. J., Head, J. D., Bembry, T. H., Mighton, H. R., Tinker, J., Galbreath, J., Holley, A. D., Goldman, L., Maynard, J. T., and Picus, N. J. Am. Chem. Soc. **68**, 1516 (1946).
9. Godchot, M. and Mousseron, M. Bull. soc. chim. France, **51**, 1277 (1932).
10. Guss, C. O. and Rosenthal, R. J. Am. Chem. Soc. **77**, 2549 (1955).
11. Hunter, L. and Marriott, J. A. J. Chem. Soc. 285 (1936).
12. Ingold, C. K. Structure and mechanism in organic chemistry. Cornell University Press, Ithaca, N.Y. 1953. p. 342.
13. Kotz, A. and Busch, G. J. prakt. Chem. [2], **119**, 1 (1928).
14. Kotz, A. and Hoffmann, W. J. prakt. Chem. [2], **110**, 101 (1925).
15. McCasland, G. E., Clark, R. K., and Carter, H. E. J. Am. Chem. Soc. **71**, 637 (1949).
16. Mousseron, M. and Granger, R. Bull. soc. chim. France, **14**, 850 (1947).
17. Osterberg, A. E. and Kendall, E. C. J. Am. Chem. Soc. **42**, 2616 (1920).
18. Petrov, K. D. and Lagucheva, E. S. Zhur. Obshcheĭ Khim. **23**, 403 (1953).
19. Potter, C. and McLaughlin, R. R. Can. J. Research, **B**, **25**, 405 (1947).
20. Rothstein, B. Ann. chim. (Paris), **14**, 461 (1930).
21. Schmidt, E., Schumacher, R., and Asmus, R. Ber. **56B**, 1239 (1923).
22. Shechter, L., Wynstra, J., and Kurkjy, R. P. Ind. Eng. Chem. **48**, 94 (1956).

Can. J. Chem. Downloaded from www.nrcresearchpress.com by 61.7.252.67 on 09/04/12
For personal use only.

23. SMITH, L. and NILSSON, T. J. prakt. Chem. **162**, 63 (1943).
24. SNYDER, H. R. and BROOKS, L. A. Organic syntheses. Collective Vol. 2. John Wiley and Sons, Inc., New York. 1943. p. 171.
25. SWARTS, F. Bull. soc. chim. Belg. **46**, 13 (1937).
26. WINSTEIN, S. J. Am. Chem. Soc. **64**, 2792 (1942).
27. WINSTEIN, S. and LUCAS, H. J. J. Am. Chem. Soc. **61**, 1576 (1939).
28. WINSTEIN, S. J. Am. Chem. Soc. **61**, 1610 (1939).
29. WINSTEIN, S. and BUCKLES, R. E. J. Am. Chem. Soc. **64**, 2780 (1942).
30. WINSTEIN, S., GRUNWALD, E., BUCKLES, R. E., and HANSON, C. J. Am. Chem. Soc. **70**, 816 (1948).
31. WINSTEIN, S. and HENDERSON, R. B. *In* Heterocyclic compounds. Vol. I. John Wiley and Sons, Inc., New York. 1950. p. 39.
32. WILSON, N. A. B. and READ, J. J. Chem. Soc. 1269 (1935).

Can. J. Chem. Downloaded from www.nrcresearchpress.com by 61.7.252.67 on 09/04/12
For personal use only.

Can. J. Chem. Downloaded from www.nrcresearchpress.com by 61.7.252.67 on 09/04/12
For personal use only.

CONFORMATIONAL EFFECTS AND THE INFLUENCE OF PRESSURE ON REACTION RATES[1]

E. WHALLEY

ABSTRACT

It has been suggested that the pressure coefficient of the rate constant of some reactions may be influenced by the formation of intermolecular or intramolecular conformations prior to reaction. This has been examined theoretically and the relevant experimental evidence has been discussed. No examples of an effect in which the conformations are at equilibrium are known with certainty, but the effect of pressure on termination in the polymerization of styrene appears to be an example of a conformational effect when the conformations are not at equilibrium.

The pressure coefficient of the rate constant for the isomerization of citraldehyde to 3,8-carvomenthenediol is not consistent with a unimolecular slow step, but it is consistent with either a bimolecular or a termolecular slow step. It is pointed out that the pressure coefficient of rate constants may be very useful in determining the molecularity of some reactions.

1. INTRODUCTION

According to the theory of absolute reaction rates (4) the rate constant k for a chemical reaction in dilute solution which goes via an activated complex is given by

$$k = \kappa(kT/h)\exp(-\Delta F^{\ddagger}/RT), \qquad [1.1]$$

where κ is the transmission coefficient, k is Boltzmann's constant, h is Planck's constant, and $\Delta F^{\ddagger}$ is the partial free energy of activation in the solution under discussion. The pressure coefficient of k is obtained by taking logarithms of equation [1.1], differentiating with respect to pressure, and using the identity

$$\partial F/\partial p = V,$$

where V is the molar volume. One finds

$$d \ln k/dp = -\Delta V^{\ddagger}/RT + d \ln \kappa/dp, \qquad [1.2]$$

where $\Delta V^{\ddagger}$ is the partial volume of activation. If $\ln \kappa$ is effectively independent of pressure—and no other assumption is fruitful at present—equation [1.2] reduces to the well-known equation

$$d \ln k/dp = -\Delta V^{\ddagger}/RT. \qquad [1.3]$$

This derivation has of course been given many times; it is included to emphasize that the variation of $\ln \kappa$ with pressure is quite unknown and introduces an uncertainty into all discussions of the pressure coefficient of reaction rate constants in terms of the activated state theory.

There are some reactions which either can or must occur in at least two stages, the first stage of which is the formation of an intermolecular or intramolecular conformation which is favorable to the reaction. For example, the reaction

$$\mathrm{A} + \mathrm{B} \rightarrow \text{products} \qquad (1.1)$$

may need or be helped by the formation of a conformation A′ of A thus

$$\mathrm{A} \rightarrow \mathrm{A}', \qquad (1.2)$$

$$\mathrm{A}' + \mathrm{B} \rightarrow \text{products}, \qquad (1.3)$$

[1]*Manuscript received September 26, 1957.*
Contribution from the Division of Applied Chemistry, National Research Council, Ottawa, Canada. Issued as N.R.C. No. 4552.

where the products of reactions (1.1) and (1.3) are identical. The term conformational effects is used in this paper to denote the effects of the conformation A′. It has been suggested several times (2, 5, 11), though without detailed examination, that the acceleration of some reactions by pressure is due to the increase in concentration with pressure of a favorable conformation. This is a very interesting suggestion and it deserves quantitative investigation, not least because the pressure coefficient of reaction rate constants can be very valuable in elucidating reaction mechanisms, and it is important to know all that may influence the pressure coefficient. The purpose of this paper is to discuss the pressure coefficients of the rate constants of reactions in which a conformational effect may occur, and in particular to examine the effect of the conformational change (1.2). The theory is discussed in Section 2 and the experimental evidence in Section 3.

2. THEORY OF CONFORMATIONAL EFFECTS

We consider the simple reaction

$$\mathrm{A} + \mathrm{B} \rightarrow \text{products}, \tag{2.1}$$

with a rate constant k_1, and assume either that it can go in one step as above or that A can take up an intramolecular or intermolecular conformation A′ which can also react with B to give the same activated state and same products as reaction (2.1). Thus the reactions

$$\mathrm{A} \rightarrow \mathrm{A}', \tag{2.2}$$

$$\mathrm{A}' \rightarrow \mathrm{A}, \tag{2.3}$$

$$\mathrm{A}' + \mathrm{B} \rightarrow \text{products}, \tag{2.4}$$

with rate constants k_2, k_3, and k_4 respectively, are also possible. We note that

$$[2.1] \qquad k_2/k_3 = K_2,$$

where K_2 is the equilibrium constant for the formation of A′, the standard state being such that the molar extensive properties are equal to the partial molar properties in the (dilute) solution under discussion. We assume that reactions (2.1) and (2.4) give the same activated complexes; if they do not, then two different reactions occur simultaneously and the analysis of the effect of pressure must take account of this. Hence the partial volumes of activation of (2.1) and (2.4), $\Delta V_1^{\ddagger}$ and $\Delta V_4^{\ddagger}$ respectively, are related to the partial volume change ΔV_2 of reaction (2.2) thus

$$[2.2] \qquad \Delta V_1^{\ddagger} = \Delta V_2 + \Delta V_4^{\ddagger}.$$

Also

$$[2.3] \qquad d \ln K_2/dp = -\Delta V_2/RT.$$

We have chosen a simple bimolecular reaction for consideration and assume that A can take up only two conformations; if the reaction is of different molecularity, or if it occurs in a number of steps, and if there are many conformations of A each with its different rate constant for reaction with B, simple modifications of the treatment will lead to results similar to those below.

The rate constant usually measured is k, where

$$\begin{aligned} \text{rate of reaction} &= k(c_{\mathrm{A}}+c_{\mathrm{A}'})c_{\mathrm{B}} \\ &= kc_{\mathrm{A}}c_{\mathrm{B}}(1+c_{\mathrm{A}'}/c_{\mathrm{A}}), \end{aligned} \qquad [2.4]$$

Can. J. Chem. Downloaded from www.nrcresearchpress.com by 61.7.252.67 on 09/04/12
For personal use only.

and c_A, $c_{A'}$, and c_B represent the concentrations of A, A′, and B. By considering reactions (2.1)–(2.4) the rate of reaction is given by

$$\text{rate of reaction} = k_1c_Ac_B+k_4c_{A'}c_B$$

$$= k_1c_Ac_B\{1+(k_4/k_1)(c_{A'}/c_A)\}. \quad [2.5]$$

By equating [2.4] and [2.5] we have

$$k = k_1\{1+(k_4/k_1)(c_{A'}/c_A)\}/\{1+(c_{A'}/c_A)\}. \quad [2.6]$$

It is convenient to let $c_{A'}/c_A$ be the fraction α of its equilibrium value K_2, so that

$$c_{A'}/c_A = \alpha K_2. \quad [2.7]$$

If $c_{A'}$ is the same as if it were independent of time a simple kinetic analysis shows that

$$\alpha = (1+c_Bk_4/k_3)^{-1}. \quad [2.8]$$

By taking logarithms of [2.6], differentiating, inserting [2.7], using equation [1.3] for k_1 and k_4, and using [2.2], which is equivalent to

$$d\ln(K_2k_4/k_1)/dp = 0, \quad [2.9]$$

we find

$$\frac{d\ln k}{dp} = \frac{d\ln k_1}{dp} + \frac{\alpha K_2k_4/k_1}{1+\alpha K_2k_4/k_1}\frac{d\ln\alpha}{dp} - \frac{d\ln(1+\alpha K_2)}{dp}. \quad [2.10]$$

This is a rather complicated equation but it simplifies quite considerably under some extreme conditions as follows.

(*a*) If A and A′ are always at equilibrium with one another, $\alpha = 1$ and [2.10] becomes

$$d\ln k/dp = d\ln k_1/dp - d\ln(1+K_2)/dp. \quad [2.11]$$

There is therefore a conformational effect contained in the second term of [2.11]. The direction of the effect is at first sight unexpected. If A′ is favored by pressure, K_2 is increased by pressure and consequently $d\ln(1+K_2)/dp$ is positive. The effect of this term in equation [2.11] is therefore to reduce or to make more negative $d\ln k/dp$. The effect of a conformation favored by pressure is therefore to reduce the pressure coefficient below that which would otherwise occur. A conformational effect of this kind, in which the conformations are at equilibrium with one another, cannot therefore be invoked to explain an apparently anomalously large pressure coefficient of k unless it is assumed that the conformations are disfavored by pressure.

If the concentration of A′ is small so that $K_2 \ll 1$, equation [2.11] becomes

$$d\ln k/dp = d\ln k_1/dp - dK_2/dp$$

$$= -\Delta V_1^{\ddagger}/RT+K_2\Delta V_2/RT. \quad [2.12]$$

The conformational effect, though present, is small unless

$$|\Delta V_2/\Delta V_1^{\ddagger}| \gg 1.$$

If the concentration of A is small so that $K_2 \gg 1$, equation [2.11] becomes

$$d\ln k/dp = d\ln k_1/dp - d\ln K_2/dp - dK_2^{-1}/dp$$

$$= -\Delta V_4^{\ddagger}/RT+(1/K_2)\Delta V_2/RT, \quad [2.13]$$

Can. J. Chem. Downloaded from www.nrcresearchpress.com by 61.7.252.67 on 09/04/12
For personal use only.

where we have used equation [2.2]. Again the conformational effect is very small unless $|\Delta V_2/\Delta V_4^{\ddagger}| \gg 1$.

Even when K_2 is at its most effective value the effect will usually be rather small because

$$d \ln(1+K_2)/dp < d \ln K_2/dp = -\Delta V_2/RT;$$

since ΔV_2 is the difference in volume between two orientations, either mutual or intramolecular, of the molecules it will usually be less than the volume of melting, which is rarely more than a few cm.^{3} mole $^{-1}$ except perhaps for very large molecules. It will consequently not be easy to distinguish it from the volume of activation, though a conformational effect probably occurs frequently since a reaction between two molecules, of which at least one is not spherically symmetrical, necessitates some prior orientation which may occur with a change of volume. No certain examples are known at present, as we shall show in Section 3.

(*b*) If A and A′ are always at equilibrium and $k_1 = 0$, the reaction will not go unless a particular conformation is first formed, and it is formed at equilibrium. Then equation [2.6] becomes, when differentiated and with the substitutions as above,

$$\begin{aligned} d \ln k/dp &= d \ln k_4/dp + d \ln K_2/dp - d \ln(1+K_2)/dp \\ &= -\Delta V_1^{\ddagger}/RT - d \ln(1+K_2)/dp. \end{aligned}$$

This is identical with equation [2.11], so the discussion which follows that equation applies to this. Even when the conformation is necessary for the reaction to go, the effect of the conformation on the pressure coefficient will usually be rather small if the conformations are present at equilibrium.

(*c*) If the reaction will not go unless a particular conformation is first formed, and the rate of formation of the conformation is the rate determining step, then

[2.14] $$k_1 = 0, \qquad k_4 \gg k_3,$$

and so

$$\alpha \sim (k_3/k_4)c_B \ll 1.$$

An example of this appears to be the diffusion into proximity of the live ends of polymer chains in the termination step in the polymerization of styrene (see Section 3). Inserting [2.14] in [2.6], differentiating, and making the usual substitutions, we find

$$k = k_2/c_B,$$

which could be obtained directly much more easily. The pressure coefficient of k is very nearly that of k_2. For this example the conformational effect may be quite large.

3. EXPERIMENTAL EVIDENCE FOR CONFORMATIONAL EFFECTS

In this section the experimental evidence for the occurrence of the conformational effects which we are discussing is reviewed.

The first suggestion that conformational effects alter the pressure coefficient of chemical reactions was made by Conant and Peterson (2) to explain the qualitative observation that aliphatic aldehydes and isoprene could be polymerized to products of high molecular weight by subjecting them to pressures of several kilobars, but no reaction took place under the same conditions at normal pressure. In their own words, "the accelerating effect of great pressures is due to the orientation of the molecules of the isoprene or the

Can. J. Chem. Downloaded from www.nrcresearchpress.com by 61.7.252.67 on 09/04/12
For personal use only.

aldehyde into a more compact bundle in which longer reaction chains would be propagated". It was realized by Conant (3) in an earlier paper that aliphatic aldehydes do not polymerize at ordinary temperatures and pressures because the chemical equilibrium between monomer and polymer is well on the side of the monomer; under pressures of several kilobars the free energy of polymerization is altered, because of the large contraction which occurs in polymerization, enough to shift the equilibrium to the side of the polymer. This is shown by the fact that the polymer depolymerizes to monomer at atmospheric pressure. Any conformational effect on the rate is secondary to the equilibrium effect, and cannot at present be distinguished from it.

The effect of pressure on the polymerization of isoprene is probably similar to its effect on the polymerization of styrene, which has recently been investigated in some detail by Nicholson and Norrish (8). The rate constants for both the propagation and termination steps are altered by pressure, but for quite different reasons. The rate constant for the propagation step,

$$M_n^{\cdot} + M \rightarrow M_{n+1}^{\cdot},$$

where $M_n^{\cdot}$ is a free radical n-mer and M is the monomer, is increased by pressure by an amount which corresponds to an apparent volume of activation of -13.4 cm.^{3} mole^{-1} (12). This is an altogether reasonable value, being about 60% of the total decrease in volume of the propagation step (10, 12), and it is not necessary to invoke conformational effects to explain it.

The rate constant for the termination step,

$$M_n^{\cdot} + M_m^{\cdot} \rightarrow M_{n+m},$$

is reduced by increasing pressure and it was shown (8) that this is probably caused by a reduction, consequent on the decrease in diffusion coefficients with increasing pressure, in the rate at which the live polymer ends can diffuse to one another. This then is an example of a conformational effect of the kind discussed in Section 2(*c*), in which the necessary conformation is the juxtaposition of two live polymer ends and the rate of formation of this conformation is the rate of reaction. The effect of pressure on the polymerization of isoprene is probably caused in part by a combination of these two effects, with the second one perhaps predominant. Hence a conformational effect probably occurs, but of a type quite different from that envisaged by Conant and Peterson.

The pressure coefficient of the rate of isomerization of citraldehyde to 3,8-carvomenthenediol (5) corresponds to a volume of activation of -24.5 cm.^{3} mole^{-1} at atmospheric pressure. This was not explicable by the mechanism proposed by Price and Dickman (9) and consequently conformational effects were invoked. In order to cyclize, citraldehyde,

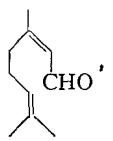

must undoubtedly take up a conformation in which the 1 and 6 carbon atoms are very close. The conformations are almost certainly in equilibrium with one another because the energy differences between them will be smaller than the activation energy for cyclization, which is 12.5 kcal. mole^{-1} (5). The arguments of Section 2(*b*) apply and show that a conformation which is favored by pressure would tend to reduce the apparent volume of activation. It is possible that conformations in which the 1 and 6 carbon atoms are

Can. J. Chem. Downloaded from www.nrcresearchpress.com by 61.7.252.67 on 09/04/12
For personal use only.

close together may be disfavored by pressure, and so contribute a little negatively to the apparent volume of activation. This is unlikely to be more than a few cm.^{3} mole^{-1} and is probably much less than this because the equilibrium constant for the formation of the cyclic conformation is probably much less than unity because of the relatively high steric hindrance in this conformation. The observed volume of activation cannot be explained as the result of conformational effects, and another explanation must be sought; it is shown in Section 4 that a slight change in mechanism is enough.

We conclude therefore that the only reaction in which conformational effects influence the pressure coefficient of the rate constant by an appreciable amount is the termination step in the polymerization of styrene. Pressure acts by reducing the rate at which the live polymer ends diffuse into juxtaposition.

4. THE EFFECT OF PRESSURE ON THE RATE OF ISOMERIZATION OF CITRALDEHYDE

Citraldehyde isomerizes in the presence of aqueous acid to 3,8-carvomenthenediol, and Price and Dickman (9) have proposed that the slow step is the unimolecular cyclization of the conjugate acid of citraldehyde as follows:

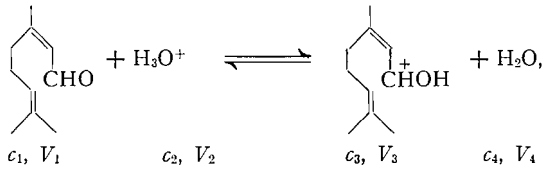

(4.1)

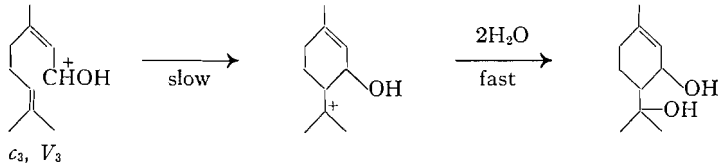

(4.2)

the concentrations and standard molar volumes are written under compounds for which they are required. The effect of pressure on the rate constant was investigated by Harris and Weale (5). They found an unexpectedly high pressure coefficient of ln k, 24.5 cm.^{3} mole^{-1}/RT at 25.2° C. and 1 atm., and this is not consistent with the above mechanism. The arguments are summarized thus: the volume change in reaction (4.1) will be rather small; the volume change in the slow step of reaction (4.2) should be very roughly 10 cm.^{3} mole^{-1} since this is about the volume lost in converting a van der Waals to a C–C valence interaction and the volume of activation will be smaller than this; the change of volume of the solvent during the reactions will be small. Consequently it is not possible to explain the measured volume of activation by a simple unimolecular slow step. Harris and Weale (5) suggested that an unspecified conformational effect was responsible. I have shown in the preceding section that this is unlikely to be correct.

There are two other likely mechanisms by which the conjugate acid of citraldehyde might be cyclized, a bimolecular reaction and a termolecular reaction, as follows:

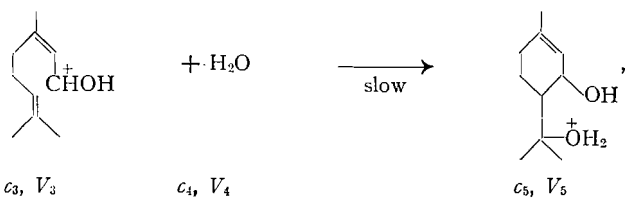

(4.3)

Can. J. Chem. Downloaded from www.nrcresearchpress.com by 61.7.252.67 on 09/04/12
For personal use only.

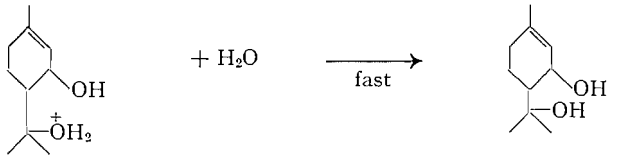

and

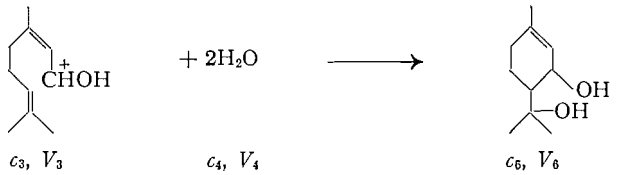

It will be shown below that both the bimolecular and the termolecular mechanisms are consistent with the measured pressure coefficient. It is less easy to distinguish between the two multimolecular mechanisms than to distinguish between these and the unimolecular mechanism. It is indeed possible that there is no formal distinction; reaction (4.4) may be so fast that the proton may leave the activated complex or may leave later depending upon the availability of a water molecule suitably oriented to accept it.

The measured rate constant k is defined by

[4.1] $$\text{rate of cyclization} = k(c_1+c_3)c_2.$$

If the reaction goes via reactions (4.3) and (4.4), then

[4.2] $$\text{rate of cyclization} = K_1k_3c_1c_2,$$

where K_1 is the equilibrium constant of reaction (4.1) and k_3 the rate constant of reaction (4.3). From equations [4.1] and [4.2] we find

[4.3] $$k = K_1k_3/(1+c_3/c_1), \quad \text{bimolecular.}$$

If the reaction goes via reaction (4.5), then

[4.4] $$\text{rate of cyclization} = K_1k_5c_1c_2c_4,$$

and from [4.1] and [4.4] we find

[4.5] $$k = K_1k_5c_4/(1+c_3/c_1), \quad \text{termolecular.}$$

In order to reduce repetition we discuss equation [4.5] in detail and later state the results of considering in a similar manner the bimolecular equation [4.3].

Taking logarithms of [4.5] and differentiating with respect to pressure, we obtain

[4.6] $$d\ln k/dp = d\ln K_1/dp + d\ln k_5/dp + d\ln c_4/dp - d\ln(1+c_3/c_1)/dp.$$

Now

[4.7] $$d\ln K_1/dp = -\Delta V_1/RT, \qquad d\ln k_5/dp = -\Delta V_5^{\ddagger}/RT,$$

where ΔV_1 is the partial volume change of reaction (4.1) and $\Delta V_5^{\ddagger}$ the partial volume of activation of reaction (4.5). K_1 is probably very small, so

[4.8] $$d\ln(1+c_3/c_1)/dp = 0 \quad \text{very nearly.}$$

The value of $d\ln c_4/dp$ depends upon the compressibility of the solution; assuming that

Can. J. Chem. Downloaded from www.nrcresearchpress.com by 61.7.252.67 on 09/04/12
For personal use only.

it is the same as that of the pure solvent (44.1% w/w ethanol in water) and using the measurements of Moesveld (7) we find

[4.9] $$d \ln c_4/dp = -49\times10^{-6} \text{ atm.}^{-1} \quad \text{at } p = 0.$$

From [4.6]–[4.9] we obtain

[4.10] $$d \ln k/dp = -(\Delta V_1+\Delta V_5^{\ddagger}+1.2 \text{ cm.}^3 \text{ mole}^{-1})/RT \quad \text{at } p = 0.$$

Let ΔV_5^* be the change in partial volume between the activated complex of reaction (4.5) and the final products and ΔV_5 be the change in partial volume of reaction (4.5) so that

[4.11] $$\Delta V_5 = \Delta V_5^{\ddagger}+\Delta V_5^*.$$

Now

$$\Delta V_1 = V_3+V_4-V_1-V_2,$$

and

$$\Delta V_5 = V_6+V_2-V_3-2V_4,$$

so by addition

[4.12] $$\Delta V_1+\Delta V_5 = V_6-V_1-V_4, = \Delta V,$$

where ΔV is the partial volume change of the whole reaction. From equations [4.10], [4.11], and [4.12] we have

[4.13] $$d \ln k/dp = -(\Delta V-\Delta V_5^*+1.2 \text{ cm.}^3 \text{ mole}^{-1})/RT.$$

The density of citraldehyde at 20° C. is 0.887 g. cm.$^{-3}$ (6) and hence

$$V_1 = 171 \text{ cm.}^3 \text{ mole}^{-1}$$

if the solution is perfect. Also

$$V_4 = 18 \text{ cm.}^3 \text{ mole}^{-1}.$$

The density of 3,8-carvomenthenediol has not, apparently, been recorded but if we assume that it is the same as that of the 6,8-diol, 1.13 g. cm.$^{-3}$ (1), we find

$$V_6 = 168 \text{ cm.}^3 \text{ mole}^{-1}.$$

Hence

$$\Delta V = -21 \text{ cm.}^3 \text{ mole}^{-1},$$

and

$$d \ln k/dp = (\Delta V_5^*+19.8 \text{ cm.}^3 \text{ mole}^{-1})/RT.$$

Experimentally $d \ln k/dp = 24.5$ cm.^{3} mole$^{-1}/RT$ at zero pressure; hence

$$\Delta V_5^* = 4.7 \text{ cm.}^3 \text{ mole}^{-1} \quad \text{at } p = 0.$$

If the termolecular mechanism is correct the final products of reaction (4.5), the 3,8-diol and H_3O^+, have a slightly higher volume than the activated complex. The value of ΔV_5^* may be somewhat in error because partial molar volumes differ from molar volumes, and the molar volume of 3,8-carvomenthenediol will differ from that of 6,8-carvomenthenediol. However, it seems safe to conclude that if reaction (4.5) is correct, the bond lengths in the activated state are close to those in the products.

If the bimolecular mechanism is correct, a similar treatment of equation [4.3] results in

$$\Delta V_4+\Delta V_3^* = 3.5 \text{ cm.}^3 \text{ mole}^{-1},$$

Can. J. Chem. Downloaded from www.nrcresearchpress.com by 61.7.252.67 on 09/04/12
For personal use only.

where ΔV_4 is the partial volume change of reaction (4.4) and ΔV_3^* is the difference in partial volume between the products and the activated complex of reaction (4.3). ΔV_4 is probably close to zero and the remarks of the preceding paragraph apply here also; if reactions (4.3)and (4.4) are correct the bond lengths in the activated state are close to those in the products.

We may note in passing that the pressure coefficient for the complete reaction is independent of the pressure coefficient of K_1. This is shown by the absence of ΔV_1 from equation [4.13] and its counterpart in the bimolecular mechanism and is due to the fact that because K_1 is small a change of ΔV_1 is exactly balanced by an equal and opposite change of ΔV_3 or ΔV_5.

The apparent volume of activation decreases rapidly with pressure from -24.5 cm.^{3} mole^{-1} at 1 atm. and 25.2° C. to -1.3 cm.^{3} mole^{-1} at 5000 atm. and the same temperature (5). If the reaction is termolecular, then by differentiating [4.13] with respect to pressure we obtain

$$[4.14] \qquad d^2\ln k/dp^2 = -(1/RT)(d\,\Delta V/dp - d\,\Delta V_5^*/dp + d^2 \ln c_4/dp^2).$$

It seems unlikely that ΔV_5^* will change much with pressure because it is already small, and $d^2\ln c_4/dp^2$ is negligible, so the major part of $d^2\ln k/dp^2$ is $d\,\Delta V/dp$. ΔV is the volume change of the reaction

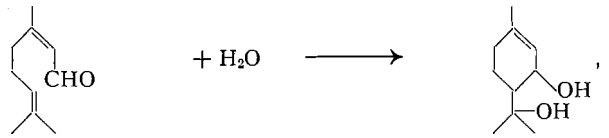

and $d\,\Delta V/dp$ depends upon the difference in compressibilities of the reactants and products. The reactants will be much more compressible than the products because two van der Waals interactions in the reactants, the intramolecular interaction between carbon atoms 1 and 6 and the intermolecular interaction between the water and the aldehyde, are converted into valence interactions which are much less compressible. Consequently $-\Delta V$ will decrease fairly rapidly with pressure, in agreement with the kinetic results. Very similar arguments hold if the slow step is bimolecular.

We conclude therefore that the kinetics of the isomerization of citraldehyde at 1 atm. together with the effect of pressure on the rate constant show that the elementary steps of the reaction are (4.1), and (4.3) and (4.4), or (4.1) and (4.5) in which the rate-controlling step is either bimolecular or termolecular. The unimolecular step (4.2) is excluded. It is likely that in the activated complex the bond lengths are close to those in the products. We note also that the effect of pressure on reaction rates may help to determine in other similar reactions whether or not the solvent is incorporated into the activated complex.

SUMMARY

1. The effect of a change of intermolecular or intramolecular conformation prior to reaction on the pressure coefficient of a reaction rate constant has been examined theoretically and the pertinent experimental evidence has been discussed.

2. If the conformations involved are at thermodynamic equilibrium with one another and if one conformation is present in much higher concentrations than the others, no effect will occur. If the concentrations of the conformations involved are of the same order of magnitude, an effect is present but it will usually be rather small.

Can. J. Chem. Downloaded from www.nrcresearchpress.com by 61.7.252.67 on 09/04/12
For personal use only.

3. If the conformations are far from equilibrium and a particular conformation is necessary for reaction to occur, the rate of formation of the necessary conformation is rate controlling and a well-defined conformational effect may occur.

4. The experimental evidence for the existence of conformational effects is reviewed and it is concluded that the only authentic example is that on the termination rate constant in the polymerization of styrene, which falls into class 3 above.

5. The apparent volume of activation for the cyclization of citraldehyde to 3,8-carvomenthenediol can be explained if the slow step is either bimolecular or termolecular but not if it is unimolecular. The bond lengths in the activated complex are close to those in the products. It is pointed out that the molecularity of other reactions may be determinable by measuring volumes of activation.

REFERENCES

1. BEILSTEINS HANDBUCH DER ORGANISCHEN CHEMIE. Vol. 6. *Edited by* B. Prager, P. Jacobsen, P. Schmidt, and D. Stern. Springer-Verlag, Berlin. 1923. p. 752.
2. CONANT, J. B. and PETERSON, W. R. J. Am. Chem. Soc. **57**, 628 (1932).
3. CONANT, J. B. and TONBERG, C. O. J. Am. Chem. Soc. **52**, 1659 (1930).
4. GLASSTONE, S., LAIDLER, K. J., and EYRING, H. Theory of rate processes. McGraw-Hill Book Company, Inc., New York. 1941.
5. HARRIS, R. T. and WEALE, K. E. J. Chem. Soc. 953 (1956).
6. HEILBRON, SIR I. and BUNBURY, H. M. Dictionary of organic compounds. Vol I. Eyre & Spottiswoode Ltd., London. 1953. p. 589.
7. MOESVELD, A. L. Th. Z. physik. Chem. **105**, 450 (1923).
8. NICHOLSON, A. E. and NORRISH, R. G. W. Discussions Faraday Soc. **22**, 104 (1956).
9. PRICE, C. C. and DICKMAN, M. L. Ind. Eng. Chem. **40**, 257 (1948).
10. STERN, A. E. and EYRING, H. Chem. Revs. **29**, 509 (1941).
11. WEALE, K. E. Discussions Faraday Soc. **22**, 145 (1956).
12. WHALLEY, E. Discussions Faraday Soc. **22**, 146 (1956).

Can. J. Chem. Downloaded from www.nrcresearchpress.com by 61.7.252.67 on 09/04/12
For personal use only.

Can. J. Chem. Downloaded from www.nrcresearchpress.com by 61.7.252.67 on 09/04/12
For personal use only.

THE PREPARATION OF AMINES AND HYDRAZO COMPOUNDS USING HYDRAZINE AND PALLADIZED CHARCOAL[1]

P. M. G. BAVIN[2]

ABSTRACT

The reduction of nitro compounds to amines by ethanolic hydrazine and palladized charcoal probably proceeds through the nitroso and hydroxylamine derivatives. This reagent is shown to be useful for the reduction of azo to hydrazo compounds.

The reduction of nitro compounds to amines using ethanolic hydrazine and Raney nickel (2, 3) or palladized charcoal (10, 24) as catalyst offers many advantages over classical reducing agents. In particular, the catalyzed hydrazine reductions are very rapid and give high yields of easily isolable amines without the use of special apparatus.

The earlier work showed that hydrazine–palladium was useful for the preparation of aniline, the toluidines, phenylenediamines, *p*-aminobenzoic acid, and aminofluorescein (24), and the amino derivatives of polynuclear hydrocarbons (10). The present work, most of which is summarized in Table I in the Experimental section, extends the usefulness of the method and points out some limitations.

The reduction of 2,2′-dinitrodiphenyl proceeded erratically, the products obtained depending on the activity of the catalyst. A highly active palladium-on-charcoal catalyst gave 2,2′-diaminodiphenyl in good yield, but a less active one gave a mixture of the diamine with benz-[*c*]-cinnoline. The latter compound could be obtained pure in 92% yield using Raney nickel of low activity[3] as catalyst.

Ortho- and *p*-chloronitrobenzene and *p*-nitrophenylacetonitrile did not give pure amines. 2,5-Dichloronitrobenzene gave, very rapidly, an excellent yield of β-(2,5-dichlorophenyl)-hydroxylamine and, more slowly, 2,5-dichloroaniline. 2-Chloro-5-nitroterephthalic acid (11) and 2-fluoro-5-nitrotoluene gave good yields of the amines.

The reduction of nitrobenzene, which has been reviewed by Sidgwick (25), is known to proceed through nitrosobenzene and β-phenylhydroxylamine to aniline, much of our knowledge being due to Haber (17) and Brand (4, 5, 6). Goldschmidt showed (13, 14, 15, 16) that the relative rates of reduction were in the order nitrosobenzene > β-phenylhydroxylamine > nitrobenzene, explaining the difficulty encountered in isolating nitrosobenzene as a reduction product except under rigorously controlled conditions. In alkaline media nitrosobenzene and β-phenylhydroxylamine condense to form azoxybenzene, giving rise to another series of reduction products.

The hydrazine–palladium reagent reduces nitro- and nitroso-benzene and β-phenylhydroxylamine to aniline, but azo- and azoxy-benzene are reduced to hydrazobenzene.[4] These facts suggest that the reduction of nitro compounds to amines by this reagent proceeds through monomeric compounds, as shown below in route I. The isolation of

[1]*Manuscript received September 5, 1957.*
Contribution from the Departments of Chemistry of the University of Ottawa, Ottawa, Canada, and (present address) the Ohio State University, Columbus 10, Ohio, U.S.A.
[2]*National Research Council of Canada Postdoctorate Fellow at the University of Ottawa, 1954–1956.*
[3]*The Raney nickel catalyst was W1 (1, 8), which had been stored for several months at 0° under absolute methanol.*
[4]*It is interesting to note that fermenting yeast will reduce nitro- and nitroso-benzene and β-phenylhydroxylamine but not azo- or azoxy-benzene, to aniline (23).*

β-(2,5-dichlorophenyl)-hydroxylamine as a reduction product of 2,5-dichloronitrobenzene lends strong support to this mechanism.

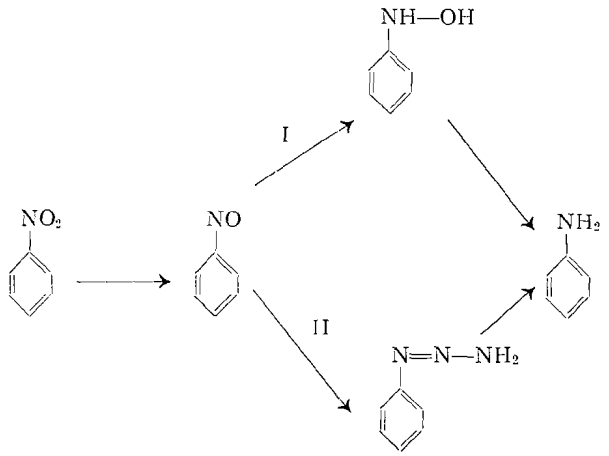

An alternative mechanism is shown, route II, based on the known easy condensation of nitrosobenzene with many amines and phenylhydrazine. Hydrazine was found to react rapidly with nitrosobenzene but the red oil obtained appeared to be stable to hydrazine–palladium, making route II improbable.

The reduction of azobenzene to hydrazobenzene by hydrazine–palladium is a considerable improvement on the usual zinc – alcoholic potash method. An excess of hydrazine is advantageous since it appears to protect the hydrazobenzene during crystallization. Hydrazo-*o*-diphenyl was also prepared in good yield, and the method may prove to be generally useful for the preparation of hydrazo compounds.

EXPERIMENTAL

Melting points are uncorrected. The active palladium-on-charcoal catalyst was 10%, supplied by Baker and Co., Newark, New Jersey; the less active catalyst was an old sample.

The reductions were carried out essentially as described by Pietra (24). Most of the results are presented in Table I. Wherever possible the identity of a product was confirmed by taking the melting point of a mixture with an authentic sample, and by taking the infrared spectrum. Many of the amines were acetylated to aid isolation.

o-Chloronitrobenzene did not give a pure product. *p*-Chloronitrobenzene gave, after several crystallizations from benzene, impure *p*-chloroacetanilide (27%), m.p. 171–175° (lit. m.p. 178° (19)).

β-(2,5-Dichlorophenyl)-hydroxylamine

Hydrazine hydrate (4 ml.) was added to a suspension of 2,5-dichloronitrobenzene (5 g.) and active 10% palladium-on-charcoal (0.1 g.) in ethanol (100 ml.). The vigorous exothermic reaction was over in 2 minutes, as shown by a pronounced slackening in the rate of nitrogen evolution. After the catalyst was removed by filtration, the solution was poured into ice water (500 ml.). A white solid separated and was collected, washed, and dried by suction. The yield was almost quantitative.

Recrystallization was achieved by dissolving the product in hot benzene (100 ml.),

Can. J. Chem. Downloaded from www.nrcresearchpress.com by 61.7.252.67 on 09/04/12
For personal use only.

TABLE I[1]

Compound	Isolated as:	%	M.p.	Lit. m.p.
Nitrobenzene	Acetanilide	91	110–112	113–114 (19)
Nitrosobenzene	Acetanilide	93	109–111	113–114 (19)
β-Phenylhydroxylamine	Acetanilide	89	112–113	113–114 (19)
Azobenzene	Hydrazobenzene	84[2]	125–126	126–127 (19)
Azoxybenzene	Hydrazobenzene	79[2]	125–126	126–127 (19)
Azoxy-*o*-diphenyl	Hydrazo-*o*-diphenyl	70[2]	172–176[3]	182 (12)
4,6-Dinitro-*m*-xylene	N,N′-Diacetyl-4,6-diamino-*m*-xylene	87	290–292	295 (19)
1-Nitro-2-naphthylamine	1,2-Diaminonaphthalene[4]	85	96–98	98.5 (19)
5-Nitro-6-amino-2-methylpyridine	5,6-Diamino-2-methylpyridine	82	64–67	69–70 (20)
o-Nitrophenol	*o*-Aminophenol	88	171–173	174 (19)
2-Nitrofluorene[7]	2-Aminofluorene	97	127–128	129 (19)
2-Fluoro-5-nitrotoluene	6-Fluoroaceto-*m*-toluidide	88	76–77	74 (7)
2-Nitrodiphenyl	2-Aminodiphenyl	89	47–49	49–50 (19)
4-Nitrodiphenyl	4-Aminodiphenyl	92	51–53	50–52 (19)
2,2′-Dinitrodiphenyl[5]	N,N′-Diacetyl-2,2′-diaminodiphenyl	88	162–164	161 (19)
6,6′-Dimethyl-2,2′-dinitrodiphenyl	6,6′-Dimethyl-2,2′-diaminodiphenyl	63[6]	133–135	136 (19)

[1] *Yield and melting point refer to crude dried product unless otherwise indicated.*
[2] *Crystallized from ethanol containing hydrazine.*
[3] *Melting point with decomposition and dependent on the rate of heating.*
[4] *Characterized by condensation with phenanthraquinone to give 1,2;3,4;5,6-tribenzphenazine, yellow prisms from xylene, m.p. 272–273° (lit. m.p. 273° (21)).*
[5] *Using a catalyst of low activity, a mixture of the diamine with benz-[c]-cinnoline, m.p. 155–156°, was obtained.*
[6] *The low yield is probably due to the use of only 0.1 g. of nitro compound.*
[7] *Raney nickel has been used as the catalyst for this reduction, a yield of 100% being claimed (22).*

adding a little anhydrous magnesium sulphate to remove traces of water, and decanting off the supernatant solution. Addition of hot heptane gave, on cooling, long white needles, m.p. 95–96° with decomposition to a black tar. The melting point depended on both the rate of heating and the crystal size, powdered samples having m.p. 93–94° (lit. m.p. 93° (9)). The melting point was not depressed when the product was mixed with an authentic sample, prepared by Lapworth's general method (18). The identity was confirmed by oxidation to 2,5-dichloronitrosobenzene, m.p. 99–100° (lit. m.p. 101° (9)), and by comparison of infrared spectra. Sharp peaks at 3600 and 3340 cm.$^{-1}$ in the spectra of dilute chloroform solutions were probably O—H and N—H stretching bands since the spectrum of β-phenylhydroxylamine was identical in that region.

Recrystallized β-(2,5-dichlorophenyl)-hydroxylamine is stable at 0° but heating a benzene solution on the steam bath for a few minutes causes extensive decomposition to a brown tar.

When the reduction was carried out for 24 hours, 2,5-dichloroaniline was obtained, m.p. and mixed m.p. 49–50° (lit. m.p. 50° (9)).

Benz-[c]-cinnoline

2,2′-Dinitrodiphenyl was reduced using the general method described by Balcom and Furst (2). After the catalyst was removed by filtration, the filtrate was concentrated to give, on cooling, benz-[c]-cinnoline as yellow prisms, m.p. 155–156° (lit. m.p. 156° (19)). The yield was consistently greater than 90% when a weakly active Raney nickel catalyst was used.

Benz-[c]-cinnoline picrate crystallized from benzene as dark yellow prisms, m.p. 194–195° (lit. m.p. 194° (19)).

Can. J. Chem. Downloaded from www.nrcresearchpress.com by 61.7.252.67 on 09/04/12
For personal use only.

NOTE ADDED IN PROOF

Since this paper was accepted for publication, two more articles have become available (26, 27) which deal with some uses of hydrazine as a reducing agent in the presence of metal catalysts.

ACKNOWLEDGMENT

The author is grateful to Doctors F. A L. Anet, M. P. Cava, and M. S. Newman for their interest and encouragement.

REFERENCES

1. ADKINS, H. and PAVLIC, A. A. J. Am. Chem. Soc. **69**, 3039 (1947).
2. BALCOM, D. and FURST, A. J. Am. Chem. Soc. **75**, 4334 (1953).
3. BAVIN, P. M. G. and DEWAR, M. J. S. J. Chem. Soc. 164 (1956).
4. BRAND, K. Die elektrochemische Reduktion organischer Nitrokorper. F. Enke, Stuttgart. 1908.
5. BRAND, K. and MAHR, J. J. prakt. Chem. **131**, 97 (1931); **142**, 153 (1935).
6. BRAND, K. and MODERSOHN, A. J. prakt. Chem. **120**, 160 (1928–1929).
7. BUU-HOÏ, N. P. and JACQUIGNON, P. J. Chem. Soc. 4173 (1952).
8. COVERT, L. W. and ADKINS, H. J. Am. Chem. Soc. **54**, 4116 (1932).
9. DE CRAUW, T. Rec. trav. chim. **50**, 753 (1931).
10. DEWAR, M. J. S. and MOLE, T. J. Chem. Soc. 2556 (1956).
11. FISHEL, D. L. Unpublished data.
12. FRIEBEL, G. and RASSOW, B. J. prakt. Chem. **63**, 459 (1901).
13. GOLDSCHMIDT, H. and ECKARDT, M. Z. physik. Chem. **56**, 385 (1906).
14. GOLDSCHMIDT, H. and INGEBRECHSTEN, K. Z. physik. Chem. **48**, 435 (1904).
15. GOLDSCHMIDT, H. and LARSEN, H. Z. physik. Chem. **71**, 437 (1910).
16. GOLDSCHMIDT, H. and SUNDE, E. Z. physik. Chem. **56**, 1 (1906).
17. HABER, F. Angew. Chem. **13**, 435 (1900); Z. physik. Chem. **32**, 193 (1900).
18. HAWORTH, R. D. and LAPWORTH, A. J. Chem. Soc. **119**, 768 (1921).
19. HEILBRON, SIR I. Dictionary of organic compounds. Oxford University Press, New York. 1953.
20. LAPPIN, G. R. and SLEZAK, F. B. J. Am. Chem. Soc. **72**, 2806 (1950).
21. LAWSON, T. A. Ber. **18**, 2426 (1885).
22. LITVNENKO, L. M. and GREKOV, A. P. Zhur. Obshcheĭ Khim. **27**, 234 (1957); Chem. Abstr. **51**, 12866e (1957).
23. NEUBERG, C. and WELDE, E. Biochem. Z. **60**, 474 (1914); **67**, 18, (1914). *See also* Advances in carbohydrate chemistry. Vol. 4. Academic Press, Inc., New York. 1949. p. 98.
24. PIETRA, S. Ann. chim. (Rome), **45**, 850 (1955).
25. SIDGWICK, N. V. The organic chemistry of nitrogen. Oxford University Press, London. 1937.
26. PIETRA, S. Ann. chim. (Rome), **47**, 410 (1957).
27. FURST, A. and MOORE, R. E. J. Am. Chem. Soc. **79**, 5492 (1957).

Can. J. Chem. Downloaded from www.nrcresearchpress.com by 61.7.252.67 on 09/04/12
For personal use only.

Can. J. Chem. Downloaded from www.nrcresearchpress.com by 61.7.252.67 on 09/04/12
For personal use only.

TRIARYLMETHANE COMPOUNDS AS REDOX INDICATORS IN THE SCHOENEMANN REACTION

III. THE DYES AND THEIR SPECTRA[1]

G. A. Grant, R. Blanchfield, and D. Morison Smith

ABSTRACT

A series of triarylmethane dyes were made by varying the substituents in the thiophene ring of the dye [4-(*p*-dimethylamino-α-2-thienylbenzylidene)-2,5-cyclohexadiene-1-ylidene]-dimethylammonium chloride. The spectra of the zinc salts of these dyes were shown to be similar to that of the dye formed in the Schoenemann reaction when the parent triarylmethane compound was used as an indicator. Neither of the absorption bands occurring in the 475 mμ or 625 mμ regions is affected by pH or buffer salts in the pH range 2.4 to 6.4 but both bands are hypsochromically shifted when the pH is lowered to 0.5. The substitution of 5-nitro and 5-acetamido groups in the thiophene ring results in the largest bathochromic and hypsochromic shifts respectively. Interpretation of the effect of substitution and pH was attempted employing existing theories on the relation between color and constitution.

INTRODUCTION

The preceding papers in this series (4, 14) described the preparation and use of some triarylmethane compounds as indicators in the Schoenemann reaction with a view to improving the method for detecting the phosphonofluoridate type of anticholinesterase compounds. As the success of the method depended greatly on the color of the dye produced it was of interest to ascertain the effect of various substituents attached to the thiophene ring on the spectra of the dyes. The effect of the replacement of the benzene nucleus by thiophene and a number of 5-substituted thiophene nuclei on triarylmethane dyes has been reported by Mason and Nord (11, 12). However, the present investigation enlarges on the previous studies by including a number of new mono- and di-substituted thienyl derivatives. The effect of pH on the spectra is also reported.

It was of interest to check the assumption that the oxidized compound produced in the Schoenemann reaction was the same as that of an authentic dye cation. Therefore spectral comparisons have been made of a number of zinc chloride salts of prepared dyes with the dyes formed in the Schoenemann reaction.

EXPERIMENTAL

Preparation of Dyes

The preparation and purification of the triarylmethane compounds from which the dyes were made have been described previously (4).

The zinc chloride salts of the dyes were prepared from the corresponding triarylmethane compounds according to the procedure of Mason and Nord (11) except that identical molar concentrations of the solutions were always used in an attempt to produce salts of the same composition. The method of Davies and Hodgson (2) was investigated but was not found to be superior to the method outlined by Mason and Nord (11) or Levi (7).

Briefly, the leuco compounds (0.04 mole) were dissolved in 2 *N* HCl (80 ml.) and the solutions were diluted with 800 ml. of water. Freshly prepared lead dioxide (0.04 mole) was added with stirring and cooling. After 2 hours sodium sulphate (0.05 mole) was

[1]*Manuscript received July 24, 1957.*
Contribution from Defence Research Board, Defence Research Chemical Laboratories, Ottawa, Ontario. Issued as D.R.C.L. Report 135C. Presented at the Annual Conference of the Chemical Institute of Canada at Vancouver in June, 1957.

added and the solution filtered. To 400 ml. of solution were added saturated zinc chloride solution (0.03 mole) and saturated brine solution (800 ml.). The precipitated dye was filtered off and the dye crystals were washed with ice water. The average yields were approximately 80%. An exception to the above procedure was the case of the dye with a nitro group in the 5-position in the thiophene ring. This leuco compound could not be made satisfactorily by the usual condensation of the nitrothiophenealdehyde with dimethylaniline (11). However, removal of the excess dimethylaniline and the oxidation of the reaction mixture by the above procedure gave the dye salt. The nitrothiophenealdehyde mentioned above was prepared from thiophenealdehyde by nitration of the aldehyde diacetate and subsequent hydrolysis according to the procedure of Patrick and Emerson (13).

The composition of some of these dyes is given in Table I.

TABLE I

ANALYSIS OF DYE SALTS

Zinc chloride salt of formula I with:			Found			Calculation (based on these analyses) for:		
R	R′	R″	% C	% H	% N	Moles $ZnCl_2$	Moles H_2O	Mol. wt.
H	H	H	45.00	4.55	—	1.24	1.15	560.5
CH_3	H	H	47.33	4.89	—	1.13	1.04	558.2
C_3H_7	H	H	58.02	5.94	5.62	0.59	0.22	497.0
CH_3	CH_3	H	52.57	5.40	5.21	0.85	0.57	525.4
CH_3	C_2H_5	H	52.60	5.95	—	0.77	1.68	547.9
C_6H_5	H	H	51.32	5.23	—	0.98	2.88	631.9
Br	CH_3	H	44.02	4.70	4.65	0.74	2.00	600.2

Spectral Measurements

On the basis of the analysis of the dyes, solutions of a definite molarity were made up in distilled water or in the appropriate Clark and Lubs buffer and the spectra were determined on a Beckman Model DU Spectrophotometer between 320 and 700 mμ. Spectra were also taken of known dyes, e.g. malachite green, for comparison purposes. Absorption spectra of the dyes produced in the Schoenemann reaction were obtained employing a test procedure as outlined previously (4). The spectra were scanned from 320 to 700 mμ in 20 mμ steps 10 minutes after the addition of all the reagents.

RESULTS AND DISCUSSION

Composition of Dyes

The analyses for the dye salts given in Table I showed that the zinc chloride salts as prepared do not have a definite composition. Mason and Nord (11) on the basis of nitrogen analyses suggested a formula with 2 moles of zinc chloride and 3 moles of water.

Spectra of Dyes Formed in the Schoenemann Reaction

A comparison was made between the spectra of the dye solutions obtained in the Schoenemann reaction and the spectra of the corresponding solutions of the zinc chloride salts of the dyes. Fig. 1 is an example of this comparison for the 4,5-dimethylthienylidene dye. Along with similar plots obtained for other compounds this supports the assumption that I is the dye formula responsible for the color in the Schoenemann reaction.

Can. J. Chem. Downloaded from www.nrcresearchpress.com by 61.7.252.67 on 09/04/12
For personal use only.

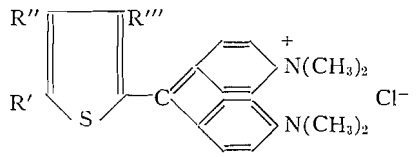

I

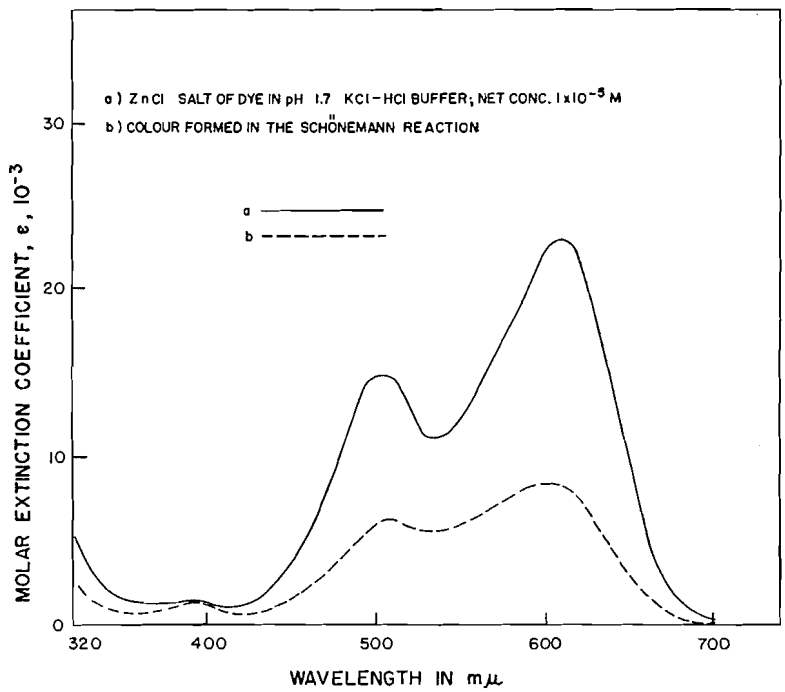

FIG. 1. Comparison of color formed in Schoenemann reaction with that of a solution of zinc chloride salt of the 4,5-dimethylthienyl substituted dye.

Effect of pH on Dye Spectra

Although a pH of approximately 2.2 or lower is necessary for the formation of the dye from the leuco compound, the pH for optimum color intensity may occur at a different pH. However, only under acid conditions would the results be of significance in the Schoenemann reaction, because the dyes are rapidly destroyed by alkaline peroxide, an excess of which is always present in this reaction.

The effect of pH was investigated over the range 0.5 to 6.4 in buffered solution. The results are reported in Table II. Neither the y band nor the x band is affected by pH or buffer salts in the pH range 2.4 to 6.4, but both bands are hypsochromically shifted for all the compounds studied except the 3-methyl and 5-acetamido derivatives when the pH is lowered to 0.5. At pH 0.5 the absorption intensity of some of the dyes decreased, and it was thought that decomposition might be taking place. The system was found to be only partially reversible, for although on the addition of alkali the color reappeared the original absorption bands were not entirely restored in intensity. All the dyes studied showed the same reversible reaction except the 3-methyl substituted compound which gave an irreversible bathochromic shift from 469 to 474 mμ when the pH was dropped from 1.60 to 0.5. Fig. 2 illustrates this decrease in intensity and shift in the absorption

Can. J. Chem. Downloaded from www.nrcresearchpress.com by 61.7.252.67 on 09/04/12
For personal use only.

TABLE II

EFFECT OF pH ON ABSORPTION BANDS

Substituent	Absorption maximum (mμ)				
	pH 0.5	pH 1.6	pH 2.4	pH 4.4	pH 6.4
	y-Absorption bands				
5-Acetamido	460	460	536	Insoluble	
4,5-Dimethyl-2-thienyl	392	504	499	499	499
4-Ethyl-5-methyl-2-thienyl	392	500	500	500	500
5-Methyl-2-thienyl	386	490	486	486	486
5-Ethyl-2-thienyl	386	488	486	486	486
5-Propyl-2-thienyl	386	486	486	486	484
5-Chloro-2-thienyl	F	476	476	476	476
5-Bromo-2-thienyl	385	474	476	476	476
5-Methyl-5-bromo-2-thienyl	F	F	476	476	476
3-Methyl-2-thienyl	474	469	469	469	469
2-Thienyl	F	F	465	465	465
	x-Absorption bands				
5-Bromo-2-thienyl	568	635	637	634	632
5-Chloro-2-thienyl	F	F	634	634	632
2-Thienyl	F	F	623	623	623
4-Methyl-5-bromo-2-thienyl	F	F	624	624	624
3-Methyl-2-thienyl	618	620	620	620	620
4-Ethyl-5-methyl-2-thienyl	552	603	620	620	620
5-Methyl-2-thienyl	534	614	616	616	616
5-Ethyl-2-thienyl	534	608	616	614	616
5-Propyl-2-thienyl	534	604	614	614	614
4,5-Dimethyl-2-thienyl	552	603	614	614	614
5-Acetamido	607	607	605	Insoluble	

F—*Unstable solution.*

curve of the 3-methyl compound when the pH value is decreased from 6.4 to 0.5. At pH 1.6 an inflection appears in the absorption curve at 555 mμ, which becomes a distinct band when the pH value is lowered to 0.5.

From pH 2.54 to 6.45 dyes with alkyl substitution in the 5-position absorb similarly to those with 3-methyl substitution, while from pH 1.6 to 2.54 they are markedly different. The appearance of the band at 540 mμ at pH 0.5 was more pronounced in the case of 5-substitution (e.g., 5-methylthienyl, Fig. 3), than with 3-substitution. The dialkyl substituted dyes responded to pH change in a similar manner to the unsubstituted and monosubstituted compounds.

The examination of the effect of pH on triarylmethane dyes containing a thienyl or substituted thienyl group showed that they were behaving as acid–base indicators similar to crystal violet. Adams and Rosenstein (1) examined the color changes of crystal violet in acid solution and showed that the absorption spectra corresponded to successive addition of positive charge to the cation. However, it is of interest to compare spectra obtained in the present investigation with those of the triphenylmethane dyes because of the difference in resonance structure between thienyl and phenyl groups. The hetero-sulphur atom in the thienyl group changes the electronic distribution and makes it impossible for the thienyl group to contribute quinoidal resonance hybrids as postulated for other triphenylmethane dyes.

In the case of crystal violet, the addition of a proton to one dimethylamino group results in the loss of the contribution of that dimethylaminophenyl group to the resonance of the molecule. The electron cloud is then redistributed between the other two dimethyl-anilino groups and the absorption spectrum becomes similar to that of malachite green.

Can. J. Chem. Downloaded from www.nrcresearchpress.com by 61.7.252.67 on 09/04/12
For personal use only.

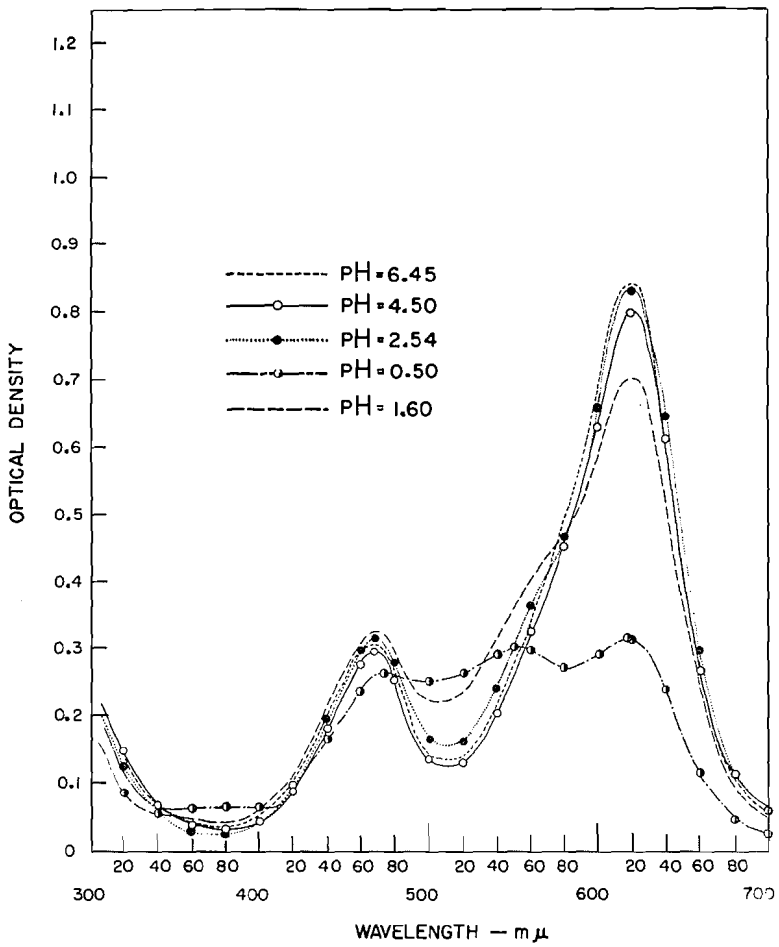

FIG. 2. Spectra at various acidities for 3-methylthienyl substituted dye.

In the case of thiophene malachite green a proton attack on one of the dimethylaminophenyl groups would substantially change the picture since the electron cloud would either be concentrated in the remaining dimethylaminophenyl group or shared between it and the 2-thienyl group. However, when the 2-thienyl group is unsubstituted or substituted only in the 3-position the resonance form showing a continuous conjugated system has a high probability.

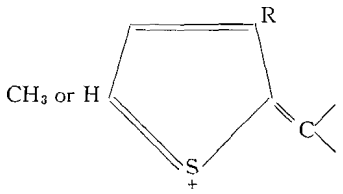

II

This structure is less likely to be subject to a proton attachment but the S=C bond may be attacked and split. This in part may account for some of the decomposition of the unsubstituted and 3-methyl substituted dyes at the lower pH. In all cases that

Can. J. Chem. Downloaded from www.nrcresearchpress.com by 61.7.252.67 on 09/04/12
For personal use only.

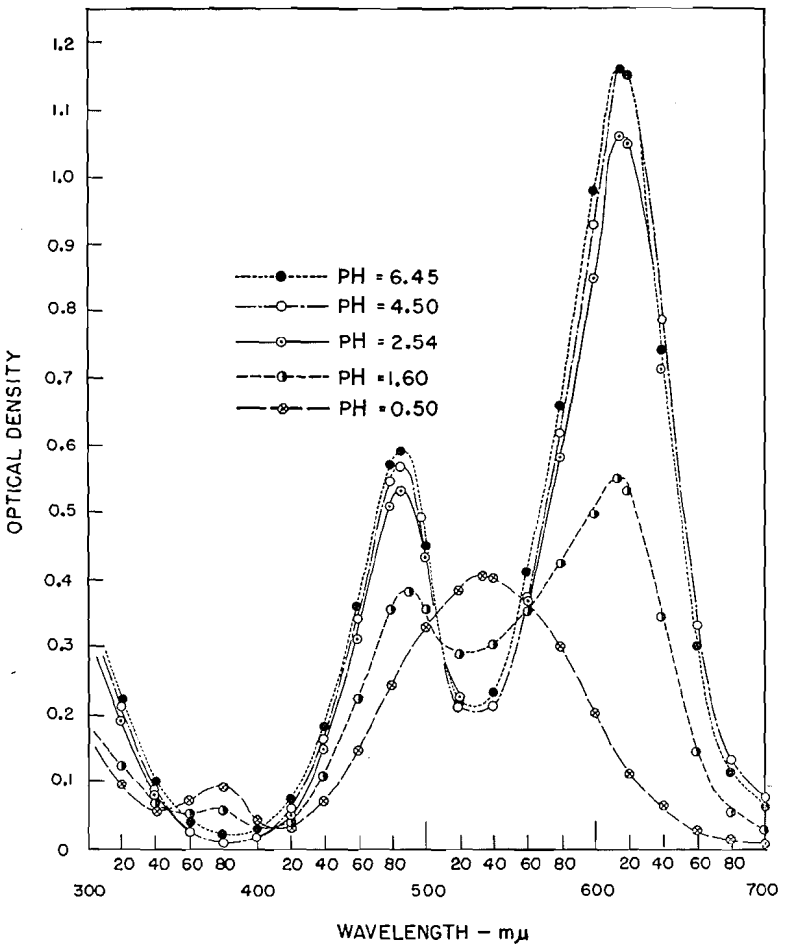

FIG. 3. Spectra at various acidities for 5-methylthienyl substituted dye.

were studied, except that of the 3-methyl-2-thienyl dye, a proton attack caused a general hypsochromic shift. The resonance hybrid of the 3-methyl substituted thienyl dye is therefore different from that obtained by disubstitution in the 4,5-positions or monosubstitution in the 5-position. That there is no shift with a proton attack on the 3-methyl substituted dye may be explained by the fact that when a methyl group is substituted in the 3-position of the thiophene ring, a larger proportion of the resonance hybrid is in the conjugated form (Formula II).

Effect of Substitution

Because of the variable composition of the zinc chloride salts the values of extinction coefficients are not reported. The wavelengths of the absorption maxima are comparable since it has been shown that the salt forming Lewis acid has little or no effect on wavelength maxima of the dye spectra (10).

For those dyes which are the same as those made previously (11, 12), the spectra and wavelength shifts obtained in this study in aqueous solution exhibit the same tendencies but are not identical in magnitude to those obtained by Mason and Nord in acetic acid solutions (12).

Can. J. Chem. Downloaded from www.nrcresearchpress.com by 61.7.252.67 on 09/04/12
For personal use only.

The relation between color and chemical constitution has been explored by Lewis (9), Knott (6), and Dewar (3). According to Lewis (9) the change from the single x absorption band of crystal violet to the x and y absorption bands of malachite green indicates the introduction of the second mode of electronic oscillation involving the unsubstituted phenyl ring. The wavelength of the x absorption of malachite green is higher than that of crystal violet because, in the malachite green case, the positive charge is distributed mainly between the two dimethylaniline rings, whereas it is distributed between three equivalent rings in the crystal violet case (8). In this degenerate case the x and y bands coincide. It would seem that the wavelength difference between the x and y bands could be used as a measure of the degree of participation of the resonance forms of the aryl portion in the aryl bis(dimethylaniline) dyes. That is, it would indicate qualitatively how close they were to the crystal violet case when there is equal participation of all three groups attached to the central carbon atom, and as well might provide a way of ranking substituted aryl rings according to their positive nature when involved in this kind of attachment. These differences are given in Table III.

TABLE III

ABSORPTION MAXIMA OF x AND y BANDS

Zinc chloride salt of (*p*-dimethylamino-*aryl*-benzylidene)-2,5-cyclohexadiene-1-ylidene dimethylammonium chloride where *aryl* is	λ_x, mμ	λ_y, mμ	$\lambda_x - \lambda_y$, mμ
5-Acetamido-2-thienyl	605*	532*	73
4-Methyl-5-ethyl-2-thienyl	614	500	114
4,5-Dimethyl-2-thienyl	614	499	115
4-Ethyl-5-methyl-2-thienyl	614	499	115
5-Methyl-2-thienyl	616	486	130
5-Ethyl-2-thienyl	616	486	130
5-Propyl-2-thienyl	614	484	130
4-Methyl-5-bromo-2-thienyl	624	476	148
3-Methyl-2-thienyl	620	468	152
5-Chloro-2-thienyl	634	476	158
5-Bromo-2-thienyl	634	476	158
p-Tolyl	600	442	158
2-Thienyl	625	465	160
2-Furyl	637	475	162
5-Phenyl-2-thienyl	632	518	174
Phenyl	617	428	189
5-Nitro-2-thienyl	662	456	216

**Taken in distilled water solution.*

Table III also includes a comparison of the wavelengths of the x and y bands of some of the triarylmethane dyes. Substitution in the 5-position, with nitro, halo, or phenyl groups, produces bathochromic shifts while alkyl or acetamido substitution produces a hypsochromic shift in the x band. The largest bathochromic and hypsochromic shifts (37 and 23 mμ respectively) result from 5-nitro and 5-acetamido substitution. The effect of substitution on y band absorption is also appreciable. Substitution of a phenyl or nitro group in the 5-position results in hypsochromic shifts of 7 and 9 mμ respectively while substitution of alkyl, acetamido, halogen groups or both alkyl and halogen groups produced bathochromic shifts.

Mason and Nord (12) reported that the hypsochromic influence exerted on the x band increased with the size of the alkyl group. The total shift was 3 mμ when the group size was increased from methyl to propyl. Our data indicate that 5-propyl thiophene

Can. J. Chem. Downloaded from www.nrcresearchpress.com by 61.7.252.67 on 09/04/12
For personal use only.

malachite green absorbs at a shorter wavelength than the 5-methyl and 5-ethyl compounds. However, there is no strong evidence to indicate that the magnitude of the hypsochromic shift increases significantly with the size of the alkyl group.

It was reported (12) that substitution of the electronegative chlorine and bromine atoms in the 2-position of the thiophene ring causes bathochromic shifts of the x and y bands. Larger bathochromic shifts of the x band were reported for the chloro compound than for the bromo compound, while the reverse was true for the y bands. The present investigation confirms that bathochromic shifts occur for the x and y bands. However, no difference in the magnitude of the shifts was noted when the less electronegative bromine atom was substituted for a chlorine atom.

It is also of interest to note that if both electron attracting and donating groups are substituted in the thiophene nucleus no appreciable shift occurs. When a methyl group is placed in the 4-position and a bromine atom in the 5-position, it is evident from the absence of wavelength shift that most of the electrons attracted by the halogen are obtained at the expense of the methyl group in the 4-position. Thus the net electronic distribution approaches that of the unsubstituted 2-thienyl nucleus.

The new members of the series are the 4,5-dialkyl, and acetamido-, nitro-, and phenyl-substituted thiophene dyes. The spectra of the 4,5-dialkyl dyes show an enhancement of the effects observed for the 5-monoalkyl dyes. These compounds possess more resonance forms with a positive charge in the thiophene ring. The 5-acetamidothienyl dye approaches most closely to the situation in crystal violet where all rings are equivalent, thus indicating possible participation of positively charged nitrogen in the amide group in the resonance of the dye. In the case of 5-nitrothienyl dye the difference between x and y peaks is much greater because the electron-attracting nitro group makes the thiophene ring system even less positive than usual. A similar effect is observed with the 5-phenylthienyl dye where the charge is dissipated over two aromatic rings, although the effect is less pronounced than in the nitro compound, because the phenyl ring, in itself, is only slightly more negative than the thiophene ring ($\lambda_x - \lambda_y = 189$ mμ for malachite green vs. 160 mμ for the thiophene analogue). With respect to this difference in x and y peaks, "furan malachite green" appears to be quite similar to the thiophene derivative. The effect of a para-methyl group in the phenyl ring (8) is about the same as the effect of a 5-methyl group in the thiophene ring, that is, $\lambda_x - \lambda_y$ is decreased by 30 mμ.

In summary, it may be noted that the leuco compounds effective as indicators in the Schoenemann reaction (14) have a wavelength difference between the absorption maxima of 110 to 150 mμ, and the order of their effectiveness increases as the wavelength difference decreases. It may also be noted that this order of substituents given in Table III corresponds to the order to be expected for Hammett's σ constants, going from negative to positive values (5), allowing for the difference to be expected between the phenyl and thienyl ring systems.

REFERENCES

1. Adams, E. Q. and Rosenstein, L. J. Am. Chem. Soc. **36**, 1452 (1914).
2. Davies, R. R. and Hodgson, H. H. J. Soc. Dyers Colourists, **59**, 196 (1943).
3. Dewar, M. J. S. J. Chem. Soc. 2329 (1950).
4. Grant, G. A., Blanchfield, R., and Smith, D. M. Can. J. Chem. **35**, 40 (1957).
5. Jaffé, H. H. Chem. Revs. **53**, 191 (1953).
6. Knott, E. B. J. Chem. Soc. 1024 (1951).
7. Levi, L. E. Ber. **20**, 517 (1887).
8. Lewis, G. N. J. Am. Chem. Soc. **67**, 770 (1945).
9. Lewis, G. N. and Bigeleisen, J. J. Am. Chem. Soc. **65**, 2102 (1943).

Can. J. Chem. Downloaded from www.nrcresearchpress.com by 61.7.252.67 on 09/04/12
For personal use only.

10. LEWIS, G. N. and BIGELEISEN, J. J. Am. Chem. Soc. **65**, 1144 (1943).
11. MASON, C. D. and NORD, F. F. J. Org. Chem. **16**, 722 (1951).
12. MASON, C. D. and NORD, F. F. J. Org. Chem. **17**, 778 (1952).
13. PATRICK, T. M. and EMERSON, W. S. J. Am. Chem. Soc. **74**, 1356 (1952).
14. SMITH, D. M., BLANCHFIELD, R., THOMPSON, J. L., and GRANT, G. A. Can. J. Chem. **35**, 156 (1957).

Can. J. Chem. Downloaded from www.nrcresearchpress.com by 61.7.252.67 on 09/04/12
For personal use only.

Can. J. Chem. Downloaded from www.nrcresearchpress.com by 61.7.252.67 on 09/04/12
For personal use only.

THE PHOTOCHEMICAL OXIDATION OF ALDEHYDES IN THE GASEOUS PHASE

PART I. THE KINETICS OF THE PHOTOCHEMICAL OXIDATION OF ACETALDEHYDE[1]

C. A. McDowell and L. K. Sharples

ABSTRACT

The photochemical oxidation of acetaldehyde has been studied in the gaseous phase at 20° C. and a wavelength of 3130 Å. It has been established that when the pressure of oxygen is between 0.5 mm. and 150 mm. the reaction obeys the kinetic law:

$$-d[CH_3CHO]/dt = (k_3/k_6^{\frac{1}{2}})(\phi_2 I_a)^{\frac{1}{2}}[CH_3CHO],$$

where k_3 is the velocity constant for the propagating reaction [3]:

$$CH_3CO_3 + CH_3CHO = CH_3CO_3H + CH_3CO, \qquad [3]$$

k_6 is the velocity constant for the terminating reaction [6]:

$$2CH_3CO_3 = (CH_3CO)_2O_2 + O_2, \qquad [6]$$

and $\phi_2 I_a$ is the rate of initiation of the photooxidation, i.e. the rate of formation of acetyl radicals, which are thought to be produced in one or both of the following ways:

$$(a) \quad CH_3CHO \overset{h\nu}{\underset{3130\text{ Å}}{=}} CH_3 + CHO,$$

$$\left.\begin{matrix} CH_3 \\ CHO \end{matrix}\right\} + O_2 = R,$$

$$R + CH_3CHO \overset{\phi_2 I_a}{=} RH + CH_3CO;$$

$$(b) \quad CH_3CHO \overset{h\nu}{\underset{3130\text{ Å}}{=}} CH_3CHO^*,$$

$$CH_3CHO^* + O_2 = CH_3CO + HO_2.$$

INTRODUCTION

Considerable progress has been made during the past decade in our knowledge of the mechanisms of the oxidation of hydrocarbons and related compounds. It has been well established that aldehydes are produced early in all hydrocarbon combustion reactions (15). Evidence has been produced which indicates that the decomposition of primary products such as peroxide radicals leads to the production of these aldehydes. It has also been shown that various aldehydes are capable of eliminating the induction periods which are observed in certain slow oxidation reactions (2, 15). Thus evidence has accumulated showing that the main course of the combustion of many hydrocarbons is largely controlled by the way aldehydes react with oxygen. In many cases it is evident that the hydrocarbon acts as a precursor of aldehyde and the combustion is largely that of the aldehyde formed early in the reaction between the hydrocarbon and oxygen (19).

It is, therefore, of considerable importance that the mechanism of the reactions between aldehydes and oxygen be thoroughly understood. There is general agreement as to the main features of the mechanism of the thermal oxidation of acetaldehyde (9, 13), and doubtless a similar mechanism is applicable to the cases of the oxidation of higher aldehydes though there have been rather few detailed studies of these latter reactions

[1]*Manuscript received July 22, 1957.*
Contribution from the Department of Inorganic and Physical Chemistry, University of Liverpool, Liverpool 7, England, and the Department of Chemistry, University of British Columbia, Vancouver 8, B.C., Canada.

(9, 17). It is, for example, generally accepted that the thermal oxidation of acetaldehyde is a chain reaction in which the acetyl radical (CH_3CO) and the peracetic radical (CH_3CO_3) play important parts. There are, however, certain details of the reactions of these radicals which have not been elucidated.

It was the aim of the work here described to discover the mechanism of the photochemical oxidation of acetaldehyde, for it is obvious that this is a very direct way to investigate the reactions of the acetyl and peracetic radicals. Furthermore, as will be seen later in Part III of this series, it is desirable to know the absolute values of the velocity constants for the propagating and terminating steps in the oxidation chain involving the acetyl and peracetic radicals, and photochemical techniques present a ready means of evaluating these constants.

The photochemical oxidation of acetaldehyde in the gaseous phase was first studied by Bowen and Tietz (6) using a flow method. It was later investigated briefly by Carruthers and Norrish (8). Bowen and Teitz found that the rate of the reaction at about 20° C. was independent of the oxygen concentration and directly proportional to the aldehyde concentration. It was also found that the rate was proportional to the square root of the light intensity. A brief investigation was also carried out later by Mignolet (14) and some preliminary studies were more recently reported briefly by McDowell and Farmer (13). The present study, which covers much of the earlier work of McDowell and Farmer, was preliminary to that reported in Part III, in which is described the determination of the absolute values of the velocity constants for the propagating and terminating steps in the photooxidation of acetaldehyde.

EXPERIMENTAL

The acetaldehyde and oxygen were prepared by the methods described previously (13). The same photochemical apparatus was used except that a "Mazda" high pressure mercury arc was used as a light source. This was supplied with power from a d.c. generator, which was driven by an a-c. synchronous motor. Calibrated fine mesh wire gauzes were used to vary the intensity of the illumination. The rate of the reaction was determined by measuring the amount of peracetic acid produced in a known time, the analytical method being that previously described (13). To obtain reproducible results it was necessary to evacuate and bake the reaction vessel at above 200° C. for more than 4 hours between runs. These precautions made it possible to obtain results reproducible to $\pm 7\%$, and any thermal or induced thermal reaction was kept to a minimum. For experiments up to $\frac{1}{2}$ hour in duration the reaction rate was accurately proportional to time.

RESULTS

The main product of the photooxidation of acetaldehyde is peracetic acid and the rate of the reaction was determined by measuring the amount of this compound formed in a given time on illuminating the reaction vessel with light of wavelength 3130 Å.

Dependence of Rate of Reaction on Acetaldehyde Concentration

The dependence of the rate of the reaction, $d[CH_3CO_3H]/dt$, on the concentration of acetaldehyde was measured at a fixed light intensity for mixtures containing 5 mm. pressure of oxygen at 20° C.; the results are given in Table I and shown graphically in Fig. 1, where we have plotted the logarithm of the corrected rate against the logarithm of the concentration of acetaldehyde. The straight line shown in Fig. 1 has a slope of 0.98. Thus it is apparent that the rate of formation of peracetic acid in the photooxidation of acetal-

Can. J. Chem. Downloaded from www.nrcresearchpress.com by 61.7.252.67 on 09/04/12
For personal use only.

TABLE I

DEPENDENCE OF RATE OF PHOTOOXIDATION OF ACETALDEHYDE ON CONCENTRATION OF ALDEHYDE

All data refer to corrected absorption of 100% and mixtures containing 5 mm. Hg pressure of oxygen at 20° C.

Acetaldehyde, mm. Hg	Duration of experiment, minutes	Corrected rate, mole $l.^{-1}$ $sec.^{-1} \times 10^8$
50	15	0.51
100	15	1.02
150	15	1.57
200	15	2.03
300	75	4.15

dehyde is directly proportional to the concentration of acetaldehyde over the sixfold variation in the concentration of the aldehyde indicated in Table I.

Dependence of the Rate of Reaction on Oxygen Concentration

The data in Table II show clearly that the rate of formation of peracetic acid in this reaction is independent of the concentration of oxygen over a 30-fold variation in concentration from 5 mm. to 150 mm. Hg.

TABLE II

DEPENDENCE OF THE RATE OF THE PHOTOOXIDATION OF ACETALDEHYDE ON THE CONCENTRATION OF OXYGEN

All data refer to mixtures containing 150 mm. Hg of acetaldehyde and were carried out at a constant light intensity at 20° C.

Oxygen, mm. Hg	Rate, mole $l.^{-1}$ $sec.^{-1} \times 10^9$
5	8.57
25	8.50
50	8.17
100	7.90
150	8.68

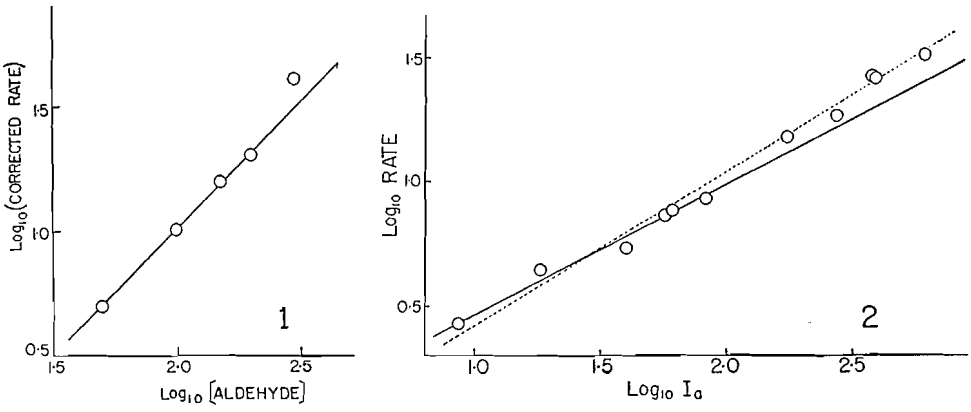

FIG. 1. Dependence of rate of photochemical oxidation of acetaldehyde on concentration of aldehyde.
FIG. 2. Dependence of rate of photochemical oxidation of acetaldehyde on intensity of absorbed radiation.

Can. J. Chem. Downloaded from www.nrcresearchpress.com by 61.7.252.67 on 09/04/12
For personal use only.

Dependence of the Rate of Reaction on the Intensity of Illumination

In Table III are given the rates of reaction observed for a mixture of 150 mm. Hg of acetaldehyde and 5 mm. Hg of oxygen at 20° C. and for different intensities of the incident radiation. In column three of this table is shown the value of the ratio "rate/square root of intensity absorbed". These data show clearly that the rate of formation of peracetic acid in this photooxidation is proportional to $I_a^{\frac{1}{2}}$. This conclusion is also demonstrated by Fig. 2, where the logarithm of the rate of reaction has been plotted against the logarithm of the absorbed intensity. The slope of the dotted line is 0.55 and that of the continuous line 0.51. It is important to note that in the experimental data listed in Table II the light intensity has been varied over a 73-fold range.

TABLE III

DEPENDENCE OF THE RATE OF THE PHOTOOXIDATION OF ACETALDEHYDE ON THE INTENSITY OF THE ILLUMINATION

All data refer to a mixture containing 150 mm. Hg of acetaldehyde and 5 mm. Hg of oxygen at 20° C.

I_a, percentage	Rate, mole $l.^{-1}$ $sec.^{-1} \times 10^9$	Rate/$I_a^{\frac{1}{2}}$
0.086	2.7	9.2
0.185	4.4	10.2
0.40	5.4	8.6
0.58	7.4	9.7
0.62	7.8	9.9
0.83	8.6	9.5
1.74	15.6	11.8
2.74	18.8	11.4
3.82	27.4	14.0
3.94	27.1	13.7
6.21	33.6	13.5

Over-all Activation Energy

It was difficult to obtain an extremely accurate value for the over-all activation energy for this reaction because above 30° C. there intervenes a troublesome thermal reaction. A value for the activation energy was, however, obtained by taking a mean of seven experiments carried out at 20° C. and a mean of a similar number carried out at 30° C. These data are set out in Table IV and there is also given the value for the activation energy E calculated from the equation $E = [RT_1T_2/(T_1 - T_2)] \ln(R_1/R_2)$, where R_1 and R_2 are relative rates of the reaction at temperatures T_1 and T_2.

TABLE IV

ACTIVATION ENERGY FOR THE PHOTOOXIDATION OF ACETALDEHYDE

Data refer to a mixture of 150 mm. Hg of acetaldehyde and 5 mm. Hg of oxygen and a light intensity of 2.05% of the total intensity

Rate at 293° K.	30.6 ± 0.7	Arbitrary units, mean of seven experiments
Rate at 303° K.	45.7 ± 1.8	
E	7.16 ± 1.0	kcal. $mole^{-1}$

DISCUSSION

The above experimental results show that the photochemical oxidation of acetaldehyde at 20° C. is governed by the kinetic equation:

$$d[CH_3CO_3H]/dt = K\, I_a^{\frac{1}{2}}[CH_3CHO].$$

Can. J. Chem. Downloaded from www.nrcresearchpress.com by 61.7.252.67 on 09/04/12
For personal use only.

There has been considerable discussion as to the nature of the primary process which occurs when acetaldehyde absorbs a quantum of radiation. Steacie (16) gives a detailed discussion of the relevant facts. Suffice it to say that Volman *et al.* (18) have shown that free radicals are produced in the direct photolysis of acetaldehyde at a wavelength of 3130 Å. There has been considerable controversy as to the primary quantum efficiencies of the two processes [1*a*] and [1*b*]:

$$CH_3CHO + h\nu = \begin{cases} \longrightarrow CH_3 + HCO, & [1a] \\ \longrightarrow CH_4 + CO. & [1b] \end{cases}$$

Early work (2, 3, 10) led to the view that at 3130 Å and moderate temperatures reaction [1*a*] predominated but the quantum yield was low. More recent studies by Calvert, Pitts, and Thompson (7) have shown that at low light intensities of 3130 Å radiation and at temperatures in excess of 250° C. the sum of all the primary efficiencies of free radical formation at 3130 Å is equal to 0.8. This conclusion is based on careful measurements of the quantum efficiencies for the formation of hydrogen at different temperatures. In this connection it is interesting to note that Lossing (12) has shown recently that in the mercury (Hg $^3P_1$) photosensitized decomposition of acetaldehyde at 55° C. the primary step is at least 95% to form methyl and formyl radicals.

The work of Leermakers (11) on the low temperature photolysis of acetaldehyde gave a quantum yield of 0.2 to 0.3. This could represent either a molecular rearrangement or a free radical non-chain reaction. Blacet and Volman's (4) results, however, indicate that at 3130 Å the primary process is entirely a free radical one.

In the case of acetaldehyde mixed with oxygen there is no reason a priori for assuming that entirely the same process or processes will occur as those which take place when pure acetaldehyde absorbs a quantum of radiation of wavelength 3130 Å. In view of the difficulties in understanding the results obtained by the photolysis of acetaldehyde in the presence of iodine (2, 3, 10), it would be unwise to assume that the presence of oxygen in the acetaldehyde would not give rise to some difficulties of interpretation.

It is to be expected that on the absorption of radiation of wavelength 3130 Å, acetaldehyde will be excited to several different states. One or more of these may dissociate to yield free radicals as in reaction [1*a*]. Energy transfer processes will probably occur from the other states; fluorescence may also occur; and by collisions with other acetaldehyde molecules some of those in excited states will be quenched. In the presence of oxygen some of these excited states may also be preferentially quenched.

The work reported in this paper does demonstrate, however, that a photolytic oxidation of acetaldehyde at a wavelength of 3130 Å does occur at 20° C. We shall, therefore, assume that this photochemical oxidation is initiated by one, or both, of the following processes:

(*a*) By the absorption of a quantum of radiation of wavelength 3130 Å the acetaldehyde, even in the presence of oxygen, undergoes the primary process [1*a*],

$$CH_3CHO \underset{3130\,\text{Å}}{\overset{h\nu}{=}} CH_3 + CHO. \qquad [1a]$$

The two radicals produced can then react with oxygen as indicated in equation [1*d*],

$$\left.\begin{matrix} CH_3 \\ CHO \end{matrix}\right\} + O_2 = R. \qquad [1d]$$

It is assumed that the radical R can then abstract a hydrogen atom from acetaldehyde to form an acetyl radical which is regarded as being the chain initiator in the thermal oxidation of acetaldehyde (13).

Can. J. Chem. Downloaded from www.nrcresearchpress.com by 61.7.252.67 on 09/04/12
For personal use only.

(*b*) The absorption of a quantum of radiation of wavelength 3130 Å can lead to excited states of acetaldehyde which may not dissociate to form radicals by reaction [1*a*]. Nevertheless, though it is possible that in the presence of oxygen some or all of these excited states may be quenched, it is at least likely that the excited acetaldehyde molecules may react with oxygen to yield free radicals which can start the oxidation chain. There is no reason why, for example, one or more of these excited states of acetaldehyde, here denoted in [1*c*] simply by CH_3CHO^*, may not react with oxygen by a process [1*f*] analogous to that thought (13) to be the mode of initiation of the thermal oxidation between ground state acetaldehyde molecules and oxygen:

$$CH_3CHO \overset{h\nu}{\underset{3130\ \text{Å}}{=}} CH_3CHO^*, \qquad [1c]$$

$$CH_3CHO^* + O_2 = CH_3CO + HO_2. \qquad [1f]$$

Reaction [1*f*] would, of course, be expected to occur at a much lower temperature than that at which the corresponding reaction between ground state acetaldehyde molecules and oxygen has a reasonable rate.

Whatever the means whereby acetyl radicals are produced following the initial absorption of radiation at 3130 Å by the acetaldehyde this radical is regarded as being the initiator of the oxidation chain and we may then write the following mechanism for the photooxidation of acetaldehyde at 3130 Å and at low temperatures (20–40° C.):

$$CH_3CHO \overset{h\nu}{\underset{3130\ \text{Å}}{=}} CH_3 + CHO \qquad [1a]$$

$$CH_3CHO \overset{h\nu}{\underset{3130\ \text{Å}}{=}} CH_3CHO^* \qquad [1c]$$

$$\left.\begin{aligned} CH_3 + O_2 &= \\ CHO + O_2 &= \end{aligned}\right\} R \qquad [1d]$$

$$\left.\begin{aligned} R + CH_3CHO &= RH + CH_3CO \\ CH_3CHO^* + O_2 &= CH_3CO + HO_2 \end{aligned}\right\} \phi_2 I_a \qquad \begin{matrix}[1e]\\[1f]\end{matrix}$$

$$CH_3CO + O_2 = CH_3CO_3 \qquad [2]$$

$$CH_3CO_3 + CH_3CHO = CH_3CO_3H + CH_3CO \qquad [3]$$

$$2CH_3CO = (CH_3CO)_2 \qquad [4]$$

$$CH_3CO + CH_3CO_3 = (CH_3CO)_2O_2 \qquad [5]$$

$$2CH_3CO_3 = (CH_3CO)_2O_2 + O_2 \qquad [6]$$

Since it has been shown that the rate of the photochemical oxidation is proportional to $I_a^{\frac{1}{2}}$, and independent of the oxygen pressure, it is probable that reaction [2] is rather fast and it is also likely that at the oxygen pressures used reactions [4] and [5] are negligible compared with reaction [6].

The application of the stationary state hypothesis to the above reaction mechanism leads to the equation

$$\frac{d[CH_3CO_3H]}{dt} = \frac{k_3(\phi_2 I_a)^{\frac{1}{2}}[CH_3CHO]}{(k_4\beta^2 + k_5\beta + k_6)^{\frac{1}{2}}},$$

where $\beta = k_3[CH_3CHO]/k_2[O_2]$. When $\beta \ll 1$, as is likely to be the case in our experiments (see above), this equation reduces to

$$d[CH_3CO_3H]/dt = (k_3/k_6^{\frac{1}{2}})(\phi_2 I_a^{\frac{1}{2}})[CH_3CHO]. \qquad [A]$$

Can. J. Chem. Downloaded from www.nrcresearchpress.com by 61.7.252.67 on 09/04/12
For personal use only.

This equation is in agreement with the experimental results reported above and it, therefore, follows that the proposed mechanism is a satisfactory one. It is, of course, similar to that shown to govern the rates of oxidation of olefins and other organic compounds in solution (5) and for aldehyde oxidations in the gas phase (9, 13).

Equation [A] and our results are in accord with the view that the main terminating step in the oxidation is the interaction of two peracetic radicals (CH_3CO_3). Thus it follows from [A] that the over-all activation energy for the photo-oxidation is $E = E_3 - \frac{1}{2}E_6$. It is in general thought that reaction [6] requires little or no activation energy. If this is so, then the value which we have obtained for the activation energy, namely, 7.16 ± 1.0 kilocalories mole^{-1} refers to E_3. It is interesting to compare this with the value of 7.5 ± 0.3 kilocalories mole^{-1} (19) for the activation energy of the corresponding reaction for the methyl radicals, namely:

$$CH_3 + CH_3CHO = CH_4 + CH_3CHO.$$

ACKNOWLEDGMENT

Most of the experimental work described in this paper was carried out in the Department of Inorganic and Physical Chemistry, University of Liverpool, and we wish to thank Professor C. E. H. Bawn, C.B.E., F.R.S., for laboratory facilities and for his interest in the work.

REFERENCES

1. BARDWELL, J. and HINSHELWOOD, Sir Cyril N. Proc. Roy. Soc. A, **205**, 375 (1951).
2. BLACET, F. E. and HELDMAN, J. D. J. Am. Chem. Soc. **64**, 889 (1942).
3. BLACET, F. E. and HOEFFER, D. E. J. Am. Chem. Soc. **64**, 893 (1942).
4. BLACET, F. E. and VOLMAN, D. A. J. Am. Chem. Soc. **60**, 1243 (1938).
5. BOLLAND, J. L. Quart. Revs. (London), **3**, 1 (1949).
6. BOWEN, E. G. and TIETZ, E. L. J. Chem. Soc. 234 (1930).
7. CALVERT, J. G., PITTS, J. N., and THOMPSON, D. D. J. Am. Chem. Soc. **78**, 4239 (1956).
8. CARRUTHERS, J. L. and NORRISH, R. G. W. J. Chem. Soc. 1036 (1936).
9. COMBE, A., NICLAUSE, M., and LETORT, M. Rev. inst. franç. pétrole, **10**, 786, 929 (1955).
10. GORIN, E. Acta Physiochim. U.R.S.S. **9**, 681 (1938); J. Chem. Phys. **7**, 256 (1939).
11. LEERMAKERS, J. A. J. Am. Chem. Soc. **56**, 1537 (1934).
12. LOSSING, F. P. Can. J. Chem. **35**, 305 (1957).
13. McDOWELL, C. A. and FARMER, J. B. Fifth Symposium (International) on Combustion. Reinhold Publishing Corp., New York. 1955. p. 453.
14. MIGNOLET, J. Bull. soc. roy. sci. Liège, **10**, 343 (1941).
15. NORRISH, R. G. W. Discussions Faraday Soc. **10**, 269 (1951).
16. STEACIE, E. W. R. Atomic and free radical reactions. 2nd ed. Reinhold Publishing Corp., New York. 1954.
17. STEACIE, E. W. R., HATCHER, W. H., and ROSENBERG, J. J. Phys. Chem. **38**, 1190 (1934).
18. VOLMAN, D. H., LEIGHTON, P. A., BLACET, F. E., and BRINTON, R. K. J. Chem. Phys. **18**, 203 (1950).
19. VOLMAN, D. H. and BRINTON, R. J. Chem. Phys. **20**, 1053 (1952).

Can. J. Chem. Downloaded from www.nrcresearchpress.com by 61.7.252.67 on 09/04/12
For personal use only.

Can. J. Chem. Downloaded from www.nrcresearchpress.com by 61.7.252.67 on 09/04/12
For personal use only.

THE PHOTOCHEMICAL OXIDATION OF ALDEHYDES IN THE GASEOUS PHASE

PART II. THE KINETICS OF THE PHOTOCHEMICAL OXIDATION OF PROPIONALDEHYDE[1]

C. A. McDowell and L. K. Sharples

ABSTRACT

The photochemical oxidation of propionaldehyde has been studied in the gaseous phase at 23° C. and a wavelength of 3130 Å. With pressures of oxygen varying from 0.3 mm. to 100 mm. Hg it has been established that the reaction obeys the same kinetic law as that found for the corresponding reaction with acetaldehyde, namely:

$$d[C_2H_5CO_3H]/dt = (k_3/k_6^{\frac{1}{2}})\ (\phi_2 I_a)^{\frac{1}{2}}[C_2H_5CHO],$$

where k_3 is the velocity constant for the propagating reaction [3]:

$$C_2H_5CO_3 + C_2H_5CHO = C_2H_5CO_3H + CH_3CO \qquad [3]$$

and k_6 is the velocity constant for the terminating reaction [6]:

$$2C_2H_5CO_3 = (C_2H_5CO)_2O_2 + O_2. \qquad [6]$$

$\phi_2 I_a$ is the rate of initiation and it is regarded as being a composite quantity representing the rate of formation of propionyl radicals, which are thought to be the initiators of the oxidation chain. The propionyl radicals are thought to be formed by two processes: (*a*) from the subsequent reactions of free radicals produced in the primary free radical process which occurs when propionaldehyde absorbs a quantum of radiation at 3130 Å, and (*b*) from the subsequent reactions, with oxygen, of excited states of propionaldehyde, which are also thought to be formed by the absorption of light of wavelength 3130 Å.

INTRODUCTION

Following the study of the photooxidation of acetaldehyde (Part I) reported in the preceding paper, it seemed desirable to study other higher aldehydes. It is important to know if the derived mechanism was of general application. It was also necessary to establish this mechanism for several aldehydes, for one of our main aims was to determine the absolute values for the propagating and terminating steps in the oxidation chain. A knowledge of the velocity constant for these oxygen-containing radicals is most important if the general features of the rates of combustion processes of hydrocarbons and other organic compounds are to be understood. Such results would also add to our available information of the factors influencing the interactions of large radicals in the gaseous phase.

Few studies have been made of the kinetics of the oxidation of aldehydes higher than acetaldehyde. Steacie *et al.* (8) investigated the gas phase thermal oxidation of propionaldehyde and showed that its kinetics were similar to those found for acetaldehyde. More recently a similar investigation (4) has largely substantiated the earlier work. Both of these studies were carried out at temperatures between 100° and 200° C. and the rates were determined by measuring pressure–time curves. It was found that the main product was perpropionic acid. Blacet and Volman (2) reported a study of the photooxidation of crotonaldehyde, but their results were not detailed enough to yield much information about the mechanism and kinetics of the reaction.

EXPERIMENTAL

Eastman-Kodak white label propionaldehyde was dried three times over anhydrous $CaSO_4$ and distilled, at a reflux ratio of 20: 1, through an efficient column in an atmosphere

[1]*Manuscript received July 22, 1957.*
Contribution from the Department of Chemistry, University of British Columbia, Vancouver 8, B.C., Canada.

of cylinder "purified" grade nitrogen. A fraction boiling at 47.9° C., comprising half of the sample, was collected. This sample was redistilled and finally bulb-to-bulb distilled 10 times on the vacuum line, each time a middle fraction being taken.

Oxygen was prepared by heating A.R. grade potassium permanganate. A trap plugged with glass wool and immersed in liquid oxygen was interposed between the oxygen reservoir and the potassium permanganate.

A sample of ethanol from a freshly opened can of "absolute" was dried over anhydrous magnesium sulphate and bulb-to-bulb distilled on the vacuum line. A sample of A.R. isopropyl alcohol was similarly purified.

A sample of A.R. acetone was dried over anhydrous potassium carbonate, refluxed with potassium permanganate, and bulb-to-bulb distilled on the vacuum line.

The apparatus was a conventional high vacuum system utilizing stopcocks lubricated with Apiezon L grease. A cylindrical quartz reaction vessel (volume 76 ml., 4 ml. of which was dead space) having optically flat ends was housed in a block aluminum furnace, the temperature of which could be readily adjusted and accurately maintained. The gases were metered into the vessel using either a calibrated, sensitive spiral gauge, or, for lower pressures, the same gauge in conjunction with a calibrated expansion volume. The reaction products were trapped in a series of cold traps, which could be plugged with glass wool, the last of which was removable to facilitate analysis of the normally liquid reaction products. A copper oxide furnace was incorporated to analyze for CO and H_2, and means was incorporated for measuring small quantities of gas, and for collecting small samples of gaseous products for analysis by mass spectrometry.

A water-cooled, General Electric AH6 mercury arc, housed in a small, water-cooled box with a 3 mm. diameter hole in one side, gave a "point" source of illumination. The input voltage to the 1000 volt transformer for the arc was stabilized at 100 volts by a Sorensen a-c. voltage regulator. The arc had a short-term stability within 5%. Liquid filters were used to isolate a fairly narrow wavelength band in the 3200 Å region. Neutral density filters made by evaporating aluminum on quartz plates were used to vary the intensity incident upon the reaction vessel. Quartz lenses were arranged so that light from the "point" source was collimated through a 5 mm. diameter hole and then into a 50 mm. diameter, very nearly parallel, beam which uniformly filled the reaction vessel. The intensity of the radiation was monitored by an electronic photometer unit utilizing a QVA39 quartz photocell as a light detector. The linearity of the response of this unit was checked occasionally and found to be good.

Perpropionic acid was estimated by the ferrous thiocyanate method, a Bausch and Lomb "Spectronic 20" absorptiometer being used to assess the intensity of the color developed by the various concentrations of peroxide. The absorptiometer was calibrated using a solution of perpropionic acid, the actual strength of which was determined iodometrically by the method of Sully (9).

The light intensity was estimated by measuring the amount of CO formed when gaseous acetone was illuminated under identical conditions to those prevailing during runs, at temperatures from 100° to 120° C. for a given length of time. The quantum yield of CO formation was found to be very nearly constant over the region 100–120° C. In calculating the intensity of our source, the quantum yield of CO from acetone was taken as being 1 (7). The estimated intensity may be in error owing to the fact that an unknown, but presumably appreciable, fraction of the light used was in the 3130–3300 Å region of the spectrum (owing to lack of sharpness of the filters and the continuous background delivered by the arc) and the precise CO quantum yield in this region is not known.

Can. J. Chem. Downloaded from www.nrcresearchpress.com by 61.7.252.67 on 09/04/12
For personal use only.

Can. J. Chem. Downloaded from www.nrcresearchpress.com by 61.7.252.67 on 09/04/12
For personal use only.

RESULTS

Initial runs showed that the main product of the reaction was perpropionic acid, with a quantum yield proportional to the square root of the absorbed intensity, $I_a^{\frac{1}{2}}$, and of the order of 50 for a medium intensity. The oxygen uptake was found to be equal to the perpropionic acid formation within experimental error. A complete analysis of the products was not carried out, but CO_2 and CO were formed in approximately equal amounts with a quantum yield of the order of 1. A very small quantity of ethane was formed, but the quantum yield was not estimated.

The reaction rate was estimated by measuring the amount of peracid formed in a given time. In all runs, except those for the determination of CO_2 and CO formation and O_2 uptake, the reaction was confined to $<0.5\%$ conversion of aldehyde.

There was found to be no measurable thermal reaction at all in a range from 20° to 40° C. and the absence of this was frequently checked. However, after about 70 runs, quite suddenly an appreciable thermal reaction became apparent and built up to a rate which was about 2% of the photochemical rate. This was only appreciable because the reactants were allowed to mix for 1 hour prior to photolysis. When the cell was removed, cleaned, and replaced, no thermal reaction took place.

No cell aging effect was noticed and runs were generally reproducible within $\pm 7\%$. A colorless, transparent polymeric substance of unknown composition was gradually deposited upon the cell walls. On being heated to 300° C. the polymer did not simply decompose and evaporate, but charred. When propionaldehyde is photolyzed, a certain amount of polymerization does take place (6); hence the polymer on the wall may be polypropionaldehyde with physically absorbed reaction products, or a polyoxypolymer formed by reaction of polypropionaldehyde with perpropionyl radicals.

Dependence of Rate of Reaction on Time

The rate of reaction remained constant up to a conversion of 0.7% of the aldehyde during a 10 minute run, indicating that there was no induction period or photochemical growth effect and no autocatalysis. See Fig. 1.

Later on in this study the apparent rate for certain runs of $<0.5\%$ conversion, but of longer duration than usual, was lower than had been anticipated. This was due to the slow decomposition or removal of perpropionic acid, and the rate of this reaction was therefore investigated.

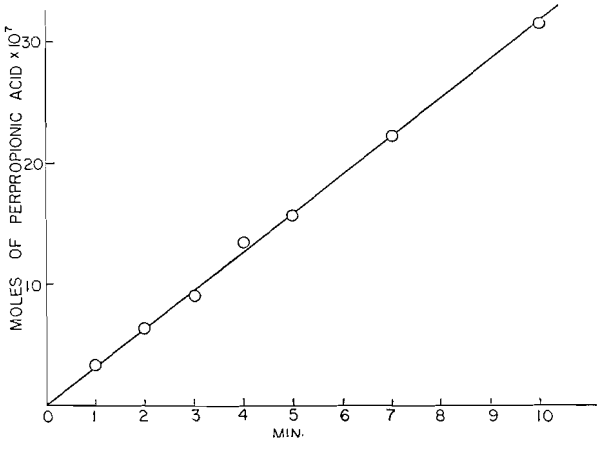

FIG. 1. Dependence of rate of photochemical oxidation of propionaldehyde on time.

Can. J. Chem. Downloaded from www.nrcresearchpress.com by 61.7.252.67 on 09/04/12
For personal use only.

Effect of Decomposition of Perpropionic Acid on Rate

The rate of peracid decomposition was not very reproducible, but it was found to be proportional to the concentration of the peracid within experimental error and roughly proportional to the reciprocal of the aldehyde pressure. It was initially thought that removal of peracid may have been due to the reaction

$$C_2H_5CO_3H + C_2H_5CHO = 2C_2H_5COOH$$

either homogeneously or at the wall, but this was obviated by the 1/[aldehyde] dependence of the rate. The rate is too slow for diffusion to be the rate-controlling step. A possible explanation is that the peracid is removed by physical absorption at the wall and the aldehyde deactivates absorption sites.

In a system where peracid is formed at a constant rate and is removed at a rate proportional to [peracid], then if P is the amount of peracid measured after t seconds, and P_1 is the amount of peracid that would have been formed in t seconds if the peracid was not being removed at all, then $P/P_1 = 1-e^{-k_p t}/k_p t$ where k_p is the rate constant of the removal step; hence the ratio of the measured rate of formation of peracid to the real rate of formation is a function of time only for a given k_p. The values of k_p were calculated for 100 mm. Hg and 35 mm. Hg of aldehyde, and the ratios P/P_1 were calculated for various times. The results are shown in Table I. The results are probably correct within $\pm 20\%$.

TABLE I

EFFECT OF TIME ON RATIO OF OBSERVED RATE TO ACTUAL RATE

Time, min.	k_p, sec.$^{-1}$	P/P_1
1	0.0011	1.00
10	0.0011	0.97
30	0.0011	0.91
60	0.0011	0.80
1	0.0023	0.99
10	0.0023	0.92
30	0.0023	0.79
60	0.0023	0.68

It is seen that the error, due to removal of peracid, in the measured rate for a 10 minute run with 100 mm. aldehyde, is about 2%; hence the only runs in this study which require correction in this respect are runs 53, 54, and 60.

Dependence of Rate of Reaction on Intensity of Absorbed Radiation

The dependence of the rate of oxidation on the light intensity was studied over a 10,000-fold range of absorbed intensity for a mixture of 100 mm. Hg of propionaldehyde and 3 mm. of O_2. It was found that over a range of I_a from 10^{-10} to 2.5×10^{-6} einstein l.$^{-1}$ sec.$^{-1}$ the rate was accurately proportional to $I_a^{\frac{1}{2}}$, but at $I_a < 10^{-10}$ einstein l.$^{-1}$ sec.$^{-1}$ this $I_a^{\frac{1}{2}}$ dependence falls off. The results are shown in Fig. 2 and Table II.

Dependence of Rate of Reaction on Pressure of Propionaldehyde

The dependence of the rate on the aldehyde pressure was studied by maintaining the oxygen pressure at 3 mm. Hg and varying the aldehyde pressure from 10 to 200 mm. Hg. As the aldehyde pressure was varied, the absorbed intensity also varied, so all these runs were carried out in the intensity region where rate is accurately proportional to $I_a^{\frac{1}{2}}$, and the tabulated results are corrected to 100% absorption of a given constant intensity (Table III). The plot of rate against aldehyde pressure was a straight line passing through

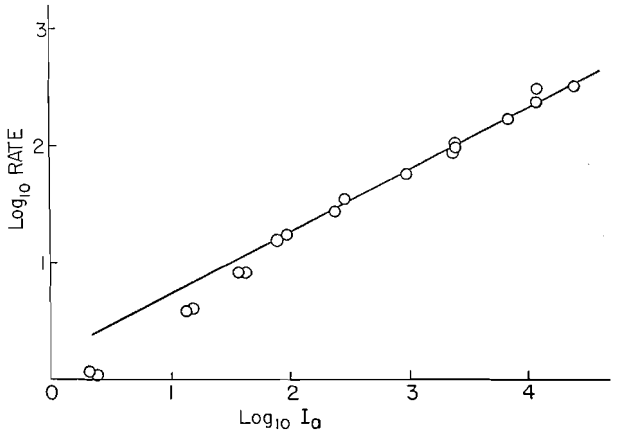

FIG. 2. Dependence of rate of photochemical oxidation of propionaldehyde on intensity of absorbed radiation.

TABLE II

DEPENDENCE OF RATE ON ABSORBED INTENSITY

These experiments were all carried out with a mixture of 100 mm. Hg of propionaldehyde, 3 mm. Hg oxygen, and at 23° C.

Run No.	I_a, ein. $l.^{-1}$ $sec.^{-1}$ $\times 10^{+12}$	Rate, mole $l.^{-1}$ $sec.^{-1}$ $\times 10^{+9}$
32	2.39×10^{3}	8.32×10
33	2.42×10^{4}	2.50×10^{2}
34	9.34×10^{2}	4.48×10
35	2.32×10^{2}	2.14×10
36	4.20×10	6.40
37	1.35×10	3.07
38	1.18×10^{4}	2.40×10^{2}
39	2.37×10^{3}	7.68×10
40	6.76×10^{3}	1.31×10^{2}
41	2.35×10^{3}	7.04×10
42	2.82×10^{2}	2.78×10
43	8.01×10	1.25×10
44	2.06	0.93
45	1.53×10	3.20
46	2.32	0.82
47	9.25×10	1.34×10
48	3.73×10	6.60
49	1.18×10^{4}	1.86×10^{2}
50	2.29×10^{3}	8.00×10

the origin, Fig. 3, but the apparent rates for low aldehyde pressure runs fall well below the straight line. This is probably due to the peracid removal step mentioned earlier, and if a correction is applied, these points fit more closely to the line.

Dependence of the Rate of Reaction on Pressure of Oxygen

The rate of oxidation was found to be independent of oxygen pressure over a range of 0.3–100 mm. Hg, in a system in which the aldehyde pressure and I_a were maintained constant. The results are shown in Table IV.

Over-all Activation Energy

In Table V are given the values of the over-all rate of the reaction at observed different temperatures for a mixture containing 3 mm. of oxygen and 5.87×10^{-3} mole $l.^{-1}$ of

Can. J. Chem. Downloaded from www.nrcresearchpress.com by 61.7.252.67 on 09/04/12
For personal use only.

TABLE III

DEPENDENCE OF RATE ON PRESSURE OF PROPIONALDEHYDE

These experiments were carried out at 23° C. with a mixture of 3.0 mm. Hg of oxygen, and the rates were corrected to an I_a of 2.14×10^{-9} einstein $l.^{-1}$ $sec.^{-1}$

Run No.	Aldehyde pressure, mm. Hg	Rate, mole $l.^{-1}$ $sec.^{-1}$ $\times10^{+8}$
51	33	3.68
52	70	8.0
53	22.5	2.24*
54	16.2	1.84*
55	100	13.2
56	200	26.7
57	41.5	5.6
58	100	13.3
59	150	20.3
60	10	1.11*

**These experiments corrected for decomposition of perpropionic acid as they exceeded 12 minutes in duration.*

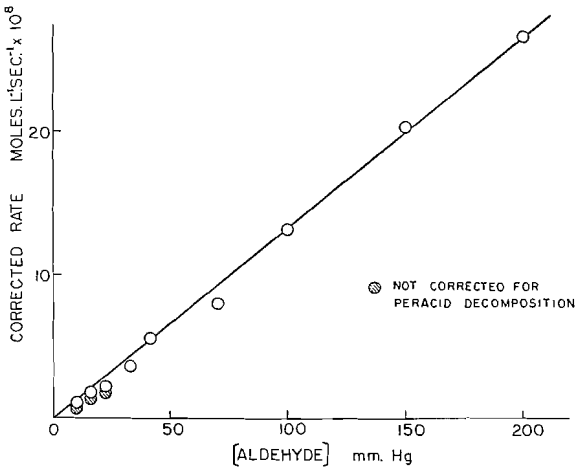

FIG. 3. Dependence of rate of photochemical oxidation of propionaldehyde on pressure of aldehyde.

TABLE IV

DEPENDENCE OF RATE ON OXYGEN PRESSURE

All experiments carried out on a mixture of 100 mm. Hg of aldehyde at 22° C., and at an I_a of 2.14×10^{-9} einstein $l.^{-1}$ $sec.^{-1}$

Run No.	Oxygen, mm. Hg	Rate, mole $l.^{-1}$ $sec.^{-1}\times10^{8}$
25	10	9.6
26	40	10.4
27	2	12.0
28	0.36	10.9
29	100	9.3
30	5	9.6
31	10	8.5

Can. J. Chem. Downloaded from www.nrcresearchpress.com by 61.7.252.67 on 09/04/12
For personal use only.

TABLE V

DEPENDENCE OF RATE ON TEMPERATURE

All experiments carried out with a mixture of 3 mm. Hg of oxygen, 5.87×10^{-3} mole $l.^{-1}$ of propionaldehyde, and at an I_a of 1.11×10^{-9} einstein $l.^{-1}$ $sec.^{-1}$

Run No.	Temp., ° C	Rate, mole $l.^{-1}$ $sec.^{-1}\times10^8$
129	19.5	5.28
130	22.6	6.08
131	27.0	8.00
132	37.5	10.6
133	21.3	6.56
134	20.0	5.92
135	39.0	11.7
136	46.5	15.0
137	34.0	9.60
138	19.5	5.75

propionaldehyde. These experiments were performed using a value of I_a of 1.11×10^{-9} einstein $l.^{-1}$ $sec.^{-1}$.

These data have been plotted in Fig. 4. From these data we have calculated by the method of least squares that the activation energy for the photooxidation of propionaldehyde is 6.75 ($\pm$0.5) kilocalories $mole^{-1}$.

DISCUSSION

The above experimental results indicate that the gas-phase photooxidation of propionaldehyde at about 23° C. is a chain process and the initial stage is governed by the kinetic equation

$$d[C_2H_5CO_3H]/dt = kI_a^{\frac{1}{2}}[C_2H_5CHO]^1[O_2]^0.$$

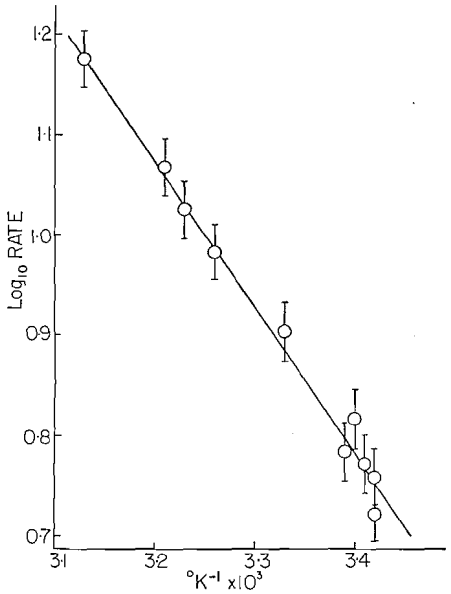

FIG. 4. Activation energy curve for the photochemical oxidation of propionaldehyde.

Can. J. Chem. Downloaded from www.nrcresearchpress.com by 61.7.252.67 on 09/04/12
For personal use only.

At low intensities this expression ceases to apply because the $I_a^{\frac{1}{2}}$ dependence falls off. Also in later stages of the oxidation, removal of the peracid becomes a significant part of the process. The $I_a^{\frac{1}{2}}$ dependence is undoubtedly due to a radical initiation process which is proportional to I_a and a chain termination process which is bimolecular. Deviation from $I_a^{\frac{1}{2}}$ dependence at low intensities indicates that the termination process is no longer solely bimolecular, but that a first-order termination starts to become important. Such a first order termination could be at the wall; which is inherently feasible, because the concentration of radicals at low I_a is small, and hence the bimolecular termination would be similarly small, thus giving radicals more chance to reach the wall.

The too low rates observed for runs at low aldehyde concentration may be due entirely to the removal of peracid at the wall, but even when a correction is applied, these rates are still somewhat low. There are two possible explanations which could account for this. At low concentrations of aldehyde and consequent low absorbed intensities, the rate of initiation of chain propagating radicals may have an aldehyde pressure dependence if there is a possible fate of the radical R other than reacting with aldehyde to yield C_2H_5CO. The radical R could react at the wall, and if it did, the wall reaction would be favored by low aldehyde pressure and low intensity, and hence under these conditions the rate would be reduced. The other possible explanation is that at low aldehyde pressure and low intensity, first-order termination of propagating radicals at the wall may become appreciable, thus reducing the observed rate.

The photolysis of propionaldehyde at a wavelength of 3130 Å has been studied by several workers (3, 5, 6). A recent detailed investigation has been made by Blacet and Pitts (1). These authors conclude that there are four separate primary processes involved:

$$C_2H_5CHO + h\nu = \begin{cases} \longrightarrow C_2H_5 + CHO & \text{(i)} \\ \longrightarrow C_2H_6 + CO & \text{(ii)} \\ \longrightarrow C_2H_4 + HCHO & \text{(iii)} \\ \longrightarrow CH_3 + CH_2CHO & \text{(iv)} \end{cases}$$

From this work it is apparent that the ratio of the primary process (ii) to primary process (i) at 3130 Å is 0.046. This result and most of the conclusions of Blacet and Pitts are based on experiments performed on mixtures of propionaldehyde and iodine. There have been some doubts expressed (see preceding paper, Part I) about the validity of some of the deductions regarding free radical mechanisms based on the use of iodine "to fix" the radical. It is to be expected that at 3130 Å propionaldehyde will form several excited states, and only some of these may dissociate to form free radicals. Further, the presence of iodine will undoubtedly quench some of these excited states of propionaldehyde by energy transfer processes (see Part I).

Our view is that it is best to regard the photolysis of propionaldehyde–oxygen mixtures as following the same processes as suggested in Part I for the case of acetaldehyde–oxygen mixtures. Namely, that the primary process (i) will undoubtedly occur, but that excited states of propionaldehyde will be formed. Some of these will undoubtedly be quenched by the oxygen, but some may react with oxygen molecules to form free radicals which should be capable of initiating the propionaldehyde oxidation chain. Thus we think that the photochemical oxidation of propionaldehyde, since it evidently obeys the same kinetic law as that of acetaldehyde as shown by our experiments, should also follow the same mechanism.

It is, therefore, assumed that the photochemical oxidation of propionaldehyde is initiated by one, or both, of the following processes:

Can. J. Chem. Downloaded from www.nrcresearchpress.com by 61.7.252.67 on 09/04/12
For personal use only.

(1) By the absorption of a quantum of radiation of wavelength 3130 Å, the primary process (i) occurs even in the presence of oxygen,

$$C_2H_5CHO \underset{3130\,Å}{\overset{h\nu}{=}} C_2H_5 + CHO. \qquad [1a]$$

These two radicals can then react with oxygen as follows:

$$\left.\begin{matrix} C_2H_5 \\ CHO \end{matrix}\right\} + O_2 = R. \qquad [1d]$$

The radical R can then abstract a hydrogen atom from propionaldehyde to form a propionyl radical, C_2H_5CO, which is regarded as being the initiation of the oxidation chain (4).

(2) Besides primary process (i) occurring, it is possible that excited states are also formed when propionaldehyde absorbs radiation of wavelength 3130 Å (equation [1*c*]). One or more of these excited states may react with oxygen molecules to form propionyl radicals as indicated in equation [1*f*] where in both [1*c*] and [1*f*] the excited states of propionaldehyde are denoted simply as $C_2H_5CHO^*$:

$$C_2H_5CHO \underset{3130\,Å}{\overset{h\nu}{=}} C_2H_5CHO^*, \qquad [1c]$$

$$C_2H_5CHO^* + O_2 = C_2H_5CO + HO_2. \qquad [1f]$$

The succeeding steps in the mechanism of the photooxidation of propionaldehyde at low temperatures are regarded as being analogous to those shown (Part I) to lead, on the application of the stationary state hypothesis, to a satisfactory explanation of the kinetics of the photochemical oxidation of acetaldehyde:†

$$C_2H_5CO + O_2 = C_2H_5CO_3 \qquad [2]$$

$$C_2H_5CO_3 + C_2H_2CHO = C_2H_5CO_3H + C_2H_5CO \qquad [3]$$

$$2C_2H_5CO = (C_2H_5CO)_2 \qquad [4]$$

$$C_2H_5CO_3 + C_2H_5CO = (C_2H_5CO)_2O_2 \qquad [5]$$

$$2C_2H_5CO_3 = (C_2H_5CO)_2O_2 + O_2 \qquad [6]$$

The application of the stationary state treatment to the above mechanism leads to the equation [A], when it is assumed (see Part I) that $k_3[C_2H_5CHO]/k_2[O_2] \ll 1$, which is likely to be the case in our experiments,

$$d[C_2H_5CO_3H]/dt = (k_3/k_6^{\frac{1}{2}})(\phi_2 I_a)^{\frac{1}{2}}[C_2H_5CHO]. \qquad [A]$$

Equation [A] agrees with the experimentally determined kinetic equation for the photochemical oxidation of propionaldehyde.

It follows from the above results and equation [A] that the over-all activation energy $E = E_3 - \frac{1}{2}E_6$. E_6, which is the activation energy for the mutual interaction of perpropionic radicals, is likely to be zero. Thus the value which we obtained for the over-all activation energy, namely 6.75 ($\pm$0.5) kilocalories mole.$^{-1}$, must equal E_3. There are no reliable values for the reaction analogous to [3] but involving the ethyl radical. Comparison of the value of E_3 for the abstraction of a hydrogen atom from propionaldehyde by

†*From the data given in the following paper (Part III) we calculate* $\phi \simeq 1.6$. *Blacet and Pitts (1) found* $\phi_{C_2H_5I}$ *and* ϕ_{HI} *in their experiments on propionaldehyde–iodine mixtures to be* $\simeq 0.45$. *Since we regard both the* C_2H_5 *and* HCO *radicals as being capable of reacting with oxygen to form a radical which can abstract a hydrogen atom from propionaldehyde to form a propionyl radical it follows that the portion of the quantum yield* ϕ_2 *which arises from the reaction of excited states of propionaldehyde [1f] is approximately* $1.6 - 0.9 = 0.7$.

Can. J. Chem. Downloaded from www.nrcresearchpress.com by 61.7.252.67 on 09/04/12
For personal use only.

the perpropionic radical with those found for the corresponding metathetical reactions with methyl (7.5 ± 0.3 kilocalories mole^{-1}) and peracetic (7.16 ± 1.0 kilocalories mole^{-1}) radical shows that it is a realistic value.

ACKNOWLEDGMENT

We are indebted to the National Research Council of Canada for a grant in aid of this work.

REFERENCES

1. BLACET, F. E. and PITTS, J. N. J. Am. Chem. Soc. **74**, 3382 (1952).
2. BLACET, F. E. and VOLMAN, D. H. J. Am. Chem. Soc. **61**, 582 (1939).
3. BLAEDEL, W. J. and BLACET, F. E. J. Am. Chem. Soc. **74**, 3382 (1952).
4. COMBE, A., NICLAUSE, M., and LETORT, M. Rev. inst. franc. pétrole, **10**, 786, 929 (1955).
5. GARRISON, W. M. and BURTON, M. J. Chem. Phys. **10**, 730 (1942).
6. LEIGHTON, P. A. and BLACET, F. E. J. Am. Chem. Soc. **54**, 3165 (1932).
7. NOYES, W. A., Jr. and HERR, D. S. J. Am. Chem. Soc. **62**, 2052 (1940).
8. STEACIE, E. W. R., HATCHER, W. H., and ROSENBERG, J. J. Phys. Chem. **38**, 1190 (1934).
9. SULLY, B. D. Analyst, **79**, 86 (1954).

Can. J. Chem. Downloaded from www.nrcresearchpress.com by 61.7.252.67 on 09/04/12
For personal use only.

Can. J. Chem. Downloaded from www.nrcresearchpress.com by 61.7.252.67 on 09/04/12
For personal use only.

THE PHOTOCHEMICAL OXIDATION OF ALDEHYDES IN THE GASEOUS PHASE

PART III. THE ABSOLUTE VALUES OF THE VELOCITY CONSTANTS FOR THE PROPAGATING AND TERMINATING STEPS IN THE PHOTOCHEMICAL OXIDATION OF ACETALDEHYDE AND PROPIONALDEHYDE[1]

C. A. McDowell and L. K. Sharples

ABSTRACT

It has been established (Parts I and II) that the photochemical oxidation of acetaldehyde and propionaldehyde obeys the kinetic expression

$$d[RCO_3H]/dt = (k_3/k_6^{\frac{1}{2}})(\phi_2 I_a)^{\frac{1}{2}}[RCHO],$$

where RCHO represents the aldehyde and RCO_3H the corresponding peracid. k_3 is the velocity constant for the propagating reaction, and k_6 that for the terminating reaction involving the mutual interaction of two RCO_3 radicals. $\phi_2 I_a$ represents the rate of initiation of the photooxidation.

Alcohols have been found to retard the photooxidation and it has been shown that the retarded reaction obeys the kinetic expression:

$$d[RCO_3H]/dt = R_i\{1+k_3[RCHO]/k_7[ROH]\}.$$

It has thus been possible to determine the rates of initiation $R_i = \phi_2 I_a$ for each of the photooxidations. Application of the rotating sector technique has enabled the lifetime of the oxidation chains to be measured. These data together with the information given in Parts I and II have been used to calculate the absolute values for the velocity constants for the propagating and terminating reactions, k_3 and k_6:

$$RCO_3 + RCHO \overset{k_3}{=} RCO_3H + RCO, \qquad [3]$$

$$2RCO_3 \overset{k_6}{=} (RCO)_2O_2 + O_2, \qquad [6]$$

in the gas-phase photooxidations of acetaldehyde and propionaldehyde.

The values of the respective velocity constants are: acetaldehyde at 20°, $k_3 = 8.05(\pm 2.04) \times 10^3$ l. mole^{-1} sec.$^{-1}$, $k_6 = 8.93(\pm 4.20) \times 10^{10}$ l. mole^{-1} sec.$^{-1}$; propionaldehyde at 22°, $k_3 = 4.35(\pm 0.9) \times 10^4$ l. mole^{-1} sec.$^{-1}$, $k_6 = 2.69(\pm 1.35) \times 10^{10}$ l. mole^{-1} sec.$^{-1}$. These values for the velocity constants for the "recombination" reactions of the peracetic and perpropionic radicals indicate that for these radicals reaction [6] is very efficient.

INTRODUCTION

The study of the combustion of hydrocarbons and related compounds has now reached a point where the main features of the over-all kinetics are apparent. It remains, however, to discover the details of the mechanisms of many of the radical reactions which control the over-all processes. It is also desirable to determine the absolute values for the velocity constants for the various radical reactions known to proceed during combustion processes.

The determination of the absolute values of the velocity constants for many radical reactions in oxidation processes has been retarded because of the need to develop sufficiently accurate experimental methods. This has been especially the case for gaseous-phase reactions. In the case of the liquid-phase oxidation of aldehydes (5), olefins (2), and some other compounds (11), it has been possible to apply photochemical techniques to determine the absolute values for the velocity constants for the propagating and terminating steps in the oxidation chains.

[1]*Manuscript received July 22, 1957.*
Contribution from the Department of Inorganic and Physical Chemistry, University of Liverpool, Liverpool 7, England, and the Department of Chemistry, University of British Columbia, Vancouver 8, B.C., Canada.

In the preceding papers, Parts I and II, we have elucidated the mechanisms of the photochemical oxidations of acetaldehyde and propionaldehyde. Both of these oxidation reactions have been shown to obey the kinetic expression:

$$d[RCO_3H]/dt = (k_3/k_6^{\frac{1}{2}})(\phi_2 I_a)^{\frac{1}{2}}[RCHO], \qquad [A]$$

in which RCO_3H represents the peracid which is the main product of the oxidation, k_3 is the velocity constant for the propagating reaction [3]:

$$RCO_3 + RCHO \overset{k_3}{=} RCO_3H + RCO, \qquad [3]$$

k_6 is the velocity constant for the interaction of two RCO_3 radicals in the terminating reaction [6]:

$$2RCO_3 \overset{k_6}{=} (RCO)_2O_2 + O_2, \qquad [6]$$

and $\phi_2 I_a = R_i$ is the rate of initiation of the photochemical oxidation at 3130 Å, the wavelength of the radiation used. Equation [A] is of the same general form as that found to be obeyed by the liquid-phase oxidation of aldehydes (5) and olefins (2), and so the application of the rotating sector technique in the present cases should enable us to determine the absolute value of the velocity constants for the reactions [3] and [6].

EXPERIMENTAL

The acetaldehyde and propionaldehyde were purified as described in Parts I and II. The alcohols were carefully purified by repeated distillations.

The photochemical apparatus was essentially the same as that employed previously. Two different sectors were used. One had two apertures of $\pi/2$ and the other had two of $\pi/4$. The former was used for the experiments with acetaldehyde and the latter in those with propionaldehyde. The light beam was focused at the sector plane so that at the point of interruption the time taken by the edge of the sector to scan the beam was less than 1/30th of the light period. Oscillographic studies showed that the light pulse was quite square. At low speeds the rotation of the sector was timed using a stop watch. An accurate gear enabled the intermediate speeds to be measured. High rotational speeds were measured accurately on a cathode ray oscillograph.

RESULTS

In a chain reaction obeying the kinetic expression [A] in which steady state conditions are quickly established (see Part I), the velocity constant for the termination step, k_6, is given by the equation

$$k_6 = 1/\tau^2 R_i, \qquad [B]$$

where R_i is the rate of initiation and τ is the lifetime of the kinetic chain. This quantity τ may in the case of the oxidation of acetaldehyde be expressed as:

$$\tau = \frac{\text{concentration of peracetic radicals}}{\text{rate of removal of peracetic radicals}}$$

with a similar expression for the lifetime of the kinetic chain in the oxidation of propionaldehyde. Thus it is seen that if R_i and τ can be determined, then the absolute value of the velocity constant, k_6, can be calculated from equation [B]. The ratio $k_3/k_6^{\frac{1}{2}}$ is readily obtainable from equation [A] once the rate of initiation $\phi_2 I_a$ is known; hence once k_6 has been determined, k_3, the absolute value of the velocity constant for the propagating step in the oxidation chain, may also be calculated.

Can. J. Chem. Downloaded from www.nrcresearchpress.com by 61.7.252.67 on 09/04/12
For personal use only.

Determination of the Rate of Initiation $R_i = \phi_2 I_a$

It is known that the oxidation of aldehydes is retarded by alcohols (3, 7) and the mechanism of this process is fairly well established. It is thought that when an alcohol, ROH, is added to a mixture of aldehyde and oxygen the ensuing retarding effect is caused by the reaction:

$$RCO_3 + ROH = RCO_3H + R'OH. \qquad [7]$$

The radical R'OH may react with a similar radical by addition or disproportionation reactions to form stable products faster than it can abstract a hydrogen atom from an aldehyde molecule. Thus the chain length of the oxidation is shortened and the reaction is retarded.

The mechanism for the retarded photochemical oxidation of acetaldehyde and propionaldehyde would then be written as:

$$RCHO \underset{3130\ Å}{\overset{h\nu}{=}} R + CHO$$

$$RCHO \underset{3130\ Å}{\overset{h\nu}{=}} RCHO^*$$

$$\left.\begin{matrix} R \\ CHO \end{matrix}\right\} + O_2 = R$$

$$\left.\begin{matrix} R + RCHO = RH + RCO \\ RCHO^* + O_2 = HO_2 + RCO \end{matrix}\right\} \phi_2 I_a$$

$$RCO + O_2 = RCO_3 \qquad [2]$$

$$RCO_3 + RCHO = RCO_3H + RCO \qquad [3]$$

$$RCO_3 + ROH = RCO_3H + R'OH \qquad [7]$$

$$2RCO_3 = (RCO)_2O_2 + O_2 \qquad [6]$$

When stationary state kinetics are applied to this mechanism the following expression results if it is assumed that $k_7[ROH][RCO_3] > k_6[RCO_3]^2$:

$$d[RCO_3H]/dt = R_i\{1+k_3[RCHO]/k_7[ROH]\}. \qquad [C]$$

In equation [C] we have written $R_i = \phi_2 I_a$. This expression implies that if the alcohol-retarded oxidation obeys the mechanism given, the rate of the retarded reaction at a constant concentration of alcohol should be directly proportional to the intensity of illumination. Furthermore, at a constant intensity of illumination the rate of the retarded oxidation is required to be directly proportional to the reciprocal of the concentration of the retarding alcohol. Thus a graph of the rate of the retarded reaction against $[ROH]^{-1}$ should be a straight line with slope $k_3[RCHO]/k_7$ and an intercept equal to the rate of initiation $\phi_2 I_a$.

Dependence of Rate of Retarded Reaction on Intensity

In Table I are given the results of experiments carried out at 20° C. on a mixture of 150 mm. Hg pressure of acetaldehyde, 5 mm. Hg pressure of oxygen, a constant concentration of ethanol (30 mm. Hg pressure), and varying intensity of illumination.

These data have been plotted in Fig. 1 and it is seen that the required dependence of the rate of retarded reaction on the intensity of illumination is found, thus substantiating the above mechanism for the retarded reaction.

Dependence of Rate of Reaction on Concentration of Retarder

In Table II are given the results of experiments carried out at 20° C. with a mixture of 150 mm. Hg pressure of acetaldehyde, 5 mm. Hg of oxygen, a constant intensity of

Can. J. Chem. Downloaded from www.nrcresearchpress.com by 61.7.252.67 on 09/04/12
For personal use only.

TABLE I

DEPENDENCE OF RATE OF RETARDED REACTION ON INTENSITY

All data refer to a mixture containing 150 mm. Hg pressure of acetaldehyde, 5 mm. Hg of oxygen, and 30 mm. Hg of ethanol at 20° C.

Absorbed intensity, percentage	Rate, mole $l.^{-1}$ $sec.^{-1} \times 10^9$
0.080	0.326
0.234	0.912
0.590	2.20
0.598	1.98
1.000	3.53
1.310	4.16
1.480	3.93

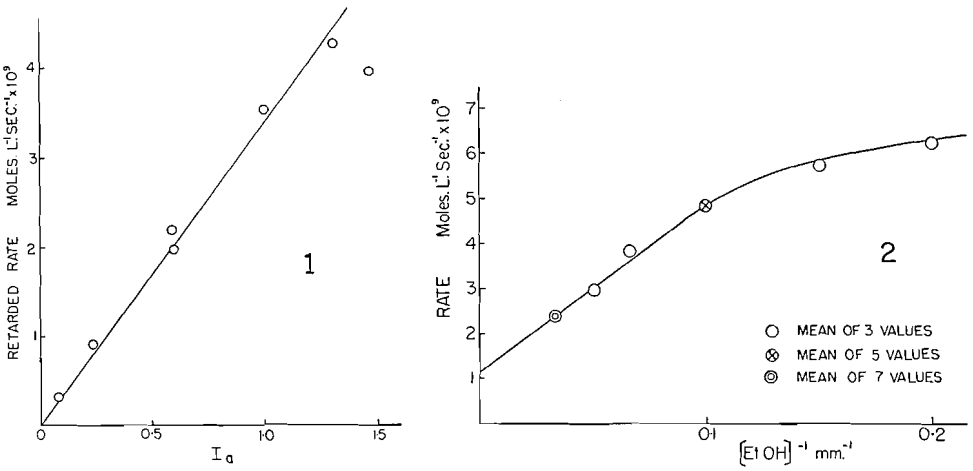

FIG. 1. Dependence of the rate of the ethanol-retarded photochemical oxidation of acetaldehyde on the intensity of the absorbed radiation.

FIG. 2. Dependence of the rate of the ethanol-retarded photochemical oxidation of acetaldehyde on the concentration of ethanol.

TABLE II

DEPENDENCE OF RATE OF ETHANOL RETARDED OXIDATION OF ACETALDEHYDE ON CONCENTRATION OF ETHANOL

All data refer to mixtures containing 150 mm. Hg pressure of acetaldehyde, 5 mm. Hg of oxygen at 20° C.; the absorbed light intensity was 0.59% of the total intensity

Ethanol concentration, mm. Hg	Rate, mole $l.^{-1}$ $sec.^{-1} \times 10^9$
0	7.93
3	7.15
5	6.50
7.5	5.85
10	4.93
15	3.92
20	3.00
30	2.39

Can. J. Chem. Downloaded from www.nrcresearchpress.com by 61.7.252.67 on 09/04/12
For personal use only.

illumination, and varying concentrations of ethanol. These data are shown graphically in Fig. 2, where the rate of the ethanol-retarded reaction is plotted against the reciprocal of the concentration of the ethanol. The linear relation at higher alcohol concentrations confirms the deductions from equation [C]. The intercept of the straight line in Fig. 2 on the rate axis gives the rate of initiation at the intensity used in these experiments as 1.12×10^{-9} mole $l.^{-1}$ $sec.^{-1}$.

Experiments were carried out to see if equation [C] was also obeyed by the alcohol-retarded photochemical oxidation of propionaldehyde. In Table III are given the results

TABLE III

DEPENDENCE OF RATE OF ETHANOL AND ISOPROPANOL RETARDED OXIDATION OF PROPIONALDEHYDE ON CONCENTRATION OF ALCOHOL

All data refer to mixtures containing 100 mm. Hg pressure of propionaldehyde, 3 mm. Hg of oxygen at 22° C., and a value of I_a of 1.12×10^{-9} einstein $l.^{-1}$ $sec.^{-1}$

Run No.	Alcohol	Alcohol pressure, mm.	Rate, mole $l.^{-1}$ $sec.^{-1}$ $\times10^9$
79	Ethyl	37.5	13.0
80	,,	18.5	22.7
81	,,	12.5	27.2
82	,,	36.0	11.9
83	,,	8.0	44.8
84	Isopropyl	10.0	15.4
85	,,	4.5	32.0
86	,,	30.0	6.08
87	,,	28.5	6.34
88	,,	6.0	21.6

of experiments carried out at 22° C. with a mixture of 100 mm. Hg pressure of propionaldehyde, 3 mm. Hg of oxygen, and varying concentrations of ethanol and isopropanol. These experiments were all performed with a light absorption of 1.12×10^{-9} einstein $l.^{-1}$ $sec.^{-1}$. The data in Table III are plotted in Fig. 3, where the rate of the alcohol-retarded reaction is again plotted against the reciprocal of the concentration of the alcohol. It is evident from the straight lines obtained that equation [C] is obeyed by the reaction. Further, it is obvious that isopropanol is a much more efficient retarder than is ethanol.

To obtain an accurate value for the rate of initiation in the case of the oxidation of propionaldehyde a series of experiments were carried out at a somewhat higher value of I_a. These results are recorded in Table IV. The data there refer to a mixture of 100 mm. Hg of propionaldehyde and 3 mm. Hg of oxygen at 22° C. The value of I_a was 1.16×10^{-8} einstein $l.^{-1}$ $sec.^{-1}$. The data are plotted in Fig. 4. The intercept of the straight line in Fig. 4 was calculated by the method of least squares using weighted means to be 1.98×10^{-8} mole $l.^{-1}$ $sec.^{-1}$, which is of course the value of the rate of initiation $\phi_2 I_a$. This value is probably correct to $\pm10\%$.

The results quoted in the above paragraphs leave little doubt that the mechanisms proposed for the alcohol-retarded photooxidation of acetaldehyde and propionaldehyde are correct. This in turn is evidence in favor of the correctness of the proposed mechanisms for the over-all photooxidations of acetaldehyde and propionaldehyde.

Measurement of the Chain Lifetimes

To measure the lifetimes of the chains in the photooxidation of acetaldehyde and propionaldehyde the usual (6) photochemical sector technique was employed. It was

Can. J. Chem. Downloaded from www.nrcresearchpress.com by 61.7.252.67 on 09/04/12
For personal use only.

TABLE IV

DEPENDENCE OF RATE OF ISOPROPANOL RETARDED OXIDATION OF PROPIONALDEHYDE ON CONCENTRATION OF ISOPROPANOL

All data refer to mixtures containing 100 mm. Hg pressure of propionaldehyde, 3 mm. Hg of oxygen at 22° C., and a value of I_a of 1.16×10^{-8} einstein $l.^{-1}$ $sec.^{-1}$

Run No.	Alcohol pressure, mm.	Rate, mole $l.^{-1}$ $sec.^{-1}$ $\times10^{8}$
89	32.5	7.26
90	30.0	7.26
91	16.7	11.80
92	12.6	14.4
93	20.0	10.25
94	10.0	16.6
95	5.0	19.9
96	0	20.5
97	32.0	6.88
98	32.0	6.40
99	10.0	18.2

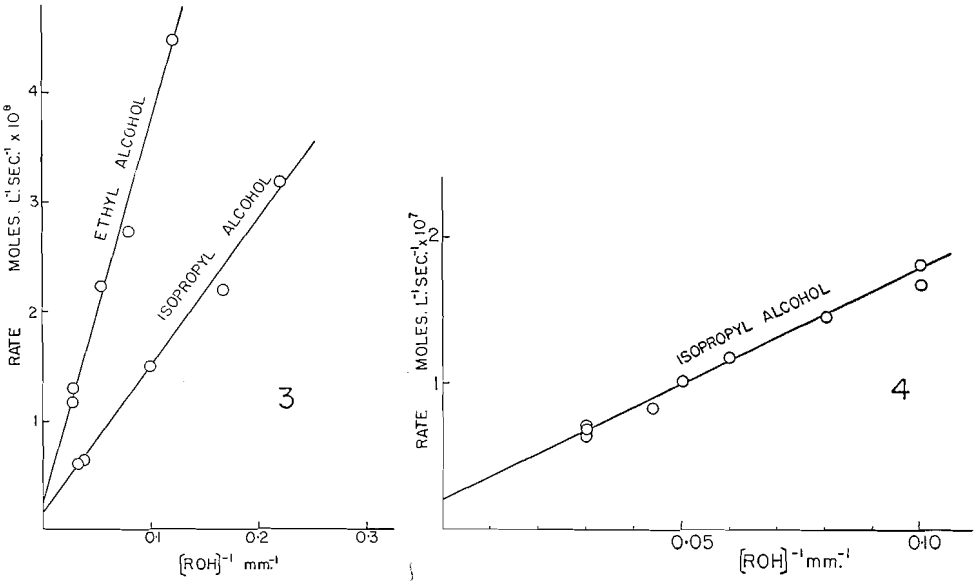

FIG. 3. Dependence of the rate of the ethanol and isopropanol retarded photochemical oxidation of propionaldehyde on the concentration of alcohol.

FIG. 4. Dependence of the rate of the isopropanol-retarded photochemical oxidation of propionaldehyde on the concentration of isopropanol. The determination of the rate of initiation of the photooxidation reaction.

confirmed experimentally that under the conditions of our studies there was no appreciable thermal oxidation and so the normal sector theory is applicable.

Series of experiments were performed for various values of the time of a single flash, t. Before and after each intermittent illumination experiment one was done under the same conditions but with continuous illumination. For each value of t, the ratio of the "intermittent" rate to the "continuous" rate, γ, was taken as ratio of the intermittent illumination rate to the average value of the continuous illumination rates of the experi-

Can. J. Chem. Downloaded from www.nrcresearchpress.com by 61.7.252.67 on 09/04/12
For personal use only.

Can. J. Chem. Downloaded from www.nrcresearchpress.com by 61.7.252.67 on 09/04/12
For personal use only.

TABLE V

ROTATING SECTOR EXPERIMENTS IN PHOTOCHEMICAL OXIDATION OF ACETALDEHYDE*

All data refer to a mixture of 150 mm. Hg pressure of acetaldehyde and 5 mm. Hg of oxygen at 20° C.; the incident intensity was 2.2% of the total intensity and I_a equal to 0.62% of total intensity

Rate, mole $l.^{-1}$ $sec.^{-1} \times 10^9$	R. intermittent / R. continuous	Flash time t, sec.
5.47	0.690	0.00174
7.93		
5.52	0.696	0.0125
7.93		
4.72	0.595	0.45
7.93		
5.39	0.679	0.112
7.93		
5.09	0.642	0.20
7.93		
5.60	0.705	0.0625
7.93		
4.66	0.588	0.875
7.93		

**The values for the "intermittent" rates quoted are mean values computed from the results of eight identical experiments. The value for the "continuous" rate quoted is a mean value of 12 identical experiments carried out between sets of eight "intermittent" experiments during the whole series of experiments.*

TABLE VI

ROTATING SECTOR EXPERIMENTS IN PHOTOCHEMICAL OXIDATION OF PROPIONALDEHYDE

All data refer to a mixture of 100 mm. Hg of propionaldehyde and 3 mm. Hg pressure of oxygen at 22° C.; the intensity of the illumination was 1.12×10^{-9} einstein $l.^{-1}$ $sec.^{-1}$

Run No.	Rate, mole $l.^{-1}$ $sec.^{-1}$ $\times 10^8$	R. intermittent / R. continuous	Flash time t, sec.
100	2.56	0.308	1.50
101	8.32	—	—
102	3.62	0.452	0.125
103	7.68	—	—
104	3.64	0.500	0.022
105	6.88	—	—
106	3.52	0.498	0.081
107	2.68	0.380	0.55
108	7.24	—	—
109	2.84	0.412	0.83
110	7.04	—	—
111	3.12	0.456	0.24
112	6.66	—	—
113	1.92	0.287	10.0
114	6.712	—	—
115	1.92	0.284	3.40
116	6.78	—	—
117	3.36	0.492	0.081
118	6.88	—	—
119	1.89	0.290	3.4
120	6.17	—	—
121	2.80	0.447	0.175
122	6.50	—	—
123	2.03	0.312	1.00

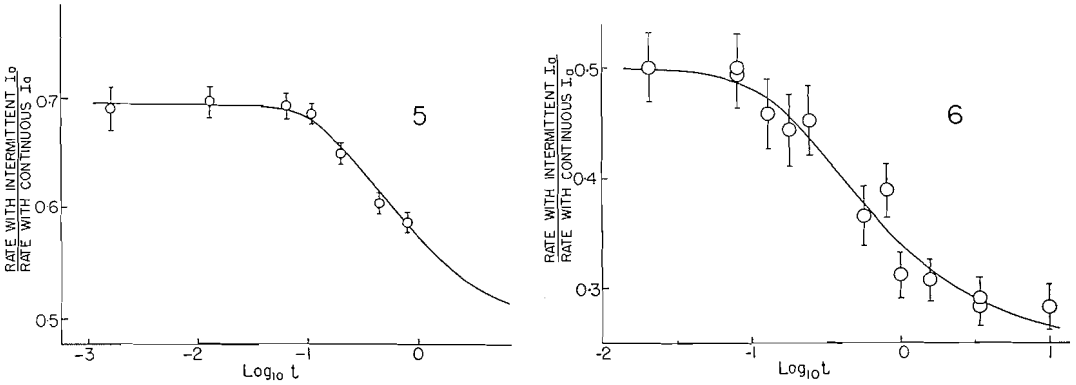

FIG. 5. Rotating sector experiment in the photochemical oxidation of acetaldehyde. Determination of the lifetime of the oxidation chain.

FIG. 6. Rotating sector experiments in the photochemical oxidation of propionaldehyde. Determination of the lifetime of the oxidation chain.

ments before and after the "intermittent" rate experiment. These data are given in Table V for the acetaldehyde oxidation, and in Table VI for the propionaldehyde.

Following the usual procedure a graph of $\log_{10}t$ against γ was plotted. Fig. 5 refers to the case of the acetaldehyde oxidation and Fig. 6 to the oxidation of propionaldehyde. In the former case a $\pi/2$ sector was used so the values of γ range from 0.5 to 0.7. In the case of the propionaldehyde oxidation a $\pi/4$ sector was used and here γ varies from 0.25 to 0.5.

Using the relevant mathematical equations given by Dickinson (6), a theoretical curve of γ against $\log_{10}b$, where $b = t/\tau$, was fitted to the experimental points. It was then possible to determine τ in each case. For the photochemical oxidation of acetaldehyde at 20° C. the data in Fig. 5 give the lifetime of the chain, τ, as 0.10 second. The data in Fig. 6 give a value of 0.14 second for the lifetime of the chain, τ, in the photochemical oxidation of propionaldehyde. These values could be in error by ± 0.05 second.

ABSOLUTE VALUES FOR THE VELOCITY CONSTANTS k_3 AND k_6 IN THE PHOTOCHEMICAL OXIDATION OF ACETALDEHYDE AND PROPIONALDEHYDE

Acetaldehyde

Using the above experimentally determined values for $R_i = \phi_2 I_a$, and τ, it is possible to calculate the absolute value of the velocity constant for the terminating reaction [6], i.e. k_6, from equations [A] and [B]. The values of 1.12×10^{-9} mole l.$^{-1}$ sec.$^{-1}$ for the rate of initiation ($= \phi_2 I_a$) and 0.10 second for τ obtained from the experiments with acetaldehyde lead to the following values for k_3 and k_6 at 20° C. in the photochemical oxidation of acetaldehyde:

$$k_3 = 8.05(\pm 2.40)\times10^3 \text{ l. mole}^{-1} \text{ sec.}^{-1},$$

$$k_6 = 8.93(\pm 4.20)\times10^{10} \text{ l. mole}^{-1} \text{ sec.}^{-1}.$$

Propionaldehyde

Our experiments lead to the values of 1.90×10^{-9} mole l.$^{-1}$ sec.$^{-1}$ for the rate of initiation ($= \phi_2 I_a$) at the light intensity of 1.12×10^{-9} einstein l.$^{-1}$ sec.$^{-1}$ used in the sector experiments, and 0.14 second for τ for the photochemical oxidation of propionaldehyde.

Can. J. Chem. Downloaded from www.nrcresearchpress.com by 61.7.252.67 on 09/04/12
For personal use only.

The substitution of these data in equations [A] and [B] leads to the following values for k_3 and k_6 at 22° C. for this reaction:

$$k_3 = 4.35(\pm 0.91)\times 10^4 \text{ l. mole}^{-1} \text{ sec.}^{-1},$$

$$k_6 = 2.69(\pm 1.35)\times 10^{10} \text{ l. mole}^{-1} \text{ sec.}^{-1}.$$

DISCUSSION

It is of considerable interest to compare these values for the velocity constants for the propagating (k_3) and terminating (k_6) steps involving peroxidic radicals derived from acetaldehyde and propionaldehyde with those for other radicals. It seems appropriate to compare the value for the velocity constant for the propagating step in the photochemical oxidation of acetaldehyde, i.e. equation [3]:

$$CH_3CO_3 + CH_3CHO \overset{k_3}{=} CH_3CO_3H + CH_3CO, \qquad [3]$$

for which we obtained the value of 8.05 $(\pm 2.40)\times 10^3$ l. mole^{-1} sec.$^{-1}$ at 20° C., with the velocity constant for the reaction [8] of the methyl radical:

$$CH_3 + CH_3CHO \overset{k_8}{=} CH_4 + CH_3CO. \qquad [8]$$

From Volman and Brinton's experiments (14) we calculate the value of 2.7×10^3 l. mole^{-1} sec.$^{-1}$ for k_3 in reaction [8] at 20° C. These data indicate that at equal concentration reaction [3] is more rapid. This must be attributed to the higher reactivity of the peracetic radical over the methyl radical. The absolute values for the velocity constant for the terminating reactions, k_6, in the photooxidation of acetaldehyde and propionaldehyde, namely $8.93(\pm 4.2)\times 10^{10}$ l. mole^{-1} sec.$^{-1}$ at 20° (acetaldehyde) and $2.89(\pm 1.35)\times 10^{10}$ l. mole^{-1} sec.$^{-1}$ at 22° C. (propionaldehyde), may be compared with the values of 2.2×10^{10} l. mole^{-1} sec.$^{-1}$ for the recombination of methyl radicals (12), and about 2.0×10^{10} l. mole^{-1} sec.$^{-1}$ (9, 4, 13) for the recombination of ethyl radicals (at 20° C.). These data indicate that the peracetic radicals "recombine" (see below) more rapidly than do methyl or ethyl radicals, and that perpropionic radicals "recombine" at about the same rate as do the hydrocarbon radicals.

It is instructive to compare the collision efficiencies for the mutual interaction of the methyl, ethyl, peracetic, and perpropionic radicals. To do this it is necessary to have the absolute values for the velocity constants for the recombination reactions and also to know the collision numbers of the radicals. It is further necessary to know if the recombination reactions require any activation energy. In nearly all the investigations of the recombination of methyl (10), trifluoromethyl (1), and ethyl radicals (4, 9, 13) there has been but little reliable evidence to show whether or not these reactions do require an activation energy. In the study of the recombination of methyl radicals by mass spectrometry (8) it has been claimed that there is a net activation energy of -1.5 kilocalories mole^{-1} and this was attributed to a third-body effect. Shepp and Kutschke (13) have recently claimed that their studies on the recombination of ethyl radicals indicate an activation energy for this process of 2.0 ± 1 kilocalories mole^{-1}. Such small activation energies as these are difficult to establish unambiguously and as the assumption that the recombination reactions require but little or zero activation energy introduces little error into our discussion, we shall therefore adopt this commonly-made assumption.

Can. J. Chem. Downloaded from www.nrcresearchpress.com by 61.7.252.67 on 09/04/12
For personal use only.

Using Shepp's (12) recalculated value for the velocity constant for the recombination of methyl radicals and the value of 3.5 Å for the collision diameter one obtained a value of about 0.3 for the collision efficiency at 125° C. In the case of trifluoromethyl radicals Ayscough (1) used a collision diameter of 4 Å and calculated a value of 0.16 for the collision efficiency of these radicals at 127° C. These values are comparable with those of 0.12 for the collision efficiency of the recombination of two ethyl radicals found by Shepp and Kutschke (13), and 0.15 for the same process obtained by Bradley, Melville, and Robb (4). We have used a value of 5.4 Å for the collision diameters of both the peracetic and perpropionic radicals—this value seemed to be the most reasonable one as judged from Courtauld models of the radicals. This leads to a collision efficiency for the mutual interaction of the peracetic radicals of 0.8 and a value of 0.29 for the collision efficiency for the mutual interaction of two perpropionic radicals. These values suggest that the mutual interactions of these peroxidic radicals are somewhat more efficient than those of comparable hydrocarbon radicals.

Chemistry of the Recombination Reaction of Peroxide Radicals

The data described in the above paragraphs show that the "recombination" reactions of peracetic and perpropionic radicals are relatively efficient. It will be recalled that the recombination or terminating step in the photooxidations is the process:

$$2RCO_3 = (RCO)_2O_2 + O_2. \qquad [6]$$

It is not easy to see why this process should be so very efficient, for it is evident from our data that one in every two collisions is effective in the case of the peracetic radical and one in every three or four is effective in the case of the perpropionic radicals. One might have thought that a rather special orientation would have been necessary before two radicals with structures like the peracetic or the perpropionic ones could have reacted.

The chemistry of process [6] is not clear. It could be that when the two peroxide radicals interact the oxygen molecule which is formed is produced by the elimination of an oxygen atom from each of the interacting radicals. This would probably be a rather complicated process and entropy considerations make us believe that it is not the mechanism of process [6].

A more likely mechanism is that the oxygen molecule which is eliminated comes wholly from one of the interacting radicals. This could be understood if the mechanism were as shown below:

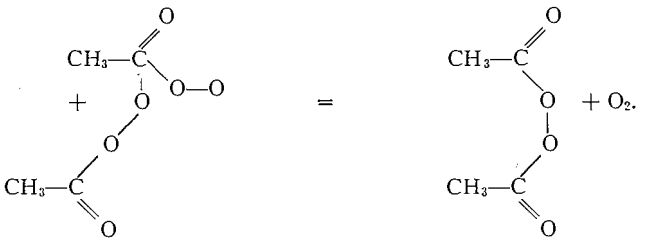

Here it is assumed that the peroxide oxygen atoms of one radical attack the second radical at the acyl carbon atom causing the attacked radical to lose two oxygen atoms to form an oxygen molecule. It is thought that the use of isotopically enriched oxygen may enable the chemistry of this process to be elucidated and we are planning to carry out such experiments.

Can. J. Chem. Downloaded from www.nrcresearchpress.com by 61.7.252.67 on 09/04/12
For personal use only.

ACKNOWLEDGMENTS

The experiments on acetaldehyde were carried out in the Department of Inorganic and Physical Chemistry, University of Liverpool, Liverpool 7, England, and we are indebted to Professor C. E. H. Bawn, C.B.E., F.R.S., for laboratory facilities and for his interest in the work. The remainder of the work was supported by a grant from the National Research Council of Canada to whom we tender our thanks.

REFERENCES

1. AYSCOUGH, P. B. J. Chem. Phys. **24**, 944 (1956).
2. BATEMAN, L. H. and GEE, G. Proc. Roy. Soc. (London), A, **195**, 376 (1948).
3. BOWEN, E. G. and TIETZ, E. L. J. Chem. Soc. 234 (1930).
4. BRADLEY, J. N., MELVILLE, H. W., and ROBB, J. C. Proc. Roy. Soc. (London), A, **236**, 333 (1956).
5. COOPER, H. R. and MELVILLE, H. W. J. Chem. Soc. 1984, 1994 (1951).
6. DICKINSON, R. G. *In* Noyes and Leighton, The photochemistry of gases. Reinhold Publishing Corp., New York. 1941.
7. FARMER, J. B. and MCDOWELL, C. A. Trans. Faraday Soc. **48**, 624 (1952).
8. INGOLD, K. U., HENDERSON, I. H. S., and LOSSING, F. P. J. Chem. Phys. **21**, 2239 (1953).
9. IVIN, K. J. and STEACIE, E. W. R. Proc. Roy. Soc. (London), A, **208**, 25 (1951).
10. KISTIAKOWSKY, G. B. and ROBERTS, E. R. J. Chem. Phys. **21**, 1637 (1953).
11. MELVILLE, H. W. and RICHARDS, S. J. Chem. Soc. 944 (1954).
12. SHEPP, A. J. Chem. Phys. **24**, 939 (1956).
13. SHEPP, A. and KUTSCHKE, K. O. J. Chem. Phys. **26**, 1020 (1957).
14. VOLMAN, D. H. and BRINTON, R. J. Chem. Phys. **20**, 1053 (1952).

Can. J. Chem. Downloaded from www.nrcresearchpress.com by 61.7.252.67 on 09/04/12
For personal use only.

The authors are thankful to Dr. A. W. Tickner for mass spectrometer analyses and to the analytical section of this division for infrared analyses and the spectrograms in Fig. 2.

1. HAAGEN-SMIT, A. J. Ind. Eng. Chem. **48**, 65 (1956).
2. NOYES, W. A., Jr. and LEIGHTON, P. A. The photochemistry of gases. Reinhold Publishing Co., New York. 1941. p. 400.
3. CVETANOVIĆ, R. J. J. Chem. Phys. **25**, 376 (1956); a more detailed account to be published.
4. CALLEAR, A. B. and CVETANOVIĆ, R. J. Can. J. Chem. **33**, 1256 (1955).
5. LEVY, N. and SCAIFE, C. W. J. Chem. Soc. 1093 (1946). BROWN, J. F., Jr. J. Am. Chem. Soc. **79**, 2480 (1957).
6. GIAUQUE, W. F. and KEMP, J. D. J. Chem. Phys. **6**, 40 (1938).
7. DICKINSON, R. G. and BAXTER, W. P. J. Am. Chem. Soc. **50**, 774 (1928).
8. NORRISH, R. G. W. J. Chem. Soc. 1604 (1929).

RECEIVED SEPTEMBER 13, 1957.
DIVISION OF APPLIED CHEMISTRY,
NATIONAL RESEARCH COUNCIL,
OTTAWA, CANADA.

ULTRAVIOLET IRRADIATION OF PYRIMIDINE DERIVATIVES
II. NOTE ON THE SYNTHESIS OF THE PRODUCT OF REVERSIBLE PHOTOLYSIS OF URACIL*

A. M. MOORE

Solutions of uracil, when irradiated with ultraviolet light (2537 Å), undergo photolysis to yield a product that lacks the absorption band (max. 2590 Å) typical of uracil but which regenerates uracil on treatment with acid (4). Several derivatives of uracil, such as uridine, uridylic acid (4, 5), and 1,3-dimethyluracil (2), exhibit a similar "reversible" photolysis.

Using 1,3-dimethyluracil as a model, Moore and Thomson (3) showed that the product of irradiation is 1,3-dimethyl-6-hydroxy-hydrouracil, resulting from the addition of a molecule of water to the 5,6 double bond. This compound has also been synthesized by reduction of 5,5-dibromo-1,3-dimethyl-6-hydroxy-hydrouracil (3) and of the 5-monobromo compound (6).

The analogous derivative of uracil has now been synthesized and compared with the "reversible" product of ultraviolet irradiation of uracil.

5,5-Dibromo-6-hydroxy-hydrouracil (I) (m.p. 136°) synthesized by the method of Wheeler and Johnson (7) was reduced with zinc dust and acetic acid (pH 4–5) using the same technique as that used for the reduction of 1,3-dimethyl-5,5-dibromo-6-hydroxy-hydrouracil (3). The product of reduction was then compared chromatographically and spectroscopically with the product of irradiation of uracil. Although the latter has not been isolated in the pure state it can readily be separated on paper chromatograms, the position of the "reversible" product on the developed chromatogram being found by exposing a test strip to HCl vapor to promote conversion of the product to uracil, which is then easily located by the ultraviolet print method of Markham and Smith (1) (Fig. 1).

Accordingly, the product of reduction was chromatographed on paper in parallel with the product of irradiation using four different solvent systems. The observed R_f values are given in Table I.

In Fig. 2 are plotted the respective relative changes in optical density that occurred when a photolyzed solution of uracil and the product of reduction of the dibromo com-

*Issued as A.E.C.L. No. 523.

Can. J. Chem. Downloaded from www.nrcresearchpress.com by 61.7.252.67 on 09/04/12
For personal use only.

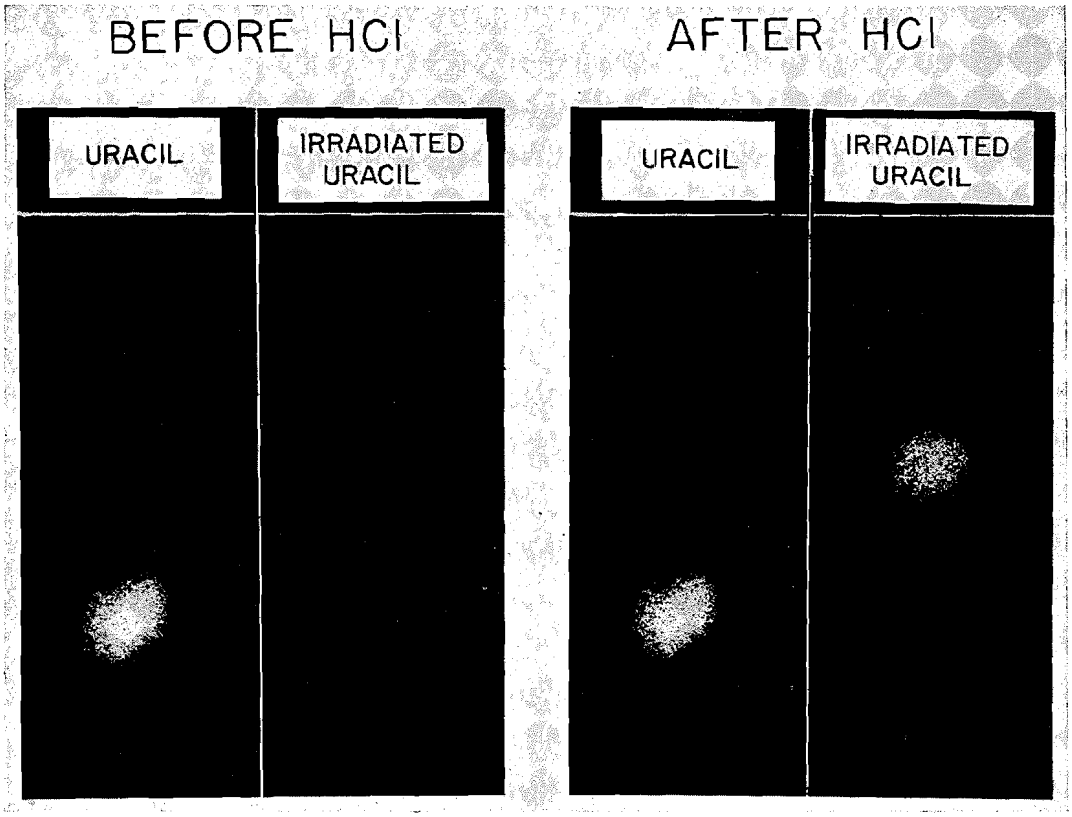

FIG. 1. Paper chromatographic separation of the "reversible" product of ultraviolet-irradiated uracil. (*n*-Butanol: water.)

TABLE I

COMPARISON OF IRRADIATION PRODUCT* WITH SYNTHETIC MATERIAL

Solvent†	Observed R_f values (mean)		
	Synthetic 6-hydroxy-hydrouracil	Product of irradiation	Uracil
(*a*)	0.22	0.22	0.35
(*b*)	0.78	0.78	0.73
(*c*)	0.42	0.42	0.50
(*d*)	0.67	0.69	0.68

**Uracil (10^{-2} M) irradiated with ultraviolet light (2537 Å) for 5 hours in the apparatus previously described (3).*

†(a) n-Butanol saturated with water. (b) Water saturated with n-butanol. (c) n-Propanol:water, 70:30 by volume. (d) Isopropanol:water, 70:50 by volume.

pound were heated with acid (100°, 5 minutes, pH 1). The agreement is good apart from the points at the three shortest wavelengths where the errors of measurement are at a maximum.

The product of reduction of 5,5-dibromo-6-hydroxy-hydrouracil presumably has the OH group at position 6. Its identity with the product of irradiation of uracil, as indicated by the very close agreement in R_f values and in spectroscopic properties of the two prepara-

Can. J. Chem. Downloaded from www.nrcresearchpress.com by 61.7.252.67 on 09/04/12
For personal use only.

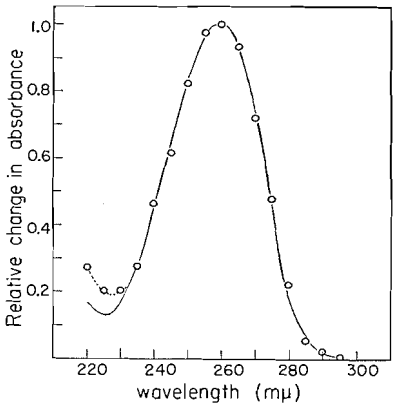

FIG. 2. Plot of $\Delta D/\Delta D_{260}$, where ΔD is the change in optical density at any wavelength and ΔD_{260} is the corresponding change at 260 mμ that occurs when the product of irradiation of uracil (solid line) or the product of the reduction of 5,5-dibromo-6-hydroxy-hydrouracil (open circles) is treated with HCl (100°, 5 minutes, pH 1). This method of presentation was chosen because the concentrations obtained in the two preparations were arbitrary.

tions, adds strong support to the suggestion made earlier (2) that the product of irradiation of uracil responsible for the acid-catalyzed regeneration phenomenon is 6-hydroxy-hydrouracil.

1. MARKHAM, R. and SMITH, J. D. Biochem. J. **45**, 294 (1949).
2. MOORE, A. M. and THOMSON, C. H. Science, **122**, 594 (1955).
3. MOORE, A. M. and THOMSON, C. H. Can. J. Chem. **35**, 163 (1957).
4. SINSHEIMER, R. L. and HASTINGS, R. Science, **110**, 525 (1949).
5. SINSHEIMER, R. L. Radiation Research, **1**, 505 (1954).
6. WANG, S. Y., APICELLA, M., and STONE, B. R. J. Am. Chem. Soc. **78**, 4180 (1956).
7. WHEELER, H. L. and JOHNSON, T. B. J. Biol. Chem. **3**, 183 (1907).

RECEIVED SEPTEMBER 13, 1957.
BIOLOGY DIVISION,
ATOMIC ENERGY OF CANADA LIMITED,
CHALK RIVER, ONTARIO.

AN ALTERNATIVE SYNTHESIS OF 2-*O*-METHYL-D-XYLOSE

W. D. S. BOWERING AND T. E. TIMELL

In studying the structure of a xylan the need arose for 2-*O*- and 3-*O*-methyl-D-xylose as reference compounds. The latter was synthesized from 1,2-*O*-isopropylidene-D-xylofuranose (1) and it was preferable to prepare the former from the same starting material if possible. Such a procedure would also obviate the necessity of using the acid-labile methyl 3,5-*O*-isopropylidene-α,β-D-xylofuranoside as described in a previous synthesis of 2-*O*-methyl-D-xylose (2).

1,2-*O*-Isopropylidene-D-xylofuranose was benzylated to give the corresponding 3,5-di-*O*-benzyl derivative, which was converted to methyl 3,5-di-*O*-benzyl-α,β-D-xylofuranoside by methanolysis. Methylation (3) of this compound yielded the 2-*O*-methyl derivative, which was then reductively debenzylated to methyl 2-*O*-methyl-α,β-D-xylofuranoside. Hydrolysis of this compound gave crystalline 2-*O*-methyl-D-xylose.

Can. J. Chem. Downloaded from www.nrcresearchpress.com by 61.7.252.67 on 09/04/12
For personal use only.

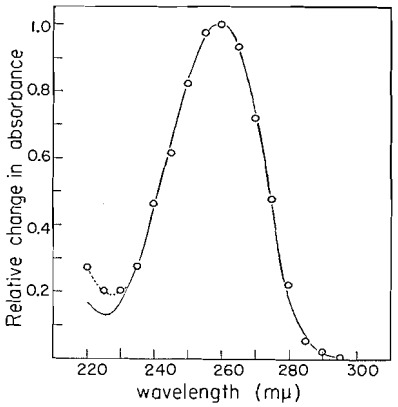

FIG. 2. Plot of $\Delta D/\Delta D_{260}$, where ΔD is the change in optical density at any wavelength and ΔD_{260} is the corresponding change at 260 mμ that occurs when the product of irradiation of uracil (solid line) or the product of the reduction of 5,5-dibromo-6-hydroxy-hydrouracil (open circles) is treated with HCl (100°, 5 minutes, pH 1). This method of presentation was chosen because the concentrations obtained in the two preparations were arbitrary.

tions, adds strong support to the suggestion made earlier (2) that the product of irradiation of uracil responsible for the acid-catalyzed regeneration phenomenon is 6-hydroxy-hydrouracil.

1. MARKHAM, R. and SMITH, J. D. Biochem. J. **45**, 294 (1949).
2. MOORE, A. M. and THOMSON, C. H. Science, **122**, 594 (1955).
3. MOORE, A. M. and THOMSON, C. H. Can. J. Chem. **35**, 163 (1957).
4. SINSHEIMER, R. L. and HASTINGS, R. Science, **110**, 525 (1949).
5. SINSHEIMER, R. L. Radiation Research, **1**, 505 (1954).
6. WANG, S. Y., APICELLA, M., and STONE, B. R. J. Am. Chem. Soc. **78**, 4180 (1956).
7. WHEELER, H. L. and JOHNSON, T. B. J. Biol. Chem. **3**, 183 (1907).

RECEIVED SEPTEMBER 13, 1957.
BIOLOGY DIVISION,
ATOMIC ENERGY OF CANADA LIMITED,
CHALK RIVER, ONTARIO.

AN ALTERNATIVE SYNTHESIS OF 2-*O*-METHYL-D-XYLOSE

W. D. S. BOWERING AND T. E. TIMELL

In studying the structure of a xylan the need arose for 2-*O*- and 3-*O*-methyl-D-xylose as reference compounds. The latter was synthesized from 1,2-*O*-isopropylidene-D-xylofuranose (1) and it was preferable to prepare the former from the same starting material if possible. Such a procedure would also obviate the necessity of using the acid-labile methyl 3,5-*O*-isopropylidene-α,β-D-xylofuranoside as described in a previous synthesis of 2-*O*-methyl-D-xylose (2).

1,2-*O*-Isopropylidene-D-xylofuranose was benzylated to give the corresponding 3,5-di-*O*-benzyl derivative, which was converted to methyl 3,5-di-*O*-benzyl-α,β-D-xylofuranoside by methanolysis. Methylation (3) of this compound yielded the 2-*O*-methyl derivative, which was then reductively debenzylated to methyl 2-*O*-methyl-α,β-D-xylofuranoside. Hydrolysis of this compound gave crystalline 2-*O*-methyl-D-xylose.

Can. J. Chem. Downloaded from www.nrcresearchpress.com by 61.7.252.67 on 09/04/12
For personal use only.

Can. J. Chem. Downloaded from www.nrcresearchpress.com by 61.7.252.67 on 09/04/12
For personal use only.

EXPERIMENTAL

*3,5-Di-O-benzyl-1,2-O-isopropylidene-*D*-xylofuranose*

1,2-*O*-Isopropylidene-D-xylofuranose, $[\alpha]_D^{21}$ −19.2° (*c*, 2.1 in water), (46.4 g.) (1) was treated with benzyl chloride (230 ml.) and powdered potassium hydroxide (57 g.) at 100° C. for 5 hours. The solution was poured into water and the sirupy material obtained on concentration was extracted with boiling ethanol. Evaporation yielded a sirup (103.2 g.) which could not be induced to crystallize, $[\alpha]_D^{22}$ +9.2° (*c*, 2.5 in ethanol). Anal.: Calc. for $C_{22}H_{26}O_5$: C, 71.3%; H, 7.1%. Found: C, 72.3%; H, 7.5%.

*Methyl 3,5-Di-O-benzyl-α,β-*D*-xylofuranoside*

A portion of the above sirup (40.0 g.) was boiled under reflux with anhydrous methanol (200 ml.) containing 1.5% hydrogen chloride. Neutralization (silver carbonate) and evaporation yielded a sirup, $[\alpha]_D^{22}$ +17.6° (*c*, 5.3 in ethanol), (37.5 g., 100.8%). Anal.: Calc. for $C_{20}H_{24}O_5$: OCH_3, 9.0%. Found: OCH_3, 8.8%.

*Methyl 3,5-Di-O-benzyl-2-O-methyl-α,β-*D*-xylofuranoside*

The above sirupy compound (37.0 g.) was dissolved in a mixture of dimethyl formamide (54 ml.) and methyl iodide (20.4 ml.). Silver oxide (20.4 g.) was added in small portions over a period of 1 hour and the mixture was shaken for 24 hours. The methylated material was recovered (3) to yield a sirup, $[\alpha]_D^{22}$ +23.7° (*c*, 3.2 in ethanol), (33.3 g., 86.5%). Anal.: Calc. for $C_{21}H_{26}O_5$: C, 70.4%; H, 7.3%; OCH_3, 17.3%. Found: C, 71.5%; H, 8.1%; OCH_3, 17.6%. An infrared spectrum of the material indicated the presence of only a trace of hydroxyl groups.

*Methyl 2-O-Methyl-α,β-*D*-xylofuranoside*

The above sirup (33.0 g.) was reductively debenzylated (4). The aqueous solution obtained was passed through a column of Amberlite IRC 50 exchange resin and the eluate was concentrated and extracted with ethanol to yield a sirup, $[\alpha]_D^{22}$ +35.4° (*c*, 2.9 in ethanol), (22.1 g.).

*2-O-Methyl-*D*-xylose*

The above material (22.0 g.) was hydrolyzed with 0.5 *N* sulphuric acid (150 ml.) by boiling under reflux for 14 hours. After neutralization with barium hydroxide and filtration through Celite, concentration of the filtrate gave a sirup (7.5 g.). Examination by paper chromatography using a system of methyl ethyl ketone – ethanol – water (20:5:2) indicated the presence of 2-*O*-methyl-D-xylose and a trace of xylose.

The crude material was added to the top of a column containing cocoanut charcoal and was eluted with 2% ethanol until the eluate gave a negative Molisch test. Evaporation yielded a white, crystalline compound, which was recrystallized from ethanol, m.p. 132–133° C. (corrected), $[\alpha]_D^{21}$ +35.1° (*c*, 3.5 in water), (3.1 g., 15.3%). Anal.: Calc. for $C_6H_{12}O_5$: OCH_3, 18.9%. Found: OCH_3, 18.9%.

1. Levene, P. A. and Raymond, A. L. J. Biol. Chem. **102**, 331 (1933).
2. Robertson, G. J. and Speedie, T. H. J. Chem. Soc. 824 (1934).
3. Kuhn, R., Trischmann, H., and Löw, I. Angew. Chem. **67**, 32 (1955).
4. Freudenberg, K. and Plankenhorn, E. Ann. **536**, 257 (1938).

Received September 17, 1957.
McGill University and
Pulp and Paper Research Institute of Canada,
Montreal, Quebec.

THE INFRARED AND RAMAN SPECTRUM OF DIMETHOXYMETHANE

J. K. WILMSHURST*

Infrared spectra of solutions of dimethoxymethane ($CH_3OCH_2OCH_3$) in CCl_4 and CS_2 have been obtained over the 3–7 μ and 7–33 μ regions respectively (Fig. 1) using a Perkin-Elmer model 112S double pass spectrometer equipped with LiF, CaF_2, NaCl, and CsBr optics. The infrared spectrum of the vapor has also been obtained around 3 μ and from 6.5 to 33 μ (Fig. 2). Although the Raman spectrum of the liquid had been recorded previously (4) a better resolved spectrum was obtained here (Fig. 3) using a White grating Raman spectrometer (7) with photoelectric recording.† Depolarization

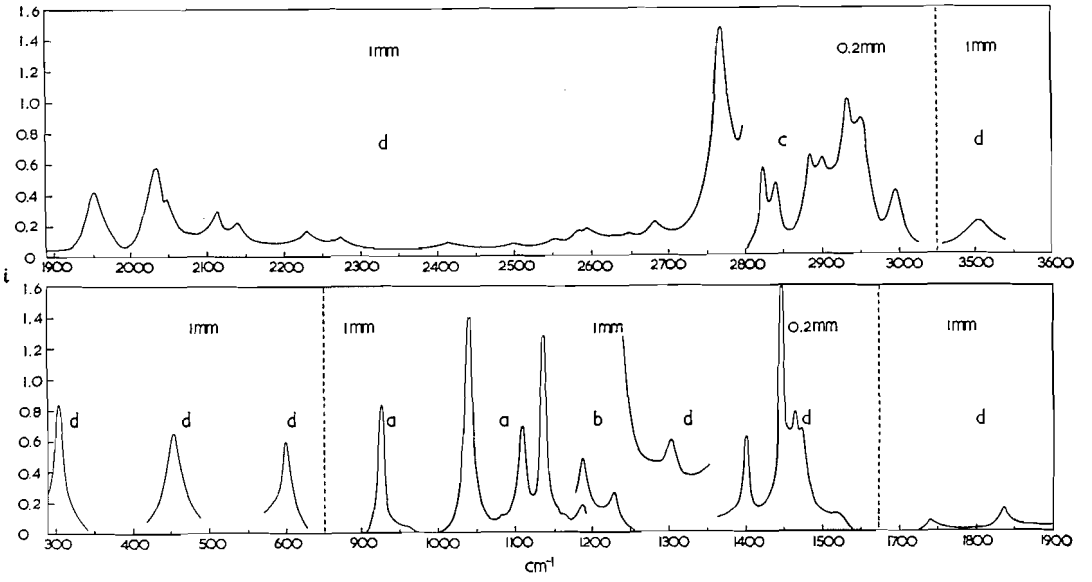

FIG. 1. The infrared spectrum of a solution of dimethoxymethane in CCl_4 (3600–1400 cm.$^{-1}$) and in CS_2 (1400–300 cm.$^{-1}$). The cell length is as shown and the concentrations (in volume) are a = 1:400, b = 1:150, c = 1:25, d = 2:25.

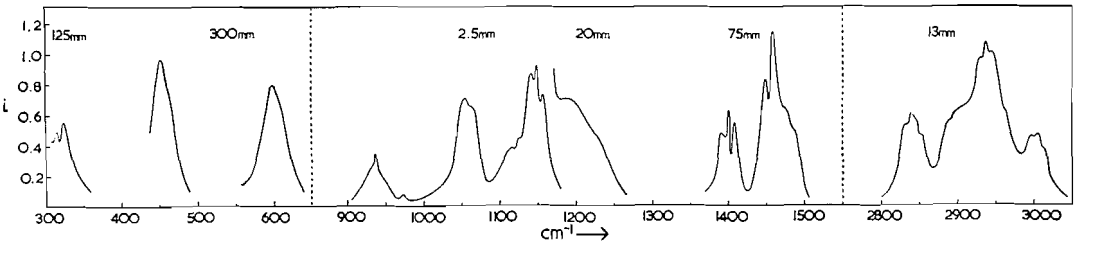

FIG. 2. The infrared spectrum of dimethoxymethane vapor in a 10-cm. cell at the pressure shown.

ratios were measured by the method of Edsall and Wilson (2) and corrected for convergence error by the method of Rank and Kagarise (6).

New Zealand University Research Fund Senior Fellow 1957.

†*The author wishes to thank Dr. H. J. Bernstein, of the National Research Council Laboratories, for the use of this instrument.*

Can. J. Chem. Downloaded from www.nrcresearchpress.com by 61.7.252.67 on 09/04/12
For personal use only.

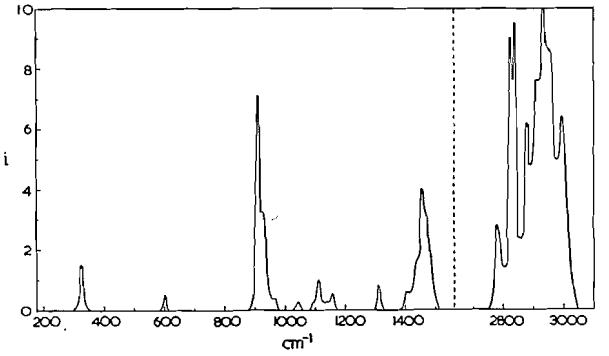

FIG. 3. The Raman spectrum of liquid dimethoxymethane.

TABLE I

THE INFRARED AND RAMAN SPECTRUM OF DIMETHOXYMETHANE

Infrared spectrum				Raman spectrum				Assignment
Solution		Vapor						
Cm.$^{-1}$	Int.	Cm.$^{-1}$	Band contour	Cm.$^{-1}$	Rel. int.	Depol. ratio	Species	Approximate description
304	m	315 324	?	325	2	0.14	a	COC bending
454	m	452 ~462	⊥				a	OCO bending
600	m	598 ~611	⊥	602	1	0.86	b	COC bending
				912	7	0.17	a	Sym. H_3C—O stretching
927	vs	~931 937 ~946	⊥	925	3	0.56	a	Sym. OCO stretching
~960	w	973	⊥?	963	0	p?		?
1042	vs	1054 1064	⊥ + ∥ hybrid	1042	0		b	Asym. H_3C—O stretching
~1084	w			~1094	0			1401 − 304 = 1097 (B)?
1110	vs	1116 ~1125	?	1111	1	0.80	b	CH_2 rocking
1138	vs	1141 1148 1156	∥	~1136	0		b	Asym. OCO stretching
~1154	w			1157	1	0.70	a	CH_3 rocking
~1165	w						b	CH_3 rocking
1188	s	~1188					b	CH_3 rocking
1229	s	~1230					a	CH_3 rocking
1303	w			1310	1	0.86	a	CH_2 twisting
1401	m	1390 1400 1408	∥	1403	1	dp	b	CH_2 wagging
				~1436	2	~0.70	a	CH_2 sym. bending
1448	m	1449 1458 —	∥	1455	4	~0.80	$a+b$	CH_3 sym. bending
1465	m	1464		1469	3	~0.80	$a+b$	CH_3 asym. bending
1473	m	1487		1483	1	~0.80	$a+b$	CH_3 asym. bending
1519	w							600+927 = 1527 (B)
1741	w							304+1448 = 1752 ($A+B$)
1836	w							912+927 = 1839 (A)
1954	m							927+1042 = 1869 (B)
2035	m							912+1138 = 2050 (B)
2049	w							927+1138 = 2065 (B)
2115	w							927+1188 = 2115 (B)
2141	w							1042+1110 = 2152 (A)

Can. J. Chem. Downloaded from www.nrcresearchpress.com by 61.7.252.67 on 09/04/12
For personal use only.

TABLE I (*concluded*)

Infrared spectrum				Raman spectrum				Assignment
Solution		Vapor						
Cm.$^{-1}$	Int.	Cm.$^{-1}$	Band contour	Cm.$^{-1}$	Rel. int.	Depol. ratio	Species	Approximate description
2231	w							1110+1138=2248 (*A*)
2275	w							2×1138=2276 (*A*)
2415	w							1110+1303=2413 (*B*)
2502	w							1042+1465=2507 (*A*+*B*)
2554	w							1110+1448=2558 (*A*+*B*)
2585	w							1138+1448=2586 (*A*+*B*)
2596	w							1138+1465=2603 (*A*+*B*)
2632	vw							1188+1448=2636 (*A*+*B*)
2650	vw							1188+1465=2653 (*A*+*B*)
2684	w							1229+1465=2694 (*A*+*B*)
2770	m			2780	3	dp		1303+1473=2776 (*A*+*B*)
2825	m	~2831 2840	⊥	2826	9	0.16	*a*	CH_2 sym. stretching
2841	m	~2846 ~2853	⊥	2841	9	0.15		2×1436=2872 (*A*)
2885	m	2889 2897 2905	∥ ?	2880	6	0.21		2×1448=2896 (*A*)
2901	m			~2914	7	0.30		1448+1465=2913 (*A*+*B*)
2934	m	2930 2938 2945	∥	2935	10	0.33	*a*+*b*	CH_3 sym. stretching
2951	m	~2964		~2956	8	0.36	*a*+*b*	CH_3 asym. stretching
2997	m	2998 3005 3013	∥	2996	6	0.53	*a*+*b* *b*	CH_3 asym. stretching CH_2 asym. stretching
3514	w							2934+600=3534 (*A*+*B*)

From dipole moment studies (5) it has been concluded that the molecule has point symmetry C_2, the two O—CH_3 bonds making angles of ~60° with the OCO plane. Electron diffraction data (1) support this model. Thus, of the 33 fundamental vibrations, 17 should be symmetric (type *a*) and 16 antisymmetric (type *b*) with respect to rotation about the symmetry axis. Calculation of the moments of inertia of the molecule* shows that it is an approximate symmetric top, the Gerhard and Dennison (3) parameter being $\beta = 2.17$. Thus, two types of bands are expected: perpendicular-type bands having a prominent *Q* branch with weaker unresolved *P* and *R* branches, and parallel-type bands having three nearly equal maxima with *PR* separation of ~17 cm.$^{-1}$. The vapor band contours observed (Fig. 2) can be seen to be essentially consistent with this, the average *PR* separation of the parallel bands being 16 cm.$^{-1}$, in agreement with the previously proposed configuration (5) for the molecule.

The type *a* modes should give rise to polarized bands in the Raman and perpendicular-type bands in the infrared, while the type *b* modes should give rise to depolarized Raman bands and either parallel or perpendicular type bands in the infrared, depending on whether the change of dipole moment is parallel to the minor axis, 0*x*, or to the major axis, 0*y* (Fig. 4). Since the two methyl groups are sufficiently far apart, the internal vibrations of one group should be independent of those of the other and, thus, the six *a*-type internal modes should have the same frequency as the corresponding six *b*-type modes. With this in mind the vibrational assignment is fairly straightforward.

**The moments of inertia were calculated (assuming* $r_{CO} = 1.44$ *Å,* $r_{CH} = 1.09$ *Å,* $\angle COC = 104°$*, and all other angles tetrahedral) to be:* $I_x = 75.6$*,* $I_y = 245.2$*, and* $I_z = 230.5 \times 10^{-40}$ *g. cm.*^{2}*, where z is the symmetry axis of the molecule and x and y axes are as shown in Fig. 4.*

Can. J. Chem. Downloaded from www.nrcresearchpress.com by 61.7.252.67 on 09/04/12
For personal use only.

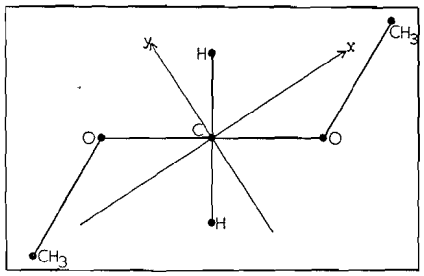

FIG. 4. Projection of the dimethoxymethane molecule on a plane perpendicular to the symmetry axis.

The polarized bands at 2996 and 2935 cm.$^{-1}$, having corresponding parallel-type infrared bands, are taken as the superimposed *a*- and *b*-type asymmetrical and symmetrical methyl stretchings respectively. The polarized band at 2956 cm.$^{-1}$ is taken as the remaining superimposed *a*- and *b*-type asymmetrical methyl stretching mode. Of the pair of intense polarized bands at 2826 and 2841 cm.$^{-1}$, the former is assigned to the symmetrical CH_2 stretching mode while the latter is assigned as 2×1436 cm.$^{-1}$, the high intensity arising from Fermi resonance with the fundamental. The asymmetrical CH_2 stretching mode is not obvious but is assigned to the infrared band at 2997 cm.$^{-1}$ coincident with the *a*- and *b*-type methyl asymmetric stretching mode.

The infrared bands at 1473 and 1465 cm.$^{-1}$ are assigned to the two superimposed *a*- and *b*-type asymmetrical methyl bending modes, while the parallel-type band at 1458 cm.$^{-1}$ is taken as the superimposed *a*- and *b*-type symmetrical methyl bending mode. The polarized band at $\sim$1436 cm.$^{-1}$ is taken as the symmetrical methylene deformation mode while the parallel-type infrared, depolarized Raman band at 1400 cm.$^{-1}$ is assigned to the methylene wagging mode. The Raman band at 1310 cm.$^{-1}$, though depolarized, is assigned to the methylene twisting vibration. From electronegativity considerations (8), the four methyl rocking modes would be expected to occur around 1150–1240 cm.$^{-1}$ and the four infrared bands observed in this region are assigned accordingly.

The intense parallel-type infrared band at 1148 cm.$^{-1}$ is assigned to the OCO asymmetric stretching mode, and the perpendicular-type infrared band at 937 cm.$^{-1}$ corresponding to a medium intensity polarized Raman band to the symmetric OCO stretching mode. The strong polarized Raman band at 912 cm.$^{-1}$, having no infrared counterpart, is taken as the symmetric CH_3—O stretching mode. From the geometry of the molecule, this latter vibration can be seen to give rise to only a small change in dipole moment and, hence, only a weak infrared band would be expected, in contrast to the stronger infrared band expected from the OCO symmetrical stretching mode at 937 cm.$^{-1}$. Of the two strong infrared bands at 1110 and 1042 cm.$^{-1}$, the former, though it appears to have a possible parallel-type band contour, is taken as the methylene rocking mode from electronegativity considerations (9), while the latter has a hybrid-type contour and is taken as the asymmetrical O—CH_3 stretching mode. The smaller difference in frequency between the two OCH_3 stretching vibrations, as compared with the difference between the two OCO stretching modes, is consistent with the expected smaller coupling constant between the two OCH_3 bonds.

The polarized band at 325 cm.$^{-1}$ is assigned to the type *a* COC bending mode, and the depolarized band at 602 cm.$^{-1}$, corresponding to a perpendicular-type infrared band, to the type *b* COC bending mode. The perpendicular-type band at 454 cm.$^{-1}$ is taken as the type *a* OCO bending mode. The four torsional vibrations would be expected to have low frequencies (<300 cm.$^{-1}$) and were not observed.

Can. J. Chem. Downloaded from www.nrcresearchpress.com by 61.7.252.67 on 09/04/12
For personal use only.

1. AOKI, K. J. Chem. Soc. Japan (Pure Chem. Sect.), **74**, 110 (1953); Chem. Abstr. **47**, 5191 (1953).
2. EDSALL, J. T. and WILSON, E. B. J. Chem. Phys. **6**, 124 (1938).
3. GERHARD, S. L. and DENNISON, D. M. Phys. Rev. **43**, 197 (1933).
4. KOHLRAUSCH, K. W. F. and YPSILANTI, P. Z. physik. Chem. B, **32**, 407 (1936).
5. MIZUSHIMA, S., MORINO, Y., and KUBO, M. Physik. Z. **38**, 459 (1937).
6. RANK, D. H. and KAGARISE, R. E. J. Opt. Soc. Am. **40**, 89 (1950).
7. WHITE, J. U., ALPERT, N., and DEBELL, A. G. J. Opt. Soc. Am. **45**, 154 (1955).
8. WILMSHURST, J. K. J. Chem. Phys. **26**, 426 (1957).
9. WILMSHURST, J. K. Can. J. Chem. **35**, 937 (1957).

RECEIVED SEPTEMBER 30, 1957.
DEPARTMENT OF CHEMISTRY,
AUCKLAND UNIVERSITY COLLEGE,
AUCKLAND, NEW ZEALAND.

Can. J. Chem. Downloaded from www.nrcresearchpress.com by 61.7.252.67 on 09/04/12
For personal use only.

Can. J. Chem. Downloaded from www.nrcresearchpress.com by 200.7.193.243 on 09/04/12
For personal use only.

Canadian Journal of Chemistry

Issued by THE NATIONAL RESEARCH COUNCIL OF CANADA

VOLUME 36 FEBRUARY 1958 NUMBER 2

DETERMINATION OF SULPHATE ACID ESTER IN UNSTABILIZED CELLULOSE NITRATE BY THE HYDROLYSIS METHOD[1]

PAUL E. GAGNON, KARL F. KEIRSTEAD,[2] AND BRIAN T. NEWBOLD[3]

ABSTRACT

The method of determining sulphate acid ester in unstabilized cellulose nitrates by hydrolysis in acetone/water solution was evaluated. The precision of duplicate determinations for cotton and wood cellulose nitrates containing about 100% sulphate ester was −0.1 to +5.9% and +0.4 to +9.2%, respectively. With cellulose nitrates containing 69–43% and 69–47% sulphate ester, it was +1.8 to +13.4% and +0.4 to +21.0%. The sulphate acid ester content of both unstabilized cotton and wood cellulose nitrates increased with decreasing nitrogen content.

INTRODUCTION

The sulphate acid ester content of cellulose acetate sulphate was estimated by ion exchange methods (5) and more recently by titration in acetone/water solution before and after hydrolysis (2). In a previous paper (3), methods were described for the determination of the sulphate ester content of unstabilized cellulose nitrates.

One of the objects of the present work was to evaluate the hydrolysis method of determining the sulphate acid ester content of unstabilized cotton and wood cellulose nitrates with a view to establishing the reproducibility of the results. The other aim was to determine the relation between the sulphate acid ester content and the nitrogen content of cotton and wood cellulose nitrates.

EXPERIMENTAL

Cellulose Nitrate

The nitrations of cotton linters and wood cellulose were performed according to the method mentioned in a recent paper (4) and the sulphate and nitrogen contents were determined by procedures previously described (3, 5).

Hydrolysis of Sulphate Ester Groups in Unstabilized Cellulose Nitrate

The sulphate acid ester content of cellulose nitrate was determined by the method given in a recent paper (3), except that in the present work the seventh aliquot removed for titration with 0.01 *N* potassium hydroxide was 50 ml. instead of 100 ml.

Zero Hydrolysis of Sulphate Ester Groups in Unstabilized Cellulose Nitrate

A moist sample (3–4 g.) of the cellulose nitrate was dissolved in 90% acetone/water solution (700 ml.) to prevent hydrolysis and the acidity was determined on aliquots (100 ml.) by titration with 0.01 *N* potassium hydroxide using a Macbeth pH meter.

[1]*Manuscript received October 17, 1957.*
Contribution from the Department of Chemistry, Laval University, Quebec, Que., with financial assistance from the Defence Research Board of Canada.
[2]*Present address: Lignosol Chemicals Limited, Quebec, Que.*
[3]*Research assistant, Department of Chemistry, Laval University.*

Evaluation of the pH Meter Titration Method of Determining Acidity

In a series of experiments, various quantities (5–50 ml.) of 0.1 *N* sulphuric acid were added to 700 ml. samples of acetone/water solution and the acidity was determined on 100 ml. aliquots by titration with 0.01 *N* potassium hydroxide and was measured on a Macbeth pH meter. The average of four determinations on each acetone/water/sulphuric acid aliquot was compared to the theoretical acidity. The mean difference from the theoretical value was −4.5%. The standard deviation was 2.8 and the 95% confidence limits were −4.5% ±6.3, as calculated by the Dean and Dixon method (1).

Determination of Sulphate Ester in Cellulose Nitrates Prepared by Duplicate Nitrations

The sulphate acid ester contents of unstabilized cotton and wood cellulose nitrates prepared by duplicate nitrations were determined using the hydrolysis method.

The precision of the ester determinations for cotton cellulose nitrate containing about 100% ester was expressed as follows: the mean difference was 11.0%, the standard deviation 6.0, and the 95% confidence limits were 11.0% ±8.8. For wood cellulose nitrate containing about 100% sulphate ester, the mean difference was 8.0%, the standard deviation 8.7, and the 95% confidence limits were 8.0% ±12.8.

RESULTS AND DISCUSSION

Evaluation of the Hydrolysis Method of Determining Sulphate Acid Ester

In the present work the sulphate acid ester, RSO_4H, contents of a wide range of cotton and wood cellulose nitrates (containing about 7 to 13% nitrogen) were determined by titration in acetone/water solution before and after hydrolysis. Determination of the ester by this method depends on the supposition that hydrolysis of the ester is completed after 24 hours and therefore the 24-hour titer value should give the total sulphate content of the cellulose nitrate. The gravimetric and 24-hour titrimetric sulphates of a series of cotton and wood unstabilized cellulose nitrates are compared in Table I.

TABLE I

COMPARISON OF GRAVIMETRIC AND TITRIMETRIC SULPHATE PERCENTAGES IN CELLULOSE NITRATES

Expt. No.	% H_2SO_4 in cellulose nitrates			
	Cotton		Wood	
	Gravimetric	Titrimetric	Gravimetric	Titrimetric
1	2.38	2.28	2.36	2.41
2	2.26	2.02	2.17	2.15
3	1.54	1.54	2.13	2.18
4	1.23	1.22	2.12	1.95
5	1.13	1.00	2.02	1.96
6	1.00	0.93	2.01	1.90
7	0.95	0.94	1.34	1.26
8	0.95	0.88	1.33	1.36
9	0.89	0.98	1.30	1.32
10	0.85	0.89	1.23	1.26
11	0.69	0.75	1.04	1.05
12	0.63	0.70	0.93	1.01
13	0.47	0.52	0.91	0.92

There is good agreement between the gravimetric and titrimetric sulphates. The differences are shown statistically in Table II, and the confidence limits for the differences were calculated by the method of Dean and Dixon (1). These results provide evidence

Can. J. Chem. Downloaded from www.nrcresearchpress.com by 200.7.193.243 on 09/04/12
For personal use only.

that hydrolysis of the sulphate acid ester was complete after 24 hours. Comparison of 24-hour and 48-hour titrimetric sulphate values, given in Table II, showed that hydrolysis continued slowly, and that the 48-hour titrimetric sulphate was always higher than the gravimetric sulphate, for instance, for cotton cellulose nitrate, about 5%. Therefore the 24-hour titrimetric sulphate was the best indication that hydrolysis of the sulphate acid ester was complete and this value was used for the ester determinations. The precision of 24- and 48-hour titrimetric sulphate determinations on duplicate samples of cellulose nitrates is shown in Table II.

TABLE II

PRECISION OF TITRIMETRIC TOTAL SULPHATE DETERMINATIONS ON CELLULOSE NITRATES

Samples		Difference, %	Standard deviation	95% Confidence limits
Nature	Time, hr.			
Cotton	24*	+0.2	8.2	+0.2 ±4.9
Wood	24*	−0.1	4.3	−0.1 ±2.6
Cotton	24 and 48	+5.2	2.5	−5.2 ±1.5
Wood	24 and 48	+4.8	4.1	−4.8 ±2.4
Cotton	24	4.0	1.6	4.0 ±1.6
Cotton	48	4.5	1.8	4.5 ±1.8
Wood	24	3.2	2.6	3.2 ±2.6
Wood	48	4.0	4.2	4.0 ±4.2

**Compared to gravimetric sulphate.*

The titration value before hydrolysis of the sulphate acid ester had started was originally determined from a rate of hydrolysis curve by extrapolation to zero time. However, more recently, experiments have been performed with 90% acetone/water solution which effectively stopped hydrolysis of the sulphate acid ester. Determinations of the ester using the zero hydrolysis titer obtained by the latter method have shown that the original zero hydrolysis figure obtained from the rate of hydrolysis curve was always too high. Thus an error of from 8 to 65% for cotton and 7 to 50% for wood cellulose nitrate was introduced into the ester determinations. The error was less when determinations were made on low ester content cellulose nitrates; thus it appears that the rate of hydrolysis when the ester is present in small amount is slower than that when a considerable amount of ester is present. It is evident that the initial hydrolysis of the sulphate acid ester, RSO_4H, is extremely rapid.

The above discussion shows that it is possible to obtain good measures of acidity for samples of cellulose nitrate in which there is no hydrolysis and others in which there is 100% hydrolysis of the sulphate acid ester; therefore the latter can be determined.

It was essential to determine the errors in the method and to establish the reproducibility of the results. The hydrolysis experiments were always performed on duplicate samples and the average results used for sulphate acid ester calculations. The precision of sulphate acid ester determinations on duplicate samples of cotton and wood cellulose nitrates containing about 100% ester is shown in Table III. It is seen that good precision can be obtained. An indication of the experimental error involved in the pH meter titration method for determining the acidity in cellulose nitrate was obtained by means of a series of acidity determinations on sulphuric acid solutions. The 95% confidence limits for the difference between the experimental and theoretical acidity were −4.5% ±6.3. Therefore in view of the latter error, the precision of the ester determinations mentioned above was

Can. J. Chem. Downloaded from www.nrcresearchpress.com by 200.7.193.243 on 09/04/12
For personal use only.

TABLE III

PRECISION OF SULPHATE ACID ESTER DETERMINATIONS ON DUPLICATE SAMPLES OF CELLULOSE NITRATES

Samples		Difference, %	Standard deviation	95% Confidence limits
Nature	Ester, %			
Cotton	100	2.9	3.0	2.9 ±3.0
Wood	100	4.8	4.4	4.8 ±4.4
Cotton	69–43	7.6	5.8	7.6 ±5.8
Wood	69–47	10.7	10.3	10.7 ±10.3

good. However, these determinations were made on cellulose nitrates containing close to the maximum amount of sulphate acid ester and therefore the precision obtained was the best possible.

It was expected that the precision of ester determinations would decrease when cellulose nitrates containing less than 70% sulphate acid ester were used. This was the case, as shown in Table III. The precision of ester determinations on cotton cellulose nitrate was better than that for those on wood cellulose nitrate. The precision of sulphate acid ester determinations on very low ester content cellulose nitrates was poor; for instance, for a cotton cellulose nitrate containing 22% sulphate acid ester the difference between duplicate determinations rose to 59%. This fact was not surprising in view of the low sulphate content, 0.47%, of the cellulose nitrate and the fact that the difference in the pH meter titration was −7.4% for the titers obtained.

Several cotton and wood cellulose nitrates were prepared by duplicate nitrations and their sulphate acid ester contents were determined. Typical nitration conditions and ester contents for wood cellulose nitrates are shown in Table IV and the precision of the ester determinations is given in the experimental part. As expected, the precision decreased for both cotton and wood cellulose nitrates.

TABLE IV

DETERMINATIONS OF SULPHATE ACID ESTER IN WOOD CELLULOSE NITRATES PREPARED BY DUPLICATE NITRATIONS

Expt. No.	Temperature, ° C.				Nitrogen, %	Ester, % of total sulphate
	Mixed acid		Drowning water			
	Initial	Maximum	Initial	Maximum		
1	26.0	29.5	25.0	43.0	11.4	81
	23.0	28.0	24.5	56.0	11.4	98
2	23.0	27.1	24.0	43.0	11.7	97
	20.0	23.4	21.0	45.0	11.8	96
3	25.0	29.0	26.0	42.5	10.8	104
	23.0	25.8	24.0	41.0	10.8	97
4	22.0	24.3	21.5	41.5	10.6	94
	20.8	24.1	20.4	40.0	10.7	99

By the hydrolysis method, sulphate acid ester can be determined on duplicate samples of cotton and wood cellulose nitrates containing about 100% sulphate acid ester, with a precision of −0.1 to +5.9% and +0.4 to +9.2%, respectively. When determinations are made on cotton cellulose nitrates containing 69–43% sulphate acid ester, the precision is +1.8 to +13.4%, and for wood cellulose nitrates containing 69–47% sulphate acid ester, +0.4 to +21.0%.

Can. J. Chem. Downloaded from www.nrcresearchpress.com by 200.7.193.243 on 09/04/12
For personal use only.

Relation between Sulphate Acid Ester and Nitrogen Content

Kullgren (6) using ion exchange studies showed that 12.57% *N* cellulose nitrate contained about three times as much sulphate acid ester as 13.05% *N* cellulose nitrate. Miles (7) reported that the proportion of sulphate ester tended to increase with decreasing nitrogen content, and Gagnon *et al.* (3) recently provided some evidence in support of the latter contention.

In the present work, the sulphate acid ester contents of a variety of unstabilized cotton and wood cellulose nitrates were determined and compared to the nitrogen contents of the cellulose nitrates. The results are shown in Fig. 1.

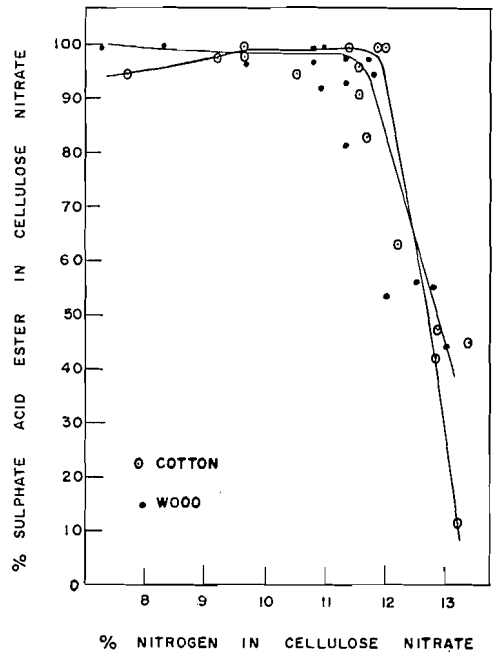

FIG. 1. Relation between sulphate acid ester and nitrogen contents of cellulose nitrate.

It is seen that for cotton cellulose nitrates containing less than 12.2% nitrogen, the sulphate acid ester content is about 100%, but for higher nitrogen contents the sulphate acid ester content rapidly decreases. Similar results were obtained for wood cellulose nitrates.

The sulphate acid ester content of both cotton and wood cellulose nitrate definitely increases with decreasing nitrogen content. This fact is very important evidence for the existence of a sulphate acid ester in unstabilized cellulose nitrate.

REFERENCES

1. DEAN, R. B. and DIXON, W. J. J. Anal. Chem. **23**, 636 (1951).
2. GAGNON, P. E., KEIRSTEAD, K. F., WALKER, J., and KAVANAUGH, K. Can. J. Technol. **34**, 71 (1956).
3. GAGNON, P. E., KEIRSTEAD, K. F., and YAMASAKI, D. Can. J. Technol. **34**, 477 (1957).
4. GAGNON, P. E., KEIRSTEAD, K. F., and NEWBOLD, B. T. Can. J. Chem. **36**, 215 (1958).
5. KEIRSTEAD, K. F. and MYERS, J. Can. J. Chem. **32**, 566 (1954).
6. KULLGREN, C. Ing. Vetenskaps Akad. Handl. No. 165 (1942).
7. MILES, F. D. Cellulose nitrate. Clarke, Irwin & Co. Ltd., Toronto. 1955.

Can. J. Chem. Downloaded from www.nrcresearchpress.com by 200.7.193.243 on 09/04/12
For personal use only.

Can. J. Chem. Downloaded from www.nrcresearchpress.com by 200.7.193.243 on 09/04/12
For personal use only.

THE REACTION OF CARBON DISULPHIDE WITH ALUMINA[1]

A. G. PINKUS AND J. S. KIM

ABSTRACT

The absorption spectrum in aqueous solution of the yellow substance formed by the reaction of carbon disulphide and alumina exhibits absorption maxima at 398 and 325 mμ. This yellow color is not due to sodium disulphide as previously proposed since the latter substance showed an entirely different spectrum with shoulders at about 360–375 mμ and 290–300 mμ. The presence of *both* water and sodium hydroxide in the alumina is necessary for the formation of the yellow color in confirmation of previous work. A study of the gain in weight of the alumina with time of contact with carbon disulphide showed that this reaction begins to level off after about 24 hours. A minimum value for the heat evolved for the alumina – carbon disulphide system was determined as 8.6 cal. per g. of alumina reacting with an excess of carbon disulphide.

INTRODUCTION

In connection with another problem, spectroscopically pure carbon disulphide was needed. A simple method of purifying many solvents is by passing them through a column of some adsorbent. For example, spectroscopically pure cyclohexane can be obtained by passing it through a column of silica gel (7, 18*a*) or alumina (19) (after shaking with a nitrating mixture), and peroxides can be removed from ethyl ether, butyl ether, or dioxane by passing through a column containing activated aluminum oxide (4, 18*b*, *c*). There are other examples making use of silica gel (18*b*). When we passed carbon disulphide through a column of activated alumina, it was observed that the entire column turned a yellow color. That this was not due to the removal of impurities from the carbon disulphide was indicated by the fact that passing the same effluent successively through several more alumina columns gave the same result. In view of the widespread use of alumina in chromatography and the use of carbon disulphide as a chromatographic solvent (1, 11) it appeared to be of importance to study this phenomenon. It is stated that the reaction of carbon disulphide with alumina at elevated temperatures produces aluminum sulphide and carbon dioxide (5). At 200° to 500° carbon disulphide reacts with water over activated alumina to produce hydrogen sulphide and carbon dioxide in 98% conversions (2) whereas under milder conditions it is reported that carbonyl sulphide (COS) is formed (16). The formation of a yellow color during the adsorption of carbon disulphide vapors by alumina gel at room temperature was first noted by Perry (15). A thorough study of the action of gaseous carbon disulphide on alumina led to the conclusion on the basis of chemical tests that the yellow color was due to sodium disulphide which was produced by the reaction of carbon disulphide with sodium hydroxide adsorbed on the alumina (13). Since the yellow color was not removed by the usual solvents for sulphur, it was concluded that no free sulphur was present. The reaction products were explained according to the following summarized equations [1]–[6]:

$$[1] \quad CS_2 + 2H_2O \rightarrow CO_2 + 2H_2S,$$

$$[2] \quad CS_2 + H_2O \rightarrow COS + H_2S,$$

$$[3] \quad COS + H_2O \rightarrow CO_2 + H_2S,$$

$$[4] \quad COS \rightarrow CO + S,$$

$$[5] \quad NaOH + H_2S \rightarrow NaHS + H_2O,$$

$$[6] \quad 2NaHS + S \rightarrow Na_2S_2 + H_2S.$$

[1]*Manuscript received May 3, 1957.*
Contribution from the Department of Chemistry, Baylor University, Waco, Texas.

The presence of sodium in the yellow aqueous extract was shown by microchemical tests and in the alumina by spectroscopic means. The presence of sodium hydroxide in the alumina (in equation [5]) was inferred by showing that alumina which had been washed with water (until the aqueous extracts showed the absence of sodium) and reactivated at 400° did not form a yellow color with carbon disulphide. The alumina had been previously saturated with carbon disulphide. In another paper (14) a quantitative study of the same reaction showed that the amount of hydrogen sulphide produced and the intensity of the yellow color qualitatively paralleled the amount of water present, there being an optimum amount (about 8%) below or above which the amount of hydrogen sulphide produced decreased. In our work we made further studies toward a characterization of the reaction of alumina with *liquid* carbon disulphide. We have used absorption spectra to check the conclusion (13) that the yellow color was due to sodium disulphide. Besides various miscellaneous observations, we have made initial studies on the rate by studying the gain in weight of the alumina and also have done some preliminary calorimetric determinations.

EXPERIMENTAL

Purification and Preparation of Materials

ACS grade carbon disulphide was purified by two methods: (*a*) a previously published procedure (18*d*, 20) and (*b*) a simple distillation. No observable differences in results were noted in using these two samples of solvent. Water used in making up solutions was redistilled from potassium permanganate in a nitrogen atmosphere and had a pH of 6.85 to 6.90. Sulphur was purified by recrystallization from redistilled ACS grade carbon disulphide and also by a previously published method (3). No apparent differences in results were detected for these two samples of sulphur. Sodium disulphide was prepared by stirring or shaking ACS analytical grade sodium sulphide ($Na_2S.9H_2O$) with the calculated weight of sulphur for about 5 hours and then adding dilute aqueous sodium hydroxide (or distilled water) in small portions with stirring or shaking until all of the solid dissolved. This solution was then diluted up to the desired concentration (approx. 0.0018 *M* for the curve reported). Sodium hydroxide was used in order to repress hydrolysis.

Several commercial grades of alumina were used in this work; however, most of the experiments were done using the same grade in order to have a better basis for comparison. Where a related series of experiments were carried out, samples from the same batch were used. The basic character of the alumina was demonstrated by the following experiments in which the pH of aqueous washings was determined. In a typical determination, a 1.000 g. sample of alumina was stirred with 50 ml. of distilled water (pH 7.00) for 1 hour. The alumina was allowed to settle, the supernatant decanted, and its pH determined by means of a Beckman glass-electrode line-operated pH meter Model H 2. The pH meter was checked at a pH of 7.0 by means of Clark and Lubs buffer mixture (10). Repeated washings with further 50 ml. portions of water showed a rapid decrease in pH from the initial value of 7.42 and then a leveling off to a pH close to 7.0. The data are plotted in Fig. 1. A quantitative estimate of the amount of base in the alumina (calculated as NaOH) was determined by titration of the washings with 0.005 *N* HCl using methyl red indicator. An asymptote was reached at about 11 washings. The total amount of NaOH calculated was 0.40%. The approximate water content of the alumina used in most of the experiments as determined by ignition to constant weight was $12.6 \pm 0.9\%$ (average of several determinations). A constant weight was attained after about 24 hours of heating.

Dilutions of the yellow reaction product from the alumina – carbon disulphide reaction

Can. J. Chem. Downloaded from www.nrcresearchpress.com by 200.7.193.243 on 09/04/12
For personal use only.

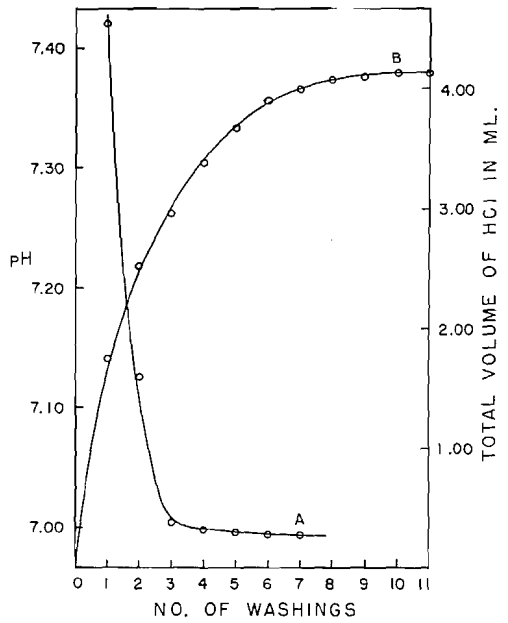

FIG. 1. A, change of pH with number of washings of alumina with water. B, total volume of 0.005 *N* HCl used to titrate washings of alumina with water using 50 ml. of water per washing.

were made by using water saturated with carbon disulphide. Carbon disulphide saturated water was used rather than distilled water alone for two reasons. Since the yellow color was found to disappear when attempts were made to remove the excess carbon disulphide from the alumina *in vacuo*, it was thought that the use of carbon disulphide saturated water would tend to repress this decolorization. Secondly, in order to observe the character of the absorption band at the lower wave lengths, it was found desirable to compensate for the excess carbon disulphide by using the saturated solution of carbon disulphide in the blank absorption cell. The carbon disulphide saturated water was freshly prepared each time just before using. It was found that when distilled water alone was used a more rapid decolorization of the solution occurred.

Various shades of color ranging from yellow to orange were obtained by the reaction of carbon disulphide with the various grades of alumina. Some of the columns themselves showed the same range of colors in different parts of the column. However, the spectra of the aqueous extracts from the various types of alumina showed remarkably similar shapes and absorption band positions. The absorption spectra for the aqueous extract of the yellow reaction product and for sodium disulphide are shown in Fig. 2. In order to show that the use of dilute sodium hydroxide in making up the solutions of sodium disulphide (to repress hydrolysis) did not greatly affect the character of the absorption curve, a curve is also shown for a solution prepared with distilled water alone. (The two are at different concentrations and are not directly comparable as to absorption intensity.)

It was of importance to investigate the possibility that different products might be formed by the reaction of alumina and carbon disulphide depending on the time of contact. In a series of experiments, it was definitely shown that the same absorption spectra were obtained regardless of the time of contact from up to 6 hours down to 1 minute contact before shaking with water and filtering. The amount of the yellow substance produced in general increased with time of contact. In order to check the possibility that the yellow

Can. J. Chem. Downloaded from www.nrcresearchpress.com by 200.7.193.243 on 09/04/12
For personal use only.

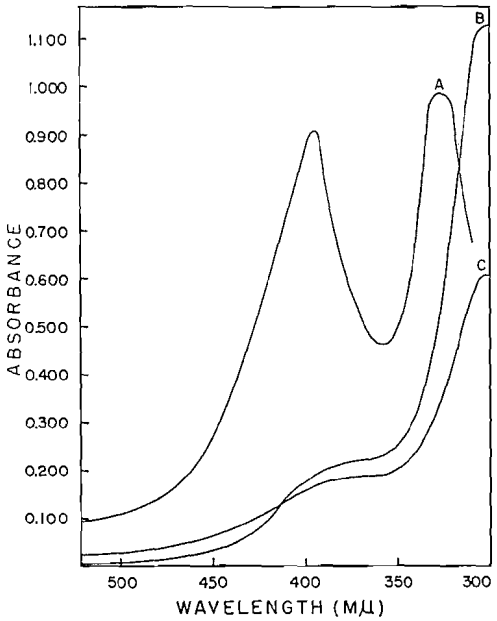

FIG. 2. A, absorption spectrum of aqueous solution of yellow color from the reaction of alumina and CS_2. B, absorption spectrum of Na_2S_2 in 0.01 *N* NaOH. C, absorption spectrum of Na_2S_2 in water.

substance formed from carbon disulphide vapor and alumina (13) might be different than when liquid carbon disulphide was used, we have also run the spectrum of the aqueous extract. The same absorption peaks were obtained.

Absorption Spectra

Absorption spectra were determined with a DK–1 Beckman spectrophotometer using matched glass-stoppered 1 cm. quartz cells. A tungsten lamp was the light source for the part of the spectra above 325 mμ and a hydrogen lamp below 375 mμ. (The overlapping parts of the spectra matched in each case.) A photomultiplier detector was used with both lamps. Absorbance (A) was calculated (6, 21) by means of the ratio $A = \log(I_0/I)$, where I_0 is the intensity of the incident light and I the intensity of the transmitted light, both in % transmission. Wavelengths were checked by comparison of accurate values reported (17) for benzene vapor. These were about 0.1 mμ higher than the reported values.

Calorimetric Studies

The evolution of heat during the passage of carbon disulphide down the column was also noted. It was hoped that a determination of the heat of reaction would aid in the elucidation of the nature of the reaction. A few preliminary calorimetric determinations were made on this reaction following a described method (8). The calorimetric constant was determined by using the reaction of standard solutions of sodium hydroxide and hydrochloric acid. In a typical run, 250 ml. (assumed to be in excess) of carbon disulphide was introduced into the Dewar flask and allowed to come to equilibrium. Then 40.00 g. of alumina was added and the mixture stirred (by using a glass stirrer or a teflon-coated stirring bar) and readings of temperature with time were taken using a Beckman differential thermometer. Since the increase in temperature was not complete even at the end of 18 hours, this indicated a slow approach to equilibrium. Since a more elaborate apparatus would be needed to determine the heat of reaction for such a long reaction period, we

Can. J. Chem. Downloaded from www.nrcresearchpress.com by 200.7.193.243 on 09/04/12
For personal use only.

discontinued these experiments at this point. On the basis of the data obtained in the longest experiment, we have calculated (9) a minimum value for the heat of reaction[2] of 8.6 cal./g. of alumina reacting with an excess of carbon disulphide (based on specific heats for alumina and carbon disulphide as deduced from the International Critical Tables).

Rate Studies

It was found that on standing the yellow color would disappear from the alumina. This decolorization would also take place when the sample was placed in a desiccator and evacuated using a water pump. This decolorization was shown not to be dependent on the presence of water since it also occurred when the sample was protected during evacuation by means of calcium chloride. Furthermore, it was shown that the alumina gained in weight even though the yellow color had disappeared. This indicated a decomposition of the yellow substance into a gaseous product which was removed leaving a non-volatile colorless product. Since this observation appeared to be an important lead in the elucidation of the nature of the yellow substance, we studied this reaction by determining the gain in weight of the alumina with time during its reaction with carbon disulphide.

In a typical experiment 0.250 g. of alumina was stirred with 25 ml. of carbon disulphide by means of a teflon-enclosed magnetic stirrer, the mixture being kept in a water bath maintained at 30°±1°. At specified times, the carbon disulphide was decanted and the alumina placed in a desiccator, which was evacuated by means of a water pump. The desiccator was protected from the water pump by means of calcium chloride. The evacuation was carried out until the weight approached a constant value (usually about 24 hours). For the next point, the decanted carbon disulphide was again added to the same alumina and the procedure repeated. The data are plotted in Fig. 3. The yellow color would disappear in about 15 minutes for experiments having a short contact time to about 6 hours for the longer times. The maximum gain in weight of the alumina in our

[2]*The referee has suggested that this probably represents a heat of wetting which varies with the activation of the alumina and the amount of water in the carbon disulphide if not anhydrous. Another possibility suggested by the referee is that it may include heat of adsorption, which is often observed with many materials. The referee has kindly furnished the following references dealing with this: J. L. Culbertson and L. L. Winter, J. Am. Chem. Soc.* **59**, *308 (1937), report a value of 6.7 cal./g. for the heat of wetting of carbon disulphide on silica gel. A. B. Lamb and E. N. Ohl, J. Am. Chem. Soc.* **57**, *2154 (1935), give values for the heat of adsorption of carbon disulphide on various substances. Bartell in Coll. Symposium Mon. VII gives 31 cal./g. for the heat of wetting of carbon disulphide on charcoal and silica gel. We have found a further reference in which heat of wetting values ranging from 2.7 to 4.7 cal./g. adsorbent are listed for various hydrocarbons on alumina: A. S. Russell, W. H. Gitzen, J. W. Newsome, R. W. Ricker, V. M. Stowe, H. C. Stumpf, J. R. Wall, and P. Wallace, Alumina properties (Technical Paper No. 10 (Revised), Aluminum Company of America, Pittsburgh, Pa., 1956), p. 42.*

The authors feel, however, that the heat of reaction contributes to a large extent to the total heat measured. In support of this, the following points can be made: (a) When carbon disulphide is passed through a column of alumina, sufficient heat is produced to make the column very noticeably warm to the touch. (b) Since we have found no such noticeable heat produced in our experiments with silica gel (see below), we conclude that the heat of wetting produced in this case is insufficient to make the column warm to the touch. (c) Since carbon disulphide dried over phosphorus pentoxide produces this noticeable heat effect, this excludes the possibility of water in the carbon disulphide. (d) Since wetting and adsorption are physical processes it would be expected that the heats of wetting and adsorption would be produced very rapidly. In our experiments we note that heat was still being produced at the end of 18 hours. This would indicate a slow exothermic chemical reaction taking place in addition. (e) Since this point was brought to our attention by the referee, we have conducted the following additional experiment. When alumina was washed free of alkali and reactivated by heating, a heat effect (to the touch) was no longer produced when carbon disulphide was passed through a column of this alumina. (It was also noted that no yellow color was produced.)

In summary we believe that in addition to the heats of wetting and adsorption, the heat of reaction contributed to a large extent to the total heat produced. Actually we have pointed out that our value is a minimum value since the reaction was still incomplete after 18 hours. Furthermore, it is probable that heat was lost during the time of measurement since our apparatus was not designed for a long period of measurement, as we have pointed out. It should be possible to obtain an estimate for the heat of reaction by measuring the heat of wetting (and adsorption) for alumina washed free of alkali and dried and subtracting this value from the total heat obtained for the alumina before washing. (This assumes that the heats of wetting and adsorption are nearly the same for the two alumina samples.) Since we do not have the equipment necessary to obtain the latter data accurately, however, we are not planning any further work along these lines. We thank the referee for bringing these points to our attention.

Can. J. Chem. Downloaded from www.nrcresearchpress.com by 200.7.193.243 on 09/04/12
For personal use only.

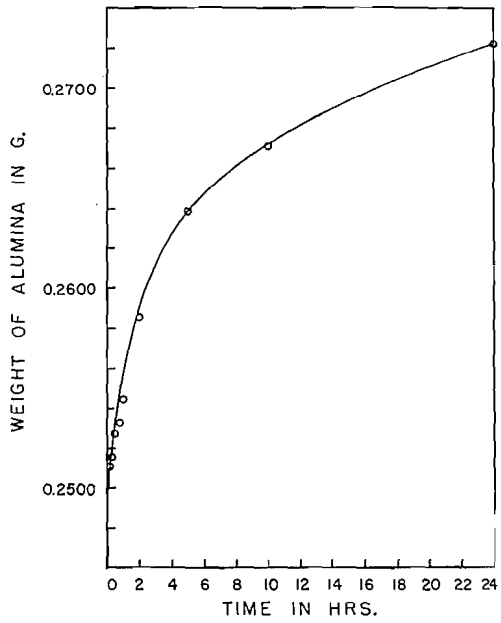

FIG. 3. Gain in weight of alumina on stirring with CS_2 for varying amounts of time using the same CS_2 each time.

experiments was 0.0045 g./0.2500 g. of alumina or 0.1800 g./10 g. of alumina. The saturation value reported by Perry (15) for the *adsorption* of carbon disulphide on alumina gel was 2.96 g./10 g. of alumina. It should be pointed out that in his work he was measuring the increase due to the yellow reaction product plus *adsorbed* carbon disulphide whereas in our work we are measuring mainly the *colorless reaction product*.

Miscellaneous Experiments and Observations

(*a*) When alumina which had been washed with water and dried was shaken with carbon disulphide, no yellow color was formed. This result confirms the previous observations (13). However, after a longer period of contact, the alumina turned a light brown color. This color, however, was not soluble in water, in contrast to the previously mentioned yellow substance, and thus appears to be a different substance. (*b*) When alumina (previously ignited to constant weight) was treated with dry carbon disulphide, no color formed even after they had been in contact for 1 week. This is in accord with the findings of Munro and McCubbin (14), who found that the catalytic activity of their alumina gel decreased to zero at zero water content of the gel. (*c*) The odor of hydrogen sulphide was quite evident from the reaction of alumina and carbon disulphide in agreement with the previous observations (13). (*d*) Silica gel did not form a yellow color with carbon disulphide, and no noticeable heat effect (to the touch) was noted when carbon disulphide was passed through a column of silica gel.

RESULTS AND DISCUSSION

The absorption spectrum for the yellow product of the reaction between alumina and carbon disulphide is shown in Fig. 2 and shows two maxima at 398 and 325 mμ. The curves for sodium disulphide (shown in the same figure) show two shoulders: 360–375 mμ and 290–300 mμ. To our knowledge the absorption spectrum of sodium disulphide below 400

Can. J. Chem. Downloaded from www.nrcresearchpress.com by 200.7.193.243 on 09/04/12
For personal use only.

Can. J. Chem. Downloaded from www.nrcresearchpress.com by 200.7.193.243 on 09/04/12
For personal use only.

mμ has not been previously reported. Recently the curves for potassium disulphide and other polysulphides were reported (12) *above* 400 mμ. However no structure is evident in this region. It is interesting that hydrolysis causes only minor differences in the spectra of the two. We have also noted that the shoulders broaden with dilution for both the basic and water solutions. For example, when the basic solution was diluted to about 0.0006 *M* the shoulder extended from about 360 to 380 mμ. In either case it is evident that these spectra differ markedly from the spectrum of the yellow reaction product from alumina and carbon disulphide. In deference to Munro and McCubbin, it should be pointed out that absorption spectra were not generally available at that time. Evidently the yellow substance must respond to the same chemical tests as sodium disulphide. This observation may be helpful in the elucidation of the nature of this substance.

It is clear from our results and those of Munro and McCubbin that *both* water and sodium hydroxide must be necessarily present in the alumina for the formation of the yellow color. Any mechanism to explain the formation of the yellow color must take these facts into account.

The studies on the gain in weight of the alumina show that equilibrium is approached after more than 24 hours of reaction. This indicates the approximate amount of time needed for a calorimetric study.

We are continuing a study of other possible compounds as the cause of the yellow color in question.

ACKNOWLEDGMENTS

The authors express their appreciation to the Texas Gulf Sulphur Co. for a research fellowship to J. S. K. under which part of this work was done and to the Aluminum Company of America for samples of activated alumina.

REFERENCES

1. ASHIZAWA, T. Repts. Lab. Okayama Univ. No. **5** (1951); Chem. Abstr. **46**, 7927 (1952).
2. BACON, R. F. and BOE, E. S. Ind. Eng. Chem. **37**, 469 (1945).
3. BACON, R. F. and FANELLI, R. Ind. Eng. Chem. **34**, 1043 (1942).
4. DASLER, W. and BAUER, C. D. Ind. Eng. Chem., Anal. Ed. **18**, 52 (1946).
5. FRÉMY, M. E. Compt. rend. **35**, 27 (1852).
6. FRIEDEL, R. A. and ORCHIN, M. Ultraviolet spectra of aromatic compounds. John Wiley & Sons, Inc., New York. 1951. p. 4.
7. HOWALD, R. A. and WILLARD, J. E. J. Am. Chem. Soc. **78**, 6217 (1956).
8. JASPER, J. J. Laboratory methods of physical chemistry. Houghton-Mifflin Co., New York. 1938. p. 163.
9. KIM, J. S. Thesis, Baylor University, Waco, Texas. 1957.
10. LANGE, N. A. Handbook of chemistry. 6th ed. Handbook Publishers, Inc., Sandusky, Ohio. 1946. p. 1103.
11. LENNARTZ, H. J. Angew. Chem. A, **59**, 158 (1947).
12. LEVI, G. R. and RIGANTI, V. Ann. chim. (Rome), **46**, 174 (1956).
13. MUNRO, L. A. and MCCUBBIN, J. W. Can. J. Research, B, **9**, 424 (1933).
14. MUNRO, L. A. and MCCUBBIN, J. W. Trans. Roy. Soc. Can., III, **28**, 29 (1934).
15. PERRY, J. H. J. Phys. Chem. **29**, 1462 (1925).
16. PHILLIPS, F. C. Am. Chem. J. **16**, 345 (1894).
17. RADLE, W. F. and BECK, C. A. J. Chem. Phys. **8**, 507 (1940).
18. RIDDICK, J. A. and TOOPS, E. E., Jr. Organic solvents. 2nd ed. Interscience Publishers, Inc., New York. 1955. (*a*) p. 307, (*b*) pp. 309–315, (*c*) p. 366, (*d*) p. 451.
19. SORENSEN, N. A. Chemist Analyst, **44**, 24 (1955).
20. STOCK, A. and SEELIG, P. Ber. **52**, 672 (1919).
21. WEST, W. *In* Weissberger's Physical methods of organic chemistry. Vol I. Part II. Interscience Publishers, Inc., New York. 1949. p. 1296.

Can. J. Chem. Downloaded from www.nrcresearchpress.com by 61.7.252.67 on 09/04/12
For personal use only.

BLOCK AND GRAFT POLYMERS

I. GRAFT POLYMERS FROM ACRYLAMIDE AND ACRYLONITRILE[1]

M. L. MILLER

ABSTRACT

Graft polymers of acrylonitrile and acrylamide with from 1 to 20 grafts have been prepared by chain transfer to polymer and by photolysis of a copolymer containing a few per cent of α-chloroacrylonitrile. The intrinsic viscosities and softening points have been measured and the dependence of these properties on the number of grafts observed.

I. INTRODUCTION

The properties of homopolymers and, to an even greater extent, those of copolymers can be changed by changing the arrangement of the monomer units in the polymer molecule. This opens up the possibility of preparing polymers with new and improved properties from old monomers and old combinations of monomers.

There are at least three ways in which monomer units A and B can be arranged in a copolymer. These three types of copolymers, random, graft, and block, are illustrated by the schematic diagrams shown below.

...AABABBBABAA...	...AAAAAAAAAA...	...AAAAABBBBBBAA...
	B B	
Random	B B	Block
	B B	
	⋮ ⋮	
	Graft	

It was the object of this series of investigations to prepare block and graft polymers with known lengths and numbers of blocks and grafts and to use these polymers to study the effect of different arrangements of monomer units on some representative physical properties. The monomer pairs chosen for this work were acrylonitrile and acrylamide and acrylic acid and acrylamide. The work falls into two parts, the preparation of the polymers and the study of their properties. This paper describes the preparation and study of graft polymers. The following paper will treat block polymers.

II. EXPERIMENTAL PREPARATION OF GRAFT POLYMERS

Two methods were used to prepare graft copolymers. These methods were: (1) chain transfer to polymer, and (2) photolysis of polymers containing a small amount of copolymerized alpha-chloroacrylonitrile.

Preparation of Graft Copolymers by Chain Transfer to Polymer

In the preparation of graft copolymers by chain transfer, the backbone polymer was dissolved in 65–70% sodium perchlorate, the second monomer added, and the grafting carried out at 55° C. with a persulphate–bisulphite catalyst. Either polyacrylonitrile or polyacrylamide could be used as the backbone polymer.

Sodium perchlorate solution was used as a solvent because it dissolves the graft copolymer and both homopolymers. Furthermore, this solvent is not a chain transfer medium

[1]*Manuscript received August 15, 1957.*
Contribution from the Stamford Laboratories, Research Division, American Cyanamid Company, Stamford, Connecticut. Presented in part before the Seventh Canadian High Polymer Forum, Sarnia, Ontario, Canada, November 8–9, 1956.

and it does not compete with the grafting reaction. A further advantage is the fact that sodium perchlorate, unlike other possible solvent salts, is not attacked by the oxidizing agent in the catalyst.

A typical preparation was as follows: 999 g. of $NaClO_4$ was dissolved in 560 g. of oxygen-free water. Eleven grams of polyacrylonitrile (molecular weight 175,000) and 33 g. of acrylamide were dissolved in this solution and the polymerization carried out at 55° C. under a blanket of CO_2 for 4 hours. 0.28 mole of ammonium persulphate and 0.07 mole of sodium metabisulphite were used as catalyst. The yield was: 20.5 g. graft polymer (containing 50 mole % acrylonitrile and 50 mole % acrylamide), 6 g. of polyacrylamide (recovered from water-solubles after dialysis to remove salts), and no dimethylformamide-soluble polymer.

By this method, polymers with as much as 50 mole per cent of the grafted monomer and with from 1 to 6.5 grafts per molecule were obtained. This method suffered from the disadvantage that excessive amounts of catalyst were required. Nevertheless, a supplementary experiment showed that the backbone polymer, when treated as in a grafting experiment but in the absence of a second monomer, suffered little or no reduction in intrinsic viscosity.

Photolysis of Copolymers of Alpha-Chloroacrylonitrile

The second and preferred method for making graft copolymers was a modification of the method used by M. H. Jones and associates (6, 7, 8). These workers brominated polystyrene to the extent of a few per cent and then photolyzed the partly brominated polystyrene in the presence of methyl methacrylate to make a graft copolymer. In our experiments, we have used for backbone polyacrylonitrile or polyacrylamide which has been copolymerized with one to three mole per cent of alpha-chloroacrylonitrile. Alpha-chloroacrylonitrile is convenient for this purpose because the copolymer containing 1–3% chloroacrylonitrile is stable to storage under ordinary laboratory conditions and to solution in and precipitation from such solvents as concentrated salt solutions and ethylene carbonate. It is less stable in dimethylformamide, but can be handled in this solvent if neutral and if the temperature is kept low. In spite of the relative stability, the presence of the nitrile on the same carbon as the chlorine acts somewhat like a second halogen and sensitizes the copolymer to photolysis (9).

The copolymers of α-chloroacrylonitrile and acrylonitrile were prepared by the following recipe:

76 cc. redistilled methanol
242 cc. oxygen-free water
5.75 cc. catalyst A (17.3 g. ammonium persulphate in 240 cc. water)
2.55 cc. catalyst B (7.68 g. sodium metabisulphite in 240 cc. water)
1.60 cc. catalyst C (0.45 g. $FeCl_3.6H_2O$ in 100 cc. water)
30 cc. acrylonitrile
1.25 cc. α-chloroacrylonitrile (b.p. 87.5–88° C. uncorr., $n_D^{25} = 1.4257$)
200 mg. sodium lauryl sulphate

The mixture was cooled to −10° to −14° C. before monomer or catalyst was added. The mixture was kept at −10° to −14° C. under a blanket of CO_2 for 120 hours. Yield 100%, molecular weight about 50,000.

In a grafting experiment, the polymer containing α-chloroacrylonitrile was dissolved in 66–70% sodium perchlorate or 50% NaSCN, the second monomer added, and the solution photolyzed for 2–4 hours at 25° to 35° C. in a quartz tube under a G.E. Sun Lamp.

Can. J. Chem. Downloaded from www.nrcresearchpress.com by 61.7.252.67 on 09/04/12
For personal use only.

An illustrative experiment used:

0.50 g. polyacrylonitrile (molecular weight 200,000, 1.5% α-chloroacrylonitrile)
50 g. of 70% $NaClO_4$ solution
2 g. acrylamide

Yield: 0.3 g. graft polymer (40 mole % acrylonitrile, 60 mole % acrylamide)
0.0 g. polyacrylonitrile
0.023 g. polyacrylamide (molecular weight 84,000)

Isolation and Characterization of Graft Polymers

After the grafting reaction was completed, the reaction mixture, whether prepared by the first or second procedure, was poured into methanol. The precipitate was extracted alternately and repeatedly with hot water and hot dimethylformamide.

Three or four extractions with each solvent were required. In each extraction, the polymer was intimately dispersed in the extracting medium. During this extraction, some polymer stuck to the glassware or was decanted with solvent. These losses resulted in a lowered over-all recovery of backbone polymer.

The graft polymer was insoluble in both dimethylformamide and water. The dimethylformamide extract contained any free polyacrylonitrile that was present. This extract was concentrated and methanol added to precipitate the polymer. The water extract contained any free polyacrylamide that was present. The water extract was concentrated, dialyzed to remove salt, and freeze-dried. In general, none of the backbone polymer was recovered ungrafted, but there was usually a relatively large amount of the homopolymer of the composition used to make the grafts. The composition of all polymers was determined by infrared examination of thin films. Films of copolymers were cast from dimethylsulphoxide and those of homopolymers from water or dimethylformamide. After evaporation of the solvent, the films were washed three times in boiling methanol and dried 16 hours at 117° C. under vacuum. A preliminary experiment showed that this treatment reduced the solvent content to less than ½%.

Because the object was to prepare graft polymers with well-defined structures, the initial backbone polymers had to be unbranched. For this reason, backbone polymers were prepared by polymerization at 0° C. Since polyacrylonitrile (11) and polyacrylamide (4) have very little branching when prepared at 50° C., polymers prepared at zero degrees can be considered essentially unbranched.

Fractions of these unbranched polymers were used as backbones. Fractions of polyacrylonitrile were prepared by precipitation from dimethylformamide by a mixture of ether and heptane (5) and fractions of polyacrylamide were prepared by precipitation from water by dioxane.

The molecular weight of polyacrylonitrile was estimated from intrinsic viscosity measured in dimethylformamide at 30° C. and calibrated against light scattering data (2, 11). The molecular weight of polyacrylamide was estimated from intrinsic viscosity measured in water at 30° C. and calibrated against molecular weights obtained by light scattering (1) and by sedimentation (13).

The chlorine-containing polymer was sensitive to degradation when attempts were made to fractionate it by the methods used with polyacrylonitrile. Therefore, it was dissolved, at 0° C., in neutral dimethylformamide to give a 1.0% solution. An equal volume of 40% ethanol was added and the clear solution fractionated by spinning in a preparative ultracentrifuge with an iced rotor at 78,000g.

The graft polymers, although insoluble in water and dimethylformamide, dissolved

Can. J. Chem. Downloaded from www.nrcresearchpress.com by 61.7.252.67 on 09/04/12
For personal use only.

readily in dimethylsulphoxide and in concentrated salt solutions. This showed that they were not cross-linked. The polymers gave optically clear films and optically clear concentrated solutions that did not show a two-phase structure when examined visually or by phase contrast microscopy. These facts are evidence that the polymers are graft polymers and not mixtures of homopolymers.

Since none of the backbone polymer was recovered ungrafted, it is evident that all of the polymer initially present has been incorporated in the graft polymer. Therefore, the molecular weight of the backbone in the graft polymer is the same as that of the dead polymer used. On this basis, the molecular weight of the graft polymer was computed from the molecular weight of the backbone polymer and the composition of the graft polymer. If we make the assumption that the molecular weight of the chains that did not become attached is the same as that of the chains that grafted on, then we can calculate the average number of grafts on the backbone chain. This assumption is reasonable and is supported by experiment (8, 10). The graft polymers shown in Table I have been characterized in this way.

TABLE I

SUMMARY OF GRAFT COPOLYMERS

Backbone polymer	Mole % acrylonitrile in graft polymer	Molecular weight of:		Number of branches	Softening point, ° C.
		Graft polymer	Branches		
Polyacrylamide	15–20	185,000	3,800	6.7	162
Polyacrylamide	20	145,000	15–25,000	1–1.5	210
Polyacrylonitrile	25	1,000,000	38,000	21	145
Polyacrylonitrile	40	600,000	84,000	4.8	162
Polyacrylonitrile	50	420,000	38,000	6.3	180
Polyacrylonitrile	50	180,000	38,000	2.7	200
Polyacrylamide	80	640,000	465,000*	1	172

**Does not check with composition.*

III. PROPERTIES OF GRAFT POLYMERS

Intrinsic Viscosity

Intrinsic viscosities were measured in 50% (by weight) aqueous sodium thiocyanate solution at 30° C. This is a solvent for graft copolymers and both homopolymers. Ostwald viscometers with flow times for the blank from 67.5 to 289.4 seconds were used. A kinetic energy correction was applied. Tests for the viscosity slope constant k' (3) were run on the graft polymers that had 2.7 and 6.3 grafts per molecule. Solutions were made up by weight and diluted by weight and the charge was weighed into the viscometer. There was no evidence for a dependence of k' on the number of grafts.

For graft polymers, linear random copolymers, and for polyacrylonitrile k' was 0.34 ± 0.02.

Table II summarizes the viscosity data. This table lists the intrinsic viscosity of the backbone polymer, of the graft polymer, and the intrinsic viscosity calculated for a hypothetical mixture of homopolymers each having the same molecular weight as the graft polymer. It will be noted that in every preparation the intrinsic viscosity of the graft polymer is greater than that of the backbone polymer. This must be true if the preparation has been carried out correctly.

In all but the first sample, the intrinsic viscosity of the graft polymer is less than that calculated for an ideal mixture of homopolymers of the same molecular weight. This is to

Can. J. Chem. Downloaded from www.nrcresearchpress.com by 61.7.252.67 on 09/04/12
For personal use only.

TABLE II

INTRINSIC VISCOSITY OF GRAFT POLYMERS IN 50% SODIUM THIOCYANATE AT 30° C.

Number of branches	Intrinsic viscosity, dl./g.		
		Graft polymer	
	Backbone	Observed	Observed/computed
1	1.35	5.1	1.13
1–1.5	1.10	1.30	0.95
2.7	0.85	1.50	0.63
4.8	2.10	4.3	0.63
6.3	2.00	3.3	0.73
6.7	1.00	1.60	0.68
21	2.10	5.6	0.58

be expected because of the branched structure. It is also to be expected that, as the number of grafts increases, the ratio of observed to computed viscosity will decrease. The last column in the table shows that this is only roughly true.

Softening Points

Softening points were measured as sticking points using a calibrated Parr melting point bar in an atmosphere of dry nitrogen. They were reproducible to ±7° C. The tests were made on films 5 to 10 mils thick that were cast from dimethylsulphoxide. After being dried in a forced draft oven at 110° C., the films were washed in boiling methanol and in boiling acetone and dried in vacuum at 117° C. for 16 hours. After this treatment, the films retained less than ½% of solvent. The films were boiled in acetone and vacuum dried another 16 hours before testing. The observed softening points are shown in Table I. Fig. 1 plots the difference between the observed softening points and a line joining the

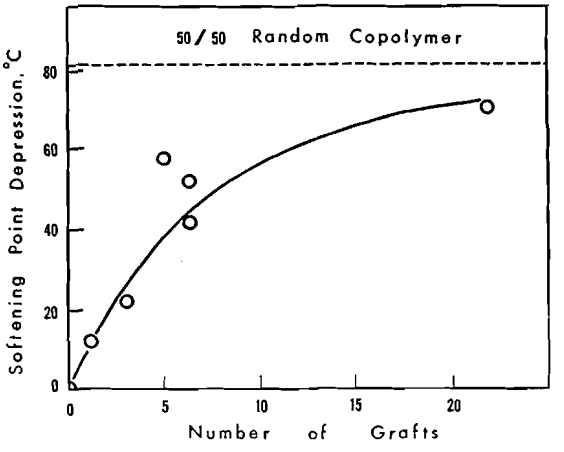

FIG. 1. Dependence of softening point depression on number of grafts.

softening points of the two homopolymers (12) against the number of grafts. Polymer 4 (Table I), for which the number of grafts is subject to some doubt, has been omitted from the figure. As the number of grafts increases, the softening point decreases and approaches, as a limit, the softening point of the 50/50 random copolymer.

Can. J. Chem. Downloaded from www.nrcresearchpress.com by 61.7.252.67 on 09/04/12
For personal use only.

ACKNOWLEDGMENTS

It is a pleasure to thank Messrs. R. Polistina, D. Roemerman, G. Yates, and R. McGrath for assistance with the experimental work and Mr. N. Colthup for the infrared analyses. Dr. R. J. Gaul kindly supplied the α-chloroacrylonitrile.

REFERENCES

1. American Cyanamid Company. New Product Bulletin on Polyacrylamide.
2. CLELAND, R. L. and STOCKMAYER, W. H. J. Polymer Sci. **17**, 473 (1955).
3. CRAGG, L. H. and BROWN, A. T. Can. J. Chem. **30**, 1033 (1952).
4. GLEASON, E. H., MILLER, M. L., and SHEATS, G. F. To be published.
5. HERRENT, P. J. Polymer Sci. **8**, 346 (1952).
6. JONES, M. H., MELVILLE, H. W., and ROBERTSON, W. G. P. Nature, **174**, 78 (1954).
7. JONES, M. H., MELVILLE, H. W., and ROBERTSON, W. G. P. Paper presented at International Symposium on Macromolecular Chemistry, Milan, September, 1954.
8. JONES, M. H. Can. J. Chem. **34**, 948 (1956).
9. MCCLOSKY, C. M. and BOND, J. Ind. Eng. Chem. **47**, 2125 (1955).
10. MERRETT, F. M. and WOOD, R. I. Rubber Chem. and Technol. **29**, 707 (1956), footnote on p. 717.
11. MILLER, M. L., BUTTON, P. A., STAMM, R. F., RAPOPORT, L., and GLEASON, E. H. Paper presented at Meeting-in-Miniature, New York Section of the American Chemical Society, March 16, 1956.
12. MILLER, M. L. Paper II in this series.
13. SCHOLTAN, W. Makromol. Chem. **14**, 169 (1954).

Can. J. Chem. Downloaded from www.nrcresearchpress.com by 61.7.252.67 on 09/04/12
For personal use only.

Can. J. Chem. Downloaded from www.nrcresearchpress.com by 61.7.252.67 on 09/04/12
For personal use only.

BLOCK AND GRAFT POLYMERS

II. BLOCK POLYMERS FROM ACRYLAMIDE AND ACRYLONITRILE AND ACRYLAMIDE AND ACRYLIC ACID[1]

M. L. MILLER

ABSTRACT

Block polymers of acrylamide and acrylonitrile and of acrylamide and acrylic acid have been prepared by photolysis of polymers with end groups that contained bromine. The intrinsic viscosities and softening points of these polymers have been measured and compared with the viscosities and softening points of random copolymers having the same composition and molecular weight.

I. INTRODUCTION

The preceding paper describes the preparation and study of graft polymers of acrylamide and acrylonitrile. This paper is concerned with block polymers of acrylamide–acrylonitrile and acrylamide – acrylic acid.

II. PREPARATION OF POLYMERS

Development of Method

Block polymers were made by a modification of the method devised by Dunn, Stead, and Melville (2). This method uses a polymer with end groups containing bromine to sensitize the photopolymerization of a second monomer. Conditions necessary to make the initial blocks of polyacrylonitrile and the block polymer were worked out on the basis of the following preliminary experiment.

In this experiment, acrylonitrile and mixtures containing equal volumes of acrylonitrile and bromoform or dibromomethane or monobromoethane were sealed in Pyrex tubes. These tubes were partly immersed in ice water and exposed to the light from a G.E. sun lamp, screened by 5 mm. of window glass for 3 hours. The glass was removed and irradiation continued for 3 hours more. The results, shown in Table I, indicate that one bromine

TABLE I

TIME REQUIRED TO POLYMERIZE ACRYLONITRILE WITH DIFFERENT PHOTOSENSITIZERS, HOURS

	Light screened*		Light unscreened†	
Additive	Trace	Thick polymer	Trace	Thick polymer
$CHBr_3$	1	2¾	—	—
CH_2Br_2	>3	Long	½	2¾
C_2H_5Br	>3	Long	2	>3
None	>3	Long	2	>3

*Cutoff 310 mμ.
†Cutoff 290 mμ.

atom is split off from the bromoform with the glass screen in place, but not from the compounds containing only one or two bromine atoms on a single carbon. With the glass removed, bromine is split off from a carbon loaded with two bromines after ½ hour exposure. A bromine atom on a carbon loaded with a single bromine is not touched before

[1]*Manuscript received August 15, 1957.*
Contribution from Stamford Laboratories, Research Division, American Cyanamid Company, Stamford, Connecticut. This paper was presented in part before the Seventh Canadian High Polymer Forum, Sarnia, Ontario, Canada, on November 8–9, 1956.

the blank, containing acrylonitrile alone, starts to polymerize. These are the conditions needed to prepare block polymers.

Preparation of Block Polymers from Acrylonitrile and Acrylamide

The initial blocks of polyacrylonitrile were made as follows. Acrylonitrile and bromoform were mixed in the proportions 25 cc. acrylonitrile to 15 cc. of bromoform. The mixture was sealed in 12 mm. i.d. Pyrex tubes containing approximately 10 cc. each. The tubes were placed in an ice bath with 5 mm. of ordinary window glass $2\frac{1}{2}$ inches above them and a G.E. sun lamp $3\frac{1}{2}$ inches above the glass. The tubes were irradiated in 15-minute exposures (with cooling and mixing between exposures) for a total of 3 hours' exposure. The tubes were opened and the contents poured into methanol. The polymer was washed with methanol three times, then with acetone, and air dried. The molecular weight was estimated from the intrinsic viscosity in dimethylformamide at 30° C. (1, 3). Two preparations by this method had molecular weights of 135,000 and 265,000.

A typical recipe for adding the polyacrylamide block was as follows. Two grams of the polyacrylonitrile (prepared as above) was dissolved in 235 cc. of 50% (by weight) sodium thiocyanate solution (prepared and kept free from oxygen by flushing and blanketing with CO_2). Three grams of acrylamide was added and the solution sealed in Pyrex tubes and exposed to the light from an unscreened sun lamp at 30–50° C. The product was worked up as described for graft polymers (4). Even though the ratio of acrylamide to polyacrylonitrile was varied within relatively wide limits, 2/1, 2/3, 2/5, 2/6, the product always had about the same composition as determined by infrared, i.e., 60 mole per cent nitrile and 40% amide. This is due, apparently, to the fact that the same solvent treatment was used for isolating the product. In one experiment, a small amount of a second block polymer containing 35 mole per cent nitrile and 65 mole per cent amide was isolated as a less soluble portion of the water solubles. Less than a third as much of this was obtained as of the main product. Little or none of the initial polyacrylonitrile block was recovered.

Preparation of Block Polymers from Acrylic Acid and Acrylamide

Blocks of polyacrylic acid were made by essentially the same method as was used for making blocks of polyacrylonitrile. Mixtures of acrylic acid and bromoform (in some experiments diluted with benzene) were irradiated as above but for only $\frac{3}{4}$ to $1\frac{1}{2}$ hours. The contents of the tubes became solid but were entirely soluble in water. After irradiation was finished the tubes were opened and the contents washed into benzene, centrifuged, and rewashed with benzene several times to remove bromoform and monomer. The polymer was dissolved in water and freeze-dried. Its molecular weight was estimated from the intrinsic viscosity measured in dioxane (5). This procedure gave polymers with molecular weights ranging from 145,000 to 540,000.

The polyacrylamide block was added to this polyacrylic acid block by the method previously used to add acrylamide to polyacrylonitrile. In an illustrative preparation, approximately $\frac{2}{3}$ of a gram of the undried or freeze-dried polyacrylic acid with end groups which contained bromine was dissolved in 100 cc. of oxygen-free water under a blanket of carbon dioxide. Two grams of acrylamide was added and the solution was sealed in tubes and irradiated by an unscreened sun lamp. Irradiation was carried out at 25° to 35° C. for 2 hours. The contents of the tubes were poured into 500 cc. of dioxane and extracted twice with hot dioxane. The flow sheet, Fig. 1, shows the work-up of the product. The over-all recovery of initial polyacid was about 40% and the ungrafted acid was 25% of the starting polyacid block.

Can. J. Chem. Downloaded from www.nrcresearchpress.com by 61.7.252.67 on 09/04/12
For personal use only.

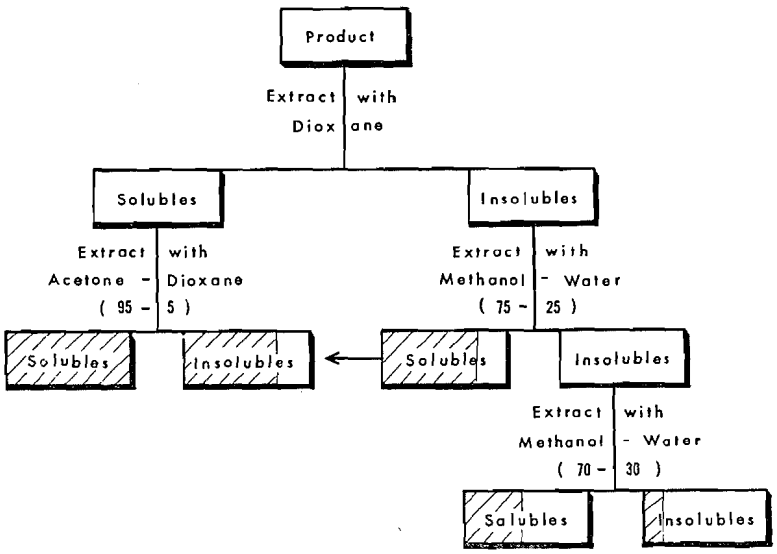

FIG. 1. Separation of block polymers of acrylic acid and acrylamide from reaction mixture. Shaded areas represent per cent of fraction that is acrylic acid.

Discussion of Preparation

In the first step, irradiation caused the photodecomposition of the bromoform,

$$\underset{}{CHBr_3} + h\nu \rightarrow \underset{(1)}{CHBr_2^{\bullet}} + \underset{(2)}{Br^{\bullet}}$$

Each of these radicals, (1) and (2), can initiate polymerization to give polymeric radicals (3) and (4):

$$\underset{(3)}{CHBr_2\text{----}^{\bullet}} \text{ and } \underset{(4)}{Br\text{----}^{\bullet}}$$

These four types of radicals can terminate by combination with one another, by disproportionation, or by chain transfer to solvent or to monomer. Although initially there are approximately equal numbers of moles of acrylonitrile and bromoform, the amount of acrylonitrile decreases very rapidly as polymerization proceeds. Thus, it is reasonable to assume that, for the bulk of the reaction, termination is by chain transfer to solvent. This mode of termination would produce two types of polymer molecules (*a*) and (*b*), i.e.,

$$CHBr_2\text{----}^{\bullet} + CHBr_3 \rightarrow \underset{(a)}{CHBr_2\text{----}Br} + CHBr_2^{\bullet}$$

$$Br\text{----}^{\bullet} + CHBr_3 \rightarrow \underset{(b)}{Br\text{----}Br} + CHBr_2^{\bullet}$$

This process would also result in the liberation of a free radical which could, in turn, initiate other chains so that the reaction could, and probably does, become autocatalytic. Molecules of type (*b*) will be unaffected by further irradiation and will be isolated as unchanged polyacrylonitrile in the work-up of the product. Molecules of type (*a*), when photolyzed, will add on acrylamide to form block polymer. These polyradicals could terminate by (1) combination with one another, (2) combination with $Br^{\bullet}$, or (3) disproportionation. Except where termination is by combination of radicals, all block polymers will consist of two blocks:

$$Br\text{----}CHBr\text{----}X$$

Can. J. Chem. Downloaded from www.nrcresearchpress.com by 61.7.252.67 on 09/04/12
For personal use only.

Here X is either Br or double bond. If there is a significant amount of combination of radicals of type (*b*) with one another, there will be polymer molecules made up of three blocks. More complex molecules are possible, but they are less probable.

III. RESULTS

Block Polymers Containing Acrylonitrile and Acrylamide

Table II summarizes the block polymers of acrylonitrile and acrylamide that have been prepared. Column 1 gives the mole per cent of nitrile, measured by infrared; column 2 the molecular weight of the block polymer as computed from the molecular weight of the initial block and the composition of the polymer; columns 3 and 4 give the intrinsic viscosity in 50% sodium thiocyanate as measured and as computed for a hypothetical mixture of homopolymers each having the same total molecular weight as the block polymer. It is seen that, except in one instance where the molecular weight is very high, the computed viscosity is in good agreement with the observed.

TABLE II

BLOCK POLYMERS FROM ACRYLONITRILE AND ACRYLAMIDE

Mole % of acrylonitrile	Molecular weight $\times 10^{-3}$	Intrinsic viscosity in 50% NaSCN at 30° C., dl./g.	
		Observed	Computed
66	196	—	
63	360	—	
60	257	2.15	2.19
62	250	2.25	2.22
60	500	—	
35	935	—	
60–65	478	3.34	3.45
70–80	276	2.75	2.71
50	620	5.2	4.0

Block Polymers Containing Acrylic Acid and Acrylamide

Table III describes two block polymers of acrylamide and acrylic acid. The molecular weight of these polymers was estimated in two ways, both of which are approximations.

In the first method the polymers were hydrolyzed until the hydrolysis stopped. The viscosity of this hydrolysis product was measured in 1 *N* NaOH and the corresponding molecular weights read from a plot of molecular weight vs. viscosity for random copolymers of the same acid contents.

TABLE III

INTRINSIC VISCOSITIES OF BLOCK POLYMERS FROM ACRYLIC ACID AND ACRYLAMIDE

Fraction No.	Acid	Molecular weight ($\times 10^{-3}$) by:		Intrinsic viscosity, dl./g.		
		Hydrolysis	Computation	Observed	Computed	Of random polymer
2	75	310	366	1.60	1.55	2.30
3	45	637	610	2.50	2.45	3.80

In the second method the molecular weight was computed from the composition of the copolymer on the assumption that the initial block of acrylic acid has not been fractionated by the processing of the mixture containing the graft polymer. The agreement of the molecular weights by the two methods is good. Columns 3 and 4 in Table III compare

Can. J. Chem. Downloaded from www.nrcresearchpress.com by 61.7.252.67 on 09/04/12
For personal use only.

the intrinsic viscosities measured in 1 *N* sodium nitrate, after neutralization, and the intrinsic viscosities computed for a hypothetical mixture of homopolymers each having the same molecular weight as the block polymer. The agreement between the observed and computed values is good.

This agreement between observed and computed viscosities for block polymers (with two or three blocks) is to be contrasted with the intrinsic viscosity of linear random copolymers. In general it is not possible to estimate the intrinsic viscosity of a linear random copolymer from measurements of the viscosity of homopolymers made from the two comonomers that were used to prepare the random polymer.

This unpredictability is illustrated by the data in column 7 of Table III which gives the intrinsic viscosity of linear random copolymers of acrylic acid and acrylamide that have the same composition and molecular weight as the block polymers. These viscosities are far greater than the computed viscosities or the viscosities of the block copolymers.

IV. PROPERTIES OF BLOCK POLYMERS

General

The properties of random copolymers from two monomers usually pass through a maximum or a minimum as the composition is changed from 100% of one comonomer to 100% of the other. If, however, the copolymer contains one long graft or, better yet, two or three long blocks the value of a given property should be very close to the value computed for a hypothetical mixture of two homopolymers each having a molecular weight equal to that of the block polymer as a whole. Preceding measurements have shown that this is true for intrinsic viscosity. It is of interest to examine the validity of this mixture rule for block copolymers with some other properties. This has been done for softening points of acrylonitrile–acrylamide copolymers and for acid dissociation constants for acrylic acid – acrylamide copolymers. The work on dissociation constants will form the subject of the third paper in this series.

Softening Points

Softening points of the copolymers of acrylamide and acrylonitrile were measured as

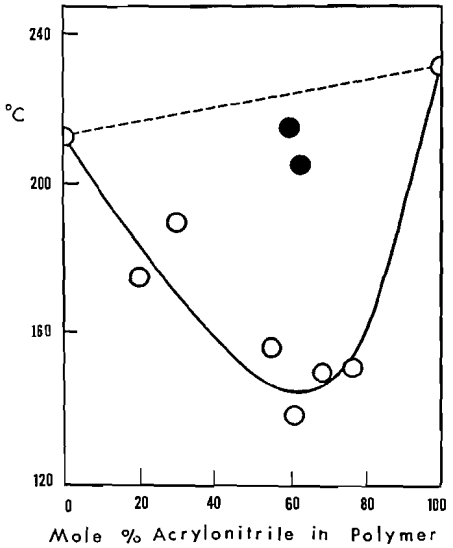

FIG. 2. Softening point of random and block copolymers of acrylamide and acrylonitrile; ○—random copolymers, ●—block copolymers.

Can. J. Chem. Downloaded from www.nrcresearchpress.com by 61.7.252.67 on 09/04/12
For personal use only.

sticking points of films using a calibrated Parr melting point bar in an atmosphere of dry nitrogen. The measurements were reproducible to ±7° C. They are to be regarded as empirical values useful for comparison. The tests were made on films 5 to 10 mils thick that were cast from dimethylsulphoxide. After being dried in a forced draft oven at 110° C., the films were washed in boiling methanol and in boiling acetone and vacuum dried at 117° C. for 16 hours. After repetition of this treatment, the films retained less than ½% of solvent. Fig. 2 plots the softening point of random copolymers of acrylonitrile and acrylamide against mole per cent of acrylonitrile. Open circles designate random copolymers and filled circles block polymers. It is seen that the softening point of random copolymers falls off very sharply as the composition is changed from 100% of one comonomer to 100% of the other. For block polymers, the softening points are very close to a line joining the softening points of the two homopolymers.

CONCLUSIONS

These experiments have shown that the softening points and intrinsic viscosities of block polymers having two or three long blocks can be computed from the corresponding properties of the homopolymers. This can be done also as a first approximation for graft polymers with only one graft (4). As the number of grafts increases, the deviations from the expected values become greater as a result of the branched structure and the increased heterogeneity.

ACKNOWLEDGMENTS

It is a pleasure to thank Miss C. A. Ederle, Mr. R. M. McGrath, and Mr. R. Polistina for assistance with the experimental work and Miss E. C. Eberling for the infrared analyses.

REFERENCES

1. CLELAND, R. L. and STOCKMAYER, W. H. J. Polymer Sci. **17**, 473 (1955).
2. DUNN, A. S., STEAD, B. D., and MELVILLE, H. W. Trans. Faraday Soc. **50**, 279 (1954).
3. MILLER, M. L., BUTTON, P. A., STAMM, R. F., RAPOPORT, L., and GLEASON, E. H. Paper presented at Meeting-in-Miniature, New York Section of the American Chemical Society, March 16, 1956.
4. MILLER, M. L. Can. J. Chem. **36**, 303 (1958).
5. NEWMAN, S., KRIGBAUM, W. R., LAUGIER, C., and FLORY, P. J. J. Polymer Sci. **14**, 451 (1954).

Can. J. Chem. Downloaded from www.nrcresearchpress.com by 61.7.252.67 on 09/04/12
For personal use only.

Can. J. Chem. Downloaded from www.nrcresearchpress.com by 200.7.193.243 on 09/04/12
For personal use only.

A MODIFICATION OF THE DIRECT CURRENT CONDUCTANCE METHOD[1]

G. D. GRAHAM AND O. MAASS

ABSTRACT

A modification in the employment of the direct current method of measuring conductivities is described. The main objective is that pure metallic probe and current carrying electrodes can be used, thus making it possible to investigate the conductivity of solutions such as hydrogen peroxide, aqua regia, etc. This necessitates a choice of electrodes which are inert to such solutions. An electrometer having an infinite resistance so as to avoid any polarization at the probes, in this case the quadrant electrometer, is described in its use as a null instrument. An accuracy as high as or greater than that of the alternating current method could be obtained. Furthermore, this method entails greater equipment economy and simplicity in apparatus required.

INTRODUCTION

In the measurement of electrolytic conductivity in water and other solvents, two main methods have been used, the alternating current method, the more common one, in which polarization is compensated for depending on frequency, capacity, and inductance, and the direct current method in which the so-called probe electrodes (as will be explained later on) bring in experimental hazards. It has been shown by Gordon (5) and co-workers that the direct current method with the experimental setup he devised will give the same accuracy in measurements that the alternating current method gives. Previous to Gordon, a number of other workers (1, 2, 3, 8) had used the direct current method, and since Gordon's publication others have substantiated his find, among them Schiff (4), Lim (7), and Ives (6).

In planning a number of investigations of electrolytic conductivity of certain systems, hydrogen peroxide solutions, so-called aqua regia solutions, and in general to make use of the direct current method, it was thought that it would be desirable to have pure metallic probe electrodes and current carrying electrodes all made of the same pure metal. For hydrogen peroxide solutions, electrodes of pure tin, which does not cause any decomposition of hydrogen peroxide, are the best to use. For aqua regia, tungsten electrodes are the best and also for every purpose in which conductivities are measured; the nature of the material of the electrodes would not diminish the accuracy of the results obtained by using the direct current method. Furthermore, the direct current method, as used by others and with certain simplifications described below, makes it possible to determine accurate conductivity data over the range of conductivities from pure solvents to highly conducting solutions without the financial expenditures for instrumentation involved in the alternating current method.

EXPERIMENTAL

As indicated above, in the direct current method, polarization of the probe electrodes has to be minimized. In this, a great deal depends on the nature of the instrument used to measure the ratio of the voltages of the electrolytic cell and the metallic resistance in series with it. If the voltage measuring instrument is to be used as an absolute one, a potentiometer will give accurate measurements but this entails having the probe electrodes of such a nature that no variable polarization will occur during the course

[1]*Manuscript received July 12, 1957.*
Contribution from the Division of Pure Chemistry, National Research Council, Ottawa, Canada.
Issued as N.R.C. No. 4583.

of the measurement. The choice of an electrometer which has an infinite resistance will have a determining advantage, as no polarization of the probe electrodes can occur owing to the infinite resistance of this electrometer. The employment of the obsolescent quadrant electrometer, which was used as a first choice of this type of instrument, is described in some detail. There the four metallic electrodes can be used.

Before going on to a detailed description of this electrometer it might be well to discuss the probe metallic electrodes. As indicated, tin electrodes were considered to be of considerable interest. When these were made by molding pure tin metal in wooden molds they were found to show an insignificant difference of potential when immersed in an aqueous solution of an electrolyte; small as this potential was it also showed no measurable variation with time and concentration of electrolyte. This potential difference, as will be elaborated on later, did not affect experimental observations. With platinum electrodes made out of foil or wire this difference in potential between two such electrodes immersed in a solution of an electrolyte was measurably large (0.1 volt), and was variable to the extent of 0.01 volt under certain experimental conditions; as the over-all voltage on the electrometer was 20 volts, the variation of 0.01 volt meant the accuracy would only be 1 part in 2000. However, if instead of platinum electrodes, platinum black electrodes are used, the difference of potential between two such electrodes in a solution containing an electrolyte is very much less, and therefore any variation in the accuracy attained is diminished. The same concept applies to any other electrodes that are used inasmuch as the probe electrodes must be made as uniform as possible, physically and chemically. Sample data for tin and platinum black electrodes are given after the description of the use of the quadrant electrometer as the measuring instrument in the direct current method.

The quadrant electrometer was originally designed as an instrument for the direct measurement of voltages and it must be kept in mind that in this work the quadrant electrometer is used as a null instrument comparing equal voltages. It then becomes an instrument giving a very high degree of precision, with which an accuracy of 1 in 10,000 can be obtained under our experimental conditions when the over-all voltage measured is 20 volts, which can be considerably enhanced with higher voltages. In using the quadrant electrometer to attain such accuracy it is important that measurements be made quickly to avoid drift owing to external electrostatic charge environment and to avoid any hysteresis effect in the suspension of the electrometer should it be subjected to sudden major changes. To countervene these effects a setup was arranged in such a way that the voltage on the electrometer was maintained continuously, except for the fractional second interval in which a double pole switch was manipulated so that small changes in the metallic resistance could be made. These only affected slightly the needle position as reflected on the scale, and were made to bring the null point register of the cell and the resistance box together.

Now for a detailed description of the experimental outlay. Referring to Fig. 1, the resistance R_1 is adjusted until it equals the cell resistance and the electrometer reading does not change when the alternating switch D is placed across the probe electrodes A,A of the cell or the resistance R_1.

An image from a Leeds and Northrup galvanometer lamp was focused on the electrometer, which was set up on a Julius suspension. The image was in turn projected onto a scale calibrated in millimeters placed 4 meters from the electrometer. A telescope was focused on this image making possible a detection of 1 part in 10,000 when a 45-volt dry cell was used in the circuit giving approximately 20 volts across the electrometer.

The electrolytic cell was placed in a water bath, the temperature of which was con-

Can. J. Chem. Downloaded from www.nrcresearchpress.com by 200.7.193.243 on 09/04/12
For personal use only.

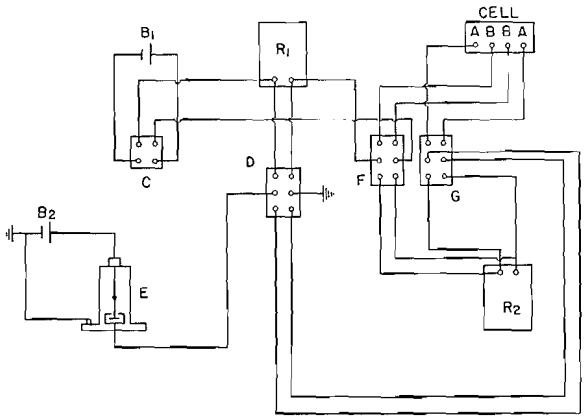

FIG. 1.

trolled to 1/100° C., and the electrodes A,A and B,B were connected. The current flowing from dry cell B_1 through switch C and resistance R_1 passes through the cell. The measurements are then made by alternating switch D from the cell side (probe electrodes A,A) to the resistance R_1 side, and then obtaining a null position on the scale by varying resistance R_1.

The simplest way of maintaining the voltage on the electrometer, and thus maintaining the image on the screen, would be to have a continuous passage of the current through the circuit including the cell. With time, electrolysis would take place owing to this continuous passage of current, although it is greatly reduced by the design of the cell (shown later). To eliminate this, switches F and G are employed, which are double pole, double throw switches connected together and reversed simultaneously. Resistance R_2 is adjusted to the cell resistance and when switches F and G are reversed the current by-passes the cell through resistance R_2. By this means the current passes through the cell only during the time when measurements are being made, which is of the order of less than 1 minute. The voltage is maintained at any time on the electrometer within the fractional second of alternating switches F and G. This makes the quadrant electrometer, with all its disposition to take up vagrant electrostatic voltages, a null instrument of the high degree of accuracy outlined above.

When the sensitivity of the electrometer is arranged to measure a variation of 1 part in 10,000, it is important that no variation in voltage occurs in the circuit during the time required for making measurements. During this time interval it was proved that the voltage of the dry cell remained constant. There remains the question of any inherent voltage between the probe electrodes, which would not affect the measurements, if it remained constant; and as was pointed out previously between tin electrodes prepared as described and between platinum black electrodes, such voltages are insignificant, and therefore no variation could be expected or was found.

Two platinum, tin, or tungsten probe electrodes when freshly cut exhibited a difference of potential in an electrolytic solution and were variable with time and external conditions; where such probes are used the accuracy of conductivity measurements may be reduced to 1 part in 500 under extreme conditions. Platinum electrodes can also be molded and would probably be as effective as molded tin. With tungsten this cannot be done, but still for most purposes where the nature of the electrolyte requires tungsten (aqua regia solutions) a sufficient degree of accuracy for the purpose of the measurements can be obtained.

Can. J. Chem. Downloaded from www.nrcresearchpress.com by 200.7.193.243 on 09/04/12
For personal use only.

Can. J. Chem. Downloaded from www.nrcresearchpress.com by 200.7.193.243 on 09/04/12
For personal use only.

CELL

In Fig. 2 the design of the cell is shown. A,A are the probe electrodes and B,B are the current carrying electrodes, all of which are made of pure tin as previously described, or of platinum black (not shown in the diagram). In this arrangement advantage is taken of the work of Ives (6) to ensure that the physical position of the probe electrodes will not affect the cell constant. The bulbs C,C below the current carrying electrodes are to ensure that any slight change in concentration due to electrolysis around the current carrying electrodes would not permeate into the main body of the cell where the conductivity is being measured. In this connection it may be recorded that it was found that over a period of 5 minutes during which a continuous current was passed through the cell, no measurable changes in resistance due to such electrolysis were found to occur. This time factor is very much below that which is involved in making our measurements.

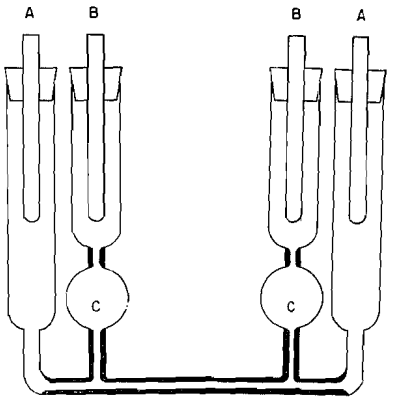

FIG. 2.

PREPARATION OF SOLUTIONS

Three solutions, 0.1, 0.05, and 0.01 *N* in potassium chloride, were made up by volume using reagent grade potassium chloride and taking all the experimental precautions which are normally taken to ensure the accuracy of the concentration. Corrections for temperature and volume showed that the solutions used had actual concentrations of 0.09990, 0.049950, and 0.009990 *N* potassium chloride. The data for aqueous potassium chloride conductivity have been well established by Shedlovsky (9) and the cell constants were calculated in the usual way using these data.

RESULTS

When the quadrant electrometer system, as outlined above, was used to measure a known metallic resistance in place of the electrolytic cell, an absolute accuracy of 1 part in 10,000 was obtained over a considerable range of resistance. The test consisted of having someone set the resistance box (replacing the cell) at a definite resistance and then having the observer make a measurement. At first, some difficulty was encountered in attaining this degree of accuracy when the electrolytic cell (replacing the metallic resistance) was measured. However, when the probe electrodes were conditioned as described, the same degree of accuracy was attained as in the measurement of the metallic resistance. It now remains to tabulate a sample set of experimental observations, which

confirm the claim that the particular experimental procedure involving probe and current carrying electrodes made of any desired material will give results to a high degree of accuracy.

In Table I are given the data which have been corrected for the conductivity of the solvent (water). This was measured conveniently by the direct current method employing a cell having a very much lower cell constant than the one used in this work. This was accomplished by using a glass tube between the probe electrodes 50 times larger in diameter than the one illustrated in Fig. 2, which was 2-millimeter capillary tubing.

It can be seen that with tin electrodes an accuracy of 1 part in 7000 and with platinum black electrodes of 1 part in 5000 was attained.

TABLE I

c	*R*	*R* average	*K*	*K* average
		Tin probes		
0.09990	27,644 27,644 27,643	27,644	356.10	
0.049950	53,445 53,443 53,446	53,445	356.08	356.10
0.009990	251,810 251,815 251,810	251,808	356.13	
		Platinum black probes		
0.09990	27,633 27,633 27,633	27,633	355.99	
0.049950	53,435 53,433 53,433	53,433	356.00	356.02
0.009990	251,655 251,650 251,650	251,652	356.06	

c—*Concentration.*
R—*Resistance.*
K—*Cell constant.*

DISCUSSION

The authors believe that an even higher degree of accuracy by the method described can be obtained if more accurate measurements are made of the conductivity of the solvent. This conductivity depends on the time that the electrolytic solution used as a standard is in contact with glass containers. A teflon cell can and has been used in certain experiments, and it is considered that if the standards are made up in teflon containers it will be possible to get reproducible results to even better than 1 part in 10,000. Taking the 0.09990 and the 0.049950 *N* solutions as in Table I, it is seen that a very high degree of relative accuracy is attained.

The accuracy required by the investigator is dependent on the fact that an accurate determination of the solvent conductivity will be of greater importance when solutions of 0.009990 *N* are used.

Can. J. Chem. Downloaded from www.nrcresearchpress.com by 200.7.193.243 on 09/04/12
For personal use only.

Instead of using a quadrant electrometer, which embodies the requirement of having an infinite resistance, a more simple device can be used. This consists of a charged metallic fiber subject to displacement between two electrodes leading to alternately the probe electrodes and the metallic resistance in series. The first electrometer of this nature showed it was possible to make null measurements giving an accuracy of 1 part in 1000. It is considered that this accuracy can be considerably enhanced by changing the dimensions involved in this instrument, and a study of this is underway.

REFERENCES

1. ANDREWS, L. V. and MARTIN, W. E. J. Am. Chem. Soc. **60**, 871 (1938).
2. BRONSTEAD, J. N. and NIELSEN, R. F. Trans. Faraday Soc. **31**, 1478 (1935).
3. EASTMAN, E. D. J. Am. Chem. Soc. **42**, 1648 (1920).
4. ELIAS, L. and SCHIFF, H. I. J. Phys. Chem. **60**, 595 (1956).
5. GUNNING, H. E. and GORDON, A. R. J. Chem. Phys. **10**, 126 (1942).
6. IVES, D. J. G. and SWARPOOPA, S. Trans. Faraday Soc. **49**, 788 (1953).
7. LIM, H. H. Australian J. Chem. **9**, 443 (1956).
8. NEWBERRY, E. J. Chem. Soc. **113**, 701 (1918).
9. SHEDLOVSKY, T. J. Am. Chem. Soc. **54**, 1411 (1932).

Can. J. Chem. Downloaded from www.nrcresearchpress.com by 200.7.193.243 on 09/04/12
For personal use only.

Can. J. Chem. Downloaded from www.nrcresearchpress.com by 61.7.252.67 on 09/04/12
For personal use only.

THE PHOTOLYSIS OF METHYL CYANIDE AT 1849 Å[1]

D. E. McElcheran,[2] M. H. J. Wijnen,[3] and E. W. R. Steacie

ABSTRACT

The photolysis of MeCN has been investigated under a considerable range of conditions and a mechanism proposed which accounts satisfactorily for the products found, viz. H_2, HCN, C_2N_2, CH_4, C_2H_6, C_2H_5CN. Two primary processes occur

$$CH_3CN \rightarrow H + CH_2CN$$
$$CH_3CN \rightarrow CH_3 + CN$$

of which the former is apparently the more important. HCN is formed predominantly by an H atom abstraction of the CN group which is believed to occur through addition to the unsaturated bond with the formation of an unstable imine radical. This and similar intermediates formed by other radicals are proposed to account for several anomalies found in the photochemistry of nitriles.

A brief investigation of the photolysis of carbonyl cyanide is reported.

INTRODUCTION

The photochemistry of the nitriles has received very little attention, undoubtedly because the nitriles are generally transparent well into the Schumann region. Certainly no direct photolysis of a nitrile has been reported previously in the literature beyond a simple spectrographic investigation of MeCN and EtCN by Terenin and Neujmin (1), who established the presence of excited CN radicals in the far ultraviolet photolysis of these molecules and concluded that excitation is followed by dissociation of the carbon–carbon bond. The possibility of a system of CN reactions parallel to those of CH_3 in which HCN and C_2N_2 would be formed in an analogous manner to the well-known methane- and ethane-forming reactions of CH_3 was of considerable interest when we undertook the present work. In view of the unsaturated nature of the CN group this conjecture was quite unjustified and the reaction proved to be considerably more complex and unusual.

EXPERIMENTAL

The ultraviolet absorption of MeCN lies entirely within the Schumann region. The 1849 Å mercury resonance line roughly coincides with the long-wave edge of a band which occurs between 1600 Å and 1800 Å (Platt and Klevens (2)). Although this marginal absorption is unfortunately weak, the mercury arc conveniently compensates by providing a relatively intense light source. The decisive advantage of the mercury arc, however, proved to be the reasonably high transparency of fused quartz to 1849 Å, which allowed the use of a conventional quartz cell; this is an important consideration because of the accumulation of polymer in the MeCN photolysis. The only effective method of removing this obscuring deposit was by heating the cell to red heat in the presence of oxygen.

The use of the 6^1P_1 mercury resonance line, of course, necessitates the complete absence of mercury vapor from the reaction cell, and a mercury-free system employing an oil

[1]*Manuscript received in original form July 27, 1956, and, as revised, September 17, 1957.*
Contribution from the Division of Pure Chemistry, National Research Council, Ottawa, Canada.
Issued as N.R.C. No. 4584.

[2]*National Research Council Postdoctorate Fellow 1954–56. Present address: Department of Physics, Laval University, Quebec.*

[3]*Present address: Celanese Corporation of America, Clarkwood, Texas.*

diffusion pump backed by a previously unused Welsh Duoseal pump was provided for the reagents and cell. The problem of transferring the reaction products to the analysis train, a separate mercury-containing vacuum system, was solved very satisfactorily by bridging the two lines with a small single-stage diffusion pump operating continuously with stable, inert Dow 703 silicone oil. The effectiveness of this arrangement in preventing back-diffusion of mercury vapor and the subsequent contamination of the reaction system was variously proved. At regular intervals both ethane and MeCN were illuminated with the 2537 Å resonance line using a Corning 7910 filter to cut off 1849 Å; at no time during the investigation was the mercury-photosensitized production of H_2 detected even after an illumination period of several days. The efficiency of the transfer diffusion pump in preventing back-diffusion was exhibited more directly, perhaps, by the complete lack of absorption of 1849 Å in the evacuated cell when the bridge section between the cell and the mercury system was opened. It should be emphasized that such drastic measures are necessary if a mercury-free system is to be obtained. The conventional use of gold foil as a mercury trap is almost totally ineffective. It is our experience that if mercury vapor has ever entered a vacuum system it can never be completely removed.

The reaction cell was the usual cylindrical quartz vessel, 15 cm. long and 252 cc. volume, mounted centrally in a split aluminum block furnace and attached to the vacuum line through a quartz–pyrex graded seal. A low pressure mercury arc, shaped into a flat spiral of somewhat greater diameter than the cell, was sealed into one end of the furnace with a solid plug of asbestos so that maximum intensity could be obtained by operating in a stream of nitrogen (to avoid absorption by oxygen). For this purpose, liquid nitrogen was boiled at a controlled rate from a 3-liter Dewar flask by an immersion heater. The cool gas was introduced into the furnace from behind the lamp, cooling it and incidentally helping to balance the temperature gradient caused by the lamp. The 1849 Å intensity is increased in this way by as much as a factor of 10, perhaps partly because of the efficiency peak of this type of lamp at about 55° C. Collimation was impracticable and for optimum operating conditions the lamp was spaced about 5 cm. from the cell window. The cell temperature, controlled through a 10-amp. Variac auto transformer operating from a Sorensen voltage stabilizer, was uniform to within 2° and stable to ±2° over long periods of time. Cell pressures were measured by a null point quartz spiral manometer with a mercury manometer reference accurate to ±0.5 mm.

The analytical line consisted of mercury cutoffs throughout with the exception of the bridge connection from the reaction cell which was isolated by a stopcock and led directly into a U-trap, which in practice was cooled with liquid nitrogen whenever the bridge stopcock was open, although it was shown that the oil diffusion pump was effective by itself in preventing mercury from diffusing into the mercury-free line. Two Leroy stills and a solid nitrogen trap followed the U-trap to effect fractional distillation of the products, which were pumped into the gas burette by a small two-stage mercury diffusion pump. The burette, which was stopcock-free, could be evacuated through cutoffs by either of two Töpler pumps, one for cycling the products through hot CuO and the other for filling sample tubes for mass spectrometric analysis. The CuO was maintained at 570° C. in a fused silica U-tube in order to oxidize methane to CO_2. At this temperature the methane oxidation rate was very slow, taking 12 hours to effect completion, while hydrogen was almost instantaneously oxidized with negligible attack on methane. This procedure permitted the convenient analysis of a mixture of H_2, CH_4, and N_2 with high accuracy as proved by standard mixtures. Dead space was kept to a minimum by using capillary tubing for the U-trap and connecting tubing. Higher CuO temperatures must be avoided to prevent O_2 production.

Can. J. Chem. Downloaded from www.nrcresearchpress.com by 61.7.252.67 on 09/04/12
For personal use only.

Methyl cyanide was treated with KOH to remove traces of HCN, distilled into the mercury-free line through P_2O_5, the middle third being preserved in a stopcocked reservoir, and thoroughly outgassed. A clean mass spectrum was obtained, but as a further precaution a sample of the MeCN was fractionated from a Leroy still into three samples which were compared on the mass spectrometer; no significant difference in the three spectra was observed.

The runs were carried out with maximum light intensity rather than constant absorbed intensity, since the intensity was generally so low that illumination periods ranged from 4 to 20 hours. Even in the longest runs less than 5% conversion of MeCN occurred. The gaseous products were identified by the mass spectrometer as HCN, C_2H_5CN, H_2, C_2N_2, CH_4, and C_2H_6 with traces of C_2H_2, C_2H_4, and C_3H_8. Of other possible products, N_2 and NH_3 were specifically sought but never detected within our range of conditions.

The products were separated by low temperature fractionation into three distinct fractions:

(1) H_2 and CH_4 were collected as the volatile fraction at $-210°$ C. and subsequently analyzed by CuO at 570° C. at which temperature H_2 was oxidized and determined by difference in a single pass. CH_4 was determined as CO_2 after 12 hours in contact with CuO as a check against the presence of N_2. The CO_2 invariably reproduced the CH_4 measurement to within 0.5%; N_2 was not observed.

TABLE I

Press., mm.	Temp., ° K.	$[CH_3CN]$, $\times 10^{-18}$ molecules per cc.	R_{CH_4}	R_{H_2}	$R_{C_2H_6}$	R_{HCN}	$R_{C_2N_2}$	$\frac{R_{H_2}}{R_{HCN}}$	$\frac{R_{C_2N_2}}{R_{HCN}}$	$\frac{R_{CH_4}}{R^{\frac{1}{2}}_{C_2H_6}[MeCN]}$, $\times 10^{14}$ molecules$^{-\frac{1}{2}}$ cc.$^{-\frac{1}{2}}$ sec.$^{\frac{1}{2}}$
			$\times 10^{-10}$ molecules/cc./sec.							
23.0	332	0.668	1.225	1.440	3.24	9.65	0.885	0.127	0.092	10.2
63.0	332	1.830	3.88	3.50	7.00	24.1	2.78	0.145	0.115	8.02
111.3	332	3.25	7.39	5.61	9.84	33.1	2.25	0.224	0.083	7.23
107.2*	332	3.12	1.12		0.714					3.04
194.7	332	5.65	12.50	8.20	11.75	39.9		0.205		6.45
26.5	373	0.686	2.60	2.25	2.23	16.9	0.54	0.133	0.032	25.4
47.0	371	1.22	6.27	3.80	6.06	27.6	1.98	0.137	0.072	20.9
61.8	369	1.62	8.52	5.20	7.31	39.2	4.50	0.133	0.115	19.4
79.2	369	2.07	11.52	6.44	8.86	47.2	4.50	0.136	0.096	18.7
105.0	375	2.705	16.00	6.92	9.03	52.1	5.13	0.133	0.099	19.6
26.2	477	0.530	13.68	2.49	1.775					194
35.1	474	0.716	24.05	4.85	2.38	44.1	4.61	0.110	0.104	218
43.4	473	0.885	34.2	6.16	4.00	63.0	6.43	0.098	0.102	193
50.5	474	1.030	41.3	7.64	4.18	66.8	7.69	0.114	0.115	201
81.0	473	1.653	67.9	11.44	5.74					171
104.0	474	2.12	82.1	13.3	6.47					153
39.0	458	0.823	23.1	4.34	2.92					164.0
71.5	450	1.536	43.0	8.42	4.78	65.0	7.20	0.130	0.111	128.5
164.5	460	3.46	77.4	11.94	5.01	95.0	14.0	0.126	0.148	99.8
242	453	5.16	128.6	19.5	7.09	145.0	18.8	0.134	0.130	93.7
290	460	6.10	150.3	22.0	4.68	165	11.4	0.146	0.069	116.0
310	456	6.56	146.3	26.2	6.42	147.5	23.2	0.177	0.158	88.2
26.7	582	0.438	43.5	5.83	0.606	37.8	7.83	0.154	0.207	1275
33.7	579	0.563	39.8	6.04	0.271	35.9	7.74	0.168	0.215	1350
46.4	582	0.770	52.4	7.13	0.252	48.1	8.72	0.148	0.181	1350
62.1	582	1.030	69.9	10.23	0.305	61.4	11.08	0.167	0.180	1230
77.6	581	1.289	98.4	12.22	0.295	79.5	14.61	0.154	0.184	1405
106.2	580	1.770	102.2	12.78	0.250	91.0	15.4	0.140	0.169	1158
133.2	583	2.21	157.8	13.80	0.417	124.0	23.1	0.111	0.186	1100

Intensity = 7% preceding run.

Can. J. Chem. Downloaded from www.nrcresearchpress.com by 61.7.252.67 on 09/04/12
For personal use only.

(2) C_2H_6 containing only traces of C_2H_4 was usually checked by the mass spectrometer.

(3) HCN and C_2N_2 were collected together for mass spectrometric analysis by distillation from the first Leroy still at a bottom temperature of $-80°$ C. through the second Leroy still at $-100°$ C. To ensure complete collection, distillation was continued well into the MeCN fraction. C_2H_5CN was always evident on the mass spectrum as it came over with the MeCN. Although it was shown to be a major product, approximately 80% of HCN concentration, satisfactory separation was not practical.

The results of a series of runs over a pressure range of 26 mm. to 300 mm. and temperatures from 55° C. to 300° C. are expressed as rates of formation in Table I.

In addition to the gaseous products some unidentified solid remained on the cell walls, except at the highest temperatures, in sufficient quantity to decrease the light intensity by as much as 20% by the end of the run. It proved necessary to burn the polymer from the cell walls by introducing air or oxygen after each run and this prevented the use of a more efficient assembly of combined lamp and cell. Furthermore it restricted experiments to a normal quartz cell and made it impracticable to use thin sucked-in windows, thus preventing investigation at shorter wavelengths.

The CO_2 formed by total combustion of the solid residue was found to be roughly equal to twice the HCN formed in the reaction; incidentally, no observable pressure change occurred during any of the runs; hence it appears likely that the solid product is largely dinitrile. Certainly little polymerization of MeCN takes place.

Accurate quantum yields were virtually impossible to obtain since I_{ab} is almost immeasurable and the incident intensity is unstable over long periods. However, using N_2O as an actinometer, ΦHCN was shown to be of the order of unity. Intensity studies suffered similarly in crudity, yet the most reliable results obtained (Fig. 1) show clearly that

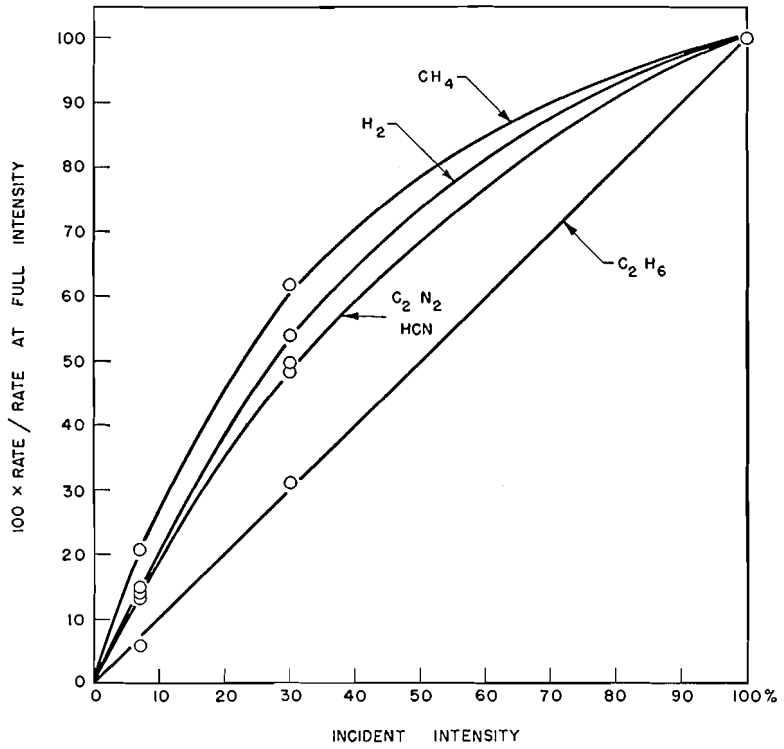

FIG. 1. Effect of intensity on formation of products.

Can. J. Chem. Downloaded from www.nrcresearchpress.com by 61.7.252.67 on 09/04/12
For personal use only.

$R_{C_2H_6}$ varies linearly with I_{ab}, in a quite different manner from the behavior of R_{HCN}, $R_{C_2N_2}$, R_{CH_4}, and R_{H_2} which are more nearly proportional to $\sqrt{I_{ab}}$. (The incident intensity is used in Fig. 1. In view of the weak absorption, however, it is strictly proportional to the absorbed intensity.)

Some experiments were made to investigate the part played by H atoms in the MeCN photolysis. H_2S and D_2S were photolyzed in the presence of MeCN using the 2537 Å region of a Hanovia S500 lamp. The mercury photosensitized decomposition of H_2 and D_2 in the presence of MeCN was also carried out in an auxiliary cell on the mercury system using the 2537 Å resonance line isolated from 1849 Å by a Corning 7910 filter. Incidentally, little direct photosensitized decomposition of MeCN occurs although the quenching cross-section is comparable to that of H_2. In both cases, all the products of the direct photolysis were found with the significant exception of C_2N_2. A material balance showed that $R_{HCN} = (R_{CH_4} + 2R_{C_2H_6})$ to within 5%, which can be accounted for only by a reaction such as

$$H + CH_3CN \rightarrow HCN + CH_3,$$

a conclusion reached also by Forst and Winkler (3).

DISCUSSION

At 1849 Å two primary processes are energetically possible:

$$CH_3CN \rightarrow CH_3 + CN,$$
$$CH_3CN \rightarrow H + CH_2CN.$$

From the nature of the products it is evident that all four radicals are involved in the reaction mechanism. Only CH_2CN would normally be expected to arise from secondary reactions as a result of H abstraction from the parent molecule; however in the present system CH_3 radicals have been proved to be liberated by an H atom attack on MeCN to form HCN.

$$H + CH_3CN \begin{cases} \nearrow H_2 + CH_2CN \\ \searrow HCN + CH_3 \end{cases}$$

On the other hand neither H atoms nor CN radicals are accounted for by secondary reactions and must be primary species. The absence of C_2N_2 in the H atom sensitization of MeCN precludes the third possibility of H atom interactions:

$$H + CH_3CN \not\rightarrow CH_4 + CN.$$

Theoretically this type of reaction is most unfavorable, since it involves the attack of a highly shielded atom and although it has been recently invoked in the reaction

$$CH_3 + CH_3COCF_3 \rightarrow C_2H_6 + COCF_3$$

(Ref. (4)), our observations are consistent with the current view. The 'abstraction' of the CN group on the other hand almost certainly results from the addition of an H atom to the group with its easily accessible π-bonds, to form an unstable imine radical. Bentley and Wijnen (5) observed a similar reaction with CH_3 radicals and in the present work there is positive evidence of the formation of C_2N_2 by 'abstraction'. It is therefore evident that the reaction is not limited to H atom attack but is of more general occurrence:

$$R + MeCN \begin{cases} \nearrow RCN + CH_3 \\ \searrow RH + CH_2CN \end{cases}$$

Can. J. Chem. Downloaded from www.nrcresearchpress.com by 61.7.252.67 on 09/04/12
For personal use only.

Both primary processes are important in the photolysis of MeCN, although the evidence favors the predominance of a C—H split. It is impossible to arrive at a unique mechanism on the basis of the information available, but the following mechanism appears reasonable and is in general agreement with the facts:

$$CH_3CN \xrightarrow{\phi' I_{ab}} H + CH_2CN$$

$$CH_3CN \xrightarrow{\phi'' I_{ab}} CH_3 + CN$$

$$H + CH_3CN \rightarrow HCN + CH_3 \quad [1]$$

$$H + CH_3CN \rightarrow H_2 + CH_2CN \quad [2]$$

$$CN + CH_3CN \rightarrow C_2N_2 + CH_3 \quad [3]$$

$$CN + CH_3CN \rightarrow HCN + CH_2CN \quad [4]$$

$$CH_3 + CH_3CN \rightarrow CH_4 + CH_2CN \quad [5]$$

$$CH_3 + CH_3 \rightarrow C_2H_6 \quad [6]$$

$$CN + CN + M? \rightarrow C_2N_2 + M? \quad [7]$$

$$CH_3 + CH_2CN \rightarrow C_2H_5CN \quad [8]$$

$$CH_3 + R \rightarrow CH_4 + M \quad [9]$$

$$CH_2CN + CH_3CN \rightarrow CNCH_2CN + CH_3 \quad [10]$$

$$CN + CH_2CN \rightarrow CNCH_2CN \quad [11]$$

$$CH_2CN + CH_2CN \rightarrow CNCH_2CH_2CN \quad [12]$$

Direct evidence for reaction [1] was obtained in the H- and D-atom investigations, as previously mentioned, and we infer from the temperature independence of the ratio R_{H_2}/R_{HCN} (Table I) that the activation energy is very close to that of reaction [2]. It can only be assumed that reactions [3] and [4] are similar in this respect also. The evidence for reaction [3] is somewhat less direct; however, it is apparent that C_2N_2 production does not kinetically parallel that of C_2H_6. The intensity dependence of $R_{C_2N_2}$ is quite different from the linear relationship of $R_{C_2H_6}$ (see Fig. 1) and is more characteristic of abstraction reactions. Furthermore, C_2N_2 production increases with higher temperatures in direct contrast to C_2H_6 production, a fact that can be explained only by a competition between a high temperature reaction [3] and a low temperature combination reaction [7] in the formation of C_2N_2.

The removal of the CN group in reactions [1] and [3] is almost certainly not a true abstraction reaction. Only the π-bonds of the nitrile group are open to radical attack resulting in an unstable excited addition complex which can either split off the CH_3 group or back-dissociate.

$$R + CH_3CN \rightleftarrows \begin{matrix} R \\ \diagdown \\ C{=}N \\ \diagup \\ H_3C \end{matrix} \rightarrow CH_3 + RCN$$

When R is H or CN the forward reaction is exothermic by 10 kcal. and 8 kcal., respectively.

The addition product intermediate, which is an imine radical, apparently has a short lifetime, since no stable imine end product has been detected. It may, however, be a source of methane by reaction [9]. It is evident from the results in Table I that reactions

Can. J. Chem. Downloaded from www.nrcresearchpress.com by 61.7.252.67 on 09/04/12
For personal use only.

[5] and [6] do not completely describe the methane–ethane relationship. There is a small but real influence of pressure on the ratio $R_{CH_4}/R^{\frac{1}{2}}_{C_2H_6}$[MeCN] (Fig. 2) which does not appear in the photosensitization of MeCN with acetone-d_6 carried out by Wijnen (6). The Arrhenius plot of Wijnen's results gives a linear slope of 10 kcal. for the abstraction of H from MeCN. In the direct photolysis a 10-kcal. slope is found only at high temperatures while at 55° C. it has tailed off to only 4 kcal. (Fig. 3). There is some parallel here to the photosensitization of HCN with acetone-d_6 by Eaton and Wijnen (7), in which an abnormally low activation energy was found for H abstraction. Apparently the same intermediate is formed by the addition of CH_3 to HCN as obtains with H and CH_3CN, which must take part in the methane reaction. Since this radical does not break down to form CH_4 and a CN radical, it must act by providing a readily abstractible hydrogen. Further evidence of a radical–radical methane step such as reaction [9] is the marked intensity dependence of $R_{CH_4}/R^{\frac{1}{2}}_{C_2H_6}$[MeCN] (Table I) at 55° C. which does not occur at higher temperature.

C_2H_5CN was identified as a product by the mass spectrometer and can be accounted for only by reaction [8], which is analogous to the $C_2H_5COCH_3$-producing reaction in the photolysis of acetone. Reactions [11] and [12] in the absence of direct identification are included in the mechanism as reasonable analogues of the acetone photolysis and of

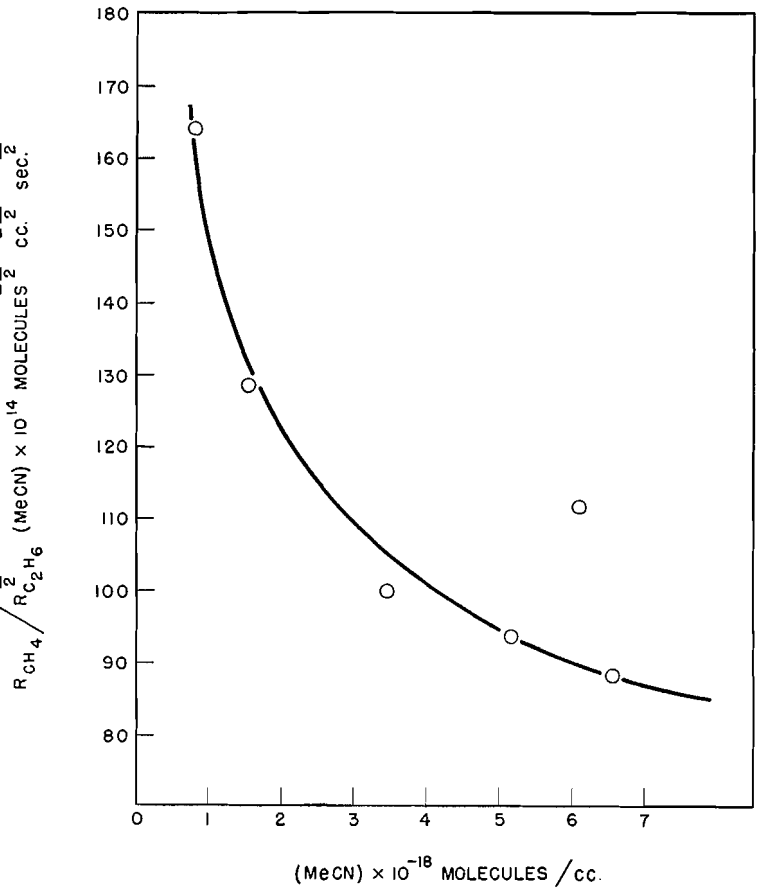

FIG. 2. Effect of pressure on production of methane and ethane. Temperature ~456° K.

Can. J. Chem. Downloaded from www.nrcresearchpress.com by 61.7.252.67 on 09/04/12
For personal use only.

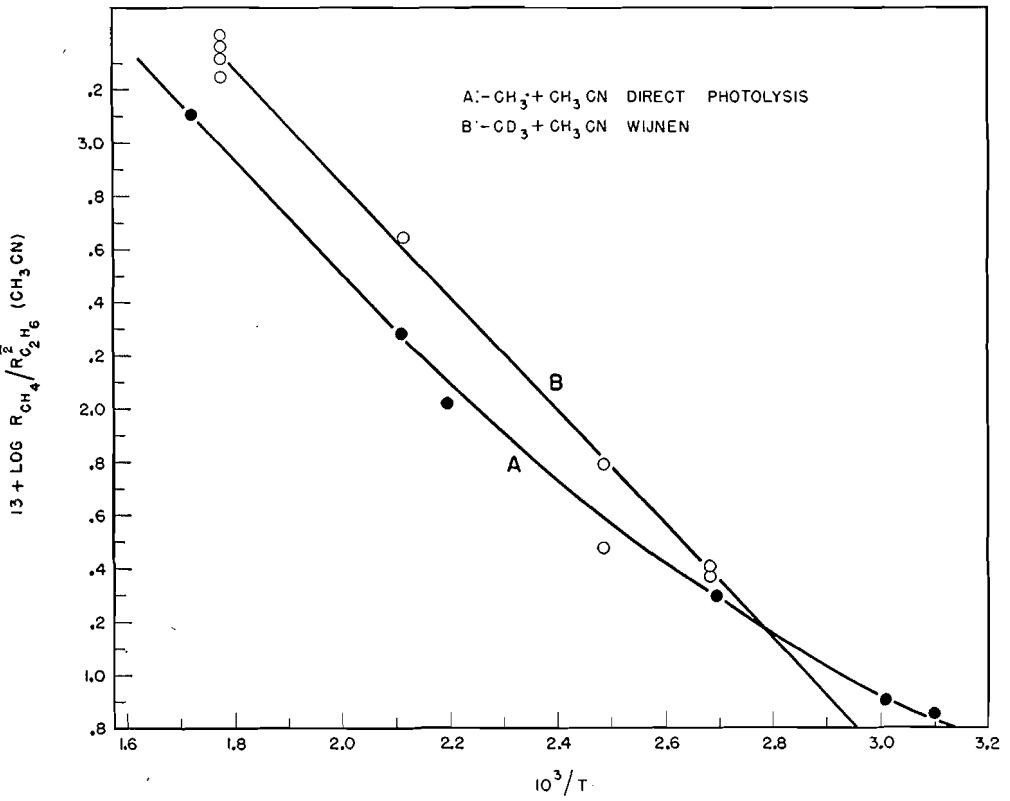

FIG. 3. Arrhenius plot for the reaction of methyl radicals with methyl cyanide.

reaction [8]. However, there is some evidence that much of the deposit on the cell walls is dinitrile. The absence of the deposit in high temperature runs is deemed significant in view of the boiling points of the two nitriles, which are of the order of 250° C. Reaction [10] has been retained for symmetry although it is unlikely to be extensive since the two carbon–carbon bonds in the intermediate would be very similar in strength.

We believe it is of interest to report on some experiments with CNCOCN, which has a similar absorption spectrum to that of acetone and which was available through the kindness of Dr. Leitch of this laboratory. It was an obvious choice as a possible source of CN radicals which would have been very useful in the present investigation. However, there are serious difficulties which render CNCOCN useless as a photosensitizing agent. Very extensive polymerization occurs in photolysis which apparently starts homogeneously since the illuminated volume of the cell becomes almost immediately filled with a fine suspension of particles. Furthermore, CNCOCN apparently undergoes a molecular reaction with water to form 1 mole of CO_2 and 2 moles of HCN. This effect appeared to be virtually inescapable as considerable care had been taken to outgas the vacuum system. C_2N_2 and CO were certainly products of the reaction. However, in view of the difficulties just mentioned, nothing can be stated regarding a mechanism.

The authors are greatly indebted to Dr. K. O. Kutschke for much helpful advice and criticism.

Can. J. Chem. Downloaded from www.nrcresearchpress.com by 61.7.252.67 on 09/04/12
For personal use only.

REFERENCES

1. TERENIN, A. and NEUJMIN, H. Nature, **134**, 255 (1934).
2. PLATT, J. R. and KLEVENS, H. B. Revs. Modern Phys. **16**, 182 (1944).
3. FORST, W. and WINKLER, C. A. Can. J. Chem. **33**, 1814 (1955).
4. SIEGER, R. A. and CALVERT, J. G. J. Am. Chem. Soc. **76**, 5197 (1954).
5. BENTLEY, A. and WIJNEN, M. H. J. To be published.
6. WIJNEN, M. H. J. J. Chem. Phys. **22**, 1074 (1954).
7. EATON, R. S. and WIJNEN, M. H. J. To be published.

Can. J. Chem. Downloaded from www.nrcresearchpress.com by 61.7.252.67 on 09/04/12
For personal use only.

Can. J. Chem. Downloaded from www.nrcresearchpress.com by 200.7.193.243 on 09/04/12
For personal use only.

THE LIMITING EQUIVALENT CONDUCTANCES OF AMMONIUM CHLORIDE, AMMONIUM BROMIDE, AND AMMONIUM NITRATE AT 35.00° C.[1]

A. N. CAMPBELL AND E. BOCK[2]

ABSTRACT

The limiting equivalent conductances of ammonium chloride, ammonium bromide, and ammonium nitrate as well as the limiting ionic conductances of the ammonium and nitrate ions were determined at 35° C. with a probable error of 0.05%. The values found were $\Lambda_{0_{NH_4Cl}}$ 180.97 mhos, $\Lambda_{0_{NH_4Br}}$ 182.73 mhos, $\Lambda_{0_{NH_4NO_3}}$ 174.21 mhos, $\lambda_{0_{NH_4^+}}$ 88.73 mhos, and $\lambda_{0_{NO_3^-}}$ 85.48 mhos. These values were obtained by the application of the Shedlovsky method of extrapolation to equivalent conductance data, which had been corrected for the hydrolysis of the ammonium ion.

Observed equivalent conductances of aqueous solutions of ammonium nitrate at 35° C., in the concentration range from 0.0002 *N* to 10 *N*, have been compared with those calculated by means of the Wishaw–Stokes and Falkenhagen–Leist equations. The Wishaw–Stokes equation was found to give better agreement with experiment than the Falkenhagen–Leist equation.

In order to apply the conductance equations of Wishaw and Stokes (1) and of Falkenhagen and Leist (2) to conductance data obtained in this laboratory for ammonium nitrate at 35° C., it is necessary to know Λ_0, the limiting conductance of ammonium nitrate at this temperature, and we therefore undertook to determine it. At the same time, we thought it would be interesting to determine the limiting conductances of the individual ions, viz. NH_4^+ and NO_3^-. This information results at once from the limiting conductance of the salt, if the transference numbers are known. Since, however, no experimental values of the transference numbers of the ions of ammonium nitrate are given in the literature (for 35° C.), we approached the problem by making experimental determinations of the limiting conductances of ammonium bromide and of ammonium chloride. Since the conductances of bromide and of chloride ions are known accurately at 35° C., it was possible to obtain the conductance of ammonium ion and of nitrate ion.

EXPERIMENTAL TECHNIQUE

The technique of measurement of conductance in very dilute solutions has been worked out in great detail, over the years, and it is to be found in works of reference. Nevertheless, some reference to the methods used by us is necessary, if only to prove that the necessary precautions were taken.

A. Purity of Materials

1. Salts

Fisher certified reagents were used; they were recrystallized twice from conductance water, dried at 90° C., and kept over sulphuric acid until needed. The potassium chloride used for cell constants was, in addition, ignited before use. Objection has been made to fusing the potassium chloride on the ground that a minute trace of hydrogen chloride may be expelled from the moist salt, leaving the residue alkaline, but direct testing showed that this did not happen with us.

2. Conductance Water

A good quality distilled water was passed through an Amberlite MB-3 ion exchange column. When the effluent water was exposed to the air, its specific conductance increased,

[1]*Manuscript received September 25, 1957.*
Contribution from the Chemistry Department of the University of Manitoba, Winnipeg, Manitoba.
[2]*Holder of the Comminco Fellowship of the Consolidated Mining and Smelting Company of Canada, to whom we are also indebted for a grant for the expenses of the research.*

rapidly at first and then more slowly, as the water became saturated with carbon dioxide from the air. The final value obtained, for the so-called "equilibrium water" (usually about 1×10^{-6} mhos), was the one used when applying the solvent correction to the observed specific conductances of the solutions, since the solutions were prepared and all measurements made in contact with the atmosphere.

B. Conductance Measurements

1. The Bridge

A Leeds and Northrup Campbell–Shakelton bridge was used, for which the makers claim an accuracy of 0.05%. A tuned telephone headpiece in series with a two-stage resistance-coupled amplifier served as detector; high sensitivity with low power input was thus obtained.

2. The Conductance Cells

Three cells were used, all of the design recommended by Jones and Bollinger (3). The electrodes were lightly platinized. The cell constants varied from 0.55032 to 46.1383.

3. Preparation of Solutions

(*a*) *Concentrations from 0.1 M to 0.005 M.*—A quantity of salt (never less than 2 g.) was weighed to 1/10 mg. The salt was transferred to a pyrex flask of 1-liter capacity, water added to give approximately the desired concentration, and the weight of the solution determined to the nearest 5 mg. All weighings were reduced to vacuum. The density was then determined.

(*b*) *Concentrations from 0.005 M to 0.0005 M.*—Twenty to fifty grams (weighed to 0.1 mg.) of a more concentrated solution were diluted with approximately 1600 g. water. The resulting solution was weighed to the nearest 5 mg., and the normality calculated from the known amounts of salt and water. It was not necessary to know the density at these concentrations, since the density of the solutions is not appreciably different from that of water.

4. Measurement of Equivalent Conductance

The cells were allowed to remain in the thermostat for $\frac{1}{2}$ hour after filling, before commencing the measurements. Readings of conductance were then taken at 5-minute intervals for another $\frac{1}{2}$ hour. For solutions stronger than 0.001 *M*, no change in conductance with time was observed, but with solutions more dilute than 0.001 *M*, as well as with conductance water, a slow but steady increase of conductance with time was observed. For the most dilute solutions the change amounted to 0.02% and for water to 0.1%.

In order to correct for the increase of conductance with time, conductance readings were plotted against time and the curve extrapolated to zero time. The extrapolated value was taken as the "true" conductance of the solution. That this procedure was sound is borne out by the fact that conductance measurements of solutions having identical concentrations showed agreement to better than 0.01%. Moreover, no less than seven determinations of the conductances of potassium chloride solutions, ranging in concentration from 0.001 *M* to 0.0005 *M*, were made and the results compared with those obtained by Gordon (4). The comparison was effected by calculating Λ_0 from the following empirical equation proposed by Gordon, using experimental concentration and conductance data:

$$\Lambda_0 = \Lambda_0' - Bc + Dc \log c. \qquad [1]$$

In all seven instances the values of Λ_0 did not differ from that reported by Gordon by more than 0.04%. In view of the fact that Gordon used a fundamentally different method of measurement (direct current method) and that equation [1] is claimed to represent conductance data to within 0.02 to 0.03%, the agreement obtained is quite satisfactory.

Can. J. Chem. Downloaded from www.nrcresearchpress.com by 200.7.193.243 on 09/04/12
For personal use only.

5. Thermostat

The thermostat was oil-filled and controlled to 0.002° C. Temperature was read on a Beckmann thermometer, which was calibrated periodically against a platinum resistance thermometer.

EXPERIMENTAL RESULTS

The main experimental results are summarized in Table I. The table contains the specific and equivalent conductances and densities of aqueous solutions of ammonium nitrate, of ammonium chloride, and of ammonium bromide at 35.00° C.

TABLE I

SPECIFIC AND EQUIVALENT CONDUCTANCES AND DENSITIES OF AQUEOUS SOLUTIONS, AT 35.00° C.

Concentration, moles/liter ×100	Specific conductance, mhos cm.$^{-1}$×10^{6}	Equivalent conductance, mhos	Density, g./ml.
	A. Ammonium nitrate		
7.7601	11584.2	149.28	0.99643
6.1204	9266.2	151.40	0.99589
5.0620	7743.9	152.98	0.99555
4.4589	6867.1	154.01	0.99545
3.6873	5733.4	155.49	0.99522
3.0658	4807.69	156.82	0.99505
2.3010	3656.50	158.91	0.99443
0.46208	771.293	166.92	—
0.21946	371.589	169.32	—
0.12959	220.960	170.50	—
0.10578	180.831	170.95	—
0.060330	104.719	171.86	—
0.058302	100.261	171.97	—
0.050534	86.929	172.02	—
0.025730	44.494	172.92	—
	B. Ammonium chloride		
8.4588	13185.881	155.88	0.99566
6.6522	10504.926	157.92	0.99533
5.0333	8056.365	160.06	0.99513
4.3262	6975.550	161.24	0.99483
3.8014	6168.520	162.27	0.99474
3.2216	5265.409	163.44	0.99462
1.7050	2856.084	167.42	0.99449
0.18328	323.517	176.52	—
0.12245	217.023	177.23	—
0.086642	154.114	177.88	—
0.079040	140.809	178.15	—
0.047689	85.291	178.85	—
0.043436	77.816	179.15	—
	C. Ammonium bromide		
7.1797	11467.8	159.72	0.99808
6.3503	10204.7	160.70	0.99770
4.8576	7904.9	162.73	0.99668
4.3820	7163.5	163.47	0.99642
3.7305	6139.5	164.58	0.99611
2.2073	3709.23	168.04	0.99519
1.9430	3280.19	168.82	0.99509
0.26811	475.137	177.22	—
0.17723	315.892	178.24	—
0.17037	303.815	178.33	—
0.096063	172.393	179.46	—
0.085742	154.112	179.74	—
0.065003	117.124	180.18	—
0.036822	66.624	180.94	—
0.025495	46.275	181.51	—

Can. J. Chem. Downloaded from www.nrcresearchpress.com by 200.7.193.243 on 09/04/12
For personal use only.

Can. J. Chem. Downloaded from www.nrcresearchpress.com by 200.7.193.243 on 09/04/12
For personal use only.

DISCUSSION OF RESULTS

Any attempt at direct determination of degree of accuracy, as apart from reproducibility, is exceedingly laborious and, in the end, the figure arrived at is always somewhat doubtful. We thought it better, therefore, to estimate our accuracy by comparing our results for the limiting conductances of potassium chloride at 25° C. and at 35° C., and for ammonium chloride at 25° C., with the values reported in the literature. These salts were chosen because their limiting conductances have been determined by highly reputable workers, who claim an experimental accuracy of 0.01%.

For the limiting conductance of potassium chloride at 25° C., Shedlovsky (5) reports a value of 149.85 mhos. Our determination gave 149.90 mhos; the discrepancy is 0.05 mhos or 0.03%. Gordon (4) obtained 180.42 mhos for potassium chloride at 35° C.; we obtained (for the limiting conductance) 180.45 mhos, a difference of 0.03 mhos or 0.02%. Finally, Longsworth (6) quotes a Λ_0 value of 149.90 mhos for ammonium chloride at 25° C. We found 149.93 mhos, a difference of 0.02%. It seems, therefore, that we may reasonably claim an accuracy of at least 0.05% in our experimental work. This claim is further supported by the fact that the difference between the limiting conductances of ammonium bromide and ammonium chloride, as determined by us, is equal, within 0.03%, to the difference between the literature values of the limiting conductances of the bromide and chloride ions.

For the determination of Λ_0, the plot of Λ against $\sqrt{c}$ proposed by Kohlrausch (7) is one of the best methods. The main difficulty in applying this method lies in the fact that the conductances of extremely dilute solutions are required (from 0.002 N to 0.0001 N) and these are difficult to measure accurately. An alternative method for the evaluation of Λ_0 was suggested by Shedlovsky (5). If the function $\Lambda_0' = (\Lambda+\alpha\sqrt{c})/(1-\beta\sqrt{c})$, where α and β are the Debye–Hückel constants, is plotted against c, the concentration, a straight line is obtained. The correct value of Λ_0 is then derived by extrapolating to zero concentration. Some exceptions to the Shedlovsky rule, however, have been observed. Thus, the function Λ_0' for the alkali nitrates and iodates and silver nitrate passes through a minimum at a concentration of about 0.005 N; this vitiates the use of the function for the determination of Λ_0 for these salts and the Kohlrausch method must be employed. The chief advantage of the Shedlovsky method lies in its applicability to a far wider concentration range than the Kohlrausch method. Whereas the latter is limited to an upper concentration of 0.002 N, the former holds up to 0.1 N. Thus, not only does the Shedlovsky method provide a wider working range but it also enhances the accuracy of determination of Λ_0, since measurements at higher concentrations are less subject to error than those at lower concentrations.

The three salts investigated (ammonium bromide, ammonium chloride, and ammonium nitrate) are hydrolyzed in aqueous solution. It was therefore necessary to apply a so-called hydrolysis correction to the experimentally determined equivalent conductances. Since the essence of the hydrolysis of ammonium ion is the replacement of ammonium ions by hydrogen ions, the conductance of the solution is increased and the increase will be the more significant the more dilute the solution. There may be some difference of opinion as to what constitutes the limiting equivalent conductance of a hydrolyzable salt but we define it as the limiting equivalent conductance derived from equivalent conductance measurements which have been corrected for hydrolysis.

The hydrolysis correction may be determined by two different methods. One method, which has been employed by McInnes and Shedlovsky (8) in their determination of the limiting conductance of the acetate ion, consists in measuring the conductance and pH

of a buffered solution. The second method, used in this work, consists in calculating x, the degree of hydrolysis, from the known value of the hydrolysis constant, i.e.,

$$x = -K_h/2c + \sqrt{[(K_h^2/4c^2)+(K_h/c)]}, \quad [2]$$

where K_h is the hydrolysis constant and c the stoichiometric concentration of the salt before hydrolysis. From x, the "true" conductance of the solution may be calculated as follows: the conductance of 1 g-equiv. of a hydrolyzed salt is made up of the conductance of $(1-x)$ equivalents of unhydrolyzed salt and x equivalents of free acid, i.e.,

$$\Lambda = (1-x)\Lambda_{corr} + x\Lambda_{0_{HA}}. \quad [3]$$

In this equation, Λ is the observed equivalent conductance of the solution, Λ_{corr} is the "true" equivalent conductance of the unhydrolyzed salt, and $\Lambda_{0_{HA}}$ is the equivalent conductance of the free acid in the salt solution. From equation [3] the "true" equivalent conductance of the unhydrolyzed salt follows as

$$\Lambda_{corr} = (\Lambda - x\Lambda_{0_{HA}})/(1-x). \quad [4]$$

$\Lambda_{0_{HA}}$ is assumed to be equal to the limiting conductance of the free acid.

The value of K_h, the hydrolysis constant, was calculated by means of the following formula, due to Bates and Pinching (9):

$$-\log K_h = A_1/T - A_2 + A_3T. \quad [5]$$

From the given values of the constants A_1, A_2, and A_3 and by inserting the appropriate value of T, viz. 308.16° K., the value of K_h for ammonium ion at 35.00° C. was found to be 1.012×10^{-9}. The values of Λ_0 for hydrochloric and hydrobromic acids were obtained from the literature (10, 11), while that of nitric acid was obtained by adding the limiting conductance of the nitrate ion, as determined by us, to the value of the limiting conductance of the hydrogen ion.

In Table II are summarized the degrees of hydrolysis and the observed and corrected equivalent conductances for the aqueous solutions of the three salts investigated. Also incorporated in this table are the values of the Shedlovsky function Λ_0' derived from the observed and from the corrected equivalent conductances.

The limiting conductances, Λ_0, of the three salts were determined by using both methods of extrapolation described above, and employing observed and corrected equivalent conductances in each case. It was observed that the function Λ_0' obtained from uncorrected equivalent conductance data passed through a minimum but, when corrected equivalent conductances were used, the minimum disappeared. It is our opinion that the increase in Λ_0' with increase in dilution observed in the low concentration region when uncorrected values are used is (in these cases) a direct consequence of hydrolysis. We also believe that the Shedlovsky method for the evaluation of Λ_0 is applicable to all three salts investigated, provided the hydrolysis effect is taken into account.

The values of the limiting equivalent conductances for the three salts at 35° C., derived from the application of the Shedlovsky extrapolation method to the corrected equivalent conductances, as well as the mean deviation of the function Λ_0' from the straight line obtained by the method of least squares, are summarized in Table III.

Application of the Kohlrausch method to observed and corrected equivalent conductances resulted in a straight plot in every case. The mean deviations from the straight line obtained by the method of least squares and the respective limiting conductances at 35° C. are summarized in Table IV. It will be observed that Λ_0 (uncorrected) is appreciably greater than Λ_0 (corrected) and this is undoubtedly due to hydrolysis.

Can. J. Chem. Downloaded from www.nrcresearchpress.com by 200.7.193.243 on 09/04/12
For personal use only.

TABLE II

CONCENTRATIONS, DEGREES OF HYDROLYSIS, OBSERVED AND CORRECTED EQUIVALENT CONDUCTANCES, AND UNCORRECTED AND CORRECTED VALUES OF AQUEOUS SOLUTIONS

Concentration, moles/liter ×100	Degree of hydrolysis ×10^4	Observed equivalent conductance, mhos	Corrected equivalent conductance, mhos	Uncorrected Λ_0'	Corrected Λ_0'
		A. Ammonium chloride			
8.4588	1.0937	155.88	155.87	190.66	190.65
6.6522	1.2333	157.92	157.88	188.65	188.60
5.0333	1.4178	160.06	160.02	186.69	186.64
4.3262	1.5294	161.24	161.19	185.88	185.83
3.8014	1.6315	162.27	162.22	185.34	185.29
3.2216	1.7722	163.44	163.38	184.66	184.59
1.7050	2.4359	167.42	167.34	182.80	182.71
0.18328	7.4180	176.52	176.29	181.54	181.31
0.12245	9.0869	177.23	176.95	181.37	181.06
0.08664	10.8017	177.88	177.54	181.30	180.99
0.07904	11.3089	178.15	177.80	181.45	181.10
0.04769	14.5663	178.85	178.40	181.23	180.96
0.04344	15.2523	179.15	178.67	181.59	181.11
		B. Ammonium nitrate			
7.7601	1.1419	149.28	149.24	182.06	181.99
6.1204	1.2857	151.40	151.36	180.40	180.35
5.0620	1.4138	152.98	152.93	179.28	179.23
4.4589	1.5064	154.01	153.96	178.68	178.62
3.6873	1.6566	155.49	155.44	177.88	177.83
3.0658	1.8168	156.82	156.76	177.21	177.15
2.3010	2.0970	158.91	158.84	176.55	176.49
0.46208	4.6787	166.92	166.77	174.79	174.64
0.21946	6.7884	169.32	169.10	174.75	174.51
0.12959	8.8329	170.50	170.22	174.67	174.38
0.10578	9.7762	170.95	170.65	174.72	174.41
0.060330	12.9433	171.86	171.46	174.72	174.30
0.058302	13.1663	171.97	171.56	174.76	174.35
0.050534	14.1413	172.02	171.58	174.62	174.18
0.025730	19.8124	172.92	172.30	174.77	174.15
		C. Ammonium bromide			
7.1797	1.1872	159.72	159.68	191.84	191.79
6.3503	1.2623	160.70	160.66	190.84	190.80
4.8576	1.4433	162.73	162.68	189.00	188.95
4.3820	1.5196	163.47	163.42	188.39	188.34
3.7305	1.6469	164.58	164.53	187.53	187.48
2.2073	2.1410	168.04	167.98	185.64	185.57
1.9430	2.2819	168.82	168.75	185.32	185.24
0.26811	6.1418	177.22	177.03	183.33	183.13
0.17723	7.5537	178.24	178.00	183.20	182.96
0.17037	7.7042	178.33	178.09	183.19	182.95
0.096063	10.2586	179.46	179.14	183.11	182.79
0.085742	10.8582	179.74	179.40	183.19	182.85
0.065003	12.4696	180.18	179.79	183.18	182.79
0.036822	16.5645	180.94	180.43	183.20	182.69
0.025495	19.9037	181.51	180.89	183.39	182.77

TABLE III

LIMITING EQUIVALENT CONDUCTANCES DERIVED BY THE SHEDLOVSKY METHOD

Salt	Λ_0	Mean deviation of Λ_0'
Ammonium chloride	180.97	0.03%
Ammonium bromide	182.73	0.02%
Ammonium nitrate	174.21	0.02%

Can. J. Chem. Downloaded from www.nrcresearchpress.com by 200.7.193.243 on 09/04/12
For personal use only.

TABLE IV

LIMITING EQUIVALENT CONDUCTANCES DERIVED BY THE KOHLRAUSCH METHOD

Salt	Mean deviation		Λ_0, mhos	
	Corr.	Uncorr.	Corr.	Uncorr.
Ammonium chloride	0.04%	0.04%	180.86	181.47
Ammonium bromide	0.03%	0.03%	182.57	183.34
Ammonium nitrate	0.02%	0.02%	173.99	174.73

A comparison of the corrected Λ_0's obtained by the two methods of extrapolation shows that the Λ_0 determinations by the Kohlrausch method are in all cases smaller than those by the Shedlovsky method. This discrepancy, amounting to about 0.1%, we believe to be due to a partial "over-correction" of the conductances in the very dilute region. Since the Kohlrausch method depends solely on conductance measurements made in the dilute region it is to be expected that Λ_0 derived by this method will be more affected by "over-correction" and therefore will be somewhat lower than the Λ_0 derived by the Shedlovsky method, which applies to a much wider concentration range. We believe that the over-correction has resulted from the use of too large a solvent correction for the measured specific conductances of the more dilute solutions. The magnitude of the solvent correction is determined by measuring the conductance of the solvent. The solvent used in this research was water saturated with carbon dioxide under its partial pressure in the laboratory atmosphere. The increase in conductance imparted to the water is due to the ionization of dissolved carbon dioxide:

$$CO_2 + H_2O \rightleftarrows H^+ + HCO_3^-.$$

The equation indicates that the ionization (and therefore the conductance of the carbon dioxide) is repressed by hydrogen ions. In dilute solutions, however, hydrogen ions are produced by hydrolysis. Therefore the ionization of the dissolved carbon dioxide is less in the salt solutions than in pure solvent and hence the magnitude of the solvent correction should be less for these solutions than that determined by measuring the conductance of the pure solvent. Since, however, it was impossible to ascertain quantitatively the extent of the decrease in the magnitude of the solvent correction, the full solvent correction had to be applied.

The limiting equivalent conductance of the ammonium ion at 35.00° C. was determined to be 88.73 mhos ±0.05 mho. This represents the average of the two values obtained by subtracting the limiting conductances of the bromide and chloride ions, as determined by Gordon (4), from the limiting conductances of ammonium bromide and ammonium chloride respectively. The limiting conductance of the nitrate ion was then obtained from the limiting conductance of ammonium nitrate. The value thus obtained for nitrate ion at 35.00° C. was 85.48 mhos ±0.05 mho.

It is customary, in the work proceeding from this laboratory, to compare experimental results with the conductances calculated by the equations of Falkenhagen and Leist (2) and of Wishaw and Stokes (1), viz.:

$$\Lambda = \Lambda_0 - \frac{e^2}{3DkT} \cdot \frac{\kappa\Lambda_0}{1+\kappa a} \cdot \frac{q}{(1+\sqrt{q})(1+\kappa a\sqrt{q})} - \frac{\eta e^2 1000\ \kappa}{3\pi c 9(1+\kappa a)10^{11}} \quad \text{(Falkenhagen and Leist)},$$

where the symbols have their usual significance and $q = \frac{1}{2}$, and

$$\Lambda = \left(\Lambda_0 - \frac{B_2\sqrt{c}}{1+B\mathring{a}\sqrt{c}}\right)\left(1 - \frac{B_1\sqrt{c}}{1+B\mathring{a}\sqrt{c}} \times F\right) \text{ (Wishaw and Stokes)},$$

Can. J. Chem. Downloaded from www.nrcresearchpress.com by 200.7.193.243 on 09/04/12
For personal use only.

where $B_1 = 8.20\times10^5/(DT)^{3/2}$, $B_2 = 82.5/\eta(DT)^{\frac{1}{2}}$, $B\mathring{a}\sqrt{c} = 50.29\mathring{a}\sqrt{c}/(DT)^{\frac{1}{2}}$,

and $$F = (\exp 0.2929\, B\mathring{a}\sqrt{c}-1)/0.2929\, B\mathring{a}\sqrt{c}.$$

The conductances of concentrated solutions of ammonium nitrate at 35.00° C. have been determined by Campbell, Gray, and Kartzmark (12) and the results compared with the results of the Wishaw–Stokes equation in a separate paper (13), but, at that time, they were unacquainted with the Falkenhagen–Leist equation and with the true value of Λ_0 for ammonium nitrate at 35.00° C. We have now recalculated with the Wishaw–Stokes equation, using the true value of Λ_0, and also we have calculated using the Falkenhagen–Leist equation. Results are given in Table V. The Wishaw–Stokes equation was found to give better agreement with experiment than the Falkenhagen–Leist equations. Moreover, the assumed value of 3.0 Å for å, the distance of closest approach of the ions,

TABLE V

OBSERVED AND CALCULATED EQUIVALENT CONDUCTANCES OF AMMONIUM NITRATE

Concentration, moles/liter ×100	Observed equivalent conductance, mhos	Corr. observed equivalent conductance, mhos	Calculated equivalent conductance			
			Wishaw–Stokes		Falkenhagen–Leist	
			å = 3.0 Å	å = 3.5 Å	å = 3.0 Å	å = 2.3 Å
1074.9	38.52		36.41	38.89	47.85	40.30
940.86	47.46		46.73	49.86	59.99	50.81
767.05	59.84		61.07	65.09	75.98	64.94
713.18	63.86		65.60	69.77	81.43	69.26
550.65	76.46		79.34	84.32	94.75	82.20
397.49	89.17		92.46	97.46	106.37	93.81
245.04	103.2		105.13	109.95	116.58	105.05
191.04	108.2		110.03	114.94	120.01	109.38
169.40	111.0		112.07	116.42	121.41	111.23
102.34	119.4		119.39	122.93	126.43	118.01
7.7601	149.28	149.24	149.47	150.33	150.52	148.94
6.1204	151.40	151.36	151.73	152.41	152.51	151.21
5.0620	152.98	152.93	153.11	153.91	154.02	152.83
4.4589	154.01	153.96	154.38	154.88	154.98	153.97
3.6873	155.49	155.44	155.83	156.26	156.33	155.47
3.0658	156.82	156.76	157.19	157.57	157.62	156.88
2.3010	158.91	158.84	159.14	159.51	159.47	158.90
0.46208	166.92	166.77	166.84	166.93	166.97	166.83
0.21946	169.32	169.10	169.03	169.07	169.09	169.02
0.12959	170.50	170.22	170.19	170.21	170.22	170.17
0.10578	170.95	170.65	170.57	170.58	170.61	170.56
0.060330	171.86	171.46	171.41	171.45	171.45	171.47
0.058302	171.97	171.56	171.48	171.49	171.50	171.48
0.050534	172.02	171.58	171.66	171.68	171.68	171.66
0.025730	172.92	172.30	172.38	172.38	172.40	172.38

is more reasonable than the 2.3 Å required by the Falkenhagen–Leist equation. Spectroscopic indications (14) that the oxygen atoms in the nitrate ion are coplanar with the nitrogen atom and surround the latter at the corners of an equilateral triangle are well supported by electron diffraction data (15). It is, therefore, not unreasonable to suppose that the distance of closest approach of the ammonium and nitrate ions is somewhat smaller (e.g. 3.0 Å) than the value of 4.0 to 6.0 Å usually encountered with ions known to be spherical, e.g., Li^+, K^+. Even, however, if the nitrate ion is assumed to have spherical shape, the distance of 3.0 Å is still less than the sum of the crystallographic radii of the ammonium ion (1.48 Å) and the calculated radius of the nitrate ion (1.34 Å).

Can. J. Chem. Downloaded from www.nrcresearchpress.com by 200.7.193.243 on 09/04/12
For personal use only.

REFERENCES

1. WISHAW, B. F. and STOKES, R. H. J. Am. Chem. Soc. **76**, 2065 (1954).
2. FALKENHAGEN, H. and LEIST, M. Naturwiss. **41**, 570 (1954).
3. JONES, L. and BOLLINGER, G. M. J. Am. Chem. Soc. **53**, 411 (1931).
4. GORDON, A. E. and BENSON, G. C. J. Chem. Phys. **13,** 473 (1945).
5. SHEDLOVSKY, T. J. Am. Chem. Soc. **54**, 1411 (1932).
6. LONGSWORTH, L. G. J. Am. Chem. Soc. **57**, 1185 (1935).
7. KOHLRAUSCH, F. and HOLBORN, L. Das Leitvermögen der Elektrolyte. Teubner, Leipzig. 1916.
8. MCINNES, D. A. and SHEDLOVSKY, T. J. Am. Chem. Soc. **54**, 1429 (1932).
9. BATES, R. G. and PINCHING, G. D. J. Research Natl. Bur. Standards, **42**, 419 (1949); J. Am. Chem. Soc. **72**, 1393 (1950).
10. OWEN, B. B. and SWEETON, F. H. J. Am. Chem. Soc. **63**, 2811 (1941).
11. OWEN, B. B. and ZELDES, H. J. Chem. Phys. **18,** 1083 (1950).
12. CAMPBELL, A. N., GRAY, A. P., and KARTZMARK, E. M. Can. J. Chem. **31**, 617 (1953).
13. CAMPBELL, A. N. and KARTZMARK, E. M. Can. J. Chem. **33**, 887 (1955).
14. MAXWELL, L. R. and MOSELY, V. N. J. Chem. Phys. **8**, 738 (1940).
15. ELLIOTT, N. J. Am. Chem. Soc. **59,** 1380 (1937).

Can. J. Chem. Downloaded from www.nrcresearchpress.com by 200.7.193.243 on 09/04/12
For personal use only.

Can. J. Chem. Downloaded from www.nrcresearchpress.com by 61.7.252.67 on 09/04/12
For personal use only.

(−)-HOMOSTACHYDRINE, A NEW ALKALOID ISOLATED FROM THE SEEDS OF MEDICAGO SATIVA L. GRIMM[1]

GERHARD WIEHLER[2] AND LÉO MARION

ABSTRACT

The seeds of *Medicago sativa* (alfalfa) have previously been shown to contain other bases besides stachydrine. One of these bases has now been isolated and found to be a homologue of stachydrine for which the name homostachydrine is suggested. (−)-Homostachydrine is shown to be identical with the (−)-methyl betaine of pipecolic acid. The synthetic racemate of the betaine of pipecolic acid has similar properties to homostachydrine, and their infrared spectra and X-ray powder diagrams are identical.

In the course of a recent study of the biogenesis of stachydrine in *Medicago sativa* L. Grimm (alfalfa), Leete, Marion, and Spenser (1) observed the presence of three unknown bases. Paper chromatography has now revealed that one of these unknown bases accompanies stachydrine through all stages of its isolation from the plant. Chromatography of the reineckates of stachydrine and this unknown base over alumina or of the bases themselves on ion-exchange resins failed to effect any separation. This behavior indicates that the new base is probably closely related to stachydrine. In the course of further experiments on the biogenesis of stachydrine, it became obvious that neither Steenbock (2), who first showed the presence of stachydrine in alfalfa, nor any of the later investigators (3) were dealing with pure stachydrine, but with a mixture.

Since our biogenetic studies with alfalfa involved feeding substances labelled with C^{14} to the growing plant and resulted in the formation of radioactive stachydrine (4), it was deemed necessary to separate the unknown base from the stachydrine and to study its structure.

Originally it had been assumed that the unknown base might be betonicine or turicine (1), but this assumption had to be abandoned, since neither of these methyl betaines of hydroxyproline[3] produced a purple spot with Dragendorff's reagent on a paper chromatogram, whereas the unknown base did, and since a hydroxyl base should separate readily from stachydrine on an alumina column.

The unknown base was more abundant in the seeds than in the leaves of alfalfa, and therefore a mixture of the unknown base and stachydrine was isolated from the seeds by a slight modification of the known procedure (1). The crystalline colorless mixture of the hydrochlorides of the bases (m.p. 212–214° decomp.) dissolved in Munier's Bc 20 solvent[4] (5) was chromatographed on a column of cellulose powder and eluted with the same solvent. In this solvent system the unknown base showed a higher R_F value than stachydrine and was eluted first. The first fractions of the eluate yielded the analytically pure hydrochloride of the new base (m.p. 216–217° decomp.) while the following fractions contained a mixture of the hydrochlorides of the new base and stachydrine. The new base hydrochloride yielded analytical figures corresponding to the empirical formula $C_8H_{15}O_2N.HCl$, which is that of a homologue of stachydrine hydrochloride ($C_7H_{13}O_2N.HCl$), and it is proposed to designate it homostachydrine.

[1]*Manuscript received October 25, 1957.*
Contribution from the Division of Pure Chemistry, National Research Council, Ottawa, Canada.
Issued as N.R.C. No. 4580.
[2]*National Research Council of Canada Postdoctoral Fellow 1956–1957.*
[3]*Samples of betonicine and turicine were given to us by Dr. B. Witkop, National Institute of Health, Bethesda, Maryland, to whom we are most grateful.*
[4]*Consists of a mixture of n-butanol, concentrated hydrochloric acid, and water, in the proportions of 100 ml.: 20 ml.: 39 ml. respectively.*

The specific optical rotation of homostachydrine hydrochloride in absolute ethanol was $[\alpha]_D$ $-13.3°$ while that of pure stachydrine hydrochloride in the same solvent was $[\alpha]_D$ $-22.2°$. Stachydrine isolated from *Galeopsis grandiflora* Lam. (6) and *Citrus aurantium* Amar. (6) appears, from the rotations reported for the hydrochloride, to have been pure since these were in agreement with the rotation of synthetic (−)-stachydrine hydrochloride (7). Steenbock (2), who first isolated stachydrine from alfalfa, reports $[\alpha]_D$ $-20.7°$ in water, which is appreciably lower than the rotation of synthetic (−)-stachydrine hydrochloride ($[\alpha]_D$ $-26.7°$ in water) (7). Since stachydrine isolated from alfalfa is always contaminated with homostachydrine, the low rotation reported by Steenbock was probably not due to racemization as he thought, but to the lower rotation of the homostachydrine, which must have been present because his method of isolation would not have separated the two bases.

Although there existed many possible structures for a homologue of stachydrine, it was thought that one of the most likely structures of homostachydrine would be that of the methyl betaine of pipecolic acid (I). Because of the small quantity of homostachydrine available no degradative experiments were tried, but a synthetic specimen of the

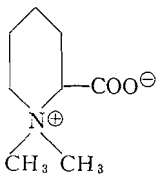

I

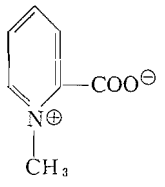

II

methyl betaine of pipecolic acid was prepared. Following the procedure of Patchett and Witkop (8) for the preparation of betonicine and turicine, the silver salt of (±)-pipecolic acid was converted to the betaine I by treatment with methyl iodide.

The synthetic (±)-betaine hydrochloride, m.p. 210–211° (decomp.), had the same properties as homostachydrine. On a paper chromatogram it showed the same red-purple spot with Dragendorff's reagent and, within the limits of error, the same R_F value. The infrared spectrum and the X-ray diffraction powder diagram of the synthetic racemate hydrochloride were identical in every respect with those of (−)-homostachydrine hydrochloride. There can be no doubt, therefore, that (−)-homostachydrine is identical with the (−)-methyl betaine of pipecolic acid (I). Attempted resolution of the synthetic racemate with *d*- and *l*-tartaric acids and with *d*-camphorsulphonic acid was unsuccessful.

Although this is the first reported occurrence of homostachydrine, pipecolic acid has been found recently in different plants (9). It has been shown that biogenetically pipecolic acid arises from lysine (10, 11, 12). The occurrence of lysine in alfalfa has been reported (3), and it can be presumed to be the precursor of homostachydrine.

Hoppe-Seyler, who first isolated homarine II from the tissues of *Arca noae* (13), mentions the possibility that it might be formed from lysine. He also assumes that ornithine is the precursor of stachydrine and since the latter occurs with homarine in *Arca noae* (13, 14), he concludes that the two bases are likely synthesized by parallel routes. Since from recent work, however, the pyridine ring does not seem to arise from lysine (15), although this amino acid is the precursor of the piperidine ring (15), it appears most improbable that lysine could be the precursor of homarine.

Can. J. Chem. Downloaded from www.nrcresearchpress.com by 61.7.252.67 on 09/04/12
For personal use only.

Can. J. Chem. Downloaded from www.nrcresearchpress.com by 61.7.252.67 on 09/04/12
For personal use only.

EXPERIMENTAL

All the melting points determined by us are corrected. The infrared absorption spectra were measured in nujol mulls on a Perkin-Elmer double beam spectrometer model 21B.

Isolation of the Mixture of Stachydrine and Homostachydrine

Air-dried alfalfa seeds (1 kg.) were ground in a Wiley mill and boiled with 70% ethanol (2 l.) for 3 hours. The mixture was filtered and the solid residue extracted twice more by boiling with 70% ethanol (1.5 l.) for 3 to 4 hours. The yellowish-brown filtrates were combined, diluted with water to a volume of 7 l., and treated with lead acetate in the usual way to remove the proteins.

The lead-free filtrate was evaporated to a brown residue (*ca.* 100 ml.), which was boiled with two successive 300-ml. portions of absolute ethanol. The combined alcoholic extract was filtered and evaporated to a brown viscous sirup. This sirup was boiled with two successive 200-ml. portions of absolute ethanol, and the combined ethanolic solutions evaporated to dryness. The residue thus obtained was dissolved in water (150 ml.) and the solution adjusted to pH 8 with dilute ammonia. A 5% reinecke salt solution in methanol was added and the mixture stored in a refrigerator for 16 hours. The precipitate was filtered off, 100 ml. of the reinecke salt solution added to the choline-free filtrate (16), and the liquor acidified with concentrated hydrochloric acid (50 ml.). A pink crystalline precipitate formed immediately, and after 30 minutes it was filtered with suction and washed with *n*-propanol, the yield of crude reineckate being 4.14 g. This crude reineckate was dissolved in acetone (200 ml.), the solution was filtered to remove some insoluble impurity and evaporated to dryness. The residue (3.87 g.) left after evaporation was dissolved in acetone (250 ml.) and the reineckate converted to the chlorides of the bases by the usual method (17) of treatment with aqueous solutions of silver sulphate (1.56 g.) and barium chloride (1.22 g.). The final filtrate obtained was evaporated to dryness. A crystalline residue resulted, which was extracted with hot absolute ethanol (25 ml.), filtered, and the filtrate evaporated to dryness. This process was repeated twice. The final filtrate was evaporated to dryness, the residue (1.28 g.) was dissolved in water (20 ml.), and the betaines precipitated with mercuric chloride (in 20% hydrochloric acid solution). The mercuric salt complex was filtered with suction, washed with the reagent solution, and decomposed with hydrogen sulphide. After filtration, the solution was evaporated to dryness *in vacuo* leaving a residue of 1.13 g. of crystalline colorless base hydrochlorides. These were dissolved in absolute ethanol (15 ml.) and precipitated by the addition of acetone (200 ml.) and ether (300 ml.). The filtered dry precipitate (0.63 g.) consisted of the pure mixture of stachydrine and homostachydrine hydrochlorides, m.p. 212–214° (decomp.).

A paper chromatogram on Whatman No. 1 paper ascending in Munier's Bc 20 solvent (5) showed two red-purple spots after spraying with a modified Dragendorff's reagent (18), R_F 0.48 (stachydrine) and R_F 0.57 (homostachydrine). The specific optical rotation of the mixture is $[\alpha]_D^{26}$ −15.5° (*c*, 1.55 in absolute ethanol).

Separation of Homostachydrine from Stachydrine

"Whatman Standard Grade" ash-free cellulose powder (200 g.) was packed dry into a column, 34 mm. by 530 mm. (19). The column was moistened with Munier's Bc 20 solvent, and a solution of 8-hydroxyquinoline (1.0 g.) in the same solvent (40 ml.) was percolated through the column. It was washed with the solvent for 48 hours, after which it was free of 8-hydroxyquinoline (no color with ferric chloride).

A methanolic solution of 500 mg. of the homostachydrine–stachydrine hydrochlorides was mixed with 10 g. of cellulose powder and dried *in vacuo*. The mixture was then ground in a mortar and conditioned by being kept for some time in an atmosphere of Munier's Bc 20 solvent. In order to indicate the position of the moving solvent front a few drops of a solution of "Orange II" (sodium salt of *p*-(2-hydroxy)-naphthylazo)-benzenesulphonic acid) were added to the top of the column. The conditioned cellulose powder containing the bases was then introduced on top of the wet cellulose column, packed carefully, and moistened with the solvent. The chromatogram was developed by passing Munier's Bc 20 solvent through the column at a rate of flow of 12 ml. per hour. The "Orange II" band reached the outlet of the column after 19 hours, and fractions of 4 ml. were collected by means of an automatic fraction collector. Altogether, 62 fractions were taken, and every fraction was tested by spotting a small amount of the eluate on a filter and spraying with Dragendorff's reagent.

Fraction 38 and all the following ones showed red-purple spots, and chromatography on Whatman No. 1 paper indicated that fractions 38–54 contained homostachydrine exclusively while the later fractions contained both homostachydrine and stachydrine. Fractions 20–54 were pooled and evaporated *in vacuo* to a volume of a few milliliters, water was added, and the evaporation *in vacuo* repeated. The residual yellow liquid was filtered and treated with mercuric chloride as already described above. The homostachydrine hydrochloride obtained after this treatment was crystallized twice from ethanol–ether. It consisted of colorless microprisms, wt. 61 mg., m.p. 216–217° (decomp.), $[\alpha]_D^{26}$ −13.3° (*c*, 1.43 in absolute ethanol). Found: C, 49.61; H, 8.33; N, 7.23; Cl, 18.31. Calc. for $C_8H_{16}O_2NCl$: C, 49.37; H, 8.21; N, 7.45; Cl, 18.29%.

The solubility of homostachydrine hydrochloride is very similar to that of stachydrine hydrochloride. Both salts are readily soluble in water and alcohol, slightly soluble in acetone, and insoluble in ether, petroleum ether, and carbon tetrachloride.

Synthesis of (±)-*Methylbetaine of Pipecolic Acid*

α-Picoline (50 g.) was oxidized with potassium permanganate (20) to α-picolinic acid, which was isolated as the hydrochloride (34 g.), m.p. 213–216° (decomp.). The α-picolinic acid hydrochloride in water was hydrogenated over platinum oxide catalyst as described by Stevens and Ellman (21). The crystalline product, after recrystallization from alcohol–benzene and methanol–acetone, consisted of 19.27 g. of pure (±)-pipecolic acid hydrochloride, m.p. 259–262° (decomp.). (±)-Pipecolic acid hydrochloride (2.58 g., 0.0156 mole) was dissolved in water (6 ml.) and, according to the procedure of Patchett and Witkop (8), silver oxide (6.95 g., 0.03 mole) was added to the solution. After 4 hours, water (4 ml.) was removed by distillation *in vacuo* and methanol (50 ml.) and methyl iodide (3.8 ml., 0.061 mole) were added to the residual mixture, which was warmed gently for a few minutes and then kept at room temperature for 1 hour. Another 3.8 ml. of methyl iodide was added, the mixture refluxed for 2.5 hours, and the precipitate filtered and washed with methanol. The combined filtrate and washings were evaporated *in vacuo* leaving the free base as an hygroscopic oil which was dissolved in absolute ethanol (50 ml.). Hydrogen chloride was passed through the solution, which was subsequently evaporated *in vacuo*. The crystalline residue was dissolved in absolute ethanol, the solution treated with charcoal and filtered, and the filtrate mixed with acetone. (±)-Pipecolic acid methylbetaine hydrochloride crystallized out (1.30 g., 0.0067 mole; yield, 43%), m.p. 208–209° (decomp.). A second crystallization from alcohol–acetone yielded 0.90 g. of the pure hydrochloride, m.p. 210–211° (decomp.). Found: C, 49.71; H, 8.44; N, 7.21. Calc. for $C_8H_{16}O_2NCl$: C, 49.61; H, 8.33; N, 7.23%.

Can. J. Chem. Downloaded from www.nrcresearchpress.com by 61.7.252.67 on 09/04/12
For personal use only.

A chromatogram on Whatman No. 1 paper developed with Munier's Bc 20 solvent showed a red-purple spot (R_F 0.56–0.58) after a spray with Dragendorff's reagent. Under the same conditions (−)-homostachydrine hydrochloride showed a red-purple spot at the same R_F value. The infrared absorption spectra in nujol mulls of both the synthetic hydrochloride and (−)-homostachydrine hydrochloride were identical in every respect, and showed a strong carbonyl absorption band at 1705 cm.$^{-1}$. The X-ray powder patterns were also identical.

ACKNOWLEDGMENTS

We wish to express our gratitude to Dr. Maria Przybylska for preparing the X-ray powder diagrams and Dr. R. Norman Jones and Mr. R. Lauzon for the infrared absorption spectra.

REFERENCES

1. LEETE, E. MARION, L., and SPENSER, I. D. J. Biol. Chem. **214**, 11 (1955).
2. STEENBOCK, H. J. Biol. Chem. **35**, 1 (1918).
3. LEAVENWORTH, C. S., WAKEMAN, A. J., and OSBORNE, T. B. J. Biol. Chem. **58**, 209 (1923). VICKERY, H. B. J. Biol. Chem. **61**, 117 (1924).
4. WIEHLER, G. and MARION, L. Unpublished results.
5. MUNIER, R. Bull. soc. chim. biol. **33**, 857 (1951). MUNIER, R. and MACHEBOEUF, M. Bull. soc. chim. biol. **32**, 192 (1950).
6. YOSHIMURA, K. and TRIER, G. Z. physiol. Chem. **77**, 290 (1912).
7. KARRER, P. and WIDMER, R. Helv. Chim. Acta, **8**, 364 (1925).
8. PATCHETT, A. A. and WITKOP, B. J. Am. Chem. Soc. **79**, 185 (1957).
9. MORRISON, R. I. Biochem. J. **50**, XIV (1952); **53**, 474 (1953). ZACHARIUS, R. M., THOMPSON, J. F., and STEWARD, F. C. J. Am. Chem. Soc. **74**, 2949 (1952); **76**, 2908 (1954). GROBBELAAR, N., ZACHARIUS, R. M., and STEWARD, F. C. J. Am. Chem. Soc. **76**, 2912 (1954).
10. LOWY, P. H. Arch. Biochem. Biophys. **47**, 228 (1953).
11. GROBBELAAR, N. and STEWARD, F. C. J. Am. Chem. Soc. **75**, 4341 (1953).
12. SCHIEDT, U. and HÖSS, H. G. Z. physiol. Chem. **308**, 179 (1957).
13. HOPPE-SEYLER, F. A. Z. physiol. Chem. **222**, 105 (1933).
14. KUTSCHER, F. and ACKERMAN, D. Z. physiol. Chem. **221**, 33 (1933).
15. LEETE, E. J. Am. Chem. Soc. **78**, 3520 (1956).
16. STRACK, E. and SCHWANEBERG, H. Z. physiol. Chem. **245**, 11 (1936). BREGOFF, H. M., ROBERTS, E., and DELWICHE, C. C. J. Biol. Chem. **205**, 565 (1936).
17. KAMPFHAMMER, J. and BISCHOFF, C. Z. physiol. Chem. **191**, 179 (1930).
18. THIES, H. and REUTHER, F. W. Naturwissenschaften, **41**, 230 (1954).
19. HOUGH, L., JONES, J. K. N., and WADMAN, W. H. Nature, **162**, 448 (1948); J. Chem. Soc. 2511 (1949). SCHMID, H., KEBRLE, J., and KARRER, P. Helv. Chim. Acta, **39**, 1864 (1952).
20. SINGER, A. W. and MCELVAIN, S. M. Org. Syntheses, **20**, 79 (1940).
21. STEVENS, C. M. and ELLMAN, P. B. J. Biol. Chem. **182**, 75 (1950).

Can. J. Chem. Downloaded from www.nrcresearchpress.com by 61.7.252.67 on 09/04/12
For personal use only.

Can. J. Chem. Downloaded from www.nrcresearchpress.com by 61.7.252.67 on 09/04/12
For personal use only.

THE PHOTOLYSIS OF AZOETHANE[1]

H. CERFONTAIN[2] AND K. O. KUTSCHKE

ABSTRACT

The photolysis of azoethane at λ 3660 Å has been reinvestigated. The quantum yield of nitrogen formation was found to be dependent on the azoethane pressure and the temperature, indicating collisional deactivation of excited azoethane molecules.

The results confirm the mechanism proposed by Ausloos and Steacie (1). For the activation energy of the addition reaction $C_2H_5+C_2H_5N_2C_2H_5$ a value of 6.0±0.3 kcal./mole has been obtained, assuming a negligible activation energy for the combination reaction of two ethyl radicals.

INTRODUCTION

The formation of nitrogen in the photooxidation of azoethane (2) was found to be greater than expected and dependent on the pressures of azoethane and oxygen, as well as on the temperature.

Weininger and Rice (3) have studied the primary process in the photolysis of azoethane and showed that the quantum yield of nitrogen formation was dependent on the azoethane pressure in a manner which is explicable in terms of an activated molecule intermediate. In their study they made the implicit assumption that the quantum yield was independent of temperature. On the other hand, Durham and Steacie (4) found the quantum yield of nitrogen formation in the photolysis of azoisopropane to be temperature dependent. This suggested that a reinvestigation of the primary process in the photolysis of azoethane would be required in order to be certain of temperature effects for the photooxidation studies.

EXPERIMENTAL

Azoethane was obtained from Merck and Company. It was distilled several times and stored behind a mercury cutoff in a blackened tube. The reaction cell, with a volume of 180 ml., was completely filled with a parallel beam of light. The total reaction cell system, including a cold finger, a magnetically driven stirrer, and connecting tubing, had a volume of 282 ml. The analytical section consisted of a solid nitrogen trap, two Ward stills, a McLeod gauge, a diffusion pump, and a combined Toepler pump and gas burette. The photolysis products were separated as follows: Nitrogen was removed at solid nitrogen temperature; C_2 hydrocarbons were separated at −165° C. and analyzed mass spectrometrically. Butane was removed at −125° C.

A Hanovia S 500 medium pressure mercury arc was used as a light source, together with a Corning filter 5860 which limited the effective radiation to the 3660 Å group of lines. Absorption measurements were made with a photocell coupled to a sensitive galvanometer. At low azoethane concentrations (<0.001 mole/l.) the absorption measurements suffered from lack of precision. In this case the light absorption was calculated from the extinction coefficient, which was estimated from the experiments at higher concentration. For the highest concentration used, about 75% of the light was absorbed. Quantum yield measurements were carried out using a potassium ferrioxalate actinometer (5, 6) according to the procedure modified by Baxendale (5). The experiments were done at room temperature in subdued light. The radiation was completely absorbed by the actinometer. For these conditions, Hatchard and Parker (6) report a quantum yield of 1.21 for the actinometer at λ 3660 Å.

[1]*Manuscript received October 4, 1957.*
Contribution from the Division of Pure Chemistry, National Research Laboratories, Ottawa, Canada.
Issued as N.R.C. No. 4586.
[2]*N.R.L. Postdoctorate Fellow 1955-57.*

Can. J. Chem. Downloaded from www.nrcresearchpress.com by 61.7.252.67 on 09/04/12
For personal use only.

RESULTS AND DISCUSSION

Primary Processes

The light intensity was measured by placing the actinometer cell before and after the reaction cell. In the first position the intensity was found to be 1.64×10^{16} and 1.70×10^{16} quanta/second; in the second position 1.16×10^{16} and 1.00×10^{16} quanta/second. This observed difference appreciably exceeds that accounted for by simple reflections only. Assuming identical absorption and scattering by the front and rear windows of the reaction cell to be the only cause of light loss, a transparency factor $\alpha = 0.85$† per window was calculated from these data. Corrections for this and for first-order reflections from quartz–gas and pyrex–gas interfaces were made for all measurements, applying the general argument of Farkas and Melville (8) to our optical system. The data for the dependence of the nitrogen formation on temperature and azoethane concentration are given in Table I. The molar extinction coefficient E was calculated

TABLE I

EFFECT OF TEMPERATURE AND PRESSURE ON QUANTUM YIELD

Temp., ° C.	Azoethane conc., mole $l.^{-1}\times10^{3}$	I_a, quanta $second^{-1}$ $\times10^{-16}$	R_{N_2}, molec. $second^{-1}$ $\times10^{-16}$	$1/\phi$	E, $l.\ mole^{-1}\ cm.^{-1}$
28	7.16	1.10	0.648	1.70	19.1
	5.08	0.93	0.608	1.53	19.3
	3.57	0.75	0.533	1.41	19.0
	2.20	0.53	0.403	1.32	19.5
	1.45	0.380	0.305	1.24	19.5
	0.68	0.202	0.172	1.17	
78	6.75	1.10	0.710	1.55	19.5
	4.53	0.91	0.630	1.43	20.2
	2.90	0.68	0.527	1.28	20.2
	1.74	0.449	0.378	1.19	19.3
	0.83	0.248	0.216	1.15	
116	6.48	1.01	0.735	1.38	20.2
	4.16	0.79	0.619	1.27	20.6
	2.76	0.59	0.495	1.18	19.6
	1.80	0.431	0.374	1.15	20.8
	0.64	0.185	0.167	1.11	
152	6.16	1.07	0.915	1.17	20.4
	3.86	0.82	0.736	1.11	20.4
	1.91	0.490	0.436	1.12	20.5
	1.48	0.402	0.390	1.03	20.8
	0.68	0.206	0.207	1.00	

from $\ln I/I_0 = -Ecd$. Fig. 1 shows the relation between the quantum yield of nitrogen formation, temperature, and pressure. The accuracy of the actinometer measurements is ±10%. This means that the uncertainty in the $1/\phi$ scale is ±10%. It should be recognized, however, that the uncertainty in the $1/\phi$ values relative to each other is much less than this.

The mechanism proposed by Weininger and Rice (3) represents the results satisfactorily:

$$A + h\nu \rightarrow A^*, \quad [1]$$

$$A^* \rightarrow N_2 + 2C_2H_5, \quad [2]$$

$$A + A^* \rightarrow 2A, \quad [3]$$

†*This* α *corresponds to* $1-A$ *of Hunt and Hill* (7).

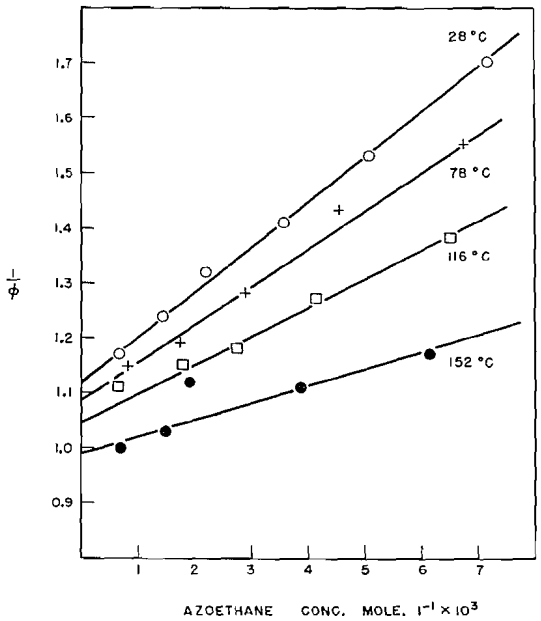

FIG. 1. Effect of pressure on reciprocal quantum yield of nitrogen formation from azoethane.

where A* represents an excited azoethane molecule. From a steady state treatment of the excited azoethane molecules, the following relation may be deduced:

$$1/\phi = 1+(k_3/k_2)\,|A|, \qquad [4]$$

where ϕ represents the quantum yield of nitrogen formation and $|A|$ the azoethane concentration.

It follows from relation [4] that a plot of $1/\phi$ against $|A|$ should be linear at each temperature with an intercept of unity, in close agreement with the experiments. By determining the slopes of these lines, values for k_3/k_2 at each temperature were derived.

The rate constant for deactivation k_3 was calculated from collision theory assuming zero activation energy and a steric factor of unity. A value of 7.0 Å was assumed for the kinetic collision diameters of normal and excited azoethane molecules. As shown in Table II, k_2 is temperature dependent. An Arrhenius plot (Fig. 2) shows the activation energy E_2 to be 2.1±0.4 kcal./mole.

TABLE II

VALUES OF RATE CONSTANTS

Temp., ° C.	k_3, molec.$^{-1}$ cm.^{3} second^{-1} $\times 10^{10}$	k_3/k_2, molec.$^{-1}$ cm.^{3} $\times 10^{19}$	k_2, second^{-1} $\times 10^{-9}$
28	2.96	1.35	2.19
78	3.20	1.13	2.84
116	3.37	0.88	3.84
152	3.52	0.515	6.8

The following observations indicate that the mechanism mentioned above is oversimplified:

Can. J. Chem. Downloaded from www.nrcresearchpress.com by 61.7.252.67 on 09/04/12
For personal use only.

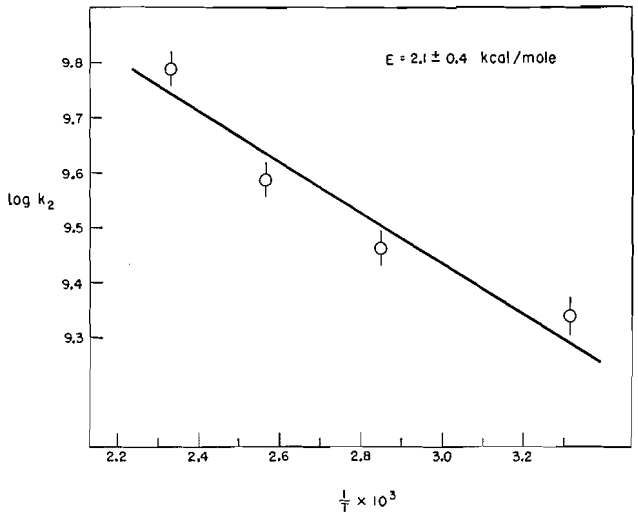

FIG. 2. Arrhenius plot of k_2.

(*a*) At higher temperatures nitrogen is formed not only by the primary process, but also by thermal decomposition of the $C_2H_4N_2C_2H_5$ radical (1),

$$C_2H_4N_2C_2H_5 \rightarrow C_2H_4 + N_2 + C_2H_5. \qquad [15]$$

An estimate of the amount of nitrogen produced by reaction [15] was made as follows: The amount of ethylene formed by disproportionation was calculated from the amount of butane, using a value of 0.12 for the ratio of disproportionation to combination of ethyl radicals (see below, *Secondary Processes*). The deviation of this amount from the total amount of ethylene formed was assumed to be due to reaction [15] only and is consequently equal to the amount of nitrogen formed by this reaction. The percentage of nitrogen formed under our experimental conditions by reaction [15] is 0.8% of the total amount at 107° C. and 2% at 152° C. This effect is very small, even at the highest temperatures employed; hence it can be neglected for the calculation of k_2.

(*b*) The intercepts of the reciprocal quantum yields of nitrogen show a small increase with a decrease in temperature.

(*c*) The curvature of the Arrhenius plot for k_2 probably exceeds experimental error.

(*d*) A fluorescence spectrogram did not indicate any fluorescence.

All these facts might well be explained by a diffusion controlled deactivation reaction of excited molecules at the wall of the reaction cell,

$$A^* + \text{wall} \rightarrow A. \qquad [5]$$

As the rate of disappearance of A* varies exponentially with temperature and the rate of diffusion varies with the square root of the temperature, an increasing deviation from unity for the reciprocal quantum yield at zero pressure may be expected with decreasing temperature. The rate of disappearance of excited molecules for wall deactivation is given by $k|A^*|/|A|$. From a steady state treatment for excited azoethane molecules one can derive

$$1/\phi = 1+(k_3/k_2)|A|+(k/k_2)|A|. \qquad [6]$$

Applying this equation, a corrected value for E_2 was calculated and found to be 2.4 ± 0.4 kcal./mole.

Can. J. Chem. Downloaded from www.nrcresearchpress.com by 61.7.252.67 on 09/04/12
For personal use only.

An alternative explanation might involve the $C_2H_5N_2$ radical, which might recombine with ethyl or decompose:

$$C_2H_5N_2C_2H_5 + h\nu \rightarrow C_2H_5N_2 + C_2H_5, \quad [7]$$

$$C_2H_5N_2 \rightarrow C_2H_5 + N_2, \quad [8]$$

$$C_2H_5N_2 + C_2H_5 \rightarrow C_2H_5N_2C_2H_5. \quad [9]$$

The stability of the $C_2H_5N_2$ radical is expected to be greatest at low temperatures, and this results in a maximum decrease in quantum yield for the nitrogen formation at these temperatures. The quantum yield of nitrogen formation should be intensity dependent in the temperature range in which the lifetime of the $C_2H_5N_2$ radical is comparable to the time between collisions of C_2H_5 and $C_2H_5N_2$ radicals. The observed quantum yield, however, (Table III) is independent of the light intensity. It may therefore be concluded that the lifetime of $C_2H_5N_2$ is short compared to the time between collisions. Reaction [9] can therefore be excluded.

TABLE III

EFFECT OF LIGHT INTENSITY ON QUANTUM YIELD AT 28° C.

Azoethane conc., mole $l.^{-1} \times 10^3$	I_a, quanta $second^{-1}$ $\times 10^{-16}$	R_{N_2}, molec. $second^{-1}$ $\times 10^{-16}$	$1/\phi$
0.75	0.242	0.215	1.12
0.75	0.0246	0.0212	1.16
0.75	0.00286	0.00248	1.15

Internal conversion of the excited azoethane molecule to another electronic state which is incapable of dissociation (9) might be considered as a third explanation,

$$A^* \rightarrow A. \quad [10]$$

From a steady state treatment of excited azoethane molecules it follows that

$$1/\phi = 1 + k_{10}/k_2 + (k_3/k_2)|A|. \quad [11]$$

The value of k_2 increases with increasing temperature (Table II) and if k_{10} is less temperature dependent, the intercept of the plot of $1/\phi$ against $|A|$ may be expected to decrease with increasing temperature, and to approach unity, as is, in fact, the case. Collisional deactivation has been observed in the photolysis of azoisopropane (4). For azomethane (10) the quantum yield of decomposition was found to be unity, independent of temperature and pressure. The difference in collisional deactivation for the three homologous azoalkanes is illustrated in Fig. 3. It is generally accepted (3) that, although the primary excitation in photochemical decompositions is mainly electronic, the mechanism of decomposition involves its transfer to vibrational energy and the accumulation of this energy in a particular bond. Hence the reasonable observation is made that collisional deactivation is negligible in the photolysis of azomethane, but is of considerable importance in the photolysis of the higher homologues because of their larger number of degrees of vibrational freedom.

Secondary Processes

The results of the photolysis are shown in Table IV. To avoid side reactions the

Can. J. Chem. Downloaded from www.nrcresearchpress.com by 61.7.252.67 on 09/04/12
For personal use only.

Can. J. Chem. Downloaded from www.nrcresearchpress.com by 61.7.252.67 on 09/04/12
For personal use only.

TABLE IV

PHOTOLYSIS OF AZOETHANE

Temp., °C.	Relative intensity	Conc., azo, molec. cm.$^{-3}$ $\times 10^{-18}$	Products, molec. cm.$^{-3}$ second^{-1} $\times 10^{-13}$				$\frac{R_{C_2H_4}}{R_{C_4H_{10}}}$	$\frac{R_{C_2H_6}+R_{C_4H_{10}}}{R_{N_2}}$	$k_{14}/k_{12}^{\frac{1}{2}}$, molec.$^{-\frac{1}{2}}$ cm.$^{3/2}$ second$^{-\frac{1}{2}}$ $\times 10^{13}$	$R_{T.E.H.}$, molec. cm.$^{-3}$ second^{-1} $\times 10^{-13}$	$k_{21}/k_{12}^{\frac{1}{2}}$, molec.$^{-\frac{1}{2}}$ cm.$^{3/2}$ second$^{-\frac{1}{2}}$ $\times 10^{13}$
			R_{N_2}	$R_{C_2H_6}$	$R_{C_2H_4}$	$R_{C_4H_{10}}$					
27	9.7	0.492	0.118	0.0166	0.0114	0.0972	0.118	0.965	1.06	0.0041	0.85
30	98	0.326	0.883	0.0972	0.0884	0.772	0.114	0.985	0.98	0.013	1.4
28	93	0.605	1.58	0.189	0.166	1.33	0.124	0.961	1.07	0.062	2.7
31	90	0.641	1.58	0.176	0.156	1.36	0.116	0.959	0.92	0.065	2.7
27	90	0.845	1.97	0.209	0.181	1.63	0.111	0.940	0.81	0.118	3.4
29	35	0.627	0.589	0.0750	0.0583	0.500	0.117	0.975	1.17	0.015	1.0
78	96	0.497	1.20	0.189	0.110	0.915	0.120	0.925	5.30	0.090	4.5
107	88	0.605	1.77	0.413	0.131	1.19	0.110	0.905	13.5	0.168	8.0
107	89	0.567	1.66	0.374	0.147	1.14	0.128	0.910	11.9	0.149	7.8
107	89	0.507	1.61	0.384	0.143	1.07	0.133	0.902	14.6	0.158	9.6
116	88	0.386	0.927	0.218	0.0722	0.628	0.115	0.912	15.2	0.082	8.4
118	90	0.381	0.944	0.236	0.0689	0.595	0.116	0.882	18.1	0.111	12.0
152	95	0.299	1.05	0.355	0.0761	0.547	0.139	0.861	40.1	0.146	20.9
175	89	0.436	1.54	0.833	0.117	0.467	0.250	0.843	76.2	0.242	25.8
175	89	0.507	1.82	0.965	0.125	0.500	0.250	0.804	74.7	0.356	31.3
175	91	0.555	1.96	1.02	0.141	0.561	0.251	0.813	67.2	0.366	27.8

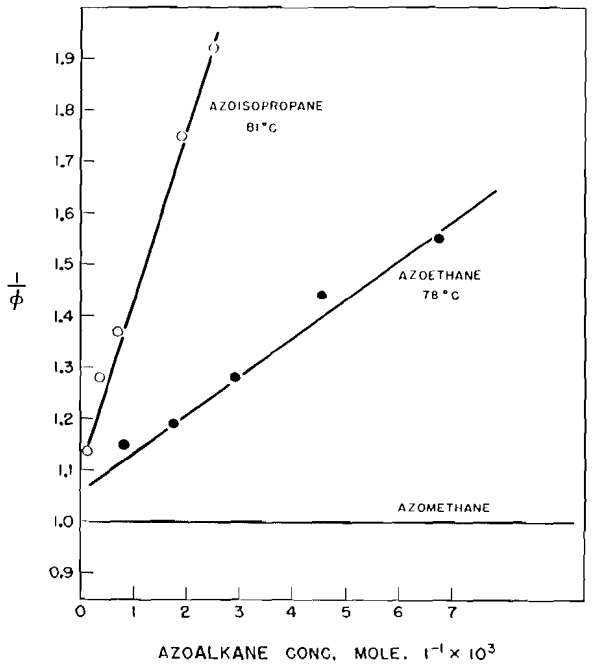

FIG. 3. Effect of pressure on reciprocal quantum yield of nitrogen formation from the lower azoalkanes.

conversion was kept below 3%. Ausloos and Steacie (1) explained their results in the photolysis of azoethane by means of the following mechanism:

$$C_2H_5N_2C_2H_5 + h\nu \rightarrow C_2H_5N_2C_2H_5^*, \quad [1]$$

$$C_2H_5N_2C_2H_5^* \rightarrow N_2 + 2C_2H_5, \quad [2]$$

$$2C_2H_5 \rightarrow C_4H_{10}, \quad [12]$$

$$2C_2H_5 \rightarrow C_2H_4 + C_2H_6, \quad [13]$$

$$C_2H_5 + C_2H_5N_2C_2H_5 \rightarrow C_2H_6 + C_2H_4N_2C_2H_5, \quad [14]$$

$$C_2H_4N_2C_2H_5 \rightarrow C_2H_4 + N_2 + C_2H_5, \quad [15]$$

$$C_2H_5 + C_2H_4N_2C_2H_5 \rightarrow C_4H_5N_2C_2H_5, \quad [16]$$

$$2C_2H_4N_2C_2H_5 \rightarrow (C_2H_4N_2C_2H_5)_2. \quad [17]$$

Assuming ethylene, ethane, and butane to be formed only by reactions [12], [13], and [14], the following relations should be obeyed:

$$\frac{R_{C_2H_4}}{R_{C_4H_{10}}} = \frac{k_{13}}{k_{12}}, \quad [18]$$

$$\frac{R_{C_2H_6} - R_{C_2H_4}}{R_{C_4H_{10}}} = \frac{k_{14}[A]}{k_{12}^{1/2} R_{C_4H_{10}}^{1/2}}, \quad [19]$$

$$\frac{R_{C_2H_6} + R_{C_2H_4}}{R_{C_4H_{10}}} = 2\frac{k_{13}}{k_{12}} + \frac{k_{14}[A]}{k_{12}^{1/2} R_{C_4H_{10}}^{1/2}}. \quad [20]$$

The ratio $R_{C_2H_4}/R_{C_4H_{10}}$ is found to be constant with a value of 0.12 ± 0.01 in the temperature range 27–118° C. This means that $E_{13} - E_{12} = 0$ (cf. Shepp and Kutschke (11)). At higher temperatures an increase in the ethylene to butane ratio is observed owing to thermal decomposition of $C_2H_4N_2C_2H_5$. In Fig. 4, $(R_{C_2H_6} + R_{C_2H_4})/R_{C_4H_{10}}$ and $(R_{C_2H_6}$

Can. J. Chem. Downloaded from www.nrcresearchpress.com by 61.7.252.67 on 09/04/12
For personal use only.

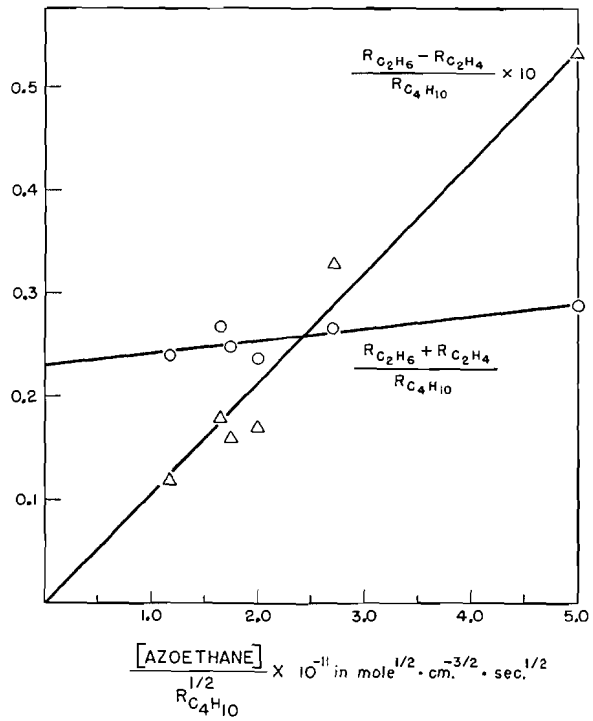

FIG. 4. Plot of $(R_{C_2H_6}+R_{C_2H_4})/R_{C_4H_{10}}$ and $(R_{C_2H_6}-R_{C_2H_6})/R_{C_4H_{10}}$ vs. $|A|/R_{C_4H_{10}}^{1/2}$.

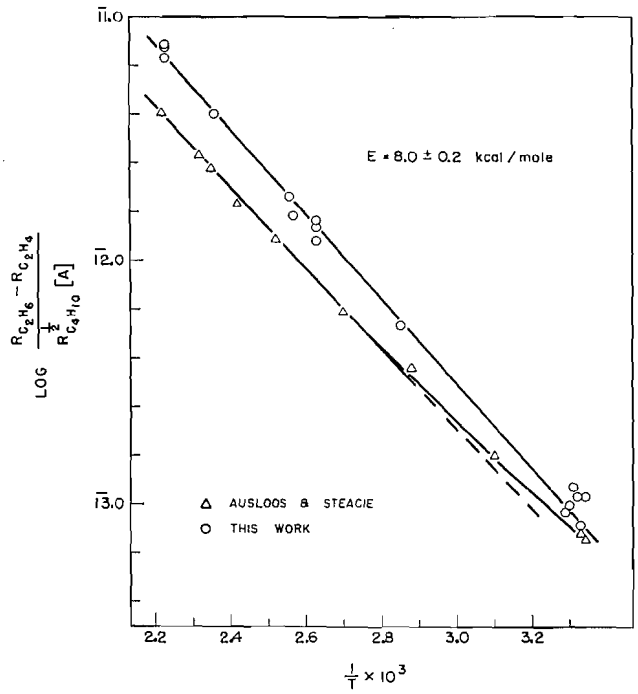

FIG. 5. Arrhenius plot of $k_{14}/k_{12}^{1/2}$.

Can. J. Chem. Downloaded from www.nrcresearchpress.com by 61.7.252.67 on 09/04/12
For personal use only.

$-R_{C_2H_4})/R_{C_4H_{10}}$ are plotted against $|A|/R_{C_4H_{10}}{}^{1/2}$ for runs at 28° C. According to relation [20] the intercept of this curve with the ordinate should be equal to $2k_{13}/k_{12}$. A value of $k_{13}/k_{12} = 0.12\pm0.01$ was obtained. Values of $k_{14}/k_{12}{}^{1/2}$ were calculated from relation [19]. By plotting log $k_{14}/k_{12}{}^{1/2}$ against $1/T$ (Fig. 5) a value of $E_{14}-\frac{1}{2}E_{12} = 8.0\pm0.2$ kcal./mole was obtained. This value is higher than that reported by Ausloos and Steacie, who estimated $E_{14}-\frac{1}{2}E_{12} = 7.5\pm0.1$ kcal./mole. This low value, as well as the curvature they observed in the Arrhenius plot below 70° C., may well be explained by a small impurity in their azoethane sample.

Some high (~20%) conversion experiments were done in order to accumulate significant quantities of heavier products for possible mass spectrometric identification; the fraction remaining after butane and higher products were removed was submitted for analysis. After subtraction of the contributions due to unreacted azoethane a large number of peaks remained between masses 28 and 150. In particular the presence of major peaks at masses 114 and 144, together with peaks corresponding to plausible fragments, suggested that ethyl butyl diimide and tetraethyl hydrazine are amongst the products. In addition, peaks at masses 56, 55, and 42, possibly corresponding to the ions $C_2H_4N_2{}^+$, $C_2H_3N_2{}^+$, and $C_2H_4N^+$ or $CH_2N_2{}^+$ respectively, suggested the presence of diazoethane. These ions might also arise as fragments in the spectrum of ethyl butyl diimide, however, and in the absence of pure standards the identification can be considered tentative only. Should diazoethane be a product, reaction [15*a*] could be suggested as a source. This is similar to the reaction thought to lead to methyl ketene in the photolysis of diethyl ketone (12),

$$C_2H_5N_2C_2H_4 \rightarrow C_2H_5 + CH_3CHN_2. \qquad [15a]$$

Since diazoethane is transparent at λ 3660 Å (13) no photolysis is expected even under conditions of high conversion.

The material balance $(R_{C_2H_6}+R_{C_4H_{10}})/R_{N_2}$ should be equal to unity if only reactions [2], [12], [13], [14], [15], and [16] are involved and should be greater than unity if reaction [15*a*] or [17] occurs as well. As can be seen from Table IV a value smaller than unity was observed, showing a decrease with increase in temperature. Since tetraethyl hydrazine is probably among the products, the following addition reactions between ethyl radicals and azoethane may be suggested:

$$C_2H_5—N{=}N—C_2H_5 + C_2H_5 \rightarrow (C_2H_5)_2N—N—C_2H_5, \qquad [21]$$

$$(C_2H_5)_2N—N—C_2H_5 + C_2H_5 \rightarrow (C_2H_5)_2N—N(C_2H_5)_2. \qquad [22]$$

The rate of formation of tetraethyl hydrazine will be equal to $R_{T.E.H.} = R_{N_2}-R_{C_4H_{10}}$ $-R_{C_2H_6}$ subject to the following assumptions:

(*a*) Reaction [21] is the rate determining step in the formation of tetraethyl hydrazine.

(*b*) Reaction [15], [15*a*], and [17] may be neglected, i.e., for every molecule of ethane formed by abstraction, a molecule of ethyl butyl diimide is formed. As pointed out before, the number of $C_2H_5N_2C_2H_4$ radicals disappearing by reaction [15] is small.

The following relation may be deduced on this basis:

$$k_{21}/k_{12}{}^{1/2} = R_{T.E.H.}/R_{C_4H_{10}}{}^{1/2}|A|. \qquad [23]$$

By plotting log $k_{21}/k_{12}{}^{1/2}$ against $1/T$ (Fig. 6) a value of $E_{21}-\frac{1}{2}E_{12} = 6.0\pm0.3$ kcal./mole was obtained. A large scatter in $R_{T.E.H.}$ and log $k_{21}/k_{12}{}^{1/2}$ may be expected at low temperatures since the material balance approaches unity under these conditions. The present value of $E_{21}-\frac{1}{2}E_{12}$ is in agreement with the activation energies for other reactions of the addition of radicals to double bonds (10, 14, 15).

Can. J. Chem. Downloaded from www.nrcresearchpress.com by 61.7.252.67 on 09/04/12
For personal use only.

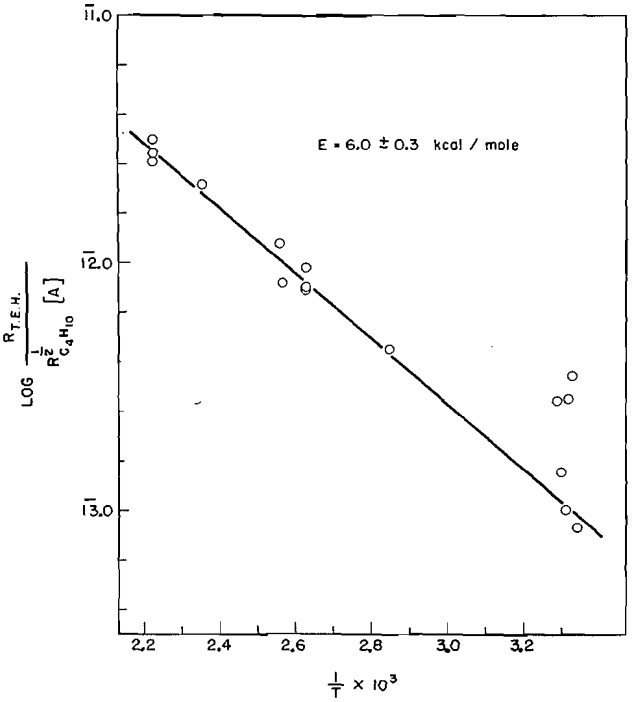

FIG. 6. Arrhenius plot of $k_{21}/k_{12}^{1/2}$.

ACKNOWLEDGMENTS

The authors are indebted to Dr. Steacie for his encouragement and interest throughout this work, and to Mrs. Frances Kutschke and Miss Bernice Thornton for the mass spectrometric analyses.

REFERENCES

1. AUSLOOS, P. and STEACIE, E. W. R. Bull. soc. chim. Belges, **63**, 87 (1954).
2. CERFONTAIN, H. and KUTSCHKE, K. O. To be published.
3. WEININGER, J. L. and RICE, O. K. J. Am. Chem. Soc. **74**, 6216 (1952).
4. DURHAM, R. W. and STEACIE, E. W. R. Can. J. Chem. **31**, 377 (1953).
5. BAXENDALE, J. H. and BRIDGE, N. K. J. Phys. Chem. **59**, 783 (1955).
6. HATCHARD, C. G. and PARKER, C. A. Proc. Roy. Soc. A, **225**, 518 (1956).
7. HUNT, R. F. and HILL, T. L. J. Chem. Phys. **15**, 111 (1947).
8. FARKAS, A. and MELVILLE, H. W. Experimental methods in gas reactions. The MacMillan Co., New York. 1939. p. 247.
9. NOYES, W. A., Jr., PORTER, G. B., and JOLLEY, E. Chem. Revs. **56**, 54 (1956).
10. JONES, M. H. and STEACIE, E. W. R. J. Chem. Phys. **21**, 1018 (1953).
11. SHEPP, A. and KUTSCHKE, K. O. J. Chem. Phys. **26**, 1020 (1957).
12. HAYNES, W. S. and GARDNER, P. D. J. Am. Chem. Soc. **73**, 3065 (1951).
13. BRINTON, R. K. and VOLMAN, D. H. J. Chem. Phys. **19**, 1394 (1951).
14. MANDELCORN, L. and STEACIE, E. W. R. Can. J. Chem. **32**, 474 (1954).
15. STEACIE, E. W. R. Atomic and free radical reactions. 2nd ed. Reinhold Publishing Corp., New York. 1954. p. 581.

Can. J. Chem. Downloaded from www.nrcresearchpress.com by 61.7.252.67 on 09/04/12
For personal use only.

Can. J. Chem. Downloaded from www.nrcresearchpress.com by 61.7.252.67 on 09/04/12
For personal use only.

TRYPTAMINES, CARBOLINES, AND RELATED COMPOUNDS

PART IV. ATTEMPTED SYNTHESIS OF THE PHYSOSTIGMINE RING SYSTEM[1,2]

R. A. ABRAMOVITCH[3]

ABSTRACT

4-Methylpiperid-2,3-dione-3-phenylhydrazone failed to undergo ring closure under Fischer-cyclization conditions but rearranged to a more stable form of the phenylhydrazone. *Cis–trans* isomerism is suggested for the two forms.

In Parts II and III (1, 2) a relatively general method of preparing tryptamines was developed which involved the hydrolysis of 1,2,3,4-tetrahydro-1-oxo-β-carbolines to tryptamine-2-carboxylic acids, followed by decarboxylation. It occurred to us that if the tryptamine-2-carboxylic acid had a 3-methyl substituent (II) decarboxylation of this indolenine carboxylic acid would give rise to an amine (III) which should cyclize readily to give the tricyclic system (IV) present in physostigmine.

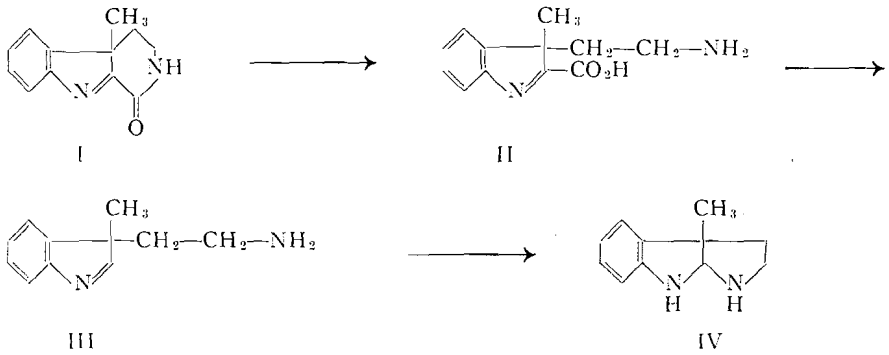

I II III IV

To this end, ethyl malonate was condensed with allyl cyanide to give diethyl (2-cyano-1-methyl)ethylmalonate (V). Allyl cyanide rearranges in the presence of alkali to crotononitrile, and it is this which undergoes the Michael addition (3). Similar reactions involving the addition of fluorene (4) and 9-monosubstituted fluorenes (5) to crotononitrile following the allylic rearrangement have been reported. The nitrile (V) was catalytically reduced under pressure to give 3-ethoxycarbonyl-4-methyl-2-oxopiperidine (VI), which was hydrolyzed to the corresponding acid. This was not isolated but its solution was treated with benzenediazonium chloride at pH 4, when it underwent the Japp–Klingemann reaction giving the phenylhydrazone (VII). The conditions of the Japp–Klingemann reaction were found, as in previous cases (1, 2), to be critical because at lower or higher pH's considerable tar formation took place.

Cyclization of the phenylhydrazone (VII) to the indolenine (I) could not be effected. Under mild conditions which effect the cyclization of unsubstituted piperidone phenylhydrazones (e.g. boiling with 90% acetic acid) VII was unchanged. If more powerful reagents were used for prolonged periods only tar formation took place. With boron trifluoride in acetic acid, or with zinc chloride, the phenylhydrazone (VII) rearranged to a

[1]*Manuscript received November 6, 1957.*
Contribution from King's College, University of London, Strand, London, W.C.2, England.
[2]*Part III: J. Chem. Soc. 4593 (1956).*
[3]*I.C.I. Research Fellow at King's College. Present address: Chemistry Department, University of Saskatchewan, Saskatoon, Sask., Canada.*

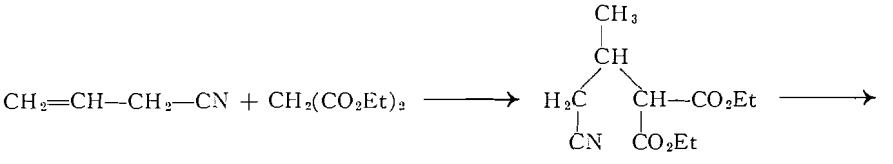

V

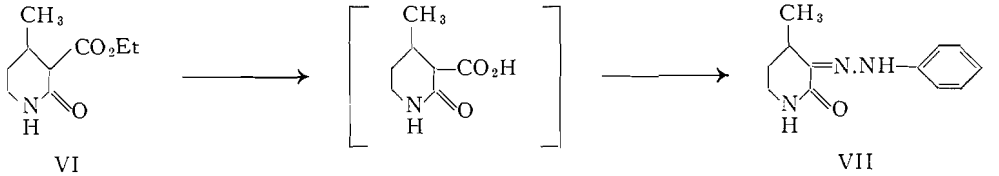

VI VII

more stable form which resisted all attempts to effect cyclization. This rearrangement of a phenylhydrazone to a more stable form, instead of undergoing cyclization, is not unique; Snyder and Smith (6) found that ethyl 4-cyano-2-oxobutyrate 2-phenylhydrazone was isomerized to a more stable form but could not be induced to cyclize. The failure of our phenylhydrazone to cyclize is somewhat surprising since Millson and Robinson (7) were able to prepare the tetrahydro-9,11-dimethylcarbazoles from the 2-methyl*cyclo*hexanone *N*-methoxyphenyl-*N*-methylhydrazones, so that possible hindrance arising from the conformation of the methyl-group does not seem to be the cause.

It seems probable that the isomerism of these hydrazones is geometrical. Recently, we have obtained evidence for the existence of such geometrical isomerism with the phenylhydrazones of pyruvamide and methyl pyruvate (8), and it had previously been observed with acetaldehyde phenylhydrazone (9) and pyruvic acid 2,4-dinitrophenylhydrazone (10). Consideration of the positions of the amide-carbonyl absorption bands in the infrared spectra of the isomeric phenylhydrazones studied here suggests that the more stable form (B) has the *anti*-configuration while the form (A) obtained from the Japp-Klingemann reaction has the *syn*-configuration.

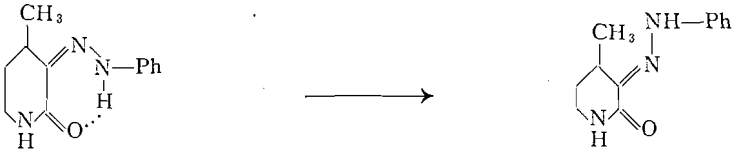

A B

The difference in the amide C=O frequencies is not, however, as large as in the other cases previously studied so that the assignments are only tentative. The *syn*-form, which has the possibility of being intramolecularly hydrogen bonded, should exhibit a lower ν_{CO} (1658 cm.$^{-1}$ in this case) than the *anti*-structure (1669 cm.$^{-1}$), where this possibility does not exist.

In view of the failure to effect cyclization at this stage the piperidone (VII) was hydrolyzed to the amino acid. This route, however, offers no advantage over well-established approaches to the physostygmine ring system and was, therefore, not pursued further.

EXPERIMENTAL

M.p.'s and b.p.'s are uncorrected. Infrared spectra were measured on a Grubb-Parsons model S4 double-beam instrument with sodium chloride optics.

Can. J. Chem. Downloaded from www.nrcresearchpress.com by 61.7.252.67 on 09/04/12
For personal use only.

Diethyl (2-Cyano-1-methyl)ethylmalonate

Ethyl malonate (16 g.) was added to a cold solution of sodium (0.5 g.) in ethanol (20 ml.). To this solution was added dropwise with stirring a solution of allyl cyanide (4 g.) in absolute ethanol (10 ml.), the temperature being maintained below 35°. The solution was kept at room temperature overnight, treated with acetic acid (1.3 g.), and the alcohol evaporated under reduced pressure. The residue was extracted with ether and the extract dried ($MgSO_4$) and evaporated, eventually *in vacuo* at 130° (water pump). The residue was distilled under reduced pressure giving the colorless ester (11.7 g.), b.p. 180° at 16 mm., 119° at 0.4 mm. Calc. for $C_{11}H_{17}O_4N$: C, 58.2; H, 7.5; N, 6.2. Found: C, 58.4; H, 7.7; N, 6.55. I.R. spectrum (liquid film) (main bands only): C≡N, 2283 cm.$^{-1}$ (w); $(CO_2Et)_2$, 1742 (s), 1730 cm.$^{-1}$ (s).

3-Ethoxycarbonyl-4-methyl-2-oxopiperidine

The above malonate (30 g.) in commercial absolute ethanol (120 ml.) was hydrogenated in the presence of Raney nickel (1 g.) at 80° and 100 atm. until hydrogen uptake was complete (*ca.* 3–4 hours). The filtered solution was evaporated, eventually under reduced pressure, on the water bath, and the cooled residue treated with light petroleum (b.p. 60–80°). Crystallization occurred immediately. The product (24 g.) was filtered, washed with cold light petroleum, and recrystallized from that solvent containing a few drops of benzene, giving colorless plates, m.p. 83–84°. Calc. for $C_9H_{15}O_3N$: C, 58.4; H, 8.2. Found: C, 58.6; H, 8.1.

4-Methylpiperid-2,3-dione-3-phenylhydrazone (A)

3-Ethoxycarbonyl-4-methyl-2-oxopiperidine (1.85 g.) in water (20 ml.) containing potassium hydroxide (0.6 g.) was kept at room temperature for 18 hours. The solution was cooled in ice and treated, with stirring, with a partially neutralized solution (30 ml.) of benzenediazonium chloride prepared from aniline (0.97 g.) and sodium nitrite (0.55 g.), and the pH of the mixture immediately adjusted to *ca.* 4 by addition of glacial acetic acid. Ammonium chloride (4 g.) was added and stirring was continued, the temperature of the solution being slowly allowed to reach room temperature. After 10 hours the solid which had separated was filtered, washed with water, and recrystallized from dilute alcohol giving the phenylhydrazone (A), m.p. 141–142°. Calc. for $C_{12}H_{15}ON_3$: C, 66.3; H, 7.0. Found: C, 66.0; H, 7.0. I.R. spectrum (Nujol mull): NH, 3185 cm.$^{-1}$ (broad); CO (amide), 1658 cm.$^{-1}$ (s); C_6H_5- 751, 702 cm.$^{-1}$ (s). The picrate separated from a small volume of alcohol as dark red needles, m.p. 105–106°.

Attempted Fisher Cyclization of the Phenylhydrazone (A)

(*a*) The phenylhydrazone (0.5 g.) in glacial acetic acid (2 ml.) was treated with a 45% ethereal solution (0.36 g.) of boron trifluoride. The solution turned red and the solid complex separated. The suspension was slowly heated to 60°, when the solid went into solution, and this was then boiled for 2 minutes, poured into cold water, and the acid neutralized with an excess of saturated aqueous sodium carbonate solution. The crude yellow product which separated was insoluble in boiling water and only sparingly soluble in boiling ethanol, but readily soluble in hot dilute ethanol, from which it was recrystallized, giving colorless flat needles (0.19 g.) of the phenylhydrazone (B), m.p. 207–208°. Calc. for $C_{12}H_{15}ON_3$: C, 66.3; H, 7.0; N, 19.3. Found: C, 66.1; H, 6.75; N, 18.8. I.R. spectrum (Nujol mull): NH 3226 cm.$^{-1}$; CO (amide) 1669 cm.$^{-1}$ (s); C_6H_5- 754, 692 cm.$^{-1}$ (s). The picrate separated from a small volume of ethanol as yellow needles, m.p. 139–140°. The filtrate from the recrystallization of the crude product was evaporated to a small volume giving crystals of the starting phenylhydrazone (A) (0.22 g.), m.p. 136–138°, undepressed on admixture with an authentic sample, m.p. 141–142°.

Can. J. Chem. Downloaded from www.nrcresearchpress.com by 61.7.252.67 on 09/04/12
For personal use only.

If the acetic acid solution was boiled for ½ hour instead of 1 minute only a dark brown gum was obtained which could not be purified. Boiling the phenylhydrazone (A) with an absolute ethanolic solution of dry hydrogen chloride for 1 minute led to recovery of starting material, whereas heating it with polyphosphoric acid led to tar formation.

(*b*) The phenylhydrazone (A) (0.5 g.) and anhydrous zinc chloride (2.5 g.) were heated to 170° (oil bath) and kept at that temperature for 1 hour. The cooled mass was treated with water and then with an excess of 15% aqueous sodium hydroxide, the residue was filtered, washed repeatedly with water, and extracted with boiling 70% ethanol. The filtered extract was evaporated down till crystallization occurred, giving the crude phenylhydrazone (B) (0.31 g.), m.p. 199–200°, raised to 207–208° on recrystallization from dilute ethanol. The I.R. spectrum was identical with that of the product obtained as under (*a*).

Alkaline Hydrolysis of Phenylhydrazone (*A*)

The hydrazone (0.5 g.) was boiled under reflux for 10 hours with a solution of potassium hydroxide (1.1 g.) in 60% ethanol (12 ml.). The alcohol was partially evaporated and replaced by water, the hot solution filtered, made just acid with glacial acetic acid, and kept overnight, when the impure amino acid, contaminated with silica, had separated. Recrystallization from a small volume of 90% ethanol gave colorless crystals (0.2 g.) of 5-amino-3-methyl-2-oxopentanoic acid 2-phenylhydrazone, m.p. 172–173° (effervescence). Calc. for $C_{12}H_{17}O_2N_3$: C, 61.3; H, 7.2. Found: C, 61.1; H, 7.3.

ACKNOWLEDGMENT

This work was carried out during the tenure of an I.C.I. Research Fellowship in the University of London.

REFERENCES

1. ABRAMOVITCH, R. A. and SHAPIRO, D. J. Chem. Soc. 4589 (1956).
2. ABRAMOVITCH, R. A. J. Chem. Soc. 4593 (1956).
3. MICHAEL, A. and ROSS, J. J. Am. Chem. Soc. **53**, 1150 (1931).
4. BRUSON, H. A. J. Am. Chem. Soc. **64**, 2457 (1942).
5. TUCKER, S. H. J. Chem. Soc. 2182 (1949).
6. SNYDER, H. R. and SMITH, C. W. J. Am. Chem. Soc. **65**, 2452 (1943).
7. MILLSON, M. F. and ROBINSON, R. J. Chem. Soc. 3362 (1955).
8. ABRAMOVITCH, R. A. and SPENSER, I. D. J. Chem. Soc. 3767 (1957).
9. LAWS, E. G. and SIDGWICK, N. V. J. Chem. Soc. **99**, 2085 (1911).
10. ISHERWOOD, F. A. and LUMLEY JONES, R. Nature, **175**, 419 (1955).

Can. J. Chem. Downloaded from www.nrcresearchpress.com by 61.7.252.67 on 09/04/12
For personal use only.

Can. J. Chem. Downloaded from www.nrcresearchpress.com by 200.7.193.243 on 09/04/12
For personal use only.

DEOXYMERCURATION[1]

O. W. Berg, W. P. Lay, A. Rodgman, and G. F Wright

ABSTRACT

The conversion of several stereoisomeric oxymercurials to alkenes (deoxymercuration) has been studied with hydrogen chloride in anhydrous and near-anhydrous methanol. In each instance the addition of water decreases the second-order rate. In benzene the addition of water to the anhydrous system first accelerates and then decreases the reaction rate. These results have been interpreted in support of molecular rather than ionic participation by hydrogen chloride. Since molecular participation requires the ↑↑ arrangement of alkoxy and chloromercuri groups for easy reaction it follows that oxymercuration also follows a molecular and not a "mercurinium ion" mechanism in the normal reaction.

The decomposition of 2-oxyorganomercuric salts to mercuric salts and alkenes has been called deoxymercuration (11). It is a much milder reaction than is the scission of simple alkylmercuric salts, some of which resist prolonged heating with strong acids. This difference must be due to the vicinal oxygen linkage. Several opinions have been expressed about the manner in which this oxygen assists the scission of the carbon–mercury link. It will be seen that these opinions are closely related to the ideas of oxymercurial formation. For this reason a decision about the manner in which deoxymercuration occurs ought to specify the mechanism of oxymercuration.

According to Whitmore (20) deoxymercuration is induced by formation of an oxonium salt, I, which then decomposes into an alcohol, an alkene, and a mercuric monocation (where X is an acid substituent bound covalently).

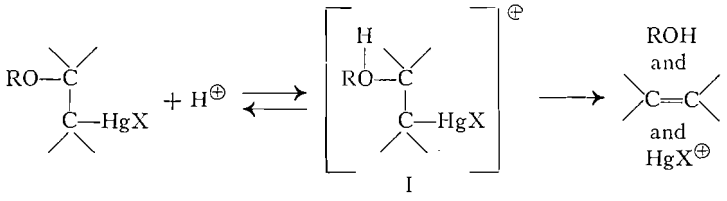

I

According to this mechanism the rate of deoxymercuration ought to be dependent on the strength of the acid used in the reaction. This dependence on acid strength has been confirmed by experiment (11).

According to another, more recent, opinion the reaction is of the "E_2 elimination" type (22) in which an anion is presumed to coordinate with the mercurial (II) to force the

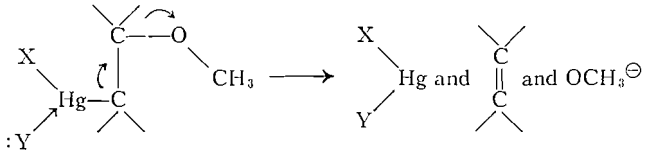

II

indicated electronic displacement. Presumably the experimental basis for this scheme lies in the early work of Sand and Breest (15) and a recent reconsideration of it (14). However these experiments were inconclusive. Moreover it has been shown (11) that deoxymercuration by hydrogen chloride in methanol is insensitive to addition of sodium chloride or mercuric chloride. Actually no factual proof of the E_2 scheme exists.

[1]*Manuscript received August 7, 1957.*
Contribution from the Department of Chemistry, University of Toronto, Toronto, Ontario.

The scheme may have been revived for several reasons. First it is essentially the reversal of a popular mechanism for oxymercuration (9). These authors propose that a mercuric monocation coordinates with an alkene to give an "alkanemercurinium" ion, III, which reacts with an alkoxide ion to yield the oxymercurial, IV.

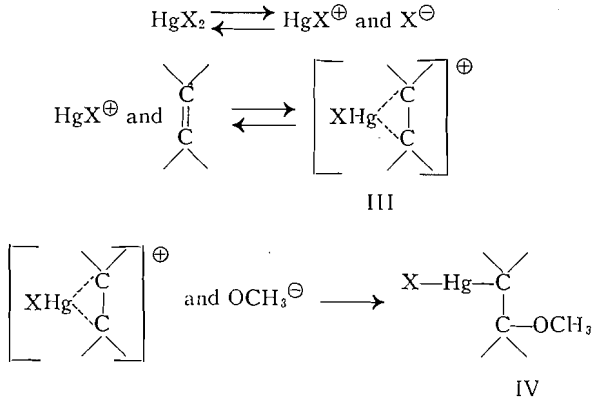

III

IV

Secondly, it may be noted that the final reaction of this series involves an inversion (postulated also for the deoxymercuration) from which a *trans* (↑↓) oxymercurial would be formed. The mechanism received strong support from an X-ray diffraction study (4) in which α-2-methoxycyclohexylmercuric chloride was assigned the ↑↓ configuration. However, it is now realized that this X-ray diffraction study is non-definitive because the ring constellation cannot be discerned adequately in the presence of several heavy atoms. If, instead of the orthodox "crown" ring, the "flexible" cyclohexane ring (8, 7) is assumed, the location of the ring substituents may be a consequence of the ring deformation rather than of substituent configuration. Attempts to refine the structures so as to locate the ring carbon atoms more concisely than in the original study have proved to be fruitless.

However, the inversion mechanism does account satisfactorily for the experimental observation that in certain circumstances the deoxymercuration is stereospecific. When the single diastereomeric oxymercurial produced from a single geoisomer is treated with concentrated hydrochloric acid the single geoisomer is regenerated without contamination (24). Inspection of the postulated mercurinium ion shows that it will be involved stereospecifically in oxymercuration, as also will the E_2 reaction specified for deoxymercuration. Moreover, the conformation required for the inversion reactions should be more favorable in one diastereomer than in another, and in many instances this difference in reactivity is observed. Thus it remains only to demonstrate that the ionic species significant to these mechanisms actually are available in the reacting systems.

There is evidence against the direct participation of ionic species in the oxymercuration of alkenes. According to these studies (12) the reacting species is a basic mercuric salt which undergoes a four-center addition to the alkene.

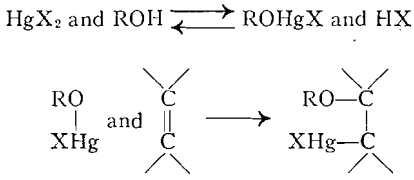

It may be seen that this mechanism also satisfies the experimental requirement of a

Can. J. Chem. Downloaded from www.nrcresearchpress.com by 200.7.193.243 on 09/04/12
For personal use only.

second-order stereospecific reaction but it differs from the ionic inversion mechanism because it involves direct (↑↑) addition rather than ↑↓ addition.

This mechanism, essentially molecular* rather than ionic, has its counterpart in deoxymercuration, where a molecule of hydrochloric acid (X = Cl) is thought to coordinate with the alkene to form a six-atom "quasi-cyclic" intermediate, V. In V the

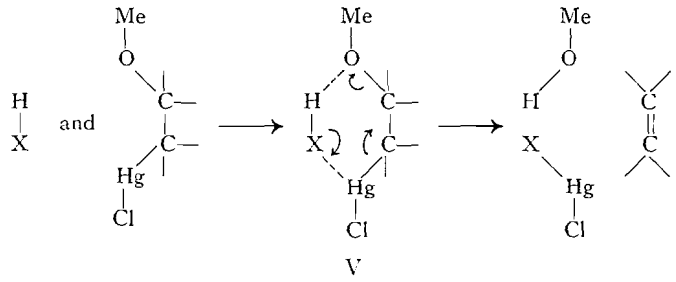

V

electronic redistribution causes scission to the products. It may be seen that these explanations that are based on direct rather than inverse addition also imply stereospecificity, either of product or of reaction rate. Actually the direct (↑↑) explanation fits better the oxymercuration of stilbene and isostilbene and the deoxymercuration of the corresponding two diastereomeric methoxymercurials than does the inverse mechanism (23). However, one essential difference in the two mechanisms involves ion participation in one but not in the other. This criterion has been evaluated in the present report.

The deoxymercurations described above have involved hydrochloric acid. To some, this might seem to involve high ion concentration although it is evident to the experimenter, by the presence of hydrogen chloride in the gas phase above these deoxymercuration systems, that molecular hydrogen chloride must be present. Moreover, the deoxymercurating agents do not need to be strong acids. For example, α-2-methoxycyclohexylmercuric chloride reacts rapidly in methanol with isopropylmercaptan. Although the K_A of this mercaptan in water is probably smaller than that of acetic acid (toward which the mercurial is reasonably stable at 25°) the precipitation of chloromercuric isopropylmercaptide is immediate. Steric convenience ought to be involved, and this effect is typified by a quasi-cyclic intermediate like IV in which HX would be isopropylmercaptan.

It is convenient to deoxymercurate in a solution consisting of methanol and concentrated hydrochloric acid but this stereospecific system may contain ionic as well as molecular species. As the water content of the system is decreased, the extent of ionization ought to become minimal. Therefore it is of interest to measure the rate of deoxymercuration in anhydrous and near-anhydrous methanol and this has been done by use of the colorimetric analysis for reacting systems of oxymercurials (3, 12).

The deoxymercurations of α-2-methoxycyclohexylmercuric halides by the appropriate halogen acids are recorded in Table I. In anhydrous methanol the reaction is second-order and very rapid but the rate is decreased markedly by the addition of a few per cent of water. Comparison of the rate constants shows that the deoxymercuration is relatively insensitive to the halide involved in the reaction although the order of reactivity is roughly paralleled by the dipole moments of the three halides in dioxane solution (2). The β-2-methoxycyclohexylmercuric chloride, which should be sterically unfavorable toward deoxymercuration, does indeed react with hydrogen chloride in anhydrous methanol at

*This term is applied to a substance which acts as a stereochemical unit and therefore will include the category of "ion-pair".

Can. J. Chem. Downloaded from www.nrcresearchpress.com by 200.7.193.243 on 09/04/12
For personal use only.

least 100 times slower than the α-diastereomer even when the concentration is increased 15-fold. However, this slow rate is decreased at least 10-fold by addition of 1% of water.

TABLE I

DEOXYMERCURATION OF α-2-METHOXYCYCLOHEXYLMERCURIC HALIDES (RHgX, 1.0×10^{-3} MOLE/LITER) BY HYDROGEN HALIDES, HX, IN 96:4 METHANOL–WATER OR METHANOL AT 25°

X	HX, $\frac{\text{mole}}{\text{liter}}\times10^{-3}$	Medium		K, $\frac{\text{liters}}{\text{mole. sec.}}$
		CH_3OH	H_2O	
Cl	1.0	100	0	3.53
Cl	1.0	96	4	0.65
Br	0.5	96	4	0.75*
Br	1.0	96	4	0.74
Br	2.0	96	4	0.76
I	0.5	96	4	0.72
I	1.0	96	4	0.70
I	2.0	96	4	0.71

**Rate constants for bromides and iodides are calculated from early stages of the reaction; the rate decays slightly in later stages.*

A similar effect is observed during the deoxymercuration of either of the diastereomeric 2-methoxy-1,2-diphenylethylmercuric chlorides. The β-diastereomer (derived from *trans*-stilbene) in anhydrous methanol follows rapid second-order kinetics (k = 2.1 liters mole^{-1} sec.$^{-1}$) and is 80% complete within an hour. Fig. 1 shows that this rate, determined by analysis after 45 minutes of reaction time, is decreased according to the amount of water present in the methanol. The α-diastereomer (derived from *cis*-stilbene) is deoxymercurated more slowly, and it is necessary to use methanol solutions four times as strong as those 0.001 molar in mercurial and in hydrogen chloride which were used for the reaction with the β-diastereomer. Fig. 2 shows that the deoxymercuration rate of the α-diastereomer also decreases with increasing amounts of water in the methanol. It may be of interest that the rate is essentially constant when more than 6% of water is present. This

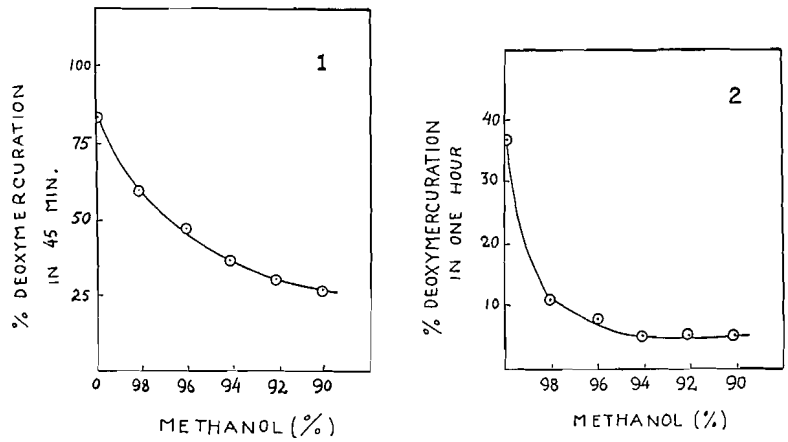

FIG. 1. Effect of water on the amount of deoxymercuration of β-1-chloromercuri-2-methoxy-1,2-diphenylethane during 45 minutes at 25°. [HCl] = [mercurial] = 0.001 mole/liter.

FIG. 2. Effect of water on the amount of deoxymercuration of α-1-chloromercuri-2-methoxy-1,2-diphenylethane during 60 minutes at 25°. [HCl] = [mercurial] = 0.004 mole/liter.

Can. J. Chem. Downloaded from www.nrcresearchpress.com by 200.7.193.243 on 09/04/12
For personal use only.

level is about the same as that reported for the minimum in limiting equivalent conductance for hydrogen chloride in aqueous methanol (16).

The following set of equations describe the chemistry which thus far has been reported here:

$$MeOH + HX \rightleftharpoons MeOH_2^{\oplus} + X^{\ominus} \quad [1]$$

$$MeOH_2^{\oplus} + MeO{-}\overset{|}{\underset{|}{C}}{-}\overset{|}{\underset{|}{C}}{-}HgX \rightleftharpoons MeO\overset{H}{\uparrow}{-}\overset{|}{\underset{|}{C}}{-}\overset{|}{\underset{|}{C}}{-}HgX^{\oplus} + MeOH \quad [2]$$

$$MeO\overset{H}{\uparrow}CH_2CH_2HgX^{\oplus} \rightarrow MeOH + \overset{|}{\underset{|}{C}}{=}\overset{|}{\underset{|}{C}} + HgX^{\oplus} \quad [3]$$

$$H_2O + HX \rightleftharpoons H_3O^{\oplus} + X^{\ominus} \quad [4]$$

$$MeOH_2^{\oplus} + H_2O \rightleftharpoons H_3O^{\oplus} + MeOH \quad [5]$$

$$H_3O^{\oplus} + MeO{-}\overset{|}{\underset{|}{C}}{-}\overset{|}{\underset{|}{C}}{-}HgX \rightarrow MeO\overset{H}{\uparrow}{-}C{-}C{-}HgX^{\oplus} + H_2O \quad [6]$$

$$HX + MeO{-}\overset{|}{\underset{|}{C}}{-}\overset{|}{\underset{|}{C}}{-}HgX \rightleftharpoons MeO{-}\overset{|}{\underset{|}{C}}{-}\overset{|}{\underset{|}{C}}{-}HgX \quad (\text{with } H{-}X \text{ bridging}) \quad [7]$$

$$MeO{-}\overset{|}{\underset{|}{C}}{-}\overset{|}{\underset{|}{C}}{-}HgX \rightarrow MeOH + \overset{|}{\underset{|}{C}}{=}\overset{|}{\underset{|}{C}}{-} + HgX_2 \quad (\text{with } H{-}X \text{ bridging}) \quad [8]$$

Among these, equations [1], [2], [3], [7], and [8] represent reactions in anhydrous media, while [4], [5], and [6] represent reactions in which water is present. Since the addition of water decreases the rates of deoxymercuration by hydrogen chloride that are described in the report, it is doubtful that equation [6] is significant to these reactions. On the other hand the diminution of molecular hydrogen chloride by increasing amounts of water according to equation [4] would account for the decreasing rate of deoxymercuration in this circumstance if equations [7] and [8] are valid. The expectation conforms with the observation of Shedlovsky and Kay (16) that the ionization of hydrogen chloride seems to decrease as the alcohol content of methanol–water systems increases.

The numerical data of this latter paper (16) indicate that 10^{-3} molar solution should contain slightly more than 1 mole per cent of molecular or ion-pair hydrogen chloride. Reaction according to the equations [7] and [8] is thus plausible. However, the experimental results may also be explained in terms of equations [1], [2], and [3], assuming that the concentration of methoxonium ion is reduced by addition of water according to equation [5]. Actually the paucity of information respecting the true composition of the methanol – hydrogen chloride system makes a choice between the two mechanisms relatively meaningless except insofar as the results may be compared with those in a solvent of lower dielectric constant.

We have chosen to use benzene for this comparison. For our studies in this solvent we have considered the following additional equations:

$$2HX \rightleftharpoons (HX)_2 \quad [9]$$

$$C_6H_5 + HX \rightleftharpoons C_6H_7^{\oplus} + X^{\ominus} \quad [10]$$

Can. J. Chem. Downloaded from www.nrcresearchpress.com by 200.7.193.243 on 09/04/12
For personal use only.

$$C_6H_7^{\oplus} + MeO-\overset{|}{\underset{|}{C}}-\overset{|}{\underset{|}{C}}-HgX \rightleftharpoons MeO\overset{H}{\uparrow}-\overset{|}{\underset{|}{C}}-\overset{|}{\underset{|}{C}}-HgX^{\oplus} + C_6H_6 \qquad [11]$$

It is evident from equations [1]–[11] inclusive that the use of benzene includes the complication that methanol is released as one of the products. Partly for this reason the kinetic data are not very reproducible and only the first stages of the reaction give useful data. The rate constants calculated from these data may be expected to be in error on the low rather than on the high side because of inadvertent admission of water vapor, even though atmospheric contamination was avoided vigorously.

According to electrical polarization studies (17) with hydrogen halides in benzene there seems to be no evidence for the phenyl cation. If it exists at all the concentration must be extremely low. Deoxymercuration in benzene via the phenyl cation ought therefore to be inordinately slow. Moreover, an initially slow rate ought to be enhanced if the reaction proceeds by an ionic mechanism because of methanol which appears as a product. Actually the rate constant for deoxymercuration of α-2-methoxycyclohexylmercuric chloride in anhydrous benzene (described below) is greater than that in anhydrous methanol; also there is no indication of autocatalysis.

The reaction of α-2-methoxycyclohexylmercuric chloride in anhydrous benzene is too fast for convenience, and solutions not stronger than 2.0×10^{-4} molar in mercurial and hydrogen chloride must be used in order to follow the reaction kinetically. Because of analytical difficulties prior to the actual colorimetric reading and because of hygroscopicity the numerical value of the second-order rate constant (5.6 liters mole^{-1} sec.$^{-1}$ at this low concentration is uncertain. However a comparison of this slope (*A*, Fig. 3) with *B* (2.2 liters mole^{-1} sec.$^{-1}$) and *C* (1.6 liters moles^{-1} sec.$^{-1}$) in which approximately 3×10^{-3} mole liter^{-1} of water is included with the benzene shows that this deoxymercuration is strongly inhibited by water.

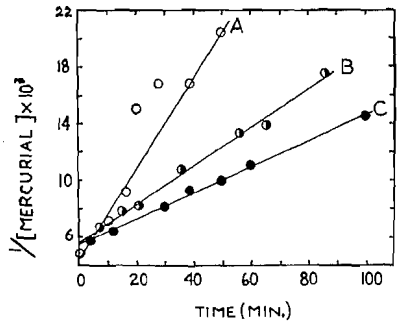

FIG. 3. Second-order rate constants (25°), deoxymercuration in benzene, anhydrous (○) or containing about 3×10^{-3} mole/liter water (◑, ●).

According to this behavior deoxymercuration in benzene does not involve freely-mobile ions which can enter into second-order rate processes. On the other hand, the alternative to a free ionic agent is not simple. Perhaps it should not be expected to be simple. The enhanced electric moment of hydrogen chloride in benzene over the moment in the gaseous state indicates association of the halide with the solvent (17), and self-association together with the solvent is not rigorously excluded. Indeed Beckmann and Lockemann in their classical study (1) show that hydrogen chloride seems to associate in anhydrous benzene and that the extent of association (1.75–2.79) decreases (to 1.16) as very small amounts

Can. J. Chem. Downloaded from www.nrcresearchpress.com by 200.7.193.243 on 09/04/12
For personal use only.

of water are added progressively. Therefore evidence for equation [9] exists and seems to be involved in deoxymercuration studies with the two 2-methoxy-1,2-diphenylethylmercuric chloride diastereomers.

The β-diastereomer of 2-methoxy-1,2-diphenylethylmercuric chloride reacts more slowly with hydrogen chloride in benzene than does α-methoxycyclohexylmercuric chloride, so solutions $1.5–2.0\times10^{-3}$ molar in the stilbene mercurial and in hydrogen chloride may be used. Although this deoxymercuration is thus easier to study in respect of water content it is, unfortunately, subject to strong catalytic acceleration by mercurous chloride. Since this β-mercurial tends spontaneously (especially in light) to decompose into mercurous chloride, and also because of the catalytic effect of liberated methanol, the reactions may be studied only qualitatively. Fig. 4 shows that the rate is decreased by

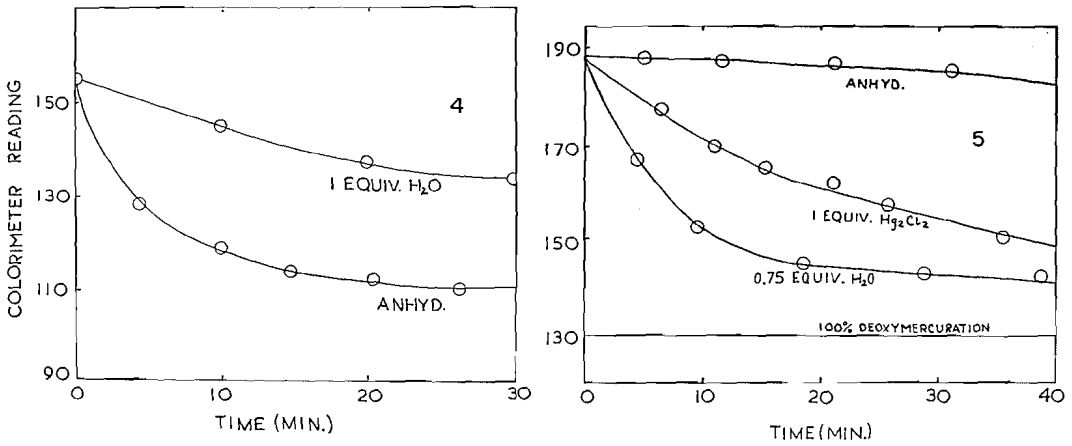

FIG. 4. Deoxymercuration of β-2-methoxy-1,2-diphenylethylmercuric chloride 2×10^{-3} molar at 25° by hydrogen chloride 2×10^{-3} molar.

FIG. 5. Deoxymercuration at 25° of β-2-methoxy-1,2-diphenylethylmercuric chloride 2.0×10^{-3} molar in benzene.

addition to the anhydrous system (2×10^{-3} molar in mercurial and acid) of a molar excess of water. On the other hand the addition of less than a molar equivalent of water to the anhydrous system causes an increase in rate. The latter behavior is shown in Fig. 5. This diagram includes also an example of the accelerating effect of mercurous chloride, which we shall not now attempt to explain. However, with respect to water it seems reasonable to suggest that the enhancement of rate by addition of 0.75 equivalent involves the reversal according to equation [9] of the association observed by Beckmann and Lockemann, while the decreased rate with one or more equivalents of water is caused by loss of molecular hydrogen chloride because of ionization according to equation [4].

The effect of water in benzene has also been studied in the deoxymercuration of α-2-methoxy-1,2-diphenylethylmercuric chloride by hydrogen chloride. In this instance the analytical method is a manometric one depending on diminution of the vapor pressure of hydrogen chloride as it is consumed in the reaction. The record (Fig. 6) of an experiment in anhydrous benzene versus a benzene solution containing less than one molar equivalent of water shows its accelerating effect to be similar to that observed for the β-diastereomer. Not shown is a curve demonstrating that mercurous chloride also accelerates the deoxymercuration of the α-diastereomer.

In summary it would seem that if deoxymercuration is faster in benzene than in methanol, if common ion effects are not found in the latter medium, and if the retarding

Can. J. Chem. Downloaded from www.nrcresearchpress.com by 200.7.193.243 on 09/04/12
For personal use only.

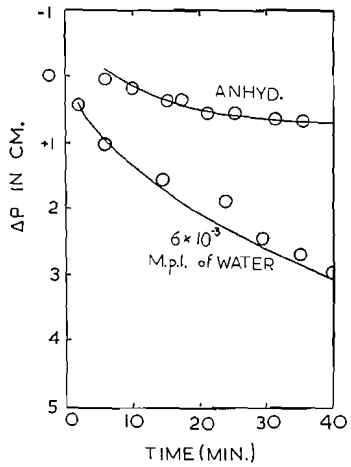

FIG. 6. Manometric analysis, deoxymercuration at 25° of α-2-methoxy-1,2-diphenylethylmercuric chloride 0.01 molar by hydrogen chloride 0.01 molar.

effect of water is comparable in both media, then the improbability of an ionic mechanism in benzene renders improbable an ionic mechanism for all of these stereospecific deoxymercurations. However, it remains to prove that the reaction in benzene is as stereospecific as it is in methanol. This similarity has now been established by isolation of *cis*-stilbene uncontaminated by the *trans* isomer when α-2-methoxy-1,2-diphenylethylmercuric chloride is treated with one equivalent of hydrogen chloride in benzene.

It should be noted that the non-ionic deoxymercuration is specified only for the stereospecific reactions. Actually we have succeeded in producing a few per cent of *trans*-stilbene from the α-diastereomer by treatment with a 1:1 mixture of concentrated hydrochloric acid in methanol. Of course we cannot attribute the slight non-stereospecificity to an ionic deoxymercuration because *cis*-stilbene might have been the initial product which then was isomerized by the acidic medium. But also the non-stereospecificity may be due to the ionic reaction specified by Whitmore.

Such an ionic reaction may also apply to the very slow deoxymercurations of some β-oxymercurials in which the configuration is unfavorable to a quasi-cyclic transition state. Likewise it may apply to deoxymercurations by acids other than the hydrogen halides. But it does not apply to the deoxymercuration which has the same stereospecific behavior as does the corresponding oxymercuration. Both of these processes seem to involve molecular reactants. Therefore both should require *cis* (↑↑) configuration in the mercurial. It follows that the "inversion" mechanism is not adequate to describe either oxymercuration or deoxymercuration, in respect of alkenes such as are considered in this report.

EXPERIMENTAL*

α-2-Isopropoxycyclohexylmercuric Chloride

To a solution of 3.18 g. (0.01 mole) of mercuric acetate in 30 ml. of propanol-2 was added 0.90 g. (0.011 mole) of cyclohexene. After 3 hours, filtration into 25 ml. of 5% aqueous sodium chloride at 0° C. precipitated 3.05 g. (80%) of the isopropoxymercurial, m.p. 90.5–91.5° C. Crystallization from absolute ethanol (20 ml./g.) raised the melting point to 94.8–95.5° C. Calc. for $C_9H_{17}ClHgO$: C, 28.7; H, 4.52; Hg, 53.2. Found: C, 28.4; H, 4.68; Hg, 52.2.

**Melting points have been corrected against reliable standards. X-Ray diffraction data have been obtained with* Cu K_α (Ni *filtered*) *radiation at d spacings in* Å *at visual relative intensities* I/I_1.

Can. J. Chem. Downloaded from www.nrcresearchpress.com by 200.7.193.243 on 09/04/12
For personal use only.

α-2-Alkoxycyclohexylmercuric Halides Used in Kinetic Studies

These oxymercurials, prepared by standard procedures, were purified to melt as shown in Table II.

TABLE II

MELTING POINTS OF 2-ALKOXYCYCLOHEXYLMERCURIC HALIDES, $ROC_6H_{10}HgX$

Diastereomer	R	X	M.p., ° C.	Reference
α	Me	Cl	115.2–116.0	(25)
β	Me	Cl	114.1–114.5	(24)
α	Et	Cl	60.8–61.5	(5)
α	Pr	Cl	57.5–58.5	(12)
α	*t*-Bu	Cl	115.0–116.0	(5)
α	$MeOC_2H_4$	Cl	121.5–122.5	(12)
α	H	Cl	153.0–153.6	(5)
α	Me	Br	114.0–114.5	(13)
α	Me	I	81.4–82.0	(6)

Deoxymercuration Using Benzoyl Chloride

A. With α-2-Methoxy-1,2-diphenylethylmercuric Chloride

To 1.12 g. (0.0025 mole) of this mercurial in 15 ml. of ethanol-free anhydrous chloroform was added 0.29 ml. (0.0025 mole) of freshly distilled benzoyl chloride, b.p. 197° C. After 96 hours, 0.66 g. (97%) of mercuric chloride was filtered off. Vacuum evaporation of the filtrate left 0.80 g. of oil with the odor of methyl benzoate. It was refluxed with 20 ml. of 10% aqueous sodium hydroxide for 270 minutes, then steam-distilled. Etherous extraction (45 ml.) of the distillate removed 0.42 g. of *cis*-stilbene (89%), m.p. 3.5–6.0° C. This geoisomer (0.0022 mole) was characterized by treatment with 0.70 g. (0.0022 mole) of mercuric acetate in 15 ml. of anhydrous methanol for 5 hours, followed by filtration into 25 ml. of 10% aqueous sodium chloride. A mixture melting point of the precipitate (0.85 g., 70%, m.p. 142.5–143.5° C.) with α-methoxydiphenylethylmercuric chloride was not lowered.

B. With β-2-Methoxy-1,2-diphenylethylmercuric Chloride

To 2.24 g. (0.005 mole) of this mercurial in 25 ml. of ethanol-free chloroform was added 0.58 ml. (0.005 ml.) of freshly-distilled benzoyl chloride, b.p. 197° C. After 1 day 1.34 g. (98%) of mercuric chloride was filtered off. Vacuum evaporation of the filtrate left a semisolid oil (1.55 g.). This was crystallized from 8 ml. of ethanol, 0.71 g. (79%) of *trans*-stilbene, m.p. 122.5–124° C., authenticated by mixture melting point.

C. With α-2-Methoxycyclohexylmercuric Chloride

To 3.49 g. (0.01 mole) of this mercurial in 25 ml. of ethanol-free chloroform was added 1.40 g. (0.01 mole) of freshly-distilled benzoyl chloride. After 18 hours, 2.58 g. (95%) of mercuric chloride was filtered off. Vacuum evaporation of the solvent left an oil which was extracted with water. The oil, 1.35 g. (99%), was then distilled at 196–198° C. This methyl benzoate (1.10 g., 81%) was characterized by saponification; acidification precipitated 0.78 g. (87%) of benzoic acid, authenticated by mixture melting point.

The use of benzoyl chloride rather than gaseous hydrogen chloride is a convenient variation for stereospecific deoxymercuration. However, there is evidence (by Mr. Paul Chu) that the reaction is not a simple one; indeed it is catalyzed by mercuric chloride, which may be present in trace amounts in the chloromercurials. In relation to the catalytic action it is of interest that the solubility of mercuric chloride in chloroform is enhanced by the presence of an organochloromercurial which is dissolved in the chloroform.

Can. J. Chem. Downloaded from www.nrcresearchpress.com by 200.7.193.243 on 09/04/12
For personal use only.

Deoxymercuration Using Hydrogen Chloride with α-2-Methoxy-1,2-diphenylethylmercuric Chloride

A. In Anhydrous Benzene

To 4.47 g. (0.01 mole) of mercurial in a 250-ml. distilling flask was added 60 ml. of a 0.195 *N* (0.012 mole) solution of hydrogen chloride in benzene during 3 minutes. Mercuric chloride was deposited during this addition; evidently reaction is rapid. After 7 minutes more the solvent was vacuum-evaporated with swirling at 25° C. In a short time the solvent was gone and the residue was quickly treated with excess of 10% aqueous alkali. The *cis*-stilbene was taken up by five washings with ether. The extract, dried by potassium carbonate, was evaporated, 1.62 g., and distilled, b.p. 140–142° C. (14 mm.), n_D^{20} 1.6217, 1.51 g. (84%), leaving no *trans*-stilbene.

B. In Aqueous Methanol

The same amount of mercurial was stirred 12 hours at 25° C. in 90 ml. of methanol plus 90 ml. of concentrated hydrochloric acid. The system, containing oil droplets, was diluted to 700 ml. with water and thrice extracted with 90-ml. lots of ether. The extract, dried by calcium chloride, was vacuum-evaporated, and the residue chromatographed from commercial hexane on a 12 cm. by 0.8 cm. alumina column (activated at 450° C.). After 90 ml. of eluate the column was extruded, the *trans*-stilbene located by permanganate streak, and removed from the zone by ether. Evaporation left 10 mg. of *trans*-stilbene, m.m.p. 120–122° C., authenticated by mixture melting point. The column eluate yielded 1.37 g. of *cis*-stilbene, which was reconverted to the α-mercurial, crude m.p. 143–144° C.

Chloromercuric Isopropylmercaptide

To a solution of 2.85 g. (0.008 mole) of α-2-methoxycyclohexylmercuric chloride in 60 ml. of methanol was added 0.99 g. (0.013 mole) of isopropylmercaptan. A voluminous white precipitate formed immediately. It was filtered off, washed with methanol (30 ml.), and then with ether (60 ml.), 3.11 g. (100%) of infusible chloromercuric isopropylmercaptide. Calc. for C_3H_7ClHgS: C, 11.6; H, 2.25. Found: C, 12.1; H, 2.41.

Identical results were obtained with ethylmercaptan. This compound was regenerated by acidification of the infusible precipitate with hydrochloric acid.

Kinetic Measurements

These were carried out at 25.0°±0.1°C.

A. Reagents

The methanol was purified under nitrogen by Lund and Bjerrum's method (10) to be peroxide-free ($TiCl_3$) and aldehyde-free (Schiff reagent). The benzene, purified by refluxing and distillation from sodium under nitrogen, was anhydrous and peroxide-free according to test with sodium benzophenone ketyl. The hydrogen chloride and hydrogen bromide were dried by passage through concentrated sulphuric acid and then through anhydrous aluminum chloride. The diphenylthiocarbazone (dithizone) was purified by the method of Winkler (21, 18).

B. The Apparatus Used for Anhydrous Reactions

The essential pieces of apparatus are shown as the storage burette in Fig. 7 and the reaction flask in Fig. 8. The storage burette, after thorough drying in a nitrogen stream, is filled with 160 ml. of benzene in the tubular absorber (195×20 mm. with fritted glass disperser) and the spherical chamber (68 mm. diameter) above it to a level just below the inlet from the top stopcock. Then hydrogen chloride is passed in through the horizontally-projecting conical joint by distillation (using a dry-ice bath as a source of heat) from a

Can. J. Chem. Downloaded from www.nrcresearchpress.com by 200.7.193.243 on 09/04/12
For personal use only.

Can. J. Chem. Downloaded from www.nrcresearchpress.com by 200.7.193.243 on 09/04/12
For personal use only.

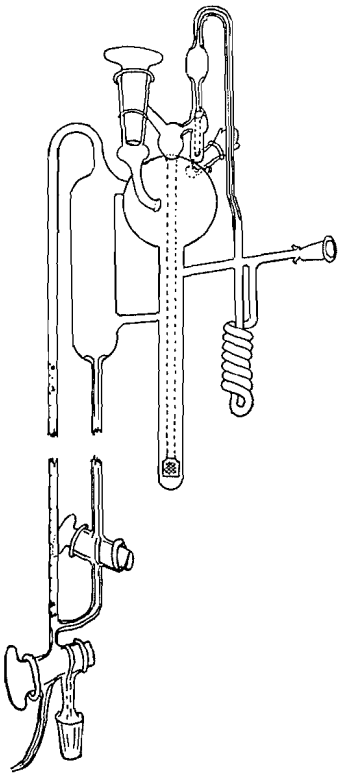

FIG. 7. The storage burette for hydrogen chloride in benzene or methanol.

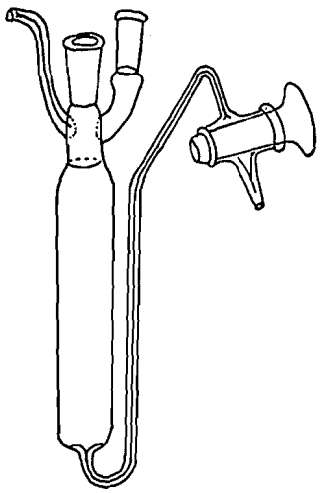

FIG. 8. The deoxymercuration vessel for kinetic studies.

trap in which the acid has been condensed by use of liquid air. When the top stopcock is closed and the three-way stopcock at the bottom of the burette is open hydrogen chloride will pass through the benzene. Finally after 30 minutes sufficient acid has been absorbed. The inlet spiral is immersed in a liquid air bath while the source of hydrogen chloride is

removed, the three-way stopcock having been closed. The latter is now reopened while a stream of dry nitrogen is passed through the horizontal inlet tube (the top stopcock being open) in order to sweep excess hydrogen chloride away from the area above the benzene solution. Then, all stopcocks being closed, the apparatus is tilted to transfer 100 ml. of the benzene solution into the storage reservoir (155×38 mm.) whence it may be standardized in the 10 ml. microburette by sample withdrawal from the plain outlet at the three-way stopcock. During all these operations the vents from the apparatus are protected from moisture by means of connections with U-tubes immersed in liquid air. All interchangeable joints are graphite-lubricated.

The reaction flask (Fig. 8) is constructed with an attachment joint to the burette, a second joint through which the solid mercurial sample is introduced by tipping from a hollow interchangeable stopper at the appropriate time, a dry-gas inlet tube and a capillary stopcock-closed outlet tube from the bottom. With these attachments the vessel does not need to be removed from the thermostat during reaction, the samples being withdrawn by rubber bulb inlet pressure which forces them out via the capillary stopcock into a cup. A definite aliquot is then withdrawn by pipette from the cup. The subsequent colorimetric procedure has been described previously (3, 12). Further detail is available in Mr. Berg's M. A. thesis.

C. The Manometric Apparatus

A differential manometer of the Warburg (19) type was modified by addition of an interconnecting stopcock between the reaction side and the compensator side in order to equilibrate the gas phase before the sample tube containing solid mercurial was inverted into the benzene – hydrogen chloride solution. Transferral of this solution to reaction and compensator flask from its preparative source (essentially the burette and reaction flask described above) was accomplished through serum caps via a hypodermic syringe.

D. Effect of Water in Methanol on Deoxymercuration

Into each of six 10 ml. volumetric flasks containing either 0, 0.2, 0.4, 0.6, 0.8, or 1.0 ml. of water was added 0.52 ml. of anhydrous methanol which was 0.0194 *N* in hydrogen chloride. Then 2 ml. of 0.005 *M* of mercurial in anhydrous methanol was added and the flask was filled quickly to volume with methanol. After brief shaking the flask was held at 20° for 5 minutes, then 1 ml. was rapidly diluted to 100 ml. with water. Ten milliliters of the diluate was thrice extracted at once by 5 ml. portions of chloroform, then 5 ml. of the aqueous layer was analyzed colorimetrically. The percentages of deoxymercuration of β-1-chloromercuri-2-methoxy-1,2-diphenylethane with increasing additions of water were 83.6, 59.5, 46.3, 36.7, 30.1, and 27.2. The corresponding percentages for the α diastereomer were 36.7, 10.7, 7.7, 5.2, 5.2, 5.2.

REFERENCES

1. BECKMANN, E. and LOCKEMANN, G. Z. physik. Chem. **60**, 385 (1907).
2. BROOK, A. G., DONOVAN, R., and WRIGHT, G. F. Can. J. Chem. **31**, 536 (1953).
3. BROOK, A. G., RODGMAN, A., and WRIGHT, G. F. J. Org. Chem. **17**, 988 (1952).
4. BROOK, A. G. and WRIGHT, G. F. Acta Cryst. **4**, 50 (1951).
5. BROOK, A. G. and WRIGHT, G. F. Can. J. Research, B, **28**, 623 (1950).
6. BROOK, A. G. and WRIGHT, G. F. J. Am. Chem. Soc. **72**, 3821 (1950).
7. GEORGE, M. V. and WRIGHT, G. F. Can. J. Chem. **36**, 189 (1958).
8. KUMLER, W. D. and HUITRIC, A. J. Am. Chem. Soc. **78**, 3369 (1956).
9. LUCAS, H. J., HEPNER, F. R., and WINSTEIN, S. J. Am. Chem. Soc. **61**, 3102 (1939).
10. LUND. H. and BJERRUM, J. Ber. **64**, 210 (1931).
11. RODGMAN, A., SHEARER, D., and WRIGHT, G. F. Can. J. Chem. **35**, 1377 (1957).
12. RODGMAN, A. and WRIGHT, G. F. J. Org. Chem. **18**, 1617 (1953).
13. ROMEYN, J. and WRIGHT, G. F. J. Am. Chem. Soc. **69**, 697 (1947).
14. ROWLAND, R. L. and KLUCHESKY, E. F. J. Am. Chem. Soc. **73**, 5490 (1951).

Can. J. Chem. Downloaded from www.nrcresearchpress.com by 200.7.193.243 on 09/04/12
For personal use only.

15. SAND, J. and BREEST, F. Z. physik. Chem. **59**, 424 (1907).
16. SHEDLOVSKY, T. and KAY, R. L. J. Phys. Chem. **60**, 151 (1956).
17. SMITH, J. W. Electric dipole moments. Butterworths Scientific Publications, London. 1955. p. 314.
18. STONESTREET, G. and WRIGHT, G. F. Can. J. Research, B, **18**, 246 (1940).
19. WARBURG, O. Biochem. Z. **152**, 51 (1924).
20. WHITMORE, F. C. Chem. Eng. News, **26**, 668 (1948).
21. WINKLER, W. O. J. Assoc. Official Agr. Chemists, **18**, 638 (1935).
22. WINSTEIN, S., TRAYLOR, T. G., and GARNER, C. S. J. Am. Chem. Soc. **77**, 3741 (1955).
23. WRIGHT, G. F. Ann. N.Y. Acad. Sci. **65**, 436 (1957); see p. 445.
24. WRIGHT, G. F. Can. J. Chem. **30**, 268 (1952).
25. WRIGHT, G. F. J. Am. Chem. Soc. **57**, 1993 (1935).

Can. J. Chem. Downloaded from www.nrcresearchpress.com by 200.7.193.243 on 09/04/12
For personal use only.

Can. J. Chem. Downloaded from www.nrcresearchpress.com by 61.7.252.67 on 09/04/12
For personal use only.

SYNTHESIS OF PORPHYRINOGEN-LIKE COMPOUNDS (MIXED QUATERENES)[1]

WILLIAM H. BROWN[2] AND WARREN N. FRENCH[3]

ABSTRACT

Three porphyrinogen-like compounds, or mixed quaterenes, have been synthesized. One quaterene contains a pyrrole and three furan residues while the others contain two pyrrole and two furan residues. The chief reaction in the preparation of these mixed quaterenes involves the condensation of a dimethylcarbinol of furan at the α-position on a furan or pyrrole ring. Several previously unknown compounds of pyrrole and furan have been prepared as necessary intermediates.

The mode of condensation of furan with acetone in the presence of hydrochloric acid has recently been investigated by Ackman, Brown, and Wright (1). They found that the end product is a cyclic compound consisting of four residues each of furan and acetone after intermolecular elimination of four molecules of water. For this compound, m.p. 243°, Ackman, Brown, and Wright (1) devised the trivial name "octamethyl-tetroxaquaterene" in which "quaterene" denotes a closed system of four cyclopentadiene nuclei linked through the 1- and 4-positions by methylene bridges.

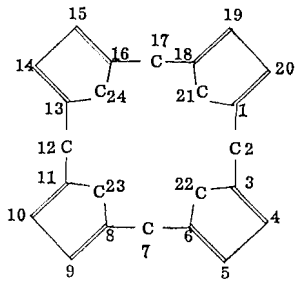

QUATERENE NUCLEUS

Similar results have been obtained in the pyrrole series in the search for compounds having porphyrinogen-like structures. In 1886, Baeyer (2) discovered the first condensation leading to such a compound; viz., the condensation of pyrrole with acetone in the presence of hydrochloric acid. The structure of the substance, m.p. 296°, was investigated by Dennstedt and Zimmerman (3) and later by Chelintzev and Tronov (4). The compound is designated as octamethyl-porphyrinogen, or 2,2,7,7,12,12,17,17-octamethyl-21,22,23,24-tetrazaquaterene in the vernacular.

We have now succeeded in preparing mixed quaterenes containing both furan and pyrrole residues. One quaterene contains one pyrrole and three furan residues (X) while two others each contain two pyrrole and two furan residues (XI, XII). The third member of the series, containing three pyrrole and one furan residue, was not obtained

[1]*Manuscript received October 30, 1957.*
Contribution from the Department of Chemistry, Ontario Agricultural College, Guelph, Ontario.
[2]*Associate Professor of Chemistry, Ontario Agricultural College, Guelph, Ontario.*
[3]*Holder of a National Research Council Bursary 1956–57. Present address: Department of Chemistry, Hamilton College, McMaster University, Hamilton, Ontario.*

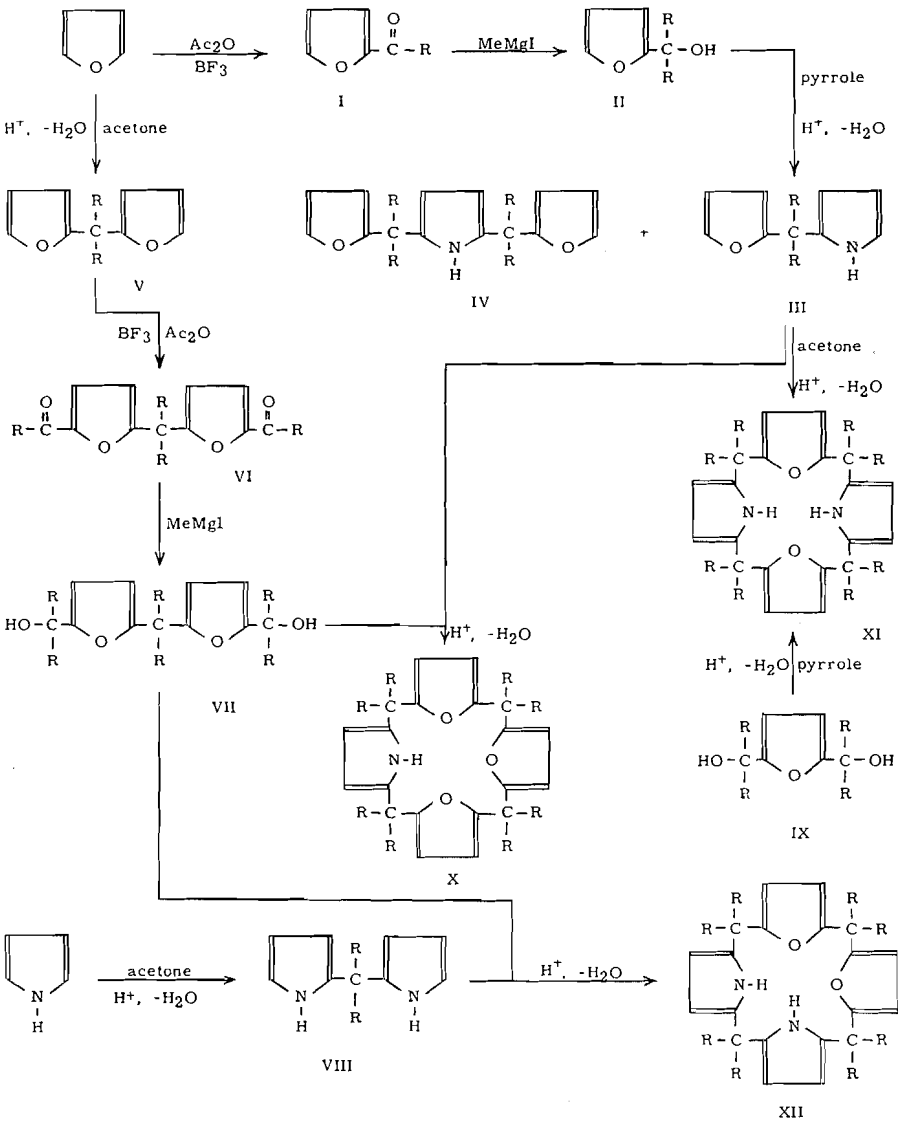

by the methods reported in this communication. The chief reaction in the preparation of these mixed quaterenes involves the condensation of a substituted furylcarbinol at the α-position on a furan or pyrrole ring.

This type of condensation has previously been demonstrated by Ackman, Brown, and Wright (1), who prepared 2,2-difurylpropane from dimethylfurylcarbinol and furan, and by Brown and Sawatzky (5), who similarly prepared difurylmethane and 1,1-difurylethane.

Since the reactions of pyrrole are, in general, similar to those of furan, it was proposed that dimethylfurylcarbinol (II) would condense with pyrrole to give an analogous product. This was indeed found to be the case. In addition to obtaining the expected

Can. J. Chem. Downloaded from www.nrcresearchpress.com by 61.7.252.67 on 09/04/12
For personal use only.

Can. J. Chem. Downloaded from www.nrcresearchpress.com by 61.7.252.67 on 09/04/12
For personal use only.

2-furyl-2-pyrrylpropane (III), a second product, thought to be 2,5-*bis*(dimethylfurfuryl)-pyrrole (IV), was isolated. Increasing the ratio of pyrrole : dimethylfurylcarbinol from 1.1 : 1.0 to 1.5 : 1.0 increases the yield of 2-furyl-2-pyrrylpropane from 20 to 40%.

Treatment of 2-furyl-2-pyrrylpropane (III) with acetone in the presence of hydrochloric acid gives 2,2,7,7,12,12,17,17-octamethyl-21,23-diaza-22,24-dioxaquaterene (XI), m.p. 230.5°. The reaction might be expected to give rise to two products, the symmetrical quaterene (XI) and the unsymmetrical quaterene (XII), but only one was isolated. Actually, the melting point of the crude product differs only a few degrees from that of the purified product. The high purity of the crude product also suggests that III reacts as a unit and not by reversion to its constituent parts. A mixture of products, which would be expected if III decomposed, is not apparent. Furthermore, it has been shown that the product formed by the condensation of III with acetone is the symmetrical quaterene (XI), since the same compound is formed by the condensation of 2,5-diisopropylolfuran (IX) with pyrrole. The unsymmetrical quaterene (XII), also containing two furan and two pyrrole residues, is formed by the condensation of 2,2-*bis*(5-isopropylolfuryl) propane (VII) with 2,2-dipyrrylpropane (VIII).

Although the condensation of pyrrole with acetone has been previously investigated, the progenitor of the reaction, 2,2-dipyrrylpropane (VIII), has not been reported. It was found that when the mole ratio of pyrrole to acetone is 2 : 1, a small amount of 2,2-dipyrrylpropane is formed, along with a greater amount of tetrazaquaterene. When the reaction is allowed to proceed slowly with a pyrrole : acetone ratio of 4 : 1, 2,2-dipyrrylpropane is obtained in about 21% yield.

The preparation of the other intermediate, 2,2-*bis*(5-isopropylolfuryl)propane (VII), utilized in the formation of 2,2,7,7,12,12,17,17-octamethyl-21,22-diaza-23,24-dioxaquaterene (XII), m.p. 260°, involved the synthesis of several previously unknown compounds. Acetylation of 2,2-difurylpropane (V) with acetic anhydride gives two products, depending on the conditions of the reaction. Under mild catalysis, such as with iodine, or when the reaction is stopped before completion under more vigorous catalysis, such as with boron trifluoride, the monoacetylated product, 2-furyl-2-(5-acetylfuryl)propane, is obtained. By allowing the reaction to proceed to completion when boron trifluoride is the catalyst, only the diacetylated product, 2,2-*bis*(5-acetylfuryl)propane (VI), results. The identity of each was established by preparing the semicarbazone; analysis for nitrogen indicated the presence of the mono- and di-acetylated compounds. Treatment of 2,2-*bis*(5-acetylfuryl)propane (VI) with methylmagnesium iodide, followed by hydrolysis, results in the expected di-tertiary alcohol (VII), which subsequently gives XII by condensation with 2,2-dipyrrylpropane (VIII).

The third mixed quaterene, 2,2,7,7,12,12,17,17-octamethyl-21-aza-22,23,24-trioxaquaterene (X), m.p. 223°, is obtained in about 13% yield from the condensation of 2,2-*bis*(5-isopropylolfuryl)furan (VII) with 2-furyl-2-pyrrylpropane (III). The preparation of X was also attempted by treating 2,5-*bis*(dimethylfurfuryl)pyrrole (IV) with 2,5-diisopropylolfuran (IX) in the presence of hydrochloric acid. However, only resinous products resulted. Similarly, Ackman, Brown, and Wright (1) obtained only resinous products by treating 2,5-*bis*(dimethylfurfuryl)furan with 2,5-diisopropylolfuran.

During the course of the investigation, several characteristics of the condensations leading to mixed quaterenes were observed. In general, it was found that the dimethylcarbinol of furan condenses with a furan nucleus to give a product in low yield (14%). However, the dimethylcarbinol of furan reacts quite readily with a pyrrole nucleus to form a product in good yield (69%). This points up the greater reactivity of pyrrole

α-hydrogen over furan α-hydrogen. It was also found that dimethylfurylcarbinol does not condense with thiophene under the conditions employed. A variety of products are formed, none of which contains a thiophene residue. Apparently, the furylcarbinol condenses with itself to form several indefinite products rather than condensing with thiophene. In view of these observations, it would appear possible to prepare other mixed quaterenes by the condensation of a substituted carbinol of thiophene with a furan or pyrrole nucleus.

EXPERIMENTAL

All melting points have been corrected against reliable standards. Molecular weights were determined by the Rast method.

Acetylfuran (I)

The compound was prepared by the method of Heid and Levine (6) involving the acetylation of furan with acetic anhydride using a boron trifluoride catalyst (B & A Code 1471).

Dimethylfurylcarbinol (II)

The method used for the preparation of the compound was that of Reichstein, Zschokke, Gehring, and Rona (7) involving the treatment of acetylfuran with methyl Grignard reagent.

2-Furyl-2-pyrrylpropane (III)

A solution of 30 g. (0.45 mole) of pyrrole in 30 ml. of commercial absolute ethanol was placed in a 125 ml. Grignard-type flask equipped with stirrer and dropping funnel and cooled to 0° in an ice-bath. Ten milliliters of 37% hydrochloric acid solution was added slowly while the solution was being stirred. To the resulting colorless solution, 48.7 g. (0.39 mole) of dimethylfurylcarbinol was added dropwise over a period of 15 minutes. The mixture turned yellow at first, then a dark green. The ice-bath was removed and the mixture stirred for 2 hours at room temperature. The addition of 100 ml. of water resulted in the formation of two liquid phases. The lower amber organic phase was separated from the upper aqueous phase, washed until neutral with 10% sodium carbonate solution, then dried over anhydrous magnesium sulphate. The excess pyrrole was removed under diminished pressure and the residual oil fractionally distilled.

The first fraction, a colorless fluorescent oil, distilled at 96–98° (2–3 mm.) and weighed 13.6 g. (20%); η_D^{20} 1.5330, d_4^{20} 1.056. Anal. Calc. for $C_{11}H_{13}NO$: N, 8.00; Mol. wt., 175. Found: N, 8.00; Mol. wt., 182.

2,5-Bis(dimethylfurfuryl)pyrrole (IV)

A second fraction from the preceding distillation, a light yellow oil, boiled at 154–156° (3 mm.) and weighed 17.1 g. (31%); η_D^{20} 1.5286, d_4^{20} 1.052. Anal. Calc. for $C_{18}H_{21}NO_2$: N, 4.94; Mol. wt., 283. Found: N, 5.00; Mol. wt., 290.

2,2-Bis(5-acetylfuryl)propane (VI)

A solution of 20 g. (0.114 mole) of 2,2-difurylpropane (V) and 24.5 g. (0.228 mole) of 95% acetic anhydride in a 125 ml. Grignard-type flask equipped with stirrer and thermometer was cooled to 0° in an ice-bath. While the solution was being stirred vigorously, 2 ml. of boron trifluoride etherate (B & A Code 1471) was added all at once. The color of the solution changed to cherry red, then to dark purple, and the temperature slowly rose to 30° and then fell. When the ice-bath was removed, the temperature slowly rose to 70°. Stirring was continued until the reaction mixture cooled to room temperature,

Can. J. Chem. Downloaded from www.nrcresearchpress.com by 61.7.252.67 on 09/04/12
For personal use only.

Can. J. Chem. Downloaded from www.nrcresearchpress.com by 61.7.252.67 on 09/04/12
For personal use only.

then 50 ml. of water was added and stirring continued for 30 minutes. The upper aqueous phase was separated from the lower organic phase and the former extracted with three 15-ml. portions of chloroform. The chloroform extracts and the lower organic phase were combined and washed with 50 ml. of 10% sodium carbonate, 50 ml. of water, and dried over anhydrous magnesium sulphate. The chloroform was flashed off and the residue distilled under diminished pressure. The product, a viscous light yellow oil, weighed 15 g. (51%) and distilled at 178–182° (2–3 mm.). On cooling in the refrigerator, the material formed a thick gel but did not crystallize.

The disemicarbazone derivative of this compound, m.p. 235° (with decomposition), was prepared in the usual manner. Anal. Calc. for $C_{17}H_{22}N_6O_4$: N, 22.4. Found: N, 22.4.

2-Furyl-2-(5-acetylfuryl)propane

A solution of 20 g. (0.114 mole) of 2,2-difurylpropane and 28.2 g. (0.262 mole) of 95% acetic anhydride was cooled to 0° by means of an ice-bath and treated with 2 ml. of boron trifluoride etherate (B & A Code 1471). The temperature of the reaction mixture rose to 34°, then fell. Stirring was continued for 30 minutes with the ice-bath still in place. After being worked up as described before, the product was fractionally distilled. The first fraction, a colorless oil which crystallized in the receiver, distilled at 123–126° (2 mm.) and weighed 5.5 g. (25%). Crystallization from an ethanol–water solution gave shiny flat plates, m.p. 84.0–84.5°. Calc. for $C_{13}H_{14}O_3$: Mol. wt., 218. Found: 210.

The semicarbazone, which was prepared in the usual manner, had a melting point of 186.5°. Anal. Calc. for $C_{14}H_{17}N_3O_3$: N, 15.3. Found: N, 15.6.

2,2-Bis(5-isopropylolfuryl)propane (VII)

An ethereal solution of 0.123 mole of methylmagnesium iodide was prepared. The solution of the Grignard reagent was cooled in an ice-bath and while it was being stirred vigorously, 15 g. (0.0577 mole) of 2,2-*bis*(5-acetylfuryl)propane was added dropwise to it over a period of 30 minutes. Stirring was continued for 2 hours at room temperature. The mixture was then poured over 150 g. of chipped ice to decompose the yellow complex. The aqueous layer was saturated with sodium carbonate and the ether decanted. After extraction with ether, the combined ether extracts were dried over anhydrous potassium carbonate. Most of the ether was removed by distillation, the remainder by passing a current of air over the cold solution. The residue was a sticky yellow solid, which was dissolved in hot hexane; the resulting solution was cooled and partially evaporated by means of a current of air. A white crystalline solid formed on the walls of the flask. After the process had been repeated three times, a total of 6.0 g. (36%) of white crystals was obtained, m.p. 91–92°.

This product was not amenable to purification for analysis by ordinary crystallization procedures since it readily decomposes with formation of an oil. The compound is assumed to be the di-tertiary alcohol based on its mode of formation and subsequent reactions. A molecular weight determination on the crude product gave a value of 308, which is in agreement with the theoretical value of 298 based on the molecular formula $C_{17}H_{24}O_4$.

2,2-Dipyrrylpropane (VIII)

A solution of 67 g. (1 mole) of pyrrole and 20 ml. of commercial absolute ethanol in a 125 ml. Grignard-type flask equipped with stirrer, dropping funnel, and thermometer was cooled to 0° in an ice-bath. While the solution was being stirred, 3 ml. of 37% hydrochloric acid solution was slowly added, followed by 14.5 g. (0.25 mole) of acetone, which was added dropwise over a period of 25 minutes. The temperature was kept at 10° throughout the addition. Stirring was continued for 2 hours during which time the

solution turned yellowish-green in color. The solution was poured into 100 ml. of water and the resulting mixture neutralized with solid sodium carbonate. The upper organic phase was removed, washed with water, and dried over anhydrous magnesium sulphate. The excess pyrrole was removed under diminished pressure and the residual oil fractionally distilled from a Claisen flask to give 13.5 g. (31%) of a light yellow oil (b.p. 146–153°, 8 mm.), which partially solidified on cooling. Fractional distillation through a column as described by Bower and Cook (8) gave 9.2 g. (21%) of a colorless fluorescent oil (b.p. 125–126°, 3 mm.), which solidified in the receiver, m.p. 59°. Crystallization from petroleum ether gave rhomboid crystals but did not change the melting point. Anal. Calc. for $C_{11}H_{14}N_2$: N, 16.1; Mol. wt., 174. Found: N, 16.3; Mol. wt., 184.

2,2,7,7,12,12,17,17-Octamethyl-21-aza-22,23,24-trioxaquaterene (*X*)

A solution of 0.50 g. (0.00172 mole) of 2,2-*bis*(5-isopropylolfuryl) propane (VII) and 0.30 g. (0.00172 mole) of 2-furyl-2-pyrrylpropane (III) in 5 ml. of absolute ethanol was cooled in an ice-bath. While the solution was being agitated, 0.4 ml. of 37% hydrochloric acid solution was added dropwise. A greenish-yellow color developed immediately, which soon changed to orange and then to dark brown. Solid material started to form in 15 minutes. After the solution was left for 15 hours, a sticky solid was removed by filtration. Crystallization from absolute ethanol gave 0.10 g. (13.5%) of light yellow needles, m.p. 217–220°. A second crystallization gave fine white needles, m.p. 223°. Yields are lower when the above reaction is carried out on a larger scale. Anal. Calc. for $C_{28}H_{33}NO_3$: N, 3.26; Mol. wt., 431. Found: N, 3.24; Mol. wt., 450.

2,2,7,7,12,12,17,17-Octamethyl-21,22-diaza-23,24-dioxaquaterene (*XII*)

A solution of 0.522 g. (0.003 mole) of 2,2-dipyrrylpropane (VIII) and 0.875 g. (0.003 mole) of 2,2-*bis*(5-isopropylolfuryl)propane (VII) in 10 ml. of absolute ethanol was cooled in an ice-bath. To this solution was added 0.15 ml. of 37% hydrochloric acid solution. A solid began to form immediately. After 3 hours, the solid was removed by filtration and washed with ethanol to give 0.89 g. (69%) of light gray needles, m.p. 255–257° (with darkening). Crystallization from benzene (15 ml./g.) gave 0.51 g. of white needles, m.p. 260° (with darkening). Anal. Calc. for $C_{28}H_{34}N_2O_2$: N, 6.50; Mol. wt., 431. Found: N, 6.58; Mol. wt., 440.

2,2,7,7,12,12,17,17-Octamethyl-21,23-diaza-22,24-dioxaquaterene (*XI*)

(*a*) *From 2-Furyl-2-pyrrylpropane and Acetone*

A solution of 2.0 g. (0.011 mole) of 2-furyl-2-pyrrylpropane (III) and 3.0 g. (0.052 mole) of acetone in 10 ml. of absolute ethanol was cooled in an ice-bath. While the solution was being swirled, 37% hydrochloric acid solution was added dropwise. The solution became orange in color, then a deep cherry red. After 2 ml. of acid had been added, an oil began to separate. The mixture was heated to 50° during which time the oil dissolved and crystals started to form. After it was left for 30 minutes, the mixture was filtered. The residue was washed with 95% ethanol until the color had been removed (about 5 ml.) leaving 0.36 g. (15%) of fine white needles, m.p. 227.5–228.5°. Crystallization from an acetone–water solution, including treatment with charcoal, gave shiny white needles, m.p. 230.5°. Anal. Calc. for $C_{28}H_{34}N_2O_2$: C, 78.1; H, 7.96; N, 6.51; Mol. wt., 431. Found: C, 78.0; H, 7.83; N, 6.73; Mol. wt., 424.

(*b*) *From 2,5-Diisopropylolfuran and Pyrrole*

The method of Ackman, Brown, and Wright (1) was used for the preparation of 2,5-diisopropylolfuran (IX) from diethyl 2,5-furandicarboxylate which had been previously prepared by the dehydration of mucic acid and esterification of the product. A

Can. J. Chem. Downloaded from www.nrcresearchpress.com by 61.7.252.67 on 09/04/12
For personal use only.

solution of 0.55 g. (0.003 mole) of 2,5-diisopropylolfuran and 0.20 g. (0.003 mole) of pyrrole in 10 ml. of absolute ethanol was cooled in an ice-bath. Then, while it was being agitated, 0.3 ml. of 37% hydrochloric acid solution was added. A white crystalline solid began to form immediately. The solution was colorless at first, then became a deep red. After 4 hours, the mixture was filtered and the residue washed with 5 ml. of 95% ethanol to give 0.090 g. (14%) of white needles, m.p. 228–229°. Crystallization from absolute ethanol (100 ml./g.) gave shiny white needles, m.p. 230.5°. A mixture melting point of this compound with that obtained in (*a*) showed no depression.

ACKNOWLEDGMENTS

We are grateful for financial assistance from the National Research Council of Canada for one of us (W.N.F.). The Du Pont Company of Canada has been most helpful by supplying generous quantities of furan and pyrrole.

REFERENCES

1. ACKMAN, R. G., BROWN, W. H., and WRIGHT, G. F. J. Org. Chem. **20**, 1147 (1955).
2. BAEYER, A. Ber. **19**, 2184 (1886).
3. DENNSTEDT, M. and ZIMMERMAN, J. Ber. **19**, 2189 (1886); **20**, 2449 (1887); **23**, 1370 (1890).
4. CHELINTZEV, V. V. and TRONOV, B. V. J. Russ. Phys. Chem. Soc. **48**, 105 (1916); Chem. Abstr. **11**, 452 (1917).
5. BROWN, W. H. and SAWATZKY, H. Can. J. Chem. **34**, 1147 (1956).
6. HEID, J. V. and LEVINE, R. J. Org. Chem. **13**, 409 (1948).
7. REICHSTEIN, T., ZSCHOKKE, H., GEHRING, R., and RONA, G. Helv. Chim. Acta, **15**, 1118 (1932).
8. BOWER, J. R. and COOK, L. M. Ind. Eng. Chem. **15**, 290 (1943).

Can. J. Chem. Downloaded from www.nrcresearchpress.com by 61.7.252.67 on 09/04/12
For personal use only.

Can. J. Chem. Downloaded from www.nrcresearchpress.com by 61.7.252.67 on 09/04/12
For personal use only.

SYNTHESIS OF GUANIDINE FROM UREA, AMMONIUM BENZENESULPHONATE, AND AMMONIUM SULPHAMATE[1]

JEAN L. BOIVIN AND MEUDE TREMBLAY

ABSTRACT

Guanidine benzenesulphonate has been obtained in yields exceeding 70% by heating urea, ammonium sulphamate, and ammonium benzenesulphonate in respective molar ratios of 1:1:0.75. The effects of temperature, proportion of reactants, and reaction time were studied batchwise. Then the process was operated on a continuous basis in a four-flask cascade reactor at temperatures between 240° and 260° C.

INTRODUCTION

The fusion of urea with ammonium sulphamate gives rise to guanidine sulphamate in relatively low yield, and even a large excess of ammonium sulphamate does not effect the transformation in yields higher than 80% (3). Moreover, the fusion is hampered by the formation of ammonium sulphate coming out of the melt at high temperature. The presence of this insoluble salt in the fusion mixture makes a continuous process impossible.

A search has been made for a guanidine salt which would be stable up to 300° C. in the fused state and could be readily transformed into either guanidine nitrate or nitroguanidine. Sulphonic acids appeared to be suitable since they are stable and, unlike sulphamic acid, are not readily hydrolyzed. Guanidine benzenesulphonate melts at 212° C. and can be fused at 300° C. without decomposition or appearance of melamine (2). Moreover, guanidine benzenesulphonate is less soluble in water than guanidine nitrate and can be crystallized from it.

Guanidine benzenesulphonate can be obtained by the reaction between urea, ammonium sulphamate, and ammonium benzenesulphonate. The fusion of urea and ammonium sulphamate gives cyanamide and ammonium sulphate (1); cyanamide then reacts with ammonium benzenesulphonate to yield guanidine benzenesulphonate according to the following equations:

$$NH_2SO_3NH_4 + NH_2CONH_2 \rightarrow NH_2CN + (NH_4)_2SO_4,$$
$$NH_2CN + NH_4SO_3C_6H_5 \rightarrow NH_2C(NH)NH_2.HSO_3C_6H_5.$$

A study of the effect of temperature, molar ratio of reactants, and reaction time was made batchwise by heating the mixture in a flask, and on a continuous basis in a four-flask cascade reactor. It was observed that the addition of ammonium sulphate to the urea – ammonium benzenesulphonate – ammonium sulphamate mixture did not appreciably change the fluidity of the melt at the synthesis temperature, because of its relative solubility in the fused mixture. The crude guanidine benzenesulphonate thus formed was isolated by crystallization from water and melted at 212° C. A mixed melting point determination with an authentic sample was not depressed.

EXPERIMENTAL AND RESULTS

Preparation of Guanidine Benzenesulphonate

Batch Process

The preliminary experiments were directed to the study of the effect of temperature, molar ratio of reactants, and time of the reaction on the yield. The reaction was carried

[1]*Manuscript received October 23, 1957.*
Contribution from Canadian Armament Research and Development Establishment, Valcartier, Quebec.

out in a three-necked flask equipped with a stirrer, a thermometer, and gas inlet. Heating was accomplished by means of a heating mantle. The mixture of ammonium sulphamate, ammonium benzenesulphonate, and urea melted at about 100° C., and at 180–200° C. an exothermic reaction took place with evolution of gases and the formation of a sublimate. The melt was heated to the desired temperature for a period of 15 to 90 minutes. The liquid was then poured into a beaker, allowed to cool, dissolved in water, and diluted to 500 cc. in a volumetric flask. The solution was analyzed for guanidine with a solution saturated with ammonium picrate and guanidine picrate.

Effect of reaction temperature.—Table I shows the results obtained at different temperatures. The maximum yield of guanidine benzenesulphonate was obtained at 240° C. after a 1-hour period of heating.

TABLE I

EFFECT OF TEMPERATURE

Urea: 15 g. (0.25 mole); ammonium sulphamate: 28.5 g. (0.25 mole); ammonium benzenesulphonate: 57.4 g. (0.25 mole)

Temp., ° C.	Time, min.	Yield from urea, %	Temp., ° C.	Time, min.	Yield from urea, %
290	30	27.0	300	60	16.0
280	"	29.6	290	"	16.5
270	"	36.3	280	"	26.3
260	"	46.3	270	"	29.7
250	"	54.9	260	"	44.0
240	"	56.2	250	"	53.3
220	"	43.0	240	"	60.0
			230	"	55.4
			220	"	53.5

Effect of molar ratio of reactants.—Results are summarized in Table II. Yields increased with excess of urea, but much decomposition occurred giving rise to a material insoluble in water. Yields increased also with the amount of ammonium sulphamate and remained practically constant as the proportion of benzenesulphonate was increased.

TABLE II

EFFECT OF MOLAR RATIO OF REACTANTS

Temperature: 240° C.; time: 1 hour

Urea		Ammonium sulphamate		Ammonium benzenesulphonate		Yield from urea, %
g.	mole	g.	mole	g.	mole	
30	0.5	28.5	0.25	57.4	0.25	79.6
24	0.4	"	"	"	"	67.9
18	0.3	"	"	"	"	62.6
15	0.25	"	"	"	"	60.0
15	0.25	34.2	0.3	57.4	0.25	57.0
"	"	42.7	0.375	"	"	61.7
"	"	57.0	0.5	"	"	67.0
15	0.25	28.5	0.25	45.8	0.2	63.4
"	"	"	"	68.7	0.3	63.1
"	"	"	"	92.2	0.4	62.3

Can. J. Chem. Downloaded from www.nrcresearchpress.com by 61.7.252.67 on 09/04/12
For personal use only.

Effect of reaction time.—The results are shown in Table III. At low temperature (240° C.) yields were practically the same, but a 30-minute period of heating was sufficient. With longer heating times some solid separated from the melt and impaired the stirring. Higher temperatures (260° C.) required shorter times.

TABLE III

EFFECT OF REACTION TIME AT 240°, 250°, AND 260° C.
Ammonium benzenesulphonate: 57.4 g. (0.25 mole); urea: 18 g. (0.3 mole); ammonium sulphamate: 57 g. (0.5 mole)

Temp., ° C.	Time, hr.	Yield from ammonium benzenesulphonate, %
240	0.5	68.2
"	1.0	66.2
"	1.5	70.3
250	0.5	66.5
"	1.0	58.9
"	1.5	60.0
260	0.5	60.4
"	1.0	53.5
"	1.5	47.5

Continuous Process

The main object of this work was to produce guanidine benzenesulphonate on a continuous basis. A cascade reactor consisting of four 500-ml. flasks was built in such a way that molten material overflows from flask 1 to flask 4 by gravity. A stream of anhydrous ammonia was introduced at the bottom of each flask to stir the molten solid while the flasks were heated by mantles.

Runs were made by adding urea, ammonium sulphamate, and ammonium benzenesulphonate in respective molar ratios of 1:1:0.9. These molar ratios were considered to be the optimum proportions to give maximum melt fluidity. The reduced molar ratio of ammonium benzenesulphonate was sufficient to form the salt of the guanidine produced in the reaction. The residence time in the reaction flasks varied from 15 to 120 minutes at the rates of feed of 20 to 5 grams per minute respectively. The mixture was first added manually at a constant rate of 5 to 15 grams per minute. Attempts were made to introduce the same mixture by means of a screw feeder to obtain a constant rate of addition but this mixture absorbed water rapidly and became tacky, causing plugging of the screw feeder. It was found that the mixture became hygroscopic owing to the presence of urea. Two screw feeders were then used to introduce respectively urea and the mixture of ammonium sulphamate and ammonium benzenesulphonate. With this arrangement two 8-hour runs were made successfully using 10 pounds of mixture each.

The mixture was melted at 160–170° C. in the first flask and allowed to overflow to the second flask where the temperature reached 250–260° C. The reaction in the second flask was exothermic with evolution of ammonia. The liquid flowed through two more flasks to complete the reaction and was finally collected in a beaker where it solidified. After solidification, a weighed sample was dissolved in the minimum of water and analyzed for guanidine. The guanidine benzenesulphonate was also crystallized, weighed, and its purity determined. Yields of about 60 to 80% were obtained depending on the rate of feed. The results given in Table IV show that the yields obtained by adding the mixture at a constant rate from 10 to 15 grams per minute were 66 to 71% by crystallization, the product obtained being about 97% pure.

Can. J. Chem. Downloaded from www.nrcresearchpress.com by 61.7.252.67 on 09/04/12
For personal use only.

TABLE IV

CONTINUOUS FUSIONS

Temperature of flask 1: 160–170° C.
Temperature of flasks 2, 3, and 4: 250° C.
Molar ratio of urea, ammonium sulphamate, and ammonium benzenesulphonate: 1: 1: 0.9

Estimated residence time of reaction, min.	Rate of feed, g./min.	Yield of guanidine from urea, %	
		By analysis	By cryst.
120	5	60.6–63.0	
90	7.5	68 –73.9	
60	10	74.5	
60	10	75.2–81.1	66.6†
60	10*	77.5	71.0
30	15*	72.4–81.5	67.4
15	20	53.4–90.0	

Using two screw feeders.
†A mixed melting point with an authentic sample of guanidine benzenesulphonate (m.p. 212° C.) was not depressed.

RECOVERY OF UNREACTED AMMONIUM SULPHAMATE

To make the synthesis more attractive, the unreacted ammonium sulphamate should be recovered. The melt obtained from the continuous reactor was dissolved in water and fractionally crystallized. Results given in Table V show that guanidine benzenesulphonate crystallized first, then on further concentration ammonium sulphate was obtained, and finally ammonium sulphamate. The separation is not very clear-cut and a more practical procedure is required to reclaim the ammonium sulphamate on a production scale.

TABLE V

FRACTIONAL CRYSTALLIZATION OF FUSION PRODUCT
Weight of melt used: 540 g.

Crop of crystals	Volume of solution, ml.	Weight of solid, g.	Composition of solid		
			Ammonium sulphate, %	Ammonium sulphamate, %	Guanidine benzenesulphonate, %
1	800	250	1.0	1.1	97.0
2	600	51.2	71.1	2.7	23.7
3	400	70.1	98.1	5.79	0.0
4	200	66.8	61.1	7.8	0.0
5	100	76.3	54.4	20.6	0.0

DISCUSSION

The results obtained by the fusion of urea, ammonium sulphamate, and ammonium benzenesulphonate are promising. The fusion stage is sufficiently exothermic to preclude any use of external heating and the conversion of urea into guanidine is high using a stoichiometric ratio of reactants. It has been shown that the proportion of ammonium benzenesulphonate could be reduced below the stoichiometric amount with equally good results.

The use of ammonium benzenesulphonate stabilizes the guanidine formed and prevents its transformation into melamine; this stabilizing effect could otherwise be

Can. J. Chem. Downloaded from www.nrcresearchpress.com by 61.7.252.67 on 09/04/12
For personal use only.

accomplished by the use of a large excess of ammonium sulphamate. The presence of ammonium benzenesulphonate in the fusion mixture also increases the fluidity of the melt and prevents the separation of ammonium sulphate.

The presence of guanidine as its benzenesulphonate salt makes possible a continuous process which has been demonstrated in a laboratory system. Guanidine benzenesulphonate was separated easily from the salts present in the fusion mixture. However, the high stability of this salt made difficult its transformation into guanidine nitrate directly by means of ammonium nitrate or nitric acid.

This fusion has the advantage of being made at atmospheric pressure. A reactor will be easily constructed from conventional materials. No difficult heat transfer problem will arise since the reaction is self-sustaining.

REFERENCES

1. BOIVIN, J. L. and LOVECY, A. L. Can. J. Chem. **33**, 1222 (1955).
2. KARRER, P. and EPPRECHT, J. Helv. Chim. Acta, **24**, 310 (1941).
3. MACKAY, J. U.S. Patent No. 2,464,247 (1949) to American Cyanamid Co.

Can. J. Chem. Downloaded from www.nrcresearchpress.com by 61.7.252.67 on 09/04/12
For personal use only.

Can. J. Chem. Downloaded from www.nrcresearchpress.com by 61.7.252.67 on 09/04/12
For personal use only.

THE PHOTOLYSIS OF ALKYL ESTERS[1,2]

P. AUSLOOS[3]

ABSTRACT

An attempt has been made to determine the primary processes in the gas and liquid phase photolysis of simple alkyl esters.

The liquid phase photolysis of methyl, ethyl, *n*-propyl, and *n*-butyl formate has been briefly investigated. Besides the dissociation processes, two intramolecular rearrangements were found to occur:

$$\begin{aligned} HCOOR + h\nu &= CO + HOR, && I \\ &= HCOOH + \text{alkene}. && II \end{aligned}$$

Process I takes place with approximately the same yield for all the formates studied. Process II occurs only when there is a β-hydrogen in the alkyl group.

An investigation of the gas and liquid phase photochemical decomposition of esters other than formates showed the existence of the following primary processes:

$$\begin{aligned} XCOOY + h\nu &= XCOOH + \text{alkene}, && VI \\ &= CH_3COOY + \text{alkene}, && VII \\ &= XCO + OY, && X \\ &= X + COOY. && XI \end{aligned}$$

Processes VI and VII require β- and γ-hydrogens, respectively, in the Y and X alkyl groups.

It was found that processes I and X occur mostly at short wavelength, while the other processes take place at long wavelengths as well.

EXPERIMENTAL

The liquids were irradiated in a quartz cell of 5 cm. diameter and 0.1 cm. depth. The cell was closed with a break seal which made it possible to attach the cell to the analysis system after each run.

Spectra taken with a Cary spectrophotometer indicated that for a 0.1 cm. path length 100% of the useful radiation was absorbed. Absorption occurred only below 2400 Å. Experiments with a Corning filter 9863, cutting off radiation below 2250 Å, reduced the rates of formation of the products by a factor of approximately 20. Absorption spectra of formates diluted with ethanol showed a maximum around 2150 Å, while the extinction coefficients were appreciably higher than those of ketones and aldehydes.

Irradiation was carried out in a quartz Dewar filled with distilled water. For a few low temperature runs, however, 3-methyl pentane was used.

The gas phase experiments were performed with a cylindrical quartz cell (5 cm. diameter, 10 cm. long) which was completely filled with a nearly parallel light beam. The low temperature runs were performed in a brass cylinder thermostat with double quartz windows. Ethyl alcohol was used as a cooling medium.

Two Hanovia (16A-13) SH type medium pressure lamps were used in the course of this work. Because a slight change in wavelength distribution changes the relative rates of formation of the products, the number of each run is preceded by a letter *a* or *b* depending on which lamp was used. Except when stated otherwise, the incident intensity was kept constant for all the runs with lamp *a*. This allows comparison of the rates of

[1]*Manuscript received August 6, 1957.*

Contribution from Département de Chimie, Université Laval, Quebec, Que., and Department of Chemistry, The University of Rochester, Rochester, N. Y.

[2]*This research was supported in part by the United States Air Force through the Air Force Office of Scientific Research of the Air Research and Development Command, under Contract No. AF18(600)1528. Reproduction in whole or in part is permitted for any purpose of the United States Government.*

[3]*Present address: Department of Chemistry, The University of Rochester, Rochester, N. Y.*

formation of the products from one table to another. All rates are given in cc./min. 10^{+4}. No absolute quantum yields were determined.

The analysis procedure was the same as described earlier (2).

The esters were obtained from Eastman Kodak Co. (White Label). Ethyl formate, methyl acetate, and methyl propionate were fractionated in a 10 plate column before distillation in the vacuum line. The other compounds were distilled and degassed in vacuum.

PART I. THE PHOTOCHEMICAL DECOMPOSITION OF FORMATES

Results

The results of runs performed in the liquid phase at constant incident intensity and varying temperatures are given in Table I.

TABLE I

LIQUID PHOTOLYSIS OF FORMATES
Variation of rate with temperature

	Run	Temp., ° C.	R_{CO}	R_{H_2}	R_{CH_4}	R_{CO_2}	
Methyl formate	*a*1	5	82.5	8.0	27.5	29.0	
	*a*2	31	82.0	8.0	186	160	
	Run	Temp., ° C.	R_{CO}	R_{H_2}	$R_{C_2H_4}$	$R_{C_2H_6}$	R_{CO_2}
Ethyl formate	*a*3	5	82.0	9.5	171	25.8	27.5
	*a*4	35	80.0	9.0	184	120	112
	*a*5	51	82.5	10.0	205	214	218
	Run	Temp., ° C.	R_{CO}	R_{H_2}	$R_{C_3H_6}$	$R_{C_3H_8}$	R_{CO_2}
n-Propyl formate	*a*6	6	74.0	7.0	305	7.0	10
	*a*7	32	77.0	7.0	302	36.0	41.5
	*a*8	50	77.0	7.0	295	70.5	84.5
	*a*9	74	83.0	8.0	297	180	206
	Run	Temp., ° C.	R_{CO}	R_{H_2}	$R_{C_4H_8}$	$R_{C_4H_{10}}$	R_{CO_2}
n-Butyl formate	*a*10	6	67.5	7.8	154	4.3	11.4
	*a*11	45	70.0	9.0	166	43.0	60.0
	*a*12	85	98.0	12.0	169	108	116

It can be seen that the rates of formation of hydrogen and of carbon monoxide change very little with temperature for each compound taken separately and show only slight variations from one compound to another.

Formates with a β-hydrogen in the alkyl groups have under these experimental conditions an alkene as most important product. The rates of formation of these alkenes vary only slightly with temperature, but, unlike the rates of formation of carbon monoxide, change considerably from one compound to another.

The only other products analyzed for were carbon dioxide and the hydrocarbons: methane, ethane, propane, butane, formed respectively in the photolysis of methyl, ethyl, propyl, butyl formate.

The results indicate that the rate of formation of carbon dioxide is roughly equal to that of the corresponding hydrocarbon. They both increase appreciably with increase in temperature.

Can. J. Chem. Downloaded from www.nrcresearchpress.com by 61.7.252.67 on 09/04/12
For personal use only.

The rates of formation of the recombination products ethane and butane, formed in the photolysis of methyl and ethyl formate, respectively, are not given in Table I because these products were always present in amounts too small to be measured accurately. The amount of ethane formed in experiments 1 and 2 was less than 1% of the carbon dioxide fraction. No attempt was made to determine the rates of formation of hexane and octane in the photolysis of propyl and butyl formate.

The results of a few more liquid phase experiments on ethyl formate are included in Table II. Runs 13, 14, and 15 were performed in order to obtain a rough idea of the effect on the products of a variation in the wavelength distribution. The temperature was

TABLE II

PHOTOLYSIS OF ETHYL FORMATE

A. Liquid phase

Run	Temp., °C.	Time, min.	R_{CO}	R_{H_2}	$R_{C_2H_4}$	$R_{C_2H_6}$	R_{CO_2}	$\frac{R_{C_2H_4}}{R_{CO}}$	I_{rel}
				Variation of wavelength					
*b*13	13	25	42.5	6.8	152	26.0	30.5	3.57	
*b*14*	13	70	13.0	1.4	112	32.5	35.0	7.80	
*b*15†	13	101	1.1	0.18	25.3	18.8	19.0	23.0	
*b*16*	−60	35	14.3	1.3	60.5	2.0	1.10	4.24	
*b*17*	−80	70	14.6	1.28	57.0	2.0	1.3	3.90	
				Variation of intensity					
*b*18	28	13	26.7	4.63	101	62.0	58.5	3.80	1500
*b*19	28	88	3.15	0.68	11.9	16.4	15.9	3.80	180
*b*20	28	705	0.405	0.08	1.32	4.68	4.5	3.25	19
*b*21	28	4700	0.023	0.0036	0.067	0.505	0.512	2.85	1

B. Gas phase

Run	Temp., °C.	Time, min.	Pressure, cm.	R_{CO}	R_{H_2}	$R_{C_2H_4}$	$R_{C_2H_6}$	R_{CO_2}	R_{CH_4}	$R_{C_3H_8}$	$R_{C_4H_{10}}$
*b*22	0	45	4.1	62.0	7.7	16.6	11.8	22.0	2.45	2.0	4.3
*b*23	29	35	4.5	80.0	8.8	16.4	15.8	31.0	5.75	3.15	4.0
*b*78§	27	20	4.5	59.0	1.35	16.0	0.5	10.6	—	—	—

**3-Methyl pentane bath.*
†Corning filter 9863.
§Iodine added 0.035 cm.

kept constant. Run 14 was done with a 3-methyl pentane bath which absorbed most of the radiation below 2150 Å. In order to cut off radiation below 2250 Å, a Corning filter 9863 was used in run 15. It follows from these experiments that a change in the wavelength distribution appreciably affects the ratio C_2H_4/CO. The rates of formation of carbon monoxide and hydrogen decrease appreciably as compared to the rate of formation of ethylene when only the longer wavelengths are absorbed by ethyl formate.

Runs 16 and 17 were done with the same experimental setup and at the same intensity as experiment 14. From the results of these experiments it follows that the rates of formation of carbon monoxide and hydrogen are practically independent of temperature, while the rate of formation of ethylene decreases with decrease in temperature. Runs 3, 4, and 5 of Table I lead to the same observation.

Can. J. Chem. Downloaded from www.nrcresearchpress.com by 61.7.252.67 on 09/04/12
For personal use only.

In the same table results are presented of runs where only the intensity has been varied. It can be seen that the carbon monoxide, hydrogen, and ethylene yields as well as the ratio C_2H_4/CO change only slightly, while the carbon dioxide and ethane yields increase markedly with diminishing intensities.

The results of the gas phase runs given in Table II indicate that addition of iodine does not affect the rate of formation of ethylene to any appreciable extent, while the rates of formation of methane, propane, and butane were reduced to negligible amounts. Increase of the temperature increases the rate of formation of the products with the exception of ethylene.

Discussion

The results of Tables I and II indicate that the following intramolecular process occurs:

$$HCOOR + h\nu = HOR + CO. \qquad I$$

The independence with respect to temperature variation of the rate of formation of carbon monoxide over a temperature range from $-80°$ to 13° C. and over a large intensity range is good evidence for the occurrence of this process. The small increase of the hydrogen and carbon monoxide yields at high temperatures and low intensities may be attributed to a thermal decomposition of formyl radicals. The fact that the less stable acetyl radicals formed in the liquid phase photolysis of methyl and ethyl acetate decompose only to a small extent agrees with the proposition that at low temperatures carbon monoxide is formed mostly by process I.

Formates with a β-hydrogen may also decompose by process II:

$$HCOOR + h\nu = HCOOH + \text{alkene}. \qquad II$$

The following facts may be cited as evidence in favor of process II:

(*a*) the independence of the ethylene yield in the liquid phase photolysis of ethyl formate over a considerable intensity range,

(*b*) the only slight variation of the rate of formation of the alkenes with temperature,

(*c*) the rate of formation of ethylene which in the gas phase photolysis of ethyl formate is unchanged upon addition of iodine.

It may be mentioned that pyrolysis studies (5) of several formates by the toluene carrier technique showed that formates with a β-hydrogen decompose by a molecular elimination process analogous to process II. Acetic anhydride may be cited as another example of the same type where photolysis (1) and pyrolysis (8) produce ketene and acetic acid in a direct process.

The ethyl formate results show that process I occurs mostly at wavelengths shorter than are required for process II. This indicates that processes I and II probably occur from different electronic levels.

Besides the intramolecular processes one or more of the following dissociative steps has to occur:

$$HCOOR + h\nu = HCO + OR, \qquad III$$

$$= H + COOR, \qquad IV$$

$$= HCOO + R. \qquad V$$

From our results little can be said about the occurrence of these processes. Analogy with the liquid phase photolysis of the acetates and propionates favors processes III and IV.

Recent studies (6) on the gas phase photolysis of acetone in the presence of methyl formate have shown that methyl radicals only abstract the hydrogen atom from the

Can. J. Chem. Downloaded from www.nrcresearchpress.com by 61.7.252.67 on 09/04/12
For personal use only.

acyl group. One carbon dioxide molecule was found for every hydrogen abstracted. In agreement with this, the pronounced increase of the rate of formation of carbon dioxide and the corresponding hydrogen with increase in temperature and diminishing intensities can be explained by the following chain propagating steps:

$$R + HCOOR = RH + COOR,$$

$$COOR = CO_2 + R.$$

The initiator may be any of the radicals formed in processes III, IV, and V.

Considering the primary processes mentioned above, hydrogen can at low temperatures only be produced by a reaction of the hydrogen atoms formed in process IV with other radicals present in the system or with formate molecules. It is perhaps surprising that the ratio H_2/CO is approximately the same for all runs done with the same lamp and at the same wavelength distribution.

It may be pointed out that at these wavelengths, hydrogen atoms cannot be formed by a primary process in which a hydrogen atom is split off from the alkyl group. This is substantiated by the fact that no hydrogen was found in the gas or liquid phase photolysis of the esters to be discussed later in this paper.

The methane and propane formed in the gas phase photolysis of ethyl formate indicate that even at room temperature the ethoxy radicals decompose to an appreciable extent into a methyl radical and formaldehyde.

PART II. THE PHOTOLYSIS OF ESTERS OTHER THAN FORMATES

Results

Liquid Phase

The results of the liquid phase photolysis of a few simple alkyl esters at varying temperatures and intensities have been summarized in Table III.

Only the volatile products have been determined quantitatively. In a few runs however some of the products were present in amounts too small to be measured with any accuracy. Except when stated otherwise, the incident intensity was the same as for the experiments given in Table I. For the runs where the intensity has been changed, the incident intensity is given relative to the constant intensity experiments. All the rates are expressed in cc./min. $\times 10^4$.

A few general features are as follows:

(*a*) Ethyl acetate and ethyl propionate give ethylene as an important product. The ethylene quantum yields are virtually not affected by a change in intensity.

(*b*) Propylene is the main volatile product in the photolysis of isopropyl and *n*-propyl acetate.

(*c*) In the photolysis of methyl *n*-butyrate a considerable amount of ethylene has been found.

(*d*) Some ethylene is also formed in the photolysis of methyl propionate. However, the rate of formation is only 10% of the rate of ethylene production in the photolysis of ethyl propionate.

(*e*) For most of these compounds a change in temperature produces a slight variation in the yields of the alkenes.

(*f*) All esters have carbon monoxide and carbon dioxide as products. The rates of formation of both compounds increase with temperature. The acetates produce less carbon monoxide, carbon dioxide, and hydrocarbons than the propionates and the butyrates.

Can. J. Chem. Downloaded from www.nrcresearchpress.com by 61.7.252.67 on 09/04/12
For personal use only.

TABLE III

LIQUID PHASE PHOTOLYSIS OF ESTERS

	Run	Temp., ° C.	Time, min.	R_{CO}	R_{CO_2}	R_{CH_4}	$R_{C_2H_6}$	$R_{C_2H_4}$	$R_{C_3H_8}$	$R_{C_4H_{10}}$
Methyl acetate	*a*24	5	85	7.3	2.47	8.80	1.42			
	*a*25	29	55	11.8	7.80	12.0	1.80			
Methyl propionate	*a*26	5	8	6.10	38.6	27.0	135	20.5	5.20	22.5
	*a*27	31	7	12.8	154	105	248	6.4	8.35	14.3
	*a*28	50	6	26.6	245	216	278	5.10	8.60	7.80
	*a*29	70	5	57.5	292	258	328	4.30	4.30	3.50
	Relative intensity 0.125									
	*a*30	5	35	0.75	7.45	6.82	26.7	2.30		
	*a*31	30	35	1.50	21.0	22.0	38.2	1.70		
	*a*32	50	30	4.45	36.5	34.5	45.8			
	*a*33	70	30	8.80	34.0	36.6	46.0			

	Run	Temp., ° C.	Time, min.	R_{CO}	R_{CO_2}	R_{CH_4}	$R_{C_3H_8}$	$R_{C_3H_6}$	$R_{C_2H_4}$
Methyl *n*-butyrate	*a*34	5	8	2.90	9.50	6.55	30.5	3.05	203
	*a*35	36	8	9.53	45.0	38.4	100	4.20	176
	*a*36	85	7	66.0	155	140	192		101

	Run	Temp., ° C.	Time, min.	R_{CO}	R_{CO_2}	R_{CH_4}	$R_{C_2H_6}$	$R_{C_2H_4}$
Ethyl acetate	*a*37	3	5	1.1		1.0		255
	*a*38	30	4	4.3	3.8	4.0		260
	*a*39	70	4	20.5	25.5	14.0	15.0	238
	Relative intensity 0.21							
	*a*40	3	122	0.34	0.90	0.30		46.0
	*a*41	26	37	1.10	2.25	0.80		55.8
	*a*42	52	41	2.80	3.15	2.05	2.70	58.0
	*a*43	74	20	4.75	5.40	4.40	4.00	47.0

	Run	Temp., ° C.	Time, min.	R_{CO}	R_{CO_2}	$R_{C_2H_6}$	$R_{C_2H_4}$	$R_{C_4H_{10}}$
Ethyl propionate	*a*44	4	4	8.40	33.2	71.0	200	34.4
	*a*45	30	3	20.5	85.0	130	176	25.0
	*a*46	30	4	19.0	87.0	135	181	22.0
	*a*47	50	3	36.0	155	227	168	19.5
	*a*48	70	3	59.2	186	315	155	16.0
	*a*49	90	3	83.5	198	384	136	10.0
	Relative intensity 0.125							
	*a*50	3	40	0.81	5.90	12.6	22.0	0.60
	*a*51	30	35	2.80	12.8	23.7	19.0	0.80
	*a*52	61	30	7.80	21.3	42.0	18.0	
	*a*53	90	30	13.0	23.5	51.0	18.0	
	Relative intensity 0.0023							
	*a*54	30	1035	0.06	0.227	0.49	0.315	

	Run	Temp., ° C.	Time, min.	R_{CO}	R_{CO_2}	R_{CH_4}	$R_{C_3H_8}$	$R_{C_3H_6}$
Isopropyl acetate	*a*55	7	6	0.40		0.50		370
	*a*56	31	6	1.40		2.60		319
	*a*57	77	6	16.0	15.0	18.0	18.5	255
n-Propyl acetate	*a*58	28	6	2.70		1.54		180
	*a*59	75	6	26.5	20.0	16.0	21.2	198

Can. J. Chem. Downloaded from www.nrcresearchpress.com by 61.7.252.67 on 09/04/12
For personal use only.

(*g*) In the photolysis of methyl and ethyl propionate, the rates of formation of carbon dioxide, methane, and ethane approach constant values at high temperatures. A decrease in intensity results in an increase of the yields of these three products. The results of the methyl propionate experiments indicate that at low intensities the rates of formation of carbon dioxide and methane are equal, while at high intensities the rate of formation of methane is somewhat less than that of carbon dioxide.

(*h*) Ethers were found to be present in the liquid phase photolysis of all the esters but their rates of formation were too small to be measured with any accuracy.

Gas Phase

Table IV represents the results of a few gas phase experiments. The incident intensity

TABLE IV

GAS PHASE PHOTOLYSIS OF ESTERS

	Run	Temp., ° C.	Pressure, cm.	Time, min.	R_{CO}	R_{CO_2}	R_{CH_4}	$R_{C_2H_6}$
Methyl acetate	*a*60	27	6.4	35	13.8	8.30	1.93	5.50
	*a*61	120	8.35	25	73.2	16.7	7.00	33.8
	*a*62	177	9.50	25	74.8	16.1	17.3	26.2

	Run	Temp., ° C.	Pressure, cm.	Time, min.	R_{CO}	R_{CO_2}	R_{CH_4}	$R_{C_2H_6}$	$R_{C_2H_4}$	$R_{C_3H_8}$	$R_{C_4H_{10}}$
Methyl propionate	*a*63	34	7.1	30	50.8	12.4	1.89	8.4	3.69	6.73	13.82
	*a*64	124	9.1	25	59.0	13.4	3.95	11.0	4.10	8.40	12.40
	*a*65	196	8.8	25	56.8	13.4	8.12	21.1	3.42	3.95	7.03
	*a*66	1	1.8	40	19.2	6.90	0.79	4.02	1.80	2.86	7.10
	*a*67	37	2.05	25	45.0	11.6	1.13	8.50	3.75	6.70	15.2

	Run	Temp., ° C.	Pressure, cm.	Time, min.	R_{CO}	R_{CO_2}	R_{CH_4}	$R_{C_2H_6}$	$R_{C_2H_4}$	$R_{C_3H_6}$	$R_{C_3H_8}$
Methyl *n*-butyrate	*b*68	29	2.85	25	55.0	15.3	1.40	1.7	4.65	3.25	9.10
	*a*69*	29	3.0	800	0.43	0.415	0.043	0.05	0.13	0.029	0.089

	Run	Temp., ° C.	Pressure, cm.	Time, min.	R_{CO}	R_{CO_2}	R_{CH_4}	$R_{C_2H_6}$	$R_{C_2H_4}$	$R_{C_3H_8}$	$R_{C_4H_{10}}$	$\frac{R_{C_2H_4}}{R_{CO_2}}$
Ethyl acetate	*b*70	−23	0.45	60	0.34	0.80	0.076	0.17	3.00	0.20	0.1	3.75
	*b*71	0	1.95	43	4.1	7.90	0.82	2.80	12.6	1.65	0.6	1.60
	*a*72	34	5.8	20	9.60	8.95	1.06	3.26	9.80	2.49	0.54	1.10
	*a*73	124	7.5	15	45.0	16.5	8.55	23.0	11.2	14.8	0.57	0.68
	*a*74	195	8.8	15	54.5	18.0	35.4	13.8	12.6	7.2		0.70
Ethyl propionate	*a*75	34	3.8	35	25.0	8.75	0.30	5.80	7.05	1.26	12.8	0.81
	*b*76†	30	3.3	1340	2.1	0.76	0.015	0.312	0.573	0.055	0.775	0.755
	*b*77*	30	3.3	1140	0.59	0.445	0.01	0.14	0.325	0.032	0.42	0.73

	Iodine present	R_{CO}	R_{CO_2}	R_{CH_4}	$R_{C_2H_6}$	$R_{C_2H_4}$	$R_{C_3H_8}$	$R_{C_4H_{10}}$
Ester–iodine mixtures.—Temperature: 28° C. Ester pressure: 2.7 cm. Iodine pressure: 0.035 cm.								
$C_2H_5COOCH_3$	No	130	34.0	5.2	22.5	9.60	18.0	36.5
	Yes	46.5	32.5	—	—	2.00	—	—
$C_2H_5COOC_2H_5$	No	90.0	33.7	0.65	17.3	29.2	3.2	41.3
	Yes	23.6	33.4	—	—	23.4	—	—
$CH_3COOC_2H_5$	No	34.0	29.0	3.3	11.0	37.0	8.5	2.1
	Yes	10.0	24.0	—	—	35.0	—	—

**Experiments carried out with Corning filter 9863.*

†*Experiment carried out at* $I_{rel} = 0.084$.

Can. J. Chem. Downloaded from www.nrcresearchpress.com by 61.7.252.67 on 09/04/12
For personal use only.

was kept the same for all experiments done with mercury arc *a*. Except for runs 69, 76, and 77, the incident intensity has been kept constant for the runs performed with lamp *b*.

It can be seen that at high temperatures and for unfiltered light, carbon monoxide is the main product for all the esters studied. Under these experimental conditions CO/CO_2 was found to be larger than 3. However, a Corning filter 9863 used in the photolysis of ethyl propionate and methyl *n*-butyrate brings this ratio close to unity, while the C_2H_4/CO_2 ratio stays practically unchanged.

The results indicate that the rates of formation of carbon monoxide and carbon dioxide decrease appreciably with decrease in temperature. In the photolysis of ethyl acetate C_2H_4/CO_2 increases gradually with diminishing temperature. At $-23°$ C. ethylene accounts for about 70% of the volatile products.

Addition of iodine to ethyl acetate and ethyl propionate causes only a slight decrease of the ethylene yield, while all the other hydrocarbons are reduced to trace amounts. In the photolysis of the methyl propionate – iodine mixture, the ethylene yield amounted to about 10% of the ethylene yield found in the photolysis of ethyl acetate and ethyl propionate. No other hydrocarbons were formed.

Except for the iodine mixtures, ethers were found in all runs but were not determined quantitatively.

Discussion

The results given in Tables III and IV indicate that the following intramolecular processes occur:

$$XCOOY + h\nu = XCOOH + \text{alkene}, \qquad \text{VI}$$

$$= CH_3COOY + \text{alkene}. \qquad \text{VII}$$

Y and X represent alkyl groups with respectively β- and γ-hydrogens.

In favor of process VI the following facts may be mentioned:

(*a*) At low temperatures ethylene is practically the only volatile product formed in both the gas and liquid phase photolysis of ethyl acetate. The other esters with a β-hydrogen in the alkoxy group have an alkene as major product. There is only slight variation with temperature of the rate of formation of the alkenes in the photolysis of these esters.

(*b*) In the liquid phase photolysis of ethyl acetate and ethyl propionate, the ethylene yields are independent of intensity.

(*c*) In the photolysis of the ethyl propionate – iodine mixture, ethylene is a major product. The decrease of the ethylene yield is probably due to the elimination of the following disproportionation reactions:

$$C_2H_5 + C_2H_5 = C_2H_4 + C_2H_6, \qquad [1]$$

$$C_2H_5 + C_2H_5O = C_2H_4 + C_2H_5OH. \qquad [2]$$

The existence of process VII is substantiated by the presence of ethylene as an important product in both the gas and liquid phase photolysis of methyl *n*-butyrate. This process is analogous to the intramolecular rearrangement which was found to occur in the photolysis of ketones and aldehydes with γ-hydrogens in the alkyl groups (7).

The small ethylene and propylene yields in the liquid phase photolysis of methyl propionate and methyl *n*-butyrate indicate that process VIII does not occur to any appreciable extent,

$$XCOOY + h\nu = HCOOY + \text{alkene}. \qquad \text{VIII}$$

Also, a considerable fraction of the ethylene and propylene may be expected to be formed in disproportionation reactions between ethyl radicals and other radicals present.

Can. J. Chem. Downloaded from www.nrcresearchpress.com by 61.7.252.67 on 09/04/12
For personal use only.

However, the small amount of ethylene found in the gas phase photolysis of the methyl propionate – iodine mixture seems to indicate that process VIII might occur to some extent. In analogy with this, recent work (4) on the gas phase photolysis of propionaldehyde and *n*-butyraldehyde showed that at 2380 and 1870 Å, these two compounds decompose to some extent into formaldehyde and the corresponding alkene. It should be pointed out, however, that the iodine runs given in Table IV were performed with unfiltered light. This may have led to the formation of ethylene by a disproportionation between ethyl radicals and iodine atoms.

The low carbon monoxide yields in the low temperature gas and liquid phase photolysis of the acetates, the very small ether yields in the liquid phase photolysis of all the compounds studied, and the absence of ethers in the iodine experiments indicate that process IX does not occur,

$$XCOOY + h\nu = XOY + CO. \qquad IX$$

Dissociation Processes

The following primary processes will be considered briefly:

$$XCOOY + h\nu = XCO + OY, \qquad X$$
$$= X + COOY, \qquad XI$$
$$= XCOO + Y. \qquad XII$$

The fact that for unfiltered light, carbon monoxide is the main product in the high temperature gas phase photolysis of all the esters indicates that under these experimental conditions process X is the most important one. It can be seen that the carbon monoxide yield for the high temperature gas phase runs is practically the same for all compounds and does not show any appreciable variation with temperature.

The decrease of the rate of formation of carbon monoxide with diminishing temperatures in both gas and liquid phase photolysis proves that only a small fraction of the XCO radicals decompose by the excess energy carried over from the primary process. In the iodine runs the CO yields are fairly high. However, it is possible that at these low iodine pressures a fraction of the XCO radicals decompose before reacting with iodine.

It is not possible to decide from the gas phase runs if the CO_2 comes from the decomposition of COOY, XCOO, or from both radicals:

$$COOY = CO_2 + Y, \qquad a$$
$$XCOO = CO_2 + X. \qquad b$$

Both radicals are considered to be fairly unstable at room temperature. However, at low temperatures the CO_2 yield decreases appreciably in both the gas and liquid phase photolysis. Although no conclusive evidence can be given, the following facts indicate that reaction *b* and consequently process XI is the most likely one to occur:

1. The rates of formation of methane and carbon dioxide in the liquid phase photolysis of methyl propionate are equal at low intensities and at all temperatures. Recombination of methyl radicals with other radicals present in the system explains the somewhat lower methane yields in the high intensity runs. The results of the liquid phase photolysis of methyl *n*-butyrate lead to the same conclusion.

2. At low temperatures $(C_2H_6+2\,C_4H_{10}+C_3H_8)/(CO+CO_2)$ is much larger than unity in the liquid phase photolysis of methyl propionate, while $C_3H_8 > (CO_2+CO)$ in the photolysis of methyl *n*-butyrate. This proves that there are COOY radicals formed which react with other species instead of decomposing.

Can. J. Chem. Downloaded from www.nrcresearchpress.com by 61.7.252.67 on 09/04/12
For personal use only.

However, the fact that the carbon dioxide yields are considerably lower for the acetates than for the propionates and butyrates remains unexplained. On the assumption that the CH_3CO_2 radicals are more stable than the $C_2H_5CO_2$ or $C_3H_7CO_2$ radicals, this observation would rather tend to favor process XII.

Cutting off short wavelengths in the gas phase photolysis of ethyl propionate and methyl *n*-butyrate reduces considerably the carbon monoxide yield as compared to the ethylene and carbon dioxide yields. This proves that process X occurs at shorter wavelengths than processes VI, VII, and XI.

After subtracting the amounts of ethylene formed in reaction [1], values of 0.66, 0.64, and 0.63 can be obtained for the ratio C_2H_4/CO_2 in the gas phase ethyl propionate runs *a*75, *b*76, and *b*77. The ethyl propionate – iodine run indicates that the contribution of reaction [2] is small. In the gas phase photolysis of methyl *n*-butyrate, values of 0.304 and 0.303 were obtained for the ratio C_2H_4/CO_2 in experiments *b*68 and *b*69. From the independence of the C_2H_4/CO_2 rates with change in wavelength, it may be concluded that processes VI and XI on the one side, and processes VII and XI on the other side, probably result from the same electronic level.

It can be seen that the value for the C_2H_4/CO_2 ratio in the liquid phase photolysis of ethyl propionate at 90° C. and low intensity, under which conditions the CO_2 yield attained a constant value, does not differ very much from the one found in the gas phase photolysis of this compound.

Summarizing the results, it may be concluded that processes I and X take place at short wavelengths, while the other intramolecular and dissociation processes occur at long wavelengths as well. In a later publication (3) it will be shown that addition of certain solvents leaves processes I and X unaffected, while the others are strongly suppressed.

ACKNOWLEDGMENTS

The author is indebted to Professors W. A. Noyes, Jr. and C. Ouellet for advice and encouragement. He also wishes to express his appreciation to the National Research Council of Canada for a University Postdoctorate Fellowship under the tenure of which much of this work was carried out.

REFERENCES

1. AUSLOOS, P. Can. J. Chem. **34**, 1709 (1956).
2. AUSLOOS, P. Can. J. Chem. (To be published).
3. AUSLOOS, P. To be published.
4. BLACET, F. E. and CRANE, R. A. J. Am. Chem. Soc. **76**, 5337 (1954).
5. BLADES, A. T. Can. J. Chem. **32**, 366 (1954).
6. KUTSCHKE, K. O. Private communication.
7. STEACIE, E. W. R. Atomic and free radical reactions. Vol. I. 2nd ed. Reinhold Publishing Corporation, New York. 1954. Chap. V.
8. SZWARC, M. and MURAWSKI, J. Trans. Faraday Soc. **47**, 269 (1951).

Can. J. Chem. Downloaded from www.nrcresearchpress.com by 61.7.252.67 on 09/04/12
For personal use only.

TREATMENT OF EXPERIMENTAL DATA IN THE STUDY OF CHELATION[1]

G. F. Atkinson and W. A. E. McBryde

ABSTRACT

Calculation from experimental formation constants of the various species of metal chelates that predominate for a given system under different experimental conditions is facilitated by the use of a digital computer. A convenient graphical representation of the results obtained in this way is proposed. From the plotted data one may select conditions for a photometric analytical procedure that will ensure the exclusive formation of a single chelate species. The changes in species that accompany changes in pH for some systems introduce a variable and appreciable contribution to the ionic strength of the solution, the magnitude of which may be estimated from the results of the foregoing calculation.

USE OF A DIGITAL COMPUTER

Many methods of attacking the problem of the stoichiometry and stability of metal chelate complexes have been reported in the literature (1, 2, 3, 4, 5). These give rise to sets of values for

p = number of ligand groups attached,
K = formation constant(s),

at particular values of

r = molar ratio of reagent to metal,
$[M]_T$ = metal concentration put in.

The choice of experimental conditions by each investigator often seems rather arbitrary.

Clearly, it is advantageous for the analytical chemist to survey the behavior of a chelate system over a range of pH and r, rather than to devise an empirical procedure closely based on the conditions of the original study. Not only may it be possible to economize on the consumption of frequently expensive reagents, but also it may be possible to arrive at an estimate of the precision needed in reproducing conditions (buffering, etc.) in successive determinations. Unfortunately, because of the number of equilibria involved in forming chelate complexes in aqueous solutions, the determination of the probable solution constituents involves exceedingly tedious calculations, and is seldom undertaken.

We have sought to reduce the labor of calculation by making use of the University of Toronto's electronic digital computer "FERUT".

The chelate system selected was iron(III) plus tiron (4,5-dihydroxybenzene-1,3-disulphonic acid). We shall employ the abbreviated formula H_4Bz for tiron, following Schwarzenbach (6). This system presents more than usual complexity for computation because of the presence in acidic solutions of both protonated and unprotonated 1:1 complexes (6). It was further felt to be an appropriate choice since K values determined for $r = 3$ and for $r = 6.4$ are in fair agreement with each other (7). Schwarzenbach's values for K were used for the calculation.

The Equations

Iron(III) is distributed according to

$$[1] \qquad [Fe]_T = [Fe_0]+[FeBz]+[FeBz_2]+[FeBz_3]+[FeHBz],$$

where $[Fe]_T$ = stoichiometric concentration of iron put in,
Fe_0 = all species not involving tiron,
Bz = "tironate" ion, $C_6H_2(SO_3)_2O_2^{-4}$.

[1]*Manuscript received October 17, 1957.*
Contribution from the Department of Chemistry, University of Toronto, Toronto, Ontario.

Can. J. Chem. Downloaded from www.nrcresearchpress.com by 200.7.193.243 on 09/04/12
For personal use only.

Tiron is distributed among the four species with iron as above, and also among Bz, HBz, and H_2Bz. So when iron is not present

$$[2] \qquad [T]_T = [T_F] = [Bz]+[HBz]+[H_2Bz]$$

and when iron is present

$$[3] \qquad \begin{aligned}[T]_T &= [T_F]+[T_C] \\ &= [Bz]+[HBz]+[H_2Bz]+[FeBz]+2[FeBz_2]+3[FeBz_3]+[FeHBz],\end{aligned}$$

where $[T]_T$ = stoichiometric concentration of tiron put in,
T_F = tiron not in species with iron,
T_C = tiron in species with iron.

Using the expressions defined by Schwarzenbach and Willi (6) for the equilibrium constants, we may set up the following equations:

$$[4] \qquad [Bz]/[T]_T = 1/(1+K_1[H]+K_1K_2[H]^2) \equiv \alpha,$$

$$[5] \qquad [HBz]/[T]_T = (1-\alpha)/(1+K_1[H]) \equiv \beta,$$

$$[6] \qquad [H_2Bz]/[T]_T = 1-(\alpha+\beta),$$

$$[7] \qquad \begin{aligned}[Fe_0]/[Fe]_T &= 1/(1+K_3[Bz]+\alpha^2K_3K_4[Bz]^2+\alpha^3K_3K_4K_5[Bz]^3+K_7[Bz]) \\ &\equiv C_0,\end{aligned}$$

$$[8] \qquad \begin{aligned}[FeBz]/[Fe]_T &= (1-C_0)/(1+\alpha K_4[Bz]+\alpha^2K_4K_5[Bz]^2+K_6[H]) \\ &\equiv C_1,\end{aligned}$$

$$[9] \qquad \begin{aligned}[FeBz_2]/[Fe]_T &= \{1-(C_0+C_1)\}/\{1+\alpha K_5[Bz]+K_6[H]/\alpha K_4[Bz]\} \\ &\equiv C_2,\end{aligned}$$

$$[10] \qquad [FeBz_3]/[Fe]_T = \{1-(C_0+C_1+C_2)\}/\{1+K_6[H]/\alpha^2K_4K_5[Bz]^2\} \equiv C_3,$$

$$[11] \qquad [FeHBz]/[Fe]_T = 1-(C_0+C_1+C_2+C_3) \equiv C_4.$$

The Calculations

The computer program was devised to evaluate these equations systematically at regularly spaced values of [Bz], pH, and $[Fe]_T$. Sets of values having $r<1$, and having $[T]_T>0.5$ molar were automatically discarded, thus limiting the output of results to a useful range. Output was presented as shown for each case:

[Bz]	pH	$[Fe]_T$		
$[T_F]$	$[T_C]$	$[T]_T$	$[T_C]/[T]_T$	
C_0	C_1	C_2	C_3	C_4

It should be pointed out that the application of this technique to all systems consisting of equivalent sets of complex species requires the writing of only one program for the computer, the various K values being supplied as number input in each application of the program. Furthermore it is apparent from the equations that minor modifications will enable the many *tris*-complex systems in which only three species are recognized (MR, MR_2, and MR_3) to be handled by the program.

PRESENTATION OF COMPUTED RESULTS

Various graphical methods of displaying the computed results are possible.

In dealing with the effect of pH on polybasic acids, the fraction of acid present in each ionic or molecular species is often plotted against pH (see, e.g., 8). Curves of this type for

Can. J. Chem. Downloaded from www.nrcresearchpress.com by 200.7.193.243 on 09/04/12
For personal use only.

several values of r are shown in Fig. 1. Their greatest usefulness is in the interpretation of experiments in which a property having a characteristic value for each species (e.g. optical absorption) is measured over a range of pH.

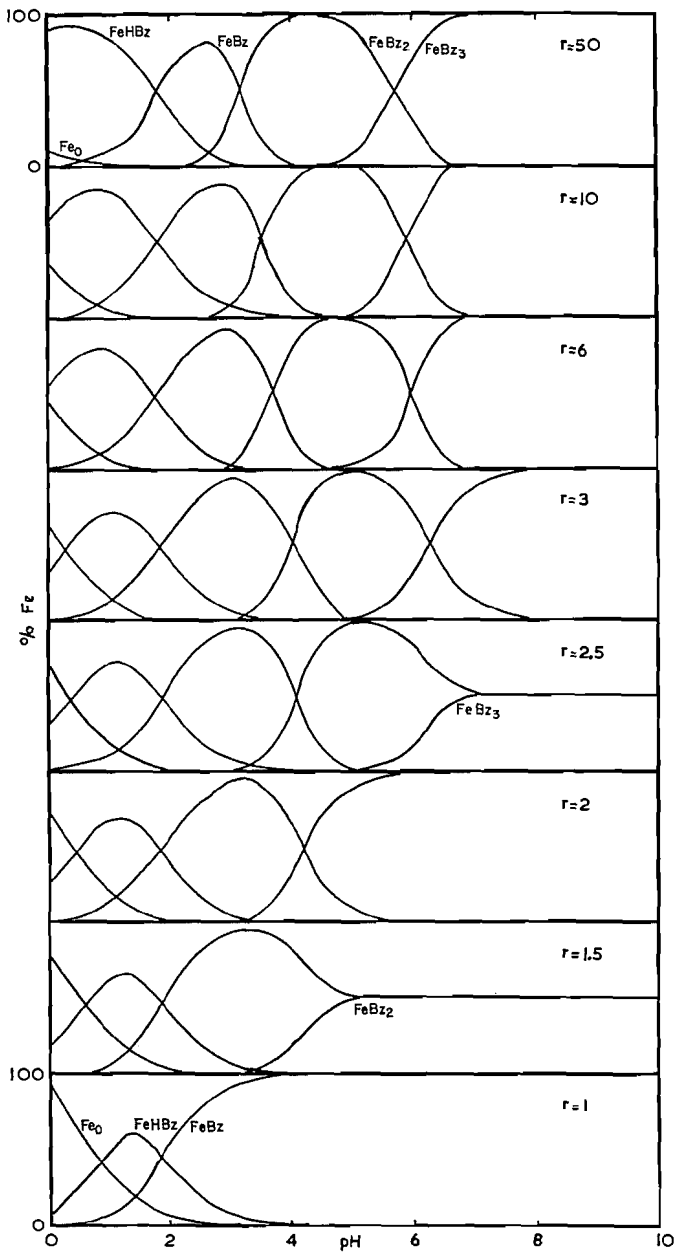

FIG. 1. Distribution of species according to pH.

Ågren (1), having drawn such diagrams with non-overlapping regions, proposes that the abscissae be made pH − pRH rather than pH, to permit the representation of conditions at more than one concentration of chelating agent.

We propose that such data may to advantage be represented as in Fig. 2(*a*), which

Can. J. Chem. Downloaded from www.nrcresearchpress.com by 200.7.193.243 on 09/04/12
For personal use only.

shows a contour map of fractions of species, plotted on axes of pH and log r. The region of greatest occurrence of each species is designated by the formula; and contours showing the percentage distribution of iron among the several species are also drawn. In Fig. 2(*b*), on the same axes, are shown areas in which stated proportions of reagent are present as species with iron. Used together, such diagrams indicate the regions of greatest interest for the development of analytical procedures, and suggest the necessary precision of pH adjustment, etc., in such procedures.

It is not difficult from such a diagram to see why different authors have differently described the color of iron(III)–tiron solutions in the vicinity of pH 4. The maintenance of constant pH by buffering does not assure the presence of a single species, changes in solution composition occurring also with variation of r, and of ionic strength. It may be added that, as far as the authors have been able to determine, the species FeBz and FeHBz have identical absorption spectra, but in order to produce these species in equivalent concentrations from solutions possessing the same content of iron(III) it has been necessary to provide solutions of equal ionic strength.

The figures reproduced here are simplified by the plotting of very few contour lines in the interest of facile reproduction, but any desired smaller interval could be selected. If this is done, it is less confusing to plot the curves for each species on a separate diagram.

These diagrams, while providing a potentially useful analysis of the solution constituents in the iron(III)–tiron system, must be applied with some restraint. For one thing, in the calculations upon which they are based it has been assumed that values of K taken from experiments in which $r = 3$ are valid for all values of r. In principle this assumption should be permissible, but it must be recalled that Freiser and co-workers have shown for *o*-aminophenol and for dimethylglyoxime that values of the apparent stability constants for certain metallic derivatives are *not* completely independent of values of r (9, 10). We therefore feel that, lacking evidence on this score, our values in the range $r > 10$ should be regarded with less confidence than those in the range $r < 10$. Care must also be taken to confine application of the data within limits for which the postulated reactions are valid. Thus, to select $r = 5$, pH = 9, for the determination of iron as its 3 : 1 tiron complex may introduce difficulty because of air-oxidation of the reagent, in which case equation [3] is no longer valid.

Strictly speaking, precise knowledge of the distribution of ferric iron among several species in solution requires that account be taken also of the formation of complex ions with any other anions in solution, particularly of any buffer present, and of hydrolysis of the metallic ion. For the latter one might incorporate the data of Hedström (11) or of Milburn and Vosburgh (12) into the calculation. As far as making allowance for other species in solution is concerned, several difficulties arise: data for interaction of ferric iron with acetate or phthalate are apparently not available (13), but even if they were the manner of using them would be complicated by the probability of formation of mixed complexes with tiron; there would then have to be as many calculations of the distribution of species as there are buffer systems selected. The data of Fig. 2 are applicable to systems including other anions only if the assumption is made that the stability constants of species formed by ferric iron with the latter are very small compared with the formation constants of the tironate species. Furthermore, since Schwarzenbach measured the formation constants upon which our calculations are based in 0.1 M chloride solutions, any use of the results of the calculations for solutions of other concentrations of chloride requires the further assumption that the reaction of ferric iron with chloride is only slight compared to that with tiron. In this connection it may be recalled that Foley and Anderson described the effect of changing the buffering constituents on the formation of ferric

Can. J. Chem. Downloaded from www.nrcresearchpress.com by 200.7.193.243 on 09/04/12
For personal use only.

Can. J. Chem. Downloaded from www.nrcresearchpress.com by 200.7.193.243 on 09/04/12
For personal use only.

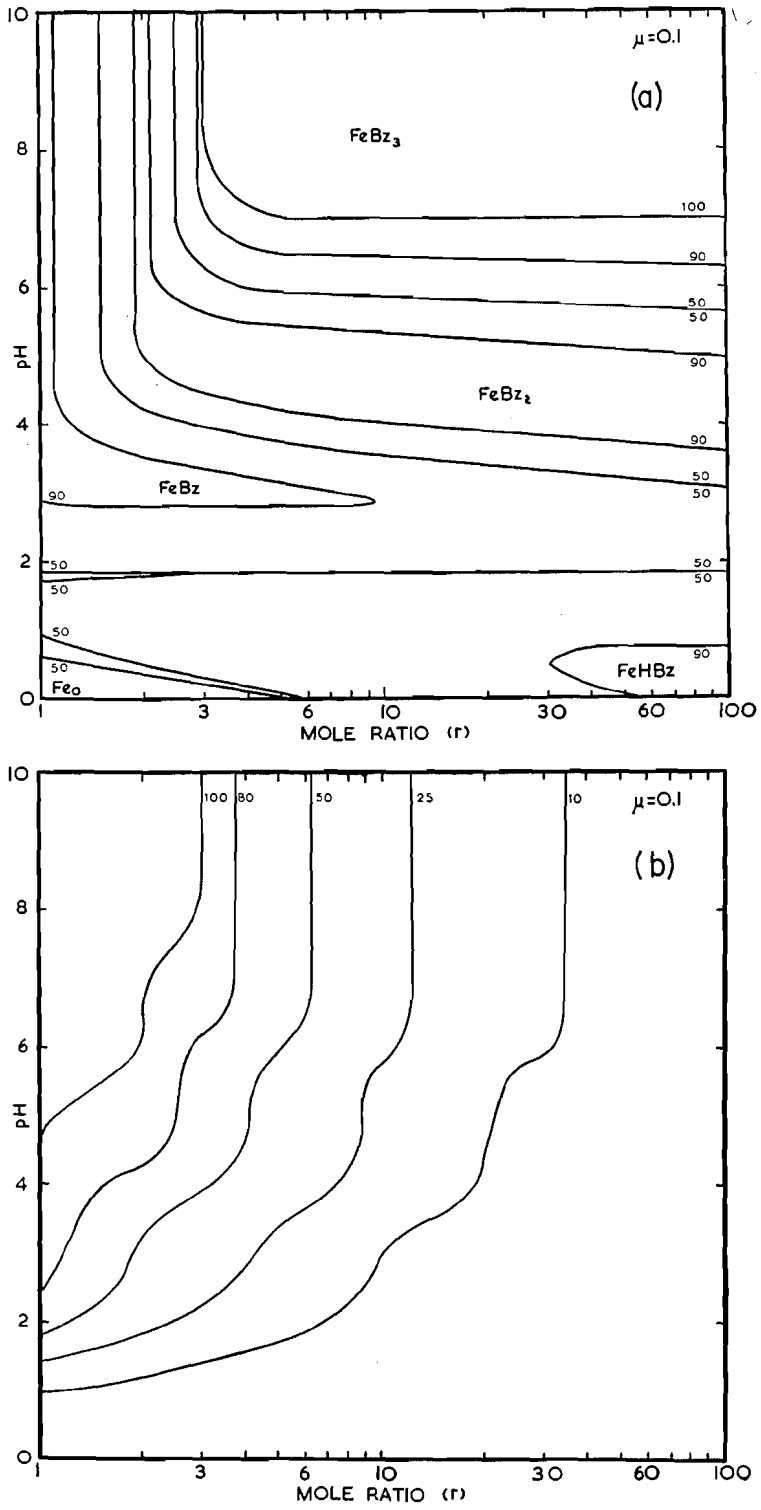

FIG. 2. Distribution of species according to pH and r; (a) percentage of iron present in stated forms, (b) percentage of tiron bound to iron.

sulphosalicylate complexes (14). However, the interpretation of these results by these authors has not been borne out by the more complete investigations of Ågren (1) or Vareille (15).

EFFECT OF CHANGES IN pH ON IONIC STRENGTH

The authors are currently investigating the effect of changes in ionic strength upon the apparent equilibrium constants for this system, and consequently upon the distribution of metal among the various species. We have already observed in spectrophotometric measurements that this effect is considerable at low pH(16).

For our experiments it would be desirable to be able to work at values of the ionic strength low enough to deny to us the convenience of adding gross amounts of indifferent electrolyte, and thereby the need arises to know rather accurately the contributions to ionic strength of all species in solution. It is apparent that the large contribution of the highly charged chelate species (in this system) will vary markedly with pH. In a similar context Olson and Simonson (17) have shown that the effects of maintaining "constant concentration of inert electrolyte" and "constant ionic strength" are not the same when the species present are changing.

By means of Fig. 2 we have computed the total contribution of species arising from ferric perchlorate and tiron for values of $r = 3$, 10, and 30. These results, plotted as log μ against pH, are shown in Fig. 3.

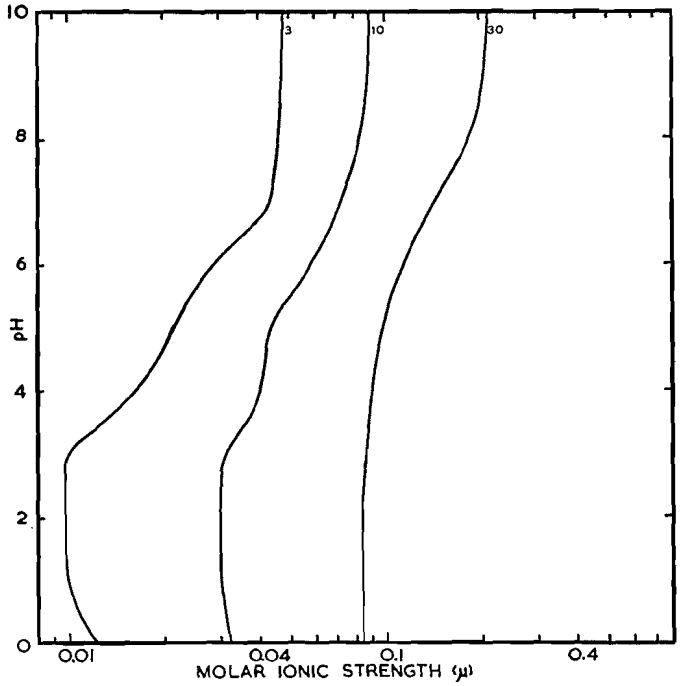

FIG. 3. Contribution to ionic strength of species from $Fe(ClO_4)_3$ and tiron. Determinant variable of curves: r.

It may be noted that Schwarzenbach's values for K were determined with $[Fe]_T = 1.11\times10^{-3}$ M, $r = 3$, and a solution of nominal ionic strength 0.1 M by addition of potassium chloride. It appears from our calculations that to this value must be added a

Can. J. Chem. Downloaded from www.nrcresearchpress.com by 200.7.193.243 on 09/04/12
For personal use only.

contribution from the several complex species amounting to as much as one-half of the nominal value, depending on pH. It follows that only in solutions of moderately high concentration of indifferent electrolyte (cf. Ågren (1)) will the ionic strength be relatively "constant" throughout the range of pH corresponding to the formation of the different complexes in this system.

ACKNOWLEDGMENT

The assistance of Dr. J. N. P. Hume, Mr. W. Kahan, and Mrs. Edith Laurie of the Computation Centre, University of Toronto, is gratefully acknowledged.

REFERENCES

1. ÅGREN, A. Acta Chem. Scand. **8**, 266 (1954).
2. BJERRUM, J. Metal ammine formation in aqueous solution. Haase, Copenhagen. 1941.
3. MARTELL, A. E. and CALVIN, M. Chemistry of the metal chelate compounds. Prentice-Hall, Inc., New York. 1952.
4. SCHWARZENBACH, G. Helv. Chim. Acta, **33**, 947 (1950).
5. VAREILLE, L. Bull. soc. chim. France, **22**, 870 (1955).
6. SCHWARZENBACH, G. and WILLI, A. Helv. Chim. Acta, **34**, 528 (1951).
7. VAREILLE, L. Bull. soc. chim. France, **22**, 1946 (1955).
8. OLSON, A. R., KOCH, C. W., and PIMENTEL, G. C. Introductory quantitative analysis. Freeman, San Fancisco. 1956.
9. CHARLES, R. G. and FREISER, H. J. Am. Chem. Soc. **74**, 1385 (1952).
10. CHARLES, R. G. and FREISER, H. Anal. Chim. Acta, **11**, 101 (1954).
11. HEDSTRÖM, B. O. A. Arkiv för Kemi, **6**, 1 (1953).
12. MILBURN, R. M. and VOSBURGH, W. C. J. Am. Chem. Soc. **77**, 1352 (1955).
13. BJERRUM, J., SCHWARZENBACH, G., and SILLÉN, L. G. Stability constants. The Chemical Society, London. 1957.
14. FOLEY, R. T. and ANDERSON, R. C. J. Am. Chem. Soc. **72**, 5609 (1950).
15. VAREILLE, L. Bull. soc. chim. France, **22**, 872 (1955).
16. ATKINSON, G. F. M. A. Thesis, University of Toronto, Toronto, Ont. 1954.
17. OLSON, A. R. and SIMONSON, T. R. J. Chem. Phys. **17**, 1322 (1949).

Can. J. Chem. Downloaded from www.nrcresearchpress.com by 200.7.193.243 on 09/04/12
For personal use only.

Can. J. Chem. Downloaded from www.nrcresearchpress.com by 200.7.193.243 on 09/04/12
For personal use only.

THE LIQUID PHASE PHOTOLYSIS OF DIETHYL KETONE AND METHYL ETHYL KETONE[1,2]

P. AUSLOOS[3]

ABSTRACT

The liquid phase photolysis of diethyl ketone has been studied in the temperature range from −35° to 95° C. The CO quantum yield at 95° C. was found to be close to unity. At 28° C. decrease in intensity and addition of heptane led to a substantial increase of the CO and the ethane yields.

The methyl ethyl ketone liquid phase photolysis at temperatures between 5° and 75° C. led to the same observations. Arrhenius plots of $R_E/R_B^{1/2}[K]$ gave for both compounds a value of 5 kcal./ mole.

Gas phase studies in the temperature range of 0° to 60° C. confirmed the low CO quantum yield reported previously and showed evidence for disproportionation and recombination reactions between ethyl and propionyl radicals.

EXPERIMENTAL

Eastman Kodak Company methyl ethyl ketone and diethyl ketone (white label) were distilled through 10 theoretical plates with rejection of large head and tail fractions. Air was removed by bulb-to-bulb distillation in the vacuum line.

Gas phase experiments were performed with a Hanovia (16A-13) SH type medium pressure lamp. The cylindrical quartz cell (5 cm. diameter, 10 cm. long) was completely filled with a nearly parallel light beam.

The liquids were irradiated in a quartz cell of 5 cm. diameter and 0.05 cm. depth. The cell was provided with two outlets, one of which was sealed after filling, while the other was closed by a break seal which made it possible to attach the cell to the analysis system after each experiment. Between runs the cell was washed out with diethyl ketone and dried at about 150° C. The irradiation was carried out in a thermostat consisting of a brass cylinder with evacuated double walls and double quartz windows. For experiments above room temperature an electric immersion heater was brought into distilled water, while for the low temperature experiments the thermostat was filled with methanol cooled by dry ice. In this way it was possible to maintain the temperature constant within half a degree.

At 3130 Å about 98% of the incident radiation is absorbed by the undiluted ketone. In order to compensate for this sharp absorption decrease throughout the cell, two Hanovia lamps were placed opposite each other with the cell fixed in the center of the nearly parallel light beam.

Except for experiments 1 and 2 Corning filters (9-53) were used to cut off wavelengths below 2800 Å. The incident intensity was varied by means of copper gratings.

After irradiation of the liquid the cell was attached to the analysis system, consisting of three traps and one modified Ward still. The CO–CH_4 fraction was removed at solid nitrogen temperature and was analyzed by combustion over hot CuO. The C_2H_6–C_2H_4 fraction was taken off at −160° C. C_2H_4 was determined by hydrogenation over a Ni

[1]*Manuscript received August 13, 1957.*
Contribution from Département de Chimie, Université Laval, Quebec, Que., and Department of Chemistry, University of Rochester, Rochester, N. Y.
[2]*This research was supported in part by the United States Air Force through the Air Force Office of Scientific Research of the Air Research and Development Command, under contract No. AF18(600)1528. Reproduction in whole or in part is permitted for any purpose of the United States Government.*
[3]*Present address: Department of Chemistry, University of Rochester, Rochester, N. Y.*

catalyst (16). The C_4H_{10} fraction was separated at about $-120°$ C. In view of the high C_2H_6/C_4H_{10} ratio, which in some experiments was higher than 100, great care was taken that no ethane was left over from the previous distillation.

RESULTS

Gas Phase

Table I represents the data of experiments performed at approximately constant diethyl ketone concentration. Runs 1 and 2 were done with an unfiltered light beam and at constant intensity. The other runs were performed with a Corning filter 9-53 and constant incident light intensity.

TABLE I

GAS PHASE PHOTOLYSIS OF DIETHYL KETONE

Run	Temp., ° C.	Time, min.	Pressure, molec./cc.10^{-17}	R_{CO}	$R_{C_2H_4}$	$R_{C_2H_6}$	$R_{C_4H_{10}}$ molec./cc./sec.10^{-11}	C_2H_4/C_4H_{10}	C_2H_6/C_4H_{10}	M.B.
				Unfiltered light						
1	0	10	2.45	51.0	11.2	11.4	72.3	0.155	0.157	1.64
2	57	10	2.45	220.0	23.4	26.5	194.0	0.120	0.136	1.00
				Corning filter 9–53						
3	0	8	2.42	13.05	2.97	3.15	17.9	0.166	0.176	1.60
4	13	12	2.48	27.0	4.27	4.60	28.5	0.149	0.162	1.22
5	25	12	2.46	43.8	5.29	5.95	41.2	0.128	0.144	1.07
6	60	12	2.45	54.8	5.50	6.98	46.4	0.119	0.150	0.96
7*	25	12	2.43	2.12	<0.1	<0.1	0.1			

**Iodine added.*

It can be seen that in both series of experiments the rates of formation of all the products decrease with temperature. In the last column M.B. stands for the material balance $[\frac{1}{2}(C_2H_4+C_2H_6)+C_4H_{10}]/CO$. This ratio increases appreciably with decrease in temperature.

Liquid Phase

All experiments given in Tables II and IV and runs 36, 39, 40, 44, 45 of Table V were conducted at the same incident intensity.

Table II shows the results of experiments done in a temperature range from $-35°$

TABLE II

LIQUID PHASE PHOTOLYSIS OF DIETHYL KETONE
Variation of rate with temperature

Run	Temp., ° C.	Time, min.	R_{CO}	$R_{C_2H_4}$	$R_{C_2H_6}$	$R_{C_4H_{10}}$ molec./cc./sec.10^{-15}	$R_E/R_B^{\frac{1}{2}}.10^{-8}$
8	−35	8	0.20	1.05	4.30	0.54	1.86
9	−14	8	0.58	1.40	11.6	0.75	4.25
10	5	6	1.26	1.62	26.0	1.02	8.20
11	28	4	4.10	3.40	70.0	2.21	14.9
12	51	4	22.0	2.73	111	1.80	26.0
13	72	2	52.0	2.07	145	1.26	40.8
14	84	2	63.0	1.91	146	0.90	48.5
15	86	2	64.2	1.58	149	0.82	52.0
16	94	2	70.0	1.25	152	0.55	65.0

Acetone at 28° C.: R_{CO}, 0.15; R_{CH_4}, 3.20; $R_{C_2H_6}$, 0.078.

Can. J. Chem. Downloaded from www.nrcresearchpress.com by 200.7.193.243 on 09/04/12
For personal use only.

to 94° C. It can be seen that the rates of formation of carbon monoxide and ethane both increase with temperature. At higher temperatures they approach constant values.

A rough measure of the quantum yield was obtained by comparing the rate of formation of carbon monoxide from the gas phase photolysis of diethyl ketone at 95° C. with the rate of formation from the liquid phase photolysis at the same temperature. The measurements were done with Corning filter 9-53 and cells of respectively 5 and 0.05 cm. depth. On the assumption that the quantum yield for CO in the vapor phase was unity, it was found that approximately 8×10^{16} quanta per second were absorbed by the liquid. This led to $\phi(CO) \sim 0.87$ at 95° C.

The rates of formation of ethylene and butane show a pronounced increase with temperature up to 28° C. followed by a gradual decrease.

In the same table are included the results of one acetone liquid phase experiment, performed at 28° C. and under the same experimental conditions as the previous runs. Comparison with the diethyl ketone results leads to a CO quantum yield roughly equal to 2×10^{-3}. This figure is somewhat higher than previous estimates (11, 15).

In Table III the results of experiments carried out at 5°, 28°, and 84° C. and at various intensities are shown. I_{rel} represents the incident intensity relative to the highest intensity run. Values of $R_{C_2H_6}/I_{rel}$ given in the last column show an increase with decrease in intensity. It can be seen from the data that this trend is even more pronounced for R_{CO}/I_{rel}. These results indicate clearly that the CO and ethane yields increase with diminishing intensity. However, this increase is much smaller at 84° C. where the quantum yield is already close to unity.

TABLE III

LIQUID PHASE PHOTOLYSIS OF DIETHYL KETONE
Variation of rate with intensity

Run	I_{rel}	Time, min.	R_{CO}	$R_{C_2H_4}$	$R_{C_2H_6}$	$R_{C_4H_{10}}$	$R_E/R_B^{\frac{1}{2}}.10^{-8}$	R_E/I_{rel}
			molec./cc./sec.10^{-15}					
				At 28° C.				
17	1	6	3.87	3.15	70.1	2.25	14.8	70.1
18	0.410	10	2.11	1.15	35.5	0.59	14.6	86.5
19	0.354	15	1.66	0.80	28.1	0.435	13.5	79.8
20	0.354	15	1.72	0.79	28.0	0.42	13.6	79.5
21	0.125	35	0.82	0.21	11.7	0.090	12.3	93.5
22	0.044	100	0.49	0.045	4.25	0.014	11.2	96.5
23	0.0055	800	0.19	0.003	0.75	~0.0009	~ 8.00	136.0
				At 5° C.				
24	1	10	1.24	1.59	26.1	1.06	8.00	26.1
25	0.354	30	0.39	0.54	11.9	0.235	7.80	33.7
26	0.125	90	0.20	0.225	6.52	0.09	6.80	52.2
				At 84° C.				
46	1	4	62.2	1.85	147.0	—	—	147
47	0.0067	504	0.0512	0.18×10^{-3}	0.103	—	—	154

In Table IV are given results of experiments made at 28° C. with *n*-heptane and *n*-octane as solvents. In the second column the percentage of light absorbed by the liquid has been given. Absorption measurements were made with a Cary absorption spectrophotometer. From the data it follows that the ratios $R_{C_2H_6}/I_{abs}$ and R_{CO}/I_{abs} increase with dilution.

Can. J. Chem. Downloaded from www.nrcresearchpress.com by 200.7.193.243 on 09/04/12
For personal use only.

TABLE IV

LIQUID PHASE PHOTOLYSIS OF DIETHYL KETONE HYDROCARBON MIXTURES AT 28° C.

Run	I_{abs}	Time, min.	Heptane molec./cc. 10^{-21}	DK molec./cc. 10^{-21}	R_{CO} molec./cc./sec. 10^{-15}	$R_{C_2H_4}$ molec./cc./sec. 10^{-15}	$R_{C_2H_6}$ molec./cc./sec. 10^{-15}	$R_{C_4H_{10}}$ molec./cc./sec. 10^{-15}	$R_E/R_B^{\frac{1}{2}}.10^{-8}$
27	95%	6	1.36	3.85	5.75	4.95	67.5	3.37	11.6
28		6	2.03	2.84	5.20	5.10	53.0	3.72	8.70
29		6	3.05	1.42	5.27	3.15	32.2	2.40	6.60
30		6	3.25	1.14	4.85	2.80	25.3	2.14	5.50
31	22%	6	3.55	0.71	4.36	2.70	19.0	2.00	4.25
32		6	3.70	0.515	3.60	2.22	14.8	1.70	3.60
33	8.5%	6	3.88	0.27	2.82	1.96	10.8	1.04	3.35
34		6	2.67*	1.14	4.40	4.00	32.5	2.76	6.18
35		6	3.25*	0.515	3.43	3.82	18.9	2.75	3.60

Octane.

In Table V are given the results of the liquid phase photochemical decomposition of methyl ethyl ketone. The experiments were done in the temperature range from 5° to 70° C. and at varying intensities. The rates of formation of carbon monoxide, methane, ethylene, ethane, and butane have been measured. Although propane was present, it could not be determined with any accuracy because it was present in an amount less than 1% of the ethane fraction.

TABLE V

LIQUID PHASE PHOTOLYSIS OF METHYL ETHYL KETONE
Variation of rate with temperature and intensity

Run	I_{rel}	Time, min.	Temp., ° C.	R_{CO} molec./cc./sec.10^{-15}	R_{CH_4} molec./cc./sec.10^{-15}	$R_{C_2H_4}$ molec./cc./sec.10^{-15}	$R_{C_2H_6}$ molec./cc./sec.10^{-15}	$R_{C_4H_{10}}$ molec./cc./sec.10^{-15}	$R_E/R_B^{\frac{1}{2}}.10^{-8}$
36	1	10	6	0.54	0.88	1.70	17.2	1.12	5.15
37	0.354	30	6	0.18	0.215	0.310	7.70	0.225	5.15
38	0.125	80	6	0.028	0.036	0.076	3.20	0.039	5.10
39	1	10	23	1.66	2.05	1.93	34.0	1.46	9.22
40	1	10	26	1.76	2.42	2.17	38.2	1.65	9.40
41	0.354	30	26	0.50	0.85	0.62	17.2	0.35	9.20
42	0.125	80	26	0.10	0.15	0.115	6.30	0.070	7.50
43	0.125	80	26	0.089	0.122	0.080	5.95	0.050	8.40
44	1	10	45	3.20	4.05	1.56	49.5	1.14	14.6
45	1	8	70	7.00	7.60	1.01	59.2	0.56	24.8

Comparison of the runs at constant intensity at varying temperatures shows that the rates of formation of carbon monoxide, methane, and ethane increase with temperature. However, the increase of the rate of formation of ethane is less pronounced at higher temperatures, where it reaches a value close to one half the value found in the liquid phase photolysis of diethyl ketone under the same experimental conditions.

The ratios C_2H_4/C_4H_{10} do not differ very much from those found in the diethyl ketone photolysis. The rates of formation of ethane and butane both go through a maximum around 28° C. Decrease of intensity leads to a substantial decrease in the CO, C_2H_4, and C_4H_{10} yields, while the C_2H_6 yields increase slightly.

Can. J. Chem. Downloaded from www.nrcresearchpress.com by 200.7.193.243 on 09/04/12
For personal use only.

DISCUSSION

Diethyl Ketone

(*a*) *Gas Phase*

The gas phase photolysis of diethyl ketone has been extensively investigated in the past (8, 9, 10, 13).

In the course of this work a few runs were performed at low temperatures in order to obtain additional information about the primary process and reactions involving the propionyl radical.

The results given in Table I indicate that at relatively high intensities, the quantum yield of the CO production drops appreciably at temperatures below 60° C. A value of 0.23 can be estimated for the CO quantum yield at 0° C., if at 60° C. the quantum yield is assumed to be 1. These results are in agreement with earlier work (13), where at 25° C. and comparable intensities a value of 0.6 was found for the quantum yield of the CO formation.

The low CO quantum yield suggests as main primary process:

$$C_2H_5COC_2H_5 + h\nu = C_2H_5CO + C_2H_5, \qquad \text{I}$$

in which the propionyl radical may eventually decompose by excess energy carried over from the primary process or by thermal reaction:

$$C_2H_5CO = C_2H_5 + CO. \qquad [1]$$

Assuming that no collisional deactivation of the excited diethyl ketone molecules occurs, run 7 as well as recent work on the photooxidation of diethyl ketone (12) suggests that at most 5% of the propionyl radicals decompose as a result of the primary process.

Besides decomposing, the propionyl radical may react with other species. Several combination and disproportionation reactions involving the propionyl radical may occur:

$$C_2H_5CO + C_2H_5 = C_2H_5COC_2H_5, \qquad [2]$$
$$= C_2H_6 + CH_3CH{=}CO, \qquad [3]$$
$$= C_2H_4 + C_2H_5CHO; \qquad [4]$$
$$C_2H_5CO + C_2H_5CO = C_2H_5COCOC_2H_5, \qquad [5]$$
$$= C_2H_5CHO + CH_3CH{=}CO; \qquad [6]$$
$$C_2H_5CO + C_2H_5COC_2H_4 = C_2H_5COC_2H_4COC_2H_5, \qquad [7]$$
$$= C_2H_5CHO + C_2H_5COCH{=}CH_2, \qquad [8]$$
$$= CH_3CH{=}CO + C_2H_5COC_2H_5. \qquad [9]$$

The increase of the C_2H_4/C_4H_{10} and C_2H_6/C_4H_{10} ratios with diminishing temperatures may be considered as good evidence for the occurrence of the reactions [3] and [4], while the fact that $(C_4H_{10}+\frac{1}{2}C_2H_4+\frac{1}{2}C_2H_6)/CO$ becomes larger than unity at low temperatures substantiates reaction [5] and perhaps also reaction [6]. Although there is no direct evidence for reactions [7], [8], and [9], it is quite likely, in view of their exothermicity, that these reactions occur.

Ethyl radicals disappear mainly by reactions [2], [3], [4], or by one of the following reactions:

$$C_2H_5 + C_2H_5COC_2H_5 = C_2H_6 + C_2H_5COC_2H_4; \qquad [10]$$
$$C_2H_5 + C_2H_5 = C_4H_{10}, \qquad [11]$$
$$= C_2H_4 + C_2H_6; \qquad [12]$$

Can. J. Chem. Downloaded from www.nrcresearchpress.com by 200.7.193.243 on 09/04/12
For personal use only.

$$C_2H_5 + C_2H_5COC_2H_4 = C_2H_5COC_4H_9, \quad [13]$$
$$= C_2H_4 + C_2H_5COC_2H_5, \quad [14]$$
$$= C_2H_6 + C_2H_5COCH{=}CH_2. \quad [15]$$

Gas phase studies led to a value of 0.12 ± 0.01 for k_{12}/k_{11} (2, 8, 13), while $E_{10} - \frac{1}{2}E_{11}$ was found to vary from 7.5 to 9 kcal./mole depending on the temperature range (3, 8, 13).

At the temperatures used in this work the pentanonyl radical does not decompose to any appreciable extent and will eventually disappear by a radical reaction such as [7], [8], [9], [13], [14], [15] or by one of the following reactions:

$$C_2H_5COC_2H_4 + C_2H_5COC_2H_4 = C_2H_5COC_2H_5 + C_2H_5COCH{=}CH_2, \quad [16]$$
$$= (C_2H_5COC_2H_4)_2. \quad [17]$$

(*b*) *Liquid Phase*

Primary process

From the results given in Table II it follows that the carbon monoxide and ethane yields approach constant values at high temperatures, which correspond to a primary quantum yield close to unity.

The fact that at room temperature the carbon monoxide yield increases appreciably with diminishing intensity and increasing dilution may be considered as evidence for a competition between reaction [1] and the radical reactions involving the propionyl radical. It is likely that infinite dilution at these temperatures may lead to a primary quantum yield equal to one.

The quantum yield determination at 95° C. is not accurate enough to decide whether any primary or secondary diffusive recombination occurs. If any recombination takes place between original partners, disproportionation ought to occur as well. From the results given in Table I, a rough estimate of 0.02 can be obtained for the ratio of the rate of the disproportionation reaction [4] to the rate of the recombination reaction [2].† From this estimate and from the amount of ethylene formed in the lowest intensity runs (Table III), it follows that under these conditions less than 20% of the ethyl radicals recombine with propionyl radicals. In view of the fact that ethylene may also be formed in several other reactions, recombination between original partners may be considered negligible.

Recent work (15) on the liquid phase photolysis of mixtures of light and heavy acetone showed that deactivation is a more likely explanation for the low quantum yield than primary or secondary diffusive recombination. In earlier work (7) diacetone alcohol was determined in the liquid phase photolysis of undiluted acetone. It was also found that addition of hydrocarbons led to a decrease of the quantum yield of the volatile products (15) and the formation of an alcohol (6, 11). These results indicate that, besides dissociation and normal deactivation by collision, the following processes involving excited acetone molecules have to be considered:

$$CH_3COCH_3^* + CH_3COCH_3 = (CH_3)_2COHCH_2COCH_3, \quad a$$
$$CH_3COCH_3^* + RH = (CH_3)_2COHR. \quad b$$

When RH is a hydrocarbon like hexane or heptane, process *b* is faster than *a*. It may be mentioned that processes of type *b* have also been found to occur in the liquid phase photolysis of esters (1).

†*In order to obtain this value the assumption was made that the* CO *quantum yield was one at 60° C., and a value of 0.12 was used for the ratio of the rate of reaction [12] to the rate of reaction [11].*

Can. J. Chem. Downloaded from www.nrcresearchpress.com by 200.7.193.243 on 09/04/12
For personal use only.

The fact that at 28° C. addition of normal heptane to diethyl ketone increases the quantum yield of the volatile products to a value close to unity indicates that at these temperatures the process analogous to process *b* does not occur. A shorter lifetime of the excited diethyl ketone molecules may explain the difference in quantum yield between the liquid phase photolysis of acetone and diethyl ketone.

In analogy with the acetone photolysis, where a decrease of the quantum yield with temperature was found in both gas (14) and liquid (15) phase, it is quite possible that the low quantum yield at temperatures below 28° C. (Table II) is partly due to deactivating processes.

It has been suggested previously (5) that, in view of the relatively high ethylene yield, the following primary process occurs:

$$C_2H_5COC_2H_5 + h\nu = C_2H_5CHO + C_2H_4.$$

The fact, however, that the ethylene yield drops appreciably with intensity means that this compound is formed mainly in a radical–radical reaction. The iodine experiments (run 7) and the lowest intensity run of Table III indicate that the quantum yield of this process has to be lower than 5×10^{-3}.

Secondary reactions

Although their relative importance may change, the same secondary reactions can be expected to occur in both gas and liquid phase photolysis. In order to explain the liquid phase results, it has to be visualized that, owing to the higher ketone concentration, alkyl radicals will react mostly with diethyl ketone itself. Consequently, reactions of the ethyl radical with other radicals will be of less importance. Indeed, it can be seen from the data of Tables II and III that ethane is the main product. The fact that at higher temperatures the amount of CO formed is about half the amount of ethane proves that at these temperatures practically all of the propionyl radicals are decomposed.

As mentioned before, the decrease of the rate of formation of ethylene and butane with intensity points to the formation of these products in a radical–radical reaction. The data of Table II show that both compounds go through maxima around 28° C. This can be explained by a competition between an increase of the ethyl radical concentration caused by a substantial increase of the quantum yield up to 28° C. and the increase in rate of the hydrogen abstraction reaction [4] which tends to decrease the stationary radical concentration.

The C_2H_4/C_4H_{10} ratio is under all conditions considerably higher than the value of 0.12 generally accepted for k_{11}/k_{12}. Because no third body is required for processes [11] and [12] (8), the ratio for the two rate constants should be the same in both gas and liquid phase. It is probable that the excess ethylene is formed in a radical–radical reaction such as [4] and [14]. Reaction [4] may be expected to be of importance at low temperatures, while reaction [14] will occur mainly in the high temperature region.

If ethane and butane are produced only by reactions [10] and [11], the following relationship exists:

$$R_E/R_B^{1/2}[K] = k_{10}/k_{11}^{1/2} = A_{10}/A_{11}^{1/2}e^{-(E_{10}-\frac{1}{2}E_{11})/RT};$$

[K], R_E, and R_B represent respectively the concentration of diethyl ketone and the rates of formation of ethane and butane.

If this relation holds, $R_E/R_B^{1/2}$ should be independent of the absorbed intensity.

Can. J. Chem. Downloaded from www.nrcresearchpress.com by 200.7.193.243 on 09/04/12
For personal use only.

The results given in Table III indicate that this ratio varies only slightly over a considerable intensity range. From this it may be concluded that ethane and butane are formed in normal kinetic processes.

In Fig. 1, log $R_E/R_B^{1/2}[K]$ calculated from the data of Table II has been plotted as a function of $1/T$. It can be seen that a good straight line is obtained which corresponds to an activation energy of 5 kcal./mole. This value may be ascribed to the activation difference $E_{10}-\frac{1}{2}E_{11}$. Gas phase studies in a temperature range from 25° to 150° C. lead to a value of 7.5 kcal./mole. The lower value obtained in the liquid phase photolysis may at least be partly due to the fact that, in a liquid, recombination of radicals may require an activation energy. In order to account for the difference between the gas and liquid phase photolysis results, a value of 5 kcal./mole has to be ascribed to the activation energy of the diffusion process.

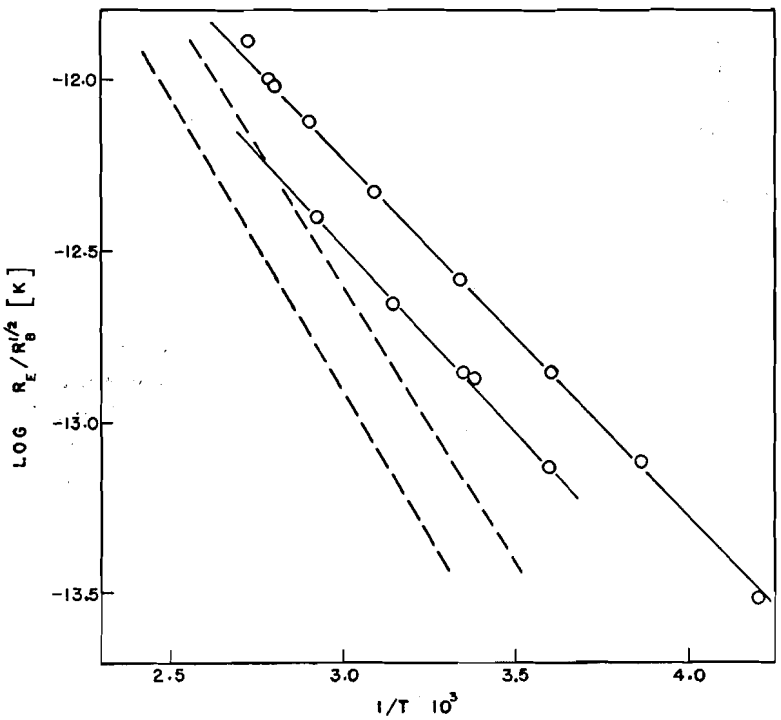

FIG. 1. Plot of log $R_E/R_B^{\frac{1}{2}}[K]$ against $1/T$ for the photolysis of diethyl ketone and methyl ethyl ketone:
——— liquid phase photolysis: upper curve—diethyl ketone,
lower curve—methyl ethyl ketone;
— — — gas phase photolysis: upper curve—diethyl ketone,
lower curve—methyl ethyl ketone.

In the above treatment, the ethane formed by reactions [3], [12], and [15] has not been taken into account. The low amount of butane formed shows reaction [12] to be unimportant. Assuming that reactions [14] and [15] on one side and [3] and [4] on the other side have comparable rates, it can be deduced from the low ethylene yield that the amount of ethane formed by reactions [3] and [15] is small compared to the amount formed by the abstraction reaction [10].

Addition of *n*-heptane and *n*-octane to diethyl ketone leads to a substantial decrease

Can. J. Chem. Downloaded from www.nrcresearchpress.com by 200.7.193.243 on 09/04/12
For personal use only.

of the ratio $R_E/R_B^{1/2}$. Increasing dilution apparently leads to a limiting constant value for this ratio which is about 22% of the one found for the undiluted diethyl ketone. These results point to an appreciably lower rate for the abstraction of a hydrogen atom from heptane and octane than from diethyl ketone itself. In agreement with this, a few gas phase photolysis experiments of equal diethyl ketone heptane mixtures at 95° C. (1) indicated that at least 80% of the ethyl radicals abstract a hydrogen atom from the diethyl ketone molecules.

Methyl Ethyl Ketone

Primary Process

Gas phase studies (17) have shown that two primary processes have to be considered:

$$CH_3COC_2H_5 + h\nu = CH_3CO + C_2H_5, \qquad \text{II}$$

$$= CH_3 + C_2H_5CO. \qquad \text{III}$$

At 3130 Å process II was found to occur about 10 times more often than process III.

The data given in Table V show that at higher temperatures, the methane and CO yields are approximately equal and appreciably lower than the ethane yields. From this it follows that in the liquid phase photolysis too, process II is the most important. The fact that at higher temperatures the ethane yield is approaching a constant value, which is approximately half that obtained in the liquid phase photolysis of diethyl ketone, indicates that in this temperature range the primary quantum yield is approximately the same for both compounds.

As in the liquid phase photolysis of diethyl ketone, the ethane yield increases slightly with decrease in intensity. From this it may be concluded that the low ethane yield at the lower temperatures is at least partly due to the disappearance of the ethyl radicals by normal radical recombination processes. However at low temperatures, diminishing intensities led to a decrease in the carbon monoxide and methane yields; this is contradictory to what was found in the liquid phase photolysis of diethyl ketone. It may be pointed out that liquid phase photolysis studies of several compounds where acetyl radicals are formed in the primary process led to the same observation (1). At high temperatures where normal thermal decomposition of acetyl radicals becomes important, an increase of the CO yield with decrease in intensity was found for all the compounds studied. Although no conclusive interpretation can be given, it is likely that at low temperatures CO and methane result from a radical–radical process.

The decrease in ethylene yield with diminishing intensity indicates that, as in the diethyl ketone photolysis, ethylene is produced mainly in a radical–radical process, instead of being formed in a primary process.

Secondary Reactions

Essentially the same reactions may be expected to occur as those described in an earlier paper on the gas phase photochemical decomposition of methyl ethyl ketone (4).

Only the following two reactions will be considered:

$$C_2H_5 + CH_3COC_2H_5 = C_2H_6 + CH_6COC_2H_4, \qquad [18]$$

$$C_2H_5 + C_2H_5 = C_4H_{10}. \qquad [11]$$

Then

$$R_E/R_B^{1/2}[K] = k_{18}/k_{11}^{1/2} = A_{18}/A_{11}^{1/2}e^{-(E_{18}-\frac{1}{2}E_{11})/RT}.$$

The data of Table V indicate that the ratio $R_E/R_B^{1/2}$ is practically independent of intensity, which substantiates the above relationship.

Can. J. Chem. Downloaded from www.nrcresearchpress.com by 200.7.193.243 on 09/04/12
For personal use only.

In Fig. 1, log $R_E/R_B^{1/2}$[K] has been plotted against $1/T$. It can be seen that this Arrhenius curve corresponds to an activation energy which is about the same as the one found for diethyl ketone. The two plots are separated by approximately 0.3 logarithmic units. The dashed lines which represent the gas phase results for the hydrogen abstraction reaction from diethyl ketone (3) and methyl ethyl ketone (4) show clearly that these plots are also approximately parallel and show the same separation as the liquid phase Arrhenius curves. These results can be explained by assuming that mainly secondary hydrogen atoms are abstracted from the ketones.

As mentioned earlier, the lower values found for the activation energy differences $E_{12}-\frac{1}{2}E_{11}$ and $E_{18}-\frac{1}{2}E_{11}$ in the liquid phase experiments may be due to the fact that diffusion of radicals in a liquid requires an activation energy. However, solvation of the reactants and activated complexes may also influence the rate of the abstraction and recombination reactions.

ACKNOWLEDGMENTS

The author wishes to thank Professors W. A. Noyes, Jr. and C. Ouellet for advice and encouragement. He also wishes to express his appreciation to the National Research Council of Canada for a University Postdoctorate Fellowship under the tenure of which part of this work was carried out.

REFERENCES

1. AUSLOOS, P. To be published.
2. AUSLOOS, P. and STEACIE, E. W. R. Bull. soc. chim. Belges, **63**, 87 (1954).
3. AUSLOOS, P. and STEACIE, E. W. R. Can. J. Chem. **32**, 593 (1954).
4. AUSLOOS, P. and STEACIE, E. W. R. Can. J. Chem. **33**, 1062 (1955).
5. BAMFORD, C. H. and NORRISH, R. G. W. J. Chem. Soc. 1531 (1938).
6. BOWEN, E. J. and HORTON, A. T. J. Chem. Soc. 1685 (1936).
7. BOWEN, E. J. and PRAUDIERE, E. L. A. E. de la. J. Chem. Soc. 1503 (1934).
8. BRINTON, R. K. and STEACIE, E. W. R. Can. J. Chem. **33**, 1840 (1955).
9. DAVIS, W., JR. Chem. Revs. **40**, 201 (1947).
10. DORFMAN, L. M. and SHELDON, Z. D. J. Chem. Phys. **17**, 511 (1949).
11. FRANKENBURG, P. E. and NOYES, W. A., JR. J. Am. Chem. Soc. **75**, 2847 (1953).
12. JOLLEY, J. E. J. Am. Chem. Soc. **79**, 1537 (1957).
13. KUTSCHKE, K. O., WIJNEN, M. H. J., and STEACIE, E. W. R. J. Am. Chem. Soc. **74**, 714 (1952).
14. NOYES, W. A., JR. and DORFMAN, L. M. J. Chem. Phys. **16**, 788 (1948).
15. PIECK, R. and STEACIE, E. W. R. Can. J. Chem. **33**, 1304 (1955).
16. SHEPP, A. and KUTSCHKE, K. O. Can. J. Chem. **32**, 1112 (1954).
17. STEACIE, E. W. R. Atomic and free radical reactions. Vol. I. 2nd ed. Reinhold Publishing Corporation, New York. 1954. p. 358–362.

Can. J. Chem. Downloaded from www.nrcresearchpress.com by 200.7.193.243 on 09/04/12
For personal use only.

Can. J. Chem. Downloaded from www.nrcresearchpress.com by 200.7.193.243 on 09/04/12
For personal use only.

THE HEMICELLULOSE OF WHITE ELM (ULMUS AMERICANA)

I. IDENTIFICATION OF 2-O-(4-O-METHYL-D-GLUCOPYRANOSYLURONIC ACID)-D-XYLOPYRANOSE[1]

J. K. GILLHAM AND T. E. TIMELL

ABSTRACT

Alkaline extraction of wood meal from white elm (*Ulmus americana*) has yielded a hemicellulose which on hydrolysis gave a sugar mixture containing xylose together with traces of galactose, glucose, mannose, and rhamnose in addition to two monouronic acids and one aldobiouronic acid. The latter was identified as 2-*O*-(4-*O*-methyl-D-glucopyranosyluronic acid)-D-xylopyranose.

This series of investigations deals with the constitution and properties of the hemicellulose portion of white elm wood. The present paper is concerned with the structure of an aldobiouronic acid obtained on partial hydrolysis of the latter.

RESULTS AND DISCUSSION

Alkaline extraction of wood meal from white elm gave a hemicellulose in a yield of 16.5%, or slightly higher than the methyl glucurono-xylan content of the wood, 15.4% (1). Hydrolysis of the crude hemicellulose yielded a sugar mixture containing six sugar acids and xylose as well as traces of galactose, glucose, mannose, and rhamnose. The acids were separated from the neutral sugars by the use of an anion exchange resin and were then resolved on a column containing the same resin by eluting with dilute acetic acid. Three main fractions were obtained, corresponding on the paper chromatogram to an aldobiouronic acid, a monouronic acid, and a methyl monouronic acid, respectively.

The methoxyl content and the equivalent weight of the aldobiouronic acid as well as chromatographic evidence suggested that it was a methoxyuronic acid linked to a pentose. A portion of the acid was converted to the methyl ester methyl glycoside, reduced with lithium aluminum hydride, and hydrolyzed. Examination on the paper chromatogram indicated the presence of 4-*O*-methyl-D-glucose and D-xylose; the latter crystallized and the former was identified through its crystalline osazone (2, 3).

The aldobiouronic acid was completely methylated and the methyl ester methyl glycoside was reduced and hydrolyzed. The two methylated sugars obtained were separated and identified through their crystalline aniline derivatives as 3,4-di-*O*-methyl-D-xylose and 2,3,4-tri-*O*-methyl-D-glucose, respectively (4, 5). The methylated aldobiouronic acid was accordingly methyl 2-*O*-(2,3,4-tri-*O*-methyl-D-glucopyranosyluronic acid)-3,4-di-*O*-methyl-D-xylopyranoside methyl ester. This conclusion was further corroborated by the fact that it gave the same infrared spectrum as a compound with this structure, previously isolated from white birch wood (6). The aldobiouronic acid was therefore 2-*O*-(4-*O*-methyl-D-glucopyranosyluronic acid)-D-xylopyranose. Confirmation of this structure was obtained from lead tetraacetate oxidation, which produced 1.2 moles of formaldehyde per mole of acid (7), a result to be expected only from a 1,2-linked disaccharide (8, 9).

The synthesis of one or both of the existing anomers of this compound is presently being attempted (10) to determine the nature of the glycosidic linkage. The high positive rotation of the compound (+110°) as well as earlier evidence (11) indicate that it is probably of the α-type.

[1]*Manuscript received October 31, 1957.*
Contribution from McGill University and Pulp and Paper Research Institute of Canada, Montreal, Quebec.

The aldobiouronic acid isolated here is identical with that obtained on partial hydrolysis of a number of other hardwood hemicelluloses, including those from trembling aspen (12), American beech (13), European beech (14), and white birch (6). It has also been tentatively identified in the hydrolyzate of hemicelluloses from Finnish birch (15), yellow birch (16), and *Eucalyptus regnans* (17).

EXPERIMENTAL

All specific rotations are equilibrium values and melting points are corrected. Evaporations were carried out *in vacuo* at 40° C.

Paper Chromatography

Solvents used for separating the sugars were (A) ethyl acetate: acetic acid: water (9: 2: 2), (B) 1-butanol: pyridine : water (10: 3: 3), and (C) 1-butanol: ethanol: water (40: 11: 19). Separations were carried out on Whatman No. 1 filter paper by the descending technique. The spray reagent was *o*-aminodiphenyl (18).

Isolation of the Hemicellulose

Extractive-free white elm wood meal (500 g., 40–60 mesh) was extracted in a nitrogen atmosphere with 4 liters of 24% (w/w) aqueous potassium hydroxide by shaking for 2 hours at room temperature. The extract was separated from the alpha-cellulose by filtration through sintered glass and was poured slowly with stirring into a mixture of glacial acetic acid (1.5 liter) and anhydrous ethanol (12 liters), cooled to −16° C. The precipitated hemicellulose was collected on a centrifuge at −20° C., was washed five times each in succession with 80% aqueous ethanol, anhydrous ethanol, and petroleum ether (b.p. 30–60° C.), and was finally dried *in vacuo* at room temperature over calcium chloride for 1 week. The yield was 82.5 g., corresponding to 16.5% of the original wood.

Acid hydrolysis and subsequent examination by paper chromatography (solvents A and B) indicated the presence of six sugar acids and xylose in addition to traces of galactose, glucose, mannose, and rhamnose.

Separation of Sugar Acids

Hemicellulose (75 g.) was partially hydrolyzed with sulphuric acid (19). After neutralization with barium carbonate and filtration through Celite, the sugar acids were adsorbed on a column of Dowex 1-4X anion exchange resin (carbonate form). Neutral sugars were removed by washing with water, after which the sugar acids were eluted with *N* sulphuric acid. The latter was removed with barium carbonate, barium ions were eliminated by treatment with Amberlite IR 120 exchange resin, and the solution was concentrated to a sirup (10 g.).

A portion of the material (7 g.) was added to the top of a column (160×5 cm.) containing Dowex 1-4X exchange resin (acetate form) and the sugar mixture was resolved by eluting with *N* acetic acid. Analysis of the fractions collected (18) indicated the presence of six sugar acids, one of which (2.5 g.) was chromatographically identical with an aldobiouronic acid previously obtained from white birch wood (6). Two others corresponded in position and color reactions to galacturonic or glucuronic acid (5–10 mg.) and 4-*O*-methyl-D-glucuronic acid (500 mg.). Anal. Calc. for $C_{12}H_{20}O_{11}$ (aldobiouronic acid): OCH_3, 9.1%; equiv. wt., 340. Found: OCH_3, 8.8%; equiv. wt. 369. $[\alpha]_D^{20}$ +110° (*c*, 2.2 in water).

Reduction and Hydrolysis of the Aldobiouronic Acid

The aldobiouronic acid (975 mg.) was converted to its methyl ester methyl glycoside by refluxing with 2% methanolic hydrogen chloride (50 ml.) for 8 hours. Neutralization

Can. J. Chem. Downloaded from www.nrcresearchpress.com by 200.7.193.243 on 09/04/12
For personal use only.

with silver carbonate and evaporation yielded a sirup which was dissolved in tetrahydrofuran (50 ml.) and reduced with a solution of lithium aluminum hydride (1.2 g.) in 75 ml. of the same solvent (20). Hydrolysis of the neutral disaccharide with *N* sulphuric acid, neutralization with barium carbonate, and concentration yielded a sirup which showed two spots of equal intensity on the paper chromatogram with solvent B, corresponding in color reaction and position to xylose and 4-*O*-methyl-D-glucose.

Identification of Hydrolysis Products

The sugar mixture was added to the top of a column (1.5×15 cm.) containing coconut charcoal. Elution with 2% and 10% aqueous ethanol yielded D-xylose (322 mg.) and 4-*O*-methyl-D-glucose (395 mg.), respectively. The xylose crystallized and had m.p. and mixed m.p. 144.5° C., $[\alpha]_D^{20}$ +18° (*c*, 3.2 in water). The 4-*O*-methyl-D-glucose was converted to its osazone derivative (2), m.p. and mixed m.p. 157° C. It was distinguished from 4-*O*-methyl-D-mannose by treatment with hydrogen bromide (21), after which glucose was the only sugar detectable on the paper chromatogram. Anal. Calc. for $C_7H_{14}O_6$: OCH_3, 16.0%. Found: OCH_3, 15.8%.

Methylation of the Aldobiouronic Acid

The aldobiouronic acid (826 mg.) was dissolved in water (10 ml.), dimethyl sulphate (10 ml.) was added, and then dropwise over a 12-hour period 30% (w/w) aqueous sodium hydroxide (30 ml.). Two further methylations were carried out with powdered sodium hydroxide (18 g.) and dimethyl sulphate (25 ml.). The material was recovered in the usual way by extraction with chloroform and was then methylated four times with methyl iodide (20 ml.) and silver oxide (6 g.) to yield a clear sirup (439 mg.). The infrared spectrum of the latter indicated the absence of any free hydroxyl groups and was identical with the spectrum of methyl 2-*O*-(2,3,4-tri-*O*-methyl-D-glucopyranosyluronic acid)-3,4-di-*O*-methyl-D-xylopyranose, previously obtained from white birch wood (6).

Reduction and Hydrolysis of the Methylated Aldobiouronic Acid

The sirup was dissolved in anhydrous ether and reduced with lithium aluminum hydride in the same solvent. The reduced material was subjected to methanolysis and was then hydrolyzed with 0.5 *N* hydrochloric acid (25 ml.) for 10 hours. The acid was removed with silver carbonate and the solution was deionized with Amberlite IR 120 and Dowex 1-4X (acetate form) exchange resins. Examination by paper chromatography revealed the presence of two components, corresponding to 2,3,4-tri-*O*-methyl-D-glucose and 3,4-di-*O*-methyl-D-xylose.

Identification of 2,3,4-Tri-O-methyl-D-glucose and 3,4-Di-O-methyl-D-xylose

The sugar mixture was resolved on a charcoal column (1.5×15 cm.) by eluting with 20% aqueous ethanol to yield chromatographically pure sirups of a tri-*O*-methyl glucose (180 mg.) and a di-*O*-methyl xylose (169 mg.) Anal. Calc. for $C_9H_{18}O_6$: OCH_3, 41.9%. Found: OCH_3, 41.5%. $[\alpha]_D^{20}$ +78° (*c*, 3.5 in water). The tri-*O*-methyl glucose was converted to the aniline derivative, 2,3,4-tri-*O*-methyl-*N*-phenyl-D-glucosylamine, m.p. 144° C. Anal. Calc. for $C_7H_{14}O_5$: OCH_3, 34.8%. Found: OCH_3, 34.3%. $[\alpha]_D^{20}$ +20.3° (*c*, 2.2 in water). The 3,4-di-*O*-methyl-*N*-phenyl-D-xylosylamine had m.p. 115–116.5° C. after recrystallization from ethyl acetate.

Oxidation of the Aldobiouronic Acid with Lead Tetraacetate

The oxidation of the aldobiouronic acid was carried out by the method of Perlin (7, 8) in the presence of potassium acetate. The formaldehyde was determined by the dimedon method, the crystalline precipitate having a m.p. of 188.5° C. (22).

Can. J. Chem. Downloaded from www.nrcresearchpress.com by 200.7.193.243 on 09/04/12
For personal use only.

ACKNOWLEDGMENTS

The authors wish to express their gratitude to Mr. C. P. J. Glaudemans for valuable help and advice. One of them (J.K.G.) is also thankful to the Allied Chemical and Dye Corporation for two fellowships and to the Pulp and Paper Research Institute of Canada for two summer stipends.

REFERENCES

1. TIMELL, T. E. Unpublished results.
2. SMITH, F. J. Chem. Soc. 2646 (1951).
3. SCHINLE, R. Ber. **65**, 315 (1932).
4. JONES, J. K. N. and HOUGH, L. J. Chem. Soc. 4349 (1952).
5. PEAT, S., SCHLÜCHTERER, E., and STACEY, M. J. Chem. Soc. 581 (1939).
6. GLAUDEMANS, C. P. J. and TIMELL, T. E. J. Am. Chem. Soc. (In press).
7. PERLIN, A. S. J. Am. Chem. Soc. **76**, 5505 (1954).
8. PERLIN, A. S. Anal. Chem. **27**, 396 (1955).
9. CHARLSON, A. J. and PERLIN, A. S. Can. J. Chem. **34**, 1200 (1956).
10. BOWERING, W. D. S. and TIMELL, T. E. Unpublished results.
11. BISHOP, C. T. Can. J. Chem. **31**, 134 (1953).
12. JONES, J. K. N. and WISE, L. E. J. Chem. Soc. 2750, 3389 (1952).
13. ADAMS, G. A. Can. J. Chem. **35**, 556 (1957).
14. ASPINALL, G. O., HIRST, E. L., and MAHOMED, R. S. J. Chem. Soc. 1734 (1954).
15. SAARNIO, J., WATHÉN, K., and GUSTAFSSON, Ch. Acta Chem. Scand. **8**, 825 (1954).
16. TIMELL, T. E. Unpublished results.
17. STEWART, C. M. and FOSTER, D. H. Nature, **171**, 792 (1953).
18. TIMELL, T. E., GLAUDEMANS, C. P. J., and CURRIE, A. L. Anal. Chem. **28**, 1916 (1954).
19. SAEMAN, J. F., MOORE, W. E., MITCHELL, R. L., and MILLETT, M. A. Tappi, **37**, 336 (1954).
20. ABDEL-AKHER, M. and SMITH, F. J. Chem. Soc. 2646 (1951).
21. HOUGH, L., JONES, J. K. N., and WADMAN, W. H. J. Chem. Soc. 1702 (1950).
22. REEVES, R. E. J. Am. Chem. Soc. **63**, 1476 (1941).

Can. J. Chem. Downloaded from www.nrcresearchpress.com by 200.7.193.243 on 09/04/12
For personal use only.

Can. J. Chem. Downloaded from www.nrcresearchpress.com by 200.7.193.243 on 09/04/12
For personal use only.

Canadian Journal of Chemistry

Issued by THE NATIONAL RESEARCH COUNCIL OF CANADA

VOLUME 36 MARCH 1958 NUMBER 3

COEXISTENCE PHENOMENA IN THE CRITICAL REGION

V. THE GRAVITY EFFECT IN THE BINARY LIQUID SYSTEM ANILINE-CYCLOHEXANE FROM LIGHT SCATTERING[1]

F. E. MURRAY[2] AND S. G. MASON

ABSTRACT

Transmittance measurements were used to investigate vertical concentration gradients, at temperatures slightly above the critical, in a binary liquid system. The gradients, which are predicted theoretically, did not begin to form during time intervals of several hours. It was found that a theoretical relation between transmittance and concentration gradient did not apply, even qualitatively, to the results obtained. The significance of these observations is discussed.

INTRODUCTION

In previous publications (3, 4), the authors reported large vertical gradients in density near the liquid–vapor critical point in one-component systems. These gradients, due to gravitational compression, were anticipated owing to the large compressibility of a fluid in the critical region.

The case of vertical concentration gradients in a binary liquid system, at temperatures slightly above the critical, forms an analogue which is not so obvious. It was, however, shown by Yvon (9) that such concentration gradients are predicted theoretically. Since Rice and Rowden (6) reported a flat apex on the coexistence curve for aniline–cyclohexane, it was of interest to see if this flat top could be ascribed to concentration gradients by analogy to the gravity effect in one-component systems (3, 4, 7, 8).

The critical solution point for a binary liquid system is defined by the conditions

$$[1] \qquad (\partial\mu_1/\partial c_1)_{T,P} = (\partial^2\mu_1/\partial c_1^2)_{T,P} = 0,$$

where μ_1 and c_1 are respectively the chemical potential and mole fraction of component 1 in the solution.

For the variation of concentration with height in a binary liquid mixture, Yvon (9) obtained an expression which may be simplified to the form

$$[2] \qquad (\partial c_1/\partial x)_T = G(x)/(\partial\mu_1/\partial c_1)_{T,P},$$

where x is distance measured positive downward and $G(x)$ is a finite function of x. From Equation [2], Yvon concluded that when the solution approaches the critical state, i.e. when $(\partial\mu_1/\partial c_1)_{T,P} \to 0$, $(\partial c_1/\partial x)_T$ becomes very large.

[1]*Manuscript received November 1, 1957.*
Contribution from the Department of Chemistry, McGill University, Montreal, Quebec.
[2]*Holder of a Fellowship from the National Research Council of Canada. Present address: British Columbia Research Council, University of British Columbia, Vancouver, B.C.*

It was considered that the light-scattering coefficient, which is highly sensitive in the critical region, might be used to reveal experimentally the composition gradients. Following the work of Einstein (1), the turbidity in a binary liquid system is given by the expression

$$\tau = B\bar{V}_1 c_2 (\partial\epsilon/\partial c_2)^2/(\partial\mu_1/\partial c_1)_{T,P}, \quad [3]$$

where B is a constant at any temperature and wave length of the incident light, $\bar{V}_1$ is the partial molar volume of component 1, ϵ is the optical dielectric constant of the fluid. By combining Equations [2] and [3] the variation of concentration with height becomes

$$(\partial c_1/\partial x)_T = B'G(x)\tau. \quad [4]$$

B' is a constant for any given concentration, temperature, and wave length of the incident light. Equation [4] is analogous to the relationship between turbidity and density gradient in a one-component system near the gas/liquid critical point.

Equation [2] predicts large vertical gradients in concentration when $(\partial\mu_1/\partial c_1)_{T,P}$ becomes very small at temperatures slightly above the critical. Equation [4] predicts that the magnitude of these gradients, at any height in the fluid column, will be directly proportional to the turbidity.

The following symbols are used to denote measured quantities:

T = temperature in degrees centigrade,
T_f = the value of T at which visible droplets form when the fluid is cooled slowly,
T_c = the highest value of T_f observed,
$\Delta T = (T - T_c)$,
V_1 = the volume fraction of aniline in the binary mixture,
I_0 = the intensity of the incident light,
I = the intensity of the transmitted light,
$\tau = 2.30 \log I_0/I$.

EXPERIMENTAL

Apparatus

The essential details of the apparatus have already been described (3, 4). In the present experiments, only the methods of filling and changing the composition of the fluid were altered.

To facilitate changing the composition of the system, the device illustrated in Fig. 1 was attached to the valve V_2 (the connection between V_2 and the bomb is illustrated in Fig. 1*a* of Reference 3). In Fig. 1, the double line denotes glass tubing and the single line metal; the open side of the valve V_5 was attached to a vacuum system. With the pinch-clamp y open and the tubing from the mercury surface to V_2 filled with cyclohexane, liquid could be forced into the bomb by opening valve V_2.

Procedures

The cyclohexane was purified by distillation from silica gel. Merck's reagent grade aniline was dried for 5 days over KOH and then fractionated. The sample fraction was collected in a glass bulb, which was sealed to valve V_2 (Fig. 1) with a Kovar glass-to-metal seal.

The aniline sample was degassed under vacuum and then forced, by mild heating, into the evacuated bomb under its own vapor pressure. The initial amount of cyclohexane was introduced in the same manner until the volume fraction of aniline was

Can. J. Chem. Downloaded from www.nrcresearchpress.com by 200.7.193.243 on 09/04/12
For personal use only.

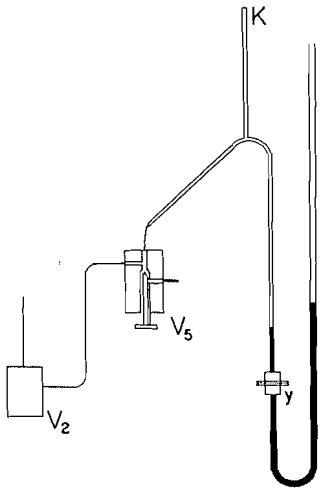

FIG. 1. Auxiliary filling system used for adding cyclohexane to the system aniline–cyclohexane.

0.416. With this initial filling, the liquid column in the bomb was about 30 cm. long.

The composition of the binary mixture was changed by allowing cyclohexane to enter the bomb by opening valve V_2 (Fig. 1). This was possible since the vapor pressure in the bomb was about 150 mm. of mercury, while the cyclohexane in the filling device was at atmospheric pressure. Volume fractions were obtained by measuring the length of the fluid column in the bomb. This procedure, which assumed no volume change on mixing, was considered sufficiently accurate for the purposes of this experiment.

RESULTS

Coexistence Curve

The curve bounding the region of two discrete phases (lower diagram, Fig. 2) was obtained by observing the first formation of visible droplets when the liquid mixture

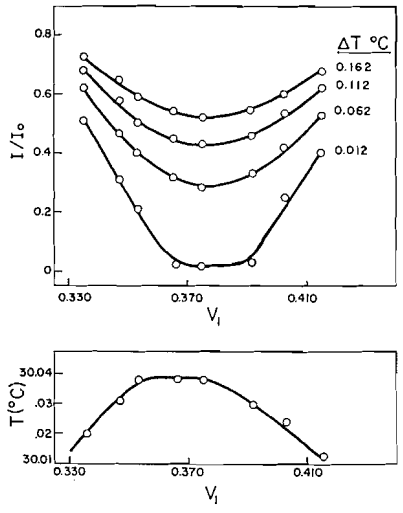

FIG. 2. The variation of optical transmittance with volume fraction of aniline at a number of temperatures above T_c (upper diagram). The coexistence curve for aniline–cyclohexane at the vapor pressure of the fluid system (lower diagram).

Can. J. Chem. Downloaded from www.nrcresearchpress.com by 200.7.193.243 on 09/04/12
For personal use only.

was cooled very slowly. The observed value of T_c was $30.04 \pm 0.02°$ C., which is slightly higher than the value 29.63° C. reported by Rice and Rowden (6). T_c was observed at three values of V_1; however, the apex of the curve could be drawn either flat or rounded within the limits of experimental error.

At T_f, the appearance of droplets occurred uniformly throughout the length (approximately 30 cm.) of the fluid column. The initial fog of condensation did not form at a particular level in the bomb, as was observed in one-component systems (3, 4, 8). This indicates that a vertical concentration gradient did not exist.

The Variation of Transmittance with Volume Fraction

The upper diagram in Fig. 2 shows the variation of optical transmittance (I/I_0) with volume fraction of aniline. The almost flat portion at the minimum of the curve at $\Delta T = 0.012°$ C. is probably due to insensitivity of measurements at this very low value of the transmittance. At all other values of ΔT, the transmittance–composition isothermals are smooth curves which pass through a minimum at a value of V_1 at which the phase volumes are equal at T_c. These isothermals are of the same form as those obtained by Zimm (10) for the binary liquid system perfluoromethylcyclohexane – carbon tetrachloride.

The Variation of Transmittance with Height

No vertical gradients in transmittance formed over periods of several hours after cessation of stirring at any value of V_1 and at various temperatures down to $\Delta T = 0.012°$ C. Since, at constant temperature, transmittance varies with composition as shown in Fig. 2 (upper diagram), it follows that no concentration gradients were formed. This was unexpected.

No extensive time-lag phenomena were observed in the binary liquid system such as were found in one-component systems near the critical point (5). When the binary liquid column, above T_c, was stirred, prestirring values of the optical transmission were re-established within 5 minutes after cessation of stirring. This time was of the order required for establishment of thermal equilibrium after the fluid had been heated by the viscous work of stirring.

The Variation of Turbidity with Temperature

Fig. 3 shows the variation of the inverse of the turbidity τ with temperature at positive values of ΔT. Results obtained for the one-component systems ethylene and xenon (4) are included for comparison.

The higher turbidities observed for the aniline–cyclohexane system show a linear dependence of τ^{-1} on ΔT right down to $\Delta T = 0$. Zimm (10) reported a similar dependence of turbidity on temperature for the system perfluoromethylcyclohexane – carbon tetrachloride.

The Effect of Radiant Energy

The action of the polychromatic light beam in passing through the fluid column caused no noticeable effect on the turbidity of one-component systems. Above T_c, in the aniline–cyclohexane mixture, the light beam caused the turbidity to slowly decrease. After about 10 minutes at a fixed level, a relatively clear path through the turbid fluid was visible at the point where the light beam had been; on moving the light source, this region of relative transparency disappeared within several minutes. The phenomenon was very pronounced at small values of ΔT. This type of behavior seems to

Can. J. Chem. Downloaded from www.nrcresearchpress.com by 200.7.193.243 on 09/04/12
For personal use only.

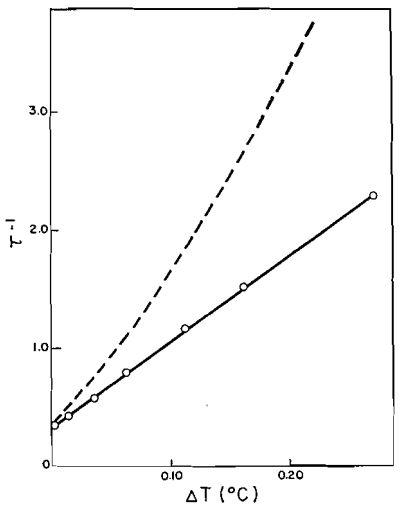

FIG. 3. Variation of the inverse of the turbidity with ΔT at the critical composition in the system aniline–cyclohexane (solid line). The broken line shows the results obtained for ethylene and xenon under similar conditions.

correspond to that observed in disperse systems, which is called "photophoresis" (2). To minimize the effect of this phenomenon on the transmission measurements, observations were recorded immediately after moving the light source. This effect is worthy of further investigation.

DISCUSSION

Since no concentration gradients are formed in the system aniline–cyclohexane at temperatures slightly above T_c, it seems that the flat apex observed by Rice and Rowden (6) on the coexistence curve for aniline–cyclohexane could not be caused by the effect of gravity. This is in contrast to the behavior in one-component systems where the flat-topped coexistence curve, observed by several authors, can be explained in terms of density gradients (4, 7, 8).

Failure to observe the gradients predicted by Equations [2], [3], and [4] may indicate that the theoretical homophase model, used in the derivation of these equations, is inadequate to describe conditions in the region of the critical solution point. Previous observations (5) indicated that molecular clusters, formed at temperatures slightly above T_c in one-component systems, have appreciable lifetimes and it may be more realistic in both cases to treat the clusters as droplets of another phase.

It must be realized that, at temperatures slightly below the classically-defined critical temperature, the difference in density and the interfacial tension between the two phases become so small that a dispersion of the two phases could be extremely stable. It may well be that the temperature T_c, now accepted as the critical temperature, is in reality the minimum temperature at which the two existing phases, of critical composition, will form a stable dispersion of minute droplets when the difference in density and the interfacial tension between the two phases have reached a very low value.

The classically-defined critical temperature, at which the difference in density and the interfacial tension between the two phases actually become zero, would be somewhat higher and could not be detected visually. It would, in fact, be extremely difficult to

Can. J. Chem. Downloaded from www.nrcresearchpress.com by 200.7.193.243 on 09/04/12
For personal use only.

detect the temperature corresponding to the classically-defined critical point owing to the continuous nature of the transition. In view of the above considerations, it may be better to refer to the temperature T_c, presently accepted as the critical temperature, as the "critical dispersion temperature".

REFERENCES

1. EINSTEIN, A. Ann. Physik, **33**, 1275 (1910).
2. HARTMAN, R. J. Colloid chemistry. Riverside Press, Cambridge, Mass. 1939. p. 287.
3. MURRAY, F. E. and MASON, S. G. Can. J. Chem. **30**, 550 (1952).
4. MURRAY, F. E. and MASON, S. G. Can. J. Chem. **33**, 1399 (1955).
5. MURRAY, F. E. and MASON, S. G. Can. J. Chem. **33**, 1408 (1955).
6. RICE, O. K. and ROWDEN, R. W. J. Chem. Phys. **19**, 1423 (1951).
7. WEINBERGER, M. A. and SCHNEIDER, W. G. Can. J. Chem. **30**, 422 (1952).
8. WHITEWAY, S. G. and MASON, S. G. Can. J. Chem. **31**, 569 (1953).
9. YVON, J. Fluctuations en densité. Actualités scientifiques et industrielles, No. 542. Hermann et Cie, Paris. 1937.
10. ZIMM, B. H. J. Phys. and Colloid Chem. **54**, 1306 (1950).

Can. J. Chem. Downloaded from www.nrcresearchpress.com by 200.7.193.243 on 09/04/12
For personal use only.

Can. J. Chem. Downloaded from www.nrcresearchpress.com by 200.7.193.243 on 09/04/12
For personal use only.

PHOTOOXIDATION OF KETONES IN AN O^{18} ENRICHED ENVIRONMENT[1]

J. R. DUNN[2] AND K. O. KUTSCHKE

ABSTRACT

A technique is described in which the origins of the products of photooxidation of ketones can be obtained in respect to whether they arise from the carbonyl or the alkyl groups of the ketone molecule. This is accomplished with the use of reactant molecular oxygen which has been enriched in the O^{18} isotope. Application of this to the photooxidation of acetone indicates that a large fraction of the carbon dioxide contains the carbonyl group of the ketone and that acetyl radicals play an important role in the oxidation to temperatures at least as high as 175° C. Propionyl radicals are much less stable, and, in the photooxidation of diethyl ketone, their reactions, other than decomposition, appear to be negligible at quite low temperatures. Some comment is made on the mechanisms of these photooxidations.

In the course of recent work on the photooxidation of azomethane it was observed that relatively small amounts of the oxides of carbon were produced (1). In particular, it has been suggested (1) that, under the conditions used in these experiments, methyl radicals are not oxidized to carbon dioxide to any large extent and that the greater amounts of the dioxide found in the photooxidation of acetone (2) must have arisen from an oxidation of the carbonyl group. Such an oxidation might occur, for example, by reactions of acetyl radicals (3) or acetonyl radicals (1) with oxygen. This disagrees with the work of Christie (4), who observed that essentially all of the carbon dioxide was radioactive when produced in the photooxidation of $C^{14}H_3COC^{14}H_3$. In view of this contradiction and of the impure acetone sample used by Christie (some unidentified material which led to unexpectedly large yields of carbon dioxide (4)), it was thought worth while to check the result by an independent method.

If oxygen enriched in O^{18} is used in these experiments, any carbon dioxide containing the methyl carbon atom will show the same O^{18} enrichment as does the reactant oxygen. Conversely, if the carbonyl group is the source of the dioxide and if it is assumed that the carbonyl group survives the reaction without rupture of the C—O carbonyl linkage, the carbon dioxide produced will show only one-half the enrichment of the reactant oxygen. By a similar argument, carbon monoxide which arises from the carbonyl group, for example by the decomposition of acetyl radicals, will possess the natural isotopic composition, while that which is formed from the terminal carbon atom will be enriched to the same extent as is the reactant oxygen. Similar considerations show that formaldehyde that arises from the carbonyl group will have the natural abundance of O^{18}, while that arising from methyl radical oxidation will be enriched.

The carbon monoxide observations also aid in the investigation of the primary products of ketone photolysis. It seems well established that methyl and acetyl radicals are the first radicals produced from the excited acetone molecule formed by light absorption at ~3130 Å (5). Acetyl radicals so formed are energy rich, and a certain fraction of them are thought to decompose before experiencing any significant number of collisions. The remainder react as acetyl radicals, the predominant reaction being decomposition into carbon monoxide and a methyl radical presumably by a quasi-unimolecular process (6), so that

[1]*Manuscript received October 29, 1957.*
Contribution from the Division of Pure Chemistry, National Research Council, Ottawa, Canada.
Issued as N.R.C. No. 4599.
[2]*National Research Council Postdoctorate Fellow 1953–55. Present address: British Rubber Research Association, Welwyn Garden City, Herts., England.*

Φ_{CO} is temperature dependent. General confirmation of this is found in the observations made here, which indicate that the extent of decomposition of the acetyl radical varies with temperature at a given oxygen pressure.

An analogous argument may be made in the case of diethyl ketone photooxidation in which the primary process is thought to differ only in degree from that in acetone (7). Substantiation for such a view may be deduced from the data presented here.

Only preliminary results appear here; more detailed investigations are reported in forthcoming publications from these laboratories. Since this work was completed, the results of Taylor and Blacet (8) appeared; these authors presented a similar treatment of biacetyl photooxidation.

EXPERIMENTAL

Experimental procedures were similar to those used previously in these laboratories (1) with a few exceptions. The reaction cell together with a magnetically driven stirrer was housed in a thermostatted air oven. A few centimeters of 8 mm. tubing were external to the oven and connected via glass float-valves to a mercury cutoff, leading to the storage and analytical systems, and to a small Toepler pump which served to "dose" oxygen into the reaction system as required to maintain the oxygen pressure constant to within some 10–15%. The system appeared to prevent the polymerization of formaldehyde during exposure since reproducible recoveries from the LeRoy still (9) were achieved for this product. The carbon monoxide – oxygen fraction, removed at −196° C., was slowly introduced into a vessel containing a fresh surface of yellow phosphorus. With sufficiently slow introduction negligible oxidation occurred; blank experiments showed no exchange during this procedure. Carbon monoxide recovered was submitted for mass spectrometric analysis. The carbon dioxide fraction, separated at −160° C., was submitted for mass analysis with no further treatment; small amounts of formaldehyde were always present. The bulk of the formaldehyde was recovered with prolonged pumping at −130° C. and submitted for isotopic analysis. Higher-boiling compounds were not investigated in the work reported here.

Analogous procedures were used with diethyl ketone; formaldehyde was absent but acetaldehyde was a major product. Some C_2 hydrocarbon was also found.

Acetone and diethyl ketone were good quality commercial products, carefully dried and outgassed. Oxygen was obtained from the slow electrolysis, *in vacuo*, of about 1 cm.^{3} of outgassed, enriched water (from Dr. L. C. Leitch of these laboratories) using a drop of sulphuric acid as an electrolyte. The oxygen was led over platinized asbestos at 300° C., and then through several liquid nitrogen traps to storage. Mass spectrometric analysis yielded a 34/32 ratio 2.90×10^{-2} (natural 0.34×10^{-2}) indicating that 2.8% of the oxygen molecules contained an atom of O^{18}. The same procedure was followed with water stated to contain 10.17% O^{18} (Dajac Laboratories); analysis of the oxygen gave 9.59 atom % O^{18}. Only a few experiments, not reported here, were made with the more highly enriched oxygen; they were in essential agreement with the results reported.

RESULTS AND DISCUSSION

With conditions of acetone and oxygen pressures, absorbed light intensity, and temperature similar to those used by earlier workers (2, 4, 10), over-all quantum yields for the production of the oxides of carbon and for the consumption of oxygen were in excellent agreement. However, the fraction of the total carbon monoxide produced which contains the carbonyl group, x_1, varies with temperature and oxygen pressure as shown in Table I.

Can. J. Chem. Downloaded from www.nrcresearchpress.com by 200.7.193.243 on 09/04/12
For personal use only.

TABLE I

ORIGIN OF THE OXIDES OF CARBON IN KETONE PHOTOOXIDATION

	O_2 (mm.)	x_1	x_2	x_3
Acetone[a]				
120° C.	0.08	0.25	0.92	
	0.17	0.22	0.92	
	0.3	0.18	0.94	
	0.5	0.0	0.83	
175° C.	0.08	0.73	0.88	
	0.56	0.12	0.82	
	0.99	0.43	0.80	
	2.0	0.12	0.80	
	14	—	0.81	
Diethyl ketone[b]				
120° C.	0.33	0.87	0.79	0.52
	0.84	—	0.79	—
	1.6	0.90	0.90	0.56
175° C.	0.4	0.88	0.74	0.32
	0.7	0.89	0.69	0.29
	1.3	0.77	0.55	0.29

[a]*Ketone pressure 13 cm.; $I_a \sim 2\times10^{12}$ quanta cm.$^{-3}$ second^{-1}; $\lambda \sim 3130$ Å; $\sim 0.5\%$ decomposition.*

[b]*Ketone pressure 3.5 cm.; $I_a \sim 1\times10^{12}$ quanta cm.$^{-3}$ second^{-1}; $\lambda \sim 3130$ Å; $\sim 1\%$ decomposition.*

The trend, aside from one experiment at 175° C., indicates that even at these temperatures acetyl radical lifetime is sufficiently long to allow a reaction with oxygen which apparently does not produce carbon monoxide. This is in agreement with the observations of McDowell and Thomas (11), who observed that acetyl radicals reacted with oxygen, rather than decomposed, as high as 200° C.

Only a small fraction $(1-x_2)$ of the carbon dioxide ever arises from the methyl group (Table I). It is felt that this conclusion is more reliable than that reached by Christie (4) in view of the uncertainty, mentioned earlier, in the latter work. Moreover, it agrees with the observation that, in the absence of carbonyl groups in the substrate molecule, carbon dioxide is a minor product of methyl radical oxidation (1).

Attempts were made to determine the origin of the formaldehyde product by observing the 32/30 ratio in its mass spectrum. The results were inconclusive, however, since the 32 residual varied in an unpredictable manner whenever formaldehyde was present in the sample chamber.

Some experiments were done on the diethyl ketone photooxidation; the data are included in Table I. Absolute values of quantum yields were again in essential agreement with those of other workers (12, 13). Two experiments at room temperature yielded negligible amounts of carbon monoxide (other workers found $\Phi_{CO} \sim 0.1$ for similar conditions); the carbon dioxide from the room temperature experiments all contained the carbonyl group. The higher values for x_1 from diethyl ketone as compared to those from acetone at the same temperature and oxygen pressure presumably reflect the greater ease with which propionyl radicals decompose. Carbon dioxide could arise in part by mechanisms analogous to those suggested earlier for acetone, but at the higher temperatures a mechanism must exist which produces carbon dioxide from the ethyl group of the ketone. This conclusion is in harmony with the carbon-14 tracer data obtained by Finkelstein and Noyes (12). It is to be noted that the mechanism proposed by Jolley (13) does not take this fact into consideration. The origin of the acetaldehyde found here (x_3 is that fraction of the aldehyde which contains the carbonyl group of the ketone—see Table I)

Can. J. Chem. Downloaded from www.nrcresearchpress.com by 200.7.193.243 on 09/04/12
For personal use only.

cannot be explained simply. The present result disagrees with the conclusion of Finkelstein and Noyes (12), who found that essentially all the acetaldehyde arose from ethyl radical oxidation. No explanation can be offered for this disagreement. The possibility of exchange between acetaldehyde and reactant oxygen (mostly O^{16}) cannot be ruled out on the basis of present data.*

Much more data are obviously required before a consistent mechanism can be written for either of these photooxidations; tracer experiments are of particular importance. It is felt that the technique outlined here presents a means whereby such data may be obtained relatively simply since the enriched oxygen is readily prepared.

ACKNOWLEDGMENTS

The authors wish to thank Dr. E. W. R. Steacie for the interest expressed throughout this work, and Mrs. June Garlick and Mrs. Frances Kutschke for the mass spectrometric analyses.

REFERENCES

1. Hoey, G. R. and Kutschke, K. O. Can. J. Chem. **33**, 496 (1955).
2. Marcotte, F. B. and Noyes, W. A., Jr. J. Am. Chem. Soc. **74**, 783 (1952); Discussions Faraday Soc. **10**, 236 (1951).
3. Hentz, R. R. J. Am. Chem. Soc. **75**, 5810 (1953).
4. Christie, M. I. J. Am. Chem. Soc. **76**, 1979 (1954).
5. Noyes, W. A., Jr. J. Phys. & Colloid Chem. **55**, 925 (1951).
6. Hoare, D. E. Trans. Faraday Soc. **53**, 791 (1957).
7. Steacie, E. W. R. Atomic and free radical reactions. Reinhold Publishing Corporation, New York. 1954.
8. Taylor, R. P. and Blacet, F. E. Ind. Eng. Chem. **48**, 1505 (1956).
9. LeRoy, D. J. Can. J. Research, B, **28**, 492 (1950).
10. Hoare, D. E. Trans. Faraday Soc. **49**, 1292 (1953).
11. McDowell, C. A. and Thomas, J. H. J. Chem. Soc. 2208, 2217 (1949); Discussions Faraday Soc. **10**, 310 (1951).
12. Finkelstein, A. and Noyes, W. A., Jr. Discussions Faraday Soc. **14**, 76 (1953).
13. Jolley, J. E. J. Am. Chem. Soc. **79**, 1537 (1957).

We are indebted to the referee for drawing our attention to this point.

Can. J. Chem. Downloaded from www.nrcresearchpress.com by 200.7.193.243 on 09/04/12
For personal use only.

RADIOCHEMICAL ANALYSIS FOR LONG-LIVED FISSION PRODUCTS IN ENVIRONMENTAL MATERIALS[1]

W. F. MERRITT

ABSTRACT

A method is described whereby radiochemical analysis for the long-lived fission products Ru^{106}, Sr^{90}, Cs^{137}, and Ce^{144} may be performed on the same sample of soil, water, or biological material. Carriers are added and the material is fused at 550° C. with KOH, KNO_3, and K_2CO_3. Ruthenium and cesium are extracted with water, strontium and cerium remaining in the melt. Ruthenium is extracted into carbon tetrachloride as ruthenium tetroxide, cesium is absorbed on Duolite C-3 cation-exchange resin from alkaline solution, strontium and cerium are extracted from the melt with acid, cerium is precipitated as the hydroxide and strontium as the carbonate. The elements are precipitated, weighed, and counted according to standard procedures.

INTRODUCTION

Low-level radioactive wastes produced at Chalk River are disposed of from seepage pits in a carefully selected disposal area. In addition, sewage and other liquid effluent streams entering the Ottawa river may contain small but measurable quantities of radioactive material. It is necessary, therefore, to monitor the drainage basin of the disposal area and the Ottawa river below the plant site for any undesirable escape of radioactivity.

The movement of activity in the disposal area is followed by drilling wells and taking soil samples, by sampling the drainage water, and by taking specimens of vegetation and animals from the surrounding area. Activity in the river is monitored by continuous sampling of the project effluents and by taking samples of bottom muds, fish, clams, aquatic plants, etc. at regular intervals. The radioactive isotopes present and important from the public health point of view are the long-lived, high-yield fission products Sr^{90}, Ru^{106}, Cs^{137}, and Ce^{144}. Since Sr^{90} is readily absorbed into the body, is fixed in the bone, and has a long half-life and energetic radiation, it is considered the most hazardous of these radioisotopes.

An analytical method was desirable which could be applied to a wide variety of natural materials and which would detect very low concentrations of the isotopes listed above in the presence of substances occurring commonly in nature.

Analytical methods for these isotopes have been described by Coryell and Sugarman (1), by Meinke (2), and by Kleinberg (3). Crouch and Cook (4) have published an excellent detailed method of separation of a large number of radioisotopes. Kahn (5) has given detailed methods for the analysis of several isotopes adsorbed on soil using acid leaching for preliminary separation from the soil. However, we have found that, in particular, Cs^{137} could not be leached quantitatively from the typical sandy soil found at Chalk River. It has been shown (6) that the cesium ions are fixed in the interlayer positions of the layer silicate minerals, and thus it is necessary to destroy the silicate structure to release them.

Standard methods for decomposing silicates are of two general classes. The first involves heating with hydrofluoric and perchloric acid so that the silicon is volatilized as the tetrafluoride. In the second the material is fused with an alkali hydroxide, carbonate,

[1]*Manuscript received September 20, 1957.*
Contribution from Health Physics Branch, Biology Division, Atomic Energy of Canada Limited, Chalk River, Ontario.
Issued as A.E.C.L. No. 540.

Can. J. Chem. Downloaded from www.nrcresearchpress.com by 200.7.193.243 on 09/04/12
For personal use only.

or peroxide. If the first method is used, ruthenium will be volatilized. In the second, the large amount of alkali added will interfere with standard cesium separations. Therefore, a different approach to the cesium analysis was needed.

Miller and Kline (7) first reported the ability of phenolic methylene–sulphonic-type cation-exchange resins to adsorb cesium from highly alkaline solutions. Ring (8) has adapted this method for separating cesium from large quantities of sodium. The method described here makes use of the ability of Duolite C-3* resin to effect a clean separation of as little as a milligram of cesium from gram quantities of potassium after alkali fusion.

PROCEDURES

Preparation of Samples

Water samples were evaporated to a few milliliters. Organic materials were wet ashed with nitric acid and hydrogen peroxide. Soil samples were ground to a fine powder with a mortar and pestle. Suitable quantities of material, determined by rough counting, were weighed or transferred into nickel crucibles, and standardized carrier solutions amounting to 20 mg. of strontium, cerium, and cesium and 10 mg. of ruthenium added by pipette. The mix was neutralized with dilute potassium hydroxide and dried under an infrared lamp. A fusion mixture of 2:1:1 by weight of potassium hydroxide, nitrate, and carbonate was added to the crucible to about 5–10 times the weight of the sample. The material was fused in a muffle at 550° C. for 2 hours, with the contents being swirled at 15-minute intervals. In this fusion the hydroxide and carbonate attack the silicate structure, and the nitrate oxidizes the ruthenium present to a soluble ruthenate. The melt was allowed to cool, and was leached twice with 10 ml. of water. The ruthenate and the cesium dissolve while the strontium and cerium remain in the melt as the insoluble carbonate and hydroxide.

Ruthenium

Potassium periodate (0.25 g.) was added to the solution to oxidize the ruthenate to ruthenium tetroxide. Zirconium, if present, will precipitate at this stage and can be removed by centrifuging. The solution was neutralized to a pH of 7 with 9 *M* sulphuric acid. Ten milliliters of redistilled carbon tetrachloride was added, and solvent extraction was started using an automatic "spitzer". The pH was reduced to 4 during the extraction by the dropwise addition of acid. Occasionally two extractions were necessary. The layers were separated and the ruthenium was stripped from the carbon tetrachloride with 6 *N* hydrochloric acid. The ruthenium was reduced to the metal with powdered magnesium as described by Kleinberg (3).

Cesium

The aqueous layer from the ruthenium solvent extraction was treated with saturated lithium hydroxide and the resulting precipitate of lithium carbonate was removed by centrifuging. A column of Duolite C-3, 60–100 mesh, 12×50 mm., was prepared in the lithium form by washing with 100 ml. of 0.5 *N* lithium hydroxide followed by 50 ml. of water. The sample solution was poured through the column and washed with 50 ml. of water. The column was then treated with 125 ml. of 0.5 *N* lithium hydroxide to elute the potassium. After a 50-ml. water wash, the lithium was eluted with 125 ml. of 0.2 *N* hydrochloric acid. The cesium was stripped off in 50 ml. of 6 *N* hydrochloric acid. Flow rates throughout were held to 2–3 ml./min.

**Chemical Process Company, Redwood City, California.*

Can. J. Chem. Downloaded from www.nrcresearchpress.com by 200.7.193.243 on 09/04/12
For personal use only.

Can. J. Chem. Downloaded from www.nrcresearchpress.com by 200.7.193.243 on 09/04/12
For personal use only.

The cesium solution was evaporated to 0.5 ml., made up to 3 ml. with water, and the cesium was precipitated with 2 ml. of 5% chloroplatinic acid.

Cerium

The solids from the original melt were treated with 10 ml. of 6 *N* nitric acid with heating. This solution was taken to dryness twice, with a few milliliters of concentrated nitric acid added, to dehydrate the silica. The dry mass was treated with 5 ml. of 6 *N* hydrochloric acid and two or three drops of 30% hydrogen peroxide to reduce any ceric ions to cerous, and the silica removed by centrifuging. The supernatant was diluted to 10 ml. and neutralized with ammonia gas to precipitate cerous hydroxide.

The cerium was then purified according to Kleinberg (3) by fluoride precipitation and by an oxidation–reduction cycle, oxidizing to Ce^{+4}, precipitating the cerium as ceric iodate, reducing to Ce^{+3}, and scavenging with zirconium iodate. The cerium was precipitated and weighed as the oxalate.

Strontium

After removal of the cerium as the hydroxide, strontium was precipitated by the addition of sodium carbonate. The precipitate was dissolved in 6 *N* nitric acid and the strontium was purified by two precipitations from fuming nitric acid. Calcium was removed by leaching the dried nitrate with alcohol–ether solution. Barium, if present, was removed by precipitation from alcoholic hydrochloric acid. The strontium salt was dissolved in water, scavenged with ferric hydroxide, and precipitated and weighed as the carbonate.

Counting

The precipitates were weighed and counted on standard 1-in. aluminum dishes. The counter used was a β scintillation counter, consisting of an anthracene crystal 1 in. in diameter and 10 thousandths of an inch thick, mounted on an RCA 6199 photomultiplier and covered with aluminized Mylar film. The unit was mounted in a 2-in. lead shield on a "Nuclear Chicago" model C110A* sample changer. The background of this system was 6 c.p.m., and the efficiency for $Sr^{90}+Y^{90}$ about 30%. The observed counting rates were corrected for background, for chemical yield based on added carrier, and for counter efficiency.

A typical set of results is shown in Table I.

TABLE I

TYPICAL RADIOCHEMICAL ANALYSIS OF DUPLICATE SAMPLES OF CONTAMINATED SOIL

Isotope	Weight of sample, mg., W	Weight of carrier, mg., A	Weight of ppt., mg., B	C.p.m. corrected for background, C	C.p.m. corrected for chemical yield, (A/B×C = D)	C.p.m. per g. of material, (D/W)×1000
Sr	24.5	18.7	12.1	50.0	77.3	3155
Sr	25.9	18.7	12.5	54.7	81.8	3159
Ru	24.5	9.9	6.6	9.4	14.4	588
Ru	25.9	9.9	7.9	10.8	13.5	522
Cs	24.5	20.1	17.2	19.6	22.9	935
Cs	25.9	20.1	15.9	17.4	22.0	850
Ce	24.5	23.2	14.7	23.2	36.6	1495
Ce	25.9	23.2	13.3	22.7	39.6	1529

**Nuclear Instrument & Chemical Corp., Chicago 10, Illinois.*

DISCUSSION

The basic procedures described have been used in the radiochemical laboratory of the Health Physics Branch of these laboratories for several months. The methods employed standard semimicroanalytical techniques. Precipitations were carried out in 50-ml. centrifuge tubes. Filtering and ignition were not required. Junior technicians achieved 50–75% yields based on added carrier.

Modifications were introduced as required. For example, it was sometimes necessary to remove silica from the insoluble portion of the melt by fuming with hydrofluoric and perchloric acids in platinum crucibles. This system was used if an analysis for ruthenium was not required. The sample was fumed with the acids, cooled, and cesium precipitated by addition of alcohol. The precipitate was dissolved in water, made alkaline with 0.5 *N* lithium hydroxide, and scavenged with 1 mg. of iron. The solution was adsorbed and eluted from an 8×30 mm. column of Duolite C-3, using reagents in the same ratio to column volume as above. The strontium and cerium were separated, purified, and precipitated as described.

For samples with a high concentration of anions (e.g. phosphate in fish specimens) it was advantageous to absorb the cations from 0.1 *N* acid solution on a Dowex 50 cation-exchange resin, wash the anions through with water, and elute the cations with 6 *N* hydrochloric acid. If an analysis of an anionic component such as P^{32} or S^{35} was required, this was a convenient method of preliminary separation.

ACKNOWLEDGMENTS

The author would like to thank Dr. Margaret Tutt, who did preliminary work on the methods, Dr. W. G. Cross, who designed and constructed the counter, and Mr. A. J. W. Hitchman for helpful discussion of the cesium method.

REFERENCES

1. CORYELL, C. D. and SUGARMAN, N. National Nuclear Energy Series, Div. IV, Vol. 9. Radiochemical studies: The fission products. McGraw-Hill Book Co., Inc., New York. 1951.
2. MEINKE, W. W. U.S. Atomic Energy Commission Report AECD-2738 (1949).
3. KLEINBERG, J. U.S. Atomic Energy Commission Report LA-1566 (1953).
4. CROUCH, E. A. C. and COOK, G. B. J. Inorg. & Nuclear Chem. **2**, 223 (1956).
5. KAHN, B. U.S. Atomic Energy Commission Report ORNL-1951 (1955).
6. EVANS, E. J. A.E.C.L., Chalk River, Ont. Private communication.
7. MILLER, H. S. and KLINE, G. E. J. Am. Chem. Soc. **73**, 2741 (1951).
8. RING, S. A. Anal. Chem. **28**, 1200 (1956).

Can. J. Chem. Downloaded from www.nrcresearchpress.com by 200.7.193.243 on 09/04/12
For personal use only.

Can. J. Chem. Downloaded from www.nrcresearchpress.com by 200.7.193.243 on 09/04/12
For personal use only.

SUR LA TRANSFORMATION DE LA DIHYDROHÉTÉROCONESSINE EN DIHYDROCONESSINE[1]

H. FAVRE ET B. MARINIER[2]

SOMMAIRE

On montre que le diperchlorate de la base résultant de la déshydrogénation de la dihydro*hétéro*conessine par l'acétate mercurique est identique à celui que l'on obtient, par ce procédé, à partir de la dihydroconessine; ce diperchlorate est réduit catalytiquement en dihydroconessine. On en conclut que la dihydro*hétéro*conessine et la dihydroconessine sont bien des épimères en position 20; la configuration du groupe méthyle dans cette position peut être déterminée par ce procédé de déshydrogénation–réhydrogénation.

La constitution de la conessine, telle que proposée par Haworth, McKenna et leurs collaborateurs (1, 2), a été confirmée par des travaux récents (3, 4, 5). Un pas décisif dans les travaux de Haworth fut l'étude du système conessine–*hétéro*conessine qui conduisit à formuler ces deux isomères comme des épimères en position 20 (2, 6).

Nous rapportons dans ce mémoire la déshydrogénation par l'acétate mercurique de la dihydroconessine (I) et de la dihydro*hétéro*conessine (II). Bien que chacune de ces bases possède un groupe méthyl-imino et un groupe diméthyl-amino capables de réagir avec l'acétate mercurique (voir (7) pour de nombreuses références bibliographiques) un seul de ces groupes semble être le siège de la réaction. En effet, lorsque 1 mole des bases I ou II est traitée par 4 moles de réactif dans les conditions opératoires habituelles (7), deux atomes d'hydrogène seulement sont éliminés (cette détermination se fait en mesurant la quantité d'acétate mercureux qui précipite). On obtient dans les deux cas une base extrêmement altérable, qui forme toutefois un diperchlorate bien cristallisé et stable. La base déshydrogénée peut être isolée sous forme solide, p.f. 100–125°; tous nos essais de purification par cristallisation n'ont conduit qu'à des huiles jaunes; nous avons cependant réussi à en obtenir un spectre infrarouge acceptable: on y décèle une bande à 1645 cm.$^{-1}$. Les diperchlorates insaturés (en provenance de I et de II) sont identiques, comme le prouvent leur pouvoir rotatoire, leur point de fusion et leur spectre infrarouge qui présente en particulier une bande à 1690 cm.$^{-1}$. Le déplacement de la bande infrarouge de 1645 à 1690 cm.$^{-1}$ par formation du diperchlorate de la base déshydrogénée est caractéristique du système

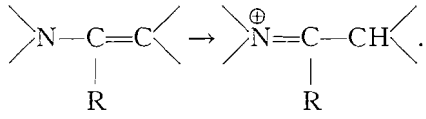

. ClO_4, quand l'amine est tertiaire (7). A la réduction catalytique (platine) le diperchlorate III (issu soit de I, soit de II) absorbe une molécule d'hydrogène et conduit spécifiquement à la dihydroconessine.

On sait, avec Haworth (2), que les bases isomères dihydroconessine (I) et dihydro*hétéro*conessine (II) se différencient uniquement par leur anneau hétérocyclique[3] et que l'ouverture de cet anneau, par dégradation selon Hofmann, supprime cette différence, comme le montre la formation de la dihydro-5,6 conessiméthine (IV) à partir de I et de II. On sait d'autre part que les bases *apo* et méthines—dont l'anneau hétérocyclique est ouvert—ont toutes une double liaison en 20–21,[4] à l'image de la base IV: ceci établit

[1]*Manuscrit reçu le 31 octobre, 1957.*
Contribution du Département de Chimie de l'Université de Montréal, Montréal, Qué.
[2]*Boursier du Conseil National de Recherches du Canada.*
[3]*Voir le travail (2) pour une discussion détaillée de ce point.*
[4]*On l'a amplement démontré (8, 9) en établissant des relations de synthèse et de dégradation entre l'apoconessine (diméthylamino-18 pregnatriène-3,5,20), la conessiméthine (bis-(diméthylamino)-3β,18 pregnadiène-5,20) et l'hydroxy-3β pregnadiène-5,20.*

indiscutablement que le carbone 17 n'est pas touché par le processus de formation de la double liaison en 20–21 et exclut l'hypothèse qui ferait de la conessine et de l'*hétéro*-conessine (par conséquent des bases I et II) des épimères en position 17. On peut donc considérer comme acquis que les bases I et II ne se distinguent ni par la position ou la configuration de leur groupe diméthylamino, ni par la configuration de leurs carbones 5 et 17.

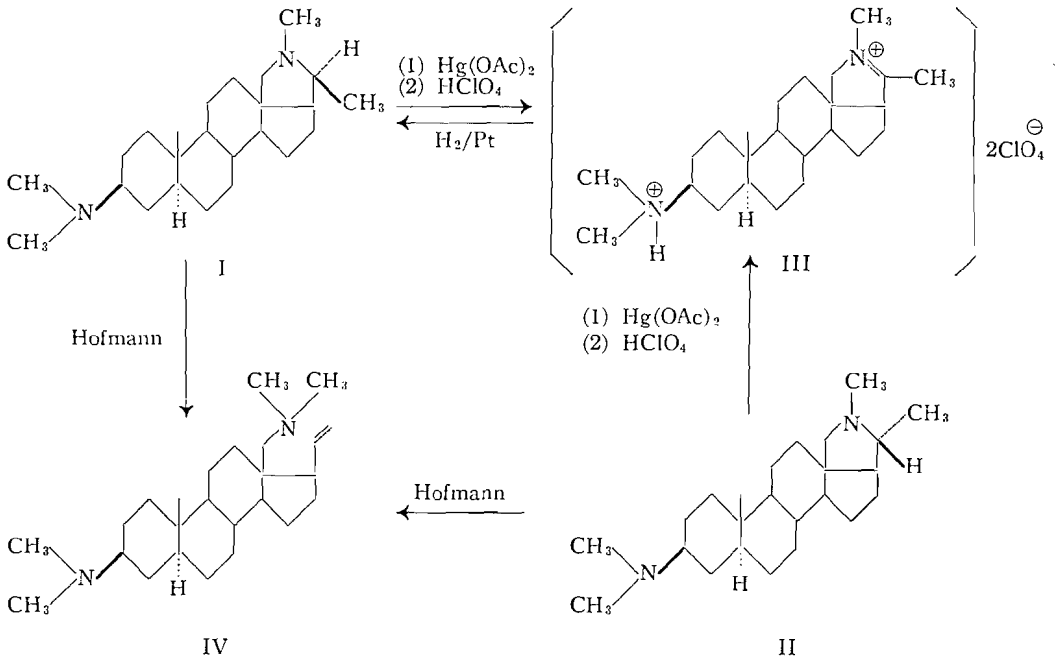

I III IV II

La présence d'un groupement $>C=\overset{\oplus}{N}<$ dans le diperchlorate obtenu par déshydrogénation, la disparition chez ce dernier de la différence qui existe entre les bases saturées I et II et la transformation de la dihydro*hétéro*conessine en dihydroconessine ne peuvent se concevoir qu'en situant la double liaison dans l'anneau hétérocyclique et en fonction des formules I et II pour les bases saturées et de la formule III pour le diperchlorate de la base déshydrogénée. Si la déshydrogénation ne s'était pas portée sur le noyau hétérocyclique nous aurions obtenu à partir de I et de II deux produits de déshydrogénation distincts, reflétant encore la différence qui existait à l'origine entre I et II. La dihydroconessine et la dihydro*hétéro*conessine, et par suite la conessine et l'*hétéro*conessine, sont donc bien des épimères en position 20.

La grande instabilité de la base déshydrogénée, correspondant au diperchlorate III, ne nous a pas permis d'approfondir pour le moment les relations qui doivent exister entre sa liaison éthylénique et celle qui est localisée en position 17–20 chez les alcaloïdes du type de la conkurchine (10, 11). Le fait que la double liaison de la base de déshydrogénation puisse se placer en position 17–20, détruisant ainsi deux centres d'asymétrie dans l'anneau hétérocyclique, n'infirme pas la conclusion que nous tirons au sujet des structures épimères en position 20 des bases I et II, puisque ces dernières ne sont pas des épimères en position 17.

Can. J. Chem. Downloaded from www.nrcresearchpress.com by 200.7.193.243 on 09/04/12
For personal use only.

Can. J. Chem. Downloaded from www.nrcresearchpress.com by 200.7.193.243 on 09/04/12
For personal use only.

Le procédé de réduction mis en oeuvre pour passer de III à I amène en règle générale la fixation de l'hydrogène sur le côté le moins empêché de la molécule (12, 13); il est raisonnable ainsi d'admettre que le groupe méthyle se trouvera au-dessus du plan de l'anneau hétérocyclique dans le produit d'hydrogénation de III—donc dans la dihydroconessine (formule I). On rejoint de cette manière les conclusions de Černý, Lábler, et Šorm (3) et de Phillips et Johnson (4) relatives à la configuration du groupe méthyle en position 20 de la conessine.

Il convient cependant de signaler quelques différences dans le mode d'action de l'acétate mercurique sur I et sur II.

Le diperchlorate III, venant de la dihydroconessine (I), se présenta d'abord sous la forme de paillettes, p.f. 317°, puis sous la forme d'une poudre, p.f. 335–337°, lorsqu'on le cristallisa. Les spectres infrarouges de ces deux variétés sont très semblables. Cette hétérogénéité montre que la déshydrogénation qui amène en majorité la formation d'une seule double liaison s'accompagne de réactions secondaires. On peut théoriquement en retenir deux: (*a*) réaction du groupe diméthylamino en position 3; (*b*) hydroxylation sur le carbone 17, comme c'est le cas pour certaines bases tertiaires dont le carbone en β de l'azote est tertiaire, par exemple la méthyl-1 décahydroquinoléine (14); cette hydroxylation pourrait justifier la présence d'une bande —OH dans le spectre infrarouge de III. Ces réactions secondaires, quelles qu'elles soient, n'ont pu être décelées avec certitude en raison de la petite quantité de base mise en oeuvre dans nos expériences.

La déshydrogénation de la dihydro*hétéro*conessine n'engendra que le diperchlorate à point de fusion élevé; le rendement en sel brut fut de 64% seulement, comparé à 85% dans le cas de la dihydroconessine. Il est raisonnable d'attribuer ces différences à l'accessibilité plus ou moins grande de l'hydrogène en position 20 chez I et II.

PARTIE EXPÉRIMENTALE[5]

Déshydrogénation de la dihydroconessine

A 1.424 g. (0.00446 mole) d'acétate mercurique dans 12 ml. d'acide acétique aqueux à 5%, on ajoute 0.400 g. (0.00114 mole) de dihydroconessine, p.f. 109°, $[\alpha]_D^{22} = +50.4°$ ($c = 3.0$; $CHCl_3$ (2, 15)). Le mélange agité mécaniquement est chauffé au bain-marie durant $1\frac{1}{2}$ heure. L'acétate mercureux apparaît après 2 à 3 minutes de chauffage. On l'élimine par essorage: 0.512 g. (soit 88.5% de ce qui est nécessaire pour éliminer deux atomes d'hydrogène); on peut déceler dans ce précipité une petite quantité de mercure. Le filtrat est saturé avec H_2S; le précipité noir est séparé du liquide par centrifugation. La solution brunâtre est recueillie, refroidie à 0° et rendue alcaline avec NaOH 50% (2–3 ml.); un solide précipite; on ajoute de l'eau et on extrait trois fois par de l'éther. Les solutions éthérées réunies sont lavées à l'eau, séchées sur du sulfate de sodium anhydre et traitées à 0° par 0.5 ml. (jusqu'au virage bleu du Congo) d'une solution faite de volumes égaux d'acide perchlorique 70% et d'éthanol 95%. Le diperchlorate précipite et après quelques heures on le recueille par essorage: 0.527 g. (85% de la théorie), poudre blanche, p.f. 307–310° (bloc Maquenne). Après une cristallisation dans l'éthanol 95% on obtient des paillettes jaune pâle, p.f. 317° (bloc), dont le spectre infrarouge: bande forte 1694 cm.$^{-1}$, $\diagdown\overset{\oplus}{\mathrm{N}}{=}\mathrm{C}\diagup$, bande moyenne 3060 cm.$^{-1}$, $-\overset{|}{\underset{\oplus}{\mathrm{N}}}\mathrm{H}-$, et

[5]*Les points de fusion (p.f.) ne sont pas corrigés; sauf indication contraire ils ont été déterminés dans un appareil de Thiele. Les spectres infrarouges ont été déterminés à l'aide d'un spectromètre "Perkin-Elmer", modèle 112, à simple faisceau et parcours double, optique* NaCl.

bande très faible 3620 cm.$^{-1}$ (présence de —OH). Une cristallisation de ces feuillets dans l'éthanol 95% donne une poudre jaune pâle, p.f. 335–337° (bloc), $[\alpha]_D^{24} = +29.9°$ ($c = 1.0$; tétrahydrofuranne–eau: 8–2). Spectre infrarouge (nujol): bande forte 1690 cm.$^{-1}$, $\rangle\overset{\oplus}{N}{=}C\langle$, bande moyenne 3110 cm.$^{-1}$, $-\underset{\oplus}{\overset{|}{N}}H-$, et bande très faible 3620 cm.$^{-1}$ (présence de —OH). Calculé pour $C_{24}H_{40}N_2.2HClO_4$: C, 51.70; H, 7.59; N, 5.02%. Trouvé[6]: C, 51.76; H, 7.60; N, 4.95%. Le rendement en diperchlorate cristallisé est de 0.303 g. (49%).

A 0.007 g. de diperchlorate en suspension dans 1 ml. d'eau on ajoute 1 ml. de NaOH 50% et 10 ml. d'eau; on extrait trois fois avec de l'éther. Après les lavages habituels, on évapore l'éther sous vide partiel; on obtient 0.004 g. d'un solide jaune très pâle, p.f. 100–125°. Cette amine est très instable et jaunit rapidement à l'air. Spectre infrarouge (nujol): bande forte à 1645 cm.$^{-1}$, $\rangle C{=}C\langle$.

Déshydrogénation de la dihydrohétéroconessine

La dihydro*hétéro*conessine (0.404 g.), p.f. 105°, $[\alpha]_D^{22} = +17°$ ($c = 1.8$; $CHCl_3$ (2, 15)), est déshydrogénée dans les conditions décrites plus haut. L'acétate mercureux commence à précipiter au bout de 5 minutes de chauffage. Il ne contient pas de mercure lorsqu'on le recueille à la fin de la réaction: 0.546 g. (94.1% de ce qui est nécessaire pour éliminer deux atomes d'hydrogène). On obtient 0.400 g. de diperchlorate brut (64.2%) sous forme de poudre blanche; après deux cristallisations dans l'éthanol 95% on a une poudre blanche: 0.187 g. (30%), p.f. 338° (bloc; ne donne pas de dépression de point de fusion avec le diperchlorate décrit plus haut, p.f. 335–337°); $[\alpha]_D^{24} = +29.7°$ ($c = 1.0$; tétrahydrofuranne–eau: 8–2). Spectre infrarouge (nujol): bande forte 1690 cm.$^{-1}$, $\rangle\overset{\oplus}{N}{=}C\langle$, bande moyenne 3110 cm.$^{-1}$, $-\underset{\oplus}{\overset{|}{N}}H-$, et bande très faible 3640 cm.$^{-1}$ (présence de —OH).

Hydrogénation catalytique des diperchlorates

(*a*) *Diperchlorate en provenance de la dihydroconessine.*—Le diperchlorate (0.100 g.) dans 2.5 ml. d'un mélange dioxanne–eau: 8–2, est hydrogéné en présence de 15 mg. de platine hydrogéné au préalable. L'absorption d'hydrogène cesse au bout d'une heure: absorbé, 4.76 ml.; calculé pour 1 H_2, 4.48 ml., pour 756 mm. et 25°. On essore le catalyseur, dilue le filtrat avec de l'eau, rend alcalin avec NaOH 50% et extrait avec de l'éther. On isole à la manière habituelle 0.062 g. (97%) de solide jaune pâle, p.f. 103°. Ce composé brut ne donne pas de dépression de p.f. en mélange avec de la dihydroconessine, mais le mélange avec la dihydro*hétéro*conessine accuse une dépression et fond à 85° environ. Après une cristallisation dans l'acétone, on retire 0.038 g. de cristaux, p.f. 106.5°, $[\alpha]_D^{25} = +49.4°$ ($c = 3$; $CHCl_3$) et 0.010 g. de cristaux, p.f. 103.5°. Le rendement total en dihydroconessine est de 0.048 g. ou 75%.

(*b*) *Diperchlorate en provenance de la dihydrohétéroconessine.*—Ce diperchlorate (0.100 g.) absorbe la quantité théorique d'hydrogène en 55 minutes dans des conditions opératoires semblables à celles décrites sous (*a*). On obtient 0.064 g. (100%) de dihydroconessine brute, p.f. 103°, et après cristallisation dans l'acétone 0.036 g., p.f. 106.5°, $[\alpha]_D^{25} = +50°$ ($c = 3$; $CHCl_3$) et 0.018 g., p.f. 104°, soit 0.054 g. ou 84.4%. Les p.f. de mélange ont été déterminés avec la dihydroconessine (aucun abaissement) et avec la dihydro*hétéro*conessine (abaissement à 89°).

[6]*L'analyse fut effectuée par M. W. Manser, Herrliberg.*

Can. J. Chem. Downloaded from www.nrcresearchpress.com by 200.7.193.243 on 09/04/12
For personal use only.

Nous remercions le Conseil National de Recherches du Canada d'une subvention de recherche (H.F.) et d'une bourse d'études (B.M.). Nous exprimons également nos remerciements au établissements Ayerst, McKenna et Harrison, Ltd., Montréal, et Merck & Cie, Ltd., Montréal, qui nous ont aidé au cours de l'extraction des alcaloïdes, ainsi qu'à M. le Professeur Sandorfy pour son aide dans l'interprétation des spectres infrarouges.

BIBLIOGRAPHIE

1. HAWORTH, R. D., MCKENNA, J., POWELL, R. G., et WHITFIELD, G. H. Chem. & Ind. (London), 215 (1952).
2. FAVRE, H., HAWORTH, R. D., MCKENNA, J., POWELL, R. G., et WHITFIELD, G. H. J. Chem. Soc. 1115 (1953).
3. ČERNÝ, C., LÁBLER, L., et ŠORM, F. Collection Czechoslov. Chem. Communs. **22**, 76 (1957).
4. PHILLIPS, D. D. et JOHNSON, A. W. Chem. & Ind. (London), 1211 (1957).
5. MCNIVEN, N. L. Chem. & Ind. (London), 1296 (1957).
6. HAWORTH, R. D. Chem. Soc. (London), Spec. Publ. **3**, 1 (1955).
7. LEONARD, N. J. et HAUCK, F. P., Jr. J. Am. Chem. Soc. **79**, 5279 (1957).
8. HAWORTH, R. D., MCKENNA, J., et WHITFIELD, G. H. J. Chem. Soc. 1102 (1953).
9. HAWORTH, R. D., MCKENNA, J., et POWELL, R. G. J. Chem. Soc. 1110 (1953).
10. TSCHESCHE, R. et ROY, A. C. Chem. Ber. **89**, 1288 (1956).
11. TSCHESCHE, R. et SNATZKE, G. Chem. Ber. **90**, 579 (1957).
12. LEONARD, N. J., THOMAS, P. D., et GASH, V. W. J. Am. Chem. Soc. **77**, 1552 (1955).
13. MARION, L. et LEONARD, N. J. Can. J. Chem. **29**, 355 (1951).
14. LEONARD, N. J., MILLER, L. A., et THOMAS, P. D. J. Am. Chem. Soc. **78**, 3463 (1956).
15. HAWORTH, R. D., MCKENNA, J., et WHITFIELD, G. H. J. Chem. Soc. 3127 (1949).

Can. J. Chem. Downloaded from www.nrcresearchpress.com by 200.7.193.243 on 09/04/12
For personal use only.

Can. J. Chem. Downloaded from www.nrcresearchpress.com by 200.7.193.243 on 09/04/12
For personal use only.

THE CHEMISTRY OF PEAT

PART I. THE STEROLS OF PEAT MOSS (SPHAGNUM)[1]

D. A. J. IVES[2] AND A. N. O'NEILL

ABSTRACT

Peat moss (*Sphagnum*) from the surface of an Atlantic peat bog has been extracted with a mixture of benzene and ethanol. The extract has been fractionated chromatographically on alumina. A mixture of sterols has been isolated from one fraction. This mixture has been proved by oxidation experiments to consist of β-sitostanol (stigmastanol) and β-sitosterol. It constituted approximately 0.2% by weight of the dried peat moss.

INTRODUCTION

A considerable amount of work has been done on the chemical composition of peat (8), lignite (brown coal) (8), and coal (8), but relatively little on the composition of peat moss (*Sphagnum*). The latter is considered to be the main precursor of peat in the Atlantic area of Canada. This work was undertaken in an effort to remedy this defect, and also to ascertain what chemical changes occur in humification. Black and his co-workers (4) carried out an extensive analysis on a sample of peat moss from Scotland and reported the presence of β-sitosterol.

The peat moss used in our experiments was a living surface moss, from Shipigan, New Brunswick, and was essentially a mixture of *Sphagnum fuscum*, *S. capillaceum*, and *S. magellanicum* with the first two predominating. It was comparatively free of other common bog plants. The moss was dried to a moisture content of approximately 5% and ground to pass through a 20-mesh screen. Only relatively small quantities of the powder could be extracted at a time, owing to its bulk. The process used was a continuous extraction method, with a constant stream of pure solvent passing through the moss.

After evaporation of the solvent, the dark brown gum (approximately 6% of the total solids) was saponified with methanolic potassium hydroxide solution and the unsaponifiable material extracted with ether. This extract (approximately 1.5% of the total solids), after evaporation, was dissolved in light petroleum and chromatographed roughly on alumina. A small portion of the gum (approximately 3%) did not dissolve in the petrol and was kept for further investigation. The eluate from the chromatogram was divided into five fractions: materials eluted progressively by (*a*) light petroleum, (*b*) benzene, (*c*) ether, (*d*) ether containing 10% methanol, and (*e*) methanol. These fractions will be described separately. The composition of fractions (*c*) and (*d*) varied from extraction to extraction and with the grade of alumina used. The ether fraction sometimes consisted of a white, low-melting solid, and the ether–methanol fraction of a colorless crystalline solid, subsequently proved to be the sterols. In the majority of extractions, however, the components were mixed and tended to be removed from the column together in fraction (*d*) as a light yellow glass. The mixture was separated into cyclic and linear aliphatic compounds by treatment with urea with which the latter formed an insoluble complex. Decomposition of the complex yielded an alcohol which has been tentatively identified as lignoceryl alcohol by melting point, mixed melting point, and molecular weight.

[1]*Manuscript received November 4, 1957.*
Contribution from the National Research Council of Canada, Atlantic Regional Laboratory, Halifax, Nova Scotia.
Issued as N.R.C. No. 4609.
[2]*National Research Council of Canada Postdoctorate Fellow 1955–57.*

Can. J. Chem. Downloaded from www.nrcresearchpress.com by 200.7.193.243 on 09/04/12
For personal use only.

The colorless crystalline material, which did not form a complex with urea, when obtained relatively pure gave a strong Liebermann–Burchard test, which indicated that it was a sterol or triterpene. The melting point was 135°–137°, but the optical rotation tended to vary from −12° to −24°. The latter depended on which fraction was taken in the chromatogram. The average value obtained was −18°. These constants were unchanged by many recrystallizations or by careful chromatographic separation into about 200 fractions. From this it was at first assumed that two sterols were present with rotations of −12° and −24°, but the infrared spectra of the two materials were identical and only differed slightly in the intensities of certain peaks. Subsequent work showed that the sterols were actually an inseparable mixture of β-sitostanol (stigmastanol) and β-sitosterol in various proportions. The infrared spectrum of the mixture indicated the presence of a secondary hydroxyl group from bands at 3584 and 1050 cm.$^{-1}$ and the presence of only one double bond from bands at 837 and 800 cm.$^{-1}$. This bond was of the type >C=CH—, and the spectrum bore a striking resemblance to that of the 5,6-double bond in cholesterol, which has bands at 839 and 800 cm.$^{-1}$. In confirmation of this the infrared spectrum of fucosterol, which has a 24,28-double bond besides the nuclear one, was markedly different from those of cholesterol and the sterols from peat moss. From this it was inferred that there was no double bond in the side chain of the sterols under investigation.

On catalytic hydrogenation the mixture gave pure β-sitostanol, identified by its melting point and rotation, and the melting points and rotations of the derived acetate and ketone. This indicated that the components of the mixture differed only in the degree or position of unsaturation. As already stated the infrared spectrum indicated a nuclear double bond and preliminary oxidation showed that this double bond was in a position to give an α,β-unsaturated ketone. There remained the possibility that some of the material had the double bond in the nucleus in a position other than the 5,6. The only remaining positions for a secondary–tertiary double bond in a six-membered ring are the 7,8-position and the 9,11-position. On attempted hydrogenation with platinum as a catalyst and in the presence of acetic acid, the 7,8-double bond will migrate to the 8,14-position (3), which is stable to hydrogenation, and requires treatment with hydrochloric acid before moving to the 14,15-position where it can be reduced (10). To date no natural sterol has been found with a 9,11-double bond. It is probable that under slightly acid conditions this bond would migrate to the 8,9-position, and attempted hydrogenation of sterols with this type of double bond will rearrange the double bond to the 8,14-position again (12, 13). Since the reduced material obtained from the hydrogenation was completely saturated, it seemed logical to assume from the above evidence that we were dealing with a mixture of β-sitostanol and β-sitosterol. This assumption has been proved correct by chemical evidence.

A further attempt to separate the mixture by chemical means failed. This involved treating the mixture with bromine and trying to recover the less soluble β-sitosterol dibromide by recrystallization. No pure crystalline dibromide was obtained however.

The composition was finally established by oxidation. The sterol mixture was oxidized with chromium trioxide in acetic acid solution. Under these conditions β-sitostanol (I) will be readily oxidized to β-sitostanone (III). β-Sitosterol, on the other hand, will form a variety of products arising from oxidation of the double bond (6). All these products will have two or more oxygen atoms, and will thus be more polar in character than β-sitostanone. In agreement, chromatography of the oxidation product first gave β-sitostanone (III), proved by melting point, rotation, and mixed melting point with an authentic specimen, followed by a series of non-crystalline oils.

Can. J. Chem. Downloaded from www.nrcresearchpress.com by 200.7.193.243 on 09/04/12
For personal use only.

Oxidation of the sterol mixture to give β-sitostenone (IV) alone was achieved by the Oppenauer method with aluminum isopropoxide. The yield, however, was poor and some oxidation of the β-sitostanol took place (7). To parallel the above work, the mixture of sterols was oxidized in such a manner as to give both β-sitostenone and β-sitostanone. This was achieved by brominating the mixture, oxidizing the β-sitosterol dibromide and β-sitostanol in a two-phase system with chromium trioxide (9), removing the bromine from the dibromide by means of sodium iodide (11), and chromatographing the resulting mixture. Both β-sitostenone and β-sitostanone were obtained, although the former was not quite as pure as desirable. From the infrared spectrum the contaminant appeared to be β-sitostanone, and the two ketones are known to be fairly difficult to separate by chromatography (7).

The proportions of β-sitostanol and β-sitosterol present in the steroid mixture obtained can be calculated directly from the rotations of the pure sterols and the rotation of the mixture. From these figures the percentage of β-sitostanol varied from 20% to 40%, with an average value of 30%. The oxidation experiments carried out to determine the chemical composition were not accurate enough to give physical composition since the yields varied and were never 100%.

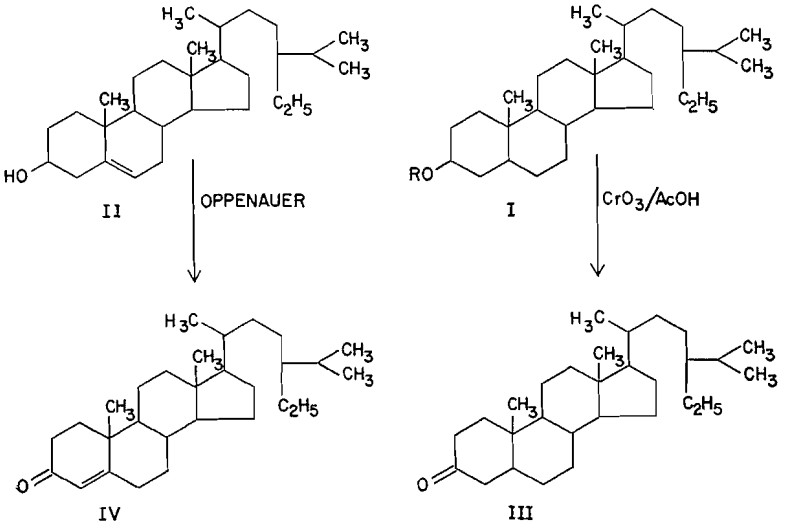

EXPERIMENTAL

All rotations were measured in a 1-dm. tube with a Rudolph polarimeter. Melting points were observed on a Kofler micro melting point apparatus and are corrected. The ultraviolet spectra were determined in ethanolic solution with a Beckman Model DU spectrophotometer. The infrared spectra were determined in carbon disulphide solution with a Baird double-beam infrared spectrophotometer model 4-55. Light petroleum refers to the fraction with boiling point 35°–60°.

Extraction of Peat Moss

The dried and ground peat moss (2.5 kg.) was loaded into a large copper percolator equipped with a pump and overflow system which permitted fresh solvent to percolate continuously through the bed. This was essentially a countercurrent extraction system. The solvent used was a mixture of benzene and ethanol (3:2, 40 liters). It was run slowly through the moss, at a rate which was controlled by a valve at the bottom of the extraction

apparatus. The extraction usually required about 12 hours. The resulting extract was concentrated to 2 liters at 50° under reduced pressure in a climbing film evaporator. Potassium hydroxide (100 g.) in methanol (500 ml.) was then added and the mixture heated under reflux for 2 hours. The mixture was diluted with water and extracted with ether, the ether extract washed and evaporated to dryness, to give the crude unsaponifiable extract. The acids were obtained by acidification of the alkali-soluble fraction followed by filtration.

Treatment of Crude Extract

The crude extract (35 g.) was dissolved in light petroleum (500 ml.). A small portion of the material which did not dissolve was removed by centrifugation for later investigation. The main bulk of the petrol solution was added to the top of a column (55×5 cm.) of alumina. The column was eluted with light petroleum (2 liters), benzene (2 liters), ether (6 liters), ether–methanol (9:1, 3 liters), and methanol (1.5 liters). The amounts of material eluted were approximately as follows: from the petrol fraction, 1 g.; benzene, 1.5 g.; ether, variable (see text, max. of 4.5 g.); ether–methanol, variable (see text, max. of 10 g.); methanol, 6–7 g.

Separation of Sterols from Crude Combined Fractions

The partly crystalline mixture (10 g.) obtained by solvent removal from the ether–methanol eluate was dissolved in light petroleum (500 ml.) and added to a mixture of urea (15 g.) made slushy with methanol. The mixture was shaken for 1 hour, and the resulting urea complex filtered off. The filtrate was again treated with a second batch of urea, but very little more material was precipitated. The petrol solution was evaporated to 250 ml., refiltered, and washed twice with distilled water to remove any remaining complex. The solution was evaporated to dryness and the product crystallized from aqueous ethanol to give a white crystalline material (4.5 g.), m.p. 135°–137°, $[\alpha]_D^{26}$ −18° (c = 1.4 in chloroform). The material complexed by the urea was recovered by treating the complex with hot water for 1 hour and extracting with benzene, washing the extract well and evaporating to dryness to give a white, waxy solid (5 g.). This was recrystallized from carbon tetrachloride, m.p. 75.5°–76.5°. It was optically inactive and a mixed melting point with lignoceryl alcohol of m.p. 74° was undepressed. Anal. Calc. for $C_{24}H_{50}O$: C, 81.27; H, 14.21; mol. wt. 354. Found: C, 81.64; H, 14.01; mol. wt. 372 (ebullioscopic in butanone), 347 (Rast). Bleyberg and Ulrich (5) report a melting point of 75.4° for lignoceryl alcohol. The alcohol was oxidized with chromic acid in acetic acid and benzene to yield an acid of melting point 81°–82°. This value is in good agreement with values reported for lignoceric acid.

Reduction of Sterols

A portion (500 mg.) of the sterol mixture obtained from the above separation was dissolved in ethyl acetate (100 ml.) and acetic acid (5 ml.). Platinum oxide (50 mg.) was added and the mixture shaken with hydrogen at a pressure of 40 p.s.i. overnight. The platinum was then filtered off and the filtrate washed free of acetic acid and evaporated to dryness. The resulting product was crystallized from aqueous ethanol to give β-sitostanol, m.p. 140°–141° (melts and resolidifies at 136°), $[\alpha]_D^{25}$ +24° (c = 1.2 in chloroform). The values recorded in the literature are m.p. 141°–142°, $[\alpha]_D$ +24° (1).

Acetylation

β-Sitostanol (100 mg.) was dissolved in pyridine (2 ml.) and acetic anhydride (3 ml.) added, and the mixture heated on the steam bath for 1 hour. The mixture was diluted with benzene, washed with dilute alkali, dilute acid, and water, and evaporated to

Can. J. Chem. Downloaded from www.nrcresearchpress.com by 200.7.193.243 on 09/04/12
For personal use only.

dryness. The product was crystallized from chloroform–methanol to give β-sitostanol acetate, m.p. 135°–136°, $[\alpha]_D^{26}$ +15° (c = 1.0 in chloroform). The values recorded in the literature are m.p. 138°–139°, $[\alpha]_D$ +15° (1).

Oxidation

β-Sitostanol (100 mg.) was dissolved in acetic acid (10 ml.), and chromium trioxide (20 mg.) in water (1 ml.) and acetic acid (10 ml.) added. The solution was allowed to stand overnight at room temperature, then diluted with water and extracted with benzene. The benzene extract was washed free of acetic acid and evaporated to dryness. The resulting crude product was dissolved in benzene and filtered through alumina. Evaporation of the solvent yielded a material which was crystallized from chloroform–methanol to give β-sitostanone, m.p. 155°–157°, $[\alpha]_D^{26}$ = +38° (c = 1.28 in chloroform). The 2,4-dinitrophenylhydrazone made in the usual manner was yellow and had m.p. 221° (dec.). For this compound Barton (2) reports m.p. 157°, $[\alpha]_D$ +38°, and the m.p. of the yellow 2,4-dinitrophenylhydrazone 223° (dec.).

Oxidation of Sterols

The sterol mixture (1 g.) was dissolved in acetic acid (15 ml.), and chromium trioxide (60 mg.) in water (1 ml.) and acetic acid (10 ml.) added. The mixture was allowed to stand at room temperature for 1 hour, then diluted with water and extracted with benzene. The benzene extract was washed well and evaporated to dryness. The crude material was chromatographed on alumina and eluted with benzene to afford β-sitostanone (50 mg.), m.p. 156°–157°, undepressed in mixed m.p. with a genuine specimen, $[\alpha]_D^{24}$ +37° (c = 1.3 in chloroform).

Oxidation of Sterols

The sterol mixture (1 g.) was dissolved in dry acetone (15 ml.), and aluminum isopropoxide (1 g.) in dry benzene (30 ml.) added. The solution was heated under reflux overnight, then diluted with water, washed twice with 2 N sulphuric acid and water, and the benzene layer evaporated to dryness. The crude oil obtained was heated on the steam bath under reduced pressure for 1 hour, then chromatographed carefully. Elution with petrol–benzene (2:1) gave a small amount of β-sitostanone (30 mg.), identified by m.p. and mixed m.p. Elution with benzene–petrol (3:1) gave β-sitostenone (120 mg.), m.p. 87°–88°, λ_{max} = 241, ϵ_{max} = 17,000. Barton and Jones (2) give m.p. 88°, λ_{max} = 240.5, ϵ_{max} = 20,000.

Oxidation of Sterols

The sterol mixture (4 g.) was dissolved in chloroform (30 ml.) and acetic acid (30 ml.). Sodium acetate (400 mg.) in acetic acid (10 ml.) was added and the solution cooled to 0°. A solution of bromine (1.5 g.) in acetic acid (10 ml.) also cooled to 0° was then added. The resulting solution was then washed with sodium thiosulphate solution to remove the excess bromine and then with water, and then evaporated to dryness. The crude material so obtained was dissolved in benzene (50 ml.) and shaken with a solution of chromium trioxide (1.5 g.) in water (15 ml.) and acetic acid (25 ml.) for 6 hours. The benzene solution was washed thoroughly to remove acetic acid and evaporated to dryness. The crude yellow oil obtained was dissolved in acetone, and sodium iodide (7 g.) in acetone (30 ml.) added. The mixture was heated under reflux for 3 hours, diluted with benzene, and washed with sodium thiosulphate solution and water, and evaporated to dryness. Chromatography of the crude oxidation product on alumina and elution with benzene gave β-sitostanone (200 mg.), identified by m.p. and mixed m.p. Elution with

Can. J. Chem. Downloaded from www.nrcresearchpress.com by 200.7.193.243 on 09/04/12
For personal use only.

benzene–ether (19:1) gave β-sitostenone (1.25 g.), m.p. 86°–87°, $[\alpha]_D^{25}$ +78° (c = 1.13 in chloroform), λ_{max} = 241, ϵ_{max} = 16,000. The value recorded in the literature for the rotation is $[\alpha]_D$ +85° (11).

REFERENCES

1. ANDERSON, R. J. and NABENHAUER, F. P. J. Am. Chem. Soc. **46**, 1953 (1924).
2. BARTON, D. H. R. and JONES, E. R. H. J. Chem. Soc. 599 (1943).
3. BARTON, D. H. R. and COX, J. D. J. Chem. Soc. 1354 (1948).
4. BLACK, W. A. P., CORNHILL, W. J., and WOODWARD, F. N. J. Appl. Chem. **5**, 484 (1955).
5. BLEYBERG, W. and ULRICH, H. Ber. **64B**, 2504 (1931).
6. FIESER, L. F. and FIESER, M. Natural products related to phenanthrene. 3rd ed. Reinhold Publishing Corporation, New York. 1949. p. 227 et seq.
7. JONES, E. R. H., WILKINSON, P. A., and KERLOGUE, R. H. J. Chem. Soc. 391 (1942).
8. KIEBLER, M. W. *In* Chemistry of coal utilization. *Edited by* H. H. Lowry. John Wiley and Sons, Inc., New York. 1945. p. 677 et seq.
9. RUZICKA, L., BRÜNGGER, H., EICHENBERGER, E., and MEYER, J. Helv. Chim. Acta, **17**, 1407 (1934).
10. SCHECK, F., BUCHHOLZ, K., and WIESE, O. Ber. **69**, 2696 (1936).
11. SCHOENHEIMER, R. J. Biol. Chem. **110**, 461 (1935).
12. WIELAND, H., RATH, F., and HESSE, H. Ann. **548**, 34 (1941).
13. WIELAND, H. and BENEND, W. Ann. **554**, 1 (1943).

Can. J. Chem. Downloaded from www.nrcresearchpress.com by 200.7.193.243 on 09/04/12
For personal use only.

Can. J. Chem. Downloaded from www.nrcresearchpress.com by 200.7.193.243 on 09/04/12
For personal use only.

ORGANIC DEUTERIUM COMPOUNDS

XIX. SYNTHESIS OF SOME DEUTERATED LAURIC ACIDS AND THEIR METHYL ESTERS[1]

M. Elaine Isabelle and L. C. Leitch

ABSTRACT

The synthesis of lauric acids deuterated in the carboxyl, the terminal methyl, and the α-methylene groups and in various combinations of these is described. The methyl and methyl-d_3 esters of each of the acids were also prepared.

Two further examples of homolytic halide addition to olefins are reported.

The reaction between alkyl halides and silver acetylides is described. A mechanism involving a new type of free radical is postulated.

In connection with studies by Jones and co-workers (9) on the infrared spectra of aliphatic fatty acids and their methyl esters it became necessary to prepare a number of deuterated lauric acids and methyl laurates. The series of compounds synthesized in this work are shown below.

$CH_3(CH_2)_{10}CO_2R$ (I) $\qquad$ $CH_3(CH_2)_9CD_2CO_2R$ (III)

$CD_3(CH_2)_{10}CO_2R$ $\qquad$ $CD_3(CH_2)_9CD_2CO_2R$

(R = H, D, CH_3, CD_3)

The compounds in the first group presented no particular problem. Lauric acid-d was obtained by decomposing lauroyl chloride with deuterium oxide. Methyl-d_3 laurate was obtained in excellent yield by heating silver laurate with methyl-d_3 bromide (14).

The synthesis of the key compound in the second series, lauric acid labelled on the terminal carbon atom of the chain, proved more difficult. Since methyl-d_3 iodide of high isotopic purity is now readily available, the preparation of the deuterolauric acid in question was attempted by the reactions shown below:

$$CD_3I + NaC{\equiv}C(CH_2)_8CO_2CH_3 \rightarrow CD_3C{\equiv}C(CH_2)_8CO_2CH_3 + NaI,$$

$$CD_3C{\equiv}C(CH_2)_8CO_2CH_3 \rightarrow CD_3(CH_2)_{10}CO_2CH_3.$$

In pilot experiments with methyl iodide, however, we were unable to methylate the sodium derivative of methyl 10-undecynoate in liquid ammonia. This observation is in agreement with that of Taylor and Strong (20), who found that the alkynes $CH_3(CH_2)_mC{\equiv}CH$ did not condense in sodamide – liquid ammonia with $I(CH_2)_nCl$ where $m < 10$ or $n < 3$. Attempts to alkylate by this method were therefore abandoned.

The reaction of deuterated alkyl iodides (and even bromides) with the silver salts of aliphatic acids is a very convenient reaction for the synthesis of deuterated esters (13) and was used above to prepare methyl-d_3 laurate. There was a possibility that silver acetylides would also react under suitable conditions, at least with methyl iodide, to give alkylacetylenes. Observations in the literature (6) relating to the inertness of silver acetylides to alkyl halides were ignored, and the silver derivative of methyl 10-undecynoate was heated to 75° C. for several hours with an excess of methyl iodide. It was an agreeable surprise to isolate methyl 10-dodecynoate although in only 40 to 50% yields. The new ester was identified by its infrared spectrum, which showed no absorption

[1]*Manuscript received August 26, 1957.*
Contribution from the Division of Pure Chemistry, National Research Council, Ottawa, Canada.
Issued as N.R.C. No. 4610.

for acetylenic hydrogen, and by the melting point of the acid; it was evidently methyl 10-dodecynoate. A similar reaction was found to take place with ethyl iodide to give methyl 10-tridecynoate. It therefore appears that silver acetylides will react with certain alkyl halides. The synthesis is particularly valuable with labelled halides owing to the ease with which unreacted halide may be recovered.*

In order to avoid using a large excess of labelled methyl iodide an experiment was next carried out in ether as a solvent. The product isolated from the reaction was not pure methyl 10-dodecynoate; its index of refraction was low, the melting point of the 10-dodecynoic acid was also low, and the ester gave a precipitate of the silver acetylide when shaken with ammoniacal silver nitrate in alcohol. The product seemed to be a mixture of methyl 10-undecynoate and 10-dodecynoate.

Several other runs were made in ether or benzene as solvent and in one case, in the absence of methyl iodide. The results of these experiments, which show the yield of ester, its index of refraction, and the melting point of the acid obtained on hydrolysis, are given in Table I.

TABLE I

INFLUENCE OF SOLVENT ON THE YIELD AND PURITY OF THE METHYL 10-DODECYNOATE

Wt. of silver derivative (g.)	Vol. of methyl iodide (ml.)	Solvent (ml.)	Yield (ml.)	n_D^{20}	M.p. of acid (°C.)
12.7	10.0	None	4.0	1.4529	51
13.7	10.0	10 ml. ether	5.4	1.4510	47
10.0	4.0	10 ml. ether	0.5	1.4500	–
6.0	5.0	10 ml. C_6H_6	1.0	1.4480	–
6.0	5.0	None	–	1.4516	50–51
6.0	None	10 ml. ether	1.0	1.4460	42–43

The formation of methyl 10-undecynoate in the presence of ether may well take place by a free radical mechanism. According to this view the silver acetylide would produce the radical $CH_3OOC(CH_2)_8C{\equiv}\dot{C}$ mentioned in reference 11, which could then give rise to the acetylenic ester by abstraction of a hydrogen atom from the solvent or from the ester itself:

$$CH_3OOC(CH_2)_8C{\equiv}CAg \rightarrow CH_3OOC(CH_2)_8C{\equiv}\dot{C} + Ag,$$

$$CH_3OOC(CH_2)_8C{\equiv}\dot{C} + C_2H_5OC_2H_5 \rightarrow CH_3OOC(CH_2)_8C{\equiv}CH + \dot{C}_2H_4OC_2H_5.$$

The following observations are submitted as evidence in favor of this mechanism. When the silver derivative of methyl 10-undecynoate was heated alone in a sealed tube, a silver mirror was formed and a small yield of methyl 10-undecynoate was obtained. Much polymeric material was found. Moreover, when the acetylide was heated in benzene-d_6, a product was isolated which had a small band in the region of the acetylenic deuterium vibration. Waters (23) is inclined to believe that silver derivatives ought to participate readily in free radical reactions because of the weak electropositive character of silver. Also, Glockling (5) has shown that the heterogeneous decomposition of iso-1-butenyl silver gives rise to iso-1-butenyl radicals, $(CH_3)_2C{=}\dot{C}H$. On the basis of all this evidence we submit that a $CH_3OOC(CH_2)_8C{\equiv}\dot{C}$ radical is involved in the present reactions and that the formation of methyl 10-undecynoate in the presence of ether takes place by abstraction of hydrogen from the solvent or from the ester itself.

**After this work was completed Davis and Schreiber (3) reported the synthesis of acetylenic ketones by reaction of the silver derivatives of 1-hexyne and 1-octyne with acid chlorides in* CCl_4.

Can. J. Chem. Downloaded from www.nrcresearchpress.com by 200.7.193.243 on 09/04/12
For personal use only.

Regarding the alkylation of the silver acetylide by methyl and ethyl iodides, one is tempted to invoke a free radical mechanism and represent the reaction by the steps shown below:

$$CH_3OOC(CH_2)_8C{\equiv}CAg \rightarrow CH_3OOC(CH_2)_8C{\equiv}\dot{C} + Ag,$$

$$CH_3I + Ag \rightarrow \dot{C}H_3 + AgI,$$

$$CH_3 + CH_3OOC(CH_2)_8C{\equiv}\dot{C} \rightarrow CH_3OOC(CH_2)_8C{\equiv}CCH_3.$$

However, the formation of methane by abstraction of hydrogen from the solvent or of ethane by dimerization, which are normal reactions of free radicals, has not been observed in these experiments.

In view of the comparative stability of the ions $R.C{\equiv}C^-$, it is possible that the alkylation takes place by a "push-pull" mechanism via the transition state shown below:

$$R.C{\equiv}C^- + CH_3I \xrightarrow{Ag^+} R.C{\equiv}C\text{- -}CH_3\text{- -}I \rightarrow R.C{\equiv}CCH_3 + AgI.$$

With methyl-d_3 iodide, methyl 10-dodecynoate deuterated on the terminal carbon atom of the chain was obtained. Reduction in an alkaline medium by the method of Schwenk *et al.* (19) gave lauric-12-d_3 acid from which methyl laurate-12-d_3 was obtained on esterification. There was no evidence of α-deuteration as judged from the infrared spectra of the acid or ester.

Lauric-12-d_3 acid was also synthesized by an alternative method. Jensen, Kharasch, and Urry have reported the peroxide induced addition of polyhalogenomethanes to olefins (7). It has now been found that addition of chloroform to methyl undecylenate gives a mediocre yield of methyl 12-trichlorolaurate. Dechlorination of the ester by means of zinc and acetic acid-*d* gave an 80% yield of methyl laurate-12-d_3. Deuterium oxide – dioxane mixtures can also be employed for the dehalogenation, and thus the necessity of preparing acetic acid-*d* can be avoided. Infrared spectra gave no evidence of α-deuteration in the acid or ester. The other members of this series of deuterated lauric acids were prepared by methods already described for lauric acid itself (7).

The third series of compounds involved the preparation of lauric acid deuterated on the α-methylene group. Interest was focused first on α-dibromolauric acid as a starting material. Textbooks on organic chemistry often make the general statement that further bromination of an α-bromo acid chloride by the Hell-Volhard method leads to the α-dibromo acid chloride. However, there are few references to these acids or their derivatives in the literature to substantiate this statement. α,α-Dibromoheptanoic acid has been reported but it was prepared from *n*-heptaldehyde diacetal (2), not from the acid. α,α-Dibromobutyric acid was supposedly formed when α-bromobutyric acid was heated with excess bromine in a sealed tube (15). Bromination of lauric acid beyond the α''-bromo stage in sealed tubes was completely unsuccessful in our hands in that inseparable mixtures of polybromobutyric acids seemed to be formed.

The required methyl ester was synthesized by making use of another peroxide induced addition to olefins. Methyl dichloroacetate was found to add readily to 1-decene to give a mediocre yield of methyl 2,2-dichlorolaurate. Dechlorination with deuterium oxide in dioxane and zinc dust gave an excellent yield of methyl laurate-2,2-d_2 (III; R=CH_3). The other members of this series were obtained as already described for the normal acid.

The final series of deuterated lauric acids and their esters (IV) were prepared from methyl laurate-12-d_3 by the following route:

Can. J. Chem. Downloaded from www.nrcresearchpress.com by 200.7.193.243 on 09/04/12
For personal use only.

$$(CO_2C_2H_5)_2 + CD_3(CH_2)_{10}CO_2CH_3 \xrightarrow{C_2H_5OK} CD_3(CH_2)_9CH(CO_2CH_3)_2$$

$$CD_3(CH_2)_9CH(CO_2CH_3)_2 \xrightarrow{^-OD} CD_3(CH_2)_9CD(CO_2D)_2$$

$$CD_3(CH_2)_9CD(CO_2D)_2 \longrightarrow CD_3(CH_2)_9CD_2CO_2D + CO_2.$$

The reactions were first carried out with the normal ester. The Claisen condensation with methyl laurate to *n*-decyl malonic ester took place readily and the yields from there on were nearly quantitative (17, 18). Similar syntheses were then carried out with the terminally labelled ester; thus lauric acid labelled on both the α-methylene and the terminal carbon atom of the chain was obtained.

An interesting observation relative to the 1420 cm.$^{-1}$ band of fatty acids in the infrared came to light on comparison of the spectra of the acids in carbon tetrachloride solution. Jones (8) has attributed the 1420 cm.$^{-1}$ band to the scissoring vibrations of the α-methylene group in $R.CH_2CO_2CH_3$. When the spectrum of α-deuterated lauric acid was examined it still showed a band of medium intensity at 1417 cm.$^{-1}$. It seemed most unlikely that deuterium would have been lost by exchange in the α-position during hydrolysis of the ester. The band was also present but of reduced intensity in the acid after exchange with deuterium oxide. However, it was entirely absent from the spectrum of the α-deuterated acid chloride. It was likewise absent from the spectrum of methyl 2,2-dichlorolaurate and 2,2-dichlorolauroyl chloride. It was present, however, in the spectrum of lauroyl chloride and lauronitrile. The absorption in the 1420 cm.$^{-1}$ region is therefore not due solely to the α-methylene but also to the hydroxyl group. The spectrum of lauric acids labelled in the methyl group showed no absorption in the 1380 cm.$^{-1}$ region. Quantitative studies on the spectra of these acids by Jones and co-workers now in progress will be reported by them in detail elsewhere.

EXPERIMENTAL

Lauroyl Chloride

Lauric acid (1.0 g.) was warmed on the steam bath with 1 ml. of thionyl chloride (purified by distillation over quinoline and linseed oil). After 4 hours' heating, excess thionyl chloride and hydrogen chloride were pumped off. The residue was then twice distilled on the vacuum line in a Späth bulb. Yields: 0.8 ml., n_D^{20} 1.4455. Its infrared spectrum showed no absorption in the 3000–3600 cm.$^{-1}$ region and the band at 1407 cm.$^{-1}$ was reduced to one-half of its intensity in the spectrum of lauric acid where it appears at 1417 cm.$^{-1}$.

Lauric Acid-d

Lauroyl chloride was warmed on the steam bath for 1 hour with 2.0 ml. of deuterium oxide. After hydrolysis the lauric acid-*d* was extracted with pentane. After one recrystallization from pentane, 0.8 g. of acid was obtained. Since the acid still showed some absorption in the 3000–3400 cm.$^{-1}$ region in the infrared, it was exchanged by being heated with 10 ml. of deuterium oxide on the steam bath overnight. The equilibrated product was worked up as already described. There was little if any change in its spectrum by this treatment. The intensity of the band at 1417 cm.$^{-1}$ was the same as that in lauroyl chloride; part of it was masked by the absorption in the 1325–1410 cm.$^{-1}$ region. There was slight absorption in the 3000–3600 cm.$^{-1}$ region due to the presence of residual OH.

Methyl-d_3 Laurate, $CH_3(CH_2)_{10}CO_2CD_3$

Silver laurate was prepared as described in reference 12 by adding at the same rate

Can. J. Chem. Downloaded from www.nrcresearchpress.com by 200.7.193.243 on 09/04/12
For personal use only.

equivalent amounts of aqueous silver nitrate and potassium laurate to hot water, with stirring. The precipitate was filtered off, washed with water, and then acetone, and dried under vacuum in the dark.

Six grams of thoroughly dry silver laurate was placed in a tube (2 cm.×15 cm.) fitted with a ground glass joint. After the tube was constricted to facilitate sealing later, 15 ml. of anhydrous ether and 1.85 g. of methyl-d_3 bromide (13) were distilled into the tube, which was then frozen in liquid nitrogen, evacuated, and sealed. The reactants were heated to 85° C. in a rocking furnace for 20 hours.

Silver iodide was filtered off and washed with anhydrous ether. The residue, after removal of the ether, was distilled in a Späth bulb placed in an air furnace at 100° C. The yield of methyl-d_3 laurate was 3.5 g. (85.7%). It was a colorless liquid melting at + 10° C., n_D^{20} 1.4329.

For ordinary methyl laurate prepared in the same manner n_D^{20} was 1.4329.

Methyl 10-Undecynoate, $HC{\equiv}C(CH_2)_8CO_2CH_3$

10-Undecynoic acid was prepared as described in reference 10. Thirty grams of the acid were esterified with methanol and a trace of sulphuric acid under reflux for 4 hours. The ester had b.p. 69–71° at 1 mm., n_D^{20} 1.4465. Yield: 32 g.

Methyl 10-Dodecynoate, $CH_3C{\equiv}C(CH_2)_8CO_2CH_3$

The silver derivative of methyl 10-undecynoate was prepared by shaking overnight 10.0 g. of the ester with 170 ml. of ammoniacal silver nitrate solution (prepared by dissolving 8.5 g. of the salt in 100 ml. of water and adding ammonium hydroxide until the precipitate of silver oxide initially formed had just dissolved). Yield: 13.2 g. of product, m.p. 76–78° C. Calc. for $C_{12}H_{19}O_2Ag$, % Ag 35.6. Found: 35.2%.

The silver derivative (12.7 g.) was heated at 75° C. in a sealed tube overnight with 10.0 ml. of methyl iodide. The solids were filtered off in a gravity funnel and washed with ether. The residue, after removal of the ether by distillation, was distilled under vacuum from a Späth bulb in an air furnace at 85° C. Yield of product n_D^{20} 1.4529 was 4.0 ml. (45% of the theoretical).

10-Undecynoic Acid, $CH_3C{\equiv}C(CH_2)_8COOH$

The methyl ester was hydrolyzed by being heated on the steam bath for a few minutes with a slight excess of alkali in 50% ethanol–water. The solution was diluted with water and acidified at 0° C. with dilute hydrochloric acid. After one recrystallization from petroleum ether the acid melted at 51° C. Neutralization equivalent, calc. for $C_{12}H_{20}O_2$: 196; found: 198.

Methyl 10-Tridecynoate, $C_2H_5C{\equiv}C(CH_2)_8CO_2CH_3$

Eight grams of the silver derivative of methyl 10-undecynoate was heated with 4.0 ml. of ethyl iodide in a sealed tube overnight at 80° C. The reaction product was worked up and purified as described for the lower homologue. Yield: 1.2 g., n_D^{20} 1.4504.

Methyl 10-Decynoate-12-d_3, $CD_3C{\equiv}C(CH_2)_8CO_2CH_3$

The silver derivative of methyl 10-undecynoate was heated in a sealed tube with 6.7 ml. of methyl-d_3 iodide (13) overnight at 65° C. The product was isolated and purified as already described. Yield: 1.8 g. (50% of the theoretical) of ester, n_D^{20} 1.4514.

Methyl 12-Trichlorolaurate, $CCl_3(CH_2)_{10}CO_2CH_3$

A solution of 45 ml. of methyl 10-undecylenate in 75 ml. of chloroform containing 0.5 g. of dissolved dibenzoyl peroxide was heated in a pressure bottle for 4 hours at

Can. J. Chem. Downloaded from www.nrcresearchpress.com by 200.7.193.243 on 09/04/12
For personal use only.

110° C. in an oven; a further 0.5 g. of peroxide was added at the end of this time and heating was resumed overnight or for another 12 to 15 hours. The bulk of the chloroform was removed on the steam bath and the residue was distilled in a Vigreux column under reduced pressure (0.5 mm.). After collection of the unchanged methyl undecenoate at 65° C. the boiling point rose rapidly to 128–130° C. at 0.5 mm. and the trichloroester began to distill. Yield: 12.0 ml., n_D^{20} 1.4695.

Methyl Laurate-12-d_3, $CD_3(CH_2)_{10}CO_2CH_3$

(*a*) *By reduction of 10-dodecynoic acid with Raney nickel.*—10-Dodecynoic acid (1.0 g.) was dissolved in 200 ml. of 2% sodium hydroxide in water, and Raney nickel alloy (10.0 g.) was added in small portions over a period of 1 hour while the mixture was being heated on the steam bath. The hot solution was then filtered and the filtrate was acidified with dilute hydrochloric acid. The melting point of the acid which was filtered off was 42–43° C. The acid was converted into the methyl ester by heating the silver salt with methyl bromide as described above.

(*b*) *By zinc dust – deuterium oxide dechlorination.*—To a suspension of 14.0 g. zinc dust (50% excess) in 150 ml. of anhydrous dioxane containing 30 ml. of deuterium oxide was added dropwise, with stirring, 15 g. of methyl trichlorolaurate. The reaction mixture was stirred overnight at 90° C. and under reflux for 4 hours. The reaction mixture was filtered and freed of dioxane by distillation under reduced pressure. The residue was taken up in ether and filtered from suspended solids. The filtrate was freed of ether and distilled in a Späth bulb yielding 8.2 g. (80.3% yield) of methyl laurate-12-d_3, n_D^{20} 1.4332.

The trichloro ester can also be dehalogenated with acetic acid-*d* and zinc dust with slightly higher yield but at the expense of preparing acetic acid-*d*.

Lauric-12-d_3 Acid, $CD_3(CH_2)_{10}COOH$

The acid was obtained by hydrolysis of the ester in nearly quantitative yield. Its infrared spectrum did not show the presence of a band for the CH_3 group at 1383 cm.$^{-1}$.

Lauric-12-d_3 Acid-d, $CD_3(CH_2)_{10}CO_2D$

This acid was prepared from the previous acid through the acid chloride.

Methyl-d_3 Laurate-12-d_3, $CD_3(CH_2)_{10}CO_2CD_3$

Silver laurate-12-d_3 prepared as described for the normal acid was heated with excess methyl-d_3 bromide in a sealed tube and the product was isolated as described in the case of methyl-d_3 laurate. The yield of distilled product, n_D^{20} 1.4337, was 92%.

Bromination of Lauric Acid

Attempts to brominate lauric acid under reflux in the presence of small amounts of phosphorus trichloride always resulted in the formation of α-bromolauric acid. No evidence of the presence of α-dibromolauric acid was ever found.

Brominations carried out at 140° C. in sealed tubes as described by Otto (15) likewise were unsatisfactory. Vast quantities of hydrogen bromide were evolved when the tubes were opened but the product boiled over a wide temperature range. Mixtures of dibrominated lauric acids were probably formed under these conditions. It is apparently not possible to introduce two bromine atoms in the α-position by this means.

Methyl 2,2-Dichlorolaurate, $CH_3(CH_2)_9CCl_2CO_2CH_3$

1-Decene (115 ml.), methyl dichloroacetate (177 g.), and 4.0 g. of dibenzoyl peroxide were heated for 15 hours on the steam bath. Unreacted decene and dichloroacetate ester were distilled off under 50 mm. pressure. After collection of a fraction (7.5 ml.) between

Can. J. Chem. Downloaded from www.nrcresearchpress.com by 200.7.193.243 on 09/04/12
For personal use only.

86° and 90° C. at 0.1 mm., methyl dichlorolaurate distilled over between 92° and 94° C. at 0.1 mm., n_D^{20} 1.4594, n_D^{23} 1.4584. The yield was only 28–30% but is offset by the ease of preparation of the ester.

Methyl Laurate-2,2-d_2, $CH_3(CH_2)_9CD_2CO_2CH_3$

Acetic acid-*d* was prepared as already described from acetyl chloride and deuterium oxide (16). To the acetic acid-*d* obtained from 26 ml. of acetyl chloride was added 6 g. of zinc dust and 5 ml. of methyl 2,2-dichlorolaurate. After the mixture had been stirred at room temperature overnight the zinc had nearly all turned white. The reaction mixture was poured into ice-water and extracted with 40 ml. of pentane. The residue, after removal of the pentane by distillation, was distilled in a Späth bulb. Yield: 3–6 g. of product, n_D^{22} 1.4342.

Reduction with deuterium oxide instead of acetic acid-*d* resulted in an impure product which showed unsaturation.

Lauric-2,2-d_2 Acid, $CH_3(CH_2)_9CD_2COOH$

The ester was hydrolyzed, isolated, and purified as described for lauric-12-d_3 acid. The yield was 2.9 g.

Lauric-2,2-d_2 Acid-d

This acid was prepared from lauric-2,2-d_2 acid via the chloride.

2,2-Dichlorolauroyl Chloride, $CH_3(CH_2)_9CCl_2COCl$

Dichloroacetyl chloride was prepared as described by Brown (1). The acid chloride (180 g.), decene-1 (53 ml.), and dibenzoyl peroxide (2.0 g.) were heated on the steam bath overnight. The reaction mixture was fractionated in a short Vigreux column under 0.06 mm. pressure. Unreacted decene and dichloroacetyl chloride were collected up to 80° C. 2,2-Dichlorolauroyl chloride then distilled at 82–83° C. Yield: 6.0 ml., n_D^{20} 1.4629.

The amide was prepared by treating a sample of the chloride with ammonia and dilute ethanol. After one recrystallization from ethanol the amide melted at 62–64° C.

2,2-Dichlorolauric Acid, $CH_3(CH_2)_9CCl_2COOH$

A mixture of 1 ml. of 2,2-dichlorolauroyl chloride and 5 ml. of water was stirred overnight at room temperature and extracted with ether. The ether solution was dried over anhydrous sodium sulphate and distilled. The residue which remained was distilled in a Späth bulb. The distillate was a colorless liquid with an odor of lauric acid. Its neutralization equivalent was somewhat low.

Methyl-d_3 Laurate-2,2-d_2, $CH_3(CH_2)_9CD_2CO_2CD_3$

The silver salt was prepared as has already been described for ordinary lauric acid and lauric-12-d_3 acid. Methyl-d_3 laurate-2,2-d_2 was prepared from the silver salt and methyl-d_3 bromide as described above.

Diethyl n-Decylmalonate, $CH_3(CH_2)_9CH(CO_2C_2H_5)_2$

"Molecular" potassium (2.0 g.) was prepared in xylene dried over sodium (21), and washed three times by decantation with absolute ether. It was then covered with 40 ml. of absolute ether and anhydrous ethanol (2.8 ml., dried by distillation over magnesium ribbon) was added. The reaction mixture was heated for 4 hours under reflux. Diethyl oxalate (9.4 ml.) and methyl laurate (9.2 ml.) were added to the ice-cold suspension of potassium ethoxide in ether. After 25 hours' stirring the reaction mixture was poured into ice-water containing a little hydrochloric acid. The ether was separated, washed

Can. J. Chem. Downloaded from www.nrcresearchpress.com by 200.7.193.243 on 09/04/12
For personal use only.

three times with water, and dried over anhydrous sodium sulphate. The ether was removed at the ordinary pressure and the residue decarboxylated by heating under vacuum at 150° C. until no further evolution of gas took place. The product began to reflux as the pressure fell to 0.5 mm. The yield of product, n_D^{20} 1.4364, b.p. 120–124° C., was 9.0 ml.

Floyd and Miller (4) report b.p. 155–158° C. at 3 mm. and n_D^{25} 1.4353 for *n*-decylmalonic ester.

n-Decylmalonic-2-d Acid-d_2, $CH_3(CH_2)_9CD(CO_2D)_2$

Sodium deuteroxide was prepared by adding 7.0 g. of clean sodium in small portions to 50 ml. of deuterium oxide stirred under an atmosphere of dry nitrogen. *n*-Decylmalonic ester was then added and the reaction mixture was stirred overnight just below the boiling point. The solution was acidified by addition of deuterium sulphate until strongly acid, and extracted with ether. On evaporation of the ether, 6.1 g. of white solid melting at 111–113° C. was obtained. According to Wallingford (22) *n*-decylmalonic acid melts at 118–119°. Recrystallization of the acid from chloroform raised its melting point to 116° C. The deuterated acid could be expected to melt at a lower temperature than the normal one (24).

Heating above its melting point converted the *n*-decylmalonic-d_2 acid-d_2 into lauric-2,2-d_2 acid-*d*.

Diethyl n-Decylmalonate-10-d_3, $CD_3(CH_2)_9CH(CO_2C_2H_5)_2$

A Claisen condensation between diethyl oxalate and methyl laurate-12-d_3 was carried out exactly as just described. From 9.3 g. of laurate ester there was obtained 9.3 ml. of malonic ester, n_D^{20} 1.4373. Hydrolysis gave 6.1 g. of acid, m.p. 111–113° C.

Lauric-2,2,12,12,12-d_5 Acid-d, $CD_3(CH_2)_9CD_2CO_2D$

This acid was obtained by decarboxylating the corresponding malonic acid in a glycerine bath at 140° C.

Methyl Laurate-2,2,12,12,12-d_5, $CD_3(CH_2)_9CD_2CO_2CH_3$

Silver laurate-2-2,12,12,12-d_5 was prepared as already described for the normal acid. It was converted into the ester by heating with methyl iodide, also as described above.

Methyl-d_3 Laurate-2,2,12,12,12-d_5, $CD_3(CH_2)_9CD_2CO_2CD_3$

This ester was prepared by the methods described above.

ACKNOWLEDGMENTS

The authors wish to thank Dr. R. N. Jones for helpful discussions and Mr. R. Lauzon for the infrared spectra of several compounds.

REFERENCES

1. Brown, H. C. J. Am. Chem. Soc. **60**, 1325 (1938).
2. Chancel, P. Bull. soc. chim. (France), 714 (1950).
3. Davis, R. B. and Schreiber, D. H. J. Am. Chem. Soc. **78**, 1675 (1956).
4. Floyd, D. E. and Miller, S. E. J. Am. Chem. Soc. **69**, 2354 (1947).
5. Glockling, F. J. Chem. Soc. 3640 (1956).
6. Jacobs, T. L. Organic reactions. Vol. V. John Wiley & Sons, Inc., New York. 1949. p. 45.
7. Jensen, E. V., Kharasch, M. S., and Urry, W. H. J. Am. Chem. Soc. **69**, 1100 (1947).
8. Jones, R. N. and Sandorfy, C. Chemical applications of spectroscopy. *Edited by* W. West. Interscience Publishers, Inc., New York. 1956. Chap. IV, p. 505.
9. Jones, R. N. To be published.
10. Khan, N. A. Organic syntheses. Vol. 32. John Wiley & Sons, Inc., New York. 1952. p. 104.

Can. J. Chem. Downloaded from www.nrcresearchpress.com by 200.7.193.243 on 09/04/12
For personal use only.

11. LEITCH, L. C. N.R.C. Review, p. 66 (1954).
12. LÜTRINGHAUS, A. and SCHADE, D. Ber. **74**, 1566 (1941).
13. NOLIN, B. Can. J. Chem. **32**, 1 (1954).
14. NOLIN, B. and LEITCH, L. C. Can. J. Chem. **31**, 153 (1953).
15. OTTO, R. Ann. **239**, 275 (1887).
16. RENAUD, R. and LEITCH, L. C. Can. J. Chem. **34**, 98 (1956).
17. ROBINSON, G. M. J. Chem. Soc. **125**, 230 (1929).
18. RUTHERFORD, K. G. and NEWMAN, M. S. J. Am. Chem. Soc. **79**, 213 (1957).
19. SCHWENK, E., PAPA, D., WHITMAN, B., and GINSBERG, H. F. J. Org. Chem. **9**, 175 (1944).
20. TAYLOR, W. R. and STRONG, F. M. J. Am. Chem. Soc. **72**, 4263 (1950).
21. VOGEL, A. Practical organic chemistry. 3rd ed. Longmans, Green & Co. Inc., New York. 1956. Chap. II, Sect. 50, p. 193.
22. WALLINGFORD, V. H., HOMEYER, A. H., and JONES, D. M. J. Am. Chem. Soc. **63**, 2056 (1941).
23. WATERS, W. A. Chemistry of free radicals in solution. Oxford University Press, London. 1948. p. 210.
24. WILSON, C. L. J. Chem. Soc. 492 (1935).

Can. J. Chem. Downloaded from www.nrcresearchpress.com by 200.7.193.243 on 09/04/12
For personal use only.

Can. J. Chem. Downloaded from www.nrcresearchpress.com by 200.7.193.243 on 09/04/12
For personal use only.

ELECTROLYTIC CONDUCTANCE IN HYDROGEN PEROXIDE – WATER MIXTURES

PART I. THE ALKALI CHLORIDES[1]

D. K. THOMAS[2] AND O. MAASS

ABSTRACT

The equivalent conductance of a series of alkali chlorides has been measured in water – hydrogen peroxide mixtures over the whole range of solvent composition. The measurements were made by a simple direct-current method, and the results obtained are interpreted in terms of the viscosity of the solvent.

INTRODUCTION

The close similarity in the values of certain of the physical constants for water and hydrogen peroxide has been appreciated for some time, and in some instances extensive studies of their variation in mixtures of the two compounds has been carried out (1, 2, 3, 4). In all cases these similarities have received adequate explanation in terms of the possession by both molecules of structures adapted to strong hydrogen bonding.

Mixtures of hydrogen peroxide and water have been found to display non-ideality in that

(*a*) there is a volume change on mixing (3),

(*b*) there is a finite heat of mixing (4),

(*c*) the vapor pressures of the solutions do not obey Raoult's law (5).

The direction of these departures from ideality is interpreted as indicating an enhancement of either the number or the force of the attractions between molecules upon forming the solutions.

One of the least-studied aspects of the hydrogen peroxide – water system has been that of its behavior as an ionizing medium, this possibly being due to the difficulty, until fairly recently, of obtaining concentrated hydrogen peroxide of a high degree of purity. Recently, measurements (6, 7) of the conductivities of a few acids and salts in solvents of compositions ranging from 100% water to 100% hydrogen peroxide have been made. In all cases it appears that addition of hydrogen peroxide to water brings about a marked reduction in the electrical conductance, and furthermore, a point is reached at which the conductance of an acid is lower than that of its potassium salt (7). No completely adequate explanation has been forthcoming to account for these results.

In the present work an attempt has been made to carry out a comprehensive study of the alkali chloride series in solvents of composition varying from 100% water to 98% hydrogen peroxide, with the object of

(*a*) seeing whether the conductance trends displayed in aqueous solution are maintained,

(*b*) attempting to account for the variation in conductance with solvent composition.

EXPERIMENTAL

The use of hydrogen peroxide as a solvent for conductivity work is beset with one major difficulty, namely its tendency to decompose at room temperature in the presence of only minute quantities of impurity. Even in the apparent absence of any catalyst sufficient

[1]*Manuscript received October 23, 1957.*
Contribution from the Division of Pure Chemistry, National Research Council, Ottawa, Canada.
Issued as N.R.C. No. 4614.
[2]*N.R.C. Postdoctorate Fellow 1956–57.*

decomposition may occur to render a conductance measurement extremely inaccurate.

All the results subsequently quoted were obtained by the use of a very simple direct-current method, in which the potential difference between two points in the solution, as measured by a pair of probe electrodes, was balanced against that across a standard resistance placed in series with the conductivity cell. This method is identical in principle to that used for the measurement of the conductance of aqueous solutions of alkali halides by Brönsted and Nielsen (8), Gunning and Gordon (9), and more recently by Ives and Swaroopa (10), and Lim (11). In the hands of these workers this direct-current method has been shown to give results closely similar to those obtained on the same systems by the use of the alternating-current method. In fact, Gunning and Gordon found that in dilute solution the results obtained from the two methods agreed to within the apparent precision of either set of measurements.

The conductivity cells used were of Pyrex glass construction, the probe electrodes and the current-carrying electrodes being molded from pure tin. All solutions were made by weight from the pure constituents and, because of their inherent instability, were used immediately. The cell constants were determined using aqueous potassium chloride solutions of concentrations 0.01 N, 0.05 N, and 0.10 N.

A typical set of values was as follows:

(a) $c = 0.01$, $K = 361.0$;
(b) $c = 0.05$, $K = 361.4$;
(c) $c = 0.10$, $K = 361.1$.

The cells were immersed in a thermostat controlled to $\pm 0.01°$ C. during all observations, and balance between the solution and the standard resistance was obtained by varying the latter until identical readings were obtained on a Keighley model 210 electrometer.

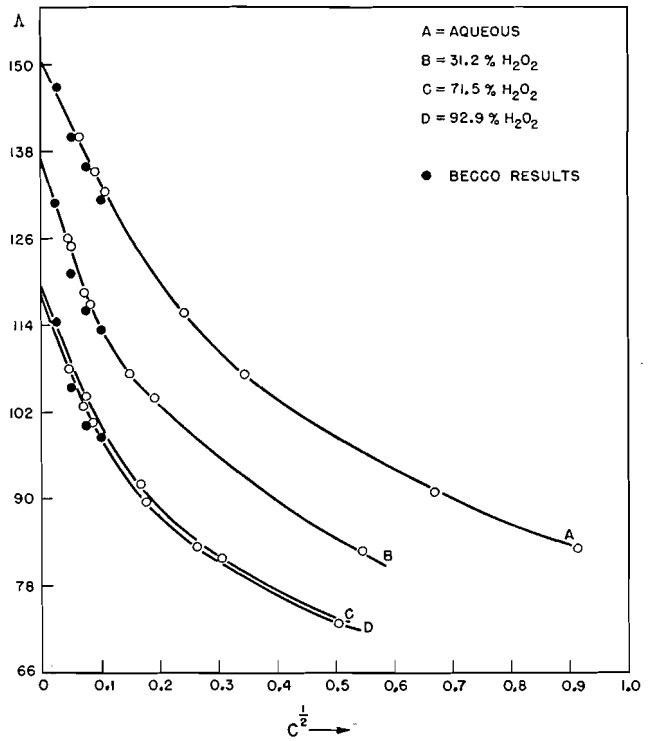

FIG. 1.

Can. J. Chem. Downloaded from www.nrcresearchpress.com by 200.7.193.243 on 09/04/12
For personal use only.

Before proceeding with the main series of measurements a study was made of the system K_2SO_4–H_2O_2–H_2O in order that a comparison could be made between the precision of the a-c. method as used by Shanley *et al.* (6, 7) and the d-c. method used in these investigations. As will be seen from Fig. 1, both methods lead to essentially the same result over the whole range of solvent composition. At the lower concentrations a solvent correction of the form $K_{\text{solute}} = K_{\text{solution}} + K_{\text{solvent}}$, where K signifies specific conductance, was applied.

It was found that the reproducibility in all the solvents used was always as good as 1%.

MATERIALS

(*i*) *Alkali Chlorides*

The alkali chlorides, i.e. those of lithium, sodium, potassium, rubidium, and cesium, were all high-grade analytical reagents, each containing only trace quantities of other alkali metals. They were dried by prolonged heating at 120° C. and stored in a desiccator until required.

(*ii*) *Hydrogen Peroxide*

Becco Chemicals 98% hydrogen peroxide was used throughout. Solvents of lower peroxide concentration were made by dilution of the concentrated material with water of specific conductance 1.5×10^{-6} mhos, and were standardized volumetrically with potassium permanganate.

(*iii*) *Tin*

The probe electrodes and current-carrying electrodes were made from pure tin, the maximum limits of impurity being as follows: As, 0.0003%; Cu, 0.002%; Te, 0.005%; Pb, 0.010%.

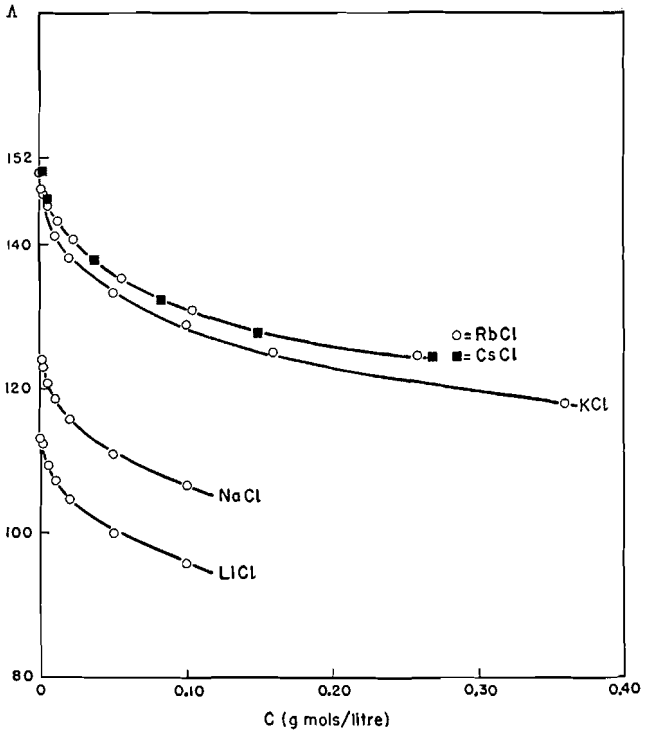

FIG. 2.

Can. J. Chem. Downloaded from www.nrcresearchpress.com by 200.7.193.243 on 09/04/12
For personal use only.

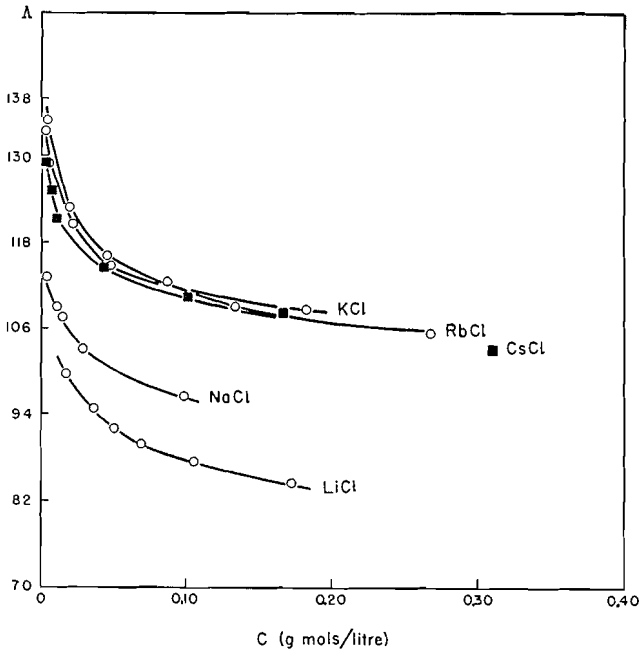

FIG. 3.

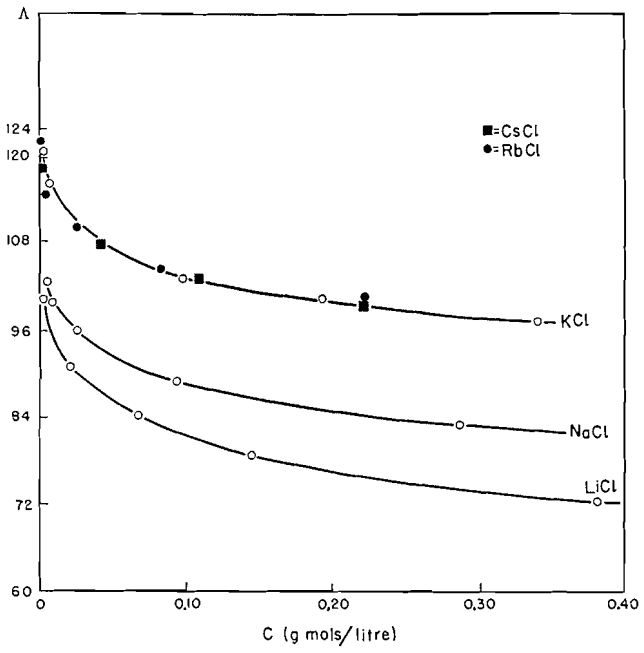

FIG. 4.

Can. J. Chem. Downloaded from www.nrcresearchpress.com by 200.7.193.243 on 09/04/12
For personal use only.

Can. J. Chem. Downloaded from www.nrcresearchpress.com by 200.7.193.243 on 09/04/12
For personal use only.

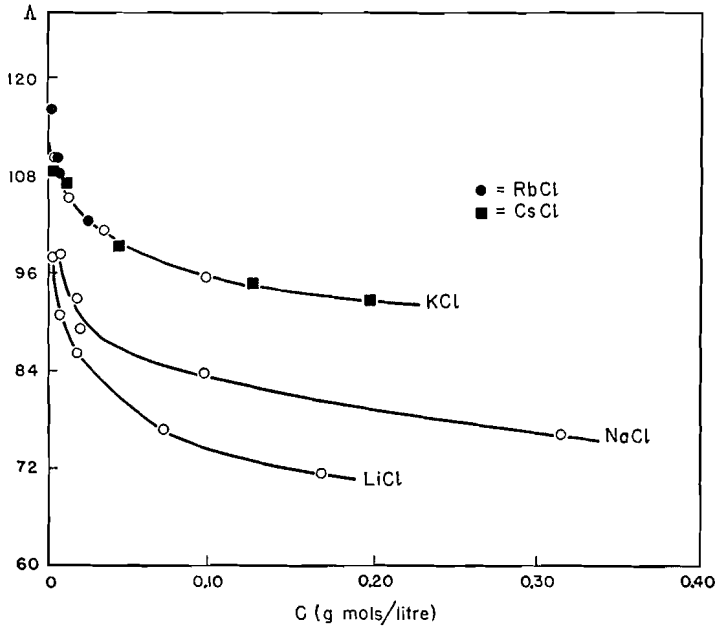

FIG. 5.

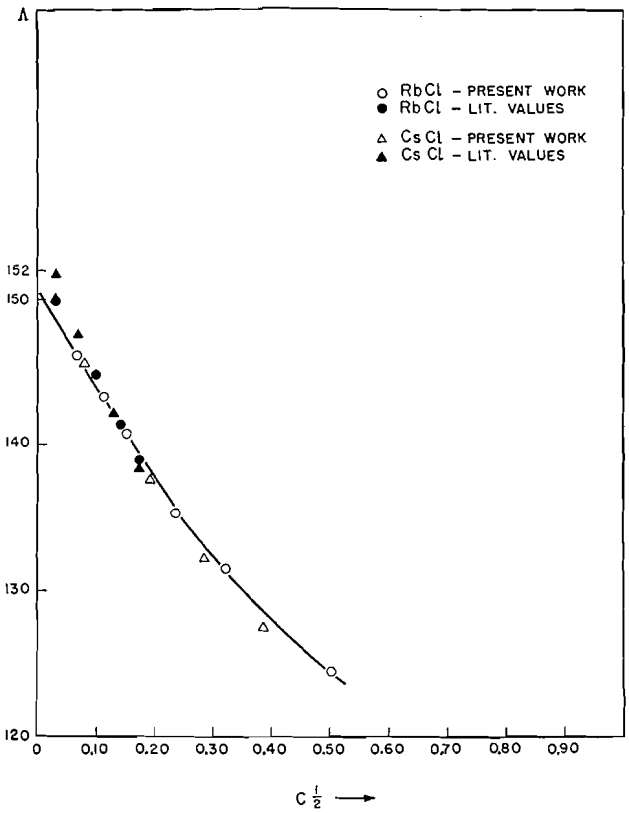

FIG. 6.

Can. J. Chem. Downloaded from www.nrcresearchpress.com by 200.7.193.243 on 09/04/12
For personal use only.

RESULTS

The results obtained are presented graphically in Figs. 2–6. Except in the cases of rubidium and cesium chloride the data for aqueous solution were obtained from the literature; for these two the only available data were those due to Boltwood (12) and Bredig (13). Since these showed the curves for equivalent conductance against concentration to cross at $C^{1/2} = 0.125$ it was felt that confirmation of these results would be in order. The measurements made did, in fact, substantiate these early observations, but deviated from them slightly at low concentration to give a value of Λ_0 different by 0.5% (see Fig. 6).

In all cases a solvent correction was applied at the lowest concentrations.

DISCUSSION

Reference to the results shows that the addition of hydrogen peroxide to the system alkali chloride – hydrogen peroxide – water leads to a reduction in the equivalent conductance of the solution. This is in accord with previous observations (6, 7). The greatest changes are effected by adding H_2O_2 to solutions containing a high percentage of water, and, in fact, once the H_2O_2 concentration exceeds about 75% by weight, further addition leads to only very small changes in conductance. A curve showing the variation of equivalent conductance with the percentage of H_2O_2 for KCl solutions is reproduced in Fig. 7, and this displays a behavior typical of all the alkali chlorides.

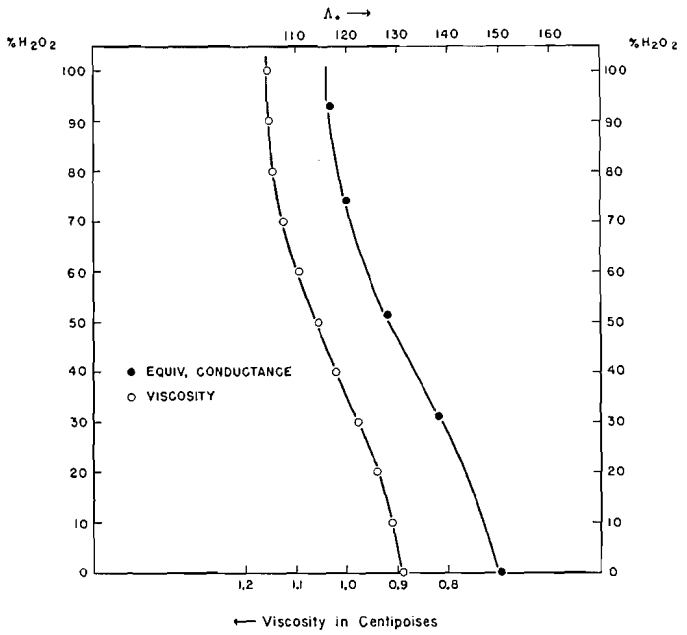

FIG. 7.

It will be seen that the sequence of conductivity values is the same as that in aqueous solution insofar as lithium chloride has the lowest value and sodium chloride the next lowest. The chlorides of potassium, rubidium, and cesium lie rather close to each other in aqueous solution, and addition of hydrogen peroxide appears to bring them even closer together until eventually, as in 98% peroxide, they are indistinguishable.

There seems little doubt that, in hydrogen peroxide as in water, the ions are solvated and that in concentrated hydrogen peroxide the relative degrees of solvation for the cations are Li > Na > K $\simeq$ Rb $\simeq$ Cs. At what particular stage the hydrogen peroxide begins to replace the water in the solvation sheath remains a matter for conjecture, but there seems good reason to suppose that, in view of its much higher dipole moment (14), there would be a tendency for this to occur. This view is supported by the work of Gorin (15), who observed a 'salting-in' of hydrogen peroxide in a number of aqueous solutions of electrolytes. Further reference to Fig. 7 shows the similarity in the variations of equivalent conductance, and of viscosity, with the percentage by weight of hydrogen peroxide in the solvent. This suggests that viscosity change is responsible for the conductance change. If that is the case, and assuming the applicability of Stokes' law to the solvated ions, the product $\Lambda_0\eta$ should be a constant. That this is indeed so may be seen by reference to Table I. The viscosity data in Table I are those of Shanley *et al.* (16).

TABLE I

Wt.% H_2O_2	Viscosity in centipoises	LiCl		NaCl		KCl		RbCl		CsCl	
		Λ_0	$\Lambda_0\eta$	Λ_0	$\Lambda_0\eta$	Λ_0	$\Lambda_0\eta$	Λ_0	$\Lambda_0\eta$	Λ_0	$\Lambda_0\eta$
0	0.00895	114.7	1.02	127.0	1.14	150.4	1.34	150.5	1.35	153.0	1.37
31	0.00970	107.8	1.05	116.6	1.13	138.0	1.33	140.0	1.36	131.2	1.27
52	0.01055	101.2	1.07	106.9	1.12	128.4	1.35	121.0	1.28	118.0	1.25
75	0.01132	99.0	1.12	102.0	1.15	117.4	1.36	117.2	1.33	108.0	1.22

CONCLUSION

The conductivity trends shown by the alkali chlorides in pure water are to a large extent maintained in hydrogen peroxide – water mixtures, and in pure hydrogen peroxide it appears that the relative degree of solvation of the alkali metal cations is Li > Na > K $\simeq$ Rb $\simeq$ Cs.

The decrease in conductance for all these salts in passing from a solvent of lower to one of higher peroxide concentration is accounted for in terms of the accompanying increase in viscosity.

ACKNOWLEDGMENTS

Thanks are due to Becco Chemicals for a gift of the hydrogen peroxide, and for valuable discussion in the early stages of the work; and to Mr. Gordon Graham for invaluable technical assistance.

REFERENCES

1. Gross, P. M. and Taylor, R. J. Am. Chem. Soc. **72**, 2075 (1950).
2. Schumb, W. C. Ind. Eng. Chem. **41**, 992 (1949).
3. Mitchell, A. G. and Wynne-Jones, W. F. Discussions Faraday Soc. **15**, 161 (1953).
4. Giguère, P. *et al.* To be published.
5. Scatchard, G., Kavanagh, G. M., and Tickner, L. B. J. Am. Chem. Soc. **74**, 3715 (1952).
6. Shanley, E. S. and Greenspan, F. P. Ind. Eng. Chem. **39**, 1536 (1947).
7. Shanley, E. S., Roth, E. M., Nichols, G. M., and Kilpatrick, M. J. Am. Chem. Soc. **78**, 5190 (1956).
8. Brönsted, J. N. and Nielsen, R. F. Trans. Faraday Soc. **31**, 1478 (1935).
9. Gunning, H. E. and Gordon, A. R. J. Chem. Phys. **10**, 126 (1942).
10. Ives, D. J. and Swaroopa, S. Trans. Faraday Soc. **49**, 788 (1953).
11. Lim, H. Australian J. Chem. **9**, No. 4 (1956).
12. Boltwood, B. B. Z. physik. Chem. **22**, 132 (1897).
13. Bredig, G. Z. physik. Chem. **13**, 191 (1894).
14. Linton, E. P. and Maass, O. Can. J. Research, **7**, 81 (1932).
15. Gorin, M. H. J. Am. Chem. Soc. **57**, 1975 (1935).
16. Shanley, E. S. and Kindson, R. Becco Chemicals. 1949 (Unpublished).

Can. J. Chem. Downloaded from www.nrcresearchpress.com by 200.7.193.243 on 09/04/12
For personal use only.

Can. J. Chem. Downloaded from www.nrcresearchpress.com by 200.7.193.243 on 09/04/12
For personal use only.

A STUDY OF THE CONDUCTIVITY OF CERTAIN ACIDS AND ALKALI HALIDES IN GLYCOL AND THE INFLUENCE OF THE ADDITION OF A SECOND SOLVENT[1]

P. KIRBY[2] AND O. MAASS

ABSTRACT

The conductivities of HCl, H_2SO_4, HNO_3, and a number of their alkali metallic salts were measured in ethylene glycol. The influence of the addition of water, methanol, and hydrogen peroxide was determined. The results are discussed on the basis of well-known theories of electrolytic conductivity involving H^+ ions.

INTRODUCTION

The conductivity of various halogen acids and alkali halides in methyl and ethyl alcoholic solutions has been studied by Goldschmidt and co-workers, and although generally the results obtained were predictable on the basis of prevailing conductivity theories, anomalous results were found on the addition of small quantities of water to the acidic solutions (1).

It was found that water gave an initial diminution of conductivity until a minimum was reached after the addition of between 1 and 2 moles of water per liter. Continued addition of water then produced a steady rise in conductivity. Similar results were found later for the addition of water to solutions of strong acids in alcoholic solution by Murray-Rust and Hartley (2), and Beznan and Verhoek (3).

Goldschmidt and Aarflot (4) also studied the effect of the addition of small quantities of methyl alcohol to an ethanolic solution of HCl, but found that it "hardly affected" the conductivity.

The present investigation describes a series of similar conductivity determinations on hydrochloric acid and alkali halides in ethylene glycol. Small quantities of water were added to both the acidic and salt solutions, and the acidic solutions showed a decrease in conductivity similar to that found by Goldschmidt and Dahll (1), although the range of water content over which this diminution was observed was much wider than that found for the solutions of acids in methanol. It was also found that addition of methanol to the solutions studied gave no decrease in conductivity. The conductivity of H_2SO_4 in glycol was decreased, however, by the addition of hydrogen peroxide.

EXPERIMENTAL

The direct-current method of conductivity determination was used in this work. The apparatus consisted of a conductivity cell, 90 v. dry cell, resistance box, and reversing switch in series. In addition, the potential difference across either the probe electrodes of the conductivity cell or the resistance box of the main circuit could be placed on the needle of a modified gold-leaf electroscope, by means of a two-way switch.

The electroscope consisted of a pair of brass plates at a separation of $\frac{1}{2}$ in., with a steady 90 v. across them; a charge could then be placed onto a gold-wire needle and the displacement observed by a microscope through a transparent window.

[1]*Manuscript received October 23, 1957.*
Contribution from the Division of Pure Chemistry, National Research Laboratories, Ottawa, Canada. Issued as N.R.C. No. 4613.
[2]*N.R.L. Postdoctorate Fellow.*

Can. J. Chem. Downloaded from www.nrcresearchpress.com by 200.7.193.243 on 09/04/12
For personal use only.

The electroscope was used as a null-point instrument, i.e. the metallic resistance in the conductivity circuit was varied until the same displacement of the needle was given by (and hence the same potential difference existed across) both the resistance box and the probes of the conductivity cell. This instrument had the great advantage of a high resistance (air gap); hence no current was drawn from the probe electrode circuit when placed across the electroscope. This in turn means that negligible polarization occurred at the probe electrodes themselves.

The conductivity cell had a capacity of 300 cc., the cell constant being determined by using three different concentrations of potassium chloride solution (four determinations were made at each of the concentrations 0.01 *N*, 0.002 *N*, and 0.001 *N*; at each concentration the agreement was within 1%; the over-all agreement was also within 1%). Using the conductivity values of Shedlovsky (5) for potassium chloride the cell constant was found to be 2.300 ± 0.003 cm.$^{-1}$. The electrodes and probes used in the conductivity cell were all of platinum.

The ethylene glycol used was reagent-grade Eastman-Kodak material ($n_4^{22} = 1.4313$). The hydrochloric acid was anhydrous and was added as a gas. The weight added was determined by a pressure-difference technique involving the freezing out of the gaseous material into a small bulb and then the evaporation of it directly into the solution.

In the nitric acid determinations, fuming nitric acid was used ($HNO_3 = 89.5\%$), but here, as with the sulphuric acid estimations ($H_2SO_4 = 96\%$), the amount of water added with the solute is so small that its effect on the conductivity of the system can be considered negligible ($\sim 0.05\%$ of the volume of solvent taken). A 0.05 *N* solution of HNO_3 in glycol was made up and allowed to stand for 7 days. During this time 25-ml. samples were withdrawn from time to time and titrated against 0.1 *N* sodium hydroxide solution. The titer was found to remain steady throughout the seven days. A similar result was obtained when 5% aqueous glycol was used as the solvent.

It was shown, therefore, that no reaction occurs between HNO_3 and ethylene glycol during the course of the conductivity determinations, which are of the duration of 45 minutes.

Hydrochloric acid was also found to give no chemical reaction with glycol by the same method.

EXPERIMENTAL RESULTS

The experimental work carried out can be divided into two sections: one, the determination of limiting values of conductivities of certain acids and salts in ethylene glycol; the other, the effect of addition of small quantities of a second solvent on the conductivity of various solutions in ethylene glycol.

As a preliminary to this work, the conductivity of ethylene glycol itself was determined and was found to be 1.28×10^{-7} cm.$^{-1}$. (Previous value recorded (6) is 2.4×10^{-7} cm.$^{-1}$.)

The authors' value was used as a solvent correction in the determination of Λ_0 for HNO_3, KNO_3, and $NaNO_3$. The values of Λ_0 to be derived by extrapolation to zero concentration of the conductivity values are determined from Table I.

The corrected values of Λ_0 found at 25° C. for these compounds are recorded in Table II. Owing to extrapolation, the accuracy of Λ_0 is a good deal less than the 1% claimed for the experimental determination, but should be within 3%.

In Table II the values for Λ_0 are given for glycol solutions. Also, for comparison, those in water (5), methanol (6), and ethanol (6) are given in Table II. It is interesting to

TABLE I

THE VARIATION OF Λ_c (CM.$^{-1}$) WITH $\sqrt{c}$ (G-MOL./LITER)$^{\frac{1}{2}}$

HNO_3		KNO_3		$NaNO_3$	
$\sqrt{c}$	Λ_c	$\sqrt{c}$	Λ_c	$\sqrt{c}$	Λ_c
0.0183	28.4	0.0104	9.43	0.0151	7.49
0.0272	27.8	0.0201	9.27	0.0279	7.35
0.0368	27.0	0.0307	8.95	0.0438	7.29
0.0538	25.7	0.0425	8.80	0.0539	7.23
0.100	22.2	0.0540	8.73	0.0642	7.19
		0.0635	8.54		

note that the conductivities of the salts are much lower compared with nitric acid in glycol than is the case in either methanol or ethanol. Glycol, in fact, gives a relationship similar to that given by water.

TABLE II

CORRECTED VALUE OF Λ_0

Comp.	Glycol	Water	MeOH	EtOH
HNO_3	29.8	421	203	88
$NaNO_3$	7.6	121	107	47
KNO_3	9.6	145	115	50

The remaining results can best be illustrated by means of Figs. 1–6; in all these figures specific conductivity has been plotted against concentration, as it was considered that this best illustrated the effects under examination.

Fig. 1 shows the effect of the addition of water to solutions of hydrochloric acid in ethylene glycol and Fig. 2 is derived from this to illustrate the effect over the range of

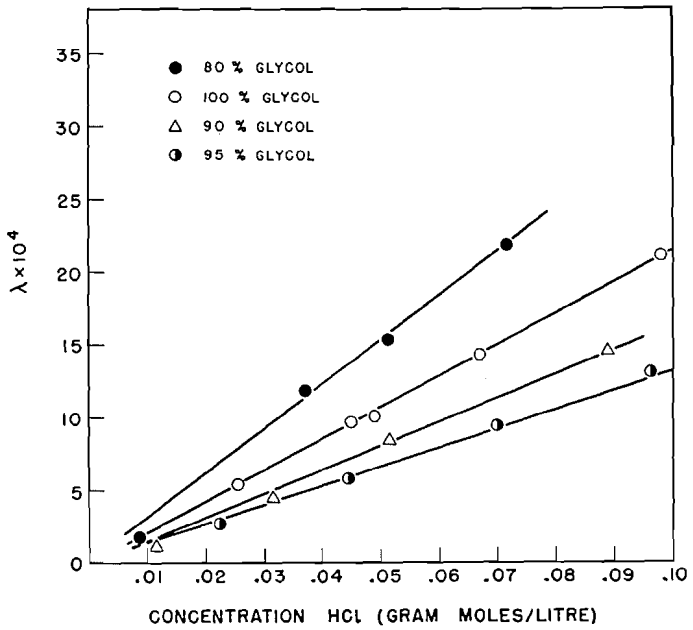

FIG. 1.

Can. J. Chem. Downloaded from www.nrcresearchpress.com by 200.7.193.243 on 09/04/12
For personal use only.

Can. J. Chem. Downloaded from www.nrcresearchpress.com by 200.7.193.243 on 09/04/12
For personal use only.

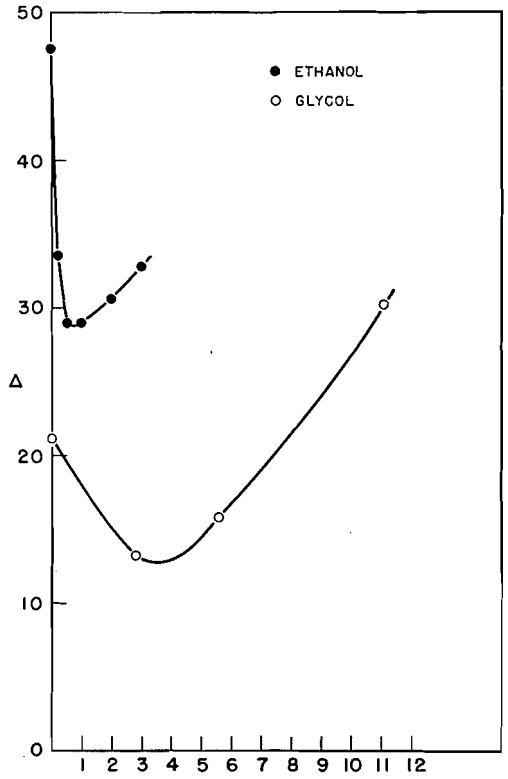

FIG. 2.

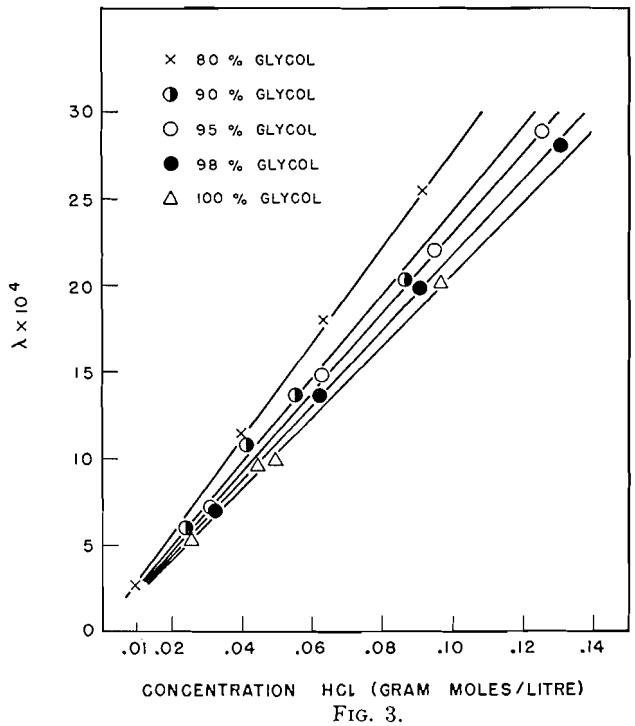

FIG. 3.

Can. J. Chem. Downloaded from www.nrcresearchpress.com by 200.7.193.243 on 09/04/12
For personal use only.

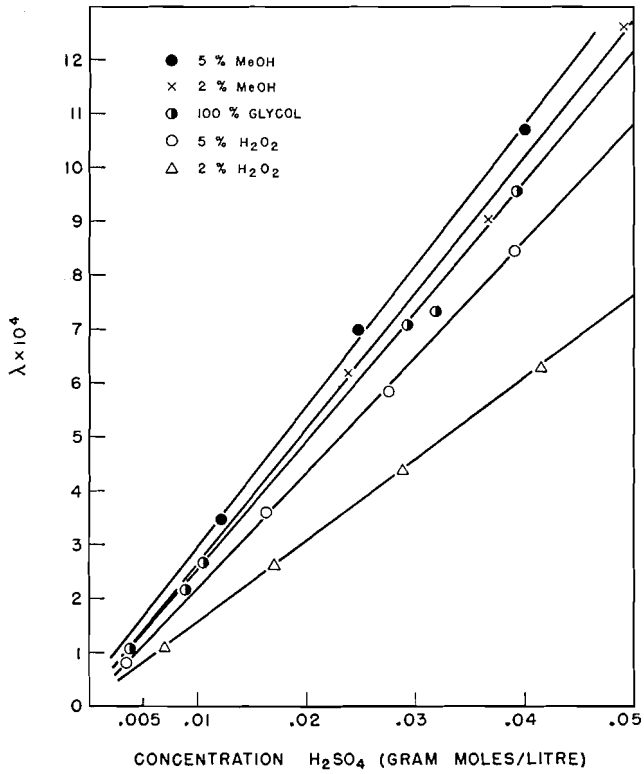

FIG. 4.

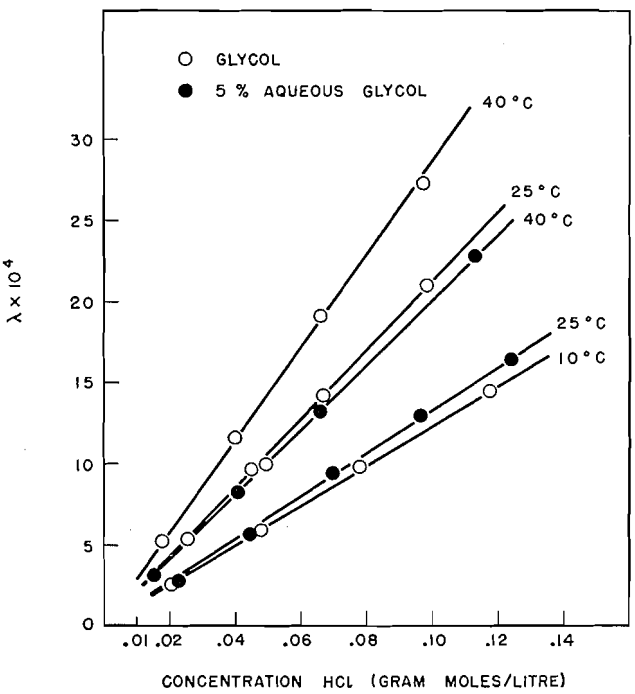

FIG. 5.

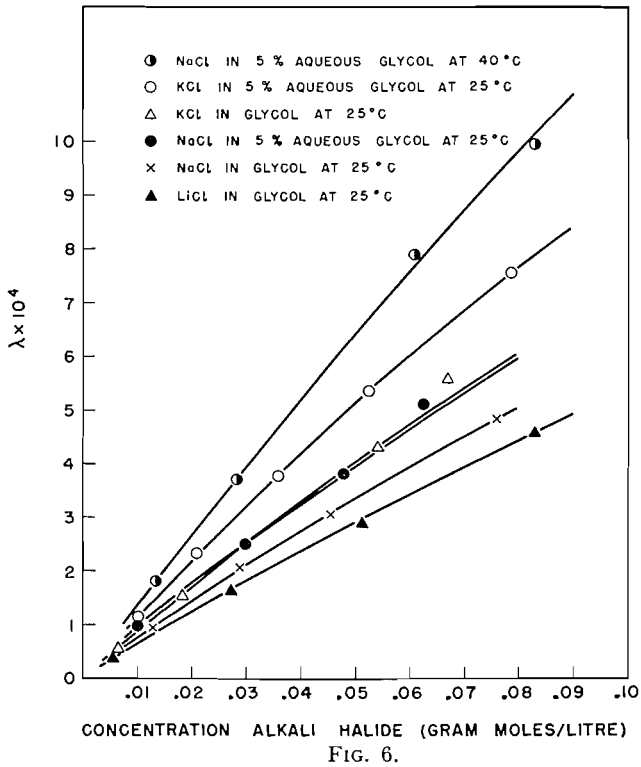

FIG. 6.

water content 0–10 g-mol./liter for a solution containing 0.05 g-mol. HCl/liter. Also in Fig. 2 is shown the curve obtained by Goldschmidt (1) for the addition of water to a solution of 0.05 g-mol. HBr/liter in ethanol. It was found that the diminution effect was much more gradual in glycol and also was evident over a much greater range of water content, although the over-all fall in conductivity was similar in either case.

Fig. 3 illustrates the effect of the addition of methanol to a glycolic HCl solution. It can be seen that an increase in conductivity was found roughly proportional to the amount of methanol added.

Fig. 4 shows the resultant conductivities for the addition of water, 98% hydrogen peroxide, and methanol to a glycolic solution of sulphuric acid. Both water and hydrogen peroxide produce a reduction of conductivity but that produced by hydrogen peroxide is less than that of water. Again, a steady increase was found on addition of methanol.

Fig. 5 deals with the temperature coefficients of hydrochloric acid both in glycol and in 5% aqueous glycol. A temperature coefficient of 2% per ° C. increase was found for the glycol solution over the range of temperature covered (25°–40°), whereas that of the 5% aqueous glycol solution was 2.3% per ° C. over the same temperature range.

Fig. 6 gives the conductivity values found for the alkali metal chlorides again in both glycol and 5% aqueous glycol at 25° C. The order of conductivity was $K^+ > Na^+ > Li^+$. The curve for NaCl in 5% aqueous glycol at 40° C. is also shown. Sodium chloride was found to have a temperature coefficient of 2.4% per ° C. between 25° and 40° C. in 5% aqueous glycol.

DISCUSSION OF RESULTS

Previous workers on the diminution of the conductivity of solutions of hydrochloric acid in organic solvents by the addition of water have always taken as a basis of their

Can. J. Chem. Downloaded from www.nrcresearchpress.com by 200.7.193.243 on 09/04/12
For personal use only.

interpretation of these results the greater stability of the H_3O^+ ion than that of the corresponding ROH_2^+ ion (1, 9, 11), which results in a certain degree of fixing of the proton, causing it to be less available as a charge carrier in slightly aqueous solutions of acids than it is in the solution of an acid in the pure solvent.

More recently a survey of the subject has been made by Conway, Bockris, and Linton (10), who suggest that the addition of water molecules to a proton-containing alcoholic solution presents an alternative route for the protons through the solution. The protons may now go to the H_2O molecules and a study of the equilibrium constants for the changes

$$H_3O^+ + ROH \rightleftharpoons ROH_2^+ + H_2O,$$

where R = Me, Et, or *n*-Pr, indicates that as soon as a trace of water is present nearly all the protons form H_3O^+ ions, and that the reverse process is improbable since it would require an increase in free energy.

When a trace of water is added to a solution of an acid in an alcoholic solution, not only are the protons mainly incorporated into the H_3O^+ ions, but so are the added water molecules. Thus proton exchanges between H_3O^+ and H_2O molecules will be infrequent owing to the smaller number of H_2O molecules present. The H_3O^+ ion rather than being involved in the transfer of protons along a chain of water molecules, as is present in aqueous solutions, will tend to remain as an independent ion, and it could be predicted that it should behave like the similarly sized K^+ ion.

To examine this prediction KCl and HCl were each studied in 0.05 g-mol./liter solution at 25° C., in a solvent of ethylene glycol containing 2.8 g-mol. water/liter, and the conductivity values were as follows:

Solvent	HCl	KCl
Aq. glycol	13.2	10.2
Water (7)	415.8	143.5
Glycol	21.2	8.1

The values for water and glycol are also given where the conductivity values are far more divergent. Further evidence for the presence of free H_3O^+ ions in solutions of acids in ethylene glycol containing small quantities of water was obtained by studying the temperature coefficients. A conductance mechanism involving proton transfer along a chain of glycol molecules should be far less sensitive to temperature than is a conductance caused by the movement of ions, since in the former case any acceleration caused by exciting the particles will be offset by the breakdown of the chain, whereas in the latter case the particles will move more quickly.

Conductivity determinations were carried out for hydrochloric acid and sodium chloride in 5% aqueous glycol at 25° C. and 40° C. and the temperature coefficients were determined.

The values are given in Table III together with those found for HCl in both glycol and water. It was found that the temperature coefficient for the conductivity of HCl was greater in 5% aqueous glycol than in either glycol itself or water; also the temperature coefficient in 5% aqueous glycol was similar to that found for NaCl in the same solvent.

Figure 2 illustrates that the decrease in conductivity found in proton-containing glycolic solutions occurred over a much larger range of water content than that found for solutions of acids in ethanol. This is no doubt a viscosity effect. In the more viscous

Can. J. Chem. Downloaded from www.nrcresearchpress.com by 200.7.193.243 on 09/04/12
For personal use only.

TABLE III

	Solvent	$\Lambda_{0.5}$ 25°	$\Lambda_{0.5}$ 40°	% dec./° C.
NaCl	5% aq. glycol	8.0	12.7	2.4
HCl	5% aq. glycol	13.2	20.1	2.3
HCl	Glycol	21.2	28.6	1.8
		25°	35°	
HCl	Water	399.09 (7)	460 (12)	1.3

glycol solution the chance of a collision between an H_3O^+ ion and a free water molecule will be much less than that in alcohol as the velocity of both particles will be reduced. Hence a minimum conductivity value is found for a 0.05 *N* solution of HBr in ethanol at 0.7 g-mol. water/liter, whereas a 0.05 *N* solution of HCl in ethylene glycol has 3.5 g-mol./liter water for a minimum conductivity.

In the runs where methyl alcohol was added to glycolic hydrochloric acid solution no decrease in conductivity was obtained. In fact, the addition seemed to produce a steady increase in conductivity dependent upon the amount of alcohol added. On the basis of previous theory this would indicate that the protons in a methanol – ethylene glycol mixture can attach themselves equally well to either type of molecule and the proton exchange mechanism is not affected.

It is interesting to note, however, that addition of hydrogen peroxide does give a decrease in conductivity. This was a considerably smaller effect than that given by water but does indicate the comparative stability of the $H_3O_2^+$ ion.

With regard to the conductivity of the alkali halides in both glycol and 5% aqueous glycol solution the order of conductivity $K^+ > Na^+ > Li^+$ is found. Thus it would seem reasonable to suppose that in both solvents solvation occurs, as the size of the unsolvate ions is in the opposite direction.

Addition of water to the alkali halide solutions in glycol gives also a steady increase in conductivity.

CONCLUSIONS

A study of the conductivity of various acids and alkali halides in solutions of glycol and aqueous glycol has shown that the behavior of these solutions supports the present theories of the diminution of conductivity caused by the addition of small amounts of water to alcoholic solution.

It was also shown that a similar, although smaller, effect was also produced by the addition of small amounts of hydrogen peroxide to acidic solutions in glycol. In the case of addition of methyl alcohol, no diminution in conductivity was observed and it was considered that this was due to the instability of the OH_2^+ ion.

To recapitulate, it is accepted that the relatively large conductivity of acids in aqueous solution is due to the formation of an H_3O^+ ion, where the proton, without any significant change in energy, can pass from one water molecule to another. While this movement from water molecule to water molecule does not involve any great change in energy, it is still recognized that the proton is always held as an H_3O^+ ion by a water molecule.

The high conductivity of acids in aliphatic alcohols is explained in a similar way, but the proton is not held so firmly in the ROH_2^+ ion. The addition of water to a solution of this type may actually decrease the conductivity because the water molecule capturing

Can. J. Chem. Downloaded from www.nrcresearchpress.com by 200.7.193.243 on 09/04/12
For personal use only.

the proton is not apt to pass it on to organic molecules as easily. It is thus taken out of circulation except insofar as it acts as a free ion. With the continued addition of water the opportunity of the proton to pass from water molecule to water molecule increases with the result that the conductivity eventually will again increase.

ACKNOWLEDGMENT

To Mr. G. Graham the authors wish to record their indebtedness for the valuable technical assistance given during the course of this research.

REFERENCES

1. GOLDSCHMIDT, H. and DAHLL, P. Z. physik. Chem. **1**, 114 (1925).
2. MURRAY-RUST, D. M. and HARTLEY, H. Proc. Roy. Soc. A, **126**, 84 (1929).
3. BEZNAN, I. and VERHOEK, F. J. Am. Chem. Soc. **67**, 1330 (1945).
4. GOLDSCHMIDT, H. and AARFLOT, H. Z. physik. Chem. **1**, 119 (1926).
5. SHEDLOVSKY, T. J. Am. Chem. Soc. **54**, 1411 (1932).
6. WALDEN, P. Z. physik. Chem. **54**, 129 (1906).
7. GLASSTONE, S. Textbook of physical chemistry. D. Van Nostrand Co., Inc., New York. 1940. p. 895.
8. GURNEY, R. W. Ionic processes in solution. McGraw-Hill Book Co., Inc., New York. 1953. p. 71.
9. BEZNAN, I. and VERHOEK, F. J. Am. Chem. Soc. **67**, 1333 (1945).
10. CONWAY, B., BOCKRIS, J. O'M., and LINTON, H. J. Chem. Phys. **24**, 834 (1956).
11. HÜCKEL, E. Z. Elektrochem. **34**, 546 (1928).
    BERNAL, J. and FOWLER, R. J. Chem. Phys. **1**, 515 (1933).
    BAKER, W. and LAMER, V. J. Chem. Phys. **3**, 406 (1935).
12. JONES, H., *et al.* Carnegie Inst., Washington, Publ. No. 17, p. 12.

Can. J. Chem. Downloaded from www.nrcresearchpress.com by 200.7.193.243 on 09/04/12
For personal use only.

Can. J. Chem. Downloaded from www.nrcresearchpress.com by 200.7.193.243 on 09/04/12
For personal use only.

NITRIMINO-(1H)PYRIDINIUM AND NITRIMINO-(3H)THIAZOLIUM INNER SALTS

THE STRUCTURE OF SOME NITRIMINES IN THE LIGHT OF INFRARED STUDY[1]

ALFRED TAURINS

ABSTRACT

Compounds previously known as nitraminopyridines and 2-nitraminothiazoles are formulated as nitrimino-(1H)pyridinium and 2-nitrimino-(3H)thiazolium inner salts on the basis of the infrared study. In the solid state, the three isomer nitriminopyridines do not exhibit any infrared absorption of the —NH group in the region 3400–3200 cm.$^{-1}$ but show a wide band at lower frequencies in the region 2880–2550 cm.$^{-1}$. 2-Nitriminothiazole shows only a wide band between 3140 and 2270 cm.$^{-1}$. These shifts of absorption bands can be correlated with structures derived from the classical nitrimino tautomeric forms in which the resonance effect stabilizes (1H)pyridinium and (3H)thiazolium cations, and a nitrimino group carrying a negative charge. *n*-Butylnitramine, a non-resonating compound, absorbs strongly at 3300 cm.$^{-1}$, indicating that nitramino groups are not associated.

INTRODUCTION

The nitration product of 2-aminopyridine reacts in two tautomeric forms, 2-nitramino- (I) and 2-nitrimino-pyridine (IA), as was postulated by Tschitschibabin and Menschikow and proved by methylation with dimethyl sulphate in alkaline medium (1), or with diazomethane in ether solution (2). A similar tautomerism can be predicted for 4-nitraminopyridine (III and IIIA) (3). However, 3-nitraminopyridine (II) cannot assume

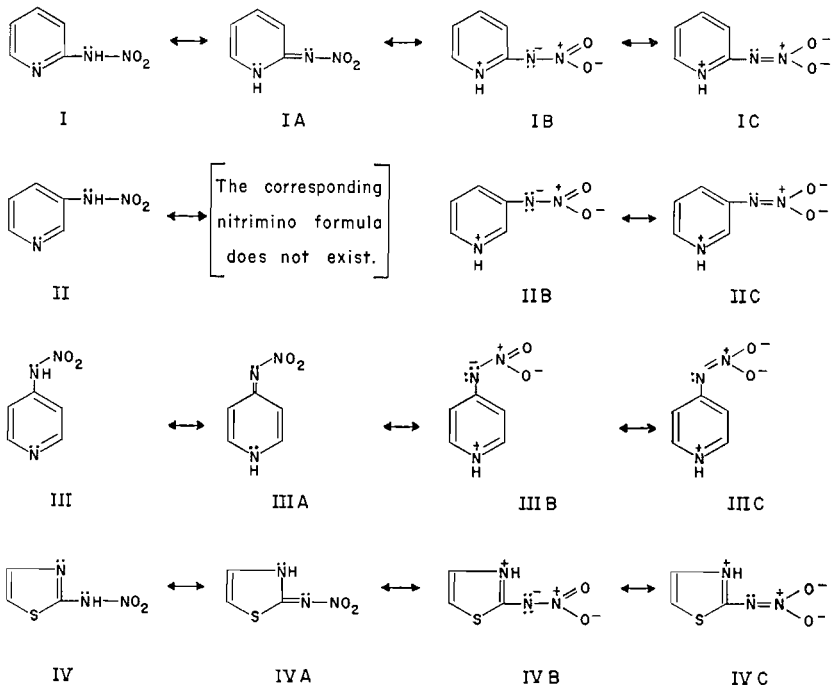

[1]*Manuscript received October 3, 1957.*
Contribution from the Department of Chemistry, McGill University, Montreal, Que. The financial support for this work was supplied by the Defence Research Board under D.R.B. Grant No. 9530-06, Project D46-95-30-06, and the National Research Council, Ottawa, Canada.

the nitrimine structure because the corresponding 3-pyridone structure is impossible (4). Also, 2-nitraminothiazole (IV) (5, 6) could exhibit a similar tautomerism to form the nitrimine (IVA).

The purpose of the present work was to study the infrared absorption spectra of the solid nitrimines of pyridine and thiazole series in order to establish the correlation between the structure and spectra. The results of the infrared study could give additional information on the structure of these substances in the crystal state. It is obvious that the structure of the solid nitrimines could differ from that established in solutions. It was expected beforehand that the presence of the heterocyclic ring in the nitrimines could greatly influence the positions of the absorption bands of the NH and NO_2 groups compared with the spectra of aliphatic nitramines. The anticipation was mainly based on facts established by several workers, that the change of a trivalent nitrogen atom to a substituted ammonium cation causes certain shifts in the infrared absorption bands (*vide infra*) (7, 8, 9, 10, 11, 12). A similar shift could be expected in the spectra of nitrimino- pyridines and -thiazoles. The nitrimino tautomeric forms IA to IVA possess resonance hybrid structures, as has been postulated by Taurins and Viron (2) for I and IA, and the most important resonance structures of the nitrimines could arise by the electron shift from the heterocyclic ring nitrogen to the nitrimino group creating a positive charge on the ring nitrogen atom. There are no resonance structures of the nitramino tautomeric form of I to IV having a positive charge on the pyridine ring nitrogen.

It is well established that resonance is present also in other compounds containing nitrimino groups and basic nitrogen atoms. On the basis of the study of electronic spectra McKay, Picard, and Brunet (13) concluded that nitroguanidine existed as a resonance hybrid of several contributing structures:

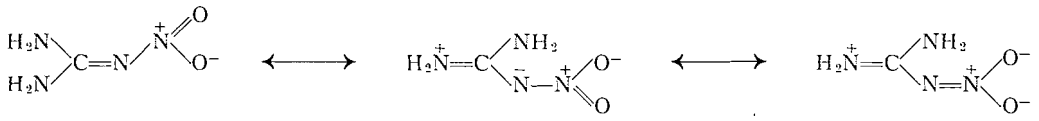

This was confirmed by Bryden, Burkardt, Hughes, and Danouhe (14) by the determination of the crystal structure of nitroguanidine. The equality of the three carbon–nitrogen distances (1.34–1.35 Å) indicated that the second structure contributes predominantly.

Resonance hybrid structures have also been considered for the anion of the monoacid salt of 5-nitraminotetrazole by Lieber, Sherman, and Pantikin (15).

Some of the papers dealing with the shift of the infrared absorption bands are mentioned here briefly. It has been found that amines and their salts absorb differently in the infrared high-frequency region (7). Heacock and Marion (8) have investigated a number of secondary amines and their salts. They found that the spectra of the salts contain several absorption bands which are absent from the spectra of the amines. The new bands in the region 1620 to 1560 cm.$^{-1}$ are characteristic of secondary amine salts, and they arise by $\overset{+}{N}H_2$ deformation vibrations. In the spectra of tertiary amine salts, the stretching vibrations of the $\overset{+}{N}$—H group are displaced towards lower frequencies. Lord and Merrifield (9) have reported that in the spectrum of pyridine hydrochloride the $\overset{+}{N}$—H stretching band at 2450 cm.$^{-1}$ is broad and structureless and that this band is accompanied by absorption maxima at 1980 and 2090 cm.$^{-1}$.

α-Amino acids, which exist in the form of dipolar ions, do not exhibit any bands in the region 3400–3300 cm.$^{-1}$ (with the exception of isovalin) (10) which could be expected

Can. J. Chem. Downloaded from www.nrcresearchpress.com by 200.7.193.243 on 09/04/12
For personal use only.

if the amino group were free. Instead, a wide and structureless band occurs between 3030 and 2546 cm.$^{-1}$, which is given by C—H and $\overset{+}{N}H_3$ stretching vibrations. In most of the spectra of α-amino acids, there is also a band at 2128 cm.$^{-1}$ present which arises by the $—\overset{+}{N}H_3$ stretching vibrations only.

From the study of the infrared spectra of myosmine and nicotine, and their mono- and di-hydrochlorides, Witkop (11) showed that it is possible to distinguish the type of substituted nitrogen cations. The substituted ammonium group 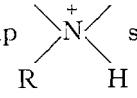 showed the absorption at 2440–2350 cm.$^{-1}$, and the immonium group 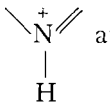 at 2095–1980 cm.$^{-1}$.

The absence of the infrared absorption at 3300 cm.$^{-1}$ by imidazole in the solid state and in concentrated solutions led Otting (12) to an explanation that, in imidazole, protons are transferred from the NH groups to the tertiary nitrogen atoms giving rise to positively and negatively charged nitrogen atoms which become associated by ionic charges:

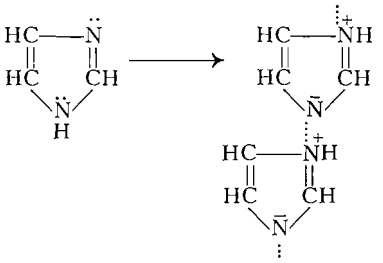

In dilute chloroform solutions, the association of imidazole is broken and the spectrum shows a maximum at 3450 cm.$^{-1}$ characteristic of the free N—H group of imidazole.

EXPERIMENTAL

The infrared spectra of nitramines were recorded with a Perkin-Elmer Model 21 double beam spectrophotometer. The settings of the instrument were as follows: resolution 927, gain 5, speed 5, response 1, suppression 0. The spectrum of *n*-butylnitramine was taken in a 0.025 mm. NaCl cell. The solid nitramino-pyridines and -thiazoles were investigated in potassium bromide pellets. The substance (1 mg.) and potassium bromide (0.4 g.) were mixed and ground by vibrating in a 1 ml. glass-stoppered tube with four steel balls for 3 minutes in a Perkin-Elmer magnetic vibrator. The pellets were pressed in a Perkin-Elmer die for 2 minutes by applying a pressure of 20,000 lb./sq. in. *n*-Butylnitramine was prepared by Mr. C. C. Bombardieri; and 2-, 3-, and 4-nitriminopyridine, and 2-nitrimino- and 4-methyl- and 4,5-dimethyl-2-nitrimino-thiazoles were made by Mr. S. Kasman. The results have been summarized in Tables I, II, and III.

RESULTS AND DISCUSSION

Region 3800–2000 cm.$^{-1}$

The infrared spectrum of the liquid *n*-butylnitramine was compared with the spectra of 2-, 3-, and 4-nitriminopyridines and 2-nitriminothiazole in the region 3800–2000

Can. J. Chem. Downloaded from www.nrcresearchpress.com by 200.7.193.243 on 09/04/12
For personal use only.

TABLE I

POSITIONS OF ABSORPTION MAXIMA ($cm.^{-1}$) IN THE INFRARED SPECTRA OF NITRIMINO-(1H)PYRIDINIUM HYDROXIDES, INNER SALTS

Assignment	2-Nitrimino-	3-Nitrimino-	4-Nitrimino-
a. $\overset{+}{N}$—H stretching	3230vw	3175vw	
	3015w	3110vw	3020w
	2800m(1)	2620(2)	2620m(3)
	2260vw	2120m	
	2020vw		2035w
	1947vw		1940w
	1882vw		
b. Pyridine ring; sym. and asym. nitrimino stretching	1625vs	1630s	1628s
	1603vs	1598s	1607s
	1543vs	1543vs	1512m
	1478s	1467s	1457s
	1427vs		1442s
	1375s	1395vs	1390s
c. Nitrimino sym. stretching	1337s	1345vs	
	1310s	1326s	1288s
	1265	1277s	
d. Pyridine ring skeletal vibrations	1225	1235s	1225vs
	1152s	1155s	1180vs
	1137m		1160vs
	1112m	1115m	1095s
		1070w	
	1045w	1060w	
	1025w(sh)	1020vw	1038w
	1007m	1005w	1007w
e. Out-of-plane vibrations: (4) C—H, (5) nitrimino group	989(4)		
	940(5)		932(5)
		895(sh)(4)	
	880w(5)	877m(5)	885s(5)
		805s(4)	882s
	770vs(4)	770m	771m(4)
	727w(4)	752m	
	672m	670s(5)	656w(5)

(1) *Wide band at 2880–2700 cm.$^{-1}$.*
(2) *Wide band at 2880–2550 cm.$^{-1}$.*
(3) *Wide band at 2800–2550 cm.$^{-1}$.*
(4),(5) *See under e. above, first column.*

TABLE II

POSITIONS OF ABSORPTION MAXIMA ($cm.^{-1}$) IN THE INFRARED SPECTRA OF 2-NITRIMINO-(3H)THIAZOLIUM HYDROXIDES, INNER SALTS

Assignment	2-Nitrimino-	2-Nitrimino-4-methyl-	2-Nitrimino-4,5-dimethyl-
a. $\overset{+}{N}$—H stretching	3140ms	3140ms	3160(sh)
	3090		3110ms
	2985	3000w(sh)	3000m
	2920		
	2870		2880(sh)
			2765(sh)
	2270		
b. Nitrimino asym. stretching	1567vs	1600ms	1625s
c. Thiazole ring	1525vs	1530w(sh)	1545sh
		1515w	1535s
		1502w(sh)	
	1476vs	1465m(sh)	1485s

Can. J. Chem. Downloaded from www.nrcresearchpress.com by 200.7.193.243 on 09/04/12
For personal use only.

TABLE II (*Concluded*)

POSITIONS OF ABSORPTION MAXIMA (cm.$^{-1}$) IN THE INFRARED SPECTRA OF 2-NITRIMINO-(3H)THIAZOLIUM HYDROXIDES, INNER SALTS (*Concluded*)

Assignment	2-Nitrimino-	2-Nitrimino-4-methyl-	2-Nitrimino-4,5-dimethyl-
d. Methyl groups		1450vs 1435ms(sh)	1445m
e. Nitrimino sym. stretching and thiazole ring	1395s	1375m	1400m 1380w
	1320s	1310s	1315m
f. Nitrimino sym. stretching	1285vs	1295vs 1280s(sh)	1272vs
	1257vs	1265s	
	1247vs	1240vs	1240vs
g. Thiazole ring skeletal vibrations	1117s	1150s	
	1068w	1040w	1030vw
	1028w		
	1008vw	1000w	
h. C—H and nitrimino out-of-plane vibrations		960w	982vw
	883s		880w
	844s	840ms	
		815ms	820m
	793m		795w
	762m	765ms	765m
	723m		
	707vs		
		675w	685m
	627vw		

TABLE III

POSITIONS OF ABSORPTION MAXIMA (cm.$^{-1}$) IN THE INFRARED SPECTRUM OF *n*-BUTYLNITRAMINE

Assignment	*n*-Butylnitramine
a. N—H stretching	3300vs 3160s(infl.)
b. CH_3 and CH_2 stretching	2920vs 2880vs
c. Nitramino asym. stretching	1580vs* 1565s(sh)
d. CH_3 asym. bending	1460m* 1405m*
e. Nitramino sym. stretching	1325vs* 1270w 1235m 1155w 1120m
f. C—H out-of-plane vibrations	775w 745

**Wide, strong bands.*

cm.$^{-1}$. The inclusion of *n*-butylnitramine in the infrared study was essential in answering the question whether the shift of —N—H absorption bands in this region arises by the association of the —N—H group with oxygen of the nitro group, or by the resonance effect. Since there is no resonance between the *n*-butyl group and nitramino group in

Can. J. Chem. Downloaded from www.nrcresearchpress.com by 200.7.193.243 on 09/04/12
For personal use only.

n-butylnitramine, the association of the —N—H group could be the only determining factor in shifting the absorption band from 3300 cm.$^{-1}$ to lower frequencies. The examination of the spectrum of *n*-butylnitramine shows that the absorption band of the N—H bonds has not been shifted but occurs at the expected position of 3300 cm.$^{-1}$. Consequently, there is no association in the liquid *n*-butylnitramine to such extent that it could influence the absorption of —N—H groups.

The analysis of the infrared spectra of the solid 2-, 3-, and 4-nitriminopyridines indicates clearly that there are no absorption bands in the region 3400–3200 cm.$^{-1}$ which could arise if the N—H group was present either in the nitramino (I to III), or nitrimino (IA to IIIA) structures. Instead of these bands, the three nitriminopyridines give wide bands between 2880 and 2550 cm.$^{-1}$. 2-Nitriminothiazole shows only a wide band between 3140 and 2270 cm.$^{-1}$, thus excluding structures IV and IVA.

These data indicate that the structures of nitriminopyridines and 2-nitriminothiazoles do not correspond to the classical formulae I to IV and IA to IVA assigned by Tschitschibabin. Since there is a very small probability that the solid heterocyclic nitrimines are associated by —N—H groups, it must be concluded that the shift of the infrared absorption bands of pyridine and thiazole nitrimines arises from the structures formed by the resonance effect. The resonance in these compounds allows the formation of pyridinium and thiazolium betaines possessing a positively charged nitrogen of the heterocyclic rings, and a negative charge located on the nitrimino group (structures IB to IVB and IC to IVC). Although nitrimino-pyridines and -thiazoles can conveniently be described as hybrids of several contributing structures, including also the IA to IVA, the infrared spectroscopic evidence points out that the structures IB to IVB and IC to IVC predominate. Accordingly, we propose to name the nitrimines of pyridine and thiazole series *nitrimino-(1H)pyridinium and nitrimino-(3H) thiazolium hydroxides, betaines (or inner salts)*. For example, the substance previously called 2-nitraminopyridine must be named 2-nitrimino-(1H)pyridinium hydroxide, betaine; the substance previously described as 4,5-dimethyl-2-nitraminothiazole must be designated 4,5-dimethyl-2-nitrimino-(3H)-thiazolium hydroxide, betaine.

The physical properties of these compounds are in good agreement with their dipolar structure. Contrary to aliphatic nitramines, which retain their old names, the heterocyclic nitrimino-(1H)pyridinium and -(3H)thiazolium hydroxides, betaines are only weakly acidic. They are insoluble in non-polar organic solvents and they possess relatively high decomposition points, without melting.

Region 1650–1235 cm.$^{-1}$, n-Butylnitramine

The infrared spectrum of *n*-butylnitramine has a very strong band at 1580 cm.$^{-1}$ which is given by the asymmetric vibrations of the nitro group. The symmetric stretching vibrations of this group produce a strong wide band at 1325 cm.$^{-1}$ accompanied by weaker bands at 1270 and 1235 cm.$^{-1}$. A band of high intensity at 1406 cm.$^{-1}$ arises by merging the absorption bands of the nitro and the methyl groups with the result of widening and intensifying of the band. There is no doubt that electronically the nitro group in *n*-butylnitramine is very similar to the nitro group in ordinary nitro compounds and therefore exhibits almost the same absorption maxima (16).

Region 1650–1375 cm.$^{-1}$, Nitrimino-(1H)pyridinium Betaines

In each of the infrared spectra of the three isomer monoaminopyridines (17), the first band in the region 1636 to 1400 cm.$^{-1}$ is shifted as much as 10 to 20 cm.$^{-1}$ towards lower frequencies, compared with the spectrum of liquid pyridine (18) which gives bands at

Can. J. Chem. Downloaded from www.nrcresearchpress.com by 200.7.193.243 on 09/04/12
For personal use only.

1636, 1584, 1485, and 1439 cm.$^{-1}$. The shift is even greater in the spectra of methylpyridines (18), the absorption beginning in the region 1604–1590 cm.$^{-1}$. Nitrimino-(1H)pyridinium betaines absorb at 1630 cm.$^{-1}$ and this band is followed by a number of peaks of high intensity in the region 1630–1375 cm.$^{-1}$ (Table I). It is obvious that the stretching vibrations of the double bonds of the pyridine ring and nitrimino group are close to each other and the final effect is the increasing of the band intensities. The nitrimino group shows its greatest effect on the bands at 1512–1543 cm.$^{-1}$ and 1478–1375 cm.$^{-1}$. It is also possible that the absorption frequency of the $\overset{+}{N}$—H group coincides with that of the pyridine ring at 1620 cm.$^{-1}$. Therefore, a very precise assignment of the band frequency to the nitrimino group is rather difficult.

Region 1000–650 cm.$^{-1}$, Nitrimino-(1H)pyridinium Betaines

In the spectra of the 2-, 3-, and 4-nitrimino-(1H)pyridinium betaines, there are bands at 672, 670, and 650 cm.$^{-1}$ respectively, which are absent in the spectra of pyridine, 2-, 3-, and 4-methylpyridines (18), and 2-aminopyridine (17). Therefore, these three bands must be considered as characteristic to the nitrimino group and can be assigned to the out-of-plane vibrations of this group. With the same type of vibrations probably are associated the strong bands at 880, 877, and 885 cm.$^{-1}$ occurring in the spectra of the three nitrimino-(1H)pyridinium betaines (Table I). This assignment is based on the observation that these bands are absent in the spectra of 2-amino- (17), 2-amino-3-methyl- (19), and 2-amino-5-methyl-pyridines (19) and they are weak in pyridine and in the three methylpyridines.

2-Nitrimino- and 4-nitrimino-(1H)pyridinium betaines possess characteristic bands at 940 and 932 cm.$^{-1}$ respectively, which are absent in the spectra of 2-, 3-, and 4-methyl-(18), 2-amino- (17), 2-amino-3-methyl- and 2-amino-5-methyl-pyridines (19).

Region 1650–1250 cm.$^{-1}$, 2-Nitrimino-(3H)thiazolium Betaines

The infrared spectrum of thiazole (20) possesses six strong absorption maxima between 1615 and 1200 cm.$^{-1}$, and in the spectrum of 2-nitrimino-(3H)thiazolium betaine there are eight bands (Table II) which are wider and more intense than the bands given by thiazole in the same region. The band at 1525 cm.$^{-1}$ exhibited by 2-nitrimino-(3H)-thiazolium betaine is characteristic of the ring vibrations of substituted thiazoles; for example, methylthiazoles (20) show absorption between 1505 and 1530 cm.$^{-1}$, and 2-aminothiazole (21) has a band at 1520 cm.$^{-1}$. The intense band at 1567 cm.$^{-1}$ given by nitrimino-(3H)thiazolium betaine must be assigned to the nitrimino group because it is wide and intense. The nitro groups of C-nitro compounds and of the nitramino group in *n*-butylnitramine absorb at the same frequency.

The skeletal vibrations of the substituted thiazole ring give bands also in the region 1210–1240 cm.$^{-1}$ and 1290–1340 cm.$^{-1}$. In the spectrum of 2-nitrimino-(3H)thiazolium betaine the corresponding bands of the thiazole ring are at 1247 cm.$^{-1}$. Some other bands at 1257, 1285, and 1320 cm.$^{-1}$ originate by the vibrations of the nitrimino group and thiazole ring. They are wide and of high intensity, similarly to the bands observed in the pyridine series.

REFERENCES

1. TSCHITSCHIBABIN, A. E. and MENSCHIKOW, G. P. Ber. deut. chem. Ges. **58**, 406 (1925).
2. TAURINS, A. and VIRON, S. J. Can. J. Chem. **31**, 1048 (1953).
3. KOENIGS, E., KINNE, G., and WEISS, W. Ber. deut. chem. Ges. **57**, 1172 (1924).
4. TSCHITSCHIBABIN, A. E. and KIRSANOW, A. W. Ber. deut. chem. Ges. **60**, 2434 (1927).
5. DICKEY, J. B., TOWNE, E. B., and WRIGHT, G. F. J. Org. Chem. **20**, 499 (1955).

Can. J. Chem. Downloaded from www.nrcresearchpress.com by 200.7.193.243 on 09/04/12
For personal use only.

6. KASMAN, S. and TAURINS, A. Can. J. Chem. **34**, 1261 (1956).
7. DEPAS, J., KHALADJI, J., and VERZOG, R. Bull. soc. chim. France, 1105 (1953).
8. HEACOCK, R. A. and MARION, L. Can. J. Chem. **34**, 1782 (1956).
9. LORD, R. C. and MERRIFIELD, R. E. J. Chem. Phys. **21**, 166 (1953).
10. KOEGEL, R. J., GREENSTEIN, J. P., WINITZ, M., BIRNBAUM, S. M., and MCCALLUM, R. A. J. Am. Chem. Soc. **77**, 5708 (1955).
11. WITKOP, B. J. Am. Chem. Soc. **76**, 5597 (1954).
12. OTTING, W. Chem. Ber. **89**, 2887 (1956).
13. MCKAY, A. F., PICARD, J. P., and BRUNET, P. E. Can. J. Chem. **29**, 746 (1951).
14. BRYDEN, J. H., BURKARDT, L. A., HUGHES, E. W., and DANOUHE, J. Acta Cryst. **9**, 573 (1956).
15. LIEBER, E., SHERMAN, E., and PANTIKIN, S. H. J. Am. Chem. Soc. **73**, 2329 (1951).
16. BROWN, J. F., Jr. J. Am. Chem. Soc. **77**, 6341 (1955).
17. ANGYAL, C. L. and WERNER, R. L. J. Chem. Soc. 2911 (1952).
18. BIDDISCOMBE, D. P., COULSON, E. A., HANDLEY, R., and HERINGTON, E. F. G. J. Chem. Soc. 1957 (1954).
19. DE SOUZA, J. E. Ph.D. Thesis, McGill University, Montreal, Que. 1954.
20. TAURINS, A., FENYES, J. G. E., and JONES, R. N. Can. J. Chem. **35**, 423 (1957).
21. RANDALL, H. M., FOWLER, R. G., FUSON, N., and DANGL, J. R. Infrared determination of organic structures. D. Van Nostrand Company, Inc., New York, N.Y. 1949. p. 210.

Can. J. Chem. Downloaded from www.nrcresearchpress.com by 200.7.193.243 on 09/04/12
For personal use only.

Can. J. Chem. Downloaded from www.nrcresearchpress.com by 200.7.193.243 on 09/04/12
For personal use only.

LYCOPODIUM ALKALOIDS

VI. REACTIONS OF THE DIPHENYL DERIVATIVE OF DESOXODIHYDROANNOTININE[1]

E. E. BETTS[2] AND DAVID B. MACLEAN

ABSTRACT

Desoxodihydroannotinine reacted with phenyl lithium to yield a diphenyl derivative, $C_{28}H_{35}O_2N$ (III). This compound yielded a ketone, $C_{28}H_{33}O_2N$ (V), upon oxidation by the Oppenauer procedure and a dihydroxyketone, $C_{28}H_{33}O_3N$ (VI), upon oxidation with chromic acid. A ketone VIII, epimeric with V, was obtained by treatment of III with potassium tertiary butoxide in cyclohexanone. Both V and VIII underwent elimination of their diphenyl carbinol groups upon treatment with potassium tertiary butoxide to yield an unsaturated ketone, $C_{15}H_{21}ON$ (IX), and benzohydrol. These reactions are discussed in relation to the recently proposed structures for the parent alkaloid, annotinine.

Annotinine, $C_{16}H_{21}O_3N$, the major alkaloid of *Lycopodium annotinum*, was first isolated by Manske and Marion (1). In a later paper they established the presence of a lactone ring and an ether ring in the molecule (2). The size of the ether ring and its relationship to the nitrogen atom were demonstrated by MacLean and Prime (3) while Wiesner *et al.* were able to relate the lactone ring to the other functions in the molecule (4). Several total structures for the alkaloid have been proposed in the past by Wiesner *et al.* (4, 5, 6) on the basis of dehydrogenation experiments on annotinine and its derivatives. In their latest publication (7) they have established the detailed structure of ring B (formula A) and have suggested that formula A adequately explains the reactions of annotinine.

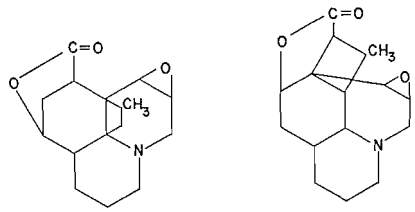

Martin-Smith, Greenhalgh, and Marion (8) have also proposed a structure for annotinine which is represented in formula B. Arguments were advanced that their structure explained the dehydrogenation reactions of annotinine equally as well as previous structures of Wiesner's. However, the seven-membered nature of ring A is not consistent with the work of Betts and MacLean (9). Nor is the structure of ring B consistent with the latest work of Wiesner *et al.* (7), nor with the results of the present study.*

Annotinine (I) was converted to desoxodihydroannotinine† (II) by the method of Manske and Marion (2). This compound has the same ring structure as annotinine but lacks the epoxide function (9). It reacted readily with phenyl lithium to yield diphenyldesoxodihydroannotinine, $C_{28}H_{35}O_2N$ (III). This compound dehydrated readily with

[1]*Manuscript received September 12, 1957.*
Contribution from the Burke Chemical Laboratories, Hamilton College, McMaster University, Hamilton, Ontario.
[2]*Holder of a National Research Council Studentship, 1956–57.*
Formula B has since been withdrawn by Marion and Przybylska (Can. J. Chem.* **35, *1075 (1957)), who have shown by an X-ray investigation that annotinine has structure A.*
†*This compound has been previously called saturated lactone A, but the present name seems more descriptive and less ambiguous in the present context.*

Can. J. Chem. Downloaded from www.nrcresearchpress.com by 200.7.193.243 on 09/04/12
For personal use only.

boiling, aqueous hydrochloric acid to yield the anhydro derivative, $C_{28}H_{33}ON$ (IV), which has an ultraviolet spectrum characteristic of a 1,1-diphenylethylene despite the fact that the compound would not absorb hydrogen at low pressures nor oxidize with ease. Oxidation of III with aluminum isopropoxide in the presence of cyclohexanone yielded the hydroxyketone, $C_{28}H_{33}O_2N$ (V), while oxidation with chromic acid in acetic acid yielded a dihydroxyketone, $C_{28}H_{33}O_3N$ (VI), also obtainable by the chromic acid oxidation of V. The new hydroxyl function in VI is probably tertiary in character; otherwise it would have been expected to oxidize in the medium. The activated positions in the molecule at which an hydroxyl group could be introduced are alpha to the carbonyl function to yield an α-hydroxyketone, or alpha to the nitrogen to yield a carbinolamine. Tests for a carbinolamine function were negative. Anhydronium salts of VI were not formed, the methiodide of VI was normal in character, and hydride reduction of VI or its hydrochloride yielded a trihydroxy compound, $C_{28}H_{35}O_3N$ (VII). Neither VI nor VII reacted with periodic acid, but VI reacted with lead tetraacetate with consumption of 3 moles of the reagent. The products of this reaction have not yet been characterized but are presently under study. The tetraacetate reaction, because of its complexity, cannot be considered evidence for an α-hydroxyketone structure in VI. However, the carbonyl absorption in the infrared of V and VI lies at 1700 cm.$^{-1}$ and 1720 cm.$^{-1}$, respectively. This shift implies a close structural relationship between the two groups in which the hydroxyl function is alpha and axial to the carbonyl function. Furthermore it has been shown in a similar series of reactions on diphenylannotinine (10) that the introduction of the new hydroxyl function is dependent on the presence of the carbonyl group. The evidence, therefore, points to an α-hydroxyketone structure for VI.

We also examined the oxidation of III with potassium tertiary butoxide and cyclohexanone. When this reaction was carried out in refluxing benzene, a ketone, $C_{28}H_{33}O_2N$ (VIII), was isolated; in refluxing toluene the reaction proceeded to yield a conjugated ketone, $C_{15}H_{21}ON$ (IX), identified through its hydrochloride and hydrobromide salts. Both V and VIII were also converted to IX by treatment with potassium tertiary butoxide in refluxing toluene.

The formation of IX directly from III or from V or VIII requires the elimination of the diphenyl carbinol group and it has been shown that it was eliminated as benzohydrol. When V was heated with potassium tertiary butoxide in an atmosphere of oxygen-free nitrogen, a quantitative recovery of benzohydrol was realized. In the presence of air some of the benzohydrol was converted to benzophenone, which was isolated as its 2,4-dinitrophenylhydrazone. In the reaction of III with potassium tertiary butoxide and cyclohexanone the presence of benzophenone was indicated in the non-basic fraction through its carbonyl absorption in the infrared at 1660 cm.$^{-1}$.

This reaction is very likely a reverse Michael reaction and can be depicted according to the sequence below:

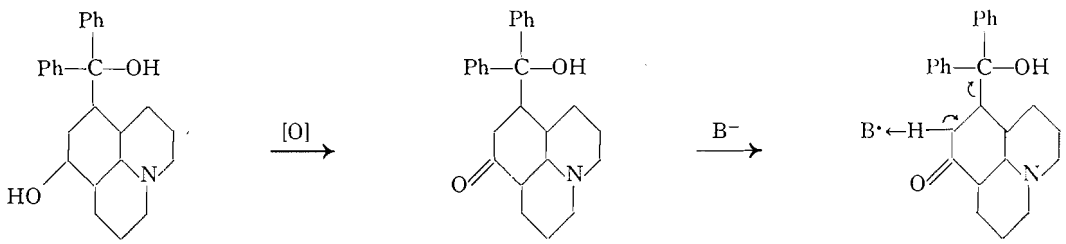

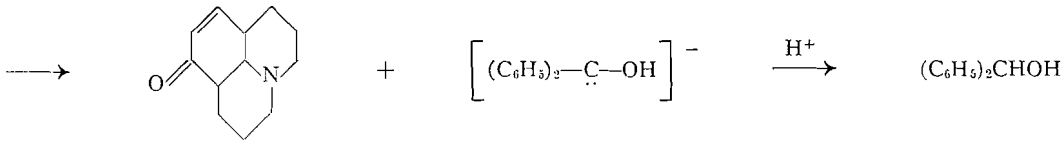

The formation of ketone VIII in the presence of potassium tertiary butoxide and ketone V in the presence of aluminum isopropoxide might suggest a more deep-seated difference between the two isomers than that of simple epimers. However, ketone V was partially converted into ketone VIII by prolonged refluxing with sodium ethoxide, a reagent which would not be expected to bring about other changes in the system. The more rapid transformation induced by potassium tertiary butoxide is likely related to its greater basic strength and greater ionic character. The two ketones V and VIII behave differently toward chromic acid in glacial acetic acid. It was pointed out previously that V was readily converted to VI by this oxidant. However, VIII was recovered unchanged upon similar treatment. This difference in behavior toward chromic acid is probably dependent on the conformation of the tertiary hydrogen in the two compounds.

The ultraviolet spectrum of IX has a peak at 2280 Å, log $\epsilon = 3.85$, which is characteristic of an α,β-unsaturated ketone with a single β-alkyl substituent (11). Thus, position "6" (formula A) must be a methylene group. The isomeric ketones V and VIII can be epimeric only at position "8" while compound VI will carry its hydroxyl function at the same position. The detailed structure of annotinine can therefore be extended to that represented by the partial formula below, which is in complete accord with the recent work of Wiesner *et al.* (7).

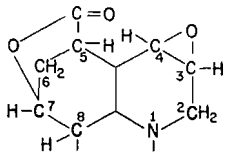

EXPERIMENTAL

Diphenyldesoxodihydroannotinine

A solution of phenyl lithium in 150 ml. ether was prepared from 4 g. of lithium and 40 g. of bromobenzene and treated with 6 g. of desoxodihydroannotinine (prepared from annotinine by the method of Manske and Marion (2)) dissolved in 100 ml. of ether. After addition was complete the mixture was refluxed for 2 hours, cooled, and decomposed in ice – hydrochloric acid. Some insoluble hydrochloride separated at this point. The ether layer was separated and washed with dilute hydrochloric acid. The acid washings and original aqueous portion were combined, made alkaline with ammonia, and extracted four times with ether. The ether extracts were dried and concentrated to yield a residue which deposited 3.5 g. of crystalline product from an acetone solution. The mother liquors were treated with concentrated hydrochloric acid to yield a crystalline hydrochloride. The total recovery as base and as hydrochloride represented a yield of 75–80%.

The base was recrystallized from acetone to yield a product which melted at 218°–220° C. Calc. for $C_{28}H_{35}O_2N$: C, 80.57; H, 8.39%. Found: C, 80.39, 80.65; H, 8.75, 8.81%.

The ultraviolet spectrum in ethanol had λ_{max} 2580 Å, log $\epsilon = 2.8$. The infrared spectrum showed hydroxyl absorption at 3600 cm.$^{-1}$ and 3150 cm.$^{-1}$ (broad) and weak phenyl absorption at 1590 cm.$^{-1}$. $[\alpha]_D^{21} = -106°$ (c, 1% in chloroform).

Can. J. Chem. Downloaded from www.nrcresearchpress.com by 200.7.193.243 on 09/04/12
For personal use only.

Dehydration of Diphenyldesoxodihydroannotinine

A solution of 0.150 g. of diphenyldesoxodihydroannotinine in 2.5 ml. of concentrated hydrochloric acid and 7.5 ml. of methanol was refluxed for 2 hours, and then evaporated to dryness. Addition of acetone yielded a crystalline hydrochloride which after recrystallization from methanol–acetone melted at 295° C. with decomposition. Calc. for $C_{28}H_{33}ON.HCl$: C, 77.15; H, 7.83; N, 3.21%. Found: C, 76.45, 76.41; H, 8.21, 7.76; N, 3.13, 3.26%.

The hydrochloride was converted to the free base by suspension in aqueous ammonia and extraction with ether. The dried ether extracts yielded a residue on evaporation, which after recrystallization from methanol melted at 189°–190° C. Calc. for $C_{28}H_{33}ON$: C, 84.21; H, 8.27; N, 3.50%. Found: C, 83.67, 83.84; H, 8.59, 8.61; N, 3.70%.

The infrared spectrum (chloroform) had hydroxyl absorption at 3630 cm.$^{-1}$ and phenyl absorption at 1600 cm.$^{-1}$ and conjugated phenyl at 1580 cm.$^{-1}$. The ultraviolet absorption spectrum had strong but broad absorption in the region 2200–2800 Å, $\log \epsilon = 3.6$–4.0. No definite band was detectable.

When this base was treated with hydrogen at 50 p.s.i.g. for 12 hours over Adam's catalyst, it failed to take up hydrogen and was recovered unchanged. It was also resistant to the action of potassium permanganate in acetone.

Oxidation of Diphenyldesoxodihydroannotinine with Aluminum Isopropoxide and Cyclohexanone

A solution of 1.2 g. of aluminum isopropoxide in 30 cc. of dry toluene was treated with 0.5 g. of compound III and 1.5 cc. of cyclohexanone. The reaction mixture was refluxed 1 hour and 15 minutes, cooled and poured on ice. The toluene layer was separated and the aqueous layer was further extracted three times with ether. The toluene and ether extracts were combined and washed four times with 10% hydrochloric acid. The acid washings were made alkaline with ammonium hydroxide and extracted with ether. The ether extracts were dried with anhydrous sodium sulphate and taken to dryness. The residue crystallized on addition of ether. The product (0.350 g.), after two recrystallizations from ether, melted sharply at 201° C. A mixed melting point with the ketone isolated from the oxidation using potassium tertiary butoxide was depressed 10°. Calc. for $C_{28}H_{33}O_2N$: C, 80.97; H, 7.95; N, 3.37%. Found: C, 80.98, 81.08; H, 7.74, 7.73; N, 3.25%.

The infrared spectrum (nujol) had phenyl absorption at 1595 cm.$^{-1}$, carbonyl absorption at 1700 cm.$^{-1}$, and a band in the hydroxyl region at 3500 cm.$^{-1}$. $[\alpha]_D^{21} = +100.7$ (c, 1% in chloroform).

Chromic Acid Oxidation of $C_{28}H_{33}O_2N$ (*V*)

A sample of compound V (0.108 g.) was dissolved in 5 cc. glacial acetic acid, the solution was warmed to 50°–60°, and excess CrO_3 in water added. After 10 minutes the excess CrO_3 was destroyed with methanol and the resulting green solution was taken to dryness under reduced pressure. Water was added to the residue, the mixture was made alkaline with ammonium hydroxide and extracted four times with ether. The combined ether extracts were dried with sodium sulphate and the ether removed. The residue (0.086 g.) was taken up in methanol and acidified with hydrochloric acid. The hydrochloride of the reaction product, after recrystallization from methanol, melted at 273°. A mixed melting point with the hydrochloride of VI was not depressed. (Yield, 50%.) The infrared spectrum was similar to that of compound VI described below.

Can. J. Chem. Downloaded from www.nrcresearchpress.com by 200.7.193.243 on 09/04/12
For personal use only.

Can. J. Chem. Downloaded from www.nrcresearchpress.com by 200.7.193.243 on 09/04/12
For personal use only.

Oxidation of Diphenyldesoxodihydroannotinine with Chromic Acid

A solution of 1.0 g. of compound III in 20 ml. of glacial acetic acid was warmed to 50°–60° and treated with concentrated aqueous solution of chromic acid in water until the dichromate color was persistent. The excess oxidizing agent was destroyed with methanol and the solution was taken to dryness under reduced pressure. The residue was taken up in water, made basic with ammonia, and exhaustively extracted with ether. The ether extracts were dried and evaporated. The residue was taken up in methanol and acidified with hydrochloric acid, whereupon the hydrochloride separated in crystalline form. Recrystallization from methanol yielded a compound which melted at 276° C. Calc. for $C_{28}H_{33}O_3N.HCl.H_2O$: C, 69.20; H, 7.48; N, 2.88%. Found: C, 69.11, 69.10; H, 7.74, 7.84; N, 2.98, 2.86%.

The infrared spectrum (nujol) had absorption at 1595 cm.$^{-1}$ (phenyl), 1720 cm.$^{-1}$ (carbonyl), and broad absorption in the region 3350–3420 cm.$^{-1}$. The ultraviolet spectrum had λ_{max} at 2600 Å, log $\epsilon = 2.69$.

The base was regenerated from the hydrochloride by treatment with aqueous ammonia and extraction with ether. It was recrystallized from methanol to yield a product which melted at 208° C. Calc. for $C_{28}H_{33}O_3N$: C, 77.94; H, 7.65; N, 3.25; act. H (2), 0.46%. Found: C, 77.94, 78.09; H, 7.81, 7.77; N, 3.65; act. H, 0.47, 0.53%.

The infrared spectrum (nujol) showed phenyl absorption at 1590 cm.$^{-1}$, carbonyl absorption at 1720 cm.$^{-1}$ (shoulder at 1728 cm.$^{-1}$), and hydroxyl absorption at 3450 cm.$^{-1}$ and 3500–3550 cm.$^{-1}$. The ultraviolet spectrum had λ_{max} at 2600 Å, log $\epsilon = 2.9$. $[\alpha]_D^{21} = +43.0$ (c, 1% in chloroform).

Compound VI (0.20 g.) was treated with 3 ml. of methyl iodide and the mixture allowed to stand at room temperature for 2 days. The crystalline solid which had separated (0.05 g.) was recrystallized from acetone and melted at 245° C. Calc. for $C_{28}H_{33}O_3N.CH_3I$: C, 60.71; H, 6.32; N, 2.44%. Found: C, 60.80, 60.67; H, 6.62, 6.38; N, 2.91%.

The infrared spectrum had phenyl absorption at 1600 cm.$^{-1}$, carbonyl absorption at 1720 cm.$^{-1}$, and a double peak in the hydroxyl region at 3250 cm.$^{-1}$ and 3430 cm.$^{-1}$.

Reduction of $C_{28}H_{33}O_3N$ *(VI) with Lithium Aluminum Hydride*

A solution of 0.4 g. of $C_{28}H_{33}O_3N$ in 40 ml. of anhydrous ether was added slowly to a solution of 1.0 g. of lithium aluminum hydride in 30 ml. of anhydrous ether. The reduction mixture was refluxed for 2.5 hours when the excess hydride was destroyed with wet ether followed by addition of a few milliliters of water. The ether solution was separated and evaporated to dryness to yield 0.34 g. of residue. The residue was dissolved in acetone and acidified with hydrochloric acid. The crystalline hydrochloride, obtained upon evaporation of the acetone, was recrystallized twice from methanol (m.p. 272° C.). The base was regenerated from the hydrochloride by extraction with ether from an aqueous ammoniacal solution. It was recrystallized twice from ether and melted at 209°. Calc. for $C_{28}H_{35}O_3N$: C, 77.56; H, 8.13%. Found: C, 77.71, 77.59; H, 8.14, 8.18%.

The infrared spectrum showed absorption at 1595 cm.$^{-1}$ (phenyl) and at 3620 cm.$^{-1}$ (slight) and 3430 cm.$^{-1}$ (broad) in the hydroxyl region.

Treatment of the hydrochloride of VI by the same procedure yielded the same product.

Reaction of $C_{28}H_{33}O_3N$ *(VI) with Lead Tetraacetate*

Compound VI (179 mg.), dissolved in 40 ml. of glacial acetic acid, was added to a mixture of 50 ml. of 0.1 N lead tetraacetate in glacial acetic acid. To this mixture 5 ml.

of water was added and the volume was made up to 100 ml. by the addition of glacial acetic acid. A blank was prepared in the same manner omitting only the sample. Aliquots of 10 ml. were withdrawn at intervals, added to 15 ml. of buffer solution containing 5 g. potassium iodide and 125 g. of potassium acetate in 250 ml. of solution. The liberated iodine was titrated with 0.02 *N* sodium thiosulphate. After about 30 hours 3 moles of reagent per mole of compound VI had been consumed, whereupon the reaction virtually ceased.

Oxidation of Diphenyldesoxodihydroannotinine with Cyclohexanone and Potassium Tertiary Butoxide

A solution of 0.2 g. of III in 20 ml. of toluene was treated with 1 ml. of cyclohexanone and 0.28 g. of freshly prepared potassium tertiary butoxide for 1 hour under reflux. The mixture was decomposed in ice water, the toluene layer separated, and the aqueous layer extracted three times with ether. The toluene and ether extracts were combined and extracted several times with 10% hydrochloric acid. The acid washings were made alkaline with ammonia and extracted with ether. The dried ether extracts yielded 0.1 g. of basic material which was dissolved in acetone and treated with concentrated hydrochloric acid. A crystalline hydrochloride separated, which after recrystallization from acetone melted at 261°–262° C. Calc. for $C_{15}H_{21}ON.HCl$: C, 67.26; H, 8.28; N, 5.27%. Found: C, 67.61, 67.62; H, 8.49, 8.77; N, 5.80, 5.80%.

The hydrobromide was prepared by a similar procedure and recrystallized from acetone–methanol. It melted at 267°–268° C. Calc. for $C_{15}H_{21}ON.HBr$: C, 57.68; H, 7.10%. Found: C, 57.54, 57.54; H, 6.89, 6.90%.

The ultraviolet spectrum of the hydrochloride showed weak absorption at 3180 Å (carbonyl) and had maximum absorption at 2280 Å, $\log \epsilon = 3.85$ (conjugated carbonyl). The infrared spectrum had peaks at 1680 cm.$^{-1}$ (conjugated carbonyl) and 1625 cm.$^{-1}$ unsaturation.

The ether–toluene mixture was examined for non-basic material. Evaporation yielded an oily residue which was mostly cyclohexanone. Examination of the infrared spectrum revealed the presence of a strong carbonyl band at 1660 cm.$^{-1}$, which corresponded to that of benzophenone, as well as the cyclohexanone carbonyl absorption at 1710 cm.$^{-1}$.

In another experiment carried out in refluxing benzene for 15 minutes, only a trace of conjugated ketone was obtained. There was isolated instead another compound which crystallized from ether and melted at 223° C. (Yield, 25%.) Calc. for $C_{28}H_{33}O_2N$: C, 80.93; H, 8.00; N, 3.30%. Found: C, 80.83, 80.67; H, 8.02, 8.03; N, 3.12%.

The infrared spectrum of this material had absorption at 1595 cm.$^{-1}$ (phenyl), 1710 cm.$^{-1}$ (carbonyl), and 3420 cm.$^{-1}$ (hydroxyl). The ultraviolet spectrum was similar to that of the starting material, $\lambda_{max} = 2580$ Å, $\log \epsilon = 2.75$. $[\alpha]_D^{21} = -60.2°$ (*c*, 1% in chloroform).

The mother liquors remaining after the separation of the above compound yielded a residue which melted over a wide range and was probably a mixture of V and VIII.

Treatment of $C_{28}H_{33}O_2N$ (*V*) *with Potassium Tertiary Butoxide in Toluene*

Compound V (0.33 g.) was dissolved in 30 ml. of dry toluene, 0.45 g. of freshly prepared potassium tertiary butoxide was added, and the mixture was refluxed for 30 minutes under an atmosphere of oxygen-free nitrogen. The reaction mixture was worked up for recovery of the conjugated ketone as described in the previous experiment. The non-basic material remaining in the toluene–ether layer was recovered by evaporation of the solvent under vacuum. The residue (0.148 g.) had an infrared spectrum identical

Can. J. Chem. Downloaded from www.nrcresearchpress.com by 200.7.193.243 on 09/04/12
For personal use only.

to authentic benzohydrol. It was recrystallized from petroleum ether and melted at 70° C. either alone or in admixture with an authentic sample of benzohydrol.

The basic material yielded a hydrochloride identical to the hydrochloride of the conjugated ketone.

When the reaction was carried out in air rather than nitrogen, the non-basic fraction was a mixture of benzohydrol and benzophenone. The latter was identified by conversion to its 2,4-dinitrophenylhydrazone.

Attempted Oxidation of VIII with Chromic Acid in Acetic Acid

About 40 mg. of VIII was dissolved in acetic acid and treated with a solution of CrO_3 in H_2O at 50°–60° for 10 minutes. After the excess CrO_3 was destroyed with methanol, the solution was taken to dryness under reduced pressure. The residue was taken up in water, the mixture was made alkaline and extracted with ether. Concentration of the dried ether extracts yielded the starting material.

Treatment of V with Sodium Ethoxide

Compound V (0.13 g.) was refluxed overnight in a dilute solution of sodium ethoxide in ethanol. The solution was evaporated to dryness, water was added, and the mixture was extracted with ether. The dried ether extracts were concentrated and seeded with a crystal of compound VIII. After 2 hours the crystalline needles (20 mg.) were separated from the solution by filtration. They melted at 220° C. and did not depress the melting point of VIII. The residual material obtained from the mother liquors melted over a wide range and was likely a mixture of V and VIII.

ACKNOWLEDGMENTS

This work was supported by grants from the National Research Council and the Ontario Research Foundation.

REFERENCES

1. MANSKE, R. H. F. and MARION, L. Can. J. Research, B, **21**, 92 (1943).
2. MANSKE, R. H. F. and MARION, L. J. Am. Chem. Soc. **69**, 2126 (1947).
3. MACLEAN, D. B. and PRIME, H. C. Can. J. Chem. **31**, 543 (1953).
4. VALENTA, Z., STONNER, F. W., BANKIEWICZ, C., and WIESNER, K. J. Am. Chem. Soc. **78**, 2867 (1956).
5. WIESNER, K., VALENTA, Z., AYER, W. A., and BANKIEWICZ, C. Chem. & Ind. 1019 (1956).
6. WIESNER, K., VALENTA, Z., and BANKIEWICZ, C. Chem. & Ind. R41 (1956).
7. WIESNER, K., AYER, W. A., FOWLER, L. R., and VALENTA, Z. Chem. & Ind. 564 (1957).
8. MARTIN-SMITH, M., GREENHALGH, R., and MARION, L. Can. J. Chem. **35**, 409 (1957).
9. BETTS, E. E. and MACLEAN, D. B. Can. J. Chem. **35**, 211 (1957).
10. PERRY, G. S. M.Sc. Thesis, McMaster University, Hamilton, Ont. May, 1956.
11. GILLAM, A. and STERN, E. S. Electronic absorption spectroscopy. Edward Arnold & Company, London. 1954. p. 94.

Can. J. Chem. Downloaded from www.nrcresearchpress.com by 200.7.193.243 on 09/04/12
For personal use only.

Can. J. Chem. Downloaded from www.nrcresearchpress.com by 200.7.193.243 on 09/04/12
For personal use only.

D-APIOSE[1]

P. A. J. GORIN AND A. S. PERLIN

ABSTRACT

Naturally-occurring apiose is shown by synthesis to be the D-isomer in the open-chain form. In this synthesis 3-*O*-benzyl-D-fructose is cyanohydrated and the resulting heptonic lactones are reduced to 3-*O*-benzyl-2-*C*-(hydroxymethyl)-D-*arabo*-hexitol. The latter is oxidized with lead tetraacetate affording 2-*O*-benzyl-3-*C*-(hydroxymethyl)-D-*glycero*-tetrose which, on debenzylation, gives 3-*C*-(hydroxymethyl)-D-*glycero*-tetrose (D-apiose).

INTRODUCTION

Apiose was first isolated by Vongerichten (1), who recognized it as a component sugar of the parsley flavone glycoside, apiin. The sugar has since been found in still other glycosides present in parsley (2, 3, 4, 5) and more recently in *Posidonia australis* (6) and in the rubber plant, *Hevea brasiliensis* (7). The researches of Vongerichten and later work by Schmidt (8), which have been reviewed by Hudson (9), established that apiose is a branched-chain pentose whose structure is represented by I. The synthesis of DL-apiose (10) provides additional confirmation of this structure. In the open-chain form the compound possesses only one asymmetric center, at carbon atom 2, for which the D-configuration has been assigned (8) by application of the salt–acid (11, 12) and phenylhydrazide and amide (12, 13) rules to the derived apionic acid and its derivatives. The present study furnishes an alternative proof for the configuration at C-2 through synthesis of D-apiose, which is found to be identical with the naturally-occurring sugar.

A ready synthetic pathway to D-apiose was suggested by the preparation of 4-*C*-(hydroxymethyl)-D-*threo*-pentose[2] (II) by Woods and Neish (14). It was apparent that D-apiose could be obtained by a one-step descent of the sugar series. However, attempts to achieve this by the Weerman degradation (15) or by partial lead tetraacetate oxidation (16) resulted in the production of only trace amounts of the desired product.

An alternative synthetic pathway, starting with 3-*O*-benzyl-D-fructose (III), was more successful. 1,2;4,5-Di-*O*-*iso*propylidene-D-fructose (17) was benzylated to give 3-*O*-benzyl-1,2;4,5-di-*O*-*iso*propylidene-D-fructose. The acetone groups were removed by acid hydrolysis, affording sirupy 3-*O*-benzyl-D-fructose (III), which was characterized by formation of 3-*O*-benzyl-D-glucose phenylosazone (18) on treatment with phenylhydrazine acetate. The 3-*O*-benzyl-D-fructose was cyanohydrated, the nitrile was hydrolyzed under alkaline conditions, and the product was acidified, yielding a mixture of the corresponding *O*-benzyl-α- and -β-D-fructoheptonic lactones (e.g., IV); the β-isomer was isolated as the crystalline γ-lactone. Reduction of the mixture with sodium borohydride (19, 20) gave the sirupy alcohol, 3-*O*-benzyl-2-*C*-(hydroxymethyl)-D-*arabo*-hexitol (V). The structure of V was confirmed by its conversion, on catalytic hydrogenolysis with palladium oxide followed by acetylation, to the known hepta-*O*-acetyl-2-*C*-(hydroxymethyl)-D-*arabo*-hexitol ("D-fructoheptitol" heptaacetate (21)).

[1]*Manuscript received November 17, 1957.*
Contribution from the National Research Council of Canada, Prairie Regional Laboratory, Saskatoon, Saskatchewan.
Issued as N.R.C. No. 4612 and Paper No. 250 on the Uses of Plant Products.
Presented at the 40th Annual Conference of the Chemical Institute of Canada, Vancouver, B.C., June 3–5, 1957.
[2]*The nomenclature of the branched-chain sugar has recently been discussed by F. Shafizadeh, Advances in carbohydrate chemistry,* **11**, *263 (1956).*

Can. J. Chem. Downloaded from www.nrcresearchpress.com by 200.7.193.243 on 09/04/12
For personal use only.

The alcohol (V) rapidly consumed approximately 2 moles of oxidant when treated with lead tetraacetate in acetic acid or aqueous periodate, but a moderately rapid over-oxidation followed, which was more pronounced with the latter reagent. Consumption of 2 moles of oxidant was expected to correspond to cleavage of the 1,2,3-triol of V affording 2-*O*-benzyl-3-*C*-(hydroxymethyl)-D-*glycero*-tetrose (2-*O*-benzyl-D-apiose) (VI), in preference to attack at the tertiary hydroxyl group (22). Accordingly, V was oxidized

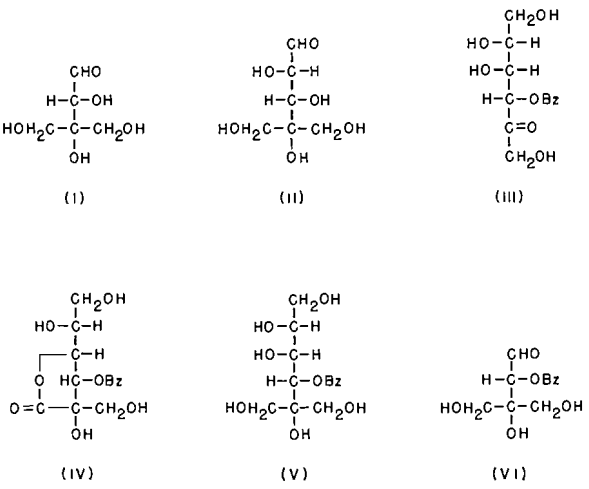

with 2 moles of lead tetraacetate in acetic acid and the product was treated with methanolic hydrogen chloride to promote formation of the methyl glycosides. The latter were debenzylated with hydrogen – palladium oxide and the product hydrolyzed with aqueous acid. The final material was found by paper chromatography to contain three components present in approximately equal proportions, the central component corresponding in its rate of travel to D-apiose (I). Presence of the faster- and slower-moving components suggests that over- and under-oxidation occur in addition to the desired reaction on treatment of IV with lead tetraacetate.

The product corresponding to D-apiose was separated as a sirup from the mixture by column chromatography on cellulose (23). Its rate of travel on a paper chromatogram was identical with that of authentic D-apiose isolated from parsley. Detected on the chromatogram with the aniline oxalate spray (24) the natural and synthetic sugars each gave a faint yellow-brown spot which exhibited a strong yellow fluorescence under ultraviolet light, a characteristic of tetroses (25). The identity of the two compounds was demonstrated further by the fact that they gave identical infrared absorption spectra and 2,5-dichlorophenylosazones (6). The specific rotation of the synthetic specimen was $[\alpha]_D$ +6.4°, which is in good agreement with the values of $[\alpha]_D$ +3.8° found by Vongerichten and Müller (26) and $[\alpha]_D$ +5.8° found by Schmidt (8) for D-apiose obtained by regeneration from the 1-benzyl-1-phenylhydrazone.

Since the configuration of carbon atom 2 of synthetic D-apiose, originally carbon atom 3 of D-fructose, is known, the present results confirm Schmidt's assignment of the D-configuration to naturally-occurring apiose.

EXPERIMENTAL

Paper chromatography was carried out on Whatman No. 1 paper using *n*-butanol–ethanol–water (40: 11: 19, v/v) as solvent. Chromatograms were developed with aniline

oxalate (24) and ammoniacal silver nitrate (27) sprays. The distance travelled by compounds on chromatograms (R_{Rh}) was measured relative to the distance travelled by L-rhamnose. Evaporations were carried out *in vacuo* at 40° C.

3-O-Benzyl-1,2;4,5-di-O-isopropylidene-D-fructose

1,2;4,5-Di-*O-iso*propylidene-D-fructose (17) (45 g.) was dissolved in a mixture of benzyl chloride (75 ml.) and xylene (50 ml.). The solution was agitated vigorously with an Ultra-Turrax stirrer (28) and powdered potassium hydroxide (180 g.) was added during a period of 0.5 hour, the reaction temperature being maintained at 85°–95° C. during this time and for an additional 1.5 hours' reaction period. The mixture was cooled, washed with water three times, and concentrated. Water was added to the resulting sirup and the suspension heated on the steam bath at 1 mm., more water was added, and the evaporation repeated. The residue was taken up in acetone, filtered through a bed of filter-cel, and concentrated, yielding a yellow, viscous sirup; n_D^{24} 1.5080. Weight 59.0 g. After distillation (135°–155° C. at 0.05 mm.) the product was colorless and had n_D^{24} 1.5033, $[\alpha]_D^{25}$ −95.0° (*c*, 4.6, ethanol). Calculated for $C_{19}H_{26}O_6$: C, 65.12%; H, 7.48%. Found: C, 65.00%; H, 7.43%.

3-O-Benzyl-D-fructose

3-*O*-Benzyl-1,2;4,5-di-*O-iso*propylidene-D-fructose (55 g.), dissolved in 50% acetic acid (200 ml.), was heated on a steam bath for 18 hours. After evaporation of the solvent, the product was found (infrared absorption) still to contain some *iso*propylidene groups and was therefore treated on a steam bath for 2 hours with 0.1 *N* sulphuric acid. The hydrolyzate was neutralized with barium carbonate and the solution filtered and concentrated, affording a pale yellow amorphous solid $[\alpha]_D^{25}$ −24.9° (*c*, 4.1, water). Weight 30.4 g. On a paper chromatogram the product gave a single spot (R_{Rh} 2.4) detected by silver nitrate. Calculated for $C_{13}H_{18}O_6$: C, 57.77%; H, 6.71%. Found: C, 57.78%; H, 6.81%.

As expected for a 3-substituted ketose, the compound consumed lead tetraacetate slowly (29).

3-O-Benzyl-D-fructose-(D-glucose)-phenylosazone

3-*O*-Benzyl-D-fructose (400 mg.) was dissolved in water (10 ml.) containing acetic acid (1.5 ml.) and phenylhydrazine (1 ml.). The solution was kept at 50° C. for 18 hours and the red-brown mass which formed was taken up in methanol. On addition of water, crystals were deposited and these were recrystallized from aqueous ethanol and then benzene. The light-yellow product (37 mg.) had m.p. 151°–152° C. Calculated for $C_{25}H_{28}O_4N_4$: C, 66.94%; H, 6.29%. Found: C, 67.14%; H, 6.20%. (Melting point of 3-*O*-benzyl-D-glucose-phenylosazone 149°–150° C. (18).)

3-O-Benzyl-2-C-hydroxymethyl-D-glucono- and -D-mannono-γ-lactones (3-O-Benzyl-α- and -β-D-fructoheptonic lactones)

In preliminary tests, cyanohydration of 3-*O*-benzyl-D-fructose with aqueous sodium cyanide at pH 9.3 was approximately 95% complete within 40 hours' reaction time, as measured by evolution of ammonia after alkaline hydrolysis. Accordingly, 3-*O*-benzyl-D-fructose (14.7 g.) in water (25 ml.) was added to a solution (200 ml.) of sodium cyanide (4.1 g.) buffered to pH 9.3 with acetic acid. The pH of the solution rose rapidly to pH 9.8 and more acetic acid was added, further additions of the acid being required during the first 5 hours' reaction time to maintain the pH at 9.3. After 48 hours at room temperature, the reaction mixture was diluted with water (200 ml.) and then concentrated, water was added again and evaporated, the procedure being repeated three times, with the last evaporation at 70° C. to promote complete hydrolysis of the nitrile. The sirup obtained

Can. J. Chem. Downloaded from www.nrcresearchpress.com by 200.7.193.243 on 09/04/12
For personal use only.

Can. J. Chem. Downloaded from www.nrcresearchpress.com by 200.7.193.243 on 09/04/12
For personal use only.

was dissolved in water, treated with Amberlite IR-120, and the hydrocyanic and acetic acids released were removed upon evaporation. After the residue was heated at 100° C. *in vacuo* over phosphorus pentoxide for 4 hours, a pale yellow amorphous solid was obtained. Weight 11.1 g. The infrared absorption spectrum of the product showed a predominance of the γ-lactone form to be present (strong absorption band at 1770 cm.$^{-1}$ (30)). The product (46.5 mg.), in water, consumed 0.26 ml. of 0.1 *N* sodium hydroxide by direct titration to a stable end point. Excess of the alkali was added, the solution heated, and back-titrated with acid. The total alkali consumed was 1.57 ml. (required, 1.55 ml.), indicating that approximately 85% of the material existed as the γ-lactone.

*3-O-Benzyl-2-C-hydroxymethyl-*D*-mannono-γ-lactone (3-O-Benzyl-β-*D*-fructoheptonic lactone)*

Partial crystallization of the lactone mixture occurred after several months. The sirup was taken up in ethyl acetate and the crystals were filtered off and recrystallized from ethyl acetate. Weight, 120 mg. from 500 mg. of the mixture. Melting point 150.5°–152.0° C., $[\alpha]_D^{27}$ +45.5° (*c*, 1.2, alcohol). Calculated for $C_{14}H_{18}O_7$: C, 56.38%; H, 6.08%. Found: C, 56.16%; H, 6.05%. The compound absorbed strongly in the infrared region at 1770 cm.$^{-1}$, which, together with the stability exhibited to alkaline hydrolysis, showed the presence of a γ-lactone structure (30). The non-crystalline fraction showed $[\alpha]_D^{27}$ +89.3° (*c*, 1.6, alcohol).

The crystalline lactone was treated with one equivalent of hot sodium hydroxide solution; the resulting sodium salt showed $[\alpha]_D^{27}$ +11.6° (*c*, 1.4). This value was altered to $[\alpha]_D^{27}$ +15.4° (*c*, 1.3) by liberation of the free acid through addition of one equivalent of hydrochloric acid. Likewise, the salt and acid prepared from the non-crystalline material had $[\alpha]_D^{27}$ −1.1° (*c*, 1.9) and $[\alpha]_D^{27}$ −5.7° (*c*, 1.7), respectively. These data are in close agreement with the results obtained (31) by application of the salt–acid rule (11, 12) to α- and β-D-fructoheptonic lactones, and indicate that the crystalline lactone is the β-(*mannono*)-isomer.

*3-O-Benzyl-2-C-(hydroxymethyl)-*D*-arabo-hexitol*

The crude mixture of *O*-benzyl-D-fructoheptonic lactones (7.5 g.) in water (15 ml.) was added slowly to a solution of sodium borohydride (1.5 g.) in water (25 ml.) (19). After 2 hours, excess of acetic acid was added, the solution passed through a column of Amberlite IR-120, and the solvent evaporated. The resulting sirup was taken up in methanol, the methanol was evaporated, and this procedure repeated five times to ensure removal of boric acid. The product contained some free acid and lactone (infrared spectrum). Accordingly the material was neutralized in methanol with ethereal diazomethane, again treated with sodium borohydride, and the product was worked up as described above. A small quantity of acid and lactone still present was removed by dissolving the product in excess hot 0.05 *N* sodium hydroxide and then treating with a mixed-bed resin of Amberlite IR-120 and IR-4B. (Reduction of the lactone was more efficient when, in a separate run, the reaction was carried out in cold methanol in the presence of sodium methoxide (20).) The final product was a colorless glass which gave a single spot (R_{Rh} 1.9) on a paper chromatogram using the ammoniacal silver nitrate spray, and was shown by its infrared spectrum to contain neither carboxyl nor lactone groups; $[\alpha]_D^{25}$ +13.7° (*c*, 2.9, water). Weight 3.0 g. Calculated for $C_{14}H_{22}O_7$: C, 55.62%; H, 7.34%. Found: C, 55.66%; H, 7.34%.

*2-C-(Hydroxymethyl)-*D*-arabo-hexitol* ("D-*Fructoheptitol*")

The *O*-benzyl heptitol was dissolved in ethanol (20 ml.) and treated at ambient temperature and pressure with hydrogen in the presence of palladium black catalyst (0.10 g.).

Approximately 1 mole of hydrogen was taken up in 2 hours' reaction time; ultraviolet absorption analysis then showed complete absence of the benzyl group. Removal of the catalyst and evaporation of the solvent afforded a sirupy product having the same R_{Rh} (0.53) on a paper chromatogram as authentic "D-fructoheptitol" (21), and an infrared absorption spectrum indistinguishable from that of the latter compound. The material was acetylated with hot acetic anhydride – sodium acetate. The sirupy acetate formed gave an infrared absorption spectrum which, except for the added presence of a weak hydroxyl band, was indistinguishable from that of "D-fructoheptitol" heptaacetate (21), and had the same specific rotation; $[\alpha]_D^{25}$ +31.0° (*c*, 6.0, chloroform) (authentic material has $[\alpha]_D^{24}$ +31.6° (21)). The product crystallized with difficulty, however, and after repeated recrystallization from ethanol–water the acetate (10 mg.) melted at 63°–67° C., undepressed by admixture with an authentic specimen (69°–70° C.). The X-ray diffraction pattern of the compound was indistinguishable from that of "D-fructoheptitol" heptaacetate. Calculated for $C_{21}H_{30}O_{14}$: C, 49.80%; H, 5.97%; acetyl, 60.8%. Found: C, 50.15%; H, 6.35%; acetyl, 60.5%.

Glycol-Cleavage Oxidations of 3-O-Benzyl-2-C-(hydroxymethyl)-D-arabo-hexitol

Oxidation of the *O*-benzyl polyol was examined using excess lead tetraacetate in acetic acid and excess sodium metaperiodate in water. At intervals, aliquots were removed from each reaction mixture and the consumption of oxidant was measured: lead tetraacetate (moles per mole)—1.85 (10 minutes), 2.20 (25 minutes), 2.55 (40 minutes); periodate (moles per mole)—2.45 (5 minutes), 2.60 (15 minutes), 2.77 (25 minutes).

3-*C*-(*Hydroxymethyl*)-D-*glycero-tetrose* (D-*Apiose*)

3-*O*-Benzyl-2-*C*-(hydroxymethyl)-D-*arabo*-hexitol (1.5 g.) was dissolved in acetic acid (20 ml.) and lead tetraacetate (4.2 g., 1.9 molar equivalents) in acetic acid (140 ml.) was added. After the oxidant has been consumed, oxalic acid (0.8 g.) in acetic acid (8.0 ml.) was added with stirring, the precipitate was filtered off, and the solvent evaporated. The sirup was extracted with ethyl acetate and the extract concentrated yielding a sirup (1.0 g.) which was treated under reflux with methanolic hydrogen chloride (0.5%, 20 ml.) for 2 hours and at room temperature for 18 hours. Acid was removed with silver carbonate and the methanolic filtrate evaporated yielding a sirup (0.88 g.) non-reducing to Fehling's solution. The product was catalytically debenzylated as described above, and then hydrolyzed with 0.3 *N* sulphuric acid for 1 hour at 95° C. The hydrolyzate was neutralized with Dowex-1 resin (bicarbonate form) and concentrated. The resulting sirup (0.40 g.), which was found by paper chromatography to contain three components (R_{Rh} 1.3, 0.9, and 0.5, respectively), was chromatographed on a cellulose column (23) using *n*-butanol half-saturated with water. The fraction corresponding to D-apiose (R_{Rh} 0.9) was collected, filtered through a Seitz bacterial filter, and concentrated. The residue was taken up in water, and the solution filtered through charcoal and concentrated giving a clear colorless sirup (94 mg.); $[\alpha]_D^{25}$ +6.4° (*c*, 1.0, water). The infrared absorption spectrum was identical with that of D-apiose isolated from parsley. Treated with 2,5-dichlorophenylhydrazine according to the procedure of Bell *et al.* (6), the product (50 mg.) gave an osazone which after two recrystallizations from aqueous ethanol (weight 47 mg.) had m.p. 194°–195.5° C. (corr.) (Bell *et al.* (6) report m.p. 188.5°–190.5° C. for D-apiose-2,5-dichlorophenylosazone). The X-ray diffraction pattern of the osazone was identical with that of the 2,5-dichlorophenylosazone prepared from D-apiose isolated according to the procedure of Vongerichten (1) from parsley. Calculated for $C_{17}H_{16}O_3N_4Cl_4$: C, 43.80%; H, 3.46%. Found: C, 44.04%; H, 3.43%.

Can. J. Chem. Downloaded from www.nrcresearchpress.com by 200.7.193.243 on 09/04/12
For personal use only.

ACKNOWLEDGMENTS

The authors express their gratitude to Dr. A. C. Neish for samples of 2-*C*-hydroxymethyl-L-xyluronic acid and D-fructoheptitol heptaacetate. They also thank Mr. J. A. Baignée for microanalyses, Mr. J. W. L. C. Christ for technical assistance, Miss A. Epp and Mr. G. B. Rennie for infrared absorption measurements, and Mr. T. M. Mallard for preparation of X-ray diffraction patterns.

REFERENCES

1. VONGERICHTEN, E. Ann. **318**, 121 (1901).
2. HEMMING, R. and OLLIS, W. D. Chem. & Ind. 85 (1953).
3. NORDSTRÖM, C. G., SWAIN, T., and HAMBLIN, A. J. Chem. & Ind. 85 (1953).
4. GUPTA, S. R. and SESHADRI, T. R. Proc. Indian Acad. Sci. A, **35**, 242 (1952).
5. FAROOQ, M. O., VARSHNEY, I. P., and RAHMAN, W. Naturwiss. **44**, 444 (1957).
6. BELL, D. J., ISHERWOOD, F. A., and HARDWICK, N. E. J. Chem. Soc. 3702 (1954).
7. PATRICK, A. D. Nature, **178**, 216 (1956).
8. SCHMIDT, O. Th. Ann. **483**, 115 (1930).
9. HUDSON, C. S. Advances in carbohydrate chemistry. Vol. 4. Academic Press, Inc., New York. 1949. p. 57.
10. RAPHAEL, R. A. and ROXBURGH, C. M. J. Chem. Soc. 3405 (1955).
11. LEVENE, P. A. J. Biol. Chem. **23**, 145 (1915).
12. LEVENE, P. A. and MEYER, G. M. J. Biol. Chem. **26**, 355 (1916).
13. HUDSON, C. S. J. Am. Chem. Soc. **39**, 462 (1917); **40**, 813 (1918).
14. WOODS, R. J. and NEISH, A. C. Can. J. Chem. **32**, 404 (1954).
15. WEERMAN, R. A. Rec. trav. chim. **37**, 16 (1917).
16. PERLIN, A. S. J. Am. Chem. Soc. **76**, 2595 (1954).
17. OHLE, H. and KOLLER, I. Ber. **57**, 1566 (1924).
18. FREUDENBERG, K., HOCHSTETTER, H. VON, and ENGELS, H. Ber. **58**, 666 (1925).
19. WOLFROM, M. L. and ANNO, K. J. Am. Chem. Soc. **74**, 5583 (1952).
20. FRUSH, H. L. and ISBELL, H. S. J. Am. Chem. Soc. **78**, 2844 (1956).
21. WOODS, R. J. and NEISH, A. C. Can. J. Chem. **31**, 471 (1953).
22. PRINS, D. A. and REICHSTEIN, T. Helv. Chim. Acta, **24**, 396 (1941).
23. HOUGH, L., JONES, J. K. N., and WADMAN, W. H. J. Chem. Soc. 2511 (1949).
24. HORROCKS, R. H. Nature, **164**, 444 (1949).
25. PERLIN, A. S. and BRICE, C. Can. J. Chem. **33**, 1216 (1955).
26. VONGERICHTEN, E. and MÜLLER, F. Ber. **39**, 241 (1906).
27. PARTRIDGE, S. M. Nature, **158**, 270 (1946).
28. PORCK, A. J. E. and CRAIG, B. M. Can. J. Chem. **33**, 1286 (1955).
29. CHARLSON, A. J. and PERLIN, A. S. Can. J. Chem. **34**, 1200 (1956).
30. BELLAMY, L. J. The infrared spectra of complex molecules. John Wiley & Sons, Inc., New York. 1954. p. 159.
31. SCHMIDT, O. TH. and WEBER-MOLSTER, C. C. Ann. **515**, 43 (1934).

Can. J. Chem. Downloaded from www.nrcresearchpress.com by 200.7.193.243 on 09/04/12
For personal use only.

Can. J. Chem. Downloaded from www.nrcresearchpress.com by 200.7.193.243 on 09/04/12
For personal use only.

SYNTHESIS OF SOME HEXANEDIOLS[1]

E. VON RUDLOFF

ABSTRACT

A general method for the preparation of 1,3-, 1,4-, and 1,5-hexanediols is described. The synthesis involves the preparation of a corresponding ketohexanoate, which is reduced to the diol with lithium aluminum hydride. Countercurrent distribution was found useful in the purification of small amounts of intermediates and end products. 1,2-, 1,6-, and 2,5-hexanediols were also prepared by known procedures. The infrared spectra of these diols have been recorded and their *p*-nitrobenzoates were prepared.

The analysis of mixtures of polyols obtained in the hydrogenolysis of methyl glucoside (1) required small amounts of various hexanediols for identification purposes. This paper describes a convenient method for preparing 3-, 4-, and 5-ketohexanoates, from which the 1,3-, 1,4-, and 1,5-hexanediols were obtained in 75–85% yield by lithium aluminum hydride reduction (2). It also describes the preparation of 1,2-, 1,6-, and 2,5-hexanediols by known procedures, and the preparation and characteristics of the *p*-nitrobenzoates. The infrared spectra of all of these hexanediols are recorded.

Hexanediols have been prepared by a variety of methods, none of which appeared to be generally applicable, and most suffered from the disadvantage that the starting materials were not readily available. Also, different types of crystalline derivatives were reported, making characterization by comparison difficult. No reference to the infrared spectra of these hexanediols could be found, although Kuhn (3) discusses the effect of hydrogen bonding on the infrared absorption band of the hydroxyl groups in 1,6-hexanediol.

The direct synthesis of hexanediols by general methods, such as the Grignard synthesis (4), did not appear feasible. A useful approach to their preparation appeared to be the synthesis of the corresponding keto- or hydroxy-acid (or ester), the latter being reduced readily to the hexanediol. When the synthesis of 4- and 5-ketohexanoic acids was attempted on a 10th molar scale by the methods of Winterfeld and Rönsberg (5), Yoho and Levine (6), and Perlin and Purves (7) only very low yields of rather impure keto-acids were obtained. Purification by fractional distillation on this scale proved unsatisfactory. The method of Cason *et al.* (8) for the preparation of keto-esters (III) was then modified according to Perlin and Purves and satisfactory results were obtained when the difficulties of purification of 5 to 10 g. reaction products had been overcome. The synthesis involves the preparation of a given carboxy acyl chloride (I), via the semi-ester of the dicarboxylic acid, which was reacted with the appropriate dialkyl cadmium (II). The latter was prepared in isopropyl ether (7) from the Grignard intermediate.

$$\underset{\text{I}}{2R'O_2C.(CH_2)_n.COCl} + \underset{\text{II}}{CdR_2} \longrightarrow \underset{\text{III}}{2R'O_2C.(CH_2)_n.\overset{\overset{O}{\|}}{C}.R} + CdCl_2$$

Provided the semi-ester was pure, the keto-ester was obtained in a satisfactory state of purity on fractional distillation. When the semi-ester was isolated impure (e.g. monoethyl malonate), neither the ketohexanoate nor the hexanediol could be purified satisfactorily

[1]*Manuscript received November 25, 1957.*
Contribution from the National Research Council of Canada, Prairie Regional Laboratory, Saskatoon, Saskatchewan.
Issued as N.R.C. No. 4616.

Can. J. Chem. Vol. 36 (1958)

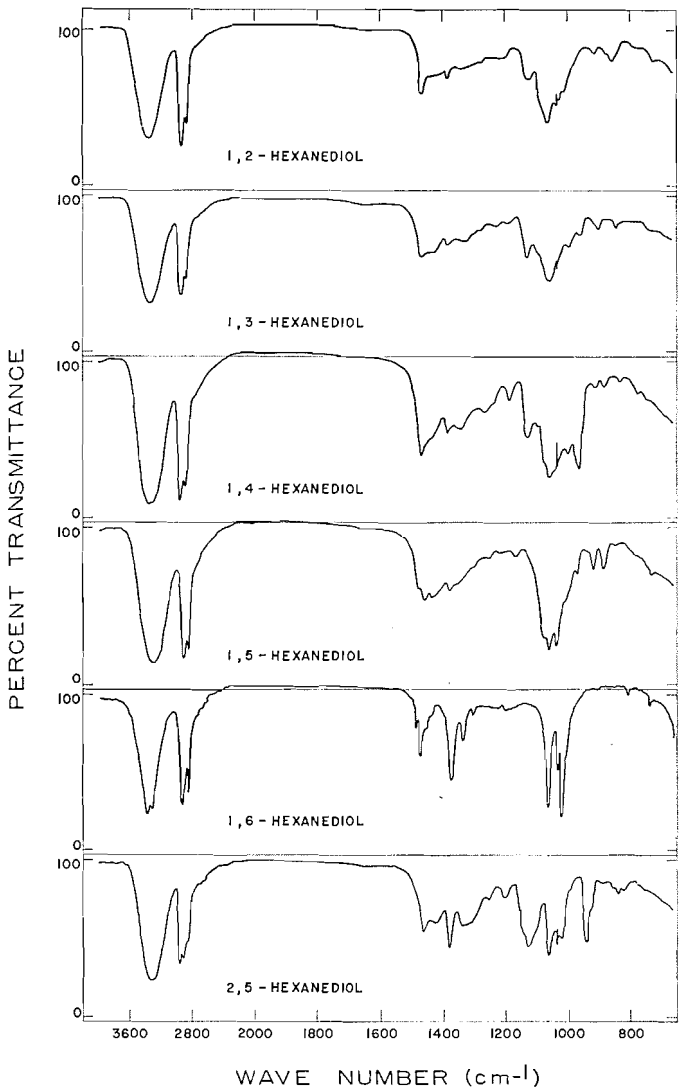

FIG. 1. Infrared spectra of hexanediols.

by fractional distillation. However, purification was possible by using countercurrent distribution. The distribution pattern of the keto-esters could not be obtained by weight analysis because of high solvent volatility. The impure keto-esters, therefore, were reduced and the reaction product was then fractionated and analyzed by countercurrent distribution, using weight analysis to obtain the distribution pattern. This analysis showed that the contaminant was the diol corresponding to the dicarboxylic acid component, indicating that the di-ester must have been present in the reaction mixture.

Reduction of the keto-esters with lithium aluminum hydride proceeded smoothly, and a good recovery of the products was obtained by salting out and extracting with ether containing 5–10% acetone. The use of methylal as solvent (9), as used in the reduction of adipic acid to 1,6-hexanediol, also gave satisfactory results. Catalytic reduction, as in the conversion of ethyl 5-ketohexanoate to 1,5-hexanediol in 85% yield by Hill and

Can. J. Chem. Downloaded from www.nrcresearchpress.com by 200.7.193.243 on 09/04/12
For personal use only.

Adkins (10), may sometimes be advantageous since the reaction can be carried out in ethanol or dioxane and larger quantities can be readily handled. The over-all yields of 1,5-, 1,4-, and 1,3-hexanediols were about 50%, 45%, and 30% respectively (based on the weight of semi-ester).

1,2-Hexanediol was prepared in about 45% over-all yield by α-bromination of caproic acid (11), hydrolysis to α-hydroxycaproic acid (12), and reduction with lithium aluminum hydride. Lithium aluminum hydride reduction of adipic acid (9) and acetonyl acetone gave 1,6- and 2,5-hexanediol, respectively, in better than 80% yield. 2,5-Hexanediol was also prepared in about 95% yield by catalytic hydrogenation of acetonyl acetone, using ethanol as solvent and copper chromium oxide as catalyst (10, 13).

Previously, it was found that hexanediols give a better yield of the *p*-nitrobenzoate than of the 3,5-dinitrobenzoate (1). Since the *p*-nitrobenzoates of hexanediols are crystalline compounds with high melting points, these were prepared as suitable derivatives. The 1,3-isomer was dimorphous, a phenomenon which was also observed with the *p*-nitrobenzoate of 1,3-propanediol.

The infrared spectra of the individual hexanediols (see Fig. 1), except those of 1,2- and 1,3-hexanediol, differ sufficiently from each other to allow identification. No significant differences were found in the spectra of the *p*-nitrobenzoates.

EXPERIMENTAL

All melting points are corrected and were measured with a Leitz heating stage microscope. The infrared spectra were recorded with a Perkin Elmer model 21 spectrometer equipped with a sodium chloride prism. Liquid compounds were mounted by the suspended film technique and solids by the potassium bromide disk technique (14). Countercurrent distribution was carried out with a 100 tube modified E.C. Apparatus Co. fractionator having 40 ml. tube capacity (20 ml. upper and 20 ml. lower phase). *p*-Nitrobenzoates were prepared by the Schotten–Baumann reaction, using pyridine as base and solvent (15), and they were recrystallized from ethyl acetate – petrol and 2-butanone–petrol (b.p. 64°–66° C.).

Semi-esters of Dicarboxylic Acids

Succinic anhydride and glutaric anhydride were prepared by refluxing the dicarboxylic acids with excess acetic anhydride (16). The anhydrides were then converted to the monomethyl esters by the method of Ruggli and Maeder (17), e.g. succinic anhydride, 25 g. (0.25 mole), was refluxed with absolute methanol, 20 ml., for ½ to 1 hour. The excess methanol was removed by evaporation in a rotary evaporator and the residue cooled to about 5° C., when it solidified. The crude material was recrystallized three times from ether to give monomethyl succinate, 29 g. (88% of theory), m.p. 58° C. Monomethyl glutarate was obtained similarly in about 80% yield and was purified by fractional distillation, b.p. 153°–155° C. at 10–11 mm.

Monoethyl malonate was prepared by saponification of the diethyl ester with the theoretical amount of potassium hydroxide (18). Diethyl malonate, 50 g. (0.31 mole), in 200 ml. absolute ethanol was added slowly to a solution of potassium hydroxide, 17.5 g. (0.31 mole), in 200 ml. absolute ethanol. The mixture was allowed to stand at room temperature until it was neutral. It was then heated and filtered hot. The potassium salt crystallized rapidly and after crystallization was complete it was filtered off, washed twice with cold ethanol and once with ether. The crystalline product was dissolved in a minimum of water and acidified in the cold with concentrated hydrochloric acid. On

Can. J. Chem. Downloaded from www.nrcresearchpress.com by 200.7.193.243 on 09/04/12
For personal use only.

standing, a little malonic acid crystallized, which was filtered off. The aqueous solution was then extracted repeatedly with ether. The ethereal extracts were washed once with water and then dried over anhydrous sodium sulphate. When the dried ethereal solution was reduced to a small volume, more malonic acid crystallized. The residue from evaporation of the filtered ethereal solution was fractionally distilled *in vacuo*, to give 29 g. monoethyl malonate (about 70% of theory), b.p. 131°–133° C. at 11–12 mm.

Synthesis of Ketohexanoates

The following is a typical example of the procedure adopted for the preparation of methyl or ethyl 3-, 4-, and 5-ketohexanoate.

To monomethyl succinate, 13.2 g. (0.10 mole), was added thionyl chloride (reagent grade), 15 g. (0.125 mole), and the mixture was left at room temperature under a reflux condenser equipped with a calcium chloride tube. After the evolution of gas had subsided, the solution was heated at 40°–45° C. for 3 to 6 hours and was left at room temperature for a further 16 hours. Excess thionyl chloride was then removed on a rotary evaporator at 15 mm. and 40°–45° C. (17). The residual acid chloride was dissolved without further purification in 25 ml. dry, peroxide-free isopropyl ether and added dropwise with stirring to a cooled mixture of the dialkyl cadmium. The latter mixture was prepared by reacting magnesium, 3.6 g. (0.15 g. atom), in isopropyl ether (7), 60–65 ml., with dry ethyl bromide, 17.4 g. (0.16 mole), in 25 ml. isopropyl ether in the normal Grignard manner, and adding to the cooled solution with vigorous stirring anhydrous cadmium chloride (dried in a vacuum oven at 70° C. for 18 to 24 hours), 14.7 g. (0.08 mole), in one portion.

After addition of the acid chloride was complete, the mixture was refluxed with stirring for 3 to 4 hours and was left at room temperature for 16 hours, and was then poured into excess ice and 10% sulphuric acid. The aqueous layer was separated and extracted three times with an equal volume of ether. The ethereal extracts were added to the isopropyl ether layer and the combined solution was washed once with 5% sodium bicarbonate solution, twice with water, and dried over anhydrous sodium sulphate. On evaporation of the ether a light brown liquid was obtained. It was distilled *in vacuo* and the fraction of b.p. 75°–78° C. at 11–12 mm. was collected. The yield of impure methyl 4-ketohexanoate was 9 g. (63% of theory).

Attempts to purify the keto-esters thus obtained by fractional distillation were unsuccessful, presumably because of the small amounts available. Countercurrent distribution, using 40 to 70% ethanol and petrol b.p. 64°–66° C. as solvent pair, gave a satisfactory separation, but about one-half of the keto-esters was lost on evaporation of the solvents. In this manner methyl 5-ketohexanoate, b.p. 100°–101° C. at 11–12 mm., was obtained in 20–25% over-all yield. Calc. for $C_7H_{12}O_3$: C, 58.31; H, 8.39%; saponification equivalent 144.17. Found: C, 58.17; H, 8.45%; saponification equivalent 145.

Reduction to Hexanediols

A solution of impure methyl 4-ketohexanoate, 4.3 g. (0.03 mole), in dry ether, 50 ml., was added dropwise with stirring to a suspension of lithium aluminum hydride, 1.9 g. (0.05 mole), in dry ether, 100 ml., which had been refluxed previously for $\frac{1}{2}$ to 1 hour. The usual precautions against moisture were taken. The mixture was refluxed for $\frac{1}{2}$ to 1 hour after addition of the ester, and, after cooling, ice water was added dropwise until excess lithium aluminum hydride had reacted. To the cold mixture was added cold 10% sulphuric acid, 10–20 ml., and after the mixture had cleared, it was saturated with potassium carbonate. The ether layer was withdrawn after adding 10 to 15 ml. acetone. The aqueous layer was then extracted exhaustively with ether containing 5–10% acetone. The ethereal

Can. J. Chem. Downloaded from www.nrcresearchpress.com by 200.7.193.243 on 09/04/12
For personal use only.

extracts were dried first over anhydrous potassium carbonate and then over anhydrous sodium sulphate. On evaporation of the ether, impure 1,4-hexanediol, 2.8 g. (80% of theory), was obtained. The mixture, 1.87 g., was fractionated by countercurrent distribution, using 2-butanone–water as solvent pair and 70 transfers. The distribution pattern was obtained by evaporating every second tube and weighing the residue in 20-ml. porcelain crucibles. Tubes 9–26 contained a viscous liquid, 0.45 g., which had an infrared spectrum identical to that of 1,4-butanediol. Calc. for $C_4H_{10}O_2$: C, 53.23; H, 11.49%. Found: C, 53.31, H, 11.19%. The *p*-nitrobenzoate, m.p. 175°–176° C., was undepressed in a mixture with an authentic specimen (m.p. 175°–176° C.). Tubes 28–40 contained 1,4-hexanediol, 1.25 g. The analytical data for this, as well as all the other hexanediols and their *p*-nitrobenzoates, are summarized in Table I.

TABLE I

	Hexanediols				*p*-Nitrobenzoates			
	B.p. at 0.3 mm. (air bath), ° C.	n_D^{20}	% C*	% H	M.p., ° C.	% C†	% H	% N
1,2-[1]	75–80	1.4431	61.11	11.75	101.5–102.5	57.79	4.87	6.63
1,3-[2]	85–90	1.4455	60.91	11.84	78–79 and 93–95.5	57.50	4.88	6.71
1,4-[3]	75–80	1.4515	60.93	11.97	124.8–125.4	57.55	4.82	6.72
1,5-[4]	85–90	1.4490	60.94	12.10	103.5–104.2	57.63	4.72	6.62
1,6-[5]	m.p. 41.0–41.8	—	61.23	12.10	121.8–122.5[6]	57.77	4.80	6.71
2,5-[7]	80–85	1.4474	60.92	11.87	170.0–171.0	57.79	4.86	6.48

*Calculated for $C_6H_{14}O_2$: C, 60.98; H, 11.94%.
†Calculated for $C_{20}H_{20}N_2O_8$: C, 57.69; H, 4.84; N, 6.73%.
[1]Levene and Haller (19): b.p. 110°–131° C. at 6 mm. (dinaphthylurethan m.p. 172°–174° C.).
[2]Glacet (20): b.p. 123°–123.4° C. at 13 mm., n_D^{22} 1.4461 (diphenylurethan m.p. 99.3° C.).
[3]Glacet (20): b.p. 127.5°–127.7° C. at 13 mm., $n_D^{16.3}$ 1.4530 (diphenylurethan m.p. 71° C.).
[4]Hill and Adkins (10): b.p. 89°–91° C. at 0.5 mm.
[5]Haworth and Perkin (21): b.p. 152° C. at 17 mm.; m.p. 42° C.
[6]Heyns and Woyrsch (22): m.p. 120° C.
[7]Duden and Lemme (23): b.p. 120°–122° C. at 12 mm.; n_D^{20} 1.4475.

In the same manner 1,5-hexanediol and 1,3-hexanediol were obtained in about 50% and 30% over-all yield respectively. In addition to 1,3-hexanediol, a considerable amount of 1,3-propanediol, *p*-nitrobenzoate, m.p. 109°–111° C. and 117°–118.5° C., mixed m.p. with an authentic specimen 111°–112° C. and 117°–118.5° C., was isolated.

Lithium aluminum hydride reduction of α-hydroxycaproic acid, adipic acid (9), and 2,5-hexanedione (acetonyl acetone) gave 1,2-, 1,6-, and 2,5-hexanediol respectively in 75–85% yield. α-Hydroxycaproic acid, m.p. 60°–62.5° C., was prepared in about 60% over-all yield by α-brominating caproic acid (11) and hydrolyzing the α-bromocaproic acid with aqueous potassium carbonate (12). Adipic acid, m.p. 151°–153° C., and 2,5-hexanediol, b.p. 192°–194° C., were obtained commercially. 2,5-Hexanediol was also prepared in better than 90% yield by hydrogenation over copper chromium oxide according to the method of Hill and Adkins (10).

ACKNOWLEDGMENTS

The author wishes to express his thanks to Mr. J. A. Baignee for the microanalyses, to Miss A. Epp and Mr. G. Rennie for recording the infrared spectra, to Mr. M. Granat for technical assistance, and to Dr. A. S. Perlin for advice and discussions.

Can. J. Chem. Downloaded from www.nrcresearchpress.com by 200.7.193.243 on 09/04/12
For personal use only.

REFERENCES

1. RUDLOFF, E. VON, STUETZ, D. E., and BAUER, H. F. Can. J. Chem. **35**, 315 (1957).
2. NYSTROM, R. F. and BROWN, W. G. J. Am. Chem. Soc. **69**, 1197 (1947).
3. KUHN, L. P. J. Am. Chem. Soc. **74**, 2492 (1952).
4. KHARASH, M. S. and REINMUTH, O. Grignard reactions of nonmetallic substances. Prentice-Hall, Inc., New York. 1954.
5. WINTERFELD, K. and RÖNSBERG, H. E. Arch. Pharm. **274**, 40 (1936).
6. YOHO, C. W. and LEVINE, R. J. Am. Chem. Soc. **74**, 5597 (1952).
7. PERLIN, A. S. and PURVES, C. B. Can. J. Chem. **31**, 227 (1953).
8. (*a*) CASON, J. J. Am. Chem. Soc. **64**, 1106 (1942).
   (*b*) CASON, J. and PROUT, F. S. J. Am. Chem. Soc. **66**, 46 (1944).
9. BERNATEK, E. Acta Chem. Scand. **8**, 874 (1954).
10. HILL, R. M. and ADKINS, H. J. Am. Chem. Soc. **60**, 1033 (1938).
11. MARVEL, C. S. *In* Organic syntheses. Vol. III. *Edited by* E. C. Horning. John Wiley & Sons, Inc., New York. 1955. p. 523.
12. HELL, C. and TWERDOMEDOFF, S. Chem. Ber. **22**, 1745 (1889).
13. ADKINS, H. and BILLICA, H. R. J. Am. Chem. Soc. **70**, 3121 (1948).
14. SCHIEDT, O. and REINWEIN, H. Z. Naturforsch. **7b**, 270 (1952).
15. SHRINER, R. L. and FUSON, R. C. The systematic identification of organic compounds. 2nd ed. John Wiley & Sons, Inc., New York. 1940. p. 137.
16. VOGEL, A. I. A textbook of practical organic chemistry. Longmans, Green & Co., Inc., New York. 1948. p. 371.
17. RUGGLI, P. and MAEDER, A. Helv. Chim. Acta, **25**, 936 (1942).
18. FREUND, M. Chem. Ber. **17**, 780 (1884).
19. LEVENE, P. A. and HALLER, H. L. J. Biol. Chem. **79**, 475 (1928).
20. GLACET, C. Compt. rend. **218**, 283 (1944).
21. HAWORTH, W. N. and PERKIN, W. H. J. Chem. Soc. **65**, 598 (1867).
22. HEYNS, K. and WOYRSCH, O. F. Chem. Ber. **86**, 76 (1953).
23. DUDEN, P. and LEMME, R. Chem. Ber. **35**, 1335 (1902).

Can. J. Chem. Downloaded from www.nrcresearchpress.com by 200.7.193.243 on 09/04/12
For personal use only.

THE COMPOUND $CaO.Ti_2O_3$[1]

NORMAN F. H. BRIGHT,[2] JOHN F. ROWLAND,[2] AND JOSEPH G. WURM[3]

ABSTRACT

By electrolyzing baths of molten $CaCl_2$ containing perovskite ($CaO.TiO_2$), a compound within the ternary Ca–Ti–O system, namely $CaO.Ti_2O_3$, has been obtained. The compound has been identified by chemical analysis, and its crystallographic data have been determined by X-ray means. Attempts to synthesize the compound apart from the electrolytic cell have, so far, failed.

INTRODUCTION

The only publications of work dealing with compounds within the ternary system Ca–Ti–O in which the titanium is in any state of valency other than the tetravalent are those of Bertaut and Blum (1, 2). In their work, the crystallography of a compound, to which is assigned the formula $CaTi_2O_4$, is described. The system CaO–TiO_2 has been studied by von Wartenberg, Reusch, and Saran (3), and their work did not indicate the existence of any compound between $CaO.TiO_2$ and TiO_2, but merely of a eutectic having a melting point of approximately 1450° C.; further, there was no indication in their work of any compound containing a lower proportion of oxygen.

In the course of work on the electrochemistry of the production of titanium, a material was encountered which forms the subject of this paper. The material was examined by chemical, X-ray diffraction, and spectrographic means and has been shown to be $CaTi_2O_4$ (or $CaO.Ti_2O_3$); some of its properties have been determined. This work was done independently and without the knowledge of the work of Bertaut and Blum. Their work was entirely crystallographic, whereas, as mentioned above, the present work includes chemical data.

EXPERIMENTAL

(*a*) *Preparation of the Compound*

When a bath composed of 300 g. of calcium chloride and containing 60 g. of calcium titanate, $CaO.TiO_2$, which is slightly soluble in the molten chloride, was electrolyzed under an inert atmosphere for 70 minutes at a current of 14 amp. at 850° C. and allowed to cool, some black, lustrous, well-formed crystals were observed close to the cathode.

(*b*) *Chemical Examination of the Compound*

Examination of the crystals under a low-power microscope showed them to be prismatic in form and very well developed. No difficulty was experienced in selecting suitable specimens for detailed X-ray crystallographic examination.

The examination of the material by semiquantitative spectrographic analysis showed that Ca and Ti were the only detectable major metallic constituents.

About 60 mg. of the material was available for chemical analysis, and the determinations shown in Table I were made.

The methods used for analysis were as follows:

Calcium.—Determined with a Perkin–Elmer flame photometer at 6200 Å, after

[1]*Manuscript received November 1, 1957.*
Contribution from the Mineral Dressing and Process Metallurgy Division, Mines Branch, Department of Mines and Technical Surveys, Ottawa, and the Faculté des Sciences, Université Laval, Québec. Published with the permission of the Director, Mines Branch, Ottawa.
[2]*Head and Scientist respectively, Physical and Crystal Chemistry Section, Mineral Dressing and Process Metallurgy Division, Mines Branch, Ottawa.*
[3]*Faculté des Sciences, Université Laval, Québec.*

Can. J. Chem. Downloaded from www.nrcresearchpress.com by 200.7.193.243 on 09/04/12
For personal use only.

TABLE I

Element	% by weight
Ca	20.3±0.2
Ti	47.0±0.1 (all trivalent)
Fe	1.05±0.05 (mean of two determinations)
C	0.07±0.02
F	None detectable

removal of iron and titanium as "cupferrides", aluminum as 8-hydroxyquinolate, and after removal of excess organic reagents.

Iron.—Determined in the chloroform solution of the "cupferride" by colorimetric means with *o*-phenanthroline, using a Coleman MK.14 spectrophotometer at $\lambda = 500\ \mu\mu$.

Titanium.—Determined in the chloroform solution of the "cupferride" by colorimetric means with hydrogen peroxide, using a Coleman MK.14 spectrophotometer at $\lambda = 410\ \mu\mu$. This gives the total titanium. The trivalent titanium was determined by dissolving the sample in aqueous sulphuric acid, and titrating against standard ferric alum, all under an argon atmosphere.

Carbon.—Determined by a standard combustion procedure.

Fluorine.—HF steam-distilled off at 135°–140° C. from an aqueous perchloric acid suspension of the sample. Fluoride estimated amperometrically at pH = 7.0 using thorium nitrate solution previously standardized against NaF.

The unestimated material, approximately 31.6%, is presumably oxygen since no major constituent other than calcium and titanium was detectable spectrographically.

An X-ray powder diffraction pattern of the crushed material was taken using CoK_α radiation and a 57.3 mm. diameter Debye-Scherrer camera. The pattern was well defined, but could not be identified by reference to either the A.S.T.M. Card Index of X-Ray Diffraction Patterns or any other source of data available to the authors.

The material showed slight signs of ferromagnetism, and certain weak lines in the X-ray diffraction pattern could be interpreted as being due to the presence of a small amount of metallic iron. It was considered, therefore, that the iron in the above chemical analysis is probably due to the presence of a small quantity of free metallic iron and that the main compound is essentially a calcium–titanium–oxygen compound. On this basis, the observed and theoretical compositions and atomic ratios of the relevant compounds are as follows:

	Ca	Ti	O
Observed	20.3±0.2%	47.0±0.1%	31.6±0.3% (by difference)
Atomic ratios	1.000	1.937±0.015	3.900±0.075
Calculated for $CaTi_2O_4$	20.1%	47.9%	32.0%
Calculated for $CaTi_2O_5$	18.6%	44.4%	37.0%

It thus seems reasonable to conclude that the compound represented by our data is, in fact, $CaO.Ti_2O_3$. It must, however, be borne in mind that the above chemical analyses were made on very small quantities of material and, in any case, the analytical procedures were not simple.

The limits of error quoted in Table I are merely those of the final stage of each estimation; with the very small quantities of material available for investigation there was no

Can. J. Chem. Downloaded from www.nrcresearchpress.com by 200.7.193.243 on 09/04/12
For personal use only.

TABLE II

Data	Present work	Data of Bertaut and Blum
Crystal system	Orthorhombic	Orthorhombic
Cell dimensions, Å	$a_0 = 9.73$	9.727
	$b_0 = 9.99$	9.976
	$c_0 = 3.14_7$	3.136
Z	4	4
Space group	$Bbmm-D_{2h}^{17}$ (V_h^{17})	$Bbmm-(D_{2h}^{17})$

TABLE III

X-RAY POWDER DIFFRACTION DATA FOR $CaO.Ti_2O_3$

Intensities assessed visually with strongest line as 100. Calculated d-spacings based on orthorhombic unit cell having dimensions $a = 9.73$, $b = 9.99$, $c = 3.14_7$ Å

Int.	d (meas.)	d (calc.)	($hk!$)	Int.	d (meas.)	d (calc.)	($hk!$)
		4.99	020	10	1.610	1.621	600
20	4.96	4.86	200	10	1.594	1.600	610
20	2.985	2.994	101			1.575	260
30	2.858	2.868	111	70	1.569	1.574	002
100	2.742	2.747	230			1.571	521
30	2.556	2.568	121	10	1.531	1.544	450
10	2.489	2.498	040			1.542	620
20	2.418	2.431	400			1.501	022
10	2.379	2.362	410	30	1.493	1.497	202
30	2.244	2.258	301			1.496	351
20	2.213	2.222	240	20	1.478	1.482	531
90	2.196	2.202	311			1.481	212
10	2.166	2.186	420	30	1.458	1.457	630
80	2.052	2.058	321			1.455	161
10	1.947	1.964	430	10	1.428	1.434	222
30	1.906	1.918	141	—	—	1.379	541
20	1.869	1.869	331	—	—	1.374	460
20	1.837	1.848	250			1.369	270
10	1.742	1.742	440	40	1.370	1.365	232
10	1.681	1.675	341		1.362	1.360	640
		1.665	060	10	1.345	1.340	361
80	1.658	1.662	151	20	1.321	1.331	042
		1.654	501			1.321	402
20	1.632	1.632	511	10	1.305	1.310	412

ready means of assessing the errors of the various stages of separation involved in these analyses; hence it is possible that the estimations, considered as a whole, may be subject to somewhat larger errors than those quoted. This being the case, a molecular formula of $CaO.2TiO_2$ (i.e., $CaTi_2O_5$) is regarded as very unlikely but not entirely impossible. Such a formula would be analogous to that of magnesium dititanate, $MgO.2TiO_2$, which is a well-established compound. This supposition is, however, in conflict with the work of von Wartenberg *et al.* (3).

Several attempts were made to synthesize both $CaO.Ti_2O_3$ and $CaO.2TiO_2$ by sintering suitable mixtures of the constituent oxides at high temperature under appropriate atmospheric conditions. In neither case was any success achieved, and all the results obtained confirmed the work of von Wartenberg *et al.*

In general, however, it may be said that the chemical evidence supports the formula $CaO.Ti_2O_3$ for the material which forms the subject of the present study, rather than the formula $CaO.2TiO_2$.

Can. J. Chem. Downloaded from www.nrcresearchpress.com by 200.7.193.243 on 09/04/12
For personal use only.

(c) Crystallographic Studies of the Compound

The following morphological data were obtained as the average of observations on two well-formed crystals, using a standard two-circle optical goniometer:

Crystal class: orthorhombic.

Axial ratio: $a:b:c = 0.916:1:0.308$.

The single crystal X-ray work included rotation photographs, zero-layer and first-layer Weissenberg photographs, and cone-axis, zero-level, and first-level precession photographs. The Weissenberg photographs were made using CoK_α radiation, with rotation about the prismatic axis, and the precession photographs were made using MoK_α radiation, with the prismatic axis as the dial axis. The cell edges were determined from these photographs; from the systematic extinctions, the space group was obtained. The results of these examinations are given in Table II.

The space group quoted is the same as for the mineral pseudobrookite, $Fe_2O_3.TiO_2$ (i.e. $TiFe_2O_5$), and for the isomorphous compound magnesium dititanate, $MgO.2TiO_2$ (i.e. $MgTi_2O_5$), referred to earlier.

The powder diffraction pattern was indexed according to our cell dimensions, as shown in Table III, and the agreement between the observed and calculated spacings is quite good; also, the axial ratios determined by optical goniometry agree well with those determined by X-ray diffraction.

DISCUSSION OF RESULTS

It has thus been possible to describe the crystallography of this compound, to which is assigned the formula $CaO.Ti_2O_3$, in a reasonably complete fashion, and to provide a chemical analysis of sufficient accuracy to indicate the molecular formula with virtual certainty, even though it was not found possible to synthesize it apart from the electrolytic method in which it was first prepared. In the work of Bertaut and Blum, the material was obtained by the electrolysis of TiO_2 in molten $CaCl_2$. Their formula is based entirely on X-ray crystallographic evidence. There is good agreement between their X-ray results and those obtained in the course of the present work. The formula, $CaTi_2O_4$, quoted by them is also in good accord with our chemical data. The fact that the titanium is in the trivalent condition, as shown by the chemical analysis, indicates that this compound is best represented by the formula $CaO.Ti_2O_3$. Thus, the present work gives additional data on the electrolytic conditions of preparation of this compound and on its chemical composition, while providing good confirmation of the X-ray crystallographic work of Bertaut and Blum.

ACKNOWLEDGMENTS

The authors wish to express their thanks to Miss E. M. Penner, Mr. L. G. Ripley, and Mr. R. C. McAdam, of the Chemical Laboratory of the Mines Branch, Ottawa, for performing the chemical analyses referred to in this publication.

REFERENCES

1. BERTAUT, E. F. and BLUM, P. J. phys. radium, **17**, 17S (1956).
2. BERTAUT, E. F. and BLUM, P. Acta Cryst. **9**, 121 (1956).
3. VON WARTENBERG, H., REUSCH, H. J., and SARAN, E. Z. anorg. Chem. **230**, 257 (1937).

Can. J. Chem. Downloaded from www.nrcresearchpress.com by 200.7.193.243 on 09/04/12
For personal use only.

Can. J. Chem. Downloaded from www.nrcresearchpress.com by 200.7.193.243 on 09/04/12
For personal use only.

AMINO ACIDS

IV. THE REACTION OF GLYCINE AND β-ALANINE WITH CARBON DISULPHIDE[1]

E. J. TARLTON AND A. F. MCKAY

ABSTRACT

Glycine and β-alanine on condensation with carbon disulphide gave the corresponding 1,3-di-(carboxyalkyl) thioureas. 1,3-Di-(carboxymethyl) thiourea is rearranged to 2-thio-3-(carboxymethyl) hydantoin by warming with hydrochloric acid solution or heating above its melting point. Evidence is presented for the reversible condensation of 2 mole equivalents of the sodium salt of 2-thio-3-(carboxymethyl) hydantoin by the elimination of water. This condensation product is obtained as well-defined pink crystals. 1,3-Di-(β-carboxyethyl) thiourea was oxidized with an alkaline solution of hydrogen peroxide or sodium hypochlorite solution to 1,3-di-(β-carboxyethyl) urea. 1,3-Di-(β-carboxyethyl) thiourea and 1,3-di-(β-carboxyethyl) urea have been cyclized by heating with *p*-toluenesulphonic acid. The products were 2-thio-3-(β-carboxyethyl) hydrouracil and 3-(β-carboxyethyl) hydrouracil respectively.

The reaction of several α-amino acids and carbon disulphide in aqueous sodium bicarbonate solution has been studied earlier by Kodama (1, 2). In most cases, he found that the only identifiable products were substituted thiohydantoins, which presumably were formed by cyclization of the intermediate 1,3-di-(carboxymethyl) thioureas. In the reaction with glycine, however, no distinct products were obtained although the copious evolution of hydrogen sulphide indicated that condensation had occurred. The reaction has now been reinvestigated in conjunction with the condensation of glycine and its homologue, β-alanine, with carbon disulphide.

Sodium glycinate and carbon disulphide were condensed in aqueous solution to yield the crude disodium salt of 1,3-di-(carboxymethyl) thiourea (I*c*). Reaction of this disodium salt with methanolic hydrogen chloride at room temperature gave 1,3-di-(carbomethoxymethyl) thiourea (I*b*) in 25% yield. The combined mother liquors on treatment with concentrated hydrochloric acid gave 2-thio-3-(carboxymethyl) hydantoin (II*a*) (m.p. 214°–215° C. dec.) in 17% yield. The latter compound was identified by analysis and by desulphurization with aqueous chloroacetic acid, to the known 3-(carboxymethyl) hydantoin (III*a*) and methyl ester of 3-(carboxymethyl) hydantoin (III*b*) (3). The methyl ester of 2-thio-3-(carboxymethyl) hydantoin (II*b*) melted at 113°–114° C.

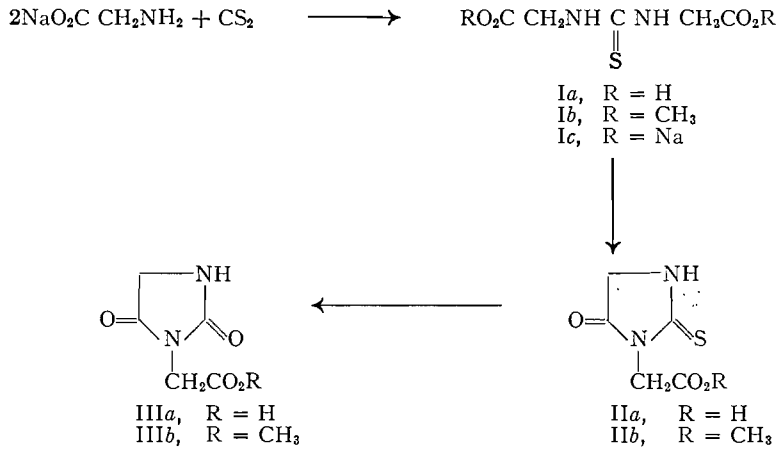

[1]*Manuscript received November 20, 1957.*
Contribution from the L. G. Ryan Research Laboratories of Monsanto Canada Limited, Montreal, Quebec.

Can. J. Chem. Downloaded from www.nrcresearchpress.com by 200.7.193.243 on 09/04/12
For personal use only.

Careful saponification of the dimethyl ester (I*b*) gave 1,3-di-(carboxymethyl) thiourea (I*a*) which melted at 164°–165° C. with loss of 1 mole of water and resolidified to form 2-thio-3-(carboxymethyl) hydantoin which then melted at 214°–215° C. with decomposition. 1,3-Di-(carboxymethyl) thiourea was previously reported (4) as melting at 170° C. with decomposition. In concurrence with previous work (4, 5) this thiourea diacid (I*a*), its dimethyl ester (I*b*), and disodium salt (I*c*) all cyclize in acid solution to give 2-thio-3-(carboxymethyl) hydantoin. As a preparative method, the reaction mixture of crude disodium 1,3-di-(carboxymethyl) thiourea (I*c*) on brief treatment with concentrated hydrochloric acid gave the thiohydantoin (II*a*) in 48% yield.

When the condensation of sodium glycinate and carbon disulphide was conducted in the usual manner and the reaction mixture was acidified at room temperature to a pH of 2 with hydrochloric acid, no precipitation of product occurred. However, the solution yielded an orange-colored product (V)[2] melting at 287°–290° C. with decomposition. A 23% yield of 2-thio-3-(carboxymethyl) hydantoin (II*a*) was obtained from the mother liquors. In another experiment, the high melting condensation product (V) appeared in 31% yield on acidification of the reaction mixture with 2.2 moles of hydrochloric acid, followed by subsequent evaporation and extraction. In this case, the residue from the mother liquors gave on methylation 2-thio-3-(carbomethoxymethyl) hydantoin (II*b*) in 7% yield. The colored condensation product (V) proved to contain chemically bound sodium but it gave a negative halogen test. Potentiometric titration of the compound in aqueous solution with standard alkali showed it to be an acid with a primary pK_a of 3.4 and a neutralization equivalent of 373, which agrees with the acid equivalent (374.31) of the empirical formula $C_{10}H_8N_4O_5S_2Na_2$. Attempts to methylate this product with methanolic hydrogen chloride gave 2-thio-3-(carbomethoxymethyl) hydantoin (II*b*) in 81% yield. Brief treatment of the condensation product (V) with concentrated hydrochloric acid gave an 84% yield of 2-thio-3-(carboxymethyl) hydantoin (II*a*), while desulphurization with aqueous chloroacetic acid followed by methylation gave 3-(carbomethoxymethyl) hydantoin (III*b*) in 25% yield. Other attempted alkylation experiments with benzyl chloride or dimethyl sulphate in the presence of aqueous base led to the isolation of 2-thio-3-(carboxymethyl) hydantoin (II*a*) and not to a derivative of the condensation product (V). Empirically, these observations indicate the condensation product (V) to be the result of an easily reversible condensation of 2 moles of the sodium salt of 2-thio-3-(carboxymethyl) hydantoin with the elimination of 1 mole of water in such a way as to leave a titratable acid function in the product. Potentiometric titration data on 2-thio-3-(carboxymethyl) hydantoin (II*a*) and the colored condensation product add additional evidence to this hypothesis.

The titration of 2-thio-3-(carboxymethyl) hydantoin (II*a*) (Fig. 1, curve A) with 0.1 *N* sodium hydroxide solution gave a typical titration curve for an acid (pK_a 3.2) with an observed neutralization equivalent of 173 (calculated, 174). At the neutralization point (n_1) the color of the solution changed from yellow to red-orange. The solution was then back-titrated with standard hydrochloric acid (Fig. 1, curve B). Again, at the neutralization point (n_2), a color change of red-orange to orange occurred. Curves A and B do not coincide and it will be observed that if the amount of sodium hydroxide solution (0 to n_1) required to neutralize 2-thio-3-(carboxymethyl) hydantoin (II*a*) is 1 mole, then the difference between n_1 and n_2 is 0.5 mole. This can be explained by consideration of the following reaction sequence:

[2]*This product is referred to hereafter as condensation product.*

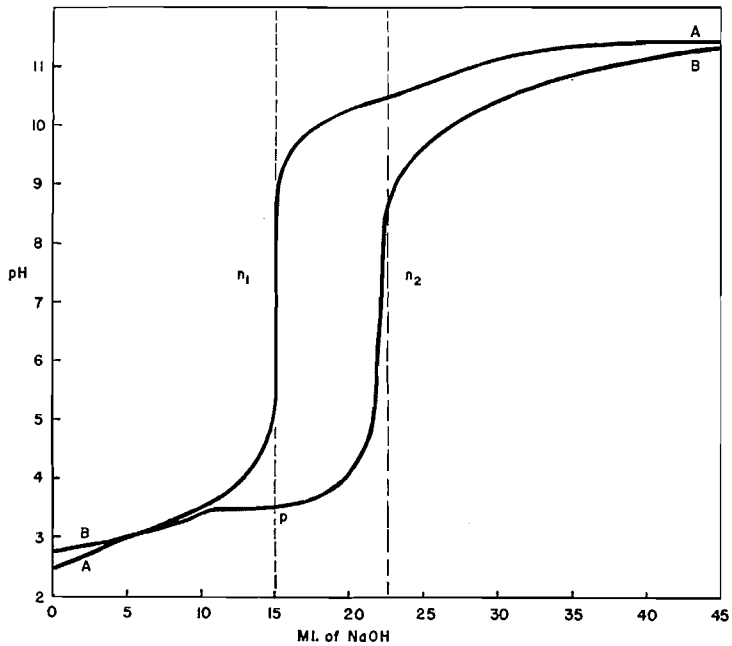

FIG. 1. Titration (*A*) and back-titration (*B*) of 2-thio-3-(carboxymethyl) hydantoin (II*a*) in aqueous solution.

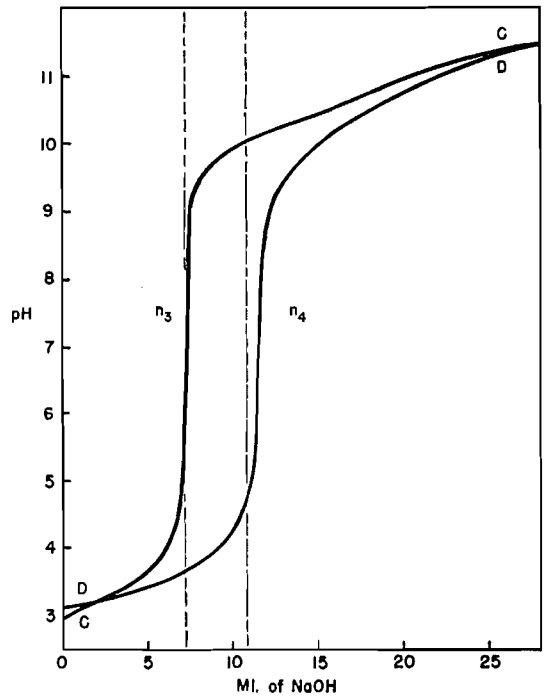

FIG. 2. Titration (*C*) and back-titration (*D*) of condensation product (V) in aqueous solution.

Can. J. Chem. Downloaded from www.nrcresearchpress.com by 200.7.193.243 on 09/04/12
For personal use only.

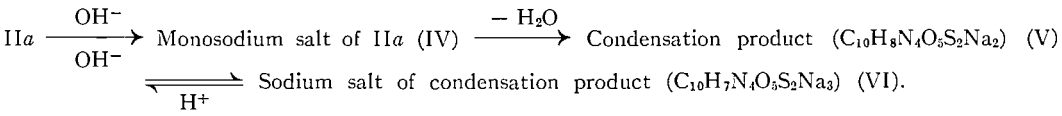

Following curve A, the conversion of 2-thio-3-(carboxymethyl) hydantoin (II*a*) into its monosodium salt (IV) is complete at n_1; at n_1, IV undergoes self-condensation with elimination of water to give the condensation product (V), which is in turn neutralized to give VI. The neutralization of V to VI requires 1 mole of base per mole of condensation product or *one-half the amount of base required to neutralize IIa originally*. On the back-titration curve B, the conversion of VI to V begins at n_2 and should be complete at p. The validity of this interpretation rests on the isolation of the condensation product (V) from the solution used in the titration and back-titration of II*a*. Experimentally, this method gave an 80% conversion of II*a* into V. The analytical values obtained for the condensation products prepared by the two methods agreed within experimental error. However, in both cases the values obtained for hydrogen were higher than the value calculated for the empirical formula $C_{10}H_8N_4O_5S_2Na_2$.

The titration and back-titration of the condensation product (V) gave the same result (Fig. 2). Again, the difference between the two curves (C and D) at n_3 and n_4 represents approximately one-half the amount of base required to reach n_3. In analogy with the titration experiments on 2-thio-3-(carboxymethyl) hydantoin (II*a*), it appears that the condensation process has again occurred.

Although there is not sufficient evidence to formulate the structure of the condensation product (V) with its two combined sodium atoms, the data suggest that the product has a free carboxyl group and that the sodium atoms are bound as salts of an enolic structure. Furthermore, the structure of the initial condensation product (V) must be such that the same mode of self-condensation can be repeated.

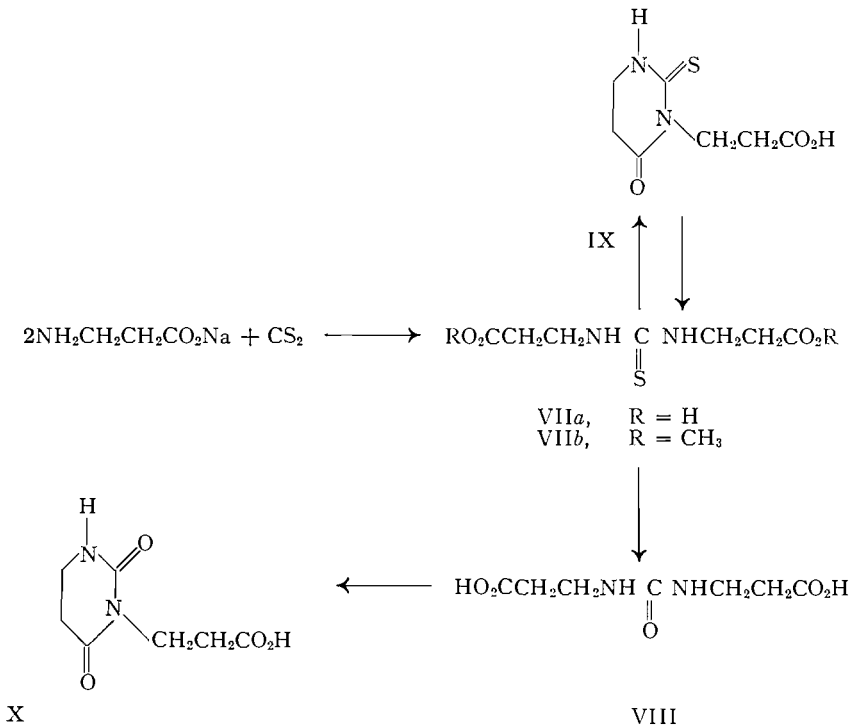

Can. J. Chem. Downloaded from www.nrcresearchpress.com by 200.7.193.243 on 09/04/12
For personal use only.

The condensation of sodium β-alaninate and carbon disulphide proceeded normally. The product, 1,3-di-(β-carboxymethyl) thiourea (VII*a*), proved to be very water soluble and hence was isolated in the form of its dimethyl ester (VII*b*) in 56% yield. Saponification of the diester (VII*b*) in aqueous base readily gave the diacid (VII*a*). This thiourea–diacid (VII*a*) was oxidized with 4 moles of aqueous sodium hypochlorite or hydrogen peroxide in the presence of 4 moles of base to 1,3-di-(β-carboxyethyl) urea (VIII).

There are numerous examples in the literature of the cyclization of β-thioureido and β-ureido alanines to hydrouracil and its derivatives. This was accomplished by the cyclizing action of acetic anhydride, hydrochloric acid, or simply heat (6, 7, 8, 9, 10, 11) on the β-ureido alanines, while others (12, 13, 14) found that the corresponding esters undergo ring closure in the presence of sodium alkoxides. When 1,3-di-(β-carboxyethyl) thiourea (VII*a*) was heated with *p*-toluenesulphonic acid at 160°–175° C., 2-thio-3-(β-carboxyethyl) hydrouracil (IX) was obtained in 85% yield. In accordance with observations on other hydrouracil derivatives (7, 15) this process was easily reversed by the action of warm aqueous base on IX. Similarly, the action of hydrochloric acid or acetic anhydride on 1,3-di-(β-carboxyethyl) urea (VIII) gave 3-(β-carboxyethyl) hydrouracil (X).

As a preparative method, the 2-thio-3-(β-carboxyethyl) hydrouracil (IX) can be prepared in 46% yield from the crude 1,3-di-(β-carboxyethyl) thiourea (VII*a*) by cyclization with *p*-toluenesulphonic acid. It is of interest to note that the cyclization of 1,3-di-(carboxymethyl) thiourea (I*a*) to yield 2-thio-3-(carboxymethyl) hydantoin (II*a*) is more facile than the ring closure of its homologue (VII*a*) to the thiohydrouracil (IX). This is demonstrated by the behavior of the two compounds on fusion. As noted above, 1,3-di-(carboxymethyl) thiourea (I*a*) loses water readily at its melting point while VII*a* remains unchanged under these conditions.

During the investigation of the cyclization of 1,3-di-(β-carboxyethyl) thiourea (VII*a*) with acetic anhydride under reflux, desulphurization as well as cyclization occurred. The product, 3-(β-carboxyethyl) hydrouracil (X), was obtained in 26% yield. To our knowledge, the desulphurization of a thiohydrouracil with acetic anhydride has not been observed previously.

EXPERIMENTAL[3]

1,3-Di-(carboxymethyl) Thiourea and 2-Thio-3-(carboxymethyl) Hydantoin

A stirred mixture of glycine (20 g., 0.26 mole), carbon disulphide (10.2 g., 0.13 mole), and water (20 ml.) was treated dropwise with a solution of sodium hydroxide (10.68 g., 0.26 mole) in water (27 ml.) over a period of 15 minutes. After the initial heat effect had abated additional carbon disulphide (2 g.) was added and the solution was held at the reflux temperature of carbon disulphide for 30 minutes. The excess carbon disulphide was evaporated and the remaining solution was refluxed for 7 hours. During this latter heating stage copious evolution of hydrogen sulphide occurred. The solution was cooled, filtered, and divided into two equal portions.

One portion of the solution was evaporated to dryness *in vacuo* on the steam bath and the residual viscous red oil was dried *in vacuo* over potassium hydroxide pellets. This residue was treated with 10% methanolic hydrogen chloride solution (100 ml.) at room temperature. A pale yellow solution containing some insoluble crystals of sodium chloride was obtained. Methylation was allowed to proceed at room temperature overnight. The filtered solution was evaporated to dryness *in vacuo* and the residue was dissolved in

[3]*All melting points are uncorrected. Microanalyses were performed by Micro Tech Laboratories, Skokie, Illinois.*

Can. J. Chem. Downloaded from www.nrcresearchpress.com by 200.7.193.243 on 09/04/12
For personal use only.

Can. J. Chem. Downloaded from www.nrcresearchpress.com by 200.7.193.243 on 09/04/12
For personal use only.

chloroform. The chloroform solution was extracted with water, dried, and then evaporated to dryness. The residue on treatment with benzene gave 3.7 g. (25%) of crude crystalline 1,3-di-(carbomethoxymethyl) thiourea (m.p. 97°–98° C.). Several crystallizations from benzene–hexane solution gave colorless platelets melting at 99°–100° C. Anal. Calc. for $C_7H_{12}N_2O_4S$: C, 38.17; H, 5.49; N, 12.72; S, 14.56%. Found: C, 38.59; H, 5.61; N, 12.81; S, 14.10%.

Part of the 1,3-di-(carbomethoxymethyl) thiourea (0.5 g., 0.002 mole) in a solution of sodium hydroxide (0.3 g., 0.007 mole) in water (7 ml.) was heated on a steam bath for 30 minutes. The solution was cooled to 0° C. and acidified with cold concentrated hydrochloric acid solution. The crystals (m.p. 157°–158° C.; resolidifies and remelts with decomposition at 214°–215° C.) were recovered by filtration, yield 0.38 g. (89%). This material was purified by solution in cold methanol and precipitation with benzene. The pure sample gave a double melting point of 164°–165° C. and 214°–215° C. with decomposition. Anal. Calc. for $C_5H_8N_2O_4S$: C, 31.25; H, 4.20; N, 14.58; S, 16.69%. Found: C, 31.49; H, 4.23; N, 14.43; S, 16.61%.

The mother liquors and washings from the preparation of 1,3-di-(carbomethoxymethyl) thiourea were combined and evaporated to dryness. The residue in concentrated hydrochloric acid solution (35 ml.) was warmed on a steam bath for 20 minutes. When the solution was cooled, 2-thio-3-(carboxymethyl) hydantoin (m.p. 210°–212° C. with decomposition) separated as pale yellow crystals, yield 2 g. (17%). Recrystallization from methanol–benzene solution raised the melting point to 214°–215° C. with decomposition. The melting points reported in the literature are 212° C. with decomposition (4) and 210°–212° C. (5). Anal. Calc. for $C_5H_6N_2O_3S$: C, 34.47; H, 3.47; N, 16.09; S, 18.41%. Found: C, 34.55; H, 3.54; N, 16.10; S, 18.21%.

A solution of 2-thio-3-(carboxymethyl) hydantoin (0.5 g., 0.003 mole) in 10% methanolic hydrogen chloride solution (10 ml.) was allowed to stand at room temperature overnight. The solvent was removed *in vacuo* at room temperature and the crystalline residue was crystallized from benzene (3 ml.) to yield 0.49 g. (91%) of 2-thio-3-(carbomethoxymethyl) hydantoin melting at 112°–113° C. One crystallization from benzene–hexane solution raised the melting point to a constant value of 113°–114° C. Anal. Calc. for $C_6H_8N_2O_3S$: C, 38.29; H, 4.28; N, 14.89; S, 17.04%. Found: C, 38.51; H, 4.37; N, 14.46; S, 16.74%.

The methyl ester of 2-thio-3-(carboxymethyl) hydantoin on hydrolysis with either 6% potassium hydroxide solution or 37% hydrochloric acid solution gave a 72% yield of 2-thio-3-(carboxymethyl) hydantoin (m.p. 214°–215° C. with decomposition). The product was identified by a mixture melting point determination with an authentic sample of 2-thio-3-(carboxymethyl) hydantoin.

The second portion of solution from the original reaction was acidified to a pH of 2 with concentrated hydrochloric acid solution. This solution was evaporated to dryness *in vacuo* and the residue was dried *in vacuo* over potassium hydroxide pellets. The dried residue was extracted with boiling methanol (2×100 ml.) and the insoluble inorganic salts were removed by filtration. After the methanolic filtrate was taken to dryness, the residue was crystallized from water (15 ml.). Orange-red crystals of condensation product (m.p. 270°–275° C. with decomposition) were obtained, yield 2.9 g. (24%). One crystallization from water (7 ml.) together with treatment with Nuchar raised the melting point to 287°–290° C. with decomposition. The product gave a negative halogen test and it gave a neutralization equivalent of 373 on titration with 0.1 *N* sodium hydroxide solution. Anal. Calc. for $C_{10}H_8N_4O_5S_2Na_2$ (mol. wt. 374.31): C, 32.09; H, 2.15; N, 14.97%. Found: C, 32.50; H, 3.13; N, 15.11; Ash, 17.53%.

The mother liquors from the condensation product were evaporated to dryness and the residue was heated with 37% hydrochloric acid solution (25 ml.) for 1 hour on the steam bath. The solution was cooled and a crystalline precipitate of 2-thio-3-(carboxymethyl) hydantoin (m.p. 210°–212° C. with decomposition) was obtained, yield 2.6 g. (23%). This product was identified by a mixed melting point determination with a known sample of 2-thio-3-(carboxymethyl) hydantoin (m.p. 214°–215° C. with decomposition).

In another experiment, after the stage of the condensation reaction, the reaction mixture was acidified with 1.1 mole of hydrochloric acid per mole of sodium hydroxide originally used. The colored condensation product (m.p. 285°–290° C. with decomposition) was obtained in 32% yield. The dry residue from the mother liquors was methylated with 10% methanolic hydrogen chloride to yield 7% of the methyl ester of 2-thio-3-(carboxymethyl) hydantoin (m.p. 112°–113° C.). This product gave no depression in melting point on admixture with an authentic sample of 2-thio-3-(carbomethoxymethyl) hydantoin (m.p. 113°–114° C.).

Direct Preparation of 2-Thio-3-(carboxymethyl) Hydantoin

A mixture of glycine (150 g., 2 moles), carbon disulphide (76 g., 1 mole), and sodium hydroxide (80 g., 2 moles) in water (350 ml.) was condensed in the above-described manner. After complete reaction, the solution was filtered and evaporated to dryness. The residue in concentrated hydrochloric acid solution (500 ml.) was heated on a steam bath for 45 minutes. The yellow solid which separated was collected and dried to give 84 g. (49%) of 2-thio-3-(carboxymethyl) hydantoin (m.p. 214°–215° C. with decomposition). This product was identified by a mixture melting point determination.

3-(Carboxymethyl) Hydantoin

2-Thio-3-(carboxymethyl) hydantoin (1.3 g., 0.007 mole) was converted into 3-(carboxymethyl) hydantoin (m.p. 183°–191° C.) in 37% yield by heating with chloroacetic acid under the conditions described by Johnson and Renfrew (5). Two crystallizations from ethanol–hexane solution raised the melting point to 197°–198° C. The melting points reported in the literature are 190°–191° C. (5), 195°–196° C. (16), and 199°–201° C. (17). Anal. Calc. for $C_5H_6N_2O_4$: C, 37.98; H, 3.83; N, 17.72%. Found: C, 38.28; H, 3.94; N, 17.95%.

A solution of 3-(carboxymethyl) hydantoin (0.1 g., 0.0006 mole) in 10% methanolic hydrogen chloride solution (8 ml.) was allowed to stand overnight. The solvent was removed *in vacuo* and the residue was crystallized from benzene–hexane solution to give 91 mg. (84%) of the methyl ester of 3-(carboxymethyl) hydantoin melting at 88°–89° C. One crystallization from acetone–hexane solution raised the melting point to 90°–91° C. The previously (3) reported melting point is 91° C.

Chemistry of the Condensation Product

(*a*) *Conversion into 2-Thio-3-(carboxymethyl) Hydantoin*

The condensation product (0.5 g., 0.0013 mole) in 37% hydrochloric acid solution (4 ml.) was heated at 100° C. for 7 minutes. The mixture was cooled and the precipitate of 2-thio-3-(carboxymethyl) hydantoin (m.p. 212°–213° C. with decomposition) was removed by filtration, yield 0.39 g. (84%). One crystallization from glacial acetic acid raised the melting point to 214°–215° C. with decomposition. This product was identified by a mixture melting point determination with a known sample of 2-thio-3-(carboxymethyl) hydantoin.

Can. J. Chem. Downloaded from www.nrcresearchpress.com by 200.7.193.243 on 09/04/12
For personal use only.

Can. J. Chem. Downloaded from www.nrcresearchpress.com by 200.7.193.243 on 09/04/12
For personal use only.

(*b*) *Conversion into 2-Thio-3-(carbomethoxymethyl) Hydantoin*

A solution of the condensation product (0.5 g., 0.0013 mole) in 10% methanolic hydrogen chloride solution (10 ml.) was allowed to stand at room temperature overnight. The solvent was removed *in vacuo* and the residue was extracted with chloroform. The chloroform extract was washed with water, dried, and evaporated to dryness. The crystalline residue was crystallized from benzene, yield 0.4 g. (81%). It melted at 112°–113.5° C. alone and on admixture with a known sample of 2-thio-3-(carbomethoxymethyl) hydantoin (m.p. 113°–114° C.).

(*c*) *Conversion into 3-(Carbomethoxymethyl) Hydantoin*

An aqueous solution (2 ml.) of the condensation product (0.5 g., 0.0013 mole) and chloroacetic acid (0.5 g., 0.005 mole) was refluxed for 1 hour. The solution was taken to dryness *in vacuo* and the residue was methylated with 10% methanolic hydrogen chloride solution (15 ml.) at room temperature overnight. The solvent was removed *in vacuo* and the residual oil was dissolved in chloroform. The chloroform solution was washed with 5% sodium bicarbonate solution and water. It was dried and the chloroform evaporated. The residue was crystallized from benzene–hexane solution (3 ml.) to give 116 mg. (25%) of 3-(carbomethoxymethyl) hydantoin melting at 89°–90° C. A sample crystallized from acetone–hexane solution melted at 90°–91° C. alone and on admixture with a known sample of 3-(carbomethoxymethyl) hydantoin.

(*d*) *Condensation Product from 2-Thio-3-(carboxymethyl) Hydantoin*

A solution of 2-thio-3-(carboxymethyl) hydantoin (5.0 g., 0.0287 mole) in water (100 ml.) was titrated with 0.1 *N* sodium hydroxide solution. After each addition of base, the pH of the solution was determined by means of a Beckman Model G pH meter equipped with external glass and calomel electrodes. At the neutralization point (288 ml. of 0.1 *N* NaOH, 0.0288 mole), the color of the solution changed from pale yellow to red. After addition of an equal amount of base, the solution was back-titrated with 118 ml. of 0.244 *N* hydrochloric acid (0.0288 mole). Again, a color change from red to orange at the equivalence point was observed when approximately half of the hydrochloric acid solution had been added. The solution was evaporated *in vacuo* until crystals began to appear. These were collected and dried to give 1.28 g. (m.p. 287°–292° C. with decomposition). A second crop (3.02 g., m.p. 270°–285° C. with decomposition) was obtained on further concentration of the mother liquor to give a total crude yield of 80%. Recrystallization of the product from water (10 ml.) together with Nuchar treatment gave orange-red crystals (2.04 g., m.p. 287°–291° C. with decomposition) which gave no depression in melting point on admixture with the condensation product (above). It gave a neutralization equivalent of 378 on titration with 0.1 *N* sodium hydroxide solution. Anal. Calc. for $C_{10}H_8N_4O_5S_2Na_2$: C, 32.09; H, 2.15; N, 14.97%. Found: C, 32.61; H, 3.36; N, 15.55; Ash, 17.47%.

(*e*) *Titration Experiments*

The titration curves (Fig. 1 and 2) were obtained by titration of aqueous solutions (1 g./100 ml.) of 2-thio-3-(carboxymethyl) hydantoin and the condensation product with 0.1 *N* sodium hydroxide solution and back-titration with standardized hydrochloric acid solution. The pH of the solution was determined by means of a Beckman Model G pH meter equipped with external glass and calomel electrodes.

1,3-Di-(β-carboxyethyl) Thiourea

A mechanically stirred mixture of β-alanine (15 g., 0.16 mole), carbon disulphide (6.4 g., 0.08 mole), and water (10 ml.) was treated dropwise with a solution of sodium

hydroxide (6.7 g., 0.17 mole) in water (17 ml.) over a period of 5 minutes. The temperature gradually rose to 30° C. and in 30 minutes all of the carbon disulphide had been consumed in the reaction. Additional carbon disulphide (2 g.) was added and the solution was heated at the reflux temperature for 30 minutes. The excess carbon disulphide was removed by distillation and the clear solution was refluxed for 7 hours. It was cooled and then filtered to remove a small amount of insoluble material. The filtrate was acidified to pH 2 with 10% hydrochloric acid solution and then evaporated to dryness *in vacuo*. The residue was extracted with hot methanol to remove the inorganic salts. The dry residue from the methanolic extract was treated with 5% methanolic hydrogen chloride solution (50 ml.) and allowed to stand at room temperature overnight. The residue from evaporation of the methanolic solution was dissolved in chloroform and the chloroform solution was washed with 5% hydrochloric acid solution, 5% sodium bicarbonate solution, and water. The dried chloroform solution was evaporated to dryness *in vacuo* and the residue was crystallized from cold benzene (60 ml.), yield 11.6 g. (56%). The melting point was raised from 69°–73° C. to 73°–74° C. by one crystallization from methanol–water solution, yield 10.4 g. Anal. Calc. for $C_9H_{16}N_2O_4S$: C, 43.53; H, 6.50; N, 11.28; S, 12.92%. Found: C, 43.93; H, 6.65; N, 11.10; S, 12.65%.

The dimethyl ester of 1,3-di-(β-carboxyethyl) thiourea (5.5 g., 0.02 mole) in a solution of potassium hydroxide (3.7 g.) in water (65 ml.) was heated on a steam bath for 45 minutes. The solution was cooled, acidified to pH 2 with 10% sulphuric acid solution, and then evaporated to dryness. The residue was extracted with acetone (2×100 ml.). After the acetone was evaporated from the combined extracts, the residue was crystallized from acetone–chloroform solution. This procedure gave 4.5 g. (93%) of 1,3-di-(β-carboxyethyl) thiourea melting at 137°–139° C. A further crystallization from the same solvent pair raised the melting point to 138°–139° C. Anal. Calc. for $C_7H_{12}N_2O_4S$: C, 38.18; H, 5.50; N, 12.73; S, 14.56%. Found: C, 38.18; H, 5.66; N, 12.45; S, 14.68%.

1,3-Di-(β-carboxyethyl) Urea

Method A

A solution of 1,3-di-(β-carboxyethyl) thiourea (1.4 g., 0.006 mole) and sodium hydroxide (1.1 g., 0.028 mole) in water (10 ml.) was treated at 20°–25° C. with 32 ml. (0.028 mole) of 0.891 *M* sodium hypochlorite solution. The addition was complete in 5 minutes and the oxidation was allowed to proceed at room temperature overnight. A small amount of insoluble sulphur was removed by filtration, and the filtrate was acidified with 10% hydrochloric acid to pH 2. It was evaporated *in vacuo* on the steam bath to a volume of 20 ml. or until white crystals began to appear. The solution was cooled and the crystals were collected, washed, and dried, yield 1.07 g. (80%). The melting point was raised from 183°–185° C. to 185°–185.5° C. by crystallization from methanol. Anal. Calc. for $C_7H_{12}N_2O_5$: C, 41.17; H, 5.93; N, 13.72%. Found: C, 41.17; H, 5.98; N, 13.68%.

Method B

A mixture of the dimethyl ester of 1,3-di-(β-carboxyethyl) thiourea (10 g., 0.04 mole) and sodium hydroxide (6.4 g., 0.16 mole) in water (70 ml.) was dissolved by slight warming on a steam bath. The solution was cooled and treated with 7.9 *M* hydrogen peroxide solution (20.4 ml., 0.16 mole) at 15°–20° C. The oxidation was allowed to proceed at room temperature overnight, after which the pH of the solution was adjusted to 2 with 37% hydrochloric acid solution. This solution was concentrated *in vacuo* until crystals began to appear. The crystals (m.p. 183°–185° C.) were removed by filtration and dried, yield 7.1 g. (86%). These crystals did not depress the melting point of 1,3-di-(β-carboxyethyl) urea (m.p. 185°–185.5° C.) prepared by Method A.

Can. J. Chem. Downloaded from www.nrcresearchpress.com by 200.7.193.243 on 09/04/12
For personal use only.

Can. J. Chem. Downloaded from www.nrcresearchpress.com by 200.7.193.243 on 09/04/12
For personal use only.

2-Thio-3-(β-carboxyethyl) Hydrouracil

β-Alanine (75 g., 0.8 mole) and carbon disulphide (35 g., 0.46 mole) in a solution of sodium hydroxide (33.7 g., 0.8 mole) in water (135 ml.) were condensed in the usual manner by refluxing for 7 hours. This solution was cooled, acidified to a pH of 2 with concentrated hydrochloric acid, and evaporated to dryness. The residue was extracted with hot methanol and the methanol extract was taken to dryness *in vacuo*. The residual oil was heated with *p*-toluenesulphonic acid monohydrate (8 g.) at 160°–175° C. *in vacuo* (15 mm.) for 30 minutes. This melt on crystallization from water (200 ml.) gave 38.8 g. (46%) of 2-thio-3-(β-carboxyethyl) hydrouracil (m.p. 163.5°–164.5° C.). Crystallization from acetone–water solution raised the melting point to 166°–167° C. Anal. Calc. for $C_7H_{10}N_2O_3S$: C, 41.57; H, 4.98; N, 13.86; S, 15.86%. Found: C, 41.80; H, 4.89; N, 14.00; S, 15.90%.

In another experiment a mixture of 1,3-di-(β-carboxyethyl) thiourea (0.5 g., 0.002 mole) and *p*-toluenesulphonic acid monohydrate (0.05 g., 0.0003 mole) was heated at 160°–175° C. for 10 minutes. The melt was cooled and crystallized from water (4 ml.) to give 0.4 g. (85%) of 2-thio-3-(β-carboxyethyl) hydrouracil melting at 166°–167° C.

2-Thio-3-(β-carboxyethyl) hydrouracil (0.5 g., 0.002 mole) was heated on a steam bath for 35 minutes in a solution of 85% potassium hydroxide (0.48 g., 0.007 mole) in water (8 ml.). This solution on acidification to pH 2 and evaporation to a small volume gave 1,3-di-(β-carboxyethyl) thiourea (m.p. 137°–138° C.) in 75% (0.41 g.) yield. The product was identified by a mixture melting point determination.

3-(β-Carboxyethyl) Hydrouracil

Method A

A mixture of 1,3-di-(β-carboxyethyl) urea (1 g., 0.005 mole) and acetic anhydride (10 ml.) was refluxed for 15 minutes. The solution was cooled, diluted with 100 ml. of water, and the excess acetic anhydride allowed to hydrolyze. Evaporation of the aqueous solution *in vacuo* on the steam bath gave a crystalline residue. The residue was crystallized from ethanol–benzene solution (10 ml.) to yield 0.59 g. of product. Concentration of the mother liquors gave another 0.1 g. of crystalline product. The total yield of 3-(β-carboxyethyl) hydrouracil (m.p. 178°–184° C.) was 76%. One crystallization raised the melting point to 183°–184° C. A sample of this compound mixed with the starting material, 1,3-di-(β-carboxyethyl) urea (m.p. 185°–185.5° C.), gave a depressed melting point. Anal. Calc. for $C_7H_{10}N_2O_4$: C, 45.16; H, 5.41; N, 15.05%. Found: C, 45.50; H, 5.48; N, 15.23%.

Method B

A solution of 1,3-di-(β-carboxyethyl) urea (0.5 g., 0.0025 mole) in 37% hydrochloric acid solution (3 ml.) was evaporated to dryness in an open beaker on a steam bath. This procedure was repeated twice and the final dry residue was extracted with hot acetone (25 ml.). After the solvent was removed by evaporation, the residue was crystallized from acetone–chloroform solution. The crystals melted at 172°–175° C., yield 0.38 g. (83%). One crystallization from methanol–benzene solution raised the melting point to 181°–182° C. A mixture melting point determination with a known sample of 3-(β-carboxyethyl) hydrouracil gave no depression.

Method C

1,3-Di-(β-carboxyethyl) thiourea (0.27 g., 0.001 mole) in acetic anhydride (5 ml.) was refluxed for 30 minutes. The solution was cooled, poured into ice-water (25 ml.), and the excess acetic anhydride was allowed to hydrolyze at room temperature. The oil remaining after evaporation of the solution was crystallized from acetone–chloroform solution. The

crude crystalline product (m.p. 179°–181° C.) was obtained in 26% (0.059 g.) yield. After two recrystallizations from the same solvent pair it melted at 183°–184° C. alone and on admixture with a known sample of 3-(β-carboxyethyl) hydrouracil (m.p. 183°–184° C.).

REFERENCES

1. KODAMA, S. J. Tokyo Chem. Soc. **41**, 951 (1920).
2. KODAMA, S. J. Chem. Soc. Japan, **42**, 1005 (1921).
3. POLICARD, A. A. Bull. soc. chim. (4), **49**, 607 (1931).
4. JEFFREYS, R. A. J. Chem. Soc. 2221 (1954).
5. JOHNSON, T. B. and RENFREW, A. G. J. Am. Chem. Soc. **47**, 240 (1925).
6. ANZIEGIN, A. and GULEWIVICH, W. Z. physiol. Chem. **158**, 32 (1926).
7. EVANS, J. and JOHNSON, T. B. J. Am. Chem. Soc. **52**, 4993 (1930).
8. GABRIEL, S. Ber. **38**, 635 (1905).
9. JOHNSON, T. B. Rec. trav. chim. **48**, 872 (1929).
10. JOHNSON, T. B. and LIVAK, J. E. J. Am. Chem. Soc. **58**, 299 (1936).
11. RODIONOV, V. M. and KURTEV, B. I. Izvest. Akad. Nauk S.S.S.R., Otdel. Khim. Nauk, 268 (1952).
12. DALMER, O., DIEHL, C., and PIEPER, H. German Patent No. 606,349; Chem. Abstr. **29**, 1583 (1935).
13. DALMER, O., DIEHL, C., and PIEPER, H. U.S. Patent No. 2,259,925; Chem. Abstr. **36**, 870 (1942).
14. TANAKA, K., KAJIURA, T., and TAKETOSHI, H. J. Pharm. Soc. Japan, **70**, 164 (1950).
15. BATT, R. D., MARTIN, J. K., PLOESER, J. McT., and MURRAY, J. J. Am. Chem. Soc. **76**, 3663 (1954).
16. GRANACHER, Ch. and LANDOLT, H. Helv. Chim. Acta, **10**, 799 (1927).
17. WESSELY, F., SCHLOGL, K., and KORGER, G. Monatsh. **83**, 1156 (1952).

Can. J. Chem. Downloaded from www.nrcresearchpress.com by 200.7.193.243 on 09/04/12
For personal use only.

Can. J. Chem. Downloaded from www.nrcresearchpress.com by 200.7.193.243 on 09/04/12
For personal use only.

PHOTOCONDUCTIVITY AND ABSORPTION AND FLUORESCENCE SPECTRA OF 9,10-DICHLOROANTHRACENE[1]

E. Bock,[2] J. Ferguson,[3] and W. G. Schneider

ABSTRACT

The spectral response, voltage, light intensity, and temperature dependences of the photocurrent generated in crystals of 9,10-dichloroanthracene have been studied as well as the absorption and fluorescence spectra. The magnitude of the measured photocurrent was 10^2–10^3 times larger than that observed in anthracene under similar conditions. The spectral response of the photocurrent in the surface cell arrangement was found to depend on the direction of the incident light relative to the electrodes. Above a certain value of the applied voltage the photocurrent was found to be ohmic. The photocurrent increased as the 0.7 or 0.8 power of the light intensity depending on whether the light was incident on the same side or opposite sides of the crystal face containing the electrodes. When the crystal was cooled the photocurrent passed through a maximum between 20° and 0° C.

The absorption edge of crystalline 9,10-dichloroanthracene as well as the absorption spectrum in chloroform solution were determined. When the crystals were cooled the fluorescence spectrum was observed to shift to longer wavelengths and the intensity increased between two and three times.

INTRODUCTION

Compton and Waddington (1) observed that anthracene crystals treated with either NO_2 or Cl_2 gas showed marked and permanent changes in the photoconduction. They attributed the changes to the formation of complexes between the anthracene and the gases. In the case of Cl_2 there is the possibility of the formation of 9,10-dichloroanthracene under the conditions of their experiments, and it was therefore decided to investigate the photoconduction of this substance in the pure crystalline state. Furthermore, 9,10-dichloroanthracene is an interesting compound in its own right since the presence of the heavy atoms should facilitate internal conversion from singlet to triplet states. The fact that the photocurrents observed were 10^2–10^3 times those usually encountered in anthracene under similar conditions suggests that this mechanism may have some importance, although it is of course not necessarily the determining factor giving rise to the enhanced photoconduction in the present case.

EXPERIMENTAL

Reagent grade 9,10-dichloroanthracene, obtained from Eastman Organic Chemicals, was purified by chromatography through alumina and was then recrystallized from light petroleum.

The crystals were grown from carbon tetrachloride solution as this solvent was found to produce the best crystals. Typical dimensions were: 1×0.2 cm. and $50\pm20\ \mu$ thick. Attempts at growing crystals by sublimation resulted in very thin needles, too fragile for handling.

X-Ray measurements showed the crystals to belong to the orthorhombic system and it was established that most, if not all, of the crystals were multiple twins. The most-developed plane was the (010) face, which is also the twinning plane. The electrodes (colloidal suspension of graphite in alcohol) were both placed on this (010) face with a separation of between 0.6 and 0.8 mm. Electrodes were considered "good" only when

[1]*Manuscript received December 5, 1957.*
Contribution from the Division of Pure Chemistry, National Research Laboratories, Ottawa, Canada.
Issued as N.R.C. No. 4617.
[2]*Summer appointment 1957.*
[3]*N.R.L. Fellow. Present address: Department of Chemistry, University of British Columbia, Vancouver, B.C.*

there was no apparent space charge associated with the photocurrent. The photocurrents were measured with a Keithley micromicroammeter and were of the order 10^{-7} to 10^{-11} amp. Since it was observed that air increased the photocurrent, all measurements were carried out in an inert atmosphere of argon. The temperature dependence of the photocurrent was measured with an almost identical arrangement to that of Kommandeur, Korinek, and Schneider (2). The absorption and fluorescence measurements were obtained with a semiautomatic Beckman DU spectrometer.

RESULTS AND DISCUSSION

A. Photoconduction

I. Photocurrent–Wavelength Relation

Fig. 1 shows that the spectral dependence for a surface cell is sensitive to the direction of the incident light. When the electrodes are carefully placed only on one (010) face of the crystal the spectral dependence with the light incident normal to this face is different to the case when the light is incident normal to the opposite (010) face of the crystal. Anthracene sublimation flakes have also been observed to show a variation of the spectral dependence with a surface cell arrangement when the direction of the incident light is changed (3), and this behavior, hitherto unnoticed, may well be quite general and should be looked for in all surface cell measurements.

Fig. 1 also shows the absorption edge of a typical crystal in polarized light. Spectral dependences were determined with polarized light but the differences between the two polarizations are not great and the curves in Fig. 1 are therefore for unpolarized light.

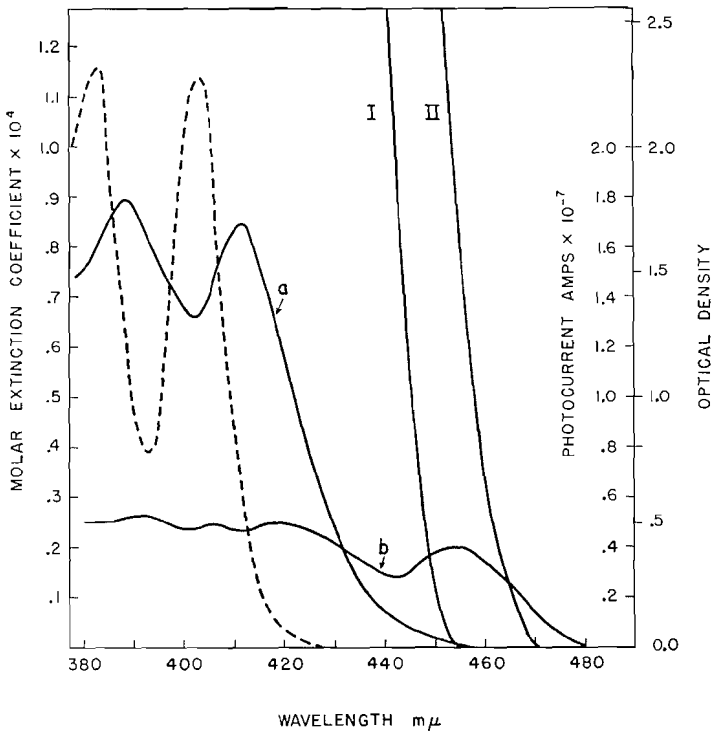

FIG. 1. Broken curve, molar extinction coefficient in $CHCl_3$. *a*, photocurrent with front face illuminated; *b*, photocurrent with back face illuminated. I and II, optical density of crystal: I, light polarized parallel to *c* axis; II, light polarized parallel to *a* axis.

Can. J. Chem. Downloaded from www.nrcresearchpress.com by 200.7.193.243 on 09/04/12
For personal use only.

When the light is incident normal to the face on which the electrodes are placed the photocurrent response curve shows two maxima, at 3875 and 4135 Å. Essentially the same spectral dependence was obtained with a total of six crystals. If the spectral dependence is compared with the absorption edge it will be seen that the maximum photocurrent is obtained only at wavelengths well below those corresponding to absorption edge optical densities of 2.0 (99% light absorbed), i.e., at 4415 and 4530 Å. However, if the light is incident on the opposite (010) face of the crystal a marked change is found in the spectral dependence. Only one peak is observed, at 4525 Å, and the response at lower wavelengths is relatively uniform. The peak appears slightly displaced to the long-wavelength side of the absorption edge. Unfortunately the crystals were far too thick to permit the determination of the complete absorption spectrum, and lacking this we cannot say whether there is any relation between the spectral dependence and the absorption spectrum for either of the two arrangements. It is however only in the *latter* arrangement, with the back crystal face illuminated, that the photocurrent reaches a maximum in the vicinity of the absorption edge.

II. Photocurrent – Light Intensity Relation

The photocurrent was found to be proportional to the 0.7 power of the light intensity when the light was incident normal to the face with the electrodes. With the light incident normal to the opposite face the relation involved the 0.8 power of the light intensity. This behavior was found over the whole spectral region from 3800 to 4700 Å, and typical results are shown in Fig. 2.

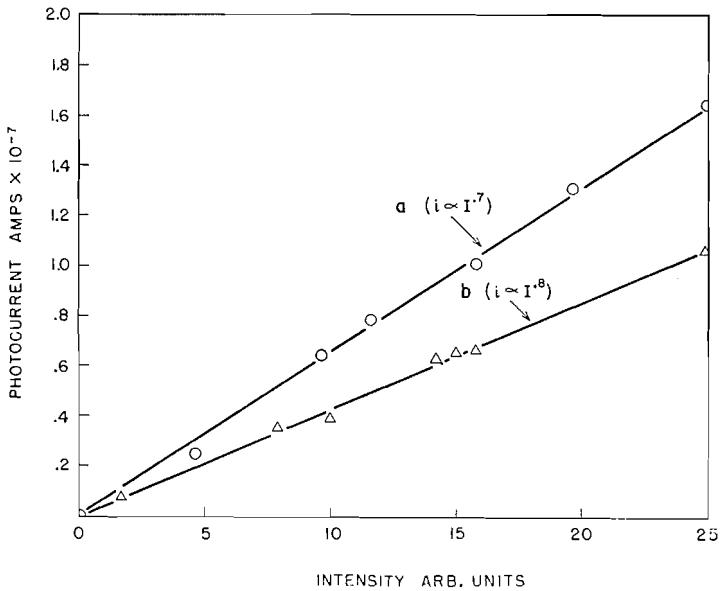

FIG. 2. Light intensity – photocurrent relation: *a*, front face illuminated; *b*, back face illuminated.

The increase of the photocurrent as a fractional power of the light intensity means that the carrier lifetime is shortened when the light intensity is increased (4), presumably by some recombination process.

III. Photocurrent–Voltage Relation

The voltage dependence was determined over the spectral region 3800 to 4700 Å. It was found to increase slowly (see Fig. 3) at low field strengths up to a value, different

Can. J. Chem. Downloaded from www.nrcresearchpress.com by 200.7.193.243 on 09/04/12
For personal use only.

for each crystal, of about 350 ± 100 v./cm.; above this point the photocurrent increased linearly with applied voltage. This behavior, which was similar when either the front or back crystal face was illuminated, was observed with all crystals measured. No saturation or deviation from linearity was found for the highest field strengths used, about 5000 v./cm.

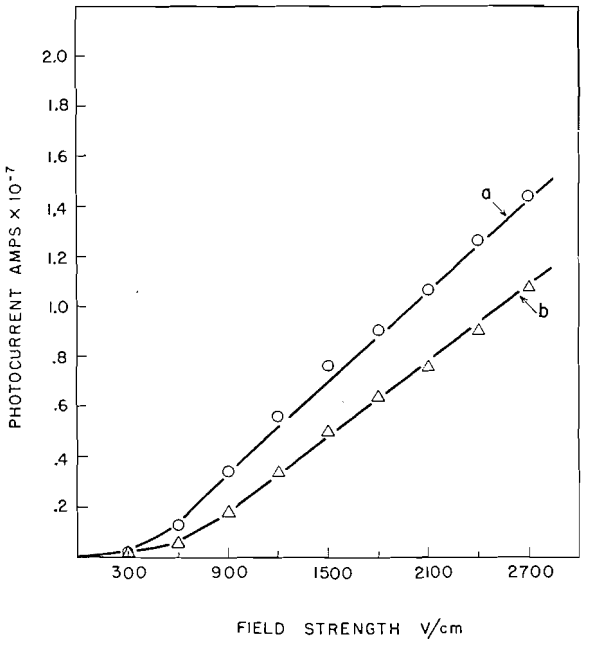

FIG. 3. Voltage–photocurrent relation: *a*, front face illuminated; *b*, back face illuminated.

IV. Photocurrent–Temperature Relation

Kommandeur, Korinek, and Schneider (2) studied the temperature dependence of the photocurrents from a number of organic crystals and they found that the photocurrents decrease exponentially with decreasing temperature. However, when 9,10-dichloroanthracene was cooled the photocurrent was observed to pass through a maximum between 20° and 0° C. On further cooling the photocurrent decreased, but as the crystals are very sensitive to thermal shock this could not be followed accurately. A similar behavior, but at higher temperature, was found by Drefahl and Henkel (5) with 4,4′-diphenylstilbene. This behavior may be related to the increase in the fluorescence efficiency that was found when the crystals were cooled (see below). This observation then supports a growing body of evidence that any process which quenches the electronic excitation energy of a crystal, whether it be energy transfer to an impurity or thermal-induced lattice quenching, leads to a decrease of the photocurrent.

B. Absorption and Fluorescence

As mentioned above in connection with the spectral dependence, all of the crystals were far too thick to penetrate the absorption band so only the absorption edge could be measured. From Fig. 1 it can be seen that this edge is at much longer wavelengths than the absorption band in solution so that intermolecular interactions are considerable.

The number of molecules in the unit cell is uncertain but from what is known about the crystal structure it seems likely that the molecules are stacked with the molecular

Can. J. Chem. Downloaded from www.nrcresearchpress.com by 200.7.193.243 on 09/04/12
For personal use only.

planes more nearly parallel to the *ab* crystal plane than any other. In addition, the short axis of the anthracene framework lies most likely closer to the *b* crystal axis than the other two. These considerations are in agreement with visual observations of the polarization of the fluorescence emitted normal to the (010) and (100) faces at room temperature, if the molecular transition is polarized along the short molecular axis. These observations are that normal to the (100) plane the fluorescence is strongly polarized parallel to the *b* crystal axis, while normal to the (010) plane the fluorescence is greater along the *a* crystal axis than along the *c*, but the ratio is not as high as in the former case.

The fluorescence spectra reported here were taken normal to the (010) face as this is the most developed. The striking feature of the fluorescence spectrum is that at room temperature the origin lies well inside the absorption edge. This is found only when the fluorescence is observed from the face which is irradiated. When the crystal is cooled the fluorescence spectrum is shifted to longer wavelengths and the relative intensities of individual bands is altered, but the total intensity of emission is increased. These changes are shown in Fig. 4, which records the *a* polarized component (the *c* component is similar

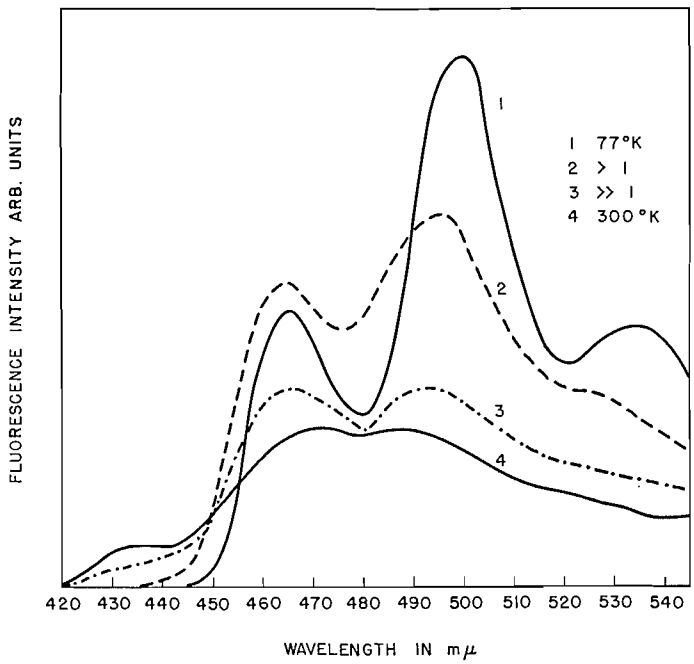

FIG. 4. Fluorescence spectrum at various temperatures: (1) 77° K., (2) >77° K., (3) ≫77° K., (4) room temp. ~290° K.

but weaker by a factor between 3 and 4) at room temperature, 77° K., and two intermediate temperatures. These spectra were all taken without moving the sample or the optical arrangement. All of the crystals examined showed the same fluorescence spectrum at 77° K. and measurements with two crystals at 4° K. produced very little further sharpening of the bands.

We are greatly indebted to Dr. M. Przybylska for crystallographic examinations of 9,10-dichloroanthracene.

Can. J. Chem. Downloaded from www.nrcresearchpress.com by 200.7.193.243 on 09/04/12
For personal use only.

REFERENCES

1. COMPTON, D. M. J. and WADDINGTON, T. C. J. Chem. Phys. **25**, 1075 (1956).
2. KOMMANDEUR, J., KORINEK, C. J., and SCHNEIDER, W. G. Can. J. Chem. **35,** 998 (1957).
3. FERGUSON, J. and SCHNEIDER, W. G. To be published.
4. ROSE, A. Proc. I.R.E. **43**, 1850 (1955).
5. DREFAHL, G. and HENKEL, H. J. Z. physik. Chem. **206**, 93 (1956).

Can. J. Chem. Downloaded from www.nrcresearchpress.com by 200.7.193.243 on 09/04/12
For personal use only.

Can. J. Chem. Downloaded from www.nrcresearchpress.com by 200.7.193.243 on 09/04/12
For personal use only.

THE CHANGE OF PHOTOCONDUCTION AND SEMICONDUCTION IN AROMATIC HYDROCARBONS ON MELTING[1]

J. KOMMANDEUR,[2] G. J. KORINEK,[3] AND W. G. SCHNEIDER

ABSTRACT

The variation of the photocurrent and dark current on melting naphthalene and biphenyl was studied. A large increase in the value of the photocurrent was observed. This change is very similar to that of the dark current. It is concluded that the increased mobilities of the charge carriers in the melt are mainly responsible for the change in both cases. The existence of photoconduction in the non-crystalline state is discussed.

INTRODUCTION

The investigation of various aspects of the photoconductivity of aromatic hydrocarbons has been reported from this laboratory (1, 2, 3). The present communication deals with the changes of the photo- and semi-conduction connected with the transition from crystal to melt.

It was observed earlier by Riehl (4) and Rabinowitch (5) that the semiconductivity of anthracene, paraffin, and naphthalene increases by a factor up to 10^3–10^4 on melting. The change is largest with pure material and single crystals and is less with the increasing amount of impurities or in polycrystalline material. This may explain why some of the earlier investigators (6) did not observe this change.

The large increase in semiconductivity of anthracene, paraffin, and naphthalene on melting is similar to that of ionic conductors. The observed ratio of σ_L, the conductivity of the liquid, to σ_S, that of the solid, is anywhere between 10 and 10^5. This change in conductivity is associated in ionic substances with the large increase in the number of lattice flaws on melting and with the fact that the expansion in volume on fusion reduces the activation energy for migration of the ions.

In contrast with ionic conductors, in metals there is a decrease in conductivity on melting, this being the result of increased scattering of electrons in the molten metal owing to the greater disorder of the atoms.

It was of interest to study the influence of melting on photoconduction, the result of which could possibly contribute to the elucidation of its mechanism. Naphthalene and diphenyl were the substances studied. Both photoconduct, are obtainable as single crystals, and have reasonably low melting points. This condition is of great importance because the semiconduction increases much faster with temperature than the photoconduction and the higher the melting point the greater is the dark current, which may completely mask any change in photocurrent.

EXPERIMENTAL

Naphthalene and biphenyl used were purified by chromatography through alumina and subsequent recrystallization from petroleum ether. The purification was carried out in the dark.

[1]*Manuscript received November 21, 1957.*
Contribution from the Division of Pure Chemistry, National Research Council, Ottawa, Canada.
Issued as N.R.C. No. 4619.
[2]*N.R.L. Postdoctorate Fellow 1955–57. Present address: National Carbon Research Laboratories, 12,600 Snow Road, Parma, Ohio.*
[3]*N.R.L. Postdoctorate Fellow 1956–57. Present address: Metals Research Laboratories, Niagara Falls, New York.*

Single crystals were used exclusively. They were grown for us by Dr. F. R. Lipsett in a Bridgman furnace (7). Only those sections of the crystals which were free of flaws were used.

APCO-15 (colloidal graphite in alcohol, supplied by APCO Industries Limited) and silver paste (Hanovia Mfg. Co.) electrodes were used first. Both these electrodes proved unsatisfactory because during the melting they contaminated the melt and increased the semiconductivity by several orders of magnitude. The only arrangement which proved feasible was to carefully melt the crystal at its edges; the melt wetted the platinum electrodes and established the contact.

Because of the known effect of gases on photoconduction all measurements were done on outgassed single crystals in vacuum ($\sim 10^{-5}$ mm. Hg).

The measurements were carried out in a properly shielded glass silica cell (see Fig. 1). The cell was designed in such a way that the field strength was practically the same for

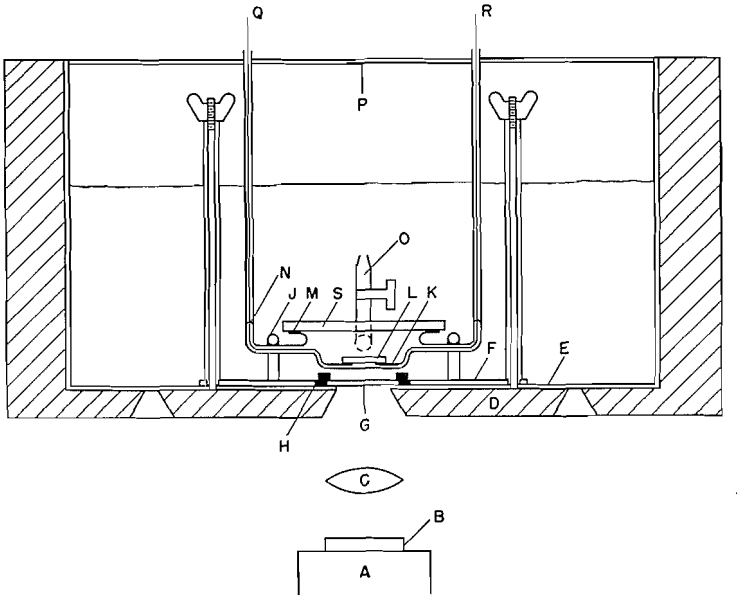

FIG. 1. Cell for the measurement of the change of semi- and photo-conduction on melting a single crystal.

A—Mercury lamp
B—Filter
C—Lens
D—Insulation
E—Brass
F—Removable carriage
G—Silica window
H—Seal
J—Clamps
K—Pt electrodes
L—Crystal
M—Ground joint
N—Kovar seal
O—Connection to vacuum
P—Cover
Q—Battery connection
R—Connection to Keithley
S—Glass cover

single crystals and the melt. Measurements were taken in the direction of increasing temperature and at temperatures ranging from 290° to 373° K., which include the melting point. The procedure could of course not be reversed, since once the single crystal was melted, subsequent cooling results in a polycrystalline mass.

The cell was mounted on a brass carriage which could at any time be removed or submerged in the water bath. This mounting provided the greatest stability and avoidance of vibrations.

The currents were measured with a Keithley micromicroammeter as described earlier

Can. J. Chem. Downloaded from www.nrcresearchpress.com by 200.7.193.243 on 09/04/12
For personal use only.

(3). In the cases where the photocurrent was substantially smaller than the dark current, the latter was "bucked out" by applying an auxiliary e.m.f. from a battery circuit. The ultraviolet light source employed was a BTH direct-current 250 w. mercury lamp, operated from a stabilized (Nobatron) d-c. power source. A filter cutting off all wavelengths shorter than 3000 Å was used.

RESULTS

Fig. 2 shows a plot of the log of the photocurrent vs. $1/T$ for naphthalene. The plot is a fairly straight line until just below the melting point, where a curvature appears. At the melting point there is a sharp rise in the photoconduction by a factor of 10^3. The graph is very similar to Fig. 3, which depicts the dependence of the semiconductivity of naphthalene on temperature. Three crystals of naphthalene yielded results similar to those shown on Figs. 2 and 3.

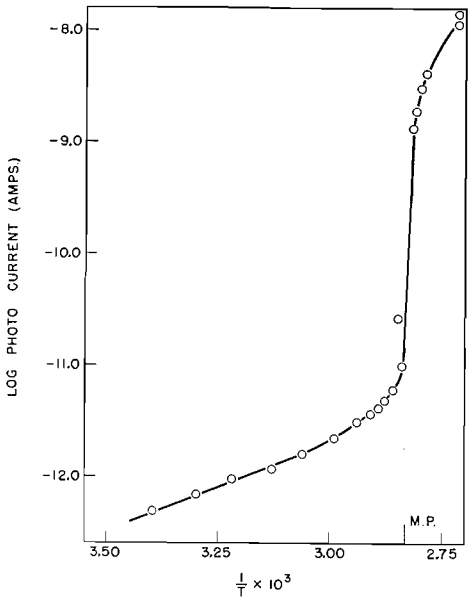

FIG. 2. Change of photocurrent of naphthalene upon melting.

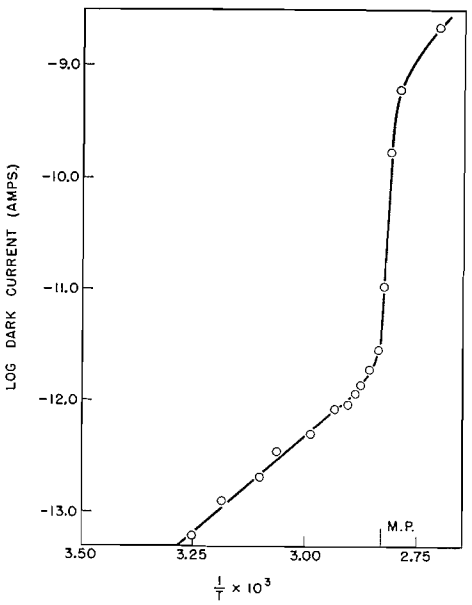

FIG. 3. Change of dark current of naphthalene upon melting.

Figs. 4 and 5 show the dependence of photo- and semi-conduction on temperature for diphenyl. In this case the log of photocurrent vs. $1/T$ dependence is hardly linear even in the intermediate region. The curvature is more pronounced and the rise at the melting point is only about a factor of 10. The logarithm of the dark current vs. the inverse temperature yields a good straight line nearly to the melting point and then a sharp increase by a factor of 10^2. A similar behavior was observed on two other crystals of biphenyl. From the slopes of the dark current vs. $1/T$ plots from room temperature until just below the melting point activation energies were determined from the relation $i = i_0 e^{-E/RT}$. Their average values are 16.5 ± 1.0 kcal. for naphthalene and 16.7 ± 0.7 kcal. for biphenyl. The value for naphthalene is close to that found by Riehl (4). The temperature dependence of the semiconduction of biphenyl has not been reported previously.

Can. J. Chem. Downloaded from www.nrcresearchpress.com by 200.7.193.243 on 09/04/12
For personal use only.

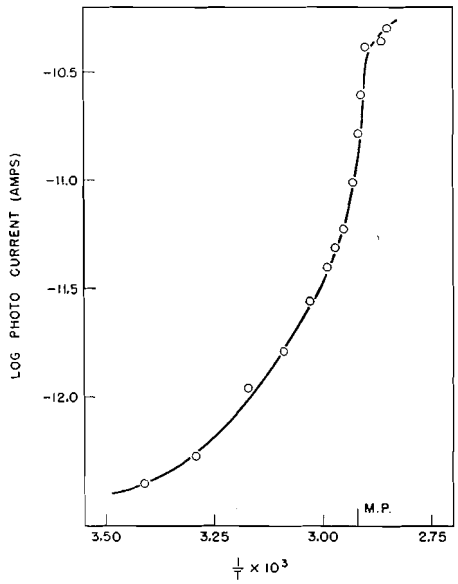

FIG. 4. Change of photocurrent of diphenyl upon melting.

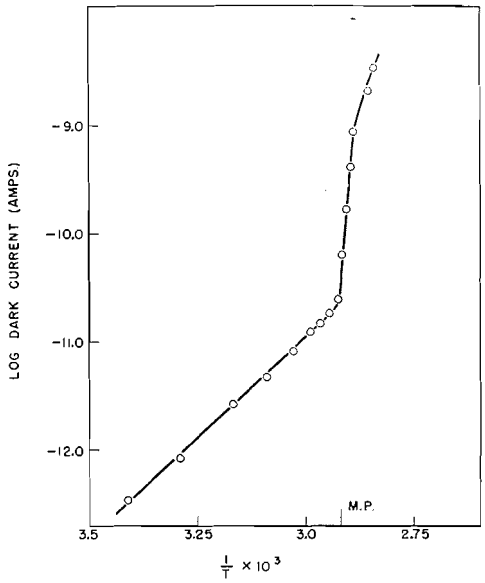

FIG. 5. Change of dark current of diphenyl upon melting.

DISCUSSION

As far as our understanding of the process of melting in the aromatic hydrocarbons goes, we can say that the melting is connected with some increase of positional disorder as evidenced, for example, by the increase in free volume. The fractional increase can be expressed as $f = (V_L - V_S)/V_S$, where V_L is the volume of melt per molecule at the melting point and V_S is the volume of solid per molecule at the melting point. It is of interest to note these values for naphthalene, biphenyl, and anthracene (8), which are: naphthalene, 16.7%; biphenyl, 12.4%; anthracene, 14.1%.

According to Riehl (9), the photoconduction of the solid at the melting point can be expressed by the equation $i_{solid} = CveFe^{-E/RT}$, where C is the concentration of the charge carriers, v the mobility, e the electronic charge, and F the applied field, and similarly in the melt $i_{melt} = C'v'eFe^{-E'/RT}$, where the symbols have the same meaning as above except that they apply to the melt.

Then in the case of naphthalene

$$\frac{i_{melt}}{i_{solid}} = 10^3 = \frac{C'v'eF}{CveF}\frac{e^{-E'/RT}}{e^{-E/RT}}.$$

The quantities which can change are C, v, and E.

The activation energy for the photoconductivity even in the crystal is very low, 2 kcal. (3), and was postulated to be connected with the transport process of the charge carriers through the crystal. Even if the value of the activation energy on going from crystal to the melt decreases to one-quarter of its value, it still cannot explain the large increase in photocurrent. Moreover, all the currents are seen to level off at higher temperatures, so there is no major permanent decrease in the activation energies. Riehl (9) showed that the activation energy for semiconduction undergoes no major change in going from the solid to the melt. Any increase in the activation energy of photoconduction will therefore also be limited. Thus $E \approx E'$.

Can. J. Chem. Downloaded from www.nrcresearchpress.com by 200.7.193.243 on 09/04/12
For personal use only.

The similarity of the changes of the photocurrent on melting with those of the dark current suggests that in both cases the pronounced change at the melting point has a common underlying cause. It is rather unlikely that the number of charge carriers would be changed by a very similar magnitude on melting irrespective of their being produced thermally as in semiconduction or optically as in photoconduction. Therefore $C = C'$. On the other hand, if on melting the transport of the charge carriers is facilitated, then it would be quite natural to expect a similar change in semiconduction and photoconduction on melting because for the transport process the way the charge carriers have been produced is of secondary importance. Thus $v' \gg v$.

The change in photocurrent as measured would involve any contribution to conductivity by movement of the molecular ions themselves which should be easier in the melt than in the solid. Nevertheless, this contribution should be rather small because (1) of the large size of molecular ions themselves (10); (2) at the melting point and at temperatures not too much above the melting point the melt is composed of clusters rather than of single molecules (8); (3) the activation energy for diffusion and migration of molecular ions should be substantially higher than that of electrons or positive holes.

We can conclude that even if there is a small contribution to the photocurrent in the melt due to the purely ionic conduction and due to the lowering of the activation energy of the charge carrier transport, the main contribution to the large increase of the photo- and semi-conductivity on melting must come from the change in the mobility of the charge carriers.

A further conclusion is that the photoconduction in aromatic hydrocarbons is not limited to the crystalline state. The existence of the photoconduction in the melt, as shown in this paper for naphthalene and biphenyl and also observed for stilbene by Henkel (11), and in a dispersion of anthracene in solid paraffin (down to concentration 2% by weight) (12) shows that an ordered arrangement of molecules in the lattice is not a necessary condition for photoconduction.

REFERENCES

1. CHYNOWETH, A. G. and SCHNEIDER, W. G. J. Chem. Phys. **22**, 1021 (1954).
2. COMPTON, D. M. J., SCHNEIDER, W. G., and WADDINGTON, T. C. J. Chem. Phys. **27**, 160 (1957).
3. KOMMANDEUR, J., KORINEK, G. J., and SCHNEIDER, W. G. Can. J. Chem. **35**, 998 (1957).
4. RIEHL, N. V. Zhur. Fiz. Khim. **29**, 959 (1955).
5. RABINOWITCH, M. Z. physik. Chem. **119**, 79 (1926).
6. KOENIGSBERGER, J. and SCHILLING, K. Ann. Physik, **32**, 179 (1910).
7. LIPSETT, F. R. Can. J. Phys. **35**, 284 (1957).
8. AL-MAHDI, A. A. K. and UBBELOHDE, A. R. Proc. Roy. Soc. (London), A, **220**, 143 (1953).
9. RIEHL, N. V. Zhur. Fiz. Khim. **29**, 1152 (1955).
10. ANDREWS, J. N. and UBBELOHDE, A. R. Proc. Roy. Soc. (London), A, **228**, 435 (1955).
11. DREHFAHL, G. and HENKEL, H. J. Z. physik. Chem. (Leipzig), **206**, 93 (1956).
12. KORINEK, G. J. and SCHNEIDER, W. G. Unpublished results.

Can. J. Chem. Downloaded from www.nrcresearchpress.com by 200.7.193.243 on 09/04/12
For personal use only.

Can. J. Chem. Downloaded from www.nrcresearchpress.com by 200.7.193.243 on 09/04/12
For personal use only.

THE SYSTEM LITHIUM NITRATE – ETHANOL – WATER AND ITS COMPONENT BINARY SYSTEMS[1]

A. N. CAMPBELL AND R. A. BAILEY[2]

ABSTRACT

The system lithium nitrate – water has been investigated by thermal analysis and by X-ray powder diffraction studies. No trace of the hemihydrate reported by Donnan and Burt was found. The X-ray powder diffraction pattern of $LiNO_3.3H_2O$ has been obtained.

The equilibrium diagram of the system ethanol–water shows an inflection at −30° C., corresponding to 40 weight per cent ethanol. This is almost certainly a true peritectic point. The formula of the hydrate formed (if there is one) is uncertain but it may be $C_2H_5OH.5H_2O$.

The system lithium nitrate – ethanol could only be studied in dilute solution (of lithium nitrate) and at temperatures near room temperature, because of high viscosity and extreme supercooling. No evidence for the existence of a solid alcoholate has been obtained.

The system lithium nitrate – ethanol – water has been investigated in the form of a series of pseudobinary systems containing water and alcohol in fixed ratios. No solid alcoholate of lithium nitrate has been found in solutions containing less than 50 weight per cent ethanol. The investigation could not be pushed beyond this alcohol content because of high viscosity and supercooling.

INTRODUCTION

This study was undertaken as a result of work on the conductance of lithium nitrate in a mixed solvent of water and ethanol (1). We think that, as the alcohol content of such a solvent is increased, the solvation of the lithium ion must change, either progressively or suddenly, from a water solvation to an alcohol solvation, with consequent increase in the effective diameter of the lithium ion. We hoped to support this view by the isolation of a solid crystalline alcoholate of lithium nitrate, analogous to the water compound $LiNO_3.3H_2O$, but it appears, as a result of the work here described, that such an alcoholate does not exist, or at least that it cannot be isolated. Despite the failure of the original aim of this work, much interesting information has resulted, particularly that relating to the important system ethanol–water.

The system lithium nitrate – ethanol – water involves the three binary systems lithium nitrate – water, ethanol–water, and lithium nitrate – ethanol. The latter system has not previously been investigated but the first two have been the subjects of several researches.

The system $LiNO_3$–H_2O was first studied in detail by Donnan and Burt (2). They reported the existence of a congruently melting trihydrate and of a hemihydrate, which decomposed into anhydrous salt and solution at 61.1° C. Campbell and Kartzmark (3) repeated the dilatometric experiments of Donnan and Burt but were unable to find any evidence for the existence of the supposed hemihydrate; neither did hemihydrate appear in their isothermal study at 25° C.

The system ethanol–water has attracted the attention of many workers but much uncertainty has always surrounded it. This system is well known for its anomalous physical behavior, and the large deviations from ideality shown by its physical properties have often been put forward as evidence of compound formation. Maxima, minima, and discontinuities on curves of various physical properties versus concentration have led to the attribution of various formulae to supposed hydrates. A bibliography of the such physical properties as density, change in volume on mixing, and viscosity, as a function of composition of the homogeneous system, it cannot be accepted as evidence

[1]*Manuscript received September 9, 1957.*
Contribution from the Chemistry Department of the University of Manitoba, Winnipeg, Manitoba.
[2]*Holder of an N.R.C. Bursary, 1956–57.*

Can. J. Chem. Downloaded from www.nrcresearchpress.com by 200.7.193.243 on 09/04/12
For personal use only.

in favor of compound formation. Anomalous physical properties can only indicate that interaction is taking place; they cannot give quantitative information about the nature of such interaction.

The soundest method of dealing with such problems is that of the phase rule and this has been applied as thermal analysis by several workers. The first systematic freezing-point determinations were carried out by Pictet (8) and by Pickering (9) but they were only interested in the point of first crystallization. Pushin and Glagoleva (10) made the first comprehensive thermal analysis and they concluded that no compounds are formed; they suggest, however, that solid solutions of ice in ethanol exist up to nearly 15 mole per cent water. Supercooling is a difficulty which has beset all investigators and this is particularly extensive in the region around 80 mole per cent ethanol.

Tarassenkov (11) repeated the thermal analysis measurements up to 75 weight per cent ethanol. He obtained an inflection on the freezing-point curve which he interpreted as evidence for the existence of a solid hydrate but he failed to obtain a peritectic halt on any cooling curve. The inflection fell at about 42 weight per cent ethanol and at $-33°$ C.

Shalberov and co-workers (12) have studied ethanol in solutions of concentration up to 53 mole per cent, as well as the ternary system ethanol – water – lithium chloride. In both systems they found a point of inflection which, for ethanol and water, fell at 34 weight per cent ethanol. Again, no peritectic halt was obtained. They suggest that the supposed hydrate has the formula $C_2H_5OH.5H_2O$.

Ross (13) determined the freezing points of a number of ethanol–water mixtures. He also obtained an inflection on the freezing-point curve at $-30°$ C. and 42 weight per cent ethanol.

The strongest indication of compound formation in the system ethanol–water is the occurrence of the point of inflection or break in the freezing-point curve but even this, without the presence of a peritectic halt on the cooling curve, cannot be accepted as truly significant unless there is further evidence that a second solid phase separates beyond this point. If this is a true peritectic point, the failure to obtain a peritectic halt is difficult to explain but the reason may lie in the persistent supercooling of alcohol–water mixtures: the peritectic halt may be hidden by the metastability of the system.

Studies of liquid ethanol at low temperatures throw some light on the physical anomalies and metastability of the system ethanol–water. Concentrated alcohol solutions supercool readily and eventually form a rigid glass near $-190°$ C. Prietzschk (14) studied the X-ray scattering at $-150°$ C. and at $-75°$ C. of liquid ethanol. From Fourier analysis he derived a radial intensity distribution curve of the pattern and from this he was able to deduce an average distribution of atoms. The structure thus determined is applicable to cold absolute alcohol and to cold alcohol containing a few per cent of water, and may be expected to give a qualitative indication of the interactions in any alcohol solution. At $-150°$ C., every oxygen atom is linked to two others, presumably by hydrogen bonding. We thus have a structure where the oxygen atoms are linked through hydrogen to form zigzag chains, the C_2H_5 groups lying at right angles to this chain. (Fig. 1 is a plane projection of such a three-dimensional chain.)

Harvey's investigation (15) of ethanol at $-75°$ C. gave the same result as that of Prietzschk. The number of nearest neighbors of each oxygen atom is found to be only older work (4, 5, 6, 7) is given but since all such work consists in the investigation of 1.2 at this temperature. This shows that the hydrogen bonding is becoming less as the temperature increases, but it is still quite appreciable at $-75°$ C.

Perfectly dry ethanol is readily crystallized but the addition of small amounts of water

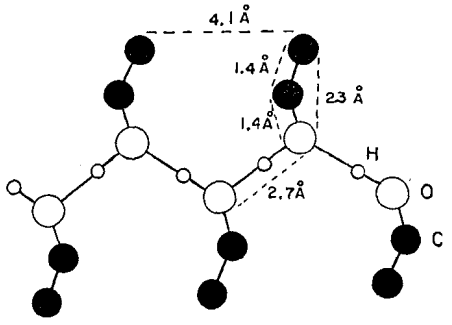

FIG. 1. Structure of absolute alcohol.

renders crystallization extremely difficult. Furthermore, at a given temperature the viscosity is sharply increased by small amounts of water, and the lower the temperature the less water is required for an increase of the same degree. Bernal and Fowler (16) have shown that at low temperatures the oxygen atom of a water molecule can be surrounded by four others, linked to it by hydrogen bonds. It is evident that the oxygen atom of water might equally well be surrounded by four oxygen atoms of ethanol. Therefore, in an alcoholic solution of low water content, we might expect that each water molecule could form the point of linkage of four alcohol chains, if the temperature were low enough. At higher temperatures dissociation would be greater and perhaps only three, or two, alcohol chains would be attached to water. Fig. 2 is a planar diagram

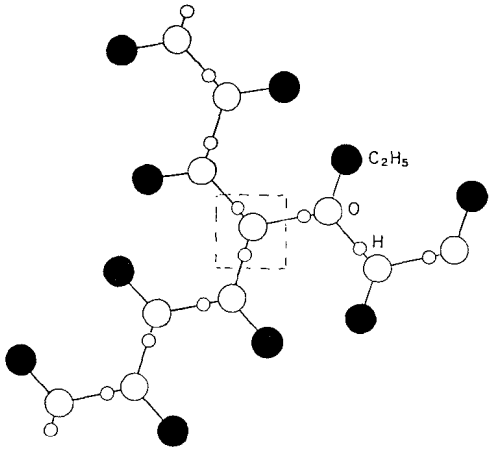

FIG. 2. Structure of "wet" alcohol.

of three ethanol chains linked to a water molecule. Prietzschk has used the viscosity data of Tammann and Hesse (17) to calculate the average length of the alcohol chains linked by water at $-130°$ C.; he finds that there are about 25 molecules of ethanol for each molecule of water, that is, each ethanol chain is six or eight molecules long, depending on whether four or three chains are linked by each water molecule at this temperature.

It is evident that there is a fundamental difference between absolute alcohol and "wet" alcohol, at low temperatures. Pure alcohol is linked only in the form of linear chains but, when water is present, an irregular three-dimensional network is formed which is analogous to the structure in silicate glasses. The lack of the three-dimensional linking in pure ethanol accounts for the comparative ease with which the material is crystallized.

Can. J. Chem. Downloaded from www.nrcresearchpress.com by 200.7.193.243 on 09/04/12
For personal use only.

Prietzschk found the powder pattern of solid ethanol to be extremely simple, consisting only of a very broad, intense line, flanked very closely on each side by a sharper but weaker line. Wahl (18) concluded that the crystals of ethanol belong to one of the low symmetry classes but he was unable to obtain further definite information.

As to the ternary system ethanol – water – lithium nitrate, there exists only the isothermal investigation of Campbell and Kartzmark (3) at 25° C., who found no evidence of compound formation between lithium nitrate and ethanol.

EXPERIMENTAL

Purity of Materials

The lithium nitrate was Fisher "Certified Reagent" and it was used without further purification. Water was removed by fusing at least twice. Grinding and transferring were done in a dry-box.

The ethanol used, when absolute alcohol was not required, was purified by distillation through a Podbelniak-type column; the middle third was the only fraction retained. Absolute ethanol was prepared from commercial material by prolonged refluxing with quicklime, followed by treatment of the distillate with magnesium according to the method described by Fieser (19). Absolute alcohol was transferred only in the dry-box. The dryness of the absolute alcohol was constantly tested with aluminum ethoxide by the method of Henle (20), and the density of each new batch was determined.

Methods of Analysis

Lithium nitrate was determined by evaporation to dryness, fusing the residue and weighing. The fusion was repeated at least once, since lithium nitrate is hygroscopic. An accuracy of about 0.1% could be obtained. The ethanol content of a mixture was determined by distilling and determining the density of the distillate.

Apparatus for Thermal Analysis

Glass cells equipped with stirrers and closed from the atmosphere were used. Temperatures were measured with copper–constantan thermocouples, whose e.m.f.'s were recorded by a Brown recording potentiometer. Double or triple copper–constantan junctions were used to increase the sensitivity to the maximum consistent with the range of the recorder. The couples were calibrated from the freezing points of purified, redistilled mercury (f.p. = −38.87° C.), of "spectro" grade carbon tetrachloride (f.p. = −22.8° C.), of reagent grade toluene (f.p. = −95.0° C.), and of "spectro" grade diethyl ether (f.p. = −116.7° C.). Calibration above 0° C. was done by comparison with a previously calibrated mercury-in-glass thermometer reading to 0.1° C.

Both types of freezing-point cell are illustrated in Fig. 3; they differed only in the method of stirring. Both consisted of an inner glass tube containing the solution and surrounded by an outer jacket which could be evacuated as required to reduce the rate of cooling. A well for the thermocouple extended into the solution near the stirrer. The first type of cell (3*a*) was stirred electromagnetically. The second type of cell (3*b*) was used when the viscosity prevented the weaker magnetic stirring of the former type from being effective; most low-temperature work was done in the latter type. Either dry-ice–acetone or liquid nitrogen was used as the cooling agent.

X-Ray Technique

A high-temperature camera of the Buerger type (21) was available and we succeeded in modifying this to take pictures at low temperatures (down to −120° C.). The manner of the modification, and particularly the method of cooling, may be of interest to others; details can be obtained from this laboratory.

Can. J. Chem. Downloaded from www.nrcresearchpress.com by 200.7.193.243 on 09/04/12
For personal use only.

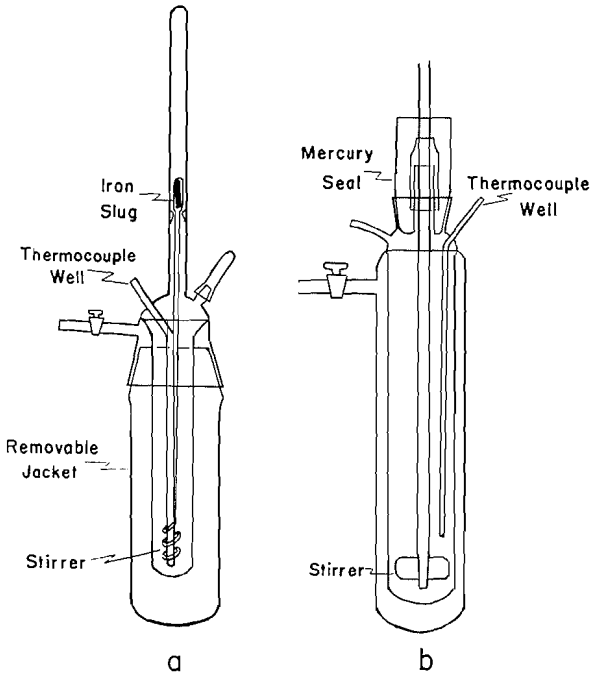

FIG. 3. Freezing-point cells.

EXPERIMENTAL PROCEDURE

The System Lithium Nitrate – Water

This system was submitted to thermal analysis. Since the results showed no indication of the existence of the peritectic point reported by Donnan and Burt (2), and since the work of Campbell and Kartzmark (3) had indicated that the hemihydrate did not exist, X-ray diffraction work was done as an additional check. Diffraction pictures of anhydrous lithium nitrate were taken at room temperature, at 45°, and at 100° C. A second picture was taken at the latter temperature, after prolonged heating, in case any phase transformation occurred slowly. A mixture of lithium nitrate and water was then made up to have a composition corresponding closely to that of the supposed hemihydrate. After this mixture had been maintained at 45° C. for some time, an X-ray diffraction photograph was taken of it.

No diffraction pattern for $LiNO_3.3H_2O$ is listed in the A.S.T.M. index of diffraction patterns, so this compound was photographed at room temperature. For all pictures, copper K_α radiation was used. The standard camera had a diameter of 57.3 mm.

The System Ethanol–Water

In the thermal analysis, little supercooling was encountered in dilute solutions, but as the alcohol content was increased, the supercooling also increased until, beyond 75 weight per cent ethanol, it became extremely difficult to obtain a freezing point at all. Little difficulty from supercooling was encountered with absolute ethanol, but as water was added supercooling increased rapidly.

To investigate the solid phase separating, X-ray diffraction photographs were taken of frozen solutions. Photographs were taken first of ice at temperatures from −20° to −80° C., as a basis of comparison. A series of pictures was also taken of solutions

Can. J. Chem. Downloaded from www.nrcresearchpress.com by 200.7.193.243 on 09/04/12
For personal use only.

containing less than 40 weight per cent ethanol, at various temperatures, particularly above the suspected peritectic temperature of −30° C. If any new phase were to appear, it was expected that it would do so beyond 40 weight per cent ethanol and photographs were taken in this region at a series of temperatures and compositions. The composition was not taken beyond 65% ethanol, since the mixture often refused to crystallize beyond this point, nor was the temperature taken below −100° C. All these pictures were taken with copper K_α radiation and an exposure time of about 1.5 hours. Diffraction pictures were also taken of absolute ethanol, both with copper and with iron radiation, at temperatures between −120° and −130° C.

The System Lithium Nitrate – Ethanol

The thermal analysis of this system could not be carried very far because all solutions were very viscous and supercooled extensively; freezing points could only be determined in solutions containing less than about 6% salt. The solubility curve was therefore determined at 50°, 30°, 20°, 0°, and −21° C. The temperature could not be carried lower than this because the extreme viscosity made sampling impossible. During a determination, sampling was made on successive days, but no change in concentration was found. At low temperatures, the mixture was chilled before stirring to prevent possible supersaturation.

The Ternary System Lithium Nitrate – Ethanol – Water

The first approach to the ternary system involved an attempt to follow the eutectic troughs inward from the lithium nitrate – water edge of the diagram but the high viscosity of the solution made sampling impossible. As an alternative a study was undertaken of a number of pseudobinary systems in each of which the ratio of alcohol to water was kept constant and the concentration of lithium nitrate varied. The freezing points of such pseudobinary systems lie on a straight line radiating from the lithium nitrate apex and cutting the ethanol–water edge at the composition of the solution used as solvent. Only the point of first crystallization may be used since, in general, the crystallization path of the solution does not lie along the line of the pseudobinary "cut". Therefore, the pseudobinary eutectic temperatures can be found accurately only if the original solution has the composition of the eutectic. Since it was not considered worth while for the purpose of this investigation to prepare mixtures having the exact pseudobinary eutectic composition, the eutectic halt of a solution near this point was used. When the solid separating is the anhydrous salt, however, the crystallization path does follow the line of the pseudobinary "cut", and true eutectic temperatures can then be obtained. The same applies to peritectic halts, under the same conditions.

Systems having a fixed lithium nitrate – water ratio can be treated in the same way. Accordingly, the freezing points of systems consisting of the hydrate, $LiNO_3.3H_2O$, to which increasing amounts of ethanol were added, were investigated. This system behaves as a true binary system between the compounds $LiNO_3.3H_2O$ and C_2H_5OH, as long as the trihydrate is the stable solid separating.

EXPERIMENTAL RESULTS

The experimental results are contained in Tables I to XIV. The headings are self-explanatory.

DISCUSSION OF RESULTS

The System Lithium Nitrate – Water

The results, as listed in Table I and shown graphically in Fig. 4, are not in complete

Can. J. Chem. Downloaded from www.nrcresearchpress.com by 200.7.193.243 on 09/04/12
For personal use only.

Can. J. Chem. Downloaded from www.nrcresearchpress.com by 200.7.193.243 on 09/04/12
For personal use only.

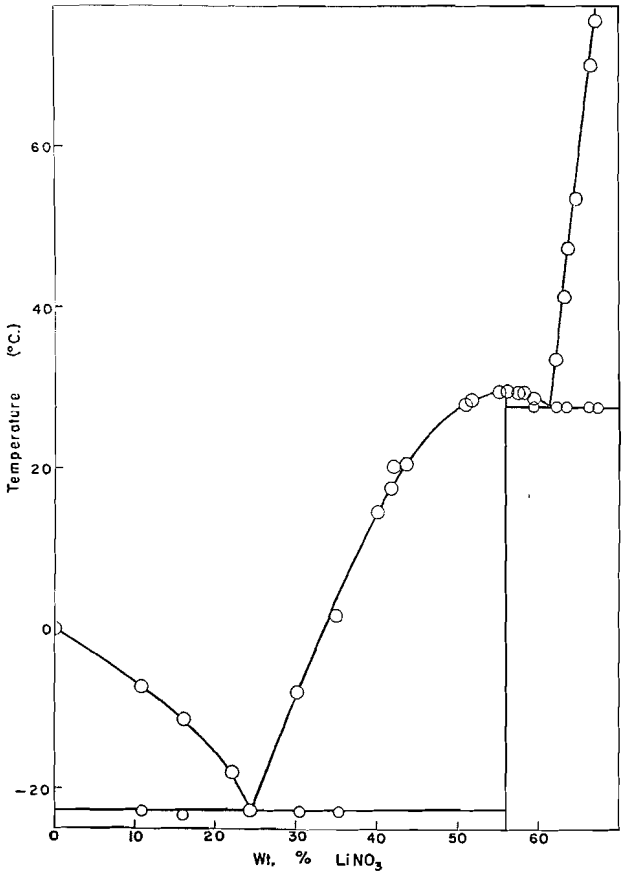

FIG. 4. The system $LiNO_3$–H_2O.

TABLE I

THERMAL ANALYSIS DATA OF THE SYSTEM LITHIUM NITRATE – WATER

Wt. % $LiNO_3$	Freezing point, ° C.	Invariant point, ° C.	Solid phases present at freezing point
10.7	−7.4	−22.8	Ice
16.0	−11.3	−23.4	"
22.3	−17.7		"
24.5		−22.9	Ice + $LiNO_3.3H_2O$
30.1	−7.9	−22.9	$LiNO_3.3H_2O$
35.1	1.5	−22.9	"
40.1	14.5		"
41.8	17.5		"
42.1	20.2		"
43.7	20.6		"
51.3	28.4		"
55.2	29.4		"
56.0	29.6		"
57.8	29.5		"
58.0	29.5		"
59.6	28.8	27.9	"
62.3	33.6	27.9	$LiNO_3$
63.4	41.3	27.9	"
63.6	47.1	27.9	"
64.6	53.7	27.9	"
66.4	70.0	27.9	"
66.9	75.6	27.9	"

agreement with those of Donnan and Burt (2). The ice–trihydrate eutectic lies at −22.9° C. and 24.5 weight per cent lithium nitrate; this is at both a lower temperature and a lower concentration than reported by Donnan and Burt (−17.8° C., 33 weight per cent lithium nitrate). The values for the higher eutectic, 27.9° C. and 61.5 weight per cent lithium nitrate, are also different from those previously accepted (29.6° C., 59 weight per cent $LiNO_3$). Here, trihydrate is in equilibrium with anhydrous lithium nitrate (and solution) and not with hemihydrate, as the previous study had supposed. The melting point of lithium nitrate trihydrate was found to be 29.6° C.

All the X-ray pictures taken on anhydrous lithium nitrate between room temperature and 100° C. were identical, showing that only one phase of anhydrous salt exists between these temperature limits. A mixture of lithium nitrate and water, corresponding in composition to the supposed hemihydrate, gave only the pattern of anhydrous salt (above 27.9° C.). This evidence, together with the observations of Campbell and Kartzmark (3), refutes the claim that a hemihydrate exists.

The X-ray powder diffraction pattern for $LiNO_3.3H_2O$ is listed in Table II. Relative intensities were estimated visually, the strongest line being assigned an intensity of 10. The trihydrate pattern has many lines in common with the anhydrous salt.

TABLE II

X-RAY POWDER DIFFRACTION PATTERN OF $LiNO_3.3H_2O$

Relative intensity	Lattice spacing, Å
2	6.13
7	4.20
3	3.47
10	2.99
2	2.79
2	2.68
1	2.53
5	2.37
8	2.13
1	2.02
1	1.90
2	1.80
3	1.71
2	1.54
	1.36

The System Ethanol–Water

The results of thermal analysis are listed in Table III and the equilibrium diagram is shown in Fig. 5. It was found that supercooling increased with ethanol content and became extremely persistent beyond 75 weight per cent ethanol, where it was impossible to detect an initial freezing point although eutectic halts could be obtained with solutions up to the eutectic composition. On the alcohol side of the eutectic, supercooling and viscosity increased with increasing water content but reasonably good freezing points could be observed up to the eutectic point. No eutectic halts were obtained in this region and this may be an indication that the solid solution formation reported by Pushin (10) does indeed exist.

Formation of solid solution is most common between substances having similar crystal structure, although this is by no means a necessary condition. Ice crystallizes in the hexagonal system but, although the structure of the ethanol molecule is known, nothing is known about the crystal structure of solid alcohol; the direct observations of Wahl

Can. J. Chem. Downloaded from www.nrcresearchpress.com by 200.7.193.243 on 09/04/12
For personal use only.

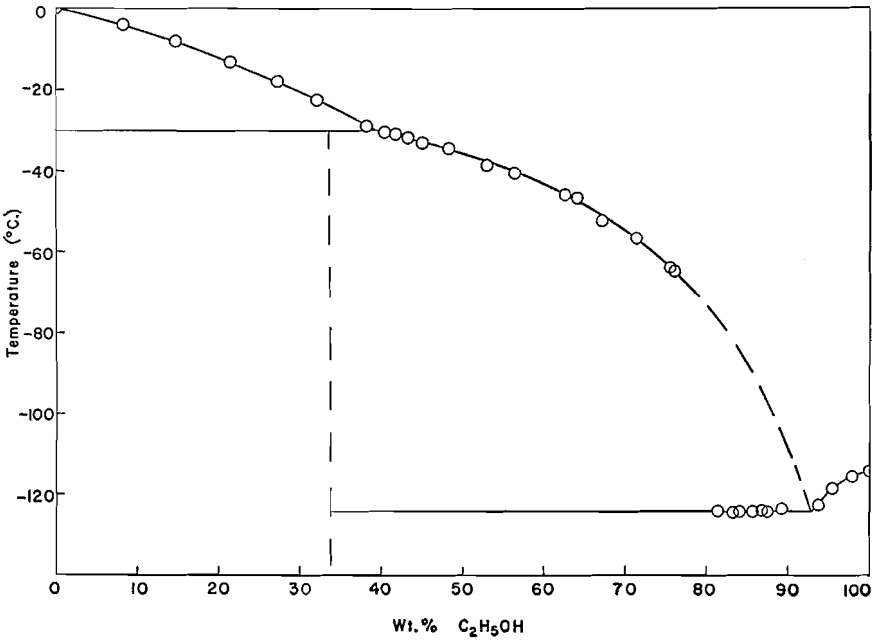

FIG. 5. The system ethanol–water.

TABLE III

THERMAL ANALYSIS DATA OF THE SYSTEM C_2H_5OH–H_2O

Composition, wt. % C_2H_5OH	Freezing point, ° C.	Invariant point, ° C.
8.1	−3.8	
14.8	−7.4	
21.4	−12.7	
27.1	−17.9	
32.1	−22.4	
38.1	−28.3	
40.4	−30.3	
41.6	−30.8	
43.2	−31.8	
45.1	−33.1	
48.3	−34.2	
53.0	−38.6	
56.3	−40.8	
62.5	−45.7	
64.0	−46.5	
67.1	−52.6	
71.3	−56.1	
75.5	−64.0	
75.8	−64.6	
81.1	—	−124.1
82.7	—	−124.4
83.9	—	−124.1
85.6	—	−124.1
86.8	—	−124.1
87.4	—	−124.6
88.1	—	−123.8
93.6	−122.9	
95.4	−118.6	
97.8	−115.7	
100.0	−114.4	

Can. J. Chem. Downloaded from www.nrcresearchpress.com by 200.7.193.243 on 09/04/12
For personal use only.

(18) indicate that solid ethanol has a very unsymmetrical form. This may easily be so, if the crystal is made up from the irregular chains of ethanol molecules which Prietzschk (14) has shown to be present in the cold liquid. It would then be possible for water to enter such a crystal lattice as part of an alcohol chain, or even as the point of linkage of two or more chains, since Prietzschk shows that such linkage certainly occurs in the "wet" liquid. Formation of solid solutions of ice in ethanol may thus be accounted for without the assumption of similar crystal structures.

The freezing-point curve shows the inflection previously found by Tarassenkov (11) and by Shalberov *et al.* (12) but no peritectic halt was ever observed. The inflection occurs at −30° C. and 39.5 weight per cent ethanol. We find the eutectic to lie at −124.1° C. and about 93.0 weight per cent ethanol, whereas Pushin and Glagoleva (10) reported the values −118° C. and 93.5 weight per cent ethanol, for this point. The freezing point of absolute ethanol was found to be −114.4° C., agreeing within the experimental error with the generally accepted value of −114.6° C.

The results of X-ray diffraction studies at low temperatures are collected in Tables IV, V, and VI, which list the spacings and intensities of the lines from diffraction photographs of ice, of dilute ethanol solutions (i.e. solutions containing less than 30% by weight of ethanol), and of more concentrated ethanol solutions, respectively. The pictures in all cases showed much background darkening and the lines were quite broad, since it

TABLE IV

X-RAY POWDER DIFFRACTION PATTERN OF ICE

Observed values (mean of 4 pictures)		Literature values	
Lattice spacing *d*, Å	Relative intensity	Lattice spacing *d*, Å	Relative intensity
4.14	Very weak	3.92	10
3.92	Medium	3.67	100
3.55	Strong	3.44	20
2.70	Medium	2.67	15
2.30	Medium	2.26	10
2.11	Strong	2.07	50
1.95	Strong	1.92	10
1.45	Very weak	1.52	15
1.39	Weak	1.37	2
1.27	Very weak	1.30	3
		1.25	3
		1.17	5

TABLE V

X-RAY POWDER DIFFRACTION PATTERN OF FROZEN SOLUTIONS CONTAINING LESS THAN 40 WT. % ETHANOL AT TEMPERATURES ABOVE −30° C.
(mean of 8 pictures)

Lattice spacing *d*, Å	Relative intensity	Number of times observed
4.18	Very weak	3
3.92	Weak	4
3.76	Very weak	3
3.54	Strong, diffuse	8
2.69	Medium	8
2.30	Strong	5
2.13	Medium	6
1.39	Weak	5

Can. J. Chem. Downloaded from www.nrcresearchpress.com by 200.7.193.243 on 09/04/12
For personal use only.

TABLE VI

X-RAY POWDER DIFFRACTION PATTERN OF FROZEN SOLUTIONS CONTAINING MORE THAN 40 WT. % ETHANOL AT TEMPERATURES FROM −30° C. TO −90° C.
(mean of 10 pictures)

Lattice spacing d, Å	Relative intensity	Number of times appearing
3.61	Weak, diffuse	6
3.32	Strong	10
2.97	Strong	8
2.64	Very weak	2

was necessary to use wide capillaries to prevent separation of the liquid column on cooling, so that no great accuracy in the measurements of the spacings could be obtained. Although the nominal diameter of the camera was 57.3 mm., the fact that the ice pattern, the mean of four pictures, has spacings consistently larger than those listed in the A.S.T.M. index and determined by Dennison (22) and by Barnes (23) indicates either that the camera is slightly smaller than the figure given above or that shrinkage of the film occurred. No attempt was made to calibrate the camera, since only comparative results were desired and, in any case, the discrepancy is not large. Neither the strong line of spacing $d = 3.67$ Å nor the weaker line at $d = 3.44$ Å could be found but a strong line was observed at $d = 3.55$ Å and this is probably equivalent to the two missing lines. A very weak line at $d = 4.14$ Å, which does not appear in the literature tabulation, also occurred.

The diffraction patterns of dilute alcohol solutions taken under such conditions that no compound could be formed (i.e., at temperatures above that of the point of inflection) were not good. The lines were quitè diffuse, largely owing to unfrozen liquid in the tests. The results agree fairly well with the literature tabulation for ice, although an additional line at $d = 3.76$ Å appeared in three cases and many of the weaker lines were absent.

The pattern given by solutions containing more than 40% by weight ethanol is listed in Table VI. A total of 10 pictures containing distinguishable lines were used. These pictures were little better than those taken in dilute solutions and the lines were particularly broad, since in general wider capillaries were required for such solutions. Few lines were obtained; only three appeared at all consistently. Of these, the first, at $d = 3.61$ Å, lies close to the position of a strong line in the ice pattern. Since this line is both weak and diffuse, there is the possibility that it is due to ice deposited on the outside of the capillary, from moisture present in the camera at the beginning of the run, but it is difficult to see how enough ice could be deposited in this way to give an observable line; it is probably a true line from the specimen. The other two lines, both strong and both nearly always present, are quite far removed from any ice lines. This is particularly true of that falling at $d = 2.97$ Å. The other line falls at $d = 3.32$ Å. These two lines were predominant on the diffraction patterns of solutions of alcohol exceeding 40 weight per cent ethanol and taken at temperatures between −35° C. and −90° C. The temperature was never taken as low as the freezing point of ethanol, so the lines cannot be due to solid alcohol. Moreover, they do not appear on any picture of ice at any temperature, or of more dilute solutions of alcohol at temperatures above −30° C. They can only be explained by the formation of a new solid phase separating from solution. They indicate that an incongruently melting hydrate of ethanol may be formed and that therefore the point of inflection on the freezing curve is a true peritectic point.

Can. J. Chem. Downloaded from www.nrcresearchpress.com by 200.7.193.243 on 09/04/12
For personal use only.

A few solutions of roughly the expected composition of the hydrate, $C_2H_5OH.5H_2O$, were made up and photographed at temperatures well below the supposed peritectic temperature. These pictures showed only the ice pattern, whereas, if a compound is formed, lines from it also should be present. This behavior can only be explained if the system cools metastably past the peritectic temperature, the reaction "ice + solution → compound" failing to take place. The absence of a peritectic halt on the cooling curve can be explained in the same way. The spacings measured from these diffraction patterns are not highly accurate and any picture alone would be of doubtful value because of the broad lines and the generally dark background. As a group, however, the results are consistent, and errors in the spacings listed are not great enough to invalidate the general conclusion.

The question of the composition of this hypothetical hydrate of ethanol cannot be answered with certainty. The position of the point of inflection corresponds to an alcohol: water ratio of 3.98, but the compound must contain more water than this. Although the formula $C_2H_5OH.4H_2O$ is possible, it is unlikely, since this composition is so close to the composition of the peritectic point. Perhaps the most probable formula is that proposed by Shalberov (12), viz. $C_2H_5OH.5H_2O$.

The diffraction photographs of absolute ethanol resulted only in a single broad line of strong intensity at $d = 3.89$ Å. This is the result of two pictures, one taken with copper, the other with iron, radiation. The latter was used in the hope that it would result in the resolution of the single line into the closely spaced triplet observed by Prietzschk (14), but it did not. The position of the single line was similar to that of the triplet in the photograph published by Prietzschk but, unfortunately, he does not indicate any spacings.

The System Lithium Nitrate – Ethanol

The results obtained by thermal analysis are shown in Table VII. Only quite dilute solutions could be frozen, the supercooling increasing with lithium nitrate content. No eutectic halt could be detected. Solubility measurements are summarized in Table VIII.

TABLE VII

THERMAL ANALYSIS DATA OF THE SYSTEM $LiNO_3$–C_2H_5OH

Composition, wt. % $LiNO_3$	Freezing point, ° C.
0.0	−114.4
0.8	−115.8
2.1	−116.7
3.8	−118.2
5.5	−118.6
6.3	−124

TABLE VIII

SOLUBILITY DATA OF THE SYSTEM $LiNO_3$–C_2H_5OH

Temperature, ° C.	Solubility, wt. % $LiNO_3$
50.0	25.6
30.1	24.7
20.1	24.0
0.0	23.0
−21	21.9

Can. J. Chem. Downloaded from www.nrcresearchpress.com by 200.7.193.243 on 09/04/12
For personal use only.

A plot of freezing point and solubility data, as in Fig. 6, shows that, in order that the two curves may intersect without compound formation, the eutectic point must lie unusually far into the diagram. For systems involving substances whose melting points are so dissimilar as are those of ethanol and lithium nitrate, it is seldom that the eutectic lies more than a short distance from the axis of the lower-melting compound. It is therefore quite possible that an alcoholate of lithium nitrate may exist in the solid state.

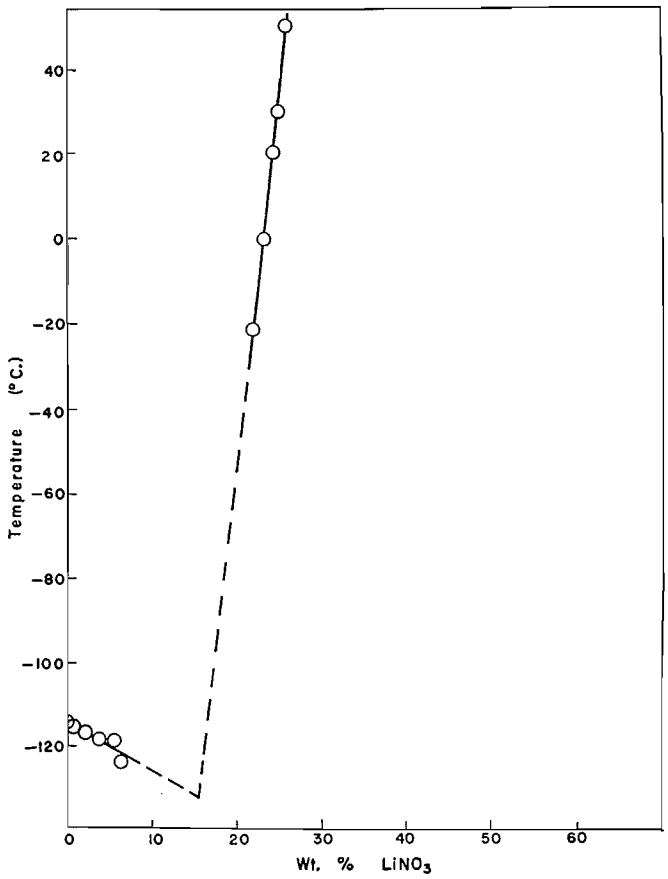

FIG. 6. The system $LiNO_3$–C_2H_5OH.

The very great viscosity of alcoholic lithium nitrate solutions at low temperatures indicates some sort of interaction between ethanol and lithium nitrate. It is very probable that the strongly electropositive lithium ion and the electronegative oxygen of the alcohol will exhibit strong electrostatic attraction, just as do lithium ion and water. Since at low temperatures the ethanol molecules are linked in chains, the lithium ions could be solvated by a number of these chains and they would, in effect, form the points of linkage of them.

The System Lithium Nitrate – Ethanol – Water

Five pseudobinary "cuts" in which lithium nitrate was dissolved in solvents of fixed ethanol: water ratio were made through the ternary system. The solvents were 27.2,

Can. J. Chem. Downloaded from www.nrcresearchpress.com by 200.7.193.243 on 09/04/12
For personal use only.

42.0, 49.7, 66.4, and 78.2 weight per cent ethanol. Tables IX to XIII give the thermal analysis data, while Figs. 7 to 11 show the freezing-point curves which were obtained. It was found that supercooling increased with alcohol content except when anhydrous lithium nitrate was the solid phase, when it was nearly negligible even in solutions containing considerable quantities of alcohol. Supercooling was especially pronounced with solutions in 78.2% ethanol, and freezing points below −20° C. could not be obtained.

The system lithium nitrate trihydrate – ethanol is shown in Fig. 12 and the thermal analysis data are given in Table XIV. Some of the points are taken from the freezing-point curves of the other pseudobinary systems.

Figs. 13 and 14 show the ternary system as a whole, so far as we have been able to determine it. In Fig. 13, a series of isothermal solubility lines are depicted. These were obtained from the various pseudobinary "cuts" by reading off the compositions corresponding to each temperature. Isothermals at 25°, 20°, 15°, 10°, 0°, −15°, −35°, and

TABLE IX

THERMAL ANALYSIS DATA OF THE PSEUDOBINARY SYSTEM
$LiNO_3$ – 27.2 WT. % C_2H_5OH

Composition, wt. % $LiNO_3$	Freezing point, ° C.	Pseudoinvariant point, ° C.
0.0	−17.8	
8.5	−25.0	
10.2	−27.1	
12.7	−30.1	
15.0	−35.3	
17.6	−26.9	−41.1
20.3	−16.6	
24.3	−4.6	
35.4	13.0	
48.6	25.0	
52.2	25.3	
57.9	50.6	22.1
56.7	38.7	22.3

TABLE X

THERMAL ANALYSIS DATA OF THE PSEUDOBINARY SYSTEM
$LiNO_3$ – 42.0 WT. % C_2H_5OH

Composition, wt. % $LiNO_3$	Freezing point, ° C.	Pseudoinvariant point, ° C.
0.0	−30.6	
5.6	−38.8	
9.7	−44.9	
12.5	−41.8	−51.0
14.1	−34.7	
33.8	15.5	
39.6	21.3	
40.3	(~21)	
42.8	22.4	
47.0	22.1	
48.7	21.6	
51.0	21.3	
52.3	35.6	20.7
54.0	46.2	21.0

Can. J. Chem. Downloaded from www.nrcresearchpress.com by 200.7.193.243 on 09/04/12
For personal use only.

−60° C. are shown, as well as the line in the ice region at −20° C. In Fig. 14, only the eutectic and peritectic troughs are shown. Again, the composition data were obtained from the pseudobinary cuts.

Some uncertain indications, not described here, have been obtained of the existence of a ternary compound (incongruently melting), such as $LiNO_3.2C_2H_5OH.H_2O$, but the evidence is extremely inconclusive.

It is reasonably certain that no alcoholate of lithium nitrate crystallizes from solutions of less than 50 weight per cent ethanol, but in more concentrated alcohol solutions the nature of the solid phase is uncertain. When the solvent contained more than 80% ethanol, pronounced supercooling made experimental study impossible.

TABLE XI

THERMAL ANALYSIS DATA OF THE PSEUDOBINARY SYSTEM $LiNO_3$ – 49.7 WT. % C_2H_5OH

Composition, wt. % $LiNO_3$	Freezing point, ° C.	Pseudoinvariant point, ° C.
0.0	−36.0	
3.0	−43.4	
8.0	−48.7	
10.4	−54.2	−58.9
14.1	−33.7	
19.7	−12.4	
36.0	18.8	
37.0	19.2	
38.5	20.1	
43.7	21.8	
45.7	21.3	
48.5	23.6	19.8
48.8	30.1	19.5

TABLE XII

THERMAL ANALYSIS DATA OF THE PSEUDOBINARY SYSTEM $LiNO_3$ – 66.4 WT. % C_2H_5OH

Composition, wt. % $LiNO_3$	Freezing point, ° C.	Pseudoinvariant, point, ° C.
0.0	−47.4	
4.9	−57.9	
6.8	−63.2	
9.0		−73.0
10.2	−62.0	
13.8	−27.0	
15.5	−18.2	
18.3	−7.8	
23.2	4.4	
26.6	10.3	
27.0	11.0	
29.6	13.8	
29.7	14.1	12.1
30.9	15.6	12.5
35.6	17.5	
35.7	17.3	
40.0	16.6	
43.0	31.1	15.0
43.9	43.1	14.6

Can. J. Chem. Downloaded from www.nrcresearchpress.com by 200.7.193.243 on 09/04/12
For personal use only.

TABLE XIII

THERMAL ANALYSIS DATA OF THE PSEUDOBINARY SYSTEM $LiNO_3$ – 78.2 WT. % C_2H_5OH

Composition, wt. % $LiNO_3$	Freezing point, ° C.	Pseudoinvariant point, ° C.
16.6	−13.2	
17.9	−6.3	
21.5	−1.3	
24.4	0.8	
26.2	1.6	
27.4	2.5	
30.6	5.4	
31.4	5.6	
32.6	(~5.2)	
32.8	11.3	
34.5	24.0	(~5)
35.1	28.8	5.7
35.2	31.9	
36.2	43.5	5.1

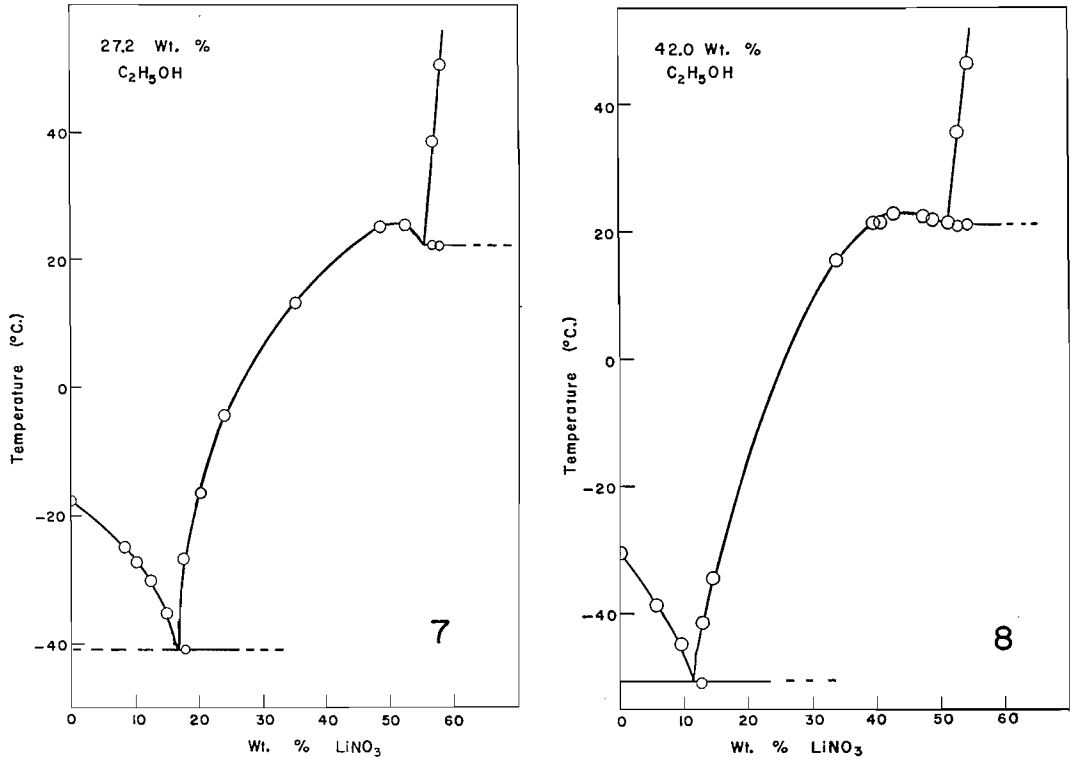

FIG. 7. The pseudobinary system.
FIG. 8. The pseudobinary system $LiNO_3$ – 42.0 wt. % C_2H_5OH.

Can. J. Chem. Downloaded from www.nrcresearchpress.com by 200.7.193.243 on 09/04/12
For personal use only.

Can. J. Chem. Downloaded from www.nrcresearchpress.com by 200.7.193.243 on 09/04/12
For personal use only.

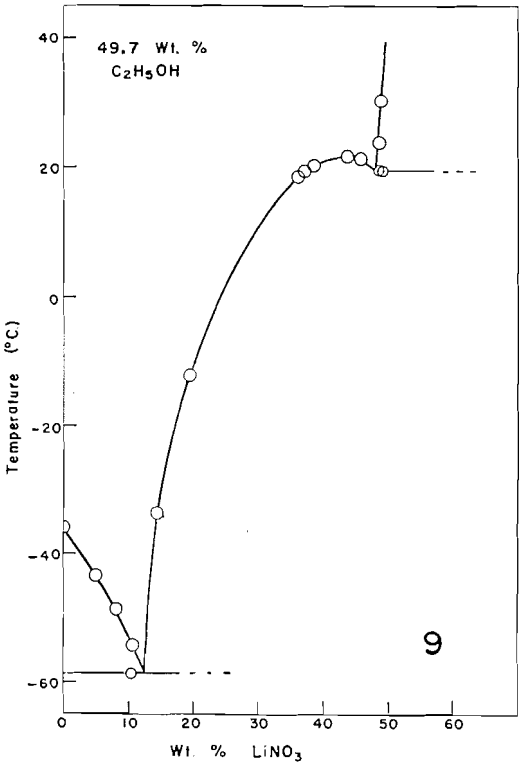

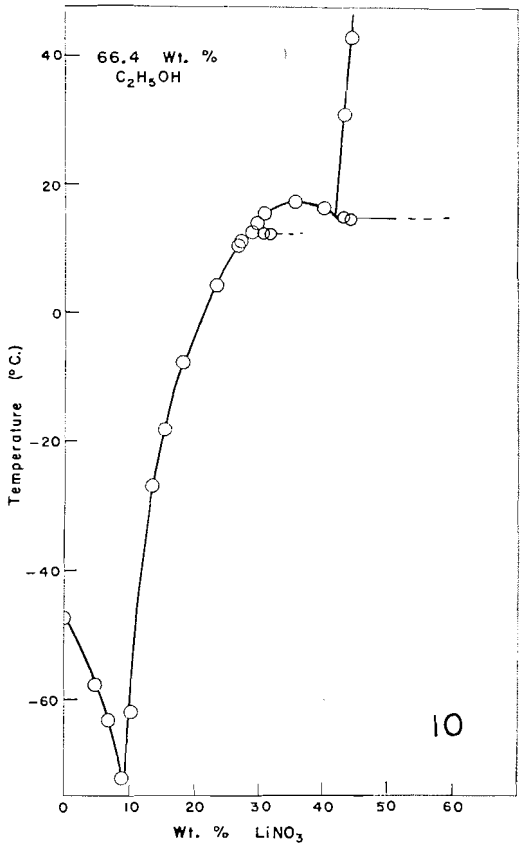

FIG. 9. The pseudobinary system $LiNO_3$ – 49.7 wt. % C_2H_5OH.
FIG. 10. The pseudobinary system $LiNO_3$ – 66.4 wt. % C_2H_5OH.

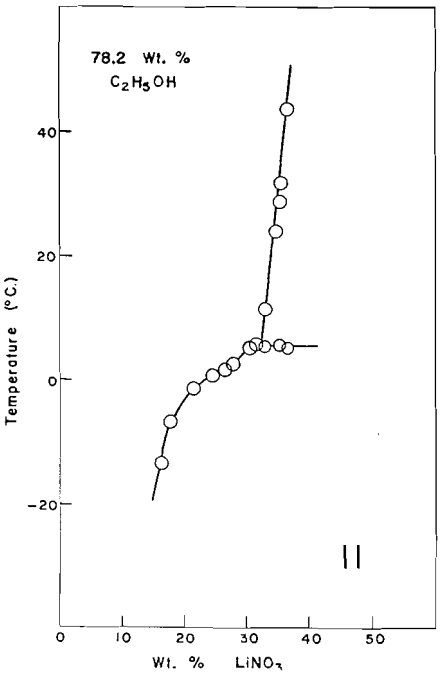

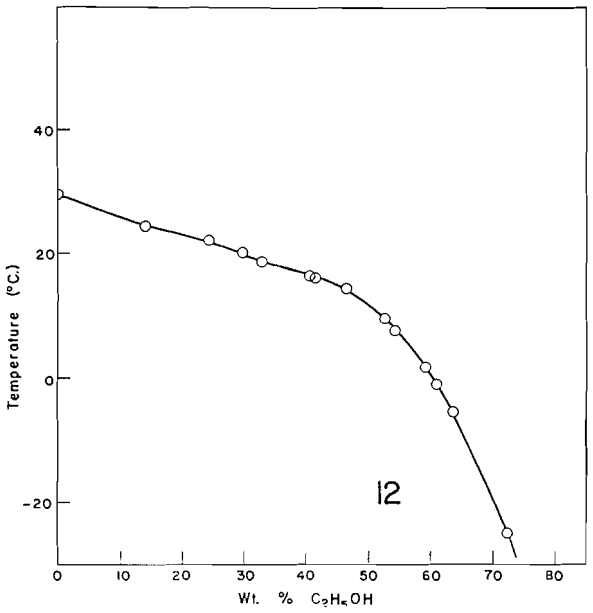

FIG. 11. The pseudobinary system $LiNO_3$ – 78.2 wt. % C_2H_5OH.
FIG. 12. The system $LiNO_3.3H_2O$–C_2H_5OH.

Can. J. Chem. Downloaded from www.nrcresearchpress.com by 200.7.193.243 on 09/04/12
For personal use only.

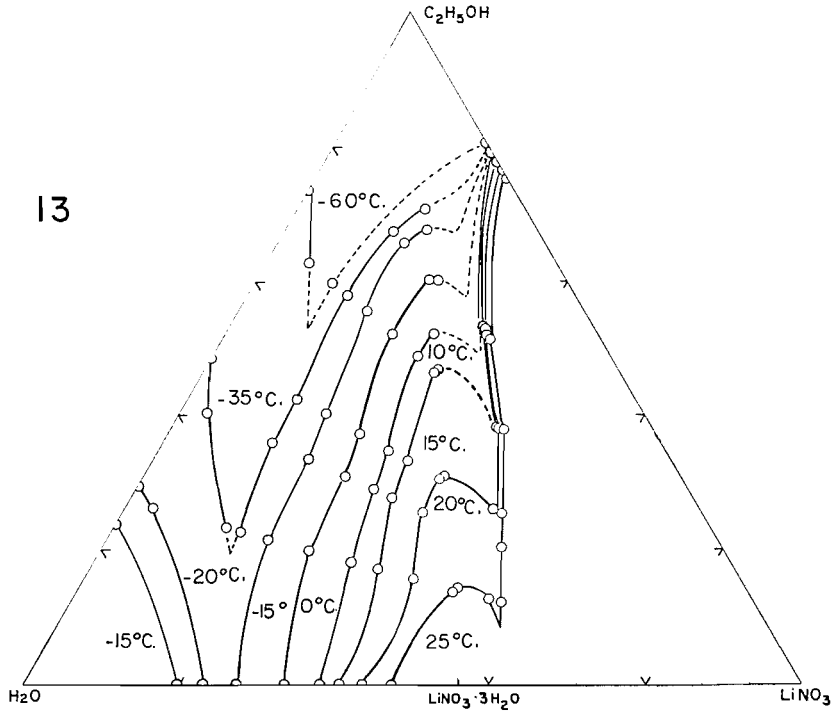

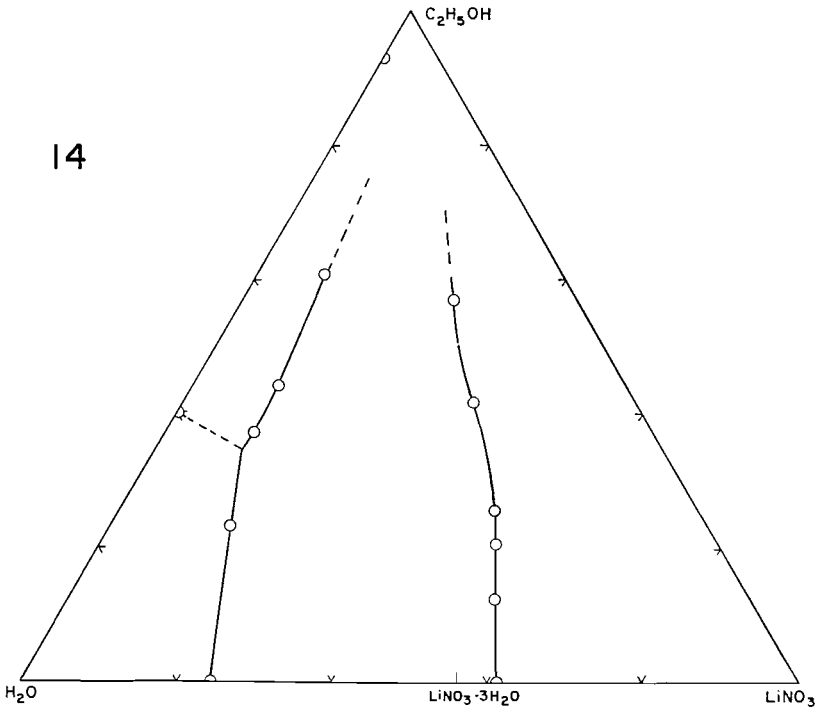

FIG. 13. Solubility isotherms in the system $LiNO_3$–C_2H_5OH–H_2O.
FIG. 14. Eutectic troughs in the system $LiNO_3$–C_2H_5OH–H_2O.

TABLE XIV

THERMAL ANALYSIS DATA OF THE SYSTEM $LiNO_3.3H_2O$–C_2H_5OH

Composition, wt. % C_2H_5OH	Freezing point, ° C.
0.0	29.6
14.2*	24.2
24.4*	22.4
30.0*	20.2
32.9	18.8
40.9	16.3
41.1	16.1
46.8*	14.5
52.6	9.7
54.4	7.7
59.0	1.7
61.8*	−1.0
67.3	−5.2
72.2	−25.0

**Values interpolated from pseudobinary cuts.*

ACKNOWLEDGMENTS

We are very greatly indebted to Dr. R. B. Ferguson, of the Department of Geology, University of Manitoba, for his assistance with the X-ray measurements, and to the National Research Council, who provided the funds for this research.

REFERENCES

1. CAMPBELL, A. N. and DEBUS, G. H. Can. J. Chem. **34**, 1232 (1956).
2. DONNAN, F. G. and BURT, B. C. J. Chem. Soc. **83**, 335 (1903).
3. CAMPBELL, A. N. and KARTZMARK, E. M. Can. J. Chem. **34**, 1405 (1956).
4. MENDELEEF, D. J. Chem. Soc. **51**, 778 (1887).
5. PICKERING, S. U. Z. physik. Chem. **6**, 10 (1890).
6. SCHMATTOLA, O. Chem. Centr. **2**, ii, 459 (1902).
7. VARENNE, E. and GODEFROY, L. Compt. rend. **137**, 993 (1903).
8. PICTET, R. Compt. rend. **119**, 678 (1894).
9. PICKERING, S. U. J. Chem. Soc. **63**, 998 (1893).
10. PUSHIN, N. A. and GLAGOLEVA, A. A. J. Russ. Phys. Chem. Soc. **47**, 100 (1915).
11. TARASSENKOV, D. N. Z. anorg. Chem. **41**, 704 (1928).
12. SHALBEROV, N. A., OSTROUNOV, V. V., and OSTROUNOV, N. M. J. Phys. Chem. (U.S.S.R.), **6**, 1398 (1935).
13. ROSS, H. K. Ind. Eng. Chem. **46**, 601 (1954).
14. PRIETZSCHK, A. Z. Physik, **117**, 1482 (1941).
15. HARVEY, G. G. J. Chem. Phys. **7**, 878 (1939).
16. BERNAL, J. D. and FOWLER, R. H. J. Chem. Phys. **1**, 518 (1933).
17. TAMMANN, G. and HESSE, W. Z. anorg. Chem. **156**, 245 (1926).
18. WAHL, W. Proc. Roy. Soc. (London), A, **89**, 327 (1914).
19. FIESER, L. F. Experiments in organic chemistry. 2nd ed. D. C. Hurst & Co. 1941. p. 359.
20. HENLE, F. Ber. **53**, 719 (1920).
21. BUERGER, M. J., BUERGER, N. W., and CHESLEY, F. G. Am. Mineralogist, **28**, 285 (1943). BUERGER, M. J. J. Appl. Phys. **16**, 501 (1945).
22. DENNISON, D. M. Phys. Rev. **17**, 20 (1921).
23. BARNES, W. H. Proc. Roy. Soc. (London), A, **125**, 670 (1929).

Can. J. Chem. Downloaded from www.nrcresearchpress.com by 200.7.193.243 on 09/04/12
For personal use only.

Can. J. Chem. Downloaded from www.nrcresearchpress.com by 200.7.193.243 on 09/04/12
For personal use only.

THE CONDENSATION OF FURAN WITH CARBONYL COMPOUNDS[1]

WILLIAM H. BROWN AND WARREN N. FRENCH[2]

ABSTRACT

A homologous series of substituted quaterenes has been synthesized by the condensation of 2,2-isopropylidene*bis*[5-(dimethylfurfuryl)furan] with keto acids and their esters. Substituted quaterenes containing chlorine have also been prepared. Only one out of the theoretically possible four geometrical isomeric quaterenes which could arise from the condensation of furan with butanone has been isolated. In all instances where more than one geometrical isomeric quaterene would be theoretically possible, only one has been isolated. Two new dinitro compounds have been prepared by the nitration of 2,2-difurylbutane and 3,3-difurylpentane.

Recently, Ackman, Brown, and Wright (1) reported the formation of difurylalkanes by the condensation of furan with the corresponding methyl ketone in the presence of hydrochloric acid. Brown and Sawatzky (2) and Beals and Brown (3) have extended the series to include the condensation of furan with aldehydes, chlorinated aldehydes and ketones, keto acids, and 3-pentanone.

The difurylalkane, 2,2-difurylpropane, has been isolated from the reaction mixture of furan with acetone. Subsequent reaction between two molecules of 2,2-difurylpropane and two molecules of acetone with the elimination of two molecules of water leads to the formation of a cyclic compound (II; R, R_1, R_2, R_3 = Me) composed of four residues each of furan and acetone. This cyclic compound has been assigned the trivial name "octamethyl-tetroxaquaterene". "Quaterene" denotes a closed system composed of four methylene-bridged 1,4-disubstituted cyclopentadienes (1). Another product of the condensation of furan with acetone is 2,2-isopropylidene*bis*[5-(dimethylfurfuryl)furan] (I; R, R_1, R_2 = Me), which condenses with one molecule of acetone to form the same octamethyl-tetroxaquaterene.

In the present investigation, two quaterenes containing chlorine were synthesized. Treatment of 2,2-isopropylidene*bis*[5-(dimethylfurfuryl)furan] [I; R, R_1, R_2 = Me) with chloroacetone in the presence of hydrochloric acid gives the expected 2-chloromethyl-2,7,7,12,12,17,17-heptamethyl-21,22,23,24-tetroxaquaterene (II; R, R_1, R_2 = Me; R_3 = CH_2Cl). The other quaterene containing chlorine, 2,12-*bis*(chloromethyl)-2,7,7,12,17,17-hexamethyl-21,22,23,24-tetroxaquaterene (II; R, R_1 = Me; R_2, R_3 = CH_2Cl), is formed by the condensation of 2,2-difurylpropane with chloroacetone. While two geometric isomers (*cis* and *trans*) of the latter quaterene are possible, only one was found. A compound having the same structure would also be expected as a result of the condensation of 2,2-difuryl-1-chloropropane with acetone. This possibility has been previously investigated (4). No reaction was observed.

The presence of halogen in the carbonyl compound appears to inhibit the above condensations since lower yields of the condensation product are obtained when chloroacetone is used in place of acetone. Chlorinated aldehydes and ketones containing two or more chlorine atoms, such as *sym*dichloroacetone, do not undergo complete condensation with I (R, R_1, R_2 = Me) to form quaterenes. The reaction probably proceeds to the carbinol stage but further condensation is prevented by the negative chlorine atoms. Carbinol formation has been demonstrated by Willard and Hamilton (5). They found that furan condenses with chloral to form 1-furyl-2,2,2-trichloroethanol.

[1]*Manuscript received October 25, 1957.*
Contribution from the Department of Chemistry, Ontario Agricultural College, Guelph, Ontario.
[2]*Holder of a National Research Council Bursary, 1956–57. Present address: Department of Chemistry, McMaster University, Hamilton, Ontario.*

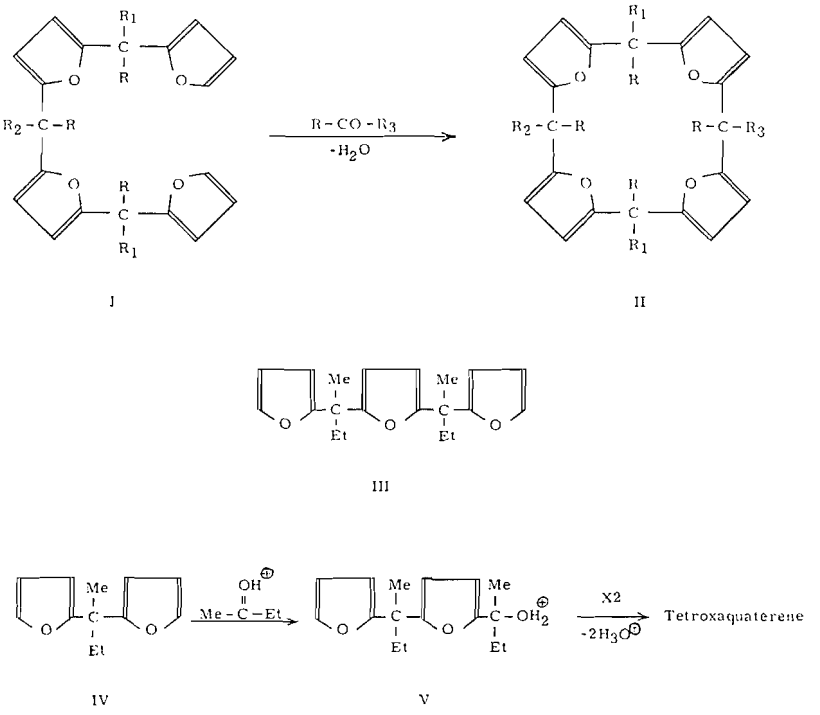

Other substituted quaterenes are formed by the condensation of keto acids or their esters with 2,2-isopropylidene*bis*[5-(dimethylfurfuryl)furan] (I; R, R_1, R_2 = Me). Thus pyruvic acid, methyl and ethyl acetoacetate, levulinic acid, and methyl levulinate react with I (R, R_1, R_2 = Me) to give the corresponding substituted tetroxaquaterenes. Since the condensations were all carried out using absolute alcohols as the reaction solvent and hydrogen chloride as the condensing agent, esterified products resulted: viz., methyl and ethyl esters. Transesterification can also occur during the reaction since the condensation of I (R, R_1, R_2 = Me) with methyl levulinate results in the formation of the corresponding ethyl ester with ethanol as the reaction solvent. The products are listed in Table I. Each

TABLE I

CONDENSATION PRODUCTS FROM 2,2-ISOPROPYLIDENE*bis*[5-(DIMETHYLFURFURYL)FURAN] AND KETO ACIDS

Substituent at the No. 2 position on the tetroxaquaterene	% yield	Melting point	Molecular formula	Analysis	
				Calc.	Found
				Methoxyl	
Carbomethoxy	15	172.5	$C_{29}H_{32}O_6$	6.51	6.42
Carbomethoxymethyl	17	179.0	$C_{30}H_{34}O_6$	6.32	6.15
Carbomethoxyethyl	34	157.5	$C_{31}H_{36}O_6$	6.15	6.13
				Ethoxyl	
Carbethoxy	39	169.5	$C_{30}H_{34}O_6$	9.19	9.22
Carbethoxymethyl*	49	165.0	$C_{31}H_{36}O_6$	8.93	8.81
Carbethoxyethyl	63	153.0	$C_{32}H_{38}O_6$	8.69	8.87
Carboxy		Decomp. 250	$C_{28}H_{30}O_6$		
Carboxymethyl		248.5–249.5	$C_{29}H_{32}O_5$		
Carboxyethyl		225.5–226.5	$C_{30}H_{34}O_6$		

**Anal. Calc. for* C, *73.8;* H, *7.19; mol. wt., 505. Found:* C, *73.8;* H, *7.18; mol. wt., 522.*

Can. J. Chem. Downloaded from www.nrcresearchpress.com by 200.7.193.243 on 09/04/12
For personal use only.

ethyl ester condensation product was hydrolyzed to the corresponding free acid and then treated with diazomethane to give the methyl ester. The same methyl ester is formed by the condensation of I (R, R_1, R_2 = Me) with a keto acid or methyl ester in methanol.

Inspection of Table I shows that the carboxyl group exerts a deactivating influence on the condensation when in proximity to the carbonyl group. Thus pyruvic acid gives a lower yield than levulinic acid under similar conditions. Yields are also lower when methanol rather than ethanol is the reaction solvent, probably owing to greater furan ring fission by methanolic hydrogen chloride than by ethanolic hydrogen chloride.

Ackman, Brown, and Wright (1) have also investigated the condensations of furan with butanone, methyl *n*-propyl ketone, methyl isobutyl ketone, and methyl *n*-amyl ketone. In each case, only one out of the possible four geometric isomers of the tetroxaquaterene has been isolated. One would expect to find more than one geometric isomer since the condensation of 2,2-difurylbutane with acetone yields the two expected geometric isomers (*cis* and *trans*) in the ratio of about 8 to 1 (1). A search for other isomers was considered to be important because of the alternative paths of formation of a tetroxaquaterene by the condensation of either I or a difurylalkane with the parent ketone.

In the present investigation, a search for additional isomeric tetroxaquaterenes was made in the reaction mixture resulting from the condensation of furan with butanone. The progenitor of the reaction, 2,2-difurylbutane, has previously been isolated (1). It condenses with butanone to form only one geometric isomer of 2,7,12,17-tetraethyl-2,7,12,17-tetramethyl-21,22,23,24-tetroxaquaterene (II; R = Me; R_1, R_2, R_3 = Et). A third product, thought to be 2,5-*bis*(ethylmethylfurfuryl)furan (III), has now been isolated from the condensation of furan with butanone. It is not a direct intermediate in the formation of the tetroxaquaterene. A fourth compound which was obtained by us is 2,2-butylidene-*bis*[5-(ethylmethylfurfuryl)furan] (I; R = Me; R_1, R_2 = Et) which condenses with butanone to yield a single tetroxaquaterene identical with the one formed from 2,2-difurylbutane and butanone. No additional isomeric tetroxaquaterenes were found in the original reaction mixture.

An inspection of the formula of I (R = Me; R_1, R_2 = Et) shows that it could exist as three diastereomers, one of which should be resolvable. Similarly, III could exist as two diastereomers, one of which should be resolvable. However, only one form of each was isolated by fractional distillation of the reaction products. Attempts to form derivatives of I (R = Me; R_1, R_2 = Et) and III having a functional group suitable for resolution purposes were unsuccessful. Nitration, aminomethylation, and acetylation reactions all gave resinous products while the condensation of I (R = Me; R_1, R_2 = Et) with keto acids gave products in insufficient yield for resolution.

The absence of possible geometric isomers of substituted quaterenes has also been noted in the pyrrole series. Chelintzev and Tronov (6) have reported that only two of the four theoretically possible isomers are obtained from the condensation of pyrrole with butanone. One geometric isomer was found to be in preponderance.

The existence of only one isomeric form of the quaterene from furan and butanone implies that the condensation is strongly influenced by steric factors which compel the reaction to proceed in such a manner as to form only one geometric isomer.

Two new dinitro compounds, 2,2-*bis*(5-nitrofuryl)butane and 3,3-*bis*(5-nitrofuryl)-pentane, have been prepared from the corresponding difurylalkanes using a nitration procedure typical for furans. The other member of the series, 2,2-*bis*(5-nitrofuryl)propane, has been previously reported (1). The data for these compounds are recorded in Table II.

Although the nitration of 1,1-difurylethane appears to proceed normally, the products are quite unstable.

Can. J. Chem. Downloaded from www.nrcresearchpress.com by 200.7.193.243 on 09/04/12
For personal use only.

TABLE II

NITRATION PRODUCTS OF DIFURYLALKANES

Compound nitrated	% yield	Melting point	Molecular formula	Analysis, % N	
				Calc.	Found
1,1-Difurylethane		No product isolated			
2,2-Difurylpropane (1)	57	135.0–135.5	$C_{11}H_{10}N_2O_6$	10.53	10.33
2,2-Difurylbutane	59	84.0–84.5	$C_{12}H_{12}N_2O_6$	10.00	9.40
3,3-Difurylpentane	67	120.0–120.5	$C_{13}H_{14}N_2O_6$	9.52	9.10

EXPERIMENTAL

All melting points have been corrected against reliable standards. Molecular weights were determined by the Rast method. A typical preparative method for the substituted quaterenes listed in Table I is given for the condensation of 2,2-isopropylidene*bis*[5-(dimethylfurfuryl)furan] (I; R, R_1, R_2 = Me) with levulinic acid and its methyl ester. The other substituted quaterenes in Table I may be obtained by a similar procedure using acetoacetic esters or pyruvic acid. The nitrated difurylalkanes were prepared by the method of Ackman, Brown, and Wright (1).

2-Chloromethyl-2,7,7,12,12,17,17-heptamethyl-21,22,23,24-tetroxaquaterene (II; R, R_1, R_2 = Me; R_3 = CH_2Cl)

A solution of 0.4 g. (0.001 mole) of 2,2-isopropylidene*bis*[5-(dimethylfurfuryl)furan] (I; R, R_1, R_2 = Me) and 0.93 g. (0.01 mole) of chloroacetone in 5 ml. of commercial absolute ethanol was saturated with anhydrous hydrogen chloride gas. The solution turned deep red and crystals began to form immediately. The solid was filtered off and washed with 5 ml. of ethanol to give 0.26 g. (56%) of crude product, m.p. 214°–216°. Crystallization from an ethanol–benzene mixture gave 0.20 g. (43%) of white needles, m.p. 219.5°–220.0°. Anal. Calc. for $C_{28}H_{31}ClO_4$: Cl, 7.60; mol. wt., 467. Found: Cl, 7.80; mol. wt., 475.

2,12-Bis(chloromethyl)-2,7,7,12,17,17-hexamethyl-21,22,23,24-tetroxaquaterene (II; R, R_1 = Me; R_2, R_3 = CH_2Cl)

A solution of 1.76 g. (0.01 mole) of 2,2-difurylpropane and 0.93 g. (0.01 mole) of chloroacetone in 10 ml. of absolute ethanol was saturated with anhydrous hydrogen chloride gas. The solution turned a deep red and solid material began forming in 2 hours. After 2 days, a sticky yellow material was filtered off and successively leached with 10-ml. portions of boiling ethanol. The first leaching contained 0.26 g. of sticky yellow material, and the following seven a total of 0.29 g. (11.5%) of white needles. Crystals from the second extract had a m.p. of 201.0°–203.5°, while those from the seventh had a m.p. of 211.0°–211.5°. The crystalline products were combined and crystallized from a 1:1 ethanol:benzene mixture (20 ml./g.) to give 0.15 g. (6.0%) of white needles, m.p. 211.0°–211.5°. Anal. Calc. for $C_{28}H_{30}Cl_2O_4$: Cl, 14.1; mol. wt., 501. Found: Cl, 14.0; mol. wt., 498.

2-Carbethoxyethyl-2,7,7,12,12,17,17-heptamethyl-21,22,23,24-tetroxaquaterene (II; R, R_1, R_2 = Me; R_3 = $CH_2CH_2COOC_2H_5$)

A solution of 1.0 g. (0.00025 mole) of 2,2-isopropylidene*bis*[5-(dimethylfurfuryl)furan] (I; R, R_1, R_2 = Me) and 0.58 g. (0.005 mole) of levulinic acid in 10 ml. of absolute ethanol was saturated with anhydrous hydrogen chloride gas. The solution became deep red and

Can. J. Chem. Downloaded from www.nrcresearchpress.com by 200.7.193.243 on 09/04/12
For personal use only.

cloudy within 3 minutes. After 20 hours, the mixture was filtered to give 0.93 g. of a yellow solid. Crystallization from ethanol gave 0.77 g. (63%) of light yellow crystals, m.p. 146.0°–147.5°. A second crystallization, including treatment with charcoal, resulted in 0.49 g. (40%) of white needles, m.p. 153°. Anal. Calc. for $C_{32}H_{38}O_6$: OC_2H_5, 8.69; mol. wt., 519. Found; OC_2H_5, 8.87; mol. wt., 517.

2-Carboxyethyl-2,7,7,12,12,17,17-heptamethyl-21,22,23,24-tetroxaquaterene (II; R, R_1, R_2 = Me; R_3 = CH_2CH_2COOH)

A solution of 0.25 g. (0.00048 mole) of the ethyl ester obtained as above in 20 ml. of *N*/1 solution of ethanolic potassium hydroxide was refluxed for 2 hours. After acidifying with glacial acetic acid, water was added until the saturation point was reached. On cooling, the resulting solid was removed by filtration and crystallized from benzene to give 0.11 g. (45%) of white needles, m.p. 225.5°–226.0°.

2-Carbomethoxyethyl-2,7,7,12,12,17,17-heptamethyl-21,22,23,24-tetroxaquaterene (II; R, R_1, R_2 = Me; R_3 = $CH_2CH_2COOCH_3$)

(*a*) *From 2,2-isopropylidenebis[5-(dimethylfurfuryl)furan] and levulinic acid in methanol.*—A solution of 0.4 g. (0.001 mole) of 2,2-isopropylidene*bis*[5-(dimethylfurfuryl)furan] and 0.58 g. (0.005 mole) of levulinic acid in 5 ml. of absolute methanol was saturated with hydrogen chloride gas. The solution slowly turned deep red with the formation of a yellow oil. Solid material began forming after 30 minutes. After 22 hours, a light yellow solid was removed by filtration. Crystallization from methanol, including treatment with charcoal, gave 0.17 g. (34%) of white needles, m.p. 157.5°. Anal. Calc. for $C_{31}H_{36}O_6$: OCH_3, 6.15. Found: OCH_3, 6.13.

(*b*) *From treatment of the acid* (II; R, R_1, R_2 = Me; R_3 = CH_2CH_2COOH) *with diazomethane.*—A solution of 0.10 g. of the acid obtained as above in ether was treated with an ethereal solution of diazomethane to give a product with a melting point of 157.5°. A mixture melting point with the methyl ester obtained in (*a*) showed no depression.

(*c*) *From 2,2-isopropylidenebis[5-(dimethylfurfuryl)furan] and methyl levulinate in methanol.*—Treatment of a solution of 0.4 g. (0.001 mole) of 2,2-isopropylidene*bis*[5-(dimethylfurfuryl)furan] and 0.65 g. (0.005 mole) of methyl levulinate in 5 ml. of absolute methanol with anhydrous hydrogen chloride gas resulted in 0.17 g. (34%) of crude product, m.p. 155.5°–156.5°. Crystallization from methanol (35 ml./g.) gave 0.09 g. (18%) of white needles, m.p. 157.7°. A mixture melting point with the compound obtained in (*a*) showed no depression. When the above reaction (*c*) was carried out using ethanol as a solvent, the ethyl ester condensation product was obtained in 47% yield.

2,2-Difurylbutane

In a three-necked 2-liter flask, fitted with reflux condenser, mechanical stirrer, and dropping funnel, were placed 340 g. (5.0 moles) of furan, 150 ml. of commercial absolute ethanol, and 100 ml. of 37% hydrochloric acid solution. To this mixture was added dropwise, while stirring, 180 g. (2.5 moles) of butanone. The addition of butanone was complete after 60 minutes, during which time no heat was evolved and the reaction mixture had taken on a reddish tinge. When stirring was discontinued after 190 hours, the mixture separated into two phases. The lower dark orange organic phase was separated from the upper pink aqueous phase and washed with 5% sodium bicarbonate solution until neutral. It was then dried over anhydrous magnesium sulphate. After the excess furan and butanone were flashed off, the residual oil was fractionally distilled under reduced pressure.

Can. J. Chem. Downloaded from www.nrcresearchpress.com by 200.7.193.243 on 09/04/12
For personal use only.

The first fraction, a colorless oil, boiled at 64°–66° (1 mm.), and weighed 71 g. (15%).

2,5-Bis(ethylmethylfurfuryl)furan (III)

A second fraction from the preceding distillation was a pale yellowish-green oil boiling at 143°–145° (1 mm.). It weighed 168 g. (43%), η_D^{20} 1.5094, d_4^{20} 1.045. Anal. Calc. for $C_{20}H_{24}O_3$: C, 76.9; H, 7.74; mol. wt., 312. Found: C, 76.6; H, 7.54; mol. wt., 327.

2,2-Butylidenebis[5-(ethylmethylfurfuryl)furan] (I; R = Me; R_1, R_2 = Et)

A third fraction from the preceding distillation, a viscous, fluorescent, yellow oil, boiled at 205°–210° (1 mm.). It weighed 82.8 g. (23%), η_D^{20} 1.5173, d_4^{20} 1.046. Anal. Calc. for $C_{28}H_{34}O_4$: C, 77.4; H, 7.89; mol. wt., 435. Found: C, 77.0; H, 7.79; mol. wt., 400.

2,7,12,17-Tetraethyl-2,7,12,17-tetramethyl-21,22,23,24-tetroxaquaterene (II; R = Me; R_1, R_2, R_3 = Et)

(*a*) *From 2,2-difurylbutane and butanone.*—The method of Ackman, Brown, and Wright (1) was used. A solution of 1.0 g. (0.0052 mole) of 2,2-difurylbutane and 3.0 g. (0.042 mole) of butanone in 10 ml. of absolute ethanol was saturated with anhydrous hydrogen chloride gas. Purification of the resulting solid resulted in 0.335 g. (27%) of white needles, m.p. 174°.

(*b*) *From 2,2-butylidenebis[5-(ethylmethylfurfuryl)furan] and butanone.*—A solution of 1.1 g. (0.025 mole) of I (R = Me; R_1, R_2 = Et) and 1.9 g. (0.025 mole) of butanone in 10 ml. of absolute ethanol was saturated with anhydrous chloride gas. The solution turned a deep cherry red and crystals began to form. On cooling, the mixture was filtered and the residue washed with 5 ml. of 95% ethanol to give 1.06 g. (87%) of light yellow needles, m.p. 169°–170°. Crystallization from absolute ethanol gave 0.78 g. (65%) of shiny white needles, m.p. 174°. A mixture melting point of this compound with the one obtained in (*a*) showed no depression.

ACKNOWLEDGMENTS

Grateful acknowledgment is made to the National Research Council for financial assistance to one of us (W.N.F.).

We are indebted to the du Pont Company of Canada for generous supplies of furan.

REFERENCES

1. Ackman, R. G., Brown, W. H., and Wright, G. F. J. Org. Chem. **20**, 1147 (1955).
2. Brown, W. H. and Sawatzky, H. Can. J. Chem. **34**, 1147 (1956).
3. Beals, R. E. and Brown, W. H. J. Org. Chem. **21**, 447 (1956).
4. Sawatzky, H. M.S.A. Thesis, University of Toronto, Toronto, Ontario. 1954.
5. Willard, J. R. and Hamilton, C. S. J. Am. Chem. Soc. **73**, 4804 (1951).
6. Chelintzev, V. V. and Tronov, B. V. J. Russ. Phys. Chem. Soc. **48**, 1197 (1916); Chem. Abstr. **11**, 1418 (1917).

Can. J. Chem. Downloaded from www.nrcresearchpress.com by 200.7.193.243 on 09/04/12
For personal use only.

THE MOLECULAR WEIGHT OF POLYVINYL ACETATE[1]

A. F. Sirianni, R. Tremblay,[2] and I. E. Puddington

ABSTRACT

The molecular weights of a series of unfractionated polyvinyl acetates of low degrees of polymerization have been measured by determining the lowering of the vapor pressure of their solutions. An approximate molecular-weight range of 5000–40,000 was examined. While most of the determinations were made in benzene solutions at 55° C., other solvents and temperatures were used. Anomalous results were obtained with one sample of fractionated material.

INTRODUCTION

A method for the determination of the molecular weights of chemical compounds based on measurements of the difference in vapor pressure between solutions of these compounds and the pure solvents has already been described (1). The previous publications dealt with the behavior of substances of known chemical constitution having molecular weights below about 1000 when examined in a variety of solvents and concentrations and over a range of temperatures.

The present communication describes results obtained with a series of commercial vinyl acetate polymers of comparatively low degree of polymerization. The individual samples, designated as Gelva 1.5, 2.5, 2.61, 7, 10, and 15, were obtained through the courtesy of Shawinigan Chemicals Ltd. The range of molecular weight covered by the series is approximately 5000 to 40,000. A single sample of fractionated polyvinyl acetate recovered from a solution was also examined.

APPARATUS AND EXPERIMENTAL

The apparatus and experimental technique have been described elsewhere (1). Molecular-weight determinations were usually carried out in benzene solution at 55° C. In some instances, however, other temperatures were used and a few determinations were made in acetone, methanol, and ethanol.

About 1 to 8 mg. of the dried polymer was weighed from the bulk sample into a 4 mm. i.d. pyrex tube and anchored to the bottom of the sample holder with a drop of distilled solvent. The occasional sample of polymer was prepared in powder form by freeze-drying its benzene solution. No difference in behavior during subsequent operations was found with samples prepared in this manner, however, and the simpler procedure was generally used. A metal stirrer about 1.5 cm. in length enclosed in a glass sheath was inserted into the tube containing the sample. The sample holder was sealed to the apparatus and the pressure reduced to about 10^{-5} mm. Hg. The apparatus was then flushed out with solvent vapor and re-evacuated. Solutions of various concentrations were prepared by condensing different amounts of solvent on the polymer sample. In this way a number of concentrations could be examined without opening the apparatus to the atmosphere. Differential vapor pressure measurements were normally begun after the solution had stood overnight with stirring. The reproducibility of these measurements was usually within 1%. The null point of the instrument was checked at the end of a series of measurements. Two or three different amounts of solute were used to obtain the entire concentration range studied.

[1]*Manuscript received October 5, 1957.*
Contribution from the Division of Applied Chemistry, National Research Council, Ottawa, Canada.
Issued as N.R.C. No. 4618.

[2]*National Research Council Postdoctorate Fellow, 1954–56. Present address: Canadian Industries Limited, Beloeil, Quebec. Paper presented in part at the sixth Canadian High Polymer Forum, St. Catharines, Ontario, April 14–15, 1955.*

Can. J. Chem. Downloaded from www.nrcresearchpress.com by 200.7.193.243 on 09/04/12
For personal use only.

Can. J. Chem. Downloaded from www.nrcresearchpress.com by 200.7.193.243 on 09/04/12
For personal use only.

RESULTS

The variation of apparent molecular weight as a function of solution concentration for a series of Gelvas in benzene at 55° C. is shown in Fig. 1. The values for the molecular weight recorded here were calculated from Raoult's law. In addition to the determinations made in benzene, results obtained with Gelva 10 in absolute ethanol at 55° C., with Gelva 1.5 in acetone and in methanol at 20° C., and with Gelva 10 and Gelva 2.5 in benzene at 42.5° C. are shown in Fig. 2. In each case good agreement was obtained when the molecular-weight values were extrapolated to zero solute concentration.

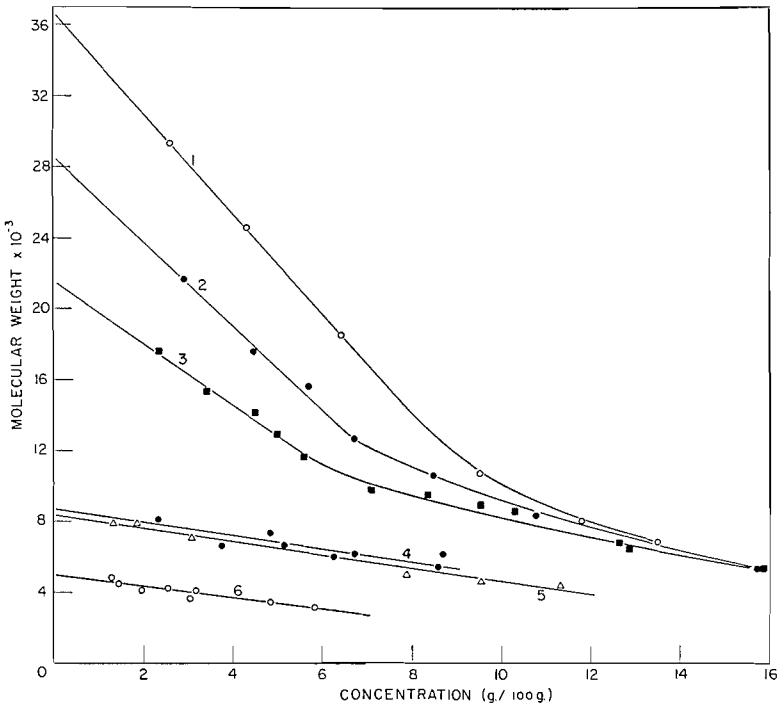

FIG. 1. Apparent molecular weight versus concentration of a series of Gelvas in benzene at 55° C. Curve 1, Gelva 15; Curve 2, Gelva 10; Curve 3, Gelva 7; Curve 4, Gelva 2.61; Curve 5, Gelva 2.5; Curve 6, Gelva 1.5.

It is evident that in most cases the apparent molecular weight is not a linear function of concentration. This is particularly obvious where the extrapolated molecular weight is in excess of 10,000. However, a straight line can be fitted reasonably well at lower concentrations, and where the molecular weight is below 10,000 the relation is quite linear up to 12% concentration.

In contrast to its behavior in benzene and in acetone, the measured molecular weight of Gelva 1.5 in absolute methanol appears to be independent of concentration over the range examined.

The behavior of the system Gelva 10 – ethanol is of considerable interest. The first determinations after fresh samples of solute were used produced a graph that was similar to that obtained with Gelva 1.5 in methanol. Subsequent determinations where the solvent was replaced by fresh ethanol gave a series of points where the molecular weight varies considerably with concentration. The extrapolated values in each case were virtually identical, however.

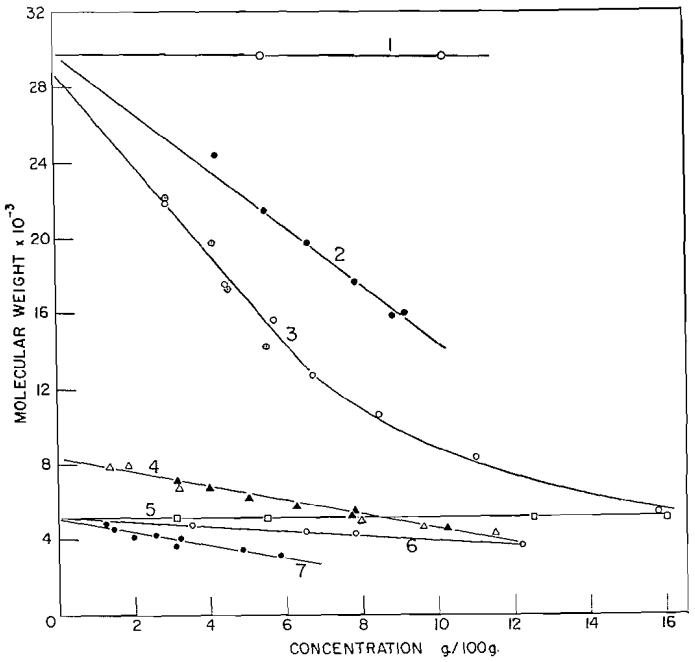

FIG. 2. Apparent molecular weight versus concentration of some Gelvas in different solvents and at various temperatures. Curve 1, Gelva 10, first determination in ethanol at 55° C.; Curve 2, Gelva 10, normal determination in ethanol at 55° C.; Curve 3, open circles, Gelva 10 in benzene at 55° C., and starred circles, at 42.5° C.; Curve 4, open triangles, Gelva 2.5 in benzene at 55° C., filled triangles, in benzene at 42.5° C., Curve 5, Gelva 1.5 in methanol at 20° C.; Curve 6, Gelva 1.5 in acetone at 20° C.; Curve 7, Gelva 1.5 in benzene at 20° C.

Since methanol is not a good solvent for polyvinyl acetate, the low degree of solute–solvent interaction may cause the solution of Gelva 1.5 to behave in the "ideal" fashion indicated. The similar behavior of fresh samples of Gelva 10 in ethanol might be ascribed to a trace of residual water in the resin which reduces solute–solvent interaction in the original solutions. If this were indeed the case, the water should be removed in subsequent operations and a higher solute–solvent interaction would be expected in succeeding solutions where the same sample of solute is used with fresh solvent.

In view of the departures of the apparent molecular weight vs. concentration curve from linearity in Fig. 1, it seemed of interest to apply an alternative method of presenting the vapor pressure data. The equation used, applicable over a wider range of concentrations provided μ_1 remains constant, is based on the theoretical equation developed by Huggins (2, 3) and by Flory (4, 5)

$$\phi \equiv (\ln a_1 - \ln V_1)/V_2 - 1 = -\bar{V}_1/\bar{V}_2 + \mu_1 V_2,$$

where

V_1, V_2 = volume fractions of components,
$\bar{V}_1$, $\bar{V}_2$ = partial molar volumes of components,
$\bar{V}_1 \simeq M_1/d_1$,
$\bar{V}_2 \simeq M_2/d_2$,
and a_1 = activity of the solvent;

M_1 and d_1, M_2 and d_2 are the molecular weight and density of the solvent and solute respectively.

Can. J. Chem. Downloaded from www.nrcresearchpress.com by 200.7.193.243 on 09/04/12
For personal use only.

A plot of ϕ vs. V_2 for the various polymers is shown in Fig. 3. In this case reasonably linear relations were found over the concentration range examined. The slopes of these graphs give the constant μ_1 directly and the molecular weight can be calculated from the intercept.

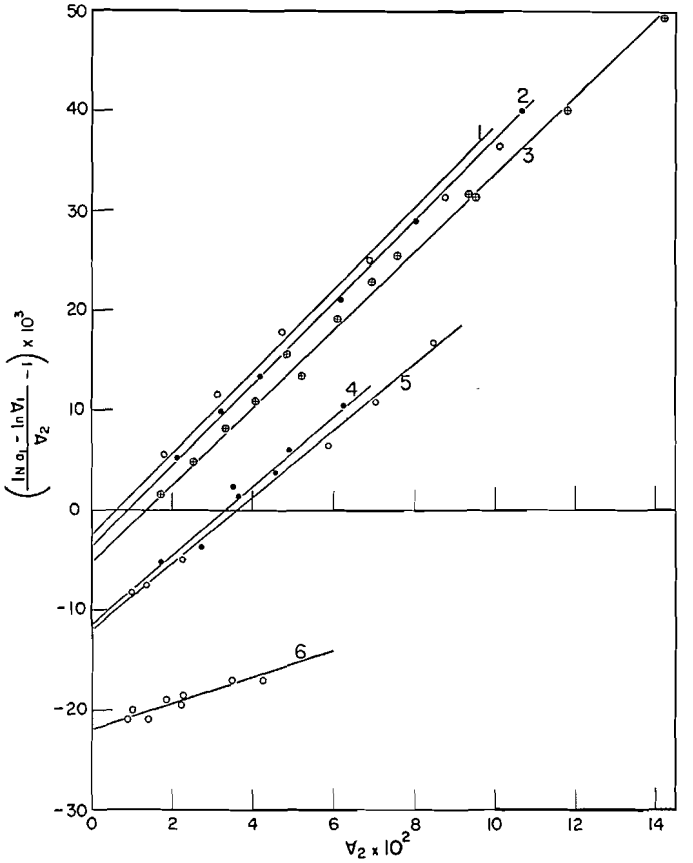

FIG. 3. Variation of $(\ln a_1 - \ln V_1)/V_2 - 1$ vs. V_2 for a series of Gelvas in benzene at 55° C. Curve 1, Gelva 15; Curve 2, Gelva 10; Curve 3, Gelva 7; Curve 4, Gelva 2.61; Curve 5, Gelva 2.5; Curve 6, Gelva 1.5.

The number-average molecular weight and the values of μ_1 for the series of Gelvas in benzene at 55° C. are given in Table I. Allowance for the non-ideal behavior of the solvent vapor has been made in calculating the concentration of the solutions. This correction amounted to about 2% on the molecular weight at infinite dilution.

TABLE I

MOLECULAR WEIGHTS OF POLYVINYL ACETATE IN BENZENE AT 55° C.

		Huggins' equation	
Gelva No.	M, Raoult's law	M	μ_1
1.5	5,100	4,960	0.134
2.5	8,500	9,010	0.333
2.61	9,000	9,560	0.347
7	22,000	21,800	0.387
10	28,600	30,300	0.401
15	36,700	45,400	0.402

Can. J. Chem. Downloaded from www.nrcresearchpress.com by 200.7.193.243 on 09/04/12
For personal use only.

In calculating the solution concentration, it was assumed that the volumes of solute and solvent are additive (6). The density of polyvinyl acetate was taken as 1.17 g./ml. for all of the fractions (7). The error involved by the change of density with molecular weight should not exceed 1%. The density of Gelva 0.9 at 20° C. has been reported as 1.159 g./ml. (8).

In addition to the work on the unfractionated polymers, several molecular-weight determinations were carried out on a sample of fractionated polyvinyl acetate made available to us through the kindness of Prof. M. Rinfret of the University of Montreal. When determined by a viscometric technique this sample had a weight-average molecular weight of 29,000. The polymer was recovered, after it had been stored for 6 months as an ethylene dichloride solution, by evaporation of the solvent under reduced pressure. It was then dissolved in benzene, filtered, and evaporated to a small volume. This concentrated solution was frozen and the solute was finally isolated as a fluffy brownish solid by subliming off the benzene.

Molecular weights were determined in ethanol and in benzene at 55° C. Two extra points were obtained in benzene solution at 65° C. The results, shown in Fig. 4, were calculated from Raoult's law.

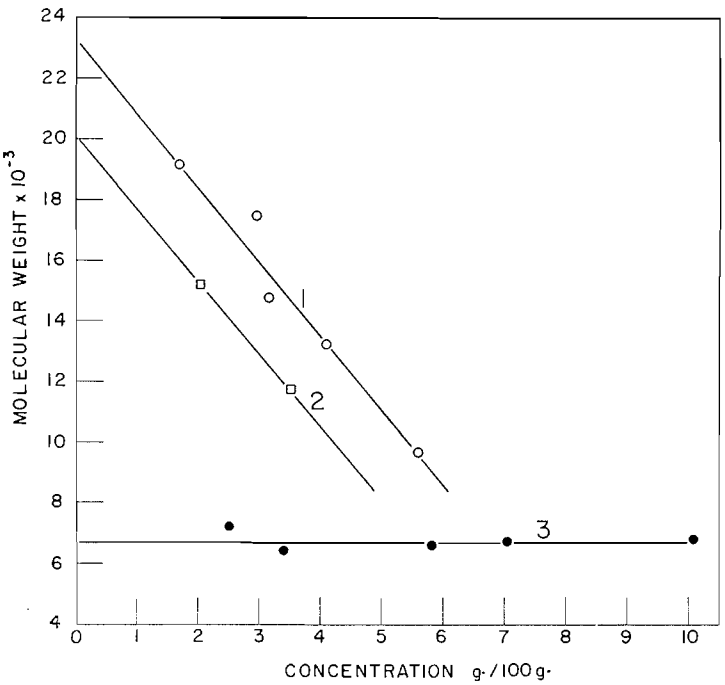

FIG. 4. Variation of apparent molecular weight versus concentration of a recovered fraction of polyvinyl acetate in benzene and in ethanol. Curve 1, in benzene at 55° C.; Curve 2, in benzene at 65° C.; Curve 3, in ethanol at 55° C.

The values obtained in ethanol solution were independent of concentration over the range used and were lower than expected. In benzene, although the molecular weight decreased as the temperature was raised from 55° C. to 65° C., the extrapolated value at both temperatures was much higher than in alcohol. While the reason for this difference is not obvious, it appears that the polymer may have become degraded during the long period of solution in the ethylene dichloride. The apparent difference in molecular weight in the polar and non-polar solvents might be ascribed to association of the solute

Can. J. Chem. Downloaded from www.nrcresearchpress.com by 200.7.193.243 on 09/04/12
For personal use only.

in the latter if any hydrolysis had occurred in the degraded polymer. Association phenomena have been observed (9, 10) with solutions of polymers containing a few hydroxyl groups in non-polar solvents and our results suggest the possibility of similar behavior. It may be added, however, that with unfractionated Gelva 10 and Gelva 2.5 there was virtually no difference in molecular weight when determinations were made in benzene at 42.5° C. and at 55° C.

DISCUSSION

The values of μ_1 are seen to decrease with decreasing molecular weight of the polymers in the series used. While this is sometimes attributed to solute impurities (3), the phenomenon has been observed for a series of polystyrene fractions in different solvents (11). Flory (12) suggested that μ_1 should be slightly dependent on molecular weight. The possibility that the variation of μ_1 with molecular weight is caused by chain branching (13) in the commercial samples (14) should not be excluded.

The values of the number-average molecular weights obtained using Raoult's law agree reasonably well with those found with Huggins' equation (2, 3) in spite of the fact that the values estimated by the latter method are very sensitive to slight changes in the slope of the curve and that rather long and possibly uncertain extrapolations were required using Raoult's law. This probably accounts for the difference found in Table I when the values obtained by the two procedures are compared.

The vapor-pressure data may also be presented as corrected π/c vs. C plots. These have not been included however, since this relationship is linear over the concentration range examined for the three polymers of the group with the lowest molecular weights only.

It is difficult to check the vapor-pressure method by calibration with known compounds of similar molecular weight since for the samples used reliable values for the degrees of polymerization are not readily available. A molecular weight of 61,000 was reported for Gelva 15 by Robertson, McIntosh, and Grummitt (15). This value was obtained by osmotic-pressure measurements on a commercial sample that had been dissolved in acetone, filtered, and precipitated in water. Since only that portion of the polymer that gathered around the glass stirrer was recovered, this treatment may have resulted in the loss of some low-molecular-weight material, and the value of 37,000 for Gelva 15 obtained in this work is perhaps not unreasonable. The distribution curves for Gelva 15 and Gelva 2.5 obtained by Blease and Tuckett (16) lend support to the molecular-weight values found here.

In favor of the vapor-pressure method, it may be pointed out that good agreement was generally obtained for the same material with different solvents and very satisfactory results were produced with pure compounds having molecular weights below 1000. Its most obvious advantage over osmotic-pressure methods, particularly where the molecular weights of the solute involved are low, is in avoiding semipermeable membranes. Its applicability over a wide temperature range is also an attractive feature.

REFERENCES

1. SIRIANNI, A. F. and PUDDINGTON, I. E. Can. J. Chem. **33**, 755 (1955).
2. HUGGINS, M. L. Ann. N.Y. Acad. Sci. **43**, 1 (1942).
3. HUGGINS, M. L. Ind. Eng. Chem. **35**, 980 (1943).
4. FLORY, P. J. J. Chem. Phys. **9**, 660 (1941).
5. FLORY, P. J. J. Chem. Phys. **10**, 52 (1942).
6. BAWN, C. E. H., FREEMAN, R. F. J., and KAMALIDDIN, A. R. Trans. Faraday Soc. **46**, 677 (1950).
7. D'AOUST, H. University of Montreal, Montreal, Que. Private communication.

Can. J. Chem. Downloaded from www.nrcresearchpress.com by 200.7.193.243 on 09/04/12
For personal use only.

8. MEARES, P. Trans. Faraday Soc. **47**, 703 (1951).
9. COTMAN, J. D., Jr. J. Am. Chem. Soc. **77**, 2290 (1955).
10. TREMENTOZZI, Q. A., STEINER, R. F., and DOTY, P. J. Am. Chem. Soc. **74**, 2070 (1952).
11. OUTER, P., CARR, C. I., and ZIMM, B. J. Chem. Phys. **17**, 830 (1950).
12. FLORY, P. J. J. Chem. Phys. **12**, 425 (1944).
13. DOTY, P., BROWNSTEIN, M., and SCHLENER, W. J. Phys. Chem. **53**, 213 (1949).
14. SAINI, G., MALDIFASSI, G., and TROSSARELLI, L. Ann. chim. **44**, 533 (1954).
15. ROBERTSON, R. E., MCINTOSH, R. L., and GRUMMITT, W. E. Can. J. Research, B, **24**, 150 (1946).
16. BLEASE, R. A. and TUCKETT, R. F. Trans. Faraday Soc. **37**, 571 (1941).

Can. J. Chem. Downloaded from www.nrcresearchpress.com by 200.7.193.243 on 09/04/12
For personal use only.

Can. J. Chem. Downloaded from www.nrcresearchpress.com by 200.7.193.243 on 09/04/12
For personal use only.

METHYLATION OF SUGAR MERCAPTALS

I. INTRODUCTION AND D-GLUCOSE DIETHYL MERCAPTAL[1]

G. G. S. DUTTON AND K. YATES

ABSTRACT

The methylation of the diethyl mercaptals of D-glucose, D-mannose, D-galactose, and L-arabinose in methyl iodide has been re-examined. The apparent lack of reactivity of the last three has been shown to be due to their insolubility in methyl iodide since appreciable methylation occurs in tetrahydrofuran. The case of D-glucose diethyl mercaptal has been examined in some detail and although polysubstitution occurs on reaction with methyl iodide in tetrahydrofuran the only monomethyl derivative formed is the 2-*O*-methyl ether. Preliminary work suggests that this is not the case with D-mannose mercaptal.

The reactions of sugar mercaptals are of particular interest in that the sugar molecule is acyclic, thus exposing an extra hydroxyl group which in the more common glycoside structure is involved in ring formation. It was reported in 1934 by Lieser and Leckzyck (1) that D-glucose diethyl mercaptal could be selectively methylated by the use of methyl iodide and silver oxide at 0° C. to give exclusively 2-*O*-methyl-D-glucose diethyl mercaptal in 52% yield. This reaction affords an easy route to 2-*O*-methyl-D-glucose and has been used by other workers (2). It was also reported by Lieser and Leckzyck that the mercaptals of D-galactose, L-arabinose, D-xylose, and L-rhamnose failed to yield methylated products when treated similarly.

It seemed to us that there was no a priori reason why other mercaptals should not react like the glucose compound. We have, therefore, re-examined this reaction to determine its generality and with the hope that it might furnish a convenient route to other partly methylated sugars such as are needed when carrying out structural studies by the methylation technique. Apart from the practical significance of such a reaction the nature of the monomethyl sugars obtained has considerable theoretical interest with respect to a study of the relative reactivity of the hydroxyl groups in an acyclic sugar derivative.

The early literature on relative reactivities of hydroxyl groups in carbohydrates has been reviewed (3) but the great majority of the examples refer to cyclic sugar structures. In 1952 there appeared a paper (4) showing that hexitols adopt a planar zigzag form resulting in selectivity in certain reactions, and it is reasonable to suppose that in some respects the acyclic mercaptals may be compared to the polyols. More recently Zinner (5, 6) has shown that in partial esterification of sugar mercaptals the terminal or primary hydroxyl group is the most reactive.

The present paper describes the qualitative paper-chromatographic examination of the products obtained on methylating the diethyl mercaptals of D-galactose, D-mannose, D-glucose, and L-arabinose. The results of a larger-scale methylation of D-glucose diethyl mercaptal and the quantitative separation of the products by column chromatography are also given.

In the initial experiments small amounts of the above mercaptals were methylated by the method of Lieser and Leckzyck (1). Upon separation of the products from excess methyl iodide and silver oxide, sirups were obtained. The sirup from the reaction of

[1]*Manuscript received November 4, 1957.*
Contribution from the Department of Chemistry, University of British Columbia, Vancouver 8, B.C., Canada. Presented in part at the 40th Annual C.I.C. Conference at Vancouver, B.C., June 3–5, 1957, and at the Northwest A.C.S. Regional Meeting at Spokane, Wash., June 13–14, 1957.

D-glucose diethyl mercaptal crystallized spontaneously to give a 46% yield of 2-*O*-methyl-D-glucose diethyl mercaptal, the others failing to yield any crystalline material except unchanged mercaptal. The mother liquor from the 2-*O*-methyl-D-glucose mercaptal and the remaining three sirups were investigated by paper partition chromatography. On development of the chromatogram with iodine vapor (7), the presence of several components was indicated as shown in Table I, indicating qualitatively that the

TABLE I

R_x VALUES OF PRODUCTS OF METHYLATION OF MERCAPTALS IN METHYL IODIDE

D-Glucose		D-Mannose		D-Galactose		L-Arabinose	
R_x*	Description	R_x	Description	R_x	Description	R_x	Description
0.13	OF	0.10	OF	0.13	OF	0.13	OF
0.21	OF	0.18	OF	0.21	OF	0.21	OF
0.36	OI	0.36	OI	0.40	OI	0.40	OI
—		—		0.47	OF	0.46	OF
—		0.94†	YI	0.95†	YF	0.95†	YI
1.00	YI	1.07	YF	1.03	YI	1.05	YF

*R_x *is based on the arbitrary standard 2-O-methyl-*D*-glucose diethyl mercaptal = 1.00* (*n*-BuOH–EtOH–H_2O = *40–10–50*).

†*These values correspond to standards of the unsubstituted mercaptals.*

KEY.—O = *orange*, Y = *yellow*, I = *intense*, F = *faint*.

reaction is more general than had been supposed. The presence of a further amount of 2-*O*-methyl-D-glucose diethyl mercaptal in the mother liquor suggested that, if desired, the yield of this product could be increased to 52% as given by the earlier workers (1). It can be seen from Table I that the reaction in each case gave products of two types; those having a high R_f value corresponded to methylated and unchanged mercaptals, while those having slower R_f's are presumably more polar compounds whose constitution is at present unknown. The latter compounds are referred to subsequently as the "slow fraction". It can, however, be stated that in these slow-moving compounds the mercaptal group has not been removed completely since they gave no spot for reducing sugar with *p*-anisidine hydrochloride (8). It is also apparent that these compounds are probably carbohydrate in nature since their R_f values varied from sugar to sugar, but on hydrolysis with acid, however, they did not regenerate the parent sugars. It was observed that the most intense of these slow spots can be produced by reacting the mercaptal with methyl iodide in the absence of silver oxide.

From the distribution and concentration of the products in Table I it appears that the reaction has been most extensive in the case of D-glucose since no unchanged mercaptal was detected. Somewhat less reaction occurs in the case of D-galactose and only a small amount in the cases of the other two mercaptals. Owing to the high R_f values of the mercaptals and consequent low degree of chromatographic separation, the products were hydrolyzed and reinvestigated by paper chromatography as the free sugars thus produced. These results are shown in Table II. From a comparison with the characteristic R_f values of known compounds it appears that the first components (from the origin) correspond to unsubstituted sugars, the second to their monomethyl derivatives, and the remainder to more highly substituted sugars. From this it can be seen that some monomethylation has occurred in each case, which is in apparent disagreement with the earlier statement that the reaction failed for sugar mercaptals other than those of D-glucose (1). Since the amount of methylation which has apparently taken place in

Can. J. Chem. Downloaded from www.nrcresearchpress.com by 200.7.193.243 on 09/04/12
For personal use only.

the case of the D-mannose and L-arabinose mercaptals is very slight and considerable polymethylation has occurred with D-galactose mercaptal, it is not surprising that no crystalline methyl derivative was isolated (1).

TABLE II

R_G* VALUES OF HYDROLYZED PRODUCTS OF METHYLATIONS IN METHYL IODIDE

D-Glucose	D-Mannose	D-Galactose	L-Arabinose
—	0.11 I	0.08 F	0.12 I
0.23 I	0.28 F	0.22 F	0.34 F
—	—	0.39 F	—
—	—	0.72 F	—
—	—	0.86 F	—

*R_G values based on 2,3,4,6-tetra-O-methyl-D-glucose = 1.00 (n–BuOH–EtOH–H_2O = 40–10–50).

During this preliminary work it was observed that there were considerable differences in the solubilities of the various mercaptals in methyl iodide. Under the conditions used it was found that the extent of methylation corresponded approximately to the degree of solubility of the particular mercaptal being reacted. D-Glucose diethyl mercaptal was found to be the most soluble of the four and its unusual reactivity appears in part to be due to the fortuitous choice of methyl iodide as a reaction solvent. Large amounts of D-mannose and L-arabinose mercaptals were found undissolved at the end of the reaction.

In order to eliminate this solubility effect it was decided to use an inert reaction solvent in which all four mercaptals had comparable solubilities and to compare the reaction of each again on a more equal basis. The most suitable of the common organic solvents which are inert to methylation was found to be tetrahydrofuran. The presence of a large amount of inert solvent necessitated the use of increased amounts of methyl iodide and silver oxide. In order to determine whether changing the original reaction temperature of 0° C. had any critical effect on the nature of the products three parallel reactions were carried out on each mercaptal at 3°, 22°, and 50° C. In the case of all four mercaptals no significant difference could be detected either in the distribution or in the intensity of the components when the reaction mixtures were examined by paper chromatography. The results of a typical methylation in tetrahydrofuran are shown in Table III. It was noted that the same "slow" products were present and the extent

TABLE III

R_x* VALUES OF PRODUCTS OF METHYLATION OF MERCAPTALS IN TETRAHYDROFURAN

D-Glucose	D-Mannose	D-Galactose	L-Arabinose
0.10	0.10	0.13	0.13
0.20	0.18	0.21	0.21
0.36	0.36	0.39	0.40
0.95	0.96	0.96	— †
1.00	1.00	1.02	1.03

*2-O-Methyl-D-glucose diethyl mercaptal = 1.00 (n–BuOH–EtOH–H_2O = 40–10–50).

†*The absence of a spot for unreacted mercaptal corresponding to the spots for* L-*arabinose produced on hydrolysis may be due to the greater sensitivity of p-anisidine.*

Can. J. Chem. Downloaded from www.nrcresearchpress.com by 200.7.193.243 on 09/04/12
For personal use only.

of methylation appeared more comparable in each case. The unusual reactivity of D-glucose diethyl mercaptal was not now so marked since unreacted mercaptal was shown to be present. In order to investigate the nature of the methylated mercaptals these were hydrolyzed and examined as the free sugars. These results are shown in Table IV, from which it is apparent that some monomethylation has taken place in all cases and that D-glucose mercaptal no longer yields exclusively monomethyl products. From these preliminary experiments it was concluded that if the methylation was carried out in a solvent it was generally applicable to the four mercaptals used and that the peculiar selectivity of the D-glucose mercaptal was no longer apparent.

TABLE IV

R_G* VALUES OF HYDROLYZED PRODUCTS OF METHYLATIONS IN TETRAHYDROFURAN

D-Glucose	D-Mannose	D-Galactose	L-Arabinose
0.09	0.13	0.08	0.12
0.23	0.26	0.20	0.32
0.42	0.45	0.38	0.44
0.47			0.50
			0.64

*R_G values based on 2,3,4,6-tetra-O-methyl-D-glucose = 1.00 (n-BuOH–EtOH–H_2O = 40–10–50).

In the light of the above results it was decided to repeat the methylation of D-glucose diethyl mercaptal on a larger scale to permit separation and identification of the reaction products. We were particularly concerned with the identification of the monomethyl fraction in order to determine if monomethylation still occurred preferentially at the 2-position. For this reason no attempt has been made at the present time to identify more highly methylated derivatives.

A large-scale methylation of D-glucose diethyl mercaptal was carried out in tetrahydrofuran at 22° C. After removal of the solvent and excess reagents the sirupy reaction product was separated on a cellulose column into two fractions: the "fast" fraction containing methylated and unreacted mercaptals and the "slow" fraction containing the unidentified products. The "fast" fraction was then hydrolyzed and the mixture of free sugars separated by chromatography on a cellulose–hydrocellulose column (9). The results of this separation are shown in Table V and the monomethyl fraction was

TABLE V

SEPARATION OF D-GLUCOSE *O*-METHYL ETHERS ON CELLULOSE–HYDROCELLULOSE (1:1) COLUMN

Classification	Tube No.	Wt. (mg.)	$[\alpha]_D^{20}$	R_f*	% OCH_3†
Hexose	238–270	23	+48° (H_2O)	0.017	—
Monomethyl	169–235	104	+59° (H_2O)	0.05	15.7
Dimethyl A	57–74	50	+82° (acetone)	0.28	26.5
Dimethyl B	86–108	47	+32° (acetone)	0.18	24.8
Dimethyl C	30–40	42	+61° (MeOH)	0.47	27.3
Trimethyl A	28–29	11	+91° (MeOH)	0.50	36.6
Trimethyl B	12–19	63	+20° (H_2O)	0.80	36.6
	Total	340			
	Recovery	84%			

*R_f values determined in methyl ethyl ketone – water azeotrope.
†Calculated methoxyl values for mono-, di-, and tri-methyl hexoses respectively are 16.0, 29.7, and 41.9%.

Can. J. Chem. Downloaded from www.nrcresearchpress.com by 200.7.193.243 on 09/04/12
For personal use only.

shown to be one component by paper chromatography and the constancy of optical rotation throughout the fraction. This fraction crystallized spontaneously and failed to depress the melting point of an authentic sample of 2-*O*-methyl-D-glucose on admixture with it. It was further characterized by the preparation of the characteristic *p*-toluidide derivative. It was thus shown that although polymethylation occurs when D-glucose diethyl mercaptal is reacted with methyl iodide in a solvent it is only the 2-monomethyl ether that is formed, thus demonstrating the superior reactivity of the 2-position.

When a large-scale methylation of D-mannose diethyl mercaptal was carried out under identical conditions two principal monomethyl derivatives were produced and these appeared to be the 5-*O*- and 6-*O*-methyl-D-mannoses. In the case of L-arabinose mercaptal, under these conditions mainly di- and tri-methylation occurred. These results and those on D-galactose mercaptal will be reported more fully at a later date.

EXPERIMENTAL

All melting points were taken by means of a Leitz electrically heated melting-point block and are corrected. All evaporations were done *in vacuo* at 40° C. Duolite A_4 anion-exchange resin is a product of Chemical Process Co., Redwood City, California.

Preparation of Diethyl Mercaptals

The four mercaptals were prepared by the method of Fischer (10) and had melting points and rotations in agreement with those given. The rotations of D-mannose diethyl mercaptal and of L-arabinose diethyl mercaptal do not appear to have been previously recorded and were found to be $[\alpha]_D^{20} = 0°$ (*c*, 0.77 in pyridine) and $-5°$ (*c*, 1.78 in pyridine).

Methylation of Mercaptals in Methyl Iodide (1)

D-Glucose diethyl mercaptal (0.94 g.) was shaken with freshly prepared silver oxide (1.5 g.) and methyl iodide (10 ml.) for 21 hours at 0° C. under anhydrous conditions. The mixture was allowed to attain room temperature (1 hour) and filtered. The residue was extracted successively with boiling chloroform, acetone, and methanol. The filtrate and extracts were combined and evaporated to a sirup, which was dissolved in a small amount of methanol. On standing, this solution deposited crystals (0.46 g.) of 2-*O*-methyl-D-glucose diethyl mercaptal, m.p. 154°–155° C. Lit. m.p. 155°–156° C. (1). Anal.: Calc. for $C_{11}H_{24}O_5S_2$: $-OCH_3 = 10.37\%$. Found: $-OCH_3 = 10.99\%$. Yield 46%.

The diethyl mercaptals of D-mannose, D-galactose, and L-arabinose were also methylated by the above procedure but the sirups obtained failed to yield any crystalline product.

Chromatographic Investigation of the Reaction Products

Chromatograms of the four reaction products above were run on Whatman No. 1 paper, using *n*-butanol–ethanol–water (40:10:50). Detection of the chromatograms with iodine vapor (5) showed the components whose R_x values are given in Table I. Duplicate chromatograms were sprayed with *p*-anisidine hydrochloride but failed to detect any reducing sugars (8).

Effect of Individual Reagents

Two samples of D-glucose diethyl mercaptal (10 mg.) were dissolved in carbon tetrachloride (5 ml.) and shaken for 21 hours at 0° C. with methyl iodide and silver oxide respectively. After they were filtered, the solutions were chromatographed with standards and detected as before. Mercaptal plus methyl iodide: three products of $R_x = 0.21, 0.35$

Can. J. Chem. Downloaded from www.nrcresearchpress.com by 200.7.193.243 on 09/04/12
For personal use only.

(intense), and 0.94 (unchanged mercaptal). Mercaptal plus silver oxide: one product of $R_x = 0.95$ (unchanged mercaptal).

Hydrolysis of Reaction Products

The sirups resulting from methylation of the four mercaptals were dissolved in 20% aqueous ethanol containing 5% hydrogen chloride. The solution was heated to reflux, a stream of nitrogen being bubbled through continuously. When chromatography of the solutions failed to detect any unchanged mercaptals (5 to 6 hours), they were passed through a column of Duolite A-4 anion-exchange resin and concentrated by evaporation. The four hydrolyzates were chromatographed on paper as before and detected with *p*-anisidine hydrochloride, the results being shown in Table II.

Methylation of Mercaptals in Tetrahydrofuran

The mercaptal (0.3 g.) was dissolved in dry peroxide-free tetrahydrofuran (20 ml.). After silver oxide (1 g.) and methyl iodide (10 ml.) were added, the whole was shaken vigorously for 22 hours. Three parallel experiments were carried out on each mercaptal at 3°, 22°, and 50° C. The products were then extracted as before, no crystalline materials being obtained. Paper chromatography of the sirups as before yielded results shown in Table III. After hydrolysis and chromatography of the free sugars the results shown in Table IV were obtained.

Large-Scale Methylation of D-*Glucose Diethyl Mercaptal*

Silver oxide (6.7 g.) and methyl iodide (67 ml.) were added to a solution of D-glucose diethyl mercaptal (2.0 g.) in purified tetrahydrofuran (100 ml.). The vessel was flushed with nitrogen, sealed, and shaken at room temperature for 22 hours. After extraction of the products there was obtained an amber sirup (2.07 g.). Paper chromatography of this sirup using methyl ethyl ketone – water azeotrope gave essentially the same results as shown in Table III. Part of the sirup (1.96 g.) was placed on a cellulose column (2.8 cm. diam. by 40 cm.) and developed with the same solvent. Fractions were collected at 1-hour intervals for 8 hours. (The time for the solvent front to pass down the column was 4 hours as judged by the addition of Sudan IV dye.) Two fractions were then collected at 2-hour intervals and the remaining material was removed by developing for a further 80 hours without any attempt at fractionation. Paper chromatographic examination of the first eight fractions in methyl ethyl ketone – water and detection with iodine vapor showed that fractions 2–5 contained all of the mercaptalated products with only slight traces of the "slow" fraction. When these fractions were combined and the solvent evaporated there was obtained a sirup (0.88 g.) designated as mercaptal fraction. The higher fractions were discarded.

The mercaptal fraction was hydrolyzed as before and yielded a sirup (0.425 g.). Duplicate chromatograms of the sirup were run in methyl ethyl ketone – water. One chromatogram was exposed to iodine vapor and the other sprayed with *p*-anisidine hydrochloride. The former showed no glucose mercaptal, indicating that hydrolysis was complete. The latter showed four components with R_f's 0.014, 0.06, 0.21, and 0.47, corresponding to the characteristic ranges of glucose and mono-, di-, and tri-methyl glucoses respectively.

A portion of the sirup (0.406 g.) in the minimum amount of methyl ethyl ketone was placed on a column (2.8×42 cm.) of cellulose–hydrocellulose (1:1) and developed with methyl ethyl ketone – water azeotrope. Fractions were collected at 30-minute intervals at a flow rate of 40 ml. per hour. After 300 fractions had been collected no

Can. J. Chem. Downloaded from www.nrcresearchpress.com by 200.7.193.243 on 09/04/12
For personal use only.

further carbohydrate material could be detected (Molisch). The results of this fractionation are shown in Table V.

All the fractions were found to be chromatographically pure except for some overlap between dimethyl glucose fractions A and B. By evaporation of the solvent from a few tubes from the beginning, middle, and end of the monomethyl fraction it was shown to have a constant rotation throughout. This monomethyl fraction yielded spontaneously, a crystalline product melting at 153°–157° C. After recrystallization, admixture with an authentic sample of 2-*O*-methyl-D-glucose gave a melting point of 154°–158° C. (2). The *p*-toluidide was prepared in poor yield by the method of Smith (11), m.p. 144°–146° C. Lit. m.p. 150°–151° C. (12).

It will be noted from Table V that the methoxyl analysis of the separate fractions is in some cases much lower than is demanded by theory. This is attributed to the difficulty of purifying small amounts of sirup from inert material from the column (cellulose?). The main significance of the methoxyl analyses was to indicate that the other components were not monomethyl glucoses.

ACKNOWLEDGMENTS

The authors wish to express their appreciation to the Research Corporation for financial support and to the National Research Council for the award of a bursary (K.Y.) and a summer research associateship (G.G.S.D.).

REFERENCES

1. LIESER, T. and LECKZYCK, E. Ann. **511**, 137 (1934).
2. WOLFROM, M. L., LEMIEUX, R. U., OLIN, S. M., and WEISBLAT, D. I. J. Am. Chem. Soc. **71**, 4057 (1949).
3. SUGIHARA, J. M. *In* Advances in carbohydrate chemistry. 8th ed. *Edited by* C. S. Hudson and M. L. Wolfrom. Academic Press Inc., New York. 1953.
4. BARKER, S. A., BOURNE, E. J., and WHIFFEN, D. H. J. Chem. Soc. 3865 (1952).
5. ZINNER, H. Angew. Chem. **69**, 238 (1957).
6. ZINNER, H. and WESSELY, K. Ber. **90**, 516 (1957).
7. GREENWAY, R. M., KENT, P. W., and WHITEHOUSE, M. W. Research (London), **6**, Suppl. No. 1, 65 (1953).
8. HOUGH, L., JONES, J. K. N., and WADMAN, W. H. J. Chem. Soc. 1702 (1950).
9. GEERDES, J. D., LEWIS, B. A., MONTGOMERY, R., and SMITH, F. Anal. Chem. **26**, 264 (1954).
10. FISCHER, E. Ber. **27**, 673 (1894).
11. SMITH, F. J. Chem. Soc. 753 (1939).
12. MITTS, E. and HIXON, R. M. J. Am. Chem. Soc. **66**, 483 (1944).

Can. J. Chem. Downloaded from www.nrcresearchpress.com by 200.7.193.243 on 09/04/12
For personal use only.

Can. J. Chem. Downloaded from www.nrcresearchpress.com by 200.7.193.243 on 09/04/12
For personal use only.

THE THERMODYNAMICS OF MUTAROTATION OF SOME SUGARS

I. MEASUREMENT OF THE HEAT OF MUTAROTATION BY MICROCALORIMETRY[1]

M. A. KABAYAMA, D. PATTERSON, AND L. PICHE

ABSTRACT

The heats of mutarotation of D-glucose, D-xylose, lactose, maltose, and cellobiose have been determined using a microcalorimeter of the Tian-Calvet type. Part I of this paper describes the experimental work and the results obtained. Discussion of these results is reserved for Part II.

INTRODUCTION

Since the discovery of the phenomenon of mutarotation, much work has been done to elucidate the kinetics and mechanism of the reaction as well as to study the stability of the various forms postulated. Some attempt has also been made to determine the heats of mutarotation of the sugars from the temperature dependence of the equilibrium constants for the mutarotations (1). The only direct measurement of a heat of mutarotation has been performed by Sturtevant (2, 3) for D-glucose using an adiabatic calorimeter. It seemed desirable, however, to have values for other sugars, particularly for those undergoing an opposing first-order mutarotation, in order to make a comparison of the appropriate thermodynamic quantities.

MATERIALS

The sugars studied were all of reagent grade purity, and were obtained as almost pure α or β anomers by slow recrystallization from slightly supersaturated aqueous or alcoholic solutions according to the method of Hudson and Dale (4).

The "purity", i.e. the percentage of α or β anomer in the "α" or "β" sugar, may be determined polarimetrically using known optical rotations. These experiments were performed at 0° C. Isbell and Pigman (5) have determined the optical rotations at 0° C. for both anomers of D-glucose and lactose and for α-D-xylose and β-maltose. They have also obtained a value at this temperature for β-cellobiose (6). The optical rotations at 20° C. for the other anomers required have been obtained by Hudson and Yanovsky (7) using an indirect method requiring the separation of only one of the anomers of the sugar. Their values have been used to find the "purity" of the sugars at 0° C. Since the "purities" of the sugars, save for cellobiose, were nearly 100%, this introduces a negligible uncertainty. In the case of cellobiose, the "purity" was sufficiently far from 100% to warrant a polarimetric run at a higher temperature.

The water used in all experiments was ordinary distilled water, saturated with CO_2, and of pH approximately 5.5. Since the rate of mutarotation of D-glucose is constant (8) between pH 2 and 7, buffering of the solution (8, 9) was deemed unnecessary for a determination of the heats of mutarotation.

EXPERIMENTAL

The Tian-Calvet microcalorimeter has been described in various publications (10, 11, 12), but an outline of its more relevant characteristics will be given here. Although arranged differentially, it consists essentially of a cell in which the reaction takes place

[1]*Manuscript received November 12, 1957.*
Contribution from the Department of Chemistry, University of Montreal, Montreal, Que.

and a block whose temperature remains constant. The temperature difference between the cell and the block is detected by a set of thermocouples and galvanometer and recorded by a photopen on a chart.

However, the heat evolved by the reaction only in part raises the temperature of the cell producing the deflection recorded on the chart. The rest of the heat is conducted down the thermocouples to the block. Nevertheless, the rate of evolution of heat is related to the deflection and the time rate of change of the deflection by the following equation:

$$W(t) = \frac{p}{g}\delta + \frac{\mu}{g}\frac{d\delta}{dt}. \qquad [1]$$

Here $W(t)$ is the rate of evolution of heat in joules/second, p is the rate of thermal conduction of heat down the thermocouples per degree temperature difference between the cell and the block, δ is the deflection on the chart in cm., g is the sensitivity of the thermocouples, galvanometer, and photopen in cm. deflection per deg. temperature difference between cell and block.

Equation [1] may be expressed as:

$$W(t) = \frac{p}{g}\Delta, \qquad [2]$$

where

$$\Delta = \delta + \frac{\mu}{p}\frac{d\delta}{dt} \qquad [3]$$

and is a "corrected" deflection related to $W(t)$ by a constant, p/g.

In the present case, the large heat of solution of the sugar had to be separated from the much smaller heat of mutarotation. This was effected by determining the evolution of heat some time after the dissolution of the sugar when the heat was due to the mutarotation alone; by extrapolation to zero time, the whole heat of mutarotation was determined. Thus, using [3], Δ was obtained graphically from the curve of the deflection δ against time commencing some 30 minutes after dissolution of the sugar. The mutarotations studied are all single first-order opposing reactions; a curve of log Δ against time was extrapolated back to zero time in an appropriate fashion, and the intercept of log Δ on the axis $t = 0$ gave the log of the total heat evolved by the mutarotation. Since the "purity" of the sample was slightly less than 100%, a correction to 100% purity was then made.

Prior to the experiment, the sugar was held in a special holder (Fig. 1) within the stainless steel reaction cell of the microcalorimeter. The holder was designed to give a low heat effect on opening. After the tension of the spring (not shown) was released, the bracket was lowered via the control wire. The hook in the center engaged the shaft to suspend the holder so that the water was allowed to circulate through the top and bottom of the cylinder to dissolve the sugar. The endothermic heat of solution was compensated by evolution of heat from a resistor within the cell in order to allow the microcalorimeter to be put as quickly as possible onto its maximum sensitivity. This was required for following the evolution of the small heat of mutarotation.

The heat of mutarotation of a sugar possessing a fast rate constant, D-lyxose, and a check on the value of D-xylose, was obtained by the so-called "ballistic" method. Dissolution of a sugar gives an immediate "ballistic" deflection on the chart which quickly

Can. J. Chem. Downloaded from www.nrcresearchpress.com by 200.7.193.243 on 09/04/12
For personal use only.

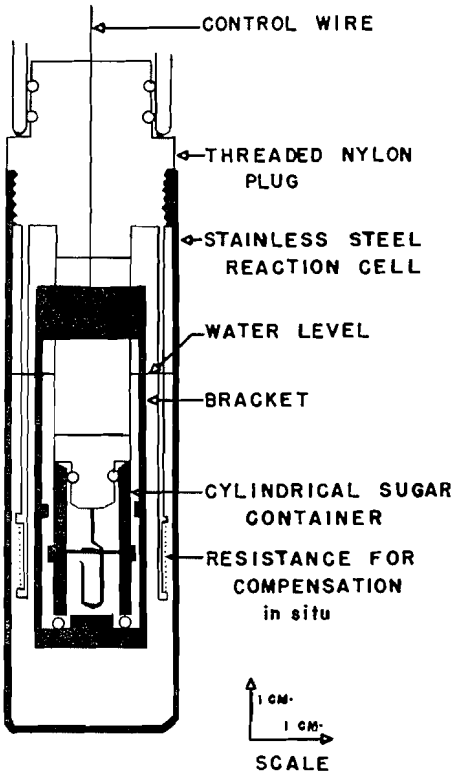

FIG. 1. Reaction cell and sugar container.

reaches a maximum and then slowly falls off. This peak deflection is almost entirely due to the heat of solution and is proportional to it. By measuring the height of the peak for the dissolution of KNO_3, whose heat of solution is well known, the instrument may be calibrated. Thus the heat of solution of the sugar may be determined. Measurement of the total area under the curve of deflection vs. time gives the heat of solution plus the heat of mutarotation. By subtracting the heat of solution, the heat of mutarotation may be obtained separately. Owing to the small size of the difference, the precision of this method is not high.

RESULTS

A typical curve of deflection vs. time as recorded on the chart is displayed in Fig. 2, with the curve of Δ against time as found by using equation [2]. A plot of $1+\log \Delta$ against time is shown in Fig. 3 with an extrapolation to zero time.

The second column of Table I shows the heat of mutarotation found for the various sugars on the basis of total conversion of the sugar from the α to the β anomer. The precision attained in the calorimetric determinations is indicated by the second number in this column. In the fourth column, the percentage β in the equilibrium mixture is found, these values (except for a small correction) having been drawn from the references cited above (5, 6, 7), which are valid at 20° C. The correction is necessary because of the temperature difference, and has been made using the Gibbs–Helmholtz equation and the experimentally determined heats of mutarotation. By the use of well-known thermodynamic relations, values of ΔF and ΔS may be found, and these are given in columns five and six. Fig. 4 presents a plot of ΔH vs. ΔS.

Can. J. Chem. Downloaded from www.nrcresearchpress.com by 200.7.193.243 on 09/04/12
For personal use only.

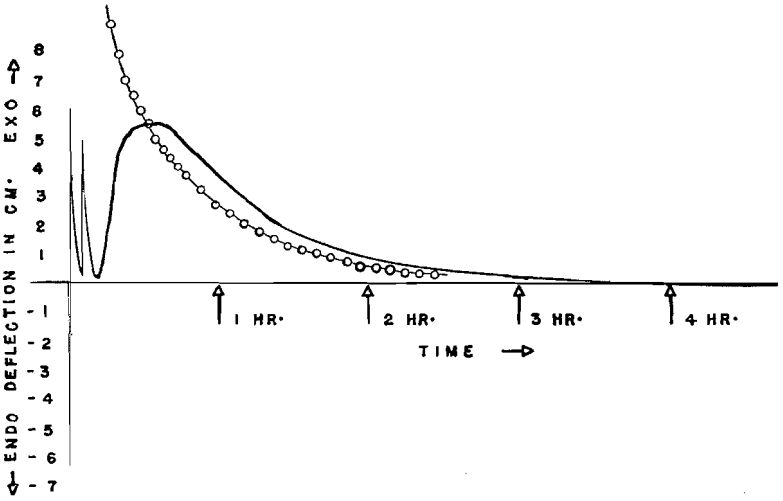

FIG. 2.

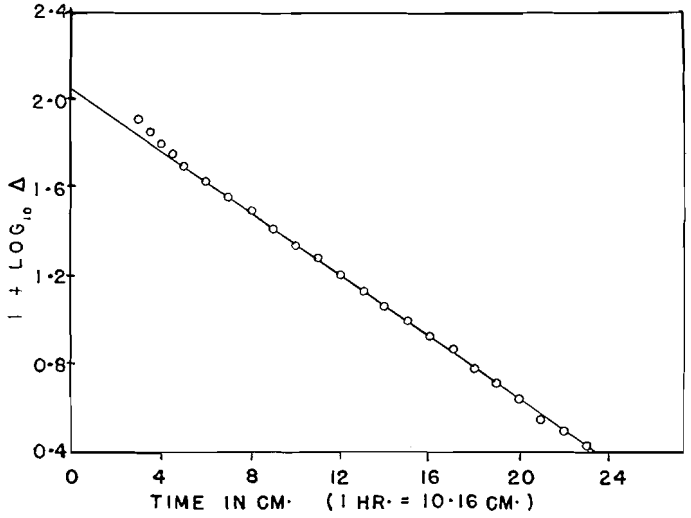

FIG. 3.

TABLE I

Sugar	ΔH, cal./deg.-mole, precision in %	Starting form	% β at 24.8° C.	ΔF, cal./mole	ΔS, e.u.	k_1+k_2, min.$^{-1}$, precision in %
D-Xylose	−535 ±3.9	α	65.5	−379	−0.52	0.038 ±10
Cellobiose	−438 ±2.0	β	64.4	−352	−0.29	0.0053 ± 2
D-Glucose	−270 ±1.4	α	63.6	−327	+0.19	0.0112 ± 4
Lactose.H_2O	−270 ±1.4	α	62.3	−297	+0.08	0.0070 ± 7
Maltose.H_2O	−126 ±7.3	β	63.9	−335	+0.70	0.0090 ±11

The accuracy of the work, as distinct from the precision, is more difficult to assess. For D-glucose and lactose, since the initial rotations of both anomers of the sugars have been determined accurately by Isbell and Pigman (5, 6), the percentage composition

Can. J. Chem. Downloaded from www.nrcresearchpress.com by 200.7.193.243 on 09/04/12
For personal use only.

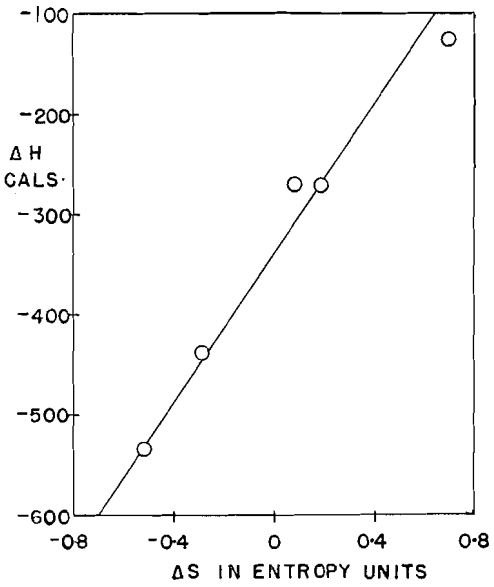

FIG. 4.

of the equilibrium solution is also known, so that the error in the values of the thermodynamic quantities should be of the order of the precision found. In fact, the value of ΔH for D-glucose agrees within 3% with that obtained by Sturtevant, viz., 277.7 cal./mole. However, in the case of the three other sugars, we are forced to rely upon the approximate values of Hudson and Yanovsky for one of the initial rotations. From a discussion of the possible uncertainty in these values, we conclude that in the case of maltose, the following limits are not unreasonable: for ΔH, $\pm 4\%$, ΔF, $\pm 10\%$, and for ΔS, $\pm 20\%$. The large relative error in the last value is due to the small value of ΔS. This introduces an uncertainty in the absolute value of 0.1 e.u. For D-xylose and cellobiose, these limits would be less.

The "ballistic" method gave a value of the heat of mutarotation of D-xylose equal to -460 cal./mole, which provides only a rough check of the value in Table I since the precision of the "ballistic" method is estimated to be $\pm 28\%$. The value obtained for D-xylose was $+312$ cal./mole with a similar precision. The positive value of ΔH is no doubt due to the axial hydrogen on $C_{(2)}$ which renders the β anomer energetically unfavored; ΔF for the mutarotation is now positive and the equilibrium composition of the sugar is 24.8% β at 25° C.

It is also possible to obtain the rate constant of the mutarotation from the slope of log $W(t)$ plotted against the time, hence from the slope of the straight line in Fig. 2. The values of k_1+k_2, the rate constant of the reaction, are shown in the last column of Table I, with the variation which was found for a series of four to seven experimental runs. The rather large variation found here seems also to occur amongst values in the literature. Isbell and Pigman (6) point out that the mutarotation is sensitive to the presence of certain metals, and it is possible that in our case, the reaction was catalyzed to some extent by brass which might have shown through the rhodium plating of the holder for the sugar. Since, however, we are interested in the heat of mutarotation between equilibrium states, any change in the rate of the reaction should not affect the thermodynamic values obtained.

Can. J. Chem. Downloaded from www.nrcresearchpress.com by 200.7.193.243 on 09/04/12
For personal use only.

The values of k_1+k_2 found by Isbell and Pigman (6) at 0° C. and 20° C. have been extrapolated to yield the following values at 24.8° C.: D-glucose, 0.0102 min.$^{-1}$; lactose.H_2O, 0.0076 min.$^{-1}$; D-xylose, 0.0381 min.$^{-1}$; maltose.H_2O, 0.0086 min.$^{-1}$. The agreement is thus seen to be satisfactory in view of the variations found.

DISCUSSION

We may note that the value of ΔH obtained for D-glucose agrees reasonably well with that obtained by Sturtevant (6), namely -278 cal./mole at 25° C.

Apart from D-lyxose, the sugars studied are identical in the neighborhood of the anomeric carbon. It is therefore surprising to find the large range of values for ΔH and ΔS shown in Table I. This is particularly so since ΔF is nearly constant for these sugars; this latter fact is reflected in the straight line obtained in Fig. 4.

A detailed discussion of these results is presented in Part II of this paper.

ACKNOWLEDGMENTS

The work described above was performed under a National Research Council research grant. Furthermore, one of us (M.A.K.) held an N.R.C. studentship during most of the period of this research and another (D.P.) was a Summer Research Associate during part of this time. We are most grateful for this financial assistance and should like to thank the National Research Council.

The award of a bursary (to M.A.K. during the early part of the research) from the Office of Scientific Research of the Province of Quebec is gratefully acknowledged.

We should also like to thank Prof. M. Rinfret for guiding us in the use of the microcalorimeter and for many helpful suggestions. We are greatly indebted to Mr. C.-E. Pion for his skilled technical assistance.

REFERENCES

1. HUDSON, C. S. J. Am. Chem. Soc. **26**, 1065 (1904).
2. STURTEVANT, J. M. J. Am. Chem. Soc. **59**, 1528 (1937).
3. STURTEVANT, J. M. J. Phys. Chem. **45**, 127 (1941).
4. HUDSON, C. S. and DALE, J. K. J. Am. Chem. Soc. **39**, 320 (1917).
5. ISBELL, H. S. and PIGMAN, W. W. J. Research Natl. Bur. Standards, **18**, 141 (1937).
6. ISBELL, H. S. and PIGMAN, W. W. Unpublished result. *Quoted by* F. J. Bates *in* Polarimetry, saccharimetry and the sugars, N.B.S. Circular C440 (1942), p. 273.
7. HUDSON, C. S. and YANOVSKY, E. J. Am. Chem. Soc. **39**, 1013 (1917).
8. LOWRY, T. M. and SMITH, G. F. J. Chem. Soc. 2539 (1927).
9. LOS, J. M. and SIMPSON, L. B. Rec. trav. chim. **73**, 941 (1954).
10. CALVET, E. Mem. serv. chim. état, **32**, 168 (1946).
11. CALVET, E. and PRAT, H. Microcalorimetrie: applications physico-chimiques et biologiques. Masson & Cie, Paris. 1956.
12. DAOUST, H. and RINFRET, M. Can. J. Chem. **32**, 492 (1954).

Can. J. Chem. Downloaded from www.nrcresearchpress.com by 200.7.193.243 on 09/04/12
For personal use only.

THE THERMODYNAMICS OF MUTAROTATION OF SOME SUGARS

II. THEORETICAL CONSIDERATIONS[1]

M. A. KABAYAMA AND D. PATTERSON

ABSTRACT

An interpretation of ΔH and ΔS for the mutarotation of D-glucose, D-xylose, maltose, lactose, and cellobiose is given in terms of changes in the hydration of the reducing hydroxyl group.

Can. J. Chem. Downloaded from www.nrcresearchpress.com by 200.7.193.243 on 09/04/12
For personal use only.

INTRODUCTION

In this part of the paper we shall attempt to give an interpretation of the experimental results shown in Table I and Fig. 4 of Part I.* We shall first consider the conformations of the sugars used in Part I and note that in all of them the neighboring groups of the reducing carbon are identical.

There is a large body of evidence for strong hydrogen bonding between the sugar hydroxyl groups and adjacent water molecules in aqueous solution. On the basis of the known conformations of the sugars and of the structure of water it is possible to come to tentative conclusions about the packing of the water molecules about the sugar molecule, and to predict that an equatorial hydroxyl group will be more strongly hydrated than an axial group. We also find that the reducing hydroxyl of the sugars of Part I is bonded to the adjacent water molecule in the same manner, with only slight variations in bond length.

The large value of ΔS for mutarotation of the various sugars can be associated with changes in the frequency of torsional oscillation of this reducing hydroxyl group about the $C_{(1)}$—O axis. On the basis of a simple model of the hydrogen bond between the group and the water molecule, the order of magnitude of this frequency can be calculated and shown to be low enough to give a large contribution to the entropy.

Using the hydrogen bond model, the order of magnitude of the variation of ΔS and ΔH amongst the sugars is calculated, and the slope of ΔH vs. ΔS in Fig. 4 of Part I can be estimated theoretically.

Finally ΔF for the mutarotation of the sugars can be viewed in the light of the free energies of interaction between adjacent hydroxyl groups in the cyclitols which have been the subject of thermodynamic study by Angyal and McHugh (1). Because the pyranose ring contains an oxygen atom, whereas the cyclitol ring does not, a difference exists between group interactions in the two cases.

CONFORMATIONS OF THE SUGARS

Reeves (2) has shown that of the two chair and six boat conformations possible for the hexopyranoses the chair conformations are normally preferred. More recent work in Reeves' laboratory (3, 4) has indicated the possibility of a boat conformation in some of the pyranoses, the tendency of hydroxyl groups to take up equatorial positions apparently overcoming the normal stereochemical preference for the chair conformation.

[1]*Manuscript received November 12, 1957.*
Contribution from the Department of Chemistry, University of Montreal, Montreal, Que.
**Preceding paper.*

D-Glucose and D-xylose, however, retain the normal C1 conformation shown for β-glucose in Fig. 1. This conformation has been confirmed by X-ray diffraction evidence for cellulose (5) and methyl β-D-xyloside (6, quoted in 5).

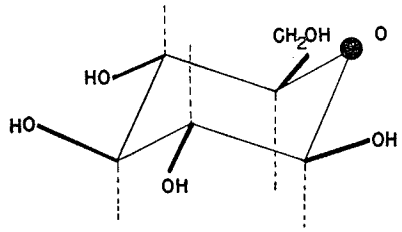

FIG. 1. The conformation of the β-D-glucose molecule.

In the disaccharides, there is no reason to suppose that the β-D-(1→4)-linked glucose residues of cellobiose are not both in the conformation found for solid cellulose. In the case of lactose, 4-*O*-(β-D-galactopyranosyl)-D-glucose, there is some evidence from X-ray diffraction work on the solid (7) that the galactose residue is distorted from the C1 conformation because of the axial OH on $C_{(4)}$ to produce a flatter molecule than would otherwise be the case. Reeves and Blouin (4) also suggest that the axial hydroxyl in galactose tends to become more equatorial distorting the C1 conformation.

The presence of a boat conformation in maltose and amylose seems to be indicated (3). Haworth (8) originally predicted that the α-D-(1→4)-linked glucose residues of amylose would lie in a boat conformation. Reeves has shown that they take up either of two boat conformations which put the α-D-(1→4) linkages in equatorial positions. Maltose, however, does not seem to have the same extent of boat conformation. Here the only steric requirement is that the 1-hydroxyl on the glycosidic residue and the 4-hydroxyl on the reducing residue be in equatorial positions to make the 1→4 linkage equatorial. This requirement is satisfied if the glycosidic residue is in a boat conformation (actually, most likely the B1), leaving the reducing glucose residue in the C1 conformation. This structure is in accord with the resemblance of the mutarotation thermodynamics of maltose to that of the other sugars shown in Fig. 4 of Part I. Such would not be the case were the reducing residue in maltose also in a boat conformation.

SOLVATION OF THE SUGARS

(*a*) *Evidence for Hydration*

Thermodynamic studies of glucose and sucrose in aqueous solution (9) show that they must be extensively hydrated, presumably by hydrogen bonding between the hydroxyl groups and the water molecules. Evidence from the intrinsic viscosities of aqueous solutions of D-glucose and sucrose shows that the van der Waals volume of these molecules is increased by a factor of about two by hydration (10).

The distances between adjacent hydroxyl groups in the pyranose ring are almost identical with those in the 1,2-cyclohexanediols. There, intramolecular hydrogen bonds can exist when the molecules are in CCl_4 solution (11), and result in decreases of the hydroxyl stretching frequency equal to 32 $cm.^{-1}$ when both hydroxyls are equatorial, and equal to 39 $cm.^{-1}$ when one is equatorial and the other axial. It is apparent from the smallness of these shifts that the intramolecular bonds are very weak. It is therefore highly probable that in aqueous solution, the sugar hydroxyls are directed outwards to oxygen atoms of adjacent water molecules, thus destroying the intramolecular hydrogen bonding between hydroxyls.

Can. J. Chem. Downloaded from www.nrcresearchpress.com by 200.7.193.243 on 09/04/12
For personal use only.

Can. J. Chem. Downloaded from www.nrcresearchpress.com by 200.7.193.243 on 09/04/12
For personal use only.

If, however, intramolecular hydrogen bonding is preserved by sugar molecules in solution, the hydroxyl stretching-frequency shift should be of the order of that observed for the 1,2-cyclohexanediols in CCl_4. On the other hand, if the hydroxyls form strong hydrogen bonds with the water oxygens, frequency shifts of several hundred cm.$^{-1}$ might be expected.

Some infrared spectroscopic observations seem pertinent to this subject, and they also give evidence of intermolecular association between sugar molecules. A Perkin-Elmer model 112 spectrometer with a NaCl prism was used to obtain spectra of a 0.1 *M* solution of α-D-glucose in pyridine and of 0.1 *M*, 0.01 *M*, and 0.002 *M* solutions of α-D-xylose in pyridine. The hydroxyl stretching-frequency band of α-D-glucose had a peak about 3250 cm.$^{-1}$ compared with the free hydroxyl value of about 3625 cm.$^{-1}$. With increasing dilution, the peak of the band for D-xylose moved from about 3300 cm.$^{-1}$ to about 3400 cm.$^{-1}$, presumably showing the effect of an association between the sugar molecules.

Since the mutarotation experiments were performed with concentrations of the order of 0.2 *M*, we must conclude that some intermolecular interaction occurred. The same may be said of the experiments of Sturtevant (12), who used concentrations of 0.15–0.3 *M* D-glucose. At low concentrations when intermolecular association was greatly reduced, the hydroxyl stretching frequency still seems too low (~3400 cm.$^{-1}$) for it to be due to intramolecularly bonded hydroxyl groups. It appears that hydroxyl groups of the sugar molecules form hydrogen bonds with the ring nitrogens of the pyridine molecules, rather than remaining intramolecularly bonded. Similarly, in water, the relatively weak intramolecular hydrogen bonds are in all probability replaced by strong bonds with the oxygen atoms of surrounding water molecules.

(*b*) *The Water Structure*

In water, the oxygen atom of each molecule is tetrahedrally coordinated by means of hydrogen bonds to the oxygen atoms of adjacent water molecules, the water structure thus resembling the SiO_2 structure. Bernal and Fowler (13) proposed the rather open tridymite SiO_2 structure for ice, and the closer-packed but still four-coordinated quartz SiO_2 structure for water at normal temperatures. X-Ray diffraction work by Morgan and Warren (14) has shown that the assumption of a quartz structure for water must be modified slightly. Recently, Pople (15) proposed a continuation of the tridymite ice structure with increasing bending of the hydrogen bonds and a movement of molecules into formerly unoccupied regions of the open ice structure.

Fig. 2(*a*) shows a plane of oxygen atoms of water molecules in the tridymite structure (16), as viewed along the hexagonal axis, each hydrogen bond between adjacent oxygen atoms containing a hydrogen atom which is not shown. The hexagons are skew and are all in the chair conformation. The atoms of the plane are repeated directly above and below those shown, but the chairs are rotated through 60°, so that atoms below the median plane of the chair are now above, and vice versa. In Fig. 2(*a*), the atoms marked ▽ and △ are joined by straight hydrogen bonds to the atoms directly above and below, respectively. In the adjacent planes above and below, the corresponding atoms would be marked △ and ▽ with the convention referred to above. The tridymite structure appears in Fig. 2(*b*) as seen from the side.

(*c*) *Hydration of the Monosaccharides*

In discussing hydration of the sugar molecules, we shall take the tridymite structure as a model for water, thus neglecting bending of the hydrogen bonds and the accompanying molecular disorder. The dimension marked on Fig. 2(*a*) for the O—O distance (2.90 Å) was found by Morgan and Warren (14) for water just above 0° C.

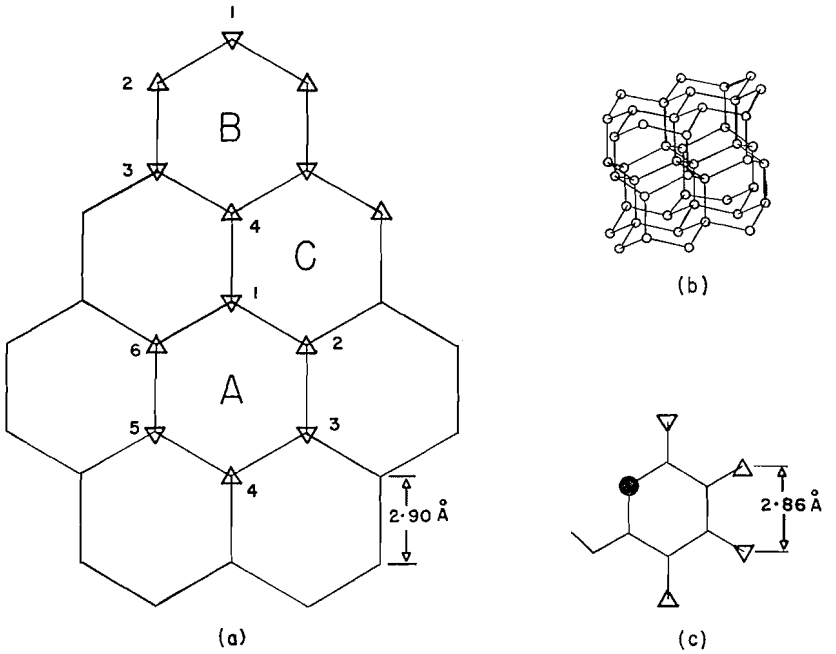

FIG. 2. (*a*) A plane of the tridymite structure in water showing direction of H bonds. (*b*) The tridymite structure. (*c*) The D-glucose molecule showing direction of possible perpendicular H bonds.

Fig. 2(*c*) shows the β-D-glucose molecule from above. The triangles mark the oxygens of hydroxyl groups on $C_{(1)}$ to $C_{(4)}$. Assuming the chair form of Fig. 1 for the β-D-glucose ring, one finds that the hydrogens of these hydroxyl groups may be placed directly above (▽) or directly below (△) the oxygens, and are thus capable of forming hydrogen bonds in these directions in a manner similar to that of the oxygen atoms in the water structure. Furthermore, the distance between adjacent oxygens of the D-glucose hydroxyls (2.86 Å) is almost identical with that between adjacent oxygens in water (2.90 Å).

It is thus apparent that the D-glucose molecule can replace a chair conformation of water oxygens in Fig. 2(*a*), e.g. the hexagon A. The oxygens on $C_{(1)}$ to $C_{(4)}$ replace oxygens marked 1 to 4 forming strong hydrogen bonds with water oxygens in planes above and below; the only distortion involved is the replacement of a hexagon of side 2.90 Å by one of side 2.86 Å. It may be seen from a model that the primary hydroxyl group on $C_{(6)}$ may form a bent hydrogen bond with an adjacent oxygen of a water molecule in the same plane as the sugar molecule. Finally, the "lone-pair" orbitals of the ring oxygen found near position 6 lie in the direction of the hydrogen atom on the adjacent oxygen in the same plane.

There is a second mode of hydration which might also occur. This involves bonding of the equatorial hydroxyls to adjacent water molecule oxygens in the same plane rather than in planes above and below. In order to do this, the molecule must be flattened as if a conformational inversion were taking place.

It seems difficult to choose between these two modes of hydration for equatorial hydroxyl groups. The energy necessary to flatten the ring would seem to favor the first mode of hydration. There seems, however, to be some evidence (17) that the glucose ring consists of five carbon atoms more or less in a plane, with an oxygen atom out of the plane, rather than the skew hexagon of the cyclohexane ring. In this case, the second mode of hydration would probably be favored.

Can. J. Chem. Downloaded from www.nrcresearchpress.com by 200.7.193.243 on 09/04/12
For personal use only.

On the other hand, if we have an axial hydroxyl, inspection of a model shows that hydrogen bonding may take place only with the oxygens of water molecules adjacent to the sugar and in the same plane. A considerably bent H bond is the result, and at the same time a partial inversion of the conformation must take place; because of the bent bond, we conclude that the hydration of an axial hydroxyl group is considerably less than that of an equatorial hydroxyl of a chair conformation. This is in conformity with the preference (as found by Reeves) of the sugars to assume those conformations having equatorial hydroxyls.

The hydration of D-xylose should take place in essentially the same manner as that outlined above for D-glucose.

(*d*) *Solvation of the Disaccharides*

The structure of the cellobiose molecule in the solid is shown from above in Fig. 3(*a*), and is identical with that of any two adjacent units of the cellulose chain (17). The C—O—C valence bond angle of the glycosidic linkage lies in the plane perpendicular to that of the paper so that the linkage appears straight. Haworth (8) originally proposed the structure of Fig. 3(*b*) as the unit of the cellulose chain. The C—O—C valence angle now lies in the plane of the paper and one residue has rotated 60° from position B to C. (In Fig. 3(*a*) appropriate bond distances are foreshortened to allow for the C—O—C valence angle.) It is interesting to note that the over-all lengths of these two different conformations are the same, viz. 10.3 Å. The triangles again show the relative directions of the hydrogen bonds, which can be directed in perpendicular directions.

A consideration of steric interferences in atomic models has led Hermans and his collaborators (18) to propose the cellobiose molecule of Fig. 3(*b*) as a unit of the cellulose chain. More recently, X-ray diffraction work (19) suggests this unit for the cellulose II (mercerized cellulose) chain while the unit of Fig. 3(*a*) is retained for cellulose I (native cellulose).

There are two reasons for supposing that, when the cellobiose molecule is in aqueous solution, the structure of Fig. 3(*a*) may transform itself into that of Fig. 3(*b*). Firstly, in order to fit the two D-glucose residues into the water lattice in the extended form, we

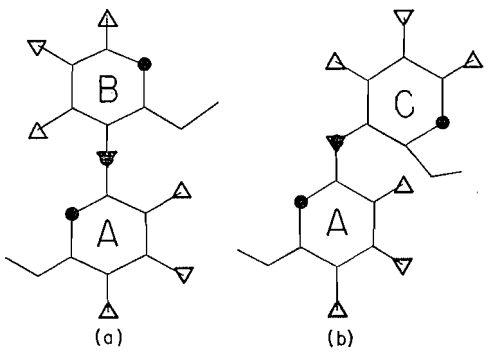

FIG. 3. Two conformations of the cellobiose molecule.

must identify the residues with the two hexagons of Fig. 2(*a*) marked A and B. In A, oxygens on $C_{(2)}$ to $C_{(4)}$ fall on points 2 to 4, and in B, oxygens on $C_{(1)}$ to $C_{(3)}$ fall on points 1 to 3. However, as shown by the positions of the triangles, the hydroxyls in D-glucose residue B cannot form hydrogen bonds in the directions required by hexagon B of the water lattice. The second point is that the over-all length of hexagons A and B in the water lattice is ~12.2 Å, whereas the corresponding cellobiose length is 10.3 Å;

Can. J. Chem. Downloaded from www.nrcresearchpress.com by 200.7.193.243 on 09/04/12
For personal use only.

this discrepancy would appear to be rather large and would result in greatly decreased hydration.

In the structure of Fig. 3(*b*), however, both residues will fit into the water lattice. Having rotated the residue B through 60° to position C, the hydrogen bonds now fit with those of hexagon C in the water lattice. Furthermore, the dimensions are such as to allow the molecule to take the place of the two adjacent hexagons A and C in the water structure without undue distortion.

As a result of these considerations, it seems likely that the cellobiose molecule takes up Haworth's Fig. 3(*b*) conformation in aqueous solution rather than retaining the conformation followed by the solid (Fig. 3(*a*)).

Presumably the same point of view will hold good for lactose. As previously mentioned, there is some evidence of distortion of the C1 galactose conformation owing to the axial 4-hydroxyl, possibly to increase hydration. This might also exist in the galactose residue in lactose.

The structure of maltose in solution may be deduced from that of amylose in solution. Haworth (8) originally proposed a conformation for amylose analogous to that which he suggested for cellulose. It is capable of forming spiral structures (20) whose dimensions have been verified by X-ray diffraction measurements on the amylose–iodine complex (21). Fig. 4 shows two units of the chain. The residue to the right must be considered to be in a boat conformation. While the dimensions of the molecule are appropriate for fitting it into the water structure, consideration of the model shows that, owing to the boat conformation, at least one of the hydrogen bonds formed by the right-hand residue must be somewhat bent. One might therefore expect that hydration of maltose would be less than that of other sugars.

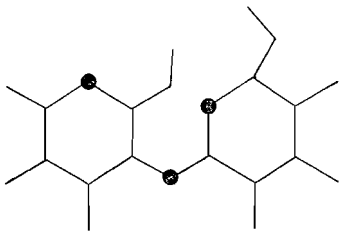

FIG. 4. The structure of the maltose molecule in solution.

As a result of the foregoing discussion of hydration, it seems likely that the packing of water molecules about the reducing hydroxyls will be much the same in D-glucose, D-xylose, cellobiose, lactose, and maltose. We have already noted the similarity of the conformations of these sugars. It thus appears that the differences in the thermodynamics of mutarotation presented in Part I must be due to rather small perturbations in the neighborhoods of the reducing carbons of these sugars.

THERMODYNAMICS OF MUTAROTATION

The negative ΔH for mutarotation of the sugars in Table I of Part I is in accord with the greater hydration for equatorial hydroxyl groups than for axial groups. Some of the values of ΔS are positive while others are negative; most would seem to be rather large as has been pointed out in Part I. Furthermore, the variation in ΔS amongst the sugars studied seems extremely large since the nearest neighbors of the reducing carbon are the same throughout, the conformations of the reducing residue being the same, in spite of small distortions of the molecules induced by the hydration. We shall first

Can. J. Chem. Downloaded from www.nrcresearchpress.com by 200.7.193.243 on 09/04/12
For personal use only.

develop a model to show that the large ΔS values are reasonable, and then use the model to discuss the relation between ΔH and ΔS manifested in Fig. 4 of Part I.

(a) The Magnitude of the Entropy Change

The entropy of a single vibrational mode is given (22) by

$$[1] \qquad S = k\left[\frac{x}{e^x-1} - \ln(1-e^{-x})\right], \qquad x = h\nu/kT,$$

where ν is the vibrational frequency,
k is Boltzmann's constant, and
h is Planck's constant.

ΔS for the mutarotation is thus given by a summation of terms as in [1] if the change of vibrational frequencies upon mutarotation is known. It seems natural to suppose ΔS to result from the changing of frequency in a relatively small number of modes per molecule. For instance, Barker, Bourne, Stacey, and Whiffen (23) have demonstrated the existence of small characteristic differences between the spectra of α and β anomers of D-pyranoses in the region of 730–960 cm.$^{-1}$. Consideration of [1] shows, however, that the contribution of a vibrational mode to the entropy diminishes with increasing frequency so that frequency changes in the above region produce a negligible contribution to the entropy change. The largest change of frequency mentioned by Barker and collaborators produces a change of about 0.032 e.u. One must therefore seek the basis of the large ΔS values in a low-frequency vibrational mode, which is thus likely to be associated with a torsional oscillation rather than a bond bending vibration. The torsional oscillation of the OH group about the $C_{(1)}$—O bond would seem to be an attractive possibility. The torsional oscillation of the free hydroxyl in CH_3OH vapor (24) was found to have a mean frequency of 225 cm.$^{-1}$. With the formation of the hydrogen bond in the liquid phase of CH_3OH, the hydroxyl oscillation gives a very wide band centering about 650 cm.$^{-1}$ (25). In the case of a sugar hydroxyl hydrogen-bonded to a water molecule, the shift in the hydroxyl stretching frequency is rather less ($\sim$200 cm.$^{-1}$) than in the case of the hydroxyl in polymeric liquid methanol (301 cm.$^{-1}$(11)).

It is therefore reasonable to suppose a smaller energy for the hydrogen bond in the D-glucose hydration case than in liquid methanol. Hence one might expect an OH torsional frequency between 225 cm.$^{-1}$ and 650 cm.$^{-1}$, and thus of the order of magnitude required to give the ΔS values found. (A torsional frequency of 400 cm.$^{-1}$ gives a contribution to the entropy, following [1], of $\sim$1 e.u.)

(b) Model of the Hydrogen Bond

The following simple model of the hydrogen bond between the reducing hydroxyl and an adjacent water oxygen atom may be used to determine the order of magnitude of the hydroxyl's frequency of torsional oscillation. We assume electrostatic forces between point charges of magnitude $-q$ and $+q$ at the O and H of the reducing hydroxyl group and a charge $-2q$ at the O of the adjacent water molecule, as shown in Fig. 5. For the simple calculation which follows, we neglect the effect of $C_{(1)}$ and the ring on

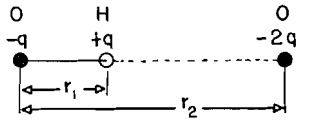

FIG. 5. Simple model of the hydrogen bond.

Can. J. Chem. Downloaded from www.nrcresearchpress.com by 200.7.193.243 on 09/04/12
For personal use only.

the charges of the hydroxyl oxygen and hydrogen. A repulsive Born–Mayer interaction also exists between the hydroxyl H and the water oxygen. This adds a term A/r^n to the energy. Verwey (26) in his simplified treatment of the hydrogen bond in water takes $n = 12$. Allowing the hydroxyl group to make small oscillations through an angle ϕ about an axis through its oxygen and perpendicular to the O—H direction, we find the torsional force constant:

$$g = [\partial^2 E/\partial\phi^2]_{\phi=0},$$

where E is the energy of the system. In this way,

$$[2] \qquad g = \frac{2q^2 r_1 r_2}{(r_2-r_1)^3}\left[1-\left\{\frac{An}{2(r_2-r_1)q^2}\right\}^{n-1}\right].$$

$(An/2q^2)^{n-1}$ has the dimensions of a (length)$^{n-1}$, or R^{n-1}. R has the physical significance of being the distance between the hydrogen and the water oxygen at which the repulsive force between these two atoms balances the attractive force. Then [2] becomes

$$[3] \qquad g = \frac{2q^2 r_1 r_2}{(r_2-r_1)^3}\left[1-\left\{\frac{R}{(r_2-r_1)}\right\}^{n-1}\right],$$

and the frequency is given by

$$\frac{1}{\lambda} = \frac{1}{2\pi c}\sqrt{\frac{g}{I}},$$

where I is the moment of inertia of the hydroxyl group about its axis of rotation. The energy of the hydrogen bond may be written as:

$$[4] \qquad E = -2q^2\left[\frac{1}{(r_2-r_1)}\left\{1-\left(\frac{1}{n}\right)\left(\frac{R}{r_2-r_1}\right)^{n-1}\right\}-\frac{1}{r_2}\right].$$

We take $q = 1.51\times10^{-10}$ e.s.u., chosen to give a dipole moment of 1.86 D. to the water molecule,

$$r_1 = 0.96 \text{ Å},$$
$$r_2 = 2.90 \text{ Å},$$
$$I = 1.236\times10^{-40} \text{ g-cm.}^2 \text{ (Ref. 24)}.$$

From the relation of ΔH to ΔS (Fig. 4, Part I), it will be found that $[R/(r_2-r_1)]^{n-1} \sim 0.7$. Using these values in [3], g becomes 5.63×10^{-13} ergs and the frequency of torsional oscillation of the OH group is 360 cm.$^{-1}$, which seems very reasonable when compared with the OH torsional frequency of methanol. The energy of the hydrogen bond between the hydroxyl group and the oxygen atom of the adjacent water molecule is ~9.7 kcal./mole, which must be considered rather high. The effect of $C_{(1)}$ would be to raise the negative charge of the hydroxyl oxygen above that assigned to it here, and therefore to lower the energy of the hydrogen bond. A more detailed calculation does not appear warranted, however, since only orders of magnitude are sought.

THE RELATION BETWEEN ΔH AND ΔS

We shall assume that ΔH and ΔS change from sugar to sugar in Fig. 4 of Part I by reason of slight perturbations in the surroundings of the reducing hydroxyl which change the length of the hydrogen bond between the hydroxyl and the adjacent water molecule. This in turn is manifested in small changes in the enthalpy and entropy of either or

Can. J. Chem. Downloaded from www.nrcresearchpress.com by 200.7.193.243 on 09/04/12
For personal use only.

both of the α and β anomers, causing a variation of ΔH and ΔS between the sugars. Furthermore, we shall use the simple model of the hydrogen bond developed above for both anomers of the sugars. Thus, supposing slight changes $\Delta r_2'$ and $\Delta r_2''$ in the lengths of the hydrogen bonds in the α and β anomers respectively, the changes in ΔH and ΔS are given by:

$$\delta\,\Delta H \simeq \left(\frac{\partial E}{\partial r_2}\right)(\Delta r_2'' - \Delta r_2') \equiv \frac{\partial E}{\partial r_2}\,\Delta r_2,$$

$$\delta\,\Delta S \simeq \left(\frac{\partial S}{\partial r_2}\right)(\Delta r_2'' - \Delta r_2') \equiv \frac{\partial S}{\partial r_2}\,\Delta r_2.$$

Here E and S are given by expressions [4] and [1] respectively. Thus,

$$[5] \qquad \delta\,\Delta H = \frac{2q^2}{(r_2-r_1)^2}\left[1-\left(\frac{R}{r_2-r_1}\right)^{n-1}-\left(\frac{r_2-r_1}{r_2}\right)^2\right]\Delta r_2$$

and

$$[6] \qquad \frac{\delta\,\Delta S}{R} = -\frac{x^2e^x}{(e^x-1)^2}\,\frac{1}{2g}\,\frac{\partial g}{\partial r_2}\,\Delta r_2.$$

In [6], using [3], and deriving g with respect to r_2, we have

$$[7] \qquad \frac{\delta\,\Delta S}{R} = -\frac{x^2e^x}{2(e^x-1)^2}\left[\frac{1}{r_2}\left\{1-\frac{3r_2}{r_2-r_1}\right\}+\frac{[(n-1)/(r_2-r_1)][R/(r_2-r_1)]^{n-1}}{1-[R/(r_2-r_1)]^{n-1}}\right]\Delta r_2.$$

Using the previously given values of the various quantities and with $[R/(r_2-r_1)]^{n-1} = 0.7$, we find $\Delta H = -2790 r_2$ cal./mole with r_2 in Å. Thus, a change of 0.1 Å produces 279 cal./mole change in ΔH. Correspondingly, $\delta\,\Delta S/R = -4.76\ \Delta r_2$ where r_2 is in Å. For $\Delta r_2 = 0.1$ Å, $\delta\,\Delta S = 0.946$ e.u. Furthermore, the slope of the line in Fig. 4 of Part I is given by

$$\mathscr{E}^* = \frac{\delta\,\Delta H}{\delta\,\Delta S/R} = 580 \text{ cal./mole.}$$

Although this figure is lower than the experimental value of 741 cal./mole, the agreement must be considered satisfactory considering the simplicity of the model. The value of $\mathscr{E}^*$ is not sensitive to the choice of $[R/(r_2-r_1)]^{n-1}$. When $[R/(r_2-r_1)]^{n-1} = 0.45$, the electrostatic attraction H . . . . . $O_{(2)}$ balances the $O_{(1)}$—$O_{(2)}$ electrostatic repulsion plus the Born–Mayer repulsion. Here $\delta\,\Delta H = 0$, and $\mathscr{E}^* = 0$. With our choice of $[R/(r_2-r_1)]^{n-1}$, we are assuming that the OH and the water oxygen are pushed slightly nearer together than this equilibrium distance.

STERIC INTERACTIONS IN THE PYRANOSE RING

Finally a word must be said about the steric interactions in the pyranose ring. Eliel and Lukach (27) have recently obtained a value for the free energy change for $OH_a \rightarrow OH_e$, and have made a comparison with other values available in the literature. There is a rather wide spread of these values, and the authors suggest a possible effect of the solvent used. Of the values mentioned, probably only that found by Angyal and McHugh (1) is relevant here, since although cyclitols rather than pyranoses were studied, their experiments were carried out in aqueous solution.

We notice that for all of the sugars in Table I of Part I, $\Delta F \sim 0.33$ kcal./mole. In each of these sugars the reducing residue is in the C1 conformation, and the change from

Can. J. Chem. Downloaded from www.nrcresearchpress.com by 200.7.193.243 on 09/04/12
For personal use only.

the α to the β anomer breaks two OH_a: H_a interactions and replaces an OH_e: OH_e interaction by an OH_e: OH_a interaction within the molecule. To a first approximation, these last two interactions may be taken as equal. At the same time, an axial group has become equatorial, changing the hydration energy of the molecule in aqueous solution. Thus, the total change of free energy may be written:

$$E - A - 2(OH_a: H_a) = 0.33 \text{ kcal./mole},$$

where E is the hydration free energy of an equatorial OH,
A is the hydration free energy of an axial OH,
OH_a: H_a is the free energy for formation of an OH_a: H_a interaction.

Thus OH_a: $H_a + \frac{1}{2}(A-E) = 0.17$ kcal./mole.

Angyal and McHugh have not taken account of hydration of the cyclitol hydroxyls explicitly. Nevertheless, of one allows for this effect, it is found that their interaction free-energy OH_a: H_a becomes OH_a: $H_a + \frac{1}{2}(A-E) = 0.45$ kcal./mole.

Thus a discrepancy exists between the two values. A tentative explanation may be advanced.

In the pyranose ring, the ring oxygen has four unpaired electrons located in two "lone-pair" orbitals on the upper side of the ring oxygen in Fig. 1. These would repel the corresponding "lone-pair" orbitals of the $C_{(1)}$ hydroxyl, and one might expect that the α anomer would be preferred to the β anomer. Such an effect has been mentioned by Edward (28). The size of the effect obviously depends on the orientation of the hydroxyl group in the α and β anomers, and hence on the manner of hydration. Two possible modes of hydration of the OH in the β anomer were considered above. It is interesting to note that the effect hardly exists for one mode of hydration, that where the hydroxyl forms a hydrogen bond with the plane of water molecules above the plane of the sugar molecule. With the other mode of hydration, that in which the hydrogen bond is directed to a water molecule in the same plane as the sugar molecule, the effect would be important Here, the lone-pair orbitals of the ring oxygen and the hydroxyl oxygen are considerably closer together in the β anomer than in the α anomer.

We may note also that the other interaction free-energies of the OH groups in the cyclitols as found by Angyal and McHugh are an indication of hydration of the cyclitols.

The interactions OH_a : OH_a and OH_e: OH_e† are found to have free energies of formation of 1.9 kcal./mole and 0.35 kcal./mole (13) respectively. In the cyclohexanediols in CCl_4, however, Kuhn finds intramolecular hydrogen bonding between pairs of OH groups and particularly in the OH_a: OH_a case. If this intramolecular hydrogen bonding were to exist for the cyclitols in aqueous solution, one would expect negative free-energies. On the other hand, hydrogen bonding of the hydroxyls to water molecules would break the intramoleculr hydrogen, turning the hydrogens of the hydroxyls outward. This would allow the "lone-pair" orbitals of the hydroxyl oxygens to interact and thus contribute towards a positive ΔF.

It may be further shown that if hydration is allowed for, we have OH_a: $OH_a + (A-E)$ = 1.9 kcal./mole,

$$OH_e: OH_e = 0.35 \text{ kcal./mole}.$$

Thus, in the case of interaction between two axial hydroxyls the essentially positive

†*Angyal and McHugh do not differentiate between* OH_e : OH_e *and* OH_a : OH_e. *However, they appear to have actually found* ΔF *for* OH_e : OH_e *interactions, the other type of interaction cancelling out of the calculation.*

Can. J. Chem. Downloaded from www.nrcresearchpress.com by 200.7.193.243 on 09/04/12
For personal use only.

term $(A-E)$ also contributes to the high positive values for the total interaction free-energy.

ACKNOWLEDGMENTS

We wish to thank Dr. C. Sandorfy of this department, who very kindly obtained the infrared spectra referred to in the paper. We are grateful to Dr. H. Favre of this department for many interesting discussions of stereochemical problems and to Dr. R. U. Lemieux for a helpful discussion of this work. Finally, we would like to acknowledge the generous financial assistance of the National Research Council for which we are extremely grateful. One of us (M.A.K.) was the recipient of an N.R.C. studentship while doing this research, and the other (D.P.) was a Summer Research Associate for part of the time.

REFERENCES

1. ANGYAL, S. J. and MCHUGH, D. J. Chem. & Ind. (London), 1147 (1956).
2. REEVES, R. E. Advances in carbohydrate chemistry. Vol. 6. Academic Press Inc., New York. 1951. p. 107.
3. REEVES, R. E. J. Am. Chem. Soc. **76**, 4594 (1954).
4. REEVES, R. E. and BLOUIN, F. A. J. Am. Chem. Soc. **79**, 2261 (1957).
5. ASTBURY, W. T. and DAVIES, M. A. Nature, **154**, 84 (1944).
6. BROWN, C. J. Ph.D. Thesis, Univ. of Birmingham (1939).
7. COX, E. G., GOODWIN, T. H., and WAGSTAFF, A. I. J. Chem. Soc. 1495 (1935).
8. HAWORTH, W. N. Rapport sur les hydrates de carbones, 10th conf. of the international union of chemistry, Paris, 1930. p. 53.
9. TAYLOR, J. B. and ROWLINSON, J. S. Trans. Faraday Soc. **51**, 1183 (1955).
10. EDWARD, J. T. Can. J. Chem. **35**, 571 (1957).
11. KUHN, L. P. J. Am. Chem. Soc. **74**, 2492 (1952).
12. STURTEVANT, J. M. J. Phys. Chem. **45**, 127 (1941).
13. BERNAL, J. D. and FOWLER, R. H. J. Chem. Phys. **1**, 515 (1933).
14. MORGAN, J. and WARREN, B. E. J. Chem. Phys. **6**, 666 (1938).
15. POPLE, J. A. Proc. Roy. Soc. (London), A, **205**, 163 (1951).
16. WELLS, A. F. Structural inorganic chemistry. 1st ed. Oxford University Press, Oxford. 1945. p. 464.
17. MARK, H. Chem. Revs. **26**, 182 (1940).
18. HERMANS, P. H., DE BOOYS, J., and MAAN, C. Kolloid Z. **102**, 169 (1943).
19. PETITPAS, T. and MERING, J. Compt. rend. **243**, 47 (1956).
20. HAWORTH, W. N. Proc. Roy. Soc. (London), A, **186**, 1 (1946).
21. RUNDLE, R. E. and FRENCH, D. J. Am. Chem. Soc. **65**, 1707 (1943).
22. WENNER, R. R. Thermochemical calculations. 1st ed. McGraw-Hill Book Co., Inc., New York and London. 1941. p. 134.
23. BARKER, S. A., BOURNE, E. J., STACEY, M., and WHIFFEN, D. H. J. Chem. Soc. 171 (1954).
24. BURKHARD, D. G. and DENNISON, D. M. Phys. Rev. **84**, 408 (1951).
25. STUART, A. V. and SUTHERLAND, G. B. B. M. J. Chem. Phys. **24**, 559 (1956).
26. VERWEY, E. J. W. Rec. trav. chim. **60**, 887 (1941).
27. ELIEL, E. L. and LUKACH, C. A. J. Am. Chem. Soc. **79**, 5986 (1957).
28. EDWARD, J. T. Chem. & Ind. (London), 1102 (1955).

Can. J. Chem. Downloaded from www.nrcresearchpress.com by 200.7.193.243 on 09/04/12
For personal use only.

Can. J. Chem. Downloaded from www.nrcresearchpress.com by 200.7.193.243 on 09/04/12
For personal use only.

SOME ANOMALOUS ELECTRICAL POLARIZATIONS[1]

PETER PODLESCHKA, LISELOTTE WESTLAND, AND GEORGE F WRIGHT

ABSTRACT

Dielectric-constant determinations of a series of solids previously reported to have high atom polarizations have not confirmed earlier opinions. Moreover, when it has been practicable to determine the change in polarization with respect to temperature, the relationship is not invariant. This variation may be, and in some instances should be, interpreted as evidence for orientation polarization. However, all such assignments cannot be certain until the change in solid dielectric constant with respect to temperature has been studied.

INTRODUCTION

This report is a continuation of recent (1) work showing that many electrical polarizations formerly attributed entirely to distortion polarization seem instead to have a component of orientation polarization in an applied field of about 1 electrostatic volt at 500 kc. These reassignments were based on dielectric constants of thin pellets pressed to maximum density from randomly oriented powders and were confirmed by determinations of the dielectric constants in benzene solutions at several temperatures. The present results, shown in Table I, also have previously been assigned abnormally high atom polarizations in lieu of orientation polarizations. These assignments seem to have been made in deference to current organic chemical theory or by analogy with another substance of the same class. It is evident from the data of Table I that the earlier opinions require revision. Each item will be discussed in order of appearance in the table.

TABLE I

DIELECTRIC CONSTANTS OF SOME SOLIDS AND SOLUTIONS IN BENZENE

Substance	d^{20}	ϵ, solid	Solution						
			Temp., °C.	$\Delta\epsilon/\Delta\omega$	$\Delta V/\Delta\omega$	P_T, cc.	P_{e+a}, cc.	P_e,* cc.	μ, D.
p,p'-Dicyanobiphenyl	1.267	3.244					68.9	61.1	
Tetramethylcyclobutanedione	1.167	2.406				47–48*	38.3	37.7	0.8*
p-Dinitrobenzene	1.617	2.887	20	0.62	0.469	53.0	40.1	38.5	0.78
			30	0.54	0.472	51.1			0.74
			40	0.48	0.477	49.7			0.69
Thorium acetylacetonate	1.753	3.056	20	0.56	0.555	175.1	145.7†	127.5	1.18
			30	0.74	0.560	198.6			1.61
			40	0.94	0.572	224.3			2.00
Zirconium acetylacetonate	1.412	2.952	20	1.08	0.385	207.6	136.0†	123.5	1.85
			30	1.28	0.411	225.5			2.10
			40	1.43	0.457	236.8			2.26

Quoted from pertinent literature (4, 5).
†*These pellets contain 2% of Koroseal.*

p,p'-Dicyanobiphenyl

In our earlier publication we doubted that the total polarization of 4,4'-dinitrobiphenyl in benzene could be due to electronic plus atomic polarization alone, because our distortion-polarization determination was only 0.8 cc. more than a reasonable value for electronic polarization. Moreover, our total polarization in benzene was about 10 cc.

[1]*Manuscript received November 20, 1957.*
Contribution from the Department of Chemistry, University of Toronto, Toronto, Ontario.

lower at 40° than that found by LeFevre and Vine (2) at 25°. The latter criterion of orientation polarization may be questionable because of the low solubility at 25°. For the same reason we would not rely on the total polarization value for the dicyano analogue in benzene, either as it was reported by LeFevre and Vine (at 25°) or on our own attempt to get a meaningful value at 40°. Therefore we cannot affirm that *p,p'*-dicyanobiphenyl has an orientation polarization. But we can say that the distortion polarization of 68.9 cc. which we found by capacitance measurements on the pelleted solid can account for only 68.9 − 61.1 = 7.8 cc. of atom polarization, in contrast to the larger value (35 cc.) previously assigned (3).

Tetramethylcyclobutanedione

The total polarization of this substance has been reported as 46.9 cc. in the vapor phase (4) and 48.5 cc. in benzene (5). Since the electronic-polarization value calculated from the latest bond constants (6) accounts for only 37.4 cc., our distortion polarization, determined experimentally, would include only 0.9 cc. of atom polarization. Thus there remains about 9 cc. of polarization indicative of a low orientation polarization for this supposedly rigid molecular structure.

p-Dinitrobenzene

The dielectric constant of pellets of this substance shows that the distortion polarization is 40.1 cc., or 1.6–1.9 cc. higher than the electronic polarization calculated from group refractions. This directly determined atom polarization is somewhat lower than that postulated (4) previously (8.2 cc.). In order to confirm our result we have determined the polarization in benzene solution at 20°, 30°, and 40° C. We find (Table I and Fig. 1) that the total polarization does vary appreciably with temperature, as would be expected if it included a component of orientation polarization. Although this interpretation is contrary to that of Coop and Sutton (4) the experimental work may not be in disagreement. From the curvature of the plot of total polarization versus the reciprocal of absolute temperature (Fig. 1) it might be expected that the polarization at 200°–255° C. would be close to the 46.5 cc. that Coop and Sutton observed in their vapor phase study.

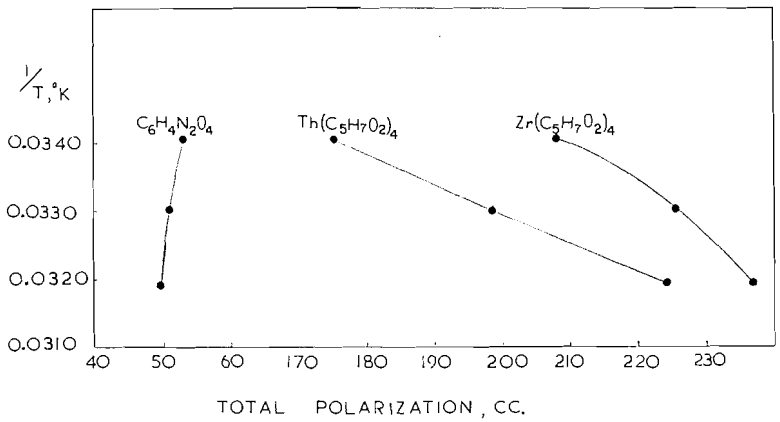

FIG. 1. Temperature coefficient of electrical polarization.

Agreement between our results and those of LeFevre and LeFevre is not as satisfactory. These workers found approximately the same polarization (46 cc.) in benzene at 25° and 45°, whereas in our apparatus (in which benzene solutions of naphthalene give

Can. J. Chem. Downloaded from www.nrcresearchpress.com by 200.7.193.243 on 09/04/12
For personal use only.

polarizations of 46.5 cc. for the latter substance both at 20° and 40°) the polarization of *p*-dinitrobenzene in benzene varies from 53.0 to 49.7 cc. over the 20° temperature range. The only difference (aside from the method of computation) apparent to us is the higher purity (m.p. 177.5°–178°) of our sublimed dinitrobenzene over that (m.p. 171°–172°) used by the earlier workers. Of course the greater precision due to improvements in electrical circuitry since 1935 may be contributory.

At any rate our results compel us to an assignment of a small but significant moment for *p*-dinitrobenzene which varies from 0.78 debye to 0.69 debye over our 20° temperature range. Since the moment decreases with increasing temperature it is unlikely to be due to out-of-plane bending of the nitro groups because of thermal agitation in a normally planar structure.

Indeed there is evidence that *p*-dinitrobenzene is normally not completely coplanar (7, 8). These structure analyses by X-ray diffraction have designated an angle of 11° 42′ between the planes of the nitro group and the benzene ring in an otherwise symmetrical molecule, but the electron density maps do not actually confirm the postulation of a centrosymmetrical molecule. In point of fact the possibility of accumulated errors (angle error ±2%) makes the X-ray diffraction study of limited value as a criterion of the out-of-plane atom distribution, which could account for the observed temperature-dependent polarization (9).

Metal Acetonylacetates

Two of these organometallic compounds have been studied. The polarizations found for thorium acetylacetonate at 20° and 30° in benzene fall in line approximately with the polarization in this solvent observed previously at 25° (10). The trend in our polarization data at 20°, 30°, and 40° is in disagreement with the previously determined vapor phase measurement, but observable decomposition (4) renders the latter observations unreliable. Of interest is the large temperature coefficient (Table I and Fig. 1) which we have observed in benzene solution. This evidence for appreciable orientation polarization (1.18–2.00 debyes from 20° to 40°) is confirmed by a separate determination of the dielectric constant of randomly distributed solid thorium acetylacetonate. Comparison of P_{e+a} (145.7 cc.) derived by this method with the P_e (127.5 cc.) calculated from refractive indices of benzene solutions (7) shows an atom polarization (P_A = 18.2 cc.) not very different from that reported for beryllium acetylacetonate (P_A = 21.2 cc.). The latter substance is the only one of the metal chelates with which a temperature–polarization study has previously been made, and the data showed that it had no permanent dipole moment (7).

Comparisons like these above are unsatisfactory in the case of zirconium tetraacetylacetonate. From the dielectric constant of the randomly oriented solid a distortion polarization (P_{e+a} = 136.0 cc.) has been calculated which is only 12.5 cc. greater than the electronic polarization calculated by Finn, Hampson, and Sutton (10). However, we are reluctant to compare any of our data for zirconium acetylacetonate with theirs. One cannot tell from the report by these authors whether their sample was pure. Neither melting point, density, nor analysis is mentioned so it is uncertain whether their sample was completely anhydrous. We have found the melting point (11) to be an unreliable criterion, but analysis for carbon, hydrogen, and water shows that our sample is pure within the limits of precision for these determinations.

The purity of our sample is important because our total solute polarizations of zirconium acetylacetonate (Table I) at 20° and 30° are both higher than that reported

Can. J. Chem. Downloaded from www.nrcresearchpress.com by 200.7.193.243 on 09/04/12
For personal use only.

(7) at 25°. Reference to Fig. 1 shows that the polarization increases markedly with increasing temperature. The line drawn through these polarization values differs from that for the thorium analogue because it is curved. This curvature might suggest a limiting temperature at which polarization is invariant.

One may be inclined to interpret these temperature-variable polarizations entirely in terms of dipole moment, but at present there is no justification for this simple interpretation. It seemed reasonable to us when we designated the temperature-dependent polarization of ferric acetylacetonate entirely in terms of dipole moment (1) because it decreased as temperature increased. Of course the opposite effect for thorium and zirconium acetylacetonates does not exclude the possiblity that these substances have dipole moments which increase because of less intramolecular hindrance at higher temperatures. In short the thorium and zirconium acetylacetonates might resemble a sterically hindered compound like 1,2-dichloroethane (3, p. 281). But also temperature-variation of atom polarization might occur as it does in substances like barium titanate (12). Such behavior would not be unexpected in these metal chelates, the molecular character of which need not entirely obliterate some salt-like properties.

It might have been expected that we would test the latter postulation by examination of the dielectric constants of the solids at different temperatures. Unfortunately we have not yet been able to devise a proper instrument for this purpose. An ultimate decision concerning the temperature-variable polarizations of thorium and zirconium acetylacetonates must await the successful construction of such apparatus.

The authors wish to thank P. Cooper, W. Boos, and M. Malaiyandi for experimental aid. The investigation could not have been made without generous financial support by the National Research Council of Canada. Mr. C. C. Meredith has given valuable advice.

EXPERIMENTAL*

Purification of Materials

The solvents used for dielectric-constant studies were purified and maintained as was described previously (1). Dicyanobiphenyl, prepared according to Ferris and Turner (13), was obtained in 70% yield, m.p. 185°–220°. After crystallization from pyridine, acetic acid, pyridine, and dioxane (m.p. 228°–232°, 39% of crude) the substance was sublimed at 180°–190° (20 mm., m.p. 232°–235°) and then crystallized (Darco) from ethanol (75 ml. per g.) to melt at 236°–237.5°. Tetramethylcyclobutanedione, synthesized from isobutyroyl chloride and triethylamine (14), was purified by repeated crystallization from benzene and finally by sublimation at 95° (750 mm.) during 4 days, repeated until a melting point of 114°–114.4° was attained. Dinitrobenzene (E.K. White Label) was sublimed repeatedly at 150°–160° (750 mm.) until it melted at 177.5°–178°. Thorium acetylacetonate (15) was crystallized from ethanol, m.p. 171°, when inserted at 155° (6° per min.). Titration with Karl Fischer reagent showed that not more than 0.15 $\pm$0.05% of water could be present.

Many crystallizations of the decahydrate of zirconium acetylacetonate (16) were required in order to remove the water. The crystallization temperature should not exceed 40°. Titration of the dehydrated form (m.p. 190°–191°) with Karl Fischer reagent showed that not more than 0.3$\pm$0.05% of water could be present. The sample used for dielectric constant determination was dried at 40° (20 mm.) for 24 hours before use. The density at 20° was found to be 1.415. According to combustion analysis the percentage of hydrogen in this sample is 5.68% as compared with 5.78% expected in $C_{20}H_{28}O_8Zr$.

Melting points have been corrected against reliable standards: Can. J. Technology, **34, 89 (1956).*

Can. J. Chem. Downloaded from www.nrcresearchpress.com by 200.7.193.243 on 09/04/12
For personal use only.

Can. J. Chem. Downloaded from www.nrcresearchpress.com by 200.7.193.243 on 09/04/12
For personal use only.

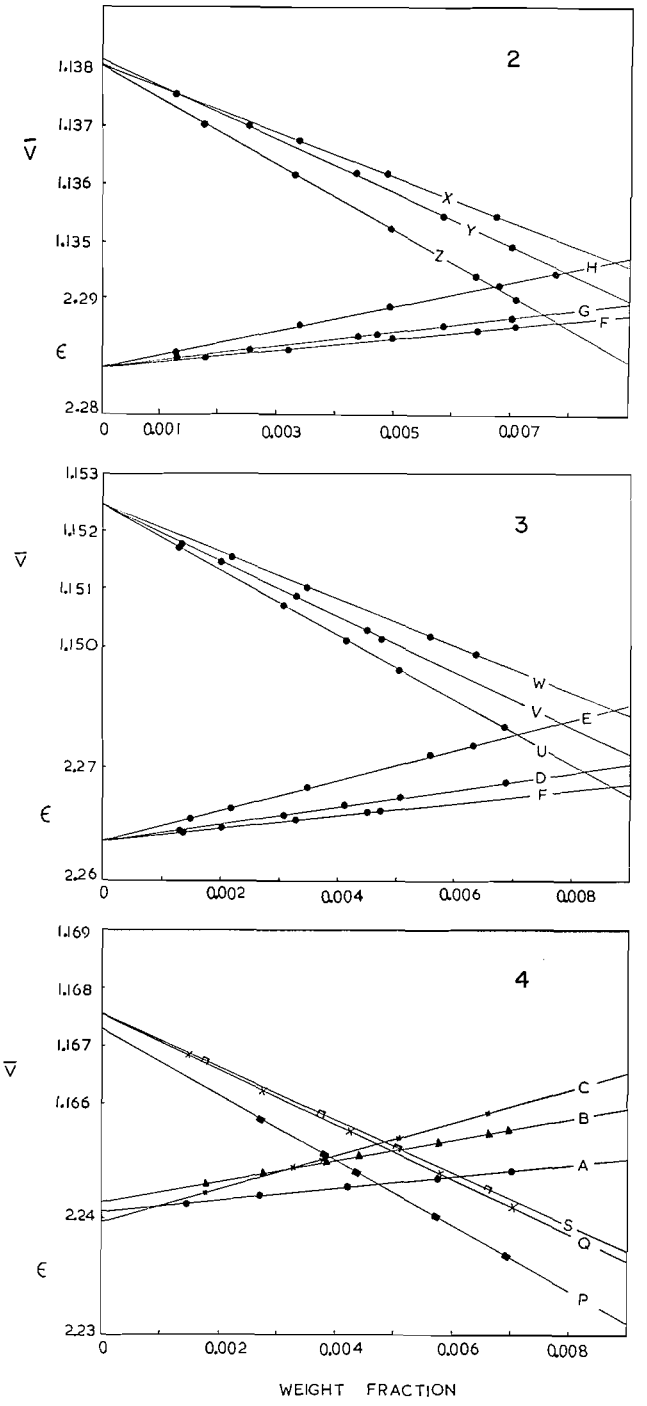

FIG. 2. Dielectric constants (*F*, *G*, *H*) and specific volumes (*Z*, *Y*, *X*) respectively for thorium acetylacetonate, *p*-dinitrobenzene, and zirconium acetylacetonate in benzene at 20°.

FIG. 3. Dielectric constants (*F*, *D*, *E*) and specific volumes (*V*, *U*, *W*) respectively for *p*-dinitrobenzene, thorium acetylacetone, and zirconium acetylacetonate in benzene at 30°.

FIG. 4. Dielectric constants (*A*, *B*, *C*) and specific volumes (*Q*, *P*, *S*) respectively for *p*-dinitrobenzene, thorium acetylacetonate, and zirconium acetylacetonate at 40°.

Density of Solids

These densities were determined by the air-displacement method described previously (17). The density determination of tetramethylcyclobutanedione was subject to error because of the significant vapor pressure of this substance. This error was evaluated and corrected after a series of analyses with samples varying in weight from 0.3 to 1.0 g.

Dielectric-Constant Measurements

The procedures and equipment described previously (1, 18) were used. A modification of the method for determination of ϵ for solids (17) involved a test capacitor built from a mild steel annulus 2.5 in. I.D. and 4 in. O.D. by 1 in. thick which was diametrically drilled for a Shardlow micrometer head at the top and a polystyrene-insulated "anvil" rigidly connected at the bottom to the ungrounded side of the VFO resonant circuit. Although this capacitor was very good for measurements at room temperature it was unsatisfactory at higher temperatures because of mechanical distortion, despite a prior normalization of the annular ring at liquid air temperatures.

The measurements in benzene solutions are shown in Figs. 2, 3, and 4. It may be seen that the dielectric constants and specific volumes are closely convergent at 20° (for benzene alone $\epsilon = 2.284$ and $\bar{V} = 1.1380$) and at 30° (for benzene alone $\epsilon = 2.263$ and $\bar{V} = 1.1525$) but at 40° (for benzene alone $\epsilon = 2.241$ and $\bar{V} = 1.1675$) two batches of benzene were used. The lack of convergence at 40° actually is less serious than is apparent. In each experiment the extrapolation to the dielectric constant and the specific volume at zero concentration is within 0.0003 and 0.0001 respectively of the values for the pure solvent (1). The differences actually are due to variations in the residual capacity following disassembly of the test capacitor. At any rate the values for the most critical of these determinations (that of the *p*-dinitrobenzene) are very close to the dielectric

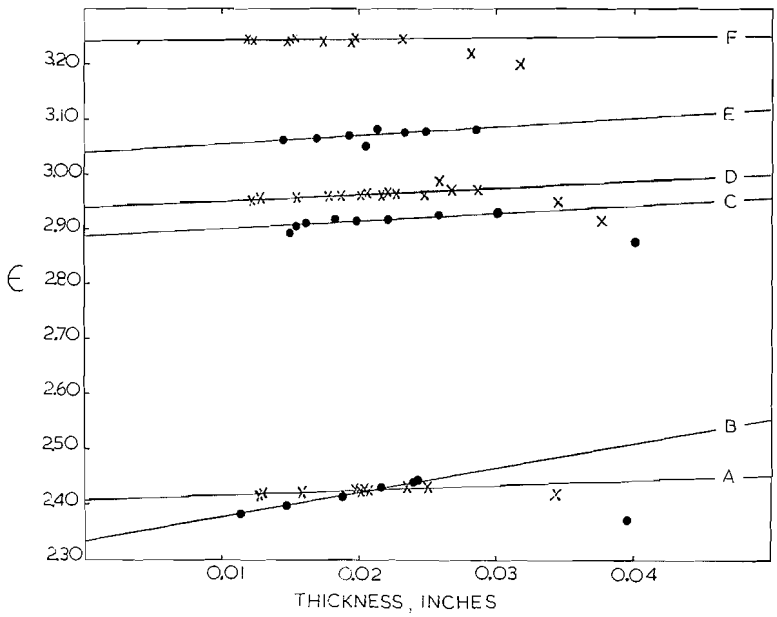

FIG. 5. Dielectric constants of solid:

A *sym*-Tetramethylcyclobutanedione
B Koroseal
C 1,4-Dinitrobenzene
D Zirconium acetylacetonate
E Thorium acetylacetonate
F 4,4-Dicyanobiphenyl

Can. J. Chem. Downloaded from www.nrcresearchpress.com by 200.7.193.243 on 09/04/12
For personal use only.

constant (2.2410) and the specific volume (1.1675) found for the pure solvent immediately after reassembly of the cell.

The dielectric constants of the solids, shown in Fig. 5, have been determined by use of gold amalgam. Included are data for the polyvinyl chloride sold under the trade name Koroseal. It is necessary to use 2% of this binder for satisfactory pelleting of some substances, such as the metal acetylacetonates marked † in Table I. In these instances a correction has been made by adding algebraically 2% of the difference between the dielectric constant of Koroseal and the mixture to the dielectric constant of the mixture.

It may be seen in Fig. 5 that the pellets of greatest thickness usually show dielectric constants lower than those falling on an extrapolatable line. It has been found by the flotation method that these pellets are less dense than those of lesser thickness. Since all pellets have been pressed at 12,000 lb. dead load, which is close to the yield-point of our dies, it is evident that thin pellets must be used for this method of determining distortion polarization.

REFERENCES

1. MEREDITH, C. C., WESTLAND, L., and WRIGHT, G. F. J. Am. Chem. Soc. **79**, 2385 (1957).
2. LEFEVRE, R. J. W. and VINE, H. J. Chem. Soc. 1878 (1938).
3. SMITH, J. W. Electric dipole moments. Butterworths Scientific Publications, London. 1955. p. 272.
4. COOP, I. E. and SUTTON, L. E. J. Chem. Soc. 1269 (1938).
5. HAMMICK, D. L., HAMPSON, G. C., and JENKINS, G. I. J. Chem. Soc. 1263 (1938).
6. VOGEL, A. I., CRESSWELL, W. T., JEFFREY, G. H., and LEICESTER, J. J. Chem. Soc. 514 (1952).
7. LLEWELLYN, F. J. J. Chem. Soc. 884 (1947).
8. ABRAHAMS, S. C. and ROBERTSON, J. M. Nature, **160**, 569 (1947).
9. LEFEVRE, C. G. and LEFEVRE, R. J. W. J. Chem. Soc. 957 (1935).
10. FINN, A. E., HAMPSON, G. C., and SUTTON, L. E. J. Chem. Soc. 1254 (1938).
11. BILTZ, W. and CLINCH, J. A. Z. anorg. Chem. **40**, 218 (1904).
12. SMYTH, C. P. Dielectric behavior and structure. McGraw-Hill Book Co., Inc., New York. 1955. p. 195.
13. FERRIS, C. V. and TURNER, E. E. J. Chem. Soc. **117**, 1140 (1920).
14. MILLER, L. L. and JOHNSON, J. R. J. Org. Chem. **1**, 135 (1936).
15. BILTZ, W. Ann. **331**, 336 (1901).
16. VON HEVESY, G. and LÖGSTRUP, M. Ber. **59**, 1890 (1926).
17. GEORGE, M. V. and WRIGHT, G. F. Can. J. Chem. **36**, 189 (1958).
18. MEREDITH, C. C. and WRIGHT, G. F. Can. J. Technol. **33**, 182 (1955).

Can. J. Chem. Downloaded from www.nrcresearchpress.com by 200.7.193.243 on 09/04/12
For personal use only.

Can. J. Chem. Downloaded from www.nrcresearchpress.com by 200.7.193.243 on 09/04/12
For personal use only.

THE SYNTHESIS OF CRYPTOPLEURINE AND RELATED PHENANTHROQUINOLIZIDINES[1]

P. MARCHINI[2] AND B. BELLEAU

ABSTRACT

The synthesis of the alkaloid cryptopleurine has been accomplished by a sequence involving as the key step the cyclization of amino acid XII. It was established that the approach is applicable to the synthesis of simpler phenanthroquinolizidines such as IV. The biogenesis of the alkaloid is briefly discussed.

INTRODUCTION

The structure of the unusual alkaloid cryptopleurine (1) was deduced by Fridrichsons and Mathieson (2) by an X-ray investigation and its chemistry examined by Gellert (3). The remarkable physiological properties of this alkaloid have been described by de La Lande (1). Recently Bradsher and Berger (4) reported on a synthesis of cryptopleurine through the application of the general method already developed by Bradsher and Beavers (5, 6) for the synthesis of polycondensed quinolizines. In an independent investigation which was completed at the time Bradsher's report appeared, we accomplished the synthesis of cryptopleurine by a different route involving a series of well-characterized intermediates. Our approach differs from that of Bradsher's in that only reduced quinolizines are involved as intermediates (Chart I).

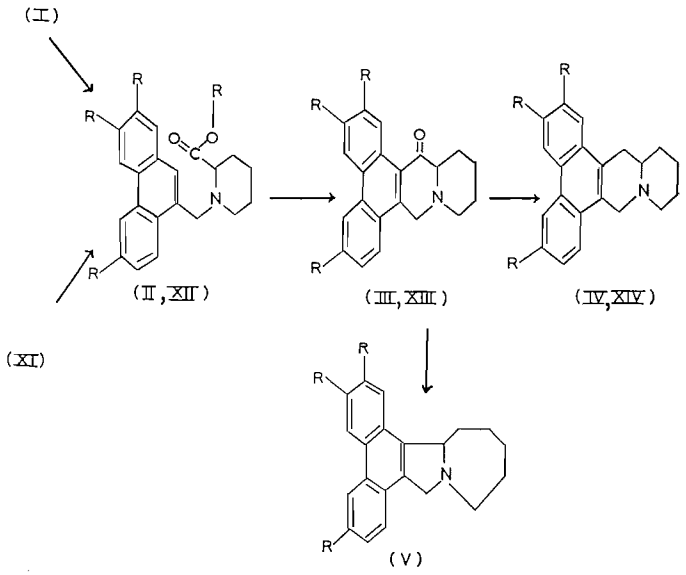

II, III, IV, V, R = H.
XII, XIII, XIV, R = CH_3O—.

CHART I.

In a model experiment, the synthesis of the phenanthroquinolizidone III was attempted through cyclization of the amino acid II, which was readily obtained from 9-chloromethylphenanthrene and methyl pipecolate followed by acid hydrolysis; this amino acid (II)

[1]*Manuscript received November 14, 1957.*
Contribution from the Department of Biochemistry, School of Medicine, Laval University, Quebec, Que.
[2]*Postdoctorate Fellow of the National Research Council of Canada (1956–1958).*

was heated to 100° in polyphosphoric acid whereupon smooth ring closure to the desired amino ketone (III) occurred in 50% yield. Optimum conditions for this conversion were studied and are given in the experimental section. Evidence for structure III is based on elemental analysis, the infrared absorption spectrum which includes a strong band at 1664 cm.$^{-1}$ characteristic of an aromatic ketone, and the ultraviolet spectrum (curve B, Fig. 1) which shows the characteristic secondary peak of 9-phenanthryl ketones at 320 mμ (7,8). Reduction of the ketone (III) by the Huang-Minlon (9) procedure afforded

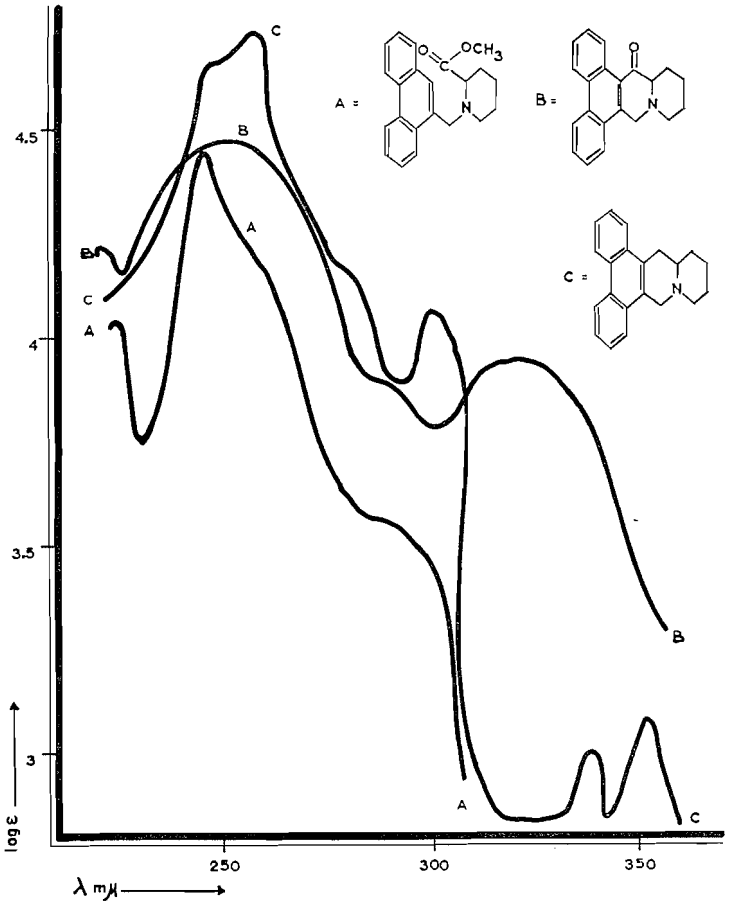

FIG. 1.

the desired phenanthroquinolizidine (IV) in high yield. Its ultraviolet absorption spectrum (curve C, Fig. 1) shows only the characteristic absorption bands of the phenanthrene nucleus, as expected. It is pertinent to note that Clemmensen reduction of the ketone (III) also produced a crystalline base in high yield of identical composition, but different from the one obtained by Wolff-Kishner reduction. Structure V is assigned to this product on the basis of the previous observations of Leonard and Wildman (10) on the reductive rearrangement of 1-quinolizidones.

With these results on hand, the synthesis of cryptopleurine itself could be considered, and a sequence of reactions also adopted by Bradsher (4) for the preparation of 9-bromomethyl-2,3,6-trimethoxyphenanthrene was carried out. Details of this synthesis are given in the experimental section and differ from Bradsher's synthesis in that only the

Can. J. Chem. Downloaded from www.nrcresearchpress.com by 200.7.193.243 on 09/04/12
For personal use only.

pure crystalline 9-chloromethyl derivative was used as a key intermediate. Reaction of the latter with methyl pipecolate followed by hydrolysis gave the amino acid (XII), which underwent smooth ring closure to 1-cryptopleurinone (XIII) when heated in polyphosphoric acid. The ultraviolet spectrum of the latter was recorded and as can be seen in Fig. 2 (curve E), the principal maxima exhibit a bathochromic shift with respect to the phenanthrene series and although the spectrum is similar to the one reported for

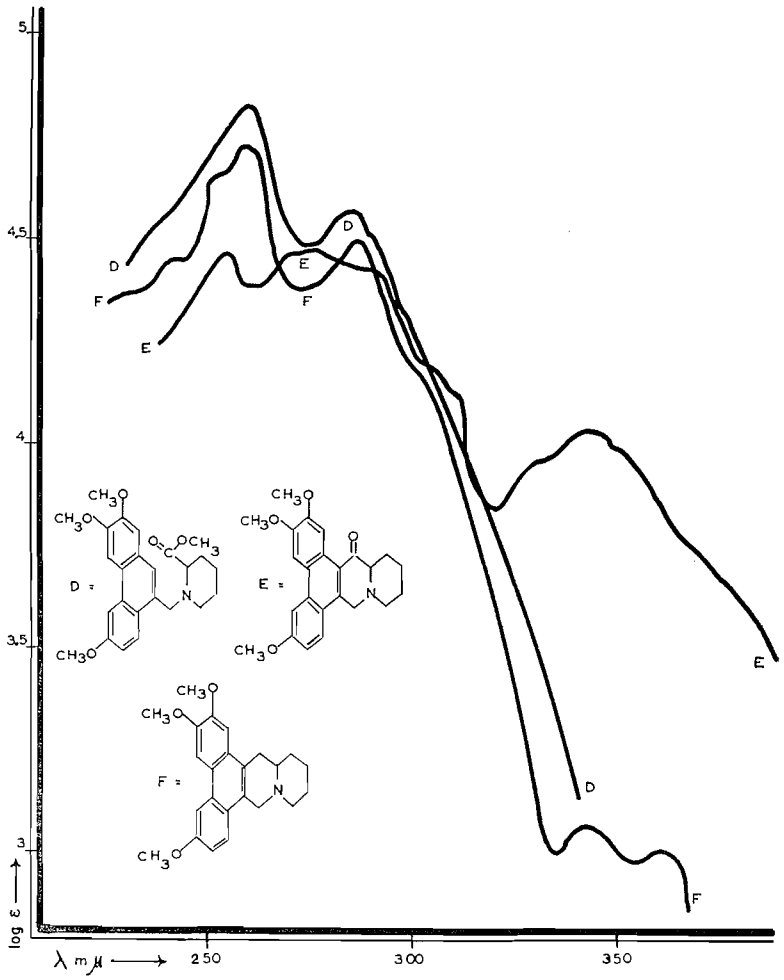

FIG. 2.

cryptopleurine, the peak at 345 mμ is of much greater intensity. Wolff-Kishner reduction of this ketone (XIII) gave rise to a mixture of phenolic compounds from which after treatment with diazomethane a small amount of crystalline material was obtained. The identity of the latter with cryptopleurine was ascertained by mixed melting point determination and by comparison of the infrared spectrum with an authentic specimen kindly provided by Dr. Bradsher. It should be noted that the spectrum was virtually superimposable on that of cryptopleurine except for the presence of a low-intensity band at 1700 cm.$^{-1}$ which is absent in the authentic specimen. It is most probable that this minor difference can be attributed to the presence of trace amounts of unchanged starting material in our sample or to deterioration of the latter on storage. The instability of

Can. J. Chem. Downloaded from www.nrcresearchpress.com by 200.7.193.243 on 09/04/12
For personal use only.

cryptopleurine has been commented upon before by Gellert (3). The small amount of material available precluded further purification or the preparation of the stable methiodide.

Additional proof of the identity of our material with cryptopleurine was obtained by comparison of the respective ultraviolet spectra, which proved to be identical in every respect (curve F, Fig. 2).

In view of Bradsher's recent report (4), no effort was made to improve the yield at the final stage of reduction although there can be little doubt that other procedures could be more successful.

The structure of cryptopleurine being of a novel type, it is of interest to attempt uncovering its biogenetical links with other classes of alkaloids. Robinson (11) suggested that the alkaloid originates from two tyrosine and one lysine unit. However, no mechanism was offered in support of this idea and we would like to suggest the scheme outlined in Chart II.

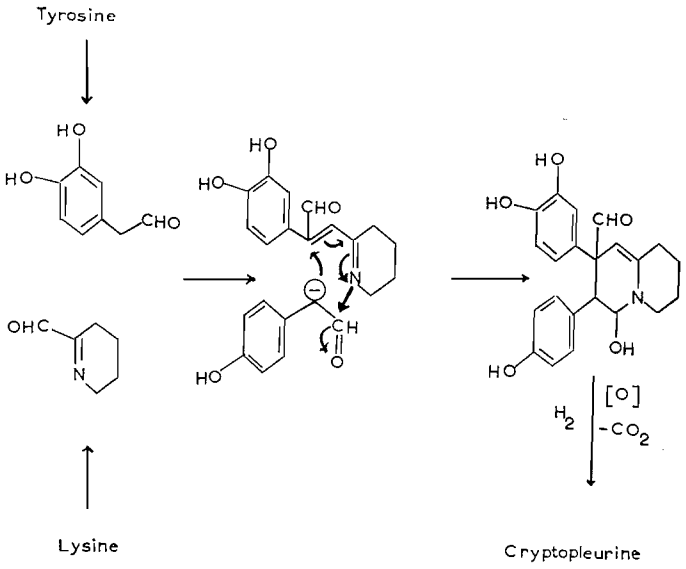

CHART II.

EXPERIMENTAL*

The spectra were determined with a Beckman spectrophotometer, Model DU, in 95% ethanol. Melting points are uncorrected and were obtained with a hot-stage microscope.

The pipecolic acid methyl ester was prepared by esterification of picolinic acid followed by hydrogenation in the presence of platinum oxide according to the procedure described by Tilford and co-workers (12).

The chloromethylphenanthrene was obtained by chloromethylation of phenanthrene as reported by Badger and co-workers (13).

Methyl N-(9-Phenanthrylmethyl)-pipecolate (1)

To a solution of 7 g. of methyl pipecolate in 150 ml. of methyl alcohol, containing 1.4 g. of potassium carbonate (freshly fused), 8.6 g. of 9-chloromethylphenanthrene was added at once. The mixture was then heated at 60°–70° and stirred for 12 hours. The suspension was evaporated almost to dryness and poured into water, and then extracted

**Microanalyses by Midwest Microlaboratories Inc., Indianapolis, Indiana, and Messrs. B. Girard and B. Mercier of our laboratories.*

Can. J. Chem. Downloaded from www.nrcresearchpress.com by 200.7.193.243 on 09/04/12
For personal use only.

with ether. The ethereal solution was washed with water, dried with sodium sulphate, and evaporated to a small volume. Treatment with dry hydrogen chloride gave a precipitate which after crystallization from acetone–ethyl acetate weighed 5 g., m.p. 177°–178°. λ_{max}: 255, 260, 289 mμ; log ε: 4.45, 4.40, 3.98 (curve A, Fig. 1). Calc. for $C_{22}H_{23}NO_2$. $HCl.H_2O$: C, 68.21; H, 6.70; N, 3.61. Found: C, 68.60; H, 6,92; N, 4.07.

Hydrolysis to the amino acid was accomplished by refluxing 5.5 g. of the ester (1) for 2 hours in 100 ml. of concentrated hydrochloric acid. After evaporation to half volume and cooling, 5.3 g. of crystalline material (II) was collected, m.p. 195°–200°. Calc. for $C_{21}H_{21}NO_2.HCl$: N, 3.9. Found: N, 3.8.

Phenanthro-(9,10;2,3)-1-quinolizidone (III)

To a solution of 10 g. of phosphorus pentoxide in 10 g. of sirupy phosphoric acid, 3 g. of the acid II was added at once. The mixture was heated to 100° for 6 hours with rapid stirring. After cooling the mixture was poured into ice-water, made alkaline with 50% sodium hydroxide solution, and extracted with chloroform.

The chloroform solution was washed with water, dried, and evaporated. The residue (III), weighing 1.4 g., crystallized from chloroform–methanol in light yellow prisms, m.p. 168°–169°. Calc. for $C_{21}H_{19}NO$: C, 83.74; H, 6.38; N, 4.64. Found: C, 83.46; H, 6.43; N, 4.62. The infrared spectrum showed (nujol mull) a strong band at 1664 $cm.^{-1}$. λ_{max}: 250, 260, 285, 320 mμ; log ε: 4.47, 4.42, 3.95, 3.95 (see Fig. 1, curve B).

Phenanthro-(9,10;2,3)-quinolizidine (IV)

To a solution of 0.6 g. of potassium hydroxide in 7 ml. ethylene glycol and 1 ml. hydrazine hydrate 0.5 g. of the ketone III was added. After refluxing for 1 hour (9), water was distilled, and distillation continued until the temperature of the vapors reached 195°; the mixture was then heated to 200° for 6 hours. The mixture was poured into water and extracted with ether. After evaporation of the solvent, the solid material was dissolved in hot ethanol and allowed to stand overnight: 0.3 g. of white needles was obtained, m.p. 169°–170° (sublimes at 155°). Calc. for $C_{21}H_{21}N$: C, 87.82; H, 7.31; N, 4.87. Found: C, 87.68; H, 7.52; N, 4.76. λ_{max}: 255, 260, 289, 330, 353 mμ; log ε: 4.48, 4.42, 3.90, 3.03, 3.07 (see Fig. 1, curve C).

3,4-Phenanthro-1-azabicyclo[0,3,5]decane (V)

To a refluxing solution of 0.4 g. of ketone III in 50 ml. of hydrochloric acid and water (3:1), 2.5 g. of zinc amalgam was added in small portions over a period of 4 hours. Every hour, 5 ml. of concentrated hydrochloric acid was added. After cooling, the solution was made alkaline and extracted with chloroform. The chloroform solution was evaporated and the residue dissolved in benzene. After filtration through a small column of basic alumina, the solution was evaporated to dryness. The solid material so obtained by crystallization from methanol gave 0.25 g. of white needles melting at 164°. Calc. for $C_{21}H_{21}N$: C, 87.82; H, 7.31; N, 4.87. Found: C, 87.46; H, 8.19; N, 5.05.

6-Nitro-3,4,4'-trimethoxy-α-phenylcinnamic Acid (VI)

Upon heating under reflux for 24 hours 58 g. of 6-nitroveratraldehyde (14) with 60 g. of homoanisic acid (15) in 300 ml. of acetic anhydride containing 5 g. of potassium acetate, 50 g. of crude product was obtained. After several crystallizations from acetic acid the m.p. was constant at 183°–184° (reported 185°–186°) (yield 38 g.).

2,3,6-Trimethoxyphenanthrene-9-carboxylic Acid (VII)

The preceding compound (37 g.) was dissolved in 112 ml. of 14% aqueous ammonia, and the resulting solution added at once to a hot solution of 228 g. of ferrous sulphate in

Can. J. Chem. Downloaded from www.nrcresearchpress.com by 200.7.193.243 on 09/04/12
For personal use only.

1 l. of 14% aqueous ammonia; the temperature was then maintained at 90° for a further 30 minutes. After cooling, careful neutralization of the mixture gave 30 g. of the corresponding amino acid. After several crystallizations from dilute ethanol, 25 g. of silky yellow crystals were obtained, m.p. 203°–204° (reported 206°–207°). Calc. for $C_{18}H_{19}NO_5$: N, 4.25%. Found: N, 4.23%.

This amino acid (23 g.) was suspended in 1400 ml. of water followed by the addition of 100 ml. of concentrated hydrochloric acid and 400 ml. dioxane. The mixture was cooled to 3°–5° and a solution of 9 g. of sodium nitrite in 100 ml. of water was added dropwise over a period of 2 hours, the temperature being kept below 5°. The clear, dark brown solution was then stirred for an additional 90 minutes.

After this time, 20 g. of activated copper bronze was added and stirring continued at room temperature for 24 hours. Evaporation *in vacuo* to half volume gave an amorphous precipitate which was collected by filtration and dissolved in chloroform. Evaporation of the solvent and crystallization of the residue from acetic acid afforded 12 g. of white crystalline material, m.p. 219°–220° (reported 222°). λ_{max}: 260, 280, 285 mμ; log ϵ: 4.58, 4.36, 4.33.

2,3,6-Trimethoxyphenanthrene-9-carboxylic Acid Methyl Ester (VIII)

The preceding acid (11.5 g.) (VIII) was heated under reflux for 2 hours in 250 ml. of methanol containing 15 ml. of sulphuric acid. The solution was then poured on ice and extracted with chloroform. Evaporation *in vacuo* left 10 g. of crude solid material. Chromatography on neutral alumina afforded in the petroleum ether eluate 5.4 g. of white crystals which crystallized from ethyl acetate – isopropyl alcohol, m.p. 156°–157°.* Calc. for $C_{19}H_{18}O_5$: C, 66.87; H, 5.52. Found: C, 66.76; H, 5.43. Extraction of the alumina with hot methanol gave 2 g. of white crystalline material, m.p. 85°–86°, which was not examined further.

2,3,6-Trimethoxy-9-phenanthrenemethanol (IX)

A solution of 5 g. of VIII in tetrahydrofuran was added dropwise with cooling to a suspension of 2.5 g. of lithium aluminum hydride in 100 ml. of ether. The mixture was then heated under reflux for 90 minutes, the excess of hydride decomposed with ethyl acetate, and the mixture poured into water and extracted with chloroform–ether. Evaporation of the solvent gave 4.5 g. of white solid mass. Crystallization from ethanol gave 4 g. of white silky needles, m.p. 186° (reported 185°–187°).

2,3,6-Trimethoxy-9-chloromethylphenanthrene (X)

To a solution of 3.7 g. of IX in 170 ml. of anhydrous chloroform containing 2.2 ml. of pyridine was added dropwise 2.96 ml. of thionyl chloride at ice temperature. The reaction was brought to completion by heating at 40°–60° while stirring for 60 minutes. The mixture was then poured on ice, and the chloroform layer separated, washed with dilute bicarbonate solution, then with water, and dried. The residue obtained by evaporation of the solvent was crystallized from benzene and weighed 3.45 g., m.p. 150°–151°. Calc. for $C_{18}H_{17}O_3Cl$: C, 68.35; H, 5.35; Cl, 11.08. Found: C, 68.11; H, 5.56; Cl, 11.30.

Methyl 2,3,6-Trimethoxy-N-9-phenanthrylmethyl-pipecolate (XI)

A mixture of 3 g. of X and 6 g. of methyl pipecolate as free base† in 100 ml. of anhydrous toluene was heated under reflux with stirring for 20 hours.

The residue obtained after evaporation of the solvent was poured into water and the

**The ethyl ester of III prepared in an analogous way was crystallized from ethanol and melted at 137° (reported 136.5°–137°).*

†The base was prepared by treatment of the hydrochloride with sodium methoxide at room temperature for 12 hours and vacuum distillation, b.p. 88°/16 mm.

Can. J. Chem. Downloaded from www.nrcresearchpress.com by 200.7.193.243 on 09/04/12
For personal use only.

pH adjusted to 9 with alkali followed by extraction with chloroform. After it was washed with water, the solution was dried and evaporated to dryness to yield a solid which was dissolved in a small volume of ether. Treatment of this solution with dry hydrogen chloride gave a precipitate which crystallized from acetone – ethyl acetate. The weight of the hydrochloride was 4.7 g., m.p. 165°–167°. λ_{max}: 250, 260, 285 mμ; log ε: 4.67, 4.80, 4.55 (see Fig. 2, curve D). Calc. for $C_{25}H_{29}O_5N.HCl.\frac{1}{2}H_2O$: C, 64.10; H, 6.41; N, 3.00. Found: C, 63.49; H, 6.84; N, 3.03.

2,3,6-Trimethoxyphenanthro-(9,10;2,3)-1-quinolizidone (XIII)

The above ester (XI) was hydrolyzed by heating for 90 minutes in 80 ml. of hydrochloric acid. After cooling a microcrystalline material was collected and dried, and without further purification, 2.4 g. of this amino acid (XII) was added to a mixture of 10 g. of phosphorus pentoxide and 10 g. of phosphoric acid and the solution heated for $3\frac{1}{2}$ hours. After cooling, the violet mixture was slowly poured on ice, and after 50% potassium hydroxide solution had been added to pH 9, the mixture was extracted with chloroform.

The solution was washed with water, dried, and evaporated *in vacuo* under nitrogen to give 1 g. of a slightly yellow solid which crystallized from acetone–methanol as yellow prisms, m.p. 154.5°–155°. λ_{max}: 255, 270, 290, 310, 345 mμ; log ε: 4.42, 4.51, 4.40, 4.02, 4.01 (see Fig. 2, curve E). Calc. for $C_{24}H_{25}O_4N$: C, 73.66; H, 6.39. Found: C, 73.87; H, 6.84.

2,3,6-Trimethoxyphenanthro-(9,10;2,3)-quinolizidine (XIV)

The reduction of 0.45 g. of XIII was effected as described above in the case of IV except that the reaction was carried out under nitrogen. The crude reaction product was chromatographed on basic alumina but no pure substance could be obtained from the various eluates. A ferric chloride test was strongly positive for all of the main fractions; a 0.25 g. portion of the brown waxy material was therefore treated in methanol–ether with a large excess of diazomethane and allowed to stand overnight.

Evaporation of the solvent *in vacuo* gave an oil which was dissolved in ether and extracted with dilute hydrochloric acid. Neutralization of the acidic solution gave a precipitate which was extracted with ether. After evaporation of the solvent, the residue was dissolved in a small volume of acetone and allowed to stand at −10°. The solution slowly deposited 5 mg. of light yellow needles which after several recrystallizations had m.p. 199°–201° (reported 197°–198° (3), 199°–200° (4)). Mixture with an authentic specimen of cryptopleurine gave no depression of the melting point. λ_{max}: 258, 286, 345, 358 mμ; log ε, 4.70, 4.47, 3.12, 2.97.

The infrared spectrum was recorded with a Baird double-beam instrument using the KBr pellet technique. The spectrum was identical to that of cryptopleurine except for the presence of a low-intensity band at 1700 $cm.^{-1}$.

ACKNOWLEDGMENTS

We express our gratitude to Dr. C. K. Bradsher for supplying an authentic specimen of cryptopleurine and to Dr. H. Hooper of Bristol Laboratories Inc. for the infrared determinations. We also express our thanks to the National Research Council of Canada for a fellowship to one of us (P.M.) and for financial assistance.

REFERENCES

1. DE LA LANDE, I. S. Australian J. Exptl. Biol. Med. Sci. **26**, 181 (1948).
2. FRIDRICHSONS, J. and MATHIESON, A. M. Acta Cryst. **8**, 761 (1955).
3. GELLERT, E. and RIGGS, N. V. Australian J. Chem. **7**, 113 (1954).

Can. J. Chem. Downloaded from www.nrcresearchpress.com by 200.7.193.243 on 09/04/12
For personal use only.

4. BRADSHER, C. K. and BERGER, H. J. Am. Chem. Soc. **79**, 3287 (1957).
5. BRADSHER, C. K. and BEAVERS, L. E. J. Am. Chem. Soc. **77**, 4812 (1955).
6. BRADSHER, C. K. and BEAVERS, L. E. J. Am. Chem. Soc. **78**, 2459 (1956).
7. JONES, R. N. J. Am. Chem. Soc. **65**, 1818 (1943).
8. JONES, R. N. J. Am. Chem. Soc. **67**, 1956 (1945).
9. HUANG-MINLON. J. Am. Chem. Soc. **68**, 2487 (1946).
10. LEONARD, N. J. and WILDMAN, W. C. J. Am. Chem. Soc. **71**, 3089 (1949).
11. ROBINSON, R. The structural relations of natural products. Clarendon Press, Oxford. 1955. p. 78.
12. TILFORD, C. H. and VAN CAMPEN, M. G., Jr. J. Am. Chem. Soc. **76**, 2431 (1954).
13. BADGER, G. M., CARRUTHER, W., COOK, J. W., and SCHOENTAL, R. J. Chem. Soc. 169 (1949).
14. Org. Syntheses, **33**, 65 (1953).
15. WENNER, W. J. Org. Chem. **15**, 548 (1950).

Can. J. Chem. Downloaded from www.nrcresearchpress.com by 200.7.193.243 on 09/04/12
For personal use only.

Can. J. Chem. Downloaded from www.nrcresearchpress.com by 200.7.193.243 on 09/04/12
For personal use only.

NOTES

THE REDUCTION OF SOME HALOGENATED COMPOUNDS BY CHROMOUS CHLORIDE

F. A. L. Anet and Elaine Isabelle

Reduction of annotinine chlorohydrin by chromous chloride gave two compounds (1, 2), (*a*) "hydroxylactone" and (*b*) "unsaturated lactone A", neither of which was the "normal" reduction product which would be formed by replacement of chlorine by hydrogen. Anet and Marion (2) suggested that these two compounds were formed by 1,2-elimination, analogous to the reduction of *vic*-dibromides to alkenes (3), and involving a chlorine atom and a β-nitrogen atom in the case of the "hydroxylactone", and a chlorine atom and a β-hydroxyl group in the case of the "unsaturated lactone A".

In order to obtain analogies for the reduction of annotinine chlorohydrin, whose structure is now firmly established (4, 5), we have studied the chromous chloride reduction of some simple β-halogenated alcohols and amines. 2-Chloroethanol was not reduced under the conditions used. 2-Bromoethanol was reduced slowly and gave 20% ethylene, isolated as the dibromide, but a considerable amount of starting product was hydrolyzed. 2-Bromoethylamine was reduced to a mixture of ethylamine, ammonia, and ethylene. In this case the "normal" reduction product, formed by simple replacement of halogen by hydrogen, was a reaction product, whereas the "normal" reduction product of annotinine chlorohydrin has not been observed. Nevertheless, the same type of reduction was found in the simple model compounds as occurred in annotinine chlorohydrin.

EXPERIMENTAL

Preparation of Aqueous Chromous Chloride Solution

Chromic chloride hexahydrate (100 g.) was dissolved in 15% hydrochloric acid (600 ml.) and reduced with amalgamated mossy zinc (100 g.) under an atmosphere of nitrogen. An apparatus of the type suggested by Lingane and Pecsok (6) was used for the reduction and storage of the reagent.

Reduction of 2-Chloroethanol

2-Chloroethanol (0.1 mole) was treated with chromous chloride solution (0.2 mole) under an atmosphere of nitrogen. The reaction mixture was heated under reflux for 3 hours and all escaping vapors were passed through an all-glass system to a series of bromine traps. During this time there was no evidence of any evolution of gas and no visible loss of blue color in the chromous solution. The bromine in the traps on being worked up yielded no trace of ethylene bromide, and distillation of the reaction mixture yielded no ethanol.

Reduction of 2-Bromoethanol

2-Bromoethanol (0.05 mole) was reduced with chromous chloride solution (*ca.* 0.1 mole). The mixture was heated under reflux in an atmosphere of nitrogen for 3 hours during the last half-hour of which a slow stream of nitrogen was allowed to pass through the system to entrain any ethylene produced and carry it to the bromide absorption traps. A trap containing water was placed before the bromide traps to scrub out any ethanol entrained.

The dibromide collected was washed with water and sodium carbonate solution until colorless. The dibromide layer was separated, the washings extracted with ether, and the combined extract, after being dried over calcium chloride, yielded on distillation 2.1 g. of pure ethylene dibromide (22% yield).

A Schotten–Baumann reaction modified (7) to detect small quantities of ethanol in aqueous solution failed to produce any ethanol derivative either from the water trap or from the initial distillate of the reaction mixture.

Control on Hydrolysis of 2-Bromoethanol

2-Bromoethanol (5 g.) was heated under reflux with 15% hydrochloric acid (30 ml.) for 3 hours. The mixture was salted out with sodium chloride and extracted five times with small quantities of ether. The ether extracts were combined, dried over magnesium sulphate, and evaporated, leaving slightly less than 1 g. of residual oil.

Reduction of 2-Bromoethylamine Hydrobromide

2-Bromoethylamine hydrobromide (0.05 mole) was reduced under nitrogen with chromous chloride solution (0.1 mole) by heating under reflux for 3 hours. The ethylene evolved was converted to the dibromide as described above, yield 4.6 g. (49%).

The residue was rendered alkaline with sodium hydroxide and steam-distilled into a dilute hydrochloric acid solution. The acidic solution was evaporated to dryness, yielding 3.49 g. of white solid. By fractional crystallization from ethanol the ammonium chloride was separated from ethylamine hydrochloride, m.p. 96°–98°, which did not depress the melting point of a known sample of ethylamine hydrochloride, and formed a benzoyl derivative, m.p. 70° (lit. m.p. 71° (8)). The ammonium chloride was estimated to comprise approximately 60% of the mixture, the ethylamine hydrochloride 40%.

ACKNOWLEDGMENT

The authors are indebted to the National Research Council for a grant in support of this work.

1. MEIER, H. L., MEISTER, P. D., and MARION, L. Can. J. Chem. **32**, 268 (1954).
2. ANET, F. A. L. and MARION, L. Can. J. Chem. **33**, 849 (1955).
3. JULIAN, P. L., COLE, W., MAGNANI, A., and MEYER, E. W. J. Am. Chem. Soc. **67**, 1728 (1945).
4. WIESNER, K., AYER, W. A., FOWLER, L. R., and VALENTA, Z. Chem. & Ind. 564 (1957).
5. MARION, L. and PRZYBYLSKA, M. Can. J. Chem. **35**, 1075 (1957).
6. LINGANE, J. J. and PECSOK, R. L. Anal. Chem. **20**, 425 (1948).
7. HENSTOCK, H. J. Chem. Soc. 216 (1933).
8. SHRINER, R. L., FUSON, R. C., and CURTIN, D. Y. The systematic identification of organic compounds. John Wiley & Sons, Inc., New York. p. 288.

RECEIVED OCTOBER 29, 1957.
DEPARTMENT OF CHEMISTRY,
UNIVERSITY OF OTTAWA,
OTTAWA, CANADA.

GAS–LIQUID PARTITION CHROMATOGRAPHY OF ORGANIC SULPHUR COMPOUNDS[1]

C. H. AMBERG

To assist in the identification of organic sulphur compounds in cracked distillates derived from Canadian crudes the relative elution times of a number of such compounds

[1]*Issued as N.R.C. No. 4615.*

Can. J. Chem. Downloaded from www.nrcresearchpress.com by 200.7.193.243 on 09/04/12
For personal use only.

The dibromide collected was washed with water and sodium carbonate solution until colorless. The dibromide layer was separated, the washings extracted with ether, and the combined extract, after being dried over calcium chloride, yielded on distillation 2.1 g. of pure ethylene dibromide (22% yield).

A Schotten–Baumann reaction modified (7) to detect small quantities of ethanol in aqueous solution failed to produce any ethanol derivative either from the water trap or from the initial distillate of the reaction mixture.

Control on Hydrolysis of 2-Bromoethanol

2-Bromoethanol (5 g.) was heated under reflux with 15% hydrochloric acid (30 ml.) for 3 hours. The mixture was salted out with sodium chloride and extracted five times with small quantities of ether. The ether extracts were combined, dried over magnesium sulphate, and evaporated, leaving slightly less than 1 g. of residual oil.

Reduction of 2-Bromoethylamine Hydrobromide

2-Bromoethylamine hydrobromide (0.05 mole) was reduced under nitrogen with chromous chloride solution (0.1 mole) by heating under reflux for 3 hours. The ethylene evolved was converted to the dibromide as described above, yield 4.6 g. (49%).

The residue was rendered alkaline with sodium hydroxide and steam-distilled into a dilute hydrochloric acid solution. The acidic solution was evaporated to dryness, yielding 3.49 g. of white solid. By fractional crystallization from ethanol the ammonium chloride was separated from ethylamine hydrochloride, m.p. 96°–98°, which did not depress the melting point of a known sample of ethylamine hydrochloride, and formed a benzoyl derivative, m.p. 70° (lit. m.p. 71° (8)). The ammonium chloride was estimated to comprise approximately 60% of the mixture, the ethylamine hydrochloride 40%.

ACKNOWLEDGMENT

The authors are indebted to the National Research Council for a grant in support of this work.

1. MEIER, H. L., MEISTER, P. D., and MARION, L. Can. J. Chem. **32**, 268 (1954).
2. ANET, F. A. L. and MARION, L. Can. J. Chem. **33**, 849 (1955).
3. JULIAN, P. L., COLE, W., MAGNANI, A., and MEYER, E. W. J. Am. Chem. Soc. **67**, 1728 (1945).
4. WIESNER, K., AYER, W. A., FOWLER, L. R., and VALENTA, Z. Chem. & Ind. 564 (1957).
5. MARION, L. and PRZYBYLSKA, M. Can. J. Chem. **35**, 1075 (1957).
6. LINGANE, J. J. and PECSOK, R. L. Anal. Chem. **20**, 425 (1948).
7. HENSTOCK, H. J. Chem. Soc. 216 (1933).
8. SHRINER, R. L., FUSON, R. C., and CURTIN, D. Y. The systematic identification of organic compounds. John Wiley & Sons, Inc., New York. p. 288.

RECEIVED OCTOBER 29, 1957.
DEPARTMENT OF CHEMISTRY,
UNIVERSITY OF OTTAWA,
OTTAWA, CANADA.

GAS–LIQUID PARTITION CHROMATOGRAPHY OF ORGANIC SULPHUR COMPOUNDS[1]

C. H. AMBERG

To assist in the identification of organic sulphur compounds in cracked distillates derived from Canadian crudes the relative elution times of a number of such compounds

[1]*Issued as N.R.C. No. 4615.*

Can. J. Chem. Downloaded from www.nrcresearchpress.com by 200.7.193.243 on 09/04/12
For personal use only.

have been measured by gas–liquid partition chromatography (GLPC). The results are recorded in the accompanying table. Few references to the separation of organic sulphur compounds by GLPC have so far appeared in the literature (1, 2, 3).

EXPERIMENTAL

The samples were eluted with nitrogen from glass columns containing tricresyl phosphate supported on Johns-Manville C-22 firebrick in the ratio 2:5 w/w. Particle sizes were 35–80 mesh for columns up to 12 ft. in length and 35–60 mesh for 18-ft. columns. The injection system consisted of a heated chamber at the column head; inside the chamber were two disks of 60-mesh stainless-steel gauze from which the liquid was flashed on to the column packing after having been introduced in the usual manner by a syringe through a self-sealing rubber cap. Flow rates were in the range 25–40 ml./min. with 1 atmosphere pressure at the column head and pressures down to 5 mm. Hg at the outlet. A thermal conductivity gauge served as monitor for the effluent stream; both the detector and reference elements were placed at the column outlet with liquid nitrogen traps interposed between the two. The traps were designed to fit directly onto a mass spectrometer. In this manner the mass spectra of separate eluate fractions could be determined.

The standard liquids indicated in Table I were benzene (B), toluene (T), and ethyl-

TABLE I

RELATIVE ELUTION TIMES OF ORGANIC SULPHUR COMPOUNDS

Compound	Column temperature, °C.	Standard liquid	Relative elution time
Mercaptans			
2-Propanethiol	85	B	0.36_2
2-Methyl-2-propanethiol	85	B	0.41_3
1-Propanethiol	85	B	0.58_1
2-Methyl-1-propanethiol	85	B	0.92
3-Methyl-1-butanethiol	85	B	1.97
1-Butanethiol	101	T	0.58_9
1-Pentanethiol	101	T	1.20
1-Hexanethiol	100	T	2.32
Sulphides			
Thiapropane	85	T	0.137
2-Thiabutane	85	T	0.272
3-Thiapentane	85	T	0.48_9
4-Thiaheptane	85	T	1.77
Thiacyclopentane	85	T	1.55
	94	T	1.52
Alkylthiophenes			
Thiophene	65	B	1.38
	85	B	1.42
2-Methylthiophene	85	T	1.18
	94	T	1.16
3-Methylthiophene	85	T	1.35
	94	T	1.33
2-Ethylthiophene	85	T	2.18
3-Ethylthiophene	85	T	2.72
2,5-Dimethylthiophene	85	T	2.11
2,4-Dimethylthiophene	85	T	2.51
2,3-Dimethylthiophene	85	T	2.82
3,4-Dimethylthiophene*	84	E	1.76
2-Methyl-5-ethylthiophene*	84	E	2.2
2,3,5-Trimethylthiophene*	85	E	2.7

Can. J. Chem. Downloaded from www.nrcresearchpress.com by 200.7.193.243 on 09/04/12
For personal use only.

benzene (E). All elution times were corrected by subtracting that of hydrogen for the same operating conditions, thus allowing for "dead volume". Compounds marked with an asterisk have been identified in petroleum distillates by boiling range and mass spectrometry only; they have so far not been confirmed by measuring the elution time of the pure compound.

ACKNOWLEDGMENTS

The author wishes to express his gratitude to Dr. J. S. Ball, Director, API Project 48A, for the gift of a high-purity sample of 3-ethylthiophene and to Dr. A. W. Tickner for determination of the mass spectra.

1. SUNNER, S., KARRMAN, K. J., and SUNDÉN, V. Mikrochim. Acta, 1144 (1956).
2. DESTY, D. H. and WHYMAN, B. H. F. Anal. Chem. **29**, 320 (1957).
3. RYCE, S. A. and BRYCE, W. A. Anal. Chem. **29**, 925 (1957).

RECEIVED NOVEMBER 28, 1957.
DIVISION OF APPLIED CHEMISTRY,
NATIONAL RESEARCH COUNCIL,
OTTAWA, CANADA.

Can. J. Chem. Downloaded from www.nrcresearchpress.com by 200.7.193.243 on 09/04/12
For personal use only.

Can. J. Chem. Downloaded from www.nrcresearchpress.com by 200.7.193.243 on 09/04/12
For personal use only.

Canadian Journal of Chemistry

Issued by THE NATIONAL RESEARCH COUNCIL OF CANADA

VOLUME 36 APRIL 1958 NUMBER 4

SYNTHESIS OF 4-AMINOBUTYRIC ACID AND 2,4-DIAMINOBUTYRIC ACID FROM BUTYROLACTONE[1,2]

GUY TALBOT, ROGER GAUDRY, AND LOUIS BERLINGUET

ABSTRACT

The ring opening of γ-butyrolactone with 1 mole of potassium phthalimide and the hydrolysis of the intermediate product gave 4-aminobutyric acid with an excellent yield. The condensation of 1 mole of potassium phthalimide with 2-bromo-4-butyrolactone gave a 2-phthalimidolactone which can also be opened by treatment with a second molecule of potassium phthalimide. This diphthalimido acid when hydrolyzed gave, with an excellent yield, 2,4-diaminobutyric acid dihydrochloride.

INTRODUCTION

4-Aminobutyric acid has long been considered as a metabolic by-product of bacteria and yeast (1, 2, 3, 4). Recently it has been isolated from proteins (5), from plants (6), and from brain tissues (7). Now we know that it is a catabolic product of glutamic acid (8, 9) and that the reaction is reversible (10).

Several methods are available for its synthesis, which are classified in four groups:

(*a*) Oxidation of piperylurethan or sparteine (11, 12).

(*b*) Condensation of potassium phthalimide or of potassium cyanide with halogenated intermediates (13, 14, 15, 16).

(*c*) Reduction of succinimide or 3-cyanopropionic acid or succinonitrile (17, 18, 19, 20, 21, 22).

(*d*) Chemical or enzymatic degradation of glutamic acid or glutarimide (23, 24, 25, 26).

Even then, the abundant supply of 4-aminobutyric acid is somewhat limited because of the nonavailability of the starting products and the four or five steps required for the synthesis.

Since γ-butyrolactone is readily available, a new synthesis starting from the lactone was considered. Bornstein and his collaborators (27) and Paris, Gaudry, and Berlinguet (28) have clearly shown that phthalide can be opened by potassium phthalimide and γ-butyrolactone can be opened by potassium cyanide.

The γ-butyrolactone ring was opened with a 73% yield by reaction with potassium phthalimide in boiling dimethylformamide.

The intermediate compound was then hydrolyzed with hydrochloric acid and the free amino acid was obtained and characterized after the usual treatment with silver car-

[1]*Manuscript received December 5, 1957.*
Contribution from the Department of Biochemistry, School of Medicine, Laval University, Quebec, Que.
[2]*Paper presented before the Division of Chemistry at the 24th Meeting of the Association Canadienne-Française pour l'Avancement des Sciences (A.C.F.A.S.), Montreal, November 4, 1956.*

bonate. The yield of 4-aminobutyric acid was 68%. It was also identified by paper chromatography. The R_f values in phenol–water and pyridine–water systems are respectively 0.76 and 0.19.

Another interesting amino acid, namely 2,4-diaminobutyric acid, was synthesized using a somewhat similar pathway from γ-butyrolactone.

This naturally occurring diamino acid has been found recently in several antibiotic polypeptides (29, 30, 31, 32). The known methods of synthesis are classified in three main groups:

(*a*) Synthesis involving a phthalimido aldehyde (33).
(*b*) Synthesis involving the Hofmann degradation of glutamic acid (34, 35, 36, 37, 38) or the Curtius and Schmidt reactions (39, 40, 41).
(*c*) Synthesis from ethyl acrylate and diazomethane (42).

The last method is by far the best even if it makes use of diazomethane and high-pressure hydrogenation.

Since Livak and his collaborators (43) have brominated very easily γ-butyrolactone, this halogenated lactone was treated with one molecule of potassium phthalimide in boiling dimethylformamide. The 2-phthalimidobutyrolactone thus obtained was opened by treatment with a second molecule of potassium phthalimide.

The total yield of 3,4-diphthalimidobutyric acid from the bromolactone was 73%. This insoluble intermediate when hydrolyzed with concentrated hydrochloric acid gave an 80% yield of the 2,4-diaminobutyric acid dihydrochloride. The over-all yield from the bromolactone was nearly 60%.

The diamino acid was characterized by paper chromatography and paper electrophoresis. R_f values in phenol–water and pyridine–water systems were respectively 0.16 and 0.04. Being a diamino acid, it migrated toward the cathode in a buffer solution of pH 8.6.

EXPERIMENTAL[3]

4-Phthalimidobutyric Acid

Potassium phthalimide (18.5 g., 0.1 mole) was added to 4-butyrolactone (10.0 g., 0.116 mole) in 50 ml. of dimethylformamide. After it was boiled for 12 hours, the mixture was poured onto ice to which had been added 30 ml. of glacial acetic acid. The solid obtained was filtered and recrystallized from water and ethanol. Yield: 17.1 g. (73%), m.p. 117°–118° (Lit. m.p. 117°–118° (44)). Anal. Calc. for $C_{12}H_{11}O_4N$: N, 6.01. Found: N, 6.09.

4-Aminobutyric Acid

4-Phthalimidobutyric acid (5.0 g., 0.021 mole) was dissolved in 100 ml. of dilute hydrochloric acid (1:1). The solution was refluxed during 5 hours, after which it was cooled. The phthalic acid was filtered and the filtrate was evaporated to dryness *in vacuo*. The residue consisted of 4-aminobutyric acid hydrochloride, which was very hygroscopic. It was treated as usual with silver carbonate, hydrogen sulphide, and charcoal. Yield: 1.5 g. (68%), m.p. 195°–196° (Lit. m.p. 196° (12)). Anal. Calc. for $C_4H_9O_2N$: N, 13.57. Found: N, 13.33.

2-Phthalimido-4-butyrolactone

Potassium phthalimide (55 g., 0.297 mole) was added to a solution of 150 ml. of dimethylformamide and 2-bromo-4-butyrolactone (43) (50 g., 0.303 mole). The well-mixed solution was heated at 100° during 12 hours, after which it was poured onto ice.

[3]*Melting points are uncorrected.*

Can. J. Chem. Downloaded from www.nrcresearchpress.com by 200.7.193.243 on 09/04/12
For personal use only.

The precipitate was collected by filtration and it was recrystallized from acetone–water. Yield: 59 g. (86%), m.p. 160°–162°. Anal. Calc. for $C_{12}H_9O_4N$: N, 6.06. Found: N, 6.15.

By acid hydrolysis, the hydrochloride of 2-amino-4-butyrolactone was obtained. It gave a yellow color when treated with ninhydrin and its R_f value in a water–pyridine system was 0.75.

2,4-Diphthalimidobutyric Acid

Potassium phthalimide (10.0 g., 0.054 mole) was added to a solution of 30 ml. of dimethylformamide and 2-phthalimido-4-butyrolactone (11.56 g., 0.05 mole). The solution was heated to reflux during 7 hours. It was then poured onto ice to which 20 ml. of glacial acetic acid had been added. The precipitate was collected by filtration. Yield: 16.0 g. (85%). It can be recrystallized from acetic acid. M.p. 177°–179°. Anal. Calc. for $C_{20}H_{14}O_6N_2$: N, 7.40. Found: N, 7.27.

2,4-Diaminobutyric Acid Dihydrochloride

2,4-Diphthalimidobutyric acid (2.0 g.) was suspended in 50 ml. of dilute hydrochloric acid (1:1). The mixture was refluxed during 12 hours, after which it was cooled. The phthalic acid was collected by filtration, and the filtrate was evaporated to dryness *in vacuo*. The residue was recrystallized from a mixture of hydrochloric acid and glacial acetic acid. Yield: 0.8 g. (79%), m.p. 206° (Lit. m.p. 202°–205° (45)). Anal. Calc. for $C_4H_{10}O_2N_2.2HCl$: Cl, 37.1; N, 14.65. Found: Cl, 36.9; N, 14.50.

ACKNOWLEDGMENTS

The authors are indebted to the National Research Council of Canada for Research Fellowships awarded to one of them (G.T.).

REFERENCES

1. ABDERHALDEN, E., FROMME, G., and HIRSCH, P. Z. physiol. Chem. **85**, 131 (1913).
2. ACKERMANN, D. Z. physiol. Chem. **69**, 273 (1910).
3. ACKERMANN, D. and KUTSCHER, F. Z. physiol. Chem. **69**, 265 (1910).
4. REED, L. J. J. Biol. Chem. **183**, 451 (1950).
5. VIRTANEN, A. I. and MIETTINEN, J. K. Biochim. et Biophys. Acta, **12**, 181 (1953).
6. DENT, C. E., STEPKA, W., and STEWARD, F. C. Nature, **160**, 682 (1947).
7. AWAPARA, J., LANDUA, A. A. J., FUERST, R., and SEALE, B. J. Biol. Chem. **187**, 35 (1950).
8. BEEVERS, A. Biochem. J. **48**, 132 (1951).
9. SCHALES, O., MIMS, V., and SCHALES, S. S. Arch. Biochem. Biophys. **10**, 455 (1946).
10. BESSMAN, S. P., ROSSEN, J., and LAYNE, E. C. J. Biol. Chem. **201**, 385 (1953).
11. SCHOTTEN, C. Ber. **16**, 643 (1883).
12. KARRER, P. and WIDMER, A. Helv. Chim. Acta, **9**, 886 (1926).
13. GABRIEL, S. Ber. **22**, 3335 (1889); **23**, 1767 (1890).
14. LEY, H. Ber. **42**, 354 (1909).
15. DE WITT, G. C. Org. Syntheses, **17**, 4 (1937).
16. ASCHAN, W. Ber. **24**, 2443 (1891).
17. TAFEL, J. and STERN, M. Ber. **33**, 2224 (1900).
18. LOB, W. Biochem. Z. **60**, 159 (1914).
19. THOMPSON, J. F., POLLARD, J. K., and STEWARD, F. C. Arch. Biochem. Biophys. **46**, 248 (1953).
20. DAKIN, H. D. Biochem. J. **11**, 79 (1917).
21. DALMER, O., DIEHL, C., FESKE, E., and PIEPER, H. Ger. Patent No. 597,305 (May 22, 1934); Chem. Abstr. **28**, 5078 (1934).
22. ARBUZOV, B. A. and POZHIL' TSOVA, E. A. Bull. acad. sci. U.R.S.S. Classe sci. chim. 65 (1946).
23. CURTIUS, T. and HECHTENBERG, W. Prakt. Chem. **105**, 319 (1923).
24. RENARD, M. and PITANCE, T. Bull. soc. roy. sci. Liège, **18**, 164 (1949).
25. CAMIEN, M. N., MCCLURE, L. E., LEPP, A., and DUNN, M. S. Arch. Biochem. Biophys. **43**, 378 (1953).
26. GALE, E. F. Biochem. J. **34**, 392 (1940).
27. BORNSTEIN, J., BEDELL, S. F., DRUMMOND, P. E., and KOSLOSKI, C. L. J. Am. Chem. Soc. **78**, 83 (1956).
28. PARIS, G., GAUDRY, R., and BERLINGUET, L. Can. J. Chem. **33**, 1724 (1955).
29. CATCH, J. R. and JONES, T. S. G. Biochem. J. **42**, lii (1948).
30. CATCH, J. R., JONES, T. S. G., and WILKINSON, S. Biochem. J. **43**, xxvii (1946).
31. GORE, R. C. and PETERSEN, E. M. Ann. N.Y. Acad. Sci. **51**, 924 (1949).

Can. J. Chem. Downloaded from www.nrcresearchpress.com by 200.7.193.243 on 09/04/12
For personal use only.

32. PETERSEN, D. H. and REINEKE, L. M. J. Biol. Chem. **181**, 95 (1949).
33. ATKINSON, R. O. and POPPELSDORF, F. J. Chem. Soc. 2448 (1952).
34. KARRER, P., ESCHER, K., and WIDMER, R. Helv. Chim. Acta, **9**, 301 (1926).
35. SYNGE, L. M. Biochem. J. **33**, 671 (1939).
36. KANEWSKAJA, S. J. Ber. **69**, 266 (1936).
37. KING, F. E. and KIDD, D. A. A. J. Chem. Soc. 3315 (1949).
38. BRUCKNER, V., KOVACS, J., and KOVACS, K. J. Chem. Soc. 1512 (1953).
39. AKABORI, S. and NUMANO, S. Bull. Chem. Soc. Japan, **11**, 208 (1936).
40. ADAMSON, D. W. J. Chem. Soc. 1564 (1939).
41. ROTHCHILD, S. and FIELDS, M. J. Org. Chem. **16**, 1080 (1951).
42. CARTER, H. E., VAN ABEELE, F. R., and ROTHROCK, J. W. J. Biol. Chem. **178**, 325 (1949).
43. LIVAK, J. E., BRITTON, E. C., VANDER WEELE, J. C., and MURRAY, M. F. J. Am. Chem. Soc. **67**, 2218 (1945).
44. GABRIEL, S. and COLMAN, J. Ber. **41**, 513 (1908).
45. WILKINSON, S. J. Chem. Soc. 104 (1951).

Can. J. Chem. Downloaded from www.nrcresearchpress.com by 200.7.193.243 on 09/04/12
For personal use only.

Can. J. Chem. Downloaded from www.nrcresearchpress.com by 200.7.193.243 on 09/04/12
For personal use only.

ARSENATES OF THE TRANSITION METALS

THE ARSENATES OF COBALT AND NICKEL[1]

J. B. TAYLOR[2] AND R. D. HEYDING

ABSTRACT

Complex oxides occurring in the systems CoO/As_2O_5 and NiO/As_2O_5 have been studied using Debye–Sherrer diagrams. The compounds were prepared either by high-temperature reaction of the oxides and subsequent pyrolysis of the products or by aqueous precipitation of arsenates followed by thermal dehydration.

The existence of compounds having metal oxide to arsenic pentoxide ratios of 1:1, 2:1, and 3:1 has been clearly demonstrated and the thermal stabilities of each *in vacuo* and in air have been studied. Corresponding compounds in the cobalt and nickel series are isostructural and unit-cell dimensions have been determined. The compounds with a 2:1 ratio could not be isolated readily although their existence is indisputable and tentative figures for the unit-cell dimensions have been obtained.

Another compound, probably with a metal oxide to arsenic pentoxide ratio of 6:1, has been observed during the pyrolysis of the 3:1 compounds. Apparently the cobalt and nickel compounds are isostructural and represent the only phase existing between the 3:1 compounds and the metal oxides.

INTRODUCTION

Continuing an investigation into the chemistry of cobalt speiss and its behavior on roasting in air we have sought to prepare and examine the so-called arsenates of cobalt and nickel which occur in the composition range between $M^{II}O.As_2O_5$ and $M^{II}O$. Previous compounds reported were in many cases hydrates and have been called meta-, pyro-, and ortho-arsenates in the usual manner. We prefer to regard the compounds which we have studied as complex oxides and accordingly will refer to them in terms of their metal oxide to arsenic pentoxide ratios.

Both cobalt and nickel occur naturally as arsenates in the form of erythrite and annabergite respectively. These compounds are of the type $3M^{II}O.As_2O_5.8H_2O$ and have been classified crystallographically as monoclinic (space group $C2/m$), having unit-cell dimensions of $a = 10.056$ Å, $b = 13.340$ Å, $c = 4.730$ Å, $\beta = 102°0'$ for the cobalt compound, and $a = 10.015$ Å, $b = 13.284$ Å, $c = 4.698$ Å, $\beta = 102°14'$ for the nickel compound (1). The structures undoubtedly contain arsenic tetrahedrally co-ordinated with oxygen (2). These compounds have been prepared synthetically together with numerous other hydrated arsenates. The latter were of little interest as far as the present work was concerned since their structures have not been established. In general it may be said that these arsenates have metal oxide to arsenic pentoxide ratios of 0.5 : 1, 1 : 1, 2 : 1, 2.5 : 1, 3 : 1, 4 : 1, and 5 : 1. They were usually prepared by one of two methods: either the reaction of metal, metal oxide, or carbonate with acid at atmospheric or high pressure (3); or the precipitation of the arsenate by addition of metal ion to arsenate ion (4).

Anhydrous complex oxides of nickel have been prepared by Guérin and Masson (5) by dehydration of a hydrated arsenate, $NiO.2As_2O_5.5H_2O$, at an elevated temperature under vacuum. They report that the product $NiO.2As_2O_5$ can be pyrolyzed *in vacuo* to give $NiO.As_2O_5$, $2NiO.As_2O_5$, and $3NiO.As_2O_5$ at 550°, 650°, and 750° C. respectively.

An alternative method of making the complex oxides involves high-temperature reaction of the metal oxide $M^{II}O$ with As_2O_5 mixed in the desired proportions. Thus

[1]*Manuscript received December 11, 1957.*
Contribution from the Division of Applied Chemistry, National Research Council, Ottawa, Canada.
Issued as N.R.C. No. 4632.
[2]*N.R.C. Postdoctorate Fellow.*

$CoO.As_2O_5$ and the isomorphous calcium, strontium, cadmium, mercury, and lead compounds have been prepared (6) as well as $CoO.Sb_2O_5$, $NiO.Sb_2O_5$ (7), and several trivalent antimony and arsenic compounds (8). The so-called 'cobalt meta-arsenate' $CoO.As_2O_5$ is reported to be hexagonal (6) (space group $P312$) with unit-cell dimensions: $a = 4.766$ Å, $c = 4.493$ Å. The structure is well established, being the same as $PbO.Sb_2O_5$ (9), and contains arsenic in octahedral co-ordination with oxygen, which appears to be an exception to the generally accepted fourfold co-ordination of arsenic. Comparison of this type of structure with that of $FePO_4$ (10) reveals a considerable difference between phosphorus and arsenic in the compounds as the structural chemistry of the former is based on PO_4 tetrahedra and is probably best compared with the SiO_4 tetrahedra in silicates.

Some crystallographic data have been reported for the 1:1 pentavalent antimony compounds of iron, cobalt, and nickel (7) and these have been found to be isostructural, with a trirutile structure $P4/mnm$. The cell dimensions of the cobalt compound are: $a = 4.64$ Å, $c = 9.25$ Å and of the nickel analogue: $a = 4.63$ Å, $c = 9.18$ Å.

MATERIALS

The arsenic pentoxide used was Mallinckrodt 'A.R.' containing 0.05% trivalent arsenic and 0.02% lead.

The nickel oxide, cobalt oxide, and cobalt sponge were obtained from Johnson, Matthey & Co. The nickel oxide contained 5 p.p.m. of iron and no cobalt. The cobalt oxide contained 2 p.p.m. of iron and was sold as Co_3O_4 but analyzed $CoO_{1.103}$. The cobalt sponge which was finally used in the preparation of cobalt monoxide contained 5 p.p.m. of iron and no nickel.

Cobalt Oxide, CoO

The CoO was prepared by thermal decomposition of the basic carbonate under vacuum as this method proved more rapid than ignition of the Johnson, Matthey oxide. Cobalt sponge was dissolved in hot 6:1 nitric acid and from this solution the basic carbonate was precipitated by addition of potassium bicarbonate solution. The carbonate was decomposed to CoO by ignition in a continuously pumped vacuum system at 1040° C. for about 2 hours. The product was analyzed for cobalt and its X-ray powder diagram compared with standards.

ANALYSIS FOR COBALT, NICKEL, AND ARSENIC

Nickel was analyzed using the dimethyl glyoxime reagent and weighing as $NiC_8H_{14}O_4N_4$ after drying at 110° C. The most satisfactory method for cobalt analysis was reduction in hydrogen at 950° C. Arsenic was determined by precipitation as silver arsenate and subsequent titration of the silver with thiocyanate. Samples which contained nickel and arsenic or cobalt and arsenic in admixture were first treated to obtain a separation of the components, and the resulting solutions estimated as above. The arsenate hydrates could be dissolved in dilute nitric acid and the metal separated by slow addition of dilute sodium hydroxide solution. Samples of the complex oxides were insoluble in mineral acids and were fused with Na_2CO_3/KNO_3 (2:1) fusion mixture. The soluble arsenate was then readily leached out and the residue containing the metal taken up by a pyrosulphate fusion.

EXPERIMENTAL

To investigate the formation of compounds of the type $xM^{II}O.As_2O_5$ by direct reaction of the oxides at a high temperature a series of nickel oxide – arsenic pentoxide mixtures

Can. J. Chem. Downloaded from www.nrcresearchpress.com by 200.7.193.243 on 09/04/12
For personal use only.

with values of x from 1 to 3 were made and sealed under vacuum in quartz ampoules. Other mixtures were also prepared containing cobalt monoxide and arsenic pentoxide in 1 : 1 admixture. The ampoules were heated in furnaces carefully maintained at 500° C., 650° C., and 800° C. for periods of up to 9 days. In all cases attack of the quartz by the As_2O_5 took place and in the samples at 800° C. this weakened the quartz to the point that several of the ampoules exploded. Reaction between the oxides occurred in all cases, resulting in a yellow or green product in the nickel experiments and a purple product for the cobalt compounds.

Several cobalt monoxide – arsenic pentoxide 1 : 1 mixtures were made taking great care to exclude as much moisture as possible. The arsenic pentoxide for this series of experiments was dried at 400° C. for 30 hours under vacuum and all operations prior to sealing the ampoules were performed in a dry box. After heating for 5 days at 460° C. no reaction had occurred between the oxides although at 800° C. some reaction was observed. The results suggest that the reaction may be partly or wholly hydrothermal and probably depends for its success on the small amount of water retained by the arsenic pentoxide when precautions to exclude it are omitted.

The complex oxides resulting from these reactions were pyrolyzed by heating in porcelain boats in quartz tube furnaces capable of being evacuated or flushed with an air stream. The progress of the thermal decomposition and loss of arsenic was followed by observing the weight loss on the sample and removing portions from time to time for X-ray analysis. Chemical analyses were also performed on some of the products.

The powder diagrams were taken in 11.46 cm. Norelco cameras with CuK_α and CoK_α radiation for the nickel and cobalt complexes respectively.

RESULTS AND DISCUSSION

$M^{II}O.As_2O_5$ *Compounds*

These were well-defined compounds formed by high-temperature oxide reactions. The cobalt compound was obtained by heating a 1 : 1 cobalt monoxide – arsenic pentoxide mixture in a quartz tube at 500° C. for 3 days and was a bright purple color. The powder diffraction pattern agrees with that obtained by Magnéli (6) and could be indexed as hexagonal with unit-cell dimensions of $a = 4.773$ Å, $c = 4.494$ Å (Table I).

Powder diagrams of the $NiO.As_2O_5$ prepared by direct reaction of the oxides at 500° C. for 10 days showed several lines which did not appear in the $CoO.As_2O_5$ pattern. However, these lines decreased gradually in intensity on heating so that after 6 hours at 700° C. under vacuum they were completely absent. It was possible to index the pattern as hexagonal with unit-cell dimensions of $a = 4.759$ Å, $c = 4.431$ Å. The diffraction patterns and density data are recorded in Table II.

The two compounds are clearly isostructural and have the $PbO.Sb_2O_5$ structure (9) previously assigned to $CoO.As_2O_5$ by Magnéli.

$2M^{II}O.As_2O_5$ *Compounds*

Reactions between cobalt or nickel oxide and arsenic pentoxide in 2 : 1 and 3 : 1 ratios at 800° C. produced mainly $M^{II}O.As_2O_5$ but the diffraction patterns showed some lines which were later attributed to the $2M^{II}O.As_2O_5$ compounds. The amount of information obtainable from these patterns was limited by contamination of the sample resulting mainly from the severe attack of the quartz by the arsenic pentoxide at the high temperature.

Vacuum pyrolysis experiments on $NiO.As_2O_5$ produced no new phase after 12 hours at 710° C. with removal, grinding, and sampling at intervals of 2 hours. A further heating

Can. J. Chem. Downloaded from www.nrcresearchpress.com by 200.7.193.243 on 09/04/12
For personal use only.

TABLE I

POWDER DIFFRACTION PATTERN OF $CoO.As_2O_5$

(Hexagonal; $a = 4.773 \pm 0.002$ Å, $c = 4.494 \pm 0.002$ Å (cf. $a = 4.766$ Å, $c = 4.493$ Å obtained by Magnéli (6)); Fe-filtered Co radiation, $\lambda_{\alpha_1} = 1.78890$ Å; camera diameter, 11.46 cm.; cutoff 20 Å; temp. 24° C.; $\rho_{calc} = 5.71$ g./cc.; $z = 1$.)

I/I_1	$hk.l$	d_{obs} (Å)	d_{calc} (Å)
20	00.1	4.46	4.49
3	10.0	4.12	4.13
100	10.1	3.06	3.04
55	11.0	2.61	2.61
5	00.2	2.24	2.25
50	11.1	2.11	2.11
40	20.1	1.88	1.88
90	11.2	1.63	1.64
60	21.1	1.470	1.475
20	10.3	1.406	1.408
65	30.0	1.375	1.378
15	30.1	1.315	1.317
25	11.3	1.268	1.269
20	20.3	1.211	1.213
20	22.0	1.191	1.193
35	30.2	1.172	1.175
20	22.1	1.152	1.153
10	00.4	1.123	1.122
50	31.1	1.111	1.111
45	21.3	1.081	1.081
70	22.2	1.053	1.054
40	11.4	1.016	1.016
25	40.1	1.007	1.007
30	22.3	0.9333	0.9332
60	32.1	0.9278	0.9279
70	31.3	0.9103	0.9104
85	41.0	0.9020	0.9020

for 5 hours at 760° C. gave a material which on X-ray powder analysis showed a series of new lines together with some NiO and $NiO.As_2O_5$. A plot of per cent loss of weight against time of pyrolysis showed no inflection at the 2 : 1 composition under these conditions. By repeating the pyrolysis at a temperature of 720° C. the necessary weight loss was achieved in 230 hours but again it was impossible to reach equilibrium conditions. Powder photographs in this composition range were ill-defined at best. Pyrolysis in air gave the same decomposition products at about 920° C. but no better diffraction patterns were obtained. The material approximating in composition to $2NiO.As_2O_5$ had an ocher-yellow color as compared with the yellow-green of the 1 : 1 compound.

Similar experiments on the pyrolysis of $CoO.As_2O_5$ gave comparable results with a rather poorly defined dark purple 2 : 1 compound after 40 hours' heating at 736° C. under vacuum.

By careful selection of lines in the powder diagrams and elimination of lines from other phases identified in the system it is possible to suggest an orthorhombic symmetry for $2CoO.As_2O_5$ and $2NiO.As_2O_5$ having unit-cell dimensions of $a = 8.16$ Å, $b = 8.56$ Å, $c = 9.16$ Å for the cobalt compound, and $a = 8.12$ Å, $b = 8.52$ Å, $c = 9.29$ Å for the nickel compound. Interplanar spacings, indices, and observed intensities of the powder diagrams are recorded in Table III.

The 2 : 1 compounds are not isostructural with $2PbO.Sb_2O_5$, which has the cubic pyrochlore form $a = 10.3$ Å (11), or with $2CaO.Sb_2O_5$, which has an orthorhombic weberite structure, $a = 7.28$ Å, $b = 7.44$ Å, $c = 10.18$ Å.

The results of these experiments do not entirely agree with those of Guérin and Masson

Can. J. Chem. Downloaded from www.nrcresearchpress.com by 200.7.193.243 on 09/04/12
For personal use only.

(5), who claimed that $NiO.As_2O_5$ decomposes *in vacuo* at 650° C. to give $2NiO.As_2O_5$ as a single phase. However, no attempt was made to substantiate their claim by published X-ray data and it may be that they also had a mixture in the 2 : 1 composition range.

TABLE II

POWDER DIFFRACTION PATTERN OF $NiO.As_2O_5$

(Hexagonal; $a = 4.759 \pm 0.002$ Å, $c = 4.431 \pm 0.002$ Å; Ni-filtered Cu radiation, $\lambda_{\alpha 1} = 1.5405$ Å; camera diameter, 11.46 cm.; cutoff 20 Å; temp. 24° C.; $\rho_{calc} = 5.82$ g./cc.; $\rho_{obs} = 5.82$ g./cc.; $z = 1$. Lines observed with I/I_1 of 15 and below are not included in the table.)

I/I_1	$hk.l$	d_{obs} (Å)	d_{calc} (Å)
60	00.1	4.41	4.42
20	10.0	4.08	4.12
100	10.1	3.00	3.02
80	11.0	2.37	2.38
80	11.1	2.09	2.10
70	20.1	1.86	1.87
90	11.2	1.62	1.62
70	21.1	1.467	1.470
25	10.3	1.388	1.390
70	30.0	1.369	1.374
20	30.1	1.310	1.312
25	11.3	1.253	1.255
20	20.3	1.200	1.200
20	22.0	1.188	1.190
25	30.2	1.166	1.168
50	31.1	1.106	1.107
40	21.3	1.072	1.072
55	22.2	1.048	1.048
55	40.1, 11.4	1.003	1.004, 1.004
25	32.1	0.9242	0.9242
20	41.0	0.8990	0.8994
20	41.1	0.8814	0.8814
30	30.4	0.8625	0.8623
70	41.2	0.8335	0.8333
40	22.4	0.8108	0.8107
40	32.3	0.7964	0.7963
40	33.0	0.7930	0.7931
35	33.1	0.7807	0.7807

TABLE III

POWDER DIFFRACTION PATTERNS OF $2CoO.As_2O_5$ AND $2NiO.As_2O_5$

($2CoO.As_2O_5$—orthorhombic; $a = 8.16 \pm 0.01$ Å, $b = 8.56 \pm 0.01$ Å, $c = 9.16 \pm 0.01$ Å; Fe-filtered Co radiation, $\lambda_{\alpha 1} = 1.7889$ Å; $2NiO.As_2O_5$—orthorhombic; $a = 8.12 \pm 0.01$ Å, $b = 8.52 \pm 0.01$ Å, $c = 9.29 \pm 0.02$ Å; Ni-filtered Cu radiation, $\lambda_{\alpha 1} = 1.5405$ Å; camera diameter, 11.46 cm.; cutoff 20 Å; temp. 24° C.)

$2CoO.As_2O_5$				$2NiO.As_2O_5$		
I/I_1	d_{obs} (Å)	d_{calc} (Å)	hkl	I/I_1	d_{obs} (Å)	d_{calc} (Å)
50	4.22	4.27	020	40	4.22	4.26
20	4.03	4.08	200	10	4.04	4.01
20	3.74	3.78	120	10	3.76	3.77
50	3.47	3.50	121	35	3.48	3.50
100	3.16	3.13	022	100	3.14	3.14
90	3.06	3.05	202	90	3.06	3.06
90	2.96	2.95	220	90	2.94	2.94
20	2.51	2.49	023	30	2.51	2.50
40	2.26	2.26	231	30	2.27	2.26
40	2.08	2.08	033	30	2.09	2.09
20	2.02	2.03	024	45	2.04	2.04
60	1.90	1.89	142	45	1.88	1.88
50	1.67	1.65	341	50	1.65	1.65

Can. J. Chem. Downloaded from www.nrcresearchpress.com by 200.7.193.243 on 09/04/12
For personal use only.

Can. J. Chem. Downloaded from www.nrcresearchpress.com by 200.7.193.243 on 09/04/12
For personal use only.

$3M^{II}O.As_2O_5$ *Compounds*

Continuing the pyrolysis by increasing the temperature, compounds appeared in both systems corresponding to a metal oxide to arsenic pentoxide ratio of 3 : 1. At 750° C. this phase is perfectly stable in contrast to the behavior of the 2 : 1 compounds.

As an alternative approach to the preparation of these compounds the hydrates $3CoO.As_2O_5.8H_2O$ (erythrite) and $3NiO.As_2O_5.8H_2O$ (annabergite) were prepared and dehydrated. These minerals were synthesized by addition of $Na_2H.AsO_4.7H_2O$ solution to hot nickel nitrate or cobalt chloride solution using 0.1 weight per cent solutions in the preparation of the cobalt compound and 5% solutions for the nickel compound.[3] Powder photographs of the synthetic minerals were in excellent agreement with those of erythrite and annabergite.

On dehydration in an open crucible at 800° C. these hydrates yielded compounds having the same powder diagrams as those obtained from pyrolysis of the 1 : 1 compounds. The diffraction patterns could be indexed as orthorhombic with a = 5.775 Å, b = 8.498 Å,

TABLE IV

POWDER DIFFRACTION PATTERN OF $3CoO.As_2O_5$

(Orthorhombic; a = 5.775±0.005 Å, b = 8.498±0.008 Å, c = 10.85±0.01 Å; Fe-filtered Co radiation, λ_{α_1} = 1.7889 Å; camera diameter, 11.46 cm.; cutoff 20 Å; temp. 24° C. All lines up to θ = 17°, then $I/I_1 > 20$ up to θ = 55° included.)

I/I_1	hkl	d_{obs} (Å)	d_{calc} (Å)
25	100	5.81	5.77
13	101	5.11	5.10
10	110	4.80	4.77
18	012	4.53	4.57
40	020, 111	4.35	4.25, 4.37
30	021	3.96	3.96
40	003	3.69	3.62
65	112	3.49	3.58
30	121	3.24	3.26
40	103	3.06	3.06
85	031, 023	2.77	2.74, 2.75
75	210	2.72	2.73
75	004	2.69	2.71
30	211	2.64	2.65
100	202	2.57	2.52
25	033	2.24	2.23
30	040	2.15	2.18, 2.12
25	230	2.01	2.02
25	142, 134 310	1.87	1.87, 1.86 1.88
40	007, 314	1.553	1.551, 1.544
50	332, 206	1.521	1.528, 1.533
30	027, 251	1.454	1.456, 1.452
25	305	1.440	1.440
25	137, 422	1.327	1.324, 1.325
25	246	1.243	1.243
25	444	1.093	1.093

[3]*The very small crystallites obtained from the more concentrated nickel solution were developed by digestion in water at 100° C. for 1 week. It may be remarked that regardless of the relative concentrations of nickel and arsenate ion in solution only annabergite was precipitated. Similarly the residue obtained by digestion of varying quantities of basic nickel carbonate with arsenic acid exhibited only the diffraction pattern of annabergite although analyses indicated nickel to arsenic ratios of from 3:2 to 6:2. The amorphous nickel compound (probably the hydroxide) retained in these residues could not be removed by chemical means. On pyrolysis at 500° C., however, a face-centered cubic pattern appeared on the Debye–Sherrer diagrams. The unit-cell dimension of this compound (approximately 4.13 Å) was less than that of* NiO *(4.177 Å). That this pattern was directly associated with the amorphous nickel compound admixed with the annabergite was shown by the increase in intensity with increasing excess nickel content. This cubic compound was converted to* NiO *on pyrolysis at 800° C., when* $3NiO.As_2O_5$ *lines also appeared resulting from the decomposition of the annabergite. We were unable to obtain this cubic pattern by any other means.*

TABLE V

POWDER DIFFRACTION PATTERN OF $3NiO.As_2O_5$

(Orthorhombic; $a = 5.693 \pm 0.005$ Å, $b = 8.30 \pm 0.01$ Å, $c = 11.04 \pm 0.02$ Å; Ni-filtered Cu radiation, $\lambda_{\alpha_1} = 1.5405$ Å; camera diameter, 11.46 cm.; cutoff 20 Å; temp. 24° C.; $\rho_{calc} = 5.76$ g./cc.; $\rho_{obs} = 5.66$ g./cc.; $z = 4$. All lines up to $\theta = 17°$, then $I/I_1 > 20$ only up to $\theta = 33°$ included.)

I/I_1	hkl	d_{obs} (Å)	d_{calc} (Å)
20	100	5.70	5.70
7	101	5.04	5.11
5	110	4.71	4.69
7	012	4.46	4.60
60	111	4.31	4.32
7	020	4.07	4.16
30	021	3.91	3.89
40	003	3.67	3.69
75	112	3.48	3.57
35	121	3.19	3.20
30	103	3.03	3.09
30	113	2.94	2.90
5	122	2.80	2.86
80	004	2.75	2.75
80	210	2.68	2.69
25	211	2.62	2.62
100	202	2.54	2.53
30	033	2.21	2.21
50	015, 124	2.13	2.13, 2.13
45	230	1.99	1.98
25	042	1.94	1.94
25	310	1.85	1.85
30	026, 240	1.676	1.675
25	126	1.623	1.615
50	206	1.545	1.545
50	314	1.525	1.537
50	117	1.493	1.492
55	305	1.440	1.439
25	127	1.430	1.427

$c = 10.85$ Å for $3CoO.As_2O_5$, and $a = 5.693$ Å, $b = 8.30$ Å, $c = 11.04$ Å for $3NiO.As_2O_5$.

Powder diffraction data and results of density measurements are given in Tables IV and V.

In agreement with Guérin and Masson we found that $3NiO.As_2O_5$ cannot be hydrated to give annabergite even under 10 atm. pressure of water vapor.

$6M^{II}O.As_2O_5$ *Compounds*

The 3 : 1 compounds decompose under vacuum at about 850° C. to give the metal oxides but it was observed that an intermediate phase appeared in both the cobalt and nickel systems. The intermediate compounds were best prepared by pyrolysis in an air stream at 1000° C. The nickel compound was a bright green as compared with the dull green of $3NiO.As_2O_5$, and the cobalt compound a dark gray color in contrast to the dark powder blue of the $3CoO.As_2O_5$. Both gave good powder diffraction patterns. As a result of observations on weight losses during their formation and determinations of nickel and arsenic percentages it was concluded that these materials had a composition corresponding to $6M^{II}O.As_2O_5$. Results of analyses on two independently prepared samples of $6NiO.As_2O_5$ are given in Table VI. Although the figures do not appear to be very accurate allowance must be made for contamination by other compounds, which were just visible on the diffraction patterns.

It was at first considered possible to index the powder diagrams on the basis of hexagonal symmetry, the nickel compound having unit-cell dimensions of $a = 10.48$ Å, $c =$

Can. J. Chem. Downloaded from www.nrcresearchpress.com by 200.7.193.243 on 09/04/12
For personal use only.

TABLE VI

ANALYSIS OF $6NiO.As_2O_5$

	Calculated	Observed (*a*)	Observed (*b*)
% Ni	50.19	48.20	50.71
% As	22.09	21.11	20.22
Ratio Ni/As	3 : 1	2.9 : 1	3.2 : 1

12.03 Å. However, the cobalt powder diagram contained a rather broad intense line that was resolved into a doublet by annealing the sample at 800° C. in an evacuated quartz tube for 5 days. These lines could not be indexed in the hexagonal system.

In view of the isostructural nature of the other nickel and cobalt arsenates in the series it seems reasonable to assume that the 6 : 1 complexes are also structurally similar, and on the basis of this assumption the hexagonal symmetry assigned to the nickel complex has been discarded. However, the diffraction patterns of both compounds can be indexed by assuming orthorhombic cells, for which it is found that the reflections giving rise to the strong doublet in the cobalt compound overlap in the nickel compound producing a rather broad line. Observed intensities, interplanar spacings, and indices for these two compounds are recorded in Tables VII and VIII.

TABLE VII

POWDER DIFFRACTION PATTERN OF $6CoO.As_2O_5$

(Orthorhombic; $a = 5.724 \pm 0.005$ Å, $b = 9.418 \pm 0.01$ Å, $c = 12.07 \pm 0.01$ Å; Fe-filtered Co radiation, $\lambda_{\alpha_1} = 1.7889$ Å; camera diameter, 11.46 cm.; cutoff 20 Å; temp. 24° C. $I/I_1 > 20$ up to 30°, and $I/I_1 > 25$ up to 48° included.)

I/I_1	*hkl*	d_{obs} (Å)	d_{calc} (Å)
20	010	9.38	9.42
25	012	5.10	5.09
50	112	3.78	3.80
25	121	3.50	3.48
40	023	3.08	3.06
50	014	2.89	2.87
60	200	2.86	2.86
40	202	2.59	2.59
60	132	2.52	2.51
40	220	2.45	2.45
100	005	2.42	2.41
40	040	2.35	2.35
100	204	2.08	2.08
40	006	2.01	2.01
40	321	1.751	1.749
40	152	1.715	1.716
40	206	1.646	1.646
30	117	1.627	1.626
40	304	1.608	1.613
75	226	1.552	1.554
85	008	1.507	1.509
60	245	1.448	1.452
80	325	1.425	1.426
30	164	1.354	1.353
25	263	1.303	1.302
40	228	1.284	1.284
30	057	1.272	1.272
25	345	1.263	1.263
40	405	1.232	1.231
30	440	1.223	1.223

Can. J. Chem. Downloaded from www.nrcresearchpress.com by 200.7.193.243 on 09/04/12
For personal use only.

TABLE VIII

POWDER DIFFRACTION PATTERN OF $6NiO.As_2O_5$

(Orthorhombic; $a = 5.594 \pm 0.005$ Å, $b = 9.27 \pm 0.01$ Å, $c = 12.04 \pm 0.01$ Å; Ni-filtered Cu radiation, $\lambda_{\alpha 1} = 1.5405$ Å; camera diameter, 11.46 cm.; cutoff 20 Å; temp. 24° C.; $\rho_{calc} = 5.41$ g./cc.; $\rho_{obs} = 5.54$ g./cc.; $z = 3$. $I/I_1 > 15$ up to 30°, and $I/I_1 > 25$ from 30° to 83° included.)

I/I_1	hkl	d_{obs} (Å)	d_{calc} (Å)
40	010	8.98	9.26
50	012	5.01	5.05
20	102	4.08	4.16
70	112	3.73	3.75
45	023	3.04	3.03
60	014	2.84	2.86
50	114	2.55	2.55
30	024, 202	2.53	2.52
60	132	2.49	2.46
75	220	2.40	2.40
75	015	2.33	2.33
15	133, 222	2.24	2.24
15	230	2.08	2.08
100	204, 223	2.05	2.05, 2.06
20	310	1.829	1.830
20	215	1.791	1.791
40	017, 152	1.690	1.690, 1.690
25	216	1.604	1.605
35	304	1.586	1.586
25	323	1.559	1.558
20	061	1.531	1.533
85	018	1.483	1.481
85	028	1.429	1.430
25	164	1.335	1.335
30	165	1.265	1.267
30	0, 0, 10	1.204	1.205
40	446	1.030	1.028
30	277	0.9827	0.9826
35	4, 2, 11	0.8477	0.8476

SUMMARY

This study of the complex oxides occurring in the CoO/As_2O_5 and NiO/As_2O_5 systems has established the compounds $M^{II}O.As_2O_5$, $2M^{II}O.As_2O_5$, $3M^{II}O.As_2O_5$, and $6M^{II}O.As_2O_5$ as the only ones existing in the composition range $M^{II}O.As_2O_5$ to $M^{II}O$.

The 1 : 1 compounds are hexagonal and the 2 : 1, 3 : 1, and 6 : 1 compounds have been tentatively assigned orthorhombic symmetry. It is interesting to note that the unit-cell volumes of the 1 : 1 and 2 : 1 complexes are just less than those calculated for a close-packed oxygen-ion system (assuming $z = 6$ for the 2 : 1 compounds). The observed unit-cell volumes for the 3 : 1 and 6 : 1 compounds are greater than those required by a close-packed oxygen-ion array.

Both cobalt and nickel compounds exhibit similar thermal stabilities in that corresponding compounds in each system were observed to be stable over the same temperature range. *In vacuo* the 1 : 1 compounds decompose at 720° C. to give 3 : 1 compounds but an intermediate structure occurs in the composition range about 2 : 1. The 3 : 1 compounds decompose to give the 6 : 1 structure at 850° C., and at 850° to 875° C. the metal oxides are formed. In air at atmospheric pressure these decompositions are observed about 150° C. higher and even at 1000° C. the 6 : 1 complexes are stable. From this it would appear that the primary process in the decomposition of the arsenates is ejection of oxygen from the lattice.

Can. J. Chem. Downloaded from www.nrcresearchpress.com by 200.7.193.243 on 09/04/12
For personal use only.

ACKNOWLEDGMENTS

We should like to thank Dr. L. D. Calvert of this Division for the great interest he has shown in this problem and the assistance he has given with the crystallographic work.

We are also indebted to Dr. S. C. Robinson of the Mineralogy Division of the Department of Mines and Technical Surveys for a powder diagram of annabergite.

REFERENCES

1. DONNAY, J. D. H. and NOWACKI, W. Crystal data. Memoir 60. The Geological Society of America. 1954. p. 191.
2. Structure Reports. International Union of Crystallography. Vol. 13. Utrecht. 1950. p. 307.
3. EPHRAIM, F. and ROSETTI, C. Helv. Chim. Acta, **12**, 1025 (1929).
4. ANDO, T. and MINAMI, S. Bull. Osaka Ind. Research Inst. **3**, 44 (1952).
5. GUÉRIN, H. and MASSON, J. Compt. rend. **241**, 415 (1955).
6. MAGNÉLI, A. Arkiv Kemi, Mineral. Geol. **15B**, No. 3 (1941).
7. BYSTRÖM, A., HÖK, B., and MASON, B. Arkiv Kimi, Mineral. Geol. **15B**, No. 4 (1941).
8. STÄHL, S. Arkiv Kemi, Mineral. Geol. **17B**, No. 5 (1943).
9. Structure Reports. International Union of Crystallography. Vol. 8. Utrecht. 1940–41. p. 156.
10. SHAFER, E. C., SHAFER, M. W., and ROY, R. Z. Krist. **107**, 263 (1956).
11. BYSTRÖM, A. Arkiv. Kemi, Mineral. Geol. **18A**, No. 21 (1945).

Can. J. Chem. Downloaded from www.nrcresearchpress.com by 200.7.193.243 on 09/04/12
For personal use only.

Can. J. Chem. Downloaded from www.nrcresearchpress.com by 200.7.193.243 on 09/04/12
For personal use only.

PHOTOCONDUCTIVITY OF SOME POLYNUCLEAR AROMATIC HYDROCARBONS[1]

J. KOMMANDEUR,[2] G. J. KORINEK,[3] AND W. G. SCHNEIDER

ABSTRACT

The spectral response, voltage dependence, and intensity dependence of the surface photocurrent in naphthalene, terphenyl, pyrene, stilbene, and azulene have been measured. Pyrene and naphthalene have a high sensitivity for photoconduction at the long-wavelength edge of the optical absorption spectrum. In the spectral response of pyrene three peaks appear at 4475 Å, 4275 Å, and 4100 Å. It is suggested that these peaks are due to weak optical absorptions to energy levels which are highly efficient in promoting conduction. It is possible that a similar effect occurs in naphthalene, where maximum photoconductivity coincides with a weak absorption reported by McClure and Schnepp. Azulene only shows photoconductivity at wavelengths corresponding to absorption to the second singlet state.

INTRODUCTION

Recently a substantial amount of work has been devoted to the photoconductive properties of anthracene and tetracene (1, 2, 3, 4). Intensity, voltage, and spectral dependence as well as rise time, decay time, and temperature dependence of the photocurrent have been investigated thoroughly. More recently Lyons and Morris (5) published a note on the spectral dependences of a number of other polycyclic hydrocarbons. As the photocurrents were extremely low, they had to restrict themselves to measurements at wavelengths where a mercury arc provided a high enough intensity, i.e. to the wavelengths of the major mercury lines. In our laboratory the temperature dependence of the photocurrent in a number of compounds has been studied (6). Recently Lyons and Morris (7) reported experiments in which they used the qualitative resemblance of the spectral response of the photocurrent to the absorption spectrum to draw conclusions about the polarization ratio and thus about the assignments of this spectrum. In our measurements of the temperature dependence of the photocurrent we observed that some compounds photoconduct at wavelengths considerably longer than those within the region of the absorption spectrum. This was the case particularly for thicker crystals. With the aid of a 1000 w. xenon lamp as a strong ultraviolet source, it was decided to try to obtain a continuous spectral response for some of the compounds studied by Lyons and Morris and for some other ones that appeared to be of interest. The results of these measurements, and particularly those for pyrene which has been studied more extensively, are given in the present paper.

EXPERIMENTAL

Naphthalene, stilbene, and terphenyl single crystals were obtained from the Harshaw Chemical Company. A number of crystals of naphthalene for comparison were kindly grown for us by Dr. F. R. Lipsett in a Bridgeman furnace (8). No dependence on the source of the crystals was found. Azulene and pyrene crystals were measured as sublimation flakes. Thicker pyrene crystals were grown from a solution of pyrene in petroleum ether.

[1]*Manuscript received November 21, 1957.*
Contribution from the Division of Pure Chemistry, National Research Council of Canada, Ottawa, Canada. Issued as N.R.C. No. 4630.
[2]*N.R.L. Postdoctorate Fellow 1955–57. Present address: National Carbon Research Laboratories, 12600 Snow Road, Parma, Ohio.*
[3]*N.R.L. Postdoctorate Fellow 1956–57. Present address: Metals Research Laboratories, Niagara Falls, N.Y.*

Can. J. Chem. Downloaded from www.nrcresearchpress.com by 200.7.193.243 on 09/04/12
For personal use only.

The light of a 1000 w. XBO 1001 (Osram) xenon lamp was passed through a Farrand 300 U.V. monochromator. The image of the exit slit of this monochromator was focused onto the specimen by means of a quartz achromat. A plane-parallel quartz plate placed in the light beam between achromat and crystal reflected part of the light onto a G.E. 935 vacuum photocell. Thus the current through the photocell is proportional to the intensity of the light incident on the crystal at any specific wavelength. The crystals were mounted on a quartz or teflon disk. Aquadag or silver paste contacts were painted round the ends of the crystal. All of the crystal and at least part of the contacts were illuminated. The teflon or quartz disks were mounted in a cell essentially the same as the one described by Chynoweth and Schneider (10), in which all insulation had been replaced by scrupulously cleaned teflon so as to prevent any spurious dark currents. From the cell went an insulated straight, rigid, and shielded lead to the input terminal of a Keithley 200 B micromicroammeter. The whole assembly was mounted on a board which slid on an optical rail and could also be adjusted in the two remaining directions; the monochromator was held in a fixed position on the same rail. With this setup currents down to about 5×10^{-14} amp. could be measured reproducibly within 2–3%.

The wavelength knob of the monochromator could be driven by a motor with gear assembly while the output of the micromicroammeter was recorded by a Varian G-10 recorder. At the beginning of each series of experiments the photoconduction assembly was replaced by a Moll thermopile (Kipp, Holland). This allowed calibration of the photocell. During a run readings of the current were continuously taken so as to allow subsequent correction for equal intensity input.

Intensity dependences were determined by placing neutral density filters between the monochromator and the deflecting quartz plate. The actual transmitted intensities could thus be read on the galvanometer of the photocell. The linearity of the photocell was checked with the thermopile and found satisfactory.

Voltage dependences were obtained by means of a 300 v. battery with a decade shunt of selected 1 meg resistances. All points for voltage and intensity dependence were taken at random.

In some pyrene crystals it was of interest to determine the absorption edge and the photoconductivity response. For these experiments the crystals were mounted on a quartz disk. The response curve was determined first and then without disturbing the crystal on the quartz disk the absorption edge was measured. These measurements were carried out in a Carey recording spectrograph. As only very small crystals were available, a condenser system was used to focus the beam from the exit slit of the Carey onto the crystal specimen. An image of the pinhole behind the crystal was focused on the entrance window of the photomultiplier. The objective lens of the condenser system was made adjustable so as to allow proper focusing outside the spectrophotometer. Lenses and specimen holder were mounted on a base which was made to fit onto the cell holder plate of the spectrophotometer compartment. For each spectrum a blank was run by removing the crystal from over the pinhole. Accurate positioning of the crystal could be carried out by looking through the objective lens, thus using it as a magnifying glass. By adjusting the slitwidths of the apparatus care was taken to ensure that about the same beamwidth was obtained in measuring spectra and spectral response curves.

RESULTS

All voltage and intensity dependences were found to be linear within the experimental error. For very low photocurrents sometimes a slight departure from the linearity of

the intensity dependence could be observed. Allowing more time between the measurements usually made any deviations disappear. Such departures from linearity could be super- or sub-linear and could never be reproduced from crystal to crystal.

The spectral dependences are given in Fig. 1. They are all corrected to an incident light intensity of about 20 μw./cm.^{2} The average beamwidth with which these curves have been measured was about 30 Å. Intensity considerations did not allow us to use polarized light in these experiments.

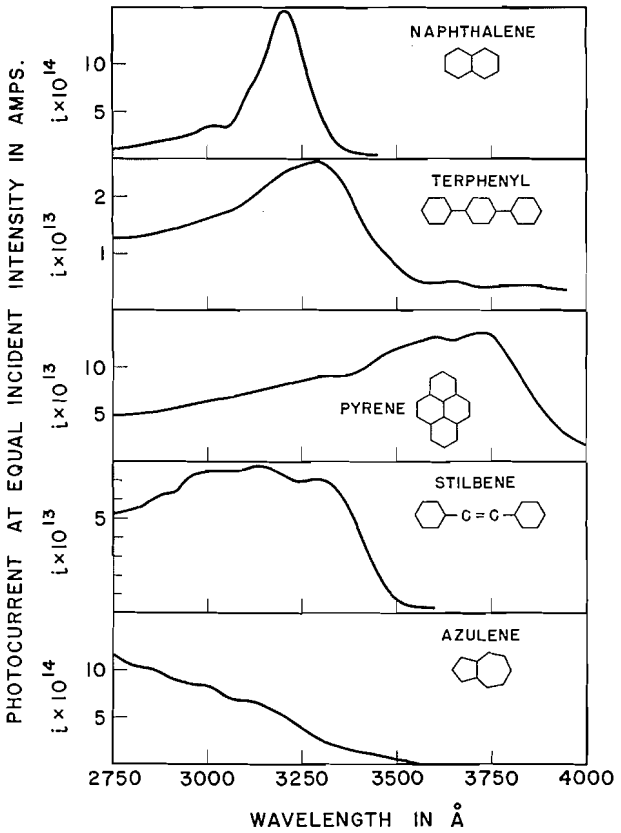

FIG. 1. Spectral response of the surface photocurrents in naphthalene, terphenyl, pyrene, stilbene, and azulene.

A feature of the spectral dependence of some of these compounds is their high sensitivity at the absorption edge. In this respect the present curves are in partial disagreement with those given by Lyons and Morris (5). However, light on the long-wavelength side of the absorption spectrum will be more strongly absorbed in the thicker crystals used in this work, and therefore lead to a higher photocurrent at these wavelengths.

The case of pyrene is most interesting, as even on the relatively thin sublimation flakes a structure in the spectral response could be observed beyond the region of the absorption spectrum of the crystal, which has its first peak at 3750 Å (11). It was therefore decided to investigate this material more closely, especially because the absorption edge lies in a spectral region where still an appreciable light intensity can be obtained without sacrificing too much resolution. It will be clear from Fig. 2 that the spectral response curves vary with the thickness of the crystals. At the long-wavelength edge of

Can. J. Chem. Downloaded from www.nrcresearchpress.com by 200.7.193.243 on 09/04/12
For personal use only.

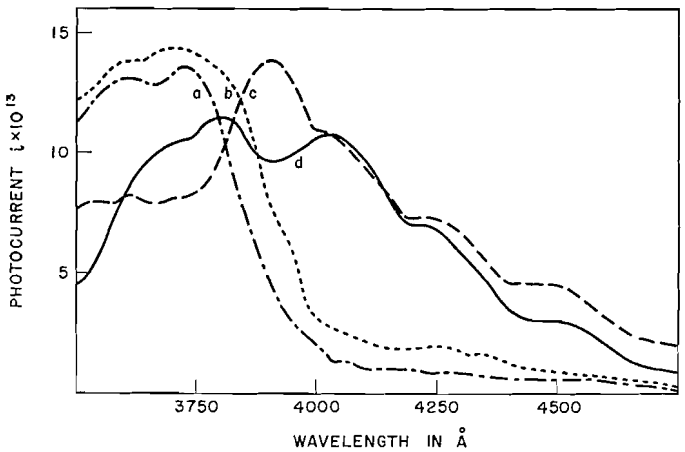

FIG. 2. Spectral response of the photocurrent of pyrene crystals of various thicknesses: (*a*) thickness 5 μ; (*b*) thickness 20 μ; (*c*) thickness 0.63 mm.; (*d*) sandwich-cell thickness 1.57 mm.

the absorption spectrum light will be absorbed throughout the crystal and contributions of deeper layers may be expected. Therefore the photocurrent at the absorption edge of the crystal will be favored with respect to the photocurrent at shorter wavelengths when the thickness of the crystals is increased. Curves *a* and *b* of Fig. 2 are for a thin (about 5 μ) and a thicker (20 μ) sublimation flake respectively. It is seen that the currents at wavelengths outside the absorption region are very low. Curve *c* applies to a crystal 0.63 mm. thick. The long-wavelength side of the curve is now very appreciable. Curve *d* is for a sandwich cell (4) of thickness 1.57 mm. with silvered contacts. Here also the long wavelengths make a greater contribution to the photocurrent. Contrary to anthracene, the bulk current in pyrene is of about the same magnitude as the surface current. A number of peaks appear at the long-wavelength side of the spectral response curves. One of these peaks is apparent. Although the curves have been calculated for an equal incident energy of 20 μw./cm.^{2} at all wavelengths, all this energy is not absorbed by the crystal. At longer wavelengths the major part is transmitted and absorbed by the black background. For this reason the absorption edges of the crystals were directly measured. Because the intensity dependence is linear the photocurrent is directly proportional to the amount of light absorbed:

$$i = \phi(I_e - I) = \phi I_0(1 - 10^{-D})$$

where i is the photocurrent, I_0 the incident intensity, I the transmitted intensity, D the optical density, and ϕ a proportionality factor we can call the "efficiency". Then:

$$\phi = (1/I_0)[i/(1 - 10^{-D})].$$

A plot of $i/(1-10^{-D})$ at constant incident intensity versus the wavelength will give a measure of the relative efficiency of the absorbed light in producing the photocurrent.

At wavelengths longer than 4100 Å no change in the absorption of a crystal could be detected. Owing to the large amount of scattered and reflected light in these thick crystals it is impossible to obtain an actual optical density at these wavelengths. As it would seem impossible for the crystal to photoconduct without the absorption of light it must be supposed that the crystals have a small but finite optical density as far out of the absorption region as 4750 Å. Fig. 3 gives a plot of $i/(1-10^{-D})$ at constant intensity

Can. J. Chem. Downloaded from www.nrcresearchpress.com by 200.7.193.243 on 09/04/12
For personal use only.

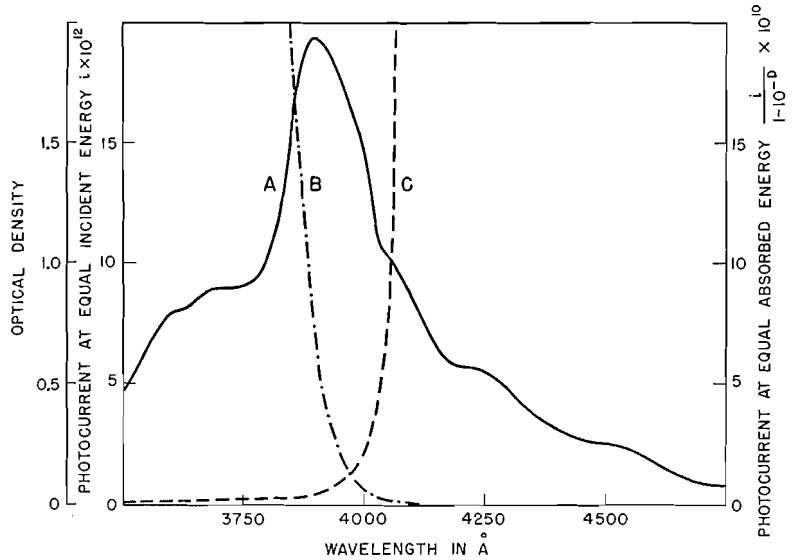

FIG. 3. Curve A shows the photocurrent as corrected for equal absorbed energy (scale at left). Curve B is the optical absorption edge (scale at left). Curve C gives the efficiency of the light in promoting photoconduction, i.e. the photocurrent corrected for equal absorbed energy (scale at right).

for a crystal with a very high apparent peak at 3900 Å. It will be seen that this peak is lost when the correction is applied. It will also be noted that light on the long-wavelength side of the absorption spectrum is very efficient in producing photoconduction. At the long-wavelength side of the response curve three peaks are observed: at 4475 Å, 4725 Å, and 4100 Å. Similar curves were obtained for a number of other crystals and within 25 Å the peak values all agree.

The fact that the 3900 Å peak is apparent could also be shown in another way. Comparison of Fig. 2 and Fig. 3 will show that its position and its magnitude changes with the thickness of the crystal. To rule out any peculiarities of the crystal, the following experiment was carried out. A crystal was mounted on a quartz disk and the spectral response curve determined with the quartz disk mounted against a black background. Then a layer of silver was evaporated on the back of the quartz plate without taking the crystal off, so as to create a mirror reflecting transmitted light and the spectral response curve was again determined. As is clear from Fig. 4 the apparent peak shifted from 3900 Å to 3950 Å.

A similar effect is observed with a background of white teflon. As the spectral response curves for the other compounds are all given for crystals on a white background it should be borne in mind that the long-wavelength side of the spectral dependence may be somewhat exaggerated.

It is of interest to note that in all materials except azulene photoconduction was detected at wavelengths where the optical absorption is negligible compared to its peak value. Stray light being ruled out by the use of suitable filters in the light beam, photoconduction was shown to take place in these materials as far out as 8000 Å, the limit of our instrument. No structure, except as mentioned for pyrene, could be observed, only a steady fall in sensitivity.

At the short-wavelength side of the spectral response curve some structure was always found. Although the accuracy at these wavelengths is rather poor owing to the low

Can. J. Chem. Downloaded from www.nrcresearchpress.com by 200.7.193.243 on 09/04/12
For personal use only.

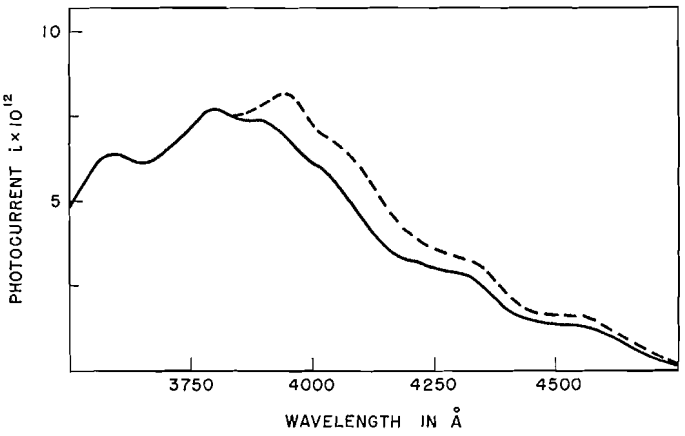

FIG. 4. Change of the spectral response of the surface photocurrent of a pyrene crystal with the reflective properties of the background. Solid curve: spectral response with a non-reflective background. Dotted curve: with a highly reflective background.

intensity of the incident light, peaks were usually observed at about 3600 Å and 3700 Å in pyrene.

In the course of obtaining absorption spectra for the pyrene crystals used in this work, it was observed that a weak absorption was present at the long-wavelength side of the absorption spectrum as given by Ferguson and Schneider (11). They observed the first main absorption band at 3750 Å. On crystals about 0.1 mm. thick, a shoulder on the main absorption was present with its center at 3832 Å.

DISCUSSION

From our results it appears that in pyrene and naphthalene light at the long-wavelength edge of the crystal absorption spectrum is very efficient in producing photoconduction. In naphthalene the peak of photoconduction appears at 3220 Å, where McClure and Schnepp (12) report a relatively weak absorption. However, in pyrene our measurements show peaks in photoconduction where there is no detectable absorption at all, even in crystals about 2 mm. thick.

There seem to be two possible explanations for this phenomenon. The first that comes to mind is the presence of an impurity. It is well known that commercial pyrene has a yellow color, and that this color persists after chromatographic purification through alumina (9). Chromatography through silica gel, however, yields completely colorless pyrene. After the first observations of the long-wavelength photoconduction, the chromatography through silica gel was repeated, but this did not change the appearance of the spectral response curve. Assuming an extinction coefficient of 10^4 for the impurity, to escape optical detection in a 1 mm. thick crystal, the concentration would have to be lower than 10^{-5} molar. If that impurity is then responsible for the photoconduction it must have a very high quantum yield. No organic photoconductors have been reported so far to possess this property. Moreover Carswell and Lyons (13) studied the influence of the addition of tetracene to anthracene on the photoconduction of anthracene. At the concentrations used (10^{-4} molar) no photoconduction by direct excitation of the tetracene could be observed. These considerations make it rather unlikely that an impurity can be held responsible for the observed effect.

We will therefore examine the other possibility, i.e. the photoconduction observed at the long-wavelength edge of the absorption spectrum is intrinsic and takes place by

Can. J. Chem. Downloaded from www.nrcresearchpress.com by 200.7.193.243 on 09/04/12
For personal use only.

direct excitation of the pyrene. Northrop and Simpson (14) have proposed levels of partly ionic character lying between the triplet and the singlet state. Terenin (15) introduced the concept of shared triplet levels, which would lie at the same energies. Lyons (16) considered the levels arising from the fact that an electron would be bound to a neutral molecule with the resulting hole on its neighbors. He thus concludes that there are a series of "ionized levels with bound electrons". For anthracene he calculated these levels to lie at energies lower and higher than the energy of the first singlet state. Murrell (17) pointed out that charge-transfer states too might be considered in this respect. All these levels have been suggested to be responsible for the electrical conduction in organic materials.

Ferguson and Schneider (11) report that the fluorescence of crystalline pyrene has its origin far below the first singlet state and propose to explain this by a charge-transfer process which would be facilitated by the close proximity of the pyrene molecules in the crystal. Contrary to naphthalene and anthracene, the molecules in the pyrene crystal lattice occur in pairs. Lyons (16) suggests that the absorption at 3339 Å as found in naphthalene (12) might be a direct observation of a transition to an ionized state.

At present it is still rather difficult to choose between the various mechanisms of photoconduction proposed by the different authors. Much more experimental work is needed to elucidate the exact nature of the transitions that can apparently take place between the ground state and some excited species with an energy lower than the singlet state. From the present work, however, the following conclusions can be drawn for crystalline pyrene:

A finite absorption exists between 4750 Å and the optically measured long-wavelength limit of the ultraviolet absorption spectrum. In this absorption, peaks appear at 4475 Å, 4275 Å, and 4100 Å. The transitions that take place in this region lead to states that are highly active in producing conduction, as is clear from the efficiency plot in Fig. 3. The peaks are at wavelengths between the absorption limit and the wavelengths of the fluorescent light as found by Ferguson and Schneider (11).

Similar conclusions can probably be drawn for naphthalene, where McClure and Schnepp (12) and various other workers reported weak absorptions in the region of maximum photoconductivity, as reported in this work.

For stilbene and terphenyl the crystal spectra so far are not available. The case of azulene is interesting because in first approximation the photoconductive response appears to coincide with the absorption to the second singlet state as measured by Sidman and McClure (18) in a solid solution of naphthalene. No photoconduction was found in the region of the absorption to the first singlet state. It is of interest to note that Beer and Longuet-Higgins (19) as well as Viswanath and Kasha (20) found that azulene does not fluoresce when it is irradiated in its first absorption band, but that it does fluoresce when irradiated in the second absorption band. Apparently the same mechanism that inhibits fluorescence also inhibits photoconduction.

The observation of photoconduction at longer wavelengths than the absorption spectrum may be useful to solve the problem of the apparent discrepancy between the thermal and optical activation energy. Pick and Wissman (21) showed that the thermal activation energy for naphthalene semiconduction in a high vacuum is 3.7 ev. This agrees well with the optical threshold energy as found in this work for naphthalene: 3400 Å $\approx$ 3.65 ev. Inokuchi (2) found for pyrene bulk currents, where gas effects will be limited, 2.4 ev., while the optical threshold appears to be at 4750 Å $\approx$ 2.61 ev. The threshold has been taken as the wavelength where the photoconductive sensitivity is approximately one hundredth of its peak value in crystals of about 1 mm. thickness. In view of the extended

Can. J. Chem. Downloaded from www.nrcresearchpress.com by 200.7.193.243 on 09/04/12
For personal use only.

long-wavelength tail, however, the concept threshold becomes rather vague, and in this respect Northrop and Simpson's idea (14) of a large number of levels, of which the higher ones contribute more to the conduction than the lower ones, becomes attractive.

ACKNOWLEDGMENTS

The authors are indebted to Dr. L. E. Lyons for the opportunity of reading his manuscript before its publication. Thanks are due to Dr. J. N. Murrell with whom we had some interesting discussions.

REFERENCES

1. Bree, A., Carswell, D. J., and Lyons, L. E. J. Chem. Soc. 1728 (1955).
2. Inokuchi, H. Bull. Chem. Soc. Japan, **29**, 131 (1956).
3. Zinszer, H. J. Z. Naturforsch. **11***a*, 306 (1956).
4. Compton, D. M. J., Waddington, T. C., and Schneider, W. G. J. Chem. Phys. **27**, 160 (1957).
5. Lyons, L. E. and Morris, G. C. Proc. Phys. Soc. (London), B, **69**, 1162 (1956).
6. Kommandeur, J., Korinek, G. J., and Schneider, W. G. Can. J. Chem. **35**, 998 (1957).
7. Lyons, L. E. and Morris, G. J. Chem. Soc. 3668 (1957).
8. Lipsett, F. R. Can. J. Phys. **35**, 284 (1957).
9. Sangster, D. C. and Irvine, J. W. J. Chem. Phys. **24**, 670 (1956).
10. Chynoweth, A. G. and Schneider, W. G. J. Chem. Phys. **22**, 1021 (1954).
11. Ferguson, J. and Schneider, W. G. J. Chem. Phys. (To be published).
12. McClure, D. S. and Schnepp, O. J. Chem. Phys. **23**, 1575 (1955).
13. Carswell, D. J. and Lyons, L. E. J. Chem. Soc. 1734 (1955).
14. Northrop, D. C. and Simpson, O. Proc. Roy. Soc. (London), A, **234**, 124 (1955).
15. Terenin, A. N. Radiotekh. i Elektron. **1**, 1127 (1956).
16. Lyons, L. E. To be published.
17. Murrell, J. N. Symposium on the structure and reactivity of electronically-excited species. University of Ottawa, Ottawa, Canada, September 5 and 6, 1957.
18. Sidman, J. W. and McClure, D. S. J. Chem. Phys. **24**, 757 (1956).
19. Beer, M. and Longuet-Higgins, H. C. J. Chem. Phys. **23**, 1390 (1955).
20. Viswanath, G. and Kasha, M. J. Chem. Phys. **24**, 579 (1956).
21. Pick, H. and Wissman, W. Z. Physik, **138**, 436 (1954).

Can. J. Chem. Downloaded from www.nrcresearchpress.com by 200.7.193.243 on 09/04/12
For personal use only.

Can. J. Chem. Downloaded from www.nrcresearchpress.com by 200.7.193.243 on 09/04/12
For personal use only.

SOME NEW FLUORIDE COMPLEXES OF TRIVALENT TITANIUM[1]

NORMAN F. H. BRIGHT[2] AND JOSEPH G. WURM[3]

ABSTRACT

Three new complex fluorides of trivalent titanium have been isolated from the products of electrolysis, under an inert atmosphere, of molten baths of KCl, NaCl, or mixtures of KCl and NaCl, containing either K_2TiF_6 or Na_2TiF_6. Electrolytic baths containing a mixture of KCl and NaCl with either K_2TiF_6 or Na_2TiF_6 yielded a violet-colored, face-centered cubic compound identified as K_2NaTiF_6, which was virtually insoluble in water and amenable to electrostatic separation from the metallic titanium also produced in the electrolysis. Baths containing molten mixtures of K_2TiF_6 and KCl gave a pale violet compound K_3TiF_6, which was slightly soluble in water. Baths containing Na_2TiF_6 and NaCl gave a deep violet-colored compound Na_3TiF_6 which was almost insoluble in water. The compounds K_3TiF_6 and Na_3TiF_6 have structures which approximate to cubic. The compounds K_2NaTiF_6 and Na_3TiF_6 are more stable to atmospheric oxidation than is K_3TiF_6. X-Ray diffraction patterns have been recorded for these compounds and some of their physical and chemical properties determined.

1. INTRODUCTION

The mechanism of titanium production by the electrolysis of fused alkali halide baths containing complex titanium salts of the type Na_2TiF_6 or K_2TiF_6 has recently been discussed by Wurm, Gravel, and Potvin (1). In the course of their work, certain products were obtained which yielded X-ray diffraction patterns corresponding to no previously published data. A preliminary notice of the isolation of the compounds giving rise to these patterns appeared in the above-mentioned publication. The present paper represents an amplification of this information and gives details of the X-ray and other data obtained on three new complex titanium fluorides which were isolated from the electrolytic products.

2. EXPERIMENTAL PROCEDURES

The alkali titanofluorides, having the formula M_2TiF_6, based on tetravalent titanium, are readily soluble in molten alkali chlorides in the temperature range 650° C. to 850° C., depending upon the particular compounds involved.

The electrolytic baths contained, at the start of the electrolysis, 20 to 30% of either Na_2TiF_6 or K_2TiF_6 in solution in a molten mixture of NaCl and KCl, having approximately the eutectic composition of 55% KCl, by weight. In certain later electrolyses, solutions of Na_2TiF_6 in NaCl and of K_2TiF_6 in KCl were used to yield products in which only one type of alkali ion was present in each case.

When these molten baths were subjected to electrolysis under an argon atmosphere, using a water-cooled stainless-steel cathode and a graphite crucible containing the melt as anode, the products of the electrolysis, examined after they had cooled and solidified, showed the following phenomena:

(*a*) Surrounding the cathode was a spherical core or "nut", composed of dendritic metallic titanium crystals embedded in a salt of deep violet color.

(*b*) Around the outside of this "nut" was the solidified salt bath, having a pale violet color.

[1]*Manuscript received November 1, 1957.*
Contribution from the Mineral Dressing and Process Metallurgy Division, Mines Branch, Department of Mines and Technical Surveys, Ottawa, and the Faculté des Sciences, Université Laval, Québec. Published with the permission of the Director, Mines Branch, Ottawa.
[2]*Head, Physical and Crystal Chemistry Section, Mineral Dressing and Process Metallurgy Division, Mines Branch, Ottawa.*
[3]*Faculté des Sciences, Université Laval, Québec.*

The cathodic "nut" was crushed and separated into its constituents by electrostatic means, yielding the titanium metal and the violet salt substantially free from each other. The crystalline salts were examined by the standard procedures of X-ray diffraction analysis, using CoK_α radiation and 57.3 mm. diameter Debye–Scherrer powder cameras. Occasionally, for greater precision in measuring line spacings, a 114.6 mm. diameter camera was used.

The solidified melt surrounding the "nut" was examined similarly, both directly as obtained and also after it was leached with boiling distilled water in the proportion of 2 g. of crushed melt to 25 ml. of water to dissolve the alkali chlorides and concentrate the remaining materials which carry the violet color. Residues of deep violet color, almost insoluble in water, were obtained by this leaching. These residues were analyzed chemically for sodium, potassium, total and trivalent titanium, chloride, and fluoride. Certain reference materials, used for preparing X-ray patterns in attempts to identify the unknown substances, were also analyzed chemically; these included the pure starting titanofluorides, Na_2TiF_6 and K_2TiF_6, and sodium titanate. All the chemical analyses referred to in this paper were done in the Chemical Laboratory of the Division of Mineral Dressing and Process Metallurgy, Mines Branch, Ottawa.

A résumé of the analytical procedures used is as follows:

Potassium and sodium.—Fluorine removed by evaporation of the sample with dilute sulphuric acid three times; titanium removed by hydrolysis of aqueous solution of product; potassium and sodium determined with a Perkin-Elmer flame photometer.

Fluorine.—HF steam-distilled off at 135°–140° C. from an aqueous perchloric acid solution of the sample. Fluorine determined amperometrically at pH = 7.0 using thorium nitrate solution previously standardized against NaF.

Chlorine.—Determined by potentiometric titration with 0.05 N $AgNO_3$ of a sulphuric/nitric acid solution of the sample. Less than one drop of reagent was required for a 0.2 g. sample, in those cases where chlorine was not expected to be present.

Titanium (total).—Residue from fluorine distillation reduced with zinc amalgam and titrated with ferric alum.

Titanium (trivalent).—Sample dissolved in aqueous sulphuric acid and titrated with ferric alum, all under an argon atmosphere. Alternatively, sample dissolved in ferric alum solution, and the reduced iron (equivalent to the trivalent titanium) titrated with standard potassium dichromate.

3. EXPERIMENTAL RESULTS

A comparison of the X-ray diffraction patterns of a considerable group of electrolytic products, using either Na_2TiF_6 or K_2TiF_6 as the starting material, in solution in mixed NaCl–KCl, showed that the principal products in all the solidified melt samples were sodium and potassium chlorides, each containing some of the other in solid solution. However, of greater interest was a group of weaker diffractions which was the same regardless of the initial material used. The violet materials, obtained as residues after the alkali chlorides were leached out, gave this same group of diffractions but in much greater strength. The same pattern was obtained from the violet material obtained from the cathodic "nut". In some of the leached products, no other pattern was detectable, and thus, presumably, the material giving rise to this set of diffractions was reasonably pure in these particular products.

The chemical analyses of the insoluble residues resulting from the water leaching of the electrolytic fusion products using K_2TiF_6 or Na_2TiF_6 with the mixed alkali chlorides are given in Table I. The two analyses obviously correspond to the same substance.

Can. J. Chem. Downloaded from www.nrcresearchpress.com by 200.7.193.243 on 09/04/12
For personal use only.

TABLE I

Element	Product using Na_2TiF_6 as starting material, % by weight	Product using K_2TiF_6 as starting material, % by weight	Theoretical for K_2NaTiF_6, % by weight
Na	9.5±0.1	9.5±0.1	8.74
K	27.5±0.1	27.4±0.1	29.72
Ti (total)	17.7±0.25	(i) 17.7±0.25 (ii) 17.6±0.25 Mean 17.7±0.25	18.21
Ti (trivalent)	17.7±0.5	17.6±0.5	18.21
F	40.2±0.25	43.1±0.25	43.33
Cl	None detectable	None detectable in 50 mg. sample	Nil

It can be seen from these analyses that the molecular formula for either material is very close to K_2NaTiF_6. The theoretical figures for this compound are also given in Table I.

From the chemical data alone, however, the material could equally well be a mixture of K_3TiF_6 and Na_3TiF_6 in the proportion of approximately 2 : 1. It therefore remained to determine whether this material (to which has been assigned the formula K_2NaTiF_6) is, in fact, a discrete compound in its own right, or merely one particular composition in a solid-solution series K_3TiF_6–Na_3TiF_6, should such a series exist. The fact that the same composition was obtained using either K_2TiF_6 or Na_2TiF_6 in molten NaCl–KCl as the starting material strongly supports the view that a single compound was present, rather than merely one particular composition in a solid-solution series. If it were a member of a solid-solution series, one might expect to obtain different compositions in the two cases. The matter was resolved with reasonable certainty by studying the products of electrolyses in which either K^+ or Na^+ ions were the sole alkali ions present.

The material obtained from the electrolysis of Na_2TiF_6 in NaCl was a deep violet in color, virtually insoluble in water, and gave the analysis given in Table II. This analysis corresponds very closely to Na_3TiF_6, and the titanium is all in the trivalent state, in accordance with the color of the material.

TABLE II

Element	% by weight	Theoretical for Na_3TiF_6
K	None detectable	Nil
Na	29.9±0.1	29.88
Ti (total)	20.2±0.25	20.74
Ti (trivalent)	20.2±0.5	20.74
F	49.7+0.25	49.38
Cl	0.034	Nil

The preparation of the corresponding potassium compound was more troublesome, since the material obtained by leaching out the KCl was readily oxidized in air. By evaporation of the water under an argon atmosphere, however, a product was obtained which contained either some unchanged or regenerated K_2TiF_6, a trace of residual KCl, and a compound of pale violet color, slightly soluble in water. In the analysis of this material, the chloride present was used as a measure of the KCl, the tetravalent titanium (i.e. total titanium minus trivalent titanium) used as a measure of the K_2TiF_6 present, and the remainder of the composition calculated accordingly. The results of this analysis are given in Table III.

The molecular formula of the compound calculated on this basis is $K_{2.997}TiF_{5.994}$,

Can. J. Chem. Downloaded from www.nrcresearchpress.com by 200.7.193.243 on 09/04/12
For personal use only.

TABLE III

Element	% by weight
Na	None detected
K	41.6±0.1
F	40.7±0.25
Cl	0.02
Ti (total)	17.1±0.25
Ti (trivalent)	15.4±0.5
Ti (tetravalent)	1.7 (by difference)

i.e. K_3TiF_6, and the composition of the product then works out at K_3TiF_6, 90.9%; K_2TiF_6, 8.4%; KCl, 0.34%.

When this product was examined by microscope, a very small amount of KCl was visible. Approximately 10% of colorless needle-shaped crystals were observed, having one refractive index $\omega = 1.475$ and the other (ϵ) slightly lower; this is in accord with the known optical properties of K_2TiF_6. The remaining material, about 90%, had a refractive index of approx. 1.406 and was slightly anisotropic. These proportions are in excellent accord with the above chemical analyses.

The material to which the formula K_2NaTiF_6 has been assigned was strictly isotropic optically and had a refractive index of 1.408. The compounds Na_3TiF_6 and K_3TiF_6 were both slightly birefringent, Na_3TiF_6 having refractive indices of $\omega = 1.387$ and $\epsilon = 1.382$, and K_3TiF_6 having refractive indices of $\omega = 1.406$ and $\epsilon =$ slightly lower than 1.406.

The mixed potassium–sodium material gave a face-centered cubic pattern based on a

TABLE IV

X-RAY POWDER DIFFRACTION PATTERN OF COMPOUND K_2NaTiF_6

(*hkl*)	Mean observed intensity*	Mean observed *d*-spacing, Å	Calculated† *d*-spacing, Å
111	35	4.8362	4.8306
002	15	4.1853	4.1835
022	100	2.9519	2.9581
113	7	2.5133	2.5227
222	50	2.4114	2.4153
004	90	2.0871	2.0917
133	3	1.9205	1.9195
024	8	1.8657	1.8709
224	50	1.7042	1.7079
115, 333	15	1.6064	1.6102
044	60	1.4766	1.4791
135	8	1.4088	1.4143
006, 244	5	1.3861	1.3945
026	25	1.3224	1.3229
335	3	1.2825 (?)	1.2759
226	10	1.2597	1.2614
444	25	1.2066	1.2077
117, 155	7	1.1704	1.1716
046	5	1.1571	1.1603
246	40	1.1167	1.1181
137, 355	5	1.0907	1.0893
008	15	1.0449	1.0459
228, 066	25	0.98562	0.98605
048	35	0.93561	0.93545
119, 357	5	0.91824	0.91839

**Strongest line assessed visually as 100.*

†*Based on a cubic cell edge of 8.3669* Å.

Can. J. Chem. Downloaded from www.nrcresearchpress.com by 200.7.193.243 on 09/04/12
For personal use only.

TABLE V

X-RAY DIFFRACTION PATTERN OF THE COMPOUND Na_3TiF_6

Line No.	Observed intensity*	Observed *d*-spacing, Å	Line No.	Observed intensity*	Observed *d*-spacing, Å
1	50	4.646	26	5	1.438
2	20	4.525	27	12	1.415‡
3	60	3.976	28	10	1.391
4	8	3.566	29	20	1.357†
5	100	2.837†	30	5	1.313
6	20	2.765	31	5	1.281
7	40	2.496	32	20	1.265
8	40	2.427	33	10	1.249
9	60	2.393	34	10	1.234
10	5	2.330	35	10	1.216
11	30	2.216	36	10	1.193
12	30	2.155	37	5	1.169
13	90	1.999	38	5	1.154
14	10	1.947†	39	5	1.137
15	5	1.854	40	5	1.125
16	27	1.812	41	10	1.112
17	30	1.793	42	10	1.073
18	30	1.769	43	10	1.052
19	10	1.719	44	5	1.038
20	70	1.650	45	5	1.027
21	80	1.618	46	5	0.9906
22	40	1.608	47	5	0.9723
23	8	1.549	48	20	0.9473
24	5	1.500	49	10	0.9385
25	7	1.467	50	20	0.9322

**Strongest line assessed visually as 100.*
†Diffuse.
‡Doublet.

TABLE VI

X-RAY DIFFRACTION PATTERN OF THE COMPOUND K_3TiF_6

Line No.	Observed intensity*	Observed *d*-spacing, Å	Line No.	Observed intensity*	Observed *d*-spacing, Å
1	35	4.978	18	7	1.678
2	20	4.355	19	5	1.629
3	40	3.076	20	5	1.544
4	100	3.024	21	30	1.517
5	5	2.761	22	10	1.383
6	5	2.643	23	5	1.340
7	10	2.496	24	5	1.246
8	10	2.403	25	3	1.187
9	5	2.308	26	5	1.169
10	10	2.263	27	3	1.158
11	40	2.186	28	3	1.122
12	17	2.106	29	3	1.031
13	10	1.994	30	3	1.012
14	5	1.902	31	3	0.9982
15	5	1.845	32	3	0.9799
16	40	1.773	33	3	0.9610
17	17	1.741	34	3	0.9504

**Strongest line assessed visually as 100.*

cell edge of 8.3669 Å. The *d*-spacings observed, together with the indices of the various reflections and the calculated *d*-spacings using the above cell edge, are given in Table IV.

The X-ray spacings for the compound Na_3TiF_6 are given in Table V. It can be shown

Can. J. Chem. Downloaded from www.nrcresearchpress.com by 200.7.193.243 on 09/04/12
For personal use only.

that the main diffractions conform approximately to a cubic arrangement but that some distortion either of cell edge or of angle has occurred to cause a departure from the true cubic structure. The crystallography was not studied further because no single crystals of this compound of sufficient size were obtained.

Similarly, the compound K_3TiF_6 gave the X-ray diffraction data shown in Table VI. These data also indicate a slight distortion from a cubic structure, though probably not in the same way as for Na_3TiF_6. Again the crystallography has not been studied further.

4. DISCUSSION

The question to be decided is whether the material to which has been assigned the formula K_2NaTiF_6 should properly be regarded as a compound in its own right, or whether it is merely one particular member in a solid-solution series of which the end members are the compounds Na_3TiF_6 and K_3TiF_6, if such a solid-solution series in fact exists.

It has been shown that both end members are slightly anisotropic optically, whereas the material containing both potassium and sodium is strictly isotropic. This is strong, though not conclusive, evidence that K_2NaTiF_6 is a definite compound, since certain cases are known in which an optically isotropic member of a solid-solution series exists where neither end member is isotropic. A notable example of this exceptional optical behavior is in the melilite solid-solution series (2); here the end members, akermanite $2CaO.MgO.2SiO_2$ (3) and gehlenite $2CaO.Al_2O_3.SiO_2$ (4), are both anisotropic but an intermediate composition of approximately 65% akermanite: 35% gehlenite is isotropic.

If this behavior were applicable in the present instance, then the refractive index of the mixed sodium–potassium material would have to lie between the values given by the two end members, Na_3TiF_6 and K_3TiF_6. This is not the case, however, as the refractive index of K_2NaTiF_6 is 1.408 whereas the values for K_3TiF_6 are 1.406 and slightly below 1.406, and the values for Na_3TiF_6 are 1.387 and 1.382. In a solid-solution series, it is normal for the refractive index of an intermediate member to approximate to the value obtained by a linear interpolation between the values for the end members. In this case the intermediate material gives a value lying outside the range of values given by the end members; hence this is not analogous to the melilite behavior. This strongly suggests that the material K_2NaTiF_6 is to be considered as a compound and not as a member of a solid-solution series.

This optical evidence is further supported by the X-ray diffraction data, which show that the pattern given by K_2NaTiF_6 can be completely indexed according to a cubic unit cell; by contrast, neither K_3TiF_6 nor Na_3TiF_6 possesses a cubic structure, although both are close to it. Thus, the fact that neither the potassium nor the sodium compound is cubic, whereas the mixed potassium–sodium material is strictly so, is a cogent argument in favor of regarding K_2NaTiF_6 as a true compound. It may be mentioned by way of contrast that in the case of the melilites, referred to above, all members of the series, including the isotropic member, have a tetragonal structure with a c/a ratio in the range 0.6 to 0.7.

The above arguments support the validity of the contention that K_2NaTiF_6 is a definite compound in its own right. The strongest evidence, however, lies in the fact that the same composition is obtained regardless of whether K_2TiF_6 or Na_2TiF_6 is used as the starting material with the NaCl/KCl eutectic in the electrolytic preparation.

There are, thus, the following arguments in favor of the K_2NaTiF_6 being a definite compound:

Can. J. Chem. Downloaded from www.nrcresearchpress.com by 200.7.193.243 on 09/04/12
For personal use only.

(*a*) Its isotropic optical behavior, as contrasted with those of K_3TiF_6 and Na_3TiF_6.

(*b*) The value of its refractive index as compared with those of K_3TiF_6 and Na_3TiF_6.

(*c*) Its cubic X-ray pattern.

(*d*) The constancy of its chemical composition, irrespective of starting material.

Additional unequivocal evidence could have been provided by conducting liquidus determinations across the system K_3TiF_6–K_2NaTiF_6–Na_3TiF_6, when, if K_2NaTiF_6 were a true compound, a peak in the liquidus curve would have been obtained at that composition. It would also have been of interest to attempt to prepare the mixed potassium–sodium material from an appropriate mixture of the pure potassium and sodium compounds. However, the small quantities of material available precluded these two lines of investigation from being followed.

It is of interest to note that an exactly analogous series of compounds is known in the complex aluminofluorides, viz. K_3AlF_6, K_2NaAlF_6, and Na_3AlF_6; in this series, the mixed potassium–sodium compound is cubic and neither the sodium nor the potassium compound alone is cubic. Thus, K_3AlF_6 (potassium cryolite) is tetragonal with $c_0 = 8.468$ Å and $a_0 = 5.944$ Å (5); K_2NaAlF_6 (elpasolite) is cubic with $a_0 = 8.109$ Å (6); and Na_3AlF_6 (cryolite) is monoclinic (almost orthorhombic, and not far removed from tetragonal) with $a_0 = 7.80$ Å, $b_0 = 5.61$ Å, $c_0 = 5.46$ Å, and $\beta = 90°11'$ (7).

In addition, many other six-coordinated complexes of transitional elements containing two different alkali elements crystallize in the cubic system. The corresponding compounds containing one alkali element only in many cases either do not exist, or are not very stable, or do not crystallize in the cubic system. This behavior is due to the greater ease of packing three alkali ions of two different sizes (two larger, and one smaller) than of packing three ions of equal size.

The three compounds described in this paper are examples of new complexes in which the titanium is present in the trivalent state. Various compounds have been described in a more or less complete manner from a chemical viewpoint, in which the titanium in the trivalent condition was the starting material, and which were supposed still to contain the titanium in that state. In no case, however, was there any specific analysis for trivalent titanium in the product, but merely for total titanium content. Also, no crystallographic data (either optical or X-ray) have been provided for such compounds. These earlier publications included the following:

(*a*) Work by Piccini (8) in which compounds designated as $(NH_4)_3TiF_6$, K_2TiF_5, and $(NH_4)_2TiF_5$ were produced by the electrolytic reduction of fluotitanates in an aqueous solution of either NH_4F or KF. These compounds were in no case obtained in the pure state.

(*b*) Work by Petersen (9) in which $(NH_4)_3TiF_6$ was obtained by the cadmium reduction of aqueous K_2TiF_6 in warm hydrochloric acid solution with subsequent addition of NH_4F.

(*c*) Work by Stähler and his co-workers (10, 11) in which hydrated complexes of titanium trihalides were produced; these workers also prepared hydrated trivalent sulphates, oxalates, acetates, formates, and thiocyanates. In all cases the titanium was considered as forming part of a coordination complex.

(*d*) Work by Schumb and Sundström (12) in which ammine complexes of titanium di- and tri-chlorides were prepared.

In a recent patent (13), complexes containing divalent and trivalent titanium are claimed, but they were not isolated nor identified precisely.

Can. J. Chem. Downloaded from www.nrcresearchpress.com by 200.7.193.243 on 09/04/12
For personal use only.

Thus, in the present work, three new compounds have been described which are complexes containing trivalent titanium. They have been characterized by chemical analysis, optical data, and X-ray crystallographic study.

ACKNOWLEDGMENTS

The authors wish to express their thanks to members of the Mines Branch staff, especially to Miss E. M. Penner, Mr. L. G. Ripley, and Mr. R. C. McAdam for the difficult and painstaking chemical analyses done in connection with this work, and to Mr. Richard H. Lake for valuable assistance with the X-ray diffraction work.

REFERENCES

1. WURM, J. G., GRAVEL, L., and POTVIN, R. J. A. J. Electrochem. Soc. **104**, 301 (1957).
2. ERVIN, G., Jr. and OSBORN, E. F. Am. Mineralogist, **34**, 717 (1949).
ANDREWS, K. W. Mineral. Mag. **28**, 374 (1948).
3. O'DANIEL, H. and TSCHEISCHWILI, L. Neues Jahrb. Mineral. Geol. u. Paläontol., Monatsh. A. Jahrg. (1945–48), p. 65.
4. RAAZ, F. Sitzber. Akad. Wiss. Wien, Math.-naturw. Kl., Abt. I, **139**, 645 (1930).
5. BROSSET, C. Arkiv Kemi, Mineral. Geol. **21A**, No. 9 (1946). *Quoted in* Crystal data *by* J. D. H. Donnay and W. Nowacki. Published by the Geological Society of America. 1954. p. 367.
6. FRONDEL, C. Am. Mineralogist, **33**, 84 (1948).
7. NARAY-SZABO, St. v. and SASVARI, K. Z. Krist. **99**, 27 (1938).
8. PICCINI, A. Compt. rend. **97**, 1064 (1883).
9. PETERSEN, E. J. prakt. Chem. **40**, 44 (1889).
10. STÄHLER, A. Ber. deut. chem. Ges. **37**, 4405 (1904).
11. STÄHLER, A. and WIRTHWEIN, H. Ber. deut. chem. Ges. **38**, 2619 (1905).
12. SCHUMB, W. C. and SUNDSTRÖM, R. F. J. Am. Chem. Soc. **55**, 596 (1933).
13. MCKENNA, Q. H. Preparation of double fluorides of titanium and an alkali metal. U.S. Patent No. 2,772,946, December 4, 1956.

Can. J. Chem. Downloaded from www.nrcresearchpress.com by 200.7.193.243 on 09/04/12
For personal use only.

Can. J. Chem. Downloaded from www.nrcresearchpress.com by 200.7.193.243 on 09/04/12
For personal use only.

MOLECULAR REARRANGEMENTS IN THE REACTIONS OF OXYGEN ATOMS WITH OLEFINS[1]

R. J. CVETANOVIĆ

ABSTRACT

Reactions of oxygen atoms with propylene, butene-1, *iso*-butene, *cis*-butene-2, *trans*-butene-2, *cis*-pentene-2, and tetramethyl ethylene have been studied at room temperature and at pressures between 50 and 600 mm. The following generalizations can be made. The oxygen atom adds predominantly to the "less-substituted" carbon atom of the olefinic double bond to form a short-lived biradical which rapidly rearranges into isomeric epoxy and carbonyl compounds. Rearrangements involve migration of radicals (including H atoms) from the carbon atom to which oxygen is attached to the other carbon atom of the original double bond. Partly inhibited rotation around the original double bond also takes place. Migration of H atoms is exclusively internal. Migration of larger radicals, such as CH_3, is only partly internal: a large fraction of these radicals become completely detached from the rest of the molecule and the particular carbonyl compound is produced both by radical combination and by internal migration. The fragmentation resulting from the splitting off of a migrating radical is pressure independent. The final addition products formed are "hot" as a result of high heats of reaction and undergo decomposition if the excess energy is not removed by collisions. This second type of fragmentation is, therefore, pressure dependent. It is very extensive in the case of ethylene and appears to be completely suppressed in the investigated pressure range in the case of more complex olefins (possessing a greater number of degrees of freedom) such as butenes and higher homologues. Propylene exhibits an intermediate behavior. For orientation of addition of oxygen atoms a carbon atom of an olefinic double bond to which CH_3 is attached is "less substituted" than a corresponding carbon atom to which C_2H_5 is attached.

INTRODUCTION

In a previous publication (1) some preliminary results of a study of the reactions of oxygen atoms with a number of butenes have been briefly reported. This investigation has two distinct objectives: (1) to establish the general mechanism and the type of products formed, and (2) to obtain information on the rates of these reactions. In the present paper the first of the two aspects of the investigation is presented in detail and is extended to some further olefins studied in the meantime.

This work is a part of a more extensive study of the reactions of oxygen atoms with different organic compounds. The reactions with ethylene (2) and acetaldehyde (3) have already been described, while the results obtained with some other types of compounds will be published at a later date. Oxygen atoms are generated by mercury-photosensitized decomposition of nitrous oxide (4) and are probably in their ground, triplet $O(^3P)$, state. The amount of nitrogen formed gives a direct quantitative measure of the oxygen atoms generated and serves as an internal actinometer.

EXPERIMENTAL

A conventional-type high-vacuum apparatus was used. It incorporated a cylindrical silica reaction cell, 5 cm. in diameter and 10 cm. long, an all-glass circulating pump supported on teflon bearings, a LeRoy still (5), and a constant volume burette with a copper oxide tube and outlets for sampling tubes connected with it. Two low-pressure mercury lamps were placed one at each end of the reaction cell and were used singly or simultaneously as the source of mercury resonance radiation.

For the analysis of products use was made of the LeRoy still (for a preliminary separation into fractions), the copper oxide tube in conjunction with the constant-volume

[1]*Manuscript received November 27, 1957.*
Contribution from the Division of Applied Chemistry, National Research Council, Ottawa, Canada.
Issued as N.R.C. No. 4638.

Can. J. Chem. Downloaded from www.nrcresearchpress.com by 200.7.193.243 on 09/04/12
For personal use only.

burette (for the analysis of the non-condensables), gas–liquid chromatography (GLC), infrared and mass spectroscopy. An attempt was made, whenever possible, to verify the qualitative identification of the products by directly comparing the GLC relative elution times (6) and the infrared and mass spectra for the unknown product (after separation on GLC) and for a standard sample of the corresponding compound. In one or two cases a standard sample was not available and the identification was based on the comparison of the mass and infrared spectra with the existing literature data. In the early stages of the investigation, before the type of products formed was established, relative elution times were determined for a number of different C_4H_8O isomers and, thus, several possibilities were readily ruled out. A 10 ft. column of dinonyl phthalate on glass spheres (passing 270 mesh) was used, and the GLC apparatus differed from the one previously described (7) in that the low pressure (*ca.* 30 mm.) at the outlet of the column was maintained constant by inserting a suitable *internal* capillary in the lead to the high-vacuum pump and not by an external leak. A better stability was obtained in this manner and a gradual deterioration in the performance of the high-vacuum pump was prevented. The inlet pressure was maintained at 14 p.s.i. and the column temperature varied from 25° to 110° C. depending on the volatility of the products.

Best available grades of reactants were used after thorough degassing and bulb-to-bulb distillation *in vacuo*. N.B.S. samples of *cis*-pentene-2 and 3-methylheptane were kindly supplied by the Stanford Research Institute. *cis*-C_4D_8-2 was prepared by Dr. L. C. Leitch of these laboratories. Molecular oxygen was produced by heating reagent grade $KMnO_4$.

In the experiments carried out a large excess of nitrous oxide was used (100 to 600 mm. N_2O and usually only a few millimeters of the olefin). The ratio of the over-all quenching efficiency of an olefin and nitrous oxide is about 2 (8). The quantum yield of decomposition of nitrous oxide, however, is quite high (3) while that of olefins is as a rule very low, especially at the high total pressures used (9). Experimental conditions, therefore, could be readily adjusted so as to eliminate complications from direct quenching decompositions of olefins. By not extending the reactions to too high conversions, secondary reactions involving the products could also be avoided. Actually no trends in the rates of formation of the products per oxygen atom consumed were observed, except at very high conversions, after most of the olefin was consumed.

RESULTS

Experiments carried out with a number of hydrocarbons have shown that in general three types of reactions may be expected between the ground-state oxygen atoms and olefins: (1) addition of atoms to the olefin to form addition products, (2) fragmentation of the initially produced addition products, and (3) hydrogen abstraction.

Hydrogen Abstraction

At room temperature at least, and with the olefins studied so far, no evidence was found of any direct hydrogen abstraction by oxygen atoms. This finding is in agreement with the observed much higher rates of addition of oxygen atoms to the olefinic double bond relative to the hydrogen abstraction from paraffins. Thus, for example, the addition of oxygen atoms to *cis*-pentene-2 was found to be 43 times faster than the reaction of oxygen atoms with 3-methylheptane. It is conceivable, however, that with certain olefins a small amount of direct hydrogen abstraction takes place even at room temperature and that at elevated temperatures the abstraction reaction might become quite important.

Reaction of Oxygen Atoms with Propylene

In the reactions reported in the present communication the observed addition compounds, isomeric epoxides and carbonyl compounds, are the major reaction products, although a certain amount of fragmentation occurs as well. In this respect propylene exhibits a behavior intermediate between that of ethylene on one side and higher alkenes on the other. In the case of ethylene (2) extensive fragmentation takes place (CO yield ≈ 0.5). At best very little ethylene oxide is formed, and while the remainder of the oxygen is recovered mainly in the form of aldehydes at least a large fraction of these results from free-radical reactions. There is, however, an indication of a pressure effect, although this is quite small: there is a slight increase in the yields of aldehyde and ethylene oxide and a decrease in CO with increasing pressure. In contrast to this, in the case of higher olefins, taking as an example butene-1, large amounts of α-butene oxide and *n*-butyraldehyde are formed by direct addition of oxygen atoms and subsequent molecular rearrangement, their yields are pressure independent between 100 and 600 mm. within the experimental error, and there is relatively little fragmentation. The main trends observed in the case of propylene are shown in Fig. 1. At higher pressures

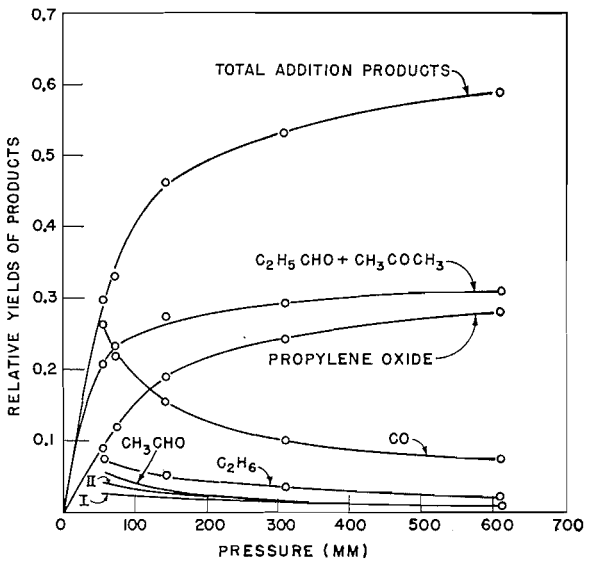

FIG. 1. Products observed in the room-temperature reaction of oxygen atoms with propylene at various total pressures. Curve I gives the yields of H_2 and also those of C_2H_4. Curve II gives the yields of CH_4. (For H_2, C_2H_4, CH_4, and CH_3CHO experimental points are not shown because of the mutual proximity and partial overlapping of the curves.)

increasing amounts of propylene oxide and propionaldehyde are formed and the character of the reaction approaches the one exhibited by butene-1, while at lower pressures fragmentation becomes more important and the reaction in many respects resembles that of ethylene. The pronounced pressure effect in the case of propylene is of particular interest and will be further discussed in the following section. With the chromatographic column used acetone could not be resolved from propionaldehyde, and total peak areas for the two compounds are plotted in Fig. 1. Infrared and mass spectra indicated large predominance and perhaps exclusive formation of the aldehyde. One separation was carried out on a 50 ft. tricresyl phosphate on firebrick column (120°) on which the two compounds completely resolved, and the ratio of the peak area of the aldehyde to that of acetone was about 9:1.

Can. J. Chem. Downloaded from www.nrcresearchpress.com by 200.7.193.243 on 09/04/12
For personal use only.

Formation of Addition Products

The addition products formed in the different reactions studied are summarized in Table I. The fractions of the addition products given in the table are based on GLC peak areas, taking the sum of the peak areas of all the addition products observed as unity. In some cases, as, for example, *cis*-β-butene oxide and *iso*-butanal as well as for *cis*-β-pentene oxide and 2-methylbutanal, the peaks partially overlapped and were approximately resolved graphically to obtain the individual peak areas. The last column in Table I gives the sum of the peak areas of all the fragmentation products observed by GLC analysis as a fraction of the total peak area of all the products (both addition and fragmentation). No attempt was made to identify the very small amounts of these fragmentation products in the cases where they were observed. In the case of butene-1 they seemed to consist largely of acetaldehyde and propionaldehyde.

TABLE I

PRODUCTS OBSERVED BY GLC ANALYSIS

(After removal of the unconsumed reactants and of any products of the same or greater volatility)

Reactant	Addition products[a]				Fragmentation products[b]
	Epoxides		Carbonyl compounds		
Propylene	Propylene oxide	0.50[c]	Propanal Acetone	0.50[c,d]	
Butene-1	α-Butene oxide	0.53	*n*-Butanal Methylethyl ketone	0.43 0.04	0.06
iso-Butene	*iso*-Butene oxide	0.54	*iso*-Butanal Methylethyl ketone	0.43 0.03	0.00
cis-Butene-2	*cis*-β-Butene oxide *trans*-β-Butene oxide	0.25 0.26	*iso*-Butanal Methylethyl ketone	0.23 0.26	0.02
trans-Butene-2	*cis*-β-Butene oxide *trans*-β-Butene oxide	0.15 0.33	*iso*-Butanal Methylethyl ketone	0.21 0.31	0.02
cis-Pentene-2	*cis*-β-Pentene oxide *trans*-β-Pentene oxide	0.23 0.31	2-Methylbutanal Methyl-*n*-propyl ketone Diethylketone	0.21 0.25[e]	0.06
Tetramethyl ethylene	Tetramethyl ethylene oxide	0.52	Pinacolone	0.48	0.08

[a] *The fractions are calculated from GLC peak areas taking the total area of all* addition *products as unity.*

[b] *The fractions are calculated from the total GLC peak area of the observed compounds other than the addition products taking the total peak area of* all *the products observed as unity.*

[c] *Extrapolated values for infinite pressure.*

[d] *Predominantly propanal (about 90%).*

[e] *Predominantly methyl-n-propyl ketone; some diethylketone is probably also formed (a small peak of the same elution time is observed; infrared and mass spectra, however, indicate a very low upper limit and perhaps absence of diethylketone).*

Formation of a restricted number of principal products in these reactions, mutually isomeric and of a molecular weight equal to that of the olefin used plus an oxygen atom, suggested strongly a direct addition of the atoms followed mainly by a molecular rearrangement rather than a free-radical process. This was substantiated by experiments in which two olefins were used simultaneously. In these experiments no new products were found but only those observed with the same two olefins when used singly, and their respective amounts were approximately proportional to the concentrations of the olefins used. Further information on the nature of these processes was obtained by studying the effect of additions of molecular oxygen.

Can. J. Chem. Downloaded from www.nrcresearchpress.com by 200.7.193.243 on 09/04/12
For personal use only.

Can. J. Chem. Downloaded from www.nrcresearchpress.com by 200.7.193.243 on 09/04/12
For personal use only.

Effect of Additions of Molecular Oxygen

Several experiments were carried out with *iso*-butene, butene-1, *cis*-butene-2, and tetramethyl ethylene in the presence of molecular oxygen. Initial pressures of 500 mm. N_2O, 7 to 15 mm. olefin, and 3 to 30 mm. O_2 were used.

In the case of *iso*-butene and butene-1 there was no or at best very little inhibition of the formation of the addition products even when the partial pressure of molecular oxygen was relatively quite high. The yields of aldehydes appeared to be slightly lowered and smaller amounts of some new products were also formed. In the case of *iso*-butene the latter amounted roughly to about 20% of the total product and probably were *tert*-butanol and acetone, although the identification was not certain. These two compounds were not found in the mercury-photosensitized reaction of *iso*-butene (60 mm.) in the presence of small amounts of O_2 but in the absence of N_2O. No attempt was made to study in detail these products or the mode of their formation.

In experiments with *cis*-butene-2 it was found that after a small amount of quenching by oxygen itself was taken into account approximately, the yields of *cis*- and *trans*-β-butene oxide and of methylethyl ketone were, within the analytical error, unaffected by the presence of molecular oxygen. On the other hand, the yield of ethane (produced normally in this reaction in small amounts, as discussed later) was rapidly suppressed and that of *iso*-butanal was reduced to about 20 to 25% of its value in the absence of oxygen and then remained independent of further oxygen additions. Simultaneously, appreciable amounts of methanol began to be formed. The effect of additions of O_2 on the composition of liquid products is shown in Table II. These results indicate that a large fraction of *iso*-butanal is formed by radical combination but that, nevertheless, a certain amount is produced by internal migration of CH_3 radicals. Similarly, one experiment with tetramethyl ethylene in the presence of about 40 mm. of O_2 showed a substantial reduction but not complete suppression of pinacolone while the yield of the epoxide appeared to be unaffected.

TABLE II

THE EFFECT OF MOLECULAR OXYGEN ON LIQUID PRODUCTS IN THE REACTION OF O ATOMS WITH *cis*-BUTENE-2 (500 mm. N_2O, 7 mm. *cis*-C_4H_8-2; irradiation time 30 min. Fractions of the sum of the observed GLC peak areas are given.)

Run	pO_2, mm.	*trans*-β-C_4H_8O	*cis*-β-C_4H_8O	$CH_3COC_2H_5$	*iso*-C_3H_7CHO	CH_3OH
264	–	0.26	0.23	0.26	0.25	–
266	3.2	0.27	0.24	0.25	0.095	0.15
265	14.6	0.27	0.22	0.24	0.052	0.21
267	41.7	0.26	0.23	0.27	0.052	0.19

Effects of Irradiation Time and of Pressure

Effects of time of irradiation and of the total pressure were checked with butene-1 and *cis*-butene-2 and, in a less systematic manner, with some of the other olefins used. Within the experimental error the rates of product formation were found to be independent of irradiation time up to relatively high conversions. The results of experiments with constant small amount of *cis*-butene-2 (about 5 mm.) and nitrous oxide varying from 80 to 600 mm. are given in Table III. There was at best only a very slight decline at low pressures in the yields per oxygen atom consumed of the addition products, and their ratios remained constant (in these experiments total peak areas of *iso*-butanal plus *cis*-β-butene oxide were measured). The yield of C_2H_6 showed a slight decline at first;

TABLE III

THE EFFECT OF PRESSURE ON THE YIELD OF PRODUCTS IN THE REACTION OF O ATOMS WITH *cis*-BUTENE-2

	Relative rates						
Pressure, mm.	CO[a]	CH_4[a]	C_2H_6[a]	C_2H_4[a]	*trans*-β-Butene oxide[b]	*iso*-C_3H_7CHO + *cis*-β-butene oxide[b]	$CH_3COC_2H_5$[b]
82	0.041	Trace	0.097	0.009	0.19	0.39	0.18
105	0.035	Trace	n.d.[c]	n.d.[c]	0.18	0.36	0.18
205	0.035	Trace	0.094	0.005	0.22	0.41	0.21
406	0.038	Trace	0.073	0.004	0.20	0.39	0.20
608	0.046	Trace	0.072	0.002	0.19	0.41	0.20

[a]*Based on manometric measurements and mass spectrometer analyses.*
[b]*Based on GLC peak areas.*
[c]*Not determined.*

there was, however, a tendency for leveling off rather than for complete suppression of this product at still higher pressures. The nitrous oxide technique is not suitable for the study of these processes at quite low pressures because of the increasing importance of secondary phenomena. In the pressure range 50 to 600 mm. the ratio of the two major products from butene-1, α-butene oxide and *n*-butanal, remained constant—their absolute yields per oxygen atom consumed appeared also to be constant although a very slight pressure dependence might have been masked by a small random run-to-run variation in GLC response. With the other olefins occasional experiments with variable pressures did not show any significant pressure effects. Of the minor products, carbon monoxide seemed to show generally a slight pressure dependence; thus, with butene-1 its yield per oxygen atom consumed decreased from about 0.06 at a total pressure of 50 mm. to 0.03 at 600 mm.

The Extent of Fragmentation

The very small amounts of fragmentation products detected by GLC analysis (Table I) were thought at first (1) to indicate that fragmentation occurred only to the extent of a few per cent. Actually, it proved difficult to establish accurately the extent of fragmentation. A number of GLC calibrations showed that the observed addition products accounted only for about 70 to 80% of the oxygen atoms consumed and in some cases even less. The quantitative aspect of this result, however, is not entirely satisfactory. Apart from the likelihood that some hydrogen abstraction may occur, there is no certainty that all the addition products formed are quantitatively recovered, in spite of all the precautions. Also, it is somewhat difficult to obtain accurate GLC calibrations with the very small amounts involved, especially so with some of the substances formed in these reactions. An attempt was, therefore, also made to estimate the extent of fragmentation from the amount of other fragmentation products detectable.

The fragmentation products more volatile than nitrous oxide were separated on the LeRoy still into the non-condensables and the "C_2" fraction and then further analyzed. The results are given in Table IV and refer to experiments in which 300 mm. N_2O and small amounts of the olefin were used. No systematic analysis could be made for products of similar volatility to that of N_2O, such as C_3H_8, C_3H_6, etc. In some cases, infrared spectra were taken of the N_2O fraction and no additional peaks were observed; minor amounts of any substances present need not have been detected in this manner. Similarly, in the GLC analysis, minor amounts of substances eluting with the original olefin or of those much less volatile than the major products observed could have escaped detection.

Can. J. Chem. Downloaded from www.nrcresearchpress.com by 200.7.193.243 on 09/04/12
For personal use only.

TABLE IV

PRODUCTS MORE VOLATILE THAN NITROUS OXIDE
(non-condensables and "C_2" hydrocarbons)

Reactant	Rates per oxygen atom consumed		
	CO	CH_4	C_2H_6[a]
Butene-1	0.04	Trace	0.00
iso-Butene	0.03	Trace	0.00
cis-Butene-2	0.04	Trace	0.08
trans-Butene-2	0.04	Trace	0.08
cis-Pentene-2	0.03	Trace	0.015
Tetramethyl ethylene	0.02	Trace	0.15

[a]*Mass spectrometer analyses of the* C_2H_6 *fraction indicated at best only trace amounts of* C_2H_4.

The appreciable amounts of ethane formed in some cases, as shown in Table IV, indicate that at least in some of the studied reactions the fragmentation is not negligible even when appreciable pressure effects are absent. With *cis*-butene-2, for example, an experiment in which a mixture of *cis*-C_4H_8-2 and a smaller amount of *cis*-C_4D_8-2 was used no C_2D_6 was formed but only CH_3CD_3 and C_2H_6. Ethane is, therefore, formed by combination of free methyl radicals. The results obtained in the presence of O_2 also showed that ethane and a large fraction of *iso*-butanal were formed by combination of free radicals, as already pointed out. On the basis of these results, the extent of fragmentation into free radicals at higher pressures can be estimated at about 30 to 35% (based on the consumption of oxygen atoms) for *cis*-butene-2 and in the case of tetramethyl ethylene probably as much as 60%. Such large fragmentation at higher pressures appears to take place when rearrangements which follow the addition of oxygen atoms involve migration of methyl radicals, but not (or at best only to a small extent) when H atoms migrate. It is significant that even when large fragmentation of this kind occurs the greater part of the free radicals recombine to form the same compound as produced by direct internal migration. Thus it would seem that the fragmentation involves entirely (or predominantly) only the splitting off of the migrating radicals.

DISCUSSION

On the basis of the comparison of the addition products formed with butene-1, *cis*-butene-2, and *iso*-butene, the mechanism of addition of oxygen atoms to a CC double bond in alkenes was generalized in the preliminary communication (1) in the form of two rules. In view of the additional information available, these rules can now be amplified. The consistency of the results obtained in all the reactions of alkenes with oxygen atoms studied so far indicates that the addition products formed can in general be explained and predicted by assuming that: (1) an oxygen atom adds to one carbon atom of the double bond to form a biradical and this addition takes place in the case of unsymmetrical alkenes predominantly at the less-substituted carbon atom, and (2) the triplet thus formed degrades to the ground-state compounds in two ways: (*a*) by forming the corresponding epoxides without any internal rearrangement except a partially restricted rotation about the original double bond, and (*b*) by forming carbonyl compounds through migration of a particle (either a hydrogen atom or a radical) attached to the carbon atom carrying the oxygen atom to the other carbon atom of the original double bond. Migrating radicals may in the course of this process become to a smaller or greater extent detached from the molecule, as will be discussed later.

Can. J. Chem. Downloaded from www.nrcresearchpress.com by 200.7.193.243 on 09/04/12
For personal use only.

The following scheme for the reaction of oxygen atoms with a generalized olefin (A) illustrates the above rules. R_1, R_2, R_3, and R_4 are alkyl radicals or hydrogen atoms. The first C atom of the double bond is assumed to be "less substituted".

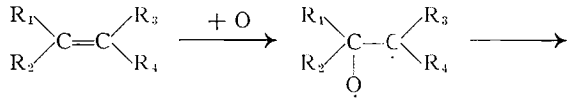

A B

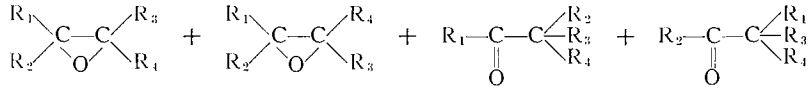

I II III IV

Each of the compounds I to IV is produced in substantial quantities: these four compounds are the main and may be the exclusive addition products formed. (Compounds III and IV will be identical if $R_1 = R_2$, and similarly I and II if either $R_1 = R_2$ or $R_3 = R_4$.) It is possible also that some addition of oxygen atoms may take place at the "more-substituted" carbon atom, in which case minor quantities of carbonyl compounds V and VI will also be formed. In all the cases studied so far, addition to the "more-substituted" carbon atom has been of minor importance inasmuch as it occurred at all.

V VI

This reaction scheme has been illustrated in the preliminary communication (1) by the example of *cis*-butene-2, a symmetrical olefin. The predicted and observed addition products in this case are *cis*- and *trans*-2,3-epoxybutane, methylethyl ketone (formed through migration of an H atom) and *iso*-butanal (formed through migration of a CH_3 radical). The same products are to be expected and have been observed with *trans*-butene-2. In the case of *iso*-butene the main addition products are *iso*-butene oxide and *iso*-butanal and, therefore, oxygen atoms add predominantly to the "less-substituted" carbon atoms of the double bond. Addition to the "more-substituted" carbon atom of the double bond would require formation of some methylethyl ketone as well; some methylethyl ketone appears to be formed but its amount is extremely small. In the case of butene-1, small amounts of methylethyl ketone besides the main addition products, 1,2-epoxybutane and *n*-butanal, indicate that minor addition to the *more*-substituted carbon atom of the double bond might be also taking place. The same is true for propylene where small amounts of acetone seem to be formed, besides the expected main addition products, propylene oxide and propanal. With tetramethyl ethylene the addition products are tetramethyl ethylene oxide and pinacolone, as expected.

The case of *cis*-pentene-2 is of particular interest since it shows that in terms of the above rules the carbon atom to which the methyl radical is attached is "*less* substituted" than the other carbon atom of the double bond to which an ethyl radical is attached. Addition of an oxygen atom to the former would lead to the formation of methyl-*n*-propyl ketone besides 2-methylbutanal and the two isomeric epoxides, *cis*- and *trans*-2,3-epoxypentane, while the addition to the latter would result in diethylketone and the same

Can. J. Chem. Downloaded from www.nrcresearchpress.com by 200.7.193.243 on 09/04/12
For personal use only.

aldehyde and epoxides. Methyl-*n*-propyl ketone is definitely the predominant ketone formed although, perhaps, small amounts of diethylketone are formed as well.

Cycloölefins represent an interesting special case. For cyclohexene, for example, the same reaction scheme would require the formation of the following compounds:

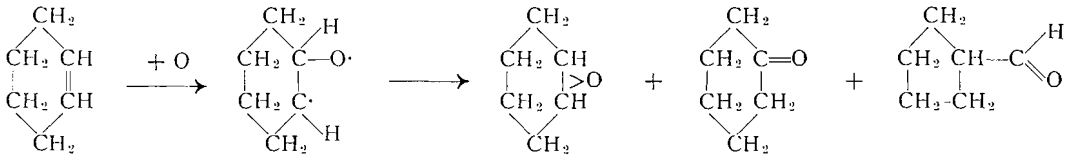

C VII VIII IX

In addition to cyclohexene oxide (VII), two carbonyl compounds would be expected to be formed: cyclohexanone (VIII) through migration of an H atom and cyclopentyl formaldehyde (IX) through migration of the "radical" attached to the carbon atom to which oxygen is attached in the biradical (C). These compounds are actually formed and no other products have been detected.*

There are indications that the intermediate biradical (B) is very short-lived. This is suggested by the difference in the ratios of *cis*- and *trans*-2,3-epoxybutane formed in the reactions of oxygen atoms with *cis*- and *trans*-butene-2, respectively. The lack of appreciable effects of the presence of molecular oxygen on the amounts of the addition products formed also supports this conclusion. It appears, therefore, that the initially formed biradical isomerizes extremely rapidly into the final addition compounds. Since these reactions, however, are very exothermic, the addition compounds carry a large excess of energy when formed (carbonyl compounds about 115 kcal./mole and epoxides probably about 90 kcal./mole). The probability of decomposition of these compounds before dissipation of the excess energy can take place will depend largely on their complexity (the number of "degrees of freedom"). The simplest olefin, ethylene, appears to undergo almost exclusive decomposition on reacting with oxygen atoms. Propylene exhibits a pronounced collisional stabilization of the addition products formed (Fig. 1), while pressure effects appear to be absent with higher alkenes in the investigated pressure range. There is, however, a certain amount of decomposition even when no pressure effects are observed, which suggests that there is an intrinsic probability of a certain fraction of the initially formed biradical undergoing fragmentation. In view of the extremely short life of the biradical, it is not surprising that this fragmentation process is pressure independent.

The nature of the two types of fragmentation processes occurring in the reactions of oxygen atoms with olefins should now be briefly discussed. The pressure-dependent fragmentation, as observed in the case of propylene (and previously with ethylene), is characterized by the formation of products which could be expected from thermal decomposition of the major addition products and is consistent with the assumption that these are initially formed in an energy-rich state. The excess energy is in most cases readily removed by collisions in the gas phase. An inspection of the data given in Tables II and IV shows that the initial act (or part of the initial act) of the pressure-independent decomposition is probably the splitting off of a radical attached to the same carbon atom to which oxygen initially adds. In other words, the same particles which migrate in the rearrangement processes may become detached from the molecule.

**Details of the experiments performed with cyclohexene and cyclopentene will be published elsewhere.*

Can. J. Chem. Downloaded from www.nrcresearchpress.com by 200.7.193.243 on 09/04/12
For personal use only.

Thus, ethane is formed only in those cases where CH_3 is a migrating particle and then a great part of the resulting product is inhibited by the additions of O_2. The remaining fraction of the molecule would probably dimerize and the amount of the dimer formed should be comparable with that of ethane. Such dimers are likely to be of too low volatility to be readily detectable by the analytical techniques employed. Their formation could explain the low material balances observed. The pressure-independent fragmentation in the case of butene-2 appears, therefore, to be similar to the pressure-independent decomposition induced in 2,3-epoxybutane by mercury photosensitization (10). It is not certain whether migrating H atoms split off to a small extent. Thus, in the case of *iso*-butene, in spite of considerable effort no products other than the addition products already described could be isolated and identified. Any free H atoms which might be produced by splitting off from the initially formed biradical would readily add to excess *iso*-butene and the tertiary butyl radicals formed would be largely converted to compounds of low volatility.

The data in Fig. 1 for the propylene reaction can be treated kinetically. Thus, a plot of the reciprocal rates of the production of propanal (plus small amounts of acetone) against reciprocal pressure gives a straight line (Fig. 2), indicating a single-stage collisional

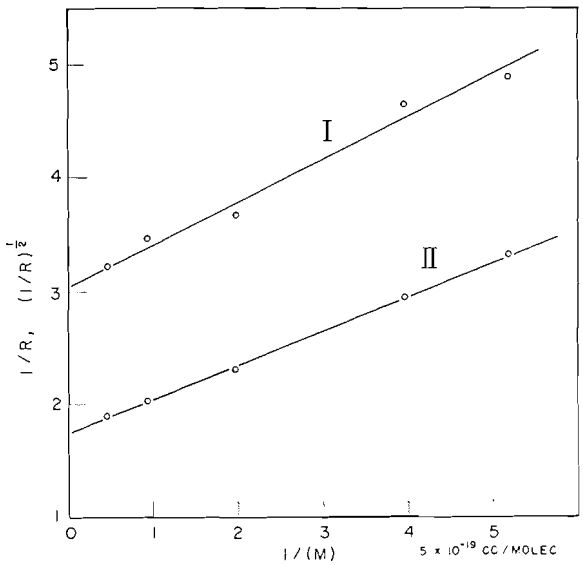

FIG. 2. I. Plot of the reciprocal relative rate $(1/R)$ of formation of propanal + acetone against the reciprocal concentration of reactants. II. Plot of the square root of the relative rate of formation of propylene oxide $(1/R)^{\frac{1}{2}}$ against the reciprocal concentration of reactants.

deactivation. A similar plot for propylene oxide shows a distinct curvature; a plot of the square root of the reciprocal rate against reciprocal pressure, on the other hand, is a straight line. Such a relationship should be expected for a two-stage collisional deactivation with decomposition occurring at both stages provided the lifetimes of the two forms are approximately equal. The following reaction scheme for the propylene reaction is probably, with minor modifications, representative of the general reaction scheme for the reactions of oxygen atoms with olefins, provided it is realized that with increasing number of degrees of freedom the energy-rich molecules formed become longer lived and the pressure-dependent fragmentation becomes less important under otherwise comparable conditions.

Can. J. Chem. Downloaded from www.nrcresearchpress.com by 200.7.193.243 on 09/04/12
For personal use only.

$$C_3H_6 + O \rightarrow CH_3 \cdot \underset{\diagdown O \diagup}{CH}—CH_2O. \quad \begin{matrix} \nearrow \\ \rightarrow \\ \searrow \end{matrix} \quad \begin{matrix} C_2H_5CHO^* \\ CH_3CH—CH_2^{**} \\ \diagdown O \diagup \end{matrix} \qquad [1] \; [2]$$

$$\text{decomposition} \qquad [3]$$

$$C_2H_5CHO^* \rightarrow \text{decomposition} \qquad [1a]$$

$$C_2H_5CHO^* + M \rightarrow C_2H_5CHO + M \qquad [1b]$$

$$CH_3CH—CH_2^{**} \rightarrow \text{decomposition} \qquad [2a]$$
$\diagdown O \diagup$

$$CH_3CH—CH_2^{**} + M \rightarrow CH_3CH—CH_2^{*} + M \qquad [2b]$$
$\diagdown O \diagup$ $\diagdown O \diagup$

$$CH_3CH—CH_2^{*} \rightarrow \text{decomposition} \qquad [2c]$$
$\diagdown O \diagup$

$$CH_3CH—CH_2^{*} + M \rightarrow CH_3CH—CH_2 + M \qquad [2d]$$
$\diagdown O \diagup$ $\diagdown O \diagup$

If, as assumed, $k_{2a}/k_{2b} = k_{2c}/k_{2d}$, the steady-state treatment leads to the relationships

$$1/R_{1b} = (1/\alpha_1)(1+k_{1a}/k_{1b}(M))$$

and

$$(1/R_{2d})^{\frac{1}{2}} = [1/(\alpha_2)]^{\frac{1}{2}}(1+k_{2a}/k_{2b}(M)),$$

where R_{1b} and R_{2d} are the rates of production of propanal and propene oxide per oxygen atom consumed, and α_1 and α_2 are the fractions of O atoms consumed in reactions (1) and (2) respectively. Taking approximately $k_{1b} = k_{2b} = k_{2d} = 10^{-10}$ cc./molec. sec., the plots in Fig. 2 indicate that the lifetimes of the energy-rich molecules $C_2H_5CHO^*$, $CH_3 \cdot \underset{\diagdown O \diagup}{CH}—CH_2^{**}$, and $CH_3 \cdot \underset{\diagdown O \diagup}{CH}—CH_2^{*}$ are between 10^{-8} and 10^{-9} second. It ought to be stressed, however, that the good straight-line plots in Fig. 2 are considerably better than should be expected in view of the likely experimental errors, and their quantitative implications should be taken with some reserve. Reaction (3) in the above scheme represents the pressure-independent fragmentation process.

The chemical reactions of oxygen atoms with olefins and the molecular rearrangements following the initial addition of the atoms exhibit certain regularities which have to be considered in the light of hyperconjugation and inductive effects. These regularities embrace: (1) systematic variation of reaction rates with the structure of the olefin, (2) specificity with respect to the position of addition of the atoms, and (3) nature of internal rearrangements which take place. These effects can best be discussed simultaneously and it is, therefore, convenient to defer their discussion until further results of the present investigations are published, particularly the relative rate constants of these reactions.

Oxygen atoms produced by the technique employed in the present study are probably in their ground, $O(^3P)$ state. This conclusion is valid provided the spin conservation rule is obeyed in the mercury-photosensitized decomposition of nitrous oxide. In this connection it is of interest that investigations now carried out in this laboratory (11) show that the course of the reaction of butene-1 with $O(^3P)$ atoms produced by photolysis of NO_2 is the same as observed in the present work.

ACKNOWLEDGMENTS

The author is indebted to Mr. L. C. Doyle for valuable assistance in the experimental work reported, to Dr. A. W. Tickner for mass spectrometer analyses, and to the Analytical Section of this Division for the infrared analyses.

Can. J. Chem. Downloaded from www.nrcresearchpress.com by 200.7.193.243 on 09/04/12
For personal use only.

REFERENCES

1. CVETANOVIĆ, R. J. J. Chem. Phys. **25**, 376 (1956).
2. CVETANOVIĆ, R. J. J. Chem. Phys. **23**, 1375 (1955).
3. CVETANOVIĆ, R. J. Can. J. Chem. **34**, 775 (1956).
4. CVETANOVIĆ, R. J. J. Chem. Phys. **23**, 1203 (1955).
5. LEROY, D. J. Can. J. Research, B, **28**, 492 (1950).
6. CVETANOVIĆ, R. J. and KUTSCHKE, K. O. Vapour phase chromatography. *Edited by* D. H. Desty. Butterworth Scientific Publications, London. 1957. p. 87.
7. CALLEAR, A. B. and CVETANOVIĆ, R. J. Can. J. Chem. **33**, 1256 (1955).
8. CVETANOVIĆ, R. J. J. Chem. Phys. **23**, 1208 (1955).
9. STEACIE, E. W. R. Atomic and free radical reactions. Vol. 1. 2nd ed. Reinhold Publishing Corporation, New York. 1954. pp. 411–456.
10. CVETANOVIĆ, R. J. and DOYLE, L. C. Can. J. Chem. **35**, 605 (1957).
11. SATO, S. and CVETANOVIĆ, R. J. To be published.

Can. J. Chem. Downloaded from www.nrcresearchpress.com by 200.7.193.243 on 09/04/12
For personal use only.

STUDIES OF THE MECHANISM OF THE FORMATION AND DECOMPOSITION OF THE MOLECULAR COMPLEX BETWEEN SOLID UREA AND *n*-OCTANE VAPOR[1]

H. G. McAdie[2] and G. B. Frost

ABSTRACT

The formation and decomposition of the molecular complex between solid urea and *n*-octane vapor, in the presence and absence of initiators, has been studied by a variety of techniques. Suggestions are made for the possible mechanism of this heterophase reaction incorporating known structural and thermodynamic data.

INTRODUCTION

It has been known for some time that when straight-chain hydrocarbon molecules are added to a concentrated solution of urea in a suitable solvent, crystallization of the urea molecules occurs in such a way that each hydrocarbon molecule becomes imprisoned in a canal formed by a hexagonal lattice of urea molecules, as contrasted with the normal tetragonal lattice of urea.

Schlenk (1) has reported that a slow formation of such molecular-inclusion complexes (frequently referred to as adducts) occurs on the mere contact of finely divided tetragonal urea crystals with certain pure liquid *n*-paraffins. Calderbank and Nikolov (2) have presented evidence that complex formation under these conditions is observable only when the particle size is less than a certain critical value.

Very little information is available regarding the formation of molecular complexes between solid (tetragonal) urea and *n*-paraffin vapor. Schlenk (1) noted that such a process could occur in air saturated with *n*-paraffin vapor if the *n*-paraffin possessed a relatively low boiling point. This type of reaction is of interest not only from the standpoint of the mechanism of complex formation under these conditions, but also since, in a more general way, it is an example of the type of heterophase reaction

$$\text{solid I} + \text{gas} \rightarrow \text{solid II}$$

for which a good deal of information is available regarding the crystallographic and energetic factors involved, and for which the changes occur in a readily accessible temperature range.

McAdie and Frost (3) attempted to carry out the process

$$\text{urea (tetragonal)} + n\text{-octane (vapor)} \rightarrow \text{complex (hexagonal)}$$

by exposing small urea crystals to *n*-octane vapor at close to its saturation vapor pressure at 25° C. for long periods of time, and were unable to observe any reaction. They found, however, that an uptake of the hydrocarbon occurred rapidly in the presence of water vapor; that if the products, so formed, were decomposed under vacuum, addition of *n*-octane then occurred rapidly in the absence of water vapor; and that cycles of decomposition and absorption of *n*-octane could then be carried out. The purpose of this paper is to report the results of some experiments which were designed to investigate these findings more extensively, and to consider the results in the light of the structural and thermodynamic data available. The experiments involve measurements of the rate of

[1]*Manuscript received September 26, 1957.*
Contribution from the Department of Chemistry, Queen's University, Kingston, Ontario.
[2]*Present address: Ontario Research Foundation, 43 Queen's Park Crescent, Toronto 5, Ontario.*

Can. J. Chem. Downloaded from www.nrcresearchpress.com by 200.7.193.243 on 09/04/12
For personal use only.

formation of the complex under various conditions in the presence and absence of water vapor, the identification of the lattice types by X-ray diffraction, the determination of changes in surface area, the effect of temperature, and other factors.

EXPERIMENTAL METHODS

Rate Studies

The apparatus is shown schematically in Fig. 1. Liquid *n*-octane was contained in a reservoir, R, the pressure of *n*-octane vapor being controlled by means of a jacket surrounding the reservoir through which water at any desired temperature could be

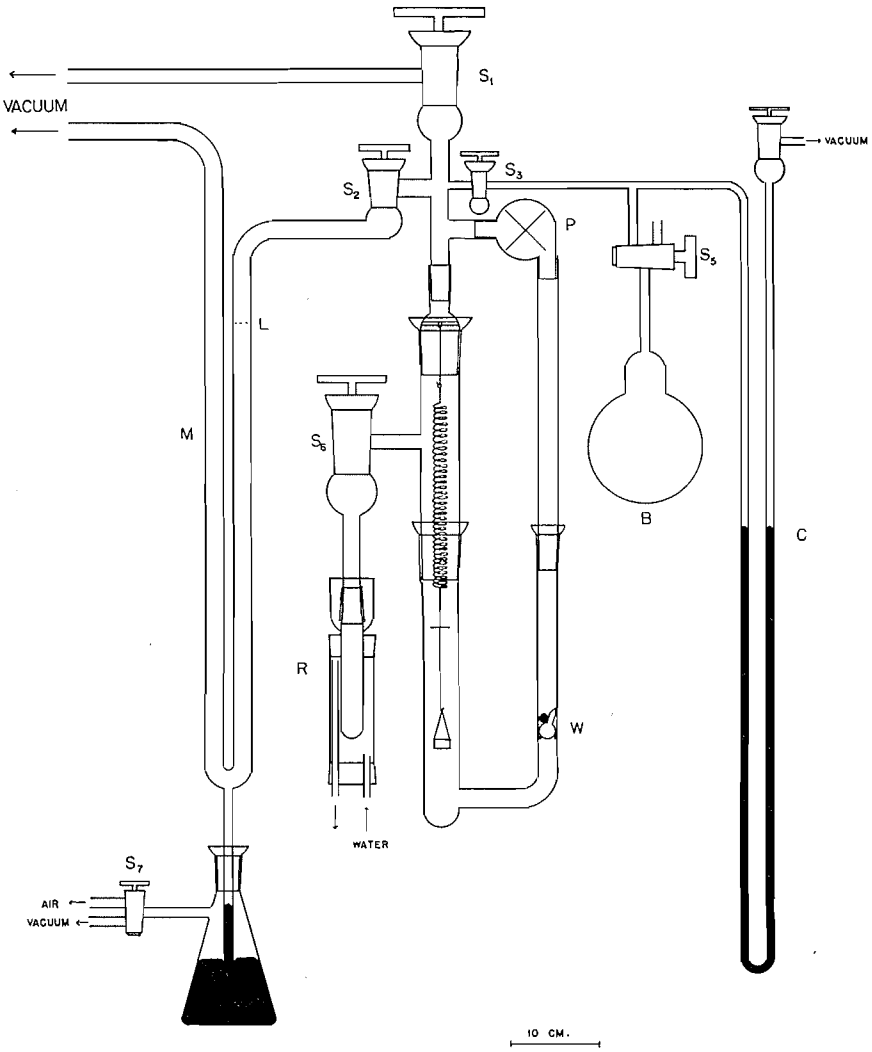

FIG. 1. Apparatus for rate studies.

rapidly circulated. Water vapor was introduced into the system by breaking a small bulb, W, containing the requisite amount of pure liquid water. The total volume of the reaction system to mark L on manometer M was found by application of the gas law in the usual way, making use of bulb B, which was of known volume, and manometer C.

Can. J. Chem. Downloaded from www.nrcresearchpress.com by 200.7.193.243 on 09/04/12
For personal use only.

Can. J. Chem. Downloaded from www.nrcresearchpress.com by 200.7.193.243 on 09/04/12
For personal use only.

To ensure mixing of the two vapors, a magnetically driven circulating pump, P, was provided. The entire apparatus was contained in a thermostatically controlled cabinet.

Reagent grade urea was recrystallized, dried, and screened, the "through 60 mesh on 80 mesh" portion being used. About 40 mg. of this material was weighed into a small copper gauze basket and suspended from a quartz spiral microbalance of sensitivity 2.006 mg. per mm. extension. The previously filled water bulb, together with a small steel ball for breaking, was placed in position. About 5 cc. of liquid *n*-octane was placed in reservoir R, with the constant-temperature jacket removed, frozen by means of liquid air, and repeatedly outgassed in the usual manner. Stopcock S_6 was then closed and the water jacket placed in position. The *n*-octane was brought to constant temperature by circulating water through the jacket. The cabinet was closed and brought to temperature.

After the urea was evacuated for 2 hours, the length of the spiral was measured to ± 0.01 mm. with a rigidly mounted twin telescope cathetometer and S_1 closed. The gas circulating pump, P, was started and S_6 opened to admit *n*-octane vapor to the system. The water bulb was broken and zero time for the reaction taken at this point. This was generally 1 to 2 minutes after the admission of the *n*-octane vapor.

Readings of spiral length, pressure on manometer M, and *n*-octane reservoir and cabinet temperatures were recorded at various intervals. The reaction was timed with an ordinary stopwatch.

When the reaction had proceeded to constant weight, S_6 was closed, S_1 opened, and the decomposition, under a pressure of 10^{-5} mm. Hg, allowed to proceed. S_6 was then carefully opened with S_1 still open and about 2 cc. of liquid *n*-octane evaporated in order to ensure removal of water vapor from the *n*-octane reservoir. S_6 was then closed and the system thoroughly evacuated. *n*-Octane was admitted to the system as described and the formation reaction in the presence of *n*-octane vapor only allowed to proceed. Subsequent decomposition and formation procedures were carried out in an identical manner.

X-Ray Diffraction Studies

Characterization, by X-ray diffraction, of the products formed during repeated formation and decomposition reactions was made by means of the apparatus shown in Fig. 2, in which the bulb below the stopcock S_3 contained water and that below S_2 contained liquid *n*-octane. This arrangement ensured adequate mixing of the vapors. A series of segments of urea were loaded into the long capillary tube, T, made of Corning 707-DG lead-free glass. After outgassing of the reactants, and evacuation of the urea for 24 hours, S_1 was closed and S_2 opened. When the equilibrium vapor pressure of *n*-octane was reached, as indicated by the manometer M, S_3 was opened until sufficient water vapor had been admitted. S_3 was then closed and reaction allowed to proceed. After 24 hours' exposure, one segment of urea was sealed off out of the center of the capillary and the X-ray diffraction pattern determined using copper K_α radiation. A central segment was chosen, so that if reaction were found to have occurred in this region, it was reasonable to assume that other segments of urea, through which the vapors had to pass before reacting with the segment in question, had reacted also. After exposure to vacuum for 24 hours at 25° C., with S_2 closed, a second segment was sealed off and its diffraction pattern determined. A similar procedure was followed after re-exposure to *n*-octane vapor only, for 24 hours, and also after re-evacuation for 24 hours.

The diffraction patterns obtained were compared with those obtained from tetragonal urea and from several known urea–*n*-paraffin complexes prepared from solution.

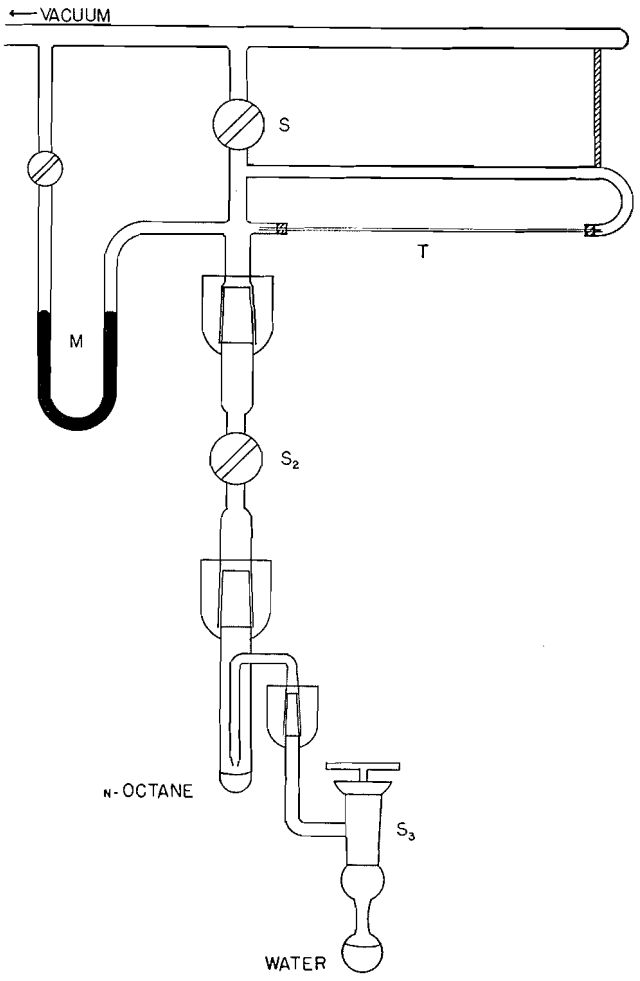

FIG. 2. Apparatus for X-ray studies.

Surface-Area Measurements

Measurements of the changes in surface area resulting from successive formation and decomposition reactions were obtained by argon adsorption at liquid-nitrogen temperatures in the usual volumetric manner. The adsorbent was contained in the annular space between two concentric cylinders of 100-mesh copper gauze. Following determination of the isotherm for urea of the particle size used in the rate experiments, the system was evacuated for 24 hours and subjected to *n*-octane and water vapors, the gas mixture being formed in an assembly similar to that shown in Fig. 2. The partial pressure of water vapor was 12.0 mm. and that of *n*-octane was 13.1 mm. The mixture was allowed to remain in contact with the urea for 5 days to ensure complete reaction. The system was then evacuated for 24 hours at room temperature (Residue I) and a second isotherm determined. The sample was exposed for 5 days to *n*-octane vapor only at its saturation pressure, the system evacuated for 24 hours (Residue II), and a third isotherm determined.

Can. J. Chem. Downloaded from www.nrcresearchpress.com by 200.7.193.243 on 09/04/12
For personal use only.

Photomicrography

Changes in the appearance of urea crystals during complex formation were followed by photomicrographic observation. Urea crystals were placed on a small glass plate ground smooth on both sides, the underside of which was painted with optical black to reduce reflections. The plate was contained in a glass tube connected to an assembly similar to that shown in Fig. 2, by means of which the urea crystals could be exposed to *n*-octane vapor and water vapor at known pressures. A small hole was blown out directly over the position of the plate, the edges ground, and a small clear glass plate cemented in position. The usual microscope and camera assembly were provided.

After evacuation of the urea for 2 hours, and outgassing of the *n*-octane and water reservoirs, the urea was photographed and exposed to a mixture of vapors. Photographs were then taken at regular intervals until the reaction was completed, as determined from earlier rate studies under identical conditions. Vacuum was then applied and the crystals photographed while undergoing decomposition.

RESULTS

Preliminary Rate Determinations

The results of a series of formation and decomposition reactions are shown in Fig. 3. These curves differ from those previously reported (3) in that diffusion effects were substantially eliminated by the gas circulating pump shown in Fig. 1. A sample of 0.0364 g. urea was exposed, at 25° C., to a mixture of *n*-octane and water vapor, the partial pressures being 13.1 mm. and 10.0 mm., respectively. An increase in weight was observed, the weight becoming constant in about 7 hours. The amount of *n*-octane taken

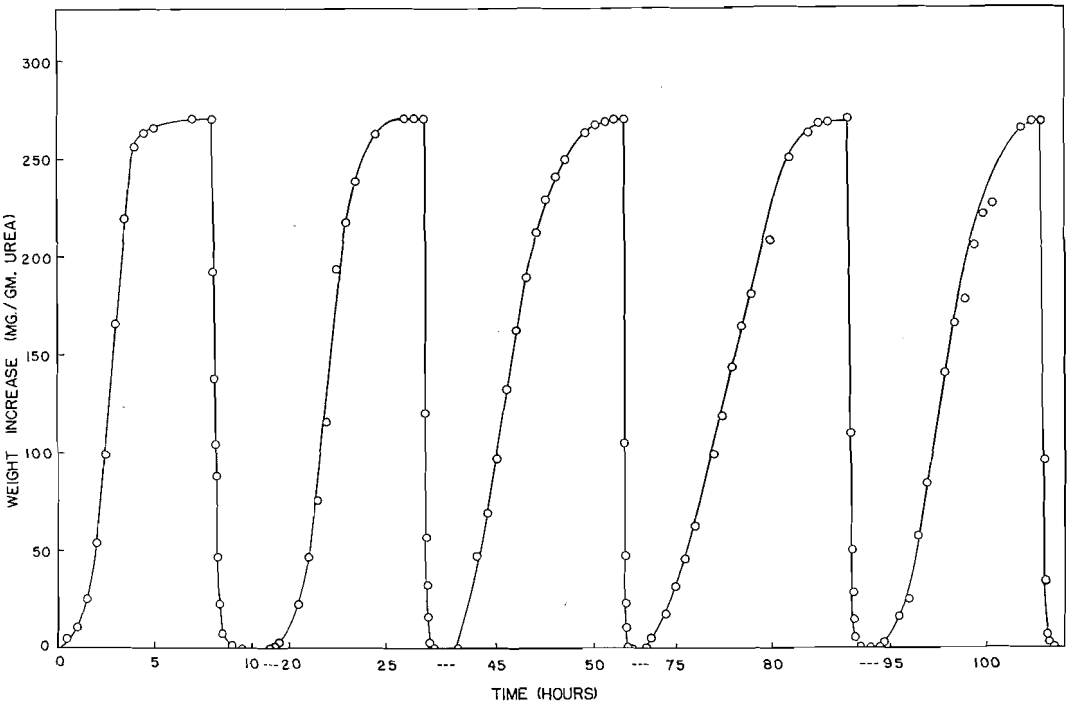

FIG. 3. Experimental results of successive formation and decomposition reactions.

Can. J. Chem. Downloaded from www.nrcresearchpress.com by 200.7.193.243 on 09/04/12
For personal use only.

up was found to be 272.3 mg. per g. urea. From the crystal structure data reported by Smith (4), the composition of the urea–*n*-octane complex is 272.7 mg. *n*-octane per g. urea. A marked swelling in the crystal mass was noted.

The system was evacuated, a rapid loss in weight being observed but no visible change in the volume of the crystal mass. The sample was next exposed to *n*-octane vapor only at 13.1 mm. pressure and an uptake of *n*-octane was observed, constant weight being attained at the same composition as before. Further decomposition and formation reactions were then carried out, no further change in the volume of the crystal mass being visible.

It is apparent that, although tetragonal urea of the particle size used is unreactive to *n*-octane vapor initially, absorption of the hydrocarbon does occur in the presence of water vapor, and that if the hydrocarbon is removed by evacuation, the residual urea is reactive to hydrocarbon and the presence of water vapor is unnecessary. The constancy of composition in successive formation reactions, and the agreement of these values with those reported by Smith (4), suggest that water is not retained in the complex in measurable amounts. From this it appears that the function of water vapor is merely to initiate the reaction.

The formation curves are all of the type characteristic of growth processes, an initial, gradual increase in rate being followed by a linear portion, this being followed in turn by a decline in rate as the reaction nears completion. No long induction periods were observed. The rate of formation, as indicated by the linear slopes of the formation curves, decreases with the number of times the reaction is carried out. It appears that the reaction proceeds to completion and is not impeded by formation of a surface layer of complex. The very rapid decomposition of the complex when subjected to vacuum, and the absence of induction periods under these conditions, are also of interest.

No change in spiral extension was observed when urea was exposed for long periods of time to water vapor only, at pressures comparable to that used in the foregoing experiment. Adsorption of water vapor at such pressures is, therefore, too small to be detected by the quartz spiral used. When the urea, so exposed to water vapor, was subjected to vacuum and then exposed to *n*-octane vapor, no reaction was observed. It is clear, therefore, that the urea crystals cannot be activated for complex formation by prior exposure to water vapor followed by evacuation, but that the reaction is initiated by water vapor in the presence of the hydrocarbon vapor.

X-Ray Diffraction Studies

The marked differences between the X-ray diffraction patterns of tetragonal urea and urea in the hexagonal complex lattice enabled the two lattices to be readily distinguished. Schlenk (1) has reported the similarity between the X-ray diffraction patterns of urea complexes of a given homologous series of reactant molecules. A number of urea–*n*-paraffin complexes, prepared from solution, confirmed this fact by giving identical diffraction patterns. All these patterns agreed with those obtained from the reaction products formed from tetragonal urea in the presence of *n*-octane vapor, with or without the presence of water vapor, thus confirming the presence of the hexagonal complex lattice. The diffraction patterns of the decomposition products formed by evacuation of the urea–*n*-octane complex conformed to that of tetragonal urea.

It is clear from these results that the complex is formed during exposure of urea to *n*-octane and water vapors, that on evacuation the lattice reverts to the tetragonal form, and that on subsequent exposure to *n*-octane vapor only, the complex is again formed, the lattice becoming hexagonal.

Can. J. Chem. Downloaded from www.nrcresearchpress.com by 200.7.193.243 on 09/04/12
For personal use only.

Surface-Area Measurements

The argon surface areas, calculated from Hüttig plots obtained from each isotherm, gave the following results:

Adsorbent	Area ($m.^2 g.^{-1}$)
Urea crystals	0.13
Residue I	1.76
Residue II	1.56

These values were found to be reproducible to about 10% although the absolute values given are not very significant in view of the relatively small areas involved. However, the 14-fold increase in the surface area of Residue I (obtained from formation of the complex in the presence of water vapor and subsequent decomposition) over that of the pure urea sample is of interest, as is the decrease in the area of Residue II (obtained by formation of the complex from Residue I in the presence of *n*-octane vapor only, and subsequent decomposition).

With successive formation and decomposition reactions, the decrease in surface area is attended by a corresponding decrease in the rate of reaction, as indicated by the slopes of the linear portions of the formation curves shown in Fig. 3. The ratio of the rates of complex formation with Residue I and Residue II is 1.32. The ratio of the corresponding surface areas is 1.13. The correlation is of interest bearing in mind the somewhat elaborate nature of the experiments and the sources of error attending them.

Photomicrography

Upon exposing urea crystals (following evacuation) to mixtures of *n*-octane vapor (about 13 mm.) and water vapor (about 16 mm.) the following observations were made:

(*a*) The reaction starts at random points, which are usually marked by the development of a slight protuberance of somewhat fuzzy appearance. The reaction spreads at first slowly and then quite rapidly through the crystal from these points.

(*b*) The time required for the initiation of the reaction is greater in some crystals than in others. The size of the crystal does not appear to be a significant factor.

(*c*) As the formation of the complex proceeds, the opaque appearance observed at the initiation of the reaction develops through the entire crystal.

(*d*) Essentially the same outward shapes of the original single crystals are retained during reaction, but some over-all expansion occurs, and the surfaces become very irregular and less clearly defined.

(*e*) No further visible change in shape or appearance occurs on evacuation, or on re-exposure to *n*-octane vapor only, although, as has been pointed out, X-ray diffraction shows that the hexagonal lattice is formed during reaction and reverts to tetragonal on evacuation.

Under the conditions of pressure employed, the reaction was complete in about 2 hours.

Effect of Water-Vapor Pressure on the Initial Formation Reaction

To determine the effect of water-vapor pressure on the rate of the initial formation of the complex, a number of experiments were performed at 25° C., using the apparatus shown in Fig. 1, at a pressure of 13.1 mm. *n*-octane. The pressures of water vapor ranged from 7.1 mm. to 16.3 mm.

A group of typical curves obtained are shown in Fig. 4. With decreasing pressure of water vapor, induction periods of increasing duration are observed, as well as decreasing slope of the linear portions of these curves. Rates, as estimated from these slopes, are

Can. J. Chem. Downloaded from www.nrcresearchpress.com by 200.7.193.243 on 09/04/12
For personal use only.

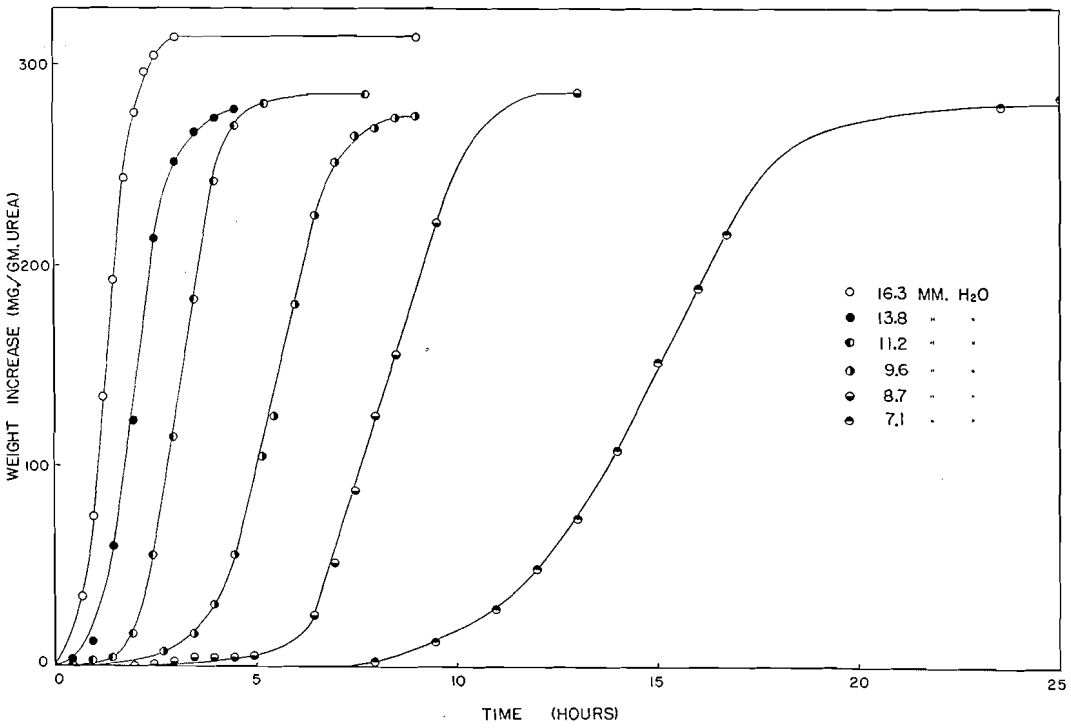

FIG. 4. Weight increase curves for constant *n*-octane pressure, constant temperature, and varying water-vapor pressure.

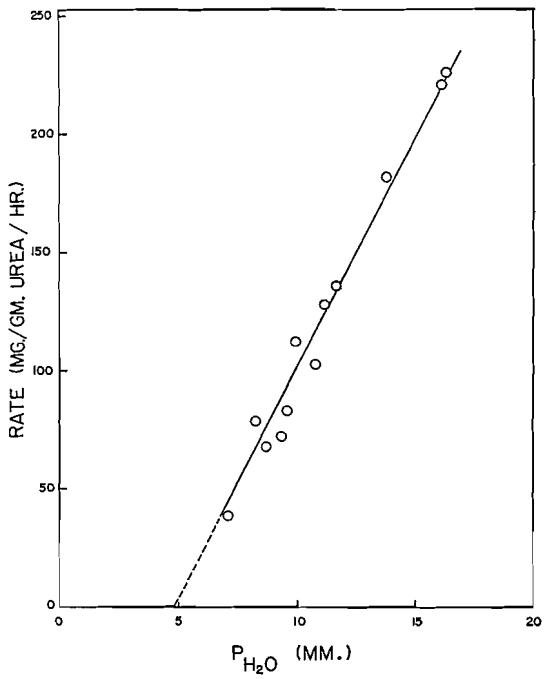

FIG. 5. Dependence of rate of initial formation reaction on water-vapor pressure.

Can. J. Chem. Downloaded from www.nrcresearchpress.com by 200.7.193.243 on 09/04/12
For personal use only.

plotted against the water-vapor pressure in Fig. 5. It will be seen that this rate is linearly dependent on the water-vapor pressure over the range of experiments. Extrapolation to zero rate suggests that a limiting pressure of 4.8 mm. of water vapor is required to initiate the complex formation reaction under these conditions. Separate experiments have shown that the reaction does not proceed at a measurable rate below this value.

The experiments at different pressures of water vapor were carried out using separate samples of urea. The composition of the end products obtained at water-vapor pressures of 11.2 mm. and 8.7 mm. is slightly higher than those shown in Fig. 3. These differences are probably due to errors inherent in the experimental method. The composition of the end product obtained at 16.3 mm. is significantly higher and may be due to adsorption of water vapor at this pressure, which is close to that of a saturated solution of urea in water.

Effect of n-Octane Pressure on the Initial Formation Reaction

A group of curves obtained at a constant water-vapor pressure of 11.5 mm., 25° C., and several *n*-octane pressures is shown in Fig. 6. The curves show the same features as those in Fig. 4, the slopes decreasing and the induction periods lengthening with decreasing *n*-octane pressure. Rates, as estimated from these slopes, are plotted against *n*-octane pressure in Fig. 7. This curve suggests that the reaction will not proceed below 7.2 mm. *n*-octane with the crystals of urea used in these experiments and in the presence of 11.5 mm. of water vapor at 25° C. A gradual leveling off in rate is observed as the *n*-octane pressure approaches the saturation pressure of 14.0 mm. at 25° C.

Effect of Temperature on the Initial Formation Reaction

A series of experiments were carried out at a constant *n*-octane pressure (9.8 mm.), a

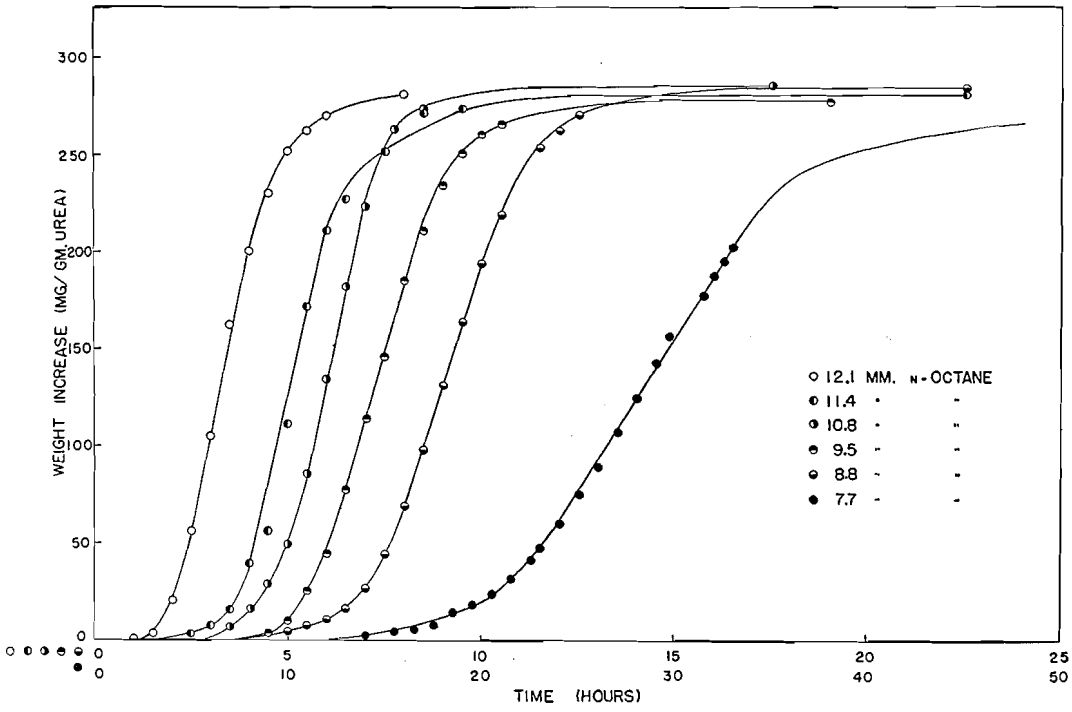

FIG. 6. Weight increase curves for constant water-vapor pressure, constant temperature, and varying *n*-octane pressure.

Can. J. Chem. Downloaded from www.nrcresearchpress.com by 200.7.193.243 on 09/04/12
For personal use only.

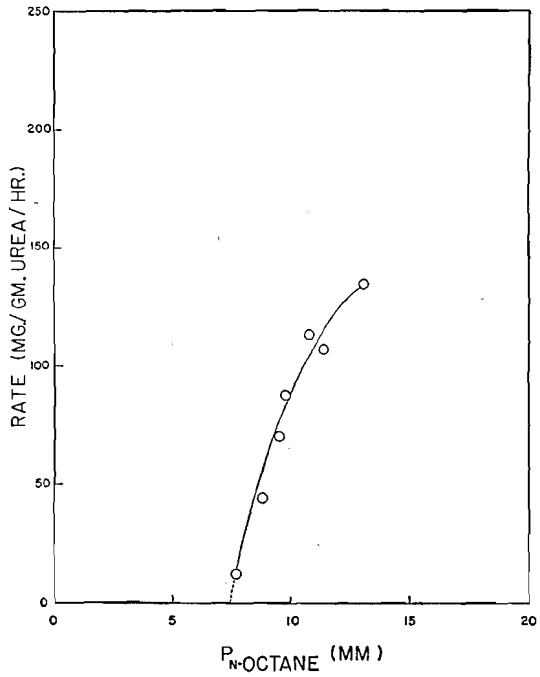

FIG. 7. Dependence of rate of initial formation reaction on *n*-octane vapor pressure.

constant water-vapor pressure (11.5 mm.), and different reaction temperatures. Weight increase versus time curves at 20.9° C., 22.4° C., and 25.0° C. are shown in Fig. 8. It will be seen that with increasing temperature over this range the induction periods lengthen markedly and the slopes of the linear portions of the curves decrease.

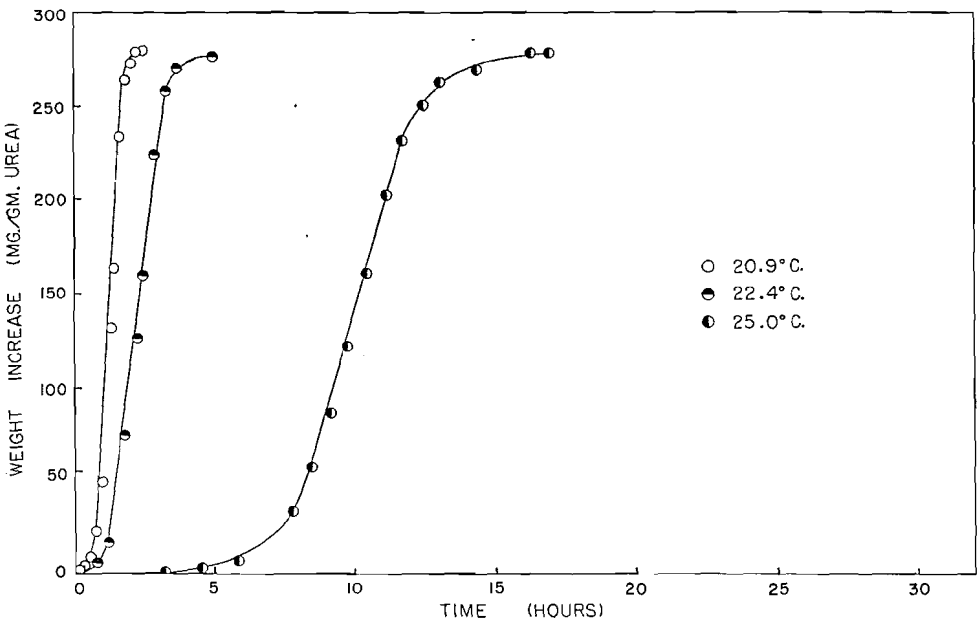

FIG. 8. Weight increase curves for constant water-vapor pressure, constant *n*-octane pressure, and varying temperature.

Can. J. Chem. Downloaded from www.nrcresearchpress.com by 200.7.193.243 on 09/04/12
For personal use only.

The dependence of rate, calculated from these slopes, on temperature is shown in Fig. 9. This indicates that under the particular experimental conditions employed, no reaction should be observed in finite time above 28.7° C. However, other conditions could conceivably alter this value.

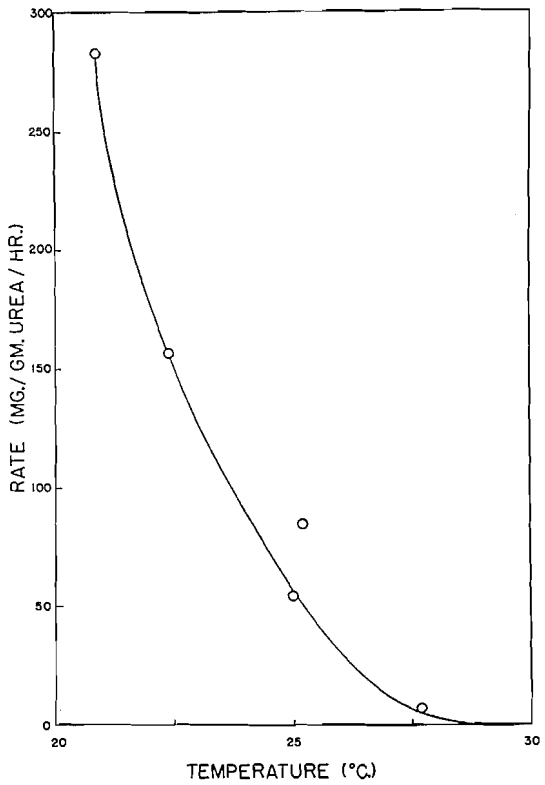

FIG. 9. Dependence of rate of initial formation reaction on temperature.

Effect of Temperature on the Second Formation Reaction

The effect of temperature on complex formation between *n*-octane vapor and the residue from a complex, previously formed in the presence of water vapor and decomposed, is shown in Fig. 10. Although the data are limited, it is significant that clearly marked induction periods are absent. However, the slopes of the linear portions of these curves decrease with temperature as in the case of the initial formation reaction.

Other Initiators

In view of the effect of water vapor in initiating the reaction between urea and *n*-octane vapor, a brief search was made for other compounds which might act in a similar manner. Two classes of compounds were considered, (*a*) those which were good solvents for urea, e.g. methanol and ethanol, and (*b*) those which are known to be highly polar e.g. nitromethane, ethylenediamine, and ammonia.

A small amount of urea, contained in a copper gauze basket, was exposed to *n*-octane vapor and the vapor of the particular compound being studied in an apparatus similar to that shown in Fig. 2. Swelling of the urea was taken as evidence of reaction, and X-ray diffraction patterns of the product were obtained as confirmation.

Can. J. Chem. Downloaded from www.nrcresearchpress.com by 200.7.193.243 on 09/04/12
For personal use only.

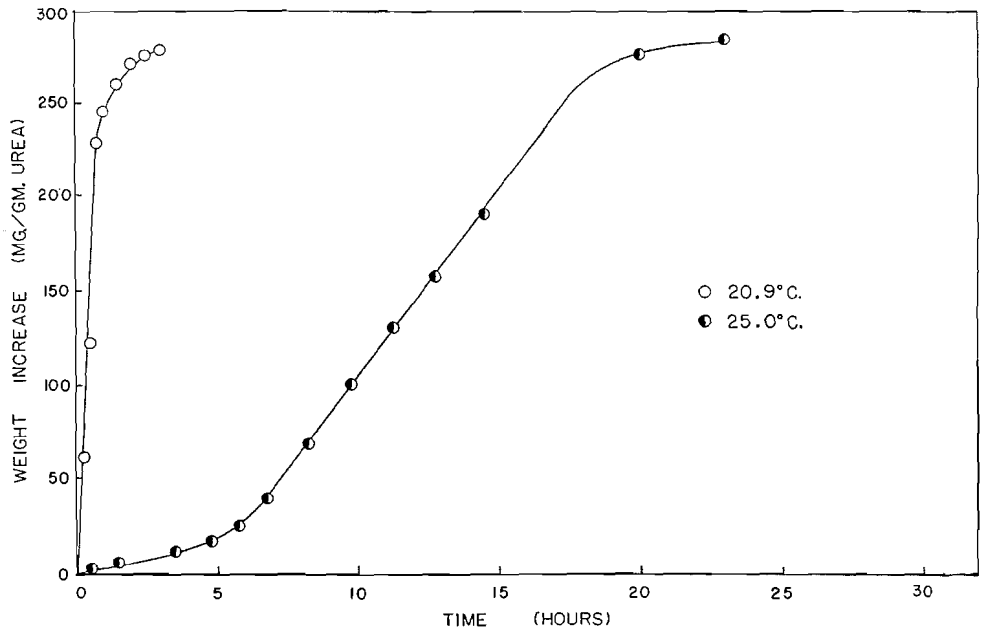

FIG. 10. Weight increase curves for the second formation reaction at constant *n*-octane pressure and varying temperature.

With methanol vapor at a pressure of about 12 mm., complex formation appeared complete after 12 hours. With ethanol vapor, at about 14 mm., about 48 hours were required. No reaction was evident with *n*-propanol vapor (10 mm.) after 1 week.

Reaction occurred in the presence of 12 mm. nitromethane vapor after about 80 hours, while with ethylenediamine at its saturation vapor pressure at room temperature, a slight swelling was observed after 5 days. No effect was found with ammonia.

In all cases, except with *n*-propanol and ammonia, X-ray diffraction patterns confirmed the presence of the hexagonal complex lattice.

DISCUSSION

Structural Factors

On the basis of X-ray (5, 6), infrared absorption (7), nuclear magnetic resonance (8, 9), and neutron-diffraction (10) data, the urea molecule may be said to possess an entirely planar structure.

The most careful determinations, by X-ray diffraction, of the crystal structures of tetragonal urea, and of urea in the hexagonal complex, have been carried out by Vaughan and Donohue (6) and by Smith (4), respectively. In the hexagonal complex, Smith (4) has shown that the molal ratio of urea to hydrocarbon is a linear function of the number of carbon atoms, n, in the hydrocarbon chain and is equal to $0.6848(n-1)+2.181$. Thus, 6.975 moles of urea are associated with 1 mole of *n*-octane in the urea–*n*-octane complex. Smith has also suggested that the configuration of the hydrocarbon molecules in the complex is very similar to that in the pure solid. Consideration of the crystal structure of these complexes shows that the hydrocarbon chains lie parallel to one another in the extended zigzag configuration.

Comparison of the tetragonal and hexagonal lattices of urea shows that the changes

Can. J. Chem. Downloaded from www.nrcresearchpress.com by 200.7.193.243 on 09/04/12
For personal use only.

in arrangement of the planar urea molecules occurring in the transition from the tetragonal to the hexagonal lattice involve the shortening of two N—H...O hydrogen bonds per urea molecule from a bond length of 2.99 Å to one of 2.93 Å. The two other N—H...O bonds per molecule of urea remain unchanged at a length of 3.04 Å. Data have recently been published on the heat of formation of N—H...O hydrogen bonds in various substances, obtained by subtracting the van der Waals energy from the total lattice energy as given by the heat of sublimation. Suzuki, Onishi, Koide, and Seki (11) suggest that the energies of N—H...O bonds will be greater in compounds where the ratio of the number of protons to the number of proton acceptors is unity, than in those compounds where it is greater than two. Examples of this latter class of compounds are urea, oxamide, and acetamide. From the data of Suzuki *et al.* (11) and the reported lengths of N—H...O bonds in oxamide (12), the heat of shortening of the N—H...O bond may be estimated to be 0.065 kcal. for a change of 0.01 Å. Thus, in the transition of urea from the tetragonal to hexagonal lattice, where two N—H...O bonds shorten by 0.06 Å each, the change in bond energy will be 0.78 kcal. mole^{-1} urea.

It has been suggested (4) that the van der Waals forces in tetragonal urea are less than normal because of the relatively open structure, while those in the complex appear to be normal. Because tetragonal urea possesses this relatively open structure, it would appear that in the tetragonal to hexagonal lattice transition there is a relaxation of the N—H...O hydrogen bond length to a state approaching the normal equilibrium distance, and not a compression of the bond to less than this distance. The process, therefore, should be exothermic, i.e. ΔH of shortening $= -0.78$ kcal. mole^{-1} urea for the tetragonal to hexagonal lattice transition.

Thermodynamic Considerations

Redlich, Gable, Dunlop, and Millar (13) have determined the equilibrium constants of a number of complex-forming reactions between urea and liquid hydrocarbons. The value of the equilibrium constant, K, corresponding to the standard free-energy change for the process

$$\text{complex (hexagonal)} \rightarrow \text{urea (tetragonal)} + \text{hydrocarbon (liquid)}$$

is p/p_0, where p is the equilibrium pressure when the coexistent phases are complex, tetragonal urea, and hydrocarbon vapor, and p_0 is the vapor pressure of the pure liquid hydrocarbon. These workers reported, in graphic form, values of $\log p/p_0$ for several hydrocarbons at various values of $1/T°$ K., the relations being found to be linear.

By interpolation from their data, and using the known values of the vapor pressure of liquid *n*-octane at various temperatures (14), values of the standard free-energy change corresponding to the change in state

$$\text{urea (tetragonal)} + n\text{-octane (vapor)} \rightarrow \text{complex (hexagonal)}$$

have been calculated, and are given in Table I.

It is seen that this reaction, under standard conditions, becomes decreasingly spontaneous with temperature increase. From the data of Table I, there is obtained: $\Delta H°$ (over the temperature range) $= -20430$ cal. mole^{-1} *n*-octane; $\Delta S°_{298° \text{ K.}} = -58.07$ cal. deg.$^{-1}$ mole^{-1} *n*-octane. The process, therefore, is markedly exothermic, the enthalpy change being opposed by a large entropy factor. Also, it may readily be calculated that at 25° C. the complex will tend to form spontaneously at *n*-octane vapor pressures above approximately 4.0 mm.

Using the above data and the molal heats of vaporization and fusion of *n*-octane

Can. J. Chem. Downloaded from www.nrcresearchpress.com by 200.7.193.243 on 09/04/12
For personal use only.

TABLE I

STANDARD FREE-ENERGY CHANGE FOR THE PROCESS

urea (solid) + *n*-octane (vapor) → complex (solid)

T, ° K.	log p/p_0	p_0, mm.	p, atm.	$\Delta F°$, cal. mole^{-1} *n*-octane
273.16	−1.2329	2.86	0.00022	−4570
278.16	−1.0964	4.04	0.00043	−4290
283.16	−0.9518	5.63	0.00083	−3990
288.16	−0.8112	7.61	0.00155	−3710
293.16	−0.6667	10.46	0.00296	−3390
298.16	−0.5502	13.98	0.0052	−3120
303.16	−0.4257	18.45	0.0091	−2830
308.16	−0.3092	23.54	0.0152	−2560
313.16	−0.1928	31.11	0.0263	−2270

(9915 cal. mole^{-1} and 4957 cal. mole^{-1}, respectively (14)), it is found that for the process:

urea (tetragonal) + *n*-octane (solid) → complex (hexagonal)

$\Delta H°_{298} = -5560$ cal. mole^{-1} *n*-octane. However, it has been pointed out that 6.975 moles of urea are associated with 1 mole of *n*-octane in the complex; hence $\Delta H°_{298} = -800$ cal. mole^{-1} urea. This value agrees with the lattice energy change due to shortening of N—H...O bonds discussed earlier. Similar calculations for the complexes of *n*-decane, *n*-dodecane, and *n*-hexadecane give $\Delta H°_{298}$ values of −748, −750, and −720 cal. mole^{-1} urea, respectively.

This agreement suggests that the spontaneous energy liberation on complex formation is almost entirely due to the shortening of the N—H...O hydrogen bonds. In other words, the process of complex formation from tetragonal urea and *n*-octane vapor is energetically accounted for by this hydrogen-bond shortening along with the heat of solidification of gaseous *n*-octane. The configuration of the hydrocarbon molecules in the complex is similar to that in the pure solid hydrocarbon, and it appears, therefore, that any changes in the van der Waals forces between hydrocarbon chains lying parallel to one another in the solid state, and those lying parallel to one another in the hexagonal urea lattice, are not energetically significant. The process of complex formation appears, then, to involve a competition between the energetically favorable arrangement of planar urea molecules in a hexagonal lattice around the hydrocarbon molecule and a reversion to the more probable tetragonal configuration.

The Effect of Water Vapor

The foregoing experiments have shown that although complex formation is energetically favorable, actually no reaction is observed when small urea crystals are exposed to *n*-octane vapor only, at close to its saturation vapor pressure at 25° C. However, complex formation occurs in the presence of water vapor and if the complex so formed is decomposed under vacuum, addition of *n*-octane then occurs rapidly and cycles of decomposition and formation may be carried out.

The function of water vapor would appear to be the freeing of separate urea molecules from their positions in the tetragonal lattice. The lattice structure of urea suggests that on adsorption of water vapor on the crystal surface two types of hydrogen bonds may be formed, depending on the disposition of the urea molecules at the surface of the crystal, namely, N—H...O bonds between NH_2 groups and the oxygen of water, and O—H...O bonds between the C=O groups and the O—H of water. Since the O—H...O

Can. J. Chem. Downloaded from www.nrcresearchpress.com by 200.7.193.243 on 09/04/12
For personal use only.

bond is one of higher energy, the molecular field in the region of the adsorption interface will be disturbed, resulting in the weakening of the N—H...O bonds in the lattice itself. Severance of urea molecules may then occur under molecular forces comparable to those involved in the solution of urea in water. This severance may occur more readily at lattice imperfections. In the presence of hydrocarbon chains, which may be imagined as crystallization nuclei, the planar urea molecules so severed will "crystallize" in a hexagonal pattern around the hydrocarbon with the energetically favorable shortening of N—H...O bonds. Since water does not enter into the composition of the complex, it must be freed from the urea molecules in this process. As the interface spreads into the tetragonal crystal, the heat liberated by the exothermic reaction will aid in freeing an increasing number of urea molecules from their tetragonal environment. Photomicrographs have shown that the reaction proceeds from isolated points on the crystals, as would be expected if lattice imperfections are favorable points for nucleation.

The presence of a limiting pressure of water vapor below which the reaction is not observed suggests that a definite (although very small) amount of water must be adsorbed at the reaction sites in order to nucleate the process, that is to provide centers from which the exothermic reaction may proceed through the crystal. In this nucleation process the presence of both water and *n*-octane vapor is necessary. The curves of Fig. 4 and Fig. 6 show that the nucleation periods progressively shorten with increase in water-vapor pressure at a constant pressure of *n*-octane, or with increase in *n*-octane pressure at a constant pressure of water vapor. The rate of uptake of *n*-octane following nucleation increases with the pressure of water vapor (Fig. 4) or with the pressure of *n*-octane vapor (Fig. 6). These rates will depend upon the extent of nucleation, and possibly upon the rate of diffusion of *n*-octane and of water vapor into the reaction zone as the reaction interface spreads into the original crystal. From the data presented, it is not possible to separate these factors for quantitative discussion.

The Decomposition of the Complex under Vacuum

When the complex is formed in the presence of water vapor, a marked increase in the volume of the entire crystal aggregate is observed. Microscopic examination reveals also an over-all increase in the size of each individual crystalline unit, which might be expected since the volume of the hexagonal unit cell is greater than that of the tetragonal. Furthermore, the surfaces become very irregular, and the appearance becomes opaque.

When the complex is subjected to vacuum, rapid decomposition occurs, the lattice reverting to the tetragonal arrangement. It is interesting to note that this process occurs without induction periods (Fig. 3). This process may be analogous to the sublimation of a solid hydrocarbon, since essentially the same configuration exists for the hydrocarbon chain in the lattice of the complex as for such chains in the solid state (4). However, since the formation of the complex appears to involve a competition between the energetically favorable formation of the hexagonal lattice around the hydrocarbon mandrel, and a reversion to the more probable tetragonal configuration, a lowering of the density of hydrocarbon molecules below the equilibrium value would result in the collapse of the hexagonal lattice without the occurrence of a preliminary escape of the hydrocarbon molecules from the hexagonal canals. Regardless, however, of the mechanism involved, rapid reversion to the tetragonal form occurs. This should be attended by a decrease in volume. However, this does not occur. Photomicrographs show that the external size and appearance of the decomposed crystal is not significantly different from the complex crystal, although the surface may be more highly pitted. The surface area (1.76 $m.^2 g.^{-1}$) is about 14-fold that of the original urea crystals. This increase would be readily accounted

Can. J. Chem. Downloaded from www.nrcresearchpress.com by 200.7.193.243 on 09/04/12
For personal use only.

for by the observed irregularity of surface. It appears possible, therefore, that during the initial reaction a honeycomb structure of hydrocarbon molecules each surrounded by a hexagonal cage develops at the reaction interface and spreads through the entire crystal. The tendency toward lattice contraction upon reversion to the tetragonal form would set up severe strains causing some areas of the crystal to buckle. Alternatively, however, the development of an opaque appearance during the initial reaction may indicate that each of the relatively large crystals of tetragonal urea breaks down into a mosaic of microcrystals which together retain essentially the same outward shape as the original single crystal. On removal of the *n*-octane, the small crystals revert to the tetragonal form with individual contraction, but with little obvious change in what was the original crystal. The X-ray diffraction lines obtained after successive formation and decomposition reactions are more clearly defined than those obtained for the original urea crystals, which suggests that such microcrystals are formed. However, diffraction lines may be obtained for microcrystals as small as 100 Å in dimensions. On this view, the surface area should be very much greater than the value obtained. It is possible that the adsorbing gas measures only the external surface of the mosaic and not that of the individual crystals, which may lie very close together.

The Reaction in the Absence of Water Vapor

It is significant that the curves of Fig. 3 and those of Fig. 10 in comparison with those of Fig. 8 show that once the complex has been formed in the presence of water vapor and then decomposed, further formations occur without clearly marked induction periods. It follows that the tetragonal material formed by decomposition of the complex can reform the hexagonal complex without extensive nucleation. If decomposition of the complex results in lattice strain and buckling, such centers might well be points of attack where separate urea molecules would become separated for complex formation. On the other hand if a mosaic of microcrystals were formed, it is possible that a few of these are much smaller than 100 Å in size, and possibly of the order of a few unit cells. At such centers the molecular process of formation of the hexagonal lattice and reversion to the tetragonal can be readily visualized.

As the complex is formed and decomposed repeatedly, there will result a gradual ordering in the repacking of the urea molecules into the tetragonal lattice. This process has been shown to be attended by a decrease in surface area, and a corresponding decrease in rate. The correlation between rate and surface area may be simply due to the fact that there is a corresponding decrease in lattice imperfections or in extremely small and reactive microcrystals. However, the over-all reaction is exothermic and if this heat is a factor in energizing the urea molecules in the tetragonal lattice for complex formation it is obvious that the rate will increase as this heat can be utilized by a greater available surface.

Comment

Some preliminary experiments have been made on the adsorption of water vapor on urea crystals. These indicate the existence of a very small but definite adsorption, and of a monolayer formation in the region of water-vapor pressure (about 4 mm.) where nucleation is just observed. Further experiments are in progress from which it is hoped that accurate adsorption isotherms of water vapor and *n*-octane vapor on urea, and heats of adsorption, can be calculated. When the results of this and other work are available, it is hoped that it will be possible to assess the foregoing possible mechanisms in a more quantitative way, and to relate the effects of other initiators to those obtained with water vapor.

Can. J. Chem. Downloaded from www.nrcresearchpress.com by 200.7.193.243 on 09/04/12
For personal use only.

ACKNOWLEDGMENTS

The award of a Canadian Industries (1954) Limited Fellowship and a Research Council of Ontario Scholarship to one of us (H.G.M.) is gratefully acknowledged. Our thanks are due to the National Research Council of Canada, and to the McLaughlin Science Fund of Queen's University for financial support.

REFERENCES

1. SCHLENK, W., JR. Ann. **565**, 204 (1949).
2. CALDERBANK, P. H. and NIKOLOV, N. S. J. Phys. Chem. **60**, 1 (1956).
3. MCADIE, H. G. and FROST, G. B. Can. J. Chem. **33**, 1275 (1955).
4. SMITH, A. E. Acta Cryst. **5**, 224 (1952).
5. KELLER, W. E. J. Chem. Phys. **16**, 1003 (1948).
6. VAUGHAN, P. and DONOHUE, J. Acta Cryst. **5**, 530 (1952).
7. WALDRON, R. D. and BADGER, R. M. J. Chem. Phys. **18**, 566 (1950).
8. ANDREW, E. R. and HYNDMAN, D. Discussions Faraday Soc. No. **10**, 195 (1955).
9. HYNDMAN, D. Acta Cryst. **7**, 690 (1954).
10. WORSHAM, J. E., JR. Acta Cryst. **10**, 319 (1957).
11. SUZUKI, K., ONISHI, S., KOIDE, T., and SEKI, S. Bull. Chem. Soc. Japan, **29**, 127 (1956).
12. ROMERS, C. Acta Cryst. **6**, 429 (1953).
13. REDLICH, O., GABLE, C. M., DUNLOP, A. K., and MILLAR, R. W. J. Am. Chem. Soc. **72**, 4161 (1950).
14. ROSSINI, F. D., PITZER, K. S., ARNETT, R. L., BROWN, R. M., and PIMENTEL, G. C. Selected values of physical and thermodynamic properties of hydrocarbons and related compounds. Carnegie Press, Carnegie Inst. of Technology, Pittsburgh, Pa. 1953.

Can. J. Chem. Downloaded from www.nrcresearchpress.com by 200.7.193.243 on 09/04/12
For personal use only.

A NEW SPOT TEST FOR NITRATE ION[1]

B. B. COLDWELL AND S. R. MCLEAN

ABSTRACT

Under the influence of short ultraviolet radiation, diphenylamine and nitrate salts react to produce a yellow-colored product. The reaction appears specific and makes it possible to detect 1 μg. of nitrate ion in 0.01 ml. of solution.

INTRODUCTION

The well-known diphenylamine and brucine tests for nitrate (1), while sensitive, are lacking in specificity. Other oxidizing agents, such as chlorates and nitrites, give the same color reaction as nitrate (1, 2). In both tests the reagent is dissolved in concentrated sulphuric acid and this prevents their use for the detection of nitrate on substrates which might be charred by the strong acid, e.g. on paper chromatograms.

This paper describes a simple, specific, and relatively sensitive test for nitrate ion which does not require concentrated acid.

METHOD

The acidity of the test solution is adjusted with dilute sodium hydroxide or hydrochloric acid so that the pH lies between 3 and 10. A convenient volume (0.05 ml. to 0.01 ml.) is transferred with a pipette to a circle of No. 30 Whatman filter paper. The spot is allowed to dry at room temperature (or with gentle warming). The same volume of reagent (1% solution of reagent grade diphenylamine in absolute or 95% ethanol or methanol) is then spotted on either side of the test solution so that the areas covered by the reagent partially overlap the area occupied by the test solution. Alternatively, the reagent may be sprayed over the area of the test solution. After the solvent has evaporated, the filter paper is exposed to short-wavelength ultraviolet light for 2 to 5 minutes. If nitrate is present, the areas of the paper covered by both reagent and test solutions will show pale to bright yellow in daylight against the faint brown color of the area occupied by the reagent alone.

The *limit of identification* of the method was 1 μg. of nitrate ion and the *dilution limit* was 1:10,000.

While the *limit of identification* was found to be 1 μg., this quantity can be built up on the filter paper by successive application of more dilute solutions. Thus, nitrate was detected in a solution containing 0.2 μg. of the anion in 0.01 ml., by making five applications of this volume to the filter paper and allowing the spot to dry between the applications.

EXPERIMENTAL RESULTS

Interference of Cations and Anions

Preliminary tests established that the yellow color was given by all colorless solutions of nitrate salts. No cation interferences were observed. The test is unsatisfactory with highly colored solutions because the yellow color is usually obscure in these cases, e.g. with solutions containing relatively large amounts of iron, cobalt, copper, and cerium salts. Aqueous solutions of the following sodium or potassium salts gave no color with

[1]*Manuscript received December 6, 1957.*
Contribution from the Crime Detection Laboratories, Royal Canadian Mounted Police, Ottawa, Canada. Published with the permission of the Commissioner, R.C.M.P., Ottawa.

Can. J. Chem. Downloaded from www.nrcresearchpress.com by 200.7.193.243 on 09/04/12
For personal use only.

diphenylamine under the conditions described above: acetate, bicarbonate, carbonate, chlorate, cyanide, thiocyanate, thiosulphate, sulphite, nitrite, chloride, iodide, "perborate", oxalate, mono- and di-hydrogen orthophosphate, sulphate, and hydroxide.

In Table I, the effect of various anions on the diphenylamine–nitrate reaction is summarized. It will be noted that only nitrite, bromate, iodate, and vanadate (ortho- and meta-) ions seriously affect the sensitivity of the reaction. Even in these instances

TABLE I

INTERFERENCE OF ANIONS WITH THE REACTION
(NO_3^- concentration = 5 μg./10^{-2} ml.)

Compound	Concn. of anion (μg./10^{-2} ml.)	Result*
NaCl	500	N.I.
KNO_2	30	S.I.
	15	N.I.
$KClO_3$	400	N.I.
NaCN	500	S.I.
	250	N.I.
Na_2CO_3	300	N.I.
$NaHCO_3$	300	N.I.
$NaHSO_4.H_2O$	1000	N.I.
$NaC_2H_3O_2.3H_2O$	500	S.I.
	250	N.I.
$Na_2S_2O_3.5H_2O$	1000	S.I.
	500	N.I.
$NaVO_3.4H_2O$	100	C.I.
	20	N.I.
$Na_3VO_4.16H_2O$	100	C.I.
	20	N.I.
NaCNS	1000	N.I.
NaI	1000	N.I.
Na_2SO_3	500	S.I.
	250	N.I.
$NaIO_3$	100	C.I.
	50	N.I.
$NaBO_3.4H_2O$	50	N.I.
$NaBrO_3$	125	C.I.
	60	N.I.
NaBr	1000	N.I.
NaOH	250	S.I.
	125	N.I.
$Na_2C_2O_4$	100	N.I.
NaF	100	N.I.
Na_2SO_4	1000	N.I.

*N.I. = *no interference, visible yellow color.*
S.I. = *slight interference, trace of yellow color.*
C.I. = *complete interference, no yellow color.*

5 μg. of nitrate ion can definitely be detected in the presence of 3 to 10 times this quantity of interfering ion. None of the compounds tested reacted with diphenylamine to give a color similar to that given by nitrates. Iodates and bromates gave a gray color, vanadates and peroxides a brown color, and mineral acids produced various shades of blue or green depending on the concentration. Nitrate was detected without difficulty in solutions made 0.1 *N* with respect to hydrobromic, molybdic, orthophosphoric, ortho- and hypo-phosphorous, hydrochloric, and sulphuric acids, in solutions containing penta- and tri-oxides of arsenic, and in sodium sulphide solutions. Thallous, stannous, and manganous ions did not interfere. If the solution was acidic, the yellow spot produced by the diphenylamine–nitrate reaction usually turned blue after several hours.

Can. J. Chem. Downloaded from www.nrcresearchpress.com by 200.7.193.243 on 09/04/12
For personal use only.

Effect of Other Factors

The ultraviolet light source used in these experiments was a Hanovia analytic model quartz lamp with type "L" burner,[2] which transmits radiations from 1849 Å into the visible spectrum. Test samples were prepared and exposed to the radiations passing the following filters:

Filter	Description*	Result
SC 5026	Range 3300–3900, maximum at 3600 Å	15 min. exposure—no yellow color
SC 5023	Range 3150–4100, maximum at 3660 Å	15 min. exposure—no yellow color
SC 5028 with SC 5025	Range 2300–4200, maximum at 3200 Å	2 min. exposure—yellow color

**Taken from transmission curves supplied by the manufacturer.*

Apparently, short-wave ultraviolet radiations are required to initiate the reaction between diphenylamine and nitrate resulting in the formation of a yellow product.

No yellow product was visible when the reaction was carried out on glass or porcelain plates. However, positive results were obtained when the reaction took place on glass wool, filter paper, or asbestos mats. Apparently the substrate is not involved in the reaction but may hinder or enhance visual detection of the yellow color. No characteristic colored product was observed when diphenylamine was replaced by diphenylbenzidine, diphenylnitrosamine, diphenylthiocarbazone, 1,3-diphenylguanidine, dipicrylamine, or brucine. α-Naphthylamine gave a yellow-orange to brown-colored product against a lilac-colored background.

Study of Yellow Substance

In the hope of characterizing the yellow-colored reaction products, large sheets of filter paper were soaked in aqueous 1% sodium nitrate solution, air-dried, and then treated with the diphenylamine reagent, air-dried, and exposed to ultraviolet light for approximately 5 minutes. Another lot of paper was treated with the reagent only and similarly exposed. In daylight, the latter had a very faint yellowish-brown tint compared to the bright yellow color of the nitrate-treated paper. Both lots of paper were extracted with ether. Drierite was added to each extract and after several days with intermittent shaking, the extracts were filtered and the filtrates concentrated to about 50 ml. The remaining ether was allowed to evaporate at room temperature and the residues were recrystallized from petroleum ether.

Microscopic examination of the products showed that the extract from the nitrate-treated paper consisted of crystals ranging in color from white through yellow to orange (product A), while the material extracted from paper treated only with diphenylamine consisted mostly of white and pale-yellow-colored crystals (product B). The melting point ranges of A, B, and diphenylamine were 49.9°–51.0° C.; 50.5°–51.5° C., and 52.5°–52.9° C., respectively. A minute orange-colored crystal from product A melted below 40° C. (All melting points are uncorrected.) Attempts to separate the yellow-colored material in product A from the rest of the mixture, by chromatographic methods, were unsuccessful.

The ultraviolet and infrared spectra of pure diphenylamine and products A and B were identical. At 397 mμ, A exhibited an absorption maximum, B gave some absorption but no pronounced maxima, while diphenylamine did not absorb (see Fig. 1).

The results suggest that diphenylamine undergoes a photochemical reaction when

[2]*Hanovia Chemical and Manufacturing Co., 100 Chestnut St., Newark 5, New Jersey.*

Can. J. Chem. Downloaded from www.nrcresearchpress.com by 200.7.193.243 on 09/04/12
For personal use only.

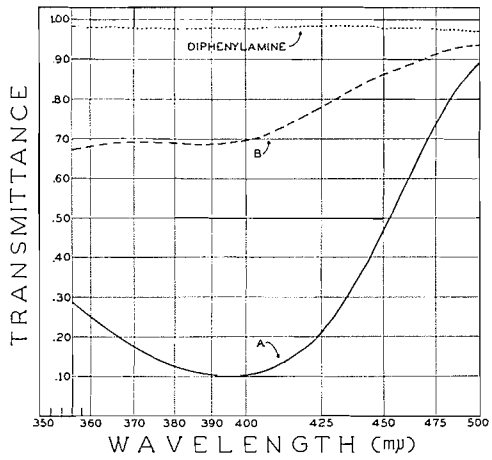

FIG. 1.

activated by short ultraviolet radiation to yield a yellow-colored product. Nitrate ions probably catalyze the reaction. The investigation is continuing.

SUMMARY

A new spot test for nitrate ion is described. The identification is based on the yellow-colored product formed when diphenylamine and nitrate, spotted on filter paper, are exposed to short-wave ultraviolet radiations. The yellow color is probably due to products formed during the photochemical reaction. The reaction appears specific and relatively sensitive, making it possible to detect 1 μg. of NO_3^- in 0.01 ml. of solution.

ACKNOWLEDGMENT

The authors are indebted to Mr. R. Lauzon for recording the infrared spectra.

REFERENCES

1. FEIGL, F. Spot tests. Vol. I. Inorganic applications. 4th English ed. Elsevier Pub. Co., New York. 1954.
2. SUTER, H. A. and SUTER, P. H. Mikrochim. Acta, **7–8**, 1136 (1956).

Can. J. Chem. Downloaded from www.nrcresearchpress.com by 200.7.193.243 on 09/04/12
For personal use only.

Can. J. Chem. Downloaded from www.nrcresearchpress.com by 200.7.193.243 on 09/04/12
For personal use only.

STRUCTURE AND PROPERTIES OF CYCLIC COMPOUNDS

XI. DISSOCIATION CONSTANTS OF THE CYANOHYDRINS OF SOME METHYLCYCLOHEXANONES[1,2]

OWEN H. WHEELER[3] AND JACOB Z. ZABICKY[4]

ABSTRACT

The dissociation constants of the cyanohydrins of a series of methylcyclohexanones have been measured. The polymethylcyclohexanone cyanohydrins show increasing instability on substitution owing to the effects of "axial crowding". The cyanohydrins of 3- and 4-methylcyclohexanone were found to be more stable than that of cyclohexanone and to explain this a new concept of "equatorial interference" is introduced.

The measurement of the dissociation constants of cyanohydrins has proved a useful method for studying the reactivities of aldehydes and ketones and has been used much (1, 2, 3, 4, 5).

As part of a general study of the effect of substitution on the reactivity of ring compounds we wished to investigate the influence of methyl groups, in various positions in the ring, on the reactivity of cyclohexanone. Accordingly, a series of methylcyclohexanones were prepared and the dissociation constants of their cyanohydrins measured (see Table I).

TABLE I

DISSOCIATION CONSTANTS OF THE CYANOHYDRINS

Cyclopentanone	149[a]	210[b]	205 ±6[c]	34.8[d]
Cyclohexanone	9.2	10	5.91±0.11	1.0
2-Methylcyclohexanone	5.9	—	10.7 ±0.3	1.8
3-Methylcyclohexanone	30	—	5.5 ±0.1	0.93
4-Methylcyclohexanone	12.7	—	3.15±0.05	0.53
2,2-Dimethylcyclohexanone	—	—	9.2 ±0.3	1.6
cis-3,5-Dimethylcyclohexanone	—	—	25.7 ±0.7	4.4
3,3-Dimethylcyclohexanone	—	—	176 ±4	30
3,3,5-Trimethylcyclohexanone	—	—	224 ±6	38
3,3,5,5-Tetramethylcyclohexanone	—	—	4690 ±120	800
Menthone	796	1300	313 ±11	53

[a]*In 96% ethanol at 20° ±0.5° (1).*
[b]*In 96% ethanol at 22°–23° (4).*
[c]*Present determinations, see Experimental.*
[d]*Ratio of dissociation constants to cyclohexanone cyanohydrin = 1.0.*

The cyanohydrin reaction has been shown to be reversible and to involve a base-catalyzed nucleophilic attack of cyanide ion on the carbon atom of the carbonyl group (6). The reaction involves a change in co-ordination number from 3 to 4 and Brown (7) has discussed such reactions in relation to the reactivity of simple cycloalkanones. Thus cyclopentanone is relatively unreactive in the cyanohydrin reaction (see Table I) since addition to the keto group gives a sterically crowded structure. However, cyclohexanone is much more reactive since a change to co-ordination number 4 relieves the angle strain in the ketone and also the small steric interference between the ketone group and the

[1]*Manuscript received November 7, 1957.*
Contribution from the Instituto de Quimica, Universidad Nacional Autonoma de Mexico, Mexico, 20, D.F. Part X, J. Org. Chem. **22**, *1153 (1957).*
[2]*A preliminary communication appeared in Chemistry and Industry, 1338 (1956).*
[3]*Present address: Department of Chemistry, Dalhousie University, Halifax, Nova Scotia.*
[4]*Present address: Department of Organic Chemistry, The Hebrew University, Jerusalem.*

Can. J. Chem. Downloaded from www.nrcresearchpress.com by 200.7.193.243 on 09/04/12
For personal use only.

adjacent hydrogen atoms (8). From the results in Table I it can be seen that the effect of placing methyl groups in the ring of cyclohexanone is to greatly reduce the stability of the cyanohydrins, except in the case of 3- and 4-methylcyclohexanone where there is a small but appreciable increase in stability.

Considering first the four dimethylcyclohexanones, the dissociation constant of 3,3-dimethylcyclohexanone cyanohydrin is much greater than either that of cyclohexanone or that of *cis*-3,5-dimethylcyclohexanone cyanohydrin. In the former case one of the methyl group must be in an axial position (9) and in the same axial direction as either a bulky cyano or a hydroxyl group. With the two large groups in this position there is considerable crowding in the cyanohydrin and consequently this readily dissociates to the ketone. This "axial crowding" effect of two bulky groups in the same axial direction is absent in *cis*-3,5-dimethylcyclohexanone cyanohydrin since both methyl groups lie in the equatorial plane (10). In the case of 2,2-dimethylcyclohexanone cyanohydrin one of the methyl groups will be in an axial position but in a direction opposite to the cyano group, and hence little "axial crowding" effect will be operative. However, the inductive effect of the methyl groups will place a partial negative charge on the carbonyl carbon atom and this will decrease the reactivity of the ketone (5) and increase the dissociation constant of the cyanohydrin. In menthone (2-isopropyl-5-methylcyclohexanone) the combined electronic and steric effects of the isopropyl group will make the cyanohydrin more unstable.

The cyanohydrin of 3,3,5-trimethylcyclohexanone is slightly less stable than that of 3,3-dimethylcyclohexanone since the extra methyl group will be in an equatorial position and exert only a small additional effect. However, in the case of 3,3,5,5-tetramethylcyclohexanone two methyl groups will be in an axial position and both in the same axial direction as the cyano (or hydroxyl) group. Consequently, there is a large "axial crowding" effect in the cyanohydrin, which is very unstable. The ratio of the stabilities of the cyanohydrins of cyclohexanone and cyclopentanone is 35:1 and the stabilities of most of the methylcyclohexanone cyanohydrins are within this range. However, in the cases of 3,3,5-tri- and 3,3,5,5-tetra-methylcyclohexanone the differences produced by the steric effects are equal to or greater than those which result from a difference in ring size.

Numerous examples exist in the literature of the instability of groups in an axial position (9) but few have demonstrated directly the presence of an "axial crowding" effect. Recently Corey and co-workers (11) have shown that while the preferred configuration of α-halogenocyclohexanones is with the halogen atoms axial, in the case of α-halogeno-4,4-dimethylcyclohexanones the halogen atoms are equatorial owing to crowding with the axial methyl group on carbon atom 4.

In the case of the monomethylcyclohexanones the 2-isomer will be subjected to the inductive effect of the methyl group, which will deactivate the ketone grouping and decrease the extent of cyanohydrin formation (5). The slightly increased reactivity of 2,2-dimethylcyclohexanone with respect to 2-methylcyclohexanone may be due to the fact that 2-methylcyclohexanone is free to assume both a methyl axial and an equatorial configuration (12) and the methyl group will have little steric effect on the ketone itself, whereas in 2,2-dimethylcyclohexanone one of the methyl groups will interfere with the ketone grouping (13) and this will favor the formation of the less-hindered staggered cyanohydrin. The cyanohydrins of both 3- and 4-methylcylcohexanone have dissociation constants which are smaller than that of cyclohexanone. The differences are not large, but are significant and suggest the operation of some other effect.

Can. J. Chem. Downloaded from www.nrcresearchpress.com by 200.7.193.243 on 09/04/12
For personal use only.

The large internal angle of the carbonyl group in cyclohexanone produces a twisting of the ring, and ring atoms 2 and 6 are pushed outwards and ring atom 4 turned inwards to the equatorial plane of the ring (8, 13). This brings the atoms on the equatorial bonds at positions 3 and 5 nearer to the equatorial bond of atom 4 and the axial bonds of atoms 2 and 6. This results in a general strain in the ring which is relieved when the co-ordination number of the carbonyl carbon atom is changed from 3 to 4 (7, 14) as in cyanohydrin formation. A substituent on carbon atom 4 will increase this strain relative to cyclohexanone itself and thus 4-methylcyclohexanone should be more reactive since the additional strain is relieved when the cyanohydrin is formed. In the case of 3-methylcyclohexanone the axial hydrogen atoms at positions 2 and 6 have some freedom of movement towards the carbonyl group and the effect will be less marked. The effect for which the term "equatorial interference" is suggested has not previously been noted. However, Brown, Fletcher, and Johannesen (14) found that in the hydrolysis of methyl-substituted 1-methyl-1-chlorocyclohexanes the order was 2-methyl > 3-methyl > 4-methyl, the reverse to that observed in the present work, and this would be expected since the reverse process of a change in co-ordination number from 4 to 3 is being measured. This distortion effect would be expected to be transferred into a second ring, and cholestan-3-one and coprostan-3-one have been found (15) to be slightly more reactive than cyclohexanone.

A quantitative comparison of the various non-bonded interactions must consider these effects in both the ketone and the cyanohydrin. Considering *cis*-3,5-dimethylcyclohexanone and 3,3,5-trimethylcyclohexanone and their cyanohydrins, interactions between the axial methyl groups and the axial hydrogen atoms will be present in both the ketones and their cyanohydrins. The principal factor contributing to the large difference between the dissociation constants of these cyanohydrins will be one non-bonded interaction between an axial methyl group and the axial cyano (or hydroxyl) group in the trimethyl ketone. The ratio of the two dissociation constants (8.7:1) gives a value of 1.3 kcal. (calculated from $\Delta F = -RT \ln(K_1/K_2)$ at 25.0°) for the free energy of interaction. Similarly the principal destabilizing effect contributing to the difference in stability of the cyanohydrins of *cis*-3,5-dimethyl- and 3,3,5,5-tetramethyl-cyclohexanone is two "non-bonded" axial interactions of methyl and cyano (or hydroxyl) groups, and the ratio of their dissociation constants (182:1) gives 1.55 kcal. for the mean interaction energy. The energy change on moving a methyl group from an axial to an equatorial position has been estimated to be about −1.8 kcal. (at 25°) (10) and found, from equilibration experiments on *cis*- and *trans*-dimethylcyclohexanes, to be about −1.5 kcal. (16). These are measurements of the repulsion energy between a methyl group in an axial position and the two hydrogen atoms in the same axial direction. Thus the individual methyl hydrogen interaction energy is about 0.8 kcal. From a study of the boric acid complexes of cyclohexanediols (17) the oxygen–oxygen axial–axial interaction energy is 1.9 kcal. The present results are thus reasonable in comparison with these other measurements.

The "equatorial interference" effect is much less than the "axial crowding" effect and in the case of 4-methylcyclohexanone increases the free energy with respect to cyclohexanone by −0.4 kcal. (ratio of dissociation constants 0.53:1). Small distortions resulting from "equatorial interference" will occur in the polymethylcyclohexanones but the effect is submerged by the much greater effects of "axial crowding". Nevertheless equatorial interactions cannot be ignored in any complete study of the influence of groups on ring reactivity, and further work is being carried out to test the hypothesis.

EXPERIMENTAL

Ketones

The ketones were initially fractionated and semicarbazones prepared from fractions of constant refractive index. The semicarbazones were recrystallized from ethanol or aqueous ethanol to constant melting point and the ketones liberated by steam distillation with phthalic anhydride (18). The regenerated ketones were carefully fractionated and middle cuts used for the equilibrium studies. The physical constants are given in Table II.

TABLE II

PHYSICAL PROPERTIES OF KETONES[a]

	Semicarbazone	B.p.[b]	n_D^{25}
Cyclopentanone	—	118°/580 mm. (129°/756 mm.)[c]	1.4328 (1.4368)[c,d]
Cyclohexanone	166° (165°)[c]	145°/580 mm. (155°/764 mm.)[c]	1.4482 (1.4498)[c,d]
2-Methylcyclohexanone	196.5° (196°)[c]	63° (165°/764 mm.)[c]	1.4449 (1.4477)[c,d]
3-Methylcyclohexanone	187.5° (191°)[c]	63° (169°/762 mm.)[c]	
4-Methylcyclohexanone	198° (197°)[c]	63° (170°/760 mm.)[c]	1.4412 (1.4457)[c,d]
2,2-Dimethylcyclohexanone	—	153°/580 mm. (169°/748 mm.)[e]	1.4453 (1.4490)[d,e]
cis-3,5-Dimethylcyclohexanone	—	151°/580 mm. (178°/760 mm.)[f]	1.4407 (1.4417)[d,f]
3,3-Dimethylcyclohexanone	210° (203°)[g]	80° (173°/750 mm.)[i]	1.4439
3,3,5-Trimethylcyclohexanone	201.5° (202°)[h]	90° (54°/11 mm.)[h]	1.4439 (1.4454)[h,i]
3,3,5,5-Tetramethylcyclohexanone	214.5° (217°–218°)[j]	95° (59°–61°/5.5 mm.)[j]	1.4509 (1.4520)[d,j]
Menthone	183° (183°)[k]	96° (98°–100°/18 mm.)[l]	1.4474

[a] *The figures in parentheses are the best literature values.*
[b] *At 23 mm. pressure, unless otherwise stated.*
[c] *Vogel, A. I. J. Chem. Soc. 1323 (1938).*
[d] n_D^{20}.
[e] *Cologne, J. and Duroux, E. Bull. soc. chim. France,* **7**, *459 (1940).*
[f] *Ungnade, H. E. and McLaren, A. D. J. Org. Chem.* **10**, *29 (1945); cf. Skita, A. and Faust, W. Ber.* **72**, *1127 (1939). They give* n_D^{20} *1.4466 for the trans-isomer.*
[g] *Blanc, H. G. Compt. rend.* **144**, *1356 (1907).*
[h] *Prizeheim, H. and Bondi, J. Ber.* **58**, *1409 (1925).*
[i] n_D^{15}.
[j] *Ref. 24.*
[k] *Neave, G. B. J. Chem. Soc.* **101**, *513 (1912).*
[l] *Ref. 20.*

Cyclopentanone, cyclohexanone, and 3- and 4-methylcyclohexanone were commercial samples (Eastman-Kodak white label grade).

2-Methylcyclohexanone and menthone were prepared by oxidation of the corresponding alcohols (19) and 2,2-dimethylcyclohexanone by methylation of 2-methylcyclohexanone (20).

cis-3,5-Dimethylcyclohexanone was obtained by hydrogenation of 3,5-dimethylcyclohexenone (21, 22) in ethanol over 5% palladium–charcoal and 3,3,5-trimethylcyclohexanone similarly from isophorone.

3,3-Dimethylcyclohexanone resulted from oxidation of 3,3-dimethylcyclohexanol (23) and 3,3,5,5-tetramethylcyclohexanone from a 1,4-addition of methylmagnesium iodide to isophorone (24).

Cyanohydrins

The solvent, 95% ethanol, was prepared by mixing 4 l. of lime-dried ethanol with 160 ml. of distilled water and had d_{25}^{25} 0.8020, d_4^{25} 0.7996.

Anhydrous hydrogen cyanide was prepared from sodium cyanide and 50% sulphuric acid (25) and dissolved in the above ethanol to give a *ca.* 0.1 *N* solution.

Aliquots of the pure ketone (0.015–0.15 g.) were dissolved in the 95% ethanol in a 50 ml. graduated flask and the hydrogen cyanide solution (10–20 ml.) added and 1 ml.

Can. J. Chem. Downloaded from www.nrcresearchpress.com by 200.7.193.243 on 09/04/12
For personal use only.

of a 2% solution of tri-*n*-propylamine in 95% ethanol. The solutions were allowed to reach equilibrium during 20–24 hours in a constant-temperature bath maintained at 25.0° ±0.2°. Samples (four of 10 ml.) were withdrawn and added to an excess of 0.1 *N* aqueous silver nitrate containing 0.5% nitric acid and the excess determined with standard 0.1 *N* potassium thiocyanate using ferric alum as indicator. All the determinations were carried out three to five times and the results, together with their mean standard deviations, are given in Table I.

The present results, obtained with highly purified specimens of ketones, differ from previous results obtained with ketones which have only been distilled.

ACKNOWLEDGMENT

The authors are grateful to the Rockefeller Foundation, New York, for financial assistance.

REFERENCES

1. LAPWORTH, A. and MANSKE, R. H. F. J. Chem. Soc. 2535 (1928); 1976 (1930).
2. BAKER, J. W. and co-workers. J. Chem. Soc. 191 (1942); 1089 (1949); 2831 (1952); 404 (1956).
3. RUZICKA, L., PLATNER, P. A., and WILD, H. Helv. Chim. Acta, **28**, 613 (1945).
4. PRELOG, V. and KOBELT, M. Helv. Chim. Acta, **32**, 1127 (1949).
5. EVANS, D. P. and YOUNG, J. R. J. Chem. Soc. 1310 (1954).
6. INGOLD, C. K. Structure and mechanism in organic chemistry. Cornell Univ. Press, Ithaca, N.Y. 1953. p. 676.
7. BROWN, H. C. J. Chem. Soc. 1248 (1956).
8. BROWN, H. C., BREWSTER, J. H., and SHECHTER, H. J. Am. Chem. Soc. **76**, 467 (1954).
9. ORLOFF, H. D. Chem. Revs. **54**, 347 (1954).
10. KILPATRICK, J. E., PITZER, D. S., and SPITZER, D. J. Am. Chem. Soc. **69**, 2483, 2491 (1947).
11. COREY, E. J. *et al.* J. Am. Chem. Soc. **75**, 2301 (1953); **77**, 5415, 5418 (1955).
12. KLYNE, W. Experientia, **12**, 119 (1956).
13. COREY, E. J. and SNEEN, R. A. J. Am. Chem. Soc. **77**, 2505 (1955).
14. BROWN, H. C., FLETCHER, R. S., and JOHANNESEN, R. B. J. Am. Chem. Soc. **73**, 212 (1951).
15. WHEELER, O. H. and MATEOS, J. L. Can. J. Chem. (In press).
16. CURTIN, D. Y. Record Chem. Progr. (Kresge-Hooker Sci. Lib.), **15**, 111 (1954).
17. ANGYAL, S. J. and MCHUGH, D. J. Chem. & Ind. (London), 1147 (1956).
18. BRAUDE, E. A., JONES, E. R. H., KOCH, H. P., RICHARDSON, R. W., SONDHEIMER, F., and TOOGOOD, J. B. J. Chem. Soc. 1890 (1949).
19. SANBORN, L. T. Organic syntheses. Collective Vol. 1. John Wiley and Sons, Inc., New York. 1932. p. 340.
20. BAILEY, W. J. and MADOFF, M. J. Am. Chem. Soc. **76**, 2708 (1954).
21. HORNING, E. C., DENEKAS, M. O., and FIELD, R. E. Org. Syntheses, **27**, 24 (1947).
22. PEPPIATT, E. G. and WICKER, R. J. Chem. & Ind. (London), 747 (1955).
23. HENSHALL, T. J. Soc. Chem. Ind. (London), **62**, 127 (1943).
24. KHARASCH, M. S. and TAWNEY, P. O. J. Am. Chem. Soc. **63**, 2308 (1941).
25. ZIEGLER, K. Organic syntheses. Collective Vol. 1. John Wiley and Sons, Inc., New York. 1932. p. 314.

Can. J. Chem. Downloaded from www.nrcresearchpress.com by 200.7.193.243 on 09/04/12
For personal use only.

Can. J. Chem. Downloaded from www.nrcresearchpress.com by 200.7.193.243 on 09/04/12
For personal use only.

HYDROGENOLYSIS OF CARBOHYDRATES

IV. 1,2-*O*-*ISO*PROPYLIDENE-D-GLUCOFURANOSE[1]

P. A. J. GORIN AND A. S. PERLIN

ABSTRACT

1,2-*O*-*Iso*propylidene-D-glucofuranose was treated with hydrogen at 180° C. and 2900 p.s.i. using copper chromium oxide catalyst and dioxane as solvent. The major isolated products were a hexanediol (2.4%), a mixture of hexanetriols (6.5%), a hexanetetrol (4.3%), and an *iso*propylidene-aldohexose (4.2%) which differed from the starting material. The latter product yielded L-idose on hydrolysis, showing clearly that isomerization of carbon 5 of monoacetone-D-glucose occurs under the reaction conditions used.

The diol and the major components of the triol mixture were found to possess a 1,2-glycol group which was derived mainly from the 5,6-glycol group of the original monoacetone-D-glucose. Thus, hydrogenolysis of 1,2-*O*-*iso*propylidene-D-glucofuranose-1-C^{14} afforded the 1,2-hexanediol and mixed triols containing only about 30% of the total specific activity in carbon 1. The tetrol was shown to be 1,2,5,6-hexanetetrol. The results suggest that the carbon–oxygen bonds at carbons 5 and 6 of *iso*propylidene-D-glucose are least prone to hydrogenolysis and that those at carbons 3 and 4 are most readily cleaved.

When methyl glycosides are subjected to hydrogenolysis in the presence of copper chromium oxide catalyst one of the major reactions involves reductive cleavage of the carbon–oxygen bond at the anomeric center with formation of an anhydro derivative (1, 2, 3). Thus methyl-β-L-arabopyranoside is attacked primarily at carbon–oxygen bonds 1, and 2 or 4, giving a mixture of 1,5-anhydro-2- and -4-deoxypentitols (*cis*- and *trans*-pyran-2,3-diols) (1). Likewise, methyl-α-D-glucopyranoside yields mainly a mixture of 1,5-anhydrodeoxyhexitols (2, 3). Sugar derivatives other than glycosides are now being examined to evaluate the stability of various substituent groups to hydrogenolysis, one objective being the possible discovery of resistant-blocking groups or of substituents easily cleaved, which may facilitate the preparation of deoxy sugars. The present paper concerns the hydrogenolysis of one of these derivatives, 1,2-*O*-*iso*propylidene-D-glucofuranose.

Under reaction conditions slightly milder than used earlier for the methyl glycosides, i.e., at about 180° C., at hydrogen pressures of 2000–3000 p.s.i., and with dioxane as solvent, the *iso*propylidene group was found to be more stable than a glycosidic methoxyl group, over half of the starting material remaining unchanged; no reaction occurred at 150° C., and at 250° C. extensive hydrogenolysis was evident. Among the reaction products obtained at 180° C. a sugar other than D-glucose was detected after hydrolytic removal of the *iso*propylidene groups. This sugar was isolated in 4.2% yield by cellulose-column chromatography (4) as a levorotatory sirup ($[\alpha]_D$ −10°) which formed a crystalline 1-benzyl-1-phenylhydrazone. The rate of movement of the sugar on a paper chromatogram (R_F = xylose) suggested that the compound might be deoxy-hexose. However, treatment of the sugar with 1.5 moles of lead tetraacetate in acetic acid and hydrolysis of the resulting formate esters gave two products which were indistinguishable from xylose and threose on a paper chromatogram. Since under the same conditions D-glucose gives D-arabinose and D-erythrose (5), it was evident that the configuration of the

[1]*Manuscript received January 2, 1958.*
Contribution from the National Research Council of Canada, Prairie Regional Laboratory, Saskatoon, Saskatchewan. Presented at the 132nd Meeting of the American Chemical Society, New York, N.Y., September, 1957. Release granted December 16, 1957.
Issued as N.R.C. No. 4651 and Paper No. 251 on the Uses of Plant Products.

hydroxyl group at carbon 5 of the D-glucose had been altered during the hydrogenation reaction. The sugar was shown, in fact, to be L-idose, for on treatment with phenylhydrazine acetate it yielded L-idose phenylosazone (L-sorbosazone) and on reduction followed by acetylation it gave L-iditol hexaacetate (6).

The conversion of D-glucose into L-idose affords a clear demonstration of a sugar isomerization promoted by catalytic hydrogenation conditions. Taken together with the recent finding (3) that dihydro-D-altral is formed from methyl-α-D-glucopyranoside and the observation (7) that under similar conditions D-xylose, D-ribose, and D- and L-lyxose are obtainable from methyl-β-L-arabopyranoside, the present results suggest that extensive isomerization may occur during hydrogenolysis reactions. Cyclic alcohols are known to isomerize in the presence of Raney nickel or platinum catalysts and hydrogen (8). It has been postulated that an intermediate ketone is formed in this reaction so that the over-all reaction represents a dehydrogenation followed by hydrogenation. A similar mechanism may be operative also in the current isomerizations of carbohydrates but, as yet, no evidence is forthcoming to support such a possibility. An apparent isomerization has recently been encountered in the catalytic hydrogenation of hexahydroxybenzene for preparation of inositols (9).

In addition to *iso*propylidene-L-idose, the hydrogenolysis of 1,2-*O*-*iso*propylidene-D-glucofuranose gave a mixture of hexanepolyols, comprising a diol, at least two triols, and a tetrol, in yields of 2.4%, 6.5%, and 4.3%, respectively, based on the weight of starting material. The tetrol, which was readily isolated from an aqueous solution after extraction of the other reaction products into chloroform, was crystalline and yielded a crystalline tetraacetate. When treated with periodate it consumed 2 moles of oxidant and liberated 2 moles of formaldehyde, but gave neither formic acid nor acetaldehyde. These properties served to characterize the tetrol as 1,2,5,6-hexanetetrol (3,4-dideoxyhexitol).

The diol and triol fractions, obtained from the chloroform extract, were separated by cellulose column chromatography. The diol, which yielded a crystalline bis-*p*-nitrobenzoate, was shown to be 1,2-hexanediol for it consumed 1 mole of periodate with production of 1 mole of formaldehyde. The sirupy triol fraction consumed almost 1 mole of oxidant and yielded close to 1 mole of formaldehyde, establishing the presence of a 1,2-diol group as a main structural feature of the triols present. Periodic acid oxidation of the triols followed by reduction with sodium borohydride (10) yielded a mixture of alcohols which could not be completely resolved into pure components via the derived *p*-nitrobenzoates. One apparently pure tris-*p*-nitrobenzoate was obtained in low yield on recrystallization from ethyl acetate. The resistance of its parent triol to periodate oxidation indicates either a 1,3,5- or a 1,3,6-hexanetriol structure, making this minor component the only hydrogenolysis product isolated which is not reconcilable with Adkins' β-hydrogenation rule (11). Because of the possibility that isomerization had occurred during formation of the various polyols, the configuration of the secondary hydroxyls cannot be assigned with certainty by reference to the parent compound, D-glucose.

The 1,2-glycol group of the diol and triols was derived principally from the 5,6-glycol group of the original D-glucose derivative. This was shown by hydrogenolysis of 1,2-*O*-*iso*propylidene-D-glucofuranose-1-C^{14}. The labelled diol and triols obtained from the latter compound were oxidized with periodate yielding formaldehyde (isolated as the dimedon derivative), which accounted for only 24% and 35%, respectively, of the

Can. J. Chem. Downloaded from www.nrcresearchpress.com by 200.7.193.243 on 09/04/12
For personal use only.

specific activity of the acetone-glucose-1-C^{14}. Further, when the diol was oxidized with the permanganate–periodate reagent (12), it yielded *n*-valeric acid possessing an activity which corresponded to 73% of that of the starting material; likewise, the mixture of pentanediols derived from the hexanetriol-C^{14} fraction by sodium periodate oxidation followed by sodium borohydride reduction accounted for 70% of the total activity. About three-quarters of the 1,2-glycol groups of the diol and triol originate from carbons 5 and 6 of the D-glucose and the remainder from carbons 1 and 2, implying that at least two different mechanisms operate in the hydrogenolysis of the *iso*propylidene group, one involving cleavage of ketal carbon–oxygen bonds, the other, of alcohol or the hemiacetal carbon–oxygen bonds.

It appears unlikely that the polyols are formed as a result of hydrolysis of the *iso*propylidene group (although the solvent was not rigorously dried, and water is a product of the reaction). This is suggested by hydrogenolysis control runs using hexitols (13), presumably the first products formed if the acetone group is hydrolyzed off, in which the variety of products was much greater than found in the present instance. The formation of these polyols is taken, rather, as an indication of the relative stability to hydrogenolysis of the various carbon–oxygen bonds in 1,2-*O*-*iso*propylidene-D-glucose. Accordingly, the bonds at carbons 3 and 4 are by far the least stable, while those at carbons 5 and 6 are most resistant to reductive cleavage. These relative stabilities may be altered substantially, however, by modification of the *iso*propylidene-D-glucose molecule. For example, the corresponding 3-*O*-methyl- and 6-deoxy-derivatives are unaffected by treatment under the same reaction conditions (13). Still other substituents at different positions may induce greater susceptibility to hydrogenolysis. The utilization of variations of this kind, it is anticipated, should extend the usefulness of catalytic hydrogenation in the synthesis of carbohydrate derivatives.

EXPERIMENTAL

Paper chromatography was carried out on Whatman No. 1 filter paper using *n*-butanol–ethanol–water (40:11:19 v/v) as solvent. Spray reagents used were *p*-anisidine hydrochloride in butanol (14), aniline oxalate (15), and ammoniacal silver nitrate (16). Melting points are uncorrected. Evaporations were carried out under reduced pressure. Optical rotations were measured at 27° C.

Radioactive samples were combusted and the specific activity of the carbon dioxide liberated was measured by the procedure of Buchanan and Nakao (17).

Hydrogenolysis of 1,2-O-Isopropylidene-D-glucofuranose-1-C^{14}

The *iso*propylidene-D-glucose-1-C^{14} (22.5 g.; 6.84 mμc./mM.) in dioxane (400 ml.) was hydrogenated at 2000–2900 p.s.i. for 6 hours at 180° C. using copper chromium oxide (6.0 g.) as catalyst. Removal of the catalyst and solvent left a colorless sirup, an aqueous solution of which was continuously extracted with chloroform.

1,2,5,6-Hexanetetrol

The aqueous solution which had been extracted with chloroform was evaporated, giving a sirup (2.0 g.) which crystallized from methanol–acetone. Two recrystallizations from the same solvent mixture gave a hexanetetrol (0.66 g.), m.p. 95°–97° C. and $[\alpha]_D$ 0° (*c*, 1.5, saturated borax) (1 dm. tube). Calculated for $C_6H_{14}O_4$: C, 47.98%; H, 9.40%. Found: C, 47.75%; H, 9.42%. The periodate equivalent, measured by the arsenite method (18), was 80 (calculated value, 75) and the formaldehyde equivalent, measured by the

Can. J. Chem. Downloaded from www.nrcresearchpress.com by 200.7.193.243 on 09/04/12
For personal use only.

chromotropic acid method (19), was 63 (calculated value, 75). No formic acid (20) or acetaldehyde (21) was formed.

Acetylated by the hot sodium acetate method the tetrol gave a tetraacetate which, after two recrystallizations from acetone – light petroleum (b.p. 60°–80° C.), had m.p. 76°–77° C. and $[\alpha]_D$ 0° (*c*, 5.5, $CHCl_3$) (1 dm. tube). Calculated for $C_{14}H_{22}O_8$: C, 52.82%; H, 6.97%. Found: C, 52.85%; H, 7.30%.

1,2-Hexanediol

The chloroform extract (above) was evaporated to a sirup, which was dissolved in hot ethyl acetate (100 ml.). On cooling, unchanged 1,2-*O*-*iso*propylidene-D-glucofuranose was deposited and the filtered mother liquor was evaporated to a sirup (6.2 g.). The latter was dissolved in 0.1 *N* sulphuric acid (50 cc.) and hydrolyzed at 100° C. for 1 hour. The acid was neutralized ($BaCO_3$), and the solution filtered and evaporated to give a sirup. Paper chromatographic examination indicated a mixture with R_F's corresponding to glucose and a deoxy-hexose (*p*-anisidine hydrochloride spray) and also a triol together with smaller amounts of diol (ammoniacal silver nitrate spray).

The mixture was fractionated on a cellulose column. Benzene–ethanol–water (500:50:1 v/v) eluted the diol, which was obtained as a mobile sirup, $[\alpha]_D$ −12° (*c*, 2.0, saturated borax), distilling at 160°–170° C. (air bath) at 1 mm., and having a specific activity of 9.28 mμc./mM. (calc. 10.2 mμc./mM.). Yield 290 mg. Calculated for $C_6H_{14}O_2$: C, 60.98%; H, 11.94%. Found: C, 60.40%; H, 12.14%. It had a periodate equivalent of 124 and a formaldehyde equivalent of 104. Calculated periodate and formaldehyde equivalents, 118. The product had an infrared spectrum identical with that of an authentic specimen (22).

The diol (67 mg.) was converted to the bis-*p*-nitrobenzoate, which after two recrystallizations from ethanol had m.p. 91°–93° C. Yield 67 mg. Racemic 1,2-hexanediol bis-*p*-nitrobenzoate has m.p. 101.5°–102.5° C. (22); the lower melting point of the current material may be due to the presence of mixed D- and L-forms or of one isomer, the diol being optically active. Calculated for $C_{20}H_{20}O_8N_2$: C, 57.69%; H, 4.84%. Found: C, 57.40%; H, 4.79%.

The diol (59 mg.) was oxidized with periodic acid (0.21 g.) in water (10 ml.), and the solution was then distilled into a solution of dimedon (0.50 g.) in 50 ml. of 0.15 *M* phosphate buffer of pH 7.0. The formaldehyde dimedon which formed was filtered off and twice recrystallized from ethanol; yield 21 mg., m.p. 190°–191° C., specific activity 0.78 mμc./mM., corresponding to an activity of 13.3 mμc./mM. for C-1. Calculated for $C_{17}H_{24}O_4$: C, 69.83%; H, 8.27%. Found: C, 70.05%; H, 8.31%.

The diol (75 mg.) was oxidized for 4 hours with a solution (150 ml.) containing potassium permanganate (14 mg.), sodium periodate (580 mg.), and potassium carbonate (183 mg.) (12), excess reagent being destroyed with sodium bisulphite and 0.1 *N* sulphuric acid. The clear solution was extracted continuously with ether and the resulting extract was neutralized with dilute sodium hydroxide and then evaporated to dryness. The residue was dissolved in water (1 ml.), ethanol (10 ml.) added, followed by *p*-bromophenacyl bromide (180 mg.). After being refluxed for 1 hour, the solution was evaporated to dryness and the product was recrystallized three times from aqueous ethanol. The product had m.p. 71° C., undepressed on admixture with *n*-valeric acid *p*-bromophenacyl ester, and a specific activity of 3.13 mμc./mM. corresponding to an activity of 40.5 mμc./mM. for C-1. Calculated for $C_{13}H_{15}O_3Br$: Br, 26.7%. Found: Br, 26.2%.

Can. J. Chem. Downloaded from www.nrcresearchpress.com by 200.7.193.243 on 09/04/12
For personal use only.

Hexanetriol Fraction

The triol fraction (0.89 g.) was eluted from the cellulose column by *n*-butanol; it had $[\alpha]_D$ −3° (*c*, 1.6, saturated borax) and a specific activity of 9.50 mμc./mM. (Calc. 10.2 mμc./mM.). Oxidation of the material with periodic acid indicated a periodate equivalent of 143 and a formaldehyde equivalent of 140.

The triol (224 mg.) was oxidized in water (10 ml.) containing periodic acid (500 mg.). After 15 minutes a slurry of barium carbonate was added to remove excess iodate and periodate and the solution was filtered. The filtrate was treated with sodium borohydride (200 mg.) and after 15 minutes the solution was acidified with dilute sulphuric acid, then continuously extracted with ether, and the extract was evaporated repeatedly with methanol to remove boric acid. A sirupy product (143 mg.) was obtained and a 55 mg. portion was converted to its *p*-nitrobenzoate by the same method as described previously. Two fractions were obtained after several fractional crystallizations from ethyl acetate and ethyl acetate – light petroleum (b.p. 50°–60° C.). The major portion (33 mg.) had m.p. 153°–156° C. (an authentic specimen of 1,5-pentanediol bis-*p*-nitrobenzoate prepared in the same way had m.p. 101°–103° C.) and an infrared spectrum similar to that of 1,5-pentanediol bis-*p*-nitrobenzoate. Calculated for $C_{19}H_{18}O_8N_2$: C, 56.71%; H, 4.51%. Found: C, 57.17%; H, 4.72%. The specific activity of the bis-*p*-nitrobenzoate was 2.11 mμc./mM. On the basis of the infrared spectrum and periodate oxidation data, the product possibly comprises a mixture of 1,5-pentanediol bis-*p*-nitrobenzoate and an impurity, thus indicating a 1,2,6-structure for the parent hexanetriol. The minor *p*-nitrobenzoate component (5 mg.) had m.p. 171°–173° C. and a tris-*p*-nitrobenzoate structure was indicated by the carbon and hydrogen microanalyses. Calculated for $C_{27}H_{23}O_{12}N_3$: C, 55.77%; H, 3.99%. Found: C, 55.49%; H, 3.93%.

L-*Idose*

Elution of the cellulose column with *n*-butanol one-quarter saturated with water gave a reducing sugar as a sirup (0.94 g.) with $[\alpha]_D$ −10° (*c*, 0.8, water). The sugar was oxidized with lead tetraacetate in acetic acid (5). After 2, 5, 10, and 30 minutes 2.02, 2.08, 2.12, and 2.14 moles/mole of reagent were consumed respectively. Oxidation of the sugar with 1.5 moles/mole of reagent gave a mixture, which, after removal of inorganic material from the solution and hydrolysis of the resulting formate esters, was indistinguishable from xylose and threose on a paper chromatogram.

The sugar (0.35 g.) was heated for 4 hours at 100° C. in an aqueous solution (20 ml.) containing phenylhydrazine (0.89 ml.) and acetic acid (1 ml.). On cooling, yellow crystals were deposited and were filtered off and recrystallized twice from methanol–benzene. The product (0.16 g.) had m.p. 170°–172° C. and $[\alpha]_D$ −13.8° (*c*, 1.0, pyridine–ethanol (1:1 v/v)) and was indistinguishable from L-sorbose phenylosazone (23) by its X-ray diffraction pattern and mixed melting point. Calculated for $C_{18}H_{22}O_4N_4$: C, 60.32%; H, 6.19%. Found: C, 60.51%; H, 6.09%.

The aldose (98 mg.) was refluxed for 15 minutes in a water (10 ml.) – ethanol (5 ml.) mixture containing 1-benzyl-1-phenylhydrazine hydrochloride (110 mg.). The solution was evaporated to a sirup which crystallized. Three recrystallizations from benzene – ethyl acetate afforded L-idose 1-benzyl-1-phenylhydrazone (104 mg.) having m.p. 113°–115° C. and $[\alpha]_D$ −19° (*c*, 1.2, ethanol). Calculated for $C_{19}H_{24}O_5N_2$: C, 63.32%; H, 6.71%. Found: C, 62.94%; H, 6.79%.

The aldose (140 mg.) was dissolved in a solution of sodium borohydride (100 mg.) in water (10 ml.). After 3 hours excess reagent was destroyed with acetic acid and the

Can. J. Chem. Downloaded from www.nrcresearchpress.com by 200.7.193.243 on 09/04/12
For personal use only.

solution then treated with Amberlite IR-120. The solution was evaporated to dryness and excess boric acid was removed by repeated evaporations of the product in methanol; yield, 126 mg., of which 104 mg. was acetylated at 100° C. in a mixture of acetic anhydride (2 ml.) and sodium acetate (0.2 g.) for 1 hour. The acetate crystallized from ethanol, and recrystallization from the same solvent gave a product (95 mg.) having m.p. 123°–124° C. and $[\alpha]_D$ −23° (*c*, 1.1, chloroform). An X-ray diffraction pattern and mixed melting point showed that the compound was L-iditol hexaacetate (6). Calculated for $C_{18}H_{26}O_{12}$: C, 49.77%; H, 6.03%. Found: C, 50.01%; H, 5.99%.

ACKNOWLEDGMENTS

The authors are grateful to the following for their assistance: Mr. J. A. Baignée for microanalyses, Mr. J. W. L. C. Christ for technical assistance, Mr. J. Dyck and Dr. A. C. Neish for specific activity estimations, Mr. T. M. Mallard for X-ray diffraction measurements, and Mr. G. B. Rennie for preparation of infrared spectra. Dr. A. C. Neish kindly supplied a sample of L-iditol hexaacetate.

REFERENCES

1. BAUER, H. F. and STUETZ, D. E. J. Am. Chem. Soc. **78**, 4097 (1956).
2. RUDLOFF, E. VON, STUETZ, D. E., and BAUER, H. F. Can. J. Chem. **35**, 315 (1957).
3. RUDLOFF, E. VON and TULLOCH, A. P. Can. J. Chem. **35**, 1504 (1957).
4. HOUGH, L., JONES, J. K. N., and WADMAN, W. H. J. Chem. Soc. 2511 (1949).
5. PERLIN, A. S. and BRICE, C. Can. J. Chem. **33**, 1216 (1955).
6. MEYER, A. S. and REICHSTEIN, T. Helv. Chim. Acta, **29**, 152 (1946).
7. PERLIN, A. S., RUDLOFF, E. VON, and TULLOCH, A. P. Unpublished.
8. WICKER, R. J. J. Chem. Soc. 2165 (1956).
9. ANGYAL, S. J. and MCHUGH, D. J. J. Chem. Soc. 3682 (1957).
10. WOLFROM, M. L. and WOOD, H. B. J. Am. Chem. Soc. **73**, 2933 (1951).
11. ADKINS, H. Reactions of hydrogen. The University of Wisconsin Press, Madison, Wis. 1946.
12. LEMIEUX, R. U. and RUDLOFF, E. VON. Can. J. Chem. **33**, 1701 (1955).
13. GORIN, P. A. J. and PERLIN, A. S. Unpublished.
14. HOUGH, L., JONES, J. K. N., and WADMAN, W. H. J. Chem. Soc. 1702 (1950).
15. HORROCKS, R. H. Nature, **164**, 444 (1949).
16. PARTRIDGE, S. M. Nature, **158**, 270 (1946).
17. BUCHANAN, D. L. and NAKAO, A. J. Am. Chem. Soc. **74**, 2389 (1952).
18. FLEURY, P. and LANGE, J. J. pharm. chim. **17**, 107 (1933).
19. LAMBERT, M. and NEISH, A. C. Can. J. Research, B, **28**, 83 (1950).
20. HALSALL, T. G., HIRST, E. L., and JONES, J. K. N. J. Chem. Soc. 1427 (1947).
21. DESNUELLE, P. and NAUDET, M. Bull. soc. chim. France, **12**, 871 (1945).
22. RUDLOFF, E. VON. Unpublished.
23. FISCHER, E. Ber. **28**, 1159 (1895).

Can. J. Chem. Downloaded from www.nrcresearchpress.com by 200.7.193.243 on 09/04/12
For personal use only.

Can. J. Chem. Downloaded from www.nrcresearchpress.com by 200.7.193.243 on 09/04/12
For personal use only.

ÉTARD REACTION

I. ITS SCOPE AND LIMITATION WITH SUBSTITUTED TOLUENES[1]

OWEN H. WHEELER[2]

ABSTRACT

The scope and limitations of the Étard oxidation of substituted toluenes to substituted benzaldehydes by chromyl chloride have been studied. The conditions of the reaction were investigated and an improved method of performing it was developed.

INTRODUCTION

Though the chromyl chloride oxidation of toluenes to benzaldehydes was discovered by Étard in 1877 (1, 2) the reaction has been little used and no systematic study has been made of its potentialities. In connection with other work it was necessary to prepare a series of substituted benzaldehydes and this method seemed the most general and convenient. Accordingly a study of its scope and limitations for the conversion of substituted toluenes to substituted benzaldehydes was carried out.

The procedure used is to add a solution of chromyl chloride to a stirred solution of the toluene. The solvents usually used are carbon tetrachloride (3, 4, 5), carbon disulphide (6, 7, 8, 9), and chloroform. Carbon disulphide has the disadvantage of a low boiling point. The chloroform must be free from preservative alcohol and also was found to give troublesome emulsions during working up. In preliminary experiments the yields were little different with each solvent and carbon tetrachloride was therefore chosen as the general solvent for the study.

A complex is formed as intermediate in the reaction and this must be hydrolyzed under reducing conditions to prevent oxidation of the benzaldehyde to a benzoic acid. Saturated aqueous sodium sulphite (3) was the most convenient, but the aqueous solution must be well cooled and stirred during addition to prevent overoxidation. It has been recommended (3) that the complex be isolated by filtration and decomposed separately. This gives a purer product, since the complex contains no unreacted toluene, but the decomposition was found to be less easily controlled than when carried out with the complex suspended in the original solvent.

During the exothermic addition of chromyl chloride to the toluene, the initial dark red color of the solution becomes dark brown to black as the complex is slowly precipitated. These observations suggest that the initial step is the formation of a π- or σ-complex between the aromatic and chromyl chloride, which is followed by the formation of the true solid complex. (Spectroscopic evidence has been obtained for the rapid formation of a soluble complex (10).) It has been the usual practice to allow the reaction mixture to stand for a period of a few days (3, 11) to several weeks (4, 8) to allow complete separation of the complex. However, if sufficient time is allowed for formation of the physical complex, it should be possible to accelerate the second step of formation of the solid complex without harm to the aromatic nucleus, by heating the reaction mixture. This has been found to be the case and the reaction time can be considerably reduced by allowing the mixture to stand a short time and then refluxing it for several hours. Reaction times of 2 to 12 hours only are then required and this makes the reaction

[1]*Manuscript received December 16, 1957.*
Contribution from the Instituto de Quimica, Universidad Nacional Autonoma de Mexico, Mexico, 20, D.F.
[2]*Present address: Department of Chemistry, Dalhousie University, Halifax, N.S.*

a very convenient one. If the reaction mixture is not initially cooled, or is heated too soon after the chromyl chloride is added, a vigorous or explosive reaction can occur.

To study the scope of the reaction with various toluenes the addition was carried out as usual and the mixture allowed to stand overnight. The product was isolated in the normal way and the aldehyde content estimated gravimetrically with 2,4-dinitrophenylhydrazine reagent. In the preparative experiments the mixture was refluxed for several hours before decomposition. The optimum conditions of reaction were generally not determined though enough data (Table I) were collected to predict them. In the case of *p*-iodotoluene the most suitable conditions are reported.

TABLE I

	Toluene	Temp.[a]	Time[b]	Yield[c]	Conversion[d]
I	*o*-Methyl	R.T.	o.n.	28	51
II	*m*-Methyl	R.T.	o.n.	32	50
III	*p*-Methyl	R.T.	o.n.	35	45
IV	*p*-Fluoro	R.T.	3 days	85	40
V	*o*-Chloro	R.T.	o.n.	79	19
VI	*o*-Chloro	Reflux	6 hr.	58	90
VII	*p*-Chloro	R.T.	2 hr.	100	0
VIII	*p*-Chloro	R.T.	3 days	86	36
IX	*p*-Chloro	Reflux	4 hr.	78	95
X	*o*-Bromo	Reflux	6 hr.	60	95
XI	*p*-Bromo	R.T.	o.n.	87	23
XII	*p*-Bromo	Reflux	6 hr.	85	92
XIII	*o*-Iodo	R.T.	3½ days	50	6
XIV	*o*-Iodo	Reflux	15 hr.	56	24
XV	*p*-Iodo	R.T.	o.n.	77	10
XVI	*p*-Iodo	R.T.	3 days	72	25
XVII	*p*-Iodo	R.T.	7 days	65	50
XVIII	*p*-Iodo	Reflux	4 hr.	90	42
XIX	*p*-Iodo	Reflux	10 hr.	83	85
XX	*o*-Nitro	Reflux	10 hr.	45	15
XXI	*p*-Nitro	Reflux	10 hr.	36	26
XXII	*p*-Methoxy	R.T.	o.n.	7	0
XXIII	*p*-Hydroxy	R.T.	o.n.	20	0
XXIV	*p*-Mercapto	R.T.	o.n.	50	0
XXV	*p*-Chloromethyl	R.T.	o.n.	32	10[e]
XXVI	*p*-Cyano	R.T.	o.n.	35	<5
XXVII	*p*-Cyano	R.T.	3 days	22	5[f]

[a]*R.T. denotes room temperature (22°–25°).*
[b]*o.n. denotes stirring overnight.*
[c]*Percentage yield of distillable product.*
[d]*Percentage of aldehyde in product.*
[e]*Derivative m.p. ca. 258°. p-Tolualdehyde 2,4-dinitrophenylhydrazone has m.p. 232.5°–234.5°, Ref. 22.*
[f]*Solid m.p. 211°–214°. p-Cyanobenzoic acid has m.p. 219°, Ref. 23.*

The three isomeric xylenes (I–III) all give tolualdehydes with oxidation of only one methyl group, as previously observed (3, 11), since the complex precipitates and further reaction is prevented. The yields and conversions are little different for all three. For the series *p*-fluoro-, *p*-chloro-, *p*-bromo-, and *p*-iodo-toluene (IV, VII, VIII, XI, XV, XVI, XVII) the yields decrease progressively for reaction at room temperature. Good conversions are obtained for *p*-chlorotoluene by refluxing for 4 hours (IX), whereas *p*-bromotoluene requires 6 hours (XII), and *p*-iodotoluene requires some 10 hours (XVIII, XIX). In these cases the yields of recovered product are all good (>80%) and the aromatic nucleus is not destroyed by prolonged refluxing. In the case of the ortho-halogenated toluenes the increasing size of the halogeno atom for the series chlorine, bromine, and iodine results in a considerably decreasing ease of oxidation (V, VI, X, XIII, XIV). Good

Can. J. Chem. Downloaded from www.nrcresearchpress.com by 200.7.193.243 on 09/04/12
For personal use only.

conversions can be obtained in the case of *o*-chloro- (V, VI) and *o*-bromo-toluene (X) by refluxing, but *o*-iodotoluene (XIII) is only oxidized very slowly, and prolonged reaction (XIV) tends to destroy the entire molecule.

p-Nitrotoluene is only slowly oxidized (XXI) and the ortho-isomer less so (XX). This must be due to the deactivating effect of a nitro group on an aromatic ring (12).

Of the other substituted toluenes investigated (XXII–XXVII), none of them gave any useful yield of a substituted benzaldehyde. Very little methoxytoluene (XXII) was recovered from its reaction with chromyl chloride. The major product was an undistillable polymer, and the chromyl chloride, which is a strong Lewis acid, must have caused polymerization. However, in the case of *p*-cresol (XXIII) and *p*-thiocresol (XXIV), though no aldehyde was formed, increased quantities of starting material could be recovered.

In the oxidation of *p*-chloromethyltoluene only some 30% of product could be obtained, but this analyzed for 10% of aldehyde. The 2,4-dinitrophenylhydrazone seemed to be that of *p*-chloromethylbenzaldehyde, since it had a higher melting point than that of *p*-tolualdehyde, the other possible product, suggesting that the methyl and not the chloromethyl group had been attacked.

p-Toluonitrile (XXVI, XXVII) was largely destroyed by reaction with chromyl chloride but a small amount of *p*-cyanobenzoic acid could be isolated.

In many cases the Étard reaction provides a simple and convenient one-step method of converting a toluene to a benzaldehyde. This gives better yields than the corresponding oxidations with manganese dioxide (3, 13) in sulphuric acid or electrolytically (3), and is simpler than the two-stage conversions of side-chain bromination and hydrolysis (14) and of oxidation with chromium trioxide in acetic anhydride followed by hydrolysis of the resulting diacetate (15).

EXPERIMENTAL

Chromyl Chloride

Chromyl chloride was a gift from the Mutual Chemical Division of the Allied Chemical Corporation, and was used as received.

Toluenes

Most of these were commercial samples, which were distilled before use. Some were made by a Sandmeyer reaction from the appropriate toluidines (16, 17).

p-Methoxytoluene

p-Cresol (21.6 g.) was dissolved in water (100 ml.) containing sodium hydroxide (8.3 g.). The mixture was cooled to 10° C. and methyl sulphate (27.0 g.) was added dropwise with stirring over 1/2 hour (18). The mixture was heated under reflux for 2 hours, cooled, diluted with water, and then extracted with ether. Isolation of the product gave 19.5 g. (80%), b.p. 163°–165° at 580 mm., n_D^{21} 1.5112 (lit. b.p. 175°–177° (19)).

p-Chloromethyltoluene

A mixture of toluene (70 g.), paraformaldehyde (6 g.), and pulverized zinc chloride (6 g.) was heated to 60°, and a stream of gaseous hydrogen chloride passed in (20) for 20 minutes. The product (25 g.) had b.p. 88°–90° at 18 mm.

Oxidations with Chromyl Chloride

In a typical experiment the toluene (1/10–1/5 mole) was dissolved in carbon tetrachloride (5–6 volumes). Chromyl chloride (0.21–0.42 mole) in an equal volume of carbon

Can. J. Chem. Downloaded from www.nrcresearchpress.com by 200.7.193.243 on 09/04/12
For personal use only.

tetrachloride was added slowly over 1 hour with stirring and external cooling in a bath of cold water so that the temperature never rose above 35°. Stirring was continued for another 2 hours and the mixture was then either allowed to stand at room temperature or refluxed with stirring for a number of hours. If the reaction is *not initially cooled* or if stirring is discontinued too soon, a *violent or explosive reaction* may take place. The reaction mixture was decomposed by pouring onto a stirred mixture of ice and saturated aqueous sodium sulphite solution. The use of insufficient ice or stirring may lead to overheating and overoxidation of the benzaldehyde to the benzoic acid. The organic layer was separated and the aqueous layer extracted several times with carbon tetrachloride. Extraction is sometimes made difficult by the precipitation of basic chromium salts, and these can best be removed by adding diluted (1:1) hydrochloric acid. The products were isolated by distillation and their content of benzaldehydes determined by treating a portion with 2,4-dinitrophenylhydrazine sulphate dissolved in aqueous methanol. The precipitates formed on warming were washed with water and cold methanol and dried at 100° before they were weighed.

p-Iodobenzaldehyde

A solution of *p*-iodotoluene (43.6 g., 0.2 mole) in carbon tetrachloride (150 ml.) was placed in a three-necked flask, immersed in ice-cold water. Chromyl chloride (65.2 g., 0.42 mole) in carbon tetrachloride (150 ml.) was allowed to run in dropwise, with good stirring, during 1 hour. The mixture was stirred at room temperature for a further 1 hour, and then heated slowly to reflux during another 1 hour. The mixture was stirred while refluxing for a further 20 hours. The cooled reaction mixture was poured slowly with vigorous stirring by hand onto sodium sulphite (60 g.) dissolved in water (300 ml.) containing ice (300 g.). Diluted (1:1) hydrochloric acid (100 ml.) was added to dissolve the basic chromium salts, and the organic layer separated and the aqueous layer extracted three times with portions of carbon tetrachloride. The combined organic solution was washed with water and dried. The residue left when the solvent was removed was distilled, giving the product, b.p. 145°–150° at 25 mm., m.p. 55°–65° (27.0–30.0 g., 58–64%). A forerun, b.p. 125°–130° at 25 mm. (3.5–5.0 g.) was largely unchanged *p*-iodotoluene. The *p*-iodobenzaldehyde can be recrystallized from aqueous ethanol to m.p. 75° (lit. m.p. 77°–78° (21)).

ACKNOWLEDGMENTS

The author is grateful to the Rockefeller Foundation, New York, for financial assistance and to the Mutual Chemical Division of the Allied Chemical and Dye Corporation, Baltimore, for generous gifts of chromyl chloride.

REFERENCES

1. ÉTARD, A. Compt. rend. **84**, 127 (1877).
2. ÉTARD, A. Ann. chim. et phys. **22**, 218 (1881).
3. LAW, H. D. and PERKIN, F. M. J. Chem. Soc. **91**, 258 (1907).
4. LAW, H. D. and PERKIN, F. M. J. Chem. Soc. **93**, 1633 (1907).
5. KATON, M. M., MASKUINA, E. P., and FLORINSKI, F. S. J. Gen. Chem. U.S.S.R. **21**, 1843 (1951).
6. RICHTER, W. VON. Ber. **19**, 1061 (1886).
7. WÖRNER, H. Ber. **29**, 153 (1896).
8. WILLSTAEDT, H. Ber. **64**, 2688 (1931).
9. SHARYGIN, P. P. and SHARYGINA, N. Y. J. Gen. Chem. U.S.S.R. **9**, 845 (1939).
10. WHEELER, O. H. Unpublished observations.
11. BOGERT, M. T., DAVIDSON, D., and APFELBAUM, P. M. J. Am. Chem. Soc. **56**, 959 (1934).
12. INGOLD, C. K. Structure and mechanism in organic chemistry. Cornell University Press, Ithaca, N.Y. 1953. Chap. VI.
13. FREUND, Z. Chem. Ztg. **51**, 803 (1927).

Can. J. Chem. Downloaded from www.nrcresearchpress.com by 200.7.193.243 on 09/04/12
For personal use only.

14. COLEMAN, G. H. and HONEYWELL, G. E. Organic syntheses. Vol. 17. John Wiley & Sons, Inc., New York. 1937. p. 20.
15. LIEBERMAN, S. V. and CONNOR, R. Organic syntheses. Vol. 18. John Wiley & Sons, Inc., New York. 1938. p. 61.
16. BIGELOW, L. A. Organic syntheses. Collective Vol. I. John Wiley & Sons, Inc., New York. 1932. p. 131.
17. CLARK, H. T. and READ, R. R. Organic syntheses. Collective Vol. I. John Wiley & Sons, Inc., New York. 1932. p. 500.
18. HIERS, G. S. and HAGER, F. D. Organic syntheses. Collective Vol. I. John Wiley & Sons, Inc., New York. 1932. p. 50.
19. BIRCH, A. J. J. Chem. Soc. 809 (1945).
20. FUSON, R. C. and MCKEEVER, C. H. Organic reactions. Vol. I. John Wiley & Sons, Inc., New York. 1942. p. 63.
21. SAH, P. P. T. J. Am. Chem. Soc. **64**, 1487 (1942).
22. HEILBRON, I. M. and BUNBURY, H. M. Dictionary of organic compounds. Eyre and Spottiswoode, Ltd., London. 1953.
23. RUPE, H. and BERNSTEIN, F. Helv. Chim. Acta, **13**, 468 (1930).

Can. J. Chem. Downloaded from www.nrcresearchpress.com by 200.7.193.243 on 09/04/12
For personal use only.

Can. J. Chem. Downloaded from www.nrcresearchpress.com by 200.7.193.243 on 09/04/12
For personal use only.

SLURRY TITRATIONS OF UNSTABILIZED CELLULOSE NITRATE[1]

PAUL E. GAGNON, KARL F. KEIRSTEAD,[2] AND BRIAN T. NEWBOLD

ABSTRACT

Slurry titrations were performed on unstabilized cotton and wood cellulose nitrates. The results for total sulphate were compared with those from gravimetric, 24-hour, and zero hydrolysis methods. The agreement was best in the case of wood cellulose nitrates. The ester sulphate contents obtained were also compared with those from 24-hour and zero hydrolysis. The agreement was again best in the case of wood cellulose nitrates. It was shown that slurry titration for the determination of sulphate acid ester could be used for wood cellulose nitrates containing not less than 100% sulphate ester, the error being −2.7 to −11.9%. For cotton cellulose nitrates, the results were not satisfactory.

INTRODUCTION

Unstabilized cellulose acetate and cellulose nitrate contain a small amount of sulphate. It has been established by Malm *et al.* (1) that the sulphate in unstabilized cellulose acetate is in the form of a sulphate acid ester, RSO_4H. The form of the sulphate content of unstabilized cellulose nitrate has for many years been a subject of discussion.

In 1942, Kullgren (2) produced some evidence for the presence of a hemiester form, RSO_4H, by means of ion-exchange studies. A few years later, support for the existence of a sulphate ester was obtained by Reeve and Giddens (3), who studied the mechanism of stabilization of cellulose nitrate by ammonia. Later, Miles (4) summarized the work done on the determination of sulphate ester in cellulose nitrate by means of titration in acetone solution. Gagnon *et al.* (5) have shown that the sulphate ester in unstabilized cellulose nitrate can be determined by titration in water, or by analysis for calcium after ion exchange, or hydrolysis in acetone/water, or determination of sulphate after treatment with 50% alcohol.

Recently, the hydrolysis method for determining the sulphate acid ester was carefully studied (6). The object of the present work was to evaluate the slurry titration of unstabilized cellulose nitrate in water and to investigate the possibility of using this type of titration for determining the sulphate acid ester content of unstabilized cellulose nitrate.

EXPERIMENTAL

Cellulose Nitrate

The preparation of the unstabilized cotton and wood cellulose nitrates was described in a previous paper (7). The sulphate content of the cellulose nitrates was determined as barium sulphate, (8), and the nitrogen by the Devarda method. In the present work, the nitrogen contents of the unstabilized cotton and wood cellulose nitrates varied from 12.1 to 7.7% and from 11.8 to 7.3%, respectively.

Slurry Titration of Unstabilized Cellulose Nitrate

The unstabilized cellulose nitrates were washed continuously with distilled water as previously described (8) and then dried to about 50% water content by centrifuging (5). Duplicate samples of moist cellulose nitrate (about 2 g. dry weight for cotton and 3 g. for wood cellulose nitrate) were placed in a beaker and distilled water (200 ml.)

[1]*Manuscript received November 14, 1957.*
Contribution from the Department of Chemistry, Laval University, Quebec, Que., with financial assistance from the Defence Research Board of Canada.
[2]*Present address: Lignosol Chemicals Limited, Quebec, Que.*

was added. The mixture was well stirred and the acidity determined by titration with 0.01 *N* potassium hydroxide using a Macbeth pH meter. Hydrolysis of the cellulose nitrate was minimized by completing the titration within 20 minutes.

In later experiments, the unstabilized cellulose nitrate obtained after centrifuging was ground with sand, so that the slurry titration could be completed within 10 minutes. "Ottawa sand"* (Standard, code 2170, 30 g.) was placed in a mortar and moist cellulose nitrate (3–5 g.) and distilled water (15–25 ml.) were added. The mixture was ground vigorously with a pestle for 10 minutes. The contents of the mortar were transferred to a beaker, the pestle and mortar washed with distilled water, and the combined washings added to the mixture in the beaker. The volume of solution was then made up to 200 ml. The change in the pH of the solution due to the presence of the sand was negligible. The mixture was well stirred and the acidity determined as before.

RESULTS AND DISCUSSION

Determination by Slurry Titration of the Total Sulphate Content of Cellulose Nitrate

Titration of unstabilized cellulose nitrate in the form of a slurry in water, when performed before hydrolysis of the nitrate begins, provides a measure of the total sulphate content. Unstabilized cellulose nitrate is thought to contain a sulphate acid ester, RSO_4H, free sulphuric acid, and possibly a very small amount of a neutral ester, R_2SO_4. The slurry titration gives the acidity due to these constituents.

In the present work, the slurry titer, expressed as milliliters 0.01 *N* potassium hydroxide, was converted to milliliters per gram of cellulose nitrate. The proportion of the slurry titer value due to sulphate acid ester can be calculated using the sulphate acid ester content obtained by the hydrolysis method (6). The portion of the slurry titer due to sulphate acid ester can be converted to sulphate, expressed as % H_2SO_4, by using 98 as the equivalent weight of the ester. An example serves to illustrate the calculations involved. For instance, a cotton cellulose nitrate was shown to contain 96% sulphate acid ester by the hydrolysis method (6). The slurry titer expressed as ml./g. was 8.90. Therefore the proportion of the latter value due to ester was 8.54 ml./g., i.e. $8.54 \times 0.01 \times 98 = 8.36$ mg. H_2SO_4 per gram of nitrocellulose, which was equivalent to 0.84% H_2SO_4. Assuming that the amount of neutral ester is negligible, the remainder of the slurry titer value, 0.36 ml./g., represents free sulphuric acid. Conversion of the latter value, using 49 as the equivalent weight, gives 0.02% H_2SO_4. Therefore the total sulphate content was 0.86% H_2SO_4. The gravimetric and slurry titration total sulphate contents of a series of cotton and wood cellulose nitrates are compared in Table I. The differences are shown statistically in Table II, together with the confidence limits for the differences, calculated by the method of Dean and Dixon (9). The precision of slurry titration total sulphates is given in Table III. The coefficients of variation by differences between duplicate results (10) for cotton and wood cellulose nitrates were 1.5 and 2.5, respectively. The slurry titration results show best agreement with the gravimetric values in the case of wood cellulose nitrates.

In cases where there was 100% sulphate acid ester present in the cellulose nitrate, the total sulphate content and the sulphate due to sulphate acid ester had the same value because of the absence of free sulphuric acid. Thus the total slurry titer represented the sulphate content due to sulphate acid ester and, using 98 only as the equivalent weight, could be converted to sulphate. For example, a wood cellulose nitrate was shown to contain 100% sulphate acid ester by the hydrolysis method (6). The slurry titer,

**General Chemical Co., New York, N.Y., U.S.A.*

Can. J. Chem. Downloaded from www.nrcresearchpress.com by 200.7.193.243 on 09/04/12
For personal use only.

expressed as ml./g., was 14.10, which was equivalent to 1.38% H_2SO_4. Four examples of slurry titration total sulphate values for cellulose nitrates containing 100% sulphate acid ester are given in Table I.

TABLE I

COMPARISON OF GRAVIMETRIC, 24-HOUR HYDROLYSIS, AND ZERO HYDROLYSIS WITH SLURRY TITRATION RESULTS FOR TOTAL SULPHATE

Expt. No.	Cotton cellulose nitrate		Wood cellulose nitrate	
	Total sulphate, % H_2SO_4		Total sulphate, % H_2SO_4	
	Grav.	Slurry	Grav.	Slurry
1	1.55	1.60	2.31	2.25*
2	0.95	0.86	2.13	2.00
3	0.89	0.89*	1.81	1.78*
4	0.85	0.82	1.79	1.68
5	0.81	0.74*	1.71	1.60
	24-hr. hydrol.	Slurry	24-hr. hydrol.	Slurry
1	1.84	1.82	2.18	2.00
2	1.42	1.49	2.11	2.07
3	1.30	1.36	2.01	1.88
4	0.98	0.89	1.64	1.68
5	0.94	0.85	1.65	1.60
	Zero hydrol.	Slurry	Zero hydrol.	Slurry
1	1.85	1.82	2.27	2.00
2	1.33	1.36	2.17	1.88
3	0.96	0.85	2.15	2.25
4	0.94	0.71	2.14	2.07
5	0.87	0.72	1.80	1.78

**100% ester content.*

The total sulphate values obtained from the 24-hour hydrolysis and slurry titers are compared in Table I. The differences are shown statistically in Table II. The coefficients of variation for cotton and wood cellulose nitrates were 2.8 and 1.0, and the Rank-correlation coefficients (11) +0.80 and +0.97, respectively. It is evident that there is good agreement between the sulphate values, especially in the case of wood cellulose nitrates.

TABLE II

DIFFERENCES BETWEEN TOTAL SULPHATES DETERMINED BY SLURRY TITRATION AND THOSE DETERMINED BY OTHER METHODS

Samples	Differences	Methods		
		Grav.	24-hr. hydrol.	Zero hydrol.
Cotton	Mean difference, %	−5.1	6.0	12.4
Wood	Mean difference, %	−3.2	5.6	5.1
Cotton	Standard deviation	10.8	4.2	8.2
Wood	Standard deviation	7.7	4.5	4.7
Cotton	95% Confidence limits	−5.1±7.5	6.0±2.8	12.4±5.7
Wood	95% Confidence limits	−3.2±5.4	5.6±3.1	5.1±3.3

Comparison of Slurry Titration and Zero Hydrolysis Total Sulphates

It has been shown recently (6) that cellulose nitrate can be titrated in 90% acetone/water solution with no hydrolysis of the sulphate acid ester occurring. Therefore zero hydrolysis and slurry titers should give the same results, expressed as milliliters 0.01 *N* potassium hydroxide per gram of cellulose nitrate. Results obtained by zero hydrolysis and slurry titrations for cotton and wood cellulose nitrates were compared. For instance,

Can. J. Chem. Downloaded from www.nrcresearchpress.com by 200.7.193.243 on 09/04/12
For personal use only.

for a wood cellulose nitrate the zero hydrolysis titer expressed as ml./g. was 14.51 and the slurry titer 14.13 ml./g. In general, there was good agreement between results, especially for wood cellulose nitrates.

The zero hydrolysis titers can be converted to total sulphate values by using sulphate acid ester contents obtained by the hydrolysis method (6) and the appropriate equivalent weights as mentioned for the slurry titration results. Total sulphate contents determined by zero hydrolysis and slurry titrations for cotton and wood cellulose nitrates are compared in Table I. The differences are shown in Table II. The coefficients of variation for cotton and wood cellulose nitrates were 6.1 and 3.2 and the Rank-correlation coefficients were +0.70 and +0.92, respectively. The precision of zero hydrolysis sulphate values is given in Table III. The Rank-correlation coefficients for cotton and wood cellulose nitrates were +0.99 and 0, respectively. It is evident that there was good agreement between zero hydrolysis and slurry titration results.

TABLE III

PRECISION OF TOTAL SULPHATE DETERMINATIONS ON DUPLICATE SAMPLES OF CELLULOSE NITRATES

		Methods	
Samples	Differences	Slurry	Zero hydrol.
Cotton	Mean difference, %	3.9	4.6
Wood	Mean difference, %	2.4	1.6
Cotton	Standard deviation	2.7	3.3
Wood	Standard deviation	4.4	1.3
Cotton	95% Confidence limits	3.9±1.9	4.6±3.3
Wood	95% Confidence limits	2.4±3.1	1.6±1.3

Total sulphates were calculated from zero hydrolysis titers of cellulose nitrates prepared by duplicate nitrations. The precision of the sulphate determinations decreased as expected. For cotton cellulose nitrate the mean difference was 11.3%, the standard deviation 12.5, and the 95% confidence limits were 11.3% ±4.8, and for wood cellulose nitrate the corresponding values were 11.1%, 7.0, and 11.1% ±8.4. Total sulphates were also calculated from slurry titers of samples prepared by duplicate nitrations but were not reproducible.

Comparison of Slurry Titration with 24-Hour Hydrolysis and Zero Hydrolysis Ester Sulphates

Ester sulphate values as determined by the hydrolysis method (6) can be compared with those calculated from slurry titration. Twenty-four hour hydrolysis and slurry titration ester sulphates are compared in Table IV. The differences are shown in Table V. The coefficients of variation for cotton and wood cellulose nitrates were 6.7 and 1.7, respectively. The precision of slurry titration ester sulphates is given in Table VI. The coefficients of variation for cotton and wood cellulose nitrates were 1.4 and 2.6 respectively.

Further comparison can be made between zero hydrolysis and slurry titration ester sulphates as shown for cotton and wood cellulose nitrates in Table IV. The differences are given in Table V. There is agreement but the best results were obtained with wood cellulose nitrates. The precision of the zero hydrolysis ester sulphates is mentioned in Table VI. It decreases markedly for results obtained from samples prepared by duplicate nitrations. For cotton cellulose nitrates, the mean difference was 15.2%, the standard deviation 9.2, and the 95% confidence limits were 15.2% ±10.9. The corresponding values for wood cellulose nitrates were 12.2%, 5.2, and 12.2% ±6.2.

Can. J. Chem. Downloaded from www.nrcresearchpress.com by 200.7.193.243 on 09/04/12
For personal use only.

TABLE IV

COMPARISON OF 24-HOUR HYDROLYSIS AND ZERO HYDROLYSIS WITH SLURRY TITRATION RESULTS FOR ESTER SULPHATE

Expt. No.	Cotton cellulose nitrate		Wood cellulose nitrate	
	Ester sulphate, % H_2SO_4		Ester sulphate, % H_2SO_4	
	24-hr. hydrol.	Slurry	24-hr. hydrol.	Slurry
1	1.42	1.52	2.31	2.25
2	0.91	0.83	2.27	2.05
3	0.89	0.89	1.98	1.92
4	0.85	0.67	1.77	1.67
5	0.81	0.74	1.76	1.68
	Zero hydrol.	Slurry	Zero hydrol.	Slurry
1	1.84	1.81	2.19	1.92
2	1.30	1.32	2.15	2.25
3	0.94	0.83	2.11	2.05
4	0.87	0.72	1.95	1.68
5	0.86	0.64	1.80	1.78

TABLE V

DIFFERENCES BETWEEN ESTER SULPHATES DETERMINED BY SLURRY TITRATION AND THOSE DETERMINED BY OTHER METHODS

Samples	Differences	Methods	
		24-hr. hydrolysis	Zero hydrolysis
Cotton	Mean difference, %	12.9	12.5
Wood	Mean difference, %	4.0	4.5
Cotton	Standard deviation	9.8	9.1
Wood	Standard deviation	2.6	4.7
Cotton	95% Confidence limits	12.9±6.3	12.5±6.3
Wood	95% Confidence limits	4.0±1.7	4.5±3.3
Cotton	Rank-correlation coeff.	0.85	0.74
Wood	Rank-correlation coeff.	0.95	0.95

TABLE VI

PRECISION OF ESTER SULPHATE DETERMINATIONS ON DUPLICATE SAMPLES OF CELLULOSE NITRATES

Samples	Differences	Methods	
		Slurry	Zero hydrolysis
Cotton	Mean difference, %	3.2	2.8
Wood	Mean difference, %	2.4	2.2
Cotton	Standard deviation	2.3	4.6
Wood	Standard deviation	4.5	2.2
Cotton	95% Confidence limits	3.2±1.1	2.8±4.6
Wood	95% Confidence limits	2.4±3.1	2.2±2.2

In general, the slurry titration results are better if obtained from wood instead of cotton cellulose nitrates. It seems that the physical form of the cellulose nitrate plays an important part in the degree of success with slurry titrations. Wood cellulose nitrate could be finely divided whereas the cotton cellulose nitrate fibers retained their thickness even after they were ground and stirred rapidly in water. The zero hydrolysis titer can be looked upon as a more reliable measure of acidity than the slurry titer, because titration of cellulose nitrate in 90% acetone/water solution presents less difficulty than a slurry titration in water.

Can. J. Chem. Downloaded from www.nrcresearchpress.com by 200.7.193.243 on 09/04/12
For personal use only.

When ester contents of cellulose nitrates determined by the hydrolysis method (6) are used to calculate total sulphate and ester sulphate values from slurry titration, the latter values compare favorably with those obtained directly by the hydrolysis method. Furthermore, slurry titration results are similar to those obtained from zero hydrolysis titrations. The fact that both slurry and zero hydrolysis results compare satisfactorily with those obtained by 24-hour hydrolysis is good evidence that the latter method is reliable.

Slurry Titration as a Method of Determining Sulphate Acid Ester in Cellulose Nitrate

Slurry titration should provide a direct method of determining sulphate acid ester in unstabilized cellulose nitrate when the sulphate content is solely in the form of sulphate acid ester. This is the case for unstabilized cellulose acetate (1), but not for unstabilized cellulose nitrate, which frequently contains some sulphate in the form of free sulphuric acid.

In the present work, several unstabilized cotton and wood cellulose nitrates containing 100% sulphate acid ester were prepared. Slurry titrations were performed on these samples. Using 98 for the equivalent weight of the sulphate acid ester, RSO_4H, the slurry titer was converted to sulphate and expressed as % H_2SO_4. The latter value represented the sulphate due to ester and was expressed as a percentage of the standard gravimetric sulphate. The per cent sulphate acid ester content thus obtained was compared to 100% (the ester content determined by the hydrolysis method, which was taken as a standard). It was found that sulphate acid ester contents determined in this way for cotton cellulose nitrates were too low. However, in the case of wood cellulose nitrates, there was better agreement; the mean difference was -7.3%, the standard deviation 5.2, and the 95% confidence limits were $-7.3\% \pm 4.6$.

The slurry titration cannot be used as a direct method for determining sulphate acid ester in cellulose nitrates which contain less than 100% ester.

REFERENCES

1. MALM, C. J., TANGHE, L. J., and LAIRD, B. C. Ind. Eng. Chem. **38**, 77 (1946).
2. KULLGREN, C. Ing. Vetenskaps Akad. Handl. No. 165 (1942).
3. REEVE, R. E. and GIDDENS, J. E. Ind. Eng. Chem. **39**, 1303 (1947).
4. MILES, F. D. Cellulose nitrate. Clarke, Irwin & Co. Ltd., Toronto. 1955.
5. GAGNON, P. E., KEIRSTEAD, K. F., and YAMASAKI, D. Can. J. Technol. **34**, 477 (1957).
6. GAGNON, P. E., KEIRSTEAD, K. F., and NEWBOLD, B. T. Can. J. Chem. **36**, 291 (1958).
7. GAGNON, P. E., KEIRSTEAD, K. F., and NEWBOLD, B. T. Can. J. Chem. **36**, 215 (1958).
8. KEIRSTEAD, K. F. and MYERS, J. Can. J. Chem. **32**, 566 (1954).
9. DEAN, R. B. and DIXON, W. J. Anal. Chem. **23**, 636 (1951).
10. WHITE, J. C., MEYER, A. S., JR., and MANNING, D. L. Anal. Chem. **28**, 959 (1956).
11. LITCHFIELD, J. T., JR. and WILCOXON, F. Anal. Chem. **27**, 299 (1955).

Can. J. Chem. Downloaded from www.nrcresearchpress.com by 200.7.193.243 on 09/04/12
For personal use only.

Can. J. Chem. Downloaded from www.nrcresearchpress.com by 200.7.193.243 on 09/04/12
For personal use only.

THE DECOMPOSITION OF NITROUS OXIDE AT LOW PRESSURES ON NICKEL OXIDE CATALYSTS[1]

J. DEWING[2] AND R. J. CVETANOVIĆ

ABSTRACT

Heterogeneous decomposition of nitrous oxide at pressures between 10^{-5} and 10^{-4} mm. on nickel oxide and doped nickel oxide catalysts has been studied in the temperature range 350° to 500° C. Under most experimental conditions the reaction is first order in nitrous oxide. The observed activation energies are considerably smaller than those observed in previous work and are decreased on doping with Li_2O and increased on adding Cr_2O_3. The results are explained by assuming that changes in the steady-state surface coverage with chemisorbed oxygen affect strongly the heats of chemisorption and, therefore, also the activation energies of the primary reactions.

INTRODUCTION

The heterogeneous decomposition of nitrous oxide has received considerable attention in the past. Studies on metallic catalysts (1, 2, 3, 4) have led to the conclusion that the decomposition is first order with respect to nitrous oxide and that the rate is reduced by the presence of oxygen. The work on metallic oxide catalysts has produced a less clear picture of the reaction kinetics (5, 6, 7, 8). In general the reaction appears to be retarded by the presence of oxygen. Some workers find a first-order dependence on nitrous oxide although a variable order and dependence on catalyst composition have also been observed (6).

In recent years the reaction has assumed considerable importance in the study of the catalytic properties of semiconductor systems with the object of correlating the electrical and catalytic properties.

In view of the apparent complexity of this decomposition we decided that it would be profitable to study the reaction at very low pressures under conditions of small percentage decomposition in an attempt to eliminate to a very large extent the effect of the products of the reaction and any diffusion effects which might interfere with the reaction.

EXPERIMENTAL

The reaction was carried out in a flow system in which nitrous oxide was streamed over the flat surface of a disk of the catalyst material at pressures between 10^{-4} and 10^{-5} mm. Hg. The rate of flow of gas over the catalyst was sufficiently fast for the transfer of gas to the internal pore structure of the catalyst to be negligibly small compared with the total flow. The undecomposed nitrous oxide was condensed in liquid nitrogen and the pressure of the noncondensable products measured continuously with a thermionic ionization gauge.

Nitrous oxide was allowed to stream through a capillary from a 5-liter reservoir filled initially to about 10^{-1} mm. The gas emerging from the capillary impinged on the surface of the catalyst and was rapidly removed by condensation in a liquid nitrogen trap placed as close to the reacting system as possible. The products nitrogen and oxygen were removed by a mercury diffusion pump with a pumping speed of 20 l./sec. They were pumped to the ionization gauge which was in turn evacuated through a narrow

[1]*Manuscript received December 4, 1957.*
Contribution from the Division of Applied Chemistry, National Research Council, Ottawa, Canada. Issued as N.R.C. No. 4655.
[2]*National Research Council Postdoctorate Fellow 1955–57. Present address: Imperial Chemical Industries Ltd., Billingham, Co. Durham, England.*

glass tubing by a second mercury diffusion pump at a rate of 0.1 l./sec. Thus the pressure of the products was increased in the region of the ionization gauge by the ratio of the pumping speeds at the catalyst and at the ionization gauge. The pumping speed at the catalyst was about 2 l./sec.

The reactor was constructed from Pyrex glass with the exception of the vacuum envelope which was of silica. The general design of the reactor was similar to the one used by Crocker (9) in the study of decomposition reactions on single crystal planes. The inlet capillary was jacketed so that the incoming gas could be held at a different temperature from that of the catalyst. It was hoped that by doing this the effect of the temperature of the incoming gas could be studied, but this was found to be impossible because of the relatively large number of secondary collisions made by the molecules before they were removed from the reaction zone. Only about 10% of the collisions with the catalyst were the initial collisions of the incoming gas. The reactor was heated by an external furnace and the catalyst temperature was measured by a Pt–Pt–Rh thermocouple pressed against the back surface of the catalyst disk. Diagrams of the reaction system and the reactor are given in Figs. 1 and 2.

The nitrous oxide was purified by the usual triple distillation procedure and was stored in a 2-liter glass bulb. Periodic repurifications were carried out to guard against possible contamination during storage over long periods of time. Pressure measurements before and after freezing out in liquid nitrogen showed a noncondensable impurity content of less than 1 p.p.m.

The catalysts were prepared from "Baker Analysed" nickel oxide. The pure nickel oxide catalysts were made by mixing a portion of the nickel oxide with distilled water, drying, and heating to 1000° C. The cake of nickel oxide was then ground in an agate mortar until it would all pass a 30-mesh screen. This powder was then pressed into a flat disk at a pressure of 700 kg./cm.^{2}, which was then sintered at 1000° C. for 3 hours. In the case of catalysts containing lithia the water was replaced by a measured amount of lithium hydroxide solution and during drying the mixture was stirred at frequent intervals to prevent concentration of the lithium at the drying surface. The rest of the

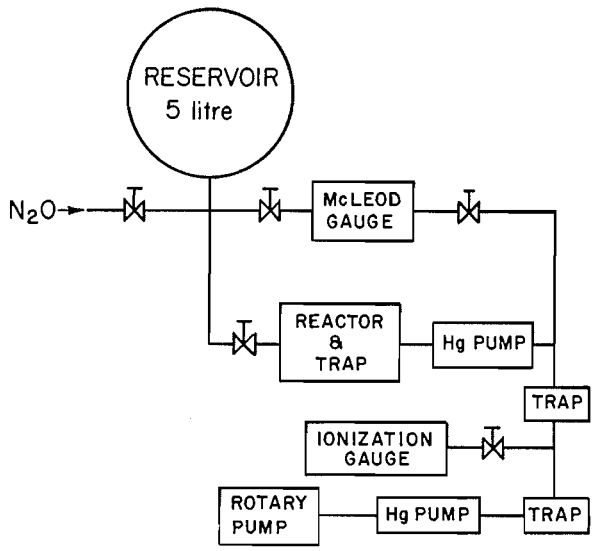

FIG. 1. Schematic diagram of the apparatus.

Can. J. Chem. Downloaded from www.nrcresearchpress.com by 200.7.193.243 on 09/04/12
For personal use only.

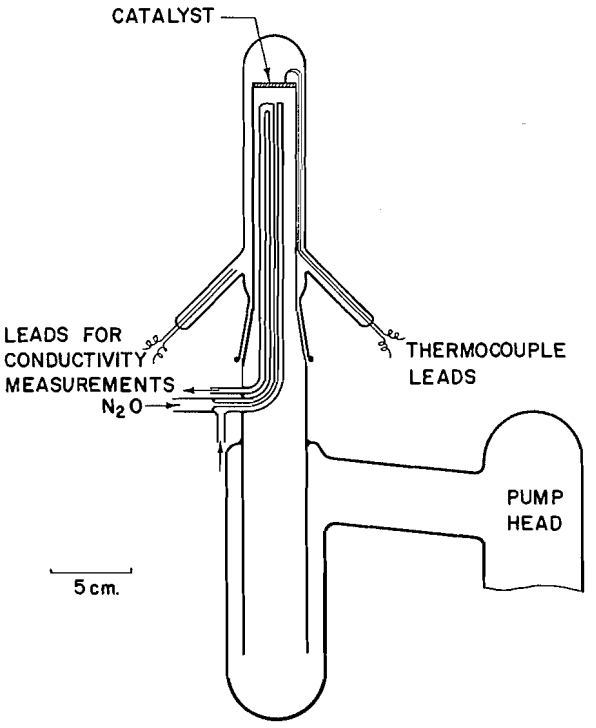

FIG. 2. Reactor. (The leads for conductivity measurements extend to the upper surface of the catalyst—this is not shown in the figure to avoid cluttering. No cooling of the capillary jacket—as indicated by the arrows—was employed in the present work, for reasons given in the text.)

preparative procedure was the same. Chromia was introduced by using a solution of ammonium dichromate.

Platinum wires were embedded in some of the catalysts before sintering to allow measurements to be made of the electrical conductivity under the reaction conditions.

RESULTS

Runs were made by filling the reservoir to a known pressure between 10^{-2} and 10^{-1} mm. with N_2O and allowing this to stream through the reactor. The pressure over the catalyst was proportional to the reservoir pressure and in a steady-state flow system the pressure of products can be taken as a measure of the rate of reaction at any instant. The reading of the ionization gauge was followed as the reservoir pressure dropped and was a measure of the variation of the rate with reactor pressure. Thus the kinetics of the reaction were easily studied even though no runs were carried out in which more than 1% decomposition occurred.

In the later runs the output of the ionization gauge was connected to a recording potentiometer. This increased the accuracy of the measurements, as it was possible to smooth the trace to reduce the effect of random fluctuations of the gauge reading.

In all experiments the apparatus was pumped down so that a reading of the order of 2×10^{-6} mm. was obtained on the ionization gauge with the catalyst at 500° C. This usually required about 16 hours when a new catalyst was used.

A typical run is shown in Fig. 3. The intercept on the axis at zero reservoir pressure represents the background pressure in the apparatus. It is clear that the reaction is first order with respect to the nitrous oxide. This first-order reaction was observed under

Can. J. Chem. Downloaded from www.nrcresearchpress.com by 200.7.193.243 on 09/04/12
For personal use only.

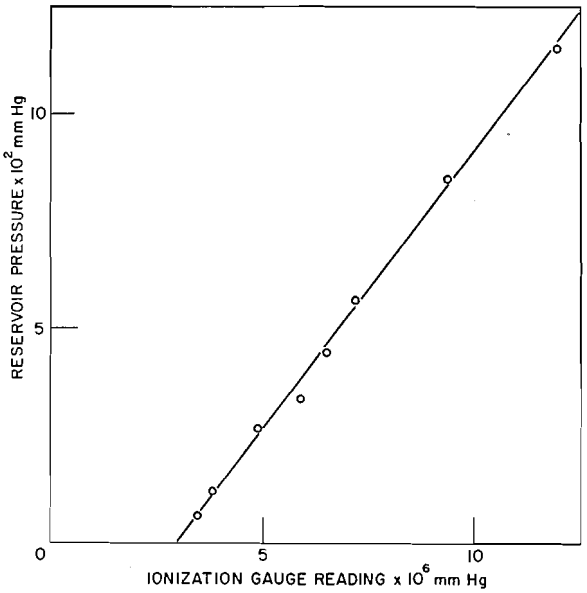

FIG. 3. Change of ionization gauge reading with reservoir pressure in a typical run (pure NiO catalyst), 442° C.

most experimental conditions. All the catalysts showed this behavior at temperatures above 400° C., but below this temperature pure NiO and NiO catalysts with up to 0.5 mole per cent lithia added showed a more complex behavior with an apparent order of reaction between 1.0 and 1.1. In cases where this complex order was observed the extrapolated rate for zero N_2O pressure was taken. This rate was found to fit well with the results taken at higher temperatures when the Arrhenius activation energy was determined.

All the results are reported in terms of the concentration of foreign ions added initially, since this appears to be the usual method of reporting such data and in terms of the surface concentrations is probably as meaningful as the analysis figures. Analysis showed, however, that about half of the added lithia distilled out of the samples during sintering.

Electrical-conductivity measurements were made on some of the catalysts during the course of the reaction using an a-c. bridge at 500 c./s. Additions of lithia had a marked effect on conductivity. One mole per cent of lithia, for example, increased the conductivity of the NiO by a factor of 10^4 at 400° C. and the apparent activation energy for conduction was lowered from 18.5 kcal. to 4.1 kcal. No attempt was made to measure the small conductivities of NiO with chromia added. There was a measurable increase in conductivity of pure NiO on admission of N_2O but this was small and tended to increase with time so that it could not be studied systematically.

The effects of the additions of foreign ions to the nickel oxide on the apparent activation energies for conduction and for the reaction are compared in Fig. 4. In the case of lithia additions the activation energy was lowered by 2 to $2\frac{1}{2}$ kcal. and the activity at 400° C. was reduced to about half that for pure NiO. Comparisons of activity are, however, of necessity very approximate since the variation is of the same order as the reproducibility of activity between different samples of catalysts of the same composition.

Additions of chromia increased the activation energy for the reaction to such an extent that a great loss of activity occurred in the temperature range used.

An attempt was made to obtain more information regarding the complex-order reaction

Can. J. Chem. Downloaded from www.nrcresearchpress.com by 200.7.193.243 on 09/04/12
For personal use only.

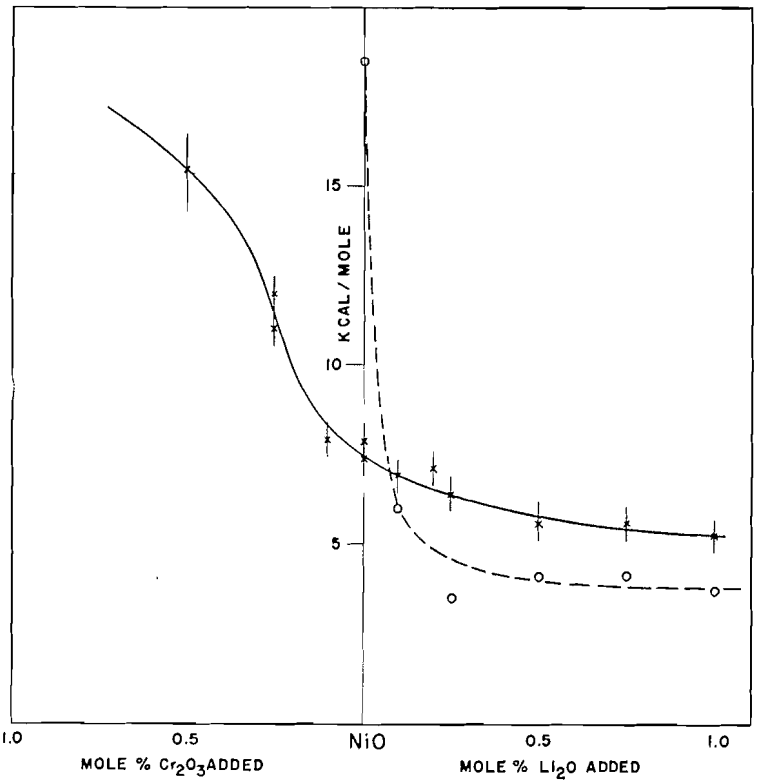

FIG. 4. Dependence of the observed activation energies for N_2O decomposition and electrical conductivity on catalyst composition. Solid line represents the activation energies for the N_2O decomposition (vertical lines indicate the probable experimental uncertainty). Broken line represents the activation energies for electrical conductivity.

occurring at lower temperatures. The results were not very reproducible but they suggested that a time-dependent loss of activity of the catalyst might be responsible for the deviation from a first-order reaction. The curvature of the plots of reaction rate against N_2O pressure was more marked after the catalyst had been evacuated at a high temperature just prior to the run. If two low-temperature runs were done consecutively, without raising the temperature in between, the first run showed a higher apparent order than the second.

DISCUSSION

Heterogeneous decomposition of nitrous oxide on a *p*-type semiconducting oxide catalyst and in the temperature region of interest in the present investigation may in general be considered in terms of the following reactions:

$$N_2O_{(g)} + S \rightleftharpoons N_2O_{(s)} \quad [1]$$

$$N_2O_{(s)} \rightarrow N_{2(g)} + O^-_{(s)} + \oplus \quad [2]$$

$$O^-_{(s)} + O^-_{(s)} + 2\oplus \rightleftharpoons O_{2(g)} \quad [3]$$

$$O^-_{(s)} + N_2O_{(g)} + \oplus \rightarrow N_{2(g)} + O_{2(g)} \quad [4]$$

$$O^-_{(s)} \rightleftarrows O^=_{(s)} + \oplus \quad [5]$$

where S represents an adsorption site on the catalyst surface, $\oplus$ a "positive hole", and subscripts (g) and (s) indicate gas phase and chemisorbed particles, respectively. All

Can. J. Chem. Downloaded from www.nrcresearchpress.com by 200.7.193.243 on 09/04/12
For personal use only.

these reactions have been considered by different authors before. The experimental conditions were, in some instances, widely different, and varying emphasis was placed on the relative importance of the individual steps in the reaction scheme.

Amphlett (8) used a great excess of oxygen, containing only 10–1000 p.p.m. of N_2O. At a constant oxygen pressure the rate expression reduces under these conditions to

$$-d(N_2O)/dt = K(N_2O)$$

and is in agreement with the observed first order in N_2O. Under conditions employed in these experiments it is likely that reaction [4] is responsible for the decomposition of N_2O. The effect of controlled impurities was not investigated. The over-all activation energy was found to be dependent on the temperature range in which the measurements were made.

Hauffe, Glang, and Engell (6) have studied the decomposition of N_2O in the presence of comparable amounts of oxygen on nickel oxide and doped nickel oxide catalysts. Percentage conversions were measured as a function of temperature and the apparent order of the reaction and the activation energy were deduced by assuming constant values of these quantities throughout the temperature ranges covered. There was a marked dependence of both the order of the reaction and the activation energy on catalyst composition. It would be difficult to explain by a detailed mechanism the wide variation of the apparent order of the reaction, although it is possible that the apparent complexity may be due to the particular method employed in evaluating this quantity. There was, however, a distinct effect of the doping on the percentage conversion, and this was interpreted by Hauffe (10) in terms of an increase in the rates of reactions [3] and [4] with increasing concentration of positive holes. These two reactions are assumed to be slow and, therefore, the rate-determining ones under most conditions.

Under most of the experimental conditions in the present work a reaction rate of first order in nitrous oxide was observed. The decomposition of N_2O amounted to less than 1%. From the observed pressure in the ionization gauge and in view of the ratio of pumping speed of the mercury diffusion pumps it is estimated that the steady-state partial pressure of gaseous oxygen over the catalyst was of the order of 10^{-6} mm. or smaller. It is, therefore, likely that under these conditions interference by secondary chemisorption of oxygen, the reverse of reaction [3], was negligibly small. Inasmuch as this assumption is correct, primary chemisorption and splitting of N_2O must play the main role in the decomposition, and the measured rates and the observed activation energies are those of the chemisorption reactions [1] and [2] and not of the desorption reactions [3] and [4]. Reactions [1] and [2] cannot be expected to be affected directly by the concentration of positive holes in the catalyst unless $N_2O_{(s)}$ is a negative ion, in which case an increase in positive-hole concentration would only tend to accelerate the reverse of reaction [1]. The dependence on doping observed in the present work is, therefore, not explainable by a direct effect of positive-hole concentration on the rates of these reactions. The indirect effect of the concentration of positive holes on the surface coverage and therefore also on the heat of adsorption, on the other hand, appears to provide a satisfactory explanation of the doping effect.

An increase in the concentration of positive holes will speed up the desorption reactions, which are dependent on electron transfer to the catalyst, and decrease the surface coverage under the steady-state reaction conditions. In our experiments the surface coverages were very small and their variations due to doping could not have significant effect on the number of available surface sites. On the other hand, these variations should affect strongly the heats of adsorption. The heat of adsorption of oxygen on NiO has

Can. J. Chem. Downloaded from www.nrcresearchpress.com by 200.7.193.243 on 09/04/12
For personal use only.

Can. J. Chem. Downloaded from www.nrcresearchpress.com by 200.7.193.243 on 09/04/12
For personal use only.

been shown to be very strongly dependent on surface coverage. Dell and Stone (11) have made calorimetric measurements of the heat of adsorption on NiO films on the surface of metallic nickel and have found values falling from 54 kcal./mole for a surface largely depleted of oxygen to 20 kcal./mole for a surface with 10% of the B.E.T. surface area covered with oxygen. The theoretical work of Takaishi (12) suggests, subject to certain assumptions, that in the case of *p*-type semiconducting oxides the decline in the heat of adsorption with increasing surface coverage should be particularly large at very low coverages. Therefore, any increase in the rate of the desorption reactions (as, for example, due to doping with Li_2O) which results in a decrease in the steady-state concentration of chemisorbed oxygen will lead to an increase in its binding energy. It is reasonable to suppose that this will result in a reduction of the potential energy of the activated complex leading to the adsorbed oxygen and thus in a lowering of the activation energy for the reaction. These views are in agreement with the observed results. Doping with Li_2O to increase the concentration of positive holes results in a decrease in the observed activation energy in the predicted manner, while additions of Cr_2O_3 have the expected opposite effect. Furthermore, the activation energies observed in the present work are much lower than have been observed by other workers. In agreement with the expressed views this provides indirect evidence for very low surface coverages under the experimental conditions employed.

The apparent complex order observed at lower temperatures is qualitatively explainable by assuming some occurrence of reaction [5] under certain conditions. Gray and Darby (13) have made a thorough study of the different processes involved in the chemisorption of oxygen on nickel oxide. They find that the rate of desorption of oxygen is extremely slow at temperatures below about 300° and requires an apparent activation energy of the order of 60 kcal./mole. At lower reaction temperatures the reverse of [5] can therefore be relatively slow and thus lead to a build-up of surface oxygen which is removed slowly on evacuation. At higher reaction temperatures deviations from the first order were not observed. Also, with NiO doped with more than about 0.5 mole per cent of Li_2O no deviations from the first order were apparent. This is in agreement with the suggested explanation since doping with Li_2O would be expected to increase the rate of the reverse reaction [5].

The trend in activation energies of conductivity shown in Fig. 4 appears to be roughly comparable with the one established by Verwey *et al.* (14). The values of the activation energies are considerably lower than those of Keier, Roginski, and Sasonov (15) at comparable atomic concentrations of lithium. The somewhat different method of catalyst preparation and the different ambient atmosphere in the present work are probably responsible for the discrepancy. At the present state of knowledge of the physical and chemical phenomena involved it would be difficult to attempt a quantitative correlation between the observed activation energies for electrical conductivity and for the decomposition reaction in terms of the mechanism proposed for the latter.

REFERENCES

1. Steacie, E. W. R. and McCubbin, J. W. J. Chem. Phys. **2**, 585 (1934).
   Steacie, E. W. R. and Folkins, H. O. Can. J. Research, B, **15**, 237 (1937).
2. Van Praagh, G. and Topley, B. Trans. Faraday Soc. **27**, 312 (1931).
3. Hinshelwood, C. N. and Pritchard, C. R. Proc. Roy. Soc. (London), A, **108**, 211 (1925).
4. Cassel, H. and Glueckauf, E. Z. physik. Chem. B, **9**, 428 (1930); **17**, 380 (1932).
5. Schwab, G. M. and Schultes, H. Z. physik. Chem. B, **25**, 411 (1934); **9**, 265 (1930).
6. Hauffe, K., Glang, R., and Engell, H.-J. Z. physik. Chem. **201**, 223 (1952).
7. Wagner, C. J. Chem. Phys. **18**, 69 (1950).

8. AMPHLETT, C. B. Trans. Faraday Soc. **50**, 273 (1954).
9. CROCKER, A. J. Ph.D. Thesis, University of London, London, England (1956).
10. HAUFFE, K. Advances in Catalysis, **7**, 213 (1955).
11. DELL, R. M. and STONE, F. S. Trans. Faraday Soc. **50**, 501 (1954).
12. TAKAISHI, T. Z. Naturforsch. **11a**, 286 (1956).
13. GRAY, T. J. and DARBY, P. W. J. Phys. Chem. **60**, 209 (1956).
14. VERWEY, E. J. W., HAAIJMAN, P. W., ROMEIJN, F. C., and VAN OOSTERHOUT, G. W. Philips Research Repts. **5**, 173 (1950).
15. KEIER, N. P., ROGINSKI, S. Z., and SASONOV, I. C. Izvest. Akad. Nauk S.S.S.R. **21**, 183 (1957).

Can. J. Chem. Downloaded from www.nrcresearchpress.com by 200.7.193.243 on 09/04/12
For personal use only.

THE NON-ENZYMATIC HYDROLYSIS OF *p*-NITROPHENYL PHOSPHATE[1]

K. A. HOLBROOK[2] AND LUDOVIC OUELLET

ABSTRACT

The kinetics of the non-enzymatic hydrolysis of *p*-nitrophenyl phosphate have been studied in aqueous solution in the pH range 2.6 to 9.0 and at temperatures from 68.0° to 82.0° C. The reaction has been followed by colorimetric measurement of the nitrophenol produced by the reaction

$$O_2NC_6H_4OPO_3H^- + H_2O \rightarrow O_2NC_6H_4OH + H_2PO_4^-.$$

The reaction is first order with respect to *p*-nitrophenyl phosphate and has an activation energy of 26.0 kcal./mole at pH 2.6. An explanation has been proposed in terms of the different rates of hydrolysis of the various ionic species of the ester present in solution.

INTRODUCTION

Studies have been made of enzymatic hydrolyses of *p*-nitrophenyl phosphate by Morton (1) using alkaline phosphatases of cow's milk and calf intestinal mucosa and by Axelrod (2) using enzymes present in citrus juices. In both cases the hydrolysis produces inorganic phosphate and *p*-nitrophenol by the simple reaction

$$O_2NC_6H_4OPO_3H^- + H_2O \rightarrow O_2NC_6H_4OH + H_2PO_4^-.$$

In view of current theories (3, 4) of organic phosphate hydrolyses it seemed desirable to make a more complete study of this reaction over a wide range of pH in the absence of enzymes.

EXPERIMENTAL

Materials

p-Nitrophenyl phosphate (disodium salt) was supplied by Mann Research Laboratories Inc. and was used without further purification. A stock solution (about 8×10^{-2} *M*) was kept in cold storage. Analysis indicated the presence of about 0.5% *p*-nitrophenol in the original phosphate.

p-Nitrophenol used for calibration purposes was purified by boiling with dilute hydrochloric acid and activated charcoal. The recrystallized material had a melting point of 114.0° C.

Buffer solutions.—The following buffer solutions were used and their pH values at 76.9° C. (given in parentheses) were measured using Beckman high-temperature electrodes: acid potassium phthalate/hydrochloric acid (2.6), acid potassium phthalate (3.8), acetic acid/sodium acetate (4.7), acid potassium phthalate/potassium hydroxide (5.8), trishydroxymethylaminomethane/hydrochloric acid (7.4), boric acid/sodium hydroxide (9.0). The concentrations of these buffers were adjusted and potassium chloride was added to make the ionic strength of the reaction mixtures 0.1.

Procedure

Kinetic runs were done using the apparatus described in a previous paper (5). The rate of reaction was measured by following colorimetrically the concentration of *p*-nitrophenol produced, the method being similar to that of Axelrod (2). One-milliliter aliquots were extracted from the reaction mixture at convenient time intervals and diluted by adding to 10 ml. *M*/6 sodium hydroxide at room temperature. This effectively stops all

[1]*Manuscript received December 16, 1957.*
Contribution from the Department of Chemistry, University of Ottawa, Ottawa, Canada.
[2]*National Research Council Postdoctorate Fellow 1956–57.*

Can. J. Chem. Downloaded from www.nrcresearchpress.com by 200.7.193.243 on 09/04/12
For personal use only.

reaction (see Fig. 2) and produces the yellow color characteristic of the *p*-nitrophenylate ion. The absorbance of the solution was measured in a Beckman model DU spectrophotometer at 400 mμ at which wavelength there is strong absorption due to the salt form (6). The addition of 1 ml. of reaction mixture did not alter the pH of the sodium hydroxide sufficiently to affect the calibration. A standard calibration graph of absorbance versus *p*-nitrophenol concentration was prepared using the purified *p*-nitrophenol described above.

RESULTS

Order of the Reaction

The reaction at 76.9° C. was found to be first order with respect to *p*-nitrophenyl

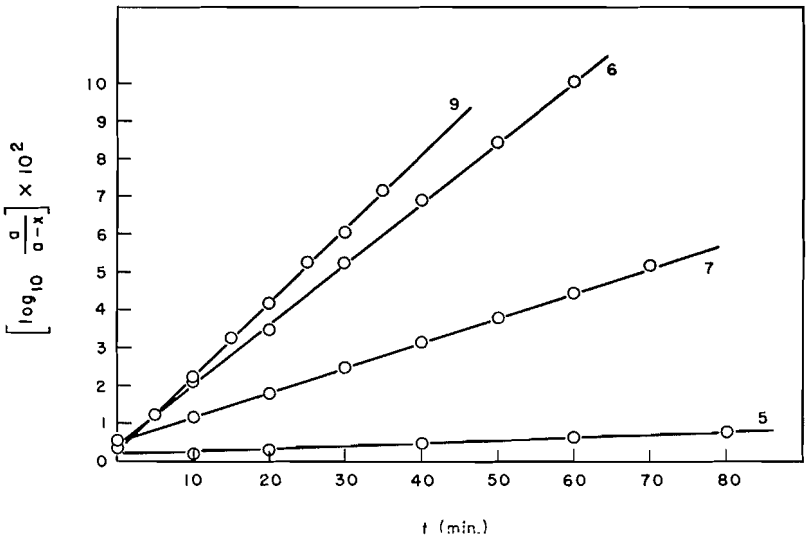

FIG. 1. Temperature = 76.9° C.

Run	5	7	6	9
Initial concn. phosphate $\times 10^3$ *M*	0.834	0.834	0.834	1.657
pH	7.4	5.8	4.7	2.7

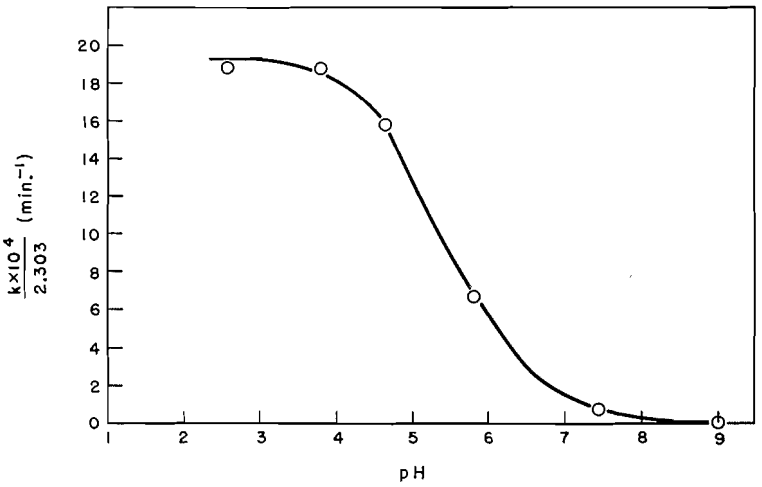

FIG. 2. Temperature = 76.9° C. *p*-Nitrophenyl phosphate = 0.834×10^{-3} *M*.

Can. J. Chem. Downloaded from www.nrcresearchpress.com by 200.7.193.243 on 09/04/12
For personal use only.

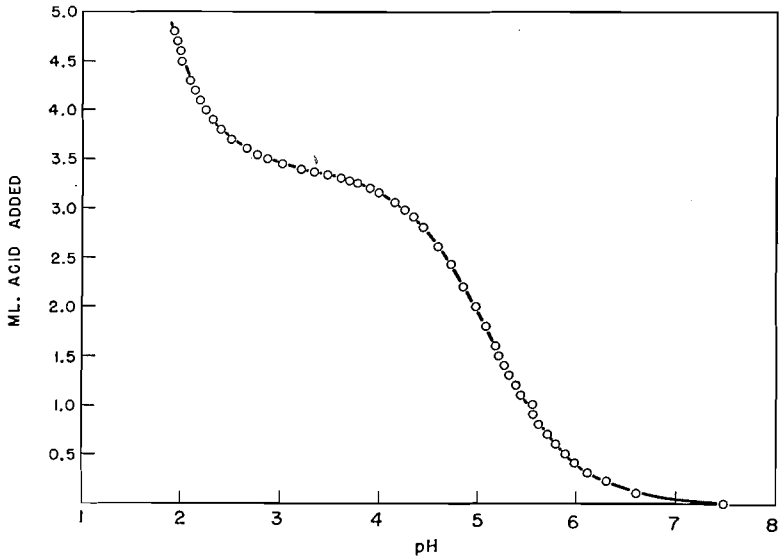

FIG. 3. Temperature = 25° C.

phosphate and first order with respect to time, over the first 10–20% hydrolysis. This is illustrated by plots of the first-order log function against time for different initial conditions of pH and phosphate concentration shown in Fig. 1.

The Effect of pH

Runs were done at different pH values from 2.6 to 9.0 at 76.9° C. and Fig. 2 shows a plot of the first-order rate constant against pH. For comparison, Fig. 3 shows a microtitration curve of *p*-nitrophenyl phosphate obtained (at 25° C.) using the standard procedure. It can be seen that the increase in rate obtained at lower pH values parallels the change in ionic form of the phosphate ester.

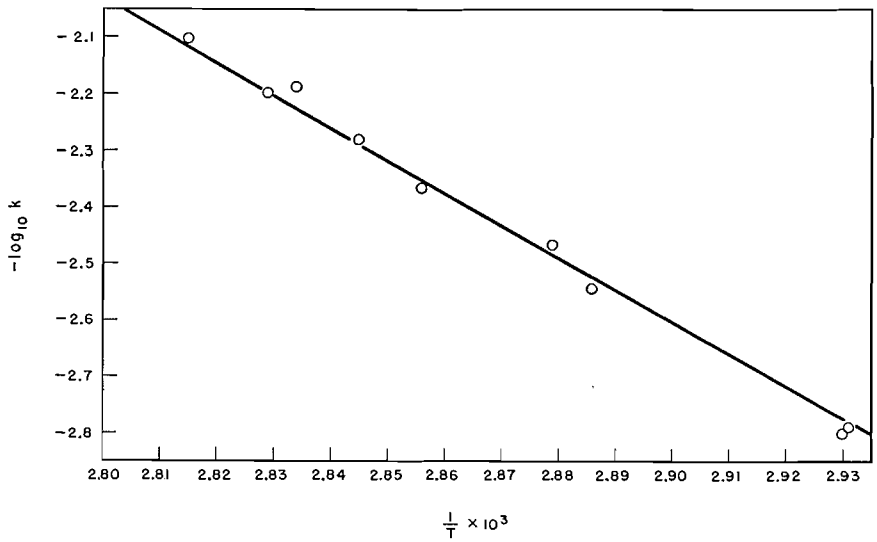

FIG. 4. pH = 2.6.

Can. J. Chem. Downloaded from www.nrcresearchpress.com by 200.7.193.243 on 09/04/12
For personal use only.

The Activation Energy

The activation energy corresponding to the first-order rate constant at pH 2.6 was obtained by measuring the rate as a function of temperature from 68.0° to 82.0° C. Fig. 4 shows a plot of $\log_{10}k$ versus $1/T°$ K.

DISCUSSION

Although the enzymatic hydrolyses of a number of organic phosphates have been studied at physiologically important pH values, relatively few attempts have been made to study these hydrolyses over a wide range of pH values in the absence of enzyme.

We have previously studied the non-enzymatic hydrolyses of ATP (7) and ADP (5) and have found that the effect of pH upon these hydrolyses could be explained in terms of the differing rates of hydrolysis of different ionic species present in solution.

The hydrolysis of *p*-nitrophenyl phosphate, which follows the simple over-all equation

$$NO_2.C_6H_4OPO_3H^- + H_2O \rightarrow NO_2.C_6H_4OH + H_2PO_4^-, \quad [1]$$

shows a similar relationship between the effect of pH (Fig. 2) and the titration curve of the ester (Fig. 3).

The inflection point in the latter at about pH 5.0 presumably corresponds to the equilibrium

$$NO_2C_6H_4OPO_3^= + H^+ \rightleftarrows NO_2C_6H_4OPO_3H^-.$$

At pH 9.0 it has been observed that the rate of hydrolysis is practically zero, when the ester is largely present as the completely ionized form $NO_2C_6H_4OPO_3^=$, whereas at pH 2.6–2.7, when the predominant ionic species present is the singly charged $NO_2C_6H_4OPO_3H^-$ (assuming no large variation in the equilibrium constant from 25° to 70° C.), the rate of hydrolysis is appreciable.

The general expression for the rate of hydrolysis between pH 2.6 and 9.0 can be written

$$\text{rate} = [H_2O]\{k_1[NO_2C_6H_4OPO_3H^-]+k_2[NO_2C_6H_4OPO_3^=]\},$$

where [*p*-nitrophenyl phosphate]$_0$ = $[NO_2C_6H_4OPO_3H^-] + [NO_2C_6H_4OPO_3^=]$. Hence under the conditions at pH 2.6, an approximation is

$$\text{rate} = k_1[H_2O]\,[p\text{-nitrophenyl phosphate}]_0.$$

At this pH, the first order of the reaction with respect to the phosphate ester has been demonstrated (Fig. 1) and the activation energy has been found to be 26.0 kcal. An entropy of activation $\Delta S_1 = -14.0$ e.u. (taking $[H_2O] = 55.5$ moles/liter) was calculated.

Whether the rate-determining hydrolysis of the singly charged species occurs by a C—O or O—P bond splitting is uncertain and could only be decided by H_2O^{18} experiments. The mechanism by which this step occurs may well involve a proton transfer as suggested by Westheimer and Kumamoto (8) for the hydrolysis of the mono anions of mono- and di-benzyl phosphates.

The entropy of activation of −14.0 e.u. is more negative than those found for the O—P splitting of the adenosine phosphates at alkaline pH values (5) although larger negative values have been reported by Friess (9) for ATP, pyrophosphoric acid, and triphosphoric acid under mildly acidic conditions. In a recent study of the hydrolyses of substituted phenyl phosphates, Chanley and Feageson (10) have noted that singly charged species tend to hydrolyze more rapidly than either the completely ionized or the uncharged species. This was explained in terms of Koshland's nucleophilic displacement mechanism (4) for such reactions.

Can. J. Chem. Downloaded from www.nrcresearchpress.com by 200.7.193.243 on 09/04/12
For personal use only.

Table I gives a comparison of the rates of hydrolysis of substituted aromatic phosphates observed by Chanley and Feageson (10) with our observed rate of hydrolysis of *p*-nitrophenyl phosphate under identical conditions. The rates are shown to increase in accordance with the increase in electrophilic character of the group attached to the phosphorus atom, as would be predicted from a nucleophilic displacement mechanism.

TABLE I

RATES OF HYDROLYSIS OF SOME AROMATIC PHOSPHATES

Compound	Dissociation constants		pH of reaction	Rate, $hr.^{-1} \times 10$, at 80° C.
	pk_1	pk_2		
Phenyl phosphate	1.00	5.88	3.83	1.16
m-Carboxyphenyl phosphate	0.85	3.91	2.36	1.61
p-Carboxyphenyl phosphate	0.88	4.20	2.31	3.07
p-Nitrophenyl phosphate	<2	~5	2.70	3.62

RÉSUMÉ

La cinétique de l'hydrolyse non-enzymatique du *p*-nitrophényl phosphate en solution aqueuse a été étudiée à des pH allant de 2.6 à 9.0 et à des températures allant de 68.0° C. à 82.0° C. La réaction a été suivie par la mesure colorimétrique du *p*-nitrophénol libéré selon la réaction

$$O_2NC_6H_4OPO_3H^- + H_2O \rightarrow O_2NC_6H_4OH + H_2PO_4^-.$$

La réaction est du premier ordre par rapport au *p*-nitrophényl phosphate et elle a une énergie d'activation de 26.0 kcal./mole à pH 2.6. On propose une explication en termes du taux d'hydrolyse des différentes espèces ioniques en solution.

REFERENCES

1. MORTON, R. K. Biochem. J. **61**, 232 (1955).
2. AXELROD, B. J. Biol. Chem. **167**, 57 (1947).
3. BARNARD, P. W. C., BUNTON, C. A., LLEWELLYN, D. R., OLDHAM, K. G., SILVER, B. L., and VERNON, C. A. Chem. & Ind. (London), 760 (1955).
4. KOSHLAND, D. E., Jr. J. Am. Chem. Soc. **74**, 2286 (1952).
5. HOLBROOK, K. A. and OUELLET, L. Can. J. Chem. **35**, 1496 (1957).
6. BIGGS, A. I. Trans. Faraday Soc. **50**, 800 (1954).
7. COUTURE, A. M. and OUELLET, L. Can. J. Chem. **35**, 1248 (1957).
8. KUMAMOTO, J. and WESTHEIMER, F. H. J. Am. Chem. Soc. **77**, 2515 (1955).
9. FRIESS, S. L. J. Am. Chem. Soc. **75**, 323 (1953).
10. CHANLEY, J. D. and FEAGESON, E. J. Am. Chem. Soc. **77**, 4002 (1955).

Can. J. Chem. Downloaded from www.nrcresearchpress.com by 200.7.193.243 on 09/04/12
For personal use only.

Can. J. Chem. Downloaded from www.nrcresearchpress.com by 200.7.193.243 on 09/04/12
For personal use only.

PHOTOLYSIS OF *n*- AND *i*-PROPYL PROPIONATE[1]

M. H. J. WIJNEN

ABSTRACT

The photolysis of *n*- and *i*-propyl propionate has been studied in the temperature range of 30° to 170° C. The results strongly indicate that the following three primary processes may occur:

$$C_2H_5COOC_3H_7 + h\nu \rightarrow C_2H_5CO + C_3H_7O, \quad [1a]$$

$$C_2H_5COOC_3H_7 + h\nu \rightarrow C_2H_5 + CO_2 + C_3H_7, \quad [1b]$$

$$C_2H_5COOC_3H_7 + h\nu \rightarrow C_2H_5COOH + C_3H_6. \quad [1c]$$

Based on these primary steps a qualitative explanation may be given for the formation of all reaction products.

INTRODUCTION

In previous investigations of methyl acetate (1), methyl d_3-acetate (2), and ethyl propionate (3) it could be shown that the main primary step in the photolysis of these esters consisted in the break of the ester into RCO and RO radicals. It was possible to obtain information on the reactivity and thermal stability of the RO radicals thus produced.

It seemed interesting to extend these investigations to higher-boiling esters. The photolysis of *n*- and *i*-propyl propionate has therefore been studied.

EXPERIMENTAL

The experimental technique is essentially the same as described elsewhere (1). A Hanovia S-500 medium pressure arc was used as the light source. The light of the S-500 arc was not filtered, and its intensity was varied by inserting wire gauze screens between reaction cell and arc. The amount of decomposition did not exceed 5% of the compound under investigation.

As reaction products of the photolysis of *n*-propyl propionate were observed: CO, CO_2, CH_2O, C_2H_4, C_2H_6, C_3H_6, C_3H_8, *n*-C_4H_{10}, *n*-C_5H_{12}, *n*-C_3H_7OH, and CH_3CH_2CHO. *n*-Propyl alcohol was determined by mass spectrometer analysis of the residue after all other products had been removed by Toepler pump at −120° C. The total volume of these products was measured, after which analysis was carried out by mass spectrometer.

The following reaction products were observed in the photolysis of *i*-propyl propionate: CO, CO_2, CH_4, C_2H_4, C_2H_6, C_3H_6, C_3H_8, *n*-C_4H_{10}, *i*-C_4H_{10}, *i*-C_5H_{12}, $\{CH(CH_3)_2\}_2$, CH_3CHO, CH_3COCH_3, $C_2H_5COCH_3$, $C_2H_5COC_2H_5$, and *i*-C_3H_7OH. The C_1 to C_5 hydrocarbons and the carbon oxides were pumped over at −130° C., measured, and analyzed by mass spectrometer. The other products such as ketones, isopropyl alcohol, and 2,3-dimethylbutane were determined by mass spectrometer analysis of the residue.

Typical results obtained at various temperatures by photolysis of *n*-propyl propionate are given in Table I, those obtained by photolysis of *i*-propyl propionate in Table II.

[1]*Manuscript received January 8, 1958.*
Contribution from the Chemical Division, Research and Development Laboratories, Celanese Corporation of America, Clarkwood, Texas.

TABLE I

PHOTOLYSIS OF *n*-PROPYL PROPIONATE AT VARIOUS TEMPERATURES

	Run number:					
	1	2	3	4	5	6
n-$PrPr_0 \times 10^{-17}$ molec./sec.	9.14	8.92	8.85	8.84	8.74	9.60
Temperature, ° C.	41	41	131	131	170	170
Intensity (relative, %)	100	9	100	9	100	9
	Rate of formation of products in molec./sec. cc. $\times 10^{-12}$					
n-Propyl alcohol	2.06	0.20	—	—	—	—
Propionaldehyde	0.10	—	—	—	—	—
n-Pentane	0.64	0.04	0.67	0.04	0.60	0.02
n-Butane	6.22	0.42	8.04	0.41	7.42	0.23
Propane	1.31	0.05	1.39	0.06	0.55	0.07
Propylene	3.93	0.25	3.26	0.23	3.50	0.20
Ethane	2.68	0.29	4.69	0.48	4.50	0.39
Ethylene	0.80	0.07	0.88	0.06	1.68	0.12
Formaldehyde	2.76	0.08	1.65	0.34	5.54	0.32
Carbon monoxide	10.48	0.74	11.08	0.91	14.08	0.90
Carbon dioxide	2.60	0.20	2.60	0.22	3.50	0.21
CO/CO_2	4.0	3.7	4.2	4.1	4.0	4.3
R_{C_3}/R_{CO_2}	2.3	1.7	2.0	1.5	1.3	1.4

TABLE II

PHOTOLYSIS OF *i*-PROPYL PROPIONATE AT VARIOUS TEMPERATURES

	Run number:					
	7	8	9	10	11	12
i-$PrPr_0 \times 10^{-17}$ molec./sec.	7.74	7.14	6.67	6.85	5.31	5.31
Temperature, ° C.	33	33	109	109	176	176
Intensity (relative, %)	100	9	100	9	100	9
	Rate of formation of products in molec./sec. cc. $\times 10^{-12}$					
i-Propyl alcohol	6.65	0.27	0.44	0.03	0.21	0.02
Acetaldehyde	7.58	0.29	10.66	0.69	7.12	0.55
Methyl ethyl ketone	1.04	0.06	—	—	—	—
Diethyl ketone	0.34	0.03	—	—	—	—
Methyl isopropyl ether	0.39	—	—	—	—	—
i-Pentane	2.23	0.13	2.63	0.19	2.18	0.15
2,3-Dimethylbutane	0.60	—	0.41	0.05	0.96	—
n-Butane	2.25	0.17	2.72	0.17	2.04	0.11
i-Butane	0.28	0.03	0.82	0.06	0.70	0.02
Propane	3.14	0.22	4.14	0.32	4.15	0.22
Propylene	5.66	0.41	6.32	0.43	5.75	0.42
Ethane	1.40	0.10	2.54	0.23	3.32	0.37
Ethylene	0.65	0.05	0.75	0.06	0.81	0.04
Methane	0.27	0.02	1.21	0.22	3.22	0.51
Carbon monoxide	9.56	0.70	10.20	0.98	10.28	0.82
Carbon dioxide	4.12	0.29	4.34	0.35	4.42	0.34
CO/CO_2	2.2	2.4	2.4	2.8	2.3	2.4

DISCUSSION OF RESULTS

n-Propyl Propionate

To explain the formation of products in the photolysis of *n*-propyl propionate the following primary steps are suggested:

$$n\text{-}C_2H_5COOC_3H_7 + h\nu \rightarrow C_2H_5CO + n\text{-}C_3H_7O, \quad [1a]$$

$$\rightarrow C_2H_5 + CO_2 + n\text{-}C_3H_7, \quad [1b]$$

$$\rightarrow C_2H_5COOH + C_3H_6. \quad [1c]$$

Can. J. Chem. Downloaded from www.nrcresearchpress.com by 200.7.193.243 on 09/04/12
For personal use only.

Can. J. Chem. Downloaded from www.nrcresearchpress.com by 200.7.193.243 on 09/04/12
For personal use only.

Steps [1*a*] and [1*b*] have been shown to occur in the photolysis of methyl acetate and ethyl propionate. Step [1*a*] produces *n*-propoxy and propionyl radicals. Propionyl radicals are known (4) to be quite unstable and decompose readily into ethyl radicals and carbon monoxide. The possibility that at 40° C. some C_2H_5CO radicals survive long enough to form diethyl ketone and possibly propyl ethyl ketone as has been observed in the case of isopropyl propionate may, however, not be excluded. Carbon monoxide is observed at all temperatures as the main reaction product. The presence of *n*-propoxy radicals is confirmed by the formation of *n*-propyl alcohol and of propionaldehyde at 40° C. Step [1*b*] produces ethyl and propyl radicals in addition to carbon dioxide. Accepting that practically all C_2H_5CO radicals decompose into C_2H_5 and CO, it would be expected that at any given temperature the ratio CO/CO_2 would be constant. This is confirmed by the results, as shown in Table I, which indicate that step [1*a*] occurs about four times as frequently as step [1*b*]. The presence of propyl radicals during the photolysis of *n*-propyl propionate is confirmed by reaction products such as propane, propylene, and pentane. The formation of butane, ethane, and ethylene confirms the presence of ethyl radicals, suggested to be formed by step [1*b*] and by step [1*a*] via the C_2H_5CO radical.

If reactions [1*a*] and [1*b*] were the only primary steps, then it would be expected that $R_{CO_2} = R_{C_3}$, where R_{C_3} is the rate of production of all compounds containing *n*-propyl radicals so that $R_{C_3} = R_{C_5H_{12}} + R_{C_3H_8} + R_{C_3H_6}$. Table I shows $R_{C_3} \gg R_{CO_2}$. This indicates that more products, containing propyl radicals, are formed than can be accounted for by step [1*b*]. To explain this, step [1*c*] has been suggested. Propionic acid in trace amounts is not detected by mass spectrometer analysis, as could be shown by adding small amounts of propionic acid to the *n*-propyl propionate residue of the photolysis before analysis. Confirmation for step [1*c*] may, however, be found (1) in the rather large amounts of propylene produced, especially if compared to the amounts of propane formed, and (2) in the fact that chemical analysis indicated the presence of an acid among the reaction products.

This investigation was mainly undertaken to obtain information regarding the *n*-propoxy radical. However, neither propyl alcohol nor propionaldehyde could be detected at 130° C. and higher temperatures. This seems to indicate that the *n*-propoxy radical is not very stable thermally. Since no hydrogen was observed among the reaction products, the results indicate that the *n*-propoxy radical decomposes into ethyl radicals and formaldehyde according to the reaction

$$n\text{-}C_3H_7O \rightarrow C_2H_5 + CH_2O. \qquad [2]$$

This type of decomposition reaction for the alkoxy radical has been suggested previously by other authors (5, 6). It is important to point out that relatively large amounts of formaldehyde were produced. In the extreme case where all *n*-propoxy radicals would decompose according to reaction [2], it would be expected that $R_{CO} = R_{CH_2O}$. This has not been observed. Since formaldehyde polymerizes easily it is probable that part of the formaldehyde was left behind in the apparatus as polymer and thus was not available for analysis.

The fact that no ethers were formed even at 40° C., which could conceivably be produced by recombination between alkyl and propoxy radicals, indicates that the concentration of propoxy radicals must be small. This is also confirmed by the fact that propionaldehyde, possibly a product of disproportionation reactions involving the propoxy radical, has only been observed in trace amounts at low temperatures.

i-Propyl Propionate

Primary steps similar to those suggested in the photolysis of *n*-propyl propionate will produce ethyl, *i*-propoxy, *i*-propyl, and propionyl radicals in addition to carbon oxides and propionic acid.

The isopropoxy radical has been suggested (6) to decompose according to the following reactions:

$$(CH_3)_2CHO \rightarrow CH_3 + CH_3CHO \quad [3]$$

and

$$(CH_3)_2CHO \rightarrow CH_3COCH_3 + H. \quad [4]$$

Reaction [3] is confirmed by the fact that large amounts of acetaldehyde were observed among the reaction products. The presence of methyl radicals is shown by the formation of methane and isobutane. Since it is not possible to decide to what extent methyl radicals are involved in the production of ethane and propane, it is difficult to draw a comparison between the amounts of acetaldehyde and methyl radicals produced by reaction [3]. No reliable data were obtained for the production of acetone although it could be established that some acetone was produced, especially at low temperatures. Since no hydrogen was observed, it is unlikely that acetone was formed by reaction [4]. More probable is the formation of acetone via disproportionation reactions involving the isopropoxy radical. Accepting primary steps [1*a*], [1*b*], [1*c*], and reaction [3], all other reaction products may be explained by abstraction, recombination, and disproportionation reactions of the radicals thus produced.

The fact that methyl ethyl ketone and diethyl ketone are found at 33° C. indicates some stability for the C_2H_5CO radical. This is in agreement with previous results for the photolysis of diethyl ketone, where a quantum yield of 0.6 (7) was observed for the production of CO at 25° C. The ratio R_{CO}/R_{CO_2} indicates that step [1*a*] occurs about 2.4 times as frequently as step [1*b*]. Comparison with the similar ratio for *n*-propyl propionate indicates that step [1*a*] is relatively more important for normal propyl propionate than it is for isopropyl propionate.

The sharp decrease of isopropyl alcohol formation with increasing temperature seems to indicate that the isopropoxy radical is not very stable thermally. In all respects our results indicate that both *n*- and *i*-propoxy radicals react very similarly and decompose readily by breakage of the carbon–carbon bond rather than by splitting off of hydrogen atoms.

ACKNOWLEDGMENTS

The author wishes to thank Dr. H. D. Medley for his constant interest in the fundamental research program of this laboratory. Special thanks are due to Mr. R. W. Jarrett and Mr. R. M. Guedin for calculation and interpretation of the mass spectrometer data.

REFERENCES

1. WIJNEN, M. H. J. J. Chem. Phys. **27**, 710 (1957).
2. WIJNEN, M. H. J. J. Chem. Phys. (To be published).
3. WIJNEN, M. H. J. 132nd National Meeting Am. Chem. Soc., New York (September 1957).
4. JOLLEY, J. E. J. Am. Chem. Soc. **79**, 1537 (1957).
5. LEVY, J. B. and ADRIAN, F. J. J. Am. Chem. Soc. **77**, 2015 (1955).
6. RUST, F. F., SEUBOLD, J. H., JR., and VAUGHAN, W. E. J. Am. Chem. Soc. **72**, 338 (1950).
7. KUTSCHKE, K. O., WIJNEN, M. H. J., and STEACIE, E. W. R. J. Am. Chem. Soc. **74**, 714 (1952).

Can. J. Chem. Downloaded from www.nrcresearchpress.com by 200.7.193.243 on 09/04/12
For personal use only.

INFLUENCE OF WATER CONCENTRATION ON THE HYDROLYSIS OF UNSTABILIZED CELLULOSE NITRATE IN ACETONE/WATER SOLUTION[1]

PAUL E. GAGNON, KARL F. KEIRSTEAD,[2] BRIAN T. NEWBOLD, AND J. THOMAS

ABSTRACT

The influence of water concentration upon the hydrolysis of the sulphate acid ester in unstabilized cotton and wood cellulose nitrates in acetone/water solution at 25°±0.1° C. has been determined. When the water content of these systems was increased, the rate of hydrolysis of the sulphate acid ester in cotton or wood cellulose nitrates decreased. This effect was greatest in the first hour of hydrolysis. The presence of more than about 2% water in the acetone/water solution prevented the completion of hydrolysis after 24 hours.

INTRODUCTION

The hydrolysis of the sulphate ester in unstabilized cellulose acetate sulphate in acetone is rapid compared to that of the acetate ester (1). Recently, it was found that hydrolysis of the sulphate acid ester, RSO_4H, in unstabilized cotton and wood cellulose nitrate in acetone was rapid compared to that of the nitrate ester (2).

The hydrolysis of the sulphate ester in cellulose acetate sulphate in acetone is greatly affected by temperature and is complete after 24 hours at 25° C. (1). There is much evidence that the rate of solvolysis of the sulphate ester in a cellulose-mixed ester depends to a great extent upon the liquid medium employed (3, 4). It was shown previously that hydrolysis of the sulphate acid ester in unstabilized cellulose nitrate proceeded rapidly in 99% acetone/water, but was stopped in 90% acetone/water solution (2).

The object of the present work was to determine the influence of water concentration upon the hydrolysis of the sulphate acid ester in unstabilized cotton and wood cellulose nitrates.

EXPERIMENTAL

Cellulose Nitrate

The unstabilized cotton and wood cellulose nitrates were prepared by the method previously mentioned (5).

Hydrolysis of Unstabilized Cellulose Nitrate

The cellulose nitrates were washed and dried. Moist samples of different weights (2–5 g. for cotton and 3–7 g. for wood) were dissolved in acetone (700 ml.) containing 0.63% water, and hydrolysis experiments were carried out at 25°±0.1° C., using the method recently given (2). The initial acidity of the cellulose nitrates before hydrolysis started was determined by titration in 90% acetone (2).

In other experiments, moist samples of equal weight (2 g. for cotton and 5 g. for wood) of cellulose nitrates were dissolved in different acetone/water solutions (700 ml.) containing 0.63 to 4.20% water.

RESULTS AND DISCUSSION

Effect of Water Content of Cellulose Nitrate upon Hydrolysis of the Sulphate Acid Ester

The rates of hydrolysis of the sulphate acid esters in unstabilized cotton and wood

[1]*Manuscript received December 20, 1957.*
Contribution from the Department of Chemistry, Laval University, Quebec, Que., with financial assistance from the Defence Research Board of Canada.
[2]*Present address: Lignosol Chemicals Limited, Quebec, Que.*

Can. J. Chem. Downloaded from www.nrcresearchpress.com by 200.7.193.243 on 09/04/12
For personal use only.

cellulose nitrates could not be strictly compared because the samples, although having the same ester content, had different water contents.

In view of the above observation it was of interest to determine the effect of water content upon the rate of hydrolysis of the sulphate acid ester in unstabilized cellulose nitrates. Accordingly, many experiments were performed using moist cotton cellulose nitrate samples of variable water content. For example, in two experiments, the rates of hydrolysis of the sulphate acid esters in 11.4% N cellulose nitrates having different water contents, 0.16 and 0.28%, were compared.

It was seen that the release of sulphuric acid was most rapid in the case of the cellulose nitrate containing least water. For instance, in the first experiment, after 5 minutes, the per cent sulphuric acid released was 1.58 whereas for the same time, in the second experiment, it was only 1.25. The difference between the water contents of the two cellulose nitrates concerned was only 0.12%. The effect of the water content was greatest upon the initial hydrolysis, that taking place in the first 15 minutes. Later, the hydrolysis proceeded normally. For instance, in the above experiments, the percentages of sulphuric acid released after 30 minutes were about the same, 2.07 and 2.13 respectively. Similar results were obtained with unstabilized wood cellulose nitrates.

It is evident that small differences in the water content had a significant effect upon the rate of hydrolysis of the sulphate acid ester, RSO_4H, as shown in Fig. 1 for two cotton cellulose nitrates containing 100% sulphate acid ester and 11.4 and 9.7% nitrogen respectively.

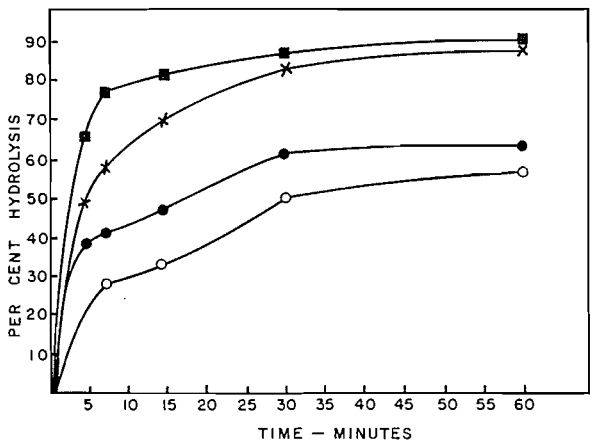

FIG. 1. Effect of water content of cellulose nitrate upon hydrolysis of sulphate acid ester.

	■	×	●	○
Nitrogen, %	11.4	11.4	9.7	9.7
Sulphate, % H_2SO_4, grav.	2.38	2.38	1.54	1.54
Water concn., % vol.	0.16	0.28	0.42	0.57

When the water content was increased, the rate of hydrolysis of the sulphate acid ester in unstabilized cotton cellulose nitrate decreased. Similar results were obtained with wood cellulose nitrate.

Effect of Water Content of Acetone upon Hydrolysis of Sulphate Acid Ester

The hydrolysis of the sulphate acid ester in both unstabilized cotton and wood cellulose nitrates was stopped in the presence of acetone containing 10% water (2).

Can. J. Chem. Downloaded from www.nrcresearchpress.com by 200.7.193.243 on 09/04/12
For personal use only.

In the present work, the effect of the water content of the acetone hydrolysis medium upon the rate of hydrolysis of the sulphate acid ester in unstabilized cellulose nitrates was carefully investigated. Hydrolysis experiments were carried out using cotton cellulose nitrate samples containing about the same amount of water, dissolved in various acetone/water solutions. For example, cellulose nitrates containing about 11.4% nitrogen, 100% sulphate acid ester, and 0.13% water, expressed as % vol. in the acetone medium, were used for hydrolysis experiments.

It was seen that the rate of hydrolysis decreased as the water content of the acetone increased. For instance, 0.54% sulphuric acid was released in the first 5 minutes of hydrolysis when the acetone contained 0.63% water, in one experiment, whereas in another none was released with 4.20% water present in the acetone. In some experiments, there was 100% hydrolysis of the sulphate acid ester, but in others the hydrolysis was not complete after 24 hours because of the presence of too much water in the acetone.

The effect of the water content of the acetone upon the rate of hydrolysis of the sulphate acid ester in an unstabilized cotton cellulose nitrate is shown in Fig. 2. It is seen that increase of water content greatly reduced the rate of hydrolysis in the first hour. For example, with only 0.63% water in the acetone medium there was about 78% hydrolysis after 1 hour, whereas with a water content of 4.20%, the corresponding value was only 6%.

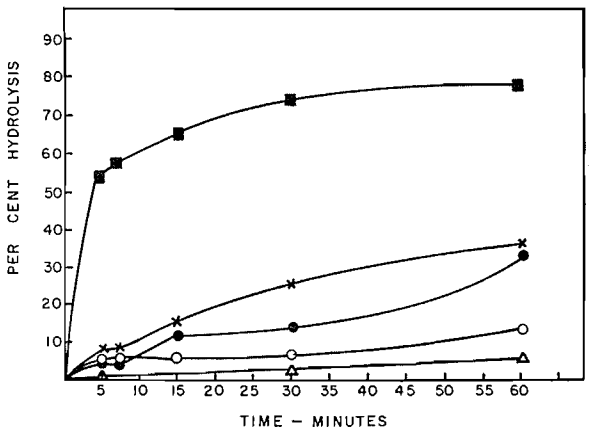

FIG. 2. Effect of water content of acetone upon hydrolysis of sulphate acid ester in cotton cellulose nitrates.

	■	×	●	○	△
Nitrogen, %	11.4	11.4	11.3	11.3	11.4
Sulphate, % H_2SO_4, grav.	0.94	0.81	0.85	0.79	0.81
Water concn., in acetone, % vol.	0.63	1.34	2.06	3.49	4.20
Sulphate acid ester, %	100	100	100	83	79

Furthermore, hydrolysis experiments were performed on unstabilized wood cellulose nitrates, and the results obtained for a sample containing about 10.7% nitrogen, 100% sulphate acid ester, and 0.35% water, expressed as % vol. in the acetone medium, were similar to those given by cotton cellulose nitrates.

The effect of the water content of the acetone medium upon the rate of hydrolysis of the sulphate acid ester in a wood cellulose nitrate is shown in Fig. 3. The results were very similar to those obtained with cotton cellulose nitrate (Fig. 2).

In the present work, cotton and wood cellulose nitrates containing 100% sulphate

Can. J. Chem. Downloaded from www.nrcresearchpress.com by 200.7.193.243 on 09/04/12
For personal use only.

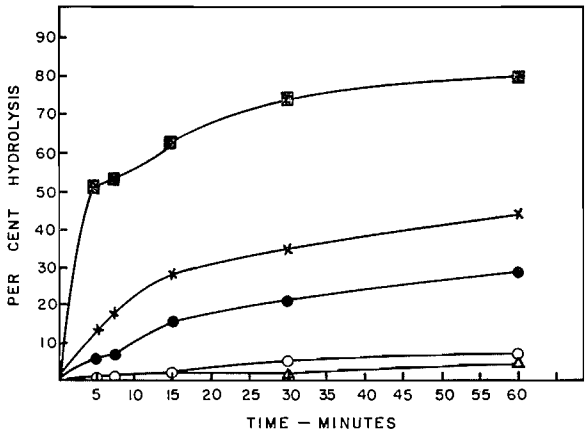

FIG. 3. Effect of water content of acetone upon hydrolysis of sulphate acid ester in wood cellulose nitrates.

	■	×	●	○	△
Nitrogen, %	10.8	10.7	10.6	10.6	10.7
Sulphate, % H_2SO_4, grav.	1.62	1.79	1.35	1.34	1.79
Water concn., in acetone, % vol.	0.63	1.34	2.06	3.49	4.20
Sulphate acid ester, %	100	99	91	67	62

acid ester were used. In some experiments, in the case of both cotton and wood cellulose nitrates, the sulphate acid ester content determined by the hydrolysis method (6) was too low in comparison to the true value, 100%. For instance, the ester contents for two cotton cellulose nitrates were 83 and 79%, and for wood cellulose nitrates, they were 67 and 62%, respectively. These low results were due to the fact that the sulphate acid ester was not completely hydrolyzed after 24 hours.

The effect of the increase in water content upon the degree of hydrolysis of the sulphate acid ester in both cotton and wood cellulose nitrates after 24 hours is shown in Fig. 4.

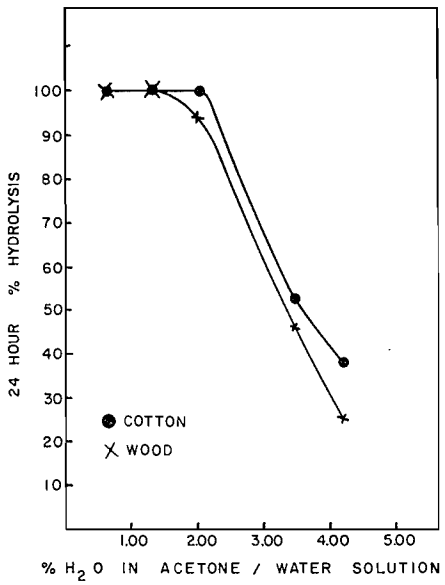

FIG. 4. Effect of water content of acetone upon the 24-hour hydrolysis of sulphate acid ester in cellulose nitrates.

Can. J. Chem. Downloaded from www.nrcresearchpress.com by 200.7.193.243 on 09/04/12
For personal use only.

It is evident that with less than 2% water in the acetone the sulphate acid ester is completely hydrolyzed after 24 hours; but with higher water contents, the degree of hydrolysis decreases rapidly.

REFERENCES

1. KEIRSTEAD, K. F. and MYERS, J. Can. J. Chem. **32**, 815 (1954).
2. GAGNON, P. E., KEIRSTEAD, K. F., and NEWBOLD, B. T. Can. J. Chem. **36**, 291 (1958).
3. MALM, C. J., TANGHE, L. J., and LAIRD, B. C. Ind. Eng. Chem. **38**, 77 (1946).
4. KEIRSTEAD, K. F. and MYERS, J. Can. J. Chem. **32**, 566 (1954).
5. GAGNON, P. E., KEIRSTEAD, K. F., and NEWBOLD, B. T. Can. J. Chem. **36**, 215 (1958).

Can. J. Chem. Downloaded from www.nrcresearchpress.com by 200.7.193.243 on 09/04/12
For personal use only.

Can. J. Chem. Downloaded from www.nrcresearchpress.com by 200.7.193.243 on 09/04/12
For personal use only.

L'ARYLATION DES QUINONES PAR LES SELS DE DIAZONIUM

I. SUR LA SYNTHÈSE DES MONOARYL-*p*-BENZOQUINONES[1]

P. BRASSARD[2] ET P. L'ÉCUYER

RÉSUMÉ

Une étude de la réaction des sels de diazonium avec la *p*-benzoquinone a été faite. Exécutée selon des conditions bien déterminées quant à la nature du solvant, la concentration de la solution tampon et la température du milieu, cette réaction constitue une excellente méthode générale de synthèse des monoaryl-*p*-benzoquinones.

INTRODUCTION

Borsche (1, 2) réussit, en 1899, la première synthèse d'une monoaryl-*p*-benzoquinone. Par l'action d'un grand excès de chlorure de benzène-diazonium sur le *p*-nitrosophénol en milieu alcalin, il parvint à isoler le 2-phényl-4-nitrosophénol et le 2,6-diphényl-4-nitrosophénol dont la réduction en aminophénols et l'oxydation de ces derniers ont fourni, avec un rendement insignifiant, les 2-phényl- et 2,6-diphényl-*p*-benzoquinones. La très sérieuse difficulté de cette préparation réside dans l'isolement et la purification du phénylnitrosophénol.

En 1924, Günther (3) rapporta la première préparation de quelques monoaryl-*p*-benzoquinones par l'action de sels de diazonium sur la *p*-benzoquinone en solution alcoolique diluée et en présence d'acétate de sodium. Enfin, en 1934, Kvalnes (4) modifia la méthode de Günther pour préparer quelques autres monoaryl-*p*-benzoquinones dont le résidu phényle est porteur d'un substituant en position 4. Il ne fait aucune mention du rendement des quinones pures.

Cette modification comporte à peu près les mêmes inconvénients que la méthode originale de Günther. En effet, l'une et l'autre ne sont réalisables qu'avec les sels de diazonium porteurs d'un substituant en position 4 ou en 3, à la condition dans ce dernier cas qu'il soit fortement électronégatif. Autrement la réaction ne marche pas, comme Kvalnes l'admet lui-même à la suite de son insuccès à préparer les *o*-nitrophényl-, 2,6-xylényl- et α-naphtyl-*p*-benzoquinones.

D'ailleurs, quelques-unes des préparations décrites par Kvalnes, lorsque reprises par Asano et Kameda (5), se sont avérées beaucoup moins efficaces tant au point de vue des rendements que de l'homogénéité du produit. Celui-ci est toujours contaminé par une certaine quantité de substances polysubstituées dont il est souvent difficile de se débarrasser.

Enfin, en 1950, Schimmelschmidt (6), en utilisant le bicarbonate de sodium en milieu aqueux, a synthétisé l'*o*-chloro-, l'*o*-nitro- et d'autres phénylquinones ayant dans le résidu aromatique plusieurs substituants dont un halogène en position 2.

Cette dernière modification constitue sous certains aspects une amélioration appréciable à la méthode de Günther. Cependant le bicarbonate de sodium donne une solution tampon alcaline dans les conditions suivies par Schimmelschmidt. Or une étude de l'influence du pH du mélange sur la réaction nous a permis de constater que le pH idéal est 5. Un pH plus élevé entraîne invariablement la formation de résines.

Il est vrai que Schimmelschmidt a obtenu un excellent rendement dans la préparation

[1]*Manuscrit reçu le 22 octobre 1957.*
Contribution du Département de Chimie, Faculté des Sciences, Université Laval, Québec, Qué. Ce mémoire est tiré de la thèse de doctorat de P. Brassard.
[2]*Adresse actuelle: Chemisches Institut der Universität, Zürich.*

Can. J. Chem. Downloaded from www.nrcresearchpress.com by 200.7.193.243 on 09/04/12
For personal use only.

TABLEAU I

INFLUENCE DU SOLVANT

Solvant organique, ml.	Eau, ml.	NaOAc.3H_2O en moles	Rdt. d'*o*-tolylquinone	
			Produit brut, %	Produit pur, %
—	1000	0.225	78	58
Ethanol (200)	50	0.300	—	0
Ethanol (200)	800	0.300	64	41
Acétone (200)	800	0.300	—	—
Formamide (150)	100	0.300	—	0

Influence de la nature et de la concentration de la solution tampon

La nature et la concentration de la solution tampon, tout comme dans la réaction de Meerwein, s'avère d'une importance primordiale. De toutes les substances déjà utilisées par Meerwein (10), Schimmelschmidt (6) et surtout Rondestvedt et Vogl (11), c'est l'acétate de sodium qu'il est préférable d'employer dans la proportion de 2 moles par mole de réactif. Le pH du mélange réactionnel est alors 5.

En faisant varier la quantité d'acétate de sodium de 2 à 5 équivalents, la vitesse de la réaction s'accélère et le rendement du produit brut s'accroît, mais sa qualité se détériore graduellement avec l'augmentation de la concentration de l'acétate. Il s'ensuit en définitive une diminution du rendement de la substance pure; car il se forme une quantité proportionnelle de produits de décomposition et on éprouve une difficulté croissante à purifier la substance recherchée (Tableau II).

TABLEAU II

INFLUENCE DE LA CONCENTRATION D'ACÉTATE DE SODIUM HYDRATÉ

Température		Poids de NaOAc. 3H_2O en grammes	Rdt. d'*o*-tolylquinone	
Initiale	Finale		Produit brut, %	Produit pur, %
10°	25°	27.2 (0.200 m.)	77	65
10°	25°	30.6 (0.225 m.)	78	62
10°	25°	34.0 (0.250 m.)	83	53
10°	25°	40.8 (0.300 m.)	89	—
20°	30°	68.0 (0.500 m.)	95	30

Influence de la température

La température initiale optimum de la réaction se situe entre 10° et 15° pour tous les sels de diazonium. A cette température le dégagement gazeux se fait à une vitesse convenable et l'aryl-*p*-benzoquinone qui précipite est relativement pure. A moins de 10°, en l'absence d'un excès d'acétate, le produit formé prend généralement une teinte verdâtre indiquant la formation de quinhydrone. Par contre, il y a avantage à laisser le mélange se réchauffer lentement et atteindre la température ambiante vers la fin de la réaction, pour que se complète heureusement la transformation du composé intermédiaire. Une baisse de température à ce moment favorise la formation de sous-produits phénoliques, tandis qu'une température initiale supérieure à 15° ou une élévation trop rapide de celle-ci entraîne invariablement la formation de goudrons (Tableau III).

Influence de la nature de l'anion du sel de diazonium

Contrairement à ce qui se produit dans la réaction de Meerwein où seul l'emploi du chlorure et, dans une plus faible mesure, du bromure est possible, le chlorure, le bromure,

Can. J. Chem. Downloaded from www.nrcresearchpress.com by 200.7.193.243 on 09/04/12
For personal use only.

TABLEAU III

INFLUENCE DE LA TEMPÉRATURE

Température		$NaOAc.3H_2O$ en moles	Rdt. d'*o*-tolylquinone	
Initiale	Finale		Produit brut, %	Produit pur, %
4°	20°	0.225	78	60
10°	25°	0.225	78	62
15°	25°	0.225	78	58
20°	30°	0.250	71	43

le phosphate et le sulfate de diazonium réagissent indifféremment avec la *p*-benzoquinone (le sulfate requiert une plus grande quantité d'acétate pour neutraliser l'ion bisulfate) sans que le rendement ne soit affecté d'une façon appréciable. Seul le nitrate s'avère insatisfaisant, en donnant lieu à la formation de produits de décomposition (Tableau IV).

TABLEAU IV

INFLUENCE DE L'ANION DU SEL DE DIAZONIUM

Température		$NaOAc.3H_2O$ en moles	Acide en mole	Rdt. d'*o*-tolylquinone	
Initiale	Finale			Produit brut, %	Produit pur, %
10°	25°	0.225	HCl (0.3)	78	62
10°	25°	0.225	HBr (0.3)	77	60
10°	25°	0.425	H_2SO_4 (0.25)	78	61
10°	25°	0.225	H_3PO_4 (0.3)	76	—
10°	25°	0.225	HNO_3 (0.3)	71	—

Influence du chlorure cuivrique comme catalyseur

Ce catalyseur, employé dans la réaction de Meerwein, nuit à la réaction. Toutefois, en opérant dans l'acétone aqueux à 20% et à pH = 3, il a été possible d'isoler de l'*o*-chlorophényl-*p*-benzoquinone à peu près exempte de goudrons. Malgré tout, la substance était encore contaminée par une certaine quantité de produits huileux provenant sans doute d'une réaction secondaire du type de celle de Sandmeyer. D'ailleurs, l'addition fréquente de quantités appréciables du catalyseur devenait essentielle au maintien d'une vitesse convenable du dégagement gazeux.

Influence de la nature et de la position de substituant

Le rendement semble peu affecté par la nature du substituant dans le sel de diazonium. L'allusion maintes fois répétée (12, 13, 14, 15, 16) à l'effet que la présence d'un groupe méthoxyle diminue le rendement dans la réaction de Meerwein ne s'applique pas ici ni dans le travail de Rondestvedt et Vogl (17).

L'arylation par les sels de diazonium substitués en position 2 s'effectue avec d'excellents rendements à la condition que le substituant ne soit ni fortement électropositif ni trop électronégatif, mais il importe d'opérer dans des conditions nettement déterminées, car autrement les rendements peuvent diminuer considérablement et la pureté du produit se déteriorer à un point où il est difficile d'en isoler une substance pure.

Lorsque le substituant en 2 est très électronégatif ou très électropositif, on obtient malgré toutes les précautions une certaine proportion de polymères, d'hydrocarbures, de phénols et même de diazoiques résultant de la copulation du sel de diazonium avec les phénols.

Can. J. Chem. Downloaded from www.nrcresearchpress.com by 200.7.193.243 on 09/04/12
For personal use only.

Can. J. Chem. Downloaded from www.nrcresearchpress.com by 200.7.193.243 on 09/04/12
For personal use only.

La plupart des phényl-*p*-benzoquinones substituées en position 2 du résidu hydrocarbonné sont très solubles dans les solvants organiques et ont un point de fusion assez bas, de sorte que leur purification présente des inconvénients et des difficultés. Il est alors préférable d'extraire le produit brut à l'éther de pétrole bouillant, d'évaporer à sec l'extrait éthéré, de traiter le résidu au noir animal et ensuite de le cristalliser ou distiller sous vide. Toutefois, même en opérant dans les conditions les plus favorables, les rendements des monoaryl-*p*-benzoquinones obtenues à partir de sels de diazonium *o*-substituées sont inférieurs de 10% à 30% à ceux qui proviennent des isomères para.

Enfin, il semble que l'encombrement stérique en 2 joue un rôle très négligeable dans la réaction. Ainsi le sel de diazonium de l'*o*-aminodiphényle donne, malgré la grosseur du substituant, un rendement de 88% d'*o*-diphényl-*p*-benzoquinone pure. De plus, il est vrai que la 2,6-diméthylaniline ne donne qu'un faible rendement même du produit brut; mais, lorsque la réactivité de cette amine est rehaussée par la bromuration en 4, la réaction procède avec facilité pour fournir un excellent rendement de 2,6-diméthyl-4-bromophényl-*p*-benzoquinone.

Quelques-unes des synthèse décrites par Kvalnes ont été répétées en tenant compte des conditions les plus favorables telles qu'établies antérieurement. Dans tous les cas, les rendements de la substance brute approchaient 100% et, après purification, le pourcentage de récupération a toujours été supérieur à 90%. Plusieurs autres monoaryl-*p*-benzoquinones, même celles qu'il serait impossible d'obtenir par la méthode de Kvalnes, ont été synthétisées avec d'excellents rendements (Tableau V).

TABLEAU V

MONOARYL-*p*-BENZOQUINONES

Groupe substituant	Rdt., %	P.f., °C.	Formule	C		H	
				Calculé	Trouvé	Calculé	Trouvé
Phényle (10)	84	113–114					
p-Hydroxyphényle	59	176–178	$C_{12}H_8O_3$	72.00	71.8	4.03	4.3
p-Anisyle (10)	93	118–120					
p-Chlorophényle	88	129.5	$C_{12}H_7O_2Cl$	65.92	65.7	3.21	3.3
p-Nitrophényle (10)	89	136–137					
3,4-Diméthoxyphényle (1)	84	134–135					
m-Tolyle	81	86–87	$C_{13}H_{10}O_2$	78.77	78.6	5.09	5.1
m-Chlorophényle	90	142–143	$C_{12}H_7O_2Cl$	65.92	66.1	3.21	3.4
m-Acétophényl	84	96–97	$C_{14}H_{10}O_3$	74.33	74.3	4.46	4.6
o-Tolyle	62	59–60	$C_{13}H_{10}O_2$	78.77	78.5	5.09	5.1
o-Anisyle	81	58–59	$C_{13}H_{10}O_3$	72.88	72.5	4.71	4.7
o-Diphényle	88	168–170	$C_{18}H_{12}O_2$	83.06	82.8	4.65	4.7
o-Chlorophényle (16)	79	82–83					
o-Bromophényle	75	98–100	$C_{12}H_7O_2Br$	54.78	54.5	2.68	2.8
o-Carbométhoxyphényle	81	107–109	$C_{14}H_{10}O_4$	69.42	69.5	4.16	4.3
o-Nitrophényle (16)	76	99–101					
2,6-Diméthyl-4-bromophényle	83	82–84	$C_{14}H_{11}O_2Br$	57.75	57.7	3.81	3.9
2,6-Dichlorophényle (16)	73	104–106					
α-Naphtyle	78	76–78	$C_{16}H_{10}O_2$	82.04	81.9	4.30	4.5
Méthane sulfonate de 2-hydroxyphényle	77	148–148.5	$C_{13}H_{10}O_5S$	56.11	56.5	3.62	3.7

PARTIE EXPÉRIMENTALE*

La synthèse des monoaryl-*p*-benzoquinones décrites dans ce mémoire a été réalisée en tenant compte des conditions optimum d'opération telles qu'établies dans la partie théorique. Comme la façon de préparer les sels de diazonium et d'effectuer leur réaction avec la *p*-benzoquinone est à peu près constamment la même pour toutes les synthèses,

**Les points de fusion ont été pris à l'aide de l'appareil de Johns. Les combustions ont été faites par les auteurs.*

nous ne la donnons en détail que pour la première, nous contentant d'en mentionner, le cas échéant, les modalités.

Un excès de 20% de quinone facilite la purification du produit de la réaction. L'excès de quinone reste en solution dans les eaux-mères. Au contraire, l'emploi de quantités équivalentes de sels de diazonium et de quinone occasionne la formation de résines.

Phényl-p-benzoquinone (*10*)

Une solution d'aniline (9.3 g., 0.1 mole) dans 25 ml. d'acide chlorhydrique concentré étendu de 100 ml. d'eau est refroidie à une température inférieure à 5° et diazotée, en agitant régulièrement, par l'addition goutte à goutte d'une solution de 7.0 g. de nitrite de sodium dans 25 ml. d'eau. On vérifie la fin de la réaction à l'aide de papier iodo-amidonné. La solution ainsi obtenue est ensuite versée d'un seul trait dans une suspension de *p*-benzoquinone (13.0 g., 0.12 mole) dans 850 ml. d'eau à 15° qui contient en solution 30.6 g. (0.225 mole) d'acétate de sodium hydraté comme tampon. On agite énergiquement au moyen d'un agitateur mécanique.

Le dégagement gazeux qui caractérise la réaction commence immédiatement et le mélange se réchauffe lentement pour atteindre finalement la température ambiante. Après une heure d'agitation la réaction est terminée. On filtre la solution et on recueille 16.9 g. de produit brut sous forme d'une poudre jaune qu'on cristallise dans l'éther de pétrole (p.é. 65°–110°). Après avoir laissé séjourner la solution pendant quelque temps au réfrigérateur à −10°, on la filtre et on recueille 15.4 g. de phényl-*p*-benzoquinone pure cristallisée en paillettes jaune doré.

p-Hydroxyphényl-p-benzoquinone

On diazote comme précédemment 10.9 g. de *p*-aminophénol dissous dans 50 ml. d'eau et 14 g. d'acide sulfurique concentré et on verse cette solution dans un mélange de 13.0 g. de *p*-benzoquinone, de 54.4 g. d'acétate de sodium hydraté et 200 ml. d'alcool éthylique, tout en agitant mécaniquement. La réaction commence immédiatement à 15° et elle est terminée à la température ordinaire après 2 heures d'agitation. Après dilution avec un assez grand volume d'eau (environ 1 litre) la majeure partie du liquide surnageant le précipité est décantée et la *p*-hydroxyphényl-*p*-benzoquinone, qui s'est séparée sous forme de cristaux rouges, est filtrée. Elle cristallise dans l'alcool dilué en fines aiguilles rouges.

p-Anisyl-p-benzoquinone (*10*)

La réaction entre le chlorure de diazonium de la *p*-anisidine (12.3 g.) et la *p*-benzoquinone (13.0 g.) se fait en 30 minutes. On cristallise dans l'acétone aqueux (2:1) et on récupère 19.9 g. de *p*-anisyl-*p*-benzoquinone sous forme de lamelles rouges.

p-Chlorophényl-p-benzoquinone

On diazote de la façon habituelle, entre 5° et 10°, de la *p*-chloraniline (12.8 g.) et on fait réagir la solution du sel de diazonium avec la *p*-benzoquinone (13.0 g.) dans 1000 ml. d'eau à la température ambiante. La réaction dure 3 heures. On obtient 21.4 g. de produit pulvérulent jaune pâle. Après cristallisation dans un mélange d'alcool éthylique et d'acétone (2:1), on recueille 19.2 g. de *p*-chlorophényl-*p*-benzoquinone pure cristallisée en aiguilles jaunes.

p-Nitrophényl-p-benzoquinone (*10*)

La *p*-benzoquinone (13.0 g.) dans 1350 ml. d'eau à 20° réagit pendant 2 heures avec le sel de diazonium de la *p*-nitraniline (13.8 g.). La réaction terminée, on filtre le précipité jaune-orangé. On cristallise dans un mélange d'éthanol et d'acétone (2:1) pour obtenir 20.3 g. de *p*-nitrophényl-*p*-benzoquinone pure sous la forme d'aiguilles jaune-orangé.

Can. J. Chem. Downloaded from www.nrcresearchpress.com by 200.7.193.243 on 09/04/12
For personal use only.

3,4-Diméthoxyphényl-p-benzoquinone (*1*)

La réaction du chlorure de diazonium de la 3,4-diméthoxy-aniline (15.3 g.) avec la *p*-benzoquinone (13.0 g.) commencée à 12°, en présence de 34.0 g. d'acétate de sodium hydraté, se termine en moins d'une heure à la température ambiante. Après refroidissement du mélange on filtre le précipité rouge et on le cristallise dans un mélange éthanol–acétone (2:1). On obtient la 3,4-diméthoxy-*p*-benzoquinone pure (20.3 g.) sous la forme de lamelles rouges.

m-Tolyl-p-benzoquinone

On fait réagir le chlorure de diazonium de la *m*-toluidine (10.7 g.) avec la *p*-benzoquinone (13.0 g.). La réaction met plusieurs heures à se compléter. On obtient, par filtration, 18.4 g. de produit jaune brunâtre. On extrait celui-ci plusieurs fois à l'éther de pétrole (p.é. 65°–110°) bouillant. On évapore à sec sous pression réduite les extraits réunis, on dissout le résidu dans un mélange d'acétone, de méthanol et d'eau (1:1:1) et on bout cette solution pendant 15 minutes avec du noir animal. Après filtration à chaud et refroidissement à $-10°$ pendant quelques jours, la *m*-tolyl-*p*-benzoquinone pure cristallise en paillettes jaune pâle.

m-Chlorophényl-p-benzoquinone

La réaction entre le chlorure de diazonium de la *m*-chloraniline (12.8 g.) et la *p*-benzoquinone (13.0 g.) se fait dans 1000 ml. d'eau. Commencée à 15° elle dure 3 heures. On recueille par filtration 21.2 g. de produit pulvérulent jaune. Cristallisée à $-10°$ dans un mélange d'éthanol et d'acétone (2:1), la *m*-chlorophényl-*p*-benzoquinone pure (19.7 g.) est obtenue sous la forme de lamelles jaune pâle.

m-Acétophényl-p-benzoquinone

La réaction du chlorure de diazonium de la *m*-acétophénone (13.5 g.) avec la *p*-benzoquinone (13.0 g.) est commencée à 10° et dure 2 heures. Le produit (21.0 g.) cristallise, après traitement à l'ébullition avec du noir animal dans un mélange d'acétone, de méthanol et d'eau (1:2:1), en aiguilles jaune-orangé.

Méthane sulfonate de la 2-hydroxyphényl-p-benzoquinone

Le méthane sulfonate d'*o*-aminophénol (9.4 g., 0.05 mole) dissous dans un mélange d'acide chlorhydrique concentré (12.5 ml.) et de 50 ml. d'eau est diazoté par une solution de 3.5 g. de nitrite de sodium dans 15 ml. d'eau et versé dans une suspension de 6.5 g. de *p*-benzoquinone dans 425 ml. d'eau à 10° et 15.3 g. d'acétate de sodium hydraté. Après cristallisation du produit de la réaction dans l'éthanol, on récupère 10.7 g. de méthane sulfonate de la 2-hydroxyphényl-*p*-benzoquinone sous la forme d'aiguilles jaune pâle.

o-Tolyl-p-benzoquinone

Un mélange de *o*-toluidine (10.7 g.) diazotée et de *p*-benzoquinone (13.0 g.) réagit pendant plusieurs heures. On isole ensuite le produit cristallin brunâtre (15.4 g.) et on l'extrait à l'éther de pétrole (p.é. 65°–110°) bouillant. Après l'évaporation à sec des extraits éthérés sous pression réduite, on dissout le résidu à chaud dans un mélange de méthanol, d'acétone et d'eau (1:1:1), on bout en présence de noir animal et on obtient, après filtration et refroidissement de la solution à $-10°$, 12.3 g. d'*o*-tolyl-*p*-benzoquinone cristallisée sous la forme de paillettes jaunes.

o-Anisyl-p-benzoquinone

Le chlorure de diazonium de l'*o*-anisidine (12.3 g.) met 3 heures à réagir avec la *p*-benzoquinone (13.0 g.). Le produit visqueux, que l'on obtient, est extrait à l'éther de pétrole

Can. J. Chem. Downloaded from www.nrcresearchpress.com by 200.7.193.243 on 09/04/12
For personal use only.

(p.é. 65°–110°) bouillant. Les extraits réunis sont évaporés à sec sous vide et le résidu est repris à l'ébullition avec du noir animal dans un mélange d'acétone, de méthanol et d'eau (1:1:1). Après cristallisation à -10°, on récupère 17.4 g. d'*o*-méthoxyphényl-*p*-benzoquinone pure sous forme d'un mélange polymorphe d'aiguilles jaune-orangé, p.f. 58°–59°, et de lamelles rouges, p.f. 64°–65°.

o-Diphényl-p-benzoquinone

Le produit brut (25 g., 96%) résultant de l'action du chlorure de diazonium de l'*o*-aminodiphényle (16.9 g.) sur la *p*-benzoquinone (13.0 g.) est isolé après 3 heures de réaction sous la forme d'une poudre jaune amorphe. On le purifie en bouillant à reflux sa solution dans l'acide acétique à 80% avec du noir animal. L'*o*-diphényl-*p*-benzoquinone pure (22.8 g.) cristallise en lamelles jaunes.

o-Chlorophényl-p-benzoquinone

Il faut agiter mécaniquement pendant 5 heures pour que la réaction entre le chlorure de diazonium de l'*o*-chloraniline (12.8 g.) et la *p*-benzoquinone (13.0 g.) se complète. Le dégagement gazeux terminé, on isole 21.1 g. de produit cristallin légèrement brunâtre. On peut le purifier selon l'une ou l'autre des façons suivantes:

Méthode A.—On extrait le produit brut jusqu'à épuisement avec plusieurs portions d'éther de pétrole (p.é. 65°–110°) bouillant et on évapore à siccité sous pression réduite les extraits réunis. On fait bouillir à reflux le résidu avec du noir animal dans un mélange de méthanol, d'acétone et d'eau (1:1:1). Après avoir éliminé le noir animal, la substance pure cristallise dans le mélange de solvants refroidi. On en récupère ainsi 18.1 g.

Méthode B.—On peut également cristalliser le résidu deux fois dans le même mélange de solvants en bouillant chaque fois la solution à reflux avec du noir animal. Le rendement de l'*o*-chlorophényl-*p*-benzoquinone pure cristallisée en paillettes jaunes est alors de 17.2 g.

o-Bromophényl-p-benzoquinone

La réaction du chlorure de diazonium de l'*o*-bromaniline (17.2 g.) avec la *p*-benzoquinone (13.0 g.) dure 6 heures. Le précipité jaune-orangé obtenu pèse 25.6 g. On le cristallise deux fois dans un mélange de méthanol, d'acétone et d'eau (1:1:1) en ayant soin chaque fois de faire bouillir la solution à reflux avec du noir animal. L'*o*-bromophényl-*p*-benzoquinone cristallise en lamelles jaunes.

o-Carbométhoxyphényl-p-benzoquinone

On fait réagir pendant 3 heures le chlorure de diazonium de l'anthranilate de méthyle (15.1 g.) et la *p*-benzoquinone (13.0 g.). Le produit brut filtré et séché pèse 22.2 g. On le cristallise à −10° dans un mélange de méthanol, d'acétone et d'eau (1:1:1) (noir animal). L'*o*-carbométhoxyphényl-*p*-benzoquinone pure (19.5 g.) s'obtient sous forme d'aiguilles jaunes.

o-Nitrophényl-p-benzoquinone

On triture 13.8 g. d'*o*-nitraniline dans 25 ml. d'acide chlorhydrique concentré jusqu'à l'obtention d'une pâte homogène; on étend alors de 100 ml. d'eau et on diazote de la façon habituelle. On fait réagir avec 13.0 g. de *p*-benzophénone. On essore 21.6 g. de produit cristallin. La quinone est isolée en faisant plusieurs extractions successives à l'éther de pétrole (p.é. 90°–110°) bouillant. Les extraits réunis sont évaporés à sec et le résidu cristallisé dans un mélange d'acétone, de méthanol et d'eau (1:2:1) (noir animal). L'*o*-nitrophényl-*p*-benzoquinone pure (17.3 g.) s'obtient en lamelles jaunes.

Can. J. Chem. Downloaded from www.nrcresearchpress.com by 200.7.193.243 on 09/04/12
For personal use only.

2,6-Diméthyl-4-bromophényl-p-benzoquinone (16)

On essore 26.8 g. du produit brut de la réaction du chlorure de diazonium de la 2,6-diméthyl-4-bromaniline (20.0 g.) et de la *p*-benzoquinone (13.0 g.) On l'extrait à l'éther de pétrole (p.é. 65°–110°) bouillant. Après l'évaporation à sec des extraits sous pression réduite, le résidu est cristallisé dans un mélange d'acétone, de méthanol et d'eau (1:2:1), après traitement au noir animal. On obtient ainsi 24.1 g. de 2,6-diméthyl-4-bromophényl-*p*-benzoquinone pure sous la forme de paillettes jaunes.

2,6-Dichlorophényl-p-benzoquinone

On obtient de la réaction du chlorure de diazonium de la 2,6-dichloraniline (16.2 g.) et de la *p*-benzoquinone (13.0 g.) 22.7 g. de produit que l'on purifie en extrayant à plusieurs reprises à l'éther de pétrole (p.é. 65°–110°) bouillant, en chassant le solvant des extraits et en cristallisant le résidu dans un mélange d'acétone, de méthanol et d'eau (1:1:1) (noir animal). La 2,6-dichlorophényl-*p*-benzoquinone pure (18.5 g.) cristallise à $-10°$ en lamelles jaunes.

α-Naphtyl-p-benzoquinone

Une suspension d'α-naphtylamine (14.3 g.) dans 300 ml. d'eau est traitée par 16.7 ml. d'acide sulfurique concentré et diazotée de la façon habituelle par 7.0 g. de nitrite de sodium dans 50 ml. d'eau. On verse ensuite cette solution dans une suspension de 13.0 g. de *p*-benzoquinone et de 30.6 g. d'acétate de sodium hydraté dans 650 ml. d'eau à 10°. On agite mécaniquement et on maintient le pH à 5 pendant toute la durée de l'expérience en ajoutant régulièrement de l'acétate de sodium en petites portions. La température s'élève lentement et l'on prend soin de la maintenir inférieure à 20° par l'addition de glace. Après plusieurs heures, on obtient une substance visqueuse qui, après la décantation de la liqueur, est séchée et extraite à la ligroine (p.é. 90°–120°) bouillante. Les extraits refroidis sont de nouveau portés à l'ébullition et décantés. On répète ce procédé jusqu'à ce qu'il ne précipite plus, à la température ordinaire, de goudrons qui restent insolubles à chaud. Les extraits sont alors évaporés à sec sous pression réduite et le résidu est cristallisé dans le méthanol. L'α-naphtyl-*p*-benzoquinone pure (12.3 g.) est obtenue en aiguilles rouges.

REMERCIEMENTS

Nous remercions le Conseil National de Recherches du Canada et la Shell Oil Company of Canada pour des bourses d'étude qu'ils ont accordées à l'un de nous (P.B.).

BIBLIOGRAPHIE

1. Borsche, W. Ber. **32**, 2935 (1899).
2. Borsche, W. Ann. **312**, 211 (1900).
3. Günther, F. Brevet allemand 508395 (1924); Frdl. **17**, 557 (1930).
4. Kvalnes, D. E. J. Am. Chem. Soc. **56**, 2478 (1934).
5. Asano, M. et Kameda, Y. J. Pharm. Soc. Japan, **59**, 768 (1939); Chem. Abstr. **34**, 2345 (1940).
6. Schimmelschmidt, K. Ann. **566**, 184 (1950).
7. Wieland, H. Ann. **514**, 145 (1934).
8. Huisgen, R. et Horeld, G. Ann. **562**, 137 (1949).
9. Akagi, M. et Hirose, K. J. Pharm. Soc. Japan, **62**, 191 (1942); Chem. Abstr. **45**, 6169 (1951).
10. Meerwein, H., Buchner, E. et Van Emster, K. J. prakt. Chem. **152**, 237 (1939).
11. Rondestvedt, C. S. et Vogl, O. J. Am. Chem. Soc. **77**, 3401 (1955).
12. Bergmann, F. et Shapiro, D. J. Org. Chem. **12**, 57 (1947).
13. Brunner, W. et Kenner, J. J. Chem. Soc. **121**, 614 (1948).
14. Brunner, W. et Kustatscher, J. Monatsch. Chem. **82**, 100 (1951).
15. L'Écuyer, P. et Olivier, C. A. Can. J. Research, B, **28**, 648 (1950).
16. Rai, J. et Mathur, K. B. L. J. Indian Chem. Soc. **24**, 413 (1947).
17. Rondestvedt, C. S. et Vogl, O. J. Am. Chem. Soc. **77**, 2313 (1955).

Can. J. Chem. Downloaded from www.nrcresearchpress.com by 200.7.193.243 on 09/04/12
For personal use only.

Can. J. Chem. Downloaded from www.nrcresearchpress.com by 200.7.193.243 on 09/04/12
For personal use only.

L'ARYLATION DES QUINONES PAR LES SELS DE DIAZONIUM

II. SUR LA SYNTHÈSE DES 2,5-BISARYL-*p*-BENZOQUINONES[1]

P. BRASSARD[2] ET P. L'ÉCUYER

RÉSUMÉ

Nous avons réussi la synthèse des 2,5-bisaryl-*p*-benzoquinones en faisant réagir des sels de diazonium avec des monoaryl-*p*-benzoquinones. Cette réaction donne des rendements fort convenables et elle constitue une méthode générale pour la préparation de cette classe de composés, quand elle est exécutée dans des conditions bien déterminées.

INTRODUCTION

Il n'existe à date aucune méthode générale de synthèse (1, 2, 3, 4, 5, 6, 7, 8, 9, 10) des 2,5-bisphénylquinones substituées dans les groupements phényles. Quoique Kvalnes (11) ait constaté qu'il n'est possible de les obtenir qu'avec de très faibles rendements et contaminées par de fortes proportions de dérivé tétrasubstitué par l'action des sels de diazonium sur la benzoquinone, il nous a semblé que la réaction de ces sels avec les monophénylquinones dans des conditions appropriées devrait pouvoir servir de méthode générale pour leur synthèse.

C'est le cas, si on opère dans un milieu qui favorise la précipitation de la 2,5-bisphénylquinone aussitôt formée et l'empêche ainsi de réagir à son tour avec le sel de diazonium. La benzoquinone réagit facilement avec les sels de diazonium en milieux aqueux (12, 13) pour donner des monophénylquinones. Celles-ci sont cependant, en général, trop insolubles dans l'eau pour réagir dans les mêmes conditions, mais elles le font dans un mélange d'un solvant organique et d'eau. L'acide acétique dilué ou l'acétone aqueux s'est révélé, selon le cas, le milieu le plus propice à l'introduction d'un deuxième résidu phényle dans la quinone.

Lorsque la phénylquinone de départ est très soluble dans les solvants organiques, il est préférable d'employer le mélange eau – acide acétique pour éviter la formation du dérivé tétrasubstitué. Par contre, avec une phénylquinone moins soluble le mélange eau–acétone donne de meilleurs résultats. Il faut toutefois dans cette dernière alternative opérer à une température inférieure à 0°.

Nous n'avons constaté aucun avantage à employer des sels cuivriques (chlorure ou acétate) comme catalyseur de la réaction. Ceci est d'autant plus surprenant que d'après Marini-Bettòlo et Rossi (14) l'addition de poudre de bronze améliore le rendement de l'arylation de la 1,4-naphtoquinone en milieu acétique.

Nous avons vérifié la généralité de cette méthode de synthèse des 2,5-bisphénylbenzoquinones en en préparant plusieurs à partir de sels de diazonium représentant toute la gamme de réactivité (Tableau I).

PARTIE EXPÉRIMENTALE

On diazote entre 0° et 5° l'amine (0.05 mole) dissoute dans un mélange de 25 ml. d'eau et de 12.5 ml. d'acide chlorhydrique concentré en ajoutant lentement une solution de 3.5 g. de nitrite de sodium dans 15 ml. d'eau. La solution du sel de diazonium est ensuite versée dans un mélange de la phénylquinone (0.045 mole), de 20.4 g. (0.15 mole)

[1]*Manuscrit reçu le 23 décembre 1957.*
Contribution du Département de Chimie de la Faculté des Sciences, Université Laval, Québec, Qué. Ce mémoire est tiré de la thèse de doctorat de P. Brassard.
[2]*Adresse actuelle: Chemisches Institut der Universität, Zürich.*

Can. J. Chem. Downloaded from www.nrcresearchpress.com by 200.7.193.243 on 09/04/12
For personal use only.

TABLEAU I

2,5-BISARYL-*p*-BENZOQUINONES

p-Benzoquinone	P.f.,°*	Rdt., %	Solvant	Forme cristalline	Formule	Analyse % calculé	Analyse % trouvé
2-Phényl-5-(*p*-anisyl)-	170–171	32	Ethanol–acétone (2:1)	Paillettes jaunes	$C_{19}H_{14}O_3$		
2-Phényl-5-(*m*-bromophényl)-	207–208	32	Butanol	Aiguilles orangées	$C_{18}H_{11}O_2Br$	C, 63.73 H, 3.27	C, 63.9 H, 3.3
2,5-Bis-(*m*-chlorophényl)-	Subl.	46	Acide acétique	Lamelles orangées	$C_{18}H_{10}O_2Cl$	C, 65.67 H, 3.06	C, 65.9 H, 3.6
2-Phényl-5-(*o*-anisyl)-	161–162	20	Ethanol-acétone (2:1)	Aiguilles orangées	$C_{19}H_{14}O_3$	C, 78.60 H, 4.86	C, 78.5 H, 5.0
2,5-Bis-(*p*-chlorophényl)-	Subl.	43	Toluène ou acide acétique	Aiguilles rouges	$C_{18}H_{10}O_2Cl_2$	C, 65.67 H, 3.06	C, 65.9 H, 3.3
2,5-Bis-(*o*-chlorophényl)-	194–196	42	Méthanol–acétone (4:1)	Aiguilles jaunes	$C_{18}H_{10}O_2Cl_2$	C, 65.67 H, 3.06	C, 65.3 H, 3.2
2,5-Bis-(*o*-bromophényl)-	217–219	40	Ethanol–butanone (2:1)	Aiguilles jaunes	$C_{18}H_{10}O_2Br_2$	C, 51.71 H, 2.41	C, 51.6 H, 2.5
2,5-Bis-(*o*-carbométhoxyphényl)-	187–188	38	Ethanol–acétone (2:1)	Lamelles jaunes	$C_{20}H_{15}O_6$		
2,5-Bis-(*o*-nitrophényl)-	208–210	50	Butanol–acétone (1:2)	Lamelles jaunes	$C_{18}H_{10}O_6N_2$	C, 61.72 H, 2.88 N, 8.00	C, 61.6 H, 2.9 N, 8.2
2-Phényl-5-(β-naphtyl)-	214	36	Butanol	Aiguilles orangées	$C_{22}H_{14}O_2$	C, 85.14 H, 4.56	C, 85.2 H, 4.5

**Les points de fusion ont été pris à l'aide de l'appareil de Johns.*

d'acétate de sodium trihydraté et de 200 à 250 ml. d'acide acétique agité mécaniquement. On ajoute alors suffisamment d'eau (environ 75 à 100 ml.) pour produire une légère précipitation de la quinone de départ. Tout en maintenant l'agitation du milieu, on peut laisser réagir à la température ambiante ou, s'il le faut, on chauffe très légèrement le mélange jusqu'à l'obtention d'un dégagement modéré d'azote sans toutefois dépasser une température de 40° à 45°.

Une fois le dégagement gazeux terminé, on étend d'eau, on isole le précipité et on le dissout dans un mélange d'acétone et de méthanol (1:4) bouillant. On laisse cristalliser la quinone en abandonnant la solution pendant quelques jours au réfrigérateur à −10°. En diluant les eaux-mères de cristallisation avec un peu de méthanol et en les laissant séjourner au réfrigérateur on augmente le rendement d'une façon appréciable. La 2,5-bisphénylquinone est obtenue presque pure. Si nécessaire, on peut la purifier davantage en la recristallisant dans les solvants appropriés.

Quand la phénylquinone de départ n'est pas assez soluble dans l'acide acétique ou lorsque le sel de diazonium l'exige, ce qui est le cas, par exemple, pour la *m*-chlorophénylquinone et le sel de diazonium de la β-naphtylamine, on dissout la phénylquinone dans l'acétone (300 ml. pour 0.045 mole), on refroidit la solution à −5° et on y verse la solution du sel de diazonium. Tout en agitant mécaniquement et en maintenant la température à −5°, on introduit l'acétate de sodium trihydraté (20.4 g. en tout) en petites portions durant une période de 20 minutes. On laisse ensuite le mélange se réchauffer à la température ambiante. L'isolement de la quinone se fait comme précédemment.

REMERCIEMENTS

Nous remercions le Conseil National de Recherches du Canada et la Shell Oil Company of Canada pour des bourses d'études qu'ils ont accordées à l'un de nous (P.B.).

BIBLIOGRAPHIE

1. MÜLLER, H. et VON PECHMANN, H. Ber. **22**, 2127 (1889).
2. PUMMERER, R., DALLY, M. et REISINGER, S. Ber. **66**, 792 (1933).
3. PUMMERER, R. et FIEDLER, H. Ber. **60**, 1439 (1927).
4. PUMMERER, R. et PRELL, E. Ber. **55**, 3105 (1922).
5. BROWNING, E. et ADAMS, R. J. Am. Chem. Soc. **52**, 4098 (1930).
6. HILL, D. W. et ADAMS, R. J. Am. Chem. Soc. **53**, 3453 (1931).
7. SCHILDNECK, P. R. et ADAMS, R. J. Am. Chem. Soc. **53**, 343 (1931).
8. SCHILDNECK, P. R. et ADAMS, R. J. Am. Chem. Soc. **53**, 2373 (1931).
9. ASANO, M. et KAMEDA, Y. J. Pharm. Soc. Japan, **59**, 768 (1939); Chem. Abstr. **34**, 2345 (1940).
10. ERDMAN, H. et NILSSON, M. Acta Chem. Scand. **10**, 735 (1956).
11. KVALNES, D. E. J. Am. Chem. Soc. **56**, 2478 (1934).
12. BRASSARD, P. et L'ÉCUYER, P. Can. J. Chem. **36**, 700 (1958).
13. SCHIMMELSCHMIDT, K. Ann. **566**, 184 (1950).
14. MARINI-BETTÒLO, G. B. et ROSSI, C. Gazz. chim. ital. **72**, 208 (1942).

Can. J. Chem. Downloaded from www.nrcresearchpress.com by 200.7.193.243 on 09/04/12
For personal use only.

Can. J. Chem. Downloaded from www.nrcresearchpress.com by 200.7.193.243 on 09/04/12
For personal use only.

REACTIVITY STUDIES ON NATURAL PRODUCTS

IV. DISSOCIATION CONSTANTS OF THE CYANOHYDRINS OF SOME STEROID KETONES[1]

OWEN H. WHEELER[2] AND JOSÉ L. MATEOS[3]

ABSTRACT

The dissociation constants of the cyanohydrins of 3-, 6-, and 7-ketocholestane, 3-keto-coprostane, Δ^4- and Δ^5-cholestenone, and Δ^7-, $\Delta^{8(9)}$-, $\Delta^{8(14)}$-, and Δ^{14}-ergosten-3-one have been measured in 80% dioxane at 25.0°. Cholestan-3-one and coprostan-3-one have essentially the same reactivity. 6- and 7-Ketocholestane show "eclipsing" effects of neighboring hydrogen atoms. Δ^4- and Δ^5-Cholestenone are less reactive than cholestanone owing to the electronic effect of the double bond, but Δ^7-, $\Delta^{8(9)}$-, $\Delta^{8(14)}$-, and Δ^{14}-ergostenone are more reactive, the effect decreasing with the distance of the double bond from the 3-keto group.

INTRODUCTION

While quantitative studies have been made on the reactivity of steroid esters and alcohols (1, 2), few quantitative data have been published on the relative reactivity towards addition reactions of a keto group in various positions of the steroid molecule, the only work of this nature being studies of the rates of oxime formation of 3-, 4-, 6-, and 7-ketocholestane (3), and of the borohydride reduction of 3- and 20-ketopregnanone (4). It is known that certain postions, e.g., 11 and 12, are unreactive with respect to a 3-keto group, but no systematic study has been made of the reactivity of groups in rings A and B, where reactivity differences would be expected to be small. The determination of ketone–cyanohydrin equilibria provides a convenient method of studying ketone reactivity towards addition reactions (5), and the dissociation constants of the cyanohydrins of 3-keto-cholestane and -coprostane (rings A/B *trans* and *cis*, respectively), 6- and 7-keto-cholestane, and 3-keto steroids with double bonds in positions 4,5,7,8(9),8(14), and 14 have been measured in 80% dioxane–water at 25.0° (see Table I), to investigate the influence of substitution in various positions, of *cis-trans* ring A/B fusion, and the effect of double bonds.

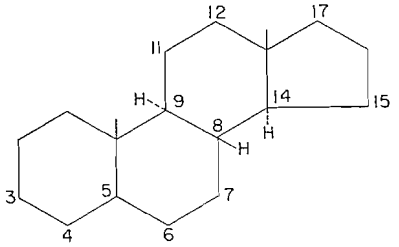

Cholestan-3-one and coprostan-3-one differ only in the nature of the ring A/B fusion. The *trans* fusion in the former case gives the molecule a continuous zigzag form, whereas the *cis* fusion, in the latter, leads to an L-shaped structure (6, 7). In cholestane the methyl group at C-10 and the 9—10 bond are *axial and equatorial* respectively (with respect to ring A), and in the second case are reversed, but in both cases the hydrogen atom at

[1]*Manuscript received November 25, 1957.*
Contribution from the Instituto de Quimica, Universidad Nacional Autonoma de Mexico, Mexico, 20, D.F. Part III, Chemistry and Industry, 395 (1957).
[2]*Present address: Department of Chemistry, Dalhousie University, Halifax, N.S.*
[3]*Present address: Department of Chemistry, University of California at Los Angeles.*

TABLE I

DISSOCIATION CONSTANTS OF CYANOHYDRINS[a]

	$K \times 10^2$	Ratio[b]
Cyclopentanone	56.0±1.0	9.3
Cyclohexanone	6.00±0.10	1.0
Cholestan-3-one	5.42±0.05	0.90
Coprostan-3-one	5.97±0.09	1.0
Cholestan-6-one	7.22±0.13	1.2
Cholestan-7-one	1.25±0.01	0.21
Δ^4-Cholesten-3-one	38.4±0.60	6.4
Δ^5-Cholesten-3-one	7.94±0.15	1.3
Δ^7-Ergosten-3-one	4.09±0.14	0.68
$\Delta^{8(9)}$-Ergosten-3-one	3.97±0.12	0.66
$\Delta^{8(14)}$-Ergosten-3-one	4.50±0.02	0.75
Δ^{14}-Ergosten-3-one	5.43±0.02	0.90

[a]*In 80% dioxane at 25.0°±0.1°.*
[b]*Ratio of dissociation constant to cyclohexanone = 1.0.*

C-5, one carbon atom nearer, is axial and the 5—6 bond equatorial and thus no large steric effect to cyanohydrin formation due to "axial crowding" (5) would be expected, and both these ketones have essentially the same cyanohydrin dissociation constant as cyclohexanone. The small increased reactivity of cholestanone with respect to cyclohexanone may be due to an "equatorial crowding" effect (5) similar to that observed in alkyl cyclohexanones, whereby the large internal carbonyl angle of the ketone distorts both rings A and B. The distortion is relieved in forming an addition product and addition is, therefore, facilitated.

6- and 7-Ketocholestane both have an extra alkyl substituent in the α-position, and this will exert an inductive effect which will increase the dissociation constant (5). However, the 6-ketone shows only a small increase while the 7-ketone actually shows a large decrease in dissociation constant and another effect must be operating. Construction of models shows that in the case of the 7-ketone the steric geometry of the steroid molecule is such that an α-hydrogen atom at C-15 is brought very close to the carbonyl group. Addition to the keto group gives a staggered structure and reduces the unfavorable oxygen–hydrogen interactions and is thus favored (8). This shielding or "eclipsing" effect has previously been observed to affect the stabilities of α-decalone and the 1,4-ketoperhydrophenanthrenes (9). In the case of the 6-ketone the small "eclipsing" effect of the hydrogen atoms on C-4 will tend to increase the extent of cyanohydrin formation, but there will be an "axial crowding" effect (5) in the cyanohydrin, between the methyl group at C-10 (2) and the cyanide (or hydroxyl) group. The net result of these opposing effects is a small decrease in reactivity, with respect to cholestan-3-one.

Δ^4- and Δ^5-Cholestan-3-one are both less reactive towards cyanohydrin formation than 3-cholestanone. In the former case, addition to the ketone grouping will destroy the resonance conjugation of the α,β-unsaturated ketone system and hence cyanohydrin formation will be difficult. (Whether addition was 1,4 as well as 1,2 was not determined. However, the reaction was unimolecular in ketone and cyanide.) The decreased reactivity of Δ^4-3-keto steriods, as compared to 3-keto steroids, towards dioxalan formation (10), ketal formation (11), and borohydride reduction (12) has previously been noted. In the Δ^5-compound there will be an inductive (or hyperconjugative) donation of electrons by the double bond to the ketone group (analogous to double-bond participation in the solvolysis of cholesteryl-*p*-toluene sulphonate (13)) and this will decrease the polarity of the ketone grouping and reduce nucleophilic attack of cyanide ion.

Can. J. Chem. Downloaded from www.nrcresearchpress.com by 200.7.193.243 on 09/04/12
For personal use only.

In contrast to the behavior of the Δ^4- and Δ^5-compounds, the four ergosten-3-ones (Δ^7, $\Delta^{8(9)}$, $\Delta^{8(14)}$, and $\Delta^{(14)}$) show increased reactivity but in an order decreasing with distance of the double bond from the ketone grouping, until no effect is apparent in the Δ^{14}-compound. This effect is probably not electronic, since the double bonds are too far removed from the keto group, and though the Δ^4- and Δ^5-ketones show displacements of ketone absorption in both the ultraviolet and the infrared (see Table II) due to electronic effects, the ergostenones are no different from cholestanone.

TABLE II

ABSORPTION SPECTRA OF KETONES

	I. R., cm.$^{-1}$	U. V.,[c] mμ
Cholestan-3-one	1716[a]	280 (73)
Coprostan-3-one	1714[a]	280 (73)
Δ^4-Cholesten-3-one	1627, 1675[a]	240.5 (18,000)[d]
		312 (100)
Δ^5-Cholesten-3-one	1683, 1724[a]	285 (100)
Δ^7-Ergosten-3-one	1712[b]	280 (59)
$\Delta^{8(9)}$-Ergosten-3-one	1715[b]	280 (57)
$\Delta^{8(14)}$-Ergosten-3-one	1718[b]	280 (56)
Δ^{14}-Ergosten-3-one	1715[b]	280 (62)

[a] *In carbon tetrachloride solution. K. Dobriner, E. R. Katzenellenbogen, and R. N. Jones. Infrared absorption spectra of steroids—An atlas. Interscience Publishers, Inc., New York, N. Y. 1953.*

[b] *Present work, as nujol mulls.*

[c] *As ethanolic solutions. Present work, unless otherwise stated.*

[d] *Ref. 40.*

Cyclohexene exists in a preferred "half-chair" conformation (14, 15), in which all the angles are slightly distorted (16), and introduction of a double bond into the steroid nucleus will lead to an over-all flattening of the rings. This will slightly distort ring A and introduce small non-bonded interactions. Cyclohexanone, itself, is a slightly distorted structure and its reactivity is due partly to the tendency to form an undistorted addition product (8). The presence of a keto group in ring A will introduce non-bonded interactions in this ring, and these will be increased by the conformational distortions produced by a double bond in a neighboring ring. Thus addition to the keto group, which will partially relieve the unfavorable interactions, will take place more readily than in the case of the saturated ketones. The effect of Δ^7 and $\Delta^{8(9)}$ double bonds, which are on either side of the C-3 to C-8 axis of rings A and B, is the same. A $\Delta^{8(14)}$ double bond, which is exocyclic to these two rings, has less effect and a Δ^{14} double bond, one more carbon atom remote and in another ring, has no measurable effect. Barton and co-workers (17, 18) have recently shown the operation of long-range effects in the mutarotation of steroid 5,6-dibromides and in the condensation of 3-keto triterpenes with benzaldehyde and has introduced the term "conformational transmission" for the transmission of distortions through a molecule by flexing of valency angles and alteration of atomic co-ordinates. Since no electronic interactions are involved and the effect is purely a steric one, it will manifest itself in an entropy term, and Barton and Head observed no difference in the energy of activation for the dibromides studied, but found small differences in the frequency factor. In the present work the maximum difference, between $\Delta^{8(9)}$-ergosten-3-one and cholestan-3-one, corresponds to a free-energy difference of only 0.18 kcal.

The ketones were generally prepared by standard methods (see Experimental), but in the course of the work some interesting observations were made. Ergosteryl acetate is

Can. J. Chem. Downloaded from www.nrcresearchpress.com by 200.7.193.243 on 09/04/12
For personal use only.

hydrogenated in ethyl acetate under ordinary conditions to Δ^7-ergostenyl acetate, but with Raney nickel at high temperature and pressure the product formed was $\Delta^{8(14)}$-ergostenyl acetate. This isomerization has previously been noted with platinum oxide in acetic acid (19). As an alternative to oxidation with chromium trioxide in acetic acid and benzene (20), or Oppenauer oxidation (21), the oxidation of some of the unsaturated alcohols with chromium trioxide in pyridine (the Sarett reagent (22)) was investigated. Cholesterol itself gave a mixture consisting largely of Δ^4-cholestenone but oxidation of Δ^7-ergostenol proceeded without rearrangement. This reagent has been recently used for the oxidation of ursa-9(11),12-dien-3-ol (23) without rearrangement of the double bond. However, it was found that use of only a small excess of chromium trioxide in acetic acid and benzene gave better yields, and this method was generally employed. The isomerization of $\Delta^{8(14)}$-ergostenone to Δ^{14}-ergostenone with hydrogen chloride in chloroform (24, 25) proved to be incomplete (26, 27). Various conditions of time and temperature were tried but the best yield obtained was only a 20% conversion. The isomerization of the corresponding acetate or alcohol gave poorer yields.

EXPERIMENTAL

Ketones

Cyclopentanone and cyclohexanone were specimens which had been previously prepared in this laboratory (5).

Cholestanone, m.p. 129°–130°, was prepared by oxidation of cholestanol (28), and coprostanone, m.p. 61°–63°, $(\alpha)_D$ +36°, by reduction of cholestenone (21) over a palladium charcoal catalyst in ethyl acetate, with the addition of two drops of piperidine. Δ^5-Cholestenone was prepared by the oxidation and subsequent zinc-dust reduction of cholesterol dibromide (29).

Cholestan-6-one

Cholesterol was converted to cholesteryl bromide, m.p. 97°–98°, $(\alpha)_D$ −20° (lit. m.p. 97°–99°, $(\alpha)_D$ −21.6° (30)), with phosphorus tribromide in benzene (31) and the bromide nitrated with fuming nitric acid and sodium nitrite to 3-bromo-6-nitrocholest-5-ene, m.p. 153°–155°, λ_{max} 262 mμ, ϵ 2200. Zinc-dust reduction (32) gave the required ketone.

Cholestan-7-one

Cholesteryl acetate was oxidized with *t*-butyl chromate (33) to 7-ketocholesteryl acetate, m.p. 157°–160°, $(\alpha)_D$ −86°, which was converted by refluxing with concentrated hydrochloric acid to $\Delta^{3,5}$-cholestadien-7-one, m.p. 112°–113° (lit. m.p. 112° (34)). Reduction of this compound with platinum oxide in ethyl acetate gave the required ketone, m.p. 116°–118°, $(\alpha)_D$ −28°, λ_{max} 292 mμ, ϵ 70 (lit. m.p. 116°–118° (35)).

Δ^7-*Ergosten-3-one*

Hydrogenation of ergosterol in ethyl acetate and ether at 30 lb. pressure with a platinum oxide catalyst gave Δ^7-ergosten-3-ol. Oxidation by the method of Oppenauer, with chromium trioxide (1.2 equiv.) in acetic acid and benzene, or by the method of Sarett, gave the ketone, m.p. 159°–160°, $(\alpha)_D$ +22° (lit. m.p. 159°, $(\alpha)_D$ +22° (36)), in about 50% yield in each case. Hydrogenation of ergosteryl acetate in ethyl acetate and acetic acid at 30 lb. pressure with a 5% palladium–charcoal catalyst, or in ethyl acetate at 1000 lb. pressure and 100° using a Raney nickel catalyst, gave $\Delta^{8(14)}$-ergostenyl acetate.

$\Delta^{8(14)}$-*Ergosten-3-one*

Oxidation of $\Delta^{8(14)}$-ergostenol with chromium trioxide in acetic acid and benzene gave

Can. J. Chem. Downloaded from www.nrcresearchpress.com by 200.7.193.243 on 09/04/12
For personal use only.

the ketone, m.p. 128°–129°, $(\alpha)_D$ +31.5° (lit. m.p. 129°–130°, $(\alpha)_D$ +30° (36)), in 70% yield. Oppenauer oxidation gave a 50% yield.

$\Delta^{8(9)}$-Ergosten-3-one

This was prepared by oxidation of $\Delta^{8(9)}$-ergostenol (37) with chromium trioxide in benzene and acetic acid, and had m.p. 118°–120°, $(\alpha)_D$ +70°.

Δ^{14}-Ergosten-3-one

This was prepared by isomerization of $\Delta^{8(14)}$-ergosten-3-one with hydrogen chloride in chloroform. The method gave only partial conversion, but the two isomers could be separated by careful chromatography on neutral alumina using hexane as eluent. The highest conversion (20%) was obtained by saturating with hydrogen chloride at 0° and allowing to stand 3–4 days in a refrigerator at *ca.* 5°. Poorer conversions were obtained with the alcohol or acetate. The pure ketone had m.p. 149°–150°, $(\alpha)_D$ +40° (lit. m.p. 149°–151°, $(\alpha)_D^{20}$ +36.4° (26)).

Solvents

Dioxane (Matheson, Coleman, and Bell) was refluxed with potassium hydroxide and fractionated from a fresh quantity. This dioxane (80 vol.) was mixed with distilled water (20 vol.), and the resulting solvent had d_4^{25} 1.0345.

Cyanohydrin Formation

Some preliminary experiments were carried out to find a suitable solvent. The steroids were not sufficiently soluble in ethanol. The dissociation constants of the cyanohydrin of cyclopentanone in anhydrous dioxane and 95% dioxane at 25° were *ca.* 700×10^{-2} and 200×10^{-2} respectively. Accordingly 80% dioxane was chosen as a solvent in which the steroids were reasonably soluble and which gave convenient dissociation constants. The procedure adopted was to dissolve the ketone (0.2–0.4 g.) in 80% dioxane in a 100 ml. graduated flask and then to add a solution of hydrogen cyanide (10 ml. of *ca.* 0.15 *N*), prepared from sodium cyanide and sulphuric acid and dissolved in 80% dioxane. A catalyst solution (1 ml.) of 2% tri-*n*-propylamine in 80% dioxane was added and the flask made up to the mark and allowed to equilibrate in a bath at 25.0°±0.1° for 6 hours. Aliquots (10 ml.) of the solution were withdrawn, added to excess silver nitrate (*ca.* 0.1 *N*) containing 0.5% nitric acid, and the excess silver nitrate titrated with potassium thiocyanate (0.05 *N*), using ferric ammonium sulphate as indicator (38, 39). Each experiment was repeated three or more times and the results, together with their mean standard deviations, are given in Table I.

ACKNOWLEDGMENTS

The authors are grateful to the Rockefeller Foundation, New York, for financial assistance.

REFERENCES

1. RUZICKA, L., FURTER, M., and GOLDBERG, M. W. Helv. Chim. Acta, **21**, 498 (1938).
2. SCHREIBER, J. and ESCHENMOSER, A. Helv. Chim. Acta, **38**, 1529 (1955).
3. DÉCOMBE, J., JACQUEMAN, R., and RABINOVITCH, J. Bull. soc. chim. France, 447 (1948).
4. GARETT, E. R. and LYTTLE, D. A. J. Am. Chem. Soc. **75**, 6051 (1953).
5. WHEELER, O. H. and ZABICKY, J. Z. Chem. & Ind. (London), 1388 (1956); Can. J. Chem. (In press).
6. TURNER, R. B. *In* Natural products related to phenanthrene. *By* L. F. Fieser and M. Fieser. Reinhold Publishing Corp., New York, N.Y. 1949. p. 620.
7. SHOPPEE, C. W. and SHOPPEE, E. *In* Chemistry of carbon compounds. Vol. IIB. *Edited by* E. H. Rodd. Elsevier Pub. Co., Inc., Amsterdam. 1953. p. 775.
8. BROWN, H. C., BREWSTER, J. H., and SHECHTER, H. J. Am. Chem. Soc. **76**, 467 (1954).

Can. J. Chem. Downloaded from www.nrcresearchpress.com by 200.7.193.243 on 09/04/12
For personal use only.

9. ROBINS, P. A. and WALKER, J. J. Chem. Soc. 1789 (1955); Chem. & Ind. (London), 772 (1955).
10. DAUBEN, H. J., LÖKEN, B., and RINGOLD, H. J. J. Am. Chem. Soc. **76**, 1359 (1954).
11. OLIVETI, E. P., GEROLD, C., and HERSHBERG, E. B. J. Am. Chem. Soc. **76**, 6113 (1954).
12. NORYMBERSKI, J. K. and WOODS, G. F. Chem. & Ind. (London), 518 (1954); J. Chem. Soc. 3426 (1955).
13. WINSTEIN, S. and ADAMS, R. J. Am. Chem. Soc. **70**, 838 (1948).
14. RAPHAEL, R. A. and STENLAKE, J. B. Chem. & Ind. (London), 1286 (1953).
15. BARTON, D. H. R., COOKSON, R. C., KLYNE, W., and SHOPPEE, C. Chem. & Ind. (London), 21 (1954).
16. COREY, E. J. and SNEEN, R. A. J. Am. Chem. Soc. **77**, 2505 (1955).
17. BARTON, D. H. R. and HEAD, A. H. J. Chem. Soc. 932 (1956).
18. BARTON, D. H. R., HEAD, A. H., and MAY, P. J. J. Chem. Soc. 935 (1957).
19. MORRISON, A. L. and SIMPSON, J. C. E. J. Chem. Soc. 1710 (1932).
20. BRUCE, W. F. Organic syntheses. Collective Vol. II. John Wiley & Sons, Inc., New York, N.Y. 1943. p. 139.
21. OPPENAUER, R. V. Org. Syntheses, **21**, 18 (1941).
22. POOS, G. I., ARTH, G. E., BEYLER, R. E., and SARETT, L. H. J. Am. Chem. Soc. **75**, 422 (1953).
23. SHAW, J. I., SPRING, F. S., and STEVENSON, R. J. Chem. Soc. 465 (1956).
24. REINDEL, F., WALTER, E., and RAUCH, H. Ann. **452**, 34 (1927).
25. REINDEL, F. and WALTER, E. Ann. **460**, 212 (1928).
26. HART, M. C. and EMERSON, H. J. Am. Chem. Soc. **54**, 1070 (1932).
27. HEILBRON, I. M. and WILKINSON, D. G. J. Chem. Soc. 1708 (1932).
28. BRUCE, W. F. Organic syntheses. Collective Vol. II. John Wiley & Sons, Inc., New York, N.Y. 1943. p. 191.
29. FIESER, L. F. J. Am. Chem. Soc. **75**, 5421 (1953).
30. BIDE, A. E., HENBEST, H. B., JONES, E. R. H., PEEVERS, R. W., and WILKINSON, P. A. J. Chem. Soc. 1783 (1948).
31. MARKER, R. E., WHITMORE, F. W., KAMM, O., OAKWOOD, T. S., and BLATTERMAN, J. M. J. Am. Chem. Soc. **58**, 338 (1936).
32. SHOPPEE, C. W. and SUMMERS, G. H. R. J. Chem. Soc. 3361 (1952).
33. HEUSLER, K. and WETTSTEIN, A. Helv. Chim. Acta, **35**, 284 (1952).
34. KARRER, P. and NAIK, A. R. Helv. Chim. Acta, **31**, 1617 (1948).
35. CREMLYN, R. J. W. and SHOPPEE, C. W. J. Chem. Soc. 3515 (1954).
36. BARTON, D. H. R. and COX, J. D. J. Chem. Soc. 783 (1948).
37. BARTON, D. H. R. and COX, J. D. J. Chem. Soc. 214 (1949).
38. LAPWORTH, A. and MANSKE, R. H. F. J. Chem. Soc. 2533 (1928).
39. EVANS, D. P. and YOUNG, J. R. J. Chem. Soc. 1310 (1954).
40. JONES, E. R. H., WILKINSON, P. A., and KERLOGUE, R. H. J. Chem. Soc. 392 (1942).

Can. J. Chem. Downloaded from www.nrcresearchpress.com by 200.7.193.243 on 09/04/12
For personal use only.

Can. J. Chem. Downloaded from www.nrcresearchpress.com by 200.7.193.243 on 09/04/12
For personal use only.

NOTES

THE DETERMINATION IN SITU OF THE CARBON CONTENT OF SOLID PRODUCTS IN REACTION VESSELS[1]

A. W. TICKNER

During an investigation of the reactions of methane in an electric discharge it was found that part of the methane was converted to a solid product which appeared as a thin film on the electrodes and, to a lesser extent, on the walls of the discharge tube. Enough of the solid was obtained by running for a long period at relatively high discharge currents to show that the composition was, very approximately, $(C_2H_3)_n$. Since the total weight of the deposit was usually of the order of 0.1 mg. and it was distributed over an area of between 10 and 100 cm.^{2} on surfaces which were not readily accessible, it was difficult to determine the total amount of carbon in the deposit by any of the standard procedures. The procedure described in this note was worked out in an effort to estimate the total carbon content of the solid product and thus to complete the material balance for the discharge reaction.

The discharge tube used was made of Pyrex tubing 4.0 cm. in diameter and was so designed that it could be surrounded by liquid nitrogen during an experiment. The electrodes were stainless steel disks 3.5 cm. in diameter mounted 3.0 cm. apart. Since direct current was used, this arrangement had the effect, at the pressures employed, of restricting the discharge to the negative glow. The total volume of the discharge system was approximately 500 cm.^{3}

After a discharge experiment with methane, the volatile products were removed, leaving the solid deposit on the electrodes and walls of the discharge tube. The discharge tube was then immersed in liquid nitrogen, and oxygen was introduced to a pressure of about 1 mm. of mercury. The discharge was turned on and run at a current of about 10 ma. until the oxygen pressure had fallen to a constant value. This constant value, which was usually about 0.3 or 0.4 mm. below the initial pressure, was attained in a few minutes and coincided with the disappearance of the last visible traces of the deposit from the cathode, where it had been deposited most heavily. The discharge was then turned off and the remaining oxygen pumped away.

Following the removal of the oxygen the discharge tube was warmed to the temperature of dry ice. This temperature was chosen in order to retain any water formed. The gas evolved was removed with a Toepler pump and its volume measured. Analysis on a mass spectrometer showed that the gas consisted of carbon dioxide and a small amount of oxygen. On the assumption that all of the carbon in the deposit had been converted into carbon dioxide, it was then possible to calculate the carbon content of the solid product obtained in the discharge reaction.

In order to test the method, a number of determinations were made using deposits consisting of measured amounts of materials of known carbon content. Each substance was made into a solution (in the case of graphite, a suspension) of known concentration, and a measured volume was evaporated on the surface of the cathode. It was estimated that the weight of a deposit produced in this way was known to within $\pm 2\%$. The

[1]*Issued as N.R.C. No. 4652.*

cathode was inserted into the discharge tube, which was evacuated and surrounded with liquid nitrogen. The deposit was then oxidized with the oxygen discharge and the products were measured and analyzed as described in the preceding paragraph.

The substances used were chosen to represent different types of compounds. All of them were required to have low volatility since the discharge tube had to be thoroughly evacuated before each experiment. The graphite used was Acheson Colloids Co. "Aquadag". Its graphite content was determined by drying a sample at 180° C. for 24 hours. It was used in the form of a suspension in distilled water. A sample of polyethylene polymer having a molecular weight of about 2500 was obtained and applied to the electrode as a toluene solution. Reagent grade *o*-terphenyl was used in benzene solution and Reagent grade sucrose in water. In addition, a luminous burner flame was used to deposit a thin but clearly visible deposit of carbon black on the cathode. The oxygen used was from a standard cylinder supply having a stated purity of 99.9%. It was passed through a trap cooled by liquid nitrogen and was used without any further purification.

The results of these determinations have been summarized in Table I. In each case the recovery of carbon as carbon dioxide was sufficiently quantitative to meet the present requirements.

TABLE I

RECOVERY OF CARBON AS CARBON DIOXIDE

Sample	Gram atoms of carbon deposited ($\times 10^6$)	Moles of carbon dioxide recovered ($\times 10^6$)	% Theoretical
Graphite	16.9	16.7	99
Polyethylene	12.4	12.0	97
o-Terphenyl	11.7	11.8	101
Sucrose	15.0	14.3	95

In addition, the experimental results showed another, and rather unexpected, correlation. As reported above, the gas recovered after the oxidation of each deposit contained some oxygen in addition to the carbon dioxide. This amount of oxygen could not be decreased even by prolonged pumping with the products of the discharge oxidation frozen out at the temperature of liquid nitrogen. A relationship appeared to exist between the percentage of oxygen in the carbon dioxide recovered and the amount of hydrogen present in the compound which had been oxidized. The values obtained for the various substances used are shown graphically in Fig. 1. On this basis the composition of the solid product formed in the discharge reaction of methane is given approximately by the formula $(CH)_n$.

No detailed explanation is offered to account for the oxygen retained in the discharge product. The 8 or 9% of oxygen found in the products of the discharge oxidation of pure carbon may represent oxygen retained in some way by the solid carbon dioxide or as an unstable carbon–oxygen compound which decomposes on being warmed to −78° C. The remainder of the oxygen, the part which appears to be related to the hydrogen content of the solid being oxidized, may be due to the formation of hydrogen–oxygen compounds which decompose on being warmed above the temperature of liquid nitrogen. Such compounds have been reported by Jones and Winkler (1) and by Giguère, Secco, and Eaton (2) as products of the decomposition of water vapor in the electric discharge.

Can. J. Chem. Downloaded from www.nrcresearchpress.com by 200.7.193.243 on 09/04/12
For personal use only.

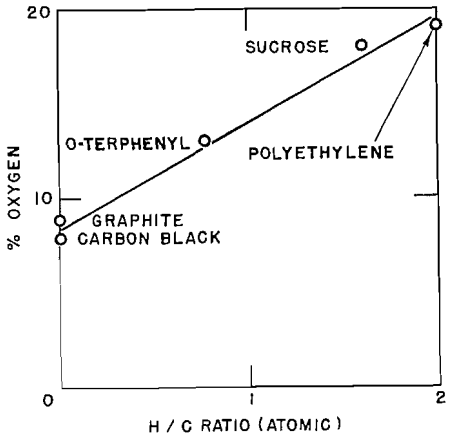

FIG. 1.

The method described above would seem to be capable of fairly wide application to situations in which it is desired to determine the carbon content of small amounts of organic solids deposited in inaccessible locations. While the work reported here has made use of a direct-current discharge in a tube with internal electrodes, it seems likely that an electrodeless discharge using radio-frequency power would also be effective. Furthermore, although the present discharge tube was arranged to allow it to be immersed in liquid nitrogen, it should be possible to carry out the oxidation successfully in a system in which the oxygen is circulated through the discharge and subsequently passed through a cold trap before being returned to the discharge chamber. With these variations it should be possible to apply the method to the determination of carbon in organic deposits in a variety of reaction vessels, including, for example, the reaction cells used in photochemical experiments. In addition, it may be possible to use the method to estimate the hydrogen content of such deposits.

1. JONES, R. A. and WINKLER, C. A. Can. J. Chem. **29**, 1010 (1951).
2. GIGUÈRE, P. A., SECCO, E. A., and EATON, R. S. Discussions Faraday Soc. No. **14**, 104 (1953).

RECEIVED DECEMBER 9, 1957.
DIVISION OF APPLIED CHEMISTRY,
NATIONAL RESEARCH COUNCIL,
OTTAWA, CANADA.

THE THERMODYNAMIC PROPERTIES OF BENZOIC ACID[1]

R. GOTON AND E. WHALLEY

Dr. R. S. Jessup has pointed out to us in a private communication that in a previous note (1) of the same title we have used the wrong value for the standard heat of combustion of benzoic acid to calculate its thermodynamic properties. The value that we used, 26,428.4±2.6 int. j. g.$^{-1}$, should be replaced by 26,420.4±2.6 int. j. g.$^{-1}$. This value has been corrected for the changed atomic weight of carbon (2) by Dr. Jessup to give 3226.99±.31 kj. mole^{-1}. In addition there are numerical errors in our table of entropies,

[1]*Issued as N.R.C. No. 4653.*

Can. J. Chem. Downloaded from www.nrcresearchpress.com by 200.7.193.243 on 09/04/12
For personal use only.

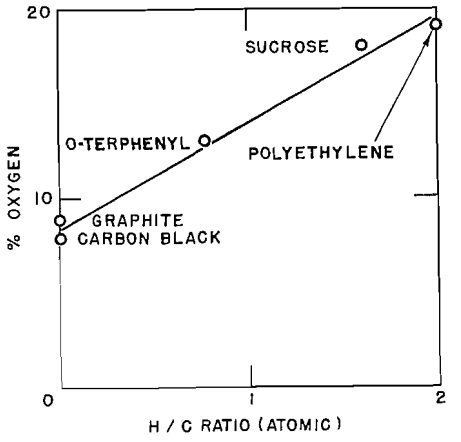

FIG. 1.

The method described above would seem to be capable of fairly wide application to situations in which it is desired to determine the carbon content of small amounts of organic solids deposited in inaccessible locations. While the work reported here has made use of a direct-current discharge in a tube with internal electrodes, it seems likely that an electrodeless discharge using radio-frequency power would also be effective. Furthermore, although the present discharge tube was arranged to allow it to be immersed in liquid nitrogen, it should be possible to carry out the oxidation successfully in a system in which the oxygen is circulated through the discharge and subsequently passed through a cold trap before being returned to the discharge chamber. With these variations it should be possible to apply the method to the determination of carbon in organic deposits in a variety of reaction vessels, including, for example, the reaction cells used in photochemical experiments. In addition, it may be possible to use the method to estimate the hydrogen content of such deposits.

1. JONES, R. A. and WINKLER, C. A. Can. J. Chem. **29**, 1010 (1951).
2. GIGUÈRE, P. A., SECCO, E. A., and EATON, R. S. Discussions Faraday Soc. No. **14**, 104 (1953).

RECEIVED DECEMBER 9, 1957.
DIVISION OF APPLIED CHEMISTRY,
NATIONAL RESEARCH COUNCIL,
OTTAWA, CANADA.

THE THERMODYNAMIC PROPERTIES OF BENZOIC ACID[1]

R. GOTON AND E. WHALLEY

Dr. R. S. Jessup has pointed out to us in a private communication that in a previous note (1) of the same title we have used the wrong value for the standard heat of combustion of benzoic acid to calculate its thermodynamic properties. The value that we used, 26,428.4±2.6 int. j. g.$^{-1}$, should be replaced by 26,420.4±2.6 int. j. g.$^{-1}$. This value has been corrected for the changed atomic weight of carbon (2) by Dr. Jessup to give 3226.99±.31 kj. mole^{-1}. In addition there are numerical errors in our table of entropies,

[1]*Issued as N.R.C. No. 4653.*

Can. J. Chem. Downloaded from www.nrcresearchpress.com by 200.7.193.243 on 09/04/12
For personal use only.

and consequently also in the free energies. The entropy relative to that at 0° K. had been calculated by Furukawa, McCoskey, and King (3), in a paper which we had overlooked; our revised values agree with theirs.

Solid benzoic acid at room temperature is composed of molecules of dimer (4) and no thermal transition has been observed between 15° K. and room temperature (3). If the hydrogen bonds in the dimer are completely disordered the zero-point entropy is $\frac{1}{2}R\ln 2$ (5). There is no experimental information on the zero-point entropies of carboxylic acids, but the disordered structure of ice and heavy water is well verified. If the maximum disorder is present in benzoic acid, and this seems likely, 0.347 should be added to $(S-S_0°)/R$ to give the entropy. The entropies thus obtained are given in the revised Table I,

TABLE I

T/° K.	$(H_T°-H_0°)/RT_0$	$S°/R$	$-(F_T°-H_0°)/RT$	$-(\Delta F_f°)/RT$
		Solid		
100	1.544	7.854	3.636	402.95
150	3.160	11.40	5.65	251.37
200	5.202	14.59	7.48	175.11
220	6.146	15.82	8.19	154.24
240	7.165	17.03	8.88	136.80
260	8.264	18.23	9.55	122.03
280	9.442	19.42	10.21	109.32
298.15	10.58	20.50	10.80	99.26
300	10.70	20.61	10.86	98.29
310	11.36	21.20	11.19	93.31
320	12.04	21.78	11.50	88.64
330	12.74	22.38	11.83	84.26
340	13.46	22.97	12.15	80.13
350	14.21	23.56	12.47	76.22
360	14.97	24.14	12.78	72.55
370	15.75	24.73	13.10	69.04
380	16.56	25.31	13.41	65.73
390	17.38	25.91	13.72	62.59
395.52	17.85	26.23	13.90	60.94
		Liquid		
395.52	25.78	31.70	13.90	60.94
400	26.27	32.04	14.10	59.68
410	27.40	32.80	14.54	56.98

herewith. The free energy and the free energy of formation have also been recalculated. The free energy of graphite was obtained by graphical interpolation of the data in Reference 6 below 300° K., and of those in Reference 7 above 300° K.

The revised heat of formation at 0° K. is $-367.75\pm.45$ kj. mole^{-1} and at 25° C. is $-385.16\pm.40$ kj. mole^{-1}. The physical constants used are from References 2 and 8, and 1 mole of benzoic acid refers to the formula $C_7H_6O_2$.

1. Goton, R. and Whalley, E. Can. J. Chem. **34**, 1506 (1956).
2. Wichers, E. J. Am. Chem. Soc. **78**, 3235 (1956).
3. Furukawa, G. T., McCoskey, R. E., and King, G. J. J. Research Natl. Bur. Standards, **47**, 256 (1951).
4. Sim, G. A., Robertson, J. M., and Goodwin, T. M. Acta Cryst. **8**, 157 (1955).
5. Pauling, L. J. Am. Chem. Soc. **57**, 2680 (1935).
6. De Sorbo, W. and Tyler, W. W. J. Chem. Phys. **21**, 1660 (1953).
7. Wagman, D. D. *et al.* J. Research Natl. Bur. Standards, **34**, 143 (1945).
8. DuMond, J. M. W. and Cohen, E. R. Revs. Modern Phys. **25**, 691 (1953).

Received July 17, 1957.
Division of Applied Chemistry,
National Research Council of Canada,
Ottawa, Canada.

Can. J. Chem. Downloaded from www.nrcresearchpress.com by 200.7.193.243 on 09/04/12
For personal use only.

1-ARYLSULPHONYL-3-*n*-BUTYL-2-METHYL-2-THIOPSEUDOUREAS

STANLEY O. WINTHROP AND GREGORY GAVIN

Compounds containing the thiopseudourea grouping have recently come under investigation in our laboratories (1). Since certain 1-arylsulphonyl-3-*n*-butylureas (I) have been shown to possess useful hypoglycemic activity, it was of interest to prepare some 1-arylsulphonyl-3-*n*-butyl-2-methyl-2-thiopseudoureas (II) for pharmacological screening. Cox (2) has reported the preparation of a series of 1-arylsulphonyl-2-methyl-2-thiopseudoureas which have shown some value as bacteriostatic agents.

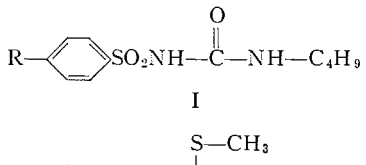

I

(*a*) R = CH_3
(*b*) R = $NHCOCH_3$
(*c*) R = NH_2

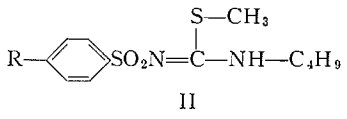

II

The sulphonylthiopseudoureas were prepared by the condensation of the appropriate sulphonyl chlorides with 1-*n*-butyl-2-methyl-2-thiopseudourea. Acid hydrolysis of 1-(*p*-acetaminobenzenesulphonyl)-3-*n*-butyl-2-methyl-2-thiopseudourea (II*b*) gave the 1-(*p*-aminobenzenesulphonyl)-3-*n*-butyl-2-methyl-2-thiopseudourea (II*c*).

The sulphonylthiopseudoureas were administered orally to rabbits which had been fasted for 24 hours. None of the compounds tested showed a significant hypoglycemic action.

EXPERIMENTAL*

1-(p-Toluenesulphonyl)-3-n-butyl-2-methyl-2-thiopseudourea

Potassium carbonate (33 g., 0.24 mole) was suspended in 90 ml. of a 3:1 acetone–water solution cooled in an ice-water bath. A well-ground mixture of *p*-toluenesulphonylchloride (12.4 g., 0.065 mole) and 1-*n*-butyl-2-methyl-2-thiopseudourea hydroiodide† (19.9 g., 0.0725 mole) was slowly added with vigorous stirring. The addition was completed after 30 minutes and the stirring was continued at room temperature for another 3 hours. The reaction contents were then added to 250 ml. of water, causing the product to separate out, 17.8 g. (91% yield), m.p. 72°–77° C. Two recrystallizations from isopropanol gave 11.5 g., m.p. 85°–86° C. Calculated for $C_{13}H_{20}N_2S_2O_2$: C, 51.97; H, 6.71; N, 9.32; S, 21.35. Found: C, 52.25; H, 6.92; N, 9.19; S, 20.93.

1-(p-Acetaminobenzenesulphonyl)-3-n-butyl-2-methyl-2-thiopseudourea

This compound was prepared in the same manner as the preceding example. Potassium carbonate (66 g., 0.48 mole), *p*-acetaminobenzenesulphonyl chloride (30.3 g., 0.13 mole), and 1-*n*-butyl-2-methyl-2-thiopseudourea hydroiodide† (39.2 g., 0.143 mole) gave 44 g. of product with m.p. 129°–135° C. Two recrystallizations from isopropanol gave 21.8 g., m.p. 141°–142° C. Calculated for $C_{14}H_{21}N_3S_2O_2$: C, 48.96; H, 6.17; N, 12.24; S, 18.67. Found: C, 49.15; H, 6.02; N, 12.11; S, 18.51.

**All melting points are uncorrected.*
†The preparation of this compound is described by Kirsten and Smith (3).

Can. J. Chem. Downloaded from www.nrcresearchpress.com by 200.7.193.243 on 09/04/12
For personal use only.

1-(p-Aminobenzenesulphonyl)-3-n-butyl-2-methyl-2-thiopseudourea

1-(*p*-Acetaminobenzenesulphonyl)-3-*n*-butyl-2-methyl-2-thiopseudourea (15.5 g., 0.045 mole) was refluxed for 2 hours in a solution consisting of 67 ml. of 7% hydrochloric acid and 30 ml. of ethanol. After cooling and addition of a large amount of water, the solution was neutralized with ammonium hydroxide, causing the product to separate out, 12.8 g. (95% yield), m.p. 158°–159° C. One recrystallization from methanol did not raise the melting point. Calculated for $C_{12}H_{19}N_3S_2O_2$: C, 47.81; H, 6.35; N, 13.94; S, 21.28. Found: C, 48.35; H, 6.72; N, 14.06; S, 21.10.

ACKNOWLEDGMENTS

The authors are grateful to Mr. W. J. Turnbull for the microanalytical data and to Dr. C. I. Chappel for the pharmacological screening.

1. WINTHROP, S. O., SYBULSKII, S., GAVIN, G., and GRANT, G. A. J. Am. Chem. Soc. **79**, 3496 (1957).
2. COX, E. H. J. Org. Chem. **7**, 307 (1942).
3. KIRSTEN, G. W. and SMITH, G. B. L. J. Am. Chem. Soc. **58**, 800 (1936).

RECEIVED DECEMBER 18, 1957.
RESEARCH AND BIOLOGICAL LABORATORIES,
AYERST, MCKENNA, & HARRISON LIMITED,
MONTREAL, QUE.

Can. J. Chem. Downloaded from www.nrcresearchpress.com by 200.7.193.243 on 09/04/12
For personal use only.

Can. J. Chem. Downloaded from www.nrcresearchpress.com by 200.7.193.243 on 09/04/12
For personal use only.

Canadian Journal of Chemistry

Issued by THE NATIONAL RESEARCH COUNCIL OF CANADA

VOLUME 36 MAY 1958 NUMBER 5

THE MOLECULAR WEIGHT OF POLYETHYLENE AND OF OTHER HIGH-MOLECULAR-WEIGHT ORGANIC COMPOUNDS[1]

R. TREMBLAY,[2] A. F. SIRIANNI, AND I. E. PUDDINGTON

ABSTRACT

The temperature range of the measurement of vapor-pressure depression using a sensitive differential mercury micromanometer has been extended, and the behavior of a series of polyethylene samples having a molecular-weight range of 2500 to 24,000 was examined in toluene solutions at 75° C. Good agreement was obtained between vapor-pressure lowering and other means of determining number-average molecular weights of several special compounds.

INTRODUCTION

Number-average molecular weights lower than about 40,000 have been determined satisfactorily for a number of compounds of known constitution and for a series of vinyl-acetate polymers, by measuring the differences in vapor pressure between solutions of these substances and the pure solvent (1, 2, 3). The present communication describes similar measurements on a series of polymers of ethylene prepared by a high-pressure process and obtained through the courtesy of Canadian Industries Limited. The individual samples designated as melt index 200,000, 20,000, 7000, 700, 2, and 0.2 cover an approximate molecular-weight range of 2500 to 24,000.

It has been shown that individual samples of polyethylene can have weight-average–number-average molecular weight ratios as high as 70 with very broad distributions of the molecular sizes (4, 5, 6, 7). Differences of 25% in number-average molecular weight, attributed to membrane permeability, have been found when the same samples were examined osmometrically and cryoscopically (8). Increases in $\bar{M}_n$ as large as 100% have been effected with no change in the melt index by mild extractive fractionation (8). It has also been suggested that the result obtained may be influenced by the solvent used in ebulliometric measurements (9). It therefore seemed worth while to test the usefulness of an additional method for measuring $\bar{M}_n$, which is not too restricted in temperature of operation and not subject to membrane permeability, in the characterization of these interesting polymers.

Since polyethylene has limited solubility in most solvents below about 70° C. (10, 11), it was necessary to raise the temperature at which the vapor-pressure measurements were made from 55° C., which was used for most of the previous work, to 75° C. A number of comparative determinations were made on polymers of ethylene oxide and an esterified

[1]*Manuscript received January 10, 1958.*
Contribution from the Division of Applied Chemistry, National Research Council, Ottawa, Canada.
Issued as N.R.C. No. 4658.
[2]*National Research Council Postdoctorate Fellow 1954–56. Present address: Canadian Industries Limited, McMasterville, Quebec.*

sucrose* that had molecular weights in the vicinity of 3000 and 1800 respectively and which had been examined by other methods.

APPARATUS AND EXPERIMENTAL

The apparatus and experimental technique have already been described (1, 2). Molecular-weight determinations on carbowax and sucrose myristate were carried out both in benzene at 42.5° C. and in toluene at 75° C. All determinations on polyethylene were made in toluene at 75° C. Solutions in all cases were optically clear and no evidence of insolubility, which would lead to fictitiously high values, was noted.

The dried polymers were stored *in vacuo* and 0.7 to 4 mg. quantities were used in preparing the solution. A drop of redistilled solvent was used to stick the newly weighed samples to their containers to reduce the danger of mechanical loss during subsequent operations. Care was taken to avoid overheating the polymers, especially when in contact with air, to minimize the possibility of molecular degradation. Solutions of the polymer were prepared in the usual way by condensing a known amount of solvent on the solid polymer after the sample holder had been sealed to the apparatus and the assembly evacuated.

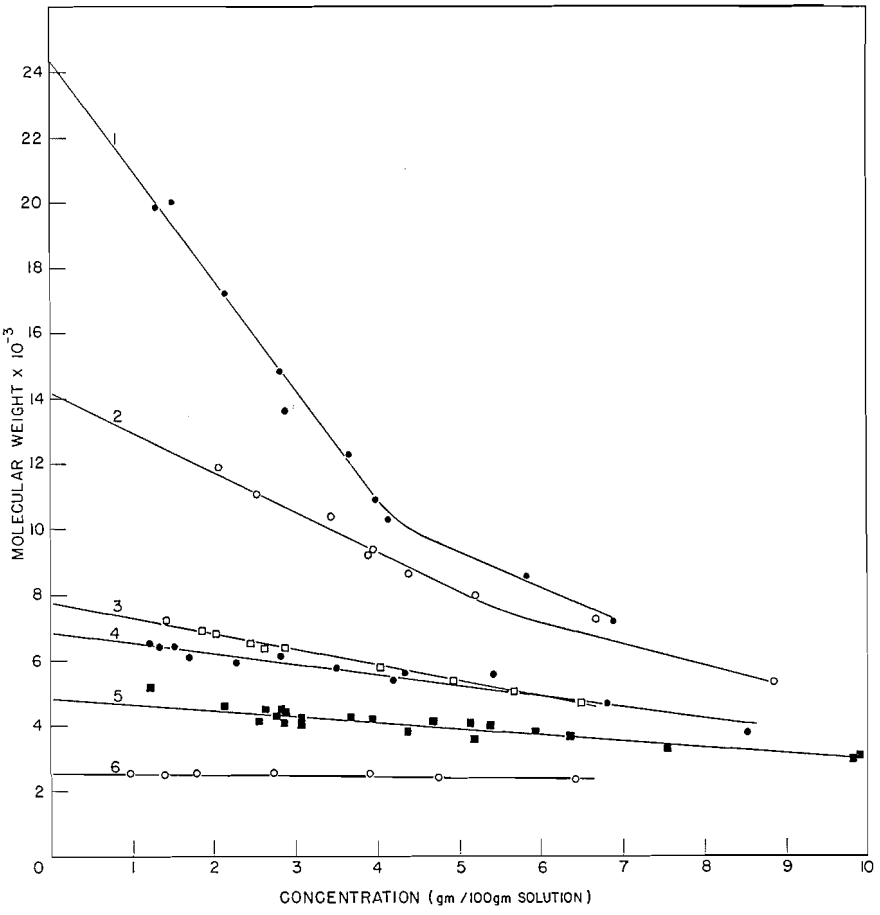

FIG. 1. Apparent molecular weight versus solute concentration for a series of polyethylene samples in toluene at 75° C. Curve 1, melt index 0.2; Curve 2, melt index 2; Curve 3, melt index 700; Curve 4, melt index 7000; Curve 5, melt index 20,000; Curve 6, melt index 200,000.

Kindly donated by Professor R. U. Lemieux, University of Ottawa, Ottawa.

Can. J. Chem. Downloaded from www.nrcresearchpress.com by 200.7.193.243 on 09/04/12
For personal use only.

Can. J. Chem. Downloaded from www.nrcresearchpress.com by 200.7.193.243 on 09/04/12
For personal use only.

RESULTS

The variation of apparent molecular weight with solution concentration for the series of polyethylenes is shown in Fig. 1. These values were calculated from Raoult's law. In estimating solution concentrations, corrections for the nonideality of the solvent vapor have been applied using Berthelot's equation of state and the critical data. However, without this correction, only a very small error is introduced in the molecular weight at infinite dilution. While it is evident that the apparent molecular weight of polyethylene samples having melt indexes of 0.2 and 2 is not a linear function of concentration over the whole range studied, a straight line fits the experimental points reasonably well at the lower concentrations. There is little evidence of curvature for all other samples and a straight line fits the experimental points over the whole concentration range covered. Similar behavior was observed for polyvinyl acetate in benzene at 55° C. (2).

The solute–solvent interaction coefficient, μ_1, of the system polyethylene–toluene was calculated from the well-known theoretical equation due to Huggins (12, 13) and Flory (14, 15)

$$\phi = (\ln a_1 - \ln V_1)/V_2 - 1 = \bar{V}_1/\bar{V}_2 + \mu_1 V_2,$$

where the symbols have their usual meaning.

The linear plots of ϕ vs. V_2 for the various polyethylene samples are shown in Fig. 2.

In calculating the solution concentration, it was assumed that the volumes of solute and solvent are additive (16) and the value for the density of ethylene polymer was taken as 0.92. The density of polyethylene in the molecular-weight range of 10,000 to 26,000 varies from 0.91 to 0.93 (17).

The molecular weights obtained from Raoult's law and those calculated from the

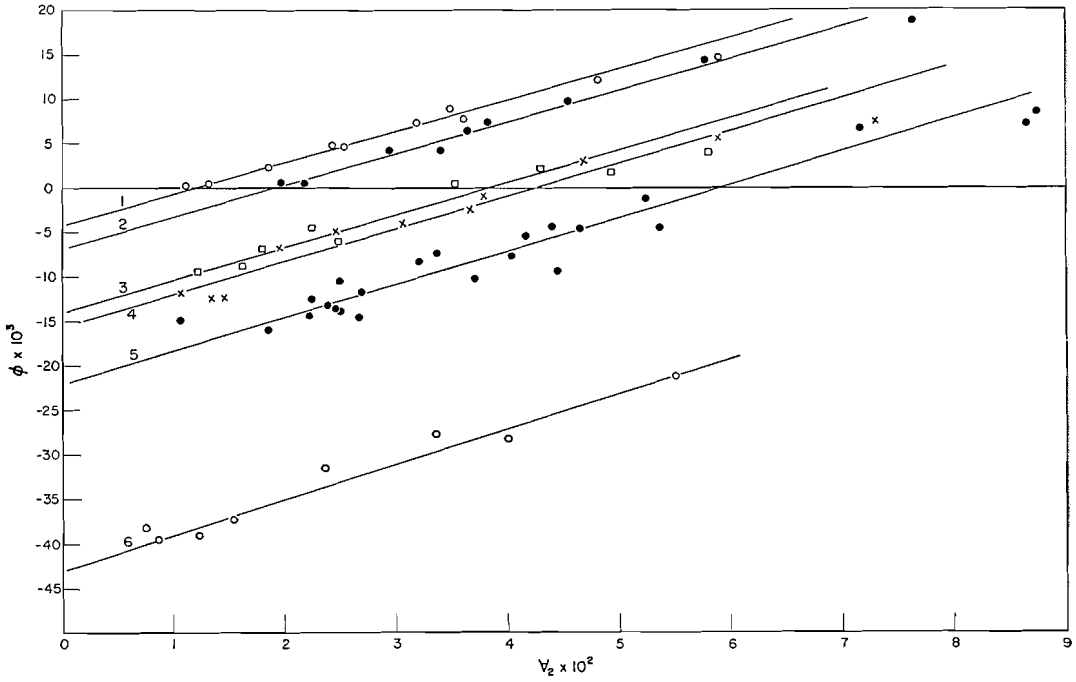

FIG. 2. ϕ vs. V_2 for a series of polyethylene samples in toluene at 75° C. Curve 1, melt index 0.2; Curve 2, melt index 2; Curve 3, melt index 700; Curve 4, melt index 7000; Curve 5, melt index 20,000; Curve 6, melt index 200,000.

Huggins–Flory equation, and values of μ_1, are shown in Table I. Also included are values obtained for the same samples in another laboratory with an ebulliometric procedure. While probably not strictly comparable some literature values of $\bar{M}_n$ are included for polyethylene of similar melt viscosity.

TABLE I

NUMBER-AVERAGE MOLECULAR WEIGHTS FOR A SERIES OF POLYETHYLENE POLYMERS

	Molecular weight				
Melt index	Raoult's law	Huggins–Flory	Ebulliometric	Literature values	μ_1
200,000	2550	2420	2500	1700[a]	0.40
20,000	4800	4720	4700	4000[a]	0.38
7,000	6850	6700	7100	5300[a]	0.37
700	7750	7410	6950	—	0.37
2	14150	14820	10400	32000[b]	0.36
				25000[c]	
				17900[d]	
0.2	24350	24420	18450		0.36

[a]*Harris (18), ebulliometric.*
[b]*Harris, osmometric.*
[c]*Smith (9), osmometric.*
[d]*Smith, ebulliometric.*

The results of the molecular-weight determinations for some other organic substances are shown in Fig. 3. Curves 1 and 2 were obtained for a sample of commercial carbowax.

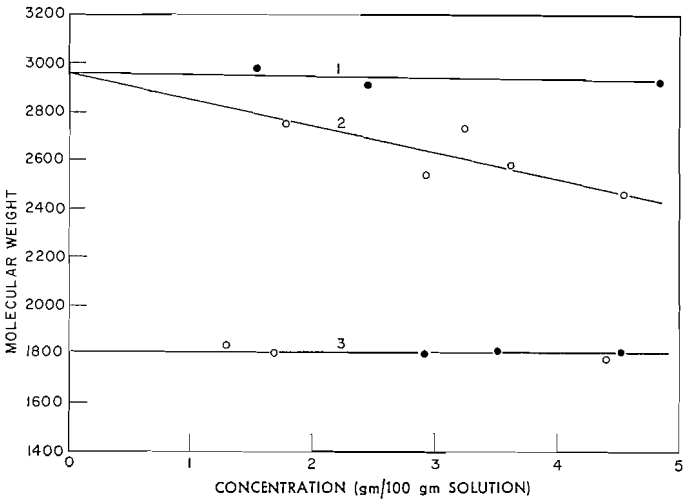

FIG. 3. Apparent molecular weight vs. solute concentration for a sample of carbowax and sucrose myristate. Curve 1, first measurements on carbowax; Curve 2, normal measurements; Curve 3, sucrose myristate (open circle, in toluene at 75° C.; closed circle, in benzene at 42.5° C.).

The first determinations were found to be independent of concentration; subsequent determinations were characterized by Curve 2. While the reason for this behavior is not too clear, the phenomenon has been observed previously with some samples of polyvinyl acetate and may be due to a slight amount of residual moisture trapped in the polymer and slightly reducing its solubility, causing the initial solutions to behave like an "ideal"

Can. J. Chem. Downloaded from www.nrcresearchpress.com by 200.7.193.243 on 09/04/12
For personal use only.

system. The molecular weight at infinite dilution was virtually identical for both curves, however. Curve 3 was obtained for a sample of sucrose myristate in benzene at 42.5° C. and in toluene at 75° C. A summary of the results for carbowax and sucrose myristate using the vapor-pressure lowering technique compared to other methods is given in Table II.

TABLE II

MOLECULAR WEIGHT OF CARBOWAX AND SUCROSE MYRISTATE OBTAINED BY DIFFERENTIAL MANOMETRY AND BY OTHER METHODS

Solute	Solvent	Mol. wt.	Method
Carbowax	Benzene	2960	Vapor pressure
Carbowax		2975	End-group analysis
Sucrose myristate	Benzene	1813	Vapor pressure
Sucrose myristate	Toluene	1813	Vapor pressure
Sucrose myristate	Benzene	1820	Cryoscopic

DISCUSSION

The similarity in the $\bar{M}_n$ values obtained when the results of cryoscopic and end-group analysis are compared to the vapor-pressure procedure lends support to the confidence that may be placed in that method. Unfortunately molecular weights of about 3000 are approaching the maximum values with which the available facilities for the former two methods are useful and it was not possible to extend the comparison.

Table I indicates satisfactory agreement between the two methods of treating the vapor-pressure data. The value of μ_1 found in this work is close to the value of 0.42 previously reported for polyethylene of melt index 200,000 in benzene at 80° C. (18). Values of 0.29 and 0.31 found for polyethylene samples having melt indexes of 20,000 and 7000 respectively in toluene at 110° C. (18) differ from the values obtained here in the expected direction when the temperature difference at which the measurements were made is considered. In contrast to the behavior of other polymers (2, 3, 13) there was virtually no dependence of the numerical value of μ_1 on molecular weight. This observation agrees with the findings of Muthana and Mark (17) and of Harris (18).

Differences between $\bar{M}_n$ values found here and those reported in the literature for polyethylene of similar melt index are not excessive in view of the variations noted recently in results obtained when the same sample of polymer is examined by different methods, and the large increase in $\bar{M}_n$ caused by the selective removal of about 1% of the sample (8).

No particular difficulty was found in the operation of the vapor-pressure apparatus at 75° C. Vapor-pressure differences normally become constant sufficiently quickly to allow check readings on the manometer at 60–90-minute intervals. It might be anticipated that volatility of mercury could become troublesome, however, if the operating temperature were raised too much higher. High-temperature operation might necessitate substitution of the mercury manometer with some form of diaphragm gauge and the cutoffs with valves. Under the present system of operation the limit on the precision of the measurement appeared to be controlled by variation in ΔP rather than by the ability of the manometer to measure these differences accurately.

The agreement between the results of the vapor-pressure and the ebulliometric procedures is excellent for the lower-molecular-weight polymers. Since several unrecorded measurements at 85° C. indicated the same molecular weight as shown for the sample of melt index 2 at 75° C., the discrepancy in the results of the two methods for the

Can. J. Chem. Downloaded from www.nrcresearchpress.com by 200.7.193.243 on 09/04/12
For personal use only.

higher-molecular-weight polymers does not appear to be due to incomplete solubility of the polymer at 75°. It may, however, be related to possible surface activity of these samples in the solvents used.

With the exception of the Huggins treatment shown in Fig. 2, the more conventional methods of presenting the experimental data offered little improvement in linearity of the curves obtained, over the plot of apparent molecular weight vs. concentration, and the simpler procedure was therefore used. It seems probable, however, that the molecular weights shown at infinite dilution may be slightly low because the linear extrapolation actually employed may not be entirely justified.

ACKNOWLEDGMENT

We are deeply indebted to Dr. W. R. Blackmore, Canadian Industries Limited, for the ebulliometric results included in Table I.

REFERENCES

1. SIRIANNI, A. F. and PUDDINGTON, I. E. Can. J. Chem. **33,** 755 (1955).
2. SIRIANNI, A. F., TREMBLAY, R., and PUDDINGTON, I. E. Can. J. Chem. **36,** 543 (1958).
3. COTTEN, G. R., SIRIANNI, A. F., and PUDDINGTON, I. E. J. Polymer Sci. (In press).
4. KOBAYACHI, T., CHITALE, A., and FRANK, H. P. J. Polymer Sci. **24,** 156 (1957).
5. MOORE, L. D., JR. J. Polymer Sci. **20,** 127 (1956).
6. NICHOLAS, L. Compt. rend. **244,** 80 (1957).
7. BILLMEYER, F. W., JR. J. Am. Chem. Soc. **75,** 6118 (1953).
8. ASHBY, C. E., REITENOUR, J. S., and HAMMER, C. F. J. Am. Chem. Soc. **79,** 5086 (1957).
9. SMITH, H. Trans. Faraday Soc. **52,** 402 (1956).
10. RICHARDS, R. D. Trans. Faraday Soc. **42,** 10 (1946).
11. RICHARDS, R. D. Trans. Faraday Soc. **42,** 17 (1946).
12. HUGGINS, M. L. Ann. N. Y. Acad. Sci. **43,** 1 (1942).
13. HUGGINS, M. L. Ind. Eng. Chem. **35,** 980 (1943).
14. FLORY, P. J. J. Chem. Phys. **9,** 660 (1941).
15. FLORY, P. J. J. Chem. Phys. **60,** 52 (1942).
16. BAWN, C. E. H., FREEMAN, R. E. J., and KAMALIDDIN, A. R. Trans. Faraday Soc. **46,** 677 (1950).
17. MUTHANA, M. S. and MARK, H. J. Polymer Sci. **4,** 527 (1949).
18. HARRIS, I. J. Polymer Sci. **8,** 353 (1952).

Can. J. Chem. Downloaded from www.nrcresearchpress.com by 200.7.193.243 on 09/04/12
For personal use only.

Can. J. Chem. Downloaded from www.nrcresearchpress.com by 200.7.193.243 on 09/04/12
For personal use only.

REACTOR NEUTRON-CAPTURE CROSS SECTION OF 18-MINUTE Rb^{88} [1]

J. C. Roy, P. J. Berry,[2] and L. P. Roy

ABSTRACT

The reactor neutron-capture cross section of 18-minute Rb^{88} has been determined by an activation method. The yield of Rb^{89} formed by successive neutron capture in Rb^{87} was determined by counting the beta rays emitted by its daughter, 51-day Sr^{89}. In these experiments Sr^{89} is also produced by the $Sr^{88}(n, \gamma)Sr^{89}$ reaction from the Sr^{88} contamination in the rubidium target and from Sr^{88} formed by the beta decay of Rb^{88}. Corrections for the contributions from these sources to the yield of Sr^{89} have been measured experimentally. The reactor neutron-capture cross section of Sr^{88} has been measured to be 5.8 mb. for the conditions of the experiment. Taking 0.12 ± 0.3 barn for the thermal cross section of Rb^{87}, the cross section of Rb^{88} was found to be 1.0 ± 0.3 barn for reactor neutrons.

INTRODUCTION

A measurement of the capture cross section of 18-minute Rb^{88} for reactor neutrons has been made using an activation method depending on successive neutron capture in Rb^{87}. Using the same technique Katcoff (1) set an upper limit of 200 barns for the thermal-neutron capture of Rb^{88}. With the advantage of much higher neutron flux than the one available to Katcoff, it has been possible to improve upon his measurement.

The following nuclear reactions occur when Rb^{87} is irradiated with neutrons:

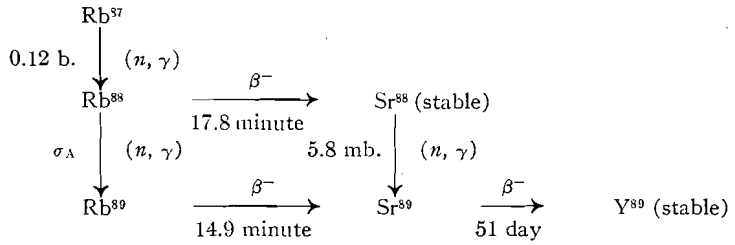

The cross section of Rb^{88} was determined by measuring the Sr^{89}, daughter of Rb^{89}, which is formed by successive neutron capture in Rb^{87}.

According to the reactions listed above three processes lead to the formation of Sr^{89}. First, Sr^{89} can be formed from strontium impurity by neutron capture in Sr^{88}. The contribution of this first-order reaction to the observed yield of Sr^{89} can be determined experimentally by irradiating a sample at a low neutron flux so that the successive neutron capture in Rb^{87} is negligible. Then the formation of Sr^{89} from Sr^{88} in the higher flux irradiations is calculated from the measured cross section of Sr^{88} using the following equation:

$$[1] \qquad N_1 = (N_K \sigma_K \phi / \lambda)(1 - e^{-\lambda t}),$$

where N_1 is the number of atoms of Sr^{89} at the end of the irradiation formed from strontium impurity,

[1]*Manuscript received January 7, 1958.*
Contribution from the Research Chemistry Branch, Atomic Energy of Canada Limited, Chalk River, Ontario. Issued as A.E.C.L. No. 564.
[2]*Present address: St. Augustine's Seminary, Toronto, Ontario.*

N_K is the number of atoms of Sr^{88} in the rubidium samples as determined by measurement at low neutron flux,
σ_K is the cross section of Sr^{88},
ϕ is the neutron flux,
t is the time of irradiation,
λ is the decay constant of Sr^{89}.

Secondly, Sr^{89} is formed by neutron capture in Sr^{88} formed by beta decay of Rb^{88} during the irradiation. The contribution of this process can be calculated using the following equation derived by Katcoff (2):

$$[2] \qquad N_2 = N_S\sigma_S\sigma_K\phi^2/\lambda^2\left[\lambda t-(1+T_A/T)(1-e^{-\lambda t})+\frac{T_A\lambda(e^{-\lambda_A t}-e^{-\lambda t})}{T(\lambda-\lambda_A)}\right],$$

where N_2 is the number of atoms of Sr^{89} at the end of the irradiation from Sr^{88} formed by beta decay of Rb^{88},
N_S is the number of atoms of Rb^{87} initially present,
σ_S is the neutron-capture cross section of Rb^{87}, taken to be 0.12 b. (3),
T_A is the half-life of Rb^{88}, taken to be 17.8 minutes (4),
T is the half-life of Sr^{89}, taken to be 51 days (5),
λ_A is the decay constant of Rb^{88}.
The other symbols have been defined under Eq. [1].

Thirdly, Sr^{89} is formed by the reaction under study: decay of Rb^{89} produced by successive neutron capture in Rb^{87}. The equation which describes this process is derived as follows: the time rate of change of Sr^{89}, dN_3/dt, is equal to its rate of production by beta decay from Rb^{89}, $\lambda_B N_B$, minus its natural disintegration rate, i.e.,

$$[3] \qquad dN_3/dt = \lambda_B N_B - \lambda N_3.$$

According to Ref. 2 N_B is given by:

$$[4] \qquad N_B = \frac{N_S\sigma_S\sigma_A\phi^2}{\lambda_A\lambda_B(\lambda_B-\lambda_A)}[\lambda_B(1-e^{-\lambda_A t})-\lambda_A(1-e^{-\lambda_B t})].$$

Substituting Eq. [4] in Eq. [3] and solving with $N_3 = 0$ at $t = 0$ gives:

$$[5] \qquad N_3 = \frac{N_S\sigma_S\sigma_A\phi^2}{\lambda_A(\lambda_B-\lambda_A)}\left[\frac{T(T_A-T_B)(1-e^{-\lambda t})}{T_AT_B}+\frac{T_AT(e^{-\lambda t}-e^{-\lambda_A t})}{T_B(T_A-T)}+\frac{T_BT(e^{-\lambda_B t}-e^{-\lambda t})}{T_A(T_B-T)}\right],$$

where N_3 is the number of atoms of Sr^{89} at the end of the irradiation, produced by decay of Rb^{89},
σ_A is the cross section to be measured,
T_B is the half-life of Rb^{89}, taken to be 14.9 minutes (6),
λ_B is the decay constant of Rb^{89}.
The other symbols have been defined under Eq. [1] and Eq. [2].

Equation [5] gives only the Sr^{89} present at the end of the irradiation. Another term should be added to take into account the formation of Sr^{89} from Rb^{89} by beta decay after the irradiation. This term is equal to N_B, the number of atoms of Rb^{89} present at the end of the irradiation, and is given by Eq. [4]. Therefore the Sr^{89} from beta decay of Rb^{89} is equal to N_3+N_B.

A re-evaluation of the neutron-capture cross section of Sr^{88} was made. A value of 5 ± 1 mb. has been reported by Seren *et al.* (7) for the thermal-neutron-capture cross

Can. J. Chem. Downloaded from www.nrcresearchpress.com by 200.7.193.243 on 09/04/12
For personal use only.

section of Sr^{88}, but considering the potential importance of the (n, γ) reaction on Sr^{88} in these experiments, this cross section was measured under conditions similar to those used in the measurement of the cross section of Rb^{88}.

A spectrographic analysis of the rubidium chloride showed that there was less than 0.02 p.p.m. of yttrium and zirconium. Therefore the formation of Sr^{89} by $Y^{89}(n, p)$ and $Zr^{92}(n, \alpha)$ processes on these two elements is ruled out.

EXPERIMENTAL

Samples of rubidium chloride were irradiated in the NRX reactor at Chalk River. The experimental conditions are given in Table I.

TABLE I

EXPERIMENTAL CONDITIONS USED FOR THE IRRADIATIONS

Experiment No.	RbCl irradiated (g.)	Irradiation time (hr.)	Neutron flux (n./cm.²/sec.)	Chemical yield (%)	Self-scattering* and self-absorption (%)
1	0.6375	16.5	6.57×10^{13}	77.0	+ 8.0
2	0.5922	16.3	6.37×10^{13}	84.2	+ 8.0
3	0.6366	16.5	6.64×10^{13}	40.2	+10.0
4	0.5528	108.8	7.83×10^{12}	53.6	+10.0
5	0.5298	109.8	3.25×10^{12}	67.9	+ 9.0

**The plus sign indicates that the net effect of self-scattering and self-absorption was an increase in the counting rate.*

The chemical purification was started about one month after the end of the irradiation. The rubidium samples were dissolved in 2–3 ml. of distilled water in the presence of 20 mg. of strontium carrier. Strontium nitrate was precipitated by addition of fuming nitric acid, centrifuged, washed with fuming nitric acid, and finally dissolved in a minimum amount of water in the presence of rubidium carrier. After this purification cycle was repeated four or five times, the strontium nitrate was dissolved in 6–8 ml. of water and several ferric hydroxide scavengings were made by addition of gaseous ammonia; the precipitates were discarded. The solution was then prepared for ion-exchange purification by precipitating strontium as carbonate. The precipitate was centrifuged and dissolved in the minimum amount of HCl, to which solution calcium and barium carriers and an equal volume of 1.5 *M* ammonium lactate were added. The solution was passed through Dowex-50 ion-exchange column using conditions similar to those described by Milton and Grummitt (8) for the separation of alkaline-earths using 1.5 *M* ammonium lactate as an eluant at pH 7. The strontium fraction was reduced in volume from 40 to 15 ml. and 2 ml. of 3 *N* sulphuric acid plus 2 ml. ethyl alcohol was added. This solution was allowed to stand overnight to let the strontium sulphate form and digest. The precipitate was centrifuged and washed with 1 ml. of water and ethyl alcohol. Finally it was transferred to a weighed aluminum counting tray, dried, weighed, and counted.

The disintegration rate of the strontium fraction was determined with an anthracene beta-counter having a window thickness of 2.16 mg./cm.² The counter was shielded with 4 inches of lead. The background was 9.7 c.p.m. and the variation during the interval over which the samples were counted was ±0.3 c.p.m. The counter efficiency was determined with a weightless source of P^{32}, mounted on an aluminum tray and prepared from a N.B.S. Standard. The efficiency found in this way was 32%. The

Can. J. Chem. Downloaded from www.nrcresearchpress.com by 200.7.193.243 on 09/04/12
For personal use only.

combined effects of self-scattering within the sources and self-absorption were determined in a separate experiment by the following method (9): To a thin layer of Sr^{89} activity, prepared by the $Sr^{88}(n, \gamma)Sr^{89}$ reaction, successive layers of inert strontium sulphate were added and the observed intensity was plotted against the weight of the inert material. The correction for self-scattering and self-absorption for a particular source thickness was then obtained from this curve after the amount of strontium sulphate present in each source was divided by two to take into account the homogeneous distribution of activity throughout the sources. The net effect was an increase in counting rates of about $9\pm3\%$.

RESULTS

Strontium-89 was identified by its maximum beta-ray energy and its decay period measured over two half-lives. The absorption curves in aluminum of the beta radiations of the activity found in experiments 1, 2, 3, and of Sr^{89}, prepared by (n, γ) reactions on strontium, were the same. A typical curve and the Sr^{89} standard curve are shown in Fig. 1. Fig. 2 shows the decay curves for the activities produced in two irradiations

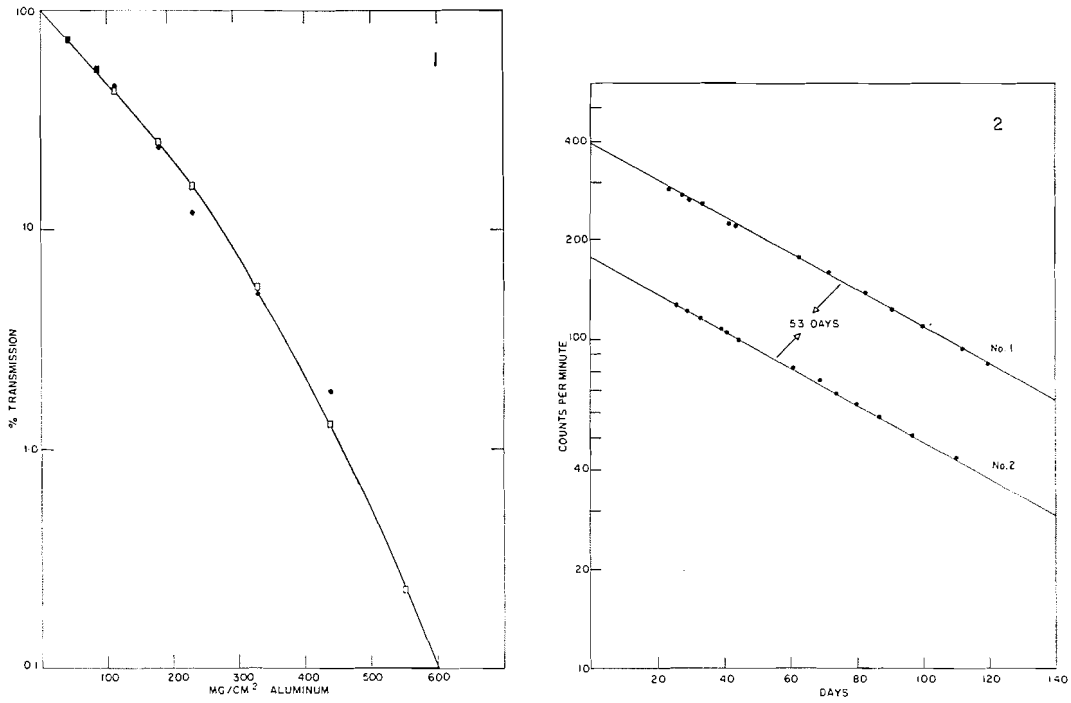

FIG. 1. Absorption curve of Sr^{89}; the circles are from the activity in the separated strontium, the squares are from a Sr^{89} standard prepared by a (n, γ) reaction in strontium.

FIG. 2. Decay curves of activities in experiments 1 and 2. The counting rates in experiment 1 have been multiplied by two.

done in a high neutron flux (expts. 1 and 2); the third one (expt. 3) is not included, because its decay has been measured for only 20 days. The measured value of the half-life in both experiments was 53 days, which, within the errors of the measurements, is in agreement with the value of 51 days for Sr^{89} (5). In experiments 4 and 5 done at low neutron flux a long-lived radioactive impurity amounting to 4 c.p.m. was found. After

Can. J. Chem. Downloaded from www.nrcresearchpress.com by 200.7.193.243 on 09/04/12
For personal use only.

this has been subtracted the remaining activity showed a 51-day half-life. This Sr^{89} activity arises mainly from neutron capture in Sr^{88} impurity present in the samples as described in the introduction.

The results are summarized in Table II. The observed counting rates were extrapolated to the end of the irradiation and absolute disintegration rates were obtained by making corrections for chemical yield, counting efficiency of the beta detector, and the combined effects of self-scattering and self-absorption within the sample.

TABLE II

NEUTRON-CAPTURE CROSS SECTION OF Rb^{88}

Experiment No.	Sr^{89} measured experimentally (dis./min.)	Sr^{89} due to Sr impurity λN_1 (dis./min.)	Sr^{89} calculated from Eq. 2 λN_2 (dis./min.)	Sr^{89} due to β decay of Rb^{89} $\lambda(N_3+N_B)$ (dis./min.)	σ_A Rb^{88} (barn)
4	209	156	23	30	
5	113	105	3	5	
1	724	320	40	364	0.96
2	608	286	34	288	0.88
3	787	323	41	423	1.1
				Average	0.98

The average value for the Sr^{88} present as an impurity in the irradiated rubidium was determined from experiments 4 and 5 to be $1.7\pm0.4\times10^{-6}$ part per atom of Rb^{87}. Its contribution to the formation of Sr^{89} was calculated using Eq. [1]. Likewise the contribution from neutron capture in Sr^{88}, formed by beta decay of Rb^{88} during the irradiation, was calculated using Eq. [2]. The contribution of these two processes, subtracted from the total activity measured in experiments 1, 2, and 3, gives the Sr^{89} formed by successive neutron capture in Rb^{87}.

The neutron flux in each experiment was determined by measuring the activity in a weighed piece of pure cobalt wire, 0.005 inch in diameter and 0.4 inch long, with an ionization chamber calibrated with standardized Co^{60} sources. A correction of 2.1% was applied to take into account the self-shielding of the cobalt wire (10). The reactor cross section of Co^{60} was calculated to be 36.6 barns, taking 36.0 ± 1.5 barns (3) for its thermal-neutron-capture cross section and 48.6 for its resonance integral (11). A value of 5.20 years (12) was taken for the half-life of Co^{60}.

By solving Eqs. [4] and [5] the cross section of Rb^{88} was obtained for each experiment and the results are given in Table II. The mean is 1.0 ± 0.25 barn. The limits of error of the measurements which contributed most to the quoted error are: $\pm20\%$ from the precision with which the amount of strontium impurity is known; $\pm7\%$ from the value of the neutron-capture cross section of Sr^{88}; $\pm8\%$ from the counting; and $\pm2\%$ for the neutron-flux determination. Combining these errors by the method of the square root of sum of squares type of addition, the resulting error in the mean value is ±0.25 barn. The assigned error of $\pm25\%$ in the value of the thermal-neutron cross section of Rb^{87} is not included in the error of the present measurement. The cross section refers to reactor spectrum neutrons, since no experiments were done to determine the epicadium contribution.

For the measurement of the neutron-capture cross section of Sr^{88} two weighed strontium carbonate samples were irradiated in two different neutron fluxes in the

Can. J. Chem. Downloaded from www.nrcresearchpress.com by 200.7.193.243 on 09/04/12
For personal use only.

NRX reactor. A few days after the end of the irradiation, the samples were dissolved in a minimum amount of dilute HCl and the volume made up to 10 ml. Weightless Sr^{89} sources were prepared for beta-counting by pipetting 50λ aliquots onto aluminum trays.

Counting and determination of the neutron flux were done by the technique described above. An absorption curve in aluminum showed the presence of a gamma component, due to 65-day Sr^{85}. This contribution amounted to 2.5% of the observed activity and was subtracted from it. Errors of 5% in the counting and of 2% in the neutron-flux determination were estimated.

The cross section was thus measured to be 5.8 ± 0.4 mb. for reactor neutrons; this is the average of the two, which agreed within 1%. Within the limits of errors quoted by Seren *et al.* (7), this value is in agreement with theirs.

REFERENCES

1. KATCOFF, S. National nuclear energy series. Div. IV, Vol. 9. McGraw-Hill Book Company, Inc., New York. 1951. Paper 222.
2. KATCOFF, S. National nuclear energy series. Div. IV, Vol. 9. McGraw-Hill Book Company, Inc., New York. 1951. Paper 220.
3. HUGHES, D. J. and HARVEY, J. A. Brookhaven Natl. Lab. Rept. BNL-325 (1955).
4. THULIN, S. Arkiv Fysik, **9**, 137 (1955).
5. KJELBERG, A. and PAPPAS, A. Nuclear Phys. **1**, 322 (1956).
6. O'KELLEY, G. D., LAZAR, N. H., and EICHLER, E. Phys. Rev. **102**, 223 (1956).
7. SEREN, L., FRIEDLANDER, H. N., and TURKEL, S. H. Phys. Rev. **72**, 888 (1947).
8. MILTON, G. M. and GRUMMITT, W. E. Can. J. Chem. **35**, 541 (1957).
9. KOHMAN, T. P. Anal. Chem. **21**, 352 (1949).
10. JERVIS, R. E. Atomic Energy of Canada Limited, Report CRDC-730 (1957).
11. MACKLIN, R. L. and POMERANCE, H. S. International conferences on the peaceful uses of atomic energy. Vol. 5. United Nations, New York. 1956. p. 96.
12. LOCKETT, E. E. and THOMAS, R. H. Nucleonics, **14** (No. 11), 127 (1956).

Can. J. Chem. Downloaded from www.nrcresearchpress.com by 200.7.193.243 on 09/04/12
For personal use only.

Can. J. Chem. Downloaded from www.nrcresearchpress.com by 200.7.193.243 on 09/04/12
For personal use only.

ALKYLGUANIDINE NITRATES AND ALKYLNITROGUANIDINES[1]

PAUL E. GAGNON, JEAN L. BOIVIN,[2] PAUL A. BOIVIN,[3] AND JOHN H. DICKSON[4]

ABSTRACT

The fusion of mixtures of alkylamine nitrates, $RR'NH.HNO_3$ ($R' = H$ when R = methyl, isopropyl, isobutyl, *n*-amyl, and phenyl, and $R' = C_2H_5$ when R = ethyl), and dicyandiamide, or calcium cyanamide, or calcium cyanamide and urea, yielded alkylguanidine nitrates. The latter were also obtained by heating solutions of alkylamine nitrates and calcium cyanamide. By treatment of the alkylguanidine nitrates with sulphuric acid, alkylnitroguanidines were prepared in good yields. A study of the effect of temperature on the yield of *n*-amyl and of time and temperature on the yields of methyl, isopropyl, and isobutyl nitroguanidine was made. The solubility of methyl, isopropyl, isobutyl, and *n*-amyl nitroguanidine in water and 10% and 20% sulphuric acid solutions at 0° C. was determined.

INTRODUCTION

Calculations based on the heat of combustion and on the empirical formula indicated that 1-methyl-3-nitroguanidine would be a more effective coolant than nitroguanidine in double base propellants. Since its density was satisfactory and it was relatively insoluble in the solvents and plasticizers used in propellant manufacture, further work was undertaken.

Davis (3) prepared alkylnitroguanidines by direct nitration of alkylguanidine sulphates in sulphuric acid and also by reacting nitroguanidine with alkylamines (2, 4). Yields were satisfactory but the preparation required nitroguanidine. McKay and Wright (6) improved this method by reacting alkylamine hydrochlorides with the potassium salt of nitroguanidine. The yield, however, did not exceed 70% based on nitroguanidine. When we consider that picrite is made in 55% yield from calcium cyanamide or 70% from dicyandiamide, the yield of alkylnitroguanidine could not be greater than 40–50%. Therefore other methods of producing this material should be considered. Methods described herein are based on calcium cyanamide, dicyandiamide, and alkylamine nitrates.

Werner and Bell (9) have stated that the fusion of dicyandiamide with alkylamine hydrochlorides gives a nearly quantitative yield of alkylguanidine hydrochlorides. This statement has been challenged by other investigators (7), who reported a yield in the order of 80%. Moreover, alkylguanidine hydrochlorides would not be of much value for the preparation of alkylnitroguanidine, since they would have to be converted into either the sulphate or the nitrate.

It was believed that methods employed to produce alkylguanidine nitrates from calcium cyanamide or dicyandiamide would give better yields if alkylamine nitrates were used in place of ammonium nitrate.

In the present work, alkylguanidine nitrates were synthesized from alkylamine nitrates and then converted into alkylnitroguanidines.

Alkylguanidine Nitrates

The alkylguanidine nitrates were synthesized by the fusion of alkylamine nitrates with

[1]*Manuscript received December 26, 1957.*
Contribution from the Department of Chemistry, Laval University, Quebec, Que., with financial assistance from the Defence Research Board of Canada. This paper constitutes part of a thesis submitted to the Graduate School, in partial fulfillment of the requirements for the degree of Doctor of Science.
[2]*Defence Research Board, C.A.R.D.E., Valcartier, Que.*
[3]*Assistant Professor of Biochemistry, Faculty of Medicine, Laval University, Quebec.*
[4]*Graduate student, holder of a Shell Oil Company of Canada Limited Scholarship in 1957–58, Laval University, Quebec.*

(*a*) dicyandiamide, (*b*) calcium cyanamide, and (*c*) calcium cyanamide and urea. They were also obtained by heating aqueous solutions of alkylamine nitrates and calcium cyanamide.

Alkylamine Nitrates and Dicyandiamide

The fusion of dicyandiamide with ammonium nitrate yielded guanidine nitrate. The reaction was mildly exothermic at 170° C. Similarly, when dicyandiamide and methylamine nitrate were fused together, an exothermic reaction took place at 170° C. but was less pronounced than in the previous case and was more easily controlled. Since alkylguanidine nitrates seemed stable in the fused state up to 190° C., when decomposition occurred, the reaction mixture, which became fluid at temperatures as low as 140° C., was maintained at a temperature of 170°–180° C. throughout the reaction.

By the reaction of 1 mole of dicyanamide (I) and 2 moles of alkylamine nitrate (II), 2 moles of alkylguanidine nitrate (III) were produced according to the following equation:

$$\underset{\text{I}}{\begin{matrix}\text{NH—CN}\\ |\\ \text{C=NH}\\ |\\ \text{NH}_2\end{matrix}} + \underset{\text{II}}{2\text{RR'NH.HNO}_3} = \underset{\text{III}}{\begin{matrix}\text{NR'R}\\ |\\ 2\text{C=NH}\\ |\\ \text{NH}_2\text{.HNO}_3\end{matrix}}$$

R′ = H when R = methyl, isopropyl, isobutyl, *n*-amyl, phenyl, and R′ = C_2H_5 when R = ethyl.

Alkylamine Nitrates and Calcium Cyanamide

The fusion of calcium cyanamide with ammonium nitrate has always been considered a hazardous process because of the high melting point of ammonium nitrate (170° C.) and its oxidizing properties when molten. However, when using alkylamine nitrates, which decomposed slightly at temperatures above 170° C., direct fusion of calcium cyanamide with alkylamine nitrates was considered practical.

By heating calcium cyanamide (55% pure) and alkylamine in a molar ratio of 1:3, alkylamines were evolved according to the following equation:

$$CaCN_2 + 3RR'NH.HNO_3 = RR'NC(NH)NH_2.HNO_3 + 2RR'NH + Ca(NO_3)_2.$$

Since calcium cyanamide contains approximately 20% of calcium oxide, more alkylamine was evolved:

$$CaO + 2RR'NH.HNO_3 = 2RR'NH + Ca(NO_3)_2 + H_2O.$$

An efficient recovery of the alkylamine evolved and of the unreacted alkylamine nitrate was necessary. Two methods were investigated in which calcium was discarded either as the carbonate or as the sulphate.

Calcium carbonate method.—By passing the alkylamine and carbon dioxide simultaneously into a solution of calcium nitrate at 60° C., precipitation of calcium carbonate commenced at pH 8.0. It was believed that calcium hydroxide was initially precipitated by alkylamine when pH 8.0 was reached:

$$Ca(NO_3)_2 + RR'NH = Ca(OH)_2 + RR'NH.HNO_3.$$

The carbon dioxide then reacted with calcium hydroxide:

$$CO_2 + Ca(OH)_2 = CaCO_3 + H_2O.$$

After the calcium carbonate was removed, the filtrate was evaporated to dryness, leaving alkylamine nitrate.

Can. J. Chem. Downloaded from www.nrcresearchpress.com by 200.7.193.243 on 09/04/12
For personal use only.

Calcium sulphate method.—This method consisted in the absorption of alkylamine in dilute sulphuric acid to form alkylamine sulphate. The solution was then added to the filtrate containing calcium nitrate. Calcium sulphate was precipitated and the filtrate evaporated to dryness to yield alkylamine nitrate according to the equation:

$$(RR'NH_2)_2SO_4 + Ca(NO_3)_2 = 2RR'NH.HNO_3 + CaSO_4.$$

Alkylamine Nitrates, Calcium Cyanamide, and Urea

Urea was used successfully in the Wright (fusion) process (5, 10), where it acted as a melting-point depressant for ammonium nitrate. When urea was added to alkylamine nitrates, fusion could be carried out effectively with calcium cyanamide at 90° C.

Alkylamine Nitrates, Calcium Cyanamide, and Water

The process patented by Burns, Gay, and I.C.I. (1) makes use of an aqueous solution of ammonium nitrate and calcium cyanamide to produce guanidine nitrate. It was considered of interest to react alkylamine nitrates and calcium cyanamide in a similar manner. By heating aqueous solutions of alkylamine nitrates and calcium cyanamide, alkylamines were evolved as before but the yields of alkylguanidine nitrates, with the exception of phenylguanidine nitrate, were lower.

Alkylnitroguanidines

Alkylnitroguanidines, $RR'NC(NH)NHNO_2$, were prepared by treatment of alkylguanidine nitrates, $RR'NC(NH)NH_2.HNO_3$, with sulphuric acid. This reaction was believed to be a dehydration process in which 1 mole of water was removed from the alkylguanidine nitrate by sulphuric acid to form a hydrate or 85% sulphuric acid. However, in the case of nitroguanidine, it was found that the guanidine nitrate – sulphuric acid mixture is a nitrating mixture in which NO_2^+ ions are present (8). A similar mechanism is probably responsible for the formation of alkylnitroguanidine from alkylguanidine nitrate.

Of the six alkylguanidine nitrates studied, the phenyl- and diethyl-nitroguanidines could not be isolated. In the case of the phenylguanidine nitrate, nitroguanidine itself was isolated.

Since these alkylnitroguanidines were crystallized from dilute sulphuric acid solutions, the solubilities of these compounds in water and 10% and 20% sulphuric acid solutions at 0° C. were determined and were found to decrease with the increasing molecular weight.

A number of experiments were performed in order to show the effects of time and temperature on the yields of methyl, isopropyl, and isobutyl nitroguanidine. When the reaction time was arbitrarily set at 21 minutes, the most efficient temperature was found to be between 0° and 5° C. as indicated in Table II. The nitration of methylguanidine nitrate was found to be almost instantaneous at 40° C. when the time was limited to 5 minutes. However, this was not true in the cases of isopropyl and isobutyl guanidine nitrate where the best yields were obtained at 0° C. with a reaction time of 5 to 15 minutes as shown in Table III.

The degrading effect of the temperature over a reaction period of 1 hour is shown in Fig. 1 where the maximum yield of 91% of *n*-amylnitroguanidine at 0° C. decreases to a yield of 15% at 30° C.

EXPERIMENTAL

Alkylamine Nitrates

Dilute nitric acid was treated with an excess of the alkylamine. The solution was

Can. J. Chem. Downloaded from www.nrcresearchpress.com by 200.7.193.243 on 09/04/12
For personal use only.

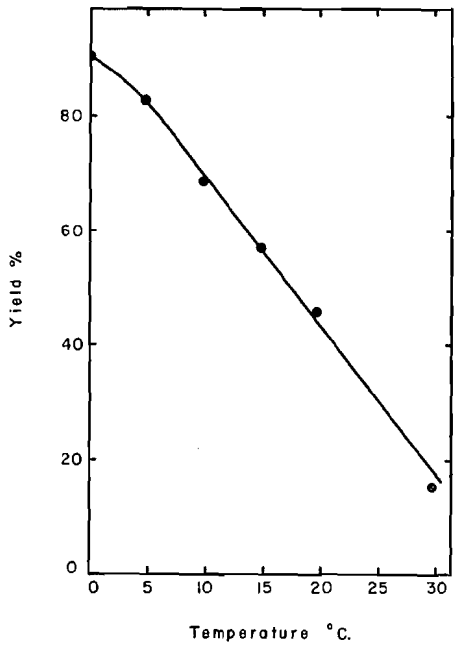

FIG. 1. Effect of temperature on the yield of *n*-amylnitroguanidine.

filtered and allowed to evaporate on a steam bath. In most cases the cooled product solidified.

Alkylguanidine Nitrates

The alkylguanidine nitrates were obtained by four different methods. The results in each case are given in Table I.

Alkylamine nitrates and dicyandiamide.—The alkylamine nitrate and dicyandiamide in a molar ratio of 2.1:1 were mixed together and heated on an oil bath. The fusion commenced at about 70° C. and the reaction mixture became clear at 135°–140° C. A temperature of 170°–180° C. was maintained for 3 hours. During this time a small amount of the alkylamine was evolved possibly owing to the decomposition of the slight excess of alkylamine nitrate employed. The reaction product, which solidified at about 35° C., was recrystallized from water.

Alkylamine nitrates and calcium cyanamide.—The alkylamine nitrate and calcium cyanamide in a molar ratio of 4:1 were mixed together and heated at 110° C. on an oil bath for 1 hour. Most of the alkylamine produced in the reaction was evolved during this time. About 40–50 ml. of hot distilled water was added to the flask and the mixture filtered while hot. In some cases more hot water was required. This necessitated the evaporation of the excess under vacuum. Finally when the solution was cooled to room temperature, the alkylguanidine crystallized, and it was recrystallized several times from water.

Alkylamine nitrates, calcium cyanamide, and urea.—The alkylamine nitrate, urea, and calcium cyanamide in a molar ratio of 4:3:1 were mixed together and heated at 90° C. for 1 hour. The alkylamine was evolved as before. The reaction products were treated with hot distilled water as described in the previous method.

Alkylamine nitrates, calcium cyanamide, and water.—An aqueous solution of alkylamine

Can. J. Chem. Downloaded from www.nrcresearchpress.com by 200.7.193.243 on 09/04/12
For personal use only.

TABLE I

ALKYLGUANIDINE NITRATES

Alkylguanidine nitrates $RR'NC(NH)NH_2.HNO_3$								
R	R′	Starting materials		M.p., °C.	Yield, %	Formula	Calc., % HNO_3	Found, % HNO_3
CH_3	H	$CH_3NH_2.HNO_3$	+ 1*	149–150	79	$C_2H_8O_3N_4$	46.3	46.1
			2		88			
			3		77			
			4		—			
C_3H_7	H	$C_3H_7NH_2.HNO_3$	+ 1	119–121	72	$C_4H_{12}O_3N_4$	38.4	38.0
			2		71			
			3		44			
			4		39			
C_4H_9	H	$C_4H_9NH_2.HNO_3$	+ 1	83–84	88	$C_5H_{14}O_3N_4$	35.4	35.3
			2		92			
			3		56			
			4		43			
C_5H_{11}	H	$C_5H_{11}NH_2.HNO_3$	+ 1	71–72	71	$C_6H_{16}O_3N_4$	32.8	32.5
			2		70			
			3		43			
			4		36			
C_6H_5	H	$C_6H_5NH_2.HNO_3$	+ 1	125–126	47	$C_7H_{10}O_3N_4$	31.8	31.7
			2		63			
			3		75			
			4		73			
C_2H_5	C_2H_5	$(C_2H_5)_2NH.HNO_3$	+ 1	170–171	65	$C_5H_{14}O_3N_4$	35.4	35.0
			2		68			
			3		41			
			4		39			

*1 = $NH_2C(NH)NH.CN$; 2 = $CaCN_2$; 3 = $CaCN_2 + CO(NH_2)_2$; 4 = $CaCN_2 + H_2O$.

TABLE II

EFFECT OF TEMPERATURE ON THE YIELDS

Temp., °C.	Starting material	Yield	
		Crude, g.	Corrected, %
0	$CH_3NHC(NH)NH_2.HNO$ (13.6 g.) and 98% H_2SO_4 (40.8 g.)	8.5	94
5		9.2	100
15		8.9	97
30		8.3	92
0	$C_3H_7NHC(NH)NH_2.HNO_3$ (5 g.) and 98% H_2SO_4 (26.0 g.)	3.3	90
5		3.2	88
10		2.9	81
25		2.9	81
0	$C_4H_9NHC(NH)NH_2.HNO_3$ (5 g.) and 98% H_2SO_4 (26.0 g.)	3.1	82
5		2.7	73
10		2.6	69
30		2.1	58

nitrate (0.29 mole) in 100 ml. of water was heated until it reached a boiling point of 100° C. Calcium cyanamide (0.07 mole) was added slowly with stirring and the reaction was continued until there was no further evolution of the alkylamine. The mixture was filtered while hot and the alkylguanidine nitrate crystallized from the cooled filtrate.

Alkylnitroguanidines

Sulphuric acid (98%) was cooled to 0° C. and alkylguanidine nitrate was added slowly

Can. J. Chem. Downloaded from www.nrcresearchpress.com by 200.7.193.243 on 09/04/12
For personal use only.

Can. J. Chem. Downloaded from www.nrcresearchpress.com by 200.7.193.243 on 09/04/12
For personal use only.

TABLE III

EFFECT OF THE REACTION TIME ON THE YIELDS

Reaction temp., °C.	Time, min.			Yield		Reaction temp., °C.	Time, min.			Yield	
	Addition	Stirring	Reaction	Crude, g.	Corrected, %		Addition	Stirring	Reaction	Crude, g.	Corrected, %
$CH_3NHC(NH)HN_2.HNO_3$ (13.6 g.) and 98% H_2SO_4 (40.8 g.)						$C_3H_7NHC(NH)NH_2.HNO_3$ (5 g.) and 98% H_2SO_4 (26 g.)					
40	2.5	0.0	1.25	8.7	96	25	2.0	15.2	16.1	3.0	83
40	2.0	4.0	5.0	9.2	100	25	2.0	25.0	26.0	2.8	79
40	2.0	10.0	11.0	8.2	92						
40	2.0	20.0	21.0	7.6	86	$C_4H_9NHC(NH)NH_2.HNO_3$ (5 g.) and 98% H_2SO_4 (26 g.)					
$C_3H_7NHC(NH)NH_2.HNO_3$ (5 g.) and 98% H_2SO_4 (26 g.)						0	2.0	0.0	1.0	2.3	65
0	2.0	1.0	1.5	1.3	45	0	2.0	5.0	6.0	2.6	71
0	2.0	5.0	6.0	3.3	90	0	2.0	10.0	11.0	3.6	84
0	2.0	10.2	11.2	3.3	90	0	2.0	14.9	16.0	3.4	89
0	2.0	15.1	16.1	3.3	90	0	2.1	24.9	25.9	3.3	87
0	2.0	25.4	26.4	3.3	90	5	2.5	0.0	1.3	2.5	67
5	2.0	0.0	1.0	2.9	81	5	2.0	5.2	6.2	2.6	71
5	2.0	5.0	6.0	2.8	79	5	2.0	10.0	11.0	2.6	71
5	2.0	10.0	11.0	2.9	81	5	1.9	15.3	16.2	2.6	71
5	2.0	15.0	16.0	3.2	88	5	2.1	25.0	26.0	2.6	71
5	2.0	25.0	26.0	2.9	81	10	2.0	0.0	1.0	2.5	67
10	2.0	0.0	1.0	3.0	79	10	2.0	5.1	6.1	3.2	82
10	2.0	5.0	6.0	2.8	79	10	2.1	10.0	11.0	3.2	82
10	2.0	10.0	11.0	2.8	79	10	2.2	16.1	17.2	3.2	82
10	2.2	15.0	16.1	2.8	79	10	2.1	25.0	26.0	2.7	71
10	2.0	25.0	26.0	2.7	77	20	2.1	0.0	1.0	2.0	56
15	2.0	0.0	1.0	2.5	72	20	2.0	5.7	6.7	2.4	64
15	2.0	5.0	6.0	2.8	79	20	2.0	10.0	11.0	2.2	60
15	2.0	10.0	11.0	2.5	72	20	1.9	15.1	16.1	2.1	58
15	2.0	15.0	16.0	2.5	72	20	2.0	25.0	26.0	2.1	58
15	2.0	25.0	26.0	2.3	67	30	2.3	0.0	1.2	2.2	62
25	2.0	0.0	1.0	2.4	70	30	1.9	5.1	6.1	2.1	58
25	2.0	5.0	6.0	3.1	88	30	2.0	10.1	11.1	1.9	56
25	2.0	10.0	11.0	3.1	85	30	2.0	15.0	16.0	2.3	64
						30	2.1	25.0	26.0	2.1	58

with stirring and cooling. After all the solid material had been added, the mixture was stirred at this temperature for 21 minutes and then poured over cracked ice. A white solid precipitated out of the diluted acid solution and was recrystallized from water. The crude yields and the yields corrected for solubility are given in Table II in grams and per cent respectively for methyl, isopropyl, and isobutyl nitroguanidine. When *n*-amylguanidine nitrate was used, the reaction time was arbitrarily set at 1 hour. The results obtained are shown in Fig. 1.

Studies were also made of the effect of the reaction time on the yields of methyl, isopropyl, and isobutyl nitroguanidines at various temperatures. The reaction time was taken as half of the addition time plus the stirring time. The results are given in Table III.

Solubility Determinations

An accurately weighed quantity of the alkylnitroguanidine was added to 50 ml. of distilled water. The solution was cooled to 0° C. and maintained at this temperature for 24 hours. After it had been filtered on a sintered glass crucible, the residue was dried over calcium chloride in a vacuum disiccator for 8 days. The weight of the insoluble material remaining as residue was subtracted from the original weight and the solubility was calculated.

The same procedure was used to determine the solubility of the alkylnitroguanidine in 10% and 20% sulphuric acid solutions. In these cases the residue was washed with a saturated solution of the alkylnitroguanidine after filtration.

The solubilities in grams at 0° C. in 100 g. of water and 10% and 20% sulphuric acid solutions for the different nitroguanidines were, respectively:

methyl —0.704, 0.977, and 1.29; isopropyl—0.502, 0.528, and 1.70;
isobutyl—0.483, 0.528, and 1.70; *n*-amyl—0.128, 0.110, and 0.13.

REFERENCES

1. Burns, R., Gay, P. F., and Imperial Chemical Industries Ltd. Brit. Patent No. 507,498 (1939).
2. Davis, T. L. and Abrams, A. J. J. Proc. Am. Acad. Arts Sci. **61**, 437 (1926).
3. Davis, T. L. and Elderfield, R. C. J. Am. Chem. Soc. **55**, 731 (1933).
4. Davis, T. L. and Luce, S. B. J. Am Chem. Soc. **49**, 2303 (1927).
5. Herring, K. F., Toombs, L. E., Stuart, R. S., and Wright, G. F. Ind. Eng. Chem. **38**, 1318 (1946).
6. McKay, A. F. and Wright, G. F. J. Am. Chem. Soc. **69**, 3028 (1947).
7. Philippi, E. and Morsch, K. Ber. **60B**, 2120 (1927).
8. Simkins, R. J. J. and Williams, G. J. Chem. Soc. 3086 (1952).
9. Werner, E. A. and Bell, J. J. Chem. Soc. **121**, 1790 (1922).
10. Wright, G. F. U.S. Patent No. 2,431,301 (1947).

Can. J. Chem. Downloaded from www.nrcresearchpress.com by 200.7.193.243 on 09/04/12
For personal use only.

Can. J. Chem. Downloaded from www.nrcresearchpress.com by 200.7.193.243 on 09/04/12
For personal use only.

ELECTROLYTIC CONDUCTANCE IN HYDROGEN PEROXIDE – WATER MIXTURES

PART II. SOME MONOBASIC AND DIBASIC ACIDS[1]

D. K. THOMAS[2] AND O. MAASS

ABSTRACT

Measurements of the equivalent conductance of sulphuric, nitric, and hydrofluoric acids were made in water – hydrogen peroxide mixtures by means of a direct-current method. It was found that in solvents containing a high percentage of hydrogen peroxide the conductivities of these acids were extremely low, and it is proposed that this results from a marked decrease in their degrees of dissociation. This proposal is supported by similar measurements made on the system water – strong acid – weak acid.

INTRODUCTION

As stated in a previous communication (1), measurements of the conductance of acids such as sulphuric and nitric in hydrogen peroxide – water mixtures (2) show that their values are considerably lower than those in aqueous solution. When the composition of the solvent is of the order of 90% to 100% hydrogen peroxide, Shanley *et al.* (2) found that when the composition of the solvent is of the order of 99% to 100% H_2O_2, sulphuric acid possesses a lower conductance than its potassium salt. They regarded the reduced conductance of the acid as being due partly to a decrease in the second dissociation step of HSO_4^- to H^+ and $SO_4^=$. The further suggestion was made that the solvated proton $H^+.H_2O_2$ showed a chain conductance in anhydrous hydrogen peroxide which was greatly reduced in the presence of water.

In the present work three acids, namely sulphuric, nitric, and hydrofluoric, have been studied at a few temperatures in solvents of composition ranging from 0 to 98 weight % of hydrogen peroxide.

EXPERIMENTAL PROCEDURE

The conductance measurements were carried out in exactly the same way as those in Part I; for the measurements on solutions of hydrofluoric acid a specially constructed Teflon cell was employed. The tin probe electrodes and current-carrying electrodes were found to be suitable for use in solutions of the concentration encountered in this work. As before, all solutions were made up by weight from the pure constituents and measurements were made with the cell immersed in a thermostat controlled to $\pm 0.01°$ C.

MATERIALS

(*i*) *Hydrogen peroxide.*—Becco chemicals 98% hydrogen peroxide was used throughout, and dilution was carried out with water of specific conductance 1.5×10^{-6}.

(*ii*) *Acids.*—The sulphuric, nitric, and hydrofluoric acids employed were all of analytical grade, the amount of metallic and other impurity being less than 0.0001%.

RESULTS

The results for the three systems studied are shown in Table I A (sulphuric acid), B (nitric acid), and C (hydrofluoric acid). The extrapolated values of Λ_0 are also given. In Fig. 1 the data of Shanley *et al.* (2) (called Becco a-c. results on the figure) for the

[1]*Manuscript received December 4, 1957.*
Contribution from the Division of Pure Chemistry, National Research Council, Ottawa, Canada.
Issued as N.R.C. No. 4675.
[2]*N.R.C. Postdoctorate Fellow 1956–57.*

TABLE I

VALUES OF Λ FOR THREE SYSTEMS AT 25°, 16°, 10° C. AND 0, 31, 78, 98 WT. % H_2O_2

	25° C.				16° C.				10° C.			
$C^{\frac{1}{2}}$	0	31	78	98	0	31	78	98	0	31	78	98
					A. System H_2SO_4–H_2O_2–H_2O							
0.020	414.8	246.0	103.0	42.0	—	207.0	94.2	37.0	—	186.0	82.0	34.5
0.050	385.0	233.0	93.0	41.2	—	198.7	86.6	35.8	—	180.0	77.5	34.0
0.075	360.2	221.2	85.6	40.5	—	191.6	80.6	35.0	—	174.0	73.0	32.7
0.100	338.4	210.0	79.8	40.0	—	184.5	75.0	34.6	—	168.5	68.5	32.0
0.150	301.2	191.0	71.7	38.4	—	170.5	63.0	33.8	—	158.0	59.6	30.0
0.200	272.0	178.0	65.0	37.0	—	156.0	—	33.0	—	146.0	51.0	29.0
Λ_0	434.2	256.0	109.6	42.5	375.0	213.0	98.7	38.2	338.0	191.0	86.0	36.0
					B. System HNO_3–H_2O_2–H_2O							
0.020	416.0	243.0	104.0	58.0	—	207.2	91.0	52.6	—	184.5	82.5	50.0
0.050	412.0	241.0	103.0	52.0	—	205.0	89.5	47.5	—	183.5	81.5	45.0
0.075	409.0	239.0	102.0	47.0	—	203.0	88.5	43.0	—	182.2	80.5	40.5
0.100	405.0	237.0	101.3	42.0	—	201.0	87.2	38.8	—	181.2	79.8	36.0
0.150	399.0	233.2	100.0	32.0	—	197.0	85.0	30.0	—	179.0	78.0	27.2
0.200	393.0	230.0	98.0	23.0	—	—	83.0	20.6	—	177.0	76.0	19.0
Λ_0	418.5	244.0	105.0	62.0	362.0	209.0	92.0	56.0	326.0	185.0	83.0	54.0
					C. System HF–H_2O_2–H_2O							
0.05	137.0	111.0	21.0	4.5					109.0	77.0	20.0	3.5
0.10	93.0	65.0	17.3	1.8					85.0	55.5	14.0	1.2
0.20	57.0	36.5	14.5	1.4					54.0	33.8	8.8	1.0
0.30	40.0	29.0	13.0	1.1					38.7	24.2	7.4	1.0
0.40	31.0	24.0	11.5	1.0					30.0	19.5	6.5	0.8
0.50	28.0	22.0	11.0	0.7					25.0	16.3	6.2	0.4

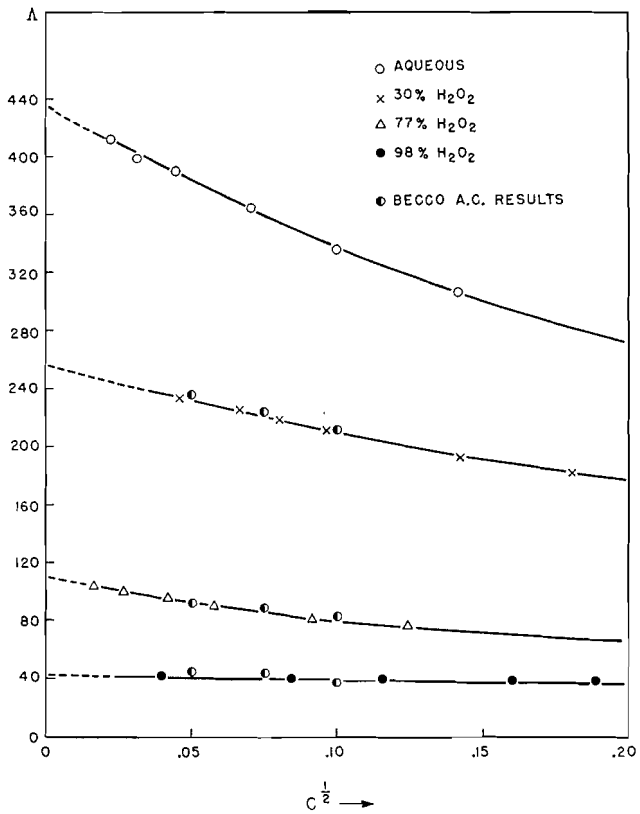

FIG. 1.

Can. J. Chem. Downloaded from www.nrcresearchpress.com by 200.7.193.243 on 09/04/12
For personal use only.

system H_2SO_4–H_2O–H_2O_2 are plotted together with the results of the present work on the same system, and this serves to demonstrate the measure of agreement attainable between the two experimental techniques.

DISCUSSION

It is of interest to record the variation in conductivity with temperature in H_2O_2–H_2O–electrolyte systems. In Table II are given such data using the relationship $\Lambda T_0 = \Lambda_{25}[1+x(T-25)]$.

TABLE II

VARIATION IN Λ WITH TEMPERATURE OVER THE RANGE 10° C. TO 25° C.

Wt. % H_2O_2	HNO_3	H_2SO_4
0	0.0145	0.0150
31	0.0161	0.0169
78	0.0134	0.0144
98	0.0086	0.0063

In Table I A, B, and C the solute concentration (C) is expressed in g-equiv. per liter, and the values quoted are equivalent conductances corrected for the solvent conductance.

The results presented in Table I A, B, and C possess one feature in common, namely that an increase in the weight % of hydrogen peroxide greatly reduces the equivalent conductance of the system H_2O–acid–H_2O_2, and in the case of almost anhydrous hydrogen peroxide the conductance has a value which is an order of magnitude less than that in aqueous solution.

Now the exceptional mobility of the proton in aqueous solution is attributed to a special mechanism of transport known as 'chain conductance'. This is made possible by the nature of the solvent itself, and requires that (*a*) the solvent molecules should possess an affinity for protons and (*b*) they should form a three-dimensional hydrogen-bonded network in the liquid state. In general, therefore, we should expect hydroxylic solvents such as the alcohols, glycols, and hydrogen peroxide to be able to sustain this 'chain conductance' process.

In the liquid state it is certain that hydrogen peroxide and water have very similar structures, both being highly associated through intermolecular hydrogen-bonding. The magnitude of the frequency shifts (3) observed in the infrared absorption spectra of the two compounds suggests that the hydrogen bond formed in hydrogen peroxide is somewhat stronger than that formed in water. Furthermore, evidence from a number of properties such as heat of mixing (4), vapor pressure (5), density (6, 7), viscosity (8, 9), and dielectric constant (10) indicates that the number, or force, of attractions increases upon the addition of the former to the latter. In other words, hydrogen bonds between water and hydrogen peroxide molecules are more stable than those between molecules of the pure substances. Thus hydrogen peroxide, which is capable of participating in twice as many intermolecular hydrogen bonds as is water, would have the effect of 'tightening' the structure of the latter, and one might anticipate that the proton mobility in H_2O–H_2O_2 mixtures would be as great as that in pure water. The fact that this supposition is so greatly at variance with the experimental results may be due to two things:

Can. J. Chem. Downloaded from www.nrcresearchpress.com by 200.7.193.243 on 09/04/12
For personal use only.

(*a*) the chain-conductance process is no longer occurring in anhydrous hydrogen peroxide and addition of peroxide to the water–acid system brings about a gradual breakdown in this process, and/or

(*b*) the number of ions present in the solution is greatly decreased as the result of a reduction in the degree of dissociation of the acid.

In view of the similarity which has been established between the liquid structures of pure water, pure hydrogen peroxide, and mixtures of the two, suggestion (*a*) above is hardly likely to be true, and an explanation of the experimental results must be sought principally in terms of effect (*b*).

The extent to which an acid will dissociate in solution is determined by the basic nature of the solvent and its dielectric properties. Referring again to pure water and almost anhydrous hydrogen peroxide, we find that the difference in dielectric constant is small but that there is an appreciable difference in their relative acidities. Measurements of the pH of mixtures of H_2O–H_2O_2 have been made and, although data from different sources (11, 12) do not agree well (see Fig. 2), they all show that the acidity increases considerably with percentage H_2O_2.

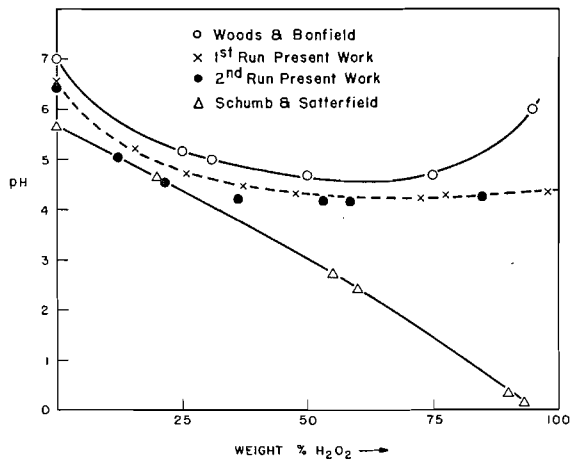

FIG. 2.

In the system H_2O–acid–H_2O_2 the following equilibria are possible:

(i) $HA + H_2O \rightleftharpoons H_3O^+ + A^-$,

(ii) $HA + H_2O_2 \rightleftharpoons H_3O_2^+ + A^-$,

(iii) $H_3O_2^+ + H_2O \rightleftharpoons H_3O^+ + H_2O_2$.

In case (i) when HA is a strong acid, the equilibrium will lie far to the right owing to the affinity of the water molecule for protons. As the basicity of the solvent molecule decreases, so too will the stability of the corresponding oxonium ion, and it is for this reason that the equilibrium position in (ii) lies well to the left. An independent measure of the relative stabilities of H_3O^+ and $H_3O_2^+$ has been given by Uri and Evans (13), who estimated a ΔH value of 4.2 kcal. per mol. for process (iii); thus assuming the entropy change to be small they find $\Delta G^\circ \simeq \Delta H^\circ = -4.2$ kcal., which gives an equilibrium constant of $K \simeq 10^3$.

As the concentration of H_2O_2 increases with respect to that of H_2O the number of ions produced by process (i) will decrease and become a minimum in almost anhydrous

Can. J. Chem. Downloaded from www.nrcresearchpress.com by 200.7.193.243 on 09/04/12
For personal use only.

hydrogen peroxide. This addition of H_2O_2 will bring about a gradual reduction in the equivalent conductance of the system, and the form of the pH curve suggests that the decrease will be most rapid for additions up to 30 weight %. Furthermore, although the degree of dissociation decreases, the mechanism of conductance remains the same as in aqueous solution, and so the temperature coefficients of conductances should also remain unchanged (except for a small change due to the effect on the dissociation constant).

These suppositions are in good agreement with the experimental results for the acids studied, and the very different behavior displayed by the alkali chlorides (1) in identical solvents adds strength to these opinions. If this is indeed a true picture of what is occurring, then similar effects should be observed in mixtures of water and any other weakly acidic substance. Conductivity measurements were therefore made in aqueous formic acid. Formic acid possesses both weakly acidic properties and a reasonably high dielectric constant (14). (It was because of its low dielectric constant that acetic acid was not used.) The effect of the reduced dielectric constant of H_2O–HCOOH mixtures as compared with that of H_2O–H_2O_2 mixtures can be assessed by measuring the conductance of KCl in a solvent of the same composition.

The results obtained are shown graphically in Figs. 3 and 4, and do indeed show that H_2SO_4 gives an over 100% lower conductance in H_2O–HCOOH than in H_2O–H_2O_2 mixtures. This would be expected from the greater acidity of HCOOH compared with H_2O_2. The results for KCl show that it behaves very much as it did in H_2O–H_2O_2 mixtures, the 7% lower values probably being due to the lower dielectric constant of the solvent.

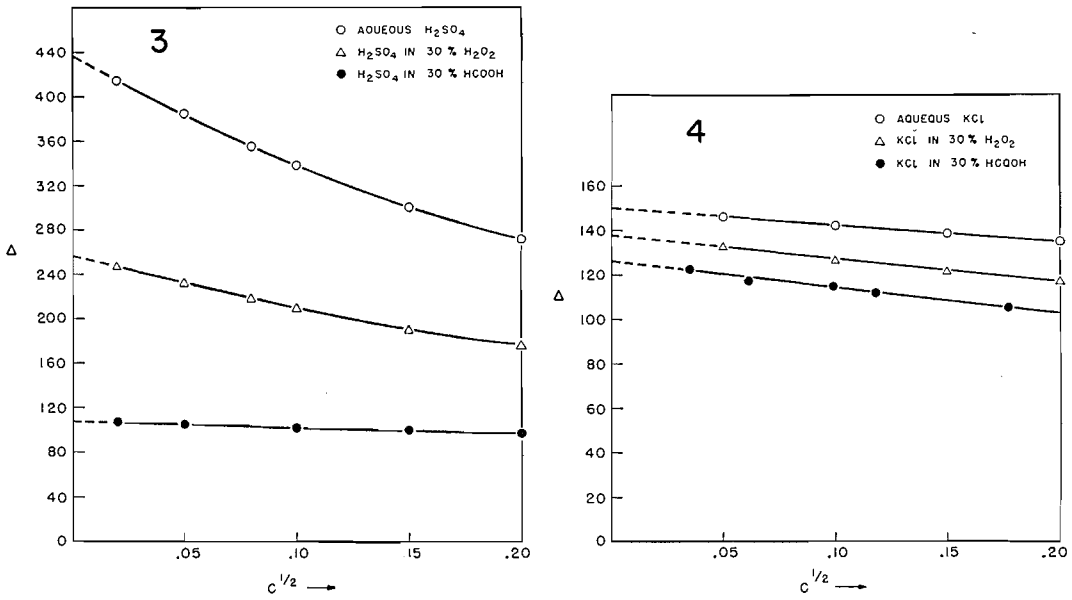

FIGS. 3 and 4.

CONCLUSION

Abnormally low values are observed for the conductance of strong acids in water – hydrogen peroxide mixtures, the value being a minimum in almost anhydrous hydrogen

Can. J. Chem. Downloaded from www.nrcresearchpress.com by 200.7.193.243 on 09/04/12
For personal use only.

peroxide. An explanation is given in terms of a decrease in the degree of dissociation of these acids with increase in concentration of hydrogen peroxide in the solvent.

The proposals made were verified by conductance measurements on sulphuric acids and potassium chloride in water – formic acid mixtures.

ACKNOWLEDGMENTS

To Dr. M. E. Bretschger and Mr. E. S. Shanley, of the Becco Chemical Division, Food Machinery and Chemical Corporation, Buffalo, New York, for advice and for their unselfish interest in helping the authors with this investigation. To Mr. Gordon Graham for his technical assistance.

REFERENCES

1. THOMAS, D. K. and MAASS, O. Can. J. Chem. **36**, 449 (1958).
2. SHANLEY, E., ROTH, E., NICHOLS, G., and KILPATRICK, M. J. Am. Chem. Soc. **78**, 5190 (1956).
3. GIGUÈRE, P. Trans. Roy. Soc. Canada (3), III, **35**, 1 (1941).
4. GIGUÈRE, P., *et al.* To be published.
5. SCATCHARD, G., KAVANAGH, G. M., and TICKNOR, L. B. J. Am. Chem. Soc. **74**, 3715 (1952).
6. KINDRON, B. and SHANLEY, E. Becco Chemical Division, Food Machinery and Chemical Corp., Buffalo, N.Y. (Unpublished, 1949.)
7. EASTON, M., MITCHELL, A., and WYNNE-JONES, W. Trans. Faraday Soc. **48**, 796 (1952).
8. KINDRON, B. and SHANLEY, E. Becco Chemical Division, Food Machinery and Chemical Corp., Buffalo, N.Y. (Unpublished, 1949.)
9. SCATTERFIELD, C., WENTWORTH, R., and DEMETRIADES, S. J. Am. Chem. Soc. **76**, 2633 (1954).
10. GROSS, P. and TAYLOR, R. J. Am. Chem. Soc. **72**, 2075 (1950).
11. WOODS, F. and BANFIELD, A. Rept. Roy. Inst. Chem. No. 2 (1954).
12. SCHUMB, A. and SATTERFIELD, C. Hydrogen peroxide. Am. Chem. Soc. Monograph, **128**, 394 (1955).
13. URI, N. and EVANS, M. Trans. Faraday Soc. **45**, 224 (1949).
14. DRUDE, P. Z. physik. Chem. **23**, 267 (1897).

Can. J. Chem. Downloaded from www.nrcresearchpress.com by 200.7.193.243 on 09/04/12
For personal use only.

Can. J. Chem. Downloaded from www.nrcresearchpress.com by 200.7.193.243 on 09/04/12
For personal use only.

SEVEN- AND EIGHT-MEMBERED RINGS CONTAINING CARBON AND TWO SULPHUR ATOMS[1]

MARSHALL KULKA

ABSTRACT

7-Chloro-2,3-dihydrobenzo(*f*)-1,4-dithiepin (IV) has been synthesized from 2-(2-chloroethylmercapto)-5-chlorobenzyl chloride (I). Attempts to synthesize the higher homologues of IV by this method failed because the required intermediates cleaved at the alkyl–sulphur bond. A reaction product of *p*-chlorothiophenol, formaldehyde, and hydrogen chloride has been identified as 2,8-dichloro-6H,12H-dibenzo(*b*,*f*)-1,5-dithiocin (VI), a tricyclic system with the eight-membered ring containing two sulphur atoms.

It has been previously shown (1, 2) that *o*-ω-chloroalkoxybenzyl isothiuronium chlorides (II, Y = O) undergo simultaneous degradation and cyclization in the presence of dilute alkali to form macrorings IV (Y = O) containing carbon, oxygen, and sulphur. It was also indicated that this reaction involves the intermediate III (Y = O). The ease with which these macrorings formed was attributed to the presence of the two heteroatoms which provided favorable bond angles.

In the present investigation it was decided to examine the preparation of rings containing two sulphur atoms. Accordingly *p*-chlorophenyl 2-chloroethyl sulphide was chloromethylated and the resulting 2-(2-chloroethylmercapto)-5-chlorobenzyl chloride (I, Y = S, $n = 2$) was treated with thiourea. This produced the required isothiuronium salt II (Y = S, $n = 2$) which when added to a large volume of hot dilute alkali yielded 7-chloro-2,3-dihydrobenzo(*f*)-1,4-dithiepin (IV, Y = S, $n = 2$). Attempts to synthesize the higher homologues of IV (Y = S, $n > 2$) failed because the required intermediates I (Y = S, $n > 2$) could not be obtained.

It was found that the sulphur–alkyl linkage of *p*-$ClC_6H_4S(CH_2)_nCl$ (where $n > 2$), unlike the ether linkage of *p*-$ClC_6H_4O(CH_2)_nCl$, was susceptible to cleavage under the acidic conditions of chloromethylation. Thus when *p*-chlorophenyl 4-chlorobutyl sulphide was subjected to the same chloromethylation conditions as were used in the preparation of 2-(2-chloroethylmercapto)-5-chlorobenzyl chloride (I, Y = S, $n = 2$) from *p*-chlorophenyl 2-chloroethyl sulphide, no reaction occurred. However, when the amount of condensing agent (zinc chloride) was increased, reaction did occur but I (Y = S, $n = 4$) was not the product. Instead, a high-melting, difficultly soluble compound was isolated. This compound was also formed when *p*-chlorothiophenol, bis(*p*-chlorophenylmercapto)-methane (3, 4), 1,2-bis(*p*-chlorophenylmercapto)ethane, and 1,4-bis(*p*-chlorophenylmercapto)butane but not 1,3-bis(*p*-chlorophenylmercapto)-2-chloropropane (5) were subjected to the more drastic chloromethylation. It became evident that *p*-chlorothiophenol was the intermediate in the formation of the high-melting compound and that the sulphides produced this intermediate by cleavage at the sulphur–alkyl bond. That 1,3-bis(*p*-chlorophenylmercapto)-2-chloropropane did not undergo cleavage under the acidic conditions of chloromethylation may be attributed to the steric hindrance offered by the alkyl chlorine atom. It is remarkable that bis(*p*-chlorophenyl) disulphide also remained unaltered under these conditions.

The structure of the unknown high-melting compound obtained from *p*-chlorothiophenol was determined in the following manner. Analyses revealed the empirical

[1]*Manuscript received January 15, 1958.*
Contribution from the Dominion Rubber Company Limited Research Laboratories, Guelph, Ontario.

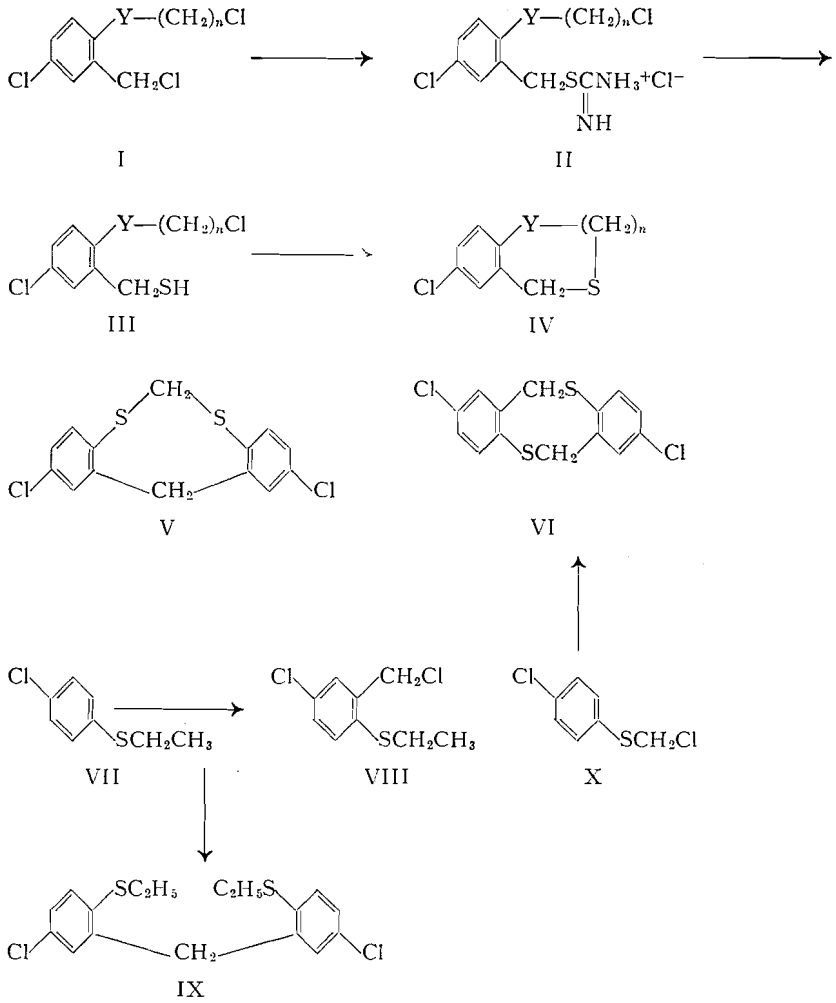

formula $C_{14}H_{10}Cl_2S_2$. A low molecular weight was indicated from the fact that the compound could be sublimed *in vacuo*, and a determination according to the method of Rast gave a figure of 315. On the basis of the properties and the origin of the compound, two possible structures, V and VI, were proposed. Further examination of the unknown compound showed that it was stable under a variety of acidic conditions and this finding eliminated the structure V, which is a mercaptal and therefore susceptible to acid hydrolysis. An attempt to synthesize V by preparing 2,2′-bis(ethylmercapto)-5,5′-dichlorodiphenylmethane (IX) from VII and VIII and subjecting it to chloromethylation resulted only in resinous material.

There are two possible routes by which the compound of structure VI could form from *p*-chlorothiophenol, formaldehyde, and hydrogen chloride in the presence of zinc chloride. Firstly, C-chloromethylation could occur to form 2-mercapto-5-chlorobenzyl chloride, two molecules of which could then react with each other in the presence of zinc chloride to form VI. Secondly, S-chloromethylation could occur to form *p*-chlorophenyl chloromethyl sulphide (X), two molecules of which could then undergo a Friedel–Crafts reaction with each other to form VI. That VI was formed via the second route was shown

Can. J. Chem. Downloaded from www.nrcresearchpress.com by 200.7.193.243 on 09/04/12
For personal use only.

by synthesis. *p*-Chlorothiophenol was treated with formaldehyde and hydrogen chloride according to the method of Scherer and Fink (6) to form *p*-chlorophenyl chloromethyl sulphide (X). Then when X was heated with zinc chloride in acetic acid 2,8-dichloro-6H,12H-dibenzo(*b*,*f*)-1,5-dithiocin (VI) was formed in high yield. On the other hand 2-ethylmercapto-5-chlorobenzyl chloride (VIII) when heated with zinc chloride in acetic acid saturated with hydrogen chloride did not produce VI.

The reaction of *p*-chlorothiophenol with formaldehyde and hydrogen chloride follows a course unlike that of its oxygen analogue. Thus when *p*-chlorophenol was treated with formaldehyde and hydrogen chloride under the conditions used in the preparation of VI, there was formed 6-chloro-8-chloromethyl-1,3-benzodioxane (7). This is obviously a reaction product of only one molecule of *p*-chlorophenol. *p*-Thiocresol did not produce a dithiocin of the type VI when subjected to chloromethylation. The product was a resin.

The chloromethylation of *p*-chlorothiophenol now provides an easy access to the ring system VI, which up to the present time was available only in the form of dibenzo(*b*,*f*)-1,5-dithiocin-6,12-dione, a dehydration product of thiosalicylic acid (8).

EXPERIMENTAL

2-(2-Chloroethylmercapto)-5-chlorobenzyl Chloride (*I*, *Y* = *S*, *n* = *2*)

A reaction mixture of acetic acid (300 ml.), paraformaldehyde (10 g.), zinc chloride (15 g.), and 2-chloroethyl *p*-chlorophenyl sulphide (60 g.) (5) was saturated with hydrogen chloride and then heated at 85°–90° for 3 days. The reaction mixture was concentrated *in vacuo* to about half its original volume and then diluted with dilute hydrochloric acid. The precipitated oil was extracted with benzene, the benzene solution washed with water, with aqueous sodium bicarbonate, and with water. The solvent was removed and the residue fractionally distilled. Fraction 1, b.p. (12 mm.) = 150°–170°, 20 g.; fraction 2, b.p. (12 mm.) = 170°–185°, 13 g.; and fraction 3, b.p. (12 mm.) = 185°–190°, 25 g. Fraction 3, which was the required product, was not purified but was used directly in the formation of the isothiuronium salt (see below).

2-(2-Chloroethylmercapto)-5-chlorobenzyl Isothiuronium Chloride (*II*, *Y* = *S*, *n* = *2*)

A solution of crude 2-(2-chloroethylmercapto)-5-chlorobenzyl chloride (fraction 3 above) (20 g.), thiourea (10 g.), and ethanol (120 ml.) was heated under reflux for 3 hours. The solvent was removed *in vacuo*, the residue dissolved in hot water (50 ml.), and the solution was allowed to cool. The white precipitate (15 g.) was filtered, washed with cold water and with benzene, and crystallized from water, yielding white prisms melting at 143°–145°. Anal. Calc. for $C_{10}H_{13}N_2Cl_3S_2$: C, 36.20; H, 3.92. Found: C, 36.01; H, 4.04.

7-Chloro-2,3-dihydrobenzo(f)-1,4-dithiepin (*IV*, *Y* = *S*, *n* = *2*)

A solution of 2-(2-chloroethylmercapto)-5-chlorobenzyl isothiuronium chloride (8 g.) in methanol (50 ml.) and water (50 ml.) was added dropwise to a stirred hot solution of sodium hydroxide (5 g.) in water (500 ml.) heated on the steam bath. The addition time was approximately $\frac{1}{2}$ hour and the reaction mixture was heated for an additional $\frac{1}{2}$ hour. The precipitated yellow oil was extracted with benzene, the solution washed with water, and the solvent removed. The residue distilled at 180°–182° (12 mm.) and the distillate when crystallized from methanol yielded golden prisms (1.9 g. or 35%) melting at 91°–92°. Anal. Calc. for $C_9H_9ClS_2$: C, 49.87; H, 4.14. Found: C, 50.23, 49.96; H, 4.15, 3.94.

p-Chlorophenyl 4-Chlorobutyl Sulphide

To a solution of potassium hydroxide (30 g.) in methanol (100 ml.) was added *p*-chlorothiophenol (73 g.) and 1,4-dichlorobutane (300 ml.), and the resulting reaction mixture

Can. J. Chem. Downloaded from www.nrcresearchpress.com by 200.7.193.243 on 09/04/12
For personal use only.

Can. J. Chem. Downloaded from www.nrcresearchpress.com by 200.7.193.243 on 09/04/12
For personal use only.

was heated on the steam bath for ½ hour. There was a slight exothermic reaction at the beginning. Water was added to dissolve the precipitated salt and the organic layer was washed with aqueous alkali and with water. The excess 1,4-dichlorobutane was removed *in vacuo* and the residue was distilled, yielding a colorless liquid (92 g.) boiling at 180° (12 mm.), n_D^{20} = 1.5793. Anal. Calc. for $C_{10}H_{12}Cl_2S$: C, 51.07; H, 5.11. Found: C, 51.58; H, 5.27.

The residue from the distillation when crystallized from methanol gave white prisms of *1,4-bis(p-chlorophenylmercapto)butane* (6 g.) melting at 73°–74°. Anal. Calc. for $C_{16}H_{16}Cl_2S_2$: C, 55.98; H, 4.67. Found: C, 55.74; H, 4.48.

2,8-Dichloro-6H,12H-dibenzo(b,f)-1,5-dithiocin (VI)

(*a*) *From p-chlorothiophenol.*—A reaction mixture of *p*-chlorothiophenol (50 g.), zinc chloride (40 g.), paraformaldehyde (20 g.), and acetic acid (350 ml.) was saturated with hydrogen chloride and then heated on the steam bath for 16 hours. The resulting white precipitate was filtered from the cooled reaction mixture, washed with acetic acid, with concentrated hydrochloric acid, and with water, and dried. The crude product (35 g.) melted at 244°–246° and was insoluble in most organic solvents. When crystallized from benzene or N,N-dimethylformamide it melted at 254°–255°. Its melting point was not depressed by the products obtained in (*b*) or (*c*) (see below). Anal. Calc. for $C_{14}H_{10}Cl_2S_2$: C, 53.68; H, 3.19; Cl, 22.70; S, 20.45. Found: C, 53.87, 53.41; H, 2.92, 3.12; Cl, 23.37; S, 20.66, 20.85.

(*b*) *From sulphides.*—When bis(*p*-chlorophenylmercapto)methane (3, 4), 1,2-bis(*p*-chlorophenylmercapto)ethane (5), and 1,4-bis(*p*-chlorophenylmercapto)butane were subjected to chloromethylation as in (*a*) in each case a product was obtained melting at 254°–255° alone or in admixture with the 2,8-dichloro-6H,12H-dibenzo(*b,f*)-1,5-dithiocin (VI) obtained in (*a*).

(*c*) *From p-chlorophenyl chloromethyl sulphide (X).*—A solution of *p*-chlorophenyl chloromethyl sulphide (X) (6) (5 g.) in acetic acid (50 ml.) and zinc chloride (20 g.) was heated on the steam bath for 2 days. The white precipitate was filtered, washed with acetic acid and with methanol, and crystallized from N,N-dimethylformamide. The white needles (3.5 g. or 86%) melted at 251°–254° alone or in admixture with the compound obtained from *p*-chlorothiophenol (see Section (*a*)).

p-Chlorophenyl Ethyl Sulphide (VII)

This was prepared in quantitative yield by treating a hot alkaline solution of *p*-chlorothiophenol with diethyl sulphate in the usual manner. It boiled at 123° (18 mm.), n_D^{20} = 1.5800. Anal. Calc. for C_8H_9ClS: C, 55.67; H, 5.22. Found: C, 56.35; H, 5.72.

2-Ethylmercapto-5-chlorobenzyl Chloride (VIII)

A mixture of *p*-chlorophenyl ethyl sulphide (45 g.), acetic acid (200 ml.), paraformaldehyde (10 g.), and zinc chloride (10 g.) was saturated with hydrogen chloride and the resulting solution was heated on the steam bath for 20 hours. The reaction mixture was concentrated *in vacuo* to about one-half of its original volume and the residue treated with water and then extracted with benzene. The benzene extract was washed with water, with aqueous sodium bicarbonate, and with water, and the solvent removed. The residue was distilled yielding three fractions: fraction 1, b.p. (11 mm.) = 110°–135°, 4 g.; fraction 2, b.p. (11 mm.) = 135°–170°, 30 g.; and fraction 3, b.p. (11 mm.) = 200°–250°, 8 g. Fraction 2 was redistilled yielding a colorless liquid (20 g.) of VIII boiling at 150°–152° (11 mm.), n_D^{20} = 1.5933. Anal. Calc. for $C_9H_{10}Cl_2S$: C, 48.87; H, 4.52. Found: C, 49.23, 49.61; H, 4.41, 4.73.

Fraction 3 was crystallized from benzene yielding white prisms (0.7 g.) melting at 250°–252° alone or in admixture with *2,8-dichloro-6H,12H-dibenzo(b,f)-1,5-dithiocin* (*VI*) prepared from *p*-chlorothiophenol.

The mother liquors from the crystallization of fraction 3 were taken to dryness and the residue crystallized from methanol yielding white prisms (1 g.) melting at 96°–98° alone or in admixture with *2,2′-bis(ethylmercapto)-5,5′-dichlorodiphenylmethane* prepared from VII and VIII (see below).

2-Ethylmercapto-5-chlorobenzyl Isothiuronium Chloride

2-Ethylmercapto-5-chlorobenzyl chloride (16 g.), thiourea (5 g.), and ethanol (100 ml.) were heated together under reflux for 3 hours. The solvent was removed *in vacuo*, the residue was dissolved in warm water (300 ml.), the solution washed with benzene and then concentrated *in vacuo* to about 25 ml. The white needles (12 g.), which precipitated when the solution was cooled, were filtered, washed, and dried, m.p. 204°–206°. Anal. Calc. for $C_{10}H_{14}N_2Cl_2S_2$: C, 40.40; H, 4.71; N, 9.42. Found: C, 40.73, 40.73; H, 4.88, 4.85; N, 9.91, 9.99.

2,2′-Bis(ethylmercapto)-5,5′-dichlorodiphenylmethane (*IX*)

A reaction mixture of 2-ethylmercapto-5-chlorobenzyl chloride (VIII) (5 g.), *p*-chlorophenyl ethyl sulphide (VII) (5 g.), zinc chloride (12 g.), and acetic acid (25 ml.) was heated under reflux for 1 hour and then poured into dilute hydrochloric acid. The precipitated oil was extracted with benzene, the benzene solution was washed with water, and the solvent removed. The residue was distilled and the fraction boiling at 175°–190° (0.5 mm.) collected. When this distillate was crystallized twice from methanol it yielded white prisms (3.5 g.) melting at 95°–97°. Anal. Calc. for $C_{10}H_{14}N_2Cl_2S_2$: C, 57.13; H, 5.04. Found: C, 57.06, 57.31; H, 5.27, 5.17.

REFERENCES

1. KULKA, M. Can. J. Chem. **33**, 1442 (1955).
2. KULKA, M. J. Org. Chem. **22**, 241 (1957).
3. FAITH, H. E. J. Am. Chem. Soc. **72**, 837 (1950).
4. MOWRY, D. T. U.S. Patent No. 2,594,480 (1952); Chem. Abstr. **46**, 7702 (1952).
5. KULKA, M. and STRYK, F. G. Can. J. Chem. **35**, 519 (1957).
6. SCHERER, O. and FINK, K. German Patent No. 845,511 (1952); Chem. Abstr. **47**, 5442 (1953).
7. BUEHLER, C. A., BASS, B. C., DARLING, R. B., and LUBS, M. E. J. Am. Chem. Soc. **62**, 890 (1940).
8. BAKER, W., EL-NAWAWY, A. S., and OLLIS, W. D. J. Chem. Soc. 3163 (1952).

Can. J. Chem. Downloaded from www.nrcresearchpress.com by 200.7.193.243 on 09/04/12
For personal use only.

Can. J. Chem. Downloaded from www.nrcresearchpress.com by 200.7.193.243 on 09/04/12
For personal use only.

STRUCTURE OF AN ARABOGALACTAN FROM WHITE SPRUCE (PICEA GLAUCA (MOENCH) VOSS)[1]

G. A. ADAMS

ABSTRACT

A water-soluble polysaccharide isolated from white spruce wood contained D-galactose, L-arabinose, and D-xylose in a molar ratio of 21:3:1. Hydrolysis of the fully methylated polysaccharide yielded 2,3,5-tri-*O*-methyl-L-arabinose (12 moles); 2,3,4,6-tetra-*O*-methyl-D-galactose (29 moles); 2,3,4-tri-*O*-methyl-D-galactose (34 moles); 2,6-di-*O*-methyl-D-galactose (0.5 moles); 2,4-di-*O*-methyl-D-galactose (45 moles); 2,3-di-*O*-methyl-D-xylose (5 moles); and monomethyl xylose (1 mole). When oxidized by periodate the polysaccharide consumed 1.18 moles of oxidant, and yielded 0.56 moles of formic acid per mole of anhydro-D-galactose. The D-xylose was attributed to the presence of a xylan mixed with the arabogalactan in the original polysaccharide preparation. The methylation and periodate oxidation data showed that the arabogalactan possessed a highly branched structure with the anhydro-D-galactose units being joined by 1→3 and 1→6 glycosidic bonds. All of the L-arabinose was present in the furanoside form as non-reducing terminal units.

Water-soluble polysaccharides of the arabogalactan type occur predominantly in the larches (1, 2, 3, 4, 5), although lesser amounts have been found in black spruce (*Picea mariana*) (6), southern yellow pine (*Pinus palustris*) (7), Jeffrey pine (*Pinus jeffreyi*) (8), and jack pine (*Pinus banksiana*) (9). The polysaccharides isolated from southern yellow pine and black spruce contained uronic acid residues in addition to arabinose and galactose. Fractionation of the water-soluble polysaccharides from the various sources has shown that some are heterogeneous. The heterogeneous nature of the polysaccharides from *Larix occidentalis* was demonstrated by Peterson *et al.* (10) and the arabogalactan from the European larch (*Larix decidua*) similarly was shown to be heterogeneous by Campbell *et al.* (11). On the other hand, the arabogalactans from Jeffrey pine (8) and jack pine (9) have been regarded as homogeneous. In an extensive investigation on the structure of the arabogalactan of western larch (*L. occidentalis*) (4, 12, 13, 14) White regarded the polysaccharide as homogeneous, a view which has been disputed by Campbell *et al.* (11).

A previous paper from this laboratory reported the isolation and composition of a

TABLE I

CHROMATOGRAPHIC SEPARATION OF METHYLATED SUGARS

Fractions from column	Methylated sugar	Yield (mg.)	$[\alpha]_D^{25}$ (water)
1 (Tube 45–88)	2,3,5-Tri-*O*-methyl-L-arabinose	242	−11°
2 (Tube 89–112)	2,3,4,6-Tetra-*O*-methyl-D-galactose	636	+94°
3 (Tube 113–138)	2,3,4,6-Tetra-*O*-methyl-D-galactose, dimethyl xylose	181	+73°
4 (Tube 139–200)	2,3,4-Tri-*O*-methyl-D-galactose	735	+104°
5 (Tube 201–214)	2,3,4-Tri-*O*-methyl-D-galactose, dimethyl galactose, monomethyl xylose	28	+70°
6 (Tube 215–218)	2,3,4-Tri-*O*-methyl-D-galactose, dimethyl galactose, monomethyl xylose	22	+64°
7 (Tube 219–234)	Impure 2,4-di-*O*-methyl-D-galactose	16	+68°
8 (Tube 235–305)	2,4-Di-*O*-methyl-D-galactose	893	+86°
9 (Tube 306–360)	Impure 2,4-di-*O*-methyl-D-galactose	83	+76°
10 (Tube 361–377)	Unknown	9	—
		2845 92% recovery	

[1]*Manuscript received January 10, 1958.*
Contribution from the Division of Applied Biology, National Research Laboratories, Ottawa, Canada. Issued as N.R.C. No. 4677.

water-soluble polysaccharide from white spruce (*Picea glauca*) (15). It contained galactose, arabinose, xylose (molar ratio, 21:3:1), and a small amount of uronic acid (3.0%), and had a specific rotation $[\alpha]_D^{25} = -7°$. Results of several fractionation procedures indicated that the polysaccharide was essentially homogeneous and this conclusion was further confirmed by electrophoretic examination.

The present investigation was concerned with the structure of the polysaccharide as shown by methylation and periodate oxidation studies. The polysaccharide was methylated and the methyl ether subjected to methanolysis and hydrolysis. The methylated sugars were separated chromatographically on a Celite column (16) into 10 fractions as shown in Table I.

Further separations of mixtures were made and the main methylated sugars were characterized by isolation of appropriate crystalline derivatives. The amounts and molar ratios of the various sugar components are shown in the following table.

TABLE II

YIELD OF METHYLATED SUGARS

Methylated sugar	Wt. (mg.)	Millimoles	Molar ratio
2,3,5-Tri-*O*-methyl-L-arabinose	236	1.23	12
2,3,4,6-Tetra-*O*-methyl-D-galactose	695	2.94	29
2,3,4-Tri-*O*-methyl-D-galactose	758	3.43	34
2,6-Di-*O*-methyl-D-galactose	10	0.05	0.5
2,4-Di-*O*-methyl-D-galactose	942	4.55	45
2,3-Di-*O*-methyl-D-xylose	89	0.50	5
Monomethyl xylose	18	0.10	1

The polysaccharide was considered to be an arabogalactan and the small amount of xylose present after hydrolysis was attributed to an admixed xylan. The methylation data showed that the xylan had the usual 1→4 linked structure with some branching present at $C_{(2)}$ and/or $C_{(3)}$. No tri-*O*-methyl-D-xylose, representative of the non-reducing end of the xylan, could be found, undoubtedly because the amount present was too small to be detected. The presence of xylan of the usual type which has a characteristically high negative rotation could account for the present polysaccharide having a slightly negative specific rotation (−7°) compared with the small positive rotation previously reported for arabogalactans (10, 8, 9).

Results of the methylation studies showed that the arabogalactan must contain the following units, in the relative amounts shown:

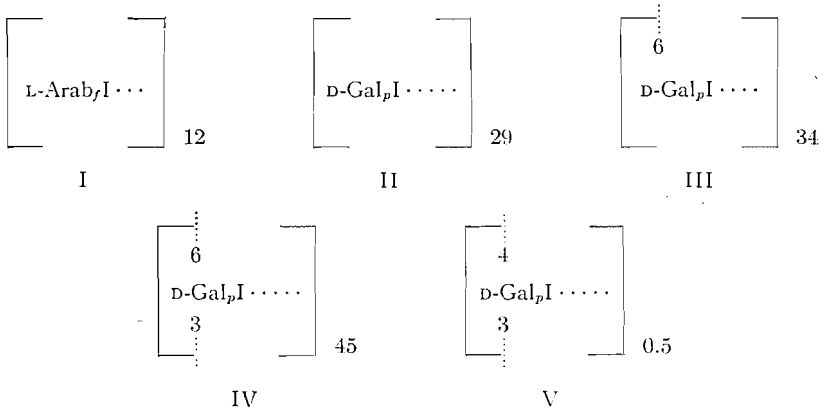

Can. J. Chem. Downloaded from www.nrcresearchpress.com by 200.7.193.243 on 09/04/12
For personal use only.

Can. J. Chem. Downloaded from www.nrcresearchpress.com by 200.7.193.243 on 09/04/12
For personal use only.

The high proportion of terminal units of arabinose (I) and galactose (II) showed that the polysaccharide molecule was highly branched, the branches occurring at positions as shown by III, IV, and V. Although the present data do not permit the assignment of a unique structure to the molecule, certain structural features are evident. The main chain or "backbone" of the molecule can be visualized as D-galactopyranose units linked 1→6. The relatively high proportion of IV showed that considerable branching occurred at $C_{(3)}$ and subsidiary chains of 1→6 linked D-galactopyranose units could be attached at this point. This arrangement provides for a branch-on-branch type of structure terminated at the non-reducing ends by unsubstituted D-galactopyranose and L-arabofuranose residues. The small amount of 2,6-di-*O*-methyl-D-galactose (0.5 moles) found in the hydrolysis products showed that a small amount of branching also occurred at $C_{(3)}$ and $C_{(4)}$ of some anhydro-D-galactose units. The number of sugar units (45.5) forming branch points (IV and V) was slightly more than the number (41) of non-reducing terminal units (I and II). The ratio of methylated arabinose to methylated galactose (12:108) found on hydrolysis was less than that in the original polysaccharide molecule (arabinose: galactose 1:7). Both of these discrepancies were probably caused by some loss of the volatile methyl glycoside of 2,3,5-tri-*O*-methyl-L-arabinose. No partially methylated arabinose units were present after hydrolysis and hence the likelihood was remote that the 2,3,5-tri-*O*-methyl-L-arabinose had its origin in an admixed araban. The absence of unoxidized arabinose units after treatment with periodate further confirmed these conclusions. The change in specific rotation on hydrolysis of the methylated polysaccharide ($[\alpha]_D^{25}$ −55 to +75°) indicated that the glycosidic bonds were mainly in the β-configuration. An arabogalactan having structural features as described should consume 1.15 moles of periodate per mole of anhydro-D-galactose and produce 0.55 moles of formic acid; the actual values of 1.18 moles of periodate and 0.56 moles of formic acid provided excellent agreement.

The structural features of the white spruce arabogalactan conform in general to those found in other arabogalactans of wood (12, 13, 14, 8, 9, 11). These structural characteristics include a high degree of branching through positions 6 and 3 of the anhydro-D-galactose units with the arabinose units attached as end groups on some of the branches. The white spruce arabogalactan resembled rather closely the arabogalactan of jack pine (9) although the latter contained proportionately less arabinose. It differed from the arabogalactan of Jeffrey pine (8) by having its arabinose units exclusively in terminal positions and also a greater proportion of the galactose units as non-reducing end groups. The arabogalactan of larch (14) differed by having more branching at position 3 of the galactose units.

The problem of heterogeneity makes positive interpretation of the methylation and periodate oxidation data difficult; the existence of a galactan admixed with the arabogalactan is a possibility that cannot be excluded.

EXPERIMENTAL

All specific rotations are equilibrium values unless otherwise stated and melting points are corrected.

Paper Chromatography

Chromatographic separations were carried out using the following solvent systems (v/v ratios): (A) pyridine:ethyl acetate:water (2:1:2); (B) methyl ethyl ketone:water (2:1); (C) ethanol:benzene:water (47:200:15); (D) *n*-butanol: ethanol:water (40:11:19); and (E) ethyl acetate:acetic acid:formic acid:water (18:3:1:4). Separations were per-

formed by the descending technique on Whatman No. 1 filter paper. Methylated sugars were located on the papers by *p*-anisidine hydrochloride spray reagent (17).

Composition of the Polysaccharide

The polysaccharide was prepared from a water-soluble extract of white spruce (*Picea glauca* (Moench) Voss) as described previously (15). The material was soluble in water and had the following analysis: D-galactose, L-arabinose, and D-xylose (molar ratio 21:3:1); Klason lignin, 3.0%; ash (sulphated), 2.5%; uronic acid 3.3% and $[\alpha]_D^{25} = -7° \pm 2.5°$ (*c*, 0.7% in 10% sodium hydroxide).

Methylation

Hemicellulose (6.40 g.) was dissolved in water (25 ml.) and methylated by the dropwise addition of dimethyl sulphate (60 ml.) and 45% sodium hydroxide solution (100 ml.) with stirring. The reagent additions required a period of 4 hours and the solution was kept alkaline at all times. After stirring for 1 hour, the foregoing methylation was repeated and the solution was stirred overnight. Complete methyl glycoside formation was indicated by a negative reduction test with Fehling's solution. A 100-ml. quantity of 45% sodium hydroxide was added at one time and further methylation carried out by the addition of dimethyl sulphate (60 ml.) over 3 hours. This treatment was repeated once more, the reaction mixture being stirred overnight and then heated at 85° C. for $1\frac{1}{2}$ hours. The solution was cooled in an ice bath and brought to pH 7.0 with acetic acid. The salts were dissolved by the addition of water and the partially methylated polysaccharide was extracted by shaking with chloroform. The extracts were dried by anhydrous sodium sulphate and evaporated to yield a glassy solid (4.10 g.). Dialysis of the extracted water phase, followed by freeze-drying of the salt-free solution, yielded a further quantity of partially methylated polysaccharide (1.74 g.). Three additional methylations of this fraction, as described above, followed by chloroform extraction, yielded a more highly methylated polysaccharide (1.04 g.). Both fractions showed a definite hydroxyl band at 3500–3600 $cm.^{-1}$ in their infrared spectra. The fractions were combined (wt. = 5.14 g.) and dissolved in tetrahydrofurane (100 ml.). Powdered sodium hydroxide (35 g.) and dimethyl sulphate (35 ml.) were added, the latter over a period of 4 hours. Recovery of the methylated polysaccharide by chloroform extraction as described before yielded a glassy solid (3.69 g.) which still showed a distinct hydroxyl band in its infrared spectrum. The partially methylated product was dissolved in methyl iodide:methanol (100:5) and methylated by addition of silver oxide (10 g.) in portions of 2 g. every hour. The solution was refluxed overnight and the methylated product was recovered by extraction with chloroform. Three additional methylations by this method were necessary to yield a product which had no hydroxyl band at 3500–3600 $cm.^{-1}$ in its infrared spectrum. The methylated polysaccharide was a yellowish solid (3.96 g.) having $[\alpha]_D^{25} = -55° \pm 1°$ (*c*, 1.0% in chloroform) and OMe 42.8% (theoretical value for $(C_9H_{16}O_5)_n$, 45.3%).

Hydrolysis of Methylated Polysaccharide

The methylated polysaccharide (3.96 g.) was heated with 8% methanolic hydrogen chloride (150 ml.) in a boiling water bath for 12 hours. Methanol was evaporated by a stream of air from a fan at room temperature, *N* hydrochloric acid (60 ml.) was added, and the methyl glycosides were hydrolyzed on a boiling water bath for 10 hours. A small insoluble precipitate was filtered off and the acidic solution was neutralized by Amberlite 1R-45 resin. The neutral solution was concentrated to a thin sirup, taken up in aqueous ethanol, clarified with charcoal, and concentrated to a thick sirup. After

Can. J. Chem. Downloaded from www.nrcresearchpress.com by 200.7.193.243 on 09/04/12
For personal use only.

Can. J. Chem. Downloaded from www.nrcresearchpress.com by 200.7.193.243 on 09/04/12
For personal use only.

further drying over calcium chloride in a desiccator *in vacuo* the product weighed 3.18 g. and had $[\alpha]_D^{25} = +75° \pm 1°$ (*c*, 1.56 in water). Chromatographic examination of the sirup on paper strips (solvent D) indicated the presence of the following methylated sugars: 2,3,5-tri-*O*-methyl-L-arabinose (R_g 0.96); 2,3,4,6-tetra-*O*-methyl-D-galactose (R_g 0.92); 2,3,4-tri-*O*-methyl-D-galactose (R_g 0.76); 2,4-di-*O*-methyl-D-galactose (R_g 0.54); 2,6-di-*O*-methyl-D-galactose (R_g 0.58); 2,3-di-*O*-methyl-D-xylose (R_f 0.50–0.52, solvent B); and a methylated uronic acid.

Separation of Methylated Sugars

The mixture of methylated sugars (3.1 g.) was separated on a Celite column using *n*-butanol saturated with water as the developing phase (16). The eluate was collected by an automatic fraction collector in 15 ml. quantities at $2\frac{1}{2}$-minute intervals. Chromatographic examination of every fifth tube on paper strips (solvent D) permitted the grouping of fractions of similar composition. The fractions were taken to dryness and weighed; Table I gives yields and the rotations of the various fractions without further purification. A small amount of uronic acid was removed from the column with water. As the amount was small and the acid was mixed with partially methylated sugars it was not examined further.

Identification of the Methylated Sugars

Fraction 1.—The sugar was dissolved in water, charcoal was added, the solution filtered and taken to dryness (236 mg.). Chromatographic examination in solvents B, C, and D showed that this sugar moved at the same rate as 2,3,5-tri-*O*-methyl-L-arabinose. Specific rotation $[\alpha]_D^{25} = -35° \pm 1°$ and OMe, 47.6% (calculated for $C_8H_{16}O_5$: OMe, 48.4%) further identified it as 2,3,5-tri-*O*-methyl-L-arabinose. The amide of the corresponding arabonic acid was prepared as follows: a portion of the sirup (140 mg.) was dissolved in water (3 ml.) and oxidized by bromine (0.5 ml.) for 50 hours at room temperature. After removal of the bromine by aeration, the solution was neutralized with silver carbonate; excess silver ions were removed by hydrogen sulphide. The solution was evaporated to dryness and 2,3,5-tri-*O*-methyl-L-arabonic acid recovered as a sirup. The acid was lactonized by distillation (bath temperature 120°–145° C. at 0.025 mm.). Addition of methanol saturated with ammonia to the lactone for 24 hours at 5° C. yielded the amide which was recovered by removal of the solvent in a desiccator. The amide crystallized on nucleation and on recrystallization from methanol–ether solution yielded pure 2,3,5-tri-*O*-methyl-L-arabonamide, m.p. 136° (undepressed with an authentic sample) and $[\alpha]_D^{25} = -18° \pm 3°$ (*c*, 1% in water); these values agree with those reported for this compound (18).

Fraction 2.—This sugar (636 mg.) was identical with 2,3,4,6-tetra-*O*-methyl-D-galactose when compared chromatographically in solvents B, C, and D. A portion of the sirup (96.4 mg.) was refluxed with aniline (50 mg.) in ethanol (5 ml.) for $2\frac{1}{2}$ hours. The aniline derivative crystallized during the heating period and after recrystallization from ethanol had a m.p. and mixed m.p. 196°–197° C. and $[\alpha]_D^{25} = -137° \pm 1°$ (*c*, 0.92 in pyridine) and thus was identified as 2,3,4,6-tetra-*O*-methyl-N-phenyl-D-galactosylamine (19).

Fraction 3.—Chromatographic evidence indicated that this sirup (181 mg.) was a mixture of 2,3,4,6-tetra-*O*-methyl-D-galactose and a dimethyl xylose. Separation was achieved on an alumina column (15 × 80 mm.) using the solvents listed below and the eluates were collected on an automatic fraction collector. The presence of the various sugars was indicated by spotting 10 drops of the eluate on paper and spraying with *p*-anisidine reagent. The results are as follows:

Fraction	Solvent	Compound	Yield (mg.)
3A (Tube 9–47)	Chloroform	2,3,4,6-Tetra-*O*-methyl-D-galactose	59
3B (Tube 48–78)	Ethanol	Dimethyl xylose	57
3C (Tube 79–100)	Water	Dimethyl xylose	32

Subfraction 3A.—This sirup was chromatographically identical in solvents B, C, and D with 2,3,4,6-tetra-*O*-methyl-D-galactose. The sirup (52 mg.) was converted as described above into its aniline derivative which had a m.p. of 196° C. and $[\alpha]_D^{25} = -137° \pm 1°$ (c, 1.0% in pyridine).

Subfraction 3B.—This sirup (57 mg.) travelled at the same rate on a paper chromatogram as 2,3-di-*O*-methyl-D-xylose in solvents B, C, and D. These solvents served to distinguish it from 2,4-di-*O*-methyl-D-xylose and also 3,4-di-*O*-methyl-D-xylose (20). A portion of the sugar (46 mg.) was heated with aniline (28.6 mg.) in ethanol (5 ml.) for 3 hours. Slow removal of the solvent in a desiccator containing calcium chloride under reduced pressure yielded crystals of 2,3-di-*O*-methyl-N-phenyl-D-xylosylamine, which on recrystallization from ethyl acetate solution had a m.p. and mixed m.p. of 126° C., reported value 126° C. (21).

Subfraction 3C.—This fraction (32 mg.) was found to be 2,3-di-*O*-methyl-D-xylose by the chromatographic separations applied to subfraction 3B.

Fraction 4.—The sirup (735 mg.) was chromatographically identical in solvents B and D with 2,3,4-tri-*O*-methyl-D-galactose. The identity of the sugar was established by formation of the amide of the corresponding galactonic acid as follows: a portion of the sirup (133.2 mg.) was dissolved in water (2 ml.) and bromine (0.5 ml.) was added and the oxidation was allowed to proceed for 50 hours. Bromine was removed by aeration and the acidity was neutralized with silver carbonate. The 2,3,4-tri-*O*-methyl-D-galactonic acid was lactonized by distillation (bath temperature 150°–170° C./0.02 mm.). Addition of methanolic ammonia yielded 2,3,4-tri-*O*-methyl-D-galactonamide, m.p. and mixed m.p. 166°–167° C. and $[\alpha]_D^{25} = 32.5° \pm 2°$ (c, 1% in water) in good agreement with the reported value (22). Further confirmation of identity was provided by preparation of the corresponding anilide by refluxing the sugar (86.4 mg.) with aniline (44.6 mg.) in ethanol (5 ml.) for 3 hours. Removal of solvent yielded crystals which on recrystallization from ethyl acetate proved to be 2,3,4-tri-*O*-methyl-N-phenyl-D-galactosylamine, m.p. and mixed m.p. 165°–166° C. and $[\alpha]_D^{25} = 40° \pm 2°$ (c, 1.2% in methanol); melting points of 164° C. and 167° C. have been reported (19, 22).

Fraction 5.—Chromatographic examination in solvents B and D showed that this sirup (28 mg.) was a mixture of a trimethyl galactose, dimethyl galactose, and a monomethyl xylose. The rate of movement in solvent D showed that the trimethyl galactose (R_g 0.73–0.75) was identical with 2,3,4-tri-*O*-methyl-D-galactose, the dimethyl-D-galactose (R_g 0.59–0.60) was identical with 2,6-di-*O*-methyl-D-galactose and different from 2,4-di-*O*-methyl-D-galactose (R_g 0.51–0.52). The monomethyl xylose was chromatographically indistinguishable in solvents B and D from 2-*O*-methyl-D-xylose and 3-*O*-methyl-D-xylose. The ratio of the three sugars in the mixture was determined, after spraying with *p*-anisidine reagent, by modifying a densitometer method described for unsubstituted sugars (23); the ratio found for the three methylated sugars was 4:1:1.

Fraction 6.—This sirup (22 mg.) was also a mixture as shown by chromatographic examination in solvents B and D and contained the same sugars as Fraction 5. The component sugars 2,3,4-tri-*O*-methyl-D-galactose, 2,6-di-*O*-methyl-D-galactose, and monomethyl xylose were present in a ratio of approximately 1:1:2.

Can. J. Chem. Downloaded from www.nrcresearchpress.com by 200.7.193.243 on 09/04/12
For personal use only.

Fraction 7.—The sirup (16 mg.) was chromatographically identical in solvents B and D with 2,4-di-*O*-methyl-D-galactose and had $[\alpha]_D^{25} = +83° \pm 1°$ constant value in 24 hours (*c*, 1% in water). This material was identical with the main Fraction 8 and no further identifications were made.

Fraction 8.—The sirup (893 mg.) crystallized when it was left standing and it corresponded chromatographically in solvents B and D to 2,4-di-*O*-methyl-D-galactose. On recrystallization from ether, 2,4-di-*O*-methyl-D-galactose monohydrate (22) was obtained, m.p. 100°–101° C. with sintering at 73°–76° C., $[\alpha]_D^{25} = +125°$ (5 minutes) $\rightarrow +84° \pm 1°$ in 24 hours (*c*, 1% in water). Anhydrous 2,4-di-*O*-methyl-D-galactose was obtained by drying the monohydrate at 55° C. at 0.1 mm. over phosphorus pentoxide for 20 hours. The anhydrous product had a m.p. and mixed m.p. 103°–104° C. (no sintering) and $[\alpha]_D^{25} = 125°$ (5 minutes) $\rightarrow +87° \pm 1°$ in 24 hours (*c*, 1% in water) in good agreement with the reported values (9). A portion of the sugar (77.0 mg.) was refluxed with aniline (40.2 mg.) in ethanol (5 ml.) for 3 hours. The aniline derivative was obtained in crystalline form on evaporation of the reaction mixture and on recrystallization from ethyl acetate yielded 2,4-di-*O*-methyl-N-phenyl-D-galactosylamine (22) having a m.p. and mixed m.p. 218°–220° C. and $[\alpha]_D^{25} = -181° \pm 4°$ (*c*, 0.92 in pyridine).

Fraction 9.—The sirup (83 mg.) partially crystallized when it was left standing and was chromatographically identical in solvents B and D with 2,4-di-*O*-methyl-D-galactose. Recrystallization from ether yielded 2,4-di-*O*-methyl-D-galactose monohydrate (40 mg.), m.p. and mixed m.p. 100°–101° C. with sintering at 73°–76° C. and $[\alpha]_D^{25} = +125°$ (5 minutes) $\rightarrow +84° \pm 1°$ in 24 hours (*c*, 1.2% in water).

Fraction 10.—The sirup (9 mg.) on chromatographic examination in solvents B and C appeared to be a monomethyl galactose. The material was not investigated further.

The amounts of the main methylated sugar components and their molar ratios are given in Table II.

Periodate Oxidation

Spruce polysaccharide (100 mg. duplicate samples) was dissolved in water (50 ml.) and oxidized by 0.1 *M* sodium periodate (50 ml.) in the dark at 16° C. Analysis for periodate consumption and formic acid production (24) gave the following results:

Time, hours	12	22	72	120	144
Formic acid, moles per $C_5H_8O_4$	0.51	0.55	0.65	0.71	0.73
Periodate consumption, moles per $C_5H_8O_4$	1.03	1.12	1.29	1.37	1.40

The time at which the oxidation was completed was found by extrapolating the flat portion of the time curve to zero time. The values of 1.15 moles of periodate per mole of anhydrogalactose residue and 0.55 moles of formic acid were obtained. In a separate experiment, 50 mg. of the polysaccharide was oxidized for 48 hours, the excess periodate was destroyed by the addition of 2,3-butanediol and the solution dialyzed. The nondialyzable solids were recovered by freeze-drying and then hydrolyzed with *N* sulphuric acid. Chromatographic examination of the neutralized solution showed galactose to be the only sugar present.

ACKNOWLEDGMENTS

The author wishes to thank A. E. Castagne for valuable technical assistance throughout the course of this investigation. Thanks are also tendered to Dr. H. Schwartz, Superintendent, Forest Product Laboratories, Ottawa, Canada, who kindly supplied an authenticated specimen of white spruce wood.

Can. J. Chem. Downloaded from www.nrcresearchpress.com by 200.7.193.243 on 09/04/12
For personal use only.

REFERENCES

1. SCHORGER, A. W. and SMITH, D. F. Ind. Eng. Chem. **8**, 494 (1916).
2. WISE, L. E. and PETERSON, F. C. Ind. Eng. Chem. **22**, 362 (1930).
3. WISE, L. E. and UNKAUF, H. C. Cellulosechemie, **14**, 20 (1933).
4. WHITE, E. V. J. Am. Chem. Soc. **63**, 2871 (1941).
5. HIRST, E. L., JONES, J. K. N., and CAMPBELL, W. G. Nature, **147**, 25 (1941).
6. BRAUNS, F. E. Science, **102**, 155 (1945).
7. FOREMAN, E. L. and ENGLES, D. T. Ind. Eng. Chem. **23**, 415 (1931).
8. WADMAN, W. H., ANDERSON, A. B., and HASSID, W. Z. J. Am. Chem. Soc. **76**, 4097 (1954).
9. BISHOP, C. T. Can. J. Chem. **35**, 1010 (1957).
10. PETERSON, F. C., BARRY, A. J., UNKAUF, H., and WISE, L. E. J. Am. Chem. Soc. **62**, 2361 (1940).
11. CAMPBELL, W. G., HIRST, E. L., and JONES, J. K. N. J. Chem. Soc. 774 (1948).
12. WHITE, E. V. J. Am. Chem. Soc. **64**, 302 (1942).
13. WHITE, E. V. J. Am. Chem. Soc. **64**, 1507 (1942).
14. WHITE, E. V. J. Am. Chem. Soc. **64**, 2838 (1942).
15. ADAMS, G. A. TAPPI, **40**, 721 (1957).
16. LEMIEUX, R. U., BISHOP, C. T., and PELLETIER, G. E. Can. J. Chem. **34**, 1365 (1956).
17. HOUGH, L., JONES, J. K. N., and WADMAN, W. H. J. Chem. Soc. 1702 (1950).
18. HUMPHREYS, R. W., PRYDE, J., and WATERS, E. T. J. Chem. Soc. 1298 (1931).
19. MCCREATH, D. and SMITH, F. J. Chem. Soc. 387 (1939).
20. WHISTLER, R. L., CONRAD, H. E., and HOUGH, L. J. Am. Chem. Soc. **76**, 1668 (1954).
21. EHRENTHAL, I., RAFIQUE, M. C., and SMITH, F. J. Am. Chem. Soc. **74**, 1341 (1952).
22. SMITH, F. J. Chem. Soc. 1724 (1939).
23. MARTIN, S. M. Chem. & Ind. 823 (1957).
24. CHANDA, S. K., HIRST, E. L., and PERCIVAL, E. G. V. J. Chem. Soc. 1240 (1951).

Can. J. Chem. Downloaded from www.nrcresearchpress.com by 200.7.193.243 on 09/04/12
For personal use only.

Can. J. Chem. Downloaded from www.nrcresearchpress.com by 200.7.193.243 on 09/04/12
For personal use only.

STUDIES IN THE WAGNER–MEERWEIN REARRANGEMENT. PART III[1]

F. A. L. Anet and P. M. G. Bavin[2]

ABSTRACT

2-(9-Methyl-9-fluorenyl)-propan-2-ol and 3-(9-ethyl-9-fluorenyl)-pentan-3-ol have been prepared and shown to give 9,10-dimethyl- and 9-10-diethylphenanthrene, respectively, when heated with polyphosphoric acid.

In Part I of this series (1), we reported that dehydration-rearrangement of 9-*t*-butyl-9-fluorenylmethanol (I, R_1 = *t*-butyl; R_2 = R_3 = hydrogen) by the action of polyphosphoric acid gave rise to a considerable amount of phenanthrene. Since 9-*t*-butylphenanthrene was stable under these conditions, loss of the alkyl group appeared to take place during the rearrangement process. Accordingly, we tried to prepare 2-(9-*t*-butyl-9-fluorenyl)-propan-2-ol (I, R_1 = *t*-butyl; R_2 = R_3 = methyl), which was expected to lead to 9,10-dimethylphenanthrene by expulsion of the *t*-butyl group and a double Wagner–Meerwein rearrangement. Our attempts to prepare this carbinol from methyl 9-*t*-butylfluorene-9-carboxylate have failed (see below), but we have made some related carbinols in which rearrangement and aromatization involved expulsion of an alkyl group.

Methyl magnesium iodide reacted with methyl 9-methylfluorene-9-carboxylate to give 2-(9-methyl-9-fluorenyl)-propan-2-ol (I, R = methyl) in 70–80% yield. Heating of this alcohol with polyphosphoric acid gave 9,10-dimethylphenanthrene. Similarly, ethyl magnesium iodide reacted with methyl 9-ethylfluorene-9-carboxylate to give 3-(9-ethyl-9-fluorenyl)-pentan-3-ol (I, R = ethyl), which gave by heating with polyphosphoric acid 9,10-diethylphenanthrene. In both reactions with polyphosphoric acid the yield of crude hydrocarbon was about 30–50%, but only about 4–10% was obtained completely pure.

These rearrangements may be represented as shown below. It is possible that a shuffling of the alkyl groups in II takes place, and this point could be examined by using suitably labelled alkyl groups.

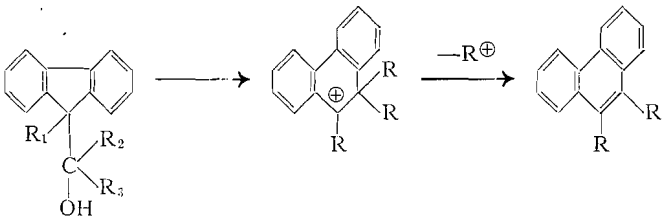

I II

The increase in resonance energy on passing from II to the 9,10-dialkylphenanthrene probably supplies the driving force for the expulsion of the alkyl group (R).

It was shown previously (1) that methyl 9-*t*-butylfluorene-9-carboxylate was saponified much more slowly than the 9-methyl compound, the difference being attributed to steric hindrance in the former compound. In agreement with this we have found that the 9-*t*-

[1]*Manuscript received January 10, 1958.*
Contribution from the Department of Chemistry, University of Ottawa, Ottawa, Canada.
[2]*National Research Council of Canada Postdoctorate Fellow, 1954–1956. Present address: the Ohio State University, Columbus 10, Ohio.*

butyl derivative was recovered unchanged after boiling for 1 hour with ethereal methyl magnesium iodide. Prolonged reaction with lithium methyl or the Grignard reagent gave a mixture which we were unable to resolve.

EXPERIMENTAL

Preparation of the Tertiary Carbinols

Methyl 9-methylfluorene-9-carboxylate (1) (3 g.) was boiled under reflux for 2 hours with ethereal methyl magnesium iodide (6 equivalents). The complex was decomposed with ice and ammonium chloride. Evaporation of chloroform extracts gave an oil which crystallized when left overnight in the ice chest under a little hexane. Recrystallization from hexane gave *2-(9-methyl-9-fluorenyl)-propan-2-ol* as long, colorless prismatic needles (2.1 g., 70%), m.p. 68°–69°. Found: C, 85.75; H, 7.52%. Calc. for $C_{17}H_{18}O$: C, 85.67; H, 7.61%.

Reaction of methyl 9-ethylfluorene-9-carboxylate (1) with ethyl magnesium iodide gave, in the same way, *3-(9-ethyl-9-fluorenyl)-pentan-3-ol* in 79% yield. It crystallized from hexane as short stout prisms, m.p. 103°–105°. Found: C, 85.55; H, 8.40%. Calc. for $C_{20}H_{24}O$: C, 85.66; H, 8.63%.

The infrared spectra of carbon disulphide solutions of the carbinols showed strong O–H stretching bands at 3615 $cm.^{-1}$. Solutions of the carbinols in cold concentrated sulphuric acid were carmine.

The crude carbinols melted over a wide range and 20°–30° below the pure compounds, although the infrared spectra did not show carbonyl absorption. It is likely that the carbinols have high molar depression constants, as have been found for other highly branched compounds (2).

Reaction of the Carbinols with Polyphosphoric Acid

The methyl carbinol (1 g.) and polyphosphoric acid (150 ml.) were heated together with stirring at 160° for 1 hour and then at 180° for 15 minutes. The cooled mixture was poured onto ice and extracted with chloroform. Evaporation left an oil which was dissolved in hexane and purified by passage through a column of alumina. Further elution and subsequent evaporation gave a colorless oil. Crystallization from methanol–acetone gave white needles, m.p. 134°–137°, raised to 142°–144° by three more crystallizations. The melting point was not depressed when the compound was mixed with authentic 9,10-dimethylphenanthrene (3), m.p. 143°–144°. Alternatively the hydrocarbon was purified through its picrate or trinitrobenzene complex.

In a similar way the ethyl carbinol gave 9,10-diethylphenanthrene, which formed glistening plates, m.p. 103°–105°, after four crystallizations from methanol–acetone. The melting point was not depressed when the compound was mixed with authentic 9,10-diethylphenanthrene (4), m.p. 106°–107°. The identities were confirmed by comparison of infrared spectra.

Attempted Preparation of 2-(9-t-Butyl-9-fluorenyl)-propan-2-ol

Methyl 9-*t*-butylfluorene-9-carboxylate (1) (12 g.) and ethereal methyl magnesium iodide (12 equivalents) were boiled under reflux for 24 hours. The product was isolated in the usual way, dissolved in hexane, and passed through a short column of activated alumina. When the product was concentrated to 15 ml. and left standing in the ice chest for 3 weeks it gave colorless prisms (7.4 g.). These were collected, washed with a little ice-cold pentane, and recrystallized from hexane (10 ml.) as before to give 4.2 g. of prisms, m.p. 70°–71°. The infrared spectrum of a chloroform solution did not show

Can. J. Chem. Downloaded from www.nrcresearchpress.com by 200.7.193.243 on 09/04/12
For personal use only.

hydroxyl or carbonyl absorption. The yield of this compound was erratic. A solution of the crude product in carbon bisulphide showed an O–H stretching band at 3618 cm.$^{-1}$.

ACKNOWLEDGMENT

The authors are grateful to Dr. D. McNeil and Dr. C. K. Bradsher for authentic samples of 9,10-dimethyl- and 9,10-diethylphenanthrene, respectively.

REFERENCES

1. ANET, F. A. L. and BAVIN, P. M. G. Can. J. Chem. **34**, 991 (1956).
2. BARTLETT, P. D. and LEFFERTS, E. B. J. Am. Chem. Soc. **77**, 2804 (1955).
3. GREENHOW, E. J., MCNEIL, D., and WHITE, E. N. J. Chem. Soc. 986 (1952).
4. BRADSHER, C. K. and BEAVERS, D. J. J. Am. Chem. Soc. **78**, 3194 (1956).

Can. J. Chem. Downloaded from www.nrcresearchpress.com by 200.7.193.243 on 09/04/12
For personal use only.

Can. J. Chem. Downloaded from www.nrcresearchpress.com by 200.7.193.243 on 09/04/12
For personal use only.

SOME STRUCTURAL FEATURES OF DELCOSINE[1]

RAGINI ANET[2] AND LÉO MARION

ABSTRACT

The alkaloid delcosine has previously been assigned tentatively the same carbon–nitrogen skeleton as lycoctonine to which it appears to be closely related in properties. Oxidation experiments now reported provide supporting evidence of the presence of two vicinal tertiary hydroxyl groups attached to a five- and a six-membered ring that are directly linked together at the two carbons carrying the hydroxyls. There is a methoxyl in a position β to the tertiary hydroxyl of the six-membered ring. Evidence is also provided as to the size of the heterocyclic ring and the presence of a methylene group next to the nitrogen.

The tentative structure I previously advanced for delcosine ($C_{24}H_{39}O_7N$) was based on an assumed relationship with the alkaloid lycoctonine, and on the possibility on this assumption[3] of explaining the nature of the oxidation products that had been described (1). We now wish to report further oxidation studies carried out with anhydrohydroxydelcosine II ($C_{24}H_{37}O_7N$), which lend support to some of the features of structure I.

Whereas lycoctonine (2) and demethylenedelpheline (3) yield oxo-derivatives that can be cleaved smoothly with periodic acid or lead tetraacetate, the corresponding bases are not oxidized in a satisfactory manner under the same conditions. Similarly, treatment of delcosine with periodic acid or sodium periodate at room temperature resulted in 4.5 moles of the reagent being consumed in 120 hours, the oxidation continuing until 21 moles had been consumed. The behavior with lead tetraacetate was equally indefinite.[4]

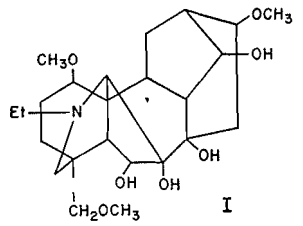

I

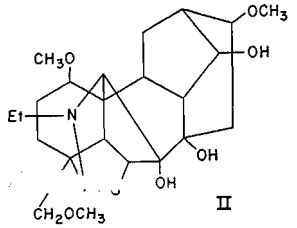

II

Anhydrohydroxydelcosine, an oxidation product which has been formulated as II, is much less basic than delcosine (1) and thus was expected to lend itself to cleavage with periodic acid more satisfactorily than the alkaloid. Indeed, it has now been found that on treatment with periodic acid at room temperature, anhydrohydroxydelcosine consumes 1 mole of the reagent in 24 hours. It has not been possible to obtain the oxidation product crystalline even after purification by chromatography on alumina, but its infrared absorption spectrum (in chloroform) contained two carbonyl bands at 1750 and 1710 cm.$^{-1}$ (no aldehyde stretching band at 2600–2800 cm.$^{-1}$) characteristic of a five- and a six-membered ketone respectively, as well as a band at 1000 cm.$^{-1}$ shown also by the spectrum of anhydrohydroxydelcosine in the same solvent. Clearly the oxidation product

[1]*Manuscript received January 21, 1958.*
Contribution from the Division of Pure Chemistry, National Research Council, Ottawa, Canada.
Issued as N.R.C. No. 4678.
[2]*National Research Council of Canada Postdoctorate Fellow.*
[3]*In the paper cited as Ref. (1), formula VII is an error. It should have been the formula of lycoctonine corresponding to the diterpenoid representation VIII. As given, VII is the formula of delcosine, and corresponds to the diterpenoid representation IX.*
[4]*These titration experiments were performed by Dr. D. W. Clayton.*

Can. J. Chem. Downloaded from www.nrcresearchpress.com by 200.7.193.243 on 09/04/12
For personal use only.

is anhydrohydroxydelcosine-*seco*diketone III formed by cleavage of a vicinal glycol system in which one of the hydroxyls is a substituent on a five-membered ring, and the other on a six-membered ring.

Although the *seco*diketone III could not be induced to crystallize, it formed a crystalline acetyl derivative IV ($C_{26}H_{37}O_8N$). In the infrared this derivative showed bands at 1763 and 1705 cm.$^{-1}$ characteristic of the carbonyls of a five-membered and a six-membered cyclic ketone, and at 1738 and 1233 cm.$^{-1}$ due to the acetate grouping. There was no absorption in the hydroxyl region. On treatment with acid under carefully controlled conditions, the acetyl derivative IV lost the elements of methanol and gave rise to desmethanol-anhydrohydroxydelcosine-*seco*diketone acetate, $C_{25}H_{33}O_7N$ (V), which in the infrared showed absorption bands at 1760, 1740, 1680, and 1615 cm.$^{-1}$. The shift in the frequency of the carbonyl band of the six-membered cyclic ketone from 1705 to 1680 cm.$^{-1}$ corresponds to the change to be expected in going from a saturated to an α,β-unsaturated ketone (4). In the ultraviolet spectrum of V the absorption at λ_{max} 232 mμ, logϵ 3.89, was somewhat higher than expected for an α,β-unsaturated-β-monosubstituted ketone (5) although the same as that occurring in the spectrum of desmethanol-hydroxylycoctonam-*seco*diketone (λ_{max} 230–233 mμ, logϵ 3.74) (6). Hence it is very probable that the double bond in V is α,β- to the carbonyl of the six-membered cyclic ketone. This parallels the chemistry of lycoctonine, and provides evidence concerning the vicinal glycol in delcosine and its environment. Consequently, on the basis of the proposed structure I, the desmethanol-derivative V can be represented as follows:

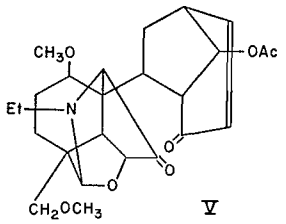

V

The amorphous anhydrohydroxydelcosine-*seco*diketone III was reduced with sodium borohydride to a compound VI ($C_{23}H_{37}O_6N$) which had lost the elements of methanol. Under the alkaline conditions of the reduction, the β-methoxyl group had been eliminated, and the carbonyls of both the six-membered and five-membered cyclic ketones had been reduced to secondary alcoholic groups. The infrared spectrum of VI showed no absorption in the carbonyl region. The presence of a double bond was confirmed by catalytic hydrogenation in the course of which 1 mole of hydrogen was absorbed smoothly. The behavior of the derivative III, on reduction, was markedly different from that of lycoctonam-*seco*diketone in which only the five-membered, but not the six-membered, ketone was reduced (2). A plausible explanation for this difference is that the internal ether present in compound V orients the carbonyls away from each other so that neither is hindered.

Hydrogenation of the *seco*diketone acetate IV, or its desmethanol-derivative V, in the presence of Adams' catalyst gave erratic results, but in the presence of palladium–charcoal in 50% acetic acid the compound V absorbed 2 moles of hydrogen in 30 minutes. No further absorption took place in the next 2 hours. The product was a crystalline compound VII ($C_{25}H_{37}O_7N$) obtained in 90% yield. Since under similar conditions anhydrohydroxydelcosine was rapidly reduced to delcosine (1), it was assumed that in the product VII the internal ether as well as the double bond had been hydrogenated. The

infrared absorption spectrum of VII contained bands at 3475 cm.$^{-1}$ indicative of a hydroxyl group; and at 1743, 1728, and 1255 cm.$^{-1}$, the first attributable to a five-membered ketone and the last two to an acetate group. The fact that no absorption occurred at 1700–1720 cm.$^{-1}$ whereas a well-resolved band in that region was present in the spectrum of the *seco*diketone acetate IV seemed to indicate that the six-membered ketone was no longer present in VII. Of the two moles of hydrogen absorbed, one was taken up by the double bond, the other must have reduced the internal ether, and therefore, the disappearance of the carbonyl of the six-membered ketone must be attributed to a rearrangement.

The reduction product VII, when oxidized with potassium permanganate in acetone containing acetic acid, gave rise to a neutral product VIII ($C_{25}H_{35}O_8N$). This neutral product had an infrared absorption spectrum containing bands in the hydroxyl region at 3470 cm.$^{-1}$ and in the carbonyl region at 1762 cm.$^{-1}$ characteristic of a five-membered cyclic ketone, at 1728 and 1255 cm.$^{-1}$ due to an acetate group, and at 1665 cm.$^{-1}$ indicative of an amide carbonyl. On vigorous alkaline hydrolysis, compound VIII produced a gum that could not be crystallized, but still showed in the infrared an absorption band at 1640 cm.$^{-1}$ (in chloroform). It has been shown previously that N-acetyl-N-desethyldelcosine is deacetylated readily under milder conditions, and hence it can be concluded that compound VIII does not contain an aliphatic amide but a lactam which from the frequency of its absorption in the infrared must be at least six-membered. This is the first evidence of the size of the heterocyclic ring in delcosine and of the presence next to the nitrogen of a methylene group consistent with the tentative structure I.

Delcosine is readily oxidized to a carbinolamine internal ether, anhydrohydroxydelcosine II, formed by elimination of water between the carbinolamine hydroxyl and one of the hydroxyls originally present in the base (1). Hence, to account for the facile oxidation of the compound VII to a lactam, it seems necessary to assume that in the course of the hydrogenation in which compound VII was produced, the hydroxyl liberated from the internal ether by reduction must have become masked. A possible explanation is that in the conversion of V to VII, this hydroxyl, set free by the hydrogenation, forms a hemiketal with the carbonyl of the six-membered ketone so that VII could be represented as follows:

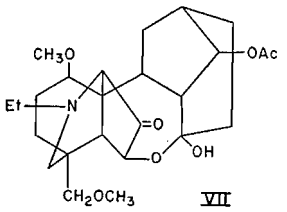

VII

The oxidation product VIII would therefore be the corresponding lactam. The infrared spectra of both VII and VIII seem to be in agreement with the presence of a hemiketal, since they contain absorption bands in the regions 1158–1190, 1124–1143, and 1063–1098 cm.$^{-1}$ (cf. 7).

EXPERIMENTAL

Ultraviolet absorption spectra were recorded with a Beckman DU spectrophotometer. The infrared absorption spectra were recorded with a Perkin-Elmer double-beam model

Can. J. Chem. Downloaded from www.nrcresearchpress.com by 200.7.193.243 on 09/04/12
For personal use only.

21 instrument with a rock salt prism. Unless otherwise mentioned the samples were suspended in nujol. All melting points were determined on a microscope hot stage and are uncorrected.

Cleavage of Anhydrohydroxydelcosine with Periodic Acid

To anhydrohydroxydelcosine (146 mg.) in water (5 ml.) 0.12 *M* periodic acid (1.5 ml.) was added and the mixture kept at room temperature in the dark for 25 hours. The aqueous solution was neutralized with sodium bicarbonate and extracted with chloroform. On evaporation, the extract yielded a gum which was dissolved in benzene and chromatographed on neutral alumina (activity III). Anhydrohydroxydelcosine-*seco*diketone was eluted from the column with benzene–ether (1:1). It consisted of a gum that could not be crystallized but was converted to an amorphous white solid in contact with petroleum ether. Its infrared absorption spectrum contained carbonyl bands at 1755 and 1710 $cm.^{-1}$.

O-Acetyl-anhydrohydroxydelcosine-secodiketone

Anhydrohydroxydelcosine (164 mg.) in periodic acid (3 ml.) was allowed to stand for 27 hours. The crude product, obtained as described above, was added to acetic anhydride (5 ml.) containing a few drops of pyridine, and left at room temperature for 18 hours. The acetic anhydride and pyridine were distilled off under reduced pressure at a temperature not exceeding 60°. The residue was dissolved in chloroform and the solution washed with dilute sodium bicarbonate and with water. The combined aqueous washings were extracted with a fresh quantity of chloroform and the combined chloroform extract dried over sodium sulphate and evaporated to dryness under reduced pressure. The residue thus obtained was an oil (90 mg.) that crystallized in contact with a little anhydrous ether. Recrystallized from acetone–ether it consisted of colorless needles, m.p. 189°–190°. Found: C, 63.64; H, 7.44; N, 2.76. Calc. for $C_{26}H_{37}O_8N$: C, 63.52; H, 7.59; N, 2.85%. $[\alpha]_D^{25}$ +131.6° (*c*, 0.38 in chloroform). The compound was very sensitive to alkali and acid and was best purified in neutral solvents. In the ultraviolet it has a maximum, λ_{max} 311 mμ, log ϵ 2.46.

Desmethanol-O-acetyl-anhydrohydroxydelcosine-secodiketone

To a solution of O-acetyl-anhydrohydroxydelcosine-*seco*diketone (200 mg.) in acetic acid (5 ml.), concentrated sulphuric acid (0.5 ml.) was added and the solution heated on the steam bath for 30 minutes. The solution turned pale yellow after 10 minutes and the color deepened slightly towards the end of the heating period. The solution was cooled, neutralized with sodium carbonate, and extracted with chloroform. The residual gum left after evaporation of the chloroform extract was dissolved in benzene and chromatographed on alumina (activity IV). Elution with benzene gave 123 mg. of a base that crystallized from acetone–ether in plates, m.p. 178.5°–179°. Further elution of the column with polar solvents did not yield any crystalline products. For analysis the product was recrystallized three times from the same solvent and dried *in vacuo* at 100°. Found: C, 65.23; H, 7.25; N, 3.11; OCH_3, 13.76. Calc. for $C_{25}H_{33}O_7N$: C, 65.34; H, 7.24; N, 3.05; $2OCH_3$, 13.51%. $[\alpha]_D^{25}$ +76.25° (*c*, 0.8 in chloroform). Ultraviolet: λ_{max} 231–232 mμ, log ϵ 3.89; λ_{max} 312 mμ, log ϵ 2.46. The crystalline desmethanol compound was sensitive to acids and alkalies and with the latter gave a soluble yellow substance which was rapidly oxidized to a tar.

Reduction of Anhydrohydroxydelcosine-secodiketone

A small quantity of the chromatographed amorphous *seco*diketone dissolved in 50%

Can. J. Chem. Downloaded from www.nrcresearchpress.com by 200.7.193.243 on 09/04/12
For personal use only.

methanol was treated with sodium borohydride at room temperature for 3 hours. Water was then added and the solution extracted with chloroform. Evaporation of the extract left an oil that crystallized from acetone in plates, m.p. 253°–254°. Found: C, 65.08; H, 8.98; N, 3.34; OCH_3, 16.42. Calc. for $C_{23}H_{37}O_6N$: C, 65.22; H, 8.81; N, 3.31; $2OCH_3$, 14.64%. $[\alpha]_D^{25}$ +34° (*c*, 0.4 in chloroform).

Hydrogenation of Desmethanol-O-acetyl-anhydrohydroxydelcosine-secodiketone

The desmethanol compound (V) (253 mg.) dissolved in 50% acetic acid (8 ml.) was hydrogenated at room temperature and atmospheric pressure in the presence of palladium–charcoal (175 mg.). Two moles of hydrogen were absorbed in 30 minutes and no further uptake was observed during the next 2 hours. The catalyst was filtered out and washed thoroughly with dilute acetic acid. The combined filtrate and washings were neutralized with sodium bicarbonate and extracted with chloroform. The extract on evaporation left a gum (240 mg.) that crystallized when triturated with ether, m.p. 178°–181° (compound VII). Chromatography and further crystallization did not raise the melting point. Found: C, 64.79; H, 7.98; N, 3.19. Calc. for $C_{25}H_{37}O_7N$: C, 64.77; H, 8.05; N, 3.02%. $[\alpha]_D^{25}$ −14° (*c*, 0.75 in chloroform).

Oxidation of Compound VII

The product VII of the catalytic hydrogenation (220 mg.) was dissolved in acetone (20 ml.) containing 50% acetic acid (1 ml.). Powdered potassium permanganate (153 mg.) was added portionwise to the solution over a period of 2 hours. The reaction mixture was allowed to stand at room temperature for 20 hours, excess permanganate destroyed by the careful addition of a saturated solution of sodium bisulphite, and the manganese dioxide filtered off and washed with acetone. The combined filtrate and washings were evaporated under diminished pressure and the residue dissolved in chloroform. The chloroform solution was washed with dilute sulphuric acid and the acid washings extracted once with chloroform. The combined chloroform solutions were dried and evaporated to dryness. There was left a froth which was dissolved in benzene and chromatographed on alumina (activity IV). The fraction eluted with chloroform yielded 130 mg. of the lactam VIII which crystallized from ether – petroleum ether as colorless prisms, m.p. 183°–184°. Found: C, 62.70; H, 7.33; N, 3.08. Calc. for $C_{25}H_{35}O_8N$: C, 62.87; H, 7.39; N, 3.08%. $[\alpha]_D^{25}$ −17° (*c*, 1.1 in chloroform).

ACKNOWLEDGMENTS

The authors wish to express their indebtedness to Dr. R. N. Jones and Mr. R. Lauzon of these laboratories for the determination of the infrared absorption spectra.

REFERENCES

1. ANET, R., CLAYTON, D. W., and MARION, L. Can. J. Chem. **35**, 397 (1957).
2. EDWARDS, O. E. and MARION, L. Can. J. Chem. **32**, 195 (1954).
3. COOKSON, R. C. and TREVETT, M. E. J. Chem. Soc. 3121 (1956).
4. BELLAMY, L. J. The infrared spectra of complex molecules. Methuen & Co. Ltd., London. 1954.
5. WOODWARD, R. B. J. Am. Chem. Soc. **63**, 1123 (1941).
6. EDWARDS, O. E., MARION, L., and STEWART, D. K. R. Can. J. Chem. **34**, 1315 (1956).
7. BERGMANN, E. D. and PINCHAS, D. Rec. trav. chim. **71**, 161 (1952).

Can. J. Chem. Downloaded from www.nrcresearchpress.com by 200.7.193.243 on 09/04/12
For personal use only.

Can. J. Chem. Downloaded from www.nrcresearchpress.com by 200.7.193.243 on 09/04/12
For personal use only.

REACTION OF TRICHLOROACETONITRILE WITH PRIMARY AND SECONDARY AMINES

PART I. PREPARATION OF SOME TRICHLOROACETAMIDINES[1]

JOHN C. GRIVAS[2] AND ALFRED TAURINS

ABSTRACT

Trichloroacetonitrile reacts with primary and secondary aliphatic and primary aromatic amines to give N-substituted trichloroacetamidines. A series of N-mono- and N-di-substituted trichloroacetamidines, $CCl_3—C(=NH)—NHR$ and $CCl_3—C(—NR_1R_2)=NH$, was prepared by carrying out the reaction in water, in water–methanol solutions, or in the absence of solvents.

INTRODUCTION

Although acetonitrile forms N-substituted acetamidines by the addition of amines only in the presence of anhydrous aluminum chloride (1), trichloroacetonitrile reacts with amines more easily. The German Patent No. 671,785 (2) reported the preparation of some trichloroacetamidines by the direct interaction of trichloroacetonitrile with aliphatic primary amines at low temperature, without giving any details. Oxley (3) prepared trichloroacetamidine and N,N-ethylene-bis-trichloroacetamidine in benzene solution. Backer and Wanmaker (4) isolated N-methyl- and N-piperidyl-trichloroacetamidine only in the form of picrates. They found that the addition of aromatic amines to trichloroacetonitrile proceeded only in the presence of methanol or acetone. The role of methanol in the reaction was explained by assuming that methanol first adds to trichloroacetonitrile to form an iminoether as an intermediate which subsequently reacts with aniline to give the amidine.

The objective of the present work was the investigation of the preparation of trichloroacetamidines by the direct addition of amines to trichloroacetonitrile without using any catalysts. In the next part, a kinetic study of the reaction will be presented, followed by the investigation of the correlation between the infrared spectra and the structure of amidines.

DISCUSSION

The preparation of the N-substituted trichloroacetamidines involved three general procedures: (*a*) the lower primary and secondary aliphatic amines were treated with trichloroacetonitrile in water solutions; (*b*) the reactions of the higher aliphatic and cyclic amines were carried out in the absence of solvents; and (*c*) the aromatic primary amines were allowed to react with trichloroacetonitrile in water–methanol solution. The results are summarized in Table I. The three procedures are characterized by their simplicity, the absence of catalysts, and the high yields of the reaction products.

The lower aliphatic N-substituted trichloroacetamidines are colorless liquids possessing an unpleasant smell. They can be distilled at low pressure in a dry nitrogen atmosphere, whereas they decompose vigorously on being heated at normal pressure. It was found

[1]*Manuscript received October 9, 1957.*
Contribution from the Department of Chemistry, McGill University, Montreal, Que., with financial assistance from the National Research Council, Ottawa, Canada.
[2]*Abstracted from a thesis submitted by J. C. Grivas to the Faculty of Graduate Studies and Research, McGill University, Montreal, Que., in partial fulfillment of the requirements for the M.Sc. degree, May, 1957.*

TABLE I

No.	Trichloro-acetamidine	Procedure	Yield, %	B.p.		Empirical formula	Nitrogen, %	
				° C.	mm. Hg		Calc.	Found[j]
1	N-Methyl-[b]	A	86	129	60	$C_3H_5Cl_3N_2$	15.96	15.85
2	N-Ethyl-[c]	A	84	62	2	$C_4H_7Cl_3N_2$	14.77	14.68
3	N-*n*-Butyl-	B	92	71–72	2	$C_6H_{11}Cl_3N_2$	12.87	12.67
4	N-*n*-Amyl-	B	94	89–90	2	$C_7H_{13}Cl_3N_2$	12.09	11.97
5	N,N-Dimethyl-[d]	A	68	51–52	2	$C_4H_7Cl_3N_2$	14.77	14.67
6	N,N-Diethyl-[e]	B	91	61–61.5	2	$C_6H_{11}Cl_3N_2$	12.87	12.69
7	N-Piperidyl-[f]	B	87	80–81	1.5	$C_7H_{11}Cl_3N_2$	12.20	12.09
8	N-Morpholyl-	B	92	89	1	$C_6H_9Cl_3N_2O$	12.10	11.99
9	N-Isopropyl-[g]	B	91	56[a]		$C_5H_9Cl_3N_2$	13.77	13.92
10	N-Benzyl-[h]	B	89	83.5[a]		$C_9H_9Cl_3N_2$	11.13	11.14
11	N-Phenyl-[i]	C	92	101–102[a]		$C_8H_7Cl_3N_2$	11.80	11.80
12	N-*p*-Ethoxyphenyl-	C	94	104[a]		$C_{10}H_{11}Cl_3N_2O$	9.95	9.90
13	N-*p*-Tolyl-	C	92	138.5[a]		$C_9H_9Cl_3N_2$	11.13	10.99
14	N-*m*-Tolyl-	C	95	100[a]		$C_9H_9Cl_3N_2$	11.13	10.96
15	N-*o*-Tolyl-	C	83	73[a]		$C_9H_9Cl_3N_2$	11.13	11.13

[a] *Melting points (° C.), corrected.*
[b] *Picrate, m.p. 163°–164°. Reported in the literature (4): m.p. 163°–164°.*
[c] *Hydrochloride, m.p. 224°–225° (decomp.).*
[d] *The yields can be increased by vigorous stirring for a longer period of time. Picrate, m.p. 162°–163°.*
[e] *Picrate, m.p. 153°.*
[f] *Picrate, m.p. 140°–140.5°. Reported in the literature (4): m.p. 139.5°–140°.*
[g] *The liquid mixture solidified in 2 minutes. The unreacted substances were evaporated in a vacuum and the solid N-isopropyl-2,2,2-trichloroacetamidine was purified by sublimation at 2 mm. pressure.*
[h] *Reported in the literature (2) but no analysis has been given. The substance was crystallized from a methanol–water mixture.*
[i] *The substance has been prepared by other authors (4, 5) using different methods. Hydrochloride, m.p. 180°–183°.*
[j] *Microanalyses by Mr. W. Manser (Herrliberg, Switzerland).*

that the salts of the primary and secondary amines do not react with trichloroacetonitrile in water solution.

The additon of the primary and secondary amines to the carbon–nitrogen triple bond seems to be an ionic reaction, which is facilitated by polar solvents, such as water and methanol. In the absence of kinetic data no proof of the mechanism is possible; however, the information obtained in this work may suggest the following scheme:

$$Cl_3C{\leftarrow}C{\equiv}\ddot{N}: + R{-}\ddot{N}H_2 \rightarrow Cl_3C{-}C{=}\ddot{N}:^- \rightarrow Cl_3C{-}C{=}\ddot{N}H$$

$$\qquad\qquad\qquad\qquad\quad H{-}N^+{-}H \qquad\qquad H{-}\ddot{N}:$$

$$\qquad\qquad\qquad\qquad\quad\ \ R \qquad\qquad\quad\ R$$

The chlorine atoms in the position α to the nitrile group increase the positive charge of the carbon atom of the nitrile group by the inductive ($-$Is) effect. The attack of the unshared electron pair of the amine nitrogen on the positive carbon is followed by the formation of a bond between these atoms, the liberation of a proton, and the subsequent addition of the proton to the negatively charged nitrogen atom. This scheme may explain the failure of the reaction between the amine salts and trichloroacetonitrile, and also the lower reactivity of the aromatic amines in which the mobility of the unshared electron pair of the nitrogen atom is decreased by the resonance effect. The ionic intermediate also explains the activating influence of water and methanol in the reaction of trichloroacetonitrile with amines.

Can. J. Chem. Downloaded from www.nrcresearchpress.com by 200.7.193.243 on 09/04/12
For personal use only.

As has been mentioned above, it has been suggested (4) that methanol is essential in the reaction of trichloroacetonitrile with aniline by forming the intermediate amidine methyl ether. Our experiments indicated that this view cannot stand, for the following reasons: (*a*) aniline reacts with trichloroacetonitrile even in the absence of methanol or other solvents; (*b*) the reaction occurs also in ethanol, which, contrary to methanol, does not react with trichloroacetonitrile.

EXPERIMENTAL

The following procedures were applied for the synthesis of N-substituted trichloroacetamidines.

Procedure A—In Water Solutions

This procedure is useful for commercial aqueous solutions of primary and secondary aliphatic amines.

N-Methyl-2,2,2-trichloroacetamidine.—Trichloroacetonitrile (8 ml.) was added dropwise with stirring over a period of 10 minutes to 15 ml. of 25% aqueous solution of methylamine. The reaction was exothermic and the flask containing the reaction mixture was cooled in an ice-water bath. The lower layer was separated, dried, and distilled. B.p. 129° at 60 mm. pressure. Yield 11.5 g., 86% of the theoretical.

N,N-Dimethyl-2,2,2-trichloroacetamidine.—Trichloroacetonitrile (7.2 g., 0.05 M.) was added to 4 ml. of an aqueous solution of dimethylamine containing 2.25 g. of the pure amine. The mixture was shaken for half an hour. The lower layer was separated, dried, and distilled. B.p. 51°–52° at 2 mm. pressure. Yield 6.45 g., 68% of the theoretical.

Procedure B—In the Absence of Solvents

This procedure can be applied successfully to the reactions of higher aliphatic primary and secondary amines, and also to piperidine and morpholine. The reaction time was 3 hours at least, and the reactions were carried out at room temperature.

N-n-Butyl-2,2,2-trichloroacetamidine.—Trichloroacetonitrile (7.2 g.) was added dropwise to 3.65 g. (0.05 M.) of pure *n*-butylamine. The temperature rose considerably and the mixture turned yellow. The distillation of the reaction product gave a colorless liquid. B.p. 71°–72° at 2 mm. pressure. Yield 9.92 g., 92% of the theoretical.

Procedure C—In Water–Methanol or Methanol Solutions at Room Temperature

This method was applied to the reactions of primary aromatic amines with trichloroacetonitrile. After a period of 3 days the reaction products were precipitated by the addition of water in almost quantitative yields. They were recrystallized from petroleum ether or water–methanol mixtures.

Reaction of Aniline and Trichloroacetonitrile

(*a*) *In the absence of solvents.*—Trichloroacetonitrile (1.44 g., 0.01 M.) was mixed with 0.93 g. of aniline (0.01 M.) and left at room temperature for 5 days. The mixture turned red, brown, and finally black, and after 48 hours crystals started to precipitate in small quantity. The mixture was diluted with 7 ml. of methanol. The reaction product was precipitated by addition of water, filtered, and crystallized from a methanol–water mixture, m.p. 101°–102°. The yield was 1.27 g. (54% of the theoretical).

(*b*) *In ethanol solution.*—Equimolar quantities of the reactants mentioned in (*a*) were dissolved in 5 ml. of ethanol and left at room temperature for 5 days. Addition of water, at the end of this period, caused the precipitation of N-phenyltrichloroacetamidine which melted at 101°–102° after crystallization from water–methanol. Yield 1.8 g. (76%).

Can. J. Chem. Downloaded from www.nrcresearchpress.com by 200.7.193.243 on 09/04/12
For personal use only.

Preparation of Picrates and Hydrochlorides

The picrates of trichloroacetamidines were obtained by the addition of equimolar quantities of the amidines and picric acid in benzene solution. The precipitated picrates were crystallized from water. Hydrochlorides of amidines were prepared by passing of a hydrogen chloride gas through solutions of amidines in dry ether.

REFERENCES

1. OXLEY, P., SHORT, F. W., and PARTRIDGE, M. J. Chem. Soc. 1110 (1947).
2. GERMAN PATENT No. 671,785 (1939); Chem. Abstr. **33**, 6345 (1939).
3. OXLEY, P., PARTRIDGE, M. W., and SHORT, F. W. J. Chem. Soc. 303 (1948).
4. BACKER, H. J. and WANMAKER, W. L. Rec. trav. chim. **70**, 638 (1951).
5. STEINKOPF, W. Ber. deut. chem. Ges. **40**, 1643 (1907); J. prakt. Chem. (2) **81**, 202 (1910).

Can. J. Chem. Downloaded from www.nrcresearchpress.com by 200.7.193.243 on 09/04/12
For personal use only.

Can. J. Chem. Downloaded from www.nrcresearchpress.com by 200.7.193.243 on 09/04/12
For personal use only.

SOME NEW SULPHONAMIDES AND DERIVATIVES OF BICYCLIC GUANIDINES[1]

M.-E. Kreling and A. F. McKay

ABSTRACT

The preparations and bacteriostatic activities of some sulphonamide derivatives of the bicyclic guanidines are described. Some 1-(2-hydroxy-3-(aryloxy)propyl)-2,3,5,6-tetrahydro-1-imidaz(1,2-*a*)imidazoles have also been prepared.

DISCUSSION

A series of arylsulphonyl derivatives of 2,3,5,6-tetrahydro-1-imidaz(1,2-*a*)imidazole (1, 2), Δ^8-hexahydro-1,4,8-pyrimidazole (3), and Δ^9-1,4,9-triazabicyclo(5.3.0)decene (3) have been prepared for evaluation as bacteriostats. Their properties are listed in Table II. An examination of Table I shows that these compounds display bacteriostatic activity against a number of organisms. Moreover, the activity of the 1-*p*-aminobenzenesulphonyl-2,3,5,6-tetrahydro-1-imidaz(1,2-*a*)imidazole is of the same order as 1-*p*-acetylaminobenzenesulphonyl-2,3,5,6-tetrahydro-1-imidaz(1,2-*a*)imidazole. Both the *p*-aminobenzenesulphonyl-derivatives are fairly toxic compounds. The LD_{50} values for mice by intraperitoneal injection lie within the range of 100–150 mg./kg.

TABLE I

Highest dilutions of sulphonamides (mg./ml.) preventing bacterial growth

Test organisms	I*	II	III	IV	V	VI
Staphylococcus pyogenes (R)	4	4	6	3	6	5
Sarcina lutea	3	<2		3	4	1
Streptococcus faecalis	4	5	6	3	6	>5
Aerobacter aerogenes	4	<2	6	3	4	3
Escherichia coli No. 198	3	3	6	3	3	4
Salmonella pullorum	4	4		3	4	4
Pseudomonas aeruginosa	4	5		3	4	4
Proteus mirabilis	5	4		3	4	>5
Proteus vulgaris	3		6	3	5	3
Staphylococcus pyogenes (S)					7	>5

*I, 1-*p*-Acetylaminobenzenesulphonyl-Δ^9-1,4,9-triazabicyclo(5.3.0)decene.
II, 1-*p*-Toluenesulphonyl-Δ^9-1,4,9-triazabicyclo(5.3.0)decene.
III, 1-*p*-Toluenesulphonyl-Δ^8-hexahydro-1,4,8-pyrimidazole.
IV, 1-*p*-Acetylaminobenzenesulphonyl-Δ^8-hexahydro-1,4,8-pyrimidazole.
V, 1-*p*-Acetylaminobenzenesulphonyl-2,3,5,6-tetrahydro-1-imidaz(1,2-*a*)imidazole.
VI, 1-*p*-Aminobenzenesulphonyl-2,3,5,6-tetrahydro-1-imidaz(1,2-*a*)imidazole.

Some substituted 2,3,5,6-tetrahydro-1-imidaz(1,2-*a*)imidazoles (I) were prepared by the reaction of 1,2-epoxy-3-aryloxypropanes with 2,3,5,6-tetrahydro-1-imidaz(1,2-*a*)imida-

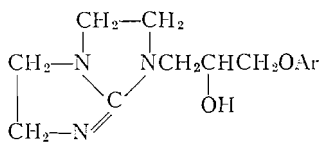

I

Ar = tolyl, *o*- or *p*-chlorophenyl, and 2,4-dichlorophenyl groups

[1]*Manuscript received November 20, 1957.*
Contribution from the L. G. Ryan Research Laboratories of Monsanto Canada Limited, Ville LaSalle, Quebec.

Can. J. Chem. Downloaded from www.nrcresearchpress.com by 200.7.193.243 on 09/04/12
For personal use only.

TABLE II

ARYLSULPHONYL DERIVATIVES OF THE BICYCLIC GUANIDINES

Compound	Yield (%)	M.p. (° C.)	Formula	C		H		N		S	
				Calc.	Found	Calc.	Found	Calc.	Found	Calc.	Found
1-*p*-Toluenesulphonyl-2,3,5,6-tetrahydro-1-imidaz(1,2-*a*)imidazole	99	182–184	$C_{12}H_{15}N_3O_2S$	54.31	54.36	5.70	5.63	15.84	16.13	12.08	11.84
1-*p*-Acetylaminobenzenesulphonyl-2,3,5,6-tetrahydro-1-imidaz(1,2,-*a*)imidazole	94.5	270–271.5	$C_{13}H_{16}N_4O_3S$	50.61	50.66	5.20	5.26	18.16	18.33	10.40	10.52
1-*p*-Toluenesulphonyl-Δ^8-hexahydro-1,4,8-pyrimidazole	99.5	174–177	$C_{13}H_{17}N_3O_2S$	55.89	56.22	6.13	6.11	15.04	15.12	11.48	11.31
1-*p*-Acetylaminobenzenesulphonyl-Δ^8-hexahydro-1,4,8-pyrimidazole	59.1	267–269	$C_{14}H_{18}N_4O_3S$	52.16	52.30	5.63	5.71	17.39	17.69	9.94	9.95
1-*p*-Toluenesulphonyl-Δ^9-1,4,9-triazabicyclo-(5.3.0)decene	86.5	110.5–111.5	$C_{14}H_{19}N_3O_2S$	57.31	57.12	6.53	6.67	14.32	14.51	10.93	11.16
1-*p*-Acetylaminobenzenesulphonyl-Δ^9-1,4,9-triazabicyclo(5.3.0)decene	72.0	236–238	$C_{15}H_{20}N_4O_3S$	53.55	53.33	5.99	6.13	16.66	16.52	9.54	9.43
1-*p*-Nitrobenzenesulphonyl-2,3,5,6-tetrahydro-1-imidaz(1,2-*a*)imidazole	97.9 67.0*	179–180 231–233 dec.	$C_{11}H_{12}N_4O_4S$ $C_{17}H_{15}N_7O_{11}S$	44.58 38.86	44.72 38.87	4.08 2.88	4.16 3.11	18.91 18.67	19.36 18.66	10.82 6.10	10.74 6.12
1-*p*-Aminobenzenesulphonyl-2,3,5,6-tetrahydro-1-imidaz(1,2-*a*)imidazole	85.8	185–186	$C_{11}H_{14}N_4O_2S$	49.60	49.23	5.30	5.36	21.04	21.09	12.04	12.05
1-*p*-Aminobenzenesulphonyl-Δ^9-1,4,9-triazabicyclo(5.3.0)decene	63.0	207–208.5	$C_{13}H_{18}N_4O_2S$	53.05	53.45	6.16	6.40	19.03	18.81	10.90	10.48

**Picrate.*

zole. 1,2-Epoxy-3-(*o*- or *p*-chlorophenoxy)propane gave the expected derivative I (Ar = *o*- or *p*-chlorophenyl) and a small amount (3.8%) of a by-product. The by-product was identified as a di-(2-hydroxy-3-(*o*- or *p*-chlorophenoxy)propyl)-2,3,5,6-tetrahydro-1-imidaz(1,2-*a*)imidazolium chloride by analysis. It gave a test for chloride ion and it formed a picrate whose analysis also agreed with this structure. This indicates that the 1,2-epoxy-3-(*o*- or *p*-chlorophenoxy)propane was contaminated with at least 3.8% of the corresponding chlorohydrin derivative, which was most likely used in the preparation of the epoxy compound.

1-(2-Hydroxy-3-(*m*-methylphenoxy)propyl)- and 1-(2-hydroxy-3-(*o*- or *p*-chlorophenoxy)propyl)-2,3,5,6-tetrahydro-1-imidaz(1,2-*a*)imidazoles gave LD_{50} values of 125–150 mg./kg. and 150–200 mg./kg. respectively on intraperitoneal injection in mice. These compounds produced convulsions at the toxic level.

EXPERIMENTAL[2]

Preparation of the Arylsulphonyl Derivatives of the Bicyclic Guanidines

Since all of the arylsulphonyl derivatives of the bicyclic guanidines were prepared in the same manner, only the preparation of 1-*p*-toluenesulphonyl-Δ^8-hexahydro-1,4,8-pyrimidazole is described in detail. The properties of the arylsulphonyl derivatives are described in Table II.

To a stirred solution of Δ^8-hexahydro-1,4,8-pyrimidazole (5.0 g., 0.04 mole) and *p*-toluenesulphonyl chloride (7.60 g., 0.04 mole) in water (25 ml.) covered with ether (20 ml.) was added a solution of sodium hydroxide (11 ml. of 3.65 *N* sodium hydroxide solution). After the dropwise addition of the sodium hydroxide solution, which required 20 minutes, the reaction mixture was stirred for an additional 40 minutes at room temperature. The product (11.06 g.) was recovered by filtration and then crystallized from ethyl acetate.

1-p-Aminobenzenesulphonyl-2,3,5,6-tetrahydro-1-imidaz(1,2-a)imidazole

A mixture of 1-(*p*-acetylaminobenzenesulphonyl)-2,3,5,6-tetrahydro-1-imidaz(1,2-*a*)-imidazole (9 g., 0.03 mole), ethanol (200 ml.), and 5 *N* sodium hydroxide solution (50 ml.) was heated under reflux for 15 minutes. The solution on cooling and dilution with water deposited crystals, yield 6.7 g. (85.5%). The crude product (m.p. 181°–184°C.) was purified by crystallizing from an acetone–hexane (4:1) solution. 1-*p*-Aminobenzenesulphonyl-Δ^9-1,4,9-triazabicyclo(5.3.0.)decene (Table II) was prepared in a similar manner from 1-*p*-acetylaminobenzenesulphonyl-Δ^9-1,4,9-triazabicyclo(5.3.0)decene.

1-(2-Hydroxy-3-(m-methylphenoxy)propyl)-2,3,5,6-tetrahydro-1-imidaz(1,2-a)imidazole

2,3,5,6-Tetrahydro-1-imidaz(1,2-*a*)imidazole (4.44 g., 0.04 mole) and 1,2-epoxy-3-(*m*-methylphenoxy)propane (6.57 g., 0.04 mole) in absolute methanol (30 ml.) were refluxed for $3\frac{1}{2}$ hours. After the solvent was removed *in vacuo* under nitrogen, a yellow oil was obtained, yield 11.05 g. (99.7%). This oil slowly crystallized over a period of several days. Recrystallization from acetone–hexane gave a 57% yield of pure product (m.p. 102.5°–104° C.). Anal. Calc. for $C_{15}H_{21}N_3O_2$: C, 65.43; H, 7.69; N, 15.27. Found: C, 65.09; H, 7.70; N, 15.42%.

A paper chromatogram of the product on No. 1 Whatman paper developed with butanol – acetic acid – water (40:10:50) gave an R_f value of 0.72 ± 0.01.

Its picrate formed in the usual manner from water melted at 127°–132° C., yield

[2]*All melting points are uncorrected. The microanalyses were determined by Micro-Tech Laboratories, Skokie, Illinois.*

Can. J. Chem. Downloaded from www.nrcresearchpress.com by 200.7.193.243 on 09/04/12
For personal use only.

85.8%. One crystallization from absolute ethanol raised the melting point to 143.5°–144° C. Anal. Calc. for $C_{21}H_{24}N_6O_9$: C, 50.00; H, 4.79; N, 16.66. Found: C, 50.10; H, 4.67; N, 16.92%.

1-(2-Hydroxy-3-(o- or p-chlorophenoxy)propyl)-2,3,5,6-tetrahydro-1-imidaz(1,2-a)imidazole

To a solution of 2,3,5,6-tetrahydro-1-imidaz(1,2-*a*)imidazole (4.44 g., 0.04 mole) in absolute methanol (35 ml.) was added 1,2-epoxy-3-(*o*- or *p*-chlorophenoxy)propane (7.35 g., 0.04 mole) and the mixture was refluxed for 3 hours. Evaporation of the solution *in vacuo* gave 11.7 g. (99%) of semicrystalline solid. A paper chromatogram on No. 1 Whatman paper, which was developed with butanol–acetic acid–water (40:10:50) solvent, gave two spots on spraying with bromcresol green solution with R_f values of 0.77±0.01 and 0.88. The two components were separated by crystallization from acetone. An acetone-insoluble fraction was obtained with an R_f value of 0.88, yield 0.78 g. (3.8%). Two crystallizations from methanol – ethyl acetate (1:5) solution raised the melting point from 183°–189° C. to a constant value of 190°–191° C. These crystals gave a positive test for chloride ion with silver nitrate solution. The analytical values agreed with those calculated for a di-(2-hydroxy-3-(*o*- or *p*-chlorophenoxy)propyl)-2,3,5,6-tetrahydro-1-imidaz-(1,2,-*a*)imidazolium chloride. Anal. Calc. for $C_{23}H_{28}Cl_3N_3O_4$: C, 53.46; H, 5.46; Cl, 20.58; N, 8.13. Found: C, 53.53; H, 5.53; Cl, 20.83; N, 8.01%.

A picrate (m.p. 162.5°–164° C.) was formed in 80% yield in the usual manner from water. The melting point was not changed by further crystallization. Anal. Calc. for $C_{29}H_{30}Cl_2N_6O_{11}$: C, 49.09; H, 4.26; Cl, 9.99; N, 11.85. Found: C, 49.01; H, 4.32; Cl, 10.06; N, 11.89%.

The acetone filtrate from above on cooling deposited 8.37 g. (71.2%) of crystals melting at 149°–153° C. Three crystallizations from acetone raised the melting point to 153.5°–154° C. (R_f, 0.77±0.01). Anal. Calc. for $C_{14}H_{18}ClN_3O_2$: C, 56.86; H, 6.13; Cl, 11.99; N, 14.21. Found: C, 57.32; H, 6.02; Cl, 12.12; N, 14.52%.

A picrate (m.p. 127°–128° C.) was formed in the usual manner from water, yield 86.2%. Two crystallizations from methanol–ether (1:1) solution raised the melting point to 129°–130° C. Anal. Calc. for $C_{20}H_{21}ClN_6O_9$: C, 45.77; H, 4.03; Cl, 6.76; N, 16.02. Found: C, 46.12; H, 4.19; Cl, 6.95; N, 16.14%.

1-(2-Hydroxy-3-(2,4-dichlorophenoxy)propyl)-2,3,5,6-tetrahydro-1-imidaz(1,2-a)imidazole

A solution of 2,3,5,6-tetrahydro-1-imidaz(1,2-*a*)imidazole (4.44 g., 0.04 mole) and 1,2-epoxy-3-(2,4-dichlorophenoxy)propane (8.79 g., 0.04 mole) in absolute methanol (35 ml.) was refluxed for 3 hours. Evaporation of the solution gave 13.04 g. (98.7%) of dark viscous oil. A paper chromatogram prepared as described above gave two basic spots with R_f values of 0.77 and 0.46. The latter value indicated the presence of unchanged 2,3,5,6-tetrahydro-1-imidaz(1,2-*a*)imidazole.

The crude oil (11.04 g.) was refluxed with water (25 ml.) and the aqueous phase was removed by decantation. This process was repeated twice to remove the unchanged starting material from the product. After the sticky residue was triturated with acetone (50 ml.), crystallization occurred, yield 2.36 g. (17.9%). The melting point of these crystals was raised from 154°–156.5° C. to 155°–156.5° C. (R_f, 0.77) by crystallizing from ethanol–water (2:3) solution. Anal. Calc. for $C_{14}H_{17}Cl_2N_3O_2$: C, 50.92; H, 5.19; Cl, 21.48; N, 12.73. Found: C, 50.96; H, 5.23; Cl, 21.83; N, 12.34%.

The picrate was prepared by dissolving a sample of the crystals in the minimum amount of methanol and adding saturated aqueous picric acid solution. The picrate (m.p. 144°–146° C.) was obtained in 66% yield. It was purified to a constant melting point

Can. J. Chem. Downloaded from www.nrcresearchpress.com by 200.7.193.243 on 09/04/12
For personal use only.

of 146°–147° C. by crystallizing from methanol–ether (2:1) solution. Anal. Calc. for $C_{20}H_{20}Cl_2N_6O_9$: C, 42.95; H, 3.61; Cl, 12.68; N, 15.03. Found: C, 42.84; H, 3.59; Cl, 13.03; N, 14.85%.

ACKNOWLEDGMENT

The bacteriostatic and acute toxicity values were determined by Drs. H. A. Baker and C. Chappel of Ayerst, McKenna, and Harrison Ltd., Montreal.

REFERENCES

1. McKAY, A. F., HATTON, W. G., and BRAUN, R. O. J. Am. Chem. Soc. **78**, 6144 (1956).
2. McKAY, A. F., KRELING, M.-E., PARIS, G. Y., BRAUN, R. O., and WHITTINGHAM, D. J. Can. J. Chem. **35**, 843 (1957).
3. McKAY, A. F. and KRELING, M.-E. Can. J. Chem. **35**, 1438 (1957).

Can. J. Chem. Downloaded from www.nrcresearchpress.com by 200.7.193.243 on 09/04/12
For personal use only.

VOLTAIC CELLS IN FUSED SALTS

PART III. THE SYSTEM SILVER - SILVER CHLORIDE, CADMIUM - CADMIUM CHLORIDE[1]

S. N. FLENGAS[2] AND T. R. INGRAHAM

ABSTRACT

Using a silver – silver chloride reference electrode, the standard electrode potential has been established for the equilibrium $Cd|Cd^{++}$ in melts containing equimolar quantities of KCl and NaCl. The experimentally obtained standard potential was greater than that calculated from theoretical thermodynamic data. This difference was attributed to the formation of a cadmium complex in the melt. A dissociation constant for the complex was calculated.

The effect of temperature on the electromotive force of the silver–cadmium voltaic cell was also measured, and the heat of the cell reaction was calculated from the data. To extend the temperature range of the cadmium data, a cadmium–lead alloy was used in the higher temperature experiments. To correlate these data with those for the pure cadmium system, the activity coefficients of cadmium in the alloy were determined electrometrically using the silver – silver chloride electrode as a reference. It was found that the activity coefficients were in agreement with previously published data obtained at lower temperatures using a pure cadmium reference electrode. The activity coefficients were virtually independent of temperature but showed large positive deviations from unity when the mole fraction of cadmium was decreased below about 0.8.

Can. J. Chem. Downloaded from www.nrcresearchpress.com by 200.7.193.243 on 09/04/12
For personal use only.

INTRODUCTION

Parts I and II of this series (1, 2) described the development and use of a reversible silver – silver chloride reference electrode for determining the electromotive forces of voltaic cells in chloride melts at high temperatures.

In this paper, experiments will be described in which the silver – silver chloride reference electrode was used to study the cadmium – cadmium chloride equilibria. An equimolar mixture of molten potassium and sodium chlorides was used as the common solvent.

These results are an additional contribution to the current program of establishing electromotive series for metals in molten salts at different temperatures.

EXPERIMENTAL

The technique used to study the Cd–Ag system was essentially the same as that previously described (1). During the preliminary experimental work it became apparent that because of the relatively high vapor pressure of molten cadmium and the inflammability of cadmium vapor in air, a closed cell operating with an inert atmosphere would be required. The complete cell design is shown in Fig. 1. The cell was constructed from silica tubing of 2 in. diameter and consisted of two sections connected by a ground silica joint. The upper section of the cell was closed with a cork stopper, into which were fitted the silver – silver chloride reference electrode, the thermocouple well, the feeding pipe with stirrer, and the gas inlet tube. The cork stopper was covered externally with Pyseal cement and then water-cooled to prevent the melting of the cement from the heat of the furnace. The inner surface of the cork stopper was covered with a close-fitting layer of asbestos. The lower section of the cell was used as a container for the molten metal indicator electrode and the molten salts. Electrical contact with the indicator electrode was made by means of a tungsten wire sealed into silica tubing and dipped into the metal pool.

[1]*Manuscript received December 31, 1957.*
Contribution from the Mineral Dressing and Process Metallurgy Division, Mines Branch, Department of Mines and Technical Surveys, Ottawa. Published with the permission of the Director, Mines Branch, Ottawa.
[2]*National Research Council Postdoctorate Fellow assigned to the Mines Branch.*

Can. J. Chem. Downloaded from www.nrcresearchpress.com by 200.7.193.243 on 09/04/12
For personal use only.

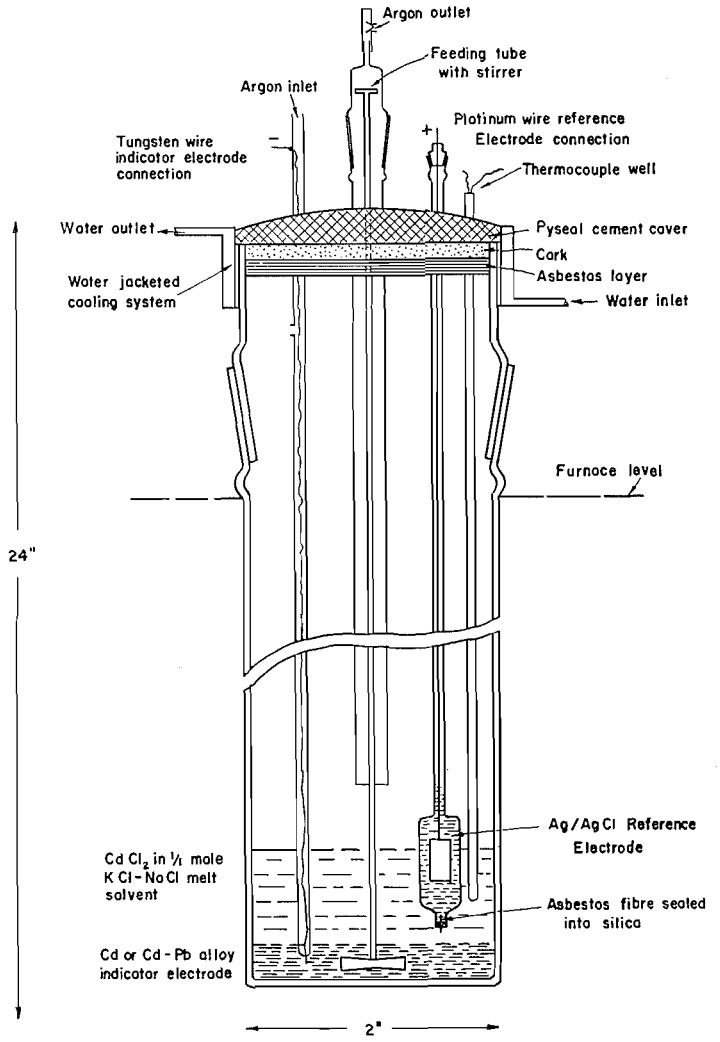

FIG. 1. All silica cell.

For potential measurements at temperatures below the boiling point of cadmium (767° C.), the indicator electrode was either pure molten cadmium metal or cadmium–lead alloy. At temperatures above 767° C., a high boiling point cadmium–lead alloy was used to determine the electromotive forces over a range of temperature in excess of 100 Centigrade degrees and thus clearly establish the linearity of the data.

To protect the contents of the cell from the atmosphere, purified argon was introduced continuously into the cell and released through a small Bunsen valve. The slight positive pressure of argon in the cell protected the contents completely over the full course of runs lasting up to 2 days.

The voltaic cell used during the experiments may be represented as follows:

$$\underset{(-)}{M} \mid \underset{\text{(indicator electrode)}}{\begin{matrix}CdCl_2\ (x_2)\\ KCl\text{–}NaCl\ (1/1\ \text{mole})\end{matrix}} \parallel \text{Asbestos fiber} \parallel \underset{\text{(reference electrode)}}{\begin{matrix}AgCl\ (x_1)\\ KCl\text{–}NaCl\ (1/1\ \text{mole})\end{matrix}} \mid \underset{(+)}{Ag}$$

where M is cadmium or a cadmium-lead alloy, and x_1 and x_2 are, respectively, the mole fractions of AgCl and $CdCl_2$ in the alkali chloride melt solvent. The cell reaction in an ideal solution should be:

$$Cd + 2Ag^+ = Cd^{++} + 2Ag.$$

The relationship between the electromotive force and the metal-ion concentration in the experimental cell is given by the Nernst equation in the form:

$$E_{cell} = (E^\circ_M - E^\circ_{Ag}) - (2.303RT/2\mathcal{F}) \log(x_2/x_1^2 a_m) \quad [1]$$

where E°_M and E°_{Ag} are, respectively, the standard electrode potentials of the half-cells $M/CdCl_2$ and $Ag/AgCl$ under the conditions of the experiment, and a_m represents the activity of cadmium in the metallic electrode. For pure cadmium, $a_m = 1$.

Determination of Metal Activities in Alloys

The use of equation [1] for the calculation of standard electrode potentials requires a knowledge of the activity (a_m) of cadmium in the cadmium–lead alloy. Since the activities of cadmium in this alloy were known only for temperatures up to 570° C. (3), it was necessary to determine these values experimentally at higher temperatures. This was done by calculating the electromotive force, ΔE, of the following hypothetical metal-alloy concentration cell:

$$Cd \left| \begin{matrix} CdCl_2\ (x) \\ KCl\text{–}NaCl\ (1/1\ mole) \end{matrix} \right| Cd(a_m)\text{–}Pb.$$

This electromotive force was derived from the difference between the potential of the experimental cell using the cadmium–lead alloy as an indicator electrode, and that of the same cell when using pure cadmium metal. The alloy was prepared *in situ* by adding small pieces of 99.9% lead to the molten cadmium electrode, or, when the equilibrium was to be approached from the pure lead side, by adding small pellets of 99.99% cadmium to the molten lead electrode. The alloy electrodes were homogenized by a small stirrer inserted through the feeding tube of the cell. The activity of cadmium in the alloy was then calculated by the equation:

$$\Delta E = 2.303RT/2\mathcal{F} \log(1/a_m). \quad [2]$$

RESULTS AND DISCUSSION

The electromotive force of the cadmium cell was measured first as a function of the metal-ion concentration and then as a function of temperature. The results of the experiments in which the concentration of the metal ion was varied at constant temperature are shown in Table I.

From equation [1] it follows that the relationship between E_{cell} and $\log(x_2/x_1^2)$ should be linear; and that when x_1 and x_2 are chosen so that the log term of this equation becomes zero, then

$$E_{cell} = E^\circ_M - E^\circ_{Ag}.$$

When the electromotive forces of the cells were plotted against $\log(x_2/x_1^2)$, as calculated from the experimental data given in Table I, the results were well represented by a straight line in agreement with the theory, as shown in Fig. 2. The slope of the experimental line agrees well with the theoretical values calculated from equation [1] for a two-electron electrode reaction. The results of these calculations are given in Table II.

Can. J. Chem. Downloaded from www.nrcresearchpress.com by 200.7.193.243 on 09/04/12
For personal use only.

TABLE I

ELECTROMOTIVE FORCES OF THE Cd–Ag VOLTAIC CELL AS A FUNCTION OF THE CADMIUM-ION CONCENTRATION IN THE INDICATOR ELECTRODE AT 680° C.

$$\begin{array}{l|l||l|l} \text{Cd} & \text{CdCl}_2 \text{ in 1/1 mole} & \text{AgCl in 1/1 mole} & \text{Ag} \\ (-) & \text{KCl–NaCl} & \text{KCl–NaCl} & (+) \end{array}$$

Mole fraction of AgCl (x_1)	Mole fraction of $CdCl_2$ (x_2)	E_{cell} (volts)
6.235×10^{-2}	2.309×10^{-3}	0.625
"	4.481×10^{-3}	0.598
"	9.047×10^{-3}	0.568
"	1.488×10^{-2}	0.550
"	2.568×10^{-2}	0.528
"	4.807×10^{-2}	0.497
"	8.348×10^{-2}	0.472

Also included in Table II are values for the standard electrode potential of cadmium derived graphically from Fig. 2. For comparison, the standard potential calculated from thermodynamic data given by Hamer, Malmberg, and Rubin (4) is also included.

TABLE II

COMPARISON OF EXPERIMENTAL AND CALCULATED RESULTS FOR THE Cd–Ag ELECTRODE SYSTEMS

		$E°_M - E°_{Ag}$ (volts)		Slope	
Cell reaction	$t°$ C.	Exptl.	Theor.	Exptl.	Theor.
$Cd + 2Ag^+ = Cd^{++} + 2Ag$	680	0.604	0.420	0.097	0.094

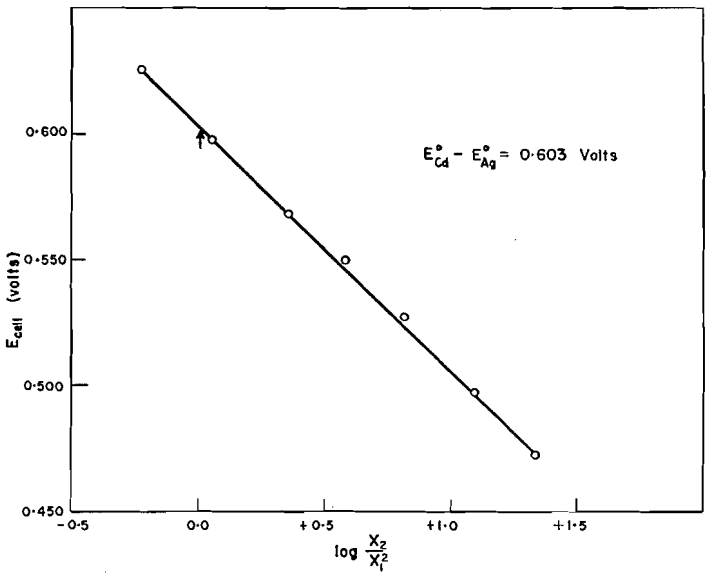

FIG. 2. Electromotive forces of the cells:

$$\begin{array}{l|l||l|l} \text{Cd} & \text{CdCl}_2 & \text{AgCl } (x_1 = 6.235\times10^{-2}) & \text{Ag} \\ (-) & \text{KCl–NaCl (1/1 mole)} & \text{KCl–NaCl (1/1 mole)} & (+) \end{array}$$

as a function of $\log(x_2/x_1^2)$ at a constant temperature of 680° C.

Can. J. Chem. Downloaded from www.nrcresearchpress.com by 200.7.193.243 on 09/04/12
For personal use only.

It is of theoretical interest to compare the experimentally obtained standard potential of the voltaic cell with the theoretical value calculated from the thermodynamic data. If the difference is entirely attributed to the presence of a cadmium complex in the alkali chloride melt solvent, the dissociation constant, K_d, of the complex can be calculated, using the method previously described (1):

$$K_d \text{ (Cd complex)} = 1.17 \times 10^{-2}.$$

The magnitude of this value indicates the presence of a fairly stable cadmium complex in the melt.

The effects of temperature change on the electromotive forces of the cadmium–lead alloy – silver and the cadmium–silver voltaic cells were investigated next. The results are shown in Table III and Fig. 3. (The procedure by which the activity a_m and the standard electrode potentials included in Table III were obtained will be described later in the text.)

TABLE III

EFFECT OF TEMPERATURE ON THE ELECTROMOTIVE FORCE OF THE CELLS

(*a*) Cd (−) | $CdCl_2$ ($x_2 = 3.875 \times 10^{-2}$) KCl–NaCl (1/1 mole) || AgCl ($x_1 = 6.103 \times 10^{-2}$) KCl–NaCl (1/1 mole) | Ag (+)

T (° K.)	E_{cell} (volts)
933	0.5255
955	0.5132
980	0.5015
1000	0.4921
1025	0.4784

(*b*) Cd(a_m)–Pb (−) | $CdCl_2$ ($x_2 = 3.785 \times 10^{-2}$) KCl–NaCl (1/1 mole) || AgCl ($x_1 = 6.103 \times 10^{-2}$) KCl–NaCl (1/1 mole) | Ag (+)

where $x_m = 0.4754$ and $a_m = 0.7654$

On heating			On cooling		
T (° K.)	E_{cell} (volts)	$E°_{Cd} - E°_{Ag}$ (volts)	T (° K.)	E_{cell} (volts)	$E°_{Cd} - E°_{Ag}$ (volts)
982	0.493	0.568	1025	0.456	0.537
984	0.479	0.557	1011	0.463	0.544
991	0.474	0.553	997	0.472	0.552
1012	0.466	0.546	985	0.476	0.555
1033	0.454	0.536	973	0.482	0.560
1065	0.438	0.523	957	0.490	0.565
1084	0.432	0.518	947	0.494	0.569
			937	0.498	0.572
			935	0.502	0.576

It is of interest to note, in Fig. 3, that the two straight lines which express the relationship between the electromotive force of the foregoing cells and temperature are essentially parallel. This shows that the activity of cadmium in a cadmium–lead alloy is almost independent of temperature. The results of experiments to determine the activities a_m of cadmium in a cadmium–lead alloy at one temperature (680° C.) are shown in Table IV. The activity coefficients were calculated using the well-known equation:

$$a_m = x_m \gamma_m \qquad [3]$$

Can. J. Chem. Downloaded from www.nrcresearchpress.com by 200.7.193.243 on 09/04/12
For personal use only.

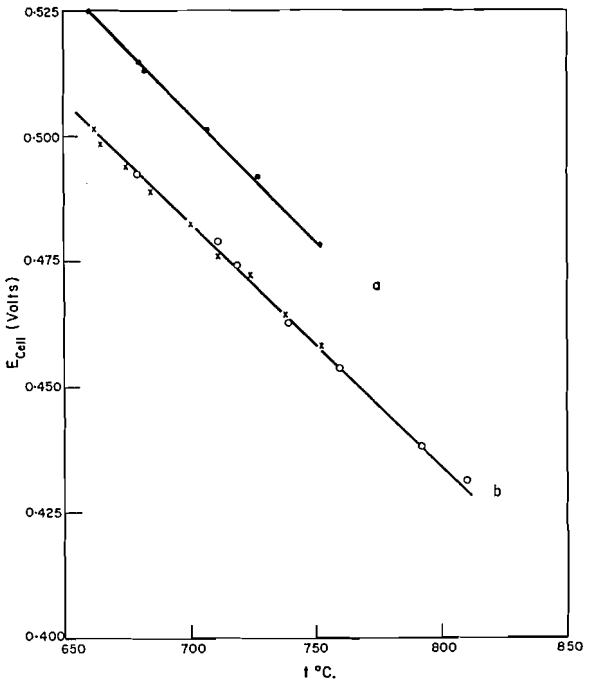

FIG. 3. The effect of temperature on the electromotive forces of the following cells:

(*a*) $\underset{(-)}{\text{Cd}} \mid \underset{\text{KCl–NaCl (1/1 mole)}}{\text{CdCl}_2\ (x_2 = 3.785\times10^{-2})} \parallel \underset{\text{KCl–NaCl (1/1 mole)}}{\text{AgCl}\ (x_1 = 6.103\times10^{-2})} \mid \underset{(+)}{\text{Ag}}$

(*b*) $\underset{(-)}{\text{Cd}(a_m = 0.7654)\text{–Pb}} \mid \underset{\text{KCl–NaCl (1/1 mole)}}{\text{CdCl}_2\ (x_2 = 3.785\times10^{-2})} \parallel \underset{\text{KCl–NaCl (1/1 mole)}}{\text{AgCl}\ (x_1 = 6.103\times10^{-2})} \mid \underset{(+)}{\text{Ag}}$

O with increasing temperature, × with decreasing temperature.

TABLE IV

MEASUREMENTS OF THE ACTIVITY OF CADMIUM METAL IN THE CADMIUM–LEAD ALLOY AT 680° C.

$\underset{(-)}{\text{Cd}(x_m)\text{–Pb}} \mid \underset{\text{KCl–NaCl (1/1 mole)}}{\text{CdCl}_2\ (x_2 = 3.285\times10^{-2})} \parallel \underset{\text{KCl–NaCl (1/1 mole)}}{\text{AgCl}\ (x_1 = 6.103\times10^{-2})} \mid \underset{(+)}{\text{Ag}}$

Mole fraction of cadmium (x_m)	E_{cell} (volts)	ΔE (volts)	Activity (a_m) of cadmium metal in the alloy	Activity coefficient (γ_m)
1.000	0.4985	−0.0000	1.0000	1.000
0.9495	0.4956	−0.0029	0.9315	0.981
0.8602	0.4920	−0.0065	0.8535	0.992
0.7873	0.4900	−0.0085	0.8128	1.032
0.6883	0.4916	−0.0069	0.8453	1.228
0.5664	0.4910	−0.0075	0.8537	1.507
0.4718	0.4878	−0.0107	0.7709	1.634
0.4712	0.4870	−0.0115	0.7551	1.602
0.3426	0.4768	−0.0217	0.5889	1.719
0.2331	0.4665	−0.0320	0.4585	1.967
0.1434	0.4524	−0.0461	0.3251	2.266
0.0801	0.4353	−0.0632	0.2143	2.675

where x_m is the mole fraction of cadmium in the alloy and γ_m is the activity coefficient.

In Table IV it can be seen that at high cadmium concentrations the cadmium–lead

Can. J. Chem. Downloaded from www.nrcresearchpress.com by 200.7.193.243 on 09/04/12
For personal use only.

alloy behaves essentially ideally. Below a mole fraction of about 0.8, deviations from ideality increase and activity coefficients greater than unity are obtained.

The variation of the activity with the mole fraction of cadmium in the cadmium–lead alloy is shown in Fig. 4.

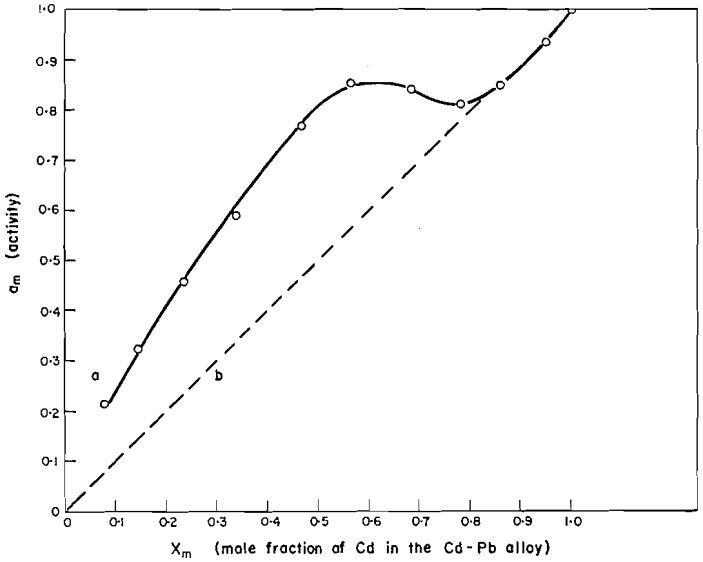

FIG. 4. The variation of the activity of cadmium in the Cd–Pb alloy, with the mole fraction of cadmium at 680° C. (*a*) Experimental data; (*b*) theoretical line for an ideal alloy.

The activity coefficient values obtained in the present investigation for a temperature of 680° C. are in good agreement with values given in the literature for lower temperatures. This is shown in Table V, where activity coefficients calculated from the data given by Taylor (3) are tabulated together with values obtained in the present investigation.

TABLE V

ACTIVITY COEFFICIENTS OF CADMIUM METAL IN CADMIUM–LEAD ALLOY AT VARIOUS TEMPERATURES AND CONCENTRATIONS

Mole fraction of cadmium in the alloy	Activity coefficient (γ_m)				
	432° C.	480° C.	544° C.	572° C.	680° C.*
0.2	2.50	2.35	2.15	2.10	2.50
0.4	1.75	1.68	1.58	1.57	1.65
0.6	1.48	1.48	1.44	1.44	1.50

* *Values obtained in the present investigation.*

It will be observed that temperature change has a very small effect on the values of the activity coefficients. This is in agreement with the previous observations on temperature effects in Fig. 3. The two lines are essentially parallel and the difference between the values of the respective electromotive forces corresponds to a $(2.303RT/2\mathcal{F})\log a_m$ term, where a_m is the activity of the cadmium in the alloy at the lower temperature of 680° C.

Can. J. Chem. Downloaded from www.nrcresearchpress.com by 200.7.193.243 on 09/04/12
For personal use only.

Having established the activities of cadmium in a cadmium–lead alloy, it was possible to use equation [1] to calculate the standard electrode potential of cadmium ($E°_{Cd} - E°_{Ag}$) at different temperatures from the data in columns 1 and 2 of Table III(b). From these standard potentials, using the well-known equations

$$\Delta F° = -nE°\mathcal{F}, \qquad [4]$$

$$\Delta F° = -2.303RT \log K,$$

the equilibrium constant for the cell reaction given in Table II was calculated for various temperatures. The results of these calculations are shown in Fig. 5, where log K was plotted against the reciprocal of the absolute temperature. The curve is linear over the

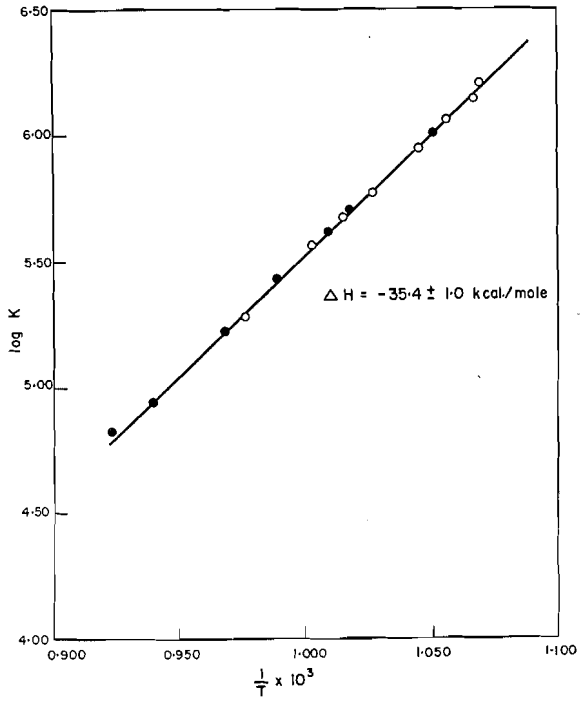

FIG. 5. The variation of log K with the reciprocal of temperature for the system:
Cd(a_m = 0.7654)–Pb | $CdCl_2$ ($x_2 = 3.785\times10^{-2}$) || AgCl ($x_1 = 6.103\times10^{-2}$) | Ag
(−) | KCl–NaCl (1/1 mole) || KCl–NaCl (1/1 mole) | (+)
○ with increasing temperature, ● with decreasing temperature.

temperature range investigated, and the best straight line through the experimental points was calculated by applying the least squares method. The heat of reaction (ΔH_r), which is the difference between the heats of formation of the respective chlorides in the melt solvent, i.e.

$$\Delta H_r = \Delta H_{f(CdCl_2 \text{ in KCl–NaCl})} - \Delta H_{f(AgCl \text{ in KCl–NaCl})}, \qquad [5]$$

can be calculated from the slope of the straight line in Fig. 5, in accordance with the van't Hoff equation,

Can. J. Chem. Downloaded from www.nrcresearchpress.com by 200.7.193.243 on 09/04/12
For personal use only.

$$d \ln K/dT = \Delta H_T/RT^2. \qquad [6]$$

The result thus obtained is:

$$\Delta H_T = -35.4 \pm 1.0 \text{ kcal.}$$

It will be noted that this value includes any effect due to the presence of the solvent.

REFERENCES

1. FLENGAS, S. N. and INGRAHAM, T. R. Can. J. Chem. **35**, 1139 (1957).
2. FLENGAS, S. N. and INGRAHAM, T. R. Can. J. Chem. **35**, 1254 (1957).
3. TAYLOR, N. W. J. Am. Chem. Soc. **45**, 2865 (1923).
4. HAMER, W., MALMBERG, M., and RUBIN, B. J. Electrochem. Soc. **103**, 1, 8 (1956).

Can. J. Chem. Downloaded from www.nrcresearchpress.com by 200.7.193.243 on 09/04/12
For personal use only.

Can. J. Chem. Downloaded from www.nrcresearchpress.com by 200.7.193.243 on 09/04/12
For personal use only.

THE EFFECT OF THE AMBIENT GASES ON THE SURFACE PHOTOCURRENT IN ANTHRACENE[1]

T. C. WADDINGTON[2] AND W. G. SCHNEIDER

ABSTRACT

Following the observation that the photocurrent in anthracene is markedly affected by an atmosphere of oxygen over the system, the behavior of anthracene in the presence of atmospheres of other gases has been investigated. The effect has been shown to be confined to the surface photocurrent, and the active gases have been shown to fall into two classes: (1) gases which are electron acceptors, e.g. BF_3, HCl, O_2, and NO, which all *increase* the photocurrent markedly; (2) gases and vapors which are electron donors, e.g. NH_3, $(CH_3)_2O$, and $(CH_3)_3N$, which all *decrease* the photocurrent markedly. The effect of the pressure of the ambient gas and of the temperature of the system on the photocurrent has also been investigated.

INTRODUCTION

Though the photoconductivity of anthracene was observed as early as 1913 by Volmer (1) it was not until the last decade that systematic investigations of its behavior were undertaken. It was recognized by Vartanyan (2) that the photoconductivity of a polycrystalline layer of anthracene was markedly affected by oxygen in contact with it, the photoconductivity being decreased on hard pumping. These observations were confirmed in this laboratory by Chynoweth (3), who transferred his attention to single crystals, because of the difficulty of outgassing multicrystalline layers and therefore of obtaining meaningful and reproducible results. The effect of oxygen on the photoconductivity of crystalline anthracene was also investigated by Bree, Carswell, and Lyons (4), working with sublimation flakes.

In view of the effect of oxygen it was decided to study the effect of other gases and vapors on the photocurrent in anthracene single crystals. A brief, preliminary account (5) of this work, which is reported here in greater detail, has already appeared. About the same time a note was published by Bree and Lyons (6) on the effect of oxygen, nitric oxide, and sulphur dioxide on the photoconductivity of anthracene. Subsequently a note (7) has appeared reporting the effects of temperature on the photoconductivity in the presence of oxygen.

EXPERIMENTAL

The photoconductivity cell was similar to that described by Chynoweth and Schneider (8). The gases used were obtained commercially and were of high purity. The nitrogen and argon were spectroscopically pure. The anthracene used in growing the crystals employed in the above experiments was purified by continuous chromatography in the manner described by Sangster and Irvine (9). Two types of crystals were employed. Large crystals were cut from long single crystals kindly grown for us by Dr. Lipsett in a Bridgeman-type furnace. Sublimation flakes were grown in an atmosphere of argon. Electrodes were painted onto the crystals with aquadag.

[1]*Manuscript received December 13, 1957.*
Contribution from the Division of Pure Chemistry, National Research Council, Ottawa, Canada.
Issued as N.R.C. No. 4679.
[2]*National Research Laboratories Postdoctorate Fellow, 1955–56. Present address: Gonville and Caius College, Cambridge, England.*

Can. J. Chem. Downloaded from www.nrcresearchpress.com by 200.7.193.243 on 09/04/12
For personal use only.

RESULTS

(*a*) *Effects of Gases on the Photocurrent in the Sandwich Cell*

Using a sandwich cell of polycrystalline anthracene Chynoweth (3) observed a large effect, with oxygen, on the photocurrent. Working with single crystals he found only a 20% to 30% increase over the hard-vacuum level of the photocurrent. In order to see if the presence of oxygen or other gases at the illuminated face of the crystal had any effect on the true bulk photocurrent in anthracene, an earthed guard ring was placed on the edge of the sandwich cell and the photocurrent measured *in vacuo* and in the presence of oxygen and of other gases. In no case could any change in the level of the photocurrent be detected. It was concluded that the gases only affected the current flowing in the surface layers of the crystal and all subsequent observations were made using the surface-cell arrangement.

(*b*) *Surface Cell—Equilibrium Behavior*

(1) *Qualitative account of the effects of various gases.*—The gases BF_3, HCl, SO_2, NO, and O_2 on admission to the photocell were all found to increase the photocurrent in the surface arrangement to a steady value well above the hard-vacuum value. Typical increases were by a factor of 20. The gases and vapors NH_3, $(CH_3)_3N$, $(CH_3)_2O$, $(C_2H_5)_2O$, C_2H_5OH, H_2O, and $(CH_3)_2CO$ were all found to decrease the photocurrent to a steady value below that of the high-vacuum value. Typical decreases were by a factor of 5 to 10. The gases and vapors CO_2, N_2, A, CH_4, and $(CH_3)_4C$ were found to have no effect on the level of the vacuum photocurrent.

(2) *The effect of the pressure of ambient gas on the level of the surface photocurrent.*—The dependence of the photocurrent on the pressure of oxygen gas has already been reported by Bree and Lyons (6). Our results are in agreement with theirs. The pressure dependence has the shape of a Langmuir adsorption isotherm, and a plot of the photocurrent minus its hard-vacuum value, i.e., $i_p - i_{vac}$, against the pressure, p, is initially linear. A plot of $p/(i_p - i_{vac})$ against p gives a good straight line. This was also found to be the case for BF_3 and HCl.

The dependence of the photocurrent on gas pressure was also studied in the presence of ammonia, of trimethylamine, and of acetone vapor. A plot of the hard-vacuum value minus the value found in the presence of ammonia, i.e., $i_p - i_{vac}$, against the pressure, p, resembled a Langmuir adsorption isotherm, being initially linear and saturating in the usual manner. A plot of $p/(i_p - i_{vac})$ against p gave a good straight line. Similar results were obtained for trimethylamine. A plot of $i_p - i_{vac}$ for acetone does not give a Langmuir isotherm, the shape of the curve resembling more nearly that for multilayer adsorption. The plots of $i_p - i_{vac}$ against p and $p/(i_p - i_{vac})$ against p are shown in Figs. 1 and 2, respectively, for BF_3 and NH_3.

(3) *The effect of temperature on the level of the surface photocurrent in the presence of an ambient gas.*—The effect of temperature (in the range $-130°$ to 55° C.) on the value of the photocurrent in the surface and sandwich cell in a hard vacuum has been reported in a previous communication (10). It takes the form of an exponential relation $i = i_0 \exp(-E/RT)$. In the presence of an ambient gas such as O_2 or BF_3 the behavior falls into two classes:

(*a*) In the case where the pressure is above the saturation value for the Langmuir isotherm, e.g., $p > p_{sat}$, the behavior is exactly the same as in the case of the hard vacuum.

(*b*) In the case where the pressure is below the saturation value for the Langmuir isotherm, e.g., $p < p_{sat}$, the behavior is different to the hard-vacuum case and the

Can. J. Chem. Downloaded from www.nrcresearchpress.com by 200.7.193.243 on 09/04/12
For personal use only.

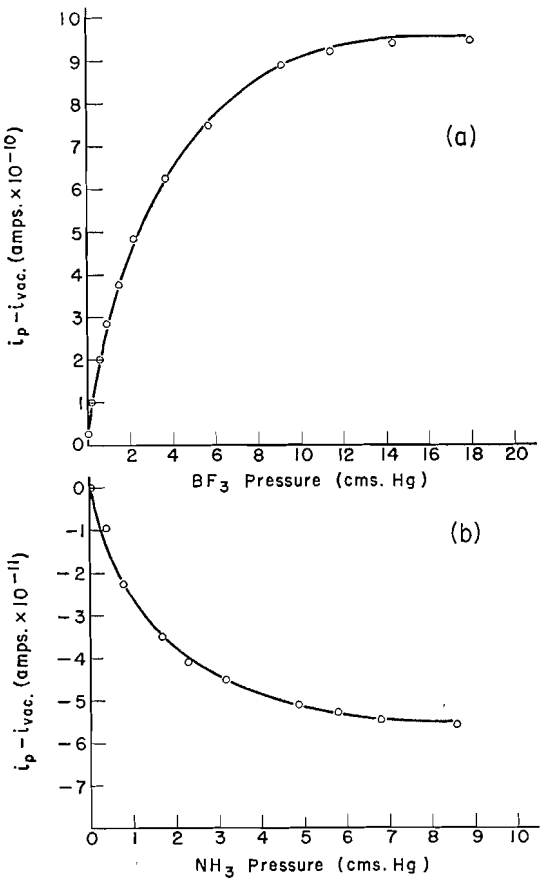

FIG. 1. (*a*) Increase of photocurrent of anthracene as a function of BF_3 gas pressure. (*b*) Decrease of photocurrent of anthracene as a function of NH_3 gas pressure.

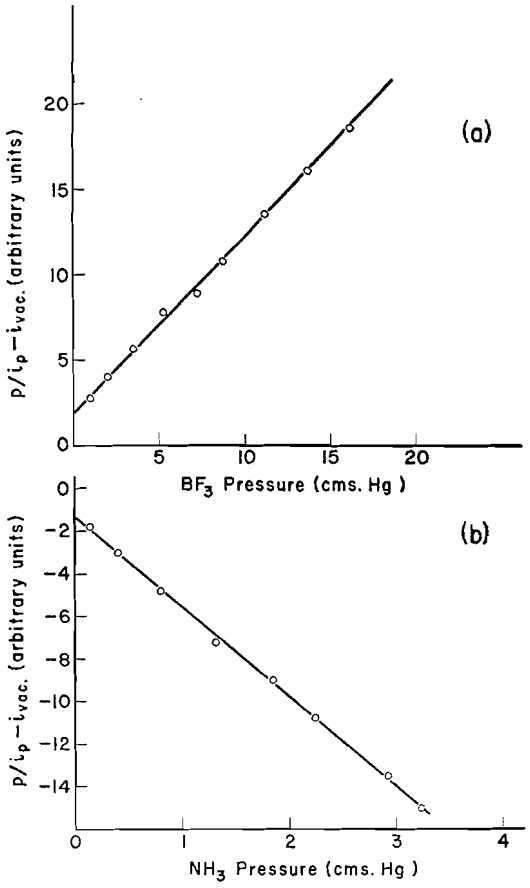

FIG. 2. Plot of $p/(i_p - i_{vac})$ vs. p for (*a*) BF_3 and (*b*) NH_3 on anthracene single crystals.

photocurrent temperature relation cannot be fitted to a simple $i = i_0 \exp(-E/RT)$ relationship.

(4) *Effect of wavelength on the photocurrent in the presence of an ambient gas.*—Some experiments were carried out on the effect of oxygen on the wavelength dependence of the photocurrent. No significant change could be found, the wavelength dependence in the surface cell showing the same type of behavior in each case.

(*c*) *Surface Cell—Non-equilibrium Behavior*

Though the effect of the ambient gases on the photocurrent is generally very rapid, there are one or two cases where the photocurrent takes an appreciable while to reach its equilibrium value. This is particularly noticeable in the case of SO_2, where several hours are required in the dark for the photocurrent to rise to a steady value after the admission of the gas to the cell. The rise is much more rapid when the crystal is illuminated than when it is in the dark. Over the somewhat limited range with which it was possible to work with SO_2 the effect was markedly dependent on temperature, the rise time being shortened by a rise in temperature.

Can. J. Chem. Downloaded from www.nrcresearchpress.com by 200.7.193.243 on 09/04/12
For personal use only.

DISCUSSION

Though at the moment sufficient information, theoretical or experimental, is not available for a detailed mechanism of the effects of ambient gases on the photoconductivity of anthracene to be given, certain definite generalizations can be made and some tentative suggestions advanced. The most important first point is that though anthracene possesses both a surface and a bulk photocurrent only the surface photocurrent is affected by the adsorbed gases. Secondly, since the wavelength dependence of the surface photocurrent is not altered by the adsorbed gases, they probably do not affect the process of carrier formation but only the movement of charge carriers.

The gases in class two, water vapor, ammonia, dimethyl ether, trimethylamine, etc., appear to be only weakly adsorbed. This is shown by the ease with which the photocurrent can be restored to its vacuum level by pumping. All these gases are electron donors of varying power, all possessing lone pairs, and they all reduce the photoconductivity. The gases in class one, oxygen, nitric oxide, boron trifluoride, etc., are all strongly adsorbed, probably chemisorbed. This is indicated by the difficulty of pumping them off the crystal as indicated by a return of the photocurrent to its hard-vacuum value. The photocurrent–pressure behavior can be fitted to a Langmuir adsorption isotherm. These gases must be interacting strongly with the π-electrons of the surface anthracene molecules, either because they possess acidic protons, e.g. HCl, or because they have a vacant orbital of low energy, e.g. boron trifluoride.

Other evidence, presented elsewhere (10), suggests that the majority charge carriers in anthracene are positive holes. Many other photoconductors show an effect due to ambient gases on the surface photocurrent and this behavior is usually explained in terms of the effect on the surface energy levels of the crystal by the gas (11, 12, 13). However, none of these materials, such as germanium, zinc sulphide, and cadmium sulphide, are as sensitive as anthracene is to the effect of adsorbed gases. If it is assumed that on the surface of an anthracene crystal *in vacuo* the energy levels of the positive-hole band are lower than in the bulk of the crystal and that the effect of the ambient gas is to raise or lower the energy levels at the surface depending on whether the gas is an electron donor or an electron acceptor relative to anthracene, then a simple phenomenological explanation is given of the behavior outlined in this paper. It is also interesting to note that if the above explanation is the correct one then the surface semiconductivity of anthracene and similar crystals might very well be expected to be affected by the presence of adsorbed gases. Pick and Wissman (14) have studied the semiconductivity of napthalene crystals and report that the pre-exponential factor and the energy of activation are altered by the presence of oxygen, the conductivity being increased.

REFERENCES

1. VOLMER, M. Ann. phys. **40**, 775 (1913).
2. VARTANYAN, A. T. Doklady Akad. Nauk, S.S.S.R. **71**(4), 641 (1950).
3. CHYNOWETH, A. G. J. Chem. Phys. **22**, 1029 (1957).
4. BREE, A., CARSWELL, D. J., and LYONS, L. E. J. Chem. Soc. 1729, 1735 (1955).
5. SCHNEIDER, W. G. and WADDINGTON, T. C. J. Chem. Phys. **25**, 358 (1956).
6. BREE, A. and LYONS, L. E. J. Chem. Phys. **25**, 384 (1956).
7. BREE, A. and LYONS, L. E. J. Chem. Phys. **25**, 1284 (1956).
8. CHYNOWETH, A. G. and SCHNEIDER, W. G. J. Chem. Phys. **22**, 1021 (1954).
9. SANGSTER, R. C. and IRVINE, J. W. J. Chem. Phys. **24**, 670 (1956).
10. COMPTON, D. M. J., SCHNEIDER, W. G., and WADDINGTON, T. C. J. Chem. Phys. **27**, 160 (1957).
11. BUBE, R. H. J. Chem. Phys. **21**, 1409 (1953).
12. LIEBSON, S. H. J. Electrochem. Soc. **101**, 359 (1954).
13. LIEBSON, S. H. and WEST, E. J. J. Chem. Phys. **23**, 977 (1955).
14. PICK, H. and WISSMAN, W. Z. Physik, **138**, 436 (1954).

Can. J. Chem. Downloaded from www.nrcresearchpress.com by 200.7.193.243 on 09/04/12
For personal use only.

NUCLEAR MAGNETIC RESONANCE MEASUREMENTS OF PROTON TRANSFERS IN ACETYLACETONE IN DIETHYLAMINE AND TRIETHYLAMINE[1]

L. W. REEVES[2] AND W. G. SCHNEIDER

ABSTRACT

Solutions of acetylacetone in triethylamine are completely enolic at all dilutions studied (0.1 to 0.85 mole fraction). The nature of the proton resonance signals in the NMR spectrum indicates a proton exchange between the OH and =CH— groups of the enol tautomer. Addition of diethylamine to acetylacetone results in the formation of a white crystalline 1:1 molecular complex which melts at 41.5° C. The NMR spectrum of the complex reveals a simultaneous proton exchange between the amine NH group and the OH and =CH— groups of the enol tautomer. The mechanism of this exchange is discussed. In effect the addition of amines to acetylacetone not only alters the keto–enol equilibrium very markedly, but also increases the keto–enol conversion rate. With diethylamine the conversion rate becomes sufficiently high to "average out" the individual NMR spectra of the two tautomers.

INTRODUCTION

The proton magnetic resonance technique provides a fruitful method for investigating systems capable of undergoing keto–enol conversion. Typical of such systems is acetylacetone, for which the keto–enol equilibrium may be represented as follows:

[1]

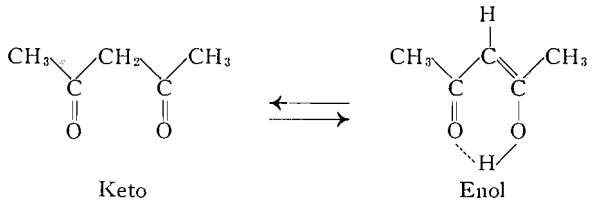

Keto ⟷ Enol

The conversion rate between the two tautomers is sufficiently slow so that the NMR spectrum of acetylacetone, under ordinary conditions, shows separate and distinct proton signals of both the keto and enol tautomers. Hence from the relative intensities of the signals the equilibrium concentrations of each of the two tautomers can be determined (1, 2). The proton resonance spectrum of acetylacetone together with the assignment of the individual proton signals is reproduced in Fig. 1.

In the sense that the keto–enol conversion involves a transfer of a proton from a carbon atom to an oxygen atom, the process may be regarded as a proton exchange phenomenon. Depending on the rate of proton exchange, the shape of the proton resonance signals may be modified in a characteristic way. If we consider a simple example of a proton capable of exchanging between two sites, A and B, we may define lifetimes, τ_A and τ_B, which are a measure of the mean time that the proton spends at each site. When the exchange is slow two separate proton signals appear in the NMR spectrum corresponding to the different environment of the proton at each of the two sites. If the rate of exchange is increased, as for example by raising the temperature, then the two proton signals may be observed to broaden, and eventually at even higher rates of exchange, to coalesce to a single averaged signal at an intermediate position.

[1]*Manuscript received December 19, 1957.*
Contribution from the Division of Pure Chemistry, National Research Council, Ottawa, Canada.
Issued as N.R.C. No. 4689.
[2]*N.R.C. Postdoctorate Fellow. Present address: Mellon Institute, University of Pittsburgh, Pittsburgh 13, Pa.*

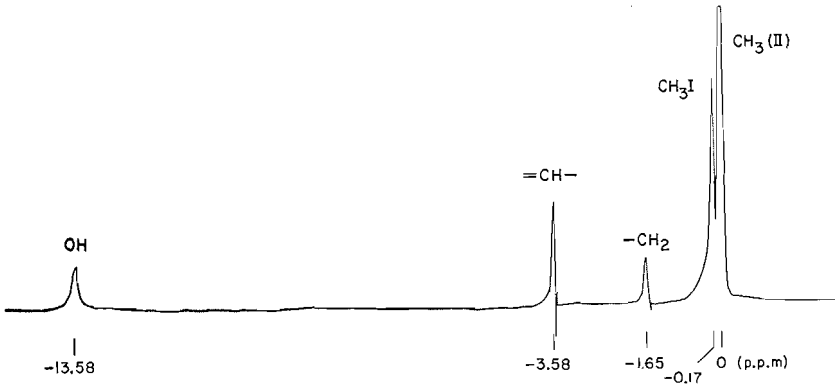

FIG. 1. Proton resonance spectrum of pure acetylacetone at 40 Mc./s. Chemical shifts are shown in p.p.m. Reading from left to right (low field to high field) the signal assignment is respectively: enol OH group, enol =CH— group, keto —CH_2— group, keto CH_3 groups, and enol CH_3 groups.

The general problem of proton exchange between two sites has been treated by Gutowsky and co-workers (3, 4, 5). If the separation of the two signals when the exchange is slow is $2\pi(\nu_A - \nu_B)$, where ν_A and ν_B are the resonance frequencies of the proton at each of the two sites, then under certain simplifying assumptions the condition for coalescence of the two signals is

$$\tau \leqslant \sqrt{2}/[2\pi(\nu_A - \nu_B)], \quad [2]$$

where $\tau = \frac{1}{2}\tau_A = \frac{1}{2}\tau_B$. This type of behavior can be observed, for example, in a 2:1 alcohol–water mixture. At room temperature two proton signals corresponding to the two different OH groups are observed, which when the temperature is raised gradually broaden and coalesce to a single signal at 72° C. (6).

Returning to the acetylacetone system, it may be noted that the separation* of the OH signal of the enol form and the —CH_2— signal of the keto form in frequency units is ~480 c./s. Thus to obtain a coalescence or averaging of these signals would require τ to be of the order of 5×10^{-4} seconds. The lifetime of the keto and enol tautomers is evidently much greater than this. Attempts to increase the conversion (exchange) rate sufficiently by heating and thus to produce a single averaged spectrum for the two tautomers were unsuccessful. When the temperature was raised to 150° C. no indication of signal coalescence, or even a noticeable signal broadening, was apparent. However, as described in the present paper, addition of triethylamine or diethylamine to acetylacetone not only disturbs the keto–enol equilibrium in a profound way, but also substantially alters the keto–enol conversion rate such that under certain conditions an "averaged" proton spectrum is observed.

EXPERIMENTAL

The method of purification of the acetylacetone used in the present work has been described previously (2). Diethylamine and triethylamine were redistilled once from C.P. material.

The proton resonance measurements were made with a V-4300 Varian high resolution spectrometer operating at a fixed frequency of 40 Mc./s. A device which was used for simultaneously spinning and heating the samples, contained in 5-mm. o.d. glass tubes, has been described elsewhere (7).

For a measuring frequency of 40 Mc./s.

Can. J. Chem. Downloaded from www.nrcresearchpress.com by 200.7.193.243 on 09/04/12
For personal use only.

Can. J. Chem. Downloaded from www.nrcresearchpress.com by 200.7.193.243 on 09/04/12
For personal use only.

RESULTS

In a previous paper (2) it was reported that acetylacetone in solution in triethylamine is completely converted to the enol tautomer. Solutions of acetylacetone in triethylamine, studied in the range 0.1 to 0.85 mole fraction acetylacetone, gave rise to proton resonance spectra which, in addition to the signals of the amine, showed only the three signals characteristic of the enol tautomer (cf. Fig. 1). It was observed, however, that the signals arising from the OH group and the =CH— group *both* showed pronounced broadening, suggesting an exchange behavior involving these protons. If this were so, heating the solution should cause further broadening and ultimate coalescence of the two signals when the exchange rate is sufficiently high. Fig. 2 shows NMR traces of the

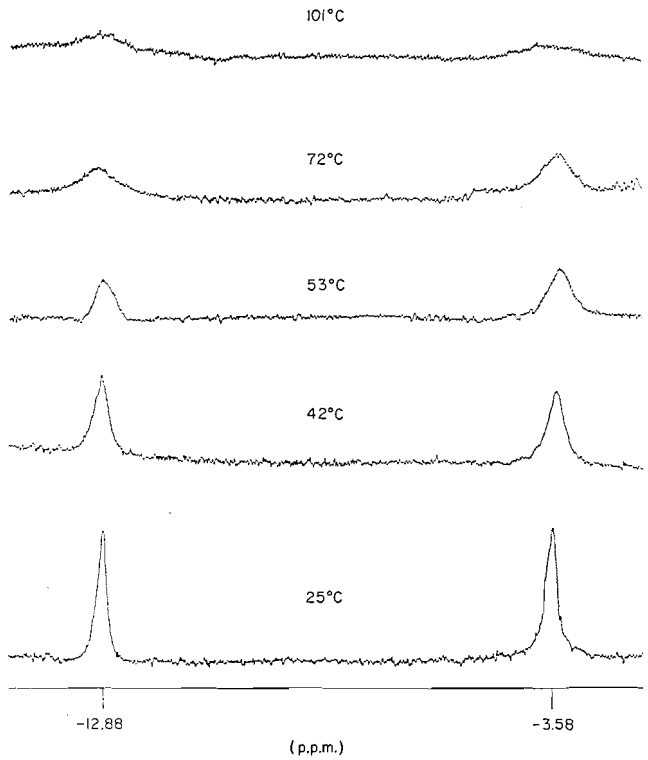

FIG. 2. NMR traces of the enol OH and =CH— group signals of acetylacetone (mole fraction 0.316) in triethylamine at various temperatures.

OH and =CH— signals of a solution of acetylacetone (mole fraction 0.316) in triethylamine at various temperatures. The increased signal broadening is evident. The solution was heated to 165° C. At this temperature the signals became so broad as to be lost in the background noise, and of course under these conditions it is difficult to avoid signal saturation. The coalesced signal, which requires still higher rates of proton exchange, must therefore appear at a much higher temperature. A further solution containing 0.703 mole fraction acetylacetone was also investigated. Apart from some chemical shift displacements in the spectrum, the same features were observed.

From the relative broadening of the signals as a function of temperature, shown in

Fig. 2, rate constants can be determined, permitting an evaluation of the activation energy for the proton exchange process. For this purpose we may employ the simple relation*

$$1/T_2' = 1/T_2 + 1/2\tau,$$

where $1/T_2'$ is related to the half-width of the broadened signal, $1/T_2$, to the corresponding half-width in the absence of exchange, and 2τ is the mean lifetime of the proton at either site. Thus, assuming negligible exchange at 25° C., values of τ at each temperature can be derived from the broadened signals. The results yield an activation energy of approximately 8 kcal./mole for the exchange process. This value is rather inaccurate, however, because of partial signal saturation broadening at the higher temperatures.

Diethylamine affects the keto–enol conversion to a much greater extent than triethylamine. In solutions of acetylacetone in diethylamine, as with triethylamine, no signals which could be assigned to the keto tautomer appear in the NMR spectrum. A specific molecular interaction between diethylamine and acetylacetone is indicated by the formation of a 1:1 molecular compound, with evolution of heat, when the two substances are mixed in equimolar quantities. The molecular complex is a white crystalline solid melting at 41.5° C. Both the amine and acetylacetone can be recovered from the complex. The complete binary freezing-point diagram of the diethylamine–acetylacetone system is shown in Fig. 3.

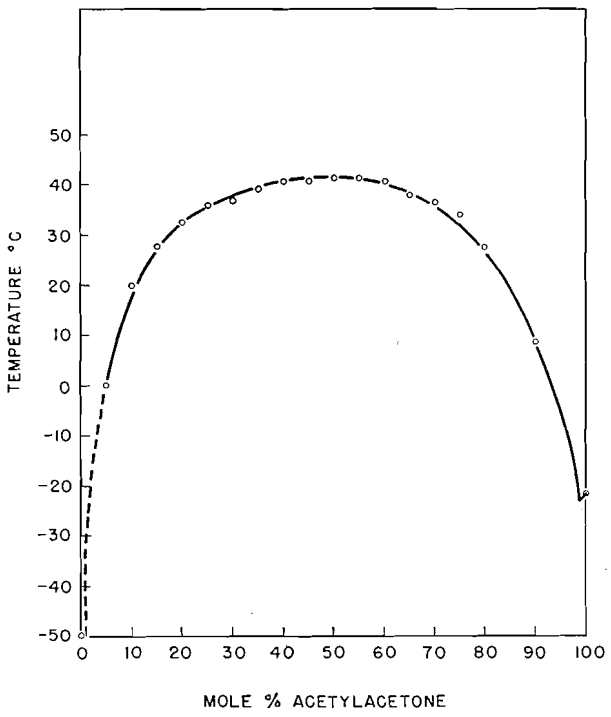

FIG. 3. The binary freezing-point diagram of acetylacetone and diethylamine.

*As pointed out by Professor H. S. Gutowsky (private communication), this relation follows from Eq. (3) of Ref. (5) with the assumption of slow exchange and no overlap of the two component signals. The derivation and application of this relation has been discussed by Grunwald, Lowenstein, and Meiboom, J. Chem. Phys. **27**, 630 (1957).*

Can. J. Chem. Downloaded from www.nrcresearchpress.com by 200.7.193.243 on 09/04/12
For personal use only.

The NMR spectrum of the 1:1 complex at a temperature just above the melting point (where a partial dissociation may be expected) is reproduced in Fig. 4. The chemical

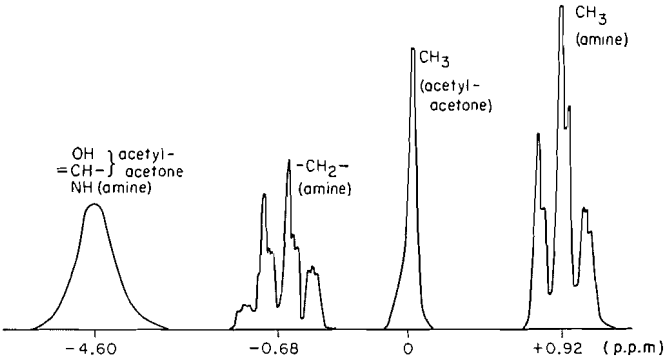

FIG. 4. NMR spectrum of 1:1 acetylacetone–diethylamine mixture (~43° C.). Chemical shifts are shown in p.p.m. The individual resonance signals were recorded at different receiver gain. The relative intensities are therefore not comparable.

shift and assignment of the individual signals are given. Thus after the two signals arising from the ethyl group of the amine are allowed for, the spectrum of the acetylacetone contains but two signals. The sharp signal on the high-field side, which was used as the reference signal in measuring the chemical shifts, must be assigned to the methyl groups of the acetylacetone. This leaves the rather broad signal at low field to account for the signals arising from the OH and =CH— groups of the enol tautomer,* as well as the NH group of the amine. The broad, structureless nature of this signal suggests that all three of these groups are simultaneously exchanging protons. This expectation was indeed confirmed by observing the proton resonance spectrum of the complex dissolved in CCl_4 at a concentration of about 15 mole per cent of complex. The spectrum was similar to that of Fig. 4 except that the low-field signal was now split into two signals having relative intensities 2:1. These two signals, shown in Fig. 5, confirm the assignment of the low-field signal in Fig. 4 as arising from *three* protons, since a 2:1 intensity ratio of the decomposed signal must involve at least three protons. Of the two signals (Fig. 5) the one at higher field, with intensity 1, can be assigned to the

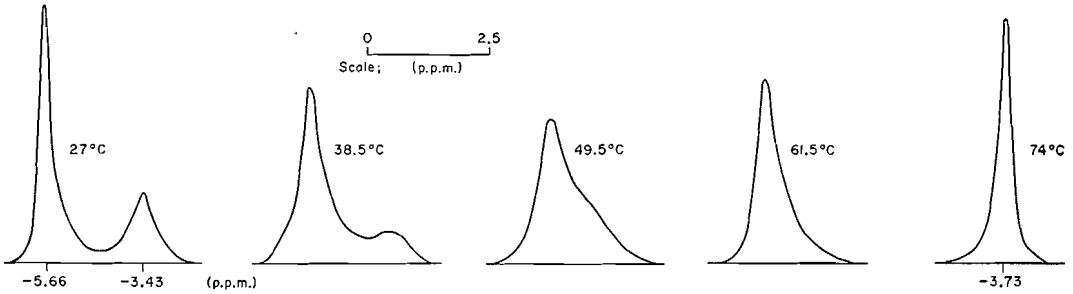

FIG. 5. NMR traces at various temperatures of the enol OH and diethylamine NH groups (low-field signal) and of the enol =CH— group (high-field signal) from 15 mole per cent solution of the 1:1 acetylacetone–diethylamine complex in CCl_4.

**This assumes, by analogy with the behavior in triethylamine, the acetylacetone spends most of its time as the enol tautomer.*

Can. J. Chem. Downloaded from www.nrcresearchpress.com by 200.7.193.243 on 09/04/12
For personal use only.

enol =CH— group, since it appears at very nearly the same position as the corresponding signal in the spectrum of acetylacetone in triethylamine. The lower field signal with intensity 2 must then be assigned to the OH group and the NH group of the amine. This observed pattern of signals suggests that these two groups are rapidly exchanging protons, but the exchange of these protons with the =CH— group is much slower when the system is diluted in CCl_4 than in the pure molecular complex of acetylacetone and diethylamine. However, as shown in Fig. 5, heating the CCl_4 solution causes an increase in the exchange rate and a coalescence of the separate signals, at which point all three protons are again undergoing rapid exchange with each other.

INTERPRETATION OF RESULTS

The most striking and perhaps surprising feature of the results is the involvement of the =CH— group of the enol tautomer in a rapid proton exchange with the OH group and also with the NH group of the diethylamine. In triethylamine, which lacks the latter group but does possess a basic N atom, this exchange is evidently considerably slower. In the presence of either amine the enol tautomer of acetylacetone predominates, suggesting a preferred interaction between the amine and this tautomer. This interaction is undoubtedly through hydrogen bonds. The internal hydrogen bond in the enol tautomer may be expected to become disrupted in the presence of the strong donor N atom of the amine, the OH group then tending to form a bond with the N atom. In general, proton exchange is greatly favored in strong hydrogen bonds, the hydrogen bond providing the exchange path (6). On this basis a fast exchange between the enol OH group and the NH group of the diethylamine can be understood in terms of hydrogen-bonded structures such as the following:

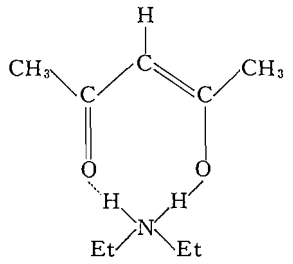

which permits a rapid transfer of protons between oxygen and nitrogen.

A simultaneous rapid exchange of the =CH— group proton under certain conditions, as indicated by the NMR results, is rather more difficult to interpret. It does in fact appear that such an exchange must take place via the keto tautomer as a short-lived intermediate state. A plausible mechanism, which can be illustrated with the aid of a molecular model shown in Fig. 6, is the following. The model of the enol tautomer in the figure shows a configuration in which the internal hydrogen bond has been broken and the OH group is rotated out of the molecular plane. In this configuration the OH proton finds itself adjacent to two electron donor sites. One electron donor site is represented by the electron lone pair of the carbonyl oxygen atom, the other by the olefinic π-bond. There is now ample evidence that the π-electrons in such bonds can act as electron donor sites for molecular interactions with H—X acceptor groups (8, 9, 10). Accordingly in the above configuration of the enol form, conditions are favorable for the NH group of a neighboring amine molecule to orient itself such that the OH group can form a hydrogen

Can. J. Chem. Downloaded from www.nrcresearchpress.com by 200.7.193.243 on 09/04/12
For personal use only.

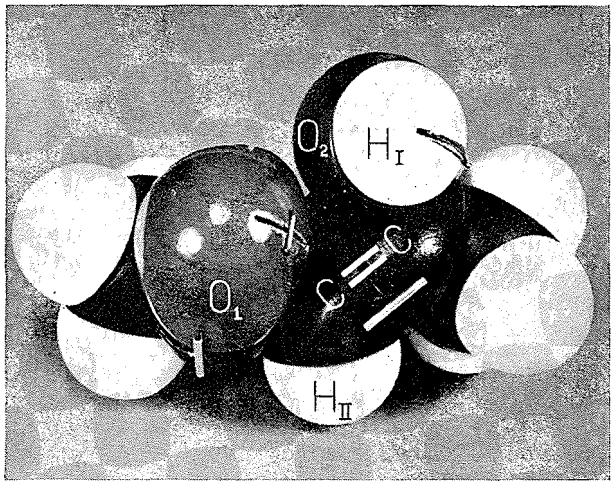

FIG. 6. Molecular model of the enol tautomer of acetylacetone.

bond to the donor lone pair electrons of the N atom, and the H atom of the NH group can bond to either of two donor sites, the carbonyl oxygen atom or the π-bond. This then permits rapid proton exchange among all sites. The individual proton exchanges taking place may be represented by:

(1) $OH\cdots N \longleftrightarrow O\cdots H{-}N$

(2) $H_{II}{-}C(=C)\cdots H{-}N \longleftrightarrow H_{II}{-}C(-C){-}H_I\cdots N$

Enol Keto

(3) $H_{II}{-}C(=C)\cdots H{-}O \longleftrightarrow H_{II}{-}C(-C){-}H_I\cdots O$

Enol Keto

Process (1) may be expected to be rapid under all conditions. Process (3) is simply the ordinary keto–enol conversion and both (2) and (3) involve the keto tautomer as an intermediate "exchange" state. However the lifetime of this state must be small, since no separate signals corresponding to the keto form are observed in the NMR spectra of the amine solutions. This together with the relatively weak donor property of the π-bond of the enol form would account for the observed lower probability of processes (2) and (3) relative to that of (1). These processes are nevertheless sufficiently rapid to average out the separate spectra of the two tautomers. The spectrum of acetylacetone in diethylamine shown in Fig. 4 can in fact be regarded as an averaged spectrum of the two tautomers. It will be noted, however, that formation of the keto tautomer as a short-lived intermediate state permits the protons H_I and H_{II} to become equivalent, and accordingly both can take part in the exchange process. In this way the exchange of the enolic =CH— group (proton$_{II}$) can be accounted for.

The conclusion indicated by the present study is that amines, by virtue of strong hydrogen bonding interactions with acetylacetone, not only alter the keto–enol equilibrium very extensively, but also greatly increase the keto–enol conversion rate. The conversion rate is more rapid in diethylamine than in triethylamine, presumably because the latter lacks an exchangeable proton of its own.

Can. J. Chem. Downloaded from www.nrcresearchpress.com by 200.7.193.243 on 09/04/12
For personal use only.

The authors are indebted to Mr. Yves Lupien for carrying out the freezing-point measurements.

REFERENCES

1. JARRET, H. S., SADLER, M. S., and SHOOLERY, J. N. J. Chem. Phys. **21**, 2092 (1953).
2. REEVES, L. W. Can. J. Chem. **35**, 1351 (1957).
3. GUTOWSKY, H. S., MCCALL, D. W., and SLICHTER, C. P. J. Chem. Phys. **21**, 279 (1953).
4. GUTOWSKY, H. S. and SAIKA, A. J. Chem. Phys. **21**, 1688 (1953).
5. GUTOWSKY, H. S. and HOLM, C. H. J. Chem. Phys. **25**, 1228 (1956).
6. SCHNEIDER, W. G. and REEVES, L. W. Ann. N.Y. Acad. Sci. (In press).
7. SCHNEIDER, W. G., BERNSTEIN, H. J., and POPLE, J. A. J. Chem. Phys. (In press).
8. BROWN, H. C. and BRADY, J. D. J. Am. Chem. Soc. **74**, 3570 (1952).
9. JOSIEN, M. L. and SOURISSEAU, G. Bull. soc. chim. France, 178 (1955).
10. COOK, D., LUPIEN, Y., and SCHNEIDER, W. G. Can. J. Chem. **34**, 957 (1956).

Can. J. Chem. Downloaded from www.nrcresearchpress.com by 200.7.193.243 on 09/04/12
For personal use only.

Can. J. Chem. Downloaded from www.nrcresearchpress.com by 200.7.193.243 on 09/04/12
For personal use only.

THE INFRARED SPECTRA OF 4-SUBSTITUTED-THIOSEMICARBAZIDES AND DIAZOTIZATION PRODUCTS[1]

EUGENE LIEBER,[2] C. N. R. RAO,[3] C. N. PILLAI,[3] J. RAMACHANDRAN,[3] AND RALPH D. HITES[4]

ABSTRACT

The infrared absorption spectra of 4-substituted-thiosemicarbazides, 5-(substituted)amino-1,2,3,4-thiatriazoles, and the corresponding isomeric tetrazolinethiones have been studied and structural assignments of importance to these systems made or suggested. Important conclusions drawn from the spectral data are: there is no suggestion of any thiol–thione tautomerism for the solid 4-substituted-thiosemicarbazides and that the thione structure predominates for these substances; that the so-called 5-thiol-tetrazoles also exist as thiones; and that the diazotization products of the 4-substituted-thiosemicarbazides yield 1,2,3,4,-thiatriazoles rather than the isomeric open chain thiocarbamyl azides. The C═S, —N—C═S, and cyclic —N—N═N— configurational assignments, which are of importance to the classes of compounds studied, are discussed.

INTRODUCTION

In a previous communication, Lieber, Pillai, and Hites (1) reported that the reaction of 4-alkyl- or 4-aryl-thiosemicarbazides, I, with nitrous acid, as well as the reaction of alkyl- or aryl-isothiocyanates, II, leads to the identical 5-(substituted)amino-1,2,3,4-thiatriazoles, III:

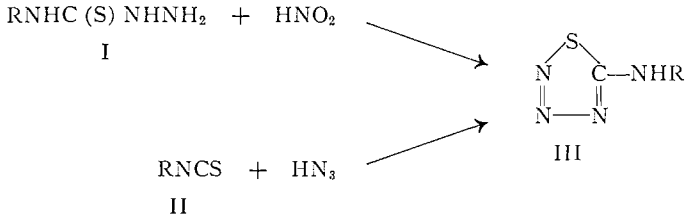

The 5-(substituted)amino-1,2,3,4-thiatriazoles (III) on treatment with base undergo two competitive reactions (1):

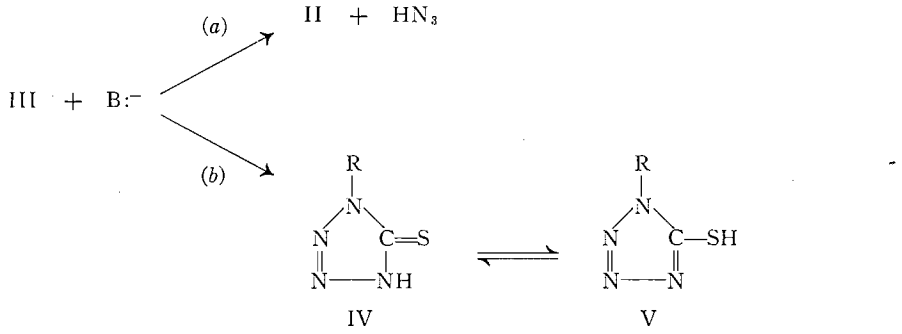

[1]*Manuscript received January 13, 1958.*
Contribution from the Departments of Chemistry of DePaul University and the Armour Research Foundation of the Illinois Institute of Technology, Chicago, Illinois.
[2]*DePaul University, Chicago 14, Illinois, U.S.A., to whom all requests for reprints and additional information should be addressed.*
[3]*DePaul University.*
[4]*Armour Research Foundation.*

the extent of mode (*a*) or (*b*) depending on the electronegativity of the substituent R.* One of the invaluable aids in treading through the pathways of these reactions involved the application of infrared absorption spectroscopy (1). Thus the chemistry of the 5-(substituted)amino-1,2,3,4-thiatriazoles, III, could be explained in terms of the isomeric thiocarbamyl azide structure, VI:

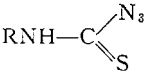

VI

except for the fact that III shows a complete absence of the azido-group frequencies in the infrared region (1). This communication reports the infrared absorption data obtained on structures I, III, and IV obtained in the course of the investigation summarized above.

EXPERIMENTAL

The spectra were recorded on a Perkin-Elmer single-beam spectrometer (Model 12C) with sodium chloride prism. The positions of the absorption maxima are listed in Tables I, II, and III with the intensities being indicated by the following symbols: s, strong; m, medium; w, weak; vw, very weak; and v, variable. The compounds studied were those reported upon in the previous communication (1). The spectra were taken in Nujol mulls.

DISCUSSION

4-Substituted-thiosemicarbazides

All of the important absorption bands of the 4-substituted-thiosemicarbazides in the region 1640–780 cm.$^{-1}$ are summarized in Table I. No SH band was found in these compounds in the region 2600–2500 cm.$^{-1}$, the range in which the SH stretching vibrations are most likely to appear (2). This clearly shows that there is no thiol–thione tautomerism in these compounds in the solid state:

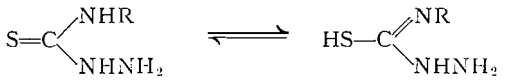

A similar conclusion has been drawn by Bogomolov and co-workers (3). All of the compounds studied showed N—H stretching modes of vibration. In general, the important infrared absorption frequencies of the 4-substituted-thiosemicarbazides can be summarized as in Table IV. The bands due to the hydrazino-, —$NHNH_2$, portion of the structure have been assigned on the basis of studies presented by Randall (4) and Lieber (5). Both the 4-methyl- (VII) and 4,4-dimethyl- (VIII) thiosemicarbazides:

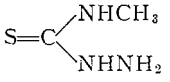

VII

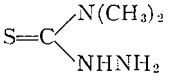

VIII

show weak absorption at 1439 cm.$^{-1}$ and 1447 cm.$^{-1}$, respectively. In agreement with Bellamy (2) these bands can be assigned to the C—H deformation mode in N—CH_3 but do not seem to be too closely defined to afford any useful correlation. The medium or

**More recently it has been found that for III (R = alkyl) a third mode of decomposition can also take place in alkaline media involving an internal oxidation–reduction leading to the formation of nitrogen, sulphur, and further degradation products. This work will be reported in a separate communication.*

Can. J. Chem. Downloaded from www.nrcresearchpress.com by 200.7.193.243 on 09/04/12
For personal use only.

TABLE I

INFRARED SPECTRA OF 4-SUBSTITUTED-THIOSEMICARBAZIDES

$R_1R_2NC(S)NHNH_2$

R_1	R_2	NH_2[a]	N—C=S	C=S	NH_2[c]	—	NH[d]	NH_2[e]	NH[f]
H	H	1642s 1619s	1524s	1362[b]	1280w	1155m	—	996s	800m
CH_3	H	1639s	1555s	1361[b]	1263s	1166m	1081m 1053m	971s	—
CH_3	CH_3	1608s	1506s	1353s	1263w	1155m	1062m	977s	—
C_2H_5	H	1632s	1540s	—	1268s	1162s	1085m 1055s 1037s	976s 934s	807m 773s
n-C_4H_9	H	1630s	1540s	1336[b]	1266s	1212s 1160m	1112w 1089m 1055s	942m	800m 738m
n-C_7H_{15}	H	1634s	1536s	1361[b]	1259s	1232m 1156w	1087w 1062m	956m	781m
$C_6H_5CH_2$	H	1610s	1488s	1370s	1266w	1227m 1188w	1076m	957s	791m
CH_2=$CHCH_2$	H	1631s	1538s	1361[b]	1272s	1232w	1094w 1070m	988w 963m	778m
C_6H_5	H	1634s	1522s	1361[b]	1279s	1212m	1065s	969s	774w
4-ClC_6H_4	H	1631s	1527s	1395w	1264s	1205s	1078s	980m	815w
2-$CH_3OC_6H_4$	H	1618s	1536s	1346w	1266s	1195m 1163w	1058m 1048m	969m	792m
4-$CH_3C_6H_4$	H	1620s	1540s	1334[b]	1300w	1198s 1118w	1060s	976s 928w 910s	842m 810s

[a] *Deformation-asymmetric.*
[b] *Seen as a shoulder on the mineral oil peak (single-beam).*
[c] *Deformation-symmetric.*
[d] *Rocking.*
[e] *Rocking.*
[f] *Bending.*

weak intensity bands observed in the region 1232–1155 cm.$^{-1}$ may be ascribed to the C—N stretching vibration (2, 4). Ueno (6) has recently assigned the region 1300–1273 cm.$^{-1}$ to the C—N stretching vibration of the para-amino group of azobenzenes. In addition to the absorption bands discussed above, bands due to other functional groups and substituted aromatic rings were also observed.

5-(Substituted)amino-1,2,3,4-thiatriazoles

The most significant observation arising out of this study of the infrared absorption spectra of a series of fourteen 5-(substituted)amino-1,2,3,4-thiatriazoles, summarized in Table II, is the absence of an absorption band in the region 2170–2080 cm.$^{-1}$. This rules out (1, 7) the presence of an azido group, supporting structure III and eliminating from consideration structure VI as proposed by Olivari-Mandala (8). Recent studies (9) have confirmed the strong absorbance for the azido group which occurs with great consistency close to 2130 cm.$^{-1}$. This intense N≡N asymmetric stretching absorption is so strong and so little altered by environmental groups as to make its absence in an infrared spectrum a guarantee that the compounds under scrutiny are free of this structural entity.* As

Lieber, Pillai, Ramachandran, and Hites (J. Org. Chem. **22, 1750 (1957)) have recently shown that the reaction products of azide ion and carbon disulphide, which have long been regarded in the literature (Audrieth, Chem. Revs. **15**, 169 (1934)) as derivatives of azidodithiocarbonic acid,*

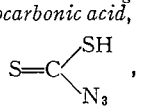

show no azido group frequency in the infrared and in reality are derivatives of the 1,2,3,4-thiatriazole ring system.

Can. J. Chem. Downloaded from www.nrcresearchpress.com by 200.7.193.243 on 09/04/12
For personal use only.

Can. J. Chem. Downloaded from www.nrcresearchpress.com by 200.7.193.243 on 09/04/12
For personal use only.

TABLE II

INFRARED ABSORPTION MAXIMA OF

5-(SUBSTITUTED)AMINO-1,2,3,4-THIATRIAZOLES

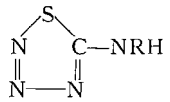

R =	Absorption bands, cm.$^{-1}$																	
H	1724m	1618s		1506m					1333w	1297w	1264w	1233w	1161w	1111m		1053m		943m	889w
CH_3	1695w		1582s					1395m		1282m		1225w		1104s		1031s		933m	
C_2H_5			1545s							1300s			1198m	1150w	1082m	1053m	932w		892w
n-C_4H_9	1724m		1538s							1290m	1247m		1181m	1144w	1086m	1053w		935s	903w
n-C_7H_{15}	1724m		1538s							1294m	1247w		1171w	1142w	1092w	1059w		935m	
CH_2=$CHCH_2$	1718w		1558s	1524s					1323w	1280m		1225w	1174m	1136w	1096m	1055w	990m	940m	911w
$CH_3(H{=}CH_3)$			1560s			1441w	1404m		1318m	1297m	1248w	1217s		1085m		1058m		951s	905s
$C_6H_5CH_2$			1539s			1440s		1370s	1348s	1292s		1220m	1168m		1093s	1032w	963w	934m	
C_6H_5		1605s	1560s		1497m					1289m		1238w	1193m	1155w	1093s	1030w	962w	946w	892w
4-$CH_3C_6H_4$	1721m	1613s	1563s	1513m						1282m		1235w	1198m	1149w	1105s	1032w	962w	950w	909w
2-$CH_3C_6H_4$	1721w	1604s	1588m	1527s	1488w	1458s				1288m				1112w	1076s				
4-$CH_3OC_6H_4$		1605m	1563m	1508s		1453s				1292m	1243s		1175w		1083m	1032m			
2-$CH_3OC_6H_4$		1608w	1588m	1539s	1486s	1464s	1411m		1325m	1292m		1236s	1171w	1117s	1084s	1047w		940w	
						1440s										1026s			
4-Cl—C_6H_4		1618s	1560s		1493s		1422m			1295m		1233w	1200s	1100s		1005w	960w		870w
													1183w						

Can. J. Chem. Downloaded from www.nrcresearchpress.com by 200.7.193.243 on 09/04/12
For personal use only.

additional confirmation of the assigned structure the characteristic absorptions for C=S and —N—C=S are also absent (Table II).

A number of the 5-(substituted)amino-1,2,3,4-thiatriazoles exhibit a band of weak or medium intensity in the region 1724–1695 cm.$^{-1}$. Randall (4) found a strong absorption band in the region 1695–1664 cm.$^{-1}$ for guanidine. Lieber (5) reported a strong absorption band in the region 1681–1661 cm.$^{-1}$ for a series of guanidine derivatives. In a few cases a band was observed a few hundredths of a micron on either side of this region. Kumler (11) repeated the infrared spectral studies of Lieber (5) on a more limited number of nitroguanidine derivatives and reported bands in the region 1663–1618 cm.$^{-1}$. All investigators (2, 4, 5, 10, 11, 12) are in agreement in assigning these bands to the C=N stretching frequency, the unit occurring in imine-type structures, >C=N—, i.e. in an open chain. Randall (4) assigned a strong 1697 cm.$^{-1}$ band to open-chain C=N linkage in N-carbethoxybenzalhydrazone and a strong band at 1694 cm.$^{-1}$ to C=N$^+$ type of linkage in phenaceturiminomethyl ether hydrochloride. It is therefore possible that the moderate to weak band in the region 1724–1695 cm.$^{-1}$ in 1,2,3,4-thiatriazole derivatives is due to an external C=N linkage. This could arise by a tautomeric shift of a proton as in structures III to IX:

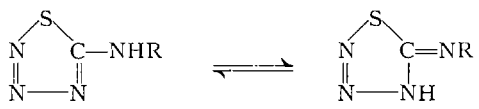

III IX

the intensity of the band depending upon the ratio of IX to III. In dimethylamino-1,2,3,4-thiatriazole, X:

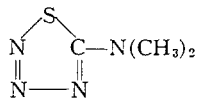

X

this tautomeric shift is not possible and the band at 1724–1695 cm.$^{-1}$ is missing, although no firm conclusion can be drawn from this since the band is also missing in those thiatriazole derivatives in which tautomeric shifts are possible.

All of the compounds listed in Table II exhibit a strong intensity band between 1618 and 1525 cm.$^{-1}$. Bellamy (2) assigns a band of variable intensity in the region 1660–1480 cm.$^{-1}$ for the C=N stretching vibration in conjugated cyclic compounds. Since the —N=N— absorption is generally weak and variable it is unlikely that the band in the 1618–1525 cm.$^{-1}$ region is due to —N=N— stretching. Ueno (6) examined a series of 17 azobenzenes and assigned the —N=N— stretching frequency to two bands of variable intensity in the 1455–1400 cm.$^{-1}$ region. On the other hand, when the nitrogen atom of the C=N bond is so substituted that it is able to take on a polar character, the characteristic frequency alters considerably. Goulden (13) quotes the region of 1659–1510 cm.$^{-1}$ for situations of this type. More recently, Clougherty (14) examined the infrared spectra of aromatic Schiff bases and ascribed the band of medium intensity in the 1631–1613 cm.$^{-1}$ region to the conjugated C=N stretching frequency. Of considerable interest is the fact that this band disappeared on reduction of the Schiff base to a secondary amine:

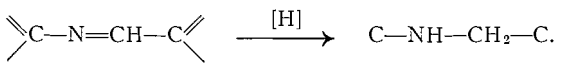

On the basis of chemical and ultraviolet spectral evidence Lieber (1) suggested that 5-(substituted)amino-1,2,3,4-thiatriazoles may possibly exist in the so-called mesoionic form, XI:

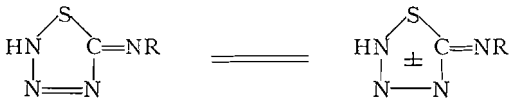

XI

Accordingly, it is possible that the two bands observed in the region 1724–1695 cm.$^{-1}$ (weak or medium intensity) and 1618–1525 cm.$^{-1}$ are due to the mesoionic structure, XI, although not enough information exists in the literature (15, 16) to firmly support this viewpoint.

The dimethylamino derivative (structure X) exhibits two weak bands at 1441 and 1404 cm.$^{-1}$ (Table II) which when combined result in a medium-intensity band at 1425 cm.$^{-1}$. The methylamino derivative (structure III, R = CH_3) exhibits a prominent shoulder at 1395 cm.$^{-1}$. These bands probably can be ascribed (2, 12) to the N—CH_3 absorption. It is also possible that the band observed in the 1217–1148 cm.$^{-1}$ region (Table II) in all of the derivatives is due to C—N vibration. All of the derivatives exhibit a medium-intensity absorption band between 1297 and 1280 cm.$^{-1}$. The significance of this region will be discussed below. From Table II it can be seen that there are a few characteristic skeletal vibration bands due to the thiatriazole ring itself in the regions 911–889 cm.$^{-1}$, 962–930 cm.$^{-1}$, 1060–1030 cm.$^{-1}$, and 1122–1090 cm.$^{-1}$.

1-Substituted-tetrazolinethiones

It has recently been found (1) that 5-(substituted)amino-1,2,3,4-thiatriazoles can be partially converted to a tetrazole derivative when the substituent was an aryl group (structure III, R = aryl). The tetrazole derivative produced could be represented in the *thione* (structure IV) or *thiol* (structure V) forms. It was found that structures of the types IV and V could easily be differentiated by a study of their infrared spectra. The results of the present study establish the *thione* (IV) structure for these compounds. Table III summarizes the important bands observed for these derivatives.

In all of the compounds studied, the —N—C=S and C=S bands are strong and are found in the regions 1500–1474 cm.$^{-1}$ and 1359–1338 cm.$^{-1}$, respectively. The more important observation for these series of compounds was the fact that the presence of the SH band in the region 2600–2550 cm.$^{-1}$ (2) was not apparent. This supports the *thione* (IV) structure rather than the *thiol* (V) structure for these compounds.

A few absorption bands are observed in the 1650–1500 cm.$^{-1}$ region. However, no differentiation of the —N=N— linkage is possible. As Ueno (6) and Bellamy (2) point out, the main difficulty is that the —N=N— absorptions are expected to appear in the double-bond region, so that they may well be merged with the conjugated and stronger aromatic ring absorptions. All of the tetrazole derivatives studied (Table III) exhibit two bands of medium intensity around 1210 cm.$^{-1}$ and 1170 cm.$^{-1}$, the former band being very weak in some cases. It is possible that these bands may be due to the C—N linkage. All of the derivatives, including 1-benzyl-tetrazoline-5-thione (IV, R =

Can. J. Chem. Downloaded from www.nrcresearchpress.com by 200.7.193.243 on 09/04/12
For personal use only.

TABLE III

INFRARED SPECTRA OF 1-SUBSTITUTED-TETRAZOLINETHIONES

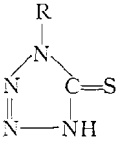

R =	N—C=S	C=S	Cyclic —N—N=N—	Skeletal				
C_6H_5	1498s	1348s	1280s	1096w	1068w	1050m		989m
4-$CH_3C_6H_4$	1500s	1350s	1280s	1115w	1080w	1042s		990m
4-$CH_3OC_6H_4$	1499s	1359m	1302w	1111w		1038s		988m
4-Cl—C_6H_4	1482s	1350s	1280m	1096m	1083m	1046s	1013m	990s
2-$CH_3C_6H_4$	1482s	1352s	1280m			1040m		985m
2-$CH_3OC_6H_4$	1483s	1347s	1280s		1078m	1046s	1018s	985s
$C_6H_5CH_2$	1474s	1338s	1287m	1089m	1075w	1053m	1024w	1000m

$C_6H_5CH_2$—), show a strong or medium intensity band around 1280 cm.$^{-1}$. The interpretation of this band is discussed below.

All of the observed frequencies in the region 1115–980 cm.$^{-1}$ have been tabulated. Although a few of the weak bands could be due to the substituted aromatic ring, it is also possible that some of the bands are characteristic skeletal vibration bands of the tetrazolinethione system:

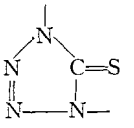

In a few cases, only two strong and/or medium-intensity bands at about 1040 and 990 cm.$^{-1}$ are found. If the small peaks in the other compounds are combined into a broad band, two maxima are invariably found at about 1085 and 1040 cm.$^{-1}$, which in addition to the 990 cm.$^{-1}$ band appear to be common to all these compounds. The results are in general agreement with the earlier observations by Lieber (5) for tetrazole derivatives.

The C=S *Frequency*

Bellamy (2) states that no adequate correlation has yet been worked out for this linkage. Colthup (17) and Thompson (18) have suggested the range 1400–1300 cm.$^{-1}$ for the C=S absorption but there is no indication of the classes of compounds on which the assignment is based. Mecke (19) in a recent study ascribed a band of strong intensity in the region 1200–1050 cm.$^{-1}$ for a series of compounds of the type:

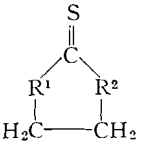

where R^1 and R^2 represented the groups CH_2, NH, O, and S, the spectral maps for ethylenethiourea ($R^1 = R^2 = NH$), oxazolthione ($R^1 = NH$, $R^2 = O$), thiopyrrolidone

Can. J. Chem. Downloaded from www.nrcresearchpress.com by 200.7.193.243 on 09/04/12
For personal use only.

(R^1 = NH, R^2 = CH_2), thiothiazolidone (R^1 = NH, R^2 = S), and ethylenetrithiocarbonate (R^1 = R^2 = S) being presented in their paper. An examination of these maps reveals bands of strong intensity in the much less variable region of 1350–1300 cm.$^{-1}$. It is more likely that this latter region corresponds to the C=S frequency and that the more variable region of 1200–1050 cm.$^{-1}$ could be assigned to either C—N, C—S, or C—O skeletal vibrations. From the data (Tables I, II, and IV) of the present investigation a frequency assignment of 1395–1338 cm.$^{-1}$ for the C=S linkage can be made.

TABLE IV

IMPORTANT INFRARED FREQUENCY ASSIGNMENTS FOR 4-SUBSTITUTED-THIOSEMICARBAZIDES

$R_1R_2NC(S)NHNH_2$

Frequency, cm.$^{-1}$	Assignment
1555–1488(s)	—N—C=S
1395–1346	C=S
Ref. (4), (5)	—$NHNH_2$ structural
1639–1610(s)	NH_2 deformation, asym.
1280–1259(v)	NH_2 deformation, sym.
1094–1058(v)	NH rocking
996–956(m/s)	NH rocking
815–774(w/m)	NH bending

The —N—C=S *Frequency*

Randall (4) has assigned a strong band to the structure R—N—C=S or R—NH—C=S in the region 1613–1471 cm.$^{-1}$. Mann (20) assigns a band at 1495 cm.$^{-1}$ for this group. Bellamy (2) feels that there is justification for a tentative assignment to the 1500–1470 cm.$^{-1}$ region. From the data of the present investigation on 4-substituted-thiosemicarbazides (Tables I and IV) and on the tetrazolinethiones (Table III) an assignment to the region 1555–1474 cm.$^{-1}$ can be made.

The 1300–1270 cm.$^{-1}$ Frequency Region

From Tables II and III it can be seen that the thiatriazole and tetrazolinethione rings exhibit a band in the 1300–1270 cm.$^{-1}$ region* of variable intensity. Since no other assignment seems possible, a tentative assignment of this frequency to the cyclic —N—N=N— linkage is suggested. It is interesting to note that the variable symmetric vibration band of the azido group, N_3, has been assigned the region of 1343–1177 cm.$^{-1}$ by Sheinker and Syrkin (21). Lieber (9) has recently assigned the 1297–1256 cm.$^{-1}$ region to this symmetric vibration band. From the results of Lieber, Levering, and Patterson (5) it can be seen that quite a large number of tetrazole derivatives show this absorption in the 1300–1270 cm.$^{-1}$ region, lending support to a cyclic —N—N=N— assignment.

ACKNOWLEDGMENTS

The authors gratefully acknowledge the receipt of research grants from the Eli Lilly

**A similar band is exhibited by substituted 1,2,3-triazoles of the configuration:*

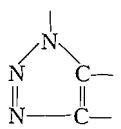

These data will be reported in a separate communication.

Can. J. Chem. Downloaded from www.nrcresearchpress.com by 200.7.193.243 on 09/04/12
For personal use only.

Company, Indianapolis, Ind., and the Research Corporation, New York, N.Y., which made this study possible.

REFERENCES

1. LIEBER, E., PILLAI, C. N., and HITES, R. D. Can. J. Chem. **35**, 832 (1957).
2. BELLAMY, L. J. The infra-red spectra of complex molecules. Methuen & Co. Ltd., London. 1954.
3. BOGOMOLOV, S. G., POSTOVSKIR, I. Y., and SHEINKER, Y. N. Doklady Akad. Nauk S.S.S.R. **91**, 1111 (1953); Chem. Abstr. **48**, 450 (1954).
4. RANDALL, H. M., FOWLER, R. G., FUSON, N., and DANGL, J. R. Infrared determination of organic structures. D. Van Nostrand Company, Inc., New York. 1949.
5. LIEBER, E., LEVERING, D. R., and PATTERSON, L. Anal. Chem. **23**, 1594 (1951).
6. UENO, K. J. Am. Chem. Soc. **79**, 3205 (1957).
7. LIEBER, E., OFTEDAHL, E., PILLAI, C. N., and HITES, R. D. J. Org. Chem. **22**, 441 (1957).
8. OLIVERI-MANDALA, E. Gazz. chim. ital. **44**, I, 670 (1914).
9. LIEBER, E., RAO, C. N. R., CHAO, T. S., and HOFFMAN, C. W. W. Anal. Chem. **29**, 916 (1957).
10. ANGELL, C. L., SHEPPARD, N., YAMAGUCHI, A., SHIMANOUCHI, T., MIYAZAWA, T., and MIZUSHIMA, S. Trans. Faraday Soc. **53**, 589 (1957).
11. KUMLER, W. D. J. Am. Chem. Soc. **76**, 814 (1954).
12. MILLER, F. A. *In* Organic chemistry. Vol. III. *Edited by* H. Gilman. John Wiley & Sons, Inc., New York. 1953.
13. GOULDEN, J. D. S. J. Chem. Soc. 997 (1953).
14. CLOUGHERTY, L. E., SOUSA, J. A., and WYMAN, G. M. J. Org. Chem. **22**, 462 (1957).
15. BAKER, W. and OLIS, W. D. Quart. Revs. (London), **11**, 15 (1957).
16. FUGGER, J., TIEN, J. M., and HUNSBERGER, I. M. J. Am. Chem. Soc. **77**, 1843 (1955).
17. COLTHUP, N. B. J. Opt. Soc. Am. **40**, 397 (1950).
18. THOMPSON, H. W., NICHOLSON, D. L., and SHORT, L. N. Discussions Faraday Soc. **9**, 222 (1950).
19. MECKE, R., MECKE, R., and LUTTRINGHAUS, A. Chem. Ber. **90**, 975 (1957).
20. MANN, J. Trans. Inst. Rubber Ind. **27**, 232 (1951).
21. SHEINKER, Y. M. and SYRKIN, Y. K. Izvest. Akad. Nauk S.S.S.R., Ser. Fiz., **14**, 478 (1950); Chem. Abstr. **45**, 3246 (1951).

Can. J. Chem. Downloaded from www.nrcresearchpress.com by 200.7.193.243 on 09/04/12
For personal use only.

RADIOCHEMICAL EVIDENCE FOR HETEROGENEITY IN WHEAT STARCH[1]

A. S. PERLIN

ABSTRACT

Wheat starches labeled with carbon-14 have been fractionated by a novel leaching procedure to give amylose, amylopectin, and a highly-branched minor fraction designated "amylopectin C". Marked differences in the specific activity of the fractions are found. Subfractionation of amylopectin also gives products of varying specific activity. These findings provide radiochemical evidence for heterogeneity in wheat starch.

Can. J. Chem. Downloaded from www.nrcresearchpress.com by 200.7.193.243 on 09/04/12
For personal use only.

Starch is composed of D-glucopyranose units joined together, chiefly by 1,4-α-glycosidic linkages, in two distinct macromolecular patterns, one linear and the other highly branched. It is generally accepted that these structural forms are represented in the starch granule by two components, amylose and amylopectin, respectively, which can be isolated and readily differentiated by chemical and physical means (1, 2). In turn, amylose and amylopectin may be subfractionated into products having characteristics substantially different from each other (1, 2, 3, 4, 5, 6), the electrophoretic examination of starch by Lewis and Smith (6) affording particularly striking evidence for such heterogeneity. However, a minority opinion (e.g. 7, 8) holds that starch is homogeneous and that amylose, amylopectin, and subfractions of these are artifacts generated by scission of unstable linkages in an indefinitely large starch molecule. These diverse views on the structure of starch are evaluated critically by Greenwood (2), who concludes that the concept of heterogeneity is favored, a conclusion reached also by Schoch (9), but underlines the difficulty in experimentally proving or disproving such postulates. The current paper provides new evidence for heterogeneity in starch based on differences in the carbon-14 content of amylose, amylopectin, and subfractions of amylopectin, which have been isolated from C^{14}-labeled wheat starches (10).

Amylose and amylopectin are most satisfactorily separated by complete dispersion of the starch in water following which the amylose is preferentially precipitated with a suitable complexing agent (1, 2). The C^{14}-labeled wheat starches were dispersed in water by autoclaving according to the procedure of Schoch (1). It was found, however, that material corresponding to amylopectin (referred to as "amylopectin B") contaminated with very little amylose ("blue values" (11) of 0.1 or less) could be separated out as a gel in a preparative-type ultracentrifuge. Addition of *n*-amyl alcohol to the supernatant solution then precipitated the amylose, which was also of relatively high purity ("blue values" of 1.0 or more). This modification of Schoch's procedure in effect constitutes a leaching process (1, 9) and in its end result resembles the method of Baum, Gilbert, and Wood (12), which employs mild heating in an oxygen-free atmosphere. After removal of the amylose a third starch fraction, referred to as "amylopectin C", was obtained from the solution by flocculation with excess ethanol.

Amylopectin C appears not to have been described by earlier workers. Its yield varied, but averaged about 5% of the total starch. On treatment with iodine the material gave a red color resembling the usual amylopectin–iodine color and, like the major amylopectin fraction ("amylopectin B"), had a "blue value" of 0.1 or less. A comparison of periodate end-group values indicated that the average unit chain lengths of amylopectins B and C

[1]*Manuscript received February 10, 1958.*
Contribution from the National Research Council of Canada, Prairie Regional Laboratory, Saskatoon, Saskatchewan.
Issued as N.R.C. No. 4686 and as Paper No. 252 on the Uses of Plant Products.

Can. J. Chem. Downloaded from www.nrcresearchpress.com by 200.7.193.243 on 09/04/12
For personal use only.

are of approximately the same order, but an accurate measure was not obtained because the polysaccharides were overoxidized. The apparent degree of hydrolysis of amylopectin C to maltose by β-amylase was 48–53%, somewhat less than the value of 55–60% found for amylopectin B. These properties, together with the fact that the material did not form an insoluble complex with *n*-amyl alcohol, served to characterize the minor starch component as a polymer closely related to amylopectin.

Two samples of amylopectin B were subfractionated, in turn, to give three products each. The first of these was obtained as a flocculus by acidifying an alkaline solution of amylopectin B. High-speed centrifugation of the opaque dispersion remaining yielded a second subfraction as a gel, and a third was precipitated from solution with ethanol. Each of these subfractions was degraded to approximately the same extent (55–60%) by β-amylase.

Marked differences in specific activity were found among the starch fractions and subfractions (Table I), the variations being dependent on the stage of plant growth at which tracer was administered. Amylose thus possessed a lower specific activity than amylopectin B if glucose-1-C^{14} or acetate-C^{14} was fed early, or higher, if a late injection was made. These observed fluctuations are thought to reflect the mode of biosynthesis of the amylose and amylopectin components of wheat starch (13). The specific activity–time pattern of labeling of the amylopectin C fractions was distinct from that of amylopectin B but closely resembled the pattern shown by amylose. Differences were found also among the subfractions of amylopectin B, subfractions 2 and 3 having similar specific activities but subfraction 1 having much higher (early injection) or lower (late injection) specific activity.

TABLE I

SPECIFIC ACTIVITY* OF STARCH FRACTIONS AND SUBFRACTIONS

Tracer:	Glucose-1-C^{14}			Acetate-1-C^{14}		Acetate-2-C^{14}		$C^{14}O_2$
Time given (days†):	67	73	79	70	85	80	85	—
Amylose	104	240	314	47	66	58	56	141
Amylopectin B	196	187	190	60	40	45	33	109
Subfraction 1	339	99						
Subfraction 2	173	215						
Subfraction 3	179	207						
Amylopectin C	116	219	377	46	69	56	65	122

*$m\mu c./mM.$ *carbon dioxide.*
†*Days after seeding.*

These variations in the quantity of carbon-14 incorporated strongly suggest that amylose and amylopectin are deposited in the kernel at far from parallel rates and that the various branched components also are not synthesized simultaneously. Accordingly, wheat starch may be considered heterogeneous in a biosynthetic sense. If starch is a giant homogeneous molecule, and the various materials isolated from it were to represent products of random degradation, differences in the specific activity of these fragments would not be expected. However, the current data do not disagree with the view that starch is an indefinitely large molecule, but require that it be built up in a stepwise manner, the stages being distinguishable by differing chemical characteristics and susceptibilities to degradation. In these terms the concept of heterogeneity in starch is meaningful even if linear and branched components are joined together at certain points within the granule by unstable linkages (7). Alternatively, if amylose and amylopectin

are to be regarded as distinct entities, the present radiochemical evidence indicates that amylopectin is itself heterogeneous and may be fractionated into components which differ in physical properties and, possibly to a lesser extent, in chemical structure.

EXPERIMENTAL

C^{14}-labeled wheat starches were isolated as described earlier (10) from the kernels of mature plants grown under field conditions, a given tracer being administered to the plants at various periods of the growing season (14).

Fractionation of Wheat Starch

The starch (0.2–1.0 g.) was extracted exhaustively with hot methanol (1) and air-dried. It was suspended in water at a concentration of 2% and gelatinized on the steam bath and then autoclaved at 18 lb./sq. in. for 4 hours (1). After cooling, the dispersion was centrifuged in a Spinco preparative ultracentrifuge at 40,000 r.p.m. for 25 minutes, giving a gelatinous sediment. The latter was washed in the centrifuge with water and recovered after dehydration with ethanol and ether (amylopectin B). The combined aqueous supernatant solutions were heated on the steam bath, amyl alcohol (1/10 volume) was added, and the suspension stirred gently and allowed to cool slowly (1). After 18 hours at 3° C., the suspension was centrifuged at 25,000 r.p.m. for 20 minutes, the precipitate was washed in the centrifuge with amyl alcohol-saturated water, then several times with ethanol and ether, and dried (amylose). Methanol (4 volumes) was added to the clear supernatant remaining after separation of amylose, and material which precipitated was recovered and dried after ethanol and ether washes (amylopectin C).

Amylose accounted for 28–33% and amylopectin B for 58–65% of the weight of the starches. The yield of amylopectin C varied widely, ranging in amount from 1 to 15% and averaging about 5% of the starches. Iodine absorption values at 610 mμ ("blue values" (11)), measured for the fractions of four starches by the procedure of McCready and Hassid (15), were as follows: amylose—1.0, 1.1, 1.2, 1.2; amylopectin B—0.08, 0.10, 0.12, 0.16; amylopectin C—0.06, 0.08, 0.10, 0.14. All amylose samples gave the typical intense blue color with iodine, and all amylopectin B and C samples a red-purple color of low intensity.

Subfractionation of Amylopectin B

Amylopectin B (0.5 g.), moistened with ethanol, was pasted in *N* sodium hydroxide (6 ml.). Boiling water (50 ml.) was added, the dispersion cooled, acidified with acetic acid, and centrifuged at 5000 r.p.m. affording a precipitate (subfraction 1). Centrifugation at 40,000 r.p.m. gave a second product as a clear gel (subfraction 2), and addition of methanol (30 ml., 1/2 volume) then yielded a bulky precipitate (subfraction 3). All three materials were recovered by washing with methanol and drying. Two samples of amylopectin B fractionated in this way gave the following percentage yields of subfractions 1, 2, and 3, respectively: 16 and 19, 23 and 21, 51 and 47.

Measurement of β-Amylase Degradation

The amylopectin sample (10 mg.) was pasted in *N* sodium hydroxide (0.2 ml.), then taken up in hot water (1 ml.), and the hydrogen-ion concentration of the cooled solution adjusted to pH 5.0 with acetic acid. An excess of a β-amylase preparation was added and the reaction allowed to proceed at room temperature. Aliquots of the solution were withdrawn at intervals and analyzed for reducing power with the Somogyi reagent (16). Hydrolysis was virtually terminated in 2–3 hours, reducing values being increased by less than 5% during a further 20 hours' reaction time. Chromatographic examination of

Can. J. Chem. Downloaded from www.nrcresearchpress.com by 200.7.193.243 on 09/04/12
For personal use only.

the hydrolyzate, after precipitation of limit dextrin with ethanol and removal of sodium ions with Amberlite IR-120, showed maltose as the single sugar produced by β-amylase degradation. The degree of hydrolysis (maltose produced in 5 hours from measure of total reducing power) of four samples of amylopectin B was 55, 58, 59, and 60%, and of four samples of amylopectin C 48, 48, 50, and 53%. Under the same reaction conditions samples of amylose were 90–95% hydrolyzed in 20 hours.

Periodate Oxidation

The starch fraction (15 mg.) was suspended in ethanol (1 ml.), 0.04 *M* sodium metaperiodate (9 ml.) was added, and the mixture stored in the dark at 19.5° C. Aliquots were withdrawn at intervals, excess periodate was destroyed with ethylene glycol, and acid formed was titrated with dilute sodium hydroxide using methyl red indicator. Acid produced (moles/mole) at 75 and 120 hours, respectively, by two samples of amylopectin B: 0.036, 0.041 and 0.052, 0.047; by two samples of amylopectin C: 0.041, 0.039 and 0.053, 0.047.

Measurement of Specific Activity

Specific activity was estimated by the method of Buchanan and Nakao (17). Samples were combusted, and the carbon dioxide liberated was estimated manometrically and its specific activity measured in a gas counter. Reproducibility of the method is ±3%.

ACKNOWLEDGMENTS

The author gratefully expresses thanks to Mr. J. W. L. C. Christ for technical assistance, Dr. W. B. McConnell for samples of starch-C^{14}, Dr. A. C. Neish and Mr. J. Dyck for specific activity measurements, and Dr. L. R. Wetter for assistance in assaying β-amylase degradation.

REFERENCES

1. SCHOCH, T. J. Advances in carbohydrate chemistry. Vol. 1. Academic Press, Inc., New York. 1945. p. 247.
2. GREENWOOD, C. T. Advances in carbohydrate chemistry. Vol. 11. Academic Press, Inc., New York. 1956. p. 335.
3. KERR, R. W. (Editor). Chemistry and industry of starch. 2nd ed. Academic Press, Inc., New York. 1950. pp. 188, 193, 206.
4. MEYER, K. H. and SETTELE, W. Helv. Chim. Acta, **36**, 197 (1953).
5. COWIE, J. M. G. and GREENWOOD, C. T. J. Chem. Soc. 4640 (1957).
6. LEWIS, B. A. and SMITH, F. J. Am. Chem. Soc. **79**, 3929 (1957).
7. PACSU, E. J. Polymer Sci. **2**, 565 (1947).
8. DUMAZERT, C. Bull. soc. chim. biol. **32**, 983 (1950).
9. SCHOCH, T. J. Starch and its derivatives. Vol. 1. *Edited by* J. A. Radley. 3rd ed. Chapman and Hall, Ltd., London. 1953. p. 123.
10. MCCONNELL, W. B. and RAMACHANDRAN, L. K. Can. J. Biochem. Physiol. **34**, 180 (1956).
11. BOURNE, E. J., HAWORTH, W. N., MACEY, A., and PEAT, S. J. Chem. Soc. 924 (1948).
12. BAUM, H., GILBERT, G. A., and WOOD, H. L. J. Chem. Soc. 4047 (1955).
13. MCCONNELL, W. B., MITRA, A. K., and PERLIN, A. S. Unpublished.
14. BILINSKI, E. and MCCONNELL, W. B. Can. J. Biochem. Physiol. **35**, 357 (1957).
15. MCCREADY, R. M. and HASSID, W. Z. J. Am. Chem. Soc. **65**, 1154 (1943).
16. SOMOGYI, M. J. Biol. Chem. **117**, 771 (1937).
17. BUCHANAN, D. L. and NAKAO, A. J. Am. Chem. Soc. **74**, 2389 (1952).

Can. J. Chem. Downloaded from www.nrcresearchpress.com by 200.7.193.243 on 09/04/12
For personal use only.

Can. J. Chem. Downloaded from www.nrcresearchpress.com by 200.7.193.243 on 09/04/12
For personal use only.

L'ARYLATION DES QUINONES PAR LES SELS DE DIAZONIUM

III. SUR LA SYNTHÈSE DES ARYL-CHLORO-*p*-BENZOQUINONES[1]

P. BRASSARD[2] ET P. L'ÉCUYER

RÉSUMÉ

La chloroquinone réagit avec les sels de benzène- et de *p*-chlorobenzène-diazonium pour donner un mélange de deux isomères monoarylés. La majeure partie du produit de la réaction est l'isomère 2,6 et le reste l'isomère 2,3.

INTRODUCTION

Les phénylbenzoquinones réagissent en solution tampon avec les sels de diazonium (1) pour donner les 2,5-bisphénylquinones correspondantes. Günther (2) a constaté que la chloroquinone réagit aussi avec les sels de diazonium et a même isolé un composé qu'il n'a pas identifié. Était-ce l'isomère 2,5? Il y avait lieu d'en douter; car la chloroquinone et la phénylquinone constituent deux systèmes dans lesquels les effets électromères devraient affecter différemment l'orientation de l'entrée du groupement phényle.

Dans le but d'établir la position du groupe phényle, nous avons effectué la réaction de la chloroquinone avec les chlorures de benzène- et de *p*-chlorobenzène-diazonium dans les mêmes conditions que nous avons établies pour la réaction de la benzoquinone avec ces sels (3), soit en milieu aqueux tamponné par l'acétate de sodium. La purification du produit de la réaction a révélé qu'il se forme dans chaque cas deux isomères au lieu d'une seule substance. Une première cristallisation a permis de les séparer grossièrement. Nous avons ensuite procédé à la purification de chacun d'eux en le cristallisant dans un solvant approprié. Dans les deux cas la purification de l'isomère le moins soluble a été facile, mais celle de l'isomère le plus soluble s'est révélée plus difficile et même impossible dans le cas particulier de l'isomère dans lequel le résidu hydrocarboné est le groupe phényle. Ce dernier composé reste toujours contaminé par une certaine quantité de l'isomère le moins soluble. Pour cette raison nous avons choisi d'identifier d'abord les deux isomères dans lesquels le résidu aryle est le groupe *p*-chlorophényle avant de caractériser l'isomère où le reste aryle est le groupement phényle.

Les analyses indiquaient que nous avions réellement affaire à deux 2-chloro-*x*-(*p*-chlorophényl)-benzoquinones isomères. Or théoriquement, il était possible d'obtenir deux des trois isomères inconnus I, II et III. En l'absence de méthode pour préparer ces derniers de façon non équivoque, la preuve de structure que nous avons établie repose essentiellement sur l'identité des *x*,*x'*-dichloro-*x''*-(*p*-chlorophényl)-benzoquinones obtenues de deux façons différentes. Selon la première, nous avons additionné de l'acide chlorhydrique aux deux 2-chloro-*x*-(*p*-chlorophényl)-benzoquinones isomères, la substance II (Ar = groupe *p*-chlorophényle), p.f. 150°, et la substance I (Ar = groupe *p*-chlorophényle), p.f. 103°, et oxydé ensuite en quinones les hydroquinones que nous avions ainsi obtenues. Selon la deuxième, nous avons fait réagir le chlorure de *p*-chlorobenzène-diazonium avec la 2,3- et la 2,6-dichlorobenzoquinone (V et IV).

La substance II (Ar = groupe *p*-chlorophényle), p.f. 150°, après l'addition de l'acide chlorhydrique et l'oxydation du produit de la réaction au chlorure ferrique, donne un mélange constitué, en majeure partie, de 2,3-dichloro-5-(*p*-chlorophényl)-benzoquinone

[1]*Manuscrit reçu le 3 février 1958.*
Contribution du Département de Chimie de la Faculté des Sciences, Université Laval, Québec, Qué.
[2]*Adresse actuelle: Chemisches Institut der Universität, Zürich.*

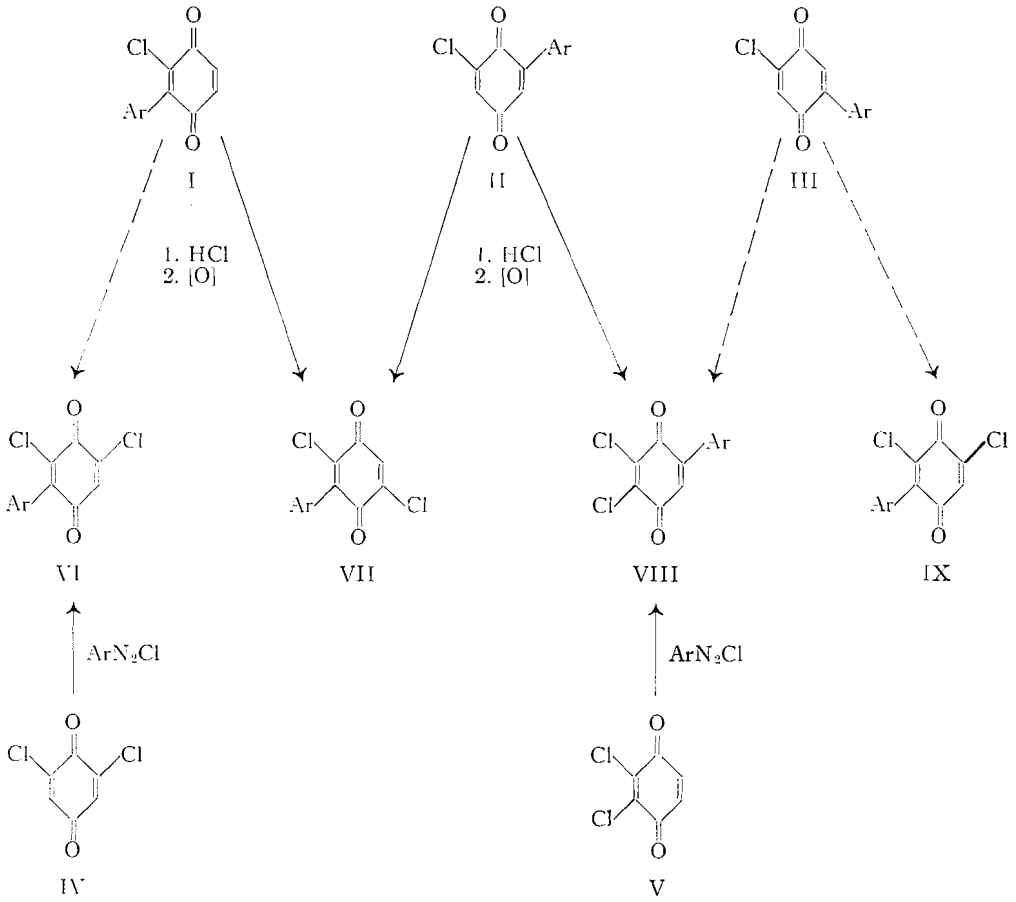

Ar = groupe phényle ou *p*-chlorophényle

(VIII), p.f. 166°–167°, composé que nous avons aussi obtenu par la condensation du chlorure de *p*-chlorobenzène-diazonium avec la 2,3-dichlorobenzoquinone (V), et d'une autre substance, p.f. 144°–145°, différente de l'isomère dichloré en 2,6 (VI), p.f. 116°–117°, et obtenue de IV (Ar = groupe *p*-chlorophényle) par réaction avec le chlorure de *p*-chlorobenzène-diazonium. Cette dernière substance ne peut être que la 2,5-dichloro-3-(*p*-chlorophényl)-benzoquinone (VII), car il ne reste pas d'autre alternative.

L'isomère I (Ar = groupe *p*-chlorophényle), p.f. 103°, soumis à la même série de réactions donne exclusivement une seule substance identique à la 2,5-dichloro-3-(*p*-chlorophényl)-benzoquinone (VII), p.f. 144°–145°, aussi obtenue de l'isomère II, tel que mentionné précédemment. Leur identité a été vérifiée par leur point de fusion mixte. Le fait que celui-ci n'est pas déprimé constitue une preuve rigide que l'isomère II est bien la 2-chloro-6-(*p*-chlorophényl)-benzoquinone et l'isomère I la 2-chloro-3-(*p*-chlorophényl)-benzoquinone.

D'ailleurs, nous avons aussi confirmé ces résultats de la façon suivante. La produit de la réaction de l'isomère II (Ar = groupe phényle), p.f. 128°–129°, avec le chlorure de benzène-diazonium et celui que l'on obtient par l'oxydation de l'hydroquinone résultant de l'addition de l'acide chlorhydrique à la 2,5-bisphénylquinone (X, Ar = groupe

Can. J. Chem. Downloaded from www.nrcresearchpress.com by 200.7.193.243 on 09/04/12
For personal use only.

phényle) ne sont qu'une seule et même substance, soit la 3-chloro-2,5-bisphénylbenzoquinone (XI, Ar = groupe phényle). Leur point de fusion est identique et n'est pas déprimé lorsque les deux produits sont mélangés. Donc l'isomère II (Ar = groupe phényle) est bien la 2-chloro-6-phénylbenzoquinone.

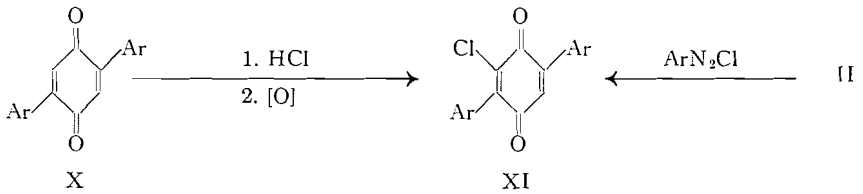

X XI

Ar = groupe phényle ou *p*-chlorophényle

L'isomère II (Ar = groupe *p*-chlorophényle), p.f. 150°, et la 2,5-bis-*p*-chlorophénylbenzoquinone (X, Ar = groupe *p*-chlorophényle) sont beaucoup plus inertes, mais donnent néanmoins par les mêmes réactions une seule et même substance, la 3-chloro-2,5-bis-*p*-chlorophénylquinone (XI, Ar = groupe *p*-chlorophényle), comme le montre le point de fusion mixte. Donc, c'est là une autre preuve que l'isomère II (Ar = groupe *p*-chlorophényle) est bien la 2-chloro-6-*p*-chlorophénylbenzoquinone.

PARTIE EXPÉRIMENTALE*

2-Chloro-6-phénylbenzoquinone (*II*, Ar = *groupe phényle*)

Une solution de chlorure de benzène-diazonium, préparée par la diazotation de 9.3 g. (0.1 mole) d'aniline dissoute dans 25 ml. d'acide chlorhydrique concentré et 100 ml. d'eau, est versée dans un mélange de 15.7 g. (0.11 mole) de chloroquinone et de 30.6 g. (0.225 mole) d'acétate de sodium trihydraté dans 1300 ml. d'eau. On agite vigoureusement à la température ambiante jusqu'à ce qu'il ne se dégage plus d'azote. On essore le précipité (18.5 g., 84% de la théorie) et on l'extrait à l'éther de pétrole bouillant. Après l'évaporation du solvant on cristallise le résidu dans l'éthanol. Une deuxième cristallisation dans le même solvant donne 11.9 g. (54%) de 2-chloro-6-phénylbenzoquinone pure sous forme de paillettes jaunes, p.f. 127°–129°. Calculé pour $C_{12}H_7O_2Cl$: C, 65.92%; H, 3.21%. Trouvé: C, 85.8%; H, 3.8%. Les eaux-mères de cristallisation contiennent un autre isomère; mais il a été impossible de le débarrasser complètement de l'isomère 2,6 qui est beaucoup moins soluble que lui dans les solvants organiques.

Pour fin d'identification l'isomère 2,6 a été préparé de la façon suivante. On fait barboter de l'acide chlorhydrique gazeux anhydre dans une suspension de 10.0 g. de phénylquinone dans 100 ml. d'acide acétique glacial; la quinone passe lentement en solution au fur et à mesure que celle-ci se sature d'acide chlorhydrique. On refroidit à la température ambiante et on ajoute d'un seul trait 100 ml. d'une solution de chlorure ferrique à 30%. On agite durant quelques secondes et on verse dans un grand volume d'eau. On essore le précipité et on le cristallise dans l'éthanol à 90%. On obtient ainsi 9.7 g. (81%) de 2-chloro-6-phénylbenzoquinone, p.f. 129°–130°. Un mélange en proportions égales de deux échantillons de la quinone obtenue par les deux méthodes différentes fond aussi à 129°–130°.

2,3-Dichloro-5-phénylbenzoquinone (*VIII*, Ar = *groupe phényle*)

En opérant comme précédemment, on additionne à la 2-chloro-6-phénylbenzoquinone (5.0 g.) dans l'acide acétique glacial (75 ml.) de l'acide chlorhydrique anhydre, on oxyde

**Les points de fusion ont été pris à l'aide de l'appareil de Johns.*

Can. J. Chem. Downloaded from www.nrcresearchpress.com by 200.7.193.243 on 09/04/12
For personal use only.

Can. J. Chem. Downloaded from www.nrcresearchpress.com by 200.7.193.243 on 09/04/12
For personal use only.

à l'aide de 50 ml. d'une solution de chlorure ferrique à 30% et on verse dans 300 ml. d'eau froide. On essore 4.4 g. (76%) de 2,3-dichloro-5-phénylbenzoquinone presque pure. Elle cristallise dans l'acool éthylique en lamelles jaunes, p.f. 166°–167°. Calculé pour $C_{12}H_6O_2Cl_2$: C, 56.95%; H, 2.39%. Trouvé: C, 56.9%; H, 2.5%.

Une solution de chlorure de benzène-diazonium, obtenue par la diazotation de 4.7 g. (0.05 mole) d'aniline dans un mélange de 12.5 ml. d'acide chlorhydrique et de 50 ml. d'eau, est versée dans une solution de 9.7 g. (0.055 mole) de 2,3-dichlorobenzoquinone dans 200 ml. d'acide acétique glacial à la température ambiante. On munit le récipient d'un agitateur mécanique et on y ajoute 15.3 g. d'acétate de sodium trihydraté dissous dans 100 ml. d'eau. Une fois la réaction terminée (environ 12 heures), le produit brut est filtré et bouilli en présence de noir animal dans un mélange de méthanol, d'acétone et d'eau (1:1:1). La solution est filtrée à chaud, refroidie et mise au réfrigérateur. On essore 8.7 g. (69% de la théorie) de 2,3-dichloro-5-phénylbenzoquinone, p.f. 166°–167°. Calculé pour $C_{12}H_6O_2Cl_2$: C, 56.95%; H, 2.39%. Trouvé: C, 57.3%; H, 2.4%. Le mélange d'un échantillon de cette quinone avec un autre de la 2,3-dichloro-5-phénylbenzoquinone obtenue de la façon décrite précédemment fond aussi à 166°–167°.

2-Chloro-6-(p-chlorophényl)-benzoquinone (*II*, Ar = *groupe p-chlorophényle*) *et 2-chloro-3-(p-chlorophényl)-benzoquinone* (*I*, Ar = *groupe p-chlorophényle*)

En condensant, dans les mêmes conditions que pour la synthèse de la 2-chloro-6-phénylquinone, le chlorure de *p*-chlorobenzène-diazonium (0.1 mole) avec la chloroquinone (0.1 mole), on recueille, la réaction terminée, 25.9 g. d'un mélange de deux isomères. On extrait le matériel brut à l'éther de pétrole (p.é. 65°–110°) bouillant et on laisse refroidir les extraits à la température ambiante. Il se sépare d'abord une huile rouge foncé, puis il se dépose des cristaux rouges. Lorsque des aiguilles jaunes commencent à apparaître, on décante la solution (qu'on conserve pour isoler l'autre isomère) et on cristallise le résidu dans l'éthanol. Après quelques cristallisations on obtient 16.0 g. (66% de la théorie) de 2-chloro-6-(*p*-chlorophényl)-benzoquinone pure sous forme d'aiguilles rouges, p.f. 150°. Calculé pour $C_{12}H_6O_2Cl_2$: C, 56.95%; H, 2.39% .Trouvé: C, 56.8%; H, 2.5%.

On évapore à sec la solution dans l'éther de pétrole qu'on a décantée dans la préparation précédente. On dissout ensuite le résidu dans un mélange bouillant de méthanol, d'acétone et d'eau (1:1:1), on traite la solution au noir animal et, après cristallisation, on essore 4.5 g. (18% de la théorie) de 2-chloro-3-(*p*-chlorophenyl)-benzoquinone pure cristallisée en paillettes jaunes, p.f. 103°. Calculé pour $C_{12}H_6O_2Cl_2$: C, 56.95%; H, 2.39%. Trouvé: C, 56.5%; H, 2.5%.

2,3-Dichloro-5-(p-chlorophényl)-benzoquinone (*VIII*, Ar = *groupe p-chlorophényle*) *et 2,5-dichloro-3-(p-chlorophényl)-benzoquinone* (*VII*, Ar = *groupe p-chlorophényle*)

On fait barboter de l'acide chlorhydrique gazeux anhydre dans une suspension de 2-chloro-6-(*p*-chlorophényl)-benzoquinone (2.0 g.) dans l'acide acétique glacial (50 ml.) jusqu'à saturation et, après avoir chassé la majeure partie du gaz chlorhydrique, on oxyde à la température ambiante à l'aide de 50 ml. d'une solution de chlorure ferrique à 30% et on verse dans 300 ml. d'eau froide. Après filtration et cristallisation du précipité dans l'éthanol, on essore 1.4 g. (61%) de 2,3-dichloro-5-(*p*-chlorophényl)-benzoquinone pure sous forme de longues aiguilles rouges, p.f. 166°–167°. Calculé pour $C_{12}H_5O_2Cl_3$: C, 50.12%; H, 1.75%. Trouvé: C, 50.3%; H, 1.9%.

En étendant d'eau les eaux-mères de cristallisation de la 2,3-dichloro-5-(*p*-chlorophényl)-benzoquinone on obtient l'isomère 2,5-dichloro-3-(*p*-chlorophényl)-benzoquinone

qui, après cristallisation dans le méthanol, donne 0.3 g. (14% de la théorie) de la substance pure sous forme d'aiguilles jaunes, p.f. 144°–145°. Calculé pour $C_{12}H_5O_2Cl_3$: C, 50.12%; H, 1.75%. Trouvé: C, 49.9%; H, 1.8%.

Dans le but d'identifier ces deux isomères, le rouge p.f. 166°–167°, et le jaune p.f. 144°–145°, nous avons préparé la 2,3-dichloro-5-(*p*-chlorophényl)-benzoquinone de la façon suivante: la *p*-choraniline (6.4 g., 0.05 mole) dissoute dans un mélange de 12.5 ml. d'acide chlorhydrique concentré et 50 ml. d'eau est diazotée et la solution du sel de diazonium est versée dans un mélange de 9.7 g. (0.055 mole) de 2,3-dichlorobenzoquinone (V) et de 20.4 g. de trihydrate d'acétate de sodium dans 200 ml. d'acide acétique à la température ambiante. Tout en agitant mécaniquement le mélange, on y verse suffisamment d'eau pour produire une légère précipitation de la quinone de départ. Une fois le dégagement gazeux terminé, on filtre et cristallise dans l'éthanol. On essore 11.6 g. (81% de la théorie) de 2,3-dichloro-5-(*p*-chorophényl)-benzoquinone pure sous la forme d'aiguilles rouges, p.f. 166°–167°. Calculé pour $C_{12}H_5O_2Cl_3$: C, 50.12%; H, 1.75%. Trouvé: C, 50.1%; H, 2.0%. Elle est identique à l'isomère rouge obtenu précédemment comme le montre le p.f. 166°–167° de leur mélange.

Une suspension de 2-chloro-3-(*p*-chlorophényl)-benzoquinone (I, Ar = groupe *p*-chlorophényle) (1.5 g.) dans l'acide acétique glacial (20 ml.) est saturée par un courant d'acide chlorhydrique sec et la solution d'hydroquinone obtenue est oxydée par l'addition de 50 ml. d'une solution de chlorure ferrique à 30%. On isole par cristallisation dans l'éthanol 1.2 g. (67% de la théorie) de 2,5-dichloro-3-(*p*-chlorophényl)-benzoquinone pure, p.f. 144°–145°. On ne décèle aucune dépression du point de fusion du mélange de cette substance avec l'isomère jaune, p.f. 144°–145°, obtenu par l'addition d'acide chlorhydrique à la 2-chloro-6-(*p*-chlorophényl)-quinone.

2,6-Dichloro-3-(p-chlorophényl)-benzoquinone (*VI*, Ar = *groupe p-chlorophényle*)

La condensation du chlorure de *p*-chlorobenzène-diazonium (0.1 mole) avec une suspension de 2,6-dichloroquinone (0.1 mole) à la température ambiante dans 300 ml. d'acide acétique en présence du trihydrate d'acétate de sodium (0.225 mole) dure 12 heures. On dilue à l'eau, on décante la liqueur et on extrait le résidu à plusieurs reprises à l'éthanol (80%) bouillant. Les extraits réunis, bouillis avec du noir animal, filtrés à chaud et refroidis donnent 18.1 g. (72% de la théorie) de 2,6-dichloro-3-(*p*-chlorophényl)-benzoquinone pure sous forme de paillettes orangées, p.f. 116°–117°. Calculé pour $C_{12}H_5O_2Cl_3$: C, 50.12%; H, 1.75%. Trouvé: C, 50.3%; H, 2.0%.

3-Chloro-2,5-bisphénylbenzoquinone (*XI*, Ar = *groupe phényle*)

En suivant la technique déjà décrite précédemment, on additionne de l'acide chlorhydrique gazeux à 2.8 g. de 2,5-bisphénylquinone (IX, Ar = groupe phényle) et on oxyde ensuite au chlorure ferrique à 30%. On obtient 2.9 g. (91%) de 3-chloro-2,5-bisphénylbenzoquinone qui cristallise dans l'acide acétique en aiguilles orangées, p.f. 188°–189°. Calculé pour $C_{18}H_{11}O_2Cl$: C, 73.35%; H, 3.76%. Trouvé: C, 73.6%; H, 3.9%.

Cette quinone s'obtient également en faisant réagir une solution de chlorure de benzènediazonium (0.05 mole) avec la 2-chloro-6-phénylbenzoquinone (0.045 mole) dans 300 ml. d'acétone à −5°. Tout en s'assurant d'une forte agitation et du maintien de la température du milieu à moins 0° on ajoute en petites portions de l'acétate de sodium trihydraté (20.4 g. en tout) durant une période de 30 minutes. On laisse ensuite le mélange prendre lentement la température ambiante. La réaction terminée, on étend d'eau, on isole le précipité et on le cristallise dans l'acide acétique. On essore la 3-chloro-2,5-bisphénylbenzoquinone (2.7 g., 20%), p.f. 188°–190°. La technique des points de fusion

Can. J. Chem. Downloaded from www.nrcresearchpress.com by 200.7.193.243 on 09/04/12
For personal use only.

mixtes montre que cette substance est identique à celle qui a été obtenue par la méthode précédente.

3-Chloro-2,5-(p-chlorophényl)-benzoquinone (*XI*, Ar = *groupe p-chlorophényle*)

On l'obtient en opérant comme pour la synthèse de la 3-chloro-2,5-bisphénylbenzoquinone par l'addition d'acide chlorhydrique à la 2,5-bis-(*p*-chlorophényl)-benzoquinone suivie de l'oxydation au chlorure ferrique et l'arylation de la 2-chloro-6-(*p*-chlorophényl)-benzoquinone par le chlorure de *p*-chlorobenzène-diazonium. La 3-chloro-2,5-bis-(*p*-chlorophényl)-benzoquinone cristallise dans l'acide acétique en aiguilles orangées de p.f. 205°–207°. Calculé pour $C_{18}H_9O_2Cl_3$: Cl, 32.16%. Trouvé: Cl, 31.9%.

REMERCIEMENTS

Nous remercions le Conseil National de Recherches du Canada et la Shell Oil Company of Canada pour des bourses d'études accordées à l'un de nous (P.B.).

BIBLIOGRAPHIE

1. BRASSARD, P. et L'ÉCUYER, P. Can. J. Chem. **36**, 700 (1958).
2. GÜNTHER, F. Brevet allemand 508,395 (1924).
3. BRASSARD, P. et L'ÉCUYER, P. Can. J. Chem. **36**, 709 (1958).

Can. J. Chem. Downloaded from www.nrcresearchpress.com by 200.7.193.243 on 09/04/12
For personal use only.

THE INFRARED SPECTRA OF ORGANO-PHOSPHORUS COMPOUNDS

II. THE 1–2.6 μ REGION[1,2]

R. A. McIvor, C. E. Hubley, G. A. Grant, and A. A. Grey

ABSTRACT

The application of near infrared spectra to the study of phosphorus compounds has been investigated. It has been found that each type of radical gives a characteristic set of bands, which are not appreciably affected by changes in the molecule more than two atoms distant. Characteristic group frequencies are given for MeO, EtO, *n*-PrO, *i*-PrO, *n*-BuO, Me, Et, Me_2N, Et_2N, and *i*-Pr_2N groups attached to phosphorus. Only the MeP bands are noticeably altered by the nature of the substitution on the phosphorus atom. Qualitative predictions of the spectra of compounds containing more than one type of C—H group may be made by summing the contributions of the components.

Can. J. Chem. Downloaded from www.nrcresearchpress.com by 200.7.193.243 on 09/04/12
For personal use only.

INTRODUCTION

In a previous paper (1) certain features of the infrared spectra of organo-phosphorus compounds were discussed and some new assignments proposed in the 2–26 μ region. In some cases useful information about the environment of the phosphorus atom was obtained by a study of the C—H bending vibrations associated with the ester groups attached to phosphorus. With the advent of commercial spectrophotometers designed to give high resolution in the 0.7–2.5 μ overtone-combination region, it was decided to examine the spectra of organo-phosphorus compounds in this region to determine whether the improved resolution would lead to more information about the environment of hydrogen-containing groups.

EXPERIMENTAL

The preparation of most of the compounds examined has been described elsewhere (2, 3).

A Cary Model 14PM double-beam recording spectrophotometer was used for all spectra. Most spectra were run as approximately 1% w/v solutions in Spectrograde carbon tetrachloride. The path lengths used were 10 cm. and 5 cm. in the 1.0–2.1 μ and 2.1–2.5 μ regions respectively. For the remaining spectra, approximately 0.5% w/v carbon tetrachloride was used in 10-cm. cells over the entire 1.0–2.5 μ region. Bands are cited to the nearest 0.001 μ, and the limits given indicate the maximum variation occurring in the compounds examined. The quoted intensities are 100 times the molar extinction coefficients. The instrumental calibration was checked by comparing the benzene spectrum with that reported by Kaye (4).

RESULTS AND DISCUSSION

Bands in the 1–2.5 μ region arise chiefly from overtones and combination bands involving hydrogen vibrations. Most of the compounds examined show two principal sets of bands at the concentration used: set A, near 1.7 μ, is attributed to the first overtone of the C—H stretching vibrations, with the 4 ν C—H bending vibrations superimposed; set B, located in the 2.2–2.5 μ region, is more intense and is attributed to binary C—H stretching and bending combinations, with lesser contributions from ternary bending

[1]*Manuscript received January 17, 1958.*
Contribution from the Defence Research Chemical Laboratories, Ottawa, Canada. Issued as D.R.C.L. Report No. 234A. Presented in part at the 16th International Conference of the International Union of Pure and Applied Chemistry, Paris, France, July, 1957.
[2]*Reference 1 is considered to be Paper No. I in this series.*

combinations and overtones. In addition, there are corresponding band groups when OH is present which exhibit marked changes as the concentration is altered.

Assignments for various types of hydrogen bands are presented in an excellent review of this field published by Kaye (4). The present work, however, is concerned with the contour of the band envelope associated with larger structural groups in the molecule (e.g. EtO, BuO, —NMe_2, etc.). We have found that the bands associated with any one of these groups are remarkably constant, being virtually insensitive to structural changes more than two atoms away, although these changes may affect the C—H fundamentals (1). Despite the variations in the slit widths and the degree of overlapping of bands, useful quantitative data can be obtained from the extinction coefficients associated with various bands in any one type of band envelope.

The various groups examined will be discussed separately. The generalized group frequencies are presented in the text, and most of the detailed examples in the Appendix.

(*a*) MeO *and* MeS *Bands*

Phosphorus compounds containing MeO (Appendix—Table XI) have, in general, two principal bands and several lesser bands in region A. The former occur at $1.680 \pm 0.002\ \mu$ (5952 $cm.^{-1}$) and $1.720 \pm 0.001\ \mu$ (5814 $cm.^{-1}$) with average intensities of 13 and 12 respectively. Similar bands occur in dimethyl carbonate and MeS compounds although MeS bands are more intense. In certain cases the concentration was too low to permit accurate readings for these weak bands, and for the additional weaker bands, one of which occurs at $1.666 \pm 0.017\ \mu$ (6002 $cm.^{-1}$).

The B region contains four principal bands up to $2.5\ \mu$. There appear to be other bands beyond $2.5\ \mu$, in particular one near $2.52\ \mu$, but not all of the compounds were investigated in that region, because of instrumental difficulties. The bands occur at $2.254 \pm 0.002\ \mu$ (4437 $cm.^{-1}$), $2.334 \pm 0.004\ \mu$ (4285 $cm.^{-1}$), $2.387 \pm 0.005\ \mu$ (4189 $cm.^{-1}$), and $2.471 \pm 0.005\ \mu$ (4047 $cm.^{-1}$) with average intensities of 174, 41, 70, and 63 per MeO group respectively. On the basis of intensities MeS seems to have all but the $2.387\ \mu$ band and both MeS-containing compounds have an additional band at $2.319\ \mu$ (4312 $cm.^{-1}$) with an intensity of 164. Dimethyl carbonate has similar bands but methanol has only two.

TABLE I

EtO bands			EtS bands		
Band position		$\epsilon \times 10^2$ per EtO group	Band position		$\epsilon \times 10^2$ per EtO group
μ	$cm.^{-1}$		μ	$cm.^{-1}$	
A region					
1.682±0.003	5945	21	1.687	5928	26
1.692±0.003	5910	26	1.695	5859	26
1.727±0.007	5790 br*	23	1.740	5757	42
1.760±0.004	5682	15			
B region					
2.262±0.007	4425	169	2.268	4409	133
2.302±0.004	4344	131	2.284	4378	121
2.342±0.006	4270	78	2.304	4340	172
2.410±0.004	4149	74	2.362	4234	101
2.453±0.005	4077	89	2.397	4172	70
2.482±0.005	4029	83	2.432	4112	26
			2.453	4077	42
			2.484	4026	51
			2.502	3997	43
			2.512	3981	50

**In this and subsequent tables*—sh = *shoulder*, wk = *weak*, br = *broad*, d = *doublet*.

Can. J. Chem. Downloaded from www.nrcresearchpress.com by 200.7.193.243 on 09/04/12
For personal use only.

Can. J. Chem. Downloaded from www.nrcresearchpress.com by 200.7.193.243 on 09/04/12
For personal use only.

(*b*) EtO *and* EtS *Bands*

Organo-phosphorus compounds whose only C—H bands are contained in ethoxy groups have four bands in the A region and six bands in the B region listed in Table I.

The ethylthio group frequencies, also given in Table I, are based on SSS-triethyl phosphorotrithioate only.

The bands of the compounds on which these characteristic frequencies are based are listed in the Appendix (Table XII), along with the bands for ethanol, ethanethiol, diethyl carbonate, and diethyl oxalate. The EtO compounds without phosphorus have spectra generally similar to the EtO—P compounds. Diethyl oxalate, in particular, has a spectrum almost indistinguishable from those of EtO—P containing compounds.

(*c*) *n*-PrO *Bands*

n-PrO—P compounds have three bands in the A region and nine bands in the B region, the frequencies for which are listed in Table II.

TABLE II

n-PrO bands			*i*-PrO bands			*n*-BuO bands		
Band position		$\epsilon\times10^2$ per *n*-PrO group	Band position		$\epsilon\times10^2$ per *i*-PrO group	Band position		$\epsilon\times10^2$ per BuO group
μ	cm.$^{-1}$		μ	cm.$^{-1}$		μ	cm.$^{-1}$	
A region								
1.698±0.001	5889	27	1.682±0.003	5945	28	1.693±0.003 sh	5907	24
1.730±0.001	5780	27	1.692±0.004	5906	37	1.703±0.001	5872	34
1.754±0.001	5701	21	1.731±0.002	5777	26	1.714±0.002	5834	31
			1.756±0.011 br	5695	14	1.732±0.005	5770	29
			1.800±0.002	5555	11	1.750±0.003	5712	28
B region								
2.269±0.004	4407	157	2.266±0.002	4413	149	2.270±0.009	4405	160
2.300±0.003	4349	153	2.295±0.005	4357	167	2.304±0.003	4340	178
2.313±0.002	4323	135	2.322±0.004	4307	172	2.348±0.002	4259	128
2.348±0.001	4259	103	2.343±0.003	4268	99	2.386±0.002	4191	116
2.366±0.003	4239	91	2.404±0.005	4160	121	2.436±0.003	4105	115
2.388±0.001	4188	80	2.432±0.005	4112	125	2.452±0.002	4078	127
2.426±0.005	4122	92	2.455±0.007	4074	116	2.485±0.003	4024	102
2.447	4087	100	2.475±0.003	4040	95	2.504±0.001	3994	94
2.487±0.001	4021	93	2.518±0.008	3971	61			
			2.551±0.007	3920	51			
			2.587±0.007	3865	49			

(*d*) *i*-PrO *Bands*

i-PrO bands have five bands in the A region and eleven bands in the B region as shown in Table II.

Isopropyl alcohol has similar bands in the A region, shifted slightly to lower frequencies, but the B region is quite different, as there are only four main bands, with numerous shoulders not recorded in the table. Isopropyl frequencies and intensities are not as constant as those due to *n*-propyl.

(*e*) *n*-BuO *Bands*

The characteristic frequencies are also listed in Table II. It is noted from the examples in the Appendix that the intensities of the bands in the B region are in general greater for compounds containing P→S than for those with P→O.

(*f*) MeP *and* MeI *Bands*

Three compounds were examined which contained only Me—P groups. These are listed in Table III along with methyl iodide. Because of the differences among MeI,

Me—P(O), and Me—P(S) type compounds, separate values are given for each class. It is interesting to note that MeI and Me—P compounds show greater dissimilarity in the 1–2.6 μ region than in the 3–16 μ region.

TABLE III

MeP AND MeI BANDS

$MePCl_2$			$MeP(O)Cl_2$			$MeP(S)Cl_2$			MeI		
μ	cm.$^{-1}$	$\epsilon\times10^2$	μ	cm.$^{-1}$	$\epsilon\times10^2$	μ	cm.$^{-1}$	$\epsilon\times10^2$	μ	cm.$^{-1}$	$\epsilon\times10^2$
A region											
1.680	5952	22	1.668	5995	19	1.670	5985	23	1.641	6094	12
1.694	5903	28	1.684	5938	40	1.686	5931	51	1.658	6031	65
1.721	5811	20	1.710	5848	21	1.717	5824	40	1.692	5910	25
1.738	5754	9	1.717	5824	25	1.730	5780	51	1.708	5855	51
1.755	5698	7	1.728	5787	26						
1.762	5675	8									
1.770	5650	7									
1.811	5522	4									
B region											
2.282	4382	134	2.277	4392	202	2.279	4388	272	2.242	4460	194
2.287	4373	137	2.312	4325	59	2.336	4281	111	2.334	4284	111
2.322	4307	21	2.339	4269	67	2.561	3905	149	2.547	3926	122
2.344	4266	113	2.566	3897	114	2.617	3821	156			
2.354	4248	82	2.629	3804	119	2.630	3802	133			
2.379	4203	13									
2.389	4186	17									
2.458	4068	33									
2.536	3943	17									
2.567	3896	20									
2.587 sh	3865	36									
2.593	3857	39									

(*g*) EtP *and* EtI *Bands*

$EtP(O)Cl_2$ and EtI had bands as listed in Table IV. As with the methyl homologues, the near infrared spectrum of EtI differs considerably from that of $EtP(O)Cl_2$.

TABLE IV

$EtP(O)Cl_2$			EtI		
μ	cm.$^{-1}$	$\epsilon\times10^2$	μ	cm.$^{-1}$	$\epsilon\times10^2$
A region					
1.651	6057	11	1.671	6984	15
1.678	5959	14	1.701	5879	36
1.688	5924	22	1.724	5800	36
1.699	5886	wk	1.748	5721	12
1.708	5855	14	1.776	5631	9
1.712	5841	14			
1.731	5777	31			
1.742	5746	41			
1.763	5672	23			
B region					
2.255	4435	112	2.266	4413	200
2.292	4363	124	2.300	4348	153
2.304	4340	131	2.330	4292	73
2.372	4216	90	2.361	4235	148
2.399	4168	53	2.386	4191	151
2.437	4103	32	2.454	4075	89
2.531	3951	76	2.504	3994	75
2.552	3918	76	2.513	3979	49

Can. J. Chem. Downloaded from www.nrcresearchpress.com by 200.7.193.243 on 09/04/12
For personal use only.

Can. J. Chem. Downloaded from www.nrcresearchpress.com by 200.7.193.243 on 09/04/12
For personal use only.

(*h*) Me_2N *Compounds*

Two compounds containing Me_2N—P and one containing Me_2N—C(O) were examined. These all are quite similar in the A region and the Me_2N—P compounds are similar in the B region. The assigned intensities listed in Table V are for the complete Me_2N grouping.

TABLE V

Me_2N GROUPS

$Me_2NP(S)Cl_2$			$Me_2NP(O)Cl_2$			$Me_2NC(O)H$			Average assignments		
μ	cm.$^{-1}$	$\epsilon\times10^2$	μ	cm.$^{-1}$	$\epsilon\times10^2$	μ	cm.$^{-1}$	$\epsilon\times10^2$	μ	cm.$^{-1}$	$\epsilon\times10^2$
A region											
1.683	5942	12	1.682	5945	15	1.684 sh	5938	20	1.683	5942	14
1.699	5886	26	1.699	5886	29	1.704	5869	39	1.699	5886	28
1.729	5784	17	1.728	5787	19	1.739	5750	27	1.729	5784	18
1.749	5718	12	1.749	5718	15				1.749	5718	14
B region											
2.254	4437	103	2.247 sh	4450	120				2.251	4442	112
2.269	4407	183	2.269	4407	200	2.282	4382	291	2.269	4409	192
2.290	4367	116	2.287	4373	149	2.302	4344	291	2.289	4369	133
2.329	4294	63	2.351	4254	108	2.348	4259	131	2.354	4248	95
2.357	4243	82				2.364	4230	134	2.454	4075	77
2.455	4073	71	2.452	4078	83	2.388	4188	114	2.502	3997	76
2.503	3995	63	2.500	4000	88	2.456	4072	139			
						2.492	4013	94			
						2.534	3946	87			

(*i*) Et_2N *Compounds*

Bands given by Et_2NPSCl_2 are compared with those from Et_3N in Table VI. Intensities given are per Et group.

TABLE VI

Et_2N GROUPS

Et_2NPSCl_2			Et_3N		
μ	cm.$^{-1}$	$\epsilon\times10^2$	μ	cm.$^{-1}$	$\epsilon\times10^2$
A region					
1.683	5942	19	1.687	5928	25
1.693	5907	23	1.697	5893	28
1.732	5774	19	1.737	5757	31
1.761	5679	12	1.766 sh	5663	20
B region					
2.266	4413	121	2.267	4411	99
2.307	4335	116	2.310	4329	141
2.337	4279	66	2.346	4263	75
2.388	4188	62	2.401	4165	85
2.414	4143	55	2.472	4045	73
2.456	4072	63			
2.476	4039	67			
2.492	4013	54			

(*j*) *i*-Pr_2N *Compounds*

Four compounds were examined which contained *i*-Pr_2N in conjunction with other alkoxy groups. A pure sample of a compound containing C—H in *i*-Pr_2N groups only has

not yet been obtained. An attempt was made to predict the spectrum of such a compound by subtracting the contributions of the alkoxy groups. The results are indicated in Table VII. The bands for these compounds are given in Appendix Table XV. Because of the similarity of *i*-PrO and *i*-Pr_2N bands the values in column 3 are probably most reliable.

TABLE VII

PREDICTED *i*-Pr_2N BANDS, μ ($\epsilon \times 10^2$), FOR FOUR COMPOUNDS

i-$Pr_2NP(S)(OEt)_2$	*i*-$PrNP(S)(O\,n\text{-}Pr)_2$	*i*-$Pr_2NP(S)(O\,i\text{-}Pr)_2$	*i*-$Pr_2NP(S)(O\,n\text{-}Bu)_2$
1.687 (56)	1.689 (90)	1.688 (46)	1.690 (37)
1.698 (58)	1.699 (69)	1.697 (46)	1.699 (36)
1.735 (58)	1.721 (26)	1.734 (48)	1.721 (26)
1.764 (28)	1.736 (47)	1.764 (33)	1.737 (37)
1.807 (29)	1.758 (34)	1.806 (16)	1.759 (29)
	1.808 (37)		1.808 (38)
2.267 (181)	2.276 (221)	2.268 (200)	2.274 (162)
2.303 (284)	2.303 (268)	2.302 (372)	2.304 (288)
2.342 (120)	2.346 (134)	2.341 (150)	2.340 (108)
2.360 (280)	2.388 (204)	2.362 (276)	2.399 (129)
2.406 (154)	2.401 (148)	2.404 (183)	2.405 (368)
2.447 (102)	2.447 (140)	2.434 (122)	2.466 (153)
2.467 (286)	2.462 ? (142)	2.462 (136)	2.545 (182)
2.482 br, sh (68)			

(*k*) *Miscellaneous*

Although the P—H group does not give rise to any sharp bands in this region, a weak diffuse band appears at about 1.892 ± 0.001 (5258 $cm.^{-1}$), with an intensity of 24 as indicated in Table VIII.

TABLE VIII

P—H VIBRATIONS

Compound	μ	$cm.^{-1}$	$\epsilon \times 10^2$
Dimethyl hydrogen phosphonate	1.892	5285	26
Diethyl hydrogen phosphonate	1.891	5288	20
Diethyl hydrogen phosphonothioate	1.893	5283	25
Dibutyl hydrogen phosphonate	1.891	5288	23

The P—SH grouping is mainly unbonded at the concentrations used and gives rise to a weak doublet at 1.970 μ (5076 $cm.^{-1}$) and 1.999 μ (5002 $cm.^{-1}$) with intensities of 19 and 19 as indicated in Table X. In contrast, diethylaminoethanethiol and ethanethiol have a band near 1.740 μ (5747 $cm.^{-1}$) in the C—H A region which might be attributed to the S—H group. Phosphorothioic acids, which appear from the 3–15 μ region to have the P(S)OH structure, have a band at 1.908 μ (5241 $cm.^{-1}$) which may arise from the P—OH grouping.

Diethyl phosphoroamidate had NH overtones at 1.481 μ (6739 $cm.^{-1}$) and 1.488 μ (6720 $cm.^{-1}$) and a combination band at 1.992 μ (5020 $cm.^{-1}$) with intensities of 50, 56, and 197 respectively whereas C—NH bands absorb at 1.531 μ (6532 $cm.^{-1}$) and 1.548 μ (6460 $cm.^{-1}$) with intensities of 72 and 73 in isopropylamine and diisopropylamine respectively. There are numerous weak combination bands in these aliphatic amines, none with intensities over 55.

Can. J. Chem. Downloaded from www.nrcresearchpress.com by 200.7.193.243 on 09/04/12
For personal use only.

TABLE IX—PREDICTIONS

A. 2EtO, 1EtS

$(EtO)_2P(O)SEt$	Predicted	$(EtO)_2P(S)SEt$
μ ($\epsilon\times10^2$)	μ ($\epsilon\times10^2$)	μ ($\epsilon\times10^2$)
1.685 (64)	1.685 (68)	1.687 (60)
1.691 (72)	1.694 (78)	1.693 (77)
1.732 (79)	1.735 (88)	1.732 (87)
1.761 (39)	1.760 (30)	1.762 (42)
2.263 (429)	2.265 (471)	2.263 (444)
	2.284 (121)	
2.302 (383)	2.302 (434)	2.305 (413)
2.345 (175)	2.342 (156)	2.344 sh (196)
2.359 (197)	2.362 (101)	2.360 (206)
2.398 sh (150)	2.397 (70)	2.397 (157)
2.411 (169)	2.410 (148)	2.412 (167)
2.453 (210)	2.453 (220)	2.452 (212)
2.483 (212)	2.483 (217)	2.482 (200)

B. MeP Compounds*

$MeP(OEt)_2$		$MeP(O)(OEt)_2$		$MeP(S)(OEt)_2$	
Predicted	Observed	Predicted	Observed	Predicted	Observed
1.681 (64)	1.681 (52)	1.668 (19)	1.672 sh (26)	1.670 (23)	1.673 (28)
1.693 (84)	1.694 (63)	1.683 (82)	1.682 (69)	1.684 (93)	1.683 (75)
1.721 (20)	1.716 sh (39)	1.692 (52)	1.692 (55)	1.692 (52)	1.692 (58)
1.727 (46)	1.727 (54)	1.714 (46)	1.714 sh (47)	1.717 (40)	1.717 sh (49)
1.739 (54)	1.736 (58)	1.728 (72)	1.728 (72)	1.728 (97)	1.728 (83)
1.758 (45)	1.757 (30)	1.760 (30)	1.759 (32)	1.760 (30)	1.760 (35)
2.262 (338)	2.269 (321)	2.270 (540)	2.271 (534)	2.271 (610)	2.271 (461)
2.285 (271)	2.280 (359)	2.303 (262)	2.304 (294)	2.303 (262)	2.302 (302)
2.303 (262)	2.305 (324)	2.312 (59)	2.324 sh (183)	2.339 (267)	2.331 (212)
2.322 (21)	2.351 (253)	2.340 (223)	2.340 (170)	2.410 (148)	2.403 (154)
2.343 (269)	2.388 wk (113)	2.410 (148)	2.411 (164)	2.453 (178)	2.452 (191)
2.354 (82)	2.403 (153)	2.453 (178)	2.458 (213)	2.482 (166)	2.482 (176)
2.384 (30)	2.453 (198)	2.482 (166)	2.482 (200)	2.561 (149)	2.565 (156)
2.400 (165)	2.482 (188)	2.566 (114)	2.571 (167)	2.617 (156)	2.617 (172)
2.456 (211)		2.629 (119)	2.619 (193)		
2.482 (166)					

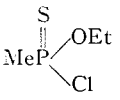	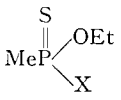	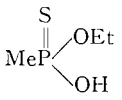	$MeP(S)(O\ i\text{-}Pr)_2$	
Observed	Predicted	Observed	Predicted	Observed
1.669 (20)	1.670 (23)	1.671 sh (20)	1.670 (23)	1.672 sh (26)
1.682 (59)	1.684 (61)	1.683 (42)	1.684 (107)	1.683 (78)
1.689 (25)	1.692 (26)	1.691 sh (28)	1.692 (74)	1.692 (66)
1.716 (43)	1.717 (40)	1.717 (32)	1.717 (40)	1.719 sh (40)
1.729 (58)	1.729 (74)	1.729 (47)	1.731 (103)	1.730 (76)
1.761 (14)	1.760 (15)	1.759 (26)	1.756 (28)	1.758 (32)
			1.800 (22)	1.801 (27)
2.261 (212)	2.262 (169)	2.262 (159)		
2.275 (348)	2.279 (272)	2.273 (241)	2.273 (580)	2.272 (380)
2.301 (151)	2.303 (131)	2.301 (127)	2.295 (334)	2.297 (312)
2.337 (157)	2.336 (111)	2.327 (124)	2.322 (344)	2.322 (348)
2.412 (79)	2.342 (78)	2.411 (84)	2.340 (309)	2.388 sh (235)
2.449 (115)	2.410 (74)	2.450 (94)	2.404 (242)	2.406 (222)
2.481 (101)	2.453 (89)	2.479 (94)	2.432 (250)	2.433 (247)
2.556 (143)	2.482 (83)	2.567 (115)	2.455 (232)	2.450 sh (215)
2.612 (156)	2.561 (149)	2.617 (122)	2.475 (190)	2.472 (181)
2.627 (196)	2.617 (156)	2.634 (120)	2.518 (122)	2.518 (137)
	2.630 (133)		2.551 (102)	2.560 (167)
			2.561 (149)	2.613 (175)
			2.617 (156)	2.628 (170)
			2.630 (133)	

**Owing to the marked differences among* MeP═, MeP(S)═, *and* MeP(O)═ *band positions, separate predictions were made depending on the nature of the* Me—P *group.*

Can. J. Chem. Downloaded from www.nrcresearchpress.com by 200.7.193.243 on 09/04/12
For personal use only.

TABLE IX (*concluded*)

C. Et—P and R_2N Compounds

$(EtO)_2P(O)Et$		$Me_2NP(O)(OEt)_2$	$Me_2N(OEt)_2$	$Me_2NP(S)(OEt)_2$
Predicted	Observed	Observed	Predicted	Observed
1.651 (11)		1.682 (53)	1.683 (56)	1.683 (55)
1.680 (56)	1.681 (52)	1.692 (70)	1.695 (80)	1.693 (72)
1.690 (74)	1.692 (69)	1.730 (67)	1.728 (64)	1.731 (69)
1.710 (28)	1.715 (30)		1.749 (14)	
1.729 (77)	1.731 (68)	1.761 (41)	1.760 (30)	1.761 (42)
1.742 (41)				
1.762 (53)	1.755 (49)	2.261 (448)	2.257 (450)	2.264sh (475)
2.259 (450)	2.260 (394)	2.267 sh (430)	2.269 (192)	2.270 (507)
2.292 (124)	2.304 (372)	2.302 (417)	2.296 (395)	2.302 (459)
2.304 (393)	2.342 (175)	2.346 sh (230)	2.342 (156)	2.347 (243)
2.342 (156)	2.371 (150)	2.356 (263)	2.354 (95)	2.360 (259)
2.372 (90)	2.416 (162)	2.383 (173)	2.410 (148)	2.387 (183)
2.405 (201)	2.450 (181)	2.410 (202)	2.454 (255)	2.412 (214)
2.437 (32)	2.483 (187)	2.457 (253)	2.482 (166)	2.453 (282)
2.453 (178)		2.480 (241)	2.502 (76)	2.480 (251)
2.482 (166)		2.498 (241)		2.501 (234)

$Me_2NP(O)(OEt)Cl$	Me_2N,OEt	$Me_2NP(S)(OEt)Cl$	$Et_2NP(S)(OEt)_2$	
Observed	Predicted	Observed	Predicted	Observed
1.681 (35)	1.683 (35)	1.682 (37)	1.683 (80)	1.688 sh (70)
1.692 (44)	1.695 (54)	1.692 (47)	1.693 (98)	1.696 (92)
1.703 (38)	1.728 (41)	1.706 (43)	1.730 (84)	1.732 (72)
1.727 (46)	1.754 (29)	1.728 (46)	1.761 (54)	1.763 (49)
1.755 (25)		1.757 (29)		
2.261 (282)	2.251 (412)	2.261 sh (340)	2.264 (580)	2.267 (531)
2.300 (233)	2.266 (361)	2.269 (363)	2.305 (494)	2.307 (532)
2.347 sh (118)	2.296 (264)	2.297 (276)	2.340 (288)	2.340 (285)
2.352 (170)	2.342 (78)	2.340 sh (150)	2.388 (124)	2.391 (209)
2.371 (106)	2.354 (75)	2.354 (189)	2.412 (258)	2.411 (230)
2.409 (115)	2.410 (74)	2.385 (117)	2.455 (304)	2.452 (290)
2.453 (154)	2.454 (166)	2.410 (130)	2.479 (300)	2.480 (298)
2.482 (157)	2.482 (83)	2.452 (179)	2.492 (108)	
2.496 (154)	2.502 (76)	2.482 (165)		
		2.498 (155)		

$Et_2NP(S)(O\,n\text{-}Pr)_2$		$Et_2NP(S)(O\,i\text{-}Pr)_2$		$Et_2NP(S)(OBu)_2$	
Predicted	Observed	Predicted	Observed	Predicted	Observed
1.683 (38)	1.688 sh (70)	1.683 (94)	1.683 (86)	1.683 (38)	1.688 (70)
1.696 (100)	1.698 (96)	1.693 (120)	1.696 (116)	1.693 (94)	1.702 (97)
1.731 (92)	1.732 (82)	1.732 (90)	1.732 (83)	1.703 (68)	1.720 (83)
1.758 (56)	1.756 (60)	1.759 (52)	1.762 (50)	1.714 (62)	1.736 (84)
		1.800 (22)	1.803 (39)	1.732 (96)	1.756 sh (75)
				1.756 (80)	
2.268 (556)	2.274 br (544)	2.266 (540)	2.268 (514)	2.268 (562)	2.272 (559)
2.304 (538)	2.306 br (543)	2.295 (234)	2.295 sh	2.306 (558)	2.307 (629)
2.313 (270)	2.348 (318)	2.307 (232) 910	2. 307 (581)	2.337 (132)	2.336 (386)
2.342 (338)	2.366 sh (265)	2.322 (344)	2.318 sh	2.348 (256)	2.350 (371)
2.366 (182)	2.391 (194)	2.337 (132)	2.340 sh (355)	2.387 (356)	2.387 (374)
2.388 (124)	2.422 (294)	2.340 (330)	2.405 (348)	2.414 (110)	2.414 sh (300)
2.420 (294)	2.452 (306)	2.409 (352)	2.435 (252)	2.436 (230)	2.438 (323)
2.452 (326)	2.486 (304)	2.432 (250)	2.458 (317)	2.454 (380)	2.452 (374)
2.476 (136)		2.476 (324)	2.471 (338)	2.476 (134)	2.473 (42)
2.489 (294)		2.492 (108)	2.492 sh (210)	2.485 (204)	2.483 (330)
		2.518 (122)	2.517 (201)		
		2.551 (102)	2.561 (161)		
		2.587 (98)	2.588 (140)		

Can. J. Chem. Downloaded from www.nrcresearchpress.com by 200.7.193.243 on 09/04/12
For personal use only.

TABLE X

P—SH AND P—OH VIBRATIONS

Compound	P—SH			P—OH		
	μ	cm.$^{-1}$	$\epsilon\times10^2$	μ	cm.$^{-1}$	$\epsilon\times10^2$
Dimethyl phosphorodithioic acid	1.970	5076	13	2.000	5000	13
Diethyl phosphorodithioic acid	1.969	5079	24	1.998	5005	24
Di-*n*-propyl phosphorodithioic acid	1.972	5071	23	2.001	4998	21
Di-isopropyl phosphorodithioic acid	1.969	5079	23	1.998	5005	23
Di-*n*-butyl phosphorodithioic acid	1.970	5076	13	2.000	5000	13
Diethylaminoethanethiol	1.738	5754	62			
Ethanethiol	1.741	5744	65			
Ethyl methylphosphonothioic acid	1.906	5247	26			
Diethyl phosphorothioic acid	1.909	5238	49			

APPLICATION

A larger number of compounds have been examined which have C—H present in more than one type of group. Spectra have been predicted for these compounds and in Table IX the observed spectra are compared with the predicted spectra. For example, the spectrum of diethyl methylphosphonate is predicted by summing the band positions and intensities for one Me—P(O) and two EtO—P groups. Where bands occur within 0.005 μ in both types of group, or at greater separations in the case of broad bands, one band is predicted at intermediate values with intensity equal to the sum of both contributing groups.

It will be apparent that spectra of compounds with more than one type of C—H containing group cannot be predicted as accurately as those with only one such group. In particular, it is difficult to know when to average positions for bands of neighboring frequencies. Sometimes an average frequency band appears with intensities close to the summed value, and sometimes shoulders appear on the main band with intensities greater than would be predicted owing to the intensity contribution of the larger band. Bands which are weak in the parent compound may be absent or may appear as weak shoulders on the side of a larger band with consequently greater than predicted intensity. It is surprising that the agreement is as good as it is considering that the original intensity assignments are based on peak heights on a band contour, without analysis of the curves. Agreement in the B region is not so good, probably because of the greater complexity, and therefore greater interference from neighboring groups.

The same type of prediction can be made instrumentally. If it is desired to know the spectrum of a compound R′R″R‴P(X), where R′, R″, and R‴ are hydrogen-containing groups, equimolar quantities of R′P(X)Y_2, R″P(X)Y_2, and R‴P(X)Y_2, where Y is any group not containing hydrogen, are placed in series in the spectrophotometer and the addition spectrum is recorded. Three examples of this type of prediction are shown in Fig. 1. The intensities on the graphs are not directly comparable as different concentrations were used in the two cases. The extinction coefficients calculated from the curves show agreement of the same order with those calculated by addition of the extinction coefficients of the component curves.

ACKNOWLEDGMENT

Diethylaminoethanethiol was kindly supplied by Dr. K. F. Jennings, formerly of these Laboratories.

Can. J. Chem. Downloaded from www.nrcresearchpress.com by 200.7.193.243 on 09/04/12
For personal use only.

Can. J. Chem. Downloaded from www.nrcresearchpress.com by 200.7.193.243 on 09/04/12
For personal use only.

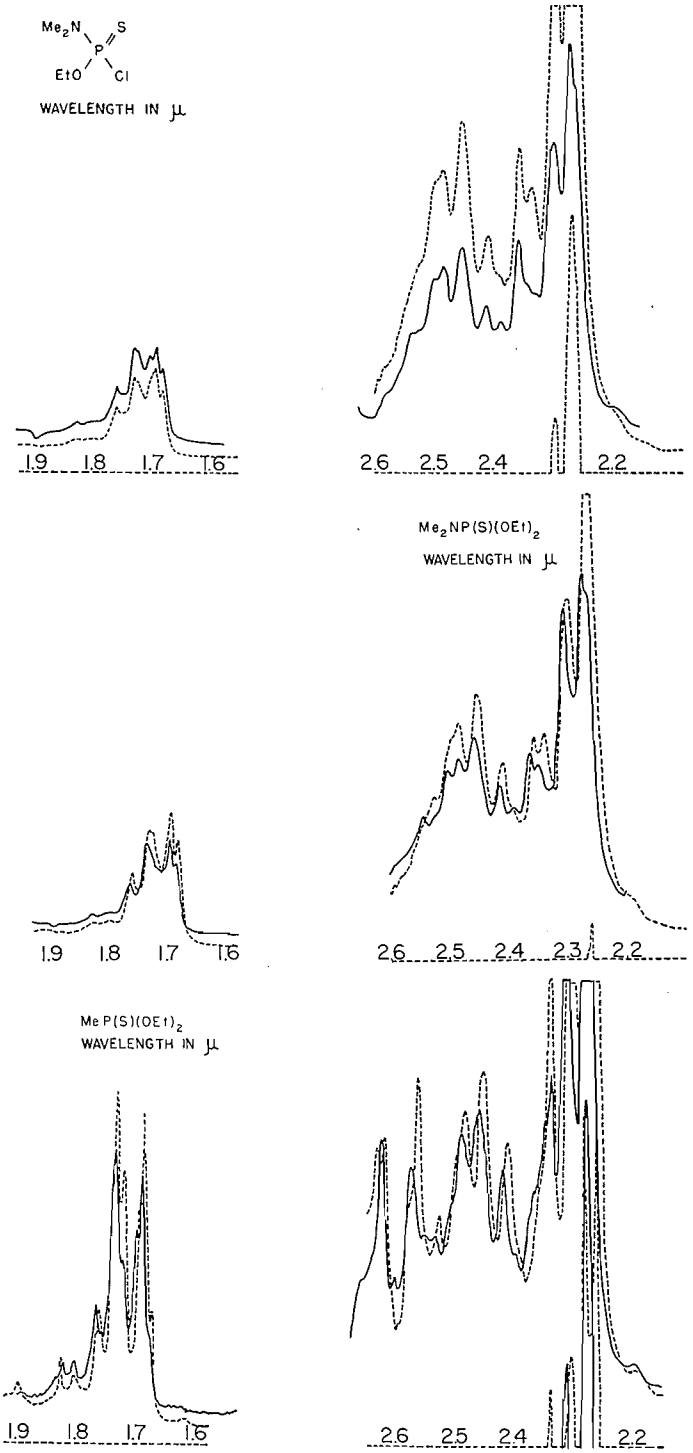

FIG. 1. Observed spectrum, ————————. Spectrum obtained by addition, - - - - - - - -.

RÉSUMÉ

On a étudié les spectres infrarouges de quelques composés phosphorés dans la région 1.0–2.6 μ. Chaque radical donne plusieurs bandes charactéristiques qui sont presque indépendants des altérations de la molécule à des distances supérieures à deux atomes. On propose des fréquences charactéristiques pour les groupements MeO, EtO, *n*-PrO, *i*-PrO, *n*-BuO, Me, Et, Me_2N, Et_2N, et *i*-Pr_2N reliés directement au phosphore. Les autres substituants de l'atome de phosphore n'affectent que les bandes attribuées au groupement Me—P. D'ailleurs, on peut prédire qualitativement l'allure des spectres des composés contenant plus qu'un type de groupement C—H, en additionnant les fréquences et les intensités des groupes composants.

REFERENCES

1. McIvor, R. A., Grant, G. A., and Hubley, C. E. Can. J. Chem. **34**, 1611 (1956).
2. McIvor, R. A., McCarthy, G. D., and Grant, G. A. Can. J. Chem. **34**, 1819 (1956).
3. McIvor, R. A. and Grant, G. A. In preparation.
4. Kaye, W. Spectrochim. Acta, **6**, 257 (1954).

APPENDIX

TABLE XI

MeO and MeS* groups

Compounds	Band positions in μ ($\epsilon \times 10^2$)		
A region			
OOS-Trimethyl phosphorothioate	1.666 (12^3)†	1.679 (26+30)†	1.720 (24+31)
OOS-Trimethyl phosphorodithioate	1.670 (10^3)	1.681 (26+44)	1.723 (24+43)
Trimethyl phosphorothionate	1.670 (14)	1.680 (16)	1.720 (15)
Dimethyl phosphorodithioic acid	1.668 (10)	1.681 (13)	1.719 (11)
Trimethyl phosphate	1.667 (8)	1.681 (10)	1.719 (9)
Dimethyl hydrogen phosphonothionate	1.669 sh? (10)	1.680 (12)	1.721 (11)
Dimethyl hydrogen phosphate	1.649 (15)	1.678 (13)	1.72 br (12)
Dimethyl carbonate	1.651 (12)	1.678 (15)	1.718 (12)
Methanol	1.664 (8)	1.69 sh (11)	1.702 (14)

	MeO				MeS
B region					
Dimethyl hydrogen phosphonothioate	2.256 (175)	2.338 (39)	2.392 (71)	2.478 (54)	
OOS-Trimethyl phosphorothioate	2.255 (178^3)	2.332 (40^3)	2.384 (75^2)	2.466 (55^3)	2.319 (153)
OOS-Trimethyl phosphorodithioate	2.253 (180^3)	2.337 (42^3)	2.390 (81^2)	2.475 (50^3)	2.319 (174)
Trimethyl phosphorothionate	2.253 (181)	2.332 (46)	2.385 (75)	2.470 (75)	
Dimethyl phosphorodithioic acid	2.253 (185)	2.336 (38)	2.387 (65)	2.470 (57)	
Trimethyl phosphate	2.253 (158)	2.332 (43)	2.385 (58)	2.466 (73)	
Dimethyl hydrogen phosphonate	2.252 (161)	2.330 (53)	2.386 (64)	2.472 (74)	
Dimethyl carbonate	2.252 (220)	2.336 (72)	2.362 (54)	2.452 (51)	2.403 (54)‡
			2.374 (55)		2.429 (42)
Methanol	2.280 (137)	2.342 (70)	2.522 (108)		

**In this and subsequent tables*—sh = *shoulder*, wk = *weak*, br = *broad*, d = *doublet*.

†12^3 *indicates the observed intensity was divided by 3, i.e. that it is assumed that all substituent groups are contributing to the band. Intensities expressed by a sum indicate an effort to assess the contributions of the* SMe *and* OMe *separately.*

‡*These unassigned bands of dimethyl carbonate are included for completeness.*

Can. J. Chem. Downloaded from www.nrcresearchpress.com by 200.7.193.243 on 09/04/12
For personal use only.

Can. J. Chem. Downloaded from www.nrcresearchpress.com by 200.7.193.243 on 09/04/12
For personal use only.

TABLE XII

EtO AND EtS

Compound	Band positions in μ ($\epsilon \times 10^2$)					
A region						
Triethyl phosphite	1.683 (18)		1.693 (22)	1.722 (20)	1.760 (12)	
Triethyl phosphorothionate	1.682 (21)		1.692 (27)	1.728 (23)	1.758 (15)	
Triethyl phosphate	1.682 (15)		1.691 (18)	1.727 (15)	1.758 (10)	
Diethyl hydrogen phosphonate	1.682 (21)		1.692 (25)	1.723 (22)	1.761 (14)	
Ethyl phosphorodichloridothionate	1.682 (24)		1.691 (27)	1.721 (27)	1.756 (15)	
Diethyl phosphoroamidate	1.683 sh (20)		1.693 (26)	1.728 (23)	1.762 (16)	
Diethyl hydrogen phosphonothioate	1.683 (20)		1.692 (26)	1.727 (23)	1.762 (15)	
Diethyl phosphorochloridothionate	1.680 (22)		1.689 (30)	1.726 (24)	1.757 (15)	
Diethyl phosphorothioic acid	1.683 (25)		1.691 (26)	1.734 (29)	1.762 (23)	
Diethyl phosphorodithioic acid	1.684 (23)		1.693 (28)	1.730 (25)	1.761 (17)	
Ethanol			1.698 (18)	1.735 br (18)	1.766 (13)	
Diethyl oxalate	1.678 (21)		1.692 (21)	1.722 (19)	1.752 (9)	
Diethyl carbonate	1.668 (22)		1.682 (23)	1.712 (20)	1.749 (12)	
SSS-Triethyl phosphorotrithioate	1.687 (26)		1.695 (26)	1.740 (42)		
Ethyl mercaptan			1.690 (33)	1.739 (65)		
B region						
Triethyl phosphite	2.265 (119)	2.305 (138)	2.344 (64)	2.411 (60)	2.453 (78)	2.482 (77)
Triethyl phosphorothionate	2.261 (199)	2.303 (145)	2.343 (78)	2.410 (47)	2.458 (58)	2.483 (60)
Triethyl phosphate	2.260 (122)	2.304 (91)	2.339 (48)	2.410 (47)	2.458 (58)	2.483 (60)
Diethyl hydrogen phosphonate	2.269 (175)	2.302 (128)	2.348 (72)	2.406 (73)	2.454 (90)	2.487 (72)
Ethyl phosphorodichloridothionate	2.258 (189)	2.298 (107)	2.340 (98)	2.410 (86)	2.449 (93)	2.483 (91)
Diethyl phosphoroamidate	2.261 (171)	2.303 (133)	2.341 (77)	2.411 (79)	2.458 (98)	2.481 (95)
Diethyl hydrogen phosphonothioate	2.261 (169)	2.302 (137)	2.341 (79)	2.412 (75)	2.450 (88)	2.477 (71)
Diethyl phosphorochloridothionate	2.258 (182)	2.302 (132)	2.338 (82)	2.409 (73)	2.451 (89)	2.481 (80)
Diethyl phosphorothioic acid	2.263 (181)	2.302 (157)	2.339 (99)	2.411 (97)	2.452 (111)	2.481 (113)
Diethyl phosphorodithioic acid	2.262 (180)	2.302 (140)	2.342 (83)	2.412 (77)	2.450 (94)	2.483 (83)
Ethanol	2.270 (110)	2.305 (137)	2.362 (72)	2.419 (59)	2.366 (87)	
Diethyl oxalate	2.257 (174)	2.302 (123)	2.346 (67)	2.408 (80)	2.441 (93)	2.483 (56)
Diethyl carbonate	2.250 (162)	2.294 (139)	2.342 (87)	2.431 (77)		2.474 (54)
		2.312 (87)	2.385 (69)			
SSS-Triethyl phosphorotrithioate	2.268 (133)	2.284 (121)	2.304 (172)	2.362 (101)	2.397 (70)	2.432 (26)
			2.453 (42)	2.484 (51)	2.502 (43)	2.512 (50)
Ethyl mercaptan	2.274 (138)	2.285 (132)	2.308 (182)	2.365 (99)	2.396 (66)	2.432 (16)
					2.455 (65)	2.488 (56)

Can. J. Chem. Downloaded from www.nrcresearchpress.com by 200.7.193.243 on 09/04/12
For personal use only.

TABLE XIII

n-PrO BANDS

Compound	Band positions in μ ($\epsilon \times 10^2$)								
A region									
Di-*n*-propyl phosphorochloridothionate			1.697 (27)		1.729 (27)		1.755 (20)		
Di-*n*-propyl phosphorodithioic acid			1.699 (26)		1.731 (26)		1.754 (20)		
n-Propyl phosphorodichloridothionate			1.698 (26)		1.729 (28)		1.753 (21)		
B region									
Di-*n*-propyl phosphoro-chloridothionate	2.268 (164)	2.302 (156)	2.314 (138)	2.348 (104)	2.365 (87)	2.389 (78)	2.431 (96)	2.447 (101)	2.488 (91)
Di-*n*-propyl phosphoro-dithioic acid	2.273 (166)	2.301 (151)	2.313 (133)	2.349 (103)	2.369 (90)	2.388 (82)	2.425 (88)	2.447 (99)	2.487 (95)
n-Propyl phosphoro-dichloridothionate	2.266 (141)	2.297 (152)	2.311 (135)	2.347 (103)	2.364 (96)	2.387 (81)	2.422 (93)	2.447 (98)	2.487 (93)

TABLE XIV

A. *i*-PrO BANDS

Compound	Band position in μ ($\epsilon \times 10^2$)							
A region								
Triisopropyl phosphite	1.684 (28)	1.696 (33)	1.733 (24)	1.767 (14)	1.799 (10)			
Diisopropyl phosphoro-chloridothionate	1.683 (26)	1.692 (36)	1.730 (26)	1.755 br (13)	1.800 (11)			
Diisopropyl phosphoro-dithioic acid	1.680 (28)	1.692 (36)	1.731 (22)	1.755 (12)	1.802 (10)			
Isopropyl phosphoro-dichloridothionate	1.679 (29)	1.689 (41)	1.729 (31)	1.752 (17)	1.798 (13)			
Isopropyl alcohol	1.687 (28)	1.699 (25)	1.736 (22)	1.767 (15)	1.824 (12)			
B region								
Triisopropyl phosphite	2.268 (140) 2.511 sh (45)	2.300 (163) 2.543 (51)	2.326 (165) 2.594 (45)	2.346 (89)	2.409 (108)	2.437 (114)	2.462 (109)	2.420 (104)
Diisopropyl phosphoro-chloridothionate	2.265 (150) 2.514 (65)	2.294 (173) 2.550 (45)	2.320 (178) 2.584 (48)	2.341 (102)	2.402 (125)	2.430 (128)	2.452 (116)	2.477 (84)
Diisopropyl phosphoro-dithioic acid	2.265 (144) 2.526 (58)	2.295 (165) 2.558 (47)	2.321 (166) 2.587 (42)	2.343 (101)	2.403 (115)	2.433 (119)	2.453 (110)	2.475 (110)
Isopropyl phosphorodi-chloridothionate	2.264 (160) 2.519 (74)	2.292 (168) 2.551 (59)	2.319 (180) 2.584 (58)	2.341 (104)	2.401 (137)	2.428 (137)	2.452 (130)	2.478 (83)
Isopropyl alcohol	2.269 (137)		2.316 (199)		2.422 (122)		2.472 (143)	

Can. J. Chem. Downloaded from www.nrcresearchpress.com by 200.7.193.243 on 09/04/12
For personal use only.

TABLE XIV (*concluded*)

B. *n*-BuO BANDS

Compound	Band positions in μ ($\epsilon \times 10^2$)							
A region								
Dibutyl hydrogen phosphonate	1.693 sh (23)	1.703 (36)	1.715 (32)	1.731 (29)	1.752 (28)			
Tributyl phosphate	1.692 sh (23)	1.702 (34)	1.716 (30)	1.732 (28)	1.752 (27)			
Tributyl phosphite	1.695 sh (22)	1.704 (32)	1.713 (33)	1.737 (26)	1.747 (28)			
Dibutyl phosphorodithioic acid	1.693 sh (25)	1.703 (35)	1.712 (31)	1.733 (30)	1.751 (28)			
Butyl phosphorodichloridothionate	1.690 sh (24)	1.703 (33)	1.712 (30) 1.718 (30)	1.730 (31)	1.747 (29)			
Dibutyl phosphorochloridothionate	1.694 sh (24)	1.702 (33)	1.713 (28) 1.721 (28)	1.731 (29)	1.750 (27)			
B region								
Dibutyl hydrogen phosphonate	2.268 (145)	2.305 (72)	2.348 (121)	2.384 (112)	2.437 (115)	2.452 (127)	2.483 (99)	2.505 (81)
Tributyl phosphate	2.268 (152)	2.304 (172)	2.347 (123)	2.386 (112)	2.437 (114)	2.450 (112)	2.488 (103)	2.504 (99)
Tributyl phosphite	2.270 (151)	2.307 (171)	2.350 (115)	2.388 (112)	2.437 (107)	2.454 (121)	2.488 (93)	2.505 (86)
Dibutyl phosphorochloridothionate	2.270 (165)	2.303 (178)	2.347 (133)	2.386 (119)	2.433 (120)	2.452 (134)	2.487 (107)	2.504 (98)
Dibutyl phosphorodithioic acid	2.271 (174)	2.305 (190) 2.285 (138)	2.348 (144)	2.384 (131)	2.437 (127)	2.451 (137)	2.482 (111)	2.503 (100)
Butyl phosphorodichloridothionate	2.266 (170)	2.301 (182)	2.348 (132)	2.385 (109)	2.437 (109)	2.450 (132)	2.485 (100)	2.503 (101)

TABLE XV

i-Pr_2N COMPOUNDS, μ ($\epsilon \times 10^2$)

i-$Pr_2NP(S)(OEt)_2$	*i*-$Pr_2NP(S)(O\ n\text{-}Pr)_2$	*i*-$Pr_2NP(S)(O\ i\text{-}Pr)_2$	*i*-$Pr_2NP(S)(O\ n\text{-}Bu)_2$
A region			
1.687 (98)	1.689 (90)	1.688 (82)	1.690 (85)
1.698 (110)	1.699 (123)	1.697 (120)	1.699 (104)
1.735 (104)	1.721 (26)	1.734 (100)	1.721 (88)
1.764 (58)	1.736 (101)	1.764 (61)	1.737 (95)
1.807 (29)	1.758 (76)	1.806 (38)	1.759 (85) br
	1.808 (37)		1.808 (38)
B region			
2.267 (519)	2.276 (535)	2.268 (498)	2.274 (482)
2.303 (646)	2.303 (674)	2.302 (706)	2.304 (644)
2.342 (276)	2.346 (340)	2.313 (600) wk, sh	2.340 (364)
2.360 (280)	2.388 (364)	2.341 (348)	2.399 (361)
2.406 (302) br	2.401 (332)	2.362 (276)	2.405 (368)
2.447 (290) br	2.447 (340)	2.404 (425)	2.443 (240)
2.467 (286)	2.462 (328)	2.434 (372)	2.466 (407)
2.482 (234)	2.587 (160) wk	2.462 (368)	2.505 (433)
2.502 (212)		2.587 (179)	2.545 (182)
2.548 (157)			
2.586 (124) wk			

Can. J. Chem. Downloaded from www.nrcresearchpress.com by 200.7.193.243 on 09/04/12
For personal use only.

SEPARATIONS OF THE PLATINUM METALS BY ION EXCHANGE[1]

S. S. Berman and W. A. E. McBryde

ABSTRACT

Distribution coefficients for the chlorides of ruthenium, rhodium, palladium, iridium(III and IV), and platinum have been determined between the anion exchanger Amberlite IRA-400 and hydrochloric acid solutions of various molarities. Separations of various combinations of rhodium, iridium, palladium, and platinum in amounts of 0.5 mg. or less are described. When, in the course of these separations, the four metals are present together, special procedures are required to ensure complete recovery of platinum.

Can. J. Chem. Downloaded from www.nrcresearchpress.com by 200.7.193.243 on 09/04/12
For personal use only.

There have been several attempts to employ ion exchange in the separation of the platinum metals, but only a limited degree of success has been achieved. MacNevin and Crummett (1) suggested that a separation of rhodium, iridium, palladium, and platinum might be possible owing to the graded stabilities of the chloride and ammine complexes of these metals, but presented no experimental data. Another report by the same authors (2) elaborated on a separation of iridium from palladium achieved by converting the palladium to a cationic diammine, leaving the iridium as an anion, and separating the two on this basis. Stevenson *et al.* (3) submitted a note on the separation of the four metals on the cation exchanger Dowex-50, based on the formation of perchlorates of these metals by fuming their solutions with perchloric acid. No data were given, but this separation is of questionable value because of the inability to keep even milligram quantities of platinum and iridium from precipitating in this medium. Blasius and Wachtel (4) achieved separations of platinum from the other three metals by adsorbing the platinum complex on the anion exchanger Permutit-ES in the hydroxide form. The other three metals were eluted by a solution of sodium hydroxide, and the platinum recovered by elution with nitric acid. MacNevin and McKay (5) have prepared spectrographically pure rhodium through the formation of a cationic rhodium species, the other metals being left as anions. This separation is not quantitative. The separations of rhodium and iridium have been discussed in a previous paper (6).

The only equilibrium data recorded concerning the behavior of platinum metal complexes toward ion exchangers are those of Kraus *et al.* (7). These workers measured the distribution coefficients of chloroplatinate (IV) and chloropalladate (II) relative to the anion exchanger Dowex-1 in hydrochloric acid solutions.

In the following report the measurement of the distribution coefficients of ruthenium, rhodium, iridium, palladium, and platinum in hydrochloric acid solutions relative to the anion exchanger Amberlite IRA-400 is described, as well as a series of separations of these metals.

EXPERIMENTAL

Standard Solutions

Palladium.—A stock solution was prepared by dissolving pure palladium sponge in aqua regia, evaporating several times to dryness with hydrochloric acid, and then dissolving the residue and diluting with 0.1 *M* hydrochloric acid. This solution was standardized gravimetrically by precipitation with salicylaldoxime (8). Analyses for palladium were generally made colorimetrically by the potassium iodide method (9),

[1]*Manuscript received December 3, 1957.*
Contribution from the Department of Chemistry, University of Toronto, Toronto 5, Ontario, Canada.

but very small amounts (less than 10 μg.) were determined by the *p*-nitrosodimethylaniline procedure (10).

Platinum.—The stock solution was prepared by the dissolution of pure platinum sponge in aqua regia and treatment similar to that described for palladium. The solution was standardized by precipitation with 4-phenylthiosemicarbazide (11). Colorimetric analyses were made by the tin(II) chloride method (12).

Ruthenium.—A stock solution was prepared in 0.5 *M* hydrochloric acid from ammonium chlororuthenate crystallized from a solution of sodium chlororuthenate in hydrochloric acid. The solution was standardized by the evaporation of a measured quantity, followed by reduction of the salt to metallic ruthenium with hydrogen. Analyses were made colorimetrically by the thiourea procedure (13).

Rhodium and Iridium.—The preparation of standard solutions of these metals is described in a previous paper (6).

The Resin and Columns

The resin used in this research was Amberlite IRA-400 in an analytical grade. The dried resin was ground to yield fractions of various degrees of fineness. The portion of mesh size 70 to 100 was used for the measurement of distribution coefficients. It was found to be hygroscopic, and was dried at 100° C. prior to weighing, and was stored over anhydrous magnesium perchlorate. The exchange capacity was found to be 3.78 meq. per gram of dry resin. This was determined for 5.00-g. samples by the procedure of Fisher and Kunin (14).

For column work the resin of <100 mesh was used. The manner of preparing the resin to rid it of fine particles has been described in a previous paper (6). The columns were of conventional design in two sizes, having internal diameters of 10 mm. and 5 mm. respectively. The depth of resin in the bed varied among the different experiments, and is stated in the description of each. The flow of liquid through the beds was maintained at about 50 ml. per hour.

Measurement of Distribution Coefficients

The distribution coefficients of chloropalladate(II), chloroplatinate(IV), chloroiridate (IV), chloroiridate(III), chlororhodate, and chlororuthenate were measured in hydrochloric acid solutions. This was done by shaking a weighed amount, approximately 0.3 g., of resin with measured quantities of platinum metal solutions in 25.0 ml. of hydrochloric acid of various molarities for 40 hours. The mixtures were filtered, and 20.0-ml. aliquots of the filtrates analyzed. The amounts of metal adsorbed on the exchanger were thus found, and the distribution coefficients (amount of metal per kilogram of resin/amount per liter of solution) were calculated. In regions of very high adsorption 300 ml. of acid solution was used, and 250-ml. aliquots taken for analysis.

TABLE I

DISTRIBUTION COEFFICIENTS

	D					
HCl, *M*	Rh	Ru	Ir(III)	Ir(IV)	Pd(II)	Pt(IV)
0.1	15	180	1050	186000	45000	44000
0.5	12	88	350	59000	15000	27000
1.0	10	40	60	32000	4300	20000
4.0	0	12	2	6000	300	2100
8.0	0	4	0	3200	75	780
12.0	0	0	0	960	35	400

Can. J. Chem. Downloaded from www.nrcresearchpress.com by 200.7.193.243 on 09/04/12
For personal use only.

The amounts of resin and solution were selected to limit loading of the resin to no more than 2% of capacity.

The results are summarized in Table I and in Fig. 1.

A comparison of these values with those obtained by Kraus *et al.* (7) for Pd(II) and Pt(IV) shows good agreement in the low-adsorption range where these workers had low degrees of loading. In the high-adsorption range where these workers allowed the loading to become large there is a marked divergence, their distribution coefficients being much lower than those given here.

It is readily seen that Pt(IV) and Ir(IV) are very strongly adsorbed throughout the whole hydrochloric acid range, and Pd(II) at low hydrochloric acid concentrations.

According to Walton (15) practically all ion-exchange distribution data can be expressed by the Rothmund–Kornfeld equation

$$M_x/M_y = K\,((x)/(y))^p,$$

where M_x and M_y are the moles of x and y per gram of exchanger and (x) and (y) are their molar concentrations in solution; K and p are constants. Then by plotting $\log(M_x/M_y)$ against $\log((x)/(y))$ one should obtain a straight line.

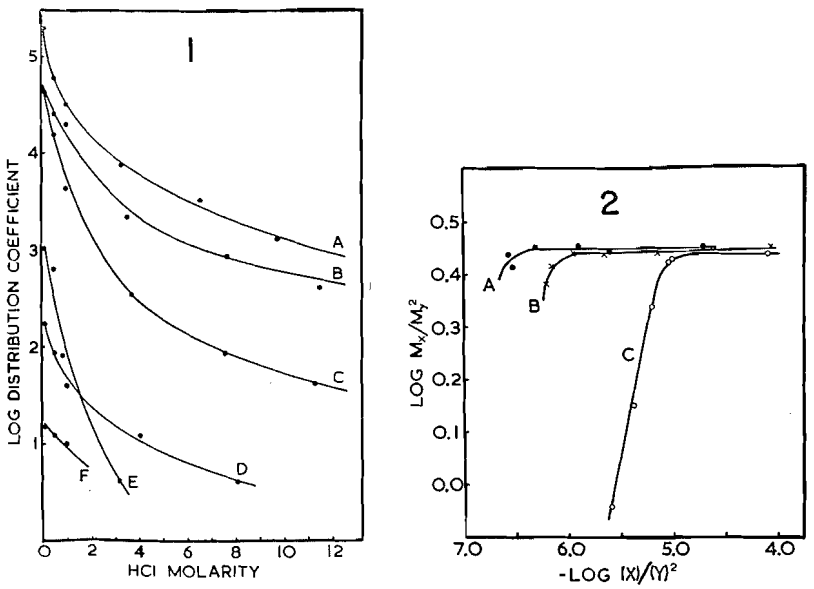

FIG. 1. The distribution coefficients of rhodium, iridium, platinum, palladium, and ruthenium in hydrochloric acid solutions. A: chloroiridate(IV), B: chloroplatinate(IV), C: chloropalladate(II), D: chlororuthenate(III), E: chloroiridate(III), F: chlororhodate.

FIG. 2. The distribution data plotted according to the Rothmund–Kornfeld equation. A: chloroiridate (IV), B: chloroplatinate(IV), C: chloropalladate(II).

This is, more or less, what happened when the data for Rh, Ru, and Ir(III) were plotted. However, the three other complexes produced interesting curves (Fig. 2). In regions of very high adsorption M_x/M_y^2 (the squared term arises since these complexes are doubly charged) is seen to be almost independent of the concentration ratio of complex to chloride in solution; i.e., $p \simeq 0$.

This might indicate that in these instances simple exchange equilibria are not taking place and that some mechanism other than ion exchange is the predominant factor.

Can. J. Chem. Downloaded from www.nrcresearchpress.com by 200.7.193.243 on 09/04/12
For personal use only.

Can. J. Chem. Downloaded from www.nrcresearchpress.com by 200.7.193.243 on 09/04/12
For personal use only.

An analogy may be seen here between this strong adsorption and the solubility of quaternary amine platinum metal chlorides. It is well known that Pt(IV) and Ir(IV) form relatively insoluble salts with quaternary amines of the type $(R_4N)_2PtCl_6$. Since the anion exchanger is in effect a polystyrenedivinylbenzene quaternary amine, it may be that the same forces that produce the insoluble salts contribute to the strong adsorption of these complexes on the resin. Palladium(II) is known to form a number of insoluble diammine dichloride complexes, the solubility of which is greater in concentrated hydrochloric acid than in neutral solution. The behavior of palladium toward the resins may be, in the same fashion, compared with the formation of ammine precipitates of this sort.

To further illustrate this analogy 5 ml. of 0.2 *M* tetrabutylammonium chloride was added to 10 mg. of each of the six complexes in 5 ml. of 0.5 *M* hydrochloric acid. Precipitates formed in the tubes containing Pd(II), Pt(IV), and Ir(IV). When 1 ml. of concentrated hydrochloric acid was added to each of these, the palladium precipitate dissolved instantly and the iridium precipitate partially dissolved. Further addition of hydrochloric acid resulted in the complete dissolution of the iridium precipitate, but the platinum precipitate could only be partially dissolved by this means.

While the above experiment does not prove that stable resin–platinum metal compounds are formed analogous to insoluble precipitates, the parallel between these observations and subsequent column experiments was striking. For example, it was possible to remove Pd(II) from the resin by elution with concentrated hydrochloric acid. Pt(IV) and Ir(IV) cannot be completely recovered by this means. The iridium complex may be removed by a hot extraction with hydrochloric acid, but even this rather violent treatment will only partially remove the platinum complex.

The Separation of Palladium and Platinum

The purpose of this research was to develop an ion-exchange procedure for this separation which could be integrated with the rhodium–iridium separation previously reported (6). Also, the recovery of Pd(II) and Pt(IV) from anion exchangers by a wet method has long been a problem and an obstacle in the application of anion exchange in the separation of platinum from base metals.

It was confirmed that Pd(II) and Pt(IV) can be quantitatively adsorbed from dilute hydrochloric acid solutions on an anion exchanger, Amberlite IRA-400.

The Recovery of Palladium

Five milliliters of 1 *M* hydrochloric acid containing approximately 500 γ of palladium were fed onto 2.5-cm. resin beds in the larger columns which had been previously washed with 25 ml. of the acid solution. Complete recovery of the palladium was achieved by 100 ml. of 12 *M* hydrochloric acid.

Number of experiments	5
Palladium taken	478 γ
Palladium recovered (range)	476–480 γ (see Fig. 3)

It was found that no platinum was eluted provided these beds were at least 2.3 cm. deep.

The work was repeated with 3-cm. beds in the smaller columns. Complete recovery was achieved by 40 ml. of 12 *M* hydrochloric acid or by 60 ml. of 9 *M* acid (see Fig. 3). The use of 6 *M* acid resulted in too much tailing to be of value. However, it was found that 40 ml. of 12 *M* hydrochloric acid eluted much platinum, whereas 60 ml. of 9 *M* acid eluted none.

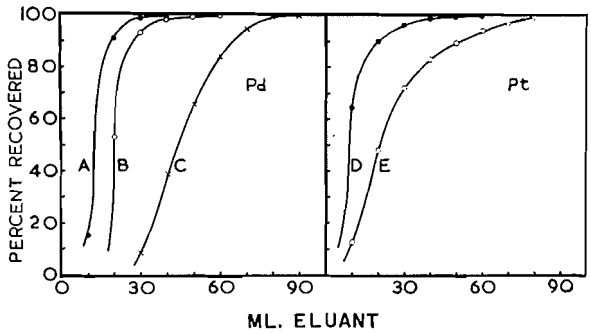

FIG. 3. Some typical elution curves for chloropalladate(II) and chloroplatinate(IV). A: chloropalladate(II) eluted with 12 *M* hydrochloric acid solution (small column), B: chloropalladate(II) eluted with 9 *M* hydrochloric acid solution (small column), C: chloropalladate(II) eluted with 12 *M* hydrochloric acid solution (large column), D: chloroplatinate(IV) eluted with 2.4 *M* perchloric acid solution (small column), E: chloroplatinate(IV) eluted with 15% (w/v) zinc chloride in 9 *M* hydrochloric acid solution at 96° C. (large column).

It was also shown that Pd(II) could be easily recovered by elution with dilute perchloric acid solutions. The recoveries observed for elution with 40 ml. of 0.5 *M* perchloric acid were as follows:

Number of experiments	3
Palladium taken	478 γ
Palladium recovered	478–481 γ

Since perchloric acid was later shown to be a good eluant for Pt(IV) this reagent cannot be used to separate the two metals.

Recovery of Platinum

Platinum was fed onto 2.5-cm. resin beds in the larger columns in a manner similar to the palladium.

It was verified that solutions of hydrochloric, nitric, or sulphuric acids, either dilute or concentrated, elute only part of the Pt(IV). The same is true for ammoniacal eluants. Working at elevated temperatures produced only minor improvements in the recoveries.

Kraus and his co-workers (7, 16) noted the high affinities of zinc and cadmium chloride in hydrochloric acid solutions toward anion exchangers. Preliminary experiments with 2.5 *M* solutions of both these salts in 9 *M* hydrochloric acid showed better recoveries of platinum than had been previously achieved. It was found that 93% of the Pt(IV) could be recovered by the zinc chloride solution, and that quantitative recoveries could be achieved if the column were surrounded with a hot-water jacket at 96° C. The following recoveries were made by elution with 90 ml. of a 15% (w/v) solution of zinc chloride in 9 *M* hydrochloric acid at 96° C. (see also Fig. 3).

Number of experiments	3
Platinum taken	490 γ
Platinum recovered	488–494 γ

Experiments showed that the Pt(IV) could also be quantitatively recovered by 90 ml. of 2.4 *M* perchloric acid. The same observation was made with 3-cm. resin beds in the smaller columns; in these cases the platinum was recovered by 60 ml. of the 2.4 *M* perchloric acid (see Fig. 3).

Number of experiments	7
Platinum taken	490 γ
Platinum recovered (4 cases)	488–492 γ (l)*
(3 cases)	488–490 γ (s)*

*l means larger column, s smaller.

Can. J. Chem. Downloaded from www.nrcresearchpress.com by 200.7.193.243 on 09/04/12
For personal use only.

Attempts to recover the Pt(IV) by a Soxhlet extraction were unsuccessful. Extraction with 6 *M* hydrochloric acid produced recoveries of only about 30%. Recoveries of about 90% were achieved with 8 *M* nitric acid.

The recovery of platinum by ashing the exchanger was also investigated. This method had previously been reported as successful by Sussman *et al.* (17) but no data were given. The resin containing the adsorbed Pt(IV) and the glass wool plug were transferred to a small crucible and dried under a heat lamp. The crucible was placed in a furnace at 300° C. and the temperature raised to 900° over the course of an hour. The crucible was removed, cooled, and set over a boiling-water bath for 1 hour after the addition of 3 or 4 ml. of aqua regia. There was no residue evident in the crucible after this treatment save for the bit of fused glass wool. Results of the analysis of this solution after filtration are given below, and indicate that this procedure is a simple and satisfactory one for the recovery of the metal.

Number of experiments	3
Platinum taken	490 γ
Platinum recovered	491–492 γ

Separation of Palladium and Platinum

Separations were carried out in both large and small columns. Mixtures of the metals containing 6 mg. of sodium chloride (to prevent baking of the metal on the bottom of the beaker) were evaporated to dryness and the residue dissolved in one or two milliliters of water. This solution was fed onto the resin bed with a dropper. The larger beds were 2.5 cm. deep and were eluted with 100 ml. of 12 *M* hydrochloric acid followed by 90 ml. of 2.4 *M* perchloric acid. The smaller columns contained resin beds 3 cm. deep, and were eluted with 60 ml. of 9 *M* hydrochloric acid followed by 75 ml. of 2.4 *M* perchloric acid. The results are summarized below:

Number of experiments	7	2
Platinum taken	490 γ	98 γ
Platinum recovered (4 cases)	487–496 γ (l)	
(3 cases)	490–491 γ (s)	97–102 γ
Palladium taken	478 γ	96 γ
Palladium recovered (4 cases)	468–480 γ (l)	
(3 cases)	476–478 γ (s)	95–96 γ

Separations of Various Mixtures of Platinum Metals in Solution

From the satisfactory results obtained in the rhodium–iridium and palladium–platinum separations it was felt that separations of all combinations of the four metals could be achieved, although separations of mixtures containing both rhodium and iridium would obviously have to be carried out in two stages. This turned out to be an overly optimistic assumption when iridium, palladium, and platinum are all present, but, generally, some very satisfactory separations were made.

Rhodium and Palladium

This separation was first done on 2.3-cm. beds in the larger columns. The beds were washed prior to use with 10 ml. of 2 *M* hydrochloric acid. A solution containing the two metals in 5 ml. of 2 *M* hydrochloric acid was fed onto the bed, and the latter eluted with 90 ml. of the acid solution to remove the rhodium. Elution was continued with 100 ml. of 12 *M* hydrochloric acid to recover the palladium. A previous experiment showed that no palladium was eluted by 90 ml. of the 2 *M* hydrochloric acid. The results of this separation are tabulated below.

Further separations were carried out in the smaller columns with 3-cm. resin beds which were previously washed with 10 ml. of 2 *M* hydrochloric acid. In this case the solutions

Can. J. Chem. Downloaded from www.nrcresearchpress.com by 200.7.193.243 on 09/04/12
For personal use only.

were evaporated to dryness with 6 mg. of sodium chloride, redissolved in one or two milliliters of water, and fed onto the bed with a dropper. Elutions were made with 50 ml. of 2 *M* hydrochloric acid followed by 50 ml. of 9 *M* hydrochloric acid. The results are included in the following table.

Number of experiments	6
Rhodium taken	499 γ
Rhodium recovered (3 cases)	499–500 γ (l)
(3 cases)	500–501 γ (s)
Palladium taken	478 γ
Palladium recovered (3 cases)	478–479 γ (l)
(3 cases)	476–478 γ (s)

It was noticed in this separation that as the rhodium was being eluted with the 2 *M* hydrochloric acid the palladium band slowly moved and diffused part way down the bed. This is the only instance in this work where a platinum metal band was seen to move. Owing to this partial migration it was possible to recover the palladium with 40 ml. of 9 *M* hydrochloric acid (Fig. 4) in contrast to the 60 ml. needed in the palladium–platinum separation.

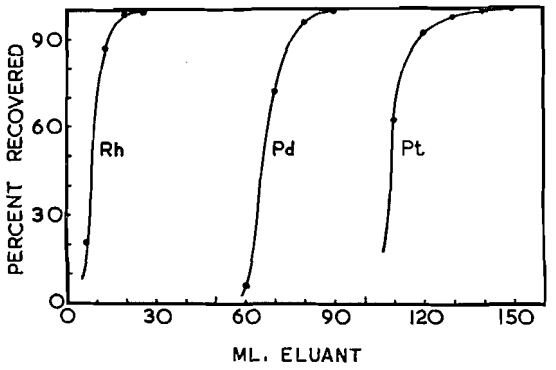

FIG. 4. Elution curves for the separation of rhodium, palladium, and platinum (small column). Rh: eluted with 50 ml. 2 *M* hydrochloric acid solution, Pd: eluted with 50 ml. 9 *M* hydrochloric acid solution, Pt: eluted with 75 ml. of 2.4 *M* perchloric acid solution.

Rhodium and Platinum

This separation was not attempted, but since the separation of rhodium, palladium, and platinum is feasible (see below) there is no reason why it should not be easily accomplished.

Iridium and Palladium

This separation was done in the larger columns in a manner similar to the separation of rhodium and palladium. The iridium was reduced to the tervalent state by hydroxylamine prior to feeding onto the column. The bed was eluted with 90 ml. of 2 *M* hydrochloric acid to recover the iridium, and then 100 ml. of 12 *M* hydrochloric acid for the palladium. The results are summarized as follows:

Number of experiments	3
Iridium taken	454 γ
Iridium recovered	452–454 γ
Palladium taken	478 γ
Palladium recovered	474–478 γ

Iridium and Platinum

This separation was not tried, but experiments described below indicate that it is quite feasible.

Can. J. Chem. Downloaded from www.nrcresearchpress.com by 200.7.193.243 on 09/04/12
For personal use only.

Rhodium, Palladium, and Platinum

One separation of these three metals was made to gather data for Fig. 4. This is the only three-metal separation that can be made with only one column. A solution containing the three metals was evaporated to dryness with 6 mg. of sodium chloride. The residue was redissolved in 2 ml. of 2 *M* hydrochloric acid solution and fed with a dropper onto a small 3-cm. resin bed which had been previously washed with 10 ml. of the acid solution. The bed was eluted with 50 ml. of 2 *M* hydrochloric acid, followed by 50 ml. of 9 *M* hydrochloric acid, and then 70 ml. of 2.4 *M* perchloric acid.

Rhodium, Iridium, and Palladium

Solutions of these three metals were evaporated to dryness with 6 mg. of sodium chloride and the residues redissolved in 1 ml. of water. The iridium was reduced with a few drops of 1% hydroxylammonium chloride solution, and the solutions fed onto 3-cm. beds in small columns. These beds had been previously washed with 10 ml. of 2 *M* hydrochloric acid. The beds were eluted with 80 ml. of the acid solution to recover the rhodium and iridium, followed by 50 ml. of 9 *M* hydrochloric acid for the palladium. The first effluents were evaporated to dryness and the residues redissolved in 2 ml. of 0.8 *M* hydrochloric acid (also containing cerium(IV) sulphate at a concentration of 0.001 *M*). These solutions were fed with a dropper onto small columns containing 3-cm. beds of resin which had been prepared with quadrivalent cerium, and the rhodium–iridium separation was carried out as described in the previous communication (6).

The procedure was repeated but the palladium was eluted with 50 ml. of 0.5 *M* perchloric acid. The rhodium and iridium were not determined in these experiments. The various results are summarized below.

Number of experiments	3
Iridium taken	454 γ
Iridium recovered	451–456 γ
Rhodium taken	499 γ
Rhodium recovered	495–500 γ
Palladium taken	478 γ
Palladium recovered	476–479 γ (eluted with HCl) 476–479 γ (3 eluted with $HClO_4$)

Rhodium, Iridium, and Platinum

The procedure was exactly as described above except that the beds were eluted with 80 ml. of 2 *M* hydrochloric acid followed by 75 ml. of 2.4 *M* perchloric acid for the platinum.

Number of experiments	3
Iridium taken	454 γ
Iridium recovered	451–456 γ
Rhodium taken	499 γ
Rhodium recovered	498–501 γ
Platinum taken	490 γ
Platinum recovered	490–492 γ

Rhodium, Iridium, Palladium, and Platinum

Solutions containing these four metals were evaporated to dryness with 6 mg. of sodium chloride, and the residues redissolved in 1 ml. of water. A few drops of hydroxylamine solution were added to reduce the iridium, and the solutions were then fed onto 3-cm. beds in small columns. The beds were eluted with 80 ml. of 2 *M* hydrochloric acid followed by 50 ml. of 9 *M* hydrochloric acid, and then with 75 ml. of 2.4 *M* perchloric acid. The first effluents were treated for a separation of rhodium and iridium as described above. Good results were obtained for the recovery of rhodium, iridium, and palladium, but the platinum recoveries were all low by about 25%.

Can. J. Chem. Downloaded from www.nrcresearchpress.com by 200.7.193.243 on 09/04/12
For personal use only.

Further examination showed that some platinum was being eluted along with the palladium but had not been noticed since this small quantity produced a negligible interference in the palladium determinations. It is believed that this early elution of the platinum was due to a partial reduction of the quadrivalent metal to the bivalent state by the hydroxylamine used to reduce the iridium. The bivalent platinum evidently has much the same affinity for the resin as the bivalent palladium.

An unsuccessful search was made for a reducing agent which would reduce the quadrivalent iridium but not any of the quadrivalent platinum. Best results (94% recovery of the platinum in the "platinum fraction") were obtained by the slow reduction of the iridium in neutral solution by sodium oxalate.

An attempt to reoxidize the platinum on the exchanger with cerium(IV) after the removal of the tervalent iridium was also unsuccessful.

One separation of the four metals was carried out in which the "palladium fraction" was evaporated to a few milliliters, boiled with nitric acid to oxidize the platinum, and evaporated twice to dryness with hydrochloric acid. The residue was dissolved in a few milliliters of 2 *M* hydrochloric acid, and this solution treated as described above for the separation of palladium and platinum. In this way platinum was completely recovered in two fractions.

	Taken	Found
Rhodium	499 γ	501 γ
Iridium	454 γ	451 γ
Palladium	478 γ	479 γ
Platinum	490 γ	363 plus 127 = 490 γ

Hydrolytic Separation of Rhodium, Iridium, and Palladium from Platinum on a Microgram Scale

The generally accepted procedure of precipitating rhodium, iridium, and palladium as hydrated oxides as a method of separating these metals from platinum has never been applied on a microgram scale. In view of the relative difficulty encountered in the four-metal separation described above it was decided to investigate the possibility of removing the platinum by this method prior to applying an ion-exchange separation for the remaining three metals.

The procedure followed was generally that described in *Applied inorganic analysis* (18), pp. 376–377, except that a carrier was employed to aid in the precipitation of the small quantities of the metals present. Both titanium(IV) sulphate and cerium(IV) sulphate were used for this purpose. The cerium salt was finally chosen because its precipitate was easier to handle.

A solution of platinum was evaporated to dryness with 6 mg. of sodium chloride in a 30-ml. beaker. The residue was dissolved in 1 ml. of 2 *M* hydrochloric acid and diluted to about 5 ml. with water. The solution was then heated to boiling and about 5 mg. of cerium(IV) sulphate was added followed by 5 ml. of a filtered solution of sodium bromate. A filtered 10% solution of sodium bicarbonate was added slowly until the first trace of a permanent precipitate formed. Then 5 ml. more of the sodium bromate solution was added. Addition of bicarbonate was continued until no further precipitation was evident. Another 5 ml. of bromate solution was added, and the mixture was boiled for 10 minutes. The mixture was allowed to cool, the precipitate to settle, and the whole was then filtered through a porcelain filter crucible of medium porosity. The precipitate was washed with 0.1 *M* sodium chloride solution. The filtrate was boiled with hydrochloric acid to destroy the bromate, and analyzed for platinum. Complete recovery of the platinum was obtained.

Can. J. Chem. Downloaded from www.nrcresearchpress.com by 200.7.193.243 on 09/04/12
For personal use only.

Solutions of the four metals were treated as above, and again all the platinum was found in the filtrates, indicating its separation from the other three metals.

The oxide precipitate from one of these experiments was dissolved in concentrated hydrochloric acid, evaporated to dryness, and the three metals separated as described above. A quantitative separation of the four metals was accomplished by this means.

	Taken	Found
Rhodium	499 γ	502 γ
Iridium	454 γ	451 γ
Palladium	478 γ	481 γ
Platinum	490 γ	492 γ

These experiments indicate that the ion-exchange separations may be integrated with a Gilchrist–Wichers type of scheme (18) for the analysis of the platinum metals on a microgram scale.

Separation of Rhodium and Ruthenium

It has been noted that this separation is of interest to radiochemists since rhodium is a daughter of ruthenium by beta decay. Some qualitative experiments were made to determine the feasibility of making the separation by ion exchange.

Ruthenium behaves toward the exchanger much like iridium. The quadrivalent complex is strongly adsorbed but appears to be partially reduced by the resin so that relatively large losses occur in the feed effluent. This can be remedied by the addition of an oxidant such as cerium(IV) to the feed solution. Attempts to elute the quadrivalent ruthenium with hydrochloric acid were unsuccessful, as was an attempt to reduce it on the resin with a 1% solution of hydroxylammonium chloride. The tervalent complex has a very low affinity for the resin, and a separation of it from tervalent rhodium does not seem to be possible.

It is possible that a procedure similar to that evolved for the separation of rhodium and iridium could be developed to separate the two metals in solution, but the problem of the quantitative removal of the quadrivalent ruthenium from the resin requires further study.

ACKNOWLEDGMENTS

This investigation was assisted by a grant from the University of Toronto's Advisory Committee on Scientific Research, for which grateful acknowledgment is made. One author (S.S.B.) was holder in 1955–56 and 1956–57 of a fellowship given to the university by Canadian Industries Ltd., for which our thanks are here recorded.

REFERENCES

1. MacNevin, W. M. and Crummett, W. B. Anal. Chem. **25**, 1628 (1953).
2. MacNevin, W. M. and Crummett, W. B. Anal. Chim. Acta, **10**, 323 (1954).
3. Stevenson, P. C., Frank, A. A., Borg, R., and Nervik, W. J. Am. Chem. Soc. **75**, 4876 (1953).
4. Blasius, E. and Wachtel, U. Z. anal. Chem. **154**, 341 (1954).
5. MacNevin, W. M. and McKay, E. S. Anal. Chem. **29**, 1220 (1957).
6. Berman, S. S. and McBryde, W. A. E. Can. J. Chem. **36**, 845 (1958).
7. Kraus, K. A., Nelson, F., and Smith, G. W. J. Phys. Chem. **58**, 11 (1954).
8. Holzer, H. Z. anal. Chem. **23**, 299 (1951).
9. Fraser, J. G., Beamish, F. E., and McBryde, W. A. E. Anal. Chem. **26**, 495 (1954).
10. Yoe, J. H. and Kirkland, J. J. Anal. Chem. **26**, 1335 (1954).
11. Fraser, J. G. M.A. Thesis, University of Toronto, Toronto, Ontario. 1951.
12. Ayres, G. H. and Meyer, A. S. Anal. Chem. **23**, 299 (1951).
13. Ayres, G. H. and Young, F. Anal. Chem. **22**, 1277 (1950).
14. Fisher, S. and Kunin, R. Anal. Chem. **27**, 1191 (1955).
15. Walton, H. F. Chap. 1. *In* Ion exchange. *Edited by* F. C. Nachod, Academic Press, Inc., New York. 1949.
16. Kraus, K. A. and Moore, G. E. J. Am. Chem. Soc. **75**, 1460 (1953).
17. Sussman, S., Nachod, F. C., and Wood, W. Ind. Eng. Chem. **37**, 618 (1945).
18. Gilchrist, R. Chap. 20. *In* Applied inorganic analysis. 2nd ed. *By* Hillebrand, Lundell, Bright, and Hoffman. John Wiley & Sons, Inc., New York. 1953.

Can. J. Chem. Downloaded from www.nrcresearchpress.com by 200.7.193.243 on 09/04/12
For personal use only.

THE SEPARATION OF RHODIUM AND IRIDIUM BY ION EXCHANGE[1]

S. S. Berman and W. A. E. McBryde

ABSTRACT

Separations of rhodium and iridium as chlorides by means of columns of the anion exchanger Amberlite IRA-400 are described. Iridium is maintained in the quadripositive state by the addition of cerium(IV), the presence of which is necessary to counteract the reducing action of the resin. The marked difference in affinity toward the resin of Ir(IV) and Rh(III) makes the separation possible. Rhodium can easily be eluted from the resin by 2 *M* hydrochloric acid. Removal of all the iridium from the resin is accomplished in a Soxhlet extractor with 6 *M* hydrochloric acid. A number of less successful procedures for this separation are discussed.

Can. J. Chem. Downloaded from www.nrcresearchpress.com by 200.7.193.243 on 09/04/12
For personal use only.

In recent years there have appeared several procedures employing ion-exchange resins for the separation of rhodium and iridium, an operation which may be regarded as the most difficult step in the analysis of the elements of the platinum metal group. Cluett *et al.* (1) proposed a method applicable to mixtures containing 10 mg. or more of each of the metals. This method can be criticized on two accounts. Removal of iridium from the exchanger required the use of large quantities of salts and acids which must be destroyed prior to the determination of the iridium. Also, losses of iridium in the feed solution indicated that attempts to use the procedure for smaller quantities of the metals would lead to relatively appreciable quantities of iridium remaining with the rhodium. The method of Berg and Senn (2) which separates the metals on the basis of oppositely-charged thiourea complexes suffers from the time-consuming necessity of destroying the thiourea prior to the analysis of the rhodium and iridium. MacNevin and McKay (3) claim to produce spectrographically pure rhodium from a rhodium–iridium mixture, but the separation is not quantitative.

The purpose of this work was to develop a relatively simple quantitative separation of the two metals which would lend itself to their subsequent analysis without difficulty. This separation is necessary, since, to date, no satisfactory specific reagent for either of these elements has been found.

The procedure described below is based, like that of Cluett *et al.*, on the strong affinity of chloroiridate(IV) toward the anion exchanger in contrast with the relatively weak affinity of the chlororhodate complex. Losses of iridium in the feed solution have been eliminated by the choice of a suitable oxidant, and a simple method of extraction of the iridium complex from the resin has been developed.

EXPERIMENTAL

Apparatus and Solutions

Stock solutions of rhodium and iridium were prepared by dissolving highly refined chloro salts, which had been obtained from the International Nickel Company of Canada, respectively in 0.05 *M* and 0.1 *M* hydrochloric acid. The rhodium solution was standardized gravimetrically (4) and the iridium solution volumetrically (5). These solutions contained approximately two milligrams of metal per milliliter of solution. They were diluted 20-fold with 0.1 *M* hydrochloric acid in the following work.

Two sizes of columns, of conventional design, were used. The larger were 10 mm. in internal diameter and about 20 cm. in height; the smaller were 5 mm. in internal diameter and about 12 cm. in height. A flow rate of about 50 ml. per hour was used.

[1]*Manuscript received December 3, 1957.*
Contribution from the Department of Chemistry, University of Toronto, Toronto 5, Ontario, Canada.

Can. J. Chem. Downloaded from www.nrcresearchpress.com by 200.7.193.243 on 09/04/12
For personal use only.

The resin used was Amberlite IRA-400 of an analytical grade. Conversion to the chloride form was ensured by stirring the resin for several hours with a large excess of 2 *M* hydrochloric acid. At the same time the resin was freed of small bits of foreign matter which usually floated on the surface of the supernatant liquid. The resin was dried at 110° C. and ground to yield two fractions, one of which was of mesh size 70 to 100 and the second of mesh size less than 100. The latter fraction was freed of very fine particles by shaking with the acid solution, allowing the bulk of the resin to settle, and pouring off the fines. This was repeated until the resin settled completely within a few minutes. The resin was stored in a solution of 2 *M* hydrochloric acid.

In some experiments the iridium was removed from the resin by a Soxhlet extraction. For this purpose a microextractor was used, Corning No. 3860.

Methods of Analysis

Determinations of rhodium were made with the colorimetric procedure employing tin(II) chloride described by Sandell (6). Dilutions were made with 2 *M* hydrochloric acid. Optical densities were measured with a Beckman Model DU spectrophotometer at 470 mμ.

Iridium was determined by the tin(II) chloride–hydrobromic acid procedure of Berman and McBryde (7).

The Adsorption of Iridium on the Exchanger

The development of a sensitive colorimetric procedure for the determination of iridium enabled the authors to carry out a more extensive study of the adsorption of quadrivalent iridium on the resin than was previously possible.

It had been previously demonstrated by Cluett *et al.* (1) that maximum adsorption of chloroiridate(IV) by the exchanger necessitated the presence of an oxidizing agent. That the resin is indeed a mild reducing agent was demonstrated by the following experiments.

A solution containing approximately 500 γ of iridium in 5 ml. of 1 *M* hydrochloric acid was fed onto a 3-cm. bed of 70–100-mesh resin, which had been previously washed with a solution of 1 *M* hydrochloric acid. A dark brown band, characteristic of chloroiridate(IV), formed at the top of the bed. After 16 hours of standing the color of the band had appreciably lightened. After 40 hours the band was no longer visible. This seemed to indicate that the quadrivalent iridium had been slowly reduced to the almost colorless tervalent complex. Elution of the resin bed with 100 ml. of 6 *M* hydrochloric acid yielded about 350 γ of iridium in the effluent, indicating that the reduction was not complete.

Ten milliliters of a 0.1 *N* solution of potassium dichromate was fed onto a resin bed, resulting in an orange-red adsorption band at the top of the bed. After a day a green solution, presumably containing tervalent chromium, was seen diffusing down through the bed.

A solution of 0.8 *M* hydrochloric acid containing about 5 mg. of cerium as cerium (IV) sulphate was passed very slowly through a resin bed. The effluent was colorless, characteristic of a solution of cerium(III).

Bromine as the Oxidant

Choice of a suitable oxidant to counteract the effect of the resin is limited by the fact that chloroiridate(IV) is itself a strong oxidant (E^0 = 1.02 v. (8)). The first choice for this purpose was bromine (E^0 = 1.09 v.). Resin beds 2.5 cm. deep were prepared by transferring the 70–100-mesh resin to the larger columns, and shaking with one or two columnfuls of 0.1 *M* hydrochloric acid containing 10% saturated bromine water by

volume. (The resin had been previously extracted with 6 *M* hydrochloric acid in a Soxhlet extractor to minimize color throwing.) Then 454 γ of iridium in 5 ml. of 0.1 *M* hydrochloric acid was fed onto the column. In most of the experiments the bed was washed with a quantity of the bromine water – hydrochloric acid solution prior to the feeding of the iridium solution. After feeding, the resin bed was washed with 20 ml. of this same solution, and was then eluted with more of the solution to simulate the removal of rhodium. The feed and wash effluents and the simulated "rhodium fraction" were collected separately and evaporated to about one milliliter in volume. A few milliliters of 30% hydrogen peroxide solution was added to each to destroy a yellow-colored material in solution which was usually present and presumably came from the resin. The solutions were boiled to expel bromine and excess hydrogen peroxide, evaporated to near dryness, and analyzed for iridium. To check whether the colored species in the iridium analysis was due to iridium and not to some interfering foreign matter, the spectral curve of each sample was examined in the vicinity of 402 mμ and compared with a known iridium spectrum.

In the following account the bromine water – hydrochloric acid solution will be referred to as the feed solution. It is evident from Table I that the losses of iridium may be considerably reduced by substantial pretreatment of the resin bed. Losses in the last three experiments amount to less than 0.25% of the iridium fed onto the bed.

TABLE I

EFFECT OF PRETREATMENT OF RESIN ON ADSORPTION OF 454 γ OF CHLOROIRIDATE(IV)

Columns of feed soln. shaken with resin	Volume of preliminary wash, ml.	Volume of eluant, ml.	Ir in feed and rinse, μg.	Ir in "Rh fraction", μg.
1	0	100	22	4
1	5	100	2.7	7.6
1	80	100	1.5	3.0
2	100	100	1.0	1.8
2	200	70	Combined — 0.0	
2	200	75	Combined — 1.1	
2	200	75	Combined — 1.1	

However, further work showed that 75 ml. of the feed solution would elute only about 90% of a 499-γ rhodium sample treated in a manner similar to the last three experiments described in Table I, and that any procedure which would quantitatively recover the rhodium resulted in a loss of 4 to 5 γ, or approximately 1% of the iridium taken.

It was also shown, by taking a 45.4-γ sample of iridium, that the loss is more or less an absolute one, and not strictly proportional to the quantity of iridium fed. This may be a serious drawback if such a procedure were to be adapted to micro separations, as the relative loss of iridium would be significant.

An explanation of why losses occur in the presence of this oxidant may be based on the following observation. It was noticed that when the bed was washed with a quantity of the feed solution prior to the feeding of the iridium, the bromine was adsorbed from the solution in a red band at the top of the resin bed. When the quadrivalent iridium was fed, the dark brown band due to this complex did not form at the top of the bed but rather directly below the bromine band, indicating that the bromine had occupied sites on the resin and had made them unavailable to the chloroiridate(IV). Since chloroiridate(IV) has an exceptionally high affinity for the resin, the bromine must indeed be very strongly bound, with a resultant decrease in its activity and in its ability to act as

Can. J. Chem. Downloaded from www.nrcresearchpress.com by 200.7.193.243 on 09/04/12
For personal use only.

a mobile oxidant toward any iridium that may have been reduced by the resin. The strong affinity of bromine for the resin was further demonstrated by the inability of a sample of resin which had been saturated with bromine to adsorb any chloroiridate(IV).

Substantially the same results were obtained when chlorine was used as the oxidant in place of bromine.

Cerium(IV) as the Oxidant

In view of the above experience with bromine it was decided that a truly effective oxidant would have to be one which would not itself be adsorbed by the exchanger, nor would oxidize chloride at the concentrations of hydrochloric acid used. The only oxidant found which met these conditions was quadrivalent cerium. The use of cerium(IV) limits the acid concentration permissible to the range of 0.5 *M* to 1 *M*. In acid solutions below this range the cerium salts hydrolyze. In solutions more concentrated than this range chloride is oxidized to chlorine.

The oxidizing solution was prepared by adding 1 ml. of 0.1 *M* cerium(IV) sulphate to 100 ml. of 0.8 *M* hydrochloric acid.

Resin beds 2.5 cm. deep were washed with 10 ml. of water and then rinsed with 10 ml. of the cerium solution. The washing with water was found to be essential for the elimination of iridium losses, although the authors can find no plausible explanation for this. Five milliliters of 0.1 *M* hydrochloric acid solution containing 454 γ of iridium was fed onto the beds, which were then eluted with a further 90 ml. of the cerium solution to simulate the removal of rhodium. The feed effluents and the "rhodium fractions" were passed through large cation-exchange beds to remove the cerium, evaporated to near dryness, and analyzed for iridium. A yellow residue was always present which was found to contain iron (presumably from the resin). Examination of the spectra in the vicinity of 402 mμ showed that no iridium was present.

Similar experiments with 499 γ of rhodium showed that this element is quantitatively recovered in the combined feed and eluate solutions. It was also established that cerium interferes but little in the colorimetric determination of rhodium, and need not be removed if a set of appropriate standards is prepared for comparison. If desired, the cerium can easily be removed by passage of the solution through a bed of Dowex-50.

The Recovery of Iridium

The recovery of iridium adsorbed on an anion exchanger has long been a problem. The metal cannot be conveniently recovered by ashing the resin as Sussman *et al.* (9) did for platinum and palladium because of the difficulty in redissolving it for the purpose of analysis. The only successful wet procedure reported is that of Cluett *et al.* (1) which is very time-consuming and extravagant of reagents.

Elution of Iridium by a Reducing Agent

Since the affinity of chloroiridate(III) for the exchanger is small in hydrochloric acid solutions more concentrated than 1 *M* it was thought that it might be possible to reduce the quadrivalent iridium complex on the resin and elute the tervalent species with hydrochloric acid. The choice of reductants is limited by three factors. Iridium is a noble metal; the determination of iridium is impossible in the presence of most metals; and, also, the reductant should not be adsorbed on the exchanger or the same type of situation may result as was experienced with bromine.

Several experiments were conducted using 1% and 4% solutions of hydroxylammonium chloride and hydrazine hydrochloride as the reductants. The iridium solutions were fed in the presence of cerium(IV) as described in the adsorption experiments. The

Can. J. Chem. Downloaded from www.nrcresearchpress.com by 200.7.193.243 on 09/04/12
For personal use only.

bed was rinsed with 20 ml. of 0.8 *M* hydrochloric acid to remove the cerium, and then 25 ml. of the reducing solution was passed through, followed by a dilute solution of hydrochloric acid. The two effluents were collected together and several milliliters of 30% hydrogen peroxide solution was added to destroy the reductant. The solutions were evaporated to near dryness to destroy most of the acid, and then were analyzed for iridium.

Results for the two reductants were much the same. Immediately they came in contact with the adsorption band, it disappeared, indicating that reduction had taken place. Recoveries of iridium ranged from 88% to 96%, and did not seem to depend on the concentration of the reducing agent or on the concentration of the hydrochloric acid eluant. It appears that some of the adsorbed iridium is not readily available for reduction. These results compare closely with those obtained with an ammoniacal elution (1) which also involves a reduction process.

Perchloric Acid as an Eluant

It was hoped that the affinity of the perchlorate anion, which is by far the strongest of all common anions for the exchanger (10), would be great enough to displace the chloroiridate(IV) complex.

The resin beds were fed with iridium as described above and then eluted with 100 ml. of a 10% (v/v) solution of perchloric acid. The bands slowly faded and the effluents were the color of chloroiridate(IV). However, recoveries of only about 80% were achieved, and they were not improved by increasing the concentration of the acid or the volume of the eluting solution.

Recovery by Soxhlet Extraction

Iridium was fed onto resin beds 2 cm. deep in small columns as described above, and the beds were washed free of cerium with 20 ml. of 0.8 *M* hydrochloric acid. The upright part of the column was removed and the beds allowed to drain. The columns were then inverted and the resin bed was shoved out, along with the glass-wool supporting pad, with a stirring rod into a specially prepared glass thimble. This thimble was made by blowing a small hole in the bottom of a soft-glass test tube, cutting the tube to the appropriate length, and pulling some glass wool through the hole so that liquids would pass through but not resin particles. (The resin used in these experiments had previously been extracted to reduce color-throwing.) The thimble was placed in the small extractor and 15 ml. of 6 *M* hydrochloric acid in the pot, and the resin extracted for ½ hour.

The solutions in the pot after the extractions were pale brown in color, not as dark as chloroiridate(IV) but far from the almost colorless chloroiridate(III). These were transferred to 30-ml. beakers, evaporated to almost dryness, and analyzed for iridium with results as follows:

Number of experiments	3
Iridium taken	454 γ
Iridium recovered (range)	452–455 γ

The recovery of iridium is quantitative by this procedure. A possible explanation for the success of this operation is that the increase in temperature enhanced the reducing properties of the resin, causing reduction of the iridium most intimately bound in the resin matrix, and making it available for leaching with the hot acid solution. It is probably this iridium that cannot be reached by conventional eluants. That partial reduction had taken place was demonstrated by the restoration of the intense chloroiridate(IV) color on the addition of a few drops of 30% hydrogen peroxide solution.

Can. J. Chem. Downloaded from www.nrcresearchpress.com by 200.7.193.243 on 09/04/12
For personal use only.

Although this operation may seem rather complicated it is in reality quite simple and quick. The recovery and analysis of the iridium can easily be done in $1\frac{1}{2}$ hours.

Separation and Analysis of Rhodium–Iridium Mixtures in Solution

The following procedure was successfully used to separate and analyze mixtures of rhodium and iridium in hydrochloric acid solution.

The samples were evaporated to dryness with a few milliliters of concentrated hydrochloric acid and 6 mg. of sodium chloride in 30-ml. beakers. The residues were dissolved in about 2 ml. of 0.8 *M* hydrochloric acid, and fed with a dropper onto 1.5-cm. beds of 70–100-mesh resin in small columns (which had been previously washed with 10 ml. of water and 10 ml. of the cerium(IV) solution as described above). The beakers were twice rinsed with 2 ml. of the acid solution, and the beds then eluted with 90 ml. of the cerium solution. The effluents were collected together, evaporated to a few milliliters, and analyzed for rhodium. The resin bed was extracted as described above and the recovered iridium determined.

Number of experiments	4	2
Iridium taken	454 γ	45.4 γ
Iridium recovered (range)	453–457 γ	45.0–45.2 γ
Rhodium taken	499 γ	49.9 γ
Rhodium recovered	500 γ	50.1–50.3 γ

Batch Separations of Rhodium and Iridium

An attempt to separate these two metals by stirring a solution containing them with a quantity of resin in the presence of an oxidant was not successful. Although conditions were found where no rhodium was adsorbed by the exchanger the rhodium always contained at least 10% of the iridium originally present.

The Separation of Chlororhodate and Chloroiridate(III)

Examination of the distribution coefficients (11) for the chlororhodate and chloroiridate(III) complexes indicates that a separation of these two species should be feasible on an anion exchanger with dilute hydrochloric acid solutions as eluants. A procedure of this nature would have the advantage of having the iridium on the resin in an easily eluted state.

Solutions containing approximately 500 γ of rhodium and iridium and 6 mg. of sodium chloride were evaporated to dryness. The residues were dissolved in 1 ml. of water, a few drops of a 1% solution of hydroxylammonium chloride added to reduce the quadrivalent iridium, and the solutions fed onto 3-cm. beds of $<$100-mesh resin in the small columns.

The rhodium complex formed a red band at the top of the bed. This band is not visible when the rhodium is fed in hydrochloric acid medium more concentrated than 0.5 *M*. The tervalent iridium band was not visible.

It was found that the rhodium could be quantitatively eluted by 80 ml. of 0.5 *M* hydrochloric acid, but that this quantity of eluant also removed significant amounts of iridium from the resin.

Elution of a bed fed with 454 γ of tervalent iridium by 100 ml. of 0.1 *M* hydrochloric acid yielded about 50 γ of iridium in the effluent. Examination of successive 10-ml. quantities of this effluent taken by a fraction collector showed that the iridium appeared shortly after the start of the elution, and that the quantity of the metal in each fraction remained almost constant at about 5 to 6 γ. This leakage of iridium could be lessened by elution with more dilute acid, but this retarded the elution of the rhodium.

It would appear that the rhodium is more strongly adsorbed than is indicated by the

Can. J. Chem. Downloaded from www.nrcresearchpress.com by 200.7.193.243 on 09/04/12
For personal use only.

distribution coefficients. Such behavior of the rhodium complex is not surprising and is in agreement with the observations of Cluett *et al.* (1), who noted that it was more difficult to remove rhodium that had been fed from a freshly prepared chlororhodate solution (which we have in this case) than from a solution that had been standing for a while.

Attempts to produce a partially hydrolyzed rhodium solution, which would have a lower affinity for the resin, by boiling, and also by adding a small quantity of urea to the solution and heating, were successful in that the ease of elution of the rhodium by 0.01 *M* hydrochloric acid was improved. However, the recoveries were still incomplete, ranging from 90% to 98% for elution with 30 ml. of the acid solution. Continued elution produced no more rhodium in the effluent. Removal of the remaining metal required an acid solution of at least 0.5 *M*. This appears to indicate that the conversion to a hydrolyzed form is not complete.

No iridium was found in the effluent on elution with 30 ml. of 0.01 *M* hydrochloric acid, but subsequent treatment with 0.5 *M* acid solution eluted small quantities of iridium.

In the face of the apparent inability to remove the rhodium without small quantities of iridium, work on this procedure was not continued.

The Separation of Partially Hydrolyzed Chlororhodate and Chloroiridate(IV)

When 5 ml. of the stock iridium solution is diluted to 100 ml. with water the resulting solution is 0.005 *M* in hydrochloric acid. It was noted that if 5 ml. of this dilute solution is fed onto a resin bed the adsorption band, while still brown in color, is not as dark as a band that is formed when the iridium is fed from a solution that has previously been boiled with hydrochloric acid or evaporated with a few milligrams of sodium chloride. Elution of the iridium adsorbed from this diluted solution with 100 ml. of 0.01 *M* hydrochloric acid produced no iridium in the effluent, but elution with 50 ml. of 6 *M* hydrochloric acid quantitatively removed the iridium.

Obviously this iridium was not in the form of chloroiridate(IV). Since the stock solution from which the diluted solution was prepared was nearly two years old, it may be assumed that the chloroiridate(IV) had undergone partial hydrolysis. Such behavior would parallel that of a chlororhodate solution (see above) except that in this case the rate of hydrolysis is probably much slower.

Repetition of this procedure with the rhodium solution showed that 25 ml. of the 0.01 *M* acid solution removed 86% to 92% of the rhodium from the resin with no more metal being removed by further elution with this solution. Removal of the rest of the rhodium could not be accomplished except under conditions which would also remove some iridium.

It was felt that if the degree of hydrolysis of the rhodium could be increased it would be possible to recover the rhodium without eluting any iridium. This was accomplished by the addition of 7 *M* ammonium hydroxide solution until a precipitate formed, and the subsequent dissolution of the precipitate with a minimum of 2 *M* hydrochloric acid. When a dilute rhodium solution was treated in this manner and fed onto a resin bed the rhodium could be completely recovered with 25 ml. of water.

Evidently this treatment produces one or more rhodium species which have no affinity for an anion exchanger. Passage of a similar solution through a cation-exchanging resin bed resulted in only partial adsorption of the rhodium, indicating that both cationic and neutral species are probably present.

Separations were carried out from the dilute, partially hydrolyzed solutions. To 5-ml. samples, each containing about 500 γ of each of the metals, were added three drops of

Can. J. Chem. Downloaded from www.nrcresearchpress.com by 200.7.193.243 on 09/04/12
For personal use only.

7 *M* ammonium hydroxide solution. The addition of the third drop produced a yellow precipitate which was redissolved by five drops of 2 *M* hydrochloric acid. The resulting solution was fed onto a 2.5-cm. resin bed of 70 to 100 mesh in a larger column, and the bed washed with 25 ml. of water followed by 50 ml. of 6 *M* hydrochloric acid. The feed and water-wash effluents were analyzed for rhodium, and the acid effluent for iridium. Quantitative separations were achieved by these means.

Unfortunately, the above separation could not be repeated when fresh rhodium and iridium solutions were used. Attempts to hydrolyze these solutions by dilution and boiling prior to the ammonia treatment resulted in maximum recoveries of 98% for rhodium and 95% for iridium. The rhodium could be completely recovered by passing the iridium fraction, after evaporation and re-treatment, through the column again. From a sample containing four times as much rhodium the same percentage loss occurred as for the smaller samples.

Although it is possible to recover all the rhodium in two stages, and presumably all the iridium by a Soxhlet extraction, the authors cannot recommend this procedure in place of the simpler and shorter method utilizing cerium(IV) described above. The one advantage of this procedure is that rhodium is produced free of other metallic elements.

By coincidence, some of this work was paralleled in the recent report by MacNevin and McKay (3), who used sodium hydroxide to precipitate the rhodium. Dissolution of this precipitate gave a solution containing almost entirely cationic rhodium, which they adsorbed on a cation exchanger to separate it from the iridium which remained in an anionic form. This reaction, like that described above, was not quantitative, and a complete separation was not achieved.

The above work demonstrates the extreme complexity of the chemistry of the platinum metals in solution, and the importance of taking into account the history of a solution sample cannot be overemphasized.

ACKNOWLEDGMENTS

This investigation was assisted by a grant from the University of Toronto's Advisory Committee on Scientific Research, for which grateful acknowledgment is made. One author (S.S.B.) was holder in 1955–56 and 1956–57 of a fellowship given to the university by Canadian Industries Ltd., for which thanks are here recorded.

REFERENCES

1. CLUETT, M. L., BERMAN, S. S., and MCBRYDE, W. A. .E Analyst, **80**, 204 (1955).
2. BERG, E. W. and SENN, W. L. Anal. Chem. **27**, 1255 (1955).
3. MACNEVIN, W. M. and MCKAY, E. S. Anal. Chem. **29**, 1220 (1957).
4. CURRAH, J. E., MCBRYDE, W. A. E., CRUIKSHANK, A. J., and BEAMISH, F. E. Ind. Eng. Chem., Anal. Ed. **18**, 120 (1946).
5. MCBRYDE, W. A. E. and CLUETT, M. L. Can. J. Research, B, **28**, 788 (1950).
6. SANDELL, E. B. Colorimetric determination of traces of metals. 2nd ed. Interscience Publishers, Inc., New York. 1950. p. 523.
7. BERMAN, S. S. and MCBRYDE, W. A. E. Analyst, **81**, 566 (1956).
8. LATIMER, W. M. Oxidation potentials. 2nd ed. Prentice-Hall, Inc., New York. 1952.
9. SUSSMAN, S., NACHOD, F. C., and WOOD, W. Ind. Eng. Chem. **37**, 618 (1945).
10. FISHER, S. and KUNIN, R. Anal. Chem. **27**, 1191 (1955).
11. BERMAN, S. S. and MCBRYDE, W. A. E. Can. J. Chem. **36**, 835 (1958).

Can. J. Chem. Downloaded from www.nrcresearchpress.com by 200.7.193.243 on 09/04/12
For personal use only.

Can. J. Chem. Downloaded from www.nrcresearchpress.com by 200.7.193.243 on 09/04/12
For personal use only.

THE CHEMISTRY OF THE "AMINOCHROMES"*

PART I. THE PREPARATION AND PAPER CHROMATOGRAPHY OF PURE ADRENOCHROME[1]

R. A. Heacock, C. Nerenberg, and A. N. Payza

ABSTRACT

The preparation of adrenochrome in a pure stable crystalline form has been carried out by the silver oxide oxidation of adrenaline in methanol with the use of an anion-exchange resin (Dowex-1(Cl^-)) to remove heavy metal ions from the reaction mixture prior to the isolation of the product. Its paper chromatographic behavior together with that of three derivatives (adrenolutin, adrenochrome monosemicarbazone, and adrenochrome monoisonicotinic acid hydrazide) in six different solvent systems has been examined. Water was found to be the best paper chromatographic solvent so far examined for this series of compounds.

Adrenochrome (I), the substance mainly responsible for the red colors produced during the mild oxidation of adrenaline (II), was first isolated from the products of an enzymatic oxidation by Green and Richter (1). Subsequently, inorganic oxidizing agents, particularly

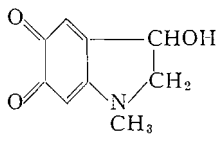

I

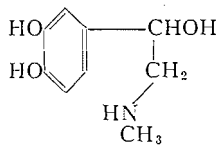

II

silver oxide, were successfully employed and it was observed that adrenochrome could be crystallized from methanol (containing a little formic acid) at −80° (cf. Veer (2); MacCarthy (3); Harley-Mason (4); Sobotka and Austin (5)). Green and Richter reported that adrenochrome was unstable both in the solid state and in solution (1); however, Sobotka and Austin claim that the dry crystalline material can be kept indefinitely at 0° (5). The stability of aqueous solutions of adrenochrome has been shown to be markedly affected by pH (cf. Zambotti and Moret (7)); under alkaline conditions and in the presence of certain metallic cations, particularly zinc, adrenochrome readily rearranges into adrenolutin (*N*-methyl-3,5,6-indoletriol, III) (cf. Lund (8); Fischer, Derouaux, Lambot, and Lecomte (9); Harley-Mason and Bu'Lock (10); Fischer and Lecomte (11)).

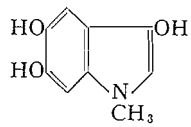

III

[1]*Manuscript received December 11, 1957.*

Contribution from the Psychiatric Research Unit, University Hospital, Saskatoon, Saskatchewan. This investigation was supported by grants from the Department of Health and Welfare, Ottawa, and the Rockefeller Foundation. This work was carried out under the auspices of the Saskatchewan Committee on Schizophrenia Research.

**The term "aminochromes" was suggested by Sobotka and Austin (5) for the highly colored cyclic oxidation products of β-(3,4-dihydroxyphenyl)-ethylamines and related compounds. These substances are often formulated as substituted 2,3-dihydroindole-5,6-quinones, although there is some uncertainty as to the existence of a true o-quinonoid structure (4, 6).*

Can. J. Chem. Downloaded from www.nrcresearchpress.com by 200.7.193.243 on 09/04/12
For personal use only.

Many samples of adrenochrome, prepared by existing methods, that were available to the authors appeared to contain varying amounts of adrenolutin (shown paper chromatographically by a method to be discussed later) and black water-insoluble melanin-like compounds. It appeared not improbable that contamination of the products by metal in a colloidal form or metallic ions, derived from the oxidizing agent, might be responsible for the deterioration of the samples and for the apparent instability of their aqueous solutions. In order to eliminate or drastically reduce the contamination by silver ions, the adrenaline – silver oxide reaction mixture in methanol was filtered through an anion-exchange resin bed in the chloride form prior to crystallization (at $-20°$) in order to remove ionic silver from solution as silver chloride. In this manner a highly crystalline product containing only traces of silver was obtained ($\gtrsim 0.01\%$).

The paper chromatographic behavior of adrenochrome and related compounds has recently been studied by Fischer using *n*-butanol: acetic acid: water (8:2:2) and *i*-propanol: 0.880 ammonia: water (8:1:1) solvent systems (12). The results reported were unsatisfactory, since some of the substances apparently decomposed in these solvents. This is not altogether surprising in view of the known sensitivity of these compounds toward acids and alkalies (7, 8, 9), and furthermore Pavolini, Gambarin, and Godenigo in a study on the action of ammonia on some 5,6-indolequinones, including adrenochrome, reported a definite reaction in this case with the formation of an unstable substance, exhibiting a yellow-green fluorescence, which rapidly turns brown (13). We have repeated Fischer's work and observed with the *i*-propanol–ammonia system that the bright red non-fluorescent adrenochrome spot rapidly turned brownish-yellow in color and exhibited a yellow-green fluorescence, even on exposure to ammonia fumes, and in contact with the solvent the spot soon became dark brown indicating that marked decomposition had occurred. In the acid solvent system, a slower but definite decomposition of the adrenochrome spot was observed during the chromatography. We have found that dilute aqueous solutions of adrenochrome prepared by our method are relatively stable and that distilled water and 2% acetic acid in water are the most suitable solvents for paper chromatography. Pure adrenochrome gave a single spot $R_f 0.8 \pm 0.02$ in water on previously washed Whatman No. 1 paper. Adrenolutin had an R_f of *ca.* 0.4 under these conditions. Contamination of adrenochrome samples with adrenolutin can easily be observed paper chromatographically, since the characteristic yellow adrenolutin spot showing a strong yellow-green fluorescence is soon visible behind the red adrenochrome spot; this can be observed very quickly as it is only necessary to allow the chromatogram to run a few inches in order to see the two spots. The adrenolutin spot is quite distinct and not a diffuse "tail" to the adrenochrome spot, indicating that the impurity was present initially and not formed by continuous isomerization of the starting material. Polymeric melanin-type impurities stay in the position of the original spot. An interesting phenomenon was observed on drying of the paper chromatograms; as the paper was allowed to dry at room temperature, the color of the adrenochrome spot gradually changed from red to yellow-brown and the spot began to exhibit the characteristic adrenolutin fluorescence. The partial formation of adrenolutin was confirmed by two-dimensional chromatography, using water as running solvent in both directions, although only one spot $R_f 0.8$ was observed in the initial run; after drying and rerunning at 90° to the original direction two distinct spots with the characteristic R_f's for adrenochrome and adrenolutin appeared.

Euler, in describing the paper chromatography of adrenaline, states that after the chromatograms have been dried adrenaline spots show an apple-green fluorescence (14, p. 16). A possible explanation of this observation would be the air-oxidation of the

spot to adrenochrome followed by isomerization to adrenolutin on the paper. Therefore it would appear that a thin film of adrenochrome on paper will spontaneously rearrange into adrenolutin. This type of behavior has also been observed by Austin, Chanley, and Sobotka with the related compound epinochrome (IV), which even in the crystalline form undergoes a slow spontaneous rearrangement to 5,6-dihydroxy-*N*-methylindole (V) (15, 16). The paper chromatography of adrenochrome, adrenolutin, adrenoxyl (adrenochrome monosemicarbazone) (VI), and adrenochrome monoisonicotinic acid hydrazide

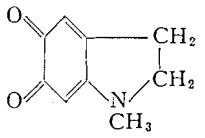

IV

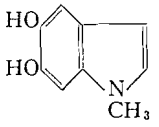

V

(VII) has been studied in six different solvent systems: (*a*) water, (*b*) 2% acetic acid in water, (*c*) 75% methanol in water, (*d*) 75% ethanol in water, (*e*) *n*-butanol: acetic acid: water (8:2:2), and (*f*) *i*-propanol: 0.880 ammonia: water (8:1:1). Although all solvents proved satisfactory for either of the two derivatives, VI and VII, only (*a*) and (*b*) were suitable for adrenochrome and possibly only (*a*) for adrenolutin, since even in (*b*), (*c*), and (*d*) the fluorescence characteristics of the compound seem to be irreversibly altered.

An attempt to purify impure preparations of adrenochrome on cellulose columns using water as solvent was disappointing, since, although pure aqueous solutions of adrenochrome were probably obtained, it was not possible to crystallize the adrenochrome from water, and all samples prepared by freeze-drying under high vacuum (a technique which gave a very finely divided product) were shown chromatographically to be contaminated to some extent with adrenolutin (fortuitously formed during the drying process).

In view of the very considerable interest that has developed, in the physiological activity of adrenochrome and related compounds, in recent years (see Bacq (17) and Hoffer (18) for lists of references) the necessity for working with the compounds in a pure and stable form has become of paramount importance.

EXPERIMENTAL

Preparation of Adrenochrome

L-Adrenaline (9.15 g.) was suspended in methanol (360 ml.) and 90% formic acid added dropwise with stirring until a clear solution was obtained (*ca.* 3.5 ml.). Freshly prepared silver oxide (36.3 g.) was added portionwise during a period of 3 minutes, the reaction temperature being maintained between 18° and 23° during the addition of the oxidant. The reaction mixture was filtered (with suction) through a Dowex-1(Cl^-) (200/400 mesh) resin bed (diam. = 6.5 cm., height = 3.7 cm.)* and the deep red filtrate was allowed to crystallize slowly at −20°. Pure adrenochrome (1.6 g.) was obtained in deep-violet needles, m.p. 112° with decomposition. Found: C, 60.30; H, 4.69; N, 7.76. Calc. for $C_9H_9O_3N$: C, 60.33; H, 5.02; N, 7.81%. The ultraviolet and visible absorption spectra were measured in aqueous solution (λ_{max}: 301, 487 mμ; λ_{mln}: 262, 361 mμ).

Samples of adrenochrome which we have prepared by repeating existing procedures contain, in our view, less well defined crystals than the product obtained as described above (rapid cooling to −80° tends to produce an amorphous product) and the products are

**The resin was prepared by extensive washing: (1) with 3N hydrochloric acid, (2) with water until neutral to litmus, and (3) finally with methanol until the washings were transparent to ultraviolet light.*

Can. J. Chem. Downloaded from www.nrcresearchpress.com by 200.7.193.243 on 09/04/12
For personal use only.

Can. J. Chem. Downloaded from www.nrcresearchpress.com by 200.7.193.243 on 09/04/12
For personal use only.

invariably more or less contaminated with adrenolutin and melanin. This has been demonstrated paper chromatographically (using Whatman No. 1 paper with water as running solvent). No particular advantage either in yield, purity, or crystalline form, appeared to attend the use of absolutely dry methanol. The silver contents of adrenochrome samples prepared in this manner and by the method of Sobotka and Austin (5) were determined by the dithizone method after complete oxidation of the organic material in the sample with a mixture of nitric and perchloric acids (cf. 19, p. 544) and were observed to be very low (not greater than *ca.* 100 parts per million) whereas preparations obtained by other routes had considerably higher silver contents (of the order of 1000 p.p.m.). Sobotka and Austin filtered the methanol reaction mixture through a sodium sulphate bed prior to crystallization. This may have fortuitously acted as an anion-exchange resin and removed silver ions from solution as the sulphate. It is conceivable that both the resin and the sodium sulphate beds would help to hold back colloidal as well as ionic silver. One possible advantage of the resin over sodium sulphate would be that it would enable the reaction to be carried out in aqueous solution if required.

The mother liquors were examined chromatographically on paper using water as solvent and there was evidence that they contained adrenochrome R_f 0.82, a little adrenolutin R_f 0.4–0.45, a non-fluorescent dark-violet unidentified compound R_f 0.92, and a non-fluorescent colorless zone R_f 0.0–0.4. All these zones gave blue colors (i.e. reduced) with the ferric chloride – potassium ferricyanide reagent (see next section). The low R_f area probably contained some unchanged adrenaline, since it gave a red color when sprayed with potassium ferricyanide or ammonium persulphate solution.

Paper Chromatography of Adrenochrome and Related Compounds

Whatman No. 1 paper was washed with distilled water for 12 hours and dried prior to use. It was observed that unwashed paper caused some decomposition of the adrenochrome. The ascending method for paper chromatography was invariably employed, and 10–20 μg. of sample were applied to the paper in each case. The results obtained are given in Table I.

In all cases, the solvent was allowed to ascend a distance of *ca.* 9 to 12 inches. There was a considerable variability in the time required for this to occur; water and 2% acetic acid having the advantage of giving considerably quicker results than the other solvent systems. The approximate times taken by the various solvents are given in Table II.

Detection of Spots

All four compounds are colored and therefore are self-indicating. Adrenolutin (III) also exhibits a marked yellow-green fluorescence in ultraviolet light. It has been previously stated that, on drying, the spots of I undergo a slow change to III; this substance, being a catechol derivative, has reducing properties and the chromatogram can be developed in the following manner (if a permanent record is required). The developing solution was prepared immediately before use, and consisted of 3% ferric chloride solution (5 ml.), 3% potassium ferricyanide solution (5 ml.), and water (90 ml.). The papers were dipped in the reagent and the reducing compounds formed permanent blue spots. The excess reagent was washed off; the papers were dipped in 2 *N* hydrochloric acid and finally excess acid was washed off. Other chromogenic reagents for adrenochrome include: (*a*) Ehrlich's reagent (violet spot), (*b*) 3% ferric chloride solution (gray-brown spot), (*c*) diazotized *p*-nitroaniline (red-brown spot), and (*d*) zinc chloride solution (yellow-green fluorescent spot in ultraviolet light).

TABLE I

R_f IN STATED SOLVENT SYSTEMS

Compound	A	B	C	D	E	F
Adrenochrome (I)	0.8 ±0.02	0.82±0.02	S. dec. (0.7–0.8)	S. dec. (0.7–0.8)	R. dec.¶	R. dec.
Adrenolutin (III)*	0.45±0.05	0.47±0.03§	S. dec. (0.7–0.8)	S. dec. (0.7–0.8)	R. dec.	R. dec.
Adrenoxyl (VI)†	0.48±0.05	0.50±0.03	0.65±0.05	0.85±0.05||	0.57±0.05**	0.58±0.05**
Adrenochrome monoisonicotinic acid hydrazide (VII)‡	0.30	0.42	0.72	0.65	0.21	0.62**

NOTE.—*A = Water. B = 2% acetic acid in water. C = Methanol:water (3:1). D = Ethanol:water (3:1). E = n-Butanol:acetic acid:water (8:2:2). F = i-Propanol:0.880 ammonia:water (8:1:1). S. dec. = slow decomposition. R. dec. = rapid decomposition.*

* = *The adrenolutin was prepared by the method of Harley-Mason and Bu'Lock (20).*

† = *Supplied by the Labaz Co.*

‡ = *Supplied by the Pfizer Co.*

§ = *In all acidic solvents adrenolutin exhibited a pink fluorescence.*

|| = *Occasionally inexplicable lower R_f's were observed for adrenoxyl with this solvent system.*

¶ = *Differing results were obtained dependent on the time taken to run the chromatogram. The red color of the spot slowly faded with the formation of a dirty yellow diffuse spot exhibiting a pink fluorescence.*

** = *These results are different from those reported previously (12); we are unable to explain these discrepancies. The R_f values quoted in Table I were obtained consistently in our investigations. Fischer's claim that adrenoxyl resolves into adrenochrome and a fluorescing spot R_f 0.88 in the ammoniacal solvent system F (12) would appear to be due to a misinterpretation of the evidence in view of known instability of adrenochrome in ammonia.*

TABLE II

Solvent system	A	B	C	D	E	F
Approximate running time (hours)	2.5–3.0	2.5–3.0	7.5	15.5–18.0	15.5–18.0	18.0–20.0

ACKNOWLEDGMENT

The authors wish to express their thanks to Dr. B. Melander, of the Kabi Co. of Stockholm, Sweden, for assistance in obtaining the microsilver analysis.

REFERENCES

1. GREEN, D. E. and RICHTER, D. Biochem. J. **31**, 596 (1937).
2. VEER, W. L. C. Rec. trav. chim. **61**, 638 (1942).
3. MACCARTHY, C. L. Chim. & ind. (Paris), **55**, 435 (1946).
4. HARLEY-MASON, J. J. Chem. Soc. 1276 (1950).
5. SOBOTKA, H. and AUSTIN, J. J. Am. Chem. Soc. **73**, 3077 (1951).
6. HARLEY-MASON, J. Experientia, **4**, 307 (1948).
7. ZAMBOTTI, V. and MORET, V. Arch. sci. biol. (Bologna), **33**, 522 (1949).
8. LUND, A. Acta Pharmacol. Toxicol. **5**, 121 (1949).
9. FISCHER, P., DEROUAUX, G., LAMBOT, H., and LECOMTE, J. Bull. soc. chim. Belges, **59**, 72 (1950).
10. HARLEY-MASON, J. and BU'LOCK, J. Nature, **166**, 1036 (1950).
11. FISCHER, P. and LECOMTE, J. Bull. soc. chim. biol. **33**, 569 (1951).
12. FISCHER, R. Naturwiss. **44**, 443 (1957).
13. PAVOLINI, T., GAMBARIN, F., and GODENIGO, A. S. Gazz. chim. ital. **81**, 527 (1951).
14. EULER, U. S. VON. Noradrenaline—chemistry, physiology, pharmacology and clinical aspects. Ryerson Press, Toronto, Ont. 1956.
15. AUSTIN, J., CHANLEY, J. D., and SOBOTKA, H. J. Am. Chem. Soc. **73**, 2395 (1951).
16. AUSTIN, J., CHANLEY, J. D., and SOBOTKA, H. J. Am. Chem. Soc. **73**, 5299 (1951).
17. BACQ, Z. M. J. Pharmacol. Exptl. Therap. **95** (ii), 1 (1949).
18. HOFFER, A. J. Clin. Exptl. Psychopathol. & Quart. Rev. Psychiat. Neurol. **18** (No. 1), 38 (1956).
19. SANDELL, E. B. Colorimetric determination of traces of metals. Interscience Publishers, Inc., New York. 1950.
20. HARLEY-MASON, J. and BU'LOCK, J. J. Chem. Soc. 703 (1951).

Can. J. Chem. Downloaded from www.nrcresearchpress.com by 200.7.193.243 on 09/04/12
For personal use only.

Can. J. Chem. Downloaded from www.nrcresearchpress.com by 200.7.193.243 on 09/04/12
For personal use only.

A STUDY OF GRAFT COPOLYMERS

I. PREPARATION AND VISCOSITY BEHAVIOR[1]

J. A. MANSON[2] AND L. H. CRAGG

ABSTRACT

Graft polymers were prepared by the redox polymerization of styrene in the presence of oxidized polystyrene or copolymers of styrene and 4-vinylcyclohexene-1; the maximum number of hydroperoxide groups per thousand monomeric units in the oxidized polymers was 18. Evidence that grafting had indeed occurred was obtained from measurements of monomer disappearance, of the decrease in hydroperoxide content of the backbone polymer during reaction, and of the infrared absorption by the polymer before and after the grafting procedure.

Although the experimental results clearly support the conclusion that branching occurred, values of Huggins' k' for both unfractionated and fractionated graft polymers were no higher than for linear polystyrene ($0.39 < k' < 0.41$ in butanone). It was concluded that, though k' is sensitive to bushy branching, Huggins' k' is not measurably affected by the presence in a polymer of a few linear branches per molecule.

INTRODUCTION

The study of branching in high polymers is important to the understanding of the relationships between molecular structure and physical properties. It is all the more important because most polymers, even ones usually assumed to be linear, are branched to some extent.

Unfortunately, the determination of the extent, or degree, of branching (that is, the average number of branches per molecule) is seldom easy. The most rigorous method is based on the fact that the size, and hence intrinsic viscosity, is less for a branched molecule than for a linear molecule of the same molecular weight (26, 29). The application of this method requires the making of viscosity and light-scattering measurements, which are tedious and which require expensive equipment. Another method for the detection of branching has been based upon the determination of Huggins' k' (14), the slope constant of the curve relating reduced viscosity to concentration; a great deal of empirical evidence has been found indicating a correlation between the presence of branching in a polymer and unusually large values of k' (10, 18, 25). Since accurate viscosity measurements can be made readily with fairly simple equipment, this method would, if generally applicable, be very useful.

Since, however, no suitable comparison of these two methods had been made, it was decided to undertake a study of the relationship between Huggins' k' and the degree of branching as determined from measurements of the intrinsic viscosity and molecular weight of branched and unbranched polymers.

In this study it was desirable to have samples of a high polymer, in some of which the molecules would all be essentially linear, while in others each of the molecules would have a known number of linear side chains attached to the main chain. However, most methods available at the time for the preparation of branched polymers with fairly high molecular weights had serious drawbacks.

If one uses polymerization methods involving chain transfer (1, 3, 13), or copolymerizes

[1]*Manuscript received January 13, 1958.*
Contribution from the Department of Chemistry, Hamilton College, McMaster University, Hamilton, Ontario, with financial assistance from the National Research Council through the Associate Committee on Synthetic Rubber Research. Based on a thesis submitted in partial fulfillment of the requirements for the degree of Doctor of Philosophy, September, 1956. Most of this work was reported at the 6th Canadian High Polymer Forum in St. Catharines, Ontario, April, 1955.
[2]*Present address: Air Reduction Company, Inc., Murray Hill, New Jersey. Holder of the R. J. Eddy Foundation Scholarship, 1953–1954.*

a monomer with a cross-linking agent, such as a divinyl compound (6, 28), or irradiates a partially halogenated polymer in the presence of its monomer (15, 16), one obtains a complex mixture of linear and branched polymers that is often difficult to resolve into its components. Moreover, these methods do not yield polymers with simple branches, but rather encourage the growth of branches on branches or the formation of gel.

The condensation of a monomer with a molecule having a known number of reactive functional groups was used by Schaefgen and Flory (24) to produce polymers having a known number of branches per molecule, but the average molecular weights obtained were rather low (less than 38,000) and the structure of the branched molecule was unusual (all branches radiating from a single "hub").

By contrast, the technique developed at the Polytechnic Institute of Brooklyn (21) for the grafting of side-chains onto a vinyl-type backbone seemed very attractive. In this method the hydroperoxide resulting from the oxidation of a vinyl polymer is used to initiate the polymerization of a vinyl monomer under redox conditions (see equations 1 and 2). As well as making possible the control of the degree of branching (by varying the degree of oxidation of the backbone polymer), this method should, in principle, yield a product free of linear material.

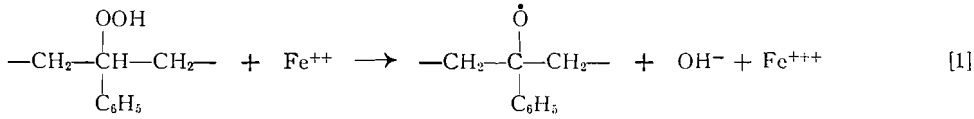

[1]

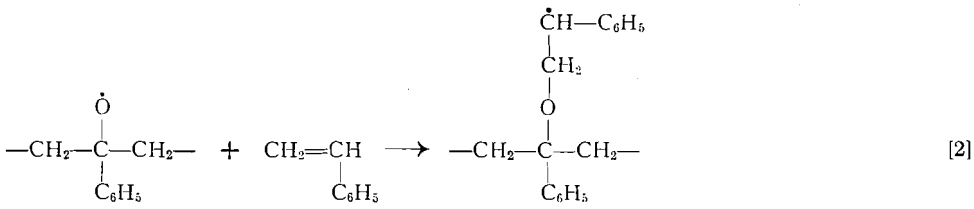

[2]

Several such graft polymerizations were carried out. The backbone polymers used were polystyrene and copolymers of styrene and 4-vinylcyclohexene-1—the latter because they were expected to oxidize more readily than styrene alone. These polymers were oxidized to varying degrees, and the products were used as initiators in the redox emulsion polymerization of styrene. Since this work was first reported at St. Catharines, Metz and Mesrobian have published a report of similar experiments (22); they were, however, unable to achieve satisfactory oxidation of polystyrene itself. Similar studies have also been described by Hahn and Lechtenböhmer (9). In neither case were measurements of Huggins' k' reported.

In this paper the preparation of the graft polymers is described and evidence that grafting did, in fact, occur is presented and discussed. Finally, measurements of intrinsic viscosity and Huggins' k' are given for the graft polymers and for their fractions.

Other more direct evidence for grafting, based on viscosity and light-scattering measurements, will be given elsewhere (19).

EXPERIMENTAL

1. Materials

Monomers were provided by the Polymer Corporation, Limited, Sarnia. Before use they were freed of inhibitor by washing with dilute aqueous potassium hydroxide, rinsed

Can. J. Chem. Downloaded from www.nrcresearchpress.com by 200.7.193.243 on 09/04/12
For personal use only.

with distilled water, and dried with Drierite. Cumene hydroperoxide (60%) was also provided by the Polymer Corporation. Phenyl-β-naphthylamine and benzoyl peroxide were both practical grade reagents supplied by the Eastman Kodak Company.

Polystyrene samples used for oxidation were prepared by a method described earlier (18); copolymers of styrene and 4-vinylcyclohexene-1 were prepared according to a similar recipe.

Tetralin, of Certified Chemical grade, was obtained from the British Drug Houses. Other solvents were of technical grade, and were used without further purification.

Inorganic reagents were of Analar grade, supplied by the British Drug Houses, or of equivalent quality. Nitrogen was purified by passing it first through Fieser's solution (8, p. 395) and then through a saturated solution of lead acetate.

2. Oxidations

Solutions of the backbone polymers in tetralin were oxidized at temperatures within the range 70° to 80° C.—usually at 75(±0.2)° C.— by passing oxygen through a sintered-glass bubbling tube in the solution at a rate sufficient to bring about rapid and thorough bubbling without excessive foaming. (No attempt was made to purify the oxygen or to regulate its flow precisely.)

Suitable concentrations ranged from 2 g./dl. for a high-molecular-weight polymer to 5 g./dl. for a low-molecular-weight one. In general, the oxidation was more successful with the lower-molecular-weight polymers.

After bubbling had been continued for a time estimated to correspond to the degree of oxidation desired the product was precipitated in methanol or ethanol. In order to remove tetralin (and its hydroperoxide), the gummy precipitate was reprecipitated several times from a solution in butanone before drying under reduced pressure at 45° C. to constant weight. The addition of Dry Ice to either the solution or the precipitant was found to help in obtaining a porous, easily dried material. Tests showed that with repeated precipitation the observed hydroperoxide content for the precipitated and reprecipitated polymers decreased rapidly at first, but then leveled off to an approximately constant value when a clear, porous product, free from the odor of tetralin, had been obtained.

3. Analysis for Hydroperoxide Content

Determination of the peroxide or hydroperoxide content of a high polymer is difficult (2, 27). Although iodometric methods should give values closer to absolute ones than do methods using ferrous ion, the most consistently reproducible results were obtained using the spectrophotometric procedure, based on the oxidation of ferrous ion, which was developed by Laitinen and Nelson (17). Provided that freshly prepared solutions were used, and that a calibration had been made recently, results for various samples of the same polymer were reproducible to within ±10% in most runs (or, at worst, to within ±20%).

In order to see whether or not the spectrophotometric method gave reliable absolute values for hydroperoxide content, the purity of a sample of 60% cumene hydroperoxide was determined. The average value, a mean of 13 determinations, was 108(±11)%, as compared to an average value of 62(±1)% obtained by means of a conventional iodometric titration (27, p. 53). Although cumene hydroperoxide is not necessarily a valid standard for the analysis of a high polymer, its structure is similar to that of the polymeric hydroperoxide. It is possible, then, that the values of hydroperoxide content found for the polymers studied are somewhat high.

In this paper hydroperoxide content is expressed as a "hydroperoxide number": the number of hydroperoxide groups per thousand monomeric styrene units.

Can. J. Chem. Downloaded from www.nrcresearchpress.com by 200.7.193.243 on 09/04/12
For personal use only.

4. Graft Polymerizations

Graft polymers were prepared in emulsion at 35(±0.2)° C. A typical recipe follows:

Oxidized polymer (in this example, one with a hydroperoxide number of 10)	2.0 g.
Monomer	15.0 g.
Soap flakes	5.0 g.
Water	90.0 g.
Potassium pyrophosphate	2.2 g.
Ferrous ammonium sulphate (hexahydrate)	0.2 g.

Thus, with 2.0 g. of a polymer of hydroperoxide number 10, the amounts of pyrophosphate and ferrous salts listed above were used; with a polymer of higher hydroperoxide content, proportionately larger amounts of the salts were used. If more than 15 ml. of styrene was required to dissolve the backbone polymer, proportionately more soap and water were used.

First, the backbone polymer was allowed to stand with enough styrene to effect solution. Then the required amount of water was divided into two portions—one for a soap solution, and one for a ferrous pyrophosphate solution. Both solutions were prepared by heating to 60° C.

As soon as the polymer had dissolved, the two hot solutions were swept out with purified nitrogen, combined, and placed with the polymer solution in a 250 ml. bottle fitted with a self-sealing cap. After the contents had been swept out again with nitrogen, the bottles were capped and, by means of a syringe, charged with nitrogen at a pressure of 10 to 15 p.s.i. The bottles were shaken vigorously in order to ensure emulsification, placed in a rack held in a constant-temperature bath, and rotated end-over-end at 33 r.p.m.

When desired, aliquot samples were withdrawn by syringe, and the polymer in them precipitated in methanol containing 0.1% hydroquinone; the percentage conversion was determined from the dry weight of the precipitated polymer. When the polymerization was judged to have proceeded to the desired degree of conversion, the contents of the bottles were poured into methanol–hydroquinone solution. After it was aged overnight, the precipitated polymer was washed with hot distilled water, rinsed three times with methanol, and dried at 45° C. under reduced pressure to constant weight.

5. Infrared Spectra

Infrared spectra were determined with a Perkin-Elmer recording spectrophotometer, Model 21. Solutions in chloroform of two graft polymers, GC-211 and GC-220, and of two blanks, GC-320 and GC-321 (prepared just as the graft polymers were, except that unoxidized polystyrene was used in place of oxidized polystyrene), were examined in calcium fluoride cells throughout the range 1200–3800 cm.$^{-1}$. Spectra for films of samples GC-210, GC-220, GC-250, and GC-320 were obtained independently in the laboratories of the Polymer Corporation, Limited.

6. Fractionation

The primary fractionation of a graft polymer was achieved by fractional precipitation, at 45° C., from a solution in butanone or in a butanone–benzene mixture, by the progressive addition of methanol or a methanol–butanone mixture. The fractions taken weighed not more than one-fourth of the original weight of the polymer fractionated, and with each polymer the fractionation was continued until at least three-fourths of the polymer had been precipitated.

After each swollen precipitate had been separated, it was carefully washed with a

Can. J. Chem. Downloaded from www.nrcresearchpress.com by 200.7.193.243 on 09/04/12
For personal use only.

small portion of solvent, and reprecipitated from a solution in butanone. The fibrous product was recovered by filtration, washed with methanol, and dried under reduced pressure at 45° C. to constant weight.

7. Viscosity Measurements

Values of intrinsic viscosity, $[\eta]$, were, unless otherwise noted, determined as described previously (18), by means of the equation of Mead and Fuoss (20):

$$(\ln \eta_r)/c = [\eta] - \beta[\eta]^2 c. \qquad [3]$$

Values of $(\ln t_r)/c$ (where t_r = flow time of solution/flow time of solvent) were determined and plotted against concentration; since Ubbelohde viscometers having negligible kinetic energy corrections were used (7), $(\ln t_r)/c$ is equivalent to $(\ln \eta_r)/c$. Values of k', the slope constant of the Huggins' equation,

$$\eta_{sp}/c = [\eta] + k'[\eta]^2 c, \qquad [4]$$

were computed from the relation $k' + \beta = 0.50$.

RESULTS AND DISCUSSION

1. Oxidations

In Fig. 1 are presented some typical results showing the effect of duration of the period of oxidation on the hydroperoxide content of low-molecular-weight polymers ($0.5 < [\eta]$ in butanone < 0.8). Lengths of the vertical lines represent approximately the error in the determination of hydroperoxide number. Although the points are rather scattered, partly because of variations in the rate of flow of oxygen, the data show that the maximum hydroperoxide content was usually reached after oxidation had proceeded for 8–12 hours.

In order to find out whether degradation had occurred during oxidation, the intrinsic

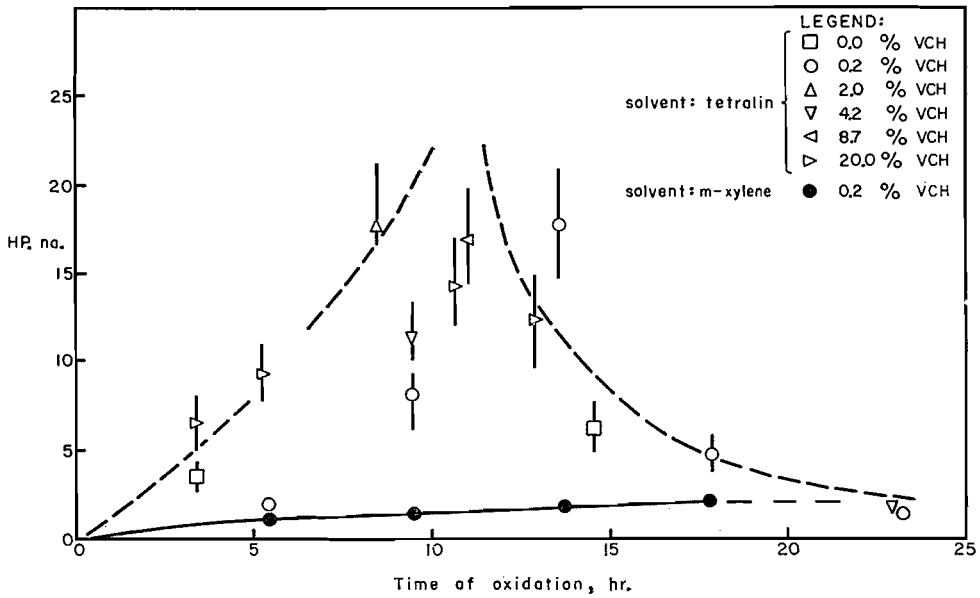

FIG. 1. Dependence of hydroperoxide content on time of oxidation and on 4-vinylcyclohexene-1 (VCH) content.

Can. J. Chem. Downloaded from www.nrcresearchpress.com by 200.7.193.243 on 09/04/12
For personal use only.

Can. J. Chem. Downloaded from www.nrcresearchpress.com by 200.7.193.243 on 09/04/12
For personal use only.

viscosities of several polymers were determined before and after oxidation. No decrease in intrinsic viscosity was observed, and it was concluded that degradation had not occurred.

The data in Fig. 1 confirm the importance of the solvent to the oxidation (22). While relatively high hydroperoxide contents were obtained for polymers oxidized in tetralin (which is itself readily oxidized to its hydroperoxide under the conditions used here), hydroperoxide numbers for polymers oxidized in *m*-xylene were very close to those found for unoxidized polymers.[3]

It is also clear that pure polystyrene is not readily oxidized by molecular oxygen (9); the highest hydroperoxide number obtained was 9, corresponding to a hydroperoxide concentration of about one mole per cent.

In the hope of obtaining higher hydroperoxide numbers, several modifications of the procedure were tried:

1. The use of copolymers of styrene and 4-vinylcyclohexene-1, the oxidation of which should be unaffected by the steric effects encountered with pure polystyrene (22).
2. The use of partially isopropylated polystyrene.
3. The use of catalysts, such as benzoyl peroxide or cumene hydroperoxide.

However, none of these modified procedures gave values of hydroperoxide content greater than 18. Although this value, the highest observed, was obtained with a styrene-vinylcyclohexene copolymer, no correlation was found between hydroperoxide number and vinylcyclohexene content.

2. Evidence for Grafting

(a) Conversion Studies

Proof that the polymeric hydroperoxides initiated the rapid polymerization of styrene was obtained from measurements of the percentage conversion of styrene to polymer as a function of time. Conversion data for a typical graft polymerization, GC-140, are given in Fig. 2; for comparison, data are included for a blank polymerization, GC-141,

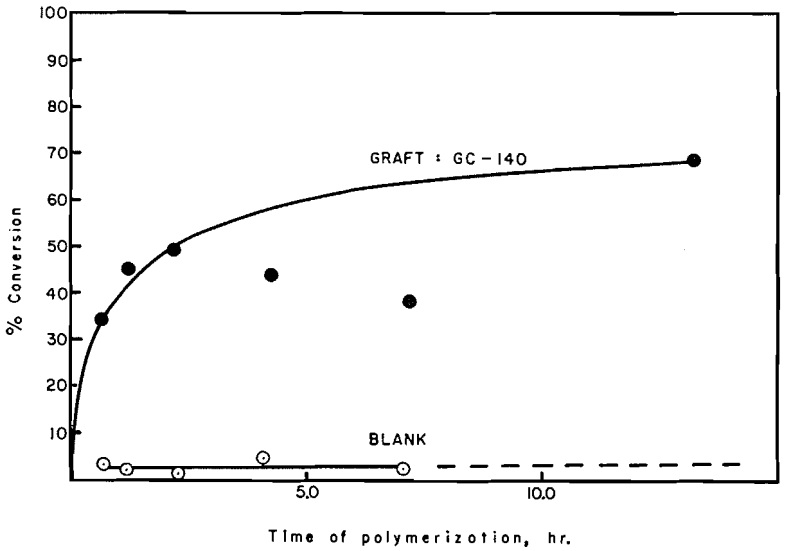

FIG. 2. Dependence of percentage conversion on time for a graft and a blank polymerization. ● Graft. ○ Blank.

[3]*As mentioned above, care was taken to remove residual tetralin from the oxidized polymers.*

a duplicate of GC-140, except for the omission of oxidized polymer from the polymerization recipe. After 1 hour of reaction, only a small amount (<3%) of the initial styrene had been polymerized in the blank, whereas in the same period more than half of the initial styrene in the graft polymerization had been polymerized.

As the polymerization proceeded, the conversion data tended to become scattered, probably because the emulsion had usually broken within the first three hours and it was consequently impossible to take truly representative samples. However, the value of percentage conversion for the total polymer (corresponding to the last point in the curve for GC-140) always fitted in well with values found for aliquot samples taken during the early stages of polymerization.

Further evidence for the initiation of polymerization by the polymeric hydroperoxides is given in Tables I and II, in which are summarized polymerization and conversion data for several series of graft polymers, and for a number of "blank" polymers prepared (with one exception, GC-141) by replacing oxidized polymer with ordinary polymer.

Without exception, a larger proportion—usually a much larger proportion—of the styrene was polymerized with oxidized than with ordinary polymer. (The relatively

TABLE I

VISCOSITY AND CONVERSION DATA FOR GRAFT POLYMERS

Sample	% VCH* in backbone	HP no. of backbone polymer	Weight, g., backbone of polymer	Weight, g., of styrene	Polymerization time, hours	Percentage conversion	[η] in benzene, dl./g. Backbone polymer	[η] in benzene, dl./g. Graft polymer
GC-100	0.8	9.5	1.5	10.2	10.0	50	1.70	7.55
GC-110	10.0	18	0.7	14.0	10.0	50	1.13	4.85
GC-140	8.3	7.7	2.0	22.7	13.5	50	1.20	6.54
GC-161	0.0	1.8	1.0	10.2	—	10	—	—
GC-162	0.0	1.8	1.0	10.2	—	10	—	—
GC-163	0.0	1.8	1.0	10.2	—	10	—	—
GC-180	10.0	1.9	1.0	22.7	8.0	10	0.92†	0.95
GC-190	0.4	3.0	1.0	16.4	11.0	10	0.78	2.96
GC-200	0.2	2.0	1.0	11.4	11.0	10	0.82	3.05
GC-210	20.0	9.0	1.0	13.6	9.0	36	0.85†	5.44
GC-211	20.0	9.0	1.0	15.0	0.5	82	0.85†	6.43
GC-220	10.0	16	1.0	13.6	9.0	38	0.92†	5.08
GC-230	0.4	7.0	1.0	18.2	9.0	40	3.90	6.05
GC-240	0.4	14	1.0	18.2	9.0	40	3.79	6.19
GC-241	0.4	14	1.0	18.2	1.0	13	3.79	4.19
GC-621	0.0	6.6	0.5	9.1	6.0	15	2.23	6.59

4-Vinylcyclohexene-1.
†*Calculated from value in butanone using relationship given in Reference 18.*

TABLE II

VISCOSITY AND CONVERSION DATA FOR BLANK POLYMERS

Sample	Weight, g. Polymer	Weight, g. Styrene	Polymerization time, hours	Percentage conversion	[η] in benzene, dl./g. Backbone polymer	[η] in benzene, dl./g. Product
GC-141*	—	22.7	13.5	2.5	—	3.40
GC-250	1.0	18.2	6.0	2.8	1.58	2.38
GC-320	1.0	9.1	5.0	5.6	0.92	1.03
GC-321	1.0	9.1	5.0	2.2	0.92	1.03
GC-322	1.0	9.1	5.0	2.2	0.92	1.02
GC-323	1.0	9.1	5.0	3.3	0.92	1.02

**This sample was prepared using the same recipe as for GC-140, except that oxidized polymer was omitted.*

Can. J. Chem. Downloaded from www.nrcresearchpress.com by 200.7.193.243 on 09/04/12
For personal use only.

low conversions in polymerizations GC-161 to GC-200 may be due to the low hydroperoxide content of the backbone polymers used in these runs, but, in general, no close relationship between percentage conversion and hydroperoxide content is evident.) These data also indicate no correlation between the vinylcyclohexene content of the backbone polymer and the percentage conversion.

(*b*) *Disappearance of Hydroperoxide Groups*

The evidence just cited indicates that, under the conditions of our grafting experiments, the formation of polymer is initiated by the hydroperoxide groups in the parent (or backbone) polymer. Other evidence of this was obtained from measurements of hydroperoxide content before and after polymerization. Results of such measurements are assembled in Table III. The formation of new polymer in the presence of the parent

TABLE III

DECREASE IN HYDROPEROXIDE CONTENT DURING GRAFTING

Sample	HP no. of backbone polymer	HP no. of graft polymer	
		Calculated*	Observed
GC-100	9.5	2.5	(2.0)†
GC-110	18.4	3.7	0.60
GC-140	7.7	1.4	0.33
GC-180	1.9	0.97	0.86
GC-190	3.0	1.5	1.1
GC-200	2.0	1.2	0.77
GC-210	9.0	2.4	0.57
GC-211	9.0	1.1	0.97
GC-220	16.0	3.4	0.64
GC-230	7.0	1.7	0.27
GC-240	14.0	2.6	0.42
GC-241	14.0	4.4	(3.6)†

**Calculated on the assumption that none of the polymeric hydroperoxide groups disappear during polymerization.*

†Appears to be anomalous.

polymer must yield a product whose hydroperoxide number (the number of hydroperoxide groups per thousand monomer units) is less than that of the parent polymer. This would be true regardless of whether or not the new polymer is attached to the old. If none of the hydroperoxide groups on the backbone chain were used up in initiating new polymer growth, the hydroperoxide number of the product would still be less because the number of monomer units in the polymer would be increased. In column 3 are listed the values of hydroperoxide number calculated on the assumption that the decrease is merely due to this "dilution" effect;[4] in column 4 are the values actually observed. Even after allowance is made for the rather imprecise results obtained in these analyses, it is clear that hydroperoxide groups do disappear in these graft polymerizations. The precautions taken to remove residual tetralin hydroperoxide were such that at worst the contribution of tetralin hydroperoxide to the hydroperoxide number of the backbone

[4]*The following expression was used for the calculation:*

$$\frac{\text{wt.}_{bb} \times \text{hydroperoxide no.}_{bb} + \text{wt.}_{ps} \times 0.50}{\text{wt. graft polymer}}$$

where the subscripts bb *and* ps *refer to backbone polymer and polymerized styrene, respectively. For convenience, it is assumed that the hydroperoxide number of the polymerized styrene is 0.50, a reasonable value slightly lower than the average of 0.55 found for the blanks GC-320, GC-321, GC-322, and GC-323; choice of an even lower value would not affect the conclusions.*

Can. J. Chem. Downloaded from www.nrcresearchpress.com by 200.7.193.243 on 09/04/12
For personal use only.

polymer would be less than 1. The polymerization must, therefore, have occurred mainly at the polymeric hydroperoxide sites.

(*c*) *Absence of Side Reactions*

So far in this discussion it has been assumed that in the presence of an excess of monomer a polymeric hydroperoxide group disappears by the series of reactions outlined in equations [1] and [2], rather than by such polar or radical side reactions as the following:

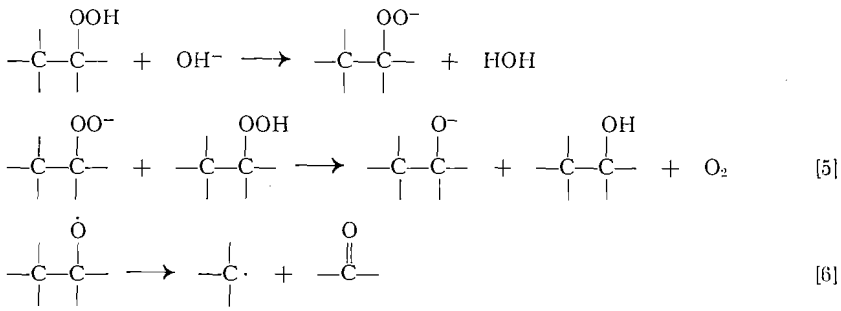

[5]

[6]

The occurrence of reactions represented by equations [5] and [6] would result in the disappearance of hydroperoxide groups, and, in the case of the free-radical reaction, in the formation of free radicals that would initiate the formation of linear polymer. Experimental evidence for the occurrence of these side reactions was sought, but in vain.

That a polar decomposition induced by the alkaline nature of the emulsion did not occur was demonstrated in the following way. Emulsions of two different polymeric hydroperoxides were prepared, following the recipe for graft polymerizations in all respects except that the ferrous salt was omitted, and these emulsions were rotated in the constant-temperature bath for 1.5 hours and 1.0 hour, respectively—times sufficient in a graft polymerization for the conversion of most of the monomer to polymer. The resulting change in hydroperoxide number was negligible: from 4.9 to 4.6 and from 5.2 to 5.6, respectively. It was concluded that the polymeric hydroperoxides used in this study were stable at the pH existing in the emulsions.

The reaction represented by equation [6] would result in the formation of terminal carbonyl groups. The infrared spectra for graft polymers GC-211 and GC-220 and for blanks GC-320 and GC-321 were carefully examined for the presence of absorption peaks corresponding to the absorption frequency of the carbonyl group (in the range 1720–1730 $cm.^{-1}$). Although the carbonyl group is detectable at low concentrations (23), no such peaks were found. The spectra for the graft polymers were in fact identical in this range with those for the blanks. These findings were confirmed by examination of the spectra for films prepared from the graft polymers GC-210 and GC-220, and from blanks GC-250 and GC-320.

These findings, though negative, constitute additional justification for our assumption that, under the conditions of our grafting experiments, hydroperoxide radicals on the parent polymer molecules initiate the growth of polymer branches.

(*d*) *Fractionation Behavior*

Finally, it should be pointed out that the fractionation behavior of the graft polymers also indicates that grafting has occurred. In carrying out a primary fractionation of linear polystyrene, it is relatively easy to control the number and size of the fractions. With the graft polymers, however, this was very difficult; once precipitation began, a very slight excess of non-solvent tended to bring down all or most of the polymer. This

Can. J. Chem. Downloaded from www.nrcresearchpress.com by 200.7.193.243 on 09/04/12
For personal use only.

is the behavior to be expected if the polymer molecules are all large and branched (as they would be if the polymer chains formed were all attached to a pre-existing backbone chain). It is not the behavior to be expected if the new polymer chains were independent molecules, for then there would be the usual wide distribution of molecular weights, and the usual wide differences in solubility.

All of this evidence is consistent with only one conclusion: that in the polymerizations described in this paper grafting had occurred, that is, branched polystyrene molecules had been formed by the growth of polystyrene chains onto a polystyrene backbone chain.

3. Viscosity Results

If every, or almost every, hydroperoxide group in the backbone polymer became a point of attachment for a branch, the graft polymer molecules must have been fairly extensively branched. For example, molecules of the backbone polymer for the graft polymer GC-210 (Table I) contained, on the average, nine hydroperoxide groups per 1000 monomer units, and hence an average molecule of the graft polymer may have had as many as nine branches per 1000 monomeric units in the backbone chain (i.e., $9 \times DP/1000$ branches, where DP is the degree of polymerization of the parent polymer).

It was expected, therefore, that Huggins' k' would have higher values for the graft polymers than for linear polystyrene. The experimental values did not, however, show this difference. In the (unfractionated) graft polymers they fell within the range characteristic of linear polystyrene (0.39–0.44 in butanone, 0.37–0.39 in benzene), and the averages of the values obtained with fractions also fell within these ranges (see Reference 19, Table IV).

Evidently k' is not measurably affected by the branching present in these polymers. This was an unexpected finding. Even a very little (i.e., 0.01%) divinylbenzene copolymerized with styrene was found to produce sufficient non-linearity in the polymer to increase k' appreciably (6, 19). Indeed, a great deal of evidence has been accumulated for many different polymers showing that non-linearity in polymers leads to high values of k'.

A careful re-examination of this evidence discloses, however, that when these increases have been observed the non-linearity of the polymer was due either to a small degree of cross-linking or to branching resulting from reactions which could have led (and probably had led) to branches that were themselves branched. Schaefgen and Flory (24) have indeed reported a very slight increase in k' for a branched condensation polymer prepared in such a way as to preclude branched branches, but in view of the errors involved in the determination of k' it is questionable whether the increase observed (average value of k' for linear polymer, 0.36, for polymer with eight branches, 0.38) is significant.

On the basis of the evidence now available, it may be concluded that k' is affected more by bushy branching than by simple branching. Indeed, it may well be that measurements of k' could afford a means of distinguishing between different types of branching.

This conclusion seems to be reasonable, for k' is a function of the segment density in the molecular coil (4), and at the same temperature and in the same solvent, the segment density for a molecule consisting of a backbone carrying a few long branches should be significantly less than that for a bushy molecule, and probably little different from that for a linear molecule of the same weight.

It would seem, then, that what affects k' is not branching per se but branching of such a type and to such a degree that the segment density in the molecular coil is significantly altered. Multiple branching (either of the bushy type or of the loose network type) is the kind most likely to increase the segment density. But if the considerable degree

Can. J. Chem. Downloaded from www.nrcresearchpress.com by 200.7.193.243 on 09/04/12
For personal use only.

of linear branching characteristic of our graft polymers does not affect k', it is to be expected that a small degree of multiple branching will not affect it. It is probably for this reason that, to cite two examples, Cragg and Brown (5) found k' to be normal for low-conversion GR-S, and Hobbs *et al.* (11, 12) found that a high-molecular-weight sample of polyvinyl acetate known to be branched (and probably with bushy branches) gave normal k' values.[5]

ACKNOWLEDGMENTS

We wish to acknowledge with thanks assistance given at various times by Mrs. D. Coleman, Mr. J. Hunt, Mr. L. Murrell, and Mr. D. M. Wiles. We are indebted to Mr. G. Perry for infrared measurements, and to Dr. H. L. Williams of the Polymer Corporation, Limited, for helpful discussions; we are also grateful to the Polymer Corporation, Limited, which provided many materials and help with infrared measurements.

REFERENCES

1. ALFREY, T. and BANDEL, D. Paper presented at the 118th meeting of the American Chemical Society, Chicago, Ill., Sept., 1950.
2. BARNARD, D. and HARGRAVE, K. Anal. Chim. Acta, **5**, 476 (1951).
3. CARLIN, R. B. and HUFFORD, D. L. J. Am. Chem. Soc. **72**, 4200 (1950).
4. CRAGG, L. H. and BIGELOW, C. C. J. Polymer Sci. **15**, 177 (1955).
5. CRAGG, L. H. and BROWN, A. T. Can. J. Chem. **30**, 1033 (1952).
6. CRAGG, L. H. and MANSON, J. A. J. Polymer Sci. **9**, 265 (1952).
7. CRAIG, A. W. and HENDERSON, D. J. Polymer Sci. **19**, 215 (1956).
8. FIESER, L. Experiments in organic chemistry. 2nd ed. D. C. Heath and Co., New York. 1941.
9. HAHN, W. and LECHTENBÖHMER, H. Makromol. Chem. **16**, 50 (1955).
10. HENDERSON, D. E. and LEGGE, N. R. Can. J. Research, B, **27**, 666 (1949).
11. HOBBS, L. M., KOTHARI, S. C., LONG, V. C., and SUTARIA, G. C. J. Polymer Sci. **22**, 123 (1956).
12. HOBBS, L. M., MANSON, J. A., and GURVITCH, M. Manuscript in preparation, University of Michigan, Ann Arbor, Mich. 1957.
13. HOUTZ, R. C. and ADKINS, H. J. Am. Chem. Soc. **55**, 1609 (1933).
14. HUGGINS, M. L. J. Am. Chem. Soc. **64**, 2716 (1942).
15. JONES, M. H. Paper presented at the 6th Canadian High Polymer Forum, St. Catharines, Ont., April, 1955; Can. J. Chem. **34**, 948, 1027 (1956).
16. JONES, M. H., MELVILLE, H. W., and ROBERTSON, W. A. P. Nature, **174**, 78 (1954).
17. LAITINEN, H. A. and NELSON, J. S. Ind. Eng. Chem., Anal. Ed. **18**, 422 (1946).
18. MANSON, J. A. and CRAGG, L. H. Can. J. Chem. **30**, 482 (1952).
19. MANSON, J. A. and CRAGG, L. H. To be published.
20. MEAD, D. and FUOSS, R. M. J. Am. Chem. Soc. **64**, 277 (1942).
21. MESROBIAN, R. B. and MARK, H. Paper presented at the 122nd meeting of the American Chemical Society, Atlantic City, N.J., Sept., 1952; see also Textile J. **23**, 294 (1953).
22. METZ, D. J. and MESROBIAN, R. B. J. Polymer Sci. **16**, 345 (1955).
23. PFANN, H. F., WILLIAMS, V. Z., and MARK, H. J. Polymer Sci. **1**, 14 (1946).
24. SCHAEFGEN, J. R. and FLORY, P. J. J. Am. Chem. Soc. **70**, 2709 (1948).
25. SPEISER, R. and WHITTENBERGER, R. T. J. Chem. Phys. **13**, 349 (1945).
26. STOCKMAYER, W. H. and FIXMAN, M. Ann. N.Y. Acad. Sci. **57**, 334 (1953).
27. TOBOLSKY, A. V. and MESROBIAN, R. B. Organic peroxides, their chemistry, decomposition, and role in polymerization. Interscience Publishers, Inc., New York. 1954.
28. WALKER, O. J. and WINKLER, C. A. Can. J. Research, B, **28**, 298 (1950).
29. ZIMM, B. H. and STOCKMAYER, W. H. J. Chem. Phys. **17**, 1301 (1949).

[5]*It has recently been reported (11) that branching may be detected, by a change in the slope of η_{sp}/c vs. c curves, when the change in k' is too small to be detected with certainty. When this method was applied to our graft polymers, an increase in slopes (over that obtained with linear polystyrene of the same intrinsic viscosity) was noted in the curves obtained with benzene solutions but not in those obtained with butanone solutions.*

Can. J. Chem. Downloaded from www.nrcresearchpress.com by 200.7.193.243 on 09/04/12
For personal use only.

Can. J. Chem. Downloaded from www.nrcresearchpress.com by 200.7.193.243 on 09/04/12
For personal use only.

LIGHT-ABSORPTION STUDIES

PART X. ULTRAVIOLET SPECTRA IN ACID AND BASIC MEDIA—SOME FURTHER OBSERVATIONS ON THE ORTHO EFFECT[1]

W. F. Forbes, Audrey S. Ralph, and
(in part) Rosemarie Gosine

ABSTRACT

The spectra of acetophenones and related compounds are obtained in acid and basic solution and are compared with previously reported spectra of substituted benzene derivatives. Evidence is adduced that the B-bands, not only in neutral solution, but also in acid or basic solution, are determined primarily by steric and mesomeric interactions.

Following previous work, the main cause of the ortho effect in the B-band of electronic spectra is ascribed to steric interactions between the vicinal substituents, and in this way, steric interactions explain the frequent similarity in the spectra of meta and ortho isomers. Other factors also play a part, and one of these, a short-range interaction between the substituent and the benzene ring, is discussed.

INTRODUCTION

In Part III (1) of this series it was stated that the B-band of orthodisubstituted benzene derivatives in neutral solution would be approximately the same as the B-band of para isomers, except for steric inhibition of resonance. This statement was based on the assumption that in the B-band the so-called mesomeric (resonance) interactions are of greater importance than inductive-type interactions. The effects of mesomeric interaction in spectra were also developed in previous papers (2, 3, 4).

The purpose of the present communication is to extend these hypotheses to spectra in acid and alkaline solution. The spectra under these conditions frequently exhibit pronounced similarity for the ortho and meta isomers. This has been noted by Doub and Vandenbelt (5), and has also received a quantum-mechanical interpretation by Förster (6). The latter interpretation, however, is inadequate for many of the compounds under investigation. It will be shown that an equally satisfactory explanation can be obtained by assuming approximate identity of the resonance interactions in ortho and para isomers in the absence of steric and other interfering interactions. The similarity of the spectra of ortho and meta isomers may then be related to the observation that frequently both spectra resemble that of one of the monosubstituted parent compounds. In this way, the frequently observed identity in monosubstituted parent compounds and ortho and meta isomers is explained, since in the meta isomer no interaction between the two substituents occurs because of the absence of suitable resonance forms; in the ortho isomer such resonance interaction is prevented because of steric interaction between the vicinal substituents.

ULTRAVIOLET ABSORPTION SPECTRA IN ACID AND BASIC MEDIA

Table I shows spectra of benzene derivatives in acid and basic media compared with the same spectra in neutral, aqueous solution. Both B- and C-bands are listed but the discussion will be limited to B-bands. This follows, because although B- and C-bands both provide a potential measure of interaction between two or more substituents in benzene derivatives, the C-band is dependent on the B-band (3) and hence less easily related

[1]*Manuscript received December 23, 1957.*
Contribution from the Memorial University of Newfoundland, St. John's, Newfoundland. This paper was presented at the New York meeting of the American Chemical Society in September, 1957.

directly to electronic interactions. The limited data available in Table I listing both B- and C-bands confirm the suggestion made in Part VIII (3) that both bands are of similar character, since comparable wavelength displacements are again observed on changing the hydrogen-ion concentration of the solvent.

TABLE I

EFFECT OF ACIDITY AND BASICITY ON SPECTRA OF BENZENE DERIVATIVES
(Values in italics represent inflections in this and subsequent tables.)

Compound	Neutral solvent		Acid (0.1 *N* HCl) solvent		Base (*N* NaOH) solvent	
	λ_{max}, mμ	ϵ_{max}	λ_{max}, mμ	ϵ_{max}	λ_{max}, mμ	ϵ_{max}
Toluene (B-band)	206	6000	206	6500		
Toluene (C-band)	260	300	260	290	260	280
Diphenyl	247	16600	247	16600	247	17700
Acetophenone (B-band)	244	12000	244	12000	244	11500
Acetophenone (C-band)	276–278	1250	277	1250	277	1250
Benzaldehyde (B-band)	248	12000	249	13500	248	10000
Benzaldehyde (C-band)	279	1400	280	1500	*279*	*1200*
Nitrobenzene	266	7800	266	7800	266	6900
Benzoic acid (B-band)	226	9500	229.5	11500	223.5	9000
Benzoic acid (C-band)	270.5	850	272	1000	267	600
Phenol (B-band)	210	6000	210	6000	234	10500
Phenol (C-band)	268	1500	268	1600	285	2700
Anisole (B-band)	217	4300	217	4900	221	3600
Anisole (C-band)	*ca.261* 267 273	*1200* 1600 1300	267 272	1700 1400	267 273	1700 1400
Aniline (B-band)	230	8000	203	7500	230	8400
Aniline (C-band)	278	1400	253	170	279	1400
p-Nitrobenzoic acid	271	10000	263.5	12500	272	10600
m-Nitrobenzoic acid	265	7000	261	7100	266	7350
o-Nitrobenzoic acid	*ca.*266	5300	*ca.*262.5	5500	267	5500
p-Aminoacetophenone	308-309	16500	*ca.*260	6000	308–309	11000
m-Aminoacetophenone	*ca.*255	3500	238	12000	*ca.*255	3500
p-Hydroxybenzoic acid*	251	12500	255	13900	280	16300
m-Hydroxybenzoic acid*	*232*	*6400*	236.5	7500	*245*	*7000*
p-Nitrophenol	313–314	9500	317.5	10000*	402.5	19200*
m-Nitrophenol	272	6000	273.5	6000*	291	4500*
p-Nitroaniline	373–377	13000	372	5600*	373–379	13000
m-Nitroaniline	278–279	4500	256	7500	278–279	4650

**See Table III and Refs. 5 and 7.*

In discussing these spectra it should first be noted that numerous "exceptional" changes occur. These exceptions may be defined as effects where the acidity or basicity causes a fundamental change in the molecular entity. Thus, the removal from the conjugated system of the unshared electron pair in the amino group by the addition of acid, and the presence of base replacing either the OH group by an ONa group or the COOH by a COONa group, represent examples of this type of change.

Similarly, the effect of acid on benzoic acid spectra is to cause a change in the molecular species present, since the equilibrium

$$C_6H_5COOH \text{ hydrate} + H_2O \rightleftharpoons C_6H_5COO^- \text{ hydrate} + H_3O^+$$

will occur in aqueous solution (cf. 8), whereas in acid media the benzoate-ion concentration will be negligible. An analogous difficulty arises in the study of benzoic acid spectra in sulphuric acid, where again the molecular entities are altered to give rise to completely ionized acids $R.CO_2H_2^+$ (cf. 9). Likewise, the actual molecular species of carbonyl compounds in concentrated sulphuric acid will be predominantly $>C{=}OH^+$, again different

Can. J. Chem. Downloaded from www.nrcresearchpress.com by 200.7.193.243 on 09/04/12
For personal use only.

Can. J. Chem. Downloaded from www.nrcresearchpress.com by 200.7.193.243 on 09/04/12
For personal use only.

from the species present in neutral solution (cf. 10). Since, when the acidity of the solvent is changed, some changes in the molecular species occur almost invariably, it is difficult to determine the effect of acidity on a single molecular species.

On the other hand, it seems incorrect to neglect completely the effects of acid or base, *qua* acid or base (for instance, the effect of a changed dielectric constant), on absorption curves of a single molecular entity. That is, although the presence of a proton, for example, may lead to a complete change in the electronic structure of the molecule, sometimes this addition will merely cause a small change in the coulomb or resonance integral of the relevant atoms. This appears to be borne out by the observation of Nagakura *et al.* (10) that absorption curves of acetone in sulphuric acid media at higher acid concentrations do not cross at the isosbestic point.

This inherent effect of acid or base, apart from the frequent ability of acid or base to change the molecular species present, usually represents a *minor* effect in electronic absorption spectra. This is illustrated in Table I by a number of spectra. For instance, the addition of dilute acid or base to aqueous solutions of diphenyl, benzaldehyde, acetophenone, or nitrobenzene, or the addition of dilute acid to aqueous solutions of phenol, does not, apparently, alter the characteristic spectra to any appreciable extent. A slight change, which is evident in Table I for the above-mentioned compounds, is a small variation in the absorption intensity as measured by the molecular extinction coefficients (ϵ). These ϵ values may show either an increase or a decrease. This change, in turn, may be related to small changes in the force constants of the central linkages, a change which has previously been shown (11) to give rise mainly to intensity changes.

Further, there appears to be some evidence that this effect is transmitted preferentially across the ends of a conjugated system particularly if mesomeric or resonance interaction is appreciable. Then this interaction may cause appreciable spectral changes. For example, the spectra of *p*-aminoacetophenone, *p*-hydroxybenzoic acid, and *p*-nitrophenol, when the pH is changed, are altered to a greater extent and differently than the spectrum of either of the two monosubstituted parent compounds with similar pH changes. A similar enhanced effect is not always observed for the corresponding meta isomers (see Table I), and it may also be noted from Lemon's data (12) that spectral changes due to alkalinity in the B-band are much more pronounced in the para isomer of *p*-hydroxybenzaldehyde than in the ortho or meta isomers.

STERIC EFFECTS IN ACID AND BASIC MEDIA

A number of spectra in sulphuric acid media have already been determined (see Part VIII (3), Table II), and it was then noted that in this medium a bathochromic shift is generally observed in both B- and C-bands, compared with the spectra in neutral solution. Such a bathochromic shift would be anticipated on theoretical grounds, since generally the more ready formation of dipolar forms, because of the greater polarity of the solvent, would be more important in the electronic excited state than in the ground state.

The sulphuric acid data also indicate that the steric effect of ortho substituents in the B-band is apparently more pronounced in acidic than in neutral solution. For example, *o*-methylbenzaldehyde compared with *p*-methylbenzaldehyde in hexane solution does not show a wavelength shift in the B-band and the intensity ratio is 0.87, while in sulphuric acid solution for the same pairs of compounds a wavelength shift of 15 mμ is observed and the intensity ratio is 0.74 (3). For *o*-methyl- and *p*-methyl-acetophenone in ethanolic solution the wavelength shift for the B-band is 10 mμ, whereas in sulphuric acid solution the wavelength shift is 16 mμ. For *o*-chloro- and *p*-chloro-benzoic acid in ethanolic

solution the wavelength shift in the B-band is 5 mμ (3), whereas in dilute acid solution the wavelength shift is 12 mμ (7). These and other examples may be rationalized by supposing that the increased polarity of the solvent will often tend to keep the molecule planar, and incidentally will more effectively dislodge a less firmly held substituent in the ortho position. In this way a methyl substituent, for example in *o*-methylacetophenone, which is held in the plane of π–π conjugation by π–σ interaction, is more readily bent in sulphuric acid solution than in ethanolic solution, presumably because π–σ conjugation, compared with π–π interaction, is less effectively strengthened by the increased polarity.

This explanation shows why steric inhibition of resonance is frequently apparently more enhanced in acid media. An additional, not unrelated, effect may also be noted. If inhibition of resonance is often more at the expense of the weaker electronic interaction, the spectra of orthodisubstituted compounds in acid media would frequently be expected to resemble that of one of the monosubstituted parent compounds. In other words, steric interactions in acid solution are more likely to cause steric effects in which conjugation is sufficiently inhibited for the molecule to absorb as two distinct entities.

Further, it may be deduced from this hypothesis that ortho and meta isomers almost invariably afford similar spectra, particularly in acid or basic media. This important observation has already been noted, and has been extremely well documented by Doub and Vandenbelt (5). On the basis of simple resonance theory and our general theory of steric inhibition of resonance (1) this ortho–meta similarity may be rationalized. This follows because in meta isomers primary resonance (mesomeric) interaction is ruled out; in ortho isomers, this same mesomeric interaction is often also ruled out because of steric interaction between the two vicinal atoms or groups (see previous paragraph). Since the B- and C-bands are determined primarily by steric and mesomeric interactions, ortho and meta isomers would be expected to be similar and an enhanced similarity would be anticipated in acid and basic media. This is in fact observed. A corollary of this hypothesis would be that for such examples of ortho–meta similarity both spectra should also resemble the spectrum of one of the monosubstituted parent compounds, except that the second substituent may exert a secondary short-range effect of the type mentioned in a previous paper (11). Some relevant examples are collected in Table II, which lists spectra of ortho- and meta-disubstituted compounds together with suitable reference compounds, and also records the wavelength displacements due to the above-mentioned short-range interaction. This latter interaction will be discussed again in the next section.

The examples chosen in Table II represent groups of spectra determined under similar conditions whenever possible. Quite frequently, however, the values in a particular group represent data obtained by different workers using a variety of instruments. Even then, the data not only show a pronounced similarity in the ortho and meta isomers, but frequently also show a similarity for the above-mentioned short-range interaction. Thus, for example, in six different hydroxysubstituted compounds the wavelength shift due to the OH group is 7 ± 1.5 mμ. Likewise, for six different methylsubstituted compounds the shift due to the methyl group is 5.5 ± 1.5 mμ (see Table II). The value for the methyl group may also be compared with the well-known observation that a methyl group usually gives rise to a bathochromic shift of about 5 mμ in a variety of ethylenic systems (14). Similar sets of values may also be obtained for other substituents, for example the values for chlorine in Table II, but for many substituents the agreement is not good, particularly if the substituent is large. Some of these data will be discussed separately elsewhere (15).

In determining the wavelength shift, because of the additional effect of the secondary substituent, the meta isomer has been used, since in the ortho isomer intramolecular

Can. J. Chem. Downloaded from www.nrcresearchpress.com by 200.7.193.243 on 09/04/12
For personal use only.

TABLE II

ABSORPTION SPECTRA OF SOME DISUBSTITUTED BENZENE DERIVATIVES AND OF THE CORRESPONDING MONOSUBSTITUTED REFERENCE COMPOUNDS

Compound	Solvent	B-band λ_{max}, mμ	B-band ϵ_{max}	Wavelength shift (disubstituted–monosubstituted) due to second substituent (in brackets), mμ
o-Methylbenzonitrile*	H_2O	228.5	11100	
m-Methylbenzonitrile*	H_2O	229.5	11000	5.5 (Me-)
Benzonitrile†	H_2O	224	13000	
o-Nitrotoluene*	H_2O	266	5300	
m-Nitrotoluene*	H_2O	273	7300	4.5 (Me-)
Nitrobenzene†	H_2O	268.5	7800	
o-Xylene*	H_2O	*210*	*8300*	
m-Xylene*	H_2O	*212*	*7200*	6 (Me-)
Toluene§	H_2O	206	6000	
o-Toluic acid‡	95% Ethanol	228	5000	
m-Toluic acid§	95% Ethanol	232	9000	6 (Me-)
Benzoic acid§	H_2O	226	9500	
o-Methylacetophenone§	Conc. H_2SO_4	293	14000	
m-Methylacetophenone§	Conc. H_2SO_4	300	21000	7 (Me-)
Acetophenone§	Conc. H_2SO_4	293	20000	
o-Toluic acid§	Conc. H_2SO_4	264	16000	
m-Toluic acid§	Conc. H_2SO_4	265	16400	5 (Me-)
Benzoic acid§	Conc. H_2SO_4	260	15500	
o-Chlorobenzoic acid*	pH 3	229	5900	
m-Chlorobenzoic acid*	pH 3	231.5	9100	2 (Cl-)
Benzoic acid§	0.1 *N* HCl	229.5	11500	
o-Chlorobenzoic acid*	0.1 *N* NaOH	Indistinct band		
m-Chlorobenzoic acid*	0.1 *N* NaOH	*228*	*6900*	4.5 (Cl-)
Benzoic acid§	*N* NaOH	223.5	9000	
o-Chloronitrobenzene*	H_2O	260	4000	
m-Chloronitrobenzene*	H_2O	264	7100	-4.5 (Cl-)
Nitrobenzene†	H_2O	268.5	7800	
o-Chloroacetophenone‡	H_2O	243	6200	
m-Chloroacetophenone‡	H_2O	245	10600	1 (Cl-)
Acetophenone§	H_2O	244	12000	
o-Chlorobenzaldehyde‡	H_2O	253	10000	
m-Chlorobenzaldehyde‡	H_2O	248.5	10800	0.5 (Cl-)
Benzaldehyde§	H_2O	248	12000	
Salicylic acid*	pH 3	237	9000	
m-Hydrobenzoic acid*	pH 3	236.5	7500	7 (OH-)
Benzoic acid§	0.1 *N* HCl	229.5	11500	
Salicylic acid*	pH 9	230.5	7200	
m-Hydroxybenzoic acid*	pH 9	*232.5*	*6400*	8.5 (OH-)
Benzoic acid§	*N* NaOH	223.5	9000	
o-Hydroxyacetophenone*	0.1 *N* HCl	252.5	10900	
m-Hydroxyacetophenone*	0.1 *N* HCl	250.5	9100	6.5 (OH-)
Acetophenone§	0.1 *N* HCl	244	12000	
o-Hydroxybenzaldehyde*	0.1 *N* HCl	256	12600	
m-Hydroxybenzaldehyde*	0.1 *N* HCl	254.5	10100	5.5 (OH-)
Benzaldehyde§	0.1 *N* HCl	249	13500	
o-Nitrophenol*	pH 3	278.5	6600	
m-Nitrophenol*	pH 3	273.5	6000	7.5 (OH-)
Nitrobenzene§	0.1 *N* HCl	266	7800	
o-Dihydroxybenzene*	pH 3	*214*	*6300*	
m-Dihydroxybenzene*	pH 3	*216*	*6800*	6 (OH-)
Phenol§	0.1 *N* HCl	210	6000	

*Ref. 5. †Ref. 7. ‡Ref. 13. §This series of papers.

Can. J. Chem. Downloaded from www.nrcresearchpress.com by 200.7.193.243 on 09/04/12
For personal use only.

hydrogen bonding, field or inductive effects, and steric effects on the primary substituent are likely to affect the absorption. An illustration of the effect of intramolecular hydrogen bonding may be provided by the spectrum of *o*-nitrophenol, which on the basis of infrared measurements (16) is believed to exist in the hydrogen-bonded form. Steric effects on the primary substituent may be assumed to occur when both ortho substituents are large. In this way, *two* steric interactions between the two vicinal substituents may occur. First, one of the two substituents may remain in the plane of the benzene ring whereas the other is twisted away from this plane. This represents a common type of steric effect as indicated both by the data recorded in the present communication and from infrared data (cf. 17). Secondly, as steric interaction further increases, the coplanarity of *both* substituents with the plane of the benzene ring may be affected. An example of this may be provided by the spectrum of *o*-chloronitrobenzene in Table II. It may be supposed that there the chloro substituent is sufficiently dislodged from the plane of the benzene ring to prevent appreciable resonance interaction between the chlorine atom and the nitro group. At the same time, the nitro group also twists in order to reduce interaction between the two vicinal substituents, and consequently the absorption of *o*-chloronitrobenzene is not that of nitrobenzene but rather that of nitrobenzene sterically hindered.

It should also be noted that the above interactions in ortho isomers may not be entirely steric in origin, since short-range inductive or field effect interactions, for example between the chloro and nitro substitutents, may contribute to the observed effect. The latter type of interaction has previously been briefly discussed for fluoro substituents (18), and may be assumed to play a part in determining spectra. Further, in this section the buttressing effect may be mentioned since it may partly account for some of the anomalous values, for example the hypsochromic shift observed in *m*-chloronitrobenzene compared with nitrobenzene (cf. 19).

THE NATURE OF THE SHORT-RANGE INTERACTION

It was shown in the previous section that sometimes the series, monosubstituted parent compound, ortho- and meta-disubstituted compound, exhibits very similar B-band maximal wavelengths (cf. for example the spectral data of acetophenone and *o*- and *m*-chloroacetophenone in Table II). In others an effect of the second substituent on the benzene ring must first be taken into account before the wavelength values are comparable. This effect has been described as a "short-range" interaction, to distinguish it from interaction which is associated with electron mobility acting along systems of conjugated bonds (mesomeric interaction). This nomenclature is based on the observation that the interaction, in the absence of other factors (see above), appears to be similar in both ortho and meta positions, and, further, the similarity of the spectra apparently still exists even if the ortho isomer is most probably non-planar (cf. for example the spectra of the toluic acids in concentrated sulphuric acid as shown in Table II).

The second point concerning the nature of this interaction is that we consider it to be of minor importance compared with the major interactions (steric and mesomeric effects) determining electronic absorption spectra. This may be deduced from the magnitude of the wavelengths shifts caused by the interactions. For example, whereas the average wavelength displacements, because of the short-range interaction, for the two substituents described in Table II are -Me 5.5 mμ, and -OH 7 mμ, the corresponding wavelength shifts caused by mesomeric interaction (as judged for shifts obtained in the parasubstituted acetophenones) are -Me 12 mμ, and -OH 14 mμ (2, 3). Even if the short-range interaction is large, as for NH_2 and O^- substituents, when wavelength shifts of up to

Can. J. Chem. Downloaded from www.nrcresearchpress.com by 200.7.193.243 on 09/04/12
For personal use only.

Can. J. Chem. Downloaded from www.nrcresearchpress.com by 200.7.193.243 on 09/04/12
For personal use only.

25 mμ are obtained, the corresponding wavelength shifts because of mesomeric interaction in the acetophenone series are 76 mμ (2) and 79 mμ (7) respectively, that is, very much larger. Further, since steric interaction can completely inhibit mesomeric interaction, both may be considered to be of similar importance in electronic spectra. Consequently, we conclude that if in substituted benzene derivatives mesomeric interaction is possible, this will normally determine predominantly the B-band of electronic absorption spectra, while the other, short-range interaction is only of secondary importance. We may also note in passing that this short-range interaction probably corresponds to the interaction deduced theoretically by Förster (6). Both these considerations point against a residual mesomeric interaction which still operates in the ortho isomer. This follows because the interaction is discernible in both ortho and meta positions to a similar extent, and is not generally more enhanced in the ortho position, as would be expected for a residual mesomeric interaction. Further, precisely such a residual mesomeric interaction may partly account for the occasional bathochromic wavelength displacement observed for the ortho isomer (see, for example, the spectra of chlorobenzaldehydes in Table II), and under these circumstances the expected bathochromic displacement relative to the meta isomer *is* obtained.

Next, it follows from theoretical considerations (cf. 20) that when both short-range and mesomeric interactions operate and when both are appreciable, the total effect will almost certainly not be simply additive but will follow a more complex pattern. This will be of importance for many paradisubstituted and, incidentally, monosubstituted benzene derivatives and may account for some of the anomalous mesomeric interactions. For example, Doub and Vandenbelt (5) found that nitro compounds frequently do not fit the normal displacement patterns; and this anomaly may be related to the relatively large short-range interaction for the nitro group (15, 21). A similar lack of additivity also prevails if more than one substituent contributes to the short-range interaction exerted on the benzene ring (cf. section on trisubstituted benzene derivatives). This again is more pronounced if the short-range interaction is large, as for example in *m*-diaminobenzene, which absorbs maximally at 240 mμ, the second amino substituent in this way causing a wavelength shift of only about 5 mμ (5).

Further, it may be noted that the order of magnitude for the short-range interaction may be related qualitatively both to the order observed for frequency displacements in some vibrational spectra and to the order of acidity constants for some aromatic acids. For example, the asymmetric stretching vibrations of nitrobenzenes are shifted to lower frequency (i.e. to longer wavelength) for meta substituents in the order $-NH_2 > -H > -NO_2$ (17), and this is qualitatively the same order as for the acidity-constant decreases in metasubstituted benzoic acids (22) and for the present short-range interactions. Generally—and this is by no means intended to rule out exceptions—all these effects will presumably be determined largely by the over-all electronegativity and hence these data may be expected to correlate also with the inductive effect. This is in fact indicated since the order for the halogens in their short-range interactions sometimes suggests the order of the inductive effects. For example, Ungnade (23) reports an order of $-F > -Cl > -Br > -I$ for the negative wave-length displacements relative to nitrobenzene. However, the inductive effect does not fully explain many of the wavelength displacements caused by the short-range interaction and hence it is preferable to consider the over-all electronegativity independently for each set of examples (15).

It also follows from the above considerations that it will normally be difficult to detect short-range interactions in the electronic absorption spectra of paradisubstituted benzene

derivatives. Exceptions may occur in compounds where the mesomeric interaction is relatively small compared with the short-range interaction. Examples of this may be provided by the various *p*-alkylsubstituted compounds which exhibit wavelength shifts in the order -*tert*-butyl > -methyl, i.e. in the order of their over-all inductive effects (cf. 24, 25).

THE B-BANDS OF TRISUBSTITUTED BENZENE DERIVATIVES

From a consideration of the previous sections it might be anticipated that the B-band spectra of trisubstituted benzene derivatives will normally be determined by the interaction of the two substituents, which when linked to the phenyl ring give rise to maximum resonance interaction and thus cause absorption at longest wavelength; the remaining substituent would be expected to exert only the short-range interaction. This expectation is supported by the observed spectra (see Table III). The data are largely those determined by Doub and Vandenbelt (13) who have already shown that the B-bands of trisubstituted benzene derivatives often closely resemble the most displaced B-band of one of the disubstituted parent compounds.

We can now relate this observation with our previous hypotheses by again postulating that one of the three substituents because of steric interactions no longer, or only partly, contributes to the observed B-band. Without introducing any additional hypotheses the data in this way correlate well with expectation. More precisely, the effects of the third substituent on the wavelength of the B-band can be classified into three types. The substituent may be almost completely dislodged, when the spectrum of the trisubstituted benzene derivative will closely resemble that of the disubstituted parent compound (see Table III, Section A). The latter is usually the para compound, but if the absorption of one of the meta or ortho isomers occurs at longer wavelength (i.e. is caused by an energetically more favorable transition) than that of the para compound, the absorption of the trisubstituted benzene derivative may resemble that of the meta or ortho isomer; the spectrum of the trisubstituted benzene derivative may also resemble that of the monosubstituted benzene derivative, if interaction between any two substituents is small. This is illustrated for a number of 2,5-disubstituted benzoic acids for which benzoic acid may be taken as the reference compound (see Table III, Section A). Sometimes also two B-bands occur for trisubstituted benzene derivatives, one corresponding to the ortho isomer and the other to the para isomer (15, cf. also 26).

Examples where some interaction with the third substituent occurs are illustrated in Section B of Table III which lists compounds where the ortho substituent makes some resonance contribution and in this way causes a bathochromic displacement of more than 5 mμ. In accordance with expectation this displacement only occurs if the vicinal ortho substituents are small, or if the interaction is essentially π–p bond interaction, which has been shown to be less direction-dependent than other interactions (3). This additional resonance interaction incidentally is assumed to include intramolecular hydrogen bonding and it should also be noted that the interaction may contribute to some of the lesser ortho effects shown in Section A of Table III. This follows because the anticipated bathochromic displacement may be cancelled out by steric effects as described in the succeeding paragraph.

Section C of Table III lists examples where the ortho substituent interferes appreciably with the resonance interaction of the reference compound and thereby gives rise to a hypsochromic wavelength displacement. This type of displacement has already been ascribed to steric effects on the primary substituent (see section on "Steric effects in acid

Can. J. Chem. Downloaded from www.nrcresearchpress.com by 200.7.193.243 on 09/04/12
For personal use only.

Can. J. Chem. Downloaded from www.nrcresearchpress.com by 200.7.193.243 on 09/04/12
For personal use only.

TABLE III

B-BANDS OF TRISUBSTITUTED BENZENE DERIVATIVES AND SUITABLE REFERENCE COMPOUNDS

Solvent	Trisubstituted derivative* Compound	λ_{max}, mμ	ϵ_{max}	Reference compound Compound	λ_{max}, mμ	ϵ_{max}
	A. B-bands of trisubstituted benzene and reference compound are within 5 mμ					
pH 3	2-Hydroxy-4-toluic acid	242	9600	*p*-Toluic acid†	241.5	14400
pH 7	3,4-Dihydroxybenzoic acid	251	7800	*p*-Hydroxybenzoic acid‡	251	12500
pH 11	2,4-Dimethoxybenzoic acid	246	8500	*p*-Anisic acid†	247	14000
pH 11	3-Amino-4-hydroxybenzoic acid	280	9200	*p*-Hydroxybenzoic acid†	280	16300
0.1 *N* HCl	3,4-Dihydroxyacetophenone	274	9900	*p*-Hydroxyacetophenone†	275	14300
pH 11	2,4-Dihydroxybenzaldehyde	331	20300	*p*-Hydroxybenzaldehyde†	330	27900
H_2O	2,5-Dimethoxynitrobenzene	273	3300	*m*-Nitroanisole§	273.5	6000
H_2O	2-Methoxy-5-chloronitrobenzene	265	3900	*m*-Chloronitrobenzene§	264	7100
pH 3	3,4-Dichlorobenzoic acid	242	13500	*p*-Chlorobenzoic acid†	241	16300
pH 11	3,4-Dichlorobenzoic acid	237	11300	*p*-Chlorobenzoic acid†	235	13600
pH 7	2-Hydroxy-4-toluic acid	238	8500	*p*-Toluic acid‡	236	14000
0.1 *N* HCl	2,4-Dihydroxybenzoic acid	256	13600	*p*-Hydroxybenzoic acid†	255	13900
pH 7	2,4-Dihydroxybenzoic acid	248	10800	*p*-Hydroxybenzoic acid‡	251	12500
pH 3	3,4-Dihydroxybenzoic acid	260	9300	*p*-Hydroxybenzoic acid†	255	13900
pH 11	3,4-Dihydroxybenzoic acid	276	8000	*p*-Hydroxybenzoic acid†	280	16300
pH 3	3-Methoxy-4-hydroxybenzoic acid	260	11100	*p*-Hydroxybenzoic acid†	255	13900
pH 7	3-Methoxy-4-hydroxybenzoic acid	251	9900	*p*-Hydroxybenzoic acid‡	251	12500
0.1 *N* NaOH	3-Methoxy-4-hydroxybenzoic acid	*280*	*13000*	*p*-Hydroxybenzoic acid†	280	16300
pH 3	2-Hydroxy-4-anisic acid	254	12400	*p*-Anisic acid†	256.5	15900
pH 7	2-Hydroxy-4-anisic acid	250	12000	*p*-Anisic acid‡	249	14000
pH 3	2,4-Dimethoxybenzoic acid	257	13100	*p*-Anisic acid†	256.5	15900
pH 7	3-Amino-4-hydroxybenzoic acid	253	6900	*p*-Hydroxybenzoic acid‡	251	12500
pH 3.6	2-Methyl-4-aminobenzoic acid	223	9600	*p*-Aminobenzoic acid†	219.5	9900
pH 11	2-Methyl-4-aminobenzoic acid	266	12200	*p*-Aminobenzoic acid†	265	14900
pH 11	2,4-Diaminobenzoic acid	266	10000	*p*-Aminobenzoic acid†	265	14900
H_2O	2,4-Dichloroacetophenone	252	8900	*p*-Chloroacetophenone*	254.5	16300
H_2O	3,4-Dichloroacetophenone	254	14600	*p*-Chloroacetophenone*	254.5	16300
pH 3	2,4-Dihydroxyacetophenone	275	13900	*p*-Hydroxyacetophenone†	275	14300
pH 11	2,4-Dihydroxyacetophenone	328	25600	*p*-Hydroxyacetophenone†	324.5	23100
pH 6	2-Hydroxy-4-aminoacetophenone	245	5700	*p*-Aminoacetophenone†	240	13000
H_2O	2,4-Dichlorobenzaldehyde	263	13700	*p*-Chlorobenzaldehyde*	259.5	17400
pH 3	2,4-Dihydroxybenzaldehyde	278	15700	*p*-Hydroxybenzaldehyde†	283.5	16000
H_2O	3,4-Dichloronitrobenzene	276	9200	*p*-Chloronitrobenzene†	280	10300
0.1 *N* HCl	2-Chloro-4-nitrophenol	317	8500	*p*-Nitrophenol†	317.5	10000
0.1 *N* NaOH	2-Chloro-4-nitrophenol	400	17400	*p*-Nitrophenol†	402.5	19200
pH 5	2-Amino-4-nitrophenol	315	5100	*p*-Nitrophenol†	317.5	10000
0.1 *N* HCl	2-Hydroxy-5-chlorobenzoic acid	233	7700	Benzoic acid‡	229.5	11500
pH 7	2-Hydroxy-5-chlorobenzoic acid	230	7900	Benzoic acid‡	226	9500
0.1 *N* HCl	2-Hydroxy-5-bromobenzoic acid	233	8400	Benzoic acid‡	229.5	11500
pH 7	2-Hydroxy-5-bromobenzoic acid	*232*	*8400*	Salicylic acid§	237	9000
0.1 *N* HCl	2,5-Dihydroxybenzoic acid	238	9300	*m*-Hydroxybenzoic acid§	236.5	7500
pH 7	2,5-Dihydroxybenzoic acid	*235*	*8300*	*m*-Hydroxybenzoic acid§	*232*	*6400*
pH 3	2-Methoxy-5-bromobenzoic acid	*234*	*9000*	Benzoic acid‡	229.5	11500
pH 3	2-Amino-5-chlorobenzoic acid	218	22000	*m*-Aminobenzoic acid§	218.5	14000
H_2O	2,5-Dichloroacetophenone	240	6200	Acetophenone‡	244	12000
0.1 *N* HCl	2,5-Dihydroxyacetophenone	256	9400	*o*-Hydroxyacetophenone§	252.5	10900
pH 3	2-Hydroxy-5-chlorobenzaldehyde	255	8900	*o*-Hydroxybenzaldehyde§	256	12600
0.1 *N* NaOH	2-Hydroxy-5-chlorobenzaldehyde	*260*	*7600*	*o*-Hydroxybenzaldehyde§	264.5	7500
H_2O	2-Methyl-5-chloronitrobenzene	262	4800	*m*-Chloronitrobenzene§	264	7100
pH 11	4-Methoxy-2-nitroaniline	285	5200	*o*-Nitroaniline	282.5	5400
	B. Orthosubstituent causes shift of more than 5 mμ towards longer wavelength					
pH 3.1	2-Hydroxy-4-aminobenzoic acid	231	8300¶	*p*-Aminobenzoic acid†	219.5	9900
pH 4.4	2,4-Diaminobenzoic acid	228	16400	*p*-Aminobenzoic acid†	219.5	9900
pH 3	2-Chloro-4-aminobenzoic acid	*225*	*9500*	*p*-Aminobenzoic acid†	219.5	9900
pH 4	2-Amino-4-chlorobenzoic acid	249	8900	*p*-Chlorobenzoic acid†	241	16300
pH 7	2-Amino-4-chlorobenzoic acid	247	8500	*p*-Chlorobenzoic acid‡	234	15000
pH 11	2,4-Dihydroxybenzoic acid	298	13000	*p*-Hydroxybenzoic acid†	280	16300
pH 11	3,4-Dihydroxyacetophenone	342	16300	*p*-Hydroxyacetophenone†	324.5	23100
0.1 *N* NaOH	2-Hydroxy-4-aminoacetophenone	348	10400	*p*-Aminoacetophenone†	311.5	17100
pH 11	2-Amino-4-nitrotoluene	293	5800	*p*-Nitrotoluene†	285	9250
pH 11	2-Amino-4-nitrophenol	446	13400	*p*-Nitrophenol†	402.5	19200
pH 7	2-Methoxy-4-nitroaniline	400	12300	*p*-Nitroaniline†	381	13500
pH 11	2-Amino-4-nitroaniline	402	9000	*p*-Nitroaniline†	381	13500
	C. Orthosubstituent causes shift of more than 5 mμ towards shorter wavelength					
pH 3	2,4-Dichlorobenzoic acid	232	7400	*p*-Chlorobenzoic acid†	241	16300
pH 11	2,4-Dichlorobenzoic acid	229	7400	*p*-Chlorobenzoic acid†	235	13600
pH 7	2-Hydroxy-4-aminobenzoic acid	265	13200	*p*-Aminobenzoic acid‡	288	19000
pH 7	2-Chloro-4-aminobenzoic acid	256	9000	*p*-Aminobenzoic acid‡	288	19000
H_2O	2,5-Dichloronitrobenzene	258	3300	*m*-Chloronitrobenzene§	264	7100

*Ref. 13.
†Ref. 7.
‡This series of papers.
§Ref. 5.
¶*Doub and Vandenbelt (13) refer to this band as the secondary primary band while designating the band at 275 mμ as the first primary band (B-band). Further in p-aminobenzoic acid the 270 mμ band is referred to (4) as the secondary band (C-band) and the band at 226.5 mμ as the first primary band. Our interpretation is to regard both the bands at 226.5 and 231 mμ as B-bands (first primary bands) and the bands at 270 and 275 mμ as C-bands (secondary bands). A similar reassignment has also been assumed for a number of other compounds in this table.*

and basic media"). The explanation now receives support since the shift is usually associated with decreased absorption intensity, and most frequently occurs if the third substituent is large or if the primary substituent is sensitive to steric interaction as for example in neutral solution (see Section C of Table III). Again steric effects of this type are also evident to a lesser extent in the other sections of Table III, particularly noticeable being the frequent loss of absorption intensity in the trisubstituted compound.

EXPERIMENTAL

All spectra were determined in duplicate on a Unicam SP. 500 spectrophotometer with 1 cm. quartz cells. Where applicable, the data obtained compared well with previous data reported in the literature.

Commercial samples, purified by crystallization or distillation, were used. Sodium hydroxide (1 *N*) was made up immediately before use from Fisher Certified pellets ($Na_2CO_3 < 0.5\%$), or when necessary from 5 *N* sodium hydroxide, volumetric solution, carbonate-free.

ACKNOWLEDGMENTS

The authors gratefully acknowledge a research grant from the National Research Council of Canada and a research fellowship (to A.S.R.) sponsored jointly by the following organizations: The Geological Survey of Newfoundland (Department of Mines and Resources), the Newfoundland and Labrador Corporation, and the British Newfoundland Corporation.

REFERENCES

1. FORBES, W. F. and MUELLER, W. A. Can. J. Chem. **34**, 1340 (1956).
2. FORBES, W. F. and MUELLER, W. A. Can. J. Chem. **35**, 488 (1957).
3. FORBES, W. F., MUELLER, W. A., RALPH, A. S., and TEMPLETON, J. F. Can. J. Chem. **35**, 1049 (1957).
4. FORBES, W. F. and RALPH, A. S. Can. J. Chem. **34**, 1447 (1956).
5. DOUB, L. and VANDENBELT, J. M. J. Am. Chem. Soc. **71**, 2414 (1949).
6. FÖRSTER, T. Z. Naturforsch. **2a**, 149 (1947).
7. DOUB, L. and VANDENBELT, J. M. J. Am. Chem. Soc. **69**, 2714 (1947).
8. UNGNADE, H. E. and LAMB, R. W. J. Am. Chem. Soc. **74**, 3789 (1952).
9. FLOWERS, R., GILLESPIE, R. J., and WASIF, S. J. Chem. Soc. 607 (1956).
10. NAGAKURA, S., MINEGISHI, A., and STANFIELD, K. J. Am. Chem. Soc. **79**, 1033 (1957).
11. FORBES, W. F. and TEMPLETON, J. F. Can. J. Chem. **36**, 180 (1958).
12. LEMON, H. W. J. Am. Chem. Soc. **69**, 2998 (1947).
13. DOUB, L. and VANDENBELT, J. M. J. Am. Chem. Soc. **77**, 4535 (1955).
14. BRAUDE, E. A. Ann. Repts. on Progr. Chem., Chem. Soc. London, **42**, 105 (1945).
15. FORBES, W. F. *et al.* Unpublished information.
16. HOYER, H. Ber. **86**, 1016 (1953); **89**, 146 (1956).
17. FRANCK, B., HÖRMANN, H., and SCHEIBE, S. Ber. **90**, 330 (1957).
18. JONES, R. N., FORBES, W. F., and MUELLER, W. A. Can. J. Chem. **35**, 504 (1957).
19. FORBES, W. F. and MUELLER, W. A. J. Am. Chem. Soc. **79**, 6495 (1957).
20. PARR, R. G. and PARISER, R. J. Chem. Phys. **23**, 711 (1955).
21. KAMLET, M. J. and GLOVER, D. J. J. Am. Chem. Soc. **77**, 5696 (1955).
22. INGOLD, C. K. Structure and mechanism in organic chemistry. Cornell University Press, Ithaca, N.Y. 1953. p. 738.
23. UNGNADE, H. E. J. Am. Chem. Soc. **76**, 1601 (1954).
24. BOWDEN, K. and BRAUDE, E. A. J. Chem. Soc. 1068 (1952).
25. BURAWOY, A. and SPINNER, E. J. Chem. Soc. 2085 (1955).
26. KANENIWA, N. J. Pharm. Soc. Japan, **76**, 253 (1956); cf. Chem. Abstracts, **50**, 13793 (1956).

Can. J. Chem. Downloaded from www.nrcresearchpress.com by 200.7.193.243 on 09/04/12
For personal use only.

Can. J. Chem. Downloaded from www.nrcresearchpress.com by 200.7.193.243 on 09/04/12
For personal use only.

NOTES

2-BENZHYDRYLIMINO-4-THIAZOLIDONES AND RELATED COMPOUNDS

STANLEY O. WINTHROP AND GREGORY GAVIN

The synthesis of a series of 1-benzhydryl-2-alkyl-2-thiopseudoureas has recently been reported from this laboratory (1). These compounds exhibited a central stimulating action when administered to experimental animals. In the present investigation, certain cyclic thiopseudoureas with a structural relationship to the above compounds were prepared and screened for their pharmacological activity. The preparation of the 1-benzhydrylthioureas used in the present study was described in the previous paper (1).

The reaction of an unsymmetrically substituted thiourea with an α-haloester may produce one of two possible isomeric 4-thiazolidones depending on the manner in which the cyclization occurs (2). Thus 1-benzhydrylthiourea and ethyl α-bromoacetate yielded either 2-benzhydrylimino-4-thiazolidone or 3-benzhydryl-2-imino-4-thiazolidone. A proof of structure was carried out by the method of Davis and Dains (3). Condensation with benzaldehyde in the presence of piperidine gave 2-benzhydrylimino-5-benzal-4-thiazolidone which was then hydrolyzed by hydrochloric acid to yield 5-benzal-2,4-thiazolidinedione, a known compound. Other 1-benzhydrylthioureas and other α-haloesters gave 2-benzhydrylimino-4-thiazolidones substituted in the 3 and the 5 positions. They are listed in Table I.

2-Benzhydrylaminothiazole has been prepared by Kaye (4) from 1-benzhydrylthiourea and dimethyl chloroacetal. In a like manner 1-benzhydrylthiourea and α-chloroacetone gave 2-benzhydrylamino-4-methylthiazole. The reaction of 1-benzhydrylthiourea with β-iodopropionic acid gave 2-benzhydrylimino-4-keto-1,3-thiazane. The preparation of some 2-alkylimino-4-keto-1,3-thiazanes by a similar procedure has been reported (5). Bose and Nandi (6) have shown that the reaction between a 1-alkylthiosemicarbazide and ethyl α-chloroacetate yields a 2-alkylimino-5-keto-1,3,4-thiadiazane and not a 2-alkylamino-3-amino-4-thiazolidone. In the present investigation, 1-benzhydrylthiosemicarbazide and ethyl α-chloroacetate gave 2-benzhydrylimino-5-keto-1,3,4-thiadiazane.

Some of the cyclic thiopseudoureas were found to be central-nervous-system depressants. This is in contrast to the stimulant properties shown by the acyclic benzhydrylthiopseudoureas.

EXPERIMENTAL*

2-Benzhydrylimino-4-thiazolidone.—A solution of 1-benzhydrylthiourea (2.42 g., 0.01 mole) and ethyl α-bromoacetate (2.5 g., 0.015 mole) in 75 ml. of ethanol was allowed to stand for 16 hours at room temperature. Ether was then added to ensure complete precipitation of the product, which was filtered off and dried to yield 2.17 g., m.p. 252°–253° C. One recrystallization from 2-propanol did not change the melting point (see Table I).

2-Benzhydrylimino-5-methyl-4-thiazolidone.—1-Benzhydrylthiourea (4.8 g., 0.02 mole) and ethyl α-bromopropionate were dissolved in 50 ml. of glacial acetic acid and the solution refluxed for 16 hours. On cooling and addition of water, the product precipitated,

**All melting points are uncorrected.*

Can. J. Chem. Downloaded from www.nrcresearchpress.com by 200.7.193.243 on 09/04/12
For personal use only.

TABLE I

2-BENZHYDRYLIMINO-4-THIAZOLIDONES

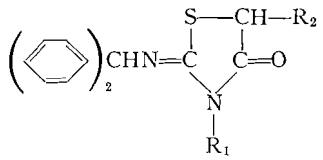

R_1	R_2	Yield, %	M.p., ° C.	Formula	Carbon		Hydrogen		Nitrogen		Sulphur	
					Calc.	Found	Calc.	Found	Calc.	Found	Calc.	Found
H	H	77	252–253	$C_{16}H_{14}N_2SO$	68.15	68.57	4.98	5.34	9.92	9.63	11.33	11.22
H	CH_3	81	245–246	$C_{17}H_{16}N_2SO$					9.45	9.44	10.82	10.71
H[a]	CH_2CH_3	81	215–216	$C_{18}H_{18}N_2SO$	69.65	69.81	5.85	5.74	9.03	8.93	10.33	10.23
H	$CH_2CH_2CH_2CH_3$	72	196–197	$C_{20}H_{22}N_2SO$					8.27	8.08	9.46	9.30
CH_3	H	54	104–105	$C_{17}H_{16}N_2SO$	68.91	69.07	5.42	5.44	9.45	9.25	10.82	10.99
CH_2CH_2OH[b]	H	51	174–175	$C_{18}H_{19}N_2SO_2Cl$[c]	59.60	59.33	5.27	5.26	7.72	7.66	8.83	8.81

[a] *Hydrobromide melts at 181°–183° C. Calculated for* $C_{18}H_{19}N_2OBrS$: N, *7.16;* Br, *20.44. Found:* N, *7.33;* Br, *20.44.*
[b] *This compound was isolated as its hydrochloride.*
[c] *Chlorine: Calc., 9.77; found, 9.84.*

4.8 g., m.p. 195°–208° C. Two recrystallizations from ethanol raised the melting point to 245°–246° C. (see Table I).

2-Benzhydrylimino-3-hydroxyethyl-4-thiazolidone hydrochloride. — 1-Benzhydryl-3-hydroxyethylthiourea (5.7 g., 0.02 mole) and α-chloroacetic acid (1.9 g., 0.02 mole) in 25 ml. of 2-propanol containing sodium acetate (1.6 g., 0.02 mole) were refluxed for 1 hour. The sodium chloride was then removed and an excess of ethereal hydrogen chloride was added to the filtrate causing the product hydrochloride to separate, 3.7 g., m.p. 168°–169° C. Two recrystallizations from a methanol–ether mixture raised the melting point to 174°–175° C. (see Table I).

2-Benzhydrylimino-5-benzal-4-thiazolidone.—2-Benzhydrylimino-4-thiazolidone (2.6 g., 0.009 mole) and benzaldehyde (0.95 g., 0.009 mole) were dissolved in 10 ml. of absolute ethanol containing a few drops of piperidine. The reaction mixture was refluxed for 2 hours. On cooling, 2.6 g. of product precipitated, m.p. 252°–257° C. Two recrystallizations from a large amount of ethanol raised the melting point to 265°–268° C. Calc. for $C_{23}H_{18}N_2SO$: N, 7.54; S, 8.65. Found: N, 7.82; S, 8.71.

5-Benzal-2,4-thiazolidinedione.—2-Benzhydrylimino-5-benzal-4-thiazolidone (0.3 g.) was dissolved in a solution of 80 ml. ethanol and 40 ml. concentrated hydrochloric acid. The reaction mixture was refluxed for 24 hours. On cooling and removal of the ethanol *in vacuo*, the product precipitated, 0.08 g., m.p. 246°–247° C. (lit. m.p. 243° C.) (3). Calc. for $C_{10}H_7NSO_2$: S, 15.62. Found: S, 15.35.

2-Benzhydrylamino-4-methylthiazole hydrochloride.—1-Benzhydrylthiourea (4.8 g., 0.02 mole) and α-chloroacetone (2.03 g., 0.022 mole) were dissolved in 150 ml. of 1:1 ether–acetone solution. The reaction mixture was allowed to stand at room temperature for 16 hours during which time the product hydrochloride precipitated, 3.3 g., m.p. 188°–189° C. One recrystallization from ethanol did not change the melting point. Calc. for $C_{17}H_{17}N_2SCl$: C, 64.39; H, 5.36; N, 8.84; S, 10.03. Found: C, 64.48; H, 5.23; N, 9.01; S, 10.03.

2-Benzhydrylimino-4-keto-1,3-thiazane hydroiodide.—1-Benzhydrylthiourea (4.8 g., 0.02 mole) and β-iodopropionic acid (4.0 g., 0.02 mole) were dissolved in 50 ml. of absolute ethanol and the solution refluxed for 4 hours. The ethanol was then removed *in vacuo* and 25 ml. of acetic anhydride added. The reaction mixture was again heated for 4 hours on a steam bath. On cooling and addition of ether, 6.1 g. of product separated out, m.p. 191°–193° C. dec. One recrystallization from acetonitrile did not change the melting point. Calc. for $C_{17}H_{17}N_2SIO$: N, 6.62; S, 7.55; I, 29.95. Found: N, 6.98; S, 7.91; I, 30.00.

2-Benzhydrylimino-5-keto-1,3,4-thiadiazane.—1-Benzhydrylthiosemicarbazide (8.9 g., 0.032 mole), α-chloroacetic acid (3.0 g., 0.032 mole), and sodium acetate (2.6 g., 0.032 mole) were added to 75 ml. of 2-propanol and refluxed for 4 hours. Water was then added causing the product to separate out as an oil, which eventually solidified to yield 7.6 g., m.p. 114°–124° C. Two recrystallizations from ethanol gave an analytically pure material, m.p. 141°–142° C. Calc. for $C_{16}H_{15}N_3SO$: C, 64.62; H, 5.09; N, 14.13; S, 10.77. Found: C, 64.80; H, 4.94; N, 14.10; S, 10.68.

ACKNOWLEDGMENTS

The authors would like to thank Dr. C. I. Chappel for the pharmacological screening, Mr. W. J. Turnbull for the analyses, and Dr. Gilles Papineau-Couture and Mrs. J. Jachner for numerous infrared spectra.

1. WINTHROP, S. O., SYBULSKII, S., GAVIN, G., and GRANT, G. A. J. Am. Chem. Soc. **79**, 3496 (1957).
2. EBERLY, F. A. and DAINS, F. B. J. Am. Chem. Soc. **58**, 2544 (1936).

Can. J. Chem. Downloaded from www.nrcresearchpress.com by 200.7.193.243 on 09/04/12
For personal use only.

3. DAVIS, J. A. and DAINS, F. B. J. Am. Chem. Soc. **57**, 2627 (1935).
4. KAYE, I. A., KOGEN, I. C., and PARRIS, C. L. J. Am. Chem. Soc. **74**, 403 (1952).
5. GASH, V. W. and WHEELER, K. W. U.S. Patent No. 2,679,500. May 25, 1954.
6. BOSE, P. K. and NANDI, B. K. J. Indian Chem. Soc. **7**, 961 (1930).

RECEIVED DECEMBER 18, 1957.
RESEARCH LABORATORIES OF AYERST, MCKENNA & HARRISON LIMITED,
MONTREAL, QUEBEC.

Can. J. Chem. Downloaded from www.nrcresearchpress.com by 200.7.193.243 on 09/04/12
For personal use only.

Can. J. Chem. Downloaded from www.nrcresearchpress.com by 200.7.193.243 on 09/04/12
For personal use only.

Canadian Journal of Chemistry

Issued by THE NATIONAL RESEARCH COUNCIL OF CANADA

VOLUME 36 JUNE 1958 NUMBER 6

HYDROGEN PEROXIDE AND ITS ANALOGUES

VIII. EXCESS FUNCTIONS FOR THE BINARY SYSTEMS H_2O–H_2O_2 AND D_2O–D_2O_2 [1]

PAUL A. GIGUÈRE, OSVALD KNOP,[2] AND MICHAEL FALK[3]

ABSTRACT

Recent volumetric and calorimetric data have been used to calculate the excess functions for mixtures of water and hydrogen peroxide over the entire concentration range. The results are compared with those for the corresponding deuterium compounds. The existing calorimetric and vapor-pressure measurements are not comprehensive nor accurate enough to support discussion of the finer details of the excess quantities. A maximum in the excess-volume curves, presumably related to the formation of the compound $H_2O_2.2H_2O$, persists in the liquid mixtures over an appreciable temperature range above the melting point of that compound. A possible crystal structure is proposed for the latter.

New density determinations were carried out on mixtures of heavy water and deuterium peroxide at 0° and 20° C. and the effect of deuterium peroxide on the temperature of maximum density of heavy water was measured and compared with that of deuterated alcohols. It is concluded that the structure of liquid water is easily penetrated by hydrogen peroxide molecules.

INTRODUCTION

Mixtures of hydrogen peroxide and water represent one of the simplest possible examples of a binary system of strongly polar liquids with extensive hydrogen bonding. So far the investigation of solutions on non-electrolytes for the purpose of testing the existing theories has been largely confined to non-polar systems. However, if the theory is to be extended to hydrogen-bonded systems, the gaps in the present experimental data on such systems will have to be lessened. With this aim in mind we are presenting here a comparative study of the associative properties, in the form of excess functions, of the binary system H_2O–H_2O_2 and its deuterated analogue D_2O–D_2O_2. The excess functions are based in part on our calorimetric measurements reported in paper VII of this series (1).*

SYMBOLS AND DEFINITIONS

T	temperature in ° K.
N_p	mole fraction of hydrogen (or deuterium) peroxide.
N_w	mole fraction of water (or heavy water).

[1]*Manuscript received January 2, 1958.*
Contribution from the Department of Chemistry, Laval University, Quebec, Que.
[2]*On leave of absence from the Nova Scotia Technical College, Halifax, N.S.*
[3]*Holder of a Shawinigan Chemicals Co. research fellowship.*

**Shortly after our data were published a new diphenyl ether calorimeter was described by R. S. Jessup of the National Bureau of Standards, Washington, D.C. (2). The calibration factor of this instrument, 18.90, is slightly different from the one we used, 19.01 cal./g. Hg (3). There is little doubt that the factor found by Jessup is more accurate, as both his apparatus and calibration technique were much more elaborate than ours. Furthermore, most causes of error will give too high a factor, and Jessup's value is the lowest of all those reported so far. The resulting uncertainty in our published results (less than 0.5%) affects in no way the present discussion.*

V_p, V_w	molar volume of peroxide and water, respectively.
V	actual volume of one mole of solution.
$V^\circ = N_w V_w + N_p V_p$	ideal volume of one mole of solution.
$V^E = V - V^\circ$	excess volume of mixing.
$\theta = -100\,V^E/V^\circ$	per cent volume contraction.
C_p	actual heat capacity of solution (average value between 0° and 26.9° C.).
$C^E_p = C_p - C^\circ_p$	excess heat capacity of solution (called $\Delta_m C_p$ in paper VII).
$H^E = H^M$	excess heat of mixing (called $\Delta_m H_{mix}$ in paper VII).
$F^E = F^M - F^\circ$	excess free energy of mixing.
$S^E = S^M - S^\circ$	excess entropy of mixing.

MOLAR VOLUMES

Several sets of density determinations on aqueous solutions of hydrogen peroxide can be found in the literature. The most recent ones, showing good mutual consistency, have been combined into cubic polynomials in either weight fraction of peroxide or temperature (4). From these expressions we have calculated the molar volumes and the excess volumes of mixing over the entire composition range and from 0° to 96° C. The temperature range was extended, though with reduced accuracy, down to the liquidus curve of the system (Table I) by including the low-temperature measurements of Giguère and Geoffrion (5). The ideal volumes below 0° C. were estimated by graphical extrapolation since the density of supercooled hydrogen peroxide is not known and that of supercooled water is known only down to −20° C.

TABLE I

EXCESS VOLUMES OF MIXING OF H_2O–H_2O_2 SOLUTIONS AT LOW TEMPERATURES

Composition		$-V^E$				
w_p	N_p	−10° C.	−20° C.	−30° C.	−40° C.	−50° C.
0.1927	0.1122	0.280	—	—	—	—
0.2954	0.1817	0.356	0.442	—	—	—
0.4123	0.2709	0.417	0.505	0.605	0.715	0.833
0.4987	0.3451	0.434	0.517	0.611	0.716	0.828
0.6837	0.5338	0.381	0.441	0.517	—	—
0.7861	0.6606	0.312	0.360	—	—	—
0.8964	0.8209	0.200	—	—	—	—

The excess volume of the mixtures is everywhere negative, as may be seen from the plots in Fig. 1. The variation of θ with temperature and composition is shown in Fig. 2. The pronounced maxima in the curves of Fig. 1 correspond to the maximum deviation from ideality, max θ. Fig. 3 illustrates the temperature dependence of the position of max θ. The equation of the best straight line fitting all the points of that curve up to 50° C. was found by least squares to be

$$\log \max \theta = -8.391\times10^{-3}T+2.512. \quad [1]$$

At higher temperatures the uncertainty in the density measurements was too great to yield reliable values of the maximum.

The position of max θ converges with decreasing temperature towards $N_p = 1/3$, that is

Can. J. Chem. Downloaded from www.nrcresearchpress.com by 200.7.193.243 on 09/04/12
For personal use only.

Can. J. Chem. Downloaded from www.nrcresearchpress.com by 200.7.193.243 on 09/04/12
For personal use only.

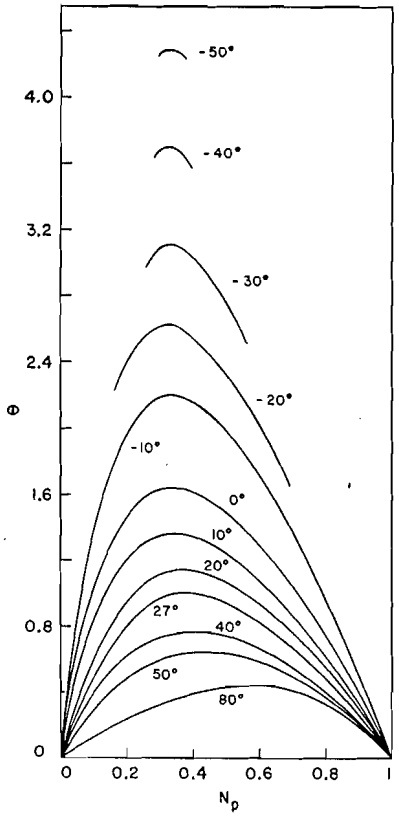

FIG. 1. Per cent volume contraction of mixtures of water and hydrogen peroxide at different temperatures.

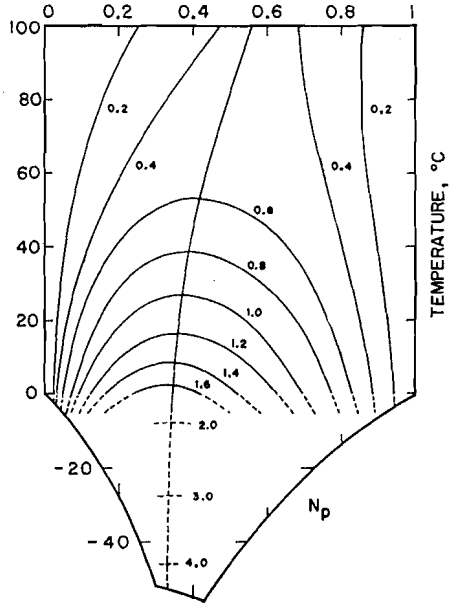

FIG. 2. Per cent volume contraction of mixtures of water and hydrogen peroxide as a function of temperature and composition.

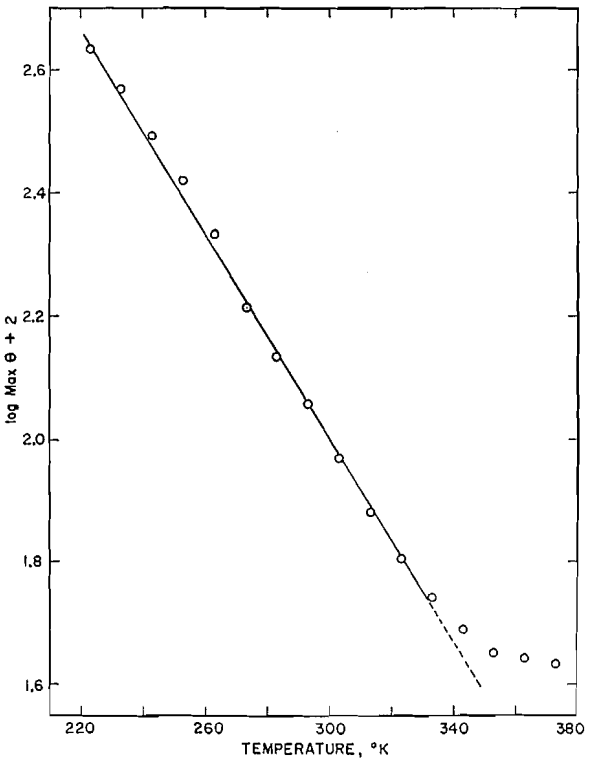

FIG. 3. Dependence of max θ on temperature.

towards the composition of the only crystalline compound, $H_2O_2.2H_2O$, in the system. The near coincidence, though not the convergence, of the position of max θ in these mixtures at ordinary temperatures with the composition of the compound had already been pointed out in somewhat different terms in a paper which recently came to our attention (6).

The experimental data for the mixtures of deuterated compounds are naturally much fewer and less accurate than for the hydrogen compounds. To supplement the first

TABLE II

DENSITIES AND EXCESS VOLUMES OF MIXING OF D_2O–D_2O_2 SOLUTIONS

	Density (g./cm.^{3})		V		$-V^E$	
N_p	0° C.	20° C.	0° C.	20° C.	0° C.	20° C.
0	1.1040	1.1050	18.131	18.113	0	0
0.1978	1.2328	1.2210	18.815	18.997	0.305	0.178
0.2498	1.2630	1.2495	19.023	19.230	0.357	0.223
0.3395	1.3089	1.2929	19.453	19.694	0.375	0.241
0.3637	1.3213	1.3034	19.563	19.832	0.386	0.233
0.4819	1.3727	1.3554	20.208	20.466	0.322	0.233
0.5236	1.3907	1.3717	20.427	20.711	0.321	0.211
0.7281	1.4693	1.4478	21.575	21.896	0.196	1.124
1	1.5577*	1.5348*	23.130*	23.479*	0	0

**Extrapolated.*

Can. J. Chem. Downloaded from www.nrcresearchpress.com by 200.7.193.243 on 09/04/12
For personal use only.

set of measurements made in this laboratory some years ago (7) we have repeated a number of determinations to define better the region of max θ. The results (Table II) show definite improvement over those of the first series owing to the larger quantity of deuterium peroxide available this time. As far as can be judged from Fig. 4, max θ occurs at the same composition in the two systems, but there is an increase in the absolute value for the deuterium system amounting to about 17% at 0° C. and about 5% at 20°.

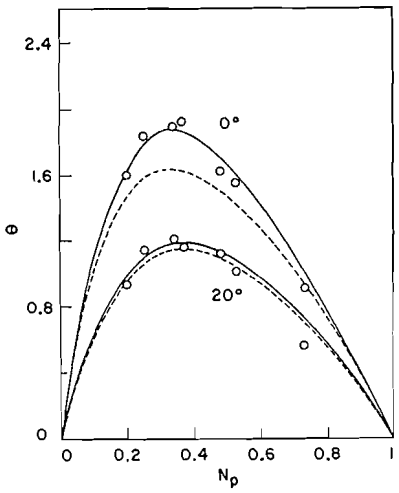

FIG. 4. Per cent volume contraction of mixtures of heavy water and deuterium peroxide at 0° and 20° C. Broken lines are the corresponding curves for the system H_2O–H_2O_2.

THERMODYNAMIC EXCESS FUNCTIONS

Another measure of the associative properties of solutions is given by the excess functions. These quantities are usually derived from vapor pressures and calorimetric data through the equations

$$F^E = RT \sum N_i \ln \gamma_i, \quad [2]$$

$$TS^E = H^E - F^E, \quad [3]$$

where the γ's are the activity coefficients. Unfortunately no complete set of data is available yet for both properties *at the same temperature.* The latest and most extensive determinations of vapor pressure and vapor composition by Scatchard *et al.* (8) were carried out at 60°, 75°, and 90° C. over a wide concentration range, and at 44.5° and 105° each for equimolar mixtures.* But the heat of mixing has been measured so far only at 0° and 26.9°, and the latter corrected to 25°. For correlation purposes one must either recalculate the H^E to 60°, 75°, and 90° or else extrapolate the vapor-pressure data down to 0° and 25°. The former procedure was deemed less reliable at this stage because it requires accurate knowledge of the heat capacity of the solutions, and the only existing set (1) consists of average values between 0° and 26.9°.

On the other hand extrapolation of the vapor pressures is not without risk. Indeed, in consolidating their results Scatchard *et al.* estimated that their vapor-composition

**However, in a paper presented at the Am. Chem. Soc. meeting in Dallas, April 1956, J. D. Floyd, J. W. Turner, and P. M. Gross, Jr. reported on measurements of vapor pressure and vapor composition of hydrogen peroxide – water mixtures at 25°, 40°, 50°, 60°, and 75° C. over the entire concentration range.*

Can. J. Chem. Downloaded from www.nrcresearchpress.com by 200.7.193.243 on 09/04/12
For personal use only.

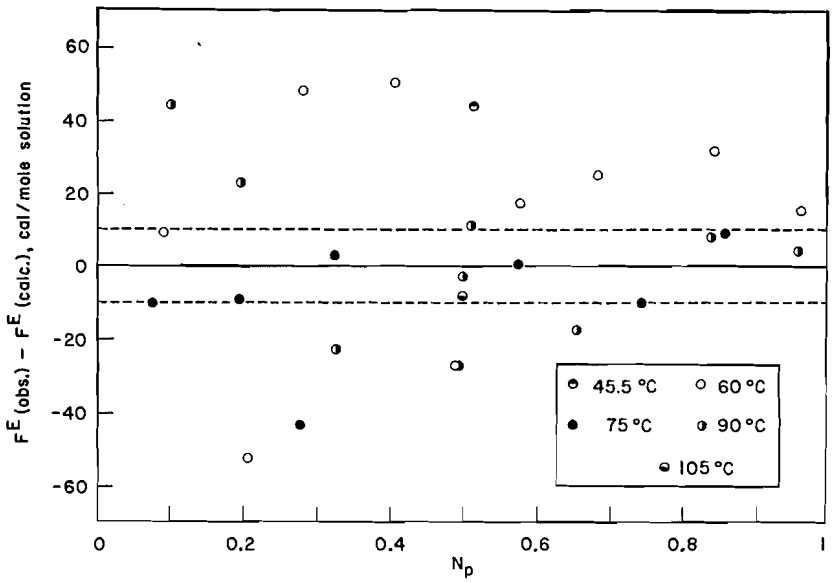

FIG. 5. Deviation of the F^E values based on individual vapor-pressure and vapor-composition measurements of Scatchard *et al.* (8) from their smoothed values obtained through equation [4].

measurements were not accurate enough for calculation of the activity coefficients.* Instead they assumed for the excess free energy an equation of the form

$$[4] \qquad F^E = N_w N_p [B_0(T) + B_1(N_p - N_w) + B_2(N_p - N_w)^2]$$

and obtained the numerical value of the B coefficients by successive graphical and analytical fitting of the experimental vapor pressures to an equation derived from [4] through the excess chemical potentials. Furthermore, in view of the rather narrow temperature range covered they used only one set of coefficients, smoothed with respect to temperature. Therefore, their calculated excess heat and entropy of mixing are temperature independent. The extent of deviation of the former quantity from our own calorimetric determinations at 0° and 26.9° has already been pointed out (Fig. 4 of paper VII). As regards the excess entropy given by their equation

$$[5] \qquad S^E = -0.97 N_p (1 - N_p)$$

it is necessarily symmetrical with respect to concentration about the middle value $N_p = 0.5$ as shown by the broken line in Fig. 6. This is to be compared with the excess-entropy curves based on our calorimetric data for 0° and 25°. Not only are they markedly unsymmetrical, but the entropy term becomes positive at 0° for dilute solutions ($N_p < 0.2$). One might be tempted to relate this feature to some property of the pure components, like the density anomaly of liquid water near the melting point. However, such inferences must be viewed with caution considering the present status of experimental evidence. Because the entropy term is obtained as the difference between two large quantities [3], even its sign in that concentration range remains uncertain pending more extensive and more accurate thermal and vapor-pressure measurements. Considerable effort will be

*In that connection it is interesting to note that although their equilibrium still was capable of greater accuracy than the static method used before by Giguère and Maass (9) their "experimental" points still show considerable spread (Fig. 5).

Can. J. Chem. Downloaded from www.nrcresearchpress.com by 200.7.193.243 on 09/04/12
For personal use only.

needed to improve significantly over the present data owing to the tendency of hydrogen peroxide to decompose spontaneously.

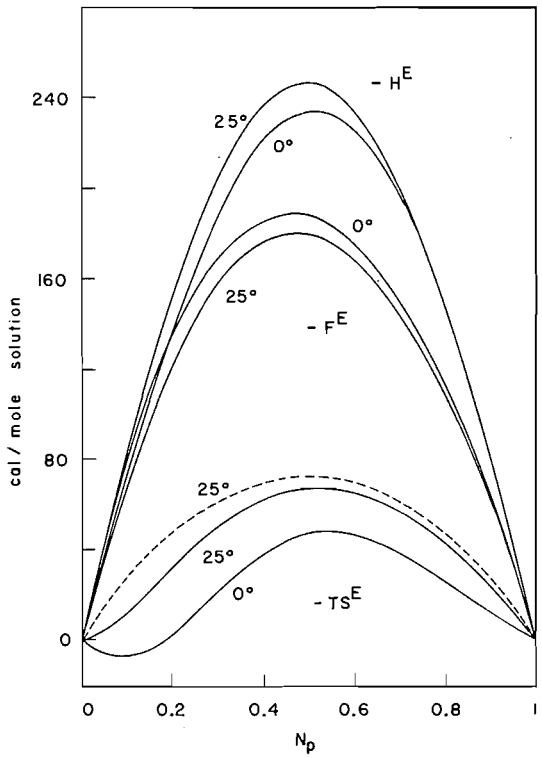

FIG. 6. Thermodynamic excess functions of aqueous solutions of hydrogen peroxide at 0° and 25° C. from calorimetric values of the heat of mixing and extrapolated vapor-pressure data.

CORRELATION OF VOLUME AND THERMODYNAMIC PROPERTIES

The excess volume of mixing is related to the other excess functions through equations

[6] $$V^E = \partial F^E/\partial p = RT \sum N_i(\partial \ln \gamma_i/\partial p)$$

and

[7] $$H^M = RT^2 \sum N_i(\partial \ln \gamma_i/\partial T).$$

Unfortunately certain information, such as the compressibility of peroxide solutions, is lacking for use in these equations, so that some sort of empirical relationship must be resorted to. A priori it seems reasonable to expect that both V^E and H^E are directly related to the number of hydrogen bonds formed on mixing. This is by no means the only factor responsible for the deviations from ideality, as proved by the fact that the curves for these two properties do not coincide. Moreover, instances are known of strongly associated binary mixtures for which the two excess quantities have opposite signs (10). However, in the present case the two are negative at all concentrations, suggesting that the assumption of proportionality to hydrogen-bond formation is tenable. Existence of such a relationship may be illustrated by plotting against composition the differences between the experimental values at 0° and at 26.9° for the three excess functions H^E, θ, and V^E, all normalized to C^E_p. Since all the points fall closely

Can. J. Chem. Downloaded from www.nrcresearchpress.com by 200.7.193.243 on 09/04/12
For personal use only.

on the same curve (Fig. 7) whatever factors, besides the number of extra hydrogen bonds formed in that temperature interval, may be responsible for the non-ideal behavior, they must affect equally the thermal and the volume excess functions of the peroxide solutions. Whether the excess heat capacity corresponds to the same modes as in the pure components cannot be decided because of the complexity of this binary system.

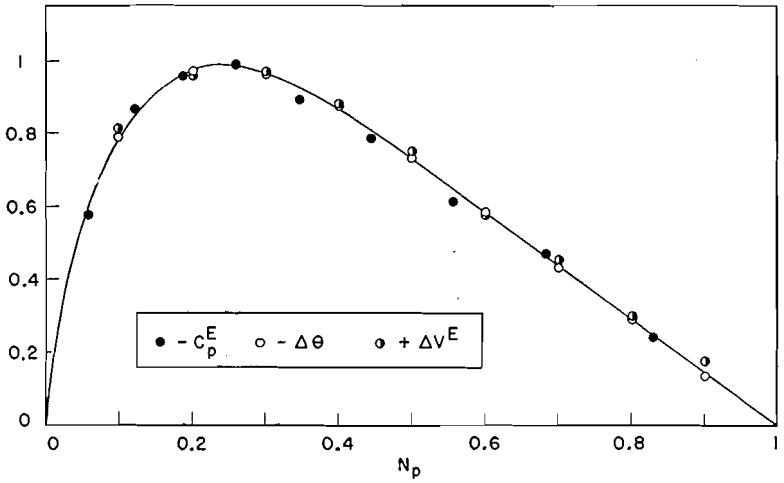

FIG. 7. Normalized values of the difference in $H^E = C_p{}^E\Delta T$, θ and V^E taken between 0° and 26.9° C.

The normalizing factor employed above in converting θ to $C^E{}_p$ may be used in turn to obtain a set of values for H^E from θ at various temperatures relative to its value at 26.9°. Obviously this procedure is open to criticism as it stands or falls with the relative

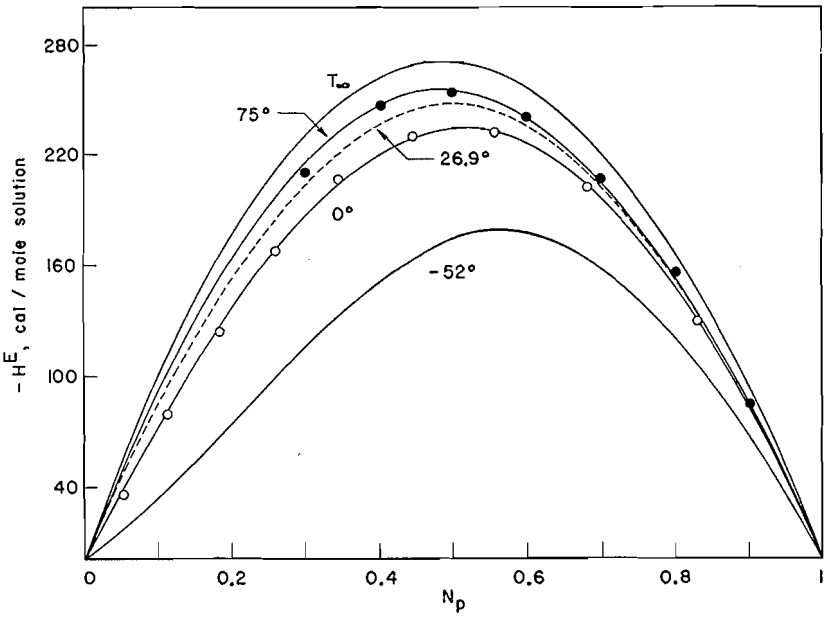

FIG. 8. Heats of mixing of water and hydrogen peroxide from the correlation of H^E and V^E. The experimental points for 75° are taken from Scatchard *et al.* (8), those at 0° from Ref. (1).

Can. J. Chem. Downloaded from www.nrcresearchpress.com by 200.7.193.243 on 09/04/12
For personal use only.

constancy of the average C^{E}_{p} at higher temperatures. Nevertheless, a fair agreement is obtained (Fig. 8) with the calculated H^{E} of Scatchard *et al.*, for 75°, their most favorable temperature. Actually the agreement is not too surprising since the excess heat of mixing is not particularly sensitive to temperature. Extension of the calculation to the high-temperature (T_{∞}) and the low-temperature limits (−52°, the melting point of the solid hydrate) gives an idea of the extent of variation of H^{E}.

Next to the number of extra hydrogen bonds, the most important factor should be the relative strength of such bonds between unlike molecules. The two factors are by no means equivalent, the former being essentially of a configurational nature. Indeed, a peroxide molecule with one site engaged in hydrogen bonding still has five other sites available for potential bond formation: either three acceptors and two donors or four acceptors and one donor. A water molecule in similar circumstances has only three sites available. Thus addition of hydrogen peroxide to water may have a cementing effect on the open, fragmentary ice structure which persists in the liquid above its melting point. This is borne out by the large effect of hydrogen peroxide in lowering the temperature of maximum density of water, as already pointed out (11), in contrast with the behavior of alcohols (Fig. 9).

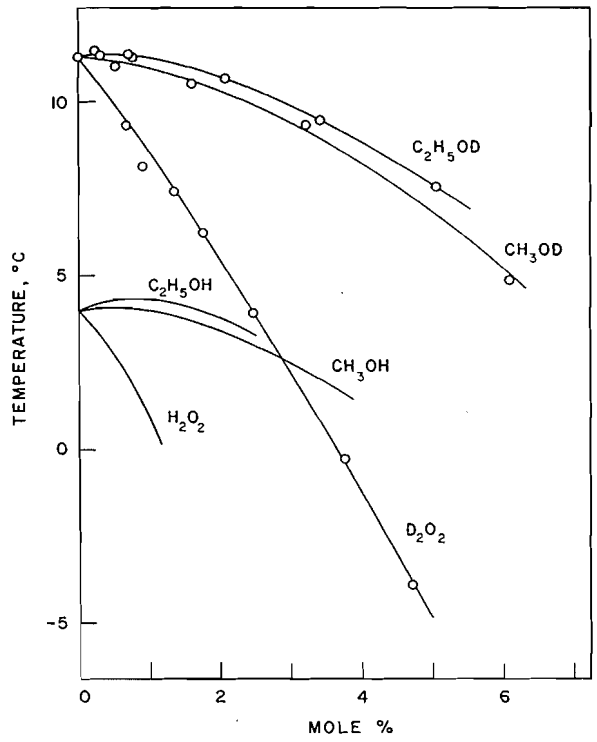

FIG. 9. Effect of different solutes on the temperatures of maximum density of water and heavy water. The curves for water are from Ref. (11).

As regards the strength of hydrogen bonds in the solutions relative to those in the pure components, the experimental evidence is meager and inconclusive. Bain (12) observed a slight shift of the O—H stretching fundamentals in the infrared spectra of peroxide solutions but he did not investigate its dependence on composition. In the

Can. J. Chem. Downloaded from www.nrcresearchpress.com by 200.7.193.243 on 09/04/12
For personal use only.

Raman spectra Taylor and Cross (13) detected a shoulder on the low-frequency side of the O—H stretching bands whose intensity increased with peroxide concentration up to a distinct maximum in the range $N_p = 0.2$ to 0.4 at $-40°$ C. At room temperature the intensity increased likewise but did not reach a maximum. The same authors also observed a concentration-dependent shift towards higher frequencies of the bending vibration ν_2 of both the water and hydrogen peroxide molecules. A systematic infrared study of these mixtures in the solid state at low temperatures (14) has confirmed these results and revealed, in addition, a number of extra bands in the low-frequency region with maximum intensity at about $N_p = 0.3$. It has been concluded (13) that an increase in the number of hydrogen bonds on mixing must be responsible for the above shifts of the bending modes towards higher frequencies, this being the experience also with other liquids. However, it is practically impossible with these methods to differentiate between varying hydrogen-bond strength and number of bonds. Refined X-ray diffraction techniques coupled with nuclear magnetic resonance investigations of the hydrate should provide useful structural data to supplement the thermodynamic arguments.

The maxima in the V^E of θ curves (Fig. 1) are obviously related in some way to the existence of the crystalline hydrate $H_2O_2.2H_2O$. In view of the presumably three-dimensional structural network and the low stability of the solid, the latter confirmed by the shape of the liquidus curve, it may not be appropriate to speak of persistence of the hydrate in the liquid above its melting point. It seems certain, however, that the packing and bonding factors are particularly favorable in liquid mixtures of water and hydrogen peroxide at N_p close to 1/3, so that optimum association ensues. The distinction between the two ways of stating the situation is mainly a matter of wording.

THE CRYSTALLINE HYDRATE

Knowledge of the structure of the solid hydrate would be valuable for interpreting the excess properties of the liquid mixtures. Unfortunately very little is known about it. Natta and Rigamonti (15) obtained an X-ray powder diffraction photograph of the solid and concluded that it had a lattice of low symmetry. The suggestion that the tetragonal symmetry of pure hydrogen peroxide degenerates progressively into monoclinic on addition of water (16) is unsubstantiated. The symmetry degeneration would entail formation of solid solutions contrary to definite experimental evidence (17). The same conclusion was already reached by Natta and Rigamonti, who failed to observe any shift in the positions of the peroxide lines in X-ray diffraction photographs of solid hydrogen peroxide containing 10 and 18% water. The extra features appearing on addition of water were assigned by them to the presence of the solid hydrate as a separate phase.

It is not difficult to visualize for that hydrate a highly organized structure which might be related to molecular aggregates of short lifetime existing in the liquid at low temperatures, and responsible for local density increases. The only requirement is the maximum engagement of the available donor and acceptor sites in hydrogen bonding. There is a total of six donor and eight acceptor sites per "molecule" of the compound, the water molecules contributing four of each kind and the peroxide molecule, two donors and four acceptors. With maximum possible engagement there will always remain two vacant acceptor sites.

The structure that we suggest here (Figs. 10 and 11) is based on the following assumptions: the unengaged acceptor sites are located on the peroxide oxygens; each peroxide molecule is surrounded by four water molecules; each water molecule is surrounded by

Can. J. Chem. Downloaded from www.nrcresearchpress.com by 200.7.193.243 on 09/04/12
For personal use only.

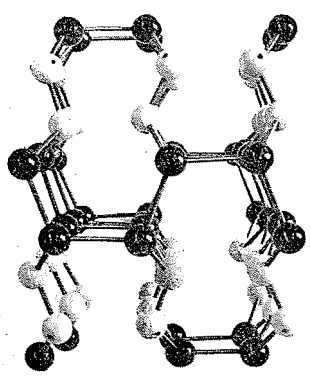

10

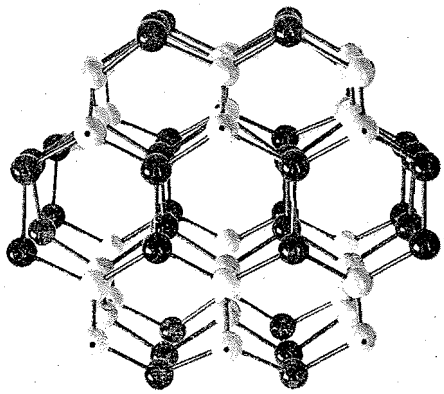

11

FIG. 10. Possible structure of the crystalline hydrate $H_2O_2.2H_2O$ viewed along the rows of peroxide molecules. (White balls, peroxide oxygens; black balls, water oxygens; hydrogen atoms not shown.)
FIG. 11. Same structure as in Fig. 10 viewed in a direction normal to the puckered water–peroxide sheets.

two water and two peroxide molecules; all hydrogen bonds are linear and of equal length; all bond angles are tetrahedral. The resulting structure is of orthorhombic symmetry with two $H_2O_2.2H_2O$ "molecules" per unit cell. Assuming 2.8 Å for the length of the hydrogen bond and 1.5 Å for the O–O distance in the peroxide molecule, the calculated density turns out to be close to the value 1.20 indicated in preliminary measurements at the melting point of the hydrate, −52° C. The structure can, in fact, be looked upon as an extreme case of the substitution process proposed by Abrahams, Collin, and Lipscomb (16). Alternate molecules in the infinite chains of pure peroxide are replaced by pairs of water molecules of appropriate orientations. The original helical peroxide chains are transformed into puckered sheets of water and peroxide molecules held in parallel stacks through hydrogen bonds normal to the sheets.

Although we assumed tetrahedral angles, this is not a necessary requirement. Even with bond angles close to their values in the free molecules the symmetry of the lattice could be preserved and the distortion would be slight. In fact, the distance between the unengaged acceptor sites of nearest peroxide oxygens would then become slightly larger than 2.8 Å, which is perhaps nearer the expected separation. Bond angle distortion in a peroxide molecule can easily take place through twisting about the O–O bond. Indeed, spectroscopic evidence indicates that the restoring force for that deformation is rather small (4); also, a recent infrared investigation of the crystalline dihydrate at low temperature leads to the conclusion that the peroxide molecule is somewhat distorted in that compound (14).

There are other ways in which the hydrogen bonds in solid $H_2O_2.2H_2O$ can be arranged into three-dimensional networks similar to the one just described. The oxygen atoms of some of such structures are roughly in the same relationship to each other as the silicon atoms in β-tridymite to those of β-cristobalite. They are all structures of equal or almost equal density, and probably also of very similar lattice energies. The similarity might account for the strong association in aqueous solutions of hydrogen peroxide, since aggregates of high local density may be formed in several, more or less equivalent ways.

Can. J. Chem. Downloaded from www.nrcresearchpress.com by 200.7.193.243 on 09/04/12
For personal use only.

Can. J. Chem. Downloaded from www.nrcresearchpress.com by 200.7.193.243 on 09/04/12
For personal use only.

COMPARISON OF THE HYDROGEN AND DEUTERIUM SYSTEMS

The pair of binary systems H_2O–H_2O_2 and D_2O–D_2O_2 offer a particularly favorable situation for investigating the effects of isotopic substitution on the thermodynamic properties of highly associated liquids. Obviously, one cannot expect any detailed information from mere determinations of bulk properties. Comparative studies of hydrogen-bonded crystals by Ubbelohde and his co-workers (18–20) have established that deuterium substitution leads to a measurable lengthening of the short bonds (shorter than about 2.65 Å) whereas for longer bonds, as in the present case, the effect is either a small contraction or is not observable at all. No such observations have been made on liquids, but the same situation may be presumed to obtain.

It is generally agreed that the zero-point energy is the main factor responsible for bond-energy difference in isotopic compounds, although the contribution of thermal energy should not be overlooked entirely. Since the extent of hydrogen bonding in associated liquids varies with temperature, comparison of the hydrogen and deuterium systems of compounds should be made at the appropriate "corresponding temperatures". We may illustrate this point by considering the effect of deuterium substitution on the temperature of maximum density of liquid water. In D_2O the temperature interval between the melting point and the maximum density (3.8° to 11.2° C.) is nearly double that for H_2O (0° to 4.1°). This anomaly in both liquids is due to persistence above the melting point of some of the residual "open structure" of ice, a structure resulting from the strongly directional character of the hydrogen bonds. Bending of these bonds is achieved mainly through rocking or "libration" of the individual water molecules about their center of gravity. Since the moments of inertia of D_2O are roughly double (1.90 times) those of H_2O, the thermal energy required for the process should therefore be double, as observed. The amount of residual ice structure must be approximately the same in water at 4.1° and in heavy water at 11.2°. This is in agreement with our observations on the effect of deuterium peroxide and deuterated alcohols on the temperature of maximum density of heavy water. As may be seen in Fig. 9 the curves for the various isotopic pairs are nearly parallel.

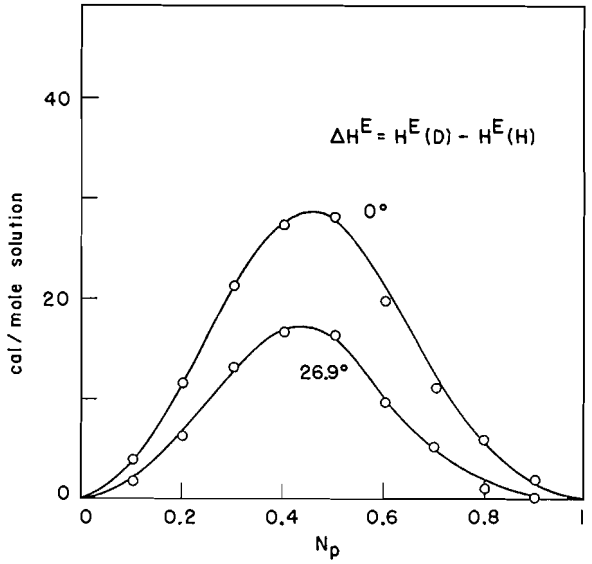

FIG. 12. Differences in the heats of mixing of the isotopic water–peroxide mixtures.

For the pure components comparison of the melting point (21), heat capacity, and heat of vaporization (1) denotes a slightly greater association of the deuterium compounds. By simple analogy we would expect correspondingly higher values of the excess functions of mixing for the deuterium system, and this is true of C^E_p and V^E. Quite unexpectedly, however, this trend is reversed in the case of H^E, the values for the deuterium compounds being significantly smaller (by nearly 10% at 25°) than for the hydrogen compounds (Fig. 12). If a temperature correction is applied to bring the two systems to the same "corresponding residual-structure states" as suggested above, namely by raising the temperature of the D_2O–D_2O_2 system by some 7°, then the two V^E curves (Fig. 4) are brought into near coincidence and the difference at the maximum in the two H^E curves is reduced by about one-third. The rest might be interpreted as an indication of weakening of the hydrogen bond on deuterium substitution. Before a more precise appraisal of the relative importance of the configurational and the other factors involved can be achieved more experimental data will be necessary, in particular on the temperature dependence of the heat capacity of the two isotopic systems. We are planning to complete such measurements at a variety of temperatures over the range 0° to 75° at all concentrations.

ACKNOWLEDGMENTS

We are indebted to the National Research Council for financial assistance, to the Shawinigan Chemical Co. for a fellowship, and to Dr. L. C. Leitch for the gift of samples of deuterated alcohols.

RÉSUMÉ

A partir de données récentes sur les propriétés volumiques et thermiques des solutions de peroxyde d'hydrogène et d'eau on a calculé les fonctions d'excès de ce système binaire. On a repris les mesures de densité des solutions de peroxyde de deutérium et d'eau lourde et on a étudié l'effet de divers composés deutérés sur la température de densité maximum de l'eau lourde. De cette étude il appert que les molécules de peroxyde d'hydrogène s'insèrent facilement dans la structure de l'eau et disloquent les traces de réseau cristallin qui y persistent encore au-dessus du point de fusion.

On propose une structure cristalline pour le composé $H_2O_2.2H_2O$.

REFERENCES

1. GIGUÈRE, P. A., MORISSETTE, B. G., OLMOS, A. W., and KNOP, O. Can. J. Chem. **33**, 804 (1955).
2. JESSUP, R. S. J. Research Natl. Bur. Standards, **55**, 317 (1955).
3. GIGUÈRE, P. A., MORISSETTE, B. G., and OLMOS, A. W. Can. J. Chem. **33**, 657 (1955).
4. SCHUMB, W. C., SATTERFIELD, C. N., and WENTWORTH, R. L. Hydrogen peroxide. Reinhold Publishing Corp., New York. 1955.
5. GIGUÈRE, P. A. and GEOFFRION, P. Can. J. Research, B, **28**, 599 (1950).
6. VOZNESENSKAJA, O. M. and ZASLAVSKIJ, I. I. J. Gen. Chem. U.S.S.R. **16**, 1189 (1946).
7. PHIBBS, M. K. and GIGUÈRE, P. A. Can. J. Chem. **29**, 173 (1951).
8. SCATCHARD, G., KAVANAGH, G. M., and TICKNOR, L. B. J. Am. Chem. Soc. **74**, 3715 (1952).
9. GIGUÈRE, P. A. and MAASS, O. Can. J. Research, B, **18**, 181 (1940).
10. FREDENHAGEN, K. Grundlagen für den Aufbau einer Theorie der Zweistoffsysteme. Akademie-Verlag, Berlin. 1950.
11. MITCHELL, A. G. and WYNNE-JONES, W. F. K. Discussions Faraday Soc. No. **15**, 161 (1953).
12. BAIN, O. Ph. D. Thesis, Laval University, Quebec, Que. 1953.
13. TAYLOR, R. C. and CROSS, P. C. J. Chem. Phys. **24**, 41 (1956).
14. HARVEY, K. B. Ph. D. Thesis, Laval University, Quebec, Que. 1956.
15. NATTA, G. and RIGAMONTI, R. Gazz. chim. ital. **66**, 762 (1936).
16. ABRAHAMS, S. C., COLLIN, R. L., and LIPSCOMB, W. N. Acta Cryst. **4**, 15 (1951).
17. FOLEY, W. T. and GIGUÈRE, P. A. Can. J. Chem. **29**, 123 (1951).
18. GALLAGHER, K. J., UBBELOHDE, A. R., and WOODWARD, I. Proc. Roy. Soc. (London), A, **222**, 195 (1954).
19. UBBELOHDE, A. R. and GALLAGHER, K. J. Acta Cryst. **8**, 71 (1955).
20. GALLAGHER, K. J., UBBELOHDE, A. R., and WOODWARD, I. Acta Cryst. **8**, 561 (1955).
21. GIGUÈRE, P. A. and SECCO, E. A. Can. J. Chem. **32**, 550 (1954).

Can. J. Chem. Downloaded from www.nrcresearchpress.com by 200.7.193.243 on 09/04/12
For personal use only.

Can. J. Chem. Downloaded from www.nrcresearchpress.com by 200.7.193.243 on 09/04/12
For personal use only.

INFLUENCE OF CALCIUM IONS ON THE MYOSIN-CATALYZED HYDROLYSIS OF ADENOSINE TRIPHOSPHATE[1]

G. E. Pelletier and Ludovic Ouellet

ABSTRACT

The activation of the myosin-catalyzed hydrolysis of adenosine triphosphate by calcium ions has been studied at pH 7.5 over a range of temperature extending from 3° to 25° C. There is evidence that the activation is due to the equilibrium formation of a complex between adenosine triphosphate and calcium ions.

From such a reaction mechanism, values of equilibrium constants are reported for the binding of adenosine triphosphate to the myosin in the presence and in the absence of calcium ions, together with stability constants for the calcium complexes of both the adenosine triphosphate and the myosin – adenosine triphosphate. The influence of hydrogen-ion concentrations on these constants is indicated.

INTRODUCTION

In the presence of myosin, a muscle protein, adenosine triphosphate (ATP) is hydrolyzed to adenosine diphosphate (ADP) and inorganic phosphate. This reaction has already been studied and related to the process of muscular contraction by Szent-Gyorgyi (1) and Engelhardt and Liubimova (2).

Various aspects of the kinetics of this reaction have been reported by Mommaerts (3, 4) including the influence of pH, magnesium, and ADP on the rate of the reaction at 27° C.

The influence of temperature on both the over-all rate and the enzyme substrate interaction constant has been reported previously (5). Pressure and ionic strength effects were studied by Laidler and Beardell (6).

This paper reports on the activation of the reaction by calcium ions at pH 7.5 over a range of temperatures. The reaction is interesting from this particular point of view as it proceeds both in the presence and in the absence of calcium ions (4).

Treatment of the Data

In the formation of enzyme–substrate–modifier complexes, the modifier (activator or inhibitor) is usually treated as being bound to an enzyme active site. If instead the modifier were bound in the complex to the substrate only, a general reaction mechanism for such a system could be represented by the following equations:

$$[1] \qquad S + M \overset{K_1}{\rightleftharpoons} SM,$$

$$[2] \qquad E + S \overset{K_2}{\rightleftharpoons} ES \overset{k_0}{\rightarrow} E + \text{Products},$$

$$[3] \qquad E + SM \overset{K_3}{\rightleftharpoons} ESM,$$

$$[4] \qquad ES + M \overset{K_4}{\rightleftharpoons} ESM \overset{k_r}{\rightarrow} E + \text{Products}.$$

In this scheme S is a substrate molecule, E and M are enzyme and modifier molecules that form with S the binary complexes ES and SM, and the ternary complex ESM. Only the complexes ES and ESM dissociate into products. The rate constants k_0 and

[1]*Manuscript received January 29, 1958.*
Contribution from the Department of Chemistry, University of Ottawa, Ottawa, Canada. Grateful acknowledgment is made to the National Research Council of Canada for financial assistance.

k_r are first-order rate constants for the breakdown of ES and ESM into enzyme and products of the reaction. All other constants are considered to be equilibrium constants.

The rapid equilibrium hypothesis yields an expression which is adequate to describe the experimental results in the kinetic behavior of the myosin – ATP – calcium ions system. As pointed out by Schwert (7), this observation does not eliminate the possibility that steady-state conditions prevail. Evidence along these lines arises from other considerations (8).

Under equilibrium conditions the rate of formation of products v in the above system can be written as

$$[5] \qquad v = \frac{k_r[\mathrm{E}]_0}{1+(1/K_2K_4[\mathrm{M}][\mathrm{S}])+(1/K_4[\mathrm{M}])} + \frac{k_0[\mathrm{E}]_0}{1+(1/K_2[\mathrm{S}])+K_4[\mathrm{M}]},$$

The different equilibrium constants can be evaluated through a proper choice of experimental conditions.

If $[\mathrm{M}] = 0$ or $K_4[\mathrm{M}] \gg 1$, equation [5] reduces to well-known Michaelis–Menten equations (9). K_2 and K_3 can then be obtained from plots of $1/v$ against $1/[\mathrm{S}]$ (10).

If $K_2[\mathrm{S}] \gg 1$ the equation can be rearranged to

$$[6] \qquad v-v_0 = \frac{(k_r-k_0)[\mathrm{E}]_0}{1+(1/K_4[\mathrm{M}])}$$

where $v_0 = k_0[\mathrm{E}]_0$. In this case a plot of $1/(v-v_0)$ against $1/[\mathrm{M}]$ gives K_4.

K_1 can be obtained from the thermodynamic relation

$$[7] \qquad K_1K_3 = K_2K_4.$$

If specific binding of the modifier on the enzyme did occur, equation [1] would become

$$[8] \qquad \mathrm{E} + \mathrm{M} \overset{K_1'}{\rightleftharpoons} \mathrm{EM}$$

and equation [3],

$$[9] \qquad \mathrm{EM} + \mathrm{S} \overset{K_3'}{\rightleftharpoons} \mathrm{EMS}.$$

Assuming equilibrium conditions, a simple expression can be derived for a system involving equations [8], [9], [2], and [4] (11). Although the expression obtained is different from equation [5], it reduces to simple Michaelis–Menten relations for both $[\mathrm{M}] = 0$ and $K_4[\mathrm{M}] \gg 1$, and to equation [6] for the cases where $K_2[\mathrm{S}]$ or $K_3[\mathrm{S}] \gg 1$. The interpretation of the constants is of course different. Evidence for the first mechanism proposed will be presented later in this paper.

EXPERIMENTAL PART

Reagents

The dipotassium salt of adenosine triphosphate (Pabst Laboratories, Milwaukee, Wis.) was used throughout these experiments. Tris(hydroxymethyl)aminomethane (THAM) (Fisher purified grade) and potassium chloride (Fisher certified reagent) were recrystallized from glass-distilled water. Calcium chloride was a certified reagent (Fisher). Acetic acid was Merck reagent grade.

Rabbit back-muscle myosin of the Weber-Edsall type was prepared according to a procedure described by Botts and Morales (12). Myosin concentrations were determined by a micro-Kjeldahl nitrogen-determination method. The myosin had a specific activity

Can. J. Chem. Downloaded from www.nrcresearchpress.com by 200.7.193.243 on 09/04/12
For personal use only.

of 5.1×10^{-6} moles of ATP hydrolyzed per second per gram of protein, at pH 7.5, in 0.6 M potassium chloride and 0.01 M calcium chloride, at 25° C.

Procedure

All reactions were carried out in buffered solutions containing 0.6 mole of potassium chloride and 0.1 mole of THAM per liter adjusted at the proper pH with acetic acid using a Beckman model G pH meter. These buffers were so adjusted at a series of temperatures, since the pH of THAM-buffered solutions varies considerably with temperature.

The solutions were kept in a constant-temperature bath (±0.1° C.) for 15 minutes, then mixed. At measured intervals of time, samples were pipetted into equal volumes of 20% trichloroacetic acid, thus precipitating the myosin which was removed by filtration through a dry filter paper. Phosphate concentrations in the filtrate were determined colorimetrically by the Fiske – Subba Row method (13), using a model DU Beckman spectrophotometer.

The rate of the reaction was measured as the number of moles of inorganic orthophosphate produced per liter per second.

RESULTS AND DISCUSSION

At constant concentration of myosin, in the presence of 5×10^{-4} moles per liter of ATP, the rate was found to increase with the concentration of calcium chloride according to equation [6]. At concentrations of calcium chloride higher than 0.01 M an already reported (4) lowering of the rate has been observed. Fig. 1 shows the results of a series of experiments at pH 7.5 and three temperatures. For the determination of the constants, the rates at zero concentration of calcium ion v_0 were subtracted from the rates obtained in the presence of calcium ions v, and the reciprocal of these values was plotted against the reciprocal of the calcium-ion concentrations. From these plots values for the constant K_4 for the binding of the calcium ions on the myosin–ATP complex were determined for each temperature. The apparent heat of reactions, $-\mathrm{R}\ d\ln K_4/d(1/T)$, was −3.5 kcal. per mole of calcium ions. The change in entropy was +3.0 e.u.

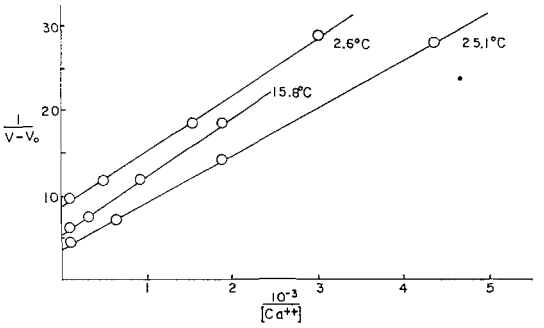

FIG. 1. Determination of K_4 in liters per mole by plotting $1/(v-v_0)$ against the reciprocal of the calcium-ion concentration in moles per liter at pH 7.5.

The pH of the solution had little effect on this constant. At 25° C. in the presence of 0.75 g. of myosin per liter K_4 was found to be 7.5×10^2 liters per mole at pH 7.5 and 8.0×10^2 liters per mole at pH 8.5. These values are consistent with data reported by Green and Mommaerts (4).

There is some evidence that the values of the experimentally determined constants

Can. J. Chem. Downloaded from www.nrcresearchpress.com by 200.7.193.243 on 09/04/12
For personal use only.

depend on the concentration of enzyme. Fig. 2 shows the effect of the enzyme concentration on the constant K_4 at 25° C. Assuming that the only effect of the enzyme is to decrease somewhat the concentration of the calcium ion in solution by non-specific binding, extrapolation to zero concentration of enzyme should give the constant K_4 independent of enzyme concentration. The extrapolated value of K_4 at 25° C. is approximately 1.5×10^3 liters per mole.

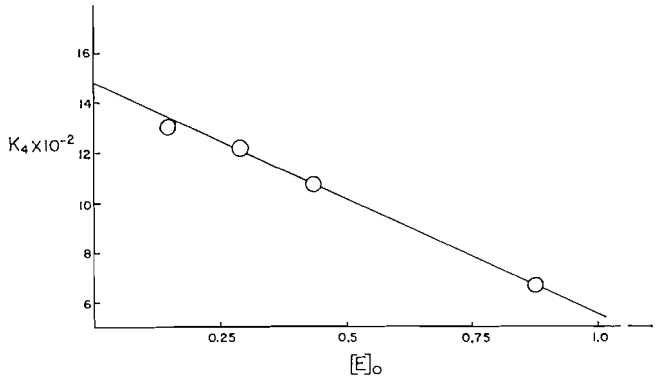

FIG. 2. Variation of the constant K_4 with enzyme concentration at 25° C. [ATP] = 5×10^{-4} M at pH 7.5.

It is interesting to note at this point that the stability constant of ATP Ca^{-2} is given by Smith and Alberty (14) as 1970 ± 280 at 25° C. and an ionic strength of 0.2. The agreement between this value and the above extrapolated value of K_4, although it could be a pure coincidence, supports the assumption made at the beginning of this paper that the activator calcium ion is bound to the ATP molecule in the ternary myosin–ATP–calcium complex. This would not of course exclude non-specific binding of calcium ions on the protein. The variation of K_4 with enzyme concentration would indeed suggest that calcium ions are bound to a considerable extent on the protein.

The constants K_2 and K_3 for the formation of the enzyme–substrate complex in the absence and in the presence of calcium ions were determined at pH 7.5 over a range of temperatures. Fig. 3 shows the results of these experiments as log K against $1/T$. The data from this figure suggest $\Delta H = +9$ kcal. per mole and $\Delta S° = 50$ e.u. The presence of calcium ions apparently does not affect to any great extent the binding of ATP on myosin. The interpretation of the above enthalpy and entropy values is complicated by contributions from hydrogen-ion concentration effects. Raising the pH from 7.0 to 9.3 lowers the value for the constant K_3 from 9.2×10^4 to 1.2×10^4 liters per mole at 25° C. (Fig. 4). A detailed description of K_3 as a function of hydrogen-ion concentration is made difficult by the fact that at high pH the enzyme is deactivated rapidly as shown by a sharp drop in the activity–pH curve around pH 9.5.

From equation [7] and the fact that $K_2 \cong K_3$, one finds that $K_1 \cong K_4$. This would imply that the calcium ion is bound just as readily to the substrate in the enzyme–substrate complex as it is to the substrate alone. As in the case of K_4 the value obtained for the constant K_1 is very close to that reported for the ATP calcium-ion stability constant (14). In an ATP – calcium ion system, there exists independently of any mechanism an equilibrium between the ATP–calcium complex and the ATP and calcium ions. The fact that this equilibrium constant has within experimental error the same value as the constant obtained in these experiments for K_1 supports the idea that K_1

Can. J. Chem. Downloaded from www.nrcresearchpress.com by 200.7.193.243 on 09/04/12
For personal use only.

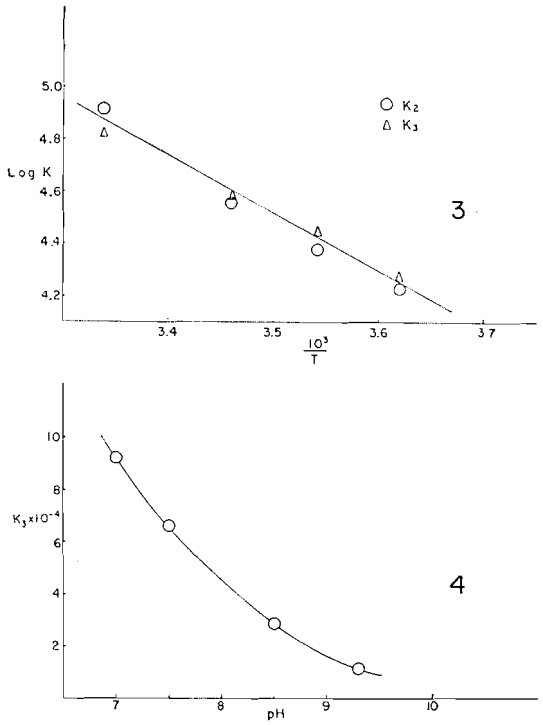

FIG. 3. Variation of the equilibrium constants for the formation of the myosin–ATP complex in the absence of calcium ions (○) and in 0.01 *M* calcium chloride solution (△).
FIG. 4. Influence of the pH on K_3 at 25° C.

actually is the equilibrium constant for the binding of calcium ions on ATP rather than the equilibrium constant for the binding of calcium ions on myosin. On the other hand, this might not be unequivocal evidence for the mechanism suggested here. As pointed out previously, the present treatment of data (equation [6]) would still describe the system if the calcium ions were bound to the active site of the enzyme.

As the variation of K_2 with temperature follows that of K_3, K_1 includes the same thermodynamic quantities as K_4, that is $\Delta H = -3.5$ kcal. per mole, $\Delta S° = +3$ e.u. These values are quite different from those reported by Smith and Alberty (14) for orthophosphate, where the formation of the calcium phosphate complex is mostly due to an increase of entropy. The behavior of ATP towards calcium ions however could be somewhat different from that of orthophosphate.

CONCLUSION

The data presented in this paper are consistent with the suggestion that the activation of the myosin-catalyzed hydrolysis of ATP by calcium ions is due to the formation of an ATP–calcium complex. The formation of such a complex would be slightly exothermic and accompanied by a small increase in entropy.

RÉSUMÉ

L'influence de la concentration des ions calcium sur le taux d'hydrolyse de l'adénosine triphosphate à été étudiée à des températures allant de 3° à 25° C. Il existe des indications que l'"activation" du système dépend de la formation d'un complexe ATP–calcium, en

Can. J. Chem. Downloaded from www.nrcresearchpress.com by 200.7.193.243 on 09/04/12
For personal use only.

état d'équilibre. Utilisant ce mécanisme, on a déterminé des constantes d'équilibre se rapportant à la formation du complexe myosine–ATP en la présence et en l'absence d'ions calcium, de même que les constantes de formation à l'équilibre des complexes des ions calcium avec l'adénosine triphosphate et l'intermédiaire myosine – adénosine triphosphate. L'influence de la concentration des ions hydrogène est mentionnée.

REFERENCES

1. SZENT-GYORGYI, A. Chemistry of muscular contraction. Academic Press, Inc., New York. 1951.
2. ENGELHARDT, V. A. and LIUBIMOVA, M. N. Nature, **144**, 668 (1939).
3. GREEN, I. and MOMMAERTS, W. F. H. M. J. Biol. Chem. **208**, 833 (1954).
4. GREEN, I. and MOMMAERTS, W. F. H. M. J. Biol. Chem. **202**, 541 (1953).
5. OUELLET, L., LAIDLER, K. J., and MORALES, M. F. Arch. Biochem. and Biophys. **39**, 37 (1952).
6. LAIDLER, K. J. and BEARDELL, A. J. Arch. Biochem. and Biophys. **55**, 138 (1955).
7. SCHWERT, G. W. Federation Proc. **13**, 971 (1954.)
8. LAIDLER, K. J. Discussions Faraday Soc. **20**, 83 (1955).
9. MICHAELIS, L. and MENTEN, M. L. Biochem. Z. **49**, 333 (1913).
10. LINEWEAVER, J. and BURK, D. J. Am. Chem. Soc. **56**, 658 (1934).
11. ALBERTY, R. A. J. Am. Chem. Soc. **75**, 1928 (1953).
12. BOTTS, J. and MORALES, M. F. J. Cellular Comp. Physiol. **37**, 27 (1951).
13. FISKE, C. H. and SUBBA ROW, J. J. Biol. Chem. **81**, 629 (1929).
14. SMITH, R. M. and ALBERTY, R. A. J. Am. Chem. Soc. **78**, 2376 (1956).

Can. J. Chem. Downloaded from www.nrcresearchpress.com by 200.7.193.243 on 09/04/12
For personal use only.

Can. J. Chem. Downloaded from www.nrcresearchpress.com by 200.7.193.243 on 09/04/12
For personal use only.

LYCODINE, A NEW ALKALOID OF LYCOPODIUM ANNOTINUM[1]

F. A. L. Anet and C. R. Eves

ABSTRACT

A new alkaloid, lycodine, $C_{17}H_{24}N_2$, m.p. 118°, has been isolated from *Lycopodium annotinum*. Lycodine is a tetracyclic diacidic base containing a secondary nitrogen atom, a 2,3-disubstituted pyridine ring, and a C-methyl group. The 2,3-disubstitution is in the form of a saturated six-membered ring.

The alkaloids of *Lycopodium annotinum* L. have been studied by several groups of workers in Canada and in Europe (1, 2, 3, 4, 5). The structure of annotinine, $C_{16}H_{21}O_3N$, which is the main alkaloid of this species, is now known (6, 7) and is of a quite novel type. It therefore becomes of interest to study the chemical structure of the minor alkaloids of this plant.

During the process of developing suitable methods for the separation of the many minor alkaloids which have been reported to occur in this *Lycopodium* species, we noticed that certain fractions possessed ultraviolet absorption characteristic of a pyridine chromophore, more or less submerged behind general absorption. This paper describes the isolation, characterization, and partial determination of the structure of a new alkaloid, lycodine, which was responsible for this characteristic absorption.

Lycodine was concentrated by countercurrent distribution of the alkaloid mother liquors from the crystallization of annotinine. Two successive countercurrent distributions were carried out, first in six large separatory funnels with the system chloroform–buffer of pH 6 and then in a 60-tube Craig machine with the system chloroform–buffer of pH 5.2. From these countercurrent distributions an alkaloid fraction was obtained which had the correct ultraviolet absorption. By chromatography of this fraction on activated alumina pure crystalline lycodine was obtained.

Lycodine, m.p. 118°, $[\alpha]_D$ −10°, had the formula $C_{17}H_{24}N_2$ and gave a characteristic dipicrate, m.p. 229°–233° (decomp.), which was sparingly soluble in methanol. Titration of the base in 50% methanol showed that the pK_a's of the base were 3.97 and 8.08. One C-methyl group was found to be present by the Kuhn–Roth method. The ultraviolet spectra of the base in neutral and in acid solutions are shown in Fig. 1, and correspond to an unconjugated pyridine chromophore in the base and salt forms respectively. A fuller discussion of these spectra will be left till after consideration of other results (see below).

The infrared spectrum of the base (in Nujol) is shown in Fig. 2; the sharp band at 3270 cm.$^{-1}$ must be due to a N—H group (8). As often happens (8) this band is of very low intensity in the spectrum (Fig. 2) of the carbon tetrachloride solution of the compound. The presence of a pyridine ring is confirmed by the band (9) at 1580 cm.$^{-1}$ (in Nujol) and that of a C-methyl group by a band (10) at 1382 cm.$^{-1}$ (in CCl_4). Acetylation of lycodine with acetic anhydride gave a N-acetyl derivative, isolated as the monopicrate. Titration of the picrate showed that the acetylated base had only one basic center (pK_a 4.95). Hydrolysis of N-acetyl lycodine gave back lycodine, thus confirming the presence of a secondary nitrogen atom in the alkaloid.

In order to determine the substitution on the pyridine ring we examined the NMR spectrum (Fig. 3) of lycodine. Under moderately high resolution there are three peaks of

[1]*Manuscript received February 6, 1958.*
Contribution from the Department of Chemistry, University of Ottawa, Ottawa, Canada.

Can. J. Chem. Downloaded from www.nrcresearchpress.com by 200.7.193.243 on 09/04/12
For personal use only.

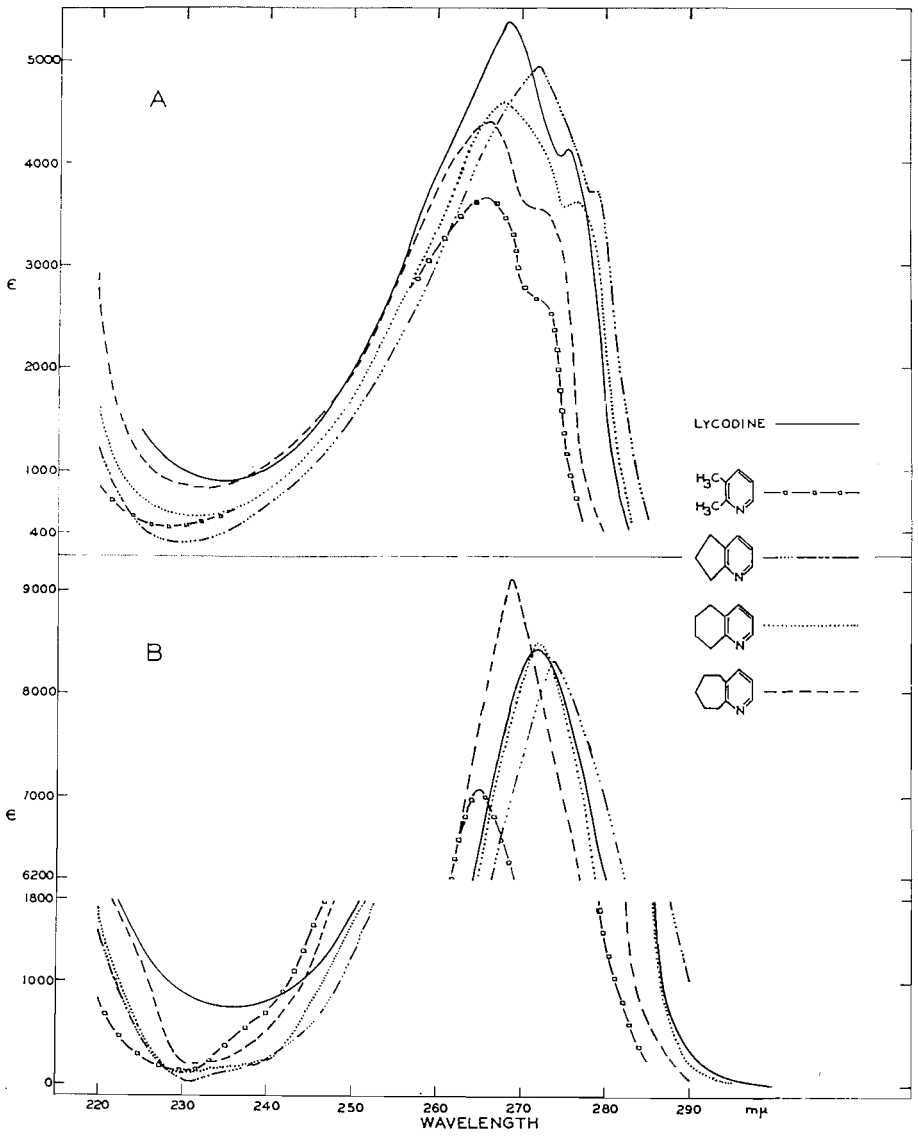

FIG. 1. Comparison of ultraviolet absorption spectra of lycodine and of 2,3-disubstituted pyridines (14). A, free bases; B, salts.

equal area at low field. These are probably due to protons on the pyridine ring (11). The sharp peak at highest field has three times the area of any of the peaks at lowest field and must correspond to the C-methyl group already found. It may be observed that the low value (61% of theoretical) found in the Kuhn–Roth estimation and the fact that the C-methyl peak in the NMR spectrum is unsplit both suggest that the methyl group is attached to a quaternary carbon atom. The other peaks in the spectrum correspond to the remaining protons in the molecule.

The spectrum of the low field part is shown at higher resolution above the main spectrum in Fig. 3. Each peak is split into four peaks, not always very well resolved.

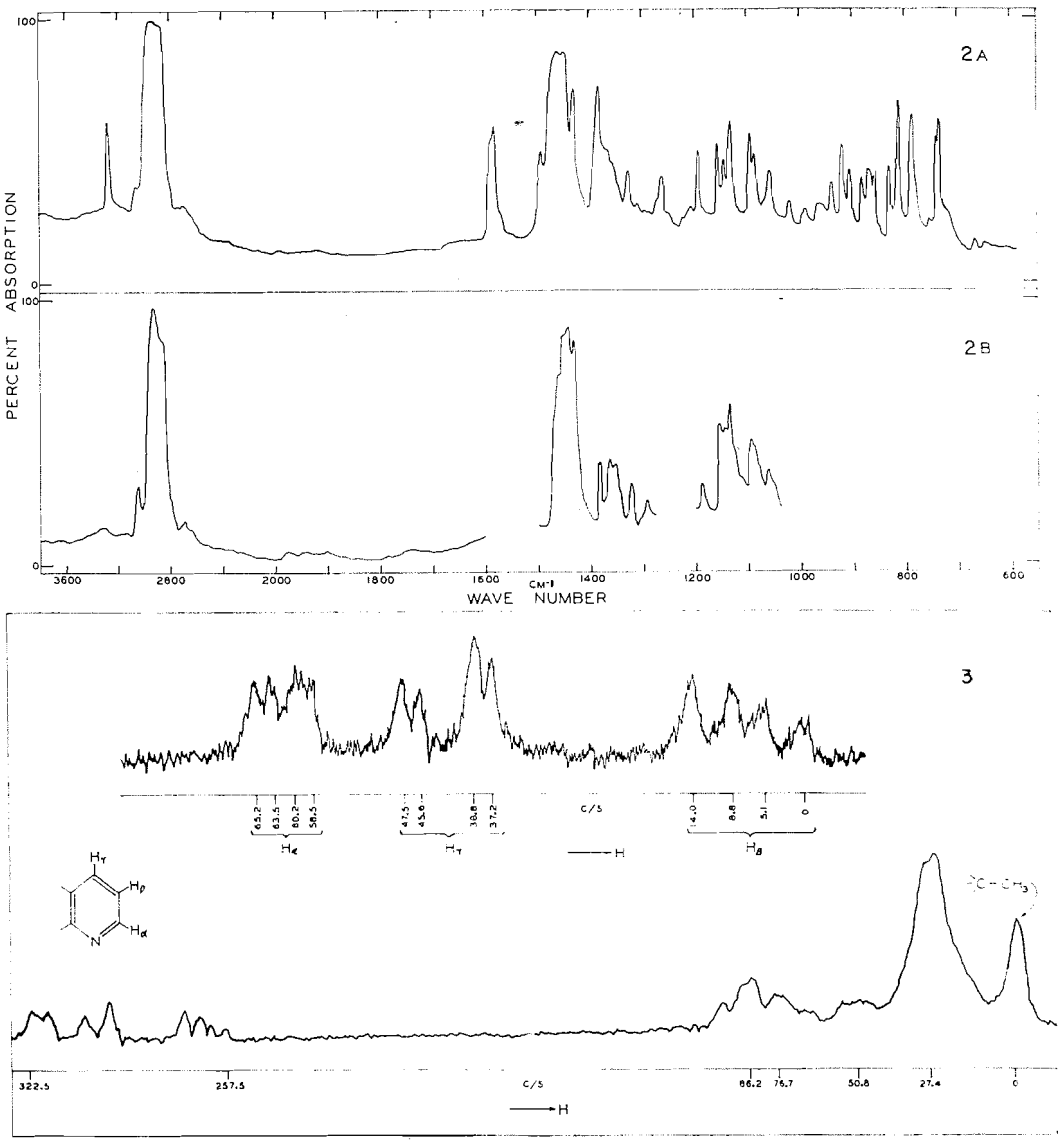

FIG. 2. Infrared absorption spectra of lycodine. A, Nujol mull; B, CCl_4 solution (1 mm. path length, 31 mg. per ml.).

FIG. 3. Nuclear magnetic resonance spectrum of lycodine. The upper curve represents the peaks at left of lower curve at higher resolution.

Bernstein, Pople, and Schneider (11, 12, 13) have recently examined the spectra of pyridine and various substituted pyridines and discussed the effect of chemical shifts and coupling constants on the spectra. From their analysis it can be seen that lycodine must be a 2,3-disubstituted pyridine, and in fact the spectrum of lycodine is very similar to that of 2,3-lutidine except for a difference in the relative chemical shift of the γ proton. The three peaks at low field may be assigned, from left to right, to the α, γ, and β protons of the pyridine ring.

The relative chemical shifts and coupling constants of the pyridine protons of lycodine

Can. J. Chem. Downloaded from www.nrcresearchpress.com by 200.7.193.243 on 09/04/12
For personal use only.

compared with those of 2,3-lutidine and pyridine are given in Table I. The observed intensities and energies of the signals from the pyridine protons of lycodine are in satisfactory agreement (Table II) with those calculated from the above parameters by the method of Bernstein, Schneider, and Pople (11). This confirms that the three peaks at low field indeed originate from the protons on the pyridine ring, and not from any other

TABLE I

CHEMICAL SHIFTS AND COUPLING CONSTANTS FOR LYCODINE AND SOME PYRIDINE DERIVATIVES (in c./sec.)

	Lycodine*	2,3-Lutidine† (11)	Pyridine† (13)
Chemical shifts			
$H\beta$–$H\alpha$	54.6	55.1	60.6
$H\gamma$–$H\alpha$	20.4	43.4	45.6
$H\gamma$–$H\beta$	34.2	11.7	15.0
Coupling constants			
$H\alpha.H\beta$	4.6	5.0	5.5
$H\beta.H\gamma$	8.6	7.35	7.5
$H\alpha.H\gamma$	2.3	1.3	1.9

**As a concentrated solution in carbon tetrachloride.*

†As pure liquids. (The effect of carbon tetrachloride on the chemical shift of these spectra is small even at infinite dilution, and is mainly on the α proton (13).)

TABLE II

OBSERVED AND CALCULATED SPECTRA FOR LYCODINE

Line	Origin of transition	Energy (c./sec.)		Relative intensity	
		Calc.	Obs.	Calc.	Obs.
1	β	0	0	0.77	0.65
2	β	5.1	5.1	0.75	0.76
3	β	8.6	8.8	1.23	1.17
4	β	13.8	14.0	1.25	1.41
5	γ	37.0	37.2	1.23	1.24
6	γ	38.5	38.8	1.25	1.54
7	γ	45.8	45.6	0.77	0.69
8	γ	47.3	47.5	0.75	0.89
9	α	58.5	58.5	1	1.85
10	α	60.3	60.2	1	
11	α	63.7	63.5	1	0.83
12	α	65.4	65.2	1	0.96

protons. The reason for the abnormal chemical shift of the γ proton of lycodine may be due to the nearness of the secondary nitrogen atom. Although, as will be shown later (see below), the secondary nitrogen atom is most probably separated from the pyridine ring by more than one carbon atom, it may still be fairly close in space to the γ proton. The abnormal chemical shift is not due to the fact that in lycodine, as will also be shown below, the 2,3-substitution is in the form of a saturated six-membered ring, since 5,6,7,8-tetrahydroquinoline gave a NMR spectrum closely similar to that of 2,3-lutidine.

We may be certain, therefore, of the presence of a 2,3-disubstituted pyridine ring in lycodine. Recently Godar and Mariella (14) have recorded the ultraviolet absorption spectra of 2,3-lutidine, 2,3-trimethylene-, 2,3-tetramethylene-, and 2,3-pentamethylene-pyridine both as free bases and as salts. Their data have been replotted in Fig. 1 using a linear ϵ scale, instead of the original log scale, which facilitates the comparison of these

Can. J. Chem. Downloaded from www.nrcresearchpress.com by 200.7.193.243 on 09/04/12
For personal use only.

curves with those of lycodine. It is clear that lycodine shows the greatest similarity to 2,3-tetramethylenepyridine (5,6,7,8-tetrahydroquinoline) and therefore that lycodine has in fact a saturated six-membered ring fused 2,3 to the pyridine ring.

The pK_a's (3.97 and 8.08) of lycodine are appreciably different from those of nicotine (3.35 and 7.70) determined under identical conditions. The difference in pK_a's of the non-pyridine nitrogen atoms may be due to the secondary nature of the nitrogen atom in one case and the tertiary nature in the other. The difference in the pK_a's of the pyridine nitrogen atoms, however, cannot be due to such an effect, but is readily understood if the saturated nitrogen atom is further (i.e. at least β) from the pyridine ring in the case of lycodine than in the case of nicotine.

Lycodine does not seem to contain unsaturation apart from the pyridine ring, as far as is shown by U.V., I.R., and NMR spectra. Therefore lycodine contains four rings, and the facts known about its constitution may be summarized by the following partial structure:

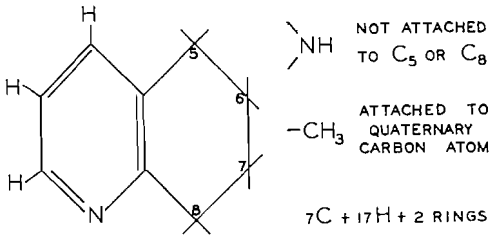

Finally, it may be mentioned that there appears to be a close similarity between lycodine and the *Lycopodium* alkaloid, β-obscurine, $C_{17}H_{24}ON_2$, which has been shown by Marion and Moore (15) to have an α-pyridone chromophore. Although the empirical formula of β-obscurine is correct for it to be the α-pyridone analogue of lycodine, the relationship between the two alkaloids cannot be so simple, for the basic nitrogen atom of β-obscurine appears to be tertiary, as the alkaloid could not be acetylated.

EXPERIMENTAL

Ultraviolet spectra were measured in methanol on a Beckman DK-2 spectrophotometer. Determinations of pK_a values were made by electrometric titrations in 50% aqueous methanol on 10–15-mg. samples. The infrared spectra of Fig. 2 (A) and (B) were measured on a Perkin-Elmer double-beam spectrometer, model 21B, with sodium chloride optics. Other infrared spectra were measured on a Perkin-Elmer single-beam double-pass instrument. The NMR spectra of compounds, as concentrated carbon tetrachloride solutions, were recorded (11) with a Varian V-4300 NMR spectrometer, equipped with field stabilizer, at a fixed frequency of 40 Mc./sec., with spinning sample tubes. Signal separations were measured by the side-band technique in the usual manner.

Isolation of Lycodine

From preliminary countercurrent distribution experiments with buffer of pH 6 and chloroform it was observed that most of the alkaloids have a high partition coefficient (conc. in buffer/conc. in $CHCl_3$) with this system, but that annotinine, lycopodine, acetyl acrifoline (alkaloid L.12), and lycodine have low partition coefficients. Alkaloids with a partition coefficient close to unity are present to only a minor extent in the batches of alkaloids used. Annotine (alkaloid L.11), which has such a partition coefficient (16), is

Can. J. Chem. Downloaded from www.nrcresearchpress.com by 200.7.193.243 on 09/04/12
For personal use only.

Can. J. Chem. Downloaded from www.nrcresearchpress.com by 200.7.193.243 on 09/04/12
For personal use only.

not present to a significant extent (16) in the crude alkaloid mixture which was available to us. On the basis of the above results the lycodine was concentrated in several stages.

(*a*) *Countercurrent distribution* (*large scale*).—The mother liquors from the crystallization of annotinine (approx. 40 g. of crude alkaloid) were first partitioned by countercurrent distribution between chloroform and concentrated citrate–phosphate buffer, pH 6 (600 ml. in each phase), using six 2-liter separatory funnels. The extraction scheme used was that of Bush and Densen (17). At each transfer the pH of the buffer was checked and corrected to pH 6, if necessary. Of the six chloroform phases (C-1 to C-6) and the six buffer phases (B-1 to B-6) obtained, the four containing lycodine (C-1 to C-4) were mixed and concentrated for the next step. The remaining fractions were retained for the separation of other alkaloids.

(*b*) *Countercurrent distribution* (*Craig machine*).—The chloroform fractions, C-1 to C-4, concentrated to 120 ml., were placed in the initial three tubes (40 ml. each) of a 60-tube Craig countercurrent machine (18) and partitioned through 60 transfers between chloroform and citrate–phosphate buffer, pH 5.2 (40 ml. in each phase). Examination of the fractions by their ultraviolet absorption disclosed the presence of lycodine in tubes 30 to 40. The alkaloids contained in both phases of these 11 tubes were then isolated in the usual manner. Paper chromatography (19) of the material by the descending technique with Whatman No. 1 paper buffered to pH 2.5, with *n*-butanol saturated with water as solvent, showed the presence of alkaloids after spraying with Dragendorff's reagent.

(*c*) *Absorption chromatography on activated alumina.*—The alkaloid mixture (2.6 g.) from tubes 30 to 40 of the Craig machine was then chromatographed on activated alumina, using *n*-pentane–benzene (1:1). The first alkaloid eluted from the column was the known alkaloid, lycopodine, followed by lycodine. A third alkaloid component, as yet uncharacterized, followed lycodine from the column upon elution wth benzene. The fractions containing lycodine were again detected by their ultraviolet absorption and by paper chromatography.

Characterization of Lycodine

Initially, lycodine was isolated as the dipicrate, which crystallized easily from methanol solution in characteristic radiating clusters of prisms, m.p. 229°–233° (decomp.). Calc. for $C_{17}H_{24}N_2.2C_6H_3O_7N_3$: C, 48.74; H, 4.23; N, 15.68%. Found: C, 48.20, 48.47; H, 4.02, 4.03; N, 15.91, 15.64%.

Lycodine dipicrate was converted to the base which was distilled at 100°–110° (air bath) (0.18 mm. Hg) to give a colorless distillate which crystallized spontaneously. The lycodine so obtained has m.p. 118°, $[\alpha]_D$ −10°±2° (*c*, 1.01 in ethanol). Calc. for $C_{17}H_{24}N_2$: C, 79.64; H, 9.43; N, 10.93; C—Me, 5.85%; M.W., 256.4. Found: C, 79.50, 79.46; H, 9.44, 9.38; N, 11.16; C—Me, 3.56%; M.W. (Rast), 246. Titration of lycodine in 50% aqueous methanol gave an equivalent weight of 255.8 (based on the strongly basic nitrogen) and pK_a's, 3.97 and 8.08.

Later, it was found that lycodine could be crystallized from *n*-pentane when seeded. This method was used to crystallize the base from the alumina fractions above, purification of the alkaloid in a number of instances being effected by means of recrystallizations of lycodine dipicrate. In all, about 400 mg. of lycodine was obtained. Attempts to obtain the monopicrate, diperchlorate, dihydrochloride, dihydroiodide, di-*p*-tolulene sulphonate, or the distyphnate in a crystalline state were unsuccessful. From the position of lycodine in the countercurrent distribution mentioned above, the distribution coefficient of the alkaloid in the system chloroform–buffer of pH 5.2 was calculated to be 1.4 (conc. in buffer/conc. in $CHCl_3$).

Acetylation of Lycodine

Lycodine (39.5 mg.) was refluxed in an excess of acetic anhydride under nitrogen for 2 hours. The solution was cooled and methanol added to react with the remaining acetic anhydride. After removal of the methyl acetate by distillation the residue was acidified with 5% hydrochloric acid and washed with ether. The aqueous solution was then made basic with sodium hydroxide solution and extracted with ether to obtain the base. N-Acetyl lycodine was isolated as the monopicrate, which crystallized from water as yellow needles, m.p. 180°–182.5° (decomp.). Calc. for $C_{19}H_{26}ON_2.C_6H_3O_7N_3$: C, 56.92; H, 5.54; N, 13.28%. Found: C, 56.58; H, 5.39; N, 13.69%. The free base was not obtained crystalline. The infrared absorption spectrum (in Nujol) of N-acetyl lycodine contained a band at 1661 cm.$^{-1}$ characteristic of an amide carbonyl, which band was not present in the spectrum of lycodine. By means of descending paper chromatography using Whatman No. 1 paper buffered at pH 3, and *n*-butanol saturated with water as the moving phase, lycodine (R_f, 0.35) was easily distinguished from N-acetyl lycodine (R_f, 0.65).

Hydrolysis of N-Acetyl Lycodine

N-Acetyl lycodine obtained from the monopicrate was refluxed in conc. hydrochloric acid for 6 hours. After cooling, the solution was rendered basic with sodium hydroxide solution and extracted with ether. The ether extractions were each washed with water and dried over anhydrous sodium sulphate before being evaporated to dryness. The residue was distilled around 125° (air bath) (0.8 mm. Hg) and the clear distillate crystallized on standing. These crystals had m.p. 118° either alone or mixed with lycodine.

Attempted Acetylation of β-Obscurine

β-Obscurine (*ca.* 1 mg.) was subjected to the same reaction conditions as used for the acetylation of lycodine. After removal of the remaining acetic anhydride, the product gave only one spot which corresponded to that of β-obscurine when it was paper chromatographed. The same result was obtained when β-obscurine was acetylated with acetic anhydride, using anhydrous sodium acetate as catalyst, for double the length of time. The neutral fraction of the product did not contain any substance having an α-pyridone chromophore.

ACKNOWLEDGMENTS

We are greatly indebted to Dr. Léo Marion, of the National Research Council, for providing us with the mother liquors from the crystallization of annotinine, to Dr. H. J. Bernstein, of the National Research Council, for taking the NMR spectra and for discussion of the results, to Dr. E. M. Godar and Dr. R. P. Mariella, of Loyola University, Chicago, Illinois, for generously providing us with a sample of tetrahydroquinoline, to Dr. D. B. McLean, of McMaster University, for a gift of obscurine, and to Mr. R. Lauzon and Dr. R. N. Jones, of the National Research Council, for the infrared spectra taken on the double-beam instrument. We wish to thank the National Research Council for a grant in aid of this work. One of the authors (C. R. E.) wishes to thank the Commissioner, Royal Canadian Mounted Police, whose kind permission and support enabled him to take part in this work.

REFERENCES

1. MARION, L. and MANSKE, R. H. F. Can. J. Research, B, **21**, 92 (1943).
2. MANSKE, R. H. F. and MARION, L. J. Am. Chem. Soc. **69**, 2126 (1947).
3. BERTHO, A. and STOLL, A. Ber. **85**, 663 (1952).

Can. J. Chem. Downloaded from www.nrcresearchpress.com by 200.7.193.243 on 09/04/12
For personal use only.

4. ACHMATOWICZ, O. and RODEWALD, W. Roczniki Chem. **29**, 509 (1955).
5. PERRY, G. S. and MACLEAN, D. B. Can. J. Chem. **34**, 1189 (1956).
6. PRZYBYLSKA, M. and MARION, L. Can. J. Chem. **35**, 1075 (1957).
7. WIESNER, K., AYER, W. A., FOWLER, L. R., and VALENTA, Z. Chem. & Ind. 564 (1957) and previous papers.
8. MARION, L., RAMSAY, D. A., and JONES, R. N. J. Am. Chem. Soc. **73**, 305 (1951).
9. BELLAMY, L. J. The infra-red spectra of complex molecules. Methuen & Co. Ltd., London. 1954. p. 234.
10. BELLAMY, L. J. The infra-red spectra of complex molecules. Methuen & Co. Ltd., London. 1954. p. 13.
11. BERNSTEIN, H. J., POPLE, J. A., and SCHNEIDER, W. G. Can. J. Chem. **35**, 65 (1957).
12. POPLE, J. A., SCHNEIDER, W. G., and BERNSTEIN, H. J. Can. J. Chem. **35**, 1060 (1957).
13. SCHNEIDER, W. G., BERNSTEIN, H. J., and POPLE, J. A. Can. J. Chem. **35**, 1487 (1957).
14. GODAR, E. and MARIELLA, R. P. J. Am. Chem. Soc. **79**, 1402 (1957).
15. MOORE, B. P. and MARION, L. Can. J. Chem. **31**, 952 (1953).
16. ANET, F. A. L. and KHAN, N. H. Unpublished results.
17. BUSH, M. T. and DENSEN, P. M. Anal. Chem. **20**, 121 (1948).
18. CRAIG, L. C. and POST, O. Anal. Chem. **21**, 500 (1949).
19. BRINDLE, H., CARLESS, J. E., and WOODHEAD, H. B. J. Pharm. and Pharmacol. **3**, 793 (1951).

Can. J. Chem. Downloaded from www.nrcresearchpress.com by 200.7.193.243 on 09/04/12
For personal use only.

Can. J. Chem. Downloaded from www.nrcresearchpress.com by 200.7.193.243 on 09/04/12
For personal use only.

THE VAPOR PRESSURE OF LITHIUM IN THE REDUCTION OF LITHIUM OXIDE BY SILICON[1]

W. MORRIS[2] AND L. M. PIDGEON

ABSTRACT

The vapor pressure of lithium over the system lithium oxide – calcium oxide – silicon has been measured using the gas entrainment method at temperatures between 970° C. and 1025° C. The experimental results are summarized in the form $4 \log P = 43.1 - (6.69/T) \times 10^4$, where P is in atmospheres and T in ° A. The reaction, as usually written,

$$2Li_2O + 2CaO + Si = 4Li(g) + 2CaO.SiO_2,$$

does not describe the process completely.

INTRODUCTION

The classical method of producing alkali metals involves electrolysis of fused chlorides, preferably a mixture of chlorides in order to utilize a low-melting-point eutectic. Lithium is so produced using LiCl–KCl mixtures. In this case, however, certain inherent disadvantages of electrolytic processes are intensified. Lithium is at the head of the electromotive series; hence, any metallic impurities present in the bath would be deposited at the cathode and find their way into the final product. The purity of the metal is dependent on the purity of the charge material.

These characteristics, together with the low electrochemical equivalent of lithium (6.94 lb. of Li per 500 amp-days of power) and the reactivity of the metal, justify the search for alternative methods in the form of thermal reduction techniques. The relative volatility of lithium metal should permit its evolution in the gaseous state from a reaction mixture consisting of the oxide and a suitable reducing agent.

Such a method has been successfully applied to magnesium, where calcined dolomite is reacted with silicon (as ferrosilicon) in the solid state, the reaction occurring being described as

$$2CaO.MgO(s) + Si(s) = 2Mg(g) + 2CaO.SiO_2(s). \quad [1]$$

Kroll and Schlechten (1) examined a number of reducing agents and decided that a reaction similar to that for magnesium was feasible and, in fact, preferable to others. For this purpose, these authors calcined mixtures of Li_2CO_3–CaO, which were subsequently briquetted with FeSi to provide the charge for their experiments. In a manner analogous to the magnesium-forming reaction, lime was added so that a calcium silicate rather than a lithium silicate would form according to the postulated reaction

$$2Li_2O(s) + 2CaO(s) + Si(s) = 4Li(g) + 2CaO.SiO_2(s). \quad [2]$$

These authors described the general procedures adopted and were not concerned with the measurement of the pressures of lithium over the system.

This paper describes measurements of the equilibrium pressures of lithium over a mixture of calcined $Li_2CO_3.CaO$ and silicon. The magnitude of this pressure is the effective driving force of the reaction, and directly controls the feasibility of a practical reduction process of this type.

[1]*Manuscript received December 23, 1957.*
Contribution from the Metallurgical Engineering Laboratory, University of Toronto, Toronto, Ontario, based on a thesis by W. Morris submitted in partial fulfillment of the requirements for the degree of Doctor of Philosophy to the Graduate School of the University of Toronto.
[2]*Now with Dow Chemical of Canada Limited, Toronto.*

Can. J. Chem. Downloaded from www.nrcresearchpress.com by 200.7.193.243 on 09/04/12
For personal use only.

EXPERIMENTAL

From preliminary experiments, it was found that the reaction pressure of lithium in the reduction process was in the order of 5 mm. Hg at 1000° C. As a result, the entrainment method was adopted, similar to that used by Pidgeon and King (2) and later by Ellingsgaeter and Rosenqvist (3) in their examination of reaction [1].

Purified argon was employed as the carrier gas, which was saturated with lithium vapor. The metal vapors were carried downstream to a point where conditions were appropriate for condensation.

Owing to the reactivity of lithium metal, the reaction tube adopted was a clean 30-inch length of black iron pipe (1 inch diameter) enclosed by a heat-resisting nickel–chromium tube. Insert condensers were troublesome, and it was decided to utilize the downstream portion of the iron reaction tube itself as condenser. At the end of an experimental run the tube was cut in two, separating the condensing section from the charge zone. The condensed product could not be weighed directly because of the rapid formation of lithium nitride in the atmosphere. As a result, the deposit was dissolved in hot distilled water, and the amount of lithium collected determined by polarographic means (4).

Clean steel wool placed at the extreme downstream section of the charge prevented the contamination of the condensing section of the reaction tube by fine particles entrapped in the gas stream. Vapor-phase condensation of the lithium vapor similar to the formation of "blue powder" in the thermal reduction of ZnO was eliminated by inserting a second piece of clean steel wool slightly downstream from the point where the bulk of the condensation occurred. This vapor-phase condensation phenomenon is caused by the "cold blanket" of carrier gas on the walls of the condenser. Steel wool serves to eliminate this phenomenon and also acts as a dust trap.

The reaction zone was equipped with baffles which maintained a 3-inch zone constant to ±1° C.

CHARGE MATERIAL

Li_2O was produced by thermal dissociation of reagent grade Li_2CO_3–CaO mixtures in vacuum according to the procedures described by Kroll and Schlechten (1). The calcined product, originally containing 60% CaO and 40% Li_2CO_3, was mixed with a 20% addition of 100% −100 mesh ferrosilicon analyzing 79% Si, and subsequently briquetted to provide particles $\frac{1}{3}$ inch in average dimension. The mixture for reduction analyzed 7.0% Li and 16.9% Si.

PROCEDURE

Reduction briquettes were charged to the reaction tube and heated to the required temperature. After the passage of a given amount of argon, sufficient to bring about 5–10% reduction (i.e., approximately 0.3 g. Li collected), the reaction tube was removed from the furnace and cooled in argon. When the tube had cooled sufficiently, it was subsequently sectioned, and the product in the condensing section was dissolved and analyzed.

From the volume of argon used, corrected to N.T.P., and the amount of lithium collected, the reaction pressure of lithium over the system was calculated.

RESULTS

A series of experiments at a temperature of 993° C. and flow rates varying from 2.0 to 8.0 cc. per second was performed. The results are shown in Table I and plotted in Fig. 1.

From the graph (Fig. 1), it can be seen that the extrapolation to zero flow rate yields

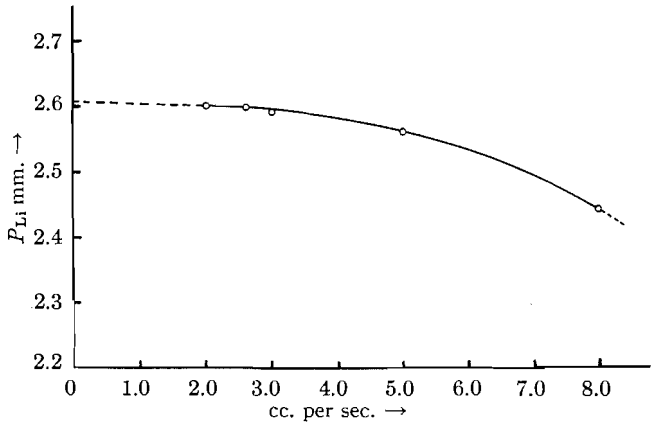

FIG. 1. Effect of flow rate on apparent vapor pressure.

TABLE I

Rate (cc./sec.)	P_{Li} mm. Hg)
2.0	2.60
2.6	2.60
3.0	2.59
5.0	2.56
8.0	2.44

a value of the vapor pressure essentially the same as the value at a flow rate of 2.6 cc. per second. At flow rates above 2.6 cc. per second saturation of the argon carrier gas was not established. This is shown by the lower values of the apparent vapor pressures at these higher rates.

The flow rate of 2.6 cc. per second is large enough to overcome thermal-diffusion effects, and small enough to establish saturation. At very low flow rates, it was observed that the iron reaction tube was bright-annealed by the lithium vapors upstream from the reaction zone, caused by the back-diffusion of lithium in the gas stream. At the saturation rates, this bright-annealing effect was not observed.

Saturation experiments were also performed at 972° C. and results similar to those at 993° C. were obtained.

EFFECT OF TEMPERATURE

At temperatures below 970° C., consistent results could not be obtained; at temperatures above 1025° C., the charge showed definite evidence of the formation of a liquid phase. Successful measurements were therefore restricted to this range of temperature.

TABLE II

P_{Li} (mm.)	log K_p (atm.)	° C.	° A.	$1/T$° K.
1.8	−10.5020	972	1245	8.032×10^{-4}
2.3	−10.0764	982	1255	7.968
2.6	− 9.8632	993	1266	7.899
2.9	− 9.6736	996	1269	7.880
3.5	− 9.3468	1005	1278	7.825
4.1	− 9.0720	1011	1284	7.788
4.5	− 8.9104	1012	1285	7.782
4.9	− 8.7624	1016	1289	7.758
6.6	− 8.2452	1025	1298	7.704

Can. J. Chem. Downloaded from www.nrcresearchpress.com by 200.7.193.243 on 09/04/12
For personal use only.

Table II summarizes the results obtained. The values quoted for the measured vapor pressure are estimated to have a probable error of 5% and represent the average of several determinations at the various temperatures.

Fig. 2 is a plot of $4 \log_{10} P_{Li}$ against $1/T°$ K.

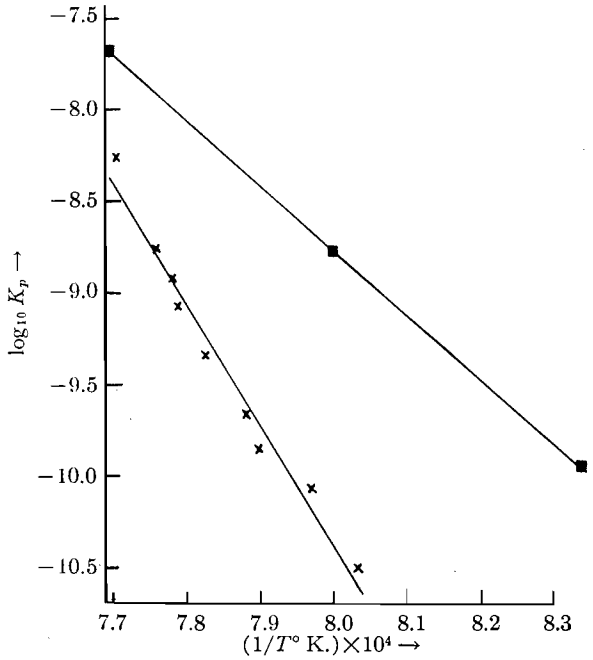

FIG. 2. Calculated and observed equilibrium constants plotted against reciprocal temperature.
■—Calculated. ×—Observed.

DISCUSSION

The reaction [2] as proposed by Kroll and Schlechten (1) served as a basis for the calculations. Experiments were performed in which the reaction was completed *in vacuo*. X-Ray diffractometer investigations on the solid residue revealed the presence of dicalcium silicate, excess CaO, and excess FeSi. The diffractometer traces also showed the presence of other compounds which could not be identified, suggesting that equation [2] is not the only reaction occurring.

The presence of the diatomic species of lithium vapor (Li_2), at a total pressure $P_{(Li+Li_2)}$ equal to 40 or 50 mm. Hg, would account for approximately 7% of the vapor phase at these temperatures (5). However, at the pressures of lithium involved in this research (in the order of 2–6 mm. Hg), the diatomic species can be shown to play a negligible role.

Assuming that the major reaction is reaction [2], equilibrium constants were computed and plotted against $1/T°$ K., both from the experimental values and from the calculated values for the reaction. The experimental values are shown in Table II and

TABLE III

P_{Li} (mm.)	log K_p (atm.)	° K.
2.46	−9.956	1200
4.94	−8.744	1250
9.25	−7.656	1300

Can. J. Chem. Downloaded from www.nrcresearchpress.com by 200.7.193.243 on 09/04/12
For personal use only.

plotted in Fig. 2. The calculated values are shown in Table III and are also plotted in Fig. 2.

For these calculations, the solids as predicted by reaction [2] were assumed to be present as pure, distinct phases; thus, their activities were equated to unity and the lithium vapors present were assumed ideal; hence, the equilibrium constant was written in the form

$$K_p = (P_{Li})^4.$$

The thermodynamic data used for the calculated values of the equilibrium constant were taken from Kubaschewski and Evans (6), Coughlin (7), and Kelley (8).

A statistical analysis of the experimental points gives the equation of the straight line in Fig. 2 in the form

$$\log_{10}K_p = 43.1 - (6.69\times10^4/T) \qquad [3]$$

corresponding to a heat of reaction of 306,000 cal. The calculated value for the heat of reaction utilizing the values shown in Table III is 164,000 cal.

The discrepancy between the calculated and the observed values is greater than either the experimental error or the uncertainty of the thermodynamic data used. The discrepancy must lie, then, in the assumption of unit activities or be due to the fact that the reaction cited (equation [2]) is an oversimplification.

It is quite probable that the formation of a lithium silicate should be accounted for, since in a series of experiments above 1025° C. the charge showed distinct evidence of the formation of a liquid phase. The melting point of pure Li_2SiO_4 is approximately 1025° C. A further possibility is the formation of the double silicate of Ca and Li.

In general, it can be stated that, if any side reaction occurs that effectively ties up any lithium, an increase in the heat of reaction would be observed.

CONCLUSIONS

1. The values of the pressure of lithium encountered in the reduction reaction are of sufficient magnitude to warrant a commercial thermal reduction process.

2. The experimental values are summarized in the form $\log_{10}P = 43.1 - (6.69/T)\times10^4$, where P is in atmospheres and T in ° K.

3. The reaction occurring, written in the form

$$2Li_2O + 2CaO + Si = 4Li + 2CaO.SiO_2,$$

is an oversimplification.

ACKNOWLEDGMENTS

The authors acknowledge financial assistance for this research in the form of an International Nickel Co. Fellowship to one of them. Reduction briquettes were supplied by courtesy of the Dominion Magnesium Limited, Haley, Ontario.

REFERENCES

1. KROLL, W. J. and SCHLECHTEN, A. W. A.I.M.M.E., Tech. Publ. No. 2179 (1947); Trans. A.I.M.M.E. **182**, 266 (1944).
2. PIDGEON, L. M. and KING, J. A. Discussions Faraday Soc. No. 4, 197 (1948).
3. ELLINGSGAETER, B. and ROSENQVIST, T. J. Metals (Aug.), 1111 (1956).
4. CLARK, W. E. J. Am. Chem. Soc. **75**, 6042 (1953).
5. DOUGLAS, T. B., EPSTEIN, L. F., DEVER, J. L., and HANLAND, W. H. J. Am. Chem. Soc. **77**, 2144 (1955).
6. KUBASCHEWSKI, O. and EVANS, E. LL. Metallurgical thermochemistry. John Wiley & Sons, Inc., New York. 1956.
7. COUGHLIN, J. P. Contribution to the data on theoretical metallurgy. III. Heats and free energy of formation of inorganic oxides. Bureau of Mines (U.S.A.), Bull. 542 (1954).
8. KELLEY, K. K. III. Free energies of vaporization and vapour pressures of inorganic substances. Bureau of Mines (U.S.A.), Bull. 383 (1935).

Can. J. Chem. Downloaded from www.nrcresearchpress.com by 200.7.193.243 on 09/04/12
For personal use only.

Can. J. Chem. Downloaded from www.nrcresearchpress.com by 200.7.193.243 on 09/04/12
For personal use only.

SUR LES RÉACTIONS DES POLYESTERS AVEC LE TÉTRACHLORURE DE TITANE

I. LA RÉACTION DE L'OXALATE DE DIÉTHYLE AVEC LE TÉTRACHLORURE DE TITANE[1]

RÉAL AUBIN[2] ET ROLAND RIVEST

SOMMAIRE

On montre dans ce mémoire que l'oxalate de diéthyle réagit avec le tétrachlorure de titane pour donner un composé d'addition moléculaire: le diéthyl oxalate-1,2 tétrachlorure de titane IV. On examine quelques propriétés de ce complexe de coordination et on propose pour ce composé la structure d'un chélate monomérique de configuration *cis*.

INTRODUCTION

Les réactions des polyesters avec le tétrachlorure de titane ont été peu étudiées; Demarçay (1) paraît en avoir donné la première description et depuis, seulement deux autres réactions (2, 3) ont été signalées. Des travaux parallèles conduits par Hieber et Reindl (4) sur le tétrachlorure d'étain et l'analyse récente menée par Archambault (5) sur les réactions acide–base du titane avec certains composés électrodotiques nous ont incités à entreprendre une étude systématique et comparée des réactions des polyesters avec le tétrachlorure de titane.

L'atome tétravalent du titane possède dans plusieurs composés connus un nombre de coordination (6). Dans le tétrachlorure, il peut donc recevoir deux doublets additionnels d'électrons venant d'une substance électrodotique appropriée. Il adopte alors une configuration octaédrique très stable de type d^2sp^3. Les diesters sont des polydentates présentant plusieurs possibilités de réaction avec le tétrachlorure de titane. Ils peuvent donner des chélates où les liaisons chimiques diester–tétrachlorure peuvent être en position *cis* ou *trans* selon la stéréochimie du diester impliqué dans la formation du composé. Il est aussi possible qu'un empêchement stérique s'oppose à la cyclisation et dans ce cas, le produit obtenu pourrait être soit un polymère, soit un composé d'addition simple.

Dans le but de vérifier ces différentes possibilités nous avons entrepris l'étude des trois types de diesters suivants:

(*a*) Les diesters à constitution $R—O—\overset{\overset{O}{\|}}{C}—(CH_2)_n—\overset{\overset{O}{\|}}{C}—O—R$, où "R" et "*n*" peuvent varier. Exemple: l'oxalate de diéthyle.

(*b*) Les polyesters du type $R—\overset{\overset{O}{\|}}{C}—O—(CH_2)_n—O—\overset{\overset{O}{\|}}{C}—R$. Exemple: le diacétate d'éthylène.

(*c*) Les polyesters aromatiques $Ar(COOR)_2$, tels l'isophthalate de diméthyle.

Comme premier terme de notre investigation, la réaction de l'oxalate de diéthyle sur le tétrachlorure de titane semblait particulièrement bien adaptée à notre projet puisque la description de Demarçay (1) et les brefs commentaires de Wurtz (7) n'avaient guère précisé la structure et les propriétés générales du complexe issu de cette réaction.

[1]*Manuscrit reçu le 27 janvier 1958.*
Contribution du Département de Chimie de l'Université de Montréal, Montréal, Qué.
[2]*Boursier de l'Office des Recherches scientifiques de la Province de Québec.*

Can. J. Chem. Downloaded from www.nrcresearchpress.com by 200.7.193.243 on 09/04/12
For personal use only.

PARTIE EXPÉRIMENTALE

Purification des produits chimiques

On utilise pour cette réaction le tétrachlorure "purifié" de la compagnie Fisher Scientific. On met en œuvre une méthode de purification achevée en appliquant le mode opératoire de Gilchrist et de ses collaborateurs (8). On obtient ainsi un produit de haute pureté sans traces de chlore ni de vanadium.

L'oxalate de diéthyle est également un produit "purifié" de Fisher Scientific. Le diester est desséché sur du sulfate de sodium anhydre et soumis à une distillation fractionnée sous pression réduite. La fraction médiane est conservée sur le sulfate de sodium anhydre.

Au cours de l'addition des deux substances concernées dans cette réaction, le tétrachlorure de carbone tient lieu de solvant usuel. Il reçoit un traitement identique à celui de l'oxalate de diéthyle sauf en ce qui a trait à la pression, lors de la distillation fractionnée.

Mode opératoire

Comme le tétrachlorure de titane réagit violemment avec certains polyesters, nous diluons les réactifs dans le tétrachlorure de carbone.

Le tétrachlorure de carbone (100 ml.) est placé dans un ballon de 250 ml. Un courant d'azote sec chasse l'air humide et prévient l'hydrolyse au cours des opérations subséquentes. Une quantité mesurée du réactif qui doit être en excès est alors ajoutée à l'aide d'une seringue graduée à aiguille de Téflon. L'agitation du mélange est provoquée par un agitateur magnétique. Une portion mesurée de l'autre réactif est alors ajoutée lentement à l'aide d'une autre seringue graduée à aiguille de Téflon. Une coloration jaune apparaît aussitôt. Bien que l'addition s'opère à température normale, la chaleur de réaction n'augmente pas trop la température du système, si l'addition est assez lente, l'agitation suffisante et les dilutions dans CCl_4 assez poussées. Bientôt le complexe précipite sous forme finement cristallisée.

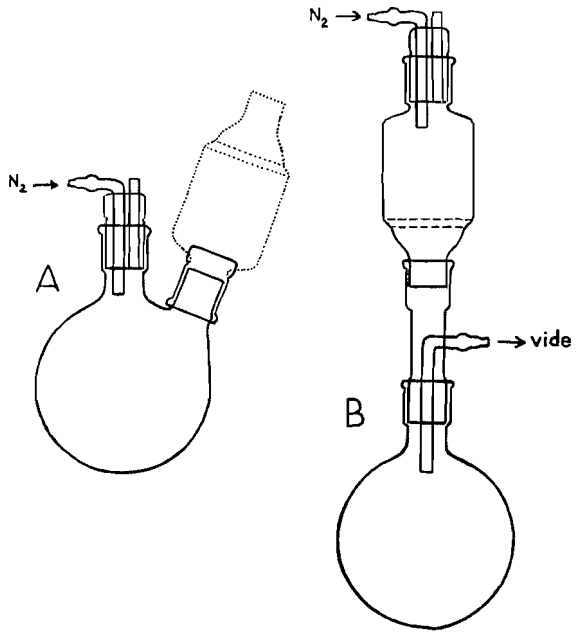

FIG. 1. Appareils utilisés: pour l'addition des réactifs (A); pour l'extraction, la purification et le séchage du complexe formé (B).

Le tout est transféré quantitativement sur un filtre de porosité moyenne. On maintient une atmosphère d'azote dans l'appareil et le précipité est lavé une dizaine de fois avec des portions de 20 ml. de CCl_4 pour le débarrasser de l'excès de réactif très soluble dans le tétrachlorure de carbone.

Le complexe cristallisé et lavé est séché durant quelques heures sous une pression inférieure à 1 mm. de mercure et à température ordinaire. Le produit est conservé dans un récipient scellé ou dans un dessiccateur renfermant du pentoxyde de phosphore.

Le schéma des appareils utilisés pour ces opérations est donné dans la figure 1.

Méthodes d'analyse

Le point de fusion (p.f.) est corrigé; il a été déterminé dans un appareil de Thiele.

Le poids moléculaire a été évalué par ébullioscopie dans le benzène anhydre chez Huffman Microanalytical Laboratories, Wheatridge, Colorado.

La détermination gravimétrique du chlore a été conduite selon le protocole analytique décrit par Vogel (9). Le titane a été déterminé gravimétriquement sous forme de TiO_2.

Les spectres infrarouges ont été déterminés à l'aide d'un spectromètre "Perkin-Elmer", modèle 112, à simple faisceau et parcours double.

RÉSULTATS ET DISCUSSION

Structure du produit de la réaction

Les travaux de Sisler et de ses collaborateurs (10) ont montré que le rapport de l'addition moléculaire dans ce genre de réaction se trouve parfois être 1:2 ou 1:1 selon qu'il y a, ou non, excès de réactif électrodotique. Nous avons voulu préciser la valeur de ce rapport dans la réaction d'addition de l'oxalate de diéthyle avec le tétrachlorure de titane; dans ce dessein, nous avons effectué plusieurs additions de l'oxalate de diéthyle dans des concentrations relatives variables par rapport au tétrachlorure de titane. C'est ainsi que nous avons utilisé l'oxalate de diéthyle en excès sur le tétrachlorure de titane, les deux réactifs en proportions équivalentes et finalement, l'oxalate de diéthyle avec un excès de tétrachlorure de titane. Le tableau I résume les résultats obtenus dans les dosages du titane et du chlore des différents composés d'addition réalisés. On voit clairement que le rapport de l'addition moléculaire demeure toujours et seulement 1:1, quelles que

TABLEAU I

TABLEAU COMPARATIF DES VALEURS (%) DE Ti ET DE Cl DANS LES COMPOSÉS THÉORIQUES 1:1 ET 1:2 ET DANS LES COMPOSÉS FORMÉS EXPÉRIMENTALEMENT

Valeurs calculées	% Ti	% Cl	Valeurs trouvées	% Ti	% Cl
$1TiCl_4.1(COOC_2H_5)_2$	14.26	42.22	Addition avec TiCl en excès	14.48	40.40
			Addition sans excès de réactif	14.40	41.27
$1TiCl_4.2(COOC_2H_5)_2$	9.93	29.41	Addition avec $(COOC_2H_5)_2$ en excès	14.48	41.38

soient les concentrations respectives de l'oxalate de diéthyle et du tétrachlorure de titane. En aucun cas, nous n'avons pu obtenir le rapport d'addition 1:2, soit $TiCl_4.2(COOC_2H_5)_2$.

Une détermination du poids moléculaire par ébullioscopie dans le benzène rigoureusement anhydre, non seulement justifie la formule brute $TiCl_4.(COOC_2H_5)_2$ pour le complexe formé, mais, également, met en évidence le caractère monomérique de la structure moléculaire recherchée; le poids moléculaire théorique 335.9 g. coïncide assez bien avec le poids moléculaire trouvé 364.

La structure cyclique ou chélatée du présent complexe de coordination est déduite

Can. J. Chem. Downloaded from www.nrcresearchpress.com by 200.7.193.243 on 09/04/12
For personal use only.

des mesures dans l'infrarouge, des vibrations du groupe C=O de la molécule du diester. Des mesures effectuées sur l'oxalate de diéthyle pur montrent une bande C=O à 1770 cm^{-1} et à 1745 cm^{-1}. Il est vrai que Randall et ses collaborateurs (11) ne mentionnent pour l'oxalate de diéthyle qu'une seule bande C=O à 1757 cm^{-1} mais, d'autre part, nos résultats rejoignent bien les mesures plus récentes de Bender (12): 1771 cm^{-1} et 1747 cm^{-1}.

L'existence d'une structure cyclique exige ici des modifications de ces deux valeurs de bande C=O; en effet, si l'on retrouve dans le complexe l'une ou l'autre de ces valeurs inchangée, alors seulement on pourra penser que l'un des groupes C=O est demeuré libre. Mais, dans ces conditions, on se demande comment les exigences du nombre de coordination maximum du titane IV pourraient être sauvegardées, le caractère monomérique du complexe et la valeur 1:1 du rapport d'addition demeurant acquis. Si, par ailleurs, les deux valeurs de bande C=O sont modifiées en passant du diester pur au complexe, il faut attribuer cette modification à une variation de la distance C=O et, pour autant, à une liaison quelconque de l'atome d'oxygène de chaque groupe C=O avec un autre atome. Puisque les deux groupes C=O habitent déjà la même molécule et que le ou les atomes liants ne peuvent se trouver que sur une seule autre molécule, on doit nécessairement envisager une structure cyclique.

Or le spectre infrarouge du complexe (émulsion dans le nujol, prisme NaCl) révèle un déplacement marqué des deux bandes C=O vers une plus grande longueur d'onde; les valeurs obtenues pour le diester pur sont disparues et remplacées par deux nouvelles bandes à 1698 cm^{-1} et à 1675 cm^{-1}, soit un décalage moyen de 71 cm^{-1} par rapport aux valeurs des bandes C=O libres. Il est donc normal de déduire une liaison nouvelle dans chacun des groupes C=O et partant, une structure cyclique.

Gordy (13) a d'ailleurs montré que la chélation du groupe C=O se traduit possiblement par un effet dans le sens que nous avons observé et Bryant et ses collaborateurs (14) ont noté que l'importance du déplacement de la bande C=O est reliée à la nature des atomes du cycle résultant et dépend aussi des substituants greffés sur le cycle.

On peut donc raisonnablement proposer une structure chélatée pour le produit de l'addition de l'oxalate de diéthyle avec le tétrachlorure de titane.

La configuration *cis* ou 1,2 doit enfin être préférée à la forme *trans* ou 1,6. On considère avec Martell et Calvin (15) qu'il est stériquement impossible pour les oxygènes de l'oxalate d'occuper deux coins opposés 1,6 de l'octaèdre du titane IV. En effet, la distance entre les deux atomes d'oxygène concernés serait très voisine de 2.73 Å pour la forme *cis* de l'oxalate de diéthyle tandis que la distance entre deux coins opposés 1,6 de l'octaèdre du titane dépasse 4.3 Å. Par contre, la distance entre deux coins voisins 1,2 de l'octaèdre du titane est de l'ordre de 3.0 Å; ces dernières positions sont donc nettement favorisées du point de vue stérique.

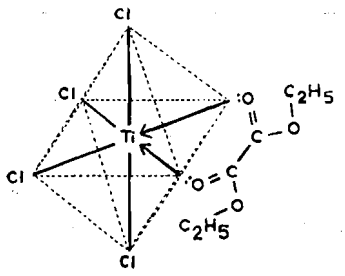

FIG. 2. Structure proposée pour $TiCl_4.(COOC_2H_5)_2$.

Can. J. Chem. Downloaded from www.nrcresearchpress.com by 200.7.193.243 on 09/04/12
For personal use only.

Dans l'évaluation de la distance entre les deux atomes d'oxygène de l'oxalate de diéthyle, il n'y a pas d'objection à postuler la forme *cis* pour le diester pur à l'état liquide car les recherches de Jatkar et Phansalkar (16) justifient l'hypothèse d'une rotation libre des deux groupes estérifiés autour de la liaison CO—CO.

Nous proposons donc la structure représentée dans la figure 2 pour le diéthyl oxalate-1,2 tétrachlorure de titane IV.

Quelques propriétés du complexe $TiCl_4.(COOC_2H_5)_2$

Le point de fusion de ce composé (p.f.) est 104–105° C.; la fusion est probablement accompagnée de décomposition partielle du complexe.

L'analyse élémentaire donne pour $TiCl_4.(COOC_2H_5)_2$:

	% Ti	% Cl
Valeurs calculées	14.26	42.22
Valeurs trouvées	14.48	41.72

Le complexe d'addition est un solide jaune pâle finement cristallisé, à odeur d'acide chlorhydrique. Il est extrêmement hygroscopique et s'hydrolyse rapidement en présence d'humidité. Quand le composé est chauffé, il donne d'abord un liquide jaune clair, puis une pâte brun foncé et finalement un résidu blanc identifié comme TiO_2. Conservé dans un récipient scellé et sous atmosphère d'azote sec, le composé conserve son état initial pendant plusieurs mois.

Nous avons étudié avec une attention particulière la solubilité de $TiCl_4.(COOC_2H_5)_2$ dans une gamme de solvants organiques usuels. Chacun de ces solvants a été séché au préalable selon le procédé le plus approprié à chaque cas. Le tableau II résume les résultats quantitatifs obtenus.

TABLEAU II

SOLUBILITÉ DE $TiCl_4.(COOC_2H_5)_2$ À TEMPÉRATURE ORDINAIRE

Nom du solvant	Formule du solvant	Solubilité en g./100 ml.
Chlorure de *n*-butyle	$CH_3—(CH_2)_2—CH_2Cl$	26.4
Dichlorure d'éthylène	$ClCH=CHCl$	49.0
Chloroforme	$CHCl_3$	64.4
Tétrachlorure de carbone	CCl_4	0.3
n-Hexane	$CH_3—(CH_2)_4—CH_3$	Insoluble
Cyclohexane	C_6H_{12}	Insoluble
Sulfure de carbone	CS_2	1.1
Éther	$C_2H_5OC_2H_5$	5.9
Dioxane	$C_4H_8O_2$	1.8
Acétone	CH_3COCH_3	87.8
Oxalate de diéthyle	$(COOC_2H_5)_2$	50.3
Acétate d'éthyle	$CH_3COOC_2H_5$	97.3
Benzène	C_6H_6	61.6
Toluène	$C_6H_5CH_3$	32.6
Xylène	$C_6H_4(CH_3)_2$	5.5
Chlorobenzène	C_6H_5Cl	43.2

On voit que le complexe est tout à fait insoluble dans les hydrocarbures saturés. Les dérivés halogénés les plus polaires sont de meilleurs solvants; si la solubilité est peu élevée dans les éthers, elle est très convenable dans les esters. Enfin, une substitution sur le noyau benzénique semble diminuer l'efficacité du solvant.

$TiCl_4.(COOC_2H_5)_2$ s'hydrolyse instantanément dans l'eau. Ce composé est soluble dans les alcools mais il réagit avec ces derniers. Il réagit aussi avec les amines et les amides.

Can. J. Chem. Downloaded from www.nrcresearchpress.com by 200.7.193.243 on 09/04/12
For personal use only.

La réaction d'addition de l'oxalate de diéthyle sur le tétrachlorure de titane réalisée dans le cyclohexane donne comme rendement de réaction: 95%.

REMERCIEMENTS

Nous tenons à adresser nos remerciements au Conseil National de Recherches du Canada pour l'aide financière accordée sous forme de subvention (R.R.) et à l'Office des Recherches scientifiques de la province de Québec pour la bourse d'études accordée (R.A.). Nous remercions aussi M. le Professeur Sandorfy et Mlle Chenon de leur collaboration dans l'étude des spectres.

BIBLIOGRAPHIE

1. DEMARÇAY, E. Bull. soc. chim. France, [2], **20**, 127 (1873).
2. SCAGLIARINI, G. et TARTARINI, G. Atti accad. nazl. Lincei, [6], **4**, 318 (1926).
3. HERTEL, E. et DEMMER, A. Ann. **499**, 134 (1932).
4. HIEBER, W. et REINDL, E. Z. Elektrochem. **46**, 559 (1940).
5. ARCHAMBAULT, J. Mémoire de maîtrise. Université de Montréal, Montréal, Québec. 1956. p. 20.
6. LEWIS, G. N. J. Franklin Inst. **226**, 293 (1938).
7. WURTZ, A. D. Dictionnaire de chimie pure et appliquée. Vol. III. Librairie Hachette & Cie, Paris. 1878. p. 425.
8. CLABAUGH, W. S., LESLIE, R. T. et GILCHRIST, R. J. Research Natl. Bur. Standards, **55**, 261 (1955).
9. VOGEL, A. I. A text-book of quantitative inorganic analysis. 2nd ed. Longmans, Green and Co., London. 1953. p. 399.
10. HAMILTON, P. M., MCBETH, R., BEKEBREDE, W. et SISLER, H. H. J. Am. Chem. Soc. **75**, 2881 (1953).
11. RANDALL, H. M., FUSON, N., FOWLER, R. G. et DAUGL, J. R. Infrared determination of organic structures. D. Van Nostrand Co., Inc., New York. 1949. p. 21.
12. BENDER, M. L. J. Am. Chem. Soc. **75**, 5986 (1953).
13. GORDY, W. J. Chem. Phys. **8**, 516 (1940).
14. BRYANT, B. E., PARIAUD, J.-C. et FERNÉLIUS, W. C. J. Org. Chem. **19**, 1889 (1954).
15. MARTELL, A. E. et CALVIN, M. Chemistry of the metal chelate compounds. Prentice-Hall, Inc., New York. 1956. p. 258.
16. JATKAR, S. K. K. et PHANSALKAR, V. K. J. Univ. Poona, Sci. Technol. No. **4**, 45 (1953).

Can. J. Chem. Downloaded from www.nrcresearchpress.com by 200.7.193.243 on 09/04/12
For personal use only.

Can. J. Chem. Downloaded from www.nrcresearchpress.com by 200.7.193.243 on 09/04/12
For personal use only.

HYDROGENOLYSIS OF CARBOHYDRATES

V. ISOMERIZATION OF METHYL β-L-ARABOPYRANOSIDE[1]

A. S. PERLIN, E. VON RUDLOFF, AND A. P. TULLOCH[2]

ABSTRACT

Treatment of methyl β-L-arabopyranoside under hydrogenolytic conditions with copper chromium oxide catalyst induces extensive isomerization. Products formed include glycosides of D-ribose, D-xylose, D-lyxose, and L-lyxose which together represent about an 80–90% conversion of starting material. Isolation of these compounds shows that carbons 2, 3, and 4 undergo isomerization, but no evidence has been obtained of anomerization. These findings possibly explain the formation of an optically *inactive* mixture of *cis*- and *trans*-tetrahydropyran-3,4-diol under slightly more drastic reaction conditions.

INTRODUCTION

The hydrogenolysis of methyl β-L-arabopyranoside (I) at 250° C. using copper chromium oxide catalyst has yielded mainly a mixture of dihydro-arabinal and -xylal (*cis*- and *trans*-3,4-dihydroxytetrahydropyran) (1). These products appeared to have been formed by reductive cleavage of the glycosidic methoxyl group and of the 2- or 4-hydroxyl group giving, respectively, the *cis*-(*arabo*-) or *trans*-(*xylo*-)isomer. However, the mixture of compounds was optically inactive and hence not the expected L-diols II and III, and it was suggested that isomerization may have occurred (1). Reinvestigation of the reaction under conditions slightly milder than used earlier has now shown, in fact, that methyl β-L-arabopyranoside readily undergoes isomerization, yielding a mixture of pentosides.

At 200° C. very little tetrahydropyrandiol was formed from methyl arabinoside although about half of the pentoside had reacted. A portion of the crude product was hydrolyzed with dilute acid, and examination of the liberated sugars by paper chromatography and electrophoresis indicated the presence in the mixture of ribose, lyxose, and xylose, the latter two being clearly distinguishable only by paper electrophoresis. In addition, an unidentified reducing material (R_{rham} 0.9) and a non-reducing product (R_{rham} 0.4) were detected on the chromatograms as minor components. The mixture of methyl pentosides proved difficult to resolve by cellulose column chromatography (2). A series of fractions was obtained, some containing predominantly one or another sugar. From one of these fractions a small quantity of a crystalline glycoside was isolated and this was shown by specific rotation, mixed melting point, and X-ray powder diagram to be methyl α-D-lyxopyranoside (IV). Chromatographic separation of the mixture of sugars after hydrolysis afforded D-xylose (V), L-lyxose (VI), and D-ribose (VII). The first two were characterized as crystalline sugars and the latter as the *p*-toluenesulphonhydrazone (3) by specific rotations, mixed melting points, and X-ray diffraction diagrams or infrared absorption spectra. Visual examination of the mixture of free pentoses on paper chromatograms and electrophoretograms suggested that lyxose and ribose were formed in about equal amounts, that approximately twice as much xylose was produced, and that these pentoses together corresponded to perhaps 40% of the starting material, i.e., to about 90% conversion.

[1]*Manuscript received February 17, 1958.*
Contribution from the National Research Council of Canada, Prairie Regional Laboratory, Saskatoon, Saskatchewan.
Issued as N.R.C. No. 4702 and as Paper No. 253 on the Uses of Plant Products.
[2]*National Research Council of Canada Postdoctorate Fellow, 1956–57.*

Other instances of hydrogenolytic isomerization of carbohydrates have recently been found in this laboratory, i.e., the formation of dihydro-D-altral from methyl α-D-glucopyranoside (4) and of *O-iso*propylidene-L-idose from 1,2-*O-iso*propylidene-D-glucose (4a). These findings suggest, therefore, that isomerization may occur frequently and may constitute an important reaction quantitatively when carbohydrates are subjected to catalytic hydrogenation conditions. Isomerization of hexitol dianhydrides (5), cyclic alcohols (6), and inositol derivatives (7) under such conditions has been established, the reactions probably involving dehydrogenation to form intermediate ketones. It is reasonable to expect that the carbohydrate isomerizations take place by a similar mechanism.

The wide variety of products obtained from methyl arabinoside by isomerization shows that the reaction involves attack at carbons 2, 3, and 4, sometimes at one carbon individually, sometimes at more than one. Thus, the formation of methyl D-xyloside requires isomerization at carbon 4, and of methyl L-lyxoside at carbon 3. Carbons 3 and 4 are both attacked in the production of methyl D-riboside and carbons 2 and 4 in the production of methyl D-lyxoside. The 2-position is least affected by isomerization; little methyl D-lyxoside is produced as indicated by the isolation of virtually pure L-lyxose from the mixture of free sugars. Since each of the secondary hydroxyl groups is affected to some degree it is possible that D-arabinose, L-xylose, and L-ribose are also products of the reaction but have not been detected. However, there is as yet no evidence for isomerization at carbon 1; the configuration at carbon 1 is retained in methyl α-D-lyxoside, the one intact glycoside isolated. Also, it may be concluded that the L-lyxoside is present in the mixture as the β-glycoside, i.e., that anomerization has not occurred, for the α-D-isomer could not have been separated from methyl α-L-lyxoside by the isolation procedure used.

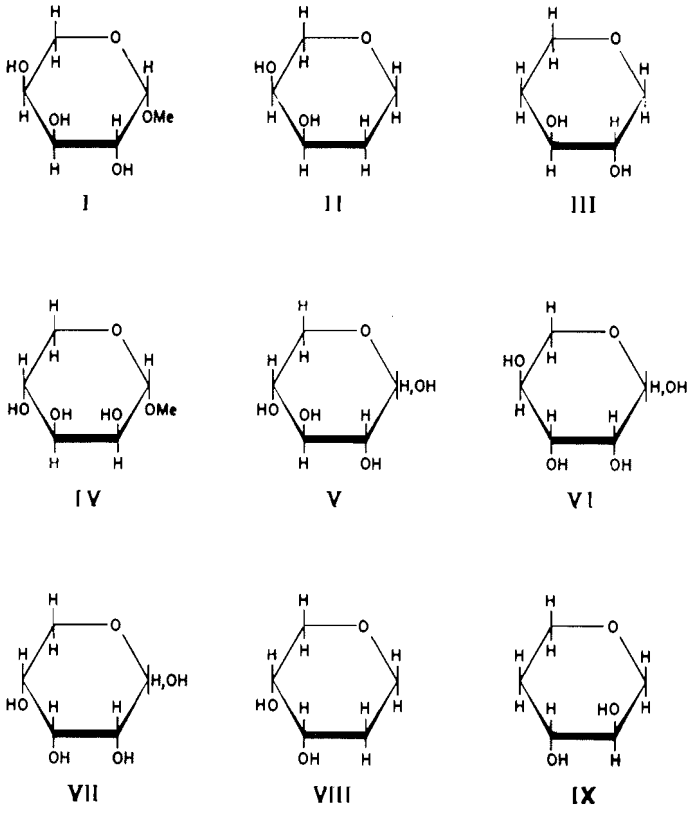

Can. J. Chem. Downloaded from www.nrcresearchpress.com by 200.7.193.243 on 09/04/12
For personal use only.

The finding that extensive isomerization can accompany the hydrogenolysis of methyl β-L-arabopyranoside points to a reaction mechanism somewhat more complex than had been indicated earlier (1). Reductive cleavage of carbon–oxygen bonds at the glycosidic center and at position 2 or 4 should yield dihydro-L-arabinal (II) and -L-xylal (III), respectively (*cis*- and *trans*-L-diol). However, with the isomeric pentosides formed as intermediates, this sequence of reactions should yield the *cis*- and *trans*-D-isomer (VIII and IX, respectively), also, as indicated in the following table:

	Product obtained when secondary position attacked	
Glycoside	2-Position	4-Position
L-Arabinoside	*cis*-L	*trans*-L
D-Xyloside	*trans*-D	*trans*-L
D-Riboside	*cis*-D	*cis*-L
L-Lyxoside	*trans*-L	*cis*-L
D-Lyxoside	*trans*-D	*cis*-D

It is seen that all four isomeric diols are obtainable by hydrogenolysis of the mixture of glycosides. Formed in the proper proportions these products could have accounted for the observation that the mixture of diols isolated was optically inactive (1). Such a possibility is increased by the fact that the rotatory power of the *cis*- and *trans*-diols is of approximately the same magnitude (dihydro-D-xylal and dihydro-D-arabinal show $[\alpha]_D$ −45° (8) and −48° (8), respectively). According to these findings, it is possible also that hydrogenolysis does not involve both positions 2 and 4. The fact that *cis*- and *trans*-diol were produced led to the early suggestion that each of these positions is attacked. A mixture of all four isomers may be obtained, however, by reductive cleavage only of the 2-hydroxyl group and the glycosidic methoxyl. By contrast, if hydrogenolysis were to occur at position 4 rather than at 2 the product would be almost exclusively a mixture of L-isomers and hence strongly dextrorotatory. The present results do not completely resolve these questions. They show, however, that isomerization can occur, which possibly leads to the formation of optically inactive hydrogenolysis products.

EXPERIMENTAL

Melting points are corrected. Infrared spectra were prepared by the potassium bromide window technique (9).

Chromatographic Methods

Paper chromatograms were developed on Whatman No. 1 paper using the following solvents: (A) phenol saturated with water (10), (B) ethyl acetate–acetic acid–water (9:2:2, v/v) (11, 12), and (C) *n*-butanol–pyridine–benzene–water (5:4:1:3 v/v) (13). None of these solvents satisfactorily resolved a sugar mixture consisting of D-ribose, D-xylose, L-arabinose, and D-lyxose. Solvent A gave a partial separation of xylose and lyxose, solvent C a good separation of ribose, xylose (or lyxose), and arabinose.

Paper electrophoresis (14) was carried out in borate buffers (pH 8–10) with a Spinco apparatus, Model R, and Whatman No. 1 paper; the current and voltage applied were 4.5 ma. and 900 volts, respectively. At pH 9.7 lyxose and xylose were completely separated (respective distances traveled in 5 hours, 3.2 cm. and 5.5 cm.) but these in turn were not as clearly separated from ribose (3.7 cm.) and arabinose (4.9 cm.). Lyxose and xylose were also separable at pH 8.0 (3.7 cm. and 4.9 cm., respectively, in 7.5 hours), but now the relative speeds of ribose and arabinose were reversed (5.4 cm. and 3.9 cm.,

Can. J. Chem. Downloaded from www.nrcresearchpress.com by 200.7.193.243 on 09/04/12
For personal use only.

respectively; compare (14)). Conditions were not found for complete resolution of the mixture.

Cellulose column chromatography was carried out using as solvents: (D) *n*-butanol one-eighth saturated with water, and (E) benzene–ethanol–water (10:1:trace).

Isomerization of Methyl β-L-Arabopyranoside

Methyl β-L-arabopyranoside (10 g.) in ethanol (100 ml.) was treated with hydrogen in the presence of copper chromium oxide catalyst (1 g.) at 200° C. and 2000 p.s.i. initial pressure for 4 hours. After removal of the catalyst a crystalline solid (2.1 g.) separated out; it was found to be slightly impure methyl arabinoside for it yielded mainly arabinose (detected chromatographically) on acid hydrolysis. A sirupy product (7.6 g.) was then obtained by evaporating the solvent. The sirup (5.4 g.) in 0.2 *N* sulphuric acid (100 ml.) was hydrolyzed on the steam bath for 4 hours, the solution was then neutralized with barium carbonate, and the filtered solution concentrated to dryness (weight 4.3 g.). Examined by paper chromatography, the residue was found to contain two minor products, one having R_{rham} 0.9 (yellow color with *p*-anisidine hydrochloride spray (12)), the other having R_{rham} 0.41 (non-reducing, detected with silver nitrate spray (10)), and major components corresponding to ribose, xylose and/or lyxose, and arabinose.

Identification of the Reaction Products

The mixture of sugars (3.5 g.) obtained on hydrolysis of the reaction product was chromatographed on a column (25 inches × $2\frac{1}{2}$ inches) of powdered cellulose using solvent D, 17 1-liter fractions were collected, and the sugars present in these were tentatively identified by paper chromatography and electrophoresis. Complete resolution of the sugar mixture was not obtained. Accordingly, those fractions found to consist chiefly of one or another sugar were selected and the products characterized as described below. The proportion of the pentoses present in each fraction was approximated visually from the intensity and area of the spots developed on the chromatograms and electrophoretograms with *p*-anisidine hydrochloride spray, a spray suited to the estimation of sugars (15). Related to the known weight of each fraction and the amount of arabinose separated earlier as the crystalline glycoside, these evaluations suggested that the ratio of arabinose–xylose–lyxose–ribose in the reaction mixture was about 5:2:1:1.

D-*Ribose.*—Fraction 8 contained only ribose. The sirup (124 mg.) obtained on removal of the solvent was treated with *p*-toluenesulphonhydrazide (120 mg.) in methanol (6 ml.) affording the corresponding hydrazone of D-ribose (93 mg.), m.p. 160°–162° C., after two recrystallizations from methanol; mixed melting point with D-ribose *p*-toluenesulphonhydrazone (m.p. 161°–163° C.) 160°–163° C., $[\alpha]_D$ 22.9° (45 minutes) → 12.5° (18 hours) (*c*, 1.0, moist pyridine). (Literature (3), $[\alpha]_D$ 42.0° (initial) → 14.0° (17 hours) (moist pyridine).) Calc. for $C_{12}H_{18}O_6N_2S$: C, 45.28%; H, 5.70%. Found: C, 45.46%; H, 5.71%. The identity of the compound was confirmed by comparison of its infrared absorption spectrum and X-ray powder diagram with those of an authentic specimen.

L-*Lyxose.*—Fraction 10 contained lyxose and a smaller proportion of xylose. On being seeded with L-lyxose the sirupy product (160 mg.) crystallized, and after recrystallization twice from ethanol – ethyl acetate and once from *n*-propanol had m.p. 104° – 106° C., undepressed on admixture with L-lyxose (m.p. 107°–108° C.), $[\alpha]_D$ 12.0° (equilibrium value) (*c*, 1.0, water). Calc. for $C_5H_{10}O_5$: C, 40.02%; H, 6.71%. Found: C, 39.89%; H, 6.71%. The X-ray powder diagram of the product and that of L-lyxose were indistinguishable.

D-*Xylose.*—Fraction 12 contained mainly xylose and a small percentage of lyxose. The sirup (170 mg.) was taken up in glacial acetic acid and crystallization promoted by

Can. J. Chem. Downloaded from www.nrcresearchpress.com by 200.7.193.243 on 09/04/12
For personal use only.

seeding with D-xylose. One recrystallization from ethanol gave a product (70 mg.) having m.p. 138°–141° C., undepressed on admixture with D-xylose, $[\alpha]_D$ 18.6° (equilibrium value) (*c*, 1.0, water). Calc. for $C_5H_{10}O_5$: C, 40.02%; H, 6.71%. Found: C, 39.80%; H, 6.71%. The infrared absorption spectrum of the compound was indistinguishable from that of D-xylose.

Methyl α-D-lyxopyranoside.—The mixture of glycosides obtained by isomerization of methyl arabinoside was chromatographed on a cellulose powder column using solvent E, a series of fractions being collected and examined chromatographically. One of these fractions, which on hydrolysis was found to contain mainly lyxose, yielded a crystalline product, m.p. 106°–107° C. after recrystallization from acetone–ether, undepressed by admixture with methyl α-D-lyxopyranoside, $[\alpha]_D$ 59.0° (*c*, 1.0, water). Calc. for $C_6H_{12}O_5$: C, 43.90%; H, 7.37%. Found: C, 44.00%; H, 7.37%. The X-ray powder diagram of the compound and that of methyl α-D-lyxopyranoside were indistinguishable.

ACKNOWLEDGMENTS

The technical assistance of Mr. M. Granat is gratefully acknowledged. The authors also thank Mr. J. A. Baignée for microanalyses, Mr. T. M. Mallard for X-ray diffraction diagrams, and Mr. G. B. Rennie for infrared absorption analyses.

REFERENCES

1. BAUER, H. F. and STUETZ, D. E. J. Am. Chem. Soc. **78**, 4097 (1956).
2. HOUGH, L., JONES, J. K. N., and WADMAN, W. H. J. Chem. Soc. 2511 (1949).
3. EASTERBY, D. G., HOUGH, L., and JONES, J. K. N. J. Chem. Soc. 3416 (1951).
4. RUDLOFF, E. VON and TULLOCH, A. P. Can. J. Chem. **35**, 1504 (1957).
4a. GORIN, P. A. J. and PERLIN, A. S. Can. J. Chem. **36**, 661 (1958).
5. FLETCHER, H. G., JR. and GOEPP, R. M., JR. J. Am. Chem. Soc. **67**, 1042 (1945).
6. WICKER, R. J. J. Chem. Soc. 2165 (1956).
7. ANGYAL, S. J. and MCHUGH, D. J. J. Chem. Soc. 3682 (1957).
8. FLETCHER, H. G., Jr. and HUDSON, C. S. J. Am. Chem. Soc. **71**, 3682 (1949).
9. SCHIEDT, U. and REINWEIN, H. Z. Naturforsch. **7b**, 270 (1952).
10. PARTRIDGE, S. M. Nature, **158**, 270 (1946).
11. JERMYN, M. A. and ISHERWOOD, F. A. Biochem. J. **44**, 402 (1949).
12. HOUGH, L., JONES, J. K. N., and WADMAN, W. H. J. Chem. Soc. 1702 (1950).
13. DE WHALLEY, H. C. S., ALBON, N., and GROSS, D. Analyst, **76**, 287 (1951).
14. CONSDEN, R. and STANIER, W. M. Nature, **169**, 783 (1952).
15. PRIDHAM, J. B. Anal. Chem. **28**, 1967 (1956).

Can. J. Chem. Downloaded from www.nrcresearchpress.com by 200.7.193.243 on 09/04/12
For personal use only.

Can. J. Chem. Downloaded from www.nrcresearchpress.com by 200.7.193.243 on 09/04/12
For personal use only.

THE CHEMISTRY OF PEAT

II. THE TRITERPENES OF PEAT MOSS (SPHAGNUM)[1]

D. A. J. IVES[2] AND A. N. O'NEILL

ABSTRACT

By further chromatographic fractionation of the unsaponifiable matter from an extract of peat moss (*Sphagnum*) three crystalline triterpenes have been isolated. They have been identified as α-amyrin, taraxerone, and taraxerol by their physical and chemical properties.

In the preceding paper (5) the method of separating the crude unsaponifiable material present in peat moss was described. Two sterols were isolated and identified. This paper deals with some of the other compounds isolated during the chromatography of the crude extract. The fraction of unsaponifiable material eluted from the alumina column with benzene represented approximately five per cent of the total. This material consisted of a light yellow oil which crystallized on standing. Attempts to purify it by crystallization from methanol or ethanol failed. However, if the material was taken up in light petroleum, a yellow sirup was dissolved leaving a white crystalline mass, which after filtration could be readily recrystallized from chloroform–methanol solution. The crystals melted at 238°–239° and had a specific rotation of +12°. The material gave a crystalline derivative with 2,4-dinitrophenylhydrazine and showed a marked peak in the infrared at 1705 cm.$^{-1}$, indicative of a carbonyl group. The infrared spectrum of this ketone from peat moss also showed the presence of a double bond by a band at 816 cm.$^{-1}$ and the position of the band indicated a trisubstituted double bond in a six-membered ring. The high melting point and comparatively few functional groups, in addition to a positive Liebermann–Burchard reaction, indicated that the compound could be a triterpene, possibly of the allobetulin series. This hypothesis was reached since derivatives of allobetulin have been found in lignite (8), a decomposition product of peat. However, analysis showed the presence of only one oxygen function, the carbonyl group, whereas allobetulin itself has two, one being an ether function. A search of the literature showed that the ketone was possibly taraxerone (I), previously isolated from *Taraxacum officinale* (3) and *Alnus glutinosa* L. (1), and further chemical evidence confirmed this. The ketone was reduced with lithium aluminum hydride to give the alcohol (II, R = H), which had the physical constants of taraxerol. This was confirmed by the preparation of the acetate in the usual way (II, R = Ac). This acetate was treated with hydrochloric acid in acetic acid (1) and the resulting product crystallized from chloroform–methanol to give β-amyrin acetate (III, R = Ac), identified by melting point and rotation and the melting point and rotation of the derived alcohol (III, R = H) β-amyrin. This rearrangement has been shown to involve the migration of a methyl group from C_{13} to C_{14} with the concomitant movement of the double bond from the 14,15-position to the 12,13-position. The process is concerted and there are no intermediates. It is also irreversible and the yield of β-amyrin is virtually 100%. The rearrangement is typical of taraxerol and some of its derivatives, and treatment of taraxerone under the same conditions afforded β-amyrone (I). Reduction by the Wolff–Kishner procedure afforded the unsaturated hydrocarbon taraxerene (VI), recently

[1]*Manuscript received February 26, 1958.*
Contribution from the National Research Council of Canada, Atlantic Regional Laboratory, Halifax, Nova Scotia.
Issued as N.R.C. No. 4717.
[2]*National Research Council of Canada Postdoctorate Fellow 1955–1957.*

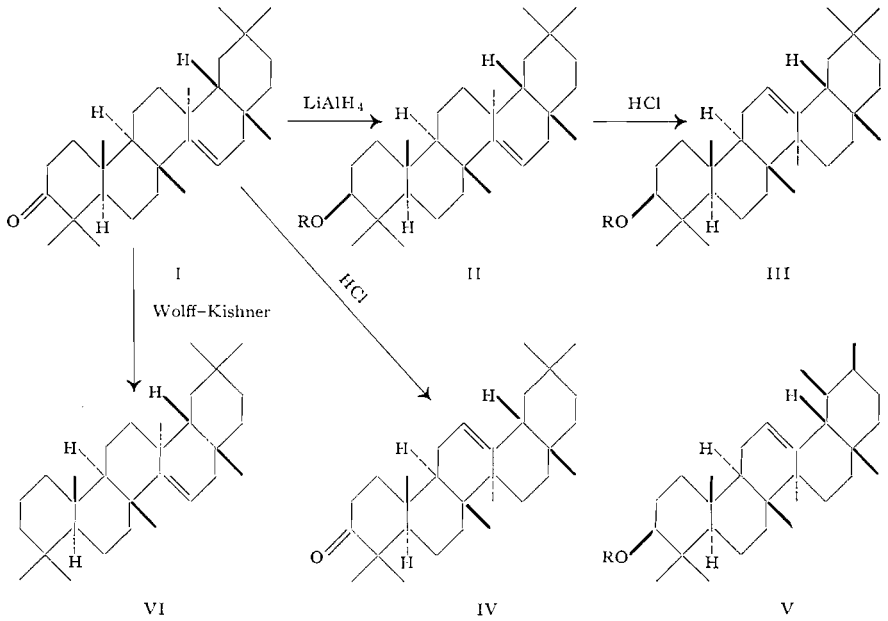

isolated from a lichen by Bruun (2). The amount of taraxerone present in the unsaponifiable extract was approximately two per cent.

The ether fraction of the crude chromatogram gave, in its earlier subfractions, a highly crystalline colorless solid. The amounts however were small, at 50–100 mg. per extraction. The material was only very slightly soluble in ethanol and ether, and could be readily recrystallized from benzene and chloroform. The same compound was also obtained from the fraction of the unsaponifiable material insoluble in light petroleum, extracted before chromatography of the crude unsaponifiable fraction. If this mixture was chromatographed roughly on alumina, elution with benzene afforded taraxerone and elution with chloroform–methanol (5:1) gave the insoluble compound. On recrystallization from chloroform–methanol this material had a melting point of 278°–279°, characterized by a change of crystalline form between 200° and 220°. The specific rotation was 0°. The infrared absorption spectrum showed the presence of a secondary hydroxyl group by bands at 3571 and 1035 cm.$^{-1}$ and the presence of a trisubstituted double bond from a band at 816 cm.$^{-1}$. The spectrum had many of the characteristics of taraxerone and the alcohol corresponded in physical constants and infrared spectrum to taraxerol (see Table I).

The material was shown to be identical with the reduced taraxerone by melting point

TABLE I

	Skimmiol (10)		Taraxerol (6)		Taraxerol*	
	M.p.	$[\alpha]_D$	M.p.	$[\alpha]_D$	M.p.	$[\alpha]_D$
Alcohol	279°–281°	+ 3°	282°–283°	+ 3°	278°–279°	0°
Acetate	298°–299°	+14°	304°–305°	+ 9°	300°–301°	+ 9°
Benzoate	287°–289°	+36°	292°–293°	+37°		
Ketone	241°–243°	+12°	240°–241°	+12°	238°–239°	+12°
Unsaturated hydrocarbon			237°–238° (2)	+ 1°	236°–238°	+ 1°

Data from Brooks, C. J. W. J. Chem. Soc. 1675 (1955).
**Constants found for materials from peat moss.*

Can. J. Chem. Downloaded from www.nrcresearchpress.com by 200.7.193.243 on 09/04/12
For personal use only.

and mixed melting point. Oxidation of the alcohol with chromium trioxide in pyridine gave taraxerone, as proved by melting point, mixed melting point, and specific rotation. The amount of taraxerol present in the extract was difficult to estimate owing to its insolubility, but it was approximately 1.5% of the unsaponifiable material or 0.02% by weight of the dried moss. It is probable that some was lost on the chromatographic column. The final proof of the identity of the material was provided by a mixed melting point with a genuine specimen of taraxerol.

The third triterpene isolated from the unsaponifiable extract was α-amyrin (V, R = H). This was not found in the preliminary extractions of the moss, possibly owing to the fact that it requires fairly careful chromatography to separate it from the sterols. However, on working up the ether–methanol fraction from the chromatography of 450 g. of unsaponifiable material, approximately 3.5 g. of α-amyrin were obtained. Chromatography of the acetylated material after the low-melting lignoceryl alcohol had been removed as previously described afforded α-amyrin acetate in the petrol–benzene (4:1) fraction and the steroid acetates in the petrol–benzene (2:1) fraction. The identity of the material was proved by the melting point and rotation of the alcohol, the derived acetate, and the derived benzoate (V, R = Ac and R = Bz respectively). The compound also had an infrared spectrum identical with that published for α-amyrin by Cole (4). A mixed melting point with an authentic specimen of α-amyrin was undepressed.

EXPERIMENTAL

All rotations were measured in a 1 dm. tube with a Rudolph polarimeter. Melting points were observed on a Kofler micromelting-point apparatus and are corrected. The infrared spectra were determined in carbon disulphide solution with a Baird double-beam infrared spectrophotometer, model 4-55. Light petroleum refers to the fraction with boiling point 35°–36°. For the method of obtaining the unsaponifiable fraction of the peat moss, see Part I (5).

Isolation of Taraxerone

The benzene fraction (1 g.) from the chromatography of the crude unsaponifiable extract was extracted with light petroleum and the white crystalline residue filtered off. Recrystallized from chloroform–methanol, it gave taraxerone (500 mg.), m.p. 238°–239°, $[\alpha]_D^{24}$ +12° (c = 1.34 in chloroform). Anal. Calc. for $C_{30}H_{48}O$: C, 84.84; H, 11.39. Found: C, 84.92; H, 11.31. The material gave a purple color in the Liebermann–Burchard test. The yellow 2,4-dinitrophenylhydrazone had m.p. 260°–262°.

Reduction of Taraxerone

Taraxerone (300 mg.) was dissolved in ether (50 ml.) and lithium aluminum hydride (500 mg.) added. The mixture was refluxed for 3 hours. The excess lithium aluminum hydride was decomposed with ethyl acetate and the ether layer washed with dilute acid and water and evaporated to dryness. The resulting product was crystallized from chloroform–methanol to give taraxerol, m.p. 279°–280°, $[\alpha]_D^{24}$ 0° (c = 1.2 in chloroform). For the constants recorded in the literature see Table I.

Acetylation

Taraxerol (200 mg.) was dissolved in pyridine (10 ml.) and acetic anhydride (3 ml.) added. The mixture was heated on the steam bath for 1 hour, then diluted with benzene and washed with dilute alkali, dilute acid, and water, and evaporated to dryness. The crude product, dissolved in benzene, was filtered through alumina and, after removal of the solvent, the material was crystallized from chloroform–methanol to give the

Can. J. Chem. Downloaded from www.nrcresearchpress.com by 200.7.193.243 on 09/04/12
For personal use only.

derived acetate with m.p. 300°–301°, $[\alpha]_D^{25}$ +9° (c = 1.56 in chloroform). Anal. Calc. for $C_{32}H_{52}O_2$: C, 81.99; H, 11.18. Found: C, 81.99; H, 11.00.

Rearrangement of Taraxerol Acetate

Taraxerol acetate (300 mg.) was suspended in acetic acid (30 ml.) and heated to 90°. Concentrated hydrochloric acid (1 ml.) was added and the mixture heated for 15 minutes on the steam bath, in which time all the taraxerol acetate went into solution. The acetic acid was distilled off under reduced pressure and the resulting product crystallized from chloroform–methanol to give β-amyrin acetate (200 mg.), m.p. 239°–240°, $[\alpha]_D^{25}$ +79° (c = 1.15 in chloroform). The values recorded in the literature for the constants are m.p. 241°, $[\alpha]_D$ +82° (11).

The β-amyrin acetate was hydrolyzed in the usual manner to give β-amyrin. Crystallized from aqueous ethanol this had m.p. 195°–196°, $[\alpha]_D^{24}$ +88° (c = 1.34 in chloroform). The values recorded in the literature for the constants are m.p. 197°, $[\alpha]_D$ +89° (11).

The rearrangement when repeated on taraxerone gave β-amyrone, with m.p. 174°–176°, $[\alpha]_D^{24}$ +109° (c = 1.41 in chloroform). The values recorded in the literature for the constants are m.p. 178° $[\alpha]_D$ +107° (7).

Wolff–Kishner Reduction of Taraxerone

Taraxerone (200 mg.) was added to a solution of sodium (500 mg.) in ethanol (5 ml.). Hydrazine hydrate (100%, 1 ml.) was added and the mixture heated in a sealed tube at 180° overnight. The mixture was diluted with benzene, washed with dilute acid and water, and evaporated to dryness. The crude product, dissolved in benzene, was filtered through alumina. After evaporation of the solvent, the resulting product was crystallized from chloroform–methanol to give taraxerene, m.p. 236°–238°, $[\alpha]_D^{24}$ +1° (c = 1.42 in chloroform). The values for the constants reported in the literature are m.p. 237°–238°, $[\alpha]_D$ +1° (2). The infrared absorption spectrum of the material showed no absorption at 1705 cm.$^{-1}$, which would indicate a carbonyl function, and no absorption at 3600 cm.$^{-1}$, which would indicate a hydroxyl group. This proved that the reduction was complete.

Isolation of Taraxerol from Peat Moss

The petrol-insoluble portion of the unsaponifiable material was dissolved in benzene and chromatographed on alumina. Elution with benzene afforded taraxerone (300 mg.), identified by its infrared spectrum. Elution with chloroform–methanol (4:1) afforded taraxerol (400 mg.), recrystallized from chloroform–methanol to give m.p. 278°–279°, $[\alpha]_D^{24}$ 0° (c = 1.17 in chloroform). The melting point was undepressed on admixture with a specimen obtained from the lithium aluminum hydride reduction of taraxerone, and also undepressed on admixture with a genuine specimen of taraxerol of like melting point. Anal. Calc. for $C_{30}H_{50}O$: C, 84.44; H, 11.81. Found: C, 84.77; H, 11.53.

Oxidation of Taraxerol

Taraxerol (500 mg.) was dissolved in pyridine (10 ml.) and the solution added to a suspension of chromium trioxide (1 g.) in pyridine (10 ml.). The mixture was allowed to stand overnight at room temperature, then diluted with water, and sulphur dioxide passed through to destroy the excess chromium trioxide. The mixture was extracted with benzene, and the benzene extract washed free of acid and evaporated to dryness. The crude product was dissolved in benzene and the solution filtered through alumina. After evaporation of the solvent, the resulting material was crystallized from chloroform–methanol to give taraxerone, identical in m.p., specific rotation, and infrared spectrum

Can. J. Chem. Downloaded from www.nrcresearchpress.com by 200.7.193.243 on 09/04/12
For personal use only.

with that isolated directly from the unsaponifiable material. This method of oxidation had to be used, since oxidation with chromium trioxide in acetic acid solution led to an impure product, which probably contained β-amyrone, owing to the acid rearrangement of taraxerone.

Isolation of α-Amyrin

The unsaponifiable material (450 g.) from the benzene–ethanol extract of 22 kg. of *Sphagnum* was chromatographed on a 60×4 in. column of alumina using the same solvents as described previously. After the ether–methanol fraction had been treated with urea to remove the lignoceryl alcohol, the residue (50 g.) was acetylated and the mixed acetates chromatographed on alumina. Elution with petrol–benzene (7:3) gave a white crystalline solid (3.5 g.), which on recrystallization from aqueous ethanol had m.p. 224°–225°, $[\alpha]_D^{25}$ +78° (c = 1.26 in chloroform). Anal. Calc. for $C_{32}H_{52}O_2$: C, 81.99; H, 11.18. Found: C, 82.69; H, 11.23. Vesterberg (11) reports m.p. 225°–226° and $[\alpha]_D$ +79° for α-amyrin acetate.

Hydrolysis

α-Amyrin acetate (500 mg.) was dissolved in dioxane (15 ml.) and methanol (20 ml.). Potassium hydroxide (1 g.) in water (3 ml.) was added and the solution heated under reflux for 1 hour. The solution was diluted with water and extracted with benzene, and the extract washed well with dilute acid and water and evaporated to dryness. The product was crystallized from methanol to give m.p. 183°–184°, undepressed on admixture with a genuine sample of α-amyrin, $[\alpha]_D^{25}$ +85° (c = 0.58 in chloroform). Anal. Calc. for $C_{30}H_{50}O$: C, 84.44; H, 11.81. Found: C, 84.56; H, 11.43. The values recorded in the literature for the constants are m.p. 186°, $[\alpha]_D$ +84° (11).

Benzoylation

α-Amyrin (250 mg.) was dissolved in pyridine (5 ml.) and benzoyl chloride (0.25 ml.) added. The mixture was heated on the steam bath for 50 minutes. The solution was diluted with benzene and washed well with dilute alkali, dilute acid, and water. It was then evaporated to dryness. The crude benzoate was dissolved in benzene and the solution filtered through alumina. After evaporation of the solvent the product was crystallized from chloroform–methanol to give α-amyrin benzoate m.p. 191°–193°, $[\alpha]_D^{25}$ +95° (c = 0.86 in chloroform). Anal. Calc. for $C_{37}H_{54}O_2$: C, 83.72; H, 10.25. Found: C, 83.81; H, 9.92. The values recorded in the literature for the constants are m.p. 193°–194°, $[\alpha]_D$ +95° (9).

ACKNOWLEDGMENT

The authors wish to thank Professor F. S. Spring, F.R.S., of the Royal Technical College, Glasgow, for his generous gifts of taraxerol and α-amyrin.

REFERENCES

1. Beaton, J. M., Spring, F. S., Stevenson, R., and Stewart, J. L. J. Chem. Soc. 2131 (1955).
2. Bruun, T. Acta Chem. Scand. **8**, 1291 (1954).
3. Burrows, S. and Simpson, J. C. E. J. Chem. Soc. 2042 (1938).
4. Cole, A. R. H. J. Chem. Soc. 3807 (1954).
5. Ives, D. A. J. and O'Neill, A. N. Can. J. Chem. **36**, 434 (1958).
6. Koller, E., Hiestand, A., Dietrich, P., and Jeger, O. Helv. Chim. Acta, **33**, 1050 (1950).
7. Rollett, A. Monatsh. **43**, 413 (1923).
8. Ruhemann, S. and Raud, H. Brennstoff-Chem. **13**, 341 (1932).
9. Ruzicka, L. and Wirz, W. Helv. Chim. Acta, **22**, 948 (1939).
10. Takeda, K. J. Pharm. Soc. Japan, **61**, 117 (1942).
11. Vesterberg, K. A. Ann. **428**, 243 (1922).

Can. J. Chem. Downloaded from www.nrcresearchpress.com by 200.7.193.243 on 09/04/12
For personal use only.

Can. J. Chem. Downloaded from www.nrcresearchpress.com by 200.7.193.243 on 09/04/12
For personal use only.

THE EFFECT OF WATER REMOVAL ON THE CRYSTALLINITY OF CELLULOSE[1]

M. KOURIS,[2] H. RUCK,[3] AND S. G. MASON

ABSTRACT

The effect of various modes of drying upon the crystallinity of cellulose has been determined by X-ray diffraction.

No change in the crystallinity index was observed when previously undried pure cellulose fibers from softwood were dried from water under a wide range of conditions, but a lower value was obtained when they were dried from benzene to which the fibers were accommodated by a series of solvent exchanges. Heat of wetting determinations on the same samples indicated changes in the accessibility with different drying methods. Qualitative variations in the degree of intrafiber bonding were also detected by a differential staining method. The X-ray measurements suggested that drying from water either produces no change in lateral order or that such changes are too small to be detectable by X-rays.

The crystallinity of cellulose prepared by dry-milling whole fibers was studied. The crystallinity was substantially reduced in a Wiley mill and obliterated in a ball mill. X-Ray diffraction showed that wetting with water and then drying restored the crystallinity, while similar treatment with other liquids yielded less definite results. However, by following the destruction of the lattice with progressive periods of milling, it was concluded that alcohols reform this lattice to a limited extent depending, among other factors, upon the swelling capacity.

INTRODUCTION

The formation of intermolecular bonds between adjacent cellulose chains by the removal of water is of considerable importance, particularly in connection with technical applications of cellulose, e.g. in textiles and in paper, and has been the subject of numerous investigations. It is now reasonably well established that most of the bonds, which can be either intra- or inter-fiber, depending upon whether or not the cellulose chains are in the same fiber, are due to hydrogen bridges (1) between hydroxyl groups of adjoining chains. As a consequence, the number of available hydroxyl groups, and therefore the accessibility of the fibers, would be reduced if additional hydrogen bridge bonds are formed.

The decrease in accessibility with evaporation-drying has been amply verified by Jayme (2, 3) and Purves *et al.* (4), the former by noting the decreased swelling capacity of dried fibers and the latter by applying the thallous-ethylation method.

Since the drying of cellulose is an irreversible process, any lateral order established by hydrogen-bonding may be expected to increase with repeated wetting and drying of the fibers, and cause a sharpening of the X-ray diffraction pattern of the crystalline portion. In this connection, it has been shown that the capacity of the fibers to reabsorb and retain the water decreases with the severity of drying conditions (3). Recently, it has been observed that freezing the wet fibers before air-drying the thawed material adversely affected the interfiber bonding of paper (5, 6). This effect was attributed to partial dehydration of the fibers as a result of freezing.

The mobility, and hence the alignment of the molecular chains in the amorphous regions of wet cellulose fibers, may be expected to be greatly reduced by freezing the water and removing it by sublimation- or freeze-drying, or by replacing the water by

[1]*Manuscript received February 19, 1958.*
Contribution from Physical Chemistry Division, Pulp and Paper Research Institute of Canada, and Department of Chemistry, McGill University, Montreal, Quebec.
[2]*Holder of the Courtaulds (Canada) Limited Fellowship 1955–57.*
[3]*Present address: Industrial Cellulose Research Limited, Hawkesbury, Ontario.*

a non-polar liquid before drying (6). Fibers dried by this means would be expected to have a higher accessibility than fibers dried by evaporation of liquid water. Although little work has been done on the accessibility of freeze-dried fibers, solvent-exchanged fibers show an increase in reactivity towards various reagents. Thus Siggia *et al.* (7) found an increased accessibility of cotton linters to HIO_4 solution, while Conrad and Scroggie (8) found the same effect towards HCl–$FeCl_3$ attack. A similar trend was observed by Brown and Purves (9) in their nitration experiments on cotton linters. In addition, several workers have shown that a reduction in interfiber bonding, during freeze-drying from water or evaporation-drying from a non-swelling liquid, may be responsible for adversely affecting paper strength. Van den Akker (5), Broughton and Wang (10), and Marchessault, Lodge, and Mason (6) demonstrated that the strength of paper handsheets dried by such methods was considerably less than the strength of normally air-dried sheets. From this it can be seen that the method of drying influences the physical properties of cellulose fibers. In turn these properties may be assumed to be closely related to the degree of hydrogen-bonding, and in turn to the lateral order introduced in the fibers by the drying operation.

In the investigation to be described the effect of different drying conditions on the crystallinity of cellulose fibers was determined by an X-ray diffraction method using the crystallinity index parameter introduced by Ant-Wuorinen (11). This parameter may be considered to be a relative (but not absolute) measure of the fraction of crystalline material. Heat of wetting determinations and a differential staining procedure were also applied to the fibers.

As the crystallinity index of whole fibers proved to be insensitive to drying, attempts were made to magnify the effects by first reducing the crystallinity by mechanical attrition and then wetting with various liquids and drying.

The almost complete destruction of crystallinity of dried cellulose I fibers by ball-milling has been shown by Hess (12) and by Hermans (13), using X-ray diffraction. These workers also showed that wetting the pulverized material resulted in partial recrystallization accompanied by a lattice modification to cellulose II. In the present investigation similar behavior was observed upon rewetting cellulose whose crystallinity had been drastically reduced by dry-grinding fibers in both a Wiley and a ball mill. However, no lattice modifications were observed on wetting. In the case of the Wiley-milled material, recrystallization was observed to occur upon exposure to water vapor of high relative humidity.

The recrystallization of mechanically degraded fibers by non-aqueous liquids has received little attention. Investigating the sorption of vapors by cellulose fibers, Kanamaru and Chao (14), Lauer (15), and Stamm and Tarkow (16) found that the sorptive capacity of cotton for the normal alcohols decreased regularly with increasing molecular weight of the homologous series. From the sparse data available, it is now generally accepted that the penetration and appreciable swelling of cellulosic material can occur only with polar liquids. Furthermore, to encourage rearrangement of the fibers and increase lateral order the swelling medium must be capable of promoting hydrogen-bonding. In this connection, it has been shown that the strength of paper handsheets made by drying from benzene was considerably less than that of handsheets dried from ethanol (10).

In the experiments described below, the variations in the crystallinity index of the mechanically degraded cellulose treated with various organic liquids appeared to parallel their sorption capacity by cellulose.

Can. J. Chem. Downloaded from www.nrcresearchpress.com by 200.7.193.243 on 09/04/12
For personal use only.

Can. J. Chem. Downloaded from www.nrcresearchpress.com by 200.7.193.243 on 09/04/12
For personal use only.

EXPERIMENTAL

1. Materials

Cellulose Fibers

Softwood dissolving-grade sulphite pulp which had never been previously dried was kindly supplied by Fraser Companies Ltd., Campbellton, N.B., together with the following analytical data:

Viscosity	25.4 cp.
Resin	0.37%
Pentosan	2.42%
Rayon yield	93.7%
10% Caustic insoluble	89.3%

Dried samples were prepared as follows:

Sample F-1.—Oven dried at 105° C.

Sample F-2.—Dried at room temperature. The drying was conducted in two stages. The pulp was first placed in a vacuum desiccator containing concentrated sulphuric acid. After about two days, when the moisture content was reduced to approximately 15%, the pulp was transferred to a desiccator containing phosphorus pentoxide and again evacuated for several days.

Sample F-3.—Cyclic wetting and oven drying. After oven drying at 105° C., the pulp was suspended in water at room temperature for 24 hours, the excess water removed under mild suction, and the pulp again dried at 105° C. This operation was repeated until the sample had been exposed to 10 complete drying cycles.

Sample F-4.—Cyclic wetting and room temperature drying. This sample was subjected to 10 wetting and drying cycles the same as for F-3, except that each drying stage was carried out at room temperature as for F-2.

Sample F-5.—Freeze-drying from water. The water-wet pulp was initially frozen at −78° C. by immersion in acetone/Dry Ice. The ice was then removed by sublimation under vacuum in a laboratory-model freeze-drier.

Sample F-6.—Freeze-drying from benzene. The water-wet pulp was suspended in 200 cc. of acetone which had previously been distilled over activated alumina to remove traces of water. The acetone was replaced several times by a fresh batch until titration of an aliquot with Karl Fischer reagent indicated the absence of water. The pulp was then suspended in 300 cc. of dry benzene, and allowed to stand for 24 hours in a stoppered flask. After a further immersion of 24 hours in a fresh batch of benzene, the latter was decanted and the pulp frozen at −78° C. The benzene (m.p. 5.3° C.) was removed by sublimation under vacuum as for F-5. It was noted that on rewetting the sample with water a strong odor of benzene was detectable. It has been shown that up to 1.5% benzene can be retained in this way (17).

Sample F-7.—Freezing in liquid nitrogen. The adverse effect of ice formation on the bonding properties of fibers has been attributed to a partial dehydration of the fibers at low temperature (6). To determine the effect of this partial dehydration on the crystallinity of cellulose, water-wet pulp was suspended in liquid nitrogen (−195.8° C.) until it had frozen solidly. It was then allowed to thaw at room temperature and finally dried as for F-2. The physical state of the dried pulp depended upon the method of drying. Evaporation of liquid water allowed the capillary forces of water to exert their influence in promoting interfiber bonding, and the fibers tended to be densely packed.

Cyclic wetting and drying produced a bulkier pulp in which the fibers were more easily separated. Pulp which had been dried either by freeze-drying, or from a non-swelling liquid such as benzene, was even less highly bonded than when cyclically dried by evaporation of water.

Wiley-Milled Cellulose

A portion of the same batch of virgin pulp used in the preceding preparation was dried at 105° C. and subsequently milled for 90 minutes in a laboratory attrition mill. An intermediate model Wiley mill was used for this purpose, with a clearance of 7.5×10^{-3} cm. between the stationary and revolving blades. Small quantities of the milled material, which was fine enough to pass a 60-mesh screen, were immersed in pure liquids, having various swelling capacities, for 24 hours at room temperature and then dried as listed in Table I.

TABLE I

TREATMENT OF WILEY-MILLED SAMPLES

Sample	
M-1	Original milled sample
M-2	M-1 immersed in water, 24 hours R.T., dried at 105° C.
M-3	Treatment for M-2 repeated 10 times
M-4	M-1 immersed in ethanol, 24 hours R.T., dried at 105° C.
M-5	Treatment for M-4 repeated 10 times
M-6	M-1 immersed in acetone, 24 hours R.T., dried at 105° C.
M-7	Treatment for M-6 repeated 10 times
M-8	M-1 exposed in a vacuum desiccator to water vapor at 93.3% R.H. for 48 hours, dried at 105° C.

Ball-Milled Cellulose

A series of ball-milled samples of dissolving grade "Rayaceta" wood pulp were kindly supplied by Dr. J. A. Howsmon of the American Viscose Corporation, Marcus Hook, Pa. The dry material had been milled for various times up to 153 hours under the following conditions:

Initial treatment of pulp	Wiley Mill, 20-mesh screen
Ball-mill charge	1200 g. steel balls, 40 g. pulp
Mill speed	47 r.p.m.

To follow the destructive action of ball-milling on the crystallinity of cellulose the samples milled for progressive periods were subjected to X-ray measurements. These samples are denoted by the letter H, followed by the number of hours milled.

In addition, small quantities of sample H-153, which was completely pulverized, were subjected to various wetting and drying treatments as outlined in Table II. Except for sample B-4, the wetting and drying procedures were as for the Wiley-milled material.

The differently treated samples prepared from both sets of milled materials remained powdery and to the eye were unchanged from the untreated material.

2. EXPERIMENTAL METHODS AND RESULTS

X-Ray Measurements

General

A transmission technique based on that of Hermans (18) was adopted for the X-ray measurements, except that air scattering was used as a reference for the incident X-ray

Can. J. Chem. Downloaded from www.nrcresearchpress.com by 200.7.193.243 on 09/04/12
For personal use only.

TABLE II

TREATMENT OF BALL-MILLED SAMPLES

Sample	
B-1	Original ball-milled sample H-153 (milled for 153 hours)
B-2	B-1 immersed in water, 24 hours R.T., dried at 105° C.
B-3	Treatment for B-2 repeated 10 times
B-4	B-1 treated as described for cellulose fibers (sample F-6) with benzene removed at 105° C.
B-5	B-1 immersed in benzene, 24 hours R.T., dried at 105° C.
B-6	B-1 immersed in ethanol, 24 hours R.T., dried at 105° C.
B-7	Treatment for B-6 repeated 10 times
B-8	B-1 immersed in acetone, 24 hours R.T., dried at 105° C.
B-9	Treatment for B-8 repeated 10 times
B-10	B-1 immersed in methanol, 24 hours R.T., dried at 105° C.
B-11	B-1 immersed in propanol, 24 hours R.T., dried at 105° C.
B-12	B-1 immersed in butanol, 24 hours R.T., dried at 105° C.

intensity instead of a Goppel (19) camera, and the samples were mounted in the form of compressed pellets which were supported in a holder during an exposure. In addition, a nickel foil was used for X-ray absorption measurements.

Fig. 1 shows the disposition of the various parts of the camera and collimating system. The nickel-filtered copper radiation was delivered by a Muller MC-50 tube. A 9×12 cm. flat film camera, manufactured commercially by R. Seifert & Co., Hamburg, Germany, was used. Its collimator was replaced by a four-pinhole system and a removable nickel foil was incorporated as shown in Fig. 1. Details of construction are to be published separately.

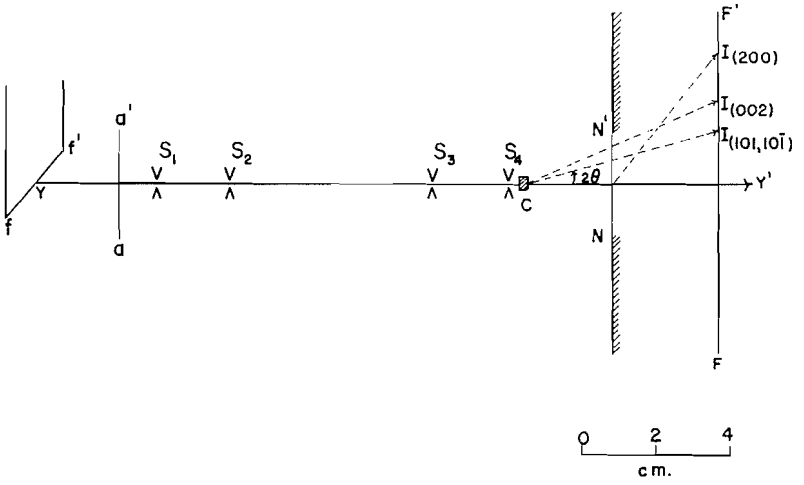

FIG. 1. Camera and collimating system. ff′ = Focal spot of tube. YY′ = Path of primary beam. aa′ = Nickel filter. S_1S_4 = Pinhole apertures, 1 mm. S_2S_3 = Pinhole apertures, 0.7 mm. C = Sample. NN′ = Nickel foil, 0.021 mm. thick, supported on metal frame. FF′ = Film. $I_{(200)}$ = Nickel interference. $I_{(101,10\bar{1})}$, I_{002} = Cellulose A_4 and A_1 interference respectively.

Mounted pellets were prepared from whole fibers by separating them with two dissecting needles until the resulting material was a mass of loosely tangled individual fibers. A weight of 3 mg. ±3% of the loose fibers was placed in a metal sample holder and compressed into a pellet by a specially-constructed press, care being taken to ensure isotropic packing in the plane of the holder. Pellets of the milled cellulose were formed in the

Can. J. Chem. Downloaded from www.nrcresearchpress.com by 200.7.193.243 on 09/04/12
For personal use only.

same manner but with no previous scraping. For an exposure to the X-ray beam, the loaded pellet holder was mounted on the collimator. The dimensions and densities of the pellets are given in Table III.

TABLE III

DIMENSIONS AND DENSITIES OF PELLETS

Pellets	Diameter, mm.	Thickness (t), mm.	Density (ρ), g./cm.^{3}
Cellulose fibers	3.0	1.7	0.25
Wiley-milled cellulose	3.0	0.5	0.85
Ball-milled cellulose	3.0	0.4	1.06

All exposures were made at room temperature and at the prevailing relative humidity, which was in the region of 50%. Ilford-B film was used throughout.

Measurements of Intensity

To determine the intensities of X-ray diffraction lines on a film, a continuous recording microdensitometer, manufactured by A. Krüss, Hamburg, Germany, was used. The sensitivity of the galvanometer was adjusted to give zero deflection in the unexposed region, and a full-scale deflection of 80 mm. when no light was transmitted through the film. Fig. 2 is a reproduction of a photometer trace of a diffraction pattern of wood

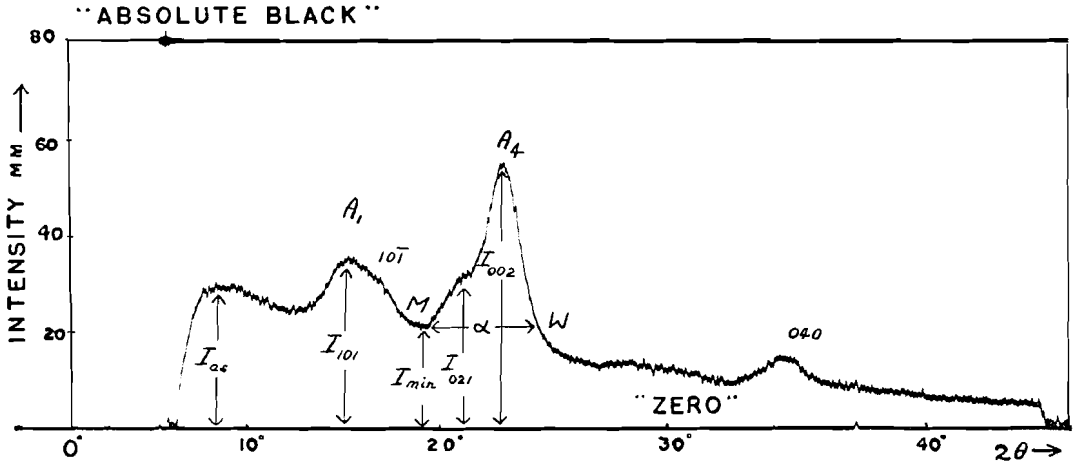

FIG. 2. Radial photometer trace of an X-ray diffraction pattern of wood pulp. I_{as} = Maximum intensity of air scattering. I_{101} = Intensity of (101) peak. I_{min} = Intensity of minimum point M. I_{021} = Intensity of (021) peak. I_{002} = Intensity of (002) peak. α = Width MW of peak (002) in radians. A_1, A_4 = Herzog designation of peaks (101) and (002), respectively.

pulp. The traces of the extreme positions of the galvanometer deflections are shown as the "zero" and "absolute black" lines. The height in mm., above the "zero" line, of any point on the trace is a measure of its intensity. The Herzog (20) designations and Miller (21) indices (hkl) of the principal planes of cellulose corresponding to the various peaks are included in Fig. 2. The maximum intensity of air scattering, I_{as}, occurs at an angle $2\theta = 7° 30'$.

Measurements of Absorption

Since sample F-6 contained entrapped benzene, measurements were made to determine

Can. J. Chem. Downloaded from www.nrcresearchpress.com by 200.7.193.243 on 09/04/12
For personal use only.

any change in its X-ray absorption coefficient, using sample F-1 as a standard. In making absorption measurements the sample was alternately placed in position and removed, and two exposures at the same intensity were made of the nickel foil NN′ (Fig. 1). From the difference in intensity of the (200) nickel interference the absorption $\mu_m \rho t$ of the sample was calculated using (see Ref. 18):

$$\ln(I_{Ni})_{air} - \ln(I_{Ni})_{cell.} = \mu_m \rho t, \quad [1]$$

where

$(I_{Ni})_{cell.}$, $(I_{Ni})_{air}$ = intensity of (200) nickel interference with and without sample in position respectively,
μ_m = mass absorption coefficient of the sample (cm.^{2}/g.),
ρ = packing density in the sample (g./cm.^{3}),
t = thickness of the sample in cm.

The resulting values of $\mu_m \rho t$ for samples F-1 and F-6, 0.383 and 0.363 respectively, agreed within experimental error indicating equal absorption coefficients. Hence, no correction was applied to the observed peak height of sample F-6; in Hermans' experiments such corrections were necessary (22).

Determination of Crystallinity Index

(*i*) *Cellulose Fibers*

Following the method of calculation used by Ant-Wuorinen (11), the per cent crystallinity index, X, is given by the following equation, which is readily derived from Ant-Wuorinen's equations:

$$X = \{1 - [80\alpha/(I_{002} - I_{min})]\} \times 100, \quad [2]$$

where, as illustrated in Fig. 2,

I_{002} = height of A_4 peak in mm.,
I_{min} = height of minimum point M above "zero" line in mm.,
α = width (MW) of peak A_4 in radians.

TABLE IV

PROCEDURE FOR IRRADIATION OF SAMPLES

Series	Samples	Pellets per sample	Exposures per pellet	Anode voltage, kv.	Anode current, ma.	Time of each exposure, min.
1	F-1 to F-7	4	1	30	20	65
2	M-1 to M-8	1	3	30	≈20	45, 80, 100
3	B-1 to B-12	1	3	30	≈20	45, 80, 100
4	H-0 to H-153	1	1	30	≈20	80

The conditions of irradiation for Series I, Table IV, produced a maximum intensity of air scattering, I_{as}, of 30 mm. and α was found to be independent of the intensity of irradiation. The results of the X-ray measurements for cellulose fibers are shown in Table V. Sample M-1 has been included for comparison.

(*ii*) *Milled Cellulose Samples*

For every sample in Series 2 and 3, Table IV, I_{as} was plotted against the corresponding values of I_{101}, I_{002}, and I_{min} obtained from the photometer trace as in Fig. 2. Excellent

Can. J. Chem. Downloaded from www.nrcresearchpress.com by 200.7.193.243 on 09/04/12
For personal use only.

TABLE V

X-RAY AND HEAT OF WETTING DATA FOR CELLULOSE FIBERS

Sample No.	Treatment	A_1 I_{101}, mm.	A_4 I_{002}, mm.	I_{min}, mm.	α, radians	X, %	Heat of wetting, cal./g.
F-1	Oven-dried at 105° C.	32.8 (1.1)†	48.8 (2.1)	21.9 (0.63)	0.0989	70.6 (1.05)	13.06
F-2	Drying at room temperature over P_2O_5	33.2 (1.03)	49.0 (2.2)	21.7 (0.97)	0.0989	71.0 (1.2)	13.90
F-3	Sample F-1, rewetted at room temperature and dried at 105° C. (10 times)	32.0 (1.3)	49.1 (2.3)	20.0 (0.53)	0.0989	72.8 (1.5)	11.80
F-4	Sample F-2, rewetted and dried at room temperature over P_2O_5 (10 times)	32.7 (1.06)	48.0 (2.4)	21.8 (1.4)	0.0989	69.8 (1.4)	12.98
F-5	Original wet sample freeze-dried	33.6 (1.2)	48.2 (2.2)	22.5 (1.1)	0.0989	69.2 (1.4)	13.68
F-6	Original wet sample solvent-exchanged to and freeze-dried from benzene	32.1 (1.05)	44.2 (1.7)	22.5 (0.76)	0.0989	63.5 (1.3)*	11.98
F-7	Original wet sample, immersed in liquid nitrogen, allowed to melt, and dried at room temperature over P_2O_5	31.2 (1.0)	44.3 (1.9)	20.3 (0.65)	0.0989	67.0 (2.0)	13.46
M-1	Original wet sample dried at 105° C. and Wiley-milled	28.0	28.0	21.5	0.0817	0.00	17.40

**Repeated 6 months later with same result.*

†Quantities in parentheses denote standard deviations from the associated mean values.

TABLE VI

X-RAY DATA FOR WILEY-MILLED CELLULOSE

Sample No.	Treatment	A_1 I_{101}, mm.	A_4 I_{002}, mm.	I_{min}, mm.	α, radians	X, %	K_{002}
M-1	Original milled sample	28.0	28.0	21.5	0.0817	0.00	0.934
M-2	M-1 water-wetted and dried	30.0	37.0	21.0	0.0989	50.5	1.230
M-3	M-1 water-wetted and dried (10 times)	30.3	40.0	19.5	0.0989	61.4	1.330
M-4	M-1 immersed in ethanol and dried	27.8	32.0	20.5	0.0946	33.8	1.065
M-5	M-1 immersed in ethanol and dried (10 times)	27.8	28.5	18.5	0.0903	28.7	0.956
M-6	M-1 immersed in acetone and dried	29.4	29.5	22.5	0.0946	—ve	0.975
M-7	M-1 immersed in acetone and dried (10 times)	29.4	30.0	21.5	0.0903	15.0	1.018
M-8	M-1 exposed to water vapor at 93.3% R.H. and dried	30.0	36.5	20.5	0.0989	50.5	1.200

straight lines of the type shown in Fig. 3 were obtained. The lines passed through the origin and the linearity was maintained up to an optical density of film blackening of 0.9. The values at I_{as} = 30 mm. were obtained from the respective graphs and X determined from Equation [2]. The same procedure was applied to samples exhibiting no interferences associated with crystallinity, except that the maximum intensity of the "amorphous" halo, I_{AmH}, was measured. Furthermore, the absence of the peaks A_4 and A_1 eliminated the minimum point M between them, and α could not be measured.

The results of the X-ray measurements on the Wiley- and ball-milled cellulose are recorded in Tables VI and VII, respectively.

For Series 4, Table IV, the values of I_{101}, I_{021}, I_{002}, I_{min}, and I_{AmH}, measured at the I_{as} of the exposure, were reduced to an I_{as} = 30 mm. by multiplying by the factor 30/measured I_{as}. The results of the X-ray experiments on the samples milled for progressive periods are recorded in Table VIII. It is interesting to note that it took more than 100 hours of ball-milling to render the photometer tracing uniform. Ellefsen *et al.* (23) report that no change was observed after 6 hours of milling in their recent experiments.

Can. J. Chem. Downloaded from www.nrcresearchpress.com by 200.7.193.243 on 09/04/12
For personal use only.

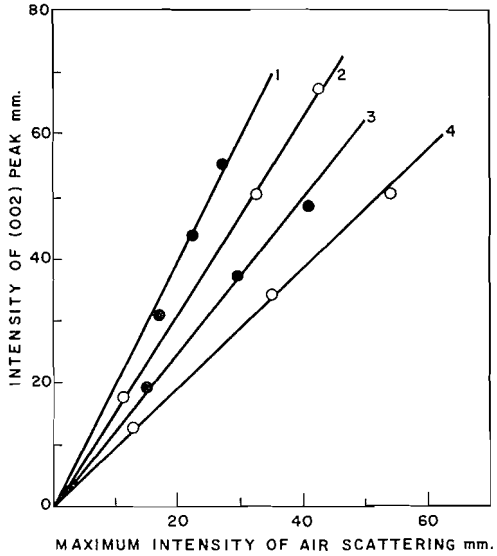

FIG. 3. Variation of intensity of (002) peak with crystallinity of cellulose and maximum intensity of air scattering. 1 = Dewaxed cotton linters. 2 = Sample F-7. 3 = Sample M-2. 4 = Sample M-1.

TABLE VII

X-RAY DATA FOR BALL-MILLED CELLULOSE

Sample No.	Treatment	A_1 I_{101}, mm.	A_4 I_{002}, mm.	I_{min}, mm.	α, radians	I_{AmH},* mm.	X, %	K_{002}
B-1	Original milled sample					28.5		
B-2	B-1 water-wetted and dried	28.0	34.0	23.0	0.0989		28.0	1.115
B-3	B-1 water-wetted and dried (10 times)	27.5	35.0	21.0	0.0946		45.9	1.170
B-4	B-1 water-wetted and dried from benzene	26.0	31.5	22.5	0.0989		12.0	1.040
B-5	B-1 immersed in benzene and dried					28.5		
B-6	B-1 immersed in ethanol and dried					26.0		
B-7	B-1 immersed in ethanol and dried (10 times)					29.0		
B-8	B-1 immersed in acetone and dried					28.0		
B-9	B-1 immersed in acetone and dried (10 times)					28.5		
B-10	B-1 immersed in methanol and dried					28.5		
B-11	B-1 immersed in propanol and dried					29.5		
B-12	B-1 immersed in butanol and dried					27.5		

*I_{AmH} = *maximum intensity of "amorphous" halo.*

TABLE VIII

X-RAY DATA FOR CELLULOSE BALL-MILLED FOR PROGRESSIVE PERIODS

Sample (hours of milling)	A_1 I_{101}, mm.	I_{021}, mm.	A_4 I_{002}, mm.	I_{AmH}, mm.	I_{min}, mm.	α, radians	X, %
H-0	32.2	29.2	45.1		22.1	0.0946	67.1
H-16	30.0	27.3	35.0		21.3	0.0946	44.8
H-32	31.0	28.4	32.3		23.7	0.0946	12.0
H-48	26.8	24.5	24.8		21.5	0.0903	
H-68	25.7	24.0	23.0		21.2	0.0860	
H-80	26.2		23.4	25.6	23.4	0.0860	
H-96	25.8			26.1	24.2		
H-114	25.7			26.2	24.8		
H-132	26.8			28.7	26.8		
H-153				28.5	25.6		

Can. J. Chem. Downloaded from www.nrcresearchpress.com by 200.7.193.243 on 09/04/12
For personal use only.

Value of K_{hkl} and Crystallinity

The ratio of a cellulose interference, I_{hkl}, and the intensity of a reference line of the Goppel (19) camera used by Hermans (18) yields a value independent of the energy of irradiation. A similar result is obtained if the Goppel interference is replaced by the maximum intensity of air scattering, I_{as}, occurring at an angle $2\theta = 7° 30'$.

Thus

$$I_{hkl}/I_{as} = K_{hkl}. \qquad [3]$$

Any variation of I_{as} with atmospheric pressure was neglected.

The air scattering peak did not contain any appreciable contribution from the cellulose. This was established by means of diffraction patterns of cellulose obtained with a Kiessig small-angle vacuum camera, both with and without a vacuum. Under vacuum the scattered intensity at 7° 30′ was negligible, a circumstance which made it possible to use air scattering for standardization.

In Table VI it is seen that in certain cases, although the diffraction pattern showed the unmistakable presence of A_1 and A_4 peaks, X failed to represent the state of crystallinity of samples subjected to severe mechanical degradation. In addition, the difficulty in measuring α caused by the broadening of the minimum between A_1 and A_4 peaks introduces an error of (0.16 to 0.20) X, when X is in the range 20 to 30%. Since the A_4 peak is more sensitive to crystallinity changes than A_1, the value of K_{002} may provide a parameter which is less susceptible to error and which is capable of continuously representing the state of crystallinity of cellulose. Assuming approximately equal size distribution of crystallites, I_{002} for a given I_{as} will be greater for a more crystalline than for a less crystalline sample.

In Tables VI and VII, K_{002} was determined from the slope of the straight lines obtained by plotting I_{as} vs. I_{002}. Fig. 3 shows the plot of I_{002} vs. I_{as} of four cellulose samples of different degrees of crystallinity. Dewaxed cotton linters, a cellulose of high crystallinity which is estimated from various methods to amount to 70% (22), was included for comparison. I_{002}, X at $I_{as} = 30$, and K_{002} are given in Table IX. Fig. 3 and Table IX show that K_{002} decreases together with X, and in addition, gives a positive value in the case of sample M-1 where X indicates somewhat misleadingly the total destruction of crystallinity.

TABLE IX

VARIATION OF I_{002}, X, AND K_{002} WITH DEGREE OF CRYSTALLINITY

No.	Sample	A_4 I_{002}, mm.	X, %	K_{002}
1	Dewaxed cotton linters	58.5	79.8	1.950
2	F-7	44.3	67.0	1.535
3	M-2	37.0	50.5	1.230
4	M-1	28.0	0.0	0.934

Heats of Wetting

Heats of wetting by liquid water were measured for samples F-1 to F-7 and M-1 using a Bunsen isothermal calorimeter with diphenyl ether as the working substance (24). The apparatus was kept in a thermostat maintained at 26.90±0.003° C. The results of these experiments are given in Table V.

Differential Staining

Differential staining of fibers provides a visual and qualitative means of demonstrating variations in the density of amorphous cellulose and the degree of fibrillation

Can. J. Chem. Downloaded from www.nrcresearchpress.com by 200.7.193.243 on 09/04/12
For personal use only.

(25). Samples F-1 to F-7 were dyed with a solution of equal parts of Benzo-Fast Yellow A and Benzo Brilliant Blue 6BS. The dyes were obtained from Bayer, Farbenfabriken, Leverkusen, Germany. The technique used by Jayme (26) was followed in its entirety. The results of the differential staining experiments are shown in Table X.

TABLE X

DIFFERENTIAL STAINING

Sample No.	Sample preparation	Color after staining
1	Sample F-2 (at room temperature over P_2O_5)	Pale green
2	Sample F-4 (10 times as No. 1)	Pale green
3	Wet (virgin) pulp	Yellowish
4	Sample F-3 (10 times as No. 8)	Blue
5	Sample F-5 (freeze-dried)	Greenish yellow
6	Sample F-7 (wet sample in liquid N dried as No. 1)	Greenish yellow
7	Sample F-6 (solvent exchanged)	Yellowish
8	Sample F-1 (dried once at 105°)	Blue to blue-green

Viscosity

To follow the effect of mechanical degradation on the degree of polymerization (D.P.), viscosity measurements were made on samples F-1 and M-1 and H-0 to H-153. The viscosity pipette procedure described in Tappi, method T-230 sm-50, was followed in its entirety.

The intrinsic viscosities were calculated from Schulz and Blaschke's (27) equation:

$$\eta_{sp}/c = [\eta](1+k'\eta_{sp}), \qquad [4]$$

where

η_{sp} = specific viscosity,
c = concentration of cellulose in g./dl.,
k' = $2.303k$,
k = 0.13 (Martin's (28) constant),
$[\eta]$ = intrinsic viscosity in dl./g.

The degree of polymerization was calculated from the equation in Ref. (29):

$$\text{D.P.} = 156[\eta]. \qquad [5]$$

The intrinsic viscosities and D.P. values are recorded in Table XI.

TABLE XI

VARIATION OF D.P. OF CELLULOSE WITH MECHANICAL TREATMENT

Sample No.	$[\eta]$, dl./g.	D.P.
F-1	2.70	422
M-1	2.49	389
H-0	4.83	755
H-16	2.68	418
H-32	2.57	402
H-48	2.41	376
H-68	2.24	350
H-80	2.08	325
H-96	1.94	303
H-114	1.79	279
H-132	1.62	253
H-153	1.53	239

Can. J. Chem. Downloaded from www.nrcresearchpress.com by 200.7.193.243 on 09/04/12
For personal use only.

Can. J. Chem. Downloaded from www.nrcresearchpress.com by 200.7.193.243 on 09/04/12
For personal use only.

DISCUSSION

Cellulose Fibers

From Table V it is seen that drying cellulose fibers under different conditions produced little change in the crystallinity index, X. Although the diffraction pattern of fibers dried by evaporation of water and freeze-drying remained unaltered, the heats of wetting varied with the method of drying. Only in sample F-6 (the results of which were duplicated) could a change in X be detected. On immersing sample F-6 in water at room temperature for 24 hours and then drying for 24 hours, it was found that X increased to 67.6% so that the increase in X due to drying from water must be considered to be real.

The results obtained for samples F-1 to F-4 and F-7 suggest that any relative changes in crystallinity, arising from variations in intrafiber bonding with the method of drying, were small compared with other changes tending to decrease the accessibility, as indicated, by the heats of wetting. Since the quantity of heat evolved when cellulose is wetted with water is believed to be primarily due to an interaction of the water molecules with free hydroxyl groups of the cellulose, it may be taken as a measure of the accessibility of these hydroxyl groups (30). On this assumption, it may be inferred that in conformity with previous findings, the vitrified regions (2) and junction points (31) established with a first drying in samples F-1 and F-2 increase with repeated wetting–drying cycles (samples F-3 and F-4) as well as with the temperature of drying. The formation of impenetrable vitreous regions and junction points would then immobilize and prevent the interaction of any available hydroxyl groups with the water molecules without necessarily increasing lateral order.

Freezing the fibers as in sample F-7 may have reduced their hydrophilic (32) character and produced the same effect on the accessibility as drying at a temperature between 105° C. and room temperature. In freeze-drying cellulose fibers the plasticizing action of water is reduced and the mobility of the molecular chains curtailed. In addition, previous work has shown that freeze-drying decreases interfiber bonding especially in the absence of hemicellulosic material (5, 6). Since benzene is a poor swelling and a poor hydrogen-bonding medium, it may be reasonable to conclude that the degree of alignment of the molecular chains in the amorphous region during drying from benzene is less than with water. Hence, any additional crystallization produced in this manner in drying from water will be absent with benzene-dried fibers. Fibers dried in this manner would be expected to have a lower X (as was found for sample F-6) and a higher value of heat of wetting than fibers dried by evaporation of water. However, since sample F-6 contained trapped benzene, the heat of wetting of 11.98 cal./g. is of doubtful validity.

An attempt was made to determine X by taking a diffraction diagram of wet (virgin) fibers, but it proved unsuccessful because it was not possible to make a quantitative separation of the X-ray scattering due to water from that due to cellulose.

Table X shows the effect of different drying procedures on the staining of cellulose fibers. The color differences resulting from the staining procedure depend upon the dyeing properties of the different components of the dyes. The main component of the yellow dye has a greater affinity for cellulose than either component of the blue dye, but the blue dye is composed of smaller molecules than the yellow dye. Hence, the blue dye can enter a capillary network into which the yellow dye, in spite of its greater affinity for cellulose, is not admitted (26). A cellulose structure having fine capillaries will be dyed blue to blue-green, while a structure in which the molecular chains are less highly bonded would stain yellow.

Can. J. Chem. Downloaded from www.nrcresearchpress.com by 200.7.193.243 on 09/04/12
For personal use only.

As could be seen under the microscope, in the virgin as well as the solvent-exchanged sample, intrafiber bonding was least and a yellow color resulted. In contrast, the highly bonded fibers resulting from the evaporation of water acquired a similar blue to blue-green color exhibited by the oven-dried sample. The color of the freeze-dried sample further indicated that drying by sublimation of water reduced intrafiber bonding to a smaller extent than drying by solvent exchange.

The variations in color became more distinct when the stained fibers were viewed in bulk. The most striking differences in color were again exhibited by the undried (virgin) and solvent-exchanged samples No. 3 and 7, respectively. Fibers dried by room-temperature evaporation of water stained pale green (No. 1) and the color did not intensify when the fibers were stained after having been wetted, and dried 10 times (No. 2). Fibers dried by evaporation of water at 105° C. stained pale blue (No. 8), while fibers which had been wetted at room temperature and dried at 105° C. exhibited a more intense blue color upon staining (No. 4). Freeze-drying (No. 5) or treatment with liquid nitrogen (No. 6) resulted in greenish-yellow fibers upon staining.

From these results it could be inferred that intrafiber bonding was least in the undried (virgin) pulp sample and greatest in sample F-3 (No. 4). Further work is in hand to measure the reflection spectra between 400 and 700 mμ of the differentially stained pulps. Preliminary measurements have indicated that a quantitative method of measuring the degree of vitrification can be worked out.

Milled Cellulose

From Tables V, VI, and VII it is seen that Wiley-milling increased the heat of wetting of cellulose fibers and reduced X to zero, while ball-milling completely destroyed the crystallinity. Figs. 4, 5, and 6 are reproductions of photometer traces of X-ray diffraction patterns of F-1, M-1 and M-2, B-1, B-2 and B-4, and B-1 (in the dry and wet state), respectively. By comparing Fig. 4(*b*) with 4(*a*), the following points may be noted:

(1) Wiley-milling reduced the intensity of the A_1 and A_4 peaks.

(2) The grinding action preferentially destroyed the $A_4(002)$ planes, reducing the A_4 peak intensity to 57% of its value in F-1, while the A_1 peak suffered a reduction of only 20%.

(3) The width α in M-1, a measure of the crystallite size, was also reduced.

In contrast, the X-ray diffraction pattern of B-1 showed only a diffuse halo, which

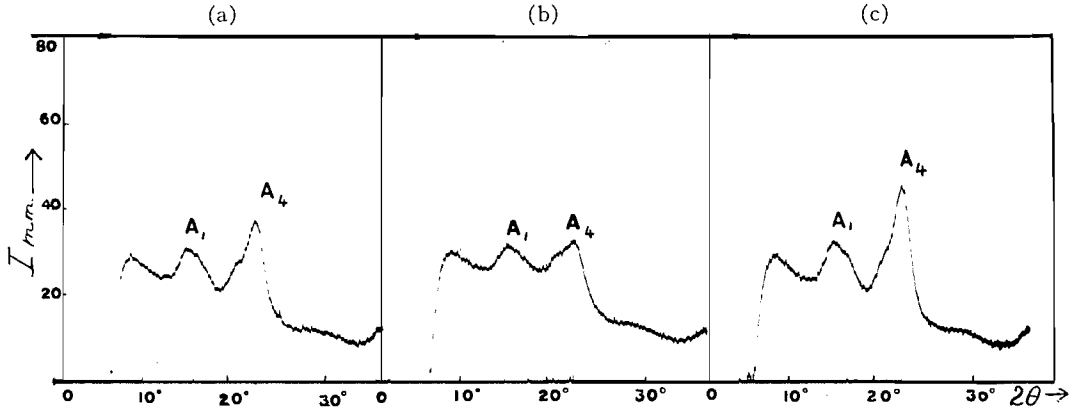

FIG. 4. Radial photometer traces of X-ray diffraction patterns of cellulose fibers and Wiley-milled cellulose. (*a*) Sample M-2. (*b*) Sample M-1. (*c*) Sample F-1.

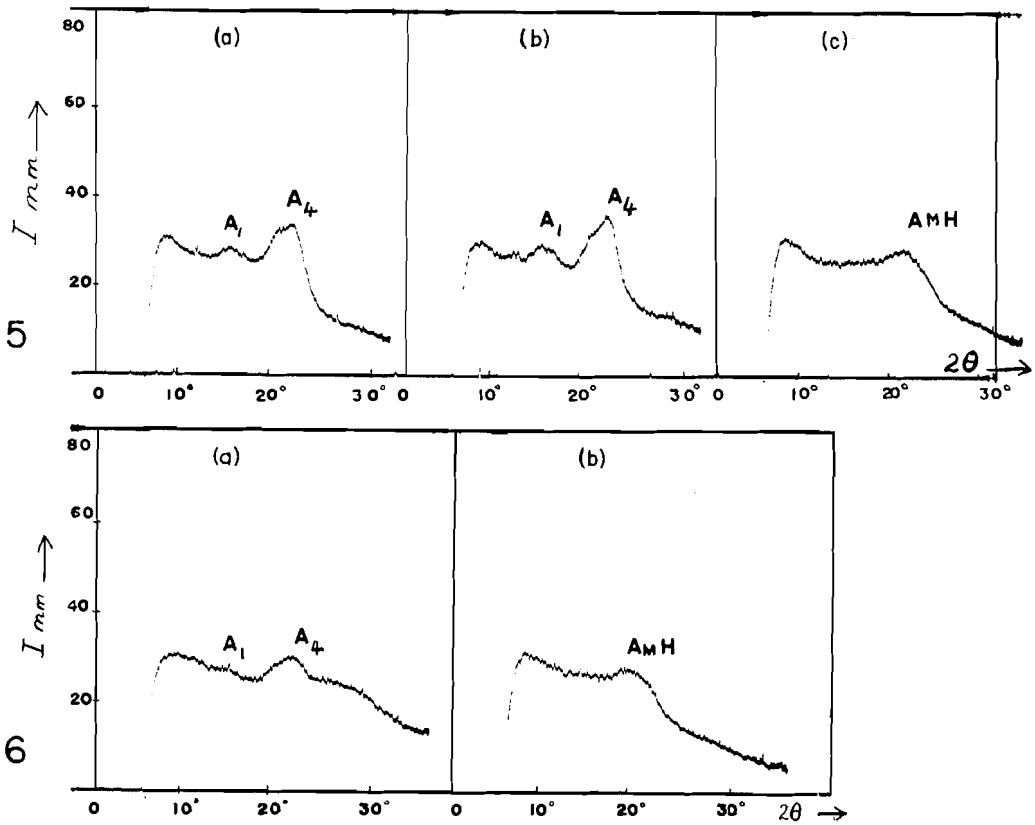

FIG. 5. Radial photometer traces of X-ray diffraction patterns of ball-milled cellulose. (*a*) Sample B-4. (*b*) Sample B-2. (*c*) Sample B-1.

FIG. 6. Radial photometer traces of X-ray diffraction patterns of dry and wet ball-milled cellulose. (*a*) Sample B-1—wet. (*b*) Sample B-1—dry.

can be seen in Fig. 5(*a*) as a broad maximum in the region previously occupied by the (021) peak.

Treatment of the milled material with water resulted in the following behavior:

(1) Partial restoration of crystallinity, Figs. 4(*c*) and 5(*b*).

(2) Exposure of the Wiley-milled product to water vapor at 93.3% R.H. resulted in the same degree of recrystallization as for M-2.

(3) Repeated wetting and drying (samples M-3 and B-3) further increased X.

(4) Recrystallization of B-1 occurred in the wet state, Figs. 6(*a*) and 6(*b*).

(5) Displacing the water from the wetted ball-milled sample with benzene and drying from the non-polar solvent resulted in a smaller degree of recrystallization than with B-2, Fig. 5(*c*).

(6) No modification to cellulose II occurred, but a slight shift was observed in the position of the A_4 peak of the treated ball-milled samples.

Treatment of the Wiley-milled samples with organic liquids gave smaller X values than with water. Because of the large error associated with such small values of X, the state of crystallinity can be better appreciated by referring to the K_{002} values. It is seen that a single wetting with ethanol gave, as expected from its greater swelling power, a larger K_{002} value than acetone. Anomalously, a lower K_{002} value was obtained

Can. J. Chem. Downloaded from www.nrcresearchpress.com by 200.7.193.243 on 09/04/12
For personal use only.

Can. J. Chem. Downloaded from www.nrcresearchpress.com by 200.7.193.243 on 09/04/12
For personal use only.

for repeated wetting and drying from ethanol than for a similar treatment using acetone, but this may have been due to contamination of the acetone with water. In contrast, treatment of the ball-milled samples with organic liquids produced no detectable X-ray interferences associated with crystallinity.

The increase in the heat of wetting of sample M-1 may be readily explained by an increase in the number of available hydroxyl groups. The disruption of the hydrogen-bonded crystalline lattice and the reduction in the degree of polymerization of the fibers with grinding (Table XI) exposed hitherto unavailable hydroxyl groups which could then react with the water molecules. Although a reduction in the size of the crystallites may be expected to produce an increase in the width α of the A_4 peak in sample M-1, the observed decrease may be attributed to a change in the distribution of the crystallite size with the larger crystallites surviving the destruction action better than the smaller ones. The progressive decrease in α with milling, observed in Table VIII, is at present inexplicable.

In order to explain the recrystallization of the milled material with water it may be assumed that mechanical degradation, in destroying the crystalline regions, also ruptures the junctions restraining normal swelling of the fibers. The plasticizing action of water, by conferring mobility on the chains, allows their realignment and the surface tension of water during drying promotes hydrogen-bonding, which increases the lateral order. Repeated wetting and drying may be expected to further extend the process of realignment and a higher degree of lateral order may be attained.

The identical results obtained for samples M-2 and M-8 may indicate that removal of the water in the earlier stages of drying contributes little to recrystallization. Upon addition of water beyond the range of "bound" water the rapid rise in the sorption isotherm in the high humidity regions cannot be explained by assuming formation of new sorption sites by swelling. In the opinion of various workers, water in the high relative humidity regions is adsorbed as multilayers (33), or by capillary condensation (34), or by solution of the non-crystalline cellulose (35).

Such water will condense within the structure with heat effects associated with normal condensation (36, 37). However, since only imbibed water can affect the intrinsic properties of the fibers and promote their rearrangement, it is reasonable to assume that recrystallization of M-8 had occurred in the range of 60–70% R.H.

Broughton and Wang (10), investigating the strength of handsheets dried from non-aqueous liquids, observed a similar behavior. Upon conditioning butanol-dried handsheets to water vapor of 85% R.H., the strength attained was found to be as great as that of a sheet initially formed from water. These authors did not discount the possibility of an increase in bonding occurring only at the onset of capillary condensation. According to Barkas (38), such condensation begins at a relative humidity of 65–70%.

By comparing values of α for the undegraded and milled material, it may be inferred that the mending action of water reproduced the same distribution of crystallite size existing before degradation. The low X and K_{002} values obtained for sample B-4 fall within expectation. Here, as in sample F-6, the mobility of the chains in benzene was greatly curtailed and there was little tendency for hydrogen-bonding, and hence on drying resulted in a low degree of lateral order. These results further confirm previous findings that drying from benzene is much less effective in bond formation in fibers than drying by sublimation of water (10).

The results obtained for samples M-4 to M-7 indicate that the amount of recrystallization occurring on drying increases with the swelling capacity of the liquid. As expected,

ethanol produced a higher lateral order than acetone, but less than for water. From the results of the ball-milled samples treated separately with benzene and acetone, it is concluded that no recrystallization is possible with these liquids. The almost complete absence of order in the ball-milled samples, and the smaller swelling capacities for cellulose of the alcohols with respect to water, may be responsible for the failure of these media to produce any detectable recrystallization. Here, it may be assumed that the relatively weaker swelling medium is unable to align the molecular chains without the initial presence of well-defined crystallites to act as anchoring points.

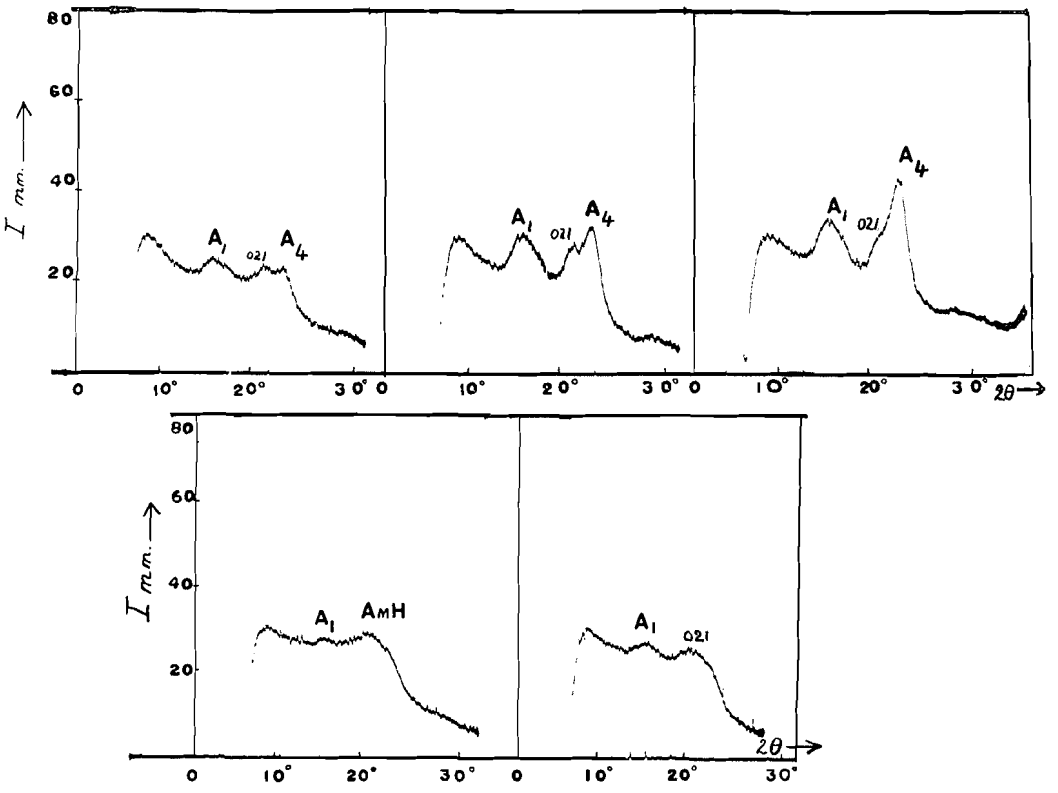

FIG. 7. Radial photometer traces of X-ray diffraction patterns of cellulose ball-milled for progressive periods. *Top*—Left: Sample H-68. Center: Sample H-32. Right: Sample H-0. *Bottom*—Left: Sample H-132. Right: Sample H-96.

Although in this case the presence of nuclei of ordered regions appears necessary for recrystallization, a further conclusion may be drawn from the variations in the intensity of the amorphous halo I_{AmH}, for the alcohol-treated samples. Fig. 7 is a reproduction of photometer traces of X-ray diffraction patterns of H-0, H-32, H-68, H-96, and H-132. From the traces and Table VIII, the following observations were made:

(1) The A_4 peak diminished steadily and disappeared after 80 hours of milling.

(2) The (021) peak also diminished and disappeared between 68 and 80 hours of milling, being replaced by an amorphous halo.

(3) The position of the maximum intensity of the amorphous halo coincided with the position of the (021) peak it replaced.

(4) The intensity of the amorphous halo increased and finally levelled out after 132 hours of milling.

Can. J. Chem. Downloaded from www.nrcresearchpress.com by 200.7.193.243 on 09/04/12
For personal use only.

(5) The A_1 peak resisted initial degradation and began to suffer only after 32 hours of milling.

(6) Table VIII shows that the intensity of I_{mln} increased with decreasing crystallinity and hence may be taken as a measure of the amorphous content.

(7) The increasing intensity of I_{mln} helped to maintain constant the intensity of the A_1 peak which merged with the background after 132 hours of milling.

Fig. 8 shows a plot of the intensity of the (021) peak against time of milling. The curve has a minimum region where the transition from the (021) peak to the amorphous halo takes place. The intensity of the (021) peak decreases gradually with milling until, after 70 hours, the intensity of the amorphous halo predominates, and increases with continued milling. After approximately 130 hours, it reaches its final value of 28.5 mm. This stage appears to mark the limiting effect of the grinding process, for although the sample probably is not completely amorphous, the intensity of the "amorphous" halo remains constant with further milling.

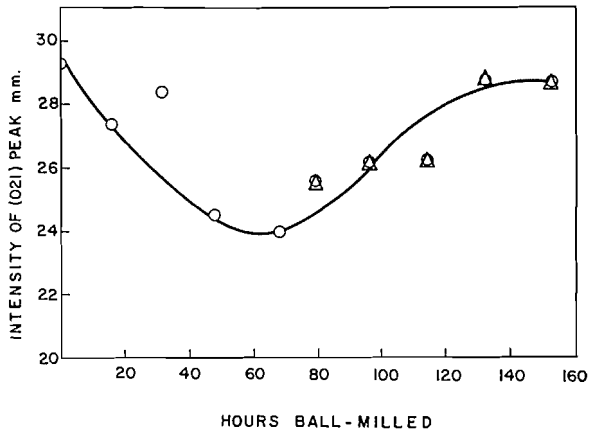

FIG. 8. Variation in intensity of (021) peak with time of ball-milling. Circles: I_{021}. Triangles: I_{AmH}.

The variations in I_{AmH} may be taken to herald the beginnings of the (021) lattice planes of cellulose I, and the I_{AmH} values for the ethanol- and methanol-treated samples may be considered to be I_{021} values on the left of the transition region in Fig. 8. It is evident that propanol and butanol are hindered (sterically or otherwise) from penetrating the degraded cellulosic structure; no (021) lattice planes are formed. Although the evidence is inconclusive, the formation of the (021) lattice planes under these conditions should not be discounted.

ACKNOWLEDGMENTS

The authors are indebted to Dr. R. M. Screaton for measuring the heats of wetting.

REFERENCES

1. CORTE, H. and SCHASCHEK, H. Das Papier, **9**, 519 (1955).
2. JAYME, G. Cellulosechemie, **21**, 73 (1943).
3. JAYME, G. Papier-Fabr. **42**, 187 (1944).
4. ASSAF, A. G., HAAS, R. H., and PURVES, C. B. J. Am. Chem. Soc. **66**, 66 (1944).
5. VAN DEN AKKER, J. A. Tappi, **35**, 13 (1952).
6. MARCHESSAULT, R. H., LODGE, W. C., and MASON, S. G. Svensk Papperstidn. **59**, 859 (1956).
7. GOLDFINGER, G., MARK, H., and SIGGIA, S. Ind. Eng. Chem. **35**, 1083 (1943).
8. CONRAD, C. G. and SCROGGIE, A. G. Ind. Eng. Chem. **37**, 592 (1945).
9. BROWN, R. K. and PURVES, C. B. Pulp & Paper Mag. Can. **48** (6), 100 (1947).

Can. J. Chem. Downloaded from www.nrcresearchpress.com by 200.7.193.243 on 09/04/12
For personal use only.

10. BROUGHTON, G. and WANG, J. P. Tappi, **38**, 412 (1955).
11. ANT-WUORINEN, O. Paperi ja Puu, **37**, 335 (1955).
12. HESS, K., KIESSIG, H., and GUNDERMANN, J. Z. physik. Chem. **49**, 64 (1941).
13. HERMANS, P. H. and WEIDINGER, A. J. Am. Chem. Soc. **68**, 2547 (1946).
14. KANAMARU, K. and CHAO, J. Kolloid-Z. **84**, 85 (1938).
15. LAUER, K. Kolloid-Z. **107**, 86 (1944).
16. STAMM, A. J. and TARKOW, H. J. Phys. & Colloid Chem. **54**, 745 (1950).
17. MARCHESSAULT, R. H., MCKNIGHT, T. S., and MASON, S. G. Pulp Paper Mag. Can. **59** (2), 81 (1958).
18. HERMANS, P. H. and WEIDINGER, A. J. Appl. Phys. **19**, 491 (1948).
19. GOPPEL, J. M. and ARLMAN, J. J. Appl. Sci. Research, A, **1**, 3 (1947).
20. MARK, H. Physik und Chemie der Cellulose. Julius Springer, Berlin. 1932. p. 140.
21. CLARK, G. L. Applied X-rays. McGraw-Hill Book Co., Inc., New York. 1955. Chap. 13.
22. HERMANS, P. H. and WEIDINGER, A. J. Polymer Sci. **4**, 135 (1949).
23. ELLEFSEN, O., LUND, E. W., TØNNESEN, B. A., and OIEN, K. Norsk Skogsind. **11**, 284, 349 (1957).
24. SCREATON, R. M. and MASON, S. G. Svensk Papperstidn. **60**, 379 (1957).
25. SIMONS, F. L. Tappi, **33**, 312 (1950).
26. JAYME, G. and HARDERS-STEINHÄUSER, M. Das Papier, **9**, 507 (1955).
27. SCHULZ, G. V. and BLASCHKE, F. J. prakt. Chem. **158**, 130 (1941).
28. DAVIS, W. E. and ELLIOTT, J. H. *In* Ott, E. and Spurlin, H. M. Cellulose and cellulose derivatives. Interscience Publishers, Inc., New York. 1955. Part III, p. 1217.
29. IMMERGUT, E. H., RANBY, B. G., and MARK, H. F. Ind. Eng. Chem. **45**, 2482 (1953).
30. REES, H. W. J. Textile Inst. **39**, T351 (1948).
31. HERMANS, P. H. Physics and chemistry of cellulose fibers. Elsevier Publishing Co., Inc., New York. 1949. p. 189.
32. KLENKOVA, N. I. J. Appl. Chem. (U.S.S.R.), **27**, 401 (1954). English translation.
33. BRUNAUER, S., EMMETT, P. H., and TELLER, E. J. Am. Chem. Soc. **60**, 309 (1938).
34. PRESTON, J. M., NIMKAR, M. V., and GUNDAVDS, S. P. J. Textile Inst. **42**, T79 (1951).
35. HERMANS, P. H. Physics and chemistry of cellulose fibers. Elsevier Publishing Co., Inc., New York. 1949. Part II, Chaps. 2 and 6; Part III, Chap. 8.
36. SMITH, S. E. J. Am. Chem. Soc. **69**, 646 (1947).
37. MAGNE, F. C., PORTAS, H. J., and WAKEHAM, H. J. Am. Chem. Soc. **69**, 1896 (1947).
38. BARKAS, W. W. The mechanical properties of wood and their relation to moisture. Interscience Publishers, Inc., New York. 1953. pp. 54–56.

Can. J. Chem. Downloaded from www.nrcresearchpress.com by 200.7.193.243 on 09/04/12
For personal use only.

Can. J. Chem. Downloaded from www.nrcresearchpress.com by 200.7.193.243 on 09/04/12
For personal use only.

ÉTARD REACTION

II. POLYCYCLIC AROMATIC AND HETEROCYCLIC COMPOUNDS[1]

OWEN H. WHEELER

ABSTRACT

Polycyclic aromatic compounds can, in a number of cases, be oxidized with chromyl chloride, whereas heterocyclic compounds are unaffected.

The Étard oxidation of a number of substituted toluenes to substituted benzaldehydes with chromyl chloride was reported in a previous publication (1). The reaction should be extendable to methyl-substituted polycyclic aromatics and possibly to heterocyclic compounds. The only such reference in the literature is the statement, without experimental details, that some substituted polycyclic aromatics are oxidized to traces of quinones (2).

In the case of many of the polycyclic aromatic compounds studied (see Table I) products could be isolated by chromatography from the tarry residues formed in the reaction.

TABLE I

Reactant	Product	Yield, %
Anthracene	Anthraquinone	12
Naphthalene	—	—
2-Methylnaphthalene	—	—
9-Methylanthracene	Anthraquinone	70
2-Methylanthracene	2-Methylanthraquinone	42
	Anthraquinone-2-aldehyde	25
9-Methylphenanthrene	9-Phenanthraldehyde	30
	Phenanthraquinone	18
9,10-Dihydroanthracene	Anthraquinone	32, 62[a]
9,10-Dihydrophenanthrene	Phenanthraquinone	35
Fluorene	Fluorenone	35
2-Picoline	—	—
2-Picoline-N-oxide	—	—
3-Methylthiophene	—	—

[a]*Time of reaction reduced to 6 hours.*

Anthracene gave 12% anthraquinone as well as a small amount of uncrystallizable oil, but naphthalene gave only traces of a dark red oil. 2-Methylnaphthalene also gave only small quantities of a yellow oil. However, 9-methylanthracene gave anthraquinone in good yield (70%). The only previous observation of the removal of a methyl group by this reagent is the conversion of isopropylbenzene to acetophenone (2, 3). The oxidation of 2-methylanthracene took place at two positions giving 2-methylanthraquinone (42%) and anthraquinone-2-aldehyde (25%). No 2-anthraldehyde was isolated and it is to be expected that the 9,10 positions would be more reactive. 9-Methylphenanthrene also gave two products: 9-phenanthraldehyde (30%) and 9,10-phenanthraquinone (18%), again with displacement of a methyl group.

Considering the high reactivity of the 9,10 positions of anthracene and phenanthrene, it should be possible to oxidize their 9,10-dihydro derivatives, and 9,10-dihydroanthracene and 9,10-dihydrophenanthrene readily gave anthraquinone and phenanthraquinone,

[1]*Manuscript received February 17, 1958.*
Contribution from the Department of Chemistry, Dalhousie University, Halifax, N.S. For Part I of this series see Can. J. Chem. **36**, *667 (1958).*

respectively. In the latter case the yield was considerably improved by reducing the reaction time, suggesting that the yields in other cases might be improved by using shorter periods of reaction. Fluorene was also converted readily into fluorenone.

2-Picoline and 2-picoline-N-oxide both formed solid complexes with chromyl chloride, but on decomposition no aldehydic products could be isolated. Continuous ether extraction of the basified aqueous extracts gave some recovered starting material and the reaction complexes must have been salts between the base and the Lewis acid, chromyl chloride. Similarly, 3-methylthiophene gave no oxidized product and was recovered unchanged. This heterocyclic could also act as a Lewis base towards chromyl chloride and complexing on the heteroatom would prevent further reaction on the methyl group.

Details of only some typical oxidations are given in the experimental section but in the other cases the identity of the isolated products was checked by mixed melting-point determinations.

EXPERIMENTAL

Many of the compounds used were commercially available samples.

2-Methylanthracene.—2-Methylanthraquinone (10 g.) in xylene (100 ml.) was refluxed with aqueous ammonia (300 ml.) and zinc dust (100 g.) added in portions during 6 hours (4). The organic layer was evaporated and the residue in benzene chromatographed on alumina using benzene–hexane mixtures as eluent. 2-Methylanthracene (5.5 g.), m.p. 206° from ethanol (lit. m.p. 207° (5)), was eluted first, followed by 2-methylanthrone (3.5 g.), m.p. *ca.* 75°. Reduction with sodium hydroxide and zinc dust gave no reaction and phosphorus and hydriodic acid gave only 2-methyloxanthranol.

9-Methylphenanthrene.—9-Phenanthraldehyde (6) was converted to its hydrazone, m.p. 102°, from ethanol. The hydrazone (16 g.) was heated with sodium (3 g.) in ethylene glycol (100 ml.) to 200° for 18 hours (7). The reaction mixture was diluted with water and extracted with ether. The residue left when the ether was evaporated was chromatographed as above and gave 9-methylphenanthrene (1.9 g.), m.p. 93–94°, from ethanol (lit. m.p. 91–92.5° (8)).

9,10-Dihydrophenanthrene was prepared by catalytic hydrogenation of purified phenanthrene (9).

2-Picoline-N-oxide resulted from peracetic acid oxidation of 2-picoline (10).

Oxidation of 9-methylanthracene.—9-Methylanthracene (0.95 g.) in carbon tetrachloride (80 ml.) was treated dropwise with chromyl chloride (1.70 g., 10% excess) in carbon tetrachloride (20 ml.) with stirring at 20–25°. The reaction was stirred for a total of 2 hours and allowed to stand overnight. The mixture was worked up by pouring into excess ice-cold aqueous sodium sulphite. The residue left after evaporation of the solvent was taken up in benzene and chromatographed on alumina using hexane, hexane–benzene mixtures, and benzene as successive eluents. The product (720 mg.) had m.p. 286°, undepressed on admixture with anthraquinone.

Oxidation of 2-methylanthracene (300 mg.) gave on chromatography 2-methylanthraquinone (145 mg.), followed by anthraquinone-2-aldehyde (95 mg.), m.p. 182–184° (lit. m.p. 188–189° (11)).

Oxidation of 9-methylphenanthrene (810 mg.) gave 9-phenanthraldehyde (260 mg.), m.p. 95–97° (lit. m.p. 100–101° (6)), and 9,10-phenanthraquinone (155 mg.), m.p. 196° (lit. m.p. 198° (12)).

ACKNOWLEDGMENTS

Dr. H. Estrada and Dr. J. Romo kindly supplied samples of 9,10-dihydroanthracene and 9-methylanthracene.

Can. J. Chem. Downloaded from www.nrcresearchpress.com by 200.7.193.243 on 09/04/12
For personal use only.

REFERENCES

1. WHEELER, O. H. Can. J. Chem. **36**, 667 (1958).
2. LAW, H. D. and PERKIN, F. M. J. Chem. Soc. **93**, 1663 (1908).
3. WHEELER, O. H. Unpublished observations.
4. BORNSTEIN, A. Ber. **15**, 1821 (1882).
5. FISCHER, F. J. prakt. Chem. **79**, 555 (1909).
6. HINKEL, L. E., AYLING, E. E., and BEYNON, J. H. J. Chem. Soc. 339 (1936).
7. FIESER, L. F. and HARTWELL, J. L. J. Am. Chem. Soc. **60**, 2555 (1938).
8. BRADSCHER, C. K. and TESS, R. W. H. J. Am. Chem. Soc. **61**, 2184 (1939).
9. DURLAND, J. R. and ADKINS, H. J. Am. Chem. Soc. **60**, 1501 (1938).
10. BOEKELHEIDE, V. and LINN, W. J. J. Am. Chem. Soc. **76**, 1286 (1954).
11. RUGGLI, P. and DISLER, A. Helv. Chim. Acta, **10**, 938 (1927).
12. SCHOLL, R. and SCHWARZER, G. Ber. **55**, 324 (1922).

Can. J. Chem. Downloaded from www.nrcresearchpress.com by 200.7.193.243 on 09/04/12
For personal use only.

Can. J. Chem. Downloaded from www.nrcresearchpress.com by 200.7.193.243 on 09/04/12
For personal use only.

MOLECULAR SIZE AND CONFIGURATION OF CELLULOSE TRINITRATE IN SOLUTION[1]

M. M. HUQUE,[2] D. A. I. GORING, AND S. G. MASON

ABSTRACT

Viscosity and light-scattering measurements were made on several fractions and two unfractionated samples of cellulose trinitrate. The samples were prepared from bleached ramie, unbleached ramie, and cotton linters. The solvents were acetone and ethyl acetate. Viscosity was measured in a multishear viscometer designed for the purpose. Light-scattering measurements were made in a Brice-Phoenix Light-scattering Photometer modified to accommodate a cell which could be ultracentrifuged.

The range of molecular weight investigated was from 6.5×10^5 to 25.0×10^5. The relationship between the z-average mean-square radius of gyration, $\overline{s_z^2}$, and the z-average molecular weight was approximately linear in both solvents. The ratio of $\overline{(s_0^2)_z}/\overline{M_z}$ (where $\overline{(s_0^2)_z}$ is the value of $\overline{s_z^2}$ in the unperturbed state) was found constant in acetone but to increase with $\overline{M_z}$ in ethyl acetate. This indicated that, whereas in acetone random coil configuration was attained, a configurational transition occurred in ethyl acetate in the molecular weight range investigated.

The value of the exponent a in the relationship between intrinsic viscosity and molecular weight was found to be lower than unity but approximately equal in both solvents.

The significance of the experimental data is discussed.

INTRODUCTION

Recent studies of the solution properties of cellulose trinitrate (designated CTN hereafter) have revealed certain unusual characteristics of the macromolecule. For example, Hunt *et al.* (1) and Holtzer *et al.* (2) showed that for CTN the ratio of the mean-square radius of gyration to the molecular weight increased with increasing molecular weight and reached a constant value at a M.W. of about 400,000. This is much higher than the value of 30,000 found for some vinyl polymers (3). This behavior was considered to arise from the unusual stiffness of the cellulose chain which attained a Gaussian configuration only at relatively high molecular weights. Holtzer *et al.* failed to observe an expected decrease in the exponent of the intrinsic viscosity – molecular weight relationship; but because of experimental difficulties these authors regarded their data for M.W.'s higher than 1.5×10^6 as unreliable. Such a decrease in the exponent has been reported by Badger and Blaker (4) and by Münster (5). There are, therefore, some anomalies and contradictions in the published data, particularly for high molecular weight material.

Apart from interest in the behavior of cellulose derivatives in solution, there is a more practical aspect of this work. Timell (6) has shown that with careful nitration the cellulose chain is made soluble without degradation. Trinitration, followed by fractionation and measurement of intrinsic viscosity, can be used to find the size distribution in any given sample of cellulose. Timell (7) has found that undegraded celluloses from a variety of sources all have rather high molecular weights ($>10^6$). In order to compute reliable values of molecular weight from intrinsic viscosities, the configurational behavior of the molecule should be understood.

The purpose of the present work was to study the configuration of high molecular weight CTN in a good (ethyl acetate) and a poor (acetone) solvent. Viscosity and light-

[1]*Manuscript received January 20, 1958.*
Contribution from the Physical Chemistry Division, Pulp and Paper Research Institute of Canada, and the Chemistry Department, McGill University, Montreal, Que.
[2]*Colombo Plan Scholar from Dacca, Pakistan.*

scattering methods were used and the results interpreted in the light of modern theories of the solution properties of polymers.

EXPERIMENTAL PART

Materials

Cellulose Nitrate

Cellulose trinitrates prepared from unbleached raw ramie, bleached ramie, and cotton linters (designated respectively by H, M, and T) were used in this investigation. The method of nitration has been described by Timell (6). The nitrogen contents are given in Table I.

TABLE I

ANALYTICAL DATA OF CELLULOSE NITRATES

Source	Nitrogen* content, % N	Degree of substitution	Base molecular weight
Unbleached raw ramie (H)	13.68	2.90	288
Bleached ramie (M)	13.80	2.93	290
Cotton linters (T)	13.57	2.88	285

**Complete nitration to cellulose trinitrate would correspond to 14.14% N with a base molecular weight of 297.*

Fractionation

The samples were fractionated by adding water to an acetone solution following the method of Mitchell (8). The exact quantities of water necessary for precipitation were ascertained from exploratory fractionations. Fractionation data for samples M and H are given in Tables II and III respectively.

TABLE II

FRACTIONATION DATA ON SAMPLE M

Fraction	Water added, cc.	Weight, g.	Yield, %
M-1	31.0	1.190	28.4
M-2A*	4.8	0.723	17.0
M-2B*	5.2	0.524	12.3
M-3	12.1	0.578	13.8
M-4		0.880	19.5
Undissolved material		0.320	7.1
Loss			1.9

**Fractions M-2A and M-2B had nearly identical intrinsic viscosities and were blended by dissolving in acetone and precipitating by addition of water. The blended sample is referred to as M-2 hereafter.*

For sample M, 4.5 g. was soaked in an acetone–water mixture (91: 9) for 24 hours and then stirred vigorously for 6 hours to yield a 0.1% solution; solutions of higher concentration were too viscous for convenient handling. The solution was then centrifuged at 500*g* for 20 minutes to remove any undissolved material. The decanted solution was placed in a 25° C. bath and distilled water added to it dropwise with vigorous stirring.

Can. J. Chem. Downloaded from www.nrcresearchpress.com by 200.7.193.243 on 09/04/12
For personal use only.

TABLE III

FRACTIONATION DATA ON SAMPLE H

Fraction	Water added, cc.	Weight, g.	Yield, %
H-1	34.0	0.369	18.5
H-2	10.3	0.548	27.4
H-3	40.0	0.397	19.8
H-4	—	0.265	13.3
H-5	—	0.340	17.0
Undissolved material		0.020	1.0
Loss			3.0

When the previously determined quantity of water had been added, the system was allowed to stand for 1 hour in the bath while the stirring was continued. The precipitate was separated by centrifuging for 20 minutes at 500*g*. The precipitate in the centrifuge cups was gel-like in appearance. It was found that addition of methanol facilitated removal of the precipitate from the cups. Excess liquid was squeezed out of the solid, which was then vacuum-dried at about 45° C. This procedure was repeated to yield four fractions (M-1, M-2A, M-2B, and M-3).

The solution remaining after separation of M-3 was evaporated to dryness to yield M-4.

Sample H was fractionated in essentially the same way from a 0.1% solution of 2 g. in acetone. The solution left after separation of the third fraction was evaporated to about one-quarter of its original volume by blowing air through it and stirring. The resulting suspension was centrifuged to take out the fourth fraction. The final fraction was obtained as before by evaporating the remaining liquid to dryness.

All fractions were stored over fused calcium chloride in a refrigerator.

Sample T, also, was fractionated after the method of Mitchell (8). Ten fractions were obtained, of which only T-6 and T-8 were used in this study. These fractions were chosen in order to extend the range to a somewhat lower molecular weight than values found for the fractions of M and H.

Finally a fraction, P, from an exploratory fractionation of bleached ramie nitrate was used to fill the gap of molecular weights between M-2 and M-3.

In the fractionation of samples M and H the solutions developed a cloudiness which increased as the fractionation proceeded. Repeated centrifugations did not remove the cloudiness. The effect seemed greater in sample H, possibly because of its lower nitrogen content. Evidently part of the precipitate remained suspended as colloidal material. It is possible that the non-sedimentable aggregates from one cycle were precipitated on the next addition of water.

Solvents

Reagent grade acetone was used for fractionation. For viscosity and light-scattering measurements reagent grade solvents were redistilled. Boiling ranges for acetone and ethyl acetate were 56.3–56.8° C. and 77–77.3° C. respectively.

Preparation of Solutions

Solutions were made up by shaking CTN in solvent for 24 hours in a wrist-action shaker. This was followed by centrifugation in stainless-steel tubes at 24,000*g* for 30 minutes to remove any undissolved material. Three-fourths of the liquid in the centrifuge

Can. J. Chem. Downloaded from www.nrcresearchpress.com by 200.7.193.243 on 09/04/12
For personal use only.

tubes was decanted into a glass-stoppered flask. This served as stock solution from which solutions were made for viscosity and light-scattering measurements. A calibrated 10-cc. hypodermic syringe was used for transfer of liquids.

It was thought possible that CTN might form aggregates on repeated cycles of dissolution, recovery (by precipitation or evaporation), and re-solution, and thus yield erroneous results from the light-scattering measurements. Such cycles were inevitable in fractionation and recovery. A careful series of experiments on approximately 0.2% solution of bleached ramie nitrate in both acetone and ethyl acetate showed, however, that the light-scattering dissymmetry did not change when such cycles were repeated. This indicated absence of significant aggregate formation.

Viscosity Measurements

Since the viscosity of solutions of high DP cellulose nitrate is shear-dependent, a standard shear rate of 500 sec.$^{-1}$ was adopted following the convention of Newman *et al.* and others (9, 10). A modified form of the suspended-level dilution capillary viscometer of Schurz and Immergut (11) was used. The viscometer had four bulbs, which enabled measurements to be made at different rates of shear calculable from the expression (12)

$$G_i = 8V_i/3\pi r^3 t_i, \quad [1]$$

where G_i = mean rate of shear corresponding to bulb i,
V_i = volume of bulb i,
t_i = efflux time of V_i,
r = radius of viscometer capillary.

Efflux times were measured at 25.00±0.01° C. to 0.1 second for each of the four bulbs for pure solvent and over a range of concentrations of the solutions obtained by progressive dilution of the solution first introduced in the viscometer. Efflux times for five or six concentrations were measured on each sample. Kinetic energy corrections (amounting to 0.2 to 3 per cent) were applied in the usual way (13) and values of the specific viscosity, η_{sp}, at shear rates calculated from Eq. [1] were obtained.

The concentration, c, of the initial solution was determined in a duplicate measurement by evaporation and weighing. The solid from 10 cc. of the solution was dried in vacuum to constant weight in a weighed aluminum cup. In determining the concentration of ethyl acetate solutions, filtered ethyl alcohol was added during evaporation to aid in the complete removal of ethyl acetate (1).

From these data, plots of log (η_{sp}/c) against log G for different concentrations were obtained. Fig. 1 shows an example. From these plots the values of η_{sp}/c for G = 500 sec.$^{-1}$ were obtained by interpolation. A plot of η_{sp}/c vs. c was then made as shown in Fig. 2. Linear extrapolation to zero concentration gave the intrinsic viscosity, $[\eta]_{500}$. In a similar manner intrinsic viscosities were obtained for a range of G values between 300 and 700 sec.$^{-1}$.

The Huggins' interaction constant (14), k'_{500}, was calculated from the slope of the η_{sp}/c vs. c line at 500 sec.$^{-1}$ using the equation

$$\eta_{sp}/c = [\eta] + k'[\eta]^2 c. \quad [2]$$

For some solutions at very low concentrations the plot η_{sp}/c vs. c deviated from linearity and showed marked upward curvature. This effect has been observed by others (15, 16)

Can. J. Chem. Downloaded from www.nrcresearchpress.com by 200.7.193.243 on 09/04/12
For personal use only.

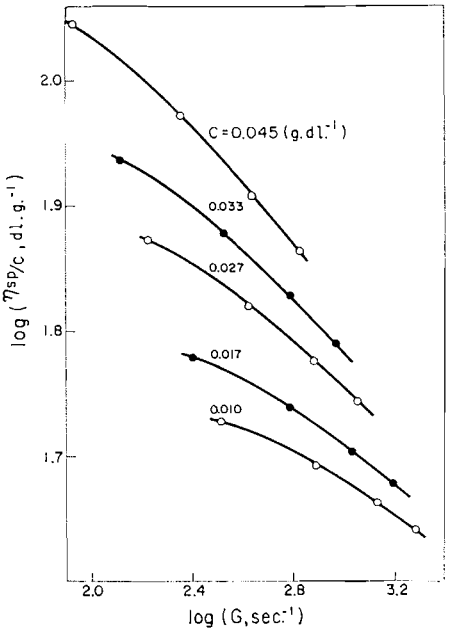

FIG. 1. Log of reduced viscosity vs. log of rate of shear at different concentrations for fraction H-2 in acetone.

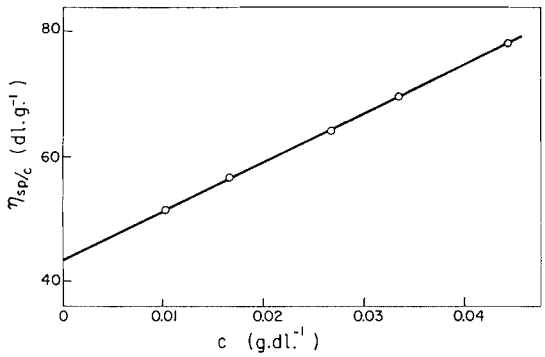

FIG. 2. Reduced viscosity vs. concentration for fraction H-2 in acetone at a shear rate of 500 sec.$^{-1}$.

and was shown by Öhrn (15) to be due to adsorption of polymer on the walls of the capillary. Extrapolation of the η_{sp}/c vs. c line to $c = 0$ was always carried out from concentrations at which the effect was negligible.

Light Scattering

Apparatus

Light-scattering measurements were made in a Brice-Phoenix photometer. The instrument was modified to accommodate cells of the type described by Dandliker and Kraut (17) in which the solution is clarified by ultracentrifugation *in situ*. This course was found necessary after attempts to remove stray dust from the solutions by conventional means such as centrifugation (outside the measuring cell) and filtration proved unsatisfactory. Despite elaborate care, the solution, clarified by centrifuging, became contaminated with dust in the transfer to the measuring cell; when ultrafine sintered-glass filters were used, the solute was retained by adsorption on the filter.

Can. J. Chem. Downloaded from www.nrcresearchpress.com by 200.7.193.243 on 09/04/12
For personal use only.

Details of the modification of the photometer are expected to be reported in a separate paper (18). After modification the intensity emitted by a dilute solution of fluorescein was constant to $\pm 1\%$ from angles of 30° to 135°. Negligible background scattering was found with toluene and acetone. Calibration with Ludox (19) was checked by measuring the excess turbidity of a 0.50% solution of Cornell standard polystyrene in toluene. The value found was 3.26×10^{-3} cm.$^{-1}$ and is in good agreement with the National Bureau of Standards' value (20) of 3.30×10^{-3} cm.$^{-1}$. The Rayleigh ratio of redistilled and filtered benzene was found to be 49.6×10^{-6} cm.$^{-1}$, also in good agreement with Maron and Lou's (21) value of 49.7×10^{-6} cm.$^{-1}$.

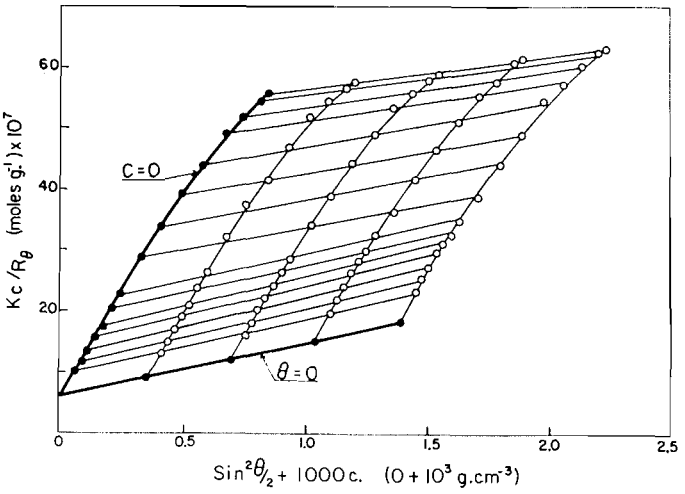

FIG. 3. Zimm plot of light-scattering data for fraction M-2 in acetone.

Zimm plots, an example of which is shown in Fig. 3, were obtained from the light-scattering data in the usual way by plotting Kc/R_θ vs. $\sin^2\theta/2+kc$, where

K = $2\pi^2 n_s^2 (dn/dc)^2/N\lambda^4$,
n_s = refractive index of solvent,
dn/dc = refractive index increment,
λ = wave length in vacuum,
θ = angle between scattered and transmitted beam,
R_θ = Rayleigh ratio at angle θ,
k = an assigned constant,
N = Avogadro's number,
c = concentration in grams per cc.

The weight-average molecular weight, $\overline{M_w}$, was obtained from the intercept from

[3] $$\overline{M_w} = 1/(Kc/R_\theta)_{c,\theta=0}$$

and the z-average radius of gyration, $\sqrt{\overline{s_z^2}}$, was computed from the initial slope of the $c = 0$ line by means of the expression

[4] $$\frac{\text{initial slope}}{\text{intercept}} = \frac{16\pi^2}{3} \cdot \overline{s_z^2} \cdot (n/\lambda)^2,$$

where n is the refractive index of the solution. The concentration dependence of the intensity can be written as

Can. J. Chem. Downloaded from www.nrcresearchpress.com by 200.7.193.243 on 09/04/12
For personal use only.

[5] $$Kc/R_\theta = [1/MP(\theta)]+2A_2c$$

where $P(\theta) = (R_\theta^\circ/R_\theta)$. R_θ° is the Rayleigh ratio if there is no intraparticle interference. A_2 is the second virial coefficient and is computed from the slope of the $(Kc/R_\theta)_{\theta=0}$ vs. c line in the Zimm plot (22).

Refractive Index Measurements

The increment of refractive index dn/dc of the solution over that of the solvent was measured by means of a Brice-Phoenix differential refractometer for $\lambda = 4358$ Å at 25° C. The instrument was calibrated with sucrose solutions of different concentrations using sodium light ($\lambda = 5890$ Å). The calibration was checked by measurement of Δn for a 4% aqueous KCl solution. The measured value was within 0.4% of the value calculated from data obtained from the International Critical Tables.

RESULTS

Viscosity and Light Scattering

The experimental results from viscosity and light-scattering measurements are listed in two tables. Table IV contains the results in acetone solution while the contents of Table V are for ethyl acetate solutions. The quantities given for each sample are the weight-average molecular weight, $\overline{M_w}$, z-average root-mean-square radius of gyration, $\sqrt{\overline{s_z^2}}$, the second virial coefficient, A_2, the intrinsic viscosity, $[\eta]_{500}$, and the Huggins' interaction constant, k'_{500}.

In order to derive the configurational parameters from the light-scattering data, certain assumptions about the molecular weight distribution were necessary since polydispersity is inevitable even in carefully fractionated material (1, 2). A suitable distribution is one

TABLE IV

RESULTS OF VISCOSITY AND LIGHT-SCATTERING MEASUREMENTS IN ACETONE

Sample	$[\eta]_{500}$, dl. g.$^{-1}$	k'_{500}	$\overline{M_w}\times10^{-5}$	$\sqrt{\overline{s_z^2}}$, Å	$A_2 \times 10^4$, mole cc. g.$^{-2}$
T-8	12.1	0.83	6.5	869	7.3
T-6	15.6	0.95	8.4	958	7.4
M-3	18.9	0.62	9.9	1060	3.2
P	20.5	0.55	11.4	1150	4.1
M	22.1	0.52	15.3	1440	4.9
M-2	26.0	0.56	16.9	1480	4.6
M-1	36.8	0.33	22.8	1610	3.8
H	43.4	0.39	23.8	1670	5.1
H-2	43.6	0.41	25.0	1730	3.8

TABLE V

RESULTS OF VISCOSITY AND LIGHT-SCATTERING MEASUREMENTS IN ETHYL ACETATE

Sample	$[\eta]_{500}$, dl. g.$^{-1}$	k'_{500}	$\overline{M_w}\times10^{-5}$	$\sqrt{\overline{s_z^2}}$, Å	$A_2 \times 10^4$, mole cc. g.$^{-2}$	$[\eta]_0$ dl. g.$^{-1}$
T-8	16.9	0.58	6.8	972	7.3	16.9
T-6	20.4	0.74	7.8	1097	7.8	20.4
M-3	24.6	0.52	9.8	1430	3.1	24.6
P	—	—	—	—	—	—
M	32.4	0.50	16.1	1520	6.6	32.9
M-2	32.8	0.55	15.9	1630	4.4	34.4
M-1	44.6	0.35	23.2	2100	4.8	46.5
H	—	—	—	—	—	—
H-2	58.6	0.27	25.0	2190	3.6	61.3

Can. J. Chem. Downloaded from www.nrcresearchpress.com by 200.7.193.243 on 09/04/12
For personal use only.

in which the z-average, weight-average, and number-average molecular weights, represented respectively by $\overline{M}_z$, $\overline{M}_w$, and $\overline{M}_n$, are related in the proportion 3:2:1. Such a distribution has been used by others (2, 22) and was assumed by Hunt *et al.* (1) for their high molecular weight samples. This proportionality will be assumed in computing $\overline{M}_z$ and $\overline{M}_n$ from the values of $\overline{M}_w$ obtained from light scattering.

The initial concentrations of solutions employed for light-scattering measurements varied from 0.12 to 0.35 g./dl. depending on the molecular weight. At the lowest concentration the solvent scattering intensity was 50% of the scattering intensity from solution. The initial concentration range in viscometry was 0.035 to 0.085 g./dl. depending on the molecular weight. The lowest concentration in viscometric measurements was a fifth or sixth of the initial concentration.

The refractive index increments, dn/dc, at 25° C. used for the calculation of K were 0.104 cc. g.$^{-1}$ and 0.105 cc. g.$^{-1}$ for ethyl acetate and acetone solution respectively. These were the mean values from solutions of bleached and unbleached (raw) ramie nitrate. The corresponding K values were 1.85×10^7 and 1.84×10^7 respectively for ethyl acetate and acetone.

Shear Dependence of Viscosity

Shear dependence of intrinsic viscosity in the range of rate of shear between 300 and 700 sec.$^{-1}$ was estimated. For the complete range of molecular weight studied $[\eta]$ was found to be independent of G in acetone solution. A typical plot of η_{sp}/c vs. c for different G is shown in Fig. 4.

In ethyl acetate solution, on the other hand, $[\eta]$ showed slight dependence on the rate of shear for the higher molecular weight samples. An example is shown in Fig. 5, where the values for H-2 have been plotted. The magnitude of the dependence decreased with decreasing molecular weight and below $[\eta] = 30$ the dependence was no longer observed. Similar results for the shear dependence in ethyl acetate solution were obtained by Timell (10).

In those cases where such dependence was noticed, $[\eta]$ values at different G were linearly related to the rate of shear. Fig. 6 shows the variation of $[\eta]$ with G for samples M, M-2, M-1, and H-2. Extrapolation of these lines gave values of the intrinsic viscosity at zero rate of shear, $[\eta]_0$ which have been included in Table V.

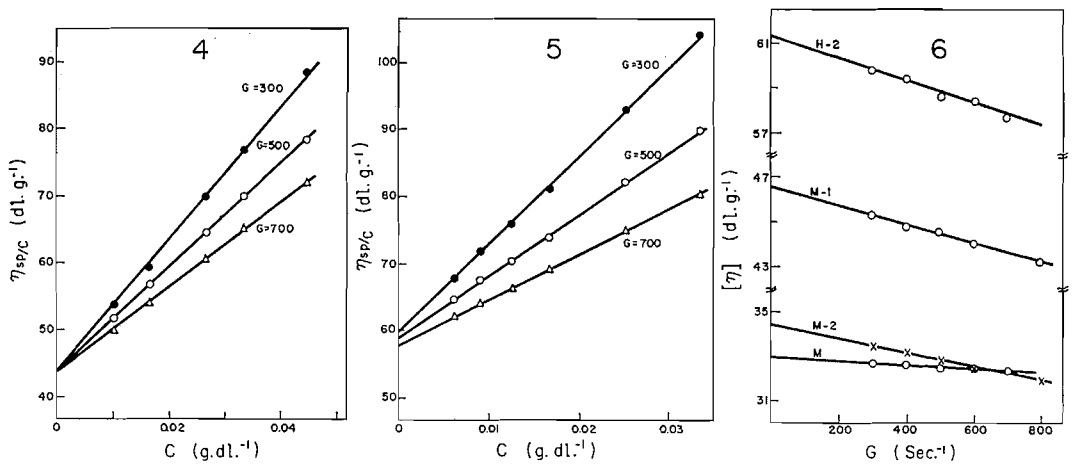

FIG. 4. Reduced viscosity vs. concentration for fraction H-2 in acetone at different rates of shear.
FIG. 5. Reduced viscosity vs. concentration for fraction H-2 in ethyl acetate at different rates of shear.
FIG. 6. Intrinsic viscosity vs. rate of shear for samples M, M-1, M-2, and H-2 in ethyl acetate.

Can. J. Chem. Downloaded from www.nrcresearchpress.com by 200.7.193.243 on 09/04/12
For personal use only.

These results show a small or no dependence of $[\eta]$ on G in the range of shear studied. As clearly shown in Figs. 4 and 5 marked shear dependence of η_{sp}/c occurs at finite concentration. This shear dependence is probably due to molecular interaction, which will increase as concentration increases, rather than to deformation or orientation of isolated molecules. A similar result has been noted recently by Nawab and Mason (23) for suspensions of model filaments. In the present work the reservation must be made that the range of shear was small, and a more marked variation of $[\eta]$ with G may have been detected had measurements been made at much lower shear rates.

Anomalous Light Scattering

Early in the work certain persistent irregularities were noted in the light-scattering measurements. In all samples the graph of Kc/R_θ vs. $\sin^2\theta/2+kc$ at $\theta = 0$ curved downwards after a certain concentration was reached and in some cases passed through a maximum. Fig. 7 is a Zimm plot showing this effect. The concentration, c_c, at which the curvature became noticeable decreased approximately linearly with increasing molecular weight. The curvature started at such low concentration with the very high molecular weight fraction H-1 in acetone solution that determination of $\overline{M_w}$ by extrapolation was not possible. The effect was also observed in solutions which were centrifuged for 1 hour or more instead of the usual 30 minutes, so that the effect was not caused by the presence of debris.

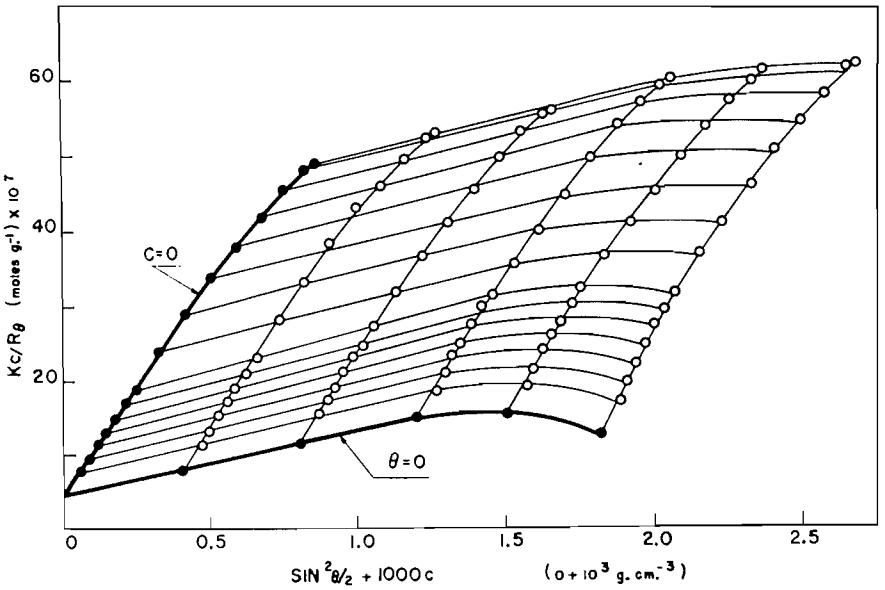

FIG. 7. Zimm plot of light-scattering data for fraction M-1 in acetone showing deviation from linearity of $(Kc/R_\theta)_{\theta=0}$ vs. c line at high concentration.

At about the same concentration at which the deviation from linearity of Zimm plots occurred, a curious optical phenomenon was noted. If the solution was centrifuged for 30 minutes at 55,000g, placed in the light-scattering apparatus and the scattered beam observed in a mirror held at low angles, quite clear vertical striations, i.e., vertical bands of scattering substance, could be seen. They were observed in nearly all samples provided that the concentration was sufficiently high.

Can. J. Chem. Downloaded from www.nrcresearchpress.com by 200.7.193.243 on 09/04/12
For personal use only.

Striations occurred only on high-speed centrifugation; none could be seen in a fresh, uncentrifuged solution. Thus the phenomenon was associated in some way with ultracentrifugation. If a centrifuged solution was allowed to stand, the striations gradually disappeared over a period of several hours, indicating that the process was reversible. In some solutions the discontinuities were not stationary but appeared to drift gradually.

The effect of striations on the scattering intensity was relatively small. A variation of intensity by about $\pm 5\%$ was found in successive measurements. No clear trend of increase or decrease in scattering intensity was noted on standing. Also the polarization of the transmitted or scattered light was unaffected.

Similar behavior for high molecular weight nitrocellulose has been reported by Holtzer *et al.* (2). These authors found that prolonged centrifugation at high speed caused the effect to disappear. However, in the present work striations were observed in a sample centrifuged at 55,000*g* for 5 hours. Also, a number of experiments were made which showed that their origin was not a trivial one, e.g. concentration or density gradients produced by sedimentation.

It is proposed to publish a separate account of deviations from linearity in Zimm-type plots and of striations.

DISCUSSION

Variation of Radius of Gyration with Molecular Weight

The radius of gyration is a characteristic dimension of the molecule in solution and, as expected, increased with increasing molecular weight (Tables IV and V). Also, for a given sample, $\sqrt{\overline{s^2}}$ was higher in ethyl acetate than in acetone, thus indicating greater extension in the former solvent.

In both solvents the relationship between $\overline{s_z^2}$ and $\overline{M_z}$ was approximately linear as shown in Figs. 8 and 9. In acetone the line passed through the origin and is expressed by the equation

$$\overline{s_z^2} = 0.80 \times \overline{M_z}. \qquad [6]$$

For ethyl acetate the relationship is

$$\overline{s_z^2} = 1.33\overline{M_z} - 3.55. \qquad [7]$$

If the data for CTN in ethyl acetate obtained by Hunt *et al.* (1) are included in Fig. 9, it is seen that below a molecular weight of about 800,000 the graph curves towards the origin. Similarly in Fig. 8 the data of Holtzer *et al.* (2) suggest a breakdown in the linearity at low molecular weight. Recently Notley and Debye (24) have noted a similar trend in the relationship between molecular dimensions and weights of polystyrene.

Configurational Change with Molecular Weight

The deviation from linearity in Figs. 8 and 9 could be expected if a transition to non-Gaussian behavior occurred at low molecular weight. Such configurational changes have been treated theoretically by Benoit and Doty (25) in terms of a stiffness parameter, the persistence length, q. The persistence length was defined originally by Porod and Kratky (26, 27) as the mean value of the projection of an infinitely long chain along the direction of the first element in the chain. The expression deduced by Benoit and Doty is

$$\overline{s_0^2} = q^2[(x/3) - 1 + (2/x) - 2(1 - e^{-x})/x^2] \qquad [8]$$

where $\sqrt{\overline{s_0^2}}$ is the unperturbed radius of gyration (described later) and x is the number of units of length q in the fully extended molecule. The value of x is given by

Can. J. Chem. Downloaded from www.nrcresearchpress.com by 200.7.193.243 on 09/04/12
For personal use only.

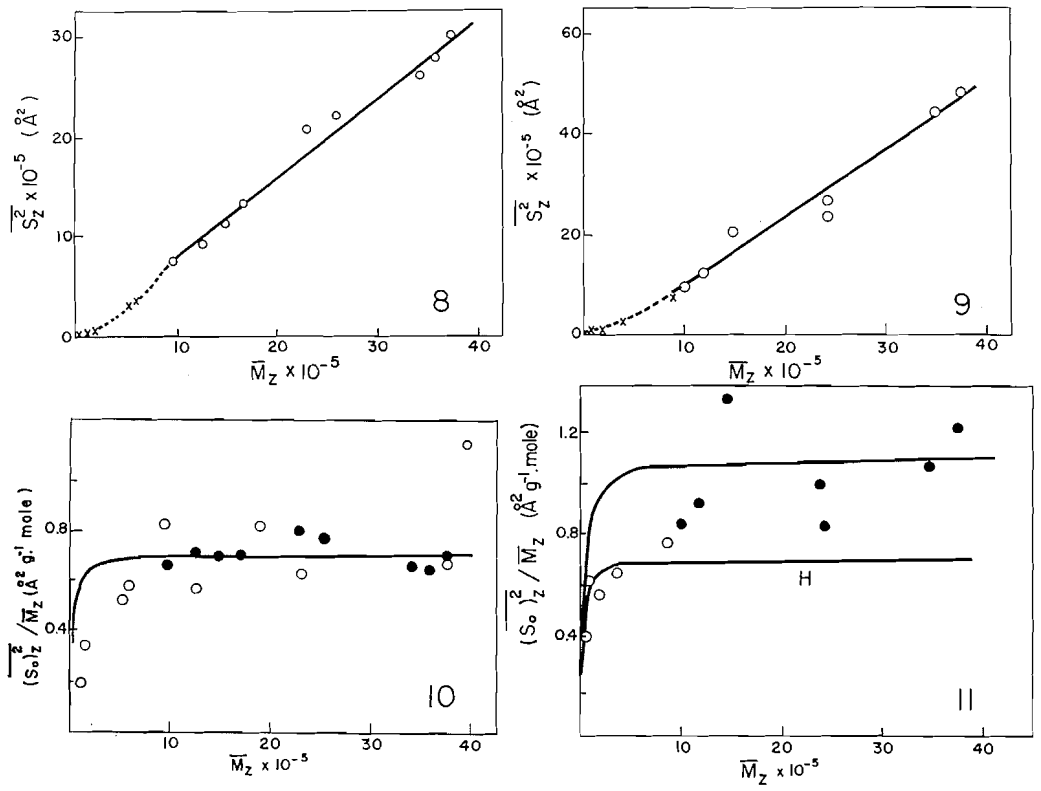

FIG. 8. Z-Average mean-square radius of gyration vs. z-average molecular weight of the CTN samples in acetone. ○—Present work. ×—Holtzer *et al.* (2).

FIG. 9. Z-Average mean-square radius of gyration vs. z-average molecular weight of the CTN samples in ethyl acetate. ○—Present work. ×—Hunt *et al.* (1).

FIG. 10. Dependence of $\overline{(s_0^2)}_z/\overline{M}_z$ on $\overline{M}_z$ for the CTN samples in acetone. The solid curve is the theoretical one based on Eq. [8]. ●—Present work. ○—Holtzer *et al.* (2).

FIG. 11. Dependence of $\overline{(s_0^2)}_z/\overline{M}_z$ on $\overline{M}_z$ for CTN samples in ethyl acetate. The upper solid curve is the theoretical one based on Eq. [8]. The solid curve H is the one proposed by Hunt *et al.* (1). ●—Present work. ○—Hunt *et al.* (1).

$$[9] \qquad x = r_{max}/q = [(DP)/q].L = (\overline{M}/M_0).(L/q),$$

r_{max} being the length of the fully extended chain and L being the length of one monomer unit which was taken as 5.15 Å. Here $\overline{M}$ is the average molecular weight and M_0 is the monomer molecular weight.

For large x (i.e., large $\overline{M}$) Eq. [8] reduces to

$$[10] \qquad \overline{s_0^2}/r_{max} = q/3,$$

which for a Gaussian coil corresponds to $(\overline{s_0^2}/\overline{M})$ being constant. For smaller x, the other terms decrease the value of $\overline{s_0^2}/\overline{M}$, indicating an approach to the rod-like configuration.

After the manner of Hunt *et al.* (1), the experimentally determined values of $(\overline{s_0^2})_z/\overline{M_z}$ may be plotted against $\overline{M_z}$ and compared with the theoretical curve deduced from Eq. [8]. The unperturbed radius of gyration was obtained from the relationship

$$[11] \qquad \sqrt{\overline{s_z^2}} = \alpha\sqrt{(\overline{s_0^2})_z},$$

Can. J. Chem. Downloaded from www.nrcresearchpress.com by 200.7.193.243 on 09/04/12
For personal use only.

where the expansion factor, α, was calculated from the second virial coefficient by the method of Orofino and Flory (28). As found by Hunt *et al.* for CTN in ethyl acetate, α was near unity for all samples in both solvents (1.03–1.09) and showed a very slight increase with increasing molecular weight. The persistence length, q, required in Eq. [8], was calculated by means of Eq. [10], from $(\overline{s_0^2})_z$ and $\overline{M}_z$ for the two highest molecular weight samples. Averages of the values of q were 115 Å and 200 Å in acetone and ethyl acetate, respectively. Hunt *et al.* (1) used a q value of 117 Å derived from the data on their three highest molecular weight samples.

In Figs. 10 and 11 $(\overline{s_0^2})_z/\overline{M}_z$ is plotted against $\overline{M}_z$ for acetone and ethyl acetate, respectively. Values of $(\overline{s_0^2})_z$ and $\overline{M}_z$ are given in Table VI. The data of Holtzer *et al.* (2) for CTN in acetone are included in Fig. 10 and the data of Hunt *et al.* (1) for CTN in ethyl acetate are included in Fig. 11.

TABLE VI

MOLECULAR AND HYDRODYNAMIC PARAMETERS

	In acetone			In ethyl acetate		
Sample	$\overline{M}_z\times10^{-6}$	$(\overline{s_0^2})_z\times10^{-6}$, Å²	$\Phi'\times10^{-22}$	$\overline{M}_z\times10^{-6}$	$(\overline{s_0^2})_z\times10^{-6}$, Å²	$\Phi'\times10^{-22}$
T-8	0.98	0.66	2.34	1.01	0.85	2.95
T-6	1.26	0.80	2.90	1.17	1.08	2.83
M-3	1.49	1.04	3.05	1.47	1.98	1.96
P	1.71	1.21	2.97	—	—	—
M	2.30	1.85	2.21	2.42	2.01	3.52
M-2	2.54	1.93	2.62	2.39	2.47	2.86
M-1	3.42	2.27	3.91	3.48	4.07	2.64
H	3.57	2.32	4.32	—	—	—
H-2	3.75	2.63	4.11	3.75	4.59	3.28

As predicted by theory, the combined data in both cases show increase of $(\overline{s_0^2})_z/\overline{M}_z$ with $\overline{M}_z$. In the case of acetone, the results from the present investigation lie in the region of constant $(\overline{s_0^2})_z/\overline{M}_z$ while at lower molecular weight the data of Holtzer *et al.* (2) show decrease in $(\overline{s_0^2})_z/\overline{M}_z$. Their results indicated that at $\overline{M}_z$ values above 10^6 the molecule behaves like a Gaussian coil. For ethyl acetate, except for one point, $(\overline{s_0^2})_z/\overline{M}_z$ increases with $\overline{M}_z$ over the complete range of molecular weights. This suggests that in the molecular weight range studied, CTN does not attain the random coil configuration in ethyl acetate. Curve *H* in Fig. 11 is the theoretical one given by Hunt *et al.*, which is based on a persistence length of 117 Å computed from the results for their three highest molecular weight samples. The points from the present investigation are well above their theoretical line. This discrepancy indicates that Hunt *et al.* (1) did not use a high enough value of $\overline{M}_z$ in computing q. It must also be noted that because of increasing trend of $(\overline{s_0^2})_z/\overline{M}_z$ with $\overline{M}_z$, the value of q computed for samples M-1 and H-2 may also be erroneously low.

The higher value of the persistence length in ethyl acetate was unexpected since, to a first approximation, q must depend only on orientation and steric factors in the chain itself. It is possible, however, that the greater solvation in ethyl acetate may cause an added inflexibility due to more extensive packing of solvent molecules around the polymer in the better solvent.

The values of x calculated from $\overline{M}_w$ by means of Eq. [9] ranged from 60 to 370. Peterlin (29) has shown that such values of x lead to perceptible downward curvature in the usual

Can. J. Chem. Downloaded from www.nrcresearchpress.com by 200.7.193.243 on 09/04/12
For personal use only.

graph of the angular distribution of light scattering intensity at zero concentration. For example, in the case of samples M-2 and M-1 (Figs. 3 and 7) the theoretical envelope for the Porod chain was deduced from the data of Peterlin (29). The envelope was assumed to deviate from the linear graph (tangential at the origin), which is expected for a completely flexible polymer with $\overline{M_z}$: $\overline{M_w}$: $\overline{M_n}$ = 3:2:1. For both sample M-2 and M-1, the theoretical curve was found to coincide almost exactly with the experimentally determined points. However no systematic analysis of the light-scattering envelopes was attempted because measurements at high angles were not precise enough.

Variation of Intrinsic Viscosity with Molecular Weight

The intrinsic viscosity is a measure of the effective hydrodynamic volume of a solute and, as expected, $[\eta]_{500}$ increased with $\overline{M_w}$. The values of the constants $\boldsymbol{K}$ and a in the intrinsic viscosity – molecular weight relationship

$$[\eta] = \boldsymbol{K}\overline{M_w}^{a} \qquad [12]$$

were obtained from plots of log $[\eta]_{500}$ vs. log $\overline{M_w}$ shown in Figs. 12 and 13 respectively for acetone and ethyl acetate solution. The values are given in Table VII along with the more recent values obtained by other workers. If $[\eta]_0$ at $G = 0$ (obtained as described previously) is used, a increases from 0.83 to 0.86 in ethyl acetate. Similar adjustment leaves a unchanged for acetone solutions since $[\eta]$ was found to be independent of G.

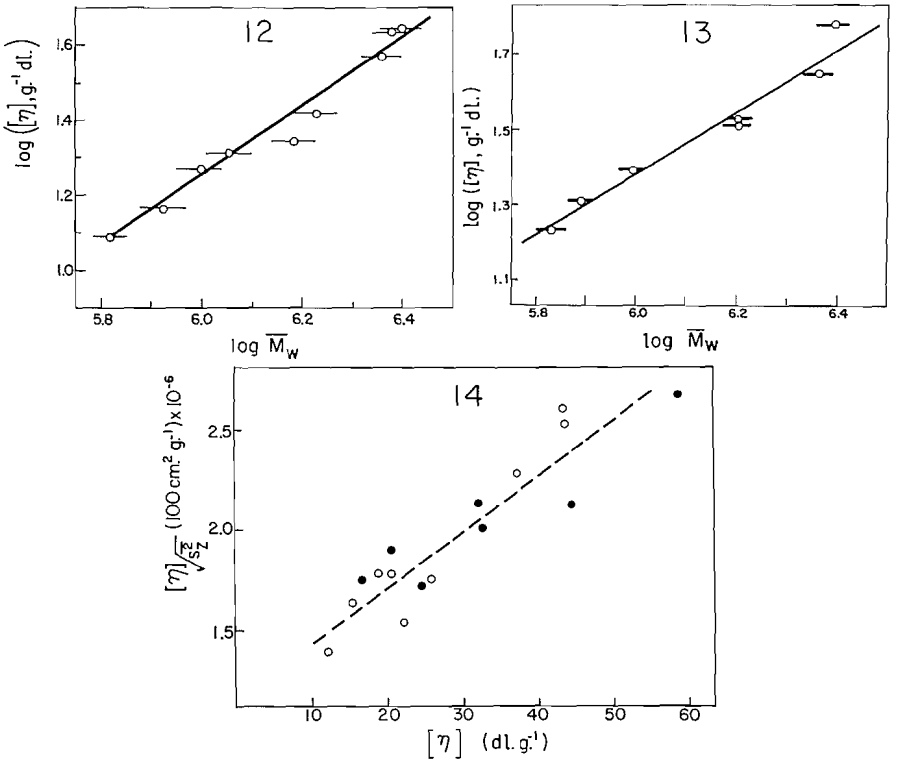

FIG. 12. Log of intrinsic viscosity at a rate of shear of 500 sec.$^{-1}$ vs. log of molecular weight for the samples in acetone.

FIG. 13. Log of intrinsic viscosity of the samples in ethyl acetate at a rate of shear of 500 sec.$^{-1}$ vs. molecular weight.

FIG. 14. Ratio of intrinsic viscosity to root-mean-square z-average radius of gyration vs. intrinsic viscosity in acetone and ethyl acetate. ●—Ethyl acetate. ○—Acetone.

Can. J. Chem. Downloaded from www.nrcresearchpress.com by 200.7.193.243 on 09/04/12
For personal use only.

TABLE VII

VALUES OF a AND K

Investigator	Solvent	Range of method, $M\times10^{-4}$		G (sec.$^{-1}$) for $[\eta]$	a	K	Ref.
Holtzer *et al.*	Acetone	7.7–264	Light scattering	0	0.99	1.73×10^{-5}	(3)
Holtzer *et al.**	Acetone	64–264	Light scattering	0	0.91	5.37×10^{-5}	(3)
Present†	Acetone	65–250	Light scattering	500	0.91	5.96×10^{-5}	
Newman *et al.*	Ethyl acetate	9.3–150	Ultracentrifuge	500	0.99	4.82×10^{-5}	(14)
Hunt *et al.*	Ethyl acetate	4.1–57.3	Light scattering	0	1.01	2.50×10^{-5}	(4)
Present	Ethyl acetate	68–250	Light scattering	500	0.83	2.60×10^{-4}	
Present	Ethyl acetate	68–250	Light scattering	0	0.86	1.66×10^{-4}	

**Values of a and K are derived from the six highest molecular weight samples.*
†The standard error in a was 0.08 in all cases.

The intrinsic viscosity of CTN has been shown to vary considerably with small changes in the nitrogen content of the sample (30, 31, 32). The intrinsic viscosity was corrected by the method of Lindsley and Frank (30) to a hypothetical value, $[\eta]^T$ corresponding to 14.14% nitrogen. The results are shown in Table VIII: $[\eta]^T$ is considerably higher than the corresponding $[\eta]$ value given in Tables IV and V. Plots of log $[\eta]^T_{500}$ vs. log $\overline{M}_w$ yield $a = 0.77$ in ethyl acetate and $a = 0.87$ in acetone. With $[\eta]^T_0$ (i.e. $[\eta]^T$ at zero rate of shear) the value of a becomes 0.82 in ethyl acetate.

TABLE VIII

VALUES OF INTRINSIC VISCOSITIES AFTER CORRECTION FOR NITROGEN CONTENT

Sample	In acetone	In ethyl acetate		% Nitrogen
	$[\eta]^T_{500}$, dl. g.$^{-1}$	$[\eta]^T_{500}$, dl. g.$^{-1}$	$[\eta]^T_0$, dl. g.$^{-1}$	
T-8	14.5	20.3	20.3	13.58
T-6	18.7	24.4	24.4	13.58
M-3	20.9	27.2	27.2	13.84
P	23.4	—	—	13.74
M	24.6	36.1	36.7	13.81
M-2	28.8	36.3	40.1	13.83
M-1	40.4	49.0	51.1	13.85
H	50.4	—	—	13.68
H-2	49.4	66.5	69.5	13.76

The value of a is influenced by two factors: (i) the configuration of the molecule and (ii) its permeability to solvent. Any increase in molecular extension would cause an increase in a whereas a change from the free-draining to the solvated (solvent immobilizing) state would cause a to decrease.

As shown in Table VII, a was lower than unity in both solvents in contrast to the results of Holtzer *et al.* (2), Hunt *et al.* (1), and Newman *et al.* (9). The lower value of a in the high molecular weight range is in conformity with the theory of Kirkwood and Riseman (32) and the data of Badger and Blaker (4) and Münster (5). Also, it is supported by the agreement between the present data and those for the six highest molecular weight samples of Holtzer *et al.* (2). Further, the low value of a is accentuated by the correction of the $[\eta]$ values for variation in nitrogen content. Thus the data support in a general way the assumption of a more coiled configuration at high molecular weights as demonstrated by the light-scattering results.

Within experimental error a was equal in both acetone and ethyl acetate in the molecular weight range studied. This applies to the work of others (2, 1, 9) as well, and is

Can. J. Chem. Downloaded from www.nrcresearchpress.com by 200.7.193.243 on 09/04/12
For personal use only.

contrary to the behavior of other polymers (e.g., polystyrene (33)) in good and bad solvents. This seeming anomaly may be due to the increased solvation in the good solvent which will decrease a by contributing to the solvent immobilizing character and compensating for extension effects. The low a in ethyl acetate may also be related to the configurational behavior discussed above. The data in Figs. 10 and 11 show that, while the configuration in acetone was constant in the present range, it changed continuously in ethyl acetate. For ethyl acetate, therefore, it is unlikely that the value of the exponent can be assigned with certainty to any model and a should remain an empirical quantity determined for various ranges of M.

The Hydrodynamic Parameter Φ

It was of interest to compute the universal hydrodynamic parameter Φ introduced by Flory (34). Following the notations of Hunt *et al.* (1) the intrinsic viscosity may be related to the chain dimensions by the equation

$$[\eta] = \Phi'(\overline{s_0^2}/\overline{M})^{3/2}\overline{M}^{1/2}\alpha^3. \qquad [13]$$

The prime is appended to Φ to indicate use of the radius of gyration instead of the end-to-end distance as customarily used (34). Values of Φ' for CTN samples in both solvents calculated according to the procedure of Hunt *et al.* are given in Table VI.

As shown in Table VI, Φ' increases with molecular weight in acetone. This is contrary to the conclusion of Holtzer, Benoit, and Doty (2) whose results suggest that Φ' is constant and approximately equal to 2.8×10^{22} in agreement with the values for our lower molecular weights. In ethyl acetate, on the other hand, Φ' is seen to be virtually constant with a mean of $2.86(\pm0.33)\times10^{22}$, which is in good agreement with the values for the two highest molecular weight samples of Hunt *et al.* (1) and close to the constant experimental value of 3.2×10^{22} obtained for the synthetic polymers.

The data can be further analyzed if Eq. [13] is written as

$$\Phi' = k[\eta]\overline{M}_z/(\overline{s_z^2})^{3/2} \qquad [14]$$

or

$$\Phi' = k.[1/(\overline{s_z^2}/\overline{M}_z)].[\eta]/\sqrt{\overline{s_z^2}}, \qquad [15]$$

where k is a constant for each solvent derived after the manner of Hunt *et al.* (1) and depends on the polydispersity. For a random coil $\overline{s_z^2}/\overline{M}_z$ is constant (α is taken as unity) according to Benoit and Doty (25) and Hunt *et al.* (1). Also, Kunst (35) has shown that $[\eta]$ is directly proportional to $\sqrt{\overline{s_z^2}}$ for polyisobutylene in different solvents. Similar direct proportionality between $[\eta]$ and $\sqrt{\overline{s_z^2}}$ can be derived from results on polystyrene (36), polymethylmethacrylate (37), and polyvinyl acetate (38), all of which have been shown to obey random flight statistics. Therefore, Φ' is constant for these polymers. In the case of CTN, $[\eta]/\sqrt{\overline{s_z^2}}$ increases with intrinsic viscosity in ethyl acetate and acetone in the range investigated, as shown in Fig. 14. Since $\overline{s_z^2}/\overline{M}_z$ is constant in acetone, Φ' will increase with increasing $\overline{M}$; whereas the increase of $\overline{s_z^2}/\overline{M}_z$ with $\overline{M}$ in ethyl acetate apparently just compensates the increase in $[\eta]/\sqrt{\overline{s_z^2}}$, leaving Φ' constant. The change of $[\eta]/\sqrt{\overline{s_z^2}}$ might be expected in ethyl acetate for which a configurational transition occurs throughout the range studied. In acetone, however, the light-scattering data suggest that a random coil configuration was attained. The increase of $[\eta]/\sqrt{\overline{s_z^2}}$ may, therefore, be related to a decreasing degree of free-draining as the molecular weight increases.

Can. J. Chem. Downloaded from www.nrcresearchpress.com by 200.7.193.243 on 09/04/12
For personal use only.

Can. J. Chem. Downloaded from www.nrcresearchpress.com by 200.7.193.243 on 09/04/12
For personal use only.

Interaction Constants

The Huggins' interaction constant, k', is an empirical quantity, but its value has been used as an indication of molecular branching (39). It was, therefore, of interest to consider the variation of k' for change of solvent and shear rate. A typical set of results is shown in Table IX. The value of k' is higher in the poor solvent, acetone, which is in agreement with the findings of Alfrey *et al.* (40) for polymethylmethacrylate in different solvents. It may also be noted that k' decreases with increasing rate of shear, in agreement with the results of Masson and Goring (41) on carrageenin—a polygalactose sulphate—and Conrad *et al.* (42) on cellulose in cuprammonium and cupriethylenediamine. In consideration of the dependence of k' on such variables as solvent and rate of shear, one must be cautious in using k' as a criterion for detecting branching, especially in the case of solutions showing non-Newtonian viscosity behavior.

TABLE IX

HUGGINS' INTERACTION CONSTANT, k', FOR FRACTION H-2 IN TWO SOLVENTS AT DIFFERENT SHEAR RATES

G (sec.$^{-1}$)	In acetone	In ethyl acetate
300	0.514	0.366
400	0.450	0.310
500	0.407	0.274
600	0.364	0.232
700	0.330	0.206

The variation of k'_{500} and A_2, the second virial coefficient in light scattering, with molecular weight is shown in Fig. 15 for both solvents. The graphs are irregular, but there is a significant decrease in k'_{500} with increase in $\overline{M}$ for both solvents. This is contrary to Huggins' (14) suggestion that it should be independent of molecular weight. Similar dependence of k'_{500} on molecular weight was found by Timell (43) for CTN in ethyl acetate and Alfrey *et al.* (40) for polymethylmethacrylate in different solvents.

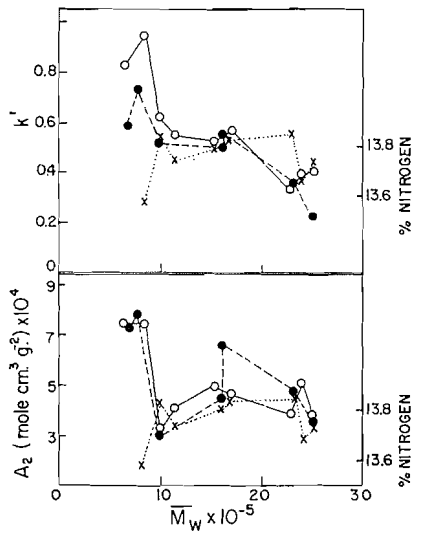

FIG. 15. The second virial coefficient, A_2, and the Huggins' interaction constant, k', vs. molecular weight of the samples in acetone and ethyl acetate. Nitrogen content of the samples have also been included in the graph. ●—Ethyl acetate. ○—Acetone. ×—Nitrogen content.

The second virial coefficient, A_2, for a polymer–solvent system should decrease slowly with increasing molecular weight. For the same polymer the value of A_2 is dependent on the nature of the solvent, being higher in a good solvent. These two general characteristics of A_2 which have been observed in the case of other polymers are not found for CTN solutions. Holtzer *et al.* (2) found negligible and irregular change of A_2 with molecular weight. In ethyl acetate, for low molecular weight fractions, Hunt *et al.* (1) obtained values of A_2 which were practically the same as found by Holtzer *et al.* except the lowest molecular weight sample for which the value was slightly higher. In the present investigation, values of A_2 were found to be the same, within experimental error, in both solvents; a slight decrease in A_2 with increase of $\overline{M_w}$ can, however, be detected.

An obvious feature of Fig. 15 is the irregularity of the data. Similar irregular results for the Huggins' constant have been reported by other workers (40, 42, 43). Irregularities in both k'_{500} and A_2 show the same trend in the two different solvents, indicating that this behavior is due to the samples rather than to experimental error. The nitrogen contents of the samples have been included in Fig. 15. Except for two points, it is seen that there is a rough correlation between the nitrogen content and the fluctuations in k'_{500} (44) and A_2. A more detailed study would be required to elucidate more clearly the source of these irregularities.

ACKNOWLEDGMENTS

The authors wish to thank Dr. T. E. Timell for kindly supplying the ramie and fractionated cotton nitrates, and Dr. R. F. Robertson for use of a Spinco preparative ultracentrifuge.

REFERENCES

1. HUNT, M. L., NEWMAN, S., SCHERAGA, H. A., and FLORY, P. J. J. Phys. Chem. **60**, 1278 (1956).
2. HOLTZER, A. M., BENOIT, H., and DOTY, P. J. Phys. Chem. **58**, 624 (1954).
3. NEWMAN, S. and FLORY, P. J. J. Polymer Sci. **10**, 121 (1953).
4. BADGER, R. M. and BLAKER, R. H. J. Phys. & Colloid Chem. **53**, 1056 (1949).
5. MÜNSTER, A. J. Polymer Sci. **8**, 633 (1952).
6. TIMELL, T. E. Ind. Eng. Chem. **47**, 2166 (1955).
7. TIMELL, T. E. Svensk Papperstidn. **60**, 836 (1957).
8. MITCHELL, R. L. Ind. Eng. Chem. **45**, 2526 (1953).
9. NEWMAN, S., LOEB, L., and CONRAD, C. M. J. Polymer Sci. **10**, 463 (1953).
10. TIMELL, T. E. Svensk Papperstidn. **57**, 777 (1954).
11. SCHURZ, J. and IMMERGUT, E. H. J. Polymer Sci. **9**, 281 (1952).
12. KROEPLIN, H. Kolloid-Z. **47**, 294 (1929).
13. DANIELS, F., MATHEWS, J. H., and WILLIAMS, J. W. Experimental physical chemistry. 4th ed. McGraw-Hill Book Company, Inc., New York. 1949. p. 434.
14. HUGGINS, M. L. J. Am. Chem. Soc. **64**, 2716 (1942).
15. ÖHRN, O. E. J. Polymer Sci. **17**, 137 (1955).
16. TAKEDA, M. and ENO, R. J. Phys. Chem. **60**, 1202 (1956).
17. DANDLIKER, W. B. and KRAUT, J. J. Am. Chem. Soc. **78**, 2380 (1956).
18. HUQUE, M. M. and GORING, D. A. I. Forthcoming publication.
19. GORING, D. A. I., SENEZ, M., MELANSON, B., and HUQUE, M. M. J. Colloid Sci. **12**, 412 (1957).
20. KUSHNER, L. M. J. Opt. Soc. Am. **44**, 155 (1954).
21. MARON, S. H. and LOU, R. H. J. Polymer Sci. **14**, 273 (1954).
22. ZIMM, B. H. J. Chem. Phys. **16**, 1093, 1099 (1948).
23. NAWAB, M. A. and MASON, S. G. Forthcoming publication.
24. NOTLEY, N. T. and DEBYE, P. J. Polymer Sci. **24**, 275 (1957).
25. BENOIT, H. and DOTY, P. J. Phys. Chem. **57**, 958 (1953).
26. KRATKY, O. and POROD, G. Rec. trav. chim. **68**, 1106 (1949).
27. POROD, G. Monatsh. **80**, 251 (1949).
28. OROFINO, T. A. and FLORY, P. J. J. Chem. Phys. **26**, 1067 (1957).
29. PETERLIN, A. Nature, **171**, 259 (1953).
30. LINDSLEY, C. H. and FRANK, M. B. Ind. Eng. Chem. **45**, 2491 (1953).
31. WANNOW, H. A. Kolloid-Z. **102**, 29 (1943).
32. KIRKWOOD, J. G. and RISEMAN, J. J. Chem. Phys. **16**, 565 (1948).

Can. J. Chem. Downloaded from www.nrcresearchpress.com by 200.7.193.243 on 09/04/12
For personal use only.

33. BAWN, C. E. H., FREEMAN, R. E. J., and KAMALIDDIN, A. R. Trans. Faraday Soc. **46**, 1107 (1950).
34. FLORY, P. J. Principles of polymer chemistry. Cornell University Press, Ithaca, N.Y. 1953.
35. KUNST, E. D. Rec. trav. chim. **69**, 125 (1950).
36. OUTER, P., CARR, C. I., and ZIMM, B. H. J. Chem. Phys. **18**, 830 (1950).
37. BISCHOFF, J. and DESREUX, V. Bull. soc. chim. Belges, **61**, 10 (1952).
38. SCHULTZ, A. R. J. Am. Chem. Soc. **76**, 3422 (1954).
39. CRAGG, L. H. and BIGELOW, C. C. J. Polymer Sci. **14**, 177 (1955).
40. ALFREY, T., GOLDBERG, A. I., and PRICE, J. A. J. Colloid Sci. **5**, 251 (1950).
41. MASSON, C. R. and GORING, D. A. I. Can. J. Chem. **33**, 895 (1955).
42. CONRAD, C. M., TRIPP, V. W., and MARES, T. J. Phys. & Colloid Chem. **55**, 1474 (1951).
43. TIMELL, T. E. Svensk Papperstidn. **57**, 913 (1954).
44. IMMERGUT, E. H., RÄNBY, B. G., and MARK, H. F. Ind. Eng. Chem. **45**, 2483 (1953).

Can. J. Chem. Downloaded from www.nrcresearchpress.com by 200.7.193.243 on 09/04/12
For personal use only.

Can. J. Chem. Downloaded from www.nrcresearchpress.com by 200.7.193.243 on 09/04/12
For personal use only.

PHOTOÖXIDATION OF BUTENE-1 AND ISOBUTENE BY NITROGEN DIOXIDE[1]

S. SATO[2] AND R. J. CVETANOVIĆ

ABSTRACT

Reactions of oxygen atoms, produced by photolysis of nitrogen dioxide at 3660 Å, with butene-1 and isobutene have been studied at room temperature. In the case of butene-1, α-butene oxide and n-butanal have been identified as the major products, and methyl ethyl ketone, propanal, acetaldehyde, and ethyl nitrate as minor products. With isobutene, isobutanal was recovered as the major product and acetone, methyl ethyl ketone, methyl nitrate, and nitromethane as minor products. The absence of isobutene oxide in the recovered products from the isobutene reaction is due to its rapid reaction with nitrogen dioxide.

The following values were obtained for the relative reaction rates of oxygen atoms with nitrogen dioxide (k_2), butene-1 (k_{4a}), and isobutene (k_{4b}): $k_2/k_{4a} = 1.9$, $k_2/k_{4b} = 0.34$, $k_{4b}/k_{4a} = 5.5$.

INTRODUCTION

The photochemical reaction between nitrogen dioxide and olefins has been studied especially from the point of view of its relation to "smog" formation in polluted atmosphere (1), but little information has been obtained about the reaction mechanism and the type of products formed. In a previous communication (2) the authors have reported a long wave length threshold for the photochemical reaction between nitrogen dioxide and butene-1. The reaction occurs at 4047 Å and shorter wave lengths, with the formation of α-butene oxide and n-butanal as the main products, but does not occur at 4358 Å and longer wave lengths. It has, therefore, been assumed that even at 4047 Å nitrogen dioxide decomposes and forms free oxygen atoms in their ground electronic state,

$$NO_2 + h\nu = NO + O(^3P). \qquad (1)$$

The photolysis of nitrogen dioxide itself has been extensively investigated (3). In the absence of foreign gases reaction (1) is followed by

$$O + NO_2 = NO + O_2. \qquad (2)$$

When an olefin is added, nitrogen dioxide and the olefin compete for the oxygen atoms formed in reaction (1).

Reactions of oxygen atoms, produced by the mercury-photosensitized decomposition of nitrous oxide, have been studied in this laboratory for some time. In the case of olefins (4), studied at pressures between about 50 and 600 mm., oxygen atoms add to the olefinic double bond, and isomeric epoxides, aldehydes, and ketones are formed as the main products when the olefins consist of more than three carbon atoms. Propylene and ethylene require a collisional stabilization of the addition products formed.

In this paper, results of a study of the photochemical reaction of nitrogen dioxide with butene-1 and isobutene at 3660 Å are reported. At this wave length oxygen atoms produced in reaction (1) are in their ground state.

EXPERIMENTAL

Nitrogen dioxide was obtained from Matheson Co., Inc., and was further purified by repeated bulb-to-bulb distillation *in vacuo* at Dry Ice temperature. The middle third was

[1]*Manuscript received February 13, 1958.*
Contribution from the Division of Applied Chemistry, National Research Council, Ottawa, Canada.
Issued as N.R.C. No. 4728.
[2]*National Research Council Postdoctorate Fellow 1956–58.*

retained and stored at liquid nitrogen temperature. The color of the solid was pure white. Butene-1 and isobutene were Phillips reagent grade products, and were purified by repeated bulb-to-bulb distillation *in vacuo*. Nitrogen gas was supplied by Linde Air Products Co., and was used without further purification.

Because of rapid reaction of nitrogen dioxide with mercury it was necessary to use a mercury-free apparatus. Stopcocks were lubricated with Myvacene-S (Dow Corning) which was not attacked by nitrogen dioxide. Pressures were measured by means of a Bourdon gauge and the compensating pressures were read on a mercury or a silicon oil manometer. The reaction cell consisted of a 300 ml. quartz cylindrical vessel with an all-glass circulating pump supported on teflon bearings and a trap for condensing the reactants attached to it. The light from a medium-pressure mercury arc (Hanovia S 500) was used with Corning glass filter 7-60 so that essentially only the monochromatic light of 3660 Å entered the reaction cell. The cell and the attachments were screened from the diffuse light in the room.

The products formed were fractionated on a LeRoy still (5). Unreacted butene was pumped off at −120° C. and the remainder was transferred into a sampling tube containing a few drops of mercury to remove the unreacted nitrogen dioxide. This tube had been previously evacuated on a second, mercury-containing, high-vacuum apparatus. After the completion of the reaction between nitrogen dioxide and mercury, the tube was evacuated again at liquid nitrogen temperature. Subsequently the products were analyzed by gas–liquid chromatography (GLC) using a 7 ft. dinonyl-phthalate-on-glass-beads column (6, 4) and helium as the carrier gas. To confirm the identity of the compounds separated by GLC, use was made of infrared and mass spectroscopy. The quantitative estimate of the products was based on GLC peak areas.

RESULTS AND DISCUSSION

Thermal Reaction

Nitrogen dioxide attacks olefins thermally and forms addition products (7). Under the conditions employed in this work, however, the thermal reaction was much slower than the photochemical reaction. Moreover, it was found that no products formed in the thermal reaction, with the exception of nitric oxide, were recorded by the GLC. The thermal reaction between nitrogen dioxide and butene was, therefore, ignored in the present work.

Photochemical Reaction

The amounts of the main products formed* at various irradiation times and constant light intensity in the reaction of 3 mm. nitrogen dioxide with 3 mm. and 30 mm. butene-1 are shown in Fig. 1(*a*), and with 3 mm. isobutene in Fig. 1(*b*). The products formed increase almost linearly with the irradiation time up to 30 minutes and the primary processes of these reactions were subsequently studied within this time interval.

The main products formed in the case of butene-1 are the same as found previously for this reaction with the use of O atoms produced by mercury-photosensitized decomposition of nitrous oxide (4). In the case of isobutene, however, isobutene oxide, one of the two main products of the reaction (4), was usually not observed (Fig. 1*b*). This was shown to be due to its rapid reaction with excess nitrogen dioxide. A sample of isobutene oxide was kindly supplied by Dr. A. M. Eastham of these laboratories and its removal

**In the presence of large excess of unreacted NO_2 no attempt could be made to analyze for NO, formed in reactions (1) and (2), and for O_2, formed in reaction (2). A knowledge of the amounts of these products, however, is not essential for the present study.*

Can. J. Chem. Downloaded from www.nrcresearchpress.com by 200.7.193.243 on 09/04/12
For personal use only.

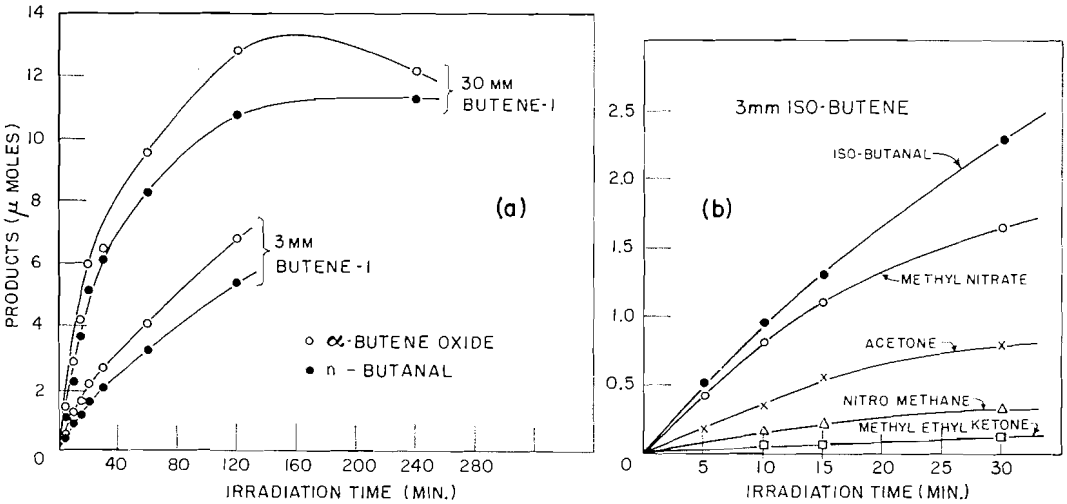

FIG. 1. Yield of the principal products as a function of irradiation time in the photoöxidation of (*a*) butene-1 and (*b*) isobutene.

in the presence of nitrogen dioxide and under conditions employed in the present experiments was demonstrated. The much greater reactivity of isobutene oxide relative to that of the 1,2-epoxides of *n*-olefins has been observed before (8).

Typical chromatograms of the reaction products are shown in Fig. 2. In the case of butene-1 (Fig. 2, A), the main products are α-butene oxide and *n*-butanal, and the minor products are methyl ethyl ketone, propanal, acetaldehyde, ethyl nitrate, and two unidentified compounds (compounds *a* and *b*). In the case of isobutene (Fig. 2, B) isobutanal appears as the only major product since isobutene oxide is removed by excess

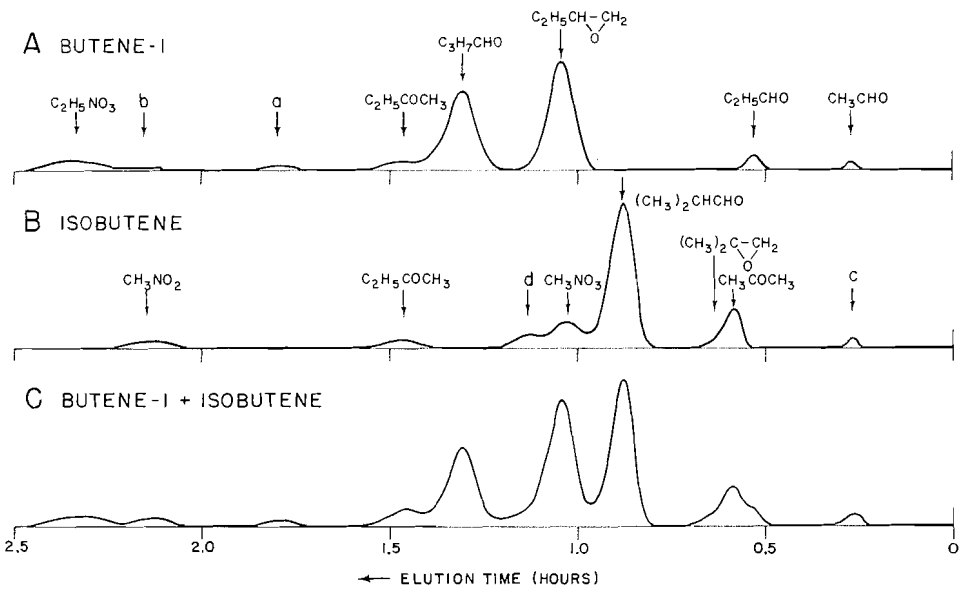

FIG. 2. Typical GLC peaks: A, photoöxidation of butene-1; B, photoöxidation of isobutene; and C, photoöxidation of mixtures of butene-1 and isobutene. (Column temperature 25° C.)

Can. J. Chem. Downloaded from www.nrcresearchpress.com by 200.7.193.243 on 09/04/12
For personal use only.

nitrogen dioxide; acetone, methyl nitrate, methyl ethyl ketone, nitromethane, and two unknown compounds (compounds *c* and *d*) are minor products. It was shown that these minor products were not formed in the thermal reaction of isobutene oxide and nitrogen dioxide.

Fig. 2, C shows the chromatogram of the products of a simultaneous photoöxidation of butene-1 and isobutene. No new products are observed but only those obtained in the reactions of the two butenes separately. This is in agreement with the previous conclusion (4) that the principal reactions under consideration do not involve a free-radical mechanism.

Effect of Pressure

Figs. 3(*a*) and 3(*b*) show the effect of pressure on the photochemical reactions of nitrogen dioxide with butene-1 and isobutene, respectively, at a constant irradiation time of 30 minutes. In both cases 1 mm. each of nitrogen dioxide and the olefin and various amounts of nitrogen were used. There is a pressure effect of the type observed previously (4) for propylene but in the present case it is confined to the pressures below about 30 mm. The lifetimes of the "hot" addition products formed appear to be an order of magnitude longer

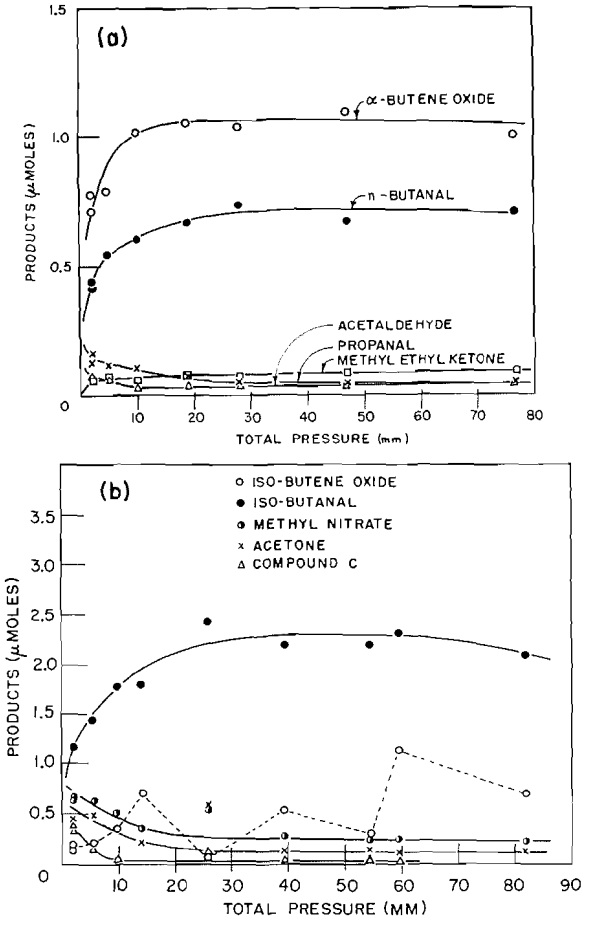

FIG. 3. Pressure effects in the photoöxidation of (*a*) butene-1 and (*b*) isobutene.

Can. J. Chem. Downloaded from www.nrcresearchpress.com by 200.7.193.243 on 09/04/12
For personal use only.

Can. J. Chem. Downloaded from www.nrcresearchpress.com by 200.7.193.243 on 09/04/12
For personal use only.

than in the case of propylene and the collisional stabilization, therefore, takes place at much smaller pressures. At pressures higher than about 70 mm. the rates of formation of the major products seem to show a tendency to decrease again. This is probably due to the additional consumption of oxygen atoms in the three-body reaction

$$O + NO_2 + M = NO_3 + M. \qquad (3)$$

No analogous decline was observed when O atoms were generated by the mercury-photosensitized decomposition of nitrous oxide (4).

In the case of butene-1 throughout the investigated pressure range the ratio of *n*-butanal to α-butene oxide was 0.40 ± 0.02 to 0.60 ± 0.02. In the case of isobutene only small and irregular quantities of isobutene oxide were recovered, for reasons already discussed. In the nitrous oxide work (4) the respective ratios of the aldehyde to the epoxide formed for the case of butene-1 and isobutene were 0.43 to 0.57 and 0.42 to 0.58.

Relative Reaction Rates of Oxygen Atoms with Nitrogen Dioxide, Butene-1, and Isobutene

Oxygen atoms are believed (4) to react with terminal monoölefins according to the following scheme:

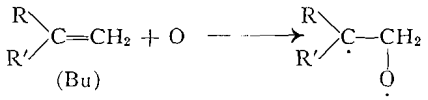

(4)

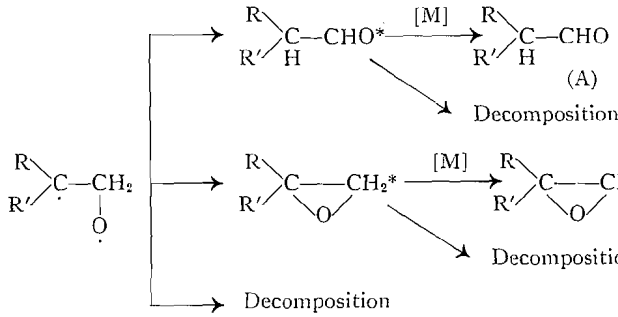

(5)
(6)
(7)
(8)
(9)

At a pressure of, for example, 40 to 50 mm. reactions (6) and (8) need not be considered. At small conversions and on applying the usual steady-state treatment to the remaining reactions and writing Bu for the butene and A for the aldehyde formed in reaction (5), the following relationship is obtained:

[1] $$\frac{\alpha\phi I[NO_2]}{R_A} = 1+\frac{k_2\,[NO_2]}{k_4\,[Bu]}\left(1+\frac{k_3}{k_2}[M]\right),$$

where $\phi I[NO_2]$ is the rate of light absorption by nitrogen dioxide (at small I and $[NO_2]$), R_A the rate of formation of the aldehyde A produced in reaction (5), and α the ratio of molecules of A formed to the number of oxygen atoms consumed in reaction (4). At constant $[NO_2]$, [M], irradiation time, and light intensity (I) a plot of reciprocal GLC peak areas of the compound A against $[NO_2]/[Bu]$ is linear. The slope-to-intercept ratio is

[2] $$m = \frac{k_2}{k_4}\left(1+\frac{k_3}{k_2}[M]\right).$$

Also

[3] $$k_{4a}/k_{4b} = m_b/m_a,$$

where the suffixes *a* and *b* refer to the butene-1 and the isobutene reaction, respectively.

The composition of the main products recovered after 15 minutes irradiation of NO_2–butene-1 mixtures at a total pressure of 50 mm. and at constant NO_2 but variable $[NO_2]/[Bu]$ ratios is shown in Table I, and for the NO_2–isobutene mixtures at a total pressure of 40 mm. in Table II.

TABLE I

YIELD OF THE PRINCIPAL PRODUCTS IN THE PHOTOÖXIDATION OF BUTENE-1 AS A FUNCTION OF THE $[NO_2]/[Bu\text{-}1]$ RATIO

(Irradiation time 15 min.)

Bu-1, mm.	NO_2, mm.	N_2, mm.	$[NO_2]/[Bu\text{-}1]$	GLC peak areas (cm.²)				
				n-BuA	α-BuO	PrA	MEK	AcA
28.9	3.1	11.3	0.11	12.9	16.2	0.3	1.5	0.3
19.4	3.1	27.6	0.16	12.6	16.0	0.5	1.0	0.4
12.9	3.1	36.7	0.24	11.2	15.9	0.6	1.3	0.4
9.2	3.1	37.0	0.34	10.8	14.3	0.5	1.1	0.5
7.1	3.1	39.2	0.44	8.4	11.9	0.5	1.0	0.5
6.0	3.1	40.7	0.52	8.1	11.1	0.4	0.8	0.4
5.0	3.1	41.3	0.62	7.4	9.4	0.5	0.8	0.4
4.5	3.1	42.4	0.69	6.0	8.1	0.4	0.8	0.3
3.9	3.1	43.2	0.79	6.6	9.1	0.4	0.6	0.3
3.3	3.0	43.3	0.91	5.9	6.2	n.d.	0.5	0.5
3.0	3.1	44.0	1.03	5.2	7.5	0.3	0.5	0.3

Bu-1 = *butene;* *n*-BuA = *n-butanal;* α-BuO = *α-butene oxide;* PrA = *propanal;* MEK = *methyl ethyl ketone;* AcA = *acetaldehyde; n.d. = not determined.*

TABLE II

YIELD OF THE PRINCIPAL PRODUCTS IN THE PHOTOÖXIDATION OF ISOBUTENE AS A FUNCTION OF THE $[NO_2]/[ISOBUTENE]$ RATIO

(Irradiation time 15 min.)

i-Bu, mm.	NO_2, mm.	N_2, mm.	$\frac{[NO_2]}{[i\text{-Bu}]}$	GLC peak areas (cm.²)							
				i-BuA	CH_3NO_3	Acetone	*i*-BuO	MEK	CH_3NO_2	Cpd. *c*	Cpd. *d*
29.2	3.1	6.7	0.11	19.2	2.5	1.7	0	0.8	1.8	0.1	1.5
9.1	3.1	26.0	0.34	17.9	2.2	2.7	0	0.8	1.0	0.2	1.4
4.8	3.1	28.0	0.65	16.2	n.d.	2.6	n.d.	n.d.	n.d.	n.d.	n.d.
3.0	3.1	33.3	1.03	12.8	2.4	2.4	0	0.3	1.0	0.3	1.4
2.0	3.1	34.3	1.6	13.4	2.5	2.5	0	0.5	0.8	0.3	1.0
1.6	3.1	34.4	2.0	11.8	2.6	1.8	0	0.4	1.0	0.3	1.2
1.5	3.1	35.6	2.1	11.7	2.1	2.0	0	0.6	0.8	0.3	1.5
1.2	3.1	38.2	2.6	11.0	1.9	1.5	0.1	0.4	0.7	0.4	1.1
0.98	3.1	38.0	3.2	9.4	1.6	1.2	0.6	0.3	1.0	0.3	1.0
0.85	3.1	39.1	3.7	8.0	1.4	1.2	0.2	0.3	0.7	0.3	1.0
0.75	3.1	39.6	4.2	7.7	2.1	1.9	0	0.2	0.5	0.2	0.7

i-Bu = *isobutene;* *i*-BuA = *isobutanal;* *i*-BuO = *isobutene oxide;* MEK = *methyl ethyl ketone; n.d. = not determined.*

The reciprocal peak areas of *n*-butanal and isobutanal, respectively, are plotted against $[NO_2]/[Bu]$ in Figs. 4(*a*) and 4(*b*). There is an appreciable scatter of experimental values and the least mean squares treatment gives $m_a = 2.1$ and $m_b = 0.38$. These quantities are approximately equal to k_2/k_{4a} and k_2/k_{4b}, respectively, since at pressures of 40 to 50 mm. the expression in the bracket in Eq. [2] does not differ much from unity. According to Ford and Endow (9), $k_3[M]/k_2 = 47.6$ [M] (where [M] is in mole/l.) so that the corrected values are

$$k_2/k_{4a} = 1.9, \text{ and } k_2/k_{4b} = 0.34.$$

Can. J. Chem. Downloaded from www.nrcresearchpress.com by 200.7.193.243 on 09/04/12
For personal use only.

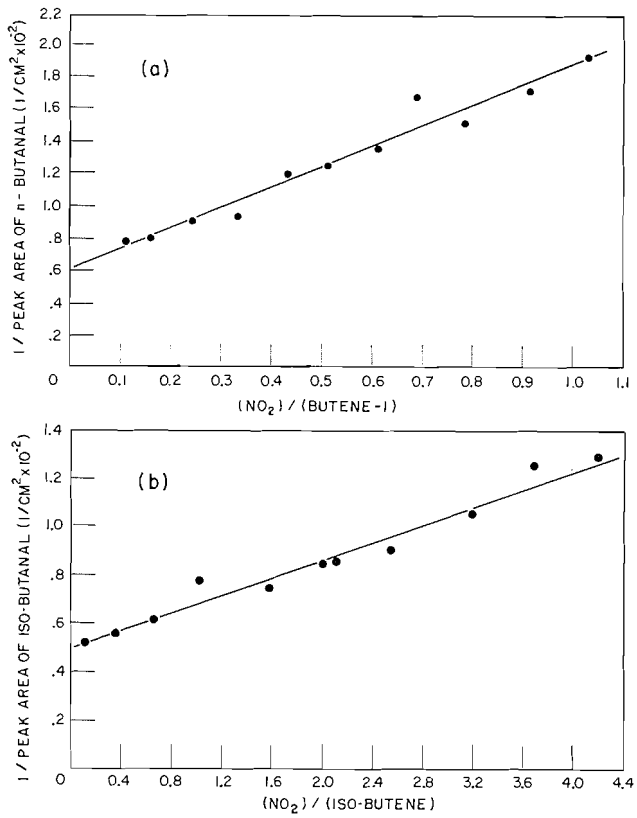

FIG. 4. (*a*) Reciprocal GLC peak areas of *n*-butanal as a function of the $[NO_2]/[\text{butene-1}]$ ratio (*b*) Reciprocal MLC peak areas of isobutanal as a function of the $[NO_2]/[\text{isobutene}]$ ratio.

The ratio of the rate constants of the reactions of oxygen atoms with butene-1 and isobutene is, therefore,

$$k_{4b}/k_{4a} = 5.5.$$

By photolyzing nitrogen dioxide in the presence of mixtures of butene-1 and isobutene, this ratio of the rate constants can be also evaluated from the relationship

$$[4] \qquad \frac{k_{4b}}{k_{4a}} = \frac{[R_A]_b}{[R_A]_a}\frac{\alpha_a}{\alpha_b}\frac{[\text{butene-1}]}{[\text{isobutene}]}.$$

Table III shows the amounts of *n*-butanal and isobutanal formed with various mixtures of butene-1 and isobutene. The two aldehydes have essentially the same molar GLC responses, as is shown in Fig. 5. Since it has also been found before (4) that $\alpha_a/\alpha_b \simeq 1$, the relative rate constant in Eq. [4] is obtained simply by multiplying the ratio of the GLC peak areas of the two aldehydes by the inverse ratio of the concentrations of the butenes. The values obtained are given in the last column of Table III. The mean value of about 5.8 agrees well with the above value of 5.5. There is, however, a considerable scatter from the mean value and perhaps also a systematic drift with the ratio of the two olefins: a decrease with decreasing isobutene to butene-1 ratio extrapolating to a limit of about 4.5 as the amount of isobutene tends to zero. In view of this and of the

Can. J. Chem. Downloaded from www.nrcresearchpress.com by 200.7.193.243 on 09/04/12
For personal use only.

TABLE III

YIELD OF ALDEHYDES IN THE PHOTOÖXIDATION OF MIXTURES OF BUTENE-1 AND ISOBUTENE

NO_2, mm.	*i*-Bu, mm.	Bu-1, mm.	N_2, mm.	Irradiation time, min.	GLC peak areas ($cm.^2$) *n*-BuA	*i*-BuA	k_{4b}/k_{4a}
3.1	0.98	3.95	31.0	15	6.8	10.1	5.9
3.2	0.81	4.97	32.3	15	7.9	6.9	5.4
3.1	1.26	3.48	31.8	15	3.9	9.1	6.4
6.2	1.00	4.10	32.1	10	6.4	9.1	5.7
3.1	0.99	4.02	31.6	15	4.8	6.8	5.8
						Average	5.8

i-Bu = *isobutene;* Bu-1 = *butene-1;* *n*-BuA = *n-butanal;* *i*-BuA = *isobutanal.*

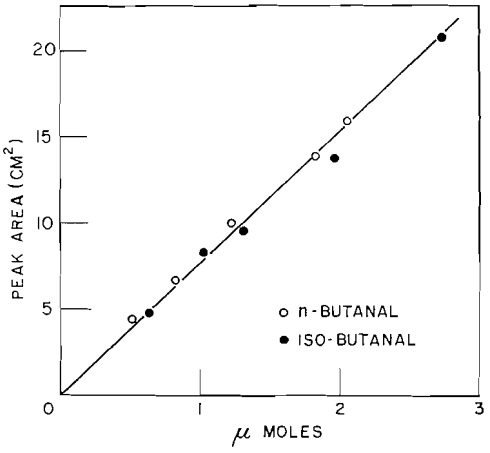

FIG. 5. GLC molar responses of *n*-butanal and isobutanal.

scatter of points in the plots in Figs. 4(*a*) and 4(*b*), it is felt that there is probably an experimental uncertainty of the order of 20 to 30 per cent in the relative rate constants determined in the present work. Previously (4) a value of 4.2 was obtained for k_{4b}/k_{4a}, which within the estimated experimental uncertainties agrees with the present value.

Formation of Minor Products

The complexity of the reactions and the incomplete analytical information preclude a detailed explanation of the method of formation of minor products.

Small amounts of methyl ethyl ketone were found in the case of both butene-1 and isobutene. The formation of this compound has been explained before (4) by addition of a small amount of oxygen atoms to the "more-substituted" carbon atom in the two butenes followed by migration of H or CH_3.

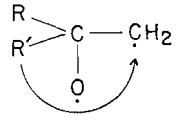

This migration is probably largely intramolecular, although the formation of nitromethane in the isobutene system suggests the presence of some free methyl radicals.

Most of the minor products increase at lower pressures, as is shown in Figs. 3(*a*) and

Can. J. Chem. Downloaded from www.nrcresearchpress.com by 200.7.193.243 on 09/04/12
For personal use only.

3(*b*). This is in agreement with an increasing importance of reactions (6) and (8) at lower pressures. However, even at higher pressures certain amounts of minor products are still formed, suggesting also the occurrence of some pressure-independent decomposition (reaction (9)).

Finally, it should be mentioned that under certain conditions in the presence of molecular oxygen propanal and acetone are formed as major products in the reactions of butene-1 and isobutene, respectively, besides the C_4 epoxides and aldehydes which are normally the only major products in these reactions. While these effects require further investigation, it is possible that oxygen produced in reaction (2) may contribute to some extent to the formation of propanal and acetone even when only nitrogen is used as diluent.

ACKNOWLEDGMENTS

The authors wish to thank Dr. E. C. Horswill for a sample of ethyl nitrate, Dr. A. W. Tickner for mass spectrometer analyses, and the Analytical Section of this Division for infrared analyses.

REFERENCES

1. THOMAS, M. D. Ind. Eng. Chem. **48**, 1522 (1956); FORD, H. W. and ENDOW, N. J. Chem. Phys. **27**, 1277 (1957).
2. SATO, S. and CVETANOVIĆ, R. J. Can. J. Chem. **36**, 279 (1958).
3. NOYES, W. A., Jr. and LEIGHTON, P. A. The photochemistry of gases. Reinhold Publishing Corp., New York. 1941. p. 400.
4. CVETANOVIĆ, R. J. J. Chem. Phys. **25**, 376 (1956); Can. J. Chem. **36**, 623 (1958).
5. LEROY, D. J. Can. J. Research, B, **28**, 492 (1950).
6. CALLEAR, A. B. and CVETANOVIĆ, R. J. Can. J. Chem. **33**, 1256 (1955).
7. LEVY, N. and SCAIFE, C. W. J. Chem. Soc. 1093 (1946); BROWN, J. F., Jr. J. Am. Chem. Soc. **79**, 2480 (1957).
8. ELTEKOW, A. Ber. **16**, 395 (1883); PRITCHARD, J. G. and LONG, F. A. J. Am. Chem. Soc. **78**, 2667 (1956).
9. FORD, H. W. and ENDOW, N. J. Chem. Phys. **27**, 1156 (1957).

Can. J. Chem. Downloaded from www.nrcresearchpress.com by 200.7.193.243 on 09/04/12
For personal use only.

CHEMICAL EFFECTS OF THE $Br^{81}(\gamma, \alpha)As^{77}$ REACTION IN BROMIDES[1]

D. H. NELSON AND K. J. MCCALLUM

ABSTRACT

An investigation has been made of the chemical forms of the arsenic produced when solid bromides, following irradiation with high-energy gamma rays, are dissolved in aqueous solution. The As^{77} is found to appear in both the pentavalent and the trivalent forms, the ratio AsV/AsIII increasing with an increase in the number of moles of water present in the hydrated solid. For the monohydrate of lithium bromide, the ratio depends upon the pH of the solution in which the solid is dissolved.

INTRODUCTION

When bromine atoms are exposed to high-energy gamma rays, one of the nuclear reactions which occurs involves the ejection of alpha particles, with the formation of As^{77}, a beta-emitting nuclide with a half-life of 39 hours (1). The present work is concerned with the chemical forms assumed by the radioactive arsenic when bromides which have been irradiated with gamma rays from a betatron are dissolved in aqueous solutions.

The As^{77} nuclide decays with the emission of a beta particle with 0.68 Mev. maximum energy to form stable Se^{77}. From the known masses of Br^{81} and Se^{77} (2), and the energy of the beta particles, the threshold energy for the $Br^{81}(\gamma, \alpha)As^{77}$ reaction can be calculated to be about 7 Mev. When betatron gamma rays of 23 Mev. peak energy are used to bring about this nuclear reaction, the maximum recoil energy imparted to the As^{77} nucleus is about 0.9 Mev.

Taylor and Haslam (3) have determined the activation and cross section curves for this reaction. From their results it can be calculated that for an irradiation dose of 10,000 roentgens with betatron gamma rays of 23 Mev. peak energy, the As^{77} produced in a 30 g. sample of KBr should have an initial decay rate equivalent to 200 disintegrations per second. This is sufficiently high to make the separation and measurement of the chemical forms of the As^{77} feasible by the carrier technique.

EXPERIMENTAL AND RESULTS

All of the bromide salts used were of reagent grade and were dried before use. The hydrated salts were prepared by the evaporation of solutions of the bromides, and drying the residue over the corresponding anhydrous salt. The water content of the hydrates so prepared did not differ by more than 2% from the theoretical quantity.

Sixty-gram samples of the bromides were exposed to radiation from a betatron operating at a peak energy of 23 Mev. for a period of 10 minutes. The intensity at the position of irradiation varied from about 1000 to 2000 roentgens per minute in different experiments. A number of different radioactive species resulted from this treatment. To determine the total amount of As^{77} produced in an irradiation a chemical separation was necessary before counting. The following procedures were used.

A weighed amount of the irradiated sample, approximately 30 g., was mixed with 40 mg. of powdered arsenic metal and the mixture was dissolved in 200 ml. of cold 6 *M* nitric acid. When the initial evolution of free bromine had ceased, the solution was then made

[1]*Manuscript received February 14, 1958.*
Contribution from the Department of Chemistry, University of Saskatchewan, Saskatoon, Saskatchewan. From a thesis submitted by D. H. Nelson in partial fulfillment of the requirements for the degree of Master of Arts.

Can. J. Chem. Downloaded from www.nrcresearchpress.com by 200.7.193.243 on 09/04/12
For personal use only.

basic with ammonia, and the arsenate precipitated as $MgNH_4AsO_4.6H_2O$. The precipitate was separated by filtration, dissolved and reprecipitated twice more. The precipitate was then mounted on filter paper, washed with a small amount of alcohol, and dried under a heat lamp. It was counted with a mica-window end-on counter under conditions of standard geometry. The weight of arsenate present in the precipitate was then determined volumetrically. The observed counts were corrected for decay. Self-scattering and self-absorption corrections were found to be negligible for the thicknesses of precipitate that were used.

The separation procedure was sufficient to separate all other radioactive nuclides present from the As^{77}, as was shown by half-life determinations on the precipitate. The measurements permitted a calculation of the total activity of the As^{77} produced per gram of bromide during the particular irradiation.

Measurements were made to determine the fraction of the As^{77} present as arsenite (AsIII) and as arsenate (AsV). A known weight of the irradiated sample, approximately 30 g., was dissolved in 100 ml. of solution containing known amounts of arsenite and arsenate carriers. After time for complete dissolution and equilibration, the arsenate fraction was removed by precipitation as $MgNH_4AsO_4.6H_2O$. This precipitate was separated by filtration, dissolved, reprecipitated, and prepared for counting in the manner previously described.

The filtrate containing the arsenite fraction was acidified to pH 2 with HCl, and the AsIII precipitated as As_2S_3 with hydrogen sulphide. The precipitate was filtered, dissolved in ammonium sulphide, and reprecipitated by acidification. The precipitate was removed and dissolved with HCl and $KClO_3$, which oxidized the arsenic to the pentavalent state. The arsenic was then precipitated and counted as $MgNH_4AsO_4.6H_2O$.

In all cases, the sum of the amounts of the As^{77} found in the AsIII and AsV fractions was equal to the total As^{77} content within experimental error. Attempts were made to detect As^{77} present as arsine by bubbling arsine through a freshly prepared solution of the irradiated bromide and then absorbing the gas on a filter paper impregnated with mercuric chloride solution. The paper was then counted but no detectable amounts of radioactivity were observed.

Experiments were carried out on the exchange of arsenic between arsenite and arsenate in the presence of high concentrations of bromide ion. Labeled arsenate ion was prepared using radioactive As^{76} produced by the (n, γ) reaction on sodium cacodylate (4). This was added to 100 ml. of a solution containing 30 g. of potassium bromide and a known amount of arsenite carrier. The solution was allowed to stand for 2 hours, and then the arsenite and arsenate fractions were separated and counted. The results indicated that at both high and low values of the pH, less than one per cent exchange had occurred.

The results obtained when irradiated samples of some bromides and bromide hydrates were dissolved in water are given in Table I. Lithium, sodium, potassium, and ammonium bromides each gave approximately 10% of the As^{77} activity in the AsV fraction, and the remainder appeared as AsIII. The monohydrate of lithium bromide gave 55% in the AsV fraction while the dihydrates of lithium and sodium bromides gave approximately 95% of the As^{77} in the AsV fraction.

The effect upon the distribution of As^{77} of the pH of the solution in which the irradiated solids were dissolved was determined. A Beckman pH meter, model N-2, was used to determine the pH values. The addition of large quantities of the solid bromides to the solutions tended to decrease the pH values. An attempt was made to keep the pH constant by the gradual addition of NaOH solution as the solid was dissolved. Table II

Can. J. Chem. Downloaded from www.nrcresearchpress.com by 200.7.193.243 on 09/04/12
For personal use only.

TABLE I

PERCENTAGE OF $As^{77}V$ FOLLOWING SOLUTION IN WATER

Compound	% $As^{77}V$
LiBr	11±1
NaBr	9±1
KBr	10±1
NH_4Br	11±1
$LiBr.H_2O$	55±2
$LiBr.2H_2O$	91±3
$NaBr.2H_2O$	92±3

TABLE II

EFFECT OF pH ON PERCENTAGE OF $As^{77}V$

Compound	pH	% $As^{77}V$
NaBr	3.0– 3.2	8±1
	10.5–10.9	9±1
	10.8–11.2	8±1
LiBr	3.0– 3.2	10±1
	10.0–10.2	9±1
	10.6–11.2	9±1
	11.0–11.6	8±1
$LiBr.H_2O$	0.5	51±1
	2.5– 2.8	55±1
	9.2– 9.6	57±2
	10.5–10.9	68±1
	10.7–11.2	72±2
	10.9–11.2	73±2
	11.1–11.6	60±2
	11.2–12.0	53±2
	12.0–13.0	54±2
$LiBr.2H_2O$	4.0– 4.2	90±3
	10.7–11.2	92±2
	13.0–14.0	96±2

gives the pH range observed during the solution of the solid, and the percentage of As^{77} appearing in the AsV fraction.

The results show that in basic solutions, anhydrous sodium and lithium bromides and the dihydrate of lithium bromide give essentially the same distribution as they do in neutral solutions. The monohydrate of lithium bromide, however, shows a peculiar behavior in that the percentage of As^{77} appearing as AsV increases to a maximum at about pH 11, and then decreases at higher pH values.

DISCUSSION

The results in Table I indicate that the distribution of As^{77} between the trivalent and pentavalent states is markedly dependent upon the amount of water contained in the crystal. For 0, 1, or 2 moles of water per mole of bromide, the percentage of As^{77} appearing as AsV is about 10, 53, and 95 respectively. An increase in the amount of water favors the formation of the more highly oxidized form. This is probably to be correlated with the corresponding increase in the percentage of oxygen in the solid.

The results given in Table II indicate that for the anhydrous salts and for the dihydrate of lithium bromide, the same results are obtained when the solids are dissolved in solutions of high pH as when they are dissolved in water. For the anhydrous bromides and the dihydrate the results can be explained by assuming that two types of As^{77}-containing

Can. J. Chem. Downloaded from www.nrcresearchpress.com by 200.7.193.243 on 09/04/12
For personal use only.

species may be present, the first reacting with water to form AsIII and the second to form AsV, the ratio of the second to the first increasing when the water content of the solid is increased from 0 to 2 moles per mole of bromide. The valence state formed on solution appears to be independent of pH.

Although the percentage of the As^{77} appearing as AsV for lithium monohydrate is intermediate between the values found for the anhydrous salts and the dihydrate, the results of Table II cannot be explained by assuming that here the same two As^{77}-containing species are present in the solid, but in intermediate proportions. The maximum in the percentage of the As^{77} appearing as AsV which occurs at about pH 11 requires the presence of at least one species in the solid whose reactions on solution depend upon the pH of the solution in a rather complicated way. This species appears to be absent or present in only small proportions when the irradiated solid is the anhydrous bromide or the dihydrate.

There is no evidence concerning the exact identity of any of the species which have been postulated to occur in the irradiated solid. The two species assumed to be present in the irradiated anhydrous bromides and in the dihydrate could contain arsenic in the trivalent and pentavalent states respectively and undergo hydrolysis upon solution to form arsenite and arsenate. The third type of species, present in addition to the other two in irradiated bromide monohydrates, could represent an intermediate type formed only at intermediate water content. If there is only one species of this intermediate type, to explain the results of Table II, one would have to assume that it undergoes three competing reactions in solution. The first would involve a reaction with water to form AsIII, the second a reaction with hydroxyl ion to form AsV, and the third a reaction of higher order with respect to hydroxyl ion to form AsIII. Other schemes to explain the results of Table II can be devised if one assumes more than one species of this intermediate type.

The results obtained are not sufficient to allow any definite conclusions to be drawn as to the chemical forms of the As^{77} in these irradiated bromides. It can be stated, however, that As^{77} is present in more than one chemical form, and that for lithium bromide monohydrate, reactions on solution involving hydroxyl ions can occur.

ACKNOWLEDGMENT

Grateful acknowledgment is made to the National Research Council for financial support.

REFERENCES

1. ERDOS, P., JORDAN, P., SCHMEUKER, J., and STOLL, P. Helv. Phys. Acta, **27**, 127 (1954).
2. COLLINS, T. L., JOHNSON, W. H., and NIER, A. O. Phys. Rev. **94**, 398 (1954).
3. TAYLOR, J. G. V. and HASLAM, R. N. H. Phys. Rev. **87**, 1138 (1952).
4. WESTERVELT, D. Phys. Rev. **92**, 531 (1953).

Can. J. Chem. Downloaded from www.nrcresearchpress.com by 200.7.193.243 on 09/04/12
For personal use only.

Can. J. Chem. Downloaded from www.nrcresearchpress.com by 200.7.193.243 on 09/04/12
For personal use only.

REACTION OF DEUTERIUM ATOMS WITH ETHANE—MECHANISM OF METHANE EXCHANGE[1]

R. Berisford[2] and D. J. Le Roy

ABSTRACT

The reaction of deuterium atoms with ethane has been studied at 25° C. by the method of mercury ($^3P_1$) photosensitization. Methane formation takes place by the addition of D atoms to methyl radicals in the presence of a third body. From the dependence of methane exchange on third-body concentration the lifetime of the excited methane molecule is estimated to be of the order of 10^{-9} sec. The lifetime of the excited ethane molecule formed by the addition of a D atom to an ethyl radical is estimated to be considerably less than 10^{-9} sec.

INTRODUCTION

The reaction between ethane and atomic hydrogen (or deuterium) has been studied under a number of different conditions and the literature has been discussed extensively by Steacie (1). There is little doubt that the primary reaction in every case is

$$H \text{ (or D)} + C_2H_6 = C_2H_5 + H_2 \text{ (or HD)}. \quad [1]$$

Methane is the main product formed at the low pressures used in the discharge tube method of Wood and Bonhoeffer (1) and the hot filament method of Berlie and Le Roy (2). It is also an important product when the H (or D) atoms are produced by mercury photosensitization, even when the initial quenching is by ethane:

$$Hg(^3P_1) + H_2 = Hg(^1S_0) + 2H, \quad [2]$$

$$Hg(^3P_1) + C_2H_6 = Hg(^1S_0) + H + C_2H_6. \quad [3]$$

Presumably, the methane arises from methyl radicals formed in the atomic cracking reaction,

$$H + C_2H_5 = 2CH_3, \quad [4]$$

followed by

$$H + CH_3 = CH_4, \quad [5]$$

$$CH_3 + H_2 = CH_4 + H, \quad [6]$$

or

$$CH_3 + C_2H_6 = CH_4 + C_2H_5. \quad [7]$$

The primary purpose of the present investigation was the elucidation of the mechanism of methane formation, particular emphasis being placed on the role of inert gases on the extent of deuterization of the methane.

EXPERIMENTAL

Reagents

Heavy water (99.83%), obtained from Atomic Energy of Canada Limited, was used to produce deuterium by the method described by Kirshenbaum (3). Ethane, obtained from the Ohio Chemical and Manufacturing Company, was subjected to numerous trap-to-trap distillations in which only the intermediate portions were retained. Carbon dioxide, obtained from commercial Dry Ice, and propane (Ohio) were treated in the same way. The four deuterated methanes, CH_3D, CH_2D_2, CHD_3, and CD_4, were obtained

[1]*Manuscript received January 30, 1958.*
Contribution from the Department of Chemistry, University of Toronto, Toronto, Ontario.
[2]*Present address: E. I. Du Pont de Nemours & Co., Inc., Newport Experimental Station, Newport, Delaware.*

from Merck & Co., Ltd., Montreal. Their purity was said to be not less than 98.0, 96.0, 96.9, and 99.4%, respectively. We were unable to detect any foreign bands in their individual infrared spectra.

Reaction System

The total volume of the reaction system was 2780 cm.^{3}, and included a buffer volume, an all-glass circulating pump, and a cylindrical quartz cell 10 cm. long and 5 cm. in diameter. Resonance radiation was provided by a 4-watt U-shaped General Electric germicidal lamp. The mercury vapor concentration in the reaction cell was the equilibrium vapor pressure at room temperature. The ethane was measured accurately in a small calibrated volume before condensing it into the reaction system.

Analysis of Products

The non-condensable products, consisting of the various hydrogens and methanes, were passed through a trap containing silica gel cooled with liquid air. This removed all of the methanes and most of the hydrogens. The methanes were finally separated in a pure state by treating the desorbed gas with copper oxide at 250° C. and then passing it through a liquid-air trap.

The condensable gases were fractionated on a low-temperature still (4). A few of the ethane fractions were subjected to infrared and mass spectrographic analysis.

Infrared analyses of the methanes formed in the reaction were made with a Perkin-Elmer Model 12-C spectrometer with sodium chloride optics, modified as described previously (5). No CH_4 was found but each of the other four methanes was present. The fundamental vibration frequencies used are given in Table I.

TABLE I

INFRARED ABSORPTION OF DEUTERATED METHANES, VALUES OF q $(=(1/P)\log I_0/I_t)$ IN MM.$^{-1}$†

cm.$^{-1}$	996	1034	1090	1156	1235	1299	1306
CH_3D	0.00	0.00	0.0045	0.0294	0.0100	0.0046	0.0227
CH_2D_2	0.00	0.0226	0.0367	0.0083	0.0215	0.0078	0.0072
CHD_3	0.0236	0.0449	0.0062	0.0034	0.0036	0.0114	0.0092
CD_4	*	*	0.00	0.00	0.00	0.00	0.00

*See text.
†For path length of 67 cm., slit width 0.250 mm.

Because of the small moments of inertia there was a considerable amount of overlapping of the bands, but of more significance was their susceptibility to pressure broadening. The observed extinction coefficient of any particular methane at one of its principal absorption frequencies was strongly dependent on the amounts of other methanes present, even when there was no overlapping of bands. This difficulty was overcome by deliberately broadening the rotational structure by the addition of large amounts of carbon dioxide. An example of the effect of carbon dioxide on optical density ($D = \log I_0/I_t$) is shown in Fig. 1. Calibration curves were obtained and analyses made using a standard pressure of 400 mm. of carbon dioxide in the absorption cell.

Under these conditions linear plots of D vs. P, the pressure in mm., were obtained for the individual methanes (except in the case of CD_4) and the values of q in the expression $D = qP$ are given in Table I; q has the units mm.$^{-1}$ and applies to the particular

Can. J. Chem. Downloaded from www.nrcresearchpress.com by 200.7.193.243 on 09/04/12
For personal use only.

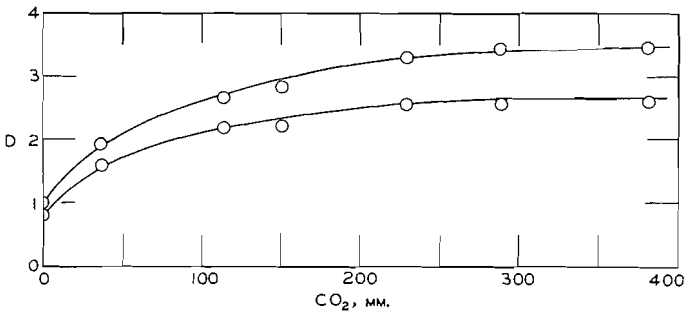

FIG. 1. Effect of carbon dioxide on the optical density, $D = \log I_0/I_t$, at 1306 cm.$^{-1}$ (upper curve) and 1235 cm.$^{-1}$ (lower curve) for a sample containing the four deuterated methanes.

optical cell used, which had a path length of 67 cm. The values of q, which are underlined in Table I, are for frequencies at which maxima occur; the remaining values indicate the magnitude of overlapping. Since D was not proportional to P for CD_4, the concentration of CD_4 in a mixture was obtained from the empirical curve of D vs. P after correcting the observed optical density at 996 cm.$^{-1}$ for the contribution due to CHD_3. The concentrations of CHD_3, CH_2D_2, and CH_3D were obtained by solving equations of the form $D = \sum q_i P_i$ for each of the appropriate frequencies.

Analytical results on three synthetic mixtures are given in Table II. Mass spectrographic analysis on sample No. 2 was done through the kindness of Dr. A. W. Tickner, Division of Applied Chemistry, National Research Council, Ottawa.

TABLE II

ANALYSIS OF SYNTHETIC MIXTURES OF THE DEUTERATED METHANES

Sample	Method	% CH_3D	% CH_2D_2	% CHD_3	% CD_4
1	Synthesis	28	30	32	10
	Infrared anal.	31	31	30	8
2	Synthesis	27.9	21.7	18.7	31.7
	Infrared anal.	29.2	21.4	19.5	29.9
	Mass spec. anal.*	30±3	22±3	21±1	24±1
3	Synthesis		37.9	52.7	9.4
	Infrared anal.		41.3	48.1	10.6

*Analysis report included 0+5% CH_4.

RESULTS AND DISCUSSION

The effect of the inert gas carbon dioxide on the relative yields of the deuterated methanes is shown in Table III. A comparison of the ethane consumed with the total methanes formed shows that these are the most important products. In a few instances analyses were made for higher products: 0.066 mm. of propane and 0.0040 mm. of butane were formed in experiment No. 6; 0.063 mm. of propane, 0.007 mm. of butane, and 0.006 mm. of hexane were formed in experiment No. 8. A mass spectrographic analysis of the residual ethane from experiment No. 12 showed that 0.36 mm. of C_2H_5D and 0.09 mm. of $C_2H_4D_2$ were formed.

It is evident from Table III that variations in the initial pressure of deuterium have

Can. J. Chem. Downloaded from www.nrcresearchpress.com by 200.7.193.243 on 09/04/12
For personal use only.

TABLE III

EFFECT OF CARBON DIOXIDE ON RELATIVE YIELDS OF THE DEUTERATED METHANES

No.	mm. $(C_2H_6)_0$	mm. $-\Delta(C_2H_6)$	mm. $(D_2)_0$	mm. (CO_2)	mm. (Methane)	% CH_3D	% CH_2D_2	% CHD_3	% CD_4
6	4.59	1.14	30.5	0	1.88	16.8	27.6	30.2	25.4
8	4.61	1.04	55.0	0	1.75	14.1	31.4	30.3	24.2
10	4.67	0.91	30.1	54.0	1.61	27.4	32.9	16.3	23.4
11	4.67	0.99	49.6	50.6	1.69	27.9	33.2	20.6	17.6
9	4.62	0.80	21.0	100.9	1.54	33.8	36.4	12.8	17.0
18	4.67	—	19.6	146.0	1.58	39.4	37.7	18.8	4.2
12	4.68	0.60	32.2	199.5	0.89	44.0	51.0	5.0	0.0

little or no effect either on the amount of total methane or on its isotopic composition. This suggests that the methyl radicals formed in [4′] do not, under the conditions of our experiments, form methane by the analogue of [6]:

$$D + C_2H_5 = CH_3 + CH_2D. \qquad [4']$$

This is further borne out by the fact that the analogue of [6] would yield only CH_3D and CH_2D_2 unless some source of CHD_2 and CD_3 radicals was provided. Reaction [7] can be eliminated since no CH_4 was produced, a fact which gives further support to the elimination of [6], since the rate constants reported for [6] and [7] are such that in the present experiments the abstraction by CH_3 radicals of D atoms from D_2 and of H atoms from C_2H_6 would proceed at approximately the same rate (6, 7).

The results in Table III show that high pressures of carbon dioxide cause an increase in the proportions of CH_3D and CH_2D_2 and a decrease in the proportions of CHD_3 and CD_4. It is evident, therefore, that reactions analogous to [5] require a third body. The following detailed mechanism is suggested:

$$D + CH_3 = CH_3D^*, \qquad [8]$$

$$CH_3D^* = CH_2D + H, \qquad [9]$$

$$CH_3D^* + M = CH_3D + M. \qquad [10]$$

Similar reactions involving $CH_2D_2^*$, CHD_3^*, and CD_4^* are assumed to occur. Defining α_1, α_2, α_3, and α_4 as the rate constants for the bimolecular formation, β_1, β_2, β_3, and β_4 for unimolecular decomposition, and γ_1, γ_2, γ_3, and γ_4 for bimolecular stabilization of these four excited molecules, expressions can be derived for the rates of formation of each of the stable deuterated methanes in terms of [4′]. The rate of [4′] will, of course, be equal to one half the total rate of formation of methane. Unimolecular decompositions of excited molecules yielding D atoms need not be taken into account, and the rate of formation of CD_4 will be given simply by $\alpha_4(D)(CD_3)$. Writing $\beta_i/\gamma_i = p_i$ and noting that the latter has the same units as M, the calculated percentage yields are as follows:

(i) $$\% CH_3D = 50[M/(p_1+M)],$$

(ii) $$\% CH_2D_2 = 50[(2p_1+M)/(p_1+M)].[M/(p_2+M)],$$

(iii) $$\% CHD_3 = 50[(2p_1+M)/(p_1+M)].[p_2/(p_2+M)].[M/(p_3+M)],$$

(iv) $$\% CD_4 = 50[(2p_1+M)/(p_1+M)].[p_2/(p_2+M)].[p_3/(p_3+M)].$$

If it is assumed that $\gamma_1 = \gamma_2 = \gamma_3 = Z$, in which Z is the collision frequency per unit concentration for the deactivating reactions, then the natural lifetimes, τ_1, τ_2, τ_3 of the activated species CH_3D^*, $CH_2D_2^*$, CHD_3^*, will be given by $\tau_1 = 1/(p_1Z)$, $\tau_2 = 1/(p_2Z)$,

Can. J. Chem. Downloaded from www.nrcresearchpress.com by 200.7.193.243 on 09/04/12
For personal use only.

$\tau_3 = 1/(p_3 Z)$. Lifetimes calculated in this way will apply, of course, only to decompositions which yield H atoms. The value of Z used, 4.3×10^{-10}, was based on that for a collision between CO_2 and CH_2D_2*, assuming a mean collision diameter of 4.42 Å, estimated from viscosity data. Taking into account reduced masses and mean collision diameters, M is given by the expression $M = (CO_2)+1.25(C_2H_6)+1.20(D_2)$; however, better correlation was obtained when the coefficient of the D_2 concentration was set at 0.6.

Since analytical errors in the determination of small percentages of CH_3D are emphasized when reciprocals are taken, the "best" value of p_1 was obtained by plotting equation (i) for various assumed values of p_1, as shown in Fig. 2. It was estimated that p_1 was approximately 60 mm. Using this value, equation (ii) was plotted for various assumed values of p_2, as shown in Fig. 3; p_2 was estimated to be approximately 85 mm. In a similar way p_3 was estimated to be approximately 50 mm. The uncertainty in p_3 was somewhat greater than that in p_2 and p_1, possibly because the analysis for CD_4 was dependent on that for CHD_3, as mentioned previously. Agreement between theory and

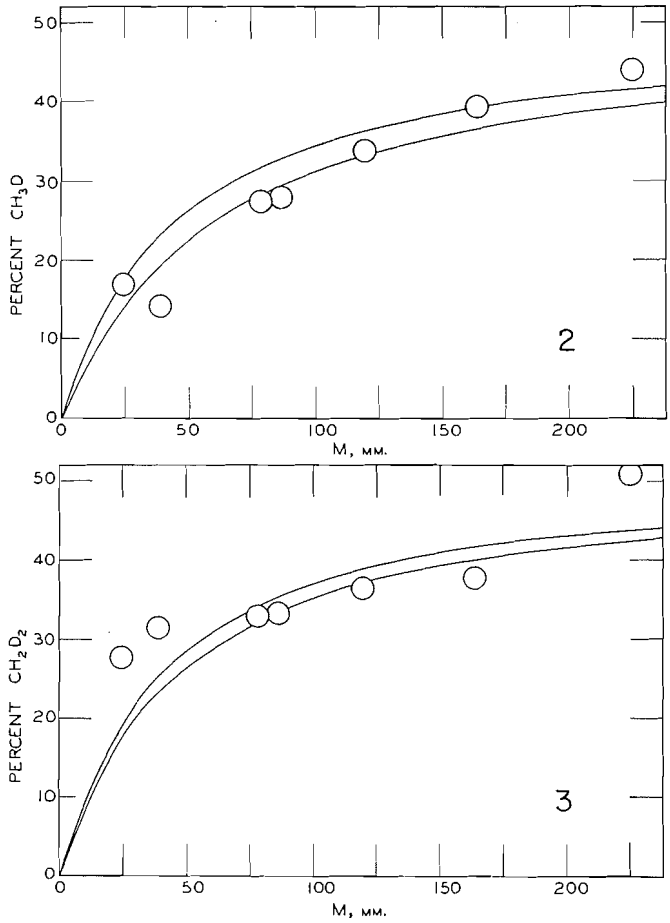

FIG. 2. Effect of third-body concentration on the proportion of CH_3D in the total methanes. Upper curve, equation (i) with $p_1 = 45$ mm.; lower curve, $p_1 = 60$ mm.

FIG. 3. Effect of third-body concentration on the proportion of CH_2D_2 in the total methanes. Upper curve, equation (ii) with $p_1 = 60$ mm., $p_2 = 85$ mm.; lower curve, $p_1 = 60$ mm., $p_2 = 95$ mm.

Can. J. Chem. Downloaded from www.nrcresearchpress.com by 200.7.193.243 on 09/04/12
For personal use only.

experiment was not improved by postulating pressure-independent exchange reactions of the type $D + CH_3 = CH_2D + H$.

In view of the limited accuracy of the determination of the individual deuterated methanes there is no justification for assigning different lifetimes to the three activated molecules. About all that can be said is that the lifetimes are of the order of 10^{-9} sec., corresponding to a p of the order of 70 mm.

It is possible to obtain a simple expression for the percentage of deuterium in the total methanes on the assumption that $p_1 = p_2 = p_3 = p$. For $p = 70$ mm. this expression agrees reasonably well with the experimental results, the average deviation being less than 4%. This would, of course, have been the only criterion of the mechanism if the methane fraction had simply been burned and the deuterium content of the water determined, but it also has some merit in the present instance since values for the individual methanes are, to some extent, interdependent.

In order to further substantiate the mechanism it is necessary to take into account the H atoms liberated in reactions such as [9]. Since no CH_4 was found the H atoms must be consumed in one or more of reactions [1], [4], and [11]:

$$H + D_2 = HD + D \qquad [11]$$

Glasstone, Laidler, and Eyring (8) have calculated that at 300° K., k_{11} will be 1.5/7.3 times the rate constant for the conversion of para to ortho hydrogen. Using the data of Geib and Harteck (8, 9) for the para–ortho conversion, k_{11} would be 2×10^7 cm.^{3} mole^{-1} sec.$^{-1}$; using the expression $10^{13.7}\ e^{-7500/RT}$, as suggested by Trotman-Dickenson (10), k_{11} would be 3.3×10^7. At the same temperature k_1 is 3.7×10^7 (2). Thus k_{11} and k_1 are of similar magnitude. Furthermore, the concentration of D_2 was from 4 to 10 times that of C_2H_6. An additional factor accounting for the absence of CH_4 is the fact that one quarter of the total atom consumption is due to reaction [1], in which the substitution of an H for a D atom would not affect the relative amounts of the deuterated methanes.

The consumption of H atoms by [4] would result in less-extensive deuterization than predicted by the mechanism. The magnitude of the decrease depends on the ratio $k_4(H)/k_{4'}(D)$ and would be more important at low values of M. By assuming a reasonable magnitude for this ratio it was concluded that the true lifetime would probably be greater than 0.5×10^{-9} sec. It is unfortunate that the experimental accuracy did not permit the use of such criteria as plotting $(CHD_3)/(CD_4)$ vs. M.

Lavrovskaia, Mardaleishvili, and Voevodskii (11, 12) have suggested a mechanism for the exchange of radicals which, in the case of CH_3, would correspond to the reaction

$$CH_3 + D_2 = CH_3D + HD \qquad [12]$$

While their results are not directly comparable to ours because they did not investigate the deuterium content of their methane, their conclusion that deuterium atoms play no role in radical exchange must be taken with reservation in view of the dependence of deuterization on third-body concentration, clearly demonstrated in the present work.

The argument that reactions such as [8], [9], and [10] cannot account, in many cases, for the amount of deuterium found in the products hinges on the relative rates of [11] and of the primary reaction of the D atoms (reaction [1] in the present instance). If the former is greater than the latter there is no difficulty in accounting for the extent of deuterization; if the rates are comparable then the extent of deuterization could increase with D_2, as found by Lavrovskaia, Mardaleishvili, and Voevodskii, even if reactions analogous to [12] did not occur.

Can. J. Chem. Downloaded from www.nrcresearchpress.com by 200.7.193.243 on 09/04/12
For personal use only.

It is of interest to compare the present results with the possible lifetime of $C_2H_5D^*$, formed in the reaction

$$D + C_2H_5 = C_2H_5D^*. \qquad [13]$$

This reaction undoubtedly precedes [4′], but the lifetime of the excited molecule must be much less than 10^{-9} sec., as shown by the following considerations.

From quenching data for D_2 (13) and CO_2 (14) the observed rates of formation of methane were corrected for quenching by CO_2. The corrected rates showed no dependence on M and hence the formation of deuterized ethane must be attributed to reactions which are independent of pressure in the range used, presumably to the combination of methyl radicals. The lifetime of $C_2H_5D^*$ formed in [13] would be expected to be much less than that of the excited methanes, in spite of the increased number of degrees of freedom, since its energy content would be about 14 kcal. per mole greater than that required for breaking the C—C bond.

The authors wish to express their thanks to the National Research Council for supporting this research.

REFERENCES

1. STEACIE, E. W. R. Atomic and free radical reactions. Reinhold Publishing Corp., New York. 1954.
2. BERLIE, M. R. and LE ROY, D. J. Discussions Faraday Soc. **14**, 50 (1953).
3. KIRSHENBAUM, I. Physical properties and analysis of heavy water. McGraw-Hill Book Company, Inc., New York. 1951.
4. LE ROY, D. J. Can. J. Research, B, **28**, 492 (1950).
5. SEFTON, V. B. and LE ROY, D. J. Can. J. Chem. **34**, 41 (1956).
6. WHITTLE, E. and STEACIE, E. W. R. J. Chem. Phys. **21**, 993 (1953).
7. TROTMAN-DICKENSON, A. F., BIRCHARD, J. R., and STEACIE, E. W. R. J. Chem. Phys. **19**, 163 (1951).
8. GLASSTONE, S., LAIDLER, K. J., and EYRING, H. The theory of rate processes. McGraw-Hill Book Company, Inc., New York. 1941.
9. GEIB, K. H. and HARTECK, P. Z. physik. Chem. (Bodenstein Festband), 849 (1931).
10. TROTMAN-DICKENSON, A. F. Gas kinetics. Butterworth Scientific Publications, London. 1955.
11. VOEVODSKII, V. V., LAVROVSKAIA, G. K., and MARDALEISHVILI, P. E. Doklady Akad. Nauk S.S.S.R., **81**, 215 (1951) (TT-358).
12. LAVROVSKAIA, G. K., MARDALEISHVILI, R. E., and VOEVODSKII, V. V. Voprosy Khimicheskoi Kinetiki, Kataliza i Reakstsionnoi Sposobnosti. Akad. Nauk S.S.S.R., Otdel. Khim. Nauk, 40 (1955) (TT-701).
13. EVANS, M. G. J. Chem. Phys. **2**, 445 (1934).
14. MITCHELL, A. C. G. and ZEMANSKY, M. W. Resonance radiation and excited atoms. Cambridge University Press, London. 1934.

Can. J. Chem. Downloaded from www.nrcresearchpress.com by 200.7.193.243 on 09/04/12
For personal use only.

Can. J. Chem. Downloaded from www.nrcresearchpress.com by 200.7.193.243 on 09/04/12
For personal use only.

THE MASS SPECTRA OF THREE DEUTERATED BUTANOLS[1]

W. H. McFadden, M. Lounsbury, and A. L. Wahrhaftig[2]

ABSTRACT

The mass spectra of 1,1-dideutero-1-butanol, 1,1,1,3,3-pentadeutero-2-butanol, and 1,1,1,2,3,3-hexadeutero-2-butanol have been obtained using 70-volt ionizing electrons. Comparison of the cracking patterns of the deuterated butanols with those of the undeuterated compounds confirms certain known features of the mass spectra of alcohols and reveals further information regarding the formation of several rearrangement ions. The strong tendency for alcohols to break at bonds beta to the hydroxyl group has been attributed to charge localization on the oxygen and this feature is used to explain the formation of many of the rearrangement ions. It is postulated that a hydrogen atom may be transferred to the electron-deficient oxygen and that the resulting structure distributes its excess energy and charge to give the activated complexes leading to the observed ions.

INTRODUCTION

The mass spectra of some deuterated ethanols (1), propanols (2, 3, 4), and butanols (5, 6) have been previously reported. In addition to being a valuable aid in kinetic studies the cracking patterns have given considerable information about the behavior of alcohols under electron bombardment. In the mass spectra of the four isomeric butanols rearrangement* ions occur at mass/charge ratio† $m/e = 33$ ($CH_3OH_2^+$) for *n*-butanol and isobutanol and at $m/e = 31$ (CH_2OH^+) for *sec*-butanol and *tert*-butanol (7). With the exception of a small amount of a mass 33 ion formed from *n*-propanol these ions are not observed in the mass spectra of other alcohols. However, many higher alcohols produce ions by loss of uncharged groups having mass 31 or 33, a notable example being formation of the abundant ion with mass 55 from 3-methyl-1-butanol. Inspection of the mass spectra of the alcohols reported by the American Petroleum Institute (7) suggests that these ions may be formed as primary daughter ions. In addition, many ions are apparently formed by loss of similar rearrangement groups such as H_3O, H_2O, CH_3OH, CH_3CH_2OH. It is clear that an activated complex in which a highly stable molecule such as H_2O or CH_3OH is partially formed will be energetically favored. It is also likely that there is some stabilization obtained by the partial formation of such radicals as OH_2 and CH_3OH_2.

From previous research (8), we had available three deuterated butanols: 1,1-dideutero-1-butanol, 1,1,1,3,3-pentadeutero-2-butanol, and 1,1,1,2,3,3-hexadeutero-2-butanol (hereafter referred to as *n*-butanol-d_2, *sec*-butanol-d_5, and *sec*-butanol-d_6 respectively). In order to investigate the formation and significance of the rearrangement ions the mass spectra of the three deuterated butanols have been obtained, along with those of the undeuterated compounds.

EXPERIMENTAL

Preparation of the three deuterated butanols has been described elsewhere (8). Originally they were collected as small "center-cut" samples from a distillation column operating with approximately eight theoretical plates. They were stored two years at Dry-Ice

[1]*Manuscript received March 4, 1958.*
Contribution from Chemistry and Metallurgy Division, Atomic Energy of Canada Limited, Chalk River, Ontario, Canada, and the Department of Chemistry, University of Utah, Salt Lake City, Utah. Presented in part at the 40th Annual Conference, Chemical Institute of Canada, Vancouver, British Columbia, June 3–5, 1957.
Issued as A.E.C.L. No. 582.
[2]*Department of Chemistry, University of Utah, Salt Lake City, Utah.*
"Rearrangement ions" refers to ions formed from an activated complex in which the molecular configuration differs from that of the original molecule owing to intramolecular transfer of atoms or groups of atoms.
†*Since this paper makes no reference to doubly charged ions the word "mass" is frequently substituted for the expression "m/e".*

temperature and about six months at room temperature. Before introduction into the mass spectrometer they were further purified by processing through a gas–liquid chromatographic column to remove traces of water and other impurities.

The mass spectra were obtained using a 90°-deflection, 6-in.-radius mass spectrometer similar to one described previously (9). The alcohols were allowed to diffuse into the ion source through a capillary leak under their own vapor pressure. The electron-accelerating potential was 70 volts and the electron current to the ionization chamber was 40 μa. The positive ions were accelerated into the analyzer tube by a potential of 2000 volts and the mass spectrum was scanned magnetically. The ion current arriving at the collector was amplified and recorded with a Speedomax Pen Recorder, Type G.

RESULTS

The mass spectra of *n*-butanol-d_0, *n*-butanol-d_2, *sec*-butanol-d_0, *sec*-butanol-d_5, and *sec*-butanol-d_6 are presented in Table I. The ion abundances, in terms of mole per cent (i.e. total ion current normalized to 100%), are the averages of two runs appropriately corrected for background contributions. The normal residual corrections were insignificant except at $m/e = 28$ where residual nitrogen contributed from 5 to 10% of that peak. However, when a sample was admitted to the mass spectrometer considerable enhancement of background was observed, which was shown to be due to the previous alcohol sample. This memory effect was reduced by mass analyzing the samples several weeks apart and by baking and flushing the mass spectrometer tube during the intervening period. Where necessary, corrections were made for the previous sample by measuring the height of a suitable ion-current peak and calculating the contribution of the contaminant to the rest of the spectrum. The maximum possible error introduced by this procedure was too small to affect the conclusions reported.

The mass spectra have not been corrected for carbon or oxygen isotopic contributions nor has any assay been made to determine the hydrogen–deuterium isotopic purity of the samples. From previous work (8) it is believed that the isotopic purity is better than 97%, and inspection of the mass spectra presented in Table I appears to confirm this. For example, the abundance ratio of the ions at $m/e = 48$ and 47 obtained from *sec*-butanol-d_5 shows the maximum possible isotopic impurity to be 3% on carbon 1. This value for the isotopic impurity would be reduced by any contribution of the ions CD_3COH^+ or CD_3CHO^+ at $m/e = 47$.

DISCUSSION

A. General

Many outstanding features of the mass spectra of alcohols have led to the conclusion that dissociation of the parent molecule–ion occurs with the ion in an electronic state in which the electron removed from the molecule is one of the non-bonding electrons of the oxygen atom. This generalization was first suggested by Cummings and Bleakney as a result of appearance-potential studies for the ions from methanol and ethanol (10). The apparent localization of charge on the oxygen causes the oxygen to behave as a trivalent atom, and as a consequence it attempts to form a bond with atoms that approach within bond-length distances. Thus, it attempts to form an additional bond with the carbon to which it is already attached and as a result the other three bonds of that carbon are weakened. Breaking of any one of these bonds, with or without transfer of the charge to the hydrocarbon fragment, gives rise to the principal ions formed by simple bond rupture. In addition to this, the trivalent oxygen also attempts to form bonds with atoms or

Can. J. Chem. Downloaded from www.nrcresearchpress.com by 200.7.193.243 on 09/04/12
For personal use only.

TABLE I

MASS SPECTRA OF DEUTERATED BUTANOLS

	n-Butanol, mole %		*sec*-Butanol, mole %		
m/e	d_0	d_2	d_0	d_5	d_6
14	0.21	0.17	0.24	0.12	0.11
15	0.88	0.51	1.07	0.36	0.29
16	0.27	0.42	0.19	0.51	0.41
17	1.15	0.79	0.08	0.96	0.55
18	4.90	3.03	0.34	2.77	1.11
19	0.58	0.23	1.57	0.17	0.22
20		0.27		0.70	0.11
21				0.64	1.14
22				0.06	0.26
27	7.41	6.02	5.03	1.34	0.98
28	6.67	6.85	4.67	4.63	4.50
29	4.45	3.68	4.61	3.80	2.30
30	0.44	2.83	0.24	2.58	4.91
31	14.9	1.25	7.72	3.65	2.60
32	0.28	1.56	0.11	4.45	4.39
33	1.27	13.8		2.06	4.14
34		0.36		0.18	0.56
35		1.32			
39	2.68	2.00	2.02	0.45	0.23
40	0.74	1.11	0.36	0.68	0.53
41	11.1	7.06	6.66	1.64	0.98
42	5.34	8.02	0.98	1.65	1.12
43	10.3	11.8	4.30	3.86	1.59
44	0.95	1.32	3.23	2.03	3.49
45	2.23	1.04	38.6	3.17	2.91
46	0.12	0.23	0.92	4.97	3.72
47		0.76		1.06	2.46
48				36.5	1.68
49				1.25	37.6
50					2.05
55	2.43	0.35	1.48	0.30	0.17
56	15.2	1.14	1.32	0.62	0.22
57	1.40	1.88	2.05	0.58	0.36
58	0.04	15.9	0.26	0.66	0.17
59	0.26	1.10	7.64	1.06	0.79
60		0.06	0.27	0.97	0.59
61		0.06		6.30	0.86
62				1.10	6.72
63				0.12	1.31
64				0.11	0.11
65					0.10
72	0.09	0.03	0.12		
73	0.30	0.10	0.67		
74	0.13(P)*	0.14	0.10(P)		
75		0.03			
76		0.11(P)			
77				0.08	0.06
78				0.51	0.27
79				0.10(P)	0.04
80					0.06(P)

*(P) = *parent ion.*

groups that come in its vicinity as a result of vibrations and internal rotations. The complexes thus formed can give rise to the various rearrangement ions observed in the mass spectra of alcohols.

These suggestions are consistent with the theory of mass spectra of polyatomic molecules presented by Rosenstock and co-workers (11, 12, 13). According to this theory, the

Can. J. Chem. Downloaded from www.nrcresearchpress.com by 200.7.193.243 on 09/04/12
For personal use only.

Can. J. Chem. Downloaded from www.nrcresearchpress.com by 200.7.193.243 on 09/04/12
For personal use only.

excited parent ion distributes its excess energy among its various degrees of freedom until a particular configuration, the activated complex, is formed. This complex then dissociates, forming a daughter ion. The redistribution of excess energy can lead to a number of different activated complexes and in addition the daughter ions can decompose to give secondary ion products. The mass spectrum is thus the result of several competing unimolecular reactions. Studies of mass spectra of polyatomic molecules show that the charge is selectively localized at various sites but it is not always possible to determine a priori where the most probable location may be. The determining factor is most generally the relative magnitudes of the ionization potentials of the two fragments but experimental data to illustrate this point for alcohols are scarce. Calculations of the mass spectra have been made using the theory of Rosenstock *et al.* for methyl, ethyl, isopropyl, and *n*-propyl alcohols (14, 15). For these calculations, charge localization on the oxygen was assumed for determinations of the principal reactions and the calculated results are in agreement with the experimental observations.

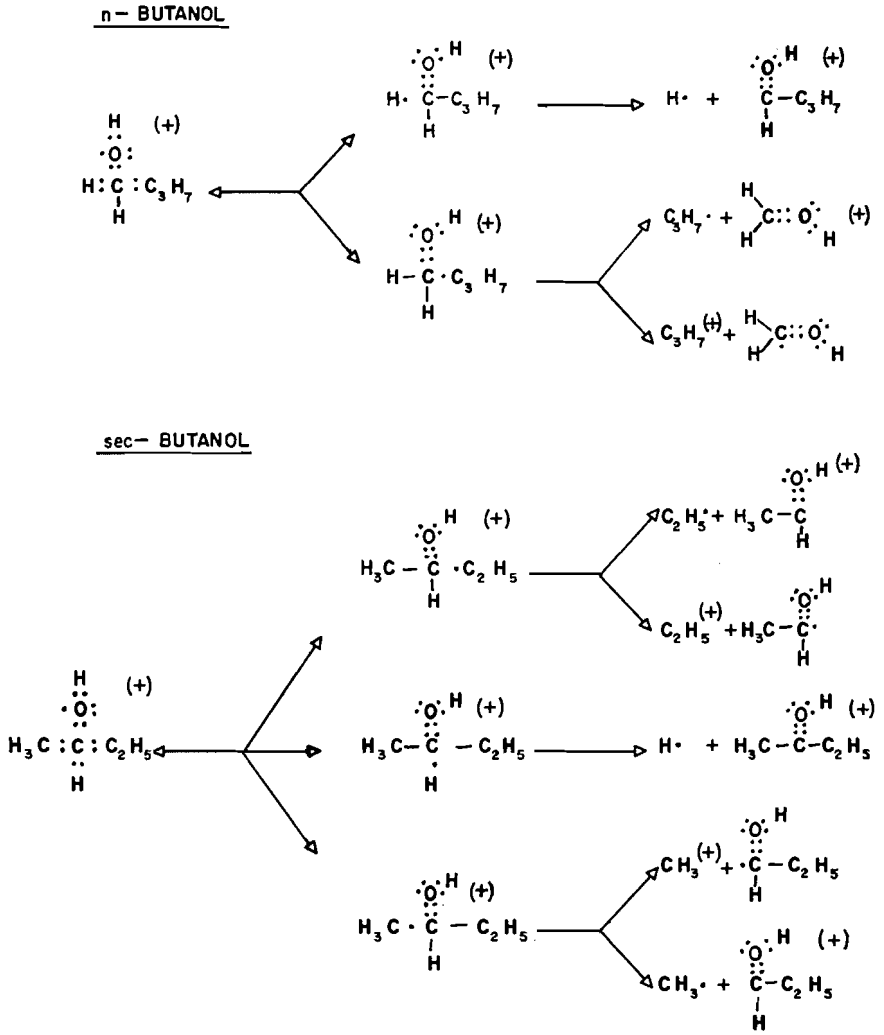

FIG. 1. Principal reactions leading to a simple bond break in *n*-butanol and *sec*-butanol.

Can. J. Chem. Downloaded from www.nrcresearchpress.com by 200.7.193.243 on 09/04/12
For personal use only.

B. Ions Formed by Simple Bond Rupture

The principal contribution of ions formed by a simple bond break to the mass spectra of alcohols arises from the rupture of bonds beta to the hydroxyl (i.e. the other bonds of the carbon to which the hydroxyl is attached). In Fig. 1 the ions formed by a simple bond break are shown for *n*-butanol and *sec*-butanol. An attempt has been made to show the important influence of charge localization by using the electron dot representation where appropriate. In Table II the data from which these reactions are deduced are shown. These data and previous experimental evidence (1, 2, 3, 4, 5, 6) indicate that this influence is not extended appreciably beyond bonds beta to the hydroxyl. During the period between ionization and decomposition the parent ion may resonate between the various structures illustrated and eventually dissociate to give the ions observed.

(*i*) *n-Butanol*

In the parent region the most abundant ion is that due to the loss of hydrogen. In Table II the mass spectrum of *n*-butanol-d_2 shows that this hydrogen is lost primarily from the carbon containing the hydroxyl for, when this carbon is deuterated, the largest ion in the parent region becomes the parent minus 2 mass units. This observation has

TABLE II

ABUNDANCES OF IONS FORMED BY A SIMPLE BOND BREAK

Ion	*n*-Butanol, mole %		*sec*-Butanol, mole %		
	d_0	d_2	d_0	d_5	d_6
Parent	0.13	0.11	0.10	0.10	0.06
P−1 (H)*	0.30	0.03	0.67	0.51	0.04
P−2 (D, H_2)	0.09	0.14	0.12	0.08	0.27
P−15 (CH_3)	0.26	0.06	7.64	0.11	0.10
P−18 (CD_3)	—	—	—	6.30	6.72
P−29 (CH_2CH_3)	2.23	0.76	38.6	—	—
P−31 (CD_2CH_3)	—	—	—	36.5	37.6
P−31 (CH_2OH)	10.3	—	—	—	—
P−33 (CD_2OH)	—	11.8	—	—	—
P−43 (C_3H_7)	14.9	13.8	—	—	—

**P refers to parent ion; P−1 refers to the parent ion minus 1 atomic mass unit (H), etc.*

been previously noted for deuterated ethanols (1) and isopropanols (2, 3, 4). Loss of $CH_3\cdot$ from *n*-butanol-d_0 can occur by a simple bond break only from a delta bond and significantly it is found that it contributes only 0.26% of the total ionization. Loss of $CH_3CH_2\cdot$ from *n*-butanol-d_0 can occur by a simple bond break of a gamma bond and contributes only 2.2% of the total. From *n*-butanol-d_2 loss of $CH_3\cdot$ or of $CH_3CH_2\cdot$ is considerably smaller (0.06% and 0.76% respectively), which may indicate that these processes occur only partly by simple rupture of gamma or delta bonds. On the other hand loss of a propyl radical to form the ion CH_2OH^+ or loss of $\cdot CH_2OH$ to form a propyl ion both contribute a considerable fraction of the total ionization of *n*-butanol and the data obtained from the mass spectrum of *n*-butanol-d_2 confirm the expectation that these ions are formed by a simple beta bond break.

(*ii*) *sec-Butanol*

The most abundant ion in the parent region is that due to loss of hydrogen, as was also noted for *n*-butanol. Again the data of Table II demonstrate that this hydrogen is

primarily from the carbon containing the hydroxyl. Loss of $CH_3\cdot$ from *sec*-butanol contributes 7.6% of the total ionization and could occur by breaking a carbon–carbon bond beta or gamma to the hydroxyl. In the d_5 and d_6 *sec*-butanols the beta methyl group is deuterated and the mass spectra show conclusively that the methyl group lost is almost entirely from the beta position. Loss of $CH_3CH_2\cdot$ may also occur as a result of a simple bond break beta to the hydroxyl and contributes 38% of the total ionization. The data of Table II indicate this to be the principal reaction with no significant indication of intramolecular rearrangements.

C. Ions Formed by Intramolecular Rearrangement

In addition to the tendency to break bonds beta to the hydroxyl, the mass spectra of alcohols show a number of important ions which are formed by intramolecular rearrangement. The existence of ions such as $CH_3OH_2^+$ from *n*-butanol indicates the possibility of an activated complex in which the rearranged group has been partly or wholly formed. It is further suggested that for certain reactions such an activated complex may lose the rearranged group as a neutral fragment by transfer of the charge to the hydrocarbon matrix. It is obvious that loss of the groups H_3O, CH_3OH_2, etc. might occur in two steps (e.g. loss of CH_3OH_2 could be the result of loss of $\cdot CH_2OH$ followed by loss of H_2) but in a homologous series no general relationship is observed between the relative abundance of the ion due to loss of $\cdot CH_2OH$ and that due to loss of CH_3OH_2. If the latter occurred principally as a two-step process one would expect the ratio (parent $-$ CH_3OH_2)/(parent $-$ $\cdot CH_2OH$) to be approximately constant. In actuality this ratio varies randomly over a range of 0.25 to 20 for the 11 alcohols cited in Table III. Alternatively it might be suggested that, since loss of H_2O gives the most abundant ion (15.2%) in the mass spectra of *n*-butanol, formation of the ion $C_3H_5^+$ could be due to loss of H_2O followed by loss of $\cdot CH_3$. However, loss of H_2O leads to the ion $C_4H_8^+$ and the most reasonable secondary step is then $C_4H_8^+ \rightarrow C_2H_4^+ + C_2H_4$. The other possibility, loss of $CH_3\cdot$ followed by loss of H_2O, seems unreasonable since the ion formed by loss of $CH_3\cdot$ at $m/e = 59$ requires breaking of a delta bond and is only 0.26% abundant.

It may reasonably be concluded that in some of the cases the CH_3OH_2 fragment is lost as a unit even though it is inherently unstable as a separate molecule. This postulate

TABLE III

RELATIVE ABUNDANCES[a] OF IONS FORMED BY LOSS OF CH_3O, CH_4O, AND CH_5O FOR BUTANOLS AND PENTANOLS

Alcohol	Minus CH_3O	Minus CH_4O	Minus CH_5O	Minus CH_5O / Minus CH_3O
1-Pentanol[b]	21.5	13.9	59.4	2.8
2-Pentanol[b]	0.81	0.72	16.0	20
3-Pentanol[b]	5.30	.43	3.00	0.57
2-Me-1-butanol[c]	*100.0*	88.2	24.5	0.25
3-Me-1-butanol[c]	30.7	12.8	*100.0*	3.3
2-Me-2-butanol[b]	1.98	1.67	32.6	16
3-Me-2-butanol[b]	1.06	0.49	9.49	9.0
2-Me-1-propanol[b]	*100.0*	57.5	57.2	0.57
2-Me-2-propanol[d]	12.1	2.7	18.3	1.5
1-Butanol[b]	60.3	31.4	61.7	1.0
2-Butanol[b]	10.5	1.77	10.8	1.0

[a] *Normalized to the most abundant ion equal to 100.*
[b] *Stanolind Oil and Gas Co., Tulsa, Oklahoma. See Ref. 7.*
[c] *University of California, Berkeley, California. See Ref. 7.*
[d] *Union Oil Co., Wilmington, California. See Ref 7.*

Can. J. Chem. Downloaded from www.nrcresearchpress.com by 200.7.193.243 on 09/04/12
For personal use only.

implies that both the rearrangement ion and the ion formed by loss of the rearranged group may result from the same activated complex. The appearance of the positive charge on either will be a statistical result of resonance between the various electronic configurations, and the ratio of the ion abundance of each species should be a function of the ionization potential of each fragment.

(*i*) *n-Butanol*

In order to explain the existence of the observed rearrangement ions it is suggested that an intramolecular rearrangement occurs whereby a hydrogen atom is transferred to the electron-deficient oxygen in the following fashion:

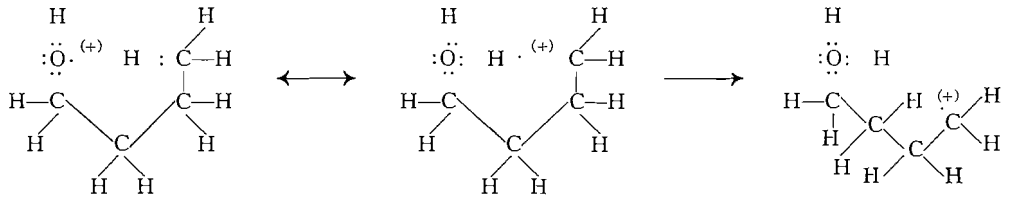

I II III

As a result of internal rotations and vibrations carbon-bonded hydrogen atoms will approach within bonding range of the oxygen and during this brief encounter establish equilibrium between structures I and II. As the molecule continues its internal motion the hydrogen may be transferred to the oxygen as shown. The resulting complex, III, would continue to distribute its excess energy and charge among the various degrees of freedom until a configuration was obtained which would lead to decomposition.

To demonstrate how a complex of this type can explain the formation of many of the rearrangement ions, specific examples are chosen for *n*-butanol. It is clear that the complex III could undergo a simple bond break to form the predominant ion $C_4H_8^+$ or the less predominant* H_2O^+. Comparison of the mass spectra of *n*-butanol-d_0 and *n*-butanol-d_2 (Table I) reveals that in the formation of H_2O^+ the hydrogen on carbon 1 is not involved to any significant extent ($<7\%$). A similar comparison for the ion formed by loss of H_2O ($C_4H_8^+$) leads to the same conclusion, i.e. that the hydrogen lost with the hydroxyl does not come from carbon 1. The mass spectrum of 1-deutero-1-butanol tabulated by Eliel and Prosser (6) confirms this conclusion and in addition the mass spectrum of their compound, 2-deutero-1-butanol, indicates that the hydrogen on carbon 2 is also not involved. These observations agree with the fact that for the rearrangements proposed, transfer of the hydrogens from carbon 3 or 4 is sterically more favorable. An alternative suggestion (16) is that the hydrogen on carbon 2 is lost after the hydroxyl, thus forming the stable ethylenic structure, but the data of Eliel and Prosser eliminate this possibility so far as *n*-butanol is concerned.

The ion $CH_3OH_2^+$, which is observed for very few alcohols and is significant only for *n*-butanol and isobutanol, could be formed from complex III by transfer of the H_2O group to the terminal methyl or alternatively by transferring another hydrogen to carbon 1. In the mass spectrum of *n*-butanol-d_2 there is an rearrangement ion of 1.32% abundance at mass 35 ($CHD_2OH_2^+$). This value is in agreement with the value of 1.27% contributed by the corresponding rearrangement ion ($CH_3OH_2^+$) formed from *n*-butanol-d_0. Since

**Although care was taken to remove H_2O from the samples it is not known whether H_2O has contributed significantly to the ions at m/e = 18 in Table I. For example, the 2.4% increase observed at this mass from sec-butanol-d_6 is probably about 40% from CD_3 and 60% from an H_2O impurity.*

Can. J. Chem. Downloaded from www.nrcresearchpress.com by 200.7.193.243 on 09/04/12
For personal use only.

the position of the deuteriums has been retained in this ion it indicates that transfer of an additional hydrogen is the predominant mechanism. The data of Eliel and Prosser for 2-deutero-1-butanol indicate furthermore that approximately one-half of the time the extra hydrogen comes from the adjacent carbon, carbon 2. It is interesting to note that although the pentanols do not form the ion $CH_3OH_2^+$ to any significant extent, several show abundant ions due to loss of 33 mass units, and in the mass spectrum of 3-methyl-1-butanol (which is structurally similar to *n*-butanol) this ion is the largest peak. An important test of the mechanisms postulated here would be a study of deuterated forms of some of these pentanols.

Formation of the ion H_3O^+ could readily occur by transfer of a second hydrogen to the H_2O group on complex III. The data indicate that this hydrogen apparently comes from the adjacent carbon (carbon 1) about one-half of the time and a similar conclusion is reached regarding loss of H_3O to form the $C_4H_7^+$ ion. In the latter case there is at present no conclusive evidence to eliminate the possibility of two consecutive reactions contributing to this ion (e.g. loss of OH followed by loss H_2), but from the arguments presented earlier these would appear to be relatively unimportant.

(ii) sec-Butanol

The mass spectrum of *sec*-butanol contains a number of rearrangement ions similar to those observed from *n*-butanol but the data obtained from the deuterated analogues do not clearly indicate simple reaction mechanisms. Secondary butanol-d_0 produces the rearrangement ion CH_2OH^+ (7.7% abundance) at mass 31. Because of the possible contribution of the deuterated ethyl ions, $CD_2CH_3^+$ and $CH_2CD_3^+$, to the peaks observed at masses 31 and 32 the reaction mechanisms are not apparent but the data indicate that several patterns may be possible. For example, the appearance of the ion CD_2OH^+ (m/e = 33) in the mass spectrum of *sec*-butanol-d_5 indicates that approximately 25% of the time the hydrogen on the carbon containing the hydroxyl (carbon 2) is not involved. (The contributions of CDH_2OH^+ and $CDHOD^+$ to the mass 33 ion are relatively small.) In addition the peak observed at mass 32 from *sec*-butanol-d_6 could not be entirely due to the deuterated ethyl ion $CD_3CH_2^+$ and it is estimated that at least one-half of the observed abundance (4.4%) would be due to the ion $CDHOH^+$. This indicates that a significant number of events involve one of the hydrogens on carbon 4. The most plausible explanation of these observations seems to be that the ion CH_2OH^+ (or its deuterated analogues) arises from the daughter ions CH_3CHOH^+ (38%) and $CH_3CH_2CHOH^+$ (7.6%), which may be in equilibrium with their various structures

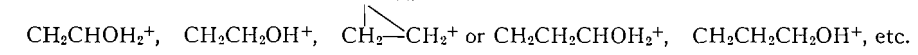

Such rearrangement ions could decompose to produce the various deuterated ions of CH_2OH^+ observed from *sec*-butanol-d_5 and *sec*-butanol-d_6. It is noteworthy that the equilibrium structures suggested might undergo a sufficient number of exchanges to give an ion with a deuterated hydroxyl. The ion abundance observed at mass 34 for both deuterated *sec*-butanols is too large to be explained as due to the C^{13} isotopic species or to a deuterated CH_3OH^+ analogue. In accordance with the foregoing postulates one may conclude that it is CD_2OD^+.

The formation of ions by loss of rearrangement groups such as CH_3OH_2, CH_2OH, cannot be deduced with any certainty because of the large expected contribution of secondary products from the abundant daughter ion CH_3CHOH^+. As indicated in Table I, the six ions with masses between 39 and 44 contribute 18% of the total ionization in the

Can. J. Chem. Downloaded from www.nrcresearchpress.com by 200.7.193.243 on 09/04/12
For personal use only.

mass spectra of *sec*-butanol-d_0. In the mass spectra of the deuterated *sec*-butanols this 18% ionization is divided quite evenly between nine ions so that one cannot reasonably determine probable reaction paths.

Ions formed by the possible loss of H_2O cannot be readily studied from the mass spectra of the two deuterated *sec*-butanols because of the excessive contribution due to the ion formed by loss of CD_3. The mechanism of the loss of H_3O to form $C_4H_7^+$ (or deuterated analogues) can be partially deduced. The data indicate that for about 60% of the events only the hydrogens from carbon 2 or carbon 4 are involved ($m/e = 59$, *sec*-butanol-d_5) while the ion at mass 60 in the spectrum of *sec*-butanol-d_6 indicates that one hydrogen from carbon 4 is involved in about 40% of the events. The formation of the hydronium ion apparently involves the hydrogens from carbon 4 less than 10% of the time ($m/e = 20$, *sec*-butanol-d_6) whereas the single hydrogen from carbon 2 can be involved about 40% ($m/e = 20$, *sec*-butanol-d_5). The appearance of the fully deuterated hydronium ion at $m/e = 22$ may indicate that H_3O^+ arises primarily from the daughter-ion structures suggested to explain the observations on the deuterated analogues of CH_2OH^+. It would seem that loss of a hydrogen and subsequent gain of three deuteriums by the oxygen would be quite unexpected except in terms of a relatively simple exchange equilibrium.

REFERENCES

1. Burr, J. G. J. Am. Chem. Soc. **79**, 751 (1957).
2. Condon, F. E. J. Am. Chem. Soc. **73**, 4675 (1951).
3. Condon, F. E., McMurray, H. L., and Thornton, V. J. Chem. Phys. **19**, 1010 (1951).
4. Friedman, L. and Turkevich, J. J. Am. Chem. Soc. **74**, 1666 (1952).
5. Eliel, E. L. and Prosser, T. J. Document number 4817, ADI Auxiliary Publications Project, Photoduplication Service, Library of Congress, Washington 25, D.C.
6. Eliel, E. L. and Prosser, T. J. J. Am. Chem. Soc. **78**, 4045 (1956).
7. Catalog of Mass Spectral Data, Am. Petroleum Inst., Research Project 44. Carnegie Institute of Technology, Pittsburgh, Pennsylvania. 1957.
8. McFadden, W. H. and Wahrhaftig, A. L. J. Am. Chem. Soc. **78**, 1572 (1956).
9. Graham, R. L., Harkness, A. L., and Thode, H. G. J. Sci. Instr. **24**, 119 (1947).
10. Cummings, C. S., II and Bleakney, W. Phys. Rev. **58**, 787 (1940).
11. Rosenstock, H. M., Wallenstein, M. B., Wahrhaftig, A. L., and Eyring, H. Proc. Natl. Acad. Sci. U.S. **38**, 667 (1952).
12. Rosenstock, H. M. Absolute rate theory for isolated systems and the mass spectra of polyatomic molecules. Doctoral thesis, University of Utah, Salt Lake City, Utah. 1952.
13. Wallenstein, M. B. The ionization and dissociation of molecules by electron impact. Doctoral thesis, University of Utah, Salt Lake City, Utah. 1951.
14. Collin, J. Bull. soc. roy. sci. Liège, 520 (1956).
15. Friedman, L., Long, F. A., and Wolfsberg, M. J. Chem. Phys. **27**, 613 (1957).
16. McLafferty, F. W. Private communication.

Can. J. Chem. Downloaded from www.nrcresearchpress.com by 200.7.193.243 on 09/04/12
For personal use only.

Can. J. Chem. Downloaded from www.nrcresearchpress.com by 200.7.193.243 on 09/04/12
For personal use only.

THE CONFIGURATION OF GLYCOSIDIC LINKAGES IN OLIGOSACCHARIDES

VI. DEGRADATION OF 4-*O*-METHYL-D-GLUCOPYRANURONOSYL-ALDOBIURONIC ACIDS TO 2-*O*-(4-*O*-METHYL-D-GLUCOPYRANOSYL)-GYCEROLS[1]

P. A. J. Gorin and A. S. Perlin

ABSTRACT

The configurations of glycosidic linkages in 4-*O*-methyl-D-glucopyranuronosyl-aldobiuronic acids can be determined by conversion to the derived 2-*O*-D-glucopyranosyl-glycerol hexamethyl ether, which is compared, by its infrared spectrum and specific rotation, with the sirupy hexamethyl ethers synthesized from 2-*O*-α- and 2-*O*-β-D-glucopyranosyl-glycerol. Thus, the configuration of 2-*O*-(4-*O*-methyl-D-glucopyranuronosyl)-D-xylose was shown to be α, since it was degraded to 2-*O*-α-D-glucopyranosyl-glycerol hexamethyl ether. The configuration of 4-*O*-(4-*O*-methyl-D-glucopyranuronosyl)-D-galactose was correlated with that of the former aldobiuronic acid, since both gave crystalline 2-*O*-α-(4-*O*-methyl-D-glucopyranosyl)-glycerol penta-*p*-nitrobenzoate.

INTRODUCTION

Parts II and IV of this series (1, 2) describe a method for determining the configuration of reducing disaccharides by degradation to one of the two possible anomeric 2-*O*-glycopyranosyl-glycerols. The present paper demonstrates the feasibility of this approach for the 4-*O*-methyl-D-glucopyranuronosyl-aldobiuronic acids, except those linked glycosidically to the primary hydroxyl group of the reducing end-unit. Two readily obtainable aldobiuronic acids, 2-*O*-(4-*O*-methyl-D-glucopyranuronosyl)-D-xylose (I) (3), from the wood of *Populus tacamahacca* Mill. (4), and 4-*O*-(4-*O*-methyl-D-glucopyranuronosyl)-D-galactose (II), from Mesquite gum (5), were examined and each found to contain the α-glycosidic linkage.

Isolated from the wood, 2-*O*-(4-*O*-methyl-D-glucopyranuronosyl)-D-xylose was converted to the D-xylitol derivative (III) by sodium borohydride reduction (6). The xylitol derivative was treated with diazomethane and the methyl ester formed was oxidized with 2.2 moles of lead tetraacetate (1) which preferentially oxidized the xylitol end-group to give 2-*O*-(4-*O*-methyl-D-glucopyranuronosyl)-L-glyceraldehyde methyl ester. Reduction of the glyceraldehyde derivative with sodium borohydride (6, 7) afforded after purification by cellulose column chromatography (8) 2-*O*-(4-*O*-methyl-D-glucopyranosyl)-glycerol (IV) ($[\alpha]_D$ +125°). All of the above-described intermediates were not crystalline. The last-named compound was methylated with sodium hydroxide – methyl sulphate to yield its hexamethyl ether ($[\alpha]_D$ +123°), which gave an infrared absorption spectrum indistinguishable from that of the sirupy hexamethyl ether ($[\alpha]_D$ +132°) prepared from the known 2-*O*-α-D-glucopyranosyl-glycerol (1). By contrast, the fully methylated sirupy derivative of the known anomeric β-glucosyl-glycerol (9, 10) showed $[\alpha]_D$ −5° and gave an infrared absorption spectrum distinctly different from that of the α-derivative. A crystalline derivative suitable for characterization of other α-(4-*O*-methyl-D-glucopyranuronosyl)-aldobiuronic acids was provided by the complete *p*-nitrobenzoylation of 2-*O*-α-(4-*O*-methyl-D-glucopyranosyl)-glycerol. This derivative may be prepared with perhaps as little as 10 mg. of the glycerol derivative and hence is more useful than the methyl ether for characterization of the α-anomer.

[1]*Manuscript received February 14, 1958.*
Contribution from the National Research Council of Canada, Prairie Regional Laboratory, Saskatoon, Saskatchewan.
Issued as N.R.C. No. 4730 and as Paper No. 254 on the Uses of Plant Products.

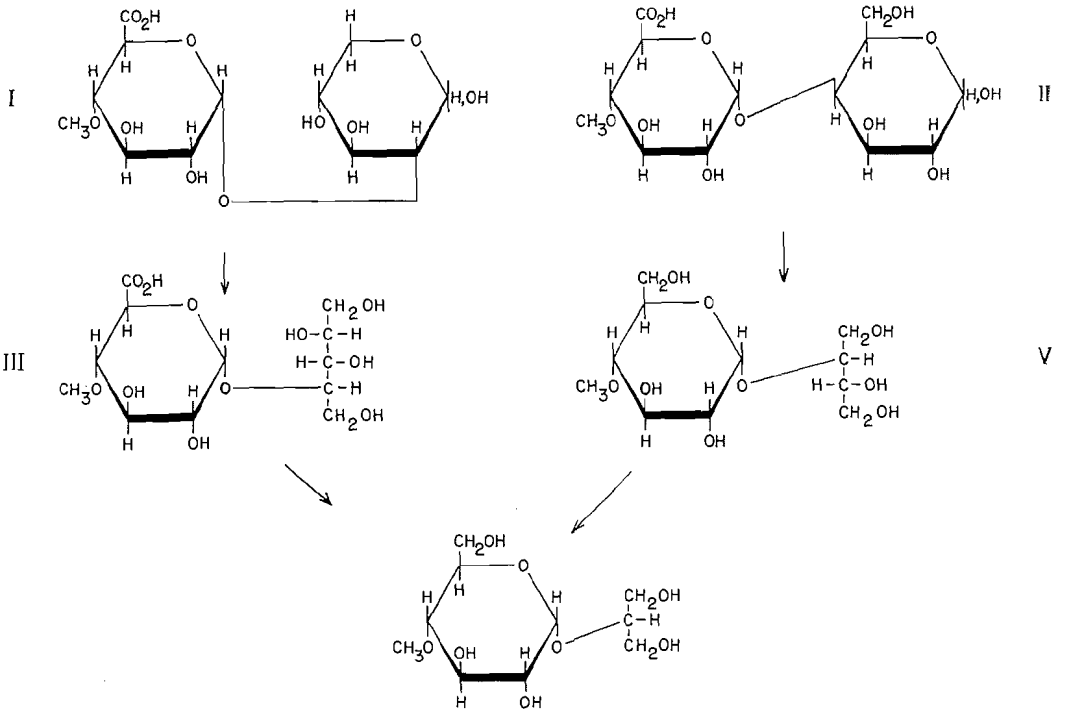

IV

The aldobiuronic acid from Mesquite gum, 4-*O*-(4-*O*-methyl-D-glucopyranuronosyl)-D-galactose, was oxidized with 2 moles of lead tetraacetate. Reduction of the D-threose derivative with sodium borohydride afforded 2-*O*-(4-*O*-methyl-D-glucopyranuronosyl)-D-threitol (V), which was not crystalline. This compound was treated with diazomethane and the methyl ester was reduced with sodium borohydride. The material thus obtained proved to be a mixture containing the required sirupy 2-*O*-(4-*O*-methyl-D-glucopyranosyl)-D-threitol, which was obtained in poor yield after fractionation on a cellulose column. The comparatively low yield is probably due to the slow rate of lead tetraacetate oxidation of 4-substituted aldoses (10). The threitol portion was found to be cleaved preferentially by 1 mole of sodium periodate (11), since formaldehyde was formed in 98% yield. The resulting glyceraldehyde derivative was reduced to 2-*O*-(4-*O*-methyl-D-glucopyranosyl)-glycerol by sodium borohydride. Removal of trace amounts of impurity by fractionation on a cellulose column furnished a material having an $[\alpha]_D$ identical with that of the known α-anomer. Confirmation of the configuration was given by *p*-nitrobenzoylation of the glycerol derivative. The penta-*p*-nitrobenzoate formed was the α-anomer, since it had the same specific rotation, melting point, mixed melting point, and X-ray diffraction pattern as 2-*O*-α-(4-*O*-methyl-D-glucopyranosyl)-glycerol penta-*p*-nitrobenzoate derived from the disaccharide obtained from *P. tacamahacca*.

EXPERIMENTAL

Optical rotations were measured at 27° C. Paper chromatography was carried out on Whatman No. 1 filter paper using *n*-butanol–ethanol–water (40:11:19 v/v) as solvent

Can. J. Chem. Downloaded from www.nrcresearchpress.com by 200.7.193.243 on 09/04/12
For personal use only.

(12) and ammoniacal silver nitrate (13) and *p*-anisidine hydrochloride (14) spray reagents. Solutions were concentrated at 50° C. under reduced pressure. Infrared absorption spectra were prepared by the potassium bromide window technique (15).

*2-O-α- and 2-O-β-*D*-Glucopyranosyl-glycerol Hexamethyl Ethers*

2-*O*-α-D-Glucopyranosyl-glycerol (2.26 g.) was dissolved in water (50 cc.) containing sodium hydroxide (20 g.), and methyl sulphate (18 cc.) was added dropwise to the stirred solution. The mixture was left overnight and the procedure repeated four times. It was then heated to 100° C. for 1 hour to destroy excess reagent, cooled, and brought to neutrality with sulphuric acid. The solution was evaporated to a solid which was extracted with ethanol. The extract was filtered and evaporated to a crust which was dissolved in water and extracted continuously with chloroform. Evaporation of the chloroform after drying with magnesium sulphate yielded a sirup which was extracted with light petroleum (b.p. 50–60° C.) (16). The petrol solution yielded the required hexamethyl ether (1.21 g.) as a sirup which had $[\alpha]_D$ +137° (*c*, 1.2, $CHCl_3$), +132° (*c*, 1.3, 2,4-lutidine), and n_D^9 1.4548. Calculated for $C_9H_{12}O_2(OCH_3)_6$: —OCH_3, 55.0%. Found: —OCH_3, 55.7%.

2-*O*-β-D-Glucopyranosyl-glycerol (145 mg.), using the same procedure, yielded the sirupy hexamethyl ether (60 mg.) which had $[\alpha]_D$ −8° (*c*, 1.2, $CHCl_3$), −5° (*c*, 1.1, 2,4-lutidine), and n_D^9 1.4532. Calculated for $C_9H_{12}O_2(OCH_3)_6$: —OCH_3, 55.0%. Found: —OCH_3, 55.3%.

*2-O-α-*D*-Glucopyranosyl-glycerol Hexamethyl Ether From 2-O-(4-O-Methyl-*D*-glucopyranuronosyl)-*D*-xylose*

The aldobiuronic acid (3.0 g.) was dissolved in water (50 cc.) and neutralized with aqueous sodium hydroxide. Sodium borohydride (1.0 g.) was added and after 2 hours excess reagent was destroyed with acetic acid. Sodium ions were removed with Amberlite IR-120 and the solution was filtered and evaporated to dryness. Boric acid was removed by repeated evaporations with methanol, the residue containing sirupy 2-*O*-α-(4-*O*-methyl-D-glucopyranuronosyl)-D-xylitol which was converted to its methyl ester (2.4 g.) using methanolic diazomethane.

The methyl ester (2.4 g.) obtained on evaporation was oxidized with 2.2 moles of lead tetraacetate for 20 hours in acetic acid (200 cc.) containing water (5 cc.). Most of the lead was removed by addition of 10% oxalic acid in acetic acid (15 cc.). The precipitate was filtered off and the solution evaporated to dryness. The 2-*O*-α-(4-*O*-methyl-D-glucopyranuronosyl)-L-glyceraldehyde methyl ester (contained in the residue) was reduced to 2-*O*-α-(4-*O*-methyl-D-glucopyranosyl)-glycerol with sodium borohydride (1.0 g.) in water (50 cc.). After 18 hours the reaction mixture was worked up by the method described above. The sirupy product (1.79 g.) gave mainly a spot on a paper chromatogram with R_{rhamnose} 0.9 and small amounts of unidentified impurities. The mixture was fractionated on a cellulose column using *n*-butanol as solvent to yield a sirup having $[\alpha]_D$ +125° (*c*, 1.0, water) and which produced 4-*O*-methyl glucose and glycerol, identified chromatographically (17) (*p*-anisidine hydrochloride and ammoniacal silver nitrate sprays), on acid hydrolysis.

Methylation of a portion of the material (403 mg.) by the method described previously gave the hexamethyl ether (221 mg.) which had $[\alpha]_D$ +123° (*c*, 1.0, 2,4-lutidine), n_D^{10} 1.4552, and an infrared absorption spectrum indistinguishable from that of the known α-hexamethyl derivative, thus identifying it as the α-anomer. Calculated for $C_9H_{12}O_2(OCH_3)_6$: —OCH_3, 55.0%. Found: —OCH_3, 55.0%.

Can. J. Chem. Downloaded from www.nrcresearchpress.com by 200.7.193.243 on 09/04/12
For personal use only.

2-O-α(4-O-Methyl-D-glucopyranosyl)-glycerol Penta-p-nitrobenzoate

The glycerol derivative (85 mg.) was heated on a steam bath for 1 hour with *p*-nitrobenzoyl chloride (600 mg.) in pyridine (4 cc.) (18). The reaction mixture was added to excess aqueous sodium bicarbonate and stirring was continued overnight. The product was filtered off and recrystallized twice from ethyl acetate. Yield, 94 mg. The crystals had m.p. 207–209° C. and $[\alpha]_D$ +95° (*c*, 1.0, 2,4-lutidine). Calculated for $C_{45}H_{35}O_{23}N_5$: C, 53.31%; H, 3.48%. Found: C, 53.17%; H, 3.42%.

2-O-α-(4-O-Methyl-D-glucopyranosyl)-glycerol Penta-p-nitrobenzoate from 4-O-(4-O-Methyl-D-glucopyranuronosyl)-D-galactose

Partially degraded Mesquite gum (50 g.) was further hydrolyzed with strong acid by the method of Smith (5), and the aldobiuronic acids obtained by treatment of the mixed barium salts (16 g.) with Amberlite IR-120 were fractionated on a cellulose column using ethyl acetate – acetic acid – water (3:1:1 v/v) as solvent. The required 4-*O*-methyl-glucuronosyl-aldobiuronic acid (2.2 g.) was thus obtained.

The acid (0.88 g.) in methanol (200 cc.) was treated with excess ethereal diazomethane. The solution was evaporated to a sirup which was oxidized for 2½ hours with 2 moles of lead tetraacetate (2.11 g.) in acetic acid (200 cc.) and water (3 cc.). Lead was removed by addition of 10% oxalic acid in acetic acid (4.5 cc.); the solution was filtered and then evaporated to dryness.

Treatment of the methyl ester derivative contained in the residue with sodium borohydride (1.5 g.) in water (100 cc.) for 18 hours afforded the reduced material (0.52 g.) after the solution was worked up in the prescribed way. Two main spots were observed on the paper chromatogram using the silver nitrate spray. They had $R_{\text{galactose}}$ 2.0 and 2.3 respectively, and the mixture was fractionated on a cellulose column using *n*-butanol one-half saturated with water as solvent. The faster material isolated (125 mg.) gave $[\alpha]_D$ +80° (*c*, 2.0, water), and was considered to be the required 2-*O*-α-(4-*O*-methyl-D-glucopyranosyl)-D-threitol. It gave spots corresponding to 4-*O*-methyl glucose and threitol on a paper chromatogram (*p*-anisidine hydrochloride and ammoniacal silver nitrate sprays) on acid hydrolysis, and consumed 1.9 moles of sodium periodate in 20 hours. Also, when oxidized with 1 molar portions of sodium periodate and lead tetraacetate, 0.98 and 0.87 moles of formaldehyde, respectively, were formed, as estimated by the chromotropic acid method (19).

Therefore, the threitol derivative (101 mg.) was oxidized with 1 mole of sodium periodate in water (10 cc.). After 18 hours the solution was treated with Amberlite IR-120, and after removal of the resin, barium carbonate was added to remove iodic and periodic acids. The insoluble material was filtered off, the filtrate evaporated to dryness, and the residue extracted with methanol. The methanolic solution was treated with sodium borohydride (25 mg.) and after it had been left for 3 hours the required 2-*O*-α-(4-*O*-methyl-D-glucopyranosyl)-glycerol was isolated. Yield, 82 mg. Minor impurities were shown to be present on a paper chromatogram and these were removed by fractionating the product on a cellulose column using *n*-butanol as solvent. The pure glycerol derivative (60 mg.) had $[\alpha]_D$ +125° (*c*, 1.0, water).

A portion (45 mg.) was characterized by conversion to its penta-*p*-nitrobenzoate derivative. Yield, 65 mg., m.p. 208–210° C., and $[\alpha]_D$ +94° (*c*, 0.8, 2,4-lutidine) after two recrystallizations from ethyl acetate. It was indistinguishable from the penta-*p*-nitrobenzoate derived from 2-*O*-α-(4-*O*-methyl-D-glucopyranuronosyl)-D-xylose by comparison of X-ray diffraction patterns; no depression of the melting point on mixing was observed. Calculated for $C_{45}H_{35}O_{23}N_5$: C, 53.32%; H, 3.48%. Found: C, 53.28%; H, 3.19%.

Can. J. Chem. Downloaded from www.nrcresearchpress.com by 200.7.193.243 on 09/04/12
For personal use only.

ACKNOWLEDGMENTS

The authors wish to thank Dr. J. R. Nunn for a gift of 4-*O*-α-(4-*O*-methyl-D-glucopyranuronosyl)-D-galactose. Also thanks are due to Mr. J. A. Baignée for microanalytical work, Mr. T. M. Mallard for determination of X-ray diffraction patterns, Mrs. Agnes Birss (Epp) for infrared absorption data, and Mr. J. W. L. C. Christ and Miss Sheila Lubin for technical assistance.

REFERENCES

1. CHARLSON, A. J., GORIN, P. A. J., and PERLIN, A. S. Can. J. Chem. **34**, 1811 (1956).
2. CHARLSON, A. J., GORIN, P. A. J., and PERLIN, A. S. Can. J. Chem. **35**, 365 (1957).
3. JONES, J. K. N. and WISE, L. E. J. Chem. Soc. 3389 (1952).
4. GORIN, P. A. J. Can. J. Chem. **35**, 595 (1957).
5. SMITH, F. J. Chem. Soc. 2646 (1951).
6. WOLFROM, M. L. and WOOD, H. B. J. Am. Chem. Soc. **73**, 2933 (1951).
7. WOLFROM, M. L. and ANNO, K. J. Am Chem. Soc. **74**, 5583 (1952).
8. HOUGH, L., JONES, J. K. N., and WADMAN, W. H. J. Chem. Soc. 2511 (1949).
9. CARTER, N. M. Ber. **63**, 1684 (1930).
10. CHARLSON, A. J. and PERLIN, A. S. Can. J. Chem. **34**, 1200 (1956).
11. CRIEGEE, R. Sitzber. Ges. Beförder. ges. Naturw. Marburg, **69**, 25 (1934); Chem. Abstr. **29**, 6820 (1935).
12. HOUGH, L. Nature, **165**, 400 (1950).
13. PARTRIDGE, S. M. Nature, **158**, 270 (1946).
14. HOUGH, L., JONES, J. K. N., and WADMAN, W. H. J. Chem. Soc. 1702 (1950).
15. SCHIEDT, U. and REINWEIN, H. Z. Naturforsch. **7b**, 270 (1952).
16. BROWN, F. and JONES, J. K. N. J. Chem. Soc. 1344 (1947).
17. PARTRIDGE, S. M. Biochem. J. **42**, 238 (1948).
18. SHRINER, R. L. and FUSON, R. C. The systematic identification of organic compounds. 2nd ed. John Wiley & Sons, Inc., New York. 1940. p. 137.
19. LAMBERT, M. and NEISH, A. C. Can. J. Research, B, **28**, 83 (1950).

Can. J. Chem. Downloaded from www.nrcresearchpress.com by 200.7.193.243 on 09/04/12
For personal use only.

Can. J. Chem. Downloaded from www.nrcresearchpress.com by 200.7.193.243 on 09/04/12
For personal use only.

THE CONDUCTANCES OF AQUEOUS SOLUTIONS OF LITHIUM CHLORATE AT 25.00° C. AND AT 131.8° C.[1]

A. N. Campbell and W. G. Paterson[2]

ABSTRACT

The conductances, densities, and viscosities of aqueous solutions of lithium chlorate have been obtained over the complete range of concentration at 131.8° C. and up to saturation (and somewhat beyond) at 25.00° C. The curve of specific conductance versus concentration passes through a maximum which does not shift noticeably in composition with change in temperature. There are no minima on the curves of equivalent conductance versus concentration. The relative viscosity of the solutions decreases with rise in temperature; this is the reverse of the effect usually observed.

The experimental results have been compared with the calculated results, obtained by the use of the equations of Wishaw and Stokes and of Falkenhagen.

An extensive study of the conductances and viscosities of concentrated aqueous electrolytic solutions has been going on in this laboratory for several years. The salts suitable for this work are such as show a wide concentration range. The salts investigated have been: ammonium nitrate at 25°, 35°, 95°, and 180° C. (1, 2, 3, 4); silver nitrate at 25°, 35°, 95°, and 221.7° C. (1, 2, 3, 4); and lithium nitrate at 25° and 110° C. (5, 6).

The conductances of aqueous solutions of lithium chlorate over a wide range of concentration and at several temperatures are reported in the literature but, for various reasons, the work is either inadequate or erroneous. Kraus and Burgess (7) give data on conductance at a series of temperatures but they were primarily interested in the conductance of lithium chlorate on the addition of small amounts of water and their data are incomplete at 25° C. Accurate measurements have been made by Scatchard (8) and co-workers in the dilute range at 10° C. The investigations of Klotschko and Grigorjew (9) cover a wide range of concentrations at six different temperatures, one of which is 25° C. These authors prefer the specific to the equivalent conductance as a basis of theoretical interpretation. When their results are plotted against concentration, it becomes evident that there is a considerable scattering of points on the graph. Their results are too inaccurate to be of any value; for example, the specific conductance of their weakest solution at 25° C. yields a value of equivalent conductance greatly in excess of the limiting conductance as calculated from the sum of the limiting ionic conductances of lithium and chlorate ions. Further, when their curves of density or viscosity versus concentration are extrapolated to zero concentration, the values for the density or viscosity of pure water so obtained are considerably different from the accepted values.

EXPERIMENTAL PROCEDURE

Lithium chlorate was prepared and dried by the method of Campbell and Griffiths (10). Since lithium chlorate is exceedingly hygroscopic, it is not possible to make up solutions of defined concentration by weighing; all solutions must be analyzed. In view of the difficulties inherent in the direct determination of lithium or chlorate radical, the following simple and satisfactory procedure was adopted for arriving at lithium chlorate content. A weighed sample of solution was treated with excess concentrated sulphuric acid and evaporated to dryness in a Vycor dish; platinum cannot be used. The resulting

[1]*Manuscript received April 1, 1957.*
Contribution from the Chemistry Department of the University of Manitoba, Winnipeg, Manitoba.
[2]*Holder of N.R.C. Bursary, 1956–57.*

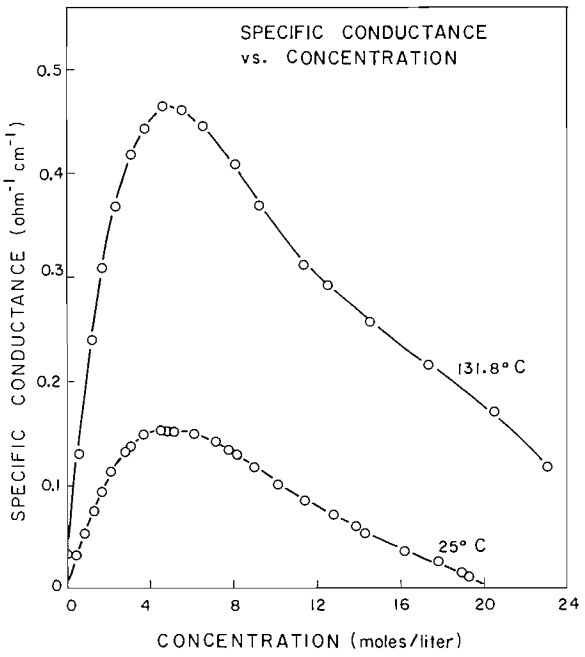

FIG. 1.

lithium sulphate was ignited to constant weight. The procedure was tested on sodium chlorate and it was found that an accuracy of 0.01% was attainable.

The density of each solution of lithium chlorate was determined and thus it was possible to plot a graph of weight per cent versus density of solution. Interpolation from this graph then became the analytical method used for the remainder of the research, with a consequent great saving of time.

Our technique of conductance measurements has been described previously (1, 2, 3, 4). In order, however, to keep down the voltage output of the audio-oscillator and avoid heating of the solution in the conductance cell, a simple triode-type amplifier was introduced in the telephone circuit.

For work at 131.8° C., where the vapor pressure of the solution exceeds 1 atm., the conductance cells were placed in a closed bomb; the technique has been described previously (4). The solvent water was distilled water having a specific conductance of less than 5×10^{-6} mhos and this is more than sufficiently low for work on concentrated solutions ($c > 0.01$ N).

The cell constants were obtained in the usual way. The standard potassium chloride solutions of Jones and Bradshaw (11) refer to 25° C. and it is not immediately obvious that cell constants obtained for 25° C. are good at other temperatures. Washburn (12), however, has shown how to calculate the cell constant at a temperature other than 25° C., from the value at 25° C. For cells constructed of Pyrex and platinum the change in cell constant is very slight. The correction for our cells for the change in temperature from 25° C. to 131.8° C. was about 0.03% and it was always applied.

Solutions were prepared from a concentrated stock solution, of known strength, by dilution with water. The exact concentration was then obtained from the density. Density was usually determined with a Weld pycnometer but for the anhydrous melt at

Can. J. Chem. Downloaded from www.nrcresearchpress.com by 200.7.193.243 on 09/04/12
For personal use only.

TABLE I

CONDUCTANCES (OBSERVED AND CALCULATED), DENSITIES, AND VISCOSITIES OF AQUEOUS SOLUTIONS OF LITHIUM CHLORATE AT 25.00° C.

Weight %	Molarity	Density, g./ml.	Relative viscosity, water = 1.000	Specific conductance, ohm^{-1} $cm.^{-1}$	Equivalent conductance, mhos	Λ_{calc} Wishaw–Stokes å = 5.3 Å	Wishaw–Stokes å = 5.5 Å	Falkenhagen å = 4.3 Å
0.1990	0.02188	0.9982	1.002	0.002044	93.31	93.34	93.41	93.22
0.9036	0.1002	1.0025	1.015	0.008495	84.78	85.09	85.29	84.92
4.519	0.5121	1.0243	1.067	0.03679	71.85	71.86	72.29	72.10
7.402	0.8532	1.0420	1.110	0.05662	66.36	66.17	66.66	66.84
10.60	1.247	1.0631	1.169	0.07677	61.58	60.73	61.26	61.86
13.68	1.640	1.0834	1.229	0.09379	57.19	56.30	56.83	57.81
17.24	2.113	1.1082	1.315	0.1108	52.45	51.34	51.86	53.23
23.01	2.928	1.1505	1.472	0.1337	45.67	44.30	44.77	46.69
24.27	3.115	1.1594	1.508	0.1374	44.11	42.94	43.40	45.42
28.39	3.742	1.1915	1.642	0.1495	39.94	38.56	38.49	41.32
33.38	4.549	1.2320	1.895	0.1546	33.90	32.58	32.97	35.47
35.49	4.908	1.2502	2.019	0.1556	31.69	30.27	30.63	33.18
36.90	5.157	1.2633	2.115	0.1556	30.17	28.69	29.04	31.60
42.58	6.199	1.3160	2.594	0.1511	24.38	22.71	22.97	25.57
47.61	7.185	1.3643	3.140	0.1420	19.76	18.27	18.49	20.99
50.36	7.762	1.3933	3.585	0.1346	17.35	15.78	15.96	18.33
51.68	8.047	1.4074	3.838	0.1312	16.30	14.63	14.80	17.10
55.71	8.947	1.4519	5.170	0.1189	13.29	10.63	10.74	12.65
60.88	10.19	1.5136	6.894	0.1031	10.11	7.723	7.752	9.441
65.82	11.49	1.5776	10.29	0.08639	7.521	5.005	5.043	6.304
70.43	12.80	1.6426	16.37	0.07189	5.618	3.035	3.055	3.953
74.09	13.93	1.7002	24.53	0.06010	4.313	1.964	1.973	2.632
75.06	14.27	1.7187	28.38	0.05644	3.955	1.681	1.690	2.271
80.66	16.15	1.8100	66.26	0.03928	2.432	0.6831	0.6850	0.9695
85.44	17.95	1.8989	166.5	0.02407	1.341	0.2577	0.2571	0.3862
88.17	19.03	1.9510	334.0	0.01644	0.8639	0.1241	0.1234	0.1920
89.03	19.33	1.9627	—	0.01487	0.7695	—	—	—

TABLE II

CONDUCTANCES (OBSERVED AND CALCULATED), DENSITIES, AND VISCOSITIES OF AQUEOUS SOLUTIONS OF LITHIUM CHLORATE AT 131.8° C.

Weight %	Molarity	Density, g./ml.	Relative viscosity, water = 1.000	Specific conductance, ohm^{-1} $cm.^{-1}$	Equivalent conductance, mhos	Λ_{calc} Wishaw–Stokes å = 3.2 Å Λ_0 = 403	Wishaw–Stokes å = 3.6 Å Λ_0 = 399	Falkenhagen å = 2.7 Å Λ_0 = 405
1.087	0.1131	0.9407	1.013	0.03438	304.02	304.62	303.76	304.29
4.987	0.5321	0.9645	1.047	0.1303	244.79	240.22	243.31	238.59
10.57	1.169	0.9994	1.110	0.2381	203.76	198.34	203.75	197.73
15.18	1.729	1.0294	1.165	0.3099	179.28	175.66	181.87	178.04
20.17	2.374	1.0641	1.257	0.3687	155.31	152.78	159.31	154.85
25.18	3.066	1.1006	1.323	0.4184	136.50	137.54	144.29	141.05
30.13	3.794	1.1382	1.408	0.4417	116.42	123.24	129.84	128.03
35.16	4.589	1.1799	1.519	0.4630	100.89	109.27	114.26	115.24
40.77	5.548	1.2302	1.686	0.4607	83.04	93.92	99.72	100.89
46.35	6.572	1.2818	1.903	0.4451	67.72	79.54	84.68	87.20
54.15	8.165	1.3630	2.364	0.4041	49.50	60.09	64.20	68.12
59.49	9.345	1.4201	2.838	0.3703	39.62	47.93	51.33	55.73
67.57	11.40	1.5251	4.263	0.3160	27.73	29.75	31.81	36.18
72.09	12.64	1.5855	5.477	0.2920	23.09	22.25	23.74	27.81
78.57	14.65	1.6860	8.836	0.2578	17.59	12.86	13.78	16.20
86.56	17.42	1.8197	17.48	0.2176	12.49	5.948	6.348	8.411
93.98	20.46	1.9681	43.38	0.1650	8.064	2.175	2.288	3.334
100.0	23.11	2.0889	113.0	0.1180	5.108	0.7684	0.7963	1.014

Can. J. Chem. Downloaded from www.nrcresearchpress.com by 200.7.193.243 on 09/04/12
For personal use only.

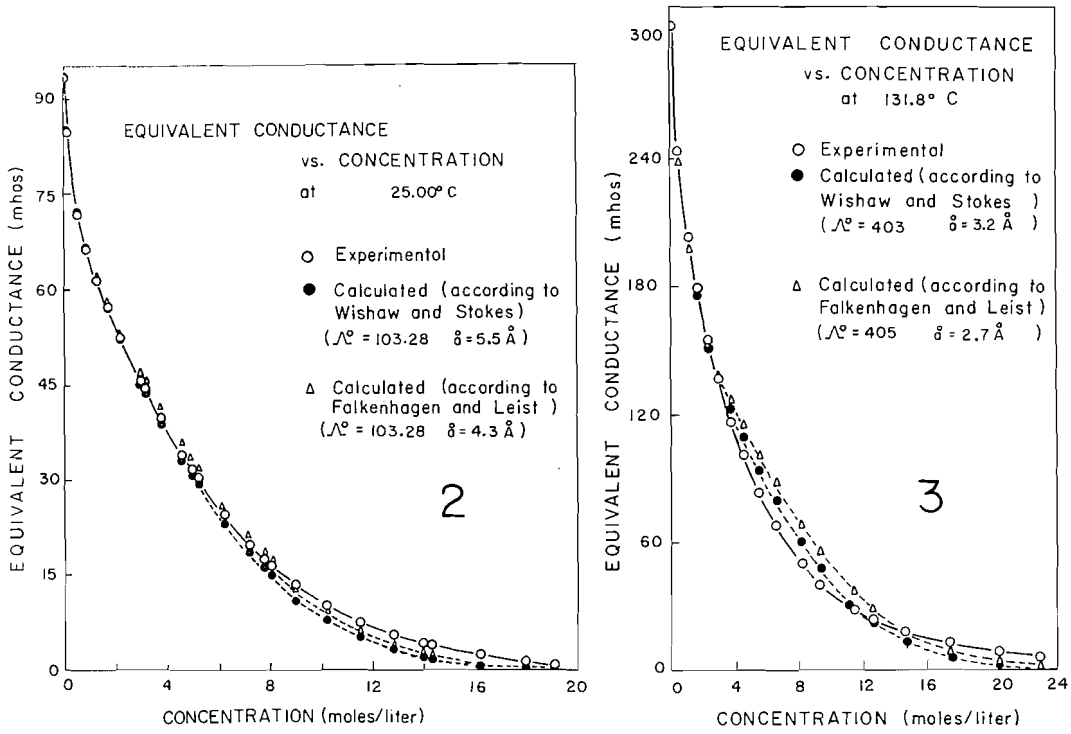

FIGS. 2 and 3.

131.8° C. a special type of filling and of pycnometer were used. This has also been described (4).

EXPERIMENTAL RESULTS

The experimental values of weight per cent, molarity, density, relative viscosity, specific conductance, and equivalent conductance, observed and calculated from the equations of Stokes and of Falkenhagen, are recorded in Tables I and II. The conductance measurements are limited to an accuracy of 0.1% and the density figures may be in error in the fourth decimal place. Plots of specific conductance and of equivalent conductance (observed and calculated) versus concentration at 25.00° C. and 131.8° C. are represented in Figs. 1 to 3. Fig. 4 is a plot of relative viscosity versus concentration at the two temperatures.

DISCUSSION OF RESULTS

The existence of maxima in the curves of specific conductance versus concentration is of interest, since it means that, for concentrations beyond that of the maximum, solutions containing more electrolyte have a lower conductance than solutions containing less electrolyte, that is, either the total number of ions is decreasing, or their mobility or both. For instance, the conductance at 131.8° C. of a 10 molar solution is the same as that of a 2 molar solution, despite a fivefold increase in electrolyte concentration. Such maxima are recorded only infrequently in the literature because of the lack of experimental investigations in the high concentration range.

The concentration corresponding to the maximum does not shift noticeably with

Can. J. Chem. Downloaded from www.nrcresearchpress.com by 200.7.193.243 on 09/04/12
For personal use only.

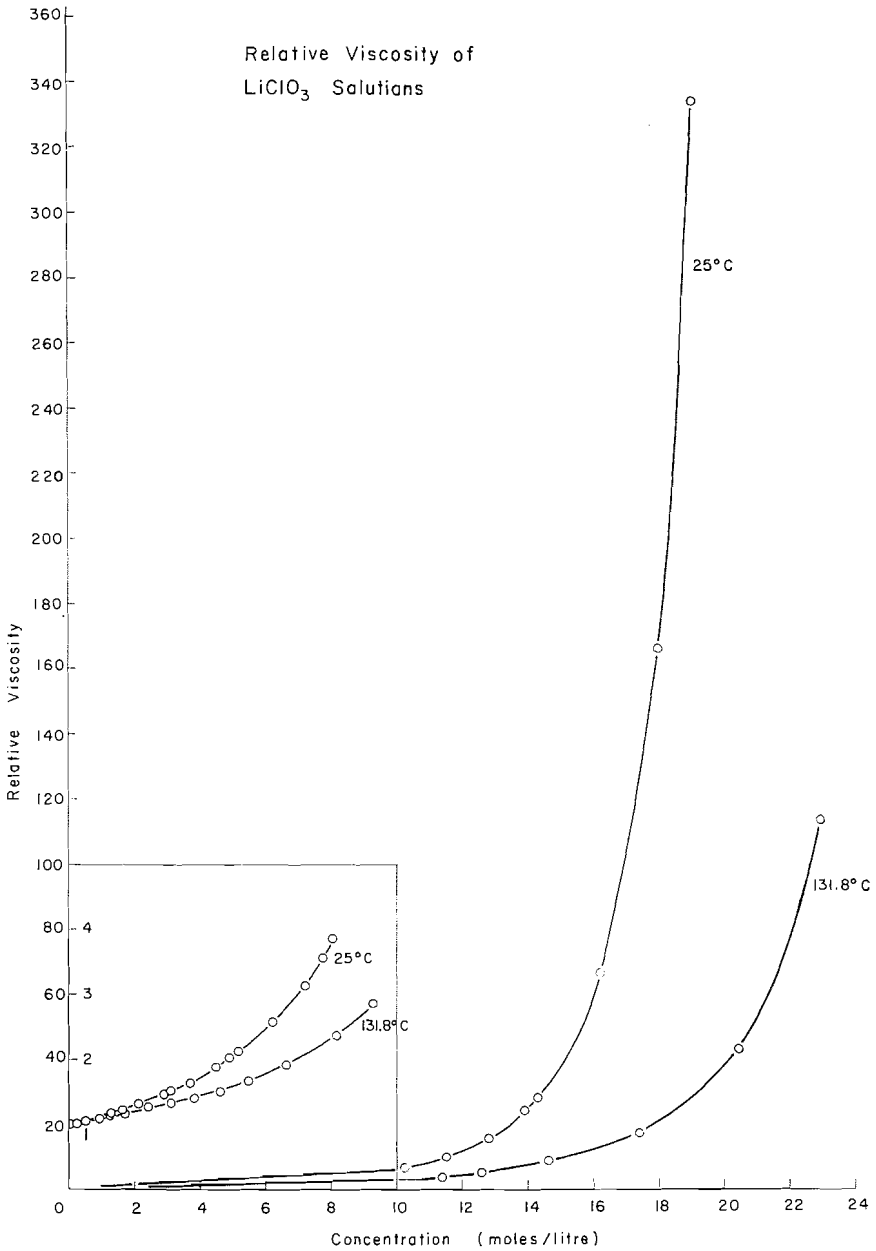

FIG. 4.

temperature, and this was observed by Klotschko and Grigorjew (9), who seek to connect this with the equilibrium diagram of the system lithium chlorate – water but there is, of course, no necessary connection whatever between the two. If it is assumed that strong electrolytes are completely ionized, no matter what the concentration, then the existence of the maximum points to a marked slowing down of the ions. Obviously, the electrical effects considered by the Debye–Hückel-Onsager theory will become very marked but the picture is complicated by changes in the hydration of the ions. At high concentrations,

Can. J. Chem. Downloaded from www.nrcresearchpress.com by 200.7.193.243 on 09/04/12
For personal use only.

all solvent molecules must be tightly held by ions; there will be little or no "free" water. This should produce, as it does, a very great increase in viscosity and this factor also tends to slow down the ions. The exact effect of viscosity on the motion of ions has not yet been formulated but it must be considerable, and is probably due in very concentrated solutions to interionic effects. Presumably, the effect is not measured simply by the bulk viscosity but there must be some connection.

The plots of equivalent conductance versus concentration (Figs. 2 and 3) show a progressive decrease in equivalent conductance with increasing concentration. At the higher temperature (131.8° C.) it was possible to cover the entire range of concentration up to anhydrous melt but no minimum is observed. Minima are found with electrolytes in solvents of relatively low dielectric constant and the meaning is discussed by Fuoss and Kraus (13). Their explanation is that non-conducting ion-pairs are first formed, followed, at high concentration, by conducting triple ions. It is apparent that, for all the salts investigated in this laboratory, no triple ions are formed. It is often contended that ion pairs cannot form in aqueous solution, because of the high dielectric constant of the medium but, in these very concentrated solutions, it becomes difficult to say what the medium is and therefore to state the dielectric constant. We think it unlikely that ion pairs will form in any lithium salt solution while there is still sufficient water present to preserve the very stable structure of the hydrated ion, but in very concentrated solutions, because of the proximity of the ions, formation of ion pairs must be considered probable. It should be pointed out that the last three figures of Table I refer to supersaturated solutions, which were easy to obtain.

The theory of extremely dilute solutions is well developed but there is no entirely satisfactory theory covering the conductance of concentrated solutions. The Debye–Hückel–Onsager theory has been extended by Fuoss and Onsager (14), by Wishaw and Stokes (15), and by Falkenhagen, Leist, and Kelbg (16). In every case, the extension consists in attributing to the ions a finite diameter, a, instead of considering them as mathematical points. In order to apply any of the above equations to more concentrated solutions, a viscosity correction must be used. Most authors, if they venture into this region at all, content themselves with dividing the calculated equivalent conductance by the relative viscosity. It has been suggested by Stokes (private communication) that it might be better to divide by some (fractional) power of the viscosity. Other workers, on the other hand, contend that because of the assumed complexity of concentrated solutions it is fruitless to pursue this line of investigation beyond, say, 0.1 N. It is our opinion, however, that solutions of moderate concentration are not so complicated in structure and that the Debye–Hückel–Onsager approach can be pursued further, if an appropriate viscosity correction can be found. It must be admitted that when the water content is reduced so low that there is not sufficient water present to hydrate the ions completely (notably in the present case of lithium chlorate) it is absurd to consider the ionic diameter as constant. It is therefore surprising that the equations of Wishaw and Stokes and of Falkenhagen to represent the general course of the equivalent conductance versus concentration curves rather well.

Papers proceeding from this laboratory have, since 1952, made extensive reference to the conductance equation of Wishaw and Stokes (15); no theoretical treatment is therefore necessary here. A somewhat similar equation is due to Falkenhagen and Leist (16); for uni-univalent electrolytes, the equation assumes the form:

$$\Lambda = \Lambda_0 \cdot \frac{\eta_0}{\eta} - \frac{e^2}{3\epsilon kT} \cdot \frac{\kappa}{1+\kappa a} \cdot \Lambda_0 \cdot \frac{\eta_0}{\eta} \cdot \frac{q}{(1+\sqrt{q})(1+\kappa a\sqrt{q})} - \frac{ne^2}{3\pi\eta_0} \cdot \frac{1000}{C\times 9\times 10^{11}} \cdot \frac{\kappa}{1+\kappa a} \cdot \frac{\eta_0}{\eta} \cdot$$

Can. J. Chem. Downloaded from www.nrcresearchpress.com by 200.7.193.243 on 09/04/12
For personal use only.

The symbols have their usual significance, except that $q = \frac{1}{2}$ for 1:1 electrolytes, n is the number of ions of a given type per cubic centimeter, and C is the concentration in moles per liter. We have used both the equations of Wishaw and Stokes and of Falkenhagen and Leist to calculate Λ for the concentrations used by us. These results are compared with our experimental results in Tables I and II and graphically in Figs. 2 and 3.

Quite recently, Professor Falkenhagen, in a private communication, has stated the most recent form of his conductance equation as:

[1] $$\Lambda = \Lambda_0 - \Lambda_I - \Lambda_{II} \qquad \text{(general formulation)}$$

where Λ_I represents the relaxation effect and Λ_{II} the electrophoretic effect:

[2] $$\Lambda_I = \frac{e^2\Lambda_0}{GD_0kT} \cdot \frac{(2-\sqrt{2})\kappa}{(1+\kappa a)(1+\frac{1}{2}\sqrt{2}\,.\,\kappa a+\frac{1}{6}\kappa^2a^2)},$$

[3] $$\Lambda_{II} = \frac{e^2L}{27\pi\times 10^{11}\eta_0} \cdot \frac{\kappa}{1+\kappa a}.$$

The symbols have their usual significance except that L = Avogadro's number. We have used this equation to calculate Λ for lithium chlorate at 25.00° C. These results, for concentrations ranging from 0.0219 M to 6.199 M, are given in Table III. We have slightly altered å from 4.3 to 4.1 Å, for this purpose. The agreement is very good. Up to 0.5121

TABLE III

COMPARISON OF OBSERVED CONDUCTANCES AND THOSE CALCULATED BY FALKENHAGEN'S MOST RECENT EQUATION: LITHIUM CHLORATE SOLUTIONS AT 25.0° C.

Concentration, M	$\Lambda_0 = 103.28$		å = 4.1 Å			
	Λ_{exp}	Λ_I	Λ_{II}	Λ^*	Λ'	% Deviation
0.0219	93.31	2.545	7.436	93.36	93.17	−0.15
0.1002	84.78	3.923	13.301	86.06	84.79	0.12
0.5121	71.85	4.694	21.961	76.63	71.82	−0.04
0.8532	66.36	4.615	24.795	73.87	66.55	0.29
1.247	61.58	4.322	26.862	72.10	61.68	0.16
1.640	57.19	4.094	28.309	70.88	57.67	0.84
2.113	52.45	3.844	29.601	69.84	53.11	1.23
2.928	45.67	3.484	31.186	68.61	46.61	2.06
3.115	44.11	3.411	31.488	68.38	45.34	2.79
3.742	39.94	3.165	32.316	67.80	41.29	3.38
4.549	33.90	2.957	33.178	67.14	35.43	4.51
4.908	31.69	2.860	33.501	66.92	33.15	4.61
5.157	30.17	2.741	33.703	66.84	31.60	4.74
6.199	24.38	2.575	34.451	66.25	25.54	4.76

$\Lambda^* = \Lambda_{calc}$ uncorrected for viscosity.
$\Lambda' = \Lambda_{calc}$ corrected for viscosity.

M, the discrepancy is negligible. After this, the error of the calculated quantity becomes increasingly positive and amounts to 4.76% of the observed result at 6.199 M. Beyond 6 M, the difference between the results of the two Falkenhagen equations is negligible, so there is no point in carrying the new calculations beyond this. Neither have we calculated for 131.8° C., with the more recent equation, because our complete ignorance of the value of Λ_0 at 131.8° makes it impossible to impose a fair test. According to Falkenhagen himself, his most recent equation is on sound theoretical ground as long as $Ka << 1$. Beyond this point, a viscosity correction must be introduced. It has always been the fashion to divide the calculated conductance by the relative viscosity and, if this is done, the following equation results:

$$\Lambda_c = (\eta_0/\eta)\{\Lambda_0 - \Lambda_I - \Lambda_{II}\}.$$

Can. J. Chem. Downloaded from www.nrcresearchpress.com by 200.7.193.243 on 09/04/12
For personal use only.

Equations such as the above, however, must at best be described as "semi-empirical", since the exact form of the viscosity correction is not known. Falkenhagen and Leist (16) test the (original) equation by using the data for the conductance of lithium chloride solutions at 18° C. Using a value of å = 4.8 Å, they obtain very good agreement with the experimental data; at a concentration of 10 molar the experimental and calculated equivalent conductances differ by less than one mho. Some of the agreement may be fortuitous, since the equation is not really justified at such high concentrations, but it does indicate that dividing by the relative viscosity is at least an approximation to the truth. For our own results Stokes' suggestion of dividing by some power of the viscosity, other than one, can very well be met by using the power 1.05, that is, by dividing the calculated conductance by $(\eta/\eta_0)^{1.05}$; calculated and observed results then agree very well up to 6 *M*. Since, however, this is a purely empirical procedure, there being no reason to use this power, or any other, of the viscosity, except to force the calculated results into agreement with the observed values, we think it better to continue the older practice of simply dividing by the relative viscosity and to attribute deviations to shortcomings in the equation. Obviously, there must be many phenomena in concentrated solutions which are not covered by the Falkenhagen treatment, which must be oversimplified for very concentrated solutions.

The new equation of Falkenhagen yields better results than that of Wishaw and Stokes (15). In all such equations, the choice of å is quite arbitrary. For example, in calculating for lithium chloride, Falkenhagen and Leist use a value of å of 4.8 Å; the calculations of Wishaw and Stokes are based on å = 5.2 Å, and Fuoss and Onsager (14) use 4.31 Å in their calculations for the dilute region.

In order to calculate Λ, Λ_0 must be known and a reasonable value for å, the distance of closest approach of the ions, must be assumed. At 25.0° C., the only uncertain parameter is the latter quantity. Two series of calculations have been made (Wishaw–Stokes equation), using slightly different values of this parameter. To obtain a good fit with the Falkenhagen equation, significantly different values of å had to be used. At the higher temperature, the difficulty of not knowing Λ_0 is an additional handicap. For each value of å, we have used a slightly different value of Λ_0. Although Stokes maintains that å is temperature independent we have used a smaller value of å for the higher temperature.

Again, all equations assume constancy of å with increasing concentration. In fact, however, and assuming again that å is a real quantity, the distance of closest approach must decrease with increasing concentration, because a concentration is eventually reached where there is no longer sufficient water in the solution to maintain extensive hydration.

ACKNOWLEDGMENTS

We are indebted to Dr. E. M. Kartzmark for her assistance in the preparation of this paper and with the calculations. As in all work proceeding from this laboratory, most of the expense of the research was borne by a research fund supplied by the National Research Council.

REFERENCES

1. CAMPBELL, A. N. and KARTZMARK, E. M. Can. J. Research, B, **28**, 43 (1950).
2. CAMPBELL, A. N., GRAY, A. P., and KARTZMARK, E. M. Can. J. Chem. **31**, 617 (1953).
3. CAMPBELL, A. N. and KARTZMARK, E. M. Can. J. Chem. **30**, 128 (1952).
4. CAMPBELL, A. N., KARTZMARK, E. M., BEDNAS, M. E., and HERRON, J. T. Can. J. Chem. **32**, 1051 (1954).
5. CAMPBELL, A. N., DEBUS, G. H., and KARTZMARK, E. M. Can. J. Chem. **33**, 1508 (1955).
6. CAMPBELL, A. N. and DEBUS, G. H. Can. J. Chem. **34**, 1232 (1956).
7. KRAUS, C. A. and BURGESS, W. M. J. Am. Chem. Soc. **49**, 1226 (1927).
8. SCATCHARD, G., PRENTISS, S. S., and JONES, P. T. J. Am. Chem. Soc. **56**, 805 (1934).

Can. J. Chem. Downloaded from www.nrcresearchpress.com by 200.7.193.243 on 09/04/12
For personal use only.

9. KLOTSCHKO, M. A. and GRIGORJEW, I. G. Akad. Wiss. (U.S.S.R.) Nachr. Abt. physik-chem. Analyse, **21**, 288 (1950). German translation.
10. CAMPBELL, A. N. and GRIFFITHS, J. E. Can. J. Chem. **34**, 1647 (1956).
11. JONES, G. and BRADSHAW, B. C. J. Am. Chem. Soc. **55**, 1780 (1933).
12. WASHBURN, E. W. J. Am. Chem. Soc. **38**, 2431 (1916).
13. FUOSS, R. M. and KRAUS, C. A. J. Am. Chem. Soc. **55**, 2387 (1933).
14. FUOSS, R. M. and ONSAGER, L. Proc. Natl. Acad. Sci. U.S. **41**, 274 (1955).
15. WISHAW, B. F. and STOKES, R. H. J. Am. Chem. Soc. **76**, 2065 (1954).
16. FALKENHAGEN, H., LEIST, M., and KELBG, G. Ann. Physik, (6), **11**, 51 (1952). FALKENHAGEN, H. and LEIST, M. Naturwiss. **24**, 570 (1954). Z. physik. Chem. **205**, 16 (1955).

Can. J. Chem. Downloaded from www.nrcresearchpress.com by 200.7.193.243 on 09/04/12
For personal use only.

Can. J. Chem. Downloaded from www.nrcresearchpress.com by 200.7.193.243 on 09/04/12
For personal use only.

SPECTRE INFRAROUGE DE HF À L'ÉTAT CRISTALLIN[1]

PAUL A. GIGUÈRE ET NUMAN ZENGIN[2]

RÉSUMÉ

On a mesuré le spectre d'absorption infrarouge entre 300 et 5000 cm.$^{-1}$ de minces films de HF cristallisé à −180° C. La vibration fondamentale produit un doublet intense à 3420 et 3060 cm.$^{-1}$ et un second, plus faible, à 3590 et 3270 cm.$^{-1}$. Toutes les caractéristiques du spectre concordent avec les données actuelles sur la structure cristalline de HF: chaînes parallèles, en zigzag, de molécules reliées par des liaisons hydrogène asymétriques. On a également déduit les dimensions approximatives suivantes:

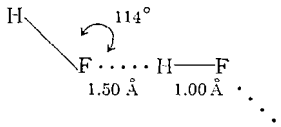

La haute polarité de la molécule et les fortes liaisons hydrogène se manifestent de plusieurs façons: largeur exceptionnelle des bandes (de 150 à 200 cm.$^{-1}$); grand espacement des diverses composantes de la fondamentale dans le cristal; abaissement considérable (quelque 700 cm.$^{-1}$) de la fréquence fondamentale en passant de la molécule libre au solide, résultant d'une diminution de la force de rappel de 8.8 à 6.3×10^5 dynes/cm.; fréquences de libration élevées (1000–1200 cm.$^{-1}$) et forces de rappel intermoléculaires allant jusqu'à 0.6×10^5 dynes/cm.

Les spectres infrarouges et Raman des cristaux moléculaires peuvent fournir des indications précieuses sur l'arrangement des molécules à l'état solide ainsi que sur les forces intermoléculaires. Cette information est particulièrement utile dans le cas des composés de l'hydrogène puisque la diffraction aux rayons X ne permet pas de localiser ces atomes avec précision. Jusqu'à présent on a étudié par ces méthodes les halogénures HCl, HBr et HI (1, 2, 3, 4) mais aucun travail n'est encore paru sur HF à l'état solide. La raison principale en est sans doute la difficulté que présente la manipulation de ce composé extrêmement corrosif. De plus sa tendance marquée à la fluorescence rend presque impossible l'étude de l'effet Raman dans les états condensés. Ainsi une étude récente du spectre Raman de l'acide liquéfié (5) n'a révélé aucune indication de la vibration fondamentale.

MÉTHODE EXPÉRIMENTALE

À cause de la grande réactivité de l'acide fluorhydrique, et en particulier de son action sur le verre, il a fallu des précautions spéciales pour préparer les échantillons. Le gaz, contenu dans un cylindre de fer, était censé pur à 99.9%.* Les seules traces d'impuretés susceptibles d'affecter les résultats (H_2O, 0.04%; H_2S, 0.02%; SO_2, 0.01%) étaient à peine visibles dans les spectres des films les plus épais. Le gaz était transféré sous pression réduite dans un réservoir de cuivre d'environ un demi-litre d'où il était admis par petites bouffées dans la cellule d'absorption. Celle-ci était en verre, du type courant (6); les parois internes étaient recouvertes d'un enduit résistant à l'acide fluorhydrique. À cette fin nous avons d'abord employé une couche suffisamment épaisse de vernis Glyptal qui offre une protection efficace mais finit par se détacher du verre après un certain temps. Par la suite nous y avons substitué la cire Halocarbon 15-00,† également inerte, qui adhère

[1]*Manuscrit reçu le 30 janvier 1958.*
Contribution du Département de Chimie, Université Laval, Québec, Qué.
[2]*Boursier postdoctoral du Conseil National de Recherches, Ottawa, Canada.*
**Produit de "The Matheson Co. Inc.", East Rutherford, New Jersey.*
†Fabriquée par "The Halocarbon Products Corp.", North Bergen, New Jersey.

indéfiniment au verre. Les fenêtres de la cellule étaient faites de disques de chlorure d'argent sauf pour les mesures au-delà de 25 μ où il fallut recourir à l'iodure de césium. Le disque central, sur lequel se condensait le film de HF, était fait des mêmes matériaux; dans le cas de l'iodure de césium un mince film de polyéthylène, suffisamment transparent jusqu'à 40 μ, empêchait l'attaque par l'acide fluorhydrique.

Les canalisations, réduites au minimum, étaient de cuivre rouge. Un robinet à pointeau en laiton permettait de contrôler le débit du gaz; un manomètre de Bourdon à capsule de cuivre indiquait la pression dans le réservoir. Le seul robinet en verre sur la cellule à absorption était lubréfié avec de la graisse Fluorolube MG.* La moindre attaque des parois par l'acide se traduisait par l'apparition dans les spectres de bandes d'absorption des fluosilicates. L'épaisseur des films, telle qu'évaluée d'après la quantité de gaz utilisé et l'étendue de la surface froide, dans l'hypothèse d'une condensation uniforme, variait entre 3 et 5 μ. Leur température n'a pas été mesurée avec précision mais elle devait être d'environ $-180°$ C. avec l'air liquide comme réfrigérant. Les spectres furent enregistrés au moyen d'un spectrographe de Perkin-Elmer, Modèle 12C à double passage. Suivant la région nous avons utilisé des prismes de LiF, NaCl et CsBr calibrés de la façon usuelle (7).

RÉSULTATS

Les bandes d'absorption infrarouges de HF cristallisé se divisent en deux groupes distincts: les fondamentales, de 2.8 à 3.5 μ (Fig. 1) et les vibrations du réseau, au-delà de 6 μ (Fig. 2). Le premier groupe comprend le doublet principal à 3420 et 3060 cm.$^{-1}$. Vu la largeur considérable de ces bandes et leur proximité relative il était difficile de déterminer avec plus de précision la position des maxima. Un second doublet beaucoup moins intense que le premier, à 3590 et 3270 cm.$^{-1}$ présente quelque difficulté d'interprétation. À première vue on pourrait l'attribuer à des combinaisons (somme-différence) des fréquences fondamentales avec une vibration du réseau de l'ordre de 200 cm.$^{-1}$. Cependant les intervalles de fréquence, soient 170, 150 et 210 cm.$^{-1}$ respectivement, ne concordent pas assez bien à cette fin. De plus on devrait s'attendre à trouver une bande semblable vers 2860 cm.$^{-1}$ alors qu'en fait on n'observe qu'un renflement à peine perceptible. Étant donnée la ressemblance générale, à des échelles différentes, des deux doublets il semble plus probable que nous avons affaire ici aux quatre composantes de la vibration fondamentale, puisqu'il y a quatre molécules de HF dans la maille cristalline (8). Normalement deux des composantes devraient être actives en infrarouge et deux en Raman. Cependant il n'est pas inconcevable que toutes quatre apparaissent en infrarouge, surtout si on considère la possibilité de désordre dans la structure du cristal (distribution statistique des liaisons hydrogène) qui détruit la symétrie des sites.

Quant à la bande très floue déjà mentionnée aux environs de 2860 cm.$^{-1}$, et visible seulement dans les échantillons les plus épais, elle peut provenir d'une combinaison d'une fondamentale avec une vibration de réseau ou encore de quelque impureté. Hornig (2) a trouvé une bande analogue à 2616 cm.$^{-1}$ dans le spectre de HCl crystallisé. L'ion H_3O^+ possède une faible bande à cet endroit dans les solutions aqueuses d'acides (9) mais comme nous n'avons pu déceler aucune trace d'absorption vers 1700 cm.$^{-1}$, cette explication se trouve éliminée. Il convient d'ajouter ici qu'aucune indication d'harmoniques ni de bandes de combinaison n'est apparue entre 4000 et 5000 cm.$^{-1}$ probablement parce que les films utilisés étaient trop minces.

Du côté des grandes longueurs d'onde outre une demi-douzaine de bandes extrêmement faibles provenant, semble-t-il, d'impuretés (SO_2, H_2S, etc.), on trouve quatre ou cinq

*Fabriquée par "Hooker Electrochemical Co.", Niagara Falls, New York.

Can. J. Chem. Downloaded from www.nrcresearchpress.com by 200.7.193.243 on 09/04/12
For personal use only.

Can. J. Chem. Downloaded from www.nrcresearchpress.com by 200.7.193.243 on 09/04/12
For personal use only.

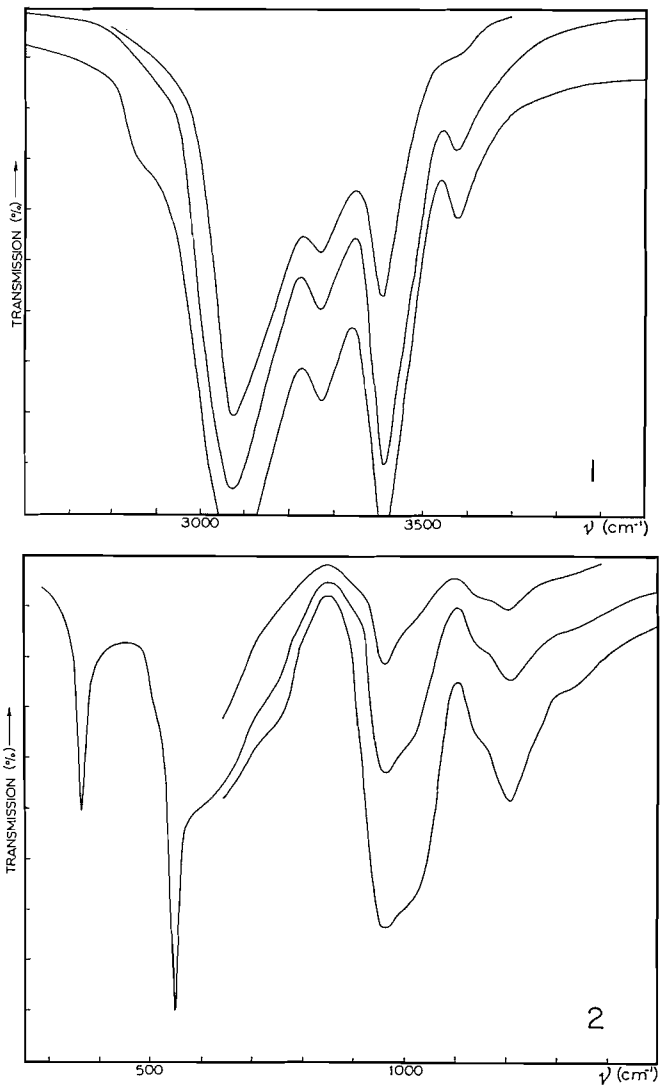

FIG. 1. Bandes d'absorption de HF à l'état cristallin dans la région de la vibration fondamentale.
FIG. 2. Bandes de vibration du réseau cristallin de HF.

bandes assez fortes à 366, 547, 955–1010 et 1204 cm.$^{-1}$. La courbe médiane dans les figures 1 et 2 a été obtenue avec le même échantillon en sorte que les intensités relatives des deux groupes de bandes sont reproduites assez fidèlement. Pour attribuer sans équivoque ces bandes aux divers modes de vibration du réseau cristallin il faudrait connaître le spectre Raman de HF cristallin. À titre d'essai on peut assigner le doublet non résolu à 955–1010 cm.$^{-1}$ ainsi que la bande assez large à 1204 cm.$^{-1}$ à des rotations gênées ou librations. A priori ces fréquences semblent passablement élevées pour de tels modes mais cette situation s'explique par la petitesse du moment d'inertie de la molécule HF ainsi que par l'énergie relativement grande des liaisons hydrogène dans cette substance. Par ailleurs le pic aigu à 366 cm.$^{-1}$ est de fréquence appropriée pour une translation comme on le verra plus loin d'après les forces de rappel intermoléculaires. Enfin l'origine de la

forte bande asymétrique surmontée d'un pic aigu à 547 cm.$^{-1}$ demeure incertaine. Sa fréquence paraît trop élevée pour une translation et un peu basse pour une libration; son intensité est également trop grande pour une harmonique de ν_T. Il se peut qu'elle provienne de mouvements de torsion des chaînes.

DISCUSSION

L'analyse de ces résultats se trouve facilitée par l'étude très poussée de Hornig et son groupe (1, 2, 3, 4) sur les spectres infrarouges de HCl, HBr et HI ainsi que par la détermination par les rayons X de la structure cristalline de HF (8). Ainsi l'on sait que ce cristal orthorhombique contient quatre molécules par maille, avec la symétrie du groupe infini $D_{24}{}^{17}$, quoique la symétrie $D_{24}{}^{16}$ ne soit pas définitivement exclue. Les molécules, reliées par des liaisons hydrogène, forment des chaînes en zigzag quasi-infinies, coplanaires et parallèles au plan 100 (Fig. 3); l'angle entre les molécules adjacentes est de 120°. Une telle structure implique des liaisons hydrogène orientées selon une direction privilégiée, ce qui semble en contradiction avec la nature essentiellement électrostatique de ce genre de liaisons. Cependant Schneider (10) a démontré récemment, en se servant du concept d'orbitale équivalente (11), le rôle important que jouent dans la formation de la liaison hydrogène les "doublets libres" sur l'atome accepteur de proton. À cause de l'hybridation des orbitales du fluor (sp^3) les molécules de HF tendent donc à s'orienter mutuellement suivant un angle à peu près tétragonal.

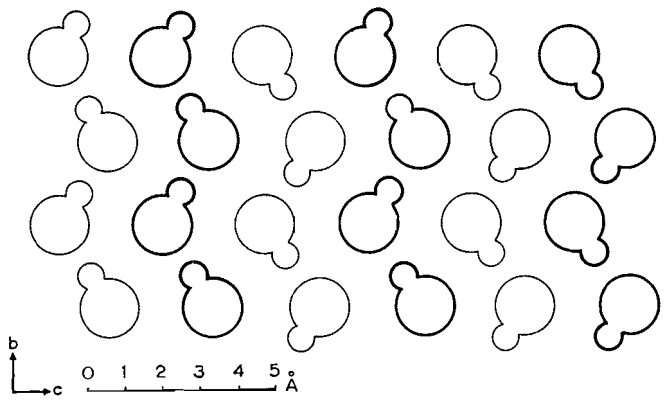

FIG. 3. Arrangement désordonné des chaînes de HF dans deux plans 100 successifs.

Les bandes fondamentales de HF cristallin sont d'abord remarquables par leur grande largeur: de 150 à 200 cm.$^{-1}$ à comparer avec 10 ou 20 cm.$^{-1}$ pour les autres halogénures HX. Cette caractéristique bien connue des composés contenant des liaisons hydrogène a suscité de nombreuses explications. Dans le cas de HF il n'est pas impossible que l'élargissement des bandes soit dû pour une part à un certain désordre dans le cristal. En effet l'analyse aux rayons X a montré la possibilité d'une distribution statistique des liaisons hydrogène, telle que représentée sur la figure 3. Les données présentes favorisent cette explication sans toutefois trancher la question; pour ce faire il faudra recourir à des méthodes plus puissantes telle la diffraction des neutrons. De toute façon ce désordre, s'il existe, ne conduit à aucune entropie résiduelle au zéro absolu puisqu'il ne fait intervenir que deux configurations différentes pour chaque chaîne (8). Contrairement aux autres halogénures d'hydrogène qui présentent à l'état solide des transitions du premier

Can. J. Chem. Downloaded from www.nrcresearchpress.com by 200.7.193.243 on 09/04/12
For personal use only.

ou du second ordre, HF garde la même structure cristalline à toute température. Il est évident qu'à cause de la grande polarité de la molécule et des fortes liaisons hydrogène les molécules n'ont pas la liberté de se réorienter dans le cristal.

La fréquence élevée des vibrations fondamentales confirme sans équivoque que la liaison F—H · · · F est asymétrique dans HF à l'état solide contrairement au cas exceptionnel de l'ion HF_2^- (10). Un calcul approximatif basé sur la règle de Badger conduit, à partir d'une fréquence moyenne de 3300 cm.$^{-1}$, à une distance H—F d'environ 1.00 Å. Comme la diffraction aux rayons X a donné 2.49 Å pour la distance minimum entre deux atomes de fluor voisins, il s'ensuit que les liaisons hydrogène sont d'à peu près 1.50 Å dans ce cristal. Dans la vapeur la distance F—H · · · F dans les polymères est de 2.55 Å (12) tandis que dans la molécule libre la distance interatomique est de 0.917 Å (13). On voit donc que les liaisons hydrogène dans HF sont notablement plus courtes, et partant plus fortes, que dans H_2O (1.75 Å); dans cette dernière substance le passage de la vapeur au solide allonge la liaison O—H de 0.96 à 1.01 Å (14).

À la suite de l'analyse de Hornig on sait que dans les cristaux des composés polaires du type HX le rapport des intensités des deux composantes fondamentales I_x et I_y dans le spectre infrarouge varie suivant l'angle α entre molécules voisines d'après la relation

$$I_x/I_y = \tan^2\alpha/2.$$

Des mesures faites sur cinq spectres différents de HF nous ont donné pour le rapport d'intensité des deux bandes à 3420 et 3060 cm.$^{-1}$ les valeurs: 2.31, 2.32, 2.38, 2.42 et 2.48 qui correspondent à des angles allant de 113° à 115°. L'accord avec le valeur trouvée par diffraction des rayons X, 120.1° (8), est satisfaisant surtout si l'on songe à l'incertitude des mesures d'intensité dans le cas présent. Par ailleurs l'écart entre ces diverses valeurs de α est beaucoup moindre que pour HCl et HBr (2). La possibilité, mentionnée par Hornig, d'une orientation partielle des films est évidemment minime pour une substance aussi polaire que HF. De toute façon on n'a jamais observé de différence notable entre les spectres de films déposés sur AgCl et sur NaCl, du moins dans la région de 300 à 1000 cm.$^{-1}$. Notons que des mesures d'intensité faites sur le doublet secondaire à 3590 et 3270 cm.$^{-1}$ conduisent à un angle voisin de 100°, bien que la précision des mesures soit évidemment assez faible ici. Ce résultat renforce l'hypothèse des deux composantes fondamentales déjà invoquée pour ces bandes.

Forces de rappel

Les présents résultats permettent d'évaluer les forces de rappel tant pour la molécule que pour le cristal. Qualitativement l'existence de forces intermoléculaires considérables

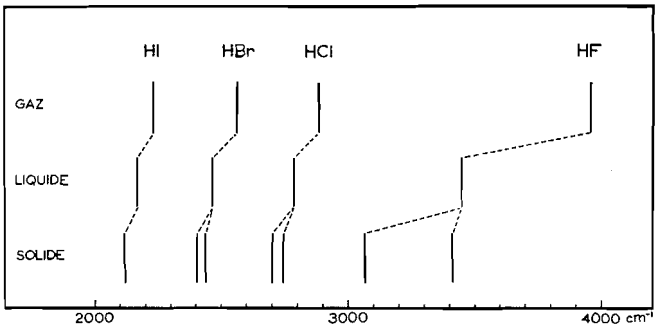

FIG. 4. Comparaison des fréquences de vibration des halogénures d'hydrogène dans les trois états physiques.

Can. J. Chem. Downloaded from www.nrcresearchpress.com by 200.7.193.243 on 09/04/12
For personal use only.

dans le cristal de HF se manifeste de trois façons: (*a*) un abaissement inusité de la vibration fondamentale en passant de la molécule libre, 3962 cm.$^{-1}$ (13) au cristal (Fig. 4); (*b*) la séparation extrêmement grande entre les composantes de la vibration fondamentale à l'état solide et enfin; (*c*) les valeurs très élevées des fréquences de libration. Ces observations sont en accord avec le caractère ionique marqué de la liaison H—F et les fortes liaisons hydrogène, 6.7 kcal./mole, selon Pauling (15), qui persistent même à l'état de vapeur.

Nous avons d'abord calculé les forces de rappel, tant principale que secondaires, à partir des quatre présumées composantes de la vibration fondamentale en supposant que le couplage entre les vibrations internes et externes des molécules dans le cristal est faible. Cette hypothèse est naturellement moins justifiable pour HF que pour les autres halogénures d'hydrogène mais elle tient encore en première approximation. En assignant arbitrairement les quatre fréquences comme suit:

$$\nu_1 = 3270 \text{ cm.}^{-1},$$
$$\nu_2 = 3060 \text{ cm.}^{-1},$$
$$\nu_3 = 3420 \text{ cm.}^{-1},$$
$$\nu_4 = 3590 \text{ cm.}^{-1},$$

on arrive aux valeurs suivantes (la notation est celle de Hornig):

$$f_{11} = 6.31\times10^5 \text{ dynes/cm.},$$
$$f_{12} = f_{34} = 0.65\times10^5 \text{ dynes/cm.},$$
$$f_{13} = f_{24} = 0.015\times10^5 \text{ dynes/cm.},$$
$$f_{14} = f_{23} = 0.36\times10^5 \text{ dynes/cm.}$$

Par contre, si on n'utilise que les deux composantes majeures on obtient des constantes assez voisines pour les deux forces principales, soient $f_{11} = 5.9$ et $f_{12} = 0.62\times10^5$ dynes/cm. Ces quantités demeurent sujettes à revision jusqu'à ce que les fréquences fondamentales dans le spectre Raman du cristal soient connues. Pour le moment il est intéressant de constater que la diminution de la force de rappel interne en passant de la molécule libre au cristal est énormément plus grande pour HF que pour les autres halogénures d'hydrogène (Tableau I). L'amortissement de la vibration de HF dans le cristal accroît son anharmonicité, laquelle se manifeste par un élargissement des bandes d'absorption.

Quant aux modes de libration des molécules dans le réseau cristallin, les fréquences trouvées ici soient 955, 1010 et 1204 cm.$^{-1}$ sont sans doute les plus hautes jamais rencontrées. Il est intéressant de les comparer à celles de la glace à 850 cm.$^{-1}$ (16). Hornig et

TABLEAU I

CONSTANTES MOLÉCULAIRES DES HALOGÉNURES D'HYDROGÈNE

	f_0	f_{11}	f_{12}	r_{H-X}	D	μ
HF	8.83	6.3	0.65	0.917	134	1.9
HCl	4.81	4.31	0.072	1.27	102	1.03
HBr	3.84	3.45	0.048	1.41	86	0.88
HI	2.93	2.66	—	1.60	70	0.38

NOTE: f_0, *constante de force de rappel (en 10^{-5} dynes/cm.) pour la molécule libre (17).*
f_{11}, *constante de force de rappel principale dans le cristal (2).*
f_{12}, *constante de force de rappel entre molécules voisines dans le cristal (2).*
r_{H-X}, *distance interatomique (en Å) dans la molécule libre (13).*
D, *énergie de dissociation de la liaison (en kcal./mole) (17).*
μ, *moment polaire (en debyes).*

Can. J. Chem. Downloaded from www.nrcresearchpress.com by 200.7.193.243 on 09/04/12
For personal use only.

Osberg (2) ont évalué à 266 cm.$^{-1}$ la fréquence de ce mode dans HCl cristallin, ce qui est en harmonie avec une valeur moyenne de 1100 cm.$^{-1}$ pour HF. Nous avons utilisé cette dernière quantité pour calculer la constante secondaire f_{12} d'après la formule usuelle

$$f = 4\pi^2\nu^2 I/r^2$$

pour une oscillation perpendiculaire à la force de rappel; nous obtenons ainsi presque exactement le même résultat (6.4×10^5 dynes/cm.) que ci-haut. Enfin un calcul très grossier de la fréquence de translation gênée ν_T d'une molécule HF par rapport à ses voisines dans l'hypothèse d'un oscillateur harmonique conduit à une valeur d'environ 330 cm.$^{-1}$.

Des deux facteurs principaux qui affectent les vibrations d'une molécule dans le cristal soient (*a*) le champ de forces créé par l'ensemble des molécules dans leur position d'équilibre et (*b*) le couplage avec les molécules adjacentes, il est clair que le second est énormément plus important dans le cas de HF. La technique dite de dilution isotopique (3) a permis à Hornig de différencier ces deux facteurs dans des "cristaux mixtes" de HCl et DCl. Vu la largeur anormale des bandes d'absorption de HF il est peu probable que cette méthode puisse révéler suffisamment de détails sur les vibrations des molécules isolées ou des paires de molécules dans les mélanges.

ABSTRACT

The infrared absorption of thin crystallized films of HF at −180° C. was measured from 300 to 5000 cm.$^{-1}$. The fundamental vibrations give rise to a strong doublet at 3420 and 3060 cm.$^{-1}$ and a weaker one at 3590 and 3270 cm.$^{-1}$. These bands are remarkably broad owing to the presence of very strong hydrogen bonds. From the intensity ratio of the fundamental components the angle between neighboring HF molecules in the zigzag chains is calculated to be about 114°. Both the splitting of the fundamental components and the vapor–solid shift are unusually large in keeping with the high polarity of the molecule and the strong hydrogen bonds. The "internal" force constant $f_{11} = 6.31 \times 10^5$ dynes/cm. is much lower than for the free molecule, and the "external" force constants are higher, by an order of magnitude, than in the other hydrogen halide crystals. Some five lattice vibrations were found between 350 and 1200 cm.$^{-1}$.

BIBLIOGRAPHIE

1. HIEBERT, G. L. et HORNIG, D. F. J. Chem. Phys. **20**, 918 (1952).
2. HORNIG, D. F. et OSBERG, W. E. J. Chem. Phys. **23**, 662 (1955).
3. HORNIG, D. F. et HIEBERT, G. L. J. Chem. Phys. **27**, 752 (1957).
4. HIEBERT, G. L. et HORNIG, D. F. J. Chem. Phys. **27**, 1216 (1957).
5. SAFARI, E. Ann. phys. **9**, 203 (1954).
6. WAGNER, E. L. et HORNIG, D. F. J. Chem. Phys. **18**, 296 (1950).
7. DOWNIE, A. R., MAGOON, M. G., PURCELL, T. et CRAWFORD, B., Jr. J. Opt. Soc. Am. **43**, 941 (1953).
8. ATOJI, M. et LIPSCOMB, W. N. Acta Cryst. **7**, 173 (1954).
9. FALK, M. et GIGUÈRE, P. A. Can. J. Chem. **35**, 1195 (1957).
10. SCHNEIDER, W. G. J. Chem. Phys. **23**, 26 (1955).
11. LENNARD-JONES, J. et POPLE, J. A. Proc. Roy. Soc. (London), A, **205**, 155 (1951).
12. BAUER, S. H., BEACH, Y. J. et SIMONS, J. H. J. Am. Chem. Soc. **61**, 19 (1939).
13. HERZBERG, G. Spectra of diatomic molecules. D. Van Nostrand Company, Inc., New York. 1950.
14. PETERSON, S. W. et LÉVY, H. A. Acta Cryst. **10**, 70 (1957).
15. PAULING, L. Nature of the chemical bond. Cornell Univ. Press, Ithaca, N.Y. 1941.
16. GIGUÈRE, P. A. et HARVEY, K. B. Can. J. Chem. **34**, 798 (1956).
17. COTTRELL, T. L. The strengths of chemical bonds. Butterworth Scientific Publications, London. 1954.

Can. J. Chem. Downloaded from www.nrcresearchpress.com by 200.7.193.243 on 09/04/12
For personal use only.

Can. J. Chem. Downloaded from www.nrcresearchpress.com by 200.7.193.243 on 09/04/12
For personal use only.

THE INFRARED CARBONYL STRETCHING BANDS OF ACETOPHENONES SUBSTITUTED IN THE METHYL GROUP[1]

R. NORMAN JONES AND ERNEST SPINNER[2]

ABSTRACT

Measurements have been made of the positions and intensities of the C=O stretching bands in the infrared spectra of compounds of the types C_6H_5—CO—CH_2X, C_6H_5—CO—CHX_2, and C_6H_5—CO—CX_3 where X = —Cl, —Br, —I, —CN, —C_6H_5, and —OH. In most cases two bands are observed, and these are attributed to *gauche* and *cis* conformations associated with hindered rotation about the CO—CH_2X and CO—CHX_2 bonds. The relative positions and intensities of these bands are discussed in terms of the steric, electrical, and mass effects of the substituents.

INTRODUCTION

Rotational isomerism has been observed repeatedly in substances containing the groups —CO—CH_2X and CO—CHX_2 (1, 2, 3, 4, 5). Rotation of the CH_2X or CHX_2 group is restricted and the preferred conformations are those in which an H or X atom eclipses the oxygen atom when the molecule is viewed along the axis of the CO—CH_2X or CO—CHX_2 bond (I, II).

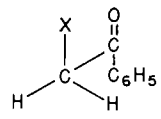

I (cis)

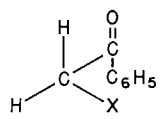

II (gauche)

Bellamy, Thomas, and Williams (4) have studied the C=O stretching bands in the infrared spectra of ω-chloroacetophenone, ω,ω-dichloroacetophenone, and ring-substituted derivatives of the former. In spectra measured in the liquid phase they observed two prominent maxima in the C=O stretching region, whereas a single band only was noted if the spectra were determined on material in the solid state. The relative intensities of the doublet peaks were temperature dependent, the lower frequency band becoming relatively more intense with rising temperature. In a later publication (5), Bellamy and Williams further established that the relative intensities of the two peaks varied with the solvent, the band at higher frequency increasing in relative intensity with change from a solvent of lower polarity (CCl_4) to one of higher polarity ($CH_3.CN$). By analogy with the influence of the C—X conformation on the C=O stretching bands of α-halogenated cyclohexanone derivatives (6, 7, 8, 9), Bellamy and collaborators assigned the doublet band of higher frequency to the *cis* form (I), and, from the temperature effect, they inferred that this is thermodynamically the more stable conformation.

This investigation extends these studies to acetophenone derivatives containing —Br, —I, —C≡N, —C_6H_5, and —OH substituents in the methyl group. The substitution effects on the integrated absorption intensities are also considered.

[1]*Manuscript received February 3, 1958.*
Contribution from the Division of Pure Chemistry, National Research Council, Ottawa, Canada. Presented in part at a meeting of the Chemical Institute of Canada, May 27, 1958.
Issued as N.R.C. No. 4739.
[2]*National Research Council Postdoctorate Fellow.*

Can. J. Chem. Downloaded from www.nrcresearchpress.com by 200.7.193.243 on 09/04/12
For personal use only.

EXPERIMENTAL

The spectra were determined in carbon tetrachloride and chloroform solutions on a Perkin-Elmer model 112 double-pass single-beam spectrometer using a calcium fluoride prism at a computed spectral slit width (S') of 1.6 cm.$^{-1}$ (10). The absolute values reported for the positions of the band maxima are correct within ± 1 cm.$^{-1}$ and the reproducibility is accurate to ± 0.5 cm.$^{-1}$. The integrated absorption intensities were determined by method II of Ramsay (11, 12); integration was performed by the use of Simpson's Rule and extended out into the wings of the band to the point where the measured optical density was 0.01. Corrections for finite spectral slit width were not applied since the ratio of S' to the half band width ($\Delta\nu_{\frac{1}{2}}^{(a)}$) was less than 0.2 in all cases except phenacyl alcohol (10). For this compound $\Delta\nu_{\frac{1}{2}}^{(a)} = 8$ cm.$^{-1}$ and the finite slit error on the basis of Ramsay's calculations would amount to about 2%.

The compounds were obtained commercially, or prepared by standard methods, and purified by fractional crystallization, vacuum distillation, vacuum sublimation, or combinations of these techniques. The melting points, boiling points, and refractive indices were consistent with values reported in the literature.

RESULTS AND DISCUSSIONS

The positions and intensities of the C=O stretching bands in both solvents are listed in Table I.

TABLE I

POSITIONS AND INTENSITIES OF THE C=O STRETCHING BANDS IN THE INFRARED SPECTRA OF SUBSTANCES C_6H_5—CO—R

	CCl_4 solution			$CHCl_3$ solution		
Group R	ν_1 (cm.$^{-1}$)	ν_2 (cm.$^{-1}$)	Integrated absorption intensity[a]	ν_1 (cm.$^{-1}$)	ν_2 (cm.$^{-1}$)	Integrated absorption intensity[a]
—CH_3	1691		*2.18, 2.26, 2.18*; 2.20	1683		2.7[b]
—CH_2Cl	1714	1694	*2.02, 1.89, 1.83*; 1.91	1707	1689	*2.16, 2.13, 2.28*; 2.19
—$CHCl_2$	1716	1693	*1.88, 1.85*; 1.87	1710	1687	*2.05, 1.97*; 2.01
—CCl_3	1717.5	—	*1.56, 1.41*; 1.49	1713	—	*1.85, 1.92*; 1.88
—CH_2Br	1709	1688	*2.07, 1.91, 1.94*; 1.97	1702	1684	*2.21, 2.18*; 2.20
—$CHBr_2$	1707	1682	*1.78, 1.84, 1.82*; 1.81	1702	1678	*1.88, 2.04*; 1.96
—CBr_3	1704	—	*1.32, 1.41, 1.44*; 1.39	1700	—	*1.61, 1.54, 1.60*; 1.58
—CH_2I	1701[c]	1683	*2.13, 2.06*; 2.10	1696	1678	*2.27, 2.19*; 2.23
—$CH_2.CN$	1709	—	*2.07, 2.18, 2.08*; 2.11	1703	—	*2.27, 2.33*; 2.30
—$CH_2.C_6H_5$	1698	1685	*2.02, 1.90, 1.98*; 1.97	—	1680	*2.08, 2.26, 2.21*; 2.18
—$CH_2.OH$	1692	—	*1.76, 1.73*; 1.75	1687	—	*2.09, 2.04*; 2.07

[a] *The intensities are expressed in units of 10^4 mole^{-1} liter cm.$^{-2}$. The individual measurements are reported in italics followed by the arithmetical mean in roman type.*
[b] *This figure is taken from the data of G. N. Barrow, J. Chem. Phys.* **21**, *2008 (1953).*
[c] *Inflection.*

Band Positions

The compounds containing the groups —CH_2Cl, —$CHCl_2$, —CH_2Br, —$CHBr_2$, —CH_2I, and —$CH_2.C_6H_5$ give two bands, designated ν_1 and ν_2. The compounds containing —$CH_2.CN$ and —$CH_2.OH$ show one band only, as do those containing —CCl_3 and —CBr_3 groups.

The doublet maxima noted for —CH_2Cl and —$CHCl_2$ agree with the observations of Bellamy and collaborators (4) on these compounds and the band positions in carbon

tetrachloride solution check with the amended values reported by these investigators in their later publication (5). In all cases where doublets are observed the band at higher frequency (ν_1) is relatively more intense in chloroform than in carbon tetrachloride solution, indicating that the ν_1 band is associated with the more polar structure. This is consistent with the assignment of the ν_1 band to the *cis* conformation I.

In any carbonyl compound, the C=O stretching frequency is determined by a combination of steric, electrical, and mass effects of the groups surrounding the C=O bond. These effects have been reviewed in a preceding publication (13). At present the relative importance of the different effects for a given structure cannot be evaluated quantitatively, though certain structures are encountered in which one or other of these effects can be recognized to exercise a dominating influence.

Substitution Effects in the gauche Conformation (Band ν_2)

The band at lower frequency falls in the range 1694–1682 cm.$^{-1}$ in carbon tetrachloride solution and 1689–1678 cm.$^{-1}$ in chloroform. Except for the chlorinated compounds, the band lies below that of acetophenone, and the frequency diminishes in the sequence:

$-CH_2Cl$	>	$-CHCl_2$	>	$-CH_3$	>	$-CH_2Br$	>	$-CH_2.C_6H_5$	>	$-CH_2I$	>	$-CHBr_2$
(49.5)		(84)		(15)		(94)		(91)		(141)		(173)

Since electron withdrawal raises the C=O frequency, this sequence shows that the polar effect of the substituent is opposed by mass and/or steric effects that act to lower the frequency. If acetophenone itself is excluded, the above sequence approximates to one of increasing mass, as is indicated by the molecular weights of the groups given above in parenthesis.

Although the mass effect may be predominant, the influence of the electrostatic and steric effects of the substituent is also apparent. The inductive effect should be strongest for chlorine; the increase in the ν_2 frequencies of the chloro compounds can be explained in this way, and it is consistent with the substitution effects of chlorine on the ν_1 band discussed below.

Steric effects should be most in evidence in the bromide and iodide. In these compounds (III) the *ortho* hydrogen atom of the benzene ring and *gauche* halogen atom appear to be in the same steric relationship as in the *ortho*-halogenated acetophenones in the *s-trans* configuration (IV), for which steric interaction effects have been demonstrated (13).

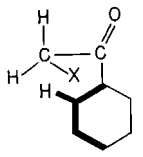

X = Br, I

III

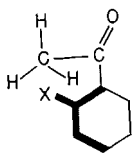

X = Br, I

IV

This steric strain can be released in a number of ways: (*a*) by a slight rotation of the methyl group about the CO—CH_2X axis; (*b*) by a slight rotation of the plane of the benzene ring about the 1,4-axis; (*c*) by increase in the angle α in

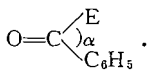

.

Can. J. Chem. Downloaded from www.nrcresearchpress.com by 200.7.193.243 on 09/04/12
For personal use only.

Of these effects (*a*) should have little effect on the ν_2 frequency and should be inoperative for the disubstituted derivatives, (*b*) should raise the C=O frequency by diminishing the resonance with the aromatic ring, and (*c*) should lower the frequency. In fact *ortho* bromination of acetophenone raises the C=O frequency by 11 cm.$^{-1}$ whereas bromination in the methyl group lowers it by 3 cm.$^{-1}$; the analogy between the steric conditions in these structures is therefore more apparent than real. The steric strain in IV would appear to be relieved largely by rotation of the whole acetyl group with respect to the ring, and the strain in III by opening of the R—CO—R angle.

Substitution Effects on the ν_1 Band

For the ν_1 band the C—O stretching frequency is in all cases greater than that of acetophenone, and diminishes in the series:

$$-CCl_3 > -CHCl_2 > -CH_2Cl > -CH_2CN > -CH_2Br > -CHBr_2 > -CBr_3 > -CH_2I > -CH_2.C_6H_5 > -CH_3.$$

Here the electronegativity of the substituent exercises the dominant influence. The trisubstituted groups $-CCl_3$ and $-CBr_3$ exhibit one band only, and since this lies well above that of acetophenone it is to be classified with the ν_1 series. For the chloro derivatives ν_1 increases with increasing substitution ($-CCl_3 > -CHCl_2 > -CH_2Cl$), whereas for bromination the sequence is reversed ($-CH_2Br > -CHBr_2 > -CBr_3$). The introduction of the first chlorine atom (in the *cis* position) changes the C=O frequency by +23 cm.$^{-1}$, while the further displacements on introduction of the second and third chlorine atoms in the *gauche* positions are +2 and +1.5 cm.$^{-1}$ respectively.* Although small, these additional positive shifts are significant, and they agree with the shifts produced by chlorination on the ν_2 band. The major shift induced by the *cis* C—Cl bond results largely from the direct dipole–dipole interaction across space, while the smaller shifts for the *gauche* C—Cl bonds are associated with the inductive effect acting through the bond system.

The "true" inductive effect of the *gauche* C—Cl bond on ν_1 must be somewhat greater than the 1 to 3 cm.$^{-1}$ actually observed. The *gauche* C—Cl bond will have a small dipole–dipole interaction with the C=O bond of opposite sign to that of the *cis* C—Cl bond. Furthermore the *gauche* C—Cl bond will have small steric and mass effects which will also act to lower the frequency. In the case of the bromo derivatives, these negative mass and steric effects are more important than the positive inductive effect of the *gauche* C—Br bond, and the reversed series is observed with the positive shift for $-CH_2Br$ (18 cm.$^{-1}$) exceeding that for $-CHBr_2$ (16 cm.$^{-1}$) and $-CBr_3$ (13 cm.$^{-1}$).

The low frequency of the single band in phenacyl alcohol suggests a *gauche* conformation, but more probably this molecule is stabilized in the *cis* conformation (V), with the hydrogen bonding being responsible for the excessive lowering of the ν_1 band. This band is symmetrical and very narrow ($\Delta\nu_{\frac{1}{2}}^{(a)} = 8$ cm.$^{-1}$), further evidence that only one molecular species is present.

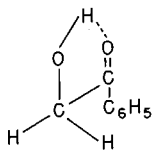

V

**All numerical data quoted in this discussion are for solutions in carbon tetrachloride unless otherwise indicated.*

Can. J. Chem. Downloaded from www.nrcresearchpress.com by 200.7.193.243 on 09/04/12
For personal use only.

Can. J. Chem. Downloaded from www.nrcresearchpress.com by 200.7.193.243 on 09/04/12
For personal use only.

Band Intensities

The integrated absorption intensity of the C=O stretching band in all types of carbonyl compounds varies over a comparatively small range between 1 and 5 intensity units.* Because the total range of intensity is so limited, it is difficult to evaluate the significance of small intensity changes associated with substitution effects. The situation is different with such bands as N—H stretch and C≡N stretch for which intensities have been observed to vary over a hundredfold range in various types of amines and nitriles (15, 16, 17).

Most of the ω-substituted acetophenones considered in this paper possess two carbonyl bands that overlap extensively. This overlap makes it impossible to evaluate the integrated absorption intensities of the ν_1 and ν_2 bands separately and only the total space integral under the complex band system can be obtained. The figures given in Table I are for this quantity.

In all cases, the integrated absorption intensity of this band system is greater in chloroform solution in carbon tetrachloride; this could indicate that the absorption of ν_1 is greater than that of ν_2, since the *gauche/cis* ratio is less in chloroform. However, the same solvent intensity effect is observed for the trichloro- and tribromo-derivatives and for acetophenone, itself, where the *gauche/cis* ratio is not involved. Most of the enhanced intensity in chloroform must therefore be attributed to a general solvent effect not dependent on the conformation.

In all cases, substitution diminishes the intensity of the carbonyl band system. The main features of these substitution effects are summarized in the series i–v listed below, where the groups are arranged in an order of diminishing band intensity. The sequence is the same in both solvents, though the quantitative differences are not.

(i) $-CH_3 > -CH_2I > -CH_2Br > -CH_2Cl$

(ii) $-CH_3 > -CH_2Cl > -CHCl_2 > -CCl_3$

(iii) $-CH_3 > -CH_2Br > -CHBr_2 > -CBr_3$

(iv) $-CH_3 > -CCl_3 > -CBr_3$

(v) $-CHCl_2 > -CHBr_2$

In series i–iii the intensity falls as the electronegativity of the functional group increases. Series iv and v, however, suggest that in the di- and tri-substituted compounds bromine is more effective than chlorine in lowering the band intensity. This effect is probably predominantly steric as it is only observed in the polysubstituted derivatives.

Substitution Effects on the gauche/cis Ratio

Because of the extensive overlap the integrated absorption intensities cannot be used to determine the equilibrium concentrations of the *gauche* and *cis* species. Some information about this equilibrium can be obtained from the ratio of the extinction coefficients at the peaks of the ν_1 and ν_2 bands. These are summarized in Table II.

The single peak of phenacyl cyanide shows little change in intensity or band width in the two solvents; from the position of the maximum (1709 cm.$^{-1}$ in CCl_4) it can be assumed that this compound exists exclusively in the *cis* conformation. The iodide shows a strong maximum at 1683 cm.$^{-1}$ in the same solvent, with a weak inflection at 1701 cm.$^{-1}$, and therefore exists predominantly, but not exclusively, in the *gauche* form. The iodide and nitrile represent the extremes of *gauche* and *cis* stabilized systems; the other compounds are listed in Table II in a sequence of increasing ratio of $\epsilon^{(a)}_{\nu_2,max}$ to $\epsilon^{(a)}_{\nu_1,max}$, and with some

**The unit of integrated absorption intensity employed here is 10^4 mole^{-1} liter cm.$^{-2}$. (See Ref. 18.)*

TABLE II

MOLECULAR EXTINCTION COEFFICIENTS OF ABSORPTION MAXIMA FOR C=O STRETCHING BANDS IN INFRARED SPECTRA OF SUBSTANCES C_6H_5—CO—R

	—CH_2OH	—CH_2CN	—$CHBr_2$	—$CHCl_2$	—CH_2Cl	—$CH_2.C_6H_5$	—CH_2Br	—CH_2I
A. CCl_4 solution								
$\epsilon^{(a)}_{\nu_1,max}$	700	400	335	245	240	220	116	60[a]
$\epsilon^{(a)}_{\nu_2,max}$	—	—	260	330	375	375	610	700
$\epsilon^{(a)}_{\nu_2,max}/\epsilon^{(a)}_{\nu_1,max}$	0	0	0.78	1.35	1.56	1.70	5.26	11.7
B. $CHCl_3$ solution								
$\epsilon^{(a)}_{\nu_1,max}$	492	444	318	290	262	*b*	145	80
$\epsilon^{(a)}_{\nu_2,max}$	—	—	148	172	214	295	384	470
$\epsilon^{(a)}_{\nu_2,max}/\epsilon^{(a)}_{\nu_1,max}$	0	0	0.47	0.59	1.22	*b*	2.65	5.9

[a] *Inflection.*
[b] *For the* —$CH_2.C_6H_5$ *group the carbonyl band envelope is particularly broad in chloroform solution and could not be resolved.*

reservations this can be identified with the sequence of increasing *gauche/cis* equilibrium ratio.

This series approximates to one of increasing stability of the *cis* form with increased electron-withdrawing effect of the X group. From III we might expect that with increase in the size of the X substituent, the increasing steric hindrance would raise the energy of the *gauche* forms, and so shift the equilibrium in favor of the *cis* conformation. In fact, the reverse appears to be true; in the iodide the equilibrium is greatly in favor of the *gauche* form, in spite of the steric hindrance associated with the large iodine atom. It is evident that we are dealing here with a complex interplay of factors which cannot be evaluated *a priori.*

VALIDITY OF THE ASSIGNMENTS

In assigning the ν_1 and ν_2 bands respectively to the *cis* and *gauche* conformations we have accepted the arguments advanced by Bellamy, Thomas, and Williams (4, 5). These in turn are based partly on an earlier generalization from this laboratory (6) that "*large positive shifts of the* C=O *stretching frequency on α-bromination in the cyclohexanone ring system in the chair configuration occur only when the bromine atom occupies an equatorial position*". This generalization was later extended to other halogens (Ref. 14, p. 478), while Corey and collaborators (7, 8, 9) have shown that conformational assignments based on this rule are consistent with those derived from thermodynamic considerations. Kumler and Huitric (19) have questioned some of Corey's conclusions because they conflicted with dipole moment data. The criticisms however were directed against Corey's assumption of a rigid chair configuration for the cyclohexanone ring in certain compounds, and not against the spectroscopic argument per se.

The existence of spectroscopic effects associated with conformational equilibria in compounds of this type was first recognized by Mizushima and co-workers (2) in chloroacetone. Initially these investigators assigned the C=O band of lower frequency to VI, which they considered thermodynamically more stable than the *gauche* structure VII. This was not consistent with the conclusions of Bellamy, Corey, and ourselves, since it required that the parallel alignment of C=O and C—Cl dipoles should produce

Can. J. Chem. Downloaded from www.nrcresearchpress.com by 200.7.193.243 on 09/04/12
For personal use only.

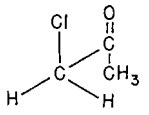

VI

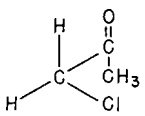

VII

a lesser spectral shift than the *gauche* arrangement. It was however in agreement with our observations in indicating greater thermodynamic stability for the *cis* conformation.

Recently Josien, Castinel, Chiurdoglu, and Vanlanduyt (20) in a reappraisal of Mizushima's data changed the assignment of the vapor-state carbonyl band of chloroacetone; this left the structural assignments for VI and VII unchanged, but indicated greater thermodynamic stability for VII over VI. This presented a complete reversal from the spectroscopic and thermodynamic behavior pattern developed by Bellamy, Corey, and ourselves for α-bromo ketones, and led Josien and collaborators to criticize our original interpretation of the α-halogenated cyclohexanone-type spectra.

The discussion of substitution effects earlier in this paper by no means fully explains the band shifts on the basis of the conformations associated with ν_1 and ν_2, but the situation is a good deal less satisfactory if the assignments are reversed. Without elaborating on this unnecessary detail, it can be noted, for example, that introduction of the first chlorine atom produces a positive displacement of $+23$ cm.$^{-1}$ for ν_1 while the additional displacements produced by the second and third chlorine atoms are $+2$ and $+1.5$ cm.$^{-1}$ respectively. If the ν_1 and ν_2 assignments are reversed this requires that the first (*gauche*) chlorine substituent produces the large displacement while the second (*gauche*) and the third (*cis*) substituents have only small effects. Difficulties of the same kind would be encountered in explaining the relatively small differences observed between mono- and di-halogenated substituents on the ν_2 band and such an assignment is quite untenable.

Finally, the recent re-examination of the spectrum of chloroacetone has led Bellamy and Williams (5) to reverse the assignments for the carbonyl bands of that compound, so that there is now complete consistency with the ω-substituted acetophenone spectra. With this change the conclusions from dipole moment measurements as well as the thermodynamic behavior of these compounds substantiate fully the hypothesis that large positive carbonyl shifts are associated with *cis*-bromination in the α-position.

ACKNOWLEDGMENTS

The acetophenone derivatives were prepared by one of us (E. S.) in the chemistry laboratories of the Manchester College of Science and Technology in connection with an investigation of their ultraviolet spectra. We wish to thank Dr. A. Burawoy for making them available to us for these studies.

REFERENCES

1. Nakagawa, I., Ichishima, I., Kuratani, K., Miyazawa, T., Shimanouchi, T., and Mizushima, S. J. Chem. Phys. **20**, 1720 (1952).
2. Mizushima, S., Shimanouchi, T., Miyazawa, T., Ichishima, I., Kuratani, K., Nakagawa, I., and Shido, N. J. Chem. Phys. **21**, 815 (1953).
3. Josien, M. L. and Calas, R. Compt. rend. **240**, 1641 (1955).
4. Bellamy, L. J., Thomas, L. C., and Williams, R. L. J. Chem. Soc. 3704 (1956).
5. Bellamy, L. J. and Williams, R. L. J. Chem. Soc. 4294 (1957).
6. Jones, R. N., Ramsay, D. A., Herling, F., and Dobriner, K. J. Am. Chem. Soc. **74**, 2828 (1952).
7. Corey, E. J. J. Am. Chem. Soc. **75**, 2301, 3297 (1953).
8. Corey, E. J., Topie, T. H., and Wozniak, W. A. J. Am. Chem. Soc. **77**, 5415 (1955).
9. Corey, E. J. and Burke, H. J. J. Am. Chem. Soc. **77**, 5418 (1955).

Can. J. Chem. Downloaded from www.nrcresearchpress.com by 200.7.193.243 on 09/04/12
For personal use only.

10. JONES, R. N. Spectrochim. Acta, **9**, 235 (1957).
11. RAMSAY, D. A. J. Am. Chem. Soc. **74**, 72 (1952).
12. JONES, R. N., RAMSAY, D. A., KEIR, D. S., and DOBRINER, K. J. Am. Chem. Soc. **74**, 80 (1952).
13. JONES, R. N., FORBES, W. F., and MUELLER, W. A. Can. J. Chem. **35**, 504 (1957).
14. JONES, R. N. and SANDORFY, C. The applications of infrared and Raman spectrometry to the eluicidation of molecular structure. *In* Technique of organic chemistry. Vol. IX. *Edited by* A. Weissberger. Interscience Publishers, Inc., New York and London. 1956.
15. RUSSELL, R. A. and THOMPSON, H. W. J. Chem. Soc. 483 (1955).
16. SKINNER, M. W. and THOMPSON, H. W. J. Chem. Soc. 487 (1955).
17. THOMPSON, H. W. and STEEL, G. Trans. Faraday Soc. **52**, 1451 (1956).
18. JONES, R. N., AUGDAHL, E., NICKON, A., ROBERTS, G., and WHITTINGHAM, D. J. Ann. N.Y. Acad. Sci. **69**, 38 (1957).
19. KUMLER, W. D. and HUITRIC, A. C. J. Am. Chem. Soc. **78**, 3369 (1956).
20. JOSIEN, M. L., CASTINEL, C., CHIURDOGLU, G., and VANLANDUYT, E. Compt. rend. **244**, 2383 (1957).

Can. J. Chem. Downloaded from www.nrcresearchpress.com by 200.7.193.243 on 09/04/12
For personal use only.

Can. J. Chem. Downloaded from www.nrcresearchpress.com by 200.7.193.243 on 09/04/12
For personal use only.

CLASSICAL APPROACH TO THE STRUCTURE OF CONDENSED-RING AROMATIC COMPOUNDS—A REJOINDER TO THE PROBLEM OF DIBENZO(*cd*,*mn*)PYRENE

LAKHBIR SINGH

According to the molecular-orbital treatment of the dibenzo(*cd*,*mn*)pyrene structure given by Lister (2), this molecule should be paramagnetic corresponding to two free electrons. It is a remarkable conclusion, as all other known hydrocarbons of this family including graphite are diamagnetic. The author of the present note, however, believes that the simple classical theory can still provide better guidance in such complicated problems. This approach can be considered reliable even today, as it is known that the earlier electronic theory was essentially correct in all its conclusions, "although expressed in a terminology which now seems old-fashioned" (1).

According to a new classical concept of the aromatic bond developed by the author (3), the π-electrons tend to form a continuous circular coupling round the benzene ring. However, the π-electron coupling in the condensed-ring aromatic compounds cannot be unique and stable, because the π-electrons on the carbon atoms which are common between two or three rings can complete the circular coupling (or the 'sextet') of only one of these rings at a time (4). Thus, the π-electron coupling in these complex molecules remains in a state of turmoil, which is responsible for their peculiar physical and chemical properties.

In naphthalene, each ring alternately becomes fully aromatic. Part of the time, the continuous aromatic coupling gets truncated in both the rings. The π-electrons at the α-positions, which do not form the continuous ring, return round these atoms to complete the π-electron coupling in the side ring. This side ring behaves more or less as a conjugated side chain (for half the time) and is the cause of greater reactivity of the napthalene

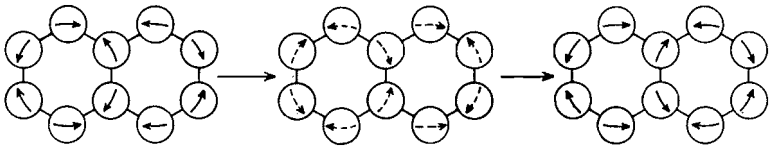

π-Electron coupling in naphthalene. The broken arrows represent the π-electrons on the lower side of the molecular plane.

molecule. In phenanthrene, most of the time a simple double bond remains in the middle ring, because of the greater tendency of the π-electrons to complete the sextets in the two outer rings. This explains the olefinic character of this C_9—C_{10} bond. In pyrene, however, a naphthalene type of coupling in the two middle rings also becomes equally

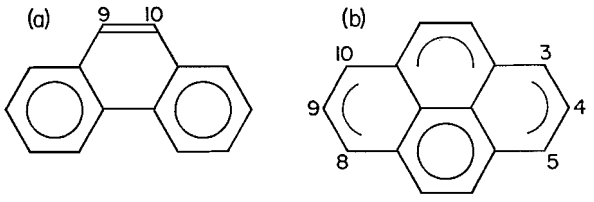

π-Electron coupling in phenanthrene (*a*) and pyrene (*b*).

effective. The transient π-electron coupling among three atoms in this molecule is supported by the reduction product 3,4,5,8,9,10-hexahydropyrene. The two π-electrons on the C_9 and C_{10} positions in the middle ring of anthracene remain uncoupled for part of the time. However, this molecule is not paramagnetic in spite of the abundant chemical evidence in favor of this partial free valence character at these two positions. This is owing to the fact that these π-electrons are not free in the usual sense of this term. They can be called free or uncoupled in a relative sense only. The π-electrons forming the

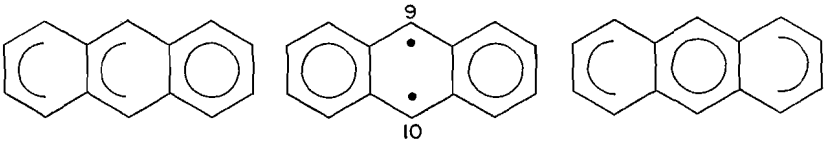

π-Electron coupling in anthracene.

aromatic bond couple on both sides of the molecular plane after each half revolution of these electrons round the carbon atoms (3). The π-electrons at the truncated ends of the aromatic bond couple after one full revolution around the carbon atoms (4) as in a simple covalent bond, while these partially free π-electrons in anthracene couple after one and a half revolutions. This situation arises only momentarily for each π-electron when it is on a C_9 or C_{10} atom. Under these circumstances the spin of the electron cannot be treated as free. These gradations in coupling are, however, reflected in the variations in chemical properties as shown by the benzene carbon atoms, the α-positions in naphthalene, and the C_9 and C_{10} positions in anthracene.

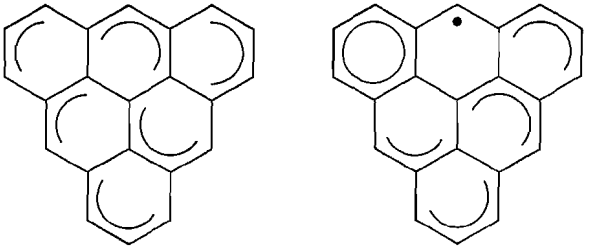

π-Electron coupling in dibenzo(*cd*,*mn*)pyrene.

On the basis of the above considerations, it can be predicted that the dibenzo(*cd*,*mn*)-pyrene hydrocarbon will not be paramagnetic. It may, however, have some free valence character of the anthracene type. The π-electron coupling in it can get truncated in many ways. The actual weight to these possibilities can be decided only after the chemical properties are known.

1. DEWAR, M. J. S. *In* Progress in organic chemistry. Vol. 2. *Edited by* J. W. Cook. Butterworths Scientific Publications, London. 1953. p. 1.
2. LISTER, M. W. Can. J. Chem. **35**, 934 (1957).
3. SINGH, L. Naturwissenschaften, **43**, 466 (1956) (in English).
4. SINGH, L. Naturwissenschaften, **44**, 111 (1957) (in English).

RECEIVED DECEMBER 23, 1957.
PHYSICAL CHEMISTRY DIVISION,
NATIONAL CHEMICAL LABORATORY,
POONA, INDIA.

Can. J. Chem. Downloaded from www.nrcresearchpress.com by 200.7.193.243 on 09/04/12
For personal use only.

Can. J. Chem. Downloaded from www.nrcresearchpress.com by 78.46.186.204 on 09/04/12
For personal use only.

Canadian Journal of Chemistry

Issued by THE NATIONAL RESEARCH COUNCIL OF CANADA

VOLUME 36 JULY 1958 NUMBER 7

THE STRUCTURE OF MITRAPHYLLINE[1]

J. C. SEATON,[2] R. TONDEUR,[2] AND LÉO MARION

ABSTRACT

Mitraphylline ($C_{21}H_{24}O_4N_2$) contains a carbomethoxyl group, and on hydrolysis gives rise to mitraphyllic acid. Spectroscopic evidence shows that the alkaloid contains two chromophores, one characteristic of an oxindole and one corresponding to the grouping $CH_3OOC—C'=CH.OR$. On treatment with dilute mineral acid the alkaloid gives rise to mitraphyllal ($C_{19}H_{24}O_3N_2$), which is a hemiacetal that no longer contains the isolated double bond and the carbomethoxyl group originally present in the alkaloid. Reduction of mitraphyllal by the Wolff–Kishner reaction gives mitraphyllane ($C_{19}H_{26}O_2N_2$). The dehydrogenation of mitraphyllal produced 3,4-diethylpyridine and 3-ethyloxindole. The action of lithium aluminum hydride on mitraphylline under mild conditions gave rise to mitraphyllol by reduction of the carbomethoxyl group, and under more vigorous conditions to dihydrodesoxy-mitraphyllol by reduction of the oxindole carbonyl as well. This last product has the properties of an aromatic amine. On the basis of the new experimental evidence, a total structure of mitraphylline is derived.

Mitraphylline has been isolated from *Mitragyna rubrostipulacea* Havil. (= *Adina rubrostipulata* K. Schuman)[3] by Michiels (1), by Denis (2), and also by Raymond-Hamet (3). Michiels (4) also isolated it from *M. stipulosa* Kuntze (= *M. macrophylla* Hiern.). In all cases except one (5) the alkaloid has been isolated in the laevorotatory form. It has been assigned the formula $C_{21}H_{24(26)}O_4N_2$, and assumed to contain a carbomethoxyl group and one C-methyl group (6). Distillation of mitraphylline hydrochloride from zinc dust under reduced pressure yields a neutral substance $C_{10}H_9ON$, 3,4-diethylpyridine, and isoquinoline (6, 7). The same neutral substance has also been obtained from rhyncophylline (8) and uncarine-A (9). It has been converted to 3-ethyloxindole by hydrogenation (7). Wenkert and Reid (10) have suggested that it was probably spiro-3,3-cyclopropyloxindole, and the identity has since been established by Kondo *et al.* (11) by direct comparison with a synthetic specimen. A monoacetyl derivative has been reported (7). Mitraphylline gives a yellow color with tetranitromethane, forms an amorphous dibromide, and when hydrogenated over Adams' catalyst absorbs 3 moles of hydrogen, but over a palladium catalyst, it is reported to absorb only 1 mole (5).

Mitraphylline has now been re-examined and sufficient additional evidence obtained to make it possible for us to advance a total structure for the alkaloid. Although many references to mitraphylline in the literature (6) include an expanded formula showing a

[1]*Manuscript received March 31, 1958.*
Contribution from the Division of Pure Chemistry, National Research Council, Ottawa, Canada.
Issued as N.R.C. No. 4745.
[2]*National Research Council of Canada Postdoctorate Fellow.*
[3]*The identity of this species seems to be controversial. Certain authors include it in the genus Mitragyna. Botanically, the two genera are very close, but it has been claimed that there are sufficient criteria to include the species in the genus Adina. The plant has been studied successively under several names. For a botanical description of the plant see J. Lebrun, Les essences forestières du Congo Belge, Publication INEAC, Vol. 2, p. 220, Brussels, 1939.*

carbomethoxyl group, the presence of such a group does not seem to have been demonstrated experimentally before. The analysis of mitraphylline and its degradative products confirm the formula $C_{21}H_{24}O_4N_2$. The base was hydrolyzed with potassium hydroxide to the crystalline mitraphyllic acid, $C_{20}H_{22}O_4N_2$. When re-esterified with methanol and hydrogen chloride the acid was partially reconverted to mitraphylline which, however, was contaminated with another product and could not be completely purified. Its X-ray powder diagram contained all the lines present in the X-ray diagram of pure mitraphylline, but a few additional faint lines were also present.

The ultraviolet spectrum of mitraphylline is identical with that of rhyncophylline, which has been shown to be made up of contributions from an oxindole chromophore and the grouping $CH_3O_2C—\acute{C}=CH.OR$ (12). The infrared absorption spectrum in chloroform shows a band at 3415 cm.$^{-1}$ indicative of an imino group, and in nujol mull it contains bands at 1725 and 1704 cm.$^{-1}$ attributable to an ester carbonyl and an oxindole carbonyl respectively, at 1626 and 755 cm.$^{-1}$ due to a benzene ring, and at 1105 cm.$^{-1}$ indicative of a cyclic ether. The intensity of the absorption at 1626 cm.$^{-1}$, however, is greater than that expected for a benzene ring, and it is probable that it also includes a contribution from a polarized double bond.

Hydrogenation of the alkaloid in acetic acid solution over a platinum catalyst yielded a hexahydroderivative $C_{21}H_{30}O_4N_2$. The absence of a band at 755 cm.$^{-1}$ in the infrared absorption spectrum of this product indicated that the benzene ring had been hydrogenated. The fact that the ultraviolet spectrum did not contain the usual absorption of an oxindole chromophore confirmed this, while the retention of the strong absorption at 239 mμ, due to the grouping $CH_3OOC—\acute{C}=CH.OR$, showed that the isolated double bond had not been affected (cf. 5). The presence of a band at 1626 cm.$^{-1}$ in the infrared spectrum of the product is also probably due to this double bond.

Reduction of mitraphylline with lithium aluminum hydride at room temperature gave rise to an alcohol, $C_{20}H_{24}O_3N_2$, that we propose to designate as mitraphyllol. Its infrared absorption spectrum contained a split oxindole carbonyl at 1730–1708 cm.$^{-1}$, and a band at 1654 cm.$^{-1}$ indicating that the enol–ether grouping was still present. The shift of the last absorption band from 1626 cm.$^{-1}$ (in the spectrum of mitraphylline) was to be expected because reduction of the ester to a primary alcohol group would remove the conjugation. The ultraviolet spectrum of mitraphyllol is that of a simple oxindole.

Under more vigorous conditions, the reduction of mitraphylline with lithium aluminum hydride produced dihydrodesoxy-mitraphyllol, $C_{20}H_{26}O_2N_2$. The infrared spectrum of this product showed no carbonyl absorption, but still contained a band at 1660 cm.$^{-1}$ due to the absorption of the enol–ether double bond. The ultraviolet spectrum was that of an aromatic amine, and indeed, dihydrodesoxy-mitraphyllol coupled with diazotized sulphanilic acid to form an indicator-type dye. Since this reduction of the oxindole carbonyl produced an amine and not an indole derivative it can be concluded that the 3-position of the oxindole system in the alkaloid must be disubstituted (13).

Acid hydrolysis of mitraphylline gave rise to a basic product (cf. 12) which could not be crystallized, but formed a crystalline picrate in methanol. The base regenerated from the picrate was a well-defined crystalline substance, $C_{20}H_{26}O_3N_2$, containing one methoxyl group. The presence of a methoxyl seemed to indicate that the expected aldehyde had, in the presence of methanol, been converted to a hemiacetal. That this was actually so became apparent when the crystalline base was obtained on treatment of the amorphous hydrolysis product with 1% methanolic hydrogen chloride. The ultraviolet spectrum of the crystalline product was that of a simple oxindole, thus indicating that the enol–ether

171537

Can. J. Chem. Downloaded from www.nrcresearchpress.com by 78.46.186.204 on 09/04/12
For personal use only.

system was no longer present. The infrared absorption spectrum contained a split oxindole carbonyl band at 1695–1730 cm.$^{-1}$, bands at 1625 and 750 cm.$^{-1}$ due to the benzene ring, and three new bands at 1180, 1140, and 1060 cm.$^{-1}$ which are reported to be characteristic of an acetal (14). The crystalline product $C_{20}H_{26}O_3N_2$, for which we suggest the name methylmitraphyllal, gave on hydrolysis a base which could not be induced to crystallize. This base contained no methoxyl group, it slowly reduced Tollens' reagent, and could be methylated in almost quantitative yield to methylmitraphyllal. Its infrared spectrum contained no absorption attributable to an aldehyde, but did contain an absorption band in the hydroxyl region, and therefore the amorphous substance must be a hemiacetal and will be designated as mitraphyllal. Further evidence that mitraphyllal was a hemiacetal was provided by the Wolff–Kishner reduction, which yielded mitraphyllane ($C_{19}H_{26}O_2N_2$), an amorphous product isolated as its crystalline picrate. As expected, the infrared absorption spectrum of mitraphyllane in chloroform contained a peak at 3600 cm.$^{-1}$ indicating the presence of a hydroxyl group.

The formation of mitraphyllal and methylmitraphyllal is consistent with the presence in the alkaloid of the cyclic system I since hydrolysis of the ester and the enol–ether group followed by decarboxylation and cyclization would result in the formation of a hemiacetal II.

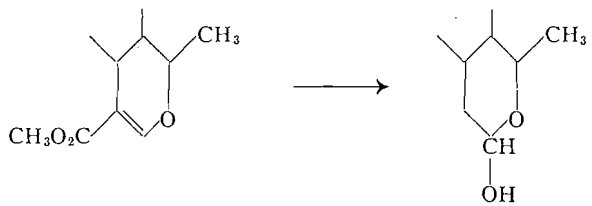

I II

Dehydrogenation of mitraphyllal with palladium–charcoal produced 3,4-diethylpyridine and 3-ethyloxindole. Hence the experimental evidence indicates the presence in the alkaloid of fragment III and either fragment IV or V. It was hoped to distinguish between IV and V by means of the dehydrogenation product of mitraphyllol, which was expected

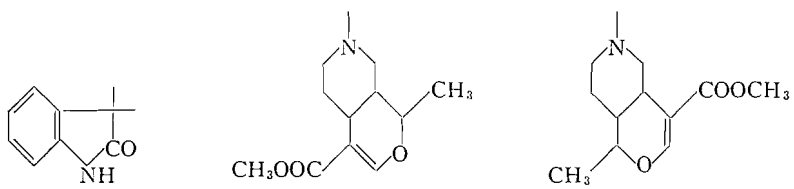

III IV V

to be 3-ethyl-4-isopropylpyridine. Unfortunately, this dehydrogenation either with selenium or with palladium produced 3,4-diethylpyridine. Biogenetically, however, structural element IV is more likely than V. Furthermore, structure IV occurs in a number of carboline alkaloids (15–18) whereas structure V has not yet been found. Also, IV definitely corresponds to the structure of rhyncophylline (12) and may legitimately be assumed to be present in mitraphylline.

The biogenetic derivation of mitraphylline is probably similar to that suggested for rhyncophylline (12) involving the same starting materials. As for rhyncophylline, the α-position of the piperidine ring would be linked to the 3-position of the oxindole system,

Can. J. Chem. Downloaded from www.nrcresearchpress.com by 78.46.186.204 on 09/04/12
For personal use only.

and therefore, the structure of mitraphylline must be that shown in formula VI (R = O, R′ = CO_2CH_3). On the basis of this formula, the structures of the various derivatives

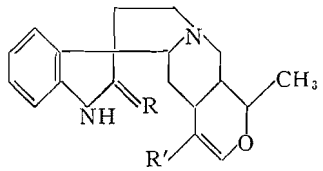

VI (R = O; R′ = CO_2CH_3)
VII (R = O; R′ = CH_2OH)
VIII (R = H_2; R′ = CH_2OH)

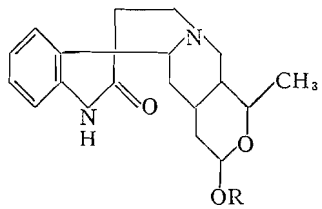

IX (R = H)
X (R = CH_3)

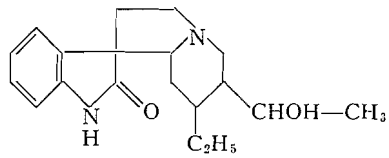

XI

of mitraphylline became obvious. Thus mitraphyllol is represented by VII, dihydrodesoxymitraphyllol by VIII, mitraphyllal by IX, methylmitraphyllal by X, and mitraphyllane by XI.

Just as rhyncophylline is the oxindole analogue of corynantheine, mitraphylline is the oxindole analogue of the four stereoisomerides ajmalacine (δ-yohimbine, tetrahydroserpentine) (15), mayumbine (16), akuammigine (17), and tetrahydroalstonine (18).

EXPERIMENTAL

The ultraviolet spectra were determined in absolute ethanol, unless otherwise stated, on a Beckmann DU spectrometer. The infrared absorption spectra were recorded with a Perkin–Elmer double beam instrument model 21. The peaks are indicated by a wave number and the percentage absorption (in parenthesis). The compounds were dispersed in mulls in nujol unless otherwise mentioned. All melting points were taken on a microscope hot stage and are uncorrected.

Mitraphylline

The alkaloid was obtained from the bark of *Mitragyna rubrostipulacea* Havil.[4] Mitraphylline consisted of colorless needles, m.p. 275–276°, $[\alpha]_D^{24}$ −3° (*c*, 1.3 in chloroform), −39° (*c*, 2.4 in 0.1 *N* hydrochloric acid), pK_a 4.6 (by titration in 80% methylcellosolve with 0.02 *N* hydrochloric acid). Found: C, 68.60; H, 6.69; N, 7.59; OCH_3, 8.46; act. H, 0.29. Calcd. for $C_{21}H_{24}O_4N_2$: C, 68.46; H, 6.57; N, 7.60; 1 OCH_3, 8.41; 1 act. H, 0.27%. Ultraviolet absorption: shoulder at 280 mμ, log ε 3.18, λ_{max} 243 mμ, log ε 4.22, λ_{min} 224 mμ, log ε 4.02. Infrared absorption: 3260(32), 1725(85), 1704(84), 1626(74), 1105(74), 755(46). In chloroform: 3415(20), 1715(81), 1625(68).

The base formed a perchlorate that crystallized from alcohol–ether as long prismatic needles, softening at 214° and melting at 240°, $[\alpha]_D^{22}$ −26°±6 (*c*, 1 in 95% ethanol). A

[4]*Collected in the Northeast section of the Experimental Station (Mulungu) of the Institut pour l'étude agronomique du Congo (INEAC) in whose chemical laboratory the isolation of the alkaloids was carried out. The extraction of the bark was done in the plant of the Cooperative Congokina, Costermansville, Belgian Congo.*

Can. J. Chem. Downloaded from www.nrcresearchpress.com by 78.46.186.204 on 09/04/12
For personal use only.

hydriodide was also prepared that consisted, after crystallization from absolute methanol, of silky needles, m.p. 233–236°, $[\alpha]_D^{22}$ −13.5° (*c*, 1.2 in absolute ethanol). Found: C, 51.31; H, 5.14. Calcd. for $C_{21}H_{24}O_4N_2.HI$: C, 50.80; H, 5.08%.

Alkaline Hydrolysis of Mitraphylline

The base (0.35 g.) was refluxed for 1 hour in methanol (9 ml.) containing water (1 ml.) and potassium hydroxide (0.5 g.). The methanol was distilled off and the aqueous solution neutralized with dilute hydrochloric acid. The mixture was then extracted with chloroform, and the extract was dried and evaporated to dryness. The residual mitraphyllic acid (150 mg.) partially crystallized when benzene was added. After several recrystallizations from ethanol, it consisted of colorless prisms (45 mg.), m.p. 301° (decomp.). $[\alpha]_D^{22}$ +21.4° (*c*, 1.17 in pyridine). Found: C, 67.66; H, 6.28; N, 7.73. Calcd. for $C_{20}H_{22}O_4N_2$: C, 67.78; H, 6.26; N, 7.91%.

Esterification of Mitraphyllic acid

The acid (66 mg.) was refluxed for 10 minutes in a saturated solution of methanolic hydrogen chloride (3 ml.). The solvent was evaporated and the base liberated with ammonium hydroxide was extracted with chloroform. The extract was washed with water, dried, and evaporated to dryness. It left a residue (49 mg.) which was chromatographed on alumina (grade II). Elution with chloroform containing 1% methanol gave mitraphylline (28 mg.), which after crystallization from methanol, melted at 257–259° either alone or in admixture with pure mitraphylline. The X-ray powder photograph confirmed the identity with mitraphylline.

Acetylmitraphylline

Mitraphylline (190 mg.) was acetylated in pyridine (2 ml.) and acetic anhydride (0.5 ml.). The acetylated product (68 mg.) after crystallization from methanol–water, melted at 171–173°. $[\alpha]_D^{23}$ −6.2 (*c*, 1.0 in ethanol). Found: C, 67.33; H, 6.21; N, 6.54; $COCH_3$, 9.96. Calcd. for $C_{23}H_{26}O_5N_2$: C, 67.30; H, 6.39; N, 6.83; 1 $COCH_3$, 10.49%. pK_a 4.3 (by titration with 0.02 *N* hydrochloric acid in 80% methylcellosolve).

Hexahydromitraphylline

Mitraphylline (108 mg.) was hydrogenated in glacial acetic acid (10 ml.) over Adams' catalyst (50 mg.) at 28° and 755 mm. of mercury. The hydrogen absorbed (23.4 ml.) corresponded to the volume calculated (21.5 ml.) to reduce three double bonds. The catalyst was filtered and the filtrate made basic with sodium carbonate solution and extracted with chloroform. The extract was dried over sodium sulphate, evaporated to dryness, and the residue crystallized from acetone from which it separated as colorless prisms (60 mg.), m.p. 276° (decomp.). $[\alpha]_D^{25}$ +15.3° (*c*, 0.97 in ethanol). Found: C, 67.29; H, 7.96; N, 7.51. Calcd. for $C_{21}H_{30}O_4N_2$: C, 67.35; H, 8.09; N, 7.48%. Ultraviolet absorption: λ_{max} 237 mμ, log ε 4.05, λ_{min} 215 mμ, log ε 3.72. Infrared absorption: 1710(89), 1698(89), 1630(70), 1105(76), 1092(77).

Acid Hydrolysis of Mitraphylline

Mitraphylline (500 mg.) was refluxed with 8% hydrochloric acid (125 ml.) for 3.5 hours, and the cooled solution neutralized with sodium bicarbonate and extracted with ether. The extract was dried over sodium sulphate and evaporated to dryness leaving the crude amorphous mitraphyllal (490 mg.), which was dissolved in absolute methanol (20 ml.). Picric acid (500 mg.) was added and the solution boiled for 30 minutes and then concentrated. The picrate crystallized as yellow prisms which after recrystallization from

Can. J. Chem. Downloaded from www.nrcresearchpress.com by 78.46.186.204 on 09/04/12
For personal use only.

methanol melted at 198–200° (decomp.). Found: C, 54.80; H, 5.03. Calcd. for $C_{20}H_{26}O_3N_2$. $C_6H_3O_7N_3$: C, 54.64; H, 5.11%. The base was regenerated on a basic resin (Amberlite IRA, 400) in methanol. The eluate on evaporation left a residue which crystallized from acetone in colorless prisms (methylmitraphyllal, 150 mg.) m.p. 224°, $[\alpha]_D^{25}$ −59.2° (*c*, 1.3 in ethanol). Found: C, 70.26; H, 7.49; N, 8.03; OCH_3, 8.43. Calcd. for $C_{20}H_{26}O_3N_2$: C, 70.15; H, 7.65; N, 8.18; 1 OCH_3, 9.05%. Ultraviolet absorption: shoulder at 780 mμ, log ε 3.18, λ_{max} 253 mμ, log ε 3.86, λ_{min} 228 mμ, log ε 3.33. Infrared absorption: 1730(94), 1696(81), 1625(56), 1183(74), 1140(71), 1060(88), 749(79).

Methylmitraphyllal

A solution of crude mitraphyllal (500 mg.) in 1% methanolic hydrogen chloride (50 ml.) was allowed to stand at room temperature overnight, refluxed for 30 minutes, and evaporated to dryness. Aqueous sodium carbonate was added to the residue and the mixture extracted with chloroform. The extract was dried over sodium sulphate, evaporated to dryness, and the residue was crystallized several times from acetone. The product (140 mg.) melted at 224° either alone or in admixture with a sample of methylmitraphyllal obtained as described above.

Hydrolysis of Methylmitraphyllal

Methylmitraphyllal (100 mg.) was refluxed with 1% hydrochloric acid (20 ml.) for 1 hour. The cooled solution was neutralized with sodium bicarbonate and extracted with ether. The extract was dried over sodium sulphate and evaporated to dryness. The residue consisted of the amorphous mitraphyllal, 95 mg. which contained no methoxyl group. Infrared absorption in chloroform: 3590(38), 3430(52), 1725(99), 1626(81). With Tollens' reagent mitraphyllal slowly formed a silver mirror. When treated with picric acid in methanol it gave an almost quantitative yield (150 mg.) of methylmitraphyllal picrate, m.p. 198–200° (decomp.).

Mitraphyllane

Mitraphyllal (100 mg.) trimethyleneglycol (2.5 ml.) and 95% hydrazine (250 mg.) were heated together at 150° for 1 hour. Potassium hydroxide (0.5 g.) was added and the excess of hydrazine evaporated while the temperature was increased to 200°. After 3 hours the mixture was cooled, water was added, and the solution extracted with ether. The extract was washed with water, dried over sodium sulphate, and evaporated to dryness. The residue was dissolved in methanol and a solution of picric acid (100 mg.) in methanol was added. The picrate was collected and recrystallized from methanol from which it separated in long yellow prisms (70 mg.) m.p. 167–169°. Found: C, 55.13; H, 5.48. Calcd. for $C_{19}H_{26}O_2N_2.C_6H_3O_7N_3$: C, 55.24; H, 5.38%. The base was regenerated on a basic resin (Amberlite IRA, 400) in methanol and was distilled at 0.1 mm. (air bath temperature 170–180°). It consisted of a colorless glass, 35 mg. $[\alpha]_D^{25}$ +39.3° (*c*, 0.89 in ethanol). Found: C, 72.42; H, 8.33. Calcd. for $C_{19}H_{26}O_2N_2$: C, 72.58; H, 8.34%. Ultraviolet absorption: shoulder at 280 mμ, log ε 3.21, λ_{max} 252 mμ, log ε 3.87, λ_{min} 229 mμ, log ε 3.60. Infrared absorption: 3200(55), 1707(92), 1625(61), 752(61). In chloroform: 3600(34), 3435(48), 1710(98), 1625(73).

Mitraphyllol

A solution of mitraphylline (500 mg.) and lithium aluminum hydride (400 mg.) in tetrahydrofuran (250 ml.) was allowed to stand at room temperature overnight. Water (3 ml.) was added, and after 30 minutes the precipitate was filtered off and washed with chloroform. The combined washings and filtrate were dried over sodium sulphate and

Can. J. Chem. Downloaded from www.nrcresearchpress.com by 78.46.186.204 on 09/04/12
For personal use only.

evaporated to dryness. The residue was crystallized from acetone from which it separated as colorless prisms (170 mg.), m.p. 227°, $[\alpha]_D^{25}$ −79.7° (*c*, 0.79 in ethanol). Found: C, 70.16; H, 6.81; N, 8.07. Calcd. for $C_{20}H_{24}O_3N_2$: C, 70.56; H, 7.11; N, 8.23%. Ultraviolet absorption: shoulder 280 mμ, log ε 3.11, λ_{max} 252 mμ, log ε 3.88, λ_{min} 230 mμ, log ε 3.57. Infrared absorption: 3270(59), 1730(89), 1708(88), 1655(62), 1626(67), 750(61).

Dihydrodesoxy-mitraphyllol

Mitraphylline (200 mg.) and lithium aluminum hydride (200 mg.) in dioxane were refluxed under nitrogen for 3 hours. Water (2 ml.) was added to the cooled solution, and after 30 minutes, the precipitate was filtered off and washed with chloroform. The combined filtrate and washings were dried over sodium sulphate and evaporated to dryness. The residue, after crystallization from ether, consisted of colorless prisms (105 mg.), m.p. 173–174°, $[\alpha]_D^{25}$ −15.9° (*c*, 1.26 in ethanol). Found: C, 73.44; H, 8.08; N, 8.66. Calcd. for $C_{20}H_{26}O_2N_2$: C, 73.59; H, 8.03; N, 8.58%. Ultraviolet absorption: λ_{max}, 295 mμ, log ε 3.45, λ_{max} 243 mμ, log ε 3.83, λ_{min} 270 mμ, log ε 3.59. Infrared absorption: 3375(48), 3180(50), 1660(56), 1615(56), 745(78).

A few drops of diazotized sulphanilic acid were added to a solution of dihydroxy-mitraphyllol in hydrochloric acid. A red color developed immediately which turned to yellow when the solution was made alkaline. The red color returned on acidification. Neither mitraphylline nor mitraphyllol coupled with diazotized sulphanilic acid.

Dehydrogenation of Mitraphyllal

Mitraphyllal (200 mg.) was heated with palladium–charcoal (30%, 200 mg.) under dry nitrogen to 290° during 1 hour. A distillate was collected which was fractionated into two portions, I, boiling below 210°, and II, boiling above 210°. Fraction I was a colorless basic liquid which formed a picrate crystallizing from methanol in yellow plates, m.p. 140–141°, not depressed on admixture with an authentic specimen of 3,4-diethylpyridine picrate. Found: C, 49.21; H, 4.25. Calcd. for $C_9H_{13}N.C_6H_3O_7N_3$: C, 49.45; H, 4.43%. The infrared spectrum was identical with that of 3,4-diethylpyridine picrate. Fraction II (boiling higher than 210°) was crystallized from hexane. It consisted of colorless prisms, m.p. 101°, not depressed on admixture with a synthetic specimen of 3-ethyloxindole. The X-ray powder diagram was identical with that of the synthetic specimen.

ACKNOWLEDGMENTS

We acknowledge our indebtedness to Mr. R. Lauzon and Dr. R. Norman Jones for recording the infrared absorption spectra, and to Dr. Maria Przybylska for the preparation of the X-ray powder diagrams. Also to the Institut pour l'étude agronomique du Congo, Mukungu, Belgian Congo, for the work done in their laboratories.

REFERENCES

1. Michiels, L. and Leroux. Bull. acad. roy. méd. Belg. **5**, 403 (1925); Michiels, L. J. pharm. Belg. **17**, 1049 (1935) (cited in Ref. 5).
2. Denis, P. Bull. acad. roy. Belg. **23**, 174 (1937).
3. Raymond-Hamet. Bull. Sci. Pharmacol. **46**, 327 (1939).
4. Michiels, L. J. pharm. Belg. **13**, 719 (1931).
5. Badger, G. M., Cook, J. W., and Ongley, P. A. J. Chem. Soc. 867 (1950).
6. Loudon, J. D. Symposium on naturally occurring nitrogen heterocyclic compounds. The Chemical Society, London. 1955.
7. Cook, J. W., Gailey, R. M., and Louden, J. W. Chem. & Ind. 640 (1953).
8. Barger, G., Dyer, E., and Sargent, L. J. J. Org. Chem. **4**, 418 (1939).
9. Ikeda, T. J. Pharm. Soc. Japan, **63**, 393 (1943).
10. Wenkert, E. and Reid, R. L. Chem. & Ind. 1390 (1953).
11. Kondo, H., Nozoye, T., and Tsukamoto, H. Ann. Rept. ITSUU Lab. Tokyo, **6**, 53 (1955).

Can. J. Chem. Downloaded from www.nrcresearchpress.com by 78.46.186.204 on 09/04/12
For personal use only.

12. SEATON, J. C. and MARION, L. Can. J. Chem. **35**, 1102 (1957).
13. JULIAN, P. L. and PRINTY, H C. J. Am. Chem. Soc. **71**, 3206 (1949).
14. BERGMANN, E. and PINCHAS, S. Rec. trav. chim. **71**, 161 (1952).
15. GOUTAREL, R. and LE HIR, A. Bull. soc. chim. France, (5), **18**, 909 (1951).
16. JANOT, M.-M., GOUTAREL, R., and MASSONNEAU, J. Compt. rend. **234**, 850 (1952).
17. ROBINSON, R. and THOMAS, A. F. J. Chem. Soc. 3479 (1954).
18. ELDERFIELD, R. C. and GRAY, A. P. J. Org. Chem. **16**, 506 (1951).

Can. J. Chem. Downloaded from www.nrcresearchpress.com by 78.46.186.204 on 09/04/12
For personal use only.

Can. J. Chem. Downloaded from www.nrcresearchpress.com by 78.46.186.204 on 09/04/12
For personal use only.

HYDROLYSIS OF SULPHATE ACID ESTER IN UNSTABILIZED CELLULOSE NITRATES[1]

PAUL E. GAGNON, KARL F. KEIRSTEAD,[2] BRIAN T. NEWBOLD, AND J. THOMAS

ABSTRACT

The rate of hydrolysis of the sulphate acid ester in unstabilized cellulose nitrates in acetone/water solution at 25° C. has been studied. The rate of hydrolysis in 90% acetone/water was too slow to produce a measurable increase in acidity during 24 hours. In 99% acetone/water solution the initial hydrolysis was very rapid and was followed by slower hydrolysis which was complete after 24 hours. Similar results were obtained with wood cellulose nitrates.

In the case of cotton cellulose nitrates, there was an indication that hydrolysis of the sulphate acid ester decreased as the nitrogen content increased. The rate of hydrolysis of the sulphate acid ester in both cotton and wood cellulose nitrates was very similar to that of the sulphate acid ester in cellulose acetate sulphate.

INTRODUCTION

It has been shown that the rate of hydrolysis of the sulphate ester of cellulose acetate sulphate depends on various factors of which the liquid medium is considered the most important (1). When cellulose acetate sulphate is dissolved in acetone the hydrolysis of the sulphate ester is rapid compared with that of the acetate ester. In 70% acetone the relative rates are reversed. At 25° C. or greater, the hydrolysis of the sulphate ester is complete after 24 hours (1). The solvolysis of both the sulphate ester and the acetate ester in acetic acid is well known (2). In water the cleavage of the acetate ester is more rapid than that of the sulphate ester (3).

Miles (4) has summarized the work done on the determination of sulphate ester in unstabilized cellulose nitrates by titration in acetone. The sulphate ester can be determined satisfactorily by titration in water, or analysis for calcium after ion exchange, or hydrolysis in acetone/water solution, or analysis for sulphate after treatment with 50% alcohol (5). Recently (6) the hydrolysis method for the determination of sulphate acid ester in acetone/water solution has been carefully studied.

The sulphate ester in unstabilized cellulose nitrate can be removed by prolonged boiling in water maintained just alkaline; the decomposition is most rapid when the boiling is carried out under slightly acid conditions (7). Spinks *et al.* (8) studied the sulphate content of unstabilized cellulose nitrate using $S^{35}O_4^=$ as a tracer, and found that it could only be removed at the expense of degradation and decomposition of the cellulose nitrate.

The object of the present work was to study the rate of hydrolysis of the sulphate acid ester in unstabilized cotton and wood cellulose nitrates in acetone/water solution.

EXPERIMENTAL

Cellulose Nitrate

The preparation of the cotton and wood unstabilized cellulose nitrates was carried out using the method mentioned in a recent publication (9). The cellulose nitrates were washed continuously for 48 hours with distilled water passed through an ion exchange column. Samples of cellulose nitrate were removed from the washing apparatus and dried

[1]*Manuscript received November 14, 1957.*
Contribution from Department of Chemistry, Laval University, Quebec, Que., with financial assistance from the Defence Research Board of Canada.
[2]*Present address: Lignosol Chemicals Limited, Quebec, Que.*

by centrifuging at 4000 r.p.m., for 5 minutes. Cotton cellulose nitrates could be dried by this method to approximately 35% moisture content and wood cellulose nitrates to about 45%. Samples were then set aside for moisture, nitrogen, and sulphate determinations (3). The per cent sulphate acid ester contents of the cellulose nitrates were determined by the hydrolysis method (6).

Hydrolysis of Sulphate Acid Ester in Unstabilized Cellulose Nitrates

The initial acidity of moist samples of cellulose nitrate in which there was no hydrolysis was determined by titration in 90% acetone/water solution, using the method recently described (6).

Hydrolysis experiments were performed on duplicate moist samples (2–3 g. dry weight) of cellulose nitrate dissolved in 99% acetone/water (700 ml.). Reagent grade acetone which contained 0.63% water, determined by an infrared absorption method, was used. The solutions were immediately placed in a constant-temperature bath controlled at 25°±0.1° C. The starting time of the experiments was taken when half the solvent had been added to the sample. Aliquots (100 ml.) were removed from the solutions at intervals and the hydrolysis stopped by dilution with distilled water (100 ml.). The increase in acidity was measured by titration with 0.01 *N* potassium hydroxide using a Macbeth pH meter.

The per cent hydrolysis was calculated directly by using the zero hydrolysis and 24-hour titers, expressed as milliliters per gram of cellulose nitrate. The 24-hour value represents the total sulphate content, because the sulphate acid ester is completely hydrolyzed. A typical example serves to illustrate the calculations involved. For a 12.1% unstabilized cotton cellulose nitrate containing 100% sulphate acid ester and 0.75% water, the zero hydrolysis titer was 5.19 ml./g. After 1 hour of hydrolysis, the titer was 11.50 ml./g. The 24-hour hydrolysis titer was 13.40 ml./g. Therefore, the percentage hydrolysis after 1 hour was $[(11.50-5.19)/(13.40-5.19)]\times 100 = (6.31/8.21)\times 100 = 77$.

RESULTS AND DISCUSSION

The difference in the rate of solvolysis of the sulphate acid ester and nitrate groups in unstabilized cellulose nitrate has been established by Gagnon *et al.* (5). In the present work, it was found that hydrolysis of the sulphate acid ester, RSO_4H, of cotton cellulose nitrate was effectively stopped by dissolving the moist cellulose nitrate in 90% acetone/water solution. The rate of hydrolysis was too slow to produce a measurable increase in acidity during 24 hours. Similar results were obtained for wood cellulose nitrates. Gagnon *et al.* (10) obtained similar results for the sulphate ester in cellulose acetate sulphate.

It was found that hydrolysis of the sulphate acid ester in unstabilized cotton cellulose nitrate could be carried out satisfactorily in 99% acetone/water solution at 25° C. In general, the initial hydrolysis of the sulphate acid ester is very rapid. For example, in one experiment, for an 11.7% N cotton cellulose nitrate containing 83% sulphate acid ester, the difference between the zero hydrolysis and 5-minute hydrolysis titers was 4.17, expressed as milliliters 0.01 *N* KOH per gram of cellulose nitrate. The difference for the 24-hour titer was 7.12 ml./g. The rate of hydrolysis slowed down considerably after 5 minutes. For instance, the difference between 5-minute and 1-hour hydrolysis titers was only 1.55 ml./g. In general, it can be said that the sulphate acid ester of unstabilized cotton cellulose nitrate is considerably hydrolyzed in the first hour.

Can. J. Chem. Downloaded from www.nrcresearchpress.com by 78.46.186.204 on 09/04/12
For personal use only.

The amount of sulphuric acid released by hydrolysis of low sulphate ester content cotton cellulose nitrates was very small. For a 13.3% N cellulose nitrate containing 46% ester, the sulphuric acid released after 24 hours was only 0.32%.

The rate of hydrolysis curves for the sulphate acid esters in four cotton cellulose nitrates, containing very similar amounts of water and sulphate ester, are shown in Fig. 1.

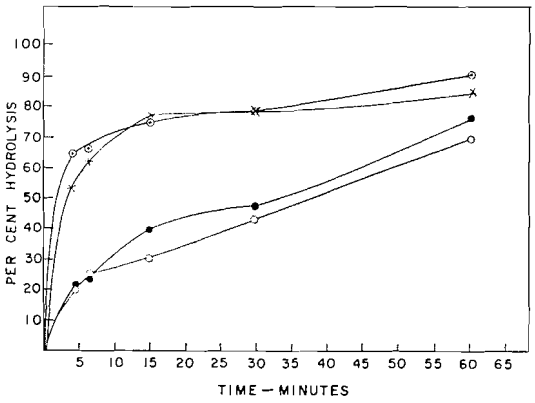

FIG. 1. Hydrolysis of the sulphate acid ester in cotton cellulose nitrates.

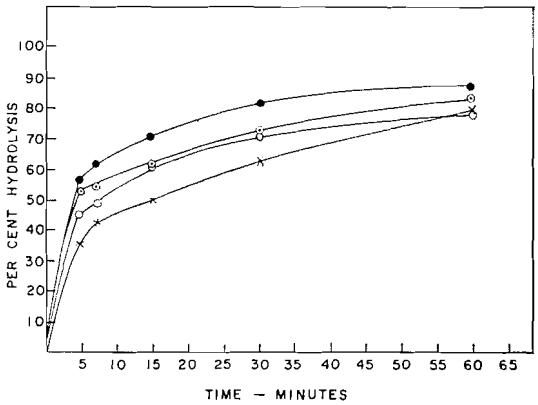

FIG. 2. Hydrolysis of the sulphate acid ester in wood cellulose nitrates.

Nitrogen, %	Sulphate acid ester, %	Sulphuric acid, %		Water concn., % vol.
		Grav.	Titrimetric	
⊙ 11.6	96	0.95	0.94	0.64
× 11.4	100	1.00	0.93	0.78
● 12.1	100	0.58	0.64	0.75
○ 11.9	100	0.69	0.75	0.77

There was 53% hydrolysis of sulphate ester in the first 5 minutes for a cellulose nitrate containing 11.4% nitrogen whereas there was only 20% hydrolysis for a 12.1% N cellulose nitrate. Similar results are shown for cellulose nitrates containing 11.6% and 11.9% nitrogen. Each curve represents the results obtained from duplicate hydrolysis experiments on the same cellulose nitrate sample. The hydrolysis values could be reproduced and the nitrogen contents were determined with good precision (9). It was very difficult to prepare cotton cellulose nitrates containing similar sulphate acid ester and water contents.

It appears that the rate of hydrolysis of the sulphate ester decreased as the nitrogen content increased (Fig. 1). This effect could be explained by the ester groups being sterically hindered by nitrate groups.

In the present work, hydrolysis experiments were also carried out on unstabilized wood cellulose nitrates. There was rapid initial hydrolysis of the sulphate acid ester, followed by slower hydrolysis up to 24 hours. For instance, in one experiment with a 12.8% N wood cellulose nitrate containing 55% sulphate acid ester and 1.26% water, the difference between zero and 5-minute hydrolysis titers was 3.00 ml./g. After 1 hour of hydrolysis, the difference rose to 6.30 and finally after 24 hours it was 8.10 ml./g.

The rate of hydrolysis curves for the sulphate esters of four wood cellulose nitrates containing similar sulphate ester and water contents are given in Fig. 2. The initial

Can. J. Chem. Downloaded from www.nrcresearchpress.com by 78.46.186.204 on 09/04/12
For personal use only.

hydrolysis was very rapid. For example, for an 11.8% N wood cellulose nitrate, there was 53% hydrolysis of the sulphate acid ester in the first 5 minutes and the corresponding value after 1 hour was 80%.

Nitrogen, %	Sulphate acid ester, %	Sulphuric acid, %		Water concn., % vol.
		Grav.	Titrimetric	
⊙ 11.8	96	1.23	1.26	0.94
× 11.7	97	1.33	1.36	0.98
● 11.4	98	2.32	2.11	0.96
○ 10.8	97	1.71	1.65	1.00

There are similarities between these curves and those obtained for cotton cellulose nitrates (Fig. 1). However, the curves cannot be strictly compared because cotton and wood cellulose nitrates having the same nitrogen content contained different amounts of moisture.

There was no striking difference between the rates of hydrolysis of wood cellulose nitrates containing different amounts of nitrogen (Fig. 2) as was the case for cotton cellulose nitrates. This fact could possibly be explained by structural differences. Wood cellulose nitrates having similar sulphate ester and moisture contents could be prepared without difficulty in contrast to cotton cellulose nitrates.

The rate of hydrolysis curves for cotton and wood cellulose nitrates (Figs. 1 and 2) are similar in shape to those given previously (10) for the hydrolysis of cellulose acetate sulphate. In general, the hydrolysis of the sulphate ester in both unstabilized cotton and wood cellulose nitrates is very similar to that of the sulphate ester in cellulose acetate sulphate.

REFERENCES

1. KEIRSTEAD, K. F. and MYERS, J. Can. J. Chem. **32**, 815 (1954).
2. MALM, C. J., TANGHE, L. J., and LAIRD, B. C. Ind. Eng. Chem. **38**, 77 (1946).
3. KEIRSTEAD, K. F. and MYERS, J. Can. J. Chem. **32**, 566 (1954).
4. MILES, F. D. Cellulose nitrate. Oliver & Boyd Ltd., London. 1955. p. 103.
5. GAGNON, P. E., KEIRSTEAD, K. F., and YAMASAKI, D. Can. J. Technol. **34**, 477 (1957).
6. GAGNON, P. E., KEIRSTEAD, K. F., and NEWBOLD, B. T. Can. J. Chem. **36**, 291 (1958).
7. DOREE, C. The methods of cellulose chemistry. Chapman & Hall, London. 1950. p. 236–237.
8. BRICKNELL, A. G., TREVOY, L. W., and SPINKS, J. W. T. Can. J. Chem. **35**, 704 (1957).
9. GAGNON, P. E., KEIRSTEAD, K. F., and NEWBOLD, B. T. Can. J. Chem. **36**, 215 (1958).
10. GAGNON, P. E., KEIRSTEAD, K. F., WALKER, J., and KAVANAUGH, K. R. Can. J. Technol. **34**, 71 (1956).

Can. J. Chem. Downloaded from www.nrcresearchpress.com by 78.46.186.204 on 09/04/12
For personal use only.

Can. J. Chem. Downloaded from www.nrcresearchpress.com by 200.7.193.243 on 09/04/12
For personal use only.

THE KINETICS OF THE THERMAL DECOMPOSITION OF ETHYL BROMIDE AND ETHYL BROMIDE-d_5[1]

ARTHUR T. BLADES

ABSTRACT

The kinetics of the pyrolysis of ethyl bromide and ethyl bromide-d_5 have been studied using the toluene carrier gas technique. Variation of the pressure in the range 0.6 to 4.4 cm. Hg reveals what is believed to be a legitimate pressure effect on the first-order rate constants. The Arrhenius rate expressions determined at 4 cm. Hg pressure are:

k(ethyl bromide) $= 8.5 \pm 1.6 \times 10^{12} e^{-52,200 \pm 300/RT}$ sec.$^{-1}$ (T = 523°–633° C.);

k(ethyl bromide-d_5) $= 2.1 \pm 0.4 \times 10^{13} e^{-54,840 \pm 300/RT}$ sec.$^{-1}$ (T = 531°–635° C.).

The differences in the two rate expressions are discussed.

INTRODUCTION

The thermal decomposition of alkyl bromides into the alkene and hydrogen bromide occurs more or less homogeneously and with few other detectable products. The effect of inhibitors on the rates of decomposition of the secondary and tertiary compounds is, in general, small, but with primary bromides the rates are reduced to a limiting value (1, 2, 3, 4, 5, 6, 7). While the order of reaction in the uninhibited pyrolysis is often obscure, the fully inhibited decomposition of all the compounds studied is believed to be unimolecular.

An example of such a decomposition is that of ethyl bromide into ethylene and hydrogen bromide. This reaction has long been known to be first order, but recent investigations of the pyrolysis by Goldberg and Daniels (2) reveal that, though the decomposition is first order, there is an induction period and the products both accelerate and retard the decomposition. They indicated that ethylene, *n*-hexane, and toluene (8) reduce the rate of decomposition to a limiting value at which the only significant reaction is the simple unimolecular decomposition:

$$C_2H_5Br \rightarrow C_2H_4 + HBr.$$

Recent studies of this decomposition in cyclohexene by Green, Harden, Maccoll, and Thomas (3) confirm this conclusion. An attempt to use the carbon isotope effect (9) to confirm the intramolecular nature of this reaction has been contested (10) on the grounds that the rate constants in the system were unusually high.

The present work was undertaken as a preliminary to a more intensive investigation of the carbon and hydrogen isotope effects in this decomposition.

EXPERIMENTAL

The toluene carrier-gas technique, in which the compound is decomposed in a large excess of toluene in a flow system, was used in this study. The apparatus was essentially a replica of that previously used (8); however, provision was made for the introduction of the toluene at higher pressures. This was achieved by the use of heated lines and a thermostatically controlled bath around both the toluene supply and the oil–mercury manometer. The ratio of toluene to ethyl bromide in the pyrolyzed gases was maintained as high as possible, consistent with the pressure and contact time requirements of each

[1]*Manuscript received March 7, 1958.*
Contribution No. 66 from the Research Council of Alberta, Edmonton, Alberta. This article is based on a paper presented at the 41st Annual Conference and Exhibition of The Chemical Institute of Canada, Toronto, May 26–28, 1958.

experiment. The reaction cell was 8 inches long and $\frac{3}{4}$ inch in diameter. Consideration for possible errors as a result of the heat load on the furnace dictated the use of contact times up to 2.2 seconds at the higher pressures. The products were condensed in a liquid nitrogen trap, and the rate constants were based on the titration of the hydrogen bromide with 0.1 N sodium hydroxide.

The commercial, ether-free ethyl bromide was distilled over phosphorus pentoxide on a 36-inch glass helix packed column; b.p. 36.1° C. at 70.2 cm. Hg. The deuterium compound, supplied by Merck and Co., was stated to be 99+% ethyl bromide-d_5 and was not further purified. The toluene was reagent grade and was distilled over sodium. All compounds were thoroughly degassed before use.

In investigating the temperature coefficients of the two pyrolyses, an attempt was made to carry out experiments on the two compounds under identical conditions so that relative rates might be plotted as a function of temperature. However, the results of such a plot indicated a difference in activation energy essentially the same as that from the individual rate expressions obtained from a least squares treatment of the data. The errors quoted are the indicated maxima from an average deviation in k of $1\frac{1}{2}$%.

RESULTS

Pressure Effect

The effect of pressure on the rate constants was investigated over the range 0.6 to 4.4 cm. Hg. Each first-order rate constant plotted in Fig. 1 represents a single analysis and must not be regarded as a limiting rate at zero conversion. No attempt was made to adjust conditions to produce uniform conversion and hence the precise shape of the curves is not too significant.

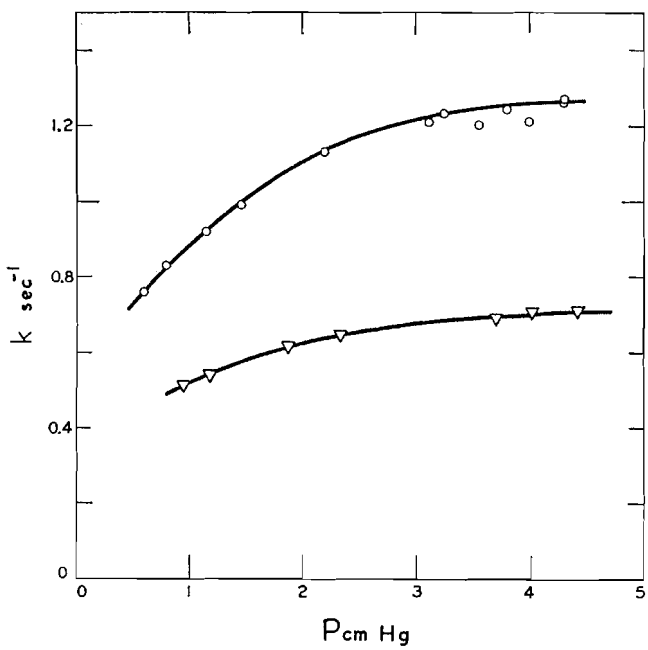

FIG. 1. The effect of pressure on the rate constant at T = 889° K.: ○ for ethyl bromide and ▽ for ethyl bromide-d_5.

Can. J. Chem. Downloaded from www.nrcresearchpress.com by 200.7.193.243 on 09/04/12
For personal use only.

TABLE I

RATE STUDIES

Expt. No.	Pressure, cm. Hg	Toluene: bromide ratio	Contact time, sec.	% Decomp.	Temp., °K.	k, sec.$^{-1}$
			A. On ethyl bromide			
60	4.00	95	0.650	75	906.0	2.11
59	4.00	90	0.645	65	897.0	1.61
42	4.01	35	1.01	74	891.0	1.33
49	4.21	58	1.02	64	882.2	1.00
58	4.00	55	1.05	48	867.9	0.617
57	4.00	54	0.675	33	867.3	0.593
51	4.09	36	1.06	31	851.3	0.347
50	4.28	60	1.05	23	841.7	0.242
52	4.05	28	2.10	26	828.4	0.145
53	4.00	18	2.16	16	815.1	0.0836
54	4.01	18	2.16	17	815.2	0.0864
55	4.04	18	2.18	11	803.9	0.0536
56	4.10	19	2.20	8.5	796.7	0.0405
			B. On ethyl bromide-d_5			
20	4.05	55	0.638	56	908.1	1.28
9	3.92	50	0.994	67	903.1	1.11
19	4.00	54	0.627	43	896.9	0.890
1	4.02	33	1.06	55	892.0	0.785
7	4.43	39	1.00	54	891.4	0.770
10	4.02	51	1.04	41	881.8	0.527
18	4.00	35	1.06	29	867.6	0.320
17	4.00	52	0.685	19	867.4	0.312
13	3.81	28	2.06	30	851.6	0.174
12	4.13	35	1.05	17	851.3	0.175
11	4.29	36	1.07	12	841.9	0.123
14	4.00	33	2.06	14	828.9	0.0732
15	4.01	17	2.15	8.5	815.4	0.0412
16	4.02	17	2.17	5.5	804.2	0.0256

Temperature Dependence

In investigating the temperature coefficient of the rate it was necessary to operate at a pressure of about 4 cm. Hg in order to obtain data in a region where errors due to non-first-order behavior would be no greater than the experimental error. The rate expressions calculated from the data in Table I were, for ethyl bromide:

$$k = 8.5\pm1.6\times10^{12}e^{-52,200\pm300/RT}\text{sec.}^{-1},$$

and for ethyl bromide-d_5:

$$k = 2.1\pm0.4\times10^{13}e^{-54,840\pm300/RT}\text{sec.}^{-1}.$$

The former compares very favorably with the previously reported expression (8) obtained by this technique,

$$k = 7.3\times10^{12}e^{-52,300/RT}\text{sec.}^{-1} \text{ at } p = 2.0\pm0.2 \text{ cm. Hg},$$

especially since the lower pressure would be expected to make the results 10% low.

An Arrhenius plot of the data is presented in Fig. 2 and a similar plot for the ratio of the rate constants is shown in Fig. 3.

DISCUSSION

The mechanism for the totally inhibited decomposition of many of the alkyl bromides

Can. J. Chem. Downloaded from www.nrcresearchpress.com by 200.7.193.243 on 09/04/12
For personal use only.

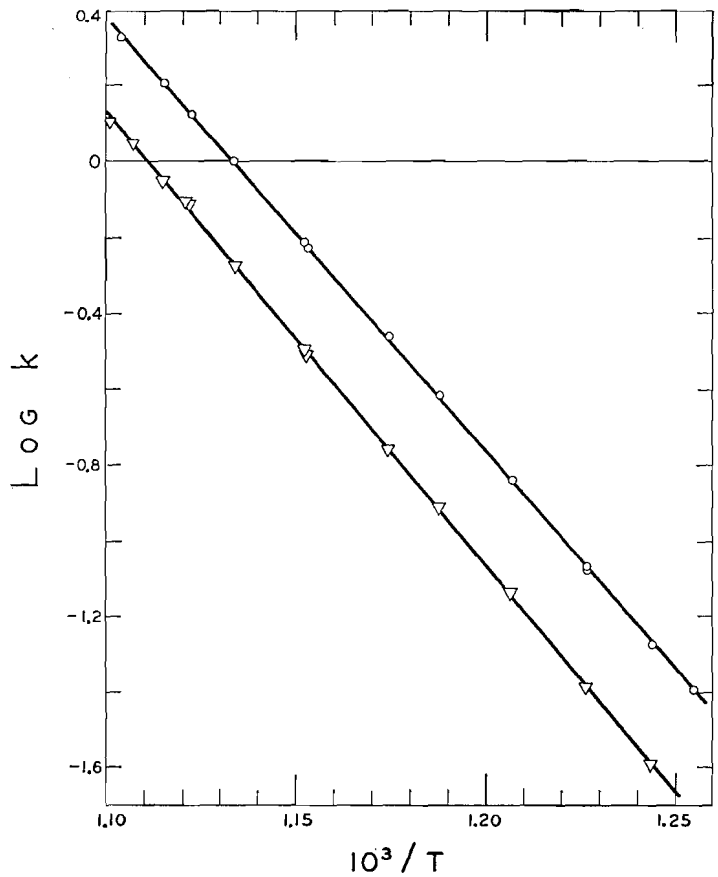

FIG. 2. Arrhenius plots for ○ ethyl bromide and ▽ ethyl bromide-d_5.

and chlorides is now generally accepted to involve the formation of a "four-centered" activated complex (8, 11).

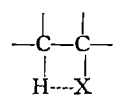

Since this is such a relatively simple mechanism, it is particularly satisfying that highly accurate and reproducible rate expressions can be obtained by the use of the toluene carrier-gas technique. Hence the decomposition of ethyl bromide seems ideal for a careful study of isotope effects in intramolecular decomposition reactions.

The effect of pressure on the rate constants for the two compounds indicates a quasi-unimolecular reaction below about 4 cm. Hg for each of them. Although this effect occurs in an atmosphere largely composed of toluene, it is likely that the collision efficiencies of the toluene and the bromides are sufficiently similar so that the pressure would be much the same as for the decomposition of the pure gases. The limited pressure range of the data for this effect renders a calculation of the Hinshelwood-Lindemann degrees-of-freedom fruitless. It is noteworthy that the pressure effect for the ethyl chloride decomposition (12) becomes apparent around 1 cm. Hg pressure despite a considerably higher frequency factor.

Can. J. Chem. Downloaded from www.nrcresearchpress.com by 200.7.193.243 on 09/04/12
For personal use only.

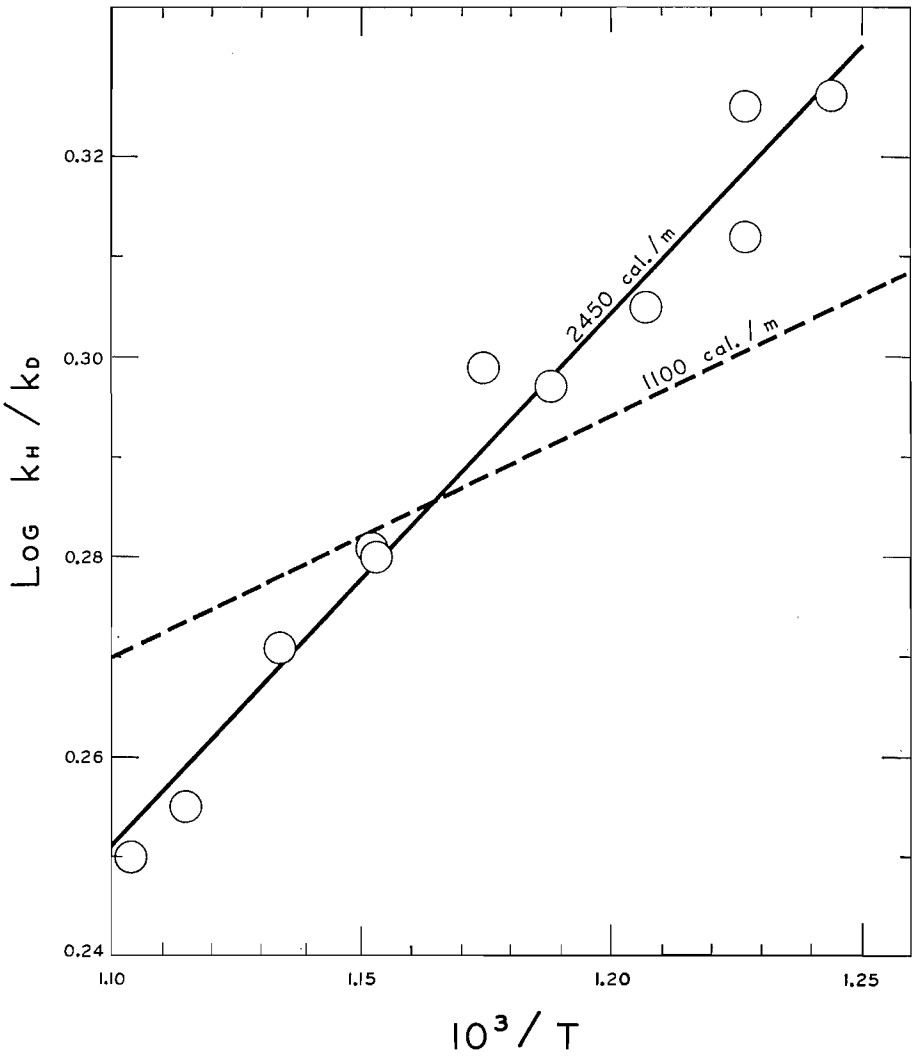

FIG. 3. Arrhenius plot for the ratio of rate constants for ethyl bromide and ethyl bromide-d_5.

The two Arrhenius rate expressions are interesting in two respects, namely, the large difference of 2600 cal./mole in the activation energies and the lower frequency factor for the hydrogen compound. Reference to the Bigeleisen (13) theory of the kinetic isotope effect suggests that the maximum difference in activation energy should be the difference in the zero-point energies in those vibrations associated with activation. Since a single carbon–hydrogen stretching frequency may account for only 1100 cal./mole, it is evident that other methyl group vibrations must be invoked to account for the observed activation energy difference.

The abnormal frequency-factor ratio of 0.4 cannot be so readily explained since the Bigeleisen theory predicts a frequency factor ratio between 1 and $\sqrt{2}$ and it would require an error of 1500 cal./mole in the activation energy difference to make the experimental rates consistent with a ratio of unity. A similarly anomalous ratio has been

Can. J. Chem. Downloaded from www.nrcresearchpress.com by 200.7.193.243 on 09/04/12
For personal use only.

observed in the relative rates of rearrangement of cyclopropane and cyclopropane-t_1 (14), and several possible explanations have been advanced which might be applicable here.

A classical rotational kinetic isotope effect occurs in these decompositions in addition to the effects discussed above. Since the activation step involves the conversion of an internal rotational degree of freedom into a less active vibration, a negative entropy of activation should result. For the ethyl bromide-d_5, however, the reduced moment of inertia about C—C bond will be almost twice as large as for the hydrogen compound, resulting in a greater entropy of internal rotation of about $(R \ln 2)/2$ and hence a greater change in entropy during activation. A maximum additional factor of $\sqrt{2}$ would be predicted for this kinetic isotope effect.

ACKNOWLEDGMENTS

The author wishes to express his appreciation to Mr. R. Tweddle for his excellent assistance in this experimental program. A National Research Council grant for fundamental research is gratefully acknowledged.

REFERENCES

1. AGIUS, P. J. and MACCOLL, A. J. Chem. Soc. 973 (1955).
2. GOLDBERG, A. E. and DANIELS, F. J. Am. Chem. Soc. **79**, 1314 (1957).
3. GREEN, J. H. S., HARDEN, G. D., MACCOLL, A., and THOMAS, P. J. J. Chem. Phys. **21**, 178 (1953).
4. HARDEN, G. D. and MACCOLL, A. J. Chem. Soc. 2454 (1955).
5. MACCOLL, A. and THOMAS, P. J. J. Chem. Soc. 979 (1955).
6. MACCOLL, A. and THOMAS, P. J. J. Chem. Soc. 2445 (1955).
7. SEMENOV, N. N., SERGEEV, G. B., and KAPRALOVA, G. A. Doklady Akad. Nauk S.S.S.R. **105**, 301 (1955).
8. BLADES, A. T. and MURPHY, G. W. J. Am. Chem. Soc. **74**, 6219 (1952).
9. FRIEDMAN, H. L., BERNSTEIN, R. B., and GUNNING, H. E. J. Chem. Phys. **23**, 109 (1955).
10. MACCOLL, A. and THOMAS, P. J. J. Chem. Phys. **23**, 1722 (1955).
11. BARTON, D. H. R. and HEAD, A. J. Trans. Faraday Soc. **46**, 114 (1950).
12. HOWLETT, K. E. J. Chem. Soc. 3695 (1952).
13. BIGELEISEN, J. J. Chem. Phys. **17**, 675 (1949).
14. WESTON, R. E. J. Chem. Phys. **26**, 975 (1957).

Can. J. Chem. Downloaded from www.nrcresearchpress.com by 200.7.193.243 on 09/04/12
For personal use only.

Can. J. Chem. Downloaded from www.nrcresearchpress.com by 78.46.186.204 on 09/04/12
For personal use only.

REACTIVITY STUDIES ON NATURAL PRODUCTS

V. RATES OF BOROHYDRIDE REDUCTION OF SOME RING A AND B STEROID KETONES[1]

OWEN H. WHEELER[2] AND JOSÉ L. MATEOS[3]

ABSTRACT

The rates of reduction of 3-, 6-, and 7-cholestanone, coprostan-3-one, Δ^4- and Δ^5-cholesten-3-one, and $\Delta^{8(14)}$-ergosten-3-one with sodium borohydride in isopropanol have been measured. The proportions of α- and β-isomers formed were determined in most cases and the corresponding rates of equatorial and axial reduction obtained. Δ^4-Cholesten-3-one and 6- and 7-cholestanone are reduced at a slower rate and Δ^5-cholesten-3-one and $\Delta^{8(14)}$-ergosten-3-one at a higher rate than the saturated 3-ketosteroids.

Sodium borohydride has been used as a selective reducing agent in steroid chemistry and preparative reductions have been reported of a 3-keto group of both allo and normal steroids, in the presence of 11- (1), 12- (2), 17- (3), and 20-keto groups (4, 5), of a 3-keto group in the presence of both 11- and 20-keto groups (5), and of a 20-keto group in preference to an 11-keto group (6) and a Δ^4-3-keto system (7). Garrett and Lyttle (8) in a kinetic study found that under their conditions the 3-keto group of pregnan-3,20-dione was reduced instantaneously and the 20-keto group at a measurable rate. All these examples of selective reduction involve positions in the steroid molecule which are known to have quite different steric environments. In the present work the reactivities of some ring A and B ketosteroids (see Table I), which would be expected to have smaller differences, have been measured.

TABLE I

KINETICS OF BOROHYDRIDE REDUCTION*

	$k \times 10^4$	Ratio†
Cyclohexanone	565±3	1.4
Cholestan-3-one	397±7	1.0
Coprostan-3-one	434±6	1.1
Cholestan-6-one	241±6	0.60
Cholestan-7-one	111±2	0.28
Δ^4-Cholesten-3-one	54.8±1.2	0.14
Δ^5-Cholesten-3-one	1320±18	3.3
$\Delta^{8(14)}$-Ergosten-3-one	610±11	1.5

*In isopropanol at 25.0°. Rate constants in liter mole^{-1} sec.$^{-1}$.
†Ratio of rate constants to cholestan-3-one = 1.0.

The solvent used by Garrett and Lyttle was aqueous dioxan but this gave very fast and irreproducible results with our very reactive ketones. Recently Brown and co-workers (9, 10) have used isopropanol for kinetic studies and this proved suitable because of the stability of borohydride in this solvent, the solubility of the steroids, and their reasonably slow rates of reduction. Although cholestan-3-one and coprostan-3-one undergo bromination at different rates (11), their rates of reduction are very similar and only a little less than that of cyclohexanone and this is to be expected since there are no large steric or strain effects influencing addition to the exocyclic double bond. However 6- and

[1]*Manuscript received February 12, 1958.*
Contribution from the Instituto de Quimica, Universidad Nacional Autonoma de Mexico, Mexico 20, D.F.
[2]*Present address: Department of Chemistry, Dalhousie University, Halifax, N.S.*
[3]*Present address: Department of Chemistry, University of California at Los Angeles.*

7-cholestanone undergo reduction at a greatly reduced rate. The principal effect decreasing the rate of reduction of the 6-ketone will be steric hindrance from the axial methyl group at C-10 (12), and the 7-ketone is hindered from attack of borohydride ion by the 'eclipsing effect' of the α-hydrogen atom on C-15 (12). Moreover, the ketone groups of both these compounds will be subject to the inductive effect of the alkyl group of the adjacent ring which will depolarize and further deactivate the carbonyl group (13), as compared to that of cholestan-3-one. Selective reduction of a 3,7-diketone should be possible, since assuming no mutual interaction, one equivalent of borohydride would reduce only 22% of the 7-keto group.

In the case of Δ^4-cholesten-3-one resonance interaction in the α,β-unsaturated ketone system will reduce the charge on the ketone group and reduce its reactivity (12). However in the case of Δ^5-cholesten-3-one there is no loss of resonance energy on reduction, but hyperconjugative interaction will stabilize the borohydride reduction intermediate and lead to an increased rate of reduction. $\Delta^{8(14)}$-Ergosten-3-one also shows an increased rate of reactivity as compared to cholestan-3-one, but it seems unlikely that this can be electronic in origin since the double bond is so remote from the keto group. The double bond in ring C will produce small distortions in the conformation of the rings which will be transmitted to ring A and this is also distorted by the keto group (11). Reduction will reduce some of the distortion in this ring and is therefore favored.

The percentages of α- and β-alcohols formed were determined for five of the ketones (Table II) and the over-all rates of reduction have been divided into the rates of formation of these α- and β-isomers (Table III) resulting from quasi-equatorial and quasi-axial attack (14) (also termed 'exo' and 'endo' attack (15)). The percentage of equatorial isomers formed from cholestan-3-one and coprostan-3-one is similar to that from 4-methylcyclohexanone (14), agreeing with the previous suggestion that 3-ketosteroids are not subject to any large steric effects.

TABLE II

PERCENTAGE OF β-ISOMER*

	Reagent		
	$LiAlH_4$	$NaBH_4$	
		In *i*-PrOH†	In aq.-MeOH‡
Cholestan-3-one	88§	85	87
Coprostan-3-one	7‡	13	17
Cholestan-7-one	69‖	58¶	27**
Δ^4-Cholesten-3-one	74‡	95	74
Δ^5-Cholesten-3-one	87‡	83	76

*Normalized to 100%. †Present work. ‡Ref. 19. §Ref. 22. ‖Ref. 23.
¶Cholestane (39%) also formed. **For 3-acetoxy-7-ketocholestane, Ref. 14.

TABLE III

RATES OF 'AXIAL' AND 'EQUATORIAL' REDUCTION

	$k^a \times 10^4$	Ratio*	$k^e \times 10^4$	Ratio†
Cholestan-3-one	60	1.0	340	1.0
Coprostan-3-one	57	1.0	380	1.1
Cholestan-7-one	48	0.8	64	0.2
Δ^4-Cholesten-3-one	2.7	0.05	52	0.15
Δ^5-Cholesten-3-one	230	3.9	1100	3.2

*Ratio of 'axial' reduction to 'axial' reduction of cholestan-3-one = 1.0.
†Ratio of 'equatorial' reduction to 'equatorial' reduction of cholestan-3-one = 1.0.

Can. J. Chem. Downloaded from www.nrcresearchpress.com by 78.46.186.204 on 09/04/12
For personal use only.

Can. J. Chem. Downloaded from www.nrcresearchpress.com by 78.46.186.204 on 09/04/12
For personal use only.

The reduction of cholestan-7-one gives a large amount of cholestane and, although the rate of 'equatorial' reduction is considerably less than that for cholestan-3-one, the rate of 'axial' reduction is only slightly reduced. This suggests that reduction of the 7-keto group by attack from the underside of the molecule is not particularly hindered, whereas reduction in the equatorial plane of the molecule is highly hindered. The principle factor seems to be the 'eclipsing effect' of the 15α-hydrogen atom (11), but the shielding of the methyl groups on carbons 10 and 13 will also decrease the rate of attack from the topside. The cholestane probably arises by steric repulsion, from the 7β-position, of the bulky carbonyl–borohydride reduction complex. Steric acceleration in the chromium trioxide oxidation of 7α-cholestanol, known to involve the attack of a chromium ester on the β-hydrogen atom, has also been observed (16).

The introduction of a double bond into a cyclohexanone ring will lead to a flattening of the ring (17). In the reduction of cholest-4-en-3-one the preferred transition state for reduction will be that leading to the formation of the equatorial alcohol, since this allows maximum interaction between the π-electrons of the double bond and the borohydride radical. β-Cholest-3-en-ol constitutes the major product and the decrease in rate is much greater for the formation of the α-alcohol.

The double bond in cholest-5-en-3-one also distorts the molecule and ring A is bent down from the equatorial planes of the other rings (18). However no large steric effects are introduced and since electronic interaction is much less than that for cholest-4-en-3-one the relative rates of equatorial and axial reduction increase equally.

A previous study of the reduction of cholest-4-en-3-one with sodium borohydride in aqueous methanol reported (19) that 74% of the β-isomer was formed. However in the present work 95% of the β-isomer was isolated and this is in agreement with the observations that cholesta-4,6-dien-3-one (20) and cholest-1-en-3-one (21) give essentially the β-isomer. In the present work 58% of cholestan-7β-ol was formed in the reduction of cholestan-7-one. However, the reduction of 3β-acetoxycholestan-7-one with sodium borohydride in aqueous methanol (14) was reported to give only 27% of cholestan-3β,7β-diol. The analysis was based on the assumption that the inseparable mixture of diols formed contained only cholestanediols. Cholestan-3β-ol was probably also formed.

EXPERIMENTAL

The ketones used were those prepared in a previous study (12).

Kinetics.—The ketone (*ca.* 0.6 g.) was dissolved in anhydrous isopropanol (90 ml.) in a flask which was allowed to equilibrate in temperature in a constant-temperature bath maintained at 25.0±0.1°. A solution (10 ml.) of sodium borohydride (98% purity, *ca.* 0.3 *N*) in isopropanol was added and the flask rapidly shaken. The halftime of addition was taken as zero time and aliquots (10 ml.) were withdrawn at definite times and added to excess potassium iodate (0.1 *N*) containing potassium iodide. The halftime of delivery of the pipette was taken as the time of sampling. Sulphuric acid (10 ml., 2 *N*) was added and the liberated iodine titrated with 0.1 *N* sodium thiosulphate using starch as indicator (9). The rate constants were calculated from a second-order rate plot and straight line graphs were obtained up to 90% reaction. Each experiment was repeated 3 or 4 times and the average results with their mean errors are given in Table I.

Isolation of products.—All the optical rotation measurements were carried out with chloroform solutions at 25°.

Cholestan-3-one.—A solution of 1.0 g. of this ketone in isopropanol (75 ml.) was mixed with sodium borohydride in isopropanol (75 ml., 0.3 *N*). After 24 hours at room temperature the solution was diluted with water and the cholestanols (1.0 g., m.p. 114–117°)

extracted with ether. The mixture was separated by chromatography on alumina into α-cholestanol (140 mg.), m.p. 180–182°, eluted with benzene and β-cholestanol (840 mg.), m.p. 135–138°, eluted with benzene–ether.

Coprostan-3-one.—Similar reduction of coprostanone (300 mg.) gave a mixture of coprostanols (205 mg.), m.p. 82–85°, which could not be separated by chromatography. Treatment with digitonine in ethanol gave a precipitate (110 mg.) corresponding to β-coprostanol (26.3. mg.), and evaporation of the mother liquor gave α-coprostanol, m.p. 118°.

Cholestan-7-one.—This ketone (500 mg.) was reduced as above and the oily product chromatographed on unwashed alumina using a proportion of 80/1. Hexane eluted cholestane (150 mg.), m.p. 77–79°. Hexane–benzene mixtures eluted successively cholestan-7α-ol (110 mg.), m.p. 74–77°, and cholestan-7β-ol (130 mg.), m.p. 114–115°.

Δ^4-*Cholesten-3-one.*—The crude product had $[\alpha]_D^{CHCl_3}$ 47.0°, corresponding to cholest-4-en-3β-ol, $[\alpha]_D$ 44°, 96%, and cholest-4-en-3α-ol, $[\alpha]_D$ 121°, 4%. It could be separated by chromatography on alumina, using hexane–benzene (4/1) as eluent, into the α-alcohol (5%), m.p. 84°, and the β-isomer (95%), m.p. 130–132°.

Δ^5-*Cholesten-3-one.*—The two isomeric alcohols formed could not be separated by chromatography, but were separated by digitonine treatment into cholesterol (83%), m.p. 148–149°, and epicholesterol (17%), m.p. 140–141°, which was recovered from the mother liquors.

ACKNOWLEDGMENT

The authors are grateful to Professor H. C. Brown for discussions on the procedure for the borohydride kinetics. The work was supported by grants from the Rockefeller Foundation, New York, and the Instituto Nacional de la Investigacion Cientifica, Mexico.

REFERENCES

1. Heymann, H. and Fieser, L. F. J. Am. Chem. Soc. **73**, 5252 (1951).
2. Djerassi, C., Lemin, A. J., Martinez, H., Rosenkrantz, G., and Sondheimer, F. J. Am. Chem. Soc. **75**, 4885 (1953).
3. Elisberg, E., Vanderhaeghe, H., and Gallagher, T. F. J. Am. Chem. Soc. **74**, 2814 (1952).
4. Mancera, O., Ringold, H. J., Djerassi, C., Rosenkrantz, G., and Sondheimer, F. J. Am. Chem. Soc. **75**, 1286 (1953).
5. Soloway, A. H., Deutsch, A. S., and Gallagher, T. F. J. Am. Chem. Soc. **75**, 2356 (1953).
6. Oliveto, E. P. and Hershberg, E. B. J. Am. Chem. Soc. **75**, 488 (1953).
7. Norymberski, J. K. and Woods, G. F. J. Chem. Soc. 3426 (1955).
8. Garrett, E. R. and Lyttle, D. A. J. Am. Chem. Soc. **75**, 6051 (1953).
9. Brown, H. C., Wheeler, O. H., and Ichikawa, K. Tetrahedron, **1**, 214 (1957).
10. Brown, H. C. and Ichikawa, K. Tetrahedron, **1**, 221 (1957).
11. Wheeler, O. H. and Mateos, J. L. J. Org. Chem. **22**, 605 (1957).
12. Wheeler, O. H. and Mateos, J. L. Can. J. Chem. **36**, 712 (1958).
13. Wheeler, O. H. and Zabicky, J. Z. Can. J. Chem. **36**, 656 (1958).
14. Dauben, W. G., Blanz, E. J., Jiu, J., and Micheli, R. A. J. Am. Chem. Soc. **78**, 3752 (1956).
15. Zimmerman, H. E. J. Org. Chem. **20**, 549 (1955).
16. Schreiber, J. and Eschenmoser, A. Helv. Chim. Acta, **28**, 1529 (1955).
17. Barton, D. H. R. and Cookson, R. C. Quart. Rev. **10**, 44 (1956).
18. Evans, D. D. and Shoppee, C. W. J. Chem. Soc. 540 (1953).
19. Dauben, W. G., Micheli, R. A., and Eastham, J. F. J. Am. Chem. Soc. **74**, 3852 (1952).
20. Schmutz, J., Schaltegger, H., and Sanz, M. Helv. Chim. Acta, **34**, 1111 (1951).
21. Bergman, W., Kita, M., and Giancala, D. J. J. Am. Chem. Soc. **76**, 4974 (1954).
22. Nace, H. R. and O'Connor, G. L. J. Am. Chem. Soc. **73**, 5824 (1954).
23. Cremlyn, R. J. W. and Shoppee, C. W. J. Chem. Soc. 3515 (1954).

Can. J. Chem. Downloaded from www.nrcresearchpress.com by 78.46.186.204 on 09/04/12
For personal use only.

Can. J. Chem. Downloaded from www.nrcresearchpress.com by 78.46.186.204 on 09/04/12
For personal use only.

THE EFFECT OF ADDITION OF POTASH TO NICKEL CHROMITE CATALYSTS[1]

H. C. ROWLINSON[2]

ABSTRACT

Experiments are described on the dehydrogenation of butene-1 in the presence of steam, over three nickel chromite catalysts. These are: (*a*) pure nickel chromite, (*b*) nickel chromite pellets impregnated with potash from solution, and (*c*) a catalyst with potash added before the nickel oxide and chromium sesquioxide are combined. The oxidation state of the catalyst largely affects the products, for overreduction causes disruption of the hydrocarbons. The effect of the potash is to prevent this overreduction and thus to improve selectivity to butadiene. There is a difference between the behavior of catalysts with surface potash (type *b*) and those where the potash is distributed through the mass (type *c*). This difference is explained by the formation of large pores on reduction of type (*c*) catalysts.

INTRODUCTION

The use of potash as a promoter has been extensively studied (1) for iron – synthetic ammonia catalysts. In addition it is widely used to encourage the water–gas reaction on dehydrogenation catalysts, and recently its effects on Cr_2O_3–Al_2O_3 have been investigated (2) for several reactions. This work reports the effect of potash additions to a nickel chromite catalyst used for the dehydrogenation of butene-1, and represents part of a larger study of olefin dehydrogenation catalysts which contain nickel chromite. In particular, the difference is emphasized, in this case, between catalysts to which the KOH has been added to the bulk of the material, and those to which it is added by impregnation from solution.

EXPERIMENTAL

Preparation of Catalysts

Three different catalysts were prepared; those of pure $NiCr_2O_4$, those with 10 wt.% K_2O "built in", and those with the K_2O added on the surface. The nickel chromite was prepared from reagent grade Cr_2O_3 powder and $Ni(NO_3)_2.6H_2O$ crystals. Upon warming of the appropriate mixture, the nitrate dissolved in its water of crystallization, and the whole was mixed to a homogeneous mush. In those catalysts where the potash was to be "built in" it was added at this stage. This mixture was then heated to 900° C. for 3 hours, cooled, powdered, and pelleted with 2% graphite. The pellets used were cylindrical, $\frac{1}{8}$ in. × $\frac{1}{8}$ in. The pellets were then fired at 1050° C. for 4 hours before use, and in the absence of KOH were shown by X-ray spectrography to be the spinel $NiCr_2O_4$. Some of the pellets were then impregnated with a potash solution by immersion of 10 g. of pellets in 10 cc. of solution containing 0.3 g. of KOH. The pellets absorbed about 6 cc. in a few minutes at room temperature and thus contained approximately 0.125 wt.% of K_2O. They were dried by heating slowly to 600° C.

Reaction Conditions

The reactor was a stainless steel (type 446) tube of internal diameter $\frac{5}{8}$ in. and has been described elsewhere (3). A flow system was used with a bed volume of 10 cc. The butene-1 feed was diluted with 10 to 12 volumes of steam preheated to 600° C., and the product gases were collected over water, and analyzed in the mass spectrograph. Flow

[1]*Manuscript received February 10, 1958.*
Contribution from the Division of Applied Chemistry, National Research Council, Ottawa.
Issued as N.R.C. No. 4774.
[2]*N.R.L. Postdoctorate Fellow, 1954–56. Present address: Canadian Industries Ltd., McMasterville, Que.*

rates of approximately 110 v/v per hr. were measured by a flow meter on the butene feed. Two estimates of the efficiency of the catalysts could thus be calculated: (*a*) percentage conversion, i.e., the mole percentage of butene that has decomposed, and (*b*) percentage selectivity, i.e., the mole percentage of the decomposed butene that is converted to butadiene. The butene in the product gas was normally the equilibrium mixture of 1- and 2-butene, although butene-1 was the feed.

RESULTS

1. Performance of the Catalysts

(*a*) *Nickel Chromite Unpromoted*

This catalyst was stable below about 590° C., and gave, for example, a conversion of 14% with a selectivity of 65% at 575° C. Above 590° C. the nickel chromite catalyst showed the phenomenon of "wildness" described by Reilly (4). This state allowed a cracking reaction to take over from the dehydrogenation, and thus caused a progressive increase in product gas, mainly H_2 and CH_4. The selectivity to butadiene fell effectively to zero, and there was a considerable lay-down of carbon.

(*b*) *Nickel Chromite Impregnated with Potash Solution*

It was not found possible to make this catalyst "wild". In addition, the selectivity to butadiene was greatly improved, as is shown by the results in Table I. The catalyst as prepared by heating in air had a great amount of surface chromate and dichromate; this

TABLE I

DEHYDROGENATION OF BUTENE-1 ON AN "IMPREGNATED" CATALYST (TYPE *b*)

Temp., ° C.	Conversion, %	Selectivity, %
587	13.1	90
613	15.5	85
613	17.7	82 feed <100 v/v per hr.
637	25.0	81
636	22.8	72 after air regeneration
630	21.6	78

was most easily shown by placing a pellet in cold water when the characteristic orange color was seen (2). Thus in the initial few minutes of the catalytic reaction the reduction of surface chromate took place with a consequent large production of CO_2. Finally it may be noted that there was very little lay-down of carbon on this catalyst. The amount of carbon lay-down was measured by burning it off with air and steam and collecting the CO_2 on "Ascarite". This burnoff was enacted every $\frac{1}{2}$ hour for the unpromoted catalyst (*a*) above, but in the presence of surface potash it was found that steam alone would restore the activity of the catalyst and even this treatment was needed only after several hours' use. Moreover, the use of air regeneration on the potash-promoted catalysts reduced its selectivity as is shown in the last two results in Table I.

(*c*) *Nickel Chromite with Potash Built In*

This catalyst also would not display "wildness", but two other characteristics distinguished it from the catalyst with potash on the surface. The first is its behavior in the initial half hour of activity. A typical plot of the rates of formation of product gas against time is given in Fig. 1. The first product is largely CO_2 and corresponds to the reduction of chromate; the subsequent rapid product-gas increase is mainly due to hydrogen formation and resembles a "wild" condition except that it tapers off to a performance

Can. J. Chem. Downloaded from www.nrcresearchpress.com by 78.46.186.204 on 09/04/12
For personal use only.

roughly equivalent to that of the impregnated catalysts, e.g., a conversion of 22% and a selectivity of 78.1 at a temperature of 622° C. This state is quite stable.

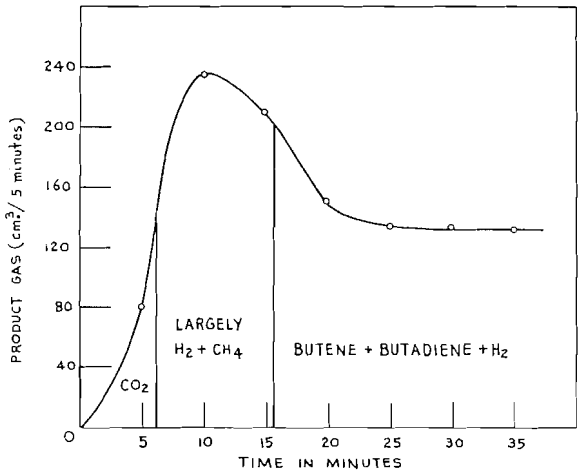

FIG. 1. Rates of product-gas formation against time for a "built-in" catalyst (type *c*). The rates are in cm.³ of gas produced over a 5-minute interval and are plotted at the end of each 5-minute interval.

The second difference between catalysts (*b*) and (*c*) is that on the latter there is considerable carbon lay-down. On a given catalyst sample the amount of this lay-down is independent of the time the catalyst is in use, and for most samples was of the order of 0.135 g. on 10 g. of catalyst (all samples contained 10 wt.% of K_2O). Experiments showed that all this carbon was laid down in the period between 5 and 15 minutes when the rate of product gas formation was large. Preliminary reduction of the catalyst with H_2 gas removed the first part of the rate of gas formation curve, but did not remove the second (large gas production) part, nor did it affect the lay-down of carbon.

2. Surface Area Measurements

Surface areas of the potash-promoted catalysts were measured by the standard B.E.T. nitrogen-adsorption method. To check that chemisorption was not occurring (5), the areas were remeasured with argon at liquid oxygen temperatures. The values of 16.2 Å² and 15.0 Å² were used for the cross-sectional areas of N_2 and A respectively (6, 7). The results of these measurements are given in Table II, and the terms "oxidized" and "reduced" are discussed below.

TABLE II

SURFACE AREAS OF POTASH PROMOTED CATALYSTS (m.²/g.)

	"Impregnated" catalyst (type *b*)		"Built-in" catalyst (type *c*)	
	With N_2	With A	With N_2	With A
Oxidized	2.19	2.20	0.672	0.646
Reduced	3.32	3.39	11.4	11.9

DISCUSSION

The most obvious effect of the addition of potash to nickel chromite catalysts is the prevention of "wildness". This state is believed to be due (3) to the reduction of nickel

Can. J. Chem. Downloaded from www.nrcresearchpress.com by 78.46.186.204 on 09/04/12
For personal use only.

oxide to nickel metal, and it is the latter that is the disruptive catalyst. It is of interest that the tendency to "wildness" disappears also in potash-free catalysts containing more Cr_2O_3 and less NiO (at approximately 75 mole % and more of Cr_2O_3). However, in this latter case reduction still takes place during catalytic action as is shown by the heat output on regeneration with air (independent of carbon burnoff). Presumably it is the agglomeration of reduced metal "ions" into metallic particles that is prevented by the excess chromia. Thus, it can be concluded that in the promoted catalysts the presence of potash on the chromia prevents either the reduction of metal oxide or the formation of metallic particles. However, the addition of potash to pure NiO does not prevent the "wildness" of this catalyst which sets in at about 520° C.

The difference between catalysts with impregnated and "built-in" potash is an unusual one; there is, for example, no similar difference in the reduction of iron oxide for synthetic ammonia catalysts (8). A possible explanation is that the formation of potassium chromate in catalyst (*c*) leaves some NiO uncombined, and that the latter behaves in a "wild" manner until covered by carbon. This explanation must be rejected, for decreasing the percentage of NiO to zero does not affect the phenomenon illustrated in Fig. 1, nor the constant carbon lay-down. Thus, it seems most likely that there is a pore effect; the reduction of the potassium chromate in the case where the potash is distributed through the mass leaves a network of tiny pores in which the butene decomposes to carbon because the butadiene cannot diffuse out. This yields the large volume of H_2 observed, and explains the constant carbon lay-down. When the pores are full of carbon the catalyst behaves like a surface-promoted one. The surface areas appear to support this explanation. For these measurements, used catalyst samples were oxidized to remove the carbon, and surface areas measured in the oxidized state. Then the samples were reduced briefly at 600° C. with hydrogen, so that there could be no lay-down of carbon, and the areas of the reduced catalysts measured. There is an increase in area by a factor of approximately 15 on reduction of the catalyst with the "built-in" potash, whereas for the surface-promoted one the factor is 1.5. This difference must be ascribed to the formation of pores in the solid mass of the catalysts of type (*c*) due to the decrease in volume of K_2CrO_4 when reduced to Cr_2O_3 and K_2O.

REFERENCES

1. EMMETT, P. H. *Editor* Catalysis. Vol. III. Hydrogenation and dehydrogenation. Reinhold Publishing Corporation, New York. 1955. pp. 171–259.
2. VOLTZ, S. E. and WELLER, S. W. J. Phys. Chem. **59**, 569 (1955).
3. ROWLINSON, H. C. and CVETANOVIĆ, R. J. Advances in Catalysis, **9**, 243 (1957).
4. REILLY, P. M. Chem. in Can. **5** (3), 25 (1953).
5. TRAPNELL, B. M. W. Chemisorption. Butterworth's Scientific Publications, London. 1955. p. 197.
6. DAVIS, R. J., JR., DEWITT, T. W., and EMMETT, P. H. J. Phys. & Colloid Chem. **51**, 1232 (1947).
7. LIVINGSTON, H. K. J. Colloid Sci. **4**, 447 (1949).
8. EMMETT, P. H. *Editor* Catalysis. Vol. III. Hydrogenation and dehydrogenation. Reinhold Publishing Corporation, New York. 1955. pp. 238–239.

Can. J. Chem. Downloaded from www.nrcresearchpress.com by 78.46.186.204 on 09/04/12
For personal use only.

Can. J. Chem. Downloaded from www.nrcresearchpress.com by 78.46.186.204 on 09/04/12
For personal use only.

THE CRYSTALLIZATION OF CALCIUM SULPHATE DIHYDRATE[1]

O. J. SCHIERHOLTZ

ABSTRACT

In this preliminary series of experiments, calcium sulphate dihydrate has been allowed to crystallize spontaneously from solutions of varying degrees of supersaturation, and induction periods and rate constants have been determined. The effect of crystal area, pH, and accelerators and retarders on this process has been examined. The degree of supersaturation has a direct effect on both the induction period and rate constant. Nucleation is affected markedly by pH. Salts having an ion in common with calcium sulphate function as accelerators. Retarders affect the induction period in proportion to their concentration, but show little, if any, effect on the rate of crystallization. The behavior of the various reagents under the conditions prevailing in these experiments is largely in accord with observations on the behavior of commercial plasters.

INTRODUCTION

The work described in this paper was undertaken because of the apparent conflict of explanations offered in the literature for some of the phenomena observed in the setting of commercial gypsum plasters, which involves the crystallization of calcium sulphate dihydrate. A clearer understanding of the function of accelerators and retarders would be of considerable value in the manipulation of commercial plasters for specific purposes.

The results of several previous studies (1, 2, 3) indicate that the hemihydrate dissolves to form a solution supersaturated with respect to the dihydrate, which then crystallizes out. Photomicrographic (1) and radioisotope (3) studies support this view, which has been discussed in relation to the theory of von Weimarn (2, 4). Some workers have suggested that the rate of solution of the hemihydrate is the controlling factor and that retarders function by affecting this rate of solution.

In this paper, the first of a series, the reactants were all in solution initially, thus eliminating any effects attributable to the surface of the hemihydrate or its rate of solution. The influence of such factors as the initial supersaturation, crystal surface area of the dihydrate, pH, and addition of accelerators and retarders was then determined. The effect of temperature was not investigated at this time, hence the calculation of activation energies has not been attempted.

EXPERIMENTAL

The first attempts to obtain solutions supersaturated with respect to calcium sulphate dihydrate were by dissolving hemihydrate at 10° C. and raising the temperature to 25° C. This was based on solubility data reported in the literature (5, 6). Because of difficulty in achieving complete, rapid solution of the hemihydrate, this method was abandoned in favor of the following.

The calcium required for any desired supersaturation was weighed out as calcium hydroxide, dispersed in a little water, the equivalent amount of standard sulphuric acid added, and the solution made to final volume of 150 cc. with water. After thorough stirring, the solution was filtered through Whatman No. 41H paper into an aluminum dish. All these operations were performed at 10° C. The temperature was then raised to 25° C. in about 15 seconds by immersion of the aluminum dish in warm water. The solution was transferred to a large scratch-free test tube, fitted with a mechanical stirrer, and

[1]*Manuscript received November 7, 1957.*
Contribution from: Department of Chemistry, Ontario Research Foundation, Toronto 5, Ontario.

suspended in a thermostat at 25° C. A 1-ml. sample was taken immediately for analysis followed by others at suitable intervals of time. The pH of these solutions was close to 4.5, as determined by Accutint papers. The glass electrode pH meter could not be used because of the tendency of calcium sulphate to crystallize on the electrode surface. Samples for analyses were pipetted through a cotton filter and titrated against standard disodium ethylenediaminetetracetate (7) using a microburette.

RESULTS AND COMMENT

A plot of the calcium content of the solution against time gave a logarithmic type of curve (Fig. 1). If c is the concentration at time t, and c_s the saturation concentration, then $\log_{10}(c-c_s)$ plotted against t will be linear provided the crystallization obeys first-order kinetics. For pure solutions of calcium sulphate, c_s was taken to be 1.53×10^{-2} moles liter^{-1} at 25° C. (6). In cases where additives were present, c_s was determined experimentally to a reasonable approximation.

The general type of curve obtained is shown in Fig. 2. Most of the experimental curves depart from linearity towards the end of the run. For purposes of analysis, the solid

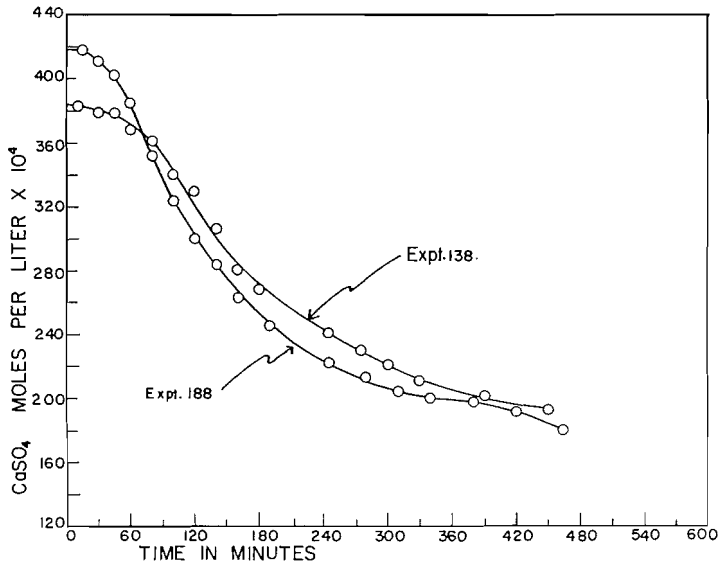

FIG. 1. Plot of concentration versus time for 150% supersaturation (Expt. 138) and 175% supersaturation (Expt. 188).

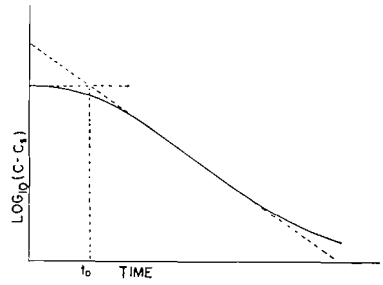

FIG. 2. Diagrammatic illustration of the plot of $\log_{10}(c-c_s)$ against time.

Can. J. Chem. Downloaded from www.nrcresearchpress.com by 78.46.186.204 on 09/04/12
For personal use only.

line has been replaced by dotted lines at both ends of the curve, and the point where the dotted line intersects the line projected horizontally at the level of the original concentration was taken as the time t_0, the approximate starting point of the linear portion of the curve. Thus, the time interval preceding t_0 is taken as the induction period.

Fig. 3 illustrates the application of this method of analysis to the cases where the initial supersaturation was varied in the series 100%, 125%, 150%, and 175%. A curve for 135% has been omitted for clarity.

A. Effect of Supersaturation on the Course of Crystallization

Starting with any given supersaturation (Fig. 3) the crystallization process appears to follow a first-order rate law over a large percentage of the reaction. This is shown by the relative constancy of the first-order rate coefficients calculated for various time intervals during a typical experiment (Table I). It is also apparent that the process does not follow a second-order rate law. The first-order rate constants, calculated over the linear portions of the curves in Fig. 3, are given in Table II.

The ends of the curves in Fig. 3 deviate considerably, indicating a more complicated process in the early and final stages. The deviation in the final stages may reflect the

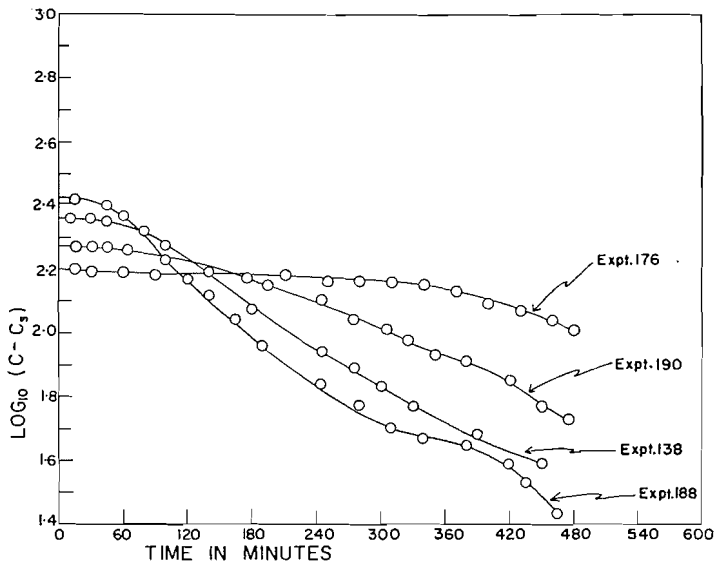

FIG. 3. Plot of $\log_{10}(c-c_s)$ versus time for the following supersaturations: Expt. 176, 100%; Expt. 190, 125%; Expt. 138, 150%; Expt. 188, 175%.

TABLE I

FIRST- AND SECOND-ORDER RATE CONSTANTS FOR CRYSTALLIZATION FROM A 175% SUPERSATURATED SOLUTION

Time intervals, min.	t_2-t_1, min.	$(c_1-c_s)\times10^4$, moles liter^{-1}	$(c_2-c_s)\times10^4$, moles liter^{-1}	$k_1\times10^3$, min.$^{-1}$	$k_2\times10^5$, liter moles^{-1} sec.$^{-1}$
45 to 140	95	249	131	6.7	3.8
165 to 245	80	109.5	68.5	5.9	6.8
280 to 340	60	59.5	47.0	4.0	7.5
380 to 465	85	45.0	27.0	6.0	17.4

Can. J. Chem. Downloaded from www.nrcresearchpress.com by 78.46.186.204 on 09/04/12
For personal use only.

TABLE II

EFFECT OF INITIAL SUPERSATURATION ON t_0 AND k

Expt. No.	Initial super-saturation, %	$c_s \times 10^4$, moles liter^{-1}	$c \times 10^4$, moles liter^{-1}	$(c-c_s) \times 10^4$, moles liter^{-1}	t_0, min.	k, min.$^{-1}$
176	103.6	153	311.5	158.5	300	0.0023
190	123.9	153	342.5	189.5	124	0.0034
189	132.4	153	355.5	202.5	110	0.0037
138	152.6	153	386.5	233.5	62	0.0051
188	175.2	153	418	265	40	0.0072

lower solubility of larger crystals, but a more refined analytical method is required at these lower calcium concentrations to investigate this aspect with assurance.

Close control of nucleation experiments is difficult to achieve. Within one set of experiments, e.g. Fig. 3 or Fig. 6, the curves obtained are reasonably reproducible and change in a logical fashion with systematic change in conditions. Unfortunately, quantitative comparison between experiments performed at widely different times is poor. For example, Expt. 188 (Fig. 3) and Expt. 71 (Fig. 6) do not agree in rate coefficient although made under nominally the same conditions several months apart.

In general, however, the observed effect of supersaturation on rate coefficient appears to be in accord with von Weimarn's theory that the initial velocity of nucleus formation is proportional to the relative supersaturation. It is possible that the results obtained might be explained by assuming that the crystals are growing in one direction only, i.e. deposition on a constant surface area. However, much more experimental data is needed to substantiate this.

The crystals produced in this series of experiments were all mixtures of the acicular and twinned types (Fig. 4), as found by earlier workers. There was some variation in the proportion of the two types, but no regular trend was found, as would be expected if the supersaturation were the dominant influence.

B. Effect of Crystal Surface Area on Crystallization

In a series of experiments the area of crystal surface in contact with the crystallizing liquid was varied. Apparently calcium sulphate behaves normally in this respect. The results, shown in Table III, suggest that the area for crystal growth is substantially constant over the linear portion of the $\log_{10}(c-c_s)$ vs. time curve, which may be a consequence of the acicular nature of the crystals with growth occurring predominantly on one face and that the process is diffusion controlled with the film of solution immediately in contact with a growing face being only slightly supersaturated.

TABLE III

EFFECT OF CRYSTAL SURFACE AREA ON k

Expt. No.	Modification	Point of modification	k, min.$^{-1}$
188	None	—	0.0072
185	Crystals added	27% Crystallized	0.0113
192	Crystals crushed	30% Crystallized	0.0110
187	Crystals removed	27% Crystallized	0.0034

C. Effect of pH on Crystallization Rate

Most of the experiments reported in this paper were made at pH 4.5. However, a

Can. J. Chem. Downloaded from www.nrcresearchpress.com by 78.46.186.204 on 09/04/12
For personal use only.

Can. J. Chem. Downloaded from www.nrcresearchpress.com by 78.46.186.204 on 09/04/12
For personal use only.

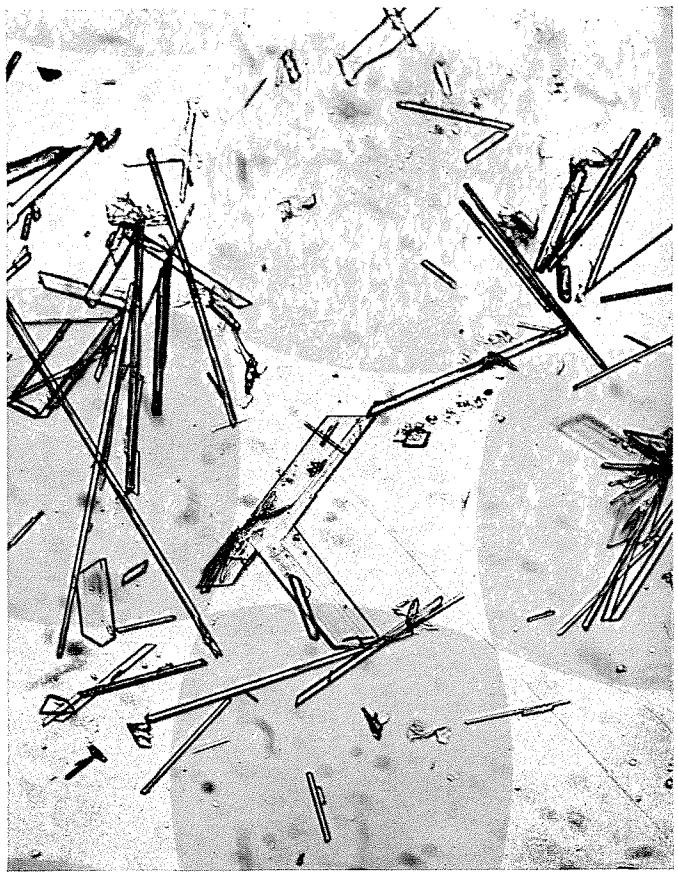

FIG. 4. Acicular and twinned types of crystals found throughout these experiments. 200 ×

number of experiments at higher pH gave rather striking results, shown in Table IV and Fig. 5. All pH adjustment was made by adding the required additional amount of calcium hydroxide.

TABLE IV

EFFECT OF pH ON t_0 AND k

Expt. No.	% Supersaturation	pH	t_0, min.	k, min.$^{-1}$
138	150	4.5	62	0.0051
170	150	5.5	314	0.0023
181	150	6.6	375	0.0017
191	175	4.5–6.6	42	0.0072
188	175	4.5	40	0.0072

It is apparent that the length of the induction period and, to a lesser extent, the rate constant are markedly affected as the pH approaches the neutral value. In Expt. 191, pH 4.5 was maintained until about 27% of the material had crystallized out and the normal rate for the prevailing conditions had been established. Adjustment of the pH to 6.6 at this stage had a negligible effect on the rate, giving further indication that the rate constant is determined by conditions existing at the end of the induction period.

D. Effect of Accelerators, Retarders, and Salts Having No Common Ion

A series of experiments were made, starting with pure calcium sulphate solution at 175% supersaturation, with the additions shown in Table V. The quantities of reagents were chosen arbitrarily, but were of such a magnitude as to clearly show their effects in these solutions. They are not particularly related to quantities used in commercial plasters.

TABLE V

EFFECT OF ADDITIONS ON t_0 AND k

Expt. No.	Addition	Concn. of addition, moles liter^{-1}	$c_s \times 10^4$ moles liter^{-1}	t_0, min.	k, min.$^{-1}$
72	K_2SO_4	(23×10^{-3})	112.4	6	0.0432
92	$CaCl_2$	(4.4×10^{-3})	139	6	0.0177
71	Control		153	50	0.0096
96	NaCl	(59×10^{-3})	195	60	0.0092
109	Retarder	(2.75×10^{-3})	153	98	0.0080
104	Retarder	(5.5×10^{-3})	153	182	0.0082

In the results shown in Table V and Fig. 6, the values of c_s were determined by experiment. These values for Expts. 92 and 96 agree well with values interpolated from the literature, although that for Expt. 72 is possibly 10 units lower than the corresponding value inferred from the literature. However, in this case the data are very scarce.

Inorganic salts added to a solution of calcium sulphate 175% supersaturated with respect to the dihydrate may affect the course of events by (*a*) changing c_s and thus the initial supersaturation, (*b*) by affecting nucleation in other ways, or (*c*) by affecting the rate constant other than through the change in initial supersaturation.

Salts containing a common cation or anion functioned as accelerators, producing a short induction period and high rate constant. The value of c_s is decreased, thus increasing the initial supersaturation, but extrapolation of the data of Table II by plotting

Can. J. Chem. Downloaded from www.nrcresearchpress.com by 78.46.186.204 on 09/04/12
For personal use only.

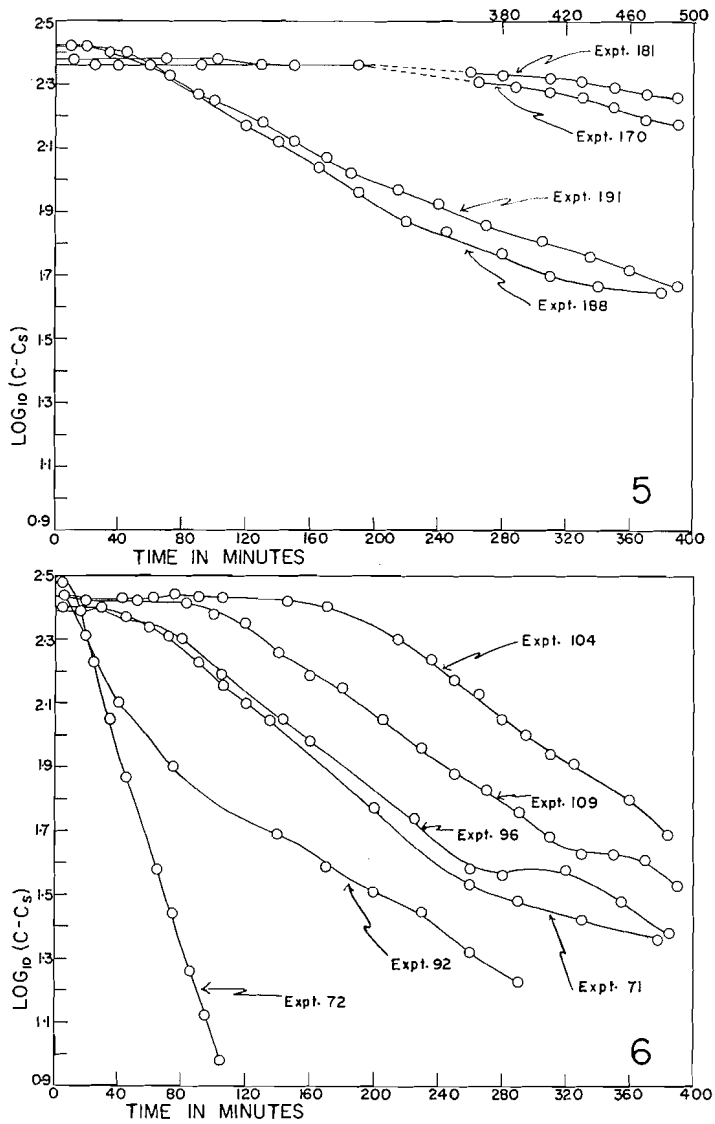

FIG. 5. Plot of $\log_{10}(c-c_s)$ versus time for various pH conditions.
FIG. 6. Plot of $\log_{10}(c-c_s)$ versus time for solutions containing various additives.

$\log_{10} k$ against (c_i-c_s), where c_i is the initial concentration, indicates that this would account for only part of the high k value found (0.0113 min.$^{-1}$ of 0.0432 min.$^{-1}$). This extrapolation involves the assumption that the same relation between initial supersaturation and k holds for both pure and salted solutions.

Salts having no ion in common with calcium sulphate showed little effect on the induction period or the value of k. The c_s value was markedly increased, hence the initial supersaturation reduced. Extrapolation of data, as above, indicates a k value of 0.0046 min.$^{-1}$ instead of 0.0092 min.$^{-1}$ for Expt. 96. Thus it might be argued that sodium chloride, for example, has an accelerating effect on the crystallization process which is offset by an increase in solubility of calcium sulphate. Sodium chloride did

Can. J. Chem. Downloaded from www.nrcresearchpress.com by 78.46.186.204 on 09/04/12
For personal use only.

not act as an accelerator in the same sense as did potassium sulphate, nor did it behave analogously to aluminum sulphate, which is widely used as an accelerator in commercial plaster.

Where retarders are present, the induction period is considerably greater and roughly proportional to the amount of retarder used. When crystallization finally begins, it proceeds at a rate not greatly different from that of the control sample. This behavior tends to support the view that retarders function by covering the nuclei as they form, until the supply of retarder is exhausted. Nucleation and subsequent crystallization then proceed unhindered. Evidently the retarder is not acting by interfering with diffusion.

ACKNOWLEDGMENTS

Grateful acknowledgment is made to Dr. A. E. R. Westman, Dr. M. H. Jones, Dr. D. B. DeLury, and Dr. H. G. McAdie for helpful suggestions, and to Douglas Renton for his painstaking assistance on the experimental work.

REFERENCES

1. THOMSON, G. M. Living mineral crystals—from birth to maturity. Address to Royal Canadian Institute, Toronto, Ontario. Feb. 4th, 1933.
2. WEISER, H. B. and MORELAND, F. B. J. Phys. Chem. **36**, 1 (1932).
3. BIRSS, F. W. and THORVALDSON, T. Can. J. Chem. **33**, 870 (1955).
4. CUNNINGHAM, W. A., DUNHAM, R. M., and ANTES, L. L. Ind. Eng. Chem. **44**, 2402 (1952).
5. RIDDELL, W. C. Rock Prods. **53** (No. 5), 68–71, 102 (1950).
6. KRUIS, A. and SPÄTH, H. Research and progress in the gypsum industry since 1939. Tonind.-Ztg. Special Reprint No. 56 (1951).
7. AMERICAN PUBLIC HEALTH ASSOCIATION, INC. Standard methods for the examination of water, sewage, and industrial wastes. 10th ed. New York. 1955. p.112.

Can. J. Chem. Downloaded from www.nrcresearchpress.com by 78.46.186.204 on 09/04/12
For personal use only.

Can. J. Chem. Downloaded from www.nrcresearchpress.com by 78.46.186.204 on 09/04/12
For personal use only.

THE SYSTEM KOH–K_2CO_3–H_2O AT LOW TEMPERATURES

I. PHASE EQUILIBRIA[1]

A. A. Lang and A. J. Sukava

ABSTRACT

Phase diagrams for the system KOH–K_2CO_3–H_2O were determined for 25°, 10°, 0°, −10°, −20°, −40°, and −60°. The stable hydrates of potassium hydroxide were the di- and tetra-hydrates; those of potassium carbonate were the sesqui- and hexa-hydrates. No compound formation between KOH and K_2CO_3 was detected.

INTRODUCTION

Very few data for the ternary system KOH–K_2CO_3–H_2O are found in the literature. It is known (1) that at 30° this system is univariant when the solution contains 55.14% potassium hydroxide and 2.05% potassium carbonate, the equilibrium solid phases being $KOH.2H_2O$ and $K_2CO_3.3/2H_2O$. The hydrate $K_2CO_3.6H_2O$ exists at −18° in equilibrium with a solution containing 8.80% potassium hydroxide and 36.11% potassium carbonate (2).

According to some of the older published data for the binary system KOH–H_2O (3, 4, 5, 6), anhydrous potassium hydroxide is stable above 143°. Below this temperature the successive stable forms are the mono-, sesqui-, di-, and tetra-hydrates at intervals down to a eutectic at −66°, at which point the tetrahydrate is in equilibrium with ice and a solution containing 30% potassium hydroxide. In partial contradiction, a more recent report (7) claims that potassium hydroxide hydrates with 5, 6, 8, and 18 moles of water also exist, and that the binary eutectic lies at −82.5° with the hexa- and octa-hydrates in equilibrium with a solution containing 31.2% potassium hydroxide.

Published data for the binary system K_2CO_3–H_2O show quite conclusively that the stable hydrates of potassium carbonate are the mono-, sesqui-, and hexa-hydrates. The hexahydrate exists down to a eutectic with ice at −36.5° (2, 8, 9, 10).

The results reported in the present paper arise from part of a study of some physical properties of aqueous solutions containing potassium hydroxide and potassium carbonate in the temperature range from 25° to −60°, a study which constitutes part of a more general investigation of the properties of alkaline battery electrolytes. Ternary phase-equilibrium data are presented for this temperature range.

EXPERIMENTAL

The temperature from 25° to −10° was kept constant to within ±0.02° with a Townson and Mercer X-27 bath. A Kelvinator refrigerating unit served as cooling equipment. Water and ethylene glycol – water solutions were used as bath liquids. A Townson and Mercer X-160/U bath was used for temperature control from −20° to −60°. This bath employed petroleum ether as bath liquid, with a Dry Ice – acetone cooling mixture surrounding the heat exchanger. It held the temperature constant to within ±0.05°.

The thermometers employed were mercury-in-glass and toluene-in-glass for the higher and lower temperatures respectively. These were calibrated against certified standards. The calibration and reading of the thermometers are considered the major sources of

[1]*Manuscript received January 21, 1958.*
Contribution from the Department of Chemistry, University of Western Ontario, London, Ontario, based on research sponsored by the Defence Research Board, Ottawa, under Grant No. 5480-10, Project D 52-54-80-10.

error in the temperature measurements. By our estimation the maximum accuracy of these measurements probably varies from about ±0.05° at 25° to about ±0.5° at −60°, despite the more precise temperature control.

All the saturated solutions were prepared from reagent grade chemicals and distilled water. The mixtures were stirred in covered Pyrex vessels held in the temperature bath, with the stirring usually prolonged for 2 or 3 days to ensure equilibrium. Samples of liquid and wet solid phases were separated by suction through sintered-glass filters and weighed quantities of these were analyzed by titration with hydrochloric acid. The compositions of equilibrium solids were determined by the "wet residue" method.

RESULTS AND DISCUSSION

The analytical data and composition of equilibrium solids are given in Table I. Typical phase diagrams are shown in Figs. 1*a* and *b* and 2. Fig. 3 shows all the liquidus curves. Some of the univariant points, or isobaric triple points, were determined by direct analysis of the equilibrium solutions, while others were found by extrapolation as indicated.

The course and shape of the liquidus curves in Fig. 3 seem to suggest that the extrapolated values for the two equilibria, (i) $KOH.4H_2O$ – $K_2CO_3.6H_2O$ – saturated solution at −40° and (ii) $KOH.4H_2O$ – ice – saturated solution at −60°, probably lie in metastable regions. No attempt was made to investigate these small regions by actual experiment.

The narrow range of liquid composition in equilibrium with potassium hydroxide dihydrate at 25°, 10°, and 0° was not investigated. The solubilities of pure potassium hydroxide were obtained from existing literature (1) and are shown as such in the tables.

The data for −10° show that potassium carbonate sesquihydrate is readily obtained in metastable equilibrium at this temperature with solutions containing less than about 7% potassium hydroxide. The rate of transition of the potassium carbonate sesquihydrate to the stable hexahydrate was found to be very slow even at temperatures 10° to 15° below the known transition point (−6.2° (2)). Seeding with hexahydrate crystals was necessary to promote the transformation. These results are in agreement with those of other studies (2).

A special effort was made to detect the hydrates $KOH.5H_2O$ and $KOH.18H_2O$, which have been reported (7). According to this report, the range of existence of the pentahydrate is supposed to be from −43° to −62.5°, with equilibrium solutions ranging from 38.5 to 33.7% potassium hydroxide. That of the octodecahydrate is supposed to be from −32° to −75.5°, with solutions ranging from 22.5 to 30.2% potassium hydroxide. If these hydrates do indeed exist, as claimed, their presence should have been shown by our data for −40° and −60°, especially since the results of our analyses were usually reproducible to within ±0.2%. We found no such evidence. In particular, it would appear that steric effects would preclude the existence of a hydrate with 18 moles of water per mole of potassium hydroxide. It is noteworthy too that extrapolation of our ternary data to 0% potassium carbonate (to give the solubility curve for pure potassium hydroxide in water) will show a trend which supports the older arguments (3, 4, 5, 6) according to which the eutectic for the binary KOH–H_2O system lies at −66°, with the hydrate $KOH.4H_2O$ and ice in equilibrium.

It should also be noted that, since our data do not extend below −60°, the possible existence of a sharp ternary eutectic with a low concentration of potassium carbonate cannot be discounted on present evidence. Such a possibility might indeed offer at least a partial explanation of the −82.5° value reported as the eutectic temperature for the

Can. J. Chem. Downloaded from www.nrcresearchpress.com by 78.46.186.204 on 09/04/12
For personal use only.

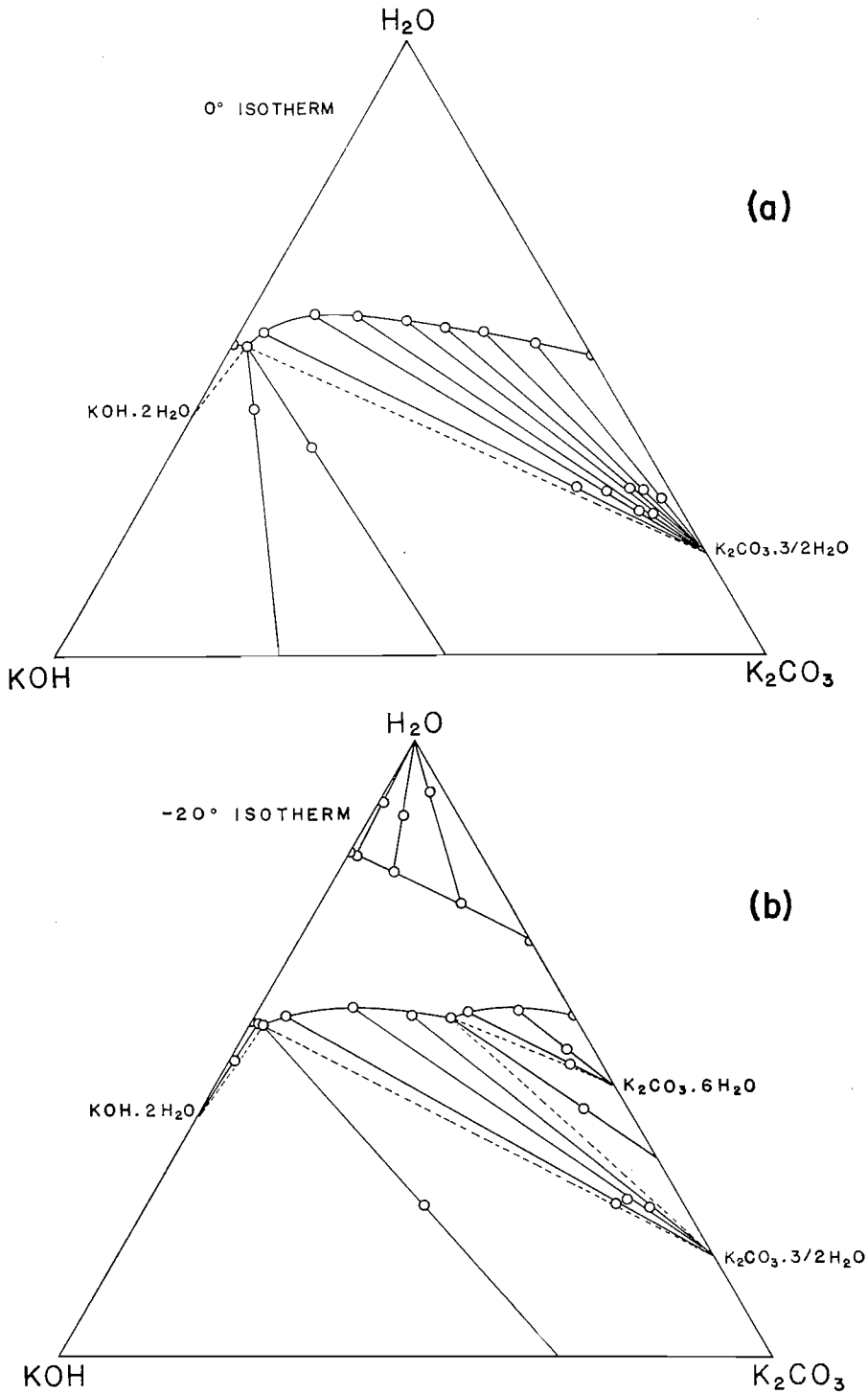

FIG. 1. The system $KOH–K_2CO_3–H_2O$ at (*a*) 0° C. and (*b*) −20° C.

Can. J. Chem. Downloaded from www.nrcresearchpress.com by 78.46.186.204 on 09/04/12
For personal use only.

Can. J. Chem. Downloaded from www.nrcresearchpress.com by 78.46.186.204 on 09/04/12
For personal use only.

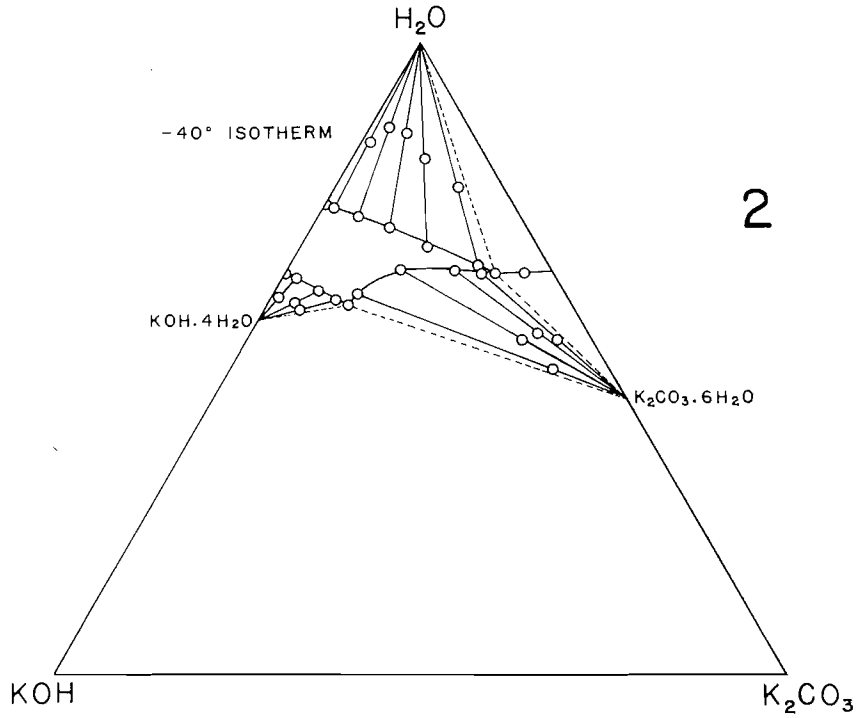

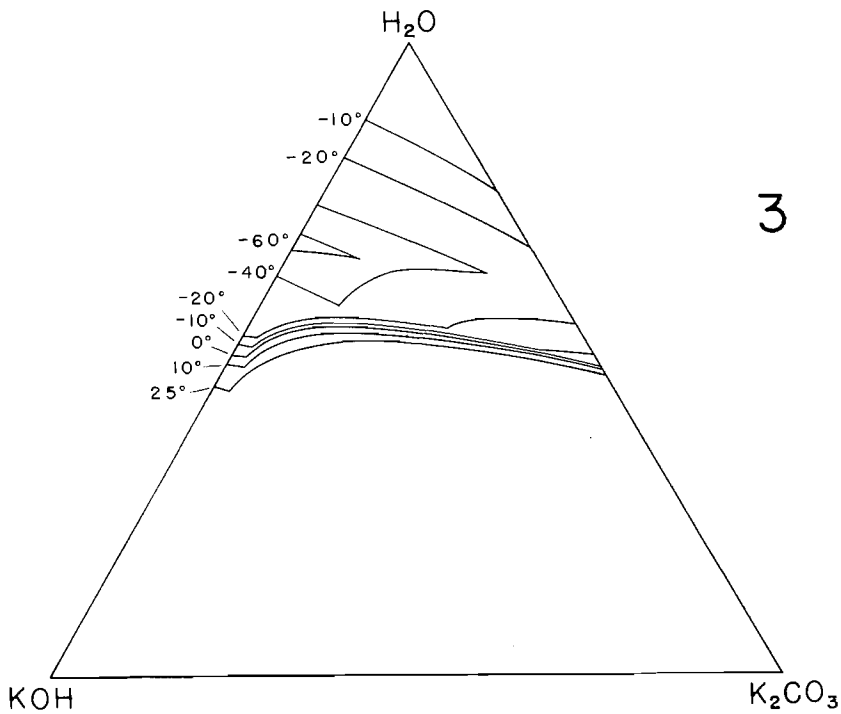

FIG. 2. The system $KOH–K_2CO_3–H_2O$ at −40° C.
FIG. 3. Liquidus curves for the system $KOH–K_2CO_3–H_2O$, from 25° to −60° C.

TABLE I

Liquid phase		Wet residue		Solid phase
% KOH	% K_2CO_3	% KOH	% K_2CO_3	
		A. Isotherm for 25° C.		
0	52.80			$K_2CO_3.3/2H_2O$
10.77	39.45	4.42	64.00	"
14.41	34.84	6.40	62.83	"
22.83	24.87	4.93	70.47	"
28.83	18.05	7.10	67.32	"
37.02	11.10	15.0	54.2	"
46.33	4.28	24.53	41.55	"
50.41	2.91	22.46	47.47	"
52.46	2.41	51.30	9.84	$K_2CO_3.3/2H_2O$ and $KOH.2H_2O$
52.50	2.36	45.93	18.80	$K_2CO_3.3/2H_2O$ and $KOH.2H_2O$
54.0*	0			$KOH.2H_2O$
		B. Isotherm for 10° C.		
0	51.9			$K_2CO_3.3/2H_2O$
9.76	39.15	2.6	73.2	"
20.08	26.93	5.4	68.5	"
29.51	16.40	6.0	70.2	"
35.82	10.05	9.3	64.3	"
42.55	5.10	13.0	59.5	"
48.92	2.18	42.4	32.7	$K_2CO_3.3/2H_2O$ and $KOH.2H_2O$
49.03	2.20	62.8	17.0	$K_2CO_3.3/2H_2O$ and $KOH.2H_2O$
50.7†	0			$KOH.2H_2O$
		C. Isotherm for 0° C.		
0	51.25			$K_2CO_3.3/2H_2O$
6.94	42.50	1.90	72.71	"
13.20	34.30	3.84	69.44	"
18.20	28.45	5.61	67.23	"
23.10	22.47	4.53	72.70	"
29.60	15.13	6.01	70.60	"
35.43	9.04	8.99	64.32	"
44.04	3.24	12.99	59.85	"
47.51	2.09	46.87	19.16	$K_2CO_3.3/2H_2O$ and $KOH.2H_2O$
47.45	2.11	51.70	8.03	$K_2CO_3.3/2H_2O$ and $KOH.2H_2O$
49.2†	0			$KOH.2H_2O$
		D. Isotherm for −10° C.		
12.1‡	0			Ice
11.05	1.72	6.20	1.03	"
9.61	4.67	4.50	2.15	"
5.68	11.80	2.88	5.95	"
0	23.60			"
0	49.40			$K_2CO_3.6H_2O$
0	49.37			"
3.88	45.16	2.00	50.5	"
6.90	41.90	4.00	48.2	"
6.9	41.9			$K_2CO_3.6H_2O$ and $K_2CO_3.3/2H_2O$
0	50.50			$K_2CO_3.3/2H_2O$§
0	50.80			"§§
5.09	44.21	2.42	66.2	"§§
13.45	33.60	3.54	71.2	"
16.40	29.72	4.12	70.1	$K_2CO_3.3/2H_2O$§
20.00	25.45	4.38	70.2	"
21.75	23.50	7.73	61.1	"
36.70	7.32	13.16	56.3	"
42.92	3.33	17.05	51.4	"
45.58	2.01	41.2	35.0	$K_2CO_3.3/2H_2O$ and $KOH.2H_2O$
45.70	1.90	56.8	26.5	"
46.40	0.92	55.7	0.44	$KOH.2H_2O$
47.0‡	0			"
		E. Isotherm for −20° C.		
18.0‡	0			Ice
17.39	1.14	9.4	0.5	"
13.68	7.63	7.8	4.3	"
6.84	19.85	2.1	6.2	"
0	32.52			"
0	44.62			$K_2CO_3.6H_2O$
7.47	36.24	3.9	46.2	"
14.68	29.50	4.5	48.0	"
17.52	27.41	6.2	53.6	$K_2CO_3.6H_2O$ and $K_2CO_3.3/2H_2O$
22.80	21.83	5.0	70.8	$K_2CO_3.3/2H_2O$
30.40	12.86	7.6	67.0	"
40.54	4.09	9.3	65.8	"
44.60	1.73	36.4	39.0	$K_2CO_3.3/2H_2O$ and $KOH.2H_2O$
44.90	1.42	51.2	0.70	$KOH.2H_2O$
46.3‡	0			"
		F. Isotherm for −40° C.		
25.5‡	0			Ice
24.84	1.22	14.5	1.05	"
22.04	5.40	10.8	2.6	"
18.71	10.65	9.0	5.2	"
15.12	17.16	8.4	10.0	"
9.62	25.65	6.1	16.7	"
7.99	28.62	3.9	32.4	Ice and $K_2CO_3.6H_2O$
9.88	26.60	4.8	42.1	$K_2CO_3.6H_2O$
13.12	22.95	6.9	39.0	"
20.68	15.15	9.6	37.4	"
28.26	11.30	7.7	44.0	"
30.5‡	11.0‡			$K_2CO_3.6H_2O$ and $KOH.4H_2O$
31.75	8.87	37.5	4.85	$KOH.4H_2O$
33.40	5.92	37.7	3.60	"
35.50	1.78	39.4	0.95	"
36.6‡	0			"
		G. Isotherm for −60° C.		
30.1‡	0			Ice
29.22	1.30	16.5	0.80	"
28.50	2.48	17.8	1.50	"
26.75	5.43	20.4	4.00	"
24‡	10‡			Ice and $KOH.4H_2O$
27.50	5.83	36.6	2.95	$KOH.4H_2O$
29.42	3.35	35.0	1.90	"
31.36	1.23	37.5	0.72	"
32.8‡	0			"

*From Seidell (1), by interpolation. †From Seidell (1). ‡Extrapolated. §Metastable.

Can. J. Chem. Downloaded from www.nrcresearchpress.com by 78.46.186.204 on 09/04/12
For personal use only.

$KOH–H_2O$ system (7). This seems the more likely, since reagent grade potassium hydroxide, unless intensively purified, is liable to contain a small percentage of carbonate, and since the investigators reporting this low eutectic point probably used such unpurified hydroxide. The possible absorption of atmospheric carbon dioxide by the potassium hydroxide solutions might also have been overlooked.

We recognize the obvious inadequacy of our data for the temperature range between $-20°$ and $-60°$. Plans are being made to complete these data at some future date, by investigating this system at $-30°$ and $-50°$.

REFERENCES

1. SEIDELL, A. Solubilities of inorganic and organic substances. 2nd ed. D. Van Nostrand Company, Inc., New York. 1919.
2. HILL, A. E. and MILLER, F. W. J. Am. Chem. Soc. **49**, 669 (1927).
3. FERCHLAND, P. Z. anorg. Chem. **30**, 133 (1902).
4. HÖLZL, F. Z. Elektrochem. **43**, 302 (1937).
5. PICKERING, S. U. J. Chem. Soc. **63**, 908 (1893).
6. SHIBATA, E., ODA, S., and FURUKAVA, S. J. Chem. Soc. Japan, **51**, 278 (1930).
7. MALLORY COMPANY. First Quart. Progr. Rept. on (U.S.) Signal Corps, Eng. Labs. Contract W-36-039-SC-38137 (1948).
8. APPLEBEY, M. P. and LEISHMAN, M. A. J. Chem. Soc. **40**, 1603 (1932).
9. MELLOR, J. W. A comprehensive treatise on inorganic and theoretical chemistry. Vol. 2. Longmans, Green and Co., Ltd., London. 1922.
10. MEYERHÖFFER, W. Z. phys. Chem. **53**, 513 (1905).

Can. J. Chem. Downloaded from www.nrcresearchpress.com by 78.46.186.204 on 09/04/12
For personal use only.

Can. J. Chem. Downloaded from www.nrcresearchpress.com by 200.7.193.243 on 09/04/12
For personal use only.

THE POLARIZED FLUORESCENCE OF VERY THIN ANTHRACENE CRYSTALS[1,2]

J. FERGUSON[3] AND W. G. SCHNEIDER

ABSTRACT

The polarized fluorescence from anthracene sublimation flakes has been measured at 300°, 77°, and 4° K. A recording spectrometer was used to measure accurately the relative intensity of the two crystal polarizations and also to determine changes in the spectrum between 77° and 4° K. The polarization ratio (b/a) was found to decrease with increasing wavelength and measurements made at 77° and 4° K. indicate that there is more than one emitting level and that these have different polarization properties. The fluorescence arises from regions of weak absorption in the crystal and it is suggested that these regions occur in the neighborhood of imperfections. In addition the polarized fluorescence excited from anthracene sublimation flakes containing traces of tetracene has been determined and changes were found in the transfer efficiency between 77° and 4° K., again suggesting the presence of more than one emitting level. No depolarization of the tetracene fluorescence was observed at low temperatures.

INTRODUCTION

The optical spectra of crystalline anthracene are important for the development of a theory of molecular crystal spectra and also to help in the elucidation of the mechanism of photoconduction. The purpose of the present communication is to report new studies of the fluorescence emitted from crystals of anthracene both at room temperature and low temperatures and to re-examine the interpretation of the origin of this fluorescence. For this pure single sublimation flakes of anthracene were used as well as single flakes deliberately contaminated with tetracene.

Previous measurements of anthracene crystal fluorescence at low temperatures have been made by the following workers: Obreimov, Prikhot'ko, and Shabaldas (1), Pesteil and Barbaron (2), Tsujikawa and Kanda (3), and Sidman (4). All these authors noticed the development of "fine" structure at very low temperatures and Pesteil and Barbaron have measured some 115 of these "lines". Perhaps more important than the appearance of this structure is the polarization ratio, here defined as the ratio of the intensity of the fluorescence vibrating parallel to the b crystal axis to that vibrating parallel to the a axis. The earliest measurements of polarization ratio were made by Obreimov, Prikhot'ko, and Shabaldas (1) and with a rather crude visual method they obtained a b/a ratio of 5.5:1, measurements being made at room temperature and low temperatures. Ganguly and Chaudhuri (5) have made measurements at room temperature but as mentioned in our earlier communication (6) their result suffers from the use of large crystals and subsequent diminution of the polarization ratio by reabsorption. Pesteil (7) has reported polarization ratios for anthracene single crystal at room temperature, but these are referred to the axes of the optical indicatrix and two of these axes vary with wavelength.

In our earlier communication (6) we reported that the polarization ratio at room temperature is about 5:1 and suggested that the reason for this is because the emitting levels are predominantly those regions of the crystal where lattice symmetry is disturbed. The present work reports more fully these results and extends them to low temperatures.

[1]*Manuscript received February 3, 1958.*
Contribution from the Division of Pure Chemistry, National Research Council, Ottawa, Canada.
Issued as N.R.C. No. 4762.
[2]*Presented at the Symposium on Molecular Structure and Spectroscopy, Ohio State University, June, 1957.*
[3]*N.R.C. Postdoctorate Fellow, now at Chemistry Department, University of British Columbia, Vancouver 8, B.C.*

Can. J. Chem. Downloaded from www.nrcresearchpress.com by 200.7.193.243 on 09/04/12
For personal use only.

EXPERIMENTAL

In order to measure quickly and accurately the fluorescence spectra a photomultiplier was used in place of the photocell compartment and cell block of a Beckman DU Spectrometer. The crystal and necessary optical accessories were placed on an optical bench running at right angles to the length of the spectrometer. The fluorescence was excited by a BTH high-pressure mercury lamp and two filters were used to obtain only 3650 Å radiation (Corning 9863 and 5860).

The power supply and amplifier were provided by a Photovolt Photometer No. 520M and a Varian G10 recorder was used in series. A constant-speed motor through a system of gears was used to drive the wavelength knob of the Beckman spectrometer at such a speed that the wavelength range 5000–4000 Å was covered in 5 minutes. Continuous recording of fluorescence spectra could therefore be made.

For room temperature measurements single anthracene sublimation flakes were mounted on a very clean silica disk. This disk was then placed over a pinhole so that it was possible to rotate the crystal centrosymmetrically through 180°. At first a Wollaston prism was used as an analyzer (placed between the crystal and the slit of the monochromator) but this was later replaced with a piece of polaroid equally satisfactory and more convenient.

For the low-temperature measurements a liquid-helium cell of the type described by Duerig and Mador (8) was used, minor modifications being made in the cell piece. The sublimation flakes were mounted on small silica disks and these fitted into copper pieces which slide into slots in the cell block at right angles to the light beam. A good portion of each crystal was selected and the remaining parts of the silica disk were painted over with Aquadag. In this way it was possible also to determine the absorption spectrum of each crystal. The cell was designed so that two crystals could be used in each assemblage of the apparatus. As it was not possible to rotate the crystals, the polaroid analyzer was rotated in order to obtain the two crystal polarizations. This necessitated a calibration of the spectrometer plus photomultiplier in order to compensate for slight changes in transmission of polarized radiation as the plane of polarization is changed.

A final calibration of the unit was obtained with a tungsten strip filament operated at known color temperature. In all cases the slit width of the spectrometer was kept constant during the recording of a spectrum and was normally about 0.2 mm.

Liquid nitrogen and liquid helium were used to cool the crystals. With liquid helium a small amount of helium gas (about 10^{-3} mm.) was momentarily introduced into the cell to act as thermal exchange gas to reduce the temperature of the sample to 4° K. No direct measurements of the temperature of the crystals were made.

The sublimation flakes were grown in a metal crucible in an atmosphere of carbon dioxide in the absence of light. The crystals grew on a filter paper placed over the mouth of the crucible and suitable ones were transferred to the silica disks with a sewing needle mounted in cork.

RESULTS

A. Room Temperature Measurements

Pure Anthracene

Fluorescence spectra from a number of single crystals were recorded. The spectra are similar to two reported elsewhere (9) and have not been included here. Only the polarization properties will be mentioned.

Fluorescence emitted normal to the *ab* plane is strongly polarized with maximum intensity (I_b) when the electric vector is parallel to the *b* crystal axis and minimum intensity (I_a) parallel to the *a* crystal axis. If the crystal is rotated and the intensity of the fluorescence is measured through an analyzer, held fixed, the resultant intensity will be given by $I_b\cos^2\theta + I_a\sin^2\theta$, where θ is the angle between the *b* crystal axis and the electric vector direction of the analyzer. The maximum and minimum correspond respectively to I_b and I_a and the ratio I_b/I_a is the polarization ratio.

Fig. 1(*a*) shows two such curves, one measured at 420 mμ, the other at 445 mμ (two maxima in the fluorescence spectrum). They represent typical results for thin anthracene sublimation flakes and correspond to polarization ratios of 5.3:1 (420 mμ) and 4.2:1 (445 mμ). This variation of polarization ratio with wavelength is important and will be discussed later.

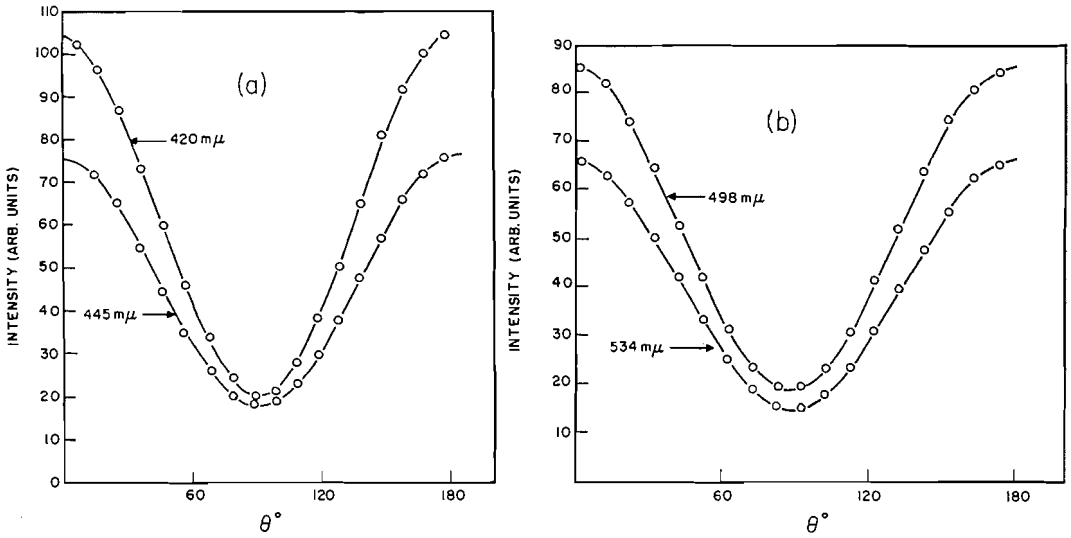

FIG. 1. Variation of fluorescence intensity as a function of θ, the angle between the electric-vector direction of the analyzer and the *b* crystal axis: (*a*) anthracene fluorescence spectrum, 420 and 445 mμ maxima; (*b*) tetracene fluorescence spectrum, 498 and 534 mμ maxima.

The measurements at room temperature can be summarized thus:

(*a*) Spectra emitted from different crystals, on the whole, are similar, showing only slight variations, mainly in the amount of reabsorption which depends on crystal thickness.

(*b*) The polarization ratio is not constant and decreases with increasing wavelength. For the 420 mμ maximum it is in the range 5.0:1–5.5:1.

(*c*) Even for very thin crystals the first maximum in the *a*-polarized spectrum (about 400 mμ) is less intense than the second maximum (about 420 mμ). There is thus evidence of an abnormal distribution of intensity in the *a*-polarized fluorescence.

Anthracene Containing Tetracene

When very small amounts of tetracene are included in anthracene the fluorescence of the latter is strongly quenched giving rise to the bright green-yellow fluorescence of the former (10).

The fluorescence from a single crystal of anthracene containing tetracene is also strongly polarized and Fig. 1(*b*) shows typical results obtained. The two curves are analogous to those of Fig. 1(*a*) and correspond to the first and second maxima in the

Can. J. Chem. Downloaded from www.nrcresearchpress.com by 200.7.193.243 on 09/04/12
For personal use only.

tetracene fluorescence spectrum. The polarization ratios are 4.5:1 and 4.4:1 respectively and unlike anthracene, therefore, the polarization ratio does not change with wavelength.

B. Low Temperature Measurements

Pure Anthracene

Obreimov, Prikhot'ko, and Shabaldas (1) conclude that "different crystals produce different fluorescence spectra. The lines in the spectrum differ in width and, perhaps, in relation to intensity. Curiously the widest bands were found in the spectrum of a crystal supposedly "blue" i.e., of a pure crystal. Spectra of green crystals are composed of narrow bands".

These conclusions were substantiated in the present work, although the poor dispersion of the spectrometer did not allow resolution of the spectrum into "lines", but indications of these were obtained in one or two favorable cases.

Because of the variation in the fluorescence spectra from different crystals it is necessary to include a number of spectra and these have been chosen to emphasize particular

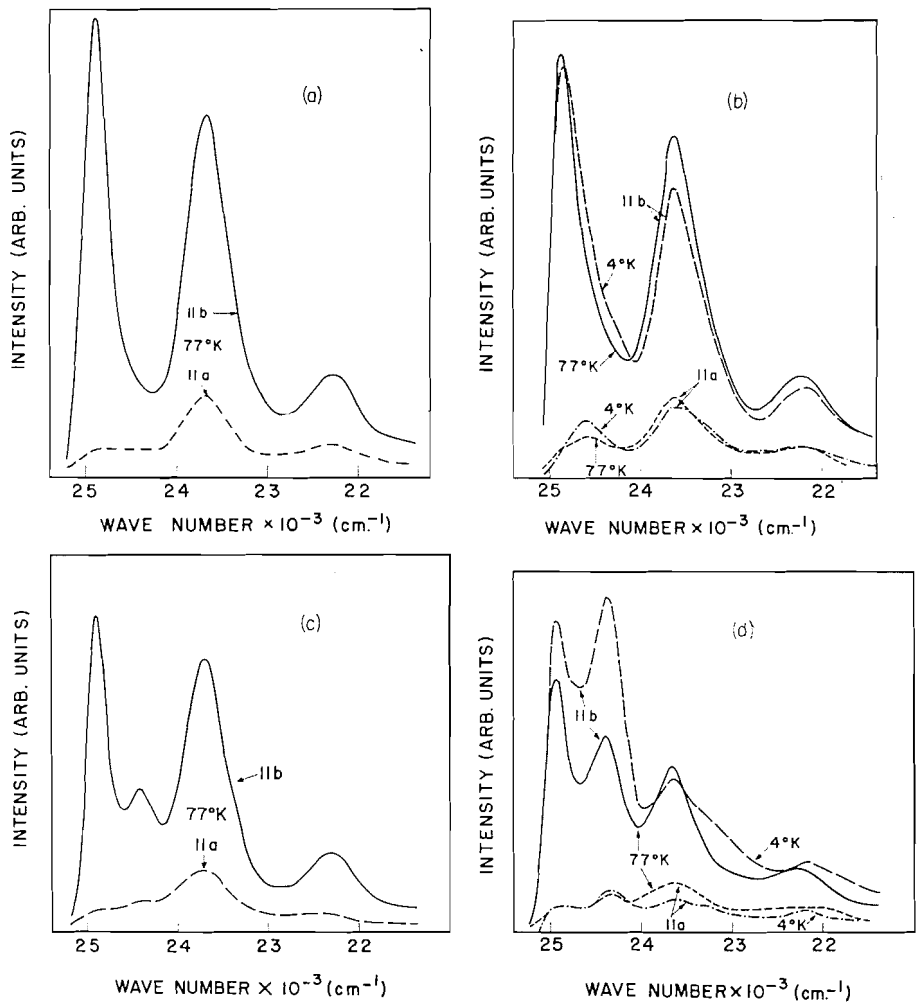

FIG. 2. Examples of the variation in the fluorescence spectrum excited from crystals about 0.2 μ thick.

Can. J. Chem. Downloaded from www.nrcresearchpress.com by 200.7.193.243 on 09/04/12
For personal use only.

differences. The spectra shown in Fig. 2(*a*) were obtained at 77° K. As can be seen, the spectrum parallel to the *b* crystal axis is more intense than that parallel to the *a* crystal axis. In addition, the polarization ratio is not constant, but decreases with decreasing energy (increasing wavelength). As at room temperature the intensity distribution in the *a* polarization is abnormal and most of the intensity is carried in the second maximum.

Fig. 2(*b*) shows spectra obtained from another crystal, measured at 77° and 4° K. The effect of lowering the temperature is to alter slightly the intensity distribution in both crystal polarizations and decrease the over-all polarization ratio but not uniformly throughout the spectrum. The highest energy *b*-polarized band is broader than the similar band in Fig. 2(*a*) and the effect of lowering the temperature is mainly to increase the intensity of the low-energy side of this band.

Fig. 2(*c*) shows the spectrum of a crystal having an absorption spectrum nearly identical with that in Fig. 2(*a*). As can be seen from a comparison with Fig. 2(*a*) the fluorescence spectra are different. This crystal has a new maximum appearing at about 24,400 cm.$^{-1}$ in both polarizations. The measurements were taken at 77° K.

Fig. 2(*d*) shows an example of the marked changes that some crystals exhibit when cooled from 77° to 4° K. The spectrum at 77° K. is similar to that in Fig. 2(*c*) except for a redistribution of intensity.

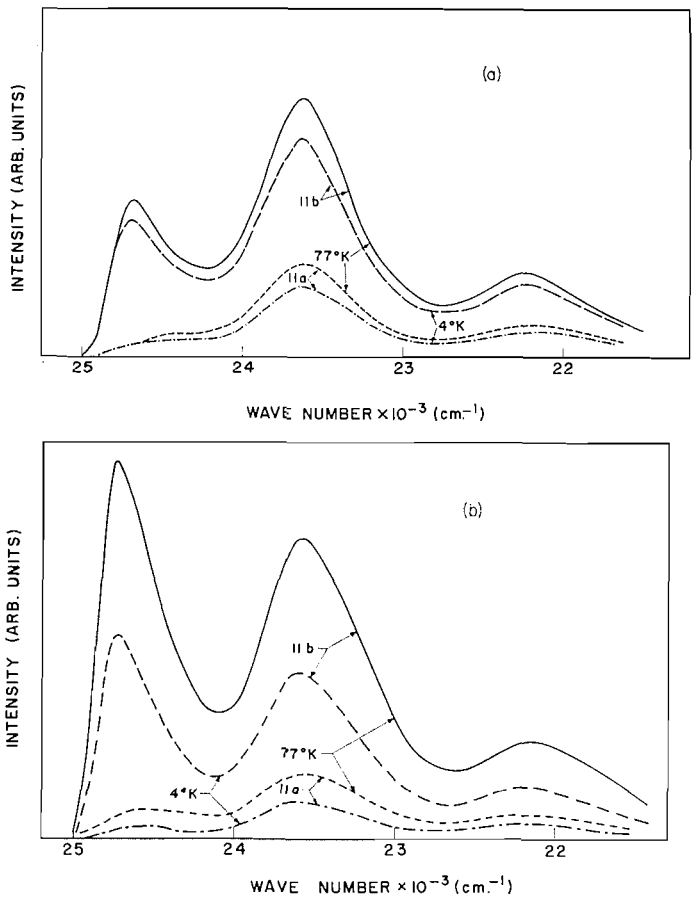

FIG. 3. Examples of the variation in the fluorescence spectrum excited from crystals 2–3 μ thick.

Can. J. Chem. Downloaded from www.nrcresearchpress.com by 200.7.193.243 on 09/04/12
For personal use only.

Examples of fluorescence spectra from thicker crystals are shown in Fig. 3. The individual variations in spectra are not so marked as with the thinner crystals and the bands are broader.

Anthracene Containing Tetracene

Because of the variation observed in the fluorescence of pure anthracene crystals it was decided to deliberately introduce tetracene in very small quantities and study the effect of temperature on both the anthracene and tetracene fluorescence, the latter

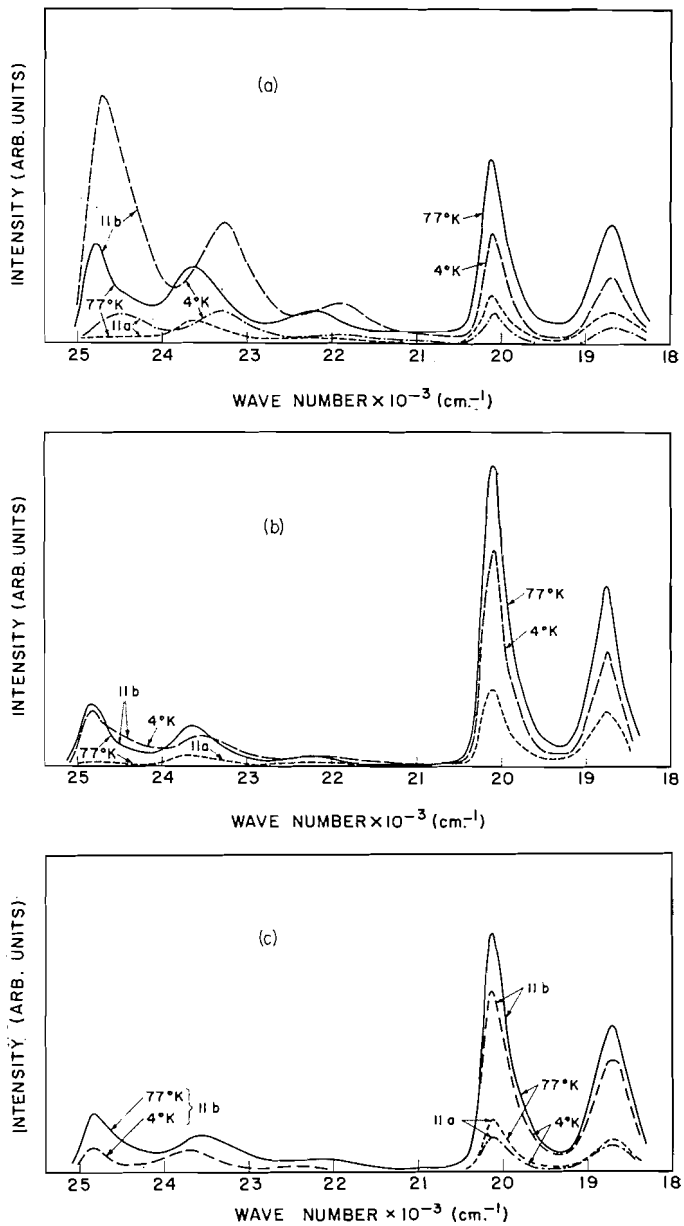

FIG. 4. Examples of the variation with temperature of the fluorescence spectrum of anthracene crystals containing traces of tetracene.

Can. J. Chem. Downloaded from www.nrcresearchpress.com by 200.7.193.243 on 09/04/12
For personal use only.

acting as an "internal standard". Previous measurements with anthracene crystals containing tetracene at 20° K., by Sidman (11), were made on crystals in which the tetracene concentration was so high that nearly all of the fluorescence came from the tetracene, and the anthracene fluorescence was not photographed.

Fig. 4(*a*) shows a most marked effect of temperature on the transfer efficiency as well as a simultaneous alteration of the anthracene spectrum, observed with a crystal about 10^{-5} M./M. At 77° K. the anthracene emission amounts to 0.50 of the whole, while at 4° K. this fraction is 0.79.

Fig. 4(*b*) shows a result similar to that in Fig. 4(*a*), obtained with a crystal containing slightly more tetracene (about 2×10^{-5} M./M.). In this case the fraction of the energy emitted by the anthracene is 0.25 at 77° K. and 0.35 at 4° K. Again there is a change in the anthracene spectrum but it is less marked.

As well as a decrease in transfer efficiency at 4° K. some crystals showed an increase and Fig. 4(*c*) is an example of the fluorescence emitted from such a crystal. The fraction of energy emitted by anthracene is 0.32 at 77° K. and 0.18 at 4° K. Again there is a change in the anthracene spectrum.

Before proceeding with a discussion of the results we shall summarize the observations with pure anthracene crystals.

(1) Fluorescence spectra from different crystals are different, as reported earlier by Obreimov, Prikhot'ko, and Shabaldas (1). In addition it should be noted that the bands are sharper with very thin crystals (about 0.2 μ). For thicker crystals the bands are broader.

(2) In most very thin crystals a considerable rearrangement of the intensity occurs when the crystal is cooled from 77° to 4° K.

(3) As well as the rearrangement of the intensity which occurs between 77° and 4° there is a change between room temperature and 77° K. In both cases the effect is to decrease the fluorescence occurring at lower energies relative to that nearer the origin so that an approximate mirror-image intensity relation to the absorption spectrum is lost.

(4) The polarization ratio is not constant and at the high energy region of the spectrum it is greater than 7:1.

(5) The spectra are all displaced to lower energies at low temperatures but the displacement is not the same for each crystal, the thinnest crystals being displaced the least.

(6) The changes in intensity which occur in some crystals when they are cooled from 77° to 4° K. indicate the presence of more than one emitting level with different polarization properties, e.g. Fig. 2(*c*).

DISCUSSION

Craig (12) has extended the theory developed by Davydov (13) to include crystal-induced mixing of the $^1B_{2u}$ and $^1B_{3u}$ molecular states of anthracene. He showed that when second-order crystal-field perturbations are included in the crystal wave functions the polarization ratio for the 3800 Å anthracene system is reduced from 7:1 (*b*:*a*), given by first-order theory (identical with the oriented gas model), to about 3:1. A subsequent detailed measurement of the extinction coefficients of the *a*- and *b*-polarized absorption in anthracene single crystals at room temperature by Bree and Lyons (14) has substantiated the theory of Craig.

Although theory satisfactorily interprets the absorption spectrum, except in the

Can. J. Chem. Downloaded from www.nrcresearchpress.com by 200.7.193.243 on 09/04/12
For personal use only.

region of the *b*-polarized absorption edge (considered in a later publication), it predicts the wrong polarization ratio for the fluorescence spectrum. This quantity should be about 3:1 and furthermore it should be constant throughout the spectrum. The reason for this failure will now be discussed but first we must consider an interpretation of the fluorescence spectrum at low temperatures advanced by Sidman (4). Sidman has suggested that emission originates from trapped exciton levels postulated by Frenkel (15) and that these levels are observed both in absorption and fluorescence. The reasons advanced for this interpretation are: (*a*) the absorption in the *b*-polarized edge of the absorption spectrum (origin of the fluorescence spectrum) is weak because the transition is to a trapped exciton state and involves lattice relaxation around an excited molecule; (*b*) the condition $|D_{mk}| >> |J_{mk}|$ given by Frenkel is fulfilled.

As regards (*a*), such a non-vertical low probability transition should *increase* the decay-time of the fluorescence emission as the temperature is decreased to 4° K. because all of the emission comes from these levels at this temperature. However, Elliot, Liebson, and Ravilious (16) find the decay-time to be *decreased* by a factor easily explained by the reduced overlap between absorption and fluorescence spectra as the temperature is lowered. As the emission at very low temperatures has a decay-time only slightly changed from the room-temperature value we must not, therefore, look for an explanation for the weak absorption in the absorption edge in terms of a low-transition probability to these levels.

The condition $|D_{mk}| >> |J_{mk}|$ given by Frenkel for the formation of trapped excitons is an approximation made for the particular type of crystals that he considered, i.e. ionic crystals. Frenkel has made it clear that if the excitation energy remains on an atom or molecule in the lattice the others will adjust themselves to the new conditions and this will correspond to a smaller potential energy than for the case when the energy is transferred before the lattice relaxation takes place. Frenkel assumed that this change in energy is of the order of $|D_{mk}|$ (the change in energy of interaction between an atom or molecule and the surrounding ones when it is brought into an excited state), but the same assumption grossly overestimates the energy of relaxation of the lattice around an excited molecule such as anthracene where the interaction forces are of the van der Waals type. In view of this and the lifetime measurements we must look further than the trapped exciton treated theoretically by Frenkel.

As we are dealing with real crystals the crystal wave functions will be of two types: those having the symmetry of the 3-dimensional space group (or closely approximating this) and those which do not have this symmetry, i.e., surfaces and various imperfections. In the case of the experimental absorption spectrum the energy levels of the former case will dominate the over-all crystal absorption and good agreement is to be expected between theory and experiment. However, for fluorescence, the levels of lowest energy are important in view of the large mean free path of the exciton, and if crystal levels of the latter type exist with energy less than the former type then these will be expected to dominate the fluorescence process in spite of their low concentration. It should be pointed out here that the trapped exciton envisaged by Frenkel applies to the perfect lattice and transitions to and from these levels would be expected to have the same energy in different crystals, i.e., fluorescence spectra from different crystals should be identical. Fluorescence arising from imperfections of course corresponds to trapped excitons in the broad sense but not in the sense used by Frenkel.

In this communication we shall not attempt a quantitative calculation of the changes to be expected in the characteristics of the emission from surfaces and imperfections but

Can. J. Chem. Downloaded from www.nrcresearchpress.com by 200.7.193.243 on 09/04/12
For personal use only.

shall limit ourselves to some qualitative conclusions. The two sets of molecules in the anthracene lattice are so oriented that the total interaction which determines the splitting between the two energy levels corresponding to a single molecular B_{2u} level is nearly zero, although some individual interactions are large. We might expect therefore that slight perturbations to the lattice structure will in some cases upset this balance and split the levels to a much greater extent than occurs in regions where the crystal symmetry approximates to the 3-dimensional space group. In other cases where the effect of the perturbation is larger it is probable that a very small number of anthracene molecules have energy levels lying below the level of the perfect lattice and, providing sufficiently low temperatures are used, these molecules will not be able to exchange their excitation energy with the neighboring molecules of the lattice and the fluorescence will show a fine structure as is observed when anthracene is an impurity in another lattice, e.g., in phenanthrene and in naphthalene (17). Such a model explains the appearance of fine structure which is seen at about 20° K. and also that the width of these "lines" varies from crystal to crystal.

Although the effect of imperfections on the energy levels must be somewhat complex, *in all cases the polarization ration will be changed from the crystal-induced value of 3:1 towards the oriented gas value of about 7:1.*

As well as emission arising from imperfections we must consider also the possibility of emission from exciton levels with wavenumber vector (k) greater than zero for the case that the level corresponding to $k = 0$ is not the one of least energy. Such an emission process requires the simultaneous creation of a phonon with wavenumber equal to the difference between the wavenumbers of the emitted photon and the exciton. The fluorescence arising in this manner will occur at lower energies than the optically allowed absorption to the level $k = 0$ as is observed; however, the polarization ratio in this case should be very close to the value in absorption. As the emission spectrum of the crystal is complex we must not overlook such a mechanism for at least a part of the total emission.

If the observations summarized at the end of the results section are now consulted it will be seen that these are consistent with the emission arising mainly from imperfections. It is possible to go further and deduce that some of these levels correspond to considerably distorted regions of the lattice. This must be so in order to explain the movement of intensity towards the origin of the fluorescence (e.g. Fig. 2(*c*)) and the subsequent loss of a mirror-image intensity relation to the absorption spectrum observed in solution (9). In such regions the potential energy surfaces of the excited state must lie more nearly over those of the ground state than is the case for the normal lattice. In addition, from the very high polarization ratio near the origin of the fluorescence the emission from these levels is mainly *b* polarized.

In principle we can distinguish between two types of imperfection that might be present in the crystals used but unfortunately no control over the presence of the second of these was possible. The two types are growth imperfections and those introduced into the crystal by mounting on silica. The latter must be important as the flakes adhere strongly to the silica surface and the strain involved must be considerable, particularly in thin crystals where the large variation in the fluorescence is no doubt explained in part by the imperfections introduced by mounting. In view of this it would be difficult to set up any satisfactory model to examine quantitatively the effect of imperfections.

The interpretation of the fluorescence from pure anthracene is substantiated by measurements made on crystals containing tetracene. Obviously the introduction of tetracene constitutes an imperfection and one that is a very efficient trap for anthracene

Can. J. Chem. Downloaded from www.nrcresearchpress.com by 200.7.193.243 on 09/04/12
For personal use only.

excitation energy so it is necessary to keep the concentration very low in order to detect fluorescence from the anthracene. If the regions close to the included tetracene represent the only imperfections in the anthracene lattice we would not expect to find any change in the transfer efficiency when the temperature is changed from 77° to 4° K. provided the thermal degradation of the excess energy is not altered. However, the results shown in Figs. 4(*a*) and 4(*b*) indicate that there must be imperfections at considerable distances from the tetracene molecules. We can say this because the transfer efficiency is decreased in going from 77° to 4° and from earlier work (9) we know that the critical intermolecular distance for transfer of energy between anthracene and tetracene is about 44 Å so that in these crystals excitation energy must be trapped by anthracene (imperfections) at distances greater than 44 Å at the lower temperature. The striking feature about this process is that the fluorescence from the latter regions is markedly different in intensity distribution and energy from the fluorescence observed at 77° K., as can be seen.

It is possible therefore to detect more than one emitting level in these crystals, but it must not be assumed that these on the average are always located at considerable distances from the tetracene impurity and this is shown by Fig. 4(*c*). In this case where the transfer efficiency is increased between 77° and 4° K. most of the anthracene levels of lowest energy must lie within the critical distance from the tetracene so that energy trapped in these levels is transferred to the tetracene with higher efficiency. The anthracene fluorescence is again changed but this time in the opposite direction to the other crystals, as is expected, since the energy normally coming from the lowest levels is now transferred to the tetracene. In all of these cases the changes which take place with decrease of temperature are perfectly reversible.

In the crystals examined no anomalous behavior of the tetracene fluorescence was found when the temperature was reduced to 4° K. Sidman (11) has recently reported that the fluorescence from tetracene in anthracene is depolarized at 20° K., but in the crystals studied in the present work no such depolarization was detected and, in fact, the polarization ratio at 4° K. averages about 4:1. The concentration of tetracene was considerably lower by at least a factor of 100 than for the crystals used by Sidman, and in addition his crystals were large ones grown from the melt. Sidman (17) has also reported a similar depolarization of the fluorescence of anthracene in phenanthrene, again with crystals grown from the melt. Here again, however, measurements made at 20° K. with sublimation flakes of phenanthrene containing anthracene by Obreimov, Prikhot'ko, and Shabaldas (1) show that the anthracene fluorescence is strongly polarized. At present there seems no satisfactory explanation for the results reported by Sidman but it is possible that this will lie in the different method of preparation of the crystals.

While there appears to be considerable evidence for the presence of imperfections in anthracene sublimation flakes it must not be assumed that these will play such a dominant role in the emission from other molecular crystals. The significant quantity indicative of emission from imperfections is the polarization ratio and this must be measured both in absorption and emission for other crystals before the importance of imperfections can be estimated.

REFERENCES

1. Obreimov, I. V., Prikhot'ko, A. F., and Shabaldas, K. G. J. Exptl. Theoret. Phys. (U.S.S.R.), **6**, 1062 (1936).
2. Pesteil, P. and Barbaron, M. J. Phys. radium, **15**, 92 (1954).
3. Tsujikawa, I. and Kanda, E. Sci. Repts. Research Inst. Tohoku Univ. Ser. A, **4**, 471 (1952).
4. Sidman, J. W. Phys. Rev. **102**, 96 (1956).
5. Ganguly, S. C. and Chaudhuri, N. K. J. Chem. Phys. **19**, 617 (1951).

Can. J. Chem. Downloaded from www.nrcresearchpress.com by 200.7.193.243 on 09/04/12
For personal use only.

6. FERGUSON, J. and SCHNEIDER, W. G. J. Chem. Phys. **25**, 780 (1956).
7. PESTEIL, P. Compt. rend. **234**, 2532 (1952).
8. DUERIG, W. H. and MADOR, I. L. Rev. Sci. Instr. **23**, 421 (1952).
9. FERGUSON, J. Australian J. Chem. **9**, 160 (1956).
10. BOWEN, E. J. Nature, **142**, 1081 (1938).
11. SIDMAN, J. W. J. Chem. Phys. **25**, 122 (1956).
12. CRAIG, D. P. J. Chem. Soc. 2302 (1955).
13. DAVYDOV, A. S. J. Exptl. Theoret. Phys. (U.S.S.R.), **18**, 210 (1948).
14. BREE, A. V. and LYONS, L. E. J. Chem. Soc. 2662 (1956).
15. FRENKEL, J. Physik. Z. Sowjetunion, **9**, 158 (1936).
16. ELLIOT, J. O., LEIBSON, S. H., and RAVILIOUS, C. F. Phys. Rev. **79**, 393 (1950).
17. SIDMAN, J. W. J. Chem. Phys. **25**, 115 (1956).

Can. J. Chem. Downloaded from www.nrcresearchpress.com by 200.7.193.243 on 09/04/12
For personal use only.

Can. J. Chem. Downloaded from www.nrcresearchpress.com by 78.46.186.204 on 09/04/12
For personal use only.

KINETIC LAWS FOR SURFACE REACTIONS IN FLOW SYSTEMS[1]

K. J. LAIDLER

ABSTRACT

A general differential equation is set up for the flow of reactant gases through a catalytic reactor, account being taken of changes in volume as the reaction proceeds and of the possibility that the catalyst surface is not completely available. Integrated solutions are given for three special cases and are presented in graphical form: (1) first-order reaction, the result being applicable whether the surface is completely available or not (Fig. 1); (2) second-order reaction with the surface completely available (Fig. 2); (3) second-order reaction with only a small fraction of the surface available (Fig. 3). The treatment is related to previous treatments of Hulburt, Thiele, and Wheeler.

INTRODUCTION

The general kinetic laws applicable to flow systems have been well worked out, but when the reactor contains a granulated porous catalyst certain complications arise. The object of the present paper is to develop the kinetic equations for such systems in forms that take into account these complexities. The main matters that give difficulty are:

(i) the question of the correct kinetic equations to use for systems of variable volume,
(ii) the corrections required when the reaction is accompanied by a volume change, and
(iii) the incomplete availability of the surface under certain conditions.

Of these (i) was treated many years ago by Benton (1), while (ii) has been discussed in detail by Hulburt (2). Various workers, in particular Thiele (3) and Wheeler (4), have discussed (iii). In the present paper all three factors will be considered together, and general kinetic equations will be developed which give the fraction of reaction occurring in a reactor as a function of the properties of the reaction system.

THEORETICAL

The Steady-State Equation

Benton's treatment leads to the conclusion that for a surface-catalyzed reaction of αth order the number of moles dn disappearing in time dt in an element of volume dV is given by

$$-dn = k_v c^\alpha \, dV dt, \qquad [1]$$

where c is the concentration of reactant in the slab and k_v is a rate coefficient. The exact form of k_v is considered later; it depends on certain characteristics of the catalyst granules, the diffusion constant within the pores, and in general on the concentration (not, however, when $\alpha = 1$ or when the catalyst surface is completely available).

Consider a thin slab of the reaction system, of volume $dV = Adx$, where A is the cross-sectional area and dx the thickness. If c is the concentration at the point x, and $c+dc$ that at $x+dx$, and if the volume of gas passing the point x per second is R, the steady-state equation for the slab is

$$Rcdt = (R+dR)(c+dc)\, dt + k_v c^\alpha \, dV dt. \qquad [2]$$

With the neglect of the term in $dVdcdt$ this equation reduces to

$$Rdc + cdR + k_v c^\alpha \, dV = 0. \qquad [3]$$

[1]*Manuscript received March 21, 1958.*
Contribution from the Department of Chemistry, University of Ottawa, Ottawa, Canada.

In order to solve this, one must have an explicit expression for R as a function of the extent to which reaction has occurred.

The Volume Rate of Flow, R

If there is no change in the total number of molecules during the reaction, R is constant; the second term in Eq. [3] then drops out and the equation is readily integrated. Suppose, however, that the stoichiometry of the reaction is such that 1 mole of reactants gives rise to ν moles of products. Then if initially a volume V_1^* of gas contains n_1 moles of reactant molecules, after some reaction has occurred, there are n moles of reactants and $\nu(n_1-n)$ moles of product. The volume occupied by this is

$$V^* = V_1^*[\nu-(\nu-1)(n/n_1)]. \quad [4]$$

It is convenient at this stage to introduce the dimensionless variables

$$f = n/n_1 \quad [5]$$

and

$$\xi = V/V_0, \quad [6]$$

where n_1 is the number of moles of gas entering the reactor in the volume V_1, V_0 is the total volume of the reactor, and V is the volume that has been traversed at any time. Eq. [4] may then be written as

$$V^* = V_1^*[\nu-(\nu-1)f], \quad [7]$$

whence

$$R = R_1[\nu-(\nu-1)f], \quad [8]$$

where R is the volume rate of flow at any point and R_1 the volume rate of flow of the entering gas. From [8] it follows that

$$dR = -(\nu-1)\, R_1\, df. \quad [9]$$

The General Dimensionless Rate Equation

Since $c = n/V^*$ and $c_1 = n_1/V_1^*$ it follows that

$$c = c_1(V_1^*/V^*)(n/n_1) \quad [10]$$

$$= c_1\{f/[\nu-(\nu-1)f]\} \quad [11]$$

and that

$$dc = c_1\{\nu/[\nu-(\nu-1)f]^2\}df. \quad [12]$$

Introduction of these expressions into Eq. [3], and using Eqs. [8] and [9], gives rise, after some reduction, to

$$\{[\nu-(\nu-1)f\,]^\alpha/f^\alpha\}df+(k_v\, V_0\, c_1^{\alpha-1}/R_1)d\xi = 0. \quad [13]$$

This equation may be written as

$$\{[\nu-(\nu-1)f]^\alpha/f^\alpha\}df+bd\xi = 0, \quad [14]$$

where b is defined by

$$b = k_v\, V_0\, c_1^{\alpha-1}/R_1. \quad [15]$$

Can. J. Chem. Downloaded from www.nrcresearchpress.com by 78.46.186.204 on 09/04/12
For personal use only.

Equations [14] and [15] can be applied to the determination of the order of reaction and the activation energy without proceeding with the integrations. Suppose, for example, that c_i is varied and, by trial and error, R_i is simultaneously varied so as to keep the f–ξ relationship the same, i.e., so that the same fraction of reaction occurs in the reactor. If this is so it follows that the ratio $c_i^{\alpha-1}/R_i$ is unchanged; α can therefore be determined. If the reaction is of the first order it will not be necessary to change R_i in order to maintain b constant as c_i is varied; if it is of the second order R_i must be varied in proportion to c_i, and so on.

The procedure for determining the activation energy is similar. The temperature is varied, and either c_i or R_i varied so as to keep b constant (i.e., so that the extent of reaction remains the same). If R_i is varied its relationship with the temperature is the same as that of k_v, and the activation energy can therefore be obtained from an Arrhenius plot of log R_i against $1/T$. A similar procedure can be used for c_i.

In general, k_v, and therefore b, is a function of f, and the dependence is discussed later. In some situations, however, as when the surface is completely available to the reaction system (when the catalyst pores are sufficiently large) b is a constant. The parameter b can also be shown to be a constant for any first-order reaction whether the surface is completely available or not. The integrated form of Eq. [14] will first be considered for this case of constant b, after which the general dependence of b on f will be discussed, and an integrated solution obtained.

The Case in which b Is Constant

It does not appear to be possible to obtain an explicit general solution of Eq. [14], but solutions for certain special cases of interest are readily obtained. The solutions for $\alpha = 1$ and $\alpha = 2$ will be given.

The integrated form of Eq. [14] for $\alpha = 1$, subject to the boundary conditon $\xi = 0$, $f = 1$, is

$$\nu \ln f + (\nu - 1)(1 - f) + b\xi = 0. \qquad [16]$$

The fraction f_t of reactant remaining at the outlet of the reactor, when $\xi = 1$, is therefore defined by

$$\nu \ln f_t + (\nu - 1)(1 - f_t) + b = 0. \qquad [17]$$

Figure 1 shows $1 - f_t$, the fractional yield of product from the reactor, plotted against the parameter b, for various values of ν. This figure permits a graphical evaluation of b from the results of an experiment in a reactor. If it is known that the surface is completely available (see below) the rate constant k_v can then be calculated using Eq. [12].

The corresponding solutions for the second-order case ($\alpha = 2$) are

$$\nu^2(1 - 1/f) - 2(\nu - 1)\ln f - (\nu - 1)(1 - f) + b\xi = 0 \qquad [18]$$

and

$$\nu^2(1 - 1/f_t) - 2(\nu - 1)\ln f_t - (\nu - 1)(1 - f_t) + b = 0. \qquad [19]$$

Figure 2 shows $1 - f_t$ plotted against b for various values of ν.

It will now be shown that Eqs. [16] and [17] apply to any first-order reaction, whether the surface is completely available or not. If the surface is completely available the rate constant k_v is given by

$$k_v = k\rho_b S_g, \qquad [20]$$

Can. J. Chem. Downloaded from www.nrcresearchpress.com by 78.46.186.204 on 09/04/12
For personal use only.

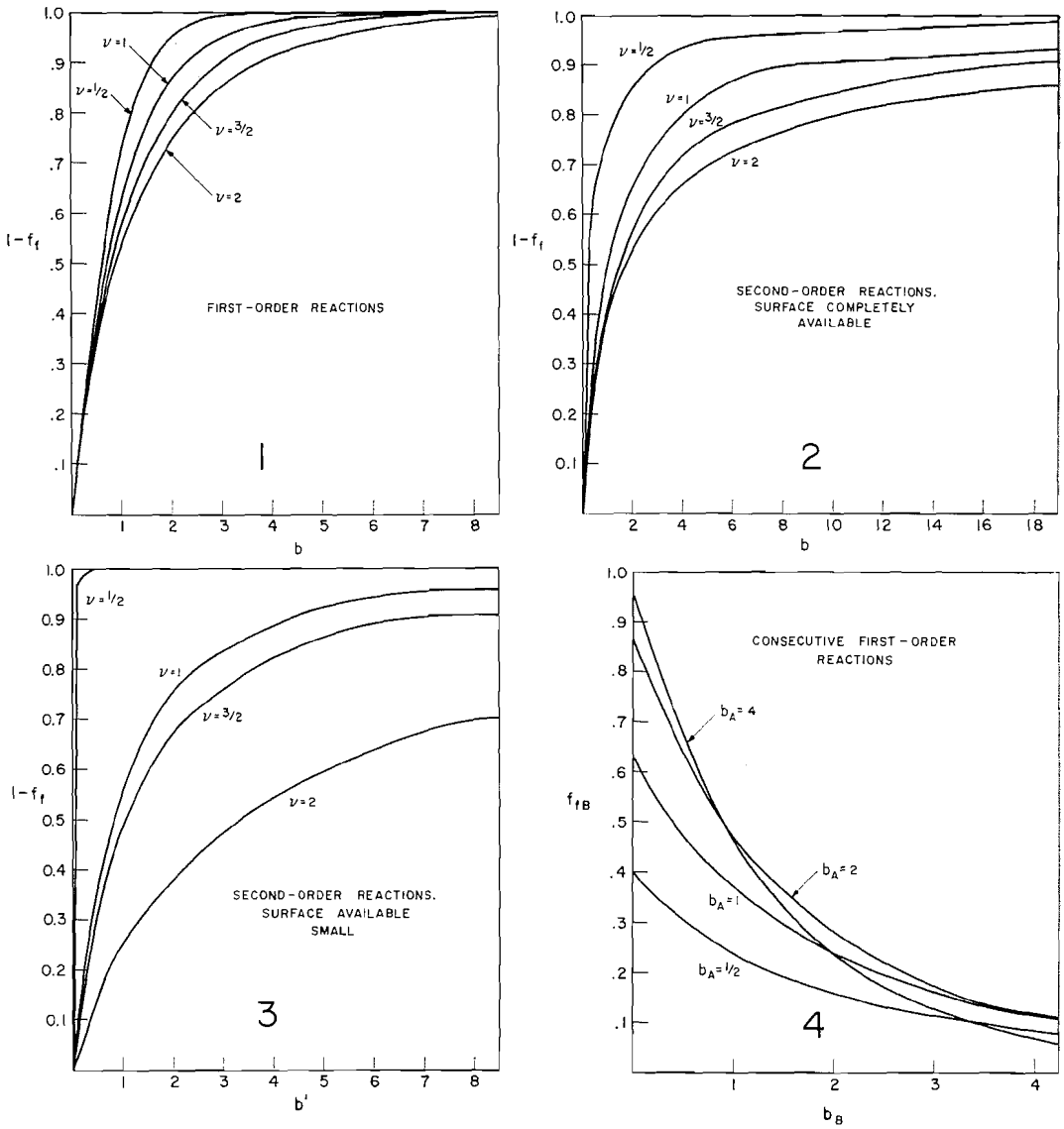

FIG. 1. The fractional yield of product plotted against the parameter b, defined by Eq. [15] in the text, for various values of ν. These curves apply to first-order reactions.

FIG. 2. The fractional yield of product plotted against b, for second-order reactions; these curves apply only when b is independent of f, i.e. when the surface is completely available.

FIG. 3. The fractional yield of product plotted against b', for second-order reactions in which the fraction of surface available is small.

FIG. 4. The fractional yield of an intermediate B, in the case of consecutive first-order reactions, plotted against the parameter b_A for various values of the parameter b_B.

where k is the intrinsic rate constant with respect to unit surface area, ρ_b is the bulk density of the catalyst (the mass per unit over-all volume), and S_g is the surface area per gram of catalyst. The parameter b is therefore in this case given by

$$b = k\rho_b S_g V_0 c_1^{\alpha-1}/R_1, \qquad [21]$$

so that if b is determined experimentally, in the manner indicated above, k can be calculated using the known characteristics of the system.

Can. J. Chem. Downloaded from www.nrcresearchpress.com by 78.46.186.204 on 09/04/12
For personal use only.

If the surface of the catalyst is not completely available to the reaction system the treatment of Thiele (3) combined with that of Wheeler (4) leads to the result that for a first-order reaction

[22] $$k_v = k\rho_b S_g(\tanh h)/h,$$

where h is defined by

[23] $$h = L(2k/Dr)^{1/2}.$$

D is the diffusion constant for the reaction system, L the mean half-length of the pores, and r the mean radius of the pores. Wheeler (4) has proposed useful methods of estimating L and r in terms of easily-measured quantities, and has discussed the magnitude of D. When h is sufficiently small (less than 0.2) $(\tanh h)/h$ is close to unity, and Eq. [22] approaches Eq. [20]. Otherwise k_v is reduced to the fraction $(\tanh h)/h$, which is therefore the fraction of surface available. Wheeler (4) has shown how this fraction can be determined from the experimental data.

Eqs. [18] and [19], and indeed the corresponding equations for any reaction of other than the first order, apply only when the surface is completely available. In such cases k_v is always given by Eq. [20] and b is therefore constant. Otherwise k_v and b are functions of f and the integrated equations then assume different forms, some of which are discussed below.

The Case in which b Is a Function of f

Thiele's treatment (3) does not lead to explicit solutions for other than first-order reactions. However, a combination of Wheeler's (4) and Thiele's (3) procedures leads to the conclusion that the fraction of surface available is approximately

$$(\tanh h)/h,$$

where h is now defined by

[24] $$h = L(2k/rD)^{1/2}\, c^{(\alpha-1)/2}.$$

This reduces to Eq. [23] when $\alpha = 1$. The parameter b is now a function of c, and therefore of f.

General solutions again appear to be impossible. The integration may, however, be carried out for a second-order reaction in which the fraction of surface available is small; in this case $\tanh h \approx 1$, so that $(\tanh h)/h$ is approximately equal to $1/h$. When this is so, k_v is given by (with $\alpha = 2$)

[25] $$k_v = (k\rho_b S_g/L)(rD/2k)^{1/2}\, c^{-1/2}$$

and b by

[26] $$b = (k\rho_b S_g V_0 c_1/R_1 L)(rD/2k)^{1/2}\, c^{-1/2}.$$

Using Eq. [11] this becomes

[27] $$b = (k\rho_b S_g V_0 c_1^{1/2}/R_1 L)(rD/2k)^{1/2} f^{-1/2}[\nu-(\nu-1)f]^{1/2}.$$

Equation [14] then becomes, with $\alpha = 2$,

[28] $$\{[\nu-(\nu-1)\,f]^{3/2}/f^{3/2}\}df + b'\,d\xi = 0,$$

where

[29] $$b' = (k\rho_b S_g V_0 c_1^{1/2}/R_1 L)(rD/2k)^{1/2}.$$

Comparison of Eq. [28] with Eq. [14] shows that Eq. [28] corresponds to a system having

Can. J. Chem. Downloaded from www.nrcresearchpress.com by 78.46.186.204 on 09/04/12
For personal use only.

an apparent order of three halves. This is shown by the index to which f is raised and by the fact that, to maintain b' constant, the ratio $c_1^{\frac{1}{2}}/R_1$, viz. $c_1^{\alpha-1}/R_1$ with $\alpha=3/2$, must be kept constant.

The solutions of Eq. [28] take different forms according to the values of ν. The simplest case is when $\nu = 1$, and the solution using the boundary condition $f = 1$, $\xi = 0$ is

$$2(1-1/f^{1/2})+b'\xi = 0. \qquad [30]$$

The solution for $\nu = 1/2$ is

$$\sqrt{2}\left(\frac{3}{4}\ln\frac{\sqrt{(1-f)}+\sqrt{(2-f)}}{\sqrt{(2-f)}-\sqrt{(1-f)}}+\tfrac{1}{2}\sqrt{[(1-f)(2-f)]}-\sqrt{\frac{1-f}{2-f}}\right)+b'\xi = 0. \qquad [31]$$

That for $\nu = 3/2$ is

$$3/2\,\{\sqrt{2}+3/2.\sin^{-1}\sqrt{\tfrac{1}{3}}-\sqrt{[(3-f)/f]}-3/2.\sin^{-1}\sqrt{\tfrac{1}{3}f}-\tfrac{1}{6}\sqrt{[f(3-f)]}\}+b'\xi = 0 \qquad [32]$$

while for $\nu = 2$.

$$\sqrt{2}.\{10+3\pi-8\sqrt{[(2-f)/f]}-12\sin^{-1}\sqrt{\tfrac{1}{2}f}-2\sqrt{[f(2-f)]}\}+b'\xi = 0. \qquad [33]$$

The plots of $1-f_t$ against b' (for $\xi = 1$) are shown in Fig. 3 for the four values of ν.

Consecutive Reactions

It is frequently the case that reactions occur in two stages, and the treatment of the flow kinetics in such systems is of some interest. If the intermediate is the desirable product, for example, it is important to know the conditions under which it will be produced in maximum amounts.

Attention will be confined to the case of two consecutive first-order reactions, represented by the scheme

$$\mathrm{A} \xrightarrow{k_{v1}} \mathrm{B} \xrightarrow{k_{v2}} \mathrm{C}.$$

The rate equations are:

$$-dn_A = k_{v1}\,c_A\,dVdt, \qquad [34]$$

$$-dn_B = k_{v2}\,c_B\,dVdt - k_{v1}\,c_A\,dVdt, \qquad [35]$$

$$-dn_C = k_{v2}\,c_B\,dVdt. \qquad [36]$$

The steady-state equations for the slab of volume dV are, for A

$$Rc_A\,dt = (R+dR)(c_A+dc_A)dt+k_{v1}\,c_A\,dVdt, \qquad [37]$$

and for B

$$Rc_B\,dt = (R+dR)(c_B+dc_B)dt+k_{v2}\,c_B\,dVdt-k_{v1}\,c_A\,dVdt. \qquad [38]$$

With the neglect of terms of the type $d\,Rdcdt$ these equations reduce to

$$Rdc_A+c_A\,dR+k_{v1}\,c_A\,dV = 0, \qquad [39]$$

$$Rdc_B+c_B\,dR+k_{v2}\,c_B\,dV-k_{v1}\,c_A\,dV = 0. \qquad [40]$$

The corresponding equations for C need not be written down, since when solutions for A and B have been obtained that for C follows at once.

The fact that both reactions are of the first order does not necessarily imply that their

Can. J. Chem. Downloaded from www.nrcresearchpress.com by 78.46.186.204 on 09/04/12
For personal use only.

stoichiometry corresponds to the equation written above. In general 1 mole of A gives rise to ν moles of B, and 1 mole of B produces μ moles of C. If initially a volume V_1^* of gas contains n_{A_1} moles of A, after some reaction has occurred there are n_A moles of A, n_B moles of B, and n_C moles of C, and

$$n_A+(n_B/\nu)+(n_C/\nu\mu) = n_{A1}. \quad [41]$$

The total number of moles present is

$$\sum n = n_A+n_B+n_C, \quad [42]$$

and this, using Eq. [41], is equal to

$$\sum n = \nu\mu\, n_{A1}-(\nu\mu-1)n_A-(\mu-1)n_B. \quad [43]$$

The volume occupied by this is

$$V^* = V_1^*[\nu\mu-(\nu\mu-1)f_A-(\mu-1)f_B], \quad [44]$$

where f_A and f_B are defined by

$$f_A = n_A/n_{A1} \quad [45]$$

and

$$f_B = n_B/n_{B1}. \quad [46]$$

The volume rate of flow, R, at any point is therefore related to the initial rate by

$$R = R_1[\nu\mu-(\nu\mu-1)f_A-(\mu-1)f_B], \quad [47]$$

whence

$$dR = -(\nu\mu-1)R_1\, df_A-(\mu-1)R_1\, df_B. \quad [48]$$

The concentrations c_A and c_B are given by

$$c_A = c_{A1}(V_1^*/V^*)(n_A/n_{A1}) = c_{A1}f_B/[\nu\mu-(\nu\mu-1)f_A-(\mu-1)f_B] \quad [49]$$

and

$$c_B = c_{A1}(V_1^*/V^*)(n_B/n_{A1}) = c_{A1}f_B/[\nu\mu-(\nu\mu-1)f_A-(\mu-1)f_B]. \quad [50]$$

An explicit solution of these equations appears not to be possible in the general case. The solution for $\nu = \mu = 1$ is simple, however, and proceeds as follows. Under these circumstances

$$f_A = c_A/c_{A1}, \qquad f_B = c_B/c_{A1}, \quad [51]$$

$$R = R_1, \qquad dR = 0, \quad [52]$$

$$\xi = V/V_0. \quad [53]$$

Equations [39] and [40] become

$$R_1\, df_A+k_{v1}\, V_0 f_A d\xi = 0, \quad [54]$$

$$R_1\, df_B+k_{v2}\, V_0 f_B d\xi-k_{v1}\, V_0 f_A d\xi = 0. \quad [55]$$

The solution of [54], with the boundary condition $\xi = 0, f_A = 1$, is

$$f_A = e^{-b_A\xi} \quad [56]$$

where b_A is defined by

Can. J. Chem. Downloaded from www.nrcresearchpress.com by 78.46.186.204 on 09/04/12
For personal use only.

[57] $$b_A = k_{v1} V_0/R_1.$$

This equation is equivalent to Eq. [16] with $\nu = 1$, as of course it must be as the law for the disappearance of A is independent of the subsequent fate of B.

Insertion of [56] into [55] gives

[58] $$df_B + b_B f_B \, d\xi - b_A e^{-b_A \xi} \, d\xi = 0$$

where b_B is defined by

[59] $$b_B = k_{v2} V_0/R_1.$$

The solution of [58], with the boundary condition $\xi = 0, f_B = 0$, is

[60] $$f_B = [b_A/(b_B - b_A)] (e^{-b_A \xi} - e^{-b_B \xi}).$$

Figure 4 shows f_{tB} (the fraction of B present at the outlet, when $\xi = 1$) as a function of b_B for various values of b_A.

DISCUSSION

The equations derived above, and the corresponding plots, are useful in the analysis of kinetic data for flow systems, particularly when it is desired to know the intrinsic activity k of the catalyst surface. A possible procedure is as follows:

(1) First determine the apparent order of the reaction, by varying concentrations and rates of flow in the manner described above.

(2) Investigate the extent to which the total surface area is utilized; this can be done by comparing the rates when the catalyst is in different states of granulation, and seeing whether the rate falls in line with the B.E.T. area or the number of pore mouths.

On the basis of the above tests it will in many cases be possible to conclude that the system belongs to one of the cases considered in Figs. 1 to 4. From a value of $1 - f_t$ it is then possible to determine b or b' and hence, using the appropriate expression for b or b', the value of k. The calculation of k of course requires a knowledge of the volume rate of flow, the bulk density, and the surface area per gram. In addition, if the surface is not completely available, it is necessary to determine (tanh h)/h in the manner suggested by Wheeler (4).

A variant of the above method is necessary if consecutive reactions are involved. A possible procedure is now to determine b_A, and hence k_1, from the disappearance of A. The values of b_B and k_2 can then be determined from the appearance of B, using Fig. 4. More complicated systems can be treated by suitable extensions of the above methods.

ACKNOWLEDGMENTS

The author is grateful to Dr. D. S. Montgomery and Dr. H. M. Hulburt for valuable discussions, to Professor A. Cormac Smith for advice on mathematical questions, and to Mr. T. Zawidzki for help with the numerical work.

REFERENCES

1. BENTON, A. F. J. Am. Chem. Soc. **53**, 2984 (1931); cf. also LAIDLER, K. J. *In* Catalysis. Vol. 1. *Edited by* P. H. Emmett. Reinhold Publishing Corp., New York. 1954. p. 124.
2. HULBURT, H. M. Ind. Eng. Chem. **36**, 1012 (1944); **37**, 1063 (1945).
3. THIELE, E. W. Ind. Eng. Chem. **31**, 916 (1939).
4. WHEELER, A. Advances in Catalysis, **1**, 249 (1951); *In* Catalysis. Vol. 3. *Edited by* P. H. Emmett. Reinhold Publishing Corp., New York. 1955. p. 105.

Can. J. Chem. Downloaded from www.nrcresearchpress.com by 78.46.186.204 on 09/04/12
For personal use only.

THE NATURE OF THE CADMIUM IONS IN HYDROXIDE AND CARBONATE SOLUTIONS[1]

PHYLLIS E. LAKE AND J. M. GOODINGS[2]

ABSTRACT

The nature and concentration of the cadmium-containing ions in potassium hydroxide and potassium carbonate solutions have been studied polarographically. The co-ordination number for the hydroxide–cadmium complex is 4 and its dissociation constant 2×10^{-10}. The co-ordination number for the carbonate–cadmium complex is 3 and its dissociation constant 6×10^{-7}.

INTRODUCTION

From a study of the electrolytic oxidation of cadmium in carbonate and hydroxide solutions (1) it became apparent that cadmium must exist in solution as an intermediate step in the oxidation. According to Latimer (2) the solubility products of $Cd(OH)_2$ and $CdCO_3$ are 2×10^{-14} and 5×10^{-12} respectively. These data show that no appreciable concentration of cadmium can exist in these solutions as a simple Cd^{+2} ion.

The object of this work was to measure the concentration of cadmium in potassium hydroxide and potassium carbonate solutions in equilibrium with solid CdO, $Cd(OH)_2$, and $CdCO_3$ and to determine the nature and properties of the cadmium-containing ion.

The method used was that described by Lingane (3). After it was established that the reduction of the complexes was reversible, measurements of half-wave potential as a function of concentration of complexing ion were made. From these results co-ordination numbers and dissociation constants were calculated.

EXPERIMENTAL

Preparation of Saturated Solutions

Solutions of KOH ranging from 1 to 13 *N*, of K_2CO_3 ranging from 1 to 10 *N* (10 *N* is supersaturated but remained stable over a period of 8 months), and mixtures of the two having a total normality of about 7 and containing varying proportions of OH^- and CO_3^{-2} were prepared. One series of these solutions was saturated with CdO, another with $Cd(NO_3)_2.4H_2O$. Approximately one gram of the cadmium compound was added to each 500-ml. sample. The solutions were allowed to stand in contact with the solid, and shaken vigorously from time to time. One set of solutions was allowed to stand at each of the following temperatures: 0° C., 25° C., and 50° C. The $Cd(NO_3)_2.4H_2O$ was converted rapidly to either $Cd(OH)_2$ or $CdCO_3$ depending on the solution. The solid phase in contact with the mixed solutions was not analyzed but was probably a mixture of $Cd(OH)_2$ and $CdCO_3$. The brown CdO gradually became lighter in color and conversion to the hydroxide and carbonate occurred slowly. Samples of the clear liquid were removed from time to time and analyzed polarographically for cadmium. When two successive samples showed no change in diffusion current, the solutions were assumed to be saturated.

Analytical Technique

A Leeds and Northrup "Electrochemograph type E" was used for all the analyses. A drop time of 4 seconds and a polarizing rate of 50 mv./min. were used throughout. One arm of the H-shaped test cell contained the reference electrode, the other the test solution.

[1]*Manuscript received April 1, 1958.*
Issued as D.R.C.L. Report No. 276.
[2]*Summer student. Present address: University of Toronto, Toronto, Ontario.*

Can. J. Chem. Downloaded from www.nrcresearchpress.com by 78.46.186.204 on 09/04/12
For personal use only.

Can. J. Chem. Downloaded from www.nrcresearchpress.com by 78.46.186.204 on 09/04/12
For personal use only.

The center portion contained a fritted-glass disk and an agar plug. The reference electrode was saturated calomel and all potentials quoted in the tables are referred to this reference. Approximately 10-ml. samples were used. Oxygen-free nitrogen was bubbled through the cell for at least 10 minutes before the analysis was carried out. Approximately 0.005% gelatin was added to the test solution to avoid maxima.

A calibration curve of diffusion current vs. cadmium concentration was drawn covering the range 1×10^{-5} to 1×10^{-2} mole/l. of cadmium nitrate in a 1.5 *N* KNO_3 supporting electrolyte. Variation of the KNO_3 concentration from 1 normal to saturated had little effect (about 1% over the whole range) on the diffusion current and half-wave potential. Potassium nitrate was chosen as a supporting electrolyte, because nitrate ion does not form a complex with cadmium (4).

Cadmium concentrations in the test samples were determined as follows: after a solution had been saturated with cadmium a small amount of the clear liquid was pipetted off and stored at the temperature of the original solution to allow for settling of any suspended material. A sample for analysis was then pipetted from this second solution and allowed to come to room temperature. A part of this solution was titrated with standard 0.1 *N* HCl to determine the final OH^- and/or CO_3^{-2} concentration. The remainder was neutralized with concentrated nitric acid and diluted or concentrated to a convenient volume so that the KNO_3 concentration was 1–2 normal. Concentrated nitric acid was chosen in preference to dilute acid to avoid volume dilution of the original sample below polarographically detectable concentrations of cadmium. The neutralized solution was analyzed polarographically, and the cadmium concentration as Cd^{+2} ion was determined from the calibration curve.

Polarograms were drawn for all the unneutralized solutions at 25° C. in order to measure the effect of OH^- and CO_3^{-2} activity on half-wave potential.

Results

The dependence of cadmium concentration on KOH and/or K_2CO_3 concentration is shown in Figs. 1, 2, and 3. The half-wave potentials for these solutions (at 25°) are shown in Table I.

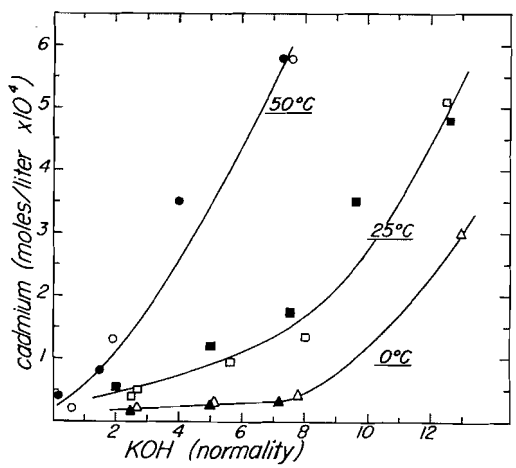

FIG. 1. Concentration of cadmium in potassium hydroxide solutions. (In all figures the open symbols refer to solutions saturated with respect to CdO, the closed symbols to solutions saturated with respect to $Cd(OH)_2$ and/or $CdCO_3$.)

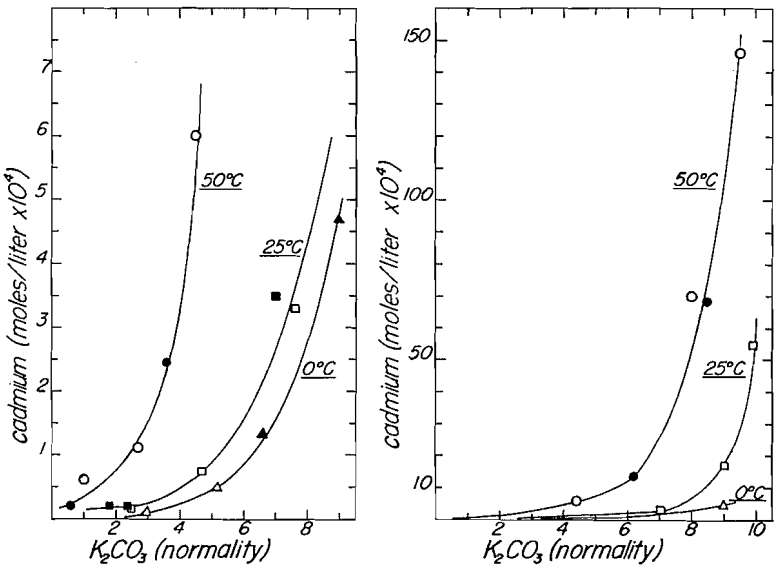

FIG. 2. Concentration of cadmium in potassium carbonate solutions.

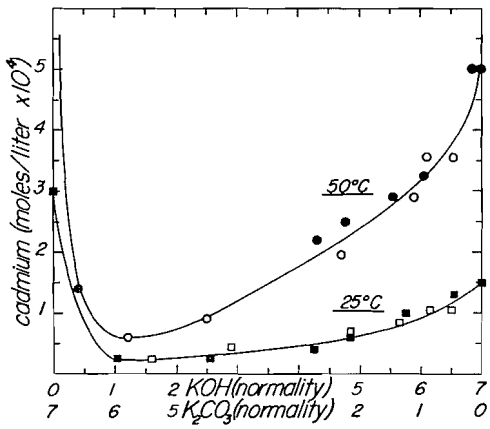

FIG. 3. Concentration of cadmium in mixed solutions.

No attempt was made to measure the rate of dissolution of the CdO, $Cd(OH)_2$, and $CdCO_3$, but the results indicate that a period of approximately two weeks was necessary to attain equilibrium at 25° C. and 4–6 weeks at 0° C.

Experimental Accuracy

The total error in determination of concentration of cadmium, considering variations in drop size from one capillary to another, and in temperature, error in regulating drop time, error in measuring i_d, and in construction and reading the calibration curve may amount to as much as ±10%. Errors in determining final OH^- and CO_3^{-2} concentration might be ±5%. Half-wave potential values were reproducible within ±5 mv.

Can. J. Chem. Downloaded from www.nrcresearchpress.com by 78.46.186.204 on 09/04/12
For personal use only.

TABLE I

HALF-WAVE POTENTIALS FOR CADMIUM COMPLEXES

Solution number		Saturating substance	Final concentration, N		$E_{\frac{1}{2}}$ average, volts	Final activity ($a\pm$)	Log activity ($a\pm$)
			A. Potassium hydroxide				
KOH	1	$Cd(OH)_2$	12.6		−0.997	19.5	1.290
	1	CdO	12.5		−0.993	19.2	1.285
	2	$Cd(OH)_2$	9.3		−0.969	8.95	0.950
	2	CdO	9.5		−0.964	9.5	0.975
	3	$Cd(OH)_2$	7.5		−0.951	6.0	0.775
	3	CdO	8.1		−0.948	6.6	0.825
	4	$Cd(OH)_2$	5.0		−0.925	3.2	0.485
	4	CdO	5.4		−0.926	4.0	0.510
	5	$Cd(OH)_2$	2.25		−0.892	1.4	0.165
	5	CdO	2.7		−0.893	1.7	0.225
	6	$Cd(OH)_2$	0.5		−0.853	0.54	−0.270
			B. Potassium carbonate				
K_2CO_3	1	$CdCO_3$	9.1		−0.855	7.5	0.875
	1	CdO	9.7		−0.860	8.5	0.929
	2	$CdCO_3$	6.9		−0.819	3.02	0.484
	2	CdO	7.5		−0.824	3.75	0.574
	3	$CdCO_3$	4.7		−0.814	1.45	0.162
	3	CdO	4.9		−0.794	1.55	0.190
	4	$CdCO_3$	2.3		−0.754	0.62	−0.207
	4	CdO	2.4		−0.760	0.66	−0.187
	5	CdO	1.0		−0.725	0.29	−0.538
			C. Mixed solutions				
Mix	1	$Cd(OH)_2$–$CdCO_3$	6.5 OH^-	0.5 CO_3^{-2}	−0.927		
	1	CdO	6.6	0.3	−0.927		
	2	$Cd(OH)_2$–$CdCO_3$	5.8	1.2	−0.928		
	2	CdO	6.3	0.7	−0.926		
	3	$Cd(OH)_2$–$CdCO_3$	5.6	1.4	−0.925		
	3	CdO	5.8	1.2	−0.921		
	4	$Cd(OH)_2$–$CdCO_3$	4.9	2.0	−0.916		
	4	CdO	4.9	2.1	−0.916		
	5	$Cd(OH)_2$–$CdCO_3$	4.3	2.7	−0.910		
	5	CdO	4.0	3.0	−0.910		
	6	$Cd(OH)_2$–$CdCO_3$	2.7	4.2	−0.899		
	6	CdO	2.6	4.3	−0.896		
	7	$Cd(OH)_2$–$CdCO_3$	1.3	5.7	−0.863		

DISCUSSION

Activities

Because of the high concentrations of K_2CO_3 and KOH used in the solubility determinations it was necessary to use activity instead of concentration and to take into account the liquid junction potentials before determining co-ordination numbers and dissociation constants.

The activity coefficients for the KOH solutions were determined using the data of Akerlof and Bender (5). Activity coefficients for K_2CO_3 were found in Landolt-Börnstein Tabellen (6).

Liquid Junction Potentials

The liquid junction potentials were calculated using both the Henderson and the Planck equations. In both cases the values obtained for the K_2CO_3 solutions were always <3 mv. and thus are within the limits of experimental error. Therefore no correction was made to the measured values of $E_{\frac{1}{2}}$ for the carbonate case. Liquid junction potentials calculated for KOH solutions were considerably larger (11–30 mv.) and could not be

Can. J. Chem. Downloaded from www.nrcresearchpress.com by 78.46.186.204 on 09/04/12
For personal use only.

neglected. Potentials corrected according to both the Planck and the Henderson equations are shown in Table II. It was felt that the "constrained diffusion junction" described by the Planck equation represented better the conditions present in the test cell; therefore, these corrections were used in the subsequent calculations.

TABLE II

CORRECTED VALUES FOR $E_{\frac{1}{2}}$ IN KOH SOLUTIONS

Concn., N	Log $a\pm$	$E_{\frac{1}{2}}$ meas., volts	$E_{\frac{1}{2}}$ corrected using Henderson eq., volts	$E_{\frac{1}{2}}$ corrected using Planck eq., volts
12.6	1.29	−0.997	−1.020	−1.014
12.5	1.285	−0.993	−1.016	−1.010
9.3	0.950	−0.969	−0.989	−0.986
9.5	0.975	−0.964	−0.984	−0.980
7.5	0.775	−0.951	−0.970	−0.967
8.1	0.825	−0.948	−0.967	−0.967
5.0	0.485	−0.925	−0.941	−0.941
5.4	0.510	−0.926	−0.942	−0.942
2.25	0.165	−0.892	−0.902	−0.903
2.7	0.225	−0.893	−0.903	−0.904
0.5	−0.270	−0.852	−0.856	−0.855

Reversibility

Lingane (3, 7) has shown that if the dissociation of the metal ion complex and its reduction at the dropping electrode are rapid and reversible then the equation for a wave, at 25° C. in the presence of an excess of complex-forming substance, is

$$[1] \qquad E_{\text{d.e.}} = E_{\frac{1}{2}} - (0.0591/n) \log\{i/(i_d - i)\},$$

where i is the current and $E_{\text{d.e.}}$ the voltage of the dropping electrode at any time, $E_{\frac{1}{2}}$ is the half-wave potential, i_d the diffusion current, and n is the number of Faradays associated with the electrode process. From Eq. [1] it is evident that, for a reversible wave,

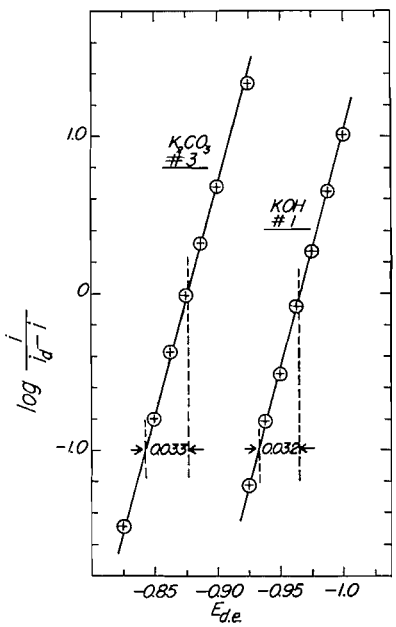

FIG. 4. Test for reversibility of reductions.

Can. J. Chem. Downloaded from www.nrcresearchpress.com by 78.46.186.204 on 09/04/12
For personal use only.

a plot of log $i/(i_d - i)$ against $E_{d.e.}$ will yield a straight line of slope $-0.0591/n$. The reversibility of the reductions was tested in this manner. Two examples are shown in Fig. 4. The points fall on straight lines of slopes -0.032 ± 0.003 and -0.033 ± 0.003 in good agreement with -0.030, the theoretical value for a reversible reduction where $n = 2$.

Co-ordination Number

The half-wave potential for reduction of a complex metal ion is independent of the concentration of the metal ion, but shifts with changing activity of the complexing ion according to the equation

$$[2] \qquad E_{\frac{1}{2}}/\log C_x f_x = -p\,(0.0591/n),$$

where p is the co-ordination number and C_x and f_x the concentration and activity coefficient of the complexing ion (3, 7). Since it is impossible to determine individual values for a_{OH^-} and $a_{CO_3^{-2}}$ the mean ion activities $a\pm$ were used in the following calculations.

In accordance with Eq. [2] the half-wave potentials for cadmium in caustic solutions (corrected for E_{lj} according to the Planck equation) are plotted against the log of the mean ion activity of KOH in Fig. 5. The slope of the line $E_{\frac{1}{2}}$ vs. log $a\pm$ is -0.108 ± 0.01. The theoretical slope for $n = 2$, $p = 4$ is -0.118. Since liquid junction potential corrections are so large the agreement is better than would be expected. The empirical formula for the cadmiate ion, then, is $Cd(OH)_4^{-2}$.

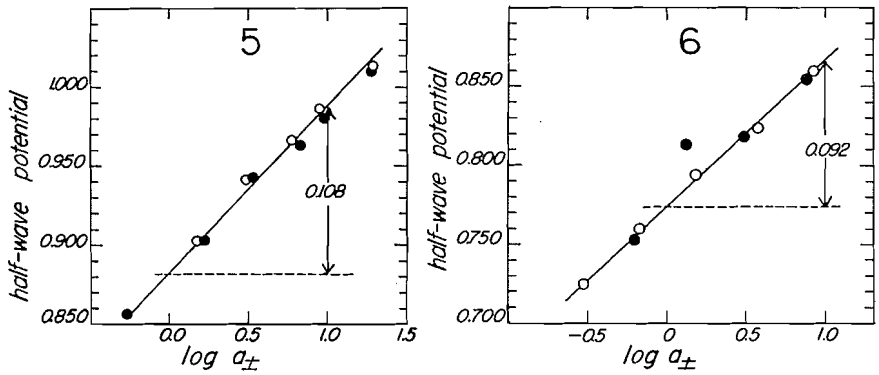

FIG. 5. Determination of p for cadmium complex in potassium hydroxide solutions.
FIG. 6. Determination of p for cadmium complex in potassium carbonate solutions.

Scholder and Staufenbiel (8) prepared and isolated disodium cadmiate ($Na_2Cd(OH)_4$) by refluxing a suspension of $Cd(OH)_2$ in concentrated NaOH solutions, but were unable to obtain the complex salt using hydroxide concentrations lower than 14 N. It appears, however, that the cadmiate ion exists in solution at concentrations as low as 1 normal with respect to hydroxide. This formula for the cadmiate complex is similar to that determined by e.m.f. measurements for the zincate ion ($Zn(OH)_4^{-2}$) (9).

The half-wave potentials for cadmium in carbonate solutions are plotted against log of the mean ion activity for K_2CO_3 in Fig. 6. The slope of the line is -0.092 ± 0.005, while the theoretical slope for $n = 2$, $p = 3$ is -0.090. Hence the co-ordination number for the carbonate complex is 3, and its empirical formula $Cd(CO_3)_3^{-4}$.

No evaluation of p can be made from the half-wave potentials for the mixed solutions because of present lack of knowledge of the activity coefficients in the mixed solutions. It

Can. J. Chem. Downloaded from www.nrcresearchpress.com by 78.46.186.204 on 09/04/12
For personal use only.

is interesting to note that, although the ionic strength of the solutions increases as the proportion of CO_3^{-2} ion increases, both the shift of $E_{\frac{1}{2}}$ and the solubility of cadmium decrease. That is, in the mixed solutions the effect of the hydroxide ion appears to be more important than that of the carbonate ion. This is consistent with the observation made previously (1) that after anodic oxidation of cadmium in similar mixed solutions, the final product is always pure $Cd(OH)_2$ if the hydroxide concentration is $\geqslant 0.7$ N.

Dissociation Constants

The half-wave potential for the reduction of a metal ion complex depends on the logarithm of the dissociation constant (K_c) and is more negative the smaller the value of K_c, that is, the more stable the complex ion. The approximate equation for the relation of $E_{\frac{1}{2}}$ to log K_c given by Lingane (3, 7) is

$$[3] \qquad (E_{\frac{1}{2}})_c - (E_{\frac{1}{2}})_s \cong (0.0591/n) \log K_c - p(0.0591/n) \log C_x f_x,$$

where $(E_{\frac{1}{2}})_c$ and $(E_{\frac{1}{2}})_s$ are the half-wave potentials for the complex and simple metal ions. Because of the wide variation of activity coefficients over the range of concentrations of KOH and K_2CO_3 used in this work, the activity coefficient f_x could not be neglected. The half-wave potential for a simple cadmium ion in 1.5 N KNO_3 is -0.0591 v. The liquid junction potential correction in this value is smaller than the experimental error. Using Eq. [3] the dissociation constants were calculated for both the hydroxide and carbonate complexes at a number of different concentrations of complexing ion. The results are shown in Table III. The dissociation constant of the cadmiate complex ($Cd(OH)_4^{-2} \rightleftharpoons Cd^{+2} + 4OH^-$) is $\sim 2\times10^{-10}$ and of the carbonate–cadmium complex ($Cd(CO_3)_3^{-4} \rightleftharpoons Cd^{+2} + 3CO_3^{-2}$) is $\sim 6\times10^{-7}$.

TABLE III

CALCULATION OF DISSOCIATION CONSTANTS

Solution		Log $a\pm$	$(E_{\frac{1}{2}})_c$, volts	log K_c	K_c
			A. Potassium hydroxide, $p = 4$		
KOH	1 $Cd(OH)_2$	1.290	−1.014	−9.53	2.9×10^{-10}
	2 $Cd(OH)_2$	0.950	−0.986	−9.85	1.4×10^{-10}
	3 $Cd(OH)_2$	0.775	−0.967	−9.80	1.6×10^{-10}
	4 $Cd(OH)_2$	0.485	−0.941	−9.90	1.3×10^{-10}
	5 $Cd(OH)_2$	0.165	−0.903	−9.85	1.4×10^{-10}
	6 $Cd(OH)_2$	−0.270	−0.855	−10.0	1.0×10^{-10}
	1 CdO	1.285	−1.010	−9.45	3.5×10^{-10}
	2 CdO	0.975	−0.980	−9.53	2.9×10^{-10}
	3 CdO	0.825	−0.964	−9.53	2.9×10^{-10}
	4 CdO	0.510	−0.942	−9.85	1.4×10^{-10}
	5 CdO	−0.225	−0.904	−9.66	2.2×10^{-10}
				Average K_c =	2×10^{-10}
			B. Potassium carbonate, $p = 3$		
K_2CO_3	1 $CdCO_3$	0.875	−0.855V	−6.32	4.7×10^{-7}
	2 $CdCO_3$	0.484	−0.819	−6.25	5.6×10^{-7}
	3 $CdCO_3$	0.162	−0.814	−6.20	6.3×10^{-7}
	4 $CdCO_3$	−0.207	−0.754	−6.15	7.1×10^{-7}
	1 CdO	0.929	−0.860	−6.32	4.7×10^{-7}
	2 CdO	0.574	−0.824	−6.20	6.3×10^{-7}
	3 CdO	0.190	−0.794	−6.30	5.0×10^{-7}
	4 CdO	−0.187	−0.760	−6.25	5.6×10^{-7}
	5 CdO	−0.538	−0.725	−6.18	6.7×10^{-7}
				Average K_c =	5.8×10^{-7}

Can. J. Chem. Downloaded from www.nrcresearchpress.com by 78.46.186.204 on 09/04/12
For personal use only.

CONCLUSIONS

Cadmium can exist in finite concentrations in concentrated hydroxide and carbonate solutions in the form of complex ions $Cd(OH)_4^{-2}$ and $Cd(CO_3)_3^{-4}$ respectively. The hydroxide–cadmium complex is the more stable of the two.

REFERENCES

1. LAKE, P. E. and CASEY, E. J. J. Electrochem. Soc. **105**, 52 (1958).
2. LATIMER, W. M. Oxidation potentials. 2nd ed. Prentice Hall Inc., New York. 1953.
3. LINGANE, J. J. Chem. Revs. **29**, 1 (1941).
4. LINGANE, J. J. J. Am. Chem. Soc. **61**, 2099 (1939).
5. AKERLOF, G. C. and BENDER, P. J. Am. Chem. Soc. **70**, 2366 (1948).
6. LANDOLT-BÖRNSTEIN TABELLEN III. Springer-Verlag, Berlin. 1936. p. 2147.
7. KOLTOFF, I. M. and LINGANE, J. J. Polarography. 2nd ed. Interscience Publishers, Inc., New York. 1952.
8. SCHOLDER, R. and STAUFENBIEL, E. Z. anorg. u. allgem. Chem. **247**, 259 (1941).
9. DIRKSE, T. P. J. Electrochem. Soc. **101**, 328 (1954).

Can. J. Chem. Downloaded from www.nrcresearchpress.com by 78.46.186.204 on 09/04/12
For personal use only.

Can. J. Chem. Downloaded from www.nrcresearchpress.com by 200.7.193.243 on 09/04/12
For personal use only.

THE INTERRELATION OF DELPHELINE AND LYCOCTONINE[1]

O. E. Edwards, Léo Marion, and K. H. Palmer[2]

ABSTRACT

Lycoctonine has been converted to a derivative of delpheline, thus establishing a common diterpenoid skeleton and identical points of nuclear substitution for the two alkaloids.

The chemistry of the delphinium alkaloid lycoctonine is for the most part understandable on the basis of the diterpenoid structure I (1, 2, 3). Cookson and Trevett, in an excellent study of the reactions of the alkaloid delpheline, have shown that these find ready interpretation if the skeleton and position of nuclear substitution is the same as that of lycoctonine (4, 5). Hence demethylenedelpheline has been assigned structure II.

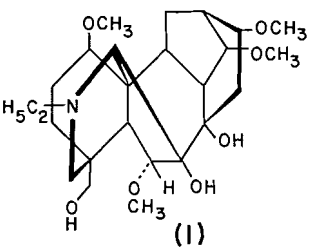

(I)

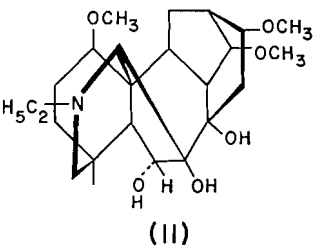

(II)

It was desirable to prove or disprove this suggested relationship. A number of routes involving conversion of lycoctonine and delpheline to a common degradation product seemed plausible. However, since delpheline was not readily available to us, we undertook instead to convert lycoctonine to a known delpheline derivative.

Three possible routes to this goal appeared promising:

(*a*) Interrelation through the monobasic dicarboxylic acid from delpheline (4) as suggested earlier (3).

(*b*) Since the methoxyl α to the ketone carbonyl in the "desoxymethyleneiso" compound from lycoctonine can be hydrolyzed readily (6), the "desoxyiso" compound III should on similar treatment give IV. Cleavage of IV with periodic acid would lead to the triketone V possibly identical with dehydrodemethyleneoxodelpheline *seco*diketone (5).

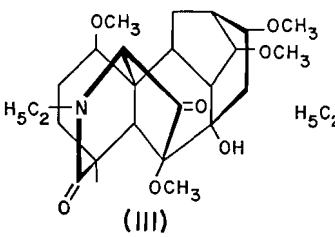

(III)

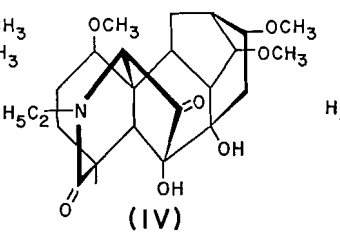

(IV)

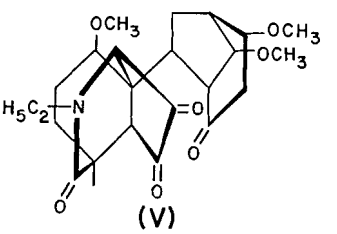

(V)

[1]*Manuscript received April, 1, 1958.*
Contribution from the Division of Pure Chemistry, National Research Council of Canada, Ottawa, Canada. Issued as N.R.C. No. 4780. Presented in part at the Ninth Seminar in the Chemistry of Natural Products, Fredericton, New Brunswick, October 23–25, 1957.
[2]*National Research Council of Canada Postdoctorate Fellow.*

(*c*) The reductive removal of the methoxyl α to the ketone carbonyl in anhydrodesoxylycoctonam VI would give VII, which could then be oxidized to the diketone VIII.[3] This is the structure suggested for dehydrodemethyleneoxodelpheline pinacone (4).

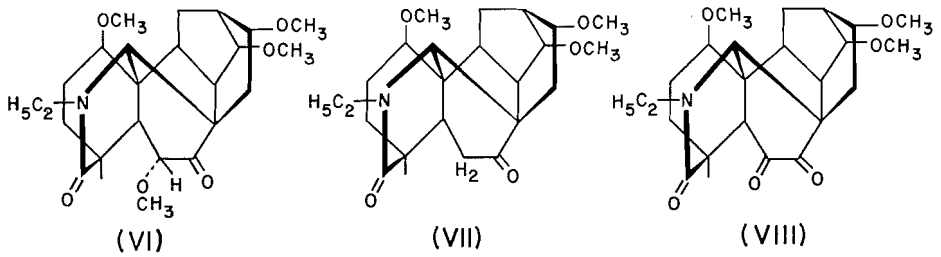

Since method (*c*) was attempted first and proved successful the others were not investigated. This approach became very attractive when we became aware of the reductive removal of alkoxy and aryloxy groups from the carbon α to a ketone by sodium amalgam (7, 8). The reduction probably proceeds by direct electron transfer from the metal surface, as illustrated.[4]

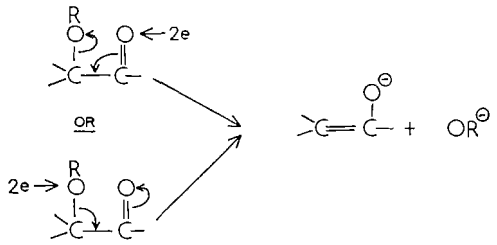

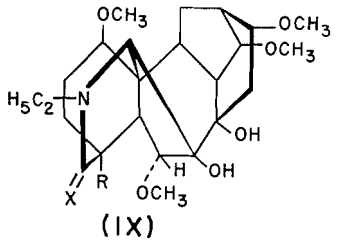

IX *a*, X = H_2, R = CH_2OH
IX *b*, X = H_2, R = CHO
IX *c*, X = H_2, R = CH_3
IX *d*, X = O, R = CH_3

In order to obtain compound VIII, lycoctonine (IX *a*) was oxidized to lycoctonal (IX *b*), which was then reduced to desoxylycoctonine (IX *c*). This was oxidized to desoxylycoctonam (IX *d*) by permanganate.[5] The conversion of IX *d* to anhydrodesoxylycoctonam VI was accomplished in high yield using the sulphuric acid in acetic acid technique (12). Treatment of an ethanol solution of VI with sodium amalgam gave an 80% yield of de(methoxy)anhydrodesoxylycoctonam (the keto lactam VII). This compound when treated in dioxane at 180° with selenium dioxide gave the α-diketone X.

The product had a melting point and X-ray powder diffraction pattern identical with those of the α-diketone from delpheline (4) and a mixed melting point with this compound showed no depression. The infrared spectra (nujol mull and in chloroform solution) were

[3]*We are grateful to Dr. Ragini Anet, who suggested this possible approach to the interrelation.*
[4]*A similar mechanism for reduction of α-ketols and α-haloketones has been put forward by Brewster (9) and in the case of α-acetoxy ketones by Rosenfeld (10).*
[5]*Modification of the procedure described earlier (11) led to improved results.*

Can. J. Chem. Downloaded from www.nrcresearchpress.com by 200.7.193.243 on 09/04/12
For personal use only.

superimposable except for small intensity differences. However, the rotation of our compound was $[\alpha]_D^{27}$ $-58\pm4°$ instead of the reported $-72°$ (4). The very kind co-operation of Professor R. C. Cookson in providing a sample of demethyleneoxodelpheline pinacone acetate enabled us to prepare sufficient delpheline α-diketone to remeasure the optical rotation. Samples of varying purity melting between 200° and 209° all had a rotation $[\alpha]_D^{27}$ $-60\pm4°$; hence we now consider the identity completely established.

The α-diketone proved to be a very sensitive compound, heating in order to concentrate a solution in ethanol or ethyl acetate being sufficient to cause a drop of 10° in the melting point. The selenium dioxide oxidation proved difficult to reproduce. The best result was obtained using an old sample of purified dioxane. Preliminary experiments on the acetoxylation of VII using lead tetraacetate in hot acetic acid gave poor yields of an amorphous acetate and were therefore abandoned.

Since the bulk of this reported work was completed[1] Carmack *et al.* (13) have converted delpheline into a known lycoctonine derivative, hence establishing the same relationship that we have proved.

The close relation between delpheline, deltaline (13), and lycoctonine and that between ajaconine, atidine, and atisine (14, 15) suggests that the great variety of delphinium and aconite alkaloids represent variations in substitution on relatively few modified diterpenoid skeletons.

EXPERIMENTAL

Unless otherwise stated, melting points (uncorrected) were determined on a micro-Kofler hot stage, rotations were measured in absolute ethanol, ultraviolet spectra in 95% ethanol, and infrared spectra using the nujol mull technique. The alumina[6] was standardized after Brockman (16).

Desoxylycoctonam

Desoxylycoctonine (1.739 g.) was dissolved in acetone (70 ml.) containing acetic acid (0.7 ml.), and to this was added finely powdered potassium permanganate (1 g.) in small portions (50 mg.). The last portion persisted for 3 hours. Excess oxidant was reduced by the addition of a saturated solution of sulphur dioxide in acetone (0.5 ml.) and the slurry was filtered. An acid–base–neutral separation of the residue left after evaporation of the acetone solution gave mainly neutral material (1.580 g.). This was chromatographed on an alumina column (activity 3, 31.6 g.).

Fractions	Eluting solvent	Wt., in mg.
1–2	Benzene	84.5
3–6	Benzene–chloroform (1:1)	749
7–8	Benzene–chloroform (1:3)	142.5
9–14	Chloroform	145
15–16	Methanol	225

Fractions 2–10 when crystallized from ether gave colorless tabular needles (865 mg.) of desoxylycoctonam. Melting point and mixed melting point with authentic material 166–168° C.

Anhydrodesoxylycoctonam (VI)

A solution of desoxylycoctonam (700 mg.) in glacial acetic acid (containing 0.1% v/v of sulphuric acid) (8 ml.) was heated at 80° C. for 70 minutes. The warm solution

[6]*Woelm brand neutral alumina.*

Can. J. Chem. Downloaded from www.nrcresearchpress.com by 200.7.193.243 on 09/04/12
For personal use only.

was poured onto crushed ice, neutralized with an ice-cold solution of potassium hydroxide (20%), and extracted with chloroform. The extract after evaporation of the chloroform gave a white froth (700 mg.) which crystallized from ether–acetone or hexane–acetone in colorless square plates (0.318 mg.), m.p. 166–168° C. Chromatography on alumina (8 g., activity 2) of the mother liquors gave a further quantity (100 mg.) of anhydrodesoxylycoctonam after crystallization of the residue (201 mg.) obtained from the chloroform–benzene (1:1) eluate. $[\alpha]_D^{23}$ −8.4 (*c*, 1.48), $[M]_D^{23}$ −37; λ_{min} 2640 Å (log ϵ 1.16), λ_{max} 3040 Å (log ϵ 1.92). Infrared max. 1729 cm.$^{-1}$ (ketone), 1646 cm.$^{-1}$ (lactam). Found: C, 67.15; H, 8.22; OCH_3, 27.45. Calc. for $C_{25}H_{37}O_6N$: C, 67.17; H, 8.34; $4OCH_3$, 27.77.

De(methoxy)anhydrodesoxylycoctonam (VII)

Sodium amalgam (5%, 2.66 g.) was added to a solution of anhydrodesoxylycoctonam (400 mg.) in absolute ethanol (5 ml.), the mixture shaken for 3 hours, then filtered through Hyflo-Supercel, and diluted with water (15 ml.). The residue (0.39 g.) after evaporation of a chloroform extract of this solution crystallized from acetone–ether or acetone–hexane in long colorless needles (270 mg.), m.p. 158–159° C. A mixture with starting material melted at 145° C. The residue (120 mg.) obtained by evaporation of the mother liquors was dissolved in ethanol (1.5 ml.), 5% sodium amalgam (440 mg.) added, and the whole experiment repeated as above. A further amount (70 mg.) of VI was obtained after chromatography of the reaction product on alumina (activity 3). $[\alpha]_D^{23}$ −5° (*c*, 1.86), $[M]_D^{23}$ −21°, λ_{min} 2580 Å (log ϵ 1.35), λ_{max} 2810 Å (log ϵ 1.66). Infrared spectrum: 1725 cm.$^{-1}$ (ketone), 1646 cm.$^{-1}$ (lactam). Found: C, 69.00; H, 8.59; N, 3.23; OCH_3, 22.4. Calc. for $C_{24}H_{35}O_5N$: C, 69.12; H, 8.46; N, 3.36; $3OCH_3$, 22.33.

Acetoxylation of De(methoxy)anhydrodesoxylycoctonam

De(methoxy)anhydrodesoxylycoctonam (20 mg.) was dissolved in glacial acetic acid (1 ml.) and heated to 100°. A saturated solution of lead tetraacetate (44.5 mg.) in glacial acetic acid (1.39 ml.) was added and the mixture heated at 100° C. for 3 hours. After it was cooled, the excess lead tetraacetate was destroyed with sodium metabisulphite. A 5% methanolic solution of potassium hydroxide (5 ml.) was added and the resulting pale yellow solution heated under reflux for 2 hours. The bulk of the methanol was removed under reduced pressure, *N* sulphuric acid was added to give a pH of 5.0, and the solution was extracted with chloroform. The pale yellow residue from the chloroform (18 mg.) was chromatographed on alumina (activity 2) (400 mg.). Benzene and benzene–chloroform (9:1) eluted unchanged starting material. Chloroform–methanol (9:1) eluted only a small quantity of material (3 mg.). This was then acetylated as described by Cookson and Trevett for their ketol (4). The pale yellow neutral product (3 mg.) could not be crystallized but had a broad absorption band at 1730 cm.$^{-1}$ ($OCO.CH_3$) in the infrared spectrum.

Oxidation of De(methoxy)anhydrodesoxylycoctonam

Freshly sublimed selenium dioxide (400 mg.) was added to a solution of de(methoxy)-anhydrodesoxylycoctonam (52 mg.) in dioxan (2.5 ml.) contained in a Carius tube. The tube was sealed and heated at 180° C. for 2 hours. The contents of the cooled tube was filtered through Hyflo-Supercel, diluted with a solution of potassium hydroxide (20%), and the resultant pale yellow solution was extracted with chloroform. The residue after evaporation of the chloroform gave a pale yellow froth (54 mg.) which was dissolved in benzene and shaken with a globule of mercury for 15 minutes. The precipitate of black mercury selenide and the mercury were filtered off and the solution evaporated under

Can. J. Chem. Downloaded from www.nrcresearchpress.com by 200.7.193.243 on 09/04/12
For personal use only.

reduced pressure to a pale yellow froth (52 mg.). This was chromatographed on an alumina column (1 g., activity 2) and the fractions crystallized from ether or acetone–hexane.

Fractions	Eluting solvent	Wt., in mg.	M.p.
1	Benzene	9.5	204–205° C.
2	Benzene–chloroform 9:1	7	204–205° C.
3–4	Benzene–chloroform 3:1	14.5	202–209° C.
5	Benzene–chloroform 2:1	5	205–209° C.
6	Benzene–chloroform 1:1	2	205–209° C.

Fractions 3 and 4 were combined and recrystallized from ether/acetone giving pale yellow needles, m.p. 211–213.5° C. A mixed melting point with these crystals and those of the α-diketone derived from demethyleneoxodelpheline pinacone (3) melted at 211–214.5° C. Fractions 1–6 were combined and recrystallized from acetone–ether or acetone–hexane giving pale yellow needles or prisms, m.p. 214–216° C. The compound had $[\alpha]_D^{27}$ $-58\pm4°$ (*c*, 0.4 in $CHCl_3$). Infrared max. (in CS_2) 1758 cm.$^{-1}$, 1722 cm.$^{-1}$ (α-diketone), and 1658 cm.$^{-1}$ (lactam); (in $CHCl_3$) 1756 cm.$^{-1}$, 1722 cm.$^{-1}$, and 1650 cm.$^{-1}$. Infrared max. (nujol mull) 1759(74.5), 1725(75), 1650(94), 1325(51), 1300(54), 1280(49), 1240(51), 1221(58), 1192(57), 1175(47), 1130(83), 1098(92), 1065 S (48), 1040(42), 1012(44), 990(46), 920(42). The X-ray powder diffraction pattern of the diketone (prisms) and the recrystallized α-diketone from delpheline (prisms) were completely superimposable (35 lines). Found: C, 66.89; H, 7.58. Calc. for $C_{24}H_{33}O_6N$: C, 66.80; H, 7.71. Further experiments using pure dry dioxane, acetic acid, acetic acid – acetic anhydride gave markedly lower yields.

Delpheline α-Diketone

Samples obtained from Professor Cookson or prepared from demethyleneoxodelpheline pinacone acetate (3) crystallized in needles from methanol–water, or as pale yellow prisms from ethyl acetate. The melting point could not be raised above 199° with these solvents if the solutions were concentrated by heat. The compound was readily eluted from a column containing a 20-fold ratio of alumina (activity 2) with benzene and benzene–ether, giving fractions melting between 207–211°. Recrystallization with heating lowered the melting point. A sample with melting point 209° had an $[\alpha]_D^{27}$ -60 ± 4 (*c*, 1.09 in $CHCl_3$). Another sample with melting point 202° had $[\alpha]_D^{27}$ -60 ± 3 (*c*, 0.80 in $CHCl_3$). Infrared max. (in $CHCl_3$) 1756 cm.$^{-1}$, 1722 cm.$^{-1}$ (α-diketone), and 1650 cm.$^{-1}$ (lactam). Infrared max. (nujol mull) 1759(73), 1725(71), 1650(92), 1325(46), 1300(48), 1280(42), 1240(46), 1220(52), 1192(51), 1175(39), 1130(80), 1098(89), 1065 S (39), 1040(35), 1012(38), 988(34), 920(38).

ACKNOWLEDGMENTS

We are grateful to Professor R. C. Cookson for his very kind co-operation in providing us with delpheline derivatives and to Dr. Ragini Anet for her valuable suggestion.[3] We wish to thank Dr. M. Przybylska for obtaining the X-ray powder diffraction patterns, Mr. R. Lauzon for taking the infrared spectra, and Mr. H. Seguin for the analyses.

REFERENCES

1. PRZYBYLSKA, M. and MARION, L. Can. J. Chem. **34**, 185 (1956).
2. EDWARDS, O. E., MARION, L., and STEWART, D. K. R. Can. J. Chem. **34**, 1315 (1956).
3. EDWARDS, O. E., MARION, L., and PALMER, K. H. J. Org. Chem. **22**, 1372 (1957).
4. COOKSON, R. C. and TREVETT, M. E. J. Chem. Soc. 3864 (1956).

Can. J. Chem. Downloaded from www.nrcresearchpress.com by 200.7.193.243 on 09/04/12
For personal use only.

5. COOKSON, R. C. and TREVETT, M. E. J. Chem. Soc. 3121 (1956).
6. EDWARDS, O. E. and MARION, L. Can. J. Chem. **32**, 195 (1954).
7. KONDO, H. and OCHIAI, E. Ann. **470**, 224 (1929).
8. GOTO, K. and SUDZUKI, A. Bull. Soc. Chem. Japan, **4**, 244 (1929).
9. BREWSTER, J. H. J. Am. Chem. Soc. **76**, 6361 (1954).
10. ROSENFELD, R. S. J. Am. Chem. Soc. **79**, 5540 (1957).
11. EDWARDS, O. E. and MARION, L. Can. J. Chem. **30**, 627 (1952).
12. EDWARDS, O. E., MARION, L., and MCIVOR, R. A. Can. J. Chem. **32**, 708 (1954).
13. CARMACK, M., FERRIS, J. P., HARVEY, J., Jr., MAGAT, P. L., MARTIN, E. W., and MAYO, D. W. J. Am. Chem. Soc. **80**, 497 (1958).
14. DVORNIK, D. and EDWARDS, O. E. Chem. & Ind. 952 (1957).
15. PELLETIER, S. W. Chem. & Ind. 1670 (1957).
16. BROCKMAN, H. and SCHODDER, H. Ber. **74**, 73 (1941).

Can. J. Chem. Downloaded from www.nrcresearchpress.com by 200.7.193.243 on 09/04/12
For personal use only.

Can. J. Chem. Downloaded from www.nrcresearchpress.com by 78.46.186.204 on 09/04/12
For personal use only.

VOLTAIC CELLS IN FUSED SALTS

PART IV. ELECTRODE POTENTIALS OF THE SYSTEMS: Tl/TlCl (KCl–NaCl), Cu/CuCl (KCl–NaCl), Cu/$CuCl_2$ (KCl–NaCl), Cr/$CrCl_2$ (KCl–NaCl), AND Cr/$CrCl_3$ (KCl–NaCl). REDOX POTENTIALS OF THE SYSTEMS: Pt/CuCl, $CuCl_2$ (KCl–NaCl), AND Pt/$CrCl_2$, $CrCl_3$ (KCl–NaCl)[1]

S. N. Flengas[2] and T. R. Ingraham

ABSTRACT

Using a Ag/AgCl (KCl–NaCl) reference electrode, the standard electrode potentials of the systems Tl/TlCl (KCl–NaCl), Cu/CuCl (KCl–NaCl), Cu/$CuCl_2$ (KCl–NaCl), Cr/$CrCl_2$ (KCl–NaCl), and Cr/$CrCl_3$ (KCl–NaCl) were measured and found to be: 0.650 volt at 680° C., and 0.250, −0.175, 0.755, and 0.423 at 700° C. respectively. The standard redox potentials of the systems Pt/$CuCl_2$, CuCl (KCl–NaCl), and Pt/$CrCl_3$, $CrCl_2$ (KCl–NaCl) were also measured at 700° C. and found to be 0.600 and 0.240 volt respectively. The effect of temperature on the electromotive forces of the above cells was measured and the heats of the cell reactions were calculated from the data.

INTRODUCTION

In previous publications (1, 2, 3) in this series, standard potentials for several electrode systems in fused salts were reported. To make these measurements, an equimolar mixture of sodium and potassium chlorides was used as the solvent for the metal chloride in the system investigated, and a silver – silver chloride electrode, developed earlier in this work (1), was used as a reference in determining the electrode potential.

In the present investigation, the method has been applied to thallium, copper, and chromium. Both copper and chromium yield ions with two or more stable valency states at high temperatures. The potentials for each of the valence states and the associated redox potentials were determined.

These results are an additional contribution to the program in these laboratories of establishing an electromotive series of metals in molten salts at different temperatures.

When a metal, M, yields two positive ions, M^{n_1+} and M^{n_2+}, where $n_2 > n_1$, there are three standard potentials associated with the system. These are the potentials $E°_1$ and $E°_2$ of the electrodes M/M^{n_1+} and M/M^{n_2+} respectively, and the oxidation–reduction potential $E°_{1,2}$ of the system M^{n_1+}/M^{n_2+}. The relationship between these three potentials can be seen from the following cyclic diagram:

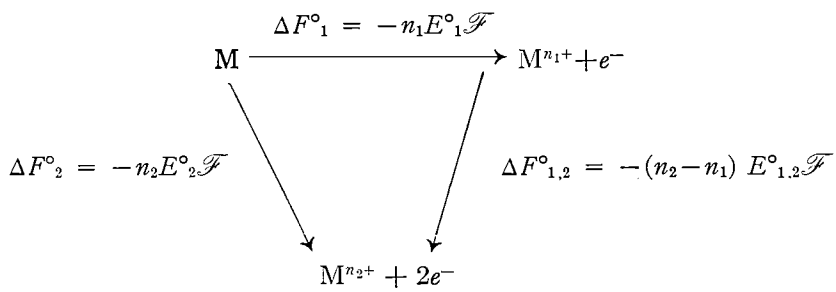

The equation relating these potentials is:

$$[1] \qquad n_2\, E°_2 - n_1\, E°_1 = (n_2 - n_1)\, E°_{1,2}.$$

[1]*Manuscript received March 11, 1958.*
Contribution from the Mines Branch Laboratories, Department of Mines and Technical Surveys, Ottawa.
[2]*National Research Council Postdoctorate Fellow, assigned to Mines Branch.*

When any two of the three potentials are known (i.e. one electrode potential $E°_1$, and the standard redox potential $E°_{1,2}$) the unknown electrode potential $E°_2$ can be calculated.

This method was applied to obtain the standard electrode potentials of the systems copper – cupric chloride and chromium – chromic chloride, neither of which could be measured directly because of the reactivity of the metals with their metal chlorides in solution.

EXPERIMENTAL

In the course of the experimental work, two different types of cells were used for determining potentials:

(a) Cells for Measurements of Metal Electrode Potentials

These were of the type

$$\begin{array}{c|c|c|c|c|c|c} \text{M} & & \text{MCl}_{n_1}\ (x_2) & & \text{AgCl}\ (x_1) & & \text{Ag} \\ (-) & | & \text{KCl–NaCl (1/1 mole)} & \| \quad \text{Asbestos fiber} \quad \| & \text{KCl–NaCl (1/1 mole)} & | & (+) \end{array}$$

where M was respectively thallium, copper, or chromium metal, and MCl_{n_1} was respectively TlCl, CuCl, or $CrCl_2$, at a mole fraction x_2.

The reaction in voltaic cells of this type is:

$$\text{M} + n_1\,\text{Ag}^+ = \text{M}^{n_1+} + n_1\text{Ag}.$$

The relationship between the electromotive force and the metal ion concentration in the cell is given by the Nernst equation in the form:

$$[2] \qquad E_{\text{cell}} = (E°_{\text{M}/\text{M}^{n_1+}} - E°_{\text{Ag}/\text{Ag}^+}) - (2.303RT/n_1\mathcal{F})\log(x_2/x_1{}^{n_1}),$$

where $E°_{\text{M}/\text{M}^{n_1+}}$ and $E°_{\text{Ag}/\text{Ag}^+}$ are respectively the standard electrode potentials of the half-cells Cu/CuCl, Cr/$CrCl_2$, or Ag/AgCl, under the conditions of the experiment. It will be observed that in equation [2], mole fractions are used in preference to activities. The simplification is justified, as will be shown by the subsequent data, when the activity coefficients or the complexity constants of the species involved in the cell reaction, or both, remain constant over the concentration range investigated. Thus, standard electrode potentials calculated from equation [2] will include the effects due to both activities and complex formation.

(b) Cells for the Measurement of Redox Potentials

These were of the type:

$$\begin{array}{c|c|c|c|c|c|c} \text{Ag} & & \text{AgCl}\ (x_1) & & \text{MCl}_{n_1}\ (x_2) & & \text{Pt} \\ (-) & | & \text{KCl–NaCl (1/1 mole)} & \| \quad \text{Asbestos fiber} \quad \| & \text{MCl}_{n_2} & | & (+) \\ & & & & \text{KCl–NaCl (1/1 mole)} & & \end{array}$$

where MCl_{n_1} was respectively CuCl or $CrCl_2$ at mole fraction x_2, and MCl_{n_2} was respectively $CuCl_2$ or $CrCl_3$ at mole fraction x_3.

The reaction in redox cells of this type is:

$$\text{Ag} + \text{M}^{n_2+} = \text{M}^{n_1+} + \text{Ag}^+$$

where $n_2 - n_1 = 1$.

The relationship between the redox electromotive force and the metal ion concentrations is given by the Nernst equation in the form:

$$[3] \qquad E_{\text{cell}} = (E°_{\text{Ag}/\text{Ag}^+} - E°_{\text{M}^{n_1+}/\text{M}^{n_2+}}) - (2.303RT/\mathcal{F})\log(x_1.x_2/x_3)$$

Can. J. Chem. Downloaded from www.nrcresearchpress.com by 78.46.186.204 on 09/04/12
For personal use only.

where $E^{\circ}_{M^{n_1+}/M^{n_2+}}$ is the standard redox potential of the half-cells Pt/CuCl, $CuCl_2$, or Pt/$CrCl_2$, $CrCl_3$, under the conditions of the experiment.

It will be noted that here, as in equation [3], mole fractions are used in preference to activities.

Preparation of Materials

Anhydrous cuprous chloride was prepared by recovery from an aqueous solution in which cupric chloride was reduced with sulphurous acid (4). The anhydrous cuprous chloride was washed with glacial acetic acid, anhydrous ether, and absolute alcohol.

Anhydrous chromic (III) chloride was prepared from the corresponding hydrated salt of analytical grade, by heating at 600° C. in the presence of carbon tetrachloride vapor (5). The compound thus obtained was in the form of violet-colored "greasy" scales, which were very stable in air. Anhydrous chromous (II) chloride was prepared by hydrogen reduction of the anhydrous chromic (III) chloride (6) in a tubular furnace heated at 550° C. To observe the end of the reduction, the HCl produced during the reaction was dissolved in water and titrated with normal sodium hydroxide solution. When purified dry hydrogen was used, the product was pure white.

All of the compounds thus prepared were pelletized and kept in closed containers in a desiccator over sulphuric acid until they were used. Analysis of the various samples of the different batches indicated that for all of the materials, a purity of over 99% had been attained.

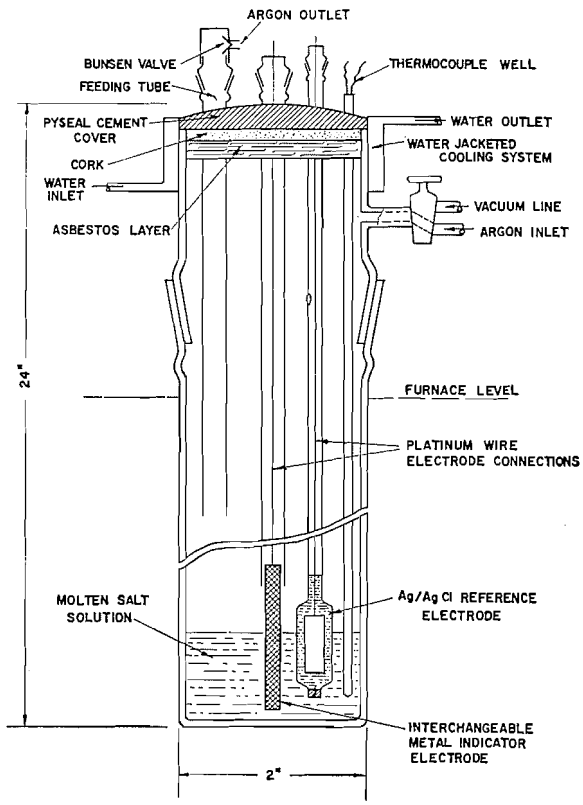

FIG. 1. All silica cell.

Can. J. Chem. Downloaded from www.nrcresearchpress.com by 78.46.186.204 on 09/04/12
For personal use only.

Apparatus and Procedure

The technique used to study the Tl–Ag, Cu–Ag, and Cr–Ag systems was essentially the same as that described in earlier papers of this series (1, 2, 3). Because the chlorides used in these experiments were reactive to both moisture and oxygen, the cell design was modified to permit evacuation to dehydrate the solvent salts before a run was begun. The modified apparatus is shown diagrammatically in Fig. 1. Slight improvements in the furnace design, over that used in previous work (1), have reduced temperature variations to ±2° C. at 900° C.

At the beginning of a run the cell was loaded with KCl–NaCl and heated for 12 hours under vacuum at 600° C. Purified argon was then introduced, the temperature increased to melt the salts, and the metal electrodes inserted into their respective positions. To protect the contents of the cell from air contamination, a small stream of argon was continuously introduced into the cell and released under a slight positive pressure through a Bunsen valve. Pellets of the metal chloride reagents were introduced, as required, through the feeding tube.

A pool of pure molten thallium metal (99.9%), copper wire of 99.99% purity or a block of 99.4% chromium metal were used as the indicator electrodes for the respective standard electrode potential measurements.

The indicator electrode for the measurement of redox potentials was a platinum tube 2 inches long and ½ inch I.D. After each addition of reagent, equilibrium was attained in 2–3 hours. In the absence of any form of stirring this was attributed either to the slow process of dissolution of the pellet in the fused-salt solvent or to the subsequent slow diffusion of the salt through the solution.

After equilibrium had been established in a cell, the potential measurements were reproducible to within one millivolt over a 2-day period.

RESULTS

The electromotive forces of the Tl–Ag, Cu–Ag, and Cr–Ag voltaic cells were measured first as a function of the metal ion concentration and then as a function of temperature. The results of the experiments in which the concentration of the metal ions was varied at constant temperature are shown in Table I.

From equation [2], it follows that when x_1 and x_2 are chosen so that the log term of this equation becomes zero, then:

$$[4] \qquad E_{cell} = E^{\circ}_{M/M^{n_1+}} - E^{\circ}_{Ag/Ag^{+}}.$$

When the electromotive forces of the cells were plotted against the log term $x_2/x_1^{n_1}$, as calculated from the data given in Table I, the results were well represented by straight lines, as shown in Fig. 2.

The slopes of the experimental lines for the Tl–Ag and Cu–Ag systems agree well with the theoretical value for a one-electron electrode process as calculated from equation [2] (0.191 and 0.196 respectively, as compared with the theoretical value 0.195 volt). That obtained with the Cr–Ag system corresponds to a two-electron electrode process (0.094, as compared with the theoretical 0.097 volt). In addition, the linearity of the curves in Fig. 2 shows that the activity coefficients or the complexity constants of TlCl, CuCl, and $CrCl_2$ in alkali chloride melt solution remain practically constant over the concentration range investigated.

The experimental standard electrode potentials for the copper, chromium, and thallium systems, as interpolated at log $(x_2/x_1^n) = 0$ on the curves in Fig. 2, are given in Table II.

Can. J. Chem. Downloaded from www.nrcresearchpress.com by 78.46.186.204 on 09/04/12
For personal use only.

Can. J. Chem. Downloaded from www.nrcresearchpress.com by 78.46.186.204 on 09/04/12
For personal use only.

TABLE I

ELECTROMOTIVE FORCES OF VOLTAIC CELLS AS A FUNCTION OF THE METAL ION CONCENTRATION AT THE INDICATOR ELECTRODE

(*a*) Tl (−) | TlCl (x_2) KCl–NaCl (1/1 mole) ‖ AgCl (x_1) KCl–NaCl (1/1 mole) | Ag (+)

Mole Fraction of AgCl (x_1)	Mole fraction of TlCl (x_2)	t,° C.	E_{cell} (volts)
6.235×10^{-2}	3.610×10^{-3}	680	0.875
6.235×10^{-2}	6.907×10^{-3}	680	0.822
6.235×10^{-2}	1.425×10^{-2}	680	0.752
6.235×10^{-2}	2.503×10^{-2}	680	0.724
6.235×10^{-2}	3.645×10^{-2}	680	0.690
6.235×10^{-2}	4.140×10^{-2}	680	0.685
6.235×10^{-2}	5.540×10^{-2}	680	0.658
6.235×10^{-2}	6.026×10^{-2}	680	0.655

(*b*) Cu (−) | CuCl (x_2) KCl–NaCl (1/1 mole) ‖ AgCl (x_1) KCl–NaCl (1/1 mole) | Ag (+)

Mole fraction of AgCl (x_1)	Mole fraction of CuCl (x_2)	t,° C.	E_{cell} (volts)
6.235×10^{-2}	1.080×10^{-3}	700	0.588
6.235×10^{-2}	3.961×10^{-3}	700	0.478
6.235×10^{-2}	1.296×10^{-2}	700	0.390
6.235×10^{-2}	2.372×10^{-2}	700	0.343
6.235×10^{-2}	3.912×10^{-2}	700	0.289

(*c*) Cr (−) | $CrCl_2$ (x_2) KCl–NaCl (1/1 mole) ‖ AgCl (x_1) KCl–NaCl (1/1 mole) | Ag (+)

Mole fraction of AgCl (x_1)	Mole fraction of $CrCl_2$ (x_2)	t,° C.	E_{cell} (volts)
6.235×10^{-2}	2.822×10^{-4}	703	0.861
6.235×10^{-2}	5.640×10^{-4}	703	0.834
6.235×10^{-2}	1.323×10^{-3}	703	0.802
6.235×10^{-2}	2.359×10^{-3}	703	0.781
6.235×10^{-2}	3.467×10^{-3}	703	0.761
6.235×10^{-2}	6.027×10^{-3}	703	0.738
6.235×10^{-2}	9.352×10^{-3}	703	0.715

In addition, the table also includes calculated (7) values for the standard potentials of the cell reactions in the absence of solvent. The significance of the differences between the experimental and calculated potentials will be discussed later in the text.

TABLE II

SUMMARY OF RESULTS

Indicator electrode	Cell reaction in molten KCl–NaCl	t,° C.	Standard potential for	Exptl.* (volts)	Calc.† (volts)
Tl, Tl^+	$Tl+AgCl=TlCl+Ag$	680	$E^\circ_{Tl/Tl^+}-E^\circ_{Ag/Ag^+}$	0.650	0.665
Cu, Cu^+	$Cu+AgCl=CuCl+Ag$	700	$E^\circ_{Cu/Cu^+}-E^\circ_{Ag/Ag^+}$	0.250	0.140
Cu, Cu^{++}	$Cu+2AgCl=CuCl_2+2Ag$	700	$E^\circ_{Cu/Cu^{++}}-E^\circ_{Ag/Ag^+}$	−0.175	(−0.410)‡
Cr, Cr^{++}	$Cr+2AgCl=CrCl_2+2Ag$	703	$E^\circ_{Cr/Cr^{++}}-E^\circ_{Ag/Ag^+}$	0.755	0.565
Cr, Cr^{+++}	$Cr+3AgCl=CrCl_3+3Ag$	703	$E^\circ_{Cr/Cr^{+++}}-E^\circ_{Ag/Ag^+}$	0.423	0.336
Cr^{+++}, Cr^{++}	$Ag+CrCl_3=AgCl+CrCl_2$	703	$E^\circ_{Ag/Ag^+}-E^\circ_{Cr^{++}/Cr^{+++}}$	0.240	0.122
Cu^{++}, Cu^+	$Ag+CuCl_2=AgCl+CuCl$	700	$E^\circ_{Ag/Ag^+}-E^\circ_{Cu^+/Cu^{++}}$	0.600	0.960

*Experimental values obtained during this investigation on voltaic cells containing alkali chloride molten salt solvent.
†Potentials calculated from existing thermodynamic data on the pure salts in the absence of any solvent.
‡Obtained by extrapolation of low temperature data.

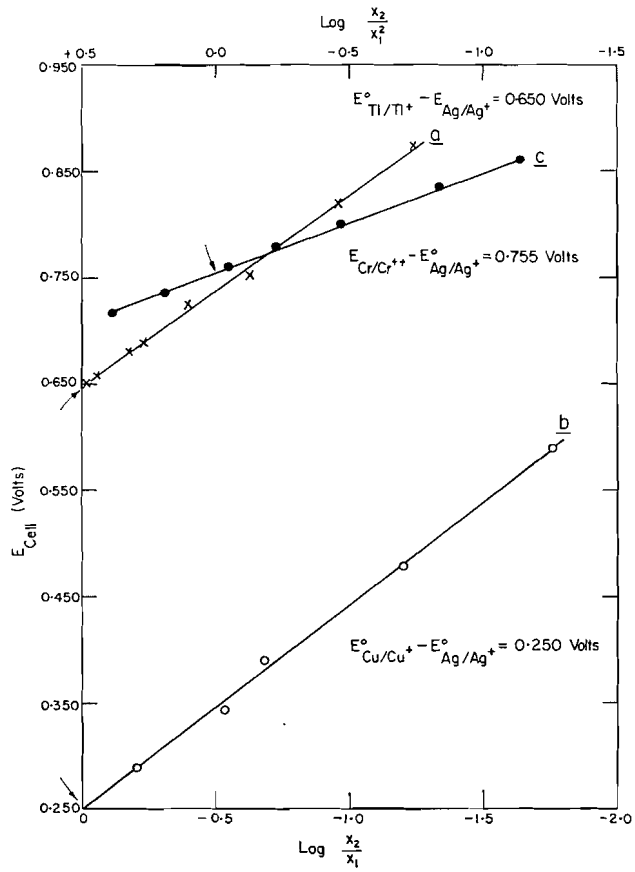

FIG. 2. Electromotive forces of the cells:

$$\begin{array}{ccccc} M & | & MCl_{n_1}\ (x_2) & \| & AgCl\ (x_1) \\ (-) & | & KCl\text{–}NaCl\ (1/1\ mole) & \| & KCl\text{–}NaCl\ (1/1\ mole) \end{array} \begin{array}{c|} \\ | \\ | \end{array} \begin{array}{c} Ag \\ (+) \end{array}$$

as a function of $\log(x_2/x_1^{n_1})$, at constant temperature.
M is (*a*) thallium, (*b*) copper, and (*c*) chromium (top scale). MCl_{n_1} is respectively TlCl, CuCl, and $CrCl_2$.

The effect of temperature change on the electromotive forces of the voltaic cells previously cited was next investigated. Because of the volatility of TlCl (b.p. 720° C.), measurements above 700° C. were not possible with the Tl–Ag voltaic cell.

The results for the Cu–Ag and Cr–Ag voltaic cells are given in Table III. Also included in Table III are values for the standard potentials at different temperatures, calculated from the data using equation [2].

From Table III it is readily seen that temperature has practically no effect on the standard potential of the Cu–Ag voltaic cell.

From the standard potentials of the Cr–Ag voltaic cell given in Table III, using the well-known equations,

$$[5] \qquad \Delta F^\circ = -n\,E^\circ\mathcal{F} = -2.303RT \log K$$

it was possible to calculate, for various temperatures, the equilibrium constants for the cell reactions given in Table II. The results of these calculations are shown in Fig. 3, where log K was plotted against the reciprocal of absolute temperature. The curve is linear over the temperature range investigated.

Can. J. Chem. Downloaded from www.nrcresearchpress.com by 78.46.186.204 on 09/04/12
For personal use only.

TABLE III

EFFECT OF TEMPERATURE ON THE ELECTROMOTIVE FORCES OF THE CELLS

(*a*) Cu (−) | CuCl ($x_2 = 3.912\times10^{-2}$) KCl–NaCl (1/1 mole) || AgCl ($x_1 = 6.235\times10^{-2}$) KCl–NaCl (1/1 mole) | Ag (+)

	T,° K	E_{cell} (volts)	$E°_{Cu/Cu^+} - E°_{Ag/Ag^+}$ (volts)
On heating			
	975	0.282	0.243
	1033	0.287	0.246
	1071	0.288	0.245
	1103	0.289	0.245
	1143	0.293	
On cooling			
	1137	0.290	0.244
	1069	0.287	0.244
	973	0.282	0.243

(*b*) Cr (−) | $CrCl_2$ ($x_2 = 3.467\times10^{-3}$) KCl–NaCl (1/1 mole) || AgCl ($x_1 = 6.235\times10^{-2}$) KCl–NaCl (1/1 mole) | Ag (+)

	T,° K.	E_{cell} (volts)	$E°_{Cr/Cr^{++}} - E°_{Ag/Ag^+}$ (volts)
On heating			
	978	0.761	0.756
	1021	0.755	0.750
	1051	0.750	0.745
	1068	0.745	0.740
	1090	0.746	0.740
	1108	0.741	0.735
	1121	0.739	0.734
	1142	0.734	0.723
On cooling			
	1023	0.755	0.750
	1008	0.757	0.752
	989	0.759	0.754
	972	0.762	0.757

The best straight line through the experimental points was calculated by applying the least-squares method.

The heat of reaction (ΔH_r) in cells of this type is the difference between the heats of formation (ΔH_f) of the respective metal chlorides in the presence of the solvent, i.e.,

[6] $$\Delta H_r = \Delta H_{f\ (CrCl_2\ \text{in KCl–NaCl})} - \Delta H_{f\ (AgCl\ \text{in KCl–NaCl})}.$$

The heat of reaction was calculated from the slope of the straight line in Fig. 3, in accordance with the van't Hoff equation,

[7] $$d \ln K/dT = \Delta H_r/RT^2.$$

The value thus obtained is:

$$\Delta H_{r(Cr,Cr^{++})} = -42.46\pm0.5 \text{ kcal./mole.}$$

In the case of the Cu–Ag voltaic cell, where it was found that $dE/dT = 0$, the heat of reaction is equal to the free energy change and can be calculated directly from equation [5]. The result of the calculation is:

$$\Delta H_{r(Cu,Cu^+)} = -6.10 \text{ kcal./mole.}$$

Can. J. Chem. Downloaded from www.nrcresearchpress.com by 78.46.186.204 on 09/04/12
For personal use only.

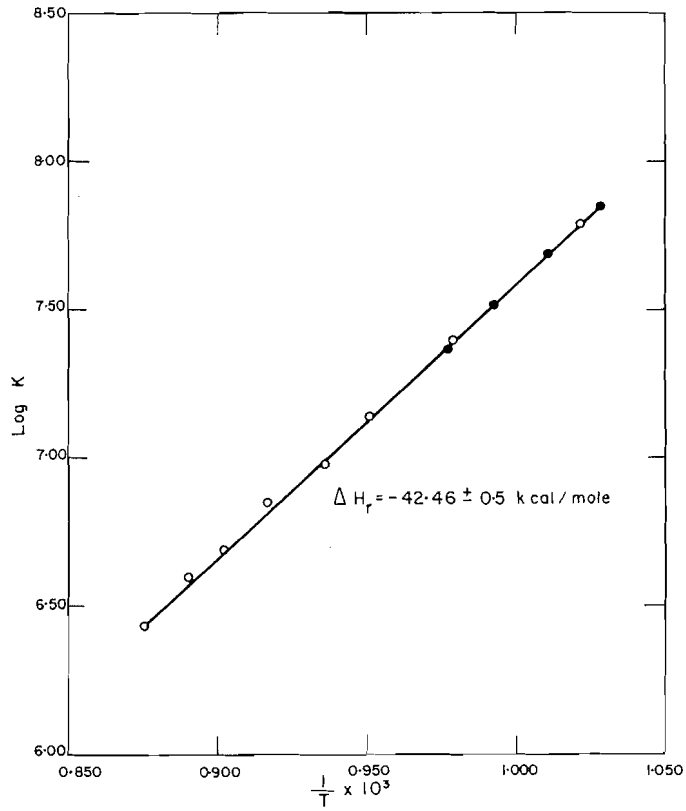

FIG. 3. The variation of log K with the reciprocal of absolute temperature for the system:

Cr	$CrCl_2$ ($x_2 = 3.467\times10^{-2}$)	AgCl ($x_1 = 6.235\times10^{-2}$)	Ag
(−)	KCl–NaCl (1/1 mole)	KCl–NaCl (1/1 mole)	(+)

○ with increasing temperature, ● with decreasing temperature.

Measurement of Redox Potentials

The electromotive forces of the Cu^+/Cu^{++} and Cr^{++}/Cr^{+++} redox cells were measured first as a function of the salt concentrations, and then as a function of temperature. The results of the experiments in which the concentration of the metal chlorides was varied at constant temperatures are shown in Table IV, and the plot of $\log(x_1.x_2/x_3)$ versus the electromotive forces is given in Fig. 4.

Following the same procedure as used previously, the standard redox potentials of the systems were obtained by graphical interpolation at zero log concentration. The results are grouped in the summary given in Table II.

It will be observed that the curves in Fig. 4 are effectively linear over the concentration range investigated, which again indicates that the activity coefficients or the complexity constants of the species involved in each of the reactions remain constant.

The slopes of the experimental lines for both redox systems agree well with the theoretical value for a one-electron reduction process (0.197 as compared with 0.195 volt) at this temperature.

The effect of temperature change on the electromotive forces of the two redox cells above was investigated next. The results are shown in Table V.

Also included in Table V are values for the standard redox potentials at different

Can. J. Chem. Downloaded from www.nrcresearchpress.com by 78.46.186.204 on 09/04/12
For personal use only.

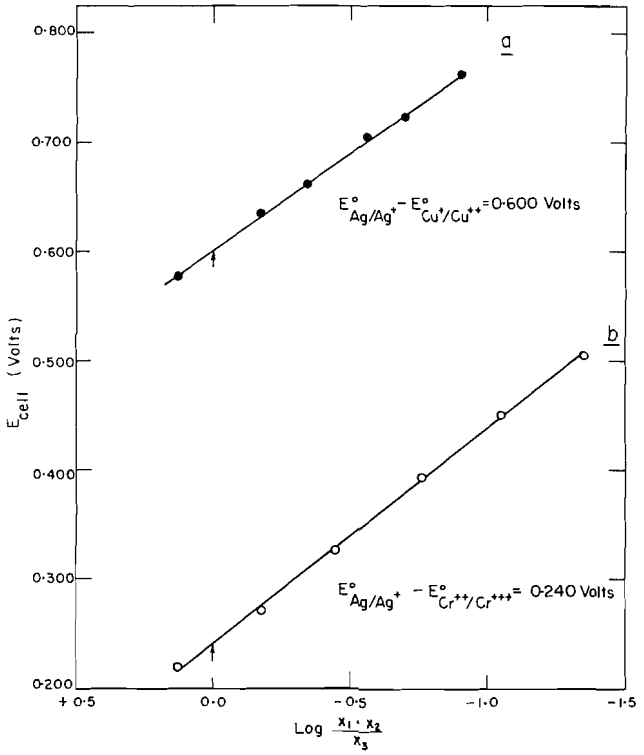

FIG. 4. Electromotive forces of the redox cells:

Ag				Pt
(−)	AgCl (x_1)	MCl_{n1} (x_2)		(+)
	KCl–NaCl (1/1 mole)	MCl_{n2} (x_3)		
		KCl–NaCl (1/1 mole)		

as a function of $\log(x_1.x_2/x_3)$, at constant temperature.
M is (*a*) copper and (*b*) chromium, and MCl_{n1} and MCl_{n2} are respectively CuCl, $CuCl_2$, and $CrCl_2$, $CrCl_3$.

temperatures, as calculated from the data using equation [3]. From these values, by applying equations [5], the effective equilibrium constants for the redox cell reactions were calculated. The results of these calculations are shown in Fig. 5, where log K was plotted against the reciprocal of the absolute temperature. The curve is linear over the temperature range investigated. For each curve the best straight line was calculated by applying the least squares method.

The heat of reaction in cells of this type is best expressed by the equation:

$$[8] \qquad \Delta H_r = \Delta H_{f(MCl_{n_2})} + \Delta H_{f(AgCl)} - \Delta H_{f(MCl_{n_1})},$$

where ΔH_f is the heat of formation of the metal chlorides in the molten alkali chloride salt solution. These heats of reactions were calculated from the slopes of the straight lines in Fig. 5, in accordance with the van't Hoff equation, and the results are:

$$\Delta H_r(Cu^{++}, Cu^{+}) = -9.15 \pm 0.6 \text{ kcal./mole}$$

$$\Delta H_r(Cr^{+++}, Cr^{++}) = +11.84 \pm 0.5 \text{ kcal./mole}$$

Having established the standard metal electrode potentials of the systems Cu/CuCl (KCl–NaCl) and Cr/$CrCl_2$ (KCl–NaCl), and the standard redox potentials of the systems $CuCl_2$/CuCl (KCl–NaCl) and $CrCl_3$/$CrCl_2$ (KCl–NaCl), equation [1] was then applied to calculate the standard electrode potentials of the systems Cu/$CuCl_2$ (KCl–NaCl)

Can. J. Chem. Downloaded from www.nrcresearchpress.com by 78.46.186.204 on 09/04/12
For personal use only.

TABLE IV

ELECTROMOTIVE FORCES OF "REDOX" CELLS AS A FUNCTION OF THE METAL ION CONCENTRATIONS AT THE INDICATOR ELECTRODE

(*a*) Ag (−) | AgCl (x_1), KCl–NaCl (1/1 mole) || CuCl (x_2), $CuCl_2$ (x_3), KCl–NaCl (1/1 mole) | Pt (+)

Mole fraction of AgCl (x_1)	Mole fraction of CuCl (x_2)	Mole fraction of $CuCl_2$ (x_3)	t,° C.	E_{cell} (volts)
6.235×10^{-2}	4.821×10^{-2}	2.242×10^{-3}	700	0.578
6.235×10^{-2}	4.810×10^{-2}	4.400×10^{-3}	700	0.634
6.235×10^{-2}	4.799×10^{-2}	7.074×10^{-3}	700	0.660
6.235×10^{-2}	4.781×10^{-2}	1.080×10^{-2}	700	0.706
6.235×10^{-2}	4.761×10^{-2}	1.471×10^{-2}	700	0.724
6.235×10^{-2}	4.721×10^{-2}	2.302×10^{-2}	700	0.761

(*b*) Ag (−) | AgCl (x_1), KCl–NaCl (1/1 mole) || $CrCl_2$ (x_2), $CrCl_3$ (x_3), KCl–NaCl (1/1 mole) | Pt (+)

Mole fraction of AgCl (x_1)	Mole fraction of $CrCl_2$ (x_2)	Mole fraction of $CrCl_3$ (x_3)	t,° C.	E_{cell} (volts)
6.235×10^{-2}	9.348×10^{-3}	4.350×10^{-4}	703	0.220
6.235×10^{-2}	9.344×10^{-3}	8.900×10^{-4}	703	0.270
6.235×10^{-2}	9.335×10^{-3}	1.649×10^{-3}	703	0.325
6.235×10^{-2}	9.319×10^{-3}	3.355×10^{-3}	703	0.393
6.235×10^{-2}	9.291×10^{-3}	6.565×10^{-3}	703	0.449
6.235×10^{-2}	9.232×10^{-3}	1.269×10^{-2}	703	0.506

TABLE V

EFFECT OF TEMPERATURE ON THE ELECTROMOTIVE FORCES OF THE REDOX CELLS

(*a*) Ag (−) | AgCl ($x_1 = 6.235\times10^{-2}$), KCl–NaCl (1/1 mole) || CuCl ($x_2 = 4.741\times10^{-2}$), $CuCl_2$ ($x_3 = 1.745\times10^{-2}$), KCl–NaCl (1/1 mole) | Pt (+)

	T,° K.	E_{cell} (volts)	$E^\circ_{Ag/Ag^+} - E^\circ_{Cu^+/Cu^{++}}$ (volts)
On heating			
	973	0.745	0.596
	1049	0.769	0.609
	1091	0.784	0.617
	1133	0.795	0.622
On cooling			
	1075	0.775	0.611
	1015	0.755	0.600
	991	0.746	0.595
	971	0.737	0.589
	947	0.729	0.584

(*b*) Ag (−) | AgCl ($x_1 = 6.235\times10^{-2}$), KCl–NaCl (1/1 mole) || $CrCl_2$ ($x_2 = 9.232\times10^{-3}$), $CrCl_3$ ($x_3 = 1.269\times10^{-2}$), KCl–NaCl (1/1 mole) | Pt (+)

	T,° K.	E_{cell} (volts)	$E^\circ_{Ag/Ag^+} - E^\circ_{Cr^{++}/Cr^{+++}}$ (volts)
On heating			
	975	0.506	0.246
	1031	0.561	0.286
	1079	0.616	0.328
	1144	0.687	0.376
On cooling			
	1128	0.663	0.363
	1073	0.610	0.324
	1011	0.547	0.278
	990	0.524	0.261
	969	0.498	0.240

Can. J. Chem. Downloaded from www.nrcresearchpress.com by 78.46.186.204 on 09/04/12
For personal use only.

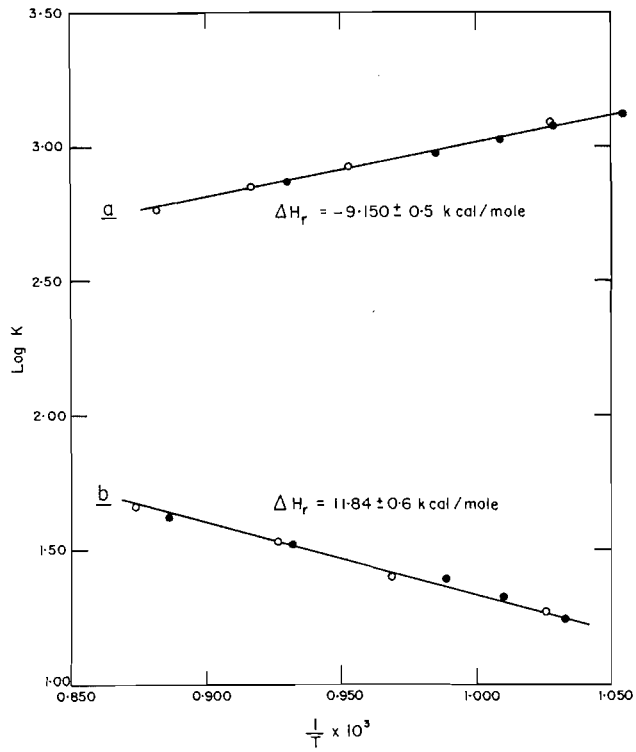

FIG. 5. The variation of log K with the reciprocal of the absolute temperature for the systems:

(*a*)	Ag (−)	AgCl ($x_1 = 6.235+10^{-2}$) KCl–NaCl (1/1 mole)	CuCl ($x_2 = 4.741\times10^{-2}$) $CuCl_2$ ($x_3 = 1.745\times10^{-2}$) KCl–NaCl (1/1 mole)	Pt (+)
(*b*)	Ag (−)	AgCl ($x_1 = 6.235\times10^{-2}$) KCl–NaCl (1/1 mole)	$CrCl_2$ ($x_2 = 9.235\times10^{-3}$) $CrCl_3$ ($x_3 = 1.269\times10^{-2}$) KCl–NaCl (1/1 mole)	Pt (+)

○ with increasing temperature, ● with decreasing temperature.

and $Cr/CrCl_3$ (KCl–NaCl), which are unobtainable by direct measurement. The results of these calculations were given previously in the summary of results in Table II. The heats of the cell reactions for these systems can be calculated by applying the equation, $\sum(\Delta H_r) = 0$, to a cyclic process similar to that used to derive equation [1]. The values thus obtained are:

$$\Delta H_{r(Cu,\ Cu^{++})} = +3.05 \text{ kcal./mole}$$

$$\Delta H_{r(Cr,\ Cr^{+++})} = -54.30 \text{ kcal./mole}$$

From the data in Table II it is also possible to calculate the free energies and the equilibrium constants of the following chemical reactions as they occur in the melt:

(1) $Cu + CuCl_2 = 2CuCl$

(2) $Cr + 2CrCl_3 = 3CrCl_2$

(3) $CuCl_2 + CrCl_2 = CrCl_3 + CuCl$

The results of these calculations are given in Table VI.

It can be readily deduced that reactions (1) and (2) will proceed effectively to completion, whilst with reaction (3) a chemical equilibrium between the reacting species will be attained.

Can. J. Chem. Downloaded from www.nrcresearchpress.com by 78.46.186.204 on 09/04/12
For personal use only.

TABLE VI

FREE ENERGIES AND EQUILIBRIUM CONSTANTS OF REACTIONS IN FUSED SALTS

Reaction at 700° C. in KCl–NaCl solvent	$\Delta F°$, kcal./mole	$K_{eq.}$
$Cu + CuCl_2 = 2CuCl$	−19.80	2.85×10^{4}
$Cr + 2CrCl_3 = 3CrCl_2$	−45.94	2.08×10^{10}
$CuCl_2 + CrCl_2 = CrCl_3 + CuCl$	− 8.30	7.33×10^{1}

DISCUSSION

It is of theoretical interest to compare the experimental electrode potentials, and the experimental heats of the cell reactions, with values calculated from thermodynamic data on the pure metal chlorides (8) without solvent. The calculations for the standard potentials are given in Table II. If the free energy change associated with the difference in standard potentials is attributed entirely to the formation of complexes in melts, the dissociation constants for these complexes can be calculated using the method previously (1) described. It must be emphasized that, in calculating dissociation constants, no assumption has been made about the structure of these compounds. Accordingly, these values could equally well represent the ratio of the activity coefficients. However, following the same procedure used previously (1, 2, 3), these values were calculated as "complex dissociation constants" and the results are:

$$K_d(\text{CuCl complex}) = 2.7\times10^{-1} \text{ at } 700° \text{ C.}$$
$$K_d(CuCl_2 \text{ complex}) = 2.9\times10^{-3} \text{ at } 700° \text{ C.}$$
$$K_d(CrCl_2 \text{ complex}) = 1.07\times10^{-2} \text{ at } 700° \text{ C.}$$
$$K_d(CrCl_3 \text{ complex}) = 4.14\times10^{-2} \text{ at } 700° \text{ C.}$$

From Table II it will be observed that in the case of TlCl, the small difference between the experimental and the calculated potential indicates almost ideal behavior.

Heats of the cell reactions calculated from existing thermodynamic data (8) on the pure metal chlorides are given in Table VII. In this table are also included values obtained experimentally in the present investigation in the presence of the KCl–NaCl solvent.

In Table VII, it will be observed that the experimental average heats of reactions are of the same order as the calculated ones.

The magnitude of the complex dissociation constants above, and the small difference between the heats of reaction, indicate that the over-all energy change which occurs when the metal ions are transferred from the solid or liquid phase of the pure metal chloride to an alkali chloride molten salt solvent is quite small.

TABLE VII

Reaction*	Heats of reaction in kcal./mole					
	Calculated* temp., ° K.					Experimental† between 973–1173° K.
	773	873	973	1073	1173	
$Cu_{(s)} + AgCl_{(l)} = CuCl_{(l)} + Ag_{(s)}$	−5.48	−4.71	−5.19	−4.86	−5.12	−6.10
$Cu_{(s)} + 2AgCl_{(l)} = CuCl_{2(l)} + 2Ag_{(s)}$	−1.44	−0.74	(−0.0)	(+1.0)	—	+3.05
$Cr_{(s)} + 2AgCl_{(l)} = CrCl_{2(s)} + 2Ag_{(s)}$	−40.13	−39.83	−39.87	−39.95	−40.58	−42.46
$Cr_{(s)} + 3AgCl_{(l)} = CrCl_{3(s)} + 3Ag_{(s)}$	−49.08	−48.92	−48.41	−48.44	−49.10	−54.30
$Ag_{(s)} + CuCl_{2(l)} = CuCl_{(l)} + AgCl_{(l)}$	−4.04	−3.91	—	—	—	−9.15
$Ag_{(s)} + CrCl_{3(s)} = CrCl_{2(s)} + AgCl_{(l)}$	+9.36	+9.10	+8.54	+8.49	+8.54	+11.84

*Heats of reaction calculated on the basis of the heats of formation of the pure salts without any solvent present.

†Average heats of reaction calculated from the experimental data in the presence of KCl–NaCl solvent.

Can. J. Chem. Downloaded from www.nrcresearchpress.com by 78.46.186.204 on 09/04/12
For personal use only.

REFERENCES

1. FLENGAS, S. N. and INGRAHAM, T. R. Can. J. Chem. **35**, 1139 (1957).
2. FLENGAS, S. N. and INGRAHAM, T. R. Can. J. Chem. **35**, 1254 (1957).
3. FLENGAS, S. N. and INGRAHAM, T. R. Can. J. Chem. **36**, 780 (1958).
4. INORGANIC SYNTHESIS. Vol. 2. McGraw-Hill Book Co., Inc., New York, London. 1946. p. 1.
5. INORGANIC SYNTHESIS. Vol. 2. McGraw-Hill Book Co., Inc., New York, London. 1946. p. 193.
6. INORGANIC SYNTHESIS. Vol. 2. McGraw-Hill Book Co., Inc., New York, London. 1946. p. 125.
7. HAMER, W., MALMBERG, M., and RUBIN, B. J. Electrochem Soc. **103**, 8 (1956).
8. GLASSNER, A. ANL-5750. The thermodynamic properties of the oxides, fluorides, and chlorides to 2500° K. Argonne National Lab. (1957).

Can. J. Chem. Downloaded from www.nrcresearchpress.com by 78.46.186.204 on 09/04/12
For personal use only.

Can. J. Chem. Downloaded from www.nrcresearchpress.com by 78.46.186.204 on 09/04/12
For personal use only.

THE STRUCTURES OF α- AND β-PARACHLORAL[1]

A. NOVAK[2] AND E. WHALLEY

ABSTRACT

The infrared and proton magnetic resonance spectra of α- and β-parachloral have been investigated and the dipole moment of α-parachloral has been determined. The results show that both isomers have the chair configuration of the ring and that α-parachloral has symmetry C_s with one axial and two equatorial CCl_3 groups and that β-parachloral has symmetry C_{3v} with three equatorial CCl_3 groups.

1. INTRODUCTION

Parachloral, the cyclic trimer of chloral, forms two stereoisomers that have been isolated by Chattaway and Kellett (1). The isomers have been designated α-parachloral, m.p. 116° C., and β-parachloral, m.p. 152° C. Their structures have not been investigated previously. In this paper the infrared and proton magnetic resonance spectra of these compounds (2) and the dipole moment of α-parachloral are used to determine the structures.

2. EXPERIMENTAL PROCEDURES AND RESULTS

α- and β-Parachloral were prepared from chloral hydrate and sulphuric acid as described by Chattaway and Kellett (1). They were purified by repeated crystallization from alcohol until their melting points were constant and in agreement with the values of Chattaway and Kellett.

The spectra were recorded with a Perkin–Elmer Infrared Spectrophotometer Model 21 equipped with a sodium chloride prism. The specimens were examined as mulls in nujol and hexachlorobutadiene, as solutions in carbon tetrachloride and carbon disulphide, and as solids in the form of thin crystalline layers between sodium chloride plates.

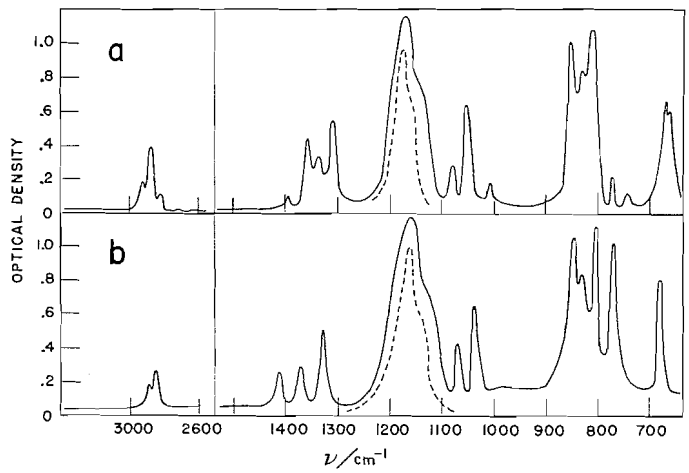

FIG. 1. Infrared spectra of solutions of (*a*) α-parachloral, (*b*) β-parachloral. Carbon tetrachloride solutions were used for the region 3600–1000 cm.$^{-1}$ and carbon disulphide solutions were used for region 1000–650 cm.$^{-1}$.

[1]*Manuscript received February 4, 1958.*
Contribution from the Division of Applied Chemistry, National Research Council, Ottawa, Canada. Issued as N.R.C. No. 4792.
[2]*National Research Council of Canada Postdoctorate Fellow 1956–58.*

The infrared spectra of α- and β-parachloral in solution are shown in Fig. 1. The wave numbers of the absorption maxima or shoulders of both the solution and the crystalline spectra and their relative intensities are listed in Table I.

The solid and solution spectra show but little difference in the position and intensity of the bands. The 1336 and 809 cm.$^{-1}$ bands of α-parachloral in solution are split in the crystal, the separation of the components being about 8 cm.$^{-1}$. If there is more than one molecule in the unit cell of the crystal the splitting can readily be explained.

TABLE I

INFRARED SPECTRA OF α- AND β-PARACHLORAL

α-Parachloral, m.p. 116° C.			β-Parachloral, m.p. 152° C.		
Wave number/cm.$^{-1}$			Wave number/cm.$^{-1}$		
Solid (mull)	Solution	Assignment	Solid (mull)	Solution	Assignment
2920 m	2920 m	ν(C—H)	2890 m	2880 sh	ν(C—H)
2880 s	2890 s	ν(C—H)	2845 s	2860 s	ν(C—H)
2830 sh	2825 m	ν(C—H)			
1394 w	1395 w	Overtone or comb. band	1412 m	1415 m	Overtone or comb. band and δ(C—H)
1358 m	1358 m	δ(C—H)	1368 m	1367 m	
1338 m, 1330 m	1336 m	δ(C—H)	1330 s	1330 s	δ(C—H)
1311 s	1310 s	δ(C—H)			
1166 vs	1166 vs	Skeletal stretching*	1150 vs	1157 vs	Skeletal stretching*
1140 sh	1140 sh		1135 sh	1135 sh	
1085 m	1080 m	γ(C—H)?	1072 s	1075 m	γ(C—H)?
1005 s	1007 s	γ(C—H)?			
1055 m	1055 w–m		1030 s	1037 s	
850 vs	845 vs		840 vs	845 vs	
830 vs	822 sh		830 vs	832 s	
814 vs, 806 vs	809 vs	Skeletal stretching	805 vs	807 vs	Skeletal stretching
767 m	770 m		762 s	771 s	
745 w	745 w				
670 s	671 s		670 s	677 s	
666 s	668 s				

*The bands near 1160, 1140, and 1050 cm.$^{-1}$ are similar to bands in paraldehyde and higher homologues (3, 4); they are probably due to mainly-ring vibrations.

The proton magnetic resonance spectra of α- and β-parachloral in chloroform solution were very kindly measured for us by W. G. Schneider and H. J. Bernstein using a Varian V-4300 NMR Spectrometer.

The dipole moment of α-parachloral in cyclohexane solution has been determined by Dr. D. W. Davidson and Miss J. Taylor of this Division. Dielectric measurements were made with a Gross-type cell of about 5 pf capacitance, using a General Radio 716 C Capacitance Bridge and 716 P Guard Circuit. The frequency was 10 kc./sec. and the temperature 25.0±0.1° C. Eastman Kodak White Label cyclohexane was used and its dielectric constant was taken to be 2.0172 (5). The capacitance with pure solvent and with solution was measured by the substitution technique using a reiteration method, and a series of 10 measurements was made by each of two observers. The results were corrected for the small effect due to the combined influence of the switch and cable capacitance, which was determined by the same reiteration process. The refractive indices (n_{25}^{D}) were measured at 25.0±0.1° C. with a Spencer Abbé Refractometer. The results are summarized in Table II.

The dipole moment was calculated using Guggenheim's equation (6) to be 1.64 Debye units, with an error, allowing for systematic effects, of ±0.1 D.

Can. J. Chem. Downloaded from www.nrcresearchpress.com by 78.46.186.204 on 09/04/12
For personal use only.

3. DISCUSSION

If all the valency angles are tetrahedral there are four likely structures for the parachlorals, shown as I to IV in Fig. 2. Structures that contain more than one axial CCl_3 group either in the chair or in a boat configuration are much less likely on steric grounds. Structure I has symmetry C_{3v} and the other structures have symmetry C_s.

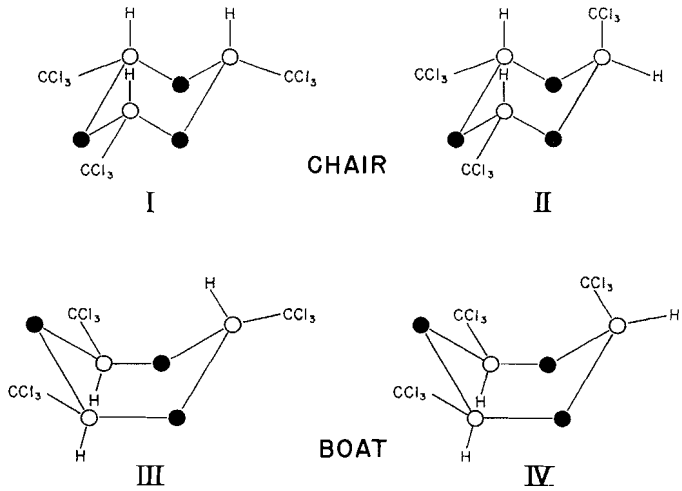

FIG. 2. Possible structures of the parachlorals. Black circles represent the oxygen, and white circles the carbon atoms.

TABLE II

α-PARACHLORAL IN CYCLOHEXANE AT 25.0° C.

10^3m/mole l.$^{-1}$	ϵ	$(\epsilon-\epsilon_0)/(10^3m$/mole l.$^{-1})$	n^2	$(n^2-n^2_0)/(10^3m$/mole l.$^{-1})$
0.1860	2.0873	0.3774	2.0395	0.0628
0.1535	2.0738	0.3686	2.0366	0.0586
0.1008	2.0537	0.3621	2.0340	0.0613
0	2.0172	0.358	2.0278	0.060

m = Concentration of α-parachloral.
ϵ, n = Dielectric constant, refractive index of solution.
ϵ_0, n_0 = Dielectric constant, refractive index of pure solvent.

Proton Magnetic Resonance Spectra

The proton magnetic resonance spectrum (2) of β-parachloral in chloroform solution has only one peak. The three protons are therefore equivalent and the molecule has a C_3 axis. Hence, the structure is I (Fig. 2). The PMR spectrum of α-parachloral has two peaks with intensities in the ratio 1:2. Two of the three protons are therefore equivalent and the molecule has C_s symmetry. Hence the structure must be either II, III, or IV.

Dipole Moment

The dipole moments for the structures I, II, III, and IV, calculated by vector addition of the bond moments by taking the moments of the C—Cl, C—O, and C—H bonds to be 1.57 (7), 0.9, and 0.2 D. (8) respectively and the valence angles to be tetrahedral, are 2.74, 1.59, 0.60, and 2.91 D. respectively. The experimentally determined dipole moment is 1.64±0.1 D. and it shows that α-parachloral has structure II (Fig. 2).

Can. J. Chem. Downloaded from www.nrcresearchpress.com by 78.46.186.204 on 09/04/12
For personal use only.

Infrared Spectra

In both C_s and C_{3v} symmetries the normal modes of vibration of parachloral, the frequencies of which are expected in the region 3500–650 cm.$^{-1}$, may, to a first approximation, be divided into 9 C—H vibrations (3 stretching, 3 bending, and 3 wagging) and 18 skeletal stretching vibrations. The C—H vibrations are classified according to symmetry species in Table III. There are five infrared-active C—H vibrations for C_{3v} and nine for C_s symmetry. The skeletal stretching vibrations for C_{3v} symmetry can be represented (9) by $4A_1+2A_2+6E$; thus 10 of them are infrared-active. All 18 vibrations ($10A'+8A''$) are active for C_s symmetry. Some frequencies of the vibrations that are mainly to the peripheral groups will probably coincide; the number of the resolved bands in the spectrum is therefore expected to be smaller than the number of the active vibrations.

TABLE III

C—H VIBRATIONS OF PARACHLORAL

Approximate type of vibration	Expected frequency range	C_{3v}			C_s	
		A_1	A_2	E	A'	A''
3 C—H stretching	3100–2700 cm.$^{-1}$	1	0	1	2	1
3 C—H bending	1500–1200 cm.$^{-1}$	1	0	1	2	1
3 C—H wagging	1300–700 cm.$^{-1}$	0	1	1	1	2
Infrared active		+	−	+	+	+

C—H Vibrations

The stretching (ν) and bending (δ) modes of CH groups are particularly suitable for confirming the symmetry classes of the parachlorals, since the corresponding bands appear in the region where other fundamentals are not expected.

In the 3 μ region α-parachloral has three bands and β-parachloral has two bands. These are too strong to be combination bands or overtones so they are almost certainly ν(C—H) fundamentals. The numbers agree with the symmetries C_s and C_{3v} respectively.

In the 1500–1300 cm.$^{-1}$ region α-parachloral has four bands. Three are expected for C_s symmetry. One of the observed bands, 1395 cm.$^{-1}$, being very weak, is probably a combination band or overtone perhaps involving C—Cl vibration; they usually give bands about here (10). β-Parachloral has three bands. Two δ(C—H) bands are expected for C_{3v} symmetry. The strong 1330 cm.$^{-1}$ band is doubtless a δ(C—H) fundamental. The two bands at 1415 and 1367 cm.$^{-1}$ are of medium and nearly equal intensity; they are probably caused by Fermi interaction of a δ(C—H) fundamental with an overtone or combination frequency, probably the analogue of the 1395 cm.$^{-1}$ band of α-parachloral.

Thus the ν(C—H) and δ(C—H) bands confirm the C_s and C_{3v} symmetries for α- and β-parachloral, respectively. The ν(C—H) and δ(C—H) bands of β-parachloral are analogous to the bands at 2900 and 2830, and 1400 and 1345 cm.$^{-1}$ in the spectrum of paraldehyde (4); paraldehyde also has C_{3v} symmetry (3, 11, 12).

The wagging (γ) C—H modes are less straightforwardly assigned. For C_{3v} symmetry only one vibration, of species E, is infrared active. This may cause the 1075 cm.$^{-1}$ band in the spectrum of β-parachloral. A similar band associated with γ(C—H) has been observed near 1025 cm.$^{-1}$ in the spectrum of chloral (13). In the α-isomer three γ(C—H) bands are expected; the two bands near 1080 and 1007 cm.$^{-1}$ may be amongst them.

Can. J. Chem. Downloaded from www.nrcresearchpress.com by 78.46.186.204 on 09/04/12
For personal use only.

Skeletal Stretching Vibrations

In the spectrum of β-parachloral there are nine strong or very strong bands near 1157, 1135, 1075, 1037, 845, 832, 807, 771, and 677 cm.$^{-1}$. If one of these, perhaps 1075 cm.$^{-1}$, is a γ(C—H) band there are eight skeletal stretching bands. This is close to the number expected for C_{3v} symmetry. The spectrum of α-parachloral in this region is very similar if one assumes that the bands at 1080 and 1007 cm.$^{-1}$ are γ(C—H) bands; the only other differences other than slight frequency shifts are that the 677 cm.$^{-1}$ band of β-parachloral is replaced by two very close bands at 671 and 668 cm.$^{-1}$ in α-parachloral and the 771 cm.$^{-1}$ band is replaced by two weaker bands at 770 and 745 cm.$^{-1}$. In both β- and α-parachloral the ring has the chair configuration so no major difference in the number of bands due to mainly-ring vibrations is expected and none is observed (Table I.) The splitting of the 677 and 771 cm.$^{-1}$ bands indicates that they are probably due mainly to peripheral groups.

The infrared spectra of β- and α-parachloral thus strongly support the assignment of structures I and II, respectively, to them.

The relative melting points agree with these structures. β-Parachloral has the more symmetrical structure and so it would be expected to pack better in its crystal and it has higher dipole moment. Both factors would tend to make β-parachloral have the higher melting point, and this is observed.

ACKNOWLEDGMENTS

We are indebted to Dr. D. W. Davidson and Miss J. Taylor for determining the dipole moment of α-parachloral and to Drs. W. G. Schneider and H. J. Bernstein for determining the proton magnetic resonance spectra.

REFERENCES

1. Chattaway, F. D. and Kellett, E. G. J. Chem. Soc. 2709 (1928).
2. Bernstein, H. J., Kullnig, R., Lemieux, R. U., and Schneider, W. G. To be published.
3. Gerding, H. and Lecomte, J. Rec. trav. chim. **58**, 614 (1939).
4. Novak, A. and Whalley, E. Unpublished work.
5. Hartshorn, L., Parry, J. V. L., and Essen, L. Proc. Phys. Soc., B, **68**, 422 (1955).
6. Guggenheim, E. A. Trans. Faraday Soc. **47**, 573 (1951).
7. Smyth, C. P. Dielectric behavior and structure. McGraw-Hill Book Co., Inc., New York. 1955. p. 293.
8. Maryott, A. A. and Acree, S. F. J. Research Natl. Bur. Standards, **33**, 71 (1944).
9. Wilson, E. B., Jr., Decius, J. C., and Cross, P. C. Molecular vibrations. McGraw-Hill Book Co., Inc., New York. 1955. p. 109.
10. Bellamy, L. J. The infrared spectra of complex molecules. Methuen & Co., Ltd., London. 1954. p. 272.
11. Le Fèvre, R. J. W. and Calderbank, K. E. J. Chem. Soc. 199 (1949).
12. Carpenter, D. C. and Brockway, L. O. J. Am. Chem. Soc. **58**, 1270 (1936).
13. Seewann-Albert, H. Acta Phys. Austriaca, **1**, 346 (1948).

Can. J. Chem. Downloaded from www.nrcresearchpress.com by 78.46.186.204 on 09/04/12
For personal use only.

Can. J. Chem. Downloaded from www.nrcresearchpress.com by 78.46.186.204 on 09/04/12
For personal use only.

ON THE NATURE OF SULPHUROUS ACID[1]

MICHAEL FALK[2] AND PAUL A. GIGUÈRE

ABSTRACT

Repeated attempts to detect by infrared spectrometry stable H_2SO_3 molecules in aqueous solutions of "sulphurous acid" or in frozen mixtures of SO_2 and H_2O have given only negative results. Sulphur dioxide dissolved in water exists mostly in the molecular state, the HSO_3^- and $HS_2O_5^-$ ions being formed in small amounts as a result of the equilibria

$$SO_2 + 2H_2O \rightleftharpoons HSO_3^- + H_3O^+ \text{ and } HSO_3^- + SO_2 \rightleftharpoons HS_2O_5^-.$$

There is very little interaction between SO_2 and H_2O molecules in condensed phases.

In spite of the major importance of aqueous solutions of sulphur dioxide in a multitude of industrial processes there remains a surprising uncertainty as to the nature of the equilibria between the molecular and ionic species in these solutions. Sulphur dioxide dissolves in water to the extent of about nine weight per cent at 25° C. and atmospheric pressure (1). The resulting solution possesses well-known acidic properties, conducts the electric current, and behaves as if it contained an acid, presumably H_2SO_3. However, although the ions H_3O^+, HSO_3^-, and SO_3^{--} are indeed present in the solution, the free acid itself has never been isolated or shown to exist. Nevertheless, its existence has been taken for granted by most chemists, the equilibria in the aqueous solutions being usually expressed as follows:

$$SO_2 + H_2O \rightarrow H_2SO_3;$$

$$H_2SO_3 + H_2O \overset{K_1}{\rightleftharpoons} H_3O^+ + HSO_3^-;$$

$$HSO_3^- + H_3O^+ \overset{K_2}{\rightleftharpoons} H_3O^+ + SO_3^{--}.$$

Assuming that these were the only equilibria involved, and that the first step is complete, i.e. that all the un-ionized sulphur dioxide in solution is combined to form H_2SO_3, the two ionization constants were calculated from electrical conductivity data to be $K_1 = 0.012$ to 0.017 (2, 3), and $K_2 = 10^{-7}$ to 10^{-6} (4, 5). The above assumptions, however, were soon proved incorrect, as evidence for the existence of unchanged SO_2 molecules in aqueous solution was obtained from ultraviolet absorption spectra (6, 7, 8, 9). Many workers attempted to calculate the ratio of H_2SO_3 to "free" SO_2 molecules in solution from the measurements of vapor pressures and electrical conductivities of the solution as a function of temperature and concentration, with widely divergent results (1, 2, 3, 10). These calculations appear to have relatively little merit, being based on such drastic assumptions as the use of Kohlrausch's law at fairly high concentrations, or the substitution of concentrations for activities. Because the individual concentrations of SO_2 and H_2SO_3 in solution were unknown, a convention was proposed by Lewis and Randall (11) setting arbitrarily the equilibrium constant

$$K = (H_2SO_3)/(SO_2)\ (H_2O) = 1.$$

With the advent of Raman spectroscopy, numerous studies were made of aqueous solutions of sulphur dioxide (12, 13, 14). In every case three Raman lines were detected,

[1]*Manuscript received March, 31, 1958.*
Contribution from the Department of Chemistry, Laval University, Quebec, Que., with financial assistance from the National Research Council.
[2]*Holder of a Cominco Fellowship.*

corresponding to essentially unchanged SO_2 molecules. The only other species detected in some cases were the HSO_4^- and SO_4^{--} ions formed by slow oxidation of aqueous SO_2, a reaction difficult to prevent during long exposures. Recently an extensive Raman study by Simon and Waldmann (15, 16, 17) revealed for the first time in these solutions some lines due to bisulphite ions, HSO_3^-, in very low concentration, as well as pyrosulphite ions, $HS_2O_5^-$, pointing to the hitherto unsuspected equilibrium $HSO_3^- + SO_2 \rightleftharpoons HS_2O_5^-$. The concentration of the sulphite ions, SO_3^{--}, is certainly much too low to be detected spectroscopically, and the H_3O^+ ion does not give rise to a measurable Raman spectrum (18). None of the Raman lines detected in aqueous solutions by Simon and Waldmann could be attributed to H_2SO_3, although these authors continue to refer to the solutions as "sulphurous acid".

In the present work we have examined the infrared spectra of sulphur dioxide solutions in water in order to supplement the evidence for the absence of H_2SO_3 in solution. We have also studied the SO_2–H_2O mixtures in the solid state, where the formation of the compound H_2SO_3 might be favored.

EXPERIMENTAL

Aqueous Solutions of SO_2

The samples were prepared simply by squeezing between a pair of silver chloride windows a drop of aqueous solution of sulphur dioxide saturated at 25° and one atmosphere. Since a pressure cell was not available, evaporation of the dissolved sulphur dioxide could not be prevented and the spectra had to be recorded in small steps. A composite spectrum, based on several overlapping runs, is reproduced in Fig. 1, together with the spectrum of pure water in the same region. The spectra were obtained with a Perkin–Elmer model 12-C instrument, using NaCl and CsBr prisms; the background noise has

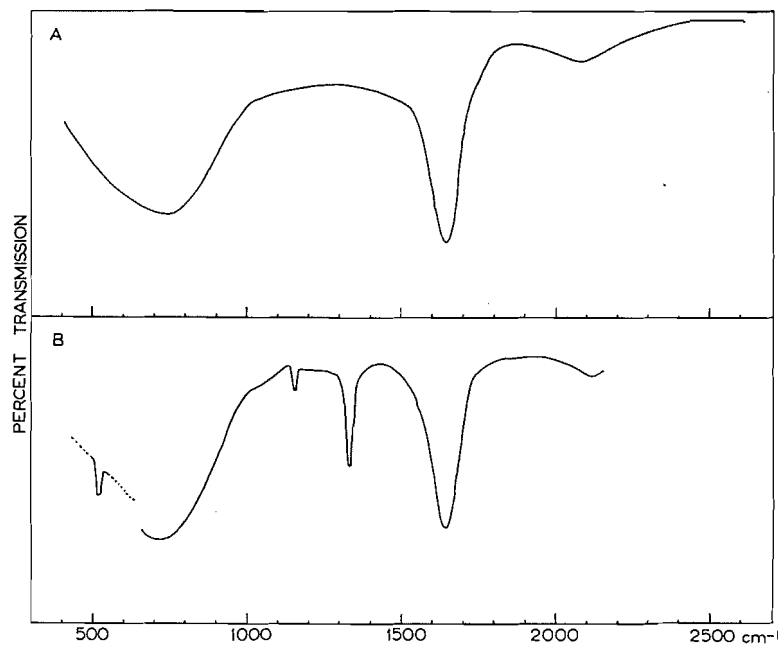

FIG. 1. A. Spectrum of a thin film of pure water in the region of NaCl and CsBr prisms. B. Spectrum of a thin film of solution of sulphur dioxide in water.

Can. J. Chem. Downloaded from www.nrcresearchpress.com by 78.46.186.204 on 09/04/12
For personal use only.

been smoothed out in replotting the spectra. In addition to the absorption bands of liquid water (ν_2 at about 710 cm.$^{-1}$, ν_2 at 1640 cm.$^{-1}$, $\nu_2 + \nu_R$ at 2120 cm.$^{-1}$, and ν_3 at 3400 cm.$^{-1}$), the spectrum of the solution contains three bands at 527, 1152, and 1334 cm.$^{-1}$, due respectively to the fundamental vibrations ν_2, ν_1, and ν_3 of the dissolved SO_2 molecules. These values are only slightly removed from the corresponding frequencies in pure liquid SO_2: 523, 1148, and 1338 cm.$^{-1}$ (19).

Solid Mixtures of SO_2 *and* H_2O

Various proportions of SO_2 and H_2O were mixed thoroughly by diffusion in the vapor phase, then condensed at liquid air temperature upon a silver chloride window in a conventional low-temperature infrared cell, and the absorption spectra recorded. The spectrum (in the range of the sodium chloride prism) of an equimolecular mixture is reproduced in Fig. 2. Included for comparison are the spectra of pure SO_2 and ice obtained in the same manner.

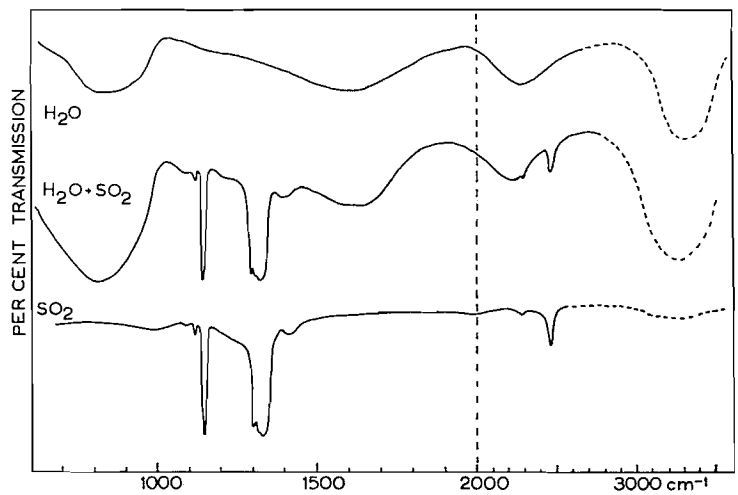

FIG. 2. Spectra in the region of NaCl prism of solid SO_2, solid H_2O, and their equimolecular mixture condensed at −190° C.

The spectrum of the mixture is essentially a superposition of the spectra of pure components. No new absorption bands appear and those of SO_2 and H_2O undergo no change of frequency, appearance, or intensity.* Variations in the composition and temperature of the deposits or irradiation with ultraviolet radiation from a Hanovia mercury lamp was without significant effect on the spectra. These results show clearly the absence of compound formation and, in particular, the absence of H_2SO_3 molecules which, if stable, would have been expected to form under these conditions. By contrast, the infrared spectra of solid mixtures of HCl or NH_3 with H_2O, condensed in an identical manner, have indicated clearly the formation of molecular compounds in those systems (21, 22).

Phase diagram studies of the SO_2–H_2O system have previously proved the existence of only one stable hydrate, $SO_2.6H_2O$ (23), apparently of the "gas hydrate" type (24). Such hydrates are characterized by very weak bonding with water, hence would have

**The shape of the ν_R band of ice appears changed somewhat in the spectrum of the mixture. It is not certain whether this effect is genuine, for the shape and intensity of the ν_R band in pure water and ice seems very sensitive to changes in film characteristics (20).*

Can. J. Chem. Downloaded from www.nrcresearchpress.com by 78.46.186.204 on 09/04/12
For personal use only.

an infrared spectrum practically identical with that of the pure components. The compound H_2SO_3, on the other hand, would give rise to a number of new absorption bands, quite different from those of SO_2. The closely related spectrum of the aqueous HSO_3^- ion contains Raman frequencies at 457, 586, 709, 1019, 1089, 1129, and 2532 cm.$^{-1}$ (15).

DISCUSSION

The present infrared spectra confirm the conclusion of earlier Raman investigations that sulphur dioxide molecules are not strongly hydrated in aqueous solution and do not form the compound H_2SO_3. The upper concentration limit of the latter, which could have escaped detection, is believed to be 0.2 *M* in the infrared spectra and about 0.1 *M* in the Raman work (Simon and Waldmann detected the strongest lines of the HSO_3^- and $HS_2O_5^-$ ions at concentrations below 0.1 *M*). Since the most concentrated solutions employed in our work contained some 8.3% SO_2, or 1.3 *M*, and those employed in the Raman study of Simon and Waldmann contained up to 17.2% SO_2, or about 3 *M* (under pressure), the upper limit for H_2SO_3 may be set at 1/30 of the sulphur dioxide concentrations. However, the actual concentration of H_2SO_3 may be expected to be very much smaller than that. Even in the solid phase, where the formation of the compound H_2SO_3 would be much more likely, it cannot be detected at all and the interaction of SO_2 and H_2O molecules appears to be very weak in all phases.

Therefore the un-ionized fraction of sulphur dioxide in "sulphurous acid" solutions exists as uncombined molecules. As for the ionic species, the electrical conductivity data indicate that the H_3O^+ ions are present at a concentration of about 0.1 *M* in a solution 1 *M* in sulphur dioxide (3). The anions, HSO_3^-, $HS_2O_5^-$, plus a much smaller amount of SO_3^{--}, must be present at the same total concentration, although the exact proportions are difficult to determine. Altogether some 10% of sulphur dioxide dissolved at n.t.p. is ionized.

Unstable H_2SO_3 molecules might be involved as short-lived intermediates in the formation of the HSO_3^- ions. However, these ions could also be formed by another mechanism such as

$$2H_2O \rightleftharpoons OH^- + H_3O^+; \; SO_2 + OH^- \rightleftharpoons HSO_3^-$$

suggested by Campbell and Maass (3) some time ago. In any event the over-all equilibrium is

$$SO_2 + 2H_2O \rightleftharpoons HSO_3^- + H_3O^+.$$

The term "sulphurous acid", like the analogous "carbonic acid" H_2CO_3, established by long tradition, will continue to be used. It should be understood, however, that these hypothetical compounds do not exist in detectable concentration even in solutions. In remarkable contrast to sulphur dioxide, selenium dioxide appears to react completely with water, forming the stable selenious acid, H_2SeO_3, both in solution and in the crystalline phase. We are now completing a similar investigation of selenious acid and expect to report the results shortly.

RÉSUMÉ

L'étude des spectres infrarouges confirme que les solutions aqueuses de SO_2 ne contiennent pas de quantités mesurables d'acide sulfureux, H_2SO_3. Dans ces solutions les molécules de SO_2 existent en majorité comme telles à côté de faibles concentrations des ions HSO_3^- et $HS_2O_5^-$ résultant des équilibres:

Can. J. Chem. Downloaded from www.nrcresearchpress.com by 78.46.186.204 on 09/04/12
For personal use only.

$$SO_2 + H_2O \rightleftharpoons HSO_3^- + H_3O^+$$

et

$$HSO_3^- + SO_2 \rightleftharpoons HS_2O_5^-.$$

Par ailleurs les spectres de mélanges solidifiés de SO_2 et H_2O n'indiquent pratiquement aucune interaction entre ces deux composés en phases condensées.

REFERENCES

1. MORGAN, C. M. and MAASS, O. Can. J. Research, **5**, 162 (1931).
2. JOHNSTONE, H. F. and LEPPLA, P. W. J. Am. Chem. Soc. **56**, 2233 (1934).
3. CAMPBELL, W. B. and MAASS, O. Can. J. Research, **2**, 42 (1930).
4. JELLINEK, K. Z. physik. Chem. **76**, 257 (1911).
5. KOLTHOFF, I. M. Chem. Weekblad, **16**, 1154 (1919).
6. WRIGHT, R. J. Chem. Soc. 2907 (1914).
7. SCHÄFFER, K. and KÖHLER, W. Z. anorg. u. allgem. Chem. **104**, 212 (1918).
8. DIETZEL, R. and GALANOS, S. Z. Electrochem. **31**, 466 (1925).
9. GETMAN, F. H. J. Phys. Chem. **30**, 266 (1926).
10. MAASS, C. E. Thesis, McGill University, Montreal, Quebec, 1929.
11. LEWIS, G. N. and RANDALL, M. Thermodynamics and the free energy of chemical substances. 1st ed. McGraw-Hill Book Co., Inc., New York. 1923. pp. 297 and 550.
12. BHAGAVANTAM, S. Indian J. Phys. **6**, 319 (1931).
13. GERDING, H. and NIJVELD, W. I. Rec. trav. chim. **56**, 968 (1937).
14. RAO, B. P. Proc. Indian Acad. Sci., A, **20**, 292 (1944).
15. SIMON, A. and WALDMANN, K. Z. anorg. u. allgem. Chem. **281**, 113, 135 (1955).
16. SIMON, A. and WALDMANN, K. Z. anorg. u. allgem. Chem. **284**, 36, 47 (1956).
17. SIMON, A. and WALDMANN, K. Z. anorg. u. allgem. Chem. **283**, 359 (1956).
18. FALK, M. and GIGUÈRE, P. A. Can. J. Chem. **35**, 1195 (1957).
19. MAYBURY, R. H., GORDON, S., and KATZ, J. J. J. Chem. Phys. **23**, 1277 (1955).
20. GIGUÈRE, P. A. and HARVEY, K. B. Can. J. Chem. **34**, 798 (1956).
21. FERRISO, C. C. and HORNIG, D. F. J. Chem. Phys. **23**, 1464 (1955).
22. WALDRON, R. D. and HORNIG, D. F. J. Am. Chem. Soc. **75**, 6079 (1953).
23. TAMMAN, G. and KRIGE, G. J. R. Z. anorg. u. allgem. Chem. **146**, 179 (1925).
24. VON STACKELBERG, M. Naturwiss. **36**, 327 (1949). Z. Electrochem. **58**, 25 (1954).

Can. J. Chem. Downloaded from www.nrcresearchpress.com by 78.46.186.204 on 09/04/12
For personal use only.

Can. J. Chem. Downloaded from www.nrcresearchpress.com by 200.7.193.243 on 09/04/12
For personal use only.

NOTES

PHYSICAL ADSORPTION IN THE BENZENE–POLYSTYRENE SYSTEM*

S. S. Barton and S. G. Mason

INTRODUCTION

Although the sorption of solvent vapors by solid polymers is usually considered as a solution process, McLaren and Cutler (1) found that when the water sorption isotherm of a water-soluble fraction of polyvinyl acetate was analyzed from the point of view of the Flory–Huggins equation, values of μ much larger than $\mu_{crit.}$ are required in the low pressure region. This phenomenon, indicating phase separation, was attributed to surface adsorption preceding solution formation at low relative pressures. On the other hand, Baughan (2) found that the sorption isotherm of benzene or polystyrene sheets fitted the Flory–Huggins equation over a benzene volume fraction of 0.07 to 0.57 with an interaction constant $\mu = 0.45$. It would appear in this case that the sorbed benzene formed a homogeneous solution with the polystyrene.

When the sorbate is not a solvent for the sorbent, the "adsorption" characteristics of the reaction can be more pronounced. The presence of strongly adsorbing sites in a polymer matrix which are saturated by initial quantities of sorbing (non-solvent) gases and vapors have been deduced by several workers (3, 4, 5).

As long as the concentration of solvent sorbate is not so high that the sorbate–sorbent complex loses its rigidity, then a certain amount of adsorption on active sites can be expected to occur in any solvent–polymer system at low relative pressures.

In the investigation described in this note, heats of sorption of small amounts of benzene on two samples of polystyrene were measured. The heats evolved were sufficiently high to be considered heats of physical adsorption, and have been taken as evidence that surface adsorption precedes solution in the benzene–polystyrene system.

EXPERIMENTAL

A conventional all-glass adsorption apparatus with mercury valves instead of stopcocks was used. Benzene vapor was measured into a calibrated volume from a reservoir containing thoroughly outgassed reagent grade benzene. The measured dose was then exposed to a fairly large (*ca.* 5 g.) sample of outgassed polystyrene, mounted in the reaction well of a large diphenyl ether isothermal calorimeter, operating at 26.9° C. (6, 7). Pressures were measured by conventional mercury manometers read to the nearest 0.5 mm.

The take-up of benzene as indicated by the falling pressure was initially rapid, but after 10–15 minutes became very slow. The slow take-up, when allowed to proceed, was observed to continue for many days. In each determination, the contribution from the slow take-up was made as small as possible by isolating the large calibrated volume from the polystyrene sample as soon as possible after the initial rapid sorption had taken place. Slow sorption could then only continue at the expense of the relatively small amount of benzene vapor in the dead space.

Heat was evolved during the initial rapid sorption, and shortly after the benzene pressure had become nearly constant, the rate of movement of the mercury thread in the

This investigation was conducted under Extra-Mural Grant No. 6 from the Defence Research Board.

dilatometer tube of the calorimeter again assumed the normal small positive drift indicating that any heat given off by the subsequent sorption was evolved too slowly to be detected by the calorimeter. The heat evolved during the rapid sorption was calculated by using the averages of the fore- and after-drifts to correct the total mercury displacement over the time of the rapid sorption. The corrected displacement figure was converted to calories by means of an electrically determined calibration constant.

Two different types of commercial polystyrene were used. Type A was in the form of a powder which passed No. 42 mesh and was supplied by Monsanto Canada Limited, who stated it to have a molecular weight of about 60,000. Type B was in the form of irregularly shaped particles of *ca.* 1.2×10^{-2} cc. The supplier, Dow Chemical Company (Midland, Mich.), stated it to have molecular weight about 270,000.

Two samples of Type A were used. Two series of heat and isotherm measurements were made on one sample and four series were made on the other. Between series, the sorbed benzene was removed by exhaustive pumping. Similarly, two samples of Type B were used in three series of measurements.

RESULTS AND DISCUSSION

Isotherms describing the "fast" adsorption of benzene on polystyrene are shown in Fig. 1. The ordinate, A_F, gives the amount of benzene adsorbed before the constant after-drift of the calorimeter was established. The slow sorption, which continued between measurements and did not affect the calorimeter, is not included. It was estimated that because of this slow sorption, the true benzene concentration in the condensed phase was about 4% higher than indicated by A_F. The relative pressure values are those observed at the end of each "fast" adsorption. No attempt was made to determine an equilibrium isotherm, since the time required, with the experimental arrangement used, would have been too long.

Fig. 1, which includes all of the isotherm points from the nine experiments, shows that within the rather large error encountered in the work it was possible to reproduce the different isotherms.

The shape of the isotherm is that of Type III or Type IV of the classification of Brunauer (8). Almost all of the benzene is sorbed over a very narrow range of pressure, and for equal amounts of sorption a higher pressure is required with Type A polystyrene than with Type B. This behavior is associated with adsorption in rather narrow size-distributions of pores (9). In fact, the present heat and isotherm data are best correlated by assuming that porous adsorption occurs. Pore radii were obtained by extrapolating the almost vertical, linear portions of each isotherm back to the pressure axis and substituting the value obtained into the simple Kelvin equation. Zero contact angle was assumed and values for the liquid density and surface tension of bulk benzene were used (10). The values obtained are given in Table I.

Fig. 2 shows the integral heat of adsorption (q_I) curves. The integral heat at any particular value of A_F is the sum of the individual amounts of heat, per gram of polystyrene, evolved up to that value of A_F.

At low values of A_F the heat curves are concave towards the A_F axis but become straight lines as A_F increases. The linear portion of the heat curve begins at roughly the same value of A_F as does the linear portion of the corresponding isotherm.

The differential heat of adsorption, q_d, is given by the slope of the integral curve. Fig. 2 shows that q_d falls fairly rapidly from an initial high value to a lower constant value as adsorption proceeds. Most of the adsorption takes place with constant q_d. Using q_L

Can. J. Chem. Downloaded from www.nrcresearchpress.com by 200.7.193.243 on 09/04/12
For personal use only.

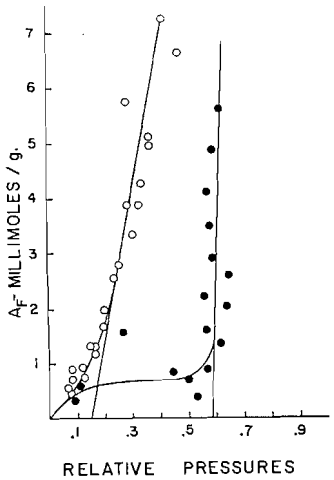

FIG. 1. "Fast" adsorption isotherms.
Type A—open circles (six isotherms).
Type B—solid circles (three isotherms).

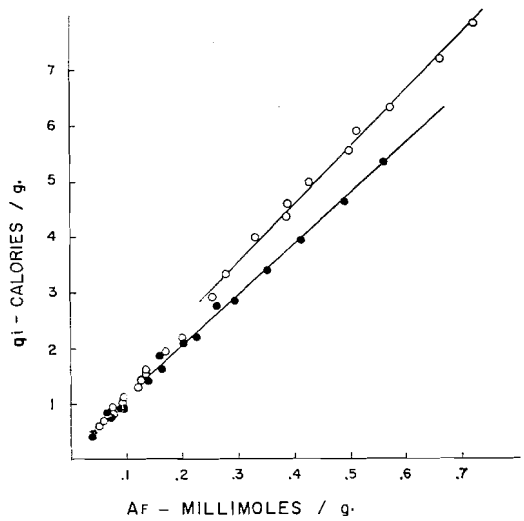

FIG. 2. Integral heat of "fast" adsorption.
Type A—open circles.
Type B—solid circles.

= 8080 cal./mole as the heat of vaporization of benzene at 27.0° C. (6) and the constant q_d values, the quantity $q_d - q_L$, the net heat associated with the adsorption of benzene on the polystyrene pore structure, has been calculated.

TABLE I

PORE SIZES AND HEATS OF ADSORPTION

Polystyrene	p_0/p	Pore radius (Å)	q_d (cal./mole)	$q_d - q_L$ (cal./mole)
A	7.36	10.1	10310	2230
B	1.75	36.2	9059	979

Taking 5.7 Å as the molecular diameter of benzene (11), it is seen that the radius of the pores in the Type A polystyrene are of the order which should give a high proportion of double-wall adsorption (12) with the benzene molecule. Also, the radii of the pores in the larger granules of Type B polystyrene are sufficiently large so that co-operative, double-wall adsorption would be very much diminished. The net heat of adsorption in the smaller pores is seen to be nearly double the net heat of adsorption in the larger pores.

Although the heat and isotherm data agree when regarded as indicating the occurrence of porous adsorption, the very small size of the pores brings into question the applicability of the simple Kelvin equation, and thus throws doubt on the whole explanation presented (13). However, the reproducibility of the isotherms indicates strongly that polystyrene can maintain its surface structure through limited adsorption and desorption cycles, and the differential heat of adsorption is of the order of magnitude associated with physical adsorption.

One of the consequences of swelling and partial solution is that any pore system will be greatly changed as the swollen structure collapses on de-swelling. It is apparent that the

Can. J. Chem. Downloaded from www.nrcresearchpress.com by 200.7.193.243 on 09/04/12
For personal use only.

amount of sorption in the experiments described was not sufficient to cause marked swelling of the polystyrene. The highest benzene volume fraction encountered here was 0.05, at the lower end of the range investigated by Baughan (2).

It is appreciated that the molecular weights of the samples were quite different. However, from the point of view adopted here, the effect of molecular weight on the amount of heat evolved or the shape of the "fast" isotherm should be of little consequence.

An alternative explanation which has been kindly suggested by the Referee does not involve capillary condensation but instead the transition from physical (surface) adsorption to solution near the surface of the substrate. In a theoretical treatment of this transition, Hill (14) has indicated that an intermediate region of sorption at an essentially constant pressure should be observed. It is possible that the nearly vertical portions in Fig. 1 may correspond to an equilibrium between benzene vapor and a saturated solution of polystyrene in benzene on the surface of the polymer. Since Type A polymer, being of lower molecular weight than Type B, is the more soluble of the two it may be expected that solution would occur at a lower relative vapor pressure for Type A. It is, however, difficult to account for the observed energies on this basis, since the (exothermic) heat of solution may be expected to increase with increasing molecular weight (15).

1. McLaren, A. D. and Cutler, J. A. J. Polymer Sci. **3**, 792 (1948).
2. Baughan, E. C. Trans. Faraday Soc. **44**, 495 (1948).
3. Heilman, W., Tammela, V., Meyer, J., Stannett, V., and Szwarc, M. Ind. Eng. Chem. **48**, 821 (1956).
4. King, G. Trans. Faraday Soc. **41**, 479 (1945).
5. Stannett, V. and Szwarc, M. J. Polymer Sci. **16**, 89 (1955).
6. Giguère, P. A., Morissette, B. G., and Olmos, A. W. Can. J. Chem. **33**, 657 (1955).
7. Screaton, R. and Mason, S. G. Svensk Papperstidn. **6**, 379 (1957).
8. Brunauer, S. The adsorption of gases and vapours. Vol. 1. Princeton University Press, Princeton. 1945. p. 150.
9. McDermot, H. L. and Arnell, J. C. J. Phys. Chem. **58**, 492 (1954).
10. International Critical Tables. McGraw-Hill Book Company, Inc., New York. 1926.
11. Weigel, O. and Steinhof, E. Z. Krist. **61**, 125 (1925).
12. Pierce, C., Wiley, J. W., and Smith, R. N. J. Phys. & Colloid Chem. **53**, 669 (1949).
13. McBain, J. W. Sorption of gases and vapours by solids. G. Routledge & Sons, London. 1932. p. 434.
14. Hill, T. L. J. Phys. Chem. **18**, 246 (1950).
15. Tager, A. A. Doklady Akad. Nauk S.S.S.R. **100**, 741 (1955).

Received March 21, 1958.
Department of Chemistry,
McGill University,
Montreal, Quebec.

THE MECHANISM OF THE PYROLYSIS OF PRIMARY ALKYL BROMIDES*

Arthur T. Blades

Considerable literature has appeared in the last few years on the pyrolysis of alkyl bromides to form the corresponding olefin and hydrogen bromide (1, 2, 3, 4, 5, 6, 7, 8). With secondary and tertiary bromides this reaction appears to involve primarily a unimolecular split and the kinetics of these reactions can be studied reasonably well without inhibitors. With primary bromides the reaction involves free radicals and it is necessary to use an inhibitor to reduce the rates to a limiting value; this residual reaction is believed to be similar to that for the secondary and tertiary compounds. This communication refers to the uninhibited pyrolysis of ethyl and *n*-propyl bromides.

**Contribution No. 67 from the Research Council of Alberta, Edmonton, Alberta.*

Can. J. Chem. Downloaded from www.nrcresearchpress.com by 200.7.193.243 on 09/04/12
For personal use only.

amount of sorption in the experiments described was not sufficient to cause marked swelling of the polystyrene. The highest benzene volume fraction encountered here was 0.05, at the lower end of the range investigated by Baughan (2).

It is appreciated that the molecular weights of the samples were quite different. However, from the point of view adopted here, the effect of molecular weight on the amount of heat evolved or the shape of the "fast" isotherm should be of little consequence.

An alternative explanation which has been kindly suggested by the Referee does not involve capillary condensation but instead the transition from physical (surface) adsorption to solution near the surface of the substrate. In a theoretical treatment of this transition, Hill (14) has indicated that an intermediate region of sorption at an essentially constant pressure should be observed. It is possible that the nearly vertical portions in Fig. 1 may correspond to an equilibrium between benzene vapor and a saturated solution of polystyrene in benzene on the surface of the polymer. Since Type A polymer, being of lower molecular weight than Type B, is the more soluble of the two it may be expected that solution would occur at a lower relative vapor pressure for Type A. It is, however, difficult to account for the observed energies on this basis, since the (exothermic) heat of solution may be expected to increase with increasing molecular weight (15).

1. McLaren, A. D. and Cutler, J. A. J. Polymer Sci. **3**, 792 (1948).
2. Baughan, E. C. Trans. Faraday Soc. **44**, 495 (1948).
3. Heilman, W., Tammela, V., Meyer, J., Stannett, V., and Szwarc, M. Ind. Eng. Chem. **48**, 821 (1956).
4. King, G. Trans. Faraday Soc. **41**, 479 (1945).
5. Stannett, V. and Szwarc, M. J. Polymer Sci. **16**, 89 (1955).
6. Giguère, P. A., Morissette, B. G., and Olmos, A. W. Can. J. Chem. **33**, 657 (1955).
7. Screaton, R. and Mason, S. G. Svensk Papperstidn. **6**, 379 (1957).
8. Brunauer, S. The adsorption of gases and vapours. Vol. 1. Princeton University Press, Princeton. 1945. p. 150.
9. McDermot, H. L. and Arnell, J. C. J. Phys. Chem. **58**, 492 (1954).
10. International Critical Tables. McGraw-Hill Book Company, Inc., New York. 1926.
11. Weigel, O. and Steinhof, E. Z. Krist. **61**, 125 (1925).
12. Pierce, C., Wiley, J. W., and Smith, R. N. J. Phys. & Colloid Chem. **53**, 669 (1949).
13. McBain, J. W. Sorption of gases and vapours by solids. G. Routledge & Sons, London. 1932. p. 434.
14. Hill, T. L. J. Phys. Chem. **18**, 246 (1950).
15. Tager, A. A. Doklady Akad. Nauk S.S.S.R. **100**, 741 (1955).

Received March 21, 1958.
Department of Chemistry,
McGill University,
Montreal, Quebec.

THE MECHANISM OF THE PYROLYSIS OF PRIMARY ALKYL BROMIDES*

Arthur T. Blades

Considerable literature has appeared in the last few years on the pyrolysis of alkyl bromides to form the corresponding olefin and hydrogen bromide (1, 2, 3, 4, 5, 6, 7, 8). With secondary and tertiary bromides this reaction appears to involve primarily a unimolecular split and the kinetics of these reactions can be studied reasonably well without inhibitors. With primary bromides the reaction involves free radicals and it is necessary to use an inhibitor to reduce the rates to a limiting value; this residual reaction is believed to be similar to that for the secondary and tertiary compounds. This communication refers to the uninhibited pyrolysis of ethyl and *n*-propyl bromides.

**Contribution No. 67 from the Research Council of Alberta, Edmonton, Alberta.*

Can. J. Chem. Downloaded from www.nrcresearchpress.com by 78.46.186.204 on 09/04/12
For personal use only.

Can. J. Chem. Downloaded from www.nrcresearchpress.com by 78.46.186.204 on 09/04/12
For personal use only.

Agius and Maccoll (10) consider that the uninhibited pyrolysis of *n*-propyl bromide is a chain reaction initiated by a break into propyl radicals and bromine atoms. A plot of the "first order" data vs. $P_0^{\frac{1}{2}}$ indicated that a 3/2 order described the data much more adequately, and an appropriate chain mechanism was devised. These observations have been confirmed by Semenov, Sergeev, and Kapralova (7), who also note the catalytic effect of bromine and hydrogen bromide. More recently, Goldberg and Daniels (8) reported similar studies on ethyl bromide, and also indicated that a chain decomposition occurs. They stated that the rate became "first order" after an induction period but that the rate constants were pressure dependent. They also found that the reaction was greatly accelerated by the addition of one of the products (hydrogen bromide), and inhibited by the other product (ethylene). It is of interest to examine the data of Goldberg and Daniels to see whether it can be reconciled with the kinetics for *n*-propyl bromide proposed by Agius and Maccoll.

The order of decomposition of ethyl bromide was inferred by Goldberg and Daniels from a plot of the logarithm of the fraction of bromide remaining, against time. However, this is not a particularly good indicator of order, especially when an induction period is observed. The fact that the rate decreased with decreasing pressure suggests that some other order might fit the data more adequately. A replot of the k vs. P_0 data in Goldberg and Daniels' Fig. 2 as k vs. $P_0^{\frac{1}{2}}$ gives a reasonably straight line with an intercept at $k = 0.6$ sec.$^{-1}$. Since a first-order decomposition corresponding to a simple molecular split is proceeding simultaneously with the chain reaction, the intercept should correspond to this rate, and it is possible to predict a value of $k = 0.5$ sec.$^{-1}$ from the data on this uncatalyzed reaction (9). Therefore, a more realistic rate expression for ethyl bromide would be:

$$r = k[C_2H_5Br] + k_1[C_2H_5Br]^{3/2}.$$

This does not imply that the mechanism proposed by Goldberg and Daniels is incorrect but it appears that some alteration must be made in their mathematical treatment of it. Their steady-state approximations are that the bromine, bromine atom, and C_2H_4Br radical concentrations become stable. As pointed out by Hirschfelder (10), the stationary-state approximation can be applied only if the rate of destruction of intermediates is many order of magnitude greater than that of the over-all reaction. For bromine, with a bond energy of 45.5 kcal./mole, this condition is not fulfilled. Insofar as this argument vitiates the steady-state treatment, their suggestion that at high bromide pressures the concentration on the wall is independent of the pressure can no longer be accepted.

Since the bromine atoms are in quasi-equilibrium with the bromine, it seems equally unlikely that this concentration would be constant but it might vary roughly according to the $\frac{1}{2}$ power of the ethyl bromide pressure as suggested by the kinetics equation of Goldberg and Daniels:

$$r = k_a[C_2H_5Br] + k_d[C_2H_5Br]\,[Br] + k_b[C_2H_5Br_{wall}]\,[HBr_{wall}].$$

In the absence of analytical data on the bromine concentration, it is impossible to properly apply the stationary-state approximation. It is possible that the molecular reaction between bromine and ethylene might alter the concentration of the former substantially.

Since Agius and Maccoll have not investigated the effect of hydrogen bromide on the *n*-propyl bromide decomposition, examination must be confined to their kinetics data. A plot of first order "k" vs. $P_0^{\frac{1}{2}}$ in their Fig. 3 and plots of $p^{-\frac{1}{2}}$ vs. time in Fig. 5 indicate a purely 3/2 order for *n*-propyl bromide. Extrapolation of data on the purely

intramolecular decomposition of this compounds to 360° C. gives a value of $k = 0.3 \times 10^{-4}$ sec.$^{-1}$ (11). This small value has been lost in their rather large experimental error, but it is sufficiently large to be included in the rate expression:

$$r = k[C_3H_7Br] + k_1[C_3H_7Br]^{3/2}.$$

Their kinetics data are then not inconsistent with the same mechanism as has been proposed for ethyl bromide.

The observation of the catalytic effect of hydrogen bromide on this decomposition (7) completes the evidence that the decompositions of ethyl and *n*-propyl bromides are mechanistically identical. The mechanism proposed by Goldberg and Daniels is the more plausible for both compounds since it explains all of the experimental facts.

If this mechanism is correct, the theories advanced by Semenov (12) and by Maccoll and Thomas (1) to explain the difference in mechanisms of decomposition of *n*-propyl and isopropyl bromides must be modified to include the possibility of the rate of reaction between hydrogen bromide and the alkyl bromide being the mechanism-controlling factor.

1. MACCOLL, A. and THOMAS, P. J. J. Chem. Soc. 979 (1955).
2. MACCOLL, A. and THOMAS, P. J. J. Chem. Soc. 2445 (1955).
3. GREEN, J. H. S. and MACCOLL, A. J. Chem. Soc. 2449 (1955).
4. HARDEN, G. D. and MACCOLL, A. J. Chem. Soc. 2454 (1955).
5. SERGEEV, G. B. Doklady Akad. Nauk S.S.S.R. **106**, 299 (1956).
6. AGIUS, P. J. and MACCOLL, A. J. Chem. Soc. 973 (1955).
7. SEMENOV, N. N., SERGEEV, G. B., and KAPRALOVA, G. A. Doklady Akad. Nauk S.S.S.R. **105**, 301 (1955).
8. GOLDBERG, A. E. and DANIELS, F. J. Am. Chem. Soc. **79**, 1314 (1957).
9. BLADES, A. T. Can. J. Chem. **36**, 1043 (1958).
10. HIRSCHFELDER, J. O. J. Chem. Phys. **26**, 271 (1957).
11. BLADES, A. T. and MURPHY, G. W. J. Am. Chem. Soc. **74**, 6219 (1952).
12. SEMENOV, N. N. Izdatel'-stvo Akad. Nauk S.S.S.R. Moscow (1954).

RECEIVED MARCH 7, 1958.
RESEARCH COUNCIL OF ALBERTA,
EDMONTON, ALBERTA.

GASEOUS AND LIQUID STATES OF AGGREGATION IN THE SUPERCRITICAL REGION

F. G. SMITH

A considerable amount of geological theory of formation of mineral deposits is dependent on the properties of water at supercritical temperatures and/or pressures. Consequently, geochemists and economic geologists are interested in physical theories of supercritical fluids, and in experimental studies of heterogeneous systems containing one or more such fluids. For example, if the volume of a liquid phase is kept constant as the temperature and pressure are increased to values above the critical temperature, and it can be shown that thermodynamic functions are continuous and uninflected, then we can extrapolate chemical properties of the liquid state into the supercritical region. There is a controversy in the geochemical literature regarding the appropriate term for designating a supercritical fluid, but it seems to be preferable to call it a liquid if it has the thermodynamic properties of a liquid, and a gas, if it has those of a gas.

In a review of data on the state of supercritical fluids of geological interest (1), it was emphasized that the liquid state is not limited by the critical temperature, but is limited

Can. J. Chem. Downloaded from www.nrcresearchpress.com by 78.46.186.204 on 09/04/12
For personal use only.

intramolecular decomposition of this compounds to 360° C. gives a value of $k = 0.3 \times 10^{-4}$ sec.$^{-1}$ (11). This small value has been lost in their rather large experimental error, but it is sufficiently large to be included in the rate expression:

$$r = k[C_3H_7Br] + k_1[C_3H_7Br]^{3/2}.$$

Their kinetics data are then not inconsistent with the same mechanism as has been proposed for ethyl bromide.

The observation of the catalytic effect of hydrogen bromide on this decomposition (7) completes the evidence that the decompositions of ethyl and *n*-propyl bromides are mechanistically identical. The mechanism proposed by Goldberg and Daniels is the more plausible for both compounds since it explains all of the experimental facts.

If this mechanism is correct, the theories advanced by Semenov (12) and by Maccoll and Thomas (1) to explain the difference in mechanisms of decomposition of *n*-propyl and isopropyl bromides must be modified to include the possibility of the rate of reaction between hydrogen bromide and the alkyl bromide being the mechanism-controlling factor.

1. MACCOLL, A. and THOMAS, P. J. J. Chem. Soc. 979 (1955).
2. MACCOLL, A. and THOMAS, P. J. J. Chem. Soc. 2445 (1955).
3. GREEN, J. H. S. and MACCOLL, A. J. Chem. Soc. 2449 (1955).
4. HARDEN, G. D. and MACCOLL, A. J. Chem. Soc. 2454 (1955).
5. SERGEEV, G. B. Doklady Akad. Nauk S.S.S.R. **106**, 299 (1956).
6. AGIUS, P. J. and MACCOLL, A. J. Chem. Soc. 973 (1955).
7. SEMENOV, N. N., SERGEEV, G. B., and KAPRALOVA, G. A. Doklady Akad. Nauk S.S.S.R. **105**, 301 (1955).
8. GOLDBERG, A. E. and DANIELS, F. J. Am. Chem. Soc. **79**, 1314 (1957).
9. BLADES, A. T. Can. J. Chem. **36**, 1043 (1958).
10. HIRSCHFELDER, J. O. J. Chem. Phys. **26**, 271 (1957).
11. BLADES, A. T. and MURPHY, G. W. J. Am. Chem. Soc. **74**, 6219 (1952).
12. SEMENOV, N. N. Izdatel'-stvo Akad. Nauk S.S.S.R. Moscow (1954).

RECEIVED MARCH 7, 1958.
RESEARCH COUNCIL OF ALBERTA,
EDMONTON, ALBERTA.

GASEOUS AND LIQUID STATES OF AGGREGATION IN THE SUPERCRITICAL REGION

F. G. SMITH

A considerable amount of geological theory of formation of mineral deposits is dependent on the properties of water at supercritical temperatures and/or pressures. Consequently, geochemists and economic geologists are interested in physical theories of supercritical fluids, and in experimental studies of heterogeneous systems containing one or more such fluids. For example, if the volume of a liquid phase is kept constant as the temperature and pressure are increased to values above the critical temperature, and it can be shown that thermodynamic functions are continuous and uninflected, then we can extrapolate chemical properties of the liquid state into the supercritical region. There is a controversy in the geochemical literature regarding the appropriate term for designating a supercritical fluid, but it seems to be preferable to call it a liquid if it has the thermodynamic properties of a liquid, and a gas, if it has those of a gas.

In a review of data on the state of supercritical fluids of geological interest (1), it was emphasized that the liquid state is not limited by the critical temperature, but is limited

Can. J. Chem. Downloaded from www.nrcresearchpress.com by 78.46.186.204 on 09/04/12
For personal use only.

approximately by the critical volume in the supercritical region of temperature and pressure. X-Ray diffraction methods allow a positive discrimination between the two states of aggregation, but simpler procedures would be more useful.

The problem is simply that of showing whether the structure of the phase is more like the continuity in all dimensions characteristic of the ideal liquid state, or more like the discontinuity of the ideal gaseous state. Since an increase in the number of chemical bonds between components of a system involves a decrease of heat content and volume, thermodynamical expressions involving these terms can be used for discrimination. Mayer and Streeter (2) discussed the use of $\Delta H/\Delta T$ and $-\Delta V/\Delta P$ relations in locating phase transitions and in discriminating between anomalous first-order and diffuse transitions.

A related method that can be applied where PVT data are available consists of analyzing isobaric thermal expansion curves. Below the critical pressure, these curves have a first-order discontinuity at the boiling temperature, but above the critical pressure, they have a diffuse first-order discontinuity. The curve of dV/dT goes to $+\infty$ at the transition when the pressure is below the critical pressure, but goes to a finite value above it. The curve of d^2V/dT^2 goes through zero at the transition, both below and above the critical pressure.

In the one-component system H_2O, the above relations are shown at 200, 500, and 1000 bars in Fig. 1. The plotted curves were drawn through values of $\Delta V/10°$ calculated from experimental data by Kennedy (3). The characteristic curvatures of the dV/dT relation in the liquid and gaseous states, respectively, are clear, at least up to pressures of the order of 1000 bars. The temperature at which d^2V/dT^2 is zero is a function of the pressure, and is such that V is between 3.0 and 3.5 cc./g. In other words, the phase transition takes place in the supercritical region near, if not exactly at, the critical

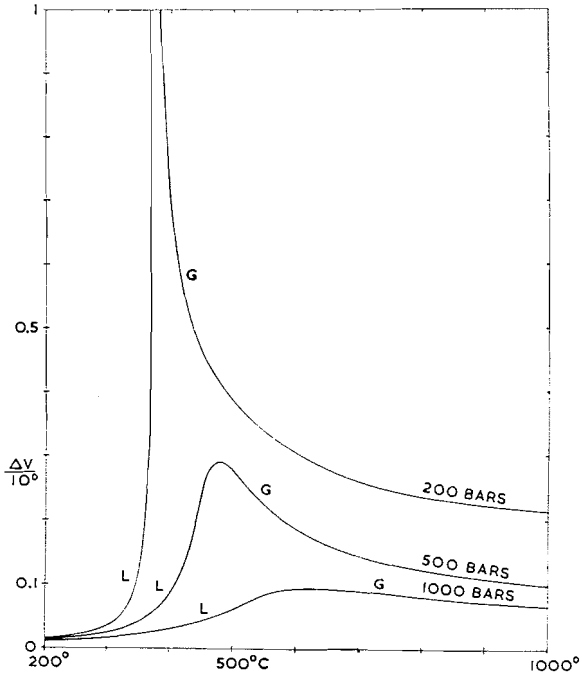

FIG. 1.

Can. J. Chem. Downloaded from www.nrcresearchpress.com by 78.46.186.204 on 09/04/12
For personal use only.

volume. There is no phase change at the critical temperature except in the special case when the pressure is exactly the critical value.

In summary, d^2V/dT^2 is positive in the liquid state and negative in the gas state, both below and above the critical pressure. In addition, the liquid–gas diffuse phase transition in the supercritical region is not at the critical temperature but near the critical volume.

1. SMITH, F. G. Econ. Geol. **48**, 14 (1953).
2. MAYER, J. E. and STREETER, S. F. J. Chem. Phys. **7**, 1019 (1939).
3. KENNEDY, G. C. Am. J. Sci. **248**, 540 (1950).

RECEIVED FEBRUARY 27, 1958.
DEPARTMENT OF GEOLOGICAL SCIENCES,
UNIVERSITY OF TORONTO,
TORONTO, ONTARIO.

Can. J. Chem. Downloaded from www.nrcresearchpress.com by 78.46.186.204 on 09/04/12
For personal use only.

Can. J. Chem. Downloaded from www.nrcresearchpress.com by 78.46.186.204 on 09/04/12
For personal use only.

Canadian Journal of Chemistry

Issued by THE NATIONAL RESEARCH COUNCIL OF CANADA

VOLUME 36 AUGUST 1958 NUMBER 8

ULTRASONIC ABSORPTION IN BUTYRIC ACID[1]

P. WHITE[2] AND G. C. BENSON

ABSTRACT

Ultrasonic absorption has been measured in pure butyric acid by a pulse technique from 0° to 40° C. and values of the relaxation frequency obtained. The activation energy of the relaxation process is shown to be 1.1 kcal./mole. These results are compared with published values for acetic and propionic acids and possible relaxation processes are discussed.

INTRODUCTION

Ultrasonic absorption measurements have been made in acetic and propionic acids over quite a wide range of temperature and at frequencies in the region of the relaxation frequency, but very little comparable information is available for other carboxylic acids. In the present paper, results are given for the absorption of ultrasound in pure butyric acid in a temperature range 0° C. to 40° C. and at frequencies from 1 to 9 Mc./second. A relaxation process has been shown to be present in acetic and propionic acids and until recently this was attributed to dimerization. Results obtained in acetic acid solutions have thrown doubt on this interpretation and it was thought that further experiments on carboxylic acids might help in deciding the mechanism of the relaxation process.

EXPERIMENTAL

Butyric acid was purified (1) and freshly distilled before use. The freezing points of samples used were in the range $-5.5°$ to $-5.7°$ C. measured using a Beckmann thermometer calibrated against a platinum resistance thermometer. Sound absorption measurements were carried out by a pulse technique at 1, 3, 5, 7, 9 Mc./second in an apparatus to be described in another publication (2).

RESULTS

Fig. 1 shows the measured value of attenuation in db./cm. with varying frequency at temperatures 0° C., 25° C., and 38.4° C. The absorption coefficient α was obtained from these values by dividing the ordinates of the graph by 8.686 (3).

For a single molecular process occurring with a relaxation time τ, the variation of absorption coefficient α with frequency ν is given by

$$\alpha = B\nu^2+[A\nu^2/\{1+(\nu/\nu_m)^2\}], \quad [1]$$

where A and B are constants and $\nu_m = 1/2\pi\tau$. Preliminary values of ν_m, A, and B were obtained by substitution of values of α at 1, 3, and 5 Mc./second in equation [1]. Further

[1]*Manuscript received April 1, 1958.*
Contribution from the Division of Pure Chemistry, National Research Council, Ottawa, Canada.
Issued as N.R.C. No. 4798.
[2]*National Research Council Postdoctorate Fellow 1956–58.*

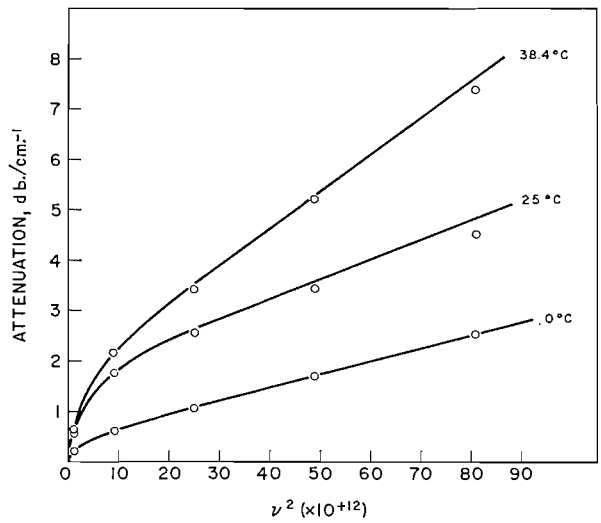

FIG. 1. Ultrasonic absorption in pure butyric acid. O—Experimental results. The solid lines were drawn using values shown in Table I.

refinement of the parameters ν_m, A, and B was carried out as described by Heasell and Lamb (4). Table I shows the values of ν_m, A, and B derived from this treatment. The solid lines in Fig. 1 were drawn using these values.

TABLE I

T, °C.	A (sec.^{2} cm.$^{-1}$) $\times 10^{17}$	B (sec.^{2} cm.$^{-1}$) $\times 10^{17}$	ν_m (sec.$^{-1}$) $\times 10^{-6}$
0	3850	300	1.13
25	9398	469	1.46
38.4	8528	804	1.64

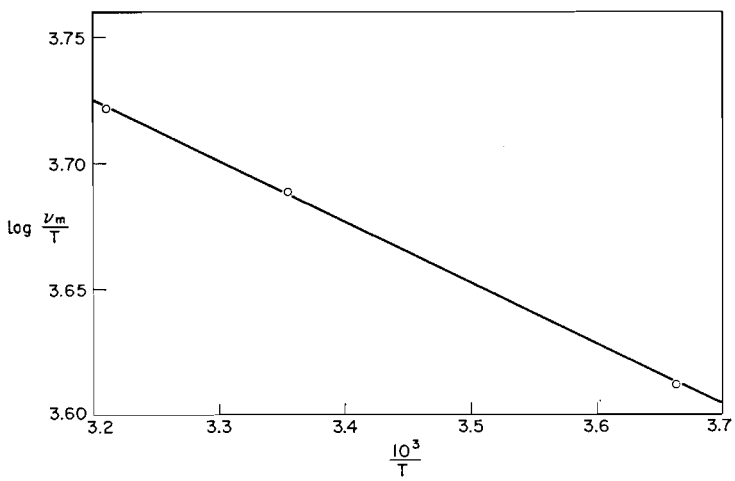

FIG. 2. Log(ν_m/T) plotted against $1/T$.

Can. J. Chem. Downloaded from www.nrcresearchpress.com by 78.46.186.204 on 09/04/12
For personal use only.

It is usual to assume that the relaxation time is given by an expression

$$\tau = (D/T) \exp(\Delta E_a/RT), \quad [2]$$

where D is a constant and ΔE_a the activation energy associated with the relaxation process. Fig. 2 shows a graph of $\log(\nu_m/T)$ against $1/T$ for butyric acid, the activation energy being $\Delta E_a = 1.11$ kcal./mole.

DISCUSSION

A comparison of the above ν_m and ΔE_a values with those already published for acetic and propionic acids (5, 6) is made in Table II. The values shown for acetic and propionic acids at 0° C. were obtained by extrapolation of $\log(\nu_m/T)$ against $1/T$ graphs. Since acetic acid is normally solid at 0° C., the value 0.18 must be regarded as that for the supercooled liquid.

TABLE II

	ν_m at 0° C. (Mc./s.)	ν_m at 25° C. (Mc./s.)	ν_m at 40° C. (Mc./s.)	ΔE_a (kcal./mole)
Acetic acid	[0.18]	0.725	1.48	8.5
Propionic acid	[0.60]	2.36	4.61	7.5
Butyric acid	1.13	1.46	1.67	1.11

Since the values of ν_m are similar for the three acids, it is possible that a similar molecular process is responsible for the relaxation in all these cases. However, the comparatively large variation in ΔE_a values between propionic and butyric acids is then difficult to understand. The results indicate that the activation energy for the process decreases as the chain length increases. It has been suggested (5, 6, 7, 8, 9) that dimerization or polymerization through hydrogen bonds was responsible for relaxation in acetic and propionic acids. Piercy and Lamb (10) recently concluded that the higher of the two relaxation frequencies ($\geqslant 15$ Mc./second) which they obtained in dilute acetic acid solutions was caused by relaxation of the monomer–dimer equilibrium. These authors suggest that the earlier work on acetic and propionic acids produces relaxation frequencies corresponding to perturbation of an equilibrium other than dimerization.

Although the results presented are interesting per se, it appears that further experiments must be conducted before the true mechanism of the relaxation process is known.

ACKNOWLEDGMENTS

We wish to thank Dr. W. G. Schneider for allowing us to use the ultrasonic equipment. We are also much indebted to Dr. Schneider and to Dr. J. E. Piercy for helpful discussions of this work and to Mr. D. Moule for technical assistance.

REFERENCES

1. VOGEL, A. I. J. Chem. Soc. 1814 (1948).
2. WHITE, P., MOULE, D., and BENSON, G. C. Trans. Faraday Soc. (In press).
3. VIGOUREUX, P. Ultrasonics. John Wiley & Sons, Inc., New York. 1951. p. 30.
4. HEASELL, E. L. and LAMB, J. Proc. Roy. Soc. (London), A, **237**, 233 (1956).
5. LAMB, J. and PINKERTON, J. M. M. Proc. Roy. Soc., A, **199**, 114 (1949).
6. LAMB, J. and HUDDART, D. H. A. Trans. Faraday Soc. **46**, 540 (1950).
7. SPAKOVSKIJ, B. G. Compt. rend. acad. sci. U.R.S.S. **18**, 173 (1938).
8. RICHARDS, W. T. Revs. Modern Phys. **11**, 36 (1939).
9. FREEDMAN, E. J. Chem. Phys. **21**, 1784 (1953).
10. PIERCY, J. E. and LAMB, J. Trans. Faraday Soc. **52**, 930 (1956).

Can. J. Chem. Downloaded from www.nrcresearchpress.com by 78.46.186.204 on 09/04/12
For personal use only.

Can. J. Chem. Downloaded from www.nrcresearchpress.com by 78.46.186.204 on 09/04/12
For personal use only.

NOTE ON THE RATE OF EVOLUTION OF HYDROGEN AT A MAGNESIUM ANODE[1]

J. H. GREENBLATT

ABSTRACT

Recent work on the mechanism of the anodic dissolution of magnesium is reviewed and additional data on the temperature dependence of the rate of hydrogen evolution at magnesium anodes during electrolysis is given. It is concluded that the results obtained and the literature on this subject are explained more logically by a kinetic mechanism involving initial solution of a univalent magnesium ion followed by subsequent reaction of this ion with water than by postulating self-corrosion with hydrogen evolved at local cathodes.

The problem of hydrogen evolution at a magnesium anode during electrolysis has received considerable attention recently (refs. 1–10) and it has been inferred from measurements of apparent valency and the ratio of reaction products that a kinetic mechanism postulating solution by a univalent ion followed by reaction of this ion with water satisfactorily accounts for the results (refs. 1–6). The basic mechanism put forward is the following (3).

$$Mg \rightarrow Mg^{+} + e \qquad [1]$$

$$2Mg^{+} + H_2O \rightarrow [Mg^{+}\,H_2O\,Mg^{+}] \rightarrow Mg^{++} + MgO + H_2 \qquad [2]$$

This mechanism explains in a logical manner the production of hydrogen and the one to one ratio between soluble and insoluble magnesium found when magnesium dissolves anodically in NaCl solutions (3). If the magnesium anode is being used in solutions containing reducible substances, such as perchlorates (1, 2), or if organic liquids that are electron acceptors are used as the anolyte (7), reduction products are obtained. The production of these can also be explained by the above mechanism.

A competing explanation to the kinetic mechanism is the assigning of the production of hydrogen and reduction products to local cathode activity as a result of self-corrosion on the magnesium anode (8, 9, 10). Although this would logically explain the production of these reduction products, it can only explain the one to one ratio of soluble to insoluble magnesium as a fortuitous event.

Recently Tomashov *et al.* (10) measured the rates of hydrogen evolution from anodes of cast technical (99.7%) magnesium and various other magnesium alloys at room temperature. They obtained a linear relation between the rate of hydrogen evolution and current density. In interpreting their findings, they ascribe the hydrogen evolution to self-corrosion and explain the linear relation as follows. Hydrogen is evolved at local cathodes that are filmed areas immediately adjacent to the active anode areas as the latter move forward during the solution process. This relates the amount of forward movement of the cathode surface to the movement of anodes over the surface as a result of dissolution of magnesium. Since the active surface is assumed proportional to the current density, the linear relationship is observed. Straumanis (8, 9) proposes an essentially similar mechanism involving the breakdown of the initial protective film with the uncovering of new cathodes. He devises a general equation for the "difference" effect, which simplifies to a linear relation between rate of hydrogen evolution and current density if the rate of formation of new cathodes is zero, or nearly so, if the overvoltage is constant and the polarization linear with current density.

[1]*Manuscript received March 12, 1958.*
Contribution from the Naval Research Establishment, Defence Research Board, Department of National Defence, Dartmouth, Nova Scotia.

The kinetic mechanism leads directly to a linear relation between the rate of hydrogen evolved and the current. If one assumes a steady state for which Mg^+ is being consumed as fast as it is produced and since $\frac{1}{2}$ mole of hydrogen gas is produced for each Mg^+ consumed, it is seen that

$$dH_2/dt = I/2F$$

is obtained, where I is the current and F the faraday.

In so far as Phelps (5) found by the rotogenerative technique that the anode areas on a corroding magnesium anode do not move over the surface as the current density is increased but merely become more intense, Tomashov's picture could be questioned. Also, the self-corrosion theory implies rate control as due to cathode area, which has been related to current density. At constant current density, or constant current, since Tomashov's work was done on samples all of the same area, rate control could be affected by other influences, such as temperature, which would affect the hydrogen overvoltage. Accordingly, rates of hydrogen evolution from anodes of pure (99.92%) magnesium and magnesium 1% manganese alloy were determined over the temperature range 0 to 75° C. to determine the effect of temperature and to determine if the temperature coefficient would give any further information as to the solution mechanism.

The rates were calculated from plots of gas evolved against time obtained by allowing the hydrogen evolved to expand into a partially evacuated volume with the pressure changes being continuously recorded. A 5% sodium chloride electrolyte was used and the cathode in the simple electrolysis cell was an Ag–AgCl electrode.

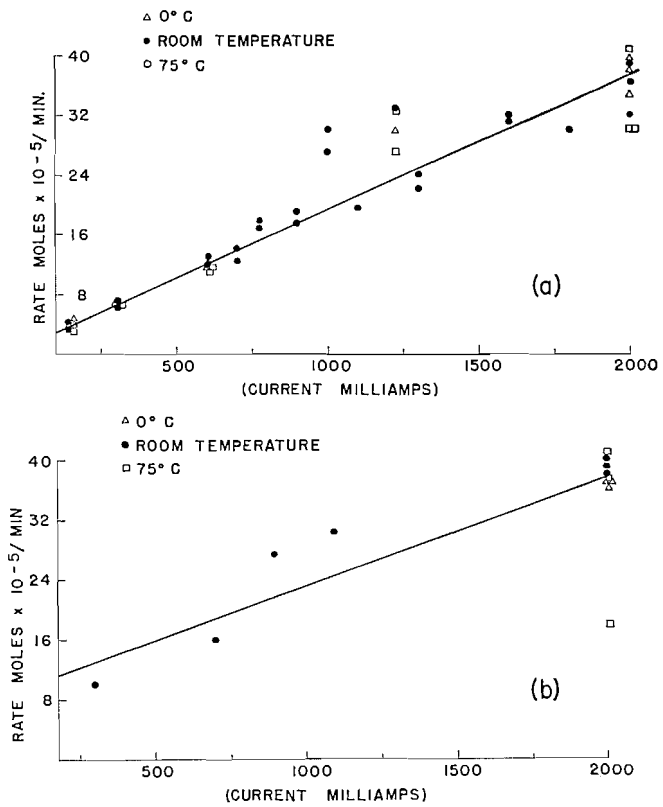

FIG. 1. Plot of the rate of evolution of hydrogen against current density for (*a*) pure magnesium and (*b*) magnesium 1% manganese alloy.

Can. J. Chem. Downloaded from www.nrcresearchpress.com by 78.46.186.204 on 09/04/12
For personal use only.

The electrode area in all cases was 23.8 cm.^{2}, and the current was varied over the range of 150 to 2000 ma. corresponding to a current density range of 0.0065 to 0.080 amp./cm.^{2}.

The results obtained are shown in Fig. 1. It is seen that at constant current (which is also equivalent to constant current density) the effect of temperature is negligible. This negligible temperature coefficient would be characteristic of the kinetic mechanism which involves essentially a free-radical mechanism, i.e., reaction between Mg^+ and water. A self-corrosion mechanism would be expected to yield a greater temperature difference because of variation of hydrogen overvoltage with temperature.

Thus, it would appear that again the kinetic mechanism explains more easily and straightforwardly the experimental results.

In passing, the rate values found agree well with Tomashov's. He lists values of 3.7, 7.3, and 16.8 ml. H_2/cm.^{2}/hr. at current densities of 10, 20, and 50 ma./cm.^{2} compared with 3.9, 7.4, and 16.1 ml. H_2/cm.^{2}/hr. at current densities of 12, 24, and 47 ma./cm.^{2}.

ACKNOWLEDGMENTS

The work reported constitutes part of Defence Research Board Project D-12-75-10-21. The author acknowledges permission of the Defence Research Board of Canada to publish. The author also acknowledges the help of Mr. W. Ritcey, who carried out the laboratory work and analysis.

REFERENCES

1. EPELBOIN, I. and FROMENT, M. Compt. rend. **238**, 2416 (1954); **239**, 1795 (1954). Colloq. intern. centre natl. recherche sci. (Paris), No. 73 (1956).
2. EPELBOIN, I. Z. Elektrochem. **59**, 689 (1955).
3. GREENBLATT, J. H. Electrochem. Soc. **103**, 539 (1956).
4. MORTON, J. M. Private communication.
5. PHELPS, S. E. H. Doctor of Philosophy Thesis, Case Institute of Technology, Cleveland, Ohio. 1955.
6. PETTY, R. L., DAVIDSON, A. W., and KLEINBERG, J. J. Am. Chem. Soc. **76**, 363 (1954).
7. RAUSCH, M. D., MCEWEN, W. E., and KLEINBERG, J. J. Am. Chem. Soc. **77**, 2093 (1955).
8. STRAUMANIS, M. E. and WANG, Y. N. J. Electrochem. Soc. **102**, 304 (1955).
9. STRAUMANIS, M. E. Uncommon valency and the difference effect. Presented at the Meeting of the Electrochemical Society, May 1957.
10. TOMASHOV, N. D., KOMMISSAROVA, V. S., and TIMONOVA, M. A. Trudy Inst. Fiz. Khim. Akad. Nauk S.S.S.R. Isseldovan Korrozii Metal, **172**, 97 (1955).

Can. J. Chem. Downloaded from www.nrcresearchpress.com by 78.46.186.204 on 09/04/12
For personal use only.

ANIONIC POLYMERIZATION OF α-METHYLSTYRENE

PART II. KINETICS[1,2]

D. J. WORSFOLD AND S. BYWATER

ABSTRACT

Dilatometric measurements have been made of the reaction rates in the reversible equilibrium anionic polymerization of α-methylstyrene initiated by sodium naphthalene in tetrahydrofuran solution, at temperatures of −10°, −40°, and −77°. The kinetic results and measurements made of the viscosity of the polymer conform with the mechanism of the reaction proposed by Szwarc *et al.*, modified by the large degree of reversibility found with this monomer at these temperatures.

The mechanism of the polymerization of certain vinyl hydrocarbons initiated by the complexes of sodium with polynuclear aromatic hydrocarbons in solution in some aliphatic ethers has recently been proposed by Szwarc *et al.* (1). They visualize an initial donation of an electron to the monomer followed by rapid dimerization of the radical ion formed to give a dicarbanion capable of growth by repeated monomer addition at both ends. In suitable solvents these carbanions are stable and no termination occurs and the chain ends remain active after the monomer has been consumed.

This latter property was made use of in demonstrating the reversible nature of the propagation step of polymerization (2). All polymers produced under these conditions should have a certain concentration of monomer in equilibrium with the active chain end (3), but in the case of α-methylstyrene this reaches appreciable amounts, even below room temperature, and profoundly changes the behavior of the system. It has been proposed that the chains are initiated rapidly and grow comparatively slowly at the expense of the monomer until the latter is reduced to its equilibrium concentration when the rate of the bimolecular forward reaction equals that of the unimolecular depolymerization. From such a scheme it is easily shown that the approach of the monomer concentration to the equilibrium concentration will, as a close approximation, follow a kinetic law first order in the initiator concentration and at a rate proportional to the excess concentration of the monomer over the equilibrium value. The polymerization of this monomer has a half-life time of the order of minutes, as opposed to seconds for other monomers, so it has been found convenient to make some kinetic measurements on this system to see if they are in accord with the scheme outlined above.

EXPERIMENTAL

The purification of the solvent (tetrahydrofuran) and the monomer have been described before (3). The method adopted for measuring the rates was dilatometric using an annulus-shaped dilatometer to minimize, as far as possible, the temperature effects inherent in reactions of this speed. The dilatometer and adjacent mixing vessel were evacuated, and the monomer and solvent condensed into the mixing vessel. The catalyst solution was formed from naphthalene solution on a sodium film under vacuum in an attached vessel. This solution was introduced into the mixing vessel by breaking a finely drawn tip by rotation of a ground joint after temperature equilibrium had been established. The reaction solution was then forced into the dilatometer under purified

[1]*Manuscript received March 17, 1958.*
Contribution from the Division of Applied Chemistry, National Research Council of Canada, Ottawa, Canada. Issued as N.R.C. No. 4800.
[2]*Part I, see reference 3.*

Can. J. Chem. Downloaded from www.nrcresearchpress.com by 78.46.186.204 on 09/04/12
For personal use only.

nitrogen (3) and the dilatometer closed by a stopcock. The contraction was measured with a mercury thread in a calibrated tube. The catalyst concentration was measured at the end of the reaction in a Fisher Electrophotometer using the dilatometer as the optical cell. The filter used had a transmission maximum at 560 mμ. A separate calibration established that Beer's Law was obeyed over the concentration range used.

Two methods were employed in the calibration of optical density against catalyst concentration. In the first, a concentrated solution of sodium naphthalene of known concentration was added in small portions from a small burette to a solution of α-methylstyrene contained in a vessel incorporating the optical cell. A small initial blank was found due to trace impurities and subtracted from the subsequent additions; the whole operation was performed under vacuum. In the second method, the vessel incorporating the optical cell was attached by means of break seals to a small vessel containing sodium naphthalene solution, another containing monomer, a longer graduated tube containing a solution of the polymer anions, and one further side vessel directly joined in which sodium naphthalene solution was made. First the solution of sodium naphthalene was rinsed all round the vessel containing the cell. It was then drained back into the side vessel and the main body rinsed by condensing the solvent into it and allowing it to drain back. When the vessel was clean, the side arm was frozen and sealed off and removed. Next, the seal to the catalyst solution was broken and the catalyst rinsed into the main vessel and then this side arm was removed. The seal to the monomer was then broken and this distilled in. Knowing all the volumes and concentrations involved, the concentration of polymer anions was known, and the optical density was measured. The solution was then diluted by distilling solvent into the solution from the graduated side tube, and the optical density found over a range of concentration.

RESULTS

As expected, each individual run was pseudo first order up to 3 half-life times, some tailing off was observed in some runs after 90% reaction. Some typical first-order plots are shown in Fig. 1. The measurements were made at three temperatures, −10°, −40°, −77°, using in the first two a glycol–water thermostat (3), in the last a dry ice – acetone slush.

The dependence of the pseudo first-order rate constant on initiator concentration at −40° is shown in Fig. 2, and appears linear with a small intercept on the rate axis. This intercept is consistent with a small amount of catalyst destruction in raising the temperature from −40° to 25°, at which the optical readings were made, the reactive polymer chain end being extremely sensitive to trace impurities. On the other hand the effect may be real and due to variations in the activity of the ionic chain ends at their relatively high ionic concentration in a solvent of such low polarity.

The rates found at the other two temperatures are shown in Table I. The constant k is calculated from the expression

$$-d[\text{monomer}]/dt = k[\text{initiator}]\{[\text{monomer}]-[\text{monomer}]_e\},$$

where $[\text{monomer}]_e$ is the equilibrium concentration. The rate constants at the three temperatures do not give a good Arrhenius plot but demonstrate that the apparent activation energy, which in this case should correspond to that of the propagation step of polymerization, is of the order of 2 to 3 kcal.

In studies of the sodium naphthalene initiated polymerization of styrene and of butadiene, Szwarc *et al.* (4) have established that a linear relationship between the logarithms

Can. J. Chem. Downloaded from www.nrcresearchpress.com by 78.46.186.204 on 09/04/12
For personal use only.

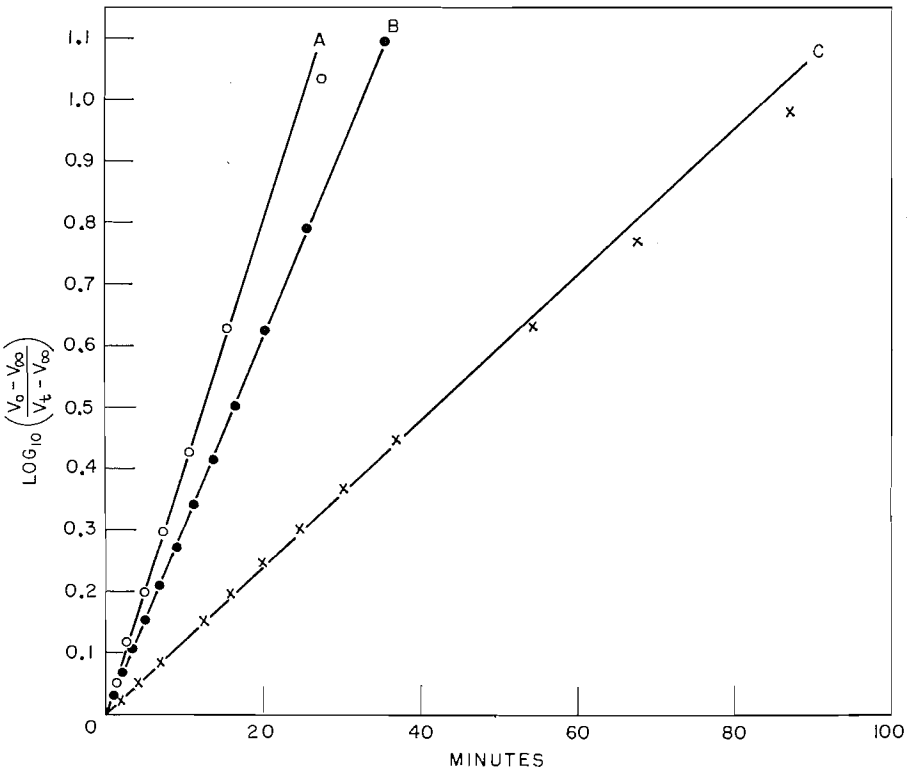

FIG. 1. Typical pseudo first-order plots at −40° C. Catalyst concentration, A = 1.53×10^{-3}, B = 1.01×10^{-3}, C = 0.25×10^{-3}.

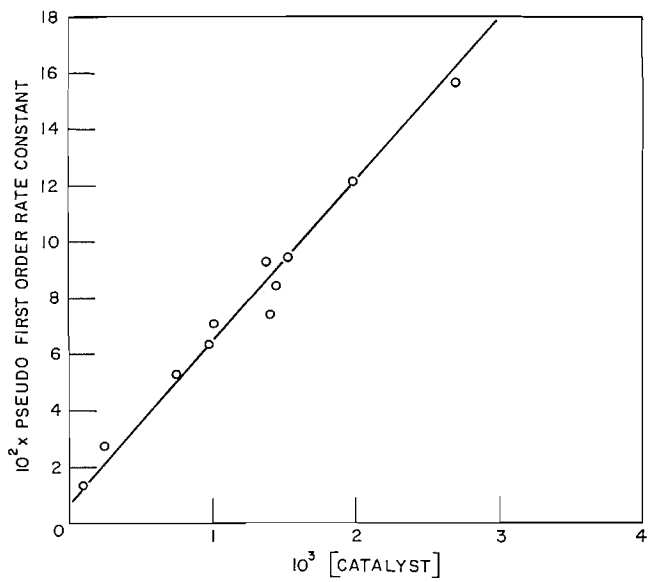

FIG. 2. Variation of pseudo first-order rate constant with catalyst concentration at −40° C.

Can. J. Chem. Downloaded from www.nrcresearchpress.com by 78.46.186.204 on 09/04/12
For personal use only.

TABLE I

PSEUDO FIRST-ORDER RATE CONSTANTS

Temp., ° C.	Catalyst concn., $\times 10^4$ moles liter^{-1}	k, liter mole^{-1}min.$^{-1}$
−10	11.8	84.5
−10	12.2	96.3
−10	13.9	85.3
−10	16.8	82.2
−10	23.6	74.1
−10	24.8	69.1
−77	16.4	20.6
−77	26.5	16.4
−77	28.2	11.2
−77	31.2	12.7
−77	50.2	14.1

of the ratio [monomer]/$\frac{1}{2}$[catalyst] and the intrinsic viscosity of the resulting polymer is achieved. This is due to the fact that the above ratio should be equivalent to the polymer chain length on the scheme suggested. The usefulness of this relation for determining molecular weights of sharply fractionated polymer samples is largely dependent on the sharp Poisson type distribution expected for the molecular weight distribution when the depolymerization reaction is not important, which for most monomers is normally true. For α-methylstyrene these conditions are more difficult to achieve because of the early onset of the depropagation reaction at temperatures above about −50° C. The calculated distribution for the equilibrium system diverges considerably from the Poisson type, and large divergences have been found for this monomer, at temperatures around 0° C.

In order to establish the Szwarc relationship, the reaction mixture, about molar in monomer and with variable catalyst, was mixed at 25°. This is above the ceiling temperature for this concentration and so no polymerization should occur. The catalyst

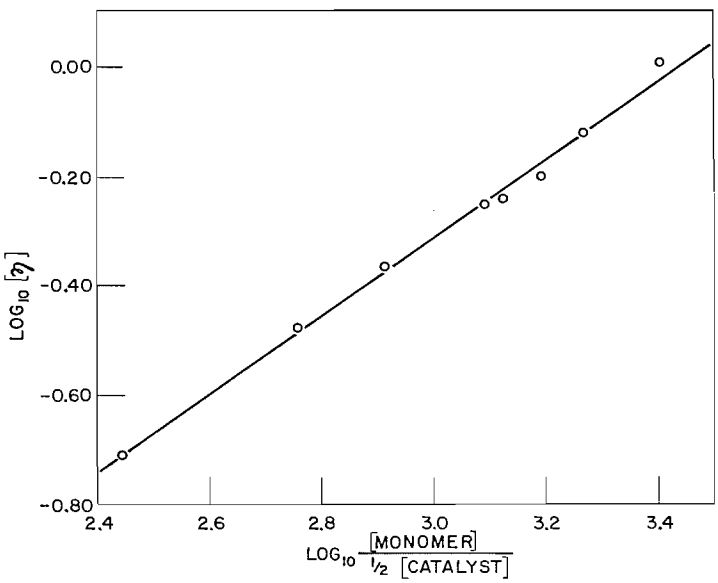

FIG. 3. Variation of intrinsic viscosity with calculated degree of polymerization.

Can. J. Chem. Downloaded from www.nrcresearchpress.com by 78.46.186.204 on 09/04/12
For personal use only.

concentration was found from the optical density, and then the reaction mixture placed in a bath at −80° C. The cooling should be rapid compared with the rate of polymerization, and at this temperature the reaction should be over 99% complete, and the resulting polymer should have a very sharp distribution. The reaction was killed after 7 half-life times with methanol at which point the influence of the depropagation should be small. The results are shown in Fig. 3 and are defined by $[\eta] = 1.16 \times 10^{-4}$ mol. wt.$^{0.714}$ by the method of least squares.

The kinetics of polymerization of α-methylstyrene catalyzed by sodium naphthalene appear therefore to conform to the scheme of Szwarc *et al.* (1) modified by the occurrence of a simultaneous depropagation reaction. The suggestion that the polymer chains grow by simultaneous addition of monomer to both ends of the chain is confirmed by preliminary results obtained in these laboratories which suggest that a very similar relationship is obtained between $[\eta]$ and molecular weight determined by light scattering and osmotic pressure measurements. Hence, the ratio Δ[monomer]/$\frac{1}{2}$[catalyst] does appear to correspond to the polymer chain length.

REFERENCES

1. SZWARC, M. Nature, **178**, 1168 (1956). SZWARC, M., LEVY, M., and MILKOVITCH, R. J. Am. Chem. Soc. **78**, 2656 (1956).
2. DAINTON, F. S. and IVIN, K. J. Nature, **162**, 705 (1948).
3. WORSFOLD, D. J. and BYWATER, S. J. Polymer Sci. **26**, 299 (1957).
4. WAUCK, R., REMBAUM, A., COOMBES, J. D., and SZWARC, M. J. Am. Chem. Soc. **79**, 2026 (1957). BRODY, H., LADACKI, M., MILKOVITCH, R., and SZWARC, M. S. J. Polymer Sci. **25**, 221 (1957).

Can. J. Chem. Downloaded from www.nrcresearchpress.com by 78.46.186.204 on 09/04/12
For personal use only.

Can. J. Chem. Downloaded from www.nrcresearchpress.com by 78.46.186.204 on 09/04/12
For personal use only.

LYCOPODIUM ALKALOIDS

VII. THE REACTION OF ANNOTININE WITH PHENYL LITHIUM[1]

G. S. PERRY,[2] DAVID B. MACLEAN, AND R. H. F. MANSKE[3]

ABSTRACT

Annotinine, $C_{16}H_{21}O_3N$, reacted with phenyl lithium to yield diphenylannotinine, $C_{23}H_{33}O_3N$, containing two hydroxyl functions. Oxidation of diphenylannotinine by the Oppenauer procedure yielded a monohydroxyketone, $C_{28}H_{31}O_3N$, while oxidation with chromic acid yielded a dihydroxyketone, $C_{28}H_{31}O_4N$. A mechanism for the formation of these compounds is discussed in relation to the chemistry of annotinine.

Annotinine, $C_{16}H_{21}O_3N$, is known to contain an epoxide function, a lactone ring, and a tertiary nitrogen atom (1). The relationship of these groups to one another has been demonstrated by Wiesner *et al.* (2) and by MacLean and Prime (3). This relationship is represented in the partial formula below.

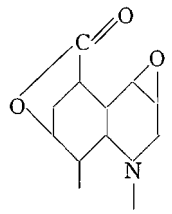

The structure of annotinine is now known (4, 5) but for the purposes of this paper the partial structure above suffices.

Some years ago we found that annotinine reacted readily with phenyl lithium to form diphenylannotinine, $C_{28}H_{33}O_3N$ (I), which was isolated at that time in an amorphous state. Diphenylannotinine did not dehydrate readily as would be expected of a diphenylcarbinol nor did it show any reactions characteristic of a compound containing an epoxide function. Our formula also differed from that of Meier and Marion (6), who proposed the formula $C_{28}H_{35}O_4N$ for the product of reaction of annotinine with phenyl lithium. Because of the anomalous behavior of diphenylannotinine and because of the difference between our results and those of Meier and Marion, we have investigated the reaction more thoroughly.

We have now obtained diphenylannotinine in crystalline form. This compound has a pronounced tendency to solvate, which may explain the formula of Meier and Marion and the difficulty in obtaining good analytical results for the base. Drastic oxidation of diphenylannotinine yielded traces of benzophenone, which indicated that both phenyl residues were attached to the same carbon atom. Oxidation by the Oppenauer procedure using potassium tertiary butoxide or aluminum isopropoxide yielded the monohydroxyketone, $C_{28}H_{31}O_3N$ (II). Both I and II were oxidized by chromic acid in acetic acid to the dihydroxyketone, $C_{28}H_{31}O_4N$ (III), which is apparently identical with the product iso-

[1]*Manuscript received in original form September 12, 1957, and, as revised, April 24, 1958.*
Contribution from the Burke Chemical Laboratories, Hamilton College, McMaster University, Hamilton, Ontario, and the Research Laboratories, Dominion Rubber Co. Ltd., Guelph, Ontario. Part of this work was taken from a thesis submitted by G. S. Perry to the Faculty of Graduate Studies in partial fulfillment of the requirements for the degree of Master of Science.
[2]*Present address: Department of Chemistry, Imperial College, London.*
[3]*Director of Research, Dominion Rubber Co. Ltd., Guelph, Ontario.*

lated by Meier and Marion (6). Compounds I, II, and III analyzed for two, one, and two active hydrogens respectively. Neither I, II, nor III underwent reactions typical of a compound containing an epoxide function. Prolonged treatment of I, II, or III with boiling concentrated hydrochloric acid or alkali resulted in the recovery of starting material. Compound I was unaffected by further treatment with phenyl lithium or with lithium aluminum hydride in ether or tetrahydrofuran. It seemed apparent therefore that the epoxide function was no longer present in the molecule and in some way it must have been destroyed in the reaction with phenyl lithium.

A plausible explanation of these results is offered in the sequence represented below:

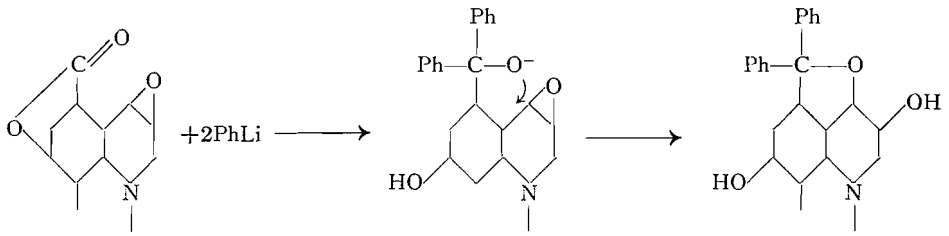

I

The formation of a new tetrahydrofuran ring results from nucleophilic attack of the intermediate tertiary alkoxide ion on the epoxide ring to yield a dihydroxy compound. This structure explains the lack of reactivity toward hydrochloric acid both as an addend to an epoxide ring and as dehydration agent toward a diphenylcarbinol. The oxidation by the Oppenauer procedure to give a single carbonyl group is not without precedent. Annotinine hydrate, which has hydroxyl groups in positions 3 and 7, yields only a C_7 ketone (2). The chromic acid oxidation is more unusual, for in this case a fourth oxygen is introduced. The fourth oxygen is apparently present as an hydroxyl group and could only be introduced at an activated position in the molecule. An indication that the carbonyl group provided the activation was afforded by a study of the behavior of acetylated diphenylannotinine toward the action of chromic acid. The acetylated compound was not affected by the oxidant under reaction conditions similar to those which oxidized diphenylannotinine. The infrared absorption spectrum of II and III tends to support the proposition that III is an α-hydroxyketone. The carbonyl absorption of II was at 1706 cm.$^{-1}$ while in III the absorption was at 1722 cm.$^{-1}$. A shift in this direction and of this magnitude is consistent with an α-hydroxyketone structure with the hydroxyl group in an axial conformation relative to the carbonyl. Compounds II and III are therefore assigned the following structures:

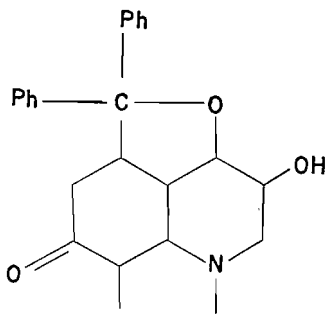

II

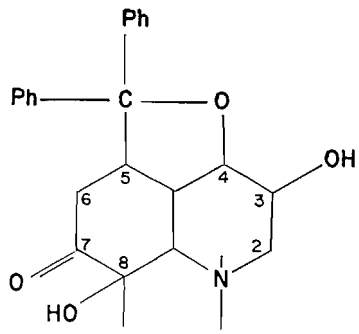

III

Can. J. Chem. Downloaded from www.nrcresearchpress.com by 78.46.186.204 on 09/04/12
For personal use only.

Position "8" is favored over position "6" as the site of the new hydroxyl function because the hydroxyl is obviously tertiary, and Wiesner *et al.* (4) have shown that position "6" is a methylene group in annotinine.

Diphenylannotinine failed to undergo elimination of its diphenylcarbinol grouping on treatment with potassium tertiary butoxide and it yielded the same ketone on treatment with potassium tertiary butoxide or aluminum isopropoxide in the presence of cyclohexanone. This contrasts with the behavior of diphenyldesoxodihydroannotinine (7). This difference in reactivity in the two series may be the result of the greater rigidity of the ring system imposed by the new tetrahydrofuran ring in diphenylannotinine.

EXPERIMENTAL

Diphenylannotinine

A solution of phenyl lithium, prepared from 1.2 g. lithium and 14.5 g. bromobenzene in 100 ml. of anhydrous ether, was treated over a period of 15 minutes with 3.0 g. of annotinine in 70 ml. of ether–benzene. The initial precipitate of a white solid soon disappeared and the mixture was refluxed for 1½ hours after the addition of annotinine. The mixture was decomposed in ice water, the organic layer separated, and the aqueous layer extracted with several portions of fresh ether. The combined extract was dried and concentrated. The residue was dissolved in benzene, adsorbed on alumina, and eluted with benzene until no more diphenyl, a by-product, was obtained. The column was then eluted with two volume per cent methanol in benzene. From this eluate 5.0 g. of a pale yellow residue was recovered which crystallized from benzene. The recovered crystals possessed a double melting point at 128° and 236° C., neither of which was particularly sharp. These crystals were apparently highly solvated, since they lost 21% of their weight on drying at 118° C. at 0.5 mm. The dried crystals, which were submitted for analysis, melted at 236° C. Calc. for $C_{28}H_{33}O_3N$: C, 77.93; H, 7.71; N, 3.25; act. H (2), 0.46. Found: C, 78.85, 78.83; H, 7.65, 7.69; N, 3.30; act. H, 0.56, 0.58%.

Recrystallization of the above sample from ether yielded a compound which had a single sharp melting point at 236°. Found: C, 77.97, 77.99; H, 7.68, 7.70%.

The infrared spectrum (nujol) contained a strong band in the hydroxyl region at 3400 cm.$^{-1}$ but only weak absorption in the aromatic region at 1600 cm.$^{-1}$. In carbon bisulphide there were two absorption bands in the hydroxyl region at 3603 cm.$^{-1}$ and 3460 cm.$^{-1}$. The three typical bands for a monosubstituted benzene were found at 3080 cm.$^{-1}$, 3052 cm.$^{-1}$, and 3021 cm.$^{-1}$.

The hydrochloride was prepared by the addition of concentrated aqueous hydrochloric acid to an acetone solution of the base from which it immediately crystallized. Recrystallization from acetone–methanol yielded a compound melting at 292–293° C. This compound was apparently a very stable hydrate and gave satisfactory analytical results only after drying over boiling xylene for 1 hour. Calc. for $C_{28}H_{33}O_3N.HCl$: C, 71.87; H, 7.27%. Found: C, 71.84, 71.51; H, 7.40, 7.27%.

The original base was regenerated from the salt by treating an aqueous suspension of the salt with ammonia and extracting with ether.

The methiodide of diphenylannotinine was prepared by heating under reflux, for 6 hours, a mixture of diphenylannotinine and methyl iodide in acetone. The crystals which separated on cooling were filtered from the mother liquor and recrystallized from ethanol. They melted at 257° C. with decomposition. Calc. for $C_{29}H_{33}O_3NI$: C, 60.73; H, 6.28%. Found: C, 60.77, 60.98; H, 6.17, 6.37%.

Diphenylannotinine was recovered unchanged after prolonged treatment with boiling

Can. J. Chem. Downloaded from www.nrcresearchpress.com by 78.46.186.204 on 09/04/12
For personal use only.

concentrated hydrochloric acid, with phenyl lithium in ether, and with lithium aluminum hydride in ether.

Oxidation of Diphenylannotinine with Chromic Acid

A solution of 0.7 g. of diphenylannotinine in 3 ml. of glacial acetic acid was mixed with a solution of 0.4 g. of chromic acid anhydride in 5 ml. of glacial acetic acid containing just enough water to effect solution. There was an immediate separation of a dark brown sludge, which soon dissolved, whereupon the mixture was poured into excess ammonia in 100 g. of ice and exhaustively extracted with chloroform. The combined chloroform extracts were dried, filtered through a pad of alumina, and taken to dryness to yield 0.38 g. of a viscous yellow oil which crystallized in contact with methanol. After several recrystallizations from methanol, the compound consisted of fine needles which melted at 242° C. Calc. for $C_{28}H_{33}O_4N$: C, 75.15; H, 7.43; N, 3.13; act. H (2), 0.44%. Found: C, 75.60, 75.36; H, 7.05, 6.81; N, 3.49; act. H, 0.42, 0.48%.

The infrared absorption spectrum (nujol) had a band in the carbonyl region at 1722 cm.$^{-1}$ and in the hydroxyl region at 3300 cm.$^{-1}$.

The starting material was recovered after treatment of this compound with boiling concentrated hydrochloric acid or alcoholic potassium hydroxide. Acetic anhydride converted this substance into an acetate from which the original base was recovered upon alkaline hydrolysis.

Oppenauer Oxidation of Diphenylannotinine

Diphenylannotinine, 1.0 g., was added to a suspension of 0.6 g. of potassium tertiary butoxide in an anhydrous mixture of 3.0 g. of cyclohexanone and 35 ml. of toluene. The mixture, which became bright yellow, was refluxed for $\frac{1}{2}$ hour. The mixture was cooled, poured on ice, the organic layer separated, and the aqueous layer extracted several times with toluene. The combined toluene extracts were extracted with three 25-ml. portions of 10% hydrochloric acid. The combined acid extracts were washed once with ether, then basified with ammonia, and exhaustively extracted with chloroform. The combined chloroform extracts were dried, concentrated, and then adsorbed on a column of alumina. Elution with two volume per cent methanol in chloroform yielded, after evaporation of the solvent, 0.61 g. of a crystalline product. After recrystallization from methanol it melted at 244–245° C. A mixture of this with the oxidation product derived from chromic acid treatment was completely liquid at 213° C. Calc. for $C_{28}H_{31}O_3N$: C, 78.29; H, 7.28; N, 3.26; act. H (1), 0.27. Found: C, 77.84, 77.81; H, 7.42, 7.45; N, 3.04, 3.02; act. H, 0.23%.

The infrared absorption spectrum (nujol) had a strong band in the carbonyl region at 1706 cm.$^{-1}$ and weak hydroxyl absorption at 3300 cm.$^{-1}$. In carbon bisulphide there was a single band in the hydroxyl region at 3595 cm.$^{-1}$.

This compound was unaffected after prolonged treatment with boiling aqueous hydrochloric acid.

Oxidation with aluminum isopropoxide as catalyst and cyclohexanone as the hydrogen acceptor also yielded compound II above.

Oxidation of $C_{28}H_{31}O_3N$ with Chromic Acid

To a solution of 0.8 g. of compound II in 5 ml. of glacial acetic acid there was added a solution of 0.7 g. of chromic acid anhydride in 8.0 ml. of glacial acetic acid containing just enough water to effect solution. After 5 minutes the reaction mixture was poured into excess ammonia in ice and extracted with chloroform. The dried extracts were filtered

Can. J. Chem. Downloaded from www.nrcresearchpress.com by 78.46.186.204 on 09/04/12
For personal use only.

through a pad of alumina and then concentrated to yield 600 mg. of a viscous oil which crystallized in contact with methanol. After several recrystallizations from methanol it melted at 241–242° C.; a mixture of this with the starting material was completely liquid at 219° C. while a mixed melting point determination with III showed no depression. The infrared spectra of III and this product were identical.

Acetylation of Diphenylannotinine and Its Attempted Oxidation with Chromic Acid

A solution of 0.5 g. of diphenylannotinine in 10 ml. of acetic anhydride was refluxed for 2 hours, cooled, and shaken with ice water to hydrolyze excess acetic anhydride. The solution was then made alkaline with sodium hydroxide and exhaustively extracted with chloroform. The dried extracts were concentrated, adsorbed on a column of alumina, and the column was eluted with chloroform to yield 0.300 g. of a glassy solid which failed to crystallize. The compound was very soluble in ether and petroleum ether. Its infrared spectrum had no bands in the hydroxyl region but contained strong bands in the acetyl region at 1746 $cm.^{-1}$ and at 1240 $cm.^{-1}$.

The above compound 0.27 g. was dissolved in glacial acetic acid and treated with chromic acid in the manner described previously. After 10 minutes the excess chromic acid was destroyed and the solution was worked up in the usual fashion. The recovered product, 0.2 g., had an infrared spectrum identical with that of the starting material.

The product from chromic acid treatment was hydrolyzed with aqueous alcoholic alkali to yield diphenylannotinine identified by its infrared spectrum.

Oxidation of Diphenylannotinine with Potassium Dichromate in Sulphuric Acid

Diphenylannotinine (1.5 g.) was added to a mixture of 5.0 g. of potassium dichromate in 20 ml. of 50% sulphuric acid. The mixture was directly steam-distilled until oily droplets no longer appeared in the distillate. Water was added continuously throughout the distillation to maintain the original concentration. The distillate was ether-extracted, the extracts dried, and concentrated to yield 30 mg. of residue. The residue was partitioned between ether and aqueous sodium bicarbonate. The ether layer yielded a viscous yellowish oil which had an infrared spectrum identical with that of benzophenone. The oil was treated with a hot solution of 2,4-dinitrophenylhydrazine to yield a yellow solid which melted at 231–235° and did not depress the melting point of authentic benzophenone 2,4-dinitrophenylhydrazone. The infrared spectra of the two hydrazones were identical.

The bicarbonate phase yielded, after acidification and extraction, benzoic acid identified by its melting point and mixed melting point with an authentic sample.

The acidic solution in the reaction mixture was basified with ammonia and extracted with chloroform. From the chloroform extracts there was isolated 20 mg. of a compound identical with III.

ACKNOWLEDGMENTS

This work was supported at McMaster University through grants from the National Research Council and the Ontario Research Foundation.

REFERENCES

1. MANSKE, R. H. F. and MARION, L. J. Am. Chem. Soc. **69**, 2126 (1947).
2. VALENTA, Z., STONNER, F. W., BANKIEWICZ, C., and WIESNER, K. J. Am. Chem. Soc. **78**, 2867 (1956).
3. MACLEAN, D. B. and PRIME, H. C. Can. J. Chem. **31**, 543 (1953).
4. WIESNER, K., AYER, W. A., FOWLER, L. R., and VALENTA, Z. Chem. & Ind. 564 (1957).
5. PRZYBYLSKA, M. and MARION, L. Can. J. Chem. **35**, 1075 (1957).
6. MEIER, H. L. and MARION, L. Can. J. Chem. **32**, 280 (1954).
7. BETTS, E. E. and MACLEAN, D. B. Can. J. Chem. **36**, 473 (1958).

Can. J. Chem. Downloaded from www.nrcresearchpress.com by 78.46.186.204 on 09/04/12
For personal use only.

Can. J. Chem. Downloaded from www.nrcresearchpress.com by 78.46.186.204 on 09/04/12
For personal use only.

A SPECTROPHOTOMETRIC DETERMINATION OF RHODIUM WITH TIN (II) BROMIDE[1]

S. S. Berman and R. Ironside

ABSTRACT

Rhodium salts react with a solution of tin (II) bromide in hydrobromic acid to produce an intense yellow color suitable for a spectrophotometric determination of rhodium. The method described is relatively simple and is the most sensitive for this metal published to date. Several factors influencing the intensity and stability of the colored species, whose nature is unknown, are described. Since the other platinum metals and base metals interfere it is necessary to isolate the rhodium prior to its determination. However, a fair estimation of rhodium can be made even when equivalent quantities of iridium are present. The procedure may be adapted, with a small loss in sensitivity, to determine rhodium in solutions which have been fumed with sulphuric acid.

INTRODUCTION

Relatively few spectrophotometric procedures have been proposed for the determination of rhodium. Of the four methods that have been developed usefully, the most satisfactory from the point of view of stability and tolerance of diverse ions is that employing tin (II) chloride as the reagent. This method, first noted in 1913 (1) and recently re-examined by several researchers (2, 3), suffers from a lack of sensitivity, an important drawback with regard to rhodium, which in all known commercial deposits of the platinum metals is present in relatively small proportions. The most sensitive method, employing sodium

TABLE I

Sensitivity of spectrophotometric methods for rhodium

Method	Molar extinction coefficient
Tin (II) chloride (2)	3.9×10^3
2-Mercaptobenzoxazole (5)	4.1×10^3
2-Mercapto-4,5-dimethylthiazole (6)	1.2×10^4
Sodium hypochlorite (4)	1.5×10^4
Tin (II) bromide	2.9×10^4

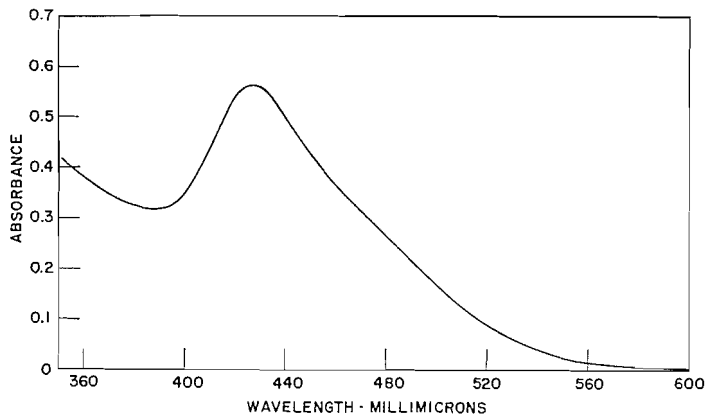

Fig. 1. Spectral curve of a rhodium solution containing 2.03 p.p.m. rhodium.

[1]*Manuscript received March 28, 1958.*
Contribution from the Division of Applied Chemistry, National Research Council of Canada, Ottawa, Canada. Issued as N.R.C. No. 4799.

hypochlorite (4), cannot be applied to solutions of rhodium in sulphuric acid, a medium in which rhodium is quite often found. A comparison of the sensitivities of these procedures and that described below is shown in Table I.

Berman and McBryde (7) noted the formation of a yellow color when tin (II) chloride in hydrobromic acid was added to solutions containing rhodium. However, this color was reported as unstable and attempts to develop a precise determination for rhodium were unsuccessful. The writers have succeeded in finding a set of conditions under which this color is quite stable, lending itself to a simple and sensitive determination of the metal. This was done primarily by the addition of a relatively large quantity of perchloric acid to the system prior to the addition of the reagent. The spectral curve produced is shown in Fig. 1. The absorption peak is at 427 mμ and the curve appears to be identical with that found by Berman and McBryde.

EXPERIMENTAL

Apparatus and Solutions

Absorption measurements were made with a Beckman Model DU quartz spectrophotometer and matched 1.00-cm. Corex-glass cells. Spectral curves and studies of the stability of the species under various conditions were made with a Beckman Model DK-1 recording spectrophotometer.

A standard rhodium solution was prepared by dissolving very pure sodium chlororhodate in 0.1 *M* hydrochloric acid. This solution was standardized gravimetrically with thiobarbituric acid (8) and found to contain 2.03 mg. of rhodium per milliliter of solution. A 5-ml. aliquot of this solution was diluted to 1000 ml. with 0.1 *M* hydrochloric acid and so contained 10.15 μg. of rhodium per milliliter of solution.

The reagent was a 20% w/v solution of tin (II) oxide dissolved in concentrated hydrobromic acid (about 40% HBr). The hydrobromic acid was redistilled before use to remove any impurities.

All other chemicals used were of analytical reagent grade.

Development of the Method

The Reagent

Preliminary experiments with the tin (II) chloride–hydrobromic acid reagent of Berman and McBryde showed that, aside from the colored species being unstable, there was formed, at room temperature, a second absorption peak at 470 mμ which slowly disappeared. This was identical with that formed using tin (II) chloride alone as the reagent and was presumably due to the high chloride concentration in the reagent. To eliminate this reaction a chloride-free reagent was prepared. This was first done by dissolving pure tin in concentrated hydrobromic acid and later by the much quicker method of dissolving tin (II) oxide in concentrated hydrobromic acid. In both these cases it is assumed that the product corresponds to a solution of tin (II) bromide in hydrobromic acid.

The intensity of the colored species was found to increase with the quantity of reagent used. However, it was noted that when more than two milliliters of reagent were used the reagent blank when measured against distilled water slowly increased in absorbancy. This, coupled with the fact that the reagent blank itself begins to absorb very strongly below 400 mμ, led to the acceptance of 2 ml. as the optimum quantity of reagent.

Effect of Hydrobromic Acid

When more than 0.5 ml. of hydrobromic acid was added to the sample the absorbancy

Can. J. Chem. Downloaded from www.nrcresearchpress.com by 78.46.186.204 on 09/04/12
For personal use only.

increased with the concentration of this acid. However, the time required to achieve maximum absorbancy was also increased. This was accompanied by a decrease in the stabilities of the colored species and the reagent blank. Except in the case of fumed sulphuric acid samples (which will be described later) no hydrobromic acid, aside from that present in the reagent, was added to the system in the final procedure.

Effect of Perchloric Acid

The addition of concentrated perchloric acid (70–72%) had the effect of stabilizing the system. Maximum absorbancy was attained within 20 minutes when 8 to 10 ml. of this acid were added to the system prior to the addition of the reagent. A precipitate sometimes formed on the addition of the reagent if the solution did not contain a few milliliters of water. This precipitate dissolved rapidly when the solution was diluted to volume. The formation and dissolution of the precipitate did not appear to affect the absorbancy of the solution. The color was stable for at least 3 hours.

It was also noted that when perchloric acid was absent the colored species was not only unstable but the rate of attainment of maximum absorbancy and the subsequent decrease in absorbancy was photosensitive.

Recommended Procedure

Transfer the solution containing the rhodium to a 25-ml. volumetric flask and dilute to about 5 ml. with water. Add 10 ml. of concentrated perchloric acid followed by 2 ml.

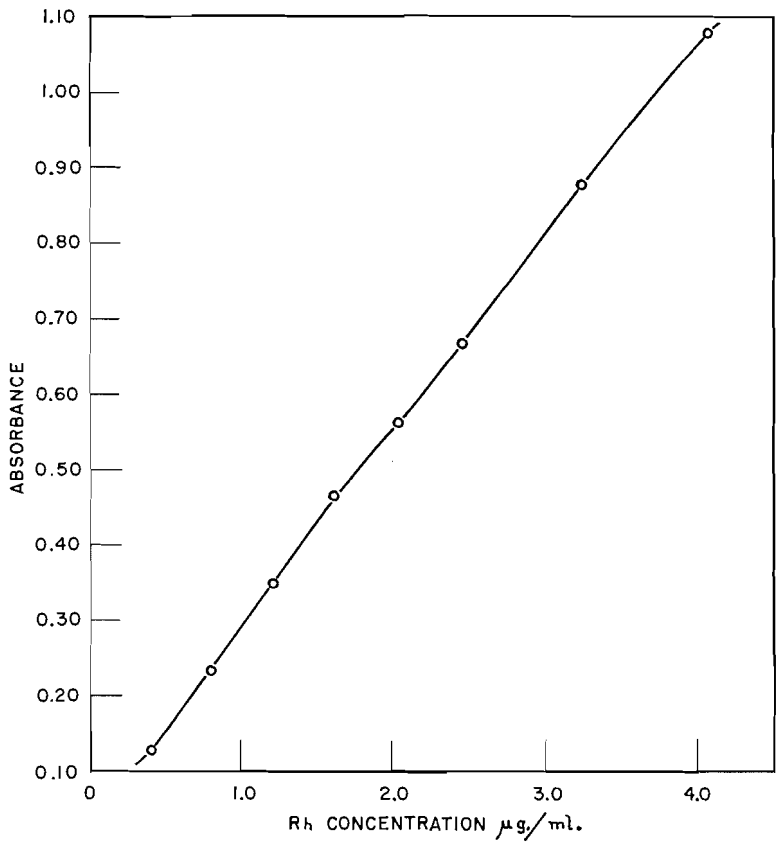

FIG. 2. Absorbance of Rh solutions at 427 mμ.

Can. J. Chem. Downloaded from www.nrcresearchpress.com by 78.46.186.204 on 09/04/12
For personal use only.

of the tin (II) bromide reagent. Dilute to volume with water. After 20 minutes measure the absorbancy at 427 mμ using a reagent blank for comparison.

Precision Attainable

The mean absorbancy of five replicate samples each containing 50.8 μg. of rhodium in a final volume of 25 ml. was 0.562. The mean deviation of these results was 0.001 or 0.2%.

Adherence to Beer's Law

The colored solutions adhere to Beer's law for concentrations ranging from 0.8 to 1.6 p.p.m. However, measurements were made over a range from 0.4 to 4.0 p.p.m. and excellent precision was attained in all cases. The deviations from Beer's law are illustrated by Fig. 2.

The recommended range for this procedure is 0.4 to 4 p.p.m. when measurements are made using 1-cm. cells.

The Determination of Rhodium in Solutions after Fuming with Sulphuric Acid

Quite often in the analysis of the platinum group metals, sulphuric acid is introduced into the system at one stage or another and the resulting solution taken to fumes of the acid. Also, in the case of rhodium, sulphuric acid is apt to be present, since it is the only single mineral acid capable of attacking this metal quantitatively. For this reason an investigation of the applicability of the procedure described above to such solutions was carried out.

Preliminary experiments with unfumed samples containing sulphuric acid showed that the presence of this acid decreased the absorbancy of the system. It was found that maximum stability accompanied by minimum reaction time occurred when 8 ml. of perchloric acid and 1 ml. of reagent were used. Under these conditions a difference of 1 ml. of concentrated sulphuric acid resulted in about a 1% change in absorbancy.

Samples were prepared by fuming solutions containing rhodium and 2 ml. of concentrated sulphuric acid.

When these samples were treated as described above in the recommended procedure no color was evident at first. A yellow color slowly formed when the sample was left standing but this never became very intense. Attempts to increase the rate of color formation by heating the sample were only partially successful.

It was found that if the fumed solution was diluted to about 5 ml. with water, 0.5 ml. of concentrated hydrobromic acid added, and the solution boiled vigorously for 5 minutes, the color developed within 8 minutes of the addition of the reagent and the absorbancy was identical with that of a similar solution that contained 2 ml. of sulphuric acid but which had not been fumed.

The following procedure was found to be quite satisfactory for samples containing between 1 and 2 milliliters of concentrated sulphuric acid. Cool the rhodium solution after fuming and add 5 ml. of water and 0.5 ml. of concentrated hydrobromic acid. Boil this solution vigorously for at least 5 minutes then allow it to cool. Add 8 ml. of concentrated perchloric acid followed by 1 ml. of the reagent. Transfer to a 25-ml. volumetric flask and dilute to volume. After 8 minutes measure the absorbancy at 427 mμ against a reagent blank containing the same quantity of sulphuric acid as the sample.

Five replicate samples, each containing 50.8 μg. of rhodium which had been fumed with 2 ml. of concentrated sulphuric acid, gave a mean absorbancy of 0.503. The mean deviation of these results was 0.001 or 0.2%.

Can. J. Chem. Downloaded from www.nrcresearchpress.com by 78.46.186.204 on 09/04/12
For personal use only.

Effect of Diverse Ions

The other platinum metals and base metals usually associated with the platinum metals interfere. Surprisingly, of the platinum metals iridium produced the least interference. A solution containing 46.4 μg. of iridium, when treated as described above, produced a colorless solution which showed no absorption peaks in the visible region. The presence of 9.3 and 46.4 μg. of iridium in solutions containing 50.8 μg. of rhodium reduced the absorbancies by about 2 and 6% respectively. It is apparent that a fair estimation of rhodium can be made even when equivalent quantities of iridium are present.

The exact intensities of the interferences of the other metals were not ascertained, as in all probability, in practice, they will depend on the history of the sample in question.

REFERENCES

1. IVANOV, V. N. J. Russ. Phys.-Chem. Soc. **50**, 460 (1913).
2. MAYNES, A. D. and MCBRYDE, W. A. E. Analyst, **79**, 230 (1954).
3. AYRES, G. H., TUFFLY, B. L., and FORRESTER, J. S. Anal. Chem. **27**, 1742 (1955).
4. AYRES, G. H. and YOUNG, F. Anal. Chem. **24**, 165 (1952).
5. RYAN, D. E. Anal. Chem. **22**, 599 (1950).
6. RYAN, D. E. Analyst, **75**, 557 (1950).
7. BERMAN, S. S. and MCBRYDE, W. A. E. Analyst, **81**, 566 (1956).
8. CURRAH, J. E., MCBRYDE, W. A. E., CRUIKSHANK, A. J., and BEAMISH, F. E. Ind. Eng. Chem., Anal. Ed. **18**, 120 (1946).

Can. J. Chem. Downloaded from www.nrcresearchpress.com by 78.46.186.204 on 09/04/12
For personal use only.

Can. J. Chem. Downloaded from www.nrcresearchpress.com by 78.46.186.204 on 09/04/12
For personal use only.

THE EXTENT OF THE ABNORMAL RECOMBINATION OF CYANISOPROPYL FREE RADICALS FROM 2,2′-AZO-BIS-ISOBUTYRONITRILE[1]

M. TALÂT-ERBEN AND A. N. ISFENDIYAROĞLU

ABSTRACT

The extent of the abnormal recombination of cyanisopropyl radicals to yield the ketenimine intermediate has been investigated at 80° C. in toluene. It is found that 54.4% of the radicals recombine this way. This value is 75% higher than that reported previously. This result makes it possible to estimate a better value for the molar extinction of intermediate, and suggests the possibility that in the decomposition of the latter both free-radical and molecular processes are co-operative.

INTRODUCTION

Talât-Erben and Bywater (3) have shown that a ketenimine intermediate is formed in the thermal decomposition of 2,2′-azo-bis-isobutyronitrile, and estimated the extent of the corresponding radical recombination to be approximately 30% of the total. This result was used to estimate the molar extinction coefficient of intermediate at maximum absorption at 287 mμ. Moreover, they used the same result to calculate the branching ratios of the two recombinations, and came to the conclusion that a decomposition step of intermediate into free radicals would be experimentally undistinguishable from a molecular process, since both assumptions give for $k_1 t_{max}$ values which are too close to be discernible. However, the above statements cannot be considered as conclusive, since the distribution ratio of the original hydrolytic product of ketenimine in toluene and 1 *N* HCl was unknown, so that there is no proof that the extraction of the product was complete. Therefore, it would be of interest to undertake a redetermination of the branching ratio under more precisely controlled experimental conditions.

EXPERIMENTAL

The azo-compound* (Westville Laboratories, Monroe, Connecticut) was recrystallized from benzene; m.p. 103° C. dec. The thermal decomposition was carried out at 80° in toluene (C.P.), in a thermostat controlled to about 0.2°, under a stream of purified nitrogen, with continual shaking. Azo-compound (1.6 to 1.9 g.) was decomposed in 50 cc. of toluene. After a definite time the solution was cooled quickly to stop the reaction, and transferred quantitatively into a separatory funnel. Fifty cubic centimeters of 1 *N* HCl were added, and the two phases were stirred rigorously for at least 20 minutes, then the emulsion-like mixture was left until the phases disengaged completely. The acid layer which contained the nitrile (II) was collected in a filter flask. The extraction was repeated at least three times with fresh portions of HCl. During extraction the ketenimine (I) hydrolyzes to the corresponding substituted amide (II), and passes into the aqueous phase. This hydrolytic step is a fast reaction owing to the unstable character of ketenimine group, as shown by Stevens and French (2).

$(CH_3)_2C{=}C{=}N{-}(CH_3)_2CN$ (I)

$(CH_3)_2CH.CO.NH.C(CH_3)_2CN$ (II)

$(CH_3)_2CH.CO.NH.C(CH_3)_2.CO.NH_2$ (III)

$(CH_3)_2CH.CO.NH.C(CH_3)_2.CO.OH$ (IV)

[1]*Manuscript received April 29, 1958.*
Contribution from the Faculty of Mining Engineering, Technical University of Istanbul, Istanbul, Turkey.
**Kindly supplied by Dr. S. Bywater of the National Research Council.*

The distribution ratio of (II) in toluene and 0.95 N HCl was found to be 1.17×10^{-2}. Therefore, after three extractions the amount left in toluene must be completely negligible; this was proved to be the case by additional extractions. The HCl extract was evaporated at 48° under reduced pressure, until all HCl was removed. The residue from evaporation, which consisted of an equimolecular mixture of (IV) and ammonium chloride, was dissolved in about 50 cc. of distilled water, and titrated against 0.1 N NaOH, potentiometrically. The fact that the end point in the neutralization was unaffected by the presence of ammonium chloride buffer has been established by titration of an authentic sample consisting of an equimolecular mixture of (IV) and NH_4Cl. This made it possible to cancel a separation step which would cause material losses. The authentic sample of (IV) had been prepared in a previous work (3) and had a melting point of 150° C. The neutralization point was taken as the inflection point of the clear S-shaped curve of the titration diagram. To check that under these conditions the hydrolysis of (II) to (IV) was complete, and that no detectable amount of (III) was ever formed, a definite amount of an authentic sample of (II) was subjected to the same conditions; the amount (in moles) of the acid formed was equal to that of the original nitrile with a great accuracy. The sample used in this experiment as well as in the determination of the distribution ratio was prepared in a previous work (4), and had a melting point of 105° C.

RESULTS AND DISCUSSION

Experiments were performed with reaction times of 25, 60, 104, 130, 180, and 240 minutes, at least two runs for each reaction time. The amount of (IV) expressed as the molar fraction of the initial amount of the azo compound changed with the reaction time in a manner very similar to that of the change of optical density with time as given in reference (3). The results are shown in Fig. 1. The maximum occurs at a point corresponding to a yield of 20.0%. This must be $1/e$th of the actual fraction of cyanisopropyl radicals that combine to form the ketenimine intermediate; this branching is thus found to be 54.4%. This result is about 75% higher than that reported in reference (3). Accordingly, the conclusion (1) that free radicals are not involved in the formation of the intermediate or in its decomposition cannot be maintained.

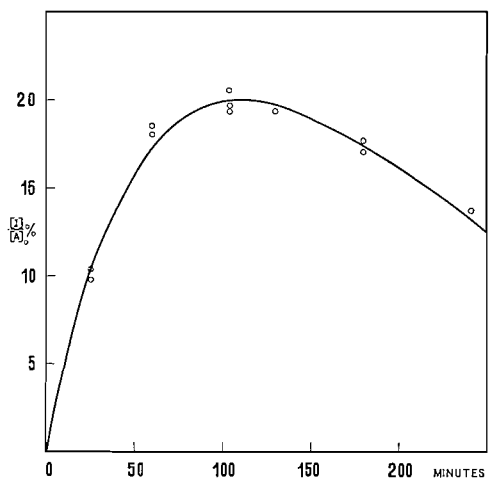

FIG. 1. Actual amounts of hydrolytic product of the intermediate as a fraction of the initial amount of azo compound versus reaction time. The curve has been calculated by using the reaction scheme of reference (3), assuming $k_4 = k_1$ and $k_3/(k_2 + k_3) = 0.544$.

Can. J. Chem. Downloaded from www.nrcresearchpress.com by 78.46.186.204 on 09/04/12
For personal use only.

By comparison of the actual amount of intermediate extracted in the form of one of its hydrolytic products in this work with the optical density data of Table I of reference (3), it is possible to predict a better value for the molar extinction of (I), namely 46 at 320 mμ. This would correspond to a molar extinction of about 150 at maximum absorption at 287 mμ, assuming that the shape of the absorption curve given by the oily fraction (3) is characteristic of the intermediate. On the other hand, in the assumption that the latter decomposes to regenerate free radicals rather than by a molecular process, $k_1 t_{max}$ would now have to be 1.5; this value would be experimentally distinguishable from the value 1.0 corresponding to the molecular decomposition. The observed value, which is in the range 1.0 to 1.2, suggests that at most both mechanisms are co-operative, with the molecular process predominating.

REFERENCES

1. ROY, J.-C., NASH, J. R., WILLIAMS, R. R., Jr., and HAMILL, W. H. J. Am. Chem. Soc. **78**, 519 (1956).
2. STEVENS, C. L. and FRENCH, J. C. J. Am. Chem. Soc. **75**, 657 (1953).
3. TALÂT-ERBEN, M. and BYWATER, S. J. Am. Chem. Soc. **77**, 3710 (1955); **77**, 3712 (1955).
4. TRUDEL, G., TALÂT-ERBEN, M., and BYWATER, S. Unpublished work.

Can. J. Chem. Downloaded from www.nrcresearchpress.com by 78.46.186.204 on 09/04/12
For personal use only.

Can. J. Chem. Downloaded from www.nrcresearchpress.com by 78.46.186.204 on 09/04/12
For personal use only.

A MASS SPECTROMETRIC STUDY OF NORMAL OXYGEN AND OXYGEN SUBJECTED TO ELECTRICAL DISCHARGE[1,2]

J. T. HERRON[3] AND H. I. SCHIFF

ABSTRACT

A mass spectrometric study was made of oxygen activated by microwave and by a-c. glow discharge. Appearance potential curves for normal oxygen at masses 16 and 32 indicated the occurrence of multiple electron impact processes. The change in the curves when the oxygen was activated could be interpreted by assuming the presence of O-atoms in the ^3P ground state, and O_2 molecules in the $^1\Delta_g$ excited state. No evidence was obtained for the presence of ozone up to pressures of 2 mm. Hg. The recombination coefficient of O-atoms on pyrex was found to be 1.1×10^{-4}. Only one oxygen atom in 21 was ionized before recombining in the mass spectrometer ion source. The rate constant for the reaction of O-atoms with N_2O is less than 1×10^{-8} cm.^{3} mole^{-1} sec.$^{-1}$, and several orders of magnitude less than this for the reaction $O(^3P) + N_2O \rightarrow 2NO$. The reaction of O-atoms with NO_2 was much faster than with NO, but no evidence was found for the formation of NO_3.

INTRODUCTION

When oxygen is subjected to electrical discharge at about 1 mm. Hg pressure, its chemical activity is greatly enhanced. The literature on the nature of the active species has recently been reviewed by Linnett and Marsden (1). They conclude that most of the oxygen is present as normal molecules and atoms. However, it may be inferred from a recent study of the thermal decomposition of ozone (2) that this compound might also be present in appreciable quantities under these conditions. The presence of ozone has also been postulated by Barth and Kaplan (3) to explain their observation of the Herzberg oxygen bands in discharges containing small quantities of nitrogen, and by Ford and Endow (4) to explain the mechanism of the NO_2 photolysis. Moreover there seem to be no compelling reasons for excluding the presence of electronically or vibrationally excited oxygen molecules.

This paper reports a mass spectrometric study of activated oxygen and some preliminary measurements of its reaction with the oxides of nitrogen. New species were identified by their mass-to-charge ratios and by their appearance potentials. To determine the appearance potentials of new species at masses 16 and 32, it was necessary to compare ionization-efficiency curves for normal and activated oxygen. The curves obtained for normal oxygen appeared to have features not previously reported. These curves are therefore also discussed.

EXPERIMENTAL

Apparatus

The mass spectrometer and the method used to measure appearance potentials have been described previously (5). Oxygen was found to reduce seriously the lifetime of the tungsten filament used as a source of electrons in the mass spectrometer. Carbon filaments were found to last longer and to give smaller CO^+ and CO_2^+ ion currents in the presence of oxygen. (For a discussion of the use of carbon filaments in mass spectrometers see ref. 6.) The only difficulty encountered with these filaments was some instability in

[1]*Manuscript received March 24, 1958.*
Contribution from the Department of Chemistry, McGill University, Montreal, Quebec.
[2]*This work was supported in part by the Geophysics Research Directorate of the Air Force Cambridge Research Center, Air Research and Development Command under Contract No. A.F. 19(604)1488, and in part by the National Research Council of Canada by a Grant-in-aid.*
[3]*Holder, National Research Council (Canada) Fellowship, 1954–56, Canadian Industries Limited Fellowship, 1956–57. Present address: Mass Spectrometry Section, National Bureau of Standards, Washington, D.C.*

electron emission caused by poor contact between the carbon and the lead wires. This difficulty was finally overcome by evaporation of gold onto the ends of the filament, which were then held by a pair of miniature screw clamps. The maximum emission from these filaments was limited by evaporation of the carbon. However, the ionizing current could be increased to values comparable to those obtained with tungsten filaments of similar dimensions by the use of a reflector shield.

Two types of electrical discharges were used, a 60-cycle glow discharge and a microwave electrodeless discharge. The glow discharge was produced in a U-shaped pyrex tube 20 mm. in diameter and 80 cm. long. The electrodes were made of 1S grade aluminum rated to have a purity of 99.5%; aluminum of lower purity was found to undergo rapid attack in an oxygen discharge. To increase the electrode life further the entire discharge tube was immersed in a water bath. The activated oxygen was withdrawn from the center of the discharge and travelled a distance of 30 cm. to the sampling leak of the mass spectrometer.

The electrodeless discharge was excited in a quartz tube, 13 mm. in outside diameter, which passed through a slot in a resonance cavity box. Power was supplied by a "Raytheon" diathermy unit operating at 2450 Mc./sec. The activated gas was pumped from the discharge over the mass spectrometer leak through 13-mm. pyrex tubing, the length of which was varied between 10 and 50 cm.

Procedure

Oxygen was flowed continuously through the discharge and over the sampling leak of the mass spectrometer. "Bone-dry" tank oxygen of 99.90% purity was used without further purification, since several experiments performed with fractionally distilled oxygen and with oxygen produced by pyrolysis of potassium permanganate gave identical results. The oxygen pressure was varied from 0.1 to 2 mm. Hg. The mass flow rate at 1 mm. Hg pressure was 25 μM./sec.; the corresponding linear flow rate was 490 cm./sec. Provision was also made for adding water vapor to the oxygen stream.

Other gas inlets were located between the discharge and the sampling leak for introduction of calibrating gases for appearance potential studies and for the nitrogen oxides. The oxides of nitrogen were purified by the method of Nightingale *et al.* (7) and the mass spectrometer conditioned for NO_2 analysis by the method suggested by Friedel *et al.* (8).

The presence of mercury vapor was avoided, since it produced a deposit of mercuric oxide on the walls which deactivated the oxygen. A mirror of mercury was deposited on the walls of a trap located above the rotary pump to prevent attack of activated oxygen on the pump oil.

RESULTS AND DISCUSSIONS

Normal Oxygen

The O_2^+ ionization efficiency curve for normal oxygen was determined in the presence of argon as the calibrating gas. The partial pressure of argon was adjusted to make the ion currents at mass numbers 40 and 32 equal when the electron energy was 60 ev. The O_2^+ curve had a smaller slope and a longer 'tail' portion than the A^+ curve, which suggested that it resulted from several ionizing processes, such as the production of O_2^+ with vibrational excitation. The present instrument was incapable of resolving energies comparable to the spacing between vibrational levels.

Fig. 1 shows a typical set of experimental points through which several straight lines have been drawn. The A^+ curve has been adjusted to make the 'linear' portion parallel

Can. J. Chem. Downloaded from www.nrcresearchpress.com by 78.46.186.204 on 09/04/12
For personal use only.

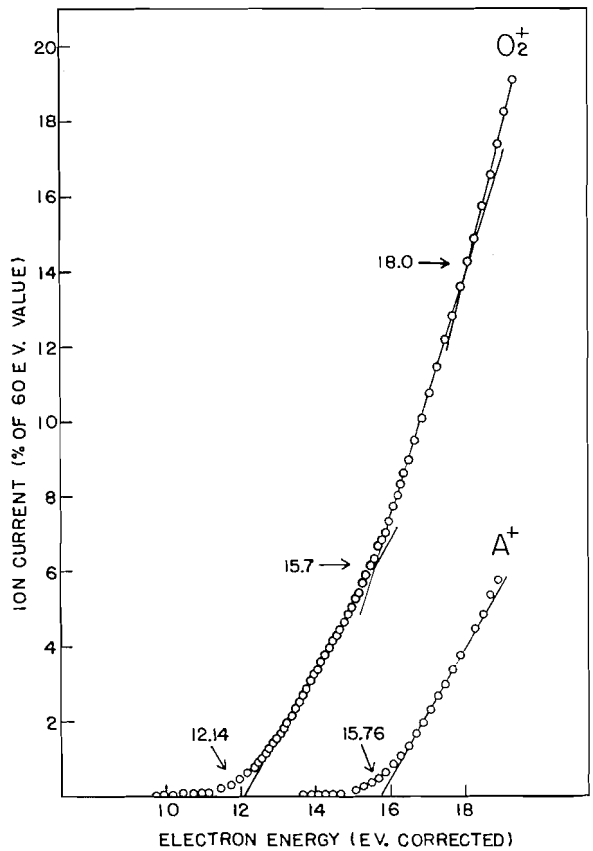

FIG. 1. Ionization efficiency curve for O_2^+ from normal oxygen.

to the lowest straight line of the O_2^+ curve. The average value of the ionization potential of O_2 obtained by extrapolation of seven such curves was 12.23±0.07 ev. A value of 12.10 ev. was obtained from a single attempt to use the extrapolated voltage difference method (9) with the adjusted A^+ curve. This method was not felt to be reliable for extrapolation of composite curves since the values obtained are very sensitive to the adjustment applied to the calibrating gas curve. However Warren (9) has used this method to obtain a value of 12.20±0.03 ev. for the ionization potential of O_2, but gave no details of the measurements. Hagstrum (10) obtained a value of 12.2±0.2 ev. using electron impact, and Watanabe reports a value of 12.075±0.010 ev. from photoionization measurements (11).

The intersections of the straight lines drawn through the O_2^+ curves gave appearance potentials of 15.7±0.5 and 18.0±0.5 ev. Herzberg (12) lists the electronic excitation energy of the $^4\pi_u$ and $^4\Sigma_g^-$ states of the O_2^+ ion as 3.95 ev. and 6.00 ev. respectively, although he indicates some uncertainty in these values. The appearance potential of these excited molecular ions formed by electron impact from ground state $^3\Sigma_g^-$ O_2 molecules can then be calculated to be 16.1 and 18.2 ev. The observed appearance potentials agree with these figures within the combined uncertainty of the spectroscopic and electron impact values.

The ionization efficiency curves obtained at mass 16 for normal oxygen indicated that

Can. J. Chem. Downloaded from www.nrcresearchpress.com by 78.46.186.204 on 09/04/12
For personal use only.

O^+ is formed by several processes. Three "linear" portions could be drawn through the lower part of the curves and appearance potentials obtained from their intersections. Since the assignment of these "linear" portions is somewhat arbitrary, averages were taken of a large number of independent measurements. These average values and the processes which can be associated with them are shown in Table I and can be seen to be in substantial agreement with those reported by Hagstrum (13) and Thorburn (14). A portion of a typical curve is plotted as filled circles in Fig. 4.

TABLE I

POSSIBLE ELECTRON IMPACT PROCESSES IN NORMAL AND ACTIVATED OXYGEN

Process	Observed appearance potential				
	Normal oxygen			Activated oxygen	Calc.
	Hagstrum	Thorburn	This work		
$O(^3P) + e \rightarrow O^+(^4S^\circ) + 2e$				13.9±0.2	13.61
$O_2(^1\Delta_g) + e \rightarrow O^+(^4S^\circ) + O^-(^2P^\circ) + e$				15.7±0.4	16.29
$O(^3P) + e \rightarrow O^+(^2D) + 2e$					16.86
$O_2(^3\Sigma_g^-) + e \rightarrow O^+(^4S^\circ) + O^-(^2P^\circ) + e$	17.2±0.2	16.9±0.2	17.1±0.2	17.2±0.2	17.27
$O_2(^1\Delta_g) + e \rightarrow O^+(^4S^\circ) + O(^3P) + 2e$				18.0±0.4	17.74
$O(^3P) + e \rightarrow O^+(^2P) + 2e$					18.54
$O_2(^3\Sigma_g^-) + e \rightarrow O^+(^4S^\circ) + O(^3P) + 2e$	19.2±0.2	18.9±0.2	18.9±0.2	18.8±0.2	18.72
$O_2(^3\Sigma_g^-) + e \rightarrow O^+(^2D^\circ) + O^-(^2P^\circ) + e^-$	20.4±0.2	20.5±0.2	20.3±0.2	20.2±0.2	20.5

Activated Oxygen

The mass spectra of normal and activated oxygen were compared over the pressure range 0.1 to 2.0 mm. Hg. Table II shows the ion currents observed at masses 16, 32, and 48 at various pressures and using both types of discharge. Small ion currents were also observed at masses 28 and 44, which were probably due to reaction of oxygen with the filament or with carbon-containing impurities in the ion source. The change in the ratio of ion intensities at mass 16 to those at mass 32, from about 0.08 to 0.03, was

TABLE II

MASS SPECTRA OF NORMAL AND ACTIVATED OXYGEN

Pressure, mm. Hg	Discharge	Ion intensity mass 16 arbitrary units	Ion intensity mass 32 arbitrary units	Ion intensity mass 48 arbitrary units	Ratio of ion intensities 16/32	% Change in ratio 16/32
0.15	Off	297	3600	0.40	8.25×10^{-2}	
0.15	A-c. glow	293	3460	0.48		2.4
0.30	Off	756	9240	1.00	8.20×10^{-2}	
0.30	A-c. glow	780	8770	1.00		8.7
0.90	Off	1476	16880	2.40	8.74×10^{-2}	
0.90	A-c. glow	1554	10380	2.40		8.5
0.34	Off	72.8	2322	0.20	3.14×10^{-2}	
0.34	Microwave	92.4	2465	0.20		19
0.50	Off	109	3468	0.50	3.14×10^{-2}	
0.50	Microwave	138	3648	0.50		19
0.90	Off	156	4920	0.98	3.12×10^{-2}	
0.90	Microwave	194	5220	0.98		17
1.80	Off	——	——	2.90	——	
1.80	Microwave			2.90		

Can. J. Chem. Downloaded from www.nrcresearchpress.com by 78.46.186.204 on 09/04/12
For personal use only.

observed when the tungsten filament was replaced by a carbon filament as a source of electrons in the mass spectrometer. This change may be due to the greater extent of pyrolysis of O_2 to O-atoms on the tungsten filament. This interpretation is supported by the longer 'tail' portion of the O^+ appearance potential curve obtained with the tungsten filament. The last column of the table shows the percentage change in the ratio of ion currents at masses 16 and 32 when the oxygen was activated. Appearance potentials were determined at these mass numbers to identify the new species present in the activated gas.

Ozone

(*a*) *Normal Oxygen*

The ion current at mass 48 in the mass spectrum of *normal* oxygen might be due to ion–molecule reactions occurring in the mass spectrometer ion source. This would agree with the observed second-order dependence of the O_3^+ ion current on pressure (cf. Table II). The possible ion–molecule reactions are listed in Table III along with the calculated heats of reaction.

TABLE III

POSSIBLE REACTIONS FOR THE FORMATION OF O_3^+ IN NORMAL OXYGEN

Process	ΔH, kcal./mole
$O_2^+(X^2\pi_g) + O_2 \rightarrow O_3^+ + O$	107.1
$O_2^+(a^4\pi_u) + O_2 \rightarrow O_3^+ + O$	16.0
$O_2^+(A^2\pi_u) + O_2 \rightarrow O_3^+ + O$	−4.0
$O_2^+(b^4\Sigma_g^-) + O_2 \rightarrow O_3^+ + O$	−31.8
$O_2^+(X^2\pi_g) + O \rightarrow O_3^+$	−10.1
$O^+ + O_2 \rightarrow O_3^+$	−42.6

The reaction $O_2^+ + O_2 \rightarrow O_3^+ + O$ is exothermic only if the O_2^+ ion is in the second or third excited state. Since Franklin has found* that only exothermic ion–molecule reactions are observable, this does not appear to be a likely source of O_3^+ ions. The analogous reaction $H_2^+ + H_2 \rightarrow H_3^+ + H$ is approximately thermally neutral and has been used to explain the H_3 ions observed in the mass spectrum of hydrogen (15).

The last two reactions shown in Table III are energetically possible, but probably require third-body stabilization. No other example of such a simple ion–molecule addition reaction has been reported.

There remains the possibility of O_3 being formed directly on the mass spectrometer filament, although the mechanism for such a reaction is not apparent. This problem can only be solved by measuring the appearance potential of the O_3^+ ion. Attempts are currently being made to improve the sensitivity of the instrument to permit such measurements.

(*b*) *Activated Oxygen*

No increase in the ion current at mass 48 was observed when the oxygen was activated. A previous mass spectrometric study of pure ozone (16) showed that the ion current at mass 48 from pure ozone is at least 0.13 times as large as the ion current at mass 32 from pure oxygen at the same pressure. From the detection limit of the mass spectrometer it can be concluded that ozone is not present in activated oxygen in concentrations greater than 0.02% up to pressures of 2 mm. Hg.

**Private communication.*

Can. J. Chem. Downloaded from www.nrcresearchpress.com by 78.46.186.204 on 09/04/12
For personal use only.

In a recent study of the pyrolysis of ozone at several hundred millimeters Hg pressure, Benson and Axworthy (2) obtained rate constants for the reactions:

$$M + O_3 \underset{k_2}{\overset{k_1}{\rightleftarrows}} M + O_2 + O$$

$$O + O_3 \xrightarrow{k_3} 2O_2.$$

These rate constants can be used to calculate the steady-state concentration of ozone, which would be expected for the experimental conditions used in the present study. The time required to reach a steady-state condition can also be shown to be the same order as the time required for the activated gas to pass from the discharge to the mass spectrometer leak. At 300° K. and 1 mm. Hg pressure the calculated steady-state concentration of ozone is 0.29%, which is at least an order of magnitude above the detection limit of the mass spectrometer. However, Benson and Axworthy's value for k_2, when the third body is O_2, is only an estimate, and might be responsible for part of the discrepancy.

This discrepancy cannot be explained by heterogeneous destruction of ozone on the walls of the tubing connecting the discharge and the mass spectrometer. Harteck and Dondes (17) have shown that ozone decomposition does not occur directly on glass but only indirectly by the recombination of the O-atoms in equilibrium with the ozone. The low recombination coefficient of O-atoms observed in this work precludes this as an important mechanism for ozone disappearance.

The presence of effective catalysts for ozone decomposition such as Hg or H_2O vapors was also carefully avoided. However, McGrath and Norrish (18) have postulated a rapid reaction between vibrationally excited O_2 and O_3 in the flash photolysis of ozone. Any ozone formed in the present study might have been rapidly destroyed by the excited O_2 (see below) found to be present in activated oxygen.

Since k_3 has an activation energy of 6.0 kcal./mole it might be argued that the steady-state ozone concentration might be lower than the calculated value, since the gas issuing from the discharge is considerably above room temperature. However, no ozone was detected when the activated gas was flowed through a 50-cm. length of tubing. The gas should then have been at 300° K. for a sufficient time to reach the steady-state concentration corresponding to this temperature.

There remains the possibility that the ozone was destroyed in the ion source. Although the sensitivity of the mass spectrometer in detecting ozone was determined using pure ozone, it is possible that at low ozone concentrations decomposition might occur more rapidly on the hot walls of the ion source. A single experiment performed with an ion source designed to prevent collisions of molecules with the metal walls did show a small increase in ion intensity at mass 48 when the oxygen was activated. However, since the mass spectrometric sensitivity for ozone with this source has not yet been determined, no estimate could be made of the ozone concentration. Further studies with this source are now in progress.

Excited Oxygen Molecules

Fig. 2 shows a typical set of curves obtained when the ion intensities at masses 40 and 32 were plotted against the electron energy. The apparent electron-energy scale was shifted to make the linear portion of the argon curve extrapolate to the spectroscopic ionization potential of argon. The argon curves obtained when the discharge was excited coincided with those obtained in the absence of the discharge. The curves at mass 32 did

Can. J. Chem. Downloaded from www.nrcresearchpress.com by 78.46.186.204 on 09/04/12
For personal use only.

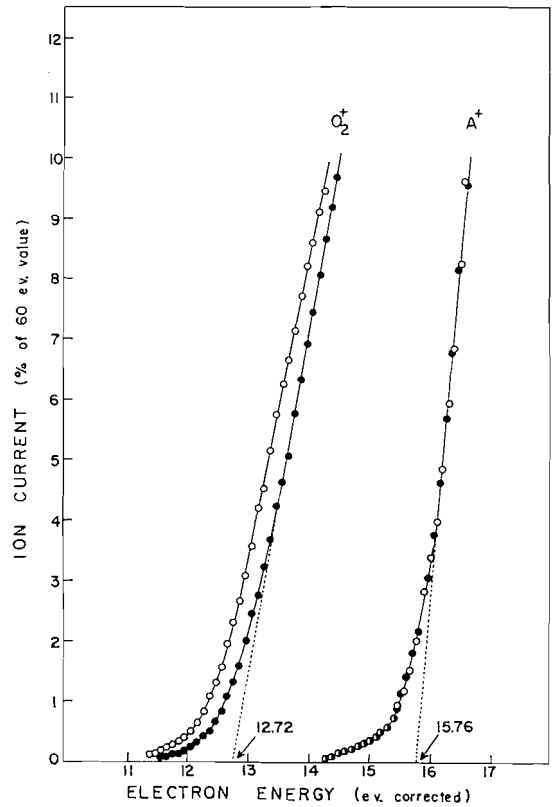

FIG. 2. Ionization efficiency curves for O_2^+ and A^+. Filled circles correspond to normal gas, open circles to activated gas.

not coincide, which suggested the presence of new species. When the difference ΔO_2^+, between the two curves, was plotted as a function of electron energy, the curve shown in Fig. 3 was obtained. The slope of the argon curve was adjusted to make it parallel to the ΔO_2^+ curve. The average of four determinations, one using xenon as the calibrating gas, indicated that the new species had an ionization potential 1.00 ± 0.03 ev. lower than normal oxygen.

Herzberg reports the excitation energy of the $^1\Delta_g$ state of oxygen to be 0.98 ev. (19). The new species may therefore be oxygen in this electronically excited state. It is unlikely that it could be oxygen in the ground state with only this amount of vibrational energy, although McGrath and Norrish (18) have proposed a long lifetime for vibrationally excited oxygen.

The concentration of excited molecules can be estimated at about 10% from a comparison of the initial slopes of the ΔO_2^+ curves and the O_2^+ curves for normal oxygen. The estimate is based on the assumption that the ionization cross sections for excited and normal oxygen are identical and that their ionization probabilities increase with excess electron energy in the same way.

Foner and Hudson (20) also obtained evidence for an excited molecular species in activated oxygen. They analyzed their ionization-efficiency curves by a mathematical procedure and obtained a value of 0.93 ± 0.10 ev. for the excitation energy. They suggested that the excited molecules were in the $^1\Delta_g$ state and estimated their concentration to be between 10 and 20%.

Can. J. Chem. Downloaded from www.nrcresearchpress.com by 78.46.186.204 on 09/04/12
For personal use only.

Several authors (21, 22, 23) have suggested the formation of excited molecules by O-atom recombination. However, it is unlikely that the excited molecules detected in this work were formed in this way. Measurements of the rate of atom recombination (see below) indicated that only a negligible proportion of the atoms would recombine during the time required for the activated gas to pass from the discharge to the mass spectrometer leak. Since the atom concentrations were of the order of 10%, appreciable quantities of excited molecules could not be formed by this mechanism. It is much more likely that they are excited by the discharge.

Oxygen Atoms

Fig. 4 shows a typical ionization efficiency curve for O^+ ions formed by electron impact with oxygen activated by the microwave discharge. Similar curves were obtained when the a-c. glow discharge was used to excite the gas. The inset in the figure shows a magnified view of the lower portion of the curve. The first appearance potential was obtained by linear extrapolation of this portion of the curve. The energy scale was corrected using krypton as the calibrating gas. The average value obtained for the appearance potential was 13.90±0.05 ev. However, in view of the ambiguities involved in the "linear" extrapolation method, the value is probably not accurate to better than ±0.2 ev.

The ionization potential of ground state $^3P_2$ oxygen atoms is 13.615 ev. (24). Since

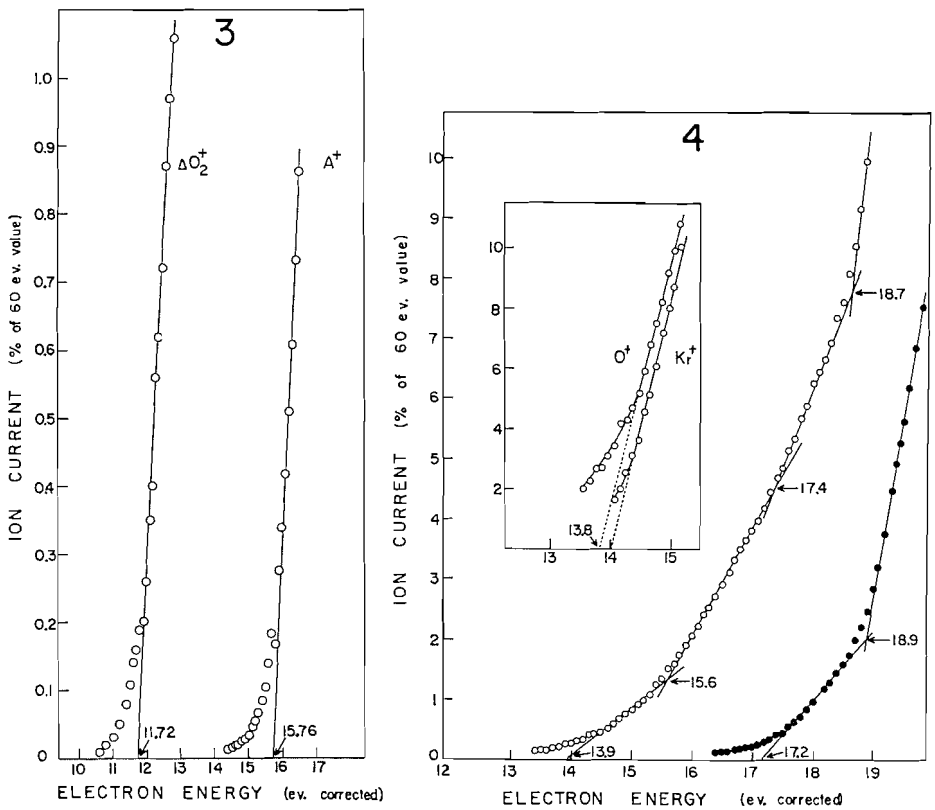

FIG. 3. Ionization efficiency curves at mass 32 for new species and at mass 40 for argon.

FIG. 4. Ionization efficiency curves for O^+ ions. Filled circles correspond to normal gas, open circles to activated gas. Inset shows lower portion of activated gas curve and curve for Kr^+ from krypton. NOTE: The numbers along the ordinate in the insert should read .2, .4, .6, .8, and 1.0.

Can. J. Chem. Downloaded from www.nrcresearchpress.com by 78.46.186.204 on 09/04/12
For personal use only.

appearance potentials obtained by linear extrapolation tend to be somewhat higher than the corresponding spectroscopic values, the agreement between these values can be considered as satisfactory evidence for the existence of ground-state atoms in activated oxygen.

Since no appearance potentials were ever observed below the ionization potential of $^3P_2$ atoms, it can be concluded that metastable atoms cannot be present in appreciable quantities.

Linear portions could also be ascribed to the O^+ ionization efficiency curves for activated oxygen. Although it was not always possible to locate all the breaks in the curve for a single experiment, average values for five higher appearance potentials could be obtained from a large number of experiments. These values are given in Table I. The appearance potentials at 15.7 and 18.0 ev. agree, within the estimated experimental uncertainty, with the values calculated for electron impact on $^1\Delta_g$ molecules in activated oxygen. The calculated values for ionization of ^3P O-atoms to excited O^+ states are somewhat outside the experimental uncertainty of the observed appearance potentials. These processes undoubtedly occur and add to the difficulty in identifying the breaks in the ionization efficiency curves.

Concentration of Oxygen Atoms

The O-atom concentration was determined by "titration" with NO_2 as originally suggested by Spealman and Rodebush (25). NO_2 was introduced into the activated oxygen stream through a mixing jet. The amount of NO_2 remaining after a reaction time of 0.5 seconds was determined as a function of initial NO_2 concentration, as shown in Fig. 5. For low NO_2 concentrations most of the NO_2 is consumed.

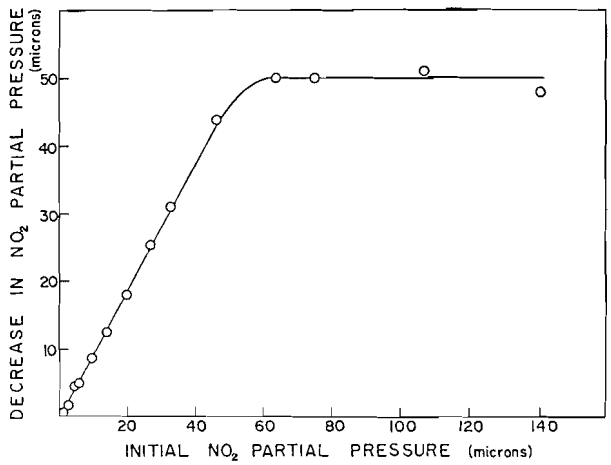

FIG. 5. Titration of O-atoms with NO_2.

This indicates that the reaction:

$$NO_2 + O \rightarrow NO + O_2 \qquad [1]$$

is very much faster than reaction:

$$NO + O + M \rightarrow NO_2 + M \qquad [2]$$

at these pressures.

Above a partial NO_2 pressure of 60 μ all the O-atoms are consumed by reaction [1]. This agrees with the observation that the chemiluminescence associated with reaction

Can. J. Chem. Downloaded from www.nrcresearchpress.com by 78.46.186.204 on 09/04/12
For personal use only.

[4] disappears above this pressure. The amount of NO_2 consumed at the "plateau" was therefore taken as a measure of the O-atom concentration.

The atom concentrations produced by both types of discharges varied from 4 to 12 mole %. The presence of water vapor in the oxygen stream greatly enhanced the atom concentration. For example, in one experiment, the atom concentration increased immediately from 4.8 to 8.6% upon addition of 0.6% water vapor. The rapidity of the change suggests that water vapor increases the discharge efficiency and does not simply act as a "poison" against wall-catalyzed recombination.

The O-atom concentration could not be estimated from the relative change in the O^+ and O_2^+ ion intensities caused by activation of the gas. Under certain conditions the O_2^+ ion intensity actually increased when the discharge was excited, although the ion intensity of argon (used here as a monitoring gas) was unaltered. This observation cannot be explained by the production of $^1\Delta_g$ molecules unless these have a much larger ionization cross section than normal oxygen. The ionization efficiency curves shown in Fig. 2 indicate that this is not the case.

Dissociation of molecules into atoms should cause a decrease in the O_2^+ ion intensity. Recombination of atoms in the ion source might not be expected to cause an increase in O_2^+ ion current above the value obtained for the undissociated gas. However, atoms will pass through the mass spectrometer leak faster than molecules, since the flow is largely non-viscous. Recombination in the ion source could then lead to a net increase in O_2^+ ion intensity relative to the monitoring gas.

An estimate can be made of the extent of atom recombination in the ion source. In a typical experiment at 0.53 mm. Hg pressure the O_2^+ ion current increased from 6820 (arbitrary units) to 7020 when the discharge was excited, the O^+ ion intensity increased from 201 to 217, while the A^+ ion intensity remained constant at 404. The O^+ ion intensity due to O-atoms was therefore:

$$217-(7020/6820\times 201)=10.$$

According to the additivity principle of ionization cross sections proposed by Stevenson and Otvos (26), oxygen atoms should have half the ionization cross section of oxygen molecules. The atom concentration for this experiment, obtained by NO_2 titration, was 6%. The ion intensity expected if no recombination had occurred in the ion source would then be:

$$0.5\times(6820+201)\times 0.06=210.$$

Thus, only 1 atom in 21 is ionized before recombining on the wall. This can be compared with LeGoff's calculation (27) that a molecule experiences an average of 50 collisions with the walls of a Nier-type source before being ionized or removed by the pump.

Recombination Coefficient of Oxygen Atoms

If it is assumed that atoms recombine exclusively on the walls, the recombination coefficient of O-atoms could also be determined by the NO_2 titration technique. The NO_2 was introduced successively at several positions along the tube connecting the discharge to the mass spectrometer leak. The O-atom concentration could then be measured as a function of time. The recombination coefficient on pyrex was found to be 1.1×10^{-4}, which agrees with the value of 1.2×10^{-4} reported by Linnett and Marsden (1).

Reactions of Activated Oxygen with Nitrogen Oxides

N_2O

The N_2O was introduced through an inlet jet. No change in mass spectrum was observed

Can. J. Chem. Downloaded from www.nrcresearchpress.com by 78.46.186.204 on 09/04/12
For personal use only.

when the oxygen was activated. The largest ion currents in the mass spectrum of pure N_2O occur at mass numbers 28, 30, and 44. This made detection of the possible reaction products, N_2 and NO, very difficult. Moreover, small changes in the parent peak were also difficult to measure, since the background CO_2^+ ion current changes when the oxygen is activated. The uncertainties in measuring these ion intensities were estimated to be about 5%. On this basis, an upper limit for the second-order rate constant for the reaction of N_2O with O-atoms can be placed at 1×10^8 cm.^{3} mole^{-1} sec.$^{-1}$.

The rate constant for the reaction

$$N_2O + O \rightarrow 2NO \qquad [3]$$

must be several orders of magnitude less than this, since no chemiluminescence was detected from the subsequent reaction

$$NO + O \rightarrow NO_2 + h\nu \qquad [4]$$

for reaction times 100 times as long as those used in the mass spectrometer measurements. The limit of detection of the chemiluminescence is also many times lower than that of the mass spectrometer.

This is in agreement with the results of Kaufman *et al.* (28), who studied the thermal decomposition of N_2O and, by an indirect calculation, estimated $k_3 = 1\times10^{11}\ e^{-15,500/RT}$ cm.^{3} mole^{-1} sec.$^{-1}$. Zelikoff and Aschenbrand (29) have proposed reaction [3] as an important step in the photolysis of N_2O at 1849 Å and at 1470 Å. This can only be reconciled with the present observations if oxygen atoms are present in excited states. This has recently been suggested by the same authors (30).

NO *and* NO_2

Reaction times of 0.02 and 0.5 seconds were used with these reactants. The only reaction products detected when either of these oxides was reacted with activated oxygen was the other oxide. No ion current at mass 62, corresponding to NO_3^+, was ever observed. The ratio of NO to NO_2 was always high, regardless of the reactant or reaction time. This would indicate that reaction [1] is much faster than reaction [2]. However, if these were the only important reactions, the ratio $[NO]/[NO_2]$ would be expected to equal k_1/k_2 [M], and should be independent of initial reactant concentration. This was not found to be the case. For example, when NO_2 was used as the reactant, the ratio of concentrations increased from 34 to 460 as the initial NO_2 concentration was increased from 0.4 to 10%. Apparently other important reactions are also occurring. These reactions are being investigated in more detail.

REFERENCES

1. LINNETT, J. W. and MARSDEN, D. G. H. Proc. Roy. Soc. (London), A, **234**, 489 (1956).
2. BENSON, S. W. and AXWORTHY, A. E. J. Chem. Phys. **26**, 1718 (1957).
3. BARTH, C. A. and KAPLAN, J. J. Chem. Phys. **26**, 506 (1957).
4. FORD, H. W. and ENDOW, N. J. Chem. Phys. **27**, 1156 (1957).
5. JACKSON, D. S. and SCHIFF, H. I. J. Chem. Phys. **23**, 2333 (1955).
6. DUVAL, X., LEGOFF, P., and VALENTIN, R. J. chim. phys. **53**, 757 (1956).
7. NIGHTINGALE, R. F., DOWNIE, A. R., ROTENBERG, D. L., CRAWFORD, B., Jr., and OGG, R. A., Jr. J. Phys. Chem. **58**, 1047 (1954).
8. FRIEDEL, R. A., SHARKEY, A. G., Jr., SHULTZ, J. L., and HUMBERT, C. R. Anal. Chem. **25**, 1314 (1953).
9. WARREN, J. W. Nature, **165**, 810 (1950).
10. HAGSTRUM, H. D. Revs. Modern Phys. **23**, 185 (1951).
11. WATANABE, K. J. Chem. Phys. **26**, 542 (1957).
12. HERZBERG, G. Spectra of diatomic molecules. D. Van Nostrand Company, Inc., New York. 1950. p. 561.
13. HAGSTRUM, H. D. J. Chem. Phys. **23**, 1178 (1955).
14. THORBURN, R. Applied mass spectrometry. The Institute of Petroleum, London. 1955. p. 185.
15. SMYTH, H. D. Revs. Modern Phys. **3**, 147 (1931).
16. HERRON, J. T. and SCHIFF, H. I. J. Chem. Phys. **24**, 1226 (1956).

Can. J. Chem. Downloaded from www.nrcresearchpress.com by 78.46.186.204 on 09/04/12
For personal use only.

17. HARTECK, P. and DONDES, S. J. Chem. Phys. **21**, 2240 (1953).
18. MCGRATH, W. D. and NORRISH, R. G. W. Proc. Roy. Soc. (London), A, **242**, 265 (1957).
19. HERZBERG, G. Spectra of diatomic molecules. D. Van Nostrand Company, Inc., New York. 1950. p. 446.
20. FONER, S. N. and HUDSON, R. L. J. Chem. Phys. **25**, 602 (1956).
21. BROIDA, H. P. and GAYDON, A. G. Proc. Roy. Soc. (London), A, **222**, 181 (1954).
22. BRANSCOMB, L. M. Phys. Rev. **86**, 258 (1952).
23. CHAPMAN, S. Proc. Roy. Soc. (London), A, **132**, 353 (1931).
24. HERZBERG, G. Atomic spectra. Prentice-Hall, Inc., New York. 1937.
25. SPEALMAN, M. L. and RODEBUSH, W. H. J. Am. Chem. Soc. **57**, 1474 (1935).
26. STEVENSON, D. P. and OTVOS, J. W. J. Am. Chem. Soc. **78**, 546 (1956).
27. LEGOFF, P. J. chim. phys. **50**, 423 (1953).
28. KAUFMAN, F., GERRI, N. J., and BOWMAN, R. E. J. Chem. Phys. **25**, 106 (1956).
29. ZELIKOFF, M. and ASCHENBRAND, L. M. J. Chem. Phys. **22**, 1680 (1954).
30. ZELIKOFF, M. and ASCHENBRAND, L. M. J. Chem. Phys. **27**, 123 (1957).

Can. J. Chem. Downloaded from www.nrcresearchpress.com by 78.46.186.204 on 09/04/12
For personal use only.

Can. J. Chem. Downloaded from www.nrcresearchpress.com by 78.46.186.204 on 09/04/12
For personal use only.

THE REACTIONS OF DIMETHYL- AND TRIMETHYL-AMINES WITH ATOMIC HYDROGEN[1]

Z. M. GEORGE, A. N. WRIGHT,[2] AND C. A. WINKLER

ABSTRACT

The reactions of hydrogen atoms with dimethyl- and trimethyl-amines produced mainly methane, together with relatively large quantities of ethane and small amounts of hydrogen cyanide. Dimethylamine was also a product of the trimethylamine reaction.

The reactions of hydrogen atoms with dimethyl- and trimethyl-amines have never been directly investigated. It was of particular interest to determine whether these reactions, like the corresponding reactions of ethylenimine and N-methylethylenimine (1), and of methyl- and ethyl-amines (2), would yield hydrogen cyanide as a product.

EXPERIMENTAL

The apparatus and techniques employed were similar to those described in the earlier papers (1, 2) from this laboratory. The total pressure of atomic and molecular hydrogen in the reaction system was 0.80 mm., with a molecular hydrogen flow rate of 7.6×10^{-5} mole per second. The hydrogen atom concentration was 5.7% at 60° C., and 4.2% at 275° C., as estimated from the amounts of reaction when ethyl chloride and hydrogen bromide were used as reactants at these temperatures (3).

RESULTS AND DISCUSSION

Figs. 1A and 2A show that both dimethyl- and trimethyl-amines react with hydrogen atoms to produce hydrogen cyanide. For both amines, the rates of production of hydrogen cyanide were linear at low flow rates of amine and increased with temperature, while at higher flow rates they passed through maxima beyond which they eventually decreased to zero.

Analyses for products other than hydrogen cyanide were made for the reactions at 60° C. The results are shown in Figs. 1 and 2, B and C. As with methylamine and ethylamine (2), free ammonia was recovered only when the total amount of base recovered exceeded the total amount of hydrogen cyanide, and conversely free hydrogen cyanide was recovered only when its amount exceeded the total recovery of base. A small amount of substance was recovered from the dimethylamine reaction which gave titration for neither base nor cyanide and defied infrared identification (cf. ref. (2)).

The maximum amounts of dimethyl- and trimethyl-amines reacted were less than the estimated hydrogen atom concentration and the amounts of reaction decreased at higher amine flow rates. As in the methylamine reaction, methane was the main product of the reactions and its amount passed through a maximum with increase in flow rate of amines. The amount of ethane produced attained a constant value in both reactions at relatively high flow rates.

The non-condensables, which consisted mainly of nitrogen and methane, were estimated mass spectrometrically for the dimethylamine reaction, and by gas chromatography (molecular sieve 5A, mesh 30–70, temperature 50° C.) for the trimethylamine reaction.

[1]*Manuscript received March 27, 1958.*
Contribution from the Physical Chemistry Laboratory, McGill University, Montreal, with financial assistance from the National Research Council of Canada, Ottawa, Canada.
[2]*Holder of N.R.C. Bursary and Studentships, 1954, 1955, 1956.*

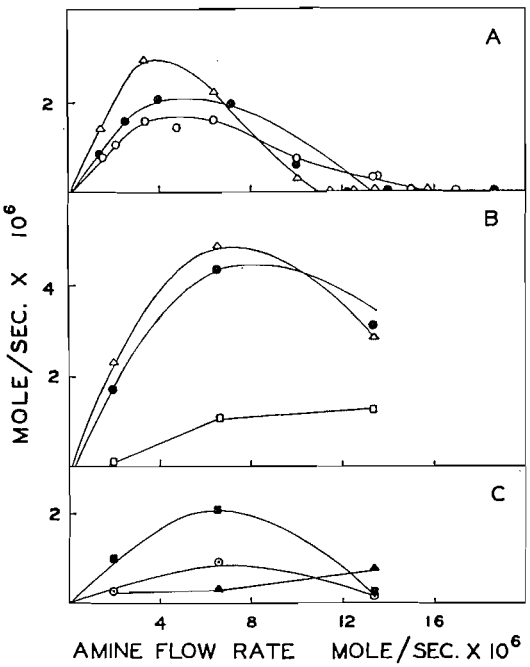

FIG. 1. Dimethylamine – hydrogen atom reaction. A—HCN production: ○ 56±5° C. ● 180±6° C. △ 284±4° C.
B and C—Amine reacted and products formed at 56±5° C.: ● Dimethylamine reacted. △ Methane. □ Ethane. ■ HCN. ⊙ "No titer". ▲ NH_3.

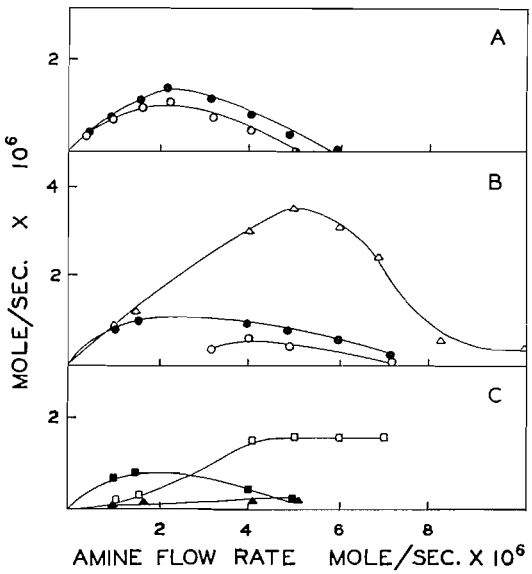

FIG. 2. Trimethylamine – hydrogen atom reaction. A—HCN production: ○ 56±3° C. ● 275±5° C. B and C—Amine reacted and products formed at 56±3° C.: ● Trimethylamine reacted. △ Methane. ○ Nitrogen. □ Ethane. ■ HCN. ▲ NH_3.

At flow rates beyond which no hydrogen cyanide was formed, the trimethylamine–hydrogen atom reaction yielded some dimethylamine, as shown by chromatographic separation (silica gel column at 50° C.) of trimethylamine from mixtures of the condensable products from which ethane and ammonia had been removed by distillation. The "recovered" trimethylamine was found to be approximately 35% dimethylamine. A series of experiments conducted with about 1% hydrogen atoms at very high flow rates of trimethylamine produced no liquid (4); the reactions appeared to follow the same course as with 5.7% hydrogen atom concentration.

Mechanisms similar to those suggested previously for the reactions of hydrogen atoms with methyl- and ethyl-amines (2) may be postulated to explain the main features of the corresponding reactions with dimethyl- and trimethyl-amines. The primary process in both reactions is probably hydrogen atom abstraction, i.e. for dimethylamine,

$$(CH_3)_2NH + H \rightarrow (CH_3)_2\dot{N} + H_2 \qquad \Delta H = -9 \text{ kcal.} \qquad [1a]$$

and

$$(CH_3)_2NH + H \rightarrow CH_3NH\dot{C}H_2 + H_2 \qquad \Delta H = -9 \text{ kcal.} \qquad [1b]$$

and for trimethylamine,

$$(CH_3)_3N + H \rightarrow (CH_3)_2N{-}\dot{C}H_2 + H_2 \qquad \Delta H = -9 \text{ kcal.} \qquad [1c]$$

Can. J. Chem. Downloaded from www.nrcresearchpress.com by 78.46.186.204 on 09/04/12
For personal use only.

The radicals formed in these reactions could react further with hydrogen atoms to form activated dimethylamine and trimethylamine molecules containing about 85 kcal. of excess energy, and these could dissociate

$$(CH_3)_2NH^* \rightarrow CH_3 + CH_3NH \qquad \Delta H = -20 \text{ kcal.} \qquad [2a]$$

$$(CH_3)_2NH^* \rightarrow CH_4 + CH_3N \qquad \Delta H = -17 \text{ kcal.} \qquad [2b]$$

and

$$(CH_3)_3N^* \rightarrow CH_3 + (CH_3)_2N \qquad \Delta H = -12 \text{ kcal.} \qquad [2c]$$

$$(CH_3)_3N^* \rightarrow CH_4 + CH_3{-}N{-}CH_2 \qquad \Delta H = -11.9 \text{ kcal.} \qquad [2d]$$

The dimethylamine radical formed in reaction [2*c*] could react with another hydrogen atom or a trimethylamine molecule to produce an activated dimethylamine molecule which could dissociate as in [2*a*] or [2*b*], but might be deactivated by collision to appear as the dimethylamine observed in the products from the trimethylamine reaction. The CH_3NH radical produced in [2*a*] could react further with hydrogen atoms to produce activated methylamine (2), followed by its dissociation to yield CH_3N radicals from which hydrogen cyanide might be formed as outlined previously,

$$CH_3N \rightarrow HCN + H_2 \qquad \Delta H = -48 \text{ kcal.} \qquad [3]$$

The only plausible reason for a decrease in hydrogen cyanide production at high flow rates of dimethyl- and trimethyl-amine appears to be recombination of CH_3N radicals, or their reaction to produce C_2H_6 and N_2, before they suffer decomposition to hydrogen cyanide.

Formation of methane as the main product of the reaction of hydrogen atoms with dimethyl- and trimethyl-amines is readily explained by reaction of methyl radicals with hydrogen atoms and hydrogen abstraction from the amines by methyl radicals. The decrease and final levelling out of methane production at high flow rates of trimethylamine might be attributed to the replacement of methyl radical – hydrogen atom reaction by the slower abstraction reactions and increased recombination of methyl radicals to form ethane, as the supply of hydrogen atoms is depleted by increased extents of the primary reactions. The apparent decrease in the amount of amine reacted at higher flow rates of amines could be attributed to the stabilization by collision of the activated amines which otherwise decompose by reactions [2*a*] to [2*d*].

REFERENCES

1. JAMIESON, J. W. S. and WINKLER, C. A. J. Phys. Chem. **60**, 1542 (1956).
2. WRIGHT, A. N., JAMIESON, J. W. S., and WINKLER, C. A. J. Phys. Chem. (In press).
3. WILES, D. M. and WINKLER, C. A. J. Phys. Chem. **61**, 620 (1957).
4. GESSER, H., MULLHAUPT, J. T., and GRIFFITHS, J. E. J. Am. Chem. Soc. **79**, 4834 (1957).

Can. J. Chem. Downloaded from www.nrcresearchpress.com by 78.46.186.204 on 09/04/12
For personal use only.

Can. J. Chem. Downloaded from www.nrcresearchpress.com by 78.46.186.204 on 09/04/12
For personal use only.

PREDICTION OF SOME THERMODYNAMIC PROPERTIES EMPLOYING THE ISOELECTRONIC PRINCIPLE[1]

P. SMITH AND C. N. R. RAO

ABSTRACT

An empirical method for predicting standard enthalpies and free energies of formation of isoelectronic molecules bearing in turn the groupings —F, —OH, —NH_2, and —CH_3 is proposed and used. It appears to be accurate to about ±10 kcal. $mole^{-1}$ or better depending on the procedure employed.

INTRODUCTION

There have been a number of useful empirical correlations between the different properties of bonds in similar molecules (1, 2, 3, 4, 5). Similar to these are the regular trends noticed in the case of the thermodynamic properties of related substances (6, 7, 8). The present paper gives a method whereby thermodynamic trends have been applied in predicting some thermodynamic quantities. Of particular interest was the prediction of the thermodynamic properties of the hypothetical substance H_2O_3, a postulated product (9) when dissociated water vapor is condensed at low temperatures.

BASIS OF THE METHOD

It is to be expected that regularities in thermodynamic quantities would be particularly evident between molecules of similar electronic structure, in harmony with the corresponding correlations of other molecular properties with electronic structure for isoelectronic molecules (10). In view of the comparative plenty of thermodynamic data on sequences of isoelectronic molecules bearing in turn the isoelectronic groupings[2] —CH_3, —NH_2, —OH, and —F attention here has been confined to them. The most convenient variable with which to relate these thermodynamic quantities[3] proved to be the atomic number of the non-hydrogen atom in the —X group,[2] owing to the paucity of data on other possible parameters for the range of molecules covered.

In general no smooth regularities are obtained if ΔH_f° or ΔF_f° values, for substances either in their standard states at 25° C. or as gases in their standard states at 25° C., are plotted against atomic number. To circumvent this difficulty these quantities were amended before use so as to relate to similar processes of formation from X_2. For example, ΔH_f° values for the HX sequence show no smooth trend with atomic number variation, but ΔH° values for the synthetic processes of the type

$$\tfrac{1}{2}H_2+\tfrac{1}{2}X_2 = HX \qquad [1]$$

do. To distinguish the value of ΔH° for step [1] with all substances in their standard states at 25° C. from that with all substances as gases in their standard states at 25° C., the former is denoted by $\Delta H_f^{\circ *}$ and the latter by $\Delta H_f^{\circ **}$. Similar notation is used for ΔF values. Fig. 1 illustrates the success achieved for this series. As might have been

[1]*Manuscript received May 5, 1958.*
Contribution from the Department of Chemistry, Purdue University, Lafayette, Indiana. Taken in part from a paper presented at a Symposium on Free Radicals: Recent Progress in Their Production and Identification, Laval University, September 10 and 11, 1956.

[2]*These will be denoted by the general symbol —X.*

[3]*All thermodynamic data used in this paper relate to 25° C. unless stated otherwise. All data are taken from the usual standard sources (11, 12) except for the values given in the Appendix and some of the values listed in Tables I and II for comparison purposes.*

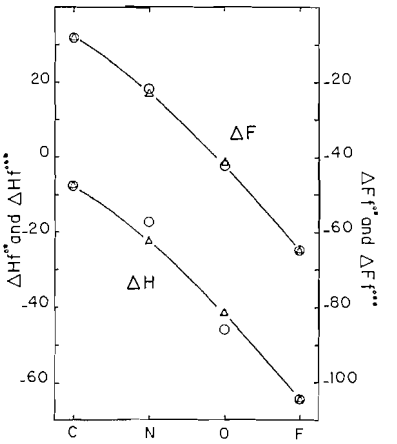

FIG. 1. $\Delta H°$ and $\Delta F°$, in kcal. mole^{-1}, for the reaction, $\frac{1}{2}H_2 + \frac{1}{2}X_2 = HX$ as a function of X. ○, $\Delta H_f°*$ or $\Delta F_f°*$; △, $\Delta H_f°**$ or $\Delta F_f°**$.

expected, the two sequences involving the all-gas-phase synthetic reaction, so reducing the effects of intermolecular forces, give the smoothest trends (which are the ones drawn). But the other two sets of points, relating to $\Delta H_f°*$ and $\Delta F_f°*$, deviate from their corresponding all-gas-phase plots by no more than ± 5 kcal. mole^{-1}, suggesting that $\Delta H_f°*$ and $\Delta F_f°*$ plots might be adequate for the many other possible sequences where gas-phase data are often lacking.

This conclusion is borne out by Fig. 2, which shows smooth trends in $\Delta H_f°*$ and $\Delta F_f°*$ for the synthetic process

$$C_6H_6 + \tfrac{1}{2}X_2 = C_6H_5X + \tfrac{1}{2}H_2. \qquad [2]$$

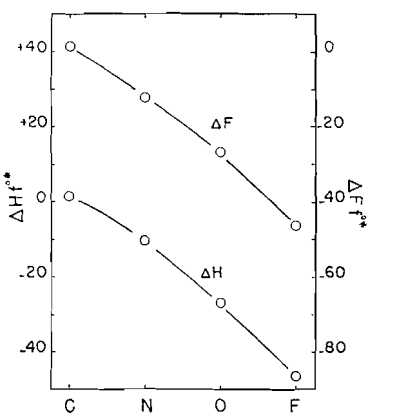

FIG. 2. $\Delta H°$ and $\Delta F°$, in kcal. mole^{-1}, for the reaction $C_6H_6 + \frac{1}{2}X_2 = C_6H_5X + \frac{1}{2}H_2$ as a function of X.

Figs. 3 and 4 indicate similar trends in $\Delta H_f°*$ for a variety of different processes. The data in these last cases are not complete. For this same reason $\Delta F_f°*$ plots are not even attempted.

PREDICTIONS

From Figs. 3 and 4 estimates of the unknown $\Delta H_f°$ values may be made. These are given in Table I together with similarly predicted values taken from Fig. 5. All estimates

Can. J. Chem. Downloaded from www.nrcresearchpress.com by 78.46.186.204 on 09/04/12
For personal use only.

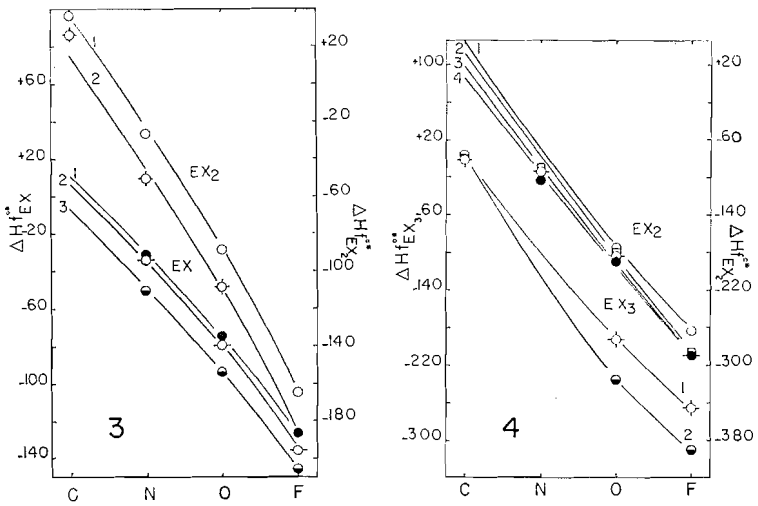

FIG. 3. $\Delta H°$, in kcal. mole^{-1}, for the reaction $E + X_2 = EX_2$ as a function of X and E; 1, E = Cd; 2, E = Zn. $\Delta H°$, in kcal. mole^{-1}, for the reaction $E + \frac{1}{2}X_2 = EX$; 1, E = Cs; 2, E = Na; 3, E = Li; the points for KX and RbX, in both cases X being —NH_2, —OH, and —F, are omitted because they lie between the corresponding Cs and Na points.

FIG. 4. $\Delta H°$, in kcal. mole^{-1}, for the reaction $E + 1\frac{1}{2}X_2 = EX_3$ as a function of X and E; 1, E = B; 2, E = Al. $\Delta H°$, in kcal. mole^{-1}, for the reaction $E + X_2 = EX_2$; 1, E = Mg; 2, E = Ba; 3, E = Sr; 4, E = Ca.

in Table I relate to the substances in their thermodynamically stable standard states at 25° C. and 1 atm. pressure. Table II lists further estimated $\Delta H_f°$ values, taken from

TABLE I

ESTIMATES OF STANDARD ENTHALPIES OF FORMATION AT 25° C.

Compound[a]	$\Delta H_f°$, kcal. mole^{-1}	$\Delta H_f°$, kcal. mole^{-1} (literature)	Reference
$LiCH_3$	−17	—	—
$NaCH_3$	−4	—	—
KCH_3	−4	—	—
$RbCH_3$	+1	—	—
$CsCH_3$	+1	—	—
$Mg(CH_3)_2$	+24	—	—
$Mg(NH_2)_2$	−56	—	—
$Ca(CH_3)_2$	−14	—	—
$Sr(CH_3)_2$	0	—	—
$Ba(CH_3)_2$	+12	—	—
$B(NH_2)_3$	−82	—	—
$Al(NH_2)_3$	−108	—	—
ZnF_2	−186	−187.9[b]	11
HCOF	−103	—	—
CH_3COF	−119	−104.4[c]	13
CH_3F	−44	−59±2[c]	21
$(HO)_2CO$	−162	−167.0[b]	11
CH_3CH_2COOH	−123	−122[d]	14
HOF	−9	—	—
NH_2F	−5	—	—

[a]Each in its thermodynamically stable state at 1 atm. pressure.

[b]Aq.

[c](g) at 16° C.; −110.6 kcal. mole^{-1} for (1) at 16° C. (13).

[d]Calculated from heat of combustion data given in the reference (14) as referring to 18–20° C.

[e]The uncertainty quoted is that given in the reference (21).

Can. J. Chem. Downloaded from www.nrcresearchpress.com by 78.46.186.204 on 09/04/12
For personal use only.

Fig. 5 and not presented in Table I, together with any related $\Delta F_f°$ data that could be deduced by this method. All predictions in Table II refer to the substances in the gaseous state because they are derived from all-gas-phase plots. The trends in Figs. 3 and 4 were taken as non-linear; those in Fig. 5 and Table II were less similar to one another and so were drawn as straight lines by the method of least squares. It is unlikely that the estimated values are uncertain by more than about ± 10 kcal. mole^{-1}. This uncertainty limit is supported by the size of the trend irregularities present in Figs. 1 to 5.

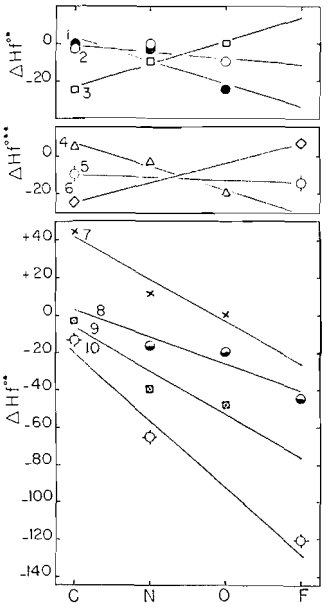

FIG. 5. $\Delta H°$, in kcal. mole^{-1}, for the reactions:

1, $\frac{1}{2}C_2H_6 + \frac{1}{2}X_2 = XCH_3$
2, $\frac{1}{2}N_2H_4 + \frac{1}{2}X_2 = XNH_2$
3, $\frac{1}{2}H_2O_2 + \frac{1}{2}X_2 = XOH$
4, $C_2H_6(g) + \frac{1}{2}X_2(g) = XC_2H_5(g) + \frac{1}{2}H_2(g)$
5, $\frac{1}{2}Cl_2(g) + \frac{1}{2}X_2(g) = XCl(g)$
6, $\frac{1}{2}O_2(g) + X_2(g) = X_2O(g)$
7, $CH_3COOH + \frac{1}{2}X_2 = CH_3COX + \frac{1}{2}H_2O_2$
8, $HCHO + \frac{1}{2}X_2 = XCHO + \frac{1}{2}H_2$
9, $CH_3COOH + \frac{1}{2}X_2 = XCH_2COOH + \frac{1}{2}H_2$
10, $CO + X_2 = COX_2$ as a function of X.

TABLE II

ESTIMATES OF STANDARD ENTHALPIES AND FREE ENERGIES OF FORMATION AT 25° C.

Compound	$\Delta H_f°$, kcal. mole^{-1}	$\Delta F_f°$, kcal. mole^{-1}
$NH_2Cl(g)$	0	—
$HOCl(g)$	-29^a	—
$(NH_2)_2O(g)$	+9	+29
$(HO)_2O(g)$	−35	-24^b
$C_2H_5F(g)$	−50	−40

[a] A recent calculation (17) of the bond dissociation energy $D°$(HO—Cl) at 25° C. gives a value for $\Delta H_f°$ HOCl(g) of -21 ± 3 kcal. mole^{-1}.

[b] Bray (18) has estimated $\Delta F_f°$ H_2O_3(aq.) and $\Delta H_f°$ 0° K. H_2O_3(g) to be not greater than −10 and −17 kcal. mole^{-1} respectively. The method used is not clear.

Can. J. Chem. Downloaded from www.nrcresearchpress.com by 78.46.186.204 on 09/04/12
For personal use only.

The agreement between the estimates by this method and the compared values given in Tables I and II is not against this assessment of the error. In the case of acetyl fluoride the two values listed in Table I are 15 kcal. mole^{-1} apart. This is probably, to some extent, because the normal boiling point of acetyl fluoride is only 4° C. below 25° C. (15); also the estimated value is obtained by extrapolation and not interpolation.[4] It is possible that the predicted data given in Table II are uncertain to only ±5 kcal. mole^{-1}, being derived from all-gas-phase plots which are also of small slope.

DISCUSSION

The trends observed in Figs. 1 to 5 appear nearly linear. The processes involved are of the types

$$RH+\tfrac{1}{2}X_2 = RX+\tfrac{1}{2}H_2, \quad [3]$$

$$\tfrac{1}{2}RR+\tfrac{1}{2}X_2 = RX, \quad [4]$$

$$E+\tfrac{1}{2}X_2 = EX, \quad [5]$$

where RH and RR are compounds and E is an atom or a molecule. These are not all that are possible. For example, [3] added to [4], taking RR as H_2, gives

$$RH+X_2 = RX+HX. \quad [6]$$

The fact that $\Delta H°$ for the reaction

$$\tfrac{1}{2}X_2(g) = X\cdot(g) \quad [7]$$

also shows a nearly linear trend (19), namely 42, 30±2, 26, and 18 kcal. mole^{-1} for methyl (11), amino (5), hydroxyl (11), and fluorine (20) respectively, implies, for example, that $\Delta H°$ for the process

$$RX(g) = R\cdot(g)+X\cdot(g), \quad [8]$$

namely $D°$(R—X), shows a similar variation with X, by virtue of the linear relation applying for [3]. This must also be so for the quantity ($\Delta H_f°$ X·(g) $-\Delta H_f°$ RX(g)) inasmuch as R· is fixed within a series. A difficulty in employing this type of dependence to estimate unknown values of $\Delta H_f°$ and unknown bond dissociation energies is the uncertainty (5) in some of the values of $\Delta H_f°$ X·(g). This could be avoided by using plots of $\Delta H_f°$ values for one complete sequence, RX(g), versus that for another, incomplete sequence R′X(g). It is of course implied above that $D°$(R—X) versus $D°$(R′—X) plots should be nearly linear also, although such plots are generally less convenient to use than the $\Delta H_f°$ RX, R′X correlations because the $D°$ values often have to be calculated from $\Delta H_f°$ data.

The fact that bond dissociation energies of isoelectronic bonds of the first row halogen-type radicals show nearly linear changes with atomic number can be appreciated qualitatively in terms of the similarity of bonding involved, as pointed out by others (19). A quantitative explanation is, so far, lacking, although the tentative, approximate formula treatment by Mulliken would appear to show promise (22). The approach used in Figs. 1 to 5 may be regarded as a limited extension to the empirical formula used by Pauling (23) for the value of $\Delta H_f°$ in kilocalories for a compound in its standard state, containing n_N and n_O atoms per molecule of nitrogen and oxygen respectively,

[4]*At the time this method was first developed $\Delta H_f°$ for liquid fluorobenzene was not known. Using the available data in Fig. 2 gave a predicted value of −38±5 kcal. mole^{-1} in agreement with the since reported (16) figure of −34.75±0.3 kcal. mole^{-1}, now plotted in Fig. 2.*

Can. J. Chem. Downloaded from www.nrcresearchpress.com by 78.46.186.204 on 09/04/12
For personal use only.

$$-\Delta H_f^\circ = 23.06 \sum(x_A - x_B)^2 - 55.1\ n_N - 24.2\ n_O, \quad [9]$$

where x_A and x_B are the electronegativities of atoms A and B making bond A—B in the compound and the summation is taken over all bonds. The present use of $\Delta H_f^{\circ **}$ or $\Delta H_f^{\circ *}$ values instead of the unamended ΔH_f° data eliminates the n_N and n_O correction terms that allow for the multiple bond character of the bonds in N_2 and O_2 and, in case [3] for example, it follows that

$$-\Delta H_f^{\circ **} = 23.06[(x_R - x_X)^2 - (x_R - x_H)^2], \quad [10]$$

where x_R and x_X are the electronegativities, on the Pauling scale, for the atoms that make the R—X bond. Now x_X varies linearly (23) with atomic number, being 2.5, 3.0, 3.5, and 4.0 respectively for C, N, O, and F. This makes equation [10] predict trends of $-\Delta H_f^{\circ **}$, or $-\Delta H_f^{\circ *}$, with atomic number much more strongly parabolic than those observed. This difference is emphasized by the fact that, from [4] for example,

$$\Delta H_f^{\circ **}\ RX(g) = D^\circ(R—X) - \tfrac{1}{2}[D^\circ(R—R) + D^\circ(X—X)] \quad [11]$$

shows a nearly linear dependence upon x_X, whereas the simple Pauling definition of electronegativity assumes a linear dependence upon $(x_X - x_R)^2$. However, the Pauling electronegativity values are based upon bond energy term data and not bond dissociation energies, so the discrepancy is not unexpected.

ACKNOWLEDGMENTS

The authors wish to thank Dr. E. J. Prosen, National Bureau of Standards, Washington, D. C., and Dr. D. W. Scott, Bureau of Mines, Bartlesville, Oklahoma, for helpful information.

REFERENCES

1. GLOCKLER, G. J. Phys. Chem. **61**, 31 (1957).
2. SMITH, R. P. J. Phys. Chem. **60**, 1293 (1956).
3. PAULING, L. J. Phys. Chem. **58**, 662 (1954).
4. BAUGHAN, E. C. Trans. Faraday Soc. **53**, 1046 (1957).
5. COTTRELL, T. L. *In* The strengths of chemical bonds. Butterworths Scientific Publications, London. 1954.
6. JANZ, G. J. Quart. Revs. (London), **9**, 229 (1955).
7. BAUGHAN, E. C. Quart. Revs. (London), **7**, 103 (1953).
8. LONG, L. H. Quart. Revs. (London), **7**, 134 (1953).
9. GHORMLEY, J. A. J. Am. Chem. Soc. **79**, 1862 (1957).
10. WALSH, A. D. *In* Progress in stereochemistry. Vol. I. *Edited by* W. Klyne. Butterworths Scientific Publications, London. 1954.
11. SELECTED VALUES OF CHEMICAL THERMODYNAMIC PROPERTIES. National Bureau of Standards Circ. No. 500. U. S. Government Printing Office, Washington, D.C. 1952.
12. SELECTED VALUES OF PROPERTIES OF HYDROCARBONS AND RELATED COMPOUNDS. American Petroleum Institute Research Project 44, Carnegie Institute of Technology, Pa. National Bureau of Standards Circ. U. S. Government Printing Office, Washington, D.C. 1952.
13. PRITCHARD, H. O. and SKINNER, H. A. J. Chem. Soc. 1099 (1950).
14. INTERNATIONAL CRITICAL TABLES. Vol. V. McGraw-Hill Book Company, Inc., New York, N.Y. 1929.
15. HANDBOOK OF CHEMISTRY AND PHYSICS. 35th ed. Chemical Rubber Publishing Company, Cleveland, Ohio. 1953.
16. SCOTT, D. W., MCCULLOUGH, J. P., GOOD, W. D., MESSERLY, J. F., PENNINGTON, R. E., KINCHELOE, T. C., HOSSENLOPP, I. A., DOUSLIN, D. R., and WADDINGTON, G. J. Am. Chem. Soc. **78**, 5457 (1956).
17. GELLES, E. Trans. Faraday Soc. **47**, 1158 (1951).
18. BRAY, W. C. J. Am. Chem. Soc. **60**, 82 (1938).
19. EVANS, M. G., WARHURST, E., and WHITTLE, E. J. Chem. Soc. 1524 (1950).
20. EVANS, W. H., MUNSON, T. R., and WAGMAN, D. D. J. Research Natl. Bur. Standards, **55**, 147 (1955).
21. MARGRAVE, J. L. J. Chem. Phys. **24**, 475, 476 (1956).
22. MULLIKEN, R. S. J. Phys. Chem. **56**, 295 (1952).
23. PAULING, L. *In* The nature of the chemical bond. Cornell University Press, Ithaca, New York, N.Y. 2nd ed. 1940. Chap. II.

Can. J. Chem. Downloaded from www.nrcresearchpress.com by 78.46.186.204 on 09/04/12
For personal use only.

24. AUDRIETH, L. F. and OGG, B. A. *In* The chemistry of hydrazine. John Wiley & Sons, Inc., New York, N.Y. 1951.
25. SCHUMB, W. C., SATTERFIELD, C. N., and WENTWORTH, R. L. *In* Hydrogen peroxide. Reinhold Publishing Corporation, New York, N.Y. 1955.
26. PARKS, G. S., MANCHESTER, K. E. M., and BAUGHAN, L. M. J. Chem. Phys. **22**, 2089 (1954).
27. PARKS, G. S., HUFFMAN, H. M., and BARMORE, M. J. Am. Chem. Soc. **55**, 2733 (1933).
28. COLE, L. G. and GILBERT, E. J. Am. Chem. Soc. **73**, 5423 (1951).
29. SNEED, M. C., MAYNARD, J. L., and BRASTED, R. C. *In* Comprehensive inorganic chemistry. Vol. III. D. Van Nostrand Company, Inc., New York, N.Y. 1954.
30. MILES, C. B. and HUNT, H. J. Phys. Chem. **45**, 1346 (1947).

APPENDIX

Table III lists thermodynamic data used that were not taken from standard compilations (11, 12).

TABLE III

THERMODYNAMIC DATA AT 25° C. NOT TAKEN FROM STANDARD COMPILATIONS (11, 12)

Compound	$\Delta H_f°$, kcal. mole^{-1}	$\Delta F_f°$, kcal. mole^{-1}	Reference
$N_2H_4(g)$	+22.70	+37.96	24
$H_2O_2(l)$	−44.85	−28.78	25
$H_2O_2(g)$	−32.52	−25.24	25
$C_6H_5OH(c)$	−38.87	−11.38	26, 27
$C_6H_5NH_2(l)$	+7.41	+35.59	27, 28
$C_6H_5F(l)$	−34.75	−16.51	16
$FCl(g)$	−13.4	—	20
$F_2O(g)$	+7.6	+11.8	20
$COF_2(g)$	−146	—	29
$(CH_3)_2CO(l)$	−59.34	—	30

Can. J. Chem. Downloaded from www.nrcresearchpress.com by 78.46.186.204 on 09/04/12
For personal use only.

Can. J. Chem. Downloaded from www.nrcresearchpress.com by 78.46.186.204 on 09/04/12
For personal use only.

HYDROGEN BONDING IN THE AMINE HYDROHALIDES

I. GENERAL ASPECTS[1, 2]

BERNADETTE CHENON[3] AND C. SANDORFY

ABSTRACT

The infrared spectra of 17 amine hydrohalides have been measured in the solid state, in aqueous solutions, and in their conjugate amine. Their NH^+ stretching and scissoring bands are discussed.

The stretching bands of hydrogen-bonded aliphatic and aromatic amine hydrohalides fall into the same part of the spectrum. In the solid state, the hydrogen bonds are of type N^+—H- - -X^-. The aliphatic amine salts usually exhibit many sharp bands, while the aromatic amine salts have broad but composite bands. Tertiary amine salts show a hypsochromic shift in the order hydrochloride, hydrobromide, hydriodide; primary and secondary aliphatic amine salts show a slight bathochromic shift in the same order. Primary and secondary aromatic amine salts behave less regularly, although in most cases the shift is hypsochromic. These facts can be explained qualitatively by considering the charge distribution in the ionized amino groups and the contribution of electrostatic and delocalization effects to the energy of the hydrogen bonds.

The anharmonicity of the potential surface which causes the appearance of strong combination bands may lead to the broadening of bands or to many sharp bands. There is no parallelism in this latter case between shift and broadening of the bands.

The assignment of a strong band which appears in many cases near 2000 cm.$^{-1}$ is discussed.

The above-mentioned characteristic band shifting is absent in the spectra of aqueous solutions and it is concluded that in this case hydrogen bonding is not of the N^+—H- - -X^- but of the N^+—H- - -O type.

INTRODUCTION

The problem of hydrogen bonding has been the subject of hundreds of publications since the notion was introduced by Moore and Winmill in 1912 (1) and since the fundamental work of Bernal and Fowler in 1933 (2), and the field has been reviewed on several occasions (3, 4, 5, 6, 7).

The most conspicuous changes in the infrared spectrum of a compound due to hydrogen bonding are the shift of the X—H stretching bands to lower wave numbers, their increased intensity, their remarkable broadness, and their splitting to two or more components in many cases. Recently a comprehensive interpretation of these phenomena was attempted by Bratož and Hadži and we shall refer to their theory frequently below (8).

The wave mechanical aspect of the hydrogen-bond problem was reviewed by Coulson (9), who considers electrostatic, delocalization, repulsion, and dispersion force contributions to the energy of the hydrogen bond. This article too will be taken as one of the bases of our discussion.

Infrared spectra of amine salts exhibit all the main characteristics of spectra of hydrogen-bonded species to a large though varying degree. Electrostatic forces should be very strong in this case, since the proton donor and the proton acceptor are here both ions with net charges. Delocalization may also be an important factor, since the ionization potential of a halide ion is very low. As Lord and Merrifield have pointed out, the amine salts constitute a test case for every theory of hydrogen bonding (10). These authors as well as Rundle and Parasol (11) have already discussed a certain number of hydrohalide spectra.

[1]*Manuscript received April 14, 1958.*
Contribution from Département de Chimie, Université de Montréal, Montreal, Quebec.

[2]*Preliminary accounts of this work were given at the Annual Symposium on Molecular Spectroscopy, June 1955, Columbus, Ohio, and at the Congress of "L'Association Canadienne-Française pour l'Avancement des Sciences", November 1955, Ottawa, Canada.*

[3]*Present address: Institut du Radium, 11, rue Pierre Curie, Paris, France.*

We have measured the infrared spectra of the hydrochlorides, hydrobromides, and hydriodides of 17 amines among which primary, secondary, and tertiary aromatic and aliphatic amines were represented. The spectra were measured in the solid state, in aqueous solution, and in the conjugate amine if the latter was a liquid.

EXPERIMENTAL

A. Preparation of the Substances

Hydrochlorides

Hydrogen chloride gas was obtained by the action of sulphuric acid on dry sodium chloride. The gas was led through sulphuric acid and anhydrous calcium chloride and then into a solution of the amine in anhydrous ether. (One part by volume of amine in three parts of ether.)

Hydrobromides

Hydrogen bromide was obtained by the action of bromine on xylene. The gas was led through cold xylene and calcium sulphate and then into a solution of the amine in anhydrous ether.

Hydrochlorides and hydrobromides obtained by this method were filtered and washed with anhydrous ether. This was done in nitrogen atmosphere whenever the salt was hygroscopic. The products were recrystallized twice or three times from absolute alcohol by slow addition of anhydrous ether.

Hydriodides

Solutions of the amines in ether were extracted with 47% hydriodic acid in several successive operations. The latter was then evaporated under vacuum on a water bath. (This operation lasted at least two hours.) The product was washed several times in anhydrous ether, then dissolved in absolute alcohol, and recrystallized in the same way as the hydrochlorides and hydrobromides. Hydriodides are much less hygroscopic than the two other salts.

The preparation of the following compounds presented certain difficulties.

N-Methyl-diphenylamine Hydrochloride

The product was oily and crystallized by friction. This product was used although it was probably not of a high degree of purity.

The hydrochloride and hydrobromide of *N*,*N*-dimethylaniline were prepared at 0° C. Since they are very hygroscopic and somewhat unstable they were kept in a desiccator over potassium hydroxide and phosphorous pentoxide.

If prepared by the general methods given above the hydrochloride and the hydrobromide of tri-*n*-butylamine are non-recrystallizable oils. In order to prepare the hydrochloride the gas was led through a third desiccant and the pure amine was used instead of a solution in ether. The white product, very hygroscopic, was recrystallized under nitrogen atmosphere.

Pure ethylamine hydriodide was obtained from a commercial sample by heating it gently with potassium hydroxide bulbs. The gaseous amine was led into 47% hydriodic acid.

B. Measurement of the Spectra

The infrared spectra were measured on a Perkin–Elmer model 112 single beam double pass instrument with a sodium chloride prism.

Can. J. Chem. Downloaded from www.nrcresearchpress.com by 78.46.186.204 on 09/04/12
For personal use only.

The spectra were taken in three different media: in the solid state, in aqueous solution, and dissolved in the conjugate amine if the latter was a liquid. The cells were filled under nitrogen atmosphere whenever the compounds were hygroscopic.

The spectra of the solids were taken in a perfluorinated paraffin oil manufactured by Hooker-Electrochemical Co. of Niagara Falls, N.Y., and labelled "fluorolube T-45". Hydrogen atoms in this oil are replaced by fluorine and chlorine in the proportion 3:1. Nujol was unsuitable because of the importance of the CH_3 and CH_2 absorption region for the present study. In many cases, however, the spectra were measured in both nujol and fluorocarbon oil and the bands not covered by the nujol bands did not show any noticeable change. We shall assume, therefore, that the influence of the halogenated mulling agent on the spectra is negligible.

The KBr pellet technique was avoided, since under the pressure applied for preparing the pellets conditions for hydrogen bonding might change.

Amine hydrohalides are usually extremely soluble in water. In the present case concentration was as high as 400 mg./ml., that is, about 1 to 3 mole/liter. The salts of diphenylamine are insoluble in water and those of *N*-methyl-diphenylamine undergo decomposition in water.

With solutions of the salts in their amine the concentration was about 100 mg./ml., that is, of the order of 0.3 to 1 mole/liter.

The compounds not listed in Table III are either unstable or insufficiently soluble in their amine for the purpose of measuring their infrared spectra.

In many cases, when a saturated solution of a salt in its amine was prepared, a solid smear resulted. In other cases such a smear was prepared by using the conjugate amine as a mulling agent. This gave very intense spectra and was used for the determination of the NH_3^+ and NH_2^+ scissoring bands, which are often weak.

We have not attempted at this stage to make quantitative measurements of intensity or extinction coefficients.

RESULTS

A. Aliphatic Compounds

I. Spectra in the Solid State (Fluorocarbon Oil)

Stretching bands due to NH_2 and NH groups between 3500 and 3100 cm.$^{-1}$ have completely disappeared. (Table I. Strong bands are indicated by the use of italics.)

Stretching bands due to the protonated amino groups appear between 2800 and 2300 cm.$^{-1}$ (first region). In addition, prominent bands appear in some salts near 2000 cm.$^{-1}$ (second region) and the scissoring bands are in the 1600–1500 cm.$^{-1}$ region (third region). We shall not be concerned in this paper with bands at lower frequencies.

First Region

Primary aliphatic amine hydrohalides (Figs.* 1, 2, 3, 4) give a series of usually well-separated, sharp, or medium broad bands in the first region. Their number varies between four and nine. In certain instances, notably tertiary butylamine and cyclohexylamine salts, these bands are remarkably sharp and well resolved. (Table I. Shoulders are not listed in the tables. Thus the number of bands is often higher than may appear from the tables. See the figures.)

There are probably more bands which coincide with the CH_3 and CH_2 bands between 3000 and 2800 cm.$^{-1}$ and which we cannot separate out in the spectra reported here.

**The region occupied by the atmospheric CO_2 band is left empty on the figures. In Fig. 18, it is approximately subtracted from the spectrum.*

Can. J. Chem. Downloaded from www.nrcresearchpress.com by 78.46.186.204 on 09/04/12
For personal use only.

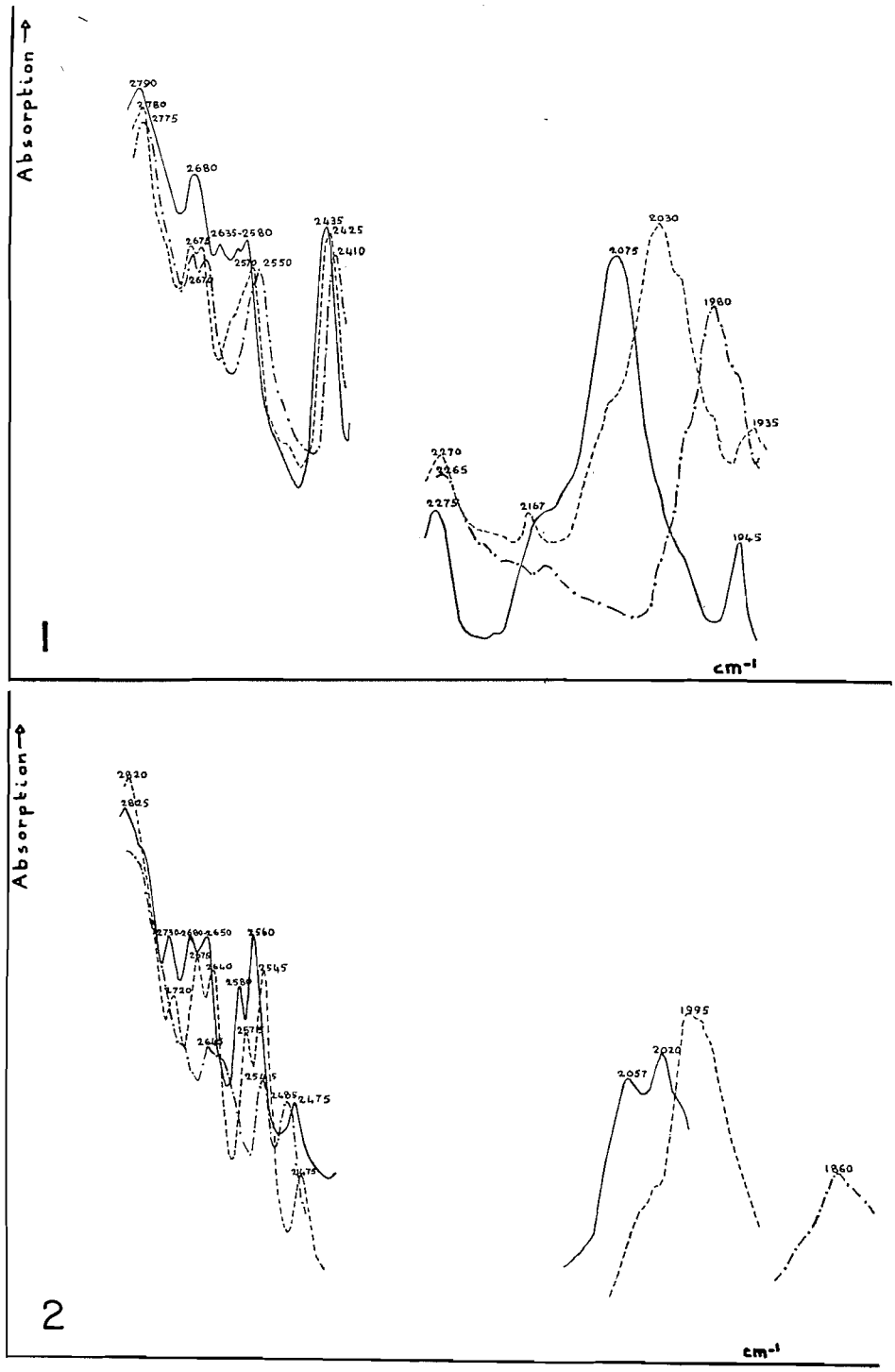

FIG. 1. Ethylamine hydrochloride ————
Ethylamine hydrobromide – – – – –
Ethylamine hydriodide — . — . —

FIG. 2. Isobutylamine hydrochloride ————
Isobutylamine hydrobromide – – – – –
Isobutylamine hydriodide — . — . —

Can. J. Chem. Downloaded from www.nrcresearchpress.com by 78.46.186.204 on 09/04/12
For personal use only.

Can. J. Chem. Downloaded from www.nrcresearchpress.com by 78.46.186.204 on 09/04/12
For personal use only.

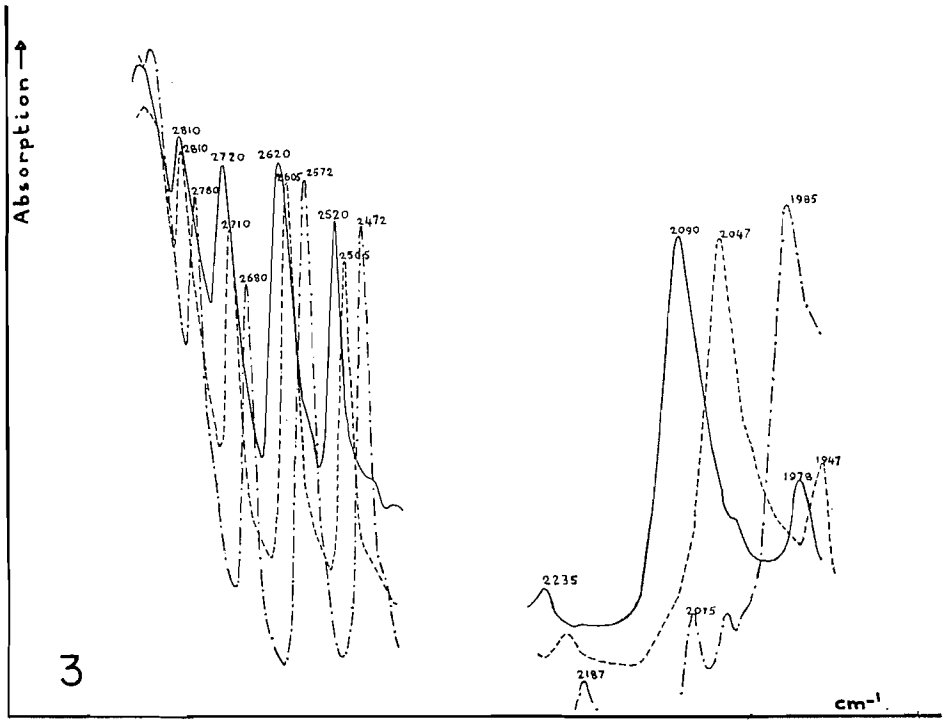

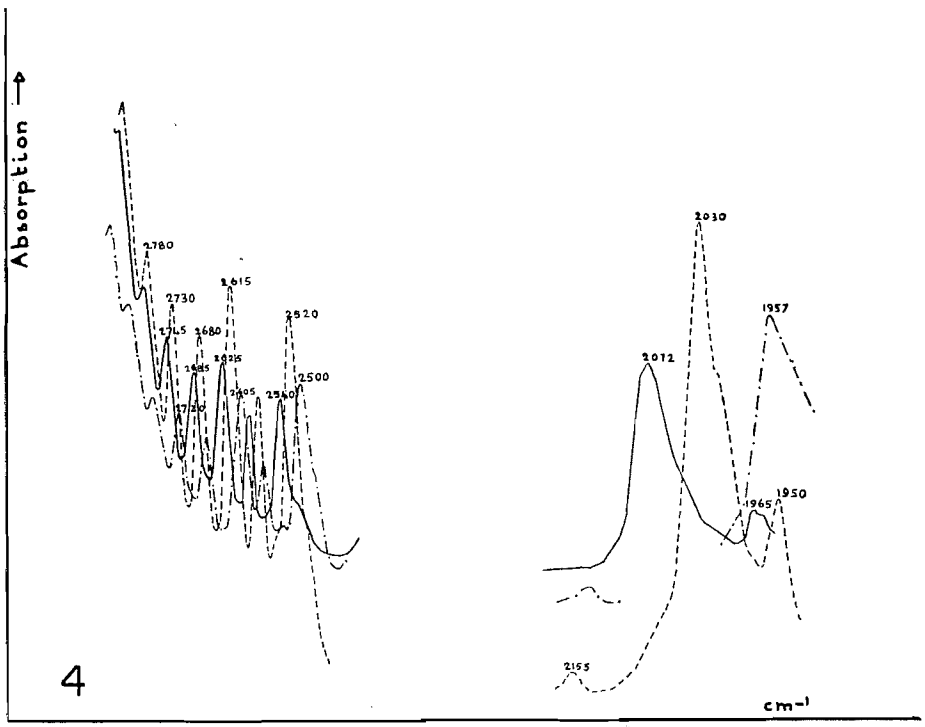

FIG. 3. Tertiary butylamine hydrochloride ————
Tertiary butylamine hydrobromide – – – – –
Tertiary butylamine hydriodide —.—.—

FIG. 4. Cyclohexylamine hydrochloride ————
Cyclohexylamine hydrobromide – – – – –
Cyclohexylamine hydriodide —.—.—

Can. J. Chem. Downloaded from www.nrcresearchpress.com by 78.46.186.204 on 09/04/12
For personal use only.

TABLE I

INFRARED SPECTRA OF AMINE HYDROHALIDES IN THE SOLID STATE

Ethylamine			*n*-Butylamine			*sec*-Butylamine			Isobutylamine			*tert*-Butylamine			Cyclohexylamine		
HCl	HBr	HI	HCl	HBr	HI	HCl	HBr	HI	HCl	HBr	HI	HCl	HBr	HI	HCl	HBr	HI
2790	2780	2775	2780	2780	2760	2805	2795	2770				*2810*	*2810*	*2780*	2835	2835	2825
															2785	2780	2775
						2735	2715	2715	2730	2720	2700	*2720*	*2710*	*2680*	2745	2730	2720
2680	*2675*	*2680*													2685	2680	2670
		2655	2650	2635	2640	*2655*	*2630*	*2595*	*2680*	*2675*	*2645*				2625	2615	2605
2635					2600	2595	2580		*2650*	*2640*		*2620*	*2605*	*2572*	2585	2580	2570
2580	*2570*	*2550*	*2540*	*2520*	*2485*	*2560*	*2535*	2515	*2580*	*2575*	*2545*				2540	2520	2500
						2510	2485	2455	*2560*	*2545*		*2520*	*2505*	*2472*			
2435	2425	2410							2475	2470					All medium strong		
														2075			
2075	*2030*	*1980*	2070	1915		2055	1995		*2057*			*2090*	*2047*	*1985*	*2072*	*2030*	*1957*
1945	*1935*								*2020*	*1995*	1860	*1975*	2010		1965	1950	
1605	1596	1592	1605	1584	1570	1606	1596	1571	1609	1601	1559	1616	1605	1592	1607	1596	1588
1477	1472			1502	1490	1517	1505	1491	1515	1502	1481	1515	1503	1498	1503	1498	1489

Diethylamine			Di-*n*-butylamine			Piperidine			Triethylamine			Tri-*n*-butylamine		
HCl	HBr	HI	HCl	HBr	HI	HCl	HBr	HI	HCl	HBr	HI	HCl	HBr	HI
2830	*2830*	*2820*	*2810*	*2810*	*2805*	2825	2830	2825	*2750*	*2755*	*2775*			*2800*
							2810	2785			*			*2760**
2775	*2780*		2755	2760	2765	2755	2750	2720						
						2655	*2645*	*2600*		*				
2570	2530	2510	*2570*	*2560*	*2550*	2605	2590	2530	*2620*	*2690*	*2700*	2600	2690	
2495	*2485*	*2455*	*2465*	*2450*	2425	*2545*	*2530*	*2480*	2550*	2550	2610		*2630*	
						2435	*2425*		*2510*	*2505*	*2500*		*2550**	
												2470		
												*2430**		
						2165	2155	2115						
						2005	2000							
						1891								
1595	1583	1544	1593	1582	1530	1592	1585	1560						
				1530										

Can. J. Chem. Downloaded from www.nrcresearchpress.com by 78.46.186.204 on 09/04/12
For personal use only.

TABLE I (*Concluded*)

INFRARED SPECTRA OF AMINE HYDROHALIDES IN THE SOLID STATE

Aniline			*N*-Methylaniline			Diphenylamine			*N*,*N*-Dimethylaniline			*N*-Methyl-diphenylamine			Pyridine		
HCl	HBr	HI	HCl	HBr	HI	HCl	HBr	HI	HCl	HBr	HI	HCl	HBr	HI	HCl	HBr	HI
*2810**	*2830**	*2870**		*2860**	*2870**	2910	2890	2880									
						2860	2840	2840							2860		*2860**
			2785	2750	2755	2815								2800			
				2725	2730	2770	2785	2780									
2610			*2620**	*2670**	*2675**	2720	2750	2740						2760			
2570	*2590*	*2580*				2675	2700	*2700*	2650	2650	*2650*						
			2450	2510	2520		2665	*			*2600**			2685		*2650**	
						2600	*2610*	*2620*	2545	2540							
							*2580**		2510	*2510*				2550			
						*2480**	2540	2545			2480			2510			
						2435	2470	*2475*		*							
									2400	*2435*	*2430*						
						2380	*2400*	*2435*						*2380**	*2400**		
						2287	2287		~2300*								
													*2245**				
2070						*2045*	2030	1990				*2050**	See Fig. 12.		See Fig. 13		
2015																	
1990						*1985*	*1945*	1935							*2110*		
															2005		
1565	1556	1548	1585	1564	1559	1562	1556	1555									
1518	1516																

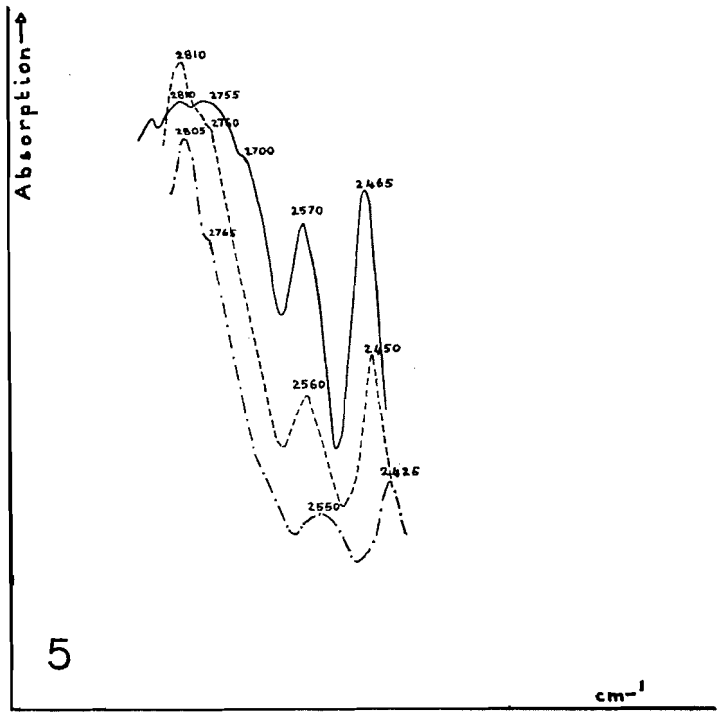

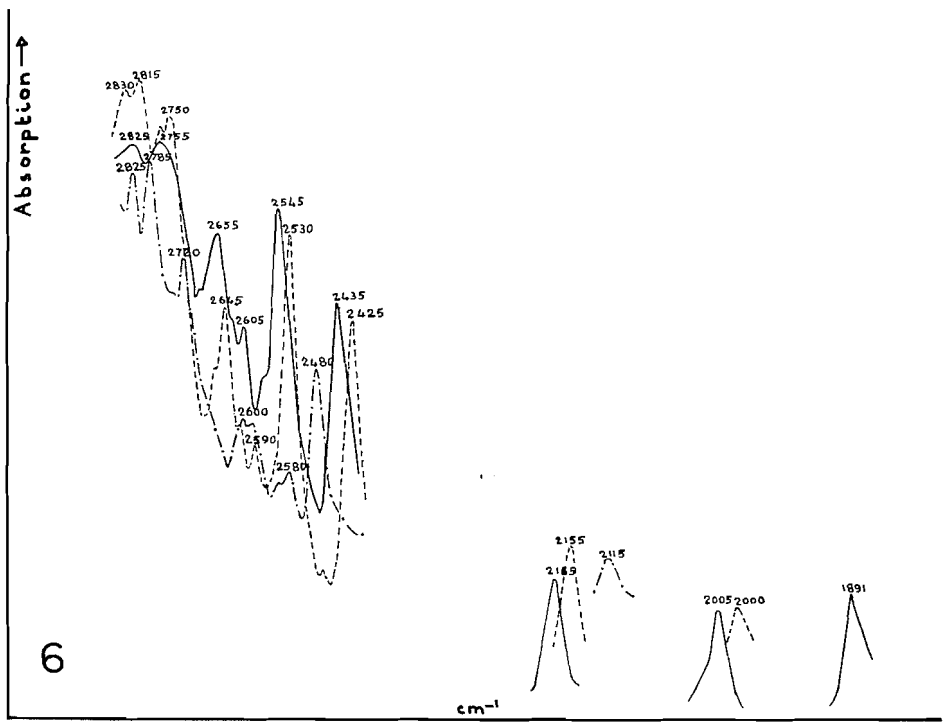

FIG. 5. Di-*n*-butylamine hydrochloride ————
Di-*n*-butylamine hydrobromide – – – – –
Di-*n*-butylamine hydriodide — . — . —

FIG. 6. Piperidine hydrochloride ————
Piperidine hydrobromide – – – – –
Piperidine hydriodide — . — . —

Can. J. Chem. Downloaded from www.nrcresearchpress.com by 78.46.186.204 on 09/04/12
For personal use only.

Can. J. Chem. Downloaded from www.nrcresearchpress.com by 78.46.186.204 on 09/04/12
For personal use only.

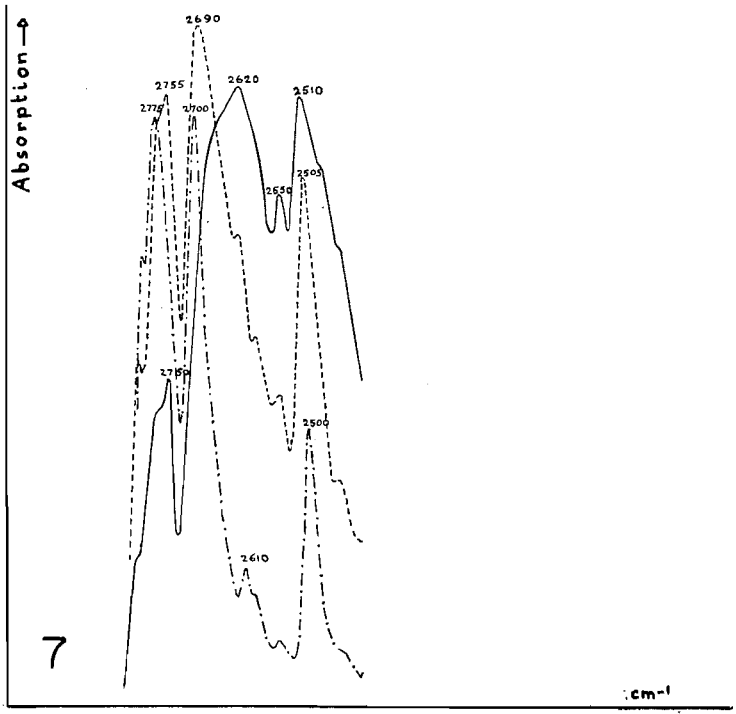

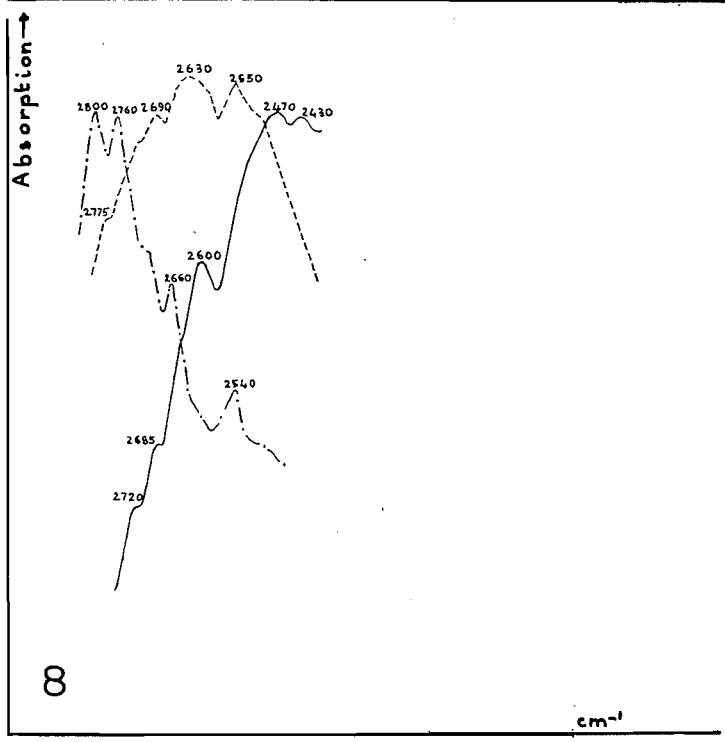

FIG. 7. Triethylamine hydrochloride ————
Triethylamine hydrobromide - - - - -
Triethylamine hydriodide — . — . —

FIG. 8. Tri-*n*-butylamine hydrochloride ————
Tri-*n*-butylamine hydrobromide - - - - -
Tri-*n*-butylamine hydriodide — . — . —

Work is going on in this laboratory in order to measure these under higher resolution.

There is, in general, a slight bathochromic shift in the order hydrochloride, hydrobromide, hydriodide, the latter having the lowest frequency. The shift amounts to 10 to 50 cm.$^{-1}$ but it could not be measured more accurately with the sodium chloride prism which was used. Band overlapping often makes it difficult to follow a band from one salt to another. The slight bathochromic shift in the above-mentioned order seems to be, however, the general rule.

Secondary aliphatic amine hydrohalides show essentially the same phenomena as the primary ones, that is, many bands (perhaps somewhat less well-resolved) between 2800 and 2400 cm.$^{-1}$ with a slight bathochromic shift from hydrochloride to hydrobromide to hydriodide (Figs. 5 and 6).

Tertiary aliphatic amine hydrohalides behave differently (Figs. 7 and 8). We find four to seven bands which are fairly well resolved in the case of triethylamine hydrohalides but less well resolved in tri-*n*-butylamine hydrohalides. Here there is a hypsochromic effect in the order hydrochloride, hydrobromide, hydriodide, and the bands become sharper in the same order. The shift is about 150 cm.$^{-1}$ from one halide to the next in the series in the case of the tri-*n*-butylamine salts and about 80 cm.$^{-1}$ for triethylamine salts. (It is not easy to see from the tables the relation between the bands of one salt and another in the series when large shifts occur. Therefore we have marked by an asterisk the approximate "center of gravity" of the bands.)

Second Region

Most hydrohalides of primary amines have one or two strong bands between 2200 and 1800 cm.$^{-1}$. These bands are strong and fairly sharp, their intensity diminishing from hydrochloride to hydrobromide to hydriodide. There is a pronounced bathochromic shift along the halide series in the same order, although in this region the shift is somewhat greater than the corresponding shift for the bands of the first region, and amounts to 30–100 cm.$^{-1}$.

In *n*-butylamine and *sec*-butylamine hydrohalides these bands are weak.

The only band we find in this area for hydrohalides of secondary and tertiary amines is for piperidine, which has three weak bands in the second region.

Third Region

In this part of the spectrum where the scissoring bands are expected we find two bands for hydrohalides of primary amines near 1600 cm.$^{-1}$ and 1510 cm.$^{-1}$. There is a regular bathochromic shift of 10 to 20 cm.$^{-1}$ in going from hydrochloride to hydrobromide and from hydrobromide to hydriodide.

Hydrohalides of secondary amines show one band near 1590 cm.$^{-1}$ with a shift in the same sense as for the primary amines, but greater in going from hydrobromide to hydriodide.

There are bands in this area for some tertiary compounds but they are unlikely to be of similar origin.

II. Spectra in Aqueous Solutions

It is important to point out that there is practically no difference between the spectra of hydrochlorides, hydrobromides, and hydriodides in aqueous solution. There is some variation of frequency in the cases of ethylamine, piperidine, and tri-*n*-butylamine but it is irregular. In all other cases the three give virtually identical spectra (Table II).

Because of the strong water absorption only the lower bands of the first region may be observed. They are somewhat broader than in the solid state but not very broad. These

Can. J. Chem. Downloaded from www.nrcresearchpress.com by 78.46.186.204 on 09/04/12
For personal use only.

TABLE II

INFRARED SPECTRA OF AMINE HYDROHALIDES IN AQUEOUS SOLUTION

	HCl		2760			*2630*			*2525*			
Ethylamine	HBr		2750			*2630*			*2520*			
	HI		2770			*2660*			*2530*			
n-Butylamine	HCl			2710			*2590*					
	HBr			2715			*2580*					
	HI			2700			*2575*					
	HCl		2765	2700			*2585*					
sec-Butylamine	HBr		2760	2695			*2585*					
	HI						*2585*					
	HCl			2730			*2600*					
Isobutylamine	HBr			2720			*2610*					
	HI			2715			*2615*					
	HCl		2770			*2645*			*2545*			
tert-Butylamine	HBr		2760			*2635*			*2540*			
	HI		2760			*2635*			*2540*			
	HCl						*2570*					
Cyclohexylamine	HBr						*2565*					
	HI						*2560*					
	HCl								*2535*			
Diethylamine	HBr								*2535*			
	HI								*2540*			
	HCl								*2505*			
Di-*n*-butylamine	HBr								*2505*			
	HI								*2505*			
	HCl						*2560*					*2410*
Piperidine	HBr						*2570*					*2450*
	HI						*2570*					*2425*
	HCl		2750						*2530*			
Triethylamine	HBr		2750						*2540*			
	HI		2755						*2540*			
	HCl			2710			2570					
Tri-*n*-butylamine	HBr			2690			2600					
	HI											
	HCl							*2640*				
Aniline	HBr							*2655*				
	HI							*2655*				
	HCl				*2750*					2520		
N-Methylaniline	HBr				*2760*					2520		
	HI				*2770*					2520		
	HCl					*2695*		2640		2540	2485	
N,N-Dimethylaniline	HBr					*2710*		2640		2540	2500	
	HI					*2710*		2640		2540	2495	
	HCl	*2890*	*2835*	2740								
Pyridine	HBr	*2890*	*2845*	2730								
	HI	*2900*		2730								

bands are always located above 2500 cm.$^{-1}$ (except for the bands for piperidine), that is, at higher frequencies than for the solids.

There is a water absorption region at about 2125 cm.$^{-1}$ and this becomes stronger when the salts are dissolved in water so the latter may have a band there.

III. Spectra of Amine Salts Dissolved in Their Amine (*Table III*)

These solutions exhibit one or two fairly sharp and strong bands between 2700 and 2450 cm.$^{-1}$. In the case of the three primary amines the bands are at about the same place as in aqueous solution; in the case of di-*n*-butylamine amine they are closer to those in the solid. The slight bathochromic shift observed in solid becomes irregular. The bands are at about the same place with slight variations. None of the tertiary aliphatic amine salts is sufficiently soluble in its amine.

There are bands, too, between 2100 and 2000 cm.$^{-1}$ but they are weak and broad. The other parts of these spectra cannot be used because of heavy amine absorption.

Can. J. Chem. Downloaded from www.nrcresearchpress.com by 78.46.186.204 on 09/04/12
For personal use only.

TABLE III

INFRARED SPECTRA OF AMINE HYDROHALIDES DISSOLVED IN THEIR AMINE

	HCl		2750		*2570*			
n-Butylamine	HBr		2775		*2565*			
	HI		2770		*2580*			
	HCl				*2580*			
sec-Butylamine	HBr				*2590*			
	HI				*2600*			
	HCl		2750		*2600*			
Isobutylamine	HBr		2750		*2605*			
	HI		2760		*2620*			
	HCl			2690	*2570*		*2470*	
Di-*n*-butylamine	HBr				*2570*		*2455*	
	HI				*2580*	*2545*	*2430*	
	HCl	*2850*	2775		*2610*			
Aniline	HBr	*2880*	2775		*2620*			
	HI	*2910*	2775		*2630*			
	HCl			2690	2600		2470	
N-Methylaniline	HBr			2685	2600		2450	
	HI			2680	2600		2425	
	HCl							*2290**
Pyridine	HBr						*2440**	
	HI				*2610**			

IV. Spectra Taken as Solid Smears of the Salts in Their Amine (Table IV)

There is a close resemblance between these spectra and the corresponding spectra of the pure salt in the solid phase. This resemblance includes the location of the bands and the significant hypsochromic shifts in the tertiary amine salts and other aromatic salts; however, the small bathochromic shift in primary and secondary aliphatic amine salts loses its regularity.

This general similarity again shows that the fluorocarbon oil used as a mulling agent for the measure of the spectra in solid state has no significant effect on the spectra.

B. AROMATIC COMPOUNDS

I. Spectra in the Solid State

First Region

In the primary and secondary amine hydrohalides two broad bands are observed (Table I) (Figs. 9 and 10). These are in the same general part of the spectrum as the more numerous bands of the aliphatic compounds. It is, however, quite clear from the appearance of the bands that none of them is simple. On the contrary, a great number of peaks and inflections shows that they are composed of several bands superimposed.

In the tertiary amine hydrohalides (Figs. 11, 12, 13) there is only one broad band which is quite clearly composite as well. This band shifts towards higher frequencies by about 100 to 200 cm.$^{-1}$ going from hydrochloride to hydrobromide to hydriodide; thus it moves in the same direction as the aliphatic tertiary amine salts. The broadness of the bands diminishes in the same order.

The bathochromic shift described previously in the aliphatic primary and secondary amine hydrohalides in the series hydrochloride, hydrobromide, and hydriodide is not observed in the primary and secondary aromatic amine salts; there is instead a hypsochromic shift. For aniline the shift is hypsochromic by about 40 cm.$^{-1}$ but only the band at higher frequency undergoes the shift. The hypsochromic effect is well pronounced in the case of diphenylamine salts (by about 100 cm.$^{-1}$ in each case) and there are other weaker bands around the main band. In the case of *N*-methylaniline the hypsochromic

Can. J. Chem. Downloaded from www.nrcresearchpress.com by 78.46.186.204 on 09/04/12
For personal use only.

Can. J. Chem. Downloaded from www.nrcresearchpress.com by 78.46.186.204 on 09/04/12
For personal use only.

TABLE IV

INFRARED SPECTRA OF SOLID SMEARS OF AMINE HYDROHALIDES IN THEIR AMINE

n-Butylamine			*sec*-Butylamine			Isobutylamine			*tert*-Butylamine			Cyclohexylamine		
HCl	HBr	HI	HCl	HBr	HI	HCl	HBr	HI	HCl	HBr	HI	HCl	HBr	HI
2785	2780	2760	2730		*2750*			*2745*	*2745*	2780		2720	2730	2725
2650	*2680*	*2640*	2660	2630		*2685*			*2665*	2700				
						2660	*2670*			*2665*	*2660*	2630	2630	2675
									2640					
										2600				
2550	*2520*	*2505*	*2560*	*2530*	*2570*	*2585*	*2575*	*2585*	*2565*	2550	*2550*	2575	2575	2570
			2515	2485	2510	*2560*	*2545*		2530	*2505*				
2450	2410	2400	2450		2425									2500
						2480	2470							
								~2380			*2425*		2415	
			2187	2160	2150				*2205*	*2105*	2187	*2185*	*2177*	*2175*
2055	2015	1960	*2057*	*2025*	*2022*	*2050*	2010	2020	*2127*	*2107*		*2135*	*2080*	
						2027					*2022*			
1607	1594	1582	1607	1594	1591	1610	1595	1587	1596	1595	1594	1608	1604	1582
					1536	1554	1555	1543	1552	1545	1541	1550	1541	1550
1512	1502	1491	1518	1507										

Diethylamine			Di-*n*-butylamine			Piperidine			Triethylamine			Tri-*n*-butylamine		
HCl	HBr	HI	HCl	HBr	HI	HCl	HBr	HI	HCl	HBr	HI	HCl	HBr	HI
		2810	2815		2815				*2810*	2810		2810	2810	*2800*
2780	2770	*2760*								2760	*2775*			*2750**
												2730	2715	
	2730	2700												2700
													2675	2650
										*2690**	*2700**			
						2655		2650	*2630**		2600	2610	*2615**	2540
						2600	*2585*	*2565*	2550	2545			2545	
2550	2535	*2500*	*2575*	2560	*2550*	*2540*		*2475*	*2510*	*2505*	*2490*	*2490**		
2490	*2480*	*2455*	*2470*	*2455*	*2430*	*2435*								
	2420													
2150		2120												
2055	2015	1965				2015								
1597	1588	1590	1593	1585		1593								
					1530									

Can. J. Chem. Downloaded from www.nrcresearchpress.com by 78.46.186.204 on 09/04/12
For personal use only.

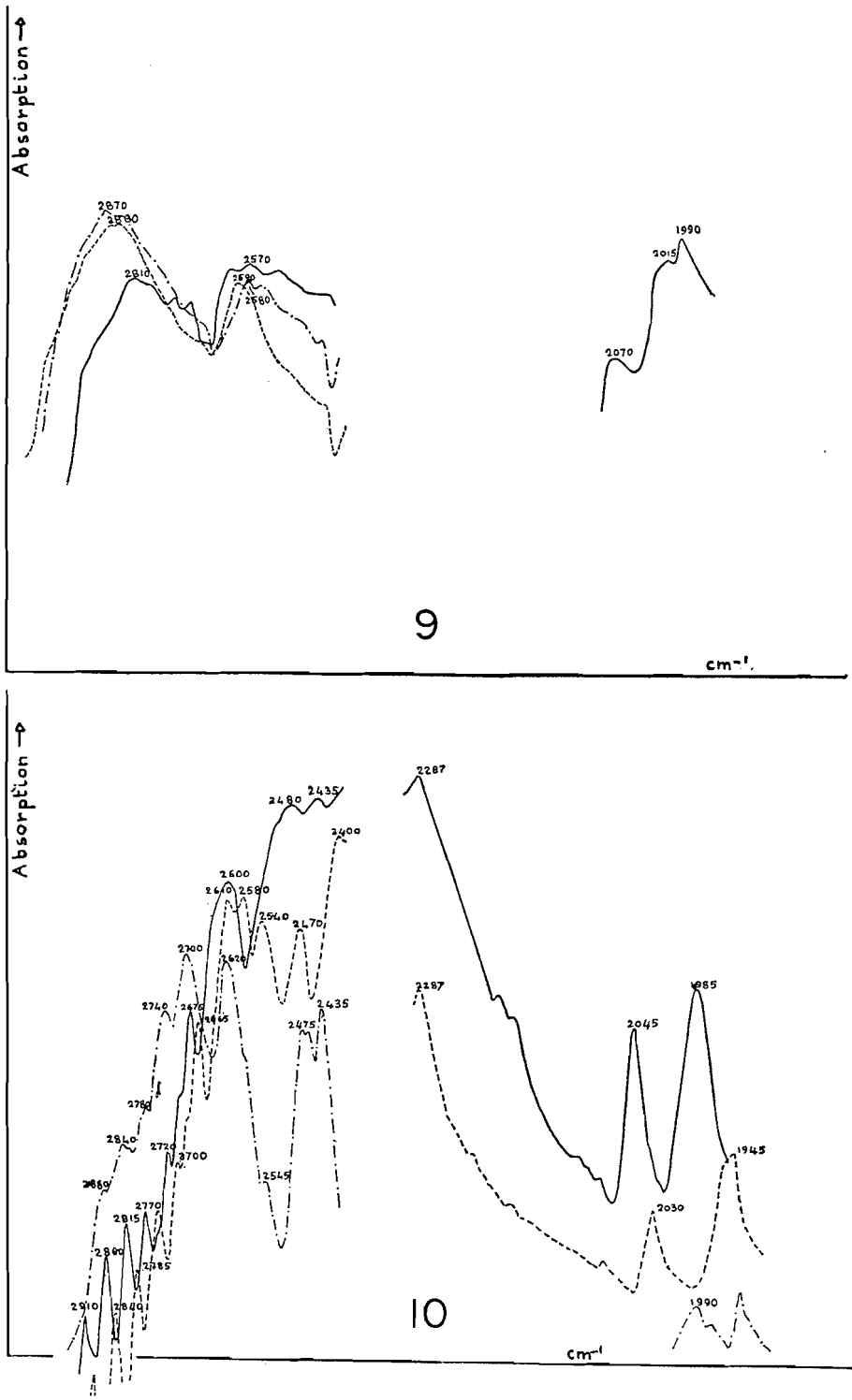

FIG. 9. Aniline hydrochloride ————
Aniline hydrobromide – – – – –
Aniline hydriodide — . — . —

FIG. 10. Diphenylamine hydrochloride ————
Diphenylamine hydrobromide – – – – –
Diphenylamine hydriodide — . — . —

Can. J. Chem. Downloaded from www.nrcresearchpress.com by 78.46.186.204 on 09/04/12
For personal use only.

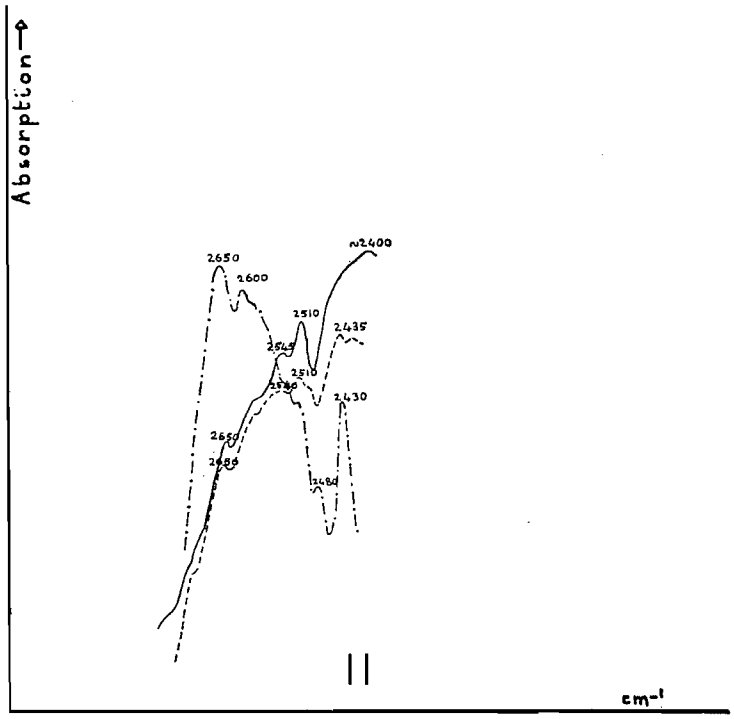

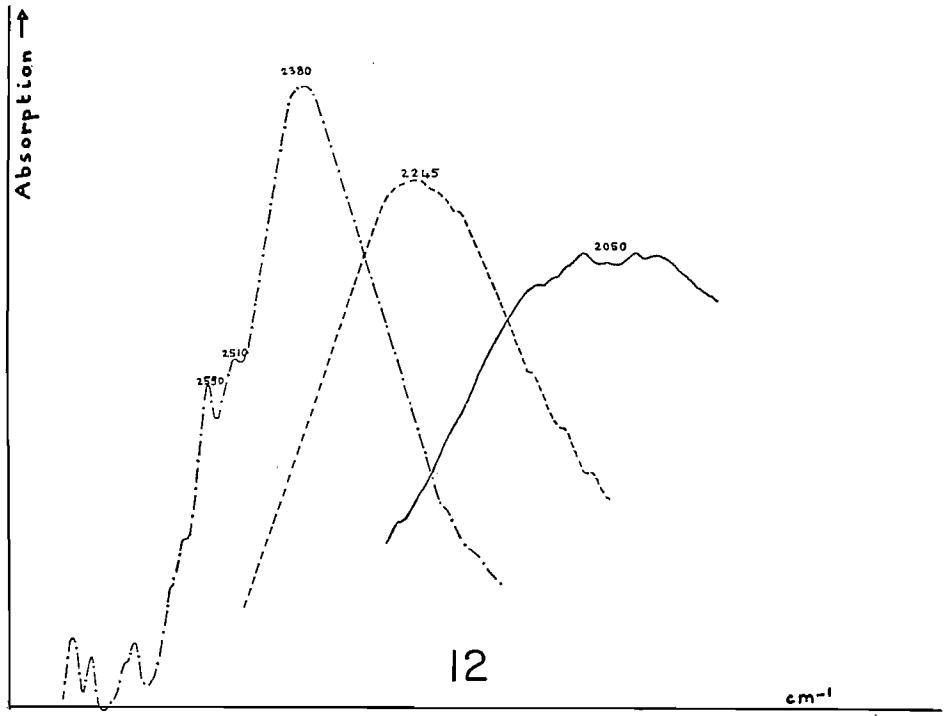

FIG. 11. *N,N*-Dimethylaniline hydrochloride ————
N,N-Dimethylaniline hydrobromide – – – – –
N,N-Dimethylaniline hydriodide — . — . —

FIG. 12. *N*-Methyl-diphenylamine hydrochloride ————
N-Methyl-diphenylamine hydrobromide – – – – –
N-Methyl-diphenylamine hydriodide — . — . —

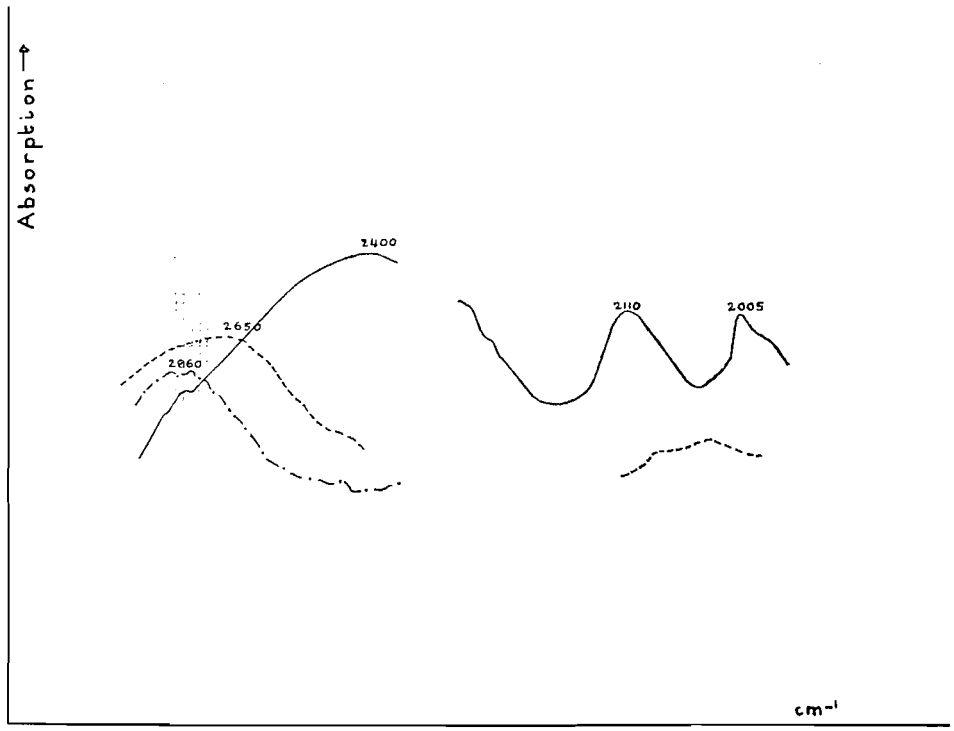

FIG. 13. Pyridine hydrochloride ————
Pyridine hydrobromide - - - - -
Pyridine hydriodide — . — . —

shift is large between hydrochloride and hydrobromide but negligible between hydrobromide and hydriodide. There are weaker bands here too.

The general tendency is thus for the hypsochromic shift with aromatic compounds.

Second Region

There are always weak overtone and combination bands between 2000 and 1600 cm.$^{-1}$ in the spectra of aromatic compounds (12) and it is necessary to distinguish from these the bands which are due to NH^+ absorption.

Hydrochlorides of aniline and pyridine show two bands between 2100 and 2000 cm.$^{-1}$ which are stronger than bands in the same region of the respective amine. The three salts of diphenylamine give two bands whose intensity diminishes from hydrochloride to hydrobromide and from hydrobromide to hydriodide and which shift towards lower frequencies in the same order.

The other compounds have no band in this region.

Third Region

Two well-known vibrations of the benzene nucleus appear at almost exactly the place where the NH_3^+ and NH_2^+ scissoring vibrations should be and thus the observation of the latter is difficult (Table I).

Aniline hydrohalides have a band near 1565 cm.$^{-1}$ and another at 1518 cm.$^{-1}$. Secondary amine hydrohalides have a band between 1580 and 1540 cm.$^{-1}$. These bands all shift bathochromically in going from hydrochloride to hydrobromide to hydriodide.

The tertiary amine salts have no band in this region.

Can. J. Chem. Downloaded from www.nrcresearchpress.com by 78.46.186.204 on 09/04/12
For personal use only.

II. Spectra of Aqueous Solutions

Hydrohalides of aniline, *N*-methylaniline, *N*,*N*-dimethylaniline, and pyridine are well soluble in water. The one band which can be observed is always higher than 2650 cm.$^{-1}$, higher than in the solid, and higher also than the corresponding bands of the aliphatic compounds (Table II).

III. Spectra of Hydrohalides Dissolved in Their Amine

Salts of aniline, *N*-methylaniline, and pyridine could be studied under these conditions. In the case of aniline the bands are 40 to 50 cm.$^{-1}$ higher than in the solid phase (Table III). The hypsochromic shift is slight in the case of the aniline salts, and also in the case of *N*-methylaniline salts but is quite pronounced in the pyridine salts.

IV. Spectra of the Hydrohalides in Solid Smears in Their Amine (Table V)

As is the case with the aliphatic amines under the same conditions, these spectra resemble those of the corresponding salts in the solid phase. The hypsochromic effect in the series hydrochloride to hydriodide is clearly observed for the tertiary compounds. However for aniline only the first band is hypsochromic and the second one is slightly bathochromic, for *N*-methylaniline the first band is stationary and the second is bathochromic.

The scissoring bands show a regular bathochromic shift. Heacock and Marion (13) have shown that the scissoring bands are of appreciable value for identification purposes and they gave data for many amines, usually of more complicated structure. We have tabulated further data in Tables I, IV, and V.

TABLE V

INFRARED SPECTRA OF SOLID SMEARS OF AMINE HYDROHALIDES IN THEIR AMINE

Aniline			*N*-Methylaniline			*N*,*N*-Dimethylaniline			Pyridine		
HCl	HBr	HI	HCl	HBr	HI	HCl	HBr	HI	HCl	HBr	HI
					*~2880**						2910
*2850**	*2870**	*2920**							2860		*2875**
			2790	2745 *	2745 2725						
			*2675**	*2675*	2670	2640	2650	*2650*		*2640**	
			2630	2630				2610*			
2625	*2605*	*2590*									
2590	2580	2570	2565	2525	2515	2540	*2560*	2530			
						2510	2515*	2480	*2460**		
			2460	2455							
				2385		2410	*2450*	*2435*			
						~2360*					
			2255	2240							
			2085								
			2010								
1568	1560	1552	1588	1563	1557						
	1518										

DISCUSSION

Number and Appearance of Bands

There is a formal analogy between $-CH_3$, $\rangle CH_2$, and $\rightarrow CH$ groups on one hand and the $-NH_3^+$, $\rangle NH_2^+$, $\rightarrow NH^+$ groups on the other hand.

CH_3 groups have an antisymmetric and a symmetric stretching vibration, the former being degenerate. CH_2 groups have two non-degenerate stretching vibrations, and CH

Can. J. Chem. Downloaded from www.nrcresearchpress.com by 78.46.186.204 on 09/04/12
For personal use only.

groups have one (14). Consequently we might expect two stretching bands for NH_3^+ or three if the C_{3v} symmetry is diminished and the degeneracy removed. This removal of the degeneracy might be caused by lower symmetry of the crystal lattice. For NH_2^+ we expect two stretching bands and for NH^+ one.

Unfortunately the free NH_3^+, NH_2^+, and NH^+ stretching frequencies are not known because of the difficulty of dissolving amine salts in non-polar solvents. Even if this were possible association by hydrogen bonding could still persist. Since the introduction of a positive charge distributed between the nitrogen and the hydrogens must weaken the N–H links we can estimate that these stretching frequencies would fall in the range 3200–3000 cm.$^{-1}$. In the solid state and in the very concentrated solutions all hydrogens should participate in hydrogen bonding except, perhaps, in a few cases of steric hindrance. This is actually what Donohue found by X-ray methods in the case of some complex amine salts (15).

While for amines the shift due to hydrogen bonding amounts to less than 100 cm.$^{-1}$ (16, 17) for their hydrohalides the shift is several hundred wave numbers showing the strength of the hydrogen bonds formed by the latter.

The main point is that we do not find three, two, or one bands, as expected on grounds of the above-mentioned formal analogy, but many more. Only in the case of some of the aromatic amine hydrohalides, such as the aniline and pyridine salts, does the rule seem to be followed; in these two compounds we find, respectively, two and one broad regions of absorption, each region, however, being composed of many bands.

In general, in the amine hydrohalides examined, there is no direct relationship between the number of bands in the first region and the number of hydrogen atoms linked to the nitrogen. It is apparent furthermore that with the aromatic compounds the bands are usually broad, while with aliphatic compounds they are usually sharp.

Although aromatic compounds give broad bands, multiple peaks and inflections reveal that they are composed of about as many component bands as we find for aliphatic compounds.

Plumb and Hornig (18) investigated ammonium fluoride crystals by both infrared and X-ray methods at room and liquid-air temperatures. They reported that "the most striking features of the NH_4F spectrum are the sharp lines and the large number of bands, shoulders, and general spectral detail" in the spectrum, especially in the low temperature spectrum. Between 3300 and 2500 cm.$^{-1}$ they found 11 peaks. The NH_4F molecule has a high symmetry, the true site symmetry being C_{3v}, but as far as the ammonium ion and its nearest neighbors are concerned the arrangement is tetrahedral (T_d). Long range interactions or coupling between the various ammonium ions may lower the symmetry but these effects are probably small as the latter are separated by a heavy atom. Thus Plumb and Hornig conclude that most of the bands are combination bands.

Amine hydrohalides may be regarded as substituted derivatives of ammonium salts. For most of them the symmetry in the crystal is probably lower and thus we might expect the degenerate stretching vibration to split in the case of primary amine salts. This, however, would not explain the many bands observed.

The striking resemblance between the spectra taken in the solid phase and in a smear in the conjugate amine of the hydrohalide, where crystallization would be at most partial and where there would be a high degree of disorder, shows that the crystal structure has generally little to do with the appearance of a great number of bands in the NH^+ stretching region. It seems likely therefore, that most of these bands are

Can. J. Chem. Downloaded from www.nrcresearchpress.com by 78.46.186.204 on 09/04/12
For personal use only.

combinations. This is in accordance with observations and suggestions of Plumb and Hornig (18) and Bratož and Hadži (8).

We have to answer, however, the following two questions:

1. Why are the bands well separated for aliphatic amine salts and melted together for aromatic amine salts?
2. What are the strong bands near 2000 cm.$^{-1}$ (second region) which appear in many cases?

The broadness of the bands is probably the key problem of theories of hydrogen bonding. The first views on this subject were that it arises from the broadening of the energy levels by intermolecular interaction (5, 19).

This early interpretation was later recognized as insufficient. Predissociation theories have been proposed by Stepanov (20, 21) and by Cannon (22). More recently it has been suggested (Lippincott and Schroeder (23) and Batuev (24)) that movement of the end atoms may constantly vary the potential under which the vibrations of the bonded hydrogen occur, and that this could be the cause of the broadening of the bands.

The unusual anharmonicity of vibrations involving hydrogen bonding has been recognized for a long time. In particular, the pronounced anharmonicity of the bands of amine hydrohalides was pointed out by Lord and Merrifield (10).

Bratož and Hadži (8) have made anharmonicity the central phenomenon in their attempt to interpret by a single theory all the characteristic properties of hydrogen bonds. According to them, intermolecular interactions would account for the moderate broadness of weakly bonded stretching bands and that of the bending bands, but to explain the large bathochromic shift and great broadness found with strong hydrogen bonds we must suppose that the part of the potential surface relevant to the stretching vibrations is highly anharmonic. This anharmonicity would account for the unusual strength of the combination bands. Bratož and Hadži have shown, too, that the effect of the displacement of the two heavy end atoms is precisely to increase anharmonicity.

In the present case there does not seem to be any reason to believe that the displacement of the end atoms affects the band width differently in the aromatic and aliphatic cases.

The fact that the absorption in the first region for aliphatic amine salts consists of a series of well-separated bands, while in the aromatic compounds the bands are broad and composite, may be connected with the availability and frequency of vibrations which combine with the NH^+ stretching vibrations. The width of the individual bands may then be related to the extent of intermolecular interactions. We should like to point out that Stark effects acting on each ion due to the electric field created by the others must be an important factor here.

It is generally believed that strong hydrogen bonds give large shifts and broad bands and that the two go together. Plumb and Hornig have pointed out (18), however, that this is not necessarily so, although it is usually the case. Our results show quite clearly that shift and broadness do not necessarily go together. Aromatics and aliphatics give bands in the same part of the spectrum but the former are broad and the latter sharp.

We may conclude that pronounced anharmonicity, which gives unusual strength to combination bands, need not lead to very broad bands; it can lead also to a great number of sharp bands. This depends on the frequencies of the vibrations combining with the NH^+ stretching vibrations but also on the width of the individual bands.

Thus we have to explain why, as seems to be the case, band broadening is greater in the case of aromatics than in the case of aliphatics. Intermolecular influences which are mainly responsible for it are unlikely to differ much between the two types. One reason may be the different charge distribution which would give more positive charge to a

Can. J. Chem. Downloaded from www.nrcresearchpress.com by 78.46.186.204 on 09/04/12
For personal use only.

hydrogen in the aromatic and tertiary cases (see the next section). Disordering in the crystal structure may be another reason for band broadening.

If we suppose that the potential surface of a hydrogen bond has two minima (see text below) and if we consider the stretching vibration as the beginning of the dissociation of a bond followed by the formation of another, we can treat this vibration as a chemical reaction and speak of an activation energy corresponding to the maximum which separates the two minima. This maximum should be lower for aromatic derivatives because for them the increasing of the N—H distance is linked with a partial return to trigonal hybridization and coplanarity and thus to a relative gain of stability, hence in this situation the bond would be more sensitive to intermolecular influences. This argument may be valid even if there are not two pronounced minima in the potential surface but only one minimum and one point of inflection as is probably the case. As in a chemical reaction there is no direct relationship between activation energy and energy of a reaction, so in the case of hydrogen bonding broadness and shift may not be directly related even if both depend on the anharmonicity of the potential surface.

Location of the Bands and Band Shifts

As we saw in the previous paragraph the hydrogen-bonded NH^+ frequencies fall into the same general spectral area for both aromatic and aliphatic amine salts. This is somewhat astonishing in view of the fact that aliphatic amines are strong basis and aromatic amines are weak basis. This is a fact we have to explain. Furthermore, as we have mentioned above, when we go from hydrochloride to hydrobromide to hydriodide we observe a significant hypsochromic shift for tertiary compounds, whether aliphatic or aromatic. For primary and secondary amine salts there is a somewhat less systematic hypsochromic shift for the aromatic compounds and a slight but systematic bathochromic shift for the aliphatic ones.

The existence of these regular shifts is a proof that the hydrogen bonds are actually of the N^+—H- - -X^- type. This applies to the solids and solutions and smears in the conjugate amines.

There is, furthermore, the appearance of the strong band (or bands) near 2000 in the case of most aliphatic primary amine salts as well as those of piperidine and pyridine. This band was first described by Randall, Fuson, Fowler, and Dangl (25) in the case of amino-acids and amino-acid hydrochlorides, and it was mentioned also by Thompson, Nicholson, and Short (26). It was clear to these authors that this band must be related to the protonated amino groups. Its assignment remained, however, an open question.

In addition to the difference in basicity between aliphatic and aromatic amines there is another simple fact we must take into account: in tertiary amine salts there are as many hydrogens as halide ions but in secondary and primary ones there are twice and three times as many, respectively. This fact may be useful especially in the absence of a knowledge of the crystal structure. It is very likely that with the secondary and primary amine hydrohalides more than one hydrogen is bonded to one halide ion.

It is generally considered that the energy of a hydrogen band comes from four different sources: attractive electrostatic forces, delocalization energy, dispersion forces, and repulsion between the interpenetrating electron clouds.

This fragmentation of the energy is of course somewhat artificial. The various contributions could correspond to the influence on the total energy of different fragments of the potential function which we find in the Hamiltonian for the system and do not represent separate physical phenomena. This language is, however, convenient for a discussion of hydrogen bonds.

Can. J. Chem. Downloaded from www.nrcresearchpress.com by 78.46.186.204 on 09/04/12
For personal use only.

For example, Lippincott and Schroeder (23, 27) and Finch and Lippincott (28) have shown that a satisfactory potential function for hydrogen-bonded systems can be set up by taking the sum of the above-mentioned contributions, and Coulson and Danielsson (29, 30) and Tsubomura (31) have introduced the notion of ionic and covalent character of hydrogen bonds. In his wave mechanical treatment of the O—H- - -O system Tsubomura considered the following five valence bond structures:

A O—H- - -O
B O^- H^+- - -O
C O^+ H^-- - -O
D O^- H—O^+
E O H^- O^+

Structures A, B, and C represent almost entirely the electrostatic effect. Structures D and E imply a charge transfer, thus a delocalization effect. Their weight, which is insignificant at large distance, increases rapidly (to as high as 11%) as the distance becomes shorter, as during a stretching vibration. Thus delocalization would explain a part of the energy of the hydrogen bond and a good part of the intensity of the related vibrational band.

In the case of amine hydrohalides we may write the following set of structures in analogy with those of Tsubomura (X = Cl, Br, or I):

A N^+—H- - -X^-
B N H^+- - -X^-
C N^{++} H^-- - -X^-
D N H—X
E N^+ H^- X

If we wish to consider this set of structures as a basis for a valence-bond calculation it is necessary that the nuclear skeleton and also the internuclear distances should be approximately the same.

Here structures B and D would represent the free amine and the acid HX, if the H—X distance was allowed to readjust to its normal value.

Let us assume that the distances are the same for all structures and that it is justified to make a qualitative valence-bond argument.

Structure A has certainly by far the highest weight. With its two opposite charges it should imply a much stronger hydrogen bond than structure A in the case of the O—H- - -O system.

If we wish to compare the hydrohalides of aliphatic and aromatic amines we, of course, have to consider the entire molecules, not only the N^+—H- - -X^- portion.

In the aromatic case the formation of the hydrohalide stabilizes the system but little because of the loss of the resonance energy due to conjugation between the approximately $2p_z$ lone pair of the nitrogen and the π-electrons of the benzene ring. The nitrogen which had approximately trigonal hybridization in the free amine will have approximately tetrahedral hybridization in the salt. Thus the energy of structure A will be relatively high. In the case of aliphatic amines there is no similar loss of resonance energy and structure A is relatively more stable.

For the aromatic hydrohalides the energies of structures B and D are stabilized relative to the energy of structure A, since they do not involve a loss of resonance energy.

Can. J. Chem. Downloaded from www.nrcresearchpress.com by 78.46.186.204 on 09/04/12
For personal use only.

In the aliphatic compounds, on the other hand, this stabilization of B and D relative to A will not occur, so that B and D will contribute less to the wave function for the hydrogen-bonded species in the aliphatic case than in the aromatic case.

To sum up, for the aliphatic amine salts structure A involves a stronger hydrogen bond and the latter is overwhelmingly electrostatic in character. Structures B and D are probably not negligible but much less important. For the aromatic salts, A involves a weaker hydrogen bond but resonance with B and D increases its stability so that the bonds are of about the same strength in both cases and the corresponding infrared NH^+ stretching bands are at about the same part of the spectrum. In the aromatic case appreciable delocalization should occur because of structure D. We have supposed in this argument that structure C is unimportant. Additional delocalization may arise because of structure E.

The qualitative valence–bond argument given above may be stated in a more chemical manner. For the aliphatic amine hydrohalides, which are strong basis, the attachment of the proton to the nitrogen can be considered as complete and the positive charge centered on the nitrogen. Therefore structure A is a good approximate representation of the system.

On the other hand, for aromatic amine salts, which arise from weak basis, the proton may not be firmly bound to the nitrogen and the positive charge may be divided between the nitrogen and the hydrogen. This implies greater weight for B and D with more delocalization.

We have now to explain the characteristic shifts from Cl^- to Br^- to I^- described in the previous section.

Our reasoning with the use of structures A, B, and D applies strictly only to tertiary amine hydrohalides where there is one hydrogen for every halide ion. Structure B should be relatively more important for them, while for primary and secondary amine salts we must suppose that structure B is less important because the positive charge is distributed among the nitrogen and three or two hydrogens. Now structure B should be more important in hydrochlorides than in hydrobromides and hydriodides, because HCl has a higher ionic character in its valence–bond description than HBr and HI (3). This would explain the large hypsochromic shift observed in this order with both aromatic and aliphatic tertiary amine hydrohalides. This tendency may be accentuated in some cases by steric effects.

Since the order of electroaffinities for the halogens is (32)

Cl	3.78 ev.,
Br	3.54 ev.,
I	3.24 ev.,

structure D, which implies delocalization, should be most important for hydriodides. Thus, whether we will observe a bathochromic or a hypsochromic shift in the series hydrochloride to hydriodide will depend upon the relative weights of structures B and D in the wave function. With tertiary amine hydrohalides we have a hypsochromic shift because structure B always has a weight which is appreciable and greater than D. This gives the strongest hydrogen bond with Cl^-. With primary and secondary *aromatic* amine hydrohalides structure B is still important (as it does not involve a loss of resonance energy) but less so than for tertiary amine salts because the fraction of positive charge on one hydrogen will be less. Therefore we still usually obtain hypsochromic shifts,

Can. J. Chem. Downloaded from www.nrcresearchpress.com by 78.46.186.204 on 09/04/12
For personal use only.

although less systematically, because of the more comparable weights of B and D. With primary and secondary *aliphatic* amine hydrohalides structure A predominates, while B and D are less important than in the aromatic case. D is more important than B, since the fraction of positive charge on one hydrogen is very small. This gives a slight bathochromic shift, the strongest hydrogen bond being formed with I^-.

As we have seen, the regularity of the slight bathochromic shift is lost in solution or smear in the conjugate amine. This is understandable too from the above argument, since the relative weights of structures B and D may be sensitive to environment.

Assignment of the Band near 2000 cm.$^{-1}$

Our next problem is the assignment of the band in the 2000 cm.$^{-1}$ area.

The following interpretations may be considered:

1. An unusually strong combination band which is a sum of the scissoring frequency and a lower internal or lattice frequency.

2. An unusually strong difference band between a stretching band and some low-lying frequency.

3. One could argue that the antisymmetric and symmetric stretching vibrations may be very far apart, the band near 2000 cm.$^{-1}$ corresponding to the latter.

4. We could assume a double minimum potential surface and a resulting splitting of the stretching bands (8, 33, 34).

There might be two reasons why the potential surface should exhibit two minima. The one would be a coupling of two (or three) vibrations where two (or three) hydrogen bonds end at the same halide ion. The other would be due to the fact that, as Plumb and Hornig (18) pointed out, there must be a point of relative stability when the hydrogen approaches the halide ion during the vibration, as this vibration can be considered the beginning of dissociation

$$R{-}NH_3^+X^- \rightleftarrows NH_3 + HX, \text{ etc.}$$

The following facts are relevant. The band at 2000 cm.$^{-1}$ always shifts bathochromically the hydriodides giving the lowest frequencies and the shift is about twice as large in most cases as for the upper bands.

We do not find this band with tertiary amine hydrohalides. The only exception is pyridine.

The band is most prominent in the spectra of aliphatic primary amines and it is interesting to note that it seems to be strong when the upper bands are well resolved, sharp bands. We find it too, however, in the spectra of piperidine, diphenylamine, pyridine, and aniline salts, but in piperidine salts it is much weaker. In pyridine and aniline it is absent or weak except for the hydrochloride. There may be some doubt whether in the latter cases the band is of the same origin. In diphenylamine salts the bands in this part of the spectrum are strong and behave like the corresponding bands in the case of the aliphatic primary amine salts.

It is usually not a single band. One can distinguish shoulders on the band contour or find two or more bands.

Now it is interesting that this band exhibits always downward shift in going from hydrochloride to hydriodide, even if the upper bands shift in the opposite direction as in the case of the diphenylamine salts. The scissoring bands behave in the same way. This would favor an interpretation of this band as an unusually strong combination of the scissoring band and a vibration which should have a frequency of about 400 cm.$^{-1}$.

Can. J. Chem. Downloaded from www.nrcresearchpress.com by 78.46.186.204 on 09/04/12
For personal use only.

Against this assignment is the fact that, as Bratož and Hadži have pointed out, the part of the potential surface involving the scissoring vibration is only moderately anharmonic. It is possible, however, that the lower frequency may be very anharmonic. This assignment is compatible with the fact that tertiary amine salts which do not have a scissoring band near 1600 cm.$^{-1}$ do not have the band near 2000 cm.$^{-1}$ either. In some of the aromatic cases (like pyridine or aniline) the supposed lower frequency may combine with benzene ring vibrations, which are always present in the same part of the spectrum, instead of with the NH_2^+ or NH_3^+ scissoring vibration.

The second interpretation (difference band) is more likely from the point of view of anharmonicity; however we must suppose again that the lower vibration is also very anharmonic if we hope to explain the fact that the band near 2000 cm.$^{-1}$ is usually much stronger than any of the higher bands. In the most typical cases, for instance that of tertiary butylamine and cyclohexylamine salts, the frequencies of the upper bands are nearly equidistant, the spacing being of the order of 100 cm.$^{-1}$. Thus these would be difference bands between the "real" stretching frequency and the overtones of a vibration of frequency 100 cm.$^{-1}$, and the band near 2000 cm.$^{-1}$ would be a difference band between the former and some very anharmonic vibration of frequency 800–700 cm.$^{-1}$. This interpretation offers no obvious reason for the absence of the band in the case of tertiary amine salts unless the lower vibration is linked to the presence of two or three hydrogens on the nitrogen atom, nor does it explain its characteristic shifting.

The third interpretation, that the upper bands are the antisymmetrical stretching band and combination bands and that the band near 2000 cm.$^{-1}$ is the symmetrical stretching band, would explain the observed strength of the latter band, since it would now be a fundamental; however it seems unlikely in view of the large separation between the two fundamentals. This separation is very large with cumulative double-bond systems but these bear little resemblance to the present case.

The general appearance of the spectra would indicate strongly an interpretation by a potential surface having two minima. The assumption of two minima because of the coupling of two of more N^+—H vibrations through a common halide ion is very unlikely because of the large weight of the latter. The other reason for the two minima (see 4 above) is more likely but this would not explain such a large splitting and it would also not explain either the absence of the band in the spectra of tertiary amine salts or the characteristic shifting of the band near 2000 cm.$^{-1}$.

More work is clearly needed but in our opinion and at the present stage the first assignment, that is, a combination between the scissoring band and a very anharmonic band near 400 cm.$^{-1}$, seems to be the most likely.

Aqueous Solutions

The spectra taken in aqueous solutions give bands which have higher frequencies than those taken in solid phase. The difference amounts to about 50–100 cm.$^{-1}$ (Table II). The case of pyridine salts seems to be exceptional; the higher frequency band lies near 2400 cm.$^{-1}$ in solid and near 2850 cm.$^{-1}$ in aqueous solution and they are very broad in both media.

It is even more important that in every case hydrochlorides, hydrobromides, and hydriodides have their bands at about the same place and we do not find the characteristic shifts found in other media. The slight variations observed in certain cases do not show any regularity.

We conclude from this that in aqueous solutions the hydrogen bonds are no longer

Can. J. Chem. Downloaded from www.nrcresearchpress.com by 78.46.186.204 on 09/04/12
For personal use only.

of the N^+—H- - -X^- type but of the N^+—H- - -O type. The water molecules might form hydrogen bonds of this type or with the halide ions or between themselves, and we can imagine other more complicated cases in these very concentrated solutions.

CONCLUSIONS

The above discussion refers to the general features we observed. Almost every amine and its salts would deserve a special study and we hope to discuss some related special problems in a second publication. This applies in particular to certain observations on amine solutions of the hydrohalides. The following facts, however, seem to be well established.

The location of the NH^+ stretching bands of the hydrogen-bonded amine hydrohalides at about the same part of the infrared spectrum for both aliphatic and aromatic molecules indicates that the energy of these hydrogen bonds comes mainly from electrostatic forces but that the charge distribution is different for the two categories and that delocalization makes a greater contribution to hydrogen bond energy in the case of the aromatic hydrohalides than in the case of the aliphatic hydrohalides.

The same factors allow a consistent qualitative explanation of regular hypsochromic or bathochromic shifts in the series hydrochloride → hydrobromide → hydriodide and of differences observed in the shifting of primary, secondary, and tertiary amine salts.

Our observations confirm the idea that the broadness of the bands is related to anharmonicity but they show too that anharmonicity might lead to broad regions of absorption and to a series of sharp bands as well, and also that shift and broadness do not necessarily go together.

Crystallographic studies would be highly desirable in order to supplement spectroscopic evidence related to the problem of hydrogen bonding in the case of amine hydrohalides.

RÉSUMÉ

Les spectres infrarouges des sels halogènes de dix-sept amines ont été mesurés à l'état solide, en solution aqueuse et en solution à l'amine même. Les vibrations de valence et de déformation des groupements NH_3^+, NH_2^+, NH^+ ont été étudiées.

Les vibrations de valence des sels des amines aliphatiques et aromatiques qui prennent part dans des associations par liaison hydrogène se trouvent dans la même partie du spectre. Les liaisons hydrogène sont du type N^+—H- - -X^-. Les composés aliphatiques ont généralement plusieurs bandes minces tandis que les composés aromatiques possèdent de vastes régions d'absorption composées de plusieurs bandes. Chez les sels des amines tertiaires les bandes se déplacent vers les ondes courtes dans l'ordre: chlorhydrate, bromhydrate, iodhydrate; chez les sels des amines aliphatiques primaires et secondaires les bandes se déplacent légerèment vers les grandes ondes. Chez les sels des amines aromatiques primaires et secondaires on observe moins de régularité mais le déplacement s'effectue généralement vers les ondes courtes. Ces faits s'expliquent qualitativement au moins si l'on prend en considération la répartition des charges dans les groupements amino ionisés, et les contributions des effets électrostatique et de délocalisation à l'énergie des liaisons hydrogène.

L'anharmonicité de la surface de potentiel qui fait apparaître des tons de combinaison forts peut conduire à l'élargissement des bandes ou à beaucoup de bandes minces. La grandeur du déplacement et l'élargissement des bandes ne vont pas toujours de pair ici.

On discute l'attribution d'une bande forte qu'on trouve près de 2000 $cm.^{-1}$ en beaucoup de cas.

Can. J. Chem. Downloaded from www.nrcresearchpress.com by 78.46.186.204 on 09/04/12
For personal use only.

Les déplacements caractéristiques observés en solide ne se reproduisent pas en solution aqueuse. On en conclut que là la liaison hydrogène n'est pas du type N^+—H- - -X^- mais du type N^+—H- - -O.

ACKNOWLEDGMENTS

The authors wish to express their thanks to Prof. Lucien Piché, Head of this Department, for his constant interest in this work.

We wish to thank Prof. D. Patterson and Prof. H. Favre for many helpful discussions.

Mrs. N. Iliesco contributed to this work at its early stage, a fact that we would like to acknowledge here.

Special thanks are due to Dr. K. Lenore McEwen for helpful discussions and help in preparation of the manuscript.

We acknowledge, too, a stimulating discussion with Dr. D. S. McClure, from Radio Corporation of America, Princeton, New Jersey.

The National Research Council of Canada and Imperial Oil Limited of Sarnia supported our research work with grants. We should like to express to them our appreciation.

REFERENCES

1. Moore, T. S. and Winmill, T. F. J. Chem. Soc. **101**, 1635 (1912).
2. Bernal, J. D. and Fowler, R. H. J. Chem. Phys. **1**, 515 (1933).
3. Pauling, L. The nature of the chemical bond. 2nd ed. Cornell Univ. Press, Ithaca, N.Y. 1945. p. 316.
4. Davies, M. M. Ann. Repts. on Progr. Chem. (Chem. Soc. London), **43**, 1 (1946).
5. Mecke, R. Discussions Faraday Soc. **9**, 161 (1950).
6. Hunter, L. Ann. Repts. on Progr. Chem. (Chem. Soc. London) **43**, 141 (1946).
7. Kellner, L. Repts. Progr. in Phys. **15**, 1 (1946).
8. Bratož, S. and Hadži, D. J. Chem. Phys. **27**, 991 (1957).
9. Coulson, C. A. Research, **10**, 149 (1957).
10. Lord, R. C. and Merrifield, R. E. J. Chem. Phys. **21**, 166 (1953).
11. Rundle, R. E. and Parasol, M. J. Chem. Phys. **20**, 1487 (1952).
12. Young, C. W., Du Vall, R. B., and Wright, N. Anal. Chem. **23**, 709 (1951).
13. Heacock, R. A. and Marion, L. Can. J. Chem. **34**, 1782 (1956).
14. Herzberg, G. Infrared and Raman spectra of polyatomic molecules. D. Van Nostrand Company, Inc., New York. 1945.
15. Donohue, J. J. Phys. Chem. **56**, 502 (1952).
16. Fuson, N., Josien, M.-L., Powell, R. L., and Utterback, E. J. Chem. Phys. **20**, 145 (1952).
17. Thompson, H. W. and Harris, G. P. J. Chem. Soc. 301 (1944).
18. Plumb, R. C. and Hornig, D. F. J. Chem. Phys. **23**, 947 (1955).
19. Bauer, E. and Magat, M. J. phys. radium, **9**, 319 (1938).
20. Stepanov, B. I. Zhur. Fiz. Khim. **19**, 507 (1945).
21. Stepanov, B. I. Zhur. Fiz. Khim. **20**, 407 (1946).
22. Cannon, C. G. Research, **4**, 439 (1951).
23. Lippincott, E. R. and Schroeder, R. J. Chem. Phys. **23**, 1099 (1955).
24. Batuev, M. I. Zhur. Fiz. Khim. **23**, 1399 (1949).
25. Randall, H. M., Fuson, N., Fowler, R. G., and Dangl, J. R. Infrared determination of organic structures. D. Van Nostrand Company, Inc., New York. 1949.
26. Thompson, H. W., Nicholson, D., and Short, L. N. Discussions Faraday Soc. **9**, 222 (1950).
27. Schroeder, R. and Lippincott, E. R. J. Phys. Chem. **61**, 921 (1957).
28. Finch, J. N. and Lippincott, E. R. J. Chem. Phys. **24**, 908 (1956).
29. Coulson, C. A. and Danielsson, U. Arkiv Fysik, **8**, 239 (1954).
30. Danielsson, U. and Coulson, C. A. Arkiv Fysik, **8**, 245 (1954).
31. Tsubomura, H. Bull. Chem. Soc. Japan, **27**, 445 (1954).
32. Pritchard, H. O. Chem. Revs. **52**, 529 (1953).
33. Baker, A. N. J. Chem. Phys. **22**, 1625 (1954).
34. Kaku, K. Kumamoto J. Sci. Ser. A, **1**, 55 (1954).

Can. J. Chem. Downloaded from www.nrcresearchpress.com by 78.46.186.204 on 09/04/12
For personal use only.

Can. J. Chem. Downloaded from www.nrcresearchpress.com by 78.46.186.204 on 09/04/12
For personal use only.

NOTES

THE POLAROGRAPHIC REDUCTION OF DIAZOTIZED AROMATIC AMINES*

R. M. ELOFSON

INTRODUCTION

The polarographic activity of diazotized aromatic amines was first reported by Elofson and Mecherly (5), who made use of it in amperometric titrations. Later Elofson and co-workers (6) reported on the polarography of diazotized amines and employed their limiting currents for analytical purposes. By comparing the total wave height with that for hydroquinone, which should have a nearly identical diffusion coefficient, it was concluded that four electrons were involved in the over-all reduction. Further support for this conclusion was cited in the fact that phenylhydrazine is produced by electrolytic reduction of diazotized amines (8) at a mercury electrode. It was therefore concluded that the net reduction occurring at a dropping mercury electrode could be described by [1].

$$ArN_2^+ + 4H^+ + 4e \rightarrow ArNHNH_3^+ \qquad [1]$$

Almost simultaneously, Atkinson and co-workers (1) reported on the detailed polarographic reduction of diazotized amines, finding that the reduction took place in two main steps, one at potentials below -0.3 volts vs. S.C.E. and a larger wave at more negative potentials. From the results of coulometric analyses performed at stirred mercury pool electrodes they concluded that only one electron was involved irrespective of whether reduction took place at the first or second plateau. No material other than phenylmercuric chloride and diphenylmercury could be isolated during the coulometric analysis. In a subsequent paper, Atkinson *et al.* (2) reported that two electrons were involved when coulometric analyses were performed at the second plateau.

Kochi (7), in a later investigation, corroborated the results of Atkinson, although he did not specify the pH at which his measurements were made.

In view of the above discrepancies and the difficulty in reconciling markedly different diffusion coefficients for diazonium ions and for hydroquinone, it was deemed desirable to reinvestigate this problem.

EXPERIMENTAL

The polarograms described in this paper were obtained with a Leeds and Northrup Electrochemograph, type E. A saturated calomel electrode was used as an anode. The temperature of the electrolysis cell was maintained at 0° C. to 2° C. At $h = 60$ cm. the capillary constants were $m = 2.62$ mg./sec. in air and $t = 3.63$ seconds at zero applied potential in 0.2 N HCl.

RESULTS

In their first paper, Elofson and Mecherly (5) noted that the lower wave was not proportional to concentration above about 4×10^{-4} M. Some results of a detailed investigation concerned with the effect of concentration of a diazotized amine in acid solution on its polarograms are illustrated in Figs. 1 and 2. It is evident that the total

Contribution No. 70 from the Research Council of Alberta, Edmonton, Alberta. Prepared for presentation at the Annual Conference of the Chemical Institute of Canada at Vancouver in June 1957.

current was proportional to the concentration to at least 2.8×10^{-3} M. On the other hand, the limiting current for the first wave reaches a constant value at a diazotized amine concentration of above 1×10^{-3} M. Very similar results were obtained in solutions buffered to pH 6.

The data in Table I illustrate the effect of varying height of the mercury column on the limiting currents. It can be seen that while the total current is very nearly proportional to the square root of the height, the magnitude of the lower wave is directly proportional to the height. This observation and the fact that the lower wave reaches a constant value indicates that the first wave is an adsorption wave. The second is diffusion controlled (4, 9).

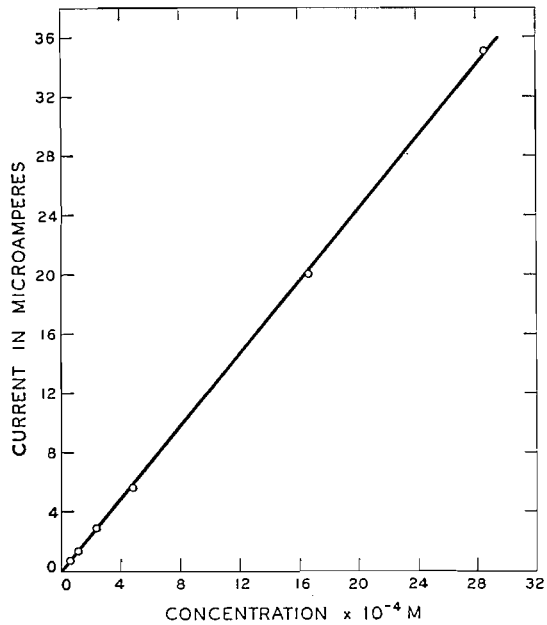

FIG. 1. Relation between total limiting current and concentration of *p*-anisidine diazo in 0.2 *N* hydrochloric acid.

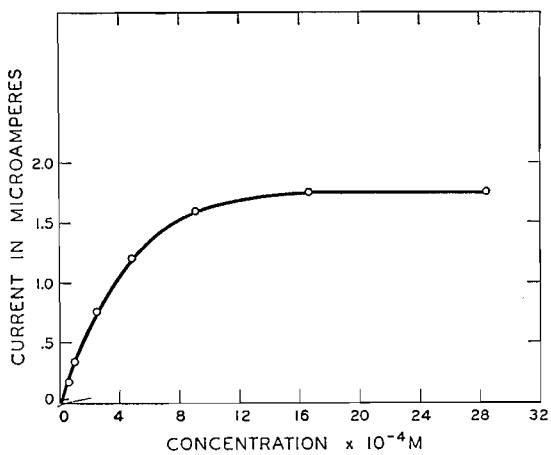

FIG. 2. Relation between limiting current for the first reduction wave and concentration of *p*-anisidine diazo in 0.2 *N* hydrochloric acid.

Can. J. Chem. Downloaded from www.nrcresearchpress.com by 78.46.186.204 on 09/04/12
For personal use only.

TABLE I

LIMITING CURRENTS FOR *p*-ANISIDINE DIAZO FOR VARYING HEIGHTS OF MERCURY

(Concentration, 2.4×10^{-4} *M* in 0.2 *N* HCl)

Height of mercury, cm.	Limiting current		First wave	Total wave
	First wave μa.	Total wave μa.	Height	Square root of height
28	0.38	1.76	0.068	1.66
56	0.74	2.58	0.066	1.70

In order to determine the value of '*n*' in the electrode reaction, *p*-methoxybenzenediazonium chloride (*p*-anisidine diazo) was selected because of its good thermal stability and low rate of coupling in side reactions (3). The work of McClure and Lowry (8) and Ruetschi and Trumpler (10) clearly indicated that only acidic solutions would actually yield hydrazines because of side reactions. Furthermore, the work of both of the above groups of workers showed that acidic solutions of benzenediazonium salts in the presence of mercury decompose to form mercuric salts according to [2].

$$ArN_2Cl + Hg \rightarrow ArHgCl + N_2 \qquad [2]$$

Coulometric analyses with stirred mercury pools were found in agreement with Atkinson (1, 2) and Kochi (7) to yield mainly phenylmercuric salts with apparent values of '*n*' less than one at either the first or second plateau. Both McClure and Lowry (8) and Ruetschi and Trumpler (10) found that rapid stirring was conducive to formation of phenylmercuric salts.

Coulometric analyses were then carried out in an ice bath in a microcell of the design shown in Fig. 3. Thermal decomposition of the diazotized amine was found to be negligible during the time required for an electrolysis. A correction was applied for the amount of the diazotized amine with mercury at zero applied potential.

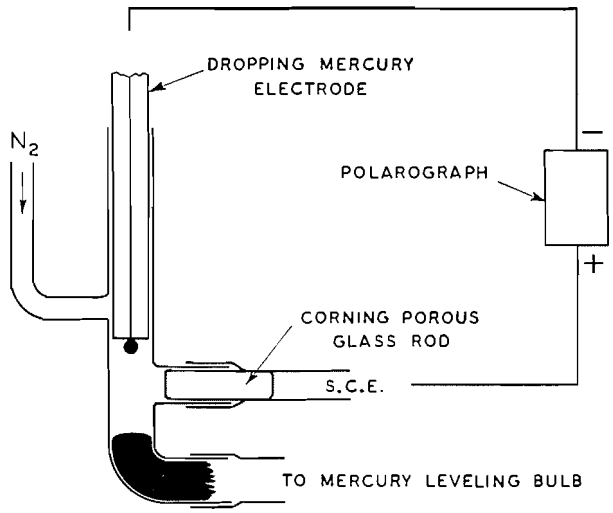

FIG. 3. Microcoulometer for controlled potential electrolyses of diazotized aromatic amines.

At a cathodic potential of −0.55 volts on the first plateau, with 0.6 ml. of 0.001 *M* solution, '*n*' was, in agreement with the results of previous workers, found to be 1.0. At −1.1 volts on the second plateau, three analyses gave a mean value for '*n*' equal to

Can. J. Chem. Downloaded from www.nrcresearchpress.com by 78.46.186.204 on 09/04/12
For personal use only.

4.1 with 0.6 ml. of 0.001 *M* solution. The solutions electrolyzed at −1.1 volts gave positive tests for the hydrazine when treated with ammonium molybdate in 5% sulphuric acid. Positive tests for the hydrazine could not be obtained when the electrolyses were carried out with stirred pool electrodes. In more concentrated solutions, 0.005 *M*, the value of '*n*' approximated four but it was difficult to obtain good measurements because the droplets would not coalesce and these droplets trapped an appreciable fraction of the cell solution. Nevertheless, confirmation of the high current efficiencies obtained by Ruetschi and Trumpler in large scale electrolyses was indicated.

DISCUSSION

The experiments described herein clearly support the claim that the over-all reaction of diazotized aromatic amines at a dropping mercury electrode involves a 4-electron reduction. The first wave in the polarographic reduction is due to an adsorption phenomenon which results from the 1-electron reduction to a free radical (1, 2, 6) according to [3], which is evidently stabilized at the mercury electrode.

$$ArN_2^+ + e \rightarrow ArN_2. \qquad [3]$$

This mechanism is also favored from the constitution of the tar isolated by Kochi (7). The stability of the adsorption complex is the principal factor which determines the potential at which the adsorption current occurs. It is therefore to be expected that the half-wave potentials for the first reduction waves of a number of diazotized aromatic amines would not correlate with electron densities in the usual way (7). It would seem desirable to correlate the half-wave potential with adsorptivities of the free radicals on the mercury electrode at various potentials.

ACKNOWLEDGMENT

The author is indebted to Dr. W. E. Harris, of the University of Alberta, for many stimulating discussions and for helpful criticism of the manuscript.

1. Atkinson, E. R., Warren, H. H., Abell, P. I., and Wing, R. E. J. Am. Chem. Soc. **72**, 915 (1950).
2. Atkinson, E. R., Garland, C. E., and Butler, A. F. J. Am. Chem. Soc. **75**, 983 (1953).
3. Atkinson, E. R., Morgan, C. R., Warren, H. H., and Manning, O. T. J. J. Am. Chem. Soc. **67**, 1513 (1945).
4. Brdicka, R. Z. Elektrochem. **48**, 278, (1942).
5. Elofson, R. M. and Mecherly, P. A. Anal. Chem. **21**, 565 (1949).
6. Elofson, R. M., Edsberg, R. L., and Mecherly, P. A. J. Electrochem. Soc. **97**, 166 (1950).
7. Kochi, J. K. J. Am. Chem. Soc. **77**, 3208 (1955).
8. McClure, R. E. and Lowry, A. Trans. Electrochem. Soc. **56**, 445 (1929).
9. Müller, O. H. Trans. Electrochem. Soc. **87**, 441 (1945).
10. Ruetschi, P. and Trumpler, G. Helv. Chim. Acta, **36**, 1649 (1953).

Received March 21, 1958.
Research Council of Alberta,
Edmonton, Alberta.

ON THE DECOMPOSITION FLAME OF OZONE AT HIGH PRESSURE*

R. Sandri

The theory of the decomposition flame in ozone–oxygen mixtures has been developed in an earlier paper of this series (1). In another paper (2), the author has shown that this theory can also be applied to high relative concentrations of ozone (up to 100%). The results were found in good agreement with measurements made by Lewis and Elbe (3) and by Streng and Grosse (4) at atmospheric pressure.

Issued as N.R.C. No. 4802.

Can. J. Chem. Downloaded from www.nrcresearchpress.com by 78.46.186.204 on 09/04/12
For personal use only.

4.1 with 0.6 ml. of 0.001 *M* solution. The solutions electrolyzed at −1.1 volts gave positive tests for the hydrazine when treated with ammonium molybdate in 5% sulphuric acid. Positive tests for the hydrazine could not be obtained when the electrolyses were carried out with stirred pool electrodes. In more concentrated solutions, 0.005 *M*, the value of '*n*' approximated four but it was difficult to obtain good measurements because the droplets would not coalesce and these droplets trapped an appreciable fraction of the cell solution. Nevertheless, confirmation of the high current efficiencies obtained by Ruetschi and Trumpler in large scale electrolyses was indicated.

DISCUSSION

The experiments described herein clearly support the claim that the over-all reaction of diazotized aromatic amines at a dropping mercury electrode involves a 4-electron reduction. The first wave in the polarographic reduction is due to an adsorption phenomenon which results from the 1-electron reduction to a free radical (1, 2, 6) according to [3], which is evidently stabilized at the mercury electrode.

$$ArN_2^+ + e \rightarrow ArN_2. \qquad [3]$$

This mechanism is also favored from the constitution of the tar isolated by Kochi (7). The stability of the adsorption complex is the principal factor which determines the potential at which the adsorption current occurs. It is therefore to be expected that the half-wave potentials for the first reduction waves of a number of diazotized aromatic amines would not correlate with electron densities in the usual way (7). It would seem desirable to correlate the half-wave potential with adsorptivities of the free radicals on the mercury electrode at various potentials.

ACKNOWLEDGMENT

The author is indebted to Dr. W. E. Harris, of the University of Alberta, for many stimulating discussions and for helpful criticism of the manuscript.

1. Atkinson, E. R., Warren, H. H., Abell, P. I., and Wing, R. E. J. Am. Chem. Soc. **72**, 915 (1950).
2. Atkinson, E. R., Garland, C. E., and Butler, A. F. J. Am. Chem. Soc. **75**, 983 (1953).
3. Atkinson, E. R., Morgan, C. R., Warren, H. H., and Manning, O. T. J. J. Am. Chem. Soc. **67**, 1513 (1945).
4. Brdicka, R. Z. Elektrochem. **48**, 278, (1942).
5. Elofson, R. M. and Mecherly, P. A. Anal. Chem. **21**, 565 (1949).
6. Elofson, R. M., Edsberg, R. L., and Mecherly, P. A. J. Electrochem. Soc. **97**, 166 (1950).
7. Kochi, J. K. J. Am. Chem. Soc. **77**, 3208 (1955).
8. McClure, R. E. and Lowry, A. Trans. Electrochem. Soc. **56**, 445 (1929).
9. Müller, O. H. Trans. Electrochem. Soc. **87**, 441 (1945).
10. Ruetschi, P. and Trumpler, G. Helv. Chim. Acta, **36**, 1649 (1953).

Received March 21, 1958.
Research Council of Alberta,
Edmonton, Alberta.

ON THE DECOMPOSITION FLAME OF OZONE AT HIGH PRESSURE*

R. Sandri

The theory of the decomposition flame in ozone–oxygen mixtures has been developed in an earlier paper of this series (1). In another paper (2), the author has shown that this theory can also be applied to high relative concentrations of ozone (up to 100%). The results were found in good agreement with measurements made by Lewis and Elbe (3) and by Streng and Grosse (4) at atmospheric pressure.

Issued as N.R.C. No. 4802.

Can. J. Chem. Downloaded from www.nrcresearchpress.com by 78.46.186.204 on 09/04/12
For personal use only.

In order to test further the validity of the formulae and to provide some assistance for experimental work, calculations have now been made predicting decomposition flame velocities at high pressures.

The formulae which have been derived for the ozone flame velocity V_0 do not contain the pressure p but only the initial relative concentration of ozone y_{30}, the initial temperature T_0, and the flame temperature T_f. For mixtures containing up to 50% ozone, T_f is practically independent of p and consequently V_0 is also independent of it. For higher values of y_{30}, however, the flame temperature becomes so high that dissociation of molecular oxygen into atomic oxygen in the "burned" gas begins to play an important role. Then, since higher pressure decreases the degree of dissociation, T_f and consequently V_0 increase appreciably with pressure. This increase is greater for higher initial temperature.

Table I shows flame velocities in pure ozone, computed for various pressures and for initial temperatures of 195° K. (temperature of dry ice) and 300° K. The corresponding flame temperatures were calculated by thermodynamic methods, using the data of the N.B.S. Circulars C461 and C564.

TABLE I

DECOMPOSITION FLAME VELOCITIES IN PURE OZONE

	Initial temperature T_0 = 195° K.				
p (atmospheres)	1	2	5	10	100
T_f (° K.)	2648	2683	2723	2748	2784
V_0 (cm./sec.)	270*	282	295	304	317
	Initial temperature T_0 = 300° K.				
p (atmospheres)	1	2	5	10	100
T_f (° K.)	2678	2716	2761	2789	2834
V_0 (cm./sec.)	444*	464	488	504	529

*Owing to improved accuracy of numerical computation, these values are slightly higher than those obtained in the earlier paper (2) of the author.

1. SANDRI, R. Can. J. Chem. **34**, 324 (1956).
2. SANDRI, R. Can. J. Chem. **35**, 474 (1957).
3. LEWIS, B. and ELBE, G. VON. J. Chem. Phys. **2**, 283 (1934).
4. STRENG, A. G. and GROSSE, A. V. VIth Intern. Symposium on Combustion, 264 (1956).

RECEIVED APRIL 25, 1958.
FUELS AND LUBRICANTS LABORATORY,
DIVISION OF MECHANICAL ENGINEERING,
NATIONAL RESEARCH COUNCIL OF CANADA,
OTTAWA, CANADA.

Can. J. Chem. Downloaded from www.nrcresearchpress.com by 78.46.186.204 on 09/04/12
For personal use only.

Can. J. Chem. Downloaded from www.nrcresearchpress.com by 78.46.186.204 on 09/04/12
For personal use only.

Canadian Journal of Chemistry

Issued by THE NATIONAL RESEARCH COUNCIL OF CANADA

VOLUME 36 SEPTEMBER 1958 NUMBER 9

PEROXIDES IN THE COMBUSTION OF ISOBUTANE[1]

G. W. TAYLOR[2]

ABSTRACT

A survey has been made of the nature of the peroxides occurring in the combustion of isobutane below and above the lower cool-flame limit. The peroxides were resolved and partially identified by paper chromatography. Below the cool-flame limit, the peroxide is found to be mostly *tert*-butyl hydroperoxide, with some hydrogen peroxide, but as the cool-flame limit is approached the proportion of *tert*-butyl hydroperoxide declines, while that of hydrogen peroxide increases. In addition, peroxides identified as aldehyde and acid peroxides increase as the cool-flame limit is approached. No *tert*-butyl hydroperoxide appears to survive the cool flame, although copious quantities of aldehyde peroxide and hydrogen peroxide remain.

INTRODUCTION

The nature and role of the peroxides occurring in the products of the non-catalyzed thermal oxidation of hydrocarbons has been the subject of considerable debate, and the problem has been complicated by the absence of a reliable analytical technique, capable of identifying peroxides in the amounts usually prevailing in the study of combustion reactions. The possible occurrence of various types of peroxides in combustion reactions has recently been considered by Tipper (1). While several unequivocal identifications have been claimed, these are for the most part confined to exceptional cases, for example the low-temperature combustion of acetaldehyde (2).

A paper chromatographic method of resolving some peroxide mixtures has recently been briefly described, and applied in the analysis of the cool-flame combustion products of ethyl benzene (3). The application of this technique has now been extended over a further range of peroxides and its use in the analysis of the combustion products of isobutane is the subject of the present paper.

Isobutane is a rather exceptional fuel, in that it possesses nine primary hydrogen atoms and only one tertiary hydrogen atom. That this latter atom is the initial point of attack by oxygen has been demonstrated by Batten, Gardner, and Ridge (4). Further, the hydroperoxide derived from isobutane, *tert*-butyl hydroperoxide, is unique among the lower alkyl hydroperoxides in its thermal stability. From the point of view of the possible identification of alkyl hydroperoxide in a hydrocarbon oxidation product, the combustion of isobutane thus appears particularly attractive. Batten, Gardner, and Ridge analyzed their combustion products in some detail and, apart from the inevitable gaseous product, found formaldehyde, a smaller amount of higher aldehyde, acetone, a little acid, and peroxides. The peroxides were further examined by polarography with successive removal of various components. Hydrogen peroxide was removed by reaction with

[1]*Manuscript received May 13, 1958.*
Contribution from the Division of Pure Chemistry, National Research Council, Ottawa, Canada.
Issued as N.R.C. No. 4813.
[2]*National Research Council Postdoctorate Fellow 1956–1958.*

titanous chloride and ammonia. Formaldehyde peroxide (and, the authors conclude, higher aldehyde peroxide also) was removed by reaction with mercury. The residual peroxide was assumed on the basis of its polarogram to be alkyl hydroperoxide. From this procedure, the authors concluded that alkyl hydroperoxide, probably *tert*-butyl hydroperoxide, could form more than 50% of the total peroxide.

An examination of their polarograms immediately reveals that the identification of the peroxide is by no means unequivocal, as the authors themselves make clear. Nevertheless, the occurrence of *tert*-butyl hydroperoxide and hydrogen peroxide appeared highly probable, the former compound especially in the induction period.

The present work entirely confirms the conclusions of Batten, Gardner, and Ridge by providing identifications which can be open to very little uncertainty.

EXPERIMENTAL

Isobutane, a gift from the British Petroleum Company Limited, contained 0.5% *n*-butane as the sole detectable impurity. Oxygen was obtained from a cylinder and was used without further treatment.

The reaction was studied using a flow system similar to that already described (3). The reaction vessel was a pyrex cone, 15 cm long, 2.5 cm maximum diameter. The fuel to oxygen ratio was 1 to 1, total pressure atmospheric. The products were passed through a trap at −80° C. At the end of a run the trap was allowed to warm up, isobutane evaporating off. The residual liquid was used in the identification of peroxides. Drops of liquid were paper chromatographed as previously described. The solvent system used was butanol–ether–water (10:10:1). The chromatograms were developed with aqueous acidified potassium iodide solution. The unknown chromatograms were compared with those of standards run on the same paper.

The standard peroxides, whose R_F values are shown in Table I, were: methoxy hydroperoxide and dimethoxyperoxide (formaldehyde peroxides); α-hydroxyethyl hydroperoxide and α,α'-dihydroxydiethyl peroxide (acetaldehyde peroxides); *tert*-butyl hydroperoxide, and hydrogen peroxide. Aldehyde peroxide was made by desiccating an aqueous mixture of aldehyde and hydrogen peroxide containing a drop of sulphuric acid, over concentrated sulphuric acid. The end product of the formaldehyde mixture was a mildly explosive, insoluble solid, shown by Rieche and Meister (5) to be tetraoxymethylene diperoxide. This contained a little material soluble in water, which was dimethoxyperoxide. A compound which was almost certainly methoxy hydroperoxide was obtained only as an intermediate in the initial stage of the reaction. A similar sequence occurred in the acetaldehyde reaction, but here polymer was not obtained. The end product was a hygroscopic, very explosive oil. In addition, butyraldehyde and caproaldehyde were shaken with hydrogen peroxide; some reaction occurred producing compounds of R_F value 0.99–1.0. In general, pure peroxides were not isolated, aqueous solutions being adequate for the present purpose.

RESULTS

The oxidation of isobutane was studied at 250, 330, 360, and 370° C. A cool flame appeared at about 350° C.

(*a*) *At 250° C, total flow 0.4 ml per sec, run time 195 minutes.*—A trace of aqueous product, strongly peroxidic, remained in the trap. The R_F values of the peroxides were 0.99 and 0.50. A smudge, of maximum density at 0.85, also was formed. The component of R_F 0.99 strongly predominated.

Can. J. Chem. Downloaded from www.nrcresearchpress.com by 78.46.186.204 on 09/04/12
For personal use only.

(*b*) *At 330° C, total flow 2.0 ml per sec, run time 30 minutes.*—The product was similar to the above. The proportion of material of R_F 0.99 was somewhat decreased, while that of R_F 0.50 increased. The smudge was also denser.

(*c*) *At 360° C, total flow 2.0 ml per sec, run time 15 minutes. Weak cool flame.*—The degree of oxidation was considerably increased, and an appreciable volume of liquid product was formed. The R_F values of the peroxides were 0.50 and 0.9; the latter spot was actually a streak, extending between 0.95 and 0.7. The component of R_F 0.99 was almost certainly absent.

(*d*) *At 370° C, total flow 2.0 ml per sec, run time 30 minutes. Bright cool flame.*—The product was treated as in (*c*). No component of R_F 0.99 was present, although the density of the 0.7–0.95 smudge was considerably increased. The component of R_F 0.50 was also present.

DISCUSSION

A comparison of the R_F values of the unknown peroxides with the R_F values of the standards shows that the unknown peroxide of R_F 0.50 is almost certainly hydrogen peroxide. It is interesting that this compound is a product of the low-temperature reaction, as it has generally been assumed to be characteristic more of a high-temperature reaction. The possibility that the hydrogen peroxide detected is actually a result of decomposition of organic peroxide during the analysis is ruled out by the fact that spots, not streaks, were obtained in the chromatography of the standards.

The spot of R_F 0.99 exactly matches that of *tert*-butyl hydroperoxide. The identification of this component as *tert*-butyl hydroperoxide is strongly substantiated by the conditions of its appearance. It is a product of the induction period, that is, a primary product, and disappears as the degree of reaction increases, that is, as the cool-flame limit is crossed. This behavior is exactly the reverse of that of aldehydes—and hence, aldehyde peroxides—which are the predominant products of cool-flame reactions (e.g. propane (6) and hexane (7)). It is improbable, therefore, that the fast-moving peroxide is a higher aldehyde peroxide possibly derived from the preferential combustion of the trace of *n*-butane in the starting material.

The material of R_F 0.7–0.95 was a minor component below the cool-flame limit, but increased markedly as the limit was crossed. A comparative study of the cool-flame oxidation of a wide variety of hydrocarbons and ethers showed that this material is a characteristic product of all the oxidations. A comparison of its chromatographic behavior with that of the standards suggests that its composition is complex, and it is believed that the material is a mixture of aldehyde and acid peroxides not completely resolved. The presence of alkyl hydroperoxides is not ruled out, but the conditions of its occurrence would appear to preclude the presence of alkyl hydroperoxides.

TABLE I

R_F VALUES OF STANDARD PEROXIDES

Peroxide	R_F
Hydrogen peroxide	0.50
Methoxyhydroperoxide	0.65
Dimethoxyperoxide	0.82
α-Hydroxyethyl hydroperoxide	0.73
α,α′-Dihydroxydiethyl peroxide	0.95
tert-Butyl hydroperoxide	0.99

Solvent: *n*-Butanol–ether–water (10:10:1 v/v).
Paper: Whatman No. 3.
Developer: Acidified potassium iodide.

Can. J. Chem. Downloaded from www.nrcresearchpress.com by 78.46.186.204 on 09/04/12
For personal use only.

It is concluded, therefore, that in the oxidation of isobutane, the peroxide products are hydrogen peroxide, *tert*-butyl hydroperoxide, and aldehyde peroxides. *Tert*-butyl hydroperoxide is the predominant product of the induction period, along with some hydrogen peroxide. As the cool-flame limit is passed, the yield of *tert*-butyl hydroperoxide suffers a catastrophic decline while the yields of aldehyde peroxides and hydrogen peroxide increase.

This behavior appears to substantiate the conclusions of Batten, Gardner, and Ridge. The decline in their total peroxide after the induction period was ended (in contrast with the present data) is probably a result of consumption of reactant in their static apparatus.

This work was done while the author was in the Department of Physical Chemistry in the University of Cambridge, England. He is indebted to Prof. R. G. W. Norrish, F.R.S., for inspiration and encouragement.

REFERENCES

1. TIPPER, C. F. H. Quart. Revs. **11**, 313 (1957).
2. MCDOWELL, C. A. and SHARPLES, L. K. Can. J. Chem. **36**, 251 (1958).
3. NORRISH, R. G. W. and TAYLOR, G. W. Proc. Roy. Soc. A, **238**, 143 (1957).
4. BATTEN, J. J., GARDNER, H. J., and RIDGE, M. J. J. Chem. Soc. 3029 (1955).
5. RIECHE, A. and MEISTER, R. Ber. deut. chem. Ges. **66**, 718 (1933).
6. KNOX, J. H. and NORRISH, R. G. W. Proc. Roy. Soc. A, **221**, 151 (1954).
7. BAILEY, H. C. and NORRISH, R. G. W. Proc. Roy. Soc. A, **212**, 311 (1952).

Can. J. Chem. Downloaded from www.nrcresearchpress.com by 78.46.186.204 on 09/04/12
For personal use only.

THE REACTIONS OF ACTIVE NITROGEN WITH CYCLOPROPANE, CYCLOBUTANE, AND CYCLOPENTANE[1]

N. V. KLASSEN,[2] M. ONYSZCHUK,[3] J. C. MCCABE,[4] AND C. A. WINKLER

ABSTRACT

Cyclopropane, cyclobutane, and cyclopentane in order of increasing reactivity with active nitrogen yielded hydrogen cyanide and ethylene as the major products. The relative proportions of ethylene to hydrogen cyanide increased with number of carbon atoms in the reactant and with increase of temperature.

Alkenes have been found (1) to react with active nitrogen more rapidly than do the corresponding alkanes, to yield a larger proportion of unsaturated hydrocarbons (other than the initial reactant) relative to hydrogen cyanide in the products. It was of interest to determine whether cycloalkanes, in their reactions with active nitrogen, would resemble the corresponding *n*-alkanes or their olefin isomers, and whether the ease of reaction would depend upon the relative stabilities of the cycloalkane rings.

EXPERIMENTAL

The apparatus, experimental techniques, and analytical methods were essentially the same as those described in previous papers (2, 3, 4). A molecular nitrogen flow of 58 micromoles/second at a pressure of 1.5 mm Hg was used in the cyclopropane and cyclobutane reactions, while in the cyclopentane reaction the molecular nitrogen flow was 100 micromoles/second at a pressure of 1.8 mm Hg. In a brief examination of the atomic hydrogen reaction with cyclopentane and ethylene the flow of hydrogen was 120 micromoles/second at a pressure of 0.95 mm Hg.

Cyclopropane of 99.5% purity was used after a single bulb-to-bulb distillation. A limited supply of cyclobutane of approximately 99% purity was obtained through the courtesy of Dr. W. D. Walters, University of Rochester. The cyclopentane used had a refractive index $n_D^{20} = 1.4062$ ($n_D^{20} = 1.4064$ for highly purified cyclopentane (5)). Low temperature fractionation failed to reveal any lower molecular weight impurities.

Analyses for HCN, $(CN)_2$, and NH_3 were made by standard titration methods (6, 7), while mass-spectrometric and gas-chromatographic methods were used for other condensible and the non-condensible products.

RESULTS

Active nitrogen appeared to react only slowly with cyclopropane, since the purple-pink reaction flame completely filled the reaction vessel, even at high reactant flow rates. The flow rate of active nitrogen was taken to be equal to the maximum flow rate of hydrogen cyanide produced in the reaction of ethylene with active nitrogen at temperatures above 250° C (1) and found to be 3.9 micromoles/second.

The recovery of HCN increased as cyclopropane flow rate increased at all temperatures (Fig. 1), hence complete consumption of active nitrogen did not take place except, perhaps, at high flow rates at 350° C. The recoveries of C_2H_4 and C_2H_2 were much smaller than that of HCN (Fig. 1), and C_2H_6 was detected only in trace amounts.

[1]*Manuscript received April 29, 1958.*
Contribution from the Physical Chemistry Laboratory, McGill University, Montreal, Que., with financial assistance from Union Carbide of Canada and the National Research Council of Canada.
[2]*Holder of a Union Carbide (Canada) Research Fellowship and a National Research Council Studentship.*
[3]*At the time, holder of a National Research Council Studentship. Now Assistant Professor, McGill University.*
[4]*Present address: Darjeeling Mission, India.*

Can. J. Chem. Downloaded from www.nrcresearchpress.com by 78.46.186.204 on 09/04/12
For personal use only.

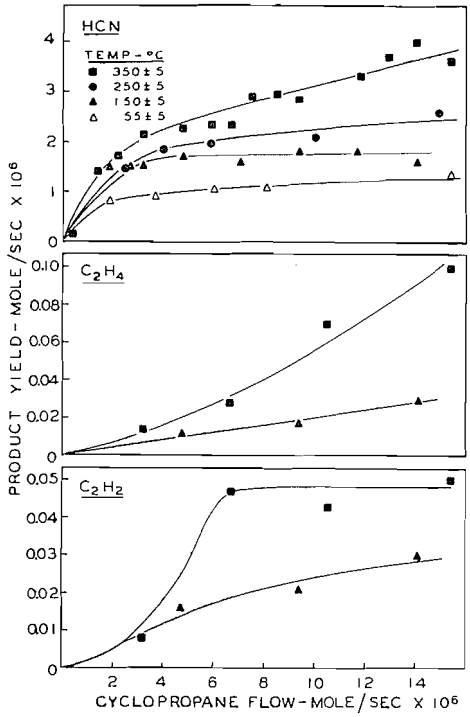

FIG. 1. Relation of cyclopropane flow rate to product yields.

At high flow rates cyclobutane reacted with a relatively intense peach-colored flame in a small volume around the hydrocarbon inlet, from which it might be inferred that cyclobutane was considerably more reactive than cyclopropane. This is confirmed by the much higher conversion to HCN (Fig. 2). Complete reaction of the active nitrogen (the flow rate of which was 5.2 micromoles/second) appeared to be attained only above 250° C and 5 micromoles/second cyclobutane flow, when the production of HCN became independent of reactant flow rate.

The yields of other products in relation to cyclobutane flow rate are also shown in Fig. 2. Propane was detected among the products, but in even smaller amounts than propylene.

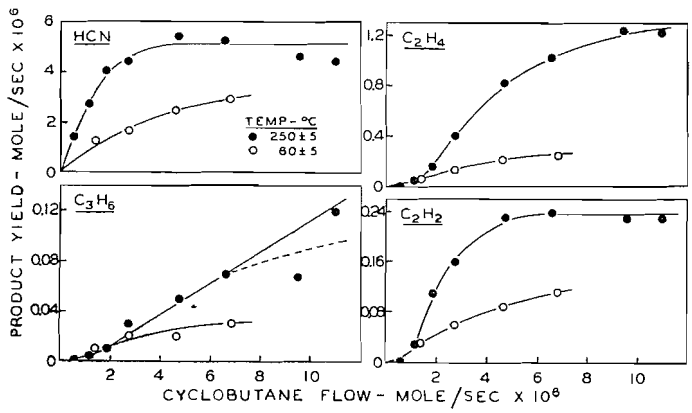

FIG. 2. Relation of cyclobutane flow rate to product yields.

Can. J. Chem. Downloaded from www.nrcresearchpress.com by 78.46.186.204 on 09/04/12
For personal use only.

Cyclopentane reacted with active nitrogen with a reddish-violet flame that was concentrated near the hydrocarbon inlet at all but the lowest flow rates, i.e. the reaction appeared to be quite fast. The limiting production of HCN (Fig. 3) was essentially equal to the active nitrogen flow rate of 13 micromoles/second. The largest observed ratio of C_2H_4 to HCN was 0.7, but this ratio would undoubtedly have increased at still higher cyclopentane flow rates (not readily attainable because of back diffusion from the reaction vessel).

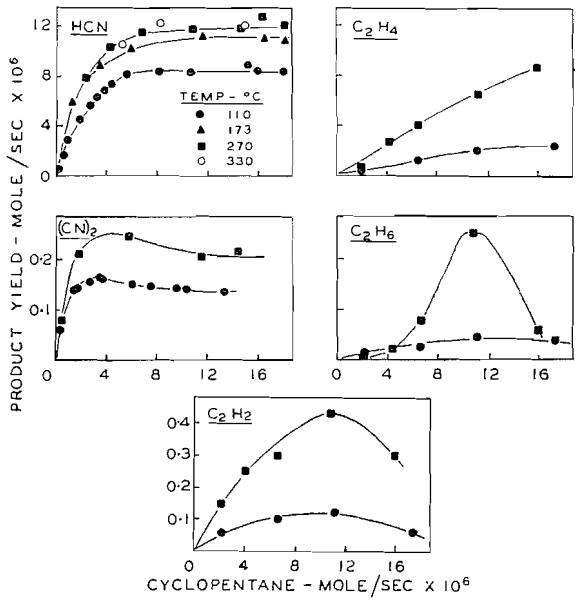

FIG. 3. Relation of cyclopentane flow rate to product yields.

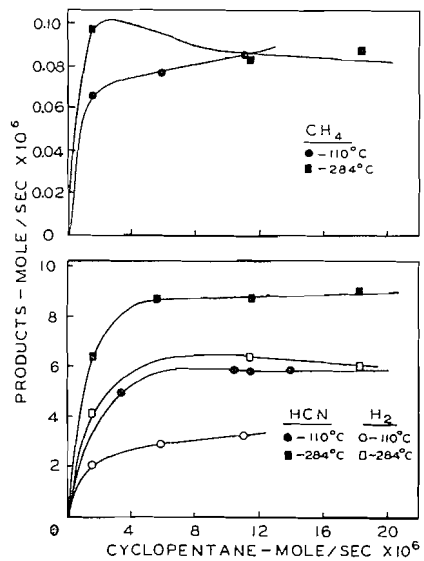

FIG. 4. Relation of cyclopentane flow rate to yields of methane and hydrogen.

Can. J. Chem. Downloaded from www.nrcresearchpress.com by 78.46.186.204 on 09/04/12
For personal use only.

The recoveries of $(CN)_2$, C_2H_6, and C_2H_2 showed maxima with cyclopentane flow rate. Ammonia and C_3 and C_4 hydrocarbons were detected in amounts less than 1% of the HCN.

In another series of experiments, with an active nitrogen flow of 9.7 micromoles/sec the productions of CH_4, H_2, and HCN were found to be related to cyclopentane flow, as shown in Fig. 4. Mass-spectrometric and gas-chromatographic analyses indicated that no product in excess of 1% of the HCN remained undetected.

To obtain information about the possible effect of atomic hydrogen on the cyclopentane – active nitrogen reaction, the relative rates of the H atom reactions with cyclopentane and ethylene were examined at 284° C. With the results shown in Table I.

TABLE I

DATA FOR THE REACTIONS OF HYDROGEN ATOMS WITH CYCLOPENTANE AND ETHYLENE AT 284° C

cyclo-C_5H_{10} input	C_2H_4 input	Argon input	C_2H_6 yield	C_2H_4 yield	C_2H_4 destroyed
12.95[a]	—	—	0.170	0.120	—
13.65	—	—	0.170	0.200	—
—	12.65	—	0.920	11.05	1.60
—	13.50	—	1.250	11.95	1.55
—	12.90	11.95	0.920	11.40	1.50
—	13.05	12.00	0.900	11.55	1.50
13.30	12.45	—	0.520	12.10	*ca.* 0.45[b]
13.20	12.85	—	0.420	12.45	*ca.* 0.45[b]

[a]All values refer to flow rates in micromoles/second.

[b]It was assumed that approximately 0.08 micromoles/second of ethylene was produced by reaction of hydrogen atoms with cyclopentane.

Since the hydrocarbon flow (13 micromoles/second) was in large excess over the H atom flow (estimated from the H atom – hydrogen iodide reaction to be about 6 micromoles/second (8)), the reaction of H atoms should have been confined largely to their initial attack on the hydrocarbon. The results obtained with a mixture of ethylene and argon indicate that physical effects in the apparatus used do not invalidate direct comparison between the reactions of hydrocarbon mixtures and the reactions of pure hydrocarbons. Hence, it may be inferred from Table I that ethylene was destroyed three times more slowly when mixed with an equal amount of cyclopentane than when it reacted alone. Therefore, the rates of the reactions of atomic hydrogen with ethylene and cyclopentane are of the same order at 284° C, and any hydrogen atoms produced in the cyclopentane – active nitrogen reaction at 270° C would be expected to react to a large extent with cyclopentane.

TABLE II

KINETIC CONSTANTS FOR THE REACTIONS OF ACTIVE NITROGEN WITH CYCLOALKANES

Cycloparaffin	Temp., ° C	k, liter $mole^{-1}sec^{-1} \times 10^{-5}$	E, kcal $mole^{-1}$	P, $\times 10^4$
Cyclopropane	50	0.8	3.2	0.6
	150	2.5		
	250	5.1		
	350	9.1		
Cyclobutane	60	1.2	4.6	4.7
	250	18.		
Cyclopentane	110	2.4	5.3	8.8
	270	19.		

Can. J. Chem. Downloaded from www.nrcresearchpress.com by 78.46.186.204 on 09/04/12
For personal use only.

Values of the second-order rate constants for the initial attack of active nitrogen on cyclopropane, cyclobutane, and cyclopentane are shown in Table II. The calculations were made for conditions of incomplete consumption of both cycloalkane and active nitrogen.

DISCUSSION

As in previous papers, it will be assumed that atomic nitrogen is the main chemically reactive species in active nitrogen (9).

It would seem that the reactions of cyclopropane, cyclobutane, and cyclopentane with nitrogen atoms can be explained by similar mechanisms, the initial steps of which are analogous to the primary reaction suggested previously (1) for the reaction of active nitrogen with saturated hydrocarbons, i.e.,

$$\text{cyclo-}C_5H_{10} + N \rightarrow HCN + H_2 + C_4H_7; \quad \Delta H = -10 \text{ to } -40 \text{ kcal.} \qquad [1]$$

$$\text{cyclo-}C_4H_8 + N \rightarrow HCN + H_2 + C_3H_5; \quad \Delta H = -58 \text{ kcal} \qquad [2]$$

$$\text{cyclo-}C_3H_6 + N \rightarrow HCN + H_2 + C_2H_3; \quad \Delta H = -29 \text{ kcal} \qquad [3]$$

An obvious alternative to reaction [1] which would permit a ratio for C_2H_4 to HCN of 0.7, but which would seem to be forbidden by its endothermicity, is the reaction

$$\text{cyclo-}C_5H_{10} + N \rightarrow HCN + 2C_2H_4 + H; \quad \Delta H = +14 \text{ kcal.} \qquad [4]$$

The reaction

$$\text{cyclo-}C_5H_{10} + N \rightarrow HCN + C_2H_4 + C_2H_5; \quad \Delta H = -25 \text{ kcal} \qquad [5]$$

is also a possible alternative to reaction [1]. However, it should be followed by very rapid reaction of C_2H_5, and subsequently CH_3 radicals with active nitrogen to form HCN (1, 10, 11). The attack of nitrogen atoms on cyclopentane almost certainly has a higher activation energy than the radical–nitrogen atom reactions, and more nitrogen atoms should therefore be consumed in the primary step at higher temperatures and cyclopentane flow rates. Consequently, the radicals should suffer correspondingly less destruction and, contrary to the experimental results, the yields of ethane and methane should increase steadily with temperature and cyclopentane flow. Hence it may be concluded that reaction [5] is also of relatively little, if any, importance in the cyclopentane–active nitrogen reaction.

The unsaturated radicals formed in reactions [1], [2], and [3] should be attacked rapidly by nitrogen atoms in reactions such as

$$C_4H_7 + N \rightarrow HCN + C_2H_4 + CH_2 \qquad [6]$$

$$C_3H_5 + N \rightarrow HCN + C_2H_4 \qquad [7]$$

$$C_2H_3 + N \rightarrow HCN + CH_2 \qquad [8]$$

together with the reactions

$$CH_2 + N \rightarrow HCN + H \qquad [9]$$

$$CH_2 + N \rightarrow CN + H_2. \qquad [10]$$

If some of the CH_2 produced in reactions such as [6] or [8] is in the triplet state, the reaction

$$CH_2^* + N \rightarrow CN + 2H \qquad [11]$$

might occur to an appreciable extent.

The large amounts of C_2H_4 formed in the cyclopentane reaction at 270° C can be explained if the previous reactions are accompanied by

Can. J. Chem. Downloaded from www.nrcresearchpress.com by 78.46.186.204 on 09/04/12
For personal use only.

$$\text{cyclo-}C_5H_{10} + H \rightarrow \text{cyclo-}C_5H_9 + H_2 \quad [12]$$

and

$$\text{cyclo-}C_5H_{10} + CN \rightarrow \text{cyclo-}C_5H_9 + HCN, \quad [13]$$

followed by

$$\text{cyclo-}C_5H_9 + N \rightarrow HCN + 2C_2H_4. \quad [14]$$

The present study has shown that the attack of cyclopentane by H atoms at 270° C and high cyclopentane flow rates is quite probable even in the presence of considerable ethylene.

The maxima in the production of CH_4 and C_2H_6 from cyclopentane at the higher temperatures may be explained if it is assumed that these arise mainly from CH_3 radicals, and that the radicals are produced as suggested previously (1, 12),

$$C_2H_4 + N \rightarrow HCN + CH_3. \quad [15]$$

The extent of reaction [15] should pass through a maximum with flow rate of cyclopentane, since it is in competition with reaction [1], and this maximum should be more pronounced at higher temperatures, as observed, since the activation energy of reaction [1] (5.3 kcal/mole) appears to be higher than that of reaction [15] (3 kcal/mole (13)). The maximum should be less pronounced for methane than for ethane production, as observed, if methane production resulted mainly from reaction of CH_3 radicals with cyclopentane, while ethane was produced by their recombination.

Recovery of acetylene in small amounts from the three hydrocarbon – N atom reactions may be explained as in an earlier paper (1), i.e. reaction of N atoms with $N \cdot C_2H_4$ complexes to bring about recombination of N atoms and production of triplet ethylene which then decomposes to yield acetylene. Cyanogen probably resulted from the recombination of CN radicals formed in reactions such as [10] and [11].

The large value of the C_2H_4: C_3H_6 ratio in the cyclobutane reaction and the increase of this ratio with temperature indicate that propylene was formed in secondary processes, perhaps by the hydrogenation of C_3H_5 radicals. Similarly, the small quantities of ethylene recovered from the cyclopropane reaction could have resulted from hydrogenation of C_2H_3 radicals, perhaps by abstraction from the parent hydrocarbon.

It is interesting to note that, of the three reactions studied, the cyclopropane reaction appears to have the lowest activation energy. This might be due to greater delocalization of carbon–carbon bond orbitals in cyclopropane (greater *p*-character), thus facilitating the approach of an electrophilic reagent such as a nitrogen atom. A similar situation exists in the ethylene – active nitrogen reaction which also has a low activation energy.

REFERENCES

1. Evans, H. G. V., Freeman, G. R., and Winkler, C. A. Can. J. Chem. **34**, 1271 (1956).
2. Blades, H. and Winkler, C. A. Can. J. Chem. **29**, 1022 (1951).
3. Forst, W. and Winkler, C. A. Can. J. Chem. **33**, 1814 (1955).
4. Gartaganis, P. A. and Winkler, C. A. Can. J. Chem. **34**, 1457 (1956).
5. Kaarsemaker, Sj. and Coops, J. Rec. trav. chim. **71**, 261 (1952).
6. Koltoff, I. M. and Sandell, E. B. Textbook of quantitative inorganic analysis. Revised ed. The Macmillan Co., New York. 1948.
7. Rhodes, F. H. J. Ind. Eng. Chem. 4, 652 (1912).
8. Wiles, D. M. and Winkler, C. A. Can. J. Chem. **35**, 1298 (1957).
9. Evans, H. G. V. and Winkler, C. A. Can. J. Chem. **34**, 1217 (1956).
10. Armstrong, D. A. and Winkler, C. A. Can. J. Chem. **33**, 1649 (1955).
11. Armstrong, D. A. and Winkler, C. A. Can. J. Chem. **34**, 885 (1956).
12. Greenblatt, J. H. and Winkler, C. A. Can. J. Research, B, **27**, 721 (1949).
13. Greenblatt, J. H. and Winkler, C. A. Can. J. Research, B, **27**, 732 (1949).

Can. J. Chem. Downloaded from www.nrcresearchpress.com by 78.46.186.204 on 09/04/12
For personal use only.

Can. J. Chem. Downloaded from www.nrcresearchpress.com by 78.46.186.204 on 09/04/12
For personal use only.

THE REACTIONS OF ACTIVE NITROGEN WITH CHLOROMETHANES[1]

S. E. Sobering[2] and C. A. Winkler

ABSTRACT

Cyanogen chloride and chlorine were the only gaseous products observed in the reaction of active nitrogen with carbon tetrachloride at 110° and 420° C. The product yields tended towards limiting values at higher reactant flow rates, and increased with increase of temperature at all flow rates. The reactions of active nitrogen with chloroform and dichloromethane at 260° and 420° C yielded hydrogen chloride, hydrogen cyanide, and cyanogen, in addition to cyanogen chloride and chlorine. The behavior of the product yields with reactant flow rates and temperature was similar to that of the products from carbon tetrachloride.

The reactions of active nitrogen with methyl-, ethyl-, propyl-, isopropyl-, and vinyl-chlorides have been discussed in earlier papers from this laboratory (1, 2). The present paper reports the results obtained in a similar study with carbon tetrachloride, chloroform, and dichloromethane, to examine the effect of different extents of halogen substitution.

EXPERIMENTAL

The apparatus and experimental procedures were essentially the same as those used in the previous studies of active nitrogen reactions (3). Standard analytical methods (4, 5, 6) were adapted without serious difficulty to the products of the reactions after they had been given appropriate preliminary separation by low-temperature distillation and chemical absorption (7).

RESULTS AND DISCUSSION

The reaction flames for the three reactions were quite bright, with an orange tint that became progressively less marked with decrease in the number of halogen atoms in the reactant molecule.

A small amount of greenish-brown polymer was formed during each of the reactions. With carbon tetrachloride, but not with the other chloromethanes, a trace of white solid was also deposited. This solid resembled hexachlorethane in its solubility in ether and in its tendency to sublime when heated. Although no chemical analyses of the polymers were made, owing to the difficulty in obtaining sufficient material, they did not behave, when heated, as if they were pure materials such as cyanuric chloride or paracyanogen. Traces of free carbon appeared to be formed in the chloroform and dichloromethane reactions.

With CCl_4, the flow rate of molecular nitrogen was 39 micromoles/second (operating pressure = 1 mm) and that of active nitrogen was estimated to be 9.3 micromoles/second, from the maximum HCN production from ethylene at 425° C (2, 3). The only gaseous products were Cl_2 and CNCl, the yields of which changed with flow rate of CCl_4 in the manner shown in Fig. 1. The ratio of Cl_2 yield to CNCl yield decreased steadily from about 3:1 to a limiting value of 1.5:1 as the flow rate of CCl_4 was increased over the range used.

With $CHCl_3$, a new pumping system was used, and the active nitrogen flow rate was estimated as 14.6 micromoles/second, with a molecular flow of 180 micromoles/second at a pressure of 1.65 mm. The gaseous products were HCl, CNCl, and Cl_2 in comparatively

[1]*Manuscript received April 29, 1958.*
Contribution from the Physical Chemistry Laboratory, McGill University, Montreal, Quebec, with financial assistance from the National Research Council.
[2]*Holder of National Research Council Studentships, 1955–57.*

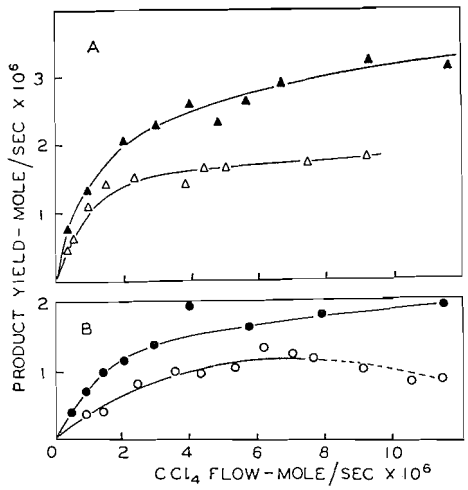

FIG. 1. Relation between carbon tetrachloride flow rate and yields of products.
A = Cl_2 production △ 90° C ▲ 420° C B = CNCl production ○ 90° C ● 420° C

large amounts, together with lesser amounts of HCN and $(CN)_2$. In Fig. 2, which depicts the relations of product yields to $CHCl_3$ flow rates, the total HCN + $(CN)_2$ yields consisted of approximately 40% HCN and 60% $(CN)_2$.

With CH_2Cl_2, the operating conditions were identical with those used for $CHCl_3$. The major products were HCl, HCN, and CNCl, production of which varied with flow rate of CH_2Cl_2 as indicated in Fig. 3. Much smaller quantities of Cl_2 (Fig. 3) and $(CN)_2$ (maximum 0.4 micromoles/second) were produced.

The reactions of active nitrogen with the three chloromethanes of the present study resemble the reaction with methyl chloride studied previously (1) in color and behavior of the reaction flames, in tendency for slight polymer formation, in exothermicity, and in production of HCl and HCN as products when possible. It should be noted that the methyl chloride reaction yielded only HCl and HCN (and hydrogen) as major products; CNCl and Cl_2 were entirely absent.

There seems to be little doubt that the active nitrogen – CCl_4 reaction occurred by

$$N + CCl_4 \rightarrow [N \cdot CCl_4] \rightarrow CNCl + Cl_2 + Cl; \quad \Delta H = -24 \text{ kcal.}$$

The alternative decomposition of the collision complex to yield CN radicals seems unlikely, since no significant quantity of cyanogen was formed.

The observed increase in Cl_2: CNCl ratio with decrease of CCl_4 flow rate suggests that, with excess N atoms, reactions occur of the type

$$N + N \cdot CCl_4 \rightarrow N_2 + CCl_4^*,$$

followed by decomposition of the excited CCl_4 to yield chlorine and perhaps CCl_3, dimerization of which would yield the traces of hexachlorethane that appeared to be formed.

The products from the reaction of chloroform with active nitrogen can be semi-quantitatively explained by the scheme

$$\begin{aligned} N + CHCl_3 \rightarrow [N \cdot CHCl_3] &\rightarrow CNCl + HCl + Cl; \quad \Delta H = -48 \text{ kcal} \\ &\rightarrow HCN + Cl_2 + Cl; \quad \Delta H = -29 \text{ kcal} \\ &\rightarrow CN + HCl + Cl_2; \quad \Delta H = -18 \text{ kcal,} \end{aligned}$$

Can. J. Chem. Downloaded from www.nrcresearchpress.com by 78.46.186.204 on 09/04/12
For personal use only.

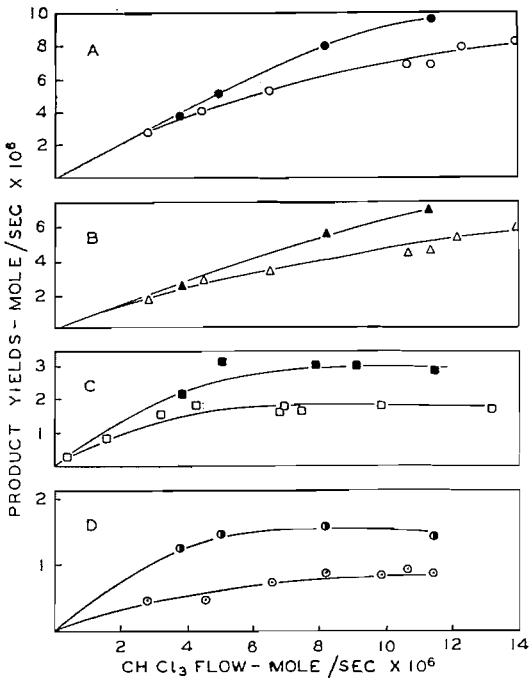

FIG. 2. Relation between chloroform flow rate and yields of products.

A = HCl production	○	260° C
	●	420° C
B = CNCl production	△	260° C
	▲	420° C
C = Cl_2 production	□	260° C
	■	420° C
D = HCN production	⊙	260° C
	◑	420° C

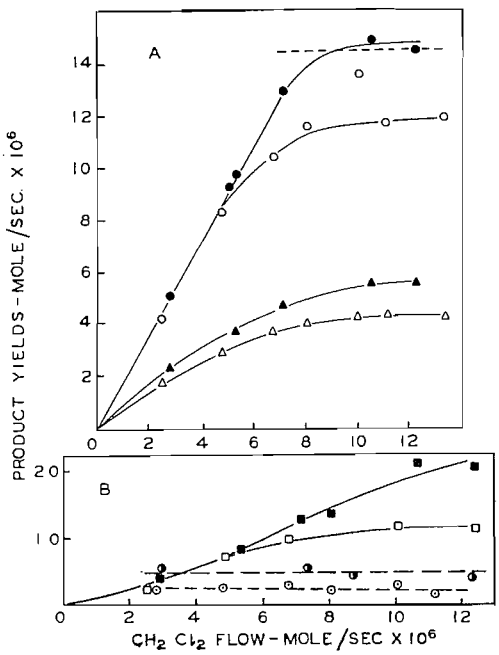

FIG. 3. Relation between dichloromethane flow rate and yields of products.

A = HCl production	○	255° C
	●	425° C
HCN production	△	255° C
	▲	425° C
B = CNCl production	□	255° C
	■	425° C
Cl_2 production	⊙	255° C
	◑	425° C

Dotted line in panel A represents yield of HCN from ethylene at high temperatures.

in which the first reaction occurs to at least three times the extent of the other two combined. However, compared with the proportions inferred from such a mechanism, there appears to be an excess of HCl and deficiency of chlorine in the products. This might result from reactions such as

$$Cl + CHCl_3 \rightarrow HCl + CCl_3; \quad \Delta H = -12 \text{ kcal}$$

followed by

$$CCl_3 + N \rightarrow CNCl + 2Cl; \quad \Delta H = -35 \text{ kcal.}$$

Other reactions that would lead to loss of chlorine at the expense of HCl production might be suggested, e.g.

$$N + N \cdot CHCl_3 \rightarrow N_2 + CHCl_3^*$$

and subsequent decomposition of the excited $CHCl_3$ to yield HCl and other products such as CCl_2, or free carbon, traces of which were observed.

The dichloromethane – active nitrogen reaction may be represented similarly to that of chloroform:

Can. J. Chem. Downloaded from www.nrcresearchpress.com by 78.46.186.204 on 09/04/12
For personal use only.

$$N + CH_2Cl_2 \rightarrow [N \cdot CH_2Cl_2] \rightarrow HCN + HCl + Cl; \quad \Delta H = -54 \text{ kcal}$$
$$\rightarrow CNCl + HCl + H; \quad \Delta H = -27 \text{ kcal}$$
$$\rightarrow CN + 2HCl; \quad \Delta H = -24 \text{ kcal.}$$

Since reaction of CN radicals with parent reactant appears not to have been appreciable (no optimum in $(CN)_2$ yield), and the amount of cyanogen formed was trivial, the third reaction must have been relatively unimportant. From the relative proportions of HCN and CNCl formed it may then be inferred that the first reaction was the predominant mode of attack.

Again, the rate of chlorine production was relatively low and HCl production relatively high. This suggests consumption of chlorine in reactions such as

$$Cl + CH_2Cl_2 \rightarrow HCl + CHCl_2$$

and HCl production in reactions such as

$$H + CH_2Cl_2 \rightarrow HCl + CH_2Cl,$$

or

$$N + [N \cdot CH_2Cl_2] \rightarrow N_2 + CH_2Cl_2^*$$

followed by

$$CH_2Cl_2^* \rightarrow 2HCl + C.$$

As with chloroform, this last possibility is supported by the apparent formation of traces of free carbon.

REFERENCES

1. DUNFORD, B., EVANS, H. G. V., and WINKLER, C. A. Can. J. Chem. **34**, 1074 (1956).
2. EVANS, H. G. V., FREEMAN, G. R., and WINKLER, C. A. Can. J. Chem. **34**, 1271 (1956).
3. GARTAGANIS, P. A. and WINKLER, C. A. Can. J. Chem. **34**, 1457 (1956).
4. VOGEL, A. I. Qualitative chemical analysis. 3rd ed. Longmans, Green and Co., Inc., New York. 1947.
5. KOLTHOFF, I. M. and SANDELL, E. B. Textbook of quantitative analysis. 3rd ed. The Macmillan Co., New York. 1952.
6. WALLIS, T. Ann. **345**, 353 (1906).
7. SOBERING, S. E. Ph.D. Thesis, McGill University, Montreal, Quebec. 1957.

Can. J. Chem. Downloaded from www.nrcresearchpress.com by 78.46.186.204 on 09/04/12
For personal use only.

REACTIONS OF ALKOXY RADICALS

V. PHOTOLYSIS OF DI-*t*-BUTYL PEROXIDE[1]

GARNETT MCMILLAN AND M. H. J. WIJNEN[2]

ABSTRACT

The photolysis of di-*t*-butyl peroxide has been investigated over the temperature range 25° to 79° C. As reaction products were observed: acetone, *t*-butyl alcohol, methyl *t*-butyl ether, *i*-butylene oxide, ethane, methane, and carbon monoxide. The following reactions, involving the *t*-butoxy radical, have been studied:

$$(CH_3)_3CO \rightarrow CH_3COCH_3 + CH_3 \quad [2]$$

$$(CH_3)_3CO + CH_3 \rightarrow (CH_3)_3COCH_3 \quad [5]$$

$$(CH_3)_3CO + DtBP \rightarrow (CH_3)_3COH + R \quad [6]$$

An activation energy difference of $E_2 - E_6 = 3$ kcal has been obtained.

INTRODUCTION

Previous work (1, 2, 3) on the photolysis of di-*t*-butyl peroxide has established that the primary process consists of the breakage of the O—O bond, thus producing two *t*-butoxy radicals. It could also be shown that the *t*-butoxy radical is relatively unstable and decomposes according to reaction [2]:

$$(CH_3)_3CO \rightarrow CH_3COCH_3 + CH_3. \quad [2]$$

As most recent values for the activation energy of reaction [2] have been reported 11.2±2 (3) and 13.2±2.4 (4) kcal.

Such a value for E_2 would, however, indicate that especially at low temperatures the *t*-butoxy radical might survive long enough to take part in abstraction and recombination reactions. While the formation of *t*-butyl alcohol through hydrogen abstraction by *t*-butoxy radicals has been reported frequently (5, 6) no information was available regarding the activation energy for the abstraction of a hydrogen atom from di-*t*-butyl peroxide. In the photolysis of di-*t*-butyl peroxide a considerable amount of ethane is produced by recombination of methyl radicals, originating from reaction [2]. It seemed, therefore, likely that especially at low temperatures some methyl *t*-butyl ether might be produced via recombination reactions, although this compound had thus far not been reported among the reaction products.

In order to clear these questions the photolysis of di-*t*-butyl peroxide has been studied again.

EXPERIMENTAL

The apparatus is essentially the same as described previously (7). As a rule, a Hanovia S-500 medium pressure arc was employed as light source. The light intensity was varied by inserting wire-gauze screens between arc and cell. In some runs, marked as such in Table I under intensity, a BH-6 lamp, made by General Electric, was used. The effective light output of the BH-6 lamp is about three times that of the Hanovia S-500 arc.

After the photolysis, the reaction products and the excess di-*t*-butyl peroxide were cooled down to about −175° C. At this temperature CO, CH_4, and C_2H_6 were removed

[1]*Manuscript received May 8, 1958.*
Contribution from the Chemical Division, Research and Development Laboratories, Celanese Corporation of America, Clarkwood, Texas.
[2]*Present address: Radiation Research Laboratories, Mellon Institute, Pittsburgh, Pa.*

Can. J. Chem. Downloaded from www.nrcresearchpress.com by 78.46.186.204 on 09/04/12
For personal use only.

TABLE I

PHOTOLYSIS OF DI-*t*-BUTYL PEROXIDE[a]

Run No.	$[DtBP]_0$ Molecules/cc $\times 10^{-17}$	Time, sec	Intensity, relative %	R_x, in molecules/(sec cc) $\times 10^{-12}$						
				$R_{CH_3COCH_3}$	$R_{(CH_3)_3COH}$	$R_{(CH_3)_3COCH_3}$	$R_{(CH_3)_2CH_2CO}$	$R_{C_2H_6}$	R_{CH_4}	R_{CO}
				Temperature, 25° C						
12	5.14	720	BH-6	46.70	2.62	n.d.	2.00*	23.80	0.09	0.51
13	5.22	1800	100	25.40	1.08	n.d.	0.83*	13.21	0.70	0.83
14	5.43	1800	100	24.40	1.08	0.18	1.08	12.90	1.00	1.20
15	5.25	1800	100	24.85	1.06	n.d.	0.97*	12.75	0.75	0.69
16	5.25	1800	100	25.40	1.33	0.20	1.34	12.90	0.65	0.54
17	5.32	1800	100	25.10	1.08	0.17	1.10	12.90	0.64	0.68
18	5.41	16080	9	2.42	0.09		0.09	1.25	0.07	0.08
20	5.29	20100	9	2.18	0.07		0.10	1.12	0.06	0.06
21	2.74	2100	100	12.08	0.45	0.06	0.36	6.70	0.53	0.68
23	5.35	6480	30	5.97	0.26	0.02	0.26	3.06	0.19	0.16
				Temperature, 55° C						
33	4.80	10560	16	4.92	0.09		0.18	2.52	0.13	0.12
34	4.22	4620	30	7.92	0.16		0.28	4.09	0.24	0.22
35	4.07	1800	100	19.50	0.43		0.70	10.00	0.57	0.54
36	4.22	16320	9	2.06	0.04		0.10	1.05	0.06	0.05
37	4.41	360	BH-6	139.01	2.13	0.39	1.74	70.52	0.29	1.34
38	2.50	420	BH-6	65.20	2.80	0.24	2.27	33.50	0.62	1.26
40	3.21	600	BH-6	58.20	0.96	0.16	1.21	29.70	0.20	0.68
41	5.04	600	BH-6	88.80	1.41	0.26	1.86	45.20	0.20	0.88
42	2.96	720	BH-6	65.25	0.83	0.13	0.48	33.40	0.15	0.78
43	3.92	600	BH-6	44.70	1.41	0.14	1.10	22.91	0.15	0.63
44	3.92	600	BH-6	37.90	0.60	0.11	0.64	19.40	0.10	0.48
				Temperature, 79° C						
24	3.86	900	BH-6	63.00	1.93	0.10	2.20	33.71	0.56	2.51
25	3.86	1800	100	31.02	0.34		1.12	16.68	0.90	1.58
26	4.32	5400	30	10.86	0.12		0.35	5.79	0.34	0.53
27	4.54	17280	9	2.52	0.04		0.11	1.31	0.08	0.09
28	4.25	15700	9	2.04	0.03		0.13	1.07	0.08	0.09
29	4.05	1740	100	22.40	0.30		0.74	11.62	0.67	0.77
30	2.74	840	BH-6	43.60	0.59		0.08	22.84	0.08	1.07
31	4.32	9180	16	4.44	0.06		0.21	2.32	0.14	0.17
32	4.32	9240	16	4.44	0.07		0.21	2.32	0.15	0.18
39	2.35	420	BH-6	53.80	0.89		0.05	28.70	0.50	2.10

[a]Open spaces indicate that, under the given conditions, this compound was formed in amounts too small to allow its determination by mass-spectrometer analysis.

NOTE: Unless marked by *, data for *i*-butylene oxide are somewhat high owing to the presence of small amounts of methyl ethyl ketone.

by Toepler pump and sampled for mass-spectrometer analysis after their total volume had been measured. The liquid products were then separated from the excess undecomposed di-*t*-butyl peroxide by gas chromatography. A 6-ft-long general-purpose column C, obtained from Perkin–Elmer, was used. The column was operated at room temperature, using helium at a pressure of 10 lb as carrier gas. Under these conditions all reaction products come over within 25 minutes after introduction of the sample, while di-*t*-butyl peroxide is retained up to 67 minutes. The reaction products, thus separated from di-*t*-butyl peroxide, were trapped out and analyzed by mass spectrometer. In this way it was possible to determine the relative ratios in which the liquid products were formed although no absolute values are obtained.

It has been established previously (2, 5) that the ratio $(2R_{C_2H_6}+R_{CH_4})/R_{CH_3COCH_3}$ is equal to unity in the thermal and photolytic decomposition of di-*t*-butyl peroxide. This is easily understood if one realizes that one methyl radical is formed for every acetone

Can. J. Chem. Downloaded from www.nrcresearchpress.com by 78.46.186.204 on 09/04/12
For personal use only.

molecule produced by the thermal decomposition of the *t*-butoxy radical, according to reaction [2]. Taking into account that some methyl radicals are produced by secondary photolysis of acetone a more correct figure for the observed rate of acetone production is obtained by $R_{CH_3COCH_3} = 2(R_{C_2H_6}-R_{CO})+R_{CH_4}$. It is thus possible to calculate the rate of acetone production from the rates of methane, ethane, and carbon monoxide production. Since the relative ratio of acetone to other liquid products is determined by mass spectrometer, the rates of formation of all other products may be calculated.

In several runs a known amount of *i*-butane was added to the liquid products before mass-spectrometer analysis. Accurate data could thus be obtained for the production of acetone and other liquid products. In all instances data thus obtained for $R_{CH_3COCH_3}$ agreed with those calculated via the formula $R_{CH_3COCH_3} = 2(R_{C_2H_6}-R_{CO})+R_{CH_4}$.

It was not possible to discriminate by mass spectrometer between methyl ethyl ketone and *i*-butylene oxide, since the only available peak, yielding good resolution is *m/e* 72, common to both compounds. It was, however, possible to stop trapping of the reaction products, leaving the gas chromatography apparatus, before the appearance of methyl ethyl ketone. In this way, accurate data for the production of *i*-butylene oxide were obtained. These data indicated that peak *m/e* 72 was mainly due to the presence of *i*-butylene oxide. Since neither of these two compounds are of extreme interest in the present discussion, data reported in Table I for *i*-butylene oxide have been calculated on the assumption that no methyl ethyl ketone was formed.

The conversion has been kept below 5% of the starting material. The di-*t*-butyl peroxide used in this investigation was obtained from Shell Chemical Corporation and was distilled under reduced pressure, a small middle fraction being retained. Gas chromatographic analysis indicated it to be more than 99% pure.

RESULTS AND DISCUSSION

Data, obtained by photolyzing di-*t*-butyl peroxide at different temperatures and light intensities are reported in Table I. The following reactions have been considered to explain the formation of acetone, *t*-butyl alcohol, methyl-*t*-butyl ether, *i*-butylene oxide, ethane, and methane:

$$(CH_3)_3COOC(CH_3)_3 + h\nu \rightarrow 2(CH_3)_3CO \quad [1]$$

$$(CH_3)_3CO \rightarrow CH_3COCH_3 + CH_3 \quad [2]$$

$$2(CH_3)_3CO \rightarrow (CH_3)_3COH + (CH_3)_2\overset{\diagdown\ \diagup}{CH_2CO} \quad [3]$$

$$CH_3 + (CH_3)_3CO \rightarrow CH_4 + (CH_3)_2\overset{\diagdown\ \diagup}{CH_2CO} \quad [4]$$

$$CH_3 + (CH_3)_3CO \rightarrow (CH_3)_3COCH_3 \quad [5]$$

$$(CH_3)_3CO + DtBP \rightarrow (CH_3)_3COH + (CH_3)_3COOC(CH_3)_2CH_2 \quad [6]$$

$$(CH_3)_3COOC(CH_3)_2CH_2 \rightarrow (CH_3)_3CO + (CH_3)_2\overset{\diagdown\ \diagup}{CH_2CO} \quad [7]$$

$$2CH_3 \rightarrow C_2H_6 \quad [8]$$

$$CH_3 + DtBP \rightarrow CH_4 + (CH_3)_3COOC(CH_3)_2CH_2 \quad [9]$$

However, in addition to the reaction products mentioned above, also carbon monoxide and traces of methyl ethyl ketone were observed. Table I clearly shows that acetone is the most abundant reaction product and it seems logical to accept, as other authors (3) did, that CO and $C_2H_5COCH_3$ are formed by secondary photolysis of acetone. The following reactions are therefore added:

Can. J. Chem. Downloaded from www.nrcresearchpress.com by 78.46.186.204 on 09/04/12
For personal use only.

$$CH_3COCH_3 + h\nu \rightarrow CH_3 + CH_3CO \quad [10]$$
$$CH_3 + CH_3CO \rightarrow CH_3COCH_3 \quad [11]$$
$$CH_3 + CH_3CO \rightarrow CH_4 + CH_2CO \quad [12]$$
$$CH_3CO \rightarrow CH_3 + CO \quad [13]$$
$$R + CH_3COCH_3 \rightarrow CH_2COCH_3 + RH \quad [14]$$
$$CH_3 + CH_2COCH_3 \rightarrow C_2H_5COCH_3 \quad [15]$$

The following equations may be derived from this mechanism:

$$R_{CH_3COCH_3} \times R^{\frac{1}{2}}_{C_2H_6}/R_{CH_3OC(CH_3)_3} = k_2k_8^{\frac{1}{2}}/k_5 \quad [I]$$

and

$$R_{(CH_3)_3COH}/R^2_{CH_3COCH_3} = k_3/k_2^2 + k_6/k_2[DtBP]/R_{CH_3COCH_3}, \quad [II]$$

where R_x is the rate of production of the compound x.

Owing to secondary reactions involving acetone, $R_{CH_3COCH_3}$ is not correctly given by measuring the observed rate of acetone production. Some of the originally formed acetone decomposed to give CO and methyl radicals, some reacted to form methyl ethyl ketone. The amount of methyl ethyl ketone is, however, smaller than 1% of the originally formed acetone and may therefore be neglected. The amount of acetone decomposed to CO and methyl radicals is given by the rate of CO production. In calculating equations [I] and [II] the rate of acetone production by reaction [2] is therefore given by the sum of the *observed* rate of acetone production and the rate of production of carbon monoxide. At room temperature a constant value was obtained for equation [I], indicating $k_2k_8^{\frac{1}{2}}/k_5 = 5.1 \pm 0.5 \times 10^8$ in molecules$^{\frac{1}{2}}$/(sec$^{\frac{1}{2}}$ cc$^{\frac{1}{2}}$). Equation [I] involves the reaction products: acetone, ethane, and methyl *t*-butyl ether. Acetone and ethane are the major reaction products in the photolysis of di-*t*-butyl peroxide. Methyl *t*-butyl ether is, however, formed in trace amounts only. As a matter of fact, the largest amount of ether observed did not exceed 3×10^{-3} ml of gas at n.t.p. This undoubtedly explains why this product was not observed by previous investigators. With increasing temperature, the production of ether decreases, mainly owing to an increased decomposition of the *t*-butoxy radical into acetone and methyl radicals via reaction [2]. The results obtained for $k_2k_8^{\frac{1}{2}}/k_5$ show, therefore, considerable scatter at 55° C, as indicated in Table II. At 79° C the amount of ether produced was too small to allow its determination by mass-spectrometer analysis.

TABLE II

RATIOS OF RATE CONSTANTS

Temperature, ° C	$10^{19}k_6/k_2$	$10^{-8}k_2k_8^{\frac{1}{2}}/k_5$, molecules$^{\frac{1}{2}}$/(cc$^{\frac{1}{2}}$ sec$^{\frac{1}{2}}$)
25	0.72	5.1
55	0.45	21±6
79	0.32	—

It is obvious that an activation energy, determined from data at two temperatures only, should be taken with the utmost reservation. It is nevertheless interesting to point out that our data indicate a value of 9±2 kcal for the activation energy of reaction [2]. This value agrees within experimental error with data obtained by Volman and Graven (3), who reported $E_2 = 11.2 \pm 2$ kcal.

Can. J. Chem. Downloaded from www.nrcresearchpress.com by 78.46.186.204 on 09/04/12
For personal use only.

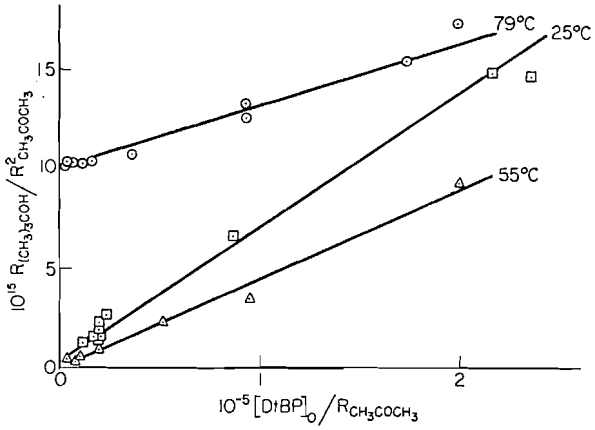

FIG. 1. Plot of $10^{15}R_{(CH_3)_3COH}/R^2_{CH_3COCH_3}$ versus $10^{-5}[DtBP]_0/R_{CH_3COCH_3}$ at various temperatures.

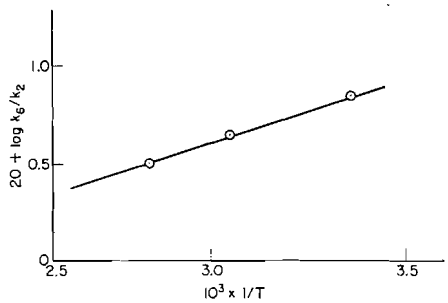

FIG. 2. Plot of $20+\log k_6/k_2$ versus $10^3\times 1/T$.

Equation [II] is plotted in Fig. 1 for the temperatures 25, 55, and 79° C. The origin on the ordinate has been displaced by 10 units for the data at 79° C. Values obtained for k_6/k_2 from Fig. 1 are given in Table II. A plot of log k_6/k_2 in Fig. 2 gives an activation energy difference of $E_2-E_6 = 3$ kcal.

No intercepts are observed when plotting equation [II] (Fig. 1) for the temperatures 55° and 79° C. It is difficult to decide whether the intercept observed at 25° C is real. The absence of an intercept would prove that reaction [3], the disproportionation of two *t*-butoxy radicals, would not occur. It may, however, be concluded that $k_3/k_2^2 \leqslant 0.5 \times 10^{-15}$ in molecules^{-1}/(sec^{-1} cc^{-1}). From this conclusion it is possible to calculate the maximum amounts of *t*-butyl alcohol and *t*-butylene oxide formed by reaction [3]. Such calculations indicate that *t*-butyl alcohol is mainly, if not only, formed by abstraction reaction [6] rather than by disproportionation of *t*-butoxy radicals. These calculations also indicate that, even at 25° C, *i*-butylene oxide is mainly, if not only, formed by decomposition of the $(CH_3)_3COO(CH_3)_2CH_2$ radical as suggested by reaction [7].

A value of 11.3 kcal has been reported (8) for the activation energy of reaction [9], the abstraction of a hydrogen atom from di-*t*-butyl peroxide by methyl radicals. Accepting our value of $E_2-E_6 = 3$ kcal and $E_2 = 11.2\pm$ kcal, as reported by Volman and Graven, the data indicate that less energy is required for the abstraction of a hydrogen atom from di-*t*-butyl peroxide by *t*-butoxy radicals than for the similar reaction by methyl radicals. A similar observation has been made regarding the case of abstraction reactions by methoxy and methyl radicals (9).

Can. J. Chem. Downloaded from www.nrcresearchpress.com by 78.46.186.204 on 09/04/12
For personal use only.

ACKNOWLEDGMENTS

The authors wish to express their sincere thanks to Dr. H. D. Medley for his constant interest in the fundamental research program of this laboratory. They also thank Mr. R. W. Jarret and Mr. R. M. Guedin for calculation and interpretation of the mass-spectrometer data.

REFERENCES

1. BELL, E. R., RUST, F. F., and VAUGHAN, W. E. J. Am. Chem. Soc. **72**, 337 (1950).
2. DORFMAN, L. M. and SALSBURG, Z. W. J. Am. Chem. Soc. **73**, 255 (1951).
3. VOLMAN, D. H. and GRAVEN, W. M. J. Am. Chem. Soc. **75**, 311 (1953).
4. BIRRS, F. W., DANBY, C. J., and HINSHELWOOD, C. Proc. Roy. Soc. **239**, 154 (1957).
5. RALEY, J. H., RUST, F. F., and VAUGHAN, W. E. J. Am. Chem. Soc. **70**, 88 (1948).
6. BROOK, J. T. H. Trans. Faraday Soc. **53**, 327 (1957).
7. KUTSCHKE, K. O., WIJNEN, M. H. J., and STEACIE, E. W. R. J. Am. Chem. Soc. **74**, 714 (1952).
8. PRITCHARD, G. O., PRITCHARD, H. O., and TROTMAN-DICKENSON, A. F. J. Chem. Soc. 1425 (1954).
9. WIJNEN, M. H. J. J. Chem. Phys. **27**, 710 (1957); **28**, 271 (1958).

Can. J. Chem. Downloaded from www.nrcresearchpress.com by 78.46.186.204 on 09/04/12
For personal use only.

Can. J. Chem. Downloaded from www.nrcresearchpress.com by 78.46.186.204 on 09/04/12
For personal use only.

THE EXTRACTION OF PLUTONIUM FROM NEUTRON-IRRADIATED URANIUM BY URANIUM TRICHLORIDE AND BY MAGNESIUM CHLORIDE[1]

D. E. McKenzie,[2] W. L. Elsdon, and J. W. Fletcher

ABSTRACT

The extraction of plutonium from neutron-irradiated uranium by uranium trichloride and by magnesium chloride has been examined in the temperature range 1150° to 1250° C. The results of the uranium trichloride experiments have been used to evaluate the standard free-energy change of the equilibrium reaction $UCl_3 + Pu \leftrightharpoons PuCl_3 + U$. These free-energy values have been used to predict the plutonium extraction in the magnesium chloride experiments on the assumption that the uranium trichloride, continuously formed from the non-equilibrium reaction $3/2MgCl_2 + U \rightarrow UCl_3 + 3/2Mg$, rapidly established the above equilibrium with the plutonium in the uranium. Agreement between predicted and experimental results supports this assumption.

A preliminary study of the kinetics of the $MgCl_2$–U reaction showed that the initial rate of reaction is controlled by the distillation of magnesium metal from the reaction zone.

INTRODUCTION

In previous papers, the separation of plutonium from neutron-irradiated uranium by volatilization (1) and by liquid silver extraction (2) was described. Another possible technique for achieving this important separation is by reaction of plutonium with molten inorganic salts, as represented in the following equilibrium expression,

$$MX + Pu \leftrightharpoons PuX + M.$$

The plutonium salt formed by the reaction enters the salt phase and is thus separated from the uranium metal. This method has been examined by a number of investigators (3, 4) using uranium fluorides. The present paper describes an investigation of the extraction of plutonium by uranium trichloride and by magnesium chloride.

High-temperature thermodynamic data may be used to predict the distribution of plutonium between the salt and metal phases. From the data on the free energy of formation, the standard free-energy change accompanying the reactions may be calculated for a given temperature. These values may be used to obtain the equilibrium constant for that temperature. Using the mass-action expression for the equilibrium constant, the distribution of plutonium between the two phases may be calculated.

Since only estimated values for the free energies of formation of liquid uranium and plutonium chlorides are available (5, 6), the distribution equilibria are a useful check on the reliability of the available data for these compounds. Besides testing the available thermodynamic data, the above calculations have been reversed to give, from the experimental data, new equilibrium constants, and hence, standard free-energy changes accompanying the reactions. A similar procedure has been used by Buyers to determine the free energy of formation of plutonium trifluoride (7). These new values have been used to predict the distribution of plutonium in the experiments with magnesium chloride.

EXPERIMENTAL

Materials and Apparatus

The neutron-irradiated uranium was cut from natural uranium fuel rods which had been irradiated in the NRX reactor and allowed to decay for 3 years. The concentration

[1]*Manuscript received May 8, 1958.*
Contribution from Chemistry and Metallurgy Division, Research Chemistry Branch, Atomic Energy of Canada Limited, Chalk River, Ontario, Canada.
Issued as A.E.C.L. No. 656.
[2]*Present address: Atomics International Division, North American Aviation Inc., P.O. Box 309, Canoga Park, California, U.S.A.*

of plutonium in this material was 0.025%. Uranium trichloride was prepared from uranium metal by passing hydrogen chloride over the hydride (8). Considerable care to exclude moisture and air was required to obtain a pure product. Anhydrous magnesium chloride was obtained by carefully heating C.P. grade ammonium magnesium chloride hexahydrate in a current of dry hydrogen chloride to remove water, followed by further heating in vacuum to remove ammonium chloride. Magnesium analyses of the product gave 25.67 and 25.35% Mg, calculated 25.54%. The chlorides were stored and handled in a dry nitrogen atmosphere.

The uranium and salt, contained in an alumina crucible ("Triangle" recrystallized alumina, Morganite Carbon Products Canada Limited, 195 Eastern Ave., Toronto 2, Ontario), were heated by a tungsten wire coil surrounded by thermal and radiation shields. The assembly was mounted in a glass bulb which could be evacuated by diffusion and mechanical pumps (1). Temperatures were measured with a platinum, platinum – 10% rhodium thermocouple which was coiled in the heating zone as a seat for the crucible containing the charge. The thermocouple was calibrated to give the temperature of the charge by melting various pure metals in the apparatus. The temperature measurements were accurate to ±5° C.

Procedure and Analyses

For an experiment, the uranium was etched in acid to remove approximately 25% of its weight for a reference solution, then washed in water and acetone. Weighed amounts of the chloride and of neutron-irradiated uranium, in an alumina crucible, were placed in the apparatus. The glass bulb was pumped down to a pressure of 10^{-5} mm Hg or less and then the crucible was heated to 300° C for further degassing. After admitting welding grade argon to a pressure of 1 atmosphere, the charge was heated to temperature. The salt and uranium were contacted for 30 minutes in all runs except those where time was the variable to be studied.

After contacting, the charge was cooled in an argon atmosphere, separated from the crucible, and the salt phase dissolved or washed away from the metal billet. In each experiment the complete phase was dissolved for analysis. The solutions were analyzed for uranium (9) and magnesium (10) spectrophotometrically; plutonium was determined using standard radiochemical procedures. Plutonium recoveries of 95% or better were obtained in all runs.

RESULTS AND DISCUSSION

The Extraction of Plutonium with Uranium Trichloride

On contacting the liquid phases of uranium trichloride and neutron-irradiated uranium the following equilibrium is established:

$$UCl_3 + Pu \leftrightharpoons PuCl_3 + U.$$

The literature values of thermodynamic data listed in Table I were used to calculate the equilibrium constants for the above equilibrium. The distribution of plutonium between salt and metal was then predicted on the assumptions that plutonium behaves ideally in molten neutron-irradiated uranium and that the product plutonium trichloride dissolves to form an ideal solution in uranium trichloride. Evidence at higher temperatures for the former assumption has been obtained in previous work (1, 3), while the isomorphism of the trichlorides and the proximity of plutonium and uranium in the actinide series are supporting evidence for the validity of the latter.

The extraction of plutonium was examined for various U/UCl_3 mole ratios (Table II)

Can. J. Chem. Downloaded from www.nrcresearchpress.com by 78.46.186.204 on 09/04/12
For personal use only.

and also at various temperatures (Table III). The proportions of the original plutonium remaining in the salt and in the metal phase are listed in the tables. The calculations using the thermodynamic data give directly the proportion of the original plutonium remaining in the uranium phase and these are listed in the last column of each table.

TABLE I

THERMODYNAMIC DATA FOR UCl_3 AND $PuCl_3$

Compound	Reference No.	$(\Delta F - \Delta H_{298})/T$(calories/degree) 500° K	1000° K	1500° K	ΔH_{298} (kcal)	Melting point (° K)
UCl_3	5	53.51 (s)	51.65 (s)	49 (l)	−213.5	1108
$PuCl_3$	6	54 (s)	53 (s)	50 (l)	−229.3	1033

Although the calculated values (Table II) for plutonium remaining in the uranium phase are close enough to the experimental values to be useful in making predictions, the experimental results at 1200° C are consistently lower (i.e. less plutonium in the uranium phase) than the predictions. Also, in Table III, there is excellent agreement for experiments at 1160° C but the data show a trend of increasing extraction with temperature, which is the reverse of that predicted by the thermodynamic data. In view of these discrepancies and the fact that the thermodynamic data were estimated, it seemed worth while to use the experimental data and the assumptions of ideality to calculate equilibrium constants and standard free-energy changes accompanying this reaction. The results of these calculations are shown in Table IV. The table shows for each temperature the "average" value for the equilibrium constant from which the standard free-energy

TABLE II

EFFECT OF MOLE RATIO U/UCl_3 ON EXTRACTION OF PLUTONIUM AT 1200° C

Wt U (g)	Wt UCl_3 (g)	Mole ratio U/UCl_3	Pu distribution (% original) Exptl. Salt	Exptl. U	Calc. U
19.100	1.000	27.63	84.8	12.7	18.3
15.928	0.883	26.10	89.2	11.5	17.4
15.057	1.000	21.78	88.2	10.6	15.0
9.289	1.002	13.41	91.1	6.9	9.8
5.909	1.186	7.20	95.0	5.6	5.5

TABLE III

EFFECT OF TEMPERATURE ON EXTRACTION OF PLUTONIUM BY URANIUM TRICHLORIDE

Mole ratio $U/UCl_3 \approx 14$

Temperature (° C)	Mole ratio U/UCl_3	Pu distribution (% original) Exptl. Salt	Exptl. U	Calc. U
1160	15.14	90.6	9.4	9.5
1160	15.00	90.5	8.9	9.4
1200	13.41	91.1	6.9	9.8
1250	14.21	93.0	7.7	12.0
1280	13.96	94.2	4.5	13.0

Can. J. Chem. Downloaded from www.nrcresearchpress.com by 78.46.186.204 on 09/04/12
For personal use only.

TABLE IV

EXPERIMENTAL VALUES FOR THE EQUILIBRIUM CONSTANTS AND $\Delta F°$'S FOR THE REACTION $UCl_3 + Pu \leftrightharpoons PuCl_3 + U$

Temperature (° C)	Equilibrium constant (K)	K_{av}	$\Delta F°$ (kcal) (Experimental)	$\Delta F°$ (kcal) (Brewer *et al.*)
1160	154	150	−14.3	−14.4
	146			
1200	191	189	−15.3	−14.1
	184			
	181			
	200			
1250	170	170	−15.5	−14.1
1280	294	294	−17.5	−14.0

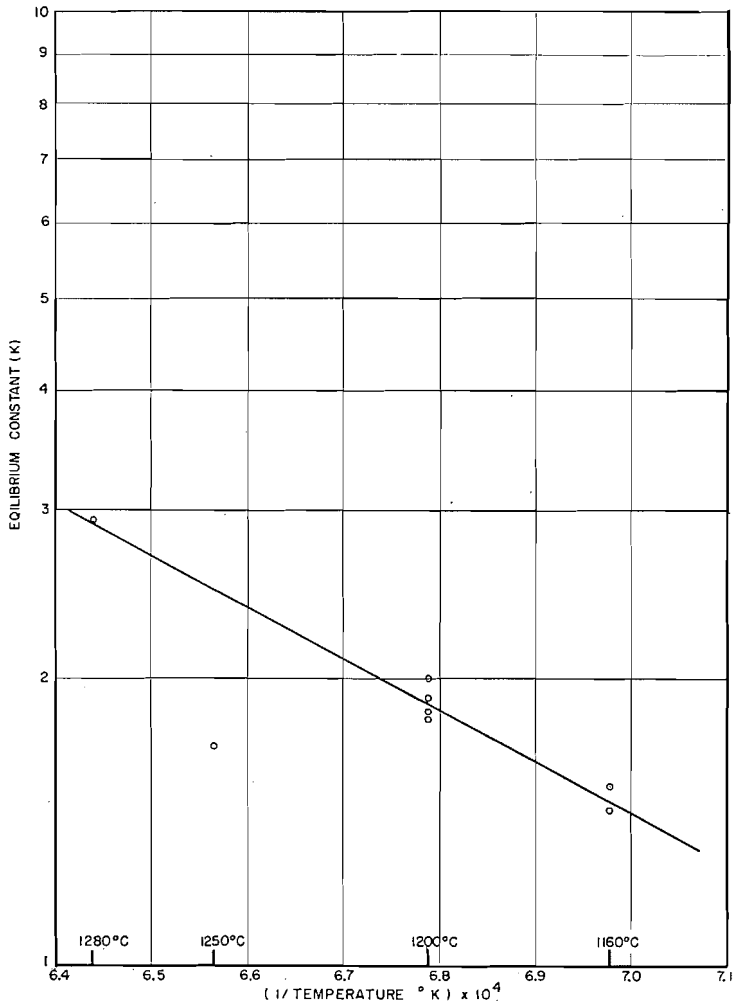

FIG. 1. The effect of temperature on the experimentally determined equilibrium constants for the reaction $UCl_3 + Pu \leftrightharpoons PuCl_3 + U$.

Can. J. Chem. Downloaded from www.nrcresearchpress.com by 78.46.186.204 on 09/04/12
For personal use only.

change for that temperature has been evaluated. This $\Delta F°$ is then compared with the previous estimate of Brewer *et al.* (5, 6). (For this comparison the estimates are listed to three significant figures although Brewer *et al.* give only two.)

As a test of the internal consistency of the data, a plot of log K vs. $1/T$ should yield a straight line. This plot is shown in Fig. 1. Although the result at 1250° C is low, the other data are reasonably consistent and may be represented, approximately, by the equation $\log K = 5.96 - (5.42 \times 10^3/T)$. From the slope of this line the enthalpy change accompanying the reaction $UCl_3 + Pu \leftrightharpoons PuCl_3 + U$ at about 1220° C is calculated to be 24.8 kcal.

The Reaction of Uranium Metal and Magnesium Chloride

Molten magnesium chloride in contact with molten uranium reacts according to the following equation:

$$3/2MgCl_2 + U \rightarrow UCl_3 + 3/2Mg.$$

Since magnesium chloride has a higher free energy of formation (i.e. more negative) than uranium trichloride, it would be expected that the reaction proceeds because the experiments were performed under conditions which permitted continuous distillation of magnesium from the reaction zone. It might be anticipated, further, that the initial rate of reaction will depend upon the surface area of uranium exposed to the salt. As the reaction proceeds, however, the rate will decrease owing to the accumulation of the reaction product, uranium trichloride, in the salt phase. These general expectations have been found to be correct.

The initial reaction rates have been measured using both neutron-irradiated uranium and natural uranium at a number of temperatures; the data are summarized in Table V and plotted as log rate (grams of U reacted/hr cm² U surface) vs. $1/T$ in Fig. 2. The results have been treated by the least squares method to give the equation: log rate (grams of U reacted/hr cm² U surface) $= 4.76 - (7.16 \times 10^3/T)$. From the slope of this line an activation energy of 32.8 kcal has been calculated for the rate-controlling step of the initial process. This activation energy may be compared with the value of 32.3 kcal per mole, the heat of vaporization of magnesium metal at 1200° C (11). This agreement is good evidence that the initial rate of the reaction of uranium metal and magnesium chloride is controlled by the distillation of magnesium metal from the reaction zone.

TABLE V

THE EFFECT OF TEMPERATURE ON THE INITIAL REACTION RATE OF $MgCl_2$ AND URANIUM METAL

Temperature (° C)	Wt U (g)	Wt $MgCl_2$ (g)	U surface area (cm²)	Time (min)	U reacted (g)	U reacted (g/hr)
Neutron-irradiated uranium						
1150	7.825	1.561	1.2	40	0.409	0.613
1200	7.302	1.517		30	0.469	0.939
1245	9.268	1.788		30	0.667	1.335
Natural uranium						
1150	12.826	2.565	1.9	30	0.495	0.991
1180	13.649	3.631		30	0.700	1.400
1200	13.391	3.754		33	0.808	1.470
1260	13.701	3.917		30	1.124	2.248
1285	12.807	3.659		30	1.362	2.725

Can. J. Chem. Downloaded from www.nrcresearchpress.com by 78.46.186.204 on 09/04/12
For personal use only.

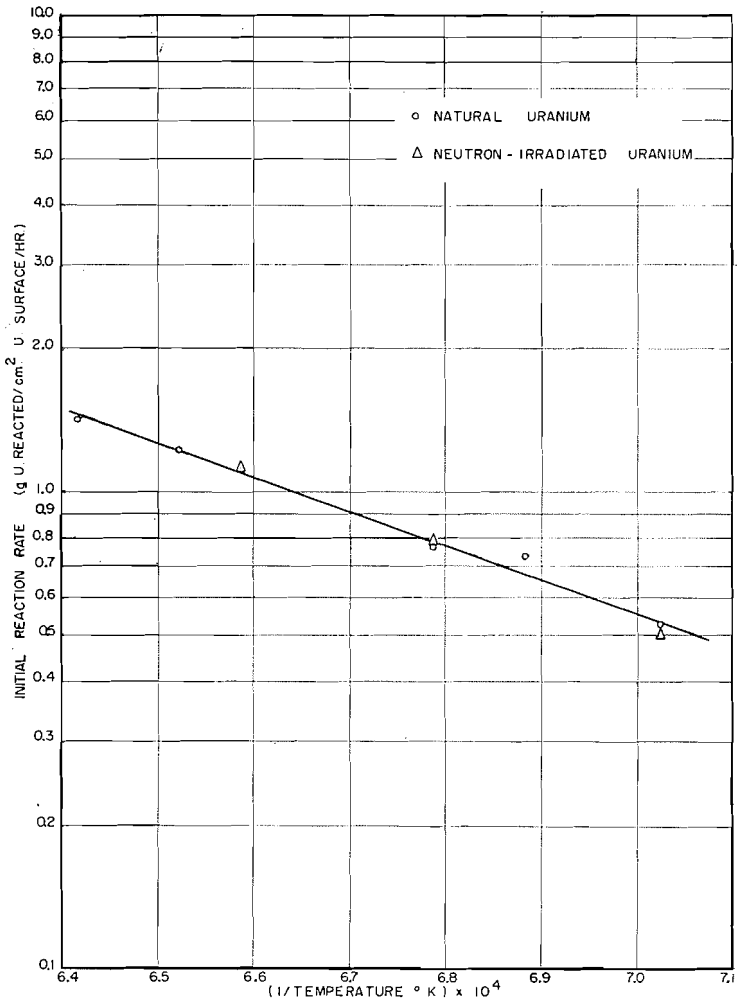

FIG. 2. The effect of temperature on the initial rate of reaction between magnesium chloride and uranium metal.

The Extraction of Plutonium in the Magnesium Chloride Experiments

For these experiments, the following reactions occur on contacting magnesium chloride with molten neutron-irradiated uranium:

$$3/2MgCl_2 + U \rightarrow UCl_3 + 3/2Mg \quad [1]$$

$$3/2MgCl_2 + Pu \rightarrow PuCl_3 + 3/2Mg \quad [2]$$

$$UCl_3 + Pu \leftrightharpoons PuCl_3 + U. \quad [3]$$

The experiments were performed under a pressure of one atmosphere of argon and at a temperature above the boiling point of magnesium metal. Thus, since the temperature of the glass bulb surrounding the reaction crucible was considerably below the melting point of magnesium, the magnesium continuously distilled from the reaction zone and equilibrium with respect to reactions [1] and [2] was not reached. To calculate the extraction of plutonium using thermodynamic data, it was assumed that reaction [3], which does no involve tvolatile components, was in equilibrium at all times, and that uranium trichloride was dissolved in an inert diluent, magnesium chloride.

Can. J. Chem. Downloaded from www.nrcresearchpress.com by 78.46.186.204 on 09/04/12
For personal use only.

On this basis, the equilibrium constants, calculated from the expression derived for the uranium trichloride experiments, were used to predict the extraction of plutonium in the magnesium chloride experiments. At the conclusion of an experiment the concentration of uranium trichloride in the salt phase was determined (by chemical analysis) and substituted into the mass-action expression to calculate the plutonium distribution, again, assuming ideal solution behavior in the salt and metal phases.

The extraction of plutonium has been examined at three temperatures (Table VI) and for various times (Table VII). The tables show the mole fraction of uranium trichloride in the salt and the proportions of original plutonium in the salt and in the metal at the end of each experiment. The latter is compared with the calculated value for plutonium remaining in the uranium.

TABLE VI

EFFECT OF TEMPERATURE ON EXTRACTION OF PLUTONIUM BY MAGNESIUM CHLORIDE

Contacting time = 30 minutes

Temperature (° C)	Wt U (g)	Wt $MgCl_2$ (g)	Final UCl_3 in salt		Pu distribution (% original)		
					Exptl.		Calc.
			% Original U	Mole fraction	Salt	U	U
1150	7.825	1.561	5.2	0.11	87.3	10.0	11.3
1200	7.302	1.517	6.4	0.13	91.4	9.0	7.0
1245	9.268	1.788	7.2	0.15	91.8	8.0	5.3

TABLE VII

EFFECT OF CONTACTING TIME ON EXTRACTION OF PLUTONIUM BY MAGNESIUM CHLORIDE AT 1200° C

Time (min)	Wt U (g)	Wt $MgCl_2$ (g)	Final UCl_3 in salt		Pu distribution (% original)		
					Exptl.		Calc.
			% Original U	Mole fraction	Salt	U	U
10	9.941	1.028	1.7	0.06	56.2	40.3	22.8
30	9.315	1.045	2.5	0.10	84.3	18.0	16.7
60	10.174	1.126	3.4	0.12	90.0	10.9	12.5
120	9.170	1.026	6.5	0.21	92.9	6.1	6.6

The reasonable agreement of the calculated and experimental results for contacting times of thirty minutes or longer provides some support for the assumptions used in making the calculations. Thus, the distribution of plutonium can be predicted from the concentration of uranium trichloride in the salt phase by assuming that the reaction between plutonium and uranium trichloride is at equilibrium even though magnesium chloride and uranium are still reacting. The results for the first experiment listed in Table VII indicate that this assumption does not hold for contacting times of less than thirty minutes.

Two additional experiments were performed at 1140° C and an argon pressure of 100 p.s.i.g. The objective in these experiments was to prevent the formation of uranium trichloride by preventing the distillation of magnesium metal. The data are summarized in Table VIII. While the application of pressure to this system did not completely prevent distillation, the results show that the rate of distillation was reduced, since there was considerably less uranium trichloride formed than in other 30-minute experiments

Can. J. Chem. Downloaded from www.nrcresearchpress.com by 78.46.186.204 on 09/04/12
For personal use only.

(e.g. Table VI). Similarly, it would be expected that the rate of reaction between magnesium chloride and plutonium would be reduced below that for experiments at one atmosphere pressure. However, the reduction in the rate of this reaction would not be expected to influence the extraction equilibrium, since it is assumed that this equilibrium is controlled by the uranium trichloride concentration. The reasonable agreement between calculated and experimental results in these experiments provides additional support for this assumption.

TABLE VIII

EXTRACTION OF PLUTONIUM BY MAGNESIUM CHLORIDE AT 1140° C AND 100 P.S.I.G. ARGON

Contacting time = 30 minutes

Wt U (g)	Wt $MgCl_2$ (g)	Final UCl_3 in salt		Pu distribution (% original)		
				Exptl.		Calc.
		% Original U	Mole fraction	Salt	U	U
9.753	2.029	1.74	0.034	65.1	33.3	30.0
13.370	2.400	1.49	0.035	60.0	39.3	33.4

ACKNOWLEDGMENT

The authors gratefully acknowledge the assistance of Mr. A. S. Denovan, who performed most of the analyses required in this study.

REFERENCES

1. MCKENZIE, D. E. Can. J. Chem. **34**, 515 (1956).
2. MCKENZIE, D. E. Can. J. Chem. **34**, 749 (1956).
3. BRUCE, F. R., FLETCHER, J. M., HEYMAN, H. H., and KATZ, J. J. Process chemistry. McGraw-Hill Book Co., Inc., New York. 1956. pp. 308–341.
4. BUYERS, A. G. Nucleonics, **15** (No. 6), 86 (1957).
5. BREWER, L., BROMLEY, L. A., GILLES, P. W., and LAFGREN, N. L. U.S. Atomic Energy Rept. MDDC-1543 (1947).
6. BREWER, L., BROMLEY, L. A., GILLES, P. W., and LAFGREN, N. L. U.S. Atomic Energy Rept. AECD-2661 (1949).
7. BUYERS, A. G. and MURBACK, E. W. Nuclear Sci. and Eng. **2**, 679 (1957).
8. KATZ, J. J. and RABINOWITCH, E. The chemistry of uranium. McGraw-Hill Book Co., Inc., New York. 1951. p. 451.
9. RODDEN, C. J. Analytical chemistry of the Manhattan project. McGraw-Hill Book Co., Inc., New York. 1950. p. 93.
10. SANDELL, E. B. Calorimetric determination of trace metals. Interscience Publishers, Inc., New York. 1950. p. 419.
11. KELLEY, K. K. U.S. Bur. Mines Bull. No. **383**, 65 (1935).

Can. J. Chem. Downloaded from www.nrcresearchpress.com by 78.46.186.204 on 09/04/12
For personal use only.

Can. J. Chem. Downloaded from www.nrcresearchpress.com by 78.46.186.204 on 09/04/12
For personal use only.

CYCLOHEXANE COMPOUNDS

II. SYNTHESIS AND STRUCTURE OF TWO STEREOISOMERIC 3-AMINO-1,2-CYCLOHEXANEDIOLS[1,2]

R. A. B. Bannard and L. R. Hawkins

ABSTRACT

The stereoisomeric 1-ethoxy-2,3-epoxycyclohexanes were prepared from 1-ethoxycyclohexene-2 via 1-ethoxycyclohexene-2 bromohydrin. Ammonolysis of the lower- and higher-boiling oxides furnished 1α-ethoxy-2β-hydroxy-3α-aminocyclohexane and 1α-ethoxy-2α-hydroxy-3β-aminocyclohexane respectively. In a similar manner, 1α-methoxy-2β-hydroxy-3α-aminocyclohexane and 1α-methoxy-2α-hydroxy-3β-aminocyclohexane were obtained from 1-methoxycyclohexene-2 via 1-methoxycyclohexene-2 bromohydrin and the stereoisomeric 1-methoxy-2,3-epoxycyclohexanes. Ether cleavage of 1α-ethoxy- and 1α-methoxy-2β-hydroxy-3α-aminocyclohexane gave 3α-amino-1α,2β-cyclohexanediol hydrobromide, from which the free base was obtained. 3β-Amino-1α,2α-cyclohexanediol was prepared similarly from 1α-ethoxy- and 1α-methoxy-2α-hydroxy-3β-aminocyclohexane. The stereochemistry of the 3-amino-1,2-cyclohexanediols, 1-alkoxy-2-hydroxy-3-aminocyclohexanes, and 1-alkoxy-2,3-epoxycyclohexanes has been elaborated.

In 1947 Mousseron and co-workers (1, 2, 3) prepared an ethoxyaminocyclohexanol of unknown structure by ammonolysis of 1-ethoxy-2,3-epoxycyclohexane, and in 1952, McCasland *et al.* (4) obtained a similar substance, m.p. 132–134°, in the same manner as Mousseron *et al.* (1, 2, 3). The compound was characterized as the N-*p*-nitrobenzoyl derivative, m.p. 201–203°, and was converted on ether cleavage with hydrobromic acid

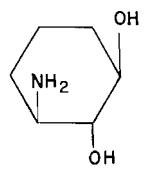

(I)

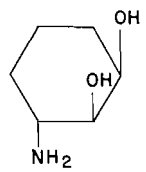

(II)

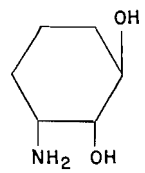

(III)

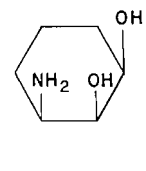

(IV)

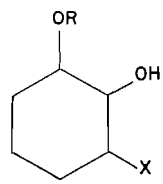

(V)

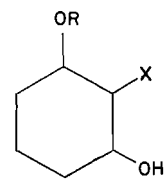

(VI)

[1]*Manuscript received April 15, 1958.*
Contribution from Defence Research Chemical Laboratories, Ottawa, Canada. Issued as D.R.C.L. Report No. 273. Presented in part at the 41st Annual Conference of the Chemical Institute of Canada, Toronto, May 26–28, 1958.
[2]*For Part I of this series see reference 12.*

to an aminocyclohexanediol hydrobromide, m.p. 167–168°. The N-*p*-nitrobenzoyl derivative of the latter compound (m.p. 182–183°) rapidly consumed 1 mole of periodate, thus showing the aminediol to be a 3-amino-1,2-cyclohexanediol. McCasland *et al.* (4) did not assign a stereochemical structure to the substance but pointed out that of the four possible structures (I to IV) only I and II are probable, since oxide ring opening usually yields *trans*-oriented products (5, 6). The present communication describes the synthesis and assignment of structure to two isomeric 3-amino-1,2-cyclohexanediols and to the 1-alkoxy-2,3-epoxycyclohexanes and 1-alkoxy-2-hydroxy-3-aminocyclohexanes used as intermediates in their preparation.

Mousseron *et al.* (1, 2, 3) and McCasland *et al.* (4) had prepared 1-ethoxy-2,3-epoxycyclohexane, either by peracid oxidation of 1-ethoxycyclohexene-2, or by the action of aqueous alkali on 1-ethoxycyclohexene-2 chlorohydrin (V or VI; R = C_2H_5, X = Cl). The chlorohydrin, which was obtained (1, 3, 4) by interaction of monochlorourea (7, 8) and 1-ethoxycyclohexene-2, was considered by McCasland *et al.* (4) to possess structure VI (R = C_2H_5, X = Cl). No proof was submitted in support of this structure nor was it demonstrated that the chlorohydrin thus obtained consists of a mixture of isomers. In 1942 Moir (9), McRae (10), and co-workers studied the reaction between 1-methoxycyclohexene-2 and monochlorourea, and found that a mixture of isomeric chlorohydrins (V or VI; R = CH_3, X = Cl) was formed together with 1-methoxycyclohexene dichloride. It did not prove possible to separate the isomeric chlorohydrins from each other or completely from the dichloride by fractional distillation. The chlorohydrin mixture on treatment with aqueous alkali yielded a mixture of stereoisomeric 1-methoxy-2,3-epoxycyclohexanes (VII and VIII; R = CH_3), demonstrating the presence of at least two isomeric chlorohydrins in the mixture. Somewhat later, but prior to the work of Mousseron *et al.* (1, 3) and McCasland *et al.* (4), Fenton (11) showed that 1-ethoxycyclohexene-2 on treatment with monochlorourea led to a mixture of isomeric chlorohydrins (V or VI; R = C_2H_5, X = Cl) which in turn gave two stereoisomeric 1-ethoxy-2,3-epoxycyclohexanes (VII and VIII; R = C_2H_5). Fenton (11) did not make it clear whether or not 1-ethoxycyclohexene dichloride was present in the chlorohydrin mixture. Repetition of Fenton's work revealed that 1-ethoxycyclohexene dichloride is indeed present. Numerous attempts to separate the chlorohydrin–dichloride mixture by fractional distillation proved fruitless (see Table III).

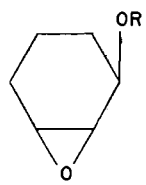

(VII)

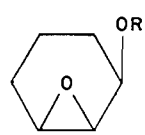

(VIII)

The presence of dichlorides in the 1-alkoxycyclohexene-2 chlorohydrins detracts from their usefulness for preparation of the corresponding oxides, since both the *trans*-, or lower-boiling, oxide (VII) and the *cis*-, or higher-boiling, oxide (VIII) were contaminated with chlorinated substances (10). Furthermore, the fact that the isomeric chlorohydrins are not readily separable makes them impractical as intermediates for preparation of

Can. J. Chem. Downloaded from www.nrcresearchpress.com by 78.46.186.204 on 09/04/12
For personal use only.

Can. J. Chem. Downloaded from www.nrcresearchpress.com by 78.46.186.204 on 09/04/12
For personal use only.

the 1-ethoxy-2-hydroxy-3-aminocyclohexanes by direct ammonolysis (12) because it has been found in the present investigation that separation of the resultant stereoisomeric amines is too laborious. Attention was therefore turned to preparation of the corresponding bromohydrins in the hope that either or both disadvantages characteristic of the chlorohydrins would be eliminated.

For many years the structures of the 1-methoxy-2,3-epoxycyclohexanes remained unassigned. Recently, however, it has been shown by Lemieux, Kullnig, and Moir (13) via proton magnetic resonance spectroscopy on the 1,3-dimethoxy-2-acetoxycyclohexanes resulting from acetylation of the products of methanolysis of the 1-methoxy-2,3-epoxycyclohexanes, that the lower-boiling isomer (the so-called α-isomer (10)) has the *trans*-configuration and the higher-boiling isomer (the so-called β-isomer (10)) the *cis*-configuration. This work, however, still left unsettled the configurations of Fenton's 1-ethoxy-2,3-epoxycyclohexanes. It will be demonstrated in the sequel that in this case also, the lower-boiling oxide is the *trans*-isomer and the higher-boiling oxide the *cis*-isomer.

1-Methoxy- and 1-ethoxycyclohexene-2 were prepared by modification of the method of Gogek *et al.* (14). 1-Methoxycyclohexene-2 on treatment with N-bromosuccinimide in aqueous suspension (cf. Guss and Rosenthal (15)) gave a mixture of isomeric 1-methoxycyclohexene-2 bromohydrins (V or VI; R = CH_3, X = Br) in 77% yield, uncontaminated with the corresponding dibromide. In a similar manner the mixed 1-ethoxycyclohexene-2 bromohydrins (V or VI; R = C_2H_5, X = Br) were obtained in 85% yield also free of dibromide. It did not prove possible to separate the isomeric bromohydrins by fractional distillation. However, the bromohydrin mixtures proved much superior to the chlorohydrin–dichloride mixtures as intermediates for preparation of the stereoisomeric 1-alkoxy-2,3-epoxycyclohexanes (VII and VIII).

1-Methoxycyclohexene-2 bromohydrin (V or VI; R = CH_3, X = Br) on treatment with aqueous sodium hydroxide gave an 84% yield of the stereoisomeric *dl*-1-methoxy-2,3-epoxycyclohexanes (VII and VIII; R = CH_3), which were readily separated by fractional distillation and were free of halogenated material (cf. McRae *et al.* (10)). On the basis of refractive index and infrared spectra of the various fractions (see Table V) it was estimated that the yield of *trans*-, or lower-boiling, oxide is 63% and that of the *cis*-, or higher-boiling, oxide is 19%. Thus, the percentages of *trans*- and *cis*-oxide in the mixture are 77% and 23% respectively, suggesting the same percentage composition for the 1-methoxycyclohexene-2 bromohydrin mixture. In a similar manner the stereoisomeric *dl*-1-ethoxy-2,3-epoxycyclohexanes (VII and VIII; R = C_2H_5) were obtained in 88% yield. The yield of *trans*-oxide was estimated to be 70.5% and that of the *cis*-oxide 17.5%, giving a distribution of 80% *trans*- and 20% *cis*-oxide in the mixture. It is evident from Table IV that fractionation of the 1-ethoxy-2,3-epoxycyclohexanes was not as clean cut as with the corresponding methoxy compounds. This result was unexpected in view of the difference in boiling points of the isomers and the high reflux ratio used.

The spectra of the 1-methoxy- and 1-ethoxy-2,3-epoxycyclohexanes are shown in Figs. 1 to 4. These substances give a strong band at 1100 cm^{-1} characteristic of the unsymmetrical C—O—C stretching vibration in aliphatic ethers (16). Absorption due to the symmetrical ring stretching vibration of the oxirane ring was observed in the characteristic 1250 cm^{-1} region (16). In each case, the *trans*-isomer showed a medium intensity band at 1245 cm^{-1} and the *cis*-isomer showed a similar band at 1255 cm^{-1}. It is possible to use the bands at 1245 and 1255 cm^{-1} as criteria of purity of the oxides but the change in intensity of these bands is not sufficiently great to permit accurate quantitative

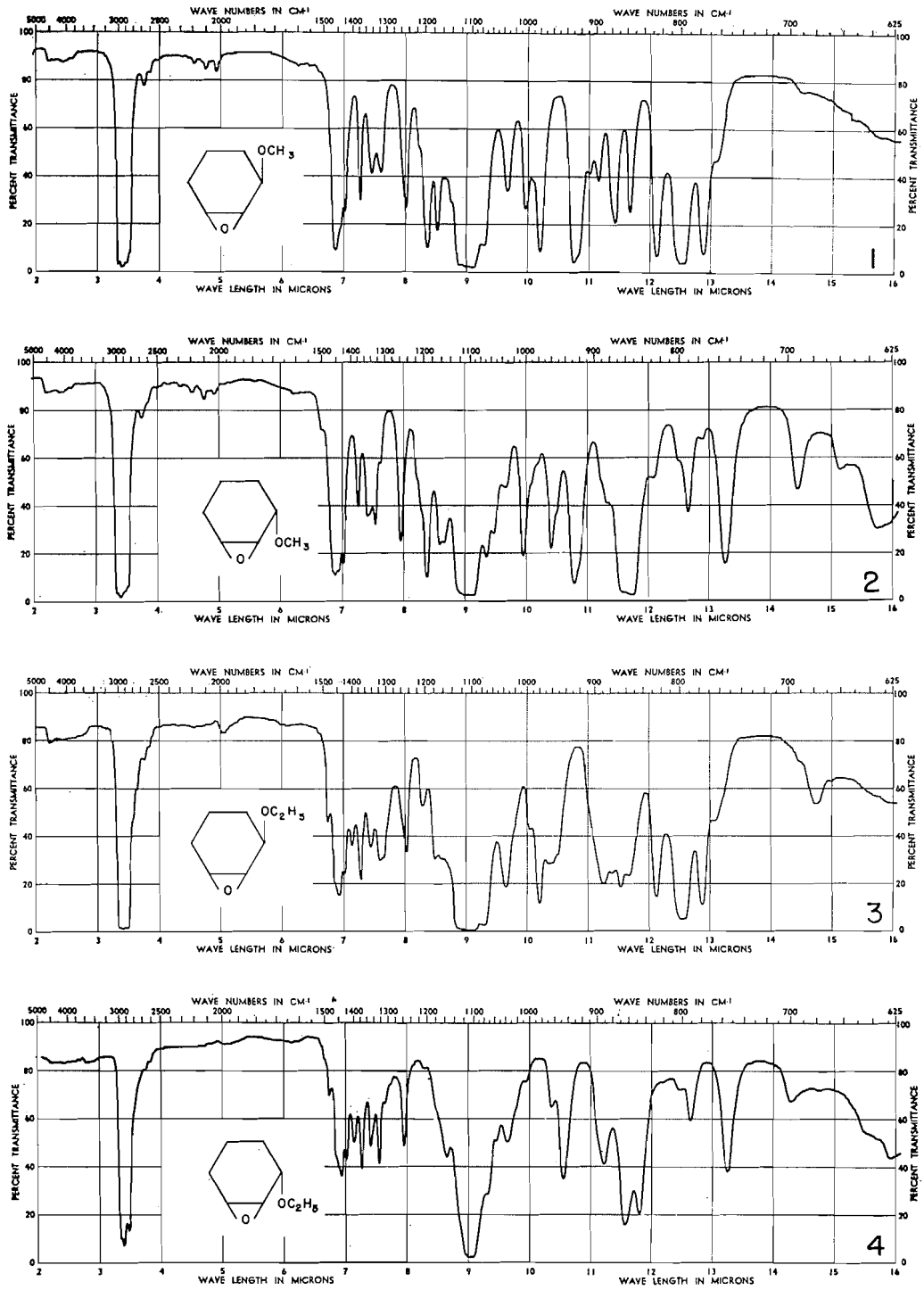

FIGS. 1–4. Infrared spectra of the 1-alkoxy-2,3-epoxycyclohexanes.

Can. J. Chem. Downloaded from www.nrcresearchpress.com by 78.46.186.204 on 09/04/12
For personal use only.

Can. J. Chem. Downloaded from www.nrcresearchpress.com by 78.46.186.204 on 09/04/12
For personal use only.

estimation of the compositions of mixtures—the refractive index gives a more sensitive method. However, there are a number of bands in the region 690–1380 cm^{-1} which show great differences in intensity as the composition of mixtures of the *trans*- and *cis*-oxides change, some of which could undoubtedly be used for quantitative estimation by means of a suitable calibration curve. The *trans*-oxides show prominent characteristic bands at 775, 795, 800, 825, 980, 1200, and 1380 cm^{-1}, whereas the *cis*-oxides show prominent characteristic bands at 690, 755, 790, 845, 865, and 1325 cm^{-1}. The forerun of each oxide contained a trace of carbonyl impurity as shown by the appearance of a weak band at 1675 cm^{-1}. This carbonyl impurity could be due to the presence of a trace of *cis*-bromohydrin in the predominantly *trans*-oriented bromohydrin mixture (17), since the action of alkali on the former would lead to ketone rather than epoxide (18, 19).

Ammonolysis of *dl*-1β-methoxy-2α,3α-epoxycyclohexane* (VII; R = CH_3) with aqueous ethanolic ammonia by Hawkins and Bannard's method (12) gave *dl*-1α-methoxy-2β-hydroxy-3α-aminocyclohexane (IX; R = CH_3), m.p. 107–108°, in 84% yield, uncontaminated with its isomer X (R = CH_3), as shown by paper chromatography. In a similar manner, ammonolysis of *dl*-1α-methoxy-2α,3α-epoxycyclohexane (VIII; R = CH_3) produced *dl*-1α-methoxy-2α-hydroxy-3β-aminocyclohexane (X; R = CH_3), m.p. 94°, in 75% yield, uncontaminated with its isomer IX (R = CH_3). The two 1-methoxy-2-hydroxy-3-aminocyclohexanes (IX and X; R = CH_3) were shown to be distinctly different by comparison of their infrared spectra, paper chromatographic behavior (see Table VI), a mixed melting-point determination (m.p. 72–92°), and preparation of their hydrobromides, and N-acetyl, N-*p*-nitrobenzoyl, and N-phenylthiourea derivatives listed in Table I.

TABLE I

DERIVATIVES OF THE 1-ALKOXY-2-HYDROXY-3-AMINOCYCLOHEXANES

Compound	Derivative	% Yield	M.p. (° C)	Analysis									
				% C		% H		% N		% Br		% S	
				Calc.	Found	Calc.	Found	Calc.	Found	Calc.	Found	Calc.	Found
dl-1α-Methoxy-2β-hydroxy-3α-aminocyclohexane	Hydrobromide	80	206 –207	37.18	37.20	7.14	7.10	6.20	6.30	35.34	35.72		
	N-Acetyl	82	115.5–116.5	57.75	57.90	9.16	9.04	7.48	7.27				
	N-*p*-Nitrobenzoyl	85	178 –179.5	57.14	57.21	6.16	5.87	9.52	9.57				
	N-Phenylthiourea	77	135 –136	59.99	60.28	7.19	7.24	10.00	10.18			11.44	11.38
dl-1α-Methoxy-2α-hydroxy-3β-aminocyclohexane	Hydrobromide	81	203 –204	37.18	37.30	7.14	7.17	6.20	6.44	35.34	35.44		
	N-Acetyl	77	154.5–155	57.75	58.00	9.16	9.32	7.48	7.41				
	N-*p*-Nitrobenzoyl	85	238.5–239	57.14	57.14	6.16	6.28	9.52	9.68				
	N-Phenylthiourea	62	155 –156	59.99	60.06	7.19	7.09	10.00	10.12			11.44	11.60
dl-1α-Ethoxy-2β-hydroxy-3α aminocyclohexane	Hydrobromide	76	194.5–196	40.00	40.18	7.55	7.59	5.83	6.04	33.27	33.18		
	N-Acetyl	77	124	59.69	59.79	9.52	9.58	6.96	6.74				
	N-*p*-Nitrobenzoyl[a]	87	203 –204	58.45	58.34	6.54	6.43	9.09	9.07				
	N-Phenylthiourea	70	133 –134	61.17	61.28	7.53	7.67	9.52	9.55			10.89	11.07
dl-1α-Ethoxy-2α-hydroxy-3β-aminocyclohexane	Hydrobromide	79	179 –180	40.00	40.22	7.55	7.59	5.83	6.08	33.27	33.14		
	N-Acetyl	82	129 –129.5	59.69	59.77	9.52	9.55	6.96	6.66				
	N-*p*-Nitrobenzoyl	84	215.5–216	58.45	53.34	6.54	6.52	9.09	9.06				
	N-Phenylthiourea	76	143 –144	61.17	61.26	7.53	7.54	9.52	9.70			10.89	10.97

[a]McCasland *et al.* (4) report m.p. 201–203°.

**The system of nomenclature used to describe the configurations of the 1-alkoxy-2,3-epoxycyclohexanes and compounds obtained on scission of the oxirane ring conforms to that used by Lemieux, Kullnig, and Moir (13).*

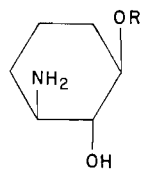

(IX)

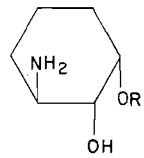

(X)

Ammonolysis of *dl*-1β-ethoxy-2α,3α-epoxycyclohexane (VII; R = C_2H_5) gave *dl*-1α-ethoxy-2β-hydroxy-3α-aminocyclohexane (IX; R = C_2H_5), m.p. 134.5–135.5°, in 77% yield, uncontaminated with its isomer X (R = C_2H_5). In one experiment in which an ammonia/oxide ratio of less than 20:1 was used, a small amount of the secondary amine α,α-bis-(2β-hydroxy-3α-ethoxycyclohexyl)amine (XI) was obtained and isolated as the hydrobromide, m.p. 313–314° (cf. Hawkins and Bannard (12)). Ammonolysis of *dl*-1α-ethoxy-2α,3α-epoxycyclohexane (VIII; R = C_2H_5) furnished *dl*-1α-ethoxy-2α-hydroxy-3β-aminocyclohexane (X; R = C_2H_5), m.p. 133–134°, in 89% yield, uncontaminated with its isomer IX (R = C_2H_5). The two 1-ethoxy-2-hydroxy-3-aminocyclohexanes (IX and X; R = C_2H_5) were shown to differ from one another by comparison of infrared spectra, paper chromatographic behavior (see Table VI), a mixed melting-point determination (m.p. 116–118°), and preparation of their hydrobromides and N-acetyl, N-*p*-nitrobenzoyl, and N-phenylthiourea derivatives given in Table I.

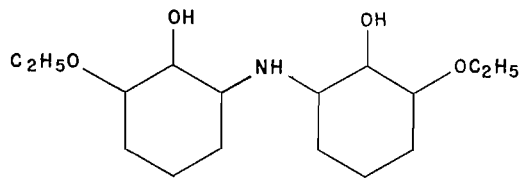

(XI)

It is evident from the melting points of the N-*p*-nitrobenzoyl derivatives of the *dl*-1-ethoxy-2-hydroxy-3-aminocyclohexanes (Table I) that McCasland *et al.* (4) obtained *dl*-1α-ethoxy-2β-hydroxy-3α-aminocyclohexane (IX; R = C_2H_5). This result was anticipated in view of the fact that the *trans*-oxide greatly predominates in the mixture of stereoisomeric oxides resulting from the action of alkali on the 1-ethoxycyclohexene-2 bromohydrins, implying that a similar situation would prevail in the case of the corresponding chlorohydrins. A similar result (i.e. predomination of *trans*-oxide) would also be expected when the oxide is prepared by peracid oxidation of 1-methoxycyclohexene-2 (1, 2, 3, 4,), since Henbest and Wilson (20, 21) have found that peracid oxidation of cyclic allylic esters or ethers yields predominantly the *trans*-oxide. It thus seems certain that Mousseron *et al.* (1, 2, 3) obtained the same compound as McCasland *et al.* (4) but in a less pure condition.

Ether cleavage of *dl*-1α-methoxy-2β-hydroxy-3α-aminocyclohexane or *dl*-1α-ethoxy-2β-hydroxy-3α-aminocyclohexane (IX; R = CH_3 or C_2H_5) with 47% hydrobromic acid gave *dl*-3α-amino-1α,2β-cyclohexanediol hydrobromide, m.p. 168–169°, in 90% yield,

Can. J. Chem. Downloaded from www.nrcresearchpress.com by 78.46.186.204 on 09/04/12
For personal use only.

which was converted to the free base I, m.p. 151°, in 87% yield. In a similar manner, ether cleavage of *dl*-1α-methoxy-2α-hydroxy-3β-aminocyclohexane or *dl*-1α-ethoxy-2α-hydroxy-3β-aminocyclohexane (X; R = CH_3 or C_2H_5) gave *dl*-3β-amino-1α,2α-cyclohexanediol hydrobromide, m.p. 165.5–167°, in 70% yield, which was converted to the free base II, m.p. 104–105°, in 95% yield. The two aminediols were shown to be quite different by a mixed melting-point determination with their hydrobromides (m.p. 145–150°), comparison of their infrared spectra and paper chromatographic behavior (see Table VI), and preparation of the N-*p*-nitrobenzoyl, N-phenylthiourea, and triacetyl derivatives listed in Table II.

TABLE II

DERIVATIVES OF THE 3-AMINO-1,2-CYCLOHEXANEDIOLS

Compound	Derivative	% Yield	M.p. (° C)	Analysis							
				% C		% H		% N		% S	
				Calc.	Found	Calc.	Found	Calc.	Found	Calc.	Found
dl-3α-Amino-1α,2β-cyclohexanediol	N-*p*-Nitrobenzoyl	74	185–187	55.71	55.39	5.75	5.77	10.00	9.89		
	N-Phenylthiourea*	98	115–117	57.65	57.06	7.74	7.70	8.97	8.81	10.26	10.31
	Triacetyl	80	193–194	56.02	56.02	7.44	7.39	5.44	5.57		
dl-3β-Amino-1α,2α-cyclohexanediol	N-*p*-Nitrobenzoyl	65	195–197	55.71	55.57	5.75	5.85	10.00	9.74		
	N-Phenylthiourea	80	151–152.5	58.61	58.66	6.81	6.86	10.52	10.84	12.03	11.88
	Triacetyl	59	148–149.5	56.02	55.80	7.44	7.56	5.44	5.22		

*Contains 1 molecule of ethanol of crystallization.

The data presented above establish the stereochemical identity of the 1-alkoxy-2-hydroxy-3-aminocyclohexanes (IX; R = CH_3 or C_2H_5) resulting from ammonolysis of the α- or lower-boiling 1-alkoxy-2,3-epoxycyclohexanes (VII; R = CH_3 or C_2H_5) and necessarily also show the stereochemical equivalence of the two oxides. Similarly the stereochemical identity of the 1-alkoxy-2-hydroxy-3-aminocyclohexanes (X; R = CH_3 or C_2H_5) resulting from ammonolysis of the β- or higher-boiling 1-alkoxy-2,3-epoxycyclohexanes (VIII; R = CH_3 or C_2H_5) has also been demonstrated and the stereochemical equivalence of the two oxides follows. Furthermore, it has been clearly shown that the α- and β-oxides differ from one another since they lead to distinctly different aminocyclohexanediols. The aminediols were shown to be 3-amino-1,2-cyclohexanediols, since the N-*p*-nitrobenzoyl derivative in each case rapidly consumed 1 mole of periodate at 25° (22). However, reaction was so rapid at this temperature that the relative rates of oxidation of the two isomers could not be observed with sufficient accuracy to permit stereochemical assignment to the diols. Repetition of the oxidation with sodium metaperiodate at 3°, however, gave the results shown in Fig. 5. Comparison of the $t_{\frac{1}{2}}$ values makes it clear that the diol group in the aminediol resulting from ammonolysis of the β-oxides must be assigned the *cis*-configuration II and the diol group in the aminediol from ammonolysis of the α-oxides must possess the *trans*-configuration I, since the N-*p*-nitrobenzoyl derivative of the former is oxidized 7.5 times more rapidly than that of the latter (23, 24, 25).

The N-phenylthiourea derivatives of the aminediols were prepared in the expectation that determination of relative rates of cleavage of the isomers with periodate would lead to confirmation of the structures assigned above. However, the periodate cleavage of these derivatives proved abnormal in that even the N-phenylthiourea derivative of

Can. J. Chem. Downloaded from www.nrcresearchpress.com by 78.46.186.204 on 09/04/12
For personal use only.

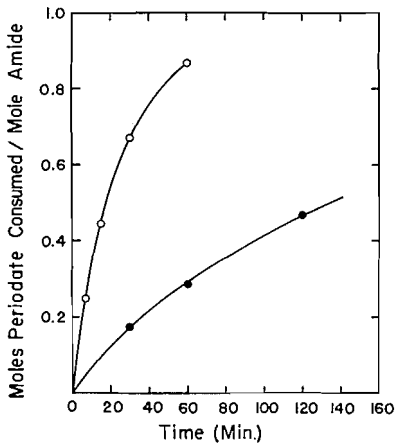

FIG. 5. Rate of periodate oxidation of the 3-*p*-nitrobenzamido-1,2-cyclohexanediols.
● 3α-*p*-Nitrobenzamido-1α,2β-cyclohexanediol
○ 3β-*p*-Nitrobenzamido-1α,2α-cyclohexanediol

trans-2-aminocyclohexanol reacted rapidly with periodate. Thus, these derivatives cannot be used to protect an amine function during diol scission with periodate.

Ionophoretic migration of *cis*-1,2-diols in borate buffer is generally considered to be associated with formation of ionized chelated complexes (25, 26) and has been used to deduce the structure of cyclitols (27). The ionophoretic mobilities of the N-*p*-nitrobenzoyl and N-phenylthiourea derivatives of the aminediols I and II in 0.1 *M* sodium tetraborate were determined. In each case (see Table VII) the derivative arising from the β- or higher-boiling 1-alkoxy-2,3-epoxycyclohexanes exhibited ionophoretic mobility, while the derivative obtained from the α- or lower-boiling 1-alkoxy-2,3-epoxycyclohexanes did not migrate, thus leading to the conclusion that derivatives obtained by oxide ring scission of the former compounds contain a *cis*-1,2-diol group (I), whereas derivatives obtained similarly from the latter compounds contain a *trans*-1,2-diol group (II). This result confirms the structural assignment made on the basis of relative rates of periodate cleavage of the aminediol N-*p*-nitrobenzoyl derivatives.

It is assumed throughout that opening of the oxirane ring under the basic conditions used is accompanied by Walden inversion at the reactive carbon atom (i.e. C_3) (4, 5, 6, 14, 28, 29), and that ether cleavage is not attended by Walden inversion (see Gogek *et al.* (14) and references there cited, also Lemieux, Kullnig, and Moir (13)). Assignment of structure I to the *trans*-diol leads to structure IX (R = CH_3 or C_2H_5) for the 3-amino-1-alkoxy-2-hydroxycyclohexanes derived from the α-oxides and hence to the *trans* structure VII (R = CH_3 or C_2H_5) for the latter, in agreement with the conclusion reached by Lemieux, Kullnig, and Moir (13) in the case of the α-methoxy oxide (VII; R = CH_3). In a similar manner, assignment of structure II to the *cis*-diol leads to structure X (R = CH_3 or C_2H_5) for the 3-amino-1-alkoxy-2-hydroxycyclohexanes derived from the β-oxides and hence to the *cis* structure VIII (R = CH_3 or C_2H_5) for the latter.

Lemieux, Kullnig, and Moir (13) have pointed out that both 1-methoxy-2,3-epoxycyclohexanes (VII and VIII; R = CH_3) show a preference for attack at position 3 by nucleophilic reagents and suggest that such preference is probably an electronic effect of the presence of the electronegative alkoxyl group, rather than a steric effect. This suggestion receives support from the results reported above on ammonolysis of the 1-methoxy- and 1-ethoxy-2,3-epoxycyclohexanes (VII and VIII; R = CH_3 or C_2H_5).

Can. J. Chem. Downloaded from www.nrcresearchpress.com by 78.46.186.204 on 09/04/12
For personal use only.

Can. J. Chem. Downloaded from www.nrcresearchpress.com by 78.46.186.204 on 09/04/12
For personal use only.

EXPERIMENTAL*, †

trans-1,2-Dibromocyclohexane

trans-1,2-Dibromocyclohexane was prepared by the method of Snyder and Brooks (30).

1-Methoxycyclohexene-2

1-Methoxycyclohexene-2 was prepared by the method of Gogek *et al.* (14), with the method of isolation modified as follows. After the solution of *trans*-1,2-dibromocyclohexane (3.88 g, 1.60 moles), sodium (90.0 g, 3.9 g-atoms), and absolute methanol (1100 ml) had been heated under reflux for 10 hours, the precipitated sodium bromide was collected by suction filtration and washed with anhydrous ether (6×50 ml). The filtrate and washings were distilled on the steam bath first at atmospheric pressure and finally at 25–30 mm pressure until a semisolid mushy residue remained. The residue was treated with water (200 ml) and the solution was extracted with ether (3×50 ml). The extracts were combined with the earlier distillates and the solution was fractionated slowly at atmospheric pressure using a 20-inch vacuum-jacketed Stedman column, yielding 134 g (74.8%) of 1-methoxycyclohexene-2 as a colorless mobile fragrant liquid, b.p. 138–139°, n_D^{25} 1.4513–1.4518. Gogek *et al.* (14) report a 60% yield of substance, b.p. 139°. Berlande (31) has reported n_D^{20} 1.4530.

1-Ethoxycyclohexene-2

1-Ethoxycyclohexene-2 was prepared by the same method as described above for 1-methoxycyclohexene-2. Yield, 58.5%, b.p. 153–154°, n_D^{25} 1.4490. Berlande (31) has reported b.p. 156°, and n_D^{20} 1.4585. Fenton (11) reported b.p. 153–153.5°.

1-Ethoxycyclohexene-2 Chlorohydrin

1-Ethoxycyclohexene-2 chlorohydrin was prepared by the method of Fenton (11) using monochlorourea as the source of hypochlorous acid. From 378 g (3.0 mole) of 1-ethoxycyclohexene-2, 358 g of colorless to pale yellow liquid, b.p. 108–113° at 11–13 mm pressure, n_D^{25} 1.4784–1.4794, was obtained. Fenton (11) reported b.p. 105–120° at 20 mm pressure and McCasland *et al.* (4) reported b.p. 110–117° at 12 mm. Refractionation at 1–2 mm pressure of 770 g of chlorohydrin prepared by the above method gave the fractions indicated in Table III.

TABLE III

FRACTIONATION OF 1-ETHOXYCYCLOHEXENE-2 CHLOROHYDRIN

Fraction No.	B.p. (° C)	Weight (g)	Refractive index n_D^{25}	Analysis[a]		
				% C	% H	% Cl
1	76 –77.5	249	1.4788	51.48	8.17	26.50
2	77.5–78	88	1.4789	52.02	7.98	25.24
3	78 –79.5	84	1.4792	52.43	8.11	24.56
4	79.5–81	92	1.4795	52.88	8.22	23.09
5	79.5–80	80	1.4798	53.23	8.48	22.15
6	80 –81	46	1.4798	53.35	8.46	21.23
7	83 –89	77	1.4800	52.38	8.21	21.10
8	Pot residue	34	1.4816	50.76	7.77	24.24

[a]Calc. for $C_8H_{15}O_2Cl$: C, 53.78; H, 8.46; Cl, 19.85%.
Calc. for $C_8H_{14}OCl_2$: C, 48.75; H, 7.16; Cl, 35.97%.

1-Ethoxycyclohexene-2 Bromohydrin

N-Bromosuccinimide (178 g, 1.00 mole), 1-ethoxycyclohexene-2 (132 g, 1.05 mole),

*All melting points and boiling points are uncorrected.
†Microanalyses by Micro-Tech Labs., Skokie, Ill., and J. G. Helie, of these laboratories.

Can. J. Chem. Downloaded from www.nrcresearchpress.com by 78.46.186.204 on 09/04/12
For personal use only.

and water (500 ml) were mixed at 25° in a 1-liter three-necked flask equipped with a "trubore" stirrer and thermometer (12). Stirring was continued until the N-bromosuccinimide dissolved (20 minutes) and a heavy colorless layer of bromohydrin separated, during which time the temperature rose to 75°. The two-phase system was allowed to cool to room temperature, the bromohydrin layer was separated, and the aqueous phase was extracted with ether (2×100 ml). The extracts and bromohydrin were combined and the ether removed by distillation *in vacuo*. The residue was kept overnight at 4°, after which the precipitated succinimide was removed by filtration. The filtrate was fractionated *in vacuo* yielding 190 g (85.2%) of 1-ethoxycyclohexene-2 bromohydrin as a colorless oil, b.p. 87.5–91.5° at 0.3 mm, n_D^{25} 1.5018–1.5025. Calc. for $C_8H_{15}O_2Br$: C, 43.07; H, 6.78; Br, 35.82%. Found: C, 42.95; H, 6.82; Br, 35.82%.

1-Methoxycyclohexene-2 Bromohydrin

1-Methoxycyclohexene-2 bromohydrin was prepared in exactly the same manner as described for 1-ethoxycyclohexene-2 bromohydrin. Yield, 161 g (77.0%) of colorless oil, b.p. 94–97° at 1 mm, n_D^{25} 1.5120–1.5131. Calc. for $C_7H_{13}O_2Br$: C, 40.22; H, 6.27; Br, 38.22%. Found: C, 40.08; H, 6.35; Br, 37.98%.

dl-1β-Ethoxy-2α,3α-epoxycyclohexane and dl-1-α-Ethoxy-2α,3α-epoxycyclohexane (VII and VIII; R = C_2H_5)

1-Ethoxycyclohexene-2 bromohydrin (234 g, 1.05 mole) was treated with aqueous sodium hydroxide (120 g, 2.94 moles, 300 ml) at 25° with mechanical stirring. The temperature rose to 35° and the lower bromohydrin layer was replaced by a supernatant layer of colorless oxide. The mixture was heated at 75° for 1 hour with continuous stirring, and cooled to room temperature; the oxide layer was then separated and the aqueous phase extracted with ether (3×100 ml). The combined oxide and ether extracts were dried over anhydrous magnesium sulphate, after which the ether was removed *in vacuo*. The colorless residue was fractionated at 10 mm pressure using a Podbielniak Whirling Heli-Band column, employing diphenylmethane as "chaser" during the final stage of fractionation, giving the results shown in Table IV.

TABLE IV

FRACTIONATION OF 1-ETHOXY-2,3-EPOXYCYCLOHEXANES

Fraction No.	B.p. (° C)	Refractive index n_D^{25}	Weight (g)	Analysis*	
				% C	% H
1	55.5–56.0	1.4484	84.2	67.52	10.01
2	56.0–56.5	1.4491	21.6	67.80	10.14
3	56.5–64.5	1.4520	2.3	67.63	9.91
4	64.5–65.5	1.4554	23.0	67.81	10.11
			131		

*Calc. for $C_8H_{14}O_2$: C, 67.58; H, 9.92%.

From Table IV it is clear that the 1-ethoxy-2,3-epoxycyclohexanes were obtained in 88.0% yield. Fraction 1 is pure *trans*-oxide, since the infrared spectrum of this compound showed the characteristic oxirane band at 1245 cm^{-1}, and fraction 4 is pure *cis*-oxide, since its infrared spectrum showed the characteristic oxirane band at 1255 cm^{-1}. Fractions 2 and 3 are mixtures of the two oxides, since both the above-mentioned bands were present in the infrared spectra. Mixtures of the pure oxides gave a linear relationship between refractive index and percentage composition and the yields of the two

oxides were estimated. The yield of *trans*-oxide is 105 g (70.4%) and that of *cis*-oxide is 26.3 g (17.6%), i.e. the mixture consists of 80% *trans*-oxide and 20% *cis*-oxide. Fenton (11) reported b.p. 82–84° at 20 mm for *trans*-oxide and 97–100° at 20 mm for *cis*-oxide. McCasland *et al.* (4) gave b.p. 79–82° at 15–16 mm and n_D^{25} 1.4530 for the oxide mixture resulting from peracid oxidation of 1-ethoxycyclohexene-2, and Mousseron *et al.* (3) gave b.p. 77–78° at 12 mm and n_D^{25} 1.4493 for a similar product.

dl-1β-Methoxy-2α,3α-epoxycyclohexane and dl-1α-Methoxy-2α,3α-epoxycyclohexane (VII and VIII; R = CH_3)

1-Methoxycyclohexene-2 bromohydrin (146 g, 0.70 mole) was treated with aqueous sodium hydroxide (84.0 g, 2.04 mole, 200 ml), as described for the preparation of the corresponding ethoxy compounds, yielding, after subsequent manipulation as described above, the fractions shown in Table V.

TABLE V

FRACTIONATION OF 1-METHOXY-2,3-EPOXYCYCLOHEXANES

Fraction No.	B.p. (° C)	Refractive index n_D^{25}	Weight (g)	Analysis*	
				% C	% H
1	54–55	1.4512	55.0	65.69	9.52
2	55–65	1.4520	0.7	65.82	9.57
3	65–69	1.4545	1.9	65.80	9.66
4	69–71	1.4585	17.4	65.71	9.56
			75		

*Calc. for $C_7H_{12}O_2$: C, 65.58; H, 9.44%.

From Table V it is evident that the yield of 1-methoxy-2,3-epoxycyclohexane mixture is 83.8%. Fraction 1 is pure *trans*-oxide and fraction 4 is pure *cis*-oxide, while fractions 2 and 3 are mixtures (infrared spectra). As in the case of the corresponding ethoxy compounds the composition of mixtures was estimated on the basis of refractive index. The yield of *trans*-oxide is thus 56.5 g (63.2%) and that of *cis*-oxide 17.4 g (19.4%), i.e. the mixture consists of approximately 77% *trans*-oxide and 23% *cis*-oxide. McRae *et al.* (10) have reported b.p. 67–69° at 15 mm and n_D^{20} 1.4532 for the *trans*-oxide and b.p. 75–85° at 12 mm and n_D^{20} 1.4603 for the *cis*-oxide.

dl-1α-Methoxy-2β-hydroxy-3α-aminocyclohexane (IX; R = CH_3)

dl-1β-Methoxy-2α,3α-epoxycyclohexane (12.8 g, 0.100 mole) was heated for 1 hour at 100° in a stainless-steel bomb with 28% aqueous ammonia (135 ml, 2 moles) and absolute ethanol (60 ml) (12). The solution was evaporated to dryness *in vacuo* and the resultant buff-colored amine was sublimed at 110–120° at 1 mm, yielding 12.1 g (83.5%) of colorless *dl*-1α-methoxy-2β-hydroxy-3α-aminocyclohexane, m.p. 107–108°. Calc. for $C_7H_{15}O_2N$: C, 57.90; H, 10.41; N, 9.65%. Found: C, 57.52; H, 10.39; N, 9.58%.

dl-1α-Methoxy-2α-hydroxy-3β-aminocyclohexane (X; R = CH_3)

dl-1α-Methoxy-2α,3α-epoxycyclohexane (15.0 g, 0.117 mole) was ammonolyzed with aqueous ethanolic ammonia under the conditions described for 1β-methoxy-2α,3α-epoxycyclohexane, yielding 12.8 g (75.3%) of *dl*-1α-methoxy-2α-hydroxy-3β-aminocyclohexane as colorless feathery needles, m.p. 94°, after recrystallization from ethanol–ether. Calc. for $C_7H_{15}O_2N$: C, 57.90; H, 10.41; N, 9.65%. Found: C, 57.47; H, 10.39; N, 9.58%.

Can. J. Chem. Downloaded from www.nrcresearchpress.com by 78.46.186.204 on 09/04/12
For personal use only.

dl-1α-Ethoxy-2β-hydroxy-3α-aminocyclohexane (IX; R = C_2H_5)

dl-1β-Ethoxy-2α,3α-epoxycyclohexane (31.1 g, 0.219 mole) was ammonolyzed with aqueous ethanolic ammonia under the conditions described for *dl*-1β-methoxy-2α,3α-epoxycyclohexane, yielding 26.8 g (77.0%) of *dl*-1α-ethoxy-2β-hydroxy-3α-aminocyclohexane as colorless platelets, m.p. 134.5–135.5°, after recrystallization from ethanol–ether. McCasland *et al.* (4) report m.p. 132–134° for this compound. Calc. for $C_8H_{17}O_2N$: C, 60.35; H, 10.76; N, 8.80%. Found: C, 60.67; H, 10.93; N, 8.72%.

In one experiment in which the ammonia–oxide ratio was less than 20:1 a small amount of α,α-bis-(2β-hydroxy-3α-ethoxycyclohexyl)amine was obtained, and isolated as the hydrobromide, m.p. 313–314°. Calc. for $C_{16}H_{32}O_4NBr$; C, 50.27; H, 8.44; N, 3.66; Br, 20.9%. Found: C, 50.36; H, 8.47; N, 4.12; Br, 20.93%.

dl-1α-Ethoxy-2α-hydroxy-3β-aminocyclohexane (X; R = C_2H_5)

dl-1α-Ethoxy-2α,3α-epoxycyclohexane (16.1 g, 0.113 mole) was ammonolyzed with aqueous ethanolic ammonia under the conditions described for *dl*-1β-methoxy-2α,3α-epoxycyclohexane, yielding 16.0 g (88.8%) of *dl*-1α-ethoxy-2α-hydroxy-3β-aminocyclohexane as fine colorless needles, m.p. 133–134°, after recrystallization from ethanol–ether. Calc. for $C_8H_{17}O_2N$: C, 60.35; H, 10.76; N, 8.80%. Found: C, 60.51; H, 10.83; N, 8.73%.

Derivatives of the dl-1-Alkoxy-2-hydroxy-3-aminocyclohexanes

The *dl*-1-alkoxy-2-hydroxy-3-aminocyclohexanes reported above were characterized as their hydrobromides and N-acetyl, N-*p*-nitrobenzoyl, and N-phenylthiourea derivatives. The hydrobromides and N-phenylthiourea derivatives were prepared by standard methods. The N-*p*-nitrobenzoyl derivatives were prepared by Leffler and Adams' procedure (32). The N-acetyl derivatives were obtained by treating the alkoxyaminocyclohexanols with a 10% excess of acetic anhydride at room temperature, followed by evaporation to dryness *in vacuo*, and recrystallization from ethanol–ether. Yields, melting points, and analytical data for the derivatives are given in Table I.

dl-3α-Amino-1α,2β-cyclohexanediol Hydrobromide

(*a*) *From dl-1α-Ethoxy-2β-hydroxy-3α-aminocyclohexane* (IX; R = C_2H_5)

dl-1α-Ethoxy-2β-hydroxy-3α-aminocyclohexane (60.0 g, 0.377 mole) was heated under reflux for 1½ hours with 48% hydrobromic acid (230 ml, 2.0 moles). Most of the excess acid was removed by distillation *in vacuo* but no attempt was made to distill to dryness (cf. McCasland *et al.* (4)). The residue was treated with ether (300 ml) and ethanol (75 ml) and evaporated *in vacuo* to small volume. This operation was repeated, after which 300 ml of ether was added, followed by just sufficient ethanol to produce a clear solution. When the solution was allowed to stand at 4°, *dl*-3α-amino-1α,2β-cyclohexanediol hydrobromide separated as colorless to light-grey rosettes. Yield, 73.1 g (91.4%), m.p. 168–169°. McCasland *et al.* (4) report m.p. 167–168°. Calc. for $C_6H_{14}O_2NBr$: C, 33.98; H, 6.65; N, 6.61; Br, 37.68%. Found: C, 33.89; H, 6.71; N, 6.66; Br, 37.64%.

(*b*) *From dl-1α-Methoxy-2β-hydroxy-3α-aminocyclohexane* (IX; R = CH_3)

dl-1α-Methoxy-2β-hydroxy-3α-aminocyclohexane (35.0 g, 0.241 mole) was subjected to ether cleavage under the conditions described above. Crystallization of the product from ethanol–ether furnished 46.3 g (90.5%) of *dl*-3α-amino-1α,2β-cyclohexanediol hydrobromide as colorless to light-grey rosettes, m.p. 167.5–169°. Admixture of this substance with that obtained in (*a*) above did not depress the melting point. The two samples gave identical infrared spectra, and moved with the same speed in paper chromatograms (R_F 0.40, see Table VI).

Can. J. Chem. Downloaded from www.nrcresearchpress.com by 78.46.186.204 on 09/04/12
For personal use only.

dl-3α-Amino-1α,2β-cyclohexanediol (I)

dl-3α-Amino-1α,2β-cyclohexanediol hydrobromide (60.0 g, 0.283 mole) was dissolved in a solution of sodium hydroxide (11.8 g, 0.286 mole in 100 ml water). Evaporation to dryness *in vacuo* gave a light-tan crystalline residue, which was sublimed at 140° at 0.5 mm to free it from inorganic material. Recrystallization of the sublimate from absolute ethanol yielded 32.4 g (87.4%) of *dl*-3α-amino-1α,2β-cyclohexanediol, m.p. 151°, as colorless prisms. Calc. for $C_6H_{13}O_2N$: C, 54.93; H, 9.99; N, 10.68%. Found: C, 55.05; H, 10.11; N, 10.71%.

dl-3β-Amino-1α,2α-cyclohexanediol Hydrobromide

(*a*) *From dl-1α-Ethoxy-2α-hydroxy-3β-aminocyclohexane* (X; R = C_2H_5)

dl-1α-Ethoxy-2α-hydroxy-3β-aminocyclohexane (14.0 g, 0.88 mole) was subjected to ether cleavage under the conditions described for its isomer. Crystallization from ethanol–ether gave 13.0 g (69.8%) of *dl*-3β-amino-1α,2α-cyclohexanediol hydrobomide as colorless rosettes, m.p. 165.5–167°. Calc. for $C_6H_{14}O_2NBr$: C, 33.98; H, 6.65; N, 6.61; Br, 37.68%. Found: C, 34.31; H, 6.86; N, 6.79; Br, 37.36%.

(*b*) *From dl-1α-Methoxy-2α-hydroxy-3β-aminocyclohexane* (X; R = CH_3)

dl-1α-Methoxy-2α-hydroxy-3β-aminocyclohexane (5.30 g, 0.0365 mole) was subjected to ether cleavage under the conditions described for *dl*-1α-ethoxy-2β-hydroxy-3α-aminocyclohexane. Crystallization from ethanol–ether gave 5.40 g (69.8%) of colorless rosettes, m.p. 165.5–167°. Admixture of this substance with the compound isolated from (*a*) above caused no depression in melting point. The two samples likewise gave identical infrared spectra and moved with the same speed in paper chromatograms (R_F 0.43, see Table VI).

dl-3β-Amino-1α,2α-cyclohexanediol (II)

dl-3β-Amino-1α,2α-cyclohexanediol hydrobromide (14.0 g, 0.066 mole) was converted to the free base by passing a 5% aqueous solution through Amberlite IRA-400 resin in the hydroxide form. Evaporation to dryness *in vacuo* followed by recrystallization from benezene gave 5.90 g (95.3%) of *dl*-3β-amino-1α,2α-cyclohexanediol, m.p. 104–105°, as colorless prisms. Calc. for $C_6H_{13}O_2N$: C, 54.93; H, 9.99; N, 10.68%. Found: C, 55.02; H, 10.00; N, 10.77%.

Derivatives of the dl-3-Amino-1,2-cyclohexanediols

The *dl*-3-amino-1,2-cyclohexanediols were characterized as their N-*p*-nitrobenzoyl, N-phenylthiourea, and triacetyl derivatives. The same methods were used as in preparation of derivatives of the 1-alkoxy-2-hydroxy-3-aminocyclohexanes, except that in preparation of the triacetyl compounds, a 10-fold excess of acetic anhydride was used. Yields, melting points, and analytical data for the derivatives are given in Table II.

N-Phenylthiourea Derivative of dl-trans-2-Aminocyclohexanol

The same method was used as for preparation of the N-phenylthiourea derivatives of the *dl*-1-alkoxy-2-hydroxy-3-aminocyclohexanes. Yield, 93%, m.p. 144.5°. Calc. for $C_{13}H_{18}N_2SO$: C, 62.37; H, 7.25; N, 11.19; S, 12.80%. Found: C, 62.09; H, 7.22; N, 11.29; S, 12.69%.

Paper Chromatography of the 3-Amino-1,2-cyclohexanediols and Derivatives

For paper chromatography 2% solutions of the compounds in water, ethanol, or acetone were applied to unwashed Whatman No. 1 paper (7.5 λ spots). The chromatograms were developed overnight in a glass tank by the descending technique using *n*-butanol – acetic acid – water (25:6:25) as developer. The air-dried chromatograms were sprayed with bromcresol green for detection of the free amines and with ammoniacal

Can. J. Chem. Downloaded from www.nrcresearchpress.com by 78.46.186.204 on 09/04/12
For personal use only.

TABLE VI

R_F VALUES OF 3-AMINO-1,2-CYCLOHEXANEDIOL DERIVATIVES IN *n*-BUTANOL – ACETIC ACID – WATER (25:6:25)

Compound	R_F
1α-Methoxy-2β-hydroxy-3α-aminocyclohexane	0.51
1α-Methoxy-2α-hydroxy-3β-aminocyclohexane	0.55
1α-Ethoxy-2β-hydroxy-3α-aminocyclohexane	0.60
1α-Ethoxy-2α-hydroxy-3β-aminocyclohexane	0.66
α,α-bis-(2β-Hydroxy-3α-ethoxycyclohexyl)amine	0.74
3α-Amino-1α,2β-cyclohexanediol	0.40
3β-Amino-1α,2α-cyclohexanediol	0.43
3α-N-*p*-Nitrobenzamido-1α,2β-cyclohexanediol	0.87
3β-N-*p*-Nitrobenzamido-1α,2α-cyclohexanediol	0.88
2β-Amino-1α-cyclohexanol	0.59

silver nitrate (33) for detection of the N-*p*-nitrobenzoyl derivatives of the aminediols. R_F values are given in Table VI.

Periodate Oxidation of dl-3α-p-Nitrobenzamido-2β,3α-cyclohexanediol and dl-3β-p-Nitrobenzamido-2α,3α-cyclohexanediol

(*a*) *At 25° C*

A 40-mg sample of each aminediol *p*-nitrobenzoyl derivative was treated with 0.1053 *N* paraperiodic acid (20.00 ml) at 25°. Iodometric titrations with sodium arsenite (22) revealed that 0.95 mole of paraperiodic acid was consumed per mole of *cis*-diol derivative in 60 minutes and 0.96 mole of paraperiodic acid was consumed per mole of *trans*-diol derivative in 90 minutes.

(*b*) *At 3° C*

A 20-mg sample of aminediol derivative was dissolved in 50 ml of water at room temperature and the solution was cooled to 3°. At time zero, sodium metaperiodate (10.00 ml, 0.0300 *N*) at 3° was pipetted into the solution, which was stirred constantly in a constant temperature bath at 3°±0.1°. The reaction was allowed to proceed for a specified length of time, after which further reaction was stopped by addition of sodium bicarbonate (2 g, A.R.), sodium arsenite (25.00 ml, 0.0200 *N*), and potassium iodide solution (1 ml, 20%). The consumption of periodate was determined by back-titration with 0.0100 *N* iodine (22) and the quantity of aminediol derivative oxidized calculated. Results are shown in Fig. 5.

Electrophoresis of 3-Amino-1,2-cyclohexanediol Derivatives on Glass Paper

The aminediol derivatives (1% solution in acetone) were spotted on 63×380 mm strips of glass fiber paper (H. Reeve Angel and Co., Inc.) together with D-glucose and 2,3,4,6-tetramethyl-D-glucose as reference compounds. The strips were placed in a water-cooled closed strip-type apparatus (E.C. Apparatus Co., Model No. 401) con-

TABLE VII

M_G VALUES OF 3-AMINO-1,2-CYCLOHEXANEDIOL DERIVATIVES

Compound		M_G
3α-Amino-1α,2β-cyclohexanediol	N-*p*-Nitrobenzoyl derivative	0.00
	N-Phenylthiourea derivative	0.00
3β-Amino-1α,2α-cyclohexanediol	N-*p*-Nitrobenzoyl derivative	0.34
	N-Phenylthiourea derivative	0.44

Can. J. Chem. Downloaded from www.nrcresearchpress.com by 78.46.186.204 on 09/04/12
For personal use only.

taining 0.1 *M* sodium tetraborate solution, and a voltage of 435 at 75 ma was applied for 1 hour. The strips were dried at 100° on a glass plate and sprayed with alkaline permanganate (34) giving yellow spots on a pink to greenish-pink background. The M_G values of the compounds studied are shown in Table VII.

ACKNOWLEDGMENTS

We are indebted to Mr. A. A. Casselman for performing the paper chromatograms described herein, to Mr. R. O. Braun for preparation of a quantity of 1-ethoxycyclohexene-2 chlorohydrin, to Dr. C. E. Hubley and Mr. A. Grey for measurement of the infrared spectra, to Dr. C. T. Bishop for assistance with the electrophoretic experiments, and to Dr. R. U. Lemieux and Dr. R. Y. Moir for a number of helpful discussions.

REFERENCES

1. Mousseron, M., Winternitz, F., and Combes, G. Bull. soc. chim. France, **14**, 79 (1947).
2. Mousseron, M. and Granger, R. Bull. soc. chim. France, **14**, 850 (1947).
3. Mousseron, M., Manon, G., and Combes, G. Bull. soc. chim. France, **16**, 396 (1949).
4. McCasland, G. E., Matchett, T. J., and Hollander, M. J. Am. Chem. Soc. **74**, 3429 (1952).
5. Winstein, S. and Henderson, R. B. *In* Heterocyclic compounds. Vol. I. John Wiley & Sons, Inc., New York. 1950. p. 29.
6. McCasland, G. E., Clark, R. K., and Carter, H. E. J. Am. Chem. Soc. **71**, 637 (1949).
7. Detoeuf, A. Bull. soc. chim. France, **31**, 102 (1922).
8. McRae, J. A., Charlesworth, E. H., and Alexander, D. S. Can. J. Research, B, **21**, 5 (1943).
9. Moir, R. Y. M.A. Thesis, Queen's University, Kingston, Ontario. 1942.
10. McRae, J. A., Moir, R. Y., Haynes, J. W., and Ripley, L. G. J. Org. Chem. **17**, 1621 (1952).
11. Fenton, S. W. M.Sc. Thesis, Queen's University, Kingston, Ontario. 1946.
12. Hawkins, L. R. and Bannard, R. A. B. Can. J. Chem. **36**, 220 (1958).
13. Lemieux, R. U., Kullnig, R. K., and Moir, R. Y. J. Am. Chem. Soc. **80**, 2237 (1958).
14. Gogek, C. J., Moir, R. Y., McRae, J. A., and Purves, C. B. Can. J. Chem. **29**, 938 (1951).
15. Guss, C. O. and Rosenthal, R. J. Am. Chem. Soc. **77**, 2549 (1955).
16. Jones, R. N. and Sandorfy, C. *In* Technique of organic chemistry. Vol. IX. Chemical applications of spectroscopy. Interscience Publishers, Inc., New York. 1956. p. 434.
17. Mousseron, M., Granger, R., Winternitz, F., and Combes, G. Bull. soc. chim. France, **13**, 610 (1946).
18. Bartlett, P. D. J. Am. Chem. Soc. **57**, 224 (1935).
19. Barton, D. H. R., Lewis, D. A., and McGhie, J. F. J. Chem. Soc. 2907 (1957).
20. Henbest, H. B. and Wilson, R. A. L. Chem. & Ind. 659 (1956).
21. Henbest, H. B. and Wilson, R. A. L. J. Chem. Soc. 1958 (1957).
22. Jackson, E. L. *In* Organic reactions. Vol. II. John Wiley & Sons, Inc., New York. 1944. Chap. 8.
23. Wasserman, H. H. *In* Steric effects in organic chemistry. *Edited by* M. S. Newman. John Wiley & Sons, Inc., New York. 1956. p. 378.
24. Price, C. C. and Knell, M. J. Am. Chem. Soc. **64**, 552 (1942).
25. Angyal, S. J. and McHugh, D. J. J. Chem. Soc. 1423 (1957).
26. Boëseken, J. Advances in Carbohydrate Chem. **4**, 189 (1949).
27. Foster, A. B. and Stacey, M. Chem. & Ind. 279 (1953).
28. Angyal, S. J. Chem. & Ind. 1230 (1954).
29. Cookson, R. C. Chem. & Ind. 223 (1954).
30. Snyder, H. R. and Brooks, L. A. Organic syntheses. Collective Vol. II. John Wiley & Sons, Inc., New York. 1943. p. 171.
31. Berlande, A. Bull. soc. chim. France, **9**, 644 (1942).
32. Leffler, M. T. and Adams, R. J. Am. Chem. Soc. **59**, 2256 (1937).
33. Hough, L. Nature, **165**, 400 (1950).
34. Briggs, D. R., Garner, E. F., and Smith, F. Nature, **178**, 154 (1956).

Can. J. Chem. Downloaded from www.nrcresearchpress.com by 78.46.186.204 on 09/04/12
For personal use only.

Can. J. Chem. Downloaded from www.nrcresearchpress.com by 78.46.186.204 on 09/04/12
For personal use only.

THE REACTION OF CYANOGEN BROMIDE WITH THE SODIUM SALTS OF CARBOXYLIC ACIDS

II. THE REACTION OF CYANOGEN BROMIDE WITH THE SODIUM SALTS OF ALIPHATIC ACIDS[1]

D. E. Douglas[2] and Anna Mary Burditt[3]

ABSTRACT

Cyanogen bromide reacts with the sodium salts of lower aliphatic acids at 250–300° C to form an α-keto isocyanate as the primary product. The latter undergoes subsequent pyrolytic decomposition to a nitrile and carbon dioxide. A mechanism is proposed to account for the observed interchange of labelled carbon atoms between the CN group of the cyanogen bromide and the carboxyl group of the salt in the over-all reaction.

INTRODUCTION

In the heterogeneous reaction between cyanogen bromide and sodium benzoate at 250–300° C, it was shown, by the use of carbon-14-labelled reactants, that an interchange of carbon atoms between the CN group of the cyanogen bromide and the carboxyl group of the benzoate occurs according to the following over-all reaction (1):

$$CNBr + RC^*OONa \rightarrow RC^*N + CO_2 + NaBr. \qquad [1]$$

Preliminary experiments with sodium salts of several aliphatic acids and cyanogen bromide under similar conditions (2) seemed to indicate that a different mechanism was in operation, since a significant portion of carbon dioxide carbon originated in the aliphatic carboxyl group. In a more detailed investigation, however, which is described in this communication, it was established that the interchange of carbon atoms in accordance with reaction [1] occurs also when R is aliphatic (R = CH_3, C_2H_5—), although other simultaneously occurring pyrolytic reactions tend to obscure this reaction.

Although the sodium salts of several aliphatic acids were employed in this study, the most significant observations were made with sodium propionate as a reactant. Upon reaction with cyanogen bromide at 250–300° C under the conditions described previously, the latter salt yielded, in addition to the expected propionitrile, carbon dioxide and sodium bromide, two other compounds. Dipropionamide collected as a sublimate in the cooler part of the apparatus.[4] The other product was collected along with propionitrile in the cold trap attached to the pyrolysis tube. Unlike a nitrile, this compound reacted readily with ammonia under anhydrous conditions. The latter material possessed the properties of propionylurea, forming carbon dioxide and acid upon alkaline hydrolysis. In an experiment in which sodium acetate was the starting material, the nitrile fraction was passed through a mixture of glass and fuller's earth at 300° C. The formation of some carbon dioxide afforded additional evidence that the primary product of the reaction of cyanogen bromide with the sodium salt of an aliphatic acid is a compound yielding nitrile and carbon dioxide on pyrolysis, and forming monoacylurea with anhydrous ammonia. This primary product is an α-keto isocyanate, on the basis of the foregoing evidence.

[1]*Manuscript received May 8, 1958.*
Contribution from the Department of Metabolism and Toxicology, The Montreal General Hospital, Montreal, Quebec.
[2]*Present Address: Department of Metabolism and Toxicology, The Montreal General Hospital, Montreal, P.Q.*
[3]*Present Address: Faculty of Medicine, Queen's University, Kingston, Ontario.*
[4]*Zappi and Bouso (3) have reported the formation of monoamides in the reaction of sodium acetate and sodium propionate with cyanogen chloride.*

The reaction of cyanogen bromide with the sodium salt of an aliphatic acid may therefore be summarized as follows:

$$CNBr + RCOONa \rightarrow RCONCO + NaBr$$

$$RCONCO \rightarrow RCN + CO_2.$$

Only with lower aliphatic acids and under high vacuum is it possible for some of the α-keto isocyanate to escape complete pyrolysis. In the previously investigated reaction of sodium benzoate with cyanogen bromide, benzoyl isocyanate is undoubtedly formed initially, but it immediately pyrolyzes because of its low volatility.

To explain the observed interchange of carbon atoms between the CN group of the cyanogen bromide and the carboxyl group, the following mechanism is postulated:

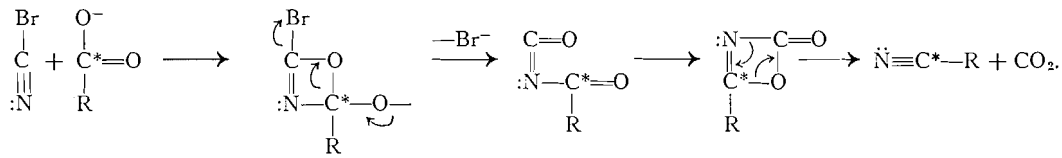

An investigation of the pyrolysis of pure propionyl (isocyanate-C^{14}) should confirm this mechanism.

EXPERIMENTAL

The apparatus and procedure have already been described in detail (1). Approximately one millimole of the aliphatic acid sodium salt was weighed out and was suspended on a mixture of 0.5 g each of ignited fuller's earth and pulverized glass (40 mesh) by evaporation of a slurry of these materials in water. When a C^{14}-labelled sodium salt was employed, a known amount of activity was added to the weighed sample of inactive sodium salt in solution, before the latter was mixed with the fuller's earth and glass. After evaporation of the slurry, the mixture was transferred to the U-tube of the pyrolysis apparatus, and was heated in a Wood's metal bath to the appropriate temperature. The pyrolysis tube was connected, through a spiral trap cooled in liquid nitrogen, to a high-vacuum line. Slightly more than the equivalent quantity of cyanogen bromide was allowed to diffuse through the contents of the U-tube, while the latter was evacuated continuously. The carbon dioxide which collected in the spiral was converted to barium carbonate after fractionation with dry ice – acetone. The nitrile fraction was partially separated from unreacted cyanogen bromide by distillation on the vacuum line, and was reduced in ethereal solution with lithium aluminum hydride for characterization and radioassay. After decomposition of the lithium aluminum complex with dilute sulphuric acid, the amine was distilled from the mixture, after the latter had been rendered alkaline with sodium hydroxide, in a semimicro-Kjeldahl apparatus. The distillate was collected in excess dilute hydrochloric acid. The amine hydrochloride remaining after evaporation of this solution was recrystallized from an appropriate solvent. Ethanol was employed for ethylamine hydrochloride, and chloroform for propylamine and higher amine hydrochlorides. Known amounts of the hydrochlorides were plated on stainless-steel planchets for radioassay. Stearonitrile was plated directly, after purification by high-vacuum sublimation. Barium carbonate was plated on aluminum disks from a slurry. Appropriate self-absorption corrections were applied where necessary (4). Counting was performed with a helium and alcohol flow-type geiger counter with an approximately 2π geometry.

Can. J. Chem. Downloaded from www.nrcresearchpress.com by 78.46.186.204 on 09/04/12
For personal use only.

Pyrolysis of Nitrile Fraction from an Experiment with Sodium Acetate

Sodium acetate (4 millimoles) was suspended on powdered glass (40 mesh), and this mixture was placed in the U-tube of the apparatus previously described. Cyanogen bromide in slight excess was passed through the U-tube while the latter was evacuated continuously. Carbon dioxide was fractionated with dry ice – acetone and converted to barium carbonate. Yield of $BaCO_3$ 0.2227 g (28% based on acetate). The liquid remaining in the spiral trap was recycled through a mixture of fuller's earth and powdered glass at 304° C under high vacuum. An additional quantity of carbon dioxide was formed during pyrolysis, yielding 0.0945 g of barium carbonate.

Alkaline Hydrolysis of Propionylurea

The liquid reaction product from two experiments in which sodium propionate-1-C^{14} was allowed to react with cyanogen bromide under the conditions previously described was treated with ammonia in ether under anhydrous conditions. To the solid obtained from this reaction was added carrier propionylurea (5), the mixture was homogenized by crystallization, and the solid was sublimed under high vacuum. To a solution of the sublimate (5.15 mg) was added carrier propionylurea (25.9 mg) and the whole was evaporated to dryness in a bomb tube. The residue was hydrolyzed with saturated barium hydroxide solution (4 ml) at 100° C in the sealed tube overnight. A quantitative yield (52.7 mg) of barium carbonate was obtained, of specific activity 22,850 counts/minute millimole. The specific activity of the material before hydrolysis was 32,800 counts/minute millimole. A small portion of the initial activity was present in the acid recovered from the hydrolysis.

PAPER CHROMATOGRAPHY OF AMINE HYDROCHLORIDES AND OTHER COMPOUNDS

The amine hydrochlorides obtained from the lithium aluminum hydride reduction of the product nitriles were chromatographed on Whatman No. 1 filter paper by the ascending technique. For comparison, authentic samples of amine hydrochlorides were run in adjacent positions. Butanol saturated with 25% aqueous acetic acid was the developing solvent. The amines were detected with ninhydrin (6).

Propionylurea could not be distinguished from propionamide when these substances were chromatographed with the butanol – acetic acid – water medium as both had R_f values of 0.74. To facilitate detection on paper, these compounds were labelled with carbon-14 by synthesis from propionic acid-1-C^{14}. The developed chromatograms were placed in contact with Eastman No-Screen X-Ray film.

Dipropionamide-1-C^{14} with butanol–water as the developing solvent had an R_f of 0.91. Several unidentified spots with R_f values less than 0.74 appeared faintly on radioautographs of chromatograms of the nitrile fraction from the sodium propionate – cyanogen bromide reaction after this fraction had been treated with anhydrous ammonia. α-Cyanopropionic acid and α-isocyanopropionic acid were shown to be absent by chromatography of these substances for comparison.

RESULTS AND DISCUSSION

Data for typical experiments are presented in Tables I and II. It is evident that a significant portion of the carbon dioxide carbon is derived from the cyanogen bromide molecule. Simultaneously occurring pyrolytic reactions, other than the formation of an α-keto isocyanate and its decomposition to a nitrile and carbon dioxide, may explain in part the distribution of radioactivity among the products. Moreover, the formation and

Can. J. Chem. Downloaded from www.nrcresearchpress.com by 78.46.186.204 on 09/04/12
For personal use only.

pyrolysis of a part of the α-keto isocyanate by a route other than the postulated one, could also account for this distribution of activity. Such reactions as decarboxylation

TABLE I

DATA FOR THE REACTION OF CNBr WITH SODIUM SALTS OF C^{14}-CARBOXYL ACIDS

Salt	Temperature, °C	Specific activities counts/minute millimole			Amine from reduction of nitrile
		Na salt	$BaCO_3$	Amine salt	
Sodium acetate	274–277	21,000	4,740	15,200	Ethylamine
		17,650	8,120	—	
		17,650	1,675	—	
Sodium propionate	267–273	48,100	6,440	47,700	Propylamine
Sodium butyrate	300–303	453,300	44,400	321,500	Butylamine
Sodium valerate	300–303	64,400	10,230	64,000	*n*-Amylamine
Sodium stearate	274–277	79,500	38,300	53,000*	

*Stearonitrile was counted directly, after purification by distillation from a Späth bulb *in vacuo*.

TABLE II

DATA FOR THE REACTION OF C^{14}-NBr WITH SODIUM SALTS OF CARBOXYLIC ACIDS

Salt	Temperature, °C	Specific activities counts/minute millimole		
		CNBr	$BaCO_3$	Amine salt
Sodium acetate	270–271	163,000	72,300	73,300
Sodium propionate	271–272	163,000	69,900	13,800
Sodium butyrate	267–274	163,000	53,100	6,060
Sodium trimethylacetate	294–297	883,000	576,000	231 counts/minute mg (Unidentified reduced product)
Sodium α-bromopropionate	287–291	318,200	29,080	—

and dehydration as well as the formation of free aliphatic acid in the presence of traces of hydrogen bromide are all possible under the experimental conditions employed, and one or more of these is probably responsible for the observed formation of a diamide. Variation in reaction conditions from one aliphatic acid to another is in part the result of the decreasing volatility of the intermediate α-keto isocyanate with increasing molecular weight. Thus, this intermediate was present in the nitrile fractions from the sodium acetate and propionate reactions, but with higher acids, and especially with benzoic acid, the α-keto isocyanate could have only a momentary existence in the hot zone of the pyrolysis apparatus. The postulated formation of an α-keto isocyanate in the reactions investigated offers a logical explanation of the observed interchange of carbon atoms between cyanogen bromide and the carboxyl group through the mechanism described earlier in this communication.

ACKNOWLEDGMENT

The authors wish to thank Dr. Karl Wiesner for his helpful criticism and advice.

REFERENCES

1. DOUGLAS, D. E., ECCLES, J., and ALMOND, A. E. Can. J. Chem. **31**, 1127 (1953).
2. DOUGLAS, D. E. and ALMOND, A. E. Unpublished results.
3. ZAPPI, E. and BOUSO, O. Anales asoc. quím. arg. **35**, 137 (1947).
4. CALVIN, M. *et al.* Isotopic carbon. John Wiley & Sons, Inc., New York. 1949.
5. STOUGHTON, R. W. J. Org. Chem. **2**, 514 (1938).
6. BLOCK, R. J., DURRUM, E. L., and ZWEIG, G. A manual of paper chromatography and paper electrophoresis. Academic Press, Inc., New York. 1956.

Can. J. Chem. Downloaded from www.nrcresearchpress.com by 78.46.186.204 on 09/04/12
For personal use only.

Can. J. Chem. Downloaded from www.nrcresearchpress.com by 78.46.186.204 on 09/04/12
For personal use only.

STUDIES ON THE MECHANISMS OF CYCLIZATION OF RING A OF STEROIDS DURING THE REFORMATSKY REACTION[1]

R. D. H. HEARD,[2] G. A. BALLA, J. R. JAMIESON,[3] AND P. ZIEGLER[4]

ABSTRACT

The Reformatsky reaction of 3,5-*seco*-5-ketocholestan-3-oic acid methyl ester with methyl bromoacetate yielded 2-carbohydroxycholestenone, cholestenone, and 4-carbomethoxycholestenone. The appearance of these products indicated that cyclization of ring A proceeded along two different paths; this conclusion was confirmed by the use of methyl bromoacetate-1-C^{14} and -2-C^{14}.

One of the earliest successful attempts (1) at introduction of radioactive carbon 14 into ring A of the steroid nucleus involved the Reformatsky reaction of 3,5-*seco*-5-ketocholestan-3-oic acid methyl ester (I*b*) with carboxyl-labelled methyl bromoacetate. In these experiments, the crude Reformatsky products were cyclized, hydrolyzed, and decarboxylated by conventional methods to provide cholestenone-3-C^{14} (XI*) in 32% yield. The molar radioactivity count of XI* was found to be the same as that of the carboxyl-labelled methyl bromoacetate used, and largely on the basis of this finding the conclusion was reached that the reaction proceeded entirely through the intermediates III*, IV*, and V*. This sequence of reactions was postulated by Turner (1) to involve abstraction of a proton from III* at position 2, followed by transannular ring closure and elimination of methoxide ion to give the keto-lactone IV*. The latter, in turn, would then lose a proton at position 4 and be transformed readily into the stable anion V*. It was also pointed out that removal of a proton, alpha to the carbomethoxy group in III*, would lead to a less stable four-membered oxygen intermediate; the latter, after hydrolysis and dehydration, would be expected to decarboxylate yielding inactive cholestenone (XI). There is considerable evidence in support of Turner's view that Reformatsky reactions of δ-ketoesters can provide intermediate lactones of the type III. Thus, it was shown (2) that methyl β-(1-methyl-2-ketocyclohexyl)propionate and ethyl bromoacetate reacted under the usual Reformatsky conditions to yield 21% of 2-keto-3-carboxy-10-methyl-$\Delta^{1,9}$-octahydronaphthalene. The isolation of this acid by extraction from the crude reaction products with 2% ammonium hydroxide can only be explained by assuming the formation of an intermediate six-membered lactone. Similarly, 1-tetralone-2-β-propionic acid methyl ester on treatment with methyl bromoacetate and zinc provided 1-acetic acid methyl ester-3,4-dihydronaphthalene-2-β-propionic acid (3). It has been known for long that γ-ketoesters undergo Reformatsky reactions to yield γ-lactones. Ethyl levulinate, for example, was found to afford amongst other products the lactone of β-hydroxy-α,β-dimethyladipate, when condensed with methyl α-bromopropionate (4). Ethyl β,β-dimethyllevulinate and ethyl bromoacetate produced over 50% of δ-carbethoxy-β,β,γ-trimethyl-γ-valerolactone (5).

The studies to be described herewith were undertaken to determine more conclusively the mechanisms of ring closure during the Reformatsky reaction of the δ-ketoester I*b*.

[1]*Manuscript received April 25, 1958.*
Contribution from the Department of Biochemistry, McGill University, Montreal, Quebec. Much of this work was done by P. Ziegler as part of the requirements for the Ph.D. degree.
[2]*Deceased.*
[3]*Present address: Charles E. Frosst & Co., Montreal, Quebec.*
[4]*Enquiries to be made to this author. Present address: Research and Development Laboratories, Canada Packers Ltd., Toronto, Ontario.*

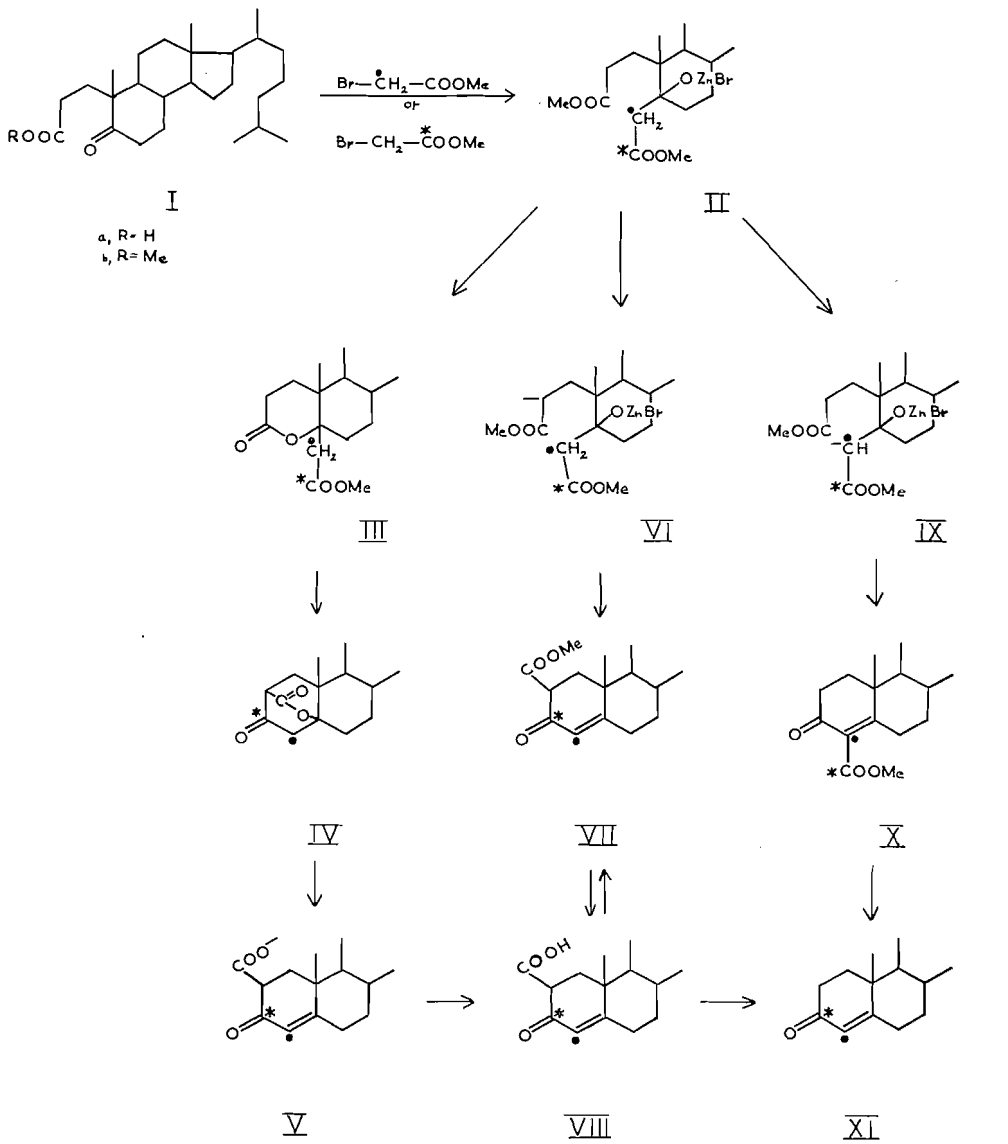

The experiments were usually carried out in refluxing benzene using tracer amounts of C^{14}-labelled methyl bromoacetate, and the products, from which zinc salts were removed by washings with dilute mineral acid, were finally chromatographed on neutral alumina. Elution from the column with hexane–benzene separated four different compounds. The first fraction consisted of cholestenone (XI* or XI•), identified by melting point, optical rotation, ultraviolet absorption, and comparison with an authentic specimen of XI. Regardless of whether methyl bromoacetate-1-C^{14} or -2-C^{14} was employed, the crystals of cholestenone proved to be radioactive. The second compound obtained from the alumina failed to crystallize and was not radioactive; it was saponified to give I*a*, and therefore represented unreacted starting material. The third fraction was a crystalline solid which was radioactive, both when methyl bromoacetate-1-C^{14} and -2-C^{14} were

Can. J. Chem. Downloaded from www.nrcresearchpress.com by 78.46.186.204 on 09/04/12
For personal use only.

used. It analyzed correctly for a carbomethoxycholestenone, and on the basis of the following evidence could be quite definitively assigned the structure of 4-carbomethoxycholestenone (X* or X•). The material exhibited maximum absorption in the ultraviolet region at 243.5 mμ (log ε = 4.14), characteristic of an α,β-unsaturated ketone. The known fact (2) that the presence of a carbomethoxy group in cross-conjugation with an α,β-unsaturated ketone does not affect the latter's absorption maximum in the ultraviolet should be noted in this case. Examination in the infrared region showed bands at 5.74 μ and at 5.95 μ, representative of the carbonyl group of an ester and a Δ^4-3-ketone respectively. The compound did not give a coloration with alcoholic ferric chloride solution and failed to react with sodium in benzene; this evidence, indicative of the absence of an active hydrogen, can be accommodated by 4-carbomethoxycholestenone (X), but not by its isomer VII. While the unknown compound, assigned structure X, was resistant to alkaline hydrolysis, probably because its resonance structures do not permit nucleophilic attack at the exocyclic carbon atom attached to C-4, it readily provided cholestenone on acid treatment. The isomer VII on the other hand would be expected to saponify in the normal fashion, since resonance in this system does not prevent carbonium ion formation at the exocyclic carbon atom attached to C-2; in fact, it was found that 2-carbomethoxycholestenone (VII) saponified readily under mild conditions. That the unknown compound was indeed 4-carbomethoxycholestenone (X) was shown conclusively by the tracer technique. It was found that acid hydrolysis of the carbomethoxycholestenone, obtained with methyl bromoacetate-2-C^{14}, gave rise to radioactive cholestenone (XI•); however, the acid hydrolysis of the intermediate obtained with methyl bromoacetate-1-C^{14} provided inactive cholestenone (XI).

The fourth and last compound eluted from the column of alumina was found to contain twice the radioactivity count of XI• (or XI*) and X• (or X*) obtained in the same experiment. It was therefore assumed that 2 moles of acetate had been incorporated into its structure. Since cholestenone could not be derived from it by acid or alkaline treatment, this compound was not examined further.

In one Reformatsky reaction, using inactive reagent, the crude products were analyzed for the presence of Δ^4-3-ketone by ultraviolet spectrophotometry, both before and after treatment with cold dilute acid. Since the two assays showed the presence of 30–35% of Δ^4-3-ketone, it was concluded that cyclization and elimination of bromozinc methoxide occurred during the Reformatsky reaction, and not on acidification or chromatography on alumina. That Dieckmann type cyclizations occur during Reformatsky reactions with δ-keto esters has previously been reported (6, 7, 8). It was of interest to note that these analytical figures agreed well with the amounts of Δ^4-3-ketones (XI plus X) usually isolated from the chromatograms. The reaction products were then separated into neutral and acidic constituents by washing with dilute sodium carbonate solution; the two fractions contained 23% and 8% of Δ^4-3-ketones respectively. The acid fraction was crystallized to yield a compound, m.p. 126–128° C, giving an intense green color with ferric chloride solution. It was assigned structure VIII on the basis of this evidence and because it provided cholestenone (XI) on pyrolysis. Methylation of VIII afforded the corresponding methyl ester (VII), which also produced a green coloration with ferric chloride solution and showed an ultraviolet absorption maximum at 244.5 mμ (log ε = 4.21). Elemental analyses for VII (and its 2,4-dinitrophenylhydrazone) were not entirely satisfactory, probably because of contamination with traces of cholestenone. On mild saponification, VII yielded VIII.

A careful examination of these results proves that, under the experimental conditions used, two different mechanisms of cyclization are operative. When the Reformatsky

Can. J. Chem. Downloaded from www.nrcresearchpress.com by 78.46.186.204 on 09/04/12
For personal use only.

reaction was carried out with methyl bromoacetate-1-C^{14}, the cholestenone (XI*) and the 4-carbomethoxycholestenone (X*), isolated from the column of alumina, were both radioactive. Since acid hydrolysis of X* yielded inactive XI, the reaction path leading to X* must be different from that leading to XI*. In other words, 4-carbomethoxycholestenone (X) is not the precursor of the cholestenone eluted from the chromatograms. The sequence of reactions leading to the formation of X is postulated to proceed by a Dieckmann cyclization of the Reformatsky ester II, via the intermediate IX. The isolation of 2-carbohydroxycholestenone (VIII) from the alkaline washings of the reaction products and the demonstration of its facile decarboxylation indicate that VIII is the precursor of the cholestenone eluted from the chromatogram. The isolation of the acid VIII lends support to Turner's hypothesis (1) of the formation of the intermediate lactonic ester III. Dieckmann cyclization of the Reformatsky ester II via VI (in the opposite sense as was postulated before) would be expected to provide VII. But since VII failed to appear amongst the isolated reaction products, the second mechanism of cyclization is believed to proceed via the intermediates III, IV, V, and VIII. In conclusion, it should be noted that the two different cyclization reactions occur to the same extent, as judged by the yields of X and XI.

EXPERIMENTAL

All melting points have been corrected. The optical rotations were determined in chloroform solution, the ultraviolet spectra in ethanol (unless otherwise stated), and the infrared spectra, obtained by Dr. R. N. Jones, of the National Research Council, Ottawa, in carbon disulphide. Microanalyses were carried out by Mr. E. Thommen, Basel, Switzerland.

Methyl bromoacetate-1-C^{14} and -2-C^{14} were kindly prepared by Dr. B. Belleau; the radioactivity counts of these reagents are not known. The radioactivities of the steroids were determined in the flow Q-gas counter (Nuclear Instrument and Chemical Corporation) and are expressed in counts per minute per milligram.

Cholestenone-4-C^{14} (XI) and 4-Carbomethoxycholestenone-4-C^{14} (X*)*

3,5-*seco*-5-Ketocholestan-3-oic acid (I*a*; 5 g; 12.3 millimoles) was treated with an ethereal solution of diazomethane, the ether was evaporated, and the residual oil dried *in vacuo*. Absolute anhydrous benzene (50 ml), a crystal of iodine, activated zinc (2.5 g), and methyl bromoacetate-2-C^{14} (3.8 g; 25 millimoles) were added to the dried residue. The mixture was refluxed for 3.5 hours, during which time a white, crystalline precipitate formed and gradually the solution turned brown. More activated zinc (1.5 g) was added during the first ½ hour of refluxing. After it had been cooled, the mixture was diluted with ether and dilute hydrochloric acid, the solvent extract was washed five times with dilute acid, then with water, dried over sodium sulphate, filtered, and evaporated to dryness. The yellow, oily residue (4.65 g) could not be crystallized; it was methylated with diazomethane and subsequently chromatographed on activated alumina (100 g), using 200 ml portions of eluant.

Fractions 5–11 were combined to yield, after recrystallization from ether–methanol, 650 mg (14%) of cholestenone-4-C^{14} (XI*), m.p. 79–80°, $[\alpha]_D^{19}$ +89.9°, showing maximum ultraviolet absorption at 242.5 mμ (log ε = 4.18) and counting at 3200.

Fractions 12–19 could not be crystallized; they were saponified for 2 hours with 5% methanolic potassium hydroxide to yield, after working up, 930 mg (19%) of crystals, m.p. 155°, giving no depression on mixed melting point with authentic 3,5-*seco*-5-ketocholestan-3-oic acid (I*a*). This recovered starting material was not radioactive.

Can. J. Chem. Downloaded from www.nrcresearchpress.com by 78.46.186.204 on 09/04/12
For personal use only.

Fraction No.	Eluant in % by volume		Eluate		
	Hexane	Benzene	Weight, mg	M.p.	Counts min^{-1} mg^{-1}
1– 4	100	0	3	oil	—
5–11	87.5	12.5	887	79–80	3200
12–19	70	30	1300	oil	0
20–26	50	50	746	154	3600
27–32	40	60	432	154	
33–38	25	75	420	155	6800
39–43	10	90	252	155	
44–47	0	100	166	153	
48–49	100 Ether		150	oil	—
50–51	100 Methanol		224	oil	—
			4580		

Fractions 20–32 were crystallized from ether–hexane to provide 850 mg (16%) of 4-carbomethoxycholestenone-4-C^{14} (X*), m.p. 154° and $[\alpha]_D^{19}$ +89.4°; this compound gave no coloration with tetranitromethane or alcoholic ferric chloride, did not react with sodium in benzene, but developed a purple color with the Zimmermann reagent; it showed an ultraviolet maximum at 243.5 mμ (log ϵ = 4.14) and in the infrared region its maxima were at 5.75 μ and 5.95 μ. Anal. Calc. for $C_{29}H_{46}O_3$: C, 78.68; H, 10.47; OCH_3, 7.01. Found: C, 78.89; H, 10.48; OCH_3, 6.90.

Fractions 33–47, crystallized from ether–hexane, yielded 650 mg (10%) of material, m.p. 155°, and gave marked depression on mixed melting point with *Ia* and X*. This material gave no color reactions with alcoholic ferric chloride, tetranitromethane, or the Zimmermann reagent and was transparent through the ultraviolet range of the spectrum. Its radioactivity count was 6800. Attempts at conversion of this compound to cholestenone by vacuum distillation, saponification, or acid hydrolysis failed. Microanalyses indicated the presence of one methoxy group and the formula $C_{31}H_{50}O_5$.

2,4-Dinitro-phenylhydrazone of X

Compound X (100 mg) and 2,4-dinitro-phenylhydrazine (300 mg) were refluxed for 15 minutes in 95% ethanol (30 ml). The hot solution was then treated with concentrated hydrochloric acid (2 ml) and refluxed for an additional 15 minutes. After it had been cooled, the precipitate was filtered off, washed with ethanol, then with hexane, and dried. The orange hydrazone had m.p. 198–200°. Anal. Calc. for $C_{35}H_{50}O_6N_4$: C, 67.50; H, 8.09; N, 9.00. Found: C, 67.49; H, 8.35; N, 9.25.

Acid Hydrolysis of 4-Carbomethoxycholestenone-4-C^{14} (X)*

Compound X* (200 mg) was refluxed for 15 hours in glacial acetic acid (12.5 ml) and concentrated hydrochloric acid (3 ml). The solution was then diluted with water, extracted with ether, and the solvent extract washed twice with water, three times with dilute sodium carbonate, and again with water. The ether solution was dried, then evaporated to yield 170 mg of an oily residue which on crystallization from ether–methanol gave 147 mg (85%) of cholestenone-4-C^{14} (XI*), m.p. 79–80°, and counting at 4000.

Saponification of 4-Carbomethoxycholestenone (X)

The ester X (200 mg) was refluxed for 2 hours in 5% methanolic potassium hydroxide (20 ml). After addition of water, most of the methanol was evaporated *in vacuo* and the residue was extracted with ether. The solvent extract, washed with water to neutrality,

Can. J. Chem. Downloaded from www.nrcresearchpress.com by 78.46.186.204 on 09/04/12
For personal use only.

yielded, after drying over sodium sulphate, filtration, and evaporation of the ether, 172 mg of material; this was crystallized from methanol to give unreacted starting material, m.p. 153–154°, no depression on mixed melting point with X.

Cholestenone-3-C^{14} (XI) and 4-Carbomethoxycholestenone-C^{14} (X*)*

The experimental procedure employed was the same as that described for the preparation of X• and XI•, except that different quantities of reagents were used and that carboxyl-labelled methyl bromoacetate was substituted for the corresponding methylene-labelled compound.

The dry residue obtained after methylation of *Ia* (3 g; 7.4 millimoles) was reacted with zinc (2 g), a crystal of iodine, and methyl bromoacetate-1-C^{14} (2.28 g; 14.9 millimoles) in benzene (35 ml). Chromatography of the products yielded 245 mg (9%) of cholestenone-3-C^{14} (XI*), m.p. 79–81°, counting at 1.5×10^4 min^{-1} mg^{-1}; 1.02 g (34%) of non-radioactive starting material (*Ia*), m.p. 153–154°; 205 mg (8%) of 4-carbomethoxycholestenone-C^{14} (X*), m.p. 154° and counting at 1.4×10^4 min^{-1} mg^{-1}; 160 mg (4%) of material, m.p. 154–155°, counting at 2.4×10^4 min^{-1} mg^{-1}.

Acid Hydrolysis of 4-Carbomethoxycholestenone-C^{14} (X)*

Compound X* (100 mg), m.p. 154° and counting at 1.4×10^4 min^{-1} mg^{-1}, was refluxed for 15 hours with glacial acetic acid (7.5 ml), concentrated hydrochloric acid (4 ml), and dioxane (2 ml). The solution was diluted with water and extracted with ether, the solvent extract was washed successively with water, dilute carbonate, and again with water. The neutral ethereal solution was dried over sodium sulphate, filtered, and evaporated to yield 98 mg of an oily residue, which was chromatographed on 5 g of alumina, using 10-ml portions of eluant. The fractions, obtained with benzene–hexane (3:7, 1:1, and 4:1), were crystallized from ether–methanol to provide 70 mg of cholestenone (XI), m.p. 80° and counting at 80 min^{-1} mg^{-1}. This very low activity could not be removed either by vacuum distillation of a sample of this cholestenone or by repeated crystallization from ether–methanol; it is attributed to slight contamination. Further elution of the alumina column with benzene and ether yielded 27 mg of residue. This material was crystallized from ether–hexane to give unreacted starting material, m.p. 149–152°, with a radioactivity of 1.5×10^4; it did not give a depression on mixed melting point with X*.

Quantitative Analysis for α,β-Unsaturated 3-Ketones in the Products of the Reformatsky Reaction by Ultraviolet Spectrophotometry

3,5-*seco*-5-Ketocholestan-3-oic acid (*Ia*; 3 g; 7.4 millimoles) was methylated with ethereal diazomethane and the ether evaporated. The residue, after thorough drying *in vacuo*, was then dissolved in anhydrous benzene (30 ml) and treated with zinc (2 g), a crystal of iodine, and methyl bromoacetate (2.28 g; 14.9 millimoles). This mixture was refluxed gently for 2 hours, then cooled. A sample (0.1 ml), pipetted out of the solution, was evaporated to remove the benzene, and then dissolved in anhydrous ether (100 ml). This ethereal solution showed an ultraviolet maximum at 243 mμ ($\log I_0/I_x = 1.44$). On the basis of molecular weight (400) and extinction coefficient (15,000), 0.96 g of Δ^4-3-ketone was calculated to be present.

The benzene solution was then diluted with ether and cold dilute hydrochloric acid, the aqueous layer was discarded, and the solvent extract washed with water. Again a sample (0.25 ml) was pipetted out of the ether–benzene extract (72 ml), the solvents were evaporated, and the residue from the sample dissolved in ethanol (100 ml). This

Can. J. Chem. Downloaded from www.nrcresearchpress.com by 78.46.186.204 on 09/04/12
For personal use only.

solution exhibited an ultraviolet maximum at 242 mμ (log $I_0/I_x = 1.2$); it was therefore calculated that 0.92 g of Δ^4-3-ketone was contained in the crude acidified Reformatsky reaction products.

The ether–benzene extract, after dilution with more ether, was washed three times with portions (30 ml) of 5% sodium carbonate solution, then with water until the washings were neutral. A sample (0.54 ml) of the neutral solvent phase (135 ml) was evaporated *in vacuo* and the residue dissolved in ethanol (100 ml). The alcoholic solution showed a maximum in the ultraviolet at 242 mμ (log $I_0/I_x = 1.05$), indicating that 0.7 g of Δ^4-3-ketone was present in the neutral solvent extract.

The carbonate washings were acidified immediately, extracted with ether, and the solvent extract washed several times with water; it was dried over sodium sulphate, filtered, and finally evaporated to dryness to yield an oily residue (275 mg). A small part (3 mg) of this residue was dissolved in 100 ml of ethanol; the resulting solution showed an ultraviolet maximum at 242 mμ (log $I_0/I_x = 0.93$), which demonstrated the presence of 230 mg of Δ^4-3-ketone in the acid fraction.

Isolation of 2-Carbohydroxycholestenone (VIII)

The acid fraction (275 mg), obtained in the preceding experiment, was crystallized from ether–hexane to yield 100 mg of material, m.p. 118–121°; recrystallization from ether gave m.p. 126–128° (the melted crystals resolidified on cooling, then remelted at 75–85°). This substance gave a yellow color with tetranitromethane, an intense green with alcoholic ferric chloride, but was negative in the Zimmermann test. It exhibited a maximum absorption in the ultraviolet at 242 mμ (log $\epsilon = 4.23$).

The mother liquor of this acid fraction on standing in aqueous ethanol gave cholestenone (XI), m.p. 81–82°, no depression on mixed melting point with authentic XI. It was therefore concluded that VIII decarboxylated partially during extraction and/or isolation procedures.

Pyrolysis of VIII

Distillation of VIII, m.p. 126–128°, *in vacuo* (0.1 mm) at 185–193° provided a distillate which readily crystallized from ether–methanol to yield quantitatively cholestenone (XI), m.p. 78–80°.

2-Carbomethoxycholestenone (VII)

Compound VIII was methylated with ethereal diazomethane, the ether solution washed with water, dried over sodium sulphate, filtered, and the filtrate evaporated *in vacuo*. The residue crystallized with difficulty from aqueous methanol to give a substance (VII) of m.p. 91–93°; recrystallization from methanol gave m.p. 102–104° and $[\alpha]_D^{19}$ +91°. This material produced a green color with ferric chloride solution, showed an ultraviolet maximum at 244.5 mμ (log $\epsilon = 4.21$), and exhibited carbonyl absorption bands in the infrared region at 5.73 μ and at 5.96 μ. Anal. Calc. for $C_{29}H_{46}O_3$: C, 78.68; H, 10.47. Found: C, 79.07; H, 10.95.

2,4-Dinitro-phenylhydrazone of VII

A solution of VII (40 mg) and 2,4-dinitro-phenylhydrazine (150 mg) in ethanol (35 ml) was refluxed for ½ hour. After cooling, concentrated hydrochloric acid (2 ml) was added and the solution was then kept at 20° for several hours. The precipitate which had formed was filtered off, washed with ethanol and hexane, and dried *in vacuo*. The orange crystals had m.p. 213–215°. Anal. Calc. for $C_{35}H_{50}O_6N_4$: C, 67.50; H, 8.09; N, 9.00. Found: C, 66.68; H, 7.91; N, 8.92.

Can. J. Chem. Downloaded from www.nrcresearchpress.com by 78.46.186.204 on 09/04/12
For personal use only.

Saponification of 2-Carbomethoxycholestenone (VII)

Compound VII (75 mg) and potassium carbonate (50 mg) were dissolved in methanol (15 ml) and water (1 ml). The solution, after standing at 20° for 48 hours, was diluted with water and extracted with ether. The solvent extract provided a neutral fraction (22 mg) which failed to crystallize; the acid fraction (50 mg), obtained from the aqueous carbonate phase, crystallized from ether, giving material of m.p. 124–125°. This substance (VIII) gave no depression on mixed melting point with VIII.

REFERENCES

1. TURNER, R. B. J. Am. Chem. Soc. **72**, 579 (1950).
2. DREIDING, A. S. and TOMASEWSKI, A. J. J. Org. Chem. **19**, 241 (1954).
3. BACHMANN, W. E. and JOHNSON, G. D. J. Am. Chem. Soc. **71**, 3463 (1949).
4. HARDING, V. J. J. Chem. Soc. 1590 (1912).
5. BAUMGARTEN, H. E. and GLEASON, D. C. J. Org. Chem. **16**, 1658 (1951).
6. MUKHERJI, P. C. Sci. and Culture, **11**, 574 (1946).
7. DUTT, P. and BANERJEE, D. K. Sci. and Culture, **12**, 507 (1947).
8. ADAMSON, P. S., MCQUILLIN, F. C., ROBINSON, R., and SIMONSEN, J. L. J. Chem. Soc. 1576 (1937).

Can. J. Chem. Downloaded from www.nrcresearchpress.com by 78.46.186.204 on 09/04/12
For personal use only.

Can. J. Chem. Downloaded from www.nrcresearchpress.com by 78.46.186.204 on 09/04/12
For personal use only.

THE SOLUBILITY OF ALUMINUM HYDROXIDE IN ACIDIC AND BASIC MEDIA AT 25° C[1, 2]

K. H. GAYER, L. C. THOMPSON, AND O. T. ZAJICEK

ABSTRACT

The solubility of $Al(OH)_3$ was measured in NaOH and $HClO_4$ solutions. Possible reactions of $Al(OH)_3$ in dilute NaOH and $HClO_4$ solutions are indicated along with the calculated constants. The amphoteric hydroxide was found to be more acidic than basic. The isoelectric point of $Al(OH)_3$ was determined to be pH 7.7.

HISTORICAL

The amphoteric nature of aluminum hydroxide has been studied by other investigators, but owing to incomplete data the extent of its amphoterism is still not entirely determined. Its isoelectric point has not been previously determined.

A number of equilibrium constant values are tabulated below:

Source	Equilibrium constant	Value
Heyrovsky (1)	Solubility product	1.06×10^{-33} at 25° C
Heyrovsky (1)	Ion product of aluminic acid	35×10^{-14} at 25° C
Kruyt and Troelstra (2)	Solubility product	1.00×10^{-32} at 25° C
Wood (3)	Acid dissociation constant	6.30×10^{-13} at 25° C
Slade (4)	Acid monobasic dissociation product approx. constant	1×10^{-10}

Hildebrand (5), in his study on the solubility of aluminum hydroxide, claimed that it dissolved as an acid. This claim was supported by the slight break in the solubility curve corresponding to the addition of another equivalent of base. Heyrovsky (6) stated that aluminum hydroxide dissolves in alkalies as follows:

$$Al(OH)_3 + OH^- \leftrightarrows Al(OH)_4^-.$$

Joseph (7) in plotting equivalent conductance against the ratio of sodium hydroxide to aluminum hydroxide obtained no sharp breaks or irregularities and, therefore, concluded that aluminate ion AlO_2^- occurs.

EXPERIMENTAL

Procedure

The general procedure is similar to that used by Garrett and Heiks (8).

Preparation of Reagents

The preparation of conductivity water is that of Gayer and Woontner (9).

Aluminum hydroxide.—Aluminum hydroxide was precipitated from aluminum chloride by means of sodium hydroxide. The precipitate was washed several times beyond that required to give a negative flame test for sodium for both the solid and the supernatant liquid. A sample of the precipitate was dried for 2 days at 50° C. Following this, it was ignited at 500° C. From the weight loss, the empirical formula was calculated to be

[1]*Manuscript received April 8, 1958.*
Contribution from the Chemistry Department, Wayne State University, Detroit, Michigan.
[2]*From a dissertation submitted by Mr. Lancelot C. Thompson in partial fulfillment of the requirements for the Doctor of Philosophy degree and a dissertation submitted by Mr. O. T. Zajicek in partial fulfillment of the requirement for the Master of Science degree.*

$Al_2O_3 \cdot 3H_2O$. An X-ray diffraction powder pattern showed the material to be crystalline. The three major d values, in order of decreasing intensity, were found to be 4.62, 4.27, and 2.20 Å.

Aluminum chloride.—Baker and Adamson reagent grade aluminum chloride crystals were used to prepare the hydroxide. Standard aluminum solutions: 1.76 g of aluminum alum was dissolved in distilled water and made up to 1 liter. The standard solution contained 0.1 mg of aluminum per milliliter. From this solution spectrophotometric determinations of aluminum were made by diluting to make solutions of 2, 4, 8, 12, 16, 20, 24, and 28 γ/ml. The standard curve was prepared by means of the Beckman Model B spectrophotometer.

Chloroform.—Reagent grade chloroform was used for the extraction of the aluminum quinolate.

8-Hydroxyquinoline.—Twenty grams of hydroxyquinoline was dissolved in 60 ml of glacial acetic acid and diluted to 1 liter with distilled water.

Colorimetric analyses.—The aluminum analyses were made with a Beckman Model B spectrophotometer using the method of Sherrington and Gentry (10). The absorbance was measured at 400 mμ against a reagent blank.

pH.—A Beckman Model G pH meter was used to determine the equilibrium values of the hydrogen and hydroxyl ion activities.

TABLE I

SOLUBILITY OF ALUMINUM HYDROXIDE IN SODIUM HYDROXIDE SOLUTIONS AT 25° C

Initial moles NaOH/1000 g $H_2O \times 10^5$	Equilibrium activity of hydroxyl ion	Equilibrium, moles aluminum/ 1000 g H_2O $\times 10^5$	$\Delta_{OH} \times 10^5$	Δ_{OH}/mole of aluminum	K
0	3.98×10^{-9}	2.97			7460.
1.04	4.17×10^{-9}	1.63			3910.
2.99	4.57×10^{-9}	1.89			4136.
12.3	1.00×10^{-8}	2.00			2000.
17.74	2.63×10^{-8}	0.78			240.
33.79	1.12×10^{-7}	0.445			40.
61.55	3.31×10^{-6}	0.667			2.02
79.28	1.62×10^{-5}	1.19	77.66	65.3	.704
95.32	4.07×10^{-5}	1.33	91.25	68.6	.327
144.9	2.09×10^{-4}	6.75	124.0	18.4	.323
295.6	8.32×10^{-4}	20.4	212.4	10.4	.245
—	1.00×10^{-3}	23.8	—	—	.240
—	1.20×10^{-3}	25.6	—	—	.210
412.4	1.48×10^{-3}	57.1	264.4	4.63	.386
1081.	5.25×10^{-3}	165.	556.0	3.4	.314
2165.	1.12×10^{-2}	227.	1045.	4.6	.202
3872.	1.41×10^{-2}	400.	2461.	6.2	.283
8440.	1.91×10^{-2}	582.	6530.	11.2	.306
30400.	—	6380.	—	—	—
60800.	—	10000.	—	—	—
91200.	—	13500.	—	—	—

Δ_{OH} = initial moles of base − equilibrium moles of base,
= base consumed by Al.

THE DATA

The data are collected in Tables I and II. The values for the activity coefficients for NaOH and $HClO_4$ are given by Robinson and Stokes (11).

From the amounts of sodium hydroxide consumed and from the ratio of consumed sodium hydroxide to dissolved aluminum, it can be concluded that a major portion of the sodium hydroxide is simply adsorbed.

Can. J. Chem. Downloaded from www.nrcresearchpress.com by 78.46.186.204 on 09/04/12
For personal use only.

TABLE II

SOLUBILITY OF ALUMINUM HYDROXIDE IN PERCHLORIC ACID SOLUTIONS OF 25° C

Initial moles of $HClO_4$/ 1000 g H_2O $\times 10^5$	Equilibrium activity of hydrogen ion	Equilibrium, moles aluminum/ 1000 g H_2O $\times 10^5$	$\Delta_{H^+} \times 10^5$	Δ_{H^+}/mole of Al	K_1	K_2	K_3
0	2.51×10^{-6}	2.97	—	—	11.8	4.7×10^{6}	1.87×10^{12}
.81	3.55×10^{-6}	2.41	.45	.187	6.79	1.9×10^{6}	5.4×10^{11}
2.30	5.62×10^{-6}	1.52	1.74	1.145	2.70	4.8×10^{5}	8.6×10^{10}
4.58	7.94×10^{-6}	5.08	3.79	.746	6.40	8.1×10^{5}	10.2×10^{10}
5.50	9.77×10^{-6}	4.75	4.52	.952	4.86	4.97×10^{5}	50.9×10^{9}
12.67	1.55×10^{-5}	5.04	11.1	2.20	3.25	2.1×10^{5}	13.5×10^{9}
21.53	2.29×10^{-5}	6.86	19.2	2.80	2.99	1.3×10^{5}	5.72×10^{9}
25.31	2.75×10^{-5}	6.30	22.6	3.59	2.29	8.3×10^{4}	3.03×10^{9}
40.50	3.09×10^{-5}	7.42	37.4	5.04	2.40	7.8×10^{4}	2.51×10^{9}
70.88	5.01×10^{-5}	12.6	65.9	5.11	2.52	5.0×10^{4}	1.00×10^{9}
109.6	6.31×10^{-5}	31.5	103.3	3.28	4.98	7.9×10^{4}	1.25×10^{9}
181.5	8.71×10^{-5}	69.7	172.8	2.48	8.00	9.2×10^{4}	1.06×10^{9}
2380.	—	2000.	—	—	—	—	—
4680.	—	2200.	—	—	—	—	—
7000.	—	3120.	—	—	—	—	—
11700.	—	3560.	—	—	—	—	—
23400.	—	4750.	—	—	—	—	—
46800.	—	5850.	—	—	—	—	—
70400.	—	6980.	—	—	—	—	—
93000.	—	7870.	—	—	—	—	—

Δ_{H^+} = initial moles of acid − equilibrium moles of acid.

In view of the constancy of the equilibrium constant values and the relatively small amounts of solid dissolved, we believe that the following reaction is predominant in the concentrations of sodium hydroxide from 0.0008 molal to 0.08 molal.

$$Al(OH)_3\,(s) + OH^- = H_2AlO_3^- + H_2O.$$

The form $H_2AlO_3^-$, rather than $Al(OH)_4^-$, was chosen since it is felt that the equation tends to better emphasize the acid-base character of the reaction. For the equation written,

$$K = a_{H_2AlO_3^-}/a_{OH^-} = M_{H_2AlO_3^-}\cdot\gamma_{H_2AlO_3^-}/a_{OH^-}.$$

According to the Debye–Hückel limiting law, the activity coefficients for 1–1 electrolytes should be equal at equal ionic strengths; hence,

$$\gamma_{H_2AlO_3^-} = \gamma_{OH^-} = \gamma_{NaOH}$$

and

$$K = M_{H_2AlO_3^-}\cdot\gamma_{NaOH}/a_{OH^-} = 2.98\times10^{-1}$$

$$\Delta F^\circ = 720 \text{ cal/mole}.$$

Using the above equilibrium constant and K_w, the ionization constant for water at 25° C, the ionization constant for the following reaction was calculated:

$$Al(OH)_3\,(s) = H^+ + H_2AlO_3^-$$

$$K = 2.98\times10^{-15}.$$

Taking into consideration (1) the amount of acid consumed to the amount of aluminum hydroxide dissolved and (2) the fair constancy of the equilibrium constants over limited ranges of acid, we can probably conclude that in very low acid concentrations from 0 to 2×10^{-4} molal, reaction [1] below predominates and in acid concentrations from

Can. J. Chem. Downloaded from www.nrcresearchpress.com by 78.46.186.204 on 09/04/12
For personal use only.

2×10^{-4} molal to 2×10^{-3} molal, and possibly higher, reaction [3] predominates. In view of the drift in values of K_2, the range of reaction [2] cannot be determined. At most, we can only conclude that it probably occurs simultaneously with reaction [3] in the intermediate concentration of acid near 2×10^{-4} molal.

$$Al(OH)_3\,(s) + H^+ = Al(OH)_2^+ + H_2O \qquad [1]$$

$$Al(OH)_3\,(s) + 2H^+ = Al(OH)^{+2} + 2H_2O \qquad [2]$$

$$Al(OH)_3\,(s) + 3H^+ = Al^{+3} + 3H_2O \qquad [3]$$

$$K_1 = a_{Al(OH)_2^+}/a_{H^+} = M_{Al(OH)_2^+}\cdot\gamma_{Al(OH)_2^+}/a_{H^+}.$$

As before,

$$\gamma_{Al(OH)_2^+} = \gamma_{HClO_4}$$

and

$$K_1 = M_{Al(OH)_2^+}\cdot\gamma_{HClO_4}/a_{H^+} = 2.52$$

$$\Delta F_1^\circ = -550 \text{ cal/mole.}$$

Since K_2 was not constant, no attempt was made to select a representative value for it.

$$K_3 = a_{Al^{+3}}/a_{H^+}^3 = M_{Al^{+3}}\cdot\gamma_{Al^{+3}}/a_{H^+}^3.$$

From the Debye–Hückel limiting law, the activity coefficient of a 1–3 electrolyte may be replaced by the cube of that for a 1–1 electrolyte; hence,

$$K_3 = M_{Al^{+3}}\cdot\gamma^3_{HClO_4}/a_{H^+}^3 = 1.10\times10^9$$

$$\Delta F_3^\circ = -12{,}300 \text{ cal/mole.}$$

Using the value obtained for K_3 above and the cube of K_w, the ionization constant for water at 25° C, the solubility product constant for the following reaction was calculated:

$$Al(OH)_3\,(s) = Al^{+3} + 3OH^-,$$

$$K = 1.10\times10^{-33}.$$

For an amphoteric hydroxide, the isoelectric point will represent the minimum solubility. Plotting the logarithm of the reciprocal of the solubility against pH gives a curve with a maximum at pH 7.7.

REFERENCES

1. Heyrovsky, J. J. Chem. Soc. **117**, 11 (1920).
2. Kruyt, H. R. and Troelstra, S. A. Kolloid-Beih. **54**, 262 (1943).
3. Wood, J. K. J. Chem. Soc. **93**, 411 (1908).
4. Slade, R. E. Z. anorg. Chem. **77**, 457 (1912).
5. Hildebrand, J. H. J. Am. Chem. Soc. **35**, 864 (1913).
6. Heyrovsky, J. J. Chem. Soc. **117**, 1013 (1920).
7. Joseph, O. J. Univ. Bombay, Sect. A, **20** (Pt. 3), 39 (1951).
8. Garrett, A. B. and Heiks, R. E. J. Am. Chem. Soc. **63**, 562 (1941).
9. Gayer, K. H. and Woontner, L. J. Chem. Educ. **33**, 296 (1956).
10. Gentry, C. H. R. and Sherrington, L. G. Analyst, **71**, 432 (1946).
11. Robinson, R. A. and Stokes, R. H. Trans. Faraday Soc. **45**, 612 (1949).

Can. J. Chem. Downloaded from www.nrcresearchpress.com by 78.46.186.204 on 09/04/12
For personal use only.

Can. J. Chem. Downloaded from www.nrcresearchpress.com by 78.46.186.204 on 09/04/12
For personal use only.

A STUDY OF SILVER NITRATE SOLUTIONS IN GAS CHROMATOGRAPHY[1]

M. E. Bednas and D. S. Russell

ABSTRACT

Silver nitrate, dissolved in some organic solvents, has formed a relatively specific medium for the gas chromatographic separation of olefins. Columns formed from ethylene glycol and glycerin solutions of silver nitrate are comparable, but those formed from the polyethylene glycol solutions are considerably less effective. These silver nitrate solutions were stable below 65° C, but began to decompose slowly at 85° C.

An aspect of gas chromatography which has received little attention in the literature has been the use of liquid phases which react with components of the sample to form unstable complexes. A solution of silver nitrate in ethylene glycol has been used to form a column of this type. It is relatively specific for olefins, retaining ethylene and propylene, for example, much longer than such higher-boiling paraffins as *n*-pentane and *n*-hexane.

The existence of unstable complexes of this type has been demonstrated by Francis (1), who isolated a compound from propylene and silver nitrate. This proved to be stable at room temperature and normal pressure, but decomposed reversibly to silver nitrate and propylene at reduced pressures or at higher temperatures. The use of silver nitrate in a gas chromatographic column was first reported by Bradford *et al.* (2). They found that a saturated solution of silver nitrate in ethylene glycol on a support of kieselguhr gave excellent separations for traces of ethane in ethylene. Tenney (3) has clearly illustrated the selective effect of silver nitrate for normal olefins from pentene-1 through to nonene-1.

The moisture which is sometimes present in ethylene glycol and similar solvents, or that which these solvents absorb from samples containing traces of water, is subsequently eluted during the chromatographic process and frequently interferes with the determination. To circumvent this problem van de Craats (4) has suggested the use of benzyl cyanide as a solvent for silver nitrate, but has not included any data on this column.

The papers referred to above have not considered the temperature stability of these columns. Keulemans (5) states that the temperature should be kept below 40° C, since above this temperature the transient adducts with silver nitrate are not formed, and the solution is not stable.

This present study was undertaken to pursue this temperature stability further and to obtain comparative results for columns of ethylene glycol, polyethylene glycol, and glycerin solutions of silver nitrate.

EXPERIMENTAL

Apparatus

A commercial chromatographic unit, the Fisher-Gulf Partitioner, was employed. The columns consisted of $\frac{1}{4}$-inch copper tubing wound into a coil 6 inches in diameter. A thermistor serves as a detector. Both the detector and the column are contained in

[1]*Manuscript received May 22, 1958.*
Contribution from the Division of Applied Chemistry, National Research Council of Canada, Ottawa, Canada. Issued as N.R.C. No. 4843.

the same air bath, which can be controlled at the following steps, 50°, 65°, 85°, 100°, 120°, and 140° C. It can also be used at its ambient temperature (27° C) but without control. In this case the drift was less than 1% of full scale deflection at full sensitivity over a period of 20 minutes. The peaks are recorded on a conventional strip-chart recorder, fitted with a ball-and-disk integrator.

In these experiments helium was the only carrier gas used.

Reagents

Silver nitrate, Mallinckrodt Analytical Reagent.
Ethylene glycol, Eimer and Amend.
Triethylene glycol (mol. wt. 200), Carbide and Carbon, "Carbowax".
Polyethylene glycol (mol. wt. 400), Carbide and Carbon, "Carbowax".
Glycerin, Baker and Adamson.

Preparation of Columns

Approximately 30 g finely pulverized silver nitrate was added slowly to 20 ml glycerin (or glycol) in a beaker while stirring vigorously with a magnetic stirrer. In some cases the beaker was placed in warm water to hasten the solution of the salt. Care was taken to keep the temperature below 50° C. After several minutes stirring the undissolved silver nitrate was separated by centrifuging for a few minutes.

Exactly 17 ml of this saturated solution was then added to 39 g (100 ml) 30–60 mesh firebrick to give a packing which contained about 40% solvent by weight. The usual care was taken to ensure a uniform mixture. The resulting material appeared to be quite dry and flowed readily.

Sufficient $\frac{1}{4}$-inch diameter copper tubing was degreased and filled with the prepared packing. Approximately 6 ml of packing was required to fill 1 foot of tubing. The tubing was carefully filled while it was suspended by one end, being shaken at intervals to produce a uniform bed. The ends were plugged with glass wool and the tubing was wound to form a coil 6 inches in diameter.

RESULTS

Columns were prepared as described containing relatively saturated solutions of silver nitrate in ethylene glycol, polyethylene glycol, and glycerin. The relative retention times

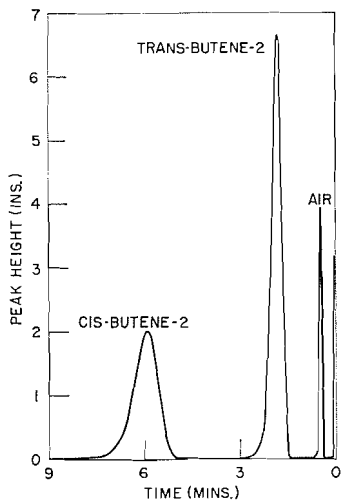

FIG. 1. Separation of *cis*- and *trans*-butene-2.

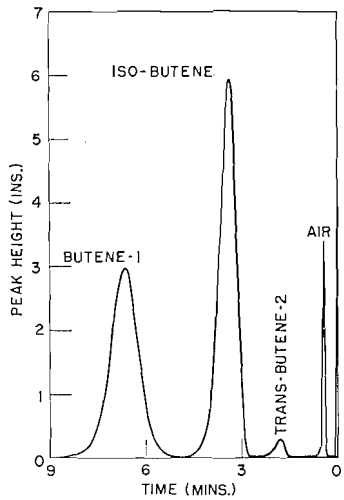

FIG. 2. Separation of butene-1 and isobutene.

Can. J. Chem. Downloaded from www.nrcresearchpress.com by 78.46.186.204 on 09/04/12
For personal use only.

which were obtained from the solutions of ethylene glycol and glycerin are given in Tables I and II. It will be observed that the *cis*- and *trans*-butene-2 are well separated as are the isobutene and the butene-1. These two pairs have been difficult to resolve with most other columns (2, 6, 7, 8, 9, 10). Their chromatograms are shown in Figs. 1 and 2.

TABLE I

RELATIVE RETENTION TIMES FOR $AgNO_3$ – ETHYLENE GLYCOL COLUMN

11-ft column
50° C
Flow rate, 25 ml/minute
Corrected retention time for ethylene, 4.5 minutes

	Retention time (ethylene = 1.00)	
n-Pentane (and lighter alkanes)	0	(Not retained)
trans-Butene-2	0.56	
trans-Pentene-2	0.89	
Ethylene	1.00	
Isobutene	1.19	
Propylene	1.22	
cis-Butene-2	2.0	
Butene-1	2.35	
Pentene-1	2.8	
cis-Pentene-2	2.95	
Hexene-1	4.2	
Heptene-1	6.1	
Octene-1	8.9	

TABLE II

RELATIVE RETENTION TIMES FOR $AgNO_3$ – GLYCERIN COLUMN

11-ft column
50° C
Flow rate, 20 ml/minute
Corrected retention time for ethylene, 4.5 minutes

	Retention time (ethylene = 1.00)	
n-Pentane (and lighter alkanes)	0	(Not retained)
trans-Butene-2	0.31	
Isobutene	0.75	
Propylene	0.91	
Ethylene	1.00	
cis-Butene-2	1.17	
Pentene-1	1.32	
Butene-1	1.42	
Ethylene dichloride	3.3	
Butadiene	6.0	
Cyclopentene	9.8	
Isopropanol	40.	
n-Propanol	60.	

The retention time for *cis*-butene-2 relative to that of *trans*-butene-2 is given in Table III for the three columns. The proportion of the silver nitrate on the firebrick is also given to demonstrate the relation between the silver nitrate concentration and the efficiency of the separation. This relation was also borne out when more dilute solutions were used and again when some of the silver nitrate was found to be decomposed in the column. With columns containing no silver nitrate (or those in which the silver nitrate was completely reduced), all olefins and paraffins containing four carbon atoms or less were not retained at all (i.e. not separated from air).

Can. J. Chem. Downloaded from www.nrcresearchpress.com by 78.46.186.204 on 09/04/12
For personal use only.

TABLE III

SELECTIVITY FOR *cis*- AND *trans*-BUTENE-2

Column	Column length, ft	% $AgNO_3$ on fire-brick	Ratio *cis/trans* 27° C	50° C		
1. $AgNO_3$ – ethylene glycol	11	24.	4.1	3.6		
2. $AgNO_3$ – polyethylene glycol	11	8.3	—	1.8		
3. $AgNO_3$ – glycerin	11	24.	4.7	4.1		
4. Formamide	6				1.18	(0° C)
5. Dimethylsulpholane	50	($\frac{3}{8}$ inch diam.)			1.17	(0° C)
6. Alumina	7				1.21	(60° C)
7. Tri-isobutylene	6				0.90	
8. Acetonyl acetone	6				0.86	(20° C)
9. $AgNO_3$ – ethylene glycol	6				0.32	
10. $AgNO_3$ – ethylene glycol ($AgNO_3$ completely decomposed)	11	*cis*- and *trans*-Butene-2 not retained				
11. Ethylene glycol	11	*cis*- and *trans*-Butene-2 not retained				

The concentration of silver nitrate found in solutions prepared as described is given in Table IV and may be regarded as relatively saturated solutions at room temperature.

TABLE IV

SOLUBILITY OF $AgNO_3$

Glycerin	95 g/100 ml solution
Ethylene glycol	85 ,, ,,
Triethylene glycol (mol. wt. 200)	48 ,, ,,
Polyethylene glycol (mol. wt. 400)	32 ,, ,,

The *cis–trans* ratios of five other columns are also included in Table III, columns 4–9, as calculated from results reported by other workers. The values reported by Bradford *et al.* (2), columns 7, 8, 9, gave ratios which were less than unity and indicate that the *cis*-butene-2 was eluted before the *trans*-butene-2. Our observations in the case of the silver nitrate – ethylene glycol column have not confirmed this fact. If, however, the values for *cis* and *trans* are interchanged in Bradford's report a *cis–trans* ratio of 3.1:1 is obtained, which is in agreement with the authors' findings.

The authors have employed "two-stage" columns (8) in an attempt to separate paraffins as well as olefins on one column. This consisted of a silver nitrate – glycerin column for separating the olefins, in series with a dinonyl phthalate column for separating the paraffins. Little success was achieved.

As an alternative, we suggest that a silver nitrate – glycerin column be employed for analysis of the olefins, and the paraffin fraction collected for subsequent analysis on a dinonyl phthalate or similar column.

Stability of Silver Nitrate Columns

The instability of the silver nitrate solutions seriously limits the use of the column to lower temperatures. It was therefore considered desirable to obtain further information concerning the temperature at which the decomposition begins, and its rate. Glycerin was also compared as a solvent in the hope that it might prove superior to ethylene glycol.

An ethylene glycol – silver nitrate column was heated to 100° C for 16 hours, and then tested for its efficiency at 35° C. No appreciable separation of *cis*- and *trans*-isomers took place, although the same column had previously shown a *cis–trans* ratio of 3.6:1

Can. J. Chem. Downloaded from www.nrcresearchpress.com by 78.46.186.204 on 09/04/12
For personal use only.

(column 1, Table III). The packing was recovered from the column and the organic phase was diluted with water. Upon titration with chloride this solution indicated the presence of little or no silver ion. The original titration for silver was obtained, however, if the packing was first digested with dilute nitric acid. From the examination of similar columns, it was found that the efficiency of the column was directly related to the concentration of silver ions present.

Ethylene glycol – silver nitrate and glycerin – silver nitrate packings were prepared on firebrick as described and kept in closed bottles. These bottles were stored in a controlled oven for periods of several days, when small samples were removed and titrated with chloride. The results which were obtained are illustrated in Fig. 3.

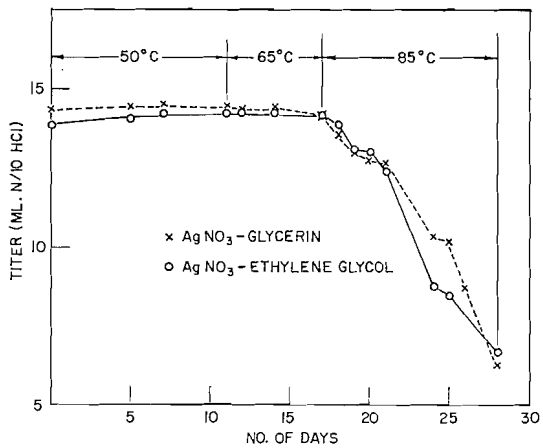

FIG. 3. Thermal stability of columns.

Both column materials were stable at least up to 65° C but decomposed slowly at 85° C. Subsequently a silver nitrate – ethylene glycol column has shown no change in relative retention times after 12 days at 65° C. It has been used intermittently at various temperatures not exceeding 65° C for 6 months, with no significant change in the relative retention times.

CONCLUSIONS

It may be concluded that the ethylene glycol and glycerin columns may be used safely up to 65° C and even at 85° C for short periods without serious damage. The glycerin – silver nitrate column had no distinct advantages, although it did show slightly better separations than its ethylene glycol counterpart. Polyethylene glycol proved less suitable probably owing to its more limited solubility of silver nitrate.

One noteworthy characteristic of these columns is their use for separating the paraffins as a group from the olefins.

REFERENCES

1. FRANCIS, A. W. J. Am. Chem. Soc. **73**, 3709 (1951).
2. BRADFORD, B. W., HARVEY, D., and CHALKLEY, D. E. J. Inst. Petrol. **41**, 80 (1955).
3. TENNEY, H. M. Anal. Chem. **30**, 3 (1958).
4. CRAATS, F. VAN DE. Anal. Chim. Acta, **14**, 136 (1956).
5. KEULEMANS, A. I. M. Gas chromatography. Reinhold Publishing Corp., New York. 1957. p. 205.
6. PODBIELNIAK, W. J. and PRESTON, S. T. Petrol. Refiner, **35**, 215 (1956).
7. KEULEMANS, A. I. M., KWANTES, A., and ZAAL, P. Anal. Chim. Acta, **13**, 357 (1955).
8. FREDERICKS, E. M. and BROOKS, F. R. Anal. Chem. **28**, 297 (1956).
9. PATON, H. W., LEWIS, J. S., and KAYE, W. J. Anal. Chem. **27**, 170 (1955).
10. RAY, N. H. J. Appl. Chem. (London), 4, 82 (1954).

Can. J. Chem. Downloaded from www.nrcresearchpress.com by 78.46.186.204 on 09/04/12
For personal use only.

Can. J. Chem. Downloaded from www.nrcresearchpress.com by 78.46.186.204 on 09/04/12
For personal use only.

THE LIMITING CONDUCTANCE OF POTASSIUM IODATE AND OF IODATE ION AT 25.00° C[1]

A. N. CAMPBELL AND E. BOCK[2]

ABSTRACT

Measurements have been made of the equivalent conductance of solutions of potassium iodate, at 25.00° C, at concentrations ranging from 0.8×10^{-4} to 16×10^{-4} *N*. From this the limiting equivalent conductance of potassium iodate is found to be 114.41 mhos and that of iodate ion 40.91 mhos. The experimental technique is described. The ionic conductances of chlorate, bromate, and iodate ions are compared.

INTRODUCTION

We are beginning, in this laboratory, an investigation of the conductances of very dilute solutions at temperatures above 25.00° C, in order to know the limiting conductances, both equivalent and ionic, above 25° C. This again has a bearing on our work on concentrated solutions, which has been appearing over the last 8 years (1, 2, 3, 4, 5, 6, 7, 8). We have already published one paper on the limiting conductances of ammonium chloride, ammonium bromide, and ammonium nitrate, at 35.00° C (9). Since then, however, we have refined our techniques and we intend this paper to be a statement of the experimental method to be used throughout the series, although, of course, as the temperature of measurement is raised further precautions will have to be taken to obtain constancy of temperature, to prevent distillation or even boiling, etc.

As a preliminary exercise, we have determined the limiting conductance of potassium iodate and of iodate ion, at 25.00° C. Apart from three rather early measurements by Harkins and Pearce (10) nothing has been done on iodate ion, although the limiting conductances of chlorate and bromate, at 25° C, have been determined with great accuracy (11, 12).

EXPERIMENTAL PROCEDURE

The electrical circuit for work of this kind is now standard. We are indebted to the International Nickel Company and to the Imperial Oil Company for the provision of a Jones bridge. The signal is amplified by a tuned amplifier. The detector is a cathode ray oscillograph; it is thus possible to differentiate between resistance and capacity imbalance. Measurements were made at the standard frequency of 1000 but measurements were also made at other frequencies to show that the apparent resistance did not vary with the frequency, as it should not if the true resistance is being measured.

Our conductance cell, of silica, is identical with that used by Shedlovsky (13). The thermostat is a double-jacketed, completely enclosed oil bath, containing 16 gal of mineral oil; the air over the bath is stirred and heated to a temperature slightly above that of the bath. Temperature is determined by a platinum resistance thermometer, and Mueller bridge.

The thermometer was obtained from the National Research Council and calibrated by them. We use a large toluene mercury regulator and thyatron control (14). The variation of temperature does not exceed 5×10^{-3} ° C. The potassium iodate was a Fisher certified reagent of the very highest purity and we felt that nothing would be gained by an additional recrystallization. Moreover, as the impurities in the salt—less than 0.01% in total—were ionic in nature, the error introduced into the conductance value

[1]*Manuscript received June 12, 1958.*
Contribution from the Chemistry Department of the University of Manitoba, Winnipeg, Manitoba.
[2]*Holder of a C.I.L. Fellowship, 1957–58.*

will be proportional to the difference in conductance of the salt investigated and the impurities; an error a great deal less than 0.01%. The salt was dried at 150° C and kept over P_2O_5 in a desiccator until needed. As for conductance water, we began by using an ion-exchange column, employing MB-3 (Fisher) ion-exchange resin. We found, however, that, although the issuing water had a very low conductance at first (2×10^{-7} mhos), this increased with time. It appears that something is extracted from the material of the column which subseqently undergoes chemical change with production of an electrolyte. The increase in conductance is small but, since the water conductance correction is considerable (about 10% of the whole for the most dilute solution used) in these very dilute solutions, it must be constant and known with accuracy. We therefore simply use the water from an electric still, from which we remove dissolved gases with bubbling nitrogen. This water has a conductance of 4.5×10^{-7} to 7×10^{-7} and it does not change with time, when preserved in a silica container. The conductance cell was subjected to a prolonged steaming operation until we were convinced, from experimental measurement, that the conductance of water stored in it did not change with time. All measurements are carried out in an atmosphere of nitrogen.

The balance used is a single-pan semimicro type, having a sensitivity of 0.01 mg. Since we do not possess a microbalance, it is not possible to make up the most dilute solutions by introducing the very small weights of dry salt directly into the cell. We have therefore used a weight burette for the purpose of obtaining a solution of known concentration. The cell constant was determined in the usual way with 1/100 demal potassium chloride. As a final test of technique, we determined some of the conductances of potassium chloride at 25.0° C (at various concentrations) and we obtained exact agreement with the results of Shedlovsky and of Gordon (13, 15).

The only previous work on potassium iodate at 25.00° C is that of Harkins and Pearce (10), who report the conductances at three rounded-off concentrations, viz., 0.2×10^{-3}, 0.5×10^{-3}, and 1×10^{-3}. From these figures, they state the limiting conductance to be 114.37 mhos, in close agreement with our figure but we do not see what justification they can have for this, since they presumably (no details are given) only made three determinations plotted. And then, again presumably, they plotted Λ versus $\sqrt{c}$, and drew a straight line, more or less at random, through the three points. Yet when such a plot is constructed the extrapolated value of Λ_0 comes to 114.20 mhos.

EXPERIMENTAL RESULTS

Our results are contained in the following table.

TABLE I

THE SPECIFIC AND EQUIVALENT CONDUCTANCES OF AQUEOUS SOLUTIONS OF POTASSIUM IODATE AT 25.00° C

Concentration, in moles/liter $\times10^4$	Specific conductance $\times10^6$, in mhos	Equivalent conductance, in mhos
0.86082	9.78064	113.62
2.05973	23.30996	113.17
3.14043	35.45545	112.90
4.69655	52.85967	112.55
6.58631	73.90498	112.21
8.66525	96.93815	111.87
10.81886	120.72765	111.59
12.92765	143.92353	111.33
14.11540	157.96544	111.19
15.64277	173.66603	111.02
16.88694	187.24239	110.88

Can. J. Chem. Downloaded from www.nrcresearchpress.com by 78.46.186.204 on 09/04/12
For personal use only.

When the above results are plotted in the form of Λ versus $\sqrt{c}$, and the best straight line drawn (by the method of least squares), it is seen that no single determination deviates from the line by more than 1/100%. The slope of the line (85.91) is very close to the theoretical Debye–Hückel slope (86.51) but is somewhat less; this is what is usually found. When the line is extrapolated to zero concentration, Λ_0 results as 114.41. Taking the limiting conductance of potassium ion to be 73.50 (15, 16) at 25.00° C, the limiting conductance of iodate ion results as 40.91.

DISCUSSION

Since the limiting conductances of chlorate, bromate, and iodate ions are now known with accuracy, there is some interest in comparing them with the dimensions of the crystallographic ions (17), thus:

TABLE II

COMPARISON OF LIMITING IONIC CONDUCTANCES WITH DIMENSIONS OF CRYSTALLOGRAPHIC IONS

Ion	Limiting conductance	Edgelength of tetrahedral ion
ClO_3^-	64.6	2.33 Å
BrO_3^-	55.74	2.73 Å
IO_3^-	40.91	3.35 Å

The ratio of conductances is 1.58:1.36:1 and that of edgelength 1.44:1:1.71 iodate, with the largest (crystallographic) ion size, has the smallest ionic conductance, but the agreement is obviously not quantitative. Indeed, similar calculations with other ions (notably the bromide ion) show that sometimes an ion may even have a greater apparent size and yet have a greater conductance. It is well known that Stokes' law does not apply to the motion of particles as small as the smaller ions. Stokes and Robinson (18) consider the problem of how large an ion must be in order that Stokes' law may be obeyed and assign a lower limit. Nevertheless though quantitative agreement with Stokes' law is not to be expected here, if the crystallographic dimensions were true measures of the sizes of the ions in solution qualitative agreement should exist.

Differences in solvation may account for the discrepancy although other explanations are possible.

REFERENCES

1. CAMPBELL, A. N. and KARTZMARK, E. M. Can. J. Research, B, **28**, 43 (1950).
2. CAMPBELL, A. N. and KARTZMARK, E. M. Can. J. Chem. **30**, 128 (1952).
3. CAMPBELL, A. N., GRAY, A. P., and KARTZMARK, E. M. Can. J. Chem. **31**, 617 (1953).
4. CAMPBELL, A. N., KARTZMARK, E. M., BEDNAS, M. E., and HERRON, J. T. Can. J. Chem. **32**, 1051 (1954).
5. CAMPBELL, A. N. and KARTZMARK, E. M. Can. J. Chem. **33**, 887 (1955).
6. CAMPBELL, A. N., DEBUS, G. H., and KARTZMARK, E. M. Can. J. Chem. **33**, 1508 (1955).
7. CAMPBELL, A. N. and ROSS, L. Can. J. Chem. **34**, 566 (1956).
8. CAMPBELL, A. N. and DEBUS, G. H. Can. J. Chem. **34**, 1232 (1956).
9. CAMPBELL, A. N. and BOCK, E. Can. J. Chem. **36**, 330 (1958).
10. HARKINS, W. D. and PEARCE, W. T. J. Am. Chem. Soc. **38**, 2679 (1916).
11. MONK, C. B. J. Am. Chem. Soc. **70**, 3281 (1948).
12. DAGGET, H. M., BAIR, E. S., and KRAUS, C. A. J. Am. Chem. Soc. **73**, 799 (1951).
13. SHEDLOVSKY, T. J. Am. Chem. Soc. **54**, 1411 (1932).
14. SWINEHART, D. F. Anal. Chem. **21**, 1577 (1949).
15. GORDON, A. R. and BENSON, G. C. J. Chem. Phys. **13**, 473 (1945).
16. OWEN, B. B. and ZELDES, H. J. Chem. Phys. **18**, 1083 (1950).
17. NARAY-SROBO, I. and NEUGEBAUER, J. J. Am. Chem. Soc. **69**, 1280 (1947).
18. STOKES, R. H. and ROBINSON, R. A. Electrolyte solutions. Butterworths Scientific Publications, London. 1955. pp. 120, 121.

Can. J. Chem. Downloaded from www.nrcresearchpress.com by 78.46.186.204 on 09/04/12
For personal use only.

Can. J. Chem. Downloaded from www.nrcresearchpress.com by 78.46.186.204 on 09/04/12
For personal use only.

DIACETYLENE: PREPARATION, PURIFICATION, AND ULTRAVIOLET SPECTRUM[1]

K. K. Georgieff and Y. Richard

ABSTRACT

Diacetylene was prepared by the reaction of 1,4-dichloro-2-butyne with sodium hydroxide. Three modifications of procedure were tried to determine which gave the highest yield and purest product. Evidence that the by-product is 2-chloro-2-butene-3-yne is presented. Several methods for purifying the diacetylene were investigated. The ultraviolet spectrum with molar extinction coefficients is given.

INTRODUCTION

A sample of very pure diacetylene was required for polymerization and spectroscopic studies. In recent years most investigators have prepared it by the dehydrochlorination of 1,4-dichloro-2-butyne with sodium hydroxide (1, 2, 3, 4, 5) but only one (4) appears to have reported that the product is not entirely pure. However, no indication of the nature of the impurity was given.

RESULTS

Several modifications of the dehydrochlorination were tried to determine which gave the highest yield and purest product. The yields were highest when 40% aqueous sodium hydroxide solution (285% of theory) was added to a 25% solution of 1,4-dichloro-2-butyne[2] in ethyl alcohol at 65–75° over a period of 1 hour (1) and the product was swept out of the reaction flask with a stream of hydrogen. However, a small percentage of a by-product having a parent peak of 86 in its mass spectrum, as well as tarry high polymers, also formed. When the procedure was reversed and the dichlorobutyne in alcohol was added to the sodium hydroxide, the yield of diacetylene was substantially lower and the fractionated product contained about the same concentration of the same impurity. When pure dichlorobutyne was added to 43% sodium hydroxide solution at 115°, the yield was still lower but the relative amount of the above impurity was lower. Some acetylene and methyl acetylene also formed and were detected by their mass spectra.

From the ratio of the 87 to the 86 mass peak, the spectrum indicates that the impurity contains four carbon atoms and the ratio of the 86 to the 88 peak is in good agreement with the known ratio of Cl_{35} to Cl_{37}. It would thus appear that its empirical formula is C_4H_3Cl. It also has a strong absorption at 224 to 245 mμ in the ultraviolet and its extinction coefficients are of a higher order than those of diacetylene, indicating two conjugated ethylenic groups or an ethylenic together with an acetylenic. From the above evidence, there would appear to be little doubt that this compound formed, even in the presence of a large excess of sodium hydroxide, by the incomplete dehydrochlorination of the dichlorobutyne and could theoretically have the structure I, II, or III.

$$CH_2Cl—C\equiv C—CH_2Cl + NaOH \rightarrow NaCl + H_2O + CH_2=CCl—C\equiv CH \quad [I]$$

$$\text{or } CHCl=CH—C\equiv CH \quad [II]$$

$$\text{or } CH_2=CH—C\equiv C—Cl \quad [III]$$

To establish its identity, its infrared spectrum was obtained and a comparison made of the out-of-plane vibrations of its olefinic hydrogens with those of four compounds

[1]*Manuscript received June 3, 1958.*
Contribution from the Research Laboratories, Shawinigan Chemicals Ltd., Shawinigan, Que.
[2]*Available from General Aniline & Film Corporation, U.S.A.*

closely related with I, II, and III, as shown in Table I. The band assignments previously published for monovinylacetylene (6, 7, 8) and 2-chloro-1,3-butadiene (9, 10) were assumed. Since only a fragmentary spectrum for 1-chloropropene-1 appears to have been previously published (10), it was first necessary to obtain samples of 1- and 2-chloropropene-1 (from K. & K. Laboratories, U.S.A.) and purify them by distillation in a Podbielniak column. Their purity was checked with the mass spectrometer.

TABLE I

ASSIGNMENT OF INFRARED BANDS (cm^{-1})

Out-of-plane vibrations of olefinic hydrogens	CH_3—CH=CHCl	CH_3—CCl=CH_2	CH_2=CH—CCl=CH_2	CH_2=CH—C≡CH	Our impurity
CH_2=CH—			974 (9, 10) 924	972 (8) 924	
CH_2=CCl—		938 929 881	878		919 862 853
R—CH=CHX (*trans*)	932				
R—CH=CHX (*cis*)	766 754				

Our impurity showed a band of medium intensity at 919 cm^{-1} and a strong doublet at 862 and 853 cm^{-1}. Both 2-chloro-1,3-butadiene and 2-chloropropene-1 show absorptions in the same regions whereas 1-chloropropene-1 shows absorption at 932 and a doublet at 766 and 754 cm^{-1}, which, in accordance with the correlations established by Kitson (10), could be attributed to *cis*- and *trans*-isomers. There is little spectral evidence in support of structure III. Neither is it probable on chemical grounds. It would thus appear that the structure of our impurity is I, CH_2=CCl—C≡CH. The shift of the chlorine atom from the 1-carbon to the 2-position is reminiscent of that of chlorobutadiene (11).

PURIFICATION

Attempts to remove the 2-chloro-2-butene-3-yne by the high vacuum, fractional distillation – condensation technique (8, 12) using distilling temperatures from −60 to −95° failed. So did distillation from solvents such as ethyl acetoacetate and methyl isobutyl ketone, as well as conventional, simple distillation at 277 mm mercury absolute. Fractional recrystallization was abandoned owing to great experimental difficulties imposed by the necessity of keeping the sample very cold and away from oxygen. Attempts to remove the impurity by partially polymerizing the sample at −6 to +13° in the absence of air and catalyst increased its concentration, thus indicating that the diacetylene polymerized more rapidly. Diluting the diacetylene with 10 to 15 volumes of hydrogen and passing it rapidly through a solution of sodium hydroxide in amyl alcohol at 138° reduced the chloro impurity from 1.5 to 0.2% but only 10–20% of the diacetylene was recovered. The remainder polymerized to tar. Gas chromatography, on the other hand, was found to produce high purity diacetylene with high recoveries. A tube (20 ft long × ¼ inch O.D.) filled with Johns-Manville C-22 firebrick (35–50 mesh) which was impregnated with 33% tricresyl phosphate was employed. Using a diacetylene vapor sample of about 5 ml (measured at 760 mm), a hydrogen flow of 67 ml per minute, and a tube temperature of 65°, the recovery was at least 93% per pass. After one or two passages through the tube, no 2-chloro-2-butene-3-yne could be detected by the mass spectrometer.

Can. J. Chem. Downloaded from www.nrcresearchpress.com by 78.46.186.204 on 09/04/12
For personal use only.

Can. J. Chem. Downloaded from www.nrcresearchpress.com by 78.46.186.204 on 09/04/12
For personal use only.

It is well known that the loss of diacetylene is substantial if it is handled by the usual laboratory techniques owing to its volatility and ease of polymerization. However, it was found that by using the high-vacuum, low-temperature-distillation technique (8, 12), such loss was reduced to a negligible value. By storing the samples (whether pure or impure) at -50 to $-78°$ under vacuum, losses due to polymerization were very small, even after 1 year without a stabilizer. The preferred procedure was to distill the diacetylene into a glass tube, cool it with liquid nitrogen, evacuate to a pressure of at least 10^{-4} mm mercury, and seal the tube. However, when the sample contained dissolved gas (usually air), it was first necessary to degas it several times by successively warming it to -20 to $0°$, cooling with liquid nitrogen, and pumping off the gas.

ULTRAVIOLET SPECTRUM

The ultraviolet spectrum of diacetylene vapor has been published by Price and Walsh (13) for the 1000 to 2000 Å region and by Woo and Chu (14, 15, 16) for the 2068 to 2970 Å region. Our spectrum was obtained with a Beckman DK-2 spectrophotometer on samples dissolved in iso-octane. There was general agreement with Woo and Chu's spectrum but there was a shift in our peaks of 7 to 9 mμ towards the lower wave lengths and some differences in the relative intensities of the maxima were apparent. The curve is given in Fig. 1 and the molar extinction coefficients in Table II. Our values are of the same order of magnitude as those obtained by Armitage *et al.* (17) on substituted diacetylenes.

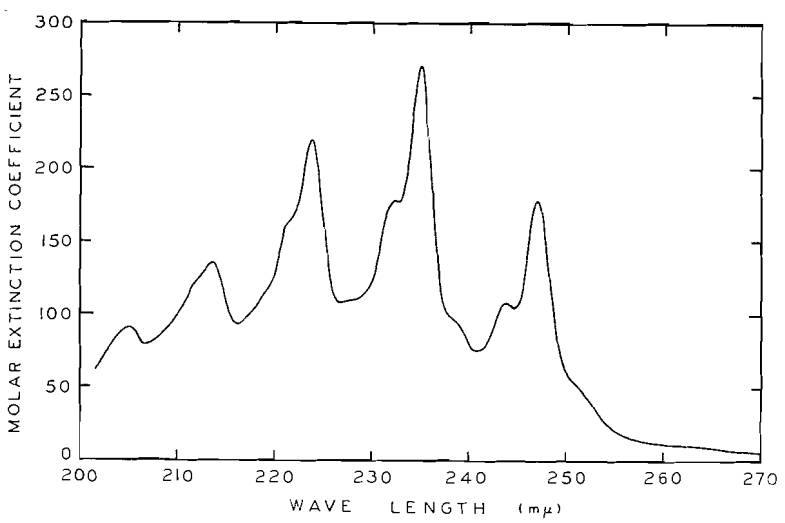

FIG. 1. Ultraviolet spectrum of diacetylene in iso-octane.

TABLE II

ULTRAVIOLET SPECTRUM OF DIACETYLENE

CONCN. = 7 TO 30 $\times 10^{-4}$ MOLES PER LITER IN ISO-OCTANE

λ_{max}, mμ	ϵ_{max}	λ_{max}, mμ	ϵ_{max}	λ_{max}, mμ	ϵ_{max}
~205	~90	223.8	222	244	110
211.3sh	117	232.5	180	247.1	180
213.5	136	234.9	270	251.5	55
221.5sh	168	238.5	101		

Extinction values were also obtained on a Beckman DU instrument and were generally 10 to 20% lower than those above. In contrast to those obtained with the DK-2, they were found to decrease rapidly with increase in concentration of diacetylene even at low optical densities (i.e. 0.1 to 0.3). A similarly great deviation from the Beer–Lambert–Bouger absorption law was noted previously with monovinylacetylene and other acetylene polymers (8).

ACKNOWLEDGMENTS

The authors wish to express their thanks to Shawinigan Chemicals Ltd. for permission to publish this paper and to Messrs. A. Dupré, E. Blais, and E. Beaulieu for their assistance.

REFERENCES

1. KEYSSNER, E. and EICHLER, E. To I. G. Farbenindustrie A. G. Ger. Patent No. 740,637 (1943).
2. JOHNSON, A. W. J. Chem. Soc. 1009 (1946).
3. ARMITAGE, J. B., JONES, E. R. H. and WHITING, M. C. J. Chem. Soc. 44 (1951).
4. POMERANTZ, P., FOOKSON, A., MEARS, T. W., ROTHBERG, S., and HOWARD, F. L. J. Research Natl. Bur. Standards, **52**, 51 (1954).
5. NAKAGAWA, M. and INUI, T. J. Chem. Soc. Japan, Pure Chem. Sect. **73**, 143 (1952).
6. SHEPPARD, N. J. Chem. Phys. **17**, 74 (1949).
7. STAMM, R. F., HALVERSON, F., and WHALEN, J. J. J. Chem. Phys. **17**, 104 (1949).
8. GEORGIEFF, K. K., CAVE, W. T., and BLAIKIE, K. G. J. Am. Chem. Soc. **76** 5494 (1954).
9. THOMPSON, H. W. and TORKINGTON, P. Proc. Roy. Soc. (London), A, **184**, 21 (1945).
10. KITSON, R. E. Anal. Chem. **25**, 1470 (1953).
11. CAROTHERS, W. H., BERCHET, G. J., and COLLINS, A. M. J. Am. Chem. Soc. **54**, 4066 (1932).
12. SANDERSON, R. T. Vacuum manipulation of volatile compounds. John Wiley & Sons, Inc., New York. 1948. p. 86,
13. PRICE, W. C. and WALSH, A. D. Trans. Faraday Soc. **41**, 381 (1945).
14. WOO, S. C. and CHU, T. C. Phys. Rev. **47**, 886 (1935).
15. WOO, S. C. and CHU, T. C. J. Chem. Phys. **3**, 541 (1935).
16. WOO, S. C. and CHU, T. C. J. Chem. Phys. **5**, 786 (1937).
17. ARMITAGE, J. B., COOK, C. L., ENTWISTLE, N., JONES, E. R. H., and WHITING, M. C. J. Chem. Soc. 1998 (1952).

Can. J. Chem. Downloaded from www.nrcresearchpress.com by 78.46.186.204 on 09/04/12
For personal use only.

Can. J. Chem. Downloaded from www.nrcresearchpress.com by 78.46.186.204 on 09/04/12
For personal use only.

SOME CHEMISTRY OF 2,6-DIETHYLANILINE[1]

P. M. G. BAVIN[2] AND J. M. W. SCOTT[3]

ABSTRACT

Orientation in the nitration and bromination of amides derived from 2,6-diethylaniline has been shown to be dependent on the acidity of the reaction medium, as found previously for the 2,6-dimethyl homologues.

The acidity of the reaction medium is known to influence the orientation of substitution products of many amines (1, 2, 3, 4, 5, 6, 7) and their derivatives, particularly anilides and sulphonamides (8, 9, 10, 11). Derivatives of 2,6-dimethylaniline (*m*-2-xylidine) have proved to be of more than usual interest (9, 10), so that the opportunity has been taken to examine some of the chemistry of 2,6-diethylaniline.

2,6-Diethylaniline was recently prepared for the first time (12). It forms nicely crystalline salts with hydrochloric, hydrobromic, and perchloric acids which, as expected for the salts of weak bases (13), are partly hydrolyzed in water. With benzaldehyde it reacts smoothly to form a Schiff's base and readily forms amides with acetic anhydride, benzoyl chloride, and *p*-toluenesulphonyl chloride. The acetamide (X) is very resistant to acid hydrolysis so that the toluenesulphonamide (I) was preferred as an intermediate.

Nitration of (I) in the presence of nitrous acid (7, 10) gave an excellent yield of pure 4-nitro derivative (II), the structure of which was proved by conversion to the known 4-nitro-2,6-diethylphenol (IV) and 2,6-diethyl-1,4-benzoquinone (V). In sulphuric acid, nitration gave a rather lower yield of the 3-nitro derivative (VI), its structure being assumed by elimination. The acetamide (X) readily yielded a dinitro compound, almost certainly (VII), and considerable difficulty was encountered in obtaining the 3-nitro derivative (VIII).

Bromination of the acetamide (X) in sulphuric acid gave the 3-bromo derivative (IX), the structure of which is assumed by analogy with previous work on the dimethyl homologue (9). In acetic acid or chloroform, the 4-isomer (XII) was obtained. This compound, the structure of which is also assumed by analogy (9), has been shown to be formed by the rearrangement of the *N*-bromoacetamide (14). Bromination of the sulphonamide (I) in sulphuric acid, chloroform, or acetic acid gave products which were not obtained pure by repeated crystallization and whose infrared spectra showed them to be essentially identical. Removal of the tosyl group followed by acetylation gave almost pure (XII), showing that bromination had occurred predominantly in the 4 position.

Aniline, the toluidines, and related compounds are very much more reactive than their salts so that the small concentration of free amine present in sulphuric acid largely controls the orientation in nitration in this medium (1, 2, 3, 4, 5, 6, 7). Derivatives of 2,6-dialkylaniline (alkyl is methyl or ethyl) offer a more complex problem. The proximity of the ortho substituents twists the amide group out of the plane of the aromatic ring,* thereby greatly reducing mesomerism between the ring and the nitrogen (10, 15, 16).

[1]*Manuscript received April 8, 1958.*
Contribution from the Department of Chemistry, University of Ottawa, Ottawa, Canada, and the Divisions of Pure and Applied Chemistry, National Research Council, Ottawa.
Issued as N.R.C. No. 4801.

[2]*National Research Council of Canada Postdoctorate Fellow, University of Ottawa, 1954–56. Present address: the Ohio State University, Columbus 10, Ohio.*
[3]*National Research Council of Canada Postdoctorate Fellow, Division of Pure and Applied Chemistry.*

**Reducing mesomerism between the ring and the nitrogen will increase the basicity of the latter, but the compression caused by the ortho substituents may nullify or even out-balance this effect ((17), pp. 214–223).*

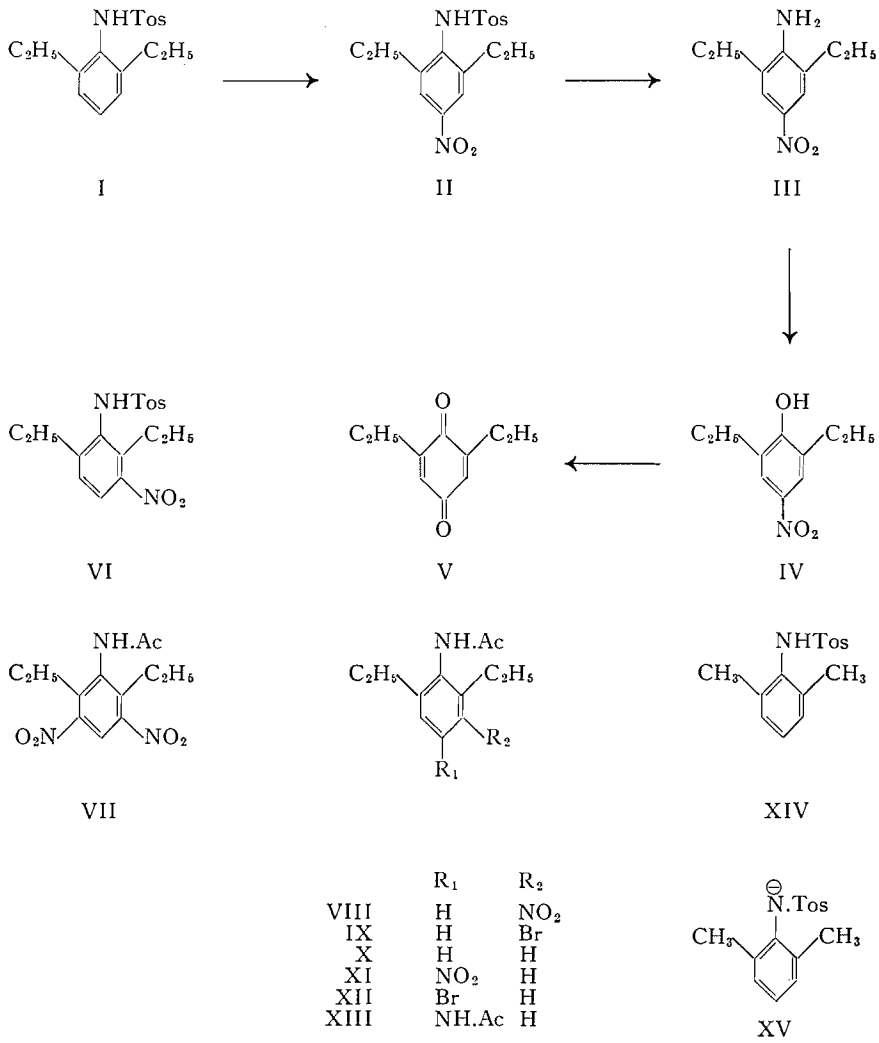

I II III IV V VI VII XIV XV

	R_1	R_2
VIII	H	NO_2
IX	H	Br
X	H	H
XI	NO_2	H
XII	Br	H
XIII	NH.Ac	H

This lowers the reactivity of the 4 position but leaves it more reactive than the 3 position (10). Since in sulphuric acid 3-derivatives are usually obtained, it appears that the protonated and unprotonated forms differ but little in reactivity at the 3 position.

The sulphonamides (I) and (XIV) and their *N*-nitroso derivatives are probably insufficiently reactive to undergo nitrosation (cf. (7)) so that (XV) has been suggested (10) as the reactive species in nitration in the presence of nitrous acid.

As expected, nitration of (I) and bromination of (X) are completely analogous to reactions of the dimethyl homologues (9, 10). That bromination of (I) in sulphuric acid gives rise to predominantly the 4-isomer may be due to the low basicity of the sulphonamide group and the greater selectivity of bromination compared with nitration (18).

It was hoped initially to confirm the structures of the bromination products by comparison of their infrared spectra with those of the corresponding nitro compounds. This hope was not realized, only approximate similarities being observed.

Can. J. Chem. Downloaded from www.nrcresearchpress.com by 78.46.186.204 on 09/04/12
For personal use only.

Can. J. Chem. Downloaded from www.nrcresearchpress.com by 78.46.186.204 on 09/04/12
For personal use only.

EXPERIMENTAL

2,6-Diethylaniline was supplied as a reddish liquid and used without purification.

Melting points are uncorrected. Most of the nitration products turned brown in light and were crystallized in covered flasks. Nitration conditions were essentially those used by Wepster for the dimethyl homologues (10).

2,6-Diethylaniline hydrochloride crystallized from dilute hydrochloric acid as colorless needles, m.p. 175–179° with decomposition. Calc. for $C_{10}H_{16}NCl$: C, 64.68; H, 8.69%. Found: C, 64.48; H, 8.44%. Crystalline salts were also formed with perchloric and hydrobromic acids but these were not characterized. The free amine separated as an oil when the salts were dissolved in warm water.

N-Benzal-2,6-diethylaniline.—On the gentle warming of a mixture of the amine (2 g.) with benzaldehyde (4 g.), water started to separate almost at once. Ethanol (2 ml.) was added and the mixture boiled under reflux for 10 minutes. The Schiff's base was obtained as a pale yellow solid by pouring the mixture into an excess of cold dilute sodium bisulphite solution. Two crystallizations from hexane afforded yellow prismatic needles (2.6 g.), m.p. 54–55°. Calc. for $C_{17}H_{19}N$: C, 86.03; H, 8.07; N, 5.90%. Found: C, 86.20; H, 8.08; N, 5.88%.

N-(2,6-Diethylphenyl)-benzamide was prepared by shaking the amine (2 g.) with benzoylchloride (3 ml.) and a solution of sodium hydroxide (5 g.) in water (10 ml.). The solid product was crystallized twice from toluene, affording slender needles (2.2 g.), m.p. 236–237°. Calc. for $C_{17}H_{19}NO$: C, 80.57; H, 7.56; N, 5.53%. Found: C, 80.73; H, 7.42; N, 5.66%.

N-(2,6-Diethylphenyl)-acetamide (X) was prepared by adding acetic anhydride (200 ml.) dropwise to the amine (100 g.) cooled in an ice bath. The reaction, which was rapid and exothermic, was completed on the steam bath. Addition of 10% sulphuric acid (500 ml.) and crushed ice precipitated the amide. Crystallization from ethanol (200 ml.) afforded white needles (110 g.), m.p. 139–140°, raised to 141–142° by two crystallizations from toluene. (Lit. m.p. 135–136°, (12).) Calc. for $C_{12}H_{17}NO$: C, 75.35; H, 8.96; N, 7.32%. Found: C, 75.56; H, 8.71; N, 7.46%.

N-(2,6-Diethylphenyl)-p-toluenesulphonamide (I).—The amine (150 g.) was dissolved in dry pyridine (500 ml.) and *p*-toluenesulphonyl chloride (210 g.) added slowly while the mixture was cooled with an ice–salt bath. Next morning, the mixture was poured onto crushed ice and the pyridine neutralized with dilute hydrochloric acid. Crystallization from methanol–acetone (Norite) afforded yellowish prisms (265 g.), m.p. 130–132°. An analytical sample was obtained as well-defined colorless prisms, m.p. 132–133°, after two crystallizations from benzene. Calc. for $C_{17}H_{21}NO_2S$: C, 67.31; H, 6.98; N, 4.62%. Found: C, 67.45; H, 6.98; N, 4.49%.

N-(4-Nitro-2,6-diethylphenyl)-p-toluenesulphonamide (II).—A mixture of the amide (I) (30 g.), acetic acid (100 ml.), fuming nitric acid (40 ml.), and sodium nitrite (2 g.) was boiled under reflux for 1 hour. Pouring onto ice precipitated a gum which soon crystallized. Successive crystallizations from methanol (Norite) and benzene–hexane afforded the nitroamide as pale yellow needles (22–25 g.), m.p. 140–141°. Calc. for $C_{17}H_{20}N_2O_4S$: N, 8.04%. Found: N, 8.18%.

4-Nitro-2,6-diethylaniline (III).—The nitroamide (II) (10 g.) was stirred overnight with sulphuric acid (30 ml.) containing water (4 ml.). Pouring onto ice precipitated the pale yellow amine sulphate, which was decomposed to the amine by neutralization with dilute ammonia solution. Two crystallizations from methanol gave long bright yellow needles of the amine, m.p. 137–138°. Calc. for $C_{10}H_{14}N_2O_2$: N, 14.42%. Found: N, 14.59%.

N-(4-Nitro-2,6-diethylphenyl)-acetamide (XI) was prepared by acetylating the amine (III). It crystallized from benzene–hexane as pale yellow needles, m.p. 195–196°. Calc. for $C_{12}H_{16}N_2O_3$: N, 11.96%. Found: N, 11.71%.

N,N-Diacetyl-2,6-diethyl-1,4-phenylenediamine (XIII).—The nitroamine (III) was reduced with hydrazine and palladized charcoal, giving the diamine as a colorless oil. Acetylation followed by two crystallizations from acetone–toluene afforded the bisamide as slender needles, m.p. 216–217°. Calc. for $C_{14}H_{20}N_2O_2$: N, 11.28%. Found: N, 11.30%.

4-Nitro-2,6-diethylphenol (IV).—To a cold (0–5°) solution of the nitroamine (III) (3 g.) in 50% sulphuric acid (40 ml.) was added sodium nitrite (2 g.). The mixture was left for 1 hour at room temperature and, after addition of urea to destroy excess nitrous acid, was maintained at 60° for 1 hour. During this time the phenol separated as a reddish solid. Attempted purification through the intensely yellow sodium salt was not successful but two crystallizations from methanol (Norite) afforded slightly reddish needles, m.p. 131–133° with decomposition. (Lit. m.p. 130–131° with decomposition (19).)

2,6-Diethyl-1,4-benzoquinone (V) was prepared by oxidizing the nitrophenol (IV) with lead tetraacetate, as described previously (19). It was obtained as bright yellow needles, m.p. 36–38°, by low temperature crystallization from pentane. (Lit. m.p. 35° (19); 39° (20).)

Attempts to oxidize the nitroamine (III) to the quinone, using chromic acid or lead tetraacetate, were not successful.

N-(3-Nitro-2,6-diethylphenyl)-p-toluenesulphonamide (VI).—A mixture of acetic acid (50 ml.), fuming nitric acid (4.5 ml., d. 1.5), and sulphuric acid (50 ml.) was added dropwise to a vigorously stirred suspension of the amide (I) (32 g.) in acetic acid (250 ml.) containing sulphuric acid (120 ml.). The addition required ½ hour during which time the temperature rose to 45°. After 6 hours the product was isolated by pouring the mixture onto crushed ice. Crystallization from aqueous ethanol (Norite) afforded buff prisms (17–26 g.), m.p. 149–151°. An analytical sample was obtained as pale yellow prisms after several crystallizations from benzene–hexane, m.p. 152–153°. Calc. for $C_{17}H_{20}N_2O_4S$: N, 8.04%. Found: N, 8.13%.

N-(3-Nitro-2,6-diethylphenyl)-acetamide (VIII).—Hydrolysis of the once-crystallized amide (VI) with 90% sulphuric acid gave the amine as a yellow oil. Acetylation followed by crystallization from methanol and then benzene–hexane afforded the acetamide as almost colorless needles, m.p. 153–154°. Calc. for $C_{12}H_{16}N_2O_3$: N, 11.96%. Found: N, 12.01%.

N-(3,5-Dinitro-2,6-diethylphenyl)-acetamide (VII) was commonly obtained when the acetamide (X) was nitrated in a mixture of acetic and sulphuric acids. It crystallized from toluene as pale yellow needles, m.p. 206–208° with some decomposition (capillary determination). On the hot stage, with a rapid rate of heating, the melting point was 211–212°. Calc. for $C_{12}H_{15}N_3O_5$: C, 51.24; H, 5.35; N, 14.94%. Found: C, 51.31; H, 5.31; N, 14.94%.

On a few occasions the mononitro compound (VIII) was obtained by nitrating (X) but reliable conditions for its preparation by this method were not found. Attempts to dinitrate the sulphonamide (I) were not successful, probably owing to hydrolysis.

N-(3-Bromo-2,6-diethylphenyl)-acetamide (IX) was prepared by shaking the acetamide (X) for several hours with a mixture of 98% sulphuric acid (400 ml.) and bromine (20 g.), during which time hydrogen bromide was steadily evolved. The product was isolated by pouring onto crushed ice, crystallization from benzene giving white needles (18 g.), m.p. 157–160°, raised to 161–162° by two crystallizations from methanol. Calc. for $C_{12}H_{16}NOBr$: C, 53.34; H, 5.18%. Found: C, 53.12; H, 5.95%.

Can. J. Chem. Downloaded from www.nrcresearchpress.com by 78.46.186.204 on 09/04/12
For personal use only.

N-(4-Bromo-2,6-diethylphenyl)-acetamide (XII) was obtained when the acetamide (X) was brominated in chloroform or acetic acid. It crystallized from methanol or benzene–hexane as long white needles, m.p. 181–182°. Addition of the 3-isomer (VII) depressed the melting point. Calc. for $C_{12}H_{16}NOBr$: C, 53.34; H, 5.97; N, 5.18; Br, 29.58%. Found: C, 53.30; H, 5.85; N, 5.13; Br, 30.25%.

Bromination of the sulphonamide (I) in chloroform (with or without addition of potassium carbonate), acetic acid, or sulphuric acid gave impure products having almost identical infrared spectra. Repeated crystallization from various solvents (methanol, acetone, ethyl acetate, benzene) gave white needles having melting points in the range 115–144°. Calc. for $C_{17}H_{20}NO_2SBr$: C, 53.41; H, 5.27%. Found: C, 53.58, 53.29; H, 5.25, 5.35%. Hydrolysis with 90% sulphuric acid gave, after acetylation, the 4-bromo-acetamide (XII), obtained after one crystallization from methanol.

INFRARED SPECTRA

The infrared spectra were obtained using potassium bromide disks and solutions in carbon disulphide or chloroform, and were calibrated against the spectrum of "Polystyrene".

The 1600–2000 cm.$^{-1}$ region, generally useful in orienting benzene derivatives (21, pp. 54–70), proved to be of little value as the acetamides showed strong carbonyl absorption at about 1650 cm.$^{-1}$. Comparison of the bands in the 700–1200 cm.$^{-1}$ region failed to reveal useful correlation with structure, and comparison of some of the spectra with those of the dimethyl homologues was also valueless.

ACKNOWLEDGMENTS

The authors are grateful to the Ethyl Corporation for generous samples of 2,6-diethylaniline and to Dr. B. M. Wepster for samples of certain derivatives of 2,6-dimethylaniline and for friendly correspondence. One of them (P. M. G. B.) is deeply indebted to Dr. F. A. L. Anet for his encouragement and interest.

REFERENCES

1. Hübner, H. and Frerichs, F. Ber. **10**, 1716 (1877).
2. Nölting, E. and Collin, A. Ber. **17**, 261 (1884).
3. Nölting, E. and Stoecklin, L. Ber. **24**, 564 (1891).
4. Nölting, E., Braun, A., and Thesmar, G. Ber. **34**, 2242 (1901).
5. Bruns, E. Ber. **28**, 1954 (1895).
6. Holleman, A. F., Hartogs, J. C., and van der Linden, T. Ber. 44, 704 (1911).
7. Hughes, E. D., Ingold, C. K. *et al.* J. Chem. Soc. 2628, 2657 (1950).
8. Scott, J. and Robinson, R. J. Chem. Soc. **121**, 844 (1922).
9. Dadswell, H. E. and Kenner, J. J. Chem. Soc. 1102 (1927).
10. Wepster, B. M. Rec. trav. chim. **73**, 809 (1954).
11. Brady, O. L., Day, J. N. E., and Rolt, W. J. W. J. Chem. Soc. **121**, 526 (1922).
12. Ecke, G. G., Napolitano, J. P., Filbey, A. H., and Kolka, A. J. J. Org. Chem. **22**, 639 (1957).
13. Beale, R. N. J. Chem. Soc. 4494 (1954).
14. Dewar, M. J. S. and Scott, J. M. W. J. Chem. Soc. 1445 (1957).
15. Klevens, H. B. and Platt, J. R. J. Am. Chem. Soc. **71**, 1714 (1949).
16. Gillois, M. and Rumpf, P. Bull. soc. chim. France, **21**, 112 (1954).
17. Badger, G. M. Structures and reactions of the organic compounds. Cambridge University Press, London. 1954.
18. Brown, H. C. and Nelson, K. L. J. Am. Chem. Soc. **75**, 6292 (1953).
19. Jones, E. C. S. and Kenner, J. J. Chem. Soc. 1851 (1931).
20. Karrer, P. and Schlöpfer, R. Helv. Chim. Acta, **24**, 298 (1941).
21. Bellamy, L. J. The infra-red spectra of complex molecules. Methuen and Co. Ltd., London. 1954.

Can. J. Chem. Downloaded from www.nrcresearchpress.com by 78.46.186.204 on 09/04/12
For personal use only.

Can. J. Chem. Downloaded from www.nrcresearchpress.com by 78.46.186.204 on 09/04/12
For personal use only.

MICROCALORIMETRIC AND KINETIC STUDIES OF THE α-CHYMOTRYPSIN – HYDROCINNAMIC ESTER – HYDROCINNAMIC ACID SYSTEM[1]

WILLIAM J. CANADY[2] AND KEITH J. LAIDLER

ABSTRACT

Using a microcalorimeter of the Tian–Calvet type the heat of binding of hydrocinnamic acid to α-chymotrypsin has been measured in aqueous solution over a range of pH values. The heat evolved was found to vary from about 5 to about 28 kcal per mole as the pH was varied from 5.1 to 7.8. In order to see whether these heats are due to the binding of the inhibitor at the active center of the enzyme, heats were also measured at pH 7.1 by a kinetic method, the inhibitor constant being determined over a range of temperatures; the heat calculated in this way was consistent with the microcalorimetric value. The kinetic work also gave rise to entropies of binding of the inhibitor and the substrate (methyl hydrocinnamate); these entropies are negative, the significance of which is discussed in terms of the mode of binding. It is suggested that the results are best explained on the hypothesis that the active center of the enzyme contains, in addition to the ordinary acidic and basic sites, a negatively charged group that interacts electrostatically with the anion of hydrocinnamic acid.

INTRODUCTION

A considerable amount of evidence has now accumulated regarding the nature of the active center in the enzyme chymotrypsin, and about the mechanisms of the reactions catalyzed by the enzyme. Since these matters have recently been reviewed and discussed (1) only the most important points will be referred to here. The work with DFP (2) and with other inhibitors (3, 4) has shown the enzyme to contain one active center per molecule. The pH dependence of the rate (5, 6) shows that the active center contains two ionizing groups, the active form of the enzyme being the one in which one of these groups is acidic and the other basic. A study of the kinetics of the hydrocinnamic acid hydrolysis in 20% methanol solution over a range of pH values and substrate concentrations (5) has shown that the pK's of the ionizing groups in the active center of the enzyme are 7.2 and 8.0, and that these groups are *not* involved in the formation of the enzyme-substrate complex but only in the subsequent steps.

The DFP work, although not entirely unequivocal, does on the whole point towards the fact (7) that the imidazole group of histidine is involved in the reaction. This group presumably corresponds to the pK value of about 7.2. The identity of the group having a pK of 8.0 (or perhaps higher, as suggested in a footnote later) is unknown, but the group might be an ω-amino group. If this is the case the ionization of the enzyme is as represented below:

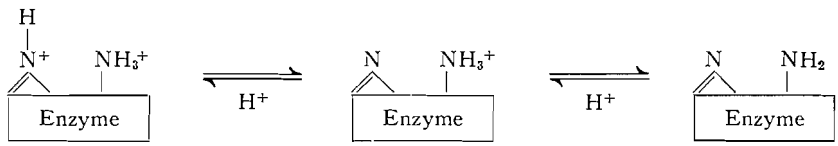

As far as reaction mechanisms are concerned, it is undoubtedly the case that a Michaelis complex is formed initially. This complex appears to be formed without the participation of the ionizing groups, and the binding may involve van der Waals and other weak

[1]*Manuscript received May 30, 1958.*
Contribution from the Department of Chemistry, the University of Ottawa, Ottawa, Canada.
[2]*Present address: Department of Biochemistry, School of Medicine, West Virginia University, Morgantown, West Virginia, U.S.A.*

forces. By analogy with the reaction with DFP and other irreversible inhibitors, it can be concluded with reasonable certainty that the enzyme is acylated at its imidazole site during the subsequent breakdown of the complex. Evidence that this is the case has been provided by the transient-phase studies of Gutfreund and Sturtevant (8, 9).

One aspect of enzyme kinetic studies that has so far been largely neglected is that involving detailed studies of the binding of inhibitors to enzymes. A few measurements of K_i values have been made, but usually at only one pH, and few ΔH and ΔS values are known for any enzyme–inhibitor system. Such studies can provide valuable information regarding reaction mechanisms, and may indeed reveal features of the active centers of enzymes that cannot be revealed by studies with substrates. The present investigation has been carried out with the object of learning about the mode of binding of the inhibitor hydrocinnamic acid to the enzyme α-chymotrypsin, over a range of pH values. Two kinds of measurement have been made. In the first place, heats of binding of the inhibitor to the enzyme have been measured directly, using a very sensitive microcalorimeter. Secondly, partly in order to see whether the heats evolved are really due to the binding of the inhibitor at the active center of the enzyme, heats of binding were also measured by a kinetic method, the inhibitor constant being measured over a range of temperatures.

Our determinations of heats of binding by microcalorimetry are, we believe, the first in which this technique has been applied to an enzyme–substrate or enzyme–inhibitor system. The results of the measurements will be seen below to provide additional knowledge of the nature of the active center and of its interaction with substrates and inhibitors.

EXPERIMENTAL

Microcalorimetry

The microcalorimeter employed is of the conduction type of Tian (10), as modified by Calvet (11, 12), and our techniques with it have been described elsewhere (13, 14). The measurements were made at 25.0° C.

The hydrocinnamic acid was supplied by Eastman Kodak and was recrystallized from hot water; m.p. 48.5° C. A solution of hydrocinnamic acid of concentration 5×10^{-2} M in $M/15$ Sørensen's phosphate buffer (15) was used throughout all of the experiments. The enzyme used was a three-times-crystallized sample of α-chymotrypsin, supplied by the Worthington Biochemical Corporation. Immediately before each experiment a fresh chymotrypsin solution of 2×10^{-4} M was made up in Sørensen buffer of the desired pH. Ten milliliters of the enzyme solution was placed in the main calorimeter cell, and 0.5 ml of the inhibitor solution was placed in the capillary bulb. After a suitable time for temperature equilibration the capillary bulb was broken, and a small rubber bulb connected to the far end of the capillary was gently squeezed to ensure mixing. A blank was run at the same time by adding inhibitor solution to a plain buffer solution of the same pH as the buffered enzyme solution. The difference between the values obtained with the blank and the enzyme is the heat evolved by the combination of inhibitor with enzyme. The final pH of the reaction mixture was checked after the heat was measured. This value was recorded as the pH at which the heat was evolved.

Kinetics

The methyl ester of hydrocinnamic acid was prepared by refluxing the acid with an excess of methanol, a few drops of concentrated sulphuric acid being used as catalyst. The product was dissolved in ether and washed with 5% sodium bicarbonate solution

Can. J. Chem. Downloaded from www.nrcresearchpress.com by 78.46.186.204 on 09/04/12
For personal use only.

and with water. It was purified by fractional distillation, the middle 20% being collected; the boiling point was 236.5° C at atmospheric pressure. The enzyme employed was the same three-times-crystallized sample used for the calorimetric investigations. The buffer employed was the Sørensen's phosphate buffer previously used in the calorimetric determinations, but at the much lower concentration of 1.7778×10^{-4} *M*. The concentration of enzyme was approximately 1×10^{-5} *M*. The same enzyme solution was always used throughout a complete set of runs. The procedure was to measure initial reaction rates over a range of substrate and inhibitor concentrations. The range of substrate concentrations employed was 0.89×10^{-3} *M* to 2.65×10^{-3} *M*, the upper limit being imposed by the low solubility of the substrate in water. The inhibitor concentration was varied from 0.659×10^{-3} to 5.27×10^{-3} *M*. In order for the ionic strength to be maintained constant all solutions were 0.1 *M* in sodium chloride. Runs were carried out at 10.0°, 15.0°, 20.0°, 25.0°, and 30.0° C, and at a pH of 7.10.

The course of the reaction was followed by potentiometric titration, using a Radiometer Automatic Titrator as a pH meter. As the reaction proceeded small amounts of 2×10^{-2} *M* sodium hydroxide were added from a syringe micropipette in order to neutralize the hydrocinnamic acid liberated and to maintain the pH constant at 7.10. The sodium hydroxide was conveyed directly to the surface of the solution by means of a bent hypodermic needle. The reaction mixture was stirred by means of a magnetic stirrer, and the temperature maintained constant by circulation of thermostatically controlled water through an outer jacket.

RESULTS

Microcalorimetry

The heats evolved per mole are shown in Table I, and a plot of ΔH against pH is given in Fig. 1.

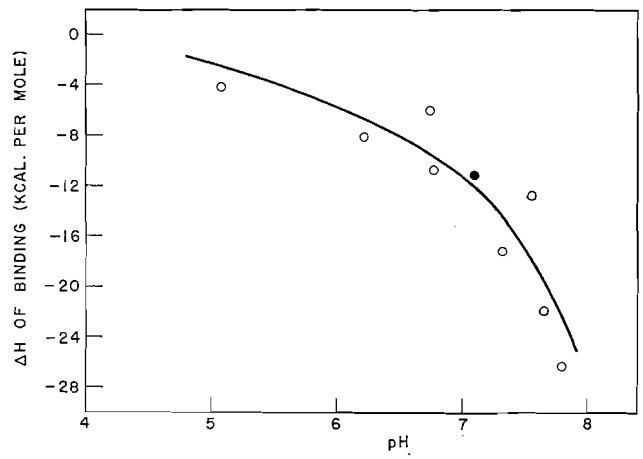

FIG. 1. Plot of ΔH of binding against pH, for the α-chromotrypsin – hydrocinnamic acid system.

Kinetics

The rates obtained at a variety of temperatures, substrate concentrations, and inhibitor concentrations are shown in Tables II and III.

Can. J. Chem. Downloaded from www.nrcresearchpress.com by 78.46.186.204 on 09/04/12
For personal use only.

TABLE I

MICROCALORIMETRIC HEATS OF BINDING FOR THE α-CHYMOTRYPSIN – HYDROCINNAMIC ACID SYSTEM

pH	ΔH (kcal per mole)
5.09	− 4.2
6.22	− 8.1
6.75	− 6.1
6.78	−10.8
7.32	−17.2
7.56	−12.8
7.65	−22.0
7.80	−26.4

TABLE II

RATES AT VARIOUS TEMPERATURES AND SUBSTRATE CONCENTRATIONS

Rates in mole liter^{-1} sec^{-1}; [S] in mole liter^{-1}

T = 10.0° C		T = 15.0° C		T = 20.0° C		T = 25.0° C		T = 30.0° C	
[S] $\times 10^3$	$v \times 10^7$	[S] $\times 10^3$	$v \times 10^7$	[S] $\times 10^3$	$v \times 10^7$	[S] $\times 10^3$	$v \times 10^7$	[S] $\times 10^3$	$v \times 10^7$
2.647	1.088	2.675	1.947	2.674	2.777	2.810	4.211	2.674	6.195
2.383	1.077	2.405	1.958	2.407	2.764	2.529	4.213	2.407	6.078
2.118	1.046	2.139	1.906	2.140	2.710	2.248	4.029	2.139	5.817
1.853	1.053	1.872	1.906	1.872	2.625	1.967	3.911	1.872	5.674
1.324	1.031	1.604	1.835	1.605	2.599	1.686	3.797	1.605	5.439
		1.337	1.787	1.337	2.485	1.405	3.699	1.337	5.101
		1.069	1.742	1.070	2.353	1.124	3.486		
				0.802	2.210	0.984	3.310		
						0.843	3.198		

TABLE III

RATES AT VARIOUS TEMPERATURES, SUBSTRATE CONCENTRATIONS, AND INHIBITOR CONCENTRATIONS

Rates in mole liter^{-1} sec^{-1}; concentrations in mole liter^{-1}

T = 10.0° C [S] = 1.337×10^{-3}		T = 15.0° C [S] = 1.337×10^{-3}		T = 20.0° C [S] = 1.604×10^{-3}		T = 25.0° C [S] = 1.405×10^{-3}		T = 25.0° C [S] = 1.967×10^{-3}		T = 25.0° C [S] = 1.124×10^{-3}		T = 30.0° C [S] = 1.324×10^{-3}	
[I] $\times 10^3$	$v \times 10^7$	[I] $\times 10^3$	$v \times 10^7$	[I] $\times 10^3$	$v \times 10^7$	[I] $\times 10^3$	$v \times 10^7$	[I] $\times 10^3$	$v \times 10^7$	[I] $\times 10^3$	$v \times 10^7$	[I] $\times 10^3$	$v \times 10^7$
0	1.004	0	1.642	0	2.136	0	4.542	0	4.834	0	3.501	0	3.272
1.315	0.830	1.318	1.397	1.318	1.907	0.659	4.159	0.659	4.554	0.659	3.238	1.319	2.819
2.629	0.721	2.637	1.169	1.637	1.653	2.637	3.170	1.319	4.222	1.319	2.803	2.637	2.486
3.944	0.633	3.955	1.042	1.955	1.506	3.956	2.739	2.637	3.811	2.637	2.455	3.956	2.293
5.259	0.570	5.274	0.902	5.274	1.312	4.615	2.681	3.956	3.444			5.274	1.959
		6.592	0.740			5.274	2.427						

Although the mechanism of the reaction is undoubtedly somewhat more complicated (8, 9) than represented by the simple Michaelis–Menten equations

$$E + S \underset{k_{-1}}{\overset{k_1}{\rightleftarrows}} ES$$

$$ES \xrightarrow{k_2} E + \text{products}$$

Can. J. Chem. Downloaded from www.nrcresearchpress.com by 78.46.186.204 on 09/04/12
For personal use only.

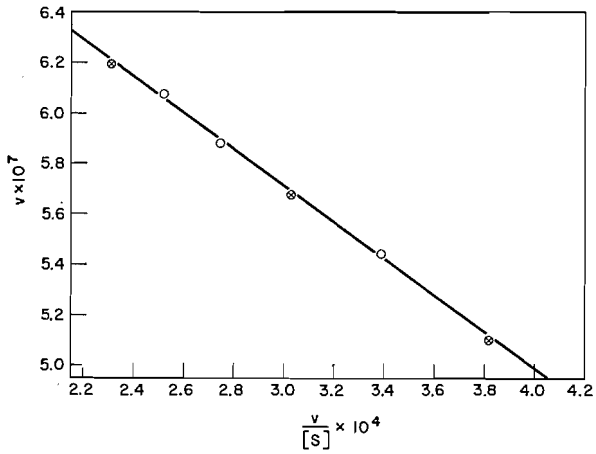

FIG. 2. Plot of v against $v/[S]$ for the hydrolysis of hydrocinnamic ester. The points with crosses represent duplicate runs.

the over-all kinetic behavior is consistent with the above mechanism; in the present treatment the above mechanism will therefore be assumed. The validity of this mechanism can be demonstrated, as first shown by Eadie (16), by plots of $v/[S]$ against v. A representative plot of this kind is shown in Fig. 2. From the slope and intercepts may be obtained the values of k_2 and $\bar{K}$; the latter is the reciprocal of the conventional Michaelis constant and is defined by

$$[1] \qquad \bar{K} = 1/K_m = k_1/(k_{-1}+k_2).$$

As referred to above there is good evidence that $k_{-1} \gg k_2$, so that $\bar{K}$ is simply the equilibrium constant for the formation of the complex.

The values of K_i were obtained from plots of v_0/v against [I]; v is the inhibited rate and v_0 the uninhibited rate. The rate equation for competitive inhibition is

$$[2] \qquad v = k_2\bar{K}[E]_0[S]/(1+\bar{K}[S]+K_i[I])$$

and from this it follows that

$$[3] \qquad v_0/v = 1+\{K_i[I]/(1+\bar{K}[S])\}.$$

The slopes of the plots were found to be proportional to $1/(1+\bar{K}[S])$; examples of such plots are shown in Fig. 3, and the lines are seen to meet the ordinate at a value of unity. The results confirm that the inhibition is indeed competitive; from the slopes, $\bar{K}$ being known, the K_i values were calculated.

Each value of $\bar{K}$ was obtained from about ten kinetic runs, every other one being made in duplicate. The values of K_i were also obtained from about ten runs. All values were calculated using the method of least squares.

Table IV shows the $\bar{K}$ and K_i values obtained in the above manner. In Fig. 4 the natural logarithms of $\bar{K}$ and of K_i are plotted against the reciprocal of the absolute temperature. The ΔH values calculated from the least-square slopes are given in Table V, together with the corresponding free energies and entropies. The second column shows the values corresponding to $\bar{K}$ and therefore related to the binding of the ester, the third column the values corresponding to K_i and related to the binding of the acid.

Can. J. Chem. Downloaded from www.nrcresearchpress.com by 78.46.186.204 on 09/04/12
For personal use only.

Can. J. Chem. Downloaded from www.nrcresearchpress.com by 78.46.186.204 on 09/04/12
For personal use only.

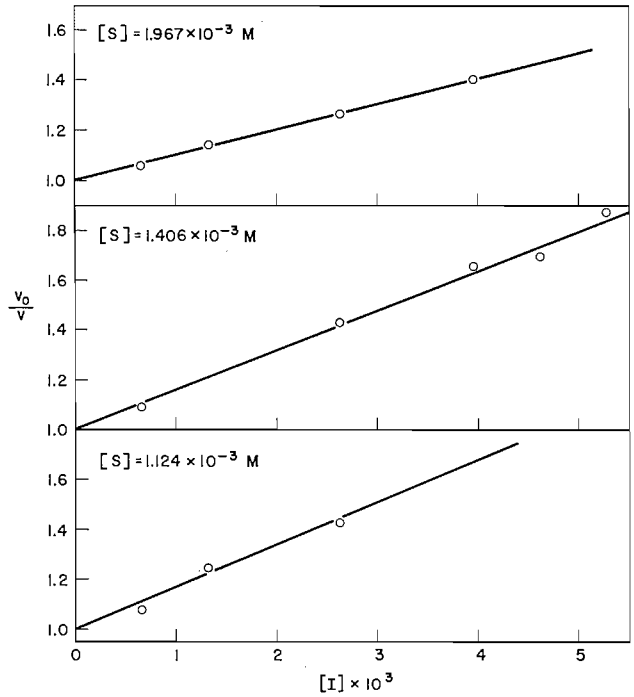

FIG. 3. Plots of v_0/v against inhibitor concentration.

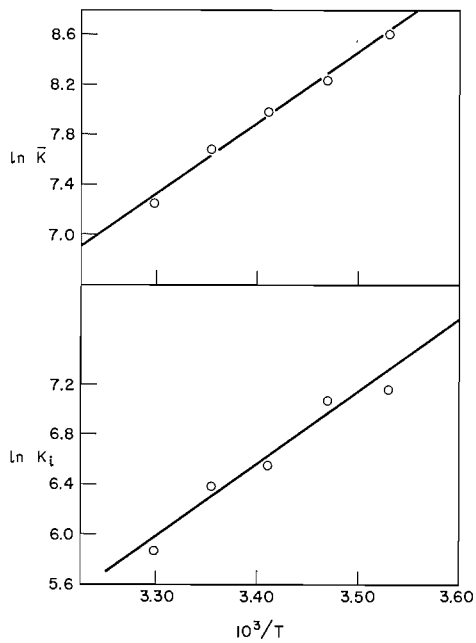

FIG. 4. Plots of the natural logarithms of $\bar{K}$ and K_i against the reciprocal of the absolute temperature.

TABLE IV

VALUES OF $\bar{K}$ AND K_i AT VARIOUS TEMPERATURES

Temperature, ° C	pH = 7.10 $\bar{K}$ (liter mole^{-1})	K_i (liter mole^{-1})
30.0	1405	356
25.0	2170	592
20.0	2831	696
15.0	3770	1179
10.0	5488	1292

TABLE V

SUMMARY OF THERMODYNAMICAL RESULTS FOR THE BINDING OF ESTER AND ACID

	pH = 7.10 Ester	Acid	
ΔG	− 4.55	− 3.78	kcal per mole
ΔH	−11.2	−11.0	kcal per mole
ΔS	−22.2	−24.3	e.u.

DISCUSSION

The result of greatest interest from the present standpoint is the fact that the heat corresponding to K_i, namely 11.0 kcal per mole, agrees quite closely with that obtained in the microcalorimetric studies. This is shown in Fig. 1, in which the heats are plotted against the pH; the open circles represent the calorimetric results, the closed circle the kinetic value obtained as described above. Since the microcalorimeter was being used at its very highest sensitivity there may well be an error of 10% or more in the calorimetric heats, and this largely accounts for the difference between the kinetic heat and the calorimetric ones. Additional reasons for differences are:

(1) the much higher enzyme concentration that had to be used in the calorimetric work (2×10^{-4} M as compared with 1×10^{-5} M),

(2) the fact that the kinetic work was done in 0.1 M sodium chloride solution.

In view of the similarity of the kinetic and calorimetric values there is no reason to doubt that the microcalorimetric values do correspond to the interaction between the active centers and the inhibitor. Further work to confirm this is, however, necessary, and is now being carried out at other pH values.

Other points that are worthy of comment are as follows. The close similarities between the ΔH, ΔS, and ΔG values for esters and inhibitor are consistent with the conclusions, strongly suggested by the pH studies in 20% methanol (5), that*

(*a*) $\bar{K}$ is actually an equilibrium constant,

(*b*) the binding between enzyme and substrate does not involve the ionizing groups on the enzyme.

Conclusion (*b*) suggests that the enzyme–substrate binding probably involves van der Waals forces between enzyme and substrate (1), and these forces are expected to remain practically the same if the ester is replaced by the acid.

**It should be mentioned that recent work (17, 18) indicates the pH behavior in aqueous solution to be slightly but significantly different from that in 20% methanol as used by Laidler and Barnard (5) and other workers. The pH optimum is 7.8 in 20% methanol but 8.4 in pure water. Stein and Laidler (17) are currently carrying out a detailed study of the influence of methanol on the kinetics of the reaction, with particular reference to the binding of irreversible inhibitors such as DFP, while Gill and Laidler (18) are studying the pH dependence in aqueous solution and are extending the present work on the binding of hydrocinnamic acid.*

Can. J. Chem. Downloaded from www.nrcresearchpress.com by 78.46.186.204 on 09/04/12
For personal use only.

A further insight into the nature of the inhibition is provided by a comparison of K_i at 25° C and at various pH values, as follows:

pH = 7.1	K_i = 592	Present work
pH = 7.8	K_i = 182	Neurath and Gladner (19)
pH = 7.9	K_i = 33	Huang and Niemann (20)
pH = 7.9	K_i = 33–50	Foster and Niemann (21)

Although the conditions (ionic strength, nature of buffer, etc.) are not the same in all cases, it seems clear that the inhibitor is much less strongly bound at the higher pH values.

The microcalorimetric studies have shown that the binding becomes more exothermic as the pH is raised; together with the K_i values, this implies that the ΔS of binding becomes considerably more negative with increasing pH. The ΔS of binding at pH 7.8 is in fact approximately -80, as compared with the value of -24.3 at pH 7.1.

Since the pK of hydrocinnamic acid is 4.66 (22) it is clear that the acid is almost entirely in the anionic form at all of the pH values of the present investigation. The variations in the thermodynamic quantities for the binding of the inhibitor must therefore be attributed to changes in the state of ionization of the enzyme. It is postulated that the enzyme possesses at its active center, in addition to the acidic and basic groups responsible for the actual hydrolysis of the substrate, a negatively charged group. This group must be largely neutralized at the pH of 7.1 (this follows from the close similarity of the thermodynamical values for the ester and the acid). At the values of 7.8–7.9, however, it must be assumed that this group is largely in the negatively charged form. As a result the binding of the acid anion is much less strong, and there is a large negative entropy of binding owing to the repulsion between the two charged groups.

ACKNOWLEDGMENTS

The authors are very much indebted to Dr. H. M. Papée, for very considerable help with the microcalorimetric determinations.

The work was supported by a grant from the Defence Research Board.

REFERENCES

1. Laidler, K. J. Discussions Faraday Soc. **20**, 83 (1955).
2. Jansen, E. F., Nutting, M. D. F., and Balls, A. K. J. Biol. Chem. **129**, 201 (1949).
3. Doherty, D. G. and Vaslow, F. J. Am. Chem. Soc. **74**, 931 (1952).
4. Loewus, M. W. and Briggs, D. R. J. Biol. Chem. **199**, 857 (1952).
5. Laidler, K. J. and Barnard, M. C. Trans. Faraday Soc. **52**, 497 (1956).
6. Cunningham, L. W. and Brown, C. S. J. Biol. Chem. **221**, 287 (1956).
7. Jandorf, B. J., Michel, H. O., Schaffer, N. K., Egan, R., and Summerson, W. H. Discussions Faraday Soc. **20**, 134 (1955).
8. Gutfreund, H. and Sturtevant, J. M. Biochem. J. **63**, 656 (1956).
9. Gutfreund, H. and Sturtevant, J. M. Proc. Natl. Acad. Sci. U.S. **47**, 719 (1956).
10. Tian, M. J. chim. phys. **30**, 665 (1933).
11. Calvet, E. Mém. serv. chim. état (Paris), **32**, 168 (1946).
12. Calvet, E. Report to the Commission on Thermochemistry. International Union of Pure and Applied Chemistry, 1952.
13. Papée, H. M., Canady, W. J., and Laidler, K. J. Can. J. Chem. **34**, 1677 (1956).
14. Canady, W. J., Papée, H. M., and Laidler, K. J. Trans. Faraday Soc. **54**, 502 (1958).
15. Clark, W. M. The determination of hydrogen ions. The Williams & Wilkins Co., Baltimore, Md. 1925.
16. Eadie, G. S. J. Biol. Chem. **146**, 85 (1942).
17. Stein, B. R. and Laidler, K. J. To be published.
18. Gill, E. K. and Laidler, K. J. To be published.
19. Neurath, H. and Gladner, J. A. J. Biol. Chem. **188**, 407 (1951).
20. Huang, H. T. and Niemann, C. J. Am. Chem. Soc. **74**, 5963 (1952).
21. Foster, R. J. and Niemann, C. J. Am. Chem. Soc. **71**, 3370 (1955).
22. Dippy, F. J. P. Chem. Revs. **25**, 151 (1939).

Can. J. Chem. Downloaded from www.nrcresearchpress.com by 78.46.186.204 on 09/04/12
For personal use only.

Can. J. Chem. Downloaded from www.nrcresearchpress.com by 78.46.186.204 on 09/04/12
For personal use only.

THE SEPARATION OF SATURATED AND UNSATURATED FATTY ACID ESTERS BY GAS–LIQUID CHROMATOGRAPHY[1]

B. M. Craig and N. L. Murty[2]

ABSTRACT

Fatty acid methyl esters are separated according to chain length by using washed silicone grease supported on 20–40 mesh C_{22} firebrick. By using a plasticizer on the firebrick support the same esters are separated according to both chain length and degree of unsaturation. Together the two procedures can be used to determine the component fatty acids in fats and oils. Nearly parallel linear relations are obtained for saturated, monoethenoid, diethenoid, and triethenoid methyl esters when the logarithm of emergence time is plotted against the carbon number of the fatty acid.

INTRODUCTION

The development of gas–liquid partition chromatography by Martin and James (1, 2) has provided a new and powerful tool for semimicro- and micro-analyses. The rapid extension of this method to fats and oils by Martin and James (1, 2, 3), Cropper and Heywood (4, 5), Dijkstra *et al.* (6), Van de Kamer *et al.* (7), Ray (8) and the improvements developed by these workers have made possible the separation of small quantities of fatty acid esters. These separations are based on chain length and include separation of esters of odd-numbered acids and branched-chain acids. Silicone grease and Apiezon grease with or without stearic or other saturated acids have been the preferred liquid phases supported on Celite or crushed firebrick. A further development has been fractionation on the basis of unsaturation in a series of esters such as stearic, oleic, linoleic, and linolenic acids. This has been accomplished by Orr and Callen (9) and by Lipsky and co-workers (10) using commercial plasticizers as liquid phases. The first used by Orr and Callen (9) is Reoplex 400, which is a commercial plasticizer and is a polyoxyalkalene adipate. The plasticizers used by Lipsky are adipic esters of diethylene glycol and the adipic ester of diethylene glycol cross-linked with pentaerythritol.

In this laboratory gas–liquid chromatography has been used with silicone and Apiezon liquid phases for the analysis of fats and oils. Reoplex 400 was found to "bleed" extensively, particularly at temperatures over 200° C. Attempts were then made to synthesize plasticizers which would effect the separation of stearic, oleic, linoleic, and linolenic acids but which would not "bleed". A number of these have been synthesized and tested and the results are given in this paper.

EXPERIMENTAL

Silicone Column

Dow–Corning High Vacuum stopcock grease was dispersed in ethyl acetate by means of an Ultra-Turrax high speed stirrer, then precipitated out by addition of methyl alcohol and treated as described by Cropper and Heywood (4, 5). The washed silicone grease was dispersed in ethyl acetate in a round-bottom flask. C_{22} firebrick (Johns Manville) was added to the suspension (a mixture of 20–30 and 30–40 mesh 1:1 (w/w)), and the solvent evaporated at 80–90° C under vacuum in a laboratory rotary evaporator.

[1]*Manuscript received March 31, 1958.*
Contribution from the National Research Council of Canada, Prairie Regional Laboratory, Saskatoon, Saskatchewan.
Issued as N.R.C. No. 4863 and Paper No. 255 on the Uses of Plant Products.
[2]*National Research Council of Canada Postdoctorate Fellow, 1957–.*

The silicone grease was applied in a 1:4 ratio (w/w) with the crushed firebrick, and was packed in a copper column $\frac{1}{4}$ inch in diameter by 12 feet in length.

Plasticizer Columns

Two plasticizers were synthesized using a dibasic acid and diethylene glycol containing 1% by weight of diglycerol to provide cross-linking. The dibasic acids were adipic and succinic and details are given for preparation of the succinic plasticizer. A mixture of 24.0 g succinic acid, 21.2 g of diethylene glycol, 0.5 g of diglycerol, and 0.2 g of *p*-toluenesulphonic acid in a round-bottom flask was heated at 130° C/2 mm for 2 hours with occasional shaking. A clear sirupy solution resulted. The plasticizer was dissolved in ethyl acetate, washed three times with water, dried over anhydrous sodium sulphate, filtered, and the solvent removed under reduced pressure. The plasticizer was dissolved in ethyl acetate and applied to 20–40 mesh C_{22} firebrick in a 1:4 ratio (w/w) as outlined for the silicone column.

Two columns, copper tubing $\frac{1}{4}$ inch by 6 feet long, using succinic and adipic plasticizers, respectively, were coupled in series, with the succinic as the fore column. Initial tests indicated that the succinic plasticizer gave a more effective separation of the esters of stearic and oleic acids and the adipic column of the esters of linolenic and arachidic acids.

Apparatus

The gas–liquid chromatographic unit of conventional design was constructed in the laboratory. Four Gow–Mac filaments were employed with two in each of the reference and sample detectors and the bridge was operated at 150 ma. Helium was used as the carrier gas and the recorder was operated at the 2.5-mv range. The apparatus was controlled at a temperature of 210° C. The silicone column was operated at a flow rate of 100 cc per minute and the plasticizer columns at 70 cc per minute, as measured by a soap bubble unit on the outlet tube. The sample sizes varied from 3 to 15 μl, depending on the particular oil, and injection was made with a precision syringe.

The materials used in the study were the methyl esters of the fatty acids from tallow, soybean oil, lard, and herring oil, which were kindly supplied by the research laboratory of Canada Packers Limited, Toronto, Canada.

RESULTS AND DISCUSSION

Figure 1, which reproduces actual recorder charts, gives the curves that resulted for lard, tallow, soybean oil, and herring oil esters with the plasticizer column and for lard and herring oil esters with the silicone column. The position of peaks representing C_{10}, C_{12}, C_{14}, C_{16}, and C_{18} saturated acids, labelled 1, 2, 3, 4, and 5, respectively, were determined by calibration with a known synthetic mixture of these acids.

The separation of palmitic, stearic, oleic, linoleic, and linolenic methyl esters in soybean oil are comparable to those obtained by Lipsky (10) using a commercial plasticizer. The plasticizer used in the present work "bled" slightly during the first runs but little or not at all at later stages and operation of the column for a period of 3 weeks indicated no decreased efficiency. The present columns using a 1:4 ratio of liquid phase have a limited capacity, e.g. approximately 10 mg of soybean esters on 20 g of column packing before evidence of overloading is indicated.

The tallow esters on a silicone column showed C_8, C_{10}, C_{12}, C_{14}, C_{15}, C_{16}, C_{17}, and C_{18} acids as well as peaks between C_{14} and C_{15} and C_{16} and C_{17}, which may have been branched-chain acids. The tallow esters from the plasticizer column showed additional peaks which may be due to unsaturated acids of various chain lengths. Herring oil esters

Can. J. Chem. Downloaded from www.nrcresearchpress.com by 78.46.186.204 on 09/04/12
For personal use only.

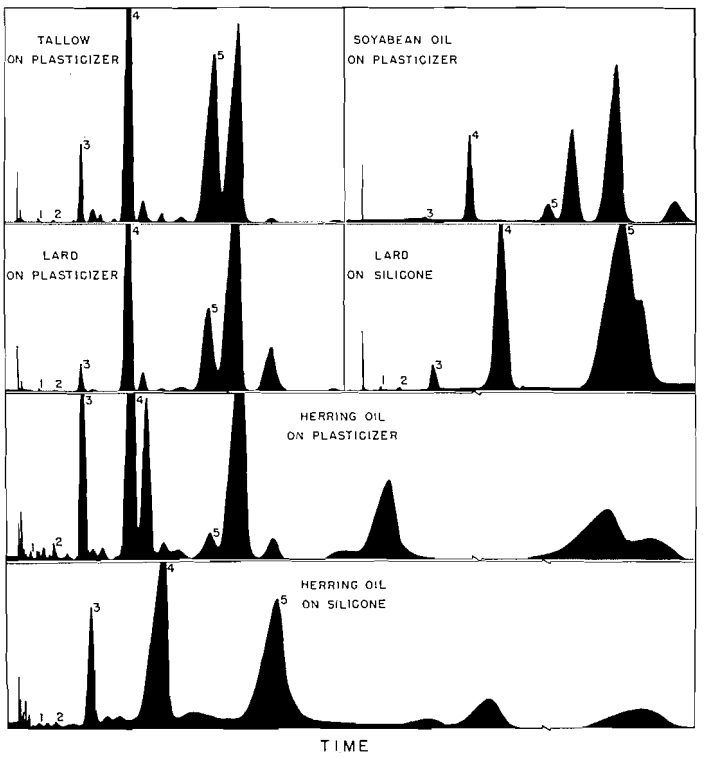

FIG. 1. Gas–liquid chromatographic separations of methyl esters of fats and oils on silicone and plasticizer columns. The numbers 1, 2, 3, 4, and 5 refer to the saturated C_{10}, C_{12}, C_{14}, C_{16}, and C_{18} acids. Peaks following these are odd-numbered or branched-chain in the case of silicone columns or unsaturated from the plasticizer column.

also showed odd-numbered fatty acids, C_9, C_{11}, C_{13}, and C_{15}, in addition to the expected even-numbered series on a silicone column. The lard esters showed even-numbered members from C_{10} to C_{20} on a silicone column and a number of unsaturated acids in each group on the plasticizer column.

Some separation of saturated and unsaturated acids took place on the silicone column within a group such as the C_{18} acids. The separation was the reverse of that accomplished by the plasticizer column in that the less unsaturated acids are retained more strongly by the liquid phase. This was proved by coupling a silicone column to a plasticizer column. The separation on the plasticizer then offset the silicone column, single peaks being obtained for each chain length. The same results were obtained with columns using Apiezon "M" as a liquid phase coupled to a plasticizer column.

The logarithm of the emergence time (time from the air peak to the sample peak) has been plotted against number of carbon atoms (Fig. 2). Peaks representing the saturated acids C_{12}, C_{14}, C_{16}, and C_{18} were plotted first and the linear relation for chain length against logarithm of retention time was established. Other peaks from various curves were plotted on the same line according to retention time only. The odd-numbered acids and compounds thought to be branched-chain acids are also represented, both from the silicone and the plasticizer columns.

The "monoethenoid" relation was made up by moving the points representing the peaks following those of palmitic, stearic, and arachidic acids, e.g. palmitoleic, oleic, and

Can. J. Chem. Downloaded from www.nrcresearchpress.com by 78.46.186.204 on 09/04/12
For personal use only.

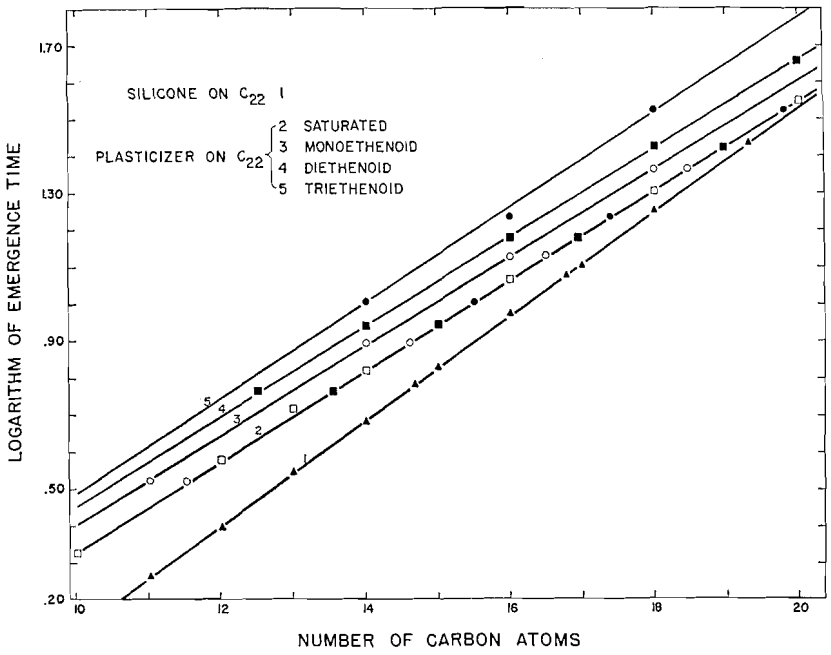

FIG. 2. Logarithm of emergence time plotted against carbon number for saturated, monoethenoid, diethenoid, and triethenoid acids from plasticizer columns and for acids from silicone column.

eicosenoic acids, to correspond to the appropriate carbon numbers. As expected, a linear relation was obtained, since the presence of one double bond would presumably have the same influence on each chain length.

The same procedure was followed for the diethenoid acids, giving a family of linear relations which are essentially parallel. The linear relation for triethenoid does not seem to be parallel to the other relations but further work needs to be done on polyethenoid acids with polyester columns to establish the slope of this line in relation to the less unsaturated acids.

Since these linear relations were established by using known esters and fatty acid esters of oils of known composition, the system is applicable for analysis of any other oil if similar conditions of temperature, flow rate, column size, and packing are used. The present system of plasticizers alone is inadequate, since the dienoic C_{16} acid has the same emergence peak as the C_{17} acid. Similarly, linolenic acid and arachidic acid examined in other oils show a simultaneous emergence. Such difficulties could be resolved by collecting the fractions from the silicone column and applying these in turn to a plasticizer column, a procedure which would require the initial separation of larger quantities of fatty acid esters.

The research on separation of saturated and unsaturated fatty acids is being continued to find liquid phases which give a more efficient separation particularly of such sequences as stearic–oleic and linolenic–arachidic acids. Preliminary results on quantitative measurements of unsaturated acids such as linoleic and linolenic which are presently done by spectrophotometric analysis indicate that the chromatographic method is equally reliable and requires considerably smaller samples.

Can. J. Chem. Downloaded from www.nrcresearchpress.com by 78.46.186.204 on 09/04/12
For personal use only.

ACKNOWLEDGMENTS

The work of Mr. T. M. Mallard, who constructed the gas–liquid chromatographic unit, and Mr. L. L. Hoffman, who aided in the analyses, is gratefully acknowledged.

REFERENCES

1. JAMES, A. T. and MARTIN, A. J. P. Biochem. J. **50**, 679 (1952).
2. JAMES, A. T. and MARTIN, A. J. P. Analyst, **77**, 915 (1952).
3. JAMES, A. T. Research, **8**, 8 (1955).
4. CROPPER, F. R. and HEYWOOD, A. Nature, **172**, 1101 (1953).
5. CROPPER, F. R. and HEYWOOD, A. Nature, **174**, 1063 (1954).
6. DIJKSTRA, G., KEPPLER, J. G., and SCHOLS, J. A. Rec. trav. chim. **74**, 805 (1955).
7. VAN DE KAMER, J. H., GERRITSMA, K. W., and WANSINK, E. J. Biochem. J. **61**, 174 (1955).
8. RAY, N. H. J. Appl. Chem. 4, 21 (1954).
9. ORR, C. H. and CALLEN, J. E. J. Am. Chem. Soc. **80**, 249 (1958).
10. LIPSKY, S. R. Chem. Eng. News, **36** (No. 5), 48 (1958).

Can. J. Chem. Downloaded from www.nrcresearchpress.com by 78.46.186.204 on 09/04/12
For personal use only.

Can. J. Chem. Downloaded from www.nrcresearchpress.com by 78.46.186.204 on 09/04/12
For personal use only.

THE ANALYSIS OF NUCLEAR MAGNETIC RESONANCE SPECTRA

IV. FOUR NUCLEI: AB_3[1]

R. J. Abraham, J. A. Pople,[2] and H. J. Bernstein

ABSTRACT

The proton magnetic resonance spectrum of methyl mercaptan has been analyzed on the basis of the nuclear grouping AB_3. The spectrum calculated for $J/\nu_0\delta = 0.324$ agrees very well with that observed.

1. INTRODUCTION

This series of papers presents detailed methods of analysis of complex nuclear magnetic resonance spectra which arise when signal separations due to chemical shifts are of the same order as the spin-coupling constants. In Part I (1), the quantum mechanical methods for setting up the problem for nuclei of spin $\frac{1}{2}$ were reviewed and a notation set up for classifying groups of nuclei which gave characteristic spectra. In this paper, we shall be concerned with four nuclei of spin $\frac{1}{2}$, three of which (type B) are in equivalent chemical positions. This means that they have the same chemical shift and the same coupling constants with the fourth nucleus (type A). According to the notation of Part I, this is described as an AB_3 group if the chemical shift is of the same order as the coupling constant. It should be noted that some groups may give spectra of this type even though the B-nuclei may not be equivalent at any one instant. If the nuclei are rearranging positions rapidly (compared with the width of the spectrum in frequency units), they will become effectively equivalent, the chemical shifts and coupling constants being replaced by mean values. An important source of AB_3 spectra is likely to be methyl groups where internal rotation carries out this rapid interchange. An example of this sort is the proton spectrum of CH_3SH at 40 Mc/sec, which is analyzed in Section 3.

2. GENERAL THEORY FOR AB_3

We shall adopt the general method and notation outlined in Part I (1). This involves the construction of matrices of the Hamiltonian using a set of basic functions chosen according to the symmetry of the nuclear group. It is necessary to combine the two spin functions of the A-nucleus with the six functions for three equivalent nuclei B_3. The latter were tabulated by McConnell, McLean, and Reilly (2) and consist of four symmetrical functions

$$[2.1] \qquad (\alpha\alpha\alpha),\ (\alpha\alpha\beta+\alpha\beta\alpha+\beta\alpha\alpha)/\sqrt{3},\ (\beta\beta\alpha+\beta\alpha\beta+\alpha\beta\beta)/\sqrt{3},\ (\beta\beta\beta)$$

and two degenerate pairs

$$[2.2] \qquad (\alpha\alpha\beta+\alpha\beta\alpha-2\beta\alpha\alpha)/\sqrt{6},\ (\alpha\alpha\beta-\alpha\beta\alpha)/\sqrt{2}$$

and

$$[2.3] \qquad (\beta\beta\alpha+\beta\alpha\beta-2\alpha\beta\beta)/\sqrt{6},\ (\beta\beta\alpha-\beta\alpha\beta)/\sqrt{2}.$$

[1]*Manuscript received June 9, 1958.*
Contribution from the Division of Pure Chemistry, National Research Council of Canada, Ottawa, Canada. Issued as N.R.C. No. 4853.
[2]*Department of Theoretical Chemistry, Cambridge, England.*

Using the group C_3, we shall call [2.1] A-functions and [2.2] and [2.3] E-functions. (The symbol A here refers to the symmetry and not to the A-nucleus.)

The next step is to construct symmetry basic functions for the complete group of four nuclei and work out the matrix of the Hamiltonian, making use of the simplifications that no mixing occurs between functions with a different total spin-component or between functions of different symmetry. Since all E-states are doubly degenerate, it is unnecessary to repeat calculations for both components, so we only consider one component of each and finally double the intensities of E-transitions. Accordingly, we shall deal only with the E basic functions $(\alpha\alpha\beta-\alpha\beta\alpha)/\sqrt{2}$ and $(\beta\beta\alpha-\beta\alpha\beta)/\sqrt{2}$.

The set of basic functions obtained by combining [2.1]-[2.3] with the functions α and β for the A-nucleus are given in Table I, together with the corresponding matrix elements of the Hamiltonian. ν_0 is the basic radio frequency employed, σ_A, σ_B, the screening constants of the two sets of nuclei, and J the A–B coupling constant. Terms involving the coupling constant between different B-nuclei are omitted, as it is known that they do not affect the observed spectrum (2). The suffix attached to each basic function gives the value of the total spin-component in the z-direction.

The determination of energies and stationary-state wave functions involves the solution of four 2×2 secular equations. We define the chemical shift δ as

$$\delta = \sigma_B - \sigma_A \qquad [2.4]$$

and introduce new positive quantities D_+, D_0, D_-, D'_0 and angles θ_+, θ_0, θ_-, θ'_0 between 0 and π, such that

$$\begin{aligned}
D_+ \cos 2\theta_+ &= \tfrac{1}{2}\nu_0\delta + \tfrac{1}{2}J \\
D_+ \sin 2\theta_+ &= \sqrt{3}\,J/2 \\
D_0 \cos 2\theta_0 &= \tfrac{1}{2}\nu_0\delta \\
D_0 \sin 2\theta_0 &= J \\
D_- \cos 2\theta_- &= \tfrac{1}{2}\nu_0\delta - \tfrac{1}{2}J \\
D_- \sin 2\theta_- &= \sqrt{3}\,J/2 \\
D'_0 \cos 2\theta'_0 &= \tfrac{1}{2}\nu_0\delta \\
D'_0 \sin 2\theta'_0 &= \tfrac{1}{2}J.
\end{aligned} \qquad [2.5]$$

TABLE I

BASIC FUNCTIONS AND MATRIX ELEMENTS OF THE HAMILTONIAN FOR FOUR NUCLEI AB_3

	Function $ABBB$	Diagonal matrix elements	Off-diagonal matrix elements
A_2	$\alpha\alpha\alpha\alpha$	$\nu_0(2-\frac{1}{2}\sigma_A-\frac{3}{2}\sigma_B)+\frac{3}{4}J$	
$1A_1$	$\alpha(\alpha\alpha\beta+\alpha\beta\alpha+\beta\alpha\alpha)/\sqrt{3}$	$\nu_0(1-\frac{1}{2}\sigma_A-\frac{1}{2}\sigma_B)+\frac{1}{4}J$	$\sqrt{3}\,J/2$
$2A_1$	$\beta\alpha\alpha\alpha$	$\nu_0(1+\frac{1}{2}\sigma_A-\frac{3}{2}\sigma_B)-\frac{3}{4}J$	
$1A_0$	$\alpha(\beta\beta\alpha+\beta\alpha\beta+\alpha\beta\beta)/\sqrt{3}$	$\nu_0(-\frac{1}{2}\sigma_A+\frac{1}{2}\sigma_B)-\frac{1}{4}J$	J
$2A_0$	$\beta(\alpha\alpha\beta+\alpha\beta\alpha+\beta\alpha\alpha)/\sqrt{3}$	$\nu_0(\frac{1}{2}\sigma_A-\frac{1}{2}\sigma_B)-\frac{1}{4}J$	
$1A_{-1}$	$\alpha\beta\beta\beta$	$\nu_0(-1-\frac{1}{2}\sigma_A+\frac{3}{2}\sigma_B)-\frac{3}{4}J$	$\sqrt{3}\,J/2$
$2A_{-1}$	$\beta(\beta\beta\alpha+\beta\alpha\beta+\alpha\beta\beta)/\sqrt{3}$	$\nu_0(-1+\frac{1}{2}\sigma_A+\frac{1}{2}\sigma_B)+\frac{1}{4}J$	
A_{-2}	$\beta\beta\beta\beta$	$\nu_0(-2+\frac{1}{2}\sigma_A+\frac{3}{2}\sigma_B)+\frac{3}{4}J$	
E_1	$\alpha\alpha(\alpha\beta-\beta\alpha)/\sqrt{2}$	$\nu_0(1-\frac{1}{2}\sigma_A-\frac{1}{2}\sigma_B)+\frac{1}{4}J$	
$1E_0$	$\alpha\beta(\beta\alpha-\alpha\beta)/\sqrt{2}$	$\nu_0(-\frac{1}{2}\sigma_A+\frac{1}{2}\sigma_B)-\frac{1}{4}J$	$-\frac{1}{2}J$
$2E_0$	$\beta\alpha(\alpha\beta-\beta\alpha)/\sqrt{2}$	$\nu_0(+\frac{1}{2}\sigma_A-\frac{1}{2}\sigma_B)-\frac{1}{4}J$	
E_{-1}	$\beta\beta(\beta\alpha-\alpha\beta)/\sqrt{2}$	$\nu_0(-1+\frac{1}{2}\sigma_A+\frac{1}{2}\sigma_B)+\frac{1}{4}J$	

Can. J. Chem. Downloaded from www.nrcresearchpress.com by 78.46.186.204 on 09/04/12
For personal use only.

The D-quantities are given directly by

$$[2.6] \qquad \begin{aligned} D_+ &= +\tfrac{1}{2}\{(\nu_0\delta)^2+2J(\nu_0\delta)+4J^2\}^{\frac{1}{2}} \\ D_0 &= +\tfrac{1}{2}\{(\nu_0\delta)^2+4J^2\}^{\frac{1}{2}} \\ D_- &= +\tfrac{1}{2}\{(\nu_0\delta)^2-2J(\nu_0\delta)+4J^2\}^{\frac{1}{2}} \\ D'_0 &= +\tfrac{1}{2}\{(\nu_0\delta)^2+J^2\}^{\frac{1}{2}}. \end{aligned}$$

The wave functions and energies of all states are now easily evaluated in terms of these quantities and it is possible to find the transition energies and intensities as outlined in Part I. These are given in Table II. A symbol such as $2A'_1$ is used for the state which reduces to the basic function $2A_1$ in the limit of large chemical shifts. The table is based on the assumption that $\sigma_B > \sigma_A$. If $\sigma_B < \sigma_A$ the spectrum is inverted, i.e. transition 1 is now $J+D_1$ to high field of $\gamma_0(1+\sigma_A/2-\sigma_B/2)$ instead of to low field etc.

TABLE II

TRANSITION ENERGIES AND INTENSITIES FOR FOUR NUCLEI AB_3

	Transition	Origin*	Energy (relative to $\nu_0(1-\frac{1}{2}\sigma_A-\frac{1}{2}\sigma_B)$)	Intensity
1.	$2A'_1 \rightarrow A_2$	A	$J+D_+$	$[\sqrt{3}\sin\theta_+-\cos\theta_+]^2$
2.	$2A'_0 \rightarrow 1A'_1$	A	$-\frac{1}{2}(\nu_0\delta)+D_+ +D_0$	$[-2\sin\theta_0\cos\theta_+ +\cos\theta_0\cos\theta_+ +\sqrt{3}\cos\theta_0\sin\theta_+]^2$
3.	$2E'_0 \rightarrow E_1$	A	$\frac{1}{2}J+D'_0$	$2[\cos\theta'_0-\sin\theta'_0]^2$
4.	$2A'_{-1} \rightarrow 1A'_0$	A	$-\frac{1}{2}(\nu_0\delta)+D_0+D_-$	$[2\sin\theta_0\cos\theta_-+\cos\theta_0\cos\theta_- \sqrt{3}\cos\theta_0\sin\theta_-]^2$
5.	$E_{-1} \rightarrow 1E'_0$	A	$-\frac{1}{2}J+D'_0$	$2[\cos\theta'_0+\sin\theta'_0]^2$
6.	$A_{-2} \rightarrow 1A'_{-1}$	A	$-J+D_-$	$[\cos\theta_-+\sqrt{3}\sin\theta_-]^2$
7.	$1A'_{-1} \rightarrow 1A'_0$	B	$-\frac{1}{2}(\nu_0\delta)+D_0-D_-$	$[\sqrt{3}\cos\theta_0\cos\theta_-+\sin\theta_-\cos\theta_0 +2\sin\theta_-\sin\theta_0]^2$
8.	$1E'_0 \rightarrow E_1$	B	$\frac{1}{2}J-D'_0$	$2[\cos\theta'_0+\sin\theta'_0]^2$
9.	$1A'_0 \rightarrow 1A'_1$	B	$-\frac{1}{2}(\nu_0\delta)+D_+-D_0$	$[2\cos\theta_0\cos\theta_++\sin\theta_0\cos\theta_+ +\sqrt{3}\sin\theta_0\sin\theta_+]^2$
10.	$1A'_1 \rightarrow A_2$	B	$J-D_+$	$[\sqrt{3}\cos\theta_++\sin\theta_+]^2$
11.	$2A'_0 \rightarrow 2A'_1$	B	$-\frac{1}{2}(\nu_0\delta)-D_++D_0$	$[\sqrt{3}\cos\theta_0\cos\theta_+-\cos\theta_0\sin\theta_+ +2\sin\theta_0\sin\theta_+]^2$
12.	$2A'_{-1} \rightarrow 2A'_0$	B	$-\frac{1}{2}(\nu_0\delta)-D_0+D_-$	$[2\cos\theta_0\cos\theta_--\sin\theta_0\cos\theta_- +\sqrt{3}\sin\theta_0\sin\theta_-]^2$
13.	$E_{-1} \rightarrow 2E'_0$	B	$-\frac{1}{2}J-D'_0$	$2[\cos\theta'_0-\sin\theta'_0]^2$
14.	$A_{-2} \rightarrow 2A'_{-1}$	B	$-J-D_-$	$[\sqrt{3}\cos\theta_--\sin\theta_-]^2$
15.	$1A'_{-1} \rightarrow 2A'_0$	Comb.	$-\frac{1}{2}(\nu_0\delta)-D_0-D_-$	$[-\sqrt{3}\sin\theta_0\cos\theta_--\sin\theta_0\sin\theta_- +2\cos\theta_0\sin\theta_-]^2$
16.	$1A'_0 \rightarrow 2A'_1$	Comb.	$-\frac{1}{2}(\nu_0\delta)-D_+-D_0$	$[-2\cos\theta_0\sin\theta_+-\sin\theta_0\sin\theta_+ +\sqrt{3}\sin\theta_0\cos\theta_+]^2$

*Based on $\sigma_B > \sigma_A$.

The shape of the spectrum (apart from scale factors) is a function only of the magnitude of the dimensionless parameters $J/(\nu_0\delta)$. Some spectra calculated for a series of values of this ratio are illustrated in Fig. 1. (The labelling of transitions assumes $\sigma_B > \sigma_A$ and $J > 0$. If $J < 0$, the appearance of the spectrum is unaltered, but the transitions would have to be renumbered.) Numerical values of the transition energies are given in Table III for a series of values of $J/(\nu_0\delta)$. The scale is adjusted so that the chemical shift is one unit.

One useful feature to note is that the spin-coupling constant is given directly by the separation between lines 3 and 5.

Can. J. Chem. Downloaded from www.nrcresearchpress.com by 78.46.186.204 on 09/04/12
For personal use only.

Can. J. Chem. Downloaded from www.nrcresearchpress.com by 78.46.186.204 on 09/04/12
For personal use only.

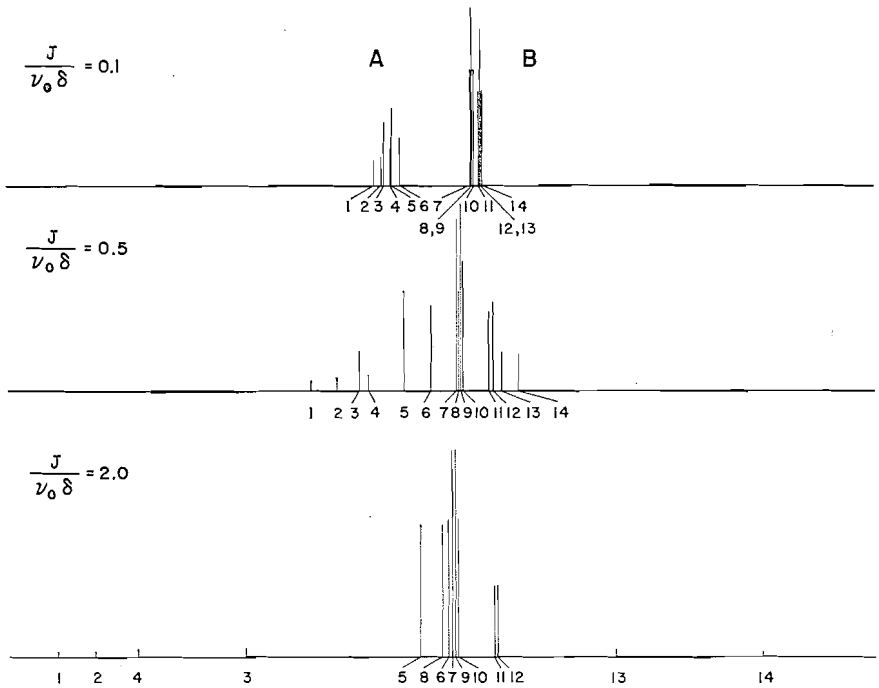

FIG. 1. Proton spectrum of CH_3SH at 40 Mc/sec. The scale is in cycles/sec and the applied field increases to the right. The frequencies are averages for several spectra to take account of drift. The numbering is that of Table II.

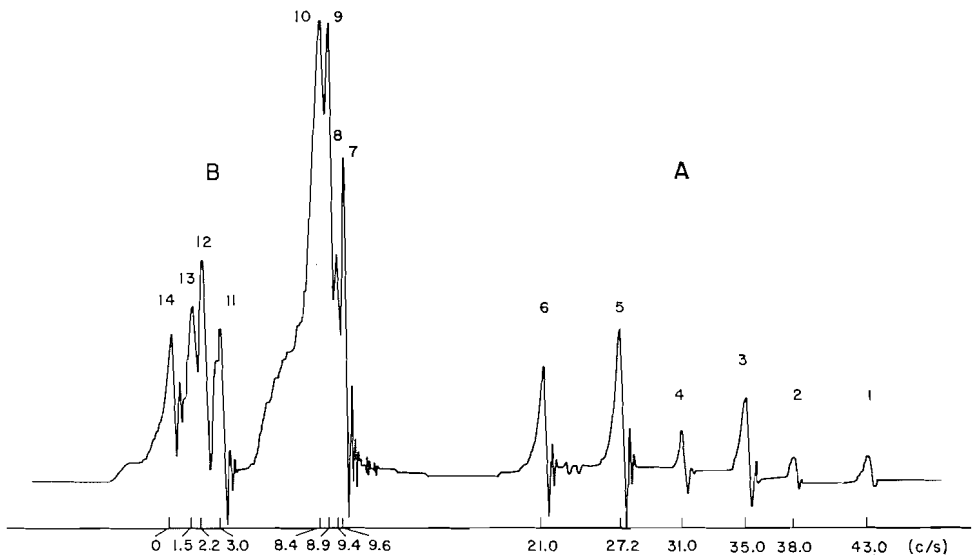

FIG. 2. Typical spectra of AB_3 group: $\sigma_B > \delta_A$ and $J > 0$. The applied field increases to the right. If $\sigma_B < \sigma_A$ the spectrum is reversed but the numbering remains the same.

TABLE III

ENERGIES OF TRANSITIONS

$J/(\nu_0\delta)$	1(A)	2(A)	3(A)	4(A)	5(A)	6(A)	7(B)	8(B)	9(B)
0	+0.500	+0.500	+0.500	+0.500	+0.500	+0.500	−0.500	−0.500	−0.500
0.1	+0.657	+0.567	+0.553	+0.468	+0.453	+0.358	−0.448	−0.453	−0.453
0.2	+0.825	+0.663	+0.620	+0.474	+0.410	+0.236	−0.397	−0.410	−0.414
0.3	+1.000	+0.783	+0.672	+0.519	+0.372	+0.136	−0.353	−0.372	−0.383
0.4	+1.181	+0.921	+0.739	+0.599	+0.339	+0.058	−0.318	−0.339	−0.359
0.5	+1.366	+1.073	+0.809	+0.707	+0.309	+0.000	−0.293	−0.309	−0.341
0.6	+1.554	+1.235	+0.883	+0.838	+0.283	−0.043	−0.276	−0.283	−0.327
0.7	+1.744	+1.404	+0.960	+0.985	+0.260	−0.076	−0.264	−0.260	−0.316
0.8	+1.936	+1.579	+1.040	+1.143	+0.240	−0.100	−0.257	−0.240	−0.308
0.9	+2.129	+1.758	+1.123	+1.311	+0.223	−0.119	−0.251	−0.223	−0.301
1.0	+2.323	+1.941	+1.207	+1.484	+0.207	−0.134	−0.248	−0.207	−0.295
1.2	+2.713	+2.313	+1.381	+1.844	+0.181	−0.156	−0.244	−0.181	−0.287
1.4	+3.106	+2.693	+1.560	+2.215	+0.160	−0.171	−0.242	−0.160	−0.281
1.6	+3.500	+3.076	+1.743	+2.594	+0.143	−0.182	−0.241	−0.143	−0.276
1.8	+3.895	+3.463	+1.930	+2.978	+0.130	−0.191	−0.241	−0.130	−0.273
2.0	+4.291	+3.853	+2.118	+3.364	+0.118	−0.197	−0.241	−0.118	−0.270

$J/(\nu_0\delta)$	10(B)	11(B)	12(B)	13(B)	14(B)	15(Comb.)	16(Comb.)
0	−0.500	−0.500	−0.500	−0.500	−0.500	−1.500	−1.500
0.1	−0.457	−0.547	−0.552	−0.553	−0.558	−1.468	−1.567
0.2	−0.425	−0.586	−0.603	−0.610	−0.636	−1.474	−1.663
0.3	−0.400	−0.617	−0.647	−0.672	−0.736	−1.519	−1.783
0.4	−0.381	−0.641	−0.682	−0.739	−0.858	−1.599	−1.921
0.5	−0.366	−0.659	−0.707	−0.809	−1.000	−1.707	−2.073
0.6	−0.354	−0.673	−0.724	−0.883	−1.157	−1.838	−2.235
0.7	−0.344	−0.684	−0.736	−0.960	−1.325	−1.985	−2.404
0.8	−0.336	−0.692	−0.743	−1.040	−1.500	−2.143	−2.579
0.9	−0.329	−0.699	−0.749	−1.123	−1.681	−2.311	−2.758
1.0	−0.323	−0.705	−0.752	−1.207	−1.866	−2.484	−2.941
1.2	−0.313	−0.713	−0.756	−1.381	−2.244	−2.844	−3.313
1.4	−0.306	−0.719	−0.758	−1.560	−2.629	−3.215	−3.693
1.6	−0.300	−0.724	−0.759	−1.743	−3.018	−3.594	−4.076
1.8	−0.295	−0.727	−0.759	−1.930	−3.409	−3.978	−4.463
2.0	−0.291	−0.730	−0.759	−2.118	−3.803	−4.364	−4.853

3. METHYL MERCAPTAN

As an example of an AB_3 spectrum we have measured the proton spectrum of CH_3SH at 40 Mc/sec. The sample of the liquid at room temperature was sealed in a spinning tube of 0.5 mm o.d. Spectra were obtained with a Varian V-4300 High Resolution Spectrometer equipped with field stabilizer. The side-band technique was used to obtain signal separations. The resonance spectrum of CH_3SH is reproduced in Fig. 2. This pattern clearly resembles the reverse of the calculated spectrum of Fig. 1 for $J/\nu_0\delta = 0.5$. The reversed spectrum corresponds to $\sigma_B < \sigma_A$ but the numbering remains the same as in Table II. The positions of the lines are easily fitted into the formulae of Table II and a good fit is obtained for

$$J = 7.85 \text{ cycles/sec}$$

$$\nu_0(\sigma_A - \sigma_B) = 24.25 \text{ cycles/sec.} \qquad [3.1]$$

Calculated transition energies and intensities using these parameters (adjusted to give agreement for line 6) are given in Table IV. The observed intensities are peak heights normalized so that the sum of the observed and theoretical intensities for the A lines are

Can. J. Chem. Downloaded from www.nrcresearchpress.com by 78.46.186.204 on 09/04/12
For personal use only.

equal and also those for the B lines. As expected, the agreement between observed and calculated intensities is much better for the well-resolved A lines than for the overlapping B lines.

TABLE IV

COMPARISON OF CALCULATED AND OBSERVED SPECTRUM FOR METHYL MERCAPTAN

	Energy		Relative intensity	
Line	Calc.	Obs.	Calc.	Obs.
1	+43.7	43.0	0.40	0.49
2	+38.2	38.0	0.51	0.42
3	+34.9	35.0	1.38	1.46
4	+31.2	31.0	0.77	0.77
5	+27.0	27.2	2.62	2.78
6	+21.0	21.0	2.32	2.09
7	+ 9.9	9.6	4.31	3.54
8	+ 9.4	9.4	2.62	2.45
9	+ 9.2	8.9	5.08	5.05
10	+ 8.4	8.4	3.60	5.08
11	+ 2.9	3.0	2.40	1.71
12	+ 2.3	2.2	2.91	2.52
13	+ 1.5	1.5	1.38	1.94
14	− 0.3	0	1.68	1.66
15	−19.0		0.007	
16	−26.0		0.002	

REFERENCES

1. BERNSTEIN, H. J., POPLE, J. A., and SCHNEIDER, W. G. Can. J. Chem. **35**, 65 (1957).
2. MCCONNELL, H. M., MCLEAN, A. D., and REILLY, C. A. J. Chem. Phys. **23**, 1152 (1955).

Can. J. Chem. Downloaded from www.nrcresearchpress.com by 78.46.186.204 on 09/04/12
For personal use only.

Can. J. Chem. Downloaded from www.nrcresearchpress.com by 78.46.186.204 on 09/04/12
For personal use only.

SECOND-ORDER UNIMOLECULAR KINETICS IN THE THERMAL DECOMPOSITION OF HYDROGEN PEROXIDE VAPOR[1]

W. FORST

ABSTRACT

The thermal decomposition of hydrogen peroxide vapor has been reinvestigated by the static method as a function of initial pressure at pressures up to 22 mm Hg, and in the presence of inert gas (helium, oxygen, and water) up to 100 mm Hg. In each case the apparent first-order rate constant increased linearly with pressure. It is demonstrated that under the present experimental conditions the pyrolysis of hydrogen peroxide shows behavior typical of an elementary unimolecular reaction in its low-pressure, second-order region. The reaction was accompanied by a heterogeneous decomposition which in the presence of foreign gas became inhibited. Helium was used as inhibitor over the temperature range 430–470° C, which permitted calculating the activation energy for activation with peroxide and with helium. The results can be satisfactorily accounted for by assuming a critical energy of 47–50 kcal and five effective classical oscillators for activation with peroxide and three with helium, provided deactivation occurs on every collision. Kinetic evidence against this assumption is briefly discussed.

INTRODUCTION

The thermal decomposition of hydrogen peroxide vapor has received close attention recently (1, 2, 3). The pressure dependence of the first-order rate constant observed by Giguère and Liu (1) suggested that under their experimental conditions the reaction behaved much like a unimolecular decomposition in its low-pressure, second-order region. As considerable interest attaches to such behavior, experimental verification appears worth while.

THEORETICAL

The general Lindemann mechanism for unimolecular reactions may be written in the form (4)

$$\mathrm{A}+\mathrm{M} \xrightarrow{a_i} \mathrm{A}_i^*+\mathrm{M}$$

$$\mathrm{A}_i^*+\mathrm{M} \xrightarrow{b_i} \mathrm{A}+\mathrm{M}$$

$$\mathrm{A}_i^* \xrightarrow{c_i} \text{products},$$

where the subscript i represents energy states of A from critical energy to infinity, the asterisk denotes a molecule of reactant possessing energy in excess of the critical amount, and M represents a molecule of reactant, product, or an inert gas. To avoid needless confusion of symbols, the notation used throughout is essentially that of Johnston (ref. 4 and later papers). From the above scheme the observed (apparent) first-order rate constant is given by

$$[\mathrm{I}] \qquad k = \frac{\text{Rate}}{[\mathrm{A}]} = \sum_i \frac{a_i c_i [\mathrm{M}]}{b_i[\mathrm{M}]+c_i},$$

where square brackets indicate concentrations.

[1]*Manuscript received June 6, 1958.*
Contribution from the Department of Chemistry, Laval University, Quebec, Que. This work was supported by the Office of Scientific Research of the U.S. Air Force under Contract No. AF 18(600)-492. Based on a paper presented at the 41st Annual Conference and Exhibition of the Chemical Institute of Canada, Toronto, May 26–28, 1958.

If $b_i[M] < c_i$ for all i this expands to

[II] $$k = [M]\left\{\sum_i a_i - \sum_i \frac{a_i b_i}{c_i}[M] + \sum_i a_i\left(\frac{b_i}{c_i}\right)^2[M]^2 - \ldots\right\}.$$

At the low-concentration limit

[III] $$b_i[M] \ll c_i \qquad \text{for all } i,$$

so that the second and higher terms in the bracket of [II] will be small compared with the leading term, and hence

[IV] $$k = \sum_i a_i[M] = a[M],$$

where a is the second-order constant for activation and [M] a properly weighted sum of the concentrations of reactant, product, and inert gas. Equation [IV] means that as long as the inequality [III] is satisfied, the plot of observed first-order rate constant k vs. [M] will be a straight line passing through the origin, i.e. the reaction will be second order. If the reaction is accompanied by a first-order heterogeneous reaction, there will be a finite intercept H on the k-axis, and [IV] becomes

$$k = a[M]+H.$$

If the inequality [III] is not satisfied, that is, if the pressure is not low enough, the second and higher terms in the bracket of [II] will not vanish and the plot of k vs. [M] will show a curvature.

The over-all reaction in the decomposition of hydrogen peroxide is

$$H_2O_2 \rightarrow H_2O + \tfrac{1}{2}O_2,$$

so that [IV] becomes in the presence of one inert foreign gas X

[V] $$k = a_1[H_2O_2]+a_2[H_2O]+a_3[O_2]+a_4[X].$$

Stoichiometry requires

$$[H_2O] = \tfrac{1}{2}[O_2] = [H_2O_2]_0 - [H_2O_2],$$

and it follows that

[VI] $$k = a_1[H_2O_2]_0+a_4[X]-(a_1-a_2-\tfrac{1}{2}a_3)([H_2O_2]_0-[H_2O_2]),$$

where the subscript zero refers to initial concentration. Define relative efficiency R_M of gas M with respect to reactant

$$R_M = a_M/a_1,$$

and the relative efficiency of products $\bar{R}$

$$\bar{R} = a_2/a_1+a_3/2a_1.$$

Substitution of $\bar{R}$ into [VI] yields

$$k = a_1[H_2O_2]_0+a_4[X]-a_1(1-\bar{R})\{[H_2O_2]_0-[H_2O_2]\},$$

which at zero time reduces to

[VII] $$k_0 = a_1[H_2O_2]_0+a_4[X],$$

so that [VI] can be written in the form (5)

[VIII] $$k = -\frac{1}{[H_2O_2]}\cdot\frac{d[H_2O_2]}{dt} = \frac{d\log[H_2O_2]}{dt} = k_0-a_1(1-\bar{R})\{[H_2O_2]_0-[H_2O_2]\}.$$

Can. J. Chem. Downloaded from www.nrcresearchpress.com by 78.46.186.204 on 09/04/12
For personal use only.

This treatment makes it clear that the simple relationship implied by [IV], i.e. that at the low-concentration limit the observed first-order rate constant k is a linear function of [M], is true only for k_0. Equation [VIII] shows that $k = k_0$ only when $\bar{R} = 1$, which in general need not be the case. Hence the proper way to test experimental data for accordance with the predictions of the theory is to calculate k_0 from initial rate, or from a plot of $d \log[H_2O_2]/dt$ vs. $[H_2O_2]_0 - [H_2O_2]$.

EXPERIMENTAL

Apparatus

The apparatus was essentially the same as that described previously (1, 6). The reaction was followed manometrically, the pressure being measured by means of a transducer, and recorded by a recording potentiometer (6). A decade resistor was incorporated in the transducer input circuit to permit adjustment of input voltage. Power source was a standard 12-v automobile storage battery of 70-amp-hr capacity which gave input voltage stable to better than one part in one thousand during the course of a run if care was taken to keep the transducer at a reasonably constant temperature (78–80° C).

The reaction vessel was a 2-liter spherical Pyrex flask properly conditioned with hydrogen peroxide (6). Temperatures were measured by an electronic resistance thermometer calibrated against a certified platinum resistance thermometer; the readings refer to the temperature of the outside wall of the reaction vessel. Temperature was constant to better than 0.1° during the course of a run, and to about ±0.2° for nonconsecutive runs. Hydrogen peroxide vapor was obtained by evaporating liquid 99%+ hydrogen peroxide at 75° C. As is usual in this type of work, difficulties were encountered in preparing hydrogen peroxide reservoirs free of catalytic activity. In one particular instance, when the usual treatments with hot fuming sulphuric acid and hot concentrated peroxide failed, hydrofluoric acid was tried as a last resort (7). This treatment was apparently successful, judging from the absence of oxygen streamers at 70° C under vacuum. However, this peroxide gave gas-phase decomposition rates that were clearly out of line, showing a steady daily drift toward higher values, until after a week and 50 runs they settled at 50% above the normal value. When a new peroxide reservoir, which did not receive the hydrofluoric acid treatment, was substituted, results returned to normal. The only explanation seems to be that the above treatment produced some volatile fluorosilicate capable of triggering off the gas-phase decomposition of peroxide.

Procedure for a Typical Experiment

Hydrogen peroxide was evaporated into a 5-liter mixing flask heated to 120° C, and this procedure was followed by the addition of a second gas in the required amount, the total pressure not exceeding 100 mm Hg. Five minutes was allowed for mixing, and then two consecutive runs were made on the same mixture. This procedure was followed also in the case of experiments with peroxide only. Immediately before an experiment the transducer input voltage was checked and the recorder zero adjusted. The mixture was then rapidly introduced through a scratched stopcock into the reaction vessel up to the required pressure as displayed on the recorder, the stopcock was closed, and the recorder rapidly switched to the lowest range 0–1 mv. This was necessary in order to magnify as far as possible the pressure increase accompanying the reaction, which in the presence of excess foreign gas was quite small. The time interval between introduction of one-half of the mixture (= zero time) and the actual start of the pressure–time record was about 10 seconds, so that a small extrapolation was necessary to obtain initial pressure.

Can. J. Chem. Downloaded from www.nrcresearchpress.com by 78.46.186.204 on 09/04/12
For personal use only.

The chart speeds used were generally high, i.e. such that the tracing showed small curvature, a condition that made extrapolation easier. Tracings which did not permit an unambiguous extrapolation were discarded. Initial rate was obtained by drawing a tangent to the pressure–time curve at zero time by means of a simple tangentimeter* of the type described by Latshaw (8). The decomposition was followed only long enough to obtain a pressure–time tracing convenient for evaluation.

RESULTS

The results are summarized in Figs. 1, 2, and 3; the captions are self-explanatory. Each experimental point represents the average of two consecutive runs. All straight lines were fitted to the equation

$$k_0 = m+n[\mathrm{X}]$$

by the method of least squares. Standard deviation was calculated for the slope and intercept of the straight-line portion of the peroxide plot at 431.5° C, the complete equation being

[IX] $$k_0 = (1.28\pm0.18)\times10^{-3}+(23.6\pm1.7)\times10^{-5}[\mathrm{H_2O_2}]_0.$$

Values of the parameters m and n for foreign-gas experiments are summarized in Table I.

TABLE I

LEAST-SQUARES FIT OF FOREIGN-GAS EXPERIMENTS TO EQUATION $k_0 = m+n[\mathrm{X}]$

Temp., ° C	[X]	$m\times10^3$ ($\mathrm{sec^{-1}}$)	$n\times10^5$ ($\mathrm{mm\ sec^{-1}}$)
431.5	H_2O	2.73	17.7
431.5	O_2	2.49	3.47
431.5	He	2.45	2.52
439.6	He	4.28	3.25
448.4	He	6.82	4.25
458.4	He	8.94	6.66
468.5	He	13.2	11.0

While all of the experiments reported there were evaluated from initial rates in the manner described, three experiments on pure peroxide were performed with the object of applying equation [VIII]. The decomposition was followed to completion for 12 half-lives (~30 minutes) and the results were replotted as $\log[\mathrm{H_2O_2}]$ vs. time. As will be shown later, in this case $\bar{R} = 0.83$ so that this plot should exhibit a curvature, which two of them in fact did. The curvature was of the right order of magnitude but in opposite directions; the third run yielded a straight line for all practical purposes. It was concluded that the data were not accurate enough to sustain the test of equation [VIII], or that complications arise if the reaction is allowed to proceed too far. For this reason it was considered safer to interpret the results on the basis of initial rate measurements only. However, it seems doubtful if equation [VIII] is useful even for data of very high accuracy because the curvature of the log(concentration) vs. time plot is very slight (unless $\bar{R}$ is very much different from unity) and consequently the difficulty of estimating accurately the small difference in slope of the tangents is considerable.

As noted previously (6), the concentration of hydrogen peroxide vapor evaporating from the liquid is subject to fluctuations, and is always less than the concentration of the

*The author is indebted to Dr. A. Sehon, of McGill University, for a loan of this instrument.

Can. J. Chem. Downloaded from www.nrcresearchpress.com by 78.46.186.204 on 09/04/12
For personal use only.

liquid itself; in addition, some decomposition occurs during the mixing time. These losses amount to about 5–10% for the two runs immediately following the mixing period, but the effect on the gas-phase decomposition rate is much less than expected, very likely because $\bar{R} = 0.83$, i.e. the collision efficiency of the products water and oxygen is quite close to the efficiency of the reactant itself. Consequently no correction was applied to hydrogen peroxide concentrations or partial pressures as determined from pressure measurements.

DISCUSSION

Basis of the interpretation of the results is equation [VII] which predicts a linear dependence of $[H_2O_2]_0$ on k_0 for $[X] = 0$, or of $[X]$ on k_0 for $[H_2O_2]_0 = \text{const}$. Inspection of Figs. 1, 2, and 3 shows that such is indeed the case for all foreign-gas experiments, and

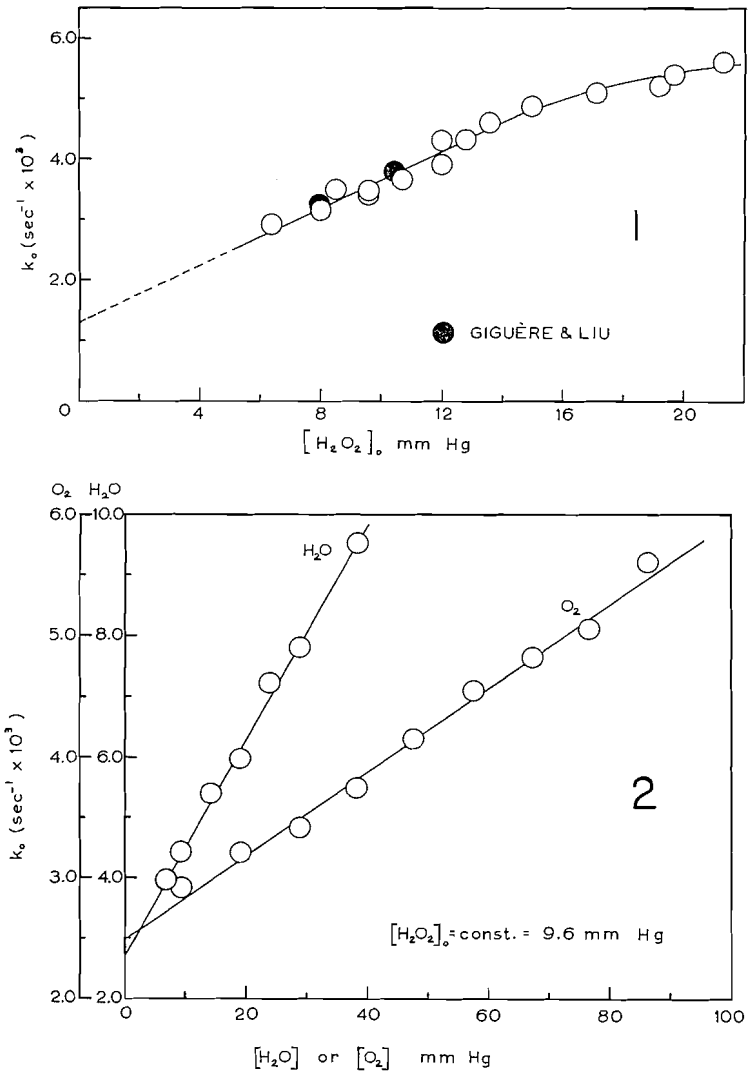

FIG. 1. Results at 431.5° C. Observed first-order rate constant k_0 plotted against initial pressure of hydrogen peroxide. Included for comparison are two points obtained by extrapolation of Giguère and Liu's results (1).

FIG. 2. Results at 431.5° C. Observed first-order rate constant k_0 plotted as a function of partial pressure of water or oxygen, with initial partial pressure of peroxide fixed at 9.6 mm Hg.

Can. J. Chem. Downloaded from www.nrcresearchpress.com by 78.46.186.204 on 09/04/12
For personal use only.

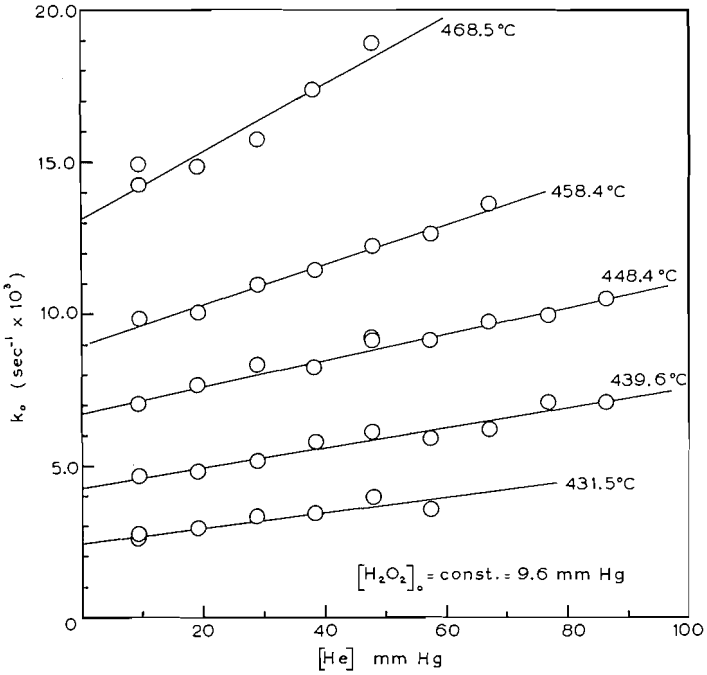

FIG. 3. Results with helium at various temperatures. Observed first-order rate constant k_0 plotted against partial pressure of helium, with initial partial pressure of peroxide fixed at 9.6 mm Hg.

for pure peroxide up to about $[H_2O_2]_0 = 15$ mm Hg. In an elementary unimolecular reaction this agreement would be sufficient proof that the reaction is in its second-order region, but the thermal decomposition of hydrogen peroxide cannot be an elementary reaction: if, as is generally conceded (1, 2), the initial step consists of a rupture of the O—O bond, it is obvious that the final products, oxygen and water, can be formed only after a more or less complex series of secondary reactions. However, by assuming a reasonable mechanism, it is easy to demonstrate that the kinetics of the gas-phase peroxide decomposition can nevertheless be simple enough to show all the essential features of an elementary unimolecular reaction.

A reasonable mechanism has been proposed by Giguère and Liu (1). It will be used here with the exception of their reaction [3]

$$2HO_2 \rightarrow H_2O_2 + O_2, \qquad [3]$$

because there is evidence, from the hydrogen–oxygen reaction, that it occurs as a first-order surface reaction (9, 10), the rate of which would be small on a clean Pyrex surface. Elimination of reaction [3] from the Giguère–Liu mechanism increases the steady-state concentration of HO_2 but has no influence on the kinetics and simplifies the algebra considerably. The reaction scheme to consider is then

$$A + M \xrightarrow{a_i} A_i^* + M$$

$$A_i^* + M \xrightarrow{b_i} A + M$$

$$A_i^* \xrightarrow{c_i} 2OH$$

Can. J. Chem. Downloaded from www.nrcresearchpress.com by 78.46.186.204 on 09/04/12
For personal use only.

$$OH+A \xrightarrow{k_2} HO_2+H_2O \qquad [2]$$

$$OH+HO_2 \xrightarrow{k_4} H_2O+O_2, \qquad [4]$$

where A represents hydrogen peroxide and the remaining symbols have their usual significance. When the usual steady-state assumption is made, the rate of disappearance of hydrogen peroxide is

$$-\frac{d[A]}{dt} = \sum_i a_i[A][M]+\sum_i \frac{a_i c_i[A][M]}{b_i[M]+c_i}-\sum_i \frac{a_i b_i[A][M]^2}{b_i[M]+c_i}.$$

If $b_i[M]<c_i$ for all i, the fractions following the summation signs may be expanded in powers of [M], and the expression for the observed first-order rate constant becomes, after some rearrangement,

$$k = -\frac{1}{[A]}\frac{d[A]}{dt} = 2[M]\left\{\sum_i a_i-\sum_i \frac{a_i b_i}{c_i}[M]+\sum_i a_i\left(\frac{b_i}{c_i}\right)^2[M]^2-\ldots\right\},$$

which is identical with [II], except for the factor 2. Consequently at the low-pressure limit

[IV′] $$k = 2\sum_i a_i[M] = 2a[M],$$

[VII′] $$k_0/2 = a_1[H_2O_2]_0+a_4[X],$$

relations analogous to [IV] and [VII]. In a similar way, it can be shown that when the pressure is high enough, $c_i \ll b_i[M]$ for all i, and

$$-\frac{d[A]}{dt} = \sum_i \frac{a_i c_i}{b_i}[A],$$

i.e. the reaction is first-order, as indeed a unimolecular reaction should be. With this demonstration the interpretation of Figs. 1, 2, and 3 in terms of equation [VII] becomes reasonably legitimate. The appearance of the factor 2 in [VII′] makes no essential difference in the arguments of this discussion.

According to equation [VII] the slopes of the straight lines in Figs. 1, 2, and 3 represent the second-order rate constant for activation; from this the relative efficiency R_M of gas M with respect to peroxide may be calculated. The results at 431.5° C are $R_{H_2O} = 0.75$, $R_{O_2} = 0.15$, $R_{He} = 0.11$. The relative efficiency of products $\bar{R}$ is then $\bar{R} = 0.75+\frac{1}{2}\times 0.15 = 0.83$, and is thus different from unity, although not sufficiently so to cause an appreciable curvature of the log(concentration) vs. time curves (see Experimental). The values for R_M reported here are comparable with efficiencies obtained in other unimolecular rate studies (11, 12), and are particularly notable for an apparent lack of correlation between the energy transfer efficiency R_M and the number of vibrational degrees of freedom (note that R_M for helium and oxygen are practically equal).

The straight line for pure peroxide (Fig. 1) does not pass through the origin; since the heterogeneous decomposition of hydrogen peroxide is known to be the first order (13), there is good reason to identify the intercept on the k-axis of the peroxide plot as representing the heterogeneous component of the reaction. On this basis, a simple calculation shows the reaction to be 65% homogeneous at 431.5° C and 10 mm Hg, compared with the estimate of 80% made by Giguère and Liu (1) for the same temperature and pressure. Presence of a heterogeneous component in the reaction requires that the inter-

Can. J. Chem. Downloaded from www.nrcresearchpress.com by 78.46.186.204 on 09/04/12
For personal use only.

cepts m in foreign-gas experiments be equal to $a_1[H_2O_2]_0+H$, i.e. there should be $m = (3.55\pm0.34)\times10^{-3}$ sec^{-1}, as determined from equation [IX] for $[H_2O_2]_0=9.6$. Comparison with the values listed in Table I for m at 431.5° C makes it at once apparent that this is not so; in fact, calculation shows that

$$m \approx a_1[H_2O_2]_0, \text{ i.e. } H \approx 0.$$

It is therefore necessary to assume that the heterogeneous reaction becomes inhibited in the presence of foreign gas, unless one is willing to make the implausible assumption that all foreign-gas experiments contain a very large systematic error in a_1 or $[H_2O_2]_0$, or both. The effective elimination of the heterogeneous reaction in foreign-gas experiments seems to be supported by the observation that reproducibility was much better in the presence of a foreign gas.

At this point it appears profitable to consider the heterogeneous decomposition of hydrogen peroxide in more detail. The sensitivity of the reaction to minute changes in surface conditions is notorious, which excludes a diffusion-controlled process. The rate-controlling process must be a reaction of absorbed species, and as such would be expected to show sensitivity to anything adsorbed on the surface, including adsorbed gases. Since adsorption of foreign gas on the surface reduces the number of surface sites available for reaction, the reaction becomes inhibited. This is apparently what happens in the case of helium, oxygen, and water. Oxygen and water are known for their inhibiting effects in other reactions (14) but a similar effect for an inert gas like helium does not seem to have been observed before. It would appear that appreciable pressures of foreign gas are needed for effective inhibition, because the amount of products (water and oxygen) formed in the course of the reaction is not sufficient for detectable self-inhibition.

If the inhibitor is strongly adsorbed, it can be shown (15) that the fractional reduction in rate of a unimolecular surface reaction is given by

$$v/v_0 = 1/K_c c_g,$$

where v = inhibited rate, v_0 = rate in absence of inhibitor, c_g = concentration of inhibitor in the gas phase, K_c = equilibrium constant for adsorption of inhibitor. For a non-localized adsorbed layer, such as would be the case with an inert gas, the expression for K_c is (16)

$$K_c = c_a/c_g = (F_a/F_g)e^{\epsilon/kT},$$

where c_a = concentration of adsorbed inhibitor, F_a, F_g = the corresponding partition functions per unit area and per unit volume, respectively, ϵ = heat of adsorption of inhibitor. Hence

$$v/v_0 = (F_g/F_a c_g)e^{-\epsilon/kT}.$$

If ϵ is small, v/v_0 will be almost temperature-independent, meaning that such inhibitor will be almost equally effective at all temperatures. The value of ϵ for helium is a few hundred calories per mole (17), which makes helium a particularly interesting inhibitor. For helium at 431.5° C,

$$H = m-a_1[H_2O_2]_0 = (0.18\pm0.16)\times10^3 \text{ sec}^{-1},$$

i.e. inhibition is very nearly complete. With a rise in temperature, v/v_0 for helium is not likely to change much; actually, inhibition is likely to become more complete, considering that temperature affects the homogeneous rate much more than the heterogeneous one owing to the difference in activation energies (~50 and 10 kcal, respectively (1)). It

Can. J. Chem. Downloaded from www.nrcresearchpress.com by 78.46.186.204 on 09/04/12
For personal use only.

seems therefore quite safe to assume that in the presence of helium $H = 0$ at temperatures above 431.5° C.

This conclusion lends a particular significance to helium experiments over a range of temperatures, as it becomes possible to obtain as a function of temperature a_1, the second-order rate constant for activation with peroxide (from the intercept m of the corresponding straight line), and a_4^{He}, the second-order rate constant for activation with helium (from slope n), and consequently also the corresponding activation energies. It would have been naturally more desirable to obtain a_1 and the corresponding activation energy more directly from peroxide experiments, but this was not possible. With rising temperature the peroxide decomposition becomes too fast to measure at higher pressures, so that the useful pressure range over which the reaction is accessible to study at higher temperatures with the present equipment is much too narrow. In addition, the effect of self-heating becomes appreciable (1).

The slopes n and intercepts m of Table I have been recalculated in terms of concentrations in moles/liter, and the results summarized in Table II. This table also includes a_1 values from oxygen and water experiments; although inhibition in these two cases does not appear quite as complete as in the case of helium, H is nevertheless roughly zero within experimental error. The data of Table II are plotted in Fig. 4 as the usual Arrhenius plot of log (rate constant) vs. reciprocal absolute temperature. The equation of each line and the standard deviation for slopes and intercepts have been calculated by the method of least squares.

The activation energy for activation with peroxide is seen to be 48.1±2.9 kcal, compared with Giguère and Liu's value of 48±3 kcal (1). Considering the wide difference

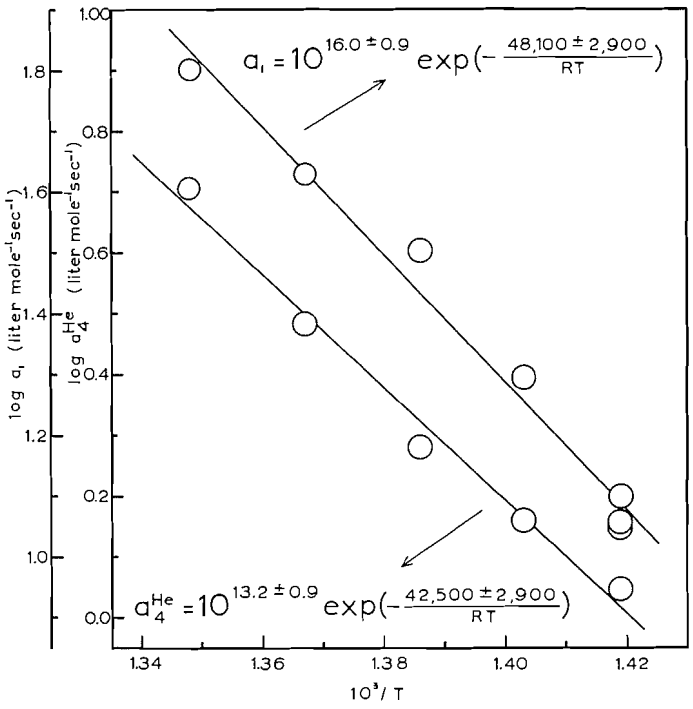

FIG. 4. Arrhenius plot for second-order rate constants for activation with peroxide (a_1) and with helium (a_4^{He}). Included is the least-squares equation of each line.

Can. J. Chem. Downloaded from www.nrcresearchpress.com by 78.46.186.204 on 09/04/12
For personal use only.

TABLE II

TEMPERATURE DEPENDENCE OF SECOND-ORDER RATE CONSTANTS FOR ACTIVATION

Temp., ° C	a_1 (liter mole^{-1} sec^{-1})	$a_4^{H_2O_2}$ (liter mole^{-1} sec^{-1})
431.5	12.5 (water)	—
431.5	11.4 (oxygen)	—
431.5	11.2 (helium)	1.11
439.6	19.8	1.44
448.4	31.9	1.91
458.4	42.4	3.04
468.5	63.3	5.08

between the two methods used for eliminating the contribution of the homogeneous reaction, this agreement is gratifying, although the closeness of the agreement is undoubtedly a coincidence. The activation energy for activation with helium is 42.5±2.9 kcal, so that, within experimental error, it equals the activation energy for activation with peroxide, as indeed in the first approximation it should because the activated state is the same in either case, namely H_2O_2*. Hence for the purpose of further discussion the two equations may be written with sufficient accuracy as

[X] $$a_1 = 10^{15} \exp(-45{,}000/RT) \text{ liter mole}^{-1} \text{ sec}^{-1},$$

[XI] $$a_4^{He} = 10^{14} \exp(-45{,}000/RT) \text{ liter mole}^{-1} \text{ sec}^{-1}.$$

It will be noted that the pre-exponential factors are larger than the kinetic collision number by a factor of 10^{-3} to 10^{-4}. If the mechanism for hydrogen peroxide decomposition proposed in this discussion is accepted, it follows from equation [VII'] that the values of the rate constants a_1 and a_4^{He} given by equations [X] and [XI] should be halved. Of course this will not affect the value of the activation energy, but will make a difference of 0.3 in the power of the pre-exponential factor.

Assuming that a non-linear molecule containing N atoms may be represented by an array of $s = 3N-6$ lightly coupled classical oscillators, one obtains from statistical mechanics (18)

[XII] $$a = Z \exp(-E_c/RT \sum_{r=0}^{r=s-1} \frac{1}{r!}\left(\frac{E_c}{RT}\right)^r,$$

which for $E_c \gg sRT$ reduces to

[XIII] $$a = Z \frac{(E_c/RT)^{s-1} \exp(-E_c/RT)}{(S-1)!},$$

where Z is the kinetic collision number; the experimental activation energy E_A is related to the critical energy E_c by the equation

$$E_A = E_c-(s-3/2)RT.$$

When the values of Z and E_c are substituted in [XIII], the value of a may be adjusted to fit experimental results expressed by equations [X] or [XI] by selecting a proper value for the parameter s. The results of these calculations are given in Table III for the two extremes of the temperature range. The best fit at either temperature seems to be for helium, $s \sim 3$, $E_c \sim 47$ kcal; for peroxide, $s \sim 5$, $E_c \sim 50$ kcal. If a_1 (equation [X]) and a_4^{He} (equation [XI]) are halved, the fit is essentially the same at either temperature. Having regard to the number of normal modes in hydrogen peroxide (six), the number of effective oscillators involved seems reasonable. If E_c may be identified with the strength

Can. J. Chem. Downloaded from www.nrcresearchpress.com by 78.46.186.204 on 09/04/12
For personal use only.

of the O—O bond, and if the latter is taken as 48 kcal (1), the values found for E_c are probably as close as one could expect. These results at the same time justify the approximation $E_c \gg sRT$ involved in [XIII].

TABLE III

NUMBER OF CLASSICAL OSCILLATORS EFFECTIVE IN ACTIVATION BY PEROXIDE AND HELIUM

$T = 431.5°$ C; $a_1 = 10.9$ (equation [X]); $a_4^{He} = 1.1$ (equation [XI])				$T = 468.5°$ C; $a_1 = 54.3$ (equation [X]); $a_4^{He} = 5.4$ (equation [XI])			
		Calc. from [XIII]				Calc. from [XIII]	
s	E_c	a_1	a_4^{He}	s	E_c	a_1	a_4^{He}
2	45.7	0.06	0.08	2	45.8	0.49	0.64
3	47.1	0.4	0.5	3	47.3	2.9	3.8
4	48.5	1.8	2.3	4	48.8	12.4	16.1
5	49.9	6.3	8.2	5	50.3	41.9	54.5
6	51.3	19.0	24.7	6	51.8	119.7	155.4

It is well to bear in mind that equation [XII] is derived for equilibrium. When [XII] is applied to a unimolecular reaction, it is implied that

$$b_i = Z,$$

or that deactivation occurs on every collision (19, 20), a proposition which has been challenged recently (12, 21, 22). In the argument against deactivation on every collision it is tacitly assumed that the distribution function $\sum_i P_i$ defined by

$$\text{[XIV]} \qquad \sum_i P_i = \sum_i \frac{A_i^*}{A} = \sum_i \frac{a_i}{b_i}$$

has a constant value independent of the nature of foreign gas (21); it is then shown that if deactivation occurred on every collision the efficiency of a foreign gas relative to reactant would be equal to the ratio of the corresponding collision numbers. As collision numbers at a given temperature do not vary much from gas to gas, the relative efficiency of all gases should not be far from unity, a consequence which is not observed.

The weakness of this argument concerns the assumed nature of the distribution function in [XIV]. The reason why this function should not depend on the nature of foreign gas is by no means obvious; actually, it would seem reasonable to assume that $\sum_i A_i^*$ could be affected by the energy transfer efficiency of the foreign gas, and hence $\sum_i P_i$ need not be a fixed quantity for all gases. In the absence of any detailed knowledge of $\sum_i P_i$ it appears that kinetic arguments alone cannot decide whether deactivation occurs on every collision or not. As a case in point, one might take equation [XIII] where an explicit form for $\sum_i P_i$ is assumed. E_A and s are experimental quantities independent of any assumption; s is an adjustable parameter, and Z a quantity about which information is desired. Clearly, unless s is known, no information can be obtained about Z. In the absence of precise knowledge of either s or Z the problem degenerates into a case of one equation and two unknowns.

ACKNOWLEDGMENT

The author wishes to express his appreciation to Prof. P. A. Giguère for his continued interest in this work.

Can. J. Chem. Downloaded from www.nrcresearchpress.com by 78.46.186.204 on 09/04/12
For personal use only.

REFERENCES

1. GIGUÈRE, P. A. and LIU, I. D. Can. J. Chem. **35**, 283 (1957).
2. SATTERFIELD, C. N. and STEIN, T. W. J. Phys. Chem. **61**, 537 (1957).
3. CONWAY, D. C. J. Phys. Chem. **61**, 1579 (1957).
4. JOHNSTON, H. S. J. Chem. Phys. **20**, 1103 (1952).
5. VOLPE, M. and JOHNSTON, H. S. J. Am. Chem. Soc. **78**, 3910 (1956).
6. FORST, W. and GIGUÈRE, P. A. J. Phys. Chem. **62**, 340 (1958).
7. HUCKABA, C. E. and KEYES, F. G. J. Am. Chem. Soc. **70**, 2578 (1948).
8. LATSHAW, M. J. Am. Chem. Soc. **47**, 793 (1925).
9. DIXON-LEWIS, G., LINNETT, J. W., and HEATH, D. F. Trans. Faraday Soc. **49**, 766 (1953).
10. WARREN, D. R. Trans. Faraday Soc. **53**, 199 (1957).
11. TROTMAN-DICKENSON, A. F. Gas kinetics. Butterworth Scientific Publications, London. 1955. p. 84.
12. VOLPE, M. and JOHNSTON, H. S. J. Am. Chem. Soc. **78**, 3903 (1956).
13. GIGUÈRE, P. A. Can. J. Research, B, **25**, 135 (1947).
14. INNES, W. B. Catalysis. *Edited by* P. H. Emmett. Vol. I. Reinhold Publishing Corp., New York. 1954. p. 245.
15. LAIDLER, K. J. Catalysis. *Edited by* P. H. Emmett. Vol. I. Reinhold Publishing Corp., New York. 1954. p. 134.
16. LAIDLER, K. J. Catalysis. *Edited by* P. H. Emmett. Vol. I. Reinhold Publishing Corp., New York. 1954. p. 97.
17. BRUNAUER, S. The adsorption of gases and vapors. Vol. I. Princeton Univ. Press, Princeton. 1943. p. 233.
18. FOWLER, R. and GUGGENHEIM, E. A. Statistical thermodynamics. Cambridge University Press, London. 1939. p. 496.
19. RICE, O. K. and RAMSPERGER, H. C. J. Am. Chem. Soc. **49**, 1617 (1927).
20. KASSEL, L. S. The kinetics of homogeneous gas reactions. The Chemical Catalog Co., Inc., New York. 1932. p. 98.
21. WILSON, D. J. and JOHNSTON, H. S. J. Am. Chem. Soc. **75**, 5763 (1953).
22. MAHAN, B. H. J. Phys. Chem. **62**, 100 (1958).

Can. J. Chem. Downloaded from www.nrcresearchpress.com by 78.46.186.204 on 09/04/12
For personal use only.

Can. J. Chem. Downloaded from www.nrcresearchpress.com by 78.46.186.204 on 09/04/12
For personal use only.

NOTES

POLYOXYETHYLENEGLYCOL ETHERS. PART II*

B. A. GINGRAS AND C. H. BAYLEY

Further to the work described in Part I (1), the three ethers $C_8H_{17}O(CH_2CH_2O)_6H$, $C_{16}H_{33}O(CH_2CH_2O)_6H$, and $C_{16}H_{33}O(CH_2CH_2O)_6C_{16}H_{33}$ have been obtained from the reaction between the mono- or di-potassium salt of the hexaoxyethyleneglycol and the appropriate alkyl chloride.

The first two ethers, with terminal hydroxyl groups, are soluble in water and in the usual organic solvents. Their infrared spectra show the typical absorption of the hydroxyl at 3 μ and the broad aliphatic ether band in the 8–9 μ region. A medium band at 13.9 μ is indicative of the paraffin chain.

The last ether, lacking a hydroxyl group, behaves like a saturated hydrocarbon, being hydrophobic and soluble in organic solvents only. Its infrared spectrum is almost identical with that of the corresponding monoether except in the region of the hydroxyl absorption.

EXPERIMENTAL

n-Octylhexaoxyethyleneglycol Ether

Metallic potassium (5.9 g, 0.15 g-atom) was added in small pieces to hexaoxyethyleneglycol (42.4 g, 0.15 mole) and the mixture was stirred and heated at 130° C. After the potassium metal had reacted completely, 1-chlorooctane (25 g, 0.17 mole, b.p. 180° at 758 mm, reported in literature, 181.5° at 765 mm) (2) was added dropwise, the stirring being continued for a further 3 hours. The mixture was then cooled, diluted with acetone, and the potassium chloride was removed by filtration.

The residue was fractionally distilled under reduced pressure, and the fraction of b.p. 150°–180° at 0.1 mm (50 g) was collected. This, when distilled, gave hexaoxyethyleneglycol (b.p. 156° at 0.02 mm, 33 g) and *n*-octylhexaoxyethyleneglycol ether (b.p. 180° at 0.07 mm, 195° at 0.3 mm, n_D^{25} 1.4499, 12.7 g, 20%). The product remained yellowish even after several distillations and it was best purified by chromatography through a silica gel column. A mixture of ethyl ether and methanol, 4:1, eluted the colorless liquid in quantitative yield. Calculated for $C_{20}H_{42}O_7$: C, 60.91%; H, 10.66%. Found: C, 60.39%; H, 10.68%.

Preparation of Hexaoxyethyleneglycol Mono- and Di-hexadecyl Ethers

The reaction was carried out as above using hexaoxyethylene–glycol (25.4 g, 0.09 mole), metallic potassium (3.5 g, 0.09 g-atom), and 1-chlorohexadexane (25 g, 0.1 mole, m.p. 12°, reported in literature 12°) (3). At the end, acetone was added to the cooled mixture and the potassium chloride removed by filtration. From the filtrate separated white crystals of hexaoxyethyleneglycol dihexadecyl ether which was recrystallized from absolute alcohol to a constant m.p. 50° C (7 g, 19%). Calculated for $C_{44}H_{90}O_7$: C, 72.33; H, 12.33. Found: C, 72.33; H, 12.40.

Issued as N.R.C. No. 4835.

The residue (24 g) was chromatographed in three portions through silica gel and there was obtained from elution with ethyl ether – methanol 9:1 mixture hexadecylhexaoxyethyleneglycol ether (18.9 g, 43%), which after recrystallization from *n*-hexane had m.p. 37° C. Calculated for $C_{28}H_{58}O_7$: C, 66.40; H, 11.46. Found: C, 66.66; H, 11.58.

1. GINGRAS, B. A. and BAYLEY, C. H. Can. J. Chem. **35**, 599 (1957).
2. VOGEL, A. I. J. Chem. Soc. 640 (1943).
3. PHILLIPS, J. W. C. and MUMFORD, S. A. J. Chem. Soc. 1732 (1931).

RECEIVED MAY 14, 1958.
TEXTILE RESEARCH SECTION,
DIVISION OF APPLIED CHEMISTRY,
NATIONAL RESEARCH COUNCIL OF CANADA,
OTTAWA, CANADA.

Can. J. Chem. Downloaded from www.nrcresearchpress.com by 78.46.186.204 on 09/04/12
For personal use only.

SEPARATION OF CARBOHYDRATES ON COCOANUT CHARCOAL COLUMNS

F. W. BARTH AND T. E. TIMELL

Chromatographic separation on columns of charcoal–Celite has been widely used for resolving mixtures of oligosaccharides (1, 2, 3, 4, 5, 6) and methylated monosaccharides (7, 8, 9). Although Celite alone has been used for separating sugars (10), its addition to the charcoal has usually only served the purpose of increasing the rate of flow of the eluate through the columns. The commonly used mixture has been that originally suggested by Whistler and Durso (1), consisting of equal parts of Darco G-60 and Celite 535 (4, 6, 9), although "activated charcoal" (3, 11) and "animal charcoal" (8) have also been employed. Recently Jermyn (6) has advocated the use of cellulose powder instead of Celite in order to obtain faster flow. Andrews, Hough, and Powell (12) have suggested the use of very short columns, supported on a sintered plate in a Büchner funnel. This technique obviates the need for the addition of Celite, which is stated to have a tendency to contaminate the fractions obtained.

In the course of an investigation on the constitution of a polysaccharide from milkweed floss (13) it was noticed that cocoanut charcoal (a product of Fisher Scientific Co., Fair Lawn, N.J.), 50–200 mesh, pretreated with 6 *N* hydrochloric acid, water, anhydrous ethanol, and again water, was an excellent material for separating both uronic acids and methylated monosaccharides. The rate of flow, even through long columns, was very rapid. The fractions obtained were very pure and the separations were sharp. When a mixture of uronic acids, obtained on partial hydrolysis of milkweed floss (13), was added to the top of a cocoanut charcoal column (4×12 cm) and eluted with 4, 7, and 15% aqueous ethanol, respectively, three main fractions were obtained, namely a chromatographically pure aldotriouronic acid (0.20 g), 2-*O*-(4-*O*-methyl-D-glucopyranosyluronic acid)-D-xylopyranose (1.30 g) and 4-*O*-methyl-D-glucuronic acid (0.45 g), the latter in admixture with some aldobiouronic acid. Addition of a mixture of sugars obtained from the methylated, reduced, and hydrolyzed aldobiouronic acid (0.57 g) to a similar column (2×10 cm) and elution with 10 and 15% aqueous ethanol gave pure 3,4-di-*O*-methyl-D-xylose and 2,3,4-tri-*O*-methyl-D-glucose, respectively. When a mixture of galactose, glucose, and 4-*O*-methyl-D-glucose was treated similarly, elution with 1.5% ethanol yielded the neutral sugars, while the 4-*O*-methyl-D-glucose was eluted with 5% ethanol.

The residue (24 g) was chromatographed in three portions through silica gel and there was obtained from elution with ethyl ether – methanol 9:1 mixture hexadecylhexaoxyethyleneglycol ether (18.9 g, 43%), which after recrystallization from *n*-hexane had m.p. 37° C. Calculated for $C_{28}H_{58}O_7$: C, 66.40; H, 11.46. Found: C, 66.66; H, 11.58.

1. GINGRAS, B. A. and BAYLEY, C. H. Can. J. Chem. **35**, 599 (1957).
2. VOGEL, A. I. J. Chem. Soc. 640 (1943).
3. PHILLIPS, J. W. C. and MUMFORD, S. A. J. Chem. Soc. 1732 (1931).

RECEIVED MAY 14, 1958.
TEXTILE RESEARCH SECTION,
DIVISION OF APPLIED CHEMISTRY,
NATIONAL RESEARCH COUNCIL OF CANADA,
OTTAWA, CANADA.

Can. J. Chem. Downloaded from www.nrcresearchpress.com by 78.46.186.204 on 09/04/12
For personal use only.

SEPARATION OF CARBOHYDRATES ON COCOANUT CHARCOAL COLUMNS

F. W. BARTH AND T. E. TIMELL

Chromatographic separation on columns of charcoal–Celite has been widely used for resolving mixtures of oligosaccharides (1, 2, 3, 4, 5, 6) and methylated monosaccharides (7, 8, 9). Although Celite alone has been used for separating sugars (10), its addition to the charcoal has usually only served the purpose of increasing the rate of flow of the eluate through the columns. The commonly used mixture has been that originally suggested by Whistler and Durso (1), consisting of equal parts of Darco G-60 and Celite 535 (4, 6, 9), although "activated charcoal" (3, 11) and "animal charcoal" (8) have also been employed. Recently Jermyn (6) has advocated the use of cellulose powder instead of Celite in order to obtain faster flow. Andrews, Hough, and Powell (12) have suggested the use of very short columns, supported on a sintered plate in a Büchner funnel. This technique obviates the need for the addition of Celite, which is stated to have a tendency to contaminate the fractions obtained.

In the course of an investigation on the constitution of a polysaccharide from milkweed floss (13) it was noticed that cocoanut charcoal (a product of Fisher Scientific Co., Fair Lawn, N.J.), 50–200 mesh, pretreated with 6 *N* hydrochloric acid, water, anhydrous ethanol, and again water, was an excellent material for separating both uronic acids and methylated monosaccharides. The rate of flow, even through long columns, was very rapid. The fractions obtained were very pure and the separations were sharp. When a mixture of uronic acids, obtained on partial hydrolysis of milkweed floss (13), was added to the top of a cocoanut charcoal column (4×12 cm) and eluted with 4, 7, and 15% aqueous ethanol, respectively, three main fractions were obtained, namely a chromatographically pure aldotriouronic acid (0.20 g), 2-*O*-(4-*O*-methyl-D-glucopyranosyluronic acid)-D-xylopyranose (1.30 g) and 4-*O*-methyl-D-glucuronic acid (0.45 g), the latter in admixture with some aldobiouronic acid. Addition of a mixture of sugars obtained from the methylated, reduced, and hydrolyzed aldobiouronic acid (0.57 g) to a similar column (2×10 cm) and elution with 10 and 15% aqueous ethanol gave pure 3,4-di-*O*-methyl-D-xylose and 2,3,4-tri-*O*-methyl-D-glucose, respectively. When a mixture of galactose, glucose, and 4-*O*-methyl-D-glucose was treated similarly, elution with 1.5% ethanol yielded the neutral sugars, while the 4-*O*-methyl-D-glucose was eluted with 5% ethanol.

An acidic solution of 3-*O*-methyl-D-xylose and 2,3,4-tri-*O*-methyl-D-glucose could also be easily resolved after the acid had been removed by washing the column with water.

The adsorptive power of cocoanut charcoal appears to be somewhat greater than that of Darco G-60, as elution with larger quantities of water is necessary for complete removal of neutral sugars (14). Addition of 1–2% aqueous ethanol usually achieves the same result much more rapidly. The use of gradient elution (6, 8) would probably improve the resolution obtainable with this type of adsorbent.

1. WHISTLER, R. L. and DURSO, D. F. J. Am. Chem. Soc. **72**, 677 (1950).
2. WHISTLER, R. L. and TU, C. C. J. Am. Chem. Soc. **74**, 3609 (1952).
3. WHELAN, W. J., BAILEY, J. M., and ROBERTS, P. J. P. J. Chem. Soc. 1293 (1953).
4. BISHOP, C. T. Can. J. Chem. **33**, 1073 (1955).
5. TU, C. C. and WARD, K., Jr. J. Am. Chem. Soc. **77**, 4938 (1955).
6. JERMYN, M. A. Australian J. Chem. **10**, 53 (1957).
7. WHELAN, W. J. and MORGAN, K. Chem. & Ind. 78 (1954).
8. LINDBERG, B. and WICKBERG, B. Acta Chem. Scand. **8**, 569 (1954).
9. GLAUDEMANS, C. P. J. and TIMELL, T. E. J. Am. Chem. Soc. **80**, 1209 (1958).
10. LEMIEUX, R. U., BISHOP, C. T., and PELLETIER, G. E. Can. J. Chem. **34**, 3609 (1956).
11. BARKER, S. A., BOURNE, E. J., and THEANDER, O. J. Chem. Soc. 4276 (1955).
12. ANDREWS, P., HOUGH, L., and POWELL, D. B. Chem. & Ind. 658 (1956).
13. BARTH, F. W. and TIMELL, T. E. To be published.
14. PAINTER, T. J. Personal communication.

RECEIVED MAY 16, 1958.
MCGILL UNIVERSITY AND
PULP AND PAPER RESEARCH INSTITUTE OF CANADA,
MONTREAL, QUEBEC.

QUENCHING AND VIBRATIONAL-ENERGY TRANSFER OF EXCITED IODINE MOLECULES

C. ARNOT AND C. A. MCDOWELL

Recent studies (1, 6) of the quenching of the fluorescence spectrum of iodine by foreign gases have led to rather different values for the quenching efficiencies of simple molecules. Polanyi's (1) results were summarized in Table I, page 127 of Can. J. Chem., **36**, 1958, and are here reproduced.

	p, mm	I_0/I_p	I_p'/I_p	$Z_p\times10^{-8}$	$\delta\times10^{-8}$	$\delta p/Z_p$	$\epsilon\times10^{-8}$	$\epsilon p/Z_p$
H_2	9.6	3.15	0.78	2.78	0.17	0.59	0.16	0.55
D_2	8.3	3.88	0.80	1.69	(0.17)	(0.83)	(0.55)	(2.7)

$\tau = 10^{-8}$ second, I_2 pressure 0.43 mm.

The values listed above for δ, the quenching constant, were obtained from data obtained by Wood (2) for hydrogen, the same value being used for deuterium. Wood studied the fluorescence excited by sunlight and not monochromatic Hg 5461 Å, and his intensity measurements were made by a visual comparative method. The iodine pressure in Wood's experiments was 0.20 mm, as opposed to Polanyi's 0.43 mm. As neither the values of δ nor ϵ were corrected by Polanyi for the reduction of the lifetime from the "ideal mean lifetime" by self-quenching, the effect of self-quenching differs in the two experiments.

Eliashevich (3) corrected his results for self-quenching, using data obtained by Stern and Volmer (4). Assuming a value of 10^{-8} second for the "ideal mean lifetime", Eliashevich

Can. J. Chem. Downloaded from www.nrcresearchpress.com by 78.46.186.204 on 09/04/12
For personal use only.

An acidic solution of 3-*O*-methyl-D-xylose and 2,3,4-tri-*O*-methyl-D-glucose could also be easily resolved after the acid had been removed by washing the column with water.

The adsorptive power of cocoanut charcoal appears to be somewhat greater than that of Darco G-60, as elution with larger quantities of water is necessary for complete removal of neutral sugars (14). Addition of 1–2% aqueous ethanol usually achieves the same result much more rapidly. The use of gradient elution (6, 8) would probably improve the resolution obtainable with this type of adsorbent.

1. WHISTLER, R. L. and DURSO, D. F. J. Am. Chem. Soc. **72**, 677 (1950).
2. WHISTLER, R. L. and TU, C. C. J. Am. Chem. Soc. **74**, 3609 (1952).
3. WHELAN, W. J., BAILEY, J. M., and ROBERTS, P. J. P. J. Chem. Soc. 1293 (1953).
4. BISHOP, C. T. Can. J. Chem. **33**, 1073 (1955).
5. TU, C. C. and WARD, K., Jr. J. Am. Chem. Soc. **77**, 4938 (1955).
6. JERMYN, M. A. Australian J. Chem. **10**, 53 (1957).
7. WHELAN, W. J. and MORGAN, K. Chem. & Ind. 78 (1954).
8. LINDBERG, B. and WICKBERG, B. Acta Chem. Scand. **8**, 569 (1954).
9. GLAUDEMANS, C. P. J. and TIMELL, T. E. J. Am. Chem. Soc. **80**, 1209 (1958).
10. LEMIEUX, R. U., BISHOP, C. T., and PELLETIER, G. E. Can. J. Chem. **34**, 3609 (1956).
11. BARKER, S. A., BOURNE, E. J., and THEANDER, O. J. Chem. Soc. 4276 (1955).
12. ANDREWS, P., HOUGH, L., and POWELL, D. B. Chem. & Ind. 658 (1956).
13. BARTH, F. W. and TIMELL, T. E. To be published.
14. PAINTER, T. J. Personal communication.

RECEIVED MAY 16, 1958.
MCGILL UNIVERSITY AND
PULP AND PAPER RESEARCH INSTITUTE OF CANADA,
MONTREAL, QUEBEC.

QUENCHING AND VIBRATIONAL-ENERGY TRANSFER OF EXCITED IODINE MOLECULES

C. ARNOT AND C. A. MCDOWELL

Recent studies (1, 6) of the quenching of the fluorescence spectrum of iodine by foreign gases have led to rather different values for the quenching efficiencies of simple molecules. Polanyi's (1) results were summarized in Table I, page 127 of Can. J. Chem., **36**, 1958, and are here reproduced.

	p, mm	I_0/I_p	I_p'/I_p	$Z_p\times10^{-8}$	$\delta\times10^{-8}$	$\delta p/Z_p$	$\epsilon\times10^{-8}$	$\epsilon p/Z_p$
H_2	9.6	3.15	0.78	2.78	0.17	0.59	0.16	0.55
D_2	8.3	3.88	0.80	1.69	(0.17)	(0.83)	(0.55)	(2.7)

$\tau = 10^{-8}$ second, I_2 pressure 0.43 mm.

The values listed above for δ, the quenching constant, were obtained from data obtained by Wood (2) for hydrogen, the same value being used for deuterium. Wood studied the fluorescence excited by sunlight and not monochromatic Hg 5461 Å, and his intensity measurements were made by a visual comparative method. The iodine pressure in Wood's experiments was 0.20 mm, as opposed to Polanyi's 0.43 mm. As neither the values of δ nor ϵ were corrected by Polanyi for the reduction of the lifetime from the "ideal mean lifetime" by self-quenching, the effect of self-quenching differs in the two experiments.

Eliashevich (3) corrected his results for self-quenching, using data obtained by Stern and Volmer (4). Assuming a value of 10^{-8} second for the "ideal mean lifetime", Eliashevich

Can. J. Chem. Downloaded from www.nrcresearchpress.com by 78.46.186.204 on 09/04/12
For personal use only.

deduced that the lifetime was reduced to 3.3×10^{-9} second at the concentration of iodine of 0.17 mm which he used. Polanyi's work can therefore be compared only with that of Eliashevich if a similar correction is made. Polanyi interpreted his results in terms of the extension of the Stern–Volmer relationship put forward by Roessler (5), which does not take into account self-quenching.

Polanyi obtained sufficient data to calculate quenching constants for hydrogen and deuterium, although for some reason he preferred to use Wood's results, which were obtained with nothing like the same precision. He states values for I_0/I_p and I_p'/I_p. The ratio of the total fluorescence intensity in the absence and in the presence of added gas (R_1), from which the quenching probability can be found, is equal to $I_0/(I_p+I_p')$.

The values of this ratio were then determined from Polanyi's data:

[1] $$R_1 = I_0/(I_p+I_p') = (I_0/I_p)/\{1+(I_p'/I_p)\}$$

Hydrogen: $I_0/I_p = 3.15$, $I_p'/I_p = 0.78$ Hence $R_1 = 3.15/1.78 = 1.77$.

Deuterium: $I_0/I_p = 3.88$, $I_p'/I_p = 0.80$ Hence $R_1 = 3.88/1.80 = 2.16$.

Polanyi's results were then interpreted in terms of the scheme put forward by Arnot and McDowell (6). Equation 24 in that paper shows:

[2] $$R_1 = (k_F+k_s[\mathrm{M}]+k_q[\mathrm{X}])/(k_F+k_s[\mathrm{M}]).$$

Rearranging,

[3] $$k_q/k_F = (R_1-1)\{1+(k_s/k_F)[\mathrm{M}]\}/[\mathrm{X}].$$

A value of 2.0×10^5 liters mole^{-1} was used for the ratio of self-quenching and fluorescence rate constants. The only other published quantitative data for self-quenching is that of Stern and Volmer (4), who found a value of 0.08 mm for the "self-quenching half pressure". On the basis of the Stern–Volmer relationship, $I_0/I = 1+\beta p$, where β is identified with k_s/k_F, this quenching half-pressure is equivalent to a value of $1/p$ for k_s/k_F, i.e. 2.25×10^5 liters mole^{-1} (1 mm Hg = 5.53×10^{-5} moles liter^{-1} at 17° C).* This value is in agreement with the value we obtained.

Substituting in equation [3]

Hydrogen: $R_1-1 = 0.77$, $k_s/k_F = 2.0\times10^5$ liters mole^{-1}, $[\mathrm{I_2}] = 0.43\times5.35\times10^{-5}$ moles liter^{-1}, $[\mathrm{M}] = 9.6\times5.35\times10^{-5}$ moles liter^{-1}

Hence $(1+k_s/k_F[\mathrm{I_2}]) = 5.60$ and $k_q/k_F = 8.4\times10^3$ liters mole^{-1}.

Deuterium: $R_1-1 = 1.16$, $(1+k_s/k_F[\mathrm{I_2}]) = 5.60$, $[D_2] = 8.3\times5.35\times10^{-5}$ moles liter^{-1}

Hence $k_q/k_F = 1.46\times10^4$ liters mole^{-1}.

Rearrangement of equation 23 in paper by Arnot and McDowell (6) yields the result

[4] $$k_T/k_F = \frac{(R_2-1)(1+[\mathrm{M}]k_s/k_F)-([\mathrm{X}]k_q/k_F)}{(1-R_3/Z)[\mathrm{X}]}.$$

Substituting for hydrogen the following values: $R_2 = 3.15$, $R_3 = 0.78$, $(1+[\mathrm{M}]k_s/k_F) = 5.60$, $k_q/k_F = 8.4\times10^3$ liters mole^{-1}, $[\mathrm{H_2}] = 9.6\times5.35\times10^{-5}$ moles liters^{-1}, $Z = 4$, we calculate

$$k_T/k_F = 1.9\times10^4 \text{ liters mole}^{-1}.$$

**Conversion factor of 1 mm = 5.35×10^{-5} moles liter^{-1} has been used here as temperature at which Polanyi's work was carried out was deduced to be ca. 27° C from his iodine pressure.*

Can. J. Chem. Downloaded from www.nrcresearchpress.com by 78.46.186.204 on 09/04/12
For personal use only.

For deuterium the following values have to be substituted in equation [4], namely: $R_2 = 3.88$, $R_3 = 0.80$, $(1+[M]k_s/k_F) = 5.60$, $k_q/k_F = 1.46\times10^4$ liters mole^{-1}, $[D_2] = 8.3\times5.35\times10^{-5}$ moles liter^{-1}. These yield the result $k_T/k_F = 2.7\times10^4$ liters mole^{-1}. The theoretical rate constants for collisions between iodine molecules and added gas molecules can be calculated from the expression:

$$[5] \qquad k = (N_0/100)\,(r_1+r_2)^2[8RT(1/M_1+1/M_2)]^{\frac{1}{2}} \text{ (liters mole}^{-1}\text{ sec}^{-1}\text{)},$$

where M_1 and M_2 are the molecular weights of the colliding species. Values of $\gamma_{I_2} = 2.7$ Å and $\gamma_{H_2} = \gamma_{D_2} = 1.1$ Å were used.

$N_0 = 6.023\times10^{23}$ molecules mole^{-1}, $R = 8.318\times10^8$ ergs/degree, $T = 300°$ K, $M_{I_2} = 254$, $M_{H_2} = 2$, $M_{D_2} = 4$, $\gamma_{I_2} = 2.7\times10^{-8}$ cm, $\gamma_{D_2} = \gamma_{H_2} = 1.1\times10^{-8}$ cm. We thus calculate

$$k_{H_2} = 4.9\times10^{11} \text{ liters mole}^{-1}\text{ sec}^{-1}$$

and

$$k_{D_2} = 3.5\times10^{11} \text{ liters mole}^{-1}\text{ sec}^{-1}.$$

On the basis of the "ideal mean lifetime" τ being 10^{-8} sec, then $k_F = 1/\tau = 10^{-8}$ sec^{-1}, and the theoretical values of k_T/k_F calculated are:

H_2 4.9×10^3 liters mole^{-1}
D_2 3.5×10^3 liters mole^{-1}.

Polanyi's experimental results interpreted this way yield values of k_T/k_F that are 3.9 times the theoretical value for H_2 and 7.7 the theoretical value for D_2 and are thus of the same order of magnitude as those found by Arnot and McDowell (6) for the quenching by other gases.

We are grateful to the National Research Council for a grant-in-aid of this research.

1. Polanyi, J. C. Can. J. Chem. **36**, 127 (1958).
2. Wood, R. W. Verhandl. deut. physik. Ges. **13**, 72 (1911).
3. Eliashevich, M. Physik. Z. Sowjetunion, **1**, 510 (1932).
4. Stern, O. and Volmer, M. Physik. Z. **20**, 184 (1919).
5. Roessler, F. Z. Physik, **96**, 251 (1935).
6. Arnot, C. and McDowell, C. A. Can. J. Chem. **36**, 114 (1958).

Received May 26, 1958.
Department of Chemistry,
The University of British Columbia,
Vancouver 8, B.C.,
Canada.

Can. J. Chem. Downloaded from www.nrcresearchpress.com by 78.46.186.204 on 09/04/12
For personal use only.

Can. J. Chem. Downloaded from www.nrcresearchpress.com by 78.46.186.204 on 09/04/12
For personal use only.

Canadian Journal of Chemistry

Issued by THE NATIONAL RESEARCH COUNCIL OF CANADA

VOLUME 36 OCTOBER 1958 NUMBER 10

CONDUCTANCES OF CONCENTRATED AQUEOUS SOLUTIONS OF MIXED ELECTROLYTES[1]

A. N. CAMPBELL, E. M. KARTZMARK, AND A. G. SHERWOOD

ABSTRACT

Equivalent conductances, viscosities, and densities were determined for solutions equimolar in two of the three salts lithium nitrate, ammonium nitrate, and silver nitrate. The three possible combinations of two salts were each studied at 25° C and at 35° C.

The observed conductances and viscosities were compared with those of the single salt solutions at the same total ion concentration. The conductances were lower than the mean of the conductances of the single salt solutions. The viscosities were also lower than the mean viscosities.

INTRODUCTION

Work in this laboratory has, for the past 8 years, been devoted to providing reliable data on the conductances of concentrated solutions of lithium, of silver, and of ammonium nitrates, and of lithium chlorate in aqueous solutions, and also, in the case of lithium nitrate, in alcohol and alcohol–water mixtures. Recently, the accumulated data have assumed an added interest with the appearance of conductance equations which purport to be valid well into the region of finite concentration. These equations are being tested and are showing encouraging results.

It was considered that a study of mixtures of electrolytes in concentrated solution would be interesting as an extension of our general scheme of work. Accordingly the nitrates of lithium, of silver, and of ammonium were investigated in pairs in aqueous solution. The conductances, viscosities, and densities of solutions, equimolar in each salt, were determined at 25° C and at 35° C.

Onsager and Fuoss (1) have extended the calculations of the Debye–Hückel–Onsager limiting law to include a mixture of ions in solution but their treatment cannot be extended, except as a qualitative analogy, to concentrated solutions. It was first observed by Bray and Hunt (2) that the conductance for a given total concentration of ions is not additive. They studied solutions of sodium chloride and hydrogen chloride and attempted to explain their results as due to incomplete dissociation.

Onsager's theory predicts that the faster ion (H^+ in the case mentioned above) will be slowed down, and the slower ion accelerated, in the mixture. This was shown to be true, experimentally, by Longsworth (3) when he determined the transference numbers of the individual ions in mixed aqueous solutions of potassium chloride and hydrogen chloride.

According to Onsager and Fuoss, of the two effects tending to retard the motion of ions in solution, only the relaxation effect will have a different value in mixed solutions from that in a solution of the single salt of the same concentration. Onsager and Fuoss have compared calculated data for solutions of sodium chloride and hydrogen chloride

[1]*Manuscript received June 3, 1958.*
Contribution from the Chemistry Department, University of Manitoba, Winnipeg, Manitoba.

with the experimental values of Bray and Hunt, and the calculated data for mixtures of barium chloride and hydrogen chloride and of potassium chloride and hydrogen chloride (all at 25° C) with the experimental values of Bennewitz, Wagner, and Küchler (4). The comparison indicates that the Onsager–Fuoss treatment is valid as a limiting law, i.e. at extreme dilution. The work of Krieger and Kilpatrick (5) on the conductance of mixed solutions of lithium chloride and potassium chloride in dilute solution also leads to the same conclusion, viz. that the Onsager–Fuoss treatment is valid for very dilute solutions.

Few measurements have been made on concentration solutions. Van Rysselberghe and Nutting (6) measured conductances of mixtures of sodium and potassium halides and nitrates, in solutions whose total concentration was 1.0 molal. They observed that the mixture rule was most nearly correct when the component salts had similar conductances. Van Rysselberghe, Grinnel, and Carson (7) measured conductances of binary mixtures of two–one, two–two, and one–one electrolytes with common anions and with concentrations ranging from 0.5 to 9.0 *N*. They found the departure from the mixture rule to be much larger for higher valence ions.

EXPERIMENTAL PROCEDURE

Our technique has been frequently described and need not be repeated here (8). All solutions were equimolar with respect to the two component salts. A dry box was introduced for the manipulation of the hygroscopic lithium nitrate. The weight concentration was known to within ±0.002%. We have recently found it convenient to adopt the thyratron relay system of temperature control, as described by Swinehart (9), in

TABLE I

DATA FOR SILVER NITRATE – AMMONIUM NITRATE SOLUTIONS

	1		2	3	4	5	6	7	8	9	10
Soln. No.	Weight per cent $AgNO_3$	Weight per cent NH_4NO_3	Total molarity	Density (g/cm³)	Specific conductance (mhos)	Equivalent conductance (Λ, mhos)	Calculated conductance (Λ (calc.), mhos)	Λ(calc.) − Λ(exp.)	$\frac{\eta-\eta_0}{\eta_0}$ (exp.)	$\frac{\eta-\eta_0}{\eta_0}$ (calc.)	$\frac{\eta-\eta_0}{\eta_0}$(calc.) − $\frac{\eta-\eta_0}{\eta_0}$(exp.)
					Temperature, 25° C						
1	0.8524	0.4016	0.1009	1.0058	0.011720	116.11	116.0	0.1	0.0018	0.002	—
2	7.8517	3.6995	1.0008	1.0827	0.08934	89.27	89.7	0.4	0.0184	0.019	0.001
3	14.5182	6.8407	1.9927	1.1659	0.15373	77.15	78.1	0.9	0.0543	0.060	0.006
4	20.6152	9.7134	3.0404	1.2528	0.20680	68.02	69.4	1.3	0.1214	0.140	0.019
5	25.4772	12.0044	3.9912	1.3307	0.24475	61.32	62.6	1.3	0.2033	0.237	0.034
6	30.2011	14.2302	5.0315	1.4152	0.2765	54.96	56.5	1.5	—	—	—
7	31.7256	14.9484	5.3961	1.4448	0.2855	52.91	54.4	1.5	0.3615	0.420	0.058
8	33.9418	15.9927	5.9509	1.4893	0.2971	49.93	51.3	1.4	0.4444	0.506	0.062
9	34.3060	16.1643	6.0452	1.4968	0.2988	49.42	50.7	1.5	0.4583	0.523	0.065
10	37.7817	17.8020	6.9939	1.5724	0.3124	44.67	45.9	1.2	0.6141	0.699	0.085
11	41.1615	19.3945	8.0137	1.6538	0.3196	39.88	40.7	0.8	0.8309	0.944	0.113
12	44.1656	20.8053	9.0029	1.7319	0.3197	35.51	36.1	0.6	1.0973	1.251	0.154
13	46.7859	22.0446	9.9482	1.8062	0.3134	31.50	—	—	1.4137	1.605	0.191
					Temperature, 35° C						
1	0.8524	0.4016	0.1006	1.0027	0.01400	139.13	140.4	1.3	0.0213	0.021	0.000
2	7.8517	3.6995	0.9973	1.0790	0.10587	106.14	107.0	0.9	0.0331	0.033	0.000
3	14.5182	6.8407	1.9838	1.1607	0.18336	92.43	91.8	−0.6	0.0827	0.087	0.004
4	20.6152	9.7134	3.0256	1.2467	0.2451	81.01	81.7	0.7	0.1591	0.169	0.010
5	25.4772	12.0044	3.9719	1.3243	0.2893	72.83	73.5	0.7	0.2497	0.271	0.022
6	30.2011	14.2302	5.0052	1.4078	0.3258	65.09	66.1	1.0	0.3771	0.409	0.032
7	31.7256	14.9484	5.3680	1.4373	0.3362	62.64	63.5	0.9	0.4341	0.469	0.035
8	33.9418	15.9927	5.9195	1.4818	0.3497	59.08	59.7	0.6	0.5083	0.557	0.049
9	34.3060	16.1643	6.0147	1.4893	0.3515	58.44	59.1	0.7	0.5292	0.576	0.047
10	37.7817	17.8020	6.9585	1.5645	0.3672	52.78	53.4	0.6	0.6897	0.777	0.087
11	41.1615	19.3945	7.9698	1.6447	0.3759	47.16	—	—	0.9150	1.031	0.116
12	44.1656	20.8053	8.9591	1.7215	0.3721	41.54	—	—	1.2187	—	—
13	46.7859	22.0446	9.9004	1.9750	0.3658	36.95	—	—	1.5471	—	—

Can. J. Chem. Downloaded from www.nrcresearchpress.com by 78.46.186.204 on 09/04/12
For personal use only.

our thermostats. The constancy of temperature control in both the thermostats (25° and 35° C) was within 0.002° C, although the absolute value of the temperature is not known to better than ±0.005° C.

EXPERIMENTAL RESULTS

The results are shown in Tables I to III. Column 6 gives the value of Λ calculated

TABLE II

DATA FOR LITHIUM NITRATE – AMMONIUM NITRATE SOLUTIONS

	1		2	3	4	5	6	7	8	9	10
Soln. No.	Weight per cent $LiNO_3$	Weight per cent NH_4NO_3	Total molarity	Density (g/cm³)	Specific conductance (mhos)	Equivalent conductance (Λ, mhos)	Calculated conductance (Λ, calc.)	Λ(calc.) – Λ(exp.)	$\frac{\eta-\eta_0}{\eta_0}$ (exp.)	$\frac{\eta-\eta_0}{\eta_0}$ (calc.)	$\frac{\eta-\eta_0}{\eta_0}$(calc.) – $\frac{\eta-\eta_0}{\eta_0}$(exp.)
					Temperature, 25° C						
14	0.3432	0.3985	0.09966	1.0009	0.01060	106.96	107.9	0.9	0.0036	0.004	0.000
15	1.8285	2.1229	0.5390	1.0163	0.04963	92.07	92.7	0.6	0.0160	0.016	0.000
16	3.1347	3.6394	0.9385	1.0303	0.07999	85.24	86.4	1.2	0.0315	0.031	0.000
17	5.9188	6.8717	1.8221	1.0613	0.1369	75.14	76.5	1.4	0.0762	0.083	0.007
18	9.4790	11.0050	3.0312	1.1024	0.1944	64.14	66.1	2.0	0.1664	0.190	0.024
19	12.1036	14.0522	3.9830	1.1344	0.2255	56.61	58.7	2.1	0.2685	0.306	0.037
20	14.8403	17.2294	5.0341	1.1694	0.2470	49.07	51.6	2.5	0.4132	0.474	0.061
21	17.4262	20.2317	6.0856	1.2039	0.2575	42.31	45.2	2.9	0.6026	0.707	0.104
22	19.7566	22.9372	7.0862	1.2365	0.2576	36.35	39.6	3.2	0.8469	0.992	0.145
23	22.0791	25.6337	8.1351	1.2702	0.2502	30.75	34.3	3.5	1.1721	1.393	0.221
24	23.7813	27.6098	8.9377	1.2956	0.2408	26.87	30.4	3.5	1.4970	1.766	0.269
25	25.7905	29.9425	9.923	1.3264	0.2236	22.53	25.8	3.3	2.0113	—	—
26	27.4651	31.8867	10.981	1.3532	0.2058	18.74	21.7	3.0	3.6197	—	—
27	29.6688	34.4452	12.124	1.4088	0.1786	14.73	—	—	4.8545	—	—
					Temperature, 35° C						
14	0.3432	0.3985	0.09933	0.9977	0.012758	128.43	130.1	1.7	0.0219	.022	0.000
15	1.8285	2.1229	0.5372	1.0129	0.059055	109.92	111.5	1.6	0.0429	0.043	0.000
16	3.1347	3.6394	0.9335	1.0266	0.09482	101.57	102.7	1.1	0.0619	0.062	0.000
17	5.9188	6.8717	1.8147	1.0569	0.16128	88.87	90.5	1.6	0.1093	0.119	0.010
18	9.4790	11.0050	3.0176	1.0975	0.22758	75.42	77.5	2.1	0.2202	0.234	0.014
19	12.1036	14.0522	3.9645	1.1292	0.26300	66.34	68.8	2.5	0.3348	0.357	0.022
20	14.8403	17.2294	5.0099	1.1638	0.28754	57.39	60.0	2.6	0.4909	0.536	0.045
21	17.4262	20.2317	6.0558	1.1980	0.29912	49.39	52.2	2.8	0.6935	0.782	0.088
22	19.7566	22.9372	7.0510	1.2304	0.29999	42.54	45.5	3.0	0.9437	1.094	0.150
23	22.0791	25.6337	8.0933	1.2637	0.29926	36.11	39.3	3.2	1.2877	1.466	0.178
24	23.7813	27.6098	8.8800	1.2873	0.28150	31.70	35.2	3.5	1.6148	—	—
25	25.7905	29.9425	9.8731	1.3197	0.26364	26.70	—	—	2.1434	—	—
26	27.4651	31.8867	10.727	1.3464	0.24449	22.79	—	—	2.7451	—	—
27	29.6688	34.4452	11.897	1.3824	0.21502	18.07	—	—	3.8916	—	—

TABLE III

DATA FOR LITHIUM NITRATE – SILVER NITRATE SOLUTIONS

	1		2	3	4	5	6	7	8	9	10
Soln. No.	Weight per cent $LiNO_3$	Weight per cent $AgNO_3$	Total molarity	Density (g/cm³)	Specific conductance (mhos)	Equivalent conductance (Λ, mhos)	Calculated conductance (Λ, calc.)	Λ(calc.) – Λ(exp.)	$\frac{\eta-\eta_0}{\eta_0}$ (exp.)	$\frac{\eta-\eta_0}{\eta_0}$ (calc.)	$\frac{\eta-\eta_0}{\eta_0}$(calc.) – $\frac{\eta-\eta_0}{\eta_0}$(exp.)
					Temperature, 25° C						
28	1.80945	4.45847	0.54923	1.0464	0.045151	82.20	82.8	0.6	0.0443	0.044	0.000
29	2.79099	6.87697	0.87025	1.0749	0.065757	75.56	76.2	0.6	0.0685	0.068	0.000
30	5.75486	14.1800	1.9540	1.1705	0.11851	60.65	61.4	0.7	0.1943	0.200	0.000
31	8.08470	19.9207	2.9466	1.2565	0.15118	51.31	52.4	1.1	0.3360	0.342	0.006
32	10.1931	25.1159	3.9768	1.3450	0.17409	43.777	44.7	0.9	0.5196	0.528	0.008
33	12.4720	30.7311	5.2672	1.4559	0.18920	35.920	37.3	1.4	0.8221	0.839	0.017
34	13.3994	33.0162	5.8441	1.5036	0.19399	33.194	34.2	1.0	0.9851	1.011	0.026
35	13.7903	33.9793	6.0976	1.5243	0.19513	32.001	32.9	.9	1.0755	1.088	0.012
					Temperature, 35° C						
28	1.80945	4.45847	0.54753	1.0428	0.053943	98.52	99.4	0.9	0.0682	0.068	0.000
29	2.79099	6.87697	0.86718	1.0711	0.078444	90.45	91.3	0.9	0.1012	0.092	−0.009
30	5.75486	14.1800	1.9460	1.1657	0.14081	72.36	73.4	1.0	0.2311	0.225	−0.006
31	8.08470	19.9207	2.9338	1.2510	0.17926	61.10	62.2	1.1	0.3822	0.370	−0.012
32	10.1931	25.1159	3.9589	1.3389	0.20579	51.98	53.1	1.1	0.5740	0.570	−0.004
33	12.4720	30.7311	5.2422	1.4490	0.22411	42.75	43.7	1.0	0.8833	0.876	−0.007
34	13.3994	33.0162	5.8166	1.4965	0.23000	39.54	40.4	0.9	1.0577	1.060	0.009
35	13.7903	33.9793	6.0687	1.5171	0.23148	38.14	39.0	0.9	1.1370	1.149	0.012

Can. J. Chem. Downloaded from www.nrcresearchpress.com by 78.46.186.204 on 09/04/12
For personal use only.

by the mixture rule from the Λ values of the individual salts in solutions of the same concentration. The mixture rule applied to conductance gives:

$$\Lambda_{mix} = x_1\Lambda_1 + x_2\Lambda_2,$$

where x_1 and x_2 are the mole fractions of salts 1 and 2 respectively and Λ_1 and Λ_2 are the equivalent conductances of the single salts at the same concentration. Since all solutions were equimolar in the two salts ($x_1 = x_2 = 0.5$), this amounts merely to taking the average of the conductances of the two single salt solutions. The values for the single salt solutions were obtained by interpolation from the previous results of this laboratory (8), and from the results for lithium nitrate at 35° C, obtained for the first time in this study and given in Table IV.

In column 7 are listed the differences between the calculated and observed equivalent conductances. Column 8 shows the increase in relative viscosity of each solution over

TABLE IV

DATA FOR LITHIUM NITRATE SOLUTIONS AT 35° C

Soln. No.	Weight per cent	Molarity	Density (g/cm³)	Relative viscosity	Specific conductance (mhos)	Equivalent conductance (mhos)
36	0.76006	0.11006	0.99843	1.0289	0.01206	109.59
37	5.73704	0.85456	1.0272	1.1212	0.07346	85.96
38	12.13645	1.8768	1.0663	1.2581	0.13172	70.32
39	17.8357	2.8538	1.1032	1.4201	0.16793	58.84
40	23.7831	3.9467	1.1442	1.6540	0.19024	48.20
41	31.8847	5.5699	1.2044	2.1411	0.19883	35.69
42	42.3407	7.9247	1.2905	3.3376	0.18141	22.89
43	50.3415	9.9537	1.3633	—	0.15549	15.62
44	56.9154	11.7966	1.4291	13.5725	0.13021	11.03

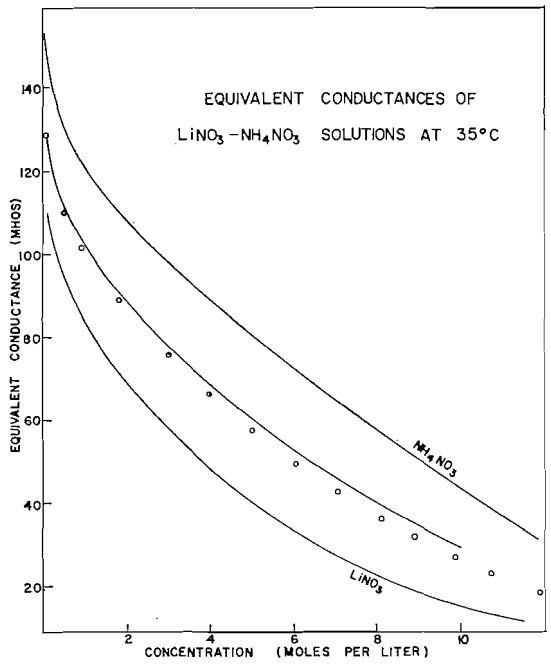

FIG. 1.

Can. J. Chem. Downloaded from www.nrcresearchpress.com by 78.46.186.204 on 09/04/12
For personal use only.

the value for water. Column 9 contains the values calculated by the mixture rule from the data for the single salts. The differences between the observed and calculated viscosity increases are listed in column 10.

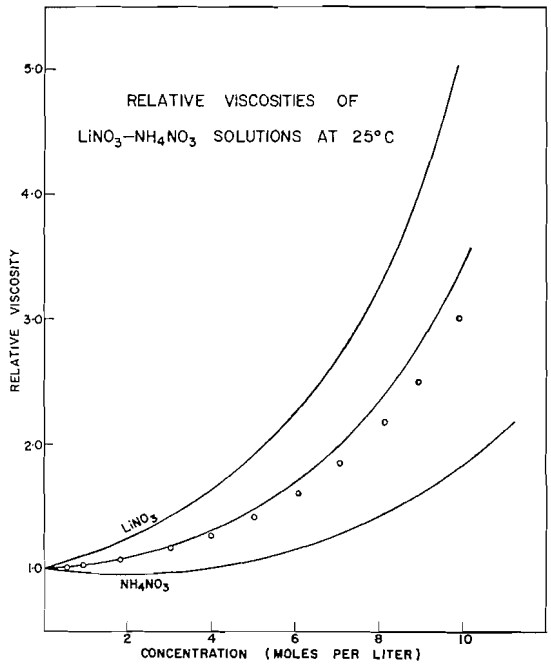

FIG. 2.

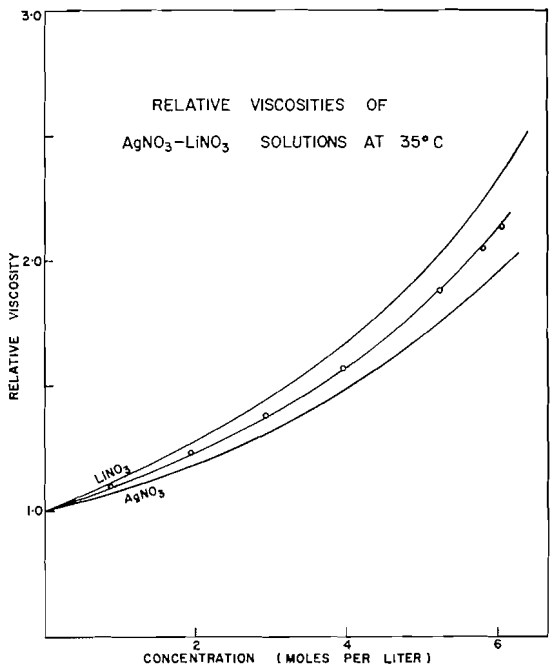

FIG. 3.

Can. J. Chem. Downloaded from www.nrcresearchpress.com by 78.46.186.204 on 09/04/12
For personal use only.

Fig. 1, a graph of equivalent conductance vs. concentration, is typical of the six sets of data. Fig. 2 illustrates graphically the relation among the viscosity of the mixed solutions, the viscosity of the single salt solutions, and the viscosity of the mixed solutions as calculated by the mixture rule, for the case of lithium nitrate – ammonium nitrate at 25° C. It can be seen from the tables of data that this type of graph is common to all the solutions, except the lithium nitrate – silver nitrate solutions at 35° C where the calculated and observed viscosities almost coincide; this graph is shown as Fig. 3. The data for lithium nitrate solutions at 35° C are given in Table IV; the graph of equivalent conductance appears in Fig. 1, and the viscosity plot in Fig. 3.

DISCUSSION OF RESULTS

The equivalent conductances of the mixed solutions were in all cases less than the values calculated by the mixture rule. If Λ_A, Λ_B, and Λ_M are the equivalent conductances of solutions of A, of B, and of an equimolar mixture of the two respectively, all at the same total ion concentration, then:

$$\Lambda_M < (\Lambda_A + \Lambda_B)/2.$$

This means that if in a solution of A one half of the A cations are replaced by B cations (the anion remaining the same), the resulting conductance will be lower than the mean conductance of the two single salt solutions. The deviations from the calculated conductances do not seem to be caused by any single ion. The deviation is large when the difference in conductances of the single salt solutions is large, and the mixture rule is more nearly applicable when the difference in conductance is small. This is in agreement with the observations of Van Rysselberghe and Nutting (6).

It is possible that differences in hydration may be concerned. For example, suppose one half of the lithium ions be replaced by ammonium ions. Since the ammonium ions are hydrated to a smaller extent than are the lithium ions, the remaining lithium ions have more water available for hydration and would therefore behave as if they were in more dilute solution. In general then, the more highly hydrated ion will be in effect in a more dilute solution. An increase in solvation and hence of the effective radius of the ion would, in the sense of Stoke's law, cause a decrease in the mobility of the ion. The increase in equivalent conductance observed on dilution of a salt solution (despite a possible increase in hydration) is due to a decrease in the interionic forces. When hydrated ions are replaced by less hydrated ions of the same charge, the number of ions presumably remains the same and the interionic forces are only slightly altered. Hence, in the case considered, the remaining lithium ions being more highly hydrated, their mobility will decrease. The contribution of the ammonium ion to conductance will be little affected, since it is only slightly hydrated. Hence it appears that the hydration effect would operate in the direction of lowering the conductance of the mixture below the value calculated by the mixture rule.

No hydration data are available for the silver ion, but from consideration of ion size and charge the primary hydration number should lie between those of sodium and potassium. Robinson and Stokes (10) from diffusion experiments assign the following values for the hydration numbers: $NH_4^+ = 0.0$; $K^+ = 0.4$; $Na^+ = 0.7$; $Li^+ = 2.3$. The nature of the experiments permits only of the determination of differences in hydration numbers but this is sufficient to show that the order of increasing hydration is $NH_4^+ < K^+ < Ag^+ < Na^+ < Li^+$. Since this is also the order of decreasing conductance, the argument developed for the lithium nitrate – ammonium nitrate solutions is consistent with our observations.

Can. J. Chem. Downloaded from www.nrcresearchpress.com by 78.46.186.204 on 09/04/12
For personal use only.

A consideration of the dielectric constant of mixed solutions leads to the same conclusion. No measurements of dielectric constant in mixed solutions have been made but certain theoretical deductions are possible. Hasted, Ritson, and Collie (11) offer the following equation to represent the change in dielectric constant of the medium with concentration of electrolyte:

$$D = D_0 + 2\bar{\delta}\sqrt{c}.$$

According to this equation, D is linear in $\sqrt{c}$. Determinations by these authors suggest that $\bar{\delta}$, the proportionality factor, is larger for smaller and more highly charged ions; this is due to the rigid orientation of the water molecules of the hydration sheath. Strict obedience to the linear equation is observed only up to a concentration of 2 molar. This is due to the inclusion of all the water molecules in the fields of the ions; the highest possible orientation of water molecules has been attained and further addition of ions can have little effect. In replacing lithium ions by ammonium ions, which are less highly hydrated, more water molecules are made available to the strong fields of the remaining lithium ions and so their power of depressing the dielectric constant is increased. Hence the dielectric constant of the mixed solution will be lower than that calculated from the mixture rule. The lower dielectric constant will increase the interionic forces and increase the tendency toward ion pair formation resulting in a lower conductance than the calculated value.

In all cases but one, the viscosities of the mixtures were lower than the values calculated by the mixture rule. The one exception, lithium nitrate – ammonium nitrate solutions at 35° C, occurs where the viscosities and conductances of the two single salt solutions are almost the same. If the viscosity were the sole factor determining conductance, this would imply that an increase in equivalent conductance would occur. Since this is not so, it is obvious that the viscosity effect is exceeded by other effects. It is difficult, however, to see why the viscosity of the solutions of two salts should be lower than the value calculated by the mixture rule. The lowering of dielectric constant, with the consequent strengthening of the interionic forces, tends to increase the viscosity. This is in agreement with the observation made by Kraus (12) in his discussion of the viscosity – dielectric constant relation. The increased hydration of the lithium ion should also increase viscosity. It therefore appears that some other factor or factors must cause this effect in mixed solutions.

REFERENCES

1. Onsager, L. and Fuoss, R. J. Phys. Chem. **36**, 2685 (1932).
2. Bray, W. C. and Hunt, F. L. J. Am. Chem. Soc. **33**, 781 (1911).
3. Longsworth, L. J. Am. Chem. Soc. **52**, 1897 (1930).
4. Bennewitz, K., Wagner, C., and Küchler, K. Physik. Z. **30**, 623 (1929).
5. Krieger, K. A. and Kilpatrick, M. J. Am. Chem. Soc. **59**, 1878 (1937).
6. Van Rysselberghe, P. and Nutting, L. J. Am. Chem. Soc. **59**, 333 (1937).
7. Van Rysselberghe, P., Grinnel, S. W., and Carson, J. M. J. Am. Chem. Soc. **59**, 336 (1937).
8. Campbell, A. N. and Kartzmark, E. M. Can. J. Chem. **28**, 43 (1950); **33**, 887 (1955). Campbell, A. N., Kartzmark, E. M., and Gray, A. P. Can. J. Chem. **31**, 617 (1953). Campbell, A. N., Kartzmark, E. M., and Debus, G. H. Can. J. Chem. **33**, 1508 (1955).
9. Swinehart, D. F. Anal. Chem. **21**, 1577 (1949).
10. Robinson, R. A. and Stokes, R. H. Electrolyte solutions. Butterworth Scientific Publications, London. 1955. p. 320.
11. Hasted, J. B., Ritson, D. M., and Collie, C. H. J. Chem. Phys. **16**, 1 (1948).
12. Kraus, C. A. Properties of electrically conducting systems. Am. Chem. Soc. Monograph Ser. The Chemical Catalog Co. Inc., New York. 1922. p. 111.

Can. J. Chem. Downloaded from www.nrcresearchpress.com by 78.46.186.204 on 09/04/12
For personal use only.

Can. J. Chem. Downloaded from www.nrcresearchpress.com by 78.46.186.204 on 09/04/12
For personal use only.

SOME THERMODYNAMIC CONSIDERATIONS OF THE EFFECTS OF STRESS ON METAL ELECTRODE POTENTIALS[1]

E. A. FLOOD

ABSTRACT

It is shown that the change in thermodynamic potential of a solid when elastically strained by the application of the principal stresses p_x, p_y, and p_z is given by the equation

$$\mu-\mu_0 = \tfrac{1}{3}\int_{0,T}^{p_x+p_y+p_z} v\,d(p_x+p_y+p_z)+\phi(q-q_0),$$

where v is the volume per unit mass and $\phi(q-q_0)$ is the shear strain work done on unit mass of the solid, at T and $(p_x+p_y+p_z)$ constant, as the relative values of p_x, p_y, and p_z vary, i.e., as the values of the principal stresses vary from their mean.

INTRODUCTION

Many modern authors of scientific papers assume that the work done upon a system constitutes a measure of the change of Gibbs free energy of the system concerned, quite regardless of how this work is done and regardless of its relation to the pertinent equilibrium conditions. Of course, it is well known that when a solid or liquid is in equilibrium with its vapor that work may be done on or by the system at constant temperature without change in the Gibbs free energy of the system, i.e., without change in the thermodynamic potential of the substance concerned.

The variation in thermodynamic potential of a substance corresponding to given variations in the various variables of the system will depend upon how these variables are involved in particular equilibrium conditions. Accordingly, in order to calculate the changes of potential which accompany given changes in the variables of a system it is essential that the mathematical operations correspond with the idealized experimental conditions.

THERMODYNAMIC POTENTIALS

The condition that a system be in reversible equilibrium with externally applied forces is that the heat absorbed during any change shall be equal to the increase in energy of the system plus the maximum work that the system can do against the externally applied forces. Thus to be in reversible equilibrium with its surroundings the work done *on* a system during a specified change will be the same as that done *by* the system during the exact reverse of the specified change. This is the oldest of the thermodynamic conditions for equilibrium and is, of course, the Carnot–Kelvin condition that a system have no tendency to change its state spontaneously. It will be noted that while both the energy and entropy changes of a system depend only on the initial and final states, the reversible work done and the net heat absorbed ($\int T\,dS$) depend upon how the change is carried out, i.e., upon the path of integration.

The Carnot–Kelvin condition for equilibrium was expressed by Gibbs in the more concise form $(\delta S)_E \leqslant 0$ or $(\delta E)_S \geqslant 0$, leading to similar expressions using the various other thermodynamic functions, the enthalpy, Helmholtz free energy, Gibbs free energy, etc.

[1]*Manuscript received June 13, 1958.*
Contribution from the Division of Pure Chemistry, National Research Council, Ottawa, Canada.
Issued as N.R.C. No. 4878.

The general condition that the various parts of an isolated system be in reversible equilibrium with one another with respect to heat transfer, as between its parts, is that the temperature of its parts shall be the same. If matter may interdiffuse between these parts independently of heat it is also necessary that the thermodynamic potentials of the various kinds of matter in these different parts of the system shall be the same.

Processes in which a given mass of material in "state 1" disappears, while at the same time an equal mass appears in "state 2", the natures and states of the masses, all their respective intensive variables, etc., remaining constant during the transformation, are essentially displacement processes. The condition that such processes be reversible is that the total thermodynamic potentials or displacement potentials of the masses in the two states shall be equal. Where the only externally applied forces involved are the temperature and hydrostatic pressures and we write $F = E - TS + pv$, the condition that the process be reversible is that $\Delta F = 0$ or that $\mu_1 = \mu_2$,* where the thermodynamic potential $\mu = (\partial F/\partial \mathrm{m})_{T,p}$. That this is equivalent to the Carnot–Kelvin equilibrium condition may readily be demonstrated as follows. Let the mass δm_1 disappear by reversible introduction into a reference system while at the same time the mass δm_2 appears as in a typical Washburn thermodynamic engine. If the nature and state of mass m_1 remain unchanged, the entropy and volume per unit mass remain unchanged. The condition that the mass m_1 be in reversible equilibrium with the externally applied forces requires that the decrease in energy δE_1 shall be equal to the heat evolved less the work done on the system by the external forces. If the only external force is the hydrostatic pressure p_1 the work done on the system is $p_1 \delta v$. Thus as the mass δm_1 disappears we have $-\delta E_1 = -T\,\delta S_1 + p_1 \delta v_1$, and similarly as δm_2 appears we have $\delta E_2 = T\,\delta S_2 - p_2 \delta v_2$ and the net effect of the operation is that the energy of the mass may have changed while a quantity of heat has been absorbed or rejected and work done by or on the system. If this work is the maximum work that can be done, the process as a whole is reversible and we can write $\delta F = T\,\delta S - W_{\mathrm{rev}}$. Evidently if $F_1 = E_1 - TS_1 + p_1 v_1$ and $F_2 = E_2 - TS_2 + p_2 v_2$ per unit masses then for the process as a whole $\Delta F = F_2 - F_1 = E_2 - E_1 - T(S_2 - S_1) + p_2 v_2 - p_1 v_1 = 0$, when $p_2 = p_1$ or when

$$\int_{p_0}^{p_2} v_2\, dp = \int_{p_0}^{p_1} v_1\, dp.$$

Thus the condition that $\Delta F = 0$ for such displacement processes at constant T and p is equivalent to the Carnot–Kelvin equilibrium condition. Thus for such processes the condition for equilibrium is that $F_1 = F_2$ or that $\mu_1 = \mu_2$ and the condition that equilibrium be preserved as F_1 and F_2 are changed is that $dF_1 = dF_2$. Hence when the temperature is constant the equilibrium condition equation is $v_1\, dp_1 = v_2\, dp_2$. Evidently in the process above

$$E_2 - E_1 = \delta E = T \int_{S(v_1)}^{S(v_2)} dS - \int_{v_1,\,T}^{v_2} p\, dv = T(S_2 - S_1) - (p_2 v_2 - p_1 v_1),$$

and $p_2 = p_1$ or if phase changes are involved

$$\int_{p_0}^{p_1} v_1\, dp = \int_{p_0}^{p_2} v_2\, dp.$$

Let us consider a case where the equilibrium between δm_1 and the reference system involves only the external pressure p_1 and T as before, but where E_1' and S_1' may differ

The subscripts refer to the "phases" or to the separate bodies of matter, not to the components as is the common convention in this respect.

Can. J. Chem. Downloaded from www.nrcresearchpress.com by 78.46.186.204 on 09/04/12
For personal use only.

from E_1 and S_1, owing to the action of some other forces (such as the presence of a gravitational field), which are not directly involved in the displacement work terms. Thus let E_1' and S_1' be given by

$$E_1'-E_1 = T\int_{x_0,T,p_1}^{x} dS-\int_{x_0,T,p_1}^{x} p\,dv-\int_{x_0,T,p_1}^{x} f(x)\,dx$$
$$= T(S_1'-S_1)-p_1(v_1'-v_1)-\phi(x_1p_1)+\phi(x_0,p_1)$$

where

$$-\int_{x_0,T,p_1}^{x} p\,dv-\int_{x_0,T,p_1}^{v} f(x)\,dx$$

is the work done by the system on changing its position from x_0 to x in a scalar potential field.*

As before, the condition for reversibility is that

$$E_2-E_1' = T(S_2-S_1')-(p_2v_2-p_1v_1')+\phi(x)-\phi(x_0)$$

and we can write,

$$F_1' = E_1'-TS_1'+p_1v_1' = E_1-TS_1+p_1v_1-\phi(x)+\phi(x_0),$$
$$F_2 = E_2-TS_2+p_2v_2,$$

or,

$$F_1'' = E_1'-TS_1'+p_1v_1'+\phi(x),$$
$$F_2'' = E_2-TS_2+p_2v_2+\phi(x_0),$$

and the condition for reversible equilibrium in such processes is again that $\Delta F = 0$.† This leads to the well-known equation for equilibrium in an isothermal potential field $v\,dp = -d\phi(x)$.

* $$\int_{x_0,T,p}^{x} f(x)\,dx = \int_0^m \frac{\partial}{\partial m}\int_{x_0,T,p}^{x} f'(x)d\,x\cdot d\,m$$

where $f'(x)$ is the force function per unit mass thus providing for variation in f with m, T, and p being constant.

†*We can derive F_1' from F_2' by integrating in two steps first from p_2 to p_1 at T and x_0, and second, from x_0 to x at p_1 and T so that*

$$F_1' = F_2'+\int_{p_2,x_0,T}^{p_1,x,T} d\,F$$

and during the first step

$$\int_{p_2,x_0,T}^{p_1} d\,F = \int_{p_2,x_0,T}^{p_1} d\,E-T\int_{p_2,x_0,T}^{p_1} d\,S+\int_{p_2,x_0,T}^{p_1} p\,dv+\int_{p_2,x_0,T}^{p_1} v\,dp$$
$$= \int_{p_2,x_0,T}^{p_1} v\,dp = \int_{p_2,x_0,T}^{p_1}\frac{\partial F}{\partial p}\,dp$$

while in the second step

$$\int_{x_0,p_1,T}^{x} d\,F = \int_{x_0,p_1,T}^{x} d\,E-T\int_{x_0,p_1,T}^{x} d\,S+\int_{x_0,p_1,T}^{x} p\,dv$$
$$= -\int_{x_0,p_1,T}^{x} f(x)\,dx = \int_{x_0,p_1,T}^{x}\frac{\partial F}{\partial x}\,dx.$$

Evidently the condition that $\Delta F = 0$ or that $F_1' = F_2'$ is that

$$\int_{p_2,x_0,T}^{p_1} v\,dp-\int_{x_0,p_1,T}^{x} f(x)\,dx = 0 = \int_{p_2,x,T}^{p_1} v\,dp-\int_{x_0,p_2,T}^{x} f(x)\,dx.$$

Can. J. Chem. Downloaded from www.nrcresearchpress.com by 78.46.186.204 on 09/04/12
For personal use only.

If we suppose that the equilibrium between the mass m_1 and the reference system necessarily involves an electric charge so that as δm_1 is forced into the reference system, reversibly, a definite electric charge is carried with it thus leaving the remaining mass with, say, a net negative charge, as in an electrolytic equilibrium where the mass is in equilibrium with positively charged ions in solution; in this case, we must write $F = E - TS + pv + \epsilon c$ where ϵ is the e.m.f. and c the charge. This leads directly to the relation

$$d\epsilon = -v\,dp/c$$

$$\epsilon - \epsilon_0 = -\frac{1}{n\mathfrak{F}}\int_{p_0}^{p} v\,dp$$

where n is the number of charges carried by the ion, $\mathfrak{F}$ is Faraday's constant, v the volume per mole, etc. Thus the potential difference between two incompressible metal electrodes which differ only in hydrostatic state of stress is $\epsilon - \epsilon_0 = -[v/n(\mathfrak{F})](p - p_0)$. Thus the electrode becomes more negative (more electropositive or less noble) as the hydrostatic pressure p increases. Of course, the electrode becomes positive (more noble) when the hydrostatic pressure p is negative.*

When the stresses acting on the electrode are not hydrostatic stresses, the situation is somewhat more complex. When the contractions $\partial x/x$, $\partial y/y$, etc., are linear functions of the normal stresses p_x, p_y, etc., and the material is isotropic, the volume change is given by the change of the sum of the normal stresses. Accordingly a definite work term is involved for given values of $(p_x + p_y + p_z)$. However, in the general case it is only when the shape remains constant that a reversible equilibrium and a definite work term can be associated with the positive or negative changes in volume which accompany the addition or removal of elements of mass. In this case, if xyz be an element of volume v, then $\delta v = yz\,dx + zx\,dy + xy\,dz$, and we can write,

$$\delta E = T\delta S - p_x yz\,dx - p_y zx\,dy - p_z xy\,dz + \mu\delta m.$$

We can integrate this equation holding T and p_x, p_y, p_z, the principal stresses, constant and obtain a definite work term only if dx, dy, and dz are related to one another in a constant manner. In this case we can write $y = a_y x$, $z = a_z x$, where a_y and a_z are constants and obtain

$$\begin{aligned}\delta E &= T\delta S - (p_x + p_y + p_z)a_y a_z x^2\,dx + \mu\delta m,\\ &= T\delta S - \tfrac{1}{3}(p_x + p_y + p_z)\delta v + \mu\delta m,\\ &= T\delta S - \bar{p}\delta v + \mu\delta m.\end{aligned}$$

This leads to

$$\epsilon - \epsilon_0 = -\frac{1}{n\mathfrak{F}}\int_{\bar{p}_0}^{\bar{p}} v\,dp$$

where $\bar{p} = \tfrac{1}{3}(p_x + p_y + p_z)$.

If, however, p_x, p_y, and p_z, the principal or normal stresses, are of relatively large magnitudes and differ from one another appreciably, shear strain energies are necessarily involved. The work term associated with the shear strain energy is not involved in the displacement work and accordingly we must add the corresponding work term to the displacement or Gibbs potential, as done above in the case of a gravitational potential

Since an electric charge on a thin wire gives rise to an appreciable mechanical stress, a term taking this into account explicitly may be necessary. The term is equivalent to $\partial\mu_1/\partial q.\delta q$ where δq is the increased charge associated with the greater ϵ.

Can. J. Chem. Downloaded from www.nrcresearchpress.com by 78.46.186.204 on 09/04/12
For personal use only.

$\phi(x)$. This work term is always positive when taken from the unsheared state, i.e., work done on the body at constant temperature as an angular deformation occurs at constant $(p_x+p_y+p_z)$, while the relative values of p_x, p_y, and p_z change. In this case we should write $F = E_{q_0}-TS+\bar{p}v+\epsilon c+\phi(q)$, where $\phi(q)$ is the shear strain energy per unit mass

$$=\int_{q_0,T,v}^{q}\phi\, dq$$

($\phi(q)$ for elastic deformations of isotropic bodies obeying Hooke's Law is $1/12M\,[(p_x-p_y)^2+(p_y-p_z)^2+(p_z-p_x)^2]$ where M is the modulus of rigidity).

Accordingly the electrode potential $\epsilon-\epsilon_0$ as a function of stress becomes,

$$\epsilon-\epsilon_0 = -\frac{1}{n\mathfrak{F}}\int_{\bar{p}_0}^{\bar{p}} v\, d\bar{p}-\int_{q_0,T,\bar{p}}^{q}\phi\, dq. \qquad [1]$$

Evidently purely compressional or dilational strain energies are not explicitly involved in the final formulae, since they are already contained in the E, TS, and pv terms. For elastic solids obeying Hooke's Law we can write approximately,

$$\epsilon-\epsilon_0 = -(v/n\mathfrak{F})(\bar{p}-\bar{p}_0)-(v/12M)[(p_x-p_y)^2+(p_y-p_z)^2+(p_z-p_x)^2]$$
$$\delta\epsilon = -(v/3n\mathfrak{F})(p_x+p_y+p_z)-(v/12M)[(p_x-p_y)^2+(p_y-p_z)^2+(p_z-p_x)^2],$$

where $\delta\epsilon$ is the voltage difference between an electrode under no stress and one with normal stresses p_x, p_y, and p_z expressed in suitable units. Thus the shear strain energy always makes the electrode more electropositive (i.e. less noble), while the displacement work terms make the electrode more electropositive when $p_x+p_y+p_z$ is positive and makes the electrode less electropositive (i.e. more noble) when the sum of the pressures or normal stresses is negative. For small positive or negative values of p_x, p_y, and p_z, the shear strain potential will be negligible, while at very large values of the stresses the shear strain potential may be dominant. If the electrode is strained beyond its elastic limit and the stress released, a term of the type $\phi(q)$ will remain so that the strained metal will in general be more electropositive (i.e. less noble) than in the unstrained state; however, in this case the magnitude of $\phi(q)$ cannot be calculated in any very simple manner. In general, in the absence of competing chemical reactions of the electrode, electrolyte, etc., lack of reversibility will tend to reduce the magnitude of the difference $\epsilon-\epsilon_0$, i.e. to reduce the magnitude of the electrical work the cell can do.

If the stress p_x arises as a result of the application of a constant force while p_y and p_z correspond to the constant hydrostatic pressure of the electrolyte, the stress p_x will vary as material dissolves or deposits on the electrode. There can be no true equilibrium in this case. However, in the case of an electrode of reasonably large diameter the variation of p_x due to dissolution or deposition will be very small, especially when the electrolyte concentrations are small. If the electrode is reasonably uniform so that all parts of it, including the surface layer, are in thermodynamic equilibrium with one another, equation 1 should hold reasonably well for small changes in stress. If the surface of the electrode which controls the ionic equilibrium consists of largely detached particles of metal so that little of the applied stress is sustained by these surface particles, the observed $\epsilon-\epsilon_0$ will be much less than that calculated. It is also possible that the outer layer, due, say, to work hardening, may be of much greater rigidity than that of the interior material and consequently that the stress sustained by the surface material is appreciably greater than that estimated from the applied force. In this case the observed $\epsilon-\epsilon_0$ may be greater than that calculated from equation 1.

Can. J. Chem. Downloaded from www.nrcresearchpress.com by 78.46.186.204 on 09/04/12
For personal use only.

The general trend of the relevant data reported in the literature, that we have seen, appears to be consistent with the views expressed above (cf. Fryxell, R. E. and Nachtrieb, N. H. J. Electrochem. Soc. **99**, 495 (1952)).

A somewhat similar problem has been discussed by Gibbs. In the paragraph following Equation (397) of his "Equilibrium of heterogeneous substances" he appears to have made a slip (!!) when he states, "the fluids in equilibrium with the solid are all supersaturated with respect to the substance of the solid, except when the solid is in a state of hydrostatic stress". This statement is only generally correct when the mean of the principal stresses of the solid is equal to or greater than the hydrostatic stress of the fluid.

APPENDIX

The basic relations may be generalized as follows:

$$dE = T\,dS - \sum P_i\,dV_i + \sum f_j\,dx_j$$

where the terms $\sum P_i dV_i$ are all work terms which are necessarily associated with the reversible addition or removal of material, its nature and state remaining constant during the process, the terms $\sum f_j\,dx_j$ are work terms which are not associated directly with the addition or removal of the material, its nature and state remaining constant.

Thus we can write,

$$\begin{aligned} dE &= T\,dS - \sum P_i\,dV_i + \left[\sum \frac{\partial}{\partial m}\int_{x_{j0}}^{x_j} f_j\,dx_j + \mu_0\right] dm \\ &= T\,dS - \sum P_i\,dV_i + \mu\,dm. \end{aligned}$$

The nature of the work terms $\sum P_i\,dV_i$ are assumed to be such that the integration of the equation holding T, the P_i's, and μ constant has a definite meaning and corresponds to an ideal physical process. Thus we can write,

$$E = TS - \sum P_i\,V_i + \mu m$$

and

$$F = E - TS + \sum P_i\,V_i = \mu m.$$

Evidently,

$$\left(\frac{\partial F}{\partial m}\right)_{T,P_i,x_j} = \left(\frac{\partial E}{\partial m}\right)_{S,V_i,x_j} = \mu$$

$$\left(\frac{\partial F}{\partial x_1}\right)_{T,P_i,m,x_2\ldots} = \left(\frac{\partial E}{\partial x_1}\right)_{S,V_i,m,x_2\ldots} = f_1$$

The condition that the μ's be the same for two separate bodies of matter is equivalent to the condition that in any transfer of matter between the two bodies, $\delta E = 0$ when S and V_i's are constant, and that $\delta E = T\delta S - \text{work}_{(\max)}$ or that $\delta F = 0$, when T and P_i's are constant.

Similar relations hold for other thermodynamic functions, thus all of the equilibrium conditions are contained in the Carnot–Kelvin condition for reversibility.

Can. J. Chem. Downloaded from www.nrcresearchpress.com by 78.46.186.204 on 09/04/12
For personal use only.

Can. J. Chem. Downloaded from www.nrcresearchpress.com by 78.46.186.204 on 09/04/12
For personal use only.

MICROCALORIMETRY OF THE ADSORPTION OF WATER VAPOR ON SODIUM CHLORIDE[1]

HENRY M. PAPÉE[2] AND KEITH J. LAIDLER

ABSTRACT

Using a microcalorimeter of the Calvet type, measurements have been made of the heats of adsorption of water vapor on microcrystals of sodium chloride, the rate of heat production being followed as a function of time. With crystals of surface areas between 1 and 15 square meters per gram it was found that three distinct processes occurred, in the following order: (1) simple adsorption of water on the surface, (2) decrease in the surface area, and (3) penetration of water into the lattice. During the second stage no adsorption could be detected. On crystals with larger surface areas there was considerable overlapping of the three phenomena, but the general mechanisms appear to be the same.

INTRODUCTION

Detailed studies of the surface enthalpies of sodium chloride crystals have been made by Benson and his co-workers (1, 2, 3), who measured the heat evolved on the solution in water of sodium chloride crystals of high surface area. The mechanism of the adsorption of water vapor on sodium chloride is a matter of considerable importance in connection with the precipitation of rain (4, 5, 6, 7), and in order to gain further knowledge of this phenomenon a microcalorimetric investigation has been made of the heat liberated when water vapor is allowed to come into contact with sodium chloride crystals of various surface areas.

EXPERIMENTAL

Materials

The sodium chloride employed was C.P., and crystals having large specific surface areas were prepared using a special apparatus and technique developed by Young and Morrison (8; cf. also ref. 2, where the same method was employed). The essential feature of the procedure is that vapor is swept from the surface of molten sodium chloride in a turbulent stream of nitrogen and is carried into an electrostatic precipitator, where the small particles are collected. Care was taken to avoid conditions that would lead to the formation of metallic sodium and of sodium nitrate (3), and tests of purity revealed the absence of contamination. The samples of salt were kept at all times in a desiccator, and all manipulations with the material were carried out at 25.0° C in an atmosphere of dry nitrogen of less than one per cent relative humidity.

In some experiments the work was done directly with samples prepared in the electrostatic precipitator. In other cases samples were prepared by controlled sintering, under vacuum at 240° C, of samples prepared in this way. Samples of low areas (from 1 to 2 $m^2 g^{-1}$) were obtained by grinding optical crystals and sieving them to -200 mesh.

Surface areas were measured by the Brunauer–Emmett–Teller method, involving the adsorption of nitrogen at relative pressures below 0.15. Tests showed that the surface areas of the samples remained constant over considerable periods of time.

All samples were heated for 12 hours at 150° C under vacuum.

Microcalorimetry

The heat measurements were carried out in a microcalorimeter of the Tian–Calvet type (9), and the general procedures were as described in previous papers (10, 11)

[1]*Manuscript received May 26, 1958.*
Contribution from the Department of Chemistry, University of Ottawa, Ottawa, Canada.
[2]*Present address: Division of Applied Chemistry, National Research Council of Canada, Ottawa, Canada.*

dealing with work with this instrument. A special device which allowed the adsorption to take place under high vacuum was designed and constructed; it is shown schematically in Fig. 1, and further details are given on p. 264 of ref. 12. Essentially it consists of two connecting cells, each one of which is fitted into a silver thimble in the microcalorimeter block. One cell contains the salt and the other, the water and a heat exchanger. When the connections between the two cells are opened the vapor diffuses into the salt, and measurements are made of both the heat evolved in the salt cell and of the heat absorbed in the water cell. The manipulations with the cells could be made from outside the calorimeter by the turning of insulated rods.

Prior to being filled with salt the interior container was outgassed under high vacuum for 5 hours at 250° C, and the whole vacuum circuit was evacuated for 5 hours, after which it was filled with dry nitrogen. The subsequent operations were carried out in a dry box in which the relative humidity was below one per cent. The sodium chloride was introduced into the cell and its weight determined by difference.

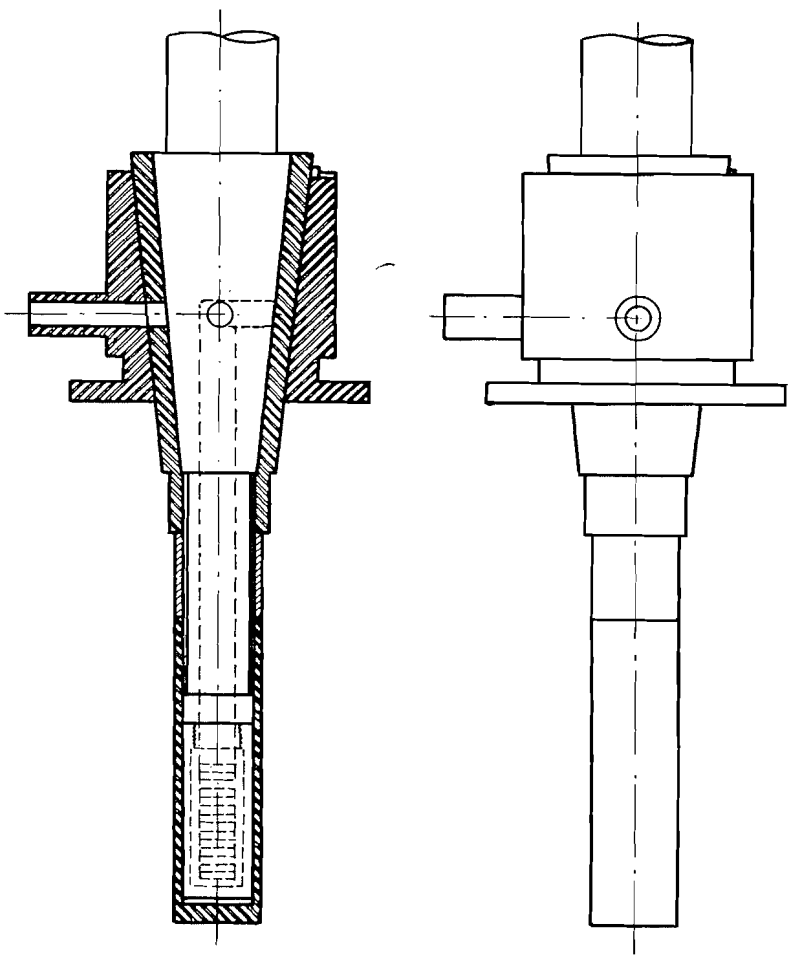

FIG. 1. Schematic representation of a high-vacuum cell for the adsorption studies. At the left is shown a section, at the right an outside view twisted through 90°. Two cells of this type are connected together by thick polythene tubing and inserted into the microcalorimeter block. The turning of valves required to connect and disconnect the two cells is performed by turning an insulated rod which comes out through the top of the apparatus.

Can. J. Chem. Downloaded from www.nrcresearchpress.com by 78.46.186.204 on 09/04/12
For personal use only.

After the introduction of the vacuum circuit into the microcalorimeter the water-containing cell was evacuated, left for 10 minutes, and the operation repeated three times. This cell was then sealed off, and the salt-containing cell was pumped down for 4 hours, using a diffusion pump. After the pump was disconnected the salt cell was sealed off and the water cell put into communication with the interconnecting bridge. The whole assembly was then left overnight to attain thermal equilibrium.

On the following day zero readings were taken over a period of several hours, and the cells then put into communication with one another. Separate recordings were made of the heat evolved in the salt cell and of the heat absorbed in the water cell. The values were corrected using results from blank experiments in which the salt container was empty but in which all other operations were identical.

All heat measurements were carried out at $25.00 \pm 0.01°$ C, and the runs were continued for a considerable number of hours in each case. The calorimeter records the rate of heat evolution (Q/t) as a function of time,* and heats are determined by mechanical integration using a planimeter. The values quoted in the present paper are 'thermochemical' calories, equal to 4.1840 joules. The instrument was calibrated electrically.

General Procedure

Two series of experiments were carried out, as follows:

Series 1.—In this group of measurements calorimetric measurements were made using different weights of a given sample of sodium chloride, the surface area being 19.68 $m^2 g^{-1}$.

Series 2.—In this series the work was done with salt samples weighing from 0.4 to 2.0 g but with specific surface areas ranging from 1 to 20 $m^2 g^{-1}$.

Work was done with various degrees of connection between the two cells, and it was found that the most useful results, in which the separate stages were distinctly revealed, were obtained when the rate of diffusion was moderate.

RESULTS

When the rate of diffusion of water vapor into the salt cell is caused to be small, points of discontinuity are observed in the record of Q/t against t for the salt cell, as shown schematically in Fig. 2. By comparing the records for the salt cell and the water cell, and using the known heat of vaporization of water, it is possible to estimate the amount of water that interacts with the salt during each of the separate processes.

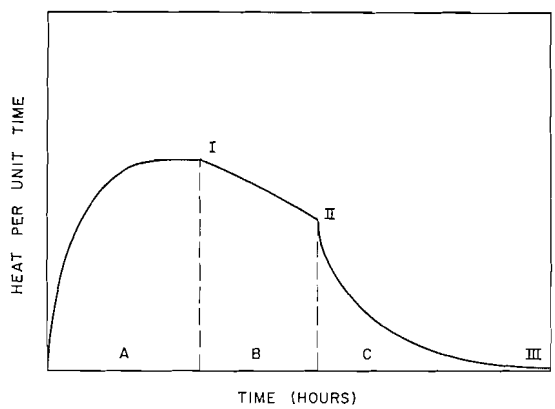

FIG. 2. Schematic plot of rate of heat production against time, showing the two inflection points observed on the microcalorimetric records.

**This is very close to the truth because of the slowness of the process.*

Can. J. Chem. Downloaded from www.nrcresearchpress.com by 78.46.186.204 on 09/04/12
For personal use only.

Fig. 2 shows that Q/t at first increases progressively with time until finally a steady value is obtained. This first process is ended by a point of discontinuity after which Q/t decreases gradually until a second point is reached. This second point could be detected only when larger crystals, with surface areas below 15 $m^2\ g^{-1}$, were used. Such points of discontinuity were well defined when the surface area was between 1 and 15 $m^2\ g^{-1}$, but difficult to detect in samples of areas of about 20 $m^2\ g^{-1}$; this was the case in experiments of series 1.

The process can therefore be regarded as occurring in three stages, corresponding to the areas A, B, and C in Fig. 2. Heats corresponding to the three stages were determined by measuring the appropriate areas.

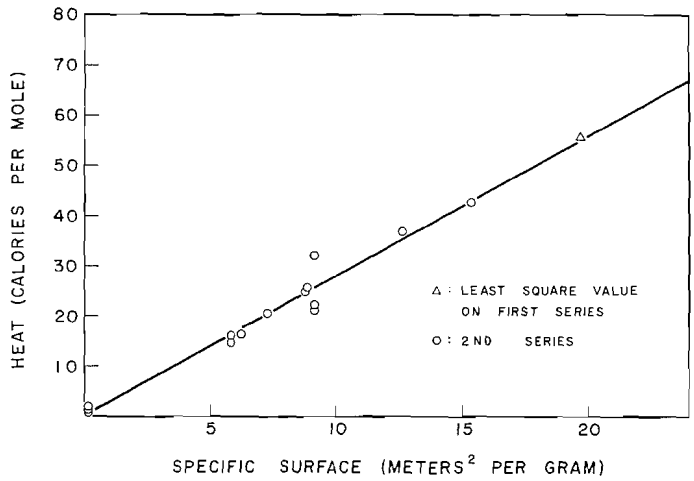

FIG. 3. Plot of heat evolved up to the first inflection point (area A in Fig. 2) against the specific surface area.

TABLE I

HEATS CORRESPONDING TO THE VARIOUS STAGES

Figure	Stage	Series of experiments	Cell	Slope
3	A	1 and 2	Salt	2.77 ± 0.06 (cal $mole^{-1}$)/($m^2\ g^{-1}$) = 0.047 ± 0.001 cal m^{-2}
4	A	1 and 2	Water	-0.75 ± 0.02 (cal $mole^{-1}$)/($m^2\ g^{-1}$) = -0.0128 ± 0.0003 cal m^{-2}
5	A + B	2	Salt	$5.91+0.08$ (cal $mole^{-1}$)/($m^2\ g^{-1}$) = 0.101 ± 0.001 cal m^{-2}
6	A + B	2	Water	-0.76 ± 0.02 (cal $mole^{-1}$)/($m^2\ g^{-1}$) = -0.0130 ± 0.0003 cal m^{-2}
7	C	1	Salt	3.93 ± 0.03 (cal $mole^{-1}$)/($m^2\ g^{-1}$) = 0.0673 ± 0.0005 cal m^{-2}
8	C	1	Water	-1.34 ± 0.17 (cal $mole^{-1}$)/($m^2\ g^{-1}$) = -0.023 ± 0.003 cal m^{-2}
9	C	2	Salt	0.30 ± 0.02 cal g^{-1}
10	C	2	Water	-0.388 ± 0.04 cal g^{-1}

Mole refers to sodium chloride.

TABLE II

SUMMARY OF RESULTS

Stage	Heat		Units	Phenomenon
	Salt cell	Water cell		
A	0.047 ± 0.001	-0.0128 ± 0.0003	cal m^{-2}	Adsorption on surface
B	0.054 ± 0.001	0.000 ± 0.0001	cal m^{-2}	Increase in surface area
C	17.5 ± 1	24.5 ± 3	cal $mole^{-1}$	Penetration of water into lattice; condensation of water on salt

Mole refers to sodium chloride.

Can. J. Chem. Downloaded from www.nrcresearchpress.com by 78.46.186.204 on 09/04/12
For personal use only.

The results are summarized in Figs. 3–10, and in Tables I and II. The figures show plots of heats against either the surface area or the weight of sample, and it is to be seen that reasonably linear behavior is found in both cases. Figs. 3, 5, 7, and 9 refer to the cell in which the salt is contained, and therefore are concerned with heat evolution; Figs. 4, 6, 8, and 10 show results for the cell from which the water was evaporating, and heat is therefore absorbed. The lines in Figs. 3–10 all appear to pass through the origin, and least-square calculations were made in such a way that the line was forced to go through the origin. The resulting slopes, and the standard deviations, are given in Table I. In the case of stage C in the second series of experiments it was found that there was no relationship between the heat and the surface area, but only between the heat and the weight of the sample.

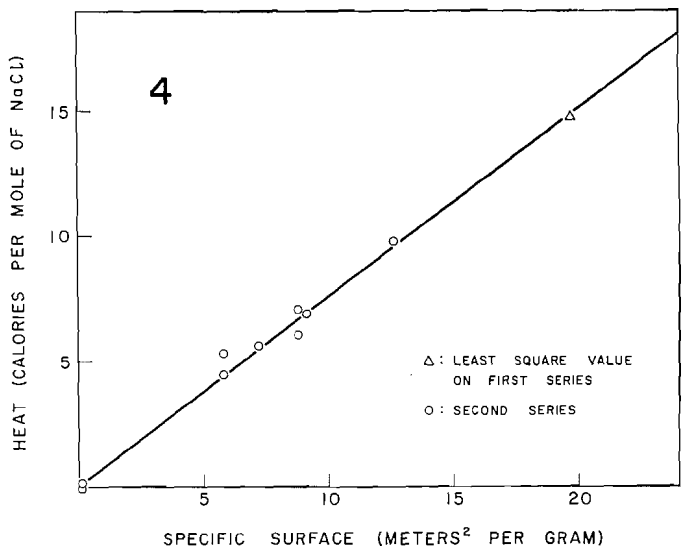

FIG. 4. Plot of heat absorbed up to the first inflection point against the specific surface area, for the cell from which the water was evaporating.

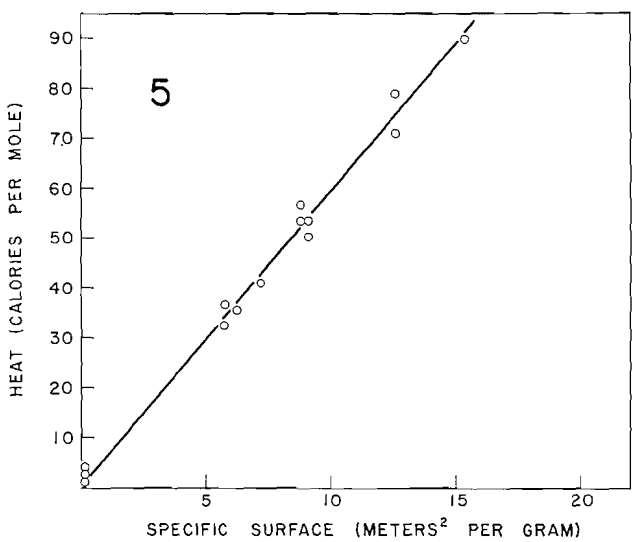

FIG. 5. Plot of heat evolved up to the second inflection point (areas A and B in Fig. 2) against the specific surface area.

Can. J. Chem. Downloaded from www.nrcresearchpress.com by 78.46.186.204 on 09/04/12
For personal use only.

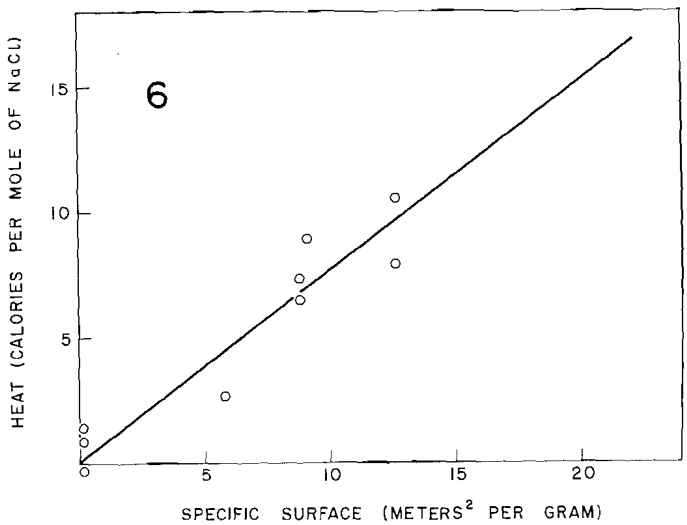

FIG. 6. Plot of heat absorbed up to the second inflection point, for the cell from which the water was evaporating.

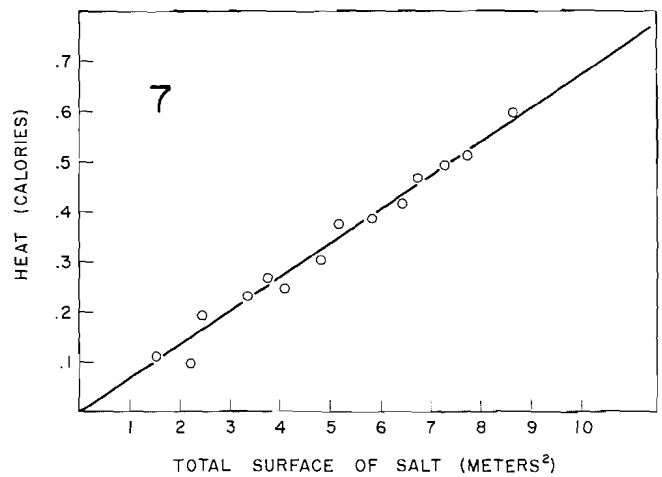

FIG. 7. Plot of heat evolved after the second inflection point (area C in Fig. 2) against the total surface area.

Table II summarizes the main results of the investigation, and shows, for each of the three stages A, B, and C, the heats evolved in the salt cell and absorbed in the water cell.

DISCUSSION

The most striking result of the present investigation is that during stage B there is, within the experimental error, no heat absorbed in the water cell. This means that there is no evaporation of water during the process and therefore no uptake of water by the salt. Stage B thus represents simply a change in the nature of the surface of the salt. The picture that therefore emerges is that the three stages are as follows:

Stage A.—Adsorption of water on the surface of the salt.

Stage B.—Change in the surface area of the salt. Presumably the salt crystals to some extent coalesce, with a decrease in surface area, and during this process there is no uptake of water.

Can. J. Chem. Downloaded from www.nrcresearchpress.com by 78.46.186.204 on 09/04/12
For personal use only.

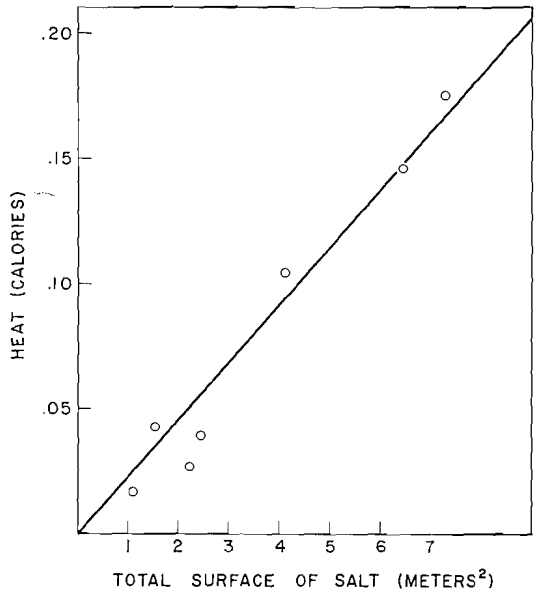

FIG. 8. Plot of heat absorbed after the second inflection point against the total surface area, for the cell from which the water was evaporating.

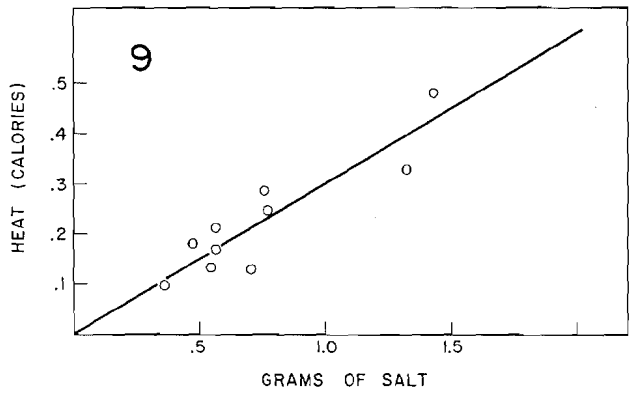

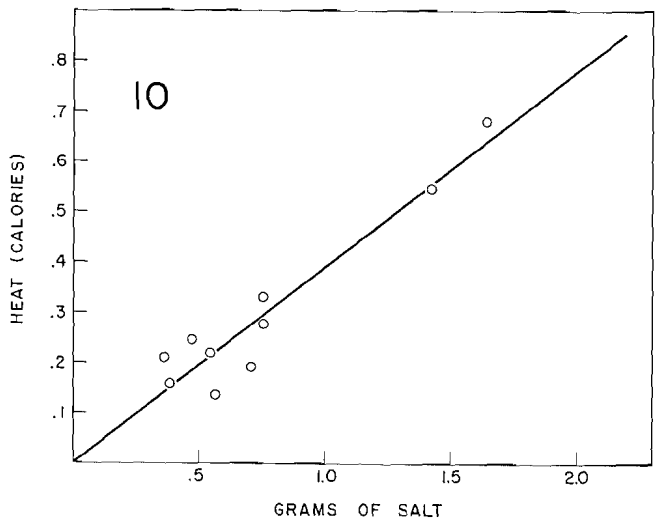

FIG. 9. Plot of heat evolved after the second inflection point against weight of salt.

FIG. 10. Plot of heat absorbed after the second inflection point against weight of salt, for the cell from which the water was evaporating.

Can. J. Chem. Downloaded from www.nrcresearchpress.com by 78.46.186.204 on 09/04/12
For personal use only.

Stage C.—Penetration of water into the crystal lattice, and condensation of additional water on the surface.

It is unlikely, however, that the stages are to be distinguished sharply. Thus the heat evolved in the salt cell during stage A is equal to about 36 kcal per mole of water, and this is too large to correspond to a simple physical adsorption; presumably some change in the surface is occurring at the same time.

It is significant that during stages A and B the heat evolution is proportional to the surface area; the heats per unit area were found to be uninfluenced by whether the material was prepared by electrostatic precipitation, by sintering, or by grinding. However, the magnitude of the heat evolved in stage C is proportional to the total weight of the sample and not to the surface area. These facts are consistent with the mechanisms proposed above for the three stages. During stage C the crystals are considered to have undergone a pronounced change in surface area, and the heat is therefore independent of the initial areas.

The amount of water evaporated in stage A, estimated from the heat absorption and the latent heat of evaporation, is found to be about one twelfth of that required to form a monolayer.* The significance of this may well be that this is the amount required to induce the crystals to undergo a structural change in which a decrease of surface occurs.

It is of interest to compare the results obtained in the present work with the value of Benson *et al.* (3) for the total surface energy of sodium chloride. Their value is

$$0.0659 \text{ cal m}^{-2}.$$

This value is seen from Table II to be greater than the value for stage A (0.047 cal m^{-2}) but less than the sum of the values for stages A and B (0.101 cal m^{-2}). This result further suggests that stages A and B are not sharply separated from one another, although it would appear that all of the surface has been broken down by the end of stage B.

ACKNOWLEDGMENTS

The authors are indebted to Mr. T. W. Zawidzki for preparing the sodium chloride of high surface area, and for help in many other ways. They are also indebted to Drs. G. C. Benson and J. A. Morrison of the National Research Council for the use of their electrostatic precipitator and for much help and valuable advice. Thanks are also due to Professor M. Proulx for the preparation of Fig. 1.

The work was performed under a contract between the U.S. Air Force Cambridge Research Center and the University of Ottawa.

REFERENCES

1. BENSON, G. C. and BENSON, G. W. Can. J. Chem. **33**, 232 (1955).
2. VAN ZEGGEREN, F., SCHREIBER, H. P., and BENSON, G. C. Can. J. Chem. **34**, 1501 (1956).
3. BENSON, G. C., SCHREIBER, H. P., and VAN ZEGGEREN, F. Can. J. Chem. **34**, 1553 (1956).
4. WOODCOCK, A. H. Artificial stimulation of rain. Pergamon Press, Ltd., New York. 1957. p. 202.
5. BYERS, H. R., SIEVERS, J. R., and TUFTS, B. J. Artificial stimulation of rain. Pergamon Press, Ltd., New York. 1957. p. 47.
6. NAKAYA, U. Artificial stimulation of rain. Pergamon Press, Ltd., New York. 1957. p. 36.
7. PAPÉE, H. M. J. Meteorol. (To be published).
8. YOUNG, D. M. and MORRISON, J. A. J. Sci. Instr. **31**, 90 (1954).
9. CALVET, E. and PRAT, H. Microcalorimetrie. Masson et Cie., Paris. 1956.
10. PAPÉE, H. M., CANADY, W. J., and LAIDLER, K. J. Can. J. Chem. **34**, 1677 (1956).
11. CANADY, W. J., PAPÉE, H. M., and LAIDLER, K. J. Trans. Faraday Soc. **54**, 502 (1958).
12. ROSSINI, R. D. Experimental thermochemistry. Interscience Publishers, Inc., New York. 1956.

**This estimate is based on a value of 10.6 Å² for the area occupied by each water molecule; a monolayer would therefore consist of 9.43×10^{18} molecules or 2.82×10^{-4} g of water per square meter. The heat absorbed in the water cell during stage A was 1.28×10^{-2} cal per square meter of salt. This corresponds to the evaporation of 2.33×10^{-5} g of water.*

Can. J. Chem. Downloaded from www.nrcresearchpress.com by 78.46.186.204 on 09/04/12
For personal use only.

Can. J. Chem. Downloaded from www.nrcresearchpress.com by 78.46.186.204 on 09/04/12
For personal use only.

L'ARYLATION DES QUINONES PAR LES SELS DE DIAZONIUM

IV. SUR LA RÉACTION DE CES SELS AVEC LA 2,5-DIHYDROXY-*p*-BENZOQUINONE ET LA SYNTHÈSE DE LA 3-HYDROXY-2,5-BISPHENYL-*p*-BENZOQUINONE[1]

P. BRASSARD[2] ET P. L'ÉCUYER

RÉSUMÉ

L'accumulation des fonctions phénoliques sur l'anneau de la *p*-benzoquinone rend la molécule particulièrement apte à la copulation avec les sels de diazonium au détriment de l'arylation. La réaction de la 2,5-dihydroxy-*p*-benzoquinone avec ces sels donne, en solution aqueuse et en présence d'un excès de 25% de la quantité stoechiométrique d'hydroxyde de potassium, la 2,5-dihydroxy-3-phénylazo-*p*-benzoquinone. Lorsqu'on effectue la réaction en présence d'au moins deux fois la quantité calculée de la base, on isole la 2,5-dihydroxy-3-phényl-6-phénylazo-*p*-benzoquinone. La 2,5-dihydroxy-3,6-bis-(*o*-tolyl)-*p*-benzoquinone est la seule 2,5-dihydroxy-3,6-bisaryl-*p*-benzoquinone que nous avons réussi à synthetiser par cette réaction. Au cours de nos travaux nous avons synthétisé la 3-hydroxy-2,5-bisphényl-*p*-benzoquinone selon un autre procédé décrit dans la partie expérimentale.

INTRODUCTION

La synthèse de la 2,5-dihydroxy-3,6-bisphényl-*p*-benzoquinone ou acide polyporique (1) et de ses dérivés naturels, l'atromentine (2) et la leucomélone (3) a été, jusqu'à présent, l'objet d'un certain nombre de travaux. Fichter (4) a d'abord réalisé la préparation de l'acide polyporique et Kögl (5) celle du diméthyléther de l'atromentine avec des rendements respectifs de 0.14 et 1.28%. Adams (6), Asano et Kameda (7), Kvalnes (8), Ghigi (9) et Fieser et Oxford (10) publièrent d'autres synthèses de l'acide polyporique, et Akagi (3) réalisa celle de la leucomélone.

Il est relativement difficile d'obtenir la 2,5-dichloro- et les 2,5-bisaryl-*p*-benzoquinones (11), les intermédiaires indispensables à la préparation des 2,5-dihydroxy-3,6-bisaryl-*p*-benzoquinones. Pour cette raison, il nous a semblé opportun de tenter d'obtenir directement ces dernières à partir de la 2,5-dihydroxy-*p*-benzoquinone en utilisant une technique analogue à celle qu'a suivie Neunhoffer (12) pour l'arylation de la 2-hydroxy-1,4-naphtoquinone avec les sels de benzène-diazonium.

La 2,5-dihydroxy-*p*-benzoquinone se prépare avec grande facilité par la méthode de Jones et Shonle (13), mais l'accumulation des fonctions phénoliques sur l'anneau de la quinone rend la molécule particulièrement apte à la copulation avec les sels de diazonium au détriment de l'arylation.

Lorsqu'on fait réagir une solution aqueuse du chlorure de diazonium avec de la 2,5-dihydroxy-*p*-benzoquinone dissoute dans de la potasse contenant 25% d'hydroxyde de potassium en excès de la quantité stoechiométrique et qu'ensuite on acidifie légèrement le mélange (pH = 5) par l'addition d'acide acétique, une certaine quantité de substances indésirables précipitent. Si on filtre alors et acidifie fortement le filtrat (pH = 2) avec de l'acide chlorhydrique on obtient la 2,5-dihydroxy-3-arylazo-*p*-benzoquinone. Il est nécessaire d'employer un excès de 25% de la quantité calculée d'hydroxyde de potassium, car autrement le rendement diminue considérablement.

Influence de la température de réaction et de la concentration d'hydroxyde de potassium

Lorsqu'on effectue la réaction du sel de diazonium avec la 2,5-dihydroxy-*p*-benzoquinone en présence de deux fois la quantité théorique d'hydroxyde de potassium, on isole de la même façon que précédemment, une autre classe de composés, soit les

[1]*Manuscrit reçu le 9 juin, 1958.*
Contribution du Département de Chimie, Université Laval, Québec, P.Q.
[2]*Adresse actuelle: Chemisches Institut der Universität, Zürich, Suisse.*

2,5-dihydroxy-3-aryl-6-arylazo-*p*-benzoquinones. En élevant la température de réaction de 50 à 85°, et en augmentant en même temps la concentration de la base jusqu'à un excès de 200%, on obtient encore les mêmes substances. Le seul effet de ces variations croissantes de la température et de la concentration de la base est de faire baisser proportionnellement les rendements (Tableau I).

TABLEAU I

INFLUENCE DE LA TEMPÉRATURE DE RÉACTION ET DE LA CONCENTRATION D'HYDROXYDE DE POTASSIUM

Réaction du chlorure de benzène-diazonium (0.1 mole) avec la 2,5-dihydroxy-*p*-benzoquinone (0.05 mole) en solution aqueuse (600 ml)

Température	% d'excès de KOH	Rendement, en %
45–50°	100	28
45–50°	150	18
45–50°	200	11
80–85°	100	20

Influence du substituant dans le sel de diazonium

Dans la synthèse des dihydroxyarylazoquinones comme dans la préparation des 2-hydroxy-3-aryl-1,4-naphtoquinones en milieu alcalin, la réactivité des sels de diazonium semble être l'inverse de celle qui se manifeste lors de la réaction normale avec la *p*-quinone en l'absence de base. Dans ce dernier cas la stabilité du sel de diazonium favorise l'arylation de la quinone non-hydroxylée. Par contre, lors de la réaction avec la 2-hydroxy-1,4-naphtoquinone d'après la méthode de Neunhoffer, l'*o*-toluidine diazotée donne un rendement de 65%, tandis que le chlorure de *p*-chlorobenzène-diazonium n'en fournit plus qu'un de 40%.

Nous avons observé la même relation dans la réaction des sels de diazonium avec la 2,5-dihydroxy-*p*-benzoquinone en milieu alcalin. Les meilleurs résultats ont été obtenus avec la *m*-toluidine diazotée tandis que le rendement est nul avec la chlorure de *p*-chlorobenzène-diazonium.

Dans un cas seulement, il nous a été possible de synthétiser une 2,5-dihydroxy-3,6-bisaryl-*p*-benzoquinone par cette réaction. C'est en utilisant un sel de diazonium particulièrement instable, le chlorure d'*o*-methylbenzène-diazonium, et en employant des quantités équimoléculaires de la quinone et du réactif diazoique. Nous avons alors obtenu la 2,5-dihydroxy-3,6-bis-(*o*-tolyl)-*p*-benzoquinone avec un rendement de 32%.

Enfin nous avons synthétisé la 3-hydroxy-2,5-bisphényl-*p*-benzoquinone, à partir de la 2,5-bisphényl-*p*-benzoquinone, en suivant la façon de procéder décrite dans la partie expérimentale.

PARTIE EXPÉRIMENTALE*

2,5-Dihydroxy-3-phénylazo-p-benzoquinone

On diazote de la façon habituelle de l'aniline (9.3 g, 0.10 mole) dissoute dans une solution diluée d'acide chlorhydrique (25 ml d'acide concentré dans 100 ml d'eau). On ajoute lentement (l'opération doit durer 5 minutes), la solution du sel de diazonium à une solution de 2,5-dihydroxy-*p*-benzoquinone (7.0 g) et d'hydroxyde de potassium (20.0 g) dans l'eau (500 ml) tout en maintenant la température entre 45 et 50° et en agitant vigoureusement. On continue d'agiter pendant 20 minutes à la même température. On

**Les points de fusion ont été pris à l'aide de l'appareil de Johns.*

Can. J. Chem. Downloaded from www.nrcresearchpress.com by 78.46.186.204 on 09/04/12
For personal use only.

dilue alors à environ 1 litre, et on acidifie à pH = 5 avec de l'acide acétique. On filtre, on rend le filtrat fortement acide par l'addition d'acide chlorhydrique et on essore le précipité. Après deux cristallisations dans le dioxane, la 2,5-dihydroxy-3-phénylazo-*p*-benzoquinone (6.2 g, 51% de la théorie), aiguilles rouges, contient du dioxane de cristallisation. Elle perd ce dioxane par séchage sous vide à 60° en se transformant en une poudre rouge vif qui se décompose entre 220 et 225°. Calculé pour $C_{12}H_8O_4N_2$: C, 59.02%; H, 3.30%; N, 11.46%. Trouvé: C, 59.0%; H, 3.3%; N, 11.2%.

2,5-Dihydroxy-3-(o-tolylazo)-p-benzoquinone

On opère exactement comme précédemment. Après deux cristallisations dans le dioxane on obtient 8.4 g (65% de la théorie) de 2,5-dihydroxy-3-(*o*-tolylazo)-*p*-benzoquinone pure sous la forme d'aiguilles brun-rouge. Après avoir éliminé le dioxane de cristallisation par chauffage sous-vide à 60° pendant 3 heures, la substance devenue pulvérulente est de couleur rouge foncé et se décompose entre 225 et 228°. Calculé pour $C_{13}H_{10}O_4N_2$: C, 60.46%; H, 3.90%; N, 10.81%. Trouvé: C, 60.7%; H, 3.8%; N, 10.7%.

2,5-Dihydroxy-3-phényl-6-phénylazo-p-benzoquinone

On procède comme pour la préparation de la 2,5-dihydroxy-3-phénylazo-*p*-benzoquinone sauf qu'on utilise 40.0 g d'hydroxyde de potassium au lieu de 20.0 g. On essore 6.9 g de produit brut. Par cristallisation dans le dioxane on obtient 4.5 g (28%) de 2,5-dihydroxy-3-phényl-6-phénylazo-*p*-benzoquinone pure sous la forme de fines aiguilles orangées. Elle se sublime au-dessus de 200°. P.f. 256–257°. Calculé pour $C_{18}H_{12}O_4N_2$: C, 67.49%; H, 3.78%; N, 8.85%. Trouvé: C, 67.7%; H, 4.0%; N, 8.9%.

2,5-Dihydroxy-3-(m-tolyl)-6-(m-tolylazo)-p-benzoquinone

On suit le même mode opératoire que pour la préparation précédente. On obtient ainsi 11.5 g de produit brut, qui après cristallisation dans le dioxane, donne 8.4 g (48% de la théorie) de 2,5-dihydroxy-3-(*m*-tolyl)-6-(*m*-tolylazo)-*p*-benzoquinone pure sous la forme d'aiguilles rouge-brun. Elle contient du dioxane de cristallisation. Elle le perd par chauffage sous vide à 60° et se transforme en une poudre brune qui se sublime au-dessus de 200°. P.f. 224–225°. Calculé pour $C_{20}H_{16}O_4N_2$: C, 68.95%; H, 4.63%; N, 8.04%. Trouvé: C, 69.2%; H, 4.6%; N, 8.0%.

2,5-Dihydroxy-2,6-bis-(o-tolyl)-p-benzoquinone

En procédant comme pour la synthèse de la 2,5-dihydroxy-3-phénylazo-*p*-benzoquinone, mais en employant 30.0 g d'hydroxyde de potassium au lieu de 20.0 g, on obtient une substance que l'on cristallise une première fois dans un mélange de dioxane et d'éthanol (1:1) et une deuxième fois dans un peu de dioxane. La 2,5-dihydroxy-3,6-bis-(*o*-tolyl)-*p*-benzoquinone pure se présente sous la forme d'aiguilles jaunes. On se débarrasse des molécules de solvant de cristallisation par chauffage sous vide à 60°. Transformée en une poudre brun-pâle, la 2,5-dihydroxy-3,6-bis-(*o*-tolyl)-*p*-benzoquinone se sublime au-dessus de 200°. P.f. 243–244°. Calculé pour $C_{20}H_{16}O_4$: C, 74.98%; H, 5.03%. Trouvé: C, 75.1%; H, 5.0%.

3-Hydroxy-2,5-bisphényl-p-benzoquinone

On laisse reposer, pendant 24 heures, un mélange d'anhydride acétique (100 ml), de 2,5-bisphényl-*p*-benzoquinone (10.0 g) et d'acide perchlorique à 40% (10 gouttes). On verse alors le mélange dans 1000 ml d'eau froide, on essore le précipité, on le dissout dans le méthanol (100 ml), on ajoute de l'acide chlorhydrique concentré (5 ml) et on bout à reflux pendant 1 heure. On refroidit la solution, on la rend alcaline par l'addition d'une solution diluée d'hydroxyde de sodium et on dilue avec de l'eau à environ 500 ml.

Can. J. Chem. Downloaded from www.nrcresearchpress.com by 78.46.186.204 on 09/04/12
For personal use only.

Le 1,3,4-trihydroxy-2,5-bisphényl-benzène s'oxyde alors spontanément à l'air. Après quelques minutes on filtre et avec de l'acide chlorhydrique dilué on acidifie à pH = 3. La 3-dihydroxy-2,5-bisphényl-*p*-benzoquinone cristallise dans le dioxane en longues aiguilles rouges qui contiennent des molécules de solvant. Elle effleurit à l'air pour donner une poudre rouge qui se sublime au-dessus de 200° sans fondre. Le rendement pour les trois étapes est excellent. Calculé pour $C_{18}H_{12}O_3$: C, 78.25%; H, 4.38%. Trouvé: C, 78.3%; H, 4.1%.

REMERCIEMENTS

Nous remercions le Conseil National de Recherches du Canada et la Shell Oil Company pour des bourses d'études accordées à l'un de nous (P.B.).

BIBLIOGRAPHIE

1. KÖGL, F. Ann. **447**, 78 (1926).
2. KÖGL, F. et BECKER, H. Ann. **465**, 211 (1928).
3. AKAGI, M. J. Pharm. Soc. Japan, **62**, 129, 202 (1942); Chem. Abstr. **45**, 2898 (1951).
4. FICHTER, F. Ann. **361**, 363 (1908).
5. KÖGL, F. Ann. **465**, 243 (1928).
6. SCHILDNECK, P. R. et ADAMS, R. J. Am. Chem. Soc. **53**, 2373 (1931).
7. ASANO, M. et KAMEDA, Y. J. Pharm. Soc. Japan, **59**, 768 (1939); Chem. Abstr. **34**, 2345 (1940).
8. KVALNES, D. E. J. Am. Chem. Soc. **56**, 2478 (1934).
9. GHIGI, E. Boll. sci. fac. chim. ind. univ. Bologna, **5**, 38 (1944–47).
10. FIESER, L. F. et OXFORD, A. E. J. Am. Chem. Soc. **64**, 2060 (1942).
11. NEUNHOFFER, O. et WEISE, J. Ber. **22**, 2127 (1889).
12. JONES, R. G. et SHONLE, H. A. J. Am. Chem. Soc. **67**, 1034 (1945).
13. BRASSARD, P. et L'ÉCUYER, P. Can. J. Chem. **36**, 709 (1958).

Can. J. Chem. Downloaded from www.nrcresearchpress.com by 78.46.186.204 on 09/04/12
For personal use only.

Can. J. Chem. Downloaded from www.nrcresearchpress.com by 78.46.186.204 on 09/04/12
For personal use only.

LIGHT ABSORPTION STUDIES

PART XI. ELECTRONIC ABSORPTION SPECTRA OF NITROBENZENES[1]

W. F. Forbes

ABSTRACT

The spectra of nitrobenzenes are discussed in terms of previously proposed hypotheses relating electronic interactions and ultraviolet absorption spectra.

INTRODUCTION

In previous parts of this series it was proposed that *B*- and *C*-bands of a large number of benzene derivatives are determined mainly by mesomeric and steric interactions and only to a lesser extent by other factors. These hypotheses, which, if true, have important implications, are consistent with a large body of data. For example, whenever primary mesomeric interactions or steric effects are assumed to operate, the spectral changes are normally much larger than the spectral changes which are ascribed to other interactions, such as field effects, inductive effects, and various types of solvent–solute interactions. The present purpose is to extend these hypotheses to nitrobenzenes. The substituent in nitrobenzene possesses a negative mesomeric effect. However, this negative mesomeric effect is greater in nitro-compounds than in the previously studied acetophenones and benzoic acids, and other interactions may also play a different part.

The spectra of nitrobenzenes have recently been described by a number of workers (for example, 1, 2, 3, 4, 5), and the spectra have been noted to cause anomalous effects (6, 7; cf. also the greater ethylenic stretching frequency at 1600 cm^{-1} in nitrobenzenes (8*a*), and the absence of the usual correlations for C–H bending vibrations in the region 1000–650 cm^{-1} (8*c*)).

ULTRAVIOLET ABSORPTION SPECTRA

Nitrobenzene

The ultraviolet absorption spectra of nitrobenzene in different solvents are listed in Table I.

A broad symmetrical absorption band, structureless even in the gas phase (3), occurs near 260 mμ, which is classified as the *B*-band, by analogy with the *B*-band near 240 mμ in acetophenones. The bands are of comparable intensity and undergo parallel changes on alteration of the dielectric constant or polarity of the solvent. The nitrobenzene band at 260 mμ will also be shown to be highly susceptible to steric effects, causing hypsochromic shifts and reduced absorption intensities, which represents a characteristic property of the *B*-band in acetophenones and benzoic acids (11).

Next, no appreciable concentration dependence could be discerned for various nitrobenzene solutions. This indicates that nitrobenzene is apparently not appreciably associated in solution within the investigated concentration range (see Table I). The observed bathochromic wavelength displacement with increased dielectric constant of the solvent is parallel, but more pronounced for nitrobenzene than for acetophenone. This suggests increased solvent stabilization of the excited state relative to the ground state and may be related to the greater contribution of dipolar excited states in nitrobenzene (cf. also ref. 3). Change of pH of the solution does not cause any additional wavelength shift,

[1]*Manuscript received in original form January 21, 1958, and, as revised, June 19, 1958.*
Contribution from the Memorial University of Newfoundland, St. John's, Newfoundland.

TABLE I

ABSORPTION SPECTRA OF NITROBENZENE

(Values in italics represent inflections in this and subsequent tables)

Solvent	*B*-Band		*C*-Band		Source
	λ_{max} (mμ)	ϵ_{max}	λ_{max} (mμ)	ϵ_{max}	
Gas phase	239.9	7600			Ref. 3
Naphtha	251	9200			Ref. 9
Cyclohexane (conc. = 2.2–88 mg/liter)	252	9000	*ca. 285*	*1500*	*
Iso-octane	252	8620	—	—	Ref. 1
Ethanol (conc. = 70 mg/liter)	257	8100	—	—	*
Ethanol (conc. = 1.75 mg/liter)	258	7700	—	—	*
95% Aqueous ethanol	260	8000			See Ref. 10
Dioxane (conc. = 90.5 mg/liter)	257–258	8400	—	—	*
Dioxane (conc. = 1.81 mg/liter)	259	7400	—	—	*
50% Aqueous dioxane	263–265	7800	—	—	*
Water (conc. = 2.4–95 mg/liter)	265–266	7900	—	—	*
N NaOH	266	6900	*ca. 304*	*2000*	*
0.1 *N* HCl	266	7800	—	—	*
Conc. H_2SO_4	287.5	8600	*ca. 302*	*7200*	*

*This series of papers.

which emphasizes the importance of the dielectric constant, compared with the presence or absence of hydrogen ions in determining the location of the *B*-band. On the other hand, media of high acidity, such as sulphuric acid (see Table I and ref. 3), have a marked effect on the spectrum.

Further, the *B*-band of nitrobenzene lies at considerably longer wavelength than that of acetophenone. Since the *B*-band of monosubstituted benzenes is predominantly determined by mesomeric interaction (cf., for example, ref. 12), it follows that in the absence of other considerations the nitro-group would be expected to exert a greater negative mesomeric interaction than the acetyl-group and in this way nitrobenzene absorbs at longer wavelength. It may be noted that the large mesomeric effect of the nitro-group can be used to explain the large frequency shift of the C–H bending vibration in nitrobenzene (13), and also the extremely high intensity of the R–NO_2 stretching vibration (8*f*) and the enhanced intensities of the aromatic bands at 1600–1500 cm^{-1} for nitrobenzenes (8*b*), since absorption intensities in the infrared region are probably largely proportional to resonance interaction (14, 15).

The *C*-band in nitrobenzene is identified only with difficulty. This is explained by the hypothesis (11) that a large mesomeric effect causes a low intensity *C*-band. There is little doubt that this band corresponds to the band in benzene at *ca.* 260 mμ (9, 11).

Para-Substituted Nitrobenzenes

The ultraviolet absorption spectra of some para-substituted nitrobenzenes are listed in Table II.

Para-disubstituted compounds provide a good method of studying mesomeric interactions because inductive-type interactions and steric effects may be assumed to be small (12) for a number of compounds of this type, and if the para-substituent is electron donating, a large mesomeric interaction would be expected. The data for this type of

Can. J. Chem. Downloaded from www.nrcresearchpress.com by 78.46.186.204 on 09/04/12
For personal use only.

TABLE II

ABSORPTION MAXIMA OF PARA-SUBSTITUTED NITROBENZENES

Substituent	Solvent	*B*-Band λ_{max} (mμ)	*B*-Band ϵ_{max}	*C*-Band λ_{max} (mμ)	*C*-Band ϵ_{max}	Source
p-Amino-	2 *N* HCl	258	8,700	—	—	Ref. 6
p-Nitro-	Methanol	258	14,700			Ref. 10
p-Acetyl-	Cyclohexane	258	14,000	*292* *308*	*2000* *1000*	*
	Ethanol	261	14,000	*ca. 298* *ca. 312*	*2200* *1200*	*
p-Carboxy-	Cyclohexane	255	13,000	*ca. 294*	*2000*	*
	Ethanol	258	12,000	*ca. 294*	*2500*	*
	Water	271	10,000			*
	0.1 *N* HCl	263.5	12,500			*
	N NaOH	272	10,600			*
p-Formyl-	Hexane	259	13,800	*ca. 284* *ca. 295* *ca. 305*	*3400* *2100* *1200*	*
	Const. boiling ethanol	265	11,400	—	—	Ref. 16
	Water	266	14,500	*ca. 301* *ca. 314*	*3000* *1800*	*
p-Fluoro-	Iso-octane	256	7,600			Ref. 17
	95% Aqueous ethanol	*ca.* 266	7,900	—	—	Ref. 4
p-Chloro-	95% Aqueous ethanol	*ca.* 272	10,000	—	—	Ref. 4
	pH 6	280	10,300	—	—	Ref. 6
p-Bromo-	95% Aqueous ethanol	*ca.* 276	11,100	—	—	Ref. 4
p-Iodo-	95% Aqueous ethanol	*ca.* 294	11,700	—	—	Ref. 4
p-Methyl-	Iso-octane	264	10,250	—	—	Ref. 1
	pH 6	285	9,250	—	—	Ref. 6
p-*i*-Propyl-	Iso-octane	265	10,430	—	—	Ref. 1
p-*t*-Butyl-	Iso-octane	265	10,720	—	—	Ref. 1
p-Hydroxy-	Cyclohexane	295	11,000	—	—	*
	Ethanol	314	13,000	—	—	Ref. 18
	Water	314	9,500			*
	pH 3	317.5	10,000	—	—	Ref. 6
	N NaOH	402.5	19,200	—	—	Ref. 6
p-Methoxy-	Ethanol	305	13,000	—	—	Ref. 18
	Water	313	10,500	—	—	*
p-Amino-	Naphtha	320	14,600			Ref. 9
	Ethanol	371	15,500	—	—	Ref. 19
	Water	373–377	13,000	—	—	*
	0.1 *N* HCl	372	5,600	—	—	*
	N NaOH	373–379	13,000	—	—	*
p-Dimethyl-amino-	Ethanol	387	18,300			See Ref. 10

*This series of papers.

compound, as discussed in the following paragraph, are in fact consistent with the hypothesis that a mesomeric type of interaction predominantly determines the spectra and that inductive and other types of interactions are again only of secondary importance (cf. Introduction). To investigate this mesomeric interaction, the data in Table II are first divided into two groups. The first group comprises the earlier values in Table II which do not show any appreciable mesomeric interaction. This is either because acid conditions prevent mesomeric interaction, as for *p*-nitroaniline in acid solution, or alternatively because primary mesomeric interaction may be negligible, as for *p*-dinitrobenzene, where by analogy with the electron-withdrawing properties of the nitro-group in the ground state, neither of the two nitro-substituents would be expected to act effectively as an electron donor in the electronic excited state.

For the latter type of example, moreover, both para-substituents will also tend to deactivate the benzene ring, that is, cause a withdrawal of π-electrons from the benzene

Can. J. Chem. Downloaded from www.nrcresearchpress.com by 78.46.186.204 on 09/04/12
For personal use only.

Can. J. Chem. Downloaded from www.nrcresearchpress.com by 78.46.186.204 on 09/04/12
For personal use only.

ring. This latter deactivation is also suggested by other data. For example, the carbonyl stretching frequencies in dilute chloroform solution for *p*-nitrobenzaldehyde (λ_{max} 1721 cm^{-1} (8*d*)) and *p*-nitroacetophenone (λ_{max} 1700 cm^{-1} (12)) are considerably displaced from those of benzaldehyde (λ_{max} 1709 cm^{-1}) and acetophenone (λ_{max} 1691 cm^{-1}) (12). This indicates that at least some of the conjugation, which causes the initial shift to lower frequency in aromatic carbonyl compounds, because of the aromatic nucleus, is no longer available. Although this argument again is evidently applicable only to the ground state, it is not unreasonable to assume that a similar deactivation occurs in the electronic excited state. Consequently, the carbonyl stretching frequencies data indirectly support the hypothesis. The supposed absence of mesomeric interaction may also be related to Hammett's observation (20) that for nitrobenzenes two different substitution constants must be used (cf. also ref. 21). Further, ultraviolet data indicate a reduced force constant in the N-nuclear bond for compounds like *p*-dinitrobenzene, since an increased extinction coefficient, as is observed in the early examples of Table II relative to nitrobenzene, may be ascribed to a reduced force constant. A number of similar examples have previously been discussed (22) and the relation between a reduced force constant and an increased extinction coefficient *in the absence of primary mesomeric interaction* has previously been suggested as a "secondary" effect in electronic spectra (22) and this hypothesis accounts well for the observed spectral changes. For example, the para-formyl group is assumed to decrease the double-bond character of the N-nuclear bond and in this way decreases the force constant of this bond, and hence increases the molecular

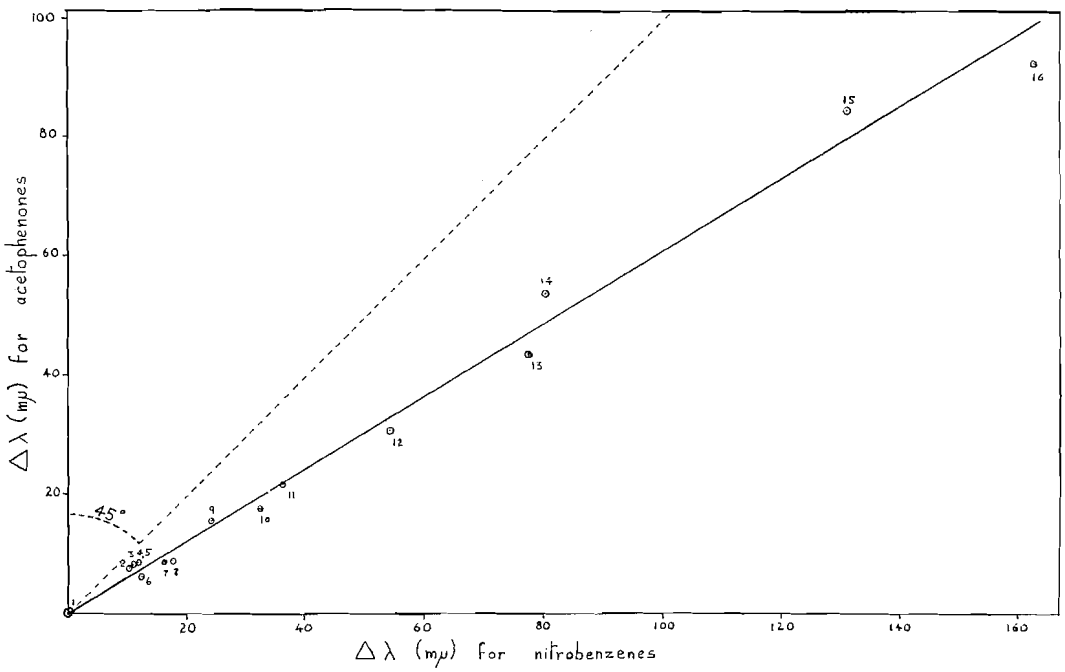

FIG. 1. Wavelength shifts ($\Delta\lambda$) of the *B*-band obtained on introducing a para-substituent in nitrobenzene and acetophenone. 1—H (gas phase); 2—Me (gas phase); 3—Et (gas phase); 4—*i*-Pr (gas phase); 5—*t*-Bu (gas phase); 6—H (hexane); 7—F (iso-octane, hexane); 8—H (ethanol); 9—Me (iso-octane, hexane); 10—Cl (95% ethanol, ethanol); 11—Br (95% ethanol, ethanol); 12—I (95% ethanol, ethanol); 13—OH (aqueous acid); 14—NH_2 (hexane, naphtha); 15—NH (ethanol); 16—OH (aqueous base). Values obtained from Table II, ref. 3, and previous papers in this series.

extinction coefficient. This decreased force constant may incidentally explain the relatively more pronounced *C*-band in compounds like *p*-nitroacetophenone (see Table II and ref. 11) compared with the *C*-band in nitrobenzene.

For the second group of data in Table II the primary mesomeric interaction which predominantly affects the electronic excited state is supposed to be the main factor determining the maximal wavelength of the *B*-band. In support of this hypothesis the following may be cited. First, an increased dielectric constant in the para-substituted nitrobenzenes, where primary mesomeric interaction is supposed to occur, causes bathochromic displacements parallel, but usually more pronounced, to those observed for nitrobenzene itself (see Tables I and II). This suggests that both changes are related to one and the same, mesomeric, interaction. Next, Fig. 1 shows that the wavelength displacements, and consequently the energy changes, for acetophenones and nitrobenzenes tend to be directly proportional to each other whenever mesomeric interaction is assumed to determine the *B*-band. This again is consistent with the hypothesis that both wavelength displacements are proportional to one electronic interaction, which is predominantly mesomeric in character.

The slope of the straight line obtained in Fig. 1 also indicates that mesomeric interaction is greater in nitro-compounds. This is ascribed to increased resonance contributions of dipolar excited states in nitrobenzene because of the greater negative mesomeric effect of the nitro-group. Two additional points may be noted. First, although the concept of resonance structures is implied in this discussion, molecular orbital theory provides, at least qualitatively, a similar picture (cf. ref. 9). Secondly, intensity values (ϵ) of para-substituted compounds compared to intensity values of unsubstituted compounds (ϵ_0) are less suitable than wavelength changes in the study of mesomeric interactions. This follows not only because overlapping of bands may interfere with the quantitative estimation of absorption intensities, but also because intensity values are more sensitive to other, secondary, interactions, such as slight changes in the force constant of the N-nuclear bond caused by solvent–solute interactions.

Meta-Substituted Nitrobenzenes

The spectra of meta-substituted nitrobenzenes are listed in Table III.

In meta-substituted nitrobenzenes primary mesomeric interaction between the meta-substituents is theoretically impossible and hence the observed *B*-bands would be expected to correspond to the *B*-bands of the two monosubstituted parent compounds. This explanation is taken to account for the frequent occurrence of two distinct *B*-bands in a meta-disubstituted benzene derivative. This is illustrated by some of the data in Table III, and the band assignment is also supported by a number of unpublished data. One of the *B*-bands, the nitrobenzene *B*-band, is usually identified without difficulty for the compounds listed in Table III. The second *B*-band is ascribed to benzenoid absorption involving the non-nitro substituent. It may be noted in passing that Doub and Vandenbelt sometimes designate this second *B*-band as a "secondary primary band" (7). For example, the maximal absorption at 251.5 mμ for *m*-nitrophenol is assumed to be a secondary primary band, whereas we would ascribe this absorption to phenolic *B*-band absorption.

However, the observed *B*-bands will not necessarily correspond closely to the *B*-bands of the mono-substituted parent compounds, since a secondary interaction also occurs between the two substituents in meta-substituted compounds. This interaction has previously been discussed in general terms (25), and we will therefore at present consider

Can. J. Chem. Downloaded from www.nrcresearchpress.com by 78.46.186.204 on 09/04/12
For personal use only.

TABLE III

ABSORPTION MAXIMA OF META-SUBSTITUTED NITROBENZENES

Substituent	Solvent	*B*-Band λ_{max} (mμ)	*B*-Band ϵ_{max}	*C*-Band λ_{max} (mμ)	*C*-Band ϵ_{max}	Source
m-Nitro-	Cyclohexane	228	20,500	*ca. 275* 283 294	*1150* 1000 770	*
	96% Aqueous ethanol	235	17,400			See Ref. 10
	Water	241.5	16,300	305	1100	Ref. 7
m-Acetyl-	Cyclohexane	224 *254*	23,000 *7000*	*288* 298	*1100* 750	*
	Ethanol	226 *ca. 260*	22,500 *6500*	*ca. 300*	*800*	*
m-Formyl-	Cyclohexane	225 *ca. 242* *ca. 252*	26,000 *11,000* *6800*	287 298	1000 700	*
	Ethanol	*ca. 256*	*7,700*	—	—	
m-Carboxy-	Cyclohexane containing 2% ether	250–251	7400	*ca. 285* *ca. 296*	*1150* *650*	*
	Ethanol	215 255	22,500 7000	—	—	*
	Water	212.5 265	20,000 7000			*
	0.1 *N* HCl	261	7100			*
	N NaOH	266	7350			*
m-Fluoro-	Iso-octane	246	7400	284	1700	Ref. 17
	95% Aqueous ethanol	*ca.* 255	7700	*ca. 300*	*1900*	Ref. 4
m-Chloro-	95% Aqueous ethanol	*ca.* 258	7200	*ca. 300*	*1500*	Ref. 4
	Water	224 264	6800 7100	313	1300	Ref. 7
m-Bromo-	95% Aqueous ethanol	*ca.* 259	6200	*ca. 303*	*1200*	Ref. 4
m-Iodo-	Light petroleum	*ca. 260*	*6200*	*ca.* 308	1000	Ref. 23
	95% Aqueous ethanol	*ca.* 262	6400	*ca.* 315	1000	Ref. 4
m-Methyl-	Iso-octane	256.5	8160	*ca. 292*	*1500*	Ref. 1
m-*t*-Butyl-	Iso-octane	258	8220	*ca. 292*	*1500*	Ref. 1
m-Hydroxy-	Cyclohexane containing *ca.* 1% ether	225–226 262	11,000 5750	319	2200	*
	Ethanol	270.5	6900	332.2	2700	Ref. 18
	Water	228 272	7600 6000	323 328	1900 1950	*
	pH 3	228.5 273.5	7900 6000	333	1960	Ref. 7
	0.1 *N* NaOH	251.5 291	11,000 4500	392	1500	Ref. 7
m-Methoxy-	Cyclohexane	223 260	13,000 6100	313	2400	*
	Ethanol	268	6400	325.2	2400	Ref. 18
	Water	228 273.5	8900 6000	330	2050	Ref. 7
m-Amino-	Ethanol	233	18,000	375	1600	Ref. 24
	Water	224 278–279	13,500 4500	350–358	1400	*
	N NaOH	224 278–279	14,000 4650	354	1400	*
	0.1 *N* HCl	256	7500			*
m-Dimethyl-amino-	Ethanol	246	23,000	400.3	1350	Ref. 24

*This series of papers.

only the effect of a meta-nitro substituent on the *B*-band of a monosubstituted benzene derivative. The relevant data (see Tables III, I, and previous parts of this series) are collected in Table IV.

Can. J. Chem. Downloaded from www.nrcresearchpress.com by 78.46.186.204 on 09/04/12
For personal use only.

TABLE IV

THE NON-NITROBENZENE *B*-BAND OF META-SUBSTITUTED NITROBENZENES, AND THE *B*-BAND OF REFERENCE COMPOUNDS

Solvent	*m*-Substituted nitrobenzene	λ_{max} (mμ)	ϵ_{max}	Reference compound	λ_{max} (mμ)	ϵ_{max}	$\Delta\lambda$ (in mμ)
Cyclohexane	*m*-Dinitrobenzene	228	20,500	Nitrobenzene	252	9000	−24
95% Aqueous ethanol	*m*-Dinitrobenzene	235	17,400	Nitrobenzene	260	8000	−25
Water	*m*-Dinitrobenzene	241.5	16,300	Nitrobenzene	265–266	7900	−24
Cyclohexane	*m*-Nitroacetophenone	224	23,000	Acetophenone	237.5	12,500	−13.5
Ethanol	*m*-Nitroacetophenone	226	22,500	Acetophenone	240	12,500	−14
Cyclohexane	*m*-Nitrobenzaldehyde	225	26,000	Benzaldehyde	241	14,000	−16
0.1 *N* NaOH	*m*-Nitroaniline	224	14,000	Aniline	230	8400	−6
Aqueous acid	*m*-Nitrophenol	228.5	7900	Phenol	210	6000	+18.5
Water	*m*-Nitrophenol	228	7600	Phenol	210	6000	+18
Aqueous NaOH	*m*-Nitrophenol	251.5	14,500	Phenol	234	10,500	+17.5
Water	*m*-Nitroanisole	228	8900	Anisole	217	4300	+11

Table IV shows that a meta-nitro substituent indeed affects the absorption band, usually giving rise to an appreciable displacement. This displacement is positive or negative, presumably depending on the dipolar forms contributing to the electronic excited state. In this way, a nitro-group apparently exerts a negative wavelength displacement on chromophores like acetophenone or nitrobenzene, but a positive wavelength displacement on chromophores like anisole or phenol. The different effect of the nitro-group in meta-disubstituted benzene derivatives may be rationalized by assuming that either structure I or II may preferentially contribute to the electronic excited state. Assuming structures of this type, one may visualize the way in which the formation of a positive or negative charge near the *m*-nitro-group may have opposite effects, as illustrated for *m*-nitrophenol and *m*-dinitrobenzene. The relatively large extinction coefficients, which are noted in the *B*-band of the meta-substituted nitrobenzenes listed in Table IV, are again tentatively ascribed to a reduced force constant caused by the electron-withdrawing effect of the nitro-substituent (cf. ref. 22).

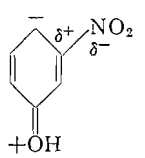

I

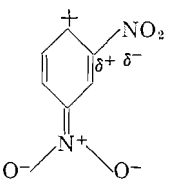

II

The nitrobenzene *B*-band is evident in most of the compounds listed in Table III, and is subject to the usual secondary interactions. One of these, the buttressing effect, would be expected to occur in meta-substituted nitrobenzenes (cf. ref. 26), and this effect would be expected to be greatest for *m*-dinitrobenzene. In this way, the buttressing effect may contribute to the variation in the observed wavelength displacement (see Table IV). The *C*-band in meta-substituted nitrobenzenes usually becomes more pronounced, an observation which has previously received an explanation (11).

Can. J. Chem. Downloaded from www.nrcresearchpress.com by 78.46.186.204 on 09/04/12
For personal use only.

Ortho-Substituted Nitrobenzenes

The ultraviolet absorption spectra of ortho-substituted nitrobenzenes are listed in Table V.

TABLE V

ABSORPTION MAXIMA OF ORTHO-SUBSTITUTED NITROBENZENES

		B-Band		*C*-Band		
Substituent	Solvent	λ_{max} (mμ)	ϵ_{max}	λ_{max} (mμ)	ϵ_{max}	Source
o-Acetyl-	Cyclohexane	254	6000	—	—	*
	Ethanol	257	6000	—	—	*
o-Formyl-	Cyclohexane	222	15300	*ca.* 285	1700	*
		247	7000			
	Ethanol	220	8500	270	3600	Ref. 16.
		252	4700			
o-Carboxy-	Cyclohexane containing *ca.* 2% ether	—	—	*ca. 278*	*1350*	*
	Ethanol	*ca. 250*	*3500*	—	—	*
	Water	*ca.* 266	5300			*
	0.1 *N* HCl	*ca.* 262.5	5500			*
	N NaOH	267	5500			*
o-Fluoro-	Iso-octane	242	7250	278	1850	Ref. 17
	95% Aqueous ethanol	*ca.* 250	6900	*ca. 285*	*2200*	Ref. 4
o-Chloro-	95% Aqueous ethanol	*ca.* 252	3500	*ca.* 290	1200	Ref. 4
	Water	228	4400	310	1400	Ref. 7
		260	4000			
o-Bromo-	95% Aqueous ethanol	*ca.* 255	3000	*ca.* 292	1300	Ref. 4
o-Iodo-	95% Aqueous ethanol	*ca. 260*	*3500*	*ca.* 310	1500	Ref. 4
o-Methyl-	Iso-octane	250	5950	*ca. 290*	*1500*	Ref. 1
o-*i*-Propyl-	Iso-octane	247	3760	*ca. 290*	*1300*	Ref. 1
o-*t*-Butyl-	Iso-octane	—	—	*ca. 275*	*700*	Ref. 1
o-Methyl-	Water	266	5300	325	1300	Ref. 7
o-Hydroxy-	Cyclohexane	269–270	7500	342	3800	*
	Ethanol	273	6600	343.5	3600	Ref. 18
	Water	*ca. 230*	*3700*	346	3000	*
		276	6350			
	pH 3	*230*	*3900*	351	3200	Ref. 7
		278.5	6600			
	0.1 *N* NaOH	*250*	*5000*	416	4800	Ref. 7
		282	4300			
o-Methoxy-	Cyclohexane	249	3400	304	2500	*
	Ethanol	258.5	3450	317.2	2850	Ref. 18
	Water	264	4300	333	2900	*
o-Amino-	Cyclohexane	227	18000	370	5000	*
		268	5000			
	Ethanol	275.2	5100	403.6	5400	Ref. 24
	Water	233	17000	400–405	4500	*
		280	5500			
	0.1 *N* NaOH	245	7000	412	4500	Ref. 7
		282.5	5400			
o-Dimethyl-amino-	Ethanol	245.5	21500	416	2950	Ref. 24

*This series of papers.

The ortho-effect of alkyl groups in nitrobenzenes has previously been ascribed to steric inhibition of resonance (1) and it was noted that the decreased intensity of absorption is qualitatively in agreement with the increased size of the substituent, i.e. *t*-butyl > *i*-propyl > methyl. For alkylnitrobenzenes in iso-octane solution a hypsochromic shift is also observed compared with the wavelength of maximal absorption in the meta-isomers. This is explained by assuming that in certain ortho-isomers not only does the alkyl group fail to contribute to mesomeric interaction between the two substituents,

Can. J. Chem. Downloaded from www.nrcresearchpress.com by 78.46.186.204 on 09/04/12
For personal use only.

but the vicinal alkyl-group also causes the nitro-group to twist about the C–NO_2 axis. Consequently, absorption in the ortho-isomer occurs at shorter wavelength, and with decreased absorption intensity (cf. ref. 25, 27).

By considering the two types of *B*-bands in ortho-isomers (cf. preceding section), we can further relate changes in the *B*-bands with the ease of dislodging a particular group from the plane of the benzene ring. For example, in *o*-nitrophenol (basic solution) the band corresponding to nitrobenzene occurs at λ_{max} 282 mμ, ϵ = 4300, similar in intensity to the band in *m*-nitrophenol, which occurs at λ_{max} 291 mμ, ϵ = 4500. The other *B*-band, which occurs in the meta-isomer at λ_{max} 251.5 mμ, ϵ = 11,000, and which is ascribed to the phenolate ion, occurs in the ortho-isomer only as an inflection at 250 mμ, ϵ = 5000. This suggests that the $-O^-$ substituent is more readily dislodged from the plane of the benzene ring than the nitro-group.

The ease of dislodging a particular group from the plane of the benzene ring may also depend on the solvent. This is illustrated in Fig. 2 for the spectrum of *o*-nitrobenzoic acid.

Fig. 2 shows that the nitrobenzene *B*-band in aqueous medium is more pronounced

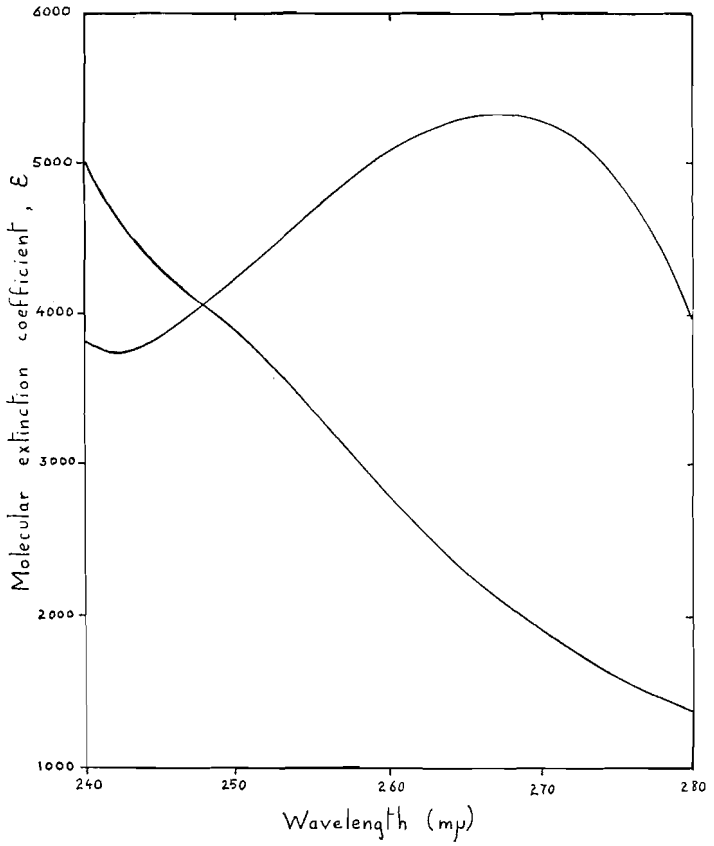

FIG. 2. The *B*-band (nitrobenzene band) of *o*-nitrobenzoic acid in 1—water; 2—cyclohexane containing 2% ether. Strictly speaking, for comparison purposes, the spectrum should have been determined in acidified aqueous solution, since in water the molecule will actually absorb as the anion and not as the undissociated acid. (We are grateful to a referee for drawing our attention to this.) However, in fact, the spectrum in acidified water also shows a similar maximum (see Table V) undergoing only the usual displacement associated with the change from neutral to acidic medium (cf. ref. 25).

Can. J. Chem. Downloaded from www.nrcresearchpress.com by 78.46.186.204 on 09/04/12
For personal use only.

and, as such, more readily recognized. This has some application from an analytical point of view (see next section). It can be explained by assuming that in aqueous solution the nitrobenzene band is strengthened at the expense of benzoic acid coplanarity. This explanation may be related to the appreciable wavelength displacement observed for nitrobenzene absorption on passing from hexane to ethanol and water, since this also suggests solvent–solute interaction between the nitro-group and the solvent. In terms of the previously proposed classification of steric effects (cf. ref. 12 and references cited there), this observation implies that *in aqueous solutions ortho-substituted nitrobenzenes will more frequently give rise to type I steric effects* (that is, an intensity decrease without appreciable wavelength displacement will be observed), *whereas in hexane media other steric effects will often be observed.*

As expected, steric interactions in ortho-substituted nitrobenzenes are also evident from a number of other physical data (cf. also ref. 5). For example, while the characteristic Raman frequency of the nitro-group is around 1367 cm^{-1}, in nitrobenzene the interaction of the nitro-group with the aromatic nucleus causes a frequency drop to 1341 cm^{-1}. In *o*-nitrotoluene some of this interaction is destroyed, and absorption again occurs at higher frequency (1345 cm^{-1}). In nitromesitylene the interaction is almost completely destroyed and the frequency occurs at 1363 cm^{-1}, close to the frequency of the unconjugated nitro-group (28; cf. also refs. 29, 30). This latter absorption may be compared with the ultraviolet absorption of nitromesitylene (1), which also indicates the virtual absence of conjugation.

Apart from steric interactions, the operation of other forces, especially intermolecular hydrogen bonding, would be expected to be evident in ortho-substituted nitrobenzenes. Examples of intermolecular hydrogen bonding may be provided by the nitrobenzene *B*-bands of nitrophenol and nitroanisole. In ethanol, the meta-isomers absorb maximally within 3 mμ (see Table III), whereas the corresponding ortho-isomers show a bathochromic shift of 14.5 mμ for the phenol (see Table V). It may be noted that this wavelength displacement is qualitatively similar to the displacement observed in the corresponding acetophenones (11) and that intramolecular hydrogen bonding in nitrobenzenes is also suggested from infrared data (cf. refs. 8*d*, 31).

The *C*-band of ortho-substituted nitrobenzenes again is normally more pronounced than that of the corresponding para-isomers, but tends to disappear in compounds where steric inhibition of resonance is large (11).

APPLICATIONS

Since the negative mesomeric effect is large for a nitro-group, the mesomeric interaction in nitrobenzene will be large, and will not be too easily inhibited by steric interactions. Consequently the prerequisite for a type I steric effect is available; namely, the electronic excited state, where mesomeric interaction is presumed to be greater than in the ground state, remains frequently at a similar energy level for the prevalent conformations in both the sterically hindered compounds and reference compounds, and hence no appreciable wavelength displacements are observed. Steric effects of type I are in fact often observed, and are found to be more probable in aqueous solution, where solvent–solute interactions are assumed to further facilitate the mesomeric interaction.

Thus, the characteristic nitrobenzene band near 260 mμ will often be evident in aqueous solution, even in a reasonably complex molecule. Conversely, the occurrence of a band near 260 mμ under those conditions, for a compound containing a nitro-group, indicates the presence of the nitrobenzene chromophore. It should be noted, however, that for

Can. J. Chem. Downloaded from www.nrcresearchpress.com by 78.46.186.204 on 09/04/12
For personal use only.

ortho- or meta-substituted nitrobenzene chromophores more than one band may occur in this region, and that for certain para-substituents the band may be considerably displaced towards longer wavelength (cf. Table II).

If a definite absorption band occurs near 260 mμ, the absorption intensity of the band can also be used to estimate steric effects. This type of spectral analysis has recently been employed in the discussion of the structures of 2-carboxy-4,5-dimethoxy-2′-nitrobiphenyl and 2-carboxy-4,5-dimethoxy-2′-nitro-3′-methylbiphenyl (26) and of (+)6,6′-dinitro-2,2′-di-(2,4-dimethylbenzoyl)biphenyl (32). Qualitative spectral investigation of the nitro-group is also possible in the infrared region (8*e*, 33), since the nitro-group causes characteristic bands near 1550 cm^{-1} and in the region 1360–1300 cm^{-1}. Lastly, the *B*-band in the ultraviolet region appears to be well suited to the quantitative determination of compounds containing a nitrobenzene chromophore. This is so, because the extinction coefficients obey Beer's law fairly accurately and in additon the absorption is not particularly sensitive to slight changes in pH. In this way, the method may offer advantages, for example, in the study of reaction mechanisms involving a nitro-substituent.

EXPERIMENTAL

The ultraviolet absorption spectra were determined in quartz cells using a Unicam SP500 spectrophotometer. For each compound at least two independent sets of observations were made. Some of the spectra, for example the acetophenone spectra used in constructing Fig. 1, have already been described in previous parts of this series. Little disagreement was found between our values and those reported elsewhere in the literature. The estimated precision of our values for extinction coefficients is $\pm 5\%$ or better. On theoretical grounds the use of oscillator strengths, *f*, would be preferred, but for practical reasons we have not used this quantity so far (cf. also Wepster (5), who has found a reasonably linear relationship between ϵ_{max} and *f*). The estimated precision of our values for the maximal wavelengths is ± 0.5 mμ.

The nitrobenzenes were purified from the commercially available compounds. Solvents also were purified by standard methods.

ACKNOWLEDGMENTS

The author gratefully acknowledges the assistance of Mr. J. C. Dearden, Miss Rosemarie Gosine, and Mr. J. F. Templeton in the experimental work, and in the preparation of the diagrams (Mr. J. C. Dearden).

Lastly, it is a pleasure to thank the National Research Council of Canada for grants supporting this work.

REFERENCES

1. Brown, W. G. and Reagan, H. J. Am. Chem. Soc. **69**, 1032 (1947).
2. Hammond, G. S. and Modic, F. C. J. Am. Chem. Soc. **75**, 1385 (1953).
3. Schubert, W. M., Robins, J., and Haun, J. L. J. Am. Chem. Soc. **79**, 910 (1957).
4. Ungnade, H. E. J. Am. Chem. Soc. **76**, 1601 (1954).
5. Wepster, B. M. Rec. trav. chim. **76**, 335 (1957).
6. Doub, L. and Vandenbelt, J. M. J. Am. Chem. Soc. **69**, 2714 (1947).
7. Doub, L. and Vandenbelt, J. M. J. Am. Chem. Soc. **71**, 2414 (1949).
8. Bellamy, L. J. The infrared spectra of complex molecules. Methuen & Co. Ltd., London. 1954. (*a*) p. 60; (*b*) p. 62; (*c*) p. 68; (*d*) p. 134; (*e*) p. 250; (*f*) p. 252.
9. Nagakura, S. J. Chem. Phys. **23**, 1441 (1955).
10. Kamlet, M. J. and Glover, D. J. J. Am. Chem. Soc. **77**, 5696 (1955).
11. Forbes, W. F., Mueller, W. A., Ralph, A. S., and Templeton, J. F. Can. J. Chem. **35**, 1049 (1957).
12. Forbes, W. F. and Mueller, W. A. Can. J. Chem. **35**, 488 (1957).

Can. J. Chem. Downloaded from www.nrcresearchpress.com by 78.46.186.204 on 09/04/12
For personal use only.

13. KROSS, R. D., FASSEL, V. A., and MARGOSHES, M. J. Am. Chem. Soc. **78**, 1332 (1956).
14. BARROW, G. M. J. Chem. Phys. **21**, 2008 (1953).
15. JONES, R. N., FORBES, W. F., and MUELLER, W. A. Can. J. Chem. **35**, 504 (1957).
16. WALKER, E. A. and YOUNG, J. R. J. Chem. Soc. 2041 (1957).
17. GRUBER, W. Can. J. Chem. **31**, 1020 (1953).
18. BURAWOY, A. and CHAMBERLAIN, J. T. J. Chem. Soc. 2310 (1952).
19. TIMMONS, C. J. J. Chem. Soc. 2613 (1957).
20. HAMMETT, L. P. Physical organic chemistry. McGraw-Hill Book Co., Inc., New York. 1940. p. 188.
21. FREEDMAN, L. D. and DOAK, G. O. J. Org. Chem. **21**, 811 (1956).
22. FORBES, W. F. and TEMPLETON, J. F. Can. J. Chem. **36**, 180 (1958).
23. FERGUSON, J. and IREDALE, T. J. Chem. Soc. 2959 (1953).
24. MORTON, R. A. and MCGOOKIN, A. J. Chem. Soc. 901 (1934).
25. FORBES, W. F. and RALPH, A. S. Can. J. Chem. **36**, 869 (1958).
26. FORBES, W. F. and MUELLER, W. A. J. Am. Chem. Soc. **79**, 6495 (1957).
27. FORBES, W. F. and MUELLER, W. A. Can. J. Chem. **34**, 1340 (1956).
28. SAUNDERS, R. H., MURRAY, M. J., and CLEVELAND, F. F. J. Am. Chem. Soc. **63**, 3121 (1941).
29. FRANCK, B., HÖRMANN, H., and SCHEIBE, S. Ber. **90**, 330 (1957).
30. LITTLEJOHN, A. C. and SMITH, J. W. J. Chem. Soc. 2476 (1957).
31. FRANCEL, R. J. J. Am. Chem. Soc. **74**, 1265 (1952).
32. FORBES, W. F., WALLENBERGER, F. T., O'CONNOR, W. F., and MORICONI, E. J. J. Org. Chem. **23**, 224 (1958).
33. HASZELDINE, R. N. J. Chem. Soc. 2525 (1953).

Can. J. Chem. Downloaded from www.nrcresearchpress.com by 78.46.186.204 on 09/04/12
For personal use only.

Can. J. Chem. Downloaded from www.nrcresearchpress.com by 78.46.186.204 on 09/04/12
For personal use only.

LIGHT ABSORPTION STUDIES

PART XII. ULTRAVIOLET ABSORPTION SPECTRA OF BENZALDEHYDES[1]

J. C. Dearden and W. F. Forbes

ABSTRACT

The electronic spectra of benzaldehydes in the region 220–360 mμ are recorded and discussed in terms of previously stated hypotheses. The formyl group is shown to endow benzene derivatives with spectral properties similar to those of the acetyl group in acetophenones, except that steric interactions are slightly modified.

INTRODUCTION

The ultraviolet absorption spectra of benzaldehydes are of interest because they provide additional examples in the study of the various interactions which determine electronic spectra. The spectra would be anticipated to be related to the previously studied spectra of acetophenones (1, 2, 3), benzoic acids (4), and nitrobenzenes (5), since in all these compounds a negative mesomeric effect operates.

The spectra of some of the benzaldehydes have previously been recorded (6, 7, 8, 9, 10), but, whenever it proved convenient, spectra were redetermined in order to obtain data under near-identical conditions. The terminology employed in this paper is identical with that employed in previous parts of this series.

THE SPECTRUM OF BENZALDEHYDE

The absorption maxima of benzaldehyde in different solvents are listed in Table I.

TABLE I

ABSORPTION MAXIMA OF BENZALDEHYDE IN DIFFERENT SOLVENTS*

		B-Band		*C*-Band	
Solvent	Concentration (mg/liter)	λ_{max} (mμ)	ϵ_{max}	λ_{max} (mμ)	ϵ_{max}
Cyclohexane	1.01	241 *247*	14,000† *11,500*	 277–278 *287*	 1200 *1000*
	40.5	241 *247*	14,500 *12,500*		
Ether	3.6	241 *ca. 247*	14,000 *12,000*	*ca. 270* 277–278 285	*1000* 1200 1000
Dioxane	41.2	243	*ca.* 12,500	278–279	1200
50% Aqueous dioxane	1.01 40.4	247 247	10,500† 12,500	279–280	1350
Water	0.98 39.1	248 248	12,000† 12,500	278–279	1400
N NaOH	1.02 40.8	248	10,000	*ca. 279*	*1200*
0.1 *N* HCl	1.03 41.2	249	13,500	280	1500
Conc. H_2SO_4	2.5	293	21,000	*ca. 330*	*2000*

*Values in italics represent inflections in this and subsequent tables.
†Intermediate values for extinction coefficients were obtained at intermediate concentrations.

[1]*Manuscript received May 5, 1958.*
Contribution from the Memorial University of Newfoundland, St. John's, Newfoundland.

Can. J. Chem. Downloaded from www.nrcresearchpress.com by 78.46.186.204 on 09/04/12
For personal use only.

Benzaldehyde in cyclohexane solution appears to show a slight concentration dependence, which may be caused by intermolecular hydrogen bonding (11). Unfortunately, the changes in the extinction coefficients are not sufficiently large to permit any conclusions at this stage. None of the *C*-bands listed in Table I shows concentration dependence within the accuracy of the experiments. Extinction coefficients are also altered on changing the solute concentration for dioxane solutions (see Table I), and some aspects of these spectral changes will be examined in a separate study. It is noticeable, however, that some interaction occurs between solvent and solute in solvents other than cyclohexane, as witnessed by the spectral changes occurring in various solvents. In particular, the characteristic doublet, observed in cyclohexane and to a small extent in ether solution, disappears in all other solvents.

This doublet is more pronounced for both *B*- and *C*-bands on reducing the temperature (12). In acetophenone, in the gas phase and in heptane, the spectrum is also reported to be slightly unsymmetrical at the *B*-band maximum and shows a small shoulder at about 7 mμ to the red of the peak. Again in all other solvents, this maximum was found to be symmetrical and the shoulder was absent. For nitrobenzenes, the *B*-band is structureless, even in the gas phase, and quite symmetrical about the maximum (13). An explanation involving hydrogen bonding cannot perhaps be ruled out completely, at least at this stage (cf. 14), but seems improbable. Any complete explanation for this fine structure effect must take into account the above and also the following observations:

(i) The fine structure occurs for all benzaldehyde *B*-bands described in this paper, with the exception of the band at 225 mμ for *m*-nitrobenzaldehyde, which exhibits no fine structure (see following sections). For this compound, the benzaldehyde band is considerably displaced.

(ii) The fine structure disappears for certain *C*-bands (see following sections).

(iii) In the *B*-band of *o*-hydroxybenzaldehyde the fine structure is slightly different inasmuch as the longer wavelength peak is more pronounced (see Table V). This is the only *B*-band for which this different band shape was noted.

The occurrence of the doublet for solutions of benzaldehyde in hexane is also of some practical importance, since it frequently allows the identification of the benzaldehyde

TABLE II

VARIATION OF ABSORPTION MAXIMA WITH DIELECTRIC CONSTANT OR ACIDITY

Solvent	Benzaldehyde		Acetophenone		Nitrobenzene	
	λ_{max} (mμ)	ϵ_{max}	λ_{max} (mμ)	ϵ_{max}	λ_{max} (mμ)	ϵ_{max}
			B-Bands			
Dioxane	243	*ca.* 12,500	239	12,000	257–259	8000
50% Aqueous dioxane	247	10,500–12,500	243	12,000	264	8000
Water	248	12,000–12,500	244	12,000	265–266	8000
N NaOH	248	10,000	244	11,500	266	7000
0.1 *N* HCl	249	13,500	244	12,000	266	8000
Conc. H_2SO_4	293	21,000	293	20,000	287.5	8500
			C-Bands			
Dioxane	278–279	1200	277	1000	—	—
50% Aqueous dioxane	279–280	1350	278	1150	—	—
Water	278–279	1400	276–278	1250	—	—
N NaOH	*ca. 279*	*1200*	277	1250	*ca. 304*	*2000*
0.1 *N* HCl	280	1500	277	1250	—	—
Conc. H_2SO_4	*ca. 330*	*2000*	*ca. 325*	*2500*	*ca. 302*	*7200*

band, not only in simple benzaldehydes (see following sections) but also in more complicated molecules (cf. 15).

Finally in this section it may be noted that the maximal absorption of the *B*-band for benzaldehyde normally occurs at longer wavelength than for acetophenone. This prompts the speculation that benzaldehyde exists, at least at room temperature, with a larger proportion of planar or near-planar conformations. This hypothesis also correlates with the known lesser susceptibility of benzaldehydes to steric interactions (cf. 1, 16). On the other hand, the carbonyl stretching frequency of benzaldehyde lies at 1709 cm^{-1} (mean integrated absorption intensity, $A = 2.56$ $mole^{-1}$. liter. $cm^{-2} \times 10^{-4}$), whereas the corresponding frequency for acetophenone under identical conditions occurs at 1691 cm^{-1} ($A = 2.20$), that is, at shorter frequency or longer wavelength (2). This wavelength shift therefore is in the reverse order from that observed in the ultraviolet spectra. An explanation of these observations may be provided if it is remembered that steric effects in the *B*-band are predominantly caused by interactions between vicinal atoms in the electronic excited state (cf. 2, 16, 17), and consequently the observed opposite wavelength displacements may represent a previously discussed type of steric effect in which ground and excited states are displaced in opposite directions compared with a non-hindered reference compound (cf. Fig. 2 in Part VII (2) of this series). Although the positions of the maximal wavelengths are displaced in opposite directions for the vibrational and electronic spectra, the integrated absorption intensities (A) of the vibrational spectra relate to the wavelength changes in the electronic spectra. This is as anticipated, since the integrated absorption intensities have been related to the resonance energies of conjugation (18), which also predominantly determine the *B*-band in electronic absorption spectra. This hypothesis, incidentally, is consistent with the observation that in sulphuric acid the two compounds absorb at identical maximal wavelength in the ultraviolet region and with similar absorption intensity. That is, it is assumed that the increased solvent–solute interaction in this solvent overcomes the steric interactions between the methyl-group and the ortho-hydrogen atoms in acetophenone.

THE SPECTRA OF PARA-SUBSTITUTED BENZALDEHYDES

The spectra of para-substituted benzaldehydes are listed in Table III and wavelength displacements compared with benzaldehyde are also related to similar wavelength displacements obtained in the acetophenone and nitrobenzene series (see Table III and Fig. 1).

Most of the values in Table III are for hexane solution, but some of the values are for ethanolic solution. In compiling the wavelength shifts for Fig. 1, the mean maximal wavelength was used. This introduces an uncertainty, since the maximum of the hypothetical "unresolved" band may not exactly coincide with this mean. However, this uncertainty does not appear to introduce any appreciable deviation from the observed relations, since Fig. 1 shows that the wavelength displacements are approximately proportional to each other, indicating that the electronic interactions are comparable for the compounds under investigation. An exception is provided by the hydroxy-compounds in alkaline ethanol, which appear to show a relatively smaller wavelength displacement for the benzaldehyde. This effect may tentatively be ascribed to the relative absence of steric interactions in benzaldehydes (see previous section), since, in this way, the alkaline medium will tend to overcome steric interactions in acetophenones and nitrobenzenes.

Table III shows that the *B*-bands of all para-substituted benzaldehydes obtained by us possess fine structure in hexane solution, except the *B*-band of *p*-nitrobenzaldehyde.

Can. J. Chem. Downloaded from www.nrcresearchpress.com by 78.46.186.204 on 09/04/12
For personal use only.

TABLE III

ABSORPTION MAXIMA OF PARA-SUBSTITUTED BENZALDEHYDES AND THE EFFECT OF PARA-SUBSTITUENTS ON THE *B*-BAND FOR BENZALDEHYDES, ACETOPHENONES, AND NITROBENZENES IN *n*-HEXANE OR CYCLOHEXANE SOLUTION

(Wavelength displacements for ethanol are given in parentheses in this and subsequent tables)

	B-Band			*C*-Band		Wavelength shifts with reference to parent compound in:			
Benzaldehyde	λ_{max} (mμ)	ϵ_{max}	Mean λ_{max}	λ_{max} (mμ)	ϵ_{max}	Benzaldehydes	Acetophenones	Nitrobenzenes	Ref.
(Benzaldehyde)	241 *247*	14,000 *12,000*	244	277–278 287	1200 1000	—	—	—	*
p-Methyl-	251 257	15,000 12,500	254	279 *284*	1200 *1000*	10	10.5	12	*, †
p-Fluoro-	244 Not given	13,000	244	Not given		3	1.5	4	*, ‡
p-Chloro-	253 *259*	19,000 *15,500*	256	276 286	1500 1000	12	10.5	14	*, ‡
p-Bromo-	257.5 Not given	18,500	257.5	Not given		16.5	14.5	18.5	*, ‡
p-Iodo-	268 275 280	19,500 16,000 14,500	274	*ca. 290*	*4000*	30 (26)	24.5 (22)	35 (34.5)	*, ‡
p-Methoxy-	265 *ca. 272* 278 286	18,500 *16,000* 12,500 5,500	275	—	—	31 (32)	27 (29)	39 (47)	*, § *, ‖
p-Hydroxy-	265–266 *ca. 274* 281 288	19,000 *15,500* 12,000 6,000	277	—	—	33 (37)	28 (35)	35 (56)	*, § *, ‖
[In alkaline ethanol	336	30,000	336	—	—	88	84	134	¶]
p-Amino-	291 296	16,300 16,100	293.5	—	—	49.5	46	69	*, **
p-Carboxy-	249 257	17,500 15,500	253	279 288 298	1650 1950 1600	9	—	3	*
p-Nitro-	[259	13,800]	—	*ca. 284* *ca. 295* *ca. 305*	*3400* *2100* *1200*	—	—	—	*
[In aqueous solution	266	14,500]		*ca. 301* *ca. 314*	*3000* *1800*				

*This series of papers. †Ref. 6. ‡Ref. 8. §Ref. 19. ‖Ref. 7. ¶Ref. 20. **Solvent: cyclohexane containing 2% ether.

Partly because of this, the *B*-band of *p*-nitrobenzaldehyde is assigned to nitrobenzene absorption. On the other hand, the spectrum of *p*-carboxybenzaldehyde shows the typical benzaldehyde doublet. The former assignment, indicated in Table III by square brackets, also receives support, since this band not only shows the absence of the characteristic benzaldehyde doublet, but also shows the characteristic properties of nitrobenzene absorption. For example, the *B*-band of *p*-nitrobenzaldehyde in aqueous solution undergoes an appreciable bathochromic wavelength displacement to 266 mμ, that is, to the wavelength associated with nitrobenzene absorption in aqueous solution (5) (see Table III). These assignments therefore suggest the absence of any appreciable interaction between two electron-withdrawing substituents in para-disubstituted benzene derivatives. Further, the assignments for para-substituted benzaldehydes may be rationalized in terms of competing mesomeric interactions, the suggested order of mesomeric interaction being $-NO_2 > -CHO > -COOH$; and this order is supported by the relative locations of the maximal absorption for nitrobenzene, benzaldehyde, and benzoic acid

Can. J. Chem. Downloaded from www.nrcresearchpress.com by 78.46.186.204 on 09/04/12
For personal use only.

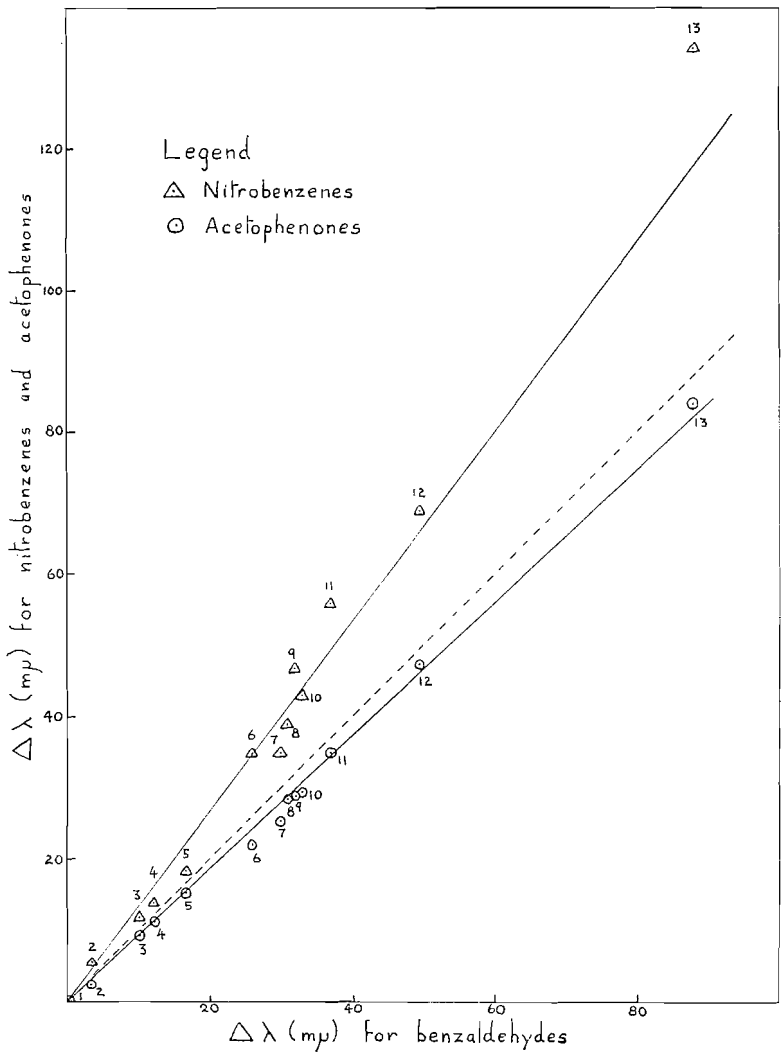

FIG. 1. Wavelength displacements ($\Delta\lambda$) in the *B*-band obtained on introducing para-substituents in benzaldehyde, acetophenone, and nitrobenzene. Values in hexane unless otherwise stated. 1—H; 2—F; 3—Me; 4—Cl; 5—Br; 6—I (in ethanol); 7—I; 8—MeO; 9—MeO (in ethanol); 10—OH; 11—OH (in ethanol); 12—NH_2; 13—OH (in alkaline ethanol) (values from Table III).

(3). This order is again suggested by the *B*-bands of ortho-substituted benzaldehydes (see Table V), since for example the fine structure of the *B*-band of *o*-carboxybenzaldehyde points to this band being due to benzaldehyde absorption. This in turn suggests that the carboxyl-group is preferentially dislocated.

Whenever the para-substituent can act as electron donor, appreciable interactions occur in para-substituted benzaldehydes and the resulting displacements to longer wavelength are shown in Fig. 1 to be directly proportional to corresponding displacements in the acetophenone and nitrobenzene series. This suggests that the displacements are proportional to one "basic" electronic interaction, which acts along the extremities of a conjugated system and which is characteristic for each substituent. This interaction

Can. J. Chem. Downloaded from www.nrcresearchpress.com by 78.46.186.204 on 09/04/12
For personal use only.

has already been associated with the mesomeric effect of a substituent, although in its assignment of the order for halogens the interaction affords a different order from that usually accepted for the mesomeric interactions of the halogens (17).

The slope of the line in Fig. 1 relating wavelength displacements in para-substituted acetophenones and benzaldehydes is less than tan 45°, whereas the slope of the line relating wavelength displacements for nitrobenzenes and benzaldehydes is greater than tan 45° (see Fig. 1). This confirms the expected order of mesomeric effect, that is $-NO_2 > -CHO$, and also suggests a mesomeric electron-withdrawing ability $-CHO > -COCH_3$. This latter observation should be related with the fact that benzaldehyde absorbs maximally at longer wavelength than acetophenone.

The *C*-band for each of the compounds listed in Table III could normally be identified only with difficulty. It disappeared in compounds where there is appreciable interaction between the two para-substituents. These tendencies have previously been noted and discussed (3).

THE SPECTRA OF META-SUBSTITUTED BENZALDEHYDES

The spectra of *m*-substituted benzaldehydes and the displacements due to the meta-substituent in benzaldehydes, acetophenones, and nitrobenzenes are listed in Table IV.

Table IV shows that the effect of substituents on the location of the benzaldehyde *B*-band is usually small and similar for benzaldehydes, acetophenones, and nitrobenzenes.

Table IV also shows that meta-substituted benzaldehydes may give rise to two distinct *B*-bands. One of these *B*-bands is the expected benzaldehyde band, somewhat modified

TABLE IV

ABSORPTION MAXIMA OF META-SUBSTITUTED BENZALDEHYDES AND THE EFFECT OF META-SUBSTITUENTS ON THE *B*-BAND FOR BENZALDEHYDES, ACETOPHENONES, AND NITROBENZENES IN *n*-HEXANE OR CYCLOHEXANE SOLUTION

	B-Band			*C*-Band		Wavelength shifts with reference to parent compound in:			
Benzaldehyde	λ_{max} (mμ)	ϵ_{max}	Mean λ_{max}	λ_{max} (mμ)	ϵ_{max}	Benzaldehydes	Acetophenones	Nitrobenzenes	Ref.
(Benzaldehyde)	241 *247*	14,000 *12,000*	244	277–278 287	1200 1000	—	—	—	*
m-Methyl-	245 251	13,500 12,000	248	280 290	1000 800	4	5 (4.5)	4.5	*, †
m-Fluoro-	238 246	12,800 11,600	242	282–283 290 *ca. 293*	2100 1750 *1700*	−2	−3.5 (−4)	−6 (−5)	*
m-Chloro-	241–242 248	11,500 10,000	245	288 298	1400 1200	1	0.5 (0)	(−2)	*
m-Bromo-							4 (0)	(−1)	*
m-Iodo-	*244* 249 *251* *253*	*8000* 7600 *7400* *6850*	249	295–296 303	1300 1235	5	9.5 (10)	(2)	*
m-Hydroxy-	244 250	10000 9500	247	302–303 *ca. 307*	2900 *2800*	3 (9)	7.5	(12.5)	*, ‡, §
m-Methoxy-	247 *ca. 251*	6800 *6500*	249	304 *ca. 313*	3000 *2700*	5 (8)	7.5	(10)	*, ‡, §
m-Amino-	*ca. 245* *ca. 256*	*9000* *7500*	250.5			6.5	7.5 (15)		*
m-Nitro-	225 [*ca. 245* ([*ca. 256*	26000 *8000*] *7700*])	225	287 298	1000 700	−19	(−25)		*, ‖

*This series of papers. †Ref. 6. ‡Ref. 8. §Ref. 7. ‖Ref. 21.

Can. J. Chem. Downloaded from www.nrcresearchpress.com by 78.46.186.204 on 09/04/12
For personal use only.

because of the secondary short-range interaction of the non-formyl substituent (5, 22). The second *B*-band corresponds to the absorption of the other substituent, with the formyl group acting as the secondary substituent. These latter bands are again indicated by square brackets. Thus, for example, in the spectrum of *m*-nitrobenzaldehyde in cyclohexane two bands occur, one at λ_{max} 225 mμ ascribed to benzaldehyde absorption and a much weaker absorption at *ca.* 245 mμ ascribed to nitrobenzene absorption. This assignment may be questioned on the grounds that the benzaldehyde band is appreciably displaced and also because the band does not show the doublet characteristic of benzaldehyde absorption in inert media. On the other hand, a nitro-group normally gives rise to appreciable changes in the spectra of meta-disubstituted benzene derivatives (5). Also, our assignment receives support from the spectrum of *m*-nitrobenzaldehyde in ethanol (see Table IV). There, the presence of ethanol would be expected to displace the nitrobenzene absorption to longer wavelength and this is in fact observed.

Steric effects in meta-substituted benzaldehydes would not be expected to be significant, since the formyl group is relatively small. However, the fairly low extinction coefficient for the *B*-band of *m*-iodobenzaldehyde may be caused, at least partly, by a buttressing interaction. Similarly, the unusual wavelength displacement, as shown in Table IV, for *m*-iodonitrobenzene compared to those for *m*-iodoacetophenone and *m*-iodobenzaldehyde also points to the operation of a buttressing effect in this type of compound (cf. 23).

The *C*-bands, as anticipated, are well defined for meta-substituted benzaldehydes (cf. 3).

THE SPECTRA OF ORTHO-SUBSTITUTED BENZALDEHYDES

The spectra of ortho-substituted benzaldehydes are listed in Table V, together with the spectra of ortho-substituted acetophenones.

All the *B*-bands, with the exception of that of *o*-nitrobenzaldehyde, occur as doublets. The *B*-band of *o*-nitrobenzaldehyde at 247 mμ is again assigned to nitrobenzene absorption, as indicated by square brackets in Table V. This is confirmed by the absorption of this compound in ethanol, which, as anticipated, occurs in the more polar solvent at longer wavelength at 252 mμ (ϵ = 4700) (21). The greatly reduced absorption intensity of the band, particularly in ethanolic solution, compared with the corresponding band in the meta-isomer, is ascribed to the increased steric interaction between the two vicinal substituents in *o*-nitrobenzaldehyde.

Information concerning the nature of the ortho-effect can also be obtained by comparing the spectra of *o*-substituted benzaldehydes with the spectra of *o*-substituted acetophenones (see Table V). At least three interpretations may be advanced for the observed ortho-effects and the data assist in deciding between these. The first interpretation is to ascribe the ortho-effect to intramolecular hydrogen bonding; a second interpretation (cf. 22) is to ascribe the ortho-effect to steric interaction between vicinal atoms or groups *with the molecule occupying only one ground state* (6); a third interpretation is to assume that the ortho-effect may also sometimes be caused by the molecule existing in more than one conformation, for example an *s-cis* and *s-trans* conformation, which however do not all contribute to the observed absorption (16).

Examination of Table V shows that an explanation based on intramolecular hydrogen bonding is consistent with the observed similarity of the *B*-bands for the *o*-hydroxy and *o*-methoxy derivatives of benzaldehyde and acetophenone. On the other hand, hydrogen bonding would not account for the generally decreased absorption intensities in the

Can. J. Chem. Downloaded from www.nrcresearchpress.com by 78.46.186.204 on 09/04/12
For personal use only.

acetophenone series, nor in particular would it account, for example, for the spectrum of *o*-chloroacetophenone, where the molecular extinction coefficient is reduced to a much greater extent than in the corresponding benzaldehyde. Therefore, steric interactions evidently also determine the ortho-effects and intramolecular hydrogen bonding is not the sole explanation for the observed ortho-effects. Experiments to differentiate between the two types of steric effects will be reported separately.

The *C*-bands show the usual changes (3), although it may be noted that in *o*-tolualdehyde and in salicylaldehyde the *C*-band does not occur as a doublet (see Table V).

TABLE V

ABSORPTION MAXIMA OF ORTHO-SUBSTITUTED BENZALDEHYDES AND ACETOPHENONES IN *n*-HEXANE OR CYCLOHEXANE SOLUTION

	Benzaldehyde				Acetophenone		
	B-Band		*C*-Band		*B*-Band		
Substituent	λ_{max} (mμ)	ϵ_{max}	λ_{max} (mμ)	ϵ_{max}	λ_{max} (mμ)	ϵ_{max}	Ref.
(Benzaldehyde)	241 *247*	14,000 *12,000*	277–278 287	1200 1000	238–239	12,500	*
o-Methyl-	243 251	12,500 13,000	291	1700	237 245.5	11,500‡ 9060	†
			284	2400			
o-Fluoro-	240 *ca. 247*	13,300 *9,700*	291 294	2000 2000	233	9500	*
o-Chloro-	246 252	11,000 8,500	292 300 302	1750 1400 1400	235	5700	*
o-Bromo-	245.5	12,500	292	2100	234–236	4900	*
o-Iodo-	*252*	*10,000*	301	1750	—	—	*
o-Hydroxy-	250 257	11,000 11,700	324–325	3600	251	9700	*, §
o-Methoxy-	246 *ca. 253*	10,500 *8500*	306 *ca. 314*	4600 *4200*	246	8000	*, §
o-Amino-	255 *ca. 262*	5600 *3500*	352	4600	252	5500	*
o-Carboxy-	224 *ca. 231*	8000 *7000*	269 276 *ca. 286*	800 850 *400*			*
o-Nitro-	222 [247 ([252	15,300 7000] 4700]	*ca. 285* 270	*1700* 3600	[254 [256	6000] 4800])	*, ‖

*This series of papers. †Ref. 6. ‡Values in isopentane, E. S. Waight, unpublished information. §Acetophenone values in ether (14). ‖ Values in constant-boiling ethanol (21).

EXPERIMENTAL

The benzaldehydes were obtained commercially or prepared by standard methods as described in the literature. The physical constants, after purification, of the compounds not previously reported in this series are listed in Table VI.

The ultraviolet absorption spectra were determined in specially calibrated quartz cells of various path lengths using a Unicam SP 500 spectrophotometer. Dioxane–water mixtures were prepared as previously described (11). For each compound at least two independent sets of observations were made. Where previous data are available, our data compare well with the published values. For the *m*- and *p*-aminobenzaldehydes the purified solutions in ether were directly diluted with cyclohexane to about 2% ether. This procedure avoided polymerization, which otherwise occurred. The spectrum was determined on each solution, and the concentration was subsequently obtained by evaporating to dryness and weighing the residue.

Can. J. Chem. Downloaded from www.nrcresearchpress.com by 78.46.186.204 on 09/04/12
For personal use only.

TABLE VI

PHYSICAL CONSTANTS OF BENZALDEHYDES

Benzaldehyde	Melting point, or boiling point and refractive index	Literature value of physical constants
(Benzaldehyde)	b.p. 41°, 1 mm, $n_D^{22.5}$ 1.5444	b.p. 62°, 10 mm, $n_D^{17.6}$ 1.5463 (24, 25)
o-Fluoro-	b.p. 51°, 11 mm, n_D^{22} 1.5212	b.p. 175° (24)
m-Fluoro-	$n_D^{21.3}$ 1.5173	b.p. 173° (24)
o-Chloro-	b.p. 213°, n_D^{22} 1.5656	b.p. 213–214°, $n_D^{21.7}$ 1.5656 (24, 25)
m-Chloro-	b.p. 55°, 1 mm, $n_D^{25.8}$ 1.5613	b.p. 213–214°, $n_D^{20.2}$ 1.5650 (25)
p-Chloro-	m.p. 47.5°	m.p. 47.5° (25)
m-Iodo-	m.p. 57°	m.p. 57° (24)
p-Iodo-	m.p. 76°	m.p. 77–78° (24)
o-Hydroxy-	b.p. 45°, 3 mm, $n_D^{22.5}$ 1.5722	b.p. 196.5°, $n_D^{19.7}$ 1.5736 (25)
m-Hydroxy-	m.p. 104°	m.p. 108° (106°) (24, 25)
p-Hydroxy-	m.p. 117°	m.p. 115–116° (24)
o-Methoxy-	b.p. 71°, 2 mm, n_D^{21} 1.5604	m.p. 36°, n_D^{20} 1.5600 (24)
m-Methoxy-	b.p. 62°, 1 mm, n_D^{25} 1.5511	b.p. 230°, n_D^{20} 1.5530 (24)
p-Methoxy-	b.p. 83°, 2 mm, n_D^{22} 1.5717	b.p. 248°, $n_D^{12.7}$ 1.5764 (24, 25)
o-Nitro-	m.p. 42°	m.p. 43–44° (24)
m-Nitro-	m.p. 57°	m.p. 58° (24)
p-Nitro-	m.p. 106°	m.p. 106° (24)
o-Carboxy-	m.p. 97.2°	m.p. 97° (25)
p-Carboxy-	m.p. *ca.* 250°	m.p. 248–250° (256°) (25)

ACKNOWLEDGMENT

The authors gratefully acknowledge the receipt of a research grant from the National Research Council of Canada.

REFERENCES

1. FORBES, W. F. and MUELLER, W. A. Can. J. Chem. **33**, 1145 (1955).
2. FORBES, W. F. and MUELLER, W. A. Can. J. Chem. **35**, 488 (1957).
3. FORBES, W. F., MUELLER, W. A., RALPH, A. S., and TEMPLETON, J. F. Can. J. Chem. **35**, 1049 (1957).
4. FORBES, W. F. and SHERATTE, M. B. Can. J. Chem. **33**, 1825 (1955).
5. FORBES, W. F. Can. J. Chem. **36**, 1350 (1958).
6. BRAUDE, E. A. and SONDHEIMER, F. J. Chem. Soc. 3754 (1955).
7. BURAWOY, A. and CHAMBERLAIN, J. T. J. Chem. Soc. 2310 (1952).
8. BURAWOY, A. and THOMPSON, A. R. J. Chem. Soc. 4314 (1956).
9. GRAMMATICAKIS, P. Compt. rend. **231**, 278 (1950).
10. GRAMMATICAKIS, P. Bull. soc. chim. France, 821 (1953).
11. FORBES, W. F. and TEMPLETON, J. F. Can. J. Chem. **36**, 180 (1958).
12. JONES, R. N., FORBES, W. F., and MUELLER, W. A. Unpublished information.
13. SCHUBERT, W. M., ROBINS, J., and HAUN, J. L. J. Am. Chem. Soc. **79**, 910 (1957).
14. MORRIS, H. H. and YOUNG, R. H. J. Am. Chem. Soc. **79**, 3408 (1957).
15. FORBES, W. F., MORICONI, E. J., WALLENBERGER, F. T., and O'CONNOR, W. F. J. Org. Chem. **23**, 224 (1958).
16. FORBES, W. F. and MUELLER, W. A. Can. J. Chem. **34**, 1347 (1956).
17. FORBES, W. F. and RALPH, A. S. Can. J. Chem. **34**, 1447 (1956).
18. BARROW, G. M. J. Chem. Phys. **21**, 2008 (1953).
19. DANNENBERG, H. Z. Naturforsch. **4b**, 327 (1949).
20. LEMON, H. W. J. Am. Chem. Soc. **69**, 2998 (1947).
21. WALKER, E. A. and YOUNG, J. R. J. Chem. Soc. 2041 (1957).
22. FORBES, W. F. and RALPH, A. S. Can. J. Chem. **36**, 869 (1958).
23. FORBES, W. F. and MUELLER, W. A. J. Am. Chem. Soc. **79**, 6495 (1957).
24. HEILBRON, Sir I. and BUNBURY, H. M. Dictionary of organic compounds. Eyre and Spottiswoode Ltd., London. 1946.
25. HODGMAN, C. D. *et al.* Handbook of chemistry and physics. 37th ed. Chemical Rubber Publishing Co., Cleveland, Ohio.

Can. J. Chem. Downloaded from www.nrcresearchpress.com by 78.46.186.204 on 09/04/12
For personal use only.

Can. J. Chem. Downloaded from www.nrcresearchpress.com by 78.46.186.204 on 09/04/12
For personal use only.

LIGHT ABSORPTION STUDIES

PART XIII. THE ELECTRONIC ABSORPTION SPECTRA OF RING-SUBSTITUTED ANILINES[1]

W. F. Forbes and I. R. Leckie

ABSTRACT

A spectral analysis of benzene derivatives in terms of steric and electronic interactions is extended to ring-substituted anilines.

INTRODUCTION

In previous parts of this series spectral analyses were carried out for substituted acetophenones, benzaldehydes, and nitrobenzenes, that is, for compounds in which one substituent possesses a *negative* mesomeric effect. The purpose of the present communication is to consider in greater detail the effect of the amino group on the electronic spectra, that is, the effect of a group which possesses a *positive* mesomeric effect.

Systematic investigations of the electronic spectra of anilines have also recently been carried out by Wepster (1) and by Klevens and Platt (2). The emphasis of our work will be to relate the available data to the hypotheses developed for other benzene derivatives in this series and, whenever convenient, we have also redetermined the reported data, in order that data would be obtained under near-identical conditions.

THE ANILINE SPECTRUM

The absorption maxima of aniline for different solvents in the region 220–300 mμ are listed in Table I.

TABLE I

Main absorption maxima of aniline in different solvents

Solvent	*B*-Band		*C*-Band		Source
	λ_{max} (mμ)	ϵ_{max}	λ_{max} (mμ)	ϵ_{max}	
Vapor phase	229		*ca.* 280		*, †
Cyclohexane	233–234	9000	286	1900	*
Ethanol	234–235	8000	284–285	1700	*
Water	230	8000	278	1400	*
0.1 *N* HCl	202	7500	247 252 258	150 170 150	*
N NaOH	230	8400	279	1400	*
Ether	238	10,000	288	1900	*
Cyclohexane containing 3% ether	234	9000	285	1800	*

*This series of papers.
†ϵ_{max} values not determined.

The two bands listed in Table I are described as *B*- and *C*-bands, implying that these bands correspond to the similar bands in acetophenone, benzaldehyde, and nitrobenzene (cf. 3, 4, 5). Consequently the corresponding electronically excited states may be visualized as involving dipolar resonance forms of type I.

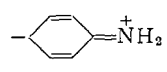

I

[1]*Manuscript received June 16, 1958.*
Contribution from the Memorial University of Newfoundland, St. John's, Newfoundland.

The *B*-band of aniline appears to be symmetrical and shows no fine structure if the spectra are determined in solution. Some fine structure occurs in cyclohexane for the *C*-band, but this is not evident in other solvents, for example in ether or water. In the vapor phase, fine structure is shown by both *B*- and *C*-bands. Further, in cyclohexane both *B*- and *C*-bands do not show any appreciable concentration dependence within the investigated concentration range (2×10^{-3} to 3.36×10^{-4} moles/liter for the *B*-band, and 1×10^{-2} to 3.36×10^{-4} moles/liter for the *C*-band). This may be related to information deduced from infrared data, which suggests that aniline in carbon tetrachloride solution occurs as the monomer up to a concentration of 10^{-2} moles/liter (6).

The data in Table I also show that although no appreciable spectral change occurs between the spectra in ethanol and cyclohexane, a more pronounced spectral change occurs between the spectra in cyclohexane and aqueous solution. Analogous wavelength displacements are observed for the spectrum of N,N-dimethylaniline in hexane, ethanol, and water (7), and this therefore suggests that the observed spectral changes are not caused by hydrogen bonding involving the nitrogen-linked hydrogen atoms. In addition, it has previously been shown that if an aqueous solution of aniline is examined within a temperature range sufficient to affect any hydrogen bonding present, no spectral changes are observed (8). Searching for a possible explanation of the spectral changes, one may note that the reduced extinction coefficient between ethanol and water for N,N-dimethylaniline, which is not observed for aniline, may be tentatively ascribed to steric interaction. Ungnade has previously pointed out (see footnote 17 of ref. 7) that it is necessary to assume a hydrate, involving the unshared electron pair, in aromatic amines in order to account for the basic properties of these substances, and that the formation of such hydrates is subject to steric effects. Consequently, the most probable explanation of the wavelength displacement is provided by assuming that in aqueous solution the molecular species $C_6H_5NH_3OH$ contributes appreciably to the observed absorption. However, this species must surely involve some form of hydrogen bonding, although it may not be the same type of hydrogen bond as will be described below. The aniline or N,N-dimethylaniline molecule presumably in some way accepts the proton of the water molecule by means of the non-bonding electrons of the nitrogen atom. It has been suggested that by partially isolating the $2p_z$ electrons of the nitrogen atom in this way, the hydrogen bond reduces the interaction between the $2p_z$ electrons and the benzene ring and thus the absorption band is displaced to shorter wavelength (9).

In aqueous solution, the equilibrium

$$C_6H_5.NH_3OH \rightleftharpoons C_6H_5.NH_3^+ + OH^-$$

may also be sufficiently displaced to the right to contribute to the observed wavelength displacements. However, within the investigated concentration range, this effect does not appear to be important. That is, the *B*-band in aqueous solution was found to be unchanged within the concentration range 2×10^{-3} to 3.25×10^{-4} moles/liter and the *C*-band was found to be unchanged within the concentration range 10^{-2} to 3.25×10^{-4} moles/liter. In acidic media, there occurs a hypsochromic wavelength displacement which may be related to the non-availability of the unshared *p*-electrons in the electronic excitation. That is, the non-bonded electrons are now predominantly involved in the nitrogen–hydrogen bond, and are consequently unable to participate in the transitions leading to the *B*-band. This wavelength displacement is incidentally quite characteristic for aniline and ring-substituted anilines (see Tables I, II, III, and IV), and may therefore be used in the identification of an amino substituent. No appreciable wavelength displacement occurs in weakly basic media (see Table I).

Can. J. Chem. Downloaded from www.nrcresearchpress.com by 78.46.186.204 on 09/04/12
For personal use only.

The observed wavelength displacement in ether solution for the *C*-band has been attributed to hydrogen bonding between the amino group and the oxygen atom of the solvent (cf. refs. 10 and 11). This wavelength displacement between heptane and ether is observed for aniline, but a similar displacement is now not observed for N,N-dimethylaniline (10) where this type of hydrogen bonding is ruled out. Further, the dipole moment increases markedly for aniline in ether, compared with the dipole moment in heptane, whereas a similar increase in dipole moment is not observed for N,N-dimethylaniline (10). On the other hand, we have found that the addition of 3% by weight of ether to a solution of aniline in cyclohexane does *not* change the absorption spectrum to a spectrum similar to that of aniline in ether (see Table I and cf. also ref. 10 for the spectrum of aniline in heptane containing various amounts of dioxane). This latter observation therefore does not support the concept of a stoichiometric, permanent, hydrogen bond. Lastly, it may be noted that the wavelength displacements observed between cyclohexane and vapor phase spectra suggest that some interaction also occurs between aniline and cyclohexane molecules.

THE SPECTRA OF PARASUBSTITUTED ANILINES

The spectra of parasubstituted anilines are listed in Table II.

TABLE II

ABSORPTION MAXIMA OF PARASUBSTITUTED ANILINES

(Values in italics represent inflections in this and subsequent tables)

		B-Band		*C*-Band		
Substituent	Solvent	λ_{max} (mμ)	ϵ_{max}	λ_{max} (mμ)	ϵ_{max}	Source
p-Hydroxy-	Cyclohexane containing 2% ether	235	7000	304	2500	*
	Water	229	6000	294	2000	*
p-Amino-	Cyclohexane	246	8500	315	2000	*
p-Methyl-	Iso-octane	237	9610	293	1910	Ref. 1
	Ethanol	236	10000			Ref. 12
p-Fluoro-	Hexane	230.5	7000			Ref. 13
	Ethanol	233.4	7000			Ref. 13
	Ethanol–HCl (99:1)	207.8	3400			Ref. 13
p-Chloro-	Hexane	241.4	12500			Ref. 13
	Ethanol	244.5	12500			Ref. 13
	Ethanol–HCl (99:1)	216.7	8000			Ref. 13
p-Bromo-	Cyclohexane	241	14000	297 *ca. 306*	1750 *1150*	*
	Ethanol	245	13300	296–297	1600	*
	Ethanol–HCl (99:1)	219	8400			Ref. 13
	0.1 *N* NaOH	239.5	12800	290	1340	Ref. 14
p-Iodo-	Hexane	246.3	17500			Ref. 13
	Ethanol	250.2	18500			Ref. 13
	Ethanol–HCl (99:1)	232.4	12500			Ref. 13
p-Acetyl-	Cyclohexane	285	19000	—	—	*
	Ethanol	316	20000	—	—	*
	Water	308–309	16500	—	—	*
	0.1 *N* HCl	*ca.* 260	6000	—	—	*
	N NaOH	308–309	11000	—	—	*
p-Formyl-	Cyclohexane containing 2% ether	291 296	16300 16100			*
p-Nitro-	Naphtha	320	14600	—	—	Ref. 15
	Ethanol	371	15500	—	—	Ref. 5
	Water	373–377	13000	—	—	*
	0.1 *N* HCl	372	5600	—	—	*
	N NaOH	373–379	13000	—	—	*
p-Carboxy-	Ether	277	20600			Ref. 16
	Ethanol	288	19000	—	—	*
	2 *N* HCl	226.5	12300	270	970	Ref. 14
	0.1 *N* NaOH	265	14900	—	—	Ref. 14

*This series of papers.

Can. J. Chem. Downloaded from www.nrcresearchpress.com by 78.46.186.204 on 09/04/12
For personal use only.

The early examples in Table II provide illustrations where both substituents are electron donating and the molecule absorbs essentially as aniline. It may be noted that for these examples the maximal extinction coefficient (ϵ_{max}) is frequently *reduced* relative to aniline, whereas in disubstituted benzene derivatives, when the substituents are electron withdrawing, the values of ϵ_{max} are usually *increased* relative to the monosubstituted parent compound (cf. 17, 18, 19).

Table II also shows that parasubstitution usually displaces the *B*-band of aniline towards longer wavelength. This is well illustrated by the spectra of the parahalogen-substituted anilines, and the magnitude of the displacements, compared with the wavelength displacements observed for meta- and ortho-isomers (see Tables III and IV), supports the postulate of dipolar forms, which may be associated with electron mobility acting along systems of conjugated bonds. However, resonance forms are evidently not entirely satisfactory in representing the relevant dipolar excited states (cf. ref. 13), although structures of type II may be used to provide a picture of the orbital delocalizations occurring in the electronic excited state.

Further, the bands are described as displaced aniline *B*-bands, but it should be noted that significant changes occur on parasubstitution. For example, whereas changing the solvent from cyclohexane to ethanol for aniline does not cause any appreciable wavelength displacement, precisely such a displacement is observed in parahalogen-substituted anilines; this displacement usually becomes increasingly pronounced with increased mesomeric interaction. Next, although normally the aniline band disappears in dilute acid media, for compounds such as *p*-nitroaniline where the mesomeric interaction is large, the band does not completely disappear, although the intensity is very greatly reduced (see Table II). Again, while for both *p*-aminoacetophenone and aniline the characteristic *hypsochromic* wavelength displacement is observed on changing the solvent from ethanol to water, in *p*-nitroaniline a *bathochromic* displacement is observed on changing the solvent from ethanol to water.

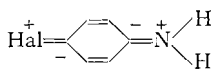

II

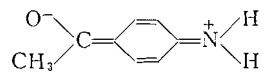

III

The absorptions at much longer wavelength for compounds like *p*-nitroaniline or *p*-aminoacetophenone may be associated with favorable resonance forms of type III contributing appreciably to the electronic excited state. The more appreciable contribution of resonance forms of type III, even in the ground state, presumably also accounts for the large dipole moments of these compounds (20) and the various effects noted by Wepster, who ascribed these effects, at least partly, to a decrease in the average angle of twist in the nitro group on substitution of an amino group in the para position (1, 21).

THE SPECTRA OF METASUBSTITUTED ANILINES

The spectra of metasubstituted anilines are listed in Table III.

For many of the spectra listed in Table III, the aniline B-band is readily discernible, as for example in *m*-methyl- or *m*-halogen-substituted anilines. It may be noted that the sensitiveness of the B-band to solvent changes is again different for metasubstituted anilines, such as *m*-aminoacetophenone, than for aniline.

As previously mentioned (18, 19), two B-bands can frequently be discerned in the spectra of metadisubstituted benzene derivatives, and these B-bands have been associated with transitions involving the two monosubstituted parent compounds. In this way, the

Can. J. Chem. Downloaded from www.nrcresearchpress.com by 78.46.186.204 on 09/04/12
For personal use only.

TABLE III

ABSORPTION MAXIMA OF METASUBSTITUTED ANILINES

Substituent	Solvent	Aniline *B*-band λ_{max} (mμ)	Aniline *B*-band ϵ_{max}	2nd *B*-band λ_{max} (mμ)	2nd *B*-band ϵ_{max}	*C*-Band λ_{max} (mμ)	*C*-Band ϵ_{max}	Source
m-Hydroxy-	Cyclohexane containing 2% ether	234	6800			283.5	2300	*
	Water	229	6400			278	1900	*
	0.1 *N* HCl	*ca. 211*	*6300*	217	6500	269	2000	*, †
						ca. 273	*1700*	
m-Amino-	Cyclohexane	*ca. 240*	*7000*	—	—	293	2600	*
	pH 9	*240*	*7300*	—	—	289	2100	Ref. 22
m-Methyl-	Cyclohexane	237	8300			289	1900	*
m-Chloro-	Cyclohexane	238	8500			289	2100	*
m-Bromo-	Cyclohexane	237–238	7800			290	2400	*
m-Iodo-	Cyclohexane	*239*	*8700*	*ca. 232*	*10400*	292	2700	*, †
						299	*2200*	
m-Acetyl-	Cyclohexane	226	26500	*246*	*9000*	320	2500	*
	Ethanol	231	23000	*ca. 255*	*7000*	338	1900	*
	Water	226	21000	*ca.* 255	7000	324	1900	*
	0.1 *N* HCl			238	12000	277	1000	*
	N NaOH	226.5	20000	*ca.* 255	7000			*
m-Formyl-	Cyclohexane containing 0.2% ether	227	17500	*ca. 243*	*9000*	327.5	2000	*
				ca. 256	*7500*			
m-Nitro-	Ethanol	233	18000			375	1600	Ref. 23
	Water	224	13500	278–279	4500	354	1400	*
	0.1 *N* HCl			256	7500			*
	N NaOH	224	14000	278–279	4650	354	1400	*
m-Carboxy-	Ethanol			*ca. 241*	*7000*	319	2100	*
	Ether			244	7800	320	2800	Ref. 16
	pH 3.73	218.5	14000	250	2400	310	650	Ref. 22
	pH 11			*241*	*7400*	300	1800	Ref. 22

*This series of papers.
†B-band assignment doubtful.

maximum at 226 mμ for *m*-aminoacetophenone in cyclohexane solution, the maximum for the same compound at 231 mμ in ethanol, the maximum at 233 mμ for *m*-nitroaniline in ethanol, and the maximum for the same compound at 224 mμ in *N* NaOH are all ascribed to aniline absorption. On the other hand, the inflections at 243 and 256 mμ for *m*-aminobenzaldehyde in cyclohexane are ascribed to the benzaldehyde chromophore, the inflection at 246 mμ for *m*-aminoacetophenone in cyclohexane is ascribed to the acetophenone chromophore, and the inflection at 241 mμ for *m*-aminobenzoic acid in ethanol is ascribed to the benzoic acid chromophore. Some typical features of the *B*-band assist in the assignments. For example, the characteristic doublet of the benzaldehyde *B*-band (cf. 19) appears in the spectrum of *m*-aminobenzaldehyde for the inflection near 250 mμ.

The meta-amino substituent, as expected, gives rise to a secondary interaction, which frequently causes an appreciable bathochromic wavelength displacement for the compounds listed in Table III (cf. 24). For example, in ethanol, the *B*-band of acetophenone at 240 mμ occurs as an inflection near 255 mμ in *m*-aminoacetophenone, and the *B*-band of benzoic acid at 227 mμ occurs as an inflection near 241 mμ in *m*-aminobenzoic acid. Similar displacements for other compounds, caused by the secondary effect of the meta-amino group, may be deduced from Table III. It is found that the wavelength displacement is reasonably constant, at least for similar compounds. Thus, whenever the non-amino substituent is electron withdrawing, the corresponding *B*-band appears to show an appreciable bathochromic wavelength displacement. An exception is provided in acid media, where the unshared electron pair of the amino substituent is presumably unable to contribute efficiently to the interaction with the benzene ring. Likewise, the

Can. J. Chem. Downloaded from www.nrcresearchpress.com by 78.46.186.204 on 09/04/12
For personal use only.

non-amino substituent affects the aniline *B*-band in a manner which seems susceptible to generalization. For example, if the non-amino substituent is electron withdrawing, the effect on the aniline absorption appears to be quite generally a displacement to shorter wavelength accompanied by increased absorption intensity (see Table III).

This relatively greater intensity of the band associated with aniline absorption suggests that the amino group gives rise to greater mesomeric interaction in the electronic excited state. Structures, which may be crudely represented by resonance forms of of type IV, would again contribute to the electronic excited state, and these resonance

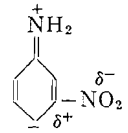

IV

forms, by analogy with the previously discussed resonance structures of that type (18), would be expected to be favored by an electron-withdrawing substituent in the meta position. On the other hand, if the meta substituent is electron donating, the band intensity of the aniline *B*-band is usually decreased (see Tables III and I). This decrease is qualitatively similar to the intensity decrease observed for the corresponding para isomers (see Table II). Both the changes may again be rationalized by resonance structures of type IV.

Since the amino group is relatively small, no appreciable buttressing interaction would be expected for metasubstituted anilines. In fact, buttressing effects are not readily discernible except possibly for the spectrum of *m*-iodoaniline (cf. 25). A buttressing interaction may also contribute to the spectral changes in the series aniline, *o*-toluidine, and 2,3-dimethylaniline. These compounds are reported to absorb in iso-octane solution at about 250 mμ with ϵ values of 9130, 8800, and 7550 respectively (1). Further, 2,3,5,6-tetramethylaniline, compared with 2,6-dimethylaniline, shows a reduced absorption intensity (1).

The *C*-band, as anticipated, is frequently more pronounced in metasubstituted anilines, compared with the *C*-band in aniline or parasubstituted anilines (26). Difficulties have arisen because of different assignments; for example, Morton and McGookin (23) note that wavelength displacements are observed in opposite senses for *m*- and *p*-nitro-N,N-dimethylaniline on changing the solvent from ethanol to water. An explanation for this apparent anomaly is provided if it is accepted that the relevant bands of the para isomer are *B*-bands, whereas the "similar" bands of the meta isomer are *C*-bands. In this way, we believe that the band of *p*-nitrodimethylaniline, which occurs in ethanol at 368.5 mμ, and the band of the same compound, which occurs in water at 422 mμ, are *B*-bands (cf. 18). On the other hand, we assume that the band of *m*-nitrodimethylaniline, which in ethanol occurs at 400.3 mμ, and which in aqueous solution is hypsochromically displaced to 385 mμ, is a *C*-band. A similar hypsochromic displacement on changing the solvent from ethanol to water is incidentally also observed for the *C*-band of *m*-nitroaniline (see Table III).

THE SPECTRA OF ORTHOSUBSTITUTED ANILINES

The spectra of orthosubstituted anilines are listed in Table IV.

The *B*-bands listed in Table IV can again be classified into the two types of *B*-bands

Can. J. Chem. Downloaded from www.nrcresearchpress.com by 78.46.186.204 on 09/04/12
For personal use only.

TABLE IV

ABSORPTION MAXIMA OF ORTHOSUBSTITUTED ANILINES

Substituent	Solvent	Aniline *B*-band		2nd *B*-band		*C*-Band		Source
		λ_{max} (mμ)	ϵ_{max}	λ_{max} (mμ)	ϵ_{max}	λ_{max} (mμ)	ϵ_{max}	
o-Hydroxy-	Cyclohexane containing 2% ether	235	7000			288	3300	*
	Water	229	6200			281	2700	*
	0.1 *N* HCl			209–210	6500	268	2100	*, †
						ca. 273	*1800*	
o-Amino-	Cyclohexane	235.5	6600	—	—	289	3500	*
	pH 9	233	6900	—	—	289	2900	Ref. 22
o-Methyl-	Cyclohexane	234	8850			283	2350	*
o-Ethyl-	Iso-octane	234	8030			286	2330	Ref. 1
o-Isopropyl-	Iso-octane	234	7780			286	2280	Ref. 1
o-Chloro-	Cyclohexane	235	8700			288	2900	*
o-Bromo-	Cyclohexane	235	8500			289	3000	*
o-Iodo-	Cyclohexane	237	8400			292	3200	*
o-Acetyl-	Cyclohexane	224	23500	252	5500	347	4350	*
	Ethanol	226	21000	254	5600	359	4350	*
	Water			254–255	5900	350	3500	*
	Dioxane			253–255	5000	354–357	4500	*
	25% Aqueous dioxane			255	5800	356–358	3800	*
o-Formyl-	Cyclohexane			255	5600	352	4700	*
				ca. 262	*3400*			
o-Nitro-	Cyclohexane	227	18000	268	5000	370	5000	*
	Ethanol	231	17000	276	5000	402	5500	Ref. 5
	Water	223	17000	280	5300	400–405	4400	*
	0.1 *N* NaOH	245	7000	282.5	5400	412	4500	Ref. 22
o-Carboxy-	Ethanol			247	6700	332	4500	*
	Ether			252	7400	333	5200	Ref. 16
	pH 3.73	216.5	18500	*248*	*3900*	327	1940	Ref. 22
	pH 11			240	7100	310	2800	Ref. 22

*This series of papers.
†B-band assignment doubtful.

as described in the previous section. Table IV then shows that both *B*-bands are frequently weakened in the ortho isomer compared with the corresponding *B*-bands in the meta isomer (see Table III). Examples of this are provided by the ortho and meta isomers of iodoaniline in cyclohexane, of aminoacetophenone in cyclohexane and ethanol, of aminobenzaldehyde in cyclohexane, and of aminobenzoic acid in ethanol and ether. In the absence of intermolecular hydrogen bonding (see below), one would expect steric effects to occur and the observed intensity decreases in the examples cited are in fact ascribed to steric interactions. Steric interactions may also occur in a number of other orthosubstituted anilines, such as *o*-toluidine and *o*-chloroaniline, for which, however, the data do not permit any definite conclusions. In this connection, it may be noted that, *compared with the B-band of the para isomer*, a hypsochromic wavelength displacement and a pronounced intensity decrease is almost invariably observed in the *B*-band of the ortho isomer. Since the resonance forms contributing to the ortho and para isomers may be regarded as similar to a first approximation, one might expect the *B*-bands of the ortho and para isomers to be similar *in the absence of steric* and other short-range *interactions*. A steric contribution to this "ortho effect" is also indicated by the fact that the decrease in absorption intensity becomes more pronounced for N,N-dimethylanilines (cf., for example, the ϵ_{max} values and integrated absorption intensities of N,N-dimethylaniline and of the corresponding *o*-methyl derivative (1)).

In the previous paragraph decreases in the absorption intensities have been used as indications of steric interactions, but unusual wavelength displacements may evidently

Can. J. Chem. Downloaded from www.nrcresearchpress.com by 78.46.186.204 on 09/04/12
For personal use only.

Can. J. Chem. Downloaded from www.nrcresearchpress.com by 78.46.186.204 on 09/04/12
For personal use only.

also indicate steric interactions. However, the wavelength displacements caused by steric interactions in this series of compounds appear to be small. For example, *o*-ethyl- and *o*-isopropyl-N,N-dimethylaniline, which presumably represent appreciably hindered compounds, still absorb maximally at 249 mμ (ϵ = 4950) and 248 mμ (ϵ = 4300) respectively, that is, at a similar maximal wavelength to N,N-dimethylaniline under identical conditions (λ_{max} 251 mμ, ϵ = 15,500) (1). This lack of an appreciable wavelength displacement, which has also recently been discussed from a theoretical viewpoint (4), may be related to the large mesomeric effect of the amino group. That is, it may be supposed that the appreciable double-bond character of the N-nuclear bond tends to keep the aniline chromophore planar and the second substituent does not contribute to the observed absorption. This mechanism has recently been described as a type III steric effect (27).

Generally, the amino group does not appear to be as sensitive to steric effects as, for example, the nitro group, which also causes appreciable mesomeric interaction. For example, an ortho-methyl group produces an appreciable intensity decrease in the *B*-band of nitrobenzene and similar compounds, whereas only a small intensity decrease is observed in the *B*-band of aniline, even compared with the *B*-band of the para isomer. Two, not mutually exclusive, explanations may account for the smaller steric effects in anilines. First, the amino group may not, because of its small size, cause appreciable steric interactions. One of the factors contributing to the relatively smaller size of the amino group may be the partial positive charge associated with excited states of the aniline chromophore. A second explanation may be that π–p electronic interaction, like π–π electronic interaction, gives rise to considerable double bond character in the N-nuclear bond, but that π–p interaction is less sensitive to steric interactions, compared with π–π electronic interaction.

Apart from steric interactions, which will tend to oppose the existence of coplanar resonance forms, other short-range interactions must also be considered. Intramolecular hydrogen bonding would be expected to be one of the most important of such interactions. For some examples, there is reasonably good evidence for an intramolecular hydrogen bond. For example, comparing the ortho and meta isomers of a number of compounds in which an intramolecular hydrogen bond would be anticipated, the following bathochromic wavelength displacements are obtained from the data listed in Tables III and IV: Aminoacetophenone in cyclohexane, *B*-band, 6 mμ; *C*-band, 27 mμ. Aminobenzoic acid in ether, *B*-band, 8 mμ; *C*-band, 13 mμ. Aminobenzoic acid in ethanol, *B*-band, 6 mμ; *C*-band, 13 mμ. Aminophenol in cyclohexane containing 2% ether, *B*-band, 1 mμ; *C*-band, 4.5 mμ. In all these compounds the ortho isomer absorbs at *longer* wavelength than the meta isomer, and the wavelength displacement may therefore be attributed, at least partly, to an intramolecular hydrogen bond.

Evidence for intramolecular hydrogen bonding may also be deduced from displaced and intensified *C*-bands in some ortho isomers, but this evidence is somewhat ambiguous (cf. ref. 26). Quite generally, and not unexpectedly, for a number of compounds the

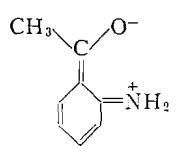

V

evidence for intramolecular hydrogen bonding from ultraviolet spectroscopy is not convincing. A number of reasons suggest themselves for this observation. For example, apart from intramolecular hydrogen bonded forms, ortho-resonance forms of type V may contribute to the ground and excited states, and this may partly account for the observed bathochromic displacements of some of the *B*-bands listed in Table IV. Next, intramolecular hydrogen bond formation may be opposed by steric interactions; the two interactions, by giving rise to opposite spectral effects, may cause different displacements depending on which interaction predominates. Further, various forms of solute–solvent interaction, including intermolecular hydrogen bonding, may interfere with intramolecular hydrogen bonding. This, in fact, is suggested by the frequent absence of the spectral effects, associated with intramolecular hydrogen bond formation, in other than inert media (cf. Tables III and IV).

The *C*-band in orthosubstituted anilines gives rise to the expected changes (see ref. 26). It is generally more pronounced in orthosubstituted anilines.

EXPERIMENTAL

The ultraviolet absorption spectra were determined by standard methods using a Unicam SP500 or a Beckman Model DU spectrophotometer. For each compound at least two independent sets of observations were made. The spectrum in the vapor phase was determined at room temperature in a 2-cm cell against air. The spectral data obtained compare well with other data whenever these were previously recorded in the literature. Where comparisons are made involving the extinction coefficients at maximal absorption (ϵ_{max}) the change in ϵ_{max} may be qualitatively related to corresponding changes in the oscillator strengths f, as far as can be discerned from the shape of the absorption bands. The precision of λ_{max} values is estimated to be ± 0.5 mμ, and the precision of ϵ_{max} values $\pm 5\%$ or better. Values were normally reproducible to $\pm 2\%$.

The physical constants, after purification, of compounds, the spectra of which have not previously been reported in this series, are listed in Table V.

TABLE V

PHYSICAL CONSTANTS OF RING-SUBSTITUTED ANILINES

Substituent	Melting point, or boiling point, and refractive index	Literature values of physical constants (28)
[Aniline	B.p. 81°, 27 mm, n_D^{23} 1.5840	B.p. 184.4°, n_D^{20} 1.5863]
m-Amino-	M.p. 62°	M.p. 62.8°
p-Amino-	M.p. 138°	M.p. 139.7°
o-Methyl-	B.p. 95.5°, 27 mm, n_D^{23} 1.5717	B.p. 200°, n_D^{20} 1.5728
m-Methyl-	B.p. 86.8°, 17 mm, n_D^{21} 1.5672	B.p. 203.3°, n_D^{22} 1.5711
o-Chloro-	B.p. 119°, 55 mm, $n_D^{24.5}$ 1.5869	B.p. 208.8°, n_D^{20} 1.5895
o-Bromo-	B.p. 152°, 117 mm, n_D^{25} 1.6165	B.p. 229°
o-Iodo-	M.p. 56°	M.p. 56.5°
o-Formyl-	M.p. 38°	M.p. 39–40°
o-Nitro-	M.p. 71.5°	M.p. 71.5°
m-Nitro-	M.p. 114°	M.p. 111.8°
p-Nitro-	M.p. 147°	M.p. 147.5°

The phenylenediamines were purified by vacuum sublimation, and the spectra of these compounds as well as the spectra of the aminophenols were determined as quickly as possible.

Can. J. Chem. Downloaded from www.nrcresearchpress.com by 78.46.186.204 on 09/04/12
For personal use only.

ACKNOWLEDGMENTS

The authors gratefully acknowledge the assistance of Mr. J. F. Templeton, in some of the preliminary work of the reported experimental data. They are also greatly indebted to the National Research Council for a research grant in support of these studies.

REFERENCES

1. WEPSTER, B. M. Rec. trav. chim. **76**, 357 (1957).
2. KLEVENS, H. B. and PLATT, J. R. J. Am. Chem. Soc. **71**, 1714 (1949).
3. MURRELL, J. N. Proc. Phys. Soc. A, **68**, 969 (1955).
4. MURRELL, J. N. J. Chem. Soc. 3779 (1956).
5. TIMMONS, C. J. J. Chem. Soc. 2613 (1957).
6. FUSON, N., JOSIEN, M. L., POWELL, R. L., and UTTERBACK, E. J. Chem. Phys. **20**, 145 (1952).
7. UNGNADE, H. E. J. Am. Chem. Soc. **75**, 432 (1953).
8. COGGESHALL, N. D. and LANG, E. M. J. Am. Chem. Soc. **70**, 3283 (1948).
9. ROBIN, M. and TRUEBLOOD, K. N. J. Am. Chem. Soc. **79**, 5138 (1957).
10. NAGAKURA, S. and BABA, H. J. Am. Chem. Soc. **74**, 5693 (1952).
11. MASAMUNE, T. J. Am. Chem. Soc. **79**, 4418 (1957).
12. BURAWOY, A. and SPINNER, E. J. Chem. Soc. 2085 (1955).
13. BURAWOY, A. and THOMPSON, A. R. J. Chem. Soc. 4314 (1956).
14. DOUB, L. and VANDENBELT, J. M. J. Am. Chem. Soc. **69**, 2714 (1947).
15. NAGAKURA, S. J. Chem. Phys. **23**, 1441 (1955).
16. DANNENBERG, H. Z. Naturforsch. **4b**, 327 (1949).
17. FORBES, W. F. and TEMPLETON, J. F. Can. J. Chem. **36**, 180 (1958).
18. FORBES, W. F. Can. J. Chem. **36**, 1350 (1958).
19. DEARDEN, J. C. and FORBES, W. F. Can. J. Chem. **36**, 1362 (1958).
20. SMITH, J. W. and WALSHAW, S. M. J. Chem. Soc. 3217 (1957).
21. WEPSTER, B. M. Rec. trav. chim. **76**, 335 (1957).
22. DOUB, L. and VANDENBELT, J. M. J. Am. Chem. Soc. **71**, 2414 (1949).
23. MORTON, R. A. and MCGOOKIN, A. J. Chem. Soc. 901 (1934).
24. FORBES, W. F. and RALPH, A. S. Can. J. Chem. **36**, 869 (1958).
25. FORBES, W. F. and MUELLER, W. A. J. Am. Chem. Soc. **79**, 6495 (1957).
26. FORBES, W. F., MUELLER, W. A., RALPH, A. S., and TEMPLETON, J. F. Can. J. Chem. **35**, 1049 (1957).
27. FORBES, W. F. The classification of steric effects in ultraviolet absorption spectra. *In* Steric effects in conjugated systems. *Edited by* G. W. Gray, Butterworth Scientific Publications, London. 1958. In press.
28. HODGMAN, C. D. *et al.* Handbook of chemistry and physics. 35th ed. Chemical Rubber Publishing Co., Cleveland, Ohio. 1953.

Can. J. Chem. Downloaded from www.nrcresearchpress.com by 78.46.186.204 on 09/04/12
For personal use only.

Can. J. Chem. Downloaded from www.nrcresearchpress.com by 78.46.186.204 on 09/04/12
For personal use only.

SUR LA SYNTHÈSE DE QUELQUES XANTHONES POLYSUBSTITUÉES[1]

R. Constantin et P. L'Écuyer

RÉSUMÉ

La synthèse de la 4,6,7-triméthoxy- et de la 1-méthyl-4,6,7-triméthoxy-9-xanthone a été réalisée en faisant agir un mélande d'anhydride acétique et d'acide sulfurique sur l'acide 6-(2′-méthoxy)- ou 6-(2′-méthoxy-5′-méthylphénoxy)-vératrique. La préparation de ces deux acides a été effectuée en condensant le 6-bromovératrate de méthyle avec le guaïacolate ou l'isocréosolate de potassium en présence de cuivre. La 1-carboxy-4,6,7-triméthoxy-9-xanthone, un produit de dégradation de la cularine, a été obtenue en oxydant la 1-méthyl-4,6,7-triméthoxy-9-xanthone par l'acide chromique en solution dans l'acide éthanoique.

Manske (1, 2) a suggéré la formule I pour la cularine en se basant sur la structure des produits de dégradation qu'il en a obtenus et, en particulier, sur celle de la 2-styrolène-4,6,7-triméthoxy-dibenz[*b*,*f*]oxépine (II), provenant de la méthylation destructive de l'alcaloïde. L'oxydation de II lui a donné, en plus de l'acide dicarboxylique correspondant, une xanthone qui, selon toute probabilité, devait être la 1-carboxy-4,6,7-triméthoxy-9-xanthone (III, R = CO_2H). Manske n'a pas synthétisé cette xanthone, parce qu'il ne

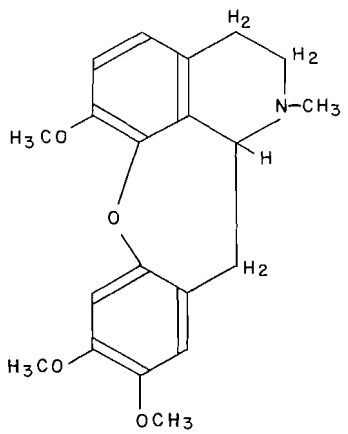

(I)

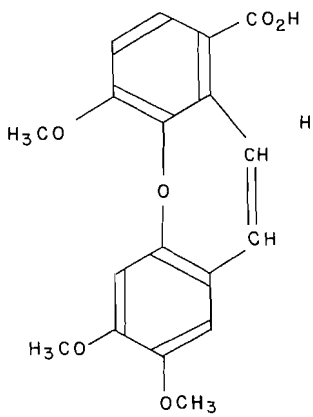

(II)

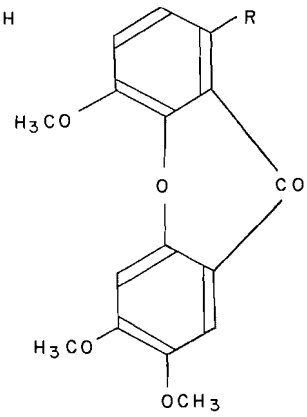

(III)

R = H, $-CH_3$ ou CO_2H

connaissait aucune méthode facile de synthèse conduisant aux xanthones polysubstituées.

Manske et Kulka (3), en appliquant la réaction de Gattermann au 2,3′,4′-triméthoxydiphényl éther et au 2,3′,4′-triméthoxy-5-méthyldiphényl éther ont déjà synthétisé les aldéhydes 6-(2′-méthoxyphénoxy)- et 6-(2′-méthoxy-5′-méthylphénoxy)-vératriques qu'ils ont transformés par oxydation en acides 6-(2′-méthoxyphénoxy)- et 6-(2′-méthoxy-5′-méthylphénoxy)-vératriques avec des rendements respectifs de 12 et 10%. En condensant le 6-bromovératrate de méthyle avec le guaïcolate ou l'isocréosolate de

[1]*Manuscrit reçu le 23 juin, 1958.*
Contribution du Département de Chimie, Faculté des Sciences, Université Laval, Québec, P.Q. Ce mémoire est tiré de la thèse de doctorat de R. Constantin.

potassium en présence de poudre de cuivre et en saponifiant les esters qui se sont formés nous avons obtenu les mêmes acides 6-(2′-méthoxyphénoxy)- et 6-(2′-méthoxy-5′-méthylphénoxy)-vératriques avec des rendements respectifs de 45 et 30%.

L'action d'un agent déshydratant sur un acide arylsalicylique constitue une méthode pratique pour la préparation d'une xanthone simple (4, 5). En faisant agir un mélange d'anhydride acétique et d'acide sulfurique sur l'acide 6-(2′-méthoxy)- ou 6-(2′-méthoxy-5′-méthylphénoxy)-vératrique nous avons pu synthétiser la 2,3,5-triméthoxy-9-xanthone (III, R = H) et la 1-méthyl-4,6,7-triméthoxy-9-xanthone (III, R = CH_3).

L'oxydation de III (R = H) par l'acide chromique dans l'acide acétique glacial nous a permis de synthétiser la 1-carboxy-4,6,7-triméthoxy-9-xanthone (III, R = CO_2H). Le point de fusion de cette xanthone mélangée à un échantillon du produit que Manske a obtenu au cours de la dégradation de la cularine n'est pas déprimé et les spectres d'absorption dans l'ultraviolet (figures 1 et 2) des deux échantillons différents de la xanthone, sont identiques. Ceci confirme donc l'exactitude de la structure que Manske a suggérée pour la xanthone qu'il a obtenue à partir de la cularine et aussi de celle qu'il a proposée pour l'alcaloïde lui-même.

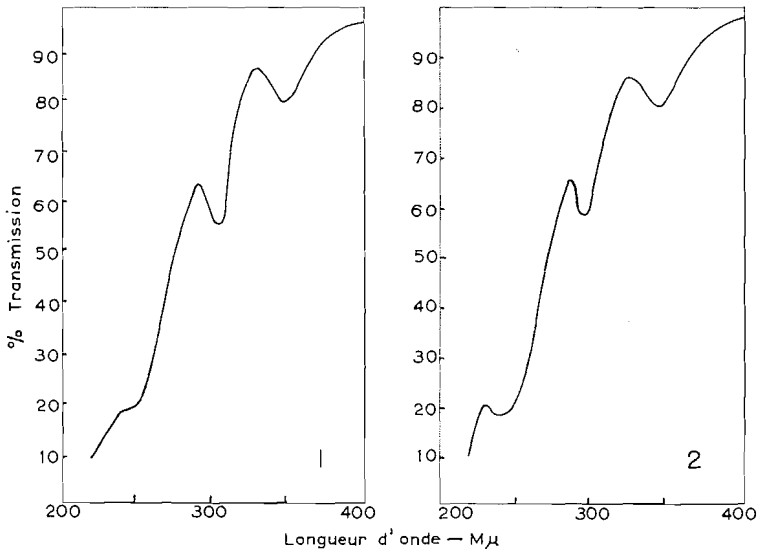

FIG. 1. Spectre d'absorption dans l'ultraviolet de la 1-carboxy-4,6,7-triméthoxy-9-xanthone synthétique.
FIG. 2. Spectre d'absorption dans l'ultraviolet de la xanthone obtenue par la dégradation de la cularine.

PARTIE EXPÉRIMENTALE*

Acides 6-(2′-méthoxyphénoxy)- et 6-(2′-méthoxy-5′-méthylphénoxy)-vératriques

On pulvérise dans un mortier un mélange de 6-bromovératrate de méthyle (0.01 mole), de guaïacolate ou d'isocréosolate de potassium (0.011 mole) et de la poudre de cuivre. On chauffe ensuite le mélange à 150° pendant 2 heures, puis à 180° pendant 15 minutes. Une fois la masse brune refroidie, on la pulvérise et on l'extrait à l'éther (3 fois avec 30 ml). Les extraits éthérés combinés sont lavés successivement à la soude 0.1 *N* et à l'eau, puis séchés et évaporés à siccité. Le résidu est saponifié en le chauffant à reflux en présence d'une solution à 3% d'hydroxyde de potassium dans le méthanol. On chasse la majeure partie du méthanol par ébullition, on dilue et on acidifie à l'acide

**Les points de fusion ont été pris à l'aide de l'appareil de Johns.*

Can. J. Chem. Downloaded from www.nrcresearchpress.com by 78.46.186.204 on 09/04/12
For personal use only.

sulfurique. Les acides 6-(2′-méthoxyphénoxy)- et 6-(2′-méthoxy-5′-méthylphénoxy)-vératriques sont essorés et cristallisés dans le benzène. Les p.f. sont respectivement 184 et 186°, et les rendements 1.37 g (45%) et 0.95 g (30% de la théorie).

4,6,7-Triméthoxy-9-xanthone (III, R = H)

A de l'acide 6-(2′-méthoxyphénoxy)-vératrique (1.6 g; 0.005 mole) dans le d'anhydride acétique (15 ml) on ajoute 2 ml d'acide sulfurique concentré. On porte la solution à 60° sur le bain-marie pendant 1 heure et on la verse ensuite sur de la glace. On essore le précipité et on le lave successivement à la soude 0.1 *N* et à l'eau. La 4,6,7-triméthoxy-9-xanthone cristallise dans le méthanol en fines aiguilles blanches de p.f. 238°. Rendement: 0.86 g (65% de la théorie). Calculé pour $C_{16}H_{14}O_5$: C, 67.11%; H, 4.92%. Trouvé: C, 66.4%; H, 5.0%.

1-Méthyl-4,6,7-triméthoxy-9-xanthone (III, R = CH_3)

On procède exactement de la même façon que pour la synthèse précédente, mais en utilisant l'acide 6-(2′-méthoxy-5′-méthylphénoxy)-vératrique comme matière première. La 1-méthyl-4,6,7-triméthoxy-9-xanthone s'obtient en fines aiguilles blanches en la cristallisant dans le méthanol ou l'éthanol. P.f. 211°. Rendement 0.26 g (40% de la théorie). Calculé pour $C_{17}H_{16}O_5$: C, 67.99%; H, 5.37%. Trouvé: C, 67.4%; H, 5.4%.

1-Carboxy-4,6,7-triméthoxy-9-xanthone (III, R = CO_2H)

On chauffe au bain-marie pendant 2 heures une solution de 1-méthyl-4,6,7-triméthoxy-9-xanthone (0.2 g) et d'oxyde chromique (0.3 g) dans l'acide acétique glacial (10 ml). On verse ensuite la solution sur de la glace et on essore le précipité qui s'est formé. La 1-carboxy-4,6,7-triméthoxy-9-xanthone cristallise dans l'acide éthanoique en fines aiguilles jaunâtres de p.f. 301°. Rendement: 0.15 g (70% de la théorie). Le p.f. mixte d'un échantillon de cette xanthone mélangée à un échantillon du produit que Manske a obtenu par la dégradation de la cularine est aussi 301°. Le spectre d'absorption dans l'ultraviolet des deux échantillons de provenance différente est aussi identique. Calculé pour $C_{17}H_{14}O_7$: C, 61.20%; H, 4.27%. Trouvé: C, 60.7%; H, 4.4%.

REMERCIEMENTS

Nous remercions le Dr. R. H. F. Manske pour nous avoir gracieusement fourni un échantillon du produit provenant de la dégradation de la cularine, puis le Conseil National de Recherches, l'office de Recherches de la Province de Québec et les Canadian Industries Limited, pour l'octroi de bourses d'études à l'un de nous (R. Constantin).

BIBLIOGRAPHIE

1. MANSKE, R. H. F. J. Am. Chem. Soc. **72**, 55 (1950).
2. MANSKE, R. H. F. et LEDINGHAM, A. E. J. Am. Chem. Soc. **72**, 4797 (1950).
3. MANSKE, R. H. F. et KULKA, M. J. Am. Chem. Soc. **75**, 1322 (1953).
4. ULLMANN, F. et ZLOKOSOFF, M. Ber. **38**, 2111 (1905).
5. ULLMANN, F. et WAGNER, C. Ann. **355**, 359 (1907).

Can. J. Chem. Downloaded from www.nrcresearchpress.com by 78.46.186.204 on 09/04/12
For personal use only.

THE KINETICS OF MOLECULAR SIEVE ACTION. SORPTION OF NITROGEN–METHANE MIXTURES BY LINDE MOLECULAR SIEVE 4A[1,2]

H. W. HABGOOD

ABSTRACT

This system illustrates "partial molecular sieve action". Methane has a higher affinity for the sorbent and hence is preferentially sorbed at equilibrium, while nitrogen diffuses through the crystal more rapidly and thus is preferentially taken up during the early stages of sorption. Measurements were made with the pure gases and with mixtures at 0° and −79.4° C. The sorption isotherms fit Langmuir equations and the isosteric heats of sorption are essentially independent of concentration. The sorption rates for the pure gases may be characterized by diffusion coefficients, D, calculated in the usual manner assuming the flux of diffusion to be proportional to the concentration gradient. The resultant values for D increase with increasing sorbate concentration. Diffusion of a mixture may be formally characterized by D's for each component. While that for methane is approximately the same as for methane alone, D for nitrogen in mixtures is much larger than for the pure gas and also varies with composition. This, as well as the existence of a temporary maximum in the amount of nitrogen sorbed, may be explained by considering the driving force for diffusion to be the gradient in chemical potential rather than in concentration.

INTRODUCTION

"Molecular sieve" behavior during sorption by dehydrated crystalline zeolites results from the small and uniform size of the intracrystalline pores left by removal of the water of hydration. Molecules having a significantly larger cross section are totally excluded but somewhat smaller molecules may be sorbed slowly. Here the rate-determining step appears to be diffusion through the crystal channels with a significant energy of activation being required. With a mixture of two such sorbates, *partial* molecular sieve action may occur. The component having the lesser affinity for the solid may move faster through the lattice and, consequently, the sorbed phase would show an initial enrichment in this substance, followed by an equilibrium enrichment in the other, more strongly sorbed, component. Since there is often a rough correlation between molecular size and adsorptive affinity, such cases should be fairly common.

Most of our knowledge of this interesting class of sorbents is from the extensive work of R. M. Barrer and his students over the past fifteen years (1). Studies by Barrer and Robins on the sorption of binary gas mixtures (2) indicate that argon–krypton mixtures with dehydrated mordenite and ethane–propane mixtures with dehydrated chabazite show the behavior described above. These experiments in which sorption was carried out in a series of finite steps from a gas phase of constant volume and hence of varying composition were not, however, amenable to detailed analysis.

The present study was intended to examine a single system in some detail, primarily to investigate the relationship between the diffusion properties of the gases individually and in mixtures. The sorption of nitrogen, methane, and their mixtures by Linde Molecular Sieve 4A* (a dehydrated synthetic crystalline zeolite) was studied. This system proved to be a very satisfactory choice. The effective collision diameters of nitrogen and methane,

[1]*Manuscript received March 17, 1958.*
Contribution No. 71 from the Research Council of Alberta, Edmonton.
[2]*Presented in part to the 40th Annual Conference of the Chemical Institute of Canada, Vancouver, June 1957.*
**Manufactured by the Linde Company, Division of Union Carbide Corporation, New York.*

Can. J. Chem. Downloaded from www.nrcresearchpress.com by 78.46.186.204 on 09/04/12
For personal use only.

3.71 Å and 3.82 Å (3), are almost the same but nitrogen would be expected to have a significantly smaller minor diameter of around 3.0 Å. Since methane is, in general, more strongly adsorbed than nitrogen, the expected behavior, if the adsorbent pores are a suitable size, is initial preferential sorption of nitrogen changing to the preferential sorption of methane at equilibrium. The present work demonstrates that such behavior does indeed occur, although, as with many other diffusion phenomena, the simple Fick's Law approach is inadequate for a complete description.

EXPERIMENTAL

Apparatus and Method

Measurements were made of the progress of sorption with time and of the equilibrium sorption for the pure gases and for mixtures. For some of the work with the pure gases a conventional constant volume system was used in which the sorption was followed by change in pressure. For all of the measurements on gas mixtures a constant pressure flow system was used.

The constant pressure apparatus, as illustrated schematically in Fig. 1, permitted a continuous gas flow in order to maintain uniform composition and pressure in the gas phase. After the gas mixture had flowed over the sample for the desired length of time, the pressure and flow being maintained constant by adjustment of the appropriate valves, the contents of the cell were isolated by closing the outlet and inlet valves. The valve from the storage tank was closed one or two seconds before the inlet valve to the cell so that the manometer read the final pressure in the cell. The cell was then heated to 200° to bring about desorption, while the gas was expanded into a calibrated glass measuring system.

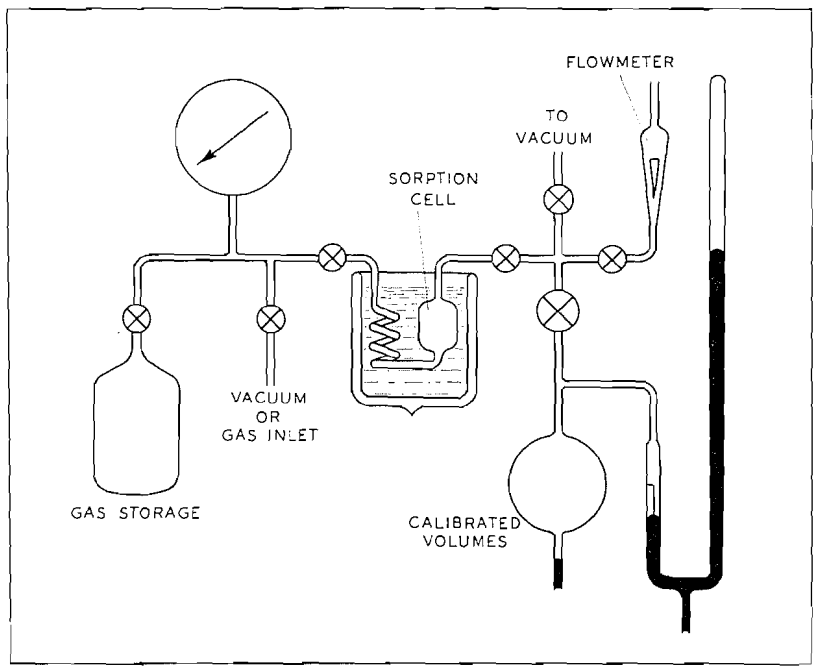

FIG. 1. Constant pressure flow system for sorption measurements.

Can. J. Chem. Downloaded from www.nrcresearchpress.com by 78.46.186.204 on 09/04/12
For personal use only.

Analysis of mixtures was by comparison of the thermal conductivity with that of a sample of the original mixture. It was necessary to mix the gas before analysis to ensure uniform composition and this was done by collection in a single bulb on charcoal at liquid air temperature followed by an hour's reheating. The thermal conductivity measurements were made with a Gow-Mac cell in a conventional bridge arrangement. It was found important to maintain the total cell current constant within 0.1% to obtain reproducible results.

A series of such measurements was carried out with different contact times. The dead space was measured both with helium and by extrapolation to zero time of the total gas volume. In calculating the amount of sorbed gas it is necessary to assume that the gas in the free space of the cell is of the same composition as the original gas mixture. A flow rate of about 10 times the average rate of sorption during the first minute appeared sufficient to ensure this, as shown by constancy of composition with varying flow rate. A higher rate would sometimes have been desirable for times less than one minute but it would then be uncertain that the gas had reached bath temperature. Measurements could be made to contact times as low as ten to fifteen seconds.

Two apparatuses of this type were used, one of glass with fritted disks at the inlet and outlet to retain the powdered zeolite and the other of metal for use at higher pressures with the zeolite in pellet form.

Gases

Purified grade nitrogen was passed through a charcoal trap cooled in dry ice – acetone. Some argon remained but this did not appear to collect on the zeolite. Phillips pure grade methane was passed through an ascarite column to remove carbon dioxide and through a charcoal trap cooled in dry ice – acetone to remove ethane.

Zeolite

The Molecular Sieve 4A was obtained as a fine crystalline powder and also in the form of extruded pellets $\frac{1}{16}$ inch diameter by about $\frac{1}{4}$ inch long. The pellets were more convenient for measurements at high pressures but the results cannot be compared with those from the powder because of differences in the total sorptive capacities and rates.

The external area of each form was determined from the B.E.T. adsorption isotherm at 0° for isobutane, which may be assumed not to penetrate the intracrystalline pores. Taking 47.4 Å^2 for the area of the isobutane molecule (4), surface areas of 10.5 and 6.9 m^2/g for pellets and powder respectively were obtained. This gives an average particle diameter for the powder of about 0.5 μ and an average intercrystalline pore diameter for the pellets of 0.1 to 0.5 μ.

The density of the dehydrated zeolite powder was determined with carbon tetrachloride (which is too large to penetrate the intracrystalline channels) to be 1.631 g/cc. The density of the hydrated crystals is given as 1.99 g/cc.

Some of the properties of this synthetic zeolite have been described by Breck *et al.* (5) and the crystal structure has been worked out by Reed and Breck (6).

Activation

The zeolite was received in essentially dehydrated form but all samples were further activated by heating under vacuum for 1 to 3 hours at 300° to 400°. The total water removed was around 1.6% and most of this came off below 300°. (The hydrated crystals contain 22.2% H_2O (5).) Activation to 400° appeared to be more reproducible than to 300°. Both the sorptive activity and the total sorptive capacity appeared to be very

Can. J. Chem. Downloaded from www.nrcresearchpress.com by 78.46.186.204 on 09/04/12
For personal use only.

sensitive to the precise degree of dehydration achieved; for example, the diffusion coefficients roughly quadrupled for activation at 400° compared to 300°. This behavior is similar to the findings of others (2, 5, 7, 8) and appears to result from the blocking action of a few residual water molecules which effectively seal off portions of the zeolite crystal. Dehydration at 400° was not sufficiently extreme to cause collapse of the crystal and decrease in adsorptive capacity, such as reported for chabazite at high temperatures (7).

Sudden sharp drops in activity often accompanying a large sorption were sometimes observed for samples with initially rather low diffusivities—e.g. those activated around 300°. A possible explanation is a non-uniform initial activation with a redistribution of the residual water, which was assisted by the local heat of sorption.

Because of this sensitivity of the zeolite and as a result of accidental exposures to air it was not possible to obtain all the information desired from a single sorbent sample. Only those results are included for which periodic repetition of some of the measurements showed the activity to be constant over the series of measurements.

RESULTS

Equilibrium Properties: Isotherms

Sorption isotherms, with one exception, gave good fits to the Langmuir equation. Some of the isotherms are shown in Fig. 2 and the Langmuir constants are given in Table I for measurements on two samples of powder at 0° and −79.4° C and on one

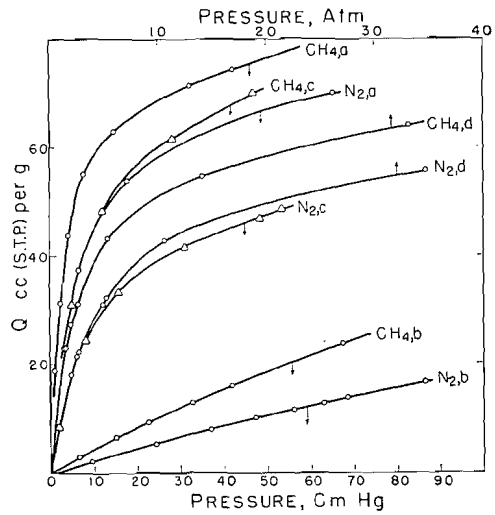

FIG. 2. Sorption isotherms. *a*—powder activated at 400° C, isotherms at 193.7° K; *b*—same sample as *a*, isotherms at 273.1° K; *c*—powder activated at 350° C, isotherms at 193.7° K; *d*—pellets activated at 400° C, isotherms at 273.1° K (upper scale).

sample of pellets at 0°. The nitrogen isotherm for the 350°-activated powder at −79.4° appears anomalous, as do the diffusion properties which were measured at the same time but there was no evident reason for this. The sorption of nitrogen at 700 mm and −78° reported by the Linde workers (5) agrees with the isotherm for the 400°-activated powder.*

**These authors also give a complete isotherm at this temperature which lies considerably above their single value and above our isotherm.*

Can. J. Chem. Downloaded from www.nrcresearchpress.com by 78.46.186.204 on 09/04/12
For personal use only.

TABLE I

SORPTION ISOTHERMS AND EQUILIBRIUM SEPARATION FACTORS

Sorbent (temp. of activation)	Temp., °K	Sorbate	Langmuir constants C_m (cc/g)	Langmuir constants b (atm^{-1})	b_{N_2}/b_{CH_4}	α equilibrium (from 10% mixture)
Powder (350°)	273.1	N_2	70.8	0.189		
		CH_4	87.1	0.362	0.52	—
	193.7	N_2	[a]	[a]		
		CH_4	77.6	10.2		—
Powder (400°)	273.1	N_2	86.8	0.210		
		CH_4	104.0	0.336	0.625	0.58[b]
	193.7	N_2	77.2	10.95		
		CH_4	79.5	25.9	0.440	0.52[b]
Pellets (400°)	273.1	N_2	60.5	0.226		
		CH_4	65.5	0.355	0.64	0.60

[a]This isotherm did not fit the Langmuir equation.

[b]The separation factor was determined on a different sample, which gave the same sorption at 1 atm.

The monolayer values are one third to one half the total capacity of the crystal for tightly packed molecules of this size. Determination of such capacity cannot be made directly by sorption of nitrogen at liquid nitrogen temperatures because of the impracticably slow rates but sorption of oxygen, or of nitrogen by the calcium-exchanged form, at liquid nitrogen temperature is around 200 cc per g (5). Since the individual 11.4 Å diameter cavities would each then contain around fifteen molecules, the lower monolayer values at higher temperatures reflect a greater average mobility. The monolayer values decrease between 0° and −79.4°, which must mean that diffusion into parts of the crystal becomes vanishingly slow. In spite of the crystalline nature of this sorbent some inhomogeneities undoubtedly remain.

While complete isotherms for mixtures of nitrogen and methane were not obtained, several individual determinations were made. According to the Langmuir theory, the separation factor for a mixture should be the ratio of the "b" values for the pure gases. This comparison is made in Table I and the agreement is reasonably good. Barrer and Robins likewise found fairly good agreement with the Langmuir theory for pure gases and mixtures in chabazite (2).

Heats of Sorption

Isosteric heats of sorption were calculated from the isotherms at 193.7° and 273.1° K for the 400°-activated powder and these are shown in Fig. 3. For both gases, the heat of sorption appears to be essentially independent of concentration—a result similar to the general conclusions of Barrer and Sutherland (9) from much more extensive work on synthetic faujasite. There is a suggestion of a slight stepwise decrease at intervals of about 12 cc per g corresponding to integral numbers of molecules per cavity. Our value for nitrogen is somewhat lower and less concentration dependent than that given by Breck *et al.* (5).

Lattice Swelling during Sorption

An attempt was made to detect any expansion of the crystal lattice accompanying sorption. Using a Norelco X-ray diffractometer with a Geiger counter scanner the 832 and 910 reflections were examined relative to the 122 quartz line which fell between them. A dehydrated sample of the zeolite was allowed slowly to hydrate in the diffracto-

Can. J. Chem. Downloaded from www.nrcresearchpress.com by 78.46.186.204 on 09/04/12
For personal use only.

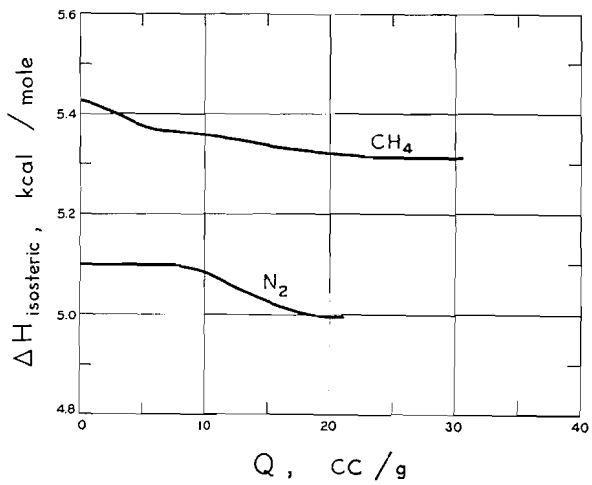

FIG. 3. Isosteric heats of sorption from isotherms at 193.7 and 273.1° K.

meter while the lines were scanned back and forth. The first measurements were taken about two minutes after the sample was opened to the air and from then until complete hydration there was no apparent change (±0.005 Å) in the unit cell spacing. (The value of 12.30 Å compares with 12.32 Å reported by Reed and Breck (6).) Observed expansions accompanying sorption of water on porous glass (10) and on carbon (11) are of the order of 0.2 to 0.3%. Other sorbates at higher pressures give similar expansion. With a maximum change of 0.05%, the crystalline zeolite appears to be more rigid than either of these amorphous materials.

Kinetic Properties—Pure Gases

As Barrer has shown (12), the slow step in these processes may be described as a process of diffusion. The amount of gas sorbed, Q, is found to be proportional to the square root of the time for as much as 50% of the total uptake. From this initial gradient, a diffusion coefficient may be calculated in the usual way according to the following equation:

$$D = \pi\left[\frac{V}{2A\,(C_0-Q_0)}\,\frac{\mathrm{d}Q}{\mathrm{d}(t^{\frac{1}{2}})}\right]^2. \qquad [1]$$

D, the diffusion coefficient, is defined by Fick's first law of diffusion

$$J = -D\,(\partial C/\partial x), \qquad [2]$$

where J is the flux of diffusing material and C is the concentration, expressed for the present work in cc (S.T.P.) per g of sorbent. C_0, the concentration at the outer surface, is taken as the equilibrium concentration from the sorption isotherm and Q_0 is the initial uniform concentration which may be zero. A and V are the external area and volume respectively of the sorbent particles. If D varies with concentration equation 1 gives an approximate average value over the concentration interval Q_0 to C_0. Crank (13) has discussed the evaluation of D as a function of C from a series of such measurements.

Obviously, for a given sample of sorbent, relative values of $D^{\frac{1}{2}}$ may be obtained from the ratio between $\mathrm{d}Q/\mathrm{d}(t^{\frac{1}{2}})$ and (C_0-Q_0).

The variation of D with concentration for each gas alone was examined for both

Can. J. Chem. Downloaded from www.nrcresearchpress.com by 78.46.186.204 on 09/04/12
For personal use only.

powder and pellets.* Results for 350°-activated powder at 0° and −79° and for 400°-activated pellets at 0° are shown in Fig. 4. Measurements with the powder were made with constant C_0 and varying Q_0 and the individual measurements are shown as light horizontal lines over the range Q_0 to C_0 together with the fitted curve of D vs. C. Over the shorter concentration ranges at 0° no variation with concentration was found. Measurements with the powder were all made for $Q_0 = 0$ and the curve of D was obtained from the individual measurements according to the method described in Crank (13). Also shown in Fig. 4 are single values at each temperature for a powder sample activated at 400°, which was used for sorption from mixtures. Pellets activated at 300° gave D values about one quarter those for the 400° material and the isotherms were about 10% lower. A similar sensitivity appeared to exist for the powder.

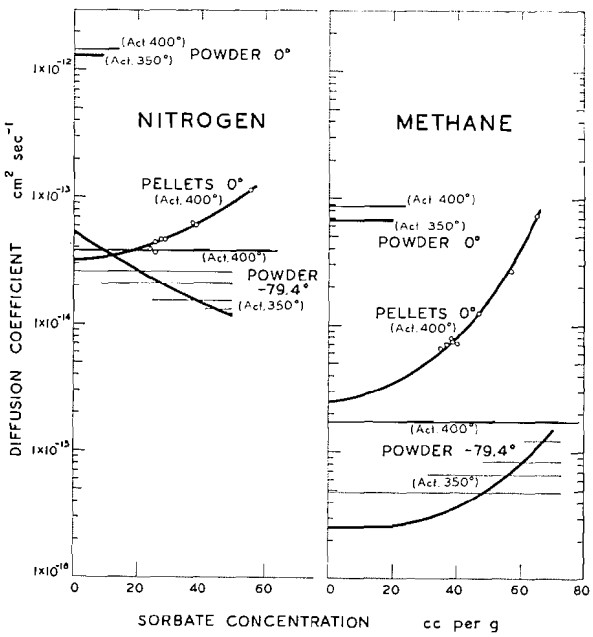

FIG. 4. Diffusion coefficients for pure nitrogen and pure methane. The light horizontal lines show individual measurements over the indicated concentration ranges. The measurements with the pellets were all made between 0 and the concentrations shown by the circles.

Diffusion coefficients for the pellets are seen to be considerably lower than for the powder. It is unlikely at these pressures (2 atmospheres and higher) that there is significant gas phase diffusional resistance in the intercrystalline pores of the pellets. All properties of the pellet form, the larger isobutane surface area, the slower rates of sorption, and the lower capacities, are consistent with the presence of some amorphous, non-sorbing binder, which, while adding to the total external surface, seals off part of the crystal surface through which sorption occurs.

**Most of the measurements with the pure gases were made under constant volume conditions where the pressure, and hence C_0, changes with time. As a result, the $Q-t^{\frac{1}{2}}$ plots begin to curve somewhat more quickly than with constant pressure sorption. The initial gradient is still given by equation 1, taking C_0 for zero time, and it can be shown (cf. ref. 13, pp. 31, 86) that the correction term to Q at time t near the beginning is approximately $(\pi t/4C_0)[dQ/d(t^{\frac{1}{2}})]_{t=0}[dC_0/d(t^{\frac{1}{2}})]$. By properly choosing the total volume of the system and the size of the sample, this correction at $t = 1$ minute can be kept within a few per cents.*

Can. J. Chem. Downloaded from www.nrcresearchpress.com by 78.46.186.204 on 09/04/12
For personal use only.

In general D increases with sorbate concentration. The one case of decreasing D was associated with an anomalous isotherm so that there is some uncertainty concerning its validity.

Relatively little has been reported previously for the concentration dependence of diffusion coefficients in dehydrated zeolites. Barrer and Brook (14) studying the sorption of several gases by chabazite found all the average diffusion coefficients to decrease with concentration—in some cases by a factor of 100. Barrer and Riley (15) for a synthetic chabazite-like zeolite found D to vary approximately as $(1-\theta)$, where θ is the fractional saturation. Tiselius (16) reported D for water in heulandite to increase rapidly with concentration and for ammonia in analcite (17) to be independent of concentration.

Activation energies for diffusion may be estimated from the diffusion coefficients for zero concentration. For the 350°-activated powder the following expressions are obtained:

$$\text{nitrogen: } D = 2.3\times10^{-9}\exp(-4070/RT),$$
$$\text{methane: } D = 5.8\times10^{-8}\exp(-7420/RT).$$

The D_0 values are of the same order as those reported for diffusion in chabazite (14).

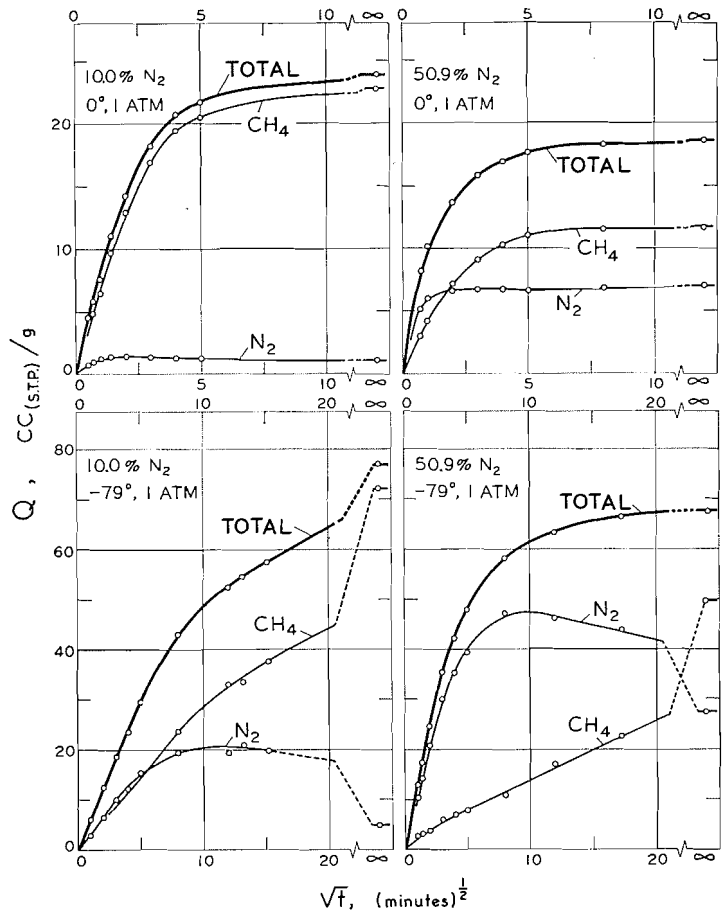

FIG. 5. Sorption from mixtures at 193.7° and 273.1° K. Zeolite powder activated at 400° C.

Can. J. Chem. Downloaded from www.nrcresearchpress.com by 78.46.186.204 on 09/04/12
For personal use only.

The activation energies are close to the 3.5 and 7.5 kcal that Kington and Laing (29) calculated as one set of possible values for diffusion in chabazite.

Mixtures

Sorption from mixtures containing 10.0% nitrogen and 50.9% nitrogen at 1 atmosphere and at 0° and −79.4° C is summarized in Figs. 5 and 6. The sample of powdered zeolite was activated at 400° C and gave equilibrium sorptions in agreement with the Langmuir isotherms in Table I. Relative diffusion coefficients for the pure gases were measured only at 1 atmosphere.

The most striking feature of these measurements is the maximum in the total nitrogen sorption, which occurs at a time prior to the establishment of complete equilibrium. This is seen in Fig. 5 only for the lower temperature, it may occur also at 0° but at a very short time where measurements are difficult to get. Measurements with samples of the pelleted zeolite (which had lower diffusion coefficients) did show a distinct maximum in the nitrogen sorption from a 10% mixture at 0°. As can be seen in Fig. 5, the initial sorption of each component is approximately linear in $t^{\frac{1}{2}}$, although less so than for the pure gases.

The degree of separation achieved by sorption from a mixture is often described by a separation factor, α, defined as follows:

$$\alpha_{N_2} = (X_{CH_4}/X_{N_2})\,(Y_{N_2}/Y_{CH_4}), \qquad [3]$$

where X and Y are the mole fractions in the gas and sorbed phases respectively. Y, of course, is an average value over the crystal, which will be uniform only at equilibrium. As shown in Fig. 6, α decreases from an initial value indicating nitrogen enrichment in the sorbed phase to an equilibrium value showing preferential sorption of methane. The value at low times is uncertain; gas diffusion resistances and depletion of the gas phase will tend to make it low; if the individual sorptions from a mixture are each truly initially linear with $t^{\frac{1}{2}}$, α should remain constant.

Fig. 7 shows plots of the variation of α with time for several experiments with the

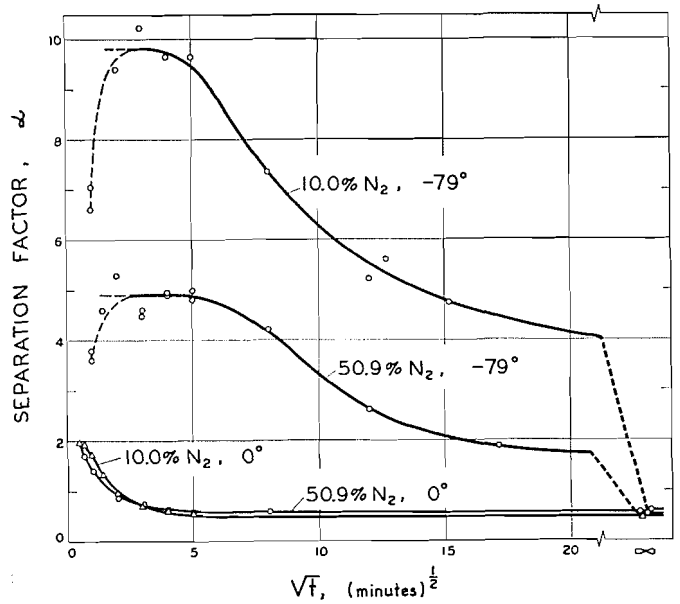

FIG. 6. Separation factors for sorption from mixtures shown in Fig. 5.

Can. J. Chem. Downloaded from www.nrcresearchpress.com by 78.46.186.204 on 09/04/12
For personal use only.

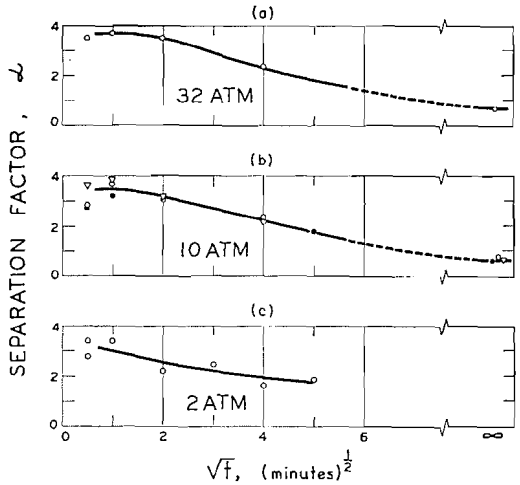

FIG. 7. Separation factors for sorption from 10.0% nitrogen mixture at 273.1° K with zeolite pellets. The different symbols for sorption at 10 atm refer to different sorbent activities.

zeolite pellets. These are very similar to those for the powder, although the actual sorption rates are much lower.

From the initial gradient of each component one may, formally at least, calculate a diffusion coefficient using equation 1 and taking for C_0 the equilibrium sorption for that component. The ratio of diffusion coefficients may also be expressed in terms of the separation factors as follows

$$\alpha_{\text{initial}} = \alpha_{\text{equilibrium}} (D_{N_2}/D_{CH_4})^{\frac{1}{2}}. \quad [4]$$

Diffusion coefficients thus determined in the mixture are compared with the values for the pure gases in Table II. It can be seen that while methane appears to have the same apparent D in the mixture as alone, nitrogen has a much enhanced value and thus the ratio is also higher. Since the increase in the apparent D for nitrogen is dependent also on the gas phase composition the simple approach of using the pure gas values for D in equation 4 is not satisfactory for predicting the behavior of mixtures.

TABLE II

DIFFUSION OF PURE GASES AND MIXTURES
Sorbent: molecular sieve 4A powder activated at 400° C

Temp., ° K	Gas	$(1/C_0)[dQ/d(t^{\frac{1}{2}})]$ min$^{-\frac{1}{2}}$	$(D_{N_2}/D_{CH_4})^{\frac{1}{2}}$	$\alpha_{\text{initial}}/\alpha_{\text{equilibrium}}$
273.1	N_2 (pure)	1.195		
	CH_4 (pure)	0.295	4.05	—
	N_2 in 10.0% mixture	1.3		
	CH_4 in 10.0% mixture	0.304	4.1	[a]
	N_2 in 50.9% mixture	1.17		
	CH_4 in 50.9% mixture	0.35	3.34	[a]
193.7	N_2 (pure)	0.194		
	CH_4 (pure)	0.0417	4.67	—
	N_2 in 10.0% mixture	0.678		
	CH_4 in 10.0% mixture	0.0402	16.9	16.0
	N_2 in 50.9% mixture	0.376		
	CH_4 in 50.9% mixture	0.0368	10.2	9.3

[a]The initial rates were too high at 273° to give an independent value of the initial separation factor.

Can. J. Chem. Downloaded from www.nrcresearchpress.com by 78.46.186.204 on 09/04/12
For personal use only.

Can. J. Chem. Downloaded from www.nrcresearchpress.com by 78.46.186.204 on 09/04/12
For personal use only.

DISCUSSION

Diffusion phenomena are usually approached from the point of view of Fick's Law (equation 2) even though in practice the resultant diffusion coefficient is markedly concentration-dependent. As a rule this is not too serious a drawback in view of the extensive experience and mathematical methods which have been accumulated to interpret measurements and to predict diffusion rates for different types of variation of D with concentration. However in the present system the Fick's Law approach is seriously inadequate. Not only are the diffusion coefficients in the mixture different from those for the pure gases but this approach can give no indication that the total sorption of the faster moving component (nitrogen) passes through a maximum before the final equilibrium is reached. The existence of such a maximum means that, in part, diffusion must be occurring under a negative Fick diffusion coefficient—a very uncommon, if not unique, situation.

It is therefore worth while to examine an alternative approach to diffusion. The chemical potential was suggested by Hartley in 1931 (18) as the fundamental driving force for electrolytic diffusion, and other sorts of diffusion have since been considered as flow under a gradient in chemical potential (19, 20, 21, 22). The chemical potential would appear also to be the driving force suggested by the methods of the thermodynamics of irreversible processes (23, 24), although this approach has not been carried through in detail for diffusion of adsorbed films. Babbitt (25, 26, 27) has approached diffusion from a hydrodynamical point of view and considers the surface diffusion of an adsorbed film as due to the gradient in spreading pressure.

The spreading pressure and the chemical potential of an adsorbed film are similar potential functions and are related as follows (28):

$$d\phi = \Gamma_A d\mu_A + \Gamma_B d\mu_B,$$

where ϕ is the spreading pressure, Γ is the concentration of adsorbate in moles per unit area, μ is the chemical potential, and A and B are two adsorbates. For a single adsorbate, the gradient in spreading pressure is therefore equal (apart from a constant factor) to the gradient in chemical potential multiplied by the adsorbate concentration. If, following other authors (18, 19, 20, 21, 22), we assume that the velocity of diffusion is proportional to the gradient in chemical potential, the two approaches are essentially equivalent in taking as the law of diffusion:

$$J = Cv = -CL\,(\partial\mu/\partial x), \qquad [5]$$

where J is the total flux of diffusing material in the x-direction in moles per unit time through unit cross-sectional area, C is the adsorbate concentration in moles per unit volume, v is the average diffusion velocity, and L is a proportionality constant.

For ideal gas diffusion or for diffusion in a mobile monolayer (27) this expression is equivalent to Fick's Law. For an adsorbed film obeying the Langmuir isotherm

$$\partial\mu/\partial x = (\partial\mu/\partial C)(dC/dx) = (RT/p)(dp/dC)(dC/dx),$$

where p is the partial pressure of the gas (assumed ideal) in equilibrium with sorbed phase of concentration C. This gives for the flux of diffusion

$$J = Cv = -[RTL/1-\theta](dC/dx), \qquad [6]$$

where $\theta = C/C_{\text{monolayer}}$. This result is identical with the one Babbitt obtained taking a constant resistive force per molecule. By comparison with equation 2 it is seen that

the Fick diffusion coefficient should accordingly vary as $1/(1-\theta)$, which is roughly what the present results show.

One might expect L to vary with concentration if, for example, there is any change in the openings in the crystal channels accompanying sorption. In view of the X-ray measurements reported above and the calculations of Kington and Laing (29) for chabazite, it is unlikely that the change in activation energy for diffusion would be more than 100 cal, or beyond experiment error. A difficulty remains of explaining the strong decrease in D which Barrer observed. He suggested, in effect, an additional entropy term (30) but this, presumably, is already included in the chemical potential function.

Mixtures

Let us now consider the sorption of a mixture of gases, A and B, as occurring under a gradient in chemical potential. The simplest approach is to assume that the flux of A is still given by equation 5, where the concentration and chemical potential are for A in the mixed sorbed phase. One could allow for an interaction with the other gas by assuming a more general expression:

$$J_A = C_A v = -C_A [L_{AA}(\partial\mu_A/\partial x)+L_{AB}(\partial\mu_B/\partial x)].$$

There is at present no evidence to justify such an extension so L_{AB} will be taken as zero. The presence of B will none the less affect the diffusion of A, since it is included in the mixed Langmuir isotherm

$$p_A = \theta_A/b_A(1-\theta_A-\theta_B).$$

Proceeding as before, using the chemical potential for the gas in equilibrium with C_A and C_B, we obtain

$$J_A = -[RTL_A/(1-\theta_A-\theta_B)] [(1-\theta_B)(dC_A/dx)+\theta_A(dC_B/dx)] \quad [7]$$

with an analogous expression for J_B, the flux of B.

This equation is adequate to explain the observed behavior in a qualitative way. Fig. 8 suggests the distribution of nitrogen and methane with distance from the external crystal surface at different times in the early stages of sorption. The relative amounts of the two substances are proportional to the actual values for a 10% nitrogen mixture at −79° C. Fig. 8 (*a*) is the hypothetical case of methane being unable to penetrate the lattice and θ_B being 0 everywhere but at the outer surface. Figs. (*b*) and (*c*) represent successive stages in the real situation. In region 1 a positive flux of A exists because although $-dC_A/dx$ is negative, $-dC_B/dx$ is strongly positive, and hence the sum of the two terms in equation 7 is positive. In the same region the flux of B will be less than that of pure B because of the negative value of $-dC_A/dx$. In region 2 $-dC_B/dx$ becomes smaller while $-dC_A/dx$ changes from negative to positive and hence a positive flux of A remains. In region 3 the situation is essentially diffusion of a single gas.

An alternative qualitative approach is to consider the equilibrium distribution of A corresponding to any given distribution of B (dashed lines in Fig. 8). The driving force for diffusion of A is a function of the gradient in the difference between this equilibrium concentration and the actual concentration. This gradient is always negative as in ordinary diffusion.

The uptake of A from a mixture is greater than from pure A at a pressure giving the same exterior surface concentration. Because of the high local concentrations the sorption of A may for a time exceed the equilibrium value at the surface, hence the observed

Can. J. Chem. Downloaded from www.nrcresearchpress.com by 78.46.186.204 on 09/04/12
For personal use only.

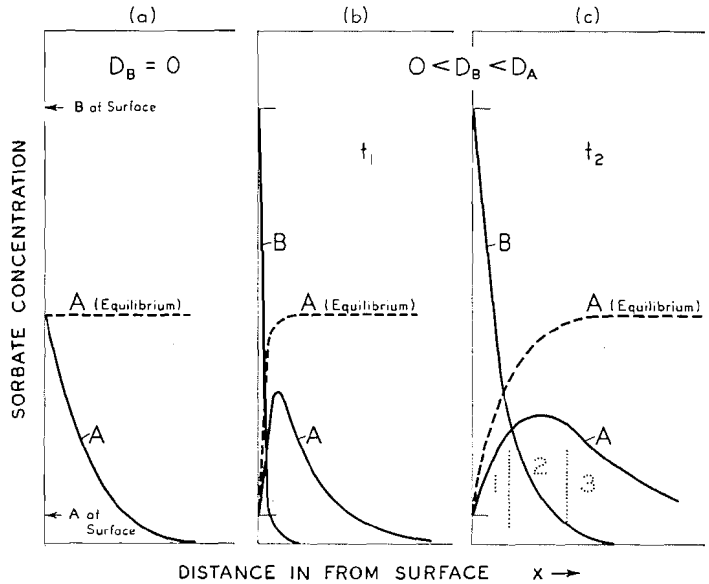

FIG. 8. Sorption from mixtures. Distribution of the sorbates within the crystal. Qualitative curves for 10% nitrogen mixture at 193.7° K. (*a*) Hypothetical case $D_{CH_4} = 0$; (*b*) and (*c*) successive distributions in the actual situation.

maximum. This maximum is more pronounced with the 10% than with the 50% nitrogen mixtures because the curvature of the isotherms gives a greater relative advantage to low partial pressures of nitrogen.

The slower gas, according to equation 7, should be somewhat retarded in the mixture. This appears to be so in the 50% mixture but the evidence is inconclusive.

In view of the complexity of the relationship between the Fick diffusion coefficient and concentration, it is somewhat surprising that the initial sorption-$t^{\frac{1}{2}}$ relationship holds as well as it does. The measurements suggest a somewhat S-shaped plot. An integration of equation 7 for the two species would be necessary to establish the precise shape and hence to quantitatively test this approach.

One may say, in general, that the distinctive feature of the diffusion of a mixture of gases into a porous solid is competition for the limited surface. Consequently, merely specifying the concentration of one sorbate is not a complete description and we may have the apparently anomalous flow of material from regions of low to high concentration. This paper has attempted to show that, qualitatively at least, these anomalies are removed by treating diffusion as flow under a gradient in chemical potential.

ACKNOWLEDGMENTS

I wish to thank R. A. Mooney, E. Dutcher, and G. A. Argue for carrying out much of the experimental work, H. Hansen and Dr. L. B. Halferdahl for assistance with the X-ray diffraction measurements.

REFERENCES

1. BARRER, R. M. Quart. Revs. (London), **3**, 293 (1949); Brennstoff-Chem. **35**, 325 (1954).
2. BARRER, R. M. and ROBINS, A. B. Trans. Faraday Soc. **49**, 807, 929 (1953).
3. HIRCHFELDER, J. O., CURTISS, C. F., and BIRD, R. B. Molecular theory of gases and liquids. John Wiley & Sons, Inc., New York. 1954. p. 1110.
4. NAY, M. A. and MORRISON, J. L. Can. J. Research, B, **27**, 205 (1949).

Can. J. Chem. Downloaded from www.nrcresearchpress.com by 78.46.186.204 on 09/04/12
For personal use only.

5. BRECK, D. W., EVERSOLE, W. G., MILTON, R. M., REED, T. B., and THOMAS, T. L. J. Am. Chem. Soc. **78**, 5963 (1956).
6. REED, T. B. and BRECK, D. W. J. Am. Chem. Soc. **78**, 5972 (1956).
7. LAMB, A. B. and WOODHOUSE, J. C. J. Am. Chem. Soc. **58**, 2637 (1936).
8. BARRER, R. M. and REES, L. V. Trans. Faraday Soc. **50**, 852, 989 (1954).
9. BARRER, R. M. and SUTHERLAND, J. W. Proc. Roy. Soc. A, **237**, 439 (1956).
10. AMBERG, C. H. and MCINTOSH, R. Can. J. Chem. **30**, 1012 (1952).
11. FLOOD, E. A. Can. J. Chem. **35**, 48 (1957).
12. BARRER, R. M. Trans. Faraday Soc. **45**, 358 (1949).
13. CRANK, J. The mathematics of diffusion. The Clarendon Press, Oxford. 1956. Chap. XI.
14. BARRER, R. M. and BROOK, D. W. Trans. Faraday Soc. **49**, 1049 (1953).
15. BARRER, R. M. and RILEY, D. W. J. Chem. Soc. 133 (1948).
16. TISELIUS, A. J. Phys. Chem. **40**, 223 (1936).
17. TISELIUS, A. Z. physik. Chem. A, **174**, 401 (1935).
18. HARTLEY, G. S. Phil. Mag. **12**, 473 (1931).
19. HARTLEY, G. D. and CRANK, J. Trans. Faraday Soc. **45**, 801 (1949).
20. HARNED, H. S. Chem. Revs. **40**, 461 (1947).
21. CARMAN, P. C. and STEIN, L. H. Trans. Faraday Soc. **52**, 619 (1956).
22. BOSWORTH, R. C. L. Transport processes in applied chemistry. John Wiley & Sons, Inc., New York. 1956. p. 118.
23. DE GROOT, S. R. Thermodynamics of irreversible processes. North-Holland Pub. Co., Amsterdam. 1951. p. 104.
24. PRIGOGINE, I. Thermodynamics of irreversible processes. Charles C. Thomas, Publisher, Springfield, Ill. 1955. p. 72.
25. BABBITT, J. D. Can. J. Research, A, **28**, 449 (1950).
26. BABBITT, J. D. Can. J. Phys. **29**, 427 (1951).
27. BABBITT, J. D. Can. J. Phys. **29**, 437 (1951).
28. FOWLER, R. and GUGGENHEIM, E. A. Statistical thermodynamics. Cambridge: The University Press, London. 1939. p. 423.
29. KINGTON, G. L. and LAING, W. Trans. Faraday Soc. **51**, 287 (1955).
30. BARRER, R. M. Trans. Faraday Soc. **37**, 590 (1941).

Can. J. Chem. Downloaded from www.nrcresearchpress.com by 78.46.186.204 on 09/04/12
For personal use only.

Can. J. Chem. Downloaded from www.nrcresearchpress.com by 78.46.186.204 on 09/04/12
For personal use only.

RADIATION CHEMISTRY OF SOLUTIONS

II. DOSE-RATE, ENERGY, AND TEMPERATURE DEPENDENCE OF A LEUCO TRIARYLMETHANE DOSIMETER SOLUTION[1]

W. A. Armstrong and G. A. Grant

ABSTRACT

The dose-rate, energy, and temperature dependence of the system 10^{-4} *M* 4,4′-(5-chloro-2-thenylidene)bis[N,N-dimethylaniline], 10^{-4} *M* ferrous ammonium sulphate, 0.1 *M* sodium chloride, and 7×10^{-3} *M* hydrochloric acid has been investigated. No energy dependence was observed in the range 0.16 to 2.0 Mev and no dose-rate dependence was observed in the range 4 to 230 rads/minute. However, with dose rates of 400 to 1200 rads/minute, postirradiation dye fading was observed. In the dosage range 0 to 1000 rads this fading is not extremely serious. The system is slightly temperature dependent at temperatures lower than 30° C and markedly dependent at higher temperatures. Dye yields of samples irradiated at 30° C were 10% higher than those of samples irradiated at 15° but 33% lower than those of samples irradiated at 45°.

INTRODUCTION

In a previous report (2), the effects of gamma radiation on acidic aqueous solutions of a number of 4,4′-thenylidene bis[N,N-dimethylaniline] compounds were described. Of the systems studied, the one best suited for dosimetric purposes consisted of 10^{-4} *M* 4,4′-(5-chloro-2-thenylidene)bis[N,N-dimethylaniline], 10^{-4} *M* ferrous ammonium sulphate, 0.1 *M* sodium chloride, and 7×10^{-3} *M* hydrochloric acid. With this system, the dye yield, as measured by the optical density at the main absorption peak of 633 mμ, increases linearly with increasing doses from zero to at least two thousand rads.

The common failing of most dosimeters developed for use in the low dosage range is their dose-rate and energy dependence. This is particularly true of systems based on acid formation from the decomposition of chlorinated hydrocarbons (4, 5, 6) where the mechanism involves a chain reaction. With this type of system it is necessary to shield out low-energy radiation and add some chain-breaking inhibitor.

Although the calculated *G* value of approximately one for the aqueous leuco system indicates the absence of chain reactions, the complicated mechanism is such that other factors might lead to dose-rate and energy effects. The present investigation was undertaken to determine the energy, dose-rate, and temperature dependence of the system.

EXPERIMENTAL

The radiation sources used to obtain the desired range of energies and dose rates are listed below:

1 curie of Cs^{137}	300 Kev Muller X-ray machine
150 curies of Co^{60}	2 Mev General Electric X-ray machine
300 curies of Co^{60}	2 curies of Cs^{137}

Procedure

The preparation of the system 10^{-4} *M* 4,4′-(5-chloro-2-thenylidene)bis[N,N-dimethylaniline], 10^{-4} *M* ferrous ammonium sulphate, 0.1 *M* sodium chloride, and 7×10^{-3} *M* hydrochloric acid has been described elsewhere (2). Solutions were found to be slightly

[1]*Manuscript received May 23, 1958.*
Contribution from Defence Research Board, Defence Research Chemical Laboratories, Ottawa, Ontario. Issued as D.R.C.L. Report No. 257.

light sensitive but blanks showed no change in color during the time required to complete an irradiation (as long as seven hours in a lighted room). Pyrex tubes of 9 mm inside diameter containing 3.3 ml of solution were used throughout. These tubes had a wall thickness of 2 mm, sufficient to ensure that electronic equilibrium was attained during the irradiations.

All dose rates were determined with Fricke ferrous sulphate, 0.8 N sulphuric acid dosimeter solution. The yield of ferric ion was measured spectrophotometrically by its own absorption at 304 mμ. Dose rates were calculated as shown below.

$$\text{Dose rate} = (\eta Fe^{+3}/t) \cdot (100/G) \cdot (1.602\times10^{-12}/100) \text{ rads/minute}$$

where t = irradiation time in minutes,
G = yield of Fe^{+3} = 15.5 molecules per 100 ev,
ηFe^{+3} = number of ferric ions per gram,
$= (6.023\times10^{23}/\epsilon\times1\times1000\times d) \cdot D_s - D_b$ ions/g,

where ϵ = molar extinction coefficient,
1 = path length of spectrophotometer cell,
D_s = optical density of irradiated sample,
D_b = optical density of blank,
d = density of solution.

Thus dose rate $= 9.649\times10^8 \cdot [(D_s-D_b)/G.\epsilon.1.d.t]$ rads/minute.

The energy absorbed in our system (E_S) can be related to the energy absorbed in the ferrous sulphate dosimeter (E_D) by the following equation:

$$E_S = E_D \cdot \mu_S/\mu_D$$

where μ_S = mass absorption coefficient of the system,
= mass absorption coefficient of 0.1 M sodium chloride.
μ_D = mass absorption coefficient of ferrous sulphate dosimeter,
= mass absorption coefficient of 0.8 N sulphuric acid.

For 160 Kev photons $\mu_S/\mu_D = 0.1479/0.1478 = 1.0007$ and for 1 Mev photons $\mu_S/\mu_D = 0.06336/0.06321 = 1.0024$. Hence for irradiations using the available sources previously mentioned $E_S = E_D$ to within 0.2%.

The housing and use of the 1-curie Cs^{137} source has been previously described (2). Eight sample tubes may be placed around this source and irradiated with gamma rays of 0.66 Mev effective energy at a dose rate of approximately five rads/minute.

The 150-curie Co^{60} source has been described by Aitken, Dyne, and Trapp (1). Three capsules, each containing about fifty curies, form a ring around the sample space. The capsules are attached to adjuster rods and the radiation flux is varied by moving the adjuster rods. Samples to be irradiated are placed on a lead piston and lowered into position. The introduction or removal of a sample requires less than one second. Samples can be irradiated at dose rates of 400 to 2000 rads/minute.

The 300-curie Co^{60} source is designed to give a narrow horizontal beam with a dose rate of 130 rads/minute at the collimator mouth. Because of the narrow field and the uncertain time required to swing the source into position, only one run was made with this source.

The Muller X-ray machine was operated at 300 kv and 10 ma. The beam was filtered to give radiation of 160 Kev effective energy, as measured in copper. With this arrangement samples can be irradiated at a maximum dose rate of 235 rads/minute.

Can. J. Chem. Downloaded from www.nrcresearchpress.com by 78.46.186.204 on 09/04/12
For personal use only.

The General Electric machine was operated at 2 Mev and 1.5 ma and the unfiltered radiation used. The dose rate from this machine is very high, being 1000 rads/minute at a distance of 45 cm from the target. As it took approximately five seconds for the machine to reach operating conditions, doses of the desired magnitude (0 to 2000 rads) could not be measured as accurately as with the other radiation sources.

The temperature-dependence studies were performed using a 2-curie Cs^{137} source. The source is placed in the center post of a lucite box. Eight sample tubes may be placed in the box around the source each tube being $1\frac{3}{4}$ in. from it. Water from a constant-temperature bath is pumped through the box during irradiation. With this arrangement samples are irradiated at a rate of approximately 250 rads per hour.

RESULTS

1. Dose-Rate Dependence

Samples were irradiated with 160 Kev X-rays at dose rates of 6, 20, 90, and 235 rads per minute. The results plotted in Fig. 1 as dye yields recorded as optical densities measured at 633 mμ against dose in rads show no dose-rate dependence in this range.

Higher dose rates were obtained with the 150-curie Co^{60} source. Irradiations were made using dose rates of 400, 790, and 1200 rads/minute. Optical densities were measured 15 minutes after irradiation and again $\frac{3}{4}$ hour later. As illustrated in Fig. 2, there is a considerable postirradiation dye fading at these dose rates. However the degree of fading is the same, within the range of experimental error, for each of these dose rates. Results obtained with a dose rate of 4 rads/minute using the 300-curie Co^{60} source are also included in Fig. 2. No dye fading was observed at this dose rate. Optical densities measured 15 minutes after irradiation at dose rates of 400 rads/minute or greater are about 8% higher than those measured after irradiation at dose rates of 4 rads/minute, while optical densities measured 1 hour after irradiation at dose rates of 400 rads/minute or greater are about 8% lower than those measured after irradiation at dose rates of 4 rads/minute. The results of a further study of postirradiation dye fading are given in Table I.

TABLE I

EFFECT OF TIME OF MEASUREMENT AND DOSE ON OPTICAL DENSITY
(Dose rate = 1200 rads/minute)

Time after irradiation, hr	Optical density, rads							
	302	604	906	1208	1510	1812	2114	2416
0.08	0.030	0.066	0.094	0.120	0.134	0.164	0.196	0.220
0.25	0.029	0.058	0.090	0.114	0.143	0.168	0.199	0.227
0.50	0.029	0.055	0.084	0.107	0.133	0.161	0.187	0.209
1.00	0.028	0.055	0.079	0.098	0.122	0.138	0.168	0.193
1.50	0.030	0.050	0.076	0.094	0.113	0.132	0.159	0.184
2.00	0.030	0.052	0.072	0.093	0.114	0.132	—	—
3.00	0.032	0.052	0.072	0.093	0.116	0.133	—	—
20.0	0.032	0.052	0.072	0.090	0.108	0.123	0.143	0.163

These results indicate that the dye concentration reaches a maximum prior to 15 minutes after irradiation, decreases for the next one to two hours, after which it changes only slightly.

A number of changes in the system were made in an attempt to decrease the after reaction. Increasing the leuco concentration from 10^{-4} M to 5×10^{-3} M increased the

Can. J. Chem. Downloaded from www.nrcresearchpress.com by 78.46.186.204 on 09/04/12
For personal use only.

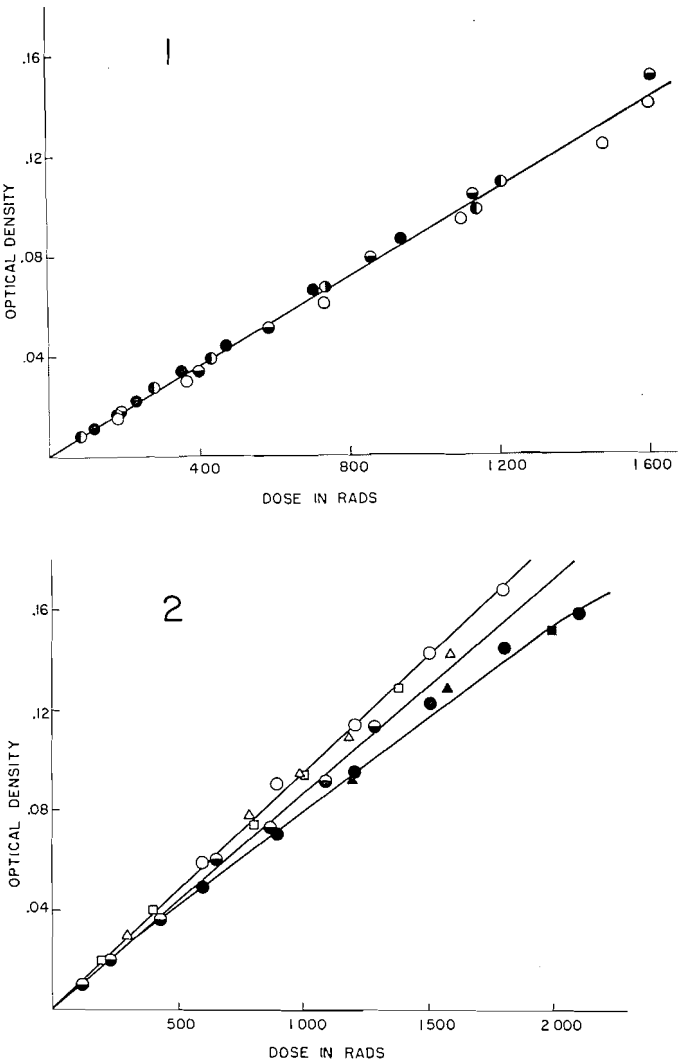

FIG. 1. Effect of dose rate with 160 kev irradiation: ○ 6 rads/minute, ◒ 20 rads/minute, ◐ 90 rads/minute, ● 235 rads/minute.

FIG. 2. Effect of dose rate with 1.25 Mev irradiation: ◒ 4 rads/minute, □ 400 rads/minute, △ 790 rads/minute, ○ 1200 rads/minute. Open symbols indicate measurements made 15 minutes after irradiation, darkened symbols 1 hour after irradiation.

amount of dye fading. With this system, the optical density of a sample which received a dose of 1000 rads at a dose rate of 1200 rads/minute decreased by 30% during the first hour following irradiation. Decreasing the sodium chloride concentration decreased greatly the sensitivity of the system and did not eliminate fading.

The effect of high dose rates on the corresponding trifluoroacetic acid system was also investigated. The system consisted of 10^{-4} *M* 4,4′-(5-chloro-2-thenylidene)bis[N,N-dimethylaniline], 10^{-4} *M* ferrous ammonium sulphate, 0.1 *M* sodium chloride, and 5×10^{-3} *M* trifluoroacetic acid. Dose-rate effects are shown in Fig. 3. As well as showing postirradiation fading, dye yields for doses received at 1200 rads/minute were about 18% lower than for doses received at 5 rads/minute.

Can. J. Chem. Downloaded from www.nrcresearchpress.com by 78.46.186.204 on 09/04/12
For personal use only.

2. Energy Dependence

In Fig. 4, dye yields recorded as optical densities are plotted against dose in rads for primary energies of 0.160, 0.660, and 1.25 Mev. Dose rates were approximately five rads/minute in each case. There is no detectable energy dependence in the range 0.160 to 1.25 Mev.

Because of the machine design, irradiation with 2 Mev X-rays at this low dose rate was not possible and dye fading at high dose rates made it difficult to compare yields with those obtained using lower-energy radiations. However, as shown in Fig. 5, optical

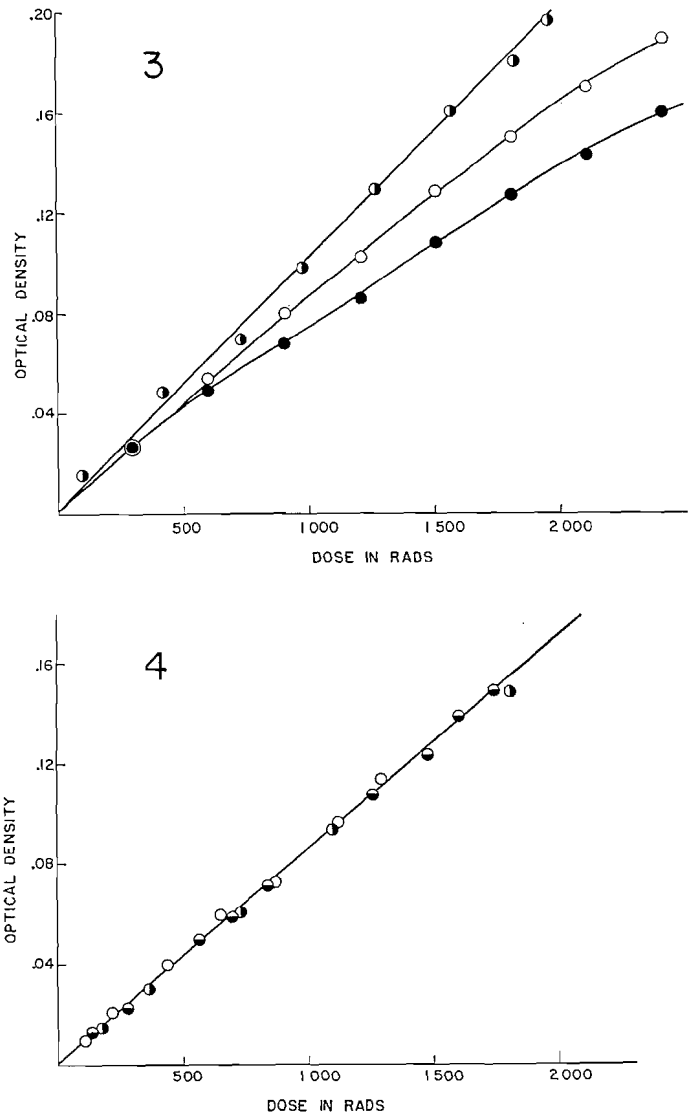

FIG. 3. Effect of high dose rate on the postirradiation stability of trifluoroacetic acid dosimeter solution: ◑ 5 rads/minute (Cs^{137} γ-rays), ○ 1200 rads/minute (Co^{60} γ-rays) (measurements made 15 minutes after irradiation), ● 1200 rads/minute (measurements made 3 hours after irradiation).

FIG. 4. Effect of energy at low dose rates (5 rads/minute): ◑ 0.16 Mev X-rays, ◒ 0.66 Mev γ-rays (Cs^{137}), ○ 1.25 Mev γ-rays (Co^{60}).

Can. J. Chem. Downloaded from www.nrcresearchpress.com by 78.46.186.204 on 09/04/12
For personal use only.

densities of solutions irradiated in one case with 1.25-Mev γ-rays at 1200 rads/minute and in the other with 2-Mev X-rays at 920 rads/minute, when remeasured at corresponding times after irradiation, show no variation attributable to energy effects.

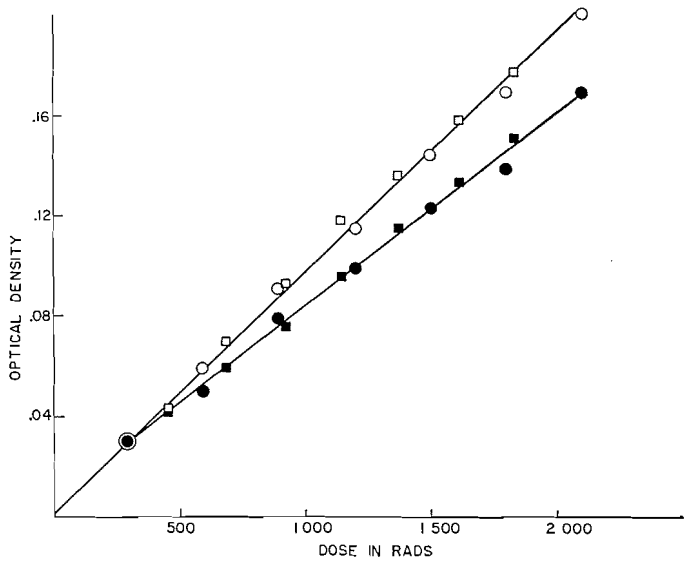

FIG. 5. Effect of energy at high dose rates (1000 rads/minute): ○ 1.25 Mev γ-rays (1200 rads/minute), □ 2 Mev X-rays (920 rads/minute). Open symbols indicate measurements made 15 minutes after irradiation, darkened symbols 1 hour after irradiation.

3. *Temperature Dependence*

Samples thermostated at temperatures from 15° to 45° C were irradiated with Cs^{137} γ-rays and optical densities measured after samples had been brought to room temperature. The optical densities of samples at various temperatures receiving given doses are listed in Table II. The slope of a plot of optical density vs. dose for each temperature is also given. The system is slightly temperature dependent at temperatures lower than 30° C and markedly dependent at higher temperatures. Raising the temperature from 20° to 30° C increases the dye yield per rad approximately 6%. However raising the temperature from 30° to 45° C increases the dye yield per rad approximately 22%.

TABLE II

EFFECT OF TEMPERATURE ON DYE YIELDS

Dose, rads	Optical density						
	15°	20°	25°	30°	35°	40°	45°
141	0.014		0.016	0.014	0.014	0.019	0.020
280	0.020	0.022	0.024	0.024	0.026	0.030	0.036
548	0.038	0.047	0.049	0.052	0.051	0.060	0.073
765	0.061	0.063	0.069	0.065	0.073	0.082	0.100
1002	0.079	0.085	0.091	0.090	0.098	0.110	0.134
1335	0.106	0.108	0.116	0.117	0.125	0.135	0.170
1639	0.128	0.133	0.138	0.142	0.152	0.170	0.213
1832	0.143	0.152	—	0.157	0.176	0.190	0.232
1919	0.153	0.155	0.169	0.165	0.182	0.194	0.236
Slope	7.85	8.15	8.63	8.63	9.40	10.55	12.87

Can. J. Chem. Downloaded from www.nrcresearchpress.com by 78.46.186.204 on 09/04/12
For personal use only.

Can. J. Chem. Downloaded from www.nrcresearchpress.com by 78.46.186.204 on 09/04/12
For personal use only.

DISCUSSION

As the mechanism of this system is not completely clear, the postirradiation fading at dose rates higher than 200 rads/minute cannot be wholly explained. Studies of the oxidation potential of the leuco compound (3) indicate that destructive oxidation of the dye occurs near the oxidation potential of the leuco compounds. Hence species formed during radiolysis which will oxidize the leuco compound may also be capable of destroying the dye. The dye fading at high dose rates is then probably due to the build-up in concentration of a dye-destroying species of relatively long life. The temperature dependence also supports the suggestion of the presence of a long-lived reactive species.

The postirradiation fading is not too serious in the range 0–1000 rads. Optical densities measured 15 minutes to 24 hours after irradiation at dose rates of 400–1200 rads/minute are within 8% of values obtained after irradiation at dose rates of 5–230 rads/minute. Optical densities measured at times greater than $1\frac{1}{2}$ hours after irradiation at high dose rates are within 2% of each other and are 6% to 8% lower than values obtained with low dose-rate exposures.

Although no temperature effects were observed when the dosimeter solution was being used at room temperature, thermostating the samples revealed a slight temperature dependence at temperatures lower than 30° and a considerable dependence at higher temperatures. A number of runs were carried out at 25° and 30° C. In all cases, dye yields for a given dose were the same. Hence only slight errors are introduced when working at room temperatures.

The system described in this report has been examined spectrophotometrically to determine the linearity of response, accuracy, reproducibility, dose-rate, energy, and temperature dependence. The results show that, in the energy range 160 kev to 2 Mev and with dose rates of 4 rads/minute to 1200 rads/minute, doses of 140 to 1000 rads absorbed at room temperature can be measured spectrophotometrically with 1-cm cells to within $\pm 8\%$. With dose rates of 4 rads/minute to 200 rads/minute, doses in this range can be measured more accurately as there are no postirradiation effects. At temperatures higher than 30° C there is a marked temperature dependence. The system should prove useful as a laboratory chemical dosimeter when employed within the limits outlined above.

ACKNOWLEDGMENTS

The authors wish to express their thanks to Dr. W. F. Baldwin and Dr. P. J. Dyne of Atomic Energy of Canada Limited for making available the 2 Mev X-ray machine and the 150-curie cobalt source as well as for valuable assistance and discussion. The authors would also like to thank Dr. J. A. Carruthers of these laboratories for the use of radiation sources.

REFERENCES

1. Aitken, P. B., Dyne, P. J., and Trapp, E. C. Nucleonics, **15** (1), 100 (1957).
2. Armstrong, W. A. and Grant, G. A. Radiation Research, **8**, 375 (1958).
3. Grant, G. A., Blanchfield, R., and Smith, D. M. Can. J. Chem. **35**, 40 (1957).
4. Taplin, G. V. The University of California School of Medicine, Atomic Energy Project Report No. UCLA 304.
5. Taplin, G. V. and Douglas, C. H. Nucleonics, **6** (6), 66 (1950).
6. Taplin, G. V., Douglas, C. H., and Sandez, B. Nucleonics, **9** (2), 73 (1951).

Can. J. Chem. Downloaded from www.nrcresearchpress.com by 78.46.186.204 on 09/04/12
For personal use only.

SYNTHESIS OF N-SUBSTITUTED DIISOPROPANOLAMINES, THEIR SEBACATE POLYESTERS AND POLYURETHANE ELASTOMERS[1]

JEAN L. BOIVIN

ABSTRACT

Several N-substituted diisopropanolamines were prepared by reacting aqueous solutions of amines with excess propylene oxide at ordinary pressure but higher N-substituted diisopropanolamines had to be prepared in an autoclave at 200° C. The ionization constants of these bases were measured and recorded as pK_a values. Their infrared absorption spectra gave bands common to all diisopropanolamines mainly at 3.04, 7.14, 7.55, 7.85, 9.45, 10.6, and 11.95 microns. Their condensation with sebacic acid gave the corresponding polyesters, which were soluble in strong acids and had molecular weights of about 1500. The hydroxyl-terminated polyesters were cured with a slight excess of 2,4-tolylene diisocyanate at 100° C for 2 days to yield elastomers of brittle temperatures in the region of −50° C.

INTRODUCTION

During the course of a research project, there were indications that elastomers containing tertiary amino derivatives in the recurring unit of the chain would be valuable elastomers with respect to their low-temperature properties and toughness. Our attention was drawn to the N-substituted diisopropanolamines[2] as starting diols in the condensation with dibasic acids. It seemed that the N-substituted diisopropanolamines have not been described in the literature, but diisopropanolamine itself has been prepared by allowing aqueous ammonia to react with propylene oxide.

Preparation of N-Substituted Diisopropanolamines

The diisopropanolamines were prepared by adding propylene oxide in excess to aqueous solutions of various primary amines. The reaction is shown by the following equation:

$$RNH_2 + 2CH_3CH\!\!-\!\!\overset{\diagdown\,O\,\diagup}{}\!\!CH_2 \longrightarrow RN\left[CH_2CH(CH_3)OH\right]_2.$$

It is believed that secondary diols were formed, since their condensation with diacids was rather slow and the reaction of their polyesters with diisocyanate required 2 days for completion. The concentration of the aqueous amine solution varying from 25 to 95% as the molecular weight of the amine increased. Reactivity with propylene oxide was observed to decrease with increasing molecular weight. The condensation was usually carried out at 60–80° C by adding propylene oxide to the amine solution. The reaction was exothermic and cooling was necessary up to amylamine, but from amylamine to decylamine the mixture had to be heated and the addition of propylene oxide was slower. From dodecylamine to octadecylamine, the reaction had to be carried out in an autoclave at 200° C. Table I shows the diisopropanolamines prepared together with their physical properties and purity as based on their acid equivalent.

Tertiary butylamine yielded the monoisopropanolamine derivative only when the reaction was run at normal pressure. The yields ranged from 90 to 100% when the amine and propylene oxide were used in the respective molar ratios of 1:2.5. The water

[1]*Manuscript received June 10, 1958.*
Contribution from the Polymer Research Group of the Canadian Armament Research and Development Establishment, Valcartier, Quebec.
This article is based on a paper presented at the 41st Annual Conference and Exhibition of the Chemical Institute of Canada, Toronto, May 26–28, 1958.
[2]*These compounds would be correctly named as N-substituted bis-(2-hydroxypropyl)-amines and for convenience the diisopropanolamine designation will be retained.*

TABLE I

N-SUBSTITUTED DIISOPROPANOLAMINES $RN\left[\begin{array}{c}CH_2CH-OH\\|\\CH_3\end{array}\right]_2$

R	B.p. (mm Hg)	Analysis* % purity	Method of preparation
Propyl	104–105 (2.0)	99.1	‖
Butyl	111–112 (1.5)	99.4	‖
Amyl	127–128 (3.0)	99.9	‖
Hexyl	144 (3.5)	98.5	‖
Octyl	144 (0.7)	99.7	‖
Decyl	152 (0.8)	99.4	‖
Dodecyl	172–174 (1.0)	96.4§	¶
Tetradecyl	185–190 (1.2)	101§	¶
Hexadecyl	205–208 (1.2)†	100§	¶
Octadecyl	210–213 (0.5)‡	102§	¶
Allyl	101–103 (0.5)	98.0	‖
Isobutyl	98–100 (1.5)	99.8	‖
tert-Butyl	122 (3.0)	99.7	¶
Benzyl	148–149 (0.5)	99.4	‖
2-Ethylhexyloxypropyl	162–164 (1.0)	99.7	‖
Dimethylaminopropyl	145 (2.8)	—§	‖
Morpholinoethyl	154–155 (0.5)	—§	‖
Morpholinopropyl	163–165 (0.5)	—§	‖

*By titration with 0.1 *N* HCl using methyl red as indicator.
†M.p. 39–40° C.
‡M.p. 38–39° C.
§Poor end point.
‖Ordinary pressure at 60–80° C.
¶In an autoclave at 200° C.

solubility of the diisopropanolamines decreased in ascending the homologue series, reaching nearly complete insolubility with the N-octadecyl compound.

Condensation products were also obtained by reacting propylene oxide with various amines; details are recorded in Table II.

Basicity of the N-Substituted Diisopropanolamines

Since the diisopropanolamines contain a tertiary nitrogen atom, they should be quite basic and have a high ionization constant (K_b). It was noticed that the determination of the purity of the base by titration with standard acid using methyl red as indicator

TABLE II

OTHER AMINE CONDENSATION PRODUCTS WITH PROPYLENE OXIDE

Compound	B.p. (mm Hg)	Analysis* % purity	Method of preparation
2-Hydroxyethyl-2-hydroxypropylmethylamine	103 (1.5)	99.0	‖
N,N′-Bis-(2-hydroxypropyl)-piperazine	130 (1.5)†	—‡	¶
tert-Butylamino-2-propanol	58 (2.5)§	99.7	‖

*By titration with 0.1 *N* HCl using methyl red as indicator.
†M.p. 70–75° C.
‡Poor end point.
§M.p. 26–27° C.
‖Ordinary pressure at 60–80° C.
¶In an autoclave at 200° C.

Can. J. Chem. Downloaded from www.nrcresearchpress.com by 78.46.186.204 on 09/04/12
For personal use only.

was erratic with the high molecular weight N-alkylated diisopropanolamines. The ionization constant of the diisopropanolamines was therefore measured by dissolving the diisopropanolamines in standard acid and back-titrating with a standard base while recording the pH.

The pK_a was given by the middle of the flat portion of the titration curve and the ionization constants are recorded for these amines using the normal acidity scale (pK_a). The results given in Table II show that the first members of the series from C_3 to C_6 inclusive have strengths similar to that of ammonium hydroxide; the higher homologues are less basic until they reach a pK_a on the acid side. It is worth while to note that

TABLE III

ELEMENTAL ANALYSIS AND pK_a VALUES OF N-SUBSTITUTED DIISOPROPANOLAMINES AND RELATED COMPOUNDS

R—N[CH$_2$CH(CH$_3$)—OH]$_2$	pK_a*	Found for:†			Calculated for:		
		C, %	H, %	N, %	C, %	H, %	N, %
Propyl	8.9	61.0	11.9	7.56	61.7	12.0	8.00
Butyl	9.3	63.6	11.7	6.98	63.5	12.2	7.40
Amyl	9.0	64.6	12.3	6.54	65.0	12.3	6.90
Hexyl	8.5	66.4	12.5	6.27	66.5	12.4	6.48
Octyl	8.3	69.0	12.9	5.84	68.6	12.6	5.72
Decyl	7.6	69.9	12.8	5.35	70.5	12.7	5.13
Dodecyl	6.2	72.0	12.9	4.81	72.0	12.9	4.65
Tetradecyl	5.6	72.6	13.0	4.52	73.1	13.1	4.25
Hexadecyl	4.8	74.2	13.0	4.09	73.8	12.5	3.93
Octadecyl	4.6	74.6	13.2	3.89	74.9	13.2	3.64
Allyl	8.2	62.1	10.9	7.33	62.5	11.0	8.11
Isobutyl	8.8	59.9	11.9	12.5	60.5	11.9	12.7
tert-Butyl	9.4	60.0	11.9	12.6	60.5	11.9	12.7
Benzyl	7.5	69.8	9.48	6.43	70.0	9.40	6.98
2-Ethylhexyloxypropyl	7.7	67.5	11.8	4.54	67.4	12.2	4.63
Dimethylaminopropyl	6.5, 9.2	59.9	11.9	12.5	60.5	11.9	12.7
Morpholinoethyl	7.9	57.8	10.6	11.5	57.0	10.4	11.3
Morpholinopropyl	5.5, 8.4	59.8	10.6	10.5	60.0	10.7	10.7
2-Hydroxyethyl-2-hydroxypropyl methylamine	8.7	54.9	11.2	9.98	54.1	11.1	10.5
tert-Butylamino-2-propanol	10.0	63.6	13.1	10.7	64.2	13.0	10.7
N,N′-Bis-(2-hydroxypropyl)-piperazine	7.1	58.4	11.9	13.3	58.6	12.1	13.6

*Determined graphically from the titration curves.
†Analysis by Micro-Tech Laboratories, Skokie, Illinois.

N-substituted monoisopropanolamines such as the N-methyl derivative are more basic than diisopropanolamine itself. Where two tertiary nitrogen atoms are present in the same molecule, two pK_a values were recorded indicating different degrees of ionization. Highly symmetrical molecules such as N,N′-bis-(2-hydroxypropyl)-piperazine exhibited only one ionization constant (pK_a of 7.1). In the case of N-morpholinoethyl diisopropanolamine the single pK_a obtained indicated that the two nitrogen atoms are equally electronegative.

Infrared Spectra

The infrared absorption spectra of all the N-substituted diisopropanolamines prepared were determined on a double beam Perkin–Elmer spectrophotometer between sodium chloride plates. They all exhibit similar absorption bands at 3.04, 7.14, 7.55, 8.85, 9.45, 10.6, and 11.95 microns excepting the CH bands.

The diisopropanolamines, which are probably associated hydroxylated compounds, exhibit an intense absorption band in the region of 3.0 to 3.04 microns which can be

Can. J. Chem. Downloaded from www.nrcresearchpress.com by 78.46.186.204 on 09/04/12
For personal use only.

attributed to the OH vibration. Most of the other bands are practically common to all the compounds studied and the N-substituents have no effect on the spectra at least for the N-alkyl derivatives. Substituents containing nitrogen or oxygen influenced the spectra in the region of 8.5 to 10 microns.

Polyesters from N-Substituted Diisopropanolamines and Sebacic Acid

The N-substituted diisopropanolamines were condensed with sebacic acid using a molar ratio of 1.1 to 1.0 at a temperature of 210–220° C for 20 hours, during which time water was eliminated. Nitrogen was passed through the melt to provide stirring and prevent oxidation. After heating for a further hour at 220° C under vacuum, the polyesters of sebacic acid were obtained and their molecular weight estimated by the hydroxyl end-group analysis after making a correction for the acidity number. Table IV shows the molecular weight, acidity number, and viscosity of the polyesters prepared. Determination of the pK_a values showed that they were weakly basic. The pK_a values range from 3 to 5.

TABLE IV

POLYESTERS OF N-SUBSTITUTED DIISOPROPANOLAMINES AND SEBACIC ACID AND THEIR 2,4-TOLYLENE DIISOCYANATE (TDI) POLYURETHANE ELASTOMERS

	Polyesters of sebacic acid and N-substituted diisopropanolamines			Polyurethanes	
N-Substituents	Mol. wt.	Viscosity at 20° C, centostokes	Acid No.*	TDI†	Gehman freeze point, ° C
Propyl	1880	—	19.6	2	−42
Butyl	1090	5450	58.8	3	−46
Amyl	1450	—	6.1	2	−51
Hexyl	1410	13400	3.4	3	−60
Octyl	1600	5580	4.5	3	−45
Decyl	2010	7690	4.0	2	−55
Dodecyl	1960	—	2.5	2	−55
Tetradecyl	1520	3000	2.8	4	−40
Hexadecyl	2450	7700	1.7	2	−40
Octadecyl	1530	2470	2.6	3	−30
Allyl	1230	—	6.2	3	−58
Isobutyl	1230	—	13.0	4	−49
Benzyl	1430	—	6.4	3	−16
tert-Butyl	1400	—	5.2	3	−42
Morpholinopropyl	1910	—	10.8	2	−32
Morpholinoethyl	1820	—	21.2	3	−28
Dimethylaminopropyl	1420	—	12.3	3	−40
2-Ethylhexyloxypropyl	1920	4200	3.5	2	−50

*Milligrams of KOH per gram of prepolymer.
†Grams per 20 grams of prepolymer.

Polyurethane Elastomers

The hydroxyl-terminated polyesters of N-substituted diisopropanolamines and sebacic acid were treated with various quantities of 2,4-tolylene diisocyanate, mixed thoroughly, and cured 48 hours at 100° C. The low-temperature brittleness of the elastomers was measured by determining the Gehman freeze point. Table IV shows the results. In most cases, the brittle point of the best specimen of elastomer was in the region of −50° C. The elastomers obtained from low molecular-weight-substituted diisopropanolamines were tough but the strength decreased in ascending the series. Owing to the high acid numbers of most polyesters prepared the elastomers were not free of bubbles.

Can. J. Chem. Downloaded from www.nrcresearchpress.com by 78.46.186.204 on 09/04/12
For personal use only.

CONCLUSION

There is an indication that N-substituted diisopropanolamine containing elastomers are slightly better at low temperature than those made from non-basic polyesters. However, these diols will be valuable intermediates to terminate any polymeric chain by secondary hydroxyl groups which are less reactive toward diisocyanates than the primary functions.

Can. J. Chem. Downloaded from www.nrcresearchpress.com by 78.46.186.204 on 09/04/12
For personal use only.

Can. J. Chem. Downloaded from www.nrcresearchpress.com by 78.46.186.204 on 09/04/12
For personal use only.

THE SPONTANEOUS PRECIPITATION OF HYDRATED ALUMINA FROM ALUMINATE SOLUTIONS[1]

T. VRBAŠKI,[2] H. IVEKOVIĆ,[3] AND D. PAVLOVIĆ[4]

ABSTRACT

The rates of spontaneous precipitation of hydrated alumina from unseeded and metastable sodium aluminate solutions of a molar relation for Na_2O/Al_2O_3 (α) ranging from 1.15 to 1.60 have been investigated. All precipitation curves showed autocatalytic characteristics with a pronounced induction period, during which no precipitation occurred, a steady state period, and a period of delayed precipitation. Empirical equations for calculating the maximum precipitation rate, for the time when this precipitation takes place, and for the amount of the precipitate at equilibrium for any of these aluminate solutions have been developed.

INTRODUCTION

The precipitation of hydrated alumina from metastable sodium aluminate solutions represents the basic reaction in the formation of alumina by the Bayer process.

This reaction has been the subject of extensive investigation using mainly hydrargillite as a seed substance (1, 2, 3, 4). Spontaneous process was also studied by Calvet *et al.* (5) and by Sato (6).

The experiments described below were carried out in order to obtain a closer insight into the kinetics of the spontaneous precipitation of hydrated alumina from unseeded aluminate solutions. The time after which first nuclei of hydrated alumina (hydrargillite) are formed in a clear solution is of greatest significance as the crystallites once formed act as seed substance (7). It is of great interest, therefore, to investigate the dependence of the induction period (6) on the molar relation (α), where $\alpha = Na_2O/Al_2O_3$, of the aluminate solution used.

As no crystallites are present in the clear solution at the beginning of the reaction, and since the precipitate formed will cause a considerable promotion of the precipitation rate, the precipitation would be expected to show autocatalytic characteristics (cf. 7). In the Bayer process such autocatalytic characteristics are masked by the action of the high concentration of seed material.

EXPERIMENTAL

Preparation of Sodium Aluminate Solutions

The solution of sodium aluminate was prepared in the way described in our previous paper (8). The aluminate solutions used were prepared by dilution of the stock solution with distilled water to a concentration of approximately one mole Al_2O_3 and 1.15 to 1.60 mole Na_2O.

The content of Al_2O_3 and Na_2O in the solution was determined by titration with 1 *N* HCl using tropeolin 00 and phenolphthalein respectively as indicators (9). The aluminate solutions were shaken continuously in stoppered Erlenmeyer flasks in a water bath at 30.0±0.1° C. When the agitation was discontinued the precipitate settled down quickly and the sample for analysis was taken from the supernatant liquid.

[1]*Manuscript received June 9, 1958.*
Contribution from the Department of Inorganic, Analytic, and Physical Chemistry, Faculty of Pharmacy, University of Zagreb, Yugoslavia.
[2]*National Research Council of Canada Postdoctorate Fellow, 1957–1959. Present address: National Research Council, Applied Chemistry, M-12.*
[3]*Professor, Department of Inorganic, Analytic, and Physical Chemistry, Faculty of Pharmacy, University of Zagreb, Yugoslavia.*
[4]*Department of Inorganic, Analytic, and Physical Chemistry, Faculty of Pharmacy, University of Zagreb, Yugoslavia.*

Can. J. Chem. Downloaded from www.nrcresearchpress.com by 78.46.186.204 on 09/04/12
For personal use only.

RESULTS

Each experiment was carried out using six different aluminate solutions. Their compositions are given in Table I.

TABLE I

THE COMPOSITION OF ALUMINATE SOLUTIONS

Solution	Al_2O_3, mole	Na_2O, mole	Initial molar relation for Na_2O/Al_2O_3 (α)	Molar relation for Na_2O/Al_2O_3 at equilibrium (α_e)
1	0.95	1.10	1.15	5.00
2	1.00	1.22	1.22	5.00
3	0.98	1.29	1.32	5.00
4	1.00	1.39	1.39	5.00
5	1.01	1.50	1.50	5.00
6	1.00	1.60	1.60	5.00

The solutions were prepared by diluting 100 ml samples of the freshly prepared stock solution to a volume of 150 ml. The molar percentage of the precipitated hydrated alumina was plotted against time. A family of curves was obtained as the molar relation for Na_2O/Al_2O_3 was varied. These are shown in Fig. 1. It was not found profitable to plot molar relation for Na_2O/Al_2O_3 against time because its values, depending on the initial molar relation, changed in a different way for each solution during the reaction.

All precipitation curves showed an autocatalytic trend with a characteristic induction period, during which no precipitation occurred, a steady state period, and a period of delayed precipitation.

(*a*) *The Induction Period*

It is evident from the Fig. 1 that the precipitation of hydrated alumina takes place

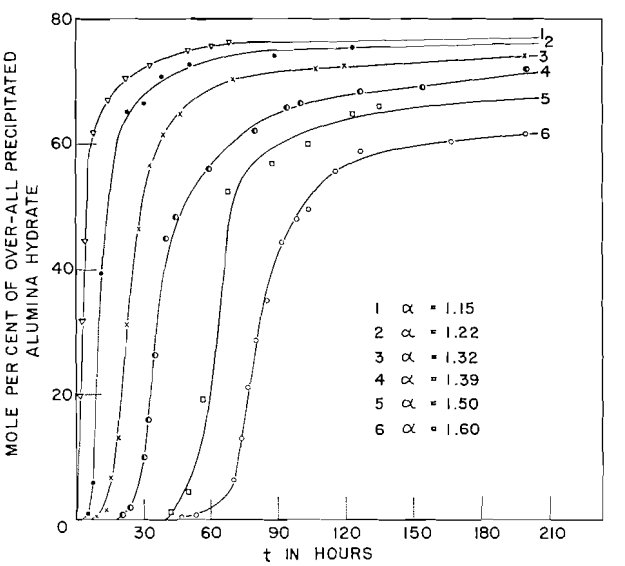

FIG. 1. Spontaneous precipitation of hydrated alumina from aluminate solutions of different molar relation for Na_2O/Al_2O_3. The volume of solutions was 150 ml, and the temperature 30.0±0.1° C.

only after an induction period, which becomes longer as the initial molar relation for Na_2O/Al_2O_3 is increased. This dependence of the induction period upon the initial molar relation is shown in Fig. 2.

The ratio of the induction period to the initial molar relation is not steady along the whole of the investigated region. The experimental curve (in Fig. 2) could be composed of two straight lines with an intersection point in S corresponding to a solution of a molar relation $\alpha = 1.385$ and an induction period of 685 minutes. Calvet *et al.* (10) found by thermochemical method of measuring the stability of solutions of sodium aluminate an instability ceiling at the same molar relation for Na_2O/Al_2O_3. This phenomenon might possibly be caused by a structural change of the aluminate solution (11) at this point. In the low molar relation region ($\alpha = 1.15$ to $\alpha = 1.40$) the increase of the induction period is slow, the slope being 62.0, i.e. only about a quarter of the succeeding slope over the region $\alpha = 1.40$ to $\alpha = 1.60$.

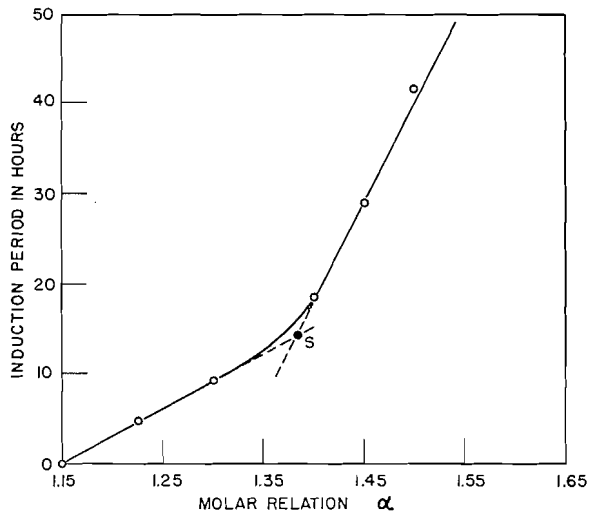

FIG. 2. The dependence of the induction period upon the initial molar relation for Na_2O/Al_2O_3.

(*b*) *The Equilibrium State*

In order to obtain data on the equilibrium state, the precipitation from solutions with higher molar relation had to be followed for up to sixty days. The amount of hydrated alumina precipitated at equilibrium was plotted against the initial molar relation. A straight line was obtained and could be expressed fairly well by the equation

$$C = 100 - 20\,\alpha, \qquad [1]$$

in which C is the molar percentage of over-all precipitated hydrated alumina and α the initial molar relation.

The molar relations established at equilibrium were found to be identical for all solutions and did not depend upon the initial molar relations used.

(*c*) *The Precipitation Rate*

The precipitation rate is higher if the initial molar relation of the aluminate solution is lower, as shown in Fig. 1. The amount of hydrated alumina precipitated in 100 minutes (ϕ) can be taken as a measure of the precipitation rate. Plotting the rates so obtained (ϕ) against time (t) we obtain a family of curves shown in Fig. 3.

Can. J. Chem. Downloaded from www.nrcresearchpress.com by 78.46.186.204 on 09/04/12
For personal use only.

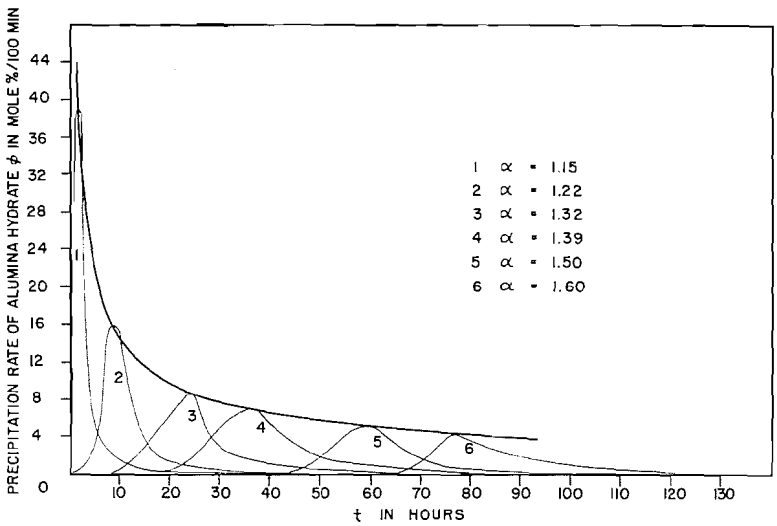

FIG. 3. Precipitation rates of hydrated alumina precipitated from aluminate solutions of various molar relations for Na_2O/Al_2O_3.

The maximum precipitation rate (ϕ_m) is higher if the initial molar relation (α) is lower. This relationship can be expressed by the equation

$$\log \phi_m = k(1/\log \alpha)^n, \quad [2]$$

where α is the initial molar relation, and n and k are constants. The average values of n and k are 0.761 ± 0.001 and 0.188 ± 0.001 respectively. They have been calculated from the equation [2] using pairs of corresponding values of α and ϕ_m. They could also be obtained graphically from a diagram in which log log ϕ_m versus log $1/(\log \alpha)$ was plotted. In the straight line so obtained n was the slope and log k the segment of the ordinate.

The maximum precipitation rate of any sodium aluminate solution of known initial molar relation can thus be readily calculated from the equation [2].

(*d*) *The Time of the Maximum Precipitation Rate*

Relationship between the maximum precipitation rate (ϕ_m) and the time of the maximum precipitation rate ($t_{\phi m}$) is obtained by connecting the peaks of the velocity curves in Fig. 3. This relationship can be expressed by the equation

$$\phi_m = k'(1/t_{\phi m})^{n'}, \quad [3]$$

where n' and k' are constants. The average n' and k' values calculated from the above equation or determined graphically, similarly as n and k values, are 0.610 ± 0.001 and 60.26 ± 0.15 respectively.

Combining [2] and [3] and eliminating ϕ_m the expression

$$t_{\phi m} = (\log k'/n') - (k/n')(1/\log \alpha)^n \quad [4]$$

is obtained.

Inserting numerical values of the constants into equation [4] we obtain

$$\log t_{\phi m} = 2.92 - 0.308(1/\log \alpha)^{0.761}. \quad [5]$$

The time of the maximum precipitation rate can thus be calculated directly from the initial molar relation for Na_2O/Al_2O_3.

Can. J. Chem. Downloaded from www.nrcresearchpress.com by 78.46.186.204 on 09/04/12
For personal use only.

Comparison of the calculated and observed values of ϕ_m and $t_{\phi m}$ is given in Table II. The differences are within $\pm 1.15\%$.*

TABLE II

COMPARISON OF CALCULATED AND OBSERVED VALUES OF ϕ_m AND $t_{\phi m}$

Initial molar relation for Na_2O/Al_2O_3 (α)	ϕ_m		$t_{\phi m}$	
	Calculated by eq. 2	Observed	Calculated by eq. 4	Observed
1.15	38.9	39.0	2.0	2.0
1.22	16.2	16.1	8.6	8.8
1.32	8.7	8.7	24.0	24.0
1.39	6.7	6.8	36.3	36.3
1.50	5.0	5.0	59.0	59.2
1.60	4.3	4.3	77.6	77.8

On the Kinetics of Precipitation of the Hydrated Alumina

The family of curves in Fig. 1 indicates that the precipitation reaction behaves more like an autocatalytic reaction at higher molar relations and less so at lower molar relations when it seems to follow a simple logarithmic law.

This phenomenon can be readily explained on the basis of the expression for the autocatalytic reaction rate†

$$+dx/dt = (k_1+k_2x)(a-x), \qquad [6]$$

where k_1 is the first-order reaction rate constant, k_2 the constant of the autocatalysis, a the initial concentration of sodium aluminate, and x the concentration of hydrated alumina, i.e. of the catalyst produced at the time t. The use of this expression is only tentative. Attributing the discussed precipitation a reaction type of a definite order is not possible at present because of lack of information.

Since the precipitation does not start if crystallization nuclei are not present, k_1 is very probably small. As soon as the reaction initiates k_1 can be neglected compared to k_2x because x increases rapidly; x and thus (k_1+k_2x) tend to reach soon a final value and the precipitation reaction seems to behave like a first-order reaction. The same conclusion will be reached if we take into consideration similar expressions proposed by other authors (13).

In the solutions of low molar relation, crystallization nuclei are rapidly formed at the very beginning of the reaction and the entire course of precipitation seems to follow the first-order reaction law. In the solutions of higher molar relation similar behavior is observed after the initial autocatalytic period.

However, if an excess of seed material is added at the beginning of the reaction the precipitation reaction is expected to behave in the same way as that in the solutions of lower molar relation. This assumption has been confirmed by recent investigations of Herrmann *et al.* (7). The authors, however, pointed out that their empirically found expression should not be considered as a simple equation for a first-order reaction rate, although this expression showed some similarity with it.

**In conclusion it should be emphasized that for generalization of equations obtained the temperature dependence of the reaction should be determined. This will be the subject of a further study.*

†This expression can be deduced from the Ostwald's expression for the first-order reaction rate if the product formed acts as a negative catalyst (12).

Can. J. Chem. Downloaded from www.nrcresearchpress.com by 78.46.186.204 on 09/04/12
For personal use only.

REFERENCES

1. VOL'F, F. F., KUZNETSOV, S. S., and SEREBRENNIKOVA, O. V. J. Appl. Chem. U.S.S.R. (English translation) **23**, 57 (1950). Zhur. Priklad. Khim. **23**, 60 (1950).
2. SATO, T. J. Chem. Soc. Japan, Ind. Chem. Sect. **55**, 66, 192 (1952); **56**, 399, 743, 840 (1953); **57**, 20, 111, 355, 540, 805 (1954); **58**, 325, 556 (1955).
3. HERRMANN, E. Z. anorg. u. allgem. Chem. **274**, 81 (1953).
4. MARIČIĆ, S. and MARKOVČIĆ, I. Arhiv Kem. **27**, 41 (1955). Z. anorg. u. allgem. Chem. **276**, 193 (1955). BOGDANOVIĆ, P., MARIČIĆ, S., and VIDAN, M. Croat. Chem. Acta, **28**, 155 (1956).
5. CALVET, É., THIBON, H., MAILLARD, A., and BOIVINET, P. Bull. soc. chim. France, 130 (1950); 402 (1951).
6. SATO, T. J. Chem. Soc. Japan, Ind. Chem. Sect. **54**, 755 (1951).
7. HERRMANN, E. and STIPETIĆ, J. Z. anorg. Chem. **262**, 258 (1950).
8. IVEKOVIĆ, H., VRBAŠKI, T., and PAVLOVIĆ, D. Croat. Chem. Acta, **28**, 41 (1956).
9. HERRMANN, E. Arhiv kem. **21**, 218 (1949).
10. CALVET, É., THIBON, H., and MAILLARD, A. Compt. rend. **228**, 928 (1949).
11. IVEKOVIĆ, H. and BAČIĆ, I. Chemiker-Ztg. **55**, 255 (1954).
12. OSTWALD, W. Allgem. Chem. **2**, II, 270 (1902). Verlag von W. Engelmann, Leipzig.
13. ADAM, N. K. Physical chemistry. Oxford University Press, London. 1956. p. 448.

Can. J. Chem. Downloaded from www.nrcresearchpress.com by 78.46.186.204 on 09/04/12
For personal use only.

Can. J. Chem. Downloaded from www.nrcresearchpress.com by 78.46.186.204 on 09/04/12
For personal use only.

AN INTERPRETATION OF THE MOISTURE DESORPTION ISOTHERM OF WHEAT[1]

H. A. Becker

ABSTRACT

It is shown that the moisture desorption isotherm of wheat can be interpreted in harmony with Cassie's theoretical assumptions regarding adsorption on localized sites by the equation

$$\frac{N}{S} = (1+K'f^n)\left(\frac{Kf}{1+Kf}\right),$$

where N is the number of adsorbed molecules per gram of wheat and S is the number of localized sites. $Kf/(1+Kf)$ is a Langmuir-type factor for adsorption of the low energy fraction of molecules, and $K'f^n$ is a factor for adsorption of the normally condensed fraction of molecules. In agreement with theory K', n, and S are independent of temperature. The dependence of K on temperature gives a value of -6.27 kcal/mole for the partial molal enthalpy of dilution of the low energy fraction of molecules, which is in the order of magnitude of a hydrogen bond. The analysis also illuminates the practice of the drying of wheat. An exact correspondence appears to exist between the calculated values of S and the apparent surface (or equilibrium) moistures observed in studying the diffusion of moisture out of wheat. The theoretical relation

$$m_s = 0.1157\ K/(1+K)$$

is therefore given for predicting apparent surface moisture contents in the vacuum drying of wheat, where

$$K = 3.05\times10^{-4}\exp(6270/RT).$$

Becker and Sallans (1) have made a comprehensive study of the moisture desorption isotherm of wheat. The isotherm was found to be sigmoid in shape and was described mathematically in three sections: at low relative vapor pressures, by the B.E.T. equation (2)

$$\frac{m}{m_L} = \frac{Kf}{1-f}\left(\frac{1}{1+(K-1)f}\right), \qquad [1]$$

where m is the moisture content, g/g dry basis, f is the relative vapor pressure, and m_L and K are constants; at intermediate relative vapor pressures, by the linear relation

$$m-m_0 = af, \qquad [2]$$

where m_0 and a are constants; and at high relative vapor pressures, by Smith's equation (3)

$$\frac{w-w_b}{w'} = \ln\frac{1}{1-f}, \qquad [3]$$

where w is the moisture content, g/g wet basis, and w_b and w' are constants. The use of the last two equations for accurate description of the isotherm was necessitated by the usual failure of the B.E.T. equation at intermediate and high relative vapor pressures. Even if put in the form for limited adsorption,

$$\frac{m}{m_L} = \frac{Kf}{1-f}\left(\frac{1-(n+1)f^n+f^{n+1}}{1+(K-1)f-Kf^{n+1}}\right), \qquad [4]$$

where n is the limiting number of layers of molecules, the B.E.T. equation will not accurately fit the data. However, the inexactness of the B.E.T. equation at all but

[1]*Manuscript received July 18, 1958.*
Contribution from the National Research Council, Prairie Regional Laboratory, Saskatoon, Saskatchewan. Issued as N.R.C. No. 4890.

low relative vapor pressures is of little consequence theoretically. The really irregular features of the data are (i) that the calculated moisture contents corresponding to a B.E.T. molecular monolayer, $m_L = 0.078$ g/g at 25° C and 0.060 g/g at 50° C, are markedly functions of temperature; and (ii) that there is no apparent relation between any of the constants in equations 1, 2, and 3 and the dynamic equilibrium moistures observed by the author (4) and by Becker and Sallans (5) in studying moisture diffusion out of the wheat kernel. It is the purpose of the present paper, therefore, to explain or eliminate these discrepancies.

THE ISOTHERM EQUATION

The B.E.T. equation was derived by Brunauer *et al.* (2) on the basis of a somewhat dubious evaporation–condensation mechanism. Cassie (6) has given the equation thermodynamic credence by derivation from statistical–thermodynamical arguments. In Cassie's view the equation is applicable to adsorption on localized sites, such as polar groups on a polymer molecule, rather than to adsorption on an unspecified surface. He postulated that the first molecule associated with each localized site is strongly adsorbed, while subsequently attached molecules are at the same energy level as in the normal liquid state. Adsorption of an essentially liquid fraction at vapor pressures below saturation is made possible by mixing with the low energy fraction. His version of the B.E.T. equation is written

$$\frac{N}{S} = \frac{Kf}{(1-f)}\left(\frac{1}{1+(K-1)f}\right), \qquad [5]$$

where N is the number of adsorbed molecules per gram of adsorbent and S is the number of localized sites. In the statistical–thermodynamical definition $K = (j_S/j_L)\exp(-\Delta\bar{H}_S/RT)$, which differs from Brunauer *et al.*'s definition by prefixing the ratio j_S/j_L where j_S and j_L are respectively the partition functions for molecules in the low energy state and in the normal liquid state; $\Delta\bar{H}_S$ is the partial molal enthalpy of dilution of the low energy (X) fraction of molecules; and R and T are respectively the gas constant and the absolute temperature. It appears that Cassie's arguments provide a reasonable and simple basis for interpretation of the moisture sorption isotherms of materials such as wheat. However, it can be expected that the course of multimolecular adsorption will rarely follow equations 1 or 4 exactly. If it is desired to obtain an accurate description of the adsorption isotherm with values of the B.E.T. constants which are consistent with their assumed behavior, then equation 4 should be written in a form which allows greater variation between the paths of adsorption of the "normally condensed" and the low energy fractions of molecules. A simple equation with flexible parameters for multimolecular adsorption, which still retains the theoretical skeleton of equation 5, can be formulated as follows.

Consider the adsorption of N molecules on X sites in a material which contains S localized sites. Following Cassie (6), we assume that X molecules are singly adsorbed, one to a site, with a constant, negative partial molal enthalpy of dilution, $\Delta\bar{H}_S$, in the order of several kilocalories. These X molecules provide the sites for adsorption of the remaining N–X molecules, which are assumed to be condensed with a zero partial molal enthalpy change. The adsorption of the X low energy molecules can reasonably be assumed, on the basis of Cassie's (6) and Enderby's (7) statistical–thermodynamical analyses, to be governed by the Langmuir form of equation 5

$$X/S = Kf/(1+Kf). \qquad [6]$$

Can. J. Chem. Downloaded from www.nrcresearchpress.com by 78.46.186.204 on 09/04/12
For personal use only.

In Cassie's argument the adsorption of the N–X condensed molecules derives from random mixing with the X low energy molecules. It is obvious, however, that this process will be complicated by various influences resulting from the physical and chemical characteristics of both adsorbate and adsorbent. Even so, it appears that the state of the normally condensed molecules should be similar in some ways to a gaseous film in which the molecules are associated, on the average, in groups of n molecules each. The equation of state of such a film is (8)

$$\pi(n\sigma) = kT, \qquad [7]$$

where π is the film pressure, $\sigma = \Sigma/N$ is the area per molecule, Σ is the area of the film, and k is Boltzmann's constant. Conjunction with Gibb's equation

$$\pi = \frac{kT}{\Sigma}\int_0^f \frac{N}{f}\,df \qquad [8]$$

gives Freundlich's isotherm (1)

$$N = K'f^n. \qquad [9]$$

We shall therefore assume that the adsorption of the N–X normally condensed molecules on X available sites can be expressed by

$$(N-X)/X = K'f^n. \qquad [10]$$

Eliminating X between equations 6 and 10 we find for the adsorption isotherm

$$\frac{N}{S} = (1+K'f^n)\left(\frac{Kf}{1+Kf}\right). \qquad [11]$$

A definite physical significance can be attached to the parameters K and K' in this equation: at saturation the Langmuir part reduces to

$$X_1/S = K/(1-K) \qquad \text{or} \qquad K = X_1/(S-X_1), \qquad [12]$$

where X_1 is the number of occupied sites. Hence K is the numerical ratio of the occupied sites to the vacant ones at the saturation vapor pressure. Putting $S = X_1(1+K)/K$, equation 11 becomes

$$\frac{N}{X_1} = (1+K'f^n)\left(\frac{(1+K)f}{1+Kf}\right) \qquad [13]$$

and at $f = 1$, $N/X_1 = 1+K'$. Therefore K' can be thought of as the average number of normally condensed molecules per occupied site toward which adsorption tends at saturation.

THE EVALUATION OF THE ISOTHERM PARAMETERS

Before discussing the evaluation of the parameters S, K, K', and n, we shall summarize the assumptions to be made as to their behavior. The following assumptions are fundamental to equation 11:

(i) The number of localized sites, S, is a constant characteristic of the adsorbent.

(ii) The parameter K is independent of concentration but is dependent on temperature. The temperature dependency should be very nearly given by

$$\frac{\partial \ln K}{\partial\, 1/T} = -\frac{\Delta\bar{H}_s}{R}. \qquad [14]$$

(iii) The parameter K' and the exponent n are independent of temperature but may be dependent on concentration.

Can. J. Chem. Downloaded from www.nrcresearchpress.com by 78.46.186.204 on 09/04/12
For personal use only.

Can. J. Chem. Downloaded from www.nrcresearchpress.com by 78.46.186.204 on 09/04/12
For personal use only.

The evaluation of the parameters may be carried out by trial and error treatment of data. A solution is obtained when the properties of the parameters are in accord with their assumed behavior. Eventually the exponent n will need to be considered as a function of the relative vapor pressure. The following cases may occur:

(i) $n = 0$. When n is equal to zero, K' will also be equal to zero, and the isotherm equation reduces to Langmuir's equation.

(ii) $n, K' =$ constants. The trial and error method should quickly yield a solution if n and K' can be treated as constants.

(iii) $K' f^n \ll 1$. In this case equation 11 reduces to Langmuir's equation.

(iv) K' and/or n are functions of relative vapor pressure. This most general case can be treated by writing equation 11 in the form

$$\frac{f(1+\phi(f))}{N} = \frac{1}{KS} + \frac{f}{S}, \qquad [15]$$

where $\phi(f) = K'f^n$. The problem then is to find a value of $\phi(f)$ which gives a linear relation between $f(1+\phi(f))/N$ and f, and a constant, temperature-independent value of S.

The general technique is illustrated by the following analyses of Bull's data (9) on the adsorption of water vapor by proteins or protein-like polymers. Figure 1 shows that a reasonably good correlation of the data on silk, wool, and gelatin is obtained by putting $1+K'f^n = 1+f+f^2$. (This substitution produces an approximation to the B.E.T. equation, since $1+f+f^2$ is an approximation to $1/1-f$.) The curves are linear in a wide region of relative vapor pressures, and the slopes of the linear regions are substantially independent of temperature. The moisture contents, m_L, corresponding to the number of localized sites, S, (m_L is given by the reciprocals of the slopes) are about 30% higher than predicted by the B.E.T. equation 1. A somewhat different relation is shown by nylon, Fig. 2, for which trial and error treatment of the data for 25° C gives

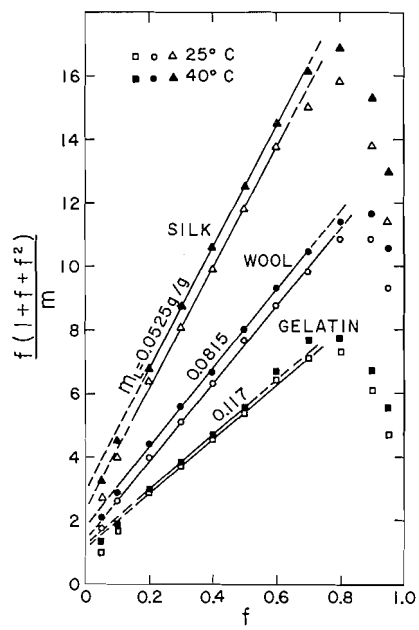

FIG. 1. Correlation of Bull's data on the adsorption of water vapor by silk, wool, and gelatin.

$K' = 5$ and $n = 2$. The data for 40° C show rather peculiar behavior at low relative vapor pressures. It may be noted that the B.E.T. equation does not fit the data on nylon at all.

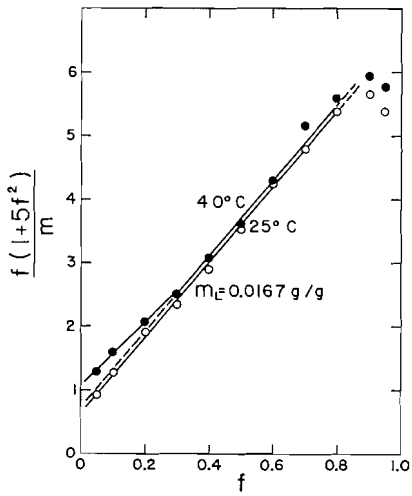

FIG. 2. Correlation of Bull's data on the adsorption of water vapor by nylon.

THE ANALYSIS OF THE MOISTURE DESORPTION ISOTHERM OF WHEAT

Becker and Sallans (1) determined the moisture desorption isotherm of wheat at temperatures of 25° and 50° C. As already noted in the introduction, the B.E.T. equation for $n = \infty$ was found to fit the data at low relative vapor pressures but gave values of the B.E.T. monolayer moisture content, m_L, which decreased markedly with increasing temperature. This discrepancy with Cassie's interpretation of m_L can be explained, most obviously, by hypothesizing an actual decrease in the number of localized sites available for adsorption. However, although the adsorptive capacity might diminish with rising temperature, owing to the exposure of non-polar areas, it is difficult to conceive of an over-all reaction which would cause a diminution of the number of polar groups exposed for water adsorption. We shall therefore accept the alternative explanation that the B.E.T. equation gives erroneous values of the parameters K and S, and assume that some form of equation 11 is applicable.

Trial and error examination of the data showed that the Langmuir form of the equation gives an excellent fit at low relative vapor pressures, Fig. 3. The values of the Langmuir parameters were thus found to be $K = 12.14$ and $m_L = 0.1157$ g/g at 25° C, and $K = 5.17$ and $m_L = 0.1178$ g/g at 50° C. As required, m_L so evaluated is constant within experimental error.

The data were subsequently analyzed to find empirical expressions for $K'f^n$. For this purpose the isotherm equation was arranged in the form

$$\frac{N}{S}\frac{1+Kf}{Kf} - 1 = K'f^n \qquad [16]$$

where $N/S = m/m_L$. Values of K' were calculated for integer values of n, and were found to have a minimum which moved toward higher vapor pressures with increasing value of n and reached the immediate neighborhood of $f = 1$ at $n = 4$. The minimum near $f = 1$, in value $K' = 2.2$, was then used to calculate values of n for a constant

Can. J. Chem. Downloaded from www.nrcresearchpress.com by 78.46.186.204 on 09/04/12
For personal use only.

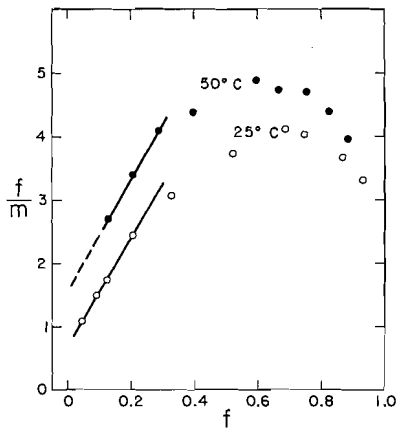

FIG. 3. Langmuir plot of moisture desorption equilibrium data on wheat.

K'. Figure 4 shows these values as a function of the relative vapor pressure. The relation is seen to be substantially independent of temperature, as it should be if the assumption of normal condensation of the multimolecularly adsorbed molecules has any truth. The calculations leading to Fig. 4 are summarized in Table I. It must be assumed that n becomes large at relative vapor pressures below 0.3 or, more likely, that K' becomes small, if the applicability of the Langmuir equation is to be retained.

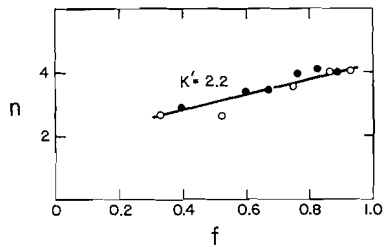

FIG. 4. Correlation of the exponent n with relative vapor pressure for $K' = 2.2$.

The rationale underlying the foregoing treatment of K' and n is as follows. The exponent n can be interpreted as being proportional to the number of normally condensed molecules on an average site. If so, it appears that n must increase with increasing relative vapor pressure and, for limited adsorption, approach constancy in the immediate neighborhood of $f = 1$. The parameter K' is in essence an equilibrium "constant", and if adsorption tends to a finite limit it is reasonable to assume that K' tends toward constancy at high relative vapor pressures. The analysis which has been given meets all of these conditions. K' is treated as a constant, and n increases with increasing relative vapor pressure and approaches constancy at $f = 1$. However, it may be seen from Table I that the assumption that K' and n are independent of temperature is fulfilled in any case, regardless of whether K' or n is treated as a constant, provided that reasonable values of K' or n are assumed.

The values found for the Langmuir constants K and S can be used directly to estimate some of the thermodynamic magnitudes involved in desorption. Equation 14 gives for K

$$K = 3.05 \times 10^{-4} \exp(6270/RT). \qquad [17]$$

Can. J. Chem. Downloaded from www.nrcresearchpress.com by 78.46.186.204 on 09/04/12
For personal use only.

TABLE I

ANALYSIS OF THE MOISTURE DESORPTION ISOTHERM OF WHEAT

				$\left(\frac{N}{S}\frac{1+Kf}{Kf}\right)-1 = K'f^n$		
				K'		n
f	m	$N/S = m/m_L$	$Kf/(1+Kf)$	$n = 3$	$n = 4$	$K' = 2.2$
			A: 25° C			
0.045	0.0421	0.364	0.353	—	—	—
0.090	0.0602	0.520	0.523	—	—	—
0.111	0.0646	0.559	0.574	—	—	—
0.203	0.0830	0.717	0.711	—	—	—
0.328	0.1068	0.924	0.799	4.41	13.40	2.64
0.520	0.1395	1.206	0.863	2.83	5.43	2.62
0.683	0.1660	1.433	0.893	1.91	2.79	3.38
0.747	0.1852	1.602	0.900	1.88	2.51	3.54
0.863	0.2351	2.03	0.913	1.89	2.19	4.00
0.930	0.2810	2.43	0.920	2.03	2.18	4.03
			B: 50° C			
0.127	0.0471	0.407	0.405	—	—	—
0.206	0.0609	0.526	0.525	—	—	—
0.286	0.0698	0.603	0.603	—	—	—
0.396	0.0907	0.785	0.690	2.44	6.15	2.89
0.596	0.1222	1.056	0.763	1.81	3.04	3.38
0.669	0.1411	1.220	0.782	1.88	2.81	3.40
0.757	0.1610	1.391	0.803	1.70	2.23	3.95
0.823	0.1878	1.623	0.815	1.78	2.17	4.09
0.884	0.2238	1.935	0.825	1.95	2.21	3.99

Hence the partial molal enthalpy of dilution of the low energy fraction of the molecules is (for desorption equilibrium) $\Delta\bar{H}_S = -6.27$ kcal/mole. This is a reasonable value for one hydrogen bond. Multiplication by the number of moles of low energy molecules adsorbed at saturation then gives an estimate of the net heat of dehydration. Equation 12 gives for the pertinent moisture content

$$m_1 = m_L\{K/(1+K)\}, \qquad [18]$$

whence $m_1 = 0.1069$ g/g at 25° C, and 0.0989 g/g at 50° C. The corresponding net heats of dehydration ($-m_1\Delta\bar{H}_S/18$) are respectively 37.2 cal and 34.5 cal per gram of moisture-free wheat. A value of 43 cal/g was previously estimated (1) for 25° C.

The values of K' in Table I indicate that adsorption tends toward a limit of about 3.2 molecules per occupied site, or toward a moisture content of about 3.2 m_1. This gives a value of 0.34 g/g for 25° C, which is in good agreement with the previous estimate (3) of 0.37 g/g.

The results of the analysis of the desorption isotherm may now be compared with previous data (4, 5) on moisture equilibria in the diffusion of moisture out of the wheat kernel. The diffusion data were correlated by application of non-stationary state, integral diffusion equations with constant diffusion coefficients. The author in his recent study has shown that the form of the equation for vacuum drying in the range of initial moistures 0.13–0.25 g/g is

$$\bar{M} = 1-(2/\sqrt{\pi})X+0.326M^*X^2 \qquad [19]$$

where

$$\bar{M} = (\bar{m}-m_{s0})/(m_0-m_{s0}),$$
$$M^* = (m_0-m_{s\infty})/(m_0-m_{s0}),$$
$$X^2 = Dt/r^2,$$

Can. J. Chem. Downloaded from www.nrcresearchpress.com by 78.46.186.204 on 09/04/12
For personal use only.

$\bar{m}$ is the average moisture content of a drying wheat kernel at time t; m_0 is the initial, uniform moisture content at time zero; r is the volume to surface ratio of the wheat kernel; and D is the diffusion coefficient. m_{s0} and $m_{s\infty}$ are the dynamic, equilibrium moistures which we wish to explain; m_{s0} is the apparent value at time zero of the moisture content, m_s, at the surface of a drying wheat kernel, and $m_{s\infty}$ is the limiting value to which m_s tends with time.

The values found for m_{s0} and $m_{s\infty}$ in vacuum drying (4) are given in Table II, and are compared with the values found in this paper for the Langmuir parameters m_L and m_1. The similarities are clear: the apparent surface moisture content (m_{s0}) at time zero

TABLE II

COMPARISON OF THE ISOTHERM PARAMETERS m_L AND m_1 WITH THE DYNAMIC EQUILIBRIUM MOISTURES IN VACUUM DRYING m_{s0} AND $m_{s\infty}$

	m_L	$m_{s\infty}$	m_1	m_{s0}
25° C	0.1157	0.1159	0.1044	0.1069
50° C	0.1178	0.1153	0.0989	0.0989

appears to be identical with the moisture content (m_1) which corresponds to the number (X_1) of sites occupied at saturation, and the value ($m_{s\infty}$) toward which the surface moisture tends with time is evidently identical with the moisture content (m_L) which corresponds to the number (S) of localized sites. It can therefore be assumed that the apparent surface moisture content for the vacuum drying of wheat in the neighborhood of time zero is given by the relation (after equation 12)

$$m_s = 0.1157K/(1+K), \qquad [20]$$

where 0.1157 g/g is the average value found by the author (2) for $m_{s\infty}$. This interpretation also provides a qualitative explanation of the observed behavior (4, 5) of the diffusion coefficient. Clearly, molecules of the low energy fraction must be much less mobile than the normally condensed ones, and hence the diffusion coefficient should decrease markedly with decreasing concentration in the neighborhood of m_1 and m_L.

REFERENCES

1. BECKER, H. A. and SALLANS, H. R. Cereal Chem. **33**, 79 (1956).
2. BRUNAUER, S., EMMETT, P. H., and TELLER, E. J. Am. Chem. Soc. **60**, 309 (1938).
3. SMITH, S. E. J. Am. Chem. Soc. **69**, 646 (1947).
4. BECKER, H. A. A general mathematical derivation of the integral diffusion equations for non-stationary state diffusion with a constant diffusion coefficient, and its application to the vacuum drying of the wheat kernel. Forthcoming publication.
5. BECKER, H. A. and SALLANS, H. R. Cereal Chem. **32**, 212 (1955).
6. CASSIE, A. B. D. Trans. Faraday Soc. **43**, 615 (1947).
7. ENDERBY, J. A. Trans. Faraday Soc. **51**, 106 (1955).
8. ADAM, N. K. The physics and chemistry of surfaces. 3rd ed. Oxford University Press, London. 1941.
9. BULL, H. J. Am. Chem. Soc. **66**, 1499 (1944).

Can. J. Chem. Downloaded from www.nrcresearchpress.com by 78.46.186.204 on 09/04/12
For personal use only.

Can. J. Chem. Downloaded from www.nrcresearchpress.com by 78.46.186.204 on 09/04/12
For personal use only.

NEUTRON CAPTURE CROSS SECTION OF I^{129} AND I^{130} [1]

J. C. Roy and D. Wuschke

ABSTRACT

The capture cross section of I^{129} for 2200 m/sec neutrons and its resonance capture integral were determined by counting the beta rays emitted by the 12.5-hour I^{130} formed by an (n, γ) reaction on I^{129}. The σ_{2200} was found to be 26.7 ± 2.0 barns and the resonance capture integral 36 ± 4.0 barns. The effective capture cross section of I^{130} for reactor neutrons was measured to be 18.0 ± 3.0 barns by counting the beta rays emitted by the 8.1-day I^{131} produced by successive neutron capture in I^{129}. The neutron fluxes were measured with cobalt monitors; the thermal cross section and the resonance capture integral of Co^{59} were taken to be 36.5 and 48.6 barns.

INTRODUCTION

This paper describes measurements of the effective capture cross section of the 12.5-hour I^{130} for reactor neutrons. An activation method has been used which depends on successive neutron capture in the long-lived radionuclide I^{129} ($t_{\frac{1}{2}} = 1.7 \times 10^7$ years (1)). Obviously, the cross section for I^{130} obtained by this technique depends on that of I^{129} for which two different values have been reported in the literature. A value of 11 ± 4 barns, an unpublished measurement credited to Oak Ridge, is found in the compilation of neutron cross sections of Hughes and Harvey (2). Purkayastha and Martin (3), as an incidental experiment to their work on the yields of I^{129} in natural and neutron induced fission of uranium, found a value of 35 barns. They do not give the errors involved in the measurement. Since it is difficult to assess which of the two values is better and furthermore considering the large discrepancy between them, it seemed necessary to re-evaluate the thermal cross section of I^{129}. The resonance capture integral of I^{129} was also measured.

Both determinations were done by counting directly the beta rays emitted by the 12.5-hour I^{130} and 8.1-day I^{131} formed respectively by single and double neutron capture in I^{129} according to the following nuclear reactions:

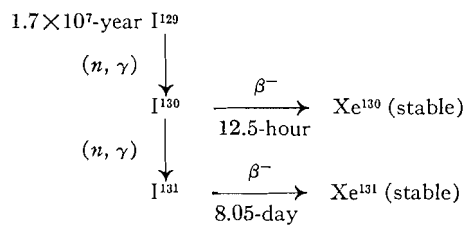

EXPERIMENTAL

(a) *Irradiation*

The I^{129} used for the irradiations was obtained from the Oak Ridge National Laboratory. A mass spectrometer analysis supplied with the material gave the following composition: 51.3% I^{129} and 48.7% I^{127}.

The samples were prepared for irradiations by precipitating the iodide as palladous iodide by the addition of 0.05 molar solution of palladous chloride to a NaI solution (3). The precipitate was washed, dried at 60° C, and transferred to one arm of a U-tube in a vacuum line. The tube was evacuated and closed off from the rest of the line. The

[1]*Manuscript received June 13, 1958.*
Contribution from Research Chemistry Branch, Atomic Energy of Canada Limited, Chalk River, Ontario. Issued as A.E.C.L. No. 679.

palladous iodide was heated to liberate the iodine and distill it into the other arm of the tube, which was made of quartz. The tube was sealed off at a constriction to form a quartz ampoule containing the elementary iodine. It was irradiated in an aluminum capsule in the NRX reactor at Chalk River.

For the measurement of the resonance capture integral the quartz ampoules were wrapped with 0.028 in. thick cadmium sheet.

To obtain the neutron flux, a piece of cobalt wire was irradiated in each capsule; the details are described in section (*e*).

(*b*) *Chemical Purification*

After the irradiation, the quartz tube was crushed under a solution of sodium bisulphite. The solution was boiled to desorb the iodine on the quartz walls. No iodine carrier was added. The iodide was oxidized with nitrous acid (4) and the iodine extracted with carbon tetrachloride. The cycle of oxidation, reduction, and extraction was repeated several times. The final iodine extract in carbon tetrachloride was washed thoroughly with water and dried with magnesium sulphate. The concentration of iodine was then measured with a Beckman spectrophotometer. The details of the method used are given in section (*d*).

The iodine was then reduced and extracted from CCl_4 with water and the resulting solution made up to a known volume. Separate experiments showed that there is a loss of $7\pm3\%$ in the reduction and extraction step following the yield determination, and the yield was corrected accordingly. The preparation of the sample for counting depended on which radioactive species was to be counted.

(*c*) *Counting Techniques*

The activities of I^{130} and I^{131} were measured with a methane-flow proportional counter having a window thickness of 2.74 mg/cm^2.

Iodine-130 was measured by taking an aliquot from the standard solution and precipitating PdI_2 on an aluminum tray. The efficiency of the detector for I^{130} was determined in one experiment by measuring an aliquot from a standard solution (5) with a 4π counter. The estimated accuracy is $\pm3\%$.

In order to measure the I^{131}, the total iodide in the standard solution was precipitated as PdI_2, filtered on a "Millipore" paper, dried, and counted as such. The yield in the precipitation had to be determined because a fraction ($\sim20\%$) of the I^{131} activity was not carried with PdI_2. It was done by the addition of iodide carrier to the filtrate, reprecipitation, filtration, and counting. This procedure was repeated until no activity was left in the filtrate.

The efficiency of the detector for I^{131} was determined in an auxiliary experiment. A source of I^{131} was obtained from the Isotope Product Division, A.E.C.L.; aliquots were measured simultaneously in the 4π and proportional counter. The accuracy of the counting of I^{131} was estimated to be $\pm5\%$.

(*d*) *Yield Determination of* I^{129}

The amounts of iodine were of the order of 0.1 mg for the measurements of the I^{129} cross section and 0.5 mg for the measurements of I^{130} cross section. They were determined at the end of the chemical purification from the measurement of the optical density of iodine in carbon tetrachloride at 516 mμ with a Beckman spectrophotometer. The instrument was calibrated with carbon tetrachloride solutions of iodine standardized with arsenious acid. The solvent used for every optical measurement was passed through a silica gel column to remove traces of unsaturated compounds which could have reacted

Can. J. Chem. Downloaded from www.nrcresearchpress.com by 78.46.186.204 on 09/04/12
For personal use only.

with iodine. No change in concentration of iodine was observed in the solutions prepared in this way over a period of several weeks. The errors were considered to be ±2% and ±5% for amounts of 0.5 and 0.1 mg of iodine respectively.

(*e*) *Neutron Flux Monitoring*

The neutron fluxes were determined by the cobalt monitoring technique developed by Jervis (6). Weighed pieces of pure cobalt wire 0.005 in. in diameter and 0.4 in. in length, wrapped in aluminum foil, were placed in each capsule for all irradiations except for those done under cadmium. In these the wire was 4 in. in length and it was coiled around the quartz ampoule. The observed activity was corrected for self-shielding in the wire. The self-shielding correction for 0.005 in. Co wire is 2.1% and 5.5% for thermal and epicadmium neutrons, respectively (7). The accuracy of the flux determination is estimated to be ±2% (6).

A value of 36.5 barns (2) was used for the thermal neutron capture cross section of Co^{59} and 48.6 barns (8) for the resonance integral. The half-life of Co^{60} was taken to be 5.28 years (2).

The thermal neutron flux $(nv_0)_{th}$ was determined from the difference in activity of the monitors irradiated with and without cadmium covers. The resonance neutron flux $(nv)_{res}$ was obtained from the activity of the monitor irradiated with cadmium covers. Thus the fluxes are defined in the way described by Cabell *et al.* (9, 10).

(*f*) *Errors*

The errors involved in the operations and measurements just described are summarized in Table I. The total error resulting from the combination of each individual error is expressed as the square root of the sum of the squares of each error.

TABLE I

SUMMARY OF THE ERRORS INVOLVED IN THE MEASUREMENTS

Radionuclide	Loss in chemical purification (%)	Counting (%)	Yield determination (%)	Neutron flux (%)	Total (%)
I^{130}	±3	±3	±5	±2	±7
I^{131}	±3	±5	±2	±2	±6.5

RESULTS

(*a*) *Cross Section of* I^{129}

The counting of I^{130} was started about 30 hours after the end of the irradiation. This delay was necessary to allow for the decay of the 25-minute I^{128}, produced by the (n, γ) reaction in I^{127}. The average of six determinations of the half-life, each followed for 10 half-lives, was 12.5±0.1 hours, in agreement with the value of 12.6 hours given in the Table of Isotopes of Hollander *et al.* (11).

The effective cross section of I^{129}, σ_{eff}, for reactor neutrons is calculated from the equation

$$[1] \qquad A = N(nv_0)_{th}\sigma_{eff}(1-e^{-\lambda t}),$$

where A is the activity of I^{130} at the end of the irradiation of an unshielded sample,
N is the number of I^{129} atoms present during the irradiation,
$(nv_0)_{th}$ is the thermal neutron flux as defined in section (*e*) of Experimental,
λ is the disintegration constant of I^{130}, and
t is the time of irradiation.

Can. J. Chem. Downloaded from www.nrcresearchpress.com by 78.46.186.204 on 09/04/12
For personal use only.

The details of the four irradiations without cadmium shielding are given in Table II.

An effective cross section under cadmium, $\sigma_{\text{eff, Cd}}$, is calculated from eq. [1] in a manner similar to σ_{eff}; A is now the I^{130} activity found under cadmium. The results of irradiations under cadmium are given in Table III.

TABLE II

EFFECTIVE CAPTURE CROSS SECTION OF I^{129} FOR REACTOR NEUTRONS

Experiment	I^{129} atoms	Time of irradiation, hours	$(nv_0)_{th}$	Activity, dis/sec	$\sigma_{\text{eff.}}$ barns
1	1.53×10^{15}	26.0	1.06×10^{13}	3.49×10^{5}	28.3
2	1.08×10^{15}	32.0	0.79×10^{13}	1.93×10^{5}	27.1
3	0.42×10^{15}	42.2	4.64×10^{13}	4.74×10^{5}	26.9
4	0.79×10^{15}	42.2	6.10×10^{13}	12.4×10^{5}	28.5
Mean	—	—	—	—	27.7

TABLE III

EFFECTIVE CAPTURE CROSS SECTION UNDER CADMIUM FOR I^{129}

Experiment	I^{129} atoms	Time of irradiation, hours	$(nv_0)_{th}$	Activity, dis/sec	$\sigma_{\text{eff, Cd.}}$ barns
5	2.72×10^{15}	7.33	1.56×10^{13}	1.23×10^{4}	0.9
6	0.96×10^{15}	13.66	1.48×10^{13}	0.81×10^{4}	1.1
Mean	—	—	—	—	1.0

The σ_{2200} m/sec neutron cross section for I^{129} is obtained by the subtraction of the effective cross section under cadmium from the effective cross section for reactor neutrons and is found to be 26.7 ± 2.0 barns.

The resonance capture integral of I^{129} is related to its cadmium ratio, R_{Cd}, by the following relationship,

$$[2] \qquad \int_{0.5}^{\infty}\sigma_c\frac{dE}{E}=\frac{(nv_0)_{\text{th}}}{(nv)_{\text{res}}}\cdot\frac{\sigma_{2200}}{(R_{\text{Cd}}-1)}$$

where $(nv_0)_{\text{th}}/(nv)_{\text{res}}$ is the ratio of the thermal flux to the resonance flux per unit interval of ln E, calculated to be 36 ± 4 from the activities of cobalt monitors inside and outside cadmium. From a Cd ratio of 28 ± 3 for I^{129}, the resonance capture integral

$$\int_{0.5}^{\infty}\sigma_c\frac{dE}{E}$$

is found to be 36 ± 4. There is therefore very little resonance capture in I^{129}.

(*b*) *Cross Section of* I^{130}

The counting of I^{131} started about 15 days after the end of the irradiation in order to allow the 12.5-hour I^{130} to decay. Iodine-131 was identified by its half-life and gamma-ray spectrum. The average of two determinations of the decay period, each followed for five half-lives, was 8.1 ± 0.1 days after the subtraction of a long-lived residual activity of 1000 counts/minute. This background represents less than 1% of the initially observed I^{131} activity and most of it can be accounted for by the radiations of I^{129}. Values of 8.04 to 8.16 days are given for the half-life of I^{131} in Hollander *et al.* (11). A decay curve of one of the two samples is given in Fig. 1.

Some I^{126} (13.3 days) is produced by the reaction $I^{127}(n, 2n)I^{126}$ during the long

Can. J. Chem. Downloaded from www.nrcresearchpress.com by 78.46.186.204 on 09/04/12
For personal use only.

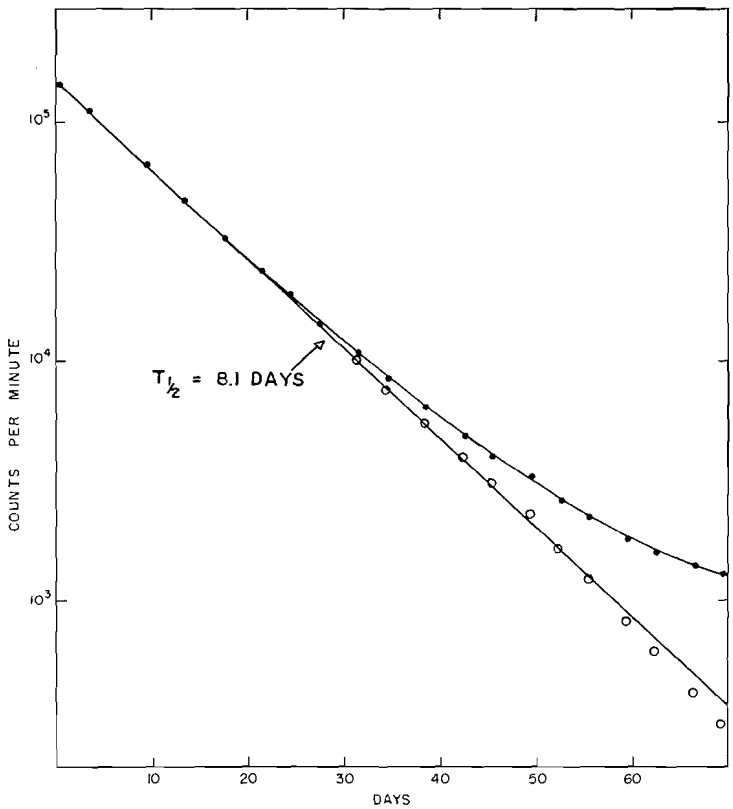

FIG. 1. Decay curve of I^{131}. A residual activity of 1000 counts/minute attributed to the radiations of I^{129} has been subtracted from the observed activity.

irradiation required to measure the I^{130} cross section. It does not interfere with the determination of the yield of I^{131}; its contribution was of the order of 2% when the counting of the samples was begun. This was shown by irradiating a known amount of natural iodine in a separate ampoule with the I^{129}. The I^{126} formed was counted under conditions identical with those used for I^{131}.

Since there were four shutdowns, each one of several hours, while the target material

TABLE IV

DETAILS OF THE IRRADIATION FOR THE FORMATION OF I^{131}

Segments x	Duration of a segment t_x (hours)	State of the reactor	Length of time from the end of segment to the end of the whole irradiation t'_x (hours)
1	26.33	On	536.3
2	7.67	Off	
3	54.75	On	473.9
4	22.65	Off	
5	248.1	On	203.2
6	22.73	Off	
7	129.4	On	51.1
8	17.5	Off	
9	33.6	On	0

Can. J. Chem. Downloaded from www.nrcresearchpress.com by 78.46.186.204 on 09/04/12
For personal use only.

Can. J. Chem. Downloaded from www.nrcresearchpress.com by 78.46.186.204 on 09/04/12
For personal use only.

was in the reactor, the calculation of σ_{eff} for I^{130} from the observed I^{131} activity becomes involved. The effect of these shutdowns on the formation of I^{131} was taken into account by assuming that the whole irradiation consisted of nine segments, the details of which are given in Table IV. The five segments characterized by the operation of the reactor are considered as separate irradiations. Then the activity of I^{131}, B, at the end of the irradiation is the sum of the activities produced during each one of these segments, namely 1, 3, 5, 7, and 9. Each activity is multiplied by a factor $e^{-\lambda_B t'}$ to take into account the decay from the end of the segment to the end of the irradiation.

$$[3] \qquad B = B_9 + B_7 e^{-\lambda_B t'_7} + B_5 e^{-\lambda_B t'_5} + B_3 e^{-\lambda_B t'_3} + B_1 e^{-\lambda_B t'_1}.$$

The I^{131} activity, B_x, formed during each segment is

$$[4] \qquad B_x = \frac{N\sigma\sigma_A (nv_0)^2_{th} T_A}{0.693(T_A - T_B)} [T_A(1-e^{-\lambda_A t_x}) - T_B(1-e^{-\lambda_B t_x})] + P,$$

$$P = \frac{N_{A(x-1)} T_A \sigma_A (nv_0)_{th}}{(T_B - T_A)} (e^{-\lambda_A t_x} - e^{-\lambda_B t_x}).$$

The first term in eq. [4] represents the formation of I^{131} by successive neutron capture in I^{129}; the second term, P, represents the formation of I^{131} by neutron capture in I^{130} formed in the previous segments of the irradiation.

N is the number of I^{129} atoms present during the irradiation,

σ is the effective cross section of I^{129} for reactor neutrons, 27.7 barns,

σ_A is the effective cross section of I^{130} for reactor neutrons to be measured,

T_A is the half-life of I^{130}, taken to be 12.5 hours,

T_B is the half-life of I^{131}, taken to be 8.1 days,

λ_A and λ_B are the disintegration constants of I^{130} and I^{131} respectively,

t_x is the duration of a segment as given in Table IV,

t'_x is the time elapsed from the end of the final irradiation to the end of a segment, x,

N_{Ax} is the number of I^{130} atoms present at the end of the 2nd, 4th, 6th, and 8th segments and is equal to

$$[5] \qquad N_{Ax} = \left[\frac{N\sigma (nv_0)_{th}}{\lambda_A} (1 - e^{-\lambda_A t_{(x-1)}}) + N_{A(x-2)} e^{-\lambda_A t_{(x-1)}} \right] e^{-\lambda_A t_x}.$$

Initially $N_A = 0$.

The experimental details and the results are given in Table V.

TABLE V

EFFECTIVE CAPTURE CROSS SECTION OF I^{130} FOR REACTOR NEUTRONS

Experiment No.	I^{129} atoms	$(nv_0)_{th}$	Activity, dis/sec	σ_{eff} (I^{130}), barns
1	7.5×10^{17}	4.76×10^{13}	3.51×10^{4}	17.1
2	8.1×10^{17}	6.30×10^{13}	7.45×10^{4}	19.2
Mean	—	—	—	18.1

The value 18.0 ± 3.0 barns is for a typical reactor neutron spectrum in a vacant fuel rod position near the center of the NRX reactor. In the two positions used in these experiments, the epicadmium neutrons are 3.5% and 4% of the thermal flux. The assigned error includes the uncertainty in the value of the cross section of I^{129}.

ACKNOWLEDGMENTS

The authors wish to thank Dr. T. A. Eastwood for helpful discussions, Mrs. J. S. Merritt and Dr. P. J. Campion for doing the 4π β-counting.

REFERENCES

1. KATCOFF, S., SCHAEFFER, O. A., and HASTINGS, J. M. Phys. Rev. **82**, 688 (1951).
2. HUGHES, D. J. and HARVEY, J. A. Brookhaven Natl. Lab. Rept. BNL-325 (1955).
3. PURKAYASTHA, B. C. and MARTIN, G. R. Can. J. Chem. **34**, 293 (1956).
4. TURK, E. H. Argonne Natl. Lab. Rept. ANL-5271 (1954).
5. PATE, B. D. and YAFFE, L. Can. J. Chem. **33**, 15, 610, 929, 1656 (1955).
6. JERVIS, R. E. Atomic Energy of Canada Limited, Rept. CRDC-730 (1957).
7. BUTLER, J. P., LOUNSBURY, M., and MERRITT, J. S. Can. J. Phys. **35**, 147 (1957).
8. MACKLIN, R. L. and POMERANCE, H. S. International conference on the peaceful uses of atomic energy. Vol. 5. United Nations, New York. 1956. p. 96.
9. CABELL, M. J., EASTWOOD, T. A., and CAMPION, P. J. Nuclear energy. (In press).
10. CABELL, M. J., EASTWOOD, T. A., and CAMPION, P. J. Atomic Energy of Canada Limited, Rept. CRC-738 (1958).
11. HOLLANDER, J. M., PERLMAN, I., and SEABORG, G. T. Revs. Modern Phys. **25**, 469 (1953).

Can. J. Chem. Downloaded from www.nrcresearchpress.com by 78.46.186.204 on 09/04/12
For personal use only.

Can. J. Chem. Downloaded from www.nrcresearchpress.com by 78.46.186.204 on 09/04/12
For personal use only.

STEREOCHEMISTRY OF REDUCTION OF KETONES BY COMPLEX METAL HYDRIDES[1]

OWEN H. WHEELER[2] AND JOSÉ L. MATEOS[3]

ABSTRACT

The stereochemistry of the reduction of a number of cyclic ketones with complex metal hydrides has been determined. In the absence of any large steric effect in the ketones, the reduction is essentially stereospecific, giving the more stable alcohol.

INTRODUCTION

The reduction of a carbonyl group by a simple metal hydride must proceed by four successive stages (1), utilizing each of the four available hydrogen atoms. Each stage probably involves two reaction steps, the initial reversible formation of a complex of the hydride ion and the carbon atom of the carbonyl group (I) and the irreversible transfer of hydrogen to this carbon atom (II).

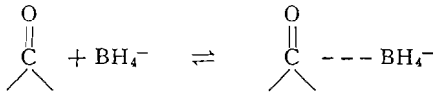

(I)

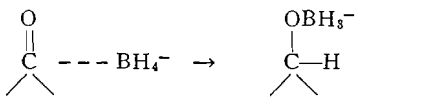

(II)

In the case of a cyclic ketone there are two possible directions of attack, pseudo equatorial and pseudo axial, giving the axial or equatorial alcohol. Dauben and co-workers (2, 3) have discussed the stereochemistry of reduction of cyclic ketones in terms of "steric approach control" to the attack of the hydride upon the ketone (stage I), and "product development control", determined by the relative thermodynamic stabilities of the two alcohols formed (and governing the relative stabilities of the two possible transition states in stage II). For a complex metal hydride substituted with bulky substituents, approach to the carbon atom of the carbonyl group, in stage I, will take place from the less hindered side. In stage II the large steric size of the reagent will favor the formation of the transition state leading to the more stable of the two products, since a bulky group is more stable in this the equatorial position. Reduction of an unhindered ketone should thus give the equatorial alcohol, whereas a sterically hindered ketone could give either isomer depending on the direction of steric hindrance.

A number of complex metal hydrides have recently been prepared and the simplest is sodium trimethoxyborohydride. However, this undergoes disproportionation in solution (4) and the reduction of 2-methylcyclohexanone with this reagent gives the same ratio of isomers as does sodium borohydride (2). Recently H. C. Brown and McFarlin (5) have developed a simple preparation of lithium tri-*tert*-butoxyaluminum hydride and we have investigated the stereochemistry of the reduction of a number of cyclic ketones (Table I) with this reagent. In all cases this reagent is considerably more stereospecific than either lithium aluminum hydride or sodium borohydride.

[1]*Manuscript received March 10, 1958.*
Contribution from the Instituto de Quimica, Universidad Nacional Autonoma de Mexico, Mexico 20, D.F. Part VI of Reactivity Studies on Natural Products. Part V, Can. J. Chem. **36**, *1049 (1958). A preliminary communication of part of this work appeared in Chem. & Ind. 395 (1957).*
[2]*Present address: Department of Chemistry, Dalhousie University, Halifax, N.S.*
[3]*Present address: Department of Chemistry, University of California, at Los Angeles.*

TABLE I
PERCENTAGE OF EQUATORIAL ISOMER*

	$LiAlH_4$	$NaBH_4$	$LiAlH(t\text{-}BuO)_3$‡	$LiAlH_4/AlCl_3$‡
Cholestan-3-one	88†	85‖	98.5	100
Coprostan-3-one	93†	87‖	96.5	94
Cholest-4-en-3-one	74†	95‖	100	—**
Cholest-5-en-3-one	87†	83‖	100	—††
Cholestan-7-one	—	58‖	86	—
Δ^5-Androsten-17-one-3β-acetate	—	—	100	—
Δ^8-Lanostenone	100‡	—	100	—
Camphor	90§	—	25	—
4-Methylcyclohexanone	81§	85¶	84	—

*Percentages normalized to 100%. †Ref. 16. ‡Present work. §Ref. 17. ‖Ref. 6. ¶Ref. 2. **Cholest-4-ene-(80%) + cholestane. ††Cholest-4-en-3-one (83%) + alcohols.

DISCUSSION

The keto group of cholestan-3-one (*IIIa*) is unhindered to attack from either an axial or equatorial direction (3, 6). In the transition state, however, the bulky alkoxide group could not occupy a pseudo-axial position, since it would be sterically hindered by the axial hydrogen atoms on carbon atoms 1 and 5. Moreover in such a position it is also sterically hindered to solvation (7), which would help to stabilize the ion. Thus the preferred transition state will be that with the alkoxy group in a pseudo-equatorial position, and the product observed is essentially that (β-cholestanol) which arises from this. Similarly coprostan-3-one (IV) is not subject to steric hindrance from either direction (6) and the equatorial (α) isomer is largely formed. A double bond at the union of rings A and B as in Δ^4- and Δ^5-cholesten-3-one will lead to a general flattening of the rings. The steric repulsion to a 3-α group will be less, since there is now no α-hydrogen at carbon-5 and the flattening of the rings moves the 3-position away from the 1-α hydrogen atom. However, electronic interaction (6) between the double bond and the pseudo-equatorial alkoxy group will greatly stabilize the transition state for formation of the equatorial alcohol, and this is formed exclusively in both cases.

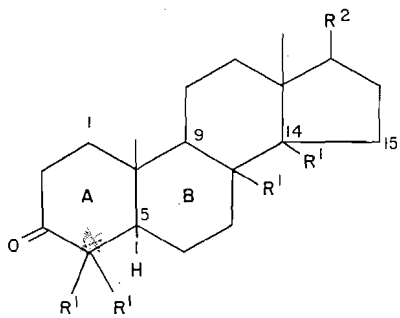

III a R^1 = H
R^2 = Isohexyl

b R^1 = Me
R^2 = Isohexyl

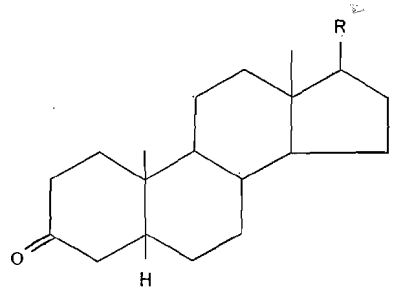

IV R = Isohexyl

Can. J. Chem. Downloaded from www.nrcresearchpress.com by 78.46.186.204 on 09/04/12
For personal use only.

The attack on the ketone group of cholestan-7-one from an axial direction will be hindered by the axial hydrogen atoms at C-5, C-9, and C-14. However, approach to the keto group from a pseudo-equatorial direction is highly hindered by the axial methyl groups at C-10 and C-13 and by the eclipsing effect of the 15-α hydrogen atom (6), and cholestan-7α-ol is only formed in 6% yield. This same eclipsing effect will tend to expel the bulky alkoxy transition complex from the 7-β position, and 57% of cholestane is formed (cf. 6).

Approach to the 17-keto steroid group from the topside of the molecule is hindered by the axial methyl group on C-18. However, approach from the underside is free and the resulting pseudo-equatorial transition complex will not be hindered by the methyl group on C-18, since the *trans*-fusion of rings C and D bends the 17-position down away from this group. Thus, Δ^5-androsten-17-one-3β-acetate gives exclusively Δ^5-androsten-3β,17β-diol.

In the case of Δ^8-lanosten-3-one (III*b*) approach to the ketone group from the upper pseudo-equatorial direction is also hindered by the axial methyl group on C-4. However, again approach from the underside is unhindered and the pseudo-equatorial transition complex (stage II) is not very hindered by either methyl group. Accordingly the β-alcohol is the sole product.

The camphor molecule (V) presents an interesting case, since one of the *gem*-dimethyl groups on the bridgehead is placed nearly above the ketone group (8). Approach from the exo (equatorial) direction is hindered and, although there is little hindrance to approach from the *endo* (axial) direction, the resulting pseudo-exo transition complex will be highly hindered. The net result of these opposing factors is that only 25% of the exo product (isoborneol) is formed.

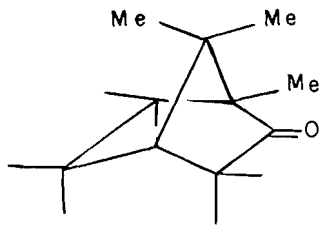

V

In the transition state of reduction of 4-methylcyclohexanone, the methyl group is free to take up either an axial or equatorial position (9), with the large alkoxy group remaining in the preferred equatorial position. Consequently lithium tri-*tert*-butoxy-aluminum hydride gives nearly the same isomer distribution as lithium aluminum hydride and sodium borohydride.

The complex of lithium aluminum hydride and excess aluminum chloride was first used for reduction by B. R. Brown (10). Aluminum hydride is formed as an intermediate (11), but the active reducing species may be AlH_2Cl (12). In the cases of the two saturated ketones, cholestan-3-one and coprostan-3-one, reduction was essentially stereospecific giving predominately the β-alcohols. Cholest-4-en-3-one, however, gave no alcohol. The product, previously reported as Δ^4-cholestene (13), was shown to be a mixture of cholestene with about 10% cholestane. Hydrogenolysis has been observed in the reduction of other compounds by this reagent (14, 15). Cholest-5-en-3-one gave a mixture which contained

Can. J. Chem. Downloaded from www.nrcresearchpress.com by 78.46.186.204 on 09/04/12
For personal use only.

cholest-4-en-3-one as well as alcohols. Because of these unfavorable observations and the uncertainty of the nature of the reducing reagent, no further work was carried out with this complex.

EXPERIMENTAL

Tetrahydrofuran and *t*-butanol were dried by refluxing with and distilling from lithium aluminum hydride and sodium, respectively. Lithium aluminum hydride and aluminum chloride were commercial samples which were finely ground. The ketones used were all analytically pure samples.

Reductions with lithium tri-tert-butoxy aluminum hydride.—In a typical experiment *t*-butanol (2 ml) was added slowly to a solution of lithium aluminum hydride (400 mg) in tetrahydrofuran (30 ml) at 0° (5). Cholestanone (1.0 g) in tetrahydrofuran (30 ml) was then added and the mixture allowed to stand at 0° for ½ hour and at room temperature for 1 hour. The mixture was then poured into excess dilute hydrochloric acid and the product extracted in the usual way. In this case the crude product was chromatographed on alumina and eluted with hexane–benzene giving α-cholestanol (14 mg), m.p. 182°–185°, and β-cholestanol (937 mg), m.p. 143°–146°. Both alcohols gave no depression on mixed melting-point determinations with authentic samples.

Coprostanone.—The product from coprostanone (200 mg) gave a precipitate with digitonin (50 mg) from which β-coprostanol (7 mg) was liberated with pyridine. α-Coprostanol (185 mg), m.p. 115°, was recovered by evaporation of the mother liquors (6).

Cholest-4-en-3-one.—Cholest-4-en-3-one (1.0 g) gave a crude product (1.0 g), m.p. 121°, which on chromatography using hexane–benzene as eluent (50 fractions) gave only cholest-4-en-3β-ol, m.p. 127°–131°, recrystallized from ether–methanol to m.p. 132°, $[\alpha]_D^{CHCl_3}$ +44°.

Cholest-5-en-3-one.—Cholest-5-en-3-one (500 mg) gave cholesterol, m.p. and mixed m.p. 148°, $[\alpha]_D^{CHCl_3}$ −42° (lit. $[\alpha]_D$ −39°, m.p. 149° (18)).

Cholestan-7-one.—Cholestan-7-one (500 mg) gave a product separated by chromatography into a fraction (243 mg) eluted with hexane, m.p. 65°–70°, recrystallized from hexane to m.p. 80°, $[\alpha]_D$ +30°. The infrared absorption showed no carbonyl or hydroxyl groups or double bond. Further elution with hexane–benzene gave 7α-cholestanol (27 mg), m.p. 92°–98° (lit. m.p. 94°–97° (19)), and 7β-cholestanol (168 mg), m.p. 103°–109° (lit. m.p. 108°–112° (19)).

Δ^5-*Androsten-17-one-3β-acetate.*—Reduction in like manner of Δ^5-androsten-17-one-3β-acetate gave a product, m.p. 183°–184°, $[\alpha]_D$ −54°. Reported for Δ^5-3β,17β-androstendiol, m.p. 182°–183°, $[\alpha]_D$ −55° (20).

Δ^8-*Lanosten-3-one.*—Δ^8-Lanosten-3-one (500 mg) gave a product, m.p. 142°–146°, recrystallized to m.p. 146°–148° and undepressed on admixture with lanostenol.

Camphor.—Two grams of this gave a product, m.p. 85°–110°, which could not be separated by chromatography on alumina (cf. 22). The mixture (500 mg) in pyridine (2 ml) was treated with *o*-nitrobenzoyl chloride and allowed to stand overnight. The pyridine was removed in vacuum and the isoborneol (106 mg), m.p. 210° from petroleum ether, separated by steam distillation (23). The residual borneol *o*-nitrobenzoate (618 mg) corresponded to borneol (322 mg).

4-Methylcyclohexanone.—Ten grams of 4-methylcyclohexanone gave a product n_D^{20} 1.4560, d_4^{30} 0.9061, which showed a small infrared ketone peak. After washing with sodium bisulphite solution the values were n_D^{20} 1.4569 and d_4^{30} 0.9063, and the compound showed no infrared carbonyl absorption. *Cis*- and *trans*-4-methylcyclohexanol have

Can. J. Chem. Downloaded from www.nrcresearchpress.com by 78.46.186.204 on 09/04/12
For personal use only.

respectively n_D^{20} 1.4614, 1.4561, and d_4^{30} 0.9173 and 0.9040 (24). The isolated product therefore contains 15% (from n_D^{20}) or 17% (from d_4^{30}) of the *cis*-isomer.

Reductions with lithium aluminum hydride – aluminum chloride.—In a typical experiment aluminum chloride (600 mg) was added to lithium aluminum hydride (135 mg) dissolved in ether (50 ml).

Cholestanone.—One gram of this ketone in ether (20 ml) was then added and the mixture allowed to stand at room temperature for at least four hours. The product (m.p. 141°–143°) was isolated by pouring the mixture into dilute hydrochloric acid. Recrystallization from ether–methanol gave β-cholestanol, m.p. 141°–142°, undepressed on admixture with an authentic sample.

Coprostanone.—Coprostanone (200 mg) gave a product from which β-coprostanol (12 mg) was isolated by digitonin separation. α-Coprostanol (180 mg) was isolated from the mother liquors, as before.

Cholest-4-en-3-one.—This gave a product, readily eluted from alumina with hexane, m.p. 65°, $[\alpha]_D^{CHCl_3}$ +56°. This rotation corresponds to Δ^4-cholestene ($[\alpha]_D$ +65°) 78% and cholestane ($[\alpha]_D$ +24°) 22%. Bromine titration showed the presence of about 85% olefin.

Cholest-5-en-3-one.—Five hundred milligrams gave a product (450 mg), which had λ_{max} 240 mμ, ε 15,700 corresponding to cholest-4-en-3-one 87%. Infrared spectra showed the presence of alcohols. No attempt was made to separate the mixture.

ACKNOWLEDGMENTS

The authors are grateful to Professor D. H. R. Barton for a gift of lanosterol and to the Rockefeller Foundation, New York, for financial assistance.

REFERENCES

1. Brown, H. C., Wheeler, O. H., and Ichikawa, K. Tetrahedron, **1**, 214 (1957).
2. Dauben, W. G., Fonken, G. J., and Noyce, D. S. J. Am. Chem. Soc. **78**, 2579 (1956).
3. Dauben, W. G., Blanz, E. J., Jiu, J., and Micheli, R. A. J. Am. Chem. Soc. **78**, 3752 (1956).
4. Brown, H. C., Mead, E. J., and Shoaf, C. J. J. Am. Chem. Soc. **78**, 3616 (1956).
5. Brown, H. C. and McFarlin, R. F. J. Am. Chem. Soc. **78**, 252 (1956).
6. Wheeler, O. H. and Mateos, J. L. Can. J. Chem. **36**, 1049 (1958).
7. Bird, C. W. and Cookson, R. C. Chem. & Ind. 1479 (1955).
8. Wheeler, O. H., Cetina, R., and Zabicky, J. Z. J. Org. Chem. **22**, 1153 (1957).
9. Winstein, S. and Holness, N. J. J. Am. Chem. Soc. **77**, 5562 (1955).
10. Brown, B. R. J. Chem. Soc. 2756 (1952).
11. Finholt, A. E., Bond, A. C., and Schlesinger, H. I. J. Am. Chem. Soc. **69**, 1199 (1947).
12. Wiberg, E. and Schmidt, M. Z. Naturforsch. **6b**, 460 (1951).
13. Broome, J. and Brown, B. R. Chem. & Ind. 1307 (1956).
14. Birch, A. J. and Slaytor, M. Chem. & Ind. 1524 (1956).
15. Brown, B. R. and White, A. M. S. J. Chem. Soc. 3755 (1957).
16. Dauben, W. G., Micheli, R. A., and Eastham, J. F. J. Am. Chem. Soc. **74**, 3852 (1952).
17. Noyce, D. S. and Denney, D. B. J. Am. Chem. Soc. **72**, 5743 (1950).
18. Fieser, L. F. and Fieser, M. Natural products related to phenanthrene. Reinhold Publishing Corp., New York. 1949. p. 95.
19. Cremlyn, R. J. W. and Shoppee, C. W. J. Chem. Soc. 3515 (1954).
20. Ruzicka, L. and Kägi, H. Helv. Chim. Acta, **18**, 1481 (1935).
21. Ruzicka, L., Denss, R., and Jeger, O. Helv. Chim. Acta, **27**, 759 (1944).
22. Vavon, G. and Gastambide, B. Compt. rend. **226**, 1201 (1948).
23. Jackman, L. M., Macbeth, A. K., and Mills, J. A. J. Chem. Soc. 2641 (1949).
24. Jackman, L. M., Macbeth, A. K., and Mills, J. A. J. Chem. Soc. 1717 (1949).

Can. J. Chem. Downloaded from www.nrcresearchpress.com by 78.46.186.204 on 09/04/12
For personal use only.

Can. J. Chem. Downloaded from www.nrcresearchpress.com by 78.46.186.204 on 09/04/12
For personal use only.

SYNTHESES OF SUBSTITUTED GUANIDINES[1]

PAUL E. GAGNON, JEAN L. BOIVIN,[2] AND JOSEPH ZAUHAR[3]

ABSTRACT

Ethyl-, propyl-, and benzyl-guanidine nitrates were prepared from amine nitrates and calcium cyanamide or dicyandiamide. Carboxyalkylguanidines were made by condensing the corresponding amino acids with guanidine carbonate in aqueous medium. All the guanidine nitrates, except the benzyl derivative, were converted into the corresponding nitroguanidines by treatment with concentrated sulphuric acid. Esters and metal salts of 1-(α-carboxyalkyl)-2-nitroguanidines were also prepared.

INTRODUCTION

Guanidine nitrate is prepared by heating ammonium nitrate with calcium cyanamide in aqueous solution (1, 2) or in the presence of urea (3), or with dicyandiamide (4, 5). Carboxyalkylguanidines have been previously made from amino acids and cyanamide in aqueous solution (6, 7) and by the action of haloaliphatic acids on guanidine (8). A more recent method for the preparation of carboxyalkylguanidines involves the use of methylisothiourea in an ammoniacal medium (9, 10). Carboxymethylguanidine was synthesized by the direct condensation of guanidine carbonate and glycine in aqueous medium (11).

RESULTS

Alkylguanidines

The methods of preparation of guanidine nitrate were extended to the syntheses of substituted guanidine nitrates in view of their nitration into the corresponding 1-substituted 2-nitroguanidines. The reaction of aqueous solutions of amine nitrates with calcium cyanamide gave the corresponding guanidine nitrates in yields ranging from 35 to 41%, as recorded in Table I.

TABLE I

ALKYLGUANIDINE NITRATES AND 1-ALKYL-2-NITROGUANIDINES

	Alkyl substituent		
	Ethyl	Propyl	Benzyl
	Nitrates		
M.p. °C	108–109	93–94	164–165
Yield, %: 1	41	38	35
2	86	67	51
3	41	41	40
4	88	67	45
	Nitroguanidines		
M.p. °C	147–148	99–100	—
Yield, %	30	57	—

1. Calcium cyanamide and amine nitrates in aqueous solution.
2. Dry mixtures of calcium cyanamide and amine nitrates.
3. Dry mixtures of calcium cyanamide, amine nitrates, and urea.
4. Dicyandiamide and amine nitrates.

[1]*Manuscript received June 2, 1958.*
Contribution from the Department of Chemistry, Laval University, Quebec, Que., with financial assistance from the Defence Research Board of Canada in 1955–56. This paper constitutes part of a thesis submitted to the Graduate School, Laval University, in partial fulfillment of the requirements for the degree of Doctor of Science.
[2]*Defence Research Board, C.A.R.D.E., Valcartier, Que.*
[3]*Graduate Student, holder of National Research Council of Canada Studentships in 1956–58.*

$$3RNH_2.HNO_3 + CaCN_2 \longrightarrow RHNC(=NH)NH_2.HNO_3 + 2RNH_2 + Ca(NO_3)_2$$

R = C_2H_5, C_3H_7, and $C_6H_5CH_2$

By heating the reactants in the solid state, instead of in aqueous solution, an increased yield was observed, namely, 86% for ethylguanidine nitrate, 67% for propylguanidine nitrate, and 51% for benzylguanidine nitrate. By adding urea to the dry reagents to depress the melting point of the mixtures, yields of about 40% were obtained. This behavior was unexpected because Wright obtained increased yields of guanidine nitrate from cyanamide (3) by using urea.

Ethyl-, propyl-, and benzyl-guanidine nitrates were also successfully synthesized by heating the amine nitrates with dicyandiamide. The over-all reaction can be expressed by the equation:

$$NCNHC(=NH)NH_2 + 2RNH_2.HNO_3 \longrightarrow 2RHNC(=NH)NH_2.HNO_3.$$

The latter method of preparation of ethyl-, propyl-, and benzyl-guanidine nitrates from amine nitrates and dicyandiamide gave yields up to 88% in some cases. In the preparation of guanidine hydrochloride from dicyandiamide and ammonium chloride (5), a biguanide hydrochloride is formed and ammonolyzed. A similar mechanism applies to the preparation of substituted guanidine nitrates from amine nitrates and dicyandiamide in which a substituted biguanide nitrate is the intermediate.

Carboxyalkylguanidines

Carboxyethylguanidine and carboxypropylguanidine were prepared from the corresponding amino acids and guanidine carbonate.

$$2H_2NCHRCOOH + [H_2NC(=NH)NH_2]_2.2H_2CO_3 \longrightarrow 2H_2NC(=NH)NHRCOOH + 2NH_3 + CO_2 + H_2O.$$

Cyclization of carboxyalkylguanidines can also take place (7, 12) in aqueous medium to form anhydro compounds.

$$2C_6H_5CH_2CH(NH_2)COOH + [H_2NC(=NH)NH_2]_2.H_2CO_3 \longrightarrow 2C_6H_5CH_2CH\text{(ring)}C{=}O + CO_2 + 3H_2O + 2NH_3$$

(ring: HN, C(=NH), NH)

Carboxyalkylguanidines when treated with a slight excess of dilute nitric acid gave the corresponding carboxyalkylguanidine nitrates. The nitrates slowly decomposed on heating in aqueous solution at temperatures above 100° C. Anhydrocarboxyphenylethylguanidine nitrate was obtained in the same manner.

Substituted Nitroguanidines

Ethyl- and propyl-nitroguanidines were obtained by a method similar to the production of nitroguanidine from guanidine nitrate using sulphuric acid (13, 14) but benzylnitroguanidine could not be obtained by this method, which confirms the results of other investigators (15). The results are shown in Table I.

Nitroguanidines substituted with an acid function were obtained by treating the corresponding carboxyalkylguanidine nitrates with concentrated sulphuric acid. The results are shown in Table II. To obtain 1-(α-carboxypropyl)-2-nitroguanidine, which was soluble in dilute sulphuric acid, the sulphate ions were eliminated and the compound was isolated as the dihydrate of the barium salt.

Can. J. Chem. Downloaded from www.nrcresearchpress.com by 78.46.186.204 on 09/04/12
For personal use only.

$$HNO_3.H_2NC(=NH)NHRCOOH \longrightarrow H_2NC(=NNO_2)NHCHRCOOH + H_2O$$

1-(α-Carboxymethyl)-2-nitroguanidine was also identified by its lead salt; it was prepared by treating an aqueous solution of the nitroguanidine with lead oxide.

The esters of 1-(α-carboxyalkyl)-2-nitroguanidines were prepared by esterification with absolute ethanol in the presence of dry hydrogen chloride. The results are shown in Table II.

TABLE II

CARBOXYALKYLGUANIDINES, NITRATES, AND NITRO DERIVATIVES

Compound	Formula	M.p., °C	Yield, %	Calculated C	Calculated H	Calculated N	Found C	Found H	Found N
Carboxyalkylguanidines									
Ethyl	$C_4H_9O_2N_3$	225–226	31	36.64	6.87	32.06	36.9	7.0	32.1
Anhydro β-phenylethyl	$C_{10}H_{11}O_1N_3$	234–235	28	63.44	5.82	22.22	63.2	5.6	21.8
Propyl	$C_5H_{11}O_2N_3$	234–235	29	41.45	7.59	28.95	41.6	7.6	29.2
Carboxyalkylguanidine nitrates									
Methyl	$C_3H_8O_5N_4$	180–181	52	(Calc. for HNO_3: 34.42. Found for HNO_3: 34.8)					
Ethyl	$C_4H_{10}O_5N_4$	149–150	51	[Ramsay, H. Ber. **41**, 4385 (1908).]					
Anhydro β-phenylethyl	$C_{10}H_{12}O_4N_4$	134–135	65	47.61	4.76	22.22	47.8	4.8	22.4
Propyl	$C_5H_{12}O_5N_4$	146–147	58	28.81	5.77	26.92	28.8	5.7	27.0
1-(α-Carboxyalkyl)-2-nitroguanidines									
1-(α-Carboxymethyl)	$C_3H_6O_4N_4$	166–167	60	22.42	3.70	34.60	22.4	3.6	34.7
1-(α-Carboxyethyl)	$C_4H_8O_4N_4$	155–157	55	27.22	4.54	31.80	27.1	4.6	31.6
Ethyl esters of 1-(α-carboxyalkyl)-2-nitroguanidines									
1-(α-Carbethoxymethyl)	$C_{15}H_{10}O_4N_4$	149–150	29	31.58	5.26	29.47	31.8	5.3	29.2
1-(α-Carbethoxyethyl)	$C_6H_{12}O_4N_4$	175–176	32	35.30	5.88	27.40	35.2	6.0	27.6

DISCUSSION

The present study has shown that the methods of syntheses of guanidine nitrate apply as well to the substituted guanidine nitrates with the difference that lower yields resulted with the use of amine nitrates. Guanidines substituted by a carboxylic group are monobasic in character and form the lead and barium salts. The solubilities of the nitro derivatives were greater than that of nitroguanidine itself or of the alkyl nitroguanidines. The esterification of 1-(α-carboxyalkyl)-2-nitroguanidines in the presence of hydrogen chloride did not yield the corresponding hydrochloride salts, which supports the view that acids combine with the free amino group to form salts.

EXPERIMENTAL PART

Alkylguanidine Nitrates

1. Syntheses from calcium cyanamide and amine nitrates in aqueous solution.—The amine nitrate (0.29 mole) was dissolved in water (100 ml) and the resulting solution was evaporated until it reached a boiling point of 100° C. Calcium cyanamide (55%, 0.05 mole) was added slowly while stirring and at that temperature the reaction occurred with frothing while some free amine was evolved. The guanidine nitrate salt crystallized from the solution on cooling. The results are shown in Table I.

2. Syntheses from amine nitrates and calcium cyanamide in the dry state.—Dry solid mixtures of amine nitrates (0.21 mole) and calcium cyanamide were heated at 110° C for 1 hour (55%, 0.05 mole), during which time free amine was liberated. The fluid

Can. J. Chem. Downloaded from www.nrcresearchpress.com by 78.46.186.204 on 09/04/12
For personal use only.

reaction products were diluted with hot water (40 ml) and the mixtures filtered while hot. On cooling, the guanidine nitrate salts crystallized and were separated by filtration. The experimental results obtained are given in Table I.

3. Syntheses from calcium cyanamide, amine nitrates, and urea.—Calcium cyanamide (55%, 0.05 mole), amine nitrates (0.21 mole), and urea (0.13 mole) were heated at 90° C for 1 hour, during which time some free amine was evolved. Hot distilled water (40 ml) was added and the mixtures were filtered while hot. The guanidine nitrate salts crystallized from the cooled filtrate and were isolated by filtration. The results are listed in Table I.

4. Syntheses from amine nitrates and dicyandiamide.—Mixtures of dicyandiamide (0.22 mole) and amine nitrates (0.44 mole) were heated in an oil bath. Fusion began at 70° C, was complete at 130–133° C, and the temperature was gradually raised to 170° C and kept there for 3 hours. Upon cooling, the crude guanidine nitrate salts crystallized from the solution and were recrystallized from water. The results obtained are given in Table I.

Alkylnitroguanidines

The substituted guanidine nitrate (0.46 mole) was slowly added to sulphuric acid (98%, 2.1 mole) and cooled to 5° C. After all the solid was added, the mixture was stirred at that temperature for 3 hours, and afterwards poured over cracked ice. A small amount of the product precipitated from the solution. The compound was separated by filtration, the filtrate neutralized with barium hydroxide, and the barium sulphate formed was filtered through charcoal. The resulting filtrate was evaporated under vacuum and a second crop of crystals was obtained. The compound was then recrystallized from ethanol. The results obtained are shown in Table I.

Carboxyalkylguanidines

An aqueous solution of guanidine carbonate (0.06 mole) was added to an aqueous solution of amino acid (0.12 mole) and the reaction vessel was heated on a sand bath for 24 hours, during which time ammonia was liberated. Upon cooling, the resulting liquid was filtered, and the filtrate evaporated under reduced pressure until a yellow viscous product remained. A mixture of absolute alcohol (50 ml) and acetone (50 ml) was added, with stirring, and the resulting solution was stored in a cool place for several hours. The carboxyalkylguanidine soon separated from the solution and after filtration and washing with ethanol, the crude product was recrystallized from water. The results are given in Table II.

Carboxyalkylguanidine Nitrates

Dilute nitric acid (0.06 mole) was added slowly to an aqueous solution of the carboxyalkylguanidine (0.05 mole) while it was being cooled and stirred, and the resulting solution was evaporated to dryness under vacuum. The product was recrystallized from water. The results are listed in Table II.

1-(α-Carboxyalkyl)-2-nitroguanidines

Concentrated sulphuric acid (98%, 0.06 mole) was cooled to 5° C and the carboxyalkylguanidine nitrate (0.01 mole) was added in small portions with continuous stirring and cooling whenever necessary. After all the nitrate salt was added, the mixture was further stirred for 15 minutes at the above temperature and then allowed to reach 20° C, where the mass was stirred for 3 hours. The sulphuric acid solution was then

Can. J. Chem. Downloaded from www.nrcresearchpress.com by 78.46.186.204 on 09/04/12
For personal use only.

poured over cracked ice, which effected precipitation, after 15 minutes, of the crude product, which separated by filtration and was recrystallized from water. The compounds prepared are shown in Table II.

Salts of 1-(α-Carboxyalkyl)-2-nitroguanidines

1-(α-Carboxymethyl)-2-nitroguanidine was also identified by its dihydrate lead salt obtained by treating 1-(α-carboxymethyl)-2-nitroguanidine with an excess of lead oxide (litharge). The compound had no melting point but decomposed above 300° C. Calc. for $C_6H_{14}O_{10}N_6Pb$: Pb, 38.50%. Found: 38.8%. 1-(α-Carboxypropyl)-2-nitroguanidine, which was soluble in sulphuric acid, was isolated by precipitating the sulphate with barium hydroxide, filtering off the barium sulphate, and evaporating the resulting filtrate under reduced pressure. The dihydrate barium salt of 1-(α-carboxypropyl)-2-nitroguanidine crystallized from the concentrated solution in colorless needles: m.p. 183–184° C. Yield, 27%. Calc. for $C_{10}H_{22}O_{10}N_8Ba$: C, 21.76; H, 4.00; N, 20.31%. Found: C, 22.2; H, 4.2; N, 19.9%.

Esters of 1-(α-Carboxyalkyl)-2-nitroguanidines

Pulverized samples of 1-(α-carboxyalkyl)-2-nitroguanidines (0.06 mole) were added to absolute ethanol (70 ml), and dry hydrogen chloride was added until the solution was saturated. The mixtures were then refluxed for 1 hour, filtered, and left to stand in a cool place. The crude esters which separated from the filtrates were recrystallized from ethanol. The compounds obtained were slightly soluble in water. The results are given in Table II.

REFERENCES

1. BURNS, R. and GAY, P. F. Brit. Patent No. 507,498 (1939).
2. DHOMMEE, R. Compt. rend. **134**, 1313 (1902).
3. WRIGHT, G. F. U.S. Patent No. 2,431,301 (1947).
4. WERNER, F. A. and BELL, J. J. Chem. Soc. **117**, 1133 (1920); **121**, 1790 (1922).
5. BLAIR, J. S. and BRAHAM, J. M. J. Am. Chem. Soc. **44**, 2342 (1922).
6. STRECKER, A. Compt. rend. **52**, 1212 (1861).
7. DUVILLIER, E. Compt. rend. **91**, 171 (1880).
8. RAMSAY, H. Ber. **41**, 4385 (1908).
9. MOURQUE, M. Bull. soc. chim. France, 181 (1948).
10. BENGERLSDORF, I. S. J. Am. Chem. Soc. **75**, 3138 (1953).
11. NENCKI, M. and SEIBER, N. J. prakt. Chem. **17**, 478 (1878).
12. ABDERHALDEN, E. and SICKEL, H. Z. physiol. Chem. **173**, 51 (1928).
13. THIELE, J. Ann. **270**, 1 (1892).
14. EWAN, T. and YOUNG, J. H. J. Chem. Ind. **40**, 109 (1921).
15. DAVIS, T. L. and ELDERFIELD, R. C. J. Am. Chem. Soc. **55**, 731, 735 (1933).

Can. J. Chem. Downloaded from www.nrcresearchpress.com by 78.46.186.204 on 09/04/12
For personal use only.

Can. J. Chem. Downloaded from www.nrcresearchpress.com by 78.46.186.204 on 09/04/12
For personal use only.

NOTES

THE ULTRAVIOLET AND INFRARED SPECTRA OF VICINAL-TRIAZOLE DERIVATIVES

E. LIEBER,[1] C. N. R. RAO,[2] T. S. CHAO,[3] AND H. RUBINSTEIN[4]

Unlike tetrazole (1, 2) vicinal-triazole absorbs in the ultraviolet region (3). Ramart-Lucas and Hoch (4) have observed that the ultraviolet spectra of the phenyltriazoles (I, $R_1 = C_6H_5$) vary according to the nature of the groups R_4 and R_5. However, they

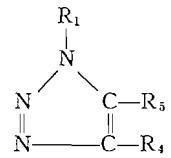

I

found that phenyltriazoles do not exhibit any absorption in the near ultraviolet region, when R_5 is H, CH_3, C_6H_5, or COOH, and R_4 is H or COOH. This appeared rather unusual because alkyl and aryl groups in 4-position have been found (3) to produce bathochromic shifts. Also, the ultraviolet spectrum of 4-phenyltriazole (I, $R_1 = R_5 = H$ and $R_4 = C_6H_5$) has been compared to that of biphenyl (3). Lieber, Rao, and Chao (5) have studied the near-ultraviolet absorption spectra of substituted aminotriazoles and have discussed the results in terms of the resonance interaction of R_1, R_4, and R_5 with triazole nucleus. We have now studied the ultraviolet spectra of a few other derivatives of vicinal-triazole. The results are summarized in Table I.

TABLE I

ULTRAVIOLET ABSORPTION SPECTRA OF VICINAL-TRIAZOLE DERIVATIVES (I)

R_1	R_4	R_5	λ_{max} (mμ)	log ϵ_{max}
C_6H_5	H	OH	235	4.03
C_6H_5	H	Cl	228	4.03
C_6H_5	COOH	Cl	231	4.03
C_6H_5	$COOCH_3$	Cl	218	4.24

The infrared spectral data on the vicinal-triazoles derivatives are limited (3, 6). We have now studied the infrared spectra of several derivatives of vicinal-triazole. All the important absorption frequencies that are common to most of the derivatives in the region 900–1310 cm^{-1} are shown in Table II. The intensities are indicated by the symbols: (s) strong; (m) medium; (w) weak; and (vw) very weak.

The syntheses of the compounds used in this study have been reported (7). The ultraviolet absorption spectra were recorded in 95% ethanol using a Cary recording

[1]*Department of Chemistry, DePaul University, Chicago 14, Illinois, U.S.A., the author to whom all correspondence should be addressed.*
[2]*Department of Chemistry, Purdue University, Lafayette, Ind., U.S.A.*
[3]*Archer-Daniels-Midland Co., Minneapolis, Minn., U.S.A.*
[4]*Wyandotte Chemical Co., Wyandotte, Mich., U.S.A.*

TABLE II

INFRARED SPECTRA OF VICINAL-TRIAZOLE DERIVATIVE (I)

R_1	R_4	R_5	Triazole vibrations (cm^{-1})			
C_6H_5	H	OH	1290(w)			
			1264(s)	1111(m)	1093(w)	990(m)
			1202(vw)		1068(w)	
C_6H_5	COOH	Cl	1277(m)	1105(w)	1081(s)	984(m)
			1230(m)			901(m)
			1198(m)			
C_6H_5	H	Cl	1290(m)	1111(m)	1053(w)	1000(m)
			1230(s)		1029(vw)	956(m)
			1203(m)			
H	H	NHC_6H_5	1302(m)			
			1236(m)	1129(w)	1081(m)	990(s)
			1176(w)		1018(s)	964(w)
			1151(w)			
C_6H_5	C_6H_5	NH_2	1297(w)	1101(w)	1067(w)	968(m)
			1235(w)		1013(w)	
p-BrC_6H_4	C_6H_5	NH_2	1280(w)	1111(w)	1082(w)	1003(m)
			1242(w)		1062(m)	974(s)
			1217(w)			
$CH_2C_6H_5$	C_6H_5	NH_2	1299(w)	1104(w)	1067(m)	999(w)
			1239(w)		1022(w)	990(w)
			1218(w)			
H	C_6H_5	NH-(*p*-$CH_3C_6H_4$)	1289(m)	1121(w)	1070(w)	996(w)
			1241(m)		1045(w)	969(m)
			1195(m)		1020(w)	911(w)
			1181(w)			

spectrophotometer. The infrared spectra were recorded using a Perkin–Elmer spectrometer (Model 21). The samples were prepared in Nujol mulls or KBr pellets.

From the results in Table I and the earlier observations (3, 5), it is found that the triazole derivatives, I, absorb in the near-ultraviolet region immaterial of the substituents in 1-, 4-, and 5-positions. These results are in variance with the earlier work of Ramart-Lucas and Hoch (4). Further, it is hard to generalize that the influence of the substituents is greater in 5- than in the 4-position (4). From the spectra of 1-substituted 4-phenyl-1,2,3-triazoles (5) it appears that the 1-(4-phenyl-5-amino)-triazolyl group is not capable of strong resonance interaction, since the effect of the substituents on the 1-phenyl group on the spectra of these derivatives is of the same magnitude as that on benzene alone. It is interesting to see that 1-phenylaminotetrazole absorbs at 225 mμ (2) compared to 221 mμ of 1-phenyl-5-amino-1,2,3-triazole (5). This difference is explained on the basis of the difference in electronegativities of the triazole and the tetrazole ring systems. Tetrazole is more electronegative than triazole, because of the greater electronegativity of nitrogen compared to carbon.

Since all the triazole derivatives had phenyl groups attached to them, it was hard to assign infrared frequencies for the N=N and the C=C links of the triazole nucleus. Some of the weak intensity bands listed in Table II may be due to the substituted aromatic groups. It is interesting to see that all the vicinal-triazole derivatives, just like the thiatriazole and tetrazole derivatives (8), exhibit a medium or weak intensity band in the region 1277–1302 cm^{-1}. This band cannot be ascribed to C—N or C_6H_4—NH or $C_6H_5N<$ linkages. It may be due to the cyclic —N—N=N— configuration (8).

From Table II it can be seen that there are at least three bands in the regions 968–1003 cm^{-1}, 1101–1129 cm^{-1}, and 1045–1093 cm^{-1} which are characteristic of the vicinal-triazole ring system. However, the possibility of one of these bands in the region 1020–1220 cm^{-1} being the C—N vibration frequency is not completely eliminated. The

Can. J. Chem. Downloaded from www.nrcresearchpress.com by 78.46.186.204 on 09/04/12
For personal use only.

characteristic frequencies for vicinal-triazoles assigned by us agree with the observation of Hartzel and Benson (3), who assigned two bands between 1136–1087 cm^{-1} and 1020–971 cm^{-1} as characteristic of *v*-triazole.

ACKNOWLEDGMENTS

The authors' thanks are due to the U. S. Office of Naval Research and the Research Corporation, New York, N.Y., U.S.A., for research grants which made this study possible.

1. SCHUELER, F. S., WANG, S. C., FEATHERSTONE, R. M., and GROSS, E. G. J. Pharmacol. Exptl. Therap. **97**, 266 (1949).
2. LIEBER, E., RAO, C. N. R., and PILLAI, C. N. Current Sci. (India), **26**, 167 (1957).
3. HARTZEL, L. W. and BENSON, F. R. J. Am. Chem. Soc. **76**, 667 (1954).
4. RAMART-LUCAS, P. and HOCH, J. Bull soc. chim. France, 451 (1949).
5. LIEBER, E., RAO, C. N. R., and CHAO, T. S. Spectrochim. Acta, **10**, 250 (1950).
6. BENSON, F. R. and SAVELL, W. L. Chem. Revs. **46**, 1 (1950).
7. LIEBER, E., CHAO, T. S., and RAO, C. N. R. J. Org. Chem. **22**, 654 (1957).
8. LIEBER, E., RAO, C. N. R., PILLAI, C. N., RAMACHANDRAN, J., and HITES, R. D. Can. J. Chem. **36**, 801 (1958).

RECEIVED JUNE 23, 1958.
DEPARTMENT OF CHEMISTRY,
DEPAUL UNIVERSITY,
CHICAGO 14, ILLINOIS.

ON THE PREPARATION AND SINTERING OF CLOUD PRECIPITATING AGENTS. LEAD DI-IODIDE MICROCRYSTALS

HENRY M. PAPÉE[1]

Lead iodide of relatively large and controlled specific surface areas had to be prepared in this laboratory in connection with a microcalorimetric study of heats of adsorption of water vapor on lead iodide surfaces (1).

EXPERIMENTAL

Attempts to prepare finely subdivided lead iodide by electrostatic precipitation of a smoke (2) failed because of considerable contamination of the product by elementary iodine, and because of low specific areas obtained. No significant improvement could be attained by varying the flow of the dry nitrogen carrying gas, the temperatures of the melt, and the potentials applied.

An entirely different method was therefore tried, and the pattern outlined by Marshall (3) was followed with some modifications. Twenty-five grams of ammonium iodide was dissolved in 700 cc of absolute ethanol, and cooled to −20° C. A boiling solution of 50 g of lead iodide in 50 cc of water was added with vigorous stirring. The resulting slurry was quickly centrifuged in a low-temperature centrifuge maintained at −15° C. The precipitate was decanted and repulped several times by means of an electromagnetic vibrator with water at 0° C and then with absolute ethanol which has been chilled to −20° C. This was followed by several repulpings with anhydrous ether at low temperatures.

The precipitate obtained was then placed in a desiccator and evacuated for 48 hours to a vacuum obtained by a 2-stage Edwards diffusion pump. The agglomerated product was ground in a mortar in an atmosphere of dry nitrogen and sieved through a 200-mesh screen. The compound was then placed again in a desiccator and again evacuated for 48

[1]*Present address: Division of Applied Chemistry, National Research Council of Canada, Ottawa, Canada.*

Can. J. Chem. Downloaded from www.nrcresearchpress.com by 78.46.186.204 on 09/04/12
For personal use only.

characteristic frequencies for vicinal-triazoles assigned by us agree with the observation of Hartzel and Benson (3), who assigned two bands between 1136–1087 cm^{-1} and 1020–971 cm^{-1} as characteristic of *v*-triazole.

ACKNOWLEDGMENTS

The authors' thanks are due to the U. S. Office of Naval Research and the Research Corporation, New York, N.Y., U.S.A., for research grants which made this study possible.

1. SCHUELER, F. S., WANG, S. C., FEATHERSTONE, R. M., and GROSS, E. G. J. Pharmacol. Exptl. Therap. **97**, 266 (1949).
2. LIEBER, E., RAO, C. N. R., and PILLAI, C. N. Current Sci. (India), **26**, 167 (1957).
3. HARTZEL, L. W. and BENSON, F. R. J. Am. Chem. Soc. **76**, 667 (1954).
4. RAMART-LUCAS, P. and HOCH, J. Bull soc. chim. France, 451 (1949).
5. LIEBER, E., RAO, C. N. R., and CHAO, T. S. Spectrochim. Acta, **10**, 250 (1950).
6. BENSON, F. R. and SAVELL, W. L. Chem. Revs. **46**, 1 (1950).
7. LIEBER, E., CHAO, T. S., and RAO, C. N. R. J. Org. Chem. **22**, 654 (1957).
8. LIEBER, E., RAO, C. N. R., PILLAI, C. N., RAMACHANDRAN, J., and HITES, R. D. Can. J. Chem. **36**, 801 (1958).

RECEIVED JUNE 23, 1958.
DEPARTMENT OF CHEMISTRY,
DEPAUL UNIVERSITY,
CHICAGO 14, ILLINOIS.

ON THE PREPARATION AND SINTERING OF CLOUD PRECIPITATING AGENTS. LEAD DI-IODIDE MICROCRYSTALS

HENRY M. PAPÉE[1]

Lead iodide of relatively large and controlled specific surface areas had to be prepared in this laboratory in connection with a microcalorimetric study of heats of adsorption of water vapor on lead iodide surfaces (1).

EXPERIMENTAL

Attempts to prepare finely subdivided lead iodide by electrostatic precipitation of a smoke (2) failed because of considerable contamination of the product by elementary iodine, and because of low specific areas obtained. No significant improvement could be attained by varying the flow of the dry nitrogen carrying gas, the temperatures of the melt, and the potentials applied.

An entirely different method was therefore tried, and the pattern outlined by Marshall (3) was followed with some modifications. Twenty-five grams of ammonium iodide was dissolved in 700 cc of absolute ethanol, and cooled to −20° C. A boiling solution of 50 g of lead iodide in 50 cc of water was added with vigorous stirring. The resulting slurry was quickly centrifuged in a low-temperature centrifuge maintained at −15° C. The precipitate was decanted and repulped several times by means of an electromagnetic vibrator with water at 0° C and then with absolute ethanol which has been chilled to −20° C. This was followed by several repulpings with anhydrous ether at low temperatures.

The precipitate obtained was then placed in a desiccator and evacuated for 48 hours to a vacuum obtained by a 2-stage Edwards diffusion pump. The agglomerated product was ground in a mortar in an atmosphere of dry nitrogen and sieved through a 200-mesh screen. The compound was then placed again in a desiccator and again evacuated for 48

[1]*Present address: Division of Applied Chemistry, National Research Council of Canada, Ottawa, Canada.*

Can. J. Chem. Downloaded from www.nrcresearchpress.com by 78.46.186.204 on 09/04/12
For personal use only.

hours. Analysis of the product showed it to be 99.8% pure, and BET surface determinations led to values of 2.05 m^2/g. The stock was then stored in a desiccator at 25.0° C, and all further manipulations of samples were done under nitrogen of a humidity below 1%, in a dry box.

Sintering by Heating

Quantities of about 8 g of lead iodide were sintered under vacuum in a glass cell of the type represented in Fig. 1. The cell was fitted directly onto the BET apparatus, and a heating unit which could be controlled within 1° C was placed around it. It was seen that the same final results were obtained at a temperature of 100° C, whether the process of heating lasted for 6 or for 48 hours. The samples were heated therefore for 24-hour periods, BET measurements taken subsequently, and the relative change between

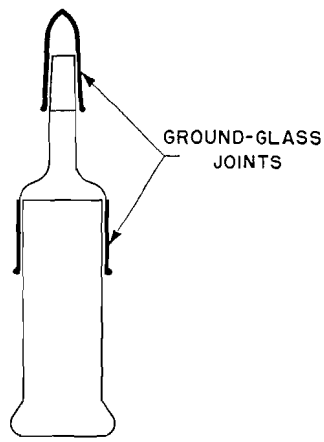

FIG. 1. Cell for storage, sintering, dispensing, and surface measurements of the product.

specific surface areas before (S_0) and after sintering (S) was plotted against the temperature of heating. Figure 2 gives the results obtained on samples originating from different batches of various initial specific areas. Each point represents a measurement taken on a different sample. It was noticed that, while salts whose area was reduced by sintering by exposure to saturated water vapor at 25° C follow the pattern of Fig. 2, samples which were presintered by heating give completely random results. The plot therefore represents measurements on crystals originating from one particular batch, and some others that were presintered by exposure to water vapor, and subsequently evacuated for long time periods.

The curve represented by Fig. 2 can be split in three parts:

(i) The ascending part, in which small variations of temperature seem to provoke considerable changes in the function and where, because of this, the error is considerable. This part has therefore been dotted.

(ii) The fairly rectilinear descending part of the curve.

(iii) The extrapolated part of the line, where there is a considerable scattering of the experimental values.

The parameters of the line in part (ii) are:

$$\text{Slope: } -0.003_2 \pm 0.0005\ (^\circ\text{C})^{-1}$$

$$\text{Intercept: } 0.50 \pm 0.06 \text{ units.}$$

Can. J. Chem. Downloaded from www.nrcresearchpress.com by 78.46.186.204 on 09/04/12
For personal use only.

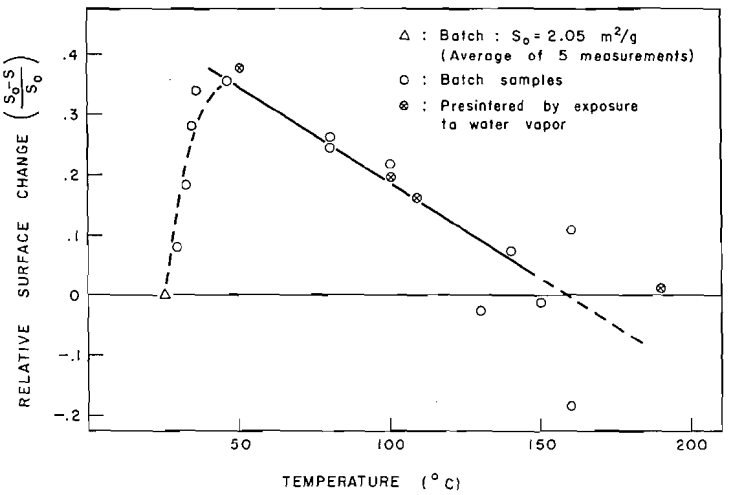

FIG. 2. Effect of sintering of lead iodide with temperature: plot of relative surface change against temperature of sintering, in degrees Centigrade.

The plot indicates a decrease of specific surface below 160° C and suggests a possible increase above that temperature of sintering.

Elementary iodine was observed in the traps during experiments which were performed in the higher temperature range. Since it was not expected that at these temperatures decomposition would set in, a separate experiment was performed at 240° C. Lead di-iodide of a specific surface of 1.5 m^2/g was placed in a long glass tube surrounded by a heating element, and was heated for 24 hours under an atmosphere of dry nitrogen at room pressure. During this time period, the salt underwent a process of stoichiometric decomposition into lead mono-iodide and elementary iodine, with the latter condensing on the colder part of the tube which protruded from the heater.

Sintering by Exposure to Water Vapor

Microcrystals of lead di-iodide, contained in the type of cell previously described, were evacuated for 12 hours by pumping with a diffusion pump. Water vapor was subsequently admitted from a cell containing distilled water at saturated vapor pressure. The cells were kept in communication for the required period of time. The cell containing the water was closed a few seconds before the end of the treatment, and, at the required time, the salt container was connected with the high-vacuum manifold. The latter was kept under vacuum by a 2-stage silicon oil diffusion pump, which was backed by a high-speed rotary mechanical pump and by a 24-liter flask branched in parallel. This was followed by 12 hours of evacuation. The whole operation was performed at 25.0° C. The surface area was then determined by BET nitrogen adsorption. Salt of an initial specific surface of 1.5_1 m^2/g was used for all of those experiments.

The results are given in Fig. 3. Two extra runs were performed with hydration times of 24 and 48 hours, and areas of 0.60_0 m^2/g were obtained in both cases. It was therefore assumed that the specific surface reached an asymptotic value of 0.60_0 m^2/g, and it was seen that under this condition the phenomenon follows first-order kinetics with respect to surface, as shown in Fig. 4. The parameters of the line are found to be:

$$\text{Slope: } -0.245 \pm 0.007 \text{ hours}^{-1}$$

$$\text{Intercept: } -0.04 \pm 0.03$$

Can. J. Chem. Downloaded from www.nrcresearchpress.com by 78.46.186.204 on 09/04/12
For personal use only.

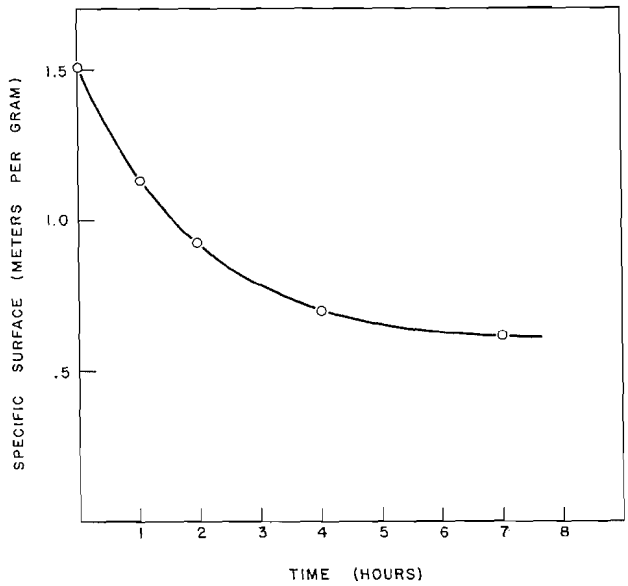

FIG. 3. Sintering of lead iodide particles with time of exposure to water vapor, at 25° C, and unit relative vapor pressure: plot of specific surface against time of exposure.

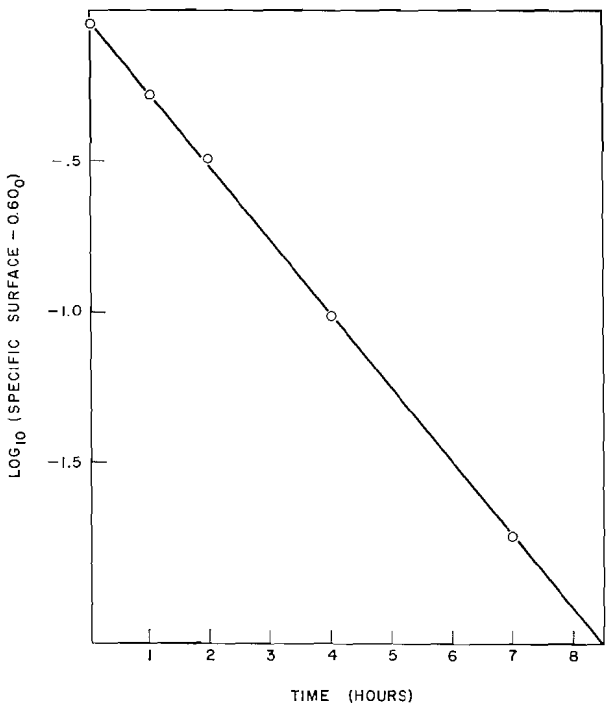

Fig. 4. Sintering of lead iodide particles with time of exposure to water vapor: plot of the decimal logarithm of the difference between the specific surface at time 't' and the asymptotic experimental value, against time of exposure.

Can. J. Chem. Downloaded from www.nrcresearchpress.com by 78.46.186.204 on 09/04/12
For personal use only.

DISCUSSION

The activity of lead iodide particles as condensation nuclei (4) and their properties toward ice nucleation (5, 6, 7) have recently resulted in investigations of the surface properties of these crystals (1, 8).

Sintering of the surface of lead di-iodide under exposure to water vapor is a slow process leading to asymptotic values. This can be visualized in terms of homogenization of initial imperfections on the surface and the absence of agglomeration between original particles. The curve of Fig. 3 follows a pattern similar to that of the curves obtained by Moffat and McIntosh (9), who studied the sintering of sodium chloride microcrystals under exposure to low partial pressures of water vapor. The pattern is, however, different from the one obtained recently by Papée (10), where sodium chloride microcrystals were sintered under exposure to water vapor at saturated vapor pressure at 25° C, and where no asymptotic values could be detected in the fast first-order process.

Experiments reported in this note indicate that the process of decrease of surface by heating under vacuum is accompanied by a contrary process of increase, and that the latter effect becomes prevalent at higher temperatures. Since no evidence indicating transition between phases, below 250°, could be found in the literature, it is assumed that the increase is due to thermal decomposition. This explains the controversial results obtained in measuring the melting point of the product (11, 12, 13). This controversy is not eliminated by data obtained by various workers who worked with purified products and knew that decomposition occurs (14), and by those who worked under inert atmospheres (15, 16) to eliminate the action of water vapor and oxygen. Similarly, measurements of vapor pressures of lead di-iodide at various temperatures seem to have led so far to controversial statements (17, 18) mainly because of misinterpretations of the experimental values and failure to analyze the final products.

The controversy noted above and the evidence of the present investigation points, however, to the conclusion that the crystals responsible for the condensation of water or for ice nucleation will have a strongly distorted lattice because of the nature of their preparation, and that this factor will possibly favor their action (19, 20). Since, furthermore, the compound can be decomposed by light (21, 22), and its over-all surface will sinter and homogenize only slowly under exposure to water vapor, as shown by experiments reported previously, a PbI_2 nucleus will probably remain active for long periods of time; even seasoned and originally inactive particles may eventually be activated photochemically.

Another surface-dependent factor that might favor condensation of water on lead iodide nuclei ought to be considered at the same time, since lead iodide gives rise to the photoelectric effect in the visible spectrum (23). It is to be expected that the nucleus will become electrically charged when illuminated, and will therefore bind water molecules by a sort of electrostriction, which, under suitable conditions, may promote coalescence (cf. ref. 24). The fact that freshly prepared lead iodide 'tires' with time towards its photoelectric properties, whether kept in moderate light or in darkness (25), may well be partly explained by the sintering of its surface when exposed to the water vapor in the atmosphere.

ACKNOWLEDGMENTS

Thanks are due to Messrs. T. W. Zawidzki and S. Tong for their help in preparing the lead iodide, and to Drs. G. C. Benson and K. J. Laidler and Mr. S. J. Birstein for many helpful discussions.

Can. J. Chem. Downloaded from www.nrcresearchpress.com by 78.46.186.204 on 09/04/12
For personal use only.

This work was performed under Contract No. A.F. 19(604)-2026 between the U.S. Air Force Cambridge Research Center and the University of Ottawa.

REFERENCES

1. PAPÉE, H. M. To be published.
2. YOUNG, D. M. and MORRISON, J. A. J. Sci. Instr. **31**, 90 (1954).
3. MARSHALL, F. H. Phys. Rev. **58**, 642 (1940).
4. SCHAEFER, V. J. J. Meteorol. **11**, 417 (1954).
5. HOSLER, C. L. and SPALDING, G. R. Artificial stimulation of rain (Symposium). Pergamon Press Ltd., New York. 1957. p. 369.
6. BIRSTEIN, S. J. and ANDERSON, C. E. J. Meteorol. **12**, 68 (1954).
7. PRUPPACHER, H. R. and SÄNGER, R. Z. angew. Math. u. Phys. **6**, 407 (1955).
8. BIRSTEIN, S. J. Geophys. Research, Paper No. 32. (1954).
9. CARNELLY, T. J. Chem. Soc. **33**, 273 (1878).
10. MOFFAT, J. B. and MCINTOSH, R. Can. J. Chem. **35**, 1511 (1957).
11. PAPÉE, H. M. J. Meteorol. To be published.
12. EHRHARDT, O. Ann. Rev. Phys. Chem. **24**, 215 (1885).
13. RAMSAY, W. and ENMORPOPULOS, M. Phil. Mag. **41**, 460 (1896).
14. CZEPINSKY, V. Z. anorg. Chem. **19**, 257 (1899).
15. SANDONINI, C. Gazz. chim. ital. **41**, II, 145 (1911).
16. TUBANDT, C. and EGGERT, S. Z. anorg. Chem. **110**, 218 (1920).
17. VON WORTENBERG, H. and BOSSES, O. Z. Elektrochem. **28**, 384 (1922).
18. JELLINEK, K. and RUDAT, A. Z. physik. Chem. A, **143**, 55 (1929).
19. TURNBULL, D. Artificial stimulation of rain (Symposium). Pergamon Press Ltd., New York. 1957. p. 356.
20. MANSON, J. E. Artificial stimulation of rain (Symposium). Pergamon Press Ltd., New York. 1957. p. 367.
21. ROUSSIEU, M. Ann. chim. et phys. **47**, 154 (1856).
22. SANYAL, A. K. and DHAR, N. R. Z. anorg. Chem. **128**, 212 (1923).
23. COBLENTZ, W. W. and ECKFORD, J. F. Sci. Papers, U.S. Bureau of Standards, 18/456.489. (1922).
24. MARSHALL, J. S. and GUNN, K. L. S. Artificial stimulation of rain, (Symposium). Pergamon Press Ltd., New York. 1957. p. 345.
25. DIMA, M. B. A. Compt. rend. **157**, 592 (1913).

RECEIVED MAY 22, 1958.
DEPARTMENT OF CHEMISTRY,
UNIVERSITY OF OTTAWA,
OTTAWA, CANADA.

Can. J. Chem. Downloaded from www.nrcresearchpress.com by 78.46.186.204 on 09/04/12
For personal use only.

Can. J. Chem. Downloaded from www.nrcresearchpress.com by 78.46.186.204 on 09/04/12
For personal use only.

Canadian Journal of Chemistry

Issued by THE NATIONAL RESEARCH COUNCIL OF CANADA

VOLUME 36 NOVEMBER 1958 NUMBER 11

FUSED HETEROCYCLICS

PART II. SYNTHESIS OF QUINOLINO-(2 : 3 : 3′: 2′)-QUINOLINE: AN ISOMER OF CALYCANINE[1, 2]

RAGINI ANET[3]

ABSTRACT

The constitution of calycanine, a dehydrogenation product of the alkaloid calycanthine, is discussed. Calycanine dipicrate has been prepared, and, on the basis of its analysis and the infrared spectrum of calycanine, a quinolinoquinoline structure has been put forward for calycanine. The synthesis of quinolino-(2 : 3 : 3′: 2′)-quinoline is described.

Calycanine is an important degradation product of the alkaloid calycanthine (1). At the time that this work was carried out, the constitution of calycanine was not known,[4] and it was decided to investigate this base as a part of the studies on calycanthine (2).

Calycanine was first prepared by Marion and Manske (4) by the selenium dehydrogenation of the alkaloid, and later by Barger, Madaniveitia, and Streuli (5) by heating calycanthine with a variety of reagents. Calycanine, m.p. 310° C after sublimation, was found to be a very stable weak base, giving faintly fluorescent solutions. It did not give any coloration with *p*-dimethylaminobenzaldehyde (Ehrlich reaction). Elementary analysis led both groups of workers to put forward a $C_{16}H_{10}N_2$ formula for calycanine. One active hydrogen and no N-methyl group was found.

Barger *et al.* (5), on the basis of their formula for calycanthine, put forward structure (I) for calycanine. Manske and Marion (6) considered that Barger's structure was inconsistent with the properties of calycanine, viz., the negative Ehrlich reaction and its basicity. As a result of further analyses of the base they proposed a $C_{21}H_{15}N_3$ or $C_{21}H_{13}N_3$ formula for calycanine, and the structures (II) or (II*a*).

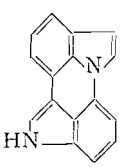

(I)

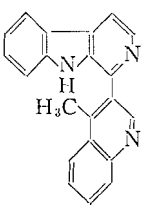

(II)

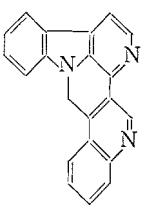

(II*a*)

[1]*Manuscript received July 23, 1958.*
Contribution from the Dyson–Perrins Laboratory, Oxford.
[2]*Somasekhara, S. and Phadké, R. J. Indian Inst. Sci. A,* **37**, *120 (1955) forms Part I.*
[3]*nee Phadké. Present address: c/o Dr. F. A. L. Anet, Department of Chemistry, University of Ottawa.*
[4]*This work was recorded in a part of a D. Phil. Thesis, Oxford University, 1952. After the completion of this work, we became aware of the unpublished work of Clark and Woodward at Harvard University, who synthesized quinolino-(3 : 4 : 4′: 3′)-quinoline and found it to be identical with calycanine (3).*

Can. J. Chem. Downloaded from www.nrcresearchpress.com by 78.46.186.204 on 09/04/12
For personal use only.

At this stage, Hargreaves reported an X-ray investigation of calycanine (7). Although the results were not conclusive, he suggested that the size of the unit cell favored a C_{16} formula and that the molecule of calycanine was centrosymmetrical (8). Later, Manske, Marion, and Kulka (9) synthesized 2-(3-lepidyl)-3-carboline (II) and found it to be different from calycanine. They discarded the C_{21} expression and proposed a $C_{15}H_{10}N_2$ formula as being in agreement with their analytical figures and with the molecular weight according to Hargreaves's data.

In the present investigation, calycanine was prepared according to Barger *et al.* (5) by the zinc dust distillation of calycanthine. Analysis of the base did not distinguish between a C_{15} and a C_{16} formula, but calycanine formed a *dipicrate* whose analysis was in better agreement with the C_{16} than with the C_{15} formula. The infrared spectrum of calycanine showed no band attributable to an —NH group, thus ruling out both Barger's structure (I) and an indoloquinoline or indoloisoquinoline structure as suggested by the Canadian workers (9). The active hydrogen in calycanine must therefore be contained in a structural feature other than an —NH group. A quinolinoquinoline system in which the two pyridine rings are fused together, would, it was felt, fulfill such a requirement. Furthermore, such a system could easily arise from two indole nuclei as follows.

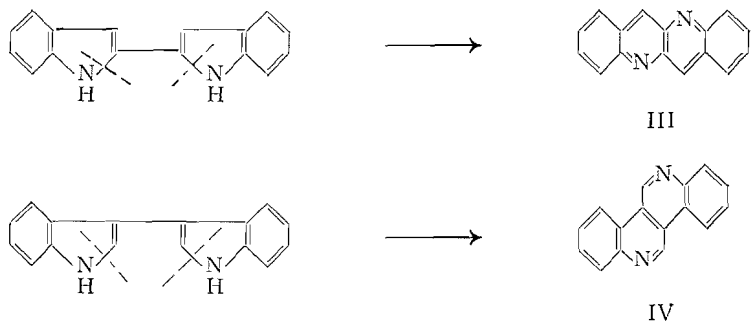

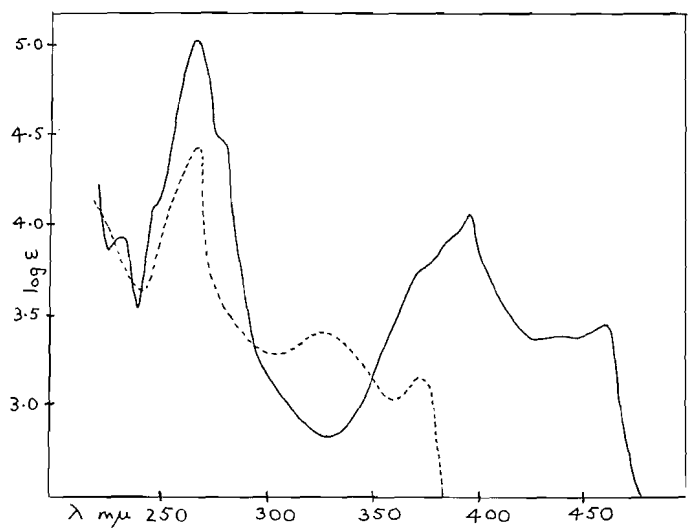

FIG. 1. Ultraviolet absorption spectra in methanol.
- - - Calycanine
—— Quinolino-(2 : 3 : 3′: 2 ′)-quinoline

Of the six quinolinoquinoline structures formed by the fusion of the two pyridine nuclei, only two, quinolino-(2:3:3′:2′)-quinoline (III) and quinolino-(3:4:4′:3′)-quinoline, are centrosymmetrical. We have now synthesized the former, and found it to be different from calycanine. By exclusion of alternatives, structure (IV) was proposed for calycanine (cf. 2).

A possible explanation for the active hydrogen found in the Zerewitinoff determination on calycanine may be that one mole of the Grignard reagent adds to the C=N linkage of one quinoline ring, and as a result, the hydrogen atom on the carbon γ to the nitrogen of the other quinoline ring is activated.

The ultraviolet absorption spectrum of calycanine is recorded in Fig. 1.

Synthesis of Quinolino-(2:3:3′:2′)-quinoline: Epindoline

Although the base itself has not been prepared previously, two of its derivatives, viz., 4:4′-dihydroxy-6:6′-dimethyl- (10) and 4:4′-dihydroxyquinolino-(2:3:3′:2′)-quinoline (11), have been synthesized. The hydroxyl groups in the quinolinoquinoline or epindoline (10) system were found to be resistant to reduction (10) or acylation (11). The synthesis of the unsubstituted base was carried out as follows.

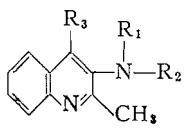

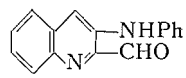

X

V. $R_1 = R_2 = H$; $R_3 = COOH$
VI. $R_1 = Ph$; $R_2 = H$; $R_3 = COOH$
VII. $R_1 = R_2 = Ph$; $R_3 = COOH$
VIII. $R_1 = Ph$; $R_2 = R_3 = H$
IX. $R_1 = R_2 = Ph$; $R_3 = H$

When 3-aminoquinaldine-4-carboxylic acid (V) (12) was heated with iodobenzene and copper catalyst under conditions described for the conversion of anthranilic acid to *o*-phenylaminobenzoic acid (13), a mixture of 3-phenylamino- and 3-diphenylamino-quinaldine-4-carboxylic acids (VI and VII respectively) was obtained. Attempts to prepare the monosubstituted acid exclusively were unsuccessful. It may be noted that 3-aminoquinaldine could not be arylated directly to give 3-arylaminoquinaldine (12, 14) and we have confirmed this difficulty in the reaction of 3-aminoquinaldine with iodobenzene. The mixture of carboxylic acids (VI and VII) could not be separated very satisfactorily, but the mixture of 3-phenylamino- and 3-diphenylamino-quinaldines (VIII and IX respectively) obtained on decarboxylation of the acids could be easily separated by chromatography over alumina.

Oxidation of 3-phenylaminoquinaldine with selenium dioxide, a reagent previously used for the oxidation of quinaldine to quinoline-2-aldehyde (15), gave 3-phenylamino-quinoline-2-aldehyde in 50% yield. It is interesting that this oxidation took place smoothly in spite of the presence of an easily oxidizable phenylamino group. Cyclization of the aldehyde to quinolino-(2:3:3′:2′)-quinoline was successful with concentrated sulphuric acid at 100° C, under the milder conditions described for the cyclization of *o*-phenylamino-benzaldehyde (13), the aldehyde (X) was recovered unchanged. The epindoline (III) was a bright yellow compound which charred but did not melt at 280° C. Its solutions in organic solvents were strongly fluorescent. The ultraviolet absorption spectrum of (III) is recorded in Fig. 1.

Can. J. Chem. Downloaded from www.nrcresearchpress.com by 78.46.186.204 on 09/04/12
For personal use only.

Can. J. Chem. Downloaded from www.nrcresearchpress.com by 78.46.186.204 on 09/04/12
For personal use only.

EXPERIMENTAL

All melting points are uncorrected. Analyses by Drs. Weiler and Strauss, Oxford.

Calycanine

This was prepared essentially according to Barger *et al.* (5) by the zinc dust distillation of calycanthine. At the same time, a neutral fraction smelling strongly of indole was obtained, but it failed to give any crystalline products. The basic portion gave calycanine, m.p. 302°–305° C, which was repeatedly sublimed to give needles from methanol, m.p. 306°–307° C. Its solution in methanol was faintly fluorescent in ultraviolet light, the fluorescence was unchanged on addition of alkali, but was slightly depressed with mineral acid. Found: C, 82.9; H, 4.4. Calc. for $C_{16}H_{10}N_2$: C, 83.5; H, 4.4%. Calc. for $C_{15}H_{10}N_2$: C, 82.5; H, 4.6%.

Calycanine Dipicrate

Chloroform solutions of calycanine and picric acid were heated together for a few minutes. On cooling, calycanine dipicrate separated as needles. It dissociated rapidly in alcohol and water but could be crystallized from chloroform containing picric acid in red needles, m.p. 238°–239° C. Found: C, 48.7; H, 2.39. Calc. for $C_{16}H_{10}N_2 \cdot 2C_6H_3N_3O_7$: C, 48.8; H, 2.32. Calc. for $C_{15}H_{10}N_2 \cdot 2C_6H_3N_3O_7$: C, 47.9; H, 2.36%.

3-Phenylaminoquinaldine-4-carboxylic Acid (VI)

Three grams of 3-aminoquinaldine-4-carboxylic acid (V) (12), 3.3 ml iodobenzene, 4.7 g freshly dried anhydrous potassium carbonate, and 0.15 g Ullmann's copper catalyst (Naturkupfer C) were refluxed in a mixture of 20 ml *cyclo*hexanol and 20 ml benzyl alcohol for 2 hours with strict exclusion of moisture. The reaction mixture was diluted with 50 ml water and steam-distilled to remove the alcohols. The solution was filtered hot and poured into dilute acetic acid. After 6–8 hours at room temperature, the flocculent precipitate was filtered (3.1 g, m.p. 250°–268° C) and extracted with a 1:1 mixture of chloroform–methanol to remove the disubstituted acid as well as some unchanged 3-amino acid. The residue (1.8 g) was crystallized from ethanol containing some pyridine in rhomboid needles, m.p. 298°–300° C with decomposition. Found: C, 73.0; H, 5.0. Calc. for $C_{17}H_{14}N_2O_2$: C, 73.4; H, 5.4%. The acid was sparingly soluble in alcohol, ether, benzene, and chloroform but easily soluble in pyridine. It did not dissolve readily in either dilute or concentrated hydrochloric acid, but gave a colorless potassium salt.

3-Phenylaminoquinaldine (VIII)

Two grams of the above acid (VI) was heated at 290°–300° C for 30 minutes. The acid melted with decomposition and some of the base sublimed into the condenser attached to the reaction flask. The melt was allowed to cool and extracted with methanolic hydrochloric acid. The acid extract was filtered, diluted with 50 ml water, and made strongly alkaline with potassium hydroxide. Ether extraction of the aqueous solution (charcoal) gave an oil which solidified on refrigeration (1.8 g, m.p. 90°–111° C). The base (VIII) was crystallized from very dilute alcohol in needles, m.p. 120°–121° C (lit. (16), m.p. 120°–121° C). Found: C, 82.1; H, 5.7. Calc. for $C_{16}H_{14}N_2$: C, 82.0; H, 6.0%. The base was very soluble in organic solvents to give non-fluorescent solutions.

The *picrate* formed in ethanol crystallized from the same solvent in golden yellow prisms, m.p. 230° C with decomposition. Found: C, 57.1; H, 3.8. Calc. for $C_{16}H_{14}N_2 \cdot 2C_6H_3N_3O_7$: C, 57.0; H, 3.7%.

3-Diphenylaminoquinaldine-4-carboxylic Acid (VII)

The chloroform–methanol extract from the preparation of the 3-phenylamino acid (VI) was evaporated to dryness and the residue repeatedly crystallized from the same solvents in stout needles, m.p. 270°–273° C with decomposition. Found: N, 7.6. Calc. for $C_{23}H_{18}N_2O_2$: N, 7.9%. The acid was soluble in chloroform and acetic acid, less so in acetone, and sparingly soluble in cold alcohol and benzene.

3-Diphenylaminoquinaldine (IX)

The diphenylamino acid (VII, 0.5 g) was decarboxylated by heating at 270°–275° C for 20 minutes. On working up the reaction mixture, as in the case of 3-phenylaminoquinaldine (VIII), the base was obtained as a yellow oil which solidified on trituration with alcohol. Crystallization from aqueous ethanol gave colorless prisms, m.p. 141°–142° C. Found: N, 9.2. Calc. for $C_{22}H_{18}N_2$: N, 9.0%. The base dissolved easily in organic solvents to give solutions with a vivid blue fluorescence.

The *picrate* prepared in ethanol formed yellow needles, m.p. 222°–223° C. Found: N, 12.8. Calc. for $C_{22}H_{18}N_2 \cdot C_6H_3N_3O_7$: N, 12.9%.

3-Phenylaminoquinoline-2-aldehyde (X)

3-Phenylaminoquinaldine (VIII, 0.9 g) and 0.45 g freshly prepared selenium dioxide were refluxed in 10 ml purified dioxan containing 1–2 drops of water. A vigorous reaction set in after 2 minutes and the solution turned dark, forming a red deposit of selenium. The heating was discontinued until the initial reaction was over, and the solution refluxed for a further 90 minutes. The dioxan was removed under reduced pressure and the black residue extracted with hot benzene (charcoal). Evaporation of the benzene extract gave an orange oil which solidified with a little cold ethanol (0.5 g, m.p. 98°–104° C). It was crystallized from dilute ethanol in needles, m.p. 109°–110° C. Found: C, 77.0; H, 4.8. Calc. for $C_{16}H_{12}N_2O$: C, 77.4; H, 4.8%. The aldehyde was very soluble in ether, benzene, and chloroform. An ethanolic solution of the aldehyde gave a deep red color with 2:4-dinitrophenylhydrazine hydrochloride in ethanol.

The *phenylhydrazone* was prepared by mixing an alcoholic solution of the aldehyde with a solution of phenylhydrazine in 50% acetic acid. On standing at room temperature for 1 hour, the phenylhydrazone separated as a red solid crystallizing from alcohol in yellow needles, m.p. 221–222° C. Found: C, 77.3; H, 5.4. Calc. for $C_{22}H_{18}N_4$: C, 77.9; H, 5.3%.

Quinolino-(2:3:3′:2′)-quinoline: Epindoline (III)

The aldehyde (X, 0.37 g) was heated with 1.4 ml concentrated sulphuric acid at 100° C under anhydrous conditions for 1 hour. The initial addition of sulphuric acid dissolved the aldehyde with evolution of heat. At the end of the reaction, the solution was poured into ice-cold water and made alkaline with ammonia. The precipitated solid (0.15 g) was extracted with 100 ml chloroform. Evaporation of chloroform gave bright yellow feathery needles, which were washed with ether to remove uncyclized aldehyde and crystallized from xylene to give stout yellow rods of epindoline which charred but did not melt at 280° C. Found: C, 83.2; H, 4.7. Calc. for $C_{16}H_{10}N_2$: C, 83.5; H, 4.4%. The base was sparingly soluble in ether, but moderately so in benzene, chloroform, and ethyl acetate. Its solutions in these solvents were bright yellow and gave a vivid green fluorescence on addition of a trace of ethanol. The solutions turned orangish and the fluorescence disappeared on addition of hydrochloric acid.

Can. J. Chem. Downloaded from www.nrcresearchpress.com by 78.46.186.204 on 09/04/12
For personal use only.

The *picrate* formed in chloroform gave red needles from alcohol containing picric acid, and melted at 308°–310° C with decomposition. Found: C, 57.3; H, 2.8. Calc. for $C_{16}H_{10}N_2 \cdot C_6H_3N_3O_7$: C, 57.5; H, 3.0%.

ACKNOWLEDGMENTS

The author is indebted to Sir Robert Robinson, O.M., F.R.S., for his advice and encouragement, and to the University of Bombay for a Sir Mangaldas Nathubhai Scholarship.

REFERENCES

1. HENRY, T. A. The plant alkaloids. J. & A. Churchill, Ltd., London. 1949. p. 485.
2. ROBINSON, R. and TEUBER, H. J. Chem. & Ind. 783 (1954).
3. SAXTON, J. E. Quart. Revs. (London), **10**, 119 (1956).
4. MARION, L. and MANSKE, R. H. F. Can. J. Research, B, **16**, 432 (1938).
5. BARGER, G., MADANIVEITIA, J., and STREULI, P. J. Chem. Soc. 510 (1939).
6. MANSKE, R. H. F. and MARION, L. Can. J. Research, B, **17**, 293 (1938).
7. HARGREAVES, A. Nature, **152**, 600 (1943).
8. HARGREAVES, A. and TAYLOR, W. H. J. Sci. Instr. **18**, 138 (1941).
9. MANSKE, R. H. F., MARION, L., and KULKA, M. Can. J. Research, B, **24**, 224 (1946).
10. AINLEY, A. D. and ROBINSON, R. J. Chem. Soc. 1508 (1934).
11. DIESBACH, H. DE, SCHURCH, A., and CAVIN, G. Helv. Chim. Acta, **31**, 716 (1948).
12. LAWSON, W., PERKIN, W. H., Jr., and ROBINSON, R. J. Chem. Soc. 635 (1924).
13. ALBERT, A. The acridines. Edward Arnold & Co., London. 1951.
14. CLEMO, G. R. and SWAN, G. A. J. Chem. Soc. 867 (1945).
15. KAPLAN, H. J. Am. Chem. Soc. **63**, 2654 (1941).
16. BRIT. PAT. No. 448,502. Chem. Abstr. **30**, 7588 (1936). U.S. Pat. 2,098,927. Chem. Abstr. **32**, 193 (1938).

Can. J. Chem. Downloaded from www.nrcresearchpress.com by 78.46.186.204 on 09/04/12
For personal use only.

Can. J. Chem. Downloaded from www.nrcresearchpress.com by 78.46.186.204 on 09/04/12
For personal use only.

ELECTROLYSIS OF LITHIUM HYDRIDE[1]

M. A. WEINBERGER, T. J. MOUSSEAU,[2] AND O. MAASS[3]

ABSTRACT

A method has been developed whereby current yields of as high as 70% of anodically discharged hydrogen can be maintained during continuous electrolysis of lithium hydride at or just below its melting point. Efforts to utilize this process for the separation of hydrogen and deuterium were unsuccessful.

INTRODUCTION

The electrolysis of heated lithium hydride was first investigated by Moers (1), who described a number of disturbing side effects which dogged his experiments. These showed up as wild fluctuations on the electrical meters monitoring the electrolysis and were ascribed by him to formation of lithium whiskers or metal fog which shorted the electrodes. This work was followed by that of Peters (2), who was able to demonstrate the validity of Faraday's laws for the separation of the electrolysis products. Optimum current efficiencies* for the electrolysis were found using solid lithium hydride at temperatures between 550 and 650° C, currents of 1–3 amp and electrolysis times of up to 3 minutes. In these experiments the hydrogen was pumped off as it was formed and corrections were made for hydrogen produced by thermal decomposition. Above the melting point, hydrogen evolution by electrolysis was found to be irregular and zero current yields were sometimes obtained. Other experiments showed that current yields dropped with increasing electrolysis times. Finally, Potter and Bockris (3) carried out electrolyses under hydrogen pressures of 1 atm to suppress thermal dissociation and showed that the electrolytically separated hydrogen was actually of anodic origin only. These workers also found that good current efficiencies (above 80%) were only obtained by electrolyzing for short times (up to $2\frac{1}{2}$ minutes) at temperatures below the melting point (570–610° C). One-half minute electrolysis at 680° C gave 27% yield, while a prolonged electrolysis (17.5 minutes) at 635° C gave only 2% of the amount of hydrogen calculated by Faraday's law. Recombination of the electrolysis products was believed to be the reason for the low efficiencies.

It appears that the liberated lithium metal is principally responsible for low electrolytic hydrogen yields and most of the apparent anomalies during the electrolyses. In the present work it was attempted to overcome this by depositing the lithium at a cathode with which it would form an alloy. Lithium alloys have been produced by electrolyzing fused lithium chloride – potassium chloride mixtures using the molten alloying metal as cathode (4). If lithium metal could in this way be prevented from spreading into or floating on the hydride and thus kept away from the hydrogen liberated at the anode, better yields should be obtainable. The choice of lithium scavenger cathode was limited to metals having a melting point below that of lithium hydride. Lead and aluminum were chosen. It was realized that because of their ability to form alloys with lithium these metals might decompose lithium hydride themselves, but it was hoped that some kind of equilibrium would be reached.

[1]*Manuscript received August 8, 1958.*
Contribution from the Defence Research Chemical Laboratories, Ottawa, Canada. Issued as D.R.C.L. Report No. 281.
[2]*Present address: Dominion Observatory, Seismology Division, Ottawa.*
[3]*National Research Council, Ottawa.*

*The current efficiency or yield is $\frac{\text{amount of product formed} \times 100\%}{\text{theoretical amount from Faraday's laws}} = \frac{\text{cc of hydrogen at n.t.p.}}{.0696 \times \text{amp minute}}\ \%$.

Can. J. Chem. Downloaded from www.nrcresearchpress.com by 78.46.186.204 on 09/04/12
For personal use only.

EXPERIMENTAL

The principal features of the electrolysis cell design were determined by the requirement that lithium deposition should occur only at the scavenger cathode. In addition, because of the corrosive nature of lithium hydride, possible cell materials were restricted to Armco iron or certain stainless steels (5), and no ceramic insulating materials could be used. The scavenger cathode then being in contact with the metallic cell walls, the latter had to be insulated from the active electrolyte to prevent lithium deposition there. This could be achieved by utilizing the poor electrical conductivity of solid lithium hydride at more than 150° below its melting point. Accordingly the cell was heated in such a way as to provide fused or nearly fused electrolyte between anode and scavenger cathode while at the same time maintaining an insulating layer of cooler solid lithium hydride on the walls of the cell not covered by the scavenger. The main heat input was therefore into the molten cathode and into the internally heated anode. By means of thermocouples, temperatures were measured in the cathode pool and at various points along the cell wall but could not be measured in the active electrolyte as the presence of metal there would have provided an auxiliary electrode.

The apparatus is shown in Fig. 1. The anode was supported by the cell lid from which it was electrically insulated and a means was provided to move it up or down in the cell. The lid and the upper part of the cell were water-cooled to protect the vacuum sealing gaskets and in addition a tube passing down the hollow anode shaft played cool nitrogen on the shaft wall opposite the teflon gasket. The temperatures of any of the gaskets never rose much above room temperature.

A conventional vacuum and gas handling system was attached to the cell.

The cell, lid, and anode were fabricated from 347 stainless steel, one of the materials recommended for use with lithium hydride (5). This material was chosen as it has a lower hydrogen permeability than pure iron. Welding was kept to a minimum and was done by the inert gas arc process. The cell after prolonged evacuation was first treated with hydrogen at 700° C. The first scavenger cathode material, reagent grade lead (7 lb), was then placed in the cell and hydrogen treatment at red heat continued. The cell was transferred to a dry box containing a helium atmosphere in which all subsequent dismantling, filling, and assembling procedures were carried out. About 280 g lithium hydride was placed in the cell, which was evacuated, filled with hydrogen, and heated. It was found that too much decomposition occurred and use of lead as cathode was abandoned, to be replaced by an aluminum–lithium mixture (15 mole % Li). The hydrogen treatment was repeated, some hydrogen being absorbed and the cell charged with 1 lb of lithium hydride (Maywood Chem. Co. 10-20 mesh). The cell was heated to 700° C, as measured by the thermocouple in the alloy. After this treatment, the cell was once again dismantled and all lithium hydride removed. A fresh 1-lb charge of hydride was placed in the cell (for later experiments the cell was almost filled with hydride to cut down dead space). When thermal decomposition had settled down to a low rate at 670–675° C, electrolysis was started using a stabilized current of 1 amp. This was obtained from storage batteries supplying 110 v d-c. by means of dropping resistors and a ballast tube. Cell voltage was not controlled but was measured. Cell temperatures were controlled manually and stability was enhanced by use of a constant voltage transformer.

Electrolyses were run for periods up to 27 minutes, during which time gas volumes of the order of 100 cc at the measured constant cell pressure (580–740 mm Hg) were collected

Can. J. Chem. Downloaded from www.nrcresearchpress.com by 78.46.186.204 on 09/04/12
For personal use only.

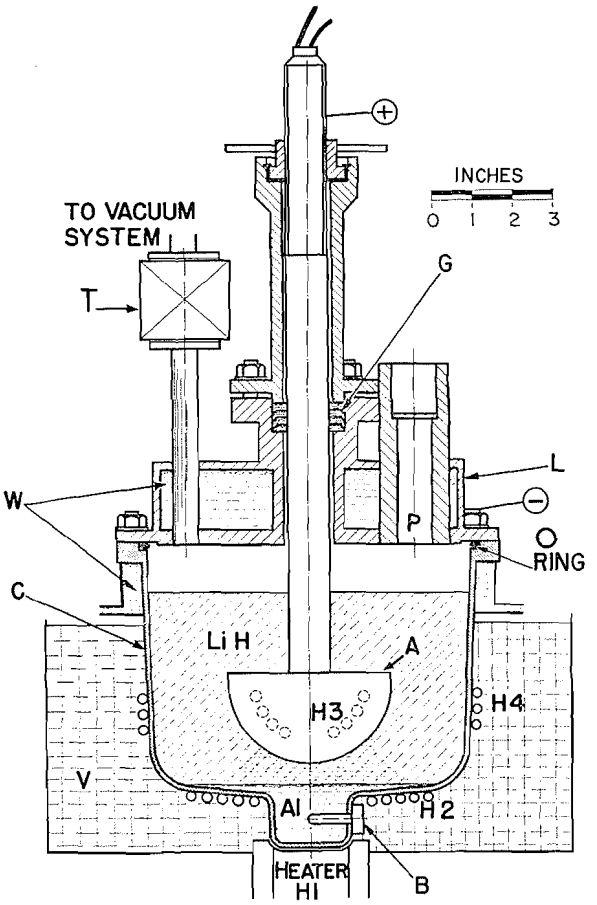

FIG. 1. Electrolysis cell.
C—Cell
L—Lid
A—Hemispherical anode
H_{1-4}—Heating elements
W—Water-cooling jackets
T—O-Ring high-vacuum valve (6)
P—Viewing port
V—Vermiculite
G—Teflon gaskets
B—Thermocouple well

in a burette. The rate of thermal decomposition or absorption was determined before and after each electrolysis and used to calculate the corrected amount of hydrogen evolved during electrolysis.

RESULTS AND DISCUSSION

With Lead as Scavenger:

Decomposition of lithium hydride shown by hydrogen evolution set in at about 350° C. Hydrogen had to be removed to keep the pressure in the system below atmospheric pressure. During subsequent cooling and reheating the onset of decomposition occurred at higher temperatures (500–550° C). The rate of gas evolution decreased somewhat as decomposition proceeded but was still high after 70% of the lithium hydride initially present had been decomposed. This system therefore does not attain hydrogen dissociation pressures below 1 atm at reasonable concentrations of lithium in the scavenger.

Can. J. Chem. Downloaded from www.nrcresearchpress.com by 78.46.186.204 on 09/04/12
For personal use only.

With Lithium–Aluminum as Scavenger:

Decomposition of lithium hydride occurred here too but after 1.2 moles had been decomposed the dissociation pressure settled down to somewhat less than an atmosphere at the operating temperatures. As the lithium content of the aluminum increased, higher temperatures were required for a given dissociation pressure. Working temperatures were chosen to give as low a rate of change of hydrogen evolution as possible, while maintaining a hydrogen pressure of 580–740 mm Hg. The other factor governing the choice of temperature was the electrical resistance of the electrolyte which with a cathode–anode separation of 1.5 cm was to be kept below 10 ohms. There was a rapid increase in resistance at temperatures below those shown in Table I. The rather large cell voltage fluctuations shown in the table for some of the runs were probably due to lack of homogeneity or local temperature instabilities in the melt. As mentioned previously the temperature measured was that of the alloy pool. In none of the experiments did the meter indications fluctuate wildly as found by Moers in the original electrolysis experiments.

From the results in Table I it appears to be rather difficult to prescribe optimum operating conditions for the electrolysis. The variables investigated were temperature, electrolysis time, and cell current. Temperature within the range studied, 670–689° C, does not seem to have too much effect. The other two variables are to some extent interrelated, since the electrolyses were run until a fixed amount of gas had been collected (100 or 127.5 cc at operating pressure), this gas, however, containing varying amounts of hydrogen produced by thermal decomposition. At first sight, the current efficiency seems to decrease with increasing duration of electrolysis, which would be in accord with the observations of Peters, and Potter and Bockris. Apparently electrolysis times of under 10 minutes correspond to yields of 60% and higher (Runs A1 to B9, E15 through F36) while electrolyses lasting for more than 20 minutes give yields of 40–50% (Runs B11 to D14). However, although the rate of electrolytic gas evolution was not usually measured, in two experiments (E16 and E17) where such measurements were made, the rate of volume increase was essentially constant for the whole period of the electrolysis. Hence the tentative supposition about a yield–time relation is not borne out in detail.

To the extent that the cell current is related to the electrolysis time, higher currents apparently correspond to better yields. This generalization does not fit experiments A1 to A8. The possibility that the higher yields in runs using 2 amp (E15 to F36) were artifacts due to thermal decomposition of the hydride by the heat liberated by the current is discounted (i) by experiments A7 and 8 where good yields were obtained with 0.29 amp, and (ii) by experiments B12 to B15 where the wattage dissipated was higher than in the 2-amp runs and much poorer yields resulted.

A possible explanation of the results discussed in the preceding paragraphs may be that the scavenger cathode is only partially effective: effective enough to make it possible to electrolyze lithium hydride near its melting point profitably for much longer periods than those used by Potter and Bockris but not quite able to prevent some lithium from getting into the melt. This would account for the apparent irregular yields and also for some of the cell voltage variations.

Hydrogen–Deuterium Separation:

Exchange of hydrogen with lithium hydride takes place slowly at room temperature (7) by means of a surface reaction and a diffusion process and would be expected to proceed much more rapidly at the working temperatures used here, where the additional mechanisms of dissociation and recombination are available. It was, however, of theoretical and practical interest to see whether one could detect any electrolytic separation

TABLE I

ELECTROLYSIS DATA

Electrolysis No.	Temperature, °C	Electrolysis time, minutes	Cell current, amp	Cell voltage, volts	Vol. of electrolytic gas at n.t.p., cc	Average thermal decomposition (absorption) rate cc/minute at n.t.p.	Current yield, %
A1	672.0→671.5	6.4	1.08	3.0→2.8*	27	7.0	56
A2	671.5	6.2	1.08	3.2	43	5.7	82
A3	672.0	10.6	0.99	4.2→4.6	75	0.2	103
A4	671.5→671.6	9.9	0.98	5.0→5.5	78	0.0	115
A5	671.6→671.7	10.0	0.98	5.9→6.2	79	0.0	115
A6	671.7	10.5	0.98	6.6→7.1	80	0.0	111
A7	671.7	10.0	0.29	2.6→2.7	23	0.1	114
A8	671.5→672.2	8.0	0.29	2.8→2.9	17	0.9	107
B9	672.8	8.1	1.00	8.4→9.5	50	3.7	89
B10	670.4	17.2	1.00		69	1.1	57
B11	670.6	20.4	1.00		62	1.2	44
B12	670.7	20.5	0.99–1.00	15→12.3	63	1.2	45
B13	671.0→671.5	21.8	0.98	14.7±2 fluc.	60	1.3	40
B14	671.0→670.3	26.8	0.98	14.0±1.6	61	1.0	33
B15	670.0→671.7	26.4	0.96	16.0±1.0	71	0.6	40
C1	677.1→677.4	21.0	1.05	4.3→5.4	63	2.2	41
C2	677.4	20.8	1.05	5.4	70	1.9	46
C3	677.6	20.8	1.05	5.6→5.4	82	1.3	54
C4	677.9	21.8	1.05	5.4→5.2	85	1.1	53
C5	677.9	20.4	1.05	5.1→5.0	86	1.1	58
C6	678.1	22.4	1.05–1.06	5.0→4.8	81	1.2	49
C7	678.3	22.0	1.06	4.8	89	0.9	55
D8	678.8	21.2	1.08–1.09	6.3±0.1	78	1.6	49
D9	678.9	22.5	1.08	6.5→5.2 fluc.	84	1.3	49
D10	679.2	23.1	1.08	5.6→5.2	84	1.2	48
D11	679.8	23.5	1.08	5.4→5.1	86	1.1	49
D12	680.0	25.6	1.08	5.0→4.8	89	0.9	46
D13	680.2	26.0	1.08	5.0→4.8	101	0.4	52
D14	680.2	27.0	1.08	5.0→4.8 fluc.	110	0.1	54
E15	684.9	10.0	2.05	6.8→6.5	94	0.7	66
E16	685.1	9.4	2.05–2.08	6.2→5.6	99	0.2	73
E17	686.0	9.4	2.07–2.09	5.6→5.0	100	0.0	74
E18	686.7	9.5	2.07–2.08	5.2→4.5	104	(0.4)	76
E19	687.6	9.7	2.08	4.9→4.2	106	(0.6)	76
E20	688.3	10.9	2.08–2.09	4.4→3.8	111	(1.0)	70
E21	688.5	9.2	2.09	4.0→3.6	108	(1.0)	81
E22	688.5	9.4	2.09	3.8→3.5	92	(0.2)	67
E23	688.5	10.8	2.09	3.8-3.6	89	0.1	57
F24	686.8	6.7	2.01	4.5→4.2	70	1.1	74
F25	686.2→685.8	7.1	2.01	4.6→4.4	69	1.0	70
F26	685.4	7.5	2.01	4.8→4.6	73	0.4	70
F27	685.4	7.7	2.01	4.9→4.6	77	0.0	72
F28	685.1	8.2	2.01	5.1→4.7	82	(0.6)	71
F29	685.1	9.3	2.01	4.8±0.4 fluc.	85	(0.9)	65
F30	685.1→684.9	9.1	2.01	5.2±0.4 fluc.	83	(0.8)	66
F31	684.9	9.1	2.01	5.5±0.5 fluc.	83	(0.8)	65
F32	684.9	9.7	2.01	6.0→5.5	83	(0.8)	61
F33	685.1	10.3	2.01	6.4→5.5±0.2 fluc.	83	(0.7)	57
F34	685.1	10.2	2.01	6.8→6.0	85	(1.0)	60
F35	685.2	8.7	2.00	7.2→6.2	87	(1.5)	72
F36	685.4	9.3	2.00	7.4→6.2	81	(0.8)	63

Electrolyses A1–B15 were carried out with different LiH filling from C1–F36. Runs between which the cell had been cooled to room temperature and sometimes evacuated are designated by different letters.

*Arrow indicates drift during an experiment.

Can. J. Chem. Downloaded from www.nrcresearchpress.com by 78.46.186.204 on 09/04/12
For personal use only.

of the hydrogen isotopes. Mass spectrometric analyses of the hydrogen produced electrolytically (i.e. 59, 65, 76, 98, and 96% of the total gas collected in electrolysis series B, C, D, E, and F respectively) did not give significantly different deuterium–hydrogen ratios from those of the hydrogen produced by thermal decomposition. Thus if any separation occurred during the electrolysis it must have been masked by exchange.

The mass spectrometer analyses also showed that the gas contained only species of mass 2 and 3 and no significant amounts of species attributable to methane (from carbon in the steel), nitrogen, etc.

ACKNOWLEDGMENTS

The authors wish to express their gratitude to Mrs. K. O. Kutschke, National Research Council, Ottawa, and Mr. D. C. Austen, Atomic Energy of Canada Limited, Chalk River, for mass spectrometric analyses. They would also like to thank Dr. H. Sheffer, Dr. R. M. Heggie, and Dr. E. J. Casey for discussions.

REFERENCES

1. MOERS, K. Z. anorg. u. allgem. Chem. **113**, 179 (1920).
2. Peters, K. Z. anorg. u. allgem. Chem. **131**, 140 (1923).
3. POTTER, E. C. and BOCKRIS, J. O'M. Colloq. intern. centre natl. recherche sci. (Paris) **39**, Electrolyse C3-C6, (1952); Chem. Abstr. **47**, 5280c (1953).
4. ROGERS, R. R. and VIENS, G. E. Trans. Can. Inst. Mining Met. **51**, 273 (1948).
5. GIBB, T. R. P., Jr. and MESSER, C. E. A survey report on lithium hydride. U.S. Atomic Energy Comm. NYO-3957 (1954).
6. STARK, J. A. and LANGSDORF, A., Jr. Rev. Sci. Instr. **25**, 188 (1954).
7. WILZBACH, K. E. and KAPLAN, L. J. Am. Chem. Soc. **72**, 5795 (1950).

Can. J. Chem. Downloaded from www.nrcresearchpress.com by 78.46.186.204 on 09/04/12
For personal use only.

Can. J. Chem. Downloaded from www.nrcresearchpress.com by 78.46.186.204 on 09/04/12
For personal use only.

DONOR ACCEPTOR REACTIONS OF TITANIUM TETRACHLORIDE WITH FORMAMIDE AND N,N-DIMETHYL FORMAMIDE[1]

JACQUES ARCHAMBAULT[2] AND ROLAND RIVEST

ABSTRACT

Co-ordination complexes of titanium tetrachloride with formamide and N,N-dimethyl formamide have been prepared. All the complexes found are explained through a co-ordination number of 6 for titanium (IV).

The infrared spectra of these compounds were measured; a negative shift observed for the carbonyl frequency and a positive shift observed for what is thought to be the C—N frequency are explained by a co-ordination through the oxygen of these molecules. Structural formulas are proposed for the compounds obtained.

INTRODUCTION

Titanium tetrachloride "A" is a very strong Lewis acid. Its reactions with donor molecules were very well summarized by Jackson (1) in 1939 and more recently by Archambault (2) in 1956. The only addition compound between "A" and an amide was prepared by Dermer and Fernelius (3). They reported the synthesis of an addition compound between "A" and N,N-diphenylacetamide, but the elementary analysis is the only evidence they have to support the proposed formula $TiCl_4.2CH_3CON(C_6H_5)_2$.

An amide, even with two donor atoms, oxygen and nitrogen, should not give a chelate with "A" because it would be a four-atom ring which is very seldom obtained (4). The bonding through both donors could lead to a polymeric species, but the molecular weight determination of one complex obtained indicated that this is not the case. So the remaining question to answer is the following: which atom in the donor molecule is complexed with "A"? Infrared spectra of some metal–urea complexes have been measured by Mizushima and Quagliano (5). They reveal that urea forms nitrogen-to-metal bonds with some transition metals and oxygen-to-metal bonds with others. Since the relative ability of the two donors is easily reversed by passing from one complex to another, it seemed to us that experimentation was the best way to get an answer to our question. N,N-dimethyl formamide was chosen for this purpose.

Furthermore, it is well known that substitution reactions occur very easily when the donor atom, oxygen or nitrogen, is combined with a more or less labile hydrogen. We had hoped that the use of formamide as a donor would give us additional information and lead to the answer of the previous question. It was also of interest to know if the strong molecular association of formamide would have any effect on the reaction.

EXPERIMENTAL

Materials and Manipulations

Reagent grade titanium tetrachloride was purified by the method of Gilchrist (6), redistilled, and used as such. The reagent grade of the amides and of the solvents used for infrared measurements was carefully dried over sodium sulphate and redistilled under completely dry atmosphere; the medium fraction was used for our experiments.

Titanium tetrachloride and its addition compounds are extremely sensitive to moisture, so all the experiments were performed under controlled atmosphere using dry nitrogen. Unless otherwise indicated, the addition of the titanium tetrachloride was made through

[1]*Manuscript received June 10, 1958.*
Contribution from the Department of Chemistry, University of Montreal, Montreal, Que.
[2]*Fellow of l'Office Provincial des Recherches Scientifiques de la Province de Québec.*

a pressure-equalizing funnel and the reaction was allowed to take place in a closed system previously flushed with nitrogen. Agitation was provided with a Teflon-enclosed magnetic stirrer.

The System: $TiCl_4$–$HCON(CH_3)_2$

A solution of $TiCl_4$ in carbon tetrachloride was added dropwise to excess dimethyl formamide diluted in the same solvent. The reaction product, washed with carbon tetrachloride and dried under vacuum, is a yellow powder, much more stable to moisture than most adducts of $TiCl_4$ with organic molecules. The high melting point of this complex (220–225° C) is another evidence of its greater stability. The compound is soluble in polar solvents with or without decomposition, according to the donor ability of the solvent molecule. The analyses for titanium and chlorine were made gravimetrically on the same sample, the titanium being weighted as TiO_2 and the chlorine as AgCl. Carbon and hydrogen were determined by the conventional microcombustion technique and nitrogen by the Kjeldal method.

	% Ti	% Cl	% N	% C	% H	Ti/Cl
Calc. for $TiCl_4.2HCON(CH_3)_2$	14.26	42.22	8.34	21.42	4.20	1/4.00
Found	14.20	41.78	8.27	21.44	4.50	1/3.97

Ebullioscopic measurements were carried out on methylene chloride solutions of the adduct, using a Swietowslavski boiling-point apparatus. The molecular weight so found (340±15) is in good agreement with the formula weight (335.9) of the monomeric species. Then the idea of a polymeric chain through both donor atoms is to be rejected. Moreover, if we are to maintain the generally admitted co-ordination number of 6 for titanium (IV), we must exclude the possibility that both nitrogen and oxygen act as donors towards the same titanium atom. This will be confirmed by infrared spectrum investigations.

The System: $TiCl_4$–$HCONH_2$

A saturated solution of formamide in methylene chloride was added dropwise to a solution of $TiCl_4$ in the same solvent, so that the reaction medium was always in excess of "A". The reaction product is a yellow powder insoluble in methylene chloride from which it was separated by filtration. After being washed many times with fresh anhydrous CH_2Cl_2, it was dried under vacuum at room temperature. This product is much less stable to moisture than its dimethyl formamide congener. It has no definite melting point, but decomposes on heating with loss of HCl. An attempt to determine nitrogen by the micro Dumas method was unsatisfactory, but the Kjeldal method gave reliable results.

	% Ti	% Cl	% N	% C	% H	Ti/Cl
Calc. for $TiCl_4.2HCONH_2$	17.12	50.69	10.01	8.58	2.16	1/4.00
Found	17.42	49.43	9.88	9.44	2.39	1/3.78

The product is soluble only in highly polar solvents in which the possibility of decomposition due to interchange with the solvent molecules is not to be disregarded. Another restriction which should not be neglected is that ebullioscopic measurements on this adduct require a low-boiling solvent in order to avoid decomposition by heat. So molecular weight determinations could not be made because of the absence of a suitable solvent either for ebullioscopic or cryoscopic experiments.

Can. J. Chem. Downloaded from www.nrcresearchpress.com by 78.46.186.204 on 09/04/12
For personal use only.

Attempts to perform the reaction between pure reactants resulted in somewhat different compounds. In a first experiment, excess $TiCl_4$ has been slowly added to pure formamide at the temperature of 0° C. The reaction, which is highly exothermic, rapidly yields a yellow spongy solid. After being thoroughly washed with CCl_4 to remove excess $TiCl_4$, and dried under vacuum, this substance yielded a hygroscopic yellow product, the composition of which changed with varying drying temperature. We have found it pretty hard to repeat our results from one experiment to the other as shown in Table I. However, at room temperature, it appears that no substitution occurs, and one finds a compound of the following formula $TiCl_4.(HCONH_2)_2.nHCONH_2$ in which "n" varies from 3.5 to 4.5. This does not imply an exception to the normal co-ordination number of 6 for titanium (IV), but simply that we are dealing with the same hexa-co-ordinated compound more or less associated through hydrogen bridging, according to the following scheme.

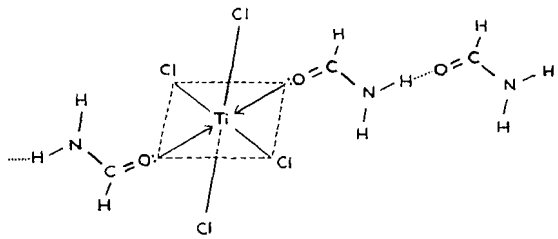

FIG. 1.

TABLE I

Drying temp.		% Ti theor.	% Ti found	% Cl theor.	% Cl found	Ti/Cl theor.	Ti/Cl found
20° C	$TiCl_4.4HCONH_2$	12.90	11.53 12.84	38.40	35.44 38.20	1/4	1/4.1 1/3.99
50° C	$TiCl_4.3HCONH_2$	14.75	14.24 14.28	43.73	40.01 40.69	1/4	1/3.79 1/3.84
100° C	$TiCl_3.HCONH.2HCONH_2$	16.28	16.22	38.90	37.81	1/3	1/3.15

If the drying temperature is increased, the composition changes gradually till one gets a ratio of Cl/Ti of 3.15 with approximately one mole of HCl and one mole of formamide pumped off.

Infrared Spectra and Structure Discussions

The infrared spectra were obtained by a Perkin–Elmer model 112 single beam spectrophotometer using NaCl prism. Characteristic absorption bands of $TiCl_4.2HCON(CH_3)_2$ are given in Table II, together with those of N,N-dimethyl formamide in different solvents.

From the spectra of $TiCl_4.2HCON(CH_3)_2$ and $HCON(CH_3)_2$ in methylene chloride and acetonitrile, the C=O stretching frequency of the complex is shown to be shifted by about 30 cm^{-1} to lower frequencies. A similar shift of the carbonyl band in complex compounds is an indication of co-ordination through the oxygen atom (5). Corresponding data for the adduct with formamide are recorded in Table III.

Once again, the carbonyl band is shifted by the amount of 28 cm^{-1} to lower frequencies. This is certainly a strong indication that co-ordination of either substituted or unsubstituted amides to titanium (IV) is made through oxygen rather than nitrogen.

Can. J. Chem. Downloaded from www.nrcresearchpress.com by 78.46.186.204 on 09/04/12
For personal use only.

TABLE II

ABSORPTION MAXIMA IN CM^{-1} OF $TiCl_4.2HCON(CH_3)_2$ AND $HCON(CH_3)_2$

Band assignment	in CH_2Cl_2			in CH_3CN		
	$TiCl_4.2HCON(CH_3)_2$	$HCON(CH_3)_2$	Frequency shift	$TiCl_4.2HCON(CH_3)_2$	$HCON(CH_3)_2$	Frequency shift
C=O stretching vibration	1646 vs	1676 vs	−30	1648 vs	1676 vs	−28
	1372±5 m	1386±5 m		—	—	—
	—	—	—	1249 m	1258 m	− 9
Possible C—N stretching vibration	1123 m	1093 m	+30	1123 m	1095 m	+28
	1062 w	1064 w	−2	—	—	—

Nevertheless, since the contribution of the tautomeric form H—C(OH)=NH to formamide is negligible (7, 8) one could argue that the loss of HCl observed on heating the formamide adduct is an evidence of co-ordination by nitrogen. Indeed, this internal rearrangement generally implies that the donor atom is bonded to a more or less labile hydrogen, but in the case of formamide, it can be accounted for otherwise in terms of the resonance theory. As pointed out by Pauling (9) and Dewar (10), amides are in resonance between the two following forms:

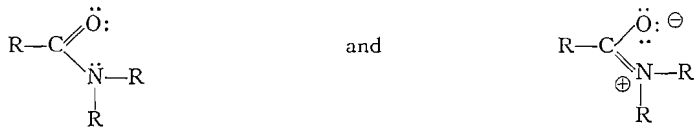

The dipolar form contributes about 15% (8). The formation of a co-ordinated link through the free electron pair of nitrogen would result in the loss of the resonance energy of the parent base which amounts to 21 kcal/mole in formamide (9). However, the formation of O→Ti bonds is expected to increase the contribution of the dipolar structure (11, 12), so the positive formal charge on nitrogen eases the departure of a proton, according to the following mechanism:

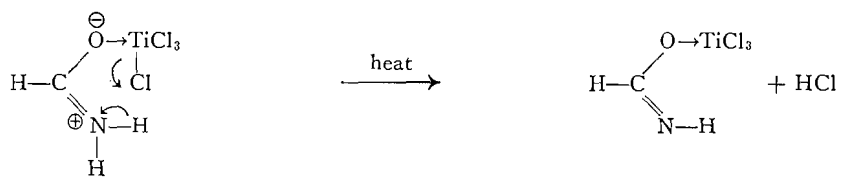

On the other hand, if the effect of a Lewis acid on amides is to result in a greater double-bond character for the nitrogen-to-carbon bond and a greater single-bond character for the carbon-to-oxygen bond, one should be able to detect these effects by infrared spectra. As we have shown above, we observed a lowering of the C=O stretching frequency in both adducts, but unfortunately, the position of the C—N stretching band is not as well

Can. J. Chem. Downloaded from www.nrcresearchpress.com by 78.46.186.204 on 09/04/12
For personal use only.

known. In fact, no data are available concerning the assignment of infrared absorption bands of N,N-dimethyl formamide.

Infrared spectrum of formamide has been more thoroughly investigated, and the position of the C—N stretching band is assumed to be at 1309 cm^{-1} in the liquid state, which is supported by the positive frequency shifts of this band accompanying the passage from vapor to liquid state and from formamide to formamide hydrochloride (13).

As shown in Table II, there is only one band of N,N-dimethyl formamide which suffers a positive shift when co-ordinating to titanium (IV), and this shift is of the same order, but opposite in direction, as the shift due to the lowering of the carbonyl frequency. This band is located at 1086 cm^{-1} in a non polar solvent like CS_2 and shifted to 1093 and 1095 cm^{-1} in CH_2Cl_2 and CH_3CN. Furthermore, its frequency increases by some 28–30 cm^{-1} when entering complexes. Such a behavior appears to be an argument in favor of its assignment to the C—N stretching vibration, although this tentative assignment needs to be checked by model compounds.

Moreover, the lack of a suitable solvent for the adduct $TiCl_4.2HCONH_2$ prevented us from finding out the exact position of its C—N band, which is well known for pure formamide. Emulsions were not too good in Nujol, and light diffusion occurred. Nevertheless, the C—N band appeared to be much broader and centered over higher frequencies, although it is difficult to estimate the value of the shift.

CONCLUSIONS

The results of elementary analysis, molecular weight determinations, and infrared measurements have led us to propose the following formulas for the compounds prepared:

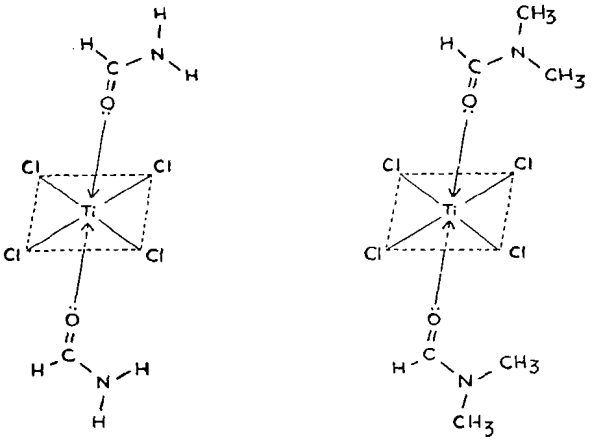

FIG. 2.

The corresponding *cis* forms are also a possibility.

ACKNOWLEDGMENTS

The authors are grateful to the following for their assistance: Prof. Camille Sandorfy for valuable discussions on the infrared spectra measured, the National Research Council of Ottawa for its financial assistance (R.R.), and l'Office Provincial des Recherches Scientifiques de la Province de Québec for a fellowship to one of us (J.A.).

Can. J. Chem. Downloaded from www.nrcresearchpress.com by 78.46.186.204 on 09/04/12
For personal use only.

TABLE III

ABSORPTION MAXIMA IN CM^{-1} OF $TiCl_4.2HCONH_2$ AND $HCONH_2$

Band assignment	Emulsions in Nujol		Solutions in CH_3CN		
	$TiCl_4.2HCONH_2$	$HCONH_2$	$TiCl_4.2HCONH_2$	$HCONH_2$	Frequency shift
NH_2 sym. and asym. vibrations	3375–3100 m	3400–3200 s	—	3467 m	
				3360 m	
C=O stretching vibration	—	1683 vs	1676 vs	1704 vs	−28
	1550±10 s	1645–1580 m			
	—	1392 s			
C—N stretching vibration	1370–1300	1312 s	—	1282 s	
	1090 m	—			
	1052 w	1052 w			

RÉSUMÉ

On a préparé des complexes de coordination du tétrachlorure de titane avec la formamide et la N,N-diméthyl formamide. Tous les complexes isolés sont expliqués en attribuant au titane (IV) le nombre de coordination 6. Les spectres infrarouges de ces composés ont été mesurés. Une variation négative de la fréquence du carbonyle et une variation positive d'une bande attribuée à la vibration C—N sont expliquées en supposant que la coordination au titane se fait par l'oxygène des molécules d'amide. On propose des formules dans l'espace pour les composés préparés.

REFERENCES

1. JACKSON, K. E. Chem. Revs. **25**, 67 (1939).
2. ARCHAMBAULT, J. Thèse de Maîtrise, Université de Montréal, Montréal, Québec. 1956.
3. DERMER, O. C. and FERNELIUS, W. C. Z. anorg. u. allgem. Chem. **221**, 83 (1934).
4. MOELLER, T. Inorganic chemistry. John Wiley & Sons, Inc., New York. 1952. p. 236.
5. PENLAND, R. B., MIZUSHIMA, S., CURRAN, C., and QUAGLIANO, J. V. J. Am. Chem. Soc. **79**, 1575 (1957).
6. CLABAUGH, W. S., LESLIE, R. T., and GILCHRIST, R. J. Research Natl. Bur. Standards, **55**, 261 (1955).
7. WHELAND, G. W. Resonance in organic chemistry. John Wiley & Sons, Inc., New York. 1955. p. 410.
8. LENORMANT, H. Bull. soc. chim. France, 33 (1948).
9. PAULING, L. Nature of the chemical bond. Cornell Univ. Press, Ithaca, N.Y. 1945. p. 207.
10. DEWAR, M. J. S. The electronic theory of organic chemistry. The Clarendon Press, Oxford. 1949. p. 96.
11. YAMAGUCHI, A. *et al.* J. Am. Chem. Soc. **80**, 527 (1958).
12. DAVIES, M., EVANS, J. C., and JONES, R. L. Trans. Faraday Soc. **51**, 761 (1955).
13. EVANS, J. C. J. Chem. Phys. **22**, 1228 (1954).

Can. J. Chem. Downloaded from www.nrcresearchpress.com by 78.46.186.204 on 09/04/12
For personal use only.

Can. J. Chem. Downloaded from www.nrcresearchpress.com by 78.46.186.204 on 09/04/12
For personal use only.

THE HEMICELLULOSE OF WHITE ELM (ULMUS AMERICANA) II. CONSTITUTION OF THE METHYL GLUCURONO-XYLAN[1]

J. K. GILLHAM AND T. E. TIMELL

ABSTRACT

The wood of white elm (*Ulmus americana*) has been found to contain less xylan than most other hardwoods. Partial hydrolysis of the hemicellulose component yielded an aldotriouronic acid, a glucuronosyl xylose, 2-*O*-(4-*O*-methyl-α-D-glucopyranosyluronic acid)-D-xylopyranose, 4-*O*-methyl-D-glucuronic acid, and galacturonic acid.

Hydrolysis of the fully methylated polysaccharide gave a mixture of 2-*O*- and 3-*O*-methyl-D-xylose, 2,3-di-*O*-methyl-D-xylose, 2,3,4-tri-*O*-methyl-D-xylose, and 2-*O*-(2,3,4-tri-*O*-methyl-α-D-glucopyranosyluronic acid)-3-*O*-methyl-D-xylopyranose in a molar ratio of 6:124:1:14. The number-average degree of polymerization of the methylated hemicellulose was 133 and that of the native polymer 185. On the basis of this and other evidence it is suggested that the xylan is linear and contains 185 1,4-linked β-D-xylopyranose residues, every seventh of which carries a single terminal side chain of 4-*O*-methyl-D-glucuronic acid attached by an α-glycosidic bond through C_2 of the xylose. The number of acid groups is larger than in other hardwood hemicelluloses so far studied.

In a previous investigation (1) it was shown that partial hydrolysis of a hemicellulose from white elm yielded a mixture of sugars containing xylose, 2-*O*-(4-*O*-methyl-α-D-glucopyranosyluronic acid)-D-xylopyranose, and several other uronic acids. The present paper is concerned with the nature of these sugar acids and with the structure and properties of the hemicellulose.

RESULTS AND DISCUSSION

Resolution of the mixture of sugar acids referred to previously (1) on a column of anion exchange resin yielded six fractions. The first acid to be eluted from the column (I) contained one methoxyl and one carboxyl group. Examination by paper chromatography after partial hydrolysis suggested the presence of xylose, a mono-*O*-methyl glucuronic acid, and the above aldobiouronic acid. Together with the equivalent weight (510) these facts indicated that I ($[\alpha]_D^{20}$ +75°) was a triouronic acid containing two xylose and one mono-*O*-methyl glucuronic acid residue. A similar triouronic acid has been isolated from trembling aspen (2), western hemlock (3), Monterey pine (4), loblolly pine (5), and milkweed floss (6).

The second acid obtained (II) was the aldobiouronic acid referred to above. The following fraction was further resolved by paper chromatography and elution from a cocoanut charcoal column (7). The first of the three acids thus obtained (III) was characterized as galacturonic acid after reduction to galactose. Acid IV contained no methoxyl group. Chromatographic examination indicated the presence in the hydrolyzate of glucuronic acid, glucuronolactone, and xylose. These results, together with the equivalent weight (354), suggested the presence of an aldobiouronic acid ($[\alpha]_D^{20}$ +85°) containing one glucuronic acid and one xylose residue. Such acids have frequently been isolated after partial hydrolysis of many non-woody plants, for example wheat straw (8). In wood, glucurone alone has so far been encountered in hydrolyzates from trembling aspen (9), black spruce (10), and white birch (11).

The next acid (V) was not further examined but the last (VI), which contained one methoxyl and one carboxyl group, was converted to the methyl ester, methyl glycoside,

[1]*Manuscript received July 14, 1958.*
Contribution from McGill University and Pulp and Paper Research Institute of Canada, Montreal, Quebec.

reduced with lithium aluminum hydride and hydrolyzed to yield 4-*O*-methyl-D-glucose, identified through its crystalline osazone. Acid VI was therefore 4-*O*-methyl-D-glucuronic acid, a common constituent of plant hemicelluloses (12). Its infrared spectrum was identical with that of an authentic specimen.

The elm wood was analyzed by standard methods (12) and found to contain cellulose (49.3), lignin (23.6), acetyl (3.9), ash (0.3), uronic anhydride (3.6), galactan (0.9), mannan (2.4), araban (0.6), and xylan (11.5%). The content of xylan was exceptionally low for a hardwood and, for example, less than half of that of white birch (13).

The hemicellulose was isolated by direct alkaline extraction of the wood as described previously (1). Earlier evidence suggested strongly that the polysaccharide possessed residues of 4-*O*-methyl-D-glucuronic acid linked to xylose. If this were so, the uronic anhydride content corresponded to 7.0 xylose residues per acid group and the methoxyl content to 7.2. The corresponding value obtained from the equivalent weight of the acidic polysaccharide was 6.8.

The fully methylated hemicellulose was subjected to methanolysis under conditions which were known to effect no cleavage of the aldobiouronic acid. The glycosides were resolved into an acidic and a neutral fraction on a column of ion exchange resin. The acidic fraction, which contained only one component, was converted to the ester glycoside, reduced, and hydrolyzed to give a mixture of reducing sugars which was resolved on a charcoal column, yielding 2,3,4-tri-*O*-methyl-D-glucose and 3-*O*-methyl-D-xylose, both of which were characterized through their aniline derivatives. The acid was accordingly 2-*O*-(2,3,4-tri-*O*-methyl-α-D-glucopyranosyluronic acid)-3-*O*-methyl-D-xylopyranose. The fact that the 4-position was unsubstituted in this acid but was substituted when the free acid itself was methylated (1) showed that its xylose moiety was linked to other sugar residues through C_4. This, in conjunction with the absence of any 3,4-di-*O*-substituted xylose, suggested that the acid side groups were attached directly to the framework of the hemicellulose.

The solution of the neutral glycosides was extracted with chloroform for removal of any highly substituted and therefore volatile xyloside (14). After concentration of the extract and the remaining aqueous solution, the glycosides were again combined and hydrolyzed and the resulting mixture of reducing sugars was resolved by fractional extraction of its aqueous solution with chloroform. The first compound to be extracted was identified as 2,3,4-tri-*O*-methyl-D-xylose through its aniline derivative. The major component, which was only sparingly soluble in chloroform, crystallized and was identified as 2,3-di-*O*-methyl-D-xylose. A mixture of two mono-*O*-methyl xyloses was recovered from the aqueous phase and resolved by paper ionophoresis to yield 2-*O*- and 3-*O*-methyl-D-xylose. The molar ratio among the mono-*O*-methyl xyloses, the 2,3-di-*O*-methyl-D-xylose, and the 2,3,4-tri-*O*-methyl-D-xylose was determined as 6 : 124 : 1 (15). The yield of the acid fragment, 14 moles per non-reducing end group, corresponded to 10 xylose residues per acid group, a value higher than expected. The reason for this was probably a loss of uronide material during the methylation. Similar observations have been made elsewhere (16, 17, 18).

The large amount of 2,3-di-*O*-methyl-D-xylose isolated indicated that the backbone of the polysaccharide was composed of xylopyranose residues linked through positions 1 and 4, while the high negative rotation (−70°) of the hemicellulose suggested that the anhydroxylose units were present in the β-configuration. The 2,3,4-tri-*O*-methyl-D-xylose evidently originated from the non-reducing end groups. The side chains consisted of 1,2-linked 4-*O*-methyl-D-glucuronic acid residues, all of which were recovered as the

Can. J. Chem. Downloaded from www.nrcresearchpress.com by 78.46.186.204 on 09/04/12
For personal use only.

partly methylated aldobiouronic acid. The presence of the mono-*O*-methylated xyloses was therefore due to either incomplete methylation, demethylation, or branching.

When the number-average molecular weight of the methylated hemicellulose was determined by osmometry (19), a value of 24,000 was obtained. Assuming one 4-*O*-methyl-D-glucuronic acid group to be associated with 10 xylose residues, this corresponded to a degree of polymerization of 133. The number of non-reducing end groups indicated a number-average D.P. of 145, thus precluding the possibility of any branching. The presence of the mono-*O*-methyl xyloses was accordingly due to incomplete methylation or demethylation. Such phenomena have frequently been encountered elsewhere (16, 18, 20).

The hemicellulose was converted to the fully substituted acetate derivative without any apparent depolymerization (21). Osmotic pressure measurements indicated a number-average molecular weight of 45,900. Assuming the presence of seven anhydroxylose units for each acidic side group, this corresponded to a number-average degree of polymerization ($\bar{P}_n$) of 185. Intrinsic viscosities ($[\eta]$) were determined in cupriethylenediamine and in dimethyl sulphoxide. Application of a relationship developed for a similar hemicellulose (19) gave $\bar{P}_n$ values of 236 and 193, respectively. These somewhat higher values were probably due to the approximate nature of the constant relating $[\eta]$ and $\bar{P}_n$.

Summarizing the above evidence, a simplified structure can now be suggested for the main hemicellulose component in white elm wood. This methyl glucurono-xylan evidently contains an average of 185 β-D-xylopyranose residues linked together by 1,4-glycosidic bonds to linear macromolecules. Every seventh, on the average, anhydroxylose unit carries a single, terminal side chain of 4-*O*-methyl-D-glucuronic acid, attached by an α-glycosidic linkage to C_2 of the xylose. In the native state most of the hydroxyl groups of the polysaccharide are probably esterified with acetic acid (22).

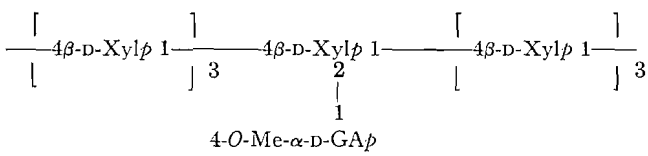

The constitution of the hemicellulose of white elm is similar, albeit not identical, to that of other methyl glucurono-xylans isolated from deciduous woods. These polysaccharides are all, with one possible exception (23), linear, and contain side chains of α-1,2-linked 4-*O*-methyl-D-glucuronic acid residues. Of the species so far studied, European (24) and American (23) beech, white birch (16), yellow birch (25), sugar maple (25), and trembling aspen (26) all contain hemicelluloses with 10–11 xylose residues per acid side group. The present hemicellulose apparently possesses relatively more acid side chains. In this respect it is, actually, more similar to the methyl araboglucurono-xylans present in coniferous woods, which contain more acid groups than the hardwood xylans. Western hemlock, for example, has been reported (27) to contain 4.3 xylose residues for each 4-*O*-methyl-D-glucuronic acid, European larch (28) 5–6, loblolly pine (29) 6–7, and Norway spruce (30) 5 and (31) 5.4, respectively. A methyl glucurono-xylan which also possesses 7 xylose residues per each 4-*O*-methyl-D-glucuronic acid is present in kapok (32), whereas another seed hair, namely milkweed floss (6), contains only half as many of the same acid groups.

It is interesting to note in this connection that white elm is more similar to softwoods than to hardwoods also in its low content of xylan (11.3%). Judging from the limited

Can. J. Chem. Downloaded from www.nrcresearchpress.com by 78.46.186.204 on 09/04/12
For personal use only.

number of species so far studied, it appears as if a relatively low content of xylan in a wood is usually associated with a larger number of acid side groups in the latter. Inspection of some recently published analytical data (13) indicates that the uronic anhydride content is rather constant for most woods in spite of the fact that the content of xylan varies considerably and is generally much lower for the conifers than for the woody angiosperms. A strict comparison is not possible, however, since a portion of the uronic anhydride is always derived from pectic material in the wood (33).

The number-average degree of polymerization of the present hemicellulose is only slightly lower than that of a similar polysaccharide from white birch, namely 197 (19), and is approximately the same as that of the methyl glucurono-xylans present in sugar maple (25) and yellow birch (25). Unfortunately, no reliable data are presently available as to the weight-average molecular weight of any native wood xylan.

EXPERIMENTAL

General experimental conditions, analytical procedures, and solvents used for separating sugars were the same as described previously (1, 12, 16). All specific rotations are equilibrium values and melting points are corrected. Evaporations were carried out *in vacuo* at temperatures not exceeding 50° C.

Preliminary Characterization of Acid I

This was the first acid to be eluted from the column of ion exchange resin referred to in the previous paper (1). Partial hydrolysis of the partly crystalline material, followed by examination by paper chromatography (solvent A), indicated the presence of xylose, 4-*O*-methyl-D-glucuronic acid, aldobiouronic acid, and unhydrolyzed triouronic acid. Anal. Calc. for $C_{17}H_{28}O_{15}\cdot 3H_2O$: OCH_3, 5.9%; equiv. wt., 472. Found: OCH_3, 4.8%; equiv. wt., 510; $[\alpha]_D^{20}$ +75° (*c*, 1.0 in water).

Separation of Acids II–V

The eluate constituting the second main fraction from the ion exchange column was evaporated to dryness (250 mg) and resolved on three large sheets of Whatman No. 1 filter paper (solvent A). In this way acid II (110 mg) and acid V (3 mg) were separated from two other acids, which were combined and resolved (7) on a cocoanut charcoal (50–200 mesh, product of Fisher Scientific Company, Fair Lawn, N.J.) column (1.5×1.5 cm). Acid II (80 mg) was eluted with 5–7% and acid IV (20 mg) with 7–8% aqueous ethanol.

Chromatographic Identification of Acid III

The rate of movement on the paper chromatogram of this acid was the same as that of galacturonic acid. The methyl ester, methyl glycoside, formed by boiling with 4% methanolic hydrogen chloride under reflux for 6 hours, was reduced with lithium aluminum hydride (34, 35). After hydrolysis, paper chromatography (solvent B) suggested the presence of galactose.

Preliminary Characterization of Acid IV

Partial hydrolysis with 0.5 *N* sulphuric acid at 100° C for 20 hours, followed by paper chromatography (solvent A), indicated the presence of unchanged IV together with glucuronic acid, glucuronolactone, and xylose. Anal. Calc. for $C_{11}H_{18}O_{11}$: OCH_3, nil; equiv. wt., 326. Found: OCH_3, nil; equiv. wt., 354; $[\alpha]_D^{20}$ +85° (*c*, 1.8 in water).

Identification of Acid VI

Acid V was not further investigated because of the paucity of material available. Acid

Can. J. Chem. Downloaded from www.nrcresearchpress.com by 78.46.186.204 on 09/04/12
For personal use only.

VI (400 mg) was converted to the ester glycoside and reduced in dry tetrahydrofuran (25 ml) with a solution of lithium aluminum hydride (1 g) in the same solvent (30 ml). The neutral glycoside was hydrolyzed to give a sirup, chromatographically (solvent B) identical with 4-*O*-methyl-D-glucuronic acid. Anal. Calc. for $C_7H_{14}O_6$: OCH_3, 16.0%. Found: OCH_3, 15.9%; $[\alpha]_D^{20}$ +63° (*c*, 2.8 in water). The phenylosazone derivative (35, 36) had m.p. and mixed m.p. 157° and an infrared spectrum identical with that of an authentic specimen.

Characterization of the Hemicellulose

The hemicellulose was isolated as described before (1). Anal. Pentosan, 78.5%; uronic anhydride, 15.2% (potassium salt); OCH_3, 2.62% (free acid); $[\alpha]_D^{20}$ −70° (*c*, 1.1 in 2% potassium hydroxide).

Methylation of the Hemicellulose

The hemicellulose (18 g) was stirred with water (75 ml) and 40% (w/w) sodium hydroxide (150 ml) was added in an atmosphere of nitrogen, followed by dimethyl sulphate (135 ml) over a period of 20 hours at a temperature of 0° C. This treatment was repeated five times. The partly methylated material was recovered in the usual way and dissolved in tetrahydrofuran (37). Powdered sodium hydroxide (200 g) was added, followed by dropwise addition of dimethyl sulphate (200 ml) over a period of 10 hours. This treatment was repeated once. After neutralization with acetic acid, tetrahydrofuran was removed by distillation and the precipitated hemicellulose was dissolved in chloroform and reprecipitated into petroleum ether. Anal. OCH_3, 36.1%.

The product was dissolved in chloroform (100 ml) and to the solution dry dimethyl formamide (100 ml), silver oxide (5 g), and methyl iodide (10 ml) were added. The mixture was shaken in the dark for 36 hours after which silver oxide (5 g) and methyl iodide (10 ml) were added and shaking was continued for another 12 hours (38). Salts were removed by filtration, chloroform was added, and the solution was extracted with water for 4 days. It was then dried over calcium sulphate, filtered through Celite, and evaporated to 100 ml. Precipitation into petroleum ether yielded white fibers (9 g). Anal. OCH_3, 38.1%; $[\alpha]_D^{20}$ −62° (*c*, 0.82 in chloroform). The infrared spectrum indicated negligible absorption at the hydroxyl frequency of 3500 cm^{-1}.

Methanolysis of the Methylated Hemicellulose and Separation of the Acidic Component

The fully methylated polysaccharide (5.0 g) was boiled under reflux with 2% methanolic hydrogen chloride (100 ml) for 8 hours. Neutralization with silver carbonate, purification with hydrogen sulphide, and filtration through Celite yielded a sirup of glycosides (5.9 g). The ester groups were saponified with *N* sodium hydroxide at room temperature for 15 hours. Acidic sugars were adsorbed on a column of Dowex 1-X4 (acetate) exchange resin which was washed with water until free of neutral sugars. The acidic component was eluted with 2 *N* acetic acid and the solution was evaporated to a brown solid (1.08 g).

Preparation, Reduction, and Hydrolysis of the Ester Glycoside of the Partially Methylated Aldobiouronic Acid

The methyl glycoside of the partially methylated acid was reconverted to the methyl ester by boiling under reflux with 2% methanolic hydrogen chloride for 8 hours. It was then reduced with lithium aluminum hydride and subjected to methanolysis followed by hydrolysis with *N* hydrochloric acid. Removal of the acid and evaporation yielded a sirup which, when examined by paper chromatography (solvent C), appeared to contain equimolar amounts of a tri-*O*-methyl glucose and a mono-*O*-methyl xylose.

Can. J. Chem. Downloaded from www.nrcresearchpress.com by 78.46.186.204 on 09/04/12
For personal use only.

Separation and Identification of 2,3,4-Tri-O-methyl-D-glucose and 3-O-Methyl-D-xylose

The above sirup was added to the top of a cocoanut charcoal column (1.5×5 cm). Elution with 10% aqueous ethanol gave a compound (263 mg) which corresponded by paper chromatography (solvent C) and paper electrophoresis in a borate buffer solution (39, 40) to 3-*O*-methyl-D-xylose. Anal. Calc. for $C_6H_{12}O_5$: OCH_3, 18.9%. Found: OCH_3, 17.9%. The 3-*O*-methyl-*N*-phenyl-D-xylosylamine, when recrystallized from ethyl acetate – petroleum ether, had m.p. 135–136° C; $[\alpha]_D^{20}$ +118° (*c*, 1.2 in ethyl acetate).

Elution with 20% aqueous ethanol gave a compound (206 mg) which was chromatographically identical with 2,3,4-tri-*O*-methyl-D-glucose. Anal. Calc. for $C_9H_{18}O_6$: OCH_3, 41.9%. Found: OCH_3, 41.0%; $[\alpha]_D^{20}$ +75° (*c*, 2.2 in water). The 2,3,4-tri-*O*-methyl-*N*-phenyl-D-glucosylamine had m.p. and mixed m.p. 146° C. Its infrared spectrum was identical with that of an authentic sample.

Separation of the Neutral Components of the Methylated Hemicellulose

The mixture of neutral glycosides (3.9 g) was extracted with chloroform and the aqueous and the chloroform solutions were concentrated separately, after which they were recombined and hydrolyzed with *N* sulphuric acid. After neutralization with barium carbonate and deionization (Amberlite IR-120 and Dowex 1-X4) the aqueous solution was exhaustively extracted with chloroform in a liquid–liquid extractor for 3 days, after which the extract was removed. Continued extraction of the aqueous solution with chloroform for 3 weeks, followed by concentration of the extract, gave a chromatographically pure di-*O*-methyl xylose. The remaining aqueous phase contained only mono-*O*-methyl xyloses. The first extract was dissolved in water and extracted with chloroform for 3 hours. Repetition of this process several times finally yielded a chromatographically pure tri-*O*-methyl xylose.

Preliminary Characterization of the Mono-O-methyl Xyloses

This fraction had a methoxyl content (18.0%) corresponding to that of a mono-*O*-methyl xylose. Ionophoresis in a borate buffer solution indicated the presence of 2-*O*- and 3-*O*-methyl-D-xylose, with the latter compound constituting the major part of the mixture.

Identification of 2,3-Di-O-methyl-D-xylose

Crystals, m.p. 78° C, formed slowly in the colorless sirup. Anal. Calc. for $C_7H_{14}O_5$: OCH_3, 34.8%. Found: OCH_3, 34.8%; $[\alpha]_D^{20}$ +23° (*c*, 2.0 in water). The 2,3-di-*O*-methyl-*N*-phenyl-D-xylosylamine, when recrystallized from ethyl acetate, had m.p. and mixed m.p. 141° C. Its infrared spectrum corresponded to that of an authentic specimen.

Partial Identification of 2,3,4-Tri-O-methyl-D-xylose

The sirup (20 mg) could not be induced to crystallize; $[\alpha]_D^{20}$ +20° (*c*, 1.3 in water). The aniline derivative, m.p. 98° C, had an infrared spectrum identical with that of an authentic sample.

Spectrophotometric Analysis of the Neutral Components of the Methylated Hemicellulose

A small portion of the mixture of methylated neutral sugars was applied to strips of filter paper which were irrigated with solvent C. The different sugars were located with guide strips, eluted with water, and adjusted to a convenient volume. Concentrations were determined by the *o*-aminodiphenyl method (15). The average value of three determinations was used. The relation between absorbance and concentrations of the three methyl sugars had been determined previously (16).

Can. J. Chem. Downloaded from www.nrcresearchpress.com by 78.46.186.204 on 09/04/12
For personal use only.

Determination of the Molecular Weight of the Methylated Hemicellulose

The osmometer used was a Zimm–Myerson (41) instrument as modified by Stabin and Immergut (42). Gel cellophane membranes, which had never been allowed to dry, were kindly supplied by American Viscose Corporation, Marcus Hook, Pa. The solvent was a 9:1 (v/v) mixture of chloroform–ethanol and the temperature was 30±0.01° C. The osmotic pressure was determined at four different concentrations by the static method and the values of the reduced osmotic pressure, h/w, as plotted against w, were extrapolated to zero concentration (Table I). The number-average molecular weight, $\bar{M}_n$, was calculated from the relationship $\bar{M}_n = 25{,}700/(h/w)_0$ and the corresponding degree of polymerization, $\bar{P}_n$, from the relationship $\bar{P}_n = \bar{M}_n \cdot n/M_R$, where n was the number of xylose residues present per acid side chain and M_R was the molecular weight of the repeating unit of the fully methylated polysaccharide.

TABLE I

OSMOMETRY DATA FOR THE METHYLATED HEMICELLULOSE

w*	h†	h/w
5.132	6.942	1.353
4.537	6.186	1.364
3.536	4.436	1.254
2.550	3.090	1.212
0	—	1.07

*Concentration in g/kg solution.
†Osmotic height in cm solvent.

Preparation of the Acetyl Derivative of the Hemicellulose

Hemicellulose (5 g) and freshly distilled formamide (200 ml) were stirred for 5 hours, after which anhydrous pyridine (250 ml) was added followed by dropwise addition of acetic anhydride over a period of 5 hours. After being stirred over night, the gelatinous reaction mixture was poured into ice water with vigorous stirring and recovered as described by Carson and Maclay (21). A second esterification was carried out in the same way although without addition of formamide. The acetyl content of the fully acetylated product was 37.8% (43).

Determination of the Molecular Weight of the Acetylated Hemicellulose

The molecular weight of the acetylated, native hemicellulose was determined as described above for the methylated polysaccharide. The results are given in Table II.

Viscosity Measurements

Relative viscosities were determined with a Craig–Henderson viscometer (44) and

TABLE II

OSMOMETRY DATA FOR THE ACETYLATED HEMICELLULOSE

w	h	h/w
3.238	2.053	0.634
2.924	1.768	0.605
2.682	1.521	0.567
2.224	1.299	0.584
1.530	0.904	0.591
0	—	0.560

Can. J. Chem. Downloaded from www.nrcresearchpress.com by 78.46.186.204 on 09/04/12
For personal use only.

extrapolated to zero concentration as described previously (19). The intrinsic viscosities in *M* cupriethylenediamine and anhydrous dimethyl sulphoxide were 1.113 and 0.557, respectively.

ACKNOWLEDGMENTS

The authors wish to express their gratitude to Dr. C. B. Purves and Dr. A. Taurins for valuable help. One of them (J.K.G.) is also thankful to the Allied Chemical and Dye Corporation for two fellowships and to the Pulp and Paper Research Institute of Canada for two summer stipends.

REFERENCES

1. GILLHAM, J. K. and TIMELL, T. E. Can. J. Chem. **36**, 410 (1958).
2. MILKS, J. E. and PURVES, C. B. J. Am. Chem. Soc. **78**, 3738 (1956).
3. HAMILTON, J. K. and THOMPSON, N. S. J. Am. Chem. Soc. **79**, 6464 (1957).
4. BRASCH, D. J. and WISE, L. E. Tappi, **39**, 581, 768 (1956).
5. PAINTER, T. J. Personal communication.
6. BARTH, F. W. and TIMELL, T. E. Unpublished results.
7. BARTH, F. W. and TIMELL, T. E. Can. J. Chem. **36**, 1321 (1958).
8. ASPINALL, G. O. and MAHOMED, R. S. J. Chem. Soc. 1731 (1954).
9. JONES, J. K. N., MERLER, E., and WISE, L. E. Can. J. Chem. **35**, 634 (1957).
10. GORROD, A. R. N. and JONES, J. K. N. J. Chem. Soc. 2522 (1954).
11. TIMELL, T. E. Unpublished results.
12. GLAUDEMANS, C. P. J. and TIMELL, T. E. J. Am. Chem. Soc. **80**, 941 (1958).
13. TIMELL, T. E. Tappi, **40**, 568 (1957).
14. DUTTON, G. G. S. and SMITH, F. J. Am. Chem. Soc. **78**, 3744 (1956).
15. TIMELL, T. E., GLAUDEMANS, C. P. J., and CURRIE, A. L. Anal. Chem. **28**, 1916 (1956).
16. GLAUDEMANS, C. P. J. and TIMELL, T. E. J. Am. Chem. Soc. **80**, 1209 (1958).
17. PAINTER, T. J. Unpublished results.
18. BARTH, F. W. and TIMELL, T. E. J. Am. Chem. Soc. (In press).
19. GLAUDEMANS, C. P. J. and TIMELL, T. E. Svensk Papperstidn. **61**, 1 (1958).
20. LINDBERG, B. Personal communication.
21. CARSON, J. F. and MACLAY, W. D. J. Am. Chem. Soc. **68**, 1015 (1946).
22. HÄGGLUND, E., LINDBERG, B., and MCPHERSON, J. Acta Chem. Scand. **10**, 1160 (1956).
23. ADAMS, G. A. Can. J. Chem. **35**, 556 (1957).
24. ASPINALL, G. O., HIRST, E. L., and MAHOMED, R. S. J. Chem. Soc. 1734 (1954).
25. TIMELL, T. E. and GLAUDEMANS, C. P. J. Unpublished results.
26. JONES, J. K. N. and WISE, L. E. J. Chem. Soc. 2750, 3389 (1952).
27. DUTTON, G. G. S. and SMITH, F. J. Am. Chem. Soc. **78**, 2505, 3744 (1956).
28. ASPINALL, G. O. and MCKAY, J. E. J. Chem. Soc. 1059 (1958).
29. JONES, J. K. N. and PAINTER, T. J. Paper presented at the 133rd meeting of the American Chemical Society. San Francisco. April 1958.
30. ASPINALL, G. O. and CARTER, M. E. J. Chem. Soc. 3744 (1956).
31. SAARNIO, J. Suomen Kemistilehti, B, **29**, 35 (1956).
32. CURRIE, A. L. and TIMELL, T. E. Unpublished results.
33. ANDERSON, E. J. Biol. Chem. **165**, 233 (1946).
34. ABDEL-AKHER, M. and SMITH, F. Nature, **166**, 1037 (1950).
35. SMITH, F. J. Chem. Soc. 2646 (1951).
36. SCHINLE, R. Ber. **65**, 315 (1932).
37. FALCONER, E. L. and ADAMS, G. A. Can. J. Chem. **34**, 338 (1956).
38. KUHN, R., TRISCHMANN, H., and LÖW, I. Angew. Chem. **67**, 32 (1955).
39. FOSTER, A. B. J. Chem. Soc. 982 (1953).
40. BOUVENG, H. and LINDBERG, B. Acta Chem. Scand. **10**, 1283 (1956).
41. ZIMM, B. H. and MYERSON, I. J. Am. Chem. Soc. **68**, 911 (1946).
42. STABIN, J. V. and IMMERGUT, E. H. J. Polymer Sci. **14**, 209 (1954).
43. GENUNG, L. B. and MALLAT, R. C. Ind. Eng. Chem., Anal. Ed. **15**, 319 (1943).
44. CRAIG, A. W. and HENDERSON, D. A. J. Polymer Sci. **19**, 215 (1956).

Can. J. Chem. Downloaded from www.nrcresearchpress.com by 78.46.186.204 on 09/04/12
For personal use only.

Can. J. Chem. Downloaded from www.nrcresearchpress.com by 78.46.186.204 on 09/04/12
For personal use only.

THE SYSTEM: NICOTINE – METHYLETHYL KETONE – WATER[1]

A. N. Campbell, E. M. Kartzmark, and W. E. Falconer[2]

ABSTRACT

The systems: nicotine–water and nicotine – methylethyl ketone were investigated by thermal analysis but the eutectic points were not obtained due to the extreme viscosity and consequent supercooling of solutions of high nicotine content.

The densities, viscosities, and refractive indices were determined for the nicotine – methylethyl ketone – water system at 25.0° C.

The mutual solubilities of nicotine, methylethyl ketone, and water were determined over the entire temperature range. A ternary critical point was found at 67.3° C, the critical composition being 27 weight per cent nicotine; 14 weight per cent methylethyl ketone.

The methylethyl ketone – water and nicotine–water solubility curves were redetermined. The existing data for the former system were confirmed but the data for the classical system nicotine–water were found to be seriously in error at the higher critical solution temperature. Thus the lower critical solution temperature was found to be 61.5° C, in good agreement with previous figures, but the upper critical solution temperature lies at 233.0° C, some twenty degrees higher than had been obtained by previous workers; the corresponding critical compositions are 36% and 40% nicotine respectively.

INTRODUCTION

The system nicotine–water presents the well-known egg-shaped diagram to be found in almost every textbook of physical chemistry. In other words this system is the classical example of a two-liquid system with both maximum and minimum critical solution temperatures. The system methylethyl ketone – water is similar in character, although the lower critical solution temperature is cut off by the occurrence of the solid phase, ice. It was thought that it would be of interest to investigate the three-component system: nicotine – methylethyl ketone – water, in order to determine the influence of one closed partial miscible region on another of the same type. There existed two main possibilities; either the third component would so increase mutual solubility that the volume of heterogeneity would shrink to a point before meeting the other volume of heterogeneity and thus two volumes of heterogeneity would exist in the solid model, or the two volumes would meet forming a tunnel. A further question was whether, in the latter case, the ternary critical solution temperatures would lie above or below those of the binary systems.

The system methylethyl ketone – water has been investigated by Rothmund (1) and by Marshall (2) but the most recent data are issued by the Shell Chemical Corporation (3). Rothmund found an upper critical solution temperature and he observed the tendency to a lower critical solution temperature but he could not realize it because of the occurrence of ice. Randall and McKenna (4) have determined the freezing curve of this system. The eutectic was found to lie at −88.88° C and the eutectic composition was 99.91 weight per cent methylethyl ketone.

Since our results differ radically (at the higher critical solution temperature) from the accepted data for the system: nicotine–water, it is necessary to deal in some detail with the literature of the subject. This system was first investigated by Hudson (5) in 1904. Neither he nor anyone else has been able to crystallize nicotine; it forms an amorphous solid on cooling. Hence the melting point is unknown.

[1]*Manuscript received May 10, 1958.*
Contribution from the Chemistry Department, University of Manitoba, Winnipeg, Manitoba.
[2]*Holder of an N.R.C. Bursary, 1957–58.*

Using the method of Alexejew, with solutions sealed in 1 mm diameter capillary tubing and heating in an air bath, Hudson determined the solubility curve for the nicotine–water system and found it to be completely closed. He found both critical compositions to be the same, viz., 32.2 weight per cent nicotine, and that the lower critical solution temperature was 61.0° C and the upper 210° C.

Tsakolotos (6) repeated the work of Hudson in 1909; he found the upper and lower critical temperatures to be 208° C and 60.8° C respectively, and both critical compositions to be 34 weight per cent nicotine. Tsakolotos claimed that the use of extremely pure nicotine did not greatly influence the form of the curve.

Leone (7), in 1926, re-examined the nicotine–water system and obtained results identical with those of Hudson, within one or two degrees. Leone used the method of Alexejew and placed his mixtures in Jena glass tubes which were heated in a double-jacketed paraffin oil bath. He found the upper critical temperature to be 213° C.

EXPERIMENTAL

All chemicals were of the highest purity. Since chemical analysis (of any degree of accuracy) was out of the question, physical analysis was used. Curves representing the behavior of any two physical properties, with respect to composition, make possible the analysis of any mixture, when plotted on a triangular diagram. In order, however, that the method may be accurate, it is necessary that the curves should intersect sharply. With this in mind, we surveyed the field by determining the viscosities, densities, refractive indices (for H_C = 6563 Å and for H_F = 4861 Å), and dispersions over the complete composition range of the ternary system. These results are given in Table I. As the result of this survey, we chose the refractive index for hydrogen red light (λ = 6563 Å) and the density.

Thermal analysis was carried out using a copper–constantan thermocouple and a Brown recording potentiometer. The two-junction thermocouple was calibrated from the freezing points of high purity materials. The available temperature range extended from 0° C to −130° C, with an accuracy of measurement of 0.5° C.

Numerous attempts were made to crystallize pure nicotine, using both slow and rapid cooling, but a glass-like mass was always obtained between −100° C and −120° C. The smooth cooling curve showed no irregularities or breaks. All solutions of water and nicotine containing more than 65 weight per cent nicotine failed to crystallize as did those solutions of methylethyl ketone – nicotine containing more than 50 weight per cent nicotine. Hence, no eutectic was observed in either system. No attempt was made to locate the ternary eutectic, since the binary eutectics were unobtainable. The freezing curve of the methylethyl ketone – water system had been determined previously (4). The freezing-point data are given in Tables II and III.

For the isothermal solubility determinations, three thermostats were used: one for the −11.4° C and 5.0° C isotherms, having a variation of ±0.3°; one operating at 25.0° C, for the analytical determinations of density and refractive index; and a third, used for all temperatures above 25° C, which had a variation of ±0.2° C. The mixtures were made up to approximately known over-all compositions, such that two equilibrium layers of more or less equal volumes would form at the temperature in question. Each layer was sampled, after 24 hours stirring, and analyzed by determining refractive index and density. A cell of heavy-walled glass was used for solutions whose vapor pressure was greater than one atmosphere and the pressure of the vapor was utilized to deliver samples of the top and bottom layers; it was possible to use this cell up to a pressure of twenty atmospheres.

Can. J. Chem. Downloaded from www.nrcresearchpress.com by 78.46.186.204 on 09/04/12
For personal use only.

Isotherms of the ternary system were determined at −11.4° C, 5.0° C, 25.0° C, 50.0° C, 65.0° C, 67.5° C, 70.0° C, 85.0° C, 115.0° C, 140.0° C, and 143.0° C and of the nicotine–water conjugate pair at 150.0° C also. The ternary system could not be investigated at 150° C because the pressure was too high. The temperature was controlled to ±0.2° C and was measured by a calibrated mercury-in-glass thermometer reading in 1/10°.

The data for all the solubility measurements are listed in Table IV and the isothermal solubility diagrams are shown in Fig. 1 (*a* and *b*).

The Alexejew Method

The method of isothermal analysis was abandoned above 143.0° C because the pressure

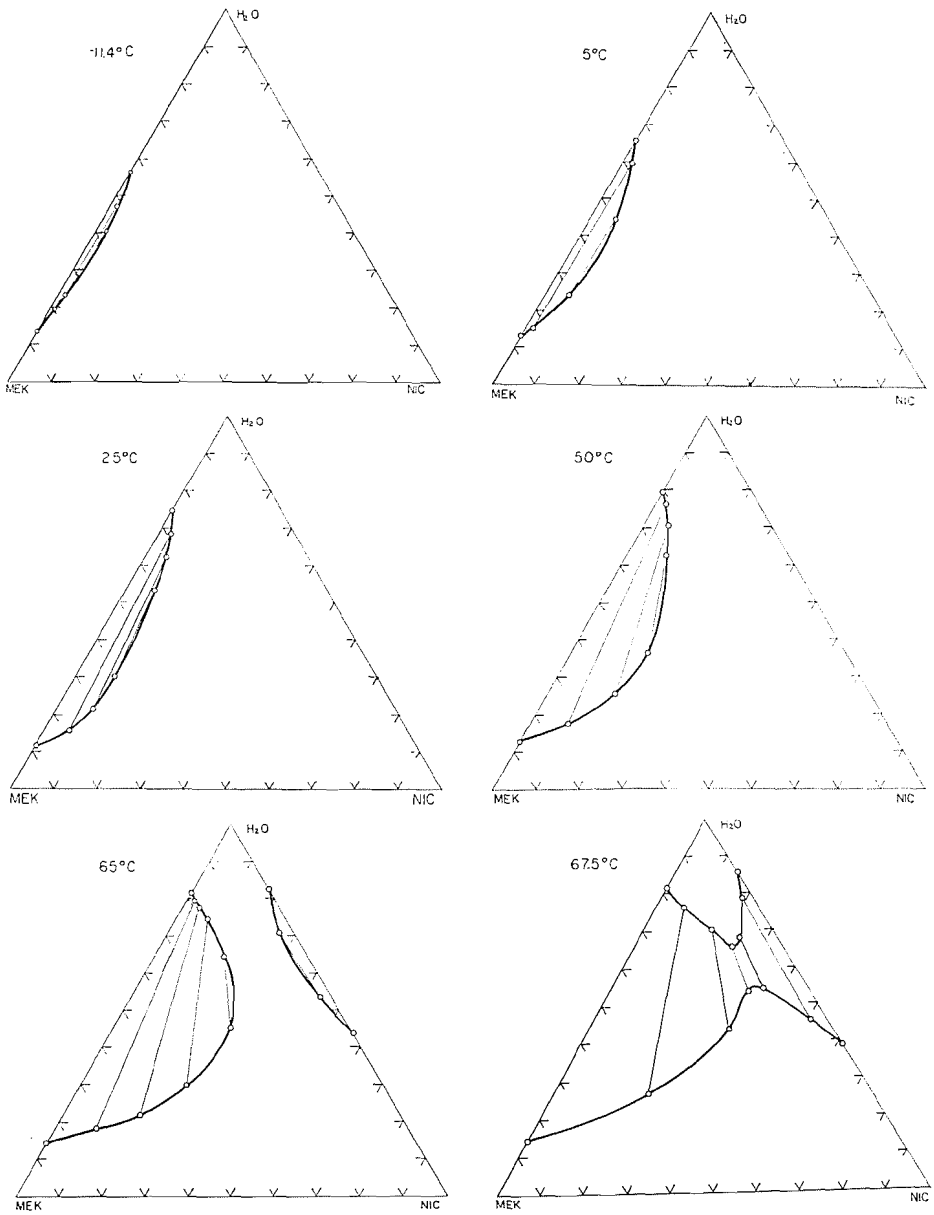

FIG. 1*a*.

Can. J. Chem. Downloaded from www.nrcresearchpress.com by 78.46.186.204 on 09/04/12
For personal use only.

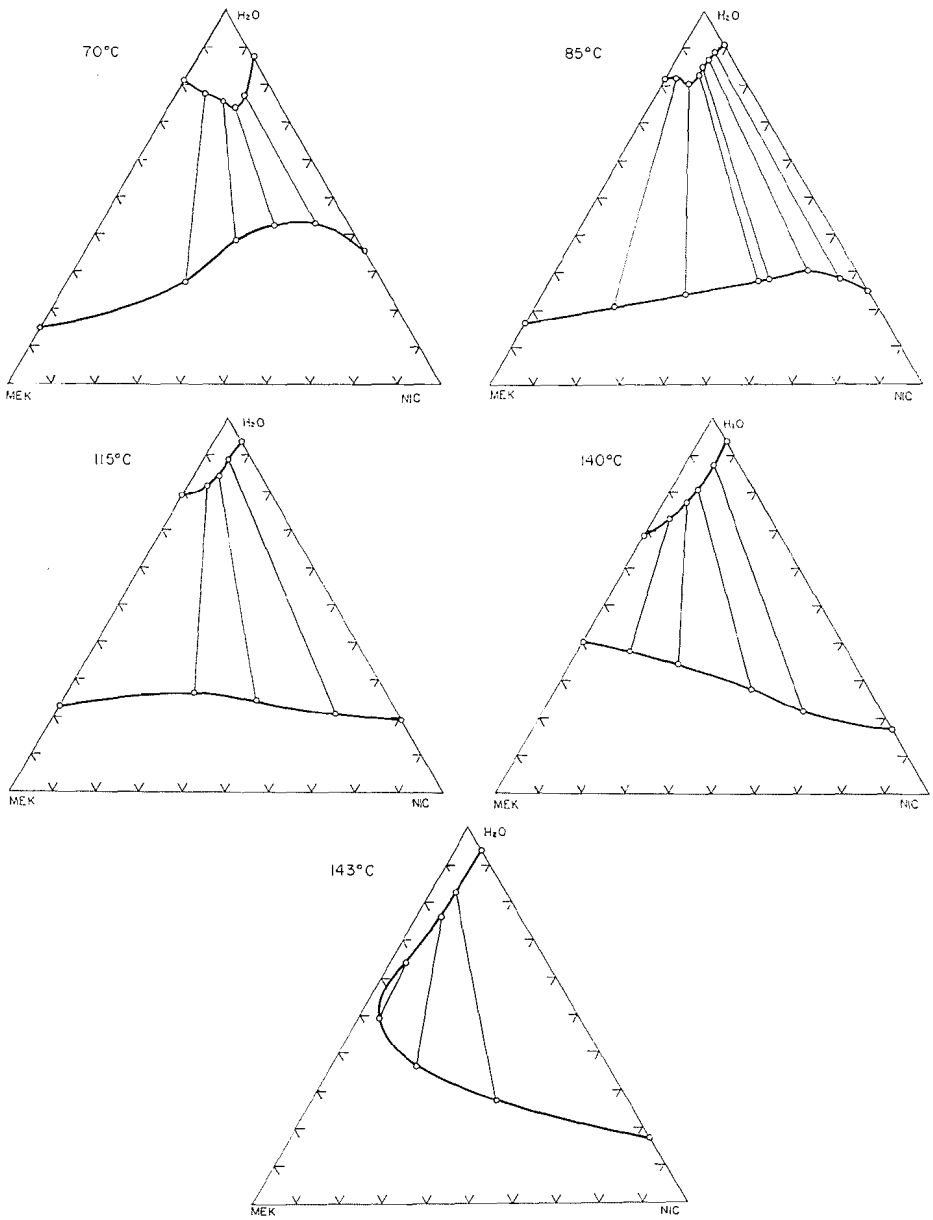

FIG. 1*b*.

developed made sampling impossible, and resort was made to the Alexejew method to complete the diagram. Our technique is described in complete detail because our results for this region differ so markedly from the accepted figures.

Mixtures of known composition by weight were placed in heavy-walled glass tubes, 8 mm in internal diameter and 12 cm in length. These tubes were filled to approximately two-thirds capacity and then sealed in the blowpipe; the liquid was kept cool to prevent evaporation and composition change during this operation. The tubes were investigated one by one, in a variable temperature bath filled with silicone oil. The temperatures at which homogeneity occurred on heating and that at which heterogeneity occurred on

Can. J. Chem. Downloaded from www.nrcresearchpress.com by 78.46.186.204 on 09/04/12
For personal use only.

cooling were noted and the mean temperature taken to be the solution temperature for the composition in question.

The bath was a glass vessel containing two gallons of silicone oil. In the neighborhood of the temperature of homogeneity it was heated at the rate of 1 degree in 5 minutes. The tubes were rotated in the bath by means of a motor and the rate of rotation was varied from 0 to 70 r.p.m. The rotation stirred the contents of the tubes thoroughly, but a speed of rotation greater than 70 r.p.m. developed sufficient centrifugal force to prevent the liquid in the tube flowing freely from end to end.

The temperatures of homogeneity or heterogeneity were measured by a single junction copper–constantan thermocouple. The couple was calibrated against the freezing points of indium (156.5° C), tin (231.9° C), and lead (327.3° C); all the metals were extremely pure. Temperature could be measured to ±0.5° C. The calibration was repeated after the series of observations was complete but no change in the calibration was observed. As a further check on the reliability of the temperature measurement a sample of pure tin was placed in a tube of the kind used for these measurements and the melting and freezing points determined by the same technique. The mean of these two temperatures agreed, within experimental error, with the literature value for the freezing point of tin.

The tubes were illuminated by a photo spotlight, mounted outside the bath. With this illumination, no difficulty was encountered in observing the condition of the mixture in the tube.

The data from these observations are listed in Table V. Fig. 2 shows temperature versus composition plots for fixed percentages of methylethyl ketone.

Finally, to check the upper critical solution temperature approximately, a few drops of nicotine–water of the upper critical composition were sealed in a piece of heavy-walled capillary tubing of 1 mm internal diameter and 25 mm in length. This was placed in an electrically heated melting-point apparatus and viewed through a magnifying lens. The thermocouple was placed in the opening along with the tube and the top of the opening plugged with asbestos wool. The total volume of the air space surrounding the tube was

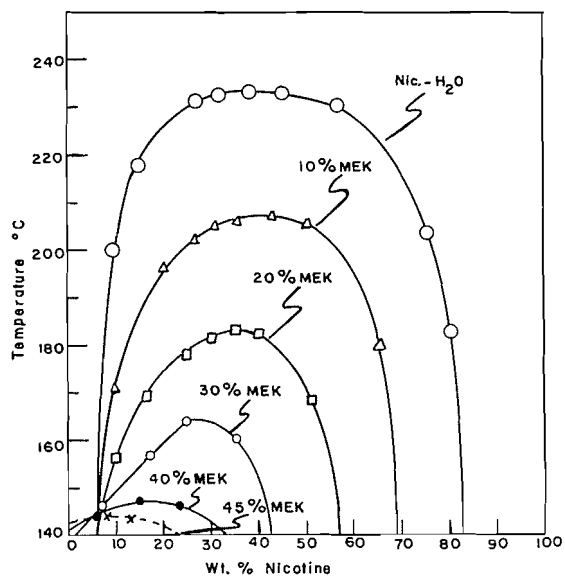

FIG. 2. Temperature versus composition plots with fixed percentages of methylethyl ketone.

Can. J. Chem. Downloaded from www.nrcresearchpress.com by 78.46.186.204 on 09/04/12
For personal use only.

between three and four milliliters. Using this apparatus the upper critical solution temperature of the nicotine–water system was found to be 234±2° C.

EXPERIMENTAL RESULTS

TABLE I

PHYSICAL PROPERTIES OF SOLUTIONS OF NICOTINE, METHYLETHYL KETONE, AND WATER AT 25° C

Composition weight per cent			Density	Relative	Relative	Refractive index	
Water	Nicotine	MEK	g/cm³	viscosity	dispersion	C, λ = 6563 Å	F, λ = 4861 Å
100	—	—	0.99706	1.0000	1.000	1.33066	1.33663
90	10	—	1.00351	1.457	0.824	1.35046	1.35722
80	20	—	1.01046	2.285	0.718	1.37127	1.37853
70	30	—	1.01718	3.693	0.617	1.39217	1.40036
60	40	—	1.02369	5.973	0.520	1.41290	1.42247
50	50	—	1.02921	9.884	0.468	1.43497	1.44428
40	60	—	1.03409	16.020	0.401	1.45649	1.46768
30	70	—	1.03525	23.376	0.345	1.47536	1.48751
25	75	—	1.03500	26.128	—	—	—
20	80	—	1.03169	25.819	0.292	1.49397	1.50705
10	90	—	1.02173	14.369	0.242	1.50867	1.52267
—	100	—	1.00677	4.285	0.192	1.52127	1.53606
90	—	10	0.98416	1.260	0.934	1.33888	1.34491
80	—	20	0.97095	1.517	0.932	1.34763	1.35287
8	—	92	0.82085	0.5570	0.735	1.37632	1.38397
—	—	100	0.79979	0.4244	0.746	1.37450	1.38115
—	10	90	0.81750	0.4777	0.681	1.38670	1.39392
—	20	80	0.83619	0.5487	0.642	1.40019	1.40775
—	30	70	0.85454	0.6326	0.579	1.41310	1.42140
—	40	60	0.87549	0.7560	0.502	1.42882	1.43842
—	50	50	0.89421	0.9089	0.449	1.44173	1.45225
—	60	40	0.91636	1.129	0.390	1.46147	1.47290
—	70	30	0.93655	1.412	0.336	1.47242	1.48479
—	80	20	0.95868	1.882	0.300	1.48752	1.50071
—	90	10	0.98181	2.696	0.239	1.50475	1.51875
60	10	30	0.95658	2.141	0.723	1.37411	1.38307
50	10	40	0.93580	2.043	0.708	1.37854	1.38565
40	10	50	0.91412	1.824	0.698	1.38298	1.38999
30	10	60	0.89191	1.460	0.698	1.38590	1.39289
20	10	70	0.86943	1.050	0.689	1.38844	1.39542
10	20	70	0.86477	0.8782	0.642	1.40218	1.40968
70	20	10	0.99595	2.669	0.684	1.37971	1.38721
20	30	50	0.91234	1.769	0.568	1.41622	1.42474
50	30	20	0.98251	3.792	0.588	1.40588	1.41434
20	50	30	0.95795	3.740	0.462	1.44546	1.45564
10	80	10	0.99742	7.293	0.307	1.49284	1.50563

TABLE II

FREEZING-POINT DATA FOR THE BINARY SYSTEM NICOTINE–WATER

Composition weight per cent		Freezing point, ° C
Water	Nicotine	
100	—	0.00
90	10	−0.854±0.003
80	20	−1.455±0.010
70	30	−2.270±0.010
60	40	−3.642±0.013
50	50	−5.9 ±0.5
40	60	−12.7 ±0.5
35	65	−22.1 ±0.5

Can. J. Chem. Downloaded from www.nrcresearchpress.com by 78.46.186.204 on 09/04/12
For personal use only.

TABLE III

FREEZING-POINT DATA FOR THE SYSTEM NICOTINE – METHYLETHYL KETONE

Composition weight per cent		Freezing point, °C
MEK	Nicotine	
100	—	−87.0±0.5
90	10	−88.3±0.5
80	20	−89.7±0.5
70	30	−91.8±0.5
60	40	−94.0±0.5
50	50	−99 ±3

TABLE IV

DATA FOR THE ISOTHERMAL SOLUBILITY MEASUREMENTS

Composition of top layer			Composition of bottom layer		
Wt. % H_2O	Wt. % Nic.	Wt. % MEK	Wt. % H_2O	Wt. % Nic.	Wt. % MEK
		−11.4° C Isotherm			
13.2	—	86.8	56.2	—	43.8
19.5	1.0	79.5	47.0	1.6	51.4
23.2	1.6	75.2	40.2	2.5	57.3
Plait point (extrapolated)			30.8	2.5	66.7
		5.0° C Isotherm			
13.0	—	87.0	65.7	—	34.3
15.0	2.0	83.0	59.5	2.2	38.3
24.1	5.7	70.2	44.4	6.0	49.6
Plait point (extrapolated)			33.0	7.0	60.0
		25.0° C Isotherm			
11.6	—	88.4	74.5	—	25.5
15.3	5.8	78.9	68.6	2.8	28.6
21.4	8.8	69.8	62.0	5.0	33.0
29.9	9.2	60.9	53.2	6.5	40.3
Plait point (extrapolated)			41.0	8.6	50.4
		50.0° C Isotherm			
12.9	—	87.1	79.4	—	20.6
17.6	8.8	73.6	76.2	2.4	21.4
25.4	16.0	58.6	70.6	5.8	23.6
36.8	17.9	45.3	62.3	9.6	28.1
Plait point (extrapolated)			49.3	14.6	36.1
		65.0° C Isotherm			
14.2	—	85.8	81.7	—	18.3
18.4	9.5	72.1	79.4	1.8	18.8
21.9	17.9	60.2	77.5	3.9	18.6
29.6	25.0	45.4	74.7	7.4	17.9
45.0	27.5	27.5	64.4	16.2	19.4
Plait point (extrapolated)			55.3	22.6	22.1
82.4	17.6	—	43.4	56.6	—
70.4	26.0	3.6	53.0	44.3	2.7
Plait point (extrapolated)			61.6	34.7	3.7
		67.5° C Isotherm			
26.5	22.3	51.2	76.1	6.6	17.3
43.4	32.8	23.8	70.0	16.0	14.0
53.6	32.1	14.3	65.4	22.8	11.8
54.1	35.4	10.5	68.0	23.2	8.8
45.7	50.5	3.8	78.4	18.9	2.7
		70.0° C Isotherm			
27.0	27.3	45.7	77.5	6.5	16.0
38.3	33.7	28.0	75.7	11.7	12.6
42.6	40.2	17.2	73.8	15.2	11.0
43.0	49.4	7.6	77.1	15.6	7.3
87.2	12.8	—	35.7	64.3	—

Can. J. Chem. Downloaded from www.nrcresearchpress.com by 78.46.186.204 on 09/04/12
For personal use only.

TABLE IV (*Concluded*)

DATA FOR THE ISOTHERMAL SOLUBILITY MEASUREMENTS

Composition of top layer			Composition of bottom layer		
Wt. % H_2O	Wt. % Nic.	Wt. % MEK	Wt. % H_2O	Wt. % Nic.	Wt. % MEK
		85.0° C Isotherm			
16.1	—	83.9	81.4	—	18.6
20.9	18.2	60.9	81.9	2.6	15.5
24.0	33.7	42.3	80.4	6.4	13.2
27.5	48.7	23.8	82.9	7.2	9.9
28.2	50.5	22.3	85.0	7.0	8.0
30.3	58.7	11.0	86.6	7.7	5.7
28.0	67.0	5.0	88.6	8.0	3.4
90.5	9.5	—	25.0	75.0	—
		115.0° C Isotherm			
23.1	—	76.9	78.9	—	21.1
26.5	29.3	44.2	81.5	4.5	14.0
24.2	44.9	30.9	84.6	5.6	9.8
20.7	64.9	14.4	88.8	5.5	5.7
19.3	80.7	—	96.8	3.2	—
		140° C Isotherm			
40.2	—	59.8	68.3	—	31.7
37.6	12.1	50.3	73.0	3.2	23.8
34.2	25.0	40.8	77.5	5.5	17.0
27.3	45.6	27.1	85.3	5.9	8.8
21.8	60.6	17.5	87.2	6.8	6.0
17.0	83.0	—	93.7	6.3	—
		143° C Isotherm			
27.6	42.5	29.9	82.6	6.0	11.4
36.8	19.6	43.6	76.3	5.7	18.0
49.1	4.9	46.0	64.0	3.7	32.3
Plait point (extrapolated)			56.0	1.7	42.3
		Nicotine–water at 62.0° C			
70	30.0	—	57.1	42.9	—
		Nicotine–water at 150.0° C			
16.8	83.2	—	94.0	6.0	—

TABLE V

DATA FOR THE ALEXEJEW MEASUREMENTS

Composition			Upper temperature limit of heterogeneous volume, ° C
Wt. % MEK	Wt. % H_2O	Wt. % Nic.	
—	20.0	80.0	183.0±0.5
—	25.0	75.0	203.5
—	32.0	68.0	219.5
—	43.0	57.0	231.0
—	54.0	46.0	232.5
—	62.0	38.0	233.0
—	68.0	32.0	232.5
—	73.0	27.0	231.5
—	85.0	15.0	218.0
—	90.0	10.0	200.0
10.0	25.0	65.0	180.0
10.0	40.0	50.0	205.5
10.0	48.0	42.0	207.0
10.0	55.0	35.0	205.5
10.0	59.0	31.0	205.0
10.0	63.0	27.0	202.0
10.0	70.0	20.0	196.0
10.0	80.0	10.0	171.0
20.0	29.0	51.0	168.5
20.0	40.0	40.0	182.5
20.0	45.0	35.0	183.0
20.0	50.0	30.0	181.0
20.0	55.0	25.0	178.0

Can. J. Chem. Downloaded from www.nrcresearchpress.com by 78.46.186.204 on 09/04/12
For personal use only.

TABLE V (*Concluded*)
DATA FOR THE ALEXEJEW MEASUREMENTS

Composition			Upper temperature limit of heterogeneous volume, °C
Wt. % MEK	Wt. % H_2O	Wt. % Nic.	
20.0	63.0	17.0	169.5
20.0	70.0	10.0	156.0
30.0	35.0	35.0	159.5
30.0	45.0	25.0	163.0
30.0	52.0	18.0	157.0
30.0	63.0	7.0	146.0
40.0	37.0	23.0	146.5
40.0	45.0	15.0	147.5
40.0	50.0	10.0	145.5
40.0*	55.0	5.0	143.5
45.0	42.0	13.0	143.5
45.0*	47.0	8.0	144.5

*These samples were made up by direct weighing, as they were heterogeneous at room temperature.

TABLE VI
DATA FOR THE MUTUAL SOLUBILITIES OF THE METHYLETHYL KETONE – WATER SYSTEM

Temperature, °C	Composition of top layer		Composition of bottom layer	
	Wt. % H_2O	Wt. % MEK	Wt. % H_2O	Wt. % MEK
−11.4	13.2	86.8	56.2	43.8
5.0	13.0	87.0	65.7	34.3
25.0	11.6	88.4	74.5	25.5
50.0	12.9	87.1	79.4	20.6
65.0	14.2	85.8	81.7	18.3
85.0	16.1	83.9	81.4	18.6
115.0	23.1	76.9	78.9	21.1
140.0	40.2	59.8	68.3	31.7
142.6 (CRIT.)	55.0	45.0	55.0	45.0

DISCUSSION OF RESULTS

The Binary System: Methylethyl Ketone – Water

At 25° C, methylethyl ketone and water are not completely miscible. Hence, the physical properties investigated, viz., density, viscosity, refractive index, and dispersion, were limited to the completely intersoluble region. The freezing-point curve of this system was not determined.

Our results for the mutual solubility of these two liquids above 0° C are in close agreement with the results of Marshall (2) and of the Shell Laboratories (3); they disagree with the earlier work of Rothmund (1). The upper critical solution temperature was found to be 142.6° C and the critical composition 45% by weight methylethyl ketone.

The lower critical solution temperature could not be obtained; at temperatures below −12° C crystallization of ice occurred though previous workers claim to have supercooled to −20° C. Our results for the solubility of water in methylethyl ketone are in exact agreement with those of Randall and McKenna (4) but our results for the solubility of methylethyl ketone in water appear to be slightly greater.

We estimate that the lower critical solution temperature, if it were realizable, would lie about −35° C and the critical composition would be about 75 weight per cent methylethyl ketone. The data for the mutual solubilities of the methylethyl ketone – water system are given in Table VI.

Can. J. Chem. Downloaded from www.nrcresearchpress.com by 78.46.186.204 on 09/04/12
For personal use only.

The Binary System: Nicotine–Water

The physical properties, density, viscosity, and refractive indices, were investigated at 10% intervals, from 0 to 100% nicotine. A maximum density was observed at 70 weight per cent nicotine and a maximum viscosity at 77% nicotine. The graphs of refractive index against composition were straight lines. The density inversion at 90° C, observed by Hudson (5), was confirmed; the water-rich layer became heavier than the nicotine-rich layer about this temperature. We estimate that the eutectic composition, if the eutectic were realizable, would be about 75 to 80% nicotine, but the measurements could not be pushed beyond 65 weight per cent.

The results for mutual solubility by the isothermal analysis method varied slightly from previous measurements and tended to flatten the lower part of the solubility curve somewhat. The so-called "rectilinear diameter" was plotted (Fig. 3). The lower critical temperature was found to be 61.5±0.2° C and the lower critical composition 36 weight per cent nicotine.

The upper half of the solubility curve differs considerably from previous results. Identical solution temperatures were obtained, independently of whether the nicotine

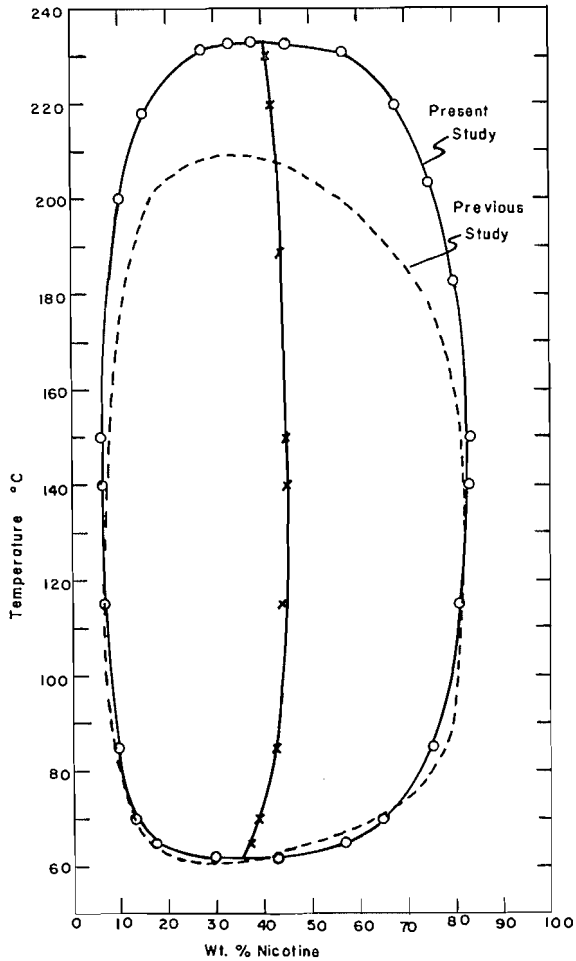

FIG. 3. Nicotine–water mutual solubility diagram.

Can. J. Chem. Downloaded from www.nrcresearchpress.com by 78.46.186.204 on 09/04/12
For personal use only.

used was old or new, freshly redistilled or not. The upper critical temperature was found to be 233.0±0.5° C, 20° higher than had previously been reported (5, 6, 7). The upper critical composition is 40% nicotine. The data for the mutual solubilities of the nicotine–water systems are given in Table VII and plotted in Fig. 3.

TABLE VII

DATA FOR THE MUTUAL SOLUBILITIES OF THE NICOTINE–WATER SYSTEM

Temperature, ° C	Composition of top layer		Composition of bottom layer	
	Wt. % H_2O	Wt. % Nic.	Wt. % H_2O	Wt. % Nic.
61.5 (CRIT.)	64.0	36.0	64.0	36.0
62.0	70.0	30.0	57.1	42.9
65.0	82.4	17.6	43.4	56.6
70.0	87.2	12.8	35.7	64.3
85.0	90.5	9.5	25.0	75.0
115.0	19.3	80.7	96.8	3.2
140.0	17.0	83.0	93.7	6.3
150.0	16.8	83.2	94.0	6.0

Composition		Upper temperature limit of heterogeneous area, ° C
Wt. % H_2O	Wt. % Nic.	
20.0	80.0	183.0±0.5
25.0	75.0	203.5
32.0	68.0	219.5
43.0	57.0	231.0
54.0	46.0	232.5
60.0 (CRIT.)	40.0	233.0
62.0	38.0	233.0
68.0	32.0	232.5
73.0	27.0	231.5
85.0	15.0	218.0
90.0	10.0	200.0

The Binary System: Methylethyl Ketone – Nicotine

Methylethyl ketone and nicotine are intersoluble at all temperatures. The densities, viscosities, and refractive indices were determined at intervals of 10% by weight. The graphs of these properties versus composition at 25° C are very nearly linear, with the exception of the viscosity curve whose slope begins to increase at a concentration of 50% nicotine, and continues to increase to a maximum at pure nicotine. The freezing curve shows no marked change of slope and therefore it is impossible to estimate the eutectic temperature and composition.

The Ternary System: Methylethyl Ketone – Nicotine – Water

At 25° C, these three substances are completely miscible except for a small region with a composition of less than 9% nicotine, and between 25 and 88% ketone. A picture of the solid model representing composition versus temperature can be visualized by imagining the isotherms of Fig. 1 to be placed vertically above one another at the appropriate distances. When this is done, a tunnel-shaped solid results. The upper part of this tunnel forms a smooth surface running from the upper critical solution temperature of the methylethyl ketone – water system to the upper critical solution temperature of the nicotine–water system, but, on the lower surface, a maximum occurs in the homogeneous volume, that is, a ternary critical solution point exists. The solubility surface rises from

Can. J. Chem. Downloaded from www.nrcresearchpress.com by 78.46.186.204 on 09/04/12
For personal use only.

the ice line of the methylethyl ketone – water system and meets a surface rising continuously from the lower critical solution temperature of the nicotine–water system. The maximum of this dent in the surface lies at a temperature of $67.3 \pm 0.2°$ C and at a composition of 27 weight per cent nicotine, and 14 weight per cent methylethyl ketone. If a corresponding critical point exists on the upper surface of the solubility model, the critical solution must contain so little nicotine, less than say one per cent, as to be non-detectable by our methods. The data for the ternary system (by the Alexejew method) are given in Table V.

Obviously, none of the systems was studied isobarically, but under the vapor pressure of the system which may be as great as twenty atmospheres. The question of what the data would be under a constant pressure of 1 atmosphere is meaningless, since the systems would cease to exist (they would vaporize completely) under this pressure.

REFERENCES

1. ROTHMUND, V. Z. physik. Chem. **26**, 433 (1898).
2. MARSHALL, A. J. Chem. Soc. **89**, 1350 (1906).
3. SHELL CHEMICAL CORPORATION. Methylethyl ketone. 1950. p. 65–67.
4. RANDALL, M. and MCKENNA, F. E. J. Am. Chem. Soc. **73**, 4859 (1951).
5. HUDSON, C. S. Z. physik. Chem. **47**, 113 (1904).
6. TSAKOLOTOS, M. D. E. Bull. soc. chim. France, **5**, 397 (1909).
7. LEONE, P. Atti congr. nazl. chim. pura ed appl. 2nd Congr. 1209 (1926).

Can. J. Chem. Downloaded from www.nrcresearchpress.com by 78.46.186.204 on 09/04/12
For personal use only.

Can. J. Chem. Downloaded from www.nrcresearchpress.com by 78.46.186.204 on 09/04/12
For personal use only.

THE DETERMINATION OF UO_3 AND U_3O_8 IN BROWN OXIDE[1]

L. G. STONHILL

ABSTRACT

Investigations leading to a method for the analysis of mixtures of the oxides UO_3, U_3O_8, and UO_2 are described.

Uranic oxide is extracted with hot ammonium citrate solution, uranic and uranous-uranic oxides are determined together by solution in phosphoric acid followed by titration of U(VI) with titanous sulphate, and uranous oxide found by difference.

INTRODUCTION

"Brown oxide" is a product consisting essentially of uranium dioxide, but with a molecular formula UO_{2+x}, where x is zero in the case of high purity brown oxide and will have larger values if oxygen is present in excess over the proportion required to form the dioxide.

It is important as an intermediate stage between refined UO_3 and uranium tetrafluoride ("green salt") in the production of uranium metal, and in addition, interest is developing in its use in reactor fuel elements without further processing.

In the Port Hope, Ontario, plant of Eldorado Mining and Refining Limited, "brown oxide" is produced by hydrogen reduction of UO_3 and then hydrofluorinated to "green salt" according to the reactions:

$$UO_3 + H_2 = UO_2 + H_2O,$$
$$UO_2 + 4HF = UF_4 + 2H_2O.$$

Owing to the difficulty of achieving complete reduction to UO_2 under plant conditions, a certain amount of U(VI) may remain in the "brown oxide" and will give uranyl fluoride by the reactions:

$$UO_3 + 2HF = UO_2F_2 + H_2O,$$
$$U_3O_8 + 8HF = 2UO_2F_2 + UF_4 + 4H_2O.$$

Therefore, as the uranyl fluoride content of "green salt" must be kept low, it is essential for control purposes to know the proportion of the higher oxides UO_3 and U_3O_8 in the "brown oxide" intended for its production; the research reported here was undertaken to provide such data.

It will be assumed in what follows that uranium is present in "brown oxide" only in the valencies IV and VI and the forms UO_2, U_3O_8, and UO_3. In the case of certain poorly reduced samples the author has made thermogravimetric observations which tend to support the latter assumption.

EXPERIMENTAL

1. *Determination of* UO_3

The loss in weight of a brown oxide sample after a 15-minute extraction with refluxing ammonium citrate solution is a method current in the industry for the estimation of UO_3 contents (1).

Under such conditions, however, U_3O_8 is markedly soluble and a source of error is thereby introduced. In the hope of overcoming this objection, qualitative tests were

[1]*Manuscript received May 20, 1958.*
Contribution from the Metallurgical Laboratories, Eldorado Mining and Refining Ltd., Ottawa, Canada.

made upon each of the three oxides with possible alternative complexants, listed in Table I. UO_3 dissolved fairly rapidly in cold solutions of some, but in other cases the application of heat was necessary; rapid dissolution then occurred.

UO_2, reduced at 500° in a mixture of hydrogen and nitrogen to simulate plant conditions, then ground to pass a 325-mesh screen, resisted the action of all the reagents under the conditions of the method described in section 4.1, and after 2 hours cold extraction (series A) or 15 minutes refluxing (series B) no dissolved uranium could be detected by the well-known peroxide test.

U_3O_8, prepared by igniting UO_2 in air at 500° followed by grinding to pass a 325-mesh screen, was detectably soluble in each reagent, and quantitative data on this solubility, obtained using the same conditions as for the UO_2 tests, are recorded in Table I. It should be noted that these are not equilibrium values but provide a comparative basis for selecting the reagent with least effect on U_3O_8.

TABLE I

SOLVENT ACTION OF VARIOUS REAGENTS ON U_3O_8

Reagent	Weight of U_3O_8 dissolved per 100 ml of reagent solution
Series A: Reaction with UO_3 fast in cold solution	
Hydrazine sulphate 5% w/v	10 mg
Oxalic acid 5% w/v	10
Sulphuric acid 2% v/v	6
Sulphosalicylic acid 5% w/v	4
Series B: Reaction with UO_3 fast in boiling solution (all solutions 5% w/v)	
Ammonium oxalate	18
Ammonium malonate	20
Ammonium succinate	19
EDTA	14
Ammonium tartrate	8.5
Ammonium citrate	8.3

Clearly, absolute specificity to UO_3 cannot be attained with the reagents so far suggested, but, of series A, sulphosalicylic and weak sulphuric acids might be of practical use, also ammonium citrate and tartrate of series B. All four are an improvement upon ammonium oxalate, and the latter's homologues, malonate and succinate, need not be further considered.

The reproducibility of results obtained using sulphosalicylic and weak sulphuric acids was found to be poor, apparently owing to their strong retention by UO_2, an effect noted elsewhere with potassium oxalate (2). On the other hand, ammonium citrate and tartrate both gave results which were reproducible and in agreement with each other within the limits of error associated with gravimetric procedures. Of this pair, ammonium citrate has been chosen for routine work but appears to have no special advantage over tartrate.

As the data in Table I imply, a 100%-pure U_3O_8 sample would be soluble to the extent of about 1.7% in both tartrate and citrate solutions under experimental conditions, but since brown oxide of good production quality contains only a few per cent U_3O_8, the latter's dissolution tendency may be expected to have no serious effect on the UO_3 values obtained in practice.

Regarding the preparation of samples for UO_3 determination, it has been found that

Can. J. Chem. Downloaded from www.nrcresearchpress.com by 78.46.186.204 on 09/04/12
For personal use only.

grinding beyond the stage at which the whole sample has been reduced below 325-mesh screen size does not significantly increase the proportion dissolved by ammonium citrate solution. Excessive grinding will in fact tend to increase the rate at which the contained U_3O_8 reacts, and should be avoided.

2. Determination of U_3O_8

For practical purposes, U_3O_8 is conveniently regarded as uranous–uranic oxide ($UO_2 \cdot 2UO_3$). Provided that it can be dissolved to give a mixture of U(VI) and U(IV) in the proportion of 2:1 expected from this formula, analysis of the resulting solution for either U(VI) or U(IV) would be a suitable method for its determination. In the present context, with both UO_3 and UO_2 also present, allowance must be made for a contribution to the quantity of both valency states arising from these other oxides because U_3O_8 cannot be specifically extracted from admixture. UO_3 present as such can be determined alone (as has been seen above) and therefore analysis of a solution of the mixed oxides for U(VI), with a correction for UO_3, would establish the amount of U_3O_8 present.

The experimental investigation was directed firstly towards a method for determining U(VI) in presence of U(IV), secondly to procedures for dissolving the mixed oxides without change in the proportions of each valency state, and finally to showing that U_3O_8 can in fact be determined in accordance with the foregoing discussion.

2.1 The Determination of U(VI)

It was quickly established that U(VI) cannot be determined spectrophotometrically in presence of U(IV). The main absorbance regions of equal concentrations of both valency states of uranium in sulphuric acid over the range of the Beckman DU instrument are such that U(VI) has no absorption wave-length unaffected by the presence of U(IV).

Attention was therefore transferred to volumetric methods. Consideration of the relevant oxidation–reduction potentials showed that either Ti(III) or Cr(III) should be suitable titrants for U(VI). Of the two, the more strongly reducing chromous ion has the operating disadvantage of instability in storage unless prepared in a highly purified state, and potentiometric titration with titanous sulphate was decided on.

The reduction of U(VI) by Ti(III) is slow at ordinary temperatures and low acidity, and in the titration of UO_3 dissolved in either hydrochloric, sulphuric, or phosphoric acids it was found necessary to increase both factors to speed up the reaction. At 80° C, and with an acid concentration of 50%, a satisfactorily sharp inflection of potential versus titrant volume was found to occur. As is usual in this type of titration (3) the addition of an ion with an intermediate redox potential to the solution being titrated speeded the attainment of a steady potential after each addition of titrant; ferrous sulphate was found satisfactory. Alternatively ammonium oxalate or citrate (4) may be used.

2.2 Dissolution of U_3O_8

While UO_3 dissolves rapidly in strong acids, U_3O_8 is rather more resistant and requires the application of heat. Phosphoric acid was found suitable as a solvent for all three oxides and is used in the recommended analytical procedure. At an early stage in these experiments it was obvious that air had to be completely excluded from hot solutions of U(IV) otherwise oxidation occurred, and special precautions were taken to ensure this. Air-free phosphoric acid was used for dissolution of the oxides, and both dissolution and titration stages were carried out in the same vessel, which was kept full of carbon dioxide throughout the analytical operations.

Can. J. Chem. Downloaded from www.nrcresearchpress.com by 78.46.186.204 on 09/04/12
For personal use only.

2.3 Stoichiometry of U_3O_8

To demonstrate that U_3O_8 does in fact dissolve in phosphoric acid giving the ratio of U(VI) to U(IV) expected from the formula ($UO_2 \cdot 2UO_3$), weighed quantities of pure U_3O_8 were dissolved in phosphoric acid and titrated with a titanous sulphate solution previously standardized with pure UO_3. Within the usual limits of experimental error, the ratio of U(VI) to total uranium content was in each case found to be 2:3.

3. Determination of UO_2

It is not possible to extract UO_2 specifically from a mixture of oxides, and an approach via a U(IV) determination would, in the presence of U_3O_8, have little value. The UO_2 content of a mixture is for present purposes, therefore, taken as the difference from 100% of the sum of the UO_3 and U_3O_8 contents. An independent method involving thermogravimetric oxidation of the UO_2 will form the subject of a later communication.

In spite of the wide variation in composition between these samples, the concordance between total uranium values obtained by independent methods is satisfactory, and particularly so in the cases of samples A, H, and J (see Table II), where the directly assayed components constitute the major fraction of the whole, and where, consequently, analytical errors would have the largest effect on the total uranium value.

4. Analytical Procedures

1. Determination of UO_3

Reagent required: dibasic ammonium citrate.

The part of the sample used for the UO_3 determination should completely pass a 325-mesh sieve. Reflux an accurately weighed quantity, about 0.5 g, with 200 ml 5% ammonium citrate solution for 15 minutes. Recover the residue by filtration through a sintered-glass filter crucible under suction; wash with hot water, followed by acetone, and dry at 80° C for 1 hour. Determine the loss in weight of the original sample. This represents its UO_3 content.

2. Determination of U_3O_8

The apparatus required is depicted in Fig. 1. Reagents required:

(*a*) Phosphoric acid 50% v/v, air-free. This solution is freed from oxygen by passing in a stream of pure nitrogen or carbon dioxide.

(*b*) Pure U_3O_8. Ignite U_3O_8, UO_3, or UO_2 in air at 750° C for 1 hour. One gram of U_3O_8 is equivalent to 0.6793 g UO_3 when its solution is used for the standardization of titanous sulphate solution.

(*c*) Titanous sulphate solution. Dilute the commercial 15% titanous sulphate solution in the ratio 1:8 with 4 *N* sulphuric acid, and store in an aspirator bottle attached to a hydrogen generator. After the solution has been left standing for 2 days, standardize it with pure U_3O_8, following the titration procedure below.

(*d*) Ferrous ammonium sulphate, reagent grade.

The procedure is as follows: Weigh accurately a quantity of powdered brown oxide containing about 200 mg U(VI) as UO_3. Add this to 50 ml air-free 50% phosphoric acid in a 500-ml three-necked flask and swirl gently to mix. Pass CO_2 into the flask at this stage and throughout the subsequent procedure to prevent entry of oxygen. Heat to boiling, and allow the acid to concentrate until a clear solution is obtained. Cool somewhat, add 150 ml more air-free 50% phosphoric acid and a glass-covered magnetic stirring bar, heat to 80–85° C, add 0.25 g ferrous ammonium sulphate, and titrate potentiometrically with the standard titanous sulphate solution, stirring continuously. The result is the U(VI) content of the sample expressed as total equivalent UO_3; subtraction of the percentage of UO_3 found to be present as such by ammonium oxalate extraction

Can. J. Chem. Downloaded from www.nrcresearchpress.com by 78.46.186.204 on 09/04/12
For personal use only.

Can. J. Chem. Downloaded from www.nrcresearchpress.com by 78.46.186.204 on 09/04/12
For personal use only.

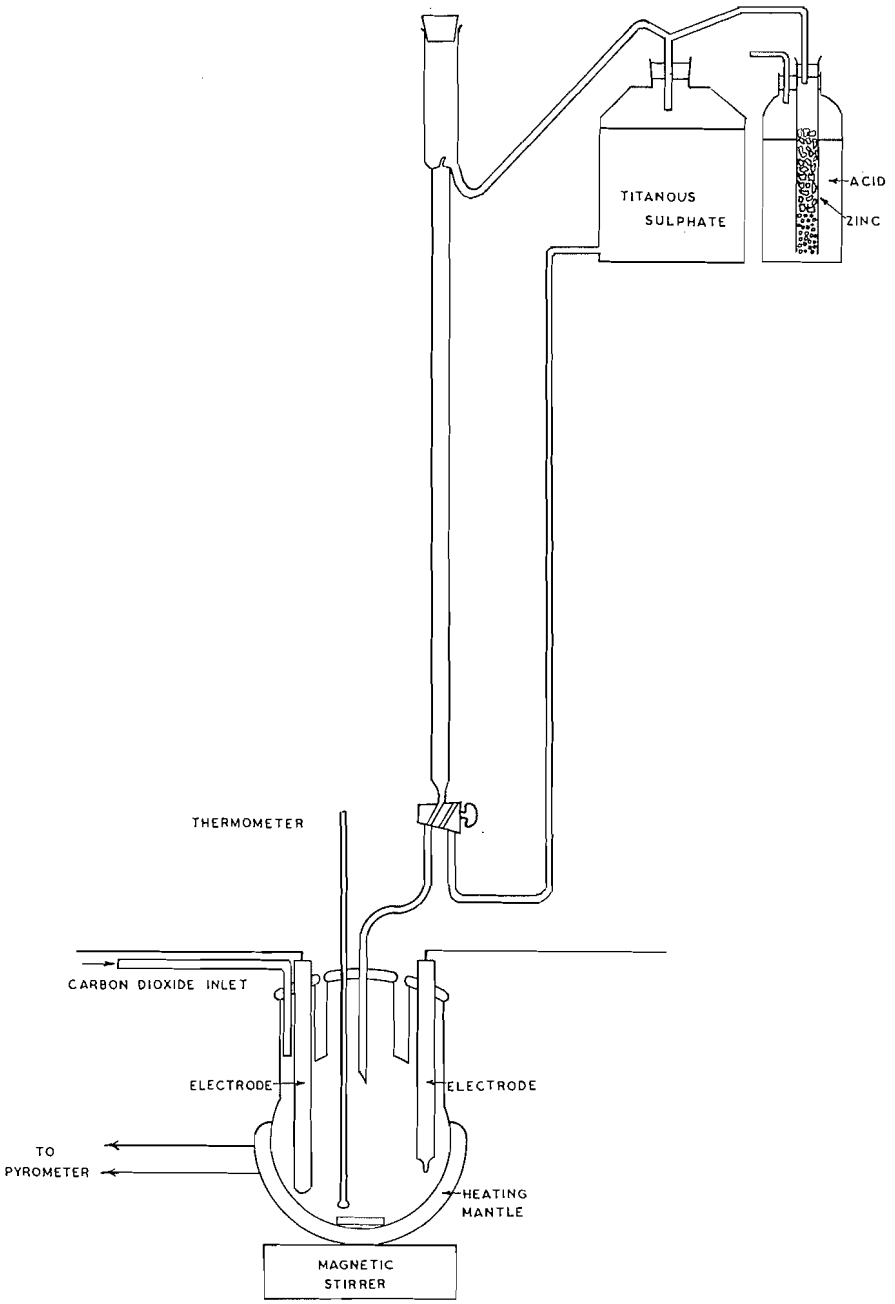

FIG. 1.

gives the percentage of the sample which is UO_3 present in U_3O_8; and the product of that figure and the factor 1.4717 is the percentage of actual U_3O_8 in the sample.

RESULTS

To test, over as wide a range of mixtures as possible, the performance of the analytical method resulting from the investigations described above, a series of brown oxide specimens of varying quality was assayed and a few of the results are shown in Table II.

TABLE II

RESULTS OF BROWN OXIDE ASSAYS

Sample	% UO_3	% U_3O_8	% UO_2 by difference
A	4.75	54.1	41.2
B	4.82	15.1	80.1
C	16.4	18.5	65.1
D	0.86	4.52	94.62
E	1.63	6.78	91.59
F	1.02	6.33	92.65
G	3.60	7.95	88.45
H	3.11	70.3	26.6
J	2.17	64.2	33.6

There is at present no alternative method for determining individual oxides in a mixture for comparison with the above results, but it is of interest to compare the total uranium content of each sample calculated from the results of the present method with that given by standard methods. The comparison is given in Table III.

TABLE III

COMPARISON OF TOTAL URANIUM VALUES

	% Uranium as given by:		
Sample	Present method	Conversion to U_3O_8	Differential colorimetry
A	86.10	85.89	86.04
B	87.41	87.21	87.25
C	86.73	86.46	86.32
D	87.96	87.65	87.97
E	87.85	87.74	87.82
F	87.89	87.70	87.52
G	87.71	87.70	87.70
H	85.65	85.41	85.45
J	85.90	85.87	85.90

REFERENCES

1. UNPUBLISHED METHOD.
2. U.S. ATOMIC ENERGY COMM. A-2912. **3**, 49 (1946).
3. KOLTHOFF, I. M. and LIVINGSTON, R. S. Ind. Eng. Chem., Anal. Ed. **7**, 209 (1935).
4. EL-SHAMY, H. F. and ZAYAN, S. EL-DIN. Analyst, **80**, 65 (1955).

Can. J. Chem. Downloaded from www.nrcresearchpress.com by 78.46.186.204 on 09/04/12
For personal use only.

Can. J. Chem. Downloaded from www.nrcresearchpress.com by 78.46.186.204 on 09/04/12
For personal use only.

THE GAS PHASE REACTIONS OF PERFLUORO-*n*-PROPYL RADICALS WITH METHANE AND ETHANE[1]

G. GIACOMETTI[2] AND E. W. R. STEACIE

ABSTRACT

The rate constants and activation energies for the reactions of C_3F_7 radicals with methane and ethane have been measured by photolyzing mixtures of $C_3F_7COC_3F_7$ and hydrocarbon with 3130 Å light. Photolysis of mixtures of the ketone, methane, and deuterium has been used to check previous measurements on the reaction of C_3F_7 and deuterium.

INTRODUCTION

The availability of completely fluorinated alkyl radicals obtained via a very simple mechanism from the photolysis of the corresponding ketones (1, 2) makes it worth while to study their reactions with simple hydrocarbons or other substrates, with the object of throwing further light on the effect of the structure of the reactants on the rate constants. The mechanism of production of n-C_3F_7 radicals from perfluoro di-*n*-propyl ketone has been investigated (2) and their reactions with hydrogen and deuterium have been subsequently studied (3).

While the mechanism of the photolysis is extremely simple in this case, especially compared with the non-fluorinated compound, there is one analytical feature of this system which complicates the situation. Owing to the very similar volatilities of the perfluoro di-*n*-propyl ketone and of the perfluoro-*n*-hexane, it is impossible to separate the latter from the bulk of the unreacted material by the usual low-temperature distillation technique.

This difficulty can be overcome, however, by taking advantage of the simplicity of the mechanism and estimating the hexane by a stoichiometric balance. This was done previously in the reaction of n-C_3F_7 with hydrogen and deuterium, although in this case some uncertainty affected the results because of ignorance of the fate of the hydrogen atoms produced in the system (3).

In this paper we present the analogous results obtained for the reactions of C_3F_7 radicals withm ethane and ethane, which are not affected by such a complication. This circumstance also permits an independent determination of the hydrogen reaction rate by performing experiments in the presence of both methane and deuterium.

EXPERIMENTAL

Apparatus

The apparatus was essentially the same as that used in the experiments on the hydrogen reaction. The light source was a B.T.H. high-pressure mercury lamp (ME/D, 250 watts) operated on stabilized 220 v d-c. The 3130 Å radiation was isolated by a standard set of filters. The quartz reaction cell was 10 cm long and had a capacity of 175 cc; it was fully illuminated by the parallel beam of light. The cell was maintained at the desired temperature by an aluminum block furnace and the temperature was constant to $\pm 1°$ C.

The filling system was of a conventional type as was the analytical line which consisted of two Ward–LeRoy stills, one solid nitrogen trap, a small mercury diffusion pump, a

[1]*Manuscript received July 27, 1958.*
Contribution from the Division of Pure Chemistry, National Research Council, Ottawa, Canada.
Issued as N.R.C. No. 4912.
[2]*National Research Council Postdoctorate Fellow 1956–58. Present address: Istituto di Chimica Fisica, Universita di Padova, Padova, Italy.*

gas burette, and a Toepler pump for sample collection. A small CuO furnace, operating at 250° C, could also be inserted in the line when necessary. All stopcocks were avoided by use of appropriate mercury cutoffs.

Materials

The ketone was supplied by Dr. L. C. Leitch of these laboratories and its purity checked by careful distillation in a Podbielniak column (b.p. 75° C) and by mass spectrometry. Deuterium was obtained from a Stuart Oxygen Company cylinder and was passed through hot palladium before storage in a 5-liter bulb connected to the line. Mass spectroscopic analysis gave a D content of 95.4% and all results have been corrected accordingly. Methane and ethane were research grade Philips products and were carefully checked for impurities in the mass spectrometer.

Procedure

After the ketone had been introduced into the cell, its pressure was measured with a constant-volume manometer. The ketone was then frozen out at liquid nitrogen temperature andm ethane or ethane was introduced at the desired pressure. The two reactants were then mixed by expanding them a few times by means of a Toepler pump. The total gas pressure was always measured as a further check. When deuterium was also present, the relative amount of the two gases was measured by reading their pressures in two separate sections of the apparatus whose volume ratio had been previously measured.

The photolysis was allowed to proceed up to 4 to 6% decomposition of the ketone. The analyses were carried out by the usual technique of low-temperature fractionation and mass spectrometry.

In the methane experiments the products of the photolysis were CO, C_3F_7H, $C_4F_7H_3$, C_2H_6, and C_6F_{14}. The first fraction was collected at −210° C and it contained all the CO together with large quantities of methane. The CO was then separated by oxidation in the CuO furnace and measured in the gas burette. Blank experiments showed that no methane was oxidized during the short time of the operation. After pumping off all the remaining methane and possible traces of ethane, a second fraction was collected at −105° C containing all the C_3F_7H and the $C_4F_7H_3$. The C_3F_7H content was estimated by the peak at mass 51 of its mass spectrum. The $C_4F_7H_3$ was estimated by difference and the main peaks of the mass spectrum of this compound are shown in Table I.

In the ethane experiments the products were CO, C_3F_7H, $C_5F_7H_5$, n-C_4H_{10}, and C_6F_{14}. CO was collected at −210° C and a few checks by oxidation in the CuO furnace showed that it did not contain ethane. Ethane was removed at −155° C. The fraction at

TABLE I

MASS SPECTRUM OF n-$C_3F_7CH_3$ (MAIN OR CHARACTERISTIC PEAKS)

Mass n	Relative height	Probable ion
169	5.6	$C_3F_7^+$
119	3.1	$C_2F_5^+$
115	1.4	$C_2F_4CH_3^+$
96	6.1	$C_2F_3CH_3^+$
77	6.0	$C_2F_2CH_3^+$
69	5.1	CF_3^+
65	100.0	$CF_2CH_3^+$
64	3.4	$CF_2CH_2^+$
45	12.9	$CFCH_2^+$

Can. J. Chem. Downloaded from www.nrcresearchpress.com by 78.46.186.204 on 09/04/12
For personal use only.

Can. J. Chem. Downloaded from www.nrcresearchpress.com by 78.46.186.204 on 09/04/12
For personal use only.

−105° C contained all the C_3F_7H, part of the $C_5F_7H_5$, and all the *n*-butane. A further fraction at −90° C contained only $C_5F_7H_5$. The mass spectrum of this compound is shown in Table II. The peak used for the analysis was the large 79 peak which does not occur with C_3F_7H, *n*-butane, or the ketone.

TABLE II

MASS SPECTRUM OF $C_3F_7C_2H_5$ (MAIN OR CHARACTERISTIC PEAKS)

Mass *n*	Relative height	Probable ion
169	27.9	$C_3F_7^+$
159	6.4	$C_3F_5C_2H_4^+$
119	20.1	$C_2F_5^+$
109	12.2	$C_2F_3C_2H_4^+$
95	8.4	$C_2F_3CH_2^+$
89	3.2	$C_2F_5C_2H_5^+$
79	100	$CF_2C_2H_5^+$
77	12.9	$CF_2C_2H_3^+$
69	75.1	CF_3^+
59	32.1	$CFC_2H_4^+$

The experiments with methane and deuterium were carried out in a manner completely analogous to that used by Miller and Steacie (3) with mixtures of hydrogen and deuterium. The peaks at mass 51 and 52 were used to measure the ratio of C_3F_7H to C_3F_7D and blank runs were performed before each experiment to check the ratio in the absence of hydrogen.

RESULTS

The results for the three sets of experiments are summarized in Tables III, IV, and V. A few runs were performed at quite different light intensities and showed that the results were independent of such changes.

TABLE III

THE REACTION OF n-C_3F_7 RADICAL WITH METHANE

	Reactants		Products			
Temp., °K	Ketone pressure, mm	CH_4 pressure, mm	CO moles $\times 10^6$	C_3F_7H moles $\times 10^6$	Time, sec	$k_3/k_2^{\frac{1}{2}}$ $cc^{\frac{1}{2}}$ $molecule^{-\frac{1}{2}}$ $sec^{-\frac{1}{2}}$ $\times 10^{13}$
439	24.0	43.4	5.20	0.606	3840	2.77
424	23.9	45.7	6.31	0.486	3780	1.83
382	21.7	42.0	5.52	0.124	3780	0.482
368	27.3	67.2	6.78	0.159	3420	0.356
343	20.2	49.3	6.48	0.052$_3$	4140	0.136
386	21.9	62.3	6.76	0.207	3840	0.497
400	26.7	66.1	8.04	0.340	4080	0.708
402	25.2	114.8	5.70	0.425	3780	0.643
355	26.8	96.5	8.56	0.121	3960	0.150
368	23.0	96.0	7.94	0.181	3960	0.244

The mechanism postulated for the reaction with methane is the following:

$$C_3F_7COC_3F_7 \rightarrow 2\ C_3F_7 + CO, \quad [1]$$

$$2\ C_3F_7 \rightarrow C_6F_{14}, \quad [2]$$

$$C_3F_7 + CH_4 \rightarrow C_3F_7H + CH_3, \quad [3]$$

$$CH_3 + CH_3 \rightarrow C_2H_6, \quad [4]$$

$$CH_3 + C_3F_7 \rightarrow C_4H_3F_7. \quad [5]$$

TABLE IV

THE REACTION OF n-C_3F_7 RADICAL WITH ETHANE

Temp., °K	Reactants: Ketone pressure, mm	Reactants: C_2H_6 pressure, mm	Products: CO moles $\times 10^6$	Products: C_3F_7H moles $\times 10^6$	Products: $C_5F_7H_5$ moles $\times 10^6$	Products: C_4H_{10} moles $\times 10^6$	Time, sec	$k_{3'}/k_2^{\frac{1}{2}}$ cc$^{\frac{1}{2}}$ molecules$^{-\frac{1}{2}}$ sec$^{-\frac{1}{2}}$ $\times 10^{13}$	$k_{3'a}/k_{3'b}$
379	22.1	20.6	7.24	1.99	(>0.730)	Negligible	3600	10.5	
423	22.1	8.9	8.16	2.76	1.49	0.031	3840	43.7	0.40
360	22.6	21.1	9.40	1.54	0.84	0.011	4200	6.17	0.40
402	26.4	22.1	12.2	5.38	2.99	0.06	4740	20.0	0.39
372	20.8	20.3	9.17	2.03	1.11	0.02	4140	8.52	0.41
400	17.3	19.6	6.98	2.95	1.58	0.047	3780	19.5	0.39
425.5	20.5	16.2	8.54	4.66	2.39	0.16	4200	37.2	0.40
433	19.4	20.1	4.96	4.06	2.31	0.24	4020	44.7	0.37
469	18.4	14.5	4.04	4.46	2.08	0.32	3720	135	0.40
455	18.9	16.5	5.30	4.12	1.87	0.30	4020	81.3	0.42

TABLE V

THE REACTION OF n-C_3F_7 RADICAL WITH DEUTERIUM–METHANE MIXTURES*

Temp., °K	CH_4 pressure/D_2 pressure	51/52 ratio corrected	$k_3/k_{3''}$
370	1.52	3.38	2.22
421	1.56	1.95	1.25
396	1.92	2.87	1.50
358	1.49	3.71	2.49
397	1.38	2.00	1.45
382	1.22	2.26	1.85
455	1.36	1.23	0.905

*Total pressures were of the order of 50–60 mm Hg-$k_3/k_{3''}$ calculated from $R_{C_3F_7H}[D_2]/R_{C_3F_7D}[CH_4]$.

Fluorine abstraction reactions are ruled out by the absence of C_3F_8 in the products and no other reaction of importance in determining the amount of products seems to be possible. The rate of production of C_6F_{14} is thus very simply given by:

$$R_{C_6F_{14}} = R_{CO} - \tfrac{1}{2}(R_{C_3F_7H} + R_{C_4H_3F_7}). \quad [1]$$

The last column of Table III shows the values of

$$k_3/k_2^{\frac{1}{2}} = R_{C_3F_7H}/R_{C_6F_{14}}^{\frac{1}{2}}[CH_4]$$

calculated in this way,* and Fig. 1 shows the Arrhenius plot obtained. Least squares fitting of this plot give:
$k_3/k_2^{\frac{1}{2}} = 1.25\times10^{-8}e^{-9.5\times10^3/RT}$ molecule$^{-\frac{1}{2}}$ cc$^{\frac{1}{2}}$ sec$^{-\frac{1}{2}}$. The value for $E_3-\frac{1}{2}E_2$ is thus 9.5 $\pm$0.5 kcal/mole.

The mechanism for the ethane reaction is somewhat more complicated owing to the possibility of disproportionation in radical–radical reactions:

$$C_3F_7 + C_2H_6 \rightarrow C_3F_7H + C_2H_5, \quad [3']$$

**Under the conditions of the experiments the quantities of $C_4H_3F_7$ were so small that no accurate analysis was possible. Their exclusion from [1] cannot affect the value of $k_3/k_2^{\frac{1}{2}}$ by more than one per cent. They have therefore been omitted from the table.*

Can. J. Chem. Downloaded from www.nrcresearchpress.com by 78.46.186.204 on 09/04/12
For personal use only.

$$C_2H_5 + C_2H_5 \rightarrow C_2H_4 + C_2H_6, \quad [4'a]$$

$$C_2H_5 + C_2H_5 \rightarrow C_4H_{10}, \quad [4'b]$$

$$C_2H_5 + C_3F_7 \rightarrow C_3F_7H + C_2H_4, \quad [5'a]$$

$$C_2H_5 + C_3F_7 \rightarrow C_5F_7H_5. \quad [5'b]$$

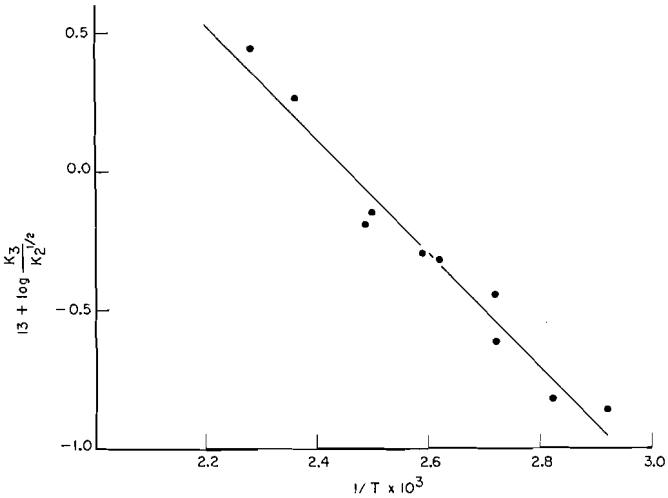

FIG. 1.

The stoichiometric balance can be carried out in this case by analyzing the products for CO, C_3F_7H, C_4H_{10}, and $C_5F_7H_5$ and assuming the ratio $k_{4'a}/k_{4'b}$ to be known. The best experimental value for the latter is 0.12, practically independent of temperature and pressure (4). The C_3F_7 radical balance will give the rate of formation of C_6F_{14} as in the former case:

$$R_{C_6F_{14}} = R_{CO} - \tfrac{1}{2}[R_{C_3F_7H} + R_{C_5F_7H_5}].$$

The balance for C_2H_5 radicals will give both the rate of formation of C_3F_7H from reaction [3'] and the ratio $k_{5'a}/k_{5'b}$:

$$(R_{C_3F_7H})_{3'} = \tfrac{1}{2}[R_{C_3F_7H} + R_{C_5F_7H_5} + 2.24\ R_{C_4H_{10}}]$$
$$k_{5'a}/k_{5'b} = [R_{C_3F_7H} - (R_{C_3F_7H})_{3'}]/R_{C_3H_5F_7}.$$

The justification of this procedure is indicated by the constancy of the value obtained for the latter expression over a range of temperatures as shown in Table IV. The table also gives the values of $k_{3'}/k_2^{\frac{1}{2}}$ obtained from

$$k_{3'}/k_2^{\frac{1}{2}} = (R_{C_3F_7H})_{3'}/R_{C_6F_{14}}^{\frac{1}{2}}\,[C_2H_6].$$

The Arrhenius plot of Fig. 2 gives for $E_{3'} - \frac{1}{2}E_2$ a value of 9.2 ± 0.5 kcal/mole and the expression for the rate is

$$k_{3'}/k_2^{\frac{1}{2}} = 2.24 \times 10^{-7}\, e^{-9.2\times 10^3/RT}\ \text{mole}^{-\frac{1}{2}}\ \text{cc}^{\frac{1}{2}}\ \text{sec}^{-\frac{1}{2}}.$$

The experiments in which methane and deuterium were put together into the reaction cell were devised to get a relative value of k_3 with respect to the rate constant of the reaction:

$$C_3F_7 + D_2 \rightarrow C_3F_7D + D. \quad [3'']$$

Can. J. Chem. Downloaded from www.nrcresearchpress.com by 78.46.186.204 on 09/04/12
For personal use only.

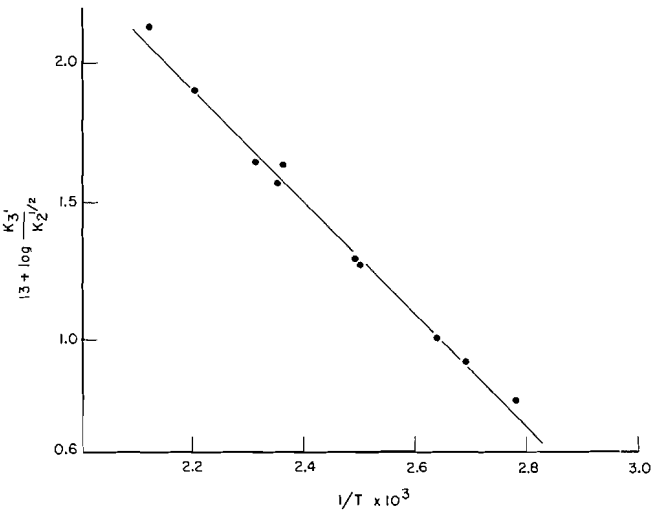

FIG. 2.

This method has already been used for the CF_3 radical by Pritchard and co-workers (5) and is simply based on the mass spectrographic estimation of the ratio RD/RH in the products. Some uncertainty arises from the fact that the fate of the D atoms produced in the abstraction is not known. In this case the possibilities are:

$$D + D + M \rightarrow D_2, \qquad [I]$$

$$D + CH_3 + M \rightarrow CH_3D, \qquad [II]$$

$$D + C_3F_7 \rightarrow C_3F_7D, \qquad [III]$$

$$D + CH_4 \rightarrow CH_3 + HD. \qquad [IV]$$

Table V gives the results of the runs performed at a total pressure of 60 to 70 mm of mercury. The Arrhenius plot is shown in Fig. 3 and the value for $E_3 - E_{3''}$ is found to be -3.4 ± 0.3 kcal/mole, the full expression for the ratio being:

$$k_3/k_{3''} = 1.99 \times 10^{-2}\, e^{3.42 \times 10^3/RT}.$$

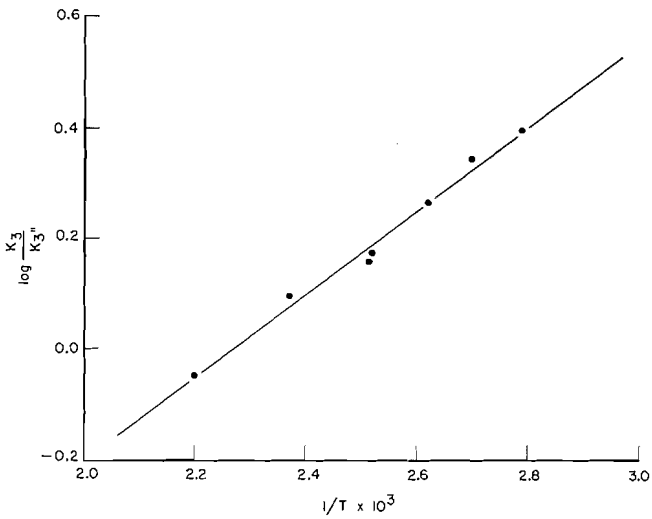

FIG. 3.

Can. J. Chem. Downloaded from www.nrcresearchpress.com by 78.46.186.204 on 09/04/12
For personal use only.

Can. J. Chem. Downloaded from www.nrcresearchpress.com by 78.46.186.204 on 09/04/12
For personal use only.

DISCUSSION

An absolute result for reaction [3″] is obtained from our data quite independently of the one obtained by Miller and Steacie (3). The value of $E_{3''} - \frac{1}{2}E_2$ obtained in the present work is 12.9±0.8 kcal/mole, which checks with the former value of 13.8±0.5, within experimental error. A comparison of the frequency factors is probably of little significance, given the somewhat large error in the activation energies. On the other hand, a comparison of the rate values in the temperature range of the experiments may be useful. At 400° K the value of Miller and Steacie (calculated assuming only reaction III to occur) is 0.24×10^{-13} molecule$^{-\frac{1}{2}}$ cc$^{\frac{1}{2}}$ sec$^{-\frac{1}{2}}$ and in the present case a reasonable agreement with that value is obtained also neglecting reaction III: 0.27×10^{-13} molecule$^{-\frac{1}{2}}$ cc$^{\frac{1}{2}}$ sec$^{-\frac{1}{2}}$. Although the uncertainty in these values is only within a factor of 2, which may be of little or no significance for these experiments, the almost complete agreement between our rate value and the former one seems to show that the same mechanism is operative in both cases. Possible occurrence of reaction IV in our case might also give a reason for the discrepancy of almost one kilocalorie per mole in our activation energy.

It is of interest to compare data for the methane, ethane, and hydrogen reactions with C_3F_7 and other radicals such as CH_3 and CF_3 for which sufficiently reliable data are available. In Table VI the activation energies, frequency factors, and the rate constants at 400° K are listed for these reactions.

TABLE VI

SUMMARY OF DATA ON REACTIONS: R′H + R → RH + R′*

R =	CH_3			CF_3			C_3F_7		
R′H	$E-\frac{1}{2}E_R$	$A/A_R^{\frac{1}{2}}\times10^8$	$k/k_R^{\frac{1}{2}}\times10^{13}$	$E-\frac{1}{2}E_R$	$A/A_R^{\frac{1}{2}}\times10^8$	$k/k_R^{\frac{1}{2}}\times10^{13}$	$E-\frac{1}{2}E_R$	$A/A_R^{\frac{1}{2}}\times10^8$	$k/k_R^{\frac{1}{2}}\times10^{13}$
H_2	10.0[a]	28.1[a]	3.0	8.8[a]	10.8[a]		12.3[c]	56.3[c]	
(D_2)	11.8[a]	16.7[a]		9.7[a]	7.5[a]		13.8[c]	77.6[c]	
CH_4	13.0[b]	3.3	0.029[b]	10.3[b]	12.5	3.5[b]	9.5[d]	1.25[d]	0.81
C_2H_6	10.4[b]	3.6	0.83[b]	7.5[b]	12.1	104[b]	9.2[d]	22.4[d]	20.4

*The subscript R refers to the recombination reaction R + R → R_2. Units for k's and A's are molecules^{-1} cc sec^{-1}. E's in kcal/mole.

[a]From ref. 5.

[b]From Steacie, E. W. R. J. Chem. Soc. 3991 (1956).

[c]From ref. 3.

[d]Obtained in the present work.

It is very difficult to find some trend in the activation energies or in the frequency factors. The only general feature is that activation energies for the D_2 reactions are always 1.5 to 2.0 kcal/mole greater than those for H_2 and this seems to be due to the zero energy effect (3).

A striking feature can be noted in the behavior of the rate constants, however. It is apparent that great changes in reactivity (over 100-fold variation) are shown by the different radicals reacting with the hydrocarbons, while the hydrogen reaction is more or less insensitive to changes in the attacking radical.

It seems that there are two quite different types of reaction. It is interesting in this respect to point out that in the case of R + H_2 there is an almost linear relationship between log A and E for the three different radicals. Such a "compensation" behavior has been found already in other cases, and there has been a recent attempt to justify it on theoretical grounds (6), especially for the case of diatomic molecules. Such a relationship does not hold for R + R′H where, on the other hand, a different regularity is

apparent. The relative reactivity of each radical toward methane and ethane is approximately constant, as shown by the ratio of the rate values of Table VI. This behavior is analogous to the findings of Smid and Szwarc for radical abstractions and additions in solution (7). It will be of interest to see if the mentioned regularities still hold in reactions with other similar radicals.

The value of the disproportionation-to-recombination ratio for the reaction between C_3F_7 and C_2H_5 is the first one reported for a reaction between a completely fluorinated radical and a completely hydrogenated one. Since C_3F_7 is seemingly more reactive toward hydrocarbons than CH_3 the ratio was expected to be greater than the one reported for $CH_3 + C_2H_5$, which is of the order of 0.03 (8); this expectation is amply justified by the value found, 0.40.

ACKNOWLEDGMENT

The authors wish to thank Miss B. Thornton for the mass spectrometric analyses.

REFERENCES

1. AYSCOUGH, P. B. and STEACIE, E. W. R. Proc. Roy. Soc. A, **234**, 476 (1956).
2. MILLER, G. H., PRITCHARD, G. O., and STEACIE, E. W. R. Z. physik. Chem. **15**, 262 (1958).
3. MILLER, G. H. and STEACIE, E. W. R. J. Am. Chem. Soc. (In press).
4. KUTSCHKE, K. O., WIJNEN, M. H. J., and STEACIE, E. W. R. J. Am. Chem. Soc. **74**, 714 (1952).
5. PRITCHARD, G. O., PRITCHARD, H. O., and TROTMAN-DICKENSON, A. F. Trans. Faraday Soc. **52**, 849 (1956).
6. RÜETSCHI, P. Z. physik. Chem. **14**, 277 (1958).
7. SMID, J. and SZWARC, M. J. Am. Chem. Soc. **79**, 1534 (1957).
8. AUSLOOS, P. and STEACIE, E. W. R. Can. J. Chem. **33**, 1062 (1955).

Can. J. Chem. Downloaded from www.nrcresearchpress.com by 78.46.186.204 on 09/04/12
For personal use only.

Can. J. Chem. Downloaded from www.nrcresearchpress.com by 78.46.186.204 on 09/04/12
For personal use only.

UNSYMMETRICALLY SUBSTITUTED 3,3′-METHYLENE BRIDGED 2,2′-DIHYDROXYCHROMONES[1,2]

R. A. Abramovitch and J. R. Gear

ABSTRACT

Unsymmetrically substituted dicoumarol derivatives* have been synthesized by taking advantage of the fact that 4-hydroxycoumarins will undergo the Mannich reaction at C_3 and also take part in Michael-type addition reactions. In the presence of methyl iodide, 4-hydroxy-3-*N*-piperidinomethylcoumarin and 4-hydroxycoumarin gave dicoumarol. By using monosubstituted 4-hydroxycoumarins a variety of unsymmetrically substituted dicoumarols have been prepared in good yield. The infrared spectra of some of the intermediates and products are reported and discussed.

A large variety of substituted derivatives of the anticoagulant dicoumarol have been prepared with a view to the production of a more active product having less side effects. These compounds fall into two main groups: (i) those bearing a substituent on the bridge methylene group are generally prepared by condensing an aldehyde or ketone with 4-hydroxycoumarin; (ii) symmetrically disubstituted dicoumarols, prepared by condensing a substituted 4-hydroxycoumarin derivative with formaldehyde, as well as combinations of (i) and (ii). Neither of these methods is amenable to the preparation of unsymmetrically substituted derivatives (I) of dicoumarol, which are of a twofold interest: (*a*) as possible physiologically active analogues of dicoumarol; (*b*) a monohydroxylated dicoumarol may be an active metabolic product of the anticoagulant but this hypothesis has never been tested owing to the unavailability of such hydroxydicoumarols. We have now developed a method which appears to be fairly general for the synthesis of this type of compound.

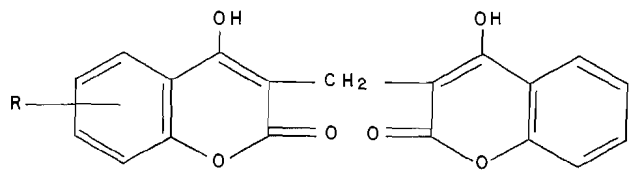

(I)

The methylene group at C_3 in 4-hydroxycoumarin is reactive and will undergo Michael addition with suitably activated double bonds. For instance, addition will take place across the double bond in ethylideneacetone (1). Sullivan *et al.* (2) suggest that formation of dicoumarol itself from formaldehyde and 4-hydroxycoumarin proceeds by this type of addition: the unstable 3-methylene-2,4-diketochroman is first formed; this is very reactive and cannot be isolated but reacts quickly with another molecule of 4-hydroxycoumarin to form dicoumarol, this last step involving a Michael addition.

[1]*Manuscript received May 15, 1958.*
Contribution from the Department of Chemistry, University of Saskatchewan, Saskatoon, Saskatchewan.
[2]*This article is based on a paper presented at the 41st Annual Conference and Exhibition of the Chemical Institute of Canada, Toronto, May 26–28, 1958.*

The chemical name for dicoumarol is 3,3′-methylenebis(2-hydroxychromone) (see p. 1506). On this basis the name of ring-monosubstituted derivatives becomes very clumsy, e.g., 2-hydroxy-7-methyl-3-chromonyl-2-hydroxy-3-chromonylmethane. We propose to use the name dicoumarol to represent the ring system of 3,3′-methylenebis(2-hydroxychromone) and this practice will be adhered to throughout this paper.

They obtained support for this suggestion by condensing 4-hydroxycoumarin (II) with an equimolar quantity of salicylaldehyde to give 3-(*o*-hydroxybenzylidene)-2,4-diketochroman (III), which could be isolated, and which reacted with 4-hydroxy-6-methylcoumarin (IV) to give (V), indicating the stepwise nature of the reaction. Incidentally, (V) was the only example of a derivative of an unsymmetrically substituted

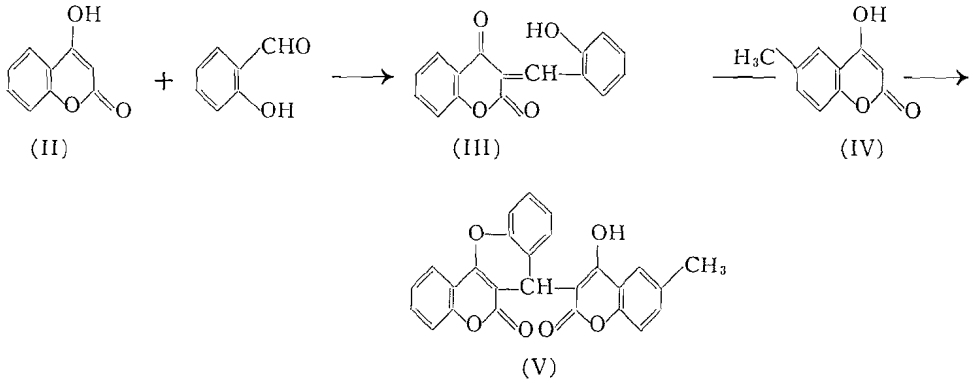

(II) (III) (IV)

(V)

dicoumarol we were able to find in the literature. If 3-methylene-2,4-diketochroman could be generated *in situ* in the presence of a substituted 4-hydroxycoumarin derivative, addition would take place to give the required type of compound. Condensation of 4-hydroxycoumarin with formaldehyde in the presence of a substituted 4-hydroxycoumarin was ruled out, since this would probably give rise to an inseparable mixture of dicoumarol derivatives. On the other hand, formation of the activated double bond *in situ* from a Mannich base was considered particularly suitable, since, by taking advantage of the active methylene at C_3, Robertson and Link (3) and also Prochazka (4) introduced a variety of aminomethyl groups in that position.

Heating together an equimolar mixture of 4-hydroxy-3-*N*-piperidinomethylcoumarin (VI) and 4-hydroxycoumarin (II) gave a highly insoluble 'addition complex' whose molecular composition corresponded to the sum of one mole of (VI) and one of (II). In view of the insolubility and instability of this complex its structure could be that of a salt of the type (VII*a*).

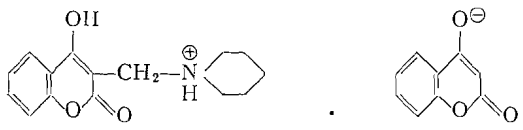

(VII*a*)

It was hoped that the infrared spectrum would shed some light onto its structure, so that it was first necessary to study the spectrum of 4-hydroxycoumarin and that of 4-hydroxy-3-*N*-piperidinomethylcoumarin, and then to see what changes took place when these two combined to form the complex.

Infrared Spectra of 4-Hydroxycoumarins

4-Hydroxycoumarin can exist in a number of tautomeric modifications, but, according to Arndt (5), because of resonance stabilization the two main forms are the 4-hydroxycoumarin (II) and the 2-hydroxychromone (VIII) structures (see also ref. 5*b*).

Can. J. Chem. Downloaded from www.nrcresearchpress.com by 78.46.186.204 on 09/04/12
For personal use only.

(II) (VIII)

As to which form predominates seems to depend on the experimental conditions and the nature of the substituents if present. From a study of the reactions of 4-hydroxycoumarin Klosa (6) concluded that the 4-hydroxycoumarin form (II) was favored but that under special conditions of solvent or acidity the chromone form could be favored. On the other hand, from a consideration of the ultraviolet spectra of 4-hydroxycoumarins in ethanol solution, Garden, Hayes, and Thomson (7) suggested that in this solvent 4-hydroxycoumarins could exist in the keto form (whether structures of types (VIII), or the diketonic structure, were meant is not clear).

It should be possible to distinguish between structures (II) and (VIII) by infrared spectroscopy: (II) should exhibit a band for an α,β-unsaturated six-membered ring lactone at *ca.* 1710 cm^{-1} (8), whereas (VIII) should have a band at *ca.* 1660 cm^{-1} corresponding to the $\alpha,\beta,\alpha',\beta'$-di-unsaturated ketone (9), and none at 1710 cm^{-1}. An elegant application of this principle is seen in the elucidation of the structures of novobiocin and its degradation products; novobiocin and 3-acetamido-7-acetoxy-4-hydroxy-8-methylcoumarin exist in the 4-hydroxycoumarin form (λ_{max} 5.92 μ) (10), whereas if a free —OH group is present at $C_{(7)}$ as in dihydronovobiocic acid (10) or in 4,7-dihydroxycoumarin (more correctly called 2,7-dihydroxychromone) (11) the chromone structure is the stable form (λ_{max} 6.0 μ). Similarly, the infrared spectra of 4-hydroxycoumarin, 4-methoxycoumarin, and 2-methoxychromone in the carbonyl region were studied by Knobloch and Prochazka (12). In dilute ethylene chloride solution 4-hydroxy- and 4-methoxycoumarin exhibited a single strong band at *ca.* 1710 cm^{-1} (with a medium intensity shoulder at 1700 cm^{-1}) corresponding to the α,β-unsaturated six-membered lactone structure, indicating that in that solvent 4-hydroxycoumarin probably exists exclusively in the 4-hydroxy form. On the other hand, 2-methoxychromone showed a single strong band at *ca.* 1650 cm^{-1} corresponding to the $\alpha,\beta,\alpha',\beta'$-di-unsaturated ketonic stretching motion. Again, Wildi (13) reports a single band at 5.90 μ for 4-hydroxy-3-phenylcoumarin in chloroform solution, together with a weak —OH stretching band at 2.87 μ.

Because of solubility and stability considerations it was only possible to measure the spectrum of the 'addition complex' obtained above as a Nujol mull so that it was desirable to study the spectrum of 4-hydroxycoumarin and 4-hydroxy-3-*N*-piperidinomethylcoumarin under such conditions. The spectrum of 4-hydroxycoumarin in the solid state is much more complex than the solution spectrum. There was no —OH band at *ca.* 2.9 μ but a medium shoulder was present at 3125 cm^{-1} together with two medium peaks at 2730 and 2560 cm^{-1}, indicating that the —OH group is strongly bonded. In the carbonyl region *two* bands were present: at 1700 (s) (with an ill-defined shoulder at 1709) and at 1673 cm^{-1}(s), the latter being the stronger of the two. The spectrum of 4-hydroxy-7-methoxycoumarin is rather similar* with bands at 3125 (sh)(m), 2760 (w), 2620 (w), 1707 (s) (medium shoulder at 1714 cm^{-1}), and 1672 cm^{-1} (ms). It seems rather unlikely

**This spectrum is very similar to that obtained by Dr. R. H. Thomson and co-workers using the* KBr *disk technique. We understand that they have made an infrared study of 4-hydroxycoumarins, which is due to be published soon, but as our limited study was necessary for an interpretation of our results we are including it here. We would like to thank Dr. Thomson for sending us a tracing of the spectrum of 4-hydroxy-7-methoxycoumarin in* KBr.

Can. J. Chem. Downloaded from www.nrcresearchpress.com by 78.46.186.204 on 09/04/12
For personal use only.

Can. J. Chem. Downloaded from www.nrcresearchpress.com by 78.46.186.204 on 09/04/12
For personal use only.

that the strong band at 1673 cm^{-1} should be due to the conjugated C=C in the 4-hydroxy form; the band for this group is probably merged with the strong broad band at 1618 cm^{-1}. There are two possible interpretations for the presence of the two carbonyl stretching bands at 1700 and 1673 cm^{-1}. One is that in the solid state the compound is a mixture of the two tautomeric modifications, (II) giving rise to the higher and (VIII) to the lower band. Alternatively, the 1673 cm^{-1} band could arise from partial intermolecular hydrogen bonding between the —OH group of one molecule and the lactone carbonyl group of another; the two bands would then be due to a mixture of chelated and unchelated lactone carbonyl groups in the solid state. In dilute ethylene chloride solution, such chelation would not take place and only the band at *ca.* 1710 cm^{-1} would be observed. This would also fit the fact that a chloroform solution of 4-hydroxy-3-phenylcoumarin has a single band at 5.90 μ and a weak —OH band at 2.87 μ (13) (though in this case the steric effect of the phenyl substituent might prevent effective intermolecular chelation). If the first interpretation is accepted one would have to assume that in ethylene chloride solution the 4-hydroxycoumarin form is stabilized with respect to the chromone structure. On the basis of the present evidence it does not seem possible as yet to decide between the two alternatives. The same remarks apply also to 4-hydroxy-7-methoxycoumarin, which again exhibits no peak at 3450 cm^{-1}; in this case the 1672 cm^{-1} peak is somewhat weaker than the 1701 cm^{-1} one and completely resolved from it.

4-Hydroxy-3-*N*-piperidinomethylcoumarin has no hydroxyl band in the 3 μ region (in Nujol mull). There are two bands at 2765 (m) and 2610 cm^{-1} (w), but only a single band is present at 1678 cm^{-1}. The Mannich base, therefore, either exists in the chromone form in the solid state, or is completely intermolecularly chelated, which is less likely. The absence of an —OH band could be due to such a chelation but could also be explained by internal salt formation (VI*a*) or internal hydrogen bonding (VI*b*).

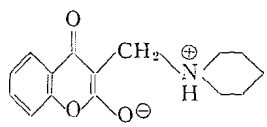

(VI*a*)

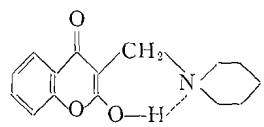

(VI*b*)

In the absence of a band at 2440–2350 cm^{-1} for an R_3NH^+ grouping (14) (VI*b*) seems the more probable structure.

The spectrum of the 'addition complex' in Nujol mull shows bands at 3170 (m) (broad) (bonded —OH), 2750 (m), 2730 (sh)(m), 2570 (m), 2470 (m) (R_3NH^+), 1719 (s) (α,β-unsaturated δ-lactone), and 1672 cm^{-1} (s) ($\alpha,\beta,\alpha',\beta'$-di-unsaturated $\rangle C{=}O$). These fit structure (VII*b*) rather well.*

The chemical evidence was also in accord with this ammonium salt structure for the

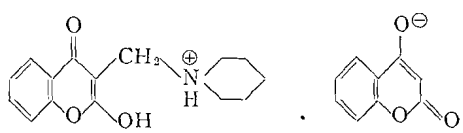

(VII*b*)

**For footnote see* NOTE *on p. 1505.*

addition complex. Thus, it could not be recrystallized without decomposition; two recrystallizations from nitromethane transformed it completely into dicoumarol, which was also obtained by heating the complex with mineral acid. These properties are in accord with the known reactivity of Mannich bases quaternary salts (15). The structure postulated for the complex led us to the expectation that if 4-hydroxy-3-*N*-piperidinomethylcoumarin was quaternized with methyl iodide before treatment with 4-hydroxycoumarin (II), then the addition complex would not be formed and heating with (II) should lead to dicoumarol readily. This was fully confirmed by experiment, no complex being formed and dicoumarol (I, R = H) being obtained in good yield.

It was now necessary to prove that the reaction had taken place by the addition of the added 4-hydroxycoumarin to the 2,4-diketo-3-methylenechroman formed *in situ* from the Mannich base, and not by a partial reversal of the Mannich condensation followed by addition of the 4-hydroxycoumarin so formed to the chroman (the yield of dicoumarol obtained in the reaction already excludes this possibility). This was readily done by treating 4-hydroxy-3-*N*-piperidinomethylcoumarin methiodide with 4-hydroxy-7-methylcoumarin to give 7-methyldicoumarol (I; R = 7–CH_3–) which could also be obtained from 4-hydroxy-7-methyl-3-*N*-piperidinomethylcoumarin methiodide and 4-hydroxycoumarin. Because of possible ambiguity owing to the closeness of analytical figures

NOTE: *Drs. K. P. Link and S. Preiss have kindly informed us that they have observed a broad band at 1635 cm^{-1} in the spectrum of the sodium salt of 4-hydroxycoumarin, presumably corresponding to the anion*

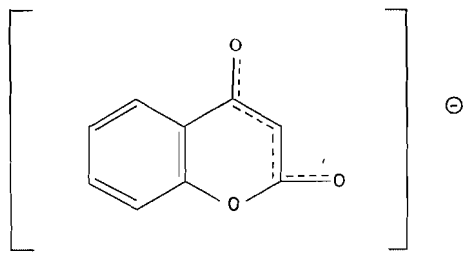

No band at 1719 cm^{-1} was observed. They suggest, therefore, that structure (VIIc) would fit the infrared data also.

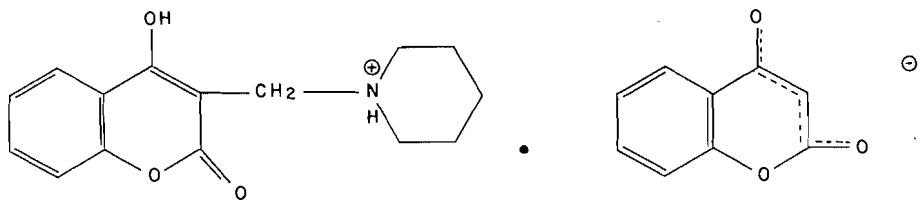

(VIIc)

The fact that we observed a sharp band at 1672 cm^{-1} for this compound at a much higher frequency than the broad band for the anion seems to speak against this possibility though it does not rule it out by any means. We would like to thank Drs. Link and Preiss for pointing the possibility out to us.

Structure

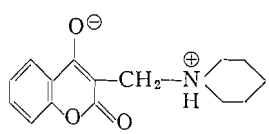

for the 3-piperidinomethyl derivative is ruled out by the absence of a band at 2440–2350 cm^{-1}.

Can. J. Chem. Downloaded from www.nrcresearchpress.com by 78.46.186.204 on 09/04/12
For personal use only.

7,7′-dimethyldicoumarol was also prepared for comparison and shown to be different from the unsymmetrical dicoumarol obtained above.

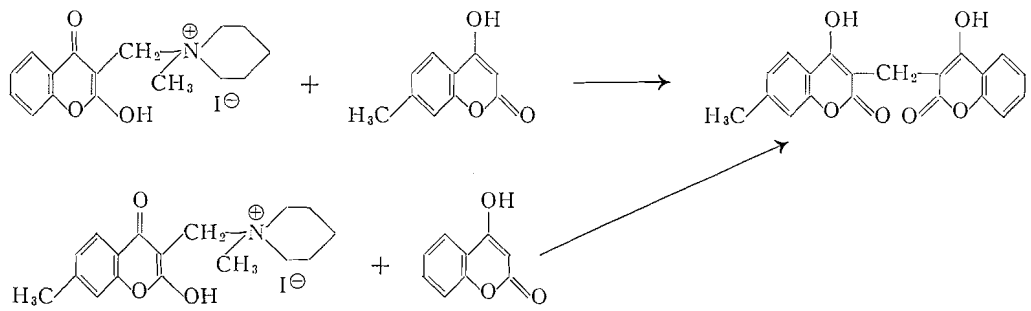

Having established the nature of the reaction, a number of unsymmetrically substituted dicoumarols were prepared to examine its scope; 6-methyl-, 6-chloro-, and 7-hydroxydicoumarol were readily obtained in good yields from 4-hydroxy-3-*N*-piperidinomethylcoumarin methiodide and the corresponding substituted 4-hydroxycoumarin. With 4-hydroxy-7-methoxycoumarin a product was readily obtained which consisted mainly of the expected 7-methoxydicoumarol, m.p. 245–248°, as shown by analysis, ultraviolet and infrared spectra, and by demethylation to the 7-hydroxydicoumarol prepared above. A small proportion of the product, however, was a highly insoluble higher melting (290–292°) substance for which good carbon and hydrogen analytical values could not be obtained. That it was a dicoumarol derivative was shown by its infrared spectrum (dicoumarols have a very characteristic type of absorption bands in the 6 μ region) which, apart from the fact that it had one extra band at 1110 cm^{-1} (m), was practically identical with that of 7-methoxydicoumarol. Also its ultraviolet absorption spectrum in dioxan solution was very similar to that of 7-methoxydicoumarol, differing only slightly in the ratios of the intensities of the peaks, indicating that the chromophoric systems were probably the same. The starting 4-hydroxy-7-methoxycoumarin was a pure compound, as shown by a comparison of its melting point and infrared spectrum with that of a specimen kindly supplied by Dr. R. H. Thomson, and also by demethylating it to the known 2,7-dihydroxychromone. The higher melting by-product was not investigated further at this stage. The infrared spectra of the dicoumarols were measured and are reported in the experimental section. They are in accord with the results of Knobloch and Prochazka (12) and will not be discussed here (dicoumarol has been represented by the 4,4′-dihydroxydicoumarin formula throughout this paper for convenience, though the infrared data indicate that the correct structure is that of a 2,2′-dihydroxydichromone with strongly intramolecularly chelated —OH groups (see ref. 12)).

The method described here for the synthesis of unsymmetrically substituted dicoumarols seems to be of general application. It is probable that it can be extended to dicoumarols bearing a substituent at the bridge methylene group by using aldehydes other than formaldehyde in the Mannich reaction.

EXPERIMENTAL

The melting points are uncorrected. Infrared spectra were measured with a Perkin–Elmer Model 21 instrument using sodium chloride optics. Ultraviolet absorption spectra were measured with a Beckmann DK 2 recording spectrophotometer.

Can. J. Chem. Downloaded from www.nrcresearchpress.com by 78.46.186.204 on 09/04/12
For personal use only.

*Reaction between 4-Hydroxycoumarin and 4-Hydroxy-3-*N*-piperidinomethylcoumarin*

4-Hydroxy-3-*N*-piperidinomethylcoumarin was best prepared by the method of Robertson and Link (3).

(*i*) *Without Methyl Iodide*

Pure 4-hydroxycoumarin (0.164 g) and 4-hydroxy-3-*N*-piperidinomethylcoumarin (0.26 g) were dissolved in hot absolute ethanol (5 ml) and the solution boiled under reflux for 10 minutes. After 3 minutes a crystalline solid began to separate out. The cooled suspension was filtered, and the addition complex (A) (0.386 g) washed with a little hot alcohol. The product, m.p. 255–257°, could not be recrystallized without decomposition. It was insoluble in ethanol, benzene, chloroform, and carbon tetrachloride but soluble in dioxan, tetrahydrofuran, acetic acid, *cyclo*hexanone, and dimethyl formamide. One recrystallization from nitromethane gave impure product, m.p. 258–260°, and a second recrystallization from the same solvent converted the material into dicoumarol, m.p. 293–295°, undepressed on admixture with an authentic specimen. For analysis purposes, (A) was washed repeatedly with hot alcohol and dried, the melting point remaining unchanged at 255–257°. Found: C, 68.35; H, 5.5. Calc. for $C_{24}H_{23}O_6N$: C, 68.3; H, 5.5%.

Heating the addition complex (0.386 g) in ethanol with concentrated hydrochloric acid (2 drops) for $1\frac{3}{4}$ hours gave dicoumarol (0.129 g, 89.5%), m.p. 290–292°.

Infrared spectrum of the addition complex (Nujol mull) (main peaks only): 3170 (m) (broad), 2750 (m), 2730 (sh) (m), 2570 (m), 2470 (m), 1719 (s), 1672 (s), 1618 (s) (broad), 915 (m), 768 (s), 684 cm^{-1} (w).

(*ii*) *Using Methyl Iodide*

4-Hydroxy-3-*N*-piperidinomethylcoumarin (0.13 g) was dissolved in absolute ethanol (3 ml) and treated with an excess of methyl iodide (1 ml; if molar quantities are used only the addition complex (A) is obtained). 4-Hydroxycoumarin (0.082 g) in hot ethanol (3 ml) was added and the solution boiled under reflux for 4 hours, during which time dicoumarol gradually separated out. The product (0.151 g) was collected and recrystallized from *cyclo*hexanone giving pure dicoumarol, m.p. 289–292°. Found: C, 68.21; H, 3.36. $C_{19}H_{12}O_6$ requires C, 68.0; H, 3.6%.

Infrared spectrum (Nujol mull) (main peaks only): 2770 (w), 2650 (w), 1663 (s), 1640 (s), 1612 (s), 1575 (s), 1555 (m), 1112 (s), 913 (m), 772 (s), 751 (m), 742 cm^{-1} (s).

*4-Hydroxy-7-methyl-3-*N*-piperidinomethylcoumarin*

A solution of piperidine (0.73 ml) and formaldehyde (0.5 ml, 38%) in absolute ethanol (5 ml) was added to a boiling solution of 4-hydroxy-7-methylcoumarin (1.0 g) in absolute ethanol (10 ml) and the mixture kept at 5° in the refrigerator for 3 days. The solid which separated (1.42 g), m.p. 177–179°, was recrystallized by dissolving it in hot ethanol and adding anhydrous ether until a turbidity appeared and then allowing to stand. After three such recrystallizations the pure base, m.p. 173–174°, was obtained. Found: C, 70.27; H, 7.04. Calc. for $C_{16}H_{19}O_3N$: C, 70.31; H, 7.01%.

7-Methyldicoumarol

(*i*) *From 4-Hydroxy-7-methylcoumarin*

A solution of 4-hydroxy-3-*N*-piperidinomethylcoumarin (0.259 g) in ethanol was treated with methyl iodide (1 ml) and after heating for a few minutes a solution of 4-hydroxy-7-methylcoumarin (0.174 g) in hot ethanol was added and the mixture boiled under reflux for 3 hours. The solid which separated (0.31 g), m.p. 256–259°, was recrystallized from *cyclo*hexanone giving 7-methyldicoumarol, m.p. 261–262°. Found: C,

Can. J. Chem. Downloaded from www.nrcresearchpress.com by 78.46.186.204 on 09/04/12
For personal use only.

68.80; H, 3.97. Calc. for $C_{20}H_{14}O_6$: C, 68.5; H, 4.03%. Infrared spectrum (Nujol mull) (main peaks only): 2755 (w), 2620 (w), 1658 (s), 1633 (s), 1613 (s), 1570 (m), 1555 (sh)(m), 1105 (s), 805 (m), 777 (m), 755 (m), 738 cm^{-1} (m).

The product was different from both dicoumarol and 7,7′-dimethyldicoumarol.

In the absence of methyl iodide the corresponding addition complex, m.p. 234–236°, was obtained in 70% yield. It, too, decomposed to give the dicoumarol on attempted recrystallization, and a specimen pure enough for analysis could not be obtained.

(*ii*) *From 4-hydroxy-7-methyl-3-N-piperidinomethylcoumarin*

Methyl iodide (1 ml) was added to a solution of 4-hydroxy-7-methyl-3-*N*-piperidinomethylcoumarin (0.273 g) in absolute ethanol, the solution heated for 5 minutes, and 4-hydroxycoumarin (0.162 g) in hot ethanol added. After boiling under reflux for 5 minutes the product began to separate. The mixture was refluxed for another $2\frac{1}{2}$ hours, cooled, filtered, and the solid (0.245 g), m.p. 255–258°, recrystallized from *cyclo*hexanone to give 7-methyldicoumarol, m.p. 255–257°, undepressed on admixture with the specimen obtained as under (i).

7,7′-Dimethyldicoumarol

Formaldehyde (2 ml, 38%) was added to a boiling solution of 4-hydroxy-7-methyldicoumarol (0.5 g) in 50% ethanol (50 ml) and the solution boiled for 5 minutes giving impure product (0.484 g), m.p. 273–293°. Recrystallization from glacial acetic acid gave 7,7′-dimethyldicoumarol, m.p. 292–294°, depressed to 260–270° on admixture with 7-methyldicoumarol. Found: C, 69.24; H, 4.47. Calc. for $C_{21}H_{16}O_6$: C, 69.2; H, 4.44%. Anschutz (16) gives m.p. 273–275° for this compound.

6-Methyldicoumarol

This was obtained in 89.4% yield from 4-hydroxy-6-methylcoumarin, 4-hydroxy-3-*N*-piperidinomethylcoumarin, and methyl iodide. It had m.p. 250–251° (from *cyclo*hexanone). Found: C, 68.57; H, 4.01. Calc. for $C_{20}H_{14}O_6$: C, 68.57; H, 4,03%.

6-Chlorodicoumarol

This was similarly obtained from 6-chloro-4-hydroxycoumarin, 4-hydroxy-3-*N*-piperidinomethylcoumarin, and methyl iodide. Yield 90.3%. Recrystallization from *cyclo*hexanone gave pure product, m.p. 266–268°. Found: C, 62.2; H, 2.93. Calc. for $C_{19}H_{11}O_6Cl$: C, 61.6; H, 3.00%. Infrared spectrum (Nujol mull) (main peaks only): 2720 (w), 2595 (w), 1657 (s), 1632 (s), 1607 (m), 1576 (m), 1500 (w), 1109 (m), 914 (w), 809 (w), 765 cm^{-1} (m).

7-Methoxydicoumarol

4-Hydroxy-7-methoxycoumarin was prepared from 2-hydroxy-4-methoxyacetophenone, diethyl carbonate, and pulverized sodium by the method of Desai and Sethna (17) and was identical in melting point (mixed melting point undepressed) and infrared spectrum with a specimen kindly supplied by Dr. R. H. Thomson (Aberdeen University, Scotland).

4-Hydroxy-3-*N*-piperidinomethylcoumarin (5.2 g) in absolute ethanol (50 ml) was treated with a large excess of methyl iodide (20 ml). 4-Hydroxy-7-methoxycoumarin (3.84 g) in ethanol (80 ml) was then added and the mixture boiled under reflux for 4 hours. The cooled suspension was filtered and the solid, m.p. 245–260°, extracted three times with boiling glacial acetic acid. On cooling, the combined extracts deposited slightly impure 7-methoxydicoumarol (5.0 g), which on recrystallization from glacial acetic acid gave product (4.9 g), m.p. 245–248°. Further recrystallizations from acetic acid did not raise the melting point. Found: C, 65.41; H, 4.05. Calc. for $C_{20}H_{14}O_7$: C, 65.57;

Can. J. Chem. Downloaded from www.nrcresearchpress.com by 78.46.186.204 on 09/04/12
For personal use only.

H, 3.85%. Infrared spectrum (Nujol mull) (main peaks): 1655 (s) (broad), 1620 (s), 1602 (s), 1565 (s), 1512 (m), 1098 (s), 835 (m), 805 (m), 775 (m), 752 (m), 740 cm^{-1} (sh)(m). Ultraviolet spectrum (in dioxan solution): λ_{max} 323 (infl.), 317, 307 (infl.), 289 $m\mu$ 10^{-3} ϵ: 35.99, 29.95, 37.52, 29.95.

The residue (0.5 g) from the acetic acid extraction was recrystallized from *cyclo*hexanone giving colorless crystals, m.p. 290–292°. Good analytical figures could not be obtained for this compound (found: C, 64.17; H, 4. 45%), which differed greatly in solubility from the 7-methoxydicoumarol, m.p. 245–248°, obtained above. The infrared spectrum was identical with that of 7-methoxydicoumarol except for a single weak peak at 1110 cm^{-1} which was absent in the spectrum of the lower melting product. The ultraviolet spectrum measured in dioxan is very similar to that of 7-methoxydicoumarol indicating that no change has occurred in the chromophoric system. λ_{max} 324 (infl.), 317, 307 (infl.), 289 $m\mu$ 10^{-3} ϵ (assuming the same molecular weight as 7-methoxydicoumarol): 35.44, 40.12, 33.70, 20.33.

4,7-Dihydroxycoumarin (2,7-Dihydroxychromone)

A mixture of 4-hydroxy-7-methoxycoumarin (0.8 g) and anhydrous aluminum chloride (4 g) in dry benzene (150 ml) was boiled under reflux for 6 hours. Crushed ice and dilute hydrochloric acid were then added to the cold mixture and the benzene evaporated off giving 4,7-dihydroxycoumarin (0.74 g), m.p. 265–268°, which could be recrystallized from dilute methanol. Bauer and Schoder (18) give m.p. 264° (decomp.) for this compound.

7-Hydroxydicoumarol

(i) 4-Hydroxy-3-*N*-piperidinomethylcoumarin (0.114 g) in absolute ethanol was treated with methyl iodide (2 ml) and then with 4,7-dihydroxycoumarin (0.75 g) and the mixture refluxed for 8 hours. Working up in the usual way gave 7-hydroxydicoumarol (0.115 g), m.p. 300–302°, which on recrystallization from glacial acetic acid had m.p. 300–302°. Found: C, 64.67; H, 3.79. Calc. for $C_{19}H_{12}O_7$: C, 64.77; H, 3.43%. Infrared spectrum (Nujol mull) (main peaks only): 3380 (m) (broad), 2740 (w), 2600 (w), 1655 (sh) (s), 1635 (s), 1608 (s), 1573 (s), 1315 (s), 1113 (s) (broad), 856 (m), 808 (m), 798 (m), 770 (s), 755 (s), 744 cm^{-1} (m).

(ii) 7-Methoxydicoumarol (0.5 g, m.p. 245–248°) and anhydrous aluminum chloride (2.5 g) in dry benzene (100 ml) were boiled under reflux for 8 hours. Cracked ice and dilute hydrochloric acid were added to the cold mixture, the benzene was removed, and the product recrystallized from glacial acetic acid giving 7-hydroxydicoumarol (0.321 g), m.p. 300–302° undepressed in admixture with material obtained as under (i) above. The infrared spectra of the two products were also identical.

ACKNOWLEDGMENTS

This work was carried out during the tenure (by J.R.G.) of a Thorvaldson Scholarship. We wish to thank Dr. R. H. Thomson (Aberdeen) for a specimen of 4-hydroxy-7-methoxycoumarin and Dr. L. Vining for the use of a Beckmann DK 2 recording spectrophotometer.

REFERENCES

1. Ikawa, M., Stahmann, M. A., and Link, K. P. J. Am. Chem. Soc. **66**, 902 (1944).
2. Sullivan, W. R., Huebner, C. F., Stahmann, M. A., and Link, K. P. J. Am. Chem. Soc. **65**, 2288 (1943).
3. Robertson, D. N. and Link, K. P. J. Am. Chem. Soc. **75**, 1883 (1953).
4. Prochazka, Z. Chem. listy, **47**, 59 (1953).

Can. J. Chem. Downloaded from www.nrcresearchpress.com by 78.46.186.204 on 09/04/12
For personal use only.

5*a*. ARNDT, F., LOEWE, L., ÜN, R., and AYCA, E. Chem. Ber. **84**, 319 (1951).
b. ARNDT, F. Problems in theoretical organic chemistry. 28th Annual Prestly Lectures. Phi Lambda Upsilon, University of Pennsylvania. 1954. p. 37.
6. KLOSA, J. Arch. Pharm. **286**, 37 (1953).
7. GARDEN, J. F., HAYES, N. F., and THOMSON, R. H. J. Chem. Soc. 3315 (1956).
8. JONES, R. N. and HERLING, F. J. Org. Chem. **19**, 1252 (1954).
9. THOMPSON, H. W. and TORKINGTON, P. J. Chem. Soc. 640 (1945).
10. STAMMER, C. H., WALTON, E., WILSON, A. N., WALKER, R. W., TRENNER, N. R., HOLLY, F. W., and FOLKERS, K. J. Am. Chem. Soc. **80**, 137 (1958).
11. SPENCER, C. F., RODIN, J. O., WALTON, E., HOLLY, F. W., and FOLKERS, K. J. Am. Chem. Soc. **80**, 140 (1958).
12. KNOBLOCH, E. and PROCHAZKA, Z. Chem. listy, **47**, 1285 (1953).
13. WILDI, B. S. J. Org. Chem. **16**, 407 (1951).
14. WITKOP, B. J. Am. Chem. Soc. **76**, 5597 (1954).
15. ADAMS, R. Organic reactions. Vol. 1. John Wiley & Sons, Inc., New York. 1942. p. 307.
16. ANSCHUTZ, R. Ann. **367**, 244 (1909).
17. DESAI, N. J. and SETHNA, S. J. Org. Chem. **22**, 388 (1957).
18. BAUER, K. G. and SCHODER, F. Arch. Pharm. **259**, 53 (1921).

Can. J. Chem. Downloaded from www.nrcresearchpress.com by 78.46.186.204 on 09/04/12
For personal use only.

Can. J. Chem. Downloaded from www.nrcresearchpress.com by 78.46.186.204 on 09/04/12
For personal use only.

RECIPROCAL SALT PAIRS, INVOLVING THE CATIONS Li_2, Na_2, AND K_2, THE ANIONS SO_4 AND Cl_2, AND WATER, AT 25° C[1]

A. N. CAMPBELL, E. M. KARTZMARK, AND E. G. LOVERING[2]

ABSTRACT

In the reciprocal salt pair Li_2, K_2, Cl_2, SO_4, and water, at 25° C there are large areas in which potassium sulphate and potassium lithium sulphate ($KLiSO_4$) are separately in equilibrium with solution. Two incongruent invariant points exist. At one of these the composition of the solution is 0.917 mole fraction chloride,* 0.437 mole fraction lithium, and 19.4 moles of water per total mole of salt, the equilibrium solid phases being potassium chloride, potassium sulphate, and the double salt. At the second, the composition of the solution is 0.967 mole fraction chloride, 0.870 mole fraction lithium, and 13.8 moles of water per mole of salt, the solid phases being potassium chloride, double salt, and lithium sulphate monohydrate. One congruent invariant point exists, at which the composition of the solution is 1.00 mole fraction chloride, 0.960 mole fraction lithium, and 9.6 moles of water per mole of salt, the solid phases being lithium sulphate monohydrate, lithium chloride monohydrate, and potassium chloride.

In the reciprocal salt pair Li_2, Na_2, Cl_2, SO_4, and water, at 25° C there is an incongruent invariant point at which the composition of the solution is 0.873 mole fraction chloride, 0.668 mole fraction lithium, and 15.1 moles water per total mole of salt, the solid phases being sodium chloride, solid solution of sodium and lithium sulphates, and lithium sulphate monohydrate. A congruent invariant point exists, at which the composition of the solution is practically entirely lithium chloride, the solid phases present being lithium chloride monohydrate, lithium sulphate monohydrate, and sodium chloride.

INTRODUCTION

The two reciprocal salt pairs

$$Li_2Cl_2 + Na_2SO_4 \rightleftarrows Li_2SO_4 + Na_2Cl_2$$

and

$$Li_2Cl_2 + K_2SO_4 \rightleftarrows Li_2SO_4 + K_2Cl_2,$$

both at 25° C, which form the subject of this paper, are part of the five-component system: Li_2, Na_2, K_2, Cl_2, SO_4, water, at 25° C, which is being studied in this department. The component ternary systems are now all known, as well as the two four-component systems: Li_2, Na_2, K_2, Cl_2, H_2O and Li_2, Na_2, K_2, SO_4, H_2O. The reciprocal salt pair:

$$Na_2Cl_2 + K_2SO_4 \rightleftarrows K_2Cl_2 + Na_2SO_4$$

is also known. Nothing has been done on the remaining two reciprocal salt pairs. A bibliography is appended to this paper (1*a*–1*i*, 2).

Particular mention should be made, however, of a recent paper by Cavalca and Nardelli (3), who claim that the double salt $Na_3Li(SO_4)_2.6H_2O$ exists at 27° C. This is not in agreement with the work of Campbell and Kartzmark (4), who found no double salt but extensive solid solution at 25° C. As a final check on this point, two experiments were carried out. Appropriate mixtures of lithium sulphate, sodium sulphate, and water were stirred for 1 week in contact with excess of solid at 25° C. The solutions and wet residues were analyzed, both by determination of sulphate as barium sulphate and by viscosity. When these results were plotted on the triangular diagram of Campbell and Kartzmark, the tie lines found by the unsatisfactory barium sulphate method crossed, while those found by the viscosity method did not. This may constitute an explanation of the results of Cavalca and Nardelli.

[1]*Manuscript received May 30, 1958.*
Contribution from the Chemistry Department, University of Manitoba, Winnipeg, Manitoba.
[2]*Cominco Fellow, University of Manitoba, 1957–58.*
**Throughout this paper mole fractions are calculated with double atomic weight for univalent ions, i.e.,* Li_2, Na_2, K_2, *and* Cl_2.

Can. J. Chem. Downloaded from www.nrcresearchpress.com by 78.46.186.204 on 09/04/12
For personal use only.

EXPERIMENTAL

All chemicals used were of the highest purity and they were not further purified by us but the sulphates were dried by fusion. Solutions and solid phases were analyzed by evaporating to dryness, igniting, and weighing. Chloride radical was determined gravimetrically as silver chloride. The remaining solid was converted to sulphate by treatment with sulphuric acid, followed by ignition. A fixed weight (10 or 20 g) of sulphate mixture was dissolved in water, made up to fixed volume (100 ml), and the viscosity determined. The value of the viscosity gave the ratio of the two cations present. Sulphate radical was determined by difference, since the gravimetric determination of sulphate, in the presence of alkali metals, is notoriously unsatisfactory, although we have occasionally been forced to use the method. The method described above works very well. It is necessary to heat the sulphated solids at 600° C, for not less than six hours, to ensure that no trace of free sulphuric acid has been left. The dried sulphate mixture was tested for the presence of free acid and chloride radical, before it was used further. Viscosity curves for the systems potassium sulphate – lithium sulphate and sodium sulphate – lithium sulphate were obtained for mixtures of known composition.

The nature of the solid phases present was revealed to some extent by the chemical analysis taken in conjunction with a knowledge of the general trend of the solubility curve under investigation, but recourse was made to other methods whenever possible. Thus, sodium sulphate decahydrate was identified by removing a few of the characteristic crystals and warming them slightly when they underwent the transition to anhydrous salt. Solid solution (in sodium salt) was suspected when the lithium content began to rise above that which might reasonably be attributed to adhering mother liquor. Lithium sulphate monohydrate was identified by its prismatic habit and the fact that it does not dehydrate on a steam bath. We found it impossible to use the polarizing microscope because it was necessary to dry the solid phase and this could change the nature of the solid phases. Similarly, X-ray diffraction photography was found to be useless here. The wet solid phases gave indefinite pictures. In the course of the X-ray work, however, it was found that the X-ray powder diffraction data for lithium sulphate monohydrate, as given in the file of the American Society for Testing Materials, were not complete. Powder pictures of this material were therefore taken and will be offered for publication elsewhere by one of us (E.G.L.).

The Jänecke method of graphical representation (5) was used. In this system of representation, ternary invariant points appear as points on the sides; water is expressed by isohydrores or lines of equal water content. Experimentally, we started from each invariant point on the sides of the diagram in turn, making sure that a plentiful excess of the two solid phases was present, and progressively added small quantities of a cation or anion which did not participate in the original equilibrium. Equilibrium was attained by stirring for 24 hours after each addition when liquid and solid phases were analyzed. Invariance in quaternary systems showed itself by the composition of the liquid phase becoming constant with further additions; it was then a question of identifying the third solid phase which had appeared. If a new ion appeared (in appreciable quantity) for the first time in the solid phase, there was seldom any doubt as to the nature of the new solid phase. Moreover, since no solid phase occurs in the quaternary systems other than those occurring in the component ternary systems, it was usually obvious when two solubility curves intersected what the new phase would be.

EXPERIMENTAL RESULTS

TABLE I

VISCOSITIES AND DENSITIES OF LITHIUM SULPHATE – POTASSIUM SULPHATE – WATER SOLUTIONS AT 25° C
(10 g salt/100 ml)

Wt. K_2SO_4 (g)	Wt. Li_2SO_4 (g)	Density (g/ml)	Viscosity (η H_2O = 1.0000)
10	0	1.0738	1.1342
9	1	1.0741	1.1751
8	2	1.0748	1.2174
7	3	1.0752	1.2594
6	4	1.0758	1.3048
5	5	1.0757	1.3460
3	7	1.0770	1.4482
2	8	1.0776	1.4999
1	9	1.0780	1.5559
0	10	1.0780	1.6141

TABLE II

VISCOSITIES AND DENSITIES OF SODIUM SULPHATE – LITHIUM SULPHATE – WATER SOLUTIONS AT 25° C
(20 g salt/100 ml)

Wt. Na_2SO_4 (g)	Wt. Li_2SO_4 (g)	Density (g/ml)	Viscosity (η H_2O = 1.0000)
20	0	1.1606	1.9057
18	2	1.1604	1.9699
16	4	1.1591	2.0369
14	6	1.1583	2.1071
12	8	1.1573	2.1817
10	10	1.1565	2.2552
8	12	1.1554	2.3356
6	14	1.1551	2.4231
4	16	1.1545	2.5163
2	18	1.1532	2.6125
0	20	1.1524	2.7016

DISCUSSION OF RESULTS

1. THE SYSTEM $K_2Cl_2 + Li_2SO_4 \rightleftarrows K_2SO_4 + Li_2Cl_2$, AT 25° C

The equilibrium diagram is shown as Fig. 1. The curves representing two solid phases in equilibrium with solution are shown as heavy lines, the lighter lines being isohydrores (lines of equal water content, expressed as moles of water per mole of total salts). The phase boundaries are usually drawn as straight lines because the experimental accuracy does not usually warrant indicating curvature. The isohydrores are very approximate, owing to lack of data, but they do indicate the course of isothermal evaporation. The stable pair of solid phases, that is, the pair of salts that can exist in contact with each other and with solution, consists of lithium sulphate monohydrate and potassium chloride. There are three invariant points. At the invariant point 8, in Fig. 1, the solid phases are potassium sulphate, potassium chloride, and double salt ($KLiSO_4$). Since the invariant point does not fall within the composition triangle, whose angular points represent the three solid phases, it is incongruent. The invariant point 17, where lithium sulphate

Can. J. Chem. Downloaded from www.nrcresearchpress.com by 78.46.186.204 on 09/04/12
For personal use only.

monohydrate, potassium chloride, and double salt are in equilibrium with solution, is also incongruent. Point 21, where the solid phases are lithium chloride monohydrate, lithium sulphate monohydrate, and potassium chloride, is congruent.

TABLE III

THE COMPOSITION OF THE SOLUTIONS AND THE NATURE OF THE SOLID PHASES IN THE SYSTEM Li_2, K_2, Cl_2, SO_4, H_2O AT 25° C

Point No.	Composition of the liquid phase: Mole fraction Cl_2	Composition of the liquid phase: Mole fraction Li_2	Moles of H_2O per mole of salt	Nature of the solid phases
1	0.959	0.140	21.9	$K_2Cl_2 + K_2SO_4$
2	0.927	0.408	19.6	$K_2Cl_2 + K_2SO_4$
3	0.167	0.594	29.2	$K_2SO_4 + LiKSO_4$
4	0.582	0.557	27.5	$K_2SO_4 + LiKSO_4$
5	0.700	0.543	26.3	$K_2SO_4 + LiKSO_4$
6	0.822	0.487	23.6	$K_2SO_4 + LiKSO_4$
7	0.467	0.880	21.0	$K_2SO_4 + LiKSO_4$
8	0.916	0.437	19.4	$K_2Cl_2 + KLiSO_4 + K_2SO_4$
9	0.917	0.435	19.4	$K_2Cl_2 + KLiSO_4 + K_2SO_4$
10	0.918	0.439	19.4	$K_2Cl_2 + KLiSO_4 + K_2SO_4$
11	0.933	0.562	18.5	$LiKSO_4 + K_2Cl_2$
12	0.956	0.698	17.1	$LiKSO_4 + K_2Cl_2$
13	0.157	0.952	17.7	$LiKSO_4 + Li_2SO_4 \cdot H_2O$
14	0.480	0.946	19.2	$LiKSO_4 + Li_2SO_4 \cdot H_2O$
15	0.740	0.933	19.0	$LiKSO_4 + Li_2SO_4 \cdot H_2O$
16	0.902	0.914	17.2	$LiKSO_4 + Li_2SO_4 \cdot H_2O$
17	0.967	0.874	13.8	$K_2Cl_2 + KLiSO_4 + Li_2SO_4 \cdot H_2O$
18	0.967	0.870	13.8	$K_2Cl_2 + KLiSO_4 + Li_2SO_4 \cdot H_2O$
19	0.966	0.870	13.8	$K_2Cl_2 + KLiSO_4 + Li_2SO_4 \cdot H_2O$
20	0.985	0.913	12.3	$K_2Cl_2 + Li_2SO_4 \cdot H_2O$
21	1.000	0.960	9.6	$Li_2Cl_2 \cdot 2H_2O + Li_2SO_4 \cdot H_2O + K_2Cl_2$

TABLE IV

THE COMPOSITION OF THE SOLUTIONS AND THE NATURE OF THE SOLID PHASES IN THE SYSTEM Li_2, Na_2, Cl_2, SO_4, H_2O AT 25° C

Point No.	Composition of the liquid phase: Mole fraction Cl_2	Composition of the liquid phase: Mole fraction Li_2	Moles of H_2O per mole of salt	Nature of the solid phases
1	0.074	0.263	18.1	$Na_2SO_4 + Na_2SO_4 \cdot 10H_2O$
2	0.149	0.212	18.0	$Na_2SO_4 + Na_2SO_4 \cdot 10H_2O$
3	0.296	0.110	17.9	$Na_2SO_4 + Na_2SO_4 \cdot 10H_2O$
4	0.777	0.112	15.7	Na_2Cl_2 + solid solution
5	0.822	0.451	15.6	Na_2Cl_2 + solid solution
6	0.846	0.592	15.4	Na_2Cl_2 + solid solution
7	0.872	0.669	15.1	$Na_2Cl_2 + Li_2SO_4 \cdot H_2O$ + solid solution
8	0.871	0.679	15.1	$Na_2Cl_2 + Li_2SO_4 \cdot H_2O$ + solid solution
9	0.880	0.660	15.2	$Na_2Cl_2 + Li_2SO_4 \cdot H_2O$ + solid solution
10	0.918	0.733	15.3	$Na_2Cl_2 + Li_2SO_4 \cdot H_2O$
11	0.890	0.695	—	$Na_2Cl_2 + Li_2SO_4 \cdot H_2O$
12	0.758	0.681	16.2	$Li_2SO_4 \cdot H_2O$ + solid solution
13	0.701	0.683	16.4	$Li_2SO_4 \cdot H_2O$ + solid solution
14	0.489	0.692	16.2	$Li_2SO_4 \cdot H_2O$ + solid solution
15	0.240	0.700	13.5	$Li_2SO_4 \cdot H_2O$ + solid solution

Can. J. Chem. Downloaded from www.nrcresearchpress.com by 78.46.186.204 on 09/04/12
For personal use only.

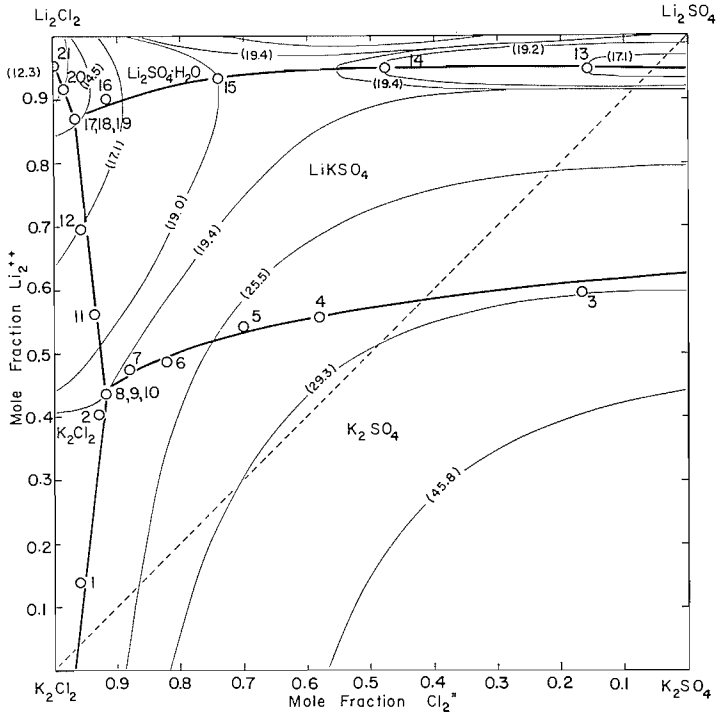

FIG. 1. The system lithium, potassium, chloride, sulphate, water, at 25° C.

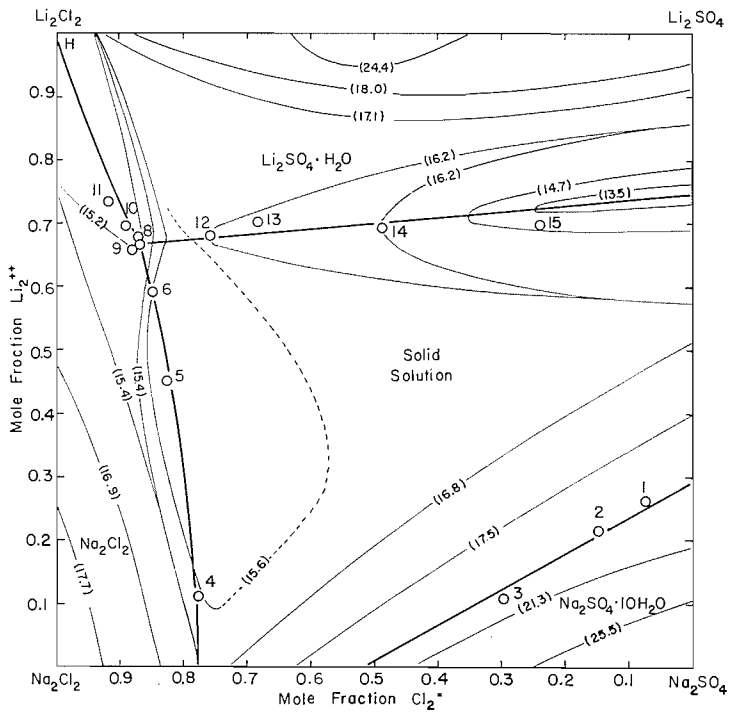

FIG. 2. The system lithium, sodium, chloride, sulphate, water, at 25° C.

Can. J. Chem. Downloaded from www.nrcresearchpress.com by 78.46.186.204 on 09/04/12
For personal use only.

Can. J. Chem. Downloaded from www.nrcresearchpress.com by 78.46.186.204 on 09/04/12
For personal use only.

2. THE SYSTEM $Na_2Cl_2 + Li_2SO_4 \rightleftarrows Na_2SO_4 + Li_2Cl_2$, AT 25° C

The equilibrium diagram is shown in Fig. 2. The stable salt pair is similar to the previous system, i.e., the coexistent salts are sodium chloride and lithium sulphate monohydrate. Since no double salt occurs in this system, there are only two invariant points, one congruent and the other not. At the incongruent invariant point (point 7), the solid phases in equilibrium with solution are lithium sulphate monohydrate, sodium chloride, and a solid solution of sodium and lithium sulphates; the amount of lithium in the solid solution increases as the concentration of lithium in the liquid phase increases. At point H, the congruent invariant point, the solid phases are lithium chloride monohydrate, lithium sulphate monohydrate, and sodium chloride; the solution is very rich in lithium chloride. It has been shown by Campbell and Kartzmark (4) that the double salt $NaLiSO_4$ exists above 29.3° C. It is conceivable that this double salt could exist, at 25° C, in contact with the solution containing lithium and sodium chlorides. If it did exist, three invariant points would appear, in place of point 7, at which the solid phases would be double salt and (1) $Li_2SO_4 \cdot H_2O$ + NaCl; (2) NaCl + solid solution; (3) solid solution + $Li_2SO_4 \cdot H_2O$. All attempts to find such invariant points failed. It is known from the ternary system, Li_2Cl_2–Li_2SO_4–H_2O that the $LiCl \cdot H_2O$ field in the quaternary diagram must be extremely narrow; it cannot be investigated experimentally or expressed graphically to scale.

ACKNOWLEDGMENTS

We are indebted to Dr. R. B. Ferguson, of the Department of Geology, for advice and assistance with the X-ray photography and to the Consolidated Mining and Smelting Company of Canada for financial assistance in the form of a Cominco Fellowship.

REFERENCES

For the following ternary systems:

Na_2Cl_2–Na_2SO_4–H_2O at 25° C

1*a*. MEYERHOFFER, W. and SAUNDERS, A. P. Z. physik. Chem. **28**, 453 (1899). SEIDELL, A. Am. Chem. J. **27**, 52 (1902). SCHREINEMAKERS, F. A. H. Proc. Roy. Soc. Amsterdam, **13**, 1163 (1911). BLASDALE, W. C. Ind. Eng. Chem. **10**, 344 (1918). TAKEGAMI, S. Mem. Coll. Sci., Kyoto Imp. Univ. **4**, 317 (1921).

NaCl–LiCl–H_2O at 25° C

1*b*. SMITS, A., ELGERSMA, J., and HARDENBURG, E. M. Rec. trav. chim. **43**, 671 (1924).

Li_2Cl_2–Li_2SO_4–H_2O at 25° C

1*c*. SCHREINEMAKERS, F. A. H. and KAYSER, G. M. A. Chem. Weekblad, **15**, 120 (1918) (at 30°). DRUZHININ, I. G. and YANKO, A. P. Doklady Akad. Nauk S.S.S.R. **94**, 481 (1954).

Li_2SO_4–Na_2SO_4–H_2O at 25° C

1*d*. CAVALCA, L. and NARDELLI, M. Gazz. chim. ital. **82**, 394 (1952). CAMPBELL, A. N. and KARTZMARK, E. M. Can. J. Chem. **36**, 171 (1958).

K_2SO_4–K_2Cl_2–H_2O at 25° C

1*e*. MEYERHOFFER, W. and SAUNDERS, A. P. Z. physik. Chem. **28**, 453 (1899). BLASDALE, W. C. Ind. Eng. Chem. **10**, 344 (1918). ANOSOV, YA. V. and BYZOVA, E. A. Izvest. Sectora Fiz.-Khim. Anal., Inst. Obshcheĭ Neorg. Khim., Akad. Nauk S.S.S.R. **15**, 118 (1947).

KCl–LiCl–H_2O at 25° C

1*f*. CAMPBELL, A. N. and KARTZMARK, E. M. Can. J. Chem. **34**, 672 (1956).

Li_2SO_4–K_2SO_4–H_2O at 25° C

1*g*. YANKO, A. P. and DRUZHININ, I. G. J. Gen. Chem. U.S.S.R. (Eng. Transl.), **25**, 13 (1955). CAMPBELL, A. N. and KARTZMARK, E. M. Can. J. Chem. **36**, 171 (1958).

NaCl–KCl–H_2O at 25° C

1*h*. BLASDALE, W. C. J. Ind. Eng. Chem. **10**, 344 (1918).

Na_2SO_4–K_2SO_4–H_2O at 25° C

1*i*. HAMID, M. A. J. Chem. Soc. 201 (1926).

For the reciprocal salt pair:

$$Na_2Cl_2 + K_2SO_4 \rightleftarrows K_2Cl_2 + Na_2SO_4 \text{ at } 25° \text{ C}$$

2. MEYERHOFFER, W. and SAUNDERS, A. P. Z. physik. Chem. **28**, 453 (1899). BLASDALE, W. C. J. Ind. Eng. Chem. **10**, 344 (1918). D'ANS, J. A. Kali, **9**, 148, 161, 177, 193, 217, 219 (1915).
3. CAVALCA, L. and NARDELLI, M. Gazz chim. ital. **82**, 394 (1952).
4. CAMPBELL, A. N. and KARTZMARK, E. M. Can. J. Chem. **36**, 171 (1958).
5. JÄNECKE, E. Z. anorg. Chem. **51**, 132 (1906); **71**, 1 (1911).

Can. J. Chem. Downloaded from www.nrcresearchpress.com by 78.46.186.204 on 09/04/12
For personal use only.

Can. J. Chem. Downloaded from www.nrcresearchpress.com by 78.46.186.204 on 09/04/12
For personal use only.

THE KINETICS OF RADICAL REACTIONS IN THE TRACKS OF FAST ELECTRONS

A DETAILED STUDY OF THE SAMUEL–MAGEE MODEL FOR THE RADIATION CHEMISTRY OF WATER[1]

P. J. Dyne and J. M. Kennedy

ABSTRACT

The kinetic behavior of a γ-ray spur produced in water, having H and OH radicals distributed spatially in the manner suggested by Samuel and Magee, has been studied using an electronic computer. The variation in yield of the molecular products H_2, H_2O_2, and H_2O with rate constants, diffusion constants, and spur size has been obtained. The model gives agreement with experiment choosing spurs with a small "radius" of the order of 10 Å. On simple assumptions, however, the model predicts no difference in the molecular yields between heavy and light water and no isotopic separation in the formation of molecular hydrogen from isotopically enriched light water. Various special assumptions needed to give agreement with experiment for these isotope effects are discussed. The observed isotopic separation in the formation of molecular hydrogen is attributed to the preferential dissociation of an H atom from an excited HDO molecule. It is found that the yield of molecular hydrogen is less sensitive to the presence of scavengers than the yield of hydrogen peroxide.

1. INTRODUCTION

The products of the radiation decomposition of water are of two types, free radicals and molecules, and it is generally supposed that the molecular products (hydrogen and hydrogen peroxide) are formed by recombination of free radicals (H and OH) in regions of high radical concentration. In the model of this process proposed by Samuel and Magee (1) it was suggested that the radicals were formed by the dissociation of excited water molecules. Consequently, both species of radicals have initially a similar spatial distribution; some of these radicals recombine to give molecular products, others escape by diffusion into the bulk of the solution where they can be detected by their reactions as radicals. Several variations of this model are discussed by Dewhurst, Samuel, and Magee (2).

While this model has been widely accepted for the interpretation of the radiation chemistry of water no detailed study of its properties has been made in which the recombination of both reacting species (H and OH) is treated. As the kinetics of recombination and diffusion cannot be handled analytically the majority of calculations hitherto have been performed on a simplified version, a "one radical" model in which the one species has the "average" properties of H and OH. These calculations have shown that the model explains many of the features of the radiation decomposition of water and on this pragmatic basis the model has been accepted.

We have surmounted the main obstacle to the study of a two-radical model, the intractable nature of the equations, by programming the problem for numerical solution on the Chalk River Datatron Computer, and this paper presents the results of these calculations. A second, equally serious, obstacle remains and this is our lack of knowledge about the rate constants and diffusion constants and other parameters of the system. We have, accordingly, adopted an approach which is essentially the converse of that of experimental chemical kinetics; the "constants" (rate constants, etc.) of the systems are treated as parameters. We derive graphical relations between these parameters and

[1]*Manuscript received July 14, 1958.*
Contribution from the Research Chemistry and Theoretical Physics Branches, Atomic Energy of Canada Limited, Chalk River, Ontario.
Issued as A.E.C.L. No. 693.

the yields of radicals and molecular products. Our conclusions comprise a qualitative picture of the kinetic properties of the model, an estimate of the range of values of the parameters which will give agreement with experiment, and a discussion of the details of the isotope effects and scavenger effects.

2. THE SAMUEL-MAGEE MODEL

In their original paper Samuel and Magee (1) suggested that the passage of a high energy (1 Mev) β-particle through liquid water initiated the following sequence of events: the β-particle ionizes water molecules at widely spaced intervals along its track, each ionization forming a "spur". The ionized electron has, on the average, an energy of about 60 ev, which is rapidly lost as it ionizes and excites some of the surrounding water molecules forming, say, three H_2O^+ ions and three electrons. The ions recapture the ionized electrons after the electrons have been thermalized by collision with surrounding molecules and form excited water molecules. These in turn dissociate to give H atoms and OH radicals. The whole process from the initial ionization to the dissociation occurs in a time of the order of 10^{-13} seconds. The radicals are distributed inside a volume which is only a few molecular diameters across. For the purposes of calculation it was assumed that the initial distribution is given by a Gaussian with a modulus of 10 Å.

Samuel and Magee solved the kinetic equations for reaction and diffusion in a spur for the case of one species of radical where the spatial distribution was assumed *always* to be a Gaussian. This technique, known as the "Prescribed Diffusion Approximation", enabled them to calculate analytically the ratio of free radicals recombining to the total formed initially. They showed that for a "reasonable" choice of parameters, the calculated value agreed with experiment. These calculations were extended to the case of α-ray decomposition and tritium β-ray decomposition. With α-rays the primary ionizations lie very close together and the initial distribution consists of a column of radicals which expands in cylindrical symmetry; with tritium β-rays the spurs overlap quite shortly after their formation and recombination occurs partly in spherical and partly in cylindrical symmetry. Agreement with experiment for both these was obtained with the choice of parameters used for the calculation on high energy β-rays.*

3. THE TRACK EQUATION FOR THE TWO-RADICAL MODEL

The calculations on the "two-radical" model described in this paper deal only with the case of high energy β-rays, i.e. spurs which expand wholly in spherical symmetry with no overlapping. From these calculations we can predict differences in the behavior of H and OH and estimate the extent of recombination to reform H_2O which is not observable experimentally and which is not distinguished in a one-radical calculation from recombination to give H_2 and H_2O_2.

We adopt the convention that the hydrogen atom is species 1 with diffusion constant D_1 and recombination rate constant k_{11} and concentration C_1 which is a function of time and space. The OH radical is species 2 with constants D_2, k_2, C_2, etc. The rate constant for the recombination of H and OH radicals is k_{12}.

The track equations governing the kinetics reaction and diffusion are:

$$\partial C_1/\partial t = D_1\nabla^2 C_1 - [(N_1-1)/N_1]\, k_{11}C_1^2 - k_{12}C_1C_2 - k_{1S}C_1C_S, \qquad [1]$$

$$\partial C_2/\partial t = D_2\nabla^2 C_2 - [(N_2-1)/N_2]\, k_{22}C_2^2 - k_{12}C_1C_2 - k_{2S}C_2C_S, \qquad [2]$$

**Note added in proof: The results of some detailed computations on a one-radical model have recently been published by Flanders and Fricke, J. Chem. Phys. 28, 1126 (1958).*

Can. J. Chem. Downloaded from www.nrcresearchpress.com by 78.46.186.204 on 09/04/12
For personal use only.

where N_1 and N_2 are the total number of radicals in the spur at time t, k_{1S} and k_{2S} are the rate constants for reaction with scavenger present in a small, uniform concentration C_S. The yields of hydrogen, hydrogen peroxide in one spur, are the values of

$$\int_0^\infty \int_0^\infty k_{11}C_1^2\, dv.dt, \int_0^\infty \int_0^\infty k_{22}C_2^2\, dv.dt, \text{ and } \int_0^\infty \int_0^\infty k_{12}C_1C_2\, dv.dt,$$

gives the amount of H_2O reformed in the spur. The quantities $(N_1-1)/N_1$ and $(N_2-1)/N_2$ are statistical factors which take into account the fact that, with a small number of radicals, the expression $k_{11}C_1^2$ must be reduced so that the bimolecular reaction of a radical with itself is not included, e.g. if there are six radicals in the spur, one particular radical can only react with five others and the rate is therefore 5/6 of the rate given by the standard kinetic expression.

The numerical method used is described in the Appendix.

4. THE INITIAL CHOICE OF CONSTANTS

Because none of the constants in the problem has been measured directly we have to estimate their order of magnitude a priori. As our object is to determine the sensitivity of the yields to variations in the constants, our initial choice is equivalent to defining the area to be explored. This is, of necessity, somewhat arbitrary.

First let $D_2 = 2\times10^{-5}$ cm^2/second (the same as the self-diffusion constant for water) (3). It seems entirely reasonable that OH and H_2O will diffuse at comparable rates. As the hydrogen atom is lighter, D_1 must necessarily be greater than D_2. Simple kinetic theory shows that the ratio $D_1/D_2 = \sqrt{(M_2/M_1)}$ where M_2 and M_1 are the masses of the two species. This gives $D_1 = 8\times10^{-5}$ cm^2/second. The use of this formula is equivalent to assuming identical scattering cross sections for the diffusion of H and OH in water. This study is confined to cases where $D_1/D_2 \approx 4$.

The initial choice of the rate constants has been made with the aid of the Smoluchowski relation

$$k_{12} = A(\sigma_1+\sigma_2)(D_1+D_2), \qquad [3]$$

where σ_1 and σ_2 are the collision diameters of the species 1 and 2. The value of A is discussed by Fricke (4) and following his arguments we have chosen a value of A so that k_{11} and k_{22} are both $\sim1\times10^{-11}$ and 1×10^{-11} cc/molecule second. With $\sigma_1 = 0.5$ Å and $\sigma_2 = 1.5$ Å we chose $k_{11} = 1.2\times10^{-11}$, $k_{12} = 3.0\times10^{-11}$, and $k_{22} = 0.9\times10^{-11}$. The larger value of k_{12} is mainly due to the statistical factor of two, which distinguishes between the collision numbers for like particles and unlike particles.

The constants k_{1S} and k_{2S} were taken as 1×10^{-11} and C_S were taken as 10^{-3} M. Two further constants which do not appear explicitly in the track equation must also be fixed. These are the initial size of spur and the number of radicals per spur. Following Samuel and Magee the *initial* concentration is taken to be a Gaussian.

$$C_1(r) = (N_1{}^0\,\beta^3/\pi^{3/2})\exp(-\beta^2r^2) \qquad [4]$$

where $1/\beta$ is the radius at which $C_1(r)$ has fallen to $1/e$ of its maximum value. No further assumption is made about the spatial distributions during the course of the reaction. We have taken $1/\beta = 10^{-7}$ cm $= 10$ Å which we denote by the symbol R. This value can be justified by noting that the spur is formed by the thermalization of a slow (50–70 ev) electron which excites, say, three to six water molecules during its lifetime. If the ex-

Can. J. Chem. Downloaded from www.nrcresearchpress.com by 78.46.186.204 on 09/04/12
For personal use only.

citation cross section is of the order of the gas kinetic cross section, the mean distance between excitations in liquid water is found to be ∽10 Å. It follows that the value of 10 Å for the modulus of a Gaussian distribution is reasonable.

No experimental evidence on the size and structure of spurs is available for water. The most relevant measurements are statistics of the number of ion pairs in spurs generated in the gas phase obtained by Wilson (5) and Beekman (6) from cloud chamber photographs. The former finds an "average" spur size of between two and three ion pairs. This is not the most probable size; according to Wilson, 40% of the spurs contains only one ion pair. Beeckman finds 60% containing one ion pair. These measurements were made in air. Taking the energy per ion pair to be 32 volts, these data suggest an average energy deposition of 65±10 volts/spur. The only direct measurement of the number of water molecules dissociated initially is obtained from Firestone's (7) studies of the radiation decomposition of water vapor where the medium is so dilute that no recombination occurs. He finds $G(-H_2O) = 11\pm1$. Combining this value with the value of 65±10 volts per spur obtained above we obtain a value of 6±1 radical pairs per spur and we have taken $N = 6$ in our calculations. Monchick, Samuel, and Magee (8) chose $N = 5$ but they did not discuss the reasons for their choice.

In this argument we assume that the "average" spur, in terms of average *energy*, is the "average" spur for the value of yields, etc., which we are interested in calculating. It is conceivable that the yields vary very sharply as a function of N so that the two averages are different. However, using some of the values of the yields calculated as a function of N and weighting these according to a distribution in N given by the above arguments we find that the "average" spur does correspond to a six-radical pair spur.

5. THE CALCULATIONS

The detailed results of the calculations are presented in Table I. The numbers to the left of the double line are the constants which specify the individual case; those to the right are the values of the yields in one spur. The yields of H_2 and H_2O_2 are expressed as the number of atoms or radicals which have recombined to give these products. The number of molecules formed is half this number. $[H_2O^*]$ is the number of water molecules reformed, $[-H_2O]$ is the net decomposition. If the number of hydrogen atoms in the spur is N_1, we have

$$N_1 = N_2 = [H_2] + [H_2O^*] + [H] = [H_2O_2] + [H_2O^*] + [OH] = [H_2O^*] + [-H_2O], \qquad [5]$$

using square brackets to symbolize the yields defined above.

From the computation of each case a plot like Fig. 1 is constructed which shows the course of the reaction as a function of time. Several features of the process are shown in this figure. A significant fraction of the total amount of recombination occurs in times of the order of 10^{-11} seconds but the process is not complete until some 10^{-8} seconds have elapsed. The scavenging reaction is, at concentrations of $\sim10^{-3}$ molar, negligible until nearly 10^{-8} seconds have elapsed. The true yields of molecular products are given by the asymptotes to the curves in Fig. 1. These can be estimated, with sufficient accuracy, by a visual extrapolation at times of $\sim10^{-8}$ seconds.

6. EXPERIMENTAL VALUES OF THE RADICAL AND MOLECULAR YIELDS

These calculations related to the decomposition of pure water; experimental G-values for this system are given in Table II. We are indebted to A. O. Allen and H. A. Schwarz

Can. J. Chem. Downloaded from www.nrcresearchpress.com by 78.46.186.204 on 09/04/12
For personal use only.

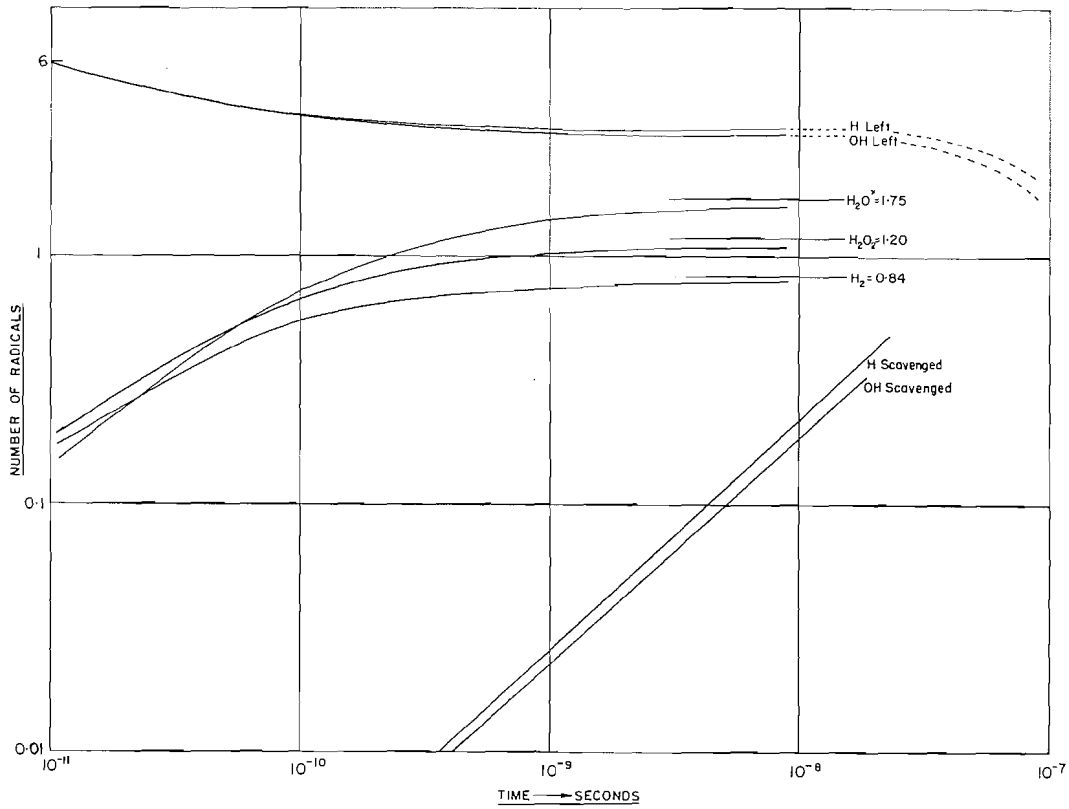

FIG. 1. Kinetics of recombination in a γ-ray spur for case I. The number of radicals which have recombined are plotted as a function of time together with the number which have not reacted. In times of the order of 10^{-7}–10^{-6} seconds the number of unreacted radicals falls sharply as they are scavenged.

(private communication) for these numbers which in their opinion represent "the best values for γ-rays acting in neutral water containing vanishingly small amounts of active solutes" which suppress the reaction of H with H_2O_2 and of OH with H_2. The second line expresses these numbers as the number of atoms or radicals of one species which have combined to give the observed yield. This is the form used in Table I.

This table contains two different kinds of information. Firstly, adopting the Samuel–Magee interpretation, it follows that of the hydrogen atoms involved in the *net* decomposition (see equation [5]) a fraction, which we shall call $f(H_2)$, recombine to give molecular hydrogen. From Table II we see that $f(H_2) = 0.90/3.7 = 0.23$ and that the analogous quantity for OH radicals $f(H_2O_2) = 1.40/3.7 = 0.38$. The second kind of information is the value of the yields per unit of energy absorbed and this is summarized by saying that $G(-H_2O) = 3.7$.

7. YIELDS AS A FUNCTION OF THE OVER-ALL VALUES OF RATE CONSTANTS AND DIFFUSION CONSTANTS

One would expect the amount of recombination to depend critically on the *ratio* of the values of the rate constants to the values of the diffusion constants. It is obvious from an inspection of the track equation that if this ratio is fixed then the yield is determined; the absolute value of the constants determines the *time* in which the recombination

Can. J. Chem. Downloaded from www.nrcresearchpress.com by 78.46.186.204 on 09/04/12
For personal use only.

TABLE I

COMPUTED MOLECULAR AND RADICAL YIELDS FOR γ-RAY SPURS

The columns to the left of the double line refer to the parameters of the spur and are explained in sections 3 and 4. The columns to the right of the double line give the computed yields which are defined in section 6.

		k_{11} $\times 10^{11}$	k_{12} $\times 10^{11}$	k_{22} $\times 10^{11}$	D_1 $\times 10^5$	D_2 $\times 10^5$	$N_1 = N_2$	$\beta_1 = \beta_2$ $\times 10^{-7}$	$k_S C_S$	$[H_2]$	$[H_2O_2]$	$[H_2O^*]$	[H]	[OH]	$[-H_2O]$
A	Initial case	1.2	3.0	0.9	8.0	2.0	6.0	1.0	6.0×10^6	0.56	1.10	2.50	2.94	2.40	3.50
B	Changing all k's and D's	0.4	1.0	0.3	$2\frac{2}{3}$	$\frac{2}{3}$	"	"	"	"	"	"	"	"	"
C	Changing all k's	"	"	"	8.0	2.0	"	"	"	0.32	0.76	1.45	4.23	3.79	4.55
D	" "	3.6	9.0	2.7	"	"	"	"	"	0.80	1.15	3.60	1.60	1.25	2.40
E	Changing both D's	1.2	3.0	0.9	3.0	0.75	"	"	"	0.78	1.15	3.50	1.72	1.35	2.50
F	" "	"	"	"	15.0	3.75	"	"	"	0.42	0.94	1.85	3.73	3.21	4.15
G	Varying k_{11}	3.6	"	"	8.0	2.0	"	"	"	1.40	1.20	2.25	2.35	2.55	3.75
H	" "	10.0	"	"	"	"	"	"	"	2.35	1.35	1.90	1.75	2.75	4.10
I	Varying k_{12}	1.2	1.0	"	"	"	"	"	"	0.84	1.20	1.75	3.41	3.05	4.25
J	" "	1.2	9.0	"	"	"	"	"	"	0.30	0.49	4.00	1.70	1.51	2.00
K	Varying k_{22}	1.2	3.0	2.7	"	"	"	"	"	0.60	2.10	2.30	3.10	1.60	3.70
L	" "	"	"	8.1	"	"	"	"	"	0.67	3.0	1.8	3.53	1.2	4.2
M	Isotope effect	0.8484	2.296	0.90	5.657	"	"	"	"	0.56	1.10	2.50	2.94	2.40	3.50
N	Vary k_{11} and D_1	0.6	3.0	0.9	4.0	"	"	"	"	0.42	0.85	3.25	2.33	1.90	2.75
O	Varying scavenger	1.2	3.0	0.9	8.0	2.0	6.0	1.0	6.0×10^5	0.56	1.10	2.50	2.04	2.30	3.50
P	Concentration	"	"	"	"	"	"	"	6×10^7	0.55	1.05	2.40	3.15	2.55	3.60
Q	"	"	"	"	"	"	"	"	6×10^8	0.49	0.79	2.10	3.31	3.11	3.80
R	"	"	"	"	"	"	"	"	6×10^9	0.33	0.39	1.32	4.35	4.29	4.38
S	Varying spur size	"	"	"	"	"	"	2.0	6×10^6	0.76	1.25	3.40	1.84	1.35	2.60
T	"	"	"	"	"	"	"	0.5	6×10^6	0.41	0.86	1.80	3.79	3.34	4.20
U	Varying no. of radicals per spur	"	"	"	"	"	2.0	1.0	"	0.056	0.13	0.49	1.45	1.38	1.51
V	"	"	"	"	"	"	3.0	"	"	0.15	0.34	0.95	1.90	1.71	2.05
W	"	"	"	"	"	"	9.0	"	"	1.10	1.90	4.40	3.50	2.70	4.60
X	"	"	"	"	"	"	15.0	"	"	2.40	3.60	8.50	4.10	2.90	6.50
Y	Vary size of spur for H atoms only	"	"	"	"	"	"	$\beta_1 = 0.65$ $\beta_2 = 1.0$	"	0.41	1.40	2.10	3.49	2.50	3.90
Z	"	"	"	"	"	"	"	$\beta_1 = 0.4$ $\beta_2 = 1.0$	"	0.28	1.70	1.41	4.31	2.89	4.59

TABLE II

G-VALUES (YIELDS/100 EV) IN PURE WATER

	$G(H_2)$	$G(H_2O_2)$	$G(H)$	$G(OH)$	$G(-H_2O)$
(*a*)	0.45	0.70	2.8	2.3	3.7
(*b*)	0.90	1.40	2.8	2.3	3.7

(*a*) Yields expressed conventionally.
(*b*) Yields expressed as number of atoms or radicals which have combined to give these species.

occurs. This is demonstrated numerically by comparing case (A) with case (B). For brevity we shall refer to cases simply by letter, e.g. (A), (B), just as we are symbolizing the yields per spur by the use of square brackets, e.g. $[H_2]$, $[-H_2O]$. In (B) all the k's and all the D's have been divided by three but the yields are unchanged.

The variation of yields as the ratio of all the k's to the D's is changed is shown by (A), (C), and (D). In these cases the ratios $k_{11}:k_{12}:k_{22}$ are unchanged as are the values of D_1 and D_2. The yields, plotted as a function of k_{12}, are shown in Fig. 2: values of $f(H_2)$ and $f(H_2O_2)$ are plotted in Fig. 3. The values of $[H_2]$ and $[H_2O_2]$ are not very sensitive to the simultaneous variation of the constants as these recombination processes are working in competition with the recombination to form H_2O. The values of $f(H_2)$ and $f(H_2O_2)$ are however very sensitive to changes in the values of the rate constants.

An inspection of Fig. 3 shows that agreement with experimental values is obtained in a

Can. J. Chem. Downloaded from www.nrcresearchpress.com by 78.46.186.204 on 09/04/12
For personal use only.

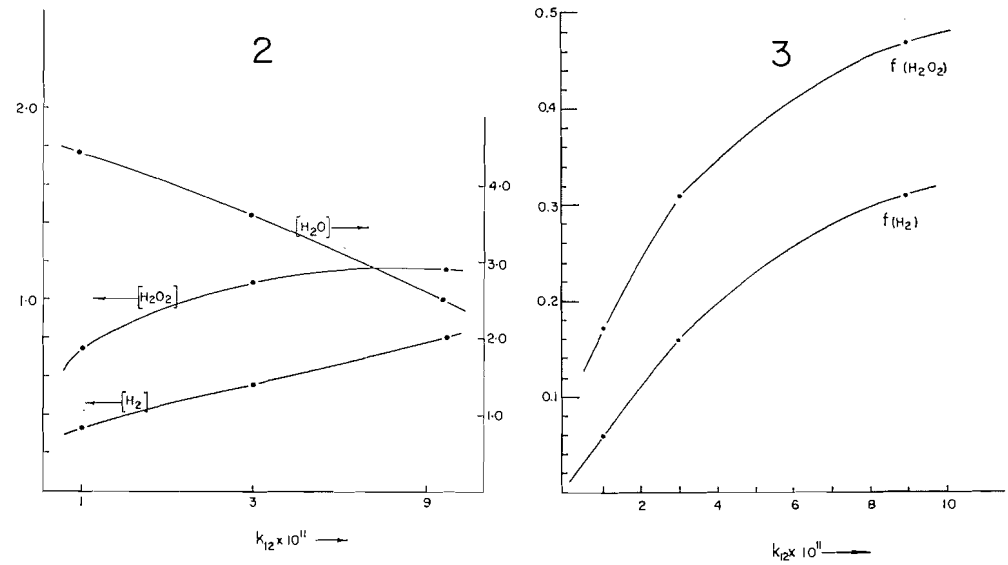

FIG. 2. Variation of yields with the over-all value of constants k_{11}, k_{12}, k_{22} plotted as a function k_{12}. Cases (A), (C), and (D). k_{12} is plotted on a logarithmic scale.

FIG. 3. Variation of $f(H_2)$ and $f(H_2O_2)$ with over-all value of constants k_{11}, k_{12}, k_{22} plotted as a function of k_{12}. Cases (A), (C), and (D).

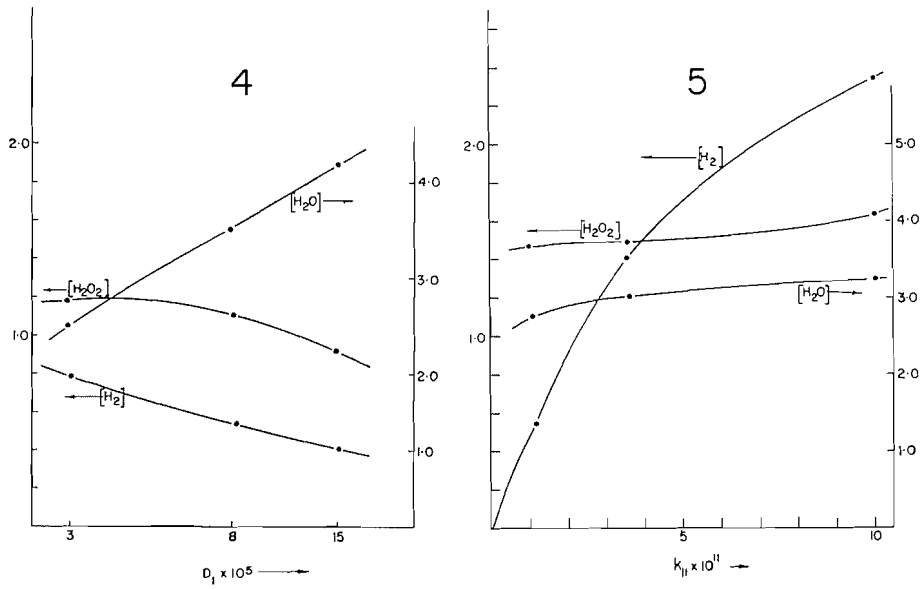

FIG. 4. Variation of yields with the over-all value of the diffusion constants, plotted against D_1. Cases (A), (E), and (F). D_1 is plotted on a logarithmic scale.

FIG. 5. Variation in yields with the value of k_{11}. Cases (A), (G), and (H).

fairly sharply defined region. The values of $f(H_2)$ and $f(H_2O_2)$ depend on the ratios k_{11}: k_{12}: k_{22} and we can only make the qualitative statement that the k's must be of the order of $2\text{–}6\times10^{-11}$ cc/molecule second to obtain agreement with experiment.

This simple point is worth re-emphasizing; for a spur of the size postulated the a

Can. J. Chem. Downloaded from www.nrcresearchpress.com by 78.46.186.204 on 09/04/12
For personal use only.

priori choice of diffusion constants and rate constants gives a strikingly sharp region of experimental agreement. The yields are, of course, a function of the initial size of the spur as discussed in Section 10.

Similar arguments apply to the over-all variation of the diffusion constants exemplified by (E), (A), and (F), whose yields are plotted in Fig. 4 as a function of D_1. This figure is a mirror image of Fig. 2—again exemplifying the fact that the yield depends only on the *ratio* of the rate constants to the diffusion constants.

Experimentally $G(H_2O_2)$ is about 80% greater than $G(H_2)$ and it is apparent from Table I that most of the cases give figures in this ratio. A similar comparison can be made for $G(H)$ and $G(OH)$. These inequalities are explained in this model by the large difference in diffusion constant between H and OH which outweighs the small difference between k_{11} and k_{22} which acts in the opposite direction ($k_{11} > k_{22}$).

8. YIELDS AS A FUNCTION OF THE INDIVIDUAL VALUES OF THE RATE CONSTANTS

Yields as a function of k_{11} are covered by (G) and (H) and plotted in Fig. 5, as a function of k_{12} are covered by (I) and (J) and plotted in Fig. 6, and as a function of k_{22} are covered by (K) and (L) and plotted in Fig. 7.

The curves show the expected form. $[H_2]$ is strongly dependent on k_{11} but not on k_{22} and $[H_2O_2]$ is similarly dependent on k_{22} but not on k_{11}.

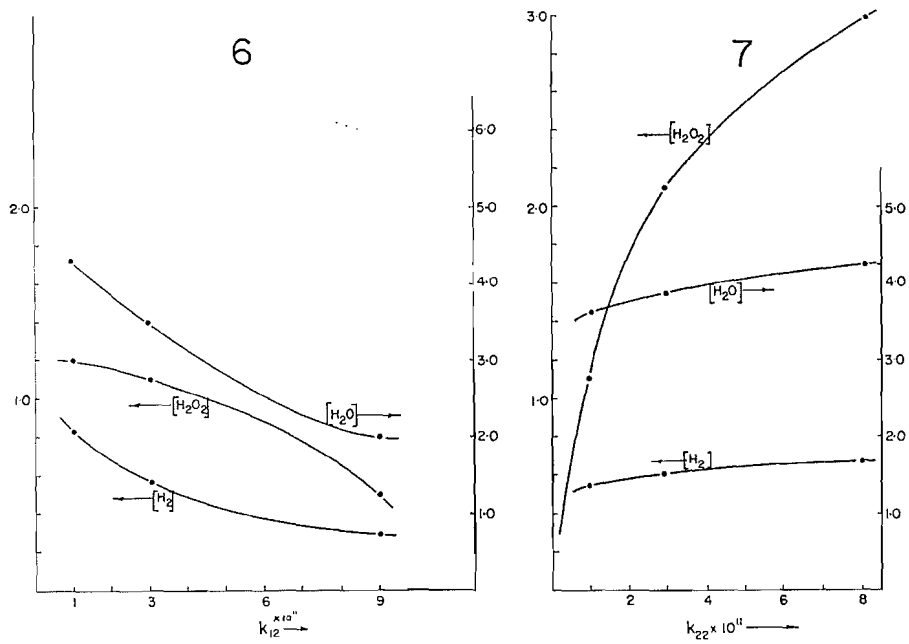

FIG. 6. Variation of yields with the values of k_{12}. Cases (A), (I), and (J).
FIG. 7. Variation in yields with a value of k_{22}. Cases (A), (K), and (L).

9. YIELDS AS A FUNCTION OF SPUR SIZE AND THE NUMBER OF RADICALS PER SPUR

There are two ways in which the variation of yield with the size of the spur can be examined. Either the relative size of the two distribution functions for the radicals or the size of both distributions may be changed. Owing to the "hot atom" effect the hydrogen atoms may be more widely dispersed than the hydroxyl radicals, i.e. $R_1 > R_2$,

Can. J. Chem. Downloaded from www.nrcresearchpress.com by 78.46.186.204 on 09/04/12
For personal use only.

where R_1 and R_2 are the characteristic radii for H atoms and OH radicals respectively. Variation of R_1, keeping R_2 constant, is followed in (Y) and (Z) and the results are plotted in Fig. 8. As R_1 is increased $[H_2]$ decreases and both $[H_2O_2]$ and $[-H_2O]$ increase.

The yields as a function of both radical distributions are followed in (S) and (T). Values of $f(H_2)$ and $f(H_2O_2)$ derived from these cases are shown in Fig. 9; they are rapidly

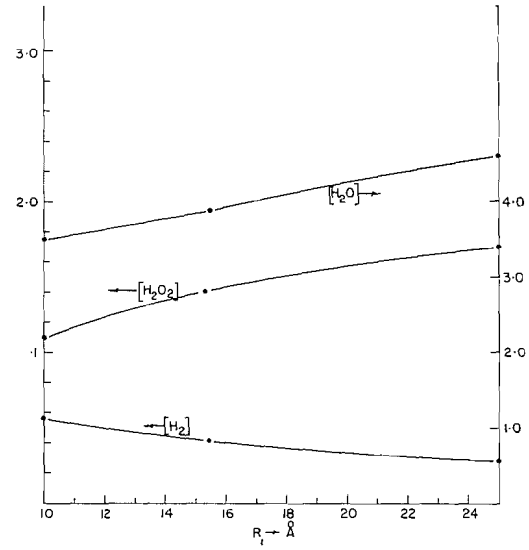

FIG. 8. Variation in yields with R_1, R_2 being unchanged. Cases (A), (Y), and (Z).

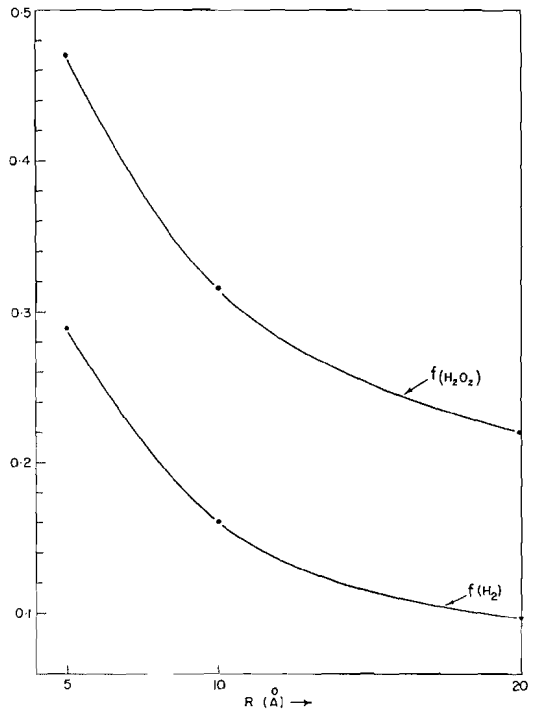

FIG. 9. Variation of $f(H_2)$ and $f(H_2O_2)$ as a function of the over-all spur size, i.e. $R_1 = R_2$. Cases (A), (S), and (T).

Can. J. Chem. Downloaded from www.nrcresearchpress.com by 78.46.186.204 on 09/04/12
For personal use only.

varying functions of size particularly for small values of the "radius". Yields as a function of the number of radicals per spur are shown in Fig. 10 for spurs of constant size (R = 10 Å) and for spurs of varying size determined by the relation $R\alpha(N)^{\frac{1}{3}}$, a radius of 10 Å being taken for the spur with N = 6. These latter values were obtained by interpolation from the changes in $f(H_2)$ and $f(H_2O_2)$ with R shown in Fig. 9. For example, the cube-root relation gives R = 11.5 Å when N = 9. From Fig. 9 we calculate the ratio of $f(H_2)$ at 10 Å to that at 11.5 Å and decrease the value of $f(H_2)$ for N = 9 by this ratio. This treatment assumes that these ratios (calculated for N = 6) are independent of N. This assumption was checked with a spot calculation for N = 15 with R = 20 Å. The calculation gave $f(H_2)$ = 0.22 and $f(H_2O_2)$ = 0.39. The interpolation technique gave $f(H_2)$ = 0.23, $f(H_2O_2)$ = 0.38.

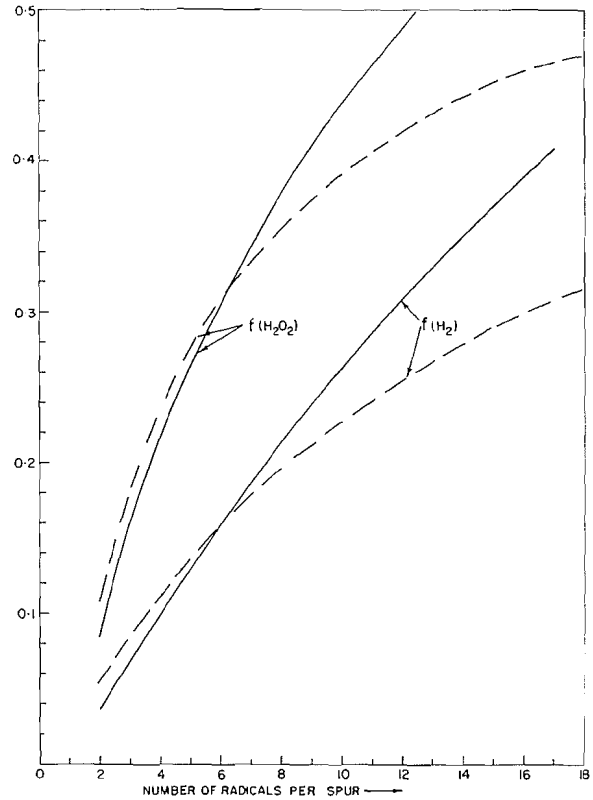

FIG. 10. Variation in $f(H_2)$ and $f(H_2O_2)$ with N, the number of radicals per spur. The full lines refer to spurs of constant size R = 10 Å. In the broken line values of $f(H_2)$ and $f(H_2O_2)$ are shown in which R varies as $\sqrt[3]{N}$ assuming that R = 10 Å when N = 6. Cases (A), (U), (V), (W), and (X).

The parameters N and R are, in a sense, complementary. If the k's and D's are fixed, we can always find values of R for any value of N which will give the experimental value of $f(H_2)$ or of $f(H_2O_2)$. This is illustrated in Fig. 11, where the solid line gives the values of N and R which give $f(H_2)$ = 0.24; the values were determined by interpolation as described in the last paragraph. The solid line corresponds to the choice of k's and D's made in (A). Another line would be generated by a different choice. For instance from Fig. 3 we find that N = 6, R = 10 Å, $k_{12} = 5.2\times10^{-10}$, $k_{11} = 2.1\times10^{-11}$, $k_{22} = 1.5\times10^{-11}$ would also give $f(H_2)$ = 0.24. This defines the circled point in Fig. 11. We can derive another line also defining $f(H_2)$ = 0.24 going through this point. This is indicated by the

Can. J. Chem. Downloaded from www.nrcresearchpress.com by 78.46.186.204 on 09/04/12
For personal use only.

broken line and which is again obtained by interpolation. It does not matter for this argument whether or not this interpolation is exact. The point is that a whole family of lines exists describing spurs with $f(H_2)$ = a constant. By interpolation from Figs. 5 and 6 two other sets of k's can be found which would generate lines essentially coincident with the dotted line. These are: $k_{12} = 3.0\times10^{-11}$, $k_{11} = 1.7\times10^{-11}$, $k_{22} = 0.9\times10^{-11}$ and $k_{12} = 0.5\times10^{-11}$, $k_{11} = 1.2\times10^{-11}$, $k_{22} = 0.9\times10^{-11}$.

The plot in Fig. 11 illustrates the fact that we can, with our present information, make no unique choice of constants which will give agreement with experiment. Plots similar to Fig. 11 could be constructed for $f(H_2O_2)$ and $[-H_2O]$ which would restrict our choice from the larger number allowed by Fig. 11. Such a search would not be very useful. Instead we choose to pick out parameters which, if fixed, would give the most valuable information for the model. The two most important parameters from this point of view are the spur size or volume and the number of radical pairs per spur. It is quite clear from Fig. 11 that the model will only work for small spurs where the characteristic length R is less than 20 Å. The figure R = 10 Å was, in fact, originally chosen by Samuel and Magee to give agreement with experiment.

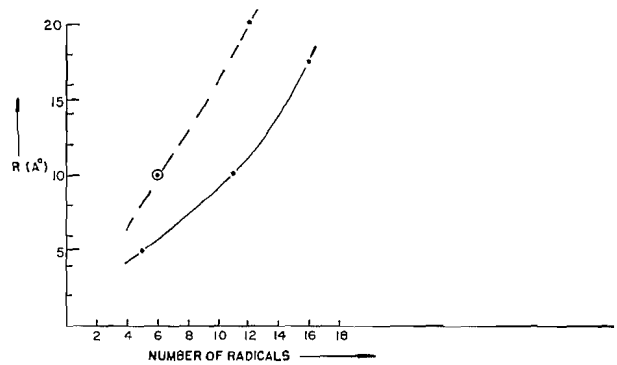

FIG. 11. Values of R, the radii, and N, number of radicals per spur, for which $f(H_2)$ = 0.24. The solid line refers to the choice of k's and D's made in (A). The dotted line refers to several choices of k's which for N = 6 and R = 10 Å also give $f(H_2)$ = 0.24.

10. ISOTOPE EFFECTS

Several workers have shown that (11, 12, and 13) the yield of deuterium gas from acidic solution in heavy water is about 25% less than the yield of hydrogen from the corresponding light water solutions. It is also known that the yield of the ferrous sulphate dosimeter is increased in heavy water solutions (14). If the stoichiometry for the oxidation of ferrous ion in light water is assumed to hold in heavy water these two observations show that, in 0.8 N H_2SO_4, $G(-D_2O)$ is greater than $G(-H_2O)$. Yields of hydrogen gas and hydrogen atoms and OH radicals and their deuterium analogues have been measured by Burton and Phung (13) in neutral solutions using benzene as a scavenger. They find that all the yields are lower than the corresponding yields in light water. The results are shown in Table III.

Burton and Phung point out that these results are not consistent with those of other workers, as may be seen by comparing Table III with Table II.

For this discussion the problem of isotope effects may be stated as follows, "Under what circumstances does the diffusion model predict a lower value of $G(D_2)$ coupled with (*a*) an increased value of $G(-D_2O)$ or (*b*) a decreased value of $G(-D_2O)$?" Following the arguments which are used in Section 4 to establish the initial choice of constants,

Can. J. Chem. Downloaded from www.nrcresearchpress.com by 78.46.186.204 on 09/04/12
For personal use only.

TABLE III

PRIMARY YIELDS IN THE RADIOLYSIS OF LIGHT AND HEAVY WATER

	$G(H_2)(D_2)$	$G(H_2O_2)(D_2O_2)$*	$G(OH)(OD)$	$G(H)(D)$	$G(-H_2O)(-D_2O)$
Light water	0.41	0.61	2.64	3.04	3.86
Heavy water	0.32	0.51	2.38	2.76	3.40

*The yield of peroxide is determined from stoichiometry.

the constants for heavy water are obtained by reducing D_1 to $1/\sqrt{2}$ of its value in (A) and adjusting k_{11} and k_{12} in accordance with the Smoluchowski relation (Section 4). This gives $k_{11} = 8.48\times10^{-12}$, $k_{12} = 2.296\times10^{-11}$, and $D_1 = 5.657\times10^{-5}$. These are the new constants for (M). It will be noted that the yields in (M) are identical with those of (A). The variation of constants required by "simple" theory produces no isotope effect. The qualitative explanation of this is that the change in k_{11} and k_{12} introduced in (M) compensates exactly for the slower diffusion of H atoms which would otherwise result in increased $[H_2]$ and $[H_2O^*]$ yields.

As the isotope effects are not explained by the "simple" choice of constants some special variation of one or more of them must be postulated. An obvious way of reducing the yield of molecular hydrogen would be to suppose that $k_{DD}/k_{HH} < 1/\sqrt{2}$. The effect of variation of k_{11} is shown in Fig. 5 and it is noted that a change in k_{11} required to reduce $[H_2]$ by $\frac{1}{4}$ leaves $[H_2O_2]$ virtually unchanged and decreases $[-H_2O]$ only slightly.

A decrease in $[-H_2O]$ could be explained by invoking the hot atom effect. As the displacement of the D atom on the dissociation of the excited D_2O molecule will be smaller than the corresponding displacement of an H atom it follows that the characteristic radii for these atoms will be different, i.e. $R_1(H) > R_1(D)$. An inspection of Fig. 8 shows that a relatively large change in R_1, of the order of 80%, is required to make the required decrease in $[H_2O_2]$ and $[-H_2O]$. This does not seem likely. It would also be necessary to postulate a further change in k_{11} large enough to affect the increase in the D_2 yield owing to the smaller characteristic radius for the deuterium atoms. A special variation in k_{11} does not therefore explain the results obtained in acidic heavy water solution and is not a very convincing explanation of the results obtained with benzene scavengers.

A choice of constants which would give a simultaneous decrease in all the molecular yields and radical yields is shown in (N). In this case both k_{11} and D_1 are smaller by a factor of two than they are in (A). k_{12} and all the other parameters are unaltered. The calculation shows that all the yields except $[H_2O^*]$ are smaller than they are in (A). When D_1 is reduced the H atoms are confined for a longer time to the region where the concentration of OH is high. $[H_2O^*]$ is therefore increased and $[-H_2O]$ is decreased. This removal of H atom and OH radicals from the central region in turn reduces $[H_2]$ and $[H_2O_2]$.

Now according to the Smoluchowski equation (Eq. [3]) k_{12} should be smaller if D_1 is smaller. By giving k_{12} the same value as in (A) we are in effect making it larger than it would be with a "simple" choice of constants. In other words a change in yields parallel to that found by Burton and Phung is obtained by increasing k_{12}. The variation of yields with k_{12} is shown in Fig. 6 and demonstrates graphically the reduction in $[H_2]$, $[H_2O_2]$, and $[-H_2O]$.

This explanation of the isotope effect in neutral solution is of interest because the arguments of Section 12 suggest that k_{12} is relatively greater in D_2O than in H_2O owing to differences in the initial spatial configuration of the radicals.

Can. J. Chem. Downloaded from www.nrcresearchpress.com by 78.46.186.204 on 09/04/12
For personal use only.

No simple variation in constants is apparent which will explain a decrease in $[H_2]$ coupled with an increase in $[-H_2O]$, as found in acid solutions. Speculations on this topic must be deferred until more detailed information on the yields in acid solutions is available. In any case the simple diffusion theory which neglects any effect of hydrogen ions and the intervention of such species as H_2^+ is not applicable to a discussion of acidic solutions.†

A second type of isotope effect is observed in the isotopic composition of molecular hydrogen evolved from dilute solution of heavy water. This has been studied by Kelly, Rigg, and Weiss (15), who measured the separation factor.

$$S = [H_2/HD]_{gas}/[H_2O/HDO]_{water} \simeq [HDO]\,[H_2]/[H_2O]\,[HD] \qquad [6]$$

for solution containing about 1 mole % deuterium and various scavengers. Deaerated ferrous sulphate solution gave $S \simeq 3.5$, close to the value of 3.8 for thermal equilibrium at room temperature. Solutions which contained efficient scavengers for hydrogen atoms, e.g. oxygen saturated ferrous sulphate and deaerated ceric sulphate, gave $S \simeq 2$. It was suggested that the hydrogen evolved from deaerated ferrous sulphate was thermally equilibrated but with solutions giving lower separation factors, exchange and equilibration were not taking place. Kelly, Rigg, and Weiss suggested that the hydrogen was produced by reactions involving excited molecules.

$$H_2O^* + H_2O^* \rightarrow H_2 + H_2O_2\ (k_1) \qquad [7]$$

$$H_2O^* + HDO^* \rightarrow HD + H_2O_2\ (k_2). \qquad [8]$$

The separation factor will be given by the ratio k_1/k_2. In their second publication (15*b*) Kelly, Rigg, and Weiss suggest that $k_1/k_2 \simeq 2$ owing to the difference in activation energy of the two reactions. A difference of 0.4 kcal, attributed to the different zero-point energies of H_2O, HDO, is postulated.

We have calculated the extent of recombination of H and D atoms in a spur to give H_2, HD, and D_2 and hence determined the separation factors predicted by the model. On "simple" assumptions the model gives $S = 1$, i.e. no separation.

Consider the statistics of the formation of HD from a spur containing $(n-1)$ H atoms and one D atom. Neglecting isotope effects in the rate constants the probability of forming an HD molecule is proportional to $(n-1)$, and the probability of forming an H_2 molecule is $(\frac{1}{2})(n-1)(n-2)$. The fraction of HD is $[HD]/([H_2] + [HD]) = 2/n$ of the total "hydrogen" produced in the spur. If the aqueous phase contains p% HDO (p is $\simeq 1$) then the percentage of spurs containing one HDO molecule is np. If the HDO dissociates statistically (this is discussed later) the percentage of spurs containing one D atom is $np/2$. The composition of all the evolved hydrogen is therefore $2/n \times np/2 = p$% HD and the separation factor is unity.

Isotope effects in the recombination and diffusion processes can be neglected because in the Samuel–Magee model, changes in rate constants and diffusion constants work in opposition to one another. We have used the "two radical" calculation to estimate the relative probabilities of recombination of H and D atoms in spurs containing six atoms in all. Putting $D_1 = 8\times10^{-5}$, $D_2 = 5.656\times10^{-5}$, $k_{11} = 1.2\times10^{-11}$, $k_{12} = 2.040\times10^{-11}$, and $k_{22} = 8.484\times10^{-12}$ and with spurs with $N_1 = 5$, $N_2 = 1$ and $N_1 = 1$, $N_2 = 5$ we find yields of $[H_2] = 0.68$ and $[HD] = 0.32$ and $[D_2] = 0.68$ and $[HD] = 0.32$, respectively. The numerical identity justifies the neglect of isotope effects and is in agree-

†*Note added in proof: A discussion of molecular and radical yields in* D_2O *which complements the present discussion has been given by Armstrong, Collinson, and Dainton, Proceedings of Second Conference on Peaceful Uses of Atomic Energy. P/1517.*

Can. J. Chem. Downloaded from www.nrcresearchpress.com by 78.46.186.204 on 09/04/12
For personal use only.

ment with the statistical ratio of $2/n = \frac{1}{3}$ for the fraction of HD in a six-radical spur.

Two tacit assumptions have been made in this discussion, firstly that hydrogen and deuterium atoms are produced, "statistically", with equal probability from an HDO molecule and secondly that no exchange reactions of the type $H + HD \rightarrow H_2 + D$ occur in the track when scavengers are present. Calculation of these 'secondary' exchange reactions would require a more elaborate computation procedure. We note that rate constants for these exchange reactions are two to three orders of magnitude smaller than the rate constants for recombination and on this basis the amount exchange which would occur in the lifetime of the spur (10^{-8} seconds) would be small.

Mass spectral data on isotopically substituted molecules such as CH_3D show that the deuterium atom is 'more firmly' held than any one hydrogen atom by a factor of two or more (16). The theoretical interpretation of these results is general and predicts in principle the same effect for HDO, i.e. the dissociation.

$$HDO^* \rightarrow H + OD \qquad [9]$$

might be about twice as probable as

$$HDO^* \rightarrow D + OH. \qquad [10]$$

Such a difference would, in the present case, reduce the number of spurs containing a D atom below the value predicted statistically and would give a separation factor greater than unity as was found experimentally by Kelly, Rigg, and Weiss.

This difference would lead to a value of less than unity for the separation factor.

$$S' = [D_2/HD]_{gas}/[D_2O/HDO]_{liq} = [HDO]\,[D_2]/[D_2O]\,[HD]$$

describing the isotopic separation of gas evolved from dilute solution of HDO in D_2O containing scavengers. A value of 0.54 has been found experimentally in this laboratory for this system with the scavengers used by Kelly, Rigg, and Weiss.

The preferential dissociation of HDO to H + OD also explains the G-values found by Bardwell and Dyne (17) for the radiation-induced exchange of hydrogen atoms between liquid water and dissolved hydrogen. The exchange was followed by a tracer technique using H_2O containing about 1% HDO. The total amount of the exchange was calculated assuming that HDO dissociated statistically. This was between $\frac{1}{2}$ and $\frac{1}{3}$ of that found by Gordon and Hart (18), who studied the system D_2, H_2O and who were consequently able to detect directly every exchange.

11. THE EFFECT OF SCAVENGER CONCENTRATION

If the concentration of scavenger is increased the yields of molecular products decrease slowly. This effect (19, 20, 21), which has been extensively studied experimentally and theoretically, is due to competition between the scavenging process and the recombination process during the time in which the latter is proceeding at a significant rate.

The scavenger effect is calculated by varying the terms $k_{1S}C_S$ and $k_{2S}C_S$. A plot of the relative yields against C_S refers only to the particular choices of k_{1S}; if k_{1S} were larger than that chosen then the same decrease in yield would be observed at a correspondingly smaller value of C_S. The relative yields plotted in Fig. 12 were obtained with $k_{1S} = k_{2S} = 1\times10^{-11}$. It is found that the $[H_2]$ yield is less sensitive to scavenger than the $[H_2O_2]$ yield.

This arises because we have put $k_{1S} = k_{2S}$. Because of the greater diffusion constant of the H atom k_{1S} will be larger than k_{2S} with the practical result that the effects of

Can. J. Chem. Downloaded from www.nrcresearchpress.com by 78.46.186.204 on 09/04/12
For personal use only.

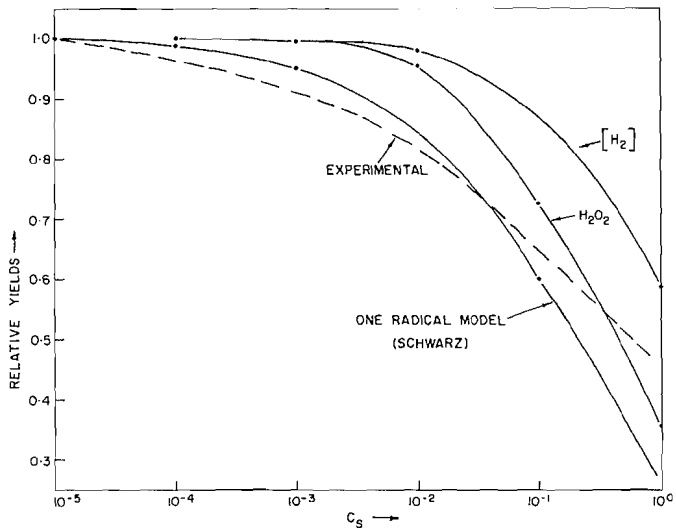

FIG. 12. Variation in relative yields with the scavenger concentration. The curves labelled H_2, H_2O_2 are from the present calculation. The calculated one radical model curve and the experimental curve are taken from Schwarz (19). Cases (A), (O), (P), (Q), and (R).

scavenger on $[H_2]$ and $[H_2O_2]$ will be more nearly equal.* Using the Smoluchowski equation to estimate the relative values of k_{1S} and k_{2S} we conclude that k_{1S} would be two or three times greater than k_{2S}. A calculation has shown that, at a concentration of 10^{-1} M with $k_{1S} = 3.0\times10^{-11}$ and $k_{2S} = 1.0\times10^{-11}$ the change in relative yields for $[H_2]$ and $[H_2O_2]$ are identical and fall on the curve for $[H_2O_2]$.

A theoretical curve calculated by Schwarz (19) is also shown in Fig. 12 together with an experimental curve. The theoretical curve was calculated analytically using a simplified one-radical model. The curve was adjusted by altering the scale on the concentration axis so that it coincided with the experimentally determined curve for the variation of $[H_2]$ with nitrite as scavenger. Schwarz showed that the data for both hydrogen and hydrogen peroxide yields for a variety of scavengers lay on similar curves. These curves could be brought into coincidence by multiplying the concentration by an empirical normalizing constant, which gives, in effect, the value of k_S relative to that for nitrite. These relative values were shown to be in agreement with experiment. The experimental curve in Fig. 12 is a curve which we have drawn from points plotted by Schwarz.

At large scavenger concentrations the experimental decrease in yield is less than that predicted. This is due to the assumption that C_S is a constant both in time and space. For $C_S = 1$ molar our numerical calculations show that three out of six radicals have reacted with scavenger in about 10^{-11} seconds. In this short time the spur has not expanded appreciably by diffusion and its effective volume is still $(10^{-7}\text{ cm})^3 = 10^{-21}\text{ cm}^3$. This volume contains less than one scavenger atom at a concentration of 1 M. It follows that there is a depletion of scavenger at high scavenger concentration inside the volume of the spur and the decrease in yield will be less than that predicted on the assumption that C_S is a constant.

At low scavenger concentrations the new theoretical curves and that given by Schwarz show a smaller decrease in yield than is observed experimentally. As this amounts to only 10%, this discrepancy may fairly be attributed to some of the simplifications

We are indebted to Dr. H. Schwarz for clarification on this point.

Can. J. Chem. Downloaded from www.nrcresearchpress.com by 78.46.186.204 on 09/04/12
For personal use only.

inherent in our treatment of the model. The nature of one of these simplifications can be seen in calculations on the same effect by Ganguly and Magee (21). They used a one-radical model but took into account the effects of overlap of spurs. This becomes more significant as the energy of the primary β-particle is decreased; for β-particles of 0.01 Mev energy a curve is obtained which falls steadily as the concentration of scavenger is increased instead of having an initial flat portion for concentrations up to 10^{-3} M. The curves calculated by Ganguly and Magee are not, unfortunately, reproduced in sufficient detail to permit a detailed comparison. The present calculations and those of Schwarz apply to spurs generated by high energy β-particles; which are so far apart that they never overlap significantly.

The curve calculated by Schwarz was adjusted to give agreement with experiment; no a priori assumptions being made as to the value of k_S. From the figure it can be seen that k_S must be $\sim 10^{-10}$ rather than $\sim 10^{-11}$ for there to be agreement between theory and experiment. Rate constants of $\sim 10^{-10}$ are approaching the values given by the kinetic theory for gas-phase reactions. Most of the normalization constants given by Schwarz are of the order of unity or somewhat larger and values of k_S are correspondingly smaller, i.e. $3\text{–}5 \times 10^{-11}$.

The fact that the experimental yields for hydrogen and hydrogen peroxide lie on one curve (Fig. 12) is good evidence that they are formed by a similar process. The agreement between the experimental and theoretical curves is again evidence that this process is a bimolecular one, occurring in a diffusion-controlled scheme of the type proposed by Samuel and Magee and which is in competition with a scavenging reaction. This evidence does not however prove that the bimolecular processes are recombinations of hydrogen atoms and hydroxyl radicals; similar experimental curves would be obtained if, for instance, the products were formed by $2H_2O^* \rightarrow H_2 + H_2O_2$ and if the excited water molecule H_2O^* reacted with the scavenger to give other products.

12. A CRITICISM OF THE MATHEMATICAL CONSTRUCTION OF THE MODEL

The equations [1] and [2] used in these calculations apply the concepts of classical chemical kinetics to reactions occurring in small volumes containing only a few molecules and occurring in very short times which are of the order of magnitude of the time between molecular jumps in a liquid. The equations deal with spatial distributions of concentration which are expressed as a continuous analytic function of the co-ordinates—no account being taken of the movements of individual radicals. A treatment of the process as a form of "random walk" is clearly more appropriate and this could conceivably be handled with a large enough computer. Leaving aside the last practical difficulty, it is difficult to devise a molecular model for the diffusion and reaction of molecules in liquid water which is not open to objections as serious as those placed against the analytical treatment. In particular the results of a random walk treatment depend on the way in which, say, the spatial movements are defined; whether the directions are random or whether some directions are preferred, whether the distances in one jump are constant or variable, etc. It is as difficult to estimate the errors involved in making assumptions of this type as it is to estimate the errors in the use of the diffusion approximation.

The model, as used in this paper, does not take into account the possible correlations in the spatial distributions of the particles. As the excited water molecules, the parents of the reactive radicals are generated along the random path of a slow electron it is proper to describe the spatial distribution of these water molecules by a distribution function which is equivalent to a concentration. The spatial distribution of the H and

Can. J. Chem. Downloaded from www.nrcresearchpress.com by 78.46.186.204 on 09/04/12
For personal use only.

OH radicals which originate from these excited water molecules will also be described by this or some similar concentration function and these functions are appropriate for calculating the probabilities of recombination $k_{11}C_1^2$, $k_{22}C_2^2$. They are not, however, necessarily applicable to the evaluation of the term $k_{12}C_1C_2$ because each hydrogen may be, on the average, much closer to the OH radical which was its original partner than it is to the nearest other hydrogen atom. In other words there is a correlation between the concentrations C_1 and C_2. In terms of the mathematical techniques used here this means that k_{12} is not a true rate constant as it will vary with time. In the case of extreme correlations between like particles k_{12} in equation [1] and [2] is initially much greater than the kinetic theory rate constant for the reaction $H + OH \rightarrow H_2O$. This is of interest in connection with the isotope effect where in section 10 we suggested that k_{12} was larger for the reaction $D + OD \rightarrow D_2O$ than it was for $H + OH \rightarrow H_2O$. The "constant" k_{12} depends initially on the separation between two radicals H, OH and D, OD. Because of the large relative difference in the masses of H and D atoms this may be significantly different. The isotope effect may be attributed to differences in the correlation functions, which are expressed in the term k_{12}.

If there is a very large correlation between H and OH, i.e. the initial separation between the dissociated atoms is small, then it follows that there is a high probability of these radicals recombining and they never really contribute to the initial number of radicals in the spur. For this reason the value of $G(-H_2O)$ given by Firestone for water vapor represents an upper limit for the initial amount of decomposition in the liquid water.

Monchick, Samuel, and Magee (8) have published a brief set of calculations on a two-radical model which includes a treatment of the correlation term. Their treatment is approximate and no significant differences are noticeable between their yield values and those obtained in these calculations which are approximate in the sense that k_{12} is taken as a constant.

In this paper we have examined the Samuel–Magee model pragmatically and have accepted its premises about primary processes in the spur without question. The model leads to reasonable interpretations of the experimental data but, with the exception of experiments on the isotope effects, it is not sufficiently well defined to allow any very critical tests. In the relatively restricted field of study we have not found any experimental data which the model cannot explain nor have we found any evidence for any "new" primary processes. Our numerical data have been presented so that they may suggest more decisive experiments and so that, when new data are available, the qualitative effect on the model can be readily estimated.

ACKNOWLEDGMENTS

We take pleasure in acknowledging the assistance of Mrs. Arden Okazaki in the writing of the detailed computer program and the benefit of many stimulating discussions with Dr. R. W. Attree, Dr. R. H. Betts, and Dr. Boris Davison.

APPENDIX

The Numerical Method

1. Analytical Transformations

The original equations for the concentrations C_1 and C_2 are

$$\partial C_i/\partial t = D_i\nabla^2 C_i - k_{ii}[(N_i-1)/N_i]C_i^2 - k_{12}C_1C_2 - k_{1S}C_iC_S \qquad [1]$$

Can. J. Chem. Downloaded from www.nrcresearchpress.com by 78.46.186.204 on 09/04/12
For personal use only.

for $i = 1, 2$. The k_{ij} are rate constants, and N_i the total number of particles in the system

$$N_i(t) = \int C_i(r,t)\, dV. \qquad [2]$$

By convention, the particles are labelled so that D_1 is the larger of the two diffusion constants.

Three transformations are applied to the variables:

(*a*) A dimensionless space variable $\rho = r/\sqrt{(D_1 t)}$ is defined in order that a fixed range in ρ corresponds to an expanding range in r as time proceeds. This is to keep pace with the outward diffusion of the particles.

(*b*) A dimensionless time variable $x = \log(t/t_0)$ is used to take account of the fact that the phenomenon can be examined on an expanded time scale as time proceeds. The choice of the initial time t_0 is discussed below.

(*c*) New dependent variables are defined by

$$Y = \rho C_1; \qquad Z = \rho C_2. \qquad [3]$$

These effectively transform the spherical geometry to plane geometry and simplify the equations.

The final form becomes

$$\frac{\partial Y}{\partial x} = \left[\frac{\partial^2 Y}{\partial \rho^2} + \frac{\rho}{2}\frac{\partial Y}{\partial \rho} + \frac{Y}{2}\right] - \frac{k_{11}t_0 e^{-x/2}Y^2}{\rho} - \frac{k_{12}t_0 e^{-x/2}YZ}{\rho} - k_{1S}t_0 e^{x} C_S Y,$$

$$\frac{\partial Z}{\partial x} = \left[\Delta\frac{\partial^2 Z}{\partial \rho^2} + \frac{\rho}{2}\frac{\partial Z}{\partial \rho} + \frac{Z}{2}\right] - \frac{k_{22}t_0 e^{-x/2}Y^2}{\rho} - \frac{k_{12}t_0 e^{-x/2}YZ}{\rho} - k_{2S}t_0 e^{x} C_S Z, \qquad [4]$$

where $\Delta = D_2/D_1$.

2. Numerical Method

The problem is the integration of the pair of equations [3] from $x = 0$, given the initial spatial distributions

$$C_i(r,0) = [N_i(0)\beta^3/\pi^{3/2}]e^{-\beta^2 r^2}. \qquad [5]$$

The space dependence is handled by replacing the functions $Y(\rho)$ and $Z(\rho)$ at any time by 40-place tables Y_n, Z_n for $\rho = nh$ ($n = 0, 1, \ldots\ldots, 39$). The derivatives are then replaced by

$$\partial^2 Y_n/\partial\rho^2 = (Y_{n+1} - 2Y_n + Y_{n-1})/h^2,$$

$$\partial Y_n/\partial\rho = (Y_{n+1} - Y_{n-1})/2h, \qquad [6]$$

and the corresponding results for Z. Thus the system reduces to 80 simultaneous first-order ordinary differential equations for the Y_n and Z_n.

Because of the definitions [3], the conditions $Y_0 = Z_0 \equiv 0$ are imposed. At the outer boundary, we set $Y_{39} = Z_{39} \equiv 0$; this implies that h is sufficiently large that no appreciable error arises from confining the phenomenon to a finite volume.

The integration in time proceeds by a step-by-step process, correct to second order in Δx. A "mid-point" procedure is used to make the evaluation of the right-hand sides necessary only once per interval.

Can. J. Chem. Downloaded from www.nrcresearchpress.com by 78.46.186.204 on 09/04/12
For personal use only.

3. The Input Data

The problem is defined by a choice of k_{11}, k_{22}, k_{12}, $k_{1S}C_S$, $k_{2S}C_S$, $N_1(0)$, $N_2(0)$, β_1, β_2, D_1, and Δ. In addition, t_0, h, and Δx must be chosen according to criteria imposed by the physics of the problem.

t_0 must be the time appropriate to the expansion of a δ-function distribution to the distribution given by $C_1(r, 0)$ when the diffusion constant is D_1; otherwise the expansion of the spatial co-ordinate will fail to keep pace with the phenomenon at subsequent times. In practice, $t_0 = \frac{1}{6}\beta_1^2 D_1$ has been used. The theoretical value, $t_0 = \frac{1}{4}\beta_1^2 D_1$ leads to an incipient instability in the mathematical treatment.

Once t_0 is chosen, the space interval h must be chosen to make the initial range of r contain all significant parts of the initial Gaussian distributions. If h is too small, the imposition of the outer boundary condition introduces errors that become magnified as time progresses; if it is too large, accuracy is lost through failure to make good use of the full 40-entry tables. With the given choice of t_0, a satisfactory value of h is 0.3.

Finally, Δx must be small enough to give reasonable accuracy in the time integrations. Experience has shown that $\Delta x = 0.22$ is reasonable for the cases run so far. An instability in the solution appears rather suddenly above $\Delta x = 0.25$.

4. Output

At the end of every step, the computer accumulates the losses of particles L_{ij} owing to each of the five recombination terms and recalculates N_1 and N_2. After every fifth or tenth step, the following information is printed:

Elapsed time:

L_{11}	L_{12}	L_{1S}	N_1	$(\text{sum})_1$
L_{22}	L_{12}	L_{2S}	N_2	$(\text{sum})_2$.

The elapsed time is $T = t_0(e^x - 1)$. The sums should remain equal to $N_1(0)$ and $N_2(0)$, within the accuracy of the calculation.

REFERENCES

1. SAMUEL, A. H. and MAGEE, J. L. J. Chem. Phys. **21**, 1080 (1953).
2. DEWHURST, H. A., SAMUEL, A. H., and MAGEE, J. L. Radiation Research, **1**, 62 (1954).
3(*a*). ORR, W. J. C. and BUTLER, J. A. V. J. Chem. Soc. 1273 (1935).
(*b*). WANG, J. H., ROBINSON, C. V., and EDELMAN, I. S. J. Am. Chem. Soc. **75**, 466 (1953).
4. FRICKE, H. Ann. N.Y. Acad. Sci. **59**, 567 (1955).
5. WILSON, C. T. R. Proc. Roy. Soc. (London), A, **104**, 192 (1923).
6. BEEKMAN, W. J. Physica, **15**, 327 (1949).
7. FIRESTONE, R. F. J. Am. Chem. Soc. **78**, 3226 (1956); **79**, 5593 (1957).
8. MONCHICK, L., MAGEE, J. L., and SAMUEL, A. H. J. Chem. Phys. **26**, 935 (1957).
9. ALLEN, A. O. Disc. Faraday Soc. No. 12, 79 (1952).
10. ALLEN, A. O. Radiation Research, **1**, 85 (1954).
11. HART, E. J., MCDONELL, W. R., and GORDON, S. Intern. Conf. on the Peaceful Uses of Atomic Energy, **7**, 576 (1955).
12. HARDWICK, T. J. Private communication.
13. PHUNG, P. V. and BURTON, M. Radiation Research, **7**, 199 (1957).
14. TRUMBORE, C. N. and VAN ATEN, A. H. W. J. Am. Chem. Soc. **78**, 4179 (1956).
15. KELLY, P., RIGG, T., and WEISS, J. (*a*) Nature, **173**, 1130 (1954); (*b*) Chemistry & Industry, 1291 (1954).
16. FIELD, F. H. and FRANKLIN, J. L. Electron impact phenomena. Academic Press Inc., New York. 1957. pp. 204–217.
17. BARDWELL, J. and DYNE, P. J. Can. J. Chem. **35**, 82 (1957).
18. GORDON, S. and HART, E. J. J. Am. Chem. Soc. **77**, 3981 (1955).
19. SCHWARZ, H. A. J. Am. Chem. Soc. **77**, 4960 (1955).
20. SWORSKI, T. J. J. Am. Chem. Soc. **76**, 4687 (1954); Radiation Research, **2**, 26 (1955).
21. GANGULY, A. K. and MAGEE, J. L. J. Chem. Phys. **25**, 129 (1956).

Can. J. Chem. Downloaded from www.nrcresearchpress.com by 78.46.186.204 on 09/04/12
For personal use only.

Can. J. Chem. Downloaded from www.nrcresearchpress.com by 78.46.186.204 on 09/04/12
For personal use only.

FATTY ACIDS OF THE SEED OIL OF CARDIOSPERMUM HALICACABUM[1]

MARY J. CHISHOLM AND C. Y. HOPKINS

ABSTRACT

The seed oil of *Cardiospermum halicacabum* L., family Sapindaceae, was found to have 11-eicosenoic acid as the major fatty acid in its glycerides. In this respect it is unique among the true natural fats. The amount of eicosenoic acid in the sample examined was 42% of the total long-chain fatty acids. The identity and amounts of the principal fatty acids of the oil were determined by gas chromatography and by distillation of the methyl esters. The estimated percentages were: palmitic 3, linolenic 8, linoleic 8, oleic 22, stearic 2, eicosenoic 42, arachidic 10. In addition, there was evidence of small proportions (1–2%) of a low-molecular-weight acid and of C_{22} acids.

In studying the occurrence of eicosenoic acid in seed oils, attention was directed to the family Sapindaceae. An unsaturated C_{20} acid has been reported as a minor component in the seed oil of three species of this family, although the acid was not completely identified in these instances (5, 6, 7).

Most of the Sapindaceae are found in tropical and subtropical regions but one genus, *Cardiospermum*, grows also in temperate climates. *Cardiospermum halicacabum* (balloon vine) was chosen for study. A previous analysis of its seed oil showed the presence of arachidic acid but not of unsaturated C_{20} acid (3). It was surprising, therefore, to find in the present work that the sample gave an oil in which 11-eicosenoic acid constituted 42% of the total fatty acids.

The other acids of the oil also differed in some respects from those of the more common seed oils.

EXPERIMENTAL

Properties of the Oil

Seed of *Cardiospermum halicacabum* L., originating in Holland, was obtained from a commercial seed house. The spherical seeds had an average weight of 0.074 g and were easily ground. The yield of oil, by extraction with petroleum ether, was 28.0% on a 10% moisture basis. Constants of the oil are shown in Table I.

TABLE I

PROPERTIES OF THE OIL

Iodine value	86.8	Acetyl value	0.9
Saponification value	206	Refractive index, 25°	1.4709
Unsaponifiable matter, %	0.4	Halphen test	Negative
Acid value	11.7		

Composition of the Fatty Acids

A sample of the oil was saponified, freed from unsaponifiable matter, and converted to methyl esters. During the removal of the solvent, after esterification, esters of any short-chain acids are volatilized. The analysis is therefore restricted to the longer-chain acids.

[1]*Manuscript received July 29, 1958.*
Contribution from the Division of Pure Chemistry, National Research Council, Ottawa, Canada.
Issued as N.R.C. No. 4767.

The esters were examined by gas chromatography, using a Perkin–Elmer fractometer, model 154-B. The detector was a thermistor type thermal conductivity cell. The column was 1 meter in length and was packed with Apiezon M stopcock grease on Celite. It was operated at 225° with a helium flow rate of 95 ml/minute at an inlet pressure of 15 p.s.i.

The proportions of the chief components were estimated from the chromatogram (Fig. 1) by chain length as follows: C_{16} 3, C_{18} 41, C_{20} 52. In addition there were minor peaks (not shown) indicating about 2% of a low-molecular weight acid and about 2% of C_{22} acid(s).

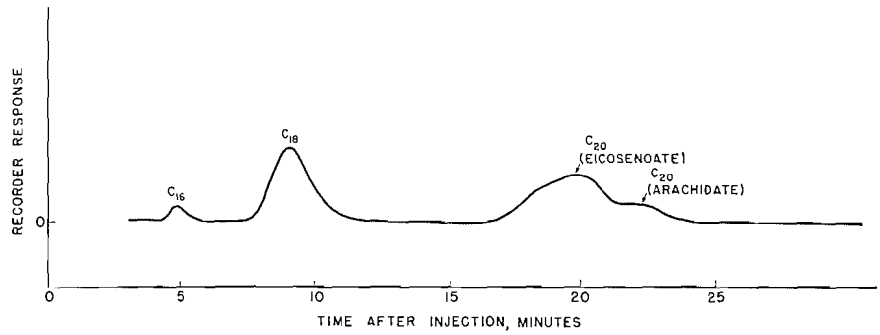

FIG. 1. Main portion of the gas chromatogram of the methyl esters. The peaks represent esters of C_{16}, C_{18}, and C_{20} acids.

A sample of the mixed esters was isomerized by alkali (45 minutes at 180° in glycerol) and examined by ultraviolet absorption. The results showed a content of 8.0% of dienoic acid and 7.6% of trienoic acid, calculated as octadecoic acids. A sample of the mixed fatty acids of the oil was brominated in ether. The insoluble bromo acid was recrystallized and identified as hexabromostearic acid (Table III).

The main portion of the oil was converted to methyl esters by methanolysis and the mixed esters (50 g) were distilled through a spinning band column at 0.5 mm pressure (Table II).

TABLE II

DISTILLATION OF METHYL ESTERS

Fraction	Temp., °C (0.5 mm)	Weight, g	Chain length	Iodine value	Refractive index, 25°
1	58–63	0.48		2.9	1.4260
2	63–114	1.16		8.0	1.4405
3	114–126	1.81		75.8	1.4490
4	126–136	1.57		119.1	1.4543
5	136–140	13.18	C_{18}	126.9	1.4558
6	140–147	2.04		95.2	1.4529
7	147–152	1.31		80.9	1.4529
8	152–156	1.36		79.2	1.4529
9	156	8.45	C_{20}	73.5	1.4524
10	156–159	13.08	C_{20}	57.1	Solid
R	Residue	4.50			

Fraction 2 was mainly palmitic ester. Fraction 5 was crystallized from acetone at −25°, giving a little methyl stearate, m.p. 38–38.5°. Oleic and linoleic acids were identified as components of the filtrate by hydroxylation with alkaline permanganate (Table III). Fraction 9 was almost pure methyl eicosenoate but yielded a little methyl arachidate, m.p. 45–45.5°. Fraction 10 gave arachidic acid in quantity. The identity of these acids was confirmed by mixed melting point in each case.

Can. J. Chem. Downloaded from www.nrcresearchpress.com by 78.46.186.204 on 09/04/12
For personal use only.

TABLE III

IDENTIFICATION OF ACIDS

Fraction	Acid	Identified as:	Melting point, °C
2	Palmitic	Palmitic acid	62–62.5
—	Linolenic	Hexabromostearic acid	180–181
5	Linoleic	*erythro,erythro*-9,10,12,13-Tetrahydroxystearic acid	171–172
5	Oleic	*erythro*-9,10–Dihydroxystearic acid	129–130
5	Stearic	Methyl stearate	38–38.5
9	11-Eicosenoic	*erythro*-11,12-Dihydroxyeicosanoic acid	129–130
		11-Eicosenoic N-hydroxyamide	69–70
10	Arachidic	Arachidic acid	74.5–75

Examination of the residue gave evidence of saturated and monounsaturated acids of chain length C_{22} (equivalent weights 343 and 342). Several of the intermediate fractions were examined further by gas chromatography.

Estimation of the fatty acid composition from all of the data gives the percentages shown in Table IV. The undetermined portion includes a low-molecular-weight acid and C_{22} acids.

TABLE IV

ESTIMATED FATTY ACID COMPOSITION (% OF TOTAL FATTY ACIDS)

Acid	%	Acid	%
Palmitic	3	Stearic	2
Linolenic	8	11-Eicosenoic	42
Linoleic	8	Arachidic	10
Oleic	22	Undetermined	5

DISCUSSION

The oil is unique in having eicosenoic acid as the chief component acid in its glycerides. The amount, 42% of the total fatty acids, is double that of the oils previously known to have a high eicosenoic acid content (18–20%) (1, 2).

As a source of this acid, the seed would compare favorably with jojoba seed (*Simmondsia californica* Nuttall), which contains a liquid wax having eicosenoic as its major fatty acid. The content of total fatty acids in jojoba wax is 50% (4) as compared to about 90% in *Cardiospermum* oil. The eicosenoic acid from all of the seed oils and jojoba wax has been identified as the Δ^{11}-isomer.

Isolation of 11-eicosenoic acid from *Cardiospermum* oil tends to confirm previous indications of a C_{20} unsaturated acid in the Sapindaceae family, viz., in species of *Nephelium* (5), *Dodonea* (6), and *Schleichera* (7). The amounts reported were 4.2, 3.1, and 8.9% of the fatty acids respectively, but the acid was not identified further in these instances. The present work shows that the family includes at least one species in which 11-eicosenoic acid is a major component of the seed oil.

The fatty acids of *C. halicacabum* include also arachidic, linolenic, and a low-molecular-weight acid, as found by Covello (3) and confirmed here.* Arachidic acid is in rather large amount (10%), and the quantity of palmitic acid is correspondingly small. This is

**Covello made a careful identification of linolenic acid by converting it to hexabromo- and hexahydroxystearic acids. However, he did not report identification of linoleic acid. His later mention of linoleic acid (ref. 3, p. 783) is manifestly a typographical error and should read "linolenic acid".*

Can. J. Chem. Downloaded from www.nrcresearchpress.com by 78.46.186.204 on 09/04/12
For personal use only.

characteristic of Sapindaceae oils. There is an appreciable content of linolenic acid. Its presence and amount, about 8%, are unusual for an oil of iodine value below 100.

REFERENCES

1. CHISHOLM, M. J. and HOPKINS, C. Y. Can. J. Chem. **31**, 1131 (1953).
2. CHISHOLM, M. J. and HOPKINS, C. Y. Can. J. Chem. **34,** 459 (1956).
3. COVELLO, M. Ann. chim. (Rome), **41**, 780 (1951).
4. ECKEY, E. W. and MILLER, L. P. Vegetable fats and oils. Reinhold Publishing Corp., New York. 1954. p. 613.
5. HILDITCH, T. P. and STAINSBY, W. J. J. Soc. Chem. Ind. **53**, 197T (1934).
6. KOCHAR, R. K. and DUTT, S. Indian Soap J. **14**, 132 (1948).
7. WEERAKOON, A. H. Thesis, University of Liverpool. 1952.

Can. J. Chem. Downloaded from www.nrcresearchpress.com by 78.46.186.204 on 09/04/12
For personal use only.

Can. J. Chem. Downloaded from www.nrcresearchpress.com by 78.46.186.204 on 09/04/12
For personal use only.

GUANIDINE COMPOUNDS

II. PREPARATION OF MONO- AND N,N-DI-ALKYLGUANIDINES[1, 2]

R. A. B. Bannard, A. A. Casselman, W. F. Cockburn, and G. M. Brown

ABSTRACT

1-Guanyl-3,5-dimethylpyrazole nitrate is superior to S-methylisothiouronium sulphate as a reagent for preparation of simple salts of mono- and N,N-di-alkylguanidines from cyclohexylamine, *trans*-2-aminocyclohexanol, pyrrolidine, and piperidine. S-Methylisothiouronium sulphate, however, gave a higher conversion in the case of dimethylamine. Cyanamide is not as useful a guanylating agent as those mentioned above. The paper chromatography of the mono- and N,N-di-alkylguanidines and the parent amines was studied using four solvent systems.

INTRODUCTION

Of the numerous methods reported in the literature for preparation of mono- and N,N-di-alkylguanidines, those which have been used most frequently are the Erlenmeyer synthesis (1), from amine salts and cyanamide (2, 3, 4, 5, 6), and the Rathke synthesis (7), from amines and an alkylisothiouronium or alkylisouronium salt (8, 9, 10, 11, 12). Both methods, however, frequently lead to poor yields of alkylguanidines, due principally to the formation of dicyandiamide by dimerization of cyanamide on the one hand (13) or hydrolysis of the alkylisouronium salt on the other (8, 14). In 1953, Scott, O'Donovan, and Reilly (15) described the preparation of a number of guanidine picrates in high yield by reaction of amines with 1-guanyl-3,5-dimethylpyrazole nitrate (I) as shown below.

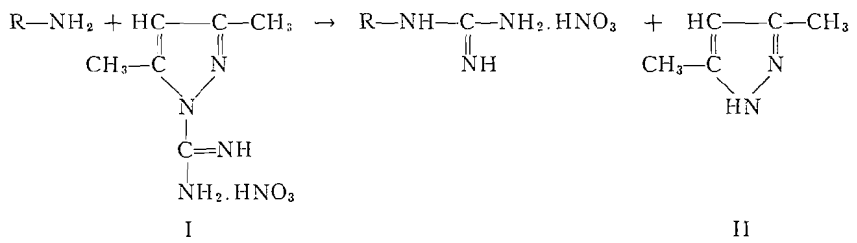

I II

The sole by-product was 3,5-dimethylpyrazole (II) and the method thus seemed a suitable candidate to replace the older methods of synthesis, provided that salts other than the picrates used (15) to simplify recovery of the alkylguanidines proved isolable in high yields. Since we required a number of alkylguanidines in connection with other studies, it seemed of interest to evaluate the usefulness of the three methods of synthesis.

RESULTS AND DISCUSSION

Several procedures for guanylation of amine salts with cyanamide in aqueous or alcoholic solution (2, 4, 5, 6) were examined but all of these in our hands gave yields of alkylguanidines in the range 0–20%. The only method found to be effective was a fusion technique due to Sugino *et al.* (16, 17), by which procedure cyclohexylguanidine hydrochloride was obtained in 48% yield. Guanylation of *trans*-2-aminocyclohexanol

[1]*Manuscript received July 23, 1958.*
Contribution from Defence Research Chemical Laboratories, Ottawa, Canada.
Issued as D.R.C.L. Report No. 284.
[2]*For Part I see ref. 27.*

hydrochloride in the same manner, however, gave an intractable mixture and the method was not studied further when it became evident that the other two processes under examination are more reliable.

For guanylation of amines with S-methylisothiouronium sulphate, Phillips and Clarke's procedure (8) was modified by using 1.5 equivalents of amine per equivalent of guanylating agent, this being the ratio of reactants best suited to facile recovery of the alkylguanidine salt in a high state of purity. Results obtained using several primary and secondary aliphatic or heterocyclic amines are given in Table I.

TABLE I

GUANYLATION OF AMINES

Amine	Product isolated	% Yield	
		Isothiouronium method[a]	Guanylpyrazole method[b]
Dimethylamine	N,N-Dimethylguanidine	89.0[c]	66.8[c, e]
Piperidine	1-Guanylpiperidine	65.4[c]	80.5[c, f]
Pyrrolidine	1-Guanylpyrrolidine	59.0[g]	80.0[c, g]
Cyclohexylamine	Cyclohexylguanidine	54.5[b]	84.8[c, f]
trans-2-Aminocyclohexanol	*trans*-2-Guanidocyclohexanol	47.6[c]	75.8[d, g]

[a]Solvent—aqueous amine, 1.5 equivalents of amine per equivalent of isothiouronium salt.
[b]10 mole amine per mole guanylpyrazole salt.
[c]Solvent—amine.
[d]Solvent—ethanol.
[e]Isolated as sulphate.
[f]Isolated as hydrochloride.
[g]Isolated as nitrate.

In the case of pyrrolidine, cyclohexylamine and *trans*-2-aminocyclohexanol separation of the guanidine sulphates from the amine sulphates formed as by-products proved troublesome. However, 1-guanylpyrrolidine and cyclohexylguanidine were readily isolated as the nitrate and hydrochloride respectively after treatment of the crude product with a strong anion exchange resin. This simple expedient did not succeed for purification of *trans*-2-guanidocyclohexanol sulphate, but for this purpose three methods proved satisfactory. A three-column ion exchange process gave a 70% recovery of *trans*-2-guanidocyclohexanol sulphate. Paper chromatography on seed-test paper (18) gave a 78% recovery but was not suitable on a preparative scale. In the most satisfactory method, the large difference in water solubility of the picrates was utilized, and after purification, *trans*-2-guanidocyclohexanol picrate was converted to the sulphate by ion exchange with an over-all recovery of 66%. It is of interest to note in this connection that Angyal and Warburton (19) were unable to convert picrates of alkylguanidines to simple salts. This observation explains our reluctance to estimate yields in guanylation reactions by conversion to the readily isoluble picrates as other workers have done (15) because we wished to obtain simple salts. The use of a strong anion exchange resin, however, now apparently assures reconversion of alkylguanidine picrates to simple salts in high yields.

For guanylation with 1-guanyl-3,5-dimethylpyrazole nitrate, procedures used by Scott, O'Donovan, and Reilly (15) were followed, but in all cases the alkylguanidines were isolated as simple salts rather than picrates. The results given in Table I make it evident that the guanylpyrazole method is clearly superior to the isothiouronium method except for preparation of N,N-dimethylguanidine sulphate. It seemed desirable to determine whether the large excess of amine employed by Scott *et al.* (15) could be

Can. J. Chem. Downloaded from www.nrcresearchpress.com by 78.46.186.204 on 09/04/12
For personal use only.

reduced to a more reasonable level without seriously impairing the yield of alkylguanidine. Accordingly, several modifications in procedure were used in guanylation of *trans*-2-aminocyclohexanol. Using ethanol as solvent, an intractable mixture resulted when equimolar quantities of reactants were used but a twofold excess of amine led to a 65% yield of *trans*-2-guanidocyclohexanol. The same substance was obtained in 56% yield when an intimate mixture of equimolar quantities of reactants was fused for 1 hour at 100°. The latter modification should prove of value for guanylation of difficultly accessible amines.

The possibility of using the Sakaguchi (20) alkaline hypochlorite – α-naphthol reaction or the Fearon (21) alkaline hypochlorite – thymol reaction to follow the appearance of guanido compounds in reaction mixtures has been examined. The Sakaguchi reaction, which is specific for monosubstituted guanidines (22), has been used for quantitative estimation of certain compounds and optimum conditions for these methods are quoted in the literature. However, these procedures are too time consuming and rapid qualitative methods for the Sakaguchi and Fearon tests are described in the experimental section. S-Methylisothiouronium sulphate, cyanamide, and dicyandiamide interfere with the color reactions and the tests are thus unsatisfactory for following the appearance of guanido compounds in reaction mixtures containing such contaminants. The Sakaguchi test is more satisfactory than the Fearon test, since the latter is both less sensitive and more subject to interference.

The paper chromatographic behavior of the mono- and N,N-di-alkylguanidines was studied in four solvent systems in relation to the behavior of the parent amines (or salts) and certain other substances containing a guanido group. The results summarized in Table II make it clear that for separation of alkylguanidines from the corresponding amines the two solvent systems containing *n*-butanol are superior but that for separation of the guanido acids the two systems containing *tert*-butanol are preferable.

TABLE II

R_F VALUES OF AMINES AND ALKYLGUANIDINES

Compound	R_F in solvent system*			
	1	2	3	4
N,N-Dimethylguanidine sulphate	0.22[a, b]	0.19	0.70	0.44
Dimethylamine hydrochloride	0.36	0.12	0.69	0.36
1-Guanylpyrrolidine nitrate	0.57	0.42	0.73	0.56
Pyrrolidine	0.51	0.21	0.74	0.48
1-Guanylpiperidine hydrochloride	0.65	0.44	0.76	0.70
Piperidine	0.59	0.27	0.77	0.55
trans-2-Guanidocyclohexanol nitrate	0.68[c]	0.47	0.78	0.72
trans-2-Aminocyclohexanol hydrochloride	0.55	0.35	0.73	0.60
Cyclohexylguanidine hydrochloride	0.80	0.60	0.83	0.84
Cyclohexylamine hydrochloride	0.73	0.50	0.81	0.82
L-Canavanine sulphate	0.05	0.02	0.09	0.16
L-Arginine	0.19	0.03	0.46	0.19
Guanidoacetic acid	0.25	0.13	0.50	0.42
α-Guanidopropionic acid	0.39	0.29	0.63	0.59
β-Guanidopropionic acid	0.41	0.21	0.66	0.52

*1. *n*-Butanol, acetic acid, water (25:6:25 v/v).
2. *n*-Butanol, 1% hydrochloric acid (5:6 v/v).
3. *tert*-Butanol, acetic acid, water (2:1:1 v/v).
4. *tert*-Butanol, 1% hydrochloric acid (3:1 v/v).

[a]All substances except canavanine gave a blue spot with bromcresol green.

[b]Weber reagent gave pink or purple spots with the guanidine compounds and a white spot with amines.

[c]Sakaguchi reagent gave a red or pink spot with monoalkylguanidines and a greenish yellow spot with canavanine.

Can. J. Chem. Downloaded from www.nrcresearchpress.com by 78.46.186.204 on 09/04/12
For personal use only.

Can. J. Chem. Downloaded from www.nrcresearchpress.com by 78.46.186.204 on 09/04/12
For personal use only.

EXPERIMENTAL[1, 2]

1-Guanyl-3,5-dimethylpyrazole Nitrate

Aminoguanidine nitrate (68.0 g, 0.500 mole) was added portionwise over a period of $1\frac{3}{4}$ hours to a refluxing solution of 2,4-pentanedione (50.0 g, 0.500 mole) in 50% aqueous ethanol (140 ml) and the resultant solution heated under reflux for $2\frac{1}{4}$ hours. The crystals which separated when the solution was allowed to stand overnight were collected, washed with ether, and dried *in vacuo*. Further crops were obtained by dilution of the filtrate with ether. Recrystallization of the combined crude substances (78.3 g) from ethanol gave 64.6 g (64.6%) of 1-guanyl-3,5-dimethylpyrazole nitrate as colorless prisms, m.p. 166–168°. Thiele and Dralle (23) report m.p. 168°. A small sample was converted to the picrate, which had m.p. 206–208.5° after recrystallization from ethanol (cf. Scott and Reilly (24)).

Aminoguanidine Nitrate

Aminoguanidine bicarbonate was converted to the nitrate salt and the crude product recrystallized from ethanol–ether. Yield, 94% m.p. 142–144°. Theile (25) reports m.p. 144°.

Cyanamide

Cyanamide obtained from the Eastman Kodak Co. was treated with anhydrous ether. The insoluble dicyandiamide was removed by filtration, and the filtrate was evaporated to dryness *in vacuo*, yielding colorless hygroscopic cyanamide, m.p. 40–41° (26).

Cyclohexylguanidine Hydrochloride

(*a*) *Guanylpyrazole method.*—1-Guanyl-3,5-dimethylpyrazole nitrate (2.01 g, 0.01 mole) and cyclohexylamine (9.92 g, 0.100 mole) were heated under reflux with mechanical stirring for $2\frac{1}{2}$ hours in a carbon-dioxide-free apparatus. The resultant pale yellow solution was evaporated to dryness *in vacuo* and the oily residue triturated with anhydrous ether (8×15 ml) to remove by-product 3,5-dimethylpyrazole. Attempts to crystallize the crude cyclohexylguanidine nitrate proved fruitless and the oily material (2.16 g) was dissolved in water (50 ml) and passed through Amberlite IRA-400 (Cl^-) resin. The resin was washed with water until the effluent gave a negative Sakaguchi test. The combined effluents were evaporated to dryness *in vacuo* and the colorless crystalline residue was recrystallized from ethanol, yielding 1.51 g (84.8%) of cyclohexylguandine hydrochloride as stout colorless needles, m.p. 228–229°. Calc. for $C_7H_{16}N_3Cl$: C, 47.32; H, 9.08; N, 23.65; Cl, 19.96%. Found: C, 47.56; H, 8.85; N, 23.40; Cl, 19.80%.

(*b*) *Isothiouronium method.*—Cyclohexylamine (14.9 g, 0.150 mole), S-methylisothiouronium sulphate (13.9 g, 0.050 mole), and water (40 ml) were mixed at 25° in a carbon-dioxide-free apparatus. On warming the mixture to 40°, brisk evolution of methyl mercaptan began and continued while the temperature was raised to 95° over a period of 3 hours and the isothiouronium salt dissolved. The colorless solution was heated under reflux for $2\frac{1}{2}$ hours, then evaporated to dryness *in vacuo*, yielding 19.0 g of colorless crystalline material. Since earlier preparations had demonstrated the difficulty of separating the cyclohexylguanidine sulphate from by-product cyclohexylamine sulphate, the crude product was converted to the corresponding mixed hydrochlorides via Amberlite IRA-400 (Cl^-) resin. The eluate from the ion-exchange process was

[1] *All melting points are uncorrected.*
[2] *Microanalyses by Micro-Tech Laboratories, Skokie, Ill., and G. J. Helie of these Laboratories.*

evaporated to dryness *in vacuo* and the crystalline residue recrystallized from ethanol, yielding 9.70 g (54.5%) of cyclohexylguanidine hydrochloride, m.p. 228–229° alone, and in admixture with an authentic sample.

(*c*) *Cyanamide fusion method.*—Cyanamide (3.15 g, 0.075 mole) and cyclohexylamine hydrochloride (6.80 g, 0.050 mole) were intimately mixed, placed in a round-bottomed flask equipped with a reflux condenser and thermometer, and the reaction vessel immersed in a mechanically stirred oil bath at 100°. The temperature of the bath was raised slowly* to 140°, at which temperature fusion of the mixture occurred, accompanied by evolution of white fumes. The temperature of the bath was held at 140–150° for 1 hour, and on cooling, the product solidified, forming a pale yellow glass. The glass was dissolved in glacial acetic acid (150 ml) and the solution was diluted with acetone to precipitate the product as a colorless solid. The latter was collected and recrystallized from ethanol yielding 4.30 g (48.4%) of stout colorless needles, m.p. 228–229° alone, and in admixture with an authentic specimen.

Cyclohexylamine Sulphate

Cyclohexylamine sulphate was obtained as by-product during preparation of cyclohexylguanidine sulphate (27) by interaction of cyclohexylamine and S-methylisothiouronium sulphate. After recrystallization from 80% aqueous ethanol it was obtained as colorless platelets, m.p. 343–346° (decomp.). Calc. for $C_{12}H_{28}N_2SO_4$: C, 48.62; H, 9.52; N, 9.45%. Found: C, 48.73; H, 9.60; N, 9.26%.

dl-trans-2-Guanidocyclohexanol Nitrate

(*a*) *Fusion method.*—A mixture of 1-guanyl-3,5-dimethylpyrazole nitrate (2.01 g, 0.010 mole) and *dl-trans*-2-aminocyclohexanol (28) (11.5 g, 0.100 mole) was heated at 100° for 2 hours with frequent agitation and exclusion of carbon dioxide. After cooling, the melt was transferred to a Soxhlet extractor and extracted with anhydrous ether for removal of the by-product 3,5-dimethylpyrazole and unreacted amine. The residue was recrystallized from acetone (25 ml), yielding 1.54 g (70.0%) of *dl-trans*-2-guanidocyclohexanol nitrate as fine colorless platelets, m.p. 137–139°. Calc. for $C_7H_{16}N_4O_4$: C, 38.19; H, 7.32; N, 25.44%. Found: C, 38.11; H, 7.34; N, 25.68%. A 57.5% recovery of the unreacted amine was obtained via isolation of the hydrochloride (28). The experiment was repeated under conditions identical with those described above except that equimolar quantities of reactants were used. Yield, 1.23 g (55.8%).

(*b*) *In ethanol.*—1-Guanyl-3,5-dimethylpyrazole nitrate (2.01 g, 0.010 mole) and *dl-trans*-2-aminocyclohexanol (11.5 g, 0.100 mole) were dissolved in ethanol (50 ml) and the solution was heated under reflux for 2 hours in a carbon-dioxide-free atmosphere. The solution was evaporated to dryness *in vacuo*, and the residue was purified as described in (*a*) above, yielding 1.67 g (75.8%) of *dl-trans*-2-guanidocyclohexanol nitrate, m.p. 137–139°. A 75.5% recovery of the unreacted amine was effected via the hydrochloride The experiment was repeated using a twofold excess of amine under otherwise the conditions specified above. Yield, 1.43 g (65.0%).

dl-trans-2-Guanidocylclohexanol Sulphate

dl-trans-2-Aminocyclohexanol (17.3 g, 0.150 mole), S-methylisothiouronium sulphate (13.9 g, 0.05 mole), and water (45 ml) were caused to react under the same conditions

**If the rate of temperature rise exceeds approximately 1° per minute as the fusion point is reached, the reaction becomes very exothermic, causing the temperature of the melt to rise to approximately 200°.*

Can. J. Chem. Downloaded from www.nrcresearchpress.com by 78.46.186.204 on 09/04/12
For personal use only.

described for preparation of cyclohexylguanidine hydrochloride. The resultant crude mixture of *dl-trans*-2-guanidocyclohexanol sulphate and *dl-trans*-2-aminocyclohexanol sulphate (21.4 g) was treated with boiling methanol (75 ml) and the insoluble crystalline platelets collected and washed with methanol (2×10 ml). This substance (5.35 g) was identified as *dl-trans*-2-aminocyclohexanol sulphate by paper chromatography. The methanolic filtrate was evaporated to dryness *in vacuo* and the resultant colorless solid triturated with anhydrous ether to remove unreacted *trans*-2-aminocyclohexanol. The insoluble material was recrystallized from methanol, yielding 14.9 g of colorless crystalline substance, m.p. 210–220°, which was shown by paper chromatography to be *dl-trans*-2-guanidocyclohexanol sulphate contaminated with a small amount of the corresponding amine sulphate. Purification via the picrate, followed by reconversion to the sulphate (see below), gave 9.80 g (54.4%) of *dl-trans*-2-guanidocyclohexanol sulphate, m.p. 223–224°, as fine colorless needles. Calc. for $C_{14}H_{32}N_6SO_6$: C, 40.76; H, 7.82; N, 20.38; S, 7.77%. Found: C, 40.96; H, 7.91; N, 19.86; S, 7.55%.

dl-trans-2-Guanidocyclohexanol Picrate

dl-trans-2-Guanidocyclohexanol nitrate was converted to the picrate in 74.5% yield, m.p. 163–165°, after recrystallization from water. Solubility, *ca.* 1.6 g/100 ml water at 4°. Calc. for $C_{13}H_{18}N_6O_8$: C, 40.41; H, 4.70; N, 21.76%. Found: C, 40.76; H, 4.82; N, 21.94%.

dl-trans-2-Aminocyclohexanol Sulphate

dl-trans-2-Aminocyclohexanol (28) was converted to the sulphate in 91.5% yield. After recrystallization from 90% ethanol the substance was obtained as colorless platelets which sintered at 265° but did not melt. Calc. for $C_{12}H_{28}N_2SO_6$: C, 43.88; H, 8.59; N, 8.53; S, 9.76%. Found: C, 44.04; H, 8.74; N, 8.24; S, 9.67%.

dl-trans-2-Aminocyclohexanol Picrate

dl-trans-2-Aminocyclohexanol was converted to the picrate in 73.5% yield, m.p. 153–155°, after recrystallization from water. Solubility *ca.* 15 g/100 ml water at 4°. Calc. for $C_{12}H_{16}N_4O_8$: C, 41.86; H, 4.68; N, 16.28%. Found: C, 41.96; H, 4.69; N, 16.32%.

Purification of dl-trans-2-Guanidocyclohexanol Sulphate Contaminated with dl-trans-2-Aminocyclohexanol Sulphate

(*a*) *Picrate separation method.*—Crude *dl-trans*-2-guanidocyclohexanol sulphate (2.74 g), m.p. 210–220°, from the isothiouronium process was converted to the picrate, yielding 3.72 g (72.4%) of *dl-trans*-2-guanidocyclohexanol picrate, m.p. 163–165°, alone and in admixture with an authentic specimen. A portion of the picrate (1.93 g, 0.0050 mole) was dissolved in methanol and passed through a column of Amberlite IRA-400 ($SO_4^=$) resin (20 ml) which had been prepared in the usual manner and solvent-exchanged with methanol. The resin was washed with water until the effluent gave a negative Sakaguchi test. The combined eluates were evaporated to dryness *in vacuo* and the residue was recrystallized from methanol, yielding 0.94 g (91.2%) of *dl-trans*-2-guanidocyclohexanol sulphate, m.p. 222–224° (recovery 66%).

(*b*) *Ion exchange method.*—An Amberlite IRA-400 (OH^-) resin column (60 ml) was connected in series to an Amberlite IRC-50 (H^+) column (9.5 ml). Crude *dl-trans*-2-guanidocyclohexanol sulphate (5.60 g), m.p. 210–220°, was dissolved in water (130 ml) and the solution passed through the resin columns. Just sufficient guanido compound was used to ensure a slight "breakthrough" of alkylguanidine from the IRC-50 column as revealed by the Sakaguchi test. The IRC-50 column was disconnected, and eluted with

Can. J. Chem. Downloaded from www.nrcresearchpress.com by 78.46.186.204 on 09/04/12
For personal use only.

5% hydrochloric acid. The eluate was evaporated to dryness *in vacuo*, the residue dissolved in water (50 ml), and the solution passed through an Amberlite IRA-400 ($SO_4^=$) column (60 ml). The eluate was evaporated to dryness *in vacuo* and the residue recrystallized from methanol, yielding 3.90 g (69.6%) of *dl-trans*-2-guanidocyclohexanol sulphate, m.p. 222–224°.

(*c*) *Paper chromatographic method.*—An 18½ in. × 22 in. sheet of Whatman seed-test paper was washed chromatographically with 0.1 *N* hydrochloric acid (3 days), with water (4 days), with *n*-butanol, 1% hydrochloric acid (5:6) (1 day), and finally with water (2 days). Crude *dl-trans*-2-guanidocyclohexanol, m.p. 210–220° (200 mg), was applied in aqueous solution (2%) as a streak on the start-line and the chromatogram was developed for 66 hours by the descending technique in a "Chromatocab" using the above-mentioned solvent system. After drying at 40° reference strips were cut from the chromatogram and sprayed with Sakaguchi reagent. The band of alkylguanidine was marked, cut out, eluted with water (100 ml), and treated with Amberlite IRA-400 ($SO_4^=$) resin to reconvert to the sulphate. The solution was evaporated to dryness *in vacuo* and the residue was recrystallized from methanol, yielding 157 mg (78%) of *dl-trans*-2-guanidocyclohexanol sulphate, m.p. 223–224°.

1-Guanylpyrrolidine Nitrate

(*a*) *Guanylpyrazole method.*—1-Guanyl-3,5-dimethylpyrazole nitrate (10.0 g, 0.0497 mole) and pyrrolidine (35.5 g, 0.498 mole) were heated under reflux for 2½ hours in a carbon-dioxide-free atmosphere. The product was isolated as described for the preparation of cyclohexylguanidine hydrochloride, except that 1-guanylpyrrolidine nitrate proved readily crystallizable from ethanol and was obtained as stout colorless prisms, m.p. 157–157.5°. Yield, 7.00 g (80.0%). Calc. for $C_5H_{12}N_4O_3$: C, 34.09; H, 6.87; N, 31.80%. Found: C, 34.20; H, 6.95; N, 32.10%.

(*b*) *Isothiouronium method.*—Pyrrolidine (10.7 g, 0.150 mole), S-methylisothiouronium sulphate (13.9 g, 0.05 mole), and water (40 ml) were caused to react under the conditions described for preparation of cyclohexylguanidine hydrochloride. The colorless mixture of 1-guanylpyrrolidine sulphate and pyrrolidine sulphate resulting from the evaporation step was dissolved in water (650 ml), the solution passed through Amberlite IRA-400 (NO_3^-) resin, and the latter washed with water until the effluent gave a negative Weber test (29). The combined eluates were evaporated to dryness *in vacuo* and the colorless residue recrystallized from ethanol, yielding 10.4 g (59.0%) of 1-guanylpyrrolidine nitrate as stout colorless prisms, m.p. 157–157.5° alone and in admixture with an authentic specimen.

1-Guanylpiperidine Hydrochloride

1-Guanyl-3,5-dimethylpyrazole nitrate (2.01 g, 0.010 mole) and piperidine (8.52 g, 0.100 mole) were caused to react under the conditions described for preparation of cyclohexylguanidine hydrochloride and the product was isolated as described in the same preparation, since the nitrate salt of 1-guanylpiperidine did not prove to be readily crystallizable. Recrystallization from ethanol–acetone gave 1.32 g (80.5%) of 1-guanylpiperidine hydrochloride as fine colorless needles, m.p. 187–188.5°. Calc. for $C_6H_{14}N_3Cl$: C, 44.03; H, 8.62; N, 25.68; Cl, 21.67%. Found: C, 44.22; H, 8.74; N, 25.18; Cl, 21.63%.

1-Guanylpiperidine Sulphate

Piperidine (12.8 g, 0.150 mole), S-methylisothiouronium sulphate (13.9 g, 0.05 mole), and water (40 ml) were caused to react under the conditions specified for preparation of

Can. J. Chem. Downloaded from www.nrcresearchpress.com by 78.46.186.204 on 09/04/12
For personal use only.

cyclohexylguanidine hydrochloride. Recrystallization of the crude product from 75% aqueous alcohol gave 11.5 g (65.4%) of 1-guanylpiperidine sulphate, as colorless stout prisms, m.p. 284–287° (decomp.). Calc. for $C_{12}H_{28}N_6SO_4$: C, 40.90; H, 8.01; N, 23.85%. Found: C, 40.80; H, 7.98; N, 24.15%. The mother liquor, on treatment with saturated aqueous picric acid gave 5.4 g of piperidine picrate, m.p. 152–153° alone and in admixture with an authentic sample.

N,N-Dimethylguanidine Sulphate

(*a*) *Guanylpyrazole method.*—1-Guanyl-3,5-dimethylpyrazole nitrate (2.01 g, 0.010 mole) and dimethylamine (18 g, 25% aqueous solution, 0.100 mole) were heated under reflux for 8 hours in a carbon-dioxide-free atmosphere, using a dry-ice condenser to prevent loss of dimethylamine. The sticky nitrate resulting from evaporation of the solution *in vacuo* was dissolved in water and converted to the sulphate via IRA-400 ($SO_4^=$) resin. Recrystallization of the crude sulphate from methanol gave 0.91 g (66.8%) of N,N-dimethylguanidine sulphate, as fine colorless crystals, m.p. 272–275°. Calc. for $C_6H_{20}N_6SO_4$: C, 26.46; H, 7.40; N, 30.86; S, 11.77%. Found: C, 26.17; H, 7.38; N, 30.67; S, 11.77%.

(*b*) *Isothiouronium method.*—To a suspension of S-methylisothiouronium sulphate (62.5 g, 0.225 mole) in water (75 ml) at 25° was added a solution of dimethylamine (122 g, 25% aqueous, 0.675 mole) in one portion. A mildly exothermic reaction occurred during which the isothiouronium salt dissolved, methyl mercaptan was evolved, the temperature rose to 35°, and loss of dimethylamine was prevented by use of a dry-ice condenser. The solution was heated under reflux for 30 minutes, then evaporated to dryness *in vacuo*, and the residue recrystallized from methanol, yielding 56.4 g, (89.0%) of N,N-dimethylguanidine sulphate, m.p. 272–275° alone, and in admixture with an authentic sample.

Sakaguchi Test for Monoalkylguanidines

For qualitative testing, the guanido compound in 1 ml of water was treated with the following reagents, in the order named, with thorough shaking between each addition. Sodium hydroxide (10% aqueous), 4 drops; α-naphthol solution (0.1% w/v in 95% ethanol), 6 drops; sodium hypochlorite (0.06 *N*, aqueous), 6 drops. The test is positive when the solution develops a pink, red-orange, or cherry-red color within 1 minute. The minimum quantity of cyclohexylguanidine detectable by the method was 5 γ. If more than 6 drops of α-naphthol or sodium hypochlorite solution are used, a yellow "blank" develops which does not interfere with the test.

Fearon Test for Monoalkylguanidines

The procedure was identical with that described for the Sakaguchi test except that it was necessary to use 12 drops of the thymol indicator (0.1% w/v in 95% ethanol). The test is positive when a golden yellow color develops within 1 minute. Three isomeric thymols were tested for usefulness as detectors. Thymol and *o*-thymol were capable of detecting 50 γ of cyclohexylguanidine hydrochloride but *p*-thymol (30) was capable of detecting only 0.5 mg or more of the same substance.

Inhibition of Sakaguchi and Fearon Tests

Cyanamide, dicyandiamide, and S-methylisothiouronium sulphate interfere with the Sakaguchi and Fearon tests. Cyanamide gives colored "blanks" (purple to Burgundy red) at concentrations greater than 0.3 mg/ml, and below this concentration 0.6 *N* hypochlorite must be used to obtain a positive reaction. S-Methylisothiouronium sulphate and dicyandiamide do not give colored blanks but their presence in concentrations

Can. J. Chem. Downloaded from www.nrcresearchpress.com by 78.46.186.204 on 09/04/12
For personal use only.

greater than 0.3 mg/ml necessitates the use of 0.6 *N* hypochlorite. Solutions containing more than 3 mg/ml of S-methylisothiouronium sulphate will not give a positive test if the concentration of guanido compound is less than 50 γ/ml.

Paper Chromatography of Amines and Guanidine Compounds

For paper chromatography, a 10 λ spot of a 2% aqueous solution of the amine or guanidine compound was applied to unwashed Whatman No. 1 paper. The chromatograms were developed for 18 hours in glass chromatographic tanks by the descending technique, using the solvent systems specified in Table II. The air-dried chromatograms were then sprayed with bromcresol green, Weber (29), or Sakaguchi reagent for detection of the substances.

REFERENCES

1. ERLENMEYER, E. Ann. **146**, 258 (1868).
2. BRAUN, C. E. J. Am. Chem. Soc. **55**, 1280 (1933).
3. KING, H. and TONKIN, I. M. J. Chem. Soc. 1063 (1946).
4. ODO, K. J. Chem. Soc. Japan, Pure Chem. Sect. **71**, 394 (1950).
5. LAWSON, A. J. Chem. Soc. 307 (1956).
6. PADEN, J. H. and MCLEAN, A. F. U. S. Pat. No. 2,425,341 (1947).
7. RATHKE, B. Ber. **14**, 1774 (1881); **17**, 297 (1884).
8. PHILLIPS, R. and CLARKE, H. T. J. Am. Chem. Soc. **45**, 1755 (1923).
9. KAPFHAMMER, J. and MULLER, H. Z. physiol. Chem. **255**, 1 (1934).
10. BRAND, E. and BRAND, F. C. Org. Syntheses, **22**, 59 (1942).
11. KURTZ, A. C. J. Biol. Chem. **180**, 1253 (1949).
12. MOURGUE, M. Bull. soc. chim. France, 181 (1948).
13. TAYLOR, T. W. J. and BAKER, W. *In* Sidgwick's organic chemistry of nitrogen. Oxford University Press, London. 1937. p. 329.
14. SCHÖBERL, A. and WAGNER, A. *In* Methoden der organischen Chemie. *Edited by* E. Müller, Georg. Theime Verlag, Stuttgart. 1955. p. 14.
15. SCOTT, F. L., O'DONOVAN, D. G., and REILLY, J. J. Am. Chem. Soc. **75**, 4053 (1953).
16. SUGINO, K., SJIRAI, K., and AOYAGI, K. Bull. Chem. Soc. Japan, **17**, 126 (1942).
17. ODO, K. and SUGINO, K. J. Chem. Soc. Japan, **63**, 336 (1942).
18. BROWNELL, H. H., HAMILTON, J. G., and CASSELMAN, A. A. Anal. Chem. **29**, 550 (1957).
19. ANGYAL, S. J. and WARBURTON, W. K. J. Chem. Soc. 2492 (1951).
20. SAKAGUCHI, S. J. Biochem. Tokyo, **5**, 13, 25 (1925).
21. FEARON, W. R. Sci. Proc. Roy. Dublin Soc. **22**, 415 (1941).
22. MOLD, J. D., LADINO, J. M., and SCHANTZ, E. J. J. Am. Chem. Soc. **75**, 6321 (1953).
23. THIELE, J. and DRALLE, E. Ann. **302**, 275 (1898).
24. SCOTT, F. L. and REILLY, J. J. Am. Chem. Soc. **74**, 4652 (1952).
25. THIELE, J. Ann. **270**, 1 (1892).
26. MIGRDICHIAN, V. The chemistry of organic cyanogen compounds. Reinhold Publishing Corp., New York. 1947. p. 15.
27. COCKBURN, W. F. and BANNARD, R. A. B. Can. J. Chem. **35**, 1285 (1957).
28. HAWKINS, L. R. and BANNARD, R. A. B. Can. J. Chem. **36**, 220 (1958).
29. WEBER, C. J. J. Biol. Chem. **78**, 465 (1948).
30. BANNARD, R. A. B. and LEITCH, L. C. Can. J. Chem. **34**, 1464 (1956)

Can. J. Chem. Downloaded from www.nrcresearchpress.com by 78.46.186.204 on 09/04/12
For personal use only.

Can. J. Chem. Downloaded from www.nrcresearchpress.com by 78.46.186.204 on 09/04/12
For personal use only.

THE CHEMISTRY OF THE "AMINOCHROMES"

PART II. THE PREPARATION, PAPER CHROMATOGRAPHY, AND SPECTROSCOPIC PROPERTIES OF PURE ADRENOLUTIN; THE INFRARED SPECTRUM OF ADRENOCHROME[1,2]

R. A. Heacock and (in part) M. E. Mahon

ABSTRACT

The preparation of adrenolutin monohydrate in pure crystalline form has been carried out by the alkaline rearrangement of aqueous solutions of adrenochrome, prepared from the silver oxide oxidation of adrenaline in aqueous solution. An anion-exchange resin (Dowex-1 (Cl^-)) was employed to remove inorganic contaminants from the reaction mixture prior to treatment with alkali. The pure anhydrous material has been prepared by the high vacuum sublimation of the monohydrate. The paper chromatographic, spectroscopic, and fluorimetric characteristics of adrenolutin have been investigated. On the basis of the infrared spectrum it is suggested that in the solid state, adrenolutin exists in the keto form, i.e. 2,3-dihydro-5,6-dihydroxy-*N*-methyl-3-ketoindole. The infrared spectrum of adrenochrome, in the solid state, agrees with the zwitterionic formulation suggested for this compound.

Adrenolutin (usually formulated as 3,5,6-trihydroxy-*N*-methylindole, I), the substance mainly responsible for the intense yellow-green fluorescence that develops in adrenaline solutions that have undergone oxidation in alkaline media, was first isolated in crystalline form and correctly identified by Lund in 1949 (1), from the alkaline rearrangement products of adrenochrome (II), although the correct structure had been assigned to the substance on theoretical grounds a year earlier (Ehrlen (2)).

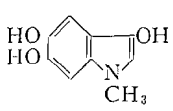

I

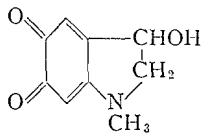

II

The structure was subsequently confirmed by an unambiguous synthesis starting from 3,4-isopropylidenedioxyaniline (Balsiger *et al.* (3)).

The preparation of adrenolutin from adrenaline oxidized with potassium ferricyanide in aqueous bicarbonate buffer, followed by rearrangement with aqueous sodium hydroxide and acidification (4), gave, in our hands, somewhat variable results, and good yields of pure product could not be consistently obtained. It appeared that the product was contaminated with inorganic residues from the oxidation mixture which probably catalyzed its decomposition. It has recently been shown that adrenochrome prepared by the oxidation of adrenaline with silver oxide was often contaminated with traces of silver, and that this contamination could be minimized by passage of the reaction mixture through an ion-exchange resin (Dowex-1 (Cl^-)) prior to isolation of the products (5). The use of this procedure to remove contaminants from adrenochrome solutions has now been extended to the preparation of adrenolutin, and gave consistently good yields of adrenolutin monohydrate in a pure crystalline form. Although the water of crystallization could be removed by drying in a vacuum desiccator, the anhydrous material was always obtained as an

[1]*Manuscript received July 21, 1958.*
Contribution from the Psychiatric Research Unit, University Hospital, Saskatoon, Saskatchewan. This investigation was supported by grants from the Federal Department of Health and Welfare, and the Rockefeller Foundation. This work was carried out under the auspices of the Saskatchewan Committee on Schizophrenia Research.
[2]*Part I—Can. J. Chem.* **36**, *853 (1958).*

amorphous brownish-green powder. However high vacuum sublimation of the hydrate gave anhydrous adrenolutin in an analytically pure form as a bright yellow crystalline solid.

The paper chromatographic behavior of this substance has already been referred to in Part I of this series (5), and the present investigation has confirmed that the use of acid-washed chromatographic paper is essential when working with adrenolutin, since traces of heavy metals and other impurities present in unwashed papers catalyze the air oxidation of adrenolutin, and on unwashed paper only dark streaks of polymeric oxidation products were observed. The best solvents for paper chromatography appeared to be water ($R_f = 0.45$) or methanol ($R_f = 0.60$). These R_f values were obtained on prewashed Whatman No. 1 paper; a somewhat lower value was observed with water on Whatman No. 54 paper. Acidic solvents caused the characteristic yellow-green fluorescence of the compound to change to a pale pinkish-orange color; alkaline solvents were quite unsuitable and caused its rapid decomposition.

The ultraviolet and visible absorption spectra obtained from samples of adrenolutin prepared as described above corresponded well with those previously published (1). The fluorescence characteristics of this substance are of considerable importance, since they have been utilized for many years in empirical methods for the estimation of adrenaline (cf. Persky (6)). The current investigation has shown that there are slight variations in the maximum wavelengths of excitation and fluorescence depending on the solvent used. The highest intensity of fluorescence emission appeared to occur when acetone was used as solvent, with excitation at 405 mμ and the fluorescence measured at 490 mμ. In alkaline solution the molecule existed in the phenoxide ion form and in this case the maximum emission was observed at 515 mμ after excitation at 405 mμ (cf. 7).

The infrared spectra of anhydrous and hydrated adrenolutin and 3,5,6-triacetoxy-*N*-methylindole ("triacetyladrenolutin") were measured in the solid state ("NUJOL" mulls). In the spectrum of the anhydrous compound, the peak at 3360 cm^{-1} was probably due to a hydrogen-bonded hydroxyl group (cf. 8, p. 84). The high-frequency region of the spectrum of the hydrate was more complicated; peaks were observed at 3480 and 2650 cm^{-1} and there were two shoulders on the "NUJOL" (C–H stretching) peak, at 3250 and 3100 cm^{-1}. These bands must presumably have arisen from the hydrogen-bonded phenolic O–H groups and the water of crystallization. It has recently been demonstrated spectroscopically that in the solid state, and in solution in chloroform and carbon disulphide certain indoxyl derivatives exist in the keto form (10). The sharp peak at 1647 cm^{-1} in the spectrum of the anhydrous compound was at a considerably lower frequency than those previously quoted for indoxyl carbonyls, both in chloroform solution and in the solid state (i.e. 1750–1710 cm^{-1}; 9, 10). However, the hydroxy groups at the 5- and 6-positions in the benzene ring would be expected to reduce the carbonyl frequency, e.g. the carbonyl stretching frequency of *p*-hydroxyacetophenone occurs at 1636 cm^{-1} in the solid state ("NUJOL" mull) and at 1653 cm^{-1} in chloroform (concentrated solution), whereas in acetophenone itself the carbonyl frequency occurs at 1686 cm^{-1} (pure liquid) (8, p. 120; 11), and this frequency is further reduced by the presence of a second hydroxy group in the benzene ring (12). Therefore, in the solid state, anhydrous adrenolutin probably exists in the keto form (III) (i.e. 2,3-dihydro-5,6-dihydroxy-*N*-methyl-3-ketoindole). In the case of the hydrate the spectrum in the "1700–1600 cm^{-1}" region was somewhat complicated, and the band at 1647 cm^{-1} was not observed, however, there were shoulders at 1632, 1610, and 1595 cm^{-1} on a main peak at 1575 cm^{-1}, but in this case no assignment of bands can be made with any degree of certainty. The triacetate exhibited well-defined bands at

Can. J. Chem. Downloaded from www.nrcresearchpress.com by 78.46.186.204 on 09/04/12
For personal use only.

1762 and 1740 cm^{-1}, the former being due to the 5,6-diacetoxy groups and the latter to the 3-acetoxy group (cf. Holt *et al.* (10)). Several attempts to measure the infrared

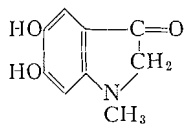

III

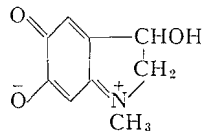

IV

spectrum of adrenochrome by the potassium bromide disk technique were unsuccessful, leading only to an ill-defined spectrum without very sharp peaks. It appeared that some decomposition and possibly some isomerization (to adrenolutin) had taken place during the preparation of the disk. However perfectly satisfactory spectra could be obtained from suspensions in "NUJOL". The results obtained can best be interpreted on the grounds of the zwitterionic structure (IV), suggested by Harley-Mason (13). There was an O–H stretching band at 3295 cm^{-1}, and in the "carbonyl region", the main band occurs at 1577 cm^{-1}; this was probably due to the $>C=\bar{O}$ group (cf. the strong band of the ionized carboxyl group occurs in this region (8); the bands at 1682, 1672, and 1622 cm^{-1} could be tentatively assigned to the $>C=\overset{+}{N}<$, $>C=O$ and the conjugated double bonds of the six-membered ring. The spectra of 2-iodoadrenochrome and six other "aminochromes" (14) were essentially the same as that of adrenochrome, indicating that all these compounds exist in the dipolar form.

EXPERIMENTAL

Preparation of Adrenolutin Monohydrate

L-Adrenaline (5.0 g) was suspended in water (150 ml) and concentrated hydrochloric acid added dropwise until a clear solution was obtained. Freshly prepared silver oxide (20.0 g) was added portionwise to the stirred solution and the stirring continued for 2 minutes. The reaction mixture was filtered through a Dowex-1 (Cl^-) (200/400 mesh) resin bed (diam. = 6.5 cm; height = 1.5 cm)* and the filtrate cooled in ice. A stream of nitrogen was passed through the filtrate, cooled in an ice bath, and 10% sodium hydroxide solution (50 ml) added. The brownish-yellow solution, which exhibited a brilliant green fluorescence, was stirred and acidified by the dropwise addition of glacial acetic acid; adrenolutin monohydrate was precipitated as a bright yellow crystalline solid (3.25 g), m.p. 232–235° with decomposition. (Found: C, 54.94; H, 5.56. Calc. for $C_9H_{11}O_4N$: C, 54.82; H, 5.62.) The product, which was dried at room temperature in a current of nitrogen, could be recrystallized from water (containing a small quantity of sodium hydrosulphite to prevent oxidation) and obtained in bright yellow prisms, m.p. 236° with decomposition.

Preparation of (Anhydrous) Adrenolutin

Adrenolutin monohydrate (0.1 g) was sublimed at 180–200°/3 mm and anhydrous adrenolutin was obtained in bright yellow prisms, m.p. 245° with decomposition. (Found: C, 60.59; H, 4.90. Calc. for $C_9H_9O_3N$: C, 60.33; H, 5.06.) Neither of these products showed any tendency to decolorize if stored at room temperature in the dry state.

**The resin was prepared by extensive washing with (1) 3 N hydrochloric acid and (2) water until neutral to litmus.*

Can. J. Chem. Downloaded from www.nrcresearchpress.com by 78.46.186.204 on 09/04/12
For personal use only.

Harley-Mason quotes melting points of 230–232° and 285°* for the monohydrate and anhydrous material respectively (4, 15). Lund states that the substance he isolated decomposes above 100° without melting (1); Balsiger *et al.*, quote melting point 195°* (anhydrous substance) (3), whilst Fischer obtained a melting point of 230–235° for the hydrate (16).

Paper Chromatography of Adrenolutin

Either Whatman No. 1 paper (washed with 2% acetic acid for 12 hours and dried prior to use) or Whatman No. 54 paper was used. Both the ascending and descending techniques were employed, each method gave approximately the same R_f values; *ca.* 20 to 30 μg of sample were applied to the paper in each case. The solvent was allowed to run a distance of *ca.* 35 cm. The solvents employed, namely water, 2% acetic acid, and methanol all ran very quickly and 2.5 to 3.5 hours were usually required for each run. The results obtained are given in Table I. Since adrenolutin is bright yellow in color its position on the developed chromatogram was usually self-indicating, however, the position of the spot could be confirmed as follows: (*a*) it showed a characteristic intense yellow-green fluorescence in ultraviolet light; (*b*) it gave a blue color with the ferric chloride – potassium ferricyanide reagent (cf. 5); (*c*) a violet color slowly developed after spraying with Ehrlich's reagent; (*d*) Gibb's reagent (*N*-2,6-trichloro-*p*-quinoneimine) gave a brown spot.

TABLE I

PAPER CHROMATOGRAPHIC CHARACTERISTICS OF ADRENOLUTIN

Solvent system	Water	2% Acetic acid in water*	Methanol
R_f of adrenolutin on:			
(*a*) Prewashed Whatman No. 1 paper	0.45±0.03	0.48±0.02	0.60±0.01
(*b*) Whatman No. 54 paper	0.35±0.01	0.43±0.03	0.60±0.02

*In acidic solvents the adrenolutin spot exhibited a pinkish-orange fluorescence.

Spectroscopic Studies on Adrenolutin, Adrenochrome, and Some Related Compounds

(*a*) *The ultraviolet and visible absorption spectra* of adrenolutin were measured on freshly prepared aqueous solutions (10 μg/ml) using a Beckman DU spectrometer (λ_{max}: 255, 285, 410 mμ; λ_{min}: 239, 272, 340 mμ).

(*b*) *The spectrophotofluorimetric characteristics* of adrenolutin were determined on a Farrand Spectrophotofluorimeter. Solutions of the anhydrous substance (10 μg/ml) in the various solvents were prepared immediately before use and the combination of wavelengths of excitation and emission giving the maximum intensity of fluorescence recorded. The results obtained are given in Table II. (The measurements were always

TABLE II

FLUORESCENCE CHARACTERISTICS OF ADRENOLUTIN SOLUTIONS[1] IN VARIOUS SOLVENTS

Solvent	Excitation maximum (wavelength, mμ)	Fluorescence maximum (wavelength, mμ)	Intensity of fluorescence (arbitrary units)
Methanol	405	490	2000
Distilled water	410	505	1400
0.01 *N* Aqueous sodium hydroxide	405	515	2400
0.01 *N* Aqueous acetic acid	405	500	1000
Acetone	405	490	3400

[1]Concentration of 10 μg/ml.

* = *with decomposition.*

Can. J. Chem. Downloaded from www.nrcresearchpress.com by 78.46.186.204 on 09/04/12
For personal use only.

made on freshly prepared solutions owing to the ease with which they undergo oxidative decomposition.)

(*c*) *The infrared spectra* of: anhydrous adrenolutin, adrenolutin monohydrate, 3,5,6-triacetoxy-*N*-methylindole (14), adrenochrome (5), and 2-iodoadrenochrome (17) were measured as "NUJOL" mulls on a Perkin–Elmer model 21 infrared spectrophotometer using a sodium chloride prism. The first two compounds were prepared as described above and the others were obtained by the methods described in the literature. The main absorption bands observed in three spectral regions are given in Table III.

TABLE III

MAIN ABSORPTION PEAKS IN SPECTRAL REGION INDICATED (IN cm^{-1})

Compound	A	B	C
Anhydrous adrenolutin	3360 (m) 3100 (m)	1647 (s) 1600 (m, sh) 1570 (s) 1545–1530 (s)	880 (m) 855 (w) 820 (w)
Adrenolutin monohydrate	3480 (m) 3250 (m, sh) 3100 (m, sh) 2650 (m, sh)	1632 (m/s, sh) 1610 (s, sh) 1595 (s, sh) 1575 (s) 1535–1525 (s) 1508 (s)	855 (m) 825 (m)
3,5,6-Triacetoxy-*N*-methylindole	—	1762 (s) 1740 (s) 1632 (w) 1547 (w)	870 (m) 854 (w) 812 (m)
Adrenochrome	3295 (m)	1682 (m/s) 1672 (m, sh) 1622 (m) 1575 (s)	900 (w) 817 (m)
2-Iodoadrenochrome	3420 (m)	1674 (m/s) 1657 (w, sh) 1612 (m) 1562 (s)	871 (m)

A = 4000–2500 cm^{-1}; B = 1800–1500 cm^{-1}; C = 900–800 cm^{-1}.
(s) = strong; (m) = medium; (w) = weak; (sh) = shoulder.

ACKNOWLEDGMENTS

The authors wish to express their thanks to Dr. A. N. Payza of this department for some useful discussion, and to Dr. R. N. Jones and Mr. R. Lauzon of the National Research Council (Ottawa) for assistance in obtaining the infrared spectrum of adrenochrome, and for some helpful suggestions on its interpretation.

REFERENCES

1. LUND, A. Acta Pharmacol. Toxicol. **5**, 75, 121 (1949).
2. EHRLEN, I. Farm. Revy, **47**, 242 (1948).
3. BALSIGER, R. W., FISCHER, R. W., HIRT, R., and GIOVANNINI, E. Helv. Chim. Acta, **36**, 708 (1953).
4. BU'LOCK, J. and HARLEY-MASON, J. J. Chem. Soc. 712 (1951).
5. HEACOCK, R. A., NERENBERG, C., and PAYZA, A. N. Can. J. Chem. **36**, 853 (1958).
6. PERSKY, H. Methods of Biochem. Anal. **2**, 57 (1955).
7. COHEN, G. and GOLDENBERG, M. J. Neurochem. **2**, 58 (1957).
8. BELLAMY, L. J. The infrared spectra of complex molecules. Methuen & Co. Ltd., London. 1954.
9. WITKOP, B. and PATRICK, J. B. J. Am. Chem. Soc. **73**, 713 (1951).
10. HOLT, S. J., KELLIE, A. E., O'SULLIVAN, D. G., and SADLER, P. W. J. Chem. Soc. 1217 (1958).
11. SOLOWAY, A. H. and FRIESS, S. L. J. Am. Chem. Soc. **73**, 5000 (1951).
12. SCROCCO, M. and LIBERTI, A. Ricerca sci. **24**, 1687 (1954).
13. HARLEY-MASON, J. Experientia, **4**, 307 (1948).
14. HEACOCK, R. A. Unpublished observations.
15. HARLEY-MASON, J. J. Chem. Soc. 1276 (1950).
16. FISCHER, P. Bull. soc. chim. Belges, **58**, 205 (1949).
17. SOBOTKA, H. and AUSTIN, J. J. Am. Chem. Soc. **73**, 3077 (1951).

Can. J. Chem. Downloaded from www.nrcresearchpress.com by 78.46.186.204 on 09/04/12
For personal use only.

Can. J. Chem. Downloaded from www.nrcresearchpress.com by 78.46.186.204 on 09/04/12
For personal use only.

THE ELECTRICAL POLARIZATIONS OF *BIS*-MERCURIALS[1]

HENRY SAWATZKY AND GEORGE F WRIGHT

ABSTRACT

Very dilute solutions of diphenylmercury in carbon tetrachloride have been found not to have orientation polarization, but in not-so-dilute carbon tetrachloride or in dioxane and benzene at any concentration there is evidence of moment. Moreover, these moments vary negatively in carbon tetrachloride and dioxane and positively in benzene with respect to temperature. The angular C–Hg–C linkage responsible for orientation polarization is also demonstrated by appreciable moments for para methylmercuri-*bis*-benzene and the homologous durene. Magnitudes comparable with the aryl analogues are found for several alkyl *bis*-mercurials, but the similarity in the moments of trifluoromethyl and methyl-*bis*-mercury as well as a temperature coefficient for moment of the latter compound indicates that the C–Hg–C linkage may vary widely and easily. However, a lower limit may be set by the moments of mercuracyclohexane and mercuracycloheptane in which the mercury angle is fixed by the cyclic structure.

INTRODUCTION

For several decades the electrical polarization of diphenylmercury has seemed to be anomalous. Originally Bergmann and Schütz found the solute polarization in benzene to be 64 cc at 14.15° and concluded that it was due entirely to electronic polarization (1). Later Hampson (2) found the polarization to be 68.8 cc at 25° in benzene. Since this value exceeded the electronic polarization, and since greater deviations from electronic polarization were found for a number of *p*-disubstituted analogues of diphenylmercury, Hampson concluded that the C–Hg–C bond was angular in these substances. Others, and most recently Armstrong, LeFevre, and LeFevre (3), consider that the data may be better interpreted in terms of abnormal atom polarization. However, a direct measurement (4) has shown that diphenylmercury has a distortion polarization which actually

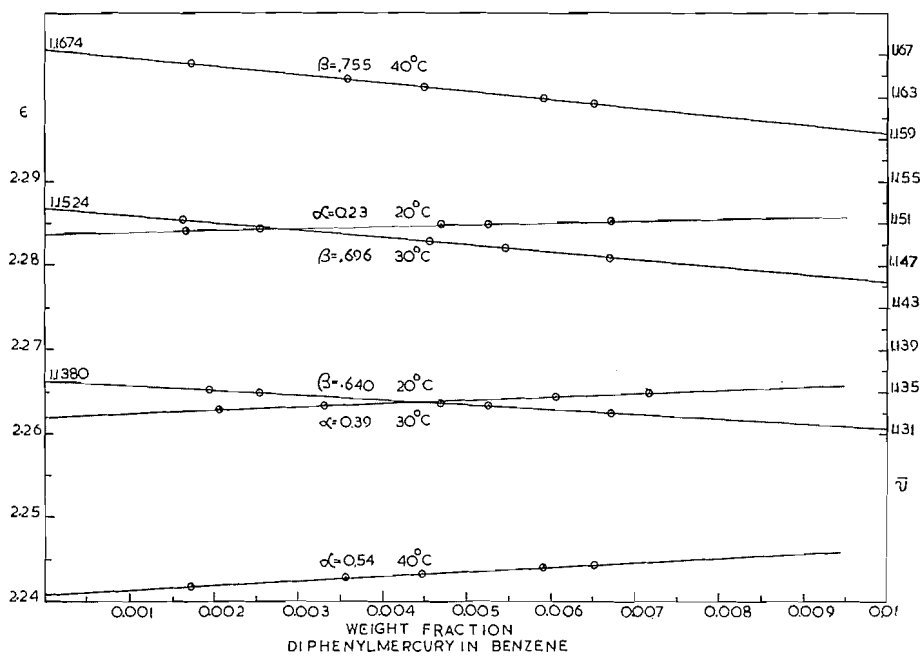

FIG. 1.

[1]*Manuscript received May 1, 1958.*
Contribution from the Department of Chemistry, University of Toronto, Toronto, Ontario, Canada.

is lower than that calculated from refractometric data. In view of this anomalous situation we have now examined a wider variety of *bis*-mercurials and of conditions under which the polarization is determined.

Diphenylmercury

The variation of electric polarization with respect to solvent, concentration, and temperature is shown in Table I. It may be seen in Fig. 1 that in benzene the relationship of both specific volume and dielectric constant is linear with respect to weight fraction even at concentrations less than 0.002, and extrapolation conforms closely with the values for the pure solvent. This seemingly normal behavior is belied by the augmentation of apparent moment as the temperature is increased from 20° to 40° (Table I). By contrast the apparent moment in dioxane (in which equally good linearity and extrapolation of $\delta\epsilon/\delta\omega$ and $\delta\bar{V}/\delta\omega$ have been observed) has shown a diminution as the temperature has been increased. Likewise with weight fractions (ω) of 0.005 to 0.01 it may be seen (Fig. 2) that the apparent moment in carbon tetrachloride decreases as the temperature rises from 20° to 40°. These variations have been plotted in Fig. 3. It is of interest that these curves (which might be straight lines within the ±0.01 D precision) intersect at about 25°.

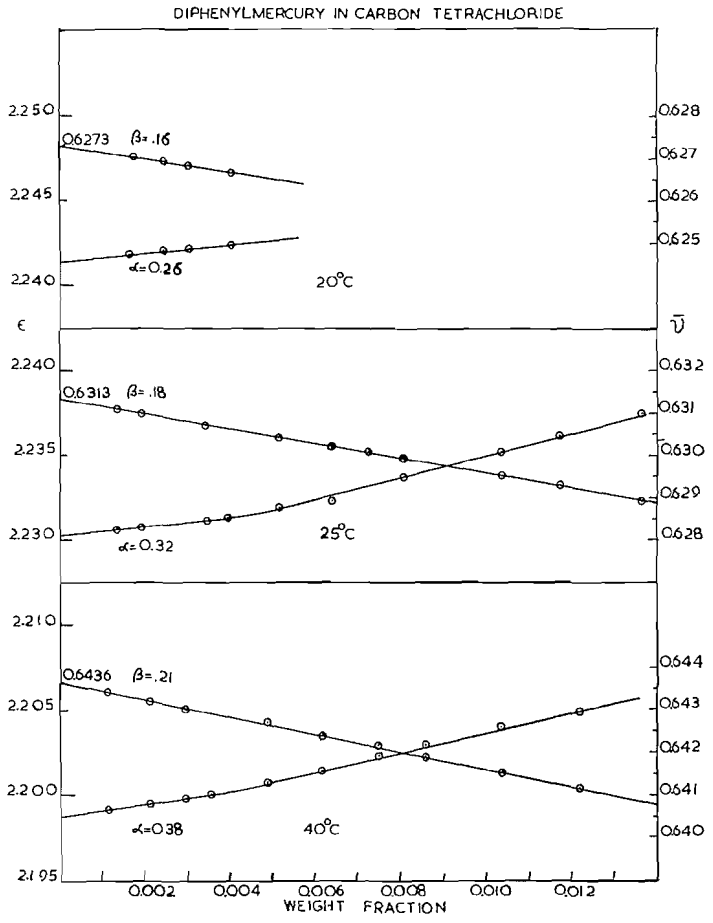

FIG. 2.

Can. J. Chem. Downloaded from www.nrcresearchpress.com by 78.46.186.204 on 09/04/12
For personal use only.

Can. J. Chem. Downloaded from www.nrcresearchpress.com by 78.46.186.204 on 09/04/12
For personal use only.

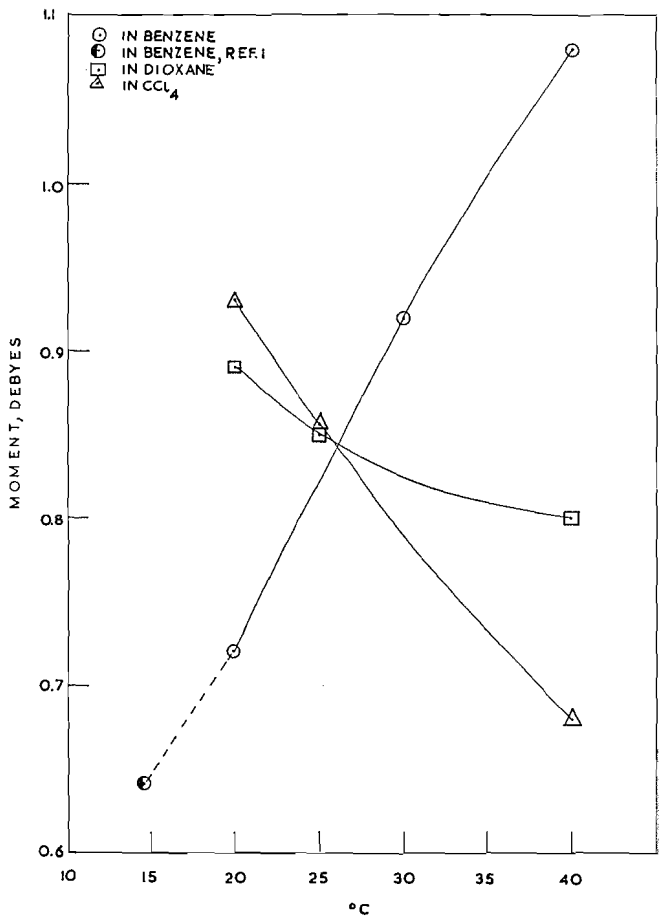

FIG. 3.

TABLE I

DIPOLE MOMENT DATA FOR DIPHENYLMERCURY

Temp., ° C	Wt. fraction range	Solvent	α	β	$P_{2\infty}$, cc	μ_1, D*
40	0–0.01	Benzene	0.54	0.755	80.1	1.08
30	0–0.015	Benzene	0.39	0.696	74.3	0.92
20	0–0.01	Benzene	0.23	0.640	68.2	0.72
40	0–0.015	Dioxane	0.40	0.536	69.8	0.80
25	0–0.010	Dioxane	0.43	0.572	72.2†	0.85
20	0–0.015	Dioxane	0.46	0.507	73.9	0.89
40	0–0.005	CCl_4	0.38	0.21	58.7	—
25	0–0.005	CCl_4	0.32	0.18	58.4	—
20	0–0.005	CCl_4	0.26	0.16	58.2	—
40	0.005–0.01	CCl_4	0.58	0.212	66.3	0.68
25	0.005–0.01	CCl_4	0.67	0.174	72.2	0.85
20	0.005–0.01	CCl_4	0.73	0.163	75.2	0.93

*The P_{e-a} of 57.1 as obtained from solid dielectric data is used for the calculations of the dipole moments.
†Contrasted to Curran's 69.02 (6).

The observed polarization at 25° in carbon tetrachloride (71.6 cc) is not far from that reported (70.2 cc) by Armstrong, LeFevre, and LeFevre (3). However, it may also be seen in Fig. 2 that the latter agreement was attained only by using the concentration range specified by the three authors (3). In the concentration range of 0–0.005 weight fraction it is apparent that a sharply different $\delta\epsilon/\delta\omega$ (α) prevails at all temperatures, although no such inflection is observed in the $\delta\bar{V}/\delta\omega$ slope. The latter evidence for the constancy of β is confirmed by isopiestic measurements which show that diphenylmercury does not associate in carbon tetrachloride.

There have been doubts (3) about the significance of the value for distortion polarization (57.1 cc) determined from the dielectric constants of solid diphenylmercury pellets. The critics considered this value to be low, but the criticism is not entirely justified in view of the total polarizations (in cc, 58.2, 58.6, and 58.7) found at 20, 30, and 40° for diphenylmercury in very dilute tetrachloride solution. An assignment of orientation polarization which exceeds these values must be erroneous. Although our measured distortion polarization (57.1 cc) is 1.1 to 1.6 cc below the total polarizations mentioned above, we cannot safely assign the differences to orientation polarization. These differences are only slightly outside our experimental error. We cannot say whether the moment of diphenylmercury in dilute carbon tetrachloride solution is zero or whether it has a very low value which cannot be defined by the present experimental techniques. But we can say that the minimal polarizations which we have observed in very dilute carbon tetrachloride solutions are contradictory rather than confirmatory to recent claims (3) of zero dipole moment for diphenylmercury, because we have set a minimum which the distortion polarization cannot exceed.

In order to arrive at these conclusions it has been necessary to give careful attention to the purity of the carbon tetrachloride. For example the use of an old sample (ϵ_0 = 2.2303 and $\bar{V}$ = 0.6312) for the polarization study of diphenylmercury shows a decrease in $\delta\epsilon/\delta\omega$ at 25° (in the concentration range ω = 0.005 to 0.01) from 0.67 (in the pure solvent where ϵ_0 = 2.2268) to 0.50 in the old solvent, although the change in $\delta\bar{V}/\delta\omega$ does not exceed 0.01. Of course, this behavior is not unprecedented (p. 130, ref. 5) when the polarity of the solvent is increased. While we have been unable to characterize the impurity which raised the dielectric constant of the old carbon tetrachloride, we have found that deliberate addition of water to our purest solvent (resultant ϵ_0 = 2.2289 at 25°) lowers $\delta\epsilon/\delta\omega$ from 0.67 to 0.48, while $\delta\bar{V}/\delta\omega$ decreases from 0.174 to 0.163. Since these differences lower the apparent moment from 0.85 D to 0.63 D it is evident that rigorously purified solvent must be used for meaningful results.

The variation in polarization with respect to concentration may indeed provide an insight into the molecular behavior of diphenylmercury, especially since the medium, carbon tetrachloride, in which this variation occurs is tetrahedrally symmetrical, with little tendency toward co-ordination. We suggest that in this medium diphenylmercury is self-polarized at the higher concentrations. We presume that the effect of this self-polarization is a reduction in the tendency for diphenylmercury molecules to execute the 360° rotation which is ineffective toward the external field. We believe that this rotation, a consequence of the mass of the central atom, is indicated by the evident perturbation in the spectral absorption at 463 cm^{-1}.

It follows that in very dilute solution more molecules, freed from self-polarization, will completely rotate. The same circumstance ought to reduce the polarization at increased temperatures. This effect is observed (Fig. 3) in carbon tetrachloride.

In this connection it is of interest to compare the dielectric constants of pure carbon

Can. J. Chem. Downloaded from www.nrcresearchpress.com by 78.46.186.204 on 09/04/12
For personal use only.

tetrachloride at the several temperatures with the extrapolation to zero solute concentration. It is evident that the extrapolations for very dilute solutions must differ from those for not-so-dilute solutions. The extrapolation of $\delta\epsilon/\delta\omega$ for very dilute solutions is essentially indistinguishable from that of the pure solvent; ϵ_0 (solvent) minus ϵ_0 (solution) is less than 0.0002. On the other hand the extrapolation of $\delta\epsilon/\delta\omega$ for not-so-dilute solution shows at 20° C that ϵ_0 (solvent) minus ϵ_0 (solution) is 0.001, but at 40° it has decreased to 0.0005. This behavior would indicate that the solvent cavities differ in the two concentration ranges, and suggests that the effectively larger cavity due to self-polarization is decreased either by separation of diphenylmercury molecules, or by thermal agitation.

Benzene is not tetrahedrally symmetrical, so interaction of diphenylmercury with this medium is not unexpected. This interaction ought to minimize self-polarization and it should prevail over the entire concentration range. This expectation is realized in the linearity of the $\delta\epsilon/\delta\omega$ graph over a weight fraction range of 0.001 to 0.008 (Fig. 1) and more.

Table I shows that the apparent moment of diphenylmercury in benzene at 20° is lower than it appears to be in not-so-dilute carbon tetrachloride solution. Assuming that the behavior in the latter medium approaches that in the gas phase the solvent effect in benzene may be called negative. According to the opinions of several workers (5, p. 47), this effect is expected when the molecule contained in a cavity of polarizable solvent has its moment axis in the long dimension of the molecule. This description may apply to a bent molecule with mercury at one end of the dipole.

However, the situation at 20° is reversed at 40° where the moment in benzene is much higher than in carbon tetrachloride. In the absence of any prior opinions (5) about dependence of solvent effect on temperature we suggest that the change of molecular shape within the polarizable solvent cage may be due to C–Hg–C bond angle variation with respect to temperature. While this effect should not be profound, it must be remembered that throughout this argument we are considering moment variations which do not exceed 0.5 debye unit.

It would seem that dioxane is intermediate in behavior between the other two solvents. Indeed the concentration effect and the solvent polarizability effect may largely be compensated in dioxane. In this connection we point again to the intersections of Fig. 3. It is unfortunate that a vapor-phase moment value at this temperature (about 25°) is not available.

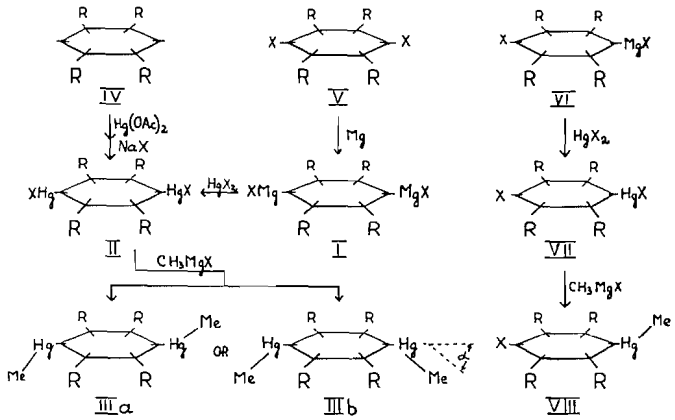

Can. J. Chem. Downloaded from www.nrcresearchpress.com by 78.46.186.204 on 09/04/12
For personal use only.

In any circumstance the data for diphenylmercury in the several solvents must be interpreted in terms of some type of induced polarization. This interpretation implies a definite dipole moment, even when it is very small (experimentally there are no negative moment values in very dilute carbon tetrachloride). The moments may be ascribed to C–Hg–C angularity and some of the differences may be due to variations in this angle. Evidence for differences in this angle will be presented in the remainder of this report.

Paradisubstituted Methylmercuribenzenes

If one assumes that benzene substituents are bonded coplanar with the ring then evidence of orientation polarization in a 1,4-dimercuribenzene ought to establish an angularity of bonding to mercury. To this end we have prepared 1,4-methylmercuri-*bis*-benzene (III*a* or *b*, R = H) by reaction of methyl chloride Grignard reagent with the 1,4-dibromomercuribenzene (II, R = H) derived from mercuric bromide and 1,4-bromomagnesium-*bis*-benzene (I, R = H).

Although the product III has a tendency toward disproportionation to dimethylmercury and a polymer it is sufficiently stable for determination of its electrical polarization at 20° in carbon disulphide. This polarization should have no orientation component if the methylmercuri group were included in the plane of the ring or if the conformation were entirely III*a* (R = H). On the other hand the substance ought to show evidence of moment if the conformation III*b* were contributory. When the additive electronic polarization (used because III will decompose partially during the time required for determination of the dielectric constant of the solid) is subtracted from the total polarization, the difference may be calculated as a moment of 0.91 debye unit.*

A further test of non-linearity has been accomplished with 1,4-methylmercuridurene (III*a* or *b*, R = Me). This substance has been synthesized by mercuration of durene (IV, R = Me), and treatment of the product II (R = Me) with methyl chloride Grignard reagent. The product III, R = Me, is only a little less prone toward disproportionation than the simpler homologue. From the total polarization in carbon disulphide at 20° is subtracted the electronic polarization, again calculated additively. The remainder represents an electric moment of 1.38 debye unit.

In order to compare the moments of the two 1,4-disubstituted phenylene mercurials it is necessary to assign a group moment to methylmercuri. Although we realize the limitation of group moment evaluations, we have used 1-bromo-4-methylmercuribenzene (VIII, R = H, X = Br) obtained by treatment of 1-bromo-4-bromomercuribenzene (VII, R = H) with methyl chloride Grignard reagent. Actually VII is a by-product in the preparation of II as a consequence of the partial Grignardization (VI) of 1,4-dibromobenzene (V, R = H).

The moment of VIII, calculated from additive electronic polarization, in carbon disulphide at 20° is 1.94 debye unit. If a value (m_1) of 1.5 debye is assumed (excluding mesomeric effects) for the 4-bromophenyl group then an equation in two unknowns, the methylmercuri moment (m_2) and its angular deviation from linearity (α), may be formulated

$$(1.94)^2 = (1.5)^2+(m_2)^2-2(1.5)(m_2)\cos\alpha.$$

**The disproportionation of the bis-mercurials described in this report is sufficiently slow that reliable polarization measurements can be made. This reliability has been demonstrated by recovery of the substance after the polarization measurement. However, the time required for analyses to be made elsewhere is detrimental. Additionally the high percentage of mercury in such compounds makes the results non-definitive. Consequently we have chosen to characterize the bis-mercurials analytically by quantitative conversion to the chloromercuri derivatives rather than by analysis of the elements.*

Can. J. Chem. Downloaded from www.nrcresearchpress.com by 78.46.186.204 on 09/04/12
For personal use only.

If one now combines this equation algebraically with the equation which defines the moment of 1,4-methylmercuri-*bis*-benzene (III, R = H)

$$(0.91)^2 = \sqrt{2} \cdot m_2 \cdot \sin \alpha,$$

then assuming that the methylmercuri group moment and the moment angle α are the same in both compounds, two sets of values may be calculated. One value ($m_2 = 0.72$ debye unit; $\alpha = 62°$) seems to be more probable than the other ($m_2 = 3.37$ debye unit, $\alpha = 10.9°$) because the methylmercuri moment ought to be much lower than the group moment (3.5 debye unit) assigned previously to the chloromercuri group (6). Actually the more probable moment value is in approximate agreement with that expected in consideration of the polarizations of diphenylmercury and dimethylmercury. Likewise the C–Hg–C angle (180° minus 62°) is comparable with that estimated for the aliphatic *bis*-mercurials described below.

It is of interest to compare the moments of methylmercuri-*bis*-benzene and the homologous durene. If the C–Hg–C linkage were linear then the moments of both compounds (III, R = H or Me) ought to be identically zero. Actually the moment of the durene (1.38 D) is found to be $\sqrt{2}$ times that (0.91 D) of the benzene. If the substituents in 1,4-methylmercuri-*bis*-benzene are simple-harmonically rotating then this ratio specifies that the substituents in the homologous durene (III, R = Me) are hindered from free rotation. Moreover, the ratio indicates that the hindrance retains the methylmercuri group on one side of the ring (III*b*, R = Me), since any contribution from III*a* (R = Me) would decrease the ratio.

This "on-side" conformation is not unexpected in view of recent observations in respect of the moment of 1,4-dinitrobenzene (7). On the other hand it must be realized that quantitative estimations of this sort are unjustified, despite their common use, and the $\sqrt{2}$ relationship may be fortuitous. For example the group moment and moment angle may differ among the compounds, the bond angle may differ from the moment angle, and the assumption of planarity of the aromatic rings with coplanarity of the substituent methyl groups is nowadays equivocal. However, the quantitative estimation does accentuate the qualitative fact that the observed moments establish the non-linearity of the C–Hg–C linkage.

Aliphatic bis-Mercurials

The electrical polarization data for a series of aliphatic *bis*-mercurials is shown in Table II. It may be seen by reference to the three solid substances with which the combined electronic-plus-atomic polarizations can be determined that the additive values for electronic polarization are not greatly in error. In no instance can a zero moment be designated. Even the polarization of hexafluorodimethylmercury in carbon tetrachloride is appreciable (*ca.* 0.3 D), although the range of concentrations ($\omega = 0.0008$ to 0.0025) is comparable with that of diphenylmercury in carbon tetrachloride where no orientation polarization can be detected.

The trend in moment among the homologous series (methyl > ethyl > propyl) is not very informative except for the unexpectedly low moment of hexafluorodimethylmercury.* In view of the high polarity of the C–F linkage a much higher polarization than has been observed, irrespective of the polarity (necessarily low) of the mercury–carbon

**We are indebted for this compound to Mr. D. Fishel, Ohio State University, who prepared it from trifluoromethyl iodide and cadmium amalgam by the procedure of Emeleus and Haszeldine (8).*

Can. J. Chem. Downloaded from www.nrcresearchpress.com by 78.46.186.204 on 09/04/12
For personal use only.

linkage, would have been expected. In the absence of this difference one may assume that the C–Hg–C angular relationship is variable in respect of the polarity of the substituent groups.

TABLE II

POLARIZATION DATA, ALIPHATIC *bis*-MERCURIALS, R_2Hg

R_2Hg	Solvent	Temp., °C	P_{total}, cc	P_{e+a}, cc	P_e additive cc	μ, D
$(CH_3)_2Hg$	Dioxane	20	33.3	—	22.6†	0.71
	Benzene	20	32.7	—	22.6	0.69
	Benzene	40	33.8	—	22.6	0.74
$(CF_3)_2Hg$	Benzene	20	47.3	27.5*	24.7	0.97
	CCl_4	20	29.2	27.5	24.7	0.29
$(C_2H_5)_2Hg$	Benzene	20	38.1	—	31.9	0.55
$(n\text{-}C_3H_7)_2Hg$	Benzene	20	47.3	—	41.1	0.54
1,7-Dioxa-4,10-mercura-cyclododecane	Benzene	20	91.0	65.7‡	62.6	1.17
Mercuracyclohexane	Benzene	20	49.8	—	34.3	0.86
Mercuracycloheptane	Carbon disulphide	20	56.0	—	38.9	0.90

*Density at 22°, 4.693.
†Additive atomic constant for mercury, 11.2 cc, as determined by Wilde.
‡Density at 22°, 3.30.

The effect of temperature on the polarization of dimethylmercury in benzene has been examined briefly. The apparent augmentation of moment with increasing temperature is similar to that found for diphenylmercury in the same solvent, but is so slight (0.05 debye unit from 20 to 40°) that it might be ascribed to experimental error. However the difference is substantiated by comparison of the moment of diethylmercury (0.55 D at 20° in benzene) with that (0.39 D) reported in the same solvent at 14.5° (1).

In view of the evidence for a C–Hg–C angularity in these aliphatic *bis*-mercurials we have sought to examine analogues in which the angularity would be intrinsic in the structure. Of the last three items in Table II the first was once thought to be 1-oxa-4-mercuracyclohexane (9) but Grdenic proved by X-ray diffraction studies (10) that it is the dimer, 1,7-dioxa-4,10-mercuracyclododecane. Because of the flexibility of a 12-membered ring and also because of a possible tendency toward co-ordination of mercury with oxygen, the substance is not the ideal example we sought for examination of rigid angularity. Nevertheless a significant orientation polarization is observed which cannot be attributed alternatively to an abnormal atom polarization. At most the latter cannot exceed 3 cc, according to the value which we have obtained for the dielectric constant of the solid substance.

When 1,5-dichloromercuripentane is treated with sodium stannite the dimer of mercuracyclohexane is formed exclusively, and this dimer seems to be the stable form. However, by treatment of 1,5-dibromopentane with sodium amalgam in ethyl acetate (11) the monomer may be obtained in varying yield. Although this monomer, $C_5H_{10}Hg$, tends to transform easily to the dimer or polymer, it may be purified for immediate use by avoidance of elevated temperatures. The moment calculated from the electric polarization in benzene (0.86 D at 20°) is closely comparable with the moments of the non-cyclic *bis*-mercurials shown in Table II.

Application of Hilpert and Gruttner's method for the preparation of mercuracyclopentane (13, 12) yields only one product which seems to be the dimer, according to an isopiestic determination of molecular weight. Since the same product is obtained by

Can. J. Chem. Downloaded from www.nrcresearchpress.com by 78.46.186.204 on 09/04/12
For personal use only.

Can. J. Chem. Downloaded from www.nrcresearchpress.com by 78.46.186.204 on 09/04/12
For personal use only.

various reductions of 1,4-dichloromercuributane it would seem that monomeric mercuracyclopentane is too unstable for isolation in sufficient purity for electric polarization studies. The polarization of the dimer (probably 1,6-dimercuracyclodecane, since it can be reconverted to 1,4-dichloromercuributane by treatment with mercuric chloride) has not been measured.

The preparation of monomeric mercuracycloheptane has been more successful, and leads from either 1,6-dibromohexane or 1,6-dichloromercurihexane to a single product which is monomeric according to isopiestic molecular weight determinations (15, 14). The product can be reconverted to 1,6-dichloromercurihexane by means of mercuric chloride. Its moment is not strictly comparable with that of mercuracyclohexane because it has been necessary to use carbon disulphide as the solvent. However, the observed moment at 20° (0.9° D) is almost identical with that of mercuracyclohexane.

From these results it would seem that the C–Hg–C angle must be greater than 108–110°, but it may be as low as 120–130° in a stable configuration. Moreover, since the observed moments are less than twice as great as that of the comparable diethyl- and dipropyl-mercury the C–Hg–C angles in the latter substances need not exceed 150°.

But this estimate should not be construed to imply a fixed C–Hg–C angle for *bis*-mercurials. Indeed the apparent anomalies which have been observed by variation of temperature and solvent with diphenyl- and dimethyl-mercury, and also the lack of correlation of moment with polarity of substituents, is a strong indication that the C–Hg–C angle is widely variable. Perhaps this variability ought to be expected with a large atom-like mercury. Conversely one might say that mercurials are poor candidates for stereochemical studies. On the other hand the behavior of *bis*-mercurials may predict the day of better precision in measurement when no polyatomic substance is known that will not be oriented by an electrical field.

The authors are grateful for studentship aid and direct grants from the National Research Council of Canada which supported this research. They wish to thank Mrs. L. Westland and Mr. F. Lautenschlaeger for aid in the experimental work. Any experimental data not presented in the paper is available in the doctoral thesis of H. Sawatzky.

EXPERIMENTAL*

1,4-Chloromercuri-bis-durene

A mixture of 5.40 g (0.04 mole) of durene, 51.2 g (0.16 mole) of mercuric acetate, 40 ml of acetic acid, and 120 ml of methanol were refluxed for 4 days. The precipitated solid was removed by hot filtration and was washed with boiling ethanol, 11.7 g. This acetoxymercurial was then dissolved in 300 ml of hot acetic acid and the partially cooled system was treated with a solution of 10 g (0.17 mole) of sodium chloride in 50 ml of water. The solid product was filtered off and washed with boiling ethanol, 11.38 g (47%). It may be crystallized from pyridine but has no melting point. X-Ray diffraction pattern is [10] 7.59; [5] 4.45; [4] 3.97; [3] 2.85; [2] 3.52, 3.33, 2.96; [1] 4.63, 3.84, 3.21, 3.01, 2.63. Anal. Calc. for $C_{10}H_{12}Hg_2Cl_2$: C, 20.0; H, 2.01. Found: C, 20.3; H, 2.00.

1,4-Methylmercuri-bis-durene

Into 15 ml (0.0189 equiv.) of stirred methyl chloride or iodide Grignard reagent under nitrogen was added 2.00 g (0.0033 mole) of 1,4-chloromercuri-*bis*-durene. To the warm

Melting points have been corrected against standards according to Can. J. Technol.* **34, *89 (1956). X-Ray diffraction is reported at relative intensities I/I_1 at d spacings in angstroms using* CuKα (Ni *filtered*) *radiation.*

suspension was added 20 ml of dry diethyl ether. After 18 hours of stirring the system was poured on 50 g of crushed ice. Then 1% aqueous sulphuric acid was added until the system was slightly acidic. After evaporation of the ether the solid (1.47 g) was filtered off and almost dissolved in hot benzene. Evaporation of the filtered solution left 1.35 g (73%) of product which did not melt. Purification may be effected by crystallization from hot benzene (25 ml per g) but prolonged heating will cause disproportionation. X-Ray diffraction pattern is [10] 7.65; [9] 3.50; [6] 6.83; [5] 4.38; [4] 5.05; [3] 4.68, 4.03, 3.64, 2.26; [2] 2.92, 2.71; [1] 6.30, 3.35. In carbon disulphide α is 0.66 and β is 0.409, so $P_{2\infty}$ is 116.9 cc. With R_D = 76.4 cc, the moment is 1.38 D. Anal. Calc. for $C_{12}H_{18}Hg_2$: C, 25.6; H, 3.22. Found: C, 25.7; H, 3.25.

When a benzene solution of this material was treated with 2 mole equivalents of mercuric chloride in ether a white precipitate could be filtered off after 20 minutes. When this precipitate (88.7% after ether washing) was treated with bromine in aqueous potassium bromide it was converted to 1,4-dibromodurene, m.p. 200–203°. The benzene filtrate left methylmercuric chloride (83%, m.p. 164–168°) when it was evaporated.

1,4-Methylmercuri-bis-benzene

To a stirred suspension of 2.40 g (0.1 atom) of magnesium in 50 ml of dry ether was added 2 ml of ethyl bromide in 50 ml of ether during 30 minutes. Then a solution of 4.72 g (0.02 mole) of *p*-dibromobenzene and 3.85 ml (total 0.06 mole) of ethyl bromide in 100 ml of ether was added during 75 minutes. Strong reflux was maintained and continued during 12 hours, then 1.2 ml more of ethyl bromide was added. After 1 hour all the magnesium was consumed, so 27.2 g (0.1 mole) of mercuric chloride was introduced during 24 hours from a soxhlet extractor.

The solid product was filtered off and washed thoroughly with water, boiling ethanol, and boiling benzene. There remained 4.88 g (38%) of 1,4-bromomercuribenzene, identified by conversion in 93% yield to 1,4-diiodobenzene, m.p. 127–129°, by means of iodine in an alcoholic suspension of the mercurial.

The filtrate from which this product was obtained was evaporated and then steam-distilled to remove 11.9 g of ethylmercuric bromide. The residue yielded 1.96 g (23% as *p*-bromophenylmercuric bromide) which may be crystallized from benzene, m.p. 234–236°. It has been converted to *p*-bromophenylmercuric acetate, m.p. 198–201°, by means of silver acetate, and subsequently to *p*-bromophenylmercuric chloride, m.p. 251–253°, by means of sodium chloride (16). Also it was converted quantitatively to *p*-dibromobenzene by treatment with bromine in aqueous potassium bromide.

To a stirred suspension of 1,4-bromomercuri-*bis*-benzene (4.30 g, 0.0074 mole) in 25 ml of dry ethyl ether at 0° under nitrogen was gradually added 20 ml (0.02 equiv.) of Grignard reagent from methyl chloride or iodide. After subsequent stirring for 90 minutes the system was poured onto 200 g of crushed ice. The ether was evaporated and the remainder was extracted by 100 ml of pure carbon disulphide. Evaporation of the extract left 2.26 g (61% of the bromomercuri-*bis*-benzene) which was crystallized from 50 ml of 1:1 benzene – diethyl ether. The melting point of this methylmercuri-*bis*-benzene is 190–193° with decomposition at 185° indicating disproportionation. It does not contain halogen; X-ray diffraction pattern is [10] 4.56; [3] 3.75, 3.63, 3.34, 3.21; [2] 5.92, 5.23; [1] 5.62. In carbon disulphide α is 0.29 and β is 0.460 so $P_{2\infty}$ is 75.7 cc. If R_D is 57.9 cc the moment is 0.91 D.

Although a satisfactory elemental analysis was not obtained the methylmercuri-*bis*-benzene was analytically characterized when a suspension of 0.044 g (0.00087 mole) in

Can. J. Chem. Downloaded from www.nrcresearchpress.com by 78.46.186.204 on 09/04/12
For personal use only.

1 ml of ethyl ether was shaken for 3 hours with a solution of 0.047 g (0.018 mole) of mercuric chloride in 5 ml of ether. The solid was filtered off and ether-washed, 0.047 g (98%) of 1,4-chloromercuri-*bis*-benzene which was converted quantitatively to 1,4-dibromobenzene. Anal. Calc. for $C_6H_4Hg_2Cl_2$: Cl, 12.93. Found: Cl, 12.97. The ether filtrate was evaporated to yield 0.0441 g (100%) of methylmercuric chloride, m.p. 168–170°, after crystallization from ethanol.

1-Bromo-4-methylmercuribenzene

A suspension of 0.87 g of *p*-bromophenylmercuric bromide (0.002 mole, obtained from the experiment reported above) in 25 ml of diethyl ether was stirred and ice-cooled under nitrogen, while 3.50 ml (0.0033 equiv.) of Grignard reagent from methyl chloride was added during 5 minutes. After 3 hours of subsequent stirring at ice-bath temperature the system was poured onto 75 g of crushed ice. The non-aqueous phase, dried by magnesium sulphate, was evaporated to leave an oil (0.63 g, 82%) which solidified when chilled to 4°. It was twice crystallized by solution (at 25°) in 1:1 ethanol–chloroform (32 ml per g) and subsequent chilling to −78°. The purified product, m.p. 52.1–52.7°, was characterized by cleavage with mercuric chloride, yielding methylmercuric chloride and *p*-bromophenylmercuric chloride, each in 100% yield. The Grignard reagent from methyl iodide cannot be used in this preparation because disproportionation occurs. In carbon disulphide this mercurial has $\alpha = 2.01$ and $\beta = 0.436$ so $P_{2\infty} = 122.9$ cc, and $\mu = 1.94$ D if $R_D = 49.9$ cc.

Mercuracycloheptane

A mixture of 450 g (0.195 atom Na) of 1% sodium amalgam, 16.5 g (0.07 mole) of 1,6-dibromohexane, 3 ml of ethyl acetate, and 25 ml of benzene was shaken at 70° (infrared lamp) for 1 day, after which time 25 ml each of benzene and water was added with agitation. After separation of the non-aqueous phase a subsequent extraction with 25 ml of benzene was accomplished. Evaporation of the benzene left 7.6 g of oily solid which was purified first by three crystallizations from chloroform (3 ml per g) from 25° to −78° and then by repeated crystallization from 4:1 ether–benzene and from 1:5 ethanol–benzene (3 ml per g) to melt at 58.5–60.2°. Anal. Calc. for $C_6H_{12}Hg$: Mol. wt., 285. Found (Willard and Blank (15)): Mol. wt., 273. Found (Barger-Rast (14)): Mol. wt., 286.

1,6-Dichloromercurihexane

A solution of 2.84 g (0.01 mole) of mercuracycloheptane in a minimum of benzene was treated with 2.72 g (0.01 mole) of mercuric chloride and then 10 ml of ethyl ether was added. The white suspension formed by stirring was filtered off and washed thoroughly with ether, 5.60 g (100%) of 1,6-dichloromercurihexane. Anal. Calc. for $C_6H_{12}Hg_2Cl_2$: Cl, 12.75. Found: Cl, 12.69. After crystallization from hot dimethylsulphoxide (15 ml per g) it melts questionably at 290° with decomposition. The X-ray powder diagram is [10] 11.72; [9] 3.31; [7] 2.65; [5] 2.38; [2] 2.99; [1] 2.25, 3.99, 4.44. Reduction of this high-melting mercurial by alkaline sodium stannite forms mercuracycloheptane, m.p. 58–60°, in 90% yield. Identity was established by mixture melting point.

Mercuracyclohexane

A mixture of 15 g (0.065 mole) of dibromopentane, 450 g (0.2 atom) of 1% sodium amalgam, 3 ml of ethyl acetate, and 50 ml of dry benzene was shaken in a stout sealed bottle at 75° for 24 hours. After treatment with 100 ml of cold water the spent amalgam

Can. J. Chem. Downloaded from www.nrcresearchpress.com by 78.46.186.204 on 09/04/12
For personal use only.

was separated and washed with 50 ml each of water and benzene. The benzene solutions, adequately dried, were vacuum evaporated leaving 8.20 g of oil. This oil was twice extracted by 5-minute reflux with 25 ml of absolute ethanol. The quickly cooled extract was filtered and further chilled to 40°. Slowly there appeared 0.53 g of crystals. Contrary to Hilpert and Gruttner the substance was found only in the extract. Three rapid crystallizations from a benzene–hexane mixture gave a product, m.p. 122.4–122.8°. The monomer seems to be very unstable thermally, and sometimes is not obtainable.

When this product was treated with mercuric chloride, a quantitative yield of 1,5-dichloromercuripentane was obtained. The X-ray diffraction pattern of this *bis*-chloromercurial is: [10] 4.33; [9] 3.34; [8] 3.18; [7] 3.56; [6] 1.97; [5] 2.71; [3] 2.11; [2] 2.45, 2.35, 2.30, 2.07; [1] 2.86, 2.17, 1.82, 1.78. Regeneration of the *bis*-mercurial by treatment with sodium stannite yielded only the dimer described by Hilpert and Gruttner (11). The monomeric *bis*-mercurial decomposed in boiling ethanol to yield an oil which seems to contain the dimer.

1,6-Dimercuracyclodecane

(*a*) *From dibromobutane.* –A mixture of 450 g (0.2 mole) of 1% sodium amalgam, 15.3 g (0.07 mole) of 1,4-dibromobutane, 3 ml of ethyl acetate, and 25 ml of benzene was shaken for 36 hours at 70°. The cooled system was then shaken with 25 ml of water and the benzene layer was separated and combined with a subsequent 25 ml benzene washing. Evaporation left an oil, 10.79 g, which was washed with cold ether leaving 3.79 g of sticky solid. Crystallization from an ether–benzene mixture gave a product, m.p. 44–45.2°.

(*b*) *From 1,4-dichloromercuributane.*—A sample of 0.50 g (10^{-4} mole) of 1,4-dichloromercuributane was treated with 40 ml of 10% aqueous sodium hydroxide and then with a solution of 1 g of stannous chloride dihydrate in 20 ml of 20% aqueous sodium hydroxide. The black suspension was filtered off when no more color change occurred. The black product was extracted with boiling xylene which was evaporated at low temperature leaving 0.17 g (66%) m.p. 37–40°. Crystallization from ether–benzene raised this melting point to 43–45°. Molecular weight determinations by the isopiestic method of Willard and Blank gave an average value of 499, while a freezing-point depression in diphenylmercury gave a value of 517. The calculated molecular weight is 513.

1,4-Dichloromercuributane

When 0.1294 g (253×10^{-6} mole) of dimercuracyclodecane in benzene is treated with 0.1390 g of mercuric chloride dissolved in a minimum of ethyl ether the resulting precipitate, washed with benzene and ether, weighs 0.253 g (93%). Its X-ray diffraction pattern is [10] 3.18; [9] 4.61; [7] 2.09; [5] 2.62; [4] 2.41; [3] 3.55, 1.78; [2] 2.53; [1] 4.00, 3.47, 2.49, 2.03 after crystallization from hot dimethylsulphoxide; m.p. 292–293° (with decomposition). Anal. Calc. for $C_4H_{10}Hg_2Cl_2$: Cl, 13.5. Found: Cl, 13.3.

Dialkylmercury Homologues

These mercurials were prepared from alkylmercuric halides according to the following general procedure. The alkylmercuric halide (0.026 mole) was dissolved and suspended in 150 ml of 10% aqueous sodium hydroxide. A solution of 8.33 g (0.035 mole) of stannous chloride dihydrate in 100 ml of aqueous sodium hydroxide was added. After 3 hours of agitation the system was steam-distilled (methyl and ethyl) or ether-extracted (propyl and butyl). All were dried with magnesium sulphate over an ether solution or (methyl)

Can. J. Chem. Downloaded from www.nrcresearchpress.com by 78.46.186.204 on 09/04/12
For personal use only.

directly by potassium hydroxide pellets and then distilled. All except dimethylmercury (m.p. −42.8 to −41.9°) are unstable in light and dibutylmercury is unstable to heat.

PHYSICAL PROPERTIES OF DIALKYLMERCURY HOMOLOGUES

Alkyl	Boiling point, °C	mm	n_D^{20}
Methyl	90.7–91.1	755	1.54512
Ethyl	50–51	16	1.54541
n-Propyl	80.0–80.6	16.5	1.51755
n-Butyl	67	0.55	1.50812
	48	0.35	

Other bis-Mercurials

Diphenylmercury was dissolved in hot 93% ethanol (40 ml per g) and allowed to cool very slowly with stirring, m.p. 125–126°. The purification of 1,7-dimercura-4,10-dioxacyclododecane (10) was effected by crystallization from chloroform, m.p. 145–146°, and its dielectric constant at 22° was found to be 2.975. Hexafluorodimethylmercury as received from Mr. Fishel was sublimed at 85–95° and 750 mm until the melting point was constant at 166–166.5°.

Purification of Solvents

Benzene was purified according to a previous description (17) and was stored over sodium under nitrogen, $\epsilon = 2.284$ and $d = 0.8788$ at 20°. Dioxane, prepared as was described previously (17), was stored under nitrogen without sodium, $\epsilon = 2.224$ and $d = 1.0336$ at 20°. Carbon disulphide was thrice-stirred during 2 hours with 100 ml of 2.5% aqueous potassium permanganate per liter, then for 5 hours with metallic mercury (250 g per liter), and finally with 2.5% aqueous mercuric chloride (100 ml per liter). After drying with phosphorus pentoxide the solvent was distilled and stored under nitrogen in the dark, $\epsilon = 2.646$ and specific volume = 0.79135. Like dioxane it is unstable. The purification of 11 liters of carbon tetrachloride was accomplished by the method of Ingold and Powell (18) by digestion at 50–60° for 3 hours with 750 ml of Fehling's solution. The non-aqueous layer was then refluxed with 5% aqueous sodium hydroxide for 3 hours, then washed with water and stirred about 15 times with 100-ml lots of concentrated sulphuric acid until coloration ceased. After being washed with aqueous sodium carbonate the carbon tetrachloride was azeotropically distilled to remove most of the water. Then it was dried with phosphorus pentoxide, distilled, and stored under nitrogen in dark bottles, $\epsilon = 2.2415$ and $V = 0.62730$ at 20°.

Dielectric Constants of Solutions

All determinations were made at 500 kc in the apparatus described previously (19). Except for the studies with diphenylmercury in carbon tetrachloride no experiment was accepted if the individual determinations did not permit linear plots of $d\epsilon/d\omega$ (α) and $dV/d\omega$ (β). Moreover, no experiment was accepted in which the extrapolations of α and β to zero concentration differed more than ± 0.0002 in specific volume and ± 0.002 in dielectric constant from the values tabulated as follows.

Dielectric Constants of Solids

The method described previously (17, 20) has been followed. The pellet thickness was measured after the determination at 5 Mc by averaging the gauged value at 4

Can. J. Chem. Downloaded from www.nrcresearchpress.com by 78.46.186.204 on 09/04/12
For personal use only.

DIELECTRIC CONSTANTS AND SPECIFIC VOLUMES OF PURE SOLVENTS

Solvent	20°		25°		30°		40°	
	ϵ	V	ϵ	V	ϵ	V	ϵ	V
Benzene	2.2849	1.1381	–	–	2.2612	1.1524	2.2395	1.1670
Dioxane	2.2206	0.9675	–	–	–	–	2.1851	0.9900
Carbon disulphide	2.6470	0.7911	–	–	–	–	–	–
Carbon tetrachloride	2.2426	0.6273	2.2306	0.6313	–	–	2.1986	0.6436
	2.2380	0.6270	2.2272	0.6310*	–	–	2.1962	0.6435

*The final six values are the best obtained for CCl_4 to date.

quadrants of the cylinder; also oftentimes the pellet was broken into halves and the center measured as well. A redetermination of the dielectric constant of diphenylmercury pellets gave a value of 57.1 cc, thus confirming the previously reported value (19).

Infrared Spectrum of Diphenylmercury

Only three absorption bands were found in the 900–300 cm^{-1} spectral region for a 10% solution of diphenylmercury in benzene, although the strong absorption of the solvent at 680 cm^{-1} may have obscured the behavior of diphenylmercury in this frequency range. The bands at 732 cm^{-1} (80% absorption) and 706 cm^{-1} (40% absorption) were symmetrical and well resolved, but the band at 463 cm^{-1} (30% absorption) was unsymmetrical, showing evidence of perturbations on the low frequency side. This band also is of interest because of its possible relationship to the angle of swing postulated by deLazlo (21) for *bis*-bromophenylmercury.

Organomercuric Halides

With the exception of the first and fourth items of Table III these substances were prepared by cleavage of *bis*-mercurials by means of mercuric chloride in ether solution. The methylmercuric chloride was crystallized (13 ml per g) from 95% ethanol, m.p. 168.7–169.6°. The ethyl analogue from 1:1 benzene – carbon tetrachloride melted at 191.8–192.9°. The propyl homologue from 95% ethanol (15 ml per g) melted at 141–143° but after sublimation melted at 142.1° to 142.7°. The butyl homologue crystallized from benzene (5 ml per g) to melt at 125.5–126.2° and then from 95% ethanol (15 ml per g) to melt at 126.9–127.2°.

The preparation of chlormethylmercuric chloride was carried out according to Hellerman and Newman (22). The 97.5% yield was crystallized from ethanol, m.p. 128.5–130°. The X-ray diffraction is [10] 10.59, 3.22; [8] 4.05, 3.26; [6] 2.65, 2.62; [4] 1.90; [2] 2.35, 3.52; [1] 4.87, 2.93, 2.43, 2.00. It is of interest that the compound also may be obtained by the action of diazomethane on 2-hydroxyorganomercuric halides.

These chloromercurials were prepared to demonstrate that the R–Hg group becomes more electropositive with increasing size in the normal homologous series. This behavior is shown in Table III.

TABLE III

POLARIZATION DATA, ORGANOMERCURIC HALIDES, RHgCl

R	Solvent	α	β	$P_{2_{\infty}}$, cc	R_D, cc	μ, D
p-Bromophenyl	Dioxane	1.32	0.690	114.8	50.1	1.75
Methyl	Dioxane	6.02	0.740	261.3	22.9	3.36
Ethyl	Dioxane	6.80	0.778	306.9	27.5	3.64
Chloromethyl	Dioxane	3.80	0.723	197.9	27.8	2.84
n-Propyl	Benzene	5.60	0.822	315.9	32.1	3.67
n-Butyl	Benzene	5.94	0.750	357.7	36.8	3.90

Can. J. Chem. Downloaded from www.nrcresearchpress.com by 78.46.186.204 on 09/04/12
For personal use only.

A study of the dielectric constants of these solid organomercurials is in progress with a view to clarify the discrepancy between the P_{e+a} values which we have measured versus the calculated values which appear in the literature (23).

REFERENCES

1. BERGMANN, E. and SCHÜTZ, W. Z. physik. Chem. B, **19**, 401 (1932).
2. HAMPSON, G. C. Trans. Faraday Soc. **30**, 877 (1934).
3. ARMSTRONG, R. S., LEFEVRE, C. G., and LEFEVRE, R. J. W. J. Chem. Soc. 371 (1957).
4. SIPOS, J., SAWATZKY, H., and WRIGHT, G. F. J. Am. Chem. Soc. **77**, 2759 (1955).
5. SMYTH, C. P. Dielectric behavior and structure. McGraw-Hill Book Co., Inc., New York. 1955. p. 39.
6. CURRAN, B. C. J. Am. Chem. Soc. **64**, 830 (1942).
7. PODLESCHKA, P., WESTLAND, L., and WRIGHT, G. F. Can. J. Chem. **36**, 574 (1958).
8. EMELEUS, H. J. and HASZELDINE, R. N. J. Chem. Soc. 2953 (1949).
9. SAND, J. Ber. **34**, 2913 (1901).
10. GRDENIC, D. Acta Cryst. **5**, 367 (1952).
11. HILPERT, S. and GRUTTNER, G. Ber. **47**, 177, 186 (1914).
12. VON BRAUN, J. Ber. **46**, 1792 (1913).
13. VON BRAUN, J. Ber. **47**, 491 (1914).
14. FRIEDRICH, A. Die Praxis der quantitativen organischen Mikroanalyse. F. Deiticke Co., Leipzig. 1933. p. 191.
15. SCHNEIDER, F. Organic qualitative microanalysis. John Wiley & Sons, Inc., New York. 1946. p. 118.
16. HANKE, M. E. J. Am. Chem. Soc. **45**, 1321 (1923).
17. MEREDITH, C. C., WESTLAND, L., and WRIGHT, G. F. J. Am. Chem. Soc. **79**, 2385 (1957).
18. INGOLD, C. K. and POWELL, W. J. J. Chem. Soc. 1222 (1921).
19. MEREDITH, C. C. and WRIGHT, G. F. Can. J. Technol. **33**, 182 (1955).
20. GEORGE, M. V. and WRIGHT, G. F. Can. J. Chem. **36**, 189 (1958).
21. DE LAZLO, H. Trans. Faraday Soc. **30**, 884 (1934).
22. HELLERMAN, L. and NEWMAN, M. D. J. Am. Chem. Soc. **54**, 2859 (1932).
23. STROHMER, W. Z. Elektrochem. **60**, 58 (1956).

Can. J. Chem. Downloaded from www.nrcresearchpress.com by 78.46.186.204 on 09/04/12
For personal use only.

Can. J. Chem. Downloaded from www.nrcresearchpress.com by 78.46.186.204 on 09/04/12
For personal use only.

THEORETICAL ASPECTS OF THE UNIMOLECULAR DECOMPOSITION OF NITROUS OXIDE[1]

E. Kerry Gill and Keith J. Laidler

ABSTRACT

The kinetic data for the unimolecular decomposition of nitrous oxide, recently analyzed by Johnston, have been considered from the standpoint of the theories of unimolecular decompositions. Particular attention is paid to the high-pressure first-order rates, the low-pressure second-order rates, and the pressure range over which the rates fall off. A normal-mode analysis is made for the molecular vibrations, and calculations are made on the basis of N. B. Slater's theory. It is found that when the change of multiplicity is taken into account the Slater theory gives a satisfactory interpretation of the high-pressure behavior, but gives rates that are much too small in the low-pressure region. The theories of Hinshelwood, Kassel, and Rice and Ramsperger account more satisfactorily for the rate of activation, and Kassel's theory accounts for the pressure fall-off. A modified theory of unimolecular reactions is proposed to explain the observed results.

INTRODUCTION

The thermal decomposition of nitrous oxide is of very special interest, since the molecule is one of the simplest capable of undergoing unimolecular breakdown. The reaction is therefore particularly suitable for testing the various theories of unimolecular reactions that have been proposed. Until recently the experimental results for the reaction have been somewhat confusing, owing to various complications such as the existence of surface effects. However Johnston (1) has recently carried out a detailed critical analysis of the various results and has shown that when the complications are eliminated the reaction represents an excellent example of a straightforward unimolecular decomposition. It is possible that Johnston slightly oversimplifies the situation (2), but it seems likely that the rate constants he deduces for the high- and low-pressure reaction are close to the true ones. They should certainly be sufficiently reliable to permit a careful test of the theories, and this is what has been done in the present paper. A similar analysis of the hydrogen peroxide decomposition has also been carried out and will be published elsewhere (3) together with a more detailed treatment of mechanisms (4).

As far as the high-pressure behavior is concerned, all modern theories of unimolecular reactions lead to approximately the same conclusions. Hinshelwood's expression (eq. [4] below) for the rate of energization together with Kassel's equation for the rate of breakdown of a critically energized molecule leads to the result that the high-pressure first-order rate constant is

$$k_\infty = k^{\ddagger} e^{-\epsilon^*/\mathbf{k}T}, \qquad [1]$$

where $k^{\ddagger}$ is of the order of magnitude of a vibrational frequency in the molecule ($\sim 10^{13}$ sec^{-1}) and ϵ^* is the energy of activation per molecule. Slater's theory (5, 6, 7, 8, 9, 10, 11) leads to the similar result that

$$k_\infty = \bar{\nu} e^{-\epsilon^*/\mathbf{k}T}, \qquad [2]$$

where $\bar{\nu}$ is a specially weighted average of the vibrational frequencies in the molecule. Eyring's absolute rate theory (12, 13) gives the relationship

$$k = \frac{\mathbf{k}T}{h} \frac{f^{\ddagger}}{f} e^{-\epsilon^*/\mathbf{k}T}, \qquad [3]$$

[1]*Manuscript received June 30, 1958.*
Contribution from the Department of Chemistry, the University of Ottawa, Ottawa 2, Canada.

where $\mathbf{k}T/h$ is close to a vibration frequency and the ratio of partition functions $f^{\ddagger}/f$ is usually close to unity. Frequency factors of 10^{13} sec^{-1} are therefore satisfactorily explained by all theories. Values significantly greater than this, of which there are a number of examples, are explained on the basis of eq. [3] in terms of a high value of $f^{\ddagger}/f$, which corresponds to a large positive entropy of activation. Modifications to equations [1], [2], and [3] are necessary when, as with nitrous oxide, the equation involves a change in multiplicity and therefore a small transmission coefficient.

As far as the low-pressure second-order behavior is concerned there are much wider divergences between the different theories of unimolecular reactions. This low-pressure rate is actually the rate of energization of the molecules, and there are two main expressions for this rate, corresponding to two fundamentally different definitions of energization. One of these expressions was first proposed by Hinshelwood (14) and has been employed in the subsequent theories of Kassel (15, 16) and of Rice and Ramsperger (17, 18). The definition of energization to which this expression applies is that the molecule contains, distributed amongst its s normal modes of vibration, at least the energy ϵ^* required for the reaction to occur. The rate of energization to this energy state is, to a good approximation,

$$k_1 = Z \frac{1}{(s-1)!} \left(\frac{\epsilon^*}{\mathbf{k}T}\right)^{s-1} e^{-\epsilon^*/\mathbf{k}T}, \qquad [4]$$

where Z is the collision number. Inherent in this treatment is the assumption that the energy can flow freely between the various modes so that provided the energy ϵ^* is in the molecule it may, after a sufficient number of vibrations, pass into one particular normal mode which is involved in the breakdown of the molecule.

In Slater's theory the contrary assumption is made that there can be no flow between the normal modes. Reaction occurs not when the energy gets into a particular mode but when the vibrations come suitably into phase, so that a critical co-ordinate becomes sufficiently extended. Not all molecules which are energized in the HKRR* sense are capable of undergoing reaction; only those which initially have the energy distributed in a particular way among the normal modes are capable of doing so. Slater's definition of energization is therefore a more stringent one than is HKRR's, and his expression for the rate of energization gives rise to much lower values. The expression is approximately

$$k_1 = Z\,(\epsilon^*/\mathbf{k}T)^{\frac{1}{2}(n-1)}(4\pi)^{\frac{1}{2}(n-1)} \prod \mu_k\, e^{-\epsilon^*/\mathbf{k}T}, \qquad [5]$$

where n is the number of normal modes concerned in the reaction and the μ's are quantities that are related to the "amplitude factors" for the various normal modes. A rigorous test of Slater's theory can only be made by carrying out a detailed vibrational analysis, a matter of considerable difficulty for all except very simple molecules. Slater's theory has been applied quantitatively to cyclopropane, which isomerizes thermally into propylene, and the results were very satisfactory (8). With hydrogen peroxide, on the other hand, the calculated low-pressure rates were much smaller than the experimental ones (3).

In the present paper both the HKRR and Slater theories are applied quantitatively to the nitrous oxide decomposition. It will be seen that Slater's expression gives much too low a rate of energization, but that the theory provides a satisfactory formulation

This abbreviation will be used to denote the point of view taken in the theories of Hinshelwood, Kassel, and Rice and Ramsperger.

Can. J. Chem. Downloaded from www.nrcresearchpress.com by 78.46.186.204 on 09/04/12
For personal use only.

for the first-order behavior. A more general treatment of unimolecular processes is outlined at the end of this paper.

THE EXPERIMENTAL DATA

Only the bare results will be stated here; for a more detailed discussion of the experimental work reference should be made to Johnston's paper (1). The rate-controlling step is believed to be

$$N_2O = N_2 + O,$$

a reaction that is endothermic by 39.5 kcal. The high-pressure activation energy of the reaction is close to 60.0 kcal. At 888° K the high-pressure first-order rate constant is

$$k_\infty = 7.47 \times 10^{-4} \text{ sec}^{-1},$$

and this corresponds to a frequency factor of

$$8.134 \times 10^{11} \text{ sec}^{-1}.$$

By extrapolation of Johnston's second-order rate coefficients to zero pressure we estimate the rate of energization to be

$$k_1 = 14.0 \text{ cc mole}^{-1} \text{ sec}^{-1}.$$

The pressure at which the first-order rate coefficient falls to one-half of its limiting value is approximately

$$p_{\frac{1}{2}} = 1.3 \times 10^4 \text{ mm}.$$

THEORY OF THE HIGH-PRESSURE RATES

The experimental frequency factor at high pressures, 8.134×10^{11} sec^{-1}, is significantly below what would be expected on the basis of equations [1], [2], and [3] above. The frequencies of vibration of the molecule are of the order of 10^{13} sec^{-1}, so that $k^{\ddagger}$ in Kassel's theory is of this magnitude. Slater's average vibrational frequency, weighted using the μ values derived below, is

$$\bar{\nu} = 4.50 \times 10^{13} \text{ sec}^{-1}.$$

The value of $\mathbf{k}T/h$ at 888° K is equal to 1.85×10^{13} sec^{-1}. It is therefore seen that the experimental value is too low by between one and two powers of 10.

The reason for this lies in the fact that the rate-controlling step involves a change of multiplicity:

$$N_2O(^1\Sigma) \rightarrow N_2(^1\Sigma) + O(^3P).$$

Since a triplet and a singlet can only give a triplet it follows that the reaction must involve a transition from one potential-energy curve to another, as represented schematically in Fig. 1. The ground state of N_2O correlates with $N_2(^1\Sigma)$ and $O(^1D)$, and the curve for this crosses the repulsive curve for $N_2(^1\Sigma) + O(^3P)$. The forms of these curves have been discussed by Stearn and Eyring (19). At the time their paper was published, however, the experimental evidence pointed to an activation energy as low as 52 kcal and a transmission coefficient of about 10^{-4}. This suggested a resonance splitting of as little as 5 cal per mole, and difficulty was experienced in explaining such a small value. The value of 10^{-1} to 10^{-2} obtained above leads to a resonance separation of the order of 500 cal per mole and this is what might reasonably be expected on the basis of spin–orbit interactions (19).

Can. J. Chem. Downloaded from www.nrcresearchpress.com by 78.46.186.204 on 09/04/12
For personal use only.

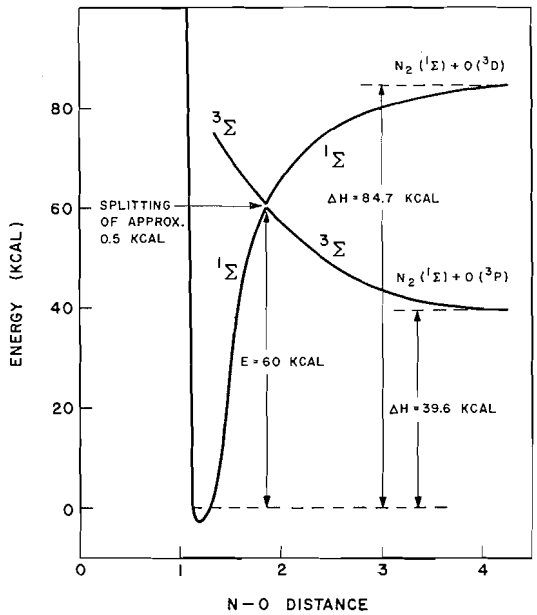

FIG. 1. Schematic potential-energy curves for the decomposition of nitrous oxide. The curves are based on those calculated by Stearn and Eyring, but are modified slightly to accommodate the latest thermochemical and kinetic values.

THEORY OF THE LOW-PRESSURE RATE

The low-pressure second-order rate constant, found experimentally to be about 14.0 cc $mole^{-1}$ sec^{-1}, is, according to all theories, the rate of energization of the molecule. This value must be explained in terms of the distribution of the energy of activation amongst the four normal modes of vibration, with or without flow of energy between the normal modes. In the calculations the collision diameter will be taken as 3.31×10^{-8} cm, as employed by Johnston (1). At 888° K this corresponds to a collision number Z of

$$3.182\times10^{-10} \text{ cc molecule}^{-1} \text{ sec}^{-1} = 1.916\times10^{14} \text{ cc mole}^{-1} \text{ sec}^{-1}.$$

The HKRR Theory

With s equal to 2 and ϵ^* equal to 60.0 kcal per mole the value of k_1 calculated using eq. [4] is 6.09 cc $mole^{-1}$ sec^{-1}, which is reasonably close to the experimental value of 14.0 cc $mole^{-1}$ sec^{-1}. This choice of s gives the best agreement; $s = 4$, for example, leads to 1.22×10^3 cc $mole^{-1}$ sec^{-1}. The reason that $s = 3$ and $s = 4$ leads to rates that are too high is presumably that there is little flow of energy between the two axial and the two bending modes (see below).

Slater's Theory

A vibrational analysis for the N_2O molecule has been carried out, and the details are given in the Appendix. The molecule is linear and the normal modes of vibration are shown in Fig. 2. Two of the frequencies, ν_1 and ν_3 in the conventional notation, correspond to axial vibrations, and one frequency, ν_2, corresponds to the doubly degenerate vibrations perpendicular to the axis. The motion of the molecule may be described in terms of three co-ordinates w, x, and y, of which w denotes the mutual displacement of the nitrogen atoms and x and y the components of the displacement of the oxygen atom relative to the center of the N–N distance; x is along the axis of the molecule and

Can. J. Chem. Downloaded from www.nrcresearchpress.com by 78.46.186.204 on 09/04/12
For personal use only.

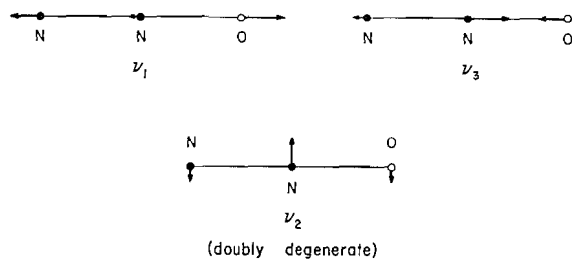

FIG. 2. The normal vibrations of nitrous oxide. The molecule is drawn to scale (equal N–N and N–O distances) and the vector lengths approximately represent the relative displacements.

y perpendicular to it. The analysis (cf. Appendix) leads to the result that the ratios of the displacements are:

$$\begin{aligned} &\text{for } \nu_1 \quad x{:}w{:}y = 1.00{:}0.429{:}0, \\ &\text{for } \nu_2 \quad x{:}w{:}y = 0{:}0{:}\text{constant}, \\ &\text{for } \nu_3 \quad x{:}w{:}y = -0.857{:}1.00{:}0. \end{aligned}$$

In applying Slater's theory we shall take as the critical co-ordinate for the dissociation into $N_2 + O$ the distance from the O to the center of mass of N–N. The variation in this co-ordinate, p, is equal simply to x; it does not involve w and y. Since the bending vibrations involve only y it follows that they do not contribute to the decomposition, so that we must take n equal to 2.* The amplitude factors, α, and the corresponding μ's, corresponding to the two axial vibrations are shown in Table I. The product of the μ's is given by

$$[6] \qquad \prod_k \mu_k = \mu_1\mu_3 = 0.3824.$$

Using eq. [5] the value of k_1 is then found to be, with $n = 2$,

$$k_1 = 1.40 \text{ cc mole}^{-1} \text{ sec}^{-1}.$$

This is below the experimental value by a factor of 10.

TABLE I

FREQUENCIES AND AMPLITUDE FACTORS (α AND μ) FOR THE TWO AXIAL MODES

i	ν_i/sec^{-1}	α_i	μ_i
1	3.864×10^{13}	1.300×10^{-3}	0.9066
3	6.709×10^{13}	-0.6048×10^{-3}	0.4218

THE FALLING-OFF OF THE HIGH-PRESSURE RATE COEFFICIENT

Figure 3 shows the experimental first-order rate coefficients as a function of pressure. The two lines to the left show the theoretical behavior based on Kassel's theory (15, 16), with s equal to 2 and to 4. These curves were constructed by numerical integration of Kassel's general rate equation

**It is readily shown using Slater's procedures that the bending vibrations do not make a contribution for any choice of axial co-ordinate.*

Can. J. Chem. Downloaded from www.nrcresearchpress.com by 78.46.186.204 on 09/04/12
For personal use only.

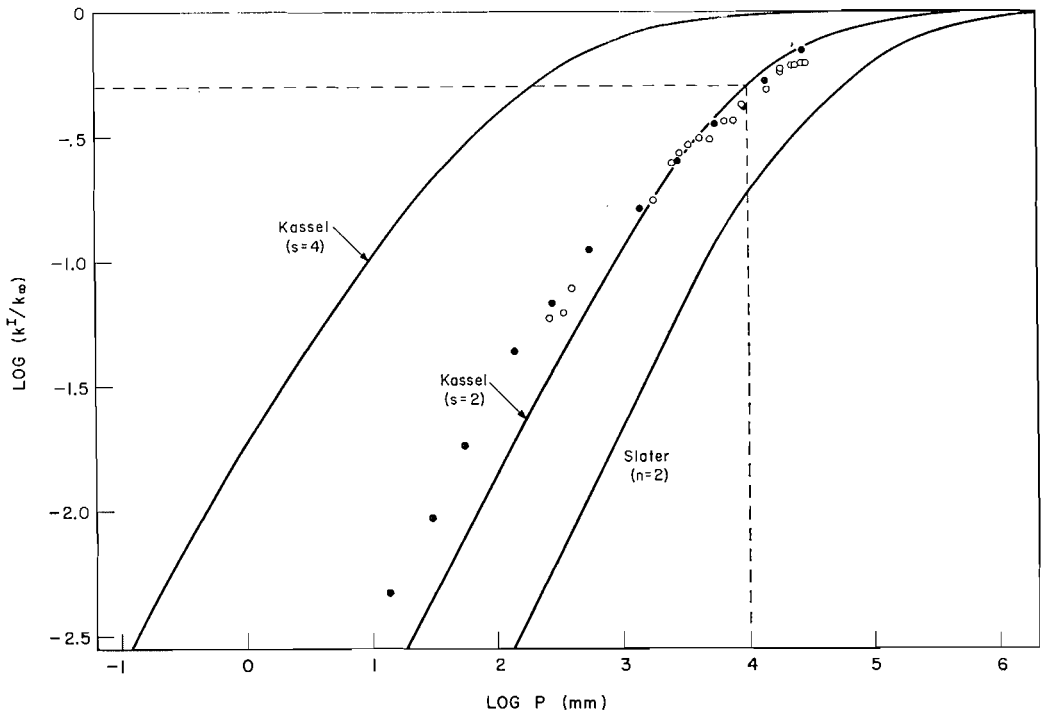

FIG. 3. Plot of the logarithm of the first-order rate coefficient against the logarithm of the pressure. The open circles represent the values given by Johnston (1), the closed circles values obtained by extrapolation. The calculated Kassel curve with $s = 2$ is seen to lie close to the experimental points, whereas Slater's curve gives rates that are too low except in the high-pressure region.

[7] $$\frac{k^I}{k_\infty} = \frac{1}{(s-1)!}\int_0^\infty \frac{x^{s-1}e^{-x}dx}{1+\dfrac{k^\ddagger}{k_{-1}[A]}\left(\dfrac{x}{b+x}\right)^{s-1}}$$

using the values

$$b = 34.63,$$
$$k^\ddagger = 7.47\times10^{-4}\ \text{sec}^{-1}\ \text{(experimental)},$$
$$k_{-1} = 3.182\times10^{10}\ \text{cc molecule}^{-1}\ \text{sec}^{-1}.$$

The curve for $s = 4$ is shown to lead to rates that are much higher than the experimental ones, but that for $s = 2$ falls very close to the experimental values. The pressure for $s = 2$ at which k^I reaches one-half the limiting rate is 1.3×10^4 mm, and this is essentially the same as the experimental value. It is of interest that the approximate relationship

[8] $$[A]_{\frac{1}{2}} = k_\infty/k_1$$

for the half pressure leads to a value of 6.78×10^3 mm.

Slater's curve is of the same shape as Kassel's, but is displaced to the right as shown in Fig. 3. The predicted half pressure is 6.3×10^4 mm, which is significantly larger than the observed value.

Can. J. Chem. Downloaded from www.nrcresearchpress.com by 78.46.186.204 on 09/04/12
For personal use only.

Can. J. Chem. Downloaded from www.nrcresearchpress.com by 78.46.186.204 on 09/04/12
For personal use only.

DISCUSSION

The main conclusion of the present work is that the Kassel treatment with s equal to 2 leads to satisfactory rates over the entire pressure range, and to a reliable estimate of the half pressure. The Slater expression, however, leads to rates that are significantly too low except in the high pressure region, and to too high a value for the half pressure.*

A similar conclusion has also been reached in the case of hydrogen peroxide (3) and other small molecules (4). Since a theoretical discussion of this problem is to be presented elsewhere (4) it will suffice at the present stage to note that in the case of small molecules there appears to be flow of energy between the normal modes, as envisaged by the HKRR theories but not by Slater's theory. Our view is that Slater is right in regarding reaction as occurring when a critical co-ordinate becomes sufficiently extended, but may be in error in prohibiting flow of energy between the modes.

A scheme of reactions that is consistent with this view is

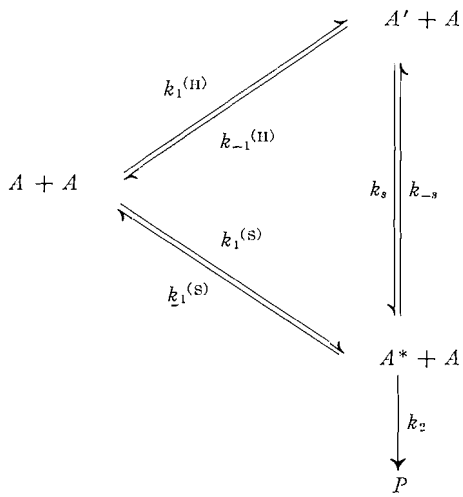

Here a distinction has been made between the two types of energized molecules, represented by A' and A^*. The A^* molecules are those that are energized in the Slater sense; they contain ϵ^* or more of energy and have it distributed between the modes in such a way that, when the vibrations come suitably into phase, there can be a sufficient extension of the critical co-ordinate. The A' molecules are energized in the less stringent HKRR sense, the energy ϵ^* or more being simply distributed between the modes and *not* being suitably distributed for reaction to occur except by a flow of energy.

This scheme of reactions leads to Slater's expression for the high-pressure rate, and in general to the HKRR formula [4] at low pressures. If there is no flow, i.e. if $k_s = k_{-s} = 0$, Slater's theory will be correct at all pressures, but otherwise the HKRR formula will apply at least over a certain range.

Further implications of the mechanism, together with a discussion of other reactions, will be discussed elsewhere (4).

**It is worth mentioning that the treatment given involves the assumption that deactivation occurs on every collision. If this is not the case the Slater and Kassell rates of energization are correspondingly reduced. The conclusion that Slater's rate of energization is too low is then true a fortiori, Kassel's rates with $s = 2$ would then be too low, but agreement might be obtained with s equal to 3 or 4.*

Can. J. Chem. Downloaded from www.nrcresearchpress.com by 78.46.186.204 on 09/04/12
For personal use only.

REFERENCES

1. JOHNSTON, H. S. J. Chem. Phys. **19**, 663 (1951).
2. TROTMAN-DICKENSON, A. F. Gas kinetics. Butterworth Scientific Publications, London. 1955. p. 72.
3. GILL, E. K. and LAIDLER, K. J. To be published.
4. LAIDLER, K. J. and GILL, E. K. To be published.
5. SLATER, N. B. Proc. Cambridge Phil. Soc. **35**, 56 (1939).
6. SLATER, N. B. Proc. Roy. Soc. A, **194**, 112 (1948).
7. SLATER, N. B. Trans. Roy. Soc. London, A, **246**, 57 (1953).
8. SLATER, N. B. Proc. Roy. Soc. A, **218**, 224 (1953).
9. SLATER, N. B. Proc. Cambridge Phil. Soc. **50**, 33 (1954).
10. SLATER, N. B. Proc. Leeds Phil. Lit. Soc. Sci. Sect. 4, 259, 268 (1955).
11. SLATER, N. B. Proc. Roy. Soc. Edinburgh, A, 44, 161 (1955).
12. EYRING, H. J. Chem. Phys. **3**, 107 (1935).
13. GLASSTONE, S., LAIDLER, K. J., and EYRING, H. The theory of rate processes. McGraw-Hill Book Co., Inc., New York. 1941. p. 286.
14. HINSHELWOOD, C. N. Proc. Roy. Soc. A, **113**, 230 (1927).
15. KASSEL, L. S. J. Phys. Chem. **32**, 225 (1928).
16. KASSEL, L. S. Kinetics of homogeneous gas reactions. Reinhold Publishing Corp., New York. 1932. Chap. 5.
17. RICE, O. K. and RAMSPERGER, H. C. J. Am. Chem. Soc. **49**, 1617 (1927).
18. RICE, O. K. and RAMSPERGER, H. C. J. Am. Chem. Soc. **50**, 617 (1928).
19. STEARN, A. E. and EYRING, H. J. Chem. Phys. **3**, 778 (1935).
20. ROSENTHAL, J. E. J. Chem. Phys. **5**, 465 (1937).
21. BARKER, E. F. Phys. Rev. **41**, 369 (1932).

APPENDIX

Vibrational Analysis

The theory of vibrations in asymmetric linear triatomic molecules, and of N_2O in particular, has been discussed by Rosenthal (20). The potential and kinetic energy functions and molecular parameters employed in that paper, along with the calculated force constants, have been used in the present investigation to compute the amplitude factors and other quantities required for Slater's treatment of unimolecular reactions.

The vibrational modes were shown above in Fig. 2. The mutual displacement of the nitrogen atoms is denoted by w, while x and y are the components of the displacement of the oxygen atom relative to the center of the two nitrogen atoms; x is the displacement along the axis and y that perpendicular to it.

The most general quadratic potential function consistent with geometrical symmetry may be written in terms of four force constants:

$$V = \tfrac{1}{2}(Ax^2+Bw^2+Cy^2+2Dxw). \quad [9]$$

If q_{NN} and q_{NO} denote the N–N and N–O distances we may define q and α by

$$q \equiv q_{NN}+q_{NO}, \quad [10]$$

$$\alpha \equiv q_{NN}/(2q_{NO}+q_{NN}), \quad [11]$$

and

$$\mu \equiv M/(M+2m), \quad [12]$$

where M and m are the masses of the oxygen and nitrogen atoms, respectively. The kinetic energy is then

$$T = \tfrac{1}{2}m\{2\mu\dot{x}^2+\tfrac{1}{2}\dot{w}^2+2\alpha^2\dot{y}^2[1+(\alpha^2/\mu)]^{-1}\}. \quad [13]$$

Using the definitions

$$E \equiv 2\mu, \quad [14]$$

[15] $$F \equiv \tfrac{1}{2},$$

[16] $$G \equiv 2\alpha^2[1+(\alpha^2/\mu)]^{-1},$$

the secular determinant is

[17] $$\begin{vmatrix} A-mE\lambda & D & 0 \\ D & B-mF\lambda & 0 \\ 0 & 0 & C-mG\lambda \end{vmatrix} = 0.$$

The observed frequencies are (21)

$$\nu_1 = 1288.7 \text{ cm}^{-1},$$
$$\nu_2 = 588.3 \text{ cm}^{-1},$$
$$\nu_3 = 2237.9 \text{ cm}^{-1},$$

and the values derived by Rosenthal (20) are:

$$\lambda_1 = 58.94\times10^{26} \qquad A = 14.72\times10^5 \text{ dynes cm}^{-1},$$
$$\lambda_3 = 1777.0\times10^{26} \qquad B = 17.20\times10^5 \text{ dynes cm}^{-1},$$
$$D = -7.08\times10^5 \text{ dynes cm}^{-1}.$$

By the use of the secular determinant [17] it is then found that

for ν_1, $x: w: y = (B-mF\lambda_1): -D: 0,$
$= 1.00: 0.429: 0;$

for ν_2, $x: w: y = 0: 0: (C-mG\lambda_2),$
$= 0: 0:$ constant;

for ν_3, $x: w: y = D: -(A-mE\lambda_3): 0,$
$= -0.857: 1.00: 0.$

In the application of Slater's method employed above, the critical co-ordinate was taken as the distance between the center of mass of the N–N system and the O atom. The variation p in this co-ordinate is equal to x, and the amplitude factor α_i is given by

[18] $$\alpha_i = \gamma_{xi} = x_i/\sqrt{V_{ii}}.$$

The calculated α's were shown in Table I above, which also gives the corresponding μ's.

The rest of the calculation is explained in the main body of the paper.

Can. J. Chem. Downloaded from www.nrcresearchpress.com by 78.46.186.204 on 09/04/12
For personal use only.

Can. J. Chem. Downloaded from www.nrcresearchpress.com by 78.46.186.204 on 09/04/12
For personal use only.

THE CONDENSATION OF RHODANINE WITH AROMATIC DIALDEHYDES AND SOME RELATED COMPOUNDS[1]

FREDERICK J. ALLAN,[2] G. GRAHAM ALLAN,[3] AND J. B. THOMSON

ABSTRACT

The condensation of rhodanine and its 3-ethyl and 3-phenyl derivatives with terephthaldehyde, pyridine-2,6-dicarboxaldehyde, and phthaldehyde has been investigated. Twenty-nine 5-arylidene-rhodanines containing an electrophilic substituent in the aromatic ring have been prepared.

Rhodanine condenses readily with a variety of aliphatic (1, 2, 3, 4), aromatic (5, 6), and heterocyclic (7, 8) aldehydes. The analogous reaction with ketones has been less extensively investigated (9, 10). Very few examples of rhodanine–diketone interaction have been described (11, 12, 13, 14, 15, 16) and we have been unable to find in the literature any reference to the condensation of rhodanine with dialdehydes. Our interest in rhodanine–dialdehyde adducts was actuated by the fungicidal and mildew-proofing properties of the 5-substituted rhodanines (I) in general, and the 5-arylidene-rhodanines (II) in particular (5, 6). In spite of the many variants of R in (II) only two compounds in which R is electrophilic have been evaluated as fungicides (5). The location of the substituent diminished or increased the fungitoxicity of (II), suggesting evaluation of electron distribution as a rationale for structure and activity. With a view to preparing further examples of this type of compound for testing we have examined the condensation of some aromatic dialdehydes with rhodanine derivatives.

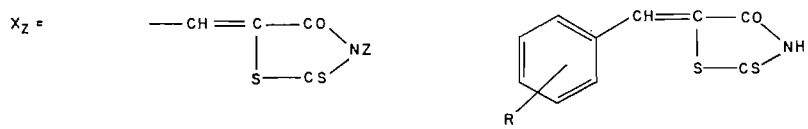

(I) (II)

in X_H (Z = H), X_{Et} (Z = C_2H_5), X_{Ph} (Z = C_6H_5).

Termolecular reaction of rhodanine and the 3-ethyl and 3-phenyl derivatives (two molecular proportions) with terephthaldehyde (III*a*) or pyridine-2,6-dicarboxaldehyde (IV*a*) (one molecular proportion) proceeds with great facility to yield the diadducts (III*b*), (III*c*), (III*d*), (IV*b*), (IV*c*), and (IV*d*) respectively, which separated from the reaction mixture in an almost pure state. The aldehyde–rhodanine derivatives were prepared using ammonia – ammonium chloride (17), acetic acid – sodium acetate (19), or acetic acid – acetic anhydride – sodium acetate (7) as condensing agents. No crystalline adducts were obtained from the reaction of phthaldehyde with either rhodanine, 3-ethyl-, or 3-phenyl-rhodanine using these reagents or with 3-ethylrhodanine under the conditions used to condense phthaldehyde with malonic ester (18). Condensation of equimolecular proportions of 3-ethyl- or 3-phenyl-rhodanine (but not rhodanine itself) with the dialdehydes (III*a*) and (IV*a*) gave readily separable mixtures of the appropriate diadducts

[1]*Manuscript received June 5, 1958.*
Contribution from the Department of Chemistry, Paisley Technical College, Paisley, Scotland.
[2]*To whom enquiries should be addressed.*
[3]*Present address: Electrochemicals Department, E. I. duPont deNemours & Co., Inc., Wilmington, Del., U.S.A.*

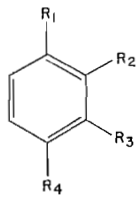

(III)

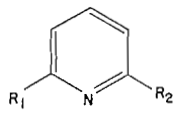

(IV)

III

a. $R_1 = R_4 = CHO$; $R_2 = R_3 = H$
b. $R_1 = R_4 = X_H$; $R_2 = R_3 = H$
c. $R_1 = R_4 = X_{Et}$; $R_2 = R_3 = H$
d. $R_1 = R_4 = X_{Ph}$; $R_2 = R_3 = H$
e. $R_1 = CHO$; $R_2 = R_3 = H$; $R_4 = X_{Et}$
f. $R_1 = CHO$; $R_2 = R_3 = H$; $R_4 = X_{Ph}$
g. $R_1 = CH{:}NOH$; $R_2 = R_3 = H$; $R_4 = X_{Ph}$
h. $R_1 = X_H$; $R_2 = NO_2$; $R_3 = R_4 = H$
i. $R_1 = X_{Et}$; $R_2 = NO_2$; $R_3 = R_4 = H$
j. $R_1 = X_{Ph}$; $R_2 = NO_2$; $R_3 = R_4 = H$
k. $R_1 = X_H$; $R_3 = NO_2$; $R_2 = R_4 = H$
l. $R_1 = X_{Et}$; $R_3 = NO_2$; $R_2 = R_4 = H$
m. $R_1 = X_{Ph}$; $R_3 = NO_2$; $R_2 = R_4 = H$
n. $R_1 = X_H$; $R_4 = NO_2$; $R_2 = R_3 = H$
o. $R_1 = X_{Et}$; $R_4 = NO_2$; $R_2 = R_3 = H$
p. $R_1 = X_{Ph}$; $R_4 = NO_2$; $R_2 = R_3 = H$
q. $R_1 = X_H$; $R_2 = CO_2H$; $R_3 = R_4 = H$
r. $R_1 = X_{Et}$; $R_2 = CO_2H$; $R_3 = R_4 = H$
s. $R_1 = X_{Ph}$; $R_2 = CO_2H$; $R_3 = R_4 = H$
t. $R_1 = X_H$; $R_4 = CO_2H$; $R_2 = R_3 = H$
u. $R_1 = X_{Et}$; $R_4 = CO_2H$; $R_2 = R_3 = H$
v. $R_1 = X_{Ph}$; $R_4 = CO_2H$; $R_2 = R_3 = H$

IV

a. $R_1 = R_2 = CHO$
b. $R_1 = R_2 = X_H$
c. $R_1 = R_2 = X_{Et}$
d. $R_1 = R_2 = X_{Ph}$
e. $R_1 = CHO$; $R_2 = X_{Et}$
f. $R_1 = CHO$; $R_2 = X_{Ph}$

described above and the related monoadducts (III*e*), (III*f*), (IV*e*), and (IV*f*). The retention of a free formyl group under the conditions of condensation is evidenced by analysis and the formation of an oxime (III*g*).

Concurrently with this study we have prepared for fungicidal and antibacterial evaluation* fifteen 5-arylidene-rhodanines (II) containing an electrophilic substituent in the benzenoid moiety and comprising two groups. The first group consists of the adducts (III*h*) to (III*p*) inclusive, containing the toxiphoric nitro group, which were synthesized by the condensation of rhodanine, its 3-ethyl and 3-phenyl homologues with 2-, 3-, and 4-nitrobenzaldehyde. The second group of adducts, (III*q*) to (III*v*) inclusive, was derived from the condensation of rhodanine and its congeners with phthaldehydic and terephthaldehydic acid; analogous derivatives of which have recently received attention as bactericidal agents (20, 21).

EXPERIMENTAL†

1,4-Phenylene-di-(5-methylenerhodanine) (III*b*)

A solution of terephthaldehyde (1.34 g, 0.01 mole) and rhodanine (2.66 g, 0.02 mole) in ethanol (20 ml) and concentrated ammonium hydroxide (7 ml, d., 0.88) was heated on the steam bath. A solution of ammonium chloride (7 g) in hot water (10 ml) was added and heating continued for 1 hour when orange needles had separated. Recrystallization from dimethylformamide gave the diadduct III*b* as fine orange needles (2.8 g, yield 77%) which did not melt below 360°. Calc. for $C_{14}H_8N_2O_2S_4$: C, 46.08; H, 2.2; N, 7.68; S, 35.25. Found: C, 45.81; H, 1.95; N, 7.31; S, 35.00%.

**Details of which we hope to publish later elsewhere.*
†*Melting points have been corrected.*

Can. J. Chem. Downloaded from www.nrcresearchpress.com by 78.46.186.204 on 09/04/12
For personal use only.

Can. J. Chem. Downloaded from www.nrcresearchpress.com by 78.46.186.204 on 09/04/12
For personal use only.

Compound*	Structure	Crystalline form†	M.p., °C	Yield %	Formula	Carbon, % Calc.	Carbon, % Found	Hydrogen, % Calc.	Hydrogen, % Found
1,4-Phenylene-di-(3-phenyl-5-methylenerhodanine)	III*d*	Fine orange needles[a]	>360	86	$C_{26}H_{16}N_2O_2S_4$	60.39	60.34	3.12	3.27
2,6-(1-Azaphenylene)-di-(3-ethyl-5-methylenerhodanine)§§	IV*c*	Fine yellow needles[b]	228–229	93	$C_{17}H_{16}N_4O_2S_4$	48.39	48.52	3.58	3.68
2,6-(1-Azaphenylene)-di-(3-phenyl-5-methylenerhodanine)|| ||	IV*d*	Fine orange needles[a]	335–336 (decomp.)	87	$C_{25}H_{16}N_4O_2S_4$	57.97	57.63	2.92	3.01
5-(2-Nitrobenzylidene)rhodanine‡	III*h*	Yellow needles[c]	204–205	71	$C_{10}H_6N_2O_3S_2$	45.09	45.31	2.27	2.13
3-Ethyl-5-(2-nitrobenzylidene)rhodanine	III*i*	Orange plates[d]	157–158	85	$C_{12}H_{10}N_2O_3S_2$	48.96	48.73	3.42	3.21
3-Phenyl-5-(2-nitrobenzylidene)rhodanine§	III*j*	Orange plates[e]	245–246	45	$C_{16}H_{10}N_2O_3S_2$	56.12	55.98	2.94	3.05
5-(3-Nitrobenzylidene)rhodanine||	III*k*	Bright yellow needles[c]	264–265	60	$C_{10}H_6N_2O_3S_2$	45.09	44.85	2.27	2.01
3-Ethyl-5-(3-nitrobenzylidene)rhodanine¶	III*l*	Golden-yellow blades[c]	194–195	58	$C_{12}H_{10}N_2O_3S_2$	48.96	48.67	3.42	3.28
3-Phenyl-5-(3-nitrobenzylidene)rhodanine**	III*m*	Orange platelets[e]	245–246	48	$C_{16}H_{10}N_2O_3S_2$	56.12	56.41	2.94	2.72
5-(4-Nitrobenzylidene)rhodanine††	III*n*	Orange-yellow needles[d]	273–274	90	$C_{10}H_6N_2O_3S_2$	45.09	44.76	2.27	2.41
3-Ethyl-5-(4-nitrobenzylidene)rhodanine	III*o*	Orange-yellow prismatic needles[d]	232–233	85	$C_{12}H_{10}N_2O_3S_2$	48.96	48.88	3.42	3.19
3-Phenyl-5-(4-nitrobenzylidene)rhodanine‡‡	III*p*	Yellow needles[e]	273–274	96	$C_{16}H_{10}N_2O_3S_2$	56.12	55.88	2.94	2.69
3-Ethyl-5-(2-carboxybenzylidene)rhodanine	III*r*	Golden-yellow rectangular plates[c]	185–187	52	$C_{13}H_{11}NO_3S_2$	53.22	52.96	3.78	3.82
3-Phenyl-5-(2-carboxybenzylidene)rhodanine	III*s*	Yellow-orange felted needles[d]	225–226	70	$C_{17}H_{11}NO_3S_2$	59.80	59.67	3.25	3.17
5-(4-Carboxybenzylidene)rhodanine	III*t*	Yellow-orange prismatic needles[b]	307–308 (decomp.)	80	$C_{11}H_7NO_3S_2$	49.79	49.61	2.65	2.53
3-Ethyl-5-(4-carboxybenzylidene)rhodanine	III*u*	Golden-yellow needles[b]	290–291	79	$C_{13}H_{11}NO_3S_2$	53.22	52.99	3.78	3.52
3-Phenyl-5-(4-carboxybenzylidene)rhodanine	III*v*	Orange-yellow prisms[a]	307–308	85	$C_{17}H_{11}NO_3S_2$	59.80	59.63	3.25	3.31

*The 17 compounds appearing in this table were similarly prepared.

†Crystallization solvents: [a]dimethylformamide, [b]acetic acid, [c]methanol, [d]acetone–methanol, [e]benzene–methanol.

‡Bondzynski (22) gives m.p. 188–189° for this compound prepared by the condensation of 2-nitrobenzaldehyde with rhodanine in ethanol containing sulphuric acid.

§Andreasch and Zipser (23) give m.p. 238° for this compound prepared by the same method.

||Bargellini (24) gives m.p. 245–255° for this compound prepared by the condensation of 3-nitrobenzaldehyde with rhodanine in ethanol containing sulphuric acid.

¶Andreasch and Zipser (25) give m.p. 188° for this compound prepared by the same method.

**Andreash and Zipser (25) give m.p. 240° for this compound prepared by the same method.

††Bondzynski (22) gives m.p. 250–252° (decomp.) for this compound prepared by the condensation of 4-nitrobenzaldehyde with rhodanine in ethanol containing sulphuric acid.

‡‡Andreasch and Zipser (25) give m.p. 240° (decomp.) for this compound prepared by the same method.

§§Nitrogen analysis: Calc., 9.96; found, 9.71%.

|| ||Nitrogen analysis: Calc., 8.11; found, 7.93%.

2,6-(1-Azaphenylene)-di-(5-methylenerhodanine) (IV*b*)*

2,6-(1-Azaphenylene)-di-(5-methylenerhodanine) (IV*b*), fine bright yellow needles (100 mg, yield 52%), from dimethylformamide, which did not melt below 360°. Calc. for $C_{13}H_7N_3O_2S_4$: C, 42.82; H, 1.94; N, 11.53. Found: C, 43.14; H, 1.94; N, 11.63%.

5-(2-Carboxybenzylidene)rhodanine (III*q*)*

5-(2-Carboxybenzylidene)rhodanine (III*q*), clusters of bright yellow needles (1.1 g, yield 42%) from aqueous ethanol, m.p. 268–270° with decomp. Calc. for $C_{11}H_7NO_3S_2$: C, 49.79; H, 2.65. Found: C, 49.58; H, 2.78%. Dijksman and Newbold (19) give m.p. 265–266° for this compound prepared by the condensation of phthaldehydic acid with rhodanine in acetic acid containing sodium acetate.

1,4-Phenylene-di-(3-ethyl-5-methylenerhodanine) (III*c*)

A mixture of terephthaldehyde (0.67 g, 0.005 mole), 3-ethylrhodanine (1.62 g, 0.01 mole), and freshly fused sodium acetate (3 g) in acetic acid (50 ml), to which acetic anhydride (1 ml) had been added, was refluxed for 1 hour during which time orange needles separated. The mixture was allowed to cool and the product collected. Recrystallization from acetic acid gave the diadduct III*c* as long prismatic orange needles (1.5 g, yield 71%) m.p. 295–296°. Calc. for $C_{18}H_{16}N_2O_2S_4$: C, 51.35; H, 3.83. Found: C, 51.42; H, 3.94%.

3-Ethyl-5-(4-formylbenzylidene)rhodanine (III*e*)

A mixture of terephthaldehyde (1.34 g, 0.01 mole), 3-ethylrhodanine (1.62 g, 0.01 mole), and freshly fused sodium acetate (3 g) in acetic acid (50 ml), to which acetic anhydride (1 ml) had been added, was refluxed for 1 hour when crystals had separated. The hot reaction mixture was filtered and the diadduct (III*c*) (1.25 g) removed. The filtrate was diluted with water (100 ml) and the yellow precipitate collected and washed with hot water. Crystallization from acetone–methanol gave 3-ethyl-5-(4-formylbenzylidene)rhodanine (550 mg, yield 20%) as orange-yellow plates, m.p. 171–172°. Calc. for $C_{13}H_{11}NO_2S_2$: C, 56.29; H, 4.0. Found: C, 56.48; H, 4.06%.

3-Phenyl-5-(4-formylbenzylidene)rhodanine (III*f*)†

3-Phenyl-5-(4-formylbenzylidene)rhodanine (III*f*), yellow needles (1.71 g, yield 53%) from benzene–ethanol, m.p. 233–234°. Calc. for $C_{17}H_{11}NO_2S_2$: C, 62.82; H, 3.41. Found: C, 62.71; H, 3.45%. The related *oxime* (III*g*) was prepared in pyridine–ethanol solution (26) and crystallized from benzene–ethanol as yellow needles, m.p. 276–278°. Calc. for $C_{17}H_{12}N_2O_2S_2$: C, 59.96; H, 3.55. Found: C, 59.77; H, 3.69%.

3-Ethyl-5-[2-(6-formyl)pyridylmethylene]rhodanine (IV*e*)†

3-Ethyl-5-[2-(6-formyl)pyridylmethylene]rhodanine (IV*e*), yellow prismatic needles (500 mg, yield 18%) from aqueous methanol, m.p. 191–192°. Calc. for $C_{12}H_{10}N_2O_2S_2$: C, 51.78; H, 3.62. Found: C, 51.53; H, 3.45%.

3-Phenyl-5-[2-(6-formyl)pyridylmethylene]rhodanine (IV*f*)†

3-Phenyl-5-[2-(6-formyl)pyridylmethylene]rhodanine (IV*f*), clusters of yellow prismatic needles (1.98 g, yield 60%) from methanol, m.p. 248–250°. Calc. for $C_{16}H_{10}N_2O_2S_2$: C, 58.88; H, 3.09. Found: C, 58.52; H, 3.01%.

**The compounds designated by * were similarly prepared.*
†*The compounds designated by † were similarly obtained.*

Can. J. Chem. Downloaded from www.nrcresearchpress.com by 78.46.186.204 on 09/04/12
For personal use only.

REFERENCES

1. NENCKI, M. Ber. **17**, 2277 (1884).
2. GRANACHER, C., GERO, M., OFNER, A., KLOPFENSTEIN, A., and SCHLATTER, E. Helv. Chim. Acta, **6**, 458 (1923).
3. ANDREASCH, R. Monatsh. **39**, 419 (1918).
4. ANDREASCH, R. Monatsh. **49**, 122 (1928).
5. BROWN, F. C., BRADSHER, C. K., and BOND, S. M. Ind. Eng. Chem. **45**, 1030 (1953).
6. BROWN, F. C., BRADSHER, C. K., BOND, S. M., and POTTER, M. J. Am. Chem. Soc. **73**, 2357 (1951) and previous references therein cited.
7. ALLAN, F. J., ALLAN, G. G., and THOMSON, J. B. J. Org. Chem. **23**, 112 (1958) and previous references therein cited.
8. NEU, R. Ber. **90**, 2638 (1957).
9. BROWN, F. C., BRADSHER, C. K., MCCALLUM, S., and POTTER, M. J. Org. Chem. **15**, 174 (1950).
10. ALLAN, G. G., MACLEAN, D., and NEWBOLD, G. T. J. Chem. Soc. 5053 (1952).
11. BUTSCHER, E. Monatsh. **32**, 9 (1911).
12. GRANACHER, C., REIS, H., and POOL, E. Helv. Chim. Acta, **5**, 382 (1922).
13. GRANACHER, C. and MAHAL, A. Helv. Chim. Acta, **6**, 467 (1923).
14. JONES, H. A. and HANN, R. M. J. Am. Chem. Soc. **50**, 2491 (1928).
15. JONES, R. V. and HENZE, H. R. J. Am. Chem. Soc. **64**, 1669 (1942).
16. KNOTT, E. B. To Kodak Ltd., Brit. Patent No. 753,648, July 25, 1956.
17. GIRARD, M. Ann. chim. **16**, 326 (1941).
18. WILEY, R. H. and HOBSON, P. H. J. Am. Chem. Soc. **71**, 2429 (1949).
19. DIJKSMAN, D. J. and NEWBOLD, G. T. J. Chem. Soc. 1213 (1951).
20. WHEELER, D. D. and YOUNG, D. C. To Dow Chemical Co., U.S. Patent Nos. 2,802,830 to 2,802,837, Aug. 13, 1957; 2,811,535, 2,811,536, Oct. 29, 1957; 2,814,627, Nov. 26, 1957; 2,817,668, Dec. 24, 1957; 2,819,286, 2,819,287, Jan. 7, 1958.
21. KAWARA, K. and KOBAYASHI, H. To Dai Nippon Drug Mfg. Co., Japan. Patent No. 2,838, April 16, 1956. Chem. Abstr. **51**, 9693 (1957).
22. BONDZYNSKI, S. Monatsh. **8**, 349 (1887).
23. ANDREASCH, R. and ZIPSER, A. Monatsh. **24**, 499 (1903).
24. BARGELLINI, G. Gazz. chim. ital. **36**, II, 129 (1906).
25. ANDREASCH, R. and ZIPSER, A. Monatsh. **25**, 176 (1904).
26. SHRINER, R. L. and FUSON, R. C. Identification of organic compounds. 2nd ed. John Wiley & Sons, Inc., New York. 1946. p. 167.

Can. J. Chem. Downloaded from www.nrcresearchpress.com by 78.46.186.204 on 09/04/12
For personal use only.

Can. J. Chem. Downloaded from www.nrcresearchpress.com by 78.46.186.204 on 09/04/12
For personal use only.

LIGHT-SCATTERING STUDIES ON ALUMINUM DISTEARATE[1]

A. E. Leger, J. C. Hyde, and H. Sheffer

ABSTRACT

A light-scattering study of aluminum distearate in dilute benzene solution suggests that it is a linear molecule of random coil shape. This is further substantiated by intrinsic viscosity – molecular weight data, the constancy of the ratio of the molecular weight to the square of the radius of gyration (Rg), the value of Φ in Flory's intrinsic viscosity – molecular weight relationship, and the close agreement between the theoretical and experimental results found for the unit length of the polymer chain. This average unit length has been calculated to be 4.46 Å.

INTRODUCTION

The fundamental structure of aluminum soaps remains rather obscure, although most authors (1, 2, 3, 4, 5, 6, 7, 8) agree that these substances dispersed in organic solvents are high polymers, the monomeric unit being the basic aluminum disoap, e.g. aluminum hydroxydistearate. Opinions differ, however, as to the nature of the chemical bonding between the monomeric units. McGee (6) and Gray and Alexander (5) have proposed an alternation of covalent and co-ordination bonds between the aluminum atom and oxygen atom of the hydroxyl radical to form the polymer chain. McBain (2) favors an association of the molecules into micelles, while McRoberts and Schulman (3) attribute the weak type of bonding exhibited by these molecules to hydrogen bonding. Recently the present authors (8) and Bauer *et al.* (7) gave evidence in favor of a structure similar to that proposed by Gray and Alexander, but with the carboxylate group also acting as a bridge between two aluminum atoms. These co-ordination bridge structures could easily be broken and could account for the changes in physical properties of solutions or gels on dilution, peptization, or on aging.

It has always been recognized that aluminum soap solutions are relatively unstable and deteriorate with time, with a gradual lowering of the molecular weight of the polymer. This instability has not as yet been fully explained but the breakdown is accelerated by moisture and in general by traces of acid or other polar compounds. The rate of change depends on the concentration, the more concentrated solutions being relatively more stable. A complete explanation of the physicochemical properties of aluminum soap solutions is impossible without a detailed knowledge of the structure of the soap molecule. It was considered important to obtain more data on molecular weight and viscosity characteristics of aluminum stearate solutions and deduce from these, if possible, the average size and shape of the molecules. It was recognized that interpretation of the results would be hampered by the instability of the polymer, so the experimental techniques employed were designed to diminish as much as possible its effect on the experimental data. Another limitation of the interpretation of the data lies in our lack of knowledge of molecular weight distribution characteristics and of any method of fractionation for this polymer.

Aluminum distearate swells in cold benzene and complete solution can be effected only by heating the mixture for some time. It would appear that the soap is a complex, probably cross-linked, polymer with relatively weak bonds. Prolonged heating causes the breakage of some of these bonds, resulting in a solution of polymer whose average molecular weight depends on the concentration.

[1]*Manuscript received July 9, 1958.*
Contribution from the Defence Research Chemical Laboratories, Ottawa, Canada.
Issued as D.R.C.L. Report No. 285.

If viscosity data are obtained for a series of solutions of differing concentration, made up by refluxing under standard conditions, a curve of the general shape OAB, as shown in Fig. 1, results. For a "starting" or refluxed solution of concentration 0.4%, point B is obtained. On dilution of this solution to 0.2% the reduced viscosity does not revert to point A but rather to point E (4), and by obtaining further points on the line BEC an intrinsic viscosity which is characteristic of the polymer in the 0.4% solution can be extrapolated. Similarly, dilution of the "starting" 0.2% solution gives the line AD and a lower intrinsic viscosity. Thus one can obtain characteristic intrinsic viscosities and corresponding average molecular weights for the polymers in the "starting" solutions. Viscosity and osmotic pressure data obtained in this manner were reported previously (4) and this paper extends the work to include light-scattering information.

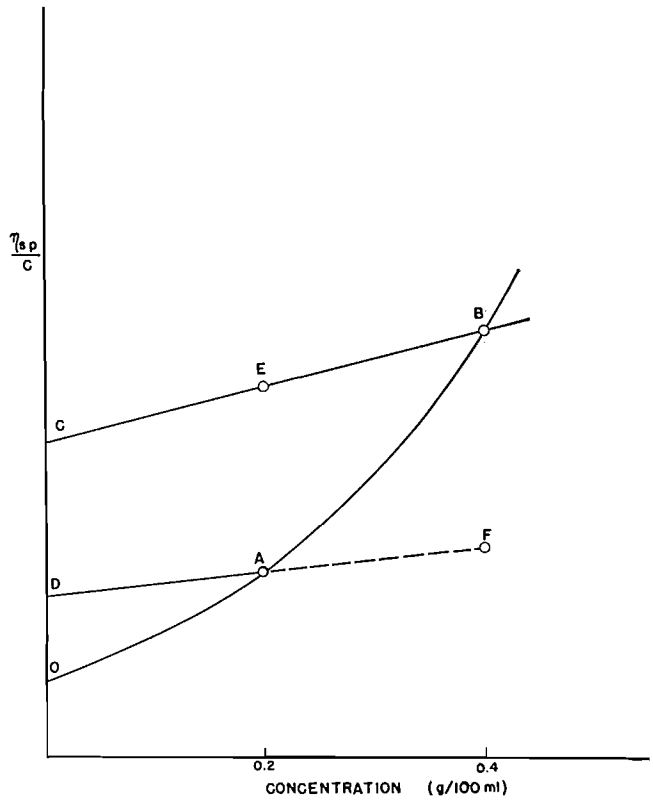

FIG. 1. A graphical representation of aluminum soap solution viscosity with changing concentration.

The fact that on dilution of solution *B* point E rather than A was obtained is an indication that the polymer is not merely an association colloid. Two other pieces of supporting evidence may be cited. One is that by melting and slowly resolidifying the soap under vacuum, material of much higher molecular weight is obtained (4) indicating that more polymer bonds are formed in the solid by this process than by association in solution. The other is concerned with the concentration of a dilute to a more concentrated one by evaporation of solution. On concentration of a 0.2% solution (point A) to 0.4%, point F on Fig. 1 is obtained rather than point B, which would be expected if the polymer were associating to larger micelles as the concentration is increased. This latter point was

Can. J. Chem. Downloaded from www.nrcresearchpress.com by 78.46.186.204 on 09/04/12
For personal use only.

checked by light-scattering technique and it was found that solution F contained polymer of molecular weight within 10% of that of solution A, while solution B contained polymer of about five times the average molecular weight of polymer in solution A.

EXPERIMENTAL

Reagents

The aluminum distearate used in this investigation was prepared by the method described previously (4) and extracted with dry acetone in a Soxhlet to remove free fatty acid. Solutions were prepared by refluxing the soap in specially dried benzene for $1\frac{1}{2}$ hours under anhydrous conditions. A small portion of the benzene was distilled at the start of the refluxing period to remove any residual moisture from the soap, solvent, and glassware.

Viscosity

Viscosity measurements were made at $30° \pm 0.01°$ C using Ostwald viscometers with a benzene flowtime of about 100 seconds, and the data were corrected for kinetic energy.

Light-Scattering Measurements

The apparatus used for the light-scattering measurements has been described previously (9). The cell in cross section is half of a regular dodecagon so that it is possible to measure scattering at 90° and at two pairs of angles about 90° (33° and 147°, 60° and 120°). The appropriate correction for reflection at the exit face (10) was made. The wavelength used was 5461 Å, obtained from a mercury-vapor lamp (General Electric AH-4) with suitable filters. Reduced intensities were plotted by the Zimm method, extrapolating the data to zero angle and infinite dilution. A typical Zimm plot of the experimental data is given in Fig. 2.

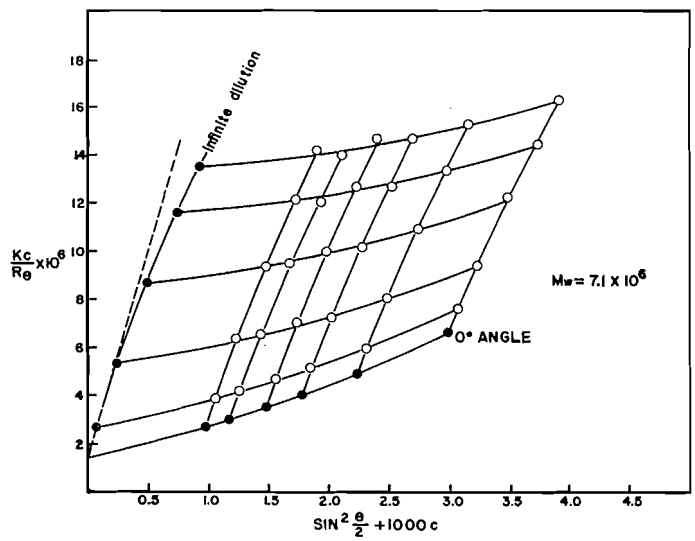

FIG. 2. A typical Zimm plot of experimental data obtained for aluminum distearate in benzene solution.

All measurements were made on aluminum distearate – benzene solutions previously cleared of dust particles by centrifuging at about 25,000 g for a few hours prior to use. A large number of "starting" solutions were prepared and the dilutions and measurements were made as fast as possible, the total time taken for each series being about 30 minutes.

Can. J. Chem. Downloaded from www.nrcresearchpress.com by 78.46.186.204 on 09/04/12
For personal use only.

Can. J. Chem. Downloaded from www.nrcresearchpress.com by 78.46.186.204 on 09/04/12
For personal use only.

RESULTS

A. Molecular Shape

The correlation of experimental data with theory is complicated by the lack of knowledge of the molecular weight distribution and by the possibility of branching of the polymer. However, it is possible to determine the radius of gyration (Rg) from the ratio of initial slope to the intercept in the Zimm plot, and the weight-average molecular weight from the reciprocal of the intercept of the infinite dilution curve. The use of the Zimm method obviates the necessity of making assumptions of the particle shape to obtain either value. The radius of gyration (Rg) and the weight-average molecular weight (Mw) are given in Table I for 21 different "starting" solutions of aluminum distearate. The ratio of the molecular weight Mw to the radius of gyration (M/Rg), to the square of the radius of gyration (M/Rg^2), and to the cube of the radius of gyration (M/Rg^3) are also given. It has previously been found (11, p. 211) that M/Rg is constant for spherical, $M/(Rg)^2$ for random-coiled, and $M/(Rg)^3$ for rod-shaped particles. As can be seen from Table I the ratio of M/Rg^2 has the greatest constancy. In making these calculations it is recognized that the absolute value of these ratios are in error as the molecular weight used is a weight average and Rg is a "Z" average length. Since, however, the "Z" and "W" average molecular weights will not have a widely varying ratio to one another, no great error is introduced in the constancy of the molecular weight radius of gyration ratio. This is especially true in the present case where the molecular weights considered are very high.

TABLE I

VALUES OF RADIUS OF GYRATION TO MOLECULAR WEIGHT RATIOS

Mw $\times 10^{-6}$	Rg Å	M/Rg $\times 10^{-2}$	$M/(Rg)^2 \times 10^{+2}$	$M/(Rg)^3 \times 10^{+5}$	$(\overline{r^2})^{\frac{1}{2}}$ Å
25.8	2790	8.95	3.20	1.13	6840
12.9	2010	6.42	3.20	1.56	4920
11.5	1800	6.39	3.54	1.97	4400
10.9	1710	6.39	3.73	2.18	4200
7.35	1510	4.86	3.22	2.14	3690
6.50	1430	4.55	3.18	2.22	3500
6.45	1580	4.09	2.59	1.64	3870
6.45	1520	4.24	2.78	1.83	3730
5.72	1490	3.84	2.58	1.73	3660
5.10	1350	3.78	2.80	2.08	3320
3.96	1270	3.12	2.46	1.94	3120
3.82	1240	3.08	2.48	2.00	3030
3.74	1150	3.25	2.82	2.46	2830
3.68	1190	3.09	2.60	2.38	2910
3.39	1220	2.78	2.28	1.87	2990
2.58	1020	2.52	2.47	2.42	2500
2.34	910	2.56	2.81	3.08	2220
1.32	750	1.76	2.35	3.14	1840
1.25	660	1.90	2.88	4.37	1660

The relative constancy of the M/Rg^2 ratio is an indication that the molecules are of the random coil type. It is known that for a random coil configuration the root-mean-square end-to-end length $(\overline{r^2})^{\frac{1}{2}}$ is equal to Rg $\sqrt{6}$. This relationship has been used to calculate the values of $(\overline{r^2})^{\frac{1}{2}}$ given in Table I.

It is also possible to correlate the light-scattering data with theoretically derived curves for spheres, coils, and rods and to determine which of these molecular shapes most closely satisfies the experimental data. The theoretical curves were calculated from the theoretical scattering functions for spheres, rods, and random coils and fitted to the experimental data to obtain the same 0° and 90° scattering. As can be seen in Fig. 3 the

experimental values are very close to the theoretical curves for random coils. Deviations of the curves could be explained by differences in polydispersity, branching, stiffness, or extension of the coils, and at the present time it would seem impossible to distinguish between these variables (12, 13).

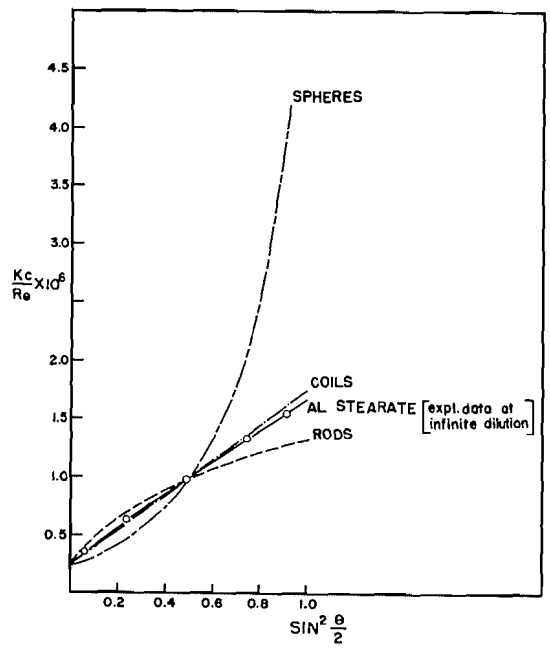

FIG. 3. A comparison of experimental data for aluminum distearate with theoretical curves for spheres, random coils, and rods.

Both the constancy of M/Rg^2 and the close agreement of the theoretical and experimental values lead to the conclusion that the molecules are indeed of the random coil type. This permits us to calculate the root-mean-square end-to-end distance as already noted and, as will be seen below, to derive some idea of the dimensions of the unit length of the molecule.

B. Viscosity – Molecular Weight Relationship

It is possible to derive some measure of the relationship between the intrinsic viscosity $[\eta]$ and the molecular weight of aluminum distearate (see Fig. 4). Although the data for extreme molecular weights introduce a curvature to the plot, for a large range of molecular weights this curve could be replaced by a straight line, within experimental error, which would correspond very closely to the theoretical value for linear molecules. This is shown by the dotted line in Fig. 4, its position having been determined by the least-squares method by neglecting the very high molecular weight and the very low viscosity values, which are less precise owing to experimental difficulties. The equation for this line is

$$[\eta] = 2.93 \times 10^{-4} M^{0.58}$$

in which the value for α in $[\eta] = KM^{\alpha}$ corresponds rather closely to the expected value of 0.5, the theoretical value for linear molecules such as polybutadiene.

Huggins' "k'" values were calculated from the slope of the reduced viscosity–concentration curves. Its average value was 0.77, but the scatter of the experimental data

Can. J. Chem. Downloaded from www.nrcresearchpress.com by 78.46.186.204 on 09/04/12
For personal use only.

made it impossible to determine any possible molecular weight dependence. This value for k' is lower and more constant than those obtained previously (4) owing to a more precise method of measuring viscosity. In general, k' values greater than 0.5 have been accounted for by branching in well-fractionated polymer samples. Interpretation of the results in aluminum soap solutions is further complicated by the known polydispersity of the polymer and it would seem impossible at this time to separate one effect from the other.

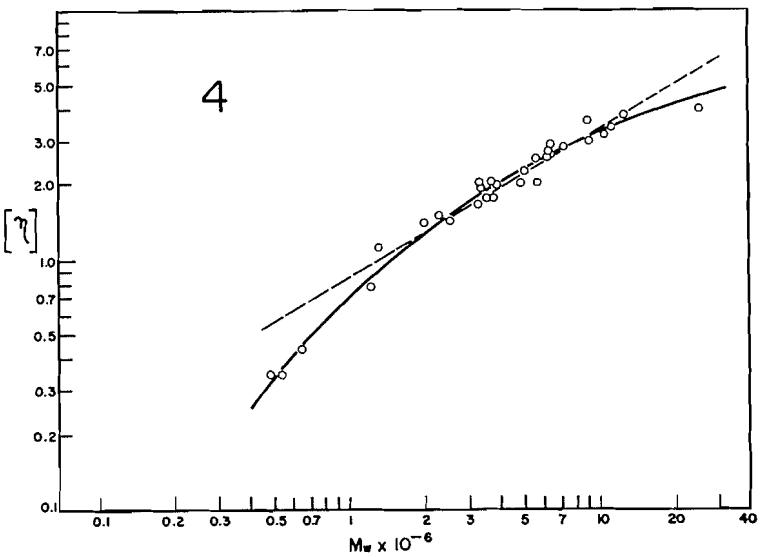

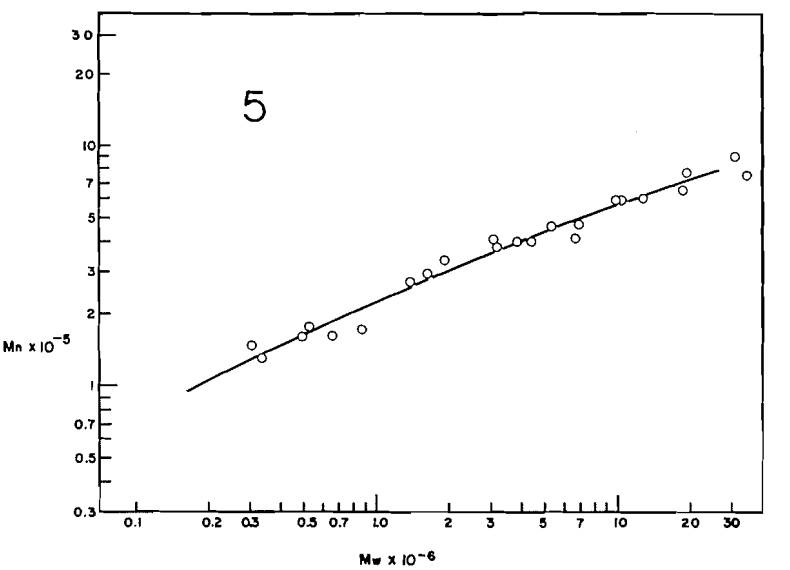

FIG. 4. Intrinsic viscosity [η] as a function of weight-average molecular weight (Mw) of aluminum distearate in benzene solution. The dotted line was obtained by neglecting three low molecular weight points and one high molecular weight point and drawing a straight line through the remainder by the method of least squares.

FIG. 5. Number-average molecular weight (Mn) as a function of weight-average molecular weight (Mw) for aluminum distearate in benzene solution.

Can. J. Chem. Downloaded from www.nrcresearchpress.com by 78.46.186.204 on 09/04/12
For personal use only.

C. Number-Average and Weight-Average Molecular Weight Correlations

Previously published data (4) gave the relationship of number-average molecular weight (Mn) as measured by the osmotic pressure method to intrinsic viscosity.

The present study gives the weight-average molecular weight (Mw) also as a function of intrinsic viscosity. It is thus possible to correlate Mn to Mw and to indicate the polydispersity of the polymer. This relationship is shown in Fig. 5. Most of the data used in the $[\eta]$–Mn curve were obtained for aluminum dilaurate, but since there did not seem to be any significant change in this relationship for other aluminum soaps, the same values were used for aluminum stearate. The ratio of Mw/Mn varies from about 30 for an Mw of 10^7 to about 3 for an Mw of 10^6. This relationship emphasizes the very wide polydispersity of the aluminum soaps and will be used below to calculate unit lengths in aluminum soap polymers.

As the polymer chains are broken down to lower molecular weight units the polydispersity decreases. Evidence was obtained to show that bond breakage does not occur near the end of the chain to form monomers or other small units. For this a Fuoss–Mead osmometer was used with a "fast" membrane, and diffusion rates through the membrane were obtained for a series of polystyrene fractions of known molecular weight. Comparing the results with those obtained for aluminum stearate solutions it was ascertained that not more than traces of soap polymer were present with molecular weight below 80,000.

D. Unit Length in Aluminum Stearate Polymer

It should be possible to derive an estimate of the unit length of the polymer chain by making certain assumptions. A molecular model for aluminum disoap has been proposed by Bauer *et al.* (7) and modified by the present authors (8).

Fig. 6 gives details of this modified model. In the actual molecular configuration, it is of course impossible for the Al—O—Al backbone to be in a straight line as the distance between succeeding Al atoms is too great for bridge formation and a zigzag configuration must be adopted (Fig. 7).

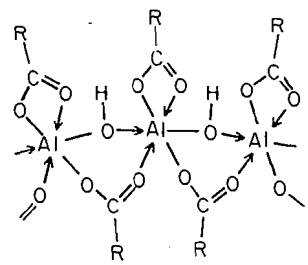

FIG. 6. Chemical formula of the aluminum soap molecule showing bridged and non-bridged carboxylate groups.

The evidence in favor of a bridge-type structure for the carboxylate group is mainly derived from experimental infrared absorption measurements. It has previously been shown (8) that in both aluminum tri- and di-soap two major absorption bands occur in the 6.1–6.4 μ region, and that these bands can be assigned to bridged and non-bridged carboxylate groups. This experimental evidence is corroborated by viscosity and molecular weight measurements. Bauer (7) has shown that peptization studies on aluminum disoaps can also be explained by a bridge-type structure.

Can. J. Chem. Downloaded from www.nrcresearchpress.com by 78.46.186.204 on 09/04/12
For personal use only.

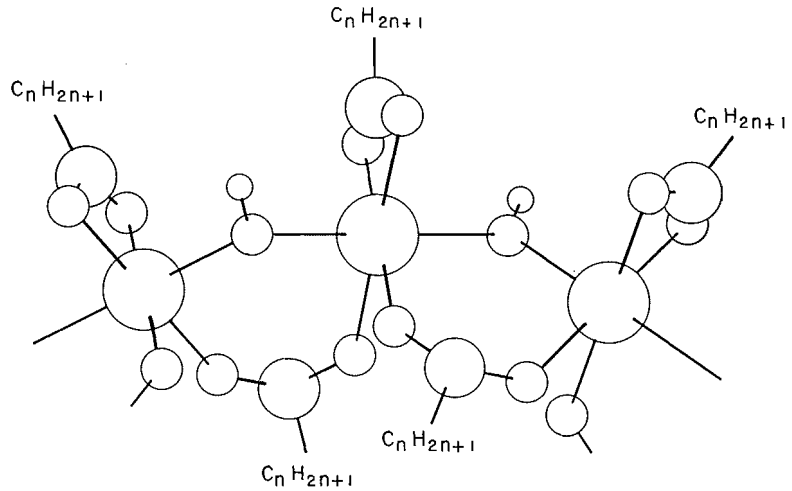

FIG. 7. Model of aluminum soap molecule showing bridged and non-bridged carboxylate groups.

The assumptions that are made in choosing this model are these:

1. The Al—O distances around the Al atoms are all equal. This assumption is probably not strictly accurate, and it is probable that the aluminum to hydroxyl bond length is greater than the aluminum–carboxylate distance, but this approximation is made to facilitate calculations in the absence of any definite value.

2. The O—O distance of a carboxylate group is taken as 2.28 Å, derived from an OCO angle of 125° and O—C bond length of 1.29 Å (14, p. 203).

3. The Al—O distance was taken as 1.92 Å, which is the sum of the covalent radii (14, p. 179). This gives a length of 2.71 Å for the O—O distance between the hydroxyl and carboxylate oxygen positions. This is higher than the 2.50 Å result found for most crystals in which aluminum–oxygen bonds are present.

The distances and angles involved in the calculation of the Al—O—Al bond angle are given in Fig. 8. The values of the Al—O—Al angle found by substituting plausible values of the O—O distance in the carboxylate group are given in Table II. These vary from a minimum of 130° to a maximum of 144°. The most probable value would probably be intermediate between all of these. For calculation purposes 135° was taken as the angle

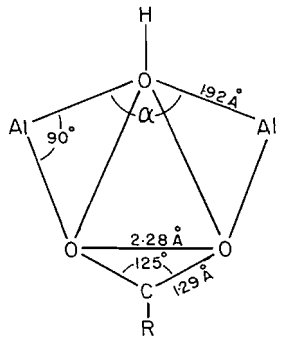

FIG. 8. Diagram of a portion of the aluminum soap molecule drawn through the Al—O—Al plane and showing its principal dimensions.

Can. J. Chem. Downloaded from www.nrcresearchpress.com by 78.46.186.204 on 09/04/12
For personal use only.

Al—O—Al. This value could be compared to 130°–160° proposed for the Si—O—Si angle in polysiloxanes (15).

TABLE II

CALCULATIONS OF BOND ANGLE

Assumed distances, Å			
Atom distance		Carboxylate group	Calculated value, angle Al—O—Al
Al—O	O—O	O—O	
1.92	2.50	1.90*	134°
	2.71	1.83*	130°
	2.50	2.28	144°
	2.71	2.28	140°
			137°

*Minimum distance of the bridge carboxylate O—O distance projected on the Al—O—Al plane as it oscillates from its average position.

It has been shown by Kuhn and others (16, Chap. X) that for polymer coils not extended by solvent–polymer interaction, the root-mean-square end-to-end distance could be related to the number and structure of the unit comprising the chain by the following relation,

$$r^2 = nl^2\,[(1+\cos\alpha)\,(1+\cos\psi)/(1-\cos\alpha)\,(1-\cos\psi)], \qquad [1]$$

where l is the unit length, i.e. the O—Al—O length; n, the number of units, $n = M_z/M_o$; α is the supplement of the valence angle Al—O—Al, i.e. $180° - 135° = 45°$; and ψ the average value of the angle between the $(i+2)^{th}$ bond and the plane of the two preceding ones. All the units must be expressed in terms of the same average. The root-mean-square end-to-end distance $(\bar{r^2})^{\frac{1}{2}}$ is derived from Rg— the radius of gyration—which as measured by light-scattering is a "Z" average value. The average number of units in the chain must also be a Z average, which means that the M in the equation must also be a Z average molecular weight. To calculate values of Mz it was assumed that the molecular weight distribution could be expressed by an exponential distribution function, especially since the molecular weight will be large (17).

$$Mn:Mw:Mz:k:k+1:k+2 \qquad [2]$$

Since the relation of Mw to Mn is given in Fig. 5, it is possible to find k, and Mz/Mn will be $(k+2)/(k+1)$. This ratio is given in Table III, together with the Mw molecular weight as derived by light-scattering measurement and from which Mz is obtained. This in turn gives n in equation [1].

The evaluation of the end-to-end distance by the relation given above [1] involves two basic steps. The first calculation—equivalent to a kinetic theory random-walk problem—gives the unit length of the polymer chains if no restriction whatsoever is imposed on the orientation of each link to its predecessor. The second, expressed in [1] as a ratio of the cosine of various angles, restricts this orientation for certain conditions imposed by steric hindrance, valency angles, and bond position. The unit length of the polymer chain without any angle restriction is about 26.3 Å, as given in Table III.

Can. J. Chem. Downloaded from www.nrcresearchpress.com by 78.46.186.204 on 09/04/12
For personal use only.

TABLE III
BOND LENGTHS IN ALUMINUM DISTEARATE

Molecular weight (W), Mw $\times 10^{-6}$	Factor $(k+2)/(k+1)$	Molecular weight (Z), Mz $\times 10^{-6}$	N = Mz/Mo $\times 10^{-4}$	$(\bar{r}^2)^{\frac{1}{2}}$ Å	Unit length	
					Uncorrected for chain angles, Å	Corrected for chain angles, Å
25.8	1.98	51.1	8.42	6840	23.5	4.02
12.9	1.95	25.2	4.13	4920	24.2	4.14
11.5	1.94	22.3	3.66	4400	23.0	3.94
10.9	1.94	21.2	3.48	4200	22.5	3.85
9.10	1.93	17.6	2.88	4020	23.7	4.05
7.35	1.93	14.2	2.33	3690	24.2	4.14
6.50	1.92	15.5	2.05	3500	24.4	4.17
6.45	1.92	12.4	2.04	3730	26.2	4.48
5.72	1.91	10.90	1.79	3660	27.4	4.68
5.10	1.91	9.74	1.59	3320	26.4	4.52
3.96	1.90	7.52	1.23	3120	28.2	4.82
3.82	1.90	7.26	1.20	3030	27.6	4.72
3.74	1.90	7.10	1.16	2830	26.3	4.50
3.68	1.90	7.00	1.15	2910	27.2	4.65
3.39	1.89	6.43	1.05	2880	28.2	4.83
2.58	1.88	4.36	0.798	2500	28.0	4.79
2.34	1.87	4.42	0.726	2220	26.0	4.44
1.32	1.72	2.27	0.371	1840	30.2	5.16
1.25	1.58	1.98	0.324	1620	28.2	4.83
					Average	4.46

The magnitude of the correction factor to be applied to this value for steric hindrance and valency angle will depend on the choice of the angles α and ψ. It has been shown that since α is the supplement of the Al—O—Al angle, it has a value of 45°. It is more difficult to choose a value for ψ. It is defined as the angle between the $(i+2)^{\text{th}}$ bond and the plane made by the preceding two bonds, and is equivalent to a restriction or rotation about the bond axis. In the case of aluminum disoap, free rotation is stopped at either 0° or 90° by the bridge structure. The average value of ψ is then 45°, which is the value used in [1].

These give an average unit length of 4.46 Å, as found in Table III. The lower values are probably more accurate as the number of units are greater and statistically more probable. This O—Al—O length is of course 2(Al—O), giving an Al—O bond length of 2.23 Å, compared with the calculated Al—O distance of 1.92 Å, as obtained from covalent radii.

Benoit (18) has shown that for polydisperse polymers made up of Gaussian chains, it is possible to obtain the number-average molecular weight and radius of gyration from the usual Zimm plot of the light-scattering data from the slope of the asymptote to the reciprocal scattering envelope at infinite dilution and at high-scattering angles. Unfortunately most of the data on aluminum stearate solutions were obtained with the dodecagonal cell, and extrapolation of this data is rather difficult with data available for only two backward angles. Several solutions were measured in a cylindrical cell with flat entrance and exit windows and the usual reflection and volume corrections made. Since the number-average molecular weight and root-mean-square end-to-end distance can both be calculated from the asymptote, no assumption need be made regarding the molecular weight distribution characteristics of the polymer. Three solutions examined in this way gave a number-average molecular weight of 2.48×10^5, 2.90×10^5, and 9.0×10^5, with an $(\overline{r_n^2})^{\frac{1}{2}}$ of 492 Å, 680 Å, and 835 Å, respectively. This leads to an

Can. J. Chem. Downloaded from www.nrcresearchpress.com by 78.46.186.204 on 09/04/12
For personal use only.

O—Al—O distance of 4.19 Å, 3.78 Å, and 3.80 Å, with the same equations and angle assumptions used previously. These bond length values are very close to those obtained by assuming a molecular weight distribution for the polymer and are a further indication of the validity of the assumptions made in the calculations.

E. Flory's Relationship

Flory (16) has postulated that for linear random coil molecules

$$[\eta] = \Phi(\bar{r}^2)^{3/2}/M$$

where $(\bar{r}^2)^{\frac{1}{2}}$ is the root-mean-square end-to-end distance of the molecule and Φ is a constant usually taken as 2.1×10^{21}.

In Fig. 9 this relationship is given as a function of Mw as determined by light-scattering. This relation has been shown to hold for various polymer systems of linear molecules. In the present case, there is a slight molecular weight dependence in Φ, probably because of the increasing polydispersity at higher molecular weights. The intercept gives the Φ value found for other systems namely 2.1×10^{21}.

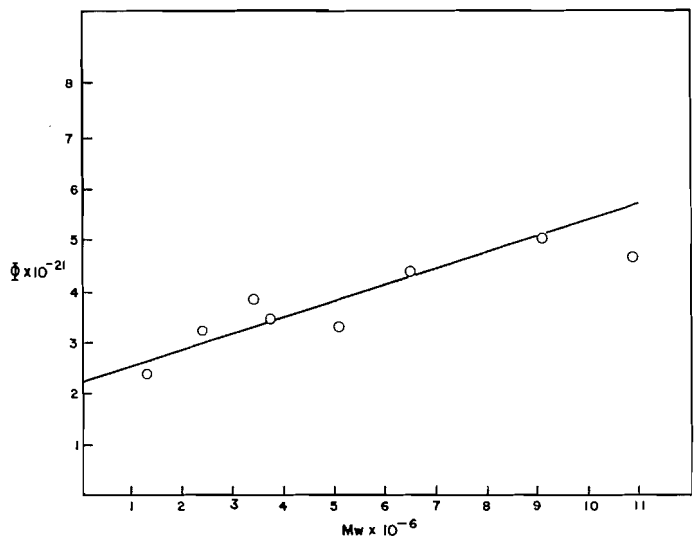

FIG. 9. Flory's Φ values as a function of weight-average molecular weight (Mn).

CONCLUSION

The results indicate that in dilute benzene solutions aluminum stearate is a linear molecule of random coil shape. In support of this conclusion, there is the expected intrinsic viscosity – molecular weight relationship, the experimental data satisfies the theoretical curves for random coils, the constancy of the ratio of the molecular weight to the square of the radius of gyration, the very close approximation of the Al—O bond length obtained by calculations based on this assumption, and expected value of Φ in the Flory intrinsic viscosity relationship.

It can also be concluded that for the aluminum distearate solutions, as prepared for our measurements, branching is not a predominant factor and the slight deviations from the usual linear molecules' behavior found above could be explained by the known very wide distribution of molecular weight.

Can. J. Chem. Downloaded from www.nrcresearchpress.com by 78.46.186.204 on 09/04/12
For personal use only.

ACKNOWLEDGMENTS

The authors wish to thank Dr. C. E. Hubley and Mr. R. L. Haines for helpful discussions and Mr. W. D. Barnes for technical assistance.

REFERENCES

1. GRAY, V. R. Trans. Faraday Soc. B, **42**, 196 (1946).
2. MCBAIN, J. W. and WORKING, E. B. J. Phys. & Colloid Chem. **51**, 974 (1947).
3. MCROBERTS, T. S. and SCHULMAN, J. H. Nature, **162**, 101 (1948).
4. SHEFFER, H. Can. J. Research, B, **26**, 481 (1948).
5. GRAY, V. R. and ALEXANDER, A. E. J. Phys. & Colloid Chem. **53**, 9, 23 (1949).
6. MCGEE, C. J. J. Am. Chem. Soc. **71**, 278 (1949).
7. SCOTT, F. A., GOLDENSON, J., WIBERLY, S. E., and BAUER, W. H. J. Phys. Chem. **58**, 61 (1954).
8. LEGER, A. E., HAINES, R. L., HUBLEY, C. E., HYDE, J. C., and SHEFFER, H. Can. J. Chem. **35**, 799 (1957).
9. HADOW, H. J., SHEFFER, H., and HYDE, J. C. Can. J. Research, B, **27**, 791 (1949).
10. SHEFFER, H. and HYDE, J. C. Can. J. Chem. **30**, 817 (1952).
11. STACEY, K. A. Light-scattering in physical chemistry. Butterworth Scientific Publications, London. 1956.
12. RICE, S. A. J. Polymer Sci. **16**, 94 (1955).
13. GOLDSTEIN, M. J. Chem. Phys. **21**, 1255 (1953).
14. PAULING, L. The nature of the chemical bond. 2nd ed. Cornell Univ. Press, Ithaca, N.Y. 1945.
15. AGGARWAL, E. H. and BAUER, S. H. J. Chem. Phys. **18**, 42 (1950).
16. FLORY, P. J. Principles of polymer chemistry. Cornell Univ. Press, Ithaca, N.Y. 1953.
17. BILLMEYER, F. W., JR. and STOCKMAYER, W. J. J. Polymer Sci. **5**, 121 (1950).
18. BENOIT, H., HOLTZER, A. M., and DOTY, P. J. Phys. Chem. **58**, 635 (1954).

Can. J. Chem. Downloaded from www.nrcresearchpress.com by 78.46.186.204 on 09/04/12
For personal use only.

Can. J. Chem. Downloaded from www.nrcresearchpress.com by 78.46.186.204 on 09/04/12
For personal use only.

NOTES

RESONANCE PARAMETERS FROM REACTIVITY CONSTANTS

C. N. RAMACHANDRA RAO* AND G. K. GOLDMAN

Recently, McDaniel and Brown (1) have compiled an extensive set of Hammett σ values based upon the ionization of benzoic acids. A number of electrophilic substituent constants, σ^+, have also been calculated based on the thermodynamic dissociation constants of benzoic acids by Brown and Okamoto (2). The σ^+ constants differ from the σ constants by an extra resonance factor resulting from the greater opportunity for resonance interaction by the substituents in electrophilic reactions. Such strong resonance interactions in electrophilic reactions occur between the electron-donating substituents and the electron-deficient centers of the reacting systems. Accordingly the σ_p^+ values differ greatly from the σ_p values for the ortho–para-directing groups. But the σ and σ^+ constants for the meta-directing substituents are very similar and the deviations fall within the limit of the estimated uncertainties of the constants (3). This is understandable, since the meta-directing groups exhibit no significant resonance interaction with the incipient carbonium ion. As one would expect, the σ_m and σ_m^+ values for groups are also similar, since the major contribution of a meta-substituent is by inductive interaction.

Although the resonance parameters of the substituents should vary with the electronic demands of the reaction, it has been possible to propose a single set of σ^+ values which would correlate the available data on electrophilic aromatic substitution and electrophilic side-chain reactions with good precision (2, 4). This suggests that the σ^+ constants can also be separated to independent inductive and resonance contributions similar to the quantitative separation of the Hammett σ constants by Taft (5),

$$\sigma^+ = \sigma_I + \sigma_R^+,$$

where σ_I and σ_R^+ are the inductive and resonance parameters respectively. The inductive

TABLE I

RESONANCE PARAMETERS FROM σ AND σ^+ CONSTANTS

	σ_I	$\sigma_R = \sigma_p - \sigma_I$	$\sigma_m - \sigma_I$	$\sigma_R^+ = \sigma_p^+ - \sigma_I$	$\sigma_m^+ - \sigma_I$
NH_2	+0.10	−0.76	−0.26	−1.40	−0.26
OH	+0.25	−0.62	−0.13	−1.17	—
OCH_3	+0.25	−0.52	−0.14	−1.03	−0.20
F	+0.52	−0.46	−0.18	−0.59	−0.17
SCH_3	+0.25	−0.25	−0.10	−0.85	−0.09
Cl	+0.47	−0.24	−0.10	−0.36	−0.07
$NHCOCH_3$	+0.28	−0.28	−0.07	−0.88	—
Br	+0.45	−0.22	−0.06	−0.30	−0.05
$(CH_3)_3C$	−0.07	−0.13	−0.03	−0.19	+0.01
I	+0.39	−0.21	−0.04	−0.26	−0.03
CH_3	−0.05	−0.12	−0.02	−0.26	−0.02
C_6H_5	+0.10	−0.11	−0.04	−0.28	−0.01
H	0.00	0.00	0.00	0.00	0.00
$\overset{+}{N}(CH_3)_3$	+0.86	−0.04	+0.02	−0.45	−0.50
CF_3	+0.41	+0.13	+0.02	+0.20	+0.11
$(CH_3)_3Si$	−0.12	+0.05	+0.08	+0.14	+0.13
CN	+0.59	+0.07	−0.03	+0.07	−0.03
$C_2H_5O_2C$	+0.32	+0.13	+0.05	+0.16	+0.05
NO_2	+0.63	+0.15	+0.08	+0.16	+0.04

*Presently at the Department of Chemistry, University of California, Berkeley, Calif.

parameters in this equation are the same as those proposed by Taft (5, 6). This is reasonable, since the inductive effect should essentially be independent of the reaction.

We have now calculated the $\sigma_p - \sigma_I$, $\sigma_m - \sigma_I$, $\sigma_p^+ - \sigma_I$ and $\sigma_m^+ - \sigma_I$ for several substituents based on the recent compilations of the σ and σ^+ values (1, 2). The results are summarized in Table I. In Fig. 1 are plotted the $\sigma_p - \sigma_I$ versus the $\sigma_p^+ - \sigma_I$ for the electron-donating groups. With the exception of $\overset{+}{N}(Me)_3$, NCOMe, SMe, and F groups, all the other groups fall on a straight line. By least-square treatment the line can be represented by the equation:

$$\sigma_R^+ = 1.91\sigma_R - 0.03.$$

This linearity further confirms the suggestion that σ_R^+ of a group is essentially a constant to a first approximation and that σ_R^+ is not a very sensitive function of ρ (4).

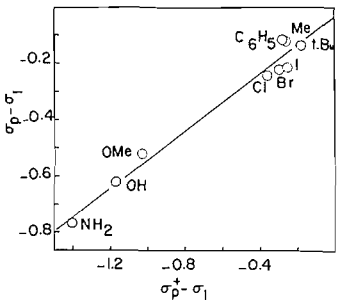

FIG. 1. Plot of σ_R^+ vs. σ_R for electron-donating groups.

ACKNOWLEDGMENT

The authors' thanks are due to Professor H. C. Brown for his kind interest.

1. McDANIEL, D. H. and BROWN, H. C. J. Org. Chem. **23**, 420 (1958).
2. BROWN, H. C. and OKAMOTO, Y. In press.
3. OKAMOTO, Y., INUKAI, T., and BROWN, H. C. In press.
4. OKAMOTO, Y. and BROWN, H. C. J. Org. Chem. **22**, 485 (1957).
5. TAFT, R. W. *In* Steric effects in organic chemistry. *Edited by* M. S. Newman, John Wiley & Sons, Inc., New York. 1956. Chap. 13.
6. TAFT, R. W. Technical Report No. 18. Office of Naval Research Contract No. 656(05), Project NRO55-328. Pennsylvania State University. 1958.

RECEIVED JULY 28, 1958.
RICHARD B. WETHERILL LABORATORY OF CHEMISTRY,
DEPARTMENT OF CHEMISTRY,
PURDUE UNIVERSITY,
LAFAYETTE, INDIANA, U.S.A.

REARRANGEMENT STUDIES WITH C^{14}
VI. THE FRIEDEL–CRAFTS ALKYLATION OF BENZENE WITH ETHYL-β-C^{14} IODIDE*

C. C. LEE, M. C. HAMBLIN, AND NADINE JAMES

In 1955, Roberts, Ropp, and Neville (1) reported that the Friedel–Crafts alkylation of benzene with ethyl-β-C^{14} chloride gave an ethylbenzene with no isotope position rearrangement in the ethyl side chain. When the ethyl-β-C^{14} chloride was allowed to stand over aluminum chloride at room temperature for 1 hour before being recovered and used to alkylate benzene, the ethylbenzene obtained showed rearrangements which

*Presented at the 41st Annual Conference of the Chemical Institute of Canada, Toronto, May 26–28, 1958.

Can. J. Chem. Downloaded from www.nrcresearchpress.com by 78.46.186.204 on 09/04/12
For personal use only.

parameters in this equation are the same as those proposed by Taft (5, 6). This is reasonable, since the inductive effect should essentially be independent of the reaction.

We have now calculated the $\sigma_p - \sigma_I$, $\sigma_m - \sigma_I$, $\sigma_p^+ - \sigma_I$ and $\sigma_m^+ - \sigma_I$ for several substituents based on the recent compilations of the σ and σ^+ values (1, 2). The results are summarized in Table I. In Fig. 1 are plotted the $\sigma_p - \sigma_I$ versus the $\sigma_p^+ - \sigma_I$ for the electron-donating groups. With the exception of $\overset{+}{N}(Me)_3$, NCOMe, SMe, and F groups, all the other groups fall on a straight line. By least-square treatment the line can be represented by the equation:

$$\sigma_R^+ = 1.91\sigma_R - 0.03.$$

This linearity further confirms the suggestion that σ_R^+ of a group is essentially a constant to a first approximation and that σ_R^+ is not a very sensitive function of ρ (4).

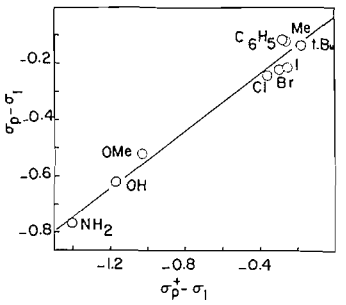

FIG. 1. Plot of σ_R^+ vs. σ_R for electron-donating groups.

ACKNOWLEDGMENT

The authors' thanks are due to Professor H. C. Brown for his kind interest.

1. McDANIEL, D. H. and BROWN, H. C. J. Org. Chem. **23**, 420 (1958).
2. BROWN, H. C. and OKAMOTO, Y. In press.
3. OKAMOTO, Y., INUKAI, T., and BROWN, H. C. In press.
4. OKAMOTO, Y. and BROWN, H. C. J. Org. Chem. **22**, 485 (1957).
5. TAFT, R. W. *In* Steric effects in organic chemistry. *Edited by* M. S. Newman, John Wiley & Sons, Inc., New York. 1956. Chap. 13.
6. TAFT, R. W. Technical Report No. 18. Office of Naval Research Contract No. 656(05), Project NRO55-328. Pennsylvania State University. 1958.

RECEIVED JULY 28, 1958.
RICHARD B. WETHERILL LABORATORY OF CHEMISTRY,
DEPARTMENT OF CHEMISTRY,
PURDUE UNIVERSITY,
LAFAYETTE, INDIANA, U.S.A.

REARRANGEMENT STUDIES WITH C^{14}
VI. THE FRIEDEL–CRAFTS ALKYLATION OF BENZENE WITH ETHYL-β-C^{14} IODIDE*

C. C. LEE, M. C. HAMBLIN, AND NADINE JAMES

In 1955, Roberts, Ropp, and Neville (1) reported that the Friedel–Crafts alkylation of benzene with ethyl-β-C^{14} chloride gave an ethylbenzene with no isotope position rearrangement in the ethyl side chain. When the ethyl-β-C^{14} chloride was allowed to stand over aluminum chloride at room temperature for 1 hour before being recovered and used to alkylate benzene, the ethylbenzene obtained showed rearrangements which

*Presented at the 41st Annual Conference of the Chemical Institute of Canada, Toronto, May 26–28, 1958.

Can. J. Chem. Downloaded from www.nrcresearchpress.com by 78.46.186.204 on 09/04/12
For personal use only.

indicated almost complete isomerization of the ethyl-β-C^{14} chloride by aluminum chloride. We have found substantially similar results for the alkylation of benzene with ethyl-β-C^{14} iodide, except that the aluminum chloride induced isomerization is much faster for the ethyl chloride (see Table I). Possibly, since chlorine is more electronegative than iodine, there may be a greater tendency for ethyl cation formation from ethyl chloride than from ethyl iodide under the influence of aluminum chloride.

TABLE I

REARRANGEMENTS IN THE FRIEDEL–CRAFTS ALKYLATION OF BENZENE WITH ETHYL-β-C^{14} IODIDE

Expt.	Reaction conditions*	Compound counted	Corrected activity†		% Rearrangement	
			Run I	Run II	Run I	Run II
A	All reactants refluxed overnight	$C_6H_5C_2H_5$	7328±96	7152±96		
		C_6H_5COOH	20±6	25±6	0.3	0.3
B	C_2H_5I and $AlCl_3$ stood at room temp. 1 hour before alkylation	$C_6H_5C_2H_5$	5040±70	5695±72		
		C_6H_5COOH	86±11	66±9	1.7	1.2
C	C_2H_5I and $AlCl_3$ refluxed 1 hour before alkylation	$C_6H_5C_2H_5$	6912±85	5422±72		
		C_6H_5COOH	1448±19	1420±19	21	26

*The reactants used were 3.0 ml C_2H_5I, 1.5 g $AlCl_3$, and 60 ml C_6H_6.

†Corrected activities in c.p.m. on a molar basis were determined by converting all compounds to barium carbonate and counted as infinitely thick samples of constant geometry in a gas flow Geiger counter. Correction for the dilution by non-labelled carbon atoms was made by multiplying the observed activity with the number of carbon atoms per molecule in the compound assayed.

The ethyl-β-C^{14} iodide was purchased from Atomic Energy of Canada Limited. The Friedel–Crafts reaction was carried out using 3.0 ml of labelled ethyl iodide, 1.5 g of anhydrous aluminum chloride, and 60 ml of redistilled benzene. The ethylbenzene obtained was oxidized with potassium permanganate to give benzoic acid, the radioactivity in which was taken as a measure of the rearrangement of the C^{14}-labelled atoms from the β- to the α-positions of the ethyl group. In Expts. B and C (Table I), the labelled ethyl iodide was treated with the aluminum chloride for 1 hour at room and reflux temperatures, respectively, before the resulting mixture was used to alkylate benzene. Similar yields of ethylbenzene, within the range of 70–75% of theoretical, were obtained in Expts. A, B, and C.

The degree of isotope position rearrangement induced by aluminum chloride on ethyl-β-C^{14} iodide is dependent on temperature as indicated by the results of Expts. B and C. It is also dependent on the length of the contact time of aluminum chloride with ethyl iodide. Mixtures of ethyl-β-C^{14} iodide (3.0 ml) and anhydrous aluminum chloride (1.5 g) were heated at 40° C for various lengths of time and the resulting material, without any fractionation, was used to alkylate an excess of benzene (60 ml). Isotope position rearrangements in the ethyl side chain of the ethylbenzene obtained are shown graphically in Fig. 1. Under these conditions, the degree of rearrangement was found to increase with length of contact time until a maximum of 50% rearrangement, corresponding to a complete equilibration of the α- and β-carbons of the ethyl group, is reached after about 42 hours.

The finding that aluminum chloride is capable of inducing isomerization in the labelled ethyl halide, while the ethylation of benzene under the usual Friedel–Crafts conditions yielded unrearranged ethylbenzene, was interpreted by Roberts, Ropp, and Neville (1) as meaning that the alkylation either follows a displacement mechanism involving no free ethyl fragments, or if a carbonium ion mechanism were operative, the ions react with the aromatic reactants so rapidly as to exclude internal hydride shifts. More recently,

Can. J. Chem. Downloaded from www.nrcresearchpress.com by 78.46.186.204 on 09/04/12
For personal use only.

Jungk, Smoot, and Brown (2) suggested that the Friedel–Crafts alkylation is another example of substitution on saturated carbon, which may have a continuum of mechanisms ranging between the extremes of a direct displacement and one involving an alkyl cation that could give rise to rearrangement. Still another possibility that rearrangement in the Friedel–Crafts alkylation may arise from a separate process which occurs before the product-forming alkylation step has been pointed out (3). Applying any one of these explanations to the present results, one would expect that the rate of the Friedel–Crafts reaction between ethyl iodide and benzene should be faster than the rate of the aluminum chloride induced rearrangement on ethyl-β-C^{14} iodide. It is thus of interest to measure the rate of the ethylation under our experimental conditions. Instead of the usual titration of the liberated hydrogen halide, we have estimated the rate of ethylbenzene formation by an isotope dilution technique. Since 1 mole of ethylbenzene is

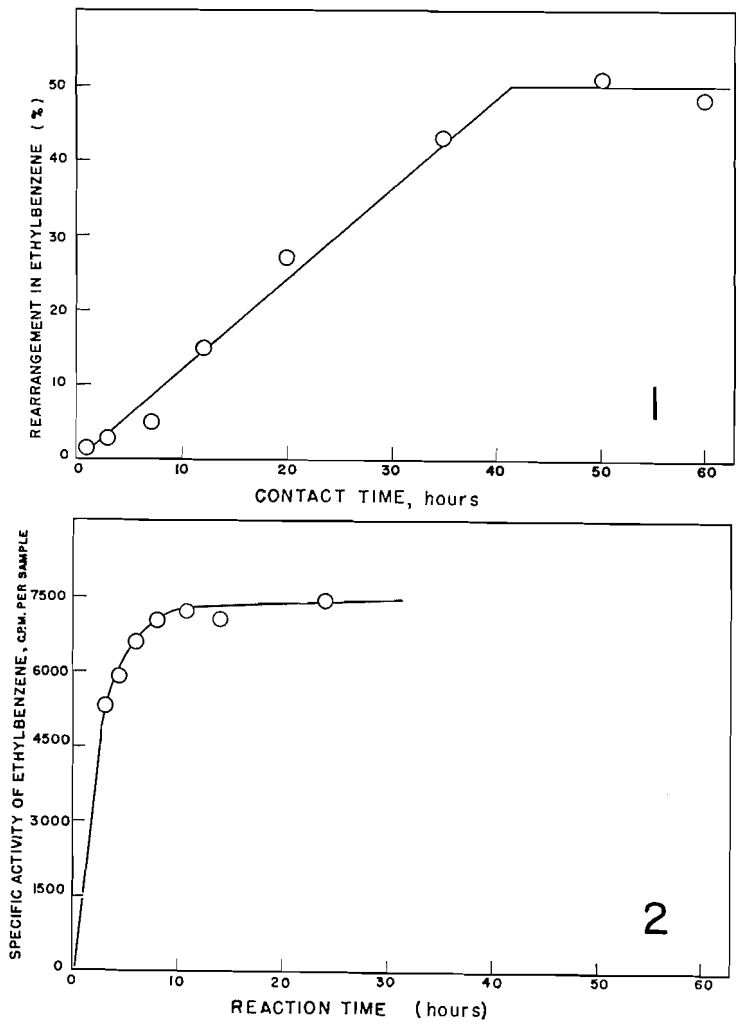

FIG. 1. Isotope position rearrangements in ethylbenzene from reaction of benzene with mixtures of labelled ethyl iodide and aluminum chloride that had been in contact at 40° for various lengths of time.

FIG. 2. Specific activities of ethylbenzene from aliquots of a Friedel–Crafts reaction at 40°, each aliquot having been diluted with a fixed amount of non-radioactive ethylbenzene.

Can. J. Chem. Downloaded from www.nrcresearchpress.com by 78.46.186.204 on 09/04/12
For personal use only.

produced from 1 mole of ethyl iodide, the activity per mole of the ethylbenzene formed should be the same as the activity per mole of the ethyl-β-C^{14} iodide used, though the total quantity of ethylbenzene produced would increase with reaction time. If aliquots of the reaction mixture were withdrawn at various time intervals and a fixed amount of non-labelled ethylbenzene added to each aliquot, the specific activity of the ethylbenzene samples recovered from these aliquots should increase with reaction time and would reach a constant maximum value after the reaction is complete. As the specific activity of the diluted ethylbenzene is a measure of the quantity of labelled ethylbenzene actually produced by the Friedel–Crafts reaction it is not necessary to have quantitative isolation of all ethylbenzene from each aliquot. The radiochemical purity of the recovered ethylbenzene can be rigorously established by showing that the specific activity of the diluted ethylbenzene from various aliquots does not change significantly on repeated distillation. Such a kinetic study was carried out at 40° C, the reactants initially present being 120 ml of benzene, 6.0 ml of ethyl-β-C^{14} iodide, and 3.0 g of aluminum chloride. The results are given graphically in Fig. 2, the plateau of constant maximum specific activity being reached in about 12 hours. Assuming the specific activity at the plateau of Fig. 2 corresponds to 100% reaction, it is possible to calculate the percentage of ethyl iodide remaining unreacted at various times before the reaction was complete. This is shown in a semilogarithmic plot in Fig. 3, indicating that the reaction, as expected, is first order with respect to ethyl iodide. The first-order specific rate constant derived from Fig. 3 is 0.81×10^{-4} sec^{-1}.

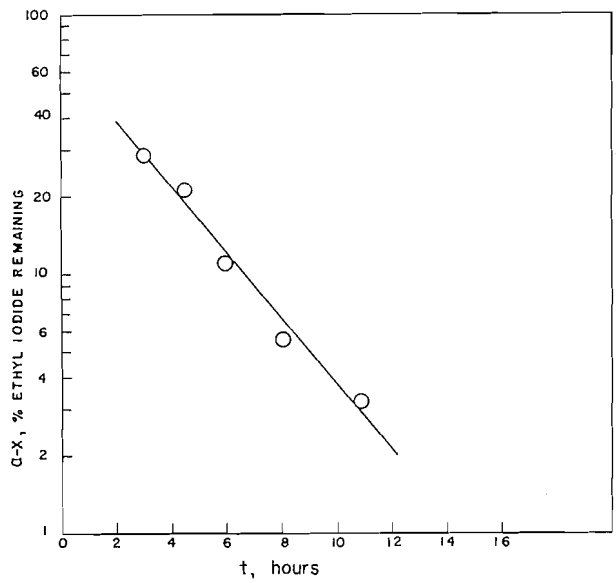

FIG. 3. First-order kinetic dependency on ethyl iodide in the formation of ethylbenzene. Calculated from Fig. 2.

Comparing Figs. 1 and 2, it is evident that at 40° C, the rate of the aluminum chloride induced rearrangement on pure ethyl iodide is slower than the rate of the Friedel–Crafts ethylation of benzene. Under the Friedel–Crafts reaction conditions, the ethyl iodide is diluted by the presence of an excess of benzene, thus the rate of the aluminum chloride induced rearrangement may be still slower. It is, therefore, reasonable to conclude that

Can. J. Chem. Downloaded from www.nrcresearchpress.com by 78.46.186.204 on 09/04/12
For personal use only.

in the Friedel–Crafts reaction between benzene and ethyl-β-C^{14} iodide, the rate of ethylbenzene formation is faster than the rate of a possible rearrangement of the ethyl iodide caused by the aluminum chloride.

1. ROBERTS, R. M., ROPP, G. A., and NEVILLE, O. K. J. Am. Chem. Soc. **77**, 1764 (1955).
2. JUNGK, H., SMOOT, C. R., and BROWN, H. C. J. Am. Chem. Soc. **78**, 2185 (1956).
3. LEE, C. C., FORMAN, A. G., and ROSENTHAL, A. Can. J. Chem. **35**, 220 (1957).

RECEIVED JUNE 24, 1958.
DEPARTMENT OF CHEMISTRY,
UNIVERSITY OF SASKATCHEWAN,
SASKATOON, SASKATCHEWAN.

Can. J. Chem. Downloaded from www.nrcresearchpress.com by 78.46.186.204 on 09/04/12
For personal use only.

Can. J. Chem. Downloaded from www.nrcresearchpress.com by 78.46.186.204 on 09/04/12
For personal use only.

Canadian Journal of Chemistry

Issued by THE NATIONAL RESEARCH COUNCIL OF CANADA

VOLUME 36 DECEMBER 1958 NUMBER 12

POTATO X VIRUS

PART I. THE SIZE AND SIZE DISTRIBUTION OF POTATO X VIRUS IN TOBACCO SAP[1]

M. E. REICHMANN

ABSTRACT

Assuming an irreversible, random, end-to-end aggregation of a small percentage of potato X virus in tobacco sap, the flow birefringence parameters of such polydisperse systems have been calculated. The extinction angles χ were evaluated for different values of the ratio G/θ_1 (G gradient, θ_1 rotary diffusion constant of non-aggregated virus) for preparations containing between 0 and 15% by weight of aggregated material. A particle length of 6200 Å for the non-aggregated virus particle was derived and an amount of 13–15% aggregated material was estimated.

A partially purified and fractionated preparation of potato X virus was also investigated and an average particle length of 5400 Å was derived. Because of the possible contribution of small fragments, this length was taken as the lower limit.

The flow birefringence – gradient curve indicated that the potato X virus behaves like a rigid particle. No evidence of flexibility was obtained from extinction angle – gradient measurements in the range 0.1–0 M phosphate buffer concentrations at pH 7.2.

INTRODUCTION

The tendency of the elongated plant viruses to aggregate irreversibly in an end-to-end fashion, in the process of isolation and purification, has made it difficult to study the shape and size of these viruses in solution (1, 2, 3, 4). The potato X virus in particular presents a difficult problem, as even the mild treatment of ultracentrifugation renders much of the material insoluble (1, 3). The value of physicochemical studies on such preparations is, therefore, somewhat dubious (5, 6). The most reliable data on the size and size distribution of this virus come from electron microscope studies of untreated plant sap (7, 8), where a uniform particle length of 500 to 525 mμ and 10 mμ thickness is indicated with a small amount of the virus material present in the form of higher end-to-end aggregates of this elementary particle. However, since the information obtained from electron microscopy is pertinent only to the non-hydrated virus and, moreover, breakage or aggregation of particles can occur during the preparation of electron microscopic specimens (9, 10, 11), an investigation of the virus size and size distribution in the hydrated form is highly desirable. This paper deals with an analysis of flow birefringence measurements made on tobacco sap infected with potato X virus. In addition, a partial purification of the virus is described. In the process the aggregated fraction present in the sap was preferentially removed. Flow birefringence measurements on this preparation made it possible to determine the lower limit of the characteristic particle size. The flow birefringence technique is particularly suitable for such studies, because of its great sensitivity to the particle length (12) and because of the absence of flow birefringent material in the sap of healthy tobacco after freezing.

[1]*Manuscript received July 6, 1958.*
Contribution No. 2, Chemistry Division, Science Service, Canada Department of Agriculture Research Laboratory, Vancouver, B.C.

Theory

In the treatment that follows, three assumptions are made: 1. The elementary virus particle (here referred to as monomer) as well as the aggregates (polymers) is sufficiently rigid to be treated as rigid ellipsoids of revolution. 2. The end-to-end aggregation occurs at random. 3. The axial ratio is greater than five. Assumptions 1 and 2 are discussed further in the last section of this paper, while assumption 3 is certainly justified by electron microscopy data (4, 7).

The flow birefringence theory for polydisperse systems has been treated by Sadron (13). The flow birefringence parameters have been evaluated for Gaussian (14) and Montroll–Simha distribution functions (15, 16). In the case of random linear aggregation the distribution function will have a different form. The problem can be treated essentially as one of a bifunctional monomer undergoing condensation polymerization. Flory has treated the distribution of x-mers in such a system, and the weight fraction of x-mers W_x is given by the following expression (17):

$$W_x = xp^{(x-1)}(1-p)^2, \tag{1}$$

where p is the total fraction of material which has undergone polymerization. In the case of rigid particles the above expression also gives the size distribution WL_x:

$$WL_x = L_x/L_1\, p^{(L_x/L_1-1)}(1-p)^2. \tag{2}$$

Here L_x is the length of the x-mer and x has been replaced by L_x/L_1. By carrying out the summation over all x's from 1 to ∞ one can see that the function is normalized. This distribution function can thus be used for a derivation of the flow birefringence parameters: the extinction angle χ and the rotary diffusion constant θ. If the axial ratio of the monomer is greater than five, the rotary diffusion constant varies inversely as the cube of the particle length (16, 18) and the following relationship applies:

$$x = L_x/L_1 = (\theta_1/\theta_x)^{\frac{1}{3}} = (\alpha_x/\alpha_1)^{\frac{1}{3}} = \gamma. \tag{3}$$

Here the α's represent the ratio of the velocity gradient G to the respective rotary diffusion constant. The distribution function can now be expressed in terms of α and p only:

$$W_\gamma = \gamma p^{(\gamma-1)}\,(1-p)^2, \tag{4}$$

$\gamma = (\alpha_x/\alpha_1)^{\frac{1}{3}}$ can only assume integer values from 1 to ∞.

The extinction angle χ in a polydisperse system is given by the following expression (14, 16):

$$\tan 2\chi = A/B,$$

where

$$A = \sum_{x=1}^{\infty} W_x f(\alpha_x) \sin 2\phi_x,\quad B = \sum_{x=1}^{\infty} W_x f(\alpha_x) \cos 2\phi_x, \tag{5}$$

ϕ_x is the extinction angle of the x-mer, and $f(\alpha_x)$ is a form factor. Both quantities can be found in the tables of Scheraga, Edsall, and Gadd (19). Introducing W_x in terms of α from [4]:

$$A = (1-p)^2 \sum_{\gamma=1}^{\infty} \gamma p^{(\gamma-1)} f(\alpha_x) \sin 2\phi_x$$

$$B = (1-p)^2 \sum_{\gamma=1}^{\infty} \gamma p^{(\gamma-1)} f(\alpha_x) \cos 2\phi_x. \tag{6}$$

Can. J. Chem. Downloaded from www.nrcresearchpress.com by 78.46.186.204 on 09/04/12
For personal use only.

For values of p not exceeding 0.15 (less than 15% aggregated material) the series converge rapidly and the fifth term ($\gamma = 5$) does not contribute more than 2% to the sum. A and B and thus χ can be evaluated by neglecting higher terms in the series. Table I gives the values of χ for $\alpha_1 = 0$–4 and for $p = 0.02$–0.15. Figure 1 represents a plot of χ vs. α_1 for various degrees of aggregation p.

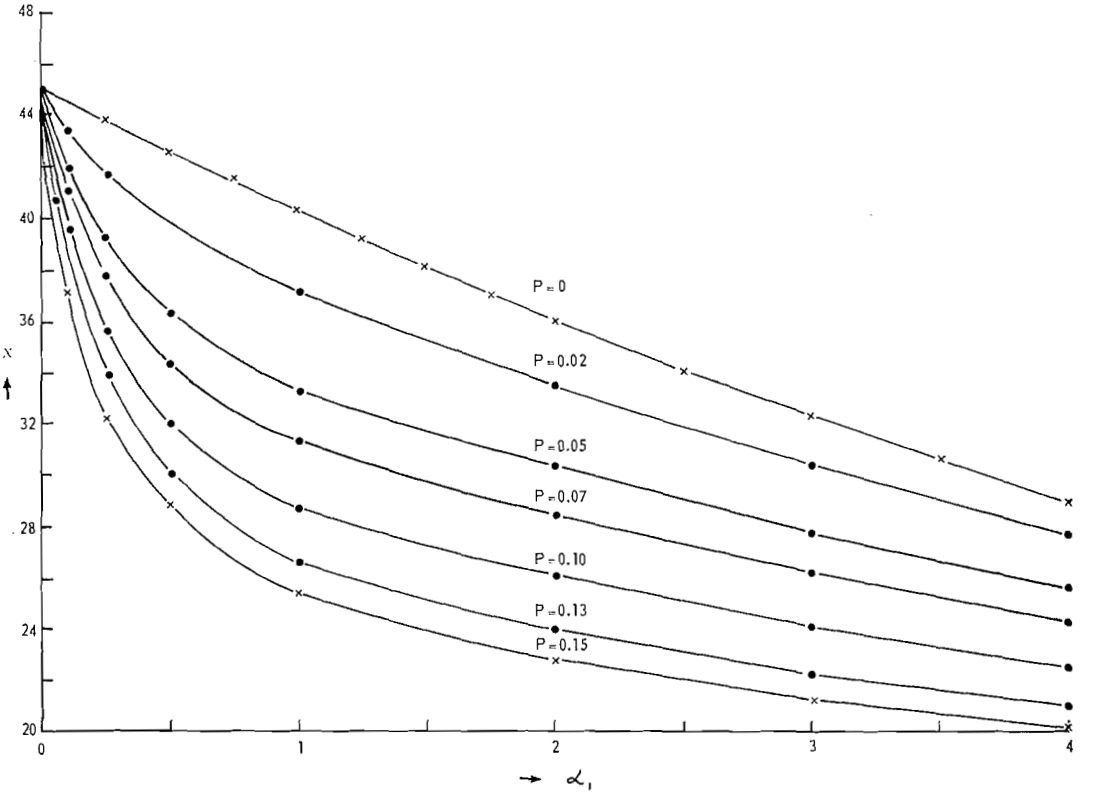

FIG. 1. Extinction angle – gradient curves for polydisperse systems with a Flory distribution function and various fractions p of aggregated material.

For values of α_1 greater than four, α_x becomes too large and the values of $f(\alpha_x)$ and ϕ_x in the tables of reference (19) are somewhat dubious. This, however, does not matter, as the largest deviations from the monodisperse curve $p = 0$ occur in the region of low α's. From the best fit of the theoretical and experimental curves in this region the amount of aggregated material p, as well as the rotary diffusion constant of the monomer, θ_1, can be determined. For prolate ellipsoids of revolution (16):

$$\theta = \frac{kT}{\pi\eta L^3}\frac{3}{2}(-1+2\ln 2\beta)$$

where k is Boltzman's constant, T is the absolute temperature, η is the solvent viscosity, and β is the axial ratio. The length of the monomeric virus particle has been calculated from this equation assuming $\beta = 60$ (4, 7). L_1 and θ_1, however, are not very sensitive to the axial ratio β, because of the logarithmic dependency.

Can. J. Chem. Downloaded from www.nrcresearchpress.com by 78.46.186.204 on 09/04/12
For personal use only.

TABLE I

VALUES OF EXTINCTION ANGLES χ AT VARIOUS VALUES OF α_1 (see text) FOR FLORY DISTRIBUTION FUNCTIONS CONTAINING A FRACTION p OF HIGHER AGGREGATES

$p = 0.02$		$p = 0.05$		$p = 0.07$	
α_1	χ	α_1	χ	α_1	χ
0.05	44.23	0.05	43.22	0.05	42.51
0.10	43.50	0.10	42.00	0.10	41.03
0.25	41.71	0.25	39.13	0.25	37.63
0.50	39.62	0.50	36.29	0.50	34.35
1.00	37.14	1.00	33.34	1.00	31.27
2.00	33.55	2.00	30.35	2.00	28.50
3.00	30.40	3.00	27.82	3.00	26.27
4.00	27.69	4.00	25.56	4.00	24.26

$p = 0.10$		$p = 0.13$		$p = 0.15$	
α_1	χ	α_1	χ	α_1	χ
0.05	41.68	0.05	40.61	0.05	40.02
0.10	39.51	0.10	38.07	0.10	37.12
0.25	35.61	0.25	33.83	0.25	32.64
0.50	32.02	0.50	30.04	0.50	28.81
1.00	28.66	1.00	26.50	1.00	25.26
2.00	26.07	2.00	23.91	2.00	22.77
3.00	24.16	3.00	22.23	3.00	21.21
4.00	22.50	4.00	21.00	4.00	20.10

MATERIAL AND METHODS

Preparation of Sap

One-month-old tobacco seedlings were infected with a severe potato X strain, isolated from a single lesion on *Gomphrena globosa*.* Two weeks after inoculation the young leaves were harvested and kept frozen overnight. They were then thawed at 5° C and squeezed in a mortar with a pestle. The sap was centrifuged for 45 minutes at 3500 r.p.m. All the operations were carried out in a cold room (0–5° C), and the brown color of the supernatant sap was not strong enough to interfere with the flow birefringence measurements. The extinction angles at various gradients were measured with a flow birefringence apparatus manufactured by the Rao Instrument Company, Brooklyn 5, New York (20, 22).

For more accurate measurements the sap was concentrated in a Petri dish in a desiccator to $\frac{1}{4}$ of its original volume. This did not change the values of the extinction angles. Dilutions were made with distilled water. The amount of birefringence was never less than 10° expressed in terms of the phase difference (which is twice the angular rotation of the Senarmont compensator). Under these conditions the isoclines were sharp enough to permit a reproducibility of at least 0.8° at gradients of 40 sec^{-1} or higher. The reproducibility on different preparations was also very good provided plants of approximately the same age were used. Sap from plants older than a month from the date of inoculation was deeper in color, and therefore no reliable data could be obtained. There was, however, some indication of the presence of more aggregated material than in younger plants.

Partial Purification and Fractionation

Fresh sap from tobacco plants infected with potato X virus was made 0.05 M in phosphate buffer pH 5.7, and centrifuged at 4000 r.p.m. for 40 minutes. Twenty-five

*The author is greatly indebted to Dr. N. S. Wright of the Plant Pathology Section of this laboratory for the supply of virus material.

Can. J. Chem. Downloaded from www.nrcresearchpress.com by 78.46.186.204 on 09/04/12
For personal use only.

grams of celite (Johns–Manville, Analytical Filter Aid) was mixed with 250 ml of supernatant sap and poured into a 45-mm diameter glass column with a fritted glass plate bottom. Mild suction was applied. The first 40 ml of sap that came through were recycled. No flow birefringence could be detected in the sap that passed through the column subsequently. The column was washed thoroughly with 0.05 *M* phosphate buffer pH 5.7. Distilled water was then used to elute the virus. Most of the virus came off the column in the first 20 ml of the eluent. About 70% of the virus was recovered. The solution was faintly yellow indicating the presence of impurities. In the Spinco ultracentrifuge a peak corresponding to the virus and a small shoulder near the meniscus were observed. This shoulder failed to separate after 45 minutes at 50,000 r.p.m. Electrophoretic patterns in 0.05 *M* phosphate buffer pH 7.0, taken with a model H Spinco Electrophoresis-Diffusion Apparatus, showed two components. In addition to a sharp, slow-moving peak corresponding to the virus, a faster-moving diffuse peak was present (Fig. 2).

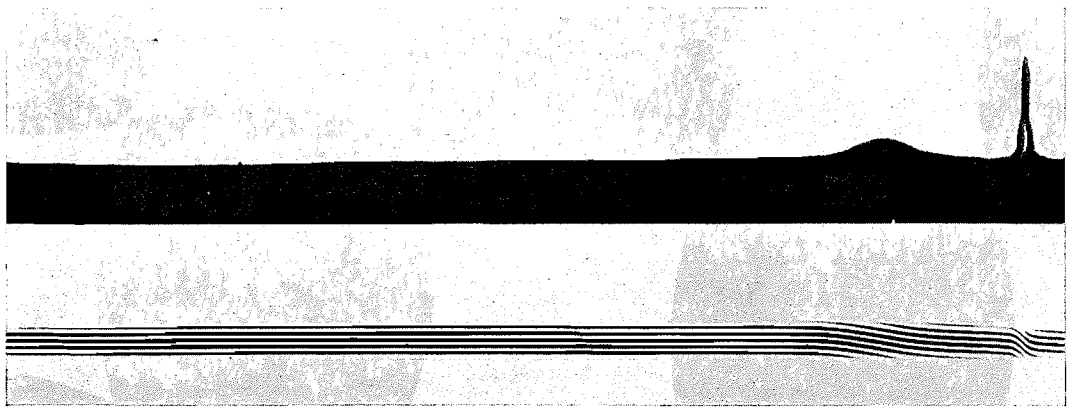

FIG. 2. Electrophoretic pattern of potato X virus after partial purification on celite column. Descending boundary, movement from right to left.

Subsequent purifications on a celite column were made by diluting the aqueous virus solution with 0.05 *M* phosphate buffer pH 5.7 to approximately the same virus concentration as in the sap, and repeating the procedure described above. The impurities present after the first purification could not be removed by additional treatment; also, the virus yields were much lower in the subsequent treatments than in the first one.

For flow birefringence measurements all solutions of the celite-treated virus were dialyzed against distilled water and centrifuged at 4000 r.p.m. for 40 minutes.

RESULTS AND DISCUSSION

Figure 3 represents a plot of the extinction angle χ as a function of gradient G for three different sap concentrations. Within experimental error the extinction angle is independent of concentration, indicating that the interactions of the virus particles with each other and with other sap constituents are negligible. Under these conditions the extinction angle is solely a function of particle length and velocity gradient. The solid lines in Fig. 3 are theoretical curves for a Flory distribution function with $\theta_1 = 70$ giving the best fit of the experimental points. The value $\theta_1 = 70$ corresponds to a length of 6200 Å for the monomer. The amount of aggregated material present in this sample can be estimated from Fig. 3 as 13 to 15%.

Can. J. Chem. Downloaded from www.nrcresearchpress.com by 78.46.186.204 on 09/04/12
For personal use only.

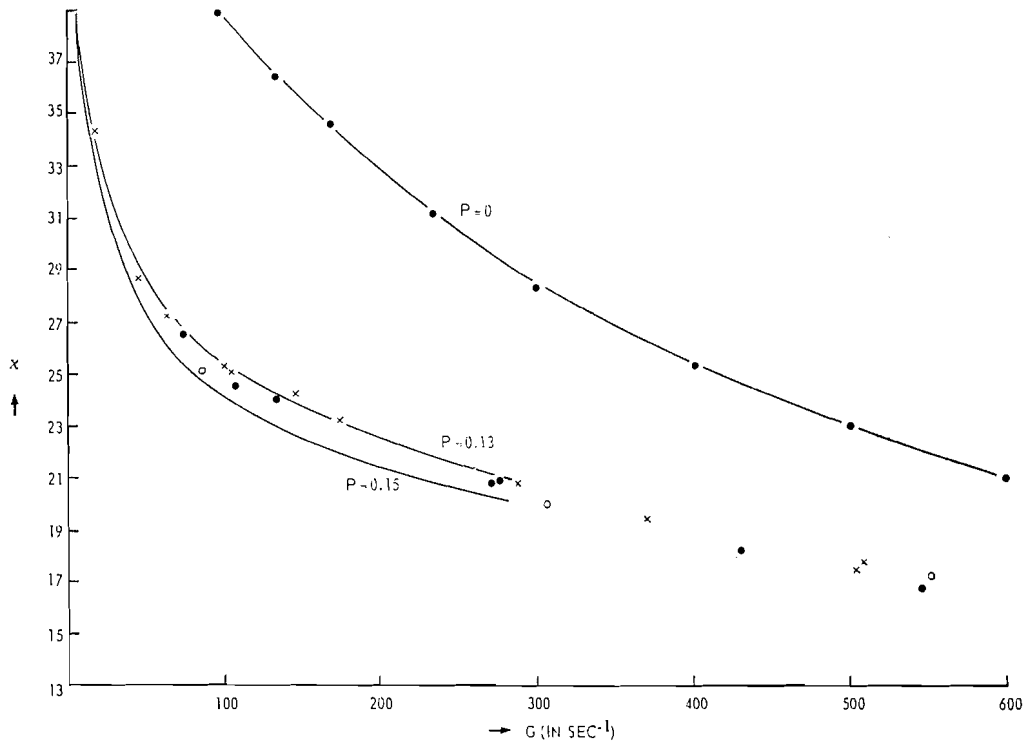

FIG. 3. Extinction angle – gradient curves of sap from potato X infected tobacco: X, four times concentrated sap; ●, one to one dilution of concentrated sap; O, one to three dilution of concentrated sap. Solid lines are theoretical curves from Fig. 1 assuming rotary diffusion constant 70.

In Fig. 4 the extinction angle as a function of gradient is plotted for partially purified potato X. Each treatment with celite caused a shift in these curves towards higher extinction angles, accompanied by a decrease in polydispersity features. After the fifth and subsequent absorptions on celite the shift became very minor.

The indication that the virus preparation was becoming less polydisperse excluded the possibility of a random breakage of virus particles. Also, the ultracentrifuge patterns remained unchanged, excluding the possibility of a splitting at specific sites. The most plausible explanation of the shift in the birefringence curves seems to be a preferential absorption of the aggregated materials by the celite column. The rotary diffusion constant of the five times celite-treated material at low gradients (100–200 sec^{-1}) is 60 to 70. Comparing this with the value of 70 derived above for the non-aggregated virus particles, it would seem that this preparation is virtually free of aggregated material. The slight polydispersity could therefore be attributed to shorter fragments present in the sap. Electron microscopy revealed the presence of short fragments in potato X preparations (4, 7, 8). The rotary diffusion constant of the five times celite-treated sample at 800 sec^{-1} is 105. This corresponds to a particle length of 5400 Å for a prolate ellipsoid of revolution. Because of the possibility of a contribution by shorter fragments, the latter value should be considered as the lower limit. Thus the characteristic hydrodynamic length of potato X virus in tobacco would be within the limits of 5400 to 6200 Å.

Curved and kinked potato X virus particles observed under the electron microscope suggested to some authors that a more flexible particle was involved than in the case

Can. J. Chem. Downloaded from www.nrcresearchpress.com by 78.46.186.204 on 09/04/12
For personal use only.

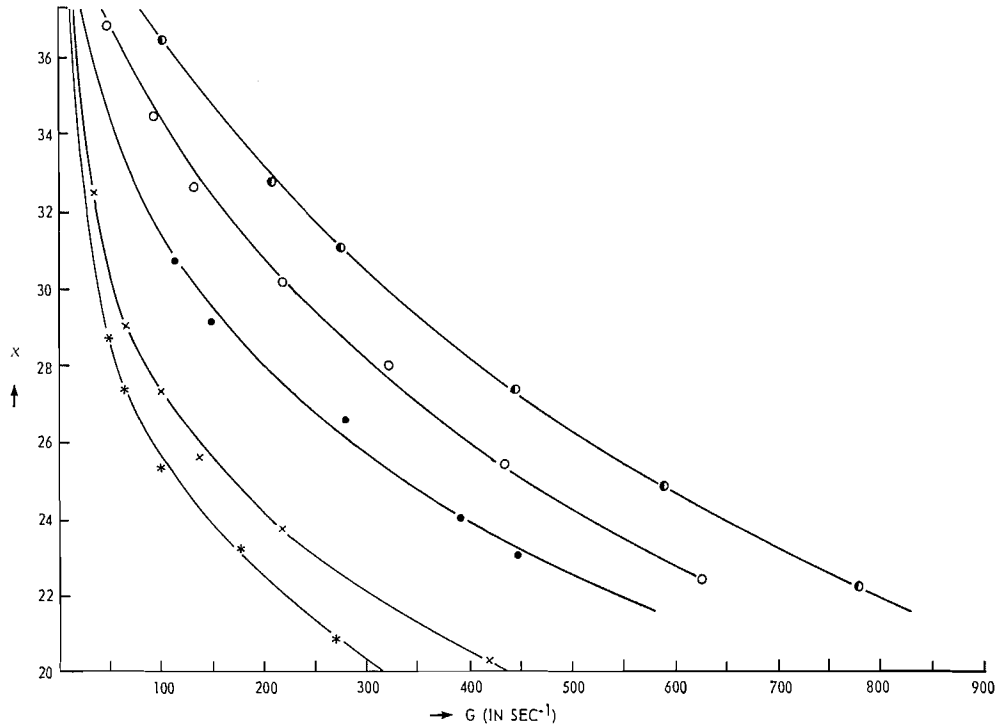

FIG. 4. Extinction angle – gradient curves of partially purified potato X virus on celite columns: *, virus in sap; X, once; ●, three times; ○, four times; and ◐, five times purified virus.

of the rigid tobacco mosaic virus (21). The difficulty encountered in an interpretation of flow birefringence data in the case of flexible particles (22) merits a closer examination of this problem. Valuable information regarding flexibility can be obtained from birefringence vs. gradient curves. In the case of rigid particles these curves have a downward curvature, the birefringence reaching a saturation value at high gradients (12). Figure 5 shows birefringence curves of potato X virus in sap, corresponding to the extinction angles in Fig. 3. The birefringence is expressed in degrees (twice the angular rotation of the Senarmont compensator), divided by relative concentrations, the most dilute sample being taken as having a concentration of one. The downward curvature is indicative of a rigid particle. Further evidence in support of inflexibility was obtained from extinction angle measurements of sap, dialyzed against distilled water and phosphate buffer pH 7.2, of varying ionic strength. The extinction angle – gradient curves remained unchanged in a range of phosphate concentrations of 0.1–0 M, indicating that no measurable stretching of the particles occurred with decreasing ionic strength.

The data on this paper confirm the conclusion from electron microscopy that a definite particle length is characteristic of the potato X virus in tobacco sap. In an earlier publication by Bode and co-workers (7) this characteristic length was given as 5600 to 5800 Å and 6000 to 6200 Å for two different strains of potato X respectively. In a later publication the first value was corrected to 5000 to 5250 Å, owing to previous errors in instrument calibration. A somewhat higher value from flow birefringence studies could be expected because of hydration and the error involved by substituting the cylindrical model with an ellipsoid of revolution (23), although a difference in the virus strains could also be a contributing factor (4, 7).

Can. J. Chem. Downloaded from www.nrcresearchpress.com by 78.46.186.204 on 09/04/12
For personal use only.

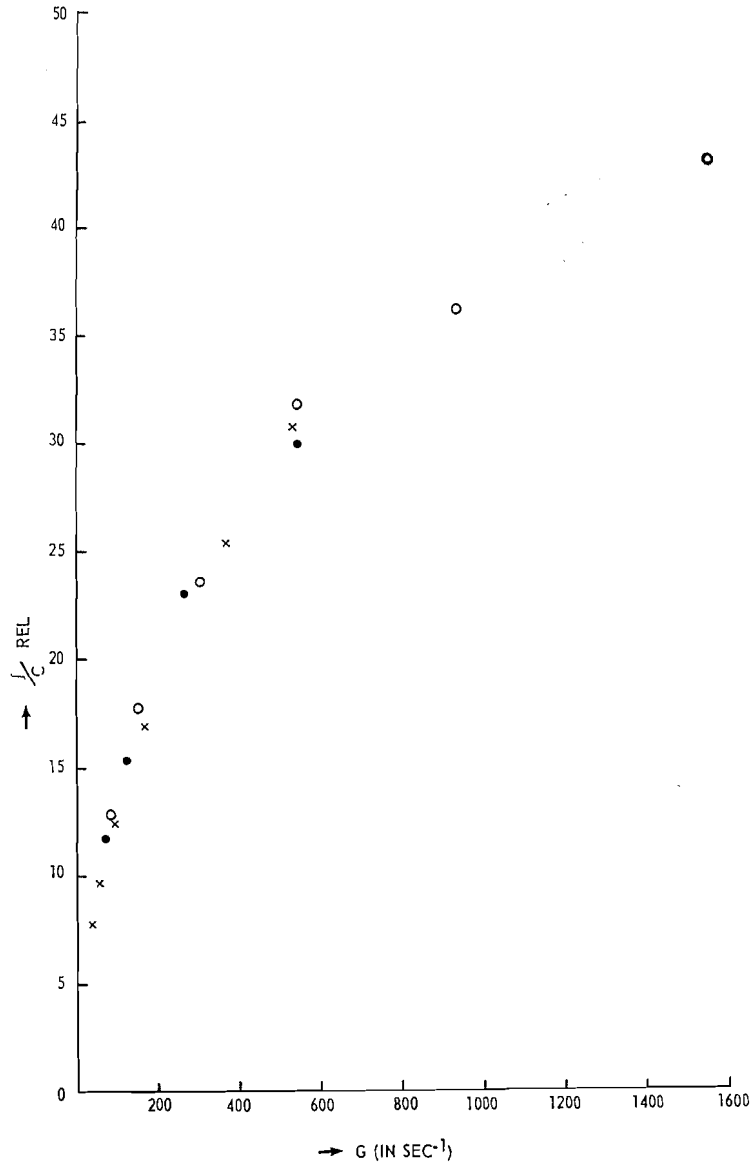

FIG. 5. Birefringence – gradient curves of potato X virus in sap. Points correspond to those given in Fig. 3.

It is difficult to make a comparison of the percentage of aggregated material reported here with that given in the literature. The wide fluctuation, from 23 particles in 651 (3.5%) (7) to 18% (8), is indicative either of great variability with growth conditions and virus strains or artefact formation during the drying processes. On the other hand, the flow birefringence value is open to criticism because of the inherent assumption of a random end-to-end aggregation. This is almost certainly an oversimplification of the mechanism involved. Furthermore the Flory distribution function does not account for fragments smaller than the monomeric unit which are present in all electron microscope mounts and for which there was evidence in the celite-fractionated material. A

Can. J. Chem. Downloaded from www.nrcresearchpress.com by 78.46.186.204 on 09/04/12
For personal use only.

close examination of the χ vs. G curves for other distribution functions will show that the curves are not very sensitive to the form of the distribution. Therefore the total amount of aggregated material determined in this way is probably a good estimate as long as the Flory distribution function is an approximate representation of the distribution.

ACKNOWLEDGMENTS

The author wishes to thank Drs. R. E. Fitzpatrick, N. S. Wright, R. Stace-Smith, and P. M. Townsley for their interest, helpful suggestions, and encouragement, and Dr. H. R. MacCarthy for reading the manuscript. The technical assistance of Mr. D. L. Hatt is gratefully acknowledged.

REFERENCES

1. BAWDEN, F. C. Plant viruses and virus diseases. Chronica Botanica Company, Waltham, Mass. 1950.
2. BANDET, J., CROISSANT, O., DERVICHIAN, D. G., JOLY, M., and MOSSE, J. Discussions Faraday Soc. **11**, 236 (1951).
3. LORING, H. S. J. Biol. Chem. **126**, 455 (1938).
4. KLECZKOWSKI, A. and NIXON, H. L. J. Gen. Microbiol. **4**, 220 (1950).
5. LORING, H. S. and WYCKOFF, R. W. G. J. Biol. Chem. **121**, 225 (1937).
6. LAUFFER, M. A. and CARTWRIGHT, T. E. Arch. Biochem. Biophys. **38**, 371 (1952).
7. BODE, O. and KÖHLER, E. Z. Naturforsch. **7b**, 598 (1952).
8. BODE, O. and PAUL, H. L. Biochem. et Biophys. Acta, **16**, 343 (1955).
9. WILLIAMS, R. C. and STEERE, R. L. J. Am. Chem. Soc. **73**, 2057 (1951).
10. RICE, R. V., KAESBERG, P., and STAHMANN, M. A. Biochim. et Biophys. Acta, **11**, 337 (1953).
11. RICE, R. V., KAESBERG, P., and STAHMANN, M. A. Biochim. et Biophys. Acta, **20**, 488 (1956).
12. CERF, R. and SCHERAGA, H. A. Chem. Revs. **51**, 185 (1952).
13. SADRON, C. J. phys. radium, **9**, 381, 384 (1938).
14. SCHERAGA, H. A. J. Chem. Phys. **19**, 983 (1951).
15. MONTROLL, E. W. and SIMHA, R. J. Chem. Phys. **8**, 721 (1940).
16. GOLDSTEIN, M. J. Chem. Phys. **20**, 677 (1952).
17. FLORY, P. J. J. Am. Chem. Soc. **58**, 1877 (1936).
18. COHN, E. J. and EDSALL, J. T. Proteins, amino acids and peptides. Reinhold Publishing Corp., New York. 1943.
19. SCHERAGA, H. A., EDSALL, J. T., and GADD, J. O. J. Chem. Phys. **19**, 1101 (1951).
20. EDSALL, J. T., RICH, A., and GOLDSTEIN, M. Rev. Sci. Instr. **23**, 695 (1952).
21. WYCKOFF, R. W. G. Electron microscopy. Interscience Publishers, Inc., New York. 1949.
22. GOLDSTEIN, M. and REICHMANN, M. E. J. Am. Chem. Soc. **76**, 3337 (1954).
23. BOEDTKER, H. and SIMMONS, N. S. J. Am. Chem. Soc. **80**, 2550 (1958).

Can. J. Chem. Downloaded from www.nrcresearchpress.com by 78.46.186.204 on 09/04/12
For personal use only.

Can. J. Chem. Downloaded from www.nrcresearchpress.com by 78.46.186.204 on 09/04/12
For personal use only.

OCCURRENCE OF β-DOLABRIN (4-ISOPROPENYLTROPOLONE) IN WESTERN RED CEDAR (THUJA PLICATA DONN.)[1]

J. A. F. GARDNER AND G. M. BARTON

ABSTRACT

The steam-volatile oil of western red cedar contains traces of a fifth tropolone, β-dolabrin (4-isopropenyltropolone), in addition to α-, β-, and γ-thujaplicin and 7-hydroxy-4-isopropyltropolone. The presence of β-dolabrin, previously obtained from Japanese "Hiba" wood by Nozoe, was detected by paper chromatography and proved by isolation of a sample from the steam-volatile oil by a combination of sodium salt precipitation, fractional crystallization, and preparative paper chromatography. The approximate composition of the steam-volatile oil from butt heartwood is given.

INTRODUCTION

The heartwood of western red cedar (*Thuja plicata* Donn.) has been shown to contain up to 1.2% by weight of the three isomeric isopropyltropolones, α-, β-, and γ-thujaplicin (1, 2, 3, 4). Recently, the presence also of a hydroxylated thujaplicin, 7-hydroxy-4-isopropyltropolone (2,7-dihydroxy-4-isopropyl-2,4,6-cycloheptatrien-1-one), was reported (5). This substance, for which the name β-thujaplicinol is now proposed, exhibits the same R_f and violet color reaction on paper chromatograms with ferric chloride as the "unknown enol" detected by Zavarin and Anderson (4) in the tropolone fractions of incense cedar (*Libocedrus decurrens* Torrey) and western red cedar. The occurrence in trace quantities in western red cedar of still another tropolone derivative, β-dolabrin (4-isopropenyltropolone), first detected by Nozoe *et al.* (6) in "Hiba" wood (*Thujopsis dolabrata* Sieb. et Zucc.), has now been proved.

During examination of the steam-volatile oil of western red cedar in this laboratory by the paper chromatographic technique of Zavarin and Anderson (4), the spot corresponding to β-thujaplicinol was observed to be usually elliptical, and sometimes, depending on temperature conditions, two barely separated spots were obtained. One of these gave the violet reaction with ferric chloride typical of β-thujaplicinol and the other of slightly greater R_f had a green-brown reaction similar to that of the thujaplicins. The R_f's and color reactions of this latter substance and its azo dye prepared by the method of Zavarin and Anderson (7) indicated it might be β-dolabrin.

In view of the importance of establishing the identity of trace components of wood extractives from the taxonomic viewpoint, proof of the presence of β-dolabrin in western red cedar was provided by isolating a sample. Because only trace quantities were involved according to the paper chromatograms, this presented considerable difficulty but was achieved by applying a combination of sodium salt precipitation and fractional crystallization to the tropolone fraction of the steam-volatile oil. This procedure provided, in addition to samples and approximate yields of the other components, residual solutions enriched in α-thujaplicin and β-dolabrin. From these, a sample of β-dolabrin was isolated by preparative paper chromatography. The material isolated had m.p. 55–56° C and showed no mixed melting point depression with an authentic sample, m.p. 56–57° C. The R_f's and ultraviolet absorption spectra of the two samples were identical. The infrared absorption spectra were also identical and showed strong bands at 1608, 1557,

[1]*Manuscript received August 1, 1958.*
Contribution from the Vancouver Laboratory, Forest Products Laboratories of Canada, a Division of the Forestry Branch, Department of Northern Affairs and National Resources. Presented at the 133rd National Meeting, American Chemical Society, San Francisco, U.S.A., April 14–18, 1958.

1470, and 1435 cm^{-1}, characteristic of the tropolone nucleus, and also two at 892 and 1407 cm^{-1}, typical of asymmetrically disubstituted ethylenes (8).

The above result shows that western red cedar as well as "Hiba" wood contains β-dolabrin. Since "Hiba" wood also contains α- and β-thujaplicin (9), there are at least three tropolones common to these species of the different genera *Thuja* and *Thujopsis* of the family Cupressaceae.

Previous analytical work (3) had shown that light-colored wood from the outer butt of mature trees had the highest content of tropolones. The composition of oil steam-distilled from freshly cut shavings of butt heartwood selected for its light straw color, estimated from yields and paper chromatographic analysis of fractions obtained, is recorded in Table I. It is, of course, to be expected that the yield and composition of the oil will vary considerably with the source of the wood (3). For optimum yields, it is necessary to distill the wood immediately after conversion to shavings because of the high volatility of the oil.

TABLE I

COMPOSITION OF STEAM-VOLATILE OIL OF WESTERN RED CEDAR BUTT HEARTWOOD (0.82% YIELD)

Components	Percentage of oil	Percentage of wood
Methyl thujate, other neutrals	21.1	0.17
Thujic acid	10.4	0.08
Tropolones	68.5	0.56
β-Thujaplicinol*	8	0.07
γ-Thujaplicin*	24	0.20
β-Thujaplicin*	35	0.30
α-Thujaplicin*	1	0.01
β-Dolabrin*	0.04	0.0003

*Figures for the individual tropolones are approximate, being derived from crude yields and quantitative paper chromatography of mother liquors.

EXPERIMENTAL

Melting points were determined on a Fisher–Johns melting point apparatus and are uncorrected. Infrared absorption spectra were determined on a Beckman Model IR-4 Infrared Spectrophotometer at the Fisheries Experimental Station, Vancouver, B.C. Ultraviolet absorption spectra were determined with a Beckman D.U. Spectrophotometer.

Steam Distillation of Light-colored Western Red Cedar Shavings

Butt-wood spalts selected for light straw color were reduced to shavings in a planer and steam-distilled immediately. Approximately 6 liters of aqueous distillate were collected per kilogram of shavings. The distillate was extracted five times with a sixth of its volume of chloroform and the extract concentrated under reduced pressure to leave a yellow oil. From 11.987 kg of shavings (moisture content 20.0%) 79 g or 0.82% based on the moisture-free wood were obtained.

Preparation of Tropolone Mixture

Steam-distilled oil (103 g) in chloroform (300 ml) was extracted with 1 *N* sodium hydroxide solution (6×50 ml) and back-extracted with chloroform. The chloroform solution was dried over anhydrous sodium sulphate and the solvent removed under reduced pressure to leave crude methyl thujate (21.8 g).

The alkaline solution was acidified and extracted with chloroform (3×100 ml). The

Can. J. Chem. Downloaded from www.nrcresearchpress.com by 78.46.186.204 on 09/04/12
For personal use only.

chloroform solution was than extracted with saturated aqueous sodium bicarbonate solution (5×50 ml). Acidification of the bicarbonate solution precipitated crude thujic acid (10.7 g). The chloroform solution, after extraction with bicarbonate, was washed with water and dried over anhydrous sodium sulphate, filtered, and the solvent removed. The residual oil was distilled under reduced pressure to yield the semicrystalline tropolones (66.0 g).

Fractionation of Tropolone Mixture

The tropolone mixture was dissolved in hot 3 *N* sodium hydroxide (350 ml) and the solution cooled. The deposited yellow sodium salts were filtered using a rubber dam to remove excess filtrate.

The caustic filtrate was acidified with 6 *N* sulphuric acid, extracted with chloroform, and the solvent removed to yield crude β-thujaplicinol.

The sodium salts were acidified with 6 *N* sulphuric acid in the presence of chloroform. Removal of the solvent from the chloroform layer left the mixed thujaplicins. The thujaplicin mixture (5.2 g approx. 40% γ-, 60% β-thujaplicin with traces of α-thujaplicin and β-dolabrin), and anhydrous sodium acetate (2.5 g) were refluxed in sodium-acetate-saturated ethanol (50 ml) for 1 hour. The solution was cooled to room temperature and the precipitated yellow sodium salt and excess sodium acetate removed by filtration. The precipitated salts were enriched with respect to γ-thujaplicin (approx. 75% γ-, 15% β-), while the filtrate was enriched with β-thujaplicin (approx. 70% β-, 30% γ-, traces of α-thujaplicin and β-dolabrin). Regeneration of the thujaplicins from the salts, and the filtrate and recrystallization from ligroin–chloroform and ligroin gave respectively γ- and β-thujaplicin. The mother liquors were combined to yield a solution, enriched with α-thujaplicin and β-dolabrin, on which the sodium acetate – sodium salt precipitation was repeated. This in turn yielded more γ- and β-thujaplicin and mother liquors which were combined for isolation of β-dolabrin.

Isolation of β-Dolabrin by Preparative Paper Chromatography

The qualitative technique of Zavarin and Anderson (4) was adapted. Sheets of Whatman No. 1 paper (6 in. × 22½ in.) were impregnated with 17% by volume of phosphoric acid, spotted with 0.2 ml of a chloroform solution (0.08 g/ml) of the residue from removal of solvent from the mother liquors above, and developed with iso-octane–toluene (3:1). The β-dolabrin zones were located by ultraviolet light, excised, and Soxhlet-extracted with petroleum ether (30–60° C) under a carbon dioxide atmosphere. Solvent removal left crystals (0.019 g from 45 sheets) which were triturated with a minimum of petroleum ether (30–60° C), filtered, and dissolved in petroleum ether (30–60° C). Slow evaporation of the solution yielded yellow crystals, m.p. 56–57° C, mixed melting point with authentic dolabrin 56–57° C. The ultraviolet and infrared absorption spectra of the isolated material and authentic β-dolabrin were identical. ν_{max}^{KBr} in cm^{-1}: 3240, 1628, 1608, 1557, 1494, 1470, 1435, 1406, 1313, 1274, 1257, 1230, 958, 911, 892, 823.

ACKNOWLEDGMENTS

The authors are indebted to MacMillan & Bloedel Ltd. and Canadian Forest Products Ltd. for samples of western red cedar, and to Professor Tetsuo Nozoe for a sample of β-dolabrin with its ultraviolet absorption spectrum. Miss Shirley McKelvey assisted with the experimental work.

REFERENCES

1. ANDERSON, A. B. and GRIPENBERG, J. Acta Chem. Scand. **2**, 644 (1948).
2. ERDTMAN, H. and GRIPENBERG, J. Acta Chem. Scand. **2**, 625 (1948).

Can. J. Chem. Downloaded from www.nrcresearchpress.com by 78.46.186.204 on 09/04/12
For personal use only.

3. MacLean, H. and Gardner, J. A. F. Forest Prods. J. **6**, 510 (1956).
4. Zavarin, E. and Anderson, A. B. J. Org. Chem. **21**, 332 (1956).
5. Gardner, J. A. F., Barton, G. M., and MacLean, H. Can. J. Chem. **35**, 1039 (1957).
6. Nozoe, T., Takase, K., and Ogata, M. Chem. & Ind. 1070 (1957).
7. Zavarin, E. and Anderson, A. B. Ber. 545 (1955).
8. Bellamy, L. J. The infrared spectra of complex molecules. Methuen & Co. Ltd., London. 1954. pp. 44, 46.
9. Nozoe, T., Yasue, A., and Yamane, K. Proc. Japan Acad. **27**, 15 (1951).

Can. J. Chem. Downloaded from www.nrcresearchpress.com by 78.46.186.204 on 09/04/12
For personal use only.

Can. J. Chem. Downloaded from www.nrcresearchpress.com by 78.46.186.204 on 09/04/12
For personal use only.

LIGHT-SCATTERING STUDIES OF COPOLYMERS

I. EFFECT OF HETEROGENEITY OF CHAIN COMPOSITION ON THE MOLECULAR WEIGHT[1]

W. BUSHUK[2] AND H. BENOÎT

ABSTRACT

The classical light-scattering theory for polymer solutions is extended to solutions of copolymers which may be polydisperse in chain composition as well as in molecular weight. It is shown that much too high molecular weights will result from light-scattering data for copolymers owing to fluctuations in chain composition; the magnitude of this effect increases rapidly as the absolute value of the refractive index increment approaches zero. The methods for determining the usual weight-average molecular weight and polydispersity of composition are described.

The theory was tested with experimental results on: (1) a mixture of polystyrene and poly(methylmethacrylate), considered as a copolymer with the highest possible polydispersity of composition; (2) a high conversion, statistical copolymer of styrene and methylmethacrylate (copolymer I); and (3) a block copolymer of the same monomers (copolymer II). The apparent molecular weight for copolymer I ($M_w = 1.83 \times 10^5$) varied markedly with refractive index increment in much the same way as the total molecular weight for the mixture. The molecular weight of copolymer II ($M_w = 1.20 \times 10^6$) remained essentially constant in the same series of solvents. The polydispersities of composition obtained were 0.72 and 0.05 for copolymer I and II respectively compared with the maximum possible value equal to 1.0.

INTRODUCTION

Since the demonstration by Debye (1) that the amount of light scattered by solutions of high polymers is related to the mass of the solute molecules, light scattering has rapidly become one of the standard methods for the determination of molecular weights of macromolecules. The application of this technique to copolymers has not been equally successful. On one occasion (2) the molecular weight obtained for a sample of GR–S (butadiene–styrene copolymer) was found to vary with refractive index of the solvent and it was suggested that this might be due to heterogeneities in the composition of the particular sample. Similar anomalous molecular weights were obtained in this laboratory for other types of copolymers (3). Accordingly, it seemed desirable to study the problem of light scattering by copolymers and the use of this technique for the determination of molecular parameters both from theoretical and experimental viewpoints.

The theoretical treatment for the molecular weights of copolymers given in this paper is similar to that indicated by Stockmayer *et al.* (4) except that the final equations are arranged in somewhat more useful form. A preliminary report of the present study has already been published (5).

To test the theory, experimental data are presented for solutions of mixtures of polystyrene (PS) and poly(methylmethacrylate) (PMM) and two types of styrene–methylmethacrylate copolymers. These polymers were selected primarily because of the large difference between the refractive indices of the two homopolymers, polystyrene and poly(methylmethacrylate).

THEORETICAL

Introduction

In a homopolymer all the scattering elements scatter in the same manner; in a copolymer there may be two or more types of scattering elements depending on the number of monomer types that make up the copolymer. The treatment given here considers

[1]*Manuscript received August 5, 1958.*
Contribution from the Centre de Recherches sur les Macromolécules, Strasbourg, France, with financial assistance from the National Research Council of Canada.
[2]*Present address: Grain Research Laboratory, Winnipeg 2, Canada.*

only the binary copolymers, although it could be readily extended to include copolymers comprising more than two monomer types. The equations derived are completely general in that they are applicable to statistical, block, or graft copolymers, which may be polydisperse in mass as well as in composition.

Specific Refractive Index Increment

It is assumed that the refractivity of a copolymer is a simple sum of the refractivities of the two component homopolymers. As pointed out by Stockmayer *et al.* (4) this should be particularly true for block copolymers and probably does not introduce a very large error when applied to statistical copolymers. Accordingly, if c_A is the concentration of type A (polymer or monomer) and c_B is the concentration of type B, the refractive index of a solution of this copolymer (or mixture of homopolymers) will take on the value:

$$n = n_0+(dn/dc)_A c_A+(dn/dc)_B c_B, \quad [1]$$

where n_0 is the index of the pure solvent and the dn/dc are the specific refractive index increments for the components indicated. In this paper the two components A and B will be taken as polystyrene and poly(methylmethacrylate) respectively.

If the total concentration is $c = c_A+c_B$, then the increment for the solution will be

$$dn/dc = (n-n_0)/c = [(dn/dc)_A c_A+(dn/dc)_B c_B]/(c_A+c_B). \quad [2]$$

As has been verified on numerous occasions, equation [2] incorporates the fact that the specific refractive index increment of a solution of polymer depends only on the weight concentration and not on the molecular weight.

To simplify the notation set $(dn/dc)_A = \nu_A$; $(dn/dc)_B = \nu_B$; and $dn/dc = \nu$; and $x = c_A/(c_A+c_B)$ the weight fraction of component A. With this notation

$$\nu = x\nu_A+(1-x)\nu_B. \quad [3]$$

Accordingly the specific refractive index for a solution of copolymer in any solvent can be calculated if the composition of the copolymer and the increments for the corresponding homopolymers for the same solvent are known accurately.

Theory for Particles Small Compared with the Wavelength of Light

General

According to classical theory on light scattering, the excess scattering due to the solute particles of mass M, concentration c, and having ν for the specific refractive index increment (expressed in terms of the usual Rayleigh ratio R, extrapolated to zero concentration) can be put in the form

$$R = K'\nu^2 cM, \quad [4]$$

where $K' = (2\pi^2\eta_0^2)/(\lambda^4 N)$, in which η_0 is the refractive index of solvent, λ is the wavelength of the incident light in vacuum, and N is Avogadro's number. If the particles are polydisperse in molecular weight, M then becomes the weight-average molecular weight.

Now consider a solution of a copolymer which may show polydispersity of chain composition in addition to polydispersity of molecular weight. Assuming additivity of scattered intensities from the different scattering elements, equation [4] can be put in the form

$$R = K'\sum \nu_i^2 c_i M_i, \quad [5]$$

where c_i is the concentration of molecules of mass M_i and composition x_i. The refractive

Can. J. Chem. Downloaded from www.nrcresearchpress.com by 78.46.186.204 on 09/04/12
For personal use only.

index increment for this composition ν_i is defined by equation [3]. To separate the effects of heterogeneity of composition and molecular weight it would probably be clearer to use a double sum in equation [5]; that is, to characterize the species of molecular weight M_i by its compositions x_{ij}. However the writing can be simplified by using a single summation without affecting the rigorousness of the mathematical treatment. It is necessary only to keep in mind that it is possible to have different values of i for the same molecular weight.

The intensity of the scattered light that is actually measured is given by

$$R = K'\nu_0^2 c M_{ap}, \qquad [6]$$

where ν_0 is the average refractive index increment that is obtained by the usual methods of measurement and M_{ap} is the molecular weight that is obtained from the data by the standard method of extrapolation to zero concentration.

Equating the intensities given by equations [5] and [6] the molecular weight takes on the value

$$M_{ap} = \sum \nu_i^2 c_i M_i / \nu_0^2 c = (1/\nu_0^2) \sum \nu_i^2 \gamma_i M_i, \qquad [7]$$

where γ_i is defined as the relative concentration of molecules of composition x_i.

Equation [7] defines the molecular weight that is obtained experimentally for a polymer for which the component molecular species may exhibit different specific refractive index increments in a single solvent. This molecular weight will be referred to henceforth as the apparent molecular weight.

The significance of equation [7] can be best demonstrated by expanding the sum for specific cases to which it can be applied. The most important of these from the viewpoint of the present investigation is the copolymer of heterogeneous chain composition. This will be discussed first. The general equations obtained will then be applied to two special cases, the copolymer of homogeneous chain composition and a binary mixture of homopolymers.

Copolymer of Heterogeneous Composition

If $\nu_i \neq \nu_0$, which is the case when the composition of different molecules is different, equation [7] can be expanded to a more practical form by substituting for ν_i its value given by equation [3]. The new equation for the apparent molecular weight becomes

$$M_{ap} = (\nu_A\nu_B/\nu_0^2)\sum\gamma_i M_i + [\nu_A(\nu_A-\nu_B)/\nu_0^2]\sum\gamma_i M_i x_i^2 + [\nu_B(\nu_B-\nu_A)/\nu_0^2]/\sum\gamma_i M_i(1-x_i)^2. \qquad [8]$$

Equation [8] can be simplified further by introducing the equalities: $\sum\gamma_i M_i = M_w$; $\sum\gamma_i M_i x_i^2 = x_0 M_A$; and $\sum\gamma_i M_i(1-x_i)^2 = (1-x_0)M_B$. M_w is the weight-average molecular weight of the copolymer, M_A and M_B are defined as the weight-average molecular weights of the parts of the copolymer formed of monomer A and B respectively, and x_0 is the over-all average weight fraction of component A.

$$M_{ap} = (\nu_A\nu_B/\nu_0^2)M_w + [\nu_A(\nu_A-\nu_B)/\nu_0^2]\, x_0 M_A + [\nu_B(\nu_B-\nu_B)/\nu_0^2](1-x_0)M_B. \qquad [9]$$

Equations [8] and [9] show that if the copolymer is of heterogeneous chain composition, the molecular weight of the particular sample, obtained from light-scattering data, will depend on the refractive index of the solvent and, as will be seen later, this dependence is related to the degree of heterogeneity. It is therefore quite possible to obtain an infinitely high apparent molecular weight as the scattering may not necessarily be zero, when the average refractive index increment is zero, owing to heterogeneity of the sample.

From measurements in three solvents it should be possible, in principle, to solve for the

Can. J. Chem. Downloaded from www.nrcresearchpress.com by 78.46.186.204 on 09/04/12
For personal use only.

three parameters M_A, M_B, and M_w from which the composition of the copolymer can be verified. From the same three sets of measurements it is also possible to obtain information on the degree of heterogeneity of composition.

The quantitative determination of the degree of polydispersity of chain composition becomes more feasible if equation [7] is expanded by a slightly different notation from that used to obtain equations [8] and [9]. In this case set

$$\delta x_i = x_i - x_0 \qquad [10]$$

where δx_i is the deviation in composition of molecules of type i from the average composition, x_0. According to this notation, equation [3] for the refractive index increment takes on the form

$$\nu_i = \nu_0 + \delta x_i(\nu_A - \nu_B) \qquad [11]$$

and the equation for the apparent molecular weight becomes

$$M_{ap} = M_w + 2(\nu_A - \nu_B)/(\nu_0)\sum\gamma_i M_i \delta x_i + (\nu_A - \nu_B)^2/(\nu_0^2)\sum\gamma_i M_i \delta x_i^2. \qquad [12]$$

It can be shown that equation [12] is equivalent to equation [9] by substituting in the former the following equalities,

$$2\sum\gamma_i M_i \delta x_i = (1-x_0)(M_w - M_B) - x_0(M_w - M_A) \qquad [13]$$

$$\sum\gamma_i M_i \delta x_i^2 = x_0(1-x_0)(M_A + M_B - M_w).$$

These relations are derived by substituting the value for δx_i given by equation [10] and expanding the sums indicated.

By introducing two new parameters P and Q, equation [12] becomes

$$M_{ap} = M_w + 2P[(\nu_A - \nu_B)/\nu_0] + Q[(\nu_A - \nu_B)/\nu_0]^2, \qquad [14]$$

in which P and Q are equal to $\sum\gamma_i M_i \delta x_i$ and $\sum\gamma_i M_i \delta x_i^2$ respectively. To plot equation [14] it is convenient to divide both sides of the equation by M_w.

According to equation [14], if M_{ap} is plotted against $(\nu_A - \nu_B)/\nu_0$, which varies with the refractive index of the solvent, the points should describe a parabola from which the values of the parameters M_w, P, and Q can be estimated. The value of M_w should agree with the value obtained from equation [9]. The other two parameters are related to the heterogeneity in composition of the sample by the definitions given above and should be constant for a particular copolymer. In general, the values of P and Q will vary between the following limits:

$$-x_0 M_w \leqslant P \leqslant (1-x_0)M_w,$$

$$0 \leqslant Q \leqslant M_w[1 - x_0(1-x_0)].$$

If the copolymer is monodisperse in mass or if the distribution of chain composition is independent of molecular weight, equation [14] simplifies further since under such conditions $P = 0$ and Q can only take on values between 0 and $x_0(1-x_0)M_w$. The maximum value of Q can only be realized with a mixture of two homopolymers.

The parameter Q/M_w for a specific copolymer may be defined as a quantitative measure of the polydispersity of chain composition. Accordingly the ratio of the value of Q/M_w, determined either graphically or by a direct calculation, to the maximum possible value, $x_0(1-x_0)$, seems to be a convenient index of the polydispersity in chain composition which can be used as an additional parameter for characterizing copolymers.

Can. J. Chem. Downloaded from www.nrcresearchpress.com by 78.46.186.204 on 09/04/12
For personal use only.

Copolymer of Homogeneous Composition

If the copolymer molecules are of uniform composition then $\nu_i = \nu_0$ for all values of i, $\delta x_i = 0$ and equation [12] gives

$$M_{ap} = M_w, \qquad [15]$$

where M_w is the usual weight-average molecular weight. That is, for a copolymer of homogeneous chain composition, the molecular weight obtained from light-scattering data will be independent of the refractive index of the solvent.

For this special case, equations [13] give $M_A = x_0 M_{ap}$ and $M_B = (1-x_0)M_{ap}$. These relations can then be used to determine the weight-average molecular weights of the two components of the copolymer.

Solution Containing Two Homopolymers

For a system comprising two homopolymers A and B, of molecular weights M_A and M_B and relative concentrations γ_A and γ_B, equations [7], [9], or [14] give

$$M_{ap} = (\nu_A^2 \gamma_A M_A + \nu_B^2 \gamma_B M_B)/\nu_0^2. \qquad [16]$$

Equation [16] shows that for a mixture of homopolymers the apparent molecular weight will depend on the refractive index of the solvent and in general will not be equal to the usual weight-average molecular weight. In a solvent with refractive index intermediate between those of the two polymers, concentrations can be selected so that the average refractive index increment will be zero. However the solution will still show positive scattering. The apparent molecular weight will then become infinite. For a solvent having the same refractive index as either component, equation [16] will give the weight-average molecular weight of the other component.

It is of interest to examine what happens to the parameters P and Q in this special case. The summations in the definitions of these parameters given above can be readily expanded to give

$$P = x_0(1-x_0)(M_A - M_B)$$
$$Q = x_0(1-x_0)[(1-x_0)M_A + x_0 M_B]. \qquad [17]$$

Equations [17] show that when the polymers are of the same mass, P will be zero as in the case of monodisperse (in mass) copolymers. If $M_A \neq M_B$, but are of the same order of magnitude, P will still be small compared with Q. This will not be true always and P can actually have values greater than those of Q when M_A and M_B are very different, that is, when the sample has a very broad distribution of molecular weight as well as of composition.

Theory for Particles of Size Comparable to the Wavelength of Light

If the dimensions of the solute molecules are greater than approximately 1/20 λ, the same type of destructive interference in the scattered light will result in the case of copolymers as with homopolymers. It is therefore necessary to make a correction for this interference in the usual manner by extrapolating to zero angle according to the method of Zimm (6). The value of the molecular weight so obtained will be the apparent molecular weight of the copolymer for the particular solvent used.

MATERIALS AND METHODS

Solvents

Solvents used for the light-scattering and the viscosity measurements were purified

Can. J. Chem. Downloaded from www.nrcresearchpress.com by 78.46.186.204 on 09/04/12
For personal use only.

by several distillations. The 1-bromonaphthalene remained slightly yellow even after two distillations; however, it did not absorb any light at the wavelength used for the light-scattering measurements. The solvents and other pertinent data are listed in Table I.

TABLE I

LIST OF SOLVENTS AND OTHER PERTINENT DATA

Solvent	$n(20°; 5460$ Å)	ν_A (PS) (cc g^{-1})	ν_B (PMM) (cc g^{-1})
Butanone	1.3856	0.220	0.111
Dioxane (*p*)	1.4280	0.168	0.068
Carbon tetrachloride	1.4677	0.146	0.023
Benzene	1.5056	0.106	−0.010
Chlorobenzene	1.5293	0.079	−0.026
Bromobenzene	1.5641	0.042	−0.058
1-Bromonaphthalene	1.6628	−0.051*	−0.147*

*Measured on the Zeiss Interferometer.

Polymers

The polystyrene used was a fraction of medium molecular weight obtained from a polydisperse polymer prepared at ordinary temperatures in the presence of an inhibitor. It was fractionated from benzene solution by precipitation by methanol. The polymer was dried in vacuum at 60° C. Its molecular weight and intrinsic viscosities in a number of solvents are listed in Table II which will be given in conjunction with a subsequent section.

The poly(methylmethacrylate) was of commercial origin (Plexiglass). It was purified by a single precipitation from a 2% solution in butanone by methanol followed by drying in vacuum at 60° C. Its molecular weight and intrinsic viscosities in a number of solvents are given in Table II.

TABLE II

SUMMARY OF RESULTS ON MIXTURES

65% PS of $M_w = 8.10\times10^5$; 35% PMM of $M_w = 6.88\times10^5$; M_w of mixture $= 7.67\times10^5$

Solvent	ν_0 (cc g^{-1})	$M_{ap}\times10^{-5}$	M_{ap}/M_w	$[\eta]$(cc g^{-1}) PS	$[\eta]$(cc g^{-1}) PMM
Butanone	0.180	7.67	1.00	82	64
Dioxane (*p*)	0.133	7.69	1.00	—	—
Benzene	0.065	9.46	1.23	168	97
Chlorobenzene	0.044	34.7	4.52	—	—
Bromobenzene	0.007*	292	38.1	124	89
1-Bromonaphthalene	−0.088†	21.4	2.80	126	92

*Calculated: $\nu_0 = 0.65(0.042)+0.35(-0.058)$.
†Measured on the Zeiss Interferometer.

Copolymer I was a statistical copolymer of styrene and methylmethacrylate prepared by using benzoyl peroxide as initiator. The copolymerization was allowed to proceed to about 95% conversion. It was then redissolved in benzene, precipitated by the addition of methanol, and dried in the usual manner. The composition of this copolymer was 68% PS and 32% PMM, as determined from the specific refractive index increments in five solvents. Combustion analysis gave its composition as 70% PS and 30% PMM.

Copolymer II was a block copolymer of styrene and methylmethacrylate. It was

Can. J. Chem. Downloaded from www.nrcresearchpress.com by 78.46.186.204 on 09/04/12
For personal use only.

prepared by the method of Szwarc (7) in which the polystyrene was the living radical. Its composition from combustion analysis (and refractive index increments) was 70% PS and 30% PMM. It was used without further purification.

Methods

Solutions were prepared by weighing a predetermined quantity of polymer directly into a volumetric flask and making up to volume with dust-free solvent. Prior to the light-scattering measurements, portions of this solution of concentration c were diluted to $\frac{2}{3}c$, $\frac{1}{2}c$, and $\frac{1}{3}c$. Two samples of pure solvent (one to rinse the pipette used to transfer the dust-free solvent and the solutions) and the four solutions were centrifuged at 25,000g, for 1 hour to remove dust. With some of the higher density solvents it was necessary to filter the solutions through a fritted-glass filter prior to centrifugation.

Light-scattering measurements were made on a photometer described by Wippler and Scheibling (8) using the green mercury line (5460 Å) and pure benzene as the calibration standard. All experiments were made at 25±1° C. After the usual refractive index and volume corrections, the data were treated according to the extrapolation method of Zimm (6) using measurements ranging from 30 to 150° to the incident at the four concentrations shown above. Except where indicated otherwise, the refractive index increments were measured on a Pulfrich Refractometer with a divided cell using the green mercury line.

Molecular weights were calculated using the value of Carr and Zimm (9) for the Rayleigh ratio of benzene (16.3×10^{-6} for 5461 Å at 25° C). It was assumed that the correction factor owing to depolarization was negligible.

Viscosities were measured in a capillary viscometer described by Vallet (10). Viscometers with capillary diameters were selected so that the flow time for the pure solvent was at least 100 seconds.

RESULTS AND DISCUSSION

The most feasible way to test the theory developed above is to study the variation of the apparent molecular weight with refractive index of the solvent. The extent of this variation, in turn, depends on the degree of heterogeneity in chain composition of the copolymer. Accordingly, it should be possible in this manner to determine the effect of the variations in chain composition on the molecular weight determined by light scattering in any specific solvent.

The first series of light-scattering experiments were made on solutions of two homopolymers, comprising 65% PS and 35% PMM of the total polymer concentration. Two features of these solutions make these experiments significant. First, they are most suitable for testing the theory, since their compositions and refractive index increments are known accurately, and second, they can be regarded as solutions of copolymer having the greatest possible heterogeneity of chain composition.

Table II gives the results for the mixture in a series of solvents. The fourth column gives the ratio of the molecular weight obtained from the Zimm plot (M_{ap}) and the weight-average molecular weight calculated from the composition and the weight-average molecular weights of the homopolymers listed at the top of Table II. The viscosities are given as an additional characterization of the polymers used.

To illustrate the variation of the apparent molecular weight with refractive index of solvent, it is convenient to plot the ratio M_{ap}/M_w as a function of the index. Figure 1 shows such a plot of the data of Table II. Experimental data are shown as circles; the solid line represents a corresponding plot for which M_{ap} was calculated from equation

Can. J. Chem. Downloaded from www.nrcresearchpress.com by 78.46.186.204 on 09/04/12
For personal use only.

[16]. The agreement between theory and experiment is satisfactory considering the large experimental errors inherent in the measurements on solutions with very small refractive index increments.

The results for the copolymer I (statistical copolymer) are summarized in Table III. In this case the ratio M_{ap}/M_w was determined using the value of M_w (given later in Table V) calculated from equation [14] with the values of M_{ap} listed in Table III. The three unknowns of equation [14], M_w, P, and Q, were evaluated by solving three simultaneous equations. The value of M_w calculated in this manner is strongly dependent on the values for the refractive index increments for the two component polymers in the series of solvents used. Determination of the latter quantities involves a fairly large experimental error particularly in the cases where the increment is very small. Accordingly, it would probably be just as correct, and less laborious, to use for M_w the value of M_{ap} obtained with the solvent having the highest index increment (butanone).

TABLE III

SUMMARY OF RESULTS ON COPOLYMER I
Composition: Combustion analysis, 70% PS+30% PMM
Index increments, 68% PS+32% PMM

Solvent	ν_0 (cc g^{-1})	$M_{ap}\times10^{-5}$	M_{ap}/M_w
Butanone	0.185	2.21	1.20
Dioxane (*p*)	0.136	2.49	1.36
Carbon tetrachloride	0.103	2.81	1.53
Benzene	0.068	3.32	1.81
Chlorobenzene	0.045	9.59	5.24
Bromobenzene	0.010*	26.4	14.42

*Calculated: $\nu_0 = 0.68(0.042)+0.32(-0.058)$.

Figure 2 gives the plots of M_{ap}/M_w as a function of the solvent refractive index. The circles represent data for copolymer I and the points those for copolymer II which will be discussed later. The lines represent points for which M_{ap}/M_w was calculated from equation [14] for the corresponding experimental conditions and the values of Q/M_w indicated. The second term of the right hand side of equation [14] was not included in the calculations for this plot, since it was found that when M_{ap} was plotted against $(\nu_A-\nu_B)/\nu_0$ the slope at $(\nu_A-\nu_B)/\nu_0 = 0$, which is equal to 2P, was essentially zero.

Figure 2 demonstrates clearly a marked variation in the apparent molecular weight of copolymer I with index of solvent. Even in the case of benzene, which is commonly used as solvent, the value of the apparent molecular weight is much higher than the true weight-average molecular weight.

Another method of plotting the data of Fig. 2 is demonstrated in Fig. 3. Here M_{ap}/M_w is plotted as a function of $(\nu_A-\nu_B)/\nu_0$. According to equation [14] the points in such a plot should fall on a parabola. One difficulty with using this plot is to find solvents that will give negative values of $(\nu_A-\nu_B)/\nu_0$. 1-Bromonaphthalene is one such solvent for styrene–methylmethacrylate copolymers; unfortunately measurements on copolymer I in this solvent could not be made owing to shortage of the copolymer. From Fig. 3 it is possible to estimate the value of Q/M_w that will best fit the experimental data. The value of this parameter for copolymer I is approximately 0.15. This result indicates an exceptionally high heterogeneity of chain composition, since the highest possible value that Q/M_w could have is 0.22.

Can. J. Chem. Downloaded from www.nrcresearchpress.com by 78.46.186.204 on 09/04/12
For personal use only.

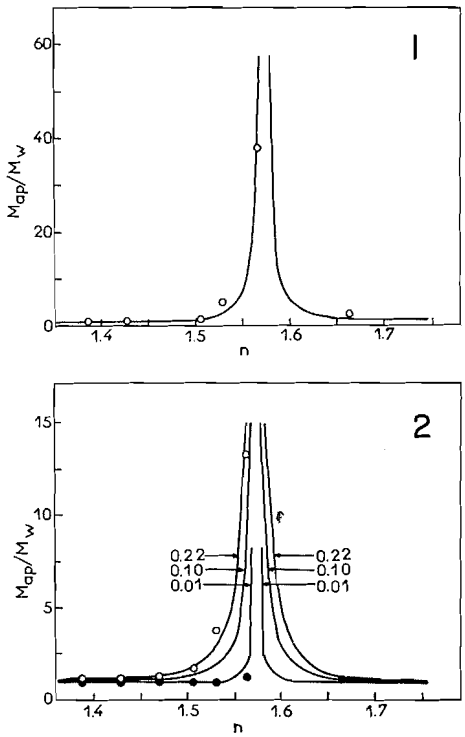

FIG. 1. Apparent (total) molecular weight of mixture comprising 65% PS and 35% PMM (expressed as M_{ap}/M_w) vs. refractive index of solvent. Circles, experimental data; lines, M_{ap} calculated from equation [16].

FIG. 2. Apparent molecular weight (M_{ap}/M_w) vs. refractive index of solvent. Experimental data: circles, copolymer I; points, copolymer II. Lines represent values of M_{ap} calculated from equation [14] with $P = 0$ and Q/M_w as indicated.

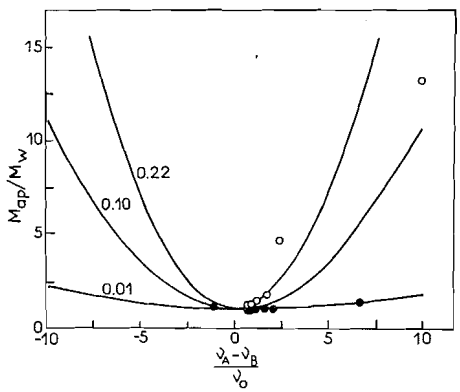

FIG. 3. Apparent molecular weight (M_{ap}/M_w) vs. $(\nu_A-\nu_B)/\nu_0$. Experimental data: circles, copolymer I; points, copolymer II. Lines represent data calculated from equation [14] with $P = 0$ and Q/M_w as indicated.

The high heterogeneity of composition found for copolymer I may seem somewhat contrary to the suggestion by Stockmayer (11) that the instantaneous distribution of chain composition of copolymers can be described by a very narrow Gaussian distribution curve. This is probably true in the case of low conversion copolymers (4); however, it

Can. J. Chem. Downloaded from www.nrcresearchpress.com by 78.46.186.204 on 09/04/12
For personal use only.

seems that high conversion copolymers may show considerable heterogeneity of chain composition. Indeed, the theory of copolymerization (12) does predict that high conversion copolymers will in general be of heterogeneous chain composition. It does not seem likely that copolymer I could be a mixture of copolymer and homopolymer of either type A or B.

A further remark is necessary regarding the merits of the two methods of plotting the experimental data shown by Figs. 2 and 3. Figure 2 gives a very striking demonstration of the extent of variation in the apparent molecular weight with the refractive index of the solvent. The deviation of M_{ap}/M_w from unity for the various solvents is related to the degree of heterogeneity of chain composition. To obtain a quantitative measure of this heterogeneity graphically, the plot of Fig. 3 is more useful than that of Fig. 2.

Table IV summarizes the light-scattering results on copolymer II (block copolymer). For this copolymer, the value of M_{ap}/M_w is equal to unity, within experimental error, for all the solvents used. Accordingly, it is concluded that copolymer II is of reasonably uniform chain composition. Whether this is generally true for copolymers prepared by the Szwarc method or whether the homogeneous composition can be attributed to the high degree of polymerization will have to be ascertained by further experiments. The results for copolymer II were plotted in Figs. 2 and 3 for the purpose of comparison.

TABLE IV

SUMMARY OF RESULTS ON COPOLYMER II

Composition: 70% PS+30% PMM

Solvent	ν_0 (cc g^{-1})	$M_{ap}\times10^{-6}$	M_{ap}/M_w
Butanone	0.195	1.42	1.18
Dioxane (p)	0.139	1.15	0.96
Carbon tetrachloride	0.116	1.39	1.16
Benzene	0.074	1.40	1.16
Chlorobenzene	0.051	1.30	1.08
Bromobenzene	0.015*	1.91	1.59
1-Bromonaphthalene	−0.096†	1.74	1.45

*Calculated: $\nu_0 = 0.70(0.042)+0.30(-0.058)$.
†Measured on the Zeiss Interferometer.

As indicated in the theoretical section, it should be possible to determine the weight-average molecular weights of the fractions comprising part A and B of the copolymer. The values obtained for the two copolymers used in this study are given in Table V. The values for M_A and M_B listed were calculated from equation [9] taking the values for M_{ap} from Fig. 2 for n equal to 1.49 where $\nu_B = 0$ and 1.61 where $\nu_A = 0$.

TABLE V

SUMMARY OF DERIVED DATA FOR COPOLYMERS I AND II

Copolymer	M_A	M_B	M_w	P/M_w	Q/M_w	Q/Q_{max}
I	1.74×10^5	0.82×10^5	1.83×10^5	0.01	0.16	0.72
II	0.84×10^6	0.36×10^6	1.20×10^6	0.00	0.01	0.05

Table V also gives the values of M_w, P/M_w, and Q/M_w. These were calculated from equation [14] using the values of M_{ap} for all the solvents used and listed in Tables III and IV.

Can. J. Chem. Downloaded from www.nrcresearchpress.com by 78.46.186.204 on 09/04/12
For personal use only.

It may be seen that for copolymer II, which seems to be of reasonably homogeneous composition, the sum of the molecular weights of the components is equal to the molecular weight of the copolymer. This is not true for copolymer I in which case M_w is related to M_A and M_B by equation [16].

As found by graphical interpolation, the value of P (actually P/M_w) for copolymer I is considerably smaller than that of Q (Q/M_w). Accordingly, omission of the term containing P when using equation [14] seems to be justified. The calculated value of Q/M_w is in satisfactory agreement with that obtained by the graphical method.

The last column of Table V gives the ratio Q/Q_{max} where Q_{max} is calculated from the relation $x_0(1-x_0)$, which for both copolymers is approximately 0.22. This ratio may be taken as the quantitative measure of the heterogeneity of chain composition as compared with the maximum possible value equal to unity. Expressed in this manner, the heterogeneity of composition values are 0.72 and 0.05 for copolymer I and II respectively.

As an application of the findings presented in this paper, it should be possible to study the variation of chain composition of copolymers as a function of conversion during copolymerization by means of light scattering. Information of this type may be of considerable value in the interpretation of copolymerization kinetics.

ACKNOWLEDGMENTS

One of the authors (W.B.) wishes to make the following grateful acknowledgments. To Professor C. Sadron, Director, Centre de Recherches sur les Macromolécules, Strasbourg, for making available the facilities of the laboratory and for his kind interest throughout the project; to the professional members and the technicians of the same laboratory for their co-operation, assistance, and advice during the period the author spent at the laboratory; to the National Research Council of Canada for the financial assistance in form of an Overseas Postdoctorate Fellowship; to the Royal Society of Canada for the Rutherford Memorial Fellowship.

The authors wish to thank Drs. Banderet and Rempp of the Centre de Recherches sur les Macromolécules for providing copolymers I and II respectively.

REFERENCES

1. DEBYE, P. J. Phys. & Colloid Chem. **51**, 18 (1947).
2. TREMBLAY, R., RINFRET, M., and RIVEST, R. J. Chem. Phys. **20**, 523 (1952).
3. WEILL, G. Private communication.
4. STOCKMAYER, W. H., MOORE, L. D., JR., FIXMAN, M., and EPSTEIN, B. N. J. Polymer Sci. **16**, 517 (1955).
5. BUSHUK, W. and BENOÎT, H. Compt. rend. **246**, 3167 (1958).
6. ZIMM, B. H. J. Chem. Phys. **16**, 1099 (1948).
7. SZWARC, M. Nature, **178**, 1168 (1956).
8. WIPPLER, C. and SCHEIBLING, G. J. chim. phys. **51**, 201 (1954).
9. CARR, C. I., JR. and ZIMM, B. H. J. Chem. Phys. **18**, 1616 (1950).
10. VALLET, G. Ph.D. Thesis, Strasbourg. 1952.
11. STOCKMAYER, W. H. J. Chem. Phys. **13**, 199 (1945).
12. ALFREY, T., JR., BOHRER, J. J., and MARK, H. Copolymerization. Interscience Publishers, Inc., New York. 1952. Chap. VII.

Can. J. Chem. Downloaded from www.nrcresearchpress.com by 78.46.186.204 on 09/04/12
For personal use only.

Can. J. Chem. Downloaded from www.nrcresearchpress.com by 78.46.186.204 on 09/04/12
For personal use only.

SUR LA SYNTHÈSE DE FORMYLDIPHÉNYL ÉTHERS POLYSUBSTITUÉS[1]

R. CONSTANTIN[2] ET P. L'ÉCUYER

RÉSUMÉ

Bon nombre de formyldiphényl éthers ont été synthétisés en faisant réagir certains phénols avec la 2-chloro-5-nitrobenzaldéhyde ou la 3-nitro-4-chlorobenzaldéhyde. Plusieurs l'ont été en condensant le tosylate de la 5-nitrovanilline ou de la 4-hydroxy-3-nitrobenzaldéhyde avec divers phénols. Ces derniers ne donnent pas d'éthers avec la 2-chloro-5-nitrobenzaldéhyde; mais, cependant, les phénolates alcalins réagissent avec cette aldéhyde en solution alcoolique diluée. Par une série de réactions, les 2,2′-diméthoxy-4,4′-diformyl-6-nitro-, 2,2′-diméthoxy-4,4′-diformyl-, 2,2′-diméthoxy- 4,4′-bis-(β-carboxyvinyl)- et 2,2′-diméthoxy-4,4′-bis-(β-carboxyéthyl)-diphényl éthers ont été préparés.

Le travail de Purves (1) sur la synthèse de la papavérine et de la papavéraldine par la méthode de Pomeranz–Fritsch nous a fait imaginer que le 2,3′,4′-triméthoxy-6-formyldiphényl éther (I) pourrait servir de matière première à la préparation de la cularine. Le désir de préparer cette aldéhyde nous a conduits à l'étude des méthodes de synthèse des formyldiphényl éthers polysubstitués.

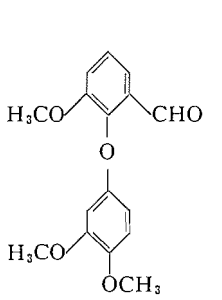

I

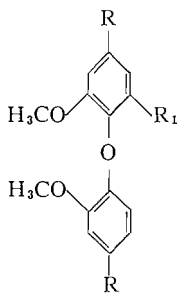

II

R = CHO, CH=CH$_2$–CO$_2$H ou CH$_2$—CH$_2$—CO$_2$H
R$_1$ = H ou NO$_2$

La préparation d'éthers diphényliques à partir d'un phénol et de chlorobenzènes convenablement activés a déjà été décrite par Grundon et Perry (2). Nous avons obtenu plusieurs formyldiphényl éthers en faisant réagir la 2-chloro-5-nitrobenzaldéhyde ou la 3-nitro-4-chlorobenzaldéhyde avec le phénol approprié en solution alcoolique diluée contenant 1 équivalent d'hydroxyde de sodium. Les rendements varient selon la nature et la position des groupes substituants (Tableau I).

Hems et quelques collaborateurs (3) avaient auparavant constaté que le tosylate du 2,4-dinitrophénol peut remplacer le 2,4-dinitrochlorobenzène dans les réactions de celui-ci avec un phénol pour donner aussi naissance à des diphényl éthers. Nous avons de cette façon préparé bon nombre de formyldiphényl éthers en condensant le tosylate de la 5-nitrovanilline ou de la 4-hydroxy-3-nitrobenzaldéhyde avec divers phénols dans la pyridine.

[1]*Manuscrit reçu le 11 juillet, 1958.*
Contribution du Département de Chimie, Faculté des Sciences, Université Laval, Québec, P.Q. Ce mémoire est tiré de la thèse de doctorat de R. Constantin.
[2]*Adresse actuelle: Département d'Agriculture, Section des Sciences, Division de la Chimie, Ottawa, Canada.*

TABLEAU I

INFLUENCE DE LA NATURE ET DE LA POSITION DES GROUPES SUBSTITUANTS DANS LE PHÉNOLATE DE SODIUM SUR LE RENDEMENT DE SES RÉACTIONS (1 HEURE) AVEC LES FORMYLNITROCHLOROBENZALDÉHYDES EN SOLUTION AQUEUSE

	Rendement, %	
Phénolate	2-Nitro-4-formylchlorobenzène	2-Formyl-4-nitrochlorobenzène
2-Méthoxy	50.5	48
4-Méthoxy	52	53
3-Formyl	48	59
4-Formyl	25	30
2-Méthoxy-5-formyl	56.5	65
2-Méthoxy-4-formyl	15	5
2-Nitro	0	—
3-Nitro	49	—
4-Nitro	0	—
2-Méthoxy-3-nitro-5-formyl	22	—

Que l'on fasse réagir avec un phénol le tosylate d'un phénol ou un chlorobenzène convenablement activé, nous avons vérifié que le rendement de la réaction dépend de la durée de celle-ci. Il augmente graduellement jusqu'à un maximum qui s'obtient pour un temps de réaction allant de 60 à 90 minutes et décroît ensuite rapidement, lorsqu'on chauffe plus longtemps (Fig. 1).

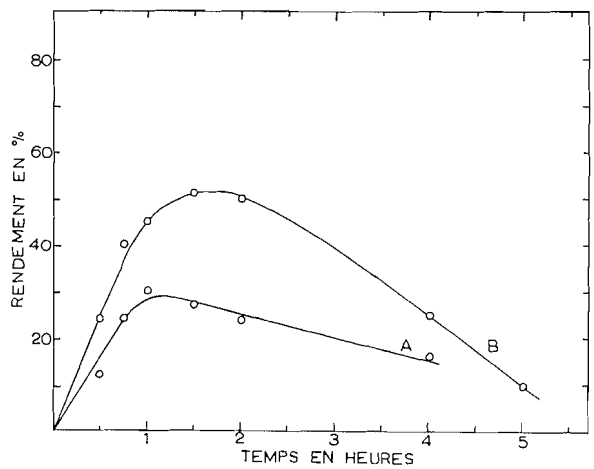

FIG. 1. Rendement de la réaction de 1 mole de guaïacol avec 3 moles de l'ester tosylique de la 5-nitrovanilline (A) ou de la 3-nitro-4-chlorobenzaldéhyde (B) en fonction du temps.

Quoique la réaction des formylchlorobenzènes ou des tosylates de phénols activés avec les phénols permette d'obtenir nombre de formyldiphényl éthers, il semble bien que la réaction de Hems ne va pas quand le groupement formyle est voisin du chlore ou du groupe oxytosyle, comme c'est le cas pour le 2-formyl-4-nitrochlorobenzène, par example. Il en est ainsi également pour la réaction d'Ullmann lorsque, en plus de la situation précédente, l'autre position voisine du chlore est occupée par un groupement méthoxyle. Par ailleurs, la réaction du tosylate de la 5-nitrovanilline ou de la 5-nitro-*o*-vanilline ne donne qu'une transestérification avec les phénolates alcalins. Nous avons cependant

Can. J. Chem. Downloaded from www.nrcresearchpress.com by 78.46.186.204 on 09/04/12
For personal use only.

réussi la condensation de la 2-chloro-5-nitrobenzaldéhyde avec les phénolates de sodium en milieu alcoolique dilué; mais nous n'avons pas réussi à obtenir la 2-chloro-3-méthoxy-5-nitrobenzaldéhyde pour préparer I.

Enfin, la condensation de la vanilline avec l'ester tosylique de la 5-nitrovanilline dans la pyridine a donné le 2,2′-diméthoxy-4,4′-diformyl-6-nitrophényl éther (II; R = CHO, $R_1 = NO_2$). Nous avons réduit celui-ci par le chlorure stanneux en 2,2′-diméthoxy-4,4′-diformyl-6-aminodiphényl éther et éliminé la fonction amine dans ce dernier en diazotant en présence d'acide hypophosphoreux pour isoler le 2,2′-diméthoxy-4,4′-diformyldiphényl éther (II; R = CHO, R_1 = H). En condensant celui-ci avec l'acide malonique dans la pyridine nous avons synthétisé le 2,2′-diméthoxy-4,4′-bis-(β-carboxy-vinyl)-diphényl éther (II; R = CH═CH—CO_2H, R_1 = H) dont la réduction par le nickel Raney a donné le 2,2′-diméthoxy-4,4′-bis-(β-carboxyéthyl)-diphényl éther (II; R = CH_2—CH_2—CO_2H, R_1 = H).

PARTIE EXPÉRIMENTALE*

Esters tosyliques de formylnitrophénols

Tout en agitant mécaniquement et en maintenant la température au-dessous de 5°, on ajoute du chlorure de *p*-toluènesulfonyle (0.11 mole) à une suspension du formyl-nitrophénol (0.1 mole) dans la pyridine (70 ml). Le tout se dissout et on abandonne la solution à la température ambiante jusqu'à ce qu'un précipité commence à se former. On verse alors le mélange dans environ 300 ml d'eau froide. On essore l'ester et on le lave à l'eau. Il cristallise dans le solvant approprié en lamelles blanches (Tableau II).

TABLEAU II

ESTERS TOSYLIQUES DE PHÉNOLS

Phénol	P.f., °C	Rdt, %	Solvant	Formule	N	
					% calculé	% trouvé
5-Nitrovanilline (2)	144–145	78	Acide acétique	$C_{15}H_{13}O_7NS$	3.98	3.9
5-Nitro-*o*-vanilline	72	74	Éthanol	$C_{15}H_{13}O_7NS$	3.98	4.1
2-Nitro-4-formylphénol	115	84	Éthanol	$C_{14}H_{16}NS$	4.36	4.5

Esters diphényliques dérivés de la 5-nitrovanilline

On bout à reflux pendant 1 heure une solution de tosylate de la 5-nitrovanilline (0.01 mole) et du phénol approprié (0.03 mole) dans de la pyridine (10 ml). On abandonne le mélange réactionnel à la température ambiante et, une fois refroidi, on le verse dans environ 100 ml d'eau froide. On extrait la suspension à l'éther, on lave l'extrait éthéré successivement à l'acide chlorhydrique et à la soude dilués, et enfin à l'eau, puis on l'évapore à siccité. On cristallise l'éther dans le solvant approprié (Tableau III).

Éthers diphényliques dérivés de la 3-nitro-4-hydroxybenzaldéhyde

On peut préparer ces éthers comme précédemment à partir du tosylate de la 3-nitro-4-hydroxybenzaldéhyde (0.01 mole) et du phénol requis (0.03 mole) dans la pyridine (10 ml) (façon de procéder (*a*)), ou bien en chauffant à reflux pendant 1 heure de la 3-nitro-4-chlorobenzaldéhyde (0.01 mole) avec le phénol approprié (0.03 mole) dans la pyridine (10 ml) (façon de procéder (*b*)), ou dans 5 ml d'eau contenant 0.4 g (1 équivalent)

**Les points de fusion ont été pris à l'aide de l'appareil de Johns.*

Can. J. Chem. Downloaded from www.nrcresearchpress.com by 78.46.186.204 on 09/04/12
For personal use only.

TABLEAU III

2-NITRO-4-FORMYL-6-MÉTHOXYPHÉNYL ARYL ÉTHERS

Groupe aryle	P.f., °C	Rdt %	Solvant	Forme cristalline	Formule	N % calculé	N % trouvé
Phényle	63	29	Éthanol	Lamelles jaunes	$C_{14}H_{11}O_5N$	5.12	4.7
2-Méthoxyphényle (2)	136–137	30	Éthanol	Aiguilles jaunes	$C_{15}H_{13}O_6N$	4.62	4.5
4-Méthoxyphényle[a]	110–111	45	Éthanol	Aiguilles jaunes	$C_{15}H_{13}O_6N$	4.62	4.6
3-Formylphényle	138	39	Éthanol	Prismes blancs	$C_{15}H_{11}O_6N$	4.65	4.8
4-Formylphényle	131.5	32	Éthanol	Prismes blancs	$C_{15}H_{11}O_6N$	4.65	4.7
2-Méthoxy-5-formyl-phényle	167	40	Acide acétique	Prismes blancs	$C_{16}H_{13}O_7N$	4.23	4.4
2-Méthoxy-4-formyl-phényle	155	48	Acide acétique	Lamelles blanches	$C_{16}H_{13}O_7N$	4.23	4.2

d'hydroxyde de sodium (façon de procéder (*c*)). Dans les deux premières façons de procéder (soit (*a*) et (*b*)) on isole les éthers comme on le fait pour les éthers dérivés de la 5-nitrovanilline, tandis que dans la dernière (soit (*c*)) on ne lave l'extrait éthéré qu'à l'eau. On cristallise les éthers dans l'éthanol (Tableau IV).

TABLEAU IV

2-NITRO-4-FORMYLPHÉNYL ARYL ÉTHERS

Groupe aryle	P.f., °C	Rdt, %	Forme cristalline	Formule	N % calculé	N % trouvé
Phényle	48	(*a*) 45	Prismes blancs	$C_{13}H_9O_4N$	5.65	5.3
2-Méthoxyphényle	101.5	(*a*) 55 (*b*) 52 (*c*) 50	Aiguilles blanches	$C_{14}H_{11}O_5N$	5.12	5.0
4-Méthoxyphényle	66	(*a*) 50 (*b*) 50 (*c*) 52	Prismes jaunes	$C_{14}H_{11}O_5N$	5.12	5.3
3-Formylphényle	99	(*a*) 45 (*b*) 45 (*c*) 48	Lamelles blanches	$C_{14}H_9O_5N$	5.16	5.1
4-Formylphényle	93.5	(*a*) 54 (*b*) 70 (*c*) 28	Lamelles blanches	$C_{14}H_9O_5N$	5.16	5.3
2-Méthoxy-5-formylphényle	127	(*a*) 70 (*b*) 65 (*c*) 56	Aiguilles blanches	$C_{15}H_{11}O_6N$	4.65	4.6
2-Méthoxy-4-formylphényle	136	(*a*) 75 (*b*) 80 (*c*) 15	Prismes jaunâtres	$C_{15}H_{11}O_6N$	4.65	4.9
3-Nitrophényle	128	(*a*) 48 (*b*) 49	Aiguilles blanches	$C_{13}H_8O_6N_2$	9.72	9.8
2-Méthoxy-3-nitro-5-formylphényle	190	(*c*) 22	Lamelles blanches	$C_{15}H_{10}O_8N_2$	8.09	8.2

Éthers diphényliques dérivés de la 5-nitrosalicylaldéhyde

Dans une solution de 2-chloro-5-nitrobenzaldéhyde (0.01 mole) dans de l'éthanol (5 ml) on verse une solution du phénol approprié (0.01 mole) dans 5 ml d'eau contenant

Can. J. Chem. Downloaded from www.nrcresearchpress.com by 78.46.186.204 on 09/04/12
For personal use only.

0.4 g (1 équivalent) d'hydroxyde de sodium et on fait bouillir à reflux pendant 1 heure. Lorsque le mélange réactionnel est à la température ambiante on le dilue avec de l'eau, on essore l'éther précipité et on le cristallise dans l'éthanol sauf pour le 2′-méthoxy-2,5′-diformyl-4-nitrodiphényl éther qu'on cristallise dans l'acide éthanoique (Tableau V).

TABLEAU V

2-FORMYL-4-NITROPHÉNYL ARYL ÉTHERS

Groupe aryle	P.f., °C	Rdt, %	Forme cristalline	Formule	N % calculé	N % trouvé
2-Méthoxyphényle	113	48	Aiguilles blanches	$C_{14}H_{11}O_5N$	5.12	5.2
4-Méthoxyphényle	105	53	Aiguilles blanches	$C_{14}H_{11}O_5N$	5.12	4.9
3-Formylphényle	119–120	59	Prismes jaunâtres	$C_{14}H_9O_5N$	5.16	5.0
4-Formylphényle	131.5	30	Prismes blancs	$C_{14}H_9O_5N$	5.16	5.3
2-Méthoxy-4-formylphényle	71	47	Aiguilles blanches	$C_{15}H_{11}O_6N$	4.65	4.9
2-Méthoxy-5-formylphényle	210	65	Lamelles blanches	$C_{15}H_{11}O_6N$	4.65	4.6

2,2′-Diméthoxy-4,4′-diformyldiphényl éther (II; R = CHO, R_1 = H)

On ajoute 9.93 g (0.03 mole) de 2,2′-diméthoxy-4,4′-diformyl-6-nitrodiphényl éther à une solution de chlorure stanneux (23.0 g) dans 25 ml d'acide chlorhydrique concentré. On agite ce mélange pendant 2 heures à la température ambiante, puis 5 minutes à 80°. On refroidit et on décompose le composé complexe en le versant dans 150 ml d'eau. On essore l'amine, on la dissout dans 50 ml d'acide chlorhydrique dilué (1:1) et on la diazote à 0° par l'addition d'une solution de nitrite de sodium (2.1 g) dans 10 ml d'eau. Tout en agitant cette solution du sel de diazonium et en la maintenant à 0°, on verse lentement 100 ml d'acide hypophosphoreux à 30% préalablement refroidi à 0° et on laisse reposer le tout à cette température pendant 20 heures. On essore le précipité qui s'est formé et on le lave successivement à la soude diluée et à l'eau. Après avoir cristallisé dans un mélange de benzène et d'éther de pétrole, on obtient 6.5 g (76% de la théorie) de 2,2′-diméthoxy-4,4′-diformyldiphényl éther pur sous la forme de prismes blancs de p.f. 123°. Calculé pour $C_{16}H_{14}O_5$: C, 66.9%; H, 4.9%. Trouvé: C, 66.7%; H, 5.1%.

2,2′-Diméthoxy-4,4′-bis-(β-carboxyvinyl)-diphényl éther (R = CH=CH—CO_2H, R_1 = H)

On chauffe au bain-marie pendent 1 heure, puis à reflux durant 5 minutes, un mélange de 2,2′-diméthoxy-4,4′-diformyldiphényl éther (5.8 g, 0.02 mole), d'acide malonique (6.5 g, 0.08 mole), de pyridine (25 ml) et de pipéridine (0.5 ml). On verse ensuite la solution froide sur de la glace (100 g) additionnée de 25 ml d'acide chlorhydrique concentré et on filtre le précipité. On cristallise dans le benzène et on essore 5.9 g (80% de la théorie) de 2,2-diméthoxy-4,4′-bis-(β-carboxyvinyl)-diphényl éther pur sous la forme de cubes jaunâtres de p.f. 225–226°. Calculé pour $C_{20}H_{18}O_7$: C, 64.8%; H, 4.8%. Trouvé: C, 64.4%; H, 4.9%.

2,2′-Diméthoxy-4,4′-bis-(β-carboxyéthyl)-diphényl éther (R = CH_2—CH_2—CO_2H, R_1 = H)

À une solution vivement agitée de 2,2′-diméthoxy-4,4′-bis-(β-carboxyvinyl)-diphényl éther (7.41 g, 0.02 mole) dans 200 ml de soude à 10%, on ajoute, en petites portions et en l'espace de 1 heure, 20.0 g de l'alliage de nickel Raney. On filtre ensuite, on lave le précipité à l'eau et on verse le filtrat dans 10 ml d'acide chlorhydrique concentré. On essore le 2,2′-diméthoxy-4,4′-bis-(β-carboxyéthyl)-diphényl éther et on le cristallise dans

Can. J. Chem. Downloaded from www.nrcresearchpress.com by 78.46.186.204 on 09/04/12
For personal use only.

l'éthanol à 50%. L'éther cristallise en aiguilles blanches de p.f. 126°. Rendement: 6.0 g (80% de la théorie). Calculé pour $C_{20}H_{22}O_7$: C, 64.1%; H. 5.9%. Trouvé: C, 63.8%; H, 6.0%.

REMERCIEMENTS

Nous remercions le Conseil National de Recherches du Canada, l'Office de Recherches de la Province de Québec et les Canadian Industries Limited pour des bourses d'études qu'ils ont accordées à l'un de nous (R.C.).

BIBLIOGRAPHIE

1. GUTHRIE, D. A., FRANK, A. W. et PURVES, C. B. Can. J. Chem. **33**, 729 (1955).
2. GRUNDON, H. F. et PERRY, H. J. H. J. Chem. Boc. 3531 (1954).
3. BORROWS, E. T., CLAYTON, J. C., HEMS, B. A. et LONG, A. G. J. Chem. Soc. S190 (1949).

Can. J. Chem. Downloaded from www.nrcresearchpress.com by 78.46.186.204 on 09/04/12
For personal use only.

Can. J. Chem. Downloaded from www.nrcresearchpress.com by 78.46.186.204 on 09/04/12
For personal use only.

ON THE SPECTRAL RESPONSE OF PHOTOCONDUCTION IN THIN SINGLE CRYSTALS OF ANTHRACENE[1]

J. FERGUSON[2] AND W. G. SCHNEIDER

ABSTRACT

The photoconduction of thin crystals of anthracene (sublimation flakes) has been studied as a function of the wavelength of the incident light as well as the geometry of the "surface cell" arrangement. With spot electrodes on one face of the crystal, the spectral response showed a very pronounced difference depending on whether the electrode face or the opposite face was illuminated. In the latter case the spectral response followed the absorption curve of the crystal, whereas when the electrode face was illuminated the photoconductivity was a minimum at wavelengths corresponding to maximum extinction coefficients of the crystal.

INTRODUCTION

Photoconduction of aromatic compounds has been the subject of a considerable number of recent publications (1–17). One important aspect of this work has been the study of the variation of the photocurrent with wavelength. Carswell (18) first noted that the spectral dependence of the photocurrent in anthracene crystals reproduced the absorption spectrum of the crystal, and Lyons and co-workers (3, 13, 14) have extended these measurements to other compounds. Lyons (4) has suggested a reason for the similarity between the absorption spectrum of the crystal and the spectral dependence of the photocurrent. During the course of an investigation of the absorption and fluorescence spectra of anthracene sublimation crystals (19, 20) we have remeasured the spectral dependence of the photocurrents in these crystals and we find that if particular care is taken to ensure that the electrode material is only on the surface on which the light falls, the spectral dependence does not reproduce the absorption spectrum. The present paper reports these measurements.

EXPERIMENTAL

The anthracene crystals were grown by sublimation in an atmosphere of carbon dioxide. Chromatographically pure anthracene which had been kept in the dark after purification was used. Crystals deliberately contaminated with tetracene were obtained by adding small amounts of tetracene to the anthracene before sublimation.

The sublimation crystals were usually transferred to a clean silica disk so that one of the developed *ab* crystal faces was in contact with the silica disk. The disk provided the necessary support for the very thin crystals. A few measurements were made on thicker crystals (about 3 μ) mounted over a slot cut in a silica disk so that only about one half of the crystal was supported by the disk. These measurements did not differ significantly from those made with the disk supporting all of the crystal.

Aquadag was initially used as the electrode material but it was found that at low light intensities the photocurrent showed an unusually long build-up time and this was eliminated by reverting to electrodes from alkadag. The electrodes were judged to be "good" if no back e.m.f. was found.

At first, electrodes were painted over each end of a crystal and also over part of the

[1]*Manuscript received May 14, 1958.*
Contribution from the Division of Pure Chemistry, National Research Council, Ottawa.
Issued as N.R.C. No. 4934.
[2]*National Research Council Postdoctorate Fellow 1955–57. Present address: Division of Industrial Chemistry, Box 4331, G.P.O., Melbourne, Victoria, Australia.*

silica disk. This produced an apparent variation of the spectral dependence of the photocurrent with crystal thickness. This variation was removed when care was taken to place the electrodes so that contact was made only with one *ab* face of the crystal. This was done by anchoring two flexible wires at diametrically opposite sides of a silica disk and making electrode contact to the exposed *ab* face with alkadag, taking particular care to prevent the electrode material from lapping over the edge of the crystal (see Fig. 1). Two arrangements were then possible, one with the light incident on the exposed *ab* face (electrode side), the other with the light incident on the opposite face.

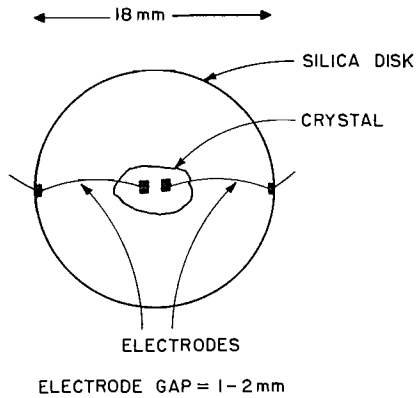

FIG. 1. Diagram of electrode arrangement. The incident light uniformly covered the electrodes and the area between the electrodes.

The silica disk was then mounted on a teflon block inside a brass cell fitted with a silica window. The cell, which could be evacuated, was clamped to a Keithley 200B micromicroammeter. Normally measurements were made in dry air but a few were made in an atmosphere of helium.

The spectral dependences were determined with a Beckman DU Spectrometer as a monochromator. The light source was a 500-watt projection lamp and the radiation was polarized by a sheet of polaroid between the exit slit and the cell. The wavelength knob of the monochromator was driven by a motor and the photocurrent was recorded by a Varian G10 recorder. The intensity dependence of the photocurrent was measured at different wavelengths by using filters of evaporated silver on silica. After the photoconduction measurements had been made the absorption spectrum in polarized light was determined in every case.

The photocurrents were usually in the range 10^{-13}–10^{-12} amp and slit widths varied from 0.05 to 0.4 mm, with 0.2 mm the usual value. No increased "resolution" was found at slit widths below this value.

RESULTS

A. Anthracene Crystals Containing Tetracene

There are two processes taking place after the absorption of light which could possibly complicate the interpretation of the spectral response of the photocurrent. These are the migration of excitation energy and reabsorption of fluorescence. It is important to demonstrate experimentally that migration of energy over a large number of lattice parameters (50–100) is not an essential factor in determining the spectral response. This

Can. J. Chem. Downloaded from www.nrcresearchpress.com by 78.46.186.204 on 09/04/12
For personal use only.

can be done simply by deliberately contaminating anthracene with small amounts of tetracene so as to quench the anthracene fluorescence and thereby reduce the mean free path of the exciton. This was done for a series of crystals with increasing tetracene concentration but no change in the polarized spectral response was observed, with either arrangement of electrodes and incident light, from that observed with pure anthracene crystals even when 90% of the emission was from the tetracene. These experiments also proved that reabsorption of fluorescence was not an important factor.

One observation, noted previously (15), is that the magnitude of the photocurrent is decreased markedly by the introduction of the tetracene. This suggests that the process leading to the production of charge carriers is one that does not take place in a time that is very short compared to the lifetime of the excited state, and the formation of charge carriers is thereby inhibited by any interaction which decreases, even slightly, the lifetime of this state.

B. Pure Anthracene Crystals

The spectral responses recorded here were all taken in dry air. Some measurements were made in which the cell was evacuated to 10^{-5} mm Hg and then dry helium introduced at atmospheric pressure. These showed that no significant changes occurred in the spectral response even after continued pumping resulting in appreciable sublimation of the crystals. As mentioned earlier, care was taken to ensure that the anthracene, after purification, was not exposed to light of high intensity so that photooxidation products on the surface of the crystals were kept to a minimum.

It was necessary to correct the spectral response in two ways. First, the intensity of the light incident on the crystal decreased with decreasing wavelengths so correction factors were calculated from the known energy distribution of the light source, the dispersion of the monochromator, and the transmission of the polaroid sheet. Measurements of the photocurrent at different wavelengths with polarized light of varying intensity showed that the photocurrent was directly proportional to the light intensity for both arrangements of light and electrodes. This result is needed to correct the response curves to equal energy input but is more important for an interpretation of the spectral response. Second, the spectral response has to be corrected in regions of the spectrum where the crystal transmits light. This occurs with very thin crystals for wavelengths within the absorption region and for all crystals at wavelengths on the absorption edge. In order to do this the absorption spectrum of each crystal was determined but no measurements of reflection losses were made. Although the latter will be small in regions where the absorption is strong (21) they are very important on the absorption edge when the optical density is less than about 0.2. As the correction factors convert the observed response to equal amounts of absorbed energy, they will be in serious error on the tail of the absorption band because the apparent absorption due to reflection is appreciable, and for this reason the corrected spectral dependences reported here cover only the wavelength region where reflection losses cause no appreciable error to the measured absorption spectrum.

As mentioned in the Experimental section, particular care is required in applying the electrode material to the crystals. If the electrodes are carefully placed only on the exposed *ab* face, then it is found that the spectral dependence depends critically on whether the incident light falls on this surface or on the opposite surface. Figs. 2 and 3 illustrate this behavior.

It was found that with light incident on the surface containing the electrodes the

Can. J. Chem. Downloaded from www.nrcresearchpress.com by 78.46.186.204 on 09/04/12
For personal use only.

Can. J. Chem. Downloaded from www.nrcresearchpress.com by 78.46.186.204 on 09/04/12
For personal use only.

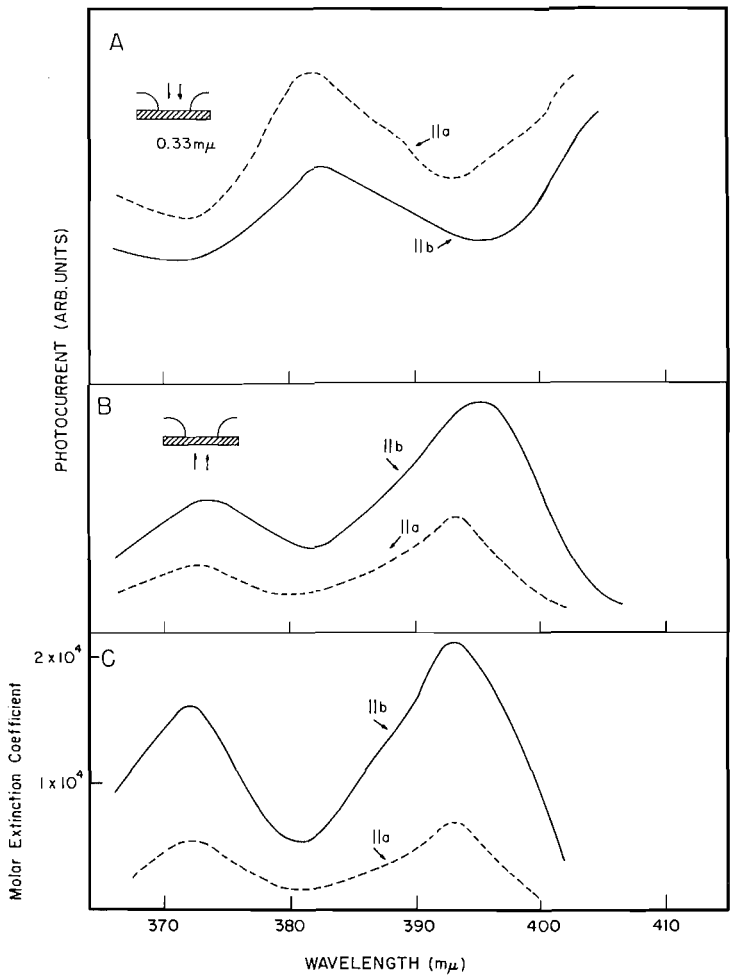

FIG. 2. The spectral dependence of the photocurrent (corrected to equal amounts of absorbed energy) in polarized light of a single anthracene crystal, thickness 0.33 μ; A, light incident on the surface containing the electrodes; B, light incident on the opposite face; C, the absorption spectrum of anthracene crystal (21).

wavelengths of maximum photocurrent correspond to wavelengths of minimum absorption coefficient, and this holds for both crystal polarizations. It is only when the light is incident on the other face that a resemblance is found between the spectral response of the photocurrent and the absorption spectrum of the crystal. In this case the wavelengths of maximum photocurrent correspond to wavelengths of maximum absorption coefficient and, although there is an apparent resemblance between the absorption spectrum and spectral response of the photocurrent, there is not a direct relation between the two. It must be assumed that in earlier reports of the spectral dependence of the surface cell the electrodes were not carefully confined to the surface on which the light was incident.

Measurements of the relative magnitudes of the photocurrents produced in the two arrangements were not made. However, with crystals of thickness about 4 μ mounted on silica and with electrodes not carefully confined to the top surface, i.e. electrode material painted over the crystal and onto the disk, the spectral response showed a resemblance to the absorption spectrum. This arrangement corresponds to electrodes simultaneously

on the front and back surfaces but with unequal distances between the electrodes. As the spectral response appeared similar to the absorption spectrum, we can assume that the arrangement with the electrodes on the back surface gives higher currents in the external circuit than the other arrangement.

A large number of measurements were made of the spectral response of a series of crystals of different thickness with the "true" surface cell arrangement, i.e. light incident

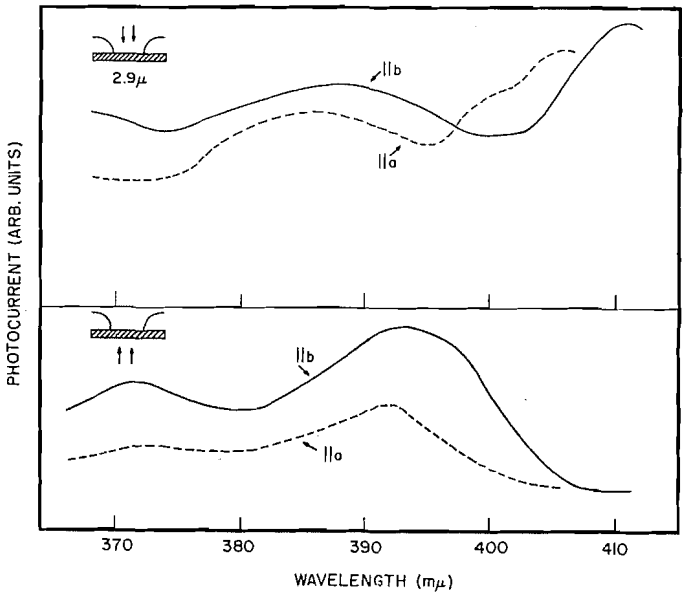

FIG. 3. The spectral dependence of the photocurrent (corrected to equal amounts of absorbed energy) in polarized light of a single anthracene crystal, thickness 2.9 μ. The top two curves were measured with the light incident on the surface containing the electrodes, the bottom two with the light incident on the opposite face.

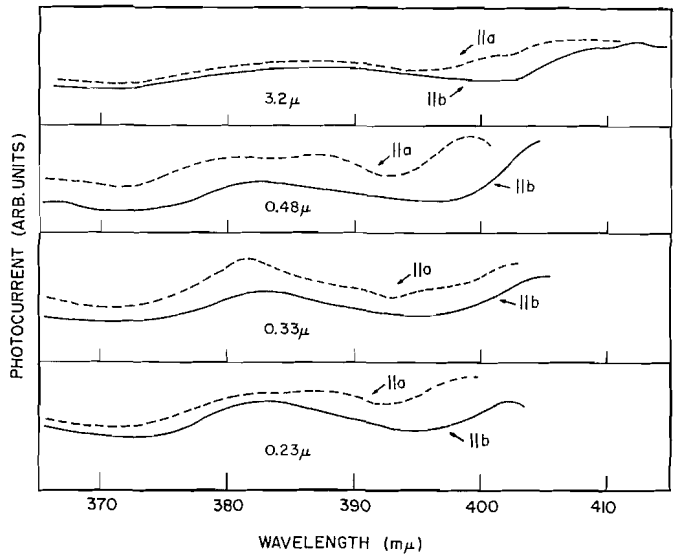

FIG. 4. The spectral dependence (corrected to equal amounts of absorbed energy) of the photocurrents in polarized light of four single anthracene crystals of different thickness, all measured with the light incident on the surface containing the electrodes.

Can. J. Chem. Downloaded from www.nrcresearchpress.com by 78.46.186.204 on 09/04/12
For personal use only.

on the face containing the electrodes. Fig. 4 shows some of the results. The crystal thickness ranges from 0.23 to 3.2 μ but there does not appear to be a dependence of the spectral response on crystal thickness. This is not strictly true for the *b* polarization, where there is seen to be a slight shift of the response to longer wavelengths for thicker crystals. This is interpreted as reflecting a modification of the surface energy levels in the thicker crystals (19), so that light absorbed near the surface is of slightly longer wavelength. The *a* polarization also shows variations in relative peak heights, as can be seen, but these show no correlation with crystal thickness.

DISCUSSION

It is apparent from Figs. 2, 3, and 4 that the wavelengths which are most strongly absorbed produce least photocurrent in the "true" surface cell arrangement. The result is striking and suggests immediately that carrier recombination limits the photocurrents in regions of high light absorption. However, the photocurrent is directly proportional to the light intensity and also, if recombination is limiting the photocurrent in these regions, then the spectral response in the arrangement where the light falls on the opposite *ab* face should be similar, whereas maximum photocurrent is found at wavelengths of high absorption coefficient.

Although the results are striking we are not able to interpret them at present. We do, however, make the suggestion that diffusion of charge carriers, hitherto neglected, should be seriously considered in any attempt at an explanation. The surface cell arrangement of electrodes must produce an inhomogeneous field within the crystal and this, coupled with diffusion of carriers, can possibly complicate the spectral dependence.

The parallelism between the spectral response within the absorption region and the absorption edge should be noted. Inside the absorption band we see that wavelengths of minimum light absorption (true surface cell arrangement) produce a higher photocurrent than wavelengths of maximum absorption. If we compare the absorption edge with the absorption band as a whole we see that the former produces a higher photocurrent than the latter, so the general rule appears to be that high photocurrents are obtained in regions of low light absorption. We must not therefore interpret the spectral response of the surface cell to mean that the absorption edge necessarily has a higher efficiency for charge carrier formation. This becomes clear when we compare the two regions in the other arrangement of the light and electrodes, the general rule here being that high photocurrents are obtained in regions of high light absorption.

We would like finally to suggest that considerable care be taken in the interpretation of spectral response curves of organic photoconductors as anthracene is not a unique case. It was shown earlier (22) that the spectral dependence of 9,10-dichloroanthracene is also critically dependent on incident light and electrode geometry. Also we note the attempt to assign the electronic states of the pyrene molecule from measurements of the polarized spectral dependence of single crystals of pyrene (14). The assignment of the lowest excited state is most likely correct but the sense of the polarization ratio as observed in the spectral dependence of the photocurrent is opposite to that found by direct absorption spectroscopy (23). This is then probably a result of some specific sensitivity of the electrode and incident light geometry.

REFERENCES

1. CHYNOWETH, A. G. and SCHNEIDER, W. G. J. Chem. Phys. **22**, 1021 (1954).
2. CHYNOWETH, A. G. J. Chem. Phys. **22**, 1029 (1954).
3. BREE, A. V. and LYONS, L. E. J. Chem. Phys. **22**, 1630 (1954).

Can. J. Chem. Downloaded from www.nrcresearchpress.com by 78.46.186.204 on 09/04/12
For personal use only.

4. LYONS, L. E. J. Chem. Phys. **23**, 220 (1955).
5. GOLDSMITH, G. J. Ph.D. Thesis, Purdue Univeristy, Lafayette, Indiana. 1955.
6. BREE, A. V., CARSWELL, D. J., and LYONS, L. E. J. Chem. Soc. 1728 (1955).
7. CARSWELL, D. J. and LYONS, L. E. J. Chem. Soc. 1734 (1955).
8. NORTHRUP, D. C. and SIMPSON, O. Proc. Phys. Soc. **68**, 974 (1955).
9. ZINZER, H. J. Z. Naturforsch. **11a**, 306 (1956).
10. INOKUCHI, H. Bull. Chem. Soc. Japan, **29**, 131 (1956).
11. SCHNEIDER, W. G. and WADDINGTON, T. C. J. Chem. Phys. **25**, 358 (1956).
12. BREE, A. V. and LYONS, L. E. J. Chem. Phys. **25**, 384, 1284 (1956).
13. LYONS, L. E. and MORRIS, G. C. Proc. Phys. Soc. **69**, 1162 (1956).
14. LYONS, L. E. and MORRIS, G. C. J. Chem. Soc. 3648, 3661 (1957).
15. COMPTON, D. M. J., SCHNEIDER, W. G., and WADDINGTON, T. C. J. Chem. Phys. **27**, 160 (1957).
16. LYONS, L. E. Australian J. Chem. **10**, 365 (1957).
17. LYONS, L. E. J. Chem. Soc. 5001 (1957).
18. CARSWELL, D. J. J. Chem. Phys. **21**, 1890 (1953).
19. FERGUSON, J. and SCHNEIDER, W. G. J. Chem. Phys. **28**, 761 (1958).
20. FERGUSON, J. and SCHNEIDER, W. G. Can. J. Chem. **36**, 1070 (1958).
21. BREE, A. V. and LYONS, L. E. J. Chem. Soc. 2663 (1956).
22. BOCK, E., FERGUSON, J., and SCHNEIDER, W. G. Can. J. Chem. **36**, 507 (1958).
23. FERGUSON, J. J. Chem. Phys. **28**, 765 (1958).

Can. J. Chem. Downloaded from www.nrcresearchpress.com by 78.46.186.204 on 09/04/12
For personal use only.

Can. J. Chem. Downloaded from www.nrcresearchpress.com by 78.46.186.204 on 09/04/12
For personal use only.

KINETICS OF EXCITED MOLECULES

I. KETENE[1]

B. T. Connelly and Gerald B. Porter

ABSTRACT

The primary quantum yield of ketene decomposition was studied as a function of pressure, temperature, and wavelength. The results show that excited vibronic states are formed which may be degraded before dissociation can occur. The ratio of the rate of collisional degradation to the rate of dissociation decreases from 164 liters/mole at 3340 Å to 16.8 liters/mole at 3130 Å.

INTRODUCTION

Previous experiments have shown that the primary quantum yield of ketene decomposition is a function of the wavelength of the absorbed radiation. At 2700 Å Strachan and Noyes (1) found the primary quantum yield to be unity within experimental error, independent of pressure and temperature. At 3650 Å (1) the primary quantum yield, extrapolated to zero pressure of ketene, is much less than unity, decreases as pressure is increased, and increases with increase in temperature.

Following the absorption of 2700 Å radiation and the formation of an excited ketene molecule, dissociation occurs in less time than that required for collision with another molecule, to give a methylene radical and a molecule of carbon monoxide. The methylene radical then attacks another ketene molecule to form ethylene and another carbon monoxide, according to the following mechanism:

$$K + h\nu\ (2700\ Å) = K^m, \qquad [1m]$$

$$K^m = CH_2 + CO, \qquad [2m]$$

$$CH_2 + K = C_2H_4 + CO, \qquad [2m]$$

where K is a ketene molecule, and K^m is a ketene molecule excited by 2700 Å radiation. For each photon absorbed, one molecule of ketene is dissociated and two molecules of carbon monoxide are formed.

Strachan and Noyes (1) found the quantum yield of carbon monoxide formation to be 2.12 ± 0.15. They also found the ratio of the quantum yield of carbon monoxide formation to the quantum yield of ethylene to be 2.2 instead of 2.0 to be expected from reactions [1*m*] and [2*m*].

It is evident therefore that some methylene radicals are involved in another reaction, such as

$$CH_2 + y\,CH_2CO = \text{polymer} + CO.$$

At 3650 Å, the low quantum yields can be attributed to collisional deactivation and internal conversion of the excited ketene molecules (2), according to the following mechanism:

$$K + h\nu\ (3650\ Å) = K^q, \qquad [1q]$$

$$K^q = \text{products}, \qquad [2q]$$

$$K^q = K, \qquad [3q]$$

$$K^q + K = 2K. \qquad [4q]$$

The energy is dissipated in processes [3*q*] and [4*q*] as heat, since no fluorescence has ever been observed.

[1]*Manuscript received July 28, 1958.*
Contribution from the Department of Chemistry, University of British Columbia, Vancouver, B.C.

It is evident from the low quantum yield that reaction [3q] is more rapid than reaction [2q]. As the pressure is increased the rate of reaction [4q] increases from zero to become the dominant process. Extrapolation to zero pressure at 26° C gives a carbon monoxide quantum yield of approximately 0.07. At 3650 Å, therefore, dissociation occurs only after a finite time interval during which the excited ketene molecule may be deactivated.

Kistiakowsky and Mahan (3) found that the primary quantum yield at 3130 Å was independent of pressure and suggested a value of unity. However, they apparently investigated the photolysis over a narrow range of pressures and their results are therefore not conclusive. Investigation of the quantum yield at a number of wavelengths provides the means of determining the relation between the rate of dissociation and the energy of the dissociating molecule. It was therefore decided to investigate the photolysis of ketene at 3130 Å more carefully over a wide range of pressures using a technique whereby quantum yields could be determined accurately. This technique would reveal any small effect of pressure on the primary quantum yield that may have escaped detection in previous work (3).

It was felt that since another mercury-arc line, 3340 Å, occurs between 3130 Å and 3650 Å, precise quantum yield determinations at this wavelength would substantially increase our understanding of the process of deactivation.

EXPERIMENTAL

A medium pressure 100-watt Hanovia mercury-arc lamp was used as the light source for runs at 3130 Å. The lamp was encased in aluminum tubing with $\frac{1}{4}$-in. diameter hole opposite the arc. The lamp was run from a constant voltage regulator (115 volts). For runs at 3340 Å a B.T.H. medium pressure mercury-arc lamp was used. The divergent light beam passed through a combination of two quartz convex lenses.

A filter cell block consisting of two compartments each 2.5 cm long and with quartz windows, together with a 2-mm Corning 9863 filter to exclude visible radiation, was placed between the lenses and the cell. The quartz reaction cell of length 14.8 cm and diameter 3.6 cm was housed in a heated aluminum block in which the temperature could be controlled to within ±0.1° C. The emergent beam was passed through another convex lens and focused on the cathode of an RCA 935 photocell.

The filter solutions used are given in Table I and the respective transmissions at the various wavelengths are shown in Fig. 1. Filters A and B were similar to those of Hunt and Davis (4), although the nickel chloride was omitted. Filter C was similar to that suggested by Kasha (5).

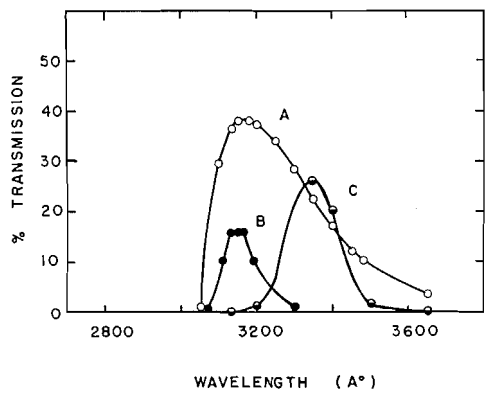

FIG. 1. Percentage transmission against wavelength for filters A, B, and C.

Can. J. Chem. Downloaded from www.nrcresearchpress.com by 78.46.186.204 on 09/04/12
For personal use only.

TABLE I
FILTER SOLUTIONS

Filter solution	Potassium biphthalate, g/100 ml 2.5-cm cell	Potassium chromate, g/100 ml 2.5-cm cell	Nickel sulphate hexahydrate, 1-cm cell	Naphthalene in methyl alcohol, g/50 ml 1-cm cell	Glass filters
A	0.08	0.008	—	—	2-cm Corning 9863
B	0.08	0.019	—	—	2-mm Corning 9863
C	—	—	Saturated solution	0.44	2-mm Corning 9863 1-mm Pyrex window

Gas Analyses

Gas analyses were carried out in an all-glass high-vacuum system evacuated by a standard-type oil pump and a single stage mercury diffusion pump. In this system mercury cutoffs were used in place of stopcocks.

The carbon monoxide analysis was performed by allowing the products to flow through successive baths cooled to −78° C, −196° C, −210° C (dry ice – acetone, liquid nitrogen, and solid nitrogen, respectively). The solid nitrogen trap was prepared by pumping on fresh liquid nitrogen for about fifteen minutes.

Ketene was condensed in the first two baths and the ethylene was collected in the solid nitrogen trap. Carbon monoxide was the only product not condensed at −210° C and was measured with a McLeod–Toepler gauge (1).

Diethyl Ketone

Diethyl ketone, used as the internal actinometer for runs at 3130 Å, was fractionally distilled (b.p. 101°). Once on the line, the diethyl ketone was distilled under vacuum and the middle third was retained.

Prior to each run, a quantity of diethyl ketone was transferred from a blackened storage bulb to a dry ice – acetone cooled trap and outgassed three times until all non-condensables and low-boiling gases were removed.

Ketene

Ketene was prepared in the vacuum system by pyrolyzing acetic anhydride (6). Trap-to-trap distillation was performed on the freshly prepared ketene and the middle third retained. Prior to each run, a quantity of ketene was thoroughly outgassed by three distillations similar to those for diethyl ketone. The ketene was stored in a trap immersed in liquid nitrogen to prevent polymerization.

Actinometry

3130 Å

Diethyl ketone was selected for experiments at 3130 Å where the quantum yield of carbon monoxide formation is 1.0 at 100° C (7). The use of an internal actinometer was found to be very convenient because it is devoid of the errors usually associated with external actinometers.

The measurement of the intensity absorbed during a run was performed by the conversion of the current from the photocell into a voltage which was continuously recorded on a 10-mv recorder. The following scale readings were taken:

R_i = cell empty,
R_t = photolyte in cell.

The recorder scale was calibrated using diethyl ketone as an internal actinometer.

Can. J. Chem. Downloaded from www.nrcresearchpress.com by 78.46.186.204 on 09/04/12
For personal use only.

Scale readings were taken before and after each run to determine the average R_i. This was necessary because of the fluctuation and decay of the lamp, and polymer formation. R_t was measured continuously during each run.

The difference $R_i - R_t = R_a$ was calibrated in terms of absolute intensity by the measurement of carbon monoxide yields from the photolysis of diethyl ketone at 100° C. It was possible to measure R_a to within $\pm 0.5\%$ and, on averaging the results of a number of diethyl ketone runs, quantum yields of carbon monoxide formation from ketene were obtained within $\pm 3\%$.

At 3130 Å, an external actinometer was also used (8), but because of the large amount of reflection from the glass–air interfaces and because of the suspected polymer on the exit wall of the reaction cell, the values for the absolute intensity of the light were considerably lower than those obtained using diethyl ketone. Twelve runs were performed using potassium ferrioxalate actinometer; consistent results indicated the need for a conversion factor to be applied when the external liquid actinometer was used to estimate the energy absorbed during runs at 3130 Å.

The intensity found from a ferrioxalate run when multiplied by this conversion factor gave the intensity incident to the cell, reproducible to within $\pm 10\%$.

3340 Å

The potassium ferrioxalate actinometer was used for runs at 3340 Å, since no internal actinometer is available for this wavelength. The intensities obtained by this actinometry when multiplied by the conversion factor found previously were used to calibrate the recorder scale. Absorbed intensities were obtained from measurements of R_i, R_t, and R_a, as described previously.

RESULTS

3130 Å

Using filter solution combination A, at low pressures of ketene, a carbon monoxide quantum yield of 1.82 was obtained, whereas at high pressures around one atmosphere, the carbon monoxide quantum yield decreased to 1.08, as shown in Table II. A decrease in the carbon monoxide quantum yield at high pressures was expected.

The results of five diethyl ketone actinometer runs, at pressures ranging from 60 to 155 mm of diethyl ketone, and interspersed between the ketene runs, gave a light intensity of approximately 5.4×10^{14} quanta per second.

Using filter solution combination B, a new series of diethyl ketone actinometer runs gave intensities of approximately 1.6×10^{14} quanta per second. The carbon monoxide quantum yield at low pressures of ketene was 2.0 within experimental error, and at 1 atmosphere a value of 1.18 was obtained as shown in Table II.

Absorbed intensities varied from 0.442×10^{14} quanta per second at 17 mm to 1.911×10^{14} quanta per second at 751 mm. All ketene runs were conducted at 37° C.

It was found that the transmissions at 3130 Å of filters A and B were appreciably lower after 2 weeks' constant use.

3340 Å

The naphthalene in methyl alcohol solutions darkened after only a few hours' exposure to the lamp and its transmission at 3340 Å decreased noticeably. Even when a pyrex window, which absorbs 50% of the light at 3130 Å and 100% of light of shorter wavelengths, was placed in front of the naphthalene solution darkening continued. This effect may have been caused by the attack of methyl alcohol on the adhesive used to bond the quartz windows to the pyrex cell.

Can. J. Chem. Downloaded from www.nrcresearchpress.com by 78.46.186.204 on 09/04/12
For personal use only.

TABLE II

PHOTOLYSIS OF KETENE

Run	Pressure of ketene, mm	Length of run, seconds	Intensity absorbed, quanta/second $\times 10^{-1}$	$\phi = \frac{1}{2}\Phi_{CO}$
	3130 Å	Cell temperature	37.0 °C	Filter A
1	35.8	3600	2.305	0.91
5	56.5	1800	2.855	0.93
4	201.6	2700	4.360	0.74
2	402.7	900	4.790	0.59
3	444.5	914	4.580	0.57
7	726.8	1800	4.290	0.54
	3130 Å	Cell temperature	37.0° C	Filter B
14	17.0	3600	0.442	1.03
13	40.8	2460	0.846	1.00
12	57.1	1800	1.029	1.00
11	135.8	2407	1.428	0.94
9	230.3	2400	1.710	0.83
10	679.1	1920	1.584	0.63
8	750.7	2400	1.911	0.59
	3340 Å	Cell temperature	37.0° C	Filter C
18	26.0	180	1.221	0.72
15	39.7	4200	0.771	0.72
16	47.0	1800	2.545	0.51
17	105.3	600	2.825	0.41
20	177.8	390	1.841	0.37
19	384.6	900	2.023	0.21
	3340 Å	Cell temperature	100.0° C	Filter C
24	26.1	180	0.811	0.80
23	56.7	240	1.239	0.74
22	121.8	255	1.579	0.58
21	299.5	600	1.920	0.37

The intensity of the beam as measured using the ferrioxalate actinometer when multiplied by the conversion factor of 2.72 gave an incident intensity of approximately 2.1×10^{15} quanta per second. When related to the recorder, this became 0.87×10^{14} quanta per second per scale division. The carbon monoxide quantum yields were determined at both 37° C and 100° C and the results are summarized in Table II.

DISCUSSION

The photolysis of ketene at 2700, 3130, 3340, and 3650 Å can be explained by the following processes:

$$K + h\nu\ (2700\ Å) = K^m \qquad [1m]$$

$$K + h\nu\ (3130\ Å) = K^n \qquad [1n]$$

$$K + h\nu\ (3340\ Å) = K^p \qquad [1p]$$

$$K + h\nu\ (3650\ Å) = K^q \qquad [1q]$$

$$K^m = \text{products} \qquad [2m]$$

$$K^n = \text{products} \qquad [2n]$$

$$K^p = \text{products} \qquad [2p]$$

$$K^q = \text{products} \qquad [2q]$$

$$K^m = K \qquad [3m]$$

Can. J. Chem. Downloaded from www.nrcresearchpress.com by 78.46.186.204 on 09/04/12
For personal use only.

$$K^n = K \quad [3n]$$
$$K^p = K \quad [3p]$$
$$K^q = K \quad [3q]$$
$$K^m + K = 2K \quad [4m]$$
$$K^n + K = 2K \quad [4n]$$
$$K^p + K = 2K \quad [4p]$$
$$K^q + K = 2K \quad [4q]$$

where K is a molecule of ketene, and K^m, K^n, K^p, and K^q are excited ketene molecules in order of decreasing vibrational energy. Reactions [1] represent activation; reactions [2] represent product formation; reactions [3] represent internal conversion; and reactions [4] represent collisional deactivation.

It is not implied that the above mechanism which represents the activation and deactivation of excited molecules K^m, K^n, K^p, and K^q formed at wavelengths 2700 Å, 3130 Å, 3340 Å, and 3650 Å is complete. It is obvious that a ketene molecule in vibronic state m can lose its excess energy by a series of vibrational cascades to states n, p, q, etc. until it eventually reaches the equilibrium vibrational state. The number of vibronic states may be 100 or more for a molecule initially in state m. The kinetics of such a process are very complicated and will be treated in a later paper (9).

For simplicity the present discussion will consider only reactions [1], [2], [3], and [4], with rate constants k_1, k_2, k_3, and k_4, to represent the activation, deactivation, and dissociation of excited ketene molecules in states m, n, p, and q.

In general,

$$1/\phi = 1+(k_3/k_2)+k_4[K]/k_2$$

represents the equation obtained by steady-state treatment; ϕ is the primary quantum yield, k_3/k_2 is the intercept in the plot $1/\phi$ against pressure, and k_4/k_2 is the slope in liters/mole.

2700 Å

Strachan and Noyes (1) found that the quantum yield of carbon monoxide formation was approximately two. According to the proposed mechanism the primary quantum yield is thus unity. It is evident, therefore, that over the range of pressures and temperatures used, internal conversion and collision deactivation of the excited ketene molecules is negligible. The only way in which these molecules can lose their excess energy is by dissociation. The observed quantum yields can be explained by the mechanism:

$$[1m], [2m].$$

That internal conversion and collisional deactivation are absent may be seen from the intercept of unity and the zero slope of the plot of $1/\phi$ against pressure.

3130 Å

The primary quantum yield of ketene decomposition at this wavelength appears as an isolated number in several papers devoted to ketene photolyses at other wavelengths (3, 9, 10, 11). However, only the recent work of Kistiakowsky and Mahan (3) gives experimental data. From the limited amount of information given it appears that photolyses were only performed at low pressures, in the region of 20 mm. It was found that the primary quantum yield was independent of pressure and possibly equal to unity.

This research has shown that when light which was not monochromatic but which contained quantities of both 3340 and 3650 Å radiation was used, primary quantum yields of 0.91 at 35.8 mm and 0.54 at 726.8 mm were obtained, as shown in Table II.

Can. J. Chem. Downloaded from www.nrcresearchpress.com by 78.46.186.204 on 09/04/12
For personal use only.

The plot of $1/\phi$ against pressure intercepts the axis at approximately 1.1 and has a positive slope. It is likely, therefore, that internal conversion and collisional deactivation of the excited ketene molecule contribute slightly to the deactivation process.

Because of the known low quantum yields at 3650 Å and the suspected low yields at 3340 Å, a new series of experiments was performed using monochromatic 3130 Å radiation. The results of these experiments are shown also in Table II. The primary quantum yield is 1.0 at pressures between 17 and 60 mm, and 0.59 and 750.7 mm.

The plot of $1/\phi$ against pressure is shown in Fig. 2; although the extrapolation to zero pressure is unity, because of experimental error the presence of internal conversion is not entirely excluded from the mechanism. The positive slope of the plot in Fig. 2 indicates the presence of collisional deactivation, and hence the mechanism: [1n], [2n], [3n], [4n] may be postulated in which the extent of reaction [3n] is very small. k_3/k_2 is approximately zero while $k_4/k_2 = 16.8$ liters/mole.

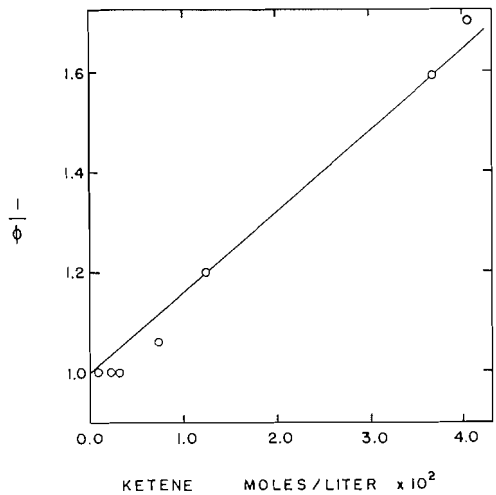

FIG. 2. Dependence of primary quantum yield on concentration at 3130 Å.

The mechanism of ketene decomposition at 3130 Å is intermediate between those postulated for 2700 Å and 3650 Å. From Table II it appears that at low pressures of ketene, every excited ketene molecule dissociates to form products, whereas, at pressures greater than approximately 60 mm, some of the excited molecules lose their energy by collision with unexcited molecules of ketene.

The photolysis at 3130 Å was not extended to higher temperatures because it was thought that little or no significant information would be obtained.

In three experiments the ethylene quantum yield was found to be 1/2.14 of the carbon monoxide quantum yield. This is approximately the same as that found at 2700 Å (1) and 3650 (1, 13).

3340 Å

This research has indicated that for photolyses at 37° C the primary quantum yield is 0.72 at 26 mm and 0.21 at 384 mm. The zero pressure intercept in Fig. 3 is 1.25. The slope of the plot is much steeper than for 3130 Å: 1.64×10^2 liters/mole. This indicates that considerable collisional deactivation of K^p occurs.

Four runs were performed at 100° C and as expected, both the slope and the intercept were smaller than for runs at 37° C. At 26.1 mm the primary quantum yield is 0.80 and

Can. J. Chem. Downloaded from www.nrcresearchpress.com by 78.46.186.204 on 09/04/12
For personal use only.

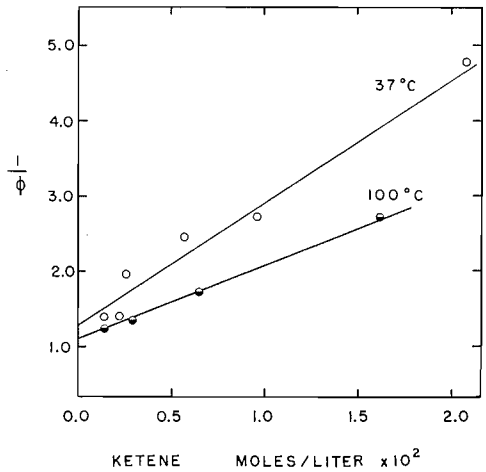

FIG. 3. Dependence of primary quantum yield on concentration at 3340 Å.

at 300 mm equals 0.37. The zero pressure intercept at 100° C is 1.1 and the slope of the straight line is 0.99×10^2 liters/mole, both obtained from Fig. 3. The ratio of the rates of internal conversion to product formation at 100° C is 0.1.

The mechanism for the activation and deactivation of K^p is: [1p], [2p], [3p], and [4p], at both 37° C and 100° C. From this information in Table II and Fig. 3, it was possible to estimate approximately the activation energy of reaction [2p] from the slope of the plot of $\log_e(k_4/k_2)$ against $1/T$. The slope is $(E_2-E_4)/R$. If E_4 is assumed to be zero, then E_2 is approximately 2 kcal/mole. This value is subject to a large uncertainty.

3650 Å

Strachan and Noyes (1) found a zero pressure intercept of 28 in the plot of reciprocal primary quantum yield against pressure. This corresponds to a primary quantum yield of approximately 0.036 at 26° C. The slope of the linear plot is 4.65×10^4 liters/mole.

Both the intercept and the slope decrease with increasing temperature. The activation energy of reaction [2q] is 4.5 kcal/mole.

k_3/k_4 as a Function of Wavelength

At 2700 Å, this ratio is indeterminant. Values of approximately 3×10^{-3}, 1.2×10^{-3}, and 6×10^{-4} all expressed in moles/liter are found for 3130 Å, 3340 Å, and 3650 Å, respectively. It must be emphasized that the values found for 3340 Å and particularly 3130 Å are subject to possible large errors.

k_2/k_4 as a Function of Wavelength

The slope of the plot of reciprocal quantum yield against pressure shows a marked dependence on wavelength, increasing from zero at 2700 Å to 4.65×10^4 liters/mole at 3650 Å. The intermediate values are 16.8 liters/mole at 3130 Å and 1.64×10^2 liters/mole at 3340 Å. It should again be pointed out that the result at 3650 Å was found at 26° C, whereas the other values were obtained at 37° C.

k_2/k_4 is thus 0.06, 0.61×10^{-2}, and 0.22×10^{-4} moles/liter at 3130, 3340, and 3650 Å respectively. In Fig. 4 these values are plotted against the energy of the exciting radiation. The slope increases rapidly as the energy of excitation increases.

If it is assumed that k_4, related to collisional deactivation, is virtually independent of the energy of the radiation, Fig. 4 represents the variation of k_2 with energy of the

Can. J. Chem. Downloaded from www.nrcresearchpress.com by 78.46.186.204 on 09/04/12
For personal use only.

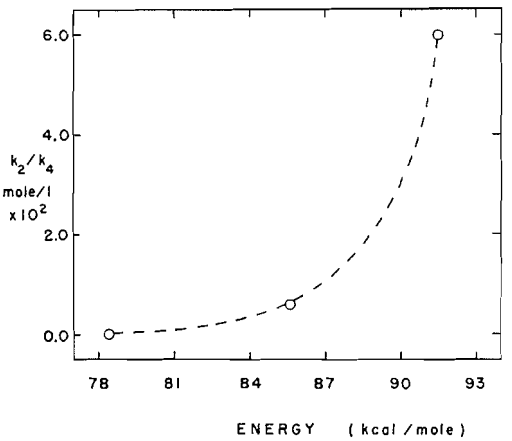

FIG. 4. Variation of k_2/k_4 with energy of excitation.

exciting radiation. It is evident, therefore, that the dissociation rate constant increases rapidly with increasing energy.

A further assumption that k_4 is the collision rate constant, 1.29×10^{11} moles^{-1} liters sec^{-1} calculated for a collision diameter of 3.5 Å, gives absolute values for k_2 of 7.74×10^{9}, 7.87×10^{8}, and 2.84×10^{6} sec^{-1} at 3130, 3340, and 3650 Å, respectively.

Energy of Activation of Reaction [2] as a Function of Wavelength

The apparent energy of activation for the dissociation reaction is 0, 2, and 4.6 (1) kcal/mole at 2700, 3340, and 3660 Å, respectively. The difference in activation energy at 3340 and 3660 Å does not correspond to the difference in energy of the absorbed quanta. The fact that the activation energy changes with wavelength implies the contribution of at least two different dissociation processes. These processes may arise from different electronic states, e.g., singlet and triplet states, whose ratio depends on wavelength. Since ketene neither fluoresces nor phosphoresces, the only evidence for the contribution of a second electronic state is the analogy with other ketones (12).

ACKNOWLEDGMENTS

This research was supported in part by a grant from the National Research Council of Canada, and in part by a grant from the President's Research Fund of the University of British Columbia. One of the authors (B.T.C.) wishes to express his appreciation to the British Columbia Sugar Refining Company for a scholarship for 1957–58.

REFERENCES

1. STRACHAN, A. N. and NOYES, W. A., JR. J. Am. Chem. Soc. **76**, 3258 (1954).
2. PORTER, G. B. J. Am. Chem. Soc. **79**, 827 (1957).
3. KISTIAKOWSKY, G. B. and MAHAN, B. H. J. Am. Chem. Soc. **78**, 2412 (1957).
4. HUNT, R. E. and DAVIES, W. J. Am. Chem. Soc. **69**, 1415 (1947).
5. KASHA, M. J. Opt. Soc. Amer. **38**, 929 (1948).
6. FISHER, G. J., MACLEAN, A. F., and SNIZER, A. W. J. Org. Chem. **18**, 1055 (1953).
7. DAVIS, W. J. Am. Chem. Soc. **70**, 1868 (1948).
8. HATCHARD, C. G. and PARKER, C. A. Proc. Roy. Soc. A, **235**, 518 (1956).
9. PORTER, G. B. and CONNELLY, B. T. To be published.
10. ROSS, W. F. and KISTIAKOWSKY, G. B. J. Am. Chem. Soc. **56**, 1112 (1934).
11. NORRISH, R. G. W., CRONE, R. G., and SALTMARSH, O. D. J. Am. Chem. Soc. **56**, 1644 (1934).
12. NOYES, W. A., JR., PORTER, G. B., and JOLLEY, J. E. Chem. Revs. **56**, 90 (1956).
13. KISTIAKOWSKY, G. B. and ROSENBERG, N. W. J. Am. Chem. Soc. **73**, 321 (1950).

Can. J. Chem. Downloaded from www.nrcresearchpress.com by 78.46.186.204 on 09/04/12
For personal use only.

THE SOLUBILITY OF URANIUM PEROXIDE IN ACIDIC AND BASIC MEDIA AT 25° C[1]

KARL H. GAYER AND LANCELOT C. THOMPSON

ABSTRACT

The solubility of uranium peroxide $UO_4 \cdot 2H_2O$ was measured in NaOH and $HClO_4$ solutions. Possible reactions of $UO_4 \cdot XH_2O$ in dilute $HClO_4$ solutions and possible reaction of $UO_4 \cdot XH_2O$ in dilute NaOH solutions are indicated along with the calculated constants. As might be expected, the several oxygens associated with the uranium atom appear to make the hydroxide more acidic than basic.

The purpose of this investigation was to obtain information regarding the reactions of uranium peroxide in dilute sodium hydroxide and dilute perchloric acid. These data should give (1) partial evidence as to the ionic species.

Uranium peroxide has not been investigated in relation to its solubility in acid or base. The literature on this substance is concerned with its preparation and composition.

EXPERIMENTAL

Procedure

The general procedure is similar to that used by Garrett and Heiks (1).

Preparation of Conductivity Water

The preparation of conductivity water is that of Gayer and Woontner (2).

Colorimetric Reagents

A standard uranium solution was prepared by dissolving uranium trioxide $UO_3 \cdot H_2O$ (prepared by hydrolysis of the uranyl acetate) in perchloric acid. Aliquot portions of this solution were used to prepare the color standards. A 10% sodium hydroxide solution was prepared from Baker and Adamson reagent pellets and distilled water. A 20% sodium carbonate solution was prepared with Baker and Adamson anhydrous reagent and distilled water. Baker and Adamson 30% hydrogen peroxide was used in preparing colorimetric solutions.

Determination of pH

The flask necks were broken while enclosed in a rubber membrane and samples were taken using a Beckman 290–78 hypodermic-type glass electrode. Measurements were made with a Beckman Model G meter which was calibrated at pH 4 with 0.05 *M* potassium acid phthalate buffer, at pH 7 with Beckman 3581 buffer, and at pH 10 with boric acid – sodium hydroxide buffer.

Uranium Analysis

The uranium analysis was made with a Beckman Model B spectrophotometer using the $NaOH–Na_2CO_3–H_2O_2$ method to produce the color, as described in *Analytical Chemistry of the Manhattan Project* (3).

Uranium Peroxide $UO_4 \cdot XH_2O$

Pure $UO_4 \cdot XH_2O$ was prepared by adding 30% hydrogen peroxide to a solution of uranium nitrate until precipitation was complete. A small amount of $NaNO_3$ was added

[1]*Manuscript received June 18, 1958.*
Contribution from the Chemistry Department, Wayne State University, Detroit, Michigan. From a dissertation submitted by Mr. Lancelot C. Thompson in partial fulfillment of the requirements for the Doctor of Philosophy degree at Wayne State University.

Can. J. Chem. Downloaded from www.nrcresearchpress.com by 78.46.186.204 on 09/04/12
For personal use only.

to the precipitate which was then washed with conductivity water until the washings gave a negative sodium flame test. This material was used in the equilibrium studies.

Uranium Peroxide $UO_4 \cdot 2H_2O$

The peroxide prepared as above was dried at 100°. Analyses of this material corresponded to the formula of the dihydrate. This material was used in the perchloric acid solubility studies and the X-ray analyses.

X-Ray Analyses

The X-ray data obtained on this material compares very favorably with that reported in the literature.

The *d* values given below were calculated from *a*, *b*, *c* values given in Katz and Rabinowitch (5).

TABLE I

Data of Watt *et al.* (4)		Gayer and Thompson				
d_{obs}	I/I^0	d_{obs}	I/I^0	d_{calc}	Index	% error
5.20	1.00	5.22	1.00	5.22	110	0.000
4.38	0.39	4.38	0.36	4.37	200	0.23
3.77	0.51	3.79	0.52	3.80	101	0.26
3.51	0.55	3.51	0.48	3.50	011	0.28
—	—	3.25	0.26	3.25	020	0.00
2.74	0.32	2.76	0.26	2.76	103	
2.65	0.31	2.66	0.26	2.66	013	
1.95	0.32	1.96	0.26	1.96	112	

Weighed samples of the peroxide prepared in the manner described above and dried at 100° were ignited to U_3O_8 and the percentages of uranium were calculated to be 70.0, 69.8, 69.8. Theoretical percentage of uranium in $UO_4 \cdot 2H_2O$ = 70.4.

From the percentage of uranium analyzed for and the X-ray data it can be seen that the compound prepared above is $UO_4 \cdot 2H_2O$.

THE DATA

The solubility data for uranium peroxide in acid and base solutions are collected in Tables II to IV. Conclusive results could not be obtained in regard to the reactions involved.

TABLE II

SOLUBILITY OF $UO_4 \cdot 2H_2O$ IN $HClO_4$ SOLUTIONS AT 25°*

Initial moles $HClO_4$/1000 g H_2O	Moles uranium/ 1000 g H_2O at equilibrium
2.3×10^{-2}	2.5×10^{-3}
7.0×10^{-2}	6.2×10^{-3}
1.2×10^{-1}	8.6×10^{-3}
1.6×10^{-1}	14.0×10^{-3}
2.0×10^{-1}	16.0×10^{-3}
2.3×10^{-1}	19.0×10^{-3}
2.8×10^{-1}	21.0×10^{-3}
4.2×10^{-1}	33.0×10^{-3}
5.8×10^{-1}	45.0×10^{-3}
8.2×10^{-1}	58.0×10^{-3}

*Each of the above values is actually the average of two experiments which agreed within 10% or less.

Can. J. Chem. Downloaded from www.nrcresearchpress.com by 78.46.186.204 on 09/04/12
For personal use only.

TABLE III

EQUILIBRIA OF $UO_4 \cdot XH_2O$ IN $HClO_4$ SOLUTION AT 25°*

Activity of H^+ ion from pH measurements at equilibrium	Moles uranium/ 1000 g H_2O at equilibrium	K_1
1.4×10^{-2}	4.2×10^{-4}	3.1×10^{-2}
1.6×10^{-2}	5.2×10^{-4}	3.3
1.7×10^{-2}	5.7×10^{-4}	3.4
2.1×10^{-2}	7.4×10^{-4}	3.4
2.3×10^{-2}	8.4×10^{-4}	3.6
2.6×10^{-2}	1.0×10^{-3}	3.9
3.4×10^{-2}	1.5×10^{-3}	4.3
		Average $K_1 = 3.6\times10^{-2}$

*Each of the above values is actually the average of two experiments which agreed within 10% or less.

Equilibria in Acid Solutions

The fair amount of constancy of the equilibrium constant values and the relatively high hydrogen ion concentration at equilibrium suggests the possibility of reaction [1] taking place in solutions of perchloric acid concentration up to about 0.03 molal. The uranium dissolved, however, is proportional to the $[H^+].1.37$. This ratio cannot simply be explained by reaction

[1] $$UO_3(OH)_2 \cdot XH_2O(s) + H^+ \leftrightharpoons UO_4H^+ \cdot XH_2O + H_2O$$

$$K_1 = m_{UO_4H \cdot XH_2O} \cdot \gamma_{UO_4H^+ \cdot XH_2O} / m_{H^+} \cdot \gamma_{H^+} = 3.6\times10^{-2}.$$

One or more competing reactions is probably taking place in the studied acid region. Possibly a peptization of the polymerized solid is taking place.

$$\Delta F^\circ_1 = 1900 \text{ cal/mole}$$

assuming that

$$\gamma_{UO_4H^+ \cdot XH_2O} / \gamma_{H^+} = 1.$$

There is considerable difference of opinion as to the correct formula which should be used for uranium peroxide. We have chosen somewhat arbitrarily $UO_3(OH)_2 \cdot XH_2O$ for the equation in this work. Actually the reactions could be shown with other formulas, since the ratio of H^+ or OH^- to uranium would not be different.

TABLE IV

EQUILIBRIA OF $UO_4 \cdot XH_2O$ IN NaOH SOLUTION AT 25°*

Initial moles NaOH/1000 g H_2O	Activity of OH^- ion per 1000 g H_2O from pH values at equilibrium	Moles uranium per 1000 g H_2O at equilibrium	K_2
5.4×10^{-2}		1.0×10^{-4}	
1.1×10^{-1}	1.3×10^{-2}	1.7×10^{-4}	1.3×10^{-2}
1.8×10^{-1}	2.5×10^{-2}	2.3×10^{-4}	0.9×10^{-2}
2.2×10^{-1}	2.6×10^{-2}	2.5×10^{-4}	0.95×10^{-2}
2.7×10^{-1}	2.8×10^{-2}	3.1×10^{-4}	1.1×10^{-2}
3.2×10^{-1}	3.2×10^{-2}	3.6×10^{-4}	1.1×10^{-2}
3.6×10^{-1}	3.2×10^{-2}	3.8×10^{-4}	1.2×10^{-2}
7.2×10^{-1}		8.2×10^{-4}	
			Average $K_2 = 1.1\times10^{-2}$

*Each of the above set of values is actually the average of two experiments which agreed within 10% or less.

Can. J. Chem. Downloaded from www.nrcresearchpress.com by 78.46.186.204 on 09/04/12
For personal use only.

Equilibria in Basic Solutions

The fair constancy of the equilibrium constant values suggests the possibility of reaction [2] in the concentration region of about 0.05 molal NaOH to 0.7 molal NaOH. The rather high equilibrium pH values would also support this contention. The excessive quantities of hydroxyl ion consumed per dissolved uranium however, precludes the possibility that reaction [2] is the only one taking place in this concentration region. Possibly a peptization of the polymerized solid is occurring. The solubility technique does not lend itself to distinguishing between competing reactions.

[2] $$UO_3(OH)_2XH_2O(s) + OH^- \leftrightharpoons HUO_5^- + XH_2O$$

$$K_2 = m_{HUO_5^-} \times \gamma_{HUO_5^-} / m_{OH^-} \times \gamma_{OH^-} = m_{HUO_5^-} / m_{OH^-} = 1.1 \times 10^{-2}$$

$$\Delta F_2 = 2700 \text{ cal/mole}$$

assuming that

$$\gamma_{HUO_5^-} / \gamma_{OH^-} = 1.$$

Water Solubility

The water solubility of $UO_4 \cdot XH_2O$ was determined from the average of three separate preparations of the oxide. (Each determination was done in duplicate so as to approach equilibrium from undersaturation and oversaturation.) Conductivity water was used as the solvent. The solubility was found to be 1.5×10^{-5} moles uranium peroxide/1000 g water.

ACKNOWLEDGMENTS

The authors gratefully wish to acknowledge the support of the U. S. Atomic Energy Commission Project No. At (11–1)–214 in sponsoring this work. They also wish to thank Mr. George McManus of the Physics Department of Wayne State University for the X-ray analyses.

REFERENCES

1. GARRETT, A. B. and HEIKS, R. E. J. Am. Chem. Soc. **63**, 562 (1941).
2. GAYER, K. H. and WOONTER, L. J. Chem. Educ. **33**, 296 (1956).
3. RODDEN, C. J. Analytical chemistry of the Manhattan project. McGraw-Hill Book Company, Inc., New York. 1950. p. 93.
4. WATT, G. W., ACHORN, S. L., and MARLEY, J. D. J. Am. Chem. Soc. **72**, 3341 (1950).
5. KATZ, J. J. and RABINOWITCH, E. The chemistry of uranium. McGraw-Hill Book Company, Inc., New York. 1951. p. 293.

Can. J. Chem. Downloaded from www.nrcresearchpress.com by 78.46.186.204 on 09/04/12
For personal use only.

Can. J. Chem. Downloaded from www.nrcresearchpress.com by 78.46.186.204 on 09/04/12
For personal use only.

PHYSICOCHEMICAL STUDIES OF LIGNINSULPHONATES

III. PROPERTIES OF FRACTIONS PREPARED BY SUCCESSIVE SULPHONATION OF PERIODATE LIGNIN[1]

D. A. I. Goring and A. Rezanowich

ABSTRACT

Periodate lignin was sulphonated in stages by a series of short bisulphite cooks. At each stage the soluble ligninsulphonate was removed and purified, and the residue was resulphonated. The 14 fractions thus obtained had constant methoxyl content and ultraviolet absorption coefficients. There was a gradual increase in the sulphur content as the integral reaction time increased, but 26% of the ligninsulphonate possessed a sulphur content of less than 3%. There was a marked increase in both the intrinsic viscosity and rate of solution with increase in reaction time. The mechanism of the sulphonation reaction is discussed in the light of these results.

INTRODUCTION

Many uses of spent sulphite liquor depend on the colloidal and polymeric properties of ligninsulphonate (1, 2, 3, 4, 5). However, information on the size, shape, and configuration of the molecule is scarce.

In an earlier paper in this series, Gardon and Mason (6) demonstrated that ligninsulphonates in spent liquor occurred in a wide range of molecular weights (from 4000 to 60,000). A similar conclusion was reached by McCarthy and co-workers (7), who obtained fractions of ligninsulphonate having molecular weights from 400 to 130,000. In the sulphite process it is possible that the lignin becomes soluble as a uniform monodisperse material. This may be either degraded or condensed during later stages of sulphonation to give the polydispersity observed. It is more likely, however, that lignins extracted at various times during the reaction will differ considerably in molecular weight. The present work is an attempt to study the properties of soluble ligninsulphonates produced at different stages of sulphonation.

The problem was simplified by use of periodate lignin prepared by a method similar to that of Purves and co-workers (8, 9). Periodate lignin, like protolignin, is insoluble in most solvents, and undergoes many of the same reactions (10). The phenyl propane chain is probably not broken during periodate oxidation, although some methoxyl is lost. As a starting material for physical studies it is probably as suitable as any other isolated lignin.

A kilogram of periodate lignin was prepared from white spruce. A large sample was cooked for successive short periods until most of the lignin was dissolved as sulphonate. After each stage of sulphonation the liquor and residue were separated. The residue was recooked and the soluble sulphonate was isolated from the liquor. The purified fractions were characterized by measurement of ultraviolet and visible absorption, methoxyl and sulphur content, and intrinsic viscosity.

A parallel investigation based on the sulphonation of wood was published by McCarthy and co-workers (11, 12) when this manuscript was in preparation. The results obtained are similar, although the present work is on an isolated lignin and is somewhat more detailed.

[1]*Manuscript received March 31, 1958.*
Contribution from the Physical Chemistry Division, Pulp and Paper Research Institute of Canada, Montreal, Que.

EXPERIMENTAL AND RESULTS

Periodate Lignin

A freshly cut, 35-year-old log of white spruce (*Picea glauca* (Moench) Voss) was reduced to a coarse sawdust with a dado circular saw. Six kilograms (dry weight) of the sawdust was subjected to cycles of periodate oxidation and alkaline hydrolysis in a 200-l stainless steel vessel at room temperature. The oxidation liquor was 2500 g of $Na_3H_2IO_6$ dissolved in 60 l of distilled water, the pH being kept at 4 with acetic acid. The hydrolysis liquor was 100 l of 0.1 *N* NaOH. There were usually two or three washings with distilled water after each oxidation and hydrolysis. After the final hydrolysis, it was necessary to neutralize the liquor before washing to reduce the high degree of swelling of the lignin.

Initially, removal of liquors and wash water was easily achieved with large bacterial filter candles. After the third hydrolysis, filtration was ineffective because the filters clogged immediately. At this stage the lignin was allowed to settle overnight when $\frac{4}{5}$ of the supernatant liquid could be removed with a siphon. The final washings were at pH 5–6. The cake of periodate lignin was frozen and the water removed by freeze-drying. The yield on a dry weight basis was 1 kg and represented 64% of the original lignin content of the wood. Some analytical data on this preparation of periodate lignin are given in Table I.

TABLE I

ANALYTICAL DATA ON PERIODATE LIGNIN

Moisture content	= 6%
Yield from wood (dry weight)	= 17.1%
Ash (dry weight)	= 2.4%
Klason lignin (dry weight; ash-free)	= 93.2%
Carbon (dry weight; ash-free)	= 60.8%
Hydrogen (dry weight; ash-free)	= 5.91%
Methoxyl (dry weight; ash-free)	= 12.8%
Sulphur	= Nil
Carbohydrate	= Nil

Sulphonation Procedure

Cooks were made in a stainless steel autoclave of 1200 cc capacity. The autoclave (Fig. 1) was designed to permit rapid heating and cooling as well as positive stirring of the reacting mixture. The vessel was heated to 130° C in 5 minutes by gas burners on the

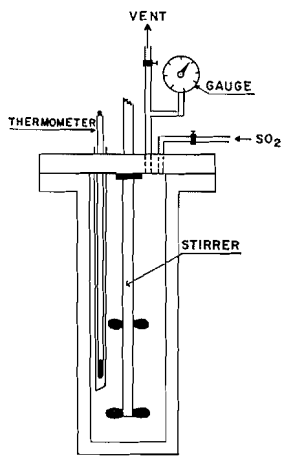

FIG. 1. Stainless steel autoclave used for sulphonation.

Can. J. Chem. Downloaded from www.nrcresearchpress.com by 78.46.186.204 on 09/04/12
For personal use only.

bottom and sides. It was cooled to room temperature in 5 minutes by being lowered into a bucket of water. From the initial application of heat to the moment of lowering the vessel into the water, cooks were 30 minutes in duration except for the final two which were for 60 minutes each. Temperature was measured with a thermometer immersed in paraffin in a stainless steel well in the cover. Constant temperature was maintained manually at 130 (±1)° C with a gas burner.

The reaction mixture was stirred with a motor-driven, twin-screw stirrer. The gland on the stirrer was a carbon disk against which a steel disk rotated, the sealing pressure being supplied by the SO_2 in the liquor. At first it was impossible to retain a constant concentration of SO_2 because of slight leakage past the gland. Accordingly, an SO_2 cylinder at 55° C was connected to the autoclave and constant pressure of SO_2 was maintained manually at 115 (±5) p.s.i.g.

The initial sample of periodate lignin, ground to pass 150 mesh, weighed 43 g. The lignin was mixed with 500 cc of distilled water, de-aerated thoroughly by successive evacuation, and soaked overnight. For sulphonation, 500 cc of sodium base acid was added which produced a final concentration of 1% Na and 6% total SO_2. Accurate control of the initial concentration of SO_2 was unnecessary, since the pressure was adjusted in the autoclave at the start of the reaction.

After each sulphonation, the reaction mixture was centrifuged. The insoluble lignin residue was washed with distilled water and recentrifuged, the washings being added to the centrifuged liquor. The residue was then washed into the autoclave with 500 g of distilled water, the liquor was added, and the cook repeated.

Purification

The object of the purification procedure was to secure a neutral sodium ligninsulphonate free from both insoluble debris and excess inorganic ions. The method finally adopted was evolved by trial and error in preliminary experiments.

Cations and anions were removed with the ion-exchange resins Dowex 50-X12 (50–100 mesh) and Dowex 1-X10 (50–100 mesh) respectively.* The centrifuged liquor was stirred with 400 g of regenerated Dowex 50. This treatment removed 90% of the sodium present. The liquor was then evaporated from 1500 cc to 50–100 cc in a rotary vacuum evaporator at 45° C, deionized on columns, neutralized with NaOH to pH 7, and freeze-dried. With some of the later fractions it was necessary to centrifuge at 25,000 *g* after passage through the columns to remove finely dispersed debris.

Fourteen successive sulphonations were made over a period of 8 hours. Cooking time was 30 minutes for fractions S-1 to S-12 and 1 hour for the final two which are designated fractions S-14 and S-16. The residue after the final reaction was 2.7% of the original weight of the lignin. The total recovery on an ash and sulphur-free basis was 86%.

The rate of solution, R, for each fraction was computed from

[1] R = wt. of fraction (sulphur-free basis)/time of cooking interval.

**In preliminary tests with a purified commercial ligninsulphonate, the columns were found to absorb less than 2% of the lignin based on optical density in the ultraviolet. However, after many of the measurements described later were made, it was found that repassage through the columns removed about 10% by weight of the ligninsulphonate. The sulphur content of the re-ion-exchanged material was virtually unchanged, while the methoxyl content increased by 0.6%. Evidently, material low in methoxyl was being absorbed by the columns. Experiments showed that it was absorbed mostly by the anion-exchange column (Dowex 1-X10) and that it could not be removed by the customary regeneration with 4% of* NaOH. *It was unlikely that the absorbed material was an inorganic sulphur-containing anion because the sulphur content of the re-ion-exchanged fraction would then decrease. No other type of inorganic anion was introduced during the cooking and purification, and as shown in Table I the ash content of the periodate lignin was relatively low. No correction was made in the original data, except in the case of the second fraction in which 33% by weight was absorbed and the methoxyl content increased from 7.6% to 11.2%.*

Can. J. Chem. Downloaded from www.nrcresearchpress.com by 78.46.186.204 on 09/04/12
For personal use only.

As shown in Fig. 2, the rate of solution showed a maximum after 4 hours' cooking. Such a maximum is in fair agreement with other studies on sulphonation. The dotted line in Fig. 2 shows some previous data (13) obtained on a different batch of periodate lignin. For this series, reactions were done in sealed glass bombs at 130° C with a bisulphite solution containing 6% total SO_2 and 1% Mg^{++}. Here the SO_2 content decreased as the sulphonation proceeded, which is probably the cause of the slower rate of solubilization. In general, however, this curve shows the same trends as those obtained in the present study.

The fractional rate of solution, R_F, was calculated from

$$R_F = R/\text{wt. of material cooked.} \qquad [2]$$

In Fig. 3 the fractional rate of solution is plotted together with intrinsic viscosity against cooking time.

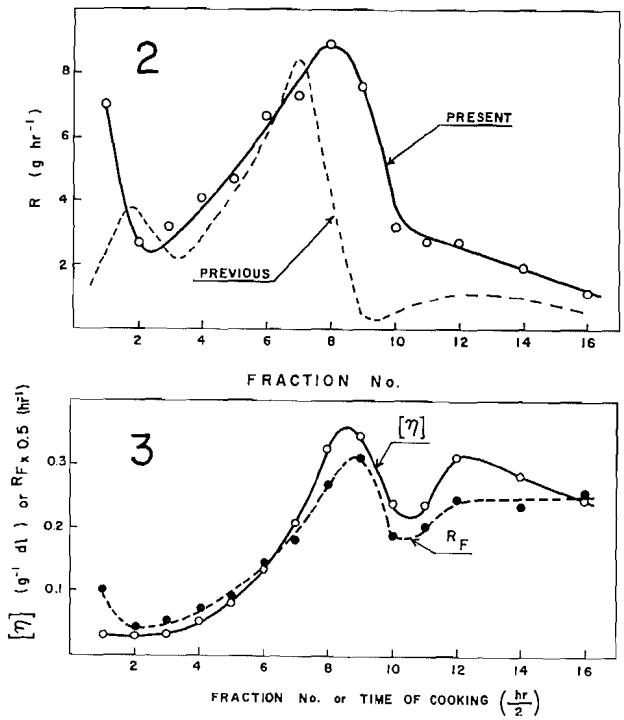

FIG. 2. Rate of solution at various stages of the sulphonation. The dotted line shows similar data from previous experiments. The abscissa units represent half-hourly and hourly intervals in the present and previous series respectively.

FIG. 3. Correlation of R_F and $[\eta]$ throughout the reaction.

Sulphur Content

Sulphur analyses were made with a Leco apparatus and the results are shown in Fig. 4. Mean error in triplicate determinations was ±2.6%. In previous experiments results with the Leco agreed within ±3% with gravimetric determinations as $BaSO_4$.

Apart from some irregularities in early fractions, there is a gradual rise in sulphur content as the cook proceeds. Some of the early fractions are soluble at a relatively low content of sulphur.

Sulphonation increases the weight of the lignin due to the replacement of —OH by —SO_3Na groups. Therefore values of yields, methoxyl content, and light absorption were adjusted to be based on the weight of unsulphonated lignin.

Can. J. Chem. Downloaded from www.nrcresearchpress.com by 78.46.186.204 on 09/04/12
For personal use only.

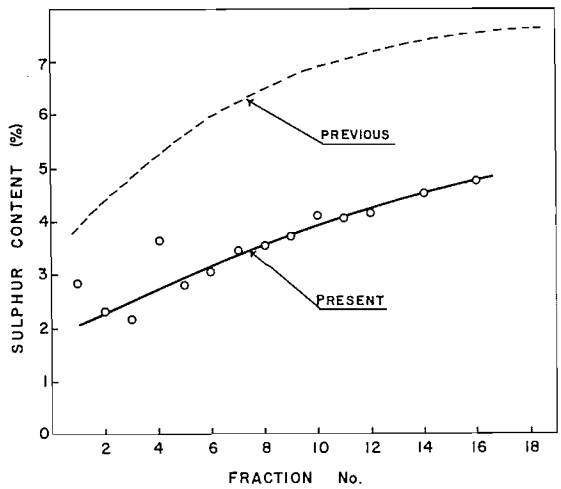

FIG. 4. Sulphur content of fractions at various stages. The dotted line shows similar data from previous experiments. The abscissa units represent half-hourly and hourly intervals in the present and previous series respectively.

Methoxyl Content

The methoxyl content was measured by TAPPI Standard Method 2M43. The mean error in duplicate determinations was ±1%. As shown in Table II the methoxyl content is fairly constant (±5%) and lies between 10 and 12%.

TABLE II

METHOXYL CONTENT AND ULTRAVIOLET ABSORPTION OF FRACTIONS

Fraction	OCH_3 (%)	ϵ_{2800}	ϵ_{2050}
S–1	10.4	12.5	92.9
S–2	11.2	14.2	88.9
S–3	9.9	12.1	87.7
S–4	11.3	13.4	101.9
S–5	10.7	13.5	99.2
S–6	11.1	13.8	99.0
S–7	11.4	15.5	107.4
S–8	11.9	14.5	109.1
S–9	11.7	14.8	102.7
S–10	11.5	14.5	101.8
S–11	11.3	13.6	104.1
S–12	10.4	13.5	100.4
S–14	11.4	14.4	97.5
S–16	9.6	12.9	108.5

Light Absorption

Optical densities were measured in the visible and the ultraviolet with a Beckman DU spectrophotometer using 1-cm quartz cells. Measurements were made in duplicate at wavelengths of 5000 Å, 2800 Å, and 2050 Å with concentrations of 0.2, 0.002, and 0.001 g dl^{-1} respectively. The solvent was 0.1 *M* NaCl.

Absorption was expressed in terms of the coefficient ϵ given by

$$\epsilon = D/cL, \quad [3]$$

where

D = optical density,
c = concentration,
L = length of cell.

Can. J. Chem. Downloaded from www.nrcresearchpress.com by 78.46.186.204 on 09/04/12
For personal use only.

As shown in Table II the ϵ values for wavelengths of 2050 Å and 2800 Å are fairly constant. Mean $\epsilon_{2050} = 100.1$ ($\pm 5\%$) cm^{-1} l g^{-1} and mean $\epsilon_{2800} = 13.8$ ($\pm 5\%$)cm^{-1} l g^{-1}. A similar constancy of ultraviolet absorption has been reported by McCarthy and co-workers (7). In the visible absorption at 5000 Å (Fig. 5) a pronounced maximum is noted after 3 hours' cooking, followed by a minimum and then a gradual increase in ϵ.

Intrinsic Viscosity

Viscosity was measured in Ubbelohde viscometers of the type described by Craig and Henderson (14). The dimensions were modified slightly to permit mounting in a Townson and Mercer water bath. Relative temperature changes were held to $\pm 0.005°$ C about the actual temperature of $25 \pm 0.05°$ C. The solvent was 0.1 *M* NaCl. Concentrations ranged from 1.5 to 0.2 g dl^{-1}.

The intrinsic viscosity, $[\eta]$, was obtained as usual by linear extrapolation of η_{sp}/c vs. c to zero concentration (Fig. 6).

The intrinsic viscosities of the fractions are shown in Fig. 3. There is a marked increase in $[\eta]$ with time of cooking up to about 4 hours, after which $[\eta]$ decreases but with another maximum at 6 hours. The correlation between $[\eta]$ and R_F will be discussed later.

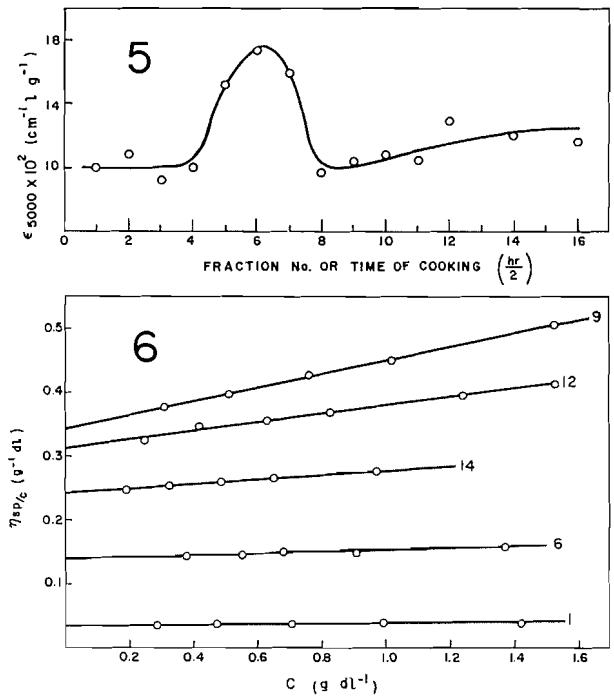

FIG. 5. Light absorption coefficient at 5000 Å at various stages.
FIG. 6. η_{sp}/c vs. c for some of the fractions: lines 1, 6, 9 etc., correspond to fractions S-1, S-6, S-9 etc.

DISCUSSION

As shown in Fig. 4 the sulphur content of the fractions increased with time of sulphonation. The curve suggests a lower rate of sulphonation in the later stages of the reaction in agreement with the results of others (15, 16). It is interesting to note that 26% of the ligninsulphonate possessed a sulphur content of less than 3%, which is generally regarded as the minimum required for solubility (17).

Can. J. Chem. Downloaded from www.nrcresearchpress.com by 78.46.186.204 on 09/04/12
For personal use only.

Can. J. Chem. Downloaded from www.nrcresearchpress.com by 78.46.186.204 on 09/04/12
For personal use only.

For comparison, the variation of sulphur content of soluble fractions with reaction time, obtained in a previous study (13), is given as the dotted line in Fig. 4. In this case the solubilized lignin was not separated from the reaction mixture but was reacted with the bisulphite solution for the full time of each cook. Both sets of data show an increase of sulphur content with time, but a higher degree of sulphonation of soluble fractions was obtained in the previous series. Rezanowich *et al.* (16) found that if the soluble and insoluble fractions from the same cook were recooked, the soluble portion was sulphonated to a higher degree than the insoluble portion. This is probably the reason why sulphur contents were higher in the previous results.

Comparison of the two series of data suggest that (*a*) some fractions are solubilized at fairly low sulphur contents ($< 3\%$) and (*b*) an appreciable portion of the sulphonation reaction occurs with the ligninsulphonate after it has been rendered soluble.

For all fractions, the ratio of ϵ_{2800} (cm^{-1} l g^{-1}) to methoxyl content (%) was 1.26 ($\pm 3\%$), which is in good agreement with the value 1.30 ($\pm 2\%$) derived for the first seven fractions of Gardon and Mason (6). These authors observed a marked increase of ultraviolet absorption and methoxyl content with molecular weight. In the present work, both ϵ_{2800} and methoxyl content remained constant to $\pm 5\%$ over a wide range of $[\eta]$ and therefore molecular weight. McCarthy and co-workers (11, 18, 19) have also found ϵ_{2800} constant for fractions prepared from non-dialyzable ligninsulphonate by precipitation with ethanol. This contradiction is probably due to a considerable portion of low methoxyl material in the low molecular weight samples of Gardon and Mason. On passing Gardon and Mason's fractions 7 and 8 through the ion-exchange columns, 42% and 70% respectively by weight was lost; methoxyl contents increased respectively from 3.3% and 2.1% to 6.9% and 6.7%. As mentioned earlier, considerably smaller increases in methoxyl content were noted after re-ion exchange of some of the fractions prepared for the present investigation.

From Table II, $\epsilon_{2050}/\epsilon_{2800}$ was 7.26 ($\pm 5\%$) for all fractions. This result supports ϵ_{2050} as a measure of lignin concentration as recommended by Kleinert and Joyce (20). In contrast to the constancy of ϵ_{2050} and ϵ_{2800}, absorption in the visible showed a pronounced maximum after 3 hours' cooking (Fig. 5). In a previous experiment (21) (not reported here in detail) it was found that prolonged cooking (24 hours) of an already sulphonated lignin increased ϵ_{5000} by a factor of 2 while ϵ_{2800} was essentially unchanged. Thus greater visible absorption would be expected in fractions isolated at the end of the reaction; the increase observed after 4 hours is probably due to this effect. However, the initial maximum in ϵ_{5000} suggests that greater visible absorption is characteristic of certain fractions of lignin. Fractions S-5, S-6, and S-7 which give rise to the maximum represented 28% of the material solubilized.

The initial increase in $[\eta]$ with fraction number (Fig. 3) indicates a marked increase in molecular weight as the lignin is made soluble. McCarthy and co-workers (11) have observed a similar increase in molecular weight for lignin sulphonates from spruce and hemlock. The maximum value of $[\eta]$ is 0.34 g^{-1} dl in fraction S-9 compared with the value of 0.075 g^{-1} dl for the highest molecular weight sample of Gardon and Mason (6). Based on the osmotic molecular weights of Gardon and Mason, the molecular weight of fraction S-9 is 250,000. On this basis, 57% of the material solubilized has a molecular weight of over 100,000. These values are somewhat higher than those found by other workers. McCarthy and co-workers (7) quote molecular weights up to 150,000 with about 2% of the lignin above 100,000. The highest value found by Gardon and Mason (6) was 58,000, although the integral distribution indicated values up to 100,000. A

possible reason for the higher molecular weights in the present series was that the lignin, once extracted, was not then subjected to further prolonged sulphonation. In an earlier experiment (21) it was noted that $[\eta]$ fell from 0.10 to 0.04 on resulphonating a lightly cooked ligninsulphonate. Felicetta and McCarthy (12) have demonstrated a similar degradation on prolonged cooking of non-dialyzable ligninsulphonates. Thus it is fairly certain that the soluble lignin is further degraded by the reaction as sulphonation proceeds. The present work indicates that relatively high molecular weights are obtained when the lignin is removed as soon as it is solubilized.

The correlation between the fractional rate of solution and $[\eta]$ (Fig. 3) lends support to the peptization theory of sulphonation proposed by Calhoun, Yorston, and Maass (22). The trends in Fig. 3 suggest that the rate at which lignin is made soluble depends on the molecular weight of the material solubilized. The initial increase in $[\eta]$ and R_F between fractions S-2 and S-9 is accompanied by an increase in the sulphur content (Fig. 4). If condensation reactions are neglected or assumed to occur rapidly, a sulphite cook may be regarded as a simultaneous sulphonation and hydrolysis of the insoluble lignin network. Fragments of lignin produced by the hydrolysis will become soluble as the sulphonation proceeds. The size of a solubilized fragment will be a function of its sulphur content because the lignin only becomes soluble when it acquires hydrophilic sulphonate groups. Thus, as the sulphur content increases, larger and larger fragments produced by the hydrolysis become soluble. The rate of solution thereby increases also.

The decrease in R_F and $[\eta]$ after fraction S-9, in spite of an increase in sulphur content, may be due to the presence of a more cross-linked lignin for which more extensive chain scission would be necessary to set fragments free. Also a more cross-linked molecule would have a lower viscosity for a given molecular weight and would be less soluble for a given sulphur content. If this explanation is correct, fractions of similar molecular weight from early and late in the cook should show clearly defined differences in molecular configuration. Light-scattering and viscometric experiments are now being carried out to investigate this possibility.

It is interesting to note that, in spite of the extremely fine subdivision of the lignin (150 mesh) and the vigorous stirring during the reaction, the rate of delignification is similar to that for the commercial cooking of wood chips. This suggests that diffusion processes have no gross effect on the rate of solution, although the rate at which the dissolved lignin diffuses out of the chip into the liquor is probably affected by the molecular weight of the ligninsulphonate.

ACKNOWLEDGMENTS

The authors wish to acknowledge the assistance of Mr. J. Jaworzyn in much of the experimental work.

REFERENCES

1. MARSHALL, H. B. Pulp Paper Mag. Can. **53**, No. 5, 125 (1952).
2. MARSHALL, H. B. and NEATE, J. M. Pulp Paper Mag. Can. **54**, No. 7, 125 (1953).
3. MARSHALL, H. B. and NEATE, J. M. Pulp Paper Mag. Can. **54**, No. 9, 113 (1953).
4. MARSHALL, H. B. and MACDONALD, A. Tappi, **38**, No. 7, 165A (1955).
5. MARSHALL, H. B. and CUNNINGHAM, A. I. Tappi, **39**, No. 7, 171A (1956).
6. GARDON, J. L. and MASON, S. G. Can. J. Chem. **33**, 1477 (1955).
7. FELICETTA, V. F., AHOLA, A., and MCCARTHY, J. L. J. Am. Chem. Soc. **78**, 1899 (1956).
8. WALD, W. J., RITCHIE, P. F., and PURVES, C. B. J. Am. Chem. Soc. **69**, 1371 (1947).
9. SMITH, D. N. and PURVES, C. B. Ind. Eng. Chem. **49**, 1394 (1957).
10. RITCHIE, P. F. and PURVES, C. B. Pulp Paper Mag. Can. **48**, No. 12, 74 (1947).
11. NOKIHARA, E., TUTTLE, J., FELICETTA, V. F., and MCCARTHY, J. L. J. Am. Chem. Soc. **79**, 4495 (1957).
12. FELICETTA, V. F. and MCCARTHY, J. L. J. Am. Chem. Soc. **79**, 4499 (1957).

Can. J. Chem. Downloaded from www.nrcresearchpress.com by 78.46.186.204 on 09/04/12
For personal use only.

13. REZANOWICH, A. Unpublished data.
14. CRAIG, A. W. and HENDERSON, D. A. J. Polymer Sci. **91**, 215 (1956).
15. ALDER, E. and LINDGREN, B. O. Svensk Papperstidn. **55**, 563 (1952).
16. REZANOWICH, A., ALLEN, G. A., and MASON, S. G. Pulp Paper Mag. Can. **58**, No. 10, 153 (1957).
17. BRAUNS, F. E. The chemistry of lignin. Academic Press, Inc., New York. 1952. p. 365–366.
18. MARKHAM, A. E., PENISTON, Q. P., and MCCARTHY, J. L. J. Am. Chem. Soc. **71**, 3599 (1949).
19. MOACANIN, J., FELICETTA, V. F., HOLLER W., and MCCARTHY, J. L. J. Am. Chem. Soc. **77**, 3470 (1955).
20. KLEINERT, T. N. and JOYCE, C. S. Pulp Paper Mag. Can. **58**, No. 10, 147 (1957).
21. GORING, D. A. I. Unpublished data.
22. CALHOUN, J. M., YORSTON, F. H., and MAASS, O. Can. J. Research, B, **17**, 121 (1939).

Can. J. Chem. Downloaded from www.nrcresearchpress.com by 78.46.186.204 on 09/04/12
For personal use only.

Can. J. Chem. Downloaded from www.nrcresearchpress.com by 78.46.186.204 on 09/04/12
For personal use only.

VOLTAIC CELLS IN FUSED SALTS

PART V. THE SYSTEMS $Sn/SnCl_2$ (KCl–NaCl), $Fe/FeCl_2$ (KCl–NaCl), and $Mn/MnCl_2$ (KCl–NaCl)[1]

S. N. Flengas and T. R. Ingraham

ABSTRACT

Using a Ag/AgCl (KCl–NaCl) reference electrode, the standard electrode potentials of the systems $Sn/SnCl_2$ (KCl–NaCl), $Fe/FeCl_2$ (KCl–NaCl), and $Mn/MnCl_2$ (KCl–NaCl) were determined at 700° C and found to be 0.370 v, 0.520 v, and 1.205 v respectively. In each of the systems the Nernst equation was found to be applicable over the range of concentrations investigated.

The effect of temperature on the electromotive forces of the above cells was measured and the heats of the cell reactions were calculated from the data.

INTRODUCTION

In previous publications in this series (1, 2, 3, 4) standard potentials for several electrode systems in fused salts were reported. To determine the potentials, a silver – silver chloride electrode was used as a null point reference electrode, and an equimolar mixture of sodium and potassium chlorides was used as the solvent for the metallic salts.

In this investigation, the method was applied to the systems tin – stannous chloride, iron – ferrous chloride, and manganese – manganous chloride. These metal chlorides were found to give stable solutions in the alkali chloride – molten salt solvent.

PREPARATION OF MATERIALS

Because the anhydrous metallic salts required in this work were not commercially available, it was necessary to prepare them.

Anhydrous stannous (II) chloride was prepared from the corresponding hydrated salt of analytical grade by heating in a tubular electric furnace at 250° C under a continuous stream of dried gaseous HCl, produced by the action of concentrated H_2SO_4 on concentrated HCl.

Anhydrous ferrous (II) chloride was prepared from National Bureau of Standards certified iron filings by dissolution in concentrated HCl, and recovery of the hydrated ferrous salt by crystallization under an oxygen-free argon cover. The product was filtered under argon and washed with ether. Finally, the light-green hydrated ferrous chloride was dried by heating at 500° C in a stream of dry HCl. In the preparations of stannous chloride and of ferrous chloride, argon was used to flush the apparatus at the beginning and the end of the drying process. The dry divalent chlorides were stable in air and were pelletized without requiring any precautions against oxidation.

Anhydrous manganous (II) chloride was prepared from the corresponding hydrated salt of analytical grade, by heating at 600° C in the presence of a carbon tetrachloride vapor stream which was produced by flash distillation.

The anhydrous salts prepared by the foregoing methods were analyzed and found to be of a purity in excess of 99%. The impurity in each of the chlorides was the corresponding metal oxide.

Very pure (99.99%) tin was used as the liquid indicator electrode in the Sn–Ag voltaic cell. A $\frac{1}{2}$-in. diameter rod of very pure electrolytic iron (99.99%) was used as the indicator

[1]*Manuscript received July 28, 1958.*
Contribution from the Mineral Dressing and Process Metallurgy Division, Mines Branch, Department of Mines and Technical Surveys, Ottawa.

electrode in the Fe–Ag voltaic cell. The manganese metal indicator electrode for the Mn–Ag voltaic cell was prepared from pure electrolytic manganese metal (99.9%) which was remelted and cast into a cylindrical form. The casting was done in a water-cooled arc furnace, operated under reduced argon gas pressure. Platinum wire or tungsten wire was used as the indicator electrode connection to the potentiometer.

EXPERIMENTAL

The experimental technique and the apparatus used to study the tin, iron, and manganese systems were the same as in the previous experiments (3, 4) with solid and liquid metal indicator electrodes and cells under inert gas cover.

The experimental cells were of the type,

M	MCl_2 (x_2)		Asbestos	AgCl (x_1)	Ag
(−)	KCl–NaCl (1/1 mole)	‖	fiber	‖ KCl–NaCl (1/1 mole)	(+)
	(indicator electrode)			(reference electrode)	

where M was respectively tin (pool of liquid metal), iron, and manganese metal, and MCl_2 was respectively $SnCl_2$, $FeCl_2$, and $MnCl_2$ at a mole fraction x_2. The reaction in cells of this type is:

[1] $$M + 2Ag^+ = M^{2+} + 2Ag.$$

The relationship between the electromotive force and the metal ion concentration in the cell is given by the Nernst equation in the form:

[2] $$E_{cell} = (E^\circ_{M/M^{2+}} - E^\circ_{Ag/Ag^+}) - (2.303RT/2\mathcal{F})\log(x_2/x_1^2)$$

where $E^\circ_{M/M^{2+}}$ and E°_{Ag/Ag^+} are respectively the standard electrode potential of the half-cells $Sn/SnCl_2$, $Fe/FeCl_2$ or $Mn/MnCl_2$, and Ag/AgCl under the conditions of the experiments.

It will be observed that in equation [2] mole fractions are used instead of activities. The simplification is justified, as will be shown by the subsequent data, only when the activity coefficients or the complexity constants of the species involved in the cell reaction, or both, remain constant over the concentration range investigated. Thus, standard potentials calculated from equation [2] will include the effects due to both activities and complex formation.

From equation [2] it follows that when $\log(x_2/x_1^2)$ is equal to zero, the cell potential is the difference in the standard electrode potentials of the system.

RESULTS

The electromotive forces of the Sn–Ag, Fe–Ag, and Mn–Ag voltaic cells were measured first as a function of the metal ion concentration and then as a function of temperature.

The results of the experiments in which the concentration of the metal ion was varied at constant temperature are given in Table I. A 15 mv correction has been included for thermoelectric effects in the Sn–Ag cell and 9 mv in the Fe–Ag cell. No correction was required in the Mn–Ag cell.

When the electromotive forces of the cells were plotted against the term $\log(x_2/x_1^2)$, as calculated from the data given in Table I, the results were well represented by straight lines as shown in Figs. 1 and 2. The slopes of the experimental lines for Sn–Ag, Fe–Ag, and Mn–Ag systems agree well with the theoretical value for a two-electron electrode process as calculated from equation [2] (0.096, 0.095, and 0.097 as compared with

Can. J. Chem. Downloaded from www.nrcresearchpress.com by 78.46.186.204 on 09/04/12
For personal use only.

TABLE I

ELECTROMOTIVE FORCES OF VOLTAIC CELLS AT CONSTANT TEMPERATURE AS A FUNCTION OF THE METAL ION CONCENTRATION AT THE INDICATOR ELECTRODE

(*a*) Sn (−) | $SnCl_2$ (x_2) KCl–NaCl (1/1mole) || AgCl (x_1) KCl–NaCl (1/1 mole) | Ag (+)

Mole fraction of AgCl (x_1)	Mole fraction of $SnCl_2$ (x_2)	t, ° C	E_{cell} (volts)
6.235×10^{-2}	6.322×10^{-4}	680	0.453
6.235×10^{-2}	1.433×10^{-3}	680	0.418
6.235×10^{-2}	2.251×10^{-3}	680	0.397
6.235×10^{-2}	4.606×10^{-3}	680	0.366
6.235×10^{-2}	7.585×10^{-3}	680	0.342
6.235×10^{-2}	1.254×10^{-2}	680	0.323

(*b*) Fe (−) | $FeCl_2$ (x_2) KCl–NaCl (1/1 mole) || AgCl (x_1) KCl–NaCl (1/1 mole) | Ag (+)

Mole fraction of AgCl (x_1)	Mole fraction of $FeCl_2$ (x_2)	t, ° C	E_{cell} (volts)
6.235×10^{-2}	8.853×10^{-4}	695	0.582
6.235×10^{-2}	2.122×10^{-3}	695	0.546
6.235×10^{-2}	3.771×10^{-3}	695	0.523
6.235×10^{-2}	7.541×10^{-3}	695	0.491
6.235×10^{-2}	1.385×10^{-2}	695	0.467

(*c*) Mn (−) | $MnCl_2$ (x_2) KCl–NaCl (1/1 mole) || AgCl (x_1) KCl–NaCl (1/1 mole) | Ag (+)

Mole fraction of AgCl (x_1)	Mole fraction of $MnCl_2$ (x_2)	t, ° C	E_{cell} (volts)
6.235×10^{-2}	5.867×10^{-4}	680	1.284
6.235×10^{-2}	1.391×10^{-3}	680	1.249
6.235×10^{-2}	2.566×10^{-3}	680	1.226
6.235×10^{-2}	4.779×10^{-3}	680	1.200
6.235×10^{-2}	1.087×10^{-2}	680	1.116

the theoretical value of 0.096). In addition, the linearity of the curves in Fig. 1 shows that the activity coefficients or the complexity constants of the species involved in the cell reaction remain constant over the range of concentrations investigated.

The experimental standard electrode potentials for the tin, iron, and manganese systems, as obtained from interpolation at $\log(x_2/x_1^2) = 0$ on the curves in Fig. 1, are given in Table II. In addition, Table II also includes, for comparison, calculated (5) values for the standard potentials of the cell reactions in the absence of solvent.

It should be noted that all potential measurements shown above are equilibrium values. Equilibrium was attained in a few minutes after each change in the metal salt

TABLE II

SUMMARY OF RESULTS

Indicator electrode	Cell reaction in molten KCl–NaCl	t, ° C	Standard potential for:	Exptl.* (volts)	Calc.† (volts)
Sn, Sn^{++}	$Sn + 2AgCl = SnCl_2 + 2Ag$	700	$E^\circ_{Sn/Sn^{++}} - E^\circ_{Ag/Ag^+}$	0.370	0.405
Fe, Fe^{++}	$Fe + 2AgCl = FeCl_2 + 2Ag$	700	$E^\circ_{Fe/Fe^{++}} - E^\circ_{Ag/Ag^+}$	0.520	0.305
Mn, Mn^{++}	$Mn + 2AgCl = MnCl_2 + 2Ag$	700	$E^\circ_{Mn/Mn^{++}} - E^\circ_{Ag/Ag^+}$	1.205	1.010

*Experimental values corrected to refer to a temperature of 700° C.

†Potentials calculated from thermodynamic data on the pure salts in the absence of any solvent.

Can. J. Chem. Downloaded from www.nrcresearchpress.com by 78.46.186.204 on 09/04/12
For personal use only.

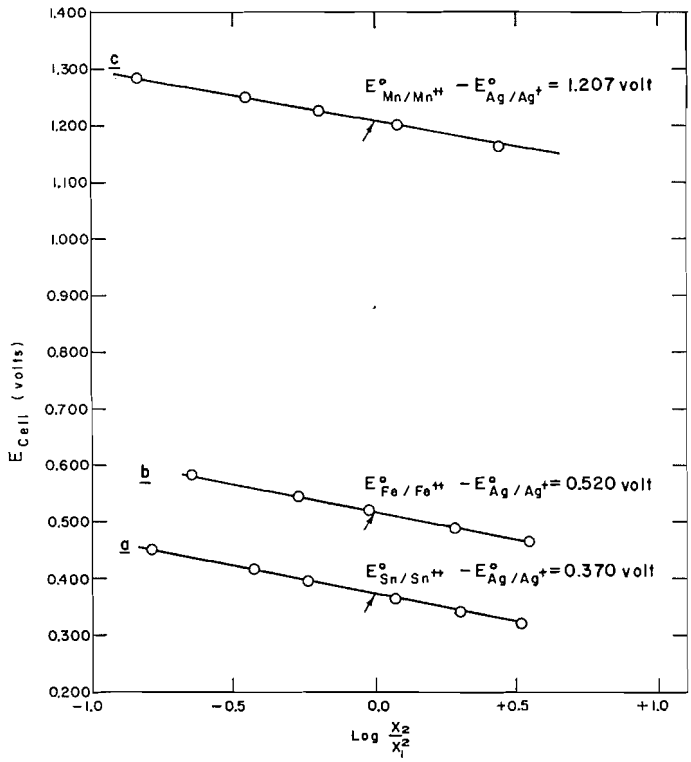

FIG. 1. Electromotive forces of the cells

M	MCl_2 (x_2)	AgCl (x_1)	Ag
(−)	KCl-NaCl (1/1 mole) ‖	KCl-NaCl (1/1 mole)	(+)

as a function of $\log(x_2/x_1^2)$, at constant temperature. M is (*a*) tin, (*b*) iron, and (*c*) manganese. MCl_2 is respectively $SnCl_2$, $FeCl_2$, and $MnCl_2$.

concentration. The potential was very steady and remained practically unchanged when the cells were left overnight.

The effect of temperature change on the electromotive forces of the tin, iron, and manganese cells was investigated next. The results of these experiments are given in Table III. The voltages have been corrected for thermoelectric effects. Also included in Table III are values for the standard potentials at different temperatures, calculated from the data, using equation [2].

From the standard potentials, using the procedure previously described (1, 2, 3, 4), it was possible to calculate for various temperatures the equilibrium constants (K) for the cell reactions given in Table II. The results of these calculations are given in Fig. 2, where $\log K$ was plotted against the reciprocal of absolute temperature. The curves are linear over the range of temperature investigated. The best straight lines were calculated by applying the least squares method.

The heat of reactions (ΔH_r) in cells of this type, as calculated according to the van't Hoff equation, is the difference between the heats of formation of the respective chlorides in the presence of the solvent.

The calculated values are:

$$\Delta H_{r(Sn/Sn^{++})} = -23.4 \pm 1.0 \text{ kcal/mole},$$
$$\Delta H_{r(Fe/Fe^{++})} = -27.8 \pm 1.4 \text{ kcal/mole},$$
$$\Delta H_{r(Mn/Mn^{++})} = -61.8 \pm 1.5 \text{ kcal/mole}.$$

Can. J. Chem. Downloaded from www.nrcresearchpress.com by 78.46.186.204 on 09/04/12
For personal use only.

TABLE III

EFFECT OF TEMPERATURE ON THE ELECTROMOTIVE FORCES OF THE CELLS

(*a*) Sn (−) | $SnCl_2$ ($x_2 = 3.93\times10^{-3}$) KCl–NaCl (1/1 mole) || AgCl ($x_1 = 6.235\times10^{-2}$) KCl–NaCl (1/1 mole) | Ag (+)

T, ° K	E_{cell} (volts)	$E^\circ_{Sn/Sn^{++}} - E^\circ_{Ag/Ag^+}$ (volts)
	On heating	
946	0.3771	0.3768
996	0.3686	0.3686
1053	0.3600	0.3597
1109	0.3470	0.3467
	On cooling	
1057	0.3598	0.3596
990	0.3710	0.3707
949	0.3779	0.3776

(*b*) Fe (−) | $FeCl_2$ ($x_2 = 3.771\times10^{-3}$) KCl–NaCl (1/1 mole) || AgCl ($x_1 = 6.235\times10^{-2}$) KCl–NaCl (1/1 mole) | Ag (+)

T, ° K	E_{cell} (volts)	$E^\circ_{Fe/Fe^{++}} - E^\circ_{Ag/Ag^+}$ (volts)
	On heating	
968	0.5231	0.5210
1018	0.5199	0.5177
1065	0.5154	0.5131
1106	0.5073	0.5049
1131	0.5047	0.5022
1159	0.5010	0.4985
	On cooling	
1091	0.5147	0.5123
1065	0.5162	0.5139
1033	0.5213	0.5130
981	0.5280	0.5258
954	0.5299	0.5278

(*c*) Mn (−) | $MnCl_2$ ($x_2 = 4.779\times10^{-3}$) KCl–NaCl (1/1 mole) || AgCl ($x_1 = 6.235\times10^{-2}$) KCl–NaCl (1/1 mole) | Ag (+)

T, ° K	E_{cell} (volts)	$E^\circ_{Mn/Mn^{++}} - E^\circ_{Ag/Ag^+}$ (volts)
	On heating	
943	1.204	1.211
953	1.200	1.208
1005	1.193	1.201
1056	1.186	1.194
1122	1.172	1.181
1153	1.168	1.177
	On cooling	
1133	1.170	1.179
1057	1.184	1.192
1037	1.188	1.196
1016	1.193	1.201
995	1.196	1.204
983	1.200	1.208

Following the same procedure, and with the same reservations, as cited previously (1, 2, 3, 4), dissociation constants of complexes of $SnCl_2$, $FeCl_2$, or $MnCl_2$, respectively, in the molten salt solvent, have been calculated as follows:

$$K_{d(SnCl_2\ complex)} = 2.3,$$
$$K_{d(FeCl_2\ complex)} = 5.9\times10^{-3},$$
$$K_{d(MnCl_2\ complex)} = 9.61\times10^{-3}.$$

Can. J. Chem. Downloaded from www.nrcresearchpress.com by 78.46.186.204 on 09/04/12
For personal use only.

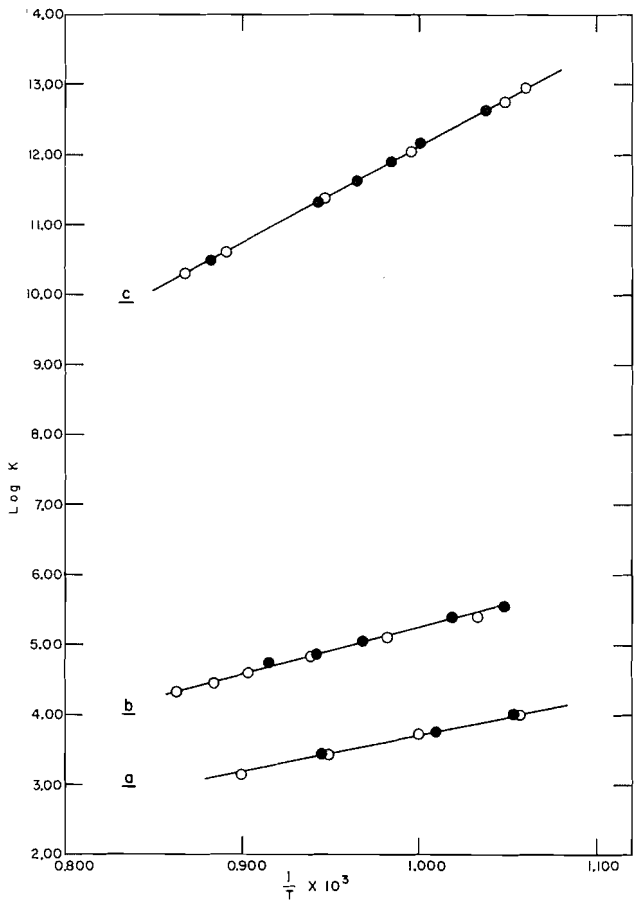

FIG. 2. The variation of log K with the reciprocal of absolute temperature for the systems:

(*a*) Sn (−) | $SnCl_2$ ($x_2 = 3.93\times10^{-3}$) KCl–NaCl (1/1 mole) || AgCl ($x_1 = 6.235\times10^{-2}$) KCl–NaCl (1/1 mole) | Ag (+)
$\Delta H = -23.4\pm1.0$ kcal.

(*b*) Fe (−) | $FeCl_2$ ($x_2 = 3.771\times10^{-3}$) KCl–NaCl (1/1 mole) || AgCl ($x_1 = 6.235\times10^{-2}$) KCl–NaCl (1/1 mole) | Ag (+)
$\Delta H = -27.8\pm1.4$ kcal.

(*c*) Mn (−) | $MnCl_2$ ($x_2 = 4.779\times10^{-3}$) KCl–NaCl (1/1 mole) || AgCl ($x_1 = 6.235\times10^{-2}$) KCl–NaCl (1/1 mole) | Ag (+)
$\Delta H = -61.8\pm1.5$ kcal.

○ with increasing temperature, ● with decreasing temperature.

It is of interest to note that both the iron and manganese complexes in the melt are substantially more stable than that formed by tin.

ACKNOWLEDGMENT

The authors wish to acknowledge the help of Mr. P. Hernandez in constructing the silica apparatus used in the foregoing experiments.

REFERENCES

1. FLENGAS, S. N. and INGRAHAM, T. R. Can. J. Chem. **35**, 1159 (1957).
2. FLENGAS, S. N. and INGRAHAM, T. R. Can. J. Chem. **35**, 1254 (1957).
3. FLENGAS, S. N. and INGRAHAM, T. R. Can. J. Chem. **36**, 780 (1958).
4. FLENGAS, S. N. and INGRAHAM, T. R. Can. J. Chem. **36**, 1103 (1958).
5. HAMER, W. J., MALMBERG, M. S., and RUBIN, B. J. Electrochem. Soc. **103**, 8 (1956).

Can. J. Chem. Downloaded from www.nrcresearchpress.com by 78.46.186.204 on 09/04/12
For personal use only.

Can. J. Chem. Downloaded from www.nrcresearchpress.com by 78.46.186.204 on 09/04/12
For personal use only.

PHOTOOXIDATION OF BUTENES BY NITROGEN DIOXIDE AT DIFFERENT WAVE LENGTHS[1]

S. SATO[2] AND R. J. CVETANOVIĆ

ABSTRACT

Photooxidation of butenes by nitrogen dioxide at room temperature has been studied at three different wave lengths: 2288, 2537, and 3261 Å. In the case of butene-1 an abrupt change in the ratios of reaction products is observed between 2537 and 2288 Å: about three times as much α-butene oxide as n-butyraldehyde is formed at 2288 Å, while the amounts of these two compounds are almost equal at the longer wave lengths. This discontinuity is ascribed to a difference in the mechanism of reaction with olefinic double bonds of the first excited state, $O(^1D)$, and the ground state, $O(^3P)$, of oxygen atoms. Experimental evidence indicates that there is collisional quenching of $O(^1D)$ to $O(^3P)$ atoms.

Reactions of *cis*- and *trans*-butene-2 and of isobutene are much less reproducible, particularly so that of isobutene, because of the much more readily occurring thermal reaction of the excess nitrogen dioxide present with the epoxides initially formed.

INTRODUCTION

The main features of the reactions between oxygen atoms and olefins have been recently established (1). Mercury-photosensitized decomposition of nitrous oxide was used as the source of oxygen atoms, which were believed to be produced in their ground electronic state. In connection with this work, a study was also made of the reactions of butene-1 and isobutene with oxygen atoms formed by photolysis of nitrogen dioxide at 3660 Å (2). At this wave length there is insufficient energy to produce electronically excited oxygen atoms and the general similarity of the two processes was taken as further evidence that ground state oxygen atoms were formed in the mercury-photosensitized decomposition of nitrous oxide.

It was thought of interest to attempt to study the behavior in similar reactions of the oxygen atoms in their first excited state, $O\ ^1D$, by photolyzing nitrogen dioxide at shorter wave lengths. It is believed (3) that at the wave lengths longer than 2450 Å, oxygen atoms are produced in this process in the ground state and at suitable wave lengths shorter than 2450 Å, in the first excited state. The long wave length threshold for this photolysis has been found to lie between 4047 and 4358 Å (4). The energy difference between 2450 and 4047 Å is 46.0 kcal/mole, which agrees with the energy difference between ^3P and ^1D states of oxygen atoms (45.2 kcal/mole).

In the present work a comparative study has been made of the photooxidation of butenes by nitrogen dioxide at 2288 and 3261 Å, obtained from a cadmium resonance lamp, and at 2537 Å, from a mercury resonance lamp. It would appear from the results obtained with butene-1 that the difference in multiplicity between ^3P and ^1D states of oxygen atoms leads to two distinct mechanisms of their interactions with olefinic double bonds. The usefulness of the reactions of the other butenes in this respect was, unfortunately, greatly reduced because of the considerably greater reactivity of the epoxide formed with excess nitrogen dioxide present and consequent poor reproducibility of the experimental results.

EXPERIMENTAL

Apparatus and experimental procedure used in the present work, as well as the method of purification of nitrogen dioxide, butene-1, isobutene, and *cis*- and *trans*-butene-2 (Phillips reagent grade products), were the same as described previously (2).

[1]*Manuscript received August 15, 1958.*
Contribution from the Division of Applied Chemistry, National Research Council, Ottawa, Canada. Issued as N.R.C. No. 4935.
[2]*National Research Council Postdoctorate Fellow 1956–58.*

Can. J. Chem. Downloaded from www.nrcresearchpress.com by 78.46.186.204 on 09/04/12
For personal use only.

A chlorine filter was used to isolate the resonance line of 2288 Å from a cadmium lamp operated at 280±5° C. The emission spectrum, taken with medium quartz Hilger spectrograph, showed that the resonance line at 2288 Å was completely isolated from the stronger resonance line at 3261 Å. A very weak line at 2537 Å was observed, probably owing to a trace of mercury taken into the lamp along with cadmium. The intensity of this mercury resonance line, however, was negligible compared to the intensity of the line at 2288 Å. The light of 3261 Å was obtained from the same cadmium lamp by using a 7–54 Corning glass filter. The light of 2537 Å was obtained from a low pressure mercury resonance lamp and using again a 7–54 Corning glass filter.

Light intensities at the three wave lengths were adjusted by varying the distances of the light sources from the reaction cell and the diameters of the circular light apertures so that almost the same amounts of total reaction products were obtained. The amounts of products were estimated from the gas–liquid chromatography peak areas (2).

A few experiments were carried out in an attempt to measure directly the relative intensities of the light absorbed by nitrogen dioxide at the three wave lengths. The light intensities were so weak that the following technique had to be applied. A very small amount (1 μmole) of nitrogen dioxide and the same amount of butene-1 were taken into the reaction cell and the intensity of transmitted light was followed by means of a photoelectric circuit. Under these conditions the consumption of nitrogen dioxide after 2-hour irradiation was essentially the same at 2288 and 3261 Å (36 and 34%, respectively). The low pressure mercury lamp was not stable enough for this type of measurement.

RESULTS AND DISCUSSION

Photooxidation of Butene-1

Mixtures of 30 mm butene-1 and 3 mm nitrogen dioxide were photolyzed at different wave lengths for 2 hours. The absolute amounts of products formed were not too reproducible and for this reason their ratios are shown in Fig. 1, where the amount of

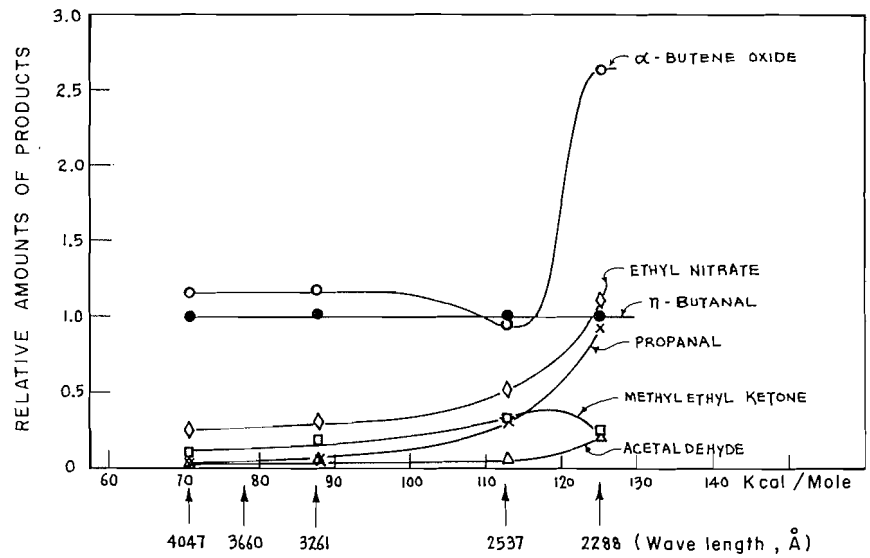

FIG. 1. Relative amounts of products (*n*-butyraldehyde taken as unity) in the photooxidation of butene-1 with nitrogen dioxide at various wave lengths (irradiation time, 2 hours; 30 mm of olefin, 3 mm NO_2; 25±2° C).

n-butyraldehyde is taken as unity.* The ratios were found to be well reproducible. The absolute amount of *n*-butyraldehyde decreased with decreasing wave length and at 2288 Å was approximately about half as great as at 3261 Å.

In Fig. 1, a discontinuity is observed between the wave lengths of 2537 Å and 2288 Å; at 2288 Å the amount of α-butene oxide is about three times as great as that of butanal, while these amounts are almost equal at longer wave lengths. The amount of methyl ethyl ketone gradually increases with decreasing wave length from 4047 Å to 2537 Å, but at 2288 Å it shows a marked decrease. The curves for ethyl nitrate, propanal, and acetaldehyde ascend monotonously with decreasing wave length. These last three compounds are secondary reaction products, while α-butene oxide, butanal, and methyl ethyl ketone are the primary addition products. These results, therefore, suggest that the mechanism of addition of oxygen atoms to butene-1 changes between 2288 Å and 2537 Å. In as much as this conclusion is correct, it can be explained by the difference in the electronic structure of oxygen atoms at the two wave lengths. The continuously increasing amounts of the secondary products, ethyl nitrate, propanal, and acetaldehyde, are, on the other hand, explainable in terms of the increasing amounts of energy with decreasing wave lengths.

The pressure dependence of photooxidation of 3 mm butene-1 by 3 mm nitrogen dioxide with various amounts of nitrogen added has been studied at 2288 Å and the results are shown in Fig. 2. Although there is a certain amount of scatter of the points, the pressure dependence in Fig. 2 is evidently quite different from that observed previously in the photooxidation of butene-1 at 3660 Å (Fig. 3*a* of ref. 2). With increasing total pressure, the amount of α-butene oxide decreases, the amounts of butanal and methyl ethyl ketone show a slight increase, and the secondary products, propanal, ethyl nitrate, and acetaldehyde, rapidly decrease. As the total pressure is increased, the ratios of all the products formed approach those observed at longer wave lengths. The rapid decrease in the

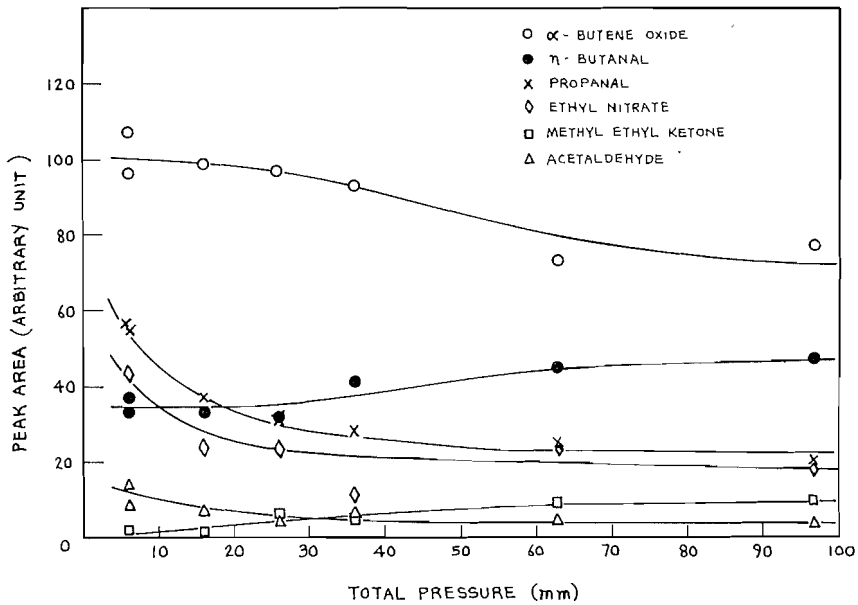

FIG. 2. Amounts of products in the photooxidation of butene-1 with nitrogen dioxide as a function of total pressure (3 mm butene-1, 3 mm NO_2, variable amounts of N_2; irradiation time, 2 hours; 25±2° C).

**The data at 4047 Å were taken from the previous work (4). The total amount of products was approximately equal to that obtained at the other three wave lengths.*

Can. J. Chem. Downloaded from www.nrcresearchpress.com by 78.46.186.204 on 09/04/12
For personal use only.

amounts of secondary products is compatible with an increased dissipation of energy by collisions at higher pressures. The trends of the addition products, on the other hand, suggest the simultaneous occurrence of the quenching reaction

$$O(^1D) + M \rightarrow O(^3P) + M. \quad [1]$$

Photooxidation of Isobutene

Experiments similar to those described for butene-1 have been carried out also with isobutene. As already reported (2), isobutene oxide, which is one of the main products of addition of oxygen atoms to isobutene, was absent because of its rapid thermal reaction with nitrogen dioxide. Moreover, this reaction seemed to be the cause of poor reproducibility. In the case of isobutene, therefore, no significant results were obtained except that with decreasing wave length there was a very pronounced increase in the amount of acetone formed, which became equal to that of isobutyraldehyde at 2288 Å. The mechanism of formation of acetone in the case of isobutene is believed to be analogous to that of propanal in the case of butene-1.

Photooxidation of cis- and trans-Butene-2

The experimental results with *cis*- and *trans*-butene-2 are less reproducible than those with butene-1 but are better than those with isobutene. This is probably because β-butene oxide, one of the main products in the case of butene-2, reacts with nitrogen dioxide at a rate intermediate between those of α-butene oxide and isobutene oxide (5).

The results are summarized in Table I where relative amounts of products are given with methyl ethyl ketone taken as unity. The absolute amount of methyl ethyl ketone appears to increase on passing from longer to the shorter wave lengths, at least in the case of *trans*-butene-2. In these reactions four main addition products are known (1) to be formed: *cis*- and *trans*-β-butene oxide, methyl ethyl ketone, and isobutyraldehyde. The greater part of isobutyraldehyde is formed by combination of free radicals. For this reason this compound would be expected to be much reduced, with simultaneous formation of large amounts of nitro compounds, in the presence of excess nitrogen dioxide used in the present work. As shown in Table I, the four addition products are formed, although *cis*-β-butene oxide and isobutyraldehyde were not separated on the gas chromatographic column used and were not estimated separately. In addition large amounts of nitromethane and methyl nitrate and smaller amounts of acetaldehyde are also formed. The

TABLE I

RELATIVE AMOUNTS OF PRODUCTS (METHYL ETHYL KETONE TAKEN AS UNITY) IN THE PHOTOOXIDATION OF *trans*-BUTENE-2 AND *cis*-BUTENE-2 WITH NITROGEN DIOXIDE

(Irradiation time 2 hours; 30 mm of olefin, 3 mm NO_2; 25±2° C)

Wave length (Å)	AcA	*trans*-BuO	*i*-BuA +*cis*-BuO	CH_3NO_3	MEK	CH_3NO_2
			A. *trans*-Butene-2			
2288	0.5	0.9	0.2	1.2	(1.0)	0.6
2537	0.4	0.8	0.3	0.8	(1.0)	0.6
3261	0.1	0.5	0.1	0.6	(1.0)	0.5
			B. *cis*-Butene-2			
2288	0.4	0.5	0.4	1.9	(1.0)	1.0
2537	0.1	0.6	0.2	0.8	(1.0)	1.0
3261	0.1	0.6	0.3	1.1	(1.0)	0.9

AcA = Acetaldehyde.
BuO = Butene oxide.
BuA = Butyraldehyde.
MEK = Methyl ethyl ketone.

Can. J. Chem. Downloaded from www.nrcresearchpress.com by 78.46.186.204 on 09/04/12
For personal use only.

secondary products tend to increase at the lowest wave length used and are similar in that respect to the secondary products observed with butene-1.

It is not possible to say conclusively whether there is an increase in stereospecificity on passing from 2537 to 2288 Å. This uncertainty is due to the relatively poor reproducibility of the figures in Table I, the unknown extent of the thermal reaction with excess nitrogen dioxide of the two epoxides produced, and the fact that *cis*-β-butene oxide was not measured separately. The mean values do suggest an increase in stereospecificity; however, these values are, unfortunately, subject to large uncertainty.

Mechanisms of Addition of Oxygen Atoms (^3P and ^1D) to a Double Bond

According to the spin conservation rule, addition of an oxygen atom in the ground state, $O(^3P)$, to an olefin, which is in a singlet state, should give a triplet state of the activated complex, while the addition of the first excited oxygen atom, $O(^1D)$, should give a singlet state of the activated complex. In agreement with this, when oxygen atoms are produced by the mercury-photosensitized decomposition of nitrous oxide they are most likely in the ^3P state and the initial step of their addition to olefins was, therefore, formulated before (1) as follows:

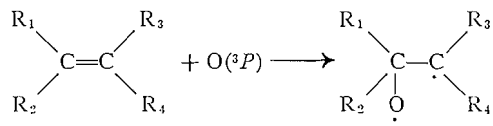

[2]

(A)

Here R stands for an alkyl radical or a hydrogen atom, and the first carbon atom of the double bond is assumed to be "less substituted". The transition complex is a stage in the formation of the biradical (A), which is presumably in the triplet state.

In the case of ^1D oxygen atoms, the activated complex is probably a stage in the following reaction,

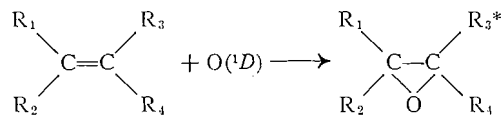

[3]

(B)

where the intermediate (B) should be in the singlet state.

The two intermediates (A) and (B) may undergo internal rearrangements (1). However, both the *cis–trans* isomerization and the migration of R_1 or R_2 to the second carbon atom of the original double bond are likely to be much easier in (A) than in (B) and, therefore, the addition of the $O(^1D)$ atoms should be more stereospecific and should lead to predominant formation of the epoxides. Thus, in the case of butene-1 (where $R_1 = R_2 = R_3 = H$ and $R_4 = C_2H_5$), the relative amount of butanal formed from (A) should be larger than that from (B). This is in agreement with the experimental observation. At the same time, the extent of stereospecificity will depend also on the extent of the quenching reaction [1]. Even when large pressures of the olefin are used and the amount of any other kind of molecules present is negligible, a certain amount of quenching by the olefin itself is likely to occur and the reaction need not be completely stereospecific if the collision yield is smaller than unity. The extent of stereospecificity will then depend on

Can. J. Chem. Downloaded from www.nrcresearchpress.com by 78.46.186.204 on 09/04/12
For personal use only.

the average number of collisions of $O(^1D)$ atoms with the olefin before an effective collision takes place. Another factor which is likely to have an effect on the stereospecificity which can be observed under conditions of the present experiments is the high exothermicity of these reactions. As pointed out before (1) the addition products at the moment when they are formed are "hot" and, therefore, the observed stereospecificity will depend to a certain extent on the relative ease of isomerization under such conditions of the particular epoxides formed. Thus, although there is a large quantitative uncertainty in the results obtained with *cis*- and *trans*-butene-2, it is certain that at least in the case of *cis*-butene-2 the addition at 2288 Å is far from being completely stereospecific, i.e. some *trans*-epoxide is still formed. In view of the preceding discussion, however, this should not be taken as an argument against the mechanism proposed here for the addition of $O(^1D)$ atoms to olefins.

Fragmentation Products

Although the complexity of the studied processes precludes a complete explanation of the formation of the fragmentation products, it may be worth while to mention that the amounts of propanal, acetone, and acetaldehyde, in the case of butene-1, isobutene, and butene-2, respectively, increase rapidly with decreasing wave length of the light used for the reaction. It is very likely that these compounds are formed in all these reactions by a similar mechanism. Their formation might perhaps be due, directly or indirectly, to the excited oxygen molecules produced by the reaction of oxygen atoms with nitrogen dioxide (6). This matter, however, requires considerable further investigation.

ACKNOWLEDGMENTS

The authors are indebted to Dr. A. W. Tickner for mass spectrometer analyses, and to the Analytical Section of this Division for the infrared analyses.

REFERENCES

1. CVETANOVIĆ, R. J. Can. J. Chem. **36**, 623 (1958).
2. SATO, S. and CVETANOVIĆ, R. J. Can. J. Chem. **36**, 970 (1958).
3. NOYES, W. A., JR. and LEIGHTON, P. A. The photochemistry of gases. Reinhold Publishing Corp., New York. 1941. p. 400.
4. SATO, S. and CVETANOVIĆ, R. J. Can. J. Chem. **36**, 279 (1958).
5. ELTEKOW, A. Ber. **16**, 395 (1883). Pritchard, J. G. and Long, F. A. J. Am. Chem. Soc. **78**, 2667 (1956).
6. LIPSCOMB, F. J., NORRISH, R. G. W., and THRUSH, B. A. Proc. Roy. Soc. A, **233**, 455 (1955).

Can. J. Chem. Downloaded from www.nrcresearchpress.com by 78.46.186.204 on 09/04/12
For personal use only.

Can. J. Chem. Downloaded from www.nrcresearchpress.com by 78.46.186.204 on 09/04/12
For personal use only.

SULPHINIC ACIDS AS ANALYTICAL REAGENTS[1]

T. P. FORREST[2] AND D. E. RYAN

ABSTRACT

The "specific" action of sulphinic acids with metal ions is not limited to compounds in which there is direct attachment of the $-SO_2H$ group to an aromatic ring. Since both aliphatic and aromatic sulphinic acids react similarly the assumption that an aromatic group is necessarily co-ordinated to the metal atom through its π system is not valid; the precipitated products are simple salts of the acids. Ferric iron yields at least two products with sulphinic acids. Ceric cerium is reduced in acid solution but an orange-yellow precipitate containing cerium is obtained from acetate-buffered solutions. Naphthalenesulphinic acid may be used to quantitatively precipitate Fe^{+++}, Th^{++++}, Zr^{++++}, U^{++++}, Ti^{++++}, Sn^{++++}, Bi^{+++}, Pd^{++}, Ag^{+}, Hg_2^{++}.

INTRODUCTION

Benzenesulphinic acid, $C_6H_5SO_2H$, and its alkali salts react with ferric salts in solutions of mineral acids to form the slightly soluble orange-yellow ferric benzenesulphinate $(C_6H_5SO_2)_3Fe$ (1). This compound has been stated (2) to be so insoluble that it is formed even in solutions containing fluoride and phosphate ions and that a distinct turbidity occurs in ferric salt solutions so dilute as to yield a scarcely perceptible pink color with thiocyanates. Although various sulphinic acids have been used for the determination and separation of ferric iron (3), Ackerman (4) and Dubsky (5) report that the determination of iron with sulphinic acids is not reproducible.

Tetravalent ions, such as cerium, thorium, uranium, tin, titanium, and zirconium, also react in acid solution to yield precipitates. Feigl (2) reported that, although the sulphinic acids are easily oxidized and ceric salts are powerful oxidizing agents, the compound $(C_6H_5SO_2)_4Ce$ is nevertheless formed in the reaction between these substances. A comparison of the reactivity of benzenesulphinic, benzylsulphinic, and cyclohexylsulphinic acids showed that only benzenesulphinic acid formed slightly soluble salts with the above-mentioned metal ions. These results led to the conclusion that direct attachment of the $-SO_2H$ group to an aromatic ring was necessary and that the phenyl group was co-ordinated to the metal atom through its system of conjugated double bonds. However, Krishna and Singh (3) precipitated ferric iron with *p*-anisylsulphinic acid in which the sulphinic acid group is separated from the aromatic ring by a methylene group.

The present work, therefore, was undertaken to determine the effect of the radical on the analytical behavior of sulphinic acids; this paper records the results of such an investigation.

COMPOUNDS INVESTIGATED

The following sulphinic acids were prepared: benzene, *p*-toluene, β-naphthalene, 2-thiophene, benzyl, cyclohexyl, *n*-hexyl, and *n*-butyl. The aromatic acids were prepared by reducing the corresponding sulphonyl chloride with sodium sulphite (3, 6). Part of the sulphinic acid was removed as a solid and the remainder was extracted with ether from the acidified reaction mixture. The aliphatic acids were prepared by the addition of sulphur dioxide to the Grignard reagent at $-50°$ C (7). The solid magnesium salt thus obtained was decomposed in acid solution and the sulphinic acid extracted with ether.

The ammonium salts, which are more stable than the acids, were prepared by bubbling

[1]*Manuscript received August 29, 1958.*
Contribution from the Department of Chemistry, Dalhousie University, Halifax, N.S., with financial assistance from the National Research Council. Abstracted from the M.Sc. thesis of T.P. Forrest.
[2]*Holder, Canadian Industries Limited Fellowship, 1957–58.*

ammonia through an ethereal solution of the acid. The salts were purified by precipitating the ferric sulphinate, washing with water, and then treating with aqueous ammonia to remove iron as the hydrous ferric oxide; the filtrate was acidified, ether extracted, and the ammonium salt reprecipitated from the ether extract with ammonia.

Properties of Compounds

The aromatic acids were obtained as white solids, the melting points of which are listed in Table I. The aliphatic acids were all obtained as oils which could be solidified at $-10°$ C. Sulphinic acids decompose relatively easily (8); they may be oxidized by air to the sulphonic acid or may disproportionate according to the following equation

$$3RSO_2H \rightarrow RSO_3H + RSOSOR + H_2O.$$

The melting points varied, therefore, due to decomposition incurred in drying the acid and in heating while melting. Benzenesulphinic acid gave melting points varying from 72° to 81° C, although consistent results of 79° to 80° were obtained; literature references (3, 9) give melting points varying from 75° to 85° C.

TABLE I

MELTING POINTS OF SULPHINIC ACIDS

Sulphinic acid	M.p., ° C
Benzene	79–80
p-Toluene	81
2-Thiophene	67
Benzyl	65–68
β-Naphthalene	104–106

The ammonium salts of the aromatic acids were white solids. The butyl and cyclohexyl ammonium sulphinates were obtained as colorless oils, although the cyclohexyl compound solidified slightly below room temperature; the hexyl derivative was obtained as a white, waxy, solid that decomposed to give off ammonia at 35° C.

Ionization constants obtained from potentiometric titration data on the acids showed that they are all fairly strong organic acids. The results obtained for benzenesulphinic acid ranged from 0.96×10^{-2} to 1.28×10^{-2} and for *p*-toluenesulphinic acid from 1.48×10^{-2} to 2.10×10^{-2}. The constants of the aliphatic acids were of the order of 10^{-3}.

Reactions with Metal Ions

Similar reactions were shown by all the sulphinic acids. The reactions were carried out by adding a 2% aqueous solution of the ammonium salt of the sulphinic acid to 0.1 *M* solutions of the metal ions. In dilute acid solution voluminous precipitates were obtained with Ag^{+}, Hg_2^{++}, Hg^{++}, Pd^{++}, Fe^{+++}, U^{++++}, Zr^{++++}. Bi^{+++}, Ti^{++++}, and Sn^{++++} gave good precipitates under these conditions with naphthalene, benzene, and *p*-toluene sulphinic acids but a higher reagent concentration was required for precipitation with the other sulphinic acids. Slight precipitation was obtained with Cu^{++}, Pb^{++}, and Pt^{++++} at reagent concentration above two per cent. From 1 *N* sulphuric acid solution ceric cerium precipitated insoluble oxidation products of the sulphinic acids but an orange-yellow precipitate containing cerium was obtained from acetate-buffered solution. The rare earths were incompletely precipitated from solutions of their salts but were not obtained from solutions above 0.5 *N* in hydrochloric acid. No color or precipitate was noted with the following: Tl^{+}, Ba^{++}, Ca^{++}, Sr^{++}, Mg^{++}, Cd^{++}, Zn^{++}, Co^{++}, Ni^{++}, Fe^{++},

Can. J. Chem. Downloaded from www.nrcresearchpress.com by 78.46.186.204 on 09/04/12
For personal use only.

$Al^{\cdot\cdot\cdot}$, $As^{\cdot\cdot\cdot}$, $Sb^{\cdot\cdot\cdot}$, $Rh^{\cdot\cdot\cdot}$, $Ir^{\cdot\cdot\cdot\cdot}$, $As^{\cdot\cdot\cdot\cdot\cdot}$, WO_4'', MoO_4'', VO_4'''. In acid solutions the orange dichromate was reduced to the green chromic ion and the pink color of permanganate was discharged.

Since all the sulphinic acids investigated exhibit the same properties for precipitating metal ions, their selective action is not due to the co-ordination of an aromatic ring to the metal atom through its system of conjugated double bonds. The only significant difference in the products obtained is in their solubilities.

THE IRON REACTION

As previously stated ferric iron has been determined by precipitation of the reportedly very insoluble ferric benzenesulphinate. Use has been made of this reaction to determine iron volumetrically by titration with a standard sulphinic acid solution with dilute thiocyanate as an external indicator (3). However, in the preliminary experiments with ferric iron it was found that, in solutions containing less than 0.5 mg of iron per milliliter, only a yellow to red color developed when the theoretical amount of reagent was added. A red color was obtained on dropwise addition of reagent to more concentrated iron solutions but this color disappeared as the orange-yellow ferric sulphinate separated from solution on the addition of more sulphinic acid; the ferric sulphinate dissolved slowly in ferric chloride solution to regenerate the red color. These results show that, in addition to the insoluble 1:3 ferric benzenesulphinate, there is at least one other product of the reaction. The volumetric method for the determination of iron by sulphinic acids cannot be recommended; although the ferric sulphinate is precipitated from solutions containing more than two milligrams of iron per milliliter the end point is poor and in more dilute solutions a soluble colored complex only is formed.

Table II shows the effects of concentration and acidity on the precipitation of ferric iron by benzenesulphinic acid. The quantity of iron remaining in solution where precipitation occurred was determined colorimetrically with *o*-phenanthroline.

TABLE II

PRECIPITATION OF FERRIC IRON WITH BENZENESULPHINIC ACID

Iron present mg/ml	Acidity	Mole ratio of reagent to iron	Results
0.05	pH 3	10:1	Yellow solution; no precipitate
0.05	pH 3	40:1	Yellow solution; slight precipitation
0.25	pH 3	10:1	Good precipitation; 3.2 p.p.m. iron in filtrate
0.25	0.2 *N* HCl	10:1	Orange solution; slight precipitation
0.40	0.2 *N* HCl	10:1	Good precipitation; 7.4 p.p.m. iron in filtrate
0.60	0.2 *N* HCl	3:1	Red solution; no precipitate
0.60	0.2 *N* HCl	10:1	Good precipitation; 3.7 p.p.m. iron in filtrate

These results show that quantitative precipitation is markedly dependent upon concentration and that best precipitation occurs from slightly acid, relatively concentrated iron solutions. However, precipitates are obtained even in solutions containing as little as 0.05 mg of iron per milliliter provided an extremely large excess of reagent is added ($>40:1$).

In view of the above results an investigation into the statements regarding the extreme insolubility of ferric benzenesulphinate and its formation in the presence of fluoride and phosphate ions was carried out. The solubility was determined by preparing a saturated aqueous solution under nitrogen at 25° C; the iron content of the filtered solution, determined colorimetrically with *o*-phenanthroline, was 4.5×10^{-4} moles per liter after 7

Can. J. Chem. Downloaded from www.nrcresearchpress.com by 78.46.186.204 on 09/04/12
For personal use only.

hours and 10^{-3} moles per liter after 4 days. Since dibenzylsulphone was obtained from solutions of ferric benzylsulphinate similarly treated, the increase in solubility on standing is undoubtedly due to some decomposition of the sulphinate. The ferric benzenesulphinate dissolved completely in 1 *M* fluoride and phosphate solutions and no precipitation occurred from neutral solutions containing 20:1 ratio of fluoride or phosphate to iron; in 0.2 *N* acid solutions, however, in which the concentrations of fluoride and phosphate complexes are small, precipitation did take place.

Similar reactions with iron were obtained with the other sulphinic acids; the most insoluble ferric sulphinate was that of naphthalenesulphinic acid. The use of this compound as an analytical reagent is discussed below.

Nature of the Solid Ferric Benzenesulphinate

Analysis of the solid product of the reaction between ferric iron and benzenesulphinic acid, after drying at 110° C, gave 11.69% iron on ignition to the oxide; the theoretical value of $Fe(C_6H_5SO_2)_3$ is 11.65%. A sample, ether-washed and dried at room temperature, lost no weight on drying at 110° C for 2 hours; this result, together with the analysis given above for the dried compound, shows the absence of water of hydration in the precipitated product.

The orange solid was insoluble in ether, ethanol, dioxane, benzene, cyclohexane, chloroform, and carbon tetrachloride but dissolved in glacial acetic acid to give a red solution having a freezing-point depression that indicated complete dissociation. The absorption spectra of this solution, between 400–500 mμ, was identical with that of a solution of ferric nitrate in glacial acetic acid; the compound, therefore, dissociates completely to form the acetate complex.

The magnetic moment of the solid was determined by means of a Guoy balance and found to be 5.7 Bohr magnetons. This value is typical of ferric compounds having five unpaired electrons and shows that no inner orbital bonding has taken place.

The above results suggest that ferric benzenesulphinate is simply a salt of benzenesulphinic acid. Alimarin and Sotnikov (10) have recently concluded, on the basis of the reactivity of benzylsulphinic acid with metal ions, that the products are typical metallic salts of the acids.

THE CERIUM REACTION

Ceric cerium has been reported to react with benzenesulphinic acid to precipitate the ceric sulphinate $Ce(C_6H_5SO_2)_4$ (2); recently, however, the reaction has been stated to be a typical oxidation–reduction reaction yielding RSO_3H and R_2SO_2 with Ce^{+3} remaining quantitatively in solution (10). Our investigation has shown that insoluble white products are obtained on the addition of sulphinic acids to ceric solutions in 1 *N* sulphuric acid; the white product from benzenesulphinic acid addition contained no cerium and recrystallized from benzene as white needles melting, with decomposition, at 192° C; the melting point of diphenyldisulphone, $(C_6H_5SO_2)_2$, is 193° C. Titration of a standard benzenesulphinic acid solution with a 0.1 *M* ceric sulphate solution (1 *N* in H_2SO_4) using ferroin indicator gave a white precipitate; the ceric solution was decolorized and the end point occurred at a molar ratio of 1.8 cerium to 1 sulphinic acid. In acid solutions ceric cerium oxidizes sulphinic acids and is not precipitated, the cerium remaining quantitatively in solution; no precipitation occurred with cerous cerium in 1 *N* sulphuric acid solution.

From ceric solutions buffered at pH 4 with ammonium acetate, however, an orange-yellow precipitate containing cerium is obtained upon addition of sulphinic acids; cerous

Can. J. Chem. Downloaded from www.nrcresearchpress.com by 78.46.186.204 on 09/04/12
For personal use only.

cerium is precipitated at pH 4 as a white precipitate. The orange-yellow product obtained from ceric solutions with benzenesulphinic acid varied in composition, part of the product being extractable into ether to give an orange solution. The ether-soluble portion was reprecipitated as an orange solid on the addition of ligroin and gave on analysis, after drying *in vacuo* over boiling methanol, 30.9% Ce. The ether-insoluble portion, after drying in the same manner, gave on analysis 18.15% Ce; the theoretical value for $Ce(C_6H_5SO_2)_4$ is 19.88% Ce. It is evident that a mixture of products is obtained on the addition of sulphinic acids to nearly neutral solutions of ceric cerium.

The reaction of cerium with sulphinic acids depends markedly on the acidity of the solution which controls the oxidation potential of the system. At low acidity ceric cerium is precipitated but not purely as the simple metallic salt of the sulphinic acid whereas in strongly acid solution it is reduced and remains in solution as cerous cerium.

NAPHTHALENESULPHINIC ACID

Since naphthalenesulphinic acid gave the most insoluble precipitates in the preliminary experiments, its usefulness as a reagent for quantitative precipitation of a number of metal ions was briefly investigated. An excess of a 2% aqueous solution of ammonium naphthalenesulphinate was added to solutions of the metal ions, under varying conditions, and the filtrates tested by means of drop reactions for the metal; for the gravimetric results recorded the precipitates were washed with dilute solutions of the reagent and then ignited to the oxide. The results are given in Table III.

TABLE III

PRECIPITATION OF METAL IONS WITH NAPHTHALENESULPHINIC ACID

Metal ion	Conditions	Results
$Fe^{\cdot\cdot\cdot}$	0.05 mg/ml at pH 3	Good precipitation; 1 p.p.m. iron left in filtrate
	0.25 mg/ml in 0.2 *N* HCl	Good precipitation; 1.3 p.p.m. iron left in filtrate
		Benzenesulphinic acid gives no precipitation under the above conditions
$Zr^{\cdot\cdot\cdot\cdot}$	0.4 mg/ml in 0.4 *N* HCl	White precipitate; no zirconium detected in filtrate with alizarin
$Th^{\cdot\cdot\cdot\cdot}$	1 mg/ml	White precipitate; quantitative in acid solutions, < 5 p.p.m. thorium left in filtrate even in 0.5 *N* HCl
	0.1 mg/ml in 0.2 *N* HCl	Thorium oxide taken, 11.82 mg; recovered 11.87 mg
$Ti^{\cdot\cdot\cdot\cdot}$	0.1 mg/ml in 0.2 *N* H_2SO_4	Yellow precipitate; no titanium detected in filtrate with chromotropic acid
	0.05 mg/ml in 0.2 *N* H_2SO_4	Titanium dioxide taken, 7.94 mg; recovered, 7.95 mg
$Sn^{\cdot\cdot\cdot\cdot}$	0.3 mg/ml in 0.25 *N* HCl	White precipitate; no tin detected in filtrate by reduction to stannous tin and testing with ferric iron and *o*-phenanthroline
	1 mg/ml in 0.6 *N* HCl	Stannic oxide taken, 12.47 mg; recovered 12.50 mg
$U^{\cdot\cdot\cdot\cdot}$	0.1 mg/ml in 0.2 *N* HCl	White precipitate; no uranium detected in filtrate with ferrocyanide
$Bi^{\cdot\cdot\cdot}$	0.1 mg/ml in 0.2 *N* HNO_3	White precipitate; < 5 p.p.m. bismuth determined with stannite and lead solutions
$Pd^{\cdot\cdot}$	0.1 mg/ml in 0.03 *N* HCl	Brown precipitate turned slowly to canary yellow; no palladium detected in filtrate with mercuric iodide in dioxane
	0.1 mg/ml in 0.2 *N* HCl	No precipitate; yellow solution
$Hg_2^{\cdot\cdot}$	0.1 mg/ml in 0.2 *N* HNO_3	White precipitate; no mercury detected in filtrate with iodide
$Ag^{\cdot}$	1 mg/ml as solution of $AgNO_3$	White precipitate; no silver detected in filtrate with N,N-dimethylaminobenzalrhodanine
	1 mg/ml in 0.5 *N* HNO_3	Greyish precipitate, indicating reduction to metallic silver; silver ion detected in filtrate with N,N-dimethylaminobenzalrhodanine

Can. J. Chem. Downloaded from www.nrcresearchpress.com by 78.46.186.204 on 09/04/12
For personal use only.

Naphthalenesulphinic acid quantitatively precipitates a number of metal ions from acid solution and should, therefore, prove useful in the separation and determination of these metals.

REFERENCES

1. THOMAS, J. J. Chem. Soc. **95**, 342 (1909).
2. FEIGL, F. *In* Specific and special reactions. Elsevier Pub. Co., New York. 1940. p. 119.
3. KRISHNA, S. and SINGH, H. J. Am. Chem. Soc. **50**, 792 (1928).
4. ACKERMAN, L. Ind. Eng. Chem., Anal. Ed. **18**, 243 (1946).
5. DUBSKY, J. V., ORAVEC, E., and LANGER, A. Chem. obzor, **12**, 41 (1937); Chem. Abstr. **31**, 5712 (1937).
6. BEATTIE, R. W. and WHITMORE, F. C. J. Am. Chem. Soc. **55**, 1567 (1933).
7. ALLEN, P. J. Org. Chem. **7**, 23 (1942).
8. GILMAN, H. *In* Organic chemistry. Vol. 1. 2nd ed. John Wiley & Sons, Inc., New York. 1947. p. 906.
9. FIELD, L. and GRUNWALD, F. A. J. Org. Chem. **16**, 946 (1951).
10. ALIMARIN, I. P. and SOTNIKOV, V. S. Doklady Akad. Nauk S.S.S.R. **113**, 150 (1957); Chem. Abstr. **51**, 11913 (1957).

Can. J. Chem. Downloaded from www.nrcresearchpress.com by 78.46.186.204 on 09/04/12
For personal use only.

Can. J. Chem. Downloaded from www.nrcresearchpress.com by 78.46.186.204 on 09/04/12
For personal use only.

INFRARED SPECTRA AND STRUCTURE OF SELENIOUS ACID[1]

MICHAEL FALK[2] AND PAUL A. GIGUÈRE

ABSTRACT

The infrared spectra of selenious acid both crystalline and in solution in water and methanol were recorded from 2 to 30 μ. Assignment of the various frequencies is made on the basis of the crystal structure as determined from X-ray data. It is shown that the molecules have the symmetrical form (*a*), the asymmetrical one (*b*) proposed by Venkateswaran being

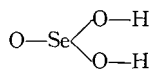

(*a*)

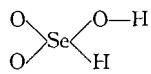

(*b*)

ruled out. The spectra of solutions in H_2O and D_2O confirm the existence of discrete H_2SeO_3 and D_2SeO_3 molecules with no indication of uncombined SeO_2 molecules even at high concentrations. This behavior is contrasted with that of SO_2 solutions.

INTRODUCTION

Recent spectroscopic investigations (1, 2) have confirmed the absence of measurable quantities of H_2SO_3 molecules in the various phases of the H_2O–SO_2 system. We have now completed a similar study of the H_2O–SeO_2 system prompted by the considerable differences between sulphurous and selenious acids. Unlike SO_2, SeO_2 combines with water to form a definite compound H_2SeO_3 stable both in solution and in the crystalline state. By X-ray diffraction Wells and Bailey (3) have shown that the crystal consists of nearly symmetrical SeO_3 pyramids linked together by strong O–H . . . O bonds. While the present work was in progress Detoni and Hadži (4) reported briefly on the infrared spectrum of the crystalline acid, interpreting their results in terms of molecules having the symmetrical form (*a*). The existence of stable H_2SeO_3 molecules in the solid phase is therefore well established.

The nature of aqueous solutions of selenious acid remained unsettled, however. By analogy with SO_2 persistence of free SeO_2 molecules in these solutions could be suspected. From a Raman study made over twenty years ago Venkateswaran (5, 6) had concluded that solutions of selenious acid present a complex system of two or three molecular species. His interpretation is now untenable as we shall see.

EXPERIMENTAL

Solid films of selenious acid were prepared by evaporating on a polished silver chloride plate solutions of selenium dioxide in chloroform or acetone and then allowing the films to hydrate in air. The latter reaction took place very readily at room temperature and at moderate humidity; once hydrated the films were indefinitely stable under these conditions, showing no tendency to effloresce. Aqueous solutions of selenious acid were prepared by adding weighed amounts of solid anhydrous SeO_2 to H_2O or D_2O. Absolute methanol was used to dissolve the pure crystalline acid. The high-purity sample of selenium dioxide was obtained through the courtesy of Dr. E. M. Elkin, Canadian Copper Refiners, Montreal East. The spectra were recorded by means of a Perkin–Elmer, Model 12-C infrared spectrometer using LiF, NaCl, and CsBr prisms.

[1]*Manuscript received August 26, 1958.*
Contribution from the Department of Chemistry, Laval University, Quebec, Que.
[2]*Present address: Division of Applied Chemistry, National Research Council, Ottawa, Canada.*

Can. J. Chem. Downloaded from www.nrcresearchpress.com by 78.46.186.204 on 09/04/12
For personal use only.

RESULTS AND DISCUSSION

The molecular spectra of crystalline selenious acid must be considered first to help decipher those of the solutions.

Solid H_2SeO_3

A composite tracing of the spectrum of selenious acid in the solid state is reproduced in Fig. 1 and the average frequency of the various maxima found in some eighteen films are listed in Table I. Both the frequencies and the relative intensities agree closely

TABLE I

INFRARED BANDS OF CRYSTALLINE H_2SeO_3 AND SeO_2

(Frequencies in cm^{-1})

H_2SeO_3			SeO_2
Ref. 4	This work	Assignments	(ref. 7)
412	403±3 w	δ OSeO	
	425 vw		
			535
			563
			591
	630±2 (sh)		
661	675±2 vs	ν Se–O	
696	715±5 (sh)	SeO_2	716
	787±5 w		
854	849±1 vs	ν Se–O	
	900±15 (sh)	SeO_2	901
			939
1134	1134±1 s	δ SeOH	
1180	1178±2 m	δ SeOH	
2290	2320±15 s	ν O–H	
2940	2900±50 vs	ν O–H	

with the results of Detoni and Hadži (4). For comparison the infrared frequencies of anhydrous SeO_2 (7) are also given. Apart from a few very weak bands presumably due to traces of SeO_2 in the acid, there is no resemblance between the two spectra; nor is there any indication of the H_2O bands in the neighborhood of 1650 and 3300 cm^{-1} usually present in molecular hydrates. Generally speaking, the frequencies below 1000 cm^{-1} may be ascribed to the SeO_3 groups and those above, to the OH groups.

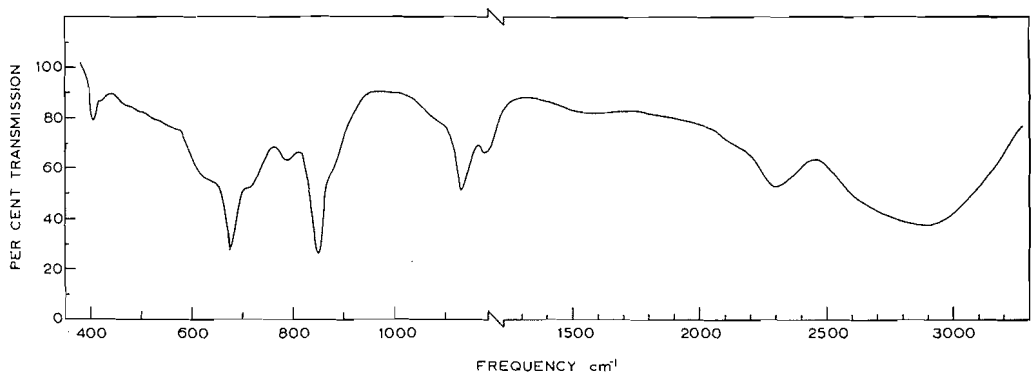

FIG. 1. Infrared absorption of crystalline selenious acid.

Can. J. Chem. Downloaded from www.nrcresearchpress.com by 78.46.186.204 on 09/04/12
For personal use only.

The two OH stretching frequencies at 2900 and 2320 cm^{-1} seem quite low compared with that of the free OH (about 3700 cm^{-1}). Such a large downward shift is indicative of strong hydrogen bonding in the crystalline acid and agrees with the short O–H · · · O distances found by X-ray diffraction, 2.56 and 2.60 Å (3). Correlations have been drawn by various authors between stretching frequencies and hydrogen bond lengths. One of the latest by Nakamoto, Margoshes, and Rundle (8) shows very good agreement for numerous compounds with O–H · · · O bonds. Taking the latter distance as 2.60 Å in H_2SeO_3, the OH stretching frequency should occur at 2500 cm^{-1}, nearly halfway between the observed values. A second relationship between frequency shift and hydrogen bond distance leads to the same approximate frequency: 3700–1200 = 2500 cm^{-1}. The large splitting between the two stretching frequencies (580 cm^{-1}) must result from the strong coupling of the two OH groups through the heavy selenium atom. In liquid H_2SO_4 the pair of corresponding bands occur at 3000 and 2430 cm^{-1} (9).

It is of interest to inquire where the hydrogen atoms are located in the H_2SeO_3 lattice. Judging from the rather low stretching frequencies one would expect an O–H bond somewhat longer than, for example, in ice: 1.01 Å (10). In fact a rough estimate based on Badgers's rule, using an average frequency of 2600 cm^{-1} leads to a distance of nearly 1.1 Å. On the other hand an empirical relationship between O–H · · · O distances and O–H bond lengths (8) yields about the same value as in ice. The discrepancy may come from the fact that the hydrogen bonds in the selenious acid crystal are not straight but bent. A neutron diffraction study of this and other mineral acids appears desirable.

The OH bending frequencies also are rather low (1178 and 1134 cm^{-1}) for such a strongly hydrogen-bonded system. Although the influence of hydrogen bonding on the deformation modes is much more complex and obscure than for the stretching modes it usually entails a slight shift toward *higher* frequencies. The situation here is somewhat reminiscent of that in tertiary alcohols (11) where a narrow association band arises near 1100 cm^{-1}. It would seem that even for a bonded hydrogen the bending frequency is strongly dependent on the "resultant mass" on the X atom in the group X–O–H · · · O.

In view of the small mass of the hydrogen atoms and the strong polarity of the O–H bonds the vibrations of the SeO_3 group can well be analyzed independently. Also for simplicity, a pyramidal configuration with C_{3v} symmetry is assumed since the three Se–O bonds are very nearly equivalent; 1.72, 1.75, and 1.76 Å (3) in the crystalline acid as a result of resonance. The normal Se–O single bond distance is about 1.81 Å (12) and the double bond, 1.68 Å (13). On the basis of that assumption one may expect a symmetrical stretching frequency and a doubly degenerate asymmetrical one. The pair of strong peaks at 849 and 675 cm^{-1} have been rightly assigned to these modes (4). The former has its equivalent at 890 cm^{-1} in the Raman spectra (5); there is, however, no trace in the infrared spectrum of the H_2SeO_3 crystal of any absorption near 600 cm^{-1} corresponding to the intense Raman shift at 597 cm^{-1}. Lastly, we assign the weak maximum at 403 cm^{-1} to a O–Se–O bending rather than a stretching mode as suggested by Detoni and Hadži (4). The other bending frequencies must lie beyond the range covered in this work.

Solutions of H_2SeO_3

The spectra of concentrated solutions of SeO_2 in H_2O and D_2O are shown in Fig. 2 and the frequency of the observed maxima are given in Table II. Progressive dilution of the solutions from 50 to 10% SeO_2 by weight resulted merely in a regular decrease of intensity for all the acid bands. The general resemblance of the spectra of H_2SeO_3 solutions and those of the crystalline acid leaves no doubt that the same species are

TABLE II

INFRARED SPECTRA OF SOLUTIONS OF SELENIOUS ACID
(Frequencies in cm^{-1})

H_2SeO_3 in CH_3OH	SeO_2 in H_2O	SeO_2 in D_2O
434±4 w		
584±4 vs		
670±10 s	682±5 s	670±8 s
920±10 s	894±5 vs	900±16 s
980±10 s	1236±5 s	
2420±20 s	2425±20 s	1820±20 s
2900±100 vs	2980±40 vs	2140±40 vs

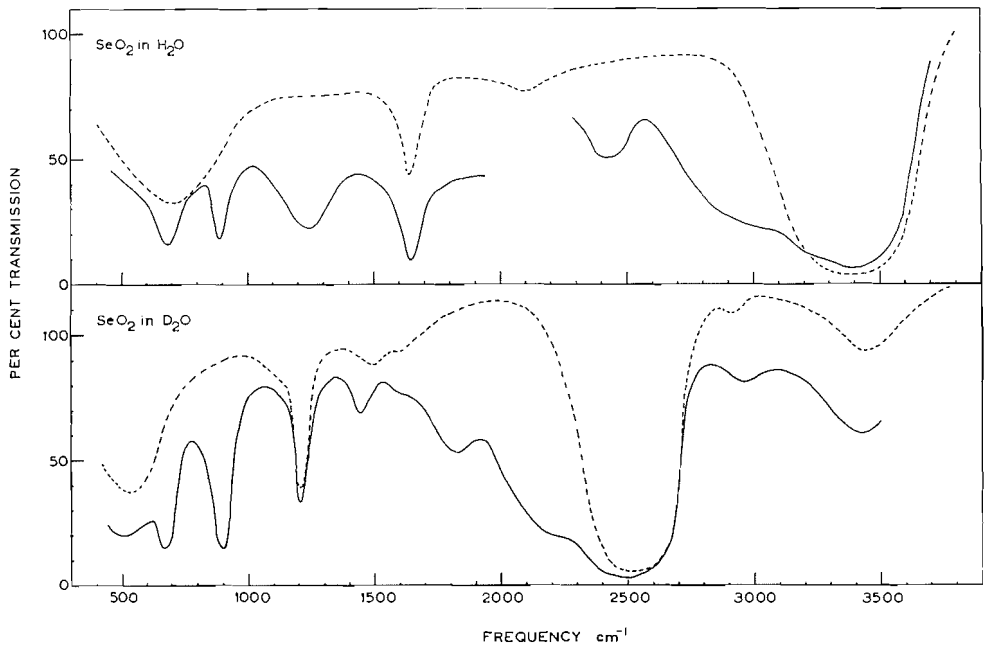

FIG. 2. Infrared spectra of 50% solutions of SeO_2 in H_2O and D_2O. Broken lines refer to the spectra of the pure solvents.

present in both cases. In particular the absence of any bands of uncombined SeO_2 in the solutions is conspicuous. In the deuterated system the OD bending frequency could not be observed as it falls in the region of strong absorption from SeO stretching near 900 cm^{-1}. Shifts of the hydrogen vibrations on passing from the crystal to solutions are not unexpected: it is, however, surprising that the deformation frequency should be shifted to the same extent (about 100 cm^{-1}) and in the same direction as the stretching frequencies.

The only peculiarity in the spectra of methanol solutions was the presence of a fairly strong absorption at 980 cm^{-1} which has no equivalent in either the aqueous solutions or in the crystalline acid. It resulted, no doubt, from oxidation of the alcohol by SeO_2, as shown by appearance, when it was left standing, of the characteristic red coloration of elemental selenium. For that reason these solutions were not studied further.

There is good agreement between our infrared frequencies and the Raman shifts reported by Venkateswaran (5, 6) for selenious acid solutions. For the crystal, however, his spectra have little in common with the present ones. Instead they resemble strangely

Can. J. Chem. Downloaded from www.nrcresearchpress.com by 78.46.186.204 on 09/04/12
For personal use only.

the Raman spectra of crystalline SeO_2 (14), which raises the suspicion that his samples were partly dehydrated by heating. From his results Venkateswaran concluded to the existence of two molecular species, a dihydroxyl, symmetrical form (*a*) and an asymmetrical one (*b*), the two being in a state of dynamic equilibrium in proportions varying

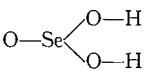

(*a*)

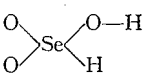

(*b*)

from phase to phase. This is obviously inconsistent with the observed permanence of all the infrared bands of selenious acid both in the solid state and in solutions over a wide range of concentration and temperature (25 to 90° C). In addition the asymmetrical form (*b*) is in contradiction with the X-ray data on the crystal (3) as well as the spectroscopic results of Detoni and Hadži (15) on a series of sulphinic and seleninic acids. Although the 2290 cm^{-1} frequency is of the right magnitude for a Se–H stretching mode (cf. 2260 and 2350 cm^{-1} in H_2Se) the fact that it is shifted to the same extent as the 2900 cm^{-1} frequency on going from crystal to solutions is sufficient proof that both vibrations involve OH groups. Selenium atoms do not normally participate in hydrogen bonding. Lastly, Venkateswaran's assignment of some of the solution bands, particularly that near 900 cm^{-1}, to the biselenite ion $HSeO_3^-$ cannot be correct in view of the very small dissociation constants of selenious acid ($k_1 = 2.4 \times 10^{-3}$ at 25° C).

In conclusion the behavior of selenium dioxide towards water may be contrasted with that of the corresponding oxides of sulphur and tellurium. Whereas SeO_2 displays high affinity for water as exemplified by a great solubility (63% by weight at ordinary temperature) and formation of a well-defined compound stable in the free state and in solutions, SO_2 is only moderately soluble (8.3% by weight) and the solutions contain no detectable amount of H_2SO_3 molecules. The greater polarity of the Se–O bond in the dioxide compared with S–O bond may be partly responsible for the marked difference in properties. This is also apparent in the existence of polymer-like chains in crystalline selenium dioxide (16). As for tellurium dioxide it is quite insoluble in water, and it is doubtful if there exists a definite tellurous acid, H_2TeO_3.

ACKNOWLEDGMENTS

The authors are grateful to the National Research Council for financial help, to the Consolidated Mining and Smelting Co. for a fellowship (M.F.), and to Dr. E. M. Elkin, for a generous sample of very pure selenium dioxide.

RÉSUMÉ

On a étudié les spectres infrarouges de l'acide sélénieux à l'état cristallin et en solution dans l'eau et le méthanol. Les résultats s'accordent avec l'existence de molécules bien définies ayant la formule symétrique

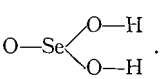

.

Les spectres des solutions ne révèlent aucune trace de bioxyde de sélénium à l'état libre contrairement au cas du bioxyde de soufre.

REFERENCES

1. Falk, M. and Giguère, P. A. Can. J. Chem. **36**, 1121 (1958).
2. Jones, L. H. and McLaren, F. J. Chem. Phys. **28**, 995 (1958).

Can. J. Chem. Downloaded from www.nrcresearchpress.com by 78.46.186.204 on 09/04/12
For personal use only.

3. WELLS, H. G. and BAILEY, M. J. Chem. Soc. 1282 (1949).
4. DETONI, S. and HADŽI, D. J. chim. phys. **53**, 760 (1956).
5. VENKATESWARAN, C. S. Proc. Indian Acad. Sci. A, **3**, 533 (1936).
6. VENKATESWARAN, C. S. Proc. Indian Acad. Sci. A, **7**, 13 (1938).
7. FALK, M. Ph.D. Thesis, Laval University, Quebec, Que. 1958.
8. NAKAMOTO, K., MARGOSHES, M., and RUNDLE, R. E. J. Am. Chem. Soc. **77**, 6480 (1955).
9. MARCUS, R. A. and FRESCO, J. M. J. Chem. Phys. **27**, 564 (1957).
10. PETERSON, S. W. and LÉVY, H. A. Acta Cryst. **10**, 70 (1957).
11. STUART, A. V. and SUTHERLAND, G. B. B. M. J. Chem. Phys. **24**, 559 (1956).
12. SCHOMAKER, V. and STEVENSON, D. P. J. Am. Chem. Soc. **63**, 37 (1941).
13. PAULING, L. Nature of the chemical bond. Cornell Univ. Press, Ithaca, N.Y. 1940.
14. GERDING, H. Rec. trav. chim. **60**, 72 (1941).
15. DETONI, S. and HADŽI, D. J. Chem. Soc. 3163 (1955).
16. MCCULLOUGH, J. D. J. Am. Chem. Soc. **59**, 789 (1937).

Can. J. Chem. Downloaded from www.nrcresearchpress.com by 78.46.186.204 on 09/04/12
For personal use only.

Can. J. Chem. Downloaded from www.nrcresearchpress.com by 78.46.186.204 on 09/04/12
For personal use only.

THE STRUCTURE OF PYRROLE SALTS AND THE BASIC STRENGTHS OF SOME SIMPLE PYRROLES[1]

E. BULLOCK[2]

ABSTRACT

The infrared spectra of hydrohalide salts of some substituted pyrroles are typical of secondary amine salts. Unlike the free base, cryptopyrrole hydrochloride is easily hydrogenated. The basic strengths of cryptopyrrole and 2,4-dimethylpyrrole are calculated from ultraviolet spectroscopic data.

Contrary to statements in some textbooks and reviews, many substituted pyrroles show considerable basicity (1, 2, 3) and form salts with halogen acids (2, 4, 7, 8). It has been suggested that salt formation is an important step in the acid-catalyzed reactions of pyrroles (1, 2, 3, 5) and the basic property of the heterocyclic nitrogen atom may be a factor in the formation of III-type porphyrins from monopyrroles (6).

The action of dry hydrogen chloride on cryptopyrrole in ether was reported to give a dimer though the conditions were not specified exactly (9). The action of chlorine on a similar solution gave a low yield of a hydrochloride of the pyrrole (8). We obtained a good yield of this stable hydrochloride on treatment of cryptopyrrole in cold ether with dry hydrogen chloride. The salt regenerated the parent base on treatment with sodium acetate solution. The hydrochlorides of 2,4- and 2,5-dimethylpyrrole were isolated similarly but were less stable, especially in contact with the mother liquor. The parent bases could be regenerated from the salts, but after 1–2 hours standing, dimeric compounds were formed. In contact with picric acid solution the picrates of 2,4-dimethylpyrrole and cryptopyrrole behaved similarly; after 4 days the former yielded only the dimer picrate and the latter a mixture of dimer and monomer picrates.

The salts of pyrroles have been formulated as I or II (2, 3, 5) rather than as secondary amine salts, by direct reference to the resonance forms of pyrrole (10). The infrared spectrum of cryptopyrrole hydrochloride (Fig. 2) shows that it is most probably III.

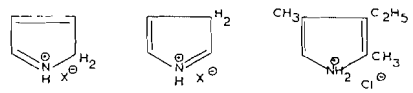

I II III

The spectrum shows no normal >NH stretching frequency (cf. Fig. 1, cryptopyrrole band at 3370 cm^{-1}) but has a broad strong band centered at 2630 cm^{-1}. The absence of "immonium" bands (11) at 2100–1980 cm^{-1}, although not conclusive, supports III rather than I or II. Coupled with the disappearance of the >NH band, a strong peak appears at 1575 cm^{-1} in the hydrochloride spectrum. Ring vibrations complicate assignments in this region but it seems likely that cryptopyrrole bands at 1597 and 1695 cm^{-1} move to 1650 and 1745 cm^{-1} respectively in the salt and that the 1575 cm^{-1} band is new. This band is considered (12) to be characteristic of the secondary amine salts. The infrared

[1]*Manuscript received August 28, 1958.*
Contribution from the Division of Pure Chemistry, National Research Council, Ottawa, Canada.
Issued as N.R.C. No. 4948.
[2]*National Research Council Postdoctorate Fellow.*

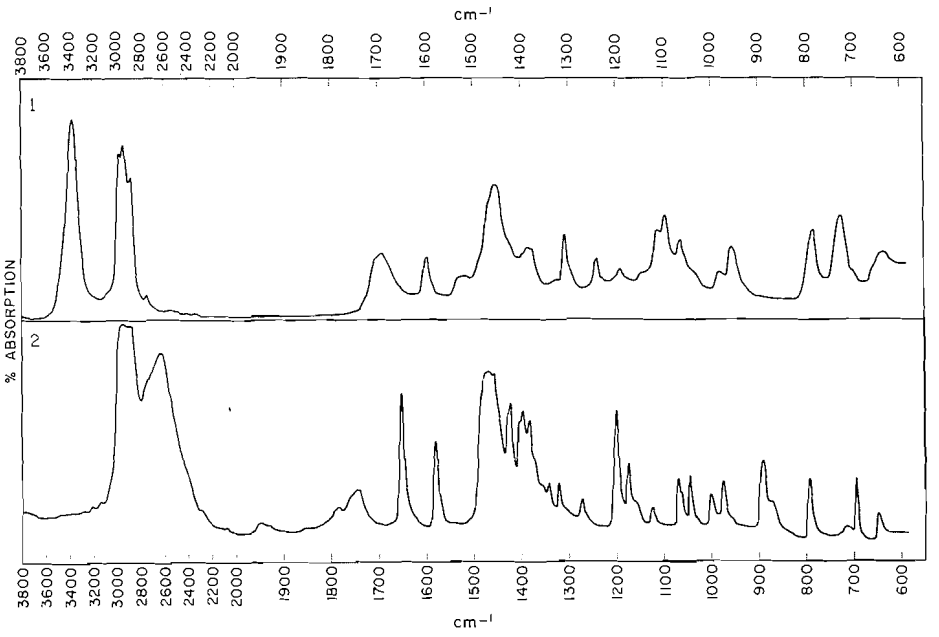

FIG. 1. Cryptopyrrole (thin film).
FIG. 2. Cryptopyrrole hydrochloride (nujol mull).

spectra of hemopyrrole- and cryptopyrrole-dicarboxylic acid hydrobromides show exactly analogous features. The picrates of 2,4-dimethylpyrrole and cryptopyrrole likewise show no normal $\rangle$NH absorption and are probably true salts.*

The ultraviolet spectra of cryptopyrrole and 2,4-dimethylpyrrole in normal hydrochloric acid are consistent with formulation of the salts as *cyclo*-pentadiene analogues (cf. 13). The additional alkyl group in cryptopyrrole causes a bathochromic shift of 11 mμ (λ_{max} 260 mμ compared with 249 mμ) in the main peak.

In neutral or alkaline solution at room temperature and atmospheric pressure, cryptopyrrole is not reduced by hydrogen over Adams' catalyst. In ethanolic hydrochloric acid under these conditions it rapidly takes up 1 mole of hydrogen, further reduction being very slow. The analysis of the product, its behavior with permanganate in acetone, and the infrared spectrum suggest that it is the Δ^3-pyrroline IV (15). As anticipated, the less basic pyrroles V and VI, whose ultraviolet spectra are unchanged by the addition of acid (cf. 14), were not reduced in similar conditions.

The pK_a's of cryptopyrrole and 2,4-dimethylpyrrole were determined by an ultraviolet spectroscopic technique (e.g. 16, 17). Solutions of the bases in various strengths of hydrochloric acid were used, rather than buffer solutions. The error introduced by

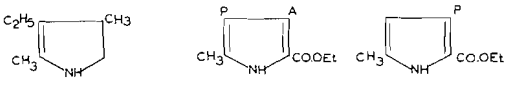

IV V VI

P = $CH_2.CH_2.CO.OEt$
A = $CH_2.CO.OEt$

The author is indebted to a referee for advice on the infrared assignments.

Can. J. Chem. Downloaded from www.nrcresearchpress.com by 78.46.186.204 on 09/04/12
For personal use only.

assuming that the pH of the solution is that of the acid is less than 2% for spectroscopic amounts of the base in 0.01 *N* acid.

The pK_a of the conjugate acid to cryptopyrrole is 2.84 and that of 2,4-dimethylpyrrole is 2.12. Allowing 0.7 units of p*K* per alkyl group and neglecting possible "positional" effects, the pK_a of pyrrole is estimated as 0.7. A previous estimate (18) gives the value 0.4. Attempts to measure the pK_a's of variously substituted alkyl pyrroles by other methods are in progress.

From these results it is concluded that: (*a*) In absence of acid, attack of electrophilic reagents may occur at the nitrogen atom of pyrroles. The known structure of the products of such reactions requires that the intermediate rearranges to give α-substituted derivatives. (*b*) In acid solution, the observed catalysis of some pyrrole reactions may be due to salt formation. The $\rangle NH_2^+$ group causes intense polarization of the diene system resulting in high electron density at the 2,5- (α-) positions.

EXPERIMENTAL

Melting points are uncorrected.

Cryptopyrrole Hydrochloride

A solution of the pyrrole (3 g) in dry ether (60 ml) was cooled in an ice bath and saturated with dry hydrogen chloride (3–5 minutes). The precipitated solid was filtered and washed with dry ether (5×20 ml) then dried in a vacuum desiccator over caustic soda. The product (3.2 g) was crystallized from alcohol–ether to large colorless needles, m.p. 109–117 (decomp.). Ehrlich reaction was positive cold. The product is stable *in vacuo* in the dark and is not deliquescent when free of cryptopyrrole (cf. 2, 7). Solutions in water and ethanol are acidic. Calc. for $C_8H_{14}NCl$ (monomer hydrochloride): Cl, 22.33. Calc. for $C_{16}H_{26}N_2Cl$ (dimer hydrochloride): Cl, 12.58. Found: Cl, 21.51. (Dried at room temperature *in vacuo*.) Infrared spectrum (nujol mull): Fig. 1. The spectroscopist reported that the sample became red during the determination. λ_{max} (1 *N* hydrochloric acid): 260 mμ; log ϵ: 3.56. The material sublimes slowly under water-pump vacuum (60–70° at 12 mm with some decomposition) to a white solid, m.p. 114–117° (decomp.), which slowly turns red on exposure to air.

Regeneration of the Parent Base

A solution of the salt in water was treated with sodium acetate and extracted with ether. The ether layer was washed with water and treated with picric acid. Yellow needles of cryptopyrrole picrate, m.p. 134° alone or mixed with an authentic sample (lit. 137° (20)), were obtained.

2,4-Dimethylpyrrole Hydrochloride

Freshly distilled 2,4-dimethylpyrrole (3.1 g) was dissolved in dry ether (60 ml) and cooled in an ice bath. A rapid stream of dry hydrogen chloride was bubbled through the solution (2–3 minutes) when a semisolid precipitate was formed. The ether was decanted and the product was washed with dry ether (3×50 ml) then taken up in water and neutralized with sodium acetate. The ethereal extract of this solution was washed with water and dried over potassium carbonate. Removal of the ether yielded an almost colorless oil (1.95 g) which distilled almost completely under reduced pressure (b.p. 56.5° at 11 mm).

A sample of the oil was converted to the picrate giving large yellow plates. The picrate is dimorphic showing signs of melting at 56°, accompanied by a collapse of the crystal structure to fine needles, m.p. 92–93° (lit. 91–92° from ethanol–ether (20)).

Can. J. Chem. Downloaded from www.nrcresearchpress.com by 78.46.186.204 on 09/04/12
For personal use only.

A sample of the oil was treated with phenyl isothiocyanate and warmed on the steam bath. After 10 minutes the solid product was crystallized from heptane to large yellow needles, m.p. 111–113° (authentic sample 112–114° (19)). Ultraviolet absorption of the pyrrole in acid, λ_{max}: 249 mμ; log ϵ: 3.43.

2,5-Dimethylpyrrole Hydrochloride

The pyrrole (4.35 g) was treated as above, the colorless oil (1.43 g) liberated from the hydrochloride distilled at 60.0° at 11 mm.

Action of Hydrogen Chloride on α-Methylpyrrole

Under the conditions described above the only product recovered was a solid, probably the dimer.

Reduction of Cryptopyrrole

(*a*) *Acid solution.*—Cryptopyrrole (3.83 g) was dissolved in ethanol (40 ml) saturated with hydrogen chloride and Adams' catalyst (75 mg) was added. The material was hydrogenated at room temperature and atmospheric pressure for 2 hours, after which time 650 ml of hydrogen (almost 50% of theoretical amount for complete reduction) had been absorbed. (In a separate experiment, the uptake was approximately 65% after 6 hours.) The platinum was filtered off over "Celite" and the alcohol removed *in vacuo*. The residue was treated with sodium hydroxide solution (50 ml, 10% w/v) and extracted with ether (3×50 ml). The ethereal extract was washed with water and then re-extracted with a near-saturated solution of potassium dihydrogen phosphate in water (3×50 ml). The yellow phosphate extract was neutralized with sodium hydroxide and the liberated base was collected by further ether extraction (3×50 ml). This ether was well washed with water (5×50 ml), fresh ether being added to maintain the volume of the ethereal layer, and dried over sodium sulphate. Removal of the ether left a pale yellow oil (3.21 g) which gave no Ehrlich reaction. Distillation gave a main fraction, b.p. 152–155° (1.26 g). Calc. for $C_8H_{15}N$: C, 76.79; H, 12.09; N, 11.20. Found: C, 76.50; H, 12.07; N, 11.27. Infrared spectrum (thin film): 3280, 2960, 2890, 1680 (shoulder), 1650, 1550, 1462, 1383, 1305, 1250, 1045, 960 cm^{-1}. α-Naphthylurethane recrystallized from aqueous ethanol. Calc. for $C_{19}H_{22}ON_2$: C, 77.51; H, 7.53; N, 9.52. Found: C, 77.01; H, 7.94; N, 8.95. The picrate, m.p. 157–159°, crystallized in thick needles from ethanol–ether.

(*b*) *Neutral solution.*—In a similar experiment to that described in (*a*) but employing 95% ethanol, no hydrogen was absorbed beyond that required for the catalyst.

(*c*) *Alkaline solution.*—In ethanolic solution containing sodium ethoxide (approximately 2% w/v) the cryptopyrrole absorbed no hydrogen.

Attempted Reduction of Carboxylated Pyrroles

In conditions similar to those given in (*a*) above, cryptopyrrole tricarboxylic acid – triethyl ester (V) and 2-methyl-5-carbcthoxypyrrole-4-propionic acid ester (VI) were not reduced.

Determination of pK_a *Values*

Solutions containing spectroscopic amounts of the pyrroles in 1 *N*, 0.1 *N*, and 0.01 *N* hydrochloric acid (0.9–1.7 mg in 25 ml of acid) were prepared and the spectra were recorded from 300 mμ to 208 mμ on a Cary self-recording instrument. The operation of the instrument required approximately 4 minutes, the total time elapsing from completion of the weighing being about 10 minutes. It was found that the spectra were substantially unchanged after 30 minutes' standing, although the solutions became slightly

Can. J. Chem. Downloaded from www.nrcresearchpress.com by 78.46.186.204 on 09/04/12
For personal use only.

colored. The spectra of the free bases were recorded in 95% ethanol and the pK_a values were calculated in the usual way (17).

Analyses are by Mr. H. Seguin and the infrared spectra were determined by Mr. R. Lauzon.

REFERENCES

1. TREIBS, A., HERRMANN, E., MEISSNER, E., and KUHN, A. Ann. **602**, 153 (1957).
2. TREIBS, A. and KOLM, H. G. Ann. **606**, 166 (1957).
3. TREIBS, A. and FRITZ, G. Ann. **611**, 162 (1957).
4. STEDMAN, R. J. and MACDONALD, S. F. Can. J. Chem. **33**, 468 (1955).
5. SMITH, G. F. and POTTS, H. A. J. Chem. Soc. 4018 (1957).
6. BULLOCK, E., JOHNSON, A. W., MARKHAM, E., and SHAW, K. B. J. Chem. Soc. 1430 (1958).
7. FISCHER, H., BAUMANN, E., and REIDLE, H. J. Ann. **475**, 205 (1929).
8. PRATESI, P. Gazz. chim. ital. **65**, 658 (1935).
9. FISCHER, H. Ber. **48**, 401 (1915).
10. INGOLD, C. K. Structure and mechanism in organic chemistry. Cornell Univ. Press, Ithaca, N.Y. 1953. p. 176.
11. WITKOP, B. J. Am. Chem. Soc. **76**, 5597 (1954). WITKOP, B., PATRICK, J. B., and KISSMAN, H. M. Chem. Ber. **85**, 949 (1952).
12. HEACOCK, R. A. and MARION, L. Can. J. Chem. **34**, 1782 (1956).
13. POWELL, J. S. and EDSON, K. C. Anal. Chem. **20**, 510 (1948).
14. COOKSON, G. H. J. Chem. Soc. 2791 (1953).
15. LEONARD, N. J. and GASH, V. W. J. Am. Chem. Soc. **76**, 2781 (1954).
16. ALBERT, A., GOLDACRE, R., and PHILLIPS, J. J. Chem. Soc. 2240 (1948).
17. FLEXSER, L. A., HAMMETT, L. P., and DINGWALL, A. J. Am. Chem. Soc. **57**, 2103 (1935).
18. HALL, N. F. J. Am. Chem. Soc. **52**, 5115 (1930).
19. BULLOCK, E. Unpublished work.
20. FISCHER, H. and BARTHOLOMAUS, E. Z. physiol. Chem. **80**, 8 (1912).

Can. J. Chem. Downloaded from www.nrcresearchpress.com by 78.46.186.204 on 09/04/12
For personal use only.

Can. J. Chem. Downloaded from www.nrcresearchpress.com by 78.46.186.204 on 09/04/12
For personal use only.

DISTRIBUTION OF NUCLEAR CHARGE IN THE PROTON-INDUCED FISSION OF Th^{232} [1]

B. D. Pate,[2] J. S. Foster, and L. Yaffe

ABSTRACT

The cross sections for the independent formation of I^{130}, I^{131}, Te^{131}, I^{132}, and I^{134} and for the cumulative formation of Te^{132}, I^{133}, and I^{135} in the proton-induced fission of Th^{232} have been measured at nine proton energies between 8 and 87 Mev. From these data and from published total chain yield data, charge distribution curves have been obtained. These are compared with published charge distribution curves for uranium fission at energies up to 480 Mev and together they show a shift of the most probable fission product charge toward stability and a widening of the distribution with increasing bombarding energy. These phenomena are interpreted in terms of current models for nuclear reactions.

INTRODUCTION

A voluminous literature exists on the distribution of nuclear mass in the fission process. In spontaneous fission (31) and in the fission of U^{233}, U^{235}, and Pu^{239} with neutrons of thermal energy, the familiar double-peaked distribution, corresponding to a preponderance of asymmetric fission modes, is observed (30). As the energy of bombarding particles is increased the mass distribution in the fission of these and other heavy nuclei becomes more and more symmetric (18, 33) and at sufficiently high energies a singly peaked distribution is observed (19).

About the nuclear charge distribution less is known. Data exist on the distribution from the fission of U^{235} with thermal neutrons (6, 7, 21) and with 14-Mev neutrons (34). Data also exist for the fission of uranium by 170-Mev protons (1), of bismuth by 190-Mev deuterons (10), and of uranium, thorium, and bismuth by 480-Mev protons (16), and there is fragmentary information from other systems. The present work was undertaken to investigate the changes that occur in the charge distribution from proton-induced fission of Th^{232} as the bombarding energy is raised from 8 to 90 Mev, the maximum proton energy of the McGill synchrocyclotron. This energy range is of interest in view of the substantial changes observed in the mass distribution (33). Also in this interval a change presumably begins in the nature of the initial step in nuclear reactions, from simple compound nucleus formation to a mechanism of direct interaction with individual nucleons (29). Thus at the lower energies studied, excitation of the nuclei at the end of the first step of the reaction will be essentially monochromatic whereas at the higher end of the bombarding energy range, a broad spectrum of excitation energies will be produced, with corresponding complexity of the reaction products observed. Ideally, in the determination of a charge distribution, one would wish to measure the independent yields of each of the nuclides in one or more fission chains. This, however, is precluded by the short half-lives of most of the members of any given mass chain. One substitutes a determination of independent yields of accessible nuclides in chains of different mass number, followed by correlation of these data. Correlation is customarily attempted by means of semiempirical or theoretical relationships (6, 7, 21, 27, 35) that

[1]*Manuscript received July 22, 1958.*
Joint contribution from the Radiochemistry Laboratory, Department of Chemistry, and the Radiation Laboratory, Department of Physics, McGill University, Montreal, Que., and the Department of Chemistry, Brookhaven National Laboratory, Upton, Long Island; with financial assistance from the Defence Research Board, the Atomic Energy Control Board of Canada, and the U.S. Atomic Energy Commission.
[2]*Present address: Department of Chemistry, Brookhaven National Laboratory, Upton, Long Island, N.Y.*

give the most probable nuclear charge, Z_p, for a given mass number A. Here Z_p is that charge value at which the peak of the charge distribution occurs, this not necessarily being an integral value. Distribution of yields around the most probable charge is usually assumed to be Gaussian and to be identical for all mass chains. These assumptions appear to be substantiated by much of the experimental evidence.

In the present experiment, yields of some iodine and tellurium nuclides in the mass region 130–135 were measured. The data have been correlated to give a charge distribution in this mass region under the assumptions that the distribution is symmetric about Z_p and that over the mass range investigated Z_p is displaced a constant amount from the Z_A value given by Pappas (21). (Z_A is that charge value, not necessarily integral, corresponding to stability for a given A.) A study over a mass range as small as six units does not provide sufficient data to test theories on the variation of Z_p with A.

EXPERIMENTAL TECHNIQUES AND RESULTS

1. Target and Irradiation

Thorium metal foil of about 190 mg/cm^2 superficial density was employed as the target material and was irradiated in the internal circulating proton beam of the McGill 82-in. synchrocyclotron. In all experiments, but the one at lowest energy, foils were irradiated in stacks of three, and the middle foil was used for the iodine yield determination. Loss of fission fragments by recoil from the target foil was thus compensated for by gain of recoils from the neighboring foils. In the lowest energy bombardment (8 Mev) energy loss considerations precluded the use of more than a single foil.

Upstream from the thorium was a monitor foil, again with a guard foil on both sides. For proton energies of 35 Mev and above, aluminum foils were used and beam intensities monitored via the $Al^{27}(p,3pn)Na^{24}$ reaction. The excitation function given by Hintz and Ramsey (13) was used with the cross-section scale reduced by a factor of 41/49, as indicated by the work of Crandall *et al.* (4). For lower energies copper monitor foils were used, the monitor reaction then being at 8 Mev, $Cu^{63}(p,n)Zn^{63}$ and at 26 Mev, $Cu^{65}(p,pn)Cu^{64}$. Here the cross-section data of Meadows (17) were used, with the appropriate scale correction. The leading edge and the top and bottom edges of the stack of six foils were aligned prior to bombardment by shearing with scissors after the foils had been clamped in the target holder.

The foils were mounted on a water-cooled probe and inserted into the cyclotron tank to a radius appropriate for the desired proton energy, using the data of Kirkaldy (15). Bombardments of 10–20 minutes and beam currents of the order of 10^{15} protons/cm^2 min were employed.

2. Chemical Processing and Measurement

After rapid removal of the target from the cyclotron probe and transfer to the radiochemistry laboratory, the thorium and monitor foils were sheared with scissors from the target clamp. This, together with the preliminary alignment described above, ensured that the monitor and target foils used in the experiment received the same flux. The middle target foil of the stack of three irradiated and likewise the middle monitor foil were selected for processing.

Three timed-separations of iodine activity from the irradiated target foil were accomplished by procedures previously described (8, 14, 34). The target foil was dissolved in concentrated hydrochloric acid, to which a known quantity of iodine (about 10 mg)

Can. J. Chem. Downloaded from www.nrcresearchpress.com by 78.46.186.204 on 09/04/12
For personal use only.

in the form of iodide had been added, and the last traces of residue were dissolved by addition of ammonium silicofluoride. The solution was then made up to volume and an aliquot taken for the first iodine separation.

The aliquot was transferred to a separatory funnel and diluted with hydrochloric acid. An equal volume of carbon tetrachloride was then added, followed dropwise by 10% hydrogen peroxide to slight excess. The iodine produced was extracted into the carbon tetrachloride and the phases separated, the time from the end of the bombardment to the separation being noted. The iodine activity was purified by three cycles of extraction of iodine from the carbon tetrachloride layer by a saturated sulphur dioxide solution, followed by acidification of the aqueous extract with 6 *M* nitric acid, reoxidation of the iodine with 1 *M* sodium nitrite solution, and re-extraction into carbon tetrachloride. The iodine was finally extracted from the organic layer with slight excess of SO_2 water, and the aqueous solution made up to volume. Aliquots (1%) were taken and mounted for 4π-counting. The mounts used were 5–10 $\mu g/cm^2$ VYNS films coated with 2–5 $\mu g/cm^2$ of gold (22). A 100 λ aliquot of the separated iodide solution was pipetted, followed by pipette washings, on to the film, followed by 100% excess of 0.1 *M* silver nitrate solution. The resulting colloidal silver iodide solution was then rapidly evaporated to dryness, the time at which the last of the solution disappeared being taken as the time of separation from xenon-daughter activities. The sample was then placed in a 4π-counter and the disintegration rate measured as a function of time by techniques described elsewhere (23, 24, 25, 26). Measurements were made first at 15-minute intervals, later less frequently, and extended for 5 to 6 weeks from the end of bombardment.

Successive 1% aliquots from the separated iodine solution were mounted at intervals, 6-hourly at first, thereafter daily until all 20-hour I^{133} had decayed and no further xenon-daughter activities were being produced.

The time from the end of the bombardment to the first iodine separation was about 20 minutes. Further iodine separations were performed on additional aliquots of the dissolved thorium solution 2–3 hours and again 2–3 days after the end of bombardment. The procedure followed in each case was the same as that described above.

After the elapse of a time interval sufficient to allow substantial decay of iodine activity, semimicrogravimetric determination of iodine as AgI was performed on each of the three iodine solutions, to establish the chemical yields in the separations. The yields averaged about 70% so that the quantity of iodine carrier originally added resulted in less than 100 μg of AgI in the samples used for disintegration rate measurements.

As soon as convenient after the end of the bombardment, the middle monitor foil was dissolved in an appropriate acid, nitric for copper, hydrochloric for aluminum. The solution was made up to volume and a suitable aliquot (0.1–1%) mounted on a VYNS film for 4π-counting, as described above. Counting-rate measurements over several days followed by decay curve analysis allowed the counting rates of 38-minute Zn^{63}, 12.8-hour Cu^{64}, and 15.0-hour Na^{24} at the end of bombardment to be determined.

It is well known that active iodine produced in the fission of uranium and thorium in the form of oxides and oxysalts does not exchange readily with carrier iodide. The chemical separation of iodine activity from uranium metal targets by a procedure involving oxidation of carrier iodide to iodine and extraction into CCl_4 is reported (14) to be 100% complete. It was felt desirable to check this behavior with thorium metal for possible use in the present work. Accordingly, an irradiated thorium metal target was dissolved as above in the presence of iodide carrier. Two aliquots were then taken

Can. J. Chem. Downloaded from www.nrcresearchpress.com by 78.46.186.204 on 09/04/12
For personal use only.

and an iodine separation was performed on each. One was treated by the procedure outlined above, and the other by the usual procedure for the separation of iodine from uranium oxysalts (8). The latter involved the oxidation of the iodine to periodate by sodium hypochlorite in sodium hydroxide solution, followed by acidification of the solution with nitric acid and reduction of the iodine to the elementary form with hydroxylamine. Yields from the two separations (after correction for carrier recoveries) were identical within experimental error. Consequently the faster separation by peroxide oxidation of the iodide was adopted, as detailed earlier.

3. Results

The iodine and xenon activities which might be expected to appear in a sample separated from the products of a fission reaction are listed, together with their decay characteristics, see Table I. The list does not include isotopes which, because of their very long or short half-lives, would not be detectable in the present experiments.

TABLE I

DECAY CHARACTERISTICS OF IODINE AND XENON ISOTOPES*

Isotopes	Mode of decay	Half-life	Beta group energies and abundances	Gamma transition energies and abundances
I^{128}	β^-, E.C.	25.0 m	1.125 Mev 2.0% 1.665 Mev 15.5% 2.120 Mev 76.0%	0.455 Mev 17.2% 0.540 Mev 1.8% 0.750 Mev 0.31% 0.990 Mev 0.29%
I^{130}	β^-	12.5 h	0.597 Mev 54% 1.02 Mev 46%	0.409 Mev 8.8% 0.528 Mev 29% 0.660 Mev 26% 0.744 Mev 24% 1.15 Mev 11.8%
I^{131}	β^-	8.05 d	0.250 Mev 2.8% 0.335 Mev 9.3% 0.608 Mev 87.2% 0.815 Mev 0.7%	0.080 Mev 2.2% 0.284 Mev 5.3% 0.364 Mev 80% 0.637 Mev 9% 0.722 Mev 3%
Xe^{131m}	IT	12.0 d	—	0.163 Mev 100%
I^{132}	β^-	2.3 h	0.73 Mev 15% 0.9 Mev 20% 1.16 Mev 23% 1.53 Mev 24% 2.12 Mev 18%	0.528 Mev 10% 0.624 Mev 2.4% 0.673 Mev 37.6% 0.777 Mev 32% 0.96 Mev 8% 1.16 Mev 3.2% 1.40 Mev 4.4% 1.96 Mev 2% 2.2 Mev 1%
I^{133}	β^-	20.9 h	0.5 Mev 6% 1.4 Mev 94%	0.53 Mev 94% 0.85 Mev 5% 1.4 Mev 1%
Xe^{133m} (Formed in 2.4% of I^{133} decays)	IT	2.3 d	conv. $e^-(\alpha_k = 4.4)$	0.233 Mev 100%
Xe^{133}	β^-	5.27 d	0.345 Mev 100%	0.081 Mev 100%
I^{134}	β^-	52.4 m	1.6 Mev 70% 2.8 Mev 30%	0.86 Mev 1.10 Mev 1.78 Mev
I^{135}	β^-	6.75 h	0.5 Mev 35% 1.0 Mev 40% 1.4 Mev 25%	1.8 Mev 1.27 Mev
Xe^{135}	β^-	9.2 h	0.55 Mev 3% 0.910 Mev 97%	0.25 Mev 96% 0.36 Mev 0.1% 0.604 Mev 3%

*These data are "best values" derived from Nuclear Science Abstracts, National Research Council, Washington, D.C.

Can. J. Chem. Downloaded from www.nrcresearchpress.com by 78.46.186.204 on 09/04/12
For personal use only.

The mixture of activities obtained from each separation was checked for radiochemical purity in two ways.

(*a*) *Gamma-radiation Measurements*

Gamma spectra were observed from suitable aliquots of the iodine activity stock solutions, by means of a $1\frac{1}{2}$ in. × 1 in. NaI (Tl) crystal with a Dumont 6292 photomultiplier, an Atomic Energy of Canada Limited amplifier (AEP 1448), and a single channel pulse-height analyzer. Figure 1 shows the spectra obtained at various times after the end of bombardment from a sample of iodine separated at 24 minutes after the end of bombardment from a thorium target irradiated with 26-Mev protons.

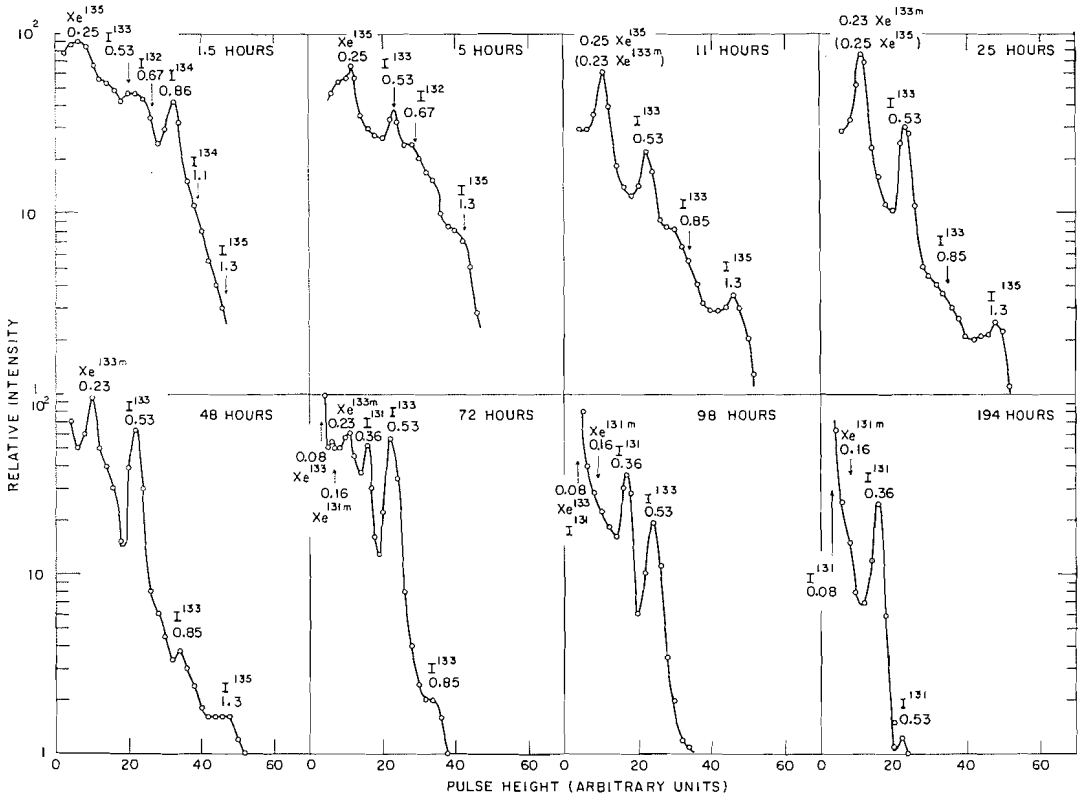

FIG. 1. Gamma spectra of iodine + xenon fission product mixture at various times after the end of bombardment.

The photopeaks are identified as to energy and isotope as indicated, and the positions at which other prominent γ lines in the decay schemes of the various iodine or xenon isotopes would be expected to appear are indicated by arrows.

It is seen that there are no features of the spectra which are inconsistent with the composition of the expected isotope mixture, either as to line energies or intensities. However, these measurements obviously do not constitute a very sensitive test for the presence or absence of activities other than those of iodine or xenon.

(*b*) *Beta-radiation Measurements*

The results of the analysis of beta-activity determinations, which are described below,

Can. J. Chem. Downloaded from www.nrcresearchpress.com by 78.46.186.204 on 09/04/12
For personal use only.

constituted a more rigorous check on the effectiveness of the iodine purification procedure. The analysis of the decay curves in terms of the published half-life values in Table I was always successful, and in no case were decay periods observed other than those corresponding to iodine or xenon isotopes. The purification procedure was consequently considered to be satisfactory.

Figure 2 shows the analysis of a typical beta-decay curve obtained with a 4π-counter from iodine samples mounted as AgI as described earlier. The data are for the first sample separated from a target irradiated with 63-Mev protons. The open circles on the curve marked "iodine + xenon activity" represent observations made on a single sample mounted shortly after the end of the separation procedure. (The data presented extend over a 2-week period, but observations continued for a further month to assure positive identification of 8.05-day I^{131}.) The closed circles on the curve marked "iodine activity" represent observations made on a series of samples (one per plotted point) freshly mounted in succession from the stock iodine solution at intervals as described earlier. Since the data plotted were obtained promptly after mounting, they give closely the iodine disintegration rates alone at the times indicated, free of xenon-daughter contributions.

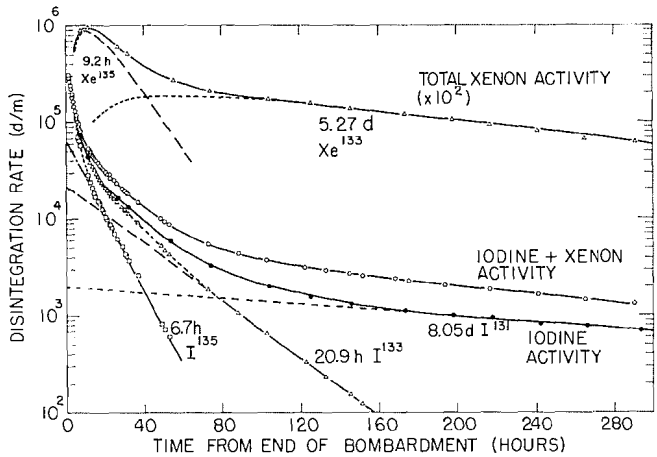

FIG. 2. Beta-decay curve of iodine + xenon fission product mixture.

The standard deviations on disintegration rate measurements were in general less than 1% and always less than the sizes of the plotted points.

The iodine + xenon data are more complete than the pure iodine data, since the mounting of successive samples was time-consuming, and more frequent preparations could not be fitted into the experimental schedule. However, the data can be combined to improve the definition of the pure iodine disintegration rate curve. The points plotted as open triangles on the curve marked "total xenon activity" are the result of the subtraction of one set of observations from the other, with the ordinate multiplied by 100 for reasons of clarity. From 120 hours after bombardment this curve exhibits an exponential decay with a half-period close to 5.27 days, corresponding to Xe^{133}. (The small scatter of the points, each representing a separate sample mounting, confirms the reproducibility of the procedure used.) From the intercept of the 5.27-day line with the ordinate, and from a knowledge of the time of separation and of parent half-life (20.9 hours), the

Can. J. Chem. Downloaded from www.nrcresearchpress.com by 78.46.186.204 on 09/04/12
For personal use only.

growth and decay curve of Xe^{133} can be calculated. The early part of this curve is shown as a broken line. Subtraction of this curve from points at abscissa values less than 120 hours gives new points which are well fitted by 9.2-hour Xe^{135} growing from 6.7-hour I^{135}, as indicated by the dashed line. Summing of these two curves gives the smooth total xenon curve. Interpolation from this curve makes possible the determination of xenon-daughter contributions to the total disintegration rate at times other than those at which fresh mountings were made. (Contribution of 2.3-day Xe^{133m} formed in a rare decay mode of I^{133} to the observed xenon activity was apparently not large enough to disturb this method of treatment of the data.)

Subtraction of the interpolated xenon activities from the iodine + xenon data now allows the pure iodine curve to be drawn accurately between the observations made. By the usual method of successive subtractions the iodine decay curves can be analyzed clearly into 8.05-day, 20.9-hour, and 6.7-hour components corresponding to I^{131}, I^{133}, and I^{135} as shown in the figure. In experiments involving proton energies in excess of 74 Mev the data are well fitted by the addition of a 12.5-hour component, corresponding to I^{130}.

After subtraction of these periods, the data at times less than 12 hours from end of bombardment showed an exponential decay with a half-life which varies between 1 and 2 hours, presumably corresponding to a mixture of 52-minute I^{134} and 2.3-hour I^{132}, which the subtraction technique cannot resolve. The resolution is effected by a method originally due to Ford (5), in which the data are fitted to the sum of two exponential terms of the form:

$$A_t = A_1^{\circ} e^{-\lambda_1 t} + A_2^{\circ} e^{-\lambda_2 t},$$

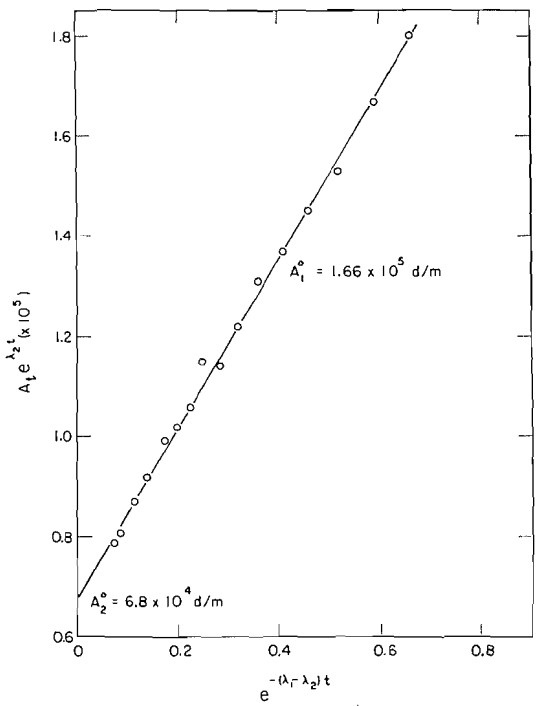

FIG. 3. Ford plot of beta-decay data for I^{132} and I^{134}.

Can. J. Chem. Downloaded from www.nrcresearchpress.com by 78.46.186.204 on 09/04/12
For personal use only.

where A_t is the combined activity at time t, and $A_1°$ and $A_2°$ are the initial activities of components 1 and 2. Then.

$$A_t\, e^{\lambda_2 t} = A_2° + A_1°\, e^{-(\lambda_1-\lambda_2)t}.$$

Therefore in a plot of $A_t\, e^{\lambda_2 t}$ versus $e^{-(\lambda_1-\lambda_2)t}$ using the disintegration rate versus time data for A_t and the appropriate decay constants of I^{132} and I^{134} for λ_1 and λ_2, the initial activities of the two isotopes are obtained as the slope of the curve and as the intercept with the ordinate axis respectively.

Figure 3 shows a typical plot of this nature. The success of the fit was in all cases shown by the linear plot obtained, indicating the absence, over the time interval studied, of activities other than the two anticipated. In particular no deviation from linearity at small t values was observed, indicating the absence of 25-minute I^{128} in the samples studied in these experiments. It should be emphasized that the success of the analysis procedure described is probably due in no small degree to the precision of the disintegration rate measurements made by the 4π-counting technique, especially the relative precision of a series of measurements made on the same sample.

TREATMENT OF THE DATA

From the experimental observations described above, two types of cross-section data were obtained. First, from the disintegration rates of given iodine isotopes, measured in samples separated from the irradiated target at times long compared with precursor half-lives, cumulative formation cross sections could be calculated. Secondly, from similar measurements made on samples separated shortly after the end of bombardment, independent formation cross sections for some iodine isotopes and cumulative formation cross sections for some tellurium isotopes could be calculated.

Our method of treatment of the data is essentially similar to that of Wahl (34). It differs in detail, because, particularly at higher bombarding energies, formation cross sections of the observed iodine isotopes are comparable with those of the tellurium precursors. This fact invalidates some of the approximations which are useful at lower energies. Likewise, in the comparison of fractional chain yields for various mass numbers, it is no longer reasonable to assume that iodine cumulative yields represented total yields of the respective masses. With increasing bombarding energies, an increasing fraction of these yields appears at atomic numbers higher than that of iodine. We have used published mass yield curves for the fission of Th^{232}, U^{235}, and U^{238} by projectiles of various energies, together with suitable interpolations and extrapolations, to obtain the variation of total chain fission yield over the mass range studied.

The generalized relationship between the activity $A_n(T, t)$ of the nth member of a decay series, at a time t after the end of a bombardment of duration T, in which the first member is formed at a constant rate r has been given by Rubinson (28) in the form:

$$A_n(T, t) = r \sum_{i=1}^{n} b_i(1-e^{-\lambda_i T})\, e^{-\lambda_i t}$$

where

$$b_i = \prod_{j \neq i} \frac{\lambda_j}{\lambda_j - \lambda_i} (j = 1, 2, \ldots, n)$$

and the λ's are appropriate decay constants.

Can. J. Chem. Downloaded from www.nrcresearchpress.com by 78.46.186.204 on 09/04/12
For personal use only.

This expression is useful in the construction of activity vs. time relationships for iodine nuclides, particularly where isomerism exists in the tellurium precursors. Thus in the generalized case of a decay scheme of the form

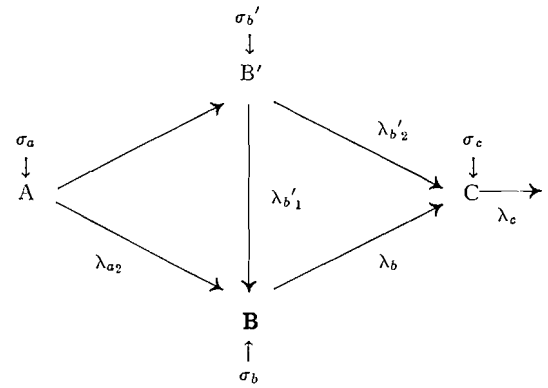

where σ's and λ's are formation cross sections and decay constants respectively (A, B, and C in the present work would be antimony, tellurium, and iodine isotopes), the appropriate expression for the activity of C after given irradiation and decay times may be obtained by summing contributions from the following decay routes:

$$\xrightarrow{\sigma_a} A \xrightarrow{\lambda_{a_1}} B' \xrightarrow{\lambda_{b'_2}} C$$

$$\xrightarrow{\sigma_a} A \xrightarrow{\lambda_{a_1}} B' \xrightarrow{\lambda_{b'_1}} B \xrightarrow{\lambda_b} C$$

$$\xrightarrow{\sigma_a} A \xrightarrow{\lambda_{a_2}} B \xrightarrow{\lambda_b} C$$

$$\xrightarrow{\sigma_{b'}} B' \xrightarrow{\lambda_{b'_2}} C$$

$$\xrightarrow{\sigma_{b'}} B' \xrightarrow{\lambda_{b'_1}} B \xrightarrow{\lambda_b} C$$

$$\xrightarrow{\sigma_b} B \xrightarrow{\lambda_b} C$$

$$\xrightarrow{\sigma_c} C$$

The assumption is implicit that the tin and earlier precursors of chains in the mass range 130–135 are too short-lived to have been observed in the present experiment. Their formation cross sections may be considered to add to those of the Sb precursors. In each case the rate of formation r in Rubinson's expression is given by

$$r_n = N\sigma_n f$$

where N and f are the number of target nuclei and bombarding particle flux respectively and σ_n is the appropriate cross section. Fortunately, however, it was possible to work with simpler expressions for reasons which will be discussed for each mass number.

A = 130.—I^{130} is shielded by stable Te^{130} from formation by decay of precursors. The activity observed at bombarding energies of 74 Mev and above was therefore due to direct formation. The independent formation cross section was calculated via the simple expression

$$\lambda_a N_a = N\sigma_a f(1-e^{-\lambda_a T})\, e^{-\lambda_a t}.$$

Can. J. Chem. Downloaded from www.nrcresearchpress.com by 78.46.186.204 on 09/04/12
For personal use only.

The failure to observe I^{130} at lower energies is assumed to have been due to the larger amounts of I^{135} formed which masked the activity.

A = 131.—The decay scheme (9, 11) of the 131 mass chain up to iodine is as follows:

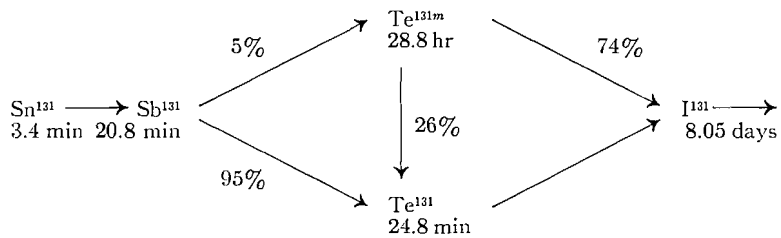

For the purposes of the present work two simplifications were made. First, the 5% branch in the decay of Sb^{131} leading to the metastable state of Te^{131} was neglected in view of the comparatively long half-life of Te^{131m}. Second, the 26% isomeric transition of Te^{131m} was ignored, and all of the decay of this body was taken to proceed directly to I^{131}. This is expected to have little effect on the calculations (34), since, at short times after the end of bombardment, little of the Te^{131m} will have decayed by either path, and after long times the effect of the 24.8-minute half-life of Te^{131} will be negligible.

Thus the approximate decay scheme is now

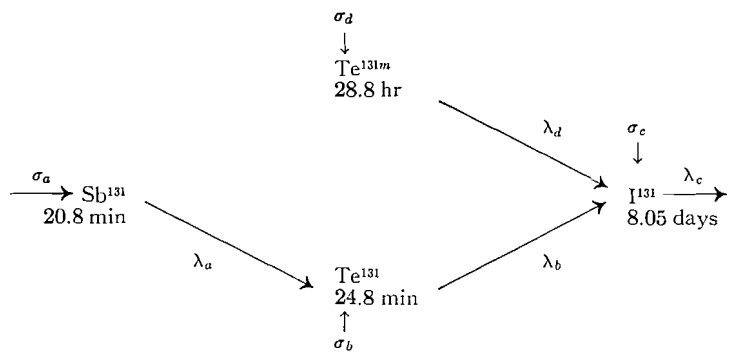

and the corresponding expression for the activity of I^{131}, obtained as outlined above:

$$\lambda_c N_c(T,t) = N\sigma_a f\left[\frac{\lambda_b\lambda_c}{(\lambda_b-\lambda_a)(\lambda_c-\lambda_a)}(1-e^{-\lambda_a T})\,e^{-\lambda_a t}+\frac{\lambda_a\lambda_c}{(\lambda_a-\lambda_b)(\lambda_c-\lambda_b)}(1-e^{-\lambda_b T})\,e^{-\lambda_b t}\right.$$
$$\left.+\frac{\lambda_a\lambda_b}{(\lambda_a-\lambda_c)(\lambda_b-\lambda_c)}(1-e^{-\lambda_c T})\,e^{-\lambda_c t}\right]$$
$$+N\sigma_b f\left[\frac{\lambda_c}{\lambda_c-\lambda_b}(1-e^{-\lambda_b T})\,e^{-\lambda_b t}+\frac{\lambda_b}{\lambda_b-\lambda_c}(1-e^{-\lambda_c T})\,e^{-\lambda_c t}\right]$$
$$+N\sigma_d f\left[\frac{\lambda_c}{\lambda_c-\lambda_d}(1-e^{-\lambda_d T})\,e^{-\lambda_d t}+\frac{\lambda_d}{\lambda_d-\lambda_c}(1-e^{-\lambda_c T})\,e^{-\lambda_c t}\right]$$
$$+N\sigma_c f(1-e^{-\lambda_c T})\,e^{-\lambda_c t}.$$

For each bombarding energy, this expression was used to obtain three equations relating σ_a, σ_b, σ_c, and σ_d by insertion of the decay-constant values for the 131 chain the irradiation time T, the measured values of N and f, and also the three measured

Can. J. Chem. Downloaded from www.nrcresearchpress.com by 78.46.186.204 on 09/04/12
For personal use only.

iodine disintegration rates corresponding to the three separation times. A unique solution for the value of σ_c was not obtainable, but an approximate value was obtained by a further series of simplifications.

First, from the data from two samples separated several hours and 3 days respectively after end of bombardment, the values of $\sigma_a+\sigma_b+\sigma_c+\sigma_d$ and of σ_d alone were calculated under the assumptions:

$$\begin{aligned}&\text{(i)} \quad \sigma_d = \sigma_a+\sigma_b+\sigma_c;\\ &\text{(ii)} \quad \sigma_d = 4\sigma_b;\ \sigma_a = 0;\\ &\text{(iii)} \quad \sigma_d = 4\sigma_b;\ \sigma_a = \sigma_b;\\ &\text{(iv)} \quad \sigma_a = \sigma_b = 4\sigma_b.\end{aligned}$$

The value of σ_d was assumed to be about four times that of σ_b, as was found by Glendenin (9) in the thermal fission of U^{235}. The value of $\sigma_a+\sigma_b+\sigma_c+\sigma_d$ was found to be unchanged from one assumption to another to within 5% and the value of σ_d to within somewhat smaller limits.

By means of an average of the values calculated, an upper limit on σ_b was now calculated under the extreme assumption that $\sigma_a = \sigma_c = 0$, and an upper limit on σ_c, under the assumption that $\sigma_a = \sigma_b = 0$. Calculations were also made for σ_b and σ_c under the intermediate assumptions $\sigma_a = \sigma_b = \sigma_c$ and $\sigma_a = 0$, $\sigma_b = \sigma_c$. From these results mean values were obtained for σ_b and σ_c together with some indication of the magnitude of the associated uncertainty. The uncertainty in the I^{131} formation cross section (σ_c) and in that for Te^{131} ($\sigma_b+\sigma_d$) from this source was far greater than the uncertainties arising from other sources in the experimental technique.

A = 132.—The decay scheme is as follows:

$$\underset{2\text{ min}}{Sb^{132}} \longrightarrow \underset{77.7\text{ hr}}{Te^{132}} \longrightarrow \underset{2.26\text{ hr}}{I^{132}}$$

In the present experiment, the time between the end of the irradiation and the first iodine separation was long compared with the Sb^{132} half-life. Consequently only a cumulative cross section for Te^{132} was obtained, together with an independent formation cross section for I^{132}. The appropriate activitity–time expression is

$$\begin{aligned}\lambda_b N_b(T,t) = N\sigma_a f\left[\frac{\lambda_b}{\lambda_b-\lambda_a}(1-e^{-\lambda_a T})\,e^{-\lambda_a t}+\frac{\lambda_a}{\lambda_a-\lambda_b}(1-e^{-\lambda_b T})\,e^{-\lambda_b t}\right]\\ +N\sigma_b f(1-e^{-\lambda_b T})\,e^{-\lambda_b t}.\end{aligned}$$

A = 133.—The 133 chain decay scheme is as follows (20):

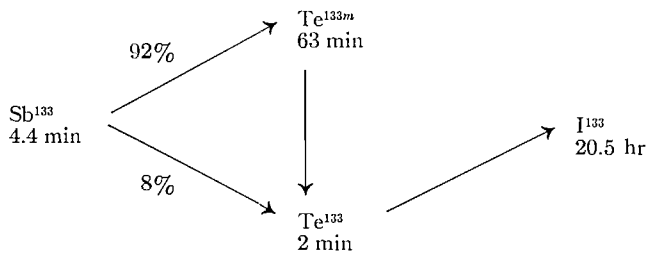

Again, the time of 20 minutes between end of bombardment and the first iodine separation made it impossible to obtain independent yield information about I^{133} or about the Te^{133}

Can. J. Chem. Downloaded from www.nrcresearchpress.com by 78.46.186.204 on 09/04/12
For personal use only.

ground state. Consequently, only cumulative formation cross sections for I^{133} were calculated, using disintegration rate data from samples separated 3 days after the end of bombardment and the expression given above under $A = 130$.

A = 134.—From the decay scheme

$$Sb^{134} \longrightarrow Te^{134} \longrightarrow I^{134}$$
$$0.8 \text{ min} \qquad 44.5 \text{ min} \qquad 52.4 \text{ min}$$

it is clear that the 20-minute separation time was in this case too long compared with the Sb^{134} half-life and indeed rather long compared with the Te^{134} half-life for the purposes of obtaining accurate independent yield data. However, the data from the 20-minute and 2–3-hour separations were analyzed using the activity–time expression given for the 132 chain, and independent formation cross sections calculated for I^{134}.

A = 135.—The precursors of I^{135} are not known and are presumably of very short half-life. Therefore, only a cumulative cross section for this isotope was obtained in this work, by means of the activity–time expression given above under $A = 130$.

RESULTS

The results of the analysis outlined above are presented in Figs. 4, 5, and 6 in the form of excitation functions, independent or cumulative formation cross sections being designated σ_{ind} or σ_{cum} respectively. Also on these figures are included, for comparison, excitation function data of Tewes and James (33) for the total proton-induced fission, with an ordinate scale as indicated to the right of the figure. The initial rise with energy of all the cross sections measured in this work is clearly associated with the corresponding rise in the total fission cross section. The decreasing cross sections at higher energies reflect the broadening and shift of the charge distribution, which will be demonstrated below.

The uncertainties associated with the cross-section data presented are estimated to

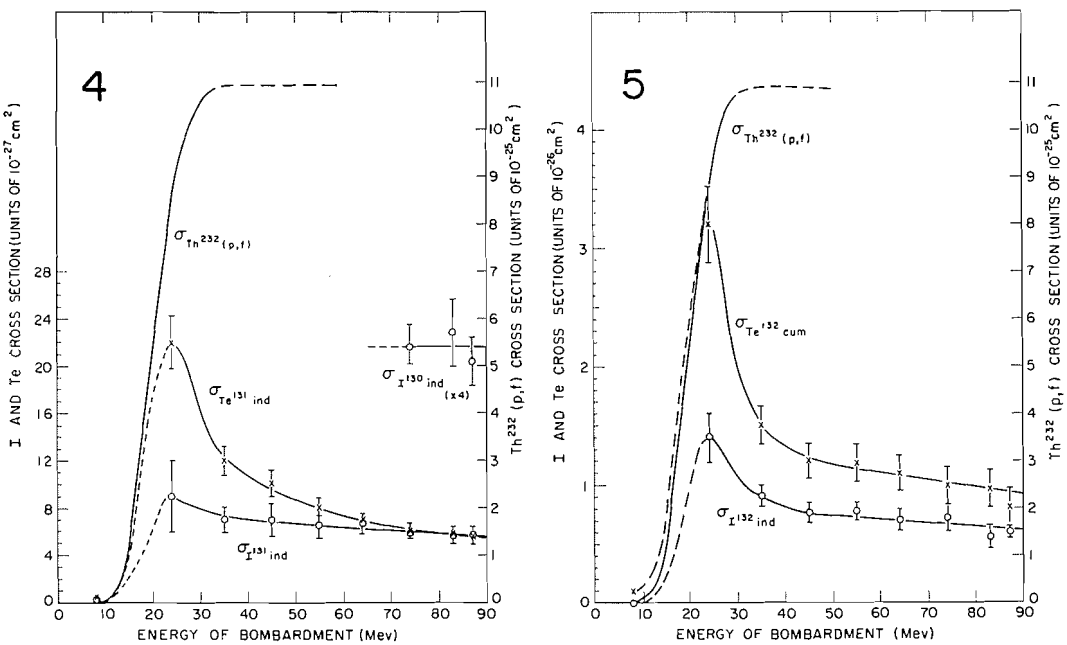

FIG. 4. Excitation functions for production of I^{130}, I^{131}, and Te^{131} in Th^{232} (p,f) reaction.
FIG. 5. Excitation functions for production of Te^{132} and I^{132} in Th^{232} (p,f) reaction.

Can. J. Chem. Downloaded from www.nrcresearchpress.com by 78.46.186.204 on 09/04/12
For personal use only.

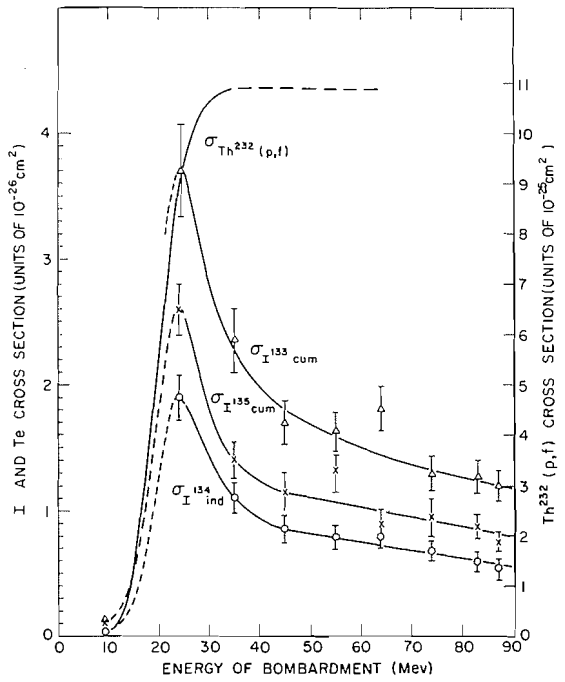

FIG. 6. Excitation functions for production of I^{133}, I^{134}, and I^{135} in Th^{232} (p,f) reaction.

be as follows: the exact proton energy at which the bombardment was made is uncertain due to energy spread in the cyclotron beam and to uncertainties in the calculated value of the energy loss in the target itself (2). Nevertheless, the beam energy was probably known to 2–5 Mev. The uncertainty in the cross-section values results from uncertainties in the original disintegration rate measurements (<1%), in the graphical decay curve analysis and associated extrapolations (5–10%), and from sources described earlier in the treatment of the activity data. The over-all uncertainty is thought to be 15–20%.

The cross-section data were converted into charge distribution curves for five bombarding energies by means of the mass yield data available in the literature and the total Th^{232} (p,f) cross-section data of Tewes and James (33) and of Steiner and Jungerman (32). The product of the fission yield for a given mass A and the total fission cross section gives the cumulative formation cross section for mass A. The division of the independent formation cross section for a given isobar of mass A by this cumulative formation cross section then gives that fraction of the mass chain formed directly as the particular isobar. These fractional values for the various iodine and tellurium nuclides were correlated in a plot versus the nuclide's displacement from stability along the isobaric chain. The assumptions implicit in such a correlation are that the distribution of yields along a chain is the same for chains of different mass, and that the displacement from stability of the charge value at which the highest yield occurs is independent of chain mass. Both assumptions are probably reasonable over the narrow region of mass (130–135) studied.

Tewes' and James' data (33) for the proton-induced fission of Th^{232} at energies of 8.0 and 21.1 Mev were used in conjunction with our data at 8 and 24 Mev, the mass yield data at 8 Mev being further checked by interpolation between the data of Wahl (34) on the 0-Mev (thermal) and 14-Mev neutron-induced fission of U^{235}. In the treatment of data in this paper at energies of 45 Mev and above, we have assumed that over the

Can. J. Chem. Downloaded from www.nrcresearchpress.com by 78.46.186.204 on 09/04/12
For personal use only.

mass range 130–135 the total chain yield was independent of mass number and energy at a value close to that indicated by Newton (18). Consideration of his results and of mass yield data at much higher energy (19) indicates that this assumption is probably not in error over the present energy range by more than $\pm 10\%$.

The error introduced by using mass yield data from projectile target systems other than the Th^{232} + proton system is probably small. The mass range studied in this work includes nuclides on the heavy peak of the fission yield curve, the position and height of which changes little with changing target mass number and like parameters.

The charge distribution curves for 8-, 24-, 45-, 64-, and 87-Mev proton energies are shown in Fig. 7, in which the fraction of the chain yield is plotted as ordinate against $Z_A - Z$ as abscissa, where Z_A is the Z-value corresponding to the minimum potential energy (maximum beta stability) for a given A (21). In this plot neutron-excess nuclides lie to the right of the figure and neutron-deficient ones to the left. The location of the Gaussian distribution plotted in each case was determined so that the area under it summed to unit total chain yield, and also so that the independent yields of Te^{132}, I^{133}, and I^{135} and their precursors, as obtained from the curve, summed to a value for the corresponding cumulative yields close to that measured experimentally. This latter is a sensitive criterion for location of the curve, and renders it much more certain than is at first apparent.

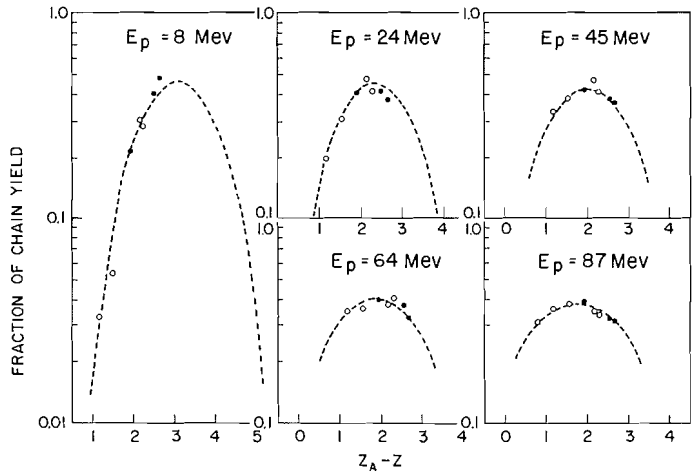

FIG. 7. Charge distribution curves in the Th^{232} (p,f) reaction at proton energies between 8 and 87 Mev.

The five charge distributions are shown assembled on Fig. 8, together with the curve of Glendenin (7) and Pappas (21) for thermal fission of U^{235}, of Wahl (34) for 14-Mev fission of U^{235}, of Aagaard *et al.* (1) for the 170-Mev proton-induced fission of uranium, and of Lavrukhina and Krasavina (16) for the 480-Mev proton-induced fission of uranium. The yield data of Aagaard *et al.* have been converted to a charge distribution in the manner outlined above, and those of Lavrukhina and Krasavina have been renormalized to give a distribution summing to unit chain yield. The position of the 170-Mev curve on the ordinate scale below the other curves is due to the fact that Aagaard *et al.* fitted their data to a wider distribution than those used by the other authors. The position of their curve on the abscissa scale in relation to the others presented, which is of more significance, is not affected by the normalization to unit chain yield.

Can. J. Chem. Downloaded from www.nrcresearchpress.com by 78.46.186.204 on 09/04/12
For personal use only.

In Table II the displacement of the maximum of the charge distribution from stability and the "half-width" of the distribution are tabulated with bombarding energy.

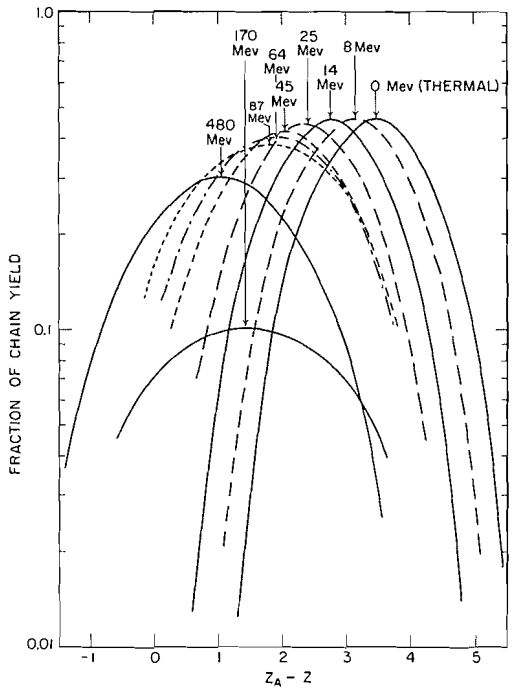

FIG. 8. Assembled charge distribution curves for thorium and uranium fission between 0 and 480 Mev bombarding energy.

DISCUSSION

The data in Table II show two effects. With increasing energy of bombarding particle, the charge distribution is observed to move towards stability, rapidly at first and then more slowly at higher energies. Secondly, while the width of the distribution remains approximately constant up to 25 Mev, at higher energies it shows evidence of increasing with increasing energies.

These effects may be rationalized in terms of a two-step model for nuclear reactions. In this model the projectile undergoes an initial rapid ($\sim 10^{-21}$ second) interaction with the target nucleus. The interaction will be predominantly the formation of a compound nucleus (3) for energies up to approximately 50 Mev. As the energy is raised above 50 Mev interaction with individual nucleons (12, 29) associated with prompt ejection of some nucleons becomes increasingly important. After this initial stage has terminated, the excitation energy deposited is dissipated in a second slower stage, largely by a particle-emission process described as nuclear evaporation, with which fission competes in heavy nuclei.

The shift of the charge distribution with increasing energy, which corresponds to a decrease in neutron/proton ratio of the fission products studied, is then interpreted as reflecting a decrease in the n/p ratio for the nuclide undergoing fission. This will be caused by increasing particle evaporation (predominantly neutron emission at moderate energies with heavy targets) prior to fission. Alternatively, the decrease in the n/p ratio of the fission products may, to some extent, be due to neutron evaporation after fission.

Can. J. Chem. Downloaded from www.nrcresearchpress.com by 78.46.186.204 on 09/04/12
For personal use only.

TABLE II

DISPLACEMENT OF CHARGE DISTRIBUTION MAXIMUM AND HALF-WIDTH OF DISTRIBUTION AS A FUNCTION OF BOMBARDING ENERGY

Bombarding energy (Mev)	Displacement of distribution maximum (units of Z)	Half-width of distribution (units of Z)
0	3.4	2.2
8	3.1	2.2
14	2.7	2.2
25	2.4	2.2
45	2.0	2.5
64	1.9	2.8
87	1.8	3.2
170	1.4	—
480	1.0	3.0

An increased width of charge distribution at higher energies is expected from the same picture, since a proliferation of both nuclear cascade and nucleon evaporation would lead to a wider distribution of fissioning nuclei and hence wider distribution of n/p values in the fission products.

Detailed interpretation in terms of calculations based on models of the nuclear cascade and nucleon evaporation processes will be presented in the succeeding paper.

REFERENCES

1. AAGAARD, P., ANDERSSON, G., BURGMAN, J. O., and PAPPAS, A. C. J. Inorg. & Nuclear Chem. **5**, 105 (1957).
2. ARON, W. A., HOFFMAN, B. G., and WILLIAMS, F. C. U.S. Atomic Energy Comm. Rept. AECU-663 (1951).
3. BOHR, N. Science, **86**, 161 (1937).
4. CRANDALL, W. E., MILLBURN, G. P., PYLE, R. V., and BIRNBAUM, W. Phys. Rev. **101**, 329 (1956).
5. FORD, G. P. Private communication to A. C. Wahl (ref. 34).
6. GLENDENIN, L. E., CORYELL, C. D., and EDWARDS, R. R. Phys. Rev. **75**, 337 (1949).
7. GLENDENIN, L. E. Ph.D. Thesis, Massachusetts Institute of Technology, Cambridge, Mass. 1949.
8. GLENDENIN, L. E. and METCALF, R. P. Natl. Nuclear Energy Ser. Vol. 9, Div. IV, Paper 278, Book 3 (1951).
9. GLENDENIN, L. E. Private communication. 1957.
10. GOECKERMANN, R. H. and PERLMAN, I. Phys. Rev. **76**, 628 (1949).
11. HEBB, E. Phys. Rev. **97**, 987 (1955).
12. HEISENBERG, W. Naturwiss. **25**, 749 (1937).
13. HINTZ, N. M. and RAMSEY, N. F. Phys. Rev. **88**, 19 (1952).
14. KATCOFF, S., DILLARD, C. R., FINSTON, H., FINKLE, B., SEILER, J. A., and SUGARMAN, N. Natl. Nuclear Energy Ser. Vol. 9, Div. IV, Paper 280, Book 3 (1951).
15. KIRKALDY, J. S. Ph.D. Thesis, McGill University, Montreal, Que. 1953.
16. LAVRUKHINA, A. K. and KRASAVINA, L. D. J. Nuclear Energy, **5**, 236 (1957).
17. MEADOWS, J. W. Phys. Rev. **91**, 885 (1953).
18. NEWTON, A. S. Phys. Rev. **75**, 17 (1949).
19. O'CONNOR, P. R. and SEABORG, G. T. Phys. Rev. **74**, 1189 (1948).
20. PAPPAS, A. C. Phys. Rev. **87**, 162 (1952).
21. PAPPAS, A. C. Ph.D. Thesis, Massachusetts Institute of Technology, Cambridge, Mass. 1953.
22. PATE, B. D. and YAFFE, L. Can. J. Chem. **33**, 15 (1955).
23. PATE, B. D. and YAFFE, L. Can. J. Chem. **33**, 610 (1955).
24. PATE, B. D. and YAFFE, L. Can. J. Chem. **33**, 929 (1955).
25. PATE, B. D. and YAFFE, L. Can. J. Chem. **33**, 1656 (1955).
26. PATE, B. D. and YAFFE, L. Can. J. Chem. **34**, 265 (1956).
27. PRESENT, R. D. Phys. Rev. **72**, 7 (1947).
28. RUBINSON, W. J. Chem. Phys. **17**, 542 (1949).
29. SERBER, R. Phys. Rev. **72**, 1114 (1947).
30. STEINBERG, E. P. and FREEDMAN, M. S. Natl. Nuclear Energy Ser. Vol. 9, Div. IV, Paper 219, Book 3 (1951).
31. STEINBERG, E. P. and GLENDENIN, L. E. Phys. Rev. **95**, 431 (1954).
32. STEINER, H. M. and JUNGERMAN, J. A. Phys. Rev. **101**, 807 (1956).
33. TEWES, H. A. and JAMES, R. A. Phys. Rev. **88**, 860 (1952).
34. WAHL, A. C. Phys. Rev. **99**, 730 (1955).
35. WAY, K. and WIGNER, E. P. Phys. Rev. **73**, 1318 (1948).

Can. J. Chem. Downloaded from www.nrcresearchpress.com by 78.46.186.204 on 09/04/12
For personal use only.

Can. J. Chem. Downloaded from www.nrcresearchpress.com by 78.46.186.204 on 09/04/12
For personal use only.

FISSION OF EXCITED HEAVY NUCLEI[1,2]

B. D. PATE

ABSTRACT

The results of published calculations on the prompt nuclear cascade and nuclear evaporation processes are combined with some assumptions regarding the nuclear fission process and fission widths to calculate the average neutron-to-proton ratios of fission products from Th + 8-Mev protons, Th + 87-Mev protons, and U + 450-Mev protons. Comparison of the results with experimental data indicates that the fission charge distribution mode characterized by the equal charge displacement hypothesis, hitherto considered a low energy phenomenon, persists in uranium and thorium up to the highest energy studied. There is also some evidence that fission occurs in excited heavy nuclei before complete de-excitation by particle emission, in agreement with other experimental work.

A. INTRODUCTION

Particle evaporation (30) and fission predominate during the de-excitation of heavy nuclei excited to energies above a few million electron volts. These two processes are expected to compete at each step during the de-excitation in the sense of the following scheme (25):

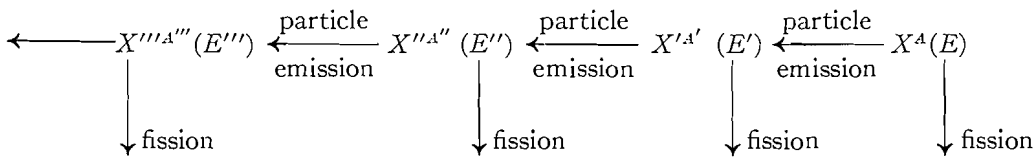

in which a nucleus of mass A excited to energy E evaporates particles to form successively nuclei of masses A', A'', etc. and energies E', E'' . . . with fission as an alternative to each particle evaporation step. The decrease in excitation energy per step, E–E', E'–E'', etc., equals the binding energy of the particle evaporated plus, in each case, the (variable) kinetic energy it carries off. The fragments from the fission of a nucleus of a given excitation energy E will themselves share in some way an excitation energy close to E, and may de-excite by further particle emission.

The relative probability that a nucleus in a given energy state de-excites via a specific reaction path is commonly described in terms of a partial "width" of the state for that reaction. Thus the competition between fission and particle emission from a given nucleus at a given energy may be expressed as a ratio Γ_f/Γ_{evap}, where Γ_f is the fission width and Γ_{evap} is a sum of particle emission widths

$$\Gamma_{evap} = \Gamma_n+\Gamma_p+\Gamma_d+\Gamma_t+\Gamma_\alpha+ \ldots \quad .$$

The ratio is expected to be a function of nuclear charge, mass, and excitation energy.

Fission-evaporation competition has been the subject of a number of previous studies, among the more recent being investigations with transuranium nuclei excited to energies up to 40 Mev (27, 28), and with thorium bombarded with protons of energies up to 100 Mev (3).

[1]*Manuscript received July 22, 1958.*
Contribution from the Chemistry Department, Brookhaven National Laboratory, Upton, Long Island, New York.
[2]*Research performed under the auspices of the U.S. Atomic Energy Commission.*

Can. J. Chem. Downloaded from www.nrcresearchpress.com by 78.46.186.204 on 09/04/12
For personal use only.

Interpretation of the experimental data is complicated by several factors aside from the complexity of a reaction scheme such as that illustrated above, for example, post-fission evaporation of nucleons from the fragments. Also a study of fission products gives only averaged information for the fission of the series of nuclei of different charge, mass, and excitation energy in the de-excitation chain.

Furthermore, as the bombarding energy is raised, the character of the initial nuclear interaction, which produces the excited nuclei whose de-excitation is to be studied, also changes. In addition to compound nucleus formation (2), characterized by the formation of a single nuclear type excited to a unique energy, reactions proceeding via direct interaction with individual nucleons (23) are observed. In some circumstances, the latter process occurs to a significant extent at energies as low as 14 Mev (14). It becomes more important with increasing energy and predominates above about 50 Mev.

Since such single nucleon reactions between target and projectile occur with the transfer of a variable amount of energy, generally less than the maximum available, and result in the prompt emission of a variable number of nucleons, de-excitation cascades such as that illustrated above begin from a range of nuclear charges, masses, and excitation energies.

Some previous attempts (1, 24) to interpret experimental data, making various assumptions regarding variation of Γ_f/Γ_{evap} with A, Z, and E, have suffered from lack of information regarding the nature of the prompt part of the nuclear interaction. The present work has the benefit of the results of detailed calculations which have been made both of the prompt initial nuclear interaction (17, 18) and of the evaporation process as it would occur in the absence of fission competition (5). It also differs from many previous studies in that it employs data on the nuclear charge distribution of fission products. The particular data used are those reported in the previous paper (20) for thorium irradiated with protons of 8- and 87-Mev energy, and those of Lavrukhina and Krasavina (15) for uranium with 480-Mev protons.

The following approach is used in the calculations. The distribution in nuclear charge, mass, and excitation energy at the end of the prompt interaction are obtained by assuming compound nucleus formation where appropriate, and elsewhere from the Monte Carlo calculations of Metropolis *et al.* (17, 18). These calculations, while being of the same general type and employing the same crude nuclear model (degenerate Fermi gas in a sharply defined nuclear potential) as previous calculations (10), nevertheless benefit from a three-dimensional relativistic treatment and good statistics. Their results are in reasonably good agreement with experiment (17, 18) and appear to be fairly reliable when used for the present purposes.

Next the Monte Carlo calculations of Dostrovsky *et al.* (5) are used to compute the course of evaporation cascades from each point in the A, Z, and E distribution at the end of the prompt cascade. These evaporation calculations have been made using the LeCouteur formalism (16) and do not take fission competition into account. The effect of the choice of input parameters for these calculations on the results obtained has not yet been completely investigated, and the results of the present analysis are uncertain to that extent. Parts (i) and (ii) of the calculations that follow (energies 8 and 87 Mev) are expected to be the least uncertain, since the nature of the evaporation reaction in heavy elements at excitation energies below 100 Mev (almost exclusively neutron emission) and the average de-excitation per particle emitted are not very sensitive to the choice of nuclear model and parameters that may reasonably be made. The same is not true for higher energies, and Part (iii) of the analysis, employing the results of

evaporation calculations for excitations of up to 480 Mev, has been made with those results obtained with a choice of parameters that seemed to lead to the best agreement with other experimental data. The parameters include a coulomb barrier independent of excitation energy with barrier penetration introduced in a manner similar to that used by LeCouteur (16), and a nuclear energy level density given by

$$w = C\, e^{2(0.1A\times E)^{\frac{1}{2}}},$$

where A is the mass number and C is a constant. The results of Part (iii) should be considered in the light of this uncertainty in the evaporation reaction calculations.

Fission competition has been introduced in the present analysis by means of three assumptions:

(1) $\Gamma_f/(\Gamma_f+\Gamma_{evap})$ increases sharply from zero to unity as the Z^2/A ratio is raised through some critical value. This step-functional behavior is illustrated in Fig. 1*a*, and it may be compared with the previously reported experimental results shown in Fig. 1*b* where the solid line is taken from the data of Seaborg (1) and the broken line from those of Huizenga (13).

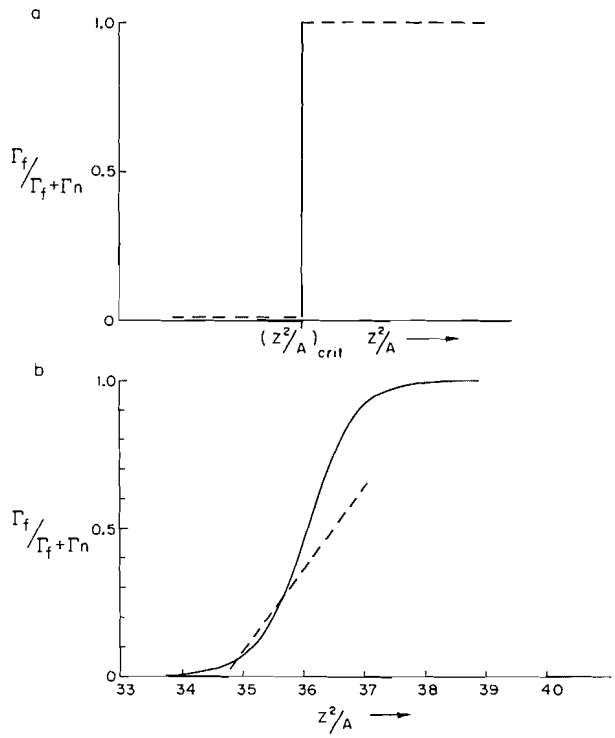

FIG. 1. Variation with Z^2/A of ratio of fission width to sum of fission and neutron widths for heavy elements. (*a*) Variation assumed in present calculations. (*b*) Experimental data (solid line from ref. (1), broken line from ref. (13)).

(2) Excitation energy of a fissioning nucleus is not (or is only to a small extent) transformed into kinetic energy of the fission fragments, or into electromagnetic radiation, but goes into excitation of the fragments (6) being divided between them in the ratio of their masses.

Can. J. Chem. Downloaded from www.nrcresearchpress.com by 78.46.186.204 on 09/04/12
For personal use only.

(3) On the average, 2.5 "fission" neutrons are emitted regardless of energy or fission mode. There is no information regarding the variation of the average number of fission neutrons ($\bar{\nu}$) with excitation energies above a few million electron volts, other than that given by Harding and Farey (11), who interpreted their experimental data for uranium bombarded with 147-Mev protons in terms of a $\bar{\nu}$ value of 2.5 ± 1.0. Further there exist few data on the variation of $\bar{\nu}$ with nuclear type (and then only for thermal energy or spontaneous fission (4, 12)) and there is no information regarding the variation of $\bar{\nu}$ with charge division mode. Thus the assumption of the constancy of $\bar{\nu}$ under all conditions seems the most reasonable working assumption that can be made at present. It should be noted that a change in $\bar{\nu}$ of unity would produce a change in fission product neutron-to-proton ratio of about 0.01 (see later).

In the calculations that follow, the results of the variation of several parameters will be investigated. These parameters include the critical Z^2/A value at which the sharp increase in the $\Gamma_f/(\Gamma_f+\Gamma_n)$ function occurs, the energy dependence of $\Gamma_f/(\Gamma_f+\Gamma_n)$ (assumed to be one of two limiting forms) and the mode of distribution of nuclear charge in fission. Experimental evidence has been cited in the literature for two charge distribution processes, namely the equal charge displacement (ECD) process (7, 8, 19) and the unchanged charge distribution (UCD) process (9). The former, observed to account well for independent yield data for the products from the fission of U^{235} at thermal energies and at 14 Mev (29), is based on the postulate that the most probable nuclear charges of complementary fragments will be equally displaced from the charge value corresponding to stability for their respective masses. That is to say

$$Z_p = Z_A - \tfrac{1}{2}[Z_A + Z_{(A_f - \bar{\nu} - A)} - Z_f],$$

where Z_p is the most probable charge for a fragment of mass A, Z_A is the stable charge for mass A, A_f and Z_f are the mass and charge of the fissioning nucleus, and $\bar{\nu}$ as before is the average number of prompt fission neutrons. This process implies a rearrangement of nucleons prior to or during the fission act, and is commonly assumed to be a low-energy process. The unchanged-charge-distribution mode of fission (first postulated by Goeckermann and Perlman (9) to occur in the fission of bismuth with 190-Mev deuterons) produces fragments whose most probable neutron-to-proton ratio is the same as that of the fissioning nucleus. This implies that the nucleonic rearrangement indicated in ECD-type fission does not take place, and UCD is considered characteristic of "fast" or "high-energy" fission (9).

Comparison between the predicted and observed neutron-to-proton ratios of primary fission products will then be made in order to determine which of the various choices of parameters best fits the data.

B. CALCULATIONS AND RESULTS

The n/p ratios resulting from calculations based on the assumptions described above are compared with the observed most probable n/p ratio for fission products in the mass range 130–135 as reported (20) for the systems

(i) Th^{232} + 8.0-Mev protons,
(ii) Th^{232} + 87-Mev protons,

and for fission products of masses 90 and 130 as reported (15) for

(iii) U^{238} + 480-Mev protons.

Can. J. Chem. Downloaded from www.nrcresearchpress.com by 78.46.186.204 on 09/04/12
For personal use only.

(*i*) Th^{232} + *8.0-Mev Protons*

The assumption of compound nucleus formation in this case is probably a good one. Consequently we must consider the de-excitation of Pa^{233} with an excitation energy

$$E^* = E_{\text{kinetic}} + E_{\text{proton binding}}$$
$$= 13.6 \text{ Mev},$$

since the proton-binding energy in Pa^{233} is 5.6 Mev (22). Thus we have the reaction scheme shown in Fig. 2; only neutron emission is considered for the evaporation reaction, since coulomb barrier effects render charged particle emission highly unlikely. The neutron-binding energies in Pa^{233} and Pa^{232} are 6.6 and 4.2 Mev (22) respectively so that formation of Pa^{231} is energetically possible. However, the evaporation calculations indicate that, in this region of charge, mass, and energy, the most probable de-excitation via neutron evaporation is greater than 9 Mev. Consequently the reaction would seldom proceed past Pa^{232}.

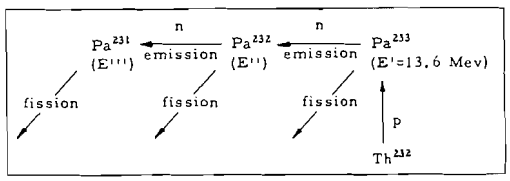

FIG. 2. De-excitation of Pa^{233} excited to 13.6 Mev.

Table I shows the n/p ratio calculated for both the ECD and the UCD mechanisms for the system of Fig. 2. The fission of Pa^{233} excited to 13.6 Mev is considered to lead to fission fragments sharing an excitation energy of about the same magnitude (see assumption (2)). Thus there is a significant probability for the evaporation of a neutron from each of the fission fragments, since the average neutron-binding energy in the iodine isotopes of mass 130–135 is about 7.4 Mev (22). This would reduce the n/p ratio calculated via ECD to 1.560 and via UCD to 1.514.

TABLE I

CALCULATED AND EXPERIMENTAL AVERAGE NEUTRON TO PROTON RATIOS FOR FRAGMENTS OF MASS 130–135 FROM THE FISSION OF Th^{232} WITH 8-MEV PROTONS

Fissioning nucleus	n/p Calculated via ECD	n/p Calculated via UCD	n/p observed
Pa^{233}	1.579	1.533	
Pa^{232}	1.570	1.522	1.566±0.004
Pa^{231}	1.560	1.511	

The experimental data in the preceding paper give a n/p ratio of 1.566±0.004. Thus they appear to be consistent with the fission of Pa^{232} via an ECD mechanism, perhaps with some contribution from ECD-type fission of Pa^{231} and Pa^{233}, and to be inconsistent with UCD-type fission.

(*ii*) Th^{232} + *87-Mev Protons*

The experimental data for this system will be compared with an analysis starting with the results of prompt cascade calculations for 83-Mev protons incident upon

Can. J. Chem. Downloaded from www.nrcresearchpress.com by 78.46.186.204 on 09/04/12
For personal use only.

U^{238}. (The difference in energy is neglected and the difference in target characteristics is taken into account by introduction of appropriate shifts in charges and masses of the reaction products.)

Figure 3 is a section of the chart of nuclides (Z plotted versus N) with the course of the reactions indicated on it. Immediately below the symbol and mass number for each nuclide are given its n/p and Z^2/A ratios. The Th^{232} target nucleus is enclosed by double lines, and the distribution of products from the prompt interaction (17) is given by the numbers (relative frequencies) in square boxes. The total number of cascades followed in the prompt interaction calculation was 1258 (in addition to those in which nuclear transparency was indicated). In addition to the number distribution given for each nuclide the excitation energy spectrum is available from the calculations (17). This is generally a continuous distribution except in the case of Pa^{233}, which is the compound nucleus product and is therefore excited to a unique energy.

The evaporation calculations (5) for heavy nuclei excited to 75 Mev indicate that 99.7% of the evaporated particles are neutrons. Consequently charged particle evaporation will be neglected. Also the average de-excitation per evaporated neutron is 9.2 Mev; the value shows no systematic trend with nuclear excitation in this energy region. Consequently a further simplification will be made, namely that all neutrons carry off exactly this energy. The evaporation reaction proceeds as indicated by the horizontal lines in Fig. 3, and leads to the final nuclide distribution shown by the unboxed numbers. (With the simplification used, the de-excitation of Pa^{233} leads to emission of $9\frac{1}{2}$ neutrons so that the 520 events are divided equally between Pa^{223} and Pa^{224}. Similar adjustments are made elsewhere as required.)

The incorporation of fission competition in the calculations must now be considered. The approximations made thus far would seem to make an analysis as sophisticated as that by Batzel (1) or Vandenbosch *et al.* (28) of doubtful value. Instead we shall examine two situations.

(1) The dependence of Γ_f/Γ_n on energy is greater than the dependence on nuclear type (specifically on the fissionability parameter Z^2/A). That is, increasing energy favors neutron emission sufficiently so that fission does not take place until the excitation energy is reduced below the neutron-binding energy at the end of the evaporation cascade.

(2) Γ_f/Γ_n is essentially independent of energy, but varies sharply with Z^2/A as described earlier and illustrated in Fig. 1*a*.

Again, both ECD- and UCD-type fission are to be considered, the n/p ratio resulting from the fission of each nuclide via the two mechanisms being calculated. The values are then weighted using the number distributions indicated for situations (1) and (2) above and averaged to give the mean n/p ratio expected for fission products of mass 130–135 in each case. The variation of total fission chain yield with mass number over the energy range and mass range considered is small enough to be neglected in the averaging.

The results of the calculation are compared with the experimental data in Table II. In Part 2 of Table II, the average n/p ratios calculated for fission fragments of mass 130–135 are listed both for the fragments initially formed by the fission act, still excited, and for these fragments after de-excitation by neutron emission. The average number of neutrons emitted was obtained by using average neutron-binding energy values appropriate to iodine nuclides in the indicated mass range (22) plus an estimated most probable

Can. J. Chem. Downloaded from www.nrcresearchpress.com by 78.46.186.204 on 09/04/12
For personal use only.

Can. J. Chem. Downloaded from www.nrcresearchpress.com by 78.46.186.204 on 09/04/12
For personal use only.

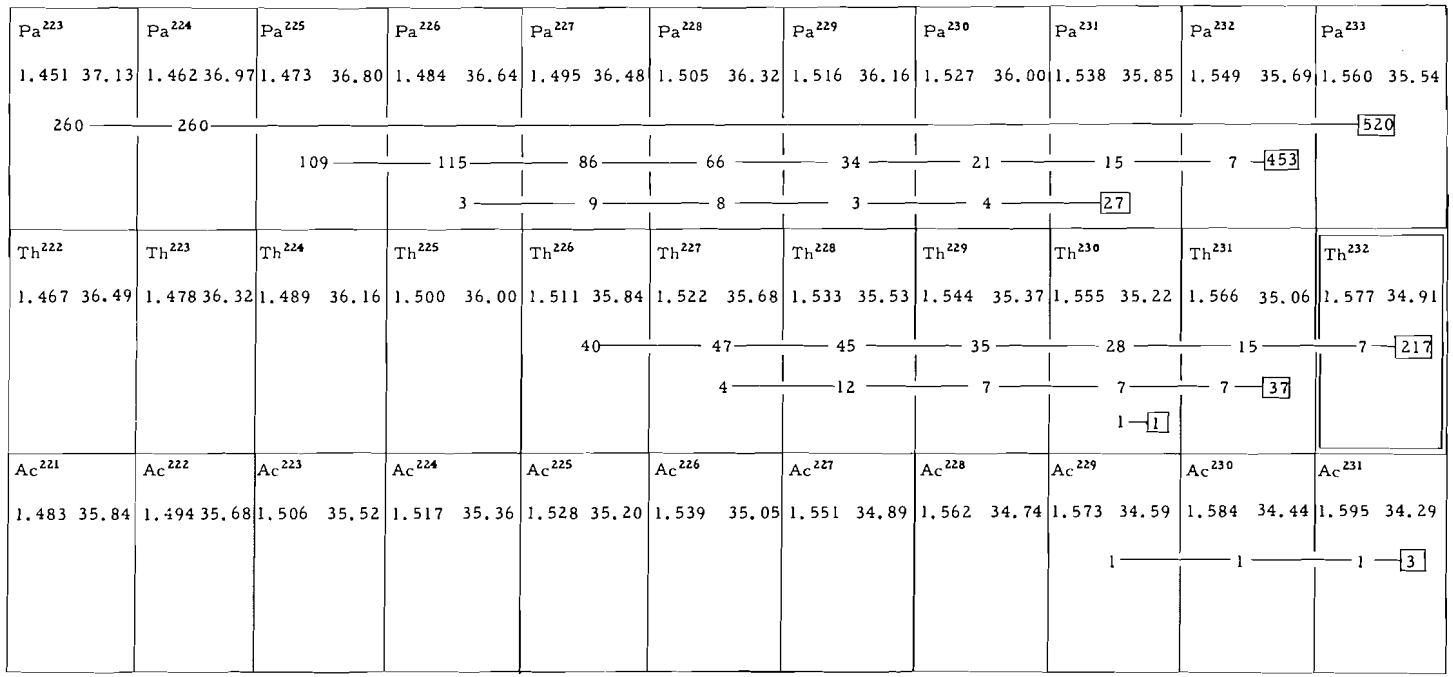

FIG. 3. Prompt cascade and evaporation reactions in thorium bombarded with 83-Mev protons.

neutron kinetic energy. In Part 1 fission is considered to take place in de-excited nuclei only, so that the fission fragments are considered to have excitation energies less than the neutron-binding energy.

TABLE II

CALCULATED AND EXPERIMENTAL AVERAGE n/p RATIOS FOR THE PRODUCTS OF THE FISSION OF Th^{232} WITH 87-MEV PROTONS—MASS NO. 130–135

1. Fission occurs after de-excitation by neutron emission in nuclides with greater than given Z^2/A value

Z^2/A greater than	ECD-type fission	UCD-type fission
37	1.478	1.423
36.6	1.491	1.435
36.3	1.497	1.441
36.0	1.499	1.445
35.5	1.506	1.450
35.0	1.511	1.458
34.5	1.512	1.459

Experimental value 1.502

2. Fission occurs at given Z^2/A value before complete de-excitation

	ECD-type fission		UCD-type fission	
Z^2/A	n/p ratio of initial fission fragments	n/p ratio of fragments after de-excitation	n/p ratio of initial fission fragments	n/p ratio of fragments after de-excitation
37.0	1.478	1.478	1.423	1.423
36.6	1.510	1.491	1.456	1.445
36.3	1.519	1.481	1.478	1.456
36.0	1.547	1.499	1.500	1.478
35.5	1.569	1.506	1.525	1.488
35.0	1.574	1.512	1.529	1.493
34.5	1.577	1.513	1.531	1.494

Experimental value 1.502

It is seen that the experimental n/p ratio is consistent with that calculated with the assumption that ECD-type fission occurs either during or at the end of de-excitation, in nuclides with Z^2/A values greater than 36.0. The n/p ratios calculated for UCD-type fission under various conditions are all inconsistent with the experimental value.

This conclusion is consistent with two other data. First, a Z^2/A value of 36.0 corresponds to a Γ_f/Γ_n value of nearly unity (1, 13), i.e. fission and neutron emission are roughly equally probable. Hence, that critical Z^2/A value of the step function assumed for $\Gamma_f/(\Gamma_f+\Gamma_n)$ which gives results most consistent with experiment, corresponds roughly to the mid-point of the $\Gamma_f/(\Gamma_f+\Gamma_n)$ functions reported previously which were based on other experimental evidence.

Second, we may calculate the cross section for the Th^{232} (p,f) reaction to be expected on the basis of the assumption that all nuclides of Z^2/A greater than 36.0 undergo fission. The total number of prompt interaction events followed in the Monte Carlo calculation (17) was 1336, of which 978 were found to give nuclides which were presumed to undergo fission. The geometric cross section for Th^{232} is 2.0×10^{-24} cm^2 for a nuclear radius parameter, $r_0 = 1.3\times10^{-13}$ cm. The fission cross section is then expected to equal

$$\sigma_f = \pi r^2 \times (978/1336)$$
$$= 1.4\times10^{-24} \text{ cm}^2$$

Can. J. Chem. Downloaded from www.nrcresearchpress.com by 78.46.186.204 on 09/04/12
For personal use only.

the value at 80 Mev is expected to be 1.1×10^{-24} cm^2 by extrapolation from published values at lower energies (26).

One further comparison with experiment may be made—namely the charge distribution for fragments of mass 130–135 may be calculated and compared with the charge distribution obtained from the mass distribution observed experimentally (20) for iodine isotopes. The calculation was made under the assumption that the charge distribution resulting from the fission of a single nuclide in this energy range is the same as that observed from the fission of U^{235} with thermal and with 14-Mev neutrons, with Z_p calculated via the ECD mechanism. The charge distribution resulting from the fission of a range of nuclides is then the sum of the separate distributions weighted by the number distribution for the fissioning nuclides (i.e. those of Z^2/A greater than 36.0) deduced from the above analysis. The calculated and observed distributions are shown in Fig. 4.

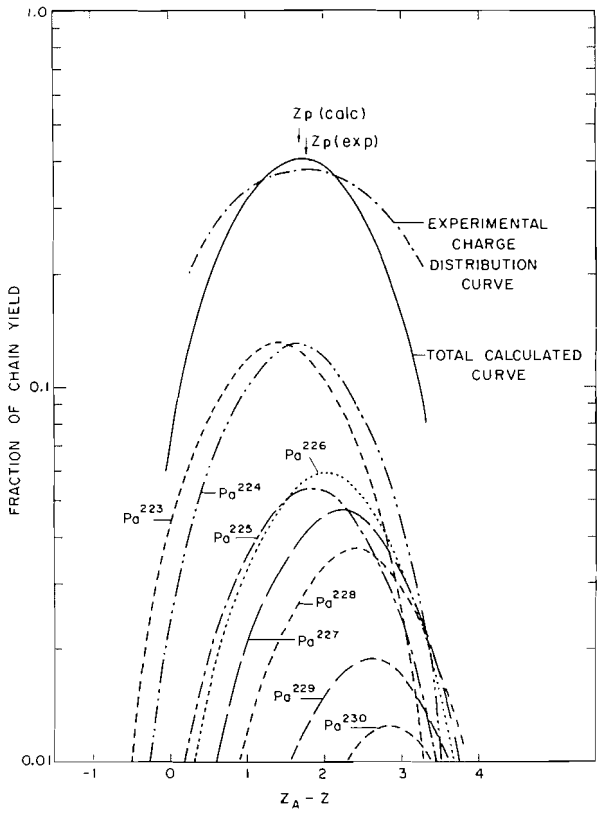

FIG. 4. Experimental and calculated fission product charge distributions in fission of Th^{232} induced by 83-Mev protons.

It is seen that the experimental distribution is wider than that calculated (although the Z_p values agree). This presumably reflects among other things the effect of one simplification made in this part of the analysis, namely that neutron-emission results in the loss of a constant amount of energy. Incorporation of a more realistic distribution of neutron-emission energies would presumably lead to a wider number distribution of fissioning nuclei, and hence a wider charge distribution.

Can. J. Chem. Downloaded from www.nrcresearchpress.com by 78.46.186.204 on 09/04/12
For personal use only.

(iii) U^{238} + *480-Mev Protons*

The experimental data for this system will be compared with the results of an analysis starting with the prompt cascade calculations for 450-Mev protons incident on U^{238} (18). Figure 5 shows again the Z versus N plot with the target nucleus enclosed in heavy lines. The frequency distribution from the prompt cascades is shown underlined in the top right-hand corner of each square.

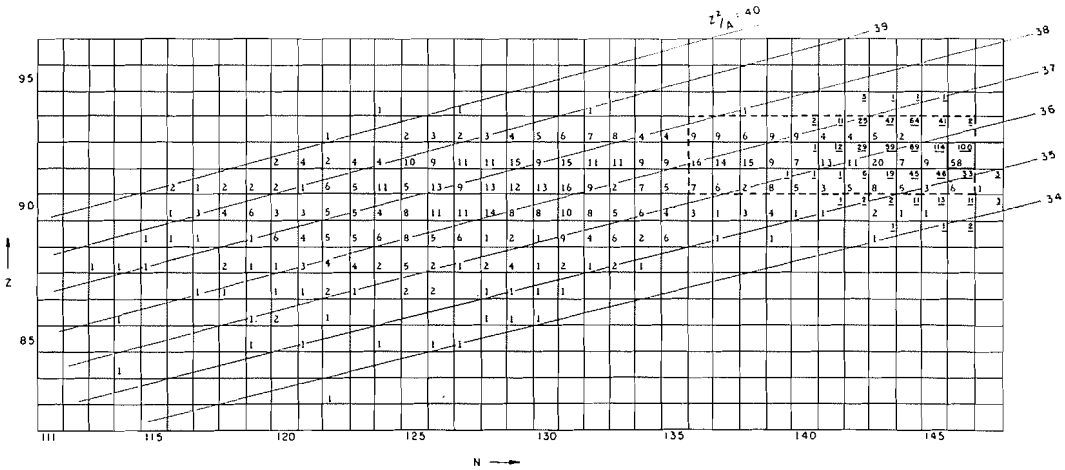

FIG. 5. Prompt cascade and evaporation reactions in uranium bombarded with 450-Mev protons.

At the excitation energies obtained in this system, charged particle emission from the product nuclei during the evaporation process is common, and no useful simplification in the treatment of that part of the reaction can be made. Consequently, from the evaporation–reaction calculations individual cascades have been chosen in which the initial A, Z, and E values match as closely as possible those for the products of individual prompt interaction cascades. These evaporation cascades have been used to specify the end product and intermediate products of the de-excitation process. The number of evaporation cascades that have been calculated is such that close matching is not difficult, and the sequence in which the data have been used is such as to ensure a random choice from among the prompt interaction and evaporation cascade data employed. The resulting number distribution of de-excited end products is shown in Fig. 5 in the bottom left-hand corner of each square. The region covered by Fig. 2 is shown enclosed in a dotted line to emphasize the much greater extent of particle emission induced at the higher bombarding energy. Also on Fig. 5 are shown lines connecting nuclides of equal Z^2/A value.

Additional information which may be obtained includes the number of de-excitation cascades which results in the transient formation of each nuclide and the spectrum of excitation energies with which it is formed.

Fission competition may now be introduced under the assumptions outlined earlier. The analysis is simplified by the general observation that the early part of a de-excitation cascade, when the excitation is highest, is characterized by emission of protons, neutrons, and alpha particles in such proportions that the evaporation "path" proceeds parallel to or towards the nuclear stability line. In the later, low-energy part of the cascade, however, coulomb effects predominate and neutron emission is favored. Consequently the Z^2/A value of nuclides successively formed in the de-excitation process generally decreases at first and then increases again, in a fairly smooth manner. Thus selection

Can. J. Chem. Downloaded from www.nrcresearchpress.com by 78.46.186.204 on 09/04/12
For personal use only.

of events producing nuclides of a given Z^2/A (particularly at the higher Z^2/A values) does not introduce serious error owing to the fact that a given event may be counted more than once.

Owing to the wide range of mass numbers produced, the variation of yield of fission fragments of a given mass with mass number can no longer be neglected. As an approximation, during the averaging of the product n/p ratios, weighting for mass yield will be accomplished using the over-all mass-yield curve given by Lavrukhina and Krasavina (15) in addition to weighting by the number distribution. The error made by use of the over-all mass-yield distribution rather than the distribution appropriate to fission of a single nucleus is probably small, since the effect of weighting for mass yield is in any case quite small.

In Part 2 of the analysis, in which fission is considered to take place from excited nuclei, it is again assumed that the total excitation of the system is unchanged during the fission process, and that, on the average, it divides among the products in the ratio of their masses. This division reduces the excitation energy per fragment in general to below 150 Mev, in which region the calculations of Dostrovsky *et al.* (5) predict a predominance of neutron emission. The de-excitation of the fission fragments is then presumed to take place in this manner with an energy loss per neutron evaporation of about 11 Mev, an average figure for this energy and mass region.

The results of the analysis are shown in Table III, with n/p ratios given for fission fragments of mass about 90 and about 130, calculated under the various parameter choices.

TABLE III

CALCULATED AVERAGE n/p RATIOS FOR THE PRODUCTS OF THE FISSION OF U^{238} WITH 450-MEV PROTONS

1. Fission occurs after de-excitation by particle evaporation in nuclides with greater than a given Z^2/A value

Z^2/A greater than	ECD-type fission		UCD-type fission	
	$A = 90$	$A = 130$	$A = 90$	$A = 130$
40	1.200	1.330	1.261	1.262
39	1.233	1.361	1.301	1.302
38	1.253	1.385	1.333	1.336
37	1.285	1.417	1.365	1.370
36	1.318	1.444	1.403	1.410
35	1.346	1.464	1.420	1.428
Experimental values:	Mass 90 ~ 1.36			
	Mass 130 ~ 1.44–1.46			

2. Fission occurs at given Z^2/A value before complete de-excitation

	ECD-type fission				UCD-type fission			
	$A = 90$		$A = 130$		$A = 90$		$A = 130$	
Z^2/A	n/p ratio of initial fragments	n/p after de-excitation	n/p before de-excitation	n/p after de-excitation	n/p before de-excitation	n/p after de-excitation	n/p before de-excitation	n/p after de-excitation
40	1.211	1.210	1.353	1.344	1.299	1.288	1.300	1.289
39	1.252	1.227	1.379	1.358	1.320	1.307	1.323	1.311
38	1.297	1.256	1.434	1.390	1.373	1.334	1.378	1.338
37	1.368	1.299	1.487	1.408	1.430	1.360	1.441	1.366
36	1.448	1.353	1.544	1.436	1.477	1.380	1.497	1.399
35	1.484	1.367	1.558	1.463	1.485	1.400	1.509	1.419
Experimental values:	Mass 90 ~ 1.36							
	Mass 130 ~ 1.44–1.46							

Can. J. Chem. Downloaded from www.nrcresearchpress.com by 78.46.186.204 on 09/04/12
For personal use only.

The most probable n/p ratios observed by Lavrukhina and Krasavina (15) are as follows: for mass 90, about 1.36; and for mass 130, 1.44 to 1.46 depending on which of the presentations of the data one uses. The agreement of the calculations with these figures is good for ECD-type fission and poor for UCD-type fission, being the best for the assumption that fission occurs before complete de-excitation and when a Z^2/A value between 35 and 36 is reached. However, a decision between the assumptions of Parts (1) and (2) of the analysis cannot be made as definitely as one between the two fission modes.

The value of Z^2/A found for best fit with experiment is close to that found in Part (ii) and is satisfactory for the same reasons.

If one calculates the fission cross section expected from the above results, in the same way as described in Section (ii), one obtains the value of 1.32 barns compared with an experimental value of 1.12 barns (15).

C. DISCUSSION

Within its limitations, the analysis described above leads to the conclusion that fission of nuclides with Z in the range 87–93 with excitation energies up to a few hundred Mev proceeds predominantly via a process described by the equal-charge displacement mechanism. There is also some indication (from Part (iii)) that fission of these nuclides begins to compete effectively with particle emission when the Z^2/A value is greater than about 36, in a fashion independent of energy. This last conclusion is generally in agreement with conclusions drawn from lower energy studies (1, 28), and in disagreement with the results of an analysis by Shamov (24).

The indication of an equal charge displacement mechanism in the fission of uranium and thorium with protons of energy up to 480 Mev, which is in disagreement with some previously published conclusions (15, 28), is at first surprising, since ECD has hitherto been considered a low-energy process. However, it may well be that ECD-type fission is characteristic of nuclides of specific charge and mass, rather than of specific energy. This is consistent with the observation by Porile and Sugarman (21) that ECD-type fission occurs when bismuth is bombarded with 450-Mev protons but that UCD-type fission occurs in tantalum bombarded with protons of the same energy.

D. ACKNOWLEDGMENTS

It is a pleasure to acknowledge the generosity of N. Metropolis *et al.* in making available to the author the material of references (17) and (18) prior to publication, and of I. Dostrovsky and G. Friedlander in providing access to the data of reference (5) prior to publication. The author is also very grateful to his colleagues in the Brookhaven National Laboratory Chemistry Department and to L. Yaffe for a number of stimulating discussions and for criticisms of the manuscript. The technical assistance of Mrs. E. McIver and Mrs. P. Payne with much of the tedious analysis is also gratefully acknowledged.

REFERENCES

1. Batzel, R. E. Univ. of Calif. Radiation Lab. Rept. UCRL 4303 (1954).
2. Bohr, N. Science, **86**, 161 (1937).
3. Bowles, B. J., Brown, F., and Butler, J. P. Phys. Rev. **107**, 751 (1957).
4. Crane, W. W. T., Higgins, G. H., and Bowman, H. R. Phys. Rev. **101**, 1804 (1956).
5. Dostrovsky, I., Rabinowitz, P., and Bivins, R. Phys. Rev. (1958) (In press).
6. Fong, P. Phys. Rev. **102**, 434 (1956).
7. Glendenin, L., Coryell, C. D., and Edwards, R. R. Phys. Rev. **75**, 337 (1949).
8. Glendenin, L. Ph.D. Thesis. Massachusetts Institute of Technology. 1949.
9. Goeckermann, R. H. and Perlman, I. Phys. Rev. **76**, 628 (1949).

Can. J. Chem. Downloaded from www.nrcresearchpress.com by 78.46.186.204 on 09/04/12
For personal use only.

10. GOLDBERGER, M. L. Phys. Rev. **74**, 1269 (1948).
11. HARDING, G. N. and FARLEY, F. J. M. Proc. Phys. Soc. (London), A, **69**, 853 (1956).
12. HICKS, D. A., ISE, J., JR., and PYLE, R. V. Phys. Rev. **101**, 1016 (1956).
13. HUIZENGA, J. R. Phys. Rev. **109**, 484 (1958).
14. IGO, G. and WEGNER, H. E. Phys. Rev. **102**, 1364 (1956).
15. LAVRUKHINA, A. K. and KRASAVINA, L. D. J. Nuclear Energy, **5**, 236 (1957).
16. LECOUTEUR, K. J. Proc. Phys. Soc. (London), A, **63**, 259 (1950).
17. METROPOLIS, N., BIVINS, R., STORM, M., TURKEVICH, A., MILLER, J. M., and FRIEDLANDER, G. Phys. Rev. **110**, 185 (1958).
18. METROPOLIS, N., BIVINS, R., STORM, M., MILLER, J. M., FRIEDLANDER, G., and TURKEVICH, A. Phys. Rev. **110**, 204 (1958).
19. PAPPAS, A. C. Ph.D. Thesis. Massachusetts Institute of Technology. 1953.
20. PATE, B. D., FOSTER, J. S., and YAFFE, L. Can. J. Chem. **36**, 1691 (1958).
21. PORILE, N. T. and SUGARMAN, N. Phys. Rev. **107**, 1410 (1957).
22. RIDDELL, J. Atomic Energy of Canada Ltd. Rept. No. CRP-654 (1956).
23. SERBER, R. Phys. Rev. **72**, 1114 (1947).
24. SHAMOV, V. P. J. Exptl. Theoret. Phys. (U.S.S.R.), **33**, 346 (1957). *Translated in* Soviet Phys. J. E. T. P. **6**, 268 (1958).
25. SPENCE, R. W. and FORD, G. P. Ann. Rev. Nuclear Sci. **2**, 399 (1953).
26. TEWES, H. A. and JAMES, R. A. Phys. Rev. **88**, 860 (1952).
27. VANDENBOSCH, R. and SEABORG, G. T. Univ. of Calif. Radiation Lab. Rept. UCRL-8047 (1957).
28. VANDENBOSCH, R., THOMAS, T. D., VANDENBOSCH, S. E., GLASS, R. A., and SEABORG, G. T. Univ. of Calif. Radiation Lab. Rept. UCRL-8032-Rev. (1958).
29. WAHL, A. C. Phys. Rev. **99**, 730 (1955).
30. WEISSKOPF, V. F. Phys. Rev. **52**, 295 (1937).

Can. J. Chem. Downloaded from www.nrcresearchpress.com by 78.46.186.204 on 09/04/12
For personal use only.

Can. J. Chem. Downloaded from www.nrcresearchpress.com by 78.46.186.204 on 09/04/12
For personal use only.

THE PREPARATION OF SOME DERIVATIVES OF D-RIBONO-1→4-LACTONE AND D-RIBITOL[1]

L. HOUGH,[2] J. K. N. JONES, AND D. L. MITCHELL[2]

ABSTRACT

Reaction of D-ribono-1→4-lactone with acetone gave the 2,3-*O*-isopropylidene derivative from which 5-*O*-methyl-D-ribitol, 5-deoxy-D-ribitol, and 2,3-*O*-isopropylidene-D-ribitol were prepared.

INTRODUCTION

5-Deoxy and 5-*O*-substituted derivatives of D-ribitol were required and consequently attempts were made to prepare from D-ribono-1→4-lactone (I) the 2,3-*O*-isopropylidene intermediate (II) for specific substitution of the primary alcohol group (e.g. methylation, tosylation), followed by reduction of the lactone function and finally hydrolysis of the ketal. D-Ribono-1→4-lactone (I) readily condensed with acetone, the reaction being catalyzed by concentrated and dilute mineral acid or anhydrous copper sulphate, although it also underwent condensation with acetone, without any added catalyst, because of the favored *cis*-configuration of the hydroxyls at carbons 2 and 3. The formation of the *O*-isopropylidene derivative was accompanied by a significant change in optical rotation which fell from an initial value of $[\alpha]_D$ 43° to an approximate value of $[\alpha]_D$ −80°. The rate and extent of the condensation reaction was dependent upon the catalyst selected and in particular on the concentration of the mineral acid. Hydrolysis of the lactone derivative (II) in water proceeded slowly in a manner typical of a 1→4 lactone, but the presence of an *O*-isopropylidene ring superimposed on the lactone ring may make this evidence unreliable. The position of the ketal ring was located by reaction of the sodium *O*-isopropylidene-D-ribonate (III), obtained by mild alkaline hydrolysis of the lactone derivative (II), with sodium metaperiodate which resulted in the consumption of 1.03 moles of oxidant and the formation of 1.02 moles of formaldehyde. The *O*-isopropylidene group must therefore be situated at carbons 2 and 3. This was confirmed by methylation of the 2,3-*O*-isopropylidene-D-ribonolactone (II), followed by mild acid hydrolysis of the mono-*O*-methyl derivative (IV) to produce in good yield 5-*O*-methyl-D-ribono-1→4-lactone (V); this compound was identical with the lactone obtained by the alkaline-bromine oxidation of 5-*O*-methyl-D-ribose (1). The methylation evidence is thus compatible with the presence of a 1→4 lactone ring in the *O*-isopropylidene derivative (II). The possibility that the change in optical rotation prior to or during ketal formation was due to a ring shift from a 1→5- to the 1→4-lactone was considered. However, the original D-ribonolactone slowly hydrolyzed in water at room temperature [$[\alpha]_D$ 17.8° (initial) → $[\alpha]_D$ 8° (13 days)], a property characteristic of 1→4-lactones (2) and the magnitude of the values recorded by Rehorst for L-ribono-1→4-lactone is similar (3). 2,3-*O*-Isopropylidene-D-ribono-1→4-lactone and D-ribonolactone possessed an infrared absorption maximum at 1790 cm^{-1} and 1793 cm^{-1} respectively, which is consistent with the 1→4-lactone structure (cf. reference 3 (*a*)). The stabilizing effect of the exocyclic double bond, thus making carbon 1 trigonal, must be a considerable influence in this case because the *cis*-hydroxyls at carbons 2 and 3 would be expected to create steric pressure as a result of the close proximity of these groups on a five-membered ring.

[1]*Manuscript received July 4, 1958.*
Contribution from the Department of Chemistry, Queen's University, Kingston, Ontario, and the Department of Organic Chemistry, The University, Bristol 8, England.
[2]*Present address: Department of Organic Chemistry, The University, Bristol 8, England.*

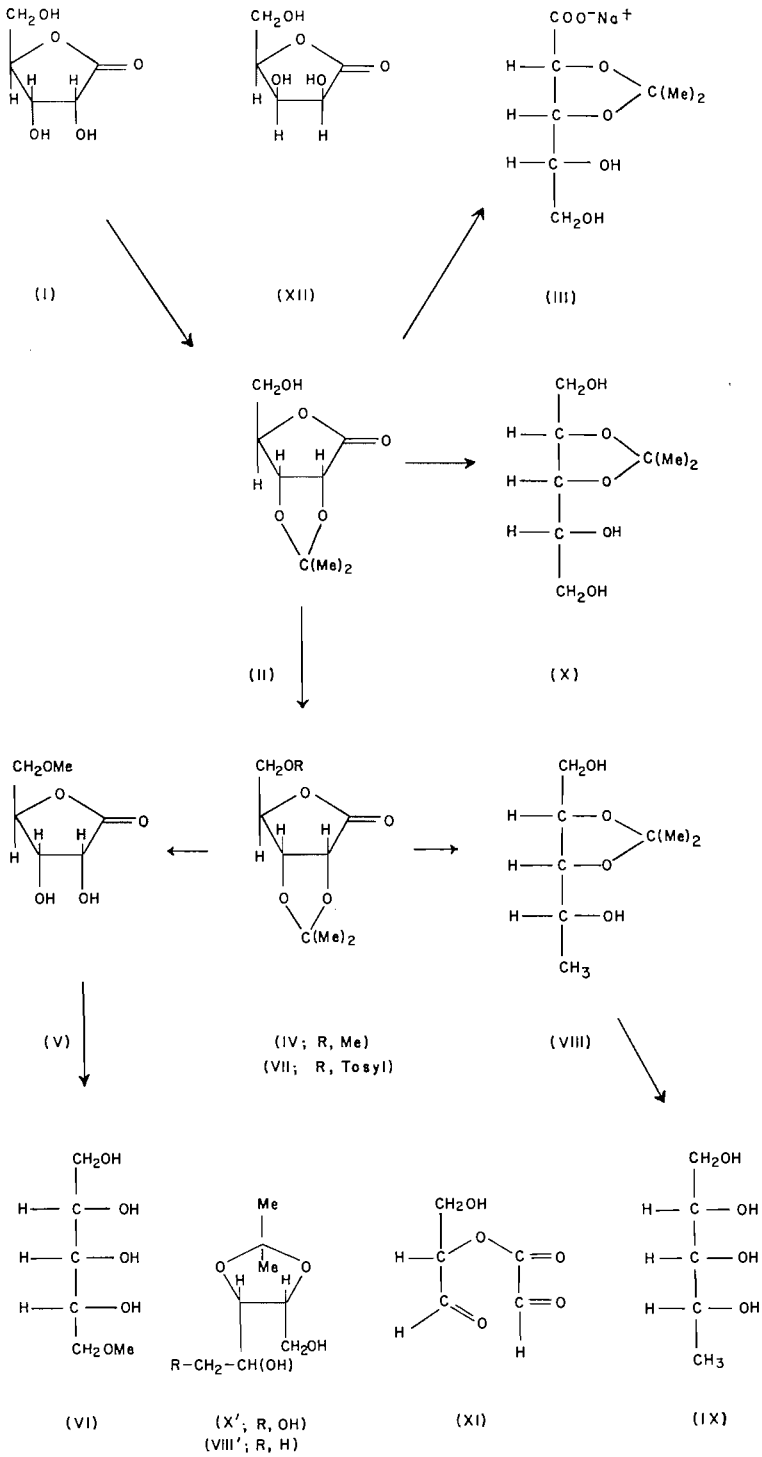

Can. J. Chem. Downloaded from www.nrcresearchpress.com by 78.46.186.204 on 09/04/12
For personal use only.

Can. J. Chem. Downloaded from www.nrcresearchpress.com by 78.46.186.204 on 09/04/12
For personal use only.

Recent studies on the periodate oxidation of monosaccharides at pH 3.6 have revealed that they are oxidized almost completely in their ring forms with the formation of esters (formyl, glycollyl, and glyoxylyl) of glyceraldehyde and glycollaldehyde, further oxidation being dependent upon the rate of hydrolysis of the ester intermediates (4, 5). Similar oxidations of 1→4- and 1→5-pentonolactones would be expected to give rise to glyoxylic acid esters of glyceraldehyde (XI) and glycollaldehyde respectively. However, the former ester should be distinguished by a fairly rapid overoxidation reaction because the electrophilic hydroxyl group (from carbon 5) neighboring the ester linkage would facilitate its hydrolysis. In accord with this theory D-ribono-1→4-lactone and its 5-*O*-methyl derivative each consumed approximately one mole of periodate rapidly, which was followed by a slower but extensive oxidation, typical of 2-*O*-esters of glyceraldehyde to the approximate theoretical values (Fig. 1). Lactobiono-1→5-lactone behaved similarly after the initial rapid reaction with 3 moles of periodate (Fig. 1). The similarity between the oxidation curves of D-ribonolactone and 5-*O*-methyl-D-ribono-1→4-lactone would suggest that the former compound was indeed oxidized as a 1→4-lactone and it therefore seems likely that the change in optical rotation during acetonation cannot be ascribed to a ring shift (1→5- to 1→4-lactone), but must actually be related to the formation of the ketal ring.

1→4-Lactones are believed to be planar or nearly planar, but some degree of ring buckling might arise in the pentono- and hexono-lactones if the molecule possesses a bulky group at carbon 5 and substituents at carbons 2 and 3 in the true *cis*-configuration (XII) (cf. reference 5 (*a*)). Deviations from planarity have been observed in the D-ribofuranosyl ring system of crystalline adenosine (6) by X-ray analysis, but 1→4-lactol and 1→4-lactone ring systems are not precisely comparable. A shift in molecular rotation which should measure approximately the extent of ring buckling has been observed for 2,3-di-*O*-methyl-D-ribono-1→4-lactone and 2,3,5-tri-*O*-methyl-D-ribono-1→4-lactone (Table I). Such an effect is probably responsible for the large molecular rotational shift in the formation of 2,3-*O*-isopropylidene-D-ribono-1→4-lactone, although buckling of the lactone ring will result in a distortion of the *O*-isopropylidene ring which will then be asymmetric (cf. D-galactose and its 1,2-3,4-di-*O*-isopropylidene derivative). Asymmetrical *O*-isopropylidene rings have been suggested as being one of the factors responsible for molecular rotational shifts between methyl *O*-isopropylidene pyranosides and the corresponding methyl pyranosides (7). The substitution of a methoxyl group for the hydroxyl group at carbon 5 of various D-ribono-1→4-lactone derivatives results in a molecular rotational shift (in the positive direction) of approximately the same magnitude for each pair (Table I).

Tosylation of 2,3-*O*-isopropylidene-D-ribono-1→4-lactone (II) at a low temperature (*ca.* −20° C; 10 hours) produced the 5-*O*-tosyl derivative (VII) in quantitative yield.

TABLE I

ROTATIONS OF DERIVATIVES OF D-RIBONO-1→4-LACTONE IN WATER

	$[\alpha]_D$	M_D	Difference	Reference
D-Ribono-1→4-lactone	17.8	2636	+1809	(*)
5-*O*-Methyl-lactone	27.4	4445		(1)
2,3-Di-*O*-methyl-lactone	−31.5	−5538	+1754	(8)
2,3,5-Tri-*O*-methyl-lactone	−19	−3784		(9)
2,3-*O*-Isopropylidene-lactone	−57.5	−10820	+1900	(*)
2,3-*O*-Isopropylidene-5-*O*-methyl-lactone	−44.1	−8920		(*)

*Present paper.

When higher reaction temperatures and longer reaction periods were employed, lower yields and tarry products were often obtained. A simultaneous reduction of the lactone function to the primary alcohol and reductive cleavage of the tosyloxy group was effected in good yield by lithium aluminum hydride in tetrahydrofuran to give 2,3-*O*-isopropylidene-5-deoxy-D-ribitol (VIII). Hydrolysis of the product with cation exchange resin (H form) afforded 5-deoxy-D-ribitol (IX). Similarly, 5-*O*-methyl-D-ribono-1→4-lactone (V) and 2,3-*O*-isopropylidene-D-ribono-1→4-lactone (II) were reduced with lithium aluminum hydride to syrupy 5-*O*-methyl-D-ribitol (VI) and syrupy 2,3-*O*-isopropylidene-D-ribitol (X) respectively. The structures were verified by periodate oxidation experiments (Table III).

2,3-*O*-Isopropylidene-D-ribitol compounds are of interest because D-erythro hydroxyls are involved in the formation of a five-membered ketal ring of the αC-type (10, 11, 12) with bulky substituents in the *cis*-configuration at carbons 2 and 3. This unfavorable conformation (VIII′ and X′) would be expected to cause the ketal ring to be labile to acid, since deformation from the preferred zigzag conformation is considerable.

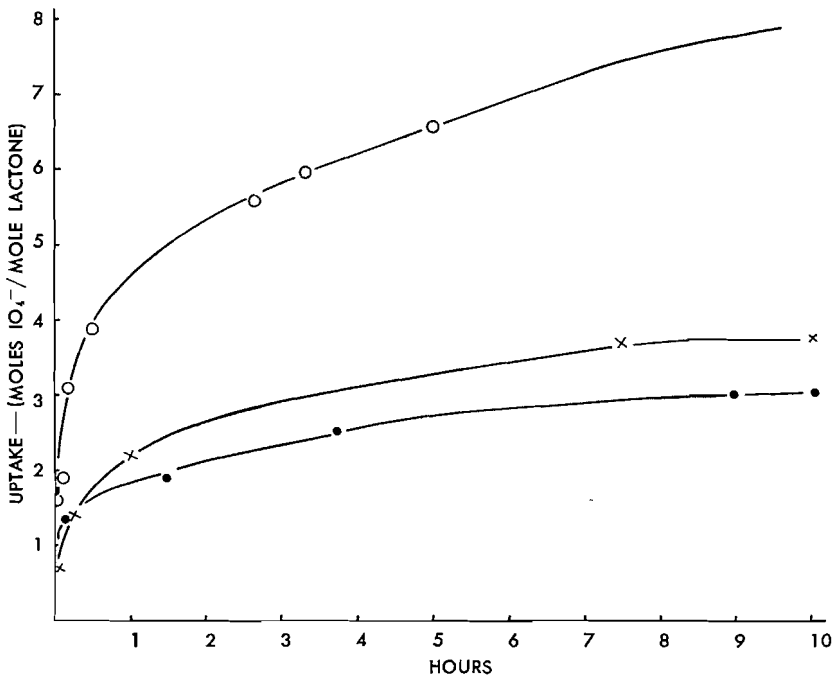

FIG. 1. Periodate oxidation of: —×— D-ribono-1→4-lactone (3.75–18.5 hours); —●— 5-*O*-methyl-D-ribono-1→4-lactone (3.05–21.0 hours); and —○— lactobiono-1→5-lactone (8.5–48 hours) (8.55–75 hours) at pH 3.7.

EXPERIMENTAL

Solutions were concentrated under reduced pressure (*ca.* 15 mm). Melting points were uncorrected and optical rotations were determined in water unless otherwise stated. Paper chromatography was carried out by the descending method (13) on Whatman No. 1 filter paper using the following solvent systems (v:v): (*a*) ethyl acetate – acetic acid – water (9:2:2); (*b*) ethyl acetate – acetic acid – formic acid – water (18:3:1:4); (*c*) butan-1-ol–ethanol–water (40:11:19); and (*d*) butan-1-ol–pyridine–water (10:3:3). Non-reducing compounds were detected on paper chromatograms with an alkaline

Can. J. Chem. Downloaded from www.nrcresearchpress.com by 78.46.186.204 on 09/04/12
For personal use only.

silver nitrate spray reagent (14). The rate of movement of the compound on paper chromatograms is quoted relative to that of the solvent front (R_f value). Wave numbers of infrared data are given to within ± 10 cm^{-1}.

*2,3-O-Isopropylidene-*D*-ribono-1→4-lactone*

(Assisted by R. J. Stoodley.) A solution of D-ribono-1→4-lactone (15 g) in acetone (600 ml) containing concentrated hydrochloric acid (6 ml) was shaken continuously for 18 hours at 25° C. The initial positive rotation decreased rapidly to reach a constant negative value (Table II). A control solution of D-ribono-1→4-lactone in dioxane and concentrated hydrochloric acid (2 drops) showed a relatively small change in optical rotation (Table II).

The solution was neutralized (silver or lead carbonate) and the inorganic salts were separated by filtration through a pad of cellulose. The combined filtrate and washings deposited crystals when concentrated. After trituration with cold acetone – light petroleum (b.p. 60–80° C), the crystals (14.0 g; 73.5%) were collected on a suction filter. They had a melting point of 138–139° C, $[\alpha]_D^{25°}$ −57.5° (initial value; *c*, 2.3) → −16.1° (20 days) and $[\alpha]_D^{24°}$ −65.7° (*c*, 2.13, pyridine; unchanged after 80 hours). ν_{max} 1790 cm^{-1} (chloroform; $C = 0$ for 1→4-lactone (15, 16)). D-Ribono-1→4-lactone gave an adsorption peak at 1793 cm^{-1} (nujol). Recrystallization from acetone–cyclohexane did not affect these constants. Anal. Calc. for $C_8H_{12}O_5$: C, 51.1; H, 6.4. Found: C, 51.4; H, 6.4.

When the condensation was catalyzed by 2 *N* hydrochloric acid (1% v:v), the rotation decreased less rapidly and reached a final rotation of $[\alpha]_D^{25°}$ −62.5° (30 hours).

A 5% solution of D-ribono-1→4-lactone in acetone revealed a polarimetric behavior similar to the acid-catalyzed reaction (Table II). After the optical rotation had reached a constant value, crystals of 2,3-*O*-isopropylidene-D-ribono-1→4-lactone were deposited, when the solution was concentrated.

TABLE II

OPTICAL ROTATION OF D-RIBONO-1→4-LACTONE IN VARIOUS SOLVENTS AT 25° C

Acidified acetone, c = 2.48	Hours:	0	0.33	0.5	2.8	3.8	15.8	18.3
	$[\alpha]_D$:	42.3°	−25°	−44.4°	−77.4°	−79°	−82.3°	−82.3°
Acidified dioxane, c = 2.5	Hours:	0	0.1	2.0	3.5	6.3	24.0	30.7
	$[\alpha]_D$:	52°	49.5°	48.5°	48°	46.8°	45°	43.6°
Water, c = 2.3	Hours:	0.25	23.0	42.5	66.2	90.5	138.5	322.8
	$[\alpha]_D$:	17.8°	17.4°	16.1°	14.8°	13.9°	11.7°	8.0°
Acetone, c = 5.0	Hours:	0.3	7	19	27	48	115	213
	$[\alpha]_D$ at 26° C:	39.8°	29.3°	7.4°	−3.9°	−24.2°	−48.7°	−65.2°

A solution of D-ribono-1→4-lactone (25 g) in acetone (500 ml) was heated under reflux in anhydrous conditions (calcium chloride tube). The optical rotation of the reaction mixture fell slowly, reaching a value of $[\alpha]_D^{25°}$ −8° after 92 hours. Anhydrous copper sulphate (5 g) was then added to the solution and the optical rotation fell to $[\alpha]_D^{25°}$ −77° (192.5 hours). The filtered solution was concentrated to a crystalline mass which was recrystallized from acetone – light petroleum (b.p. 60–80° C) to yield the *O*-isopropylidene derivative (21.5 g; 67%).

*2,3-O-Isopropylidene-5-O-methyl-*D*-ribono-1→4-lactone*

2,3-*O*-Isopropylidene-D-ribono-1→4-lactone (5.28 g) was treated three times with methyl iodide and active silver oxide (in the presence of anhydrous calcium sulphate), to aid solution chloroform was added to the first methylation. After filtration, the silver salts were thoroughly digested with chloroform. Concentration of the combined filtrates

Can. J. Chem. Downloaded from www.nrcresearchpress.com by 78.46.186.204 on 09/04/12
For personal use only.

yielded a pale yellow syrup (6.0 g) which was distilled at 90–100° C (bath temp.) and 10^{-5} mm to give the 5-*O*-methyl derivative [4.76 g; 84% with $n_D^{23°}$ 1.4490 at 90° C, $n_D^{23°}$ 1.4500 at 100° C, $[\alpha]_D^{27°}$ −56.8° (*c*, 3.0 ethanol), and $[\alpha]_D^{26°}$ −44.1° (*c*, 2.5)]. Anal. Calc. for $C_9H_{14}O_5$: C, 53.45; H, 7.0; OMe, 15.35. Found: C, 53.4; H, 7.5; OMe, 17.2.

5-O-Methyl-D-*ribono-1→4-lactone*

A mixture of a solution of 2,3-*O*-isopropylidene-5-*O*-methyl-D-ribono-1→4-lactone (4.5 g) in 40% aqueous acetone (100 ml) together with Amberlite resin IR-120 (H) (3 ml) was treated under reflux at 50° C. The initial specific rotation, $[\alpha]_D^{27°}$ −42.7°, rose to $[\alpha]_D^{27°}$ 9.5° (constant value; 60 hours). After it had been cooled, the solution was decanted from the resin, concentrated to a crystalline mass, and recrystallized from ethyl acetate to give 5-*O*-methyl-D-ribono-1→4-lactone (2.3 g; 63.5%) with m.p. 110–111° C, mixed m.p. 108.5–110° C, $[\alpha]_D^{25°}$ 26° (0.08 hours) → 19° (168 hours) (*c*, 0.94). R_f 0.71 (solvent *b*) and R_f 0.67 (solvent *d*). ν_{max} 1765 cm^{-1} (nujol) [lit. m.p. 109–110° C, $[\alpha]_D^{18°}$ 27.4° → 15.3° (7 hours; *c*, 9.0) (1)]. Anal.Calc. for $C_6H_{10}O_5$: C, 44.4; H, 6.2; OMe, 19.1. Found: C, 44.8; H, 6.2; OMe, 19.9.

5-O-Methyl-D-*ribitol*

A solution of 5-*O*-methyl-D-ribono-1→4-lactone (1.0 g) in anhydrous tetrahydrofuran (25 ml) was added dropwise to a suspension of lithium aluminum hydride (0.57 g) in tetrahydrofuran (25 ml). After the mixture had been heated under reflux for 4 hours, then cooled, ethyl acetate (2 ml) was added, followed by 70% aqueous alcohol (100 ml). The precipitate was separated by centrifugation and was washed twice with ethanol. The combined supernatants were percolated through Amberlite IR-120 (H) resin prior to concentration to a colorless syrup (0.78 g; 76%). Paper chromatographic examination of the compound revealed only a single spot with R_f 0.40 (solvent *b*), R_f 0.42 (solvent *d*), $[\alpha]_D^{25°}$ 10° (*c*, 1.0), and $n_D^{20°}$ 1.4802. Anal. Calc. for $C_6H_{14}O_5$: C, 43.4; H, 8.5; OMe, 18.7. Found: C, 43.5; H, 7.8; OMe, 20.6.

2,3-O-Isopropylidene-5-O-toluene-p-sulphonyl-D-*ribono-1→4-lactone*

2,3-*O*-Isopropylidene-D-ribono-1→4-lactone (1.13 g) was dissolved in cold (−20° C), anhydrous pyridine and toluene-*p*-sulphonyl chloride (2.38 g; 100% excess) was added in one portion. After the mixture had been kept for 10 hours at −20° C, with intermittent shaking, water (0.5 ml) was added and the solution was poured slowly into ice water (600 ml) with vigorous stirring. The crystals were collected by filtration and dried under reduced pressure at room temperature (2.07 g; 100%). Recrystallization from methanol gave prisms melting at 117.5–118° C and with $[\alpha]_D^{24°}$ −15.8° (*c*, 2.4 acetone). ν_{max} 1810 cm^{-1} (chloroform). Anal. Calc. for $C_{15}H_{18}O_7S$: C, 52.6; H, 5.3; S, 9.4. Found: C, 52.7; H, 5.3; S, 9.7.

2,3-O-Isopropylidene-5-deoxy-D-*ribitol*

To a suspension of lithium aluminum hydride (5.5 g) in anhydrous tetrahydrofuran (50 ml), a solution of 2,3-*O*-isopropylidene-5-*O*-toluene-*p*-sulphonyl-D-ribono-1→4-lactone (5.38 g) in tetrahydrofuran (50 ml) was added dropwise. The reaction mixture was heated under reflux for 5 hours, then ethyl acetate (20 ml) was slowly added dropwise, followed by 10% aqueous ethanol until the inorganic salts were precipitated. After filtration, the organic solvents were evaporated by repeated dilution with water and the product, obtained by continuous extraction with chloroform, was a syrup (2.38 g; 84%) with $n_D^{20°}$ 1.4510 and $[\alpha]_D^{27°}$ −15.5° (*c*, 2.7, ethanol). Anal. Calc. for $C_8H_{16}O_4$: C, 54.5; H, 9.15. Found: C, 52.9; H, 9.2.

Can. J. Chem. Downloaded from www.nrcresearchpress.com by 78.46.186.204 on 09/04/12
For personal use only.

Can. J. Chem. Downloaded from www.nrcresearchpress.com by 78.46.186.204 on 09/04/12
For personal use only.

TABLE III

RESULTS OF PERIODATE OXIDATION EXPERIMENTS

Compound	Determination	pH	Time (hours) 0.08	0.15	0.25	0.50	0.66	1.0	3.5	4.0	
D-Ribitol	Uptake*	7.5	4.0		4.0						(4.0–1.7 hr)
2,3-*O*-Isopropylidene-D-ribono-1→4-lactone	Uptake*	U	0.08		0.08		0.08	0.08			
Sodium 2,3-*O*-isopropylidene-D-ribonate	Uptake*	10		0.92	0.99	1.03		1.03	1.03		
	Formaldehyde*	10	0.94		0.95			1.02	1.02		
Sodium 5-*O*-methyl-D-ribonate	Uptake*		2.3		2.65	2.84		2.94	2.97	2.99	
	Formaldehyde*	10									(Nil–24 hr)
5-*O*-Methyl-D-ribono-l→4-lactone	Uptake*	3.7	1.38	1.34					2.52		(3.0–9.0 hr)
											(3.05–21 hr)
	Formaldehyde*	3.7									(Nil–13 hr)
5-*O*-Methyl-D-ribitol	Uptake*			2.23		2.38		2.48		2.50	
	Acid*									1.4	(1.5–20.5 hr)
	Formaldehyde*	U			0.88	0.88		0.89			
2,3-*O*-Isopropylidene-5-deoxy-D-ribitol	Uptake*	U		0.02	0.08	0.04		0.04			
5-Deoxy-D-ribitol	Uptake*	7.5	2.24			3.01			3.14	3.16	
	Uptake*	U	2.99			2.96					(2.96–2.0 hr)
											(2.96–22 hr)
	Acid*	U	1.78			1.85					(1.78–2.5 hr)
											(1.74–23 hr)
	Formaldehyde*	U			1.02	1.09				1.03	(0.99–16.5 hr)
2,3-*O*-Isopropylidene-D-ribitol	Uptake*	U		0.93		0.89		0.90			(0.92–18 hr)
	Formaldehyde*	U			1.05	1.0				1.0	(0.95–16 hr)

U = Unbuffered.
*In moles of periodate per mole substrate.

5-Deoxy-D-ribitol

The above *O*-isopropylidene compound (2.09 g) was hydrolyzed with Amberlite IR-120 (H) resin under the conditions previously described for the preparation of 5-*O*-methyl-D-ribono-1→4-lactone. The product (1.51 g; 93%) crystallized spontaneously when the solution was concentrated to dryness. Recrystallization from ethyl acetate – methanol (5:1 v:v) gave 5-deoxy-D-ribitol with m.p. 77–80° C. The product contained solvent of crystallization which could be removed under reduced pressure to give a product melting at 65–69° C and $[\alpha]_D^{25°}$ −10.6° (*c*, 1.7). Anal. Calc. for $C_5H_{12}O_4$: C, 44.1; H, 8.9. Found: C, 44.1; H, 8.6.

2,3-O-Isopropylidene-D-ribitol

2,3-*O*-Isopropylidene-D-ribono-1→4-lactone (1.50 g) was treated with lithium aluminum hydride by the method described for the preparation of 5-*O*-methyl-D-ribitol, except the reaction period was extended to 8 hours and the ion exchange resin, Amberlite IR-120, was used in the ammonium form. The syrupy product (1.6 g) moved on paper chromatograms as a single spot (R_f 0.39; solvent *b*) and had $[\alpha]_D^{26°}$ −4.3° (*c*, 2.8, ethanol), $n_D^{20°}$ 1.4730. Anal. Calc. for $C_8H_{16}O_5$: C, 50.0; H, 8.4. Found: C, 49.2; H, 8.0.

D-*Ribitol* (*Adonitol*)

2,3-*O*-Isopropylidene-D-ribono-1→4-lactone (130 mg) was dissolved in ethanol (5 ml) and sodium borohydride (93 mg) was added in one portion. The solution was heated at 50° C for 5 hours and then kept at room temperature overnight. After acidification with acetic acid, the solution was passed down a column of Amberlite resin IR-120 (H) and the effluent was evaporated to dryness. After removal of acetic and boric acids by repeated co-distillations with methanol, the syrupy product was hydrolyzed with 0.01 *N* sulphuric acid (10 ml, 3 hours, 95° C). The cooled solution was neutralized (barium carbonate), then filtered, and the filtrate concentrated to a syrup. Examination of the product in solvent systems (*a*) and (*c*) revealed a single component which had a rate of movement identical with that of an authentic specimen of adonitol. The syrup readily crystallized on seeding with adonitol (ribitol).

When the reduction was carried out using water as the solvent under the conditions described above, the major product was an acid (paper chromatography) and only a small amount of adonitol was detected.

Periodate Oxidation Experiments

All reactions were carried out in the dark and at room temperature (*ca.* 18°).

(i) *Determination of the Reacted Periodate*

The lactone or pentitol derivative (10–15 mg; accurately weighed) was dissolved in water or the required buffer solution containing 0.3 *M* sodium metaperiodate solution (1 or 2 ml). The total volume was made up to 10 ml with additional buffer solution. A blank was run concurrently. Aliquot portions (2 ml) were withdrawn at intervals and pipetted into phosphate buffer (pH 7.0; 25 ml) containing 20% potassium iodide solution (1–3 ml), and the liberated iodine was titrated with 0.01 *N* sodium thiosulphate solution using starch solution as indicator (17).

In some cases the lactone was hydrolyzed to the aldonic acid (sodium salt) with a slight excess of 0.01 *N* sodium hydroxide solution prior to the addition of the sodium metaperiodate solution and sufficient water to bring the total volume to 20 ml. (Buffer solutions: pH 7.5, 0.05 *M* sodium bicarbonate solution; pH 3.7, 0.05 *M* acetic acid – sodium acetate solution.)

Can. J. Chem. Downloaded from www.nrcresearchpress.com by 78.46.186.204 on 09/04/12
For personal use only.

(ii) *Estimation of the Formic Acid Produced*

Solutions containing *ca.* 5 mg of compound per milliliter of solution were oxidized with sodium metaperiodate solution under unbuffered conditions. At various intervals of time, ethylene glycol (1 ml) was added to aliquot portions (5 ml) and the acidic solution was titrated with 0.01 *N* sodium hydroxide solution using methyl red, screened with methylene blue as the indicator. A blank was run concurrently.

(iii) *Determination of the Formaldehyde Liberated*

Samples (2–4 mg; accurately weighed) were dissolved in water or buffer solution containing 0.3 *M* sodium metaperiodate solution (1 ml) and made up to 25 ml. At intervals, aliquot samples (1 ml) were withdrawn and the formaldehyde was estimated by the chromotropic acid method (18). A known weight of erythritol (periodate oxidized) was used as the source of formaldehyde for the preparation of the standard curve.

ACKNOWLEDGMENTS

The authors wish to thank Dr. G. R. Barker and Dr. D. C. C. Smith, of the University of Manchester, for a specimen of 5-*O*-methyl-D-ribono-1→4-lactone. They also wish to thank Mr. R. J. Stoodley for his assistance in the preparation of 2,3-*O*-isopropylidene-D-ribono-1→4-lactone, Messrs. B. S. Noyes and M. J. Graham for microanalyses, and Mr. M. C. B. Marshall for infrared absorption data. One of us (D.L.M.) thanks the Ontario Research Foundation for a grant which made this investigation possible.

REFERENCES

1. BARKER, G. R., NOONE, T. M., SMITH, D. C. C., and SPOORS, J. W. J. Chem. Soc. 1327 (1955).
2. DREW, H. D. K., GOODYEAR, E. H., and HAWORTH, W. N. J. Chem. Soc. 1237 (1927).
3. REHORST, K. Ann. **503**, 143 (1933). (*a*) BARKER, S. A., BOURNE, E. J., PINKARD, R. M., and WHIFFEN, D. H. Chem. & Ind. 658 (1958).
4. HOUGH, L., TAYLOR, T. J., THOMAS, G. H. S., and WOODS, B. M. J. Chem. Soc. 1212 (1958).
5. WARSI, S. A. and WHELAN, W. J. Chem. & Ind. 71 (1958). (*a*) COOKSON, R. C. Ann. Repts. (London), **54**, 173 (1957).
6. FURBERG, S. Acta Chem. Scand. **4**, 751 (1950).
7. REEVES, R. E. Advances in carbohydrate chemistry. Vol. 6. Academic Press, Inc., New York. 1951. p. 107.
8. BARKER, G. R. and SMITH, D. C. C. J. Chem. Soc. 1323 (1955).
9. LEVENE, P. A. and STILLER, E. T. J. Biol. Chem. **102**, 187 (1933).
10. BARKER, S. A. and BOURNE, E. J. J. Chem. Soc. 905 (1952).
11. BARKER, S. A., BOURNE, E. J., and WHIFFEN, D. H. J. Chem. Soc. 3865 (1952).
12. BARKER, S. A. and BOURNE, E. J. Advances in carbohydrate chemistry. Vol. 7. Academic Press, Inc., New York. 1952. p. 137.
13. PARTRIDGE, S. M. Biochem. J. **42**, 238 (1948).
14. TREVELYAN, W. E., PROCTOR, D. P., and HARRISON, J. S. Nature, **166**, 444 (1950).
15. ALI, M. E. and OWEN, L. N. J. Chem. Soc. 1074 (1958).
16. BELLAMY, L. J. The infra-red spectra of complex molecules. Methuen & Co. Ltd., London. 1954.
17. NEUMÜLLER, G. and VASSEUR, E. Arkiv Kemi, **5**, 235 (1953).
18. O'DEA, J. F. and GIBBONS, R. A. Biochem. J. **55**, 580 (1953).

Can. J. Chem. Downloaded from www.nrcresearchpress.com by 78.46.186.204 on 09/04/12
For personal use only.

Can. J. Chem. Downloaded from www.nrcresearchpress.com by 78.46.186.204 on 09/04/12
For personal use only.

THE REACTION OF 2,2-DIPHENYL-1-PICRYLHYDRAZYL WITH SECONDARY AMINES[1]

J. E. HAZELL[2] AND K. E. RUSSELL

ABSTRACT

The reaction of DPPH (2,2-diphenyl-1-picrylhydrazyl) with *N*-phenyl-1-naphthylamine, *N*-phenyl-2-naphthylamine, diphenylamine, and methylaniline has been studied and has been shown to be primarily a hydrogen abstraction process. Two moles DPPH react with 1–1.15 moles secondary amine to give 1.7–1.8 moles 2,2-diphenyl-1-picrylhydrazine and further products.

The reaction between DPPH and *N*-phenyl-1-naphthylamine is first order with respect to each reactant. The reaction of DPPH with the other amines is retarded by the major product 2,2-diphenyl-1-picrylhydrazine and the kinetics of the over-all reaction are complex. However second-order rate constants and activation energies have been obtained using initial rates of reaction. Possible reaction mechanisms are discussed.

This study of the reaction between 2,2-diphenyl-1-picrylhydrazyl (DPPH) and secondary amines forms part of a general investigation of the rates of hydrogen abstraction processes in solution using DPPH as the acceptor molecule. In spite of its existence as a stable free radical DPPH readily abstracts hydrogen atoms from mercaptans (1) and hydroaromatic compounds such as 1,4-dihydronaphthalene (2). A similar reactivity towards many secondary amines (3, 4), phenols, and hydrogen halides is observed. Rate studies on these reactions should give information concerning the influence of structure on the ease of hydrogen abstraction from the various donors.

As the acceptor molecule, DPPH has the advantage that it is a colored free radical which does not dimerize and its concentration can be estimated by its absorption in the visible region. However, it complexes with amines (3) and possibly with aromatic hydrocarbons (2) and such complexing may affect the kinetics of reaction. It may also be involved in steric effects which are not observed with small radicals.

In the present work the reactions between DPPH and certain secondary amines have been investigated with regard to stoichiometry and kinetics. It was hoped that the single hydrogen atom attached to nitrogen would be abstracted in the primary reaction. The secondary amines used were *N*-phenyl-1-naphthylamine, *N*-phenyl-2-naphthylamine, diphenylamine, and methylaniline. A few kinetic experiments were performed with di-*n*-propylamine.

EXPERIMENTAL

Materials

2,2-Diphenyl-1-picrylhydrazine and DPPH were prepared by the method of Goldschmidt and Renn (5). The hydrazyl crystals were heated to 75° *in vacuo* for 6 hours to break down a DPPH–chloroform complex.

Di-*n*-propylamine was distilled in a 20-plate column. Methylaniline was distilled under reduced pressure to give one sample. A second sample was obtained by conversion to the nitrosamine, followed by reduction with tin and hydrochloric acid and distillation. Diphenylamine was recrystallized from petroleum ether. The phenylnaphthylamines were recrystallized from 95% ethanol. The amines were stored in the dark.

[1]*Manuscript received in original form March 11, 1957, and, as revised, June 25, 1958.*
Contribution from the Department of Chemistry, Queen's University, Kingston, Ontario.
[2]*Milton Hersey Fellow 1955–56.*

Tetraphenylhydrazine was prepared by the oxidation of diphenylamine with lead dioxide (6). Diphenyldihydrophenazine was prepared by heating tetraphenylhydrazine in boiling toluene for 30 minutes (7); it was purified by dissolution in hot benzene and addition of 2 volumes of ethanol.

Alumina was deactivated by adding 500 g alumina to 20 cc water in a stoppered bottle.

Stoichiometry

Mixtures of DPPH and amine of varying ratio were made up in benzene, degassed, and heated to 55°. Reaction was virtually complete in less than an hour with the phenylnaphthylamines, but diphenylamine required some hours and methylaniline 2 days. If any significant amount of DPPH remained it gave a violet color to the solution. The results give an estimate of the number of moles DPPH reacting with 1 mole amine.

Benzene solutions of amine and DPPH, each at a known concentration (approximately 0.1 *M*), were heated to 55° until reaction was virtually complete, and were concentrated in an atmosphere of nitrogen. The products were separated on a column of deactivated alumina. Benzene was used as eluent.

The first fractions from the column contained the excess amine and part of the dehydrogenation products. The solvent was removed, and the amine was separated by careful treatment with small amounts of 95% ethanol in which the reaction products are almost insoluble; petroleum ether was used in the place of ethanol in the case of methylaniline. The phenylnaphthylamines and diphenylamine were identified by melting point and mixed melting point; methylaniline was identified by boiling point only. The excess amine was weighed in order to confirm the value of the DPPH to amine ratio determined colorimetrically.

The main fraction came down the column as a dark brown band. The solvent was removed from the eluate, the last traces of complexed benzene disappearing when the red solid was warmed *in vacuo*. The material was 1,1-diphenyl-2-picrylhydrazine, m.p. 170–171°, mixed m.p. 171–172°, and having an infrared spectrum identical with that of the pure hydrazine. It was weighed and the fraction of hydrazyl converted to hydrazine obtained. The infrared spectrum of the products in chloroform before separation on the column was compared with that of 1,1-diphenyl-2-picrylhydrazine at various concentrations. The results were consistent with the assumption that no hydrazine was produced or lost by reaction on the alumina column.

Further Products

In all cases a violet band of strongly adsorbed material appeared on the alumina column. It was removed by treating the alumina with ethanol. The yield was about 10% based on the amine reacting. The material was not identified, but a sample from the DPPH–diphenylamine reaction contained about 65% carbon suggesting that it was derived from the DPPH and was not simply a dehydrogenation product of the amine.

The first fractions from the column contained products derived from the dehydrogenated amine. The yields, based on the amine reacting, were 30%, 65%, 60%, and 40% respectively for methylaniline, diphenylamine, *N*-phenyl-1-naphthylamine, and *N*-phenyl-2-naphthylamine. In all cases some separation into bands occurred on the column, indicating the presence of more than one compound, but the separate fractions were impure judged by the wide temperature ranges over which they melted. A white solid, m.p. 128–132°, accounted for 40% of the amine reacting in the dehydrogenation of diphenylamine; the melting point was raised to 134–136° by admixture with tetra-

Can. J. Chem. Downloaded from www.nrcresearchpress.com by 78.46.186.204 on 09/04/12
For personal use only.

phenylhydrazine. Anal. Found: C, 86.37; H, 6.74. Calc. for $C_{24}H_{20}N_2$: C, 85.7; H, 6.00. Its infrared spectrum was almost identical with that of tetraphenylhydrazine; the absorption in the N–H stretching region was negligible, but weak bands below 1400 cm^{-1} indicate the possible presence of diphenyldihydrophenazine.

A yellow solid, m.p. 240–245°, accounted for 35% of the amine reacting in the dehydrogenation of *N*-phenyl-1-naphthylamine. Anal. Found: C, 87.4; H, 5.49. Calc. for $C_{32}H_{24}N_2$: C, 88.0; H, 5.54. Mol. wt. 480 (by Rast method). Oxidation of *N*-phenyl-1-naphthylamine with lead dioxide leads first to a red product and then to a yellow product, m.p. 266–268°, which gives the same analysis as the above solid. Infrared spectra of the two products are similar; a weak absorption at 3350 cm^{-1} is probably due to a minor impurity containing an N–H group. The yellow solid appears to be ultimately derived from two *N*-phenyl-1-naphthylamine molecules, but its structure is not known.

N-Phenyl-2-naphthylamine and methylaniline each gave a complex mixture of products. These were partially separated on the column but attempts to identify them were unsuccessful.

Kinetics

Reaction mixtures were prepared using measured amounts of benzene solutions of DPPH and amine. The reaction vessels were standard bore tubes of internal diameter 12 mm. The concentration of DPPH was followed by taking measurements of optical density with a Fisher electrophotometer. A 650 mμ filter was used because in this region the DPPH absorbs fairly strongly whereas the products of reaction absorb only weakly. The electrophotometer was adapted for constant temperature work by replacing the normal cell holder with a brass box with glass windows. Water from a Sargent thermostat was passed through the box by means of an Eastern Industries Circulating pump (Model B-1). Temperatures of 20°, 30°, 40°, and 50° were used and apart from the first 3 minutes of reaction the control was better than ±0.05°.

The experiments were normally performed in the presence of air. Experiments with degassed systems showed that oxygen had little or no effect on the initial rates of reaction. Degassing with the highly reactive phenylnaphthylamines was performed with the separate DPPH and amine solutions before they were mixed, so that the early stages of reaction could be observed.

For initial rate experiments, the amine concentrations used were in the range 1–5 $\times 10^{-4}$ *M* for the phenylnaphthylamines, 4–20$\times 10^{-4}$ *M* for diphenylamine, and 2–10$\times$ 10^{-3} *M* for methylaniline. The complete reactions were followed using concentrations some five times greater than these. The initial DPPH concentrations were in the range 6–30$\times 10^{-5}$ *M*.

No correction is required for the reaction of DPPH with the solvent, since experiments showed that the rate of this process is negligible at temperatures up to 50°.

TABLE I

STOICHIOMETRY OF REACTION OF DPPH WITH SECONDARY AMINES

Amine	DPPH (mM)	Amine reacting* (mM)	Amine reacting† (mM)	Hydrazine (mM)
N-Phenyl-1-naphthylamine	2.00	1.0	1.1	1.8
N-Phenyl-2-naphthylamine	2.00	1.0	1.1	1.8
Diphenylamine	2.00	1.15	1.2	1.76
Methylaniline	2.00	1.15	1.2	1.7

*From experiments involving disappearance of violet color of DPPH.
†From experiments involving isolation of excess amine.

Can. J. Chem. Downloaded from www.nrcresearchpress.com by 78.46.186.204 on 09/04/12
For personal use only.

Can. J. Chem. Downloaded from www.nrcresearchpress.com by 78.46.186.204 on 09/04/12
For personal use only.

RESULTS AND DISCUSSION

The results of the stoichiometric investigations are summarized in Table I.

The number of millimoles of amine reacting with 2 millimoles of DPPH was estimated (*a*) from experiments involving the disappearance of the violet color from reacting solutions, (*b*) from experiments involving the isolation of excess amine from solutions containing initially equimolar amounts of DPPH and amine. An uncertainty of up to 0.1 millimole arises in the first set of results because separate experiments have shown that some DPPH is removed by reaction with the products. The results of method (*b*) are maximum values, as the excess amine has probably not been completely isolated; 85–90% of the DPPH is recovered as 1,1-diphenyl-2-picrylhydrazine in each case.

The main process occurring is one of hydrogen abstraction by DPPH from the amine. In the case of diphenylamine the following evidence indicates that it is the amino hydrogen which is initially removed by the DPPH. Triphenylamine, a tertiary amine, does not react with DPPH at an appreciable rate. About 40% of the diphenylamine which reacts with DPPH is converted to tetraphenylhydrazine. Both lead dioxide and potassium permanganate oxidize diphenylamine to tetraphenylhydrazine showing that the amino hydrogen is most readily removed in related reactions. There is less definite evidence with the other amines. The yellow product from the *N*-phenyl-1-naphthylamine reaction shows only a weak N–H absorption in its infrared spectrum so that abstraction of the amino hydrogen certainly occurs in the reaction. Dimethylaniline reacts with DPPH at a very much lower rate than methylaniline. Whilst it is possible that attack by DPPH on a C–H bond does occur as a primary process in these reactions, attack on an N–H bond appears to be far more probable, and it is assumed here that it is the only important primary process.

The reactions are all retarded by the product 2,2-diphenyl-1-picrylhydrazine. Retardation is slight in the reaction of DPPH with *N*-phenyl-1-naphthylamine, but is quite considerable in other cases. For instance the addition of 2,2-diphenyl-1-picrylhydrazine at a concentration of 6×10^{-5} *M* to a solution containing *N*-phenyl-2-naphthylamine at a concentration of 5×10^{-4} *M* and DPPH at a concentration of 2×10^{-4} *M* reduces the initial rate of reaction by a factor of 3, and when the 2,2-diphenyl-1-picrylhydrazine concentration is increased to 15×10^{-5} *M* the rate is further reduced by a factor of 2. In order to obtain the rates of the unretarded reaction, the experimental results should be extrapolated back to zero reaction. However, the nature of the extrapolation is uncertain, and we have chosen to use as "initial rates" the rates of reaction after 3% reaction. These rates are close to the true values for *N*-phenyl-1-naphthylamine, but are less than the true values for the other amines.

The initial rate of reaction between DPPH and any of the amines is proportional to the concentration of DPPH and to the concentration of amine. This is readily understood if the primary process involves the attack of a molecule of DPPH on a molecule of amine, and this process is rate-determining in the initial stages of the reaction.

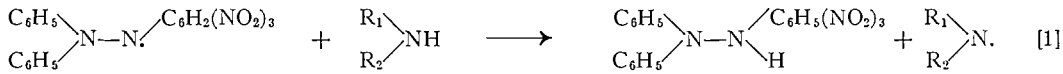

[1]

Rate constants (*k*) for this second-order reaction have been calculated from the rates of disappearance of DPPH, taking into account the stoichiometric results listed in Table I. The values of *k* at 20° have been recorded in Table II, together with activation energies (*E*) and frequency factors (*A*).

TABLE II

KINETIC RESULTS FOR THE REACTION OF DPPH WITH SECONDARY AMINES

Amine	k at 20° (cc/mole sec)	E (kcal/mole)	A (cc/mole sec)
N-Phenyl-1-naphthylamine	330	9.6	4.8×10^{9}
N-Phenyl-2-naphthylamine	580	11.0	1.1×10^{11}
Diphenylamine	53	12.8	2.3×10^{11}
Methylaniline	4.8	14.7	5.6×10^{11}

The value of E for the reaction with *N*-phenyl-1-naphthylamine is probably accurate to ±0.5 kcal/mole, but because of the difficulties associated with retardation by 2,2-diphenyl-1-picrylhydrazine, the other activation energies are not known to better than ±1 kcal/mole. The effect of structure on ease of abstraction of a hydrogen atom is clearly shown. The activation energies increase in going from the phenylnaphthylamines to methylaniline and this is associated with a considerable decrease in rate constant. Aliphatic amines are less reactive, the value of k at 20° for the reaction of DPPH with di-*n*-propylamine being approximately 0.2 cc/mole sec. The frequency factors are comparable to those obtained for reactions between DPPH and aliphatic mercaptans (1) and are of the same order as the frequency factors of hydrogen abstraction reactions involving methyl radicals (8). The relatively low value of the frequency factor for *N*-phenyl-1-naphthylamine is perhaps due to a steric effect.

The retardation of the reaction by the product 2,2-diphenyl-1-picrylhydrazine is explained by the reversal of reaction [1]; the concentration of amino radicals is reduced, and the over-all rate of reaction falls. The fall in rate can be adequately explained by the retarding effect of the diphenylpicrylhydrazine, and it is probable that complex formation between DPPH and amine, if it occurs, does not affect the kinetics of reaction.

Little information has been obtained in this study concerning the further reactions of the amino radicals. In the DPPH–diphenylamine reaction the following processes may be considered, among others:

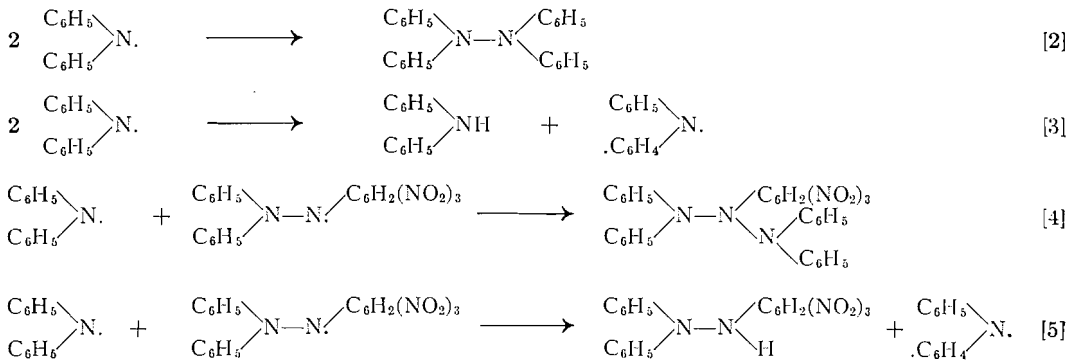

[2]

[3]

[4]

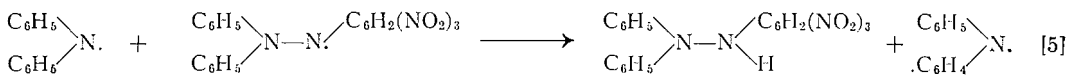

[5]

Reaction [2] occurs almost exclusively when diphenylamine is oxidized by lead dioxide at room temperature (6). It takes place to some extent in the dehydrogenation by DPPH as tetraphenylhydrazine accounts for about 40% of the products. It cannot occur exclusively, because this would require that 2 moles DPPH would react with 2 moles diphenylamine instead of the 1.2 moles diphenylamine observed experimentally. Reaction [3] involving the disproportionation of amino radicals probably occurs to some

Can. J. Chem. Downloaded from www.nrcresearchpress.com by 78.46.186.204 on 09/04/12
For personal use only.

extent at 55°, since tetraphenylhydrazine is slowly converted to diphenyldihydrophenazine in benzene solution at this temperature. Reaction [4] cannot be of great importance because 85–90% of the DPPH reacting is recovered as 2,2-diphenyl-1-picrylhydrazine. It is possible that the adduct is formed and then decomposes but infrared evidence indicates that such a decomposition does not take place on the alumina column. The disproportionation reaction [5] would help to explain the stoichiometric ratio of DPPH to diphenylamine observed experimentally. Attack at the ortho position may eventually lead to diphenyldihydrophenazine, but attack at the meta and para positions would give rise to more complex products. In the absence of a better knowledge of the dehydrogenation products further speculation on the secondary reactions does not appear to be warranted.

Two factors limit the accuracy of the kinetic results in Table II. In the first place, no allowance has been made for the possible primary attack of DPPH on C–H as well as on N–H bonds. Secondly, the retardation by 2,2-diphenyl-1-picrylhydrazine reduces the rate significantly with three of the amines even at 3% reaction, so that the rate constants quoted are less than the true values. Work in progress indicates that reactions involving phenols as donors are less subject to these limiting factors. It also shows that substituents in the aromatic ring may cause considerable changes in rates of dehydrogenation.

ACKNOWLEDGMENTS

The authors are grateful to the National Research Council and to the McLaughlin Research Fund of Queen's University for financial assistance.

REFERENCES

1. RUSSELL, K. E. J. Phys. Chem. **58**, 437 (1954).
2. BRAUDE, E. A., BROOK, A. G., and LINSTEAD, R. P. J. Chem. Soc. 3574 (1954).
3. BROOK, A. G., ANDERSON, R. J., and TISSOT VAN PATOT, J. Can. J. Chem. **36**, 159 (1958).
4. KUZ'MINSKIĬ, A. S. and ANGERT, L. G. Doklady Akad. Nauk S.S.S.R. **96**, 1187 (1954).
5. GOLDSCHMIDT, S. and RENN, K. Ber. **55**, 628 (1922).
6. WIELAND, H. and GAMBARJAN, S. Ber. **39**, 1499 (1906).
7. WIELAND, H. Ann. **381**, 200 (1911).
8. TROTMAN-DICKENSON, A. F. Quart. Revs. (London), **7**, 198 (1953).

Can. J. Chem. Downloaded from www.nrcresearchpress.com by 78.46.186.204 on 09/04/12
For personal use only.

DISSOCIATION CONSTANTS OF THE CYANOHYDRINS OF SOME TRITERPENE KETONES[1]

OWEN H. WHEELER[2] AND V. S. GAIND[3]

ABSTRACT

The reactivity of a number of triterpene ketones towards cyanohydrin formation is influenced by groups present in rings remote from the keto group. The results are interpreted as evidence of "conformational transmission" of the effects of the substituents.

INTRODUCTION

Barton and co-workers (1) have recently shown that the rate of condensation of a number of triterpene ketones with benzaldehyde is influenced by substituents in other rings. The effect does not seem to be electronic and Barton has suggested (1, 2) that the substituents cause small changes in valency angles and in the co-ordinates of the atoms, producing small distortions throughout the whole molecule, and effecting the reactivity of some substituent in the rings. The term "conformational transmission" has been introduced (3) for this new effect produced by substituents.

Similar effects have recently been observed in the formation of cyanohydrins from ring A keto steroids (4), and in their rates of reduction with sodium borohydride (5).

In the present work we have measured the dissociation constants of the cyanohydrins (in 80% dioxane–water) of a number of triterpene ketones. Most of these ketones were also used in the study of benzylidene derivative formation (1). The compounds used fall into four groups: (*a*) lanostan-3-one (I), lanost-8-en-3-one (II) and α-onoceradienedione (III), which lack an 8-methyl substituent; (*b*) germanicone (IV) and allobetulone (V), which have different substituents in ring E; (*c*) β-amyrone (VI), oleanonic acid (VII) and dehydro-β-amyrone (VIII), which have differences in rings C and D; and (*d*) α-amyra-9,11(12)-dien-3-one (IX) and α-amyra-12-en-3,11-dione (X), which have another carbon skeleton. The differences in reactivity (Table II) vary over a range of 2.1, while the corresponding values for benzylidene formation (1) differ within a range of 2.2.

DISCUSSION

If the effect was electrostatic in origin, those substituents with a greater charge separation, such as an acid or ketone group, would be expected to show the largest differences. However, oleanonic acid (VII) and allobetulone (V) are only a little more reactive than lanostan-3-one (I), in which there can be no electrostatic interaction. Moreover, the α,β-unsaturated ketone system of α-amyra-12-en-3,11-dione (X) has a smaller effect than the diene system of α-amyra-9,11(12)-dien-3-one (IX). On the other hand if the effect is due to changes in the conformation of the rings then double bonds would have the largest effect, since a double bond placed in a cyclohexane ring changes all its valency angles (6). In support of this lanost-8-en-3-one (II), β-amyrone (V), and germanicone (IV) show large differences in reactivity as compared to lanostan-3-one (I), and the greatest differences are shown by the homoannular dienes dehydro-β-amyrone (VIII) and α-amyra-9,11(12)-dien-3-one (IX).

[1]*Manuscript received May 15, 1958.*
Contribution from the Department of Chemistry, Dalhousie University, Halifax, N.S. Published as Part VII of Reactivity Studies on Natural Products. Part VI, Can. J. Chem. **36**, *1431 (1958).*
[2]*Present address: Department of Chemistry, University of Puerto Rico, Mayaguez, Puerto Rico.*
[3]*National Research Council Postdoctorate Fellow.*

Can. J. Chem. Downloaded from www.nrcresearchpress.com by 190.90.36.8 on 09/04/12
For personal use only.

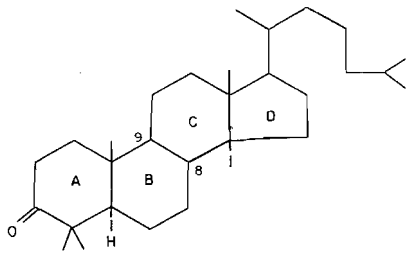

I; II $\Delta^{8(9)}$

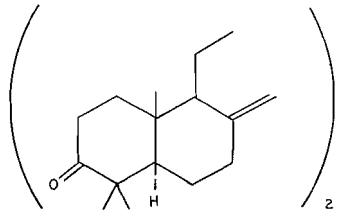

III

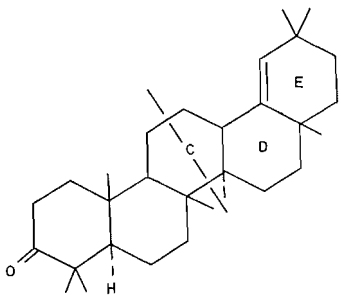

IV

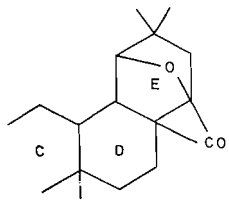

V

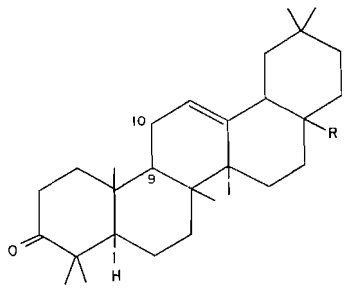

VI, R = Me

VII, R = CO_2H

VIII, $\Delta^{9(10)}$, R = Me

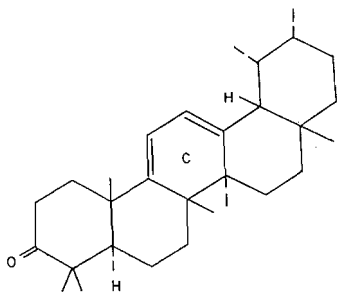

IX

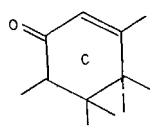

X, ring C

In cyclohexanone the α and γ axial groups are 2.37 Å apart (6), whereas in cyclohexane they are 2.53 Å apart (6). Thus in the triterpene ketones any interaction between the 4 and 10 axial methyl groups is reduced on forming the cyanohydrin, and in agreement with this lanostan-3-one (I) cyanohydrin is more stable than that of cholestanone.

A double bond placed elsewhere within the rings would be expected to increase the distortion in ring A, by "conformational transmission", and to increase the 1–3 axial methyl interference in the ketones. Such an effect would favor cyanohydrin formation

Can. J. Chem. Downloaded from www.nrcresearchpress.com by 190.90.36.8 on 09/04/12
For personal use only.

and the dissociation constants of the cyanohydrins of the unsaturated ketones are greater than those of the saturated ones. Moreover, those compounds having an axial methyl group at position 8, e.g. β-amyrone (VI), germanicone (IV), and dehydro-β-amyrone (VIII), form the more stable cyanohydrins. In these cases interaction between the 4, 10, and 8 axial methyl groups is possible.

The free-energy differences (calculated from $\Delta\Delta F = -RT \ln K_1/K$ at 25°) between the dissociation constant of the cyanohydrins of the various ketones are only small. Thus introducing a Δ^8 double bond (I and II) results in a difference of 0.11 kcal, in going from a double bond to a homoannular diene a difference of 0.17 kcal (VI and VIII), and changing a methyl group for a carboxylic acid grouping (VI and VII) a difference of 0.18 kcal. Changing the position of a double bond has little effect ($\Delta\Delta F = 0.05$ kcal for IV and VI).

The present results show a similar trend in the series of compounds studied as the results of Barton, Head, and May (1). However, the dissociation constant of the cyanohydrin of α-amyra-12-en-3,11-dione (X) shows a greater reactivity than expected. In this case the α,β-unsaturated ketone group may also have reacted with hydrogen cyanide (cf. cholest-4-en-3-one, ref. 4), and the measured dissociation constant may not be that of the 3-ketone cyanohydrin alone.

The experimental method was essentially that used in previous studies (4), but the equilibration time was increased to 20 to 25 hours. This will be more than sufficient, since Δ^8-lanosten-3-one reached equilibrium in some six hours (Table I).

TABLE I

REACTION LANOSTENONE WITH HYDROGEN CYANIDE*

Time, hours	Vol. 0.0020 N $Hg(NO_3)_2$, ml
0	0.98
1½	0.88
2½	0.85
3	0.83
3½	0.82
4½	0.78
6½	0.76
24	0.76, 0.75

*Initial concentrations, Δ^8-lanosten-3-one 0.00234 M, hydrogen cyanide, 0.00080 M, in 80% dioxane-water at 25.0°.

EXPERIMENTAL

Ketones

Many of the ketones were donated by Professor Barton.

Dehydro-β-amyrin was prepared by selenium dioxide oxidation of β-amyrin (7).

Lanost-8-en-3-one (II), β-amyrone (VI), and oleanonic acid (VII) were prepared by oxidation of the corresponding alcohols with chromium trioxide in pyridine (8).

Dissociation Constants

The triterpene ketones (25–30 mg) were dissolved in 80% aqueous dioxane (80 vol. purified dioxane + 20 vol. distilled water) (15 ml), and solutions of hydrogen cyanide (0.004 M, 5 ml) and 1% tri-*n*-propylamine (1 ml) in the 80% aqueous dioxane were added. The total volume was made up to 25 ml with the same solvent. The tightly stoppered flasks were allowed to equilibrate in a constant temperature bath, maintained at 25.0±0.1°, for 20–25 hours. Aliquots (5 ml) were then withdrawn and titrated with

Can. J. Chem. Downloaded from www.nrcresearchpress.com by 190.90.36.8 on 09/04/12
For personal use only.

aqueous mercuric nitrate solution (0.002 *N*), containing 5% nitric acid, using a capillary microburette. A freshly prepared solution of diphenylcarbazide in ethanol was used as indicator (9). The determinations were, in most cases, carried out in triplicate. The averaged results and their mean errors are given in Table II.

TABLE II

REACTIVITY OF TRITERPENE KETONES

	K_D^{HCN}*	k^{PhCHO}†
Dehydro-β-amyrone (VIII)	101±2	124
α-Amyra-9,11(12)-dien-3-one (IX)	110±1	115
Germanicone (IV)	125‡	—
β-Amyrone (VI)	135±3	108
α-Amyra-12-en-3,11-dione (X)	145±4	75
Lanost-8-en-3-one (II)	176±4	100
α-Onoceradienedione (III)	181±1	117
Allobetulone (V)	182±3	100
Oleanonic acid (VII)	185±2	97
Lanostan-3-one (I)	213±9	55
Cholestan-3-one	556±12	—

*Dissociation constants of cyanohydrins in 80% dioxane–water at 25.0°, from the present work.

†Rates of reaction with benzaldehyde at 25.0°, in 99% ethanol, relative to lanost-8-en-3-one = 100, ref. 1.

‡Only one determination.

Fredelin and 4,4-dimethylcholest-5-en-3-one were too insoluble in 80% aqueous dioxane for any measurements to be made. In aqueous dioxane containing less water, the dissociation constants were immeasurably high.

ACKNOWLEDGMENTS

The authors are very grateful to Professor D. H. R. Barton for initially suggesting this study and for generously supplying most of the compounds used. Dr. Estrada kindly furnished samples of germanicone, β-amyrin, and fredelin.

One of us (V.S.G.) is indebted to the National Research Council for the award of a Postdoctorate Fellowship.

REFERENCES

1. BARTON, D. H. R., HEAD, A. J., and MAY, P. J. J. Chem. Soc. 935 (1957).
2. BARTON, D. H. R. and HEAD, A. J. J. Chem. Soc. 932 (1956).
3. BARTON, D. H. R. XIVth Intern. Congr. Pure Appl. Chem. Experientia Suppl. II, 121 (1955).
4. WHEELER, O. H. and MATEOS, J. L. Can. J. Chem. **36**, 712 (1958).
5. WHEELER, O. H. and MATEOS, J. L. Can. J. Chem. **36**, 1049 (1958).
6. COREY, E. J. and SNEEN, R. A. J. Am. Chem. Soc. **77**, 2505 (1955).
7. RUZICKA, L. and JEGER, O. Helv. Chim. Acta, **24**, 1236 (1941).
8. POOS, G. I., ARTH, G. E., BEYLER, R. E., and SARETT, L. H. J. Am. Chem. Soc. **75**, 422 (1953).
9. PRELOG, V. and KOBELT, M. Helv. Chim. Acta, **32**, 1187 (1949).

Can. J. Chem. Downloaded from www.nrcresearchpress.com by 190.90.36.8 on 09/04/12
For personal use only.

Can. J. Chem. Downloaded from www.nrcresearchpress.com by 78.46.186.204 on 09/04/12
For personal use only.

NOTE ON THE INDUCTIVE AND MESOMERIC EFFECTS IN SUBSTITUTED BENZENE DERIVATIVES

C. SANDORFY

Inductive and mesomeric effects have become familiar terms with both organic and theoretical chemists since they were introduced by Ingold and others (1), and since the fundamental work of Wheland and Pauling (2). Among the numerous theoretical treatments we mention only those by Matsen (3, 4), who used an LCAO MO method combined with perturbation calculations, and by Murrell and Longuet-Higgins (5, 6), who used a simplified self-consistent field-molecular orbital method.

In 1949, the present author (7) published a series of diagrams of electronic charge distributions in monosubstituted benzene derivatives where, as in phenol or aniline, two electrons of the substituent can interact with the π-electrons of the benzene carbon atoms. The simple Hückel approximation of the LCAO MO method was used.

The extent of the mesomeric effect due to the addition of two more mobile electrons to the system depends in this approximation on the difference between the Coulombic integral, α_R, associated with the substituent, R, and α_C for a carbon atom. This difference is taken to be proportional to the corresponding difference in electronegativities or ionization potentials. The smaller these differences are, the easier it is for the electrons of the substituent to penetrate into the benzene ring orbitals.

The inductive effect is due to the fact that the presence of the substituent modifies the potential field in the benzene ring with the main result that the carbon linked to the substituent will have a somewhat increased electronegativity. This again may be represented by a supplement to its Coulombic integral, generally taken as a fraction of α_R.

It is interesting to see what would be the charge distribution if only the mesomeric or only the inductive effects are present. The purely mesomeric effect is obtained if we give an extra Coulombic integral to the substituent but none to the carbon linked to it. The purely inductive effect is obtained if we put the resonance integral between these two atoms, β, equal to zero and we give an extra Coulombic integral to the carbon atom linked to the substituent.

We have given $(\alpha_R - \alpha_C)$ the successive values of -2, -1, 0, 1, 2, and 3 in β units and to $(\alpha_{CR} - \alpha_C)$ one tenth of the respective values of the former difference. All the resonance integrals were taken to be the same, β (except of course the one necessary to compute the pure inductive effect).

In Fig. 1, the first row represents the pure mesomeric effect, the second row the pure inductive effect, and the third row the combined effect of the two. Electron charge densities (at the atoms) and bond orders (at the bonds) are as defined by Coulson and Longuet-Higgins (8). Overlap was neglected. The unit for the charges is the charge of an electron. Values greater than one represent partial negative charges, values smaller than one (or two for the substituent) partial positive charges. The second and third rows are taken from (7) and in the third row the last decimal is uncertain.

The diagrams in the third row having respectively $\alpha_R = 1$, 2, and 3 are probably fairly close to aniline, phenol, and fluorobenzene. $\alpha_R = -1$ would be close to phenylphosphine.

Figure 1 needs little comment. For positive values of α_R the mesomeric and inductive effects are opposed and practically additive. The positive charge on the substituent is

Can. J. Chem. Downloaded from www.nrcresearchpress.com by 78.46.186.204 on 09/04/12
For personal use only.

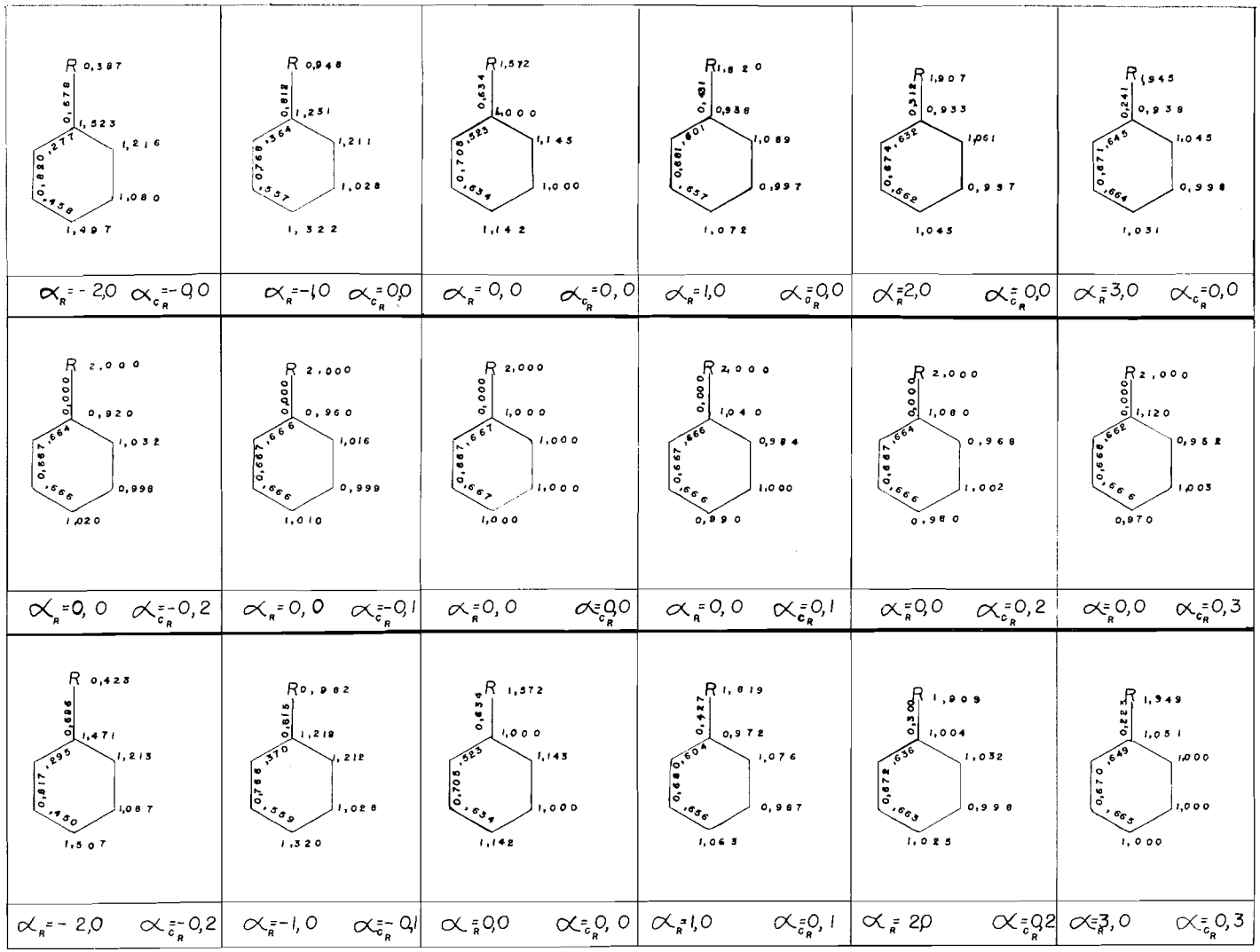

FIG. 1. First row: pure mesomeric effect. Second row: pure inductive effect. Third row: combined inductive and mesomeric effects. α_C is taken equal to zero.

determined only by the mesomeric effect, the negative charges in ortho and para by both effects. The ortho-para orienting character of the substituent is clearly brought out, as is the invariance of the meta position.

For negative values of α_R the situation is quite different. The very great positive charge appearing on the substituent because of the mesomeric effect is slightly diminished by the inductive effect, which from this point of view is again opposed to the mesomeric effect. The mesomeric effect sends a considerable negative charge into the para and ortho and even to the meta position, although much less to the last position. Curiously, the inductive effect leaves the ortho, meta, and para carbons practically unaffected.

Thus, while the inductive effect does not alter the charge on the substituent for positive values of $(\alpha_R - \alpha_C)$, it does influence the charges on the ring carbon atoms; the contrary is predicted for negative values of $(\alpha_R - \alpha_C)$ in this approximation.

The bond orders show that in the latter case, the benzene ring undergoes considerable deformation. The chemical behavior of the corresponding compounds should be interesting.

The inductive effect changes symmetrically if we change the sign of α_R but the mesomeric effect does not. The inductive effect affects not only the ortho position but also the para position.

As we know today, the simple approximation used to obtain these results is not very accurate. It has yielded, however, so many qualitatively correct results that our findings should have a relative interest even though the method does not correspond to the latest stage of development in theoretical chemistry.

The diagrams of the first row of Fig. 1 were obtained with the help of the Compution Centre of the University of Toronto. Free machine time was allotted by the National Research Council. The author wishes to express his thanks to these two institutions. Thanks are due to Professor D. Patterson for help in preparation of the manuscript.

RÉSUMÉ

Dans cet article on donne des diagrammes de répartition électronique représentant l'effet mésomère pur et l'effet inductif pur des substituants sur le noyau benzénique ainsi que leur effet simultané.

1. INGOLD, C. K. Chem. Revs. **15**, 225 (1934).
2. WHELAND, G. W. and PAULING, L. J. Am. Chem. Soc. **57**, 2086 (1935).
3. MATSEN, F. A. J. Am. Chem. Soc. **72**, 5243 (1950).
4. ROBERTSON, W. W. and MATSEN, F. A. J. Am. Chem. Soc. **72**, 5252 (1950).
5. MURRELL, J. N. and LONGUET-HIGGINS, H. C. Proc. Phys. Soc. A, **68**, 329 (1955).
6. MURRELL, J. N. Proc. Phys. Soc. A, **68**, 969 (1955).
7. SANDORFY, C. Bull. soc. chim. France, **16**, 615 (1949).
8. COULSON, C. A. and LONGUET-HIGGINS, H. C. Proc. Roy. Soc. A, **191**, 39 (1947).

RECEIVED AUGUST 18, 1958.
DEPARTMENT OF CHEMISTRY,
UNIVERSITY OF MONTREAL,
MONTREAL, QUEBEC.

THE CONFIGURATION OF GLYCOSIDIC LINKAGES IN OLIGOSACCHARIDES VII. 4-*O*-β-D-GALACTOPYRANOSYL-D-GALACTOSE FROM WHITE BIRCH WOOD*

J. K. GILLHAM, A. S. PERLIN, AND T. E. TIMELL

Partial acid hydrolysis of an α-cellulose prepared from white birch (*Betula papyrifera*) wood has led to the isolation of a new disaccharide (1). The disaccharide is now shown to be 4-*O*-β-D-galactopyranosyl-D-galactose.

**Issued as N.R.C. No. 4963 and as Paper No. 256 on the Uses of Plant Products.*

Can. J. Chem. Downloaded from www.nrcresearchpress.com by 78.46.186.204 on 09/04/12
For personal use only.

determined only by the mesomeric effect, the negative charges in ortho and para by both effects. The ortho-para orienting character of the substituent is clearly brought out, as is the invariance of the meta position.

For negative values of α_R the situation is quite different. The very great positive charge appearing on the substituent because of the mesomeric effect is slightly diminished by the inductive effect, which from this point of view is again opposed to the mesomeric effect. The mesomeric effect sends a considerable negative charge into the para and ortho and even to the meta position, although much less to the last position. Curiously, the inductive effect leaves the ortho, meta, and para carbons practically unaffected.

Thus, while the inductive effect does not alter the charge on the substituent for positive values of $(\alpha_R - \alpha_C)$, it does influence the charges on the ring carbon atoms; the contrary is predicted for negative values of $(\alpha_R - \alpha_C)$ in this approximation.

The bond orders show that in the latter case, the benzene ring undergoes considerable deformation. The chemical behavior of the corresponding compounds should be interesting.

The inductive effect changes symmetrically if we change the sign of α_R but the mesomeric effect does not. The inductive effect affects not only the ortho position but also the para position.

As we know today, the simple approximation used to obtain these results is not very accurate. It has yielded, however, so many qualitatively correct results that our findings should have a relative interest even though the method does not correspond to the latest stage of development in theoretical chemistry.

The diagrams of the first row of Fig. 1 were obtained with the help of the Compution Centre of the University of Toronto. Free machine time was allotted by the National Research Council. The author wishes to express his thanks to these two institutions. Thanks are due to Professor D. Patterson for help in preparation of the manuscript.

RÉSUMÉ

Dans cet article on donne des diagrammes de répartition électronique représentant l'effet mésomère pur et l'effet inductif pur des substituants sur le noyau benzénique ainsi que leur effet simultané.

1. INGOLD, C. K. Chem. Revs. **15**, 225 (1934).
2. WHELAND, G. W. and PAULING, L. J. Am. Chem. Soc. **57**, 2086 (1935).
3. MATSEN, F. A. J. Am. Chem. Soc. **72**, 5243 (1950).
4. ROBERTSON, W. W. and MATSEN, F. A. J. Am. Chem. Soc. **72**, 5252 (1950).
5. MURRELL, J. N. and LONGUET-HIGGINS, H. C. Proc. Phys. Soc. A, **68**, 329 (1955).
6. MURRELL, J. N. Proc. Phys. Soc. A, **68**, 969 (1955).
7. SANDORFY, C. Bull. soc. chim. France, **16**, 615 (1949).
8. COULSON, C. A. and LONGUET-HIGGINS, H. C. Proc. Roy. Soc. A, **191**, 39 (1947).

RECEIVED AUGUST 18, 1958.
DEPARTMENT OF CHEMISTRY,
UNIVERSITY OF MONTREAL,
MONTREAL, QUEBEC.

THE CONFIGURATION OF GLYCOSIDIC LINKAGES IN OLIGOSACCHARIDES VII. 4-*O*-β-D-GALACTOPYRANOSYL-D-GALACTOSE FROM WHITE BIRCH WOOD*

J. K. GILLHAM, A. S. PERLIN, AND T. E. TIMELL

Partial acid hydrolysis of an α-cellulose prepared from white birch (*Betula papyrifera*) wood has led to the isolation of a new disaccharide (1). The disaccharide is now shown to be 4-*O*-β-D-galactopyranosyl-D-galactose.

**Issued as N.R.C. No. 4963 and as Paper No. 256 on the Uses of Plant Products.*

Can. J. Chem. Downloaded from www.nrcresearchpress.com by 78.46.186.204 on 09/04/12
For personal use only.

The compound, isolated by chromatography on paper, crystallized from methanol. It had melting point 204°, $[\alpha]_D$ +68°, and a degree of polymerization (2) of 2.0. Complete acid hydrolysis with hot 0.1 *N* sulphuric acid required about 8 hours, indicative of the presence of a pyranosidic non-reducing end unit in the compound. The only detectable component sugar produced by hydrolysis was D-galactose, identified by its chromatographic behavior, specific rotation, and by conversion to crystalline galactose 1-methyl-1-phenylhydrazone.

In acetic acid solution the disaccharide consumed lead tetraacetate relatively slowly, 1.8 moles being taken up in 30 minutes, which is consistent with the oxidation of a 4-substituted aldohexose unit (3). When treated with 1.5 moles of oxidant it afforded a product which on hydrolysis yielded (chromatographic evidence) the expected products, i.e., galactose, lyxose, and threose (3, 4). In 90% acetic acid and in the presence of potassium acetate 1 mole of carbon dioxide was liberated at a rate almost identical with that for methyl α-D-galactopyranoside (5), suggesting that formic acid was produced only from the galactopyranosidic non-reducing end unit. Further, the corresponding figure for lead tetraacetate uptake was 3.9 moles, which allows for the required consumption of 2 moles by the non-reducing end unit and for degradation of the reducing end unit to a di-*O*-formyl tetrose derivative by cleavage of carbon–carbon bonds 1,2- and 2,3- (4). These data are consistent only with the formulation of a 1,4-D-galactopyranosyl-D-galactose structure for the disaccharide.

The new galactobiose is distinct from 4-*O*-D-galactopyranosyl-D-galactose derived from okra mucilage by Whistler and Conrad (6) and from pectic acid by Jones and Reid (7), since the latter disaccharide* gave a different X-ray powder diagram and has $[\alpha]_D$ +173°, in contrast to the current value of $[\alpha]_D$ +68°. It is clear, therefore, that the glycosidic linkage of galactobiose from birch possesses the β-configuration which, at the same time, confirms the presence of an α-linkage in the disaccharide from okra mucilage and pectic acid.

EXPERIMENTAL

Isolation of the Disaccharide

Alpha cellulose (400 g), prepared from white birch (*Betula papyrifera*) as described earlier (1), was heated with *N* sulphuric acid (2000 ml) at 95° C for 40 minutes. After neutralization with barium carbonate the hydrolyzate was deionized and the mixture of products formed was partially resolved by chromatography on Whatman 3 MM paper using ethyl acetate:acetic acid:water (9:2:2) as solvent. A second chromatographic separation, using butanol:pyridine:water (10:3:3), afforded five disaccharide fractions (1). After several weeks in methanol, one of these fractions (98 mg) yielded crystals (25 mg) having m.p. 204° C (corr.) and $[\alpha]_D^{20}$ +68° (equilibrium value; *c*, 1.0, water); degree of polymerization found by the end-group method of Peat, Whelan, and Roberts (2), 2.06. The X-ray powder diagram of the compound was distinct from that of 4-*O*-α-D-galactopyranosyl-D-galactose; interplanar lattice spacings in Å were as follows (relative intensities are given in parentheses): 7.85 (56), 6.56 (49), 5.40 (53), 4.50 (100), 3.76 (71), 3.50 (47), 3.05 (44), 2.7 (diffuse) (51), 2.3 (diffuse) (44), 2.15 (23), 2.05 (30), 1.84 (14), 1.60 (8), 1.46 (9), 1.40 (4).

D-*Galactose 1-Methyl-1-phenylhydrazone*

The disaccharide (2.74 mg) was taken up in 0.5 ml of 0.1 *N* sulphuric acid (found, $[\alpha]_D^{25}$ +66°, equilibrium value) and heated on the steam bath to constant rotation (α_D^{25} +0.22°±0.01°, 0.5 dm tube), which required 7.5 hours. After neutralization with Dowex-1

*The authors are grateful to Prof. R. L. Whistler for providing a sample of this compound.

Can. J. Chem. Downloaded from www.nrcresearchpress.com by 78.46.186.204 on 09/04/12
For personal use only.

resin (bicarbonate form) the hydrolyzate was examined by paper chromatography using three solvent systems, each chromatogram suggesting that galactose was the only product formed and showing the presence of a trace of unhydrolyzed disaccharide. Accordingly, the specific rotation of the sugar produced on hydrolysis was $[\alpha]_D^{25}$ +77° (*c*, 0.576, 0.1 *N* sulphuric acid); (D-galactose has $[\alpha]_D^{20}$ +80°).

To the neutral hydrolyzate 0.5 ml of ethanolic 1-methyl-1-phenylhydrazine acetate (8) was added; the solution was stored in the dark at 35° C for 12 hours and then at 4° C for 9 hours. Crystals which formed were filtered off, washed with cold ethanol, and dried. Melting point 189–190° C (corr.), undepressed on admixture with authentic D-galactose 1-methyl-1-phenylhydrazone, m.p. 190–191° C. The known and unknown derivatives gave X-ray powder diagrams which were indistinguishable from each other.

Lead Tetraacetate Oxidation of the Disaccharide

(*a*) The galactobiose (1.0 mg), in 0.04 ml of water, was taken up in acetic acid (1.0 ml) and a solution of lead tetraacetate (5.0 mg) in acetic acid (1.0 ml) was added at room temperature. At 10, 20, and 30 minutes aliquots (0.5 ml) were withdrawn and the lead tetraacetate consumption measured by microtitration. Found: 1.0, 1.5, and 1.8 moles/mole, respectively. Under the same conditions maltose consumed 0.8, 1.3, and 1.5 moles/mole, respectively.

(*b*) In another experiment the galactobiose (1.1 mg) was treated with an aliquot of the lead tetraacetate solution equivalent to 1.5 moles of oxidant/mole. A negative starch–iodide test was obtained within two hours, water (2.0 ml) was added, divalent lead was removed with excess Amberlite IR-120, and the suspension was heated on the water bath for 2 hours. Examination of the hydrolyzate on a paper chromatogram, using two solvent systems and aniline oxalate spray (9), showed the presence of products corresponding to threose, lyxose, and galactose, in addition to unhydrolyzed material.

(*c*) On oxidation in the Warburg respirometer in 90% acetic acid and in the presence of potassium acetate (5), the galactobiose (1.1 mg) yielded carbon dioxide (formic acid) at the following rate (comparative data is given for methyl α-D-galactopyranoside oxidized simultaneously), in moles/mole:

Time (minutes)	15	20	40	60	80	140
Galactobiose	0.33	0.80	0.97	1.02	1.04	1.09
Methyl galactoside	0.32	0.73	0.89	0.98	1.01	1.01

At 140 minutes the total consumption of lead tetraacetate was 4.95 moles/mole which, corrected for the oxidant used in converting formic acid to carbon dioxide (1.09 moles/mole), corresponds to a lead tetraacetate uptake of 3.86 moles/mole by the disaccharide.

1. GILLHAM, J. K. and TIMELL, T. E. Can. J. Chem. **36**, 1467 (1958).
2. PEAT, S., WHELAN, W. J., and ROBERTS, J. G. J. Chem. Soc. 2258 (1956).
3. CHARLSON, A. J. and PERLIN, A. S. Can. J. Chem. **34**, 1200 (1956).
4. PERLIN, A. S. Anal. Chem. **27**, 396 (1955).
5. PERLIN, A. S. J. Am. Chem. Soc. **76**, 5505 (1954).
6. WHISTLER, R. L. and CONRAD, H. E. J. Am. Chem. Soc. **76**, 1673 (1954).
7. JONES, J. K. N. and REID, W. W. J. Chem. Soc. 1890 (1955).
8. HIRST, E. L., JONES, J. K. N., and WOODS, E. A. J. Chem. Soc. 1048 (1947).
9. HORROCKS, R. H. Nature, **164**, 444 (1949).

RECEIVED AUGUST 1, 1958.
MCGILL UNIVERSITY AND PULP AND PAPER RESEARCH INSTITUTE OF CANADA,
MONTREAL, QUEBEC;
AND
PRAIRIE REGIONAL LABORATORY,
NATIONAL RESEARCH COUNCIL OF CANADA,
SASKATOON, SASKATCHEWAN.

Can. J. Chem. Downloaded from www.nrcresearchpress.com by 78.46.186.204 on 09/04/12
For personal use only.

Can. J. Chem. Downloaded from www.nrcresearchpress.com by 78.46.186.204 on 09/04/12
For personal use only.

ADDITION OF PYRROLES TO 1,4-BENZOQUINONE*

E. BULLOCK†

Several workers have observed the formation of colored products from quinones and pyrroles (1, 2). In the reaction, four hydrogens are lost between two molecules of pyrrole and one of quinone, hydroquinone being a by-product. The structure I (2) is incompatible with the infrared spectra of the benzoquinone adducts of 2,4-dimethylpyrrole (I*a*) and cryptopyrrole (I*b*), since these show a "bonded" NH band at 3360 cm^{-1}.

The cryptopyrrole adduct must therefore possess structure II*b* and since the ultraviolet and visible spectra of the two adducts are almost identical, the product from 2,4-dimethylpyrrole is formulated as II*a*. Structure II gives a satisfactory explanation of the intense color of the compounds and their behavior with acid.

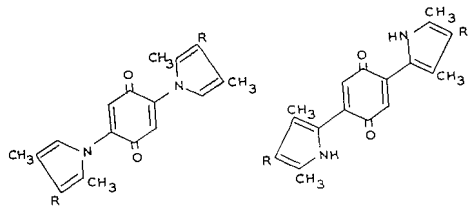

I

I*a*, R = H
I*b*, R = C_2H_5

II

II*a*, R = H
II*b*, R = C_2H_5

EXPERIMENTAL

The adducts were prepared according to Pratesi (2) and recrystallized from chloroform.

2,5-bis(2′,4′-Dimethyl-5′-pyrryl)p-benzoquinone (II*a*)

Calc. for $C_{18}H_{18}O_2N_2$: C, 73.41; H, 6.17; N, 9.97. Found: C, 73.26; H, 6.01; N, 9.55. λ_{max} (chloroform): 324, 545–552 mμ; log ϵ: 4.45, 4.37. Infrared spectrum: (saturated solution in chloroform, 1-mm cell) absorbed at 3360, 1618, 1385, 986, 965 cm^{-1}. Solution in *N,N*-dimethyl formamide was violet, turning yellow on addition of concentrated hydrochloric acid, the color being restored after neutralization.

2,5-bis(2′,4′-Dimethyl-3′-ethyl-5′-pyrryl)p-benzoquinone (II*b*)

Calc. for $C_{22}H_{26}O_2N_2$: C, 75.39; H, 7.49; N, 7.99. Found: C, 74.94; H, 7.36; N, 8.22. λ_{max} (chloroform): 327, 560–575 mμ; log ϵ: 4.49, 4.41. Infrared spectrum: (approximately 50% saturated solution in chloroform, 1-mm cell) absorbed at 3360, 1615, 1387, 1066, 993, 968 cm^{-1}.

Solution in *N,N*-dimethyl formamide was blue, turning very pale green on acidification; the solution became blue again on neutralization.

The analyses are by Mr. H. Seguin and the infrared determinations by Mr. R. Lauzon.

1. MOHLÄU, R. and REDLICH, A. Ber. **44**, 3605 (1911).
2. PRATESI, P. Gazz. chim. ital. **66**, 215 (1936).

RECEIVED AUGUST 28, 1958.
DIVISION OF PURE CHEMISTRY,
NATIONAL RESEARCH COUNCIL OF CANADA,
OTTAWA, CANADA.

*Issued as N.R.C. No. 4947.
†*National Research Council Postdoctorate Fellow.*

Can. J. Chem. Downloaded from www.nrcresearchpress.com by 190.90.36.8 on 09/04/12
For personal use only.

AN INFRARED CELL FOR SMALL GAS SAMPLES*

D. S. Russell

During the examination of some organic reaction products and the fractions from gas chromatographic separations, it was necessary to obtain the infrared spectra of very small gas samples. The conventional cylindrical gas cell usually provided for infrared work has a relatively large volume, most of which is not in the effective light path. A wedge-shaped metal cell has recently been available for small samples which provides much more efficient absorption of the light beam. Although the shape of this cell is quite satisfactory, there is no convenient method of transferring a gas sample to the cell completely from a vacuum system.

In order to overcome this problem, a glass cell was made whose volume conformed roughly to the shape of the converging light beam of a Perkin–Elmer model 21 spectrophotometer. In addition a small freeze-out tube was added to the bottom so that a small gas sample could be condensed from a vacuum system. Thus quantities of the order of 0.03 ml could be completely transferred to give satisfactory spectra in compounds which exhibited a normal absorption coefficient. Using a spectrophotometer equipped with scale expansion this limit could be extended considerably further.

The cell walls were constructed from flat pieces of pyrex glass fused together at the corners. A similar result could probably be obtained by flattening a slightly conical glass tube of appropriate dimensions. The ends were ground flat on abrasive paper on a plane surface. The sodium chloride windows were then sealed in place by a lead gasket which had been wetted with mercury. The cell assembly was clamped together in the usual way between two metal plates, and adjusted so that the light column fell on the slit when the cell was in place in the instrument.

The cell as illustrated has a light path of 5.0 cm and a total volume of 7.5 ml, which is approximately 1/10th the volume of the 5.0-cm conventional cell. Although some

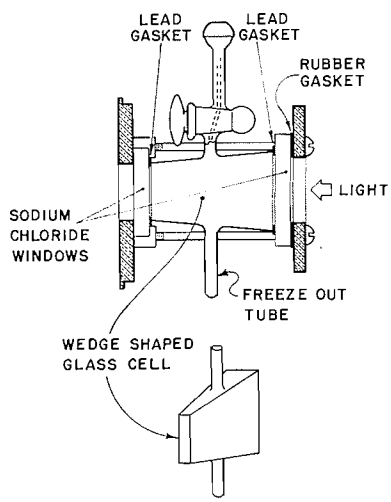

FIG. 1.

*Issued as N.R.C. No. 4940.

light was lost by the cell, it did extend the lower sample limit by at least a factor of five.

In use, packets of silica were fastened over the windows while the sample was being condensed into the cell by liquid nitrogen to prevent condensation of moisture on them.

RECEIVED SEPTEMBER 19, 1958.
DIVISION OF APPLIED CHEMISTRY,
NATIONAL RESEARCH COUNCIL,
OTTAWA, CANADA.

Can. J. Chem. Downloaded from www.nrcresearchpress.com by 190.90.36.8 on 09/04/12
For personal use only.